supported by

MINISTRY OF ENERGY AND MINERAL RESOURCES
REPUBLIC OF INDONESIA

hosted by

Indonesian Geothermal Association

THE 7th INDONESIA INTERNATIONAL
GEOTHERMAL
CONVENTION & EXHIBITION 2019
13 - 15 AUGUST 2019
JAKARTA CONVENTION CENTER

MAKING GEOTHERMAL THE ENERGY OF TODAY

PROCEEDING BOOK



endorsed by

Geothermal Resources Council GRC

IGA

www.iigce.com

Hosted by

Indonesian Geothermal Association

Supported by

Organized by

quad convex

member of Dyandra & Co.

Kompas Gramedia

MAKING GEOTHERMAL THE ENERGY OF TODAY

Proceeding

The 7th Indonesia International Geothermal Convention & Exhibition (IIGCE) 2019

13–15 August 2019, Jakarta Convention Center

Editor:

Abadi Poernomo, Aquardi Suminar
Suryantini, Ali Ashat
Doddy Astra, Grandy Bilhan Danakusumah
Marchel Christian Supijo

Reviewer:

Doddy Astra, Ginanjar
Suryantini, Christovik
Ali Ashat, Ashadi
Khasani, Yayan Sofyan
Aquardi Suminar, Ketut Sujata
Uum Komarudin, Budi Inderajaya
Riza Passiki, Fernando Pasaribu
Imam Baru Raharjo, Boyke Bratakusuma
Yunus Daud, Marino Baroek
Riki Irfan, Yudi Kusumah

Indonesian Geothermal Association

2020

MAKING GEOTHERMAL THE ENERGY OF TODAY

13 – 15 August 2019, Jakarta Convention Center

COMMITTEE

ADVISOR

F.X. Sutijastoto *(DIRJEN EBTKE)*

STEERING COMMITTEE

Ida Nuryatin Finahari *(DIR PANAS BUMI EBTKE)*
Prijandaru Effendi *(Chairman API)*
Abadi Poernomo *(API)*
Sanusi Satar *(API)*
Tafif Azimudin *(API)*
Ahmad Yuniarto *(API)*
Heribertus Dwiyudha *(API)*
Ali Mundakir *(PGE)*
Yudistian Yunis *(PLN)*
Ikbal Nur *(Geo Dipa)*

CHAIRMAN

Paul Mustakim *(SOL)*

VICE CHAIRMAN

Sapto Ciptadi *(PGE)*

SECRETARIAT

Dini (SOL)
Wini Rizkiningayu *(NZTE)*
Andry Sutanto *(API)*
Panggih Akbar *(API)*

TREASURY

Noppie Setiarto *(SOL)*
Amsal *(SE)*

MARKETING & FUND RAISING

Novan Ersytawan *(SOL)*
Mukawi Djumadin *(Tripatra)*
Win Sukardi *(Supreme)*
Vanny Widiana *(Tripatra)*

PUBLICATION/ OPENING CLOSING

Siska Tan *(Ormat)*
Ifnaldi Sikumbang *(API)*
Elvina Winda Sagala *(PGE)*

TECHNICAL PAPER

Doddy Astra *(SOL)*
Suryantini (*ITB*)
Ali Ashat *(ITB)*
Khasani *(UGM)*
Aquardi Suminar *(SEGSD)*
Uum Komarudin *(API)*
Riza Passiki *(SEGWWL)*
Imam Baru Raharjo *(PGE)*
Yunus Daud *(UI)*
Riki Irfan *(MPI)*
Ginanjar *(SEGSD)*
Christovik *(SOL)*
Ashadi *(KS Orka)*
Yayan Sofyan *(West JEC)*
Ketut Sujata *(Pertamina)*
Budi Inderajaya
Fernando Pasaribu *(PGE)*
Boyke Bratakusuma *(SEGWWL)*
Marino Baroek *(Supreme)*
Yudi Kusumah

COMMITTEE

PROTOCOL & GOVERNMENT RELATION

Kristyaningrum Yunita *(Medco)*
Rangga Wirapasa *(SOL)*
Ismoyo Aargo *(Supreme)*
Murdiono *(Ormat)*

CONVENTION & PRE-CONFERENCE WORKSHOP

Reza Arsyad *(SEGWWL)*
Amin Hantoni *(API)*

PHOTO COMPETITION

Yulnofrins *(Supreme)*
Kustiyah *(SEGSD)*
Syaiful Hidayat *(SEGWWL)*

FIELD TRIP

Iwan Azof *(SEGSD)*
Hadi Kuswoyo *(SEGSD)*
Imamul Ashuri *(SEGSD)*

Published by:
Asosiasi Panasbumi Indonesia (API)
2020

ISBN 978-602-52132-2-9

Sanksi Pelanggaran Pasal 72 Undang-Undang Nomor 19 Tahun 2002 Tentang HAK CIPTA

1. Barangsiapa dengan sengaja dan tanpa hak melakukan perbuatan sebagaimana dimaksud dalam Pasal 2 ayat (1) atau Pasal 49 ayat (1) dan ayat (2) dipidana dengan pidana penjara masing-masing paling singkat 1 (satu) bulan dan/atau denda paling sedikit Rp. 1.000.000,00 (satu juta rupiah), atau pidana penjara paling lama 7 (tujuh) tahun dan/atau denda paling banyak Rp. 5.000.000.000,00 (lima miliar rupiah).
2. Barangsiapa dengan sengaja menyiarkan, memamerkan, mengedarkan, atau menjual kepada umum suatu Ciptaan atau barang hasil pelanggaran Hak Cipta atau Hak Terkait sebagaimana dimaksud pada ayat (1) dipidana dengan pidana penjara paling lama 5 (lima) tahun dan/atau denda paling banyak Rp. 500.000.000,00 (lima ratus juta rupiah).

FOREWORD

To advance knowledge and capacity of its geothermal community, Indonesian Geothermal Association (INAGA) conducted the 19th Annual Scientific Gathering (PIT - Pertemuan Ilmiah Tahunan) in conjunction with the Annual Indonesian International Geothermal Convention & Exhibition (IIGCE) 2019.

The 7th IIGCE 2019 was held successfully on August 13th - 15th, 2019 at Assembly Hall the Jakarta Convention Center and attended by more than 1000 people around the globe. The 7th IIGCE 2019 is a continuous success of the annual events that have been held since 2013.

This year, the Committee of PIT as part of the 7th IIGCE event, has received 225 abstracts and 109 papers with various topics focusing on Earth Science, Engineering, General, Resources Management and Special Topics. Papers were presented in the Technical Papers Session during the 2 (two) days convention.

By this opportunity, I would like to express my gratitude and appreciation to the Technical Paper Committee, the Chairperson of Technical Paper Presentation, Authors, Presenters and all parties who have made the 2019 Technical Papers Session successful.

I believe that the content and the quality of all papers, with various interesting topics, were great and excellent. Therefore, on behalf of INAGA, I have the pleasure to share these papers for our geothermal community.

Yours truly,

Prijandaru Effendi
President of INAGA

This page is intentionally left blank

CONTENTS

Committee ii
Foreword v

EARTH SCIENCES 1
ENGINEERING 373
GENERAL 637
RESOURCES AND MANAGEMENT 755
SOCIAL, POLITICS, ECONOMICS, AND COMMUNITY 815

EARTH SCIENCES

OVERVIEW OF GEOTHERMAL RESOURCES OF NORTHERN ITALY 1-10
M. Verdoya, C. Pasqua, and P. Chiozzi

A CORRELATION OF MERCURY (HG) AND HYDROGEN SULFIDE (H_2S) GAS DISTRIBUTION WITH A FAULT STRUCTURE ON ULUBELU GEOTHERMAL SYSTEM 11-18
Taufiq, Atmojo J. P., Yunis, Budiraharjo S., Mujihardi B., Rozaq K., Maharani, and Saputra D. D.

A CORRELATION OF ARSENIC (AS) GAS DISTRIBUTION WITH SUBSURFACE TEMPERATURE LOG TO DETERMINE A HIGH TEMPERATURE ROCK OR STEAM ZONE ON ULUBELU GEOTHEMAL SYSTEM 19-24
Atmojo, J. P., Budiraharjo, S., Yunis, Taufiq, Mujihardi, B., Rozaq, K., Maharani, and Saputra, D. D.

THE GEOTHERMAL EXPLORATION OF THE EAST AFRICAN RIFT SYSTEM: RECENT ADVANCES 25-36
C. Pasqua, M. Verdoya, and P. Chiozzi

ABSOLUTE DATING OF THERMAL HISTORY USING THERMOLUMINESCENCE 37-44
Stephen Simamora, Dikdik Risdianto, and Nizar Muhamad Nurdin

INTEGRATING OF GEOMAGNETIC DATA AND VERTICAL ELECTRICAL SOUNDING FOR IDENTIFICATION OF RESERVOIR AND GEOTHERMAL FLUIDS IN GEOTHERMAL PROSPECT RAJABASA MOUNTAIN 45-54
Syamsurijal Rasimeng, Jakasura Leandro Tarigan, Ditha Arlinsky. Ar, and M. Ikhsan Fadhillah

THE APPLICATION OF EXPERIMENTAL DESIGN USING THREE-LEVEL FULL FACTORIAL DESIGN FOR PROBABILISTIC RESOURCE ASSESSMENT IN ATADEI GEOTHERMAL FIELD, INDONESIA 55-70
Marchel Christian Supijo, Heru Berian Pratama, and Sutopo

POWER DENSITY UPDATE OF INDONESIAN FIELDS 71-76
Maxwell Wilmarth, James Stimac, and Gugi Ganefianto

INTEGRATED ADVANCE FRACTURE ANALYSIS: A CASE STUDY FROM FALLON FORGE WELL 21-31, NEVADA USA 77-94
Pasca Siburian, Tito Perdana, Heri Tanjung, Merza Adeyosfi, Leonora Lilasari, and Sonny Wiyoga

GEOTERMAL ACTIVE MANIFESTATIONS IN NON-VOLCANIC AREA OF SOUTH EAST SULAWESI, INDONESIA 95-108
Anna Yushantarti and Dudi Hermawan

COMPREHENSIVE STUDY OF HOT SPRINGS POTENTIALS IN LOJING GEOTHERMAL COMPLEX, MALAYSIA 109-122
Mohammad Noor Akmal Anuar, Mohd Hariri Arifin, Hassan Baioumy, Che Aziz Ali, Kamal Roslan, Akma Din, Norsafina, and M. Hasiib Mansor

CHARACTERIZATION OF CHANGING SURFACE MANIFESTATIONS IN AN EXPLOITED GEOTHERMAL FIELD – HIGH ENTHALPY SYSTEM IN INDONESIA 123-130
Lily Suherlina, Maren Brehme, Juliet Newson, and M. Yustin Kamah

EVOLUTION OF BEUNGGA GEOTHERMAL SYSTEM REVEALED FROM SURFACE MANIFESTATION 131-138
Aidina Anisa, Niniek Rina Herdianita, and Dede Iim Setiawan

GEOLOGY OF MT. RATAI-PESAWARAN HYDROTHERMAL SYSTEM, LAMPUNG, INDONESIA 139-150
Tri Bagus Prabaswara and Niniek Rina Herdianita

IDENTIFYING OF GEOTHERMAL MANIFESTATION EXISTENCE AND CHARACTERIZATION OF SULPHIDATION TYPE USING LANDSAT-8 IMAGE PROCESSING RESULTS: CASE STUDY OF MOUNT PAPANDAYAN AREA, GARUT REGENCY, WEST JAVA PROVINCE 151-166
Sinatrya Diko Prayudi, Daffa Arrofi, and Rinal Khaidar Ali

AN OVERVIEW GEOCHEMISTRY IN SORIK MARAPI GEOTHERMAL FIELD 161-176
Ryan Hidayat, Ridha Hendri, and Vicky Chandra

IDENTIFICATION OF HEAT SOURCE AND STRUCTURE USING GRAVITY AND MAGNETIC DATA INTEGRATION ON NON-VOLCANIC GEOTHERMAL SYSTEM OF PARANG WEDANG 177-186
Muhammad Zaki and Nadya Noorvita

PRECISION GRAVITY MONITORING OF SALAK GEOTHERMAL FIELD: INSIGHT AND CONSTRAINTS FOR NUMERICAL SIMULATION 187-202
M. Wildan Perdana, Fikri Rahmansyah, and Gregg Nordquist

ANALYSIS OF OPTIMUM STATION SPACING IN MAGNETOTELLURIC DATA ACQUISITION BY USING 3-DIMENSIONAL FORWARD AND INVERSE MODELLING FOR GEOTHERMAL EXPLORATION 203-214
Dhara Adhnandya Kumara, Yunus Daud, Rifqa Agung Wicaksono, Wahyu Noor Iqwan, Fikri Fahmi, and Ewin Rahman Dzuhri

IDENTIFICATION OF GUCI, TEGAL, CENTRAL JAVA, GEOTHERMAL MANIFESTATION BASED ON GEOLOGICAL GUIDE 215-222
Arhananta Anggita Mahyudani, Antu Ridha Falkhan Barizi, Riko Dwi Kurniawan, Oscarino Hunaifi Ahmad, and Agus Harjanto

DETERMINATION OF GEOTHERMAL RESERVOIR CHARACTERISTIC AND HYDROTHERMAL ALTERATION MODEL BASED ON COMPREHENSIVE SURFACE MAPPING, GEOCHEMICAL, AND XRD ANALYSIS: CASE STUDY OF WIROGOMO AREA 223-234
Saifullah Fatah Al-Ayyubi, Garindra Yogiswara, Nabilah Afifah Habni Harahap, Arief Budiman Ustiawan, and Navendra Chista Yogatama

SEA EFFECT ANALYSIS IN MAGNETOTELLURIC DATA USING FORWARD AND INVERSE 3-D MODELING FOR GEOTHERMAL EXPLORATION 235-246
Ewin Rahman Dzuhri, Yunus Daud, Fikri Fahmi, Wahyu Noor Ikhwan, and Dhara Adhnandya Kumara

FAULT FRACTURE DENSITY (FFD) AND ALTERATION ZONE ANALYSIS TO DETERMINE FLUID-ROCK INTERACTIONS TO ENSURE EFFECTIVE DECISION MAKING OF PROSPECTIVE FIELDS IN MOUNT TELOMOYO, SEMARANG 247-252
Astri Yunita, Muhammad Ali Akbar, and Velayati Salim

NEW GEOTHERMAL EXPLORATION CONCEPT BASED ON CIRCULAR FEATURE OF LOW BOUGUER ANOMALY: MAGNETOTELLURIC DATA OF WEST JAVA GEOTHERMAL PROSPECT AREA AS THE EVIDENT OF NEW GEOTHERMAL EXPLORATION 253-256
Eddy Gaffar, Yayat Sudrajat, and Haryadi Permana

KEPAHIANG GEOTHERMAL VOLUMETRIC POTENTIAL USING MONTE CARLO SIMULATION 257-264
Wisnu Ardhi Nugroho, Arino Mangihut Tua Sitanggang, and Daniel Marpaung, Ivan

COMPARING HORNER & WAPLES IN TEMPERATURE PREDICTION 265-268
Muhammad Syarif Fadhlurrahman and Kris Pudyastuti

REMOTE SENSING AND GEOLOGICAL MAPPING METHOD FOR GEOTHERMAL PROSPECT ANALYSIS: CASE STUDY OF TELOMOYO GEOTHERMAL SYSTEM, CENTRAL JAVA 269-278
Lestari Butarbutar, Kristina Sarah Yuliana, and Elena Sekar Rahayu

GEOTHERMAL EXPLORATION USING APPLICATIONS GEOLOGICAL MAPPING, FFD SRTM, MODELLING CONCEPT OF STRUCTURAL CONTROL, PETROGRAPHY AND HOT WATER GEOTHERMOMETER ANALYSIS TO IDENTIFICATION AND EVALUATION POTENTIAL OF VOLCANO GEOTHERMAL ENERGY AT CANGAR, EAST JAVA 279-298
Yoyok Ragowo Siswomiharjo, Desi Kiswiranti, Venny Ayu Syafriani, Pamela Felita Adibrata, Agung Candra Setiawan, and Dessensa

DETECTING THE EXISTENCE OF ALTERATION MINERALS IN THE ACTIVE GEOTHERMAL AREA OF TANGKUBAN PERAHU MOUNTAIN AND SURROUNDING AREAS USING RESULTS OF LANDSAT-8 PROCESSING TO IDENTIFY DISTRIBUTION SURFACE CONDITION CHANGES FROM THE HYDROTHERMAL PROCESS 299-310
Sinatrya Diko Prayudi, Daffa Arrofi, and Rinal Khaidar Ali

INVESTIGATION OF GEOTHERMAL POTENTIALS OF MOUNTAIN LAMONGAN BASED ON MORPHOSTRUCTURE AND GEOCHEMICAL ANALYSIS 311-316
Arhananta, Kenny Lekatompessy, M. Alhafiq Wahyu Nabillah, Nazwa Khoiratun Hisan, and Agus Harjanto

GEOELECTRICAL STRIKE VS GEOLOGICAL STRIKE TENSOR ROTATION IN 2-D MODELLING OF MAGNETOTELLURIC DATA. STUDY CASE: BONJOL GEOTHERMAL AREA, WEST SUMATERA 317-326
Paulus Febrianto Pandu Wibowo, Wiwid Joni, and Hafiz Hamdalah

HYDROTHERMAL CYCLE ESTIMATION BASED ON RECHARGE AND DISCHARGE ZONE IDENTIFICATION USING GRAVITY METHOD AND GEOCHEMISTRY FLUID ON ARJUNO-WELIRANG COMPLEX, EAST JAVA 327-336
Bramasta Adya Dewanta, Ibanes Pramitasari, Tria Ainur Rokhis, Novia Dwi Rantikasari, and Cholisina Anik Perwita

ANALYSIS OF FAULT AND DISTRIBUTION FLUID GEOTHERMAL USING DEM SATELLITE IMAGE DATA, LANDSAT 8 OLI/TIRS AND SATELLITE GRAVITY IN THE VILLAMASIN GEOTHERMAL AREA, JAYAPURA DISTRICT, EAST OKU REGENCY 337-342
Jakasura Leonardo Tarigan and Elsadella Nindya Putri

SEA WATER DESALINATION USING DISTILLATION METHOD BY UTILIZING THE GEOTHERMAL POTENTIAL OF TEMBOKO LEHI BEACH AS A SOLUTION OF DROUGHT IN SIAU TAGULANDANG BIARO DISTRICT, NORTH SULAWESI 343-346
Nikita Christina, Ratna Pertiwi, Muhammad Rizqy Septyandy, and Nurchasanah Ananda Sari

FAULT STRUCTURE AND GEOTHERMAL SYSTEM ANALYSIS BASED ON GRAVITY INVERSION MODEL, MAGNETOTELLURIC AND GEOCHEMISTRY OF GEOTHERMAL PROSPECTING FIELD WAI SELABUNG SOUTH SUMATERA 347-362
Clara Armiliany, David Suganda Putra Manurung, Davit Manalu, Suharno, and Karyanto

GEOLOGY AND THE RELATIONSHIP OF LINEAMENT DENSITY WITH GEOTHERMAL MANIFESTATION DISTRIBUTION IN NORTHERN BAJAWA AREA, NGADA DISTRICT, EAST NUSA TENGGARA PROVINCE, INDONESIA 363-372
Astri Indra Mustika, Agung Setianto, and Agung Harijoko

ENGINEERING

REPRESENTATIVE RESULTS AND COSTS SAVED: SLIM HOLE 373-382
Ingo P.C. Rott

GEOCHEMISTRY ROLE IN GEOTHERMAL BINARY BRINE IN THE FIRST INTEGRATED COMBINE CYCLE POWER PLANT OPERATION IN INDONESIA: SARULLA CASE STUDY 383-390
Muhamad Andhika, Mona Natalia Siahaan, Sanif Isa Aritonang, Rizvy Asnin Nasution, Sahat Berutu

THERMO-HYDRO-MECHANICAL MODELING TO SIMULATE LAHENDONG GEOTHERMAL FIELD 391-400
Muhammad Qarinur, Hideaki Yasuhara, Naoki Kinoshita, Sho Ogata

THERMODYNAMICS AND PROCUREMENT COST ANALYSIS OF DEVELOPING BINARY CYCLE FROM BACK PRESSURE TURBINE POWER PLANT IN FLORES, INDONESIA 401-408
Naufal Nandaliarasyad, Dimas Taha Maulana, Reza Adiprana, Prihadi Setyo Darmanto

ORC, AN EFFICIENT AND DEPENDABLE SOLUTION FOR MODERN GEOTHERMAL APPLICATIONS, TURBODEN'S EUROPEAN EXPERIENCE 409-414
Joseph Bonafin and David Paul

DRILLING COST REDUCTION INITIATIVES FOR GEOTHERMAL DRILLING 415-422
Yudi Hartono, Ashadi, Sentanu W. Reksalegora

CORROSSION PREVENTION OF BURRIED REINJECTION PIPELINE USING GEOTHERMAL-POWERED IMPRESSED CURRENT CATHODIC PROTECTION IN LAHENDONG GEOTHERMAL AREA 423-430
Viqar Adly Gani, Achmad Ardialim, Ahmad Indra Sakti, Luhung Pravubinantaka, Albarrosyah Putra

A THERMAL CASING CONNECTION TEST FOR GEOTHERMAL WELLS IN KS ORKA 431-440
M. Fahmi.Sungkar, Hendra Simanjuntak, Boga Isa, Ashadi Ashadi, and Yudi Hartono

GEOTHERMAL CEMENTING DESIGN AND METHODOLOGY ENHANCEMENT IN WAYANG WINDU 441-448
Eric Tanoto, Allam Putra Rachimillah, Cinto Azwar, Febra Sakti Dewa, and Tommy Souvanir

OBTAINING ULTIMATE ZONAL ISOLATION IN GEOTHERMAL WELL: RECOMMENDATION & BEST PRACTICE OF GEOTHERMAL WELL CEMENTING DESIGN & OPERATION 449-454
Allam Putra Rachimillah, Eric Tanoto, and Cinto Azwar

ACHIEVEMENTS AND CHALLENGES TO UTILIZE EXPLORATION WELLS INTO DEVELOPMENT OF COMMERCIAL GEOTHERMAL POWER PLANTS, CASE STUDY ULUMBU 4 X 2.5 MW 455-466
Sugeng Triyono, Dwi Handoyo Saputro, and Budi Wibowo

FUJI GEOTHERMAL ORC POWER GENERATION SYSTEM 467-472
Hiroshi Oyama and Shigeto Yamada

UTILIZATION OF SURFACE GEOTHERMAL MANIFESTATION (STEAMING GROUND) AS SMALL-SCALE ELECTRICAL POWER PLANT IN KAWAH MATI KAMOJANG, GARUT REGENCY: THERMOELECTRIC COOLER TECHNOLOGY 473-478
Navendra Chista Yogatama, Dani Muhamad Iqbal, Hezron Christian Marbun, Kodrat Cahyo Wicaksono, and Meliana Atmika

SALAK TURBINE ROTOR SUSCEPTIBILITY ANALYSIS AGAINST SULFIDE STRESS CRACKING 479-488
Diva E. Nataprawira and Adrian Muskan

DEVELOPMENT OF THE FIRST DUAL FLASH GEOTHERMAL POWER PLANT IN INDONESIA 489-494
Munggang H. Purnanto, Stefanus Wisanto, and Ruswanto bin Nurudin Data

A SIMPLE PREDICTION AND APPROACH TO DETERMINE RESERVOIR PRESSURE 495-498
Erwandi Yanto, Gamal Hastriansyah, Ahmad Fahmi Fanani, M. Bayu Saputra, Fadiel Evan Marastio, Fernando Pasaribu, and Marihot S.P. Silaban

NITROGEN LIFTING METHOD TO DISCHARGE GEOTHERMAL WELLS 499-508
Erwandi Yanto, Gamal Hastriansyah, Ahmad Fahmi Fanani, M. Bayu Saputra, Fadiel Evan Marastio, Fernando Pasaribu, and Marihot S.P. Silaban

DESIGN AND APPLICATION OF AERATED AND FOAM DRILLING FLUID, CASE STUDY IN DRILLING OPERATION IN INDONESIA 509-518
Wisnu Adi Nugroho, Ali Imran Rangkuti, and Satria Hermawan

HYBRID DRILL BIT TECHNOLOGY, IMPROVED ROP, DRILLED INTERVAL AND CONTRIBUTED TO 96 HOURS CUMULATIVE SAVING IN ONE GEOTHERMAL WELL IN SOUTH SUMATERA OPERATION 519-530
Mohammad Khairanto Nugroho and Son N. Pham

SUPERHYDROPHOBIC SELF CLEANING LAYER IN PIPE SCALING 531-534
Cynthia Dewi Susanto, Jose Prima Boang Manalu, Ignatius Bernadi, and Roynaldo Lumban Batu

DARAJAT GEOTHERMAL POWER PLANT PROTECTION SYSTEM IMPROVEMENT 535-540
Nixon Manik and Bayu Satmoko

ANALYSIS OF PRODUCTION TEST BY USING HORIZONTAL LIP PRESSURE TEST METHOD IN Y-WELL OF K-CLUSTER IN PT. PERTAMINA GEOTHERMAL ENERGY AREA OF ULUBELU, LAMPUNG 541-546
Audiah Fadhilah, Ubaidillah Anwar Prabu, and Wenny Herlina

UNIFIED LOGGING UNIT – DIGITALIZING GEOTHERMAL DRILLING IN STAR ENERGY GEOTHERMAL 547-554
Febra Sakti Dewa, Sufian Elsaleh, Hulyadi Halim, Mousa Namavar, Charbel Oueis, Tommy Souvanir, and Doddy Darmawan

REAL TIME DECISION CENTER: DRIVING OPERATIONAL EXCELLENCE IN GEOTHERMAL DRILLING 555-568
Gatra Kusuma, Febra Sakti Dewa, Puthut Hadi Surya, Tommy Souvanir, Agus Ziyad Kurnia, and Hulyadi Halim

COMPREHENSIVE AERATED DIRECTIONAL DRILLING APPLICATION IN WAYANG WINDU GEOTHERMAL PROJECT CAMPAIGN 569-576
Agus Ziyad Kurnia, Tommy Souvanir, and Citra Christina

FOCUS IMPROVEMENT: MEASURING LEVEL OF CONDENSATE PUMP TO INCREASE UNIT RELIABILITY UP TO 98% 577-582
Richard Alexander, Argy Rigwan, Efrata Meliala, Querubin Wendell, and Kadar Aditama

OPTIMIZATION OF USING COOLING TOWER FAN IN THE GEOTHERMAL POWER PLANT OF ULUBELU UNIT 4 IN HOUSE LOAD SAVING 583-588
Nizar Muslim and Yusup Anwar Ridwan

INCIDENT INVESTIGATION AND ROOT CAUSE ANALYIS (RCA) BEST PRACTICES TO IMPROVE SAFE AND RELIABLE GEOTHERMAL PLANT OPERATIONS 589-596
U. Anang Ishak and Indra Rahmansyah

MAINTAINING THE AVAILABILITY OF STEAM SUPPLY TO GEOTHERMAL POWER PLANT UNIT 1-4 WITH PIPELINE DEBOTTLENECKING PROJECT AT PGE LAHENDONG 597-602
Achmad Sani Zahid, Mukhamad Nashir, Viqar Adly Gani, Bagus Reka Susilo, Manda Wijaya Kusumah, and Apriyansah Toni

MACHINE LEARNING MODEL FOR IMPROVING SINGLE FLASH GEOTHERMAL ENERGY PRODUCTION: A CASE OF INDONESIA 603-616
Aldi Cahya Muhammad, K. Habibul Kabir, and Adam A. Alli

STUDY CASE COMPARISON OF LONG STRING AND TIE BACK STRING IN DARAJAT FIELD 617-626
Khansa Hanifa Zahra, Suci Nur Hidayah, and Mohammad Fidi Abganis Hermawan

EFFECTIVENESS OF GEOTHERMAL OPERATOR FOR DELIVERING MAXIMIZE PLANT AVAILABILITY FACTOR 627-636
Arnaldo Napitu

GENERAL

LIFE CYCLE ANALYSIS OF GEOTHERMAL POWER PLANT SYSTEM OPERATION IN THE LAHENDONG GEOTHERMAL FIELD 637-644
Muhammad Gilang Madiantara, Ahmad Indra Sakti Harahap, Ramadoni Febriandinata

THE GEOTHERMAL CAPACITY BUILDING INITIATIVES BY THE MINISTRY OF ENERGY AND MINERAL RESOURCES 645-654
Mukhamad Faeshol Umam, Husin Setia Nugraha, Ahmad Fathoni

THE APPLICATION OF NUMERICAL SIMULATION RESULT FOR GEOTHERMAL FINANCIAL MODEL WITH PROBABILISTIC APPROACH: A COMPREHENSIVE STUDY 655-670
Nevi Cahya Winofa, Ade Lesmana, Heru Berian Pratama, Nenny Miryani Saptadji, Ali Ashat

OPTIMIZING OPERATIONAL EXPENSE BY DEVELOPING A MONITORING AND UPDATING SYSTEM OF OPERATIONAL BUDGET STATUS AT PT PGE KAMOJANG 671-678
Raka Kautsar Lahia, Reza Amaludin, Dona Febi Rosalina, A.Novi Purwono

THE BENEFIT AND ROLE OF WOMEN IN GEOTHERMAL (WING) INDONESIA ON SUPPORTING RENEWABLE ENERGY INDUSTRY 679-684
Ratih Nurruhliati, Jane Brotheridge, Jane Bydder, Pri Utami, and Kris Pudyastuti

GEOTHERMAL ENERGY DEVELOPMENT COMPARISON AMONG TOP GEOTHERMAL PRODUCERS 685-690
Dorman P. Purba, Ribka F. Asokawaty, Daniel W. Adityatama, Rany C. Putri, Riviani Kusumawardani, and Mukhamad Umam

UTILIZATION OF MULTI-CRITERIA DECISION ANALYSIS (MCDA) IN SELECTING CONTRACT TYPES FOR GEOTHERMAL EXPLORATION DRILLING PROJECT IN INDONESIA 691-706
Farhan Muhammad, Vicki Agustino, Dorman Purba, Daniel Adityatama, Ruly Husnie, Mukhamad F. Umam, Ribka Asokawaty

JAVAN LEOPARD IN SEGS CONCESSION AREA: THE HARMONY BETWEEN WILDLIFE AND GEOTHERMAL 707-716
Misbah Satria Giri, Senjaya Mercusiana, Nur Indah Ristiana, Ali Sahid, Willy Ekariyono

COMPARISON OF GLOBAL APPROACHES TO GEOTHERMAL RESOURCE RISK MITIGATION 717-728
Muchsin Chasani Abdul Qadir

RAPID ENVIRONMENTAL AND SOCIAL IMPACT ASSESSMENT TO AVOID HIGH RISK AREAS IN GEOTHERMAL EXPLORATION AND DEVELOPMENT 729-730
Agustina Parwitosari, Ninin Kania Dewi, and Muchsin Chasani Abdul Qadir

THE INVOLVEMENT OF LOCAL INSTITUTION AND COLLABORATION WITH GEOTHERMAL INDUSTRY IN INCREASING LIVELIHOOD OF THE PROJECT AFFECTED PEOPLE 731-740
Erwin Patrisa Floris and Ismoyo Argo

SROI ANALYSIS TO MEASURE THE IMPACT OF CSR PROGRAM, CASE STUDY IN STAR ENERGY GEOTHERMAL SALAK 741-744
Dali Sadli Mulia, Fernando Eka Satria, and Reva Sasistiya

BUFFERZONE PROGRAM AS A STRATEGIC IMPLEMENTATION OF COMMUNITY DEVELOPMENT PROGRAM BASED ON SECURITY IN DARAJAT FOREST AREA 745-750
Maraden H. Panggabean, Dali Sadli Mulia, and Panji Pranadikusumah

EMPOWERMENT OF QUAIL BREEDER (EAGLE FEED SUPPLIER) TO EAGLE CONSERVATION CENTER IN GEOTHERMAL KAMOJANG AREA WITH UTILIZING FECES TO BE FERTILIZER AS AN ADDITIONAL VALUE 751-754
Darussalam

RESOURCES AND MANAGEMENT

NUMERICAL MODEL OF WAYANG WINDU GEOTHERMAL SYSTEM TO OPTIMIZE PRODUCTION STRATEGY 755-764
Riza Pasikki, Boyke Bratakusuma, and Mulyadi

DARAJAT UNIT 2 AND UNIT 3 UPSTREAM PRESSURE OPTIMIZATION 765-772
Agus Riyadi and Sigit Winarno

PRE-FEASIBILITY STUDY OF WELLHEAD GENERATING UNIT IN WATER DOMINATED SYSTEM 773-788
Muhammad Alwy Dahlan, Heru Berian Pratama, and Nenny Miryani Saptadji

PROBABILISTIC METHOD: A NEW APPROACH FOR DETERMINING THE NUMBER OF MAKE-UP WELLS IN FEASIBILITY STUDY 789-802
Feri Vernando Salim, Heru Berian Pratama, and Nenny Miryani Saptadji

HOW TO MANAGE THE GEOTHERMAL FIELD IN ACHIEVING SUSTAINABLE POWER OUTPUT BASED ON RESERVOIR CHARACTERISTICS AND UNIQUE PROBLEM CASE STUDY: GEOTHERMAL FIELDS IN INDONESIA 803-814
Akbar Dwi Wahyono and Heru Berian Pratama

SOCIAL, POLITICS, ECONOMICS, AND COMMUNITY

CERTIFIED EMISSION REDUCTION ISSUANCE PROGRESS OF CLEAN DEVELOPMENT MECHANISM GEOTHERMAL PROJECT IN INDONESIA 815-822
Muhyidin

LITHIUM IN BRINE WATERS FROM THE INDONESIAN GEOTHERMAL SYSTEMS: COULD IT MEET THE NATIONAL NEEDS OF MAKING LITHIUM BATTERIES? 823-828
Niniek Rina Herdianita, I Gusti Bagus Eddy Sucipta, and Aditya Yuda Kencana

WELL TARGETTING BASED ON TEMPERATURE AND STRUCTURAL MODEL IN GEOTHERMAL FIELD BY USING PETREL SOFTWARE 829-842
S. Mulyani and D. Juandi

3D GEOLOGICAL MODELLING WORKFLOW USING LEAPFROG GEOTHERMAL: PRELIMINARY STAGE 843-850
Claudio R.I. Ponggohong, Suryantini, and Angga B. Pratama

HIV AIDS PROGRAM IN THE GEOTHREMAL COMPANY: A STRATEGIC WAY TO SUSTAINABLE GEOTHERMAL OPERATION IN FACING THE THREAT OF GLOBAL PANDEMIC 851-886
Deddi Ekaputra Rangan, Sandriana Tadjoeddin, Rahmat D. Gulo, Jedi Rijendra, Afrionaldi, and Stevano Dihart

GEOTHERMAL SALT FACTORY (GSF) DESIGN IN PARANGWEDANG GEOTHERMAL, BANTUL, SPECIAL REGION OF YOGYAKARTA 887-894
Alfian Gilang, Mohammad Hassan Jauhari, Yusril Ihza, and Maria Theresia Kristiati

THE SIGNIFICANCE OF DRILLING DATA MANAGEMENT TO IMPROVE GEOTHERMAL DRILLING OPERATION 895-906
Daniel Adityatama, Riviani Kusumawardani, Dorman Purba, Farhan Muhammad, and Ribka Asokawaty

A REVIEW OF GEOHEAT AS NEW ZEALAND'S GEOTHERMAL DIRECT USE STRATEGY 907-916
Wini Rizkiningayu

DEVELOPING INTEGRATED GEOTOURISM IN UNGARAN'S GEOTHERMAL MANIFESTATION 917-924
Dhinar Luhung Anggita and Yanuar Dian Anugrah

GEOTOURISM PROSPECT SELECTION USING ANALYTICAL HIERARCHY PROCESS (AHP): CASE STUDY IN TELOMOYO GEOTHERMAL AREA, INDONESIA 925-932
Aulia Umami and Alfath Zain

USING CONTINUOUS WAVELET TRANSFORM FOR ENHANCING MAGNETOTELLURIC DATA IN GEOTHERMAL EXPLORATION 933-938
Haidar Firdaus Avicienna, Yunus Daud, and Nauval Ivanditho

GEOTHERMAL DIRECT UTILIZATION FOR FROST PROTECTION ON POTATO CROPS IN DIENG PLATEAU, CENTRAL JAVA 939-946
Farizky Hisyam and Afifah Nurul Maulina

INDONESIA GEOTHERMAL DASHBOARD WITH PLANT INFORMATION MANAGEMENT SYSTEM (PIMS) 947-952
Kadar Aditama

I-FIELD IMPLEMENTATION FOR ENERGY EFFICIENCY IMPROVEMENT IN DARAJAT UNIT II AND III POWER PLANTS 953-964
Wibisono Yamin, Otto Hari Karyawan, and Agus Riyadi

GEOTHERMAL WELL ANALYSIS USING UNDERBALANCE DRILLING MODULE ON LANDMARK HALLIBURTON WELLPLAN SOFTWARE 965-974
Wisnu Adi Nugroho, Ali Imran Rangkuti, Fernando Marpaung, Samuel Halomoan Silitonga, Frankly Hardytanputra, Muhammad Sinar, Beno Marfianto, Randy Janitra, Muhammad Taufiq Qurrahman, and Deshinta Putri

PRODUCTION BEHAVIOR COMPARISON OF CO_2 AND WATER AS WORKING FLUID AS POSSIBILITY OF ENHANCED GEOTHERMAL SYSTEM IN SIBAYAK AND DARAJAT, INDONESIA 975-982
Roynaldo Lumban Batu, Ignatius Bernadi, Cynthia Dewi Susanto, and Jose Prima Boang Manalu

UTILIZATION OF GEOTHERMAL MANIFESTATION AS THE POTENTIAL OF THE LOMBONGO REGIONAL GEOMETIC, BONEBOLANGO REGENCY, PROVINCE OF GORONTALO 983-988
Miftahul Jannah and Muhammad Rizqy Gau

INVESTIGATION AND PRELIMINARY STUDY OF GEOTOURISM PROSPECTS IN GEOTHERMAL AREA: A CASE STUDY IN NGEBEL GEOTHERMAL PROJECT, EAST JAVA, INDONESIA 989-1000
Fathoni Tri Kurniawan, Muhamad Fauzan Tanjung, and Ilham Arifal Guntoro

INTEGRATION OF GEOTHERMAL MANIFESTATION AND GEOTOURISM AS A CATALYST TOWARDS EDUCATING SOCIETY, ECONOMIC GROWTH AND SUSTAINABLE DEVELOPMENT BASED ON GEOTHERMAL ENERGY 1001-1006
Muhammad Ali Akbar Velayati Salim, and Astri Yunita

This page is intentionally left blank

Earth Sciences



This page is intentionally left blank



OVERVIEW OF GEOTHERMAL RESOURCES OF NORTHERN ITALY

M. Verdoya[1], C. Pasqua[1,2], and P. Chiozzi[1]

[1]DISTAV Università di Genova, Viale Benedetto XV 5, I-16132 Genoa, Italy
[2]ELC Electroconsult S.p.A, Via Marostica 1, I-20146 Milan, Italy
Email: massimo.verdoya@unige.it

ABSTRACT

We present a synthesis of the geothermal resources in northern Italy by focusing on the Po Plain, the region extending between the Alps and Apennines orogenic belts. Thermal data, mostly derived from exploration oil wells, yield a picture of the temperature distribution at a depth of 2000 m across the Po Plain. With the exception of small areas, where advection takes place and originates thermo-artesian systems by the leakage of meteoric water to shallow-medium depth, the orogenic belts surrounding the Po Plain seem dominated by conductive thermal regime. In the eastern sector of the Po Plain, important thermal anomalies are controlled by the Mesozoic carbonate basement. We found that thermal convection might develop, especially at the Ferrara High and its surroundings, where widespread fracturing may have increased permeability.

Keywords: Geothermal resource, Italy

INTRODUCTION

Important geothermal resources in Italy are available and a large part of them is being used at competitive cost since several decades (see e.g. Bertani, 2010). Studies on the geothermal energy in Italy have been traditionally focused on the high-enthalpy fields scattered in the central-southern part of the country. Temperatures often exceeding 200 °C at 2-3 km depth occur within a wide and several hundred-kilometer-long belt, affected by lithosphere extension and recent magmatism (Pasquale et al., 2010), that originated geothermal fields, mainly exploited for electricity generation. (e.g. Gianelli et al., 1988; Sommaruga and Verdiani, 1991; Allegrini et al., 1995). Northern Italy has instead drawn less attention, although it exhibits in some areas promising medium enthalpy resources (Carella and Sommaruga, 2000). This region includes the Po Plain, part of the Alpine chain and the northern portion of the Apennines belt.

In the Po Plain, exploration for hydrocarbons has given the main contribution to the knowledge of the structure and the stratigraphic setting of the sedimentary sequence. Generally, up to ten exploratory wells were drilled annually during the 1930s and 1940s, and both exploration and development operations intensified in the 1950s when the analysis of seismic reflection data was refined. Early exploration was focused on the shallow Tertiary anticlines, identified from seismic data. The deeper Mesozoic, folded and faulted carbonate successions, were targeted in the 1970s and 1980s, with improved success rates achieved by the new seismic techniques (Pieri and Groppi, 1981). Since then, well logs, which often included temperature records, and regional seismic sections were integrated with magnetic and gravimetric modeling to obtain several geological cross-sections extending to the pre-Mesozoic crystalline basement (Cassano et al., 1986 and 1990).

Despite the extensive structural information, knowledge of the thermal water resources in Northern Italy is still poorly understood. In this paper, we give an overview of the thermal regime of this region and describe its relation with the hydrothermal characteristics. We also show that the analysis of available temperature data from hydrocarbon exploration wells together with structural information argue that the deep aquifer in the carbonate rocks of the Po Plain may host thermal convection.

GEOLOGICAL AND HYDROGEOLOGICAL SETTING

Northern Italy includes the Po Plain, part of the Alpine chain and the northern portion of the Apennines belt (Figure 1). Its present tectonic setting is a result of the interaction between the Africa and Europe plates. In the Mesozoic, the whole region experienced extensional events, which led to the formation of a wide carbonate platform. Subsequently, the tectonic regime turned into compressive, producing the formation since the Oligocene of south-verging thrusts in the Southern Alps and north-verging thrusts in the Northern Apennines. At present, the Mesozoic carbonate platform crops out in the Southern Alps and is buried beneath the Po Plain Cenozoic clastic sediments (Pieri and Groppi 1981), where it forms an important reservoir of geothermal fluids (Pasquale et al. 2013).

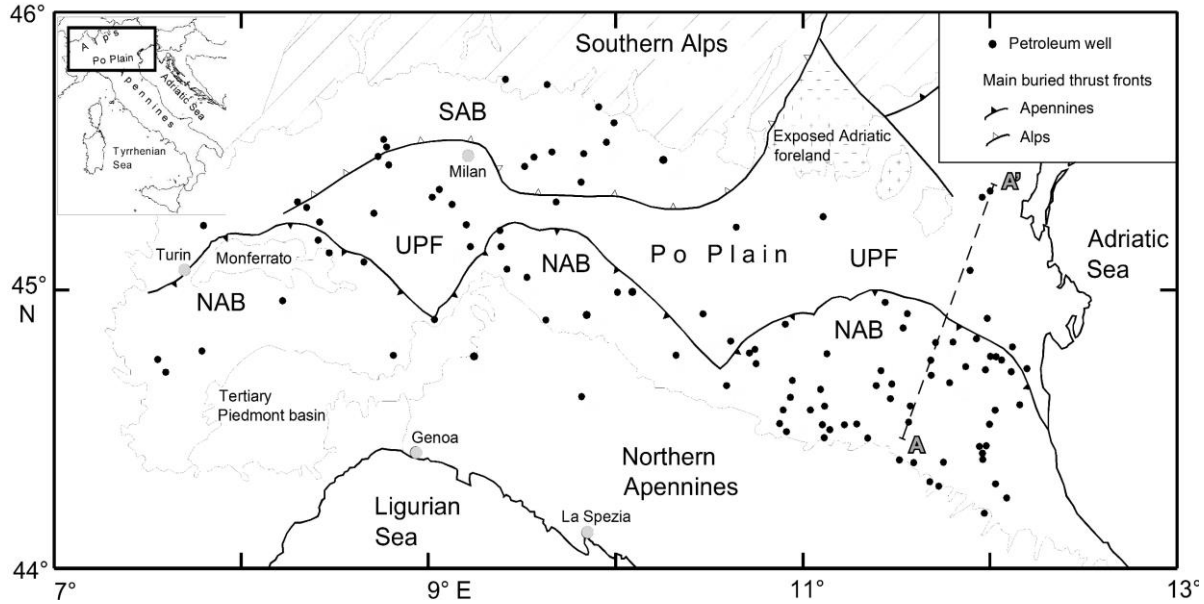


Figure 1: Tectonic sketch of northern Italy and location of petroleum wells (full circles) providing temperatures, thermal parameters and lithostratigraphic information. NAB – Northern Apennines Buried, SAB – Southern Alps Buried, UPF – Undeformed Po Foredeep units. Cross-section A-A' based on geological and geophysical data by Cassano et al. (1986).

The main structural and hydrothermal characters of northern Italy are well known from several geological and geophysical studies, both at the local and the regional scale. Moreover, drillings carried out during several years of hydrocarbon exploration and regional seismic sections, integrated with magnetic and gravimetric modelling, have given a contribution of paramount importance (see Cassano et al. 1990 and references therein). These pieces of information permit to distinguish the following tectonic units (Figure 1):

– the Southern Alps, related to the post-collisional (Oligo-Miocene) deformation of the Alpine belt. They consist of thrust sheets, partly buried beneath the Po Plain Plio-Quaternary cover (SAB). The regional detachment surface of the thrust sheets corresponds to the top of the Eocene deposits. The few thermal waters occurring in this unit are often carbonic, of shallow-medium depth origin and with rather low temperature;

– the undeformed Po foredeep (UPF), filled by terrigenous sediments deposited since Upper Eocene–Oligocene times and characterized by an impressive contribution of dismantling debris of the Alps and, only in recent times, of the Apennines. In the northern part of UPF, there occur outcrops of the carbonate basement together with Paleocene-Oligocene volcanic and subvolcanic products (exposed Adriatic foreland). With the exception of few thermal springs of minor importance, geothermal fluids seem confined in the deep carbonate basement buried beneath the terrigenous sediments;

– the Northern Apennines, consisting of thrusts sheets, which have developed since the Oligo-Miocene. Their external front is arcuate and buried beneath the Plio-Quaternary cover (NAB). The thermal springs occurring in this unit consist of either fossil, salty water, often associated with hydrocarbon reservoirs, or sulphate/sulphurous water related to the Messinian evaporitic series. Water can leak to shallow-medium depth only at few zones and originates thermo-artesian systems;

– the Western Alps, including the deformed Alpine European foreland and the Pennine thrust sheets (ophiolitic unit cover and basement thrust sheets). Thermal springs generally originate from groundwater circulating in crystalline rocks. Important thermal reservoirs occur also beneath the sedimentary cover of the Tertiary Piedmont Basin, structurally related to the Western Alps and to the Northern Apennines.

The main structural elements that characterize the sedimentary sequence and the crystalline basement of the Po Plain are depicted by the cross–section of Figure 2. The buried Apennines thrusts consist of reverse faults with dextral arrangement (Costa 2003), affecting the whole sedimentary sequence and the underlying crystalline basement. Thrusting is a result of progressive shortening caused by the opening of the Tyrrhenian Sea (e.g. Pasquale et al., 2003; Verdoya et al., 2005, and references therein). The sedimentary sequence consists mainly of terrigenous rocks, deposited on the Mesozoic carbonate successions cropping out in the Southern Alps. This denotes an important detrital contribution and remarkable subsidence, which have taken place

through two major cycles in Tertiary and Quaternary times (Dondi, 1985).

Thrust front culminates in a structural high, known as the Ferrara High, which is characterized by a reduced thickness of the Tertiary and Quaternary cover overlying the carbonate rocks. Because impermeable formations prevail in the clastic sedimentary sequence, meteoric water cannot penetrate to large depth and only a small number of thermal springs occur. Water can leak to shallow-medium depth only at few zones, located in the Southern Alps and the Northern Apennines, and originate thermo-artesian systems, such as in the Abano and Porretta districts (see above Figure 3) (Duchi et al., 2005). In the low plain, thermal springs are absent, as shallow water has low probability to leak, because the thick and impermeable sediment cover isolates the underlying aquifers making them confined.

At intermediate depth, groundwater flow may occur, due to mixing of water of shallow origin with deeper brackish water, generally causing a very slow flow (e.g. Conti et al., 2000). At larger depth, the carbonate unit might play a major hydrothermal role. There is evident that in the Pedeappennic zone, it hosts a confined and salty aquifer, whose top at structural highs can be as shallow as about one kilometer (Sommaruga and Verdiani, 1995).

THERMAL DATA

In 1980s, a few studies attempted to outline the thermal regime and geothermal flow in northern Italy (see Pasquale et al. 1986a and 1986b, Pasquale and Verdoya 1990 and references therein). These investigations were based on several thermal datasets, mainly derived from petroleum exploration wells. Rigorous analyses to test the quality of the geothermal flow data and to account for their geological meaning in relation to tectonic processes, such as sedimentation and thrusting, and deep groundwater flow were however tackled only in recent times (Pasquale et al. 2008 and 2012).

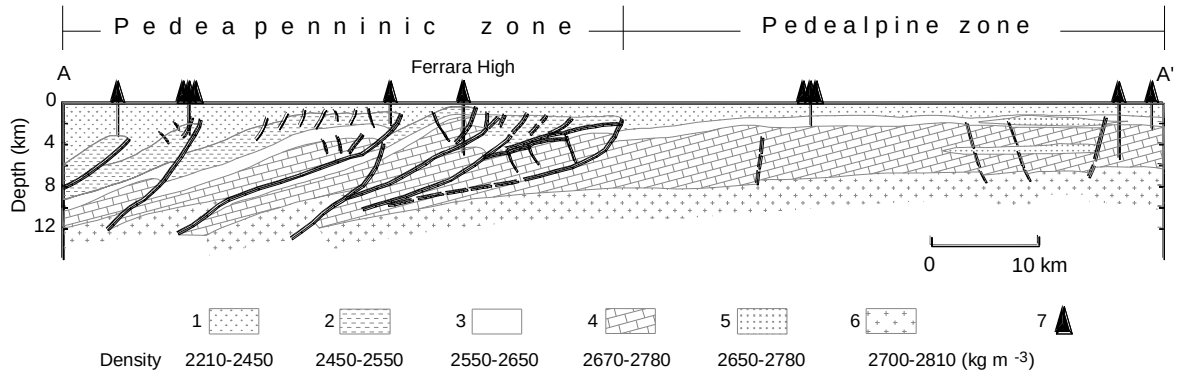


Figure 2: 1 - Sands, clayey sands, clays, 2 - Marls, silty marls, arenaceous marls, 3 - Argillaceous and marly limestones, 4 - Mudstone, wackestone, packstone, dolostone, 5 - volcanic bodies, 6 - crystalline basement, 7 - exploratory wells. Density values of the lithotypes are indicated.

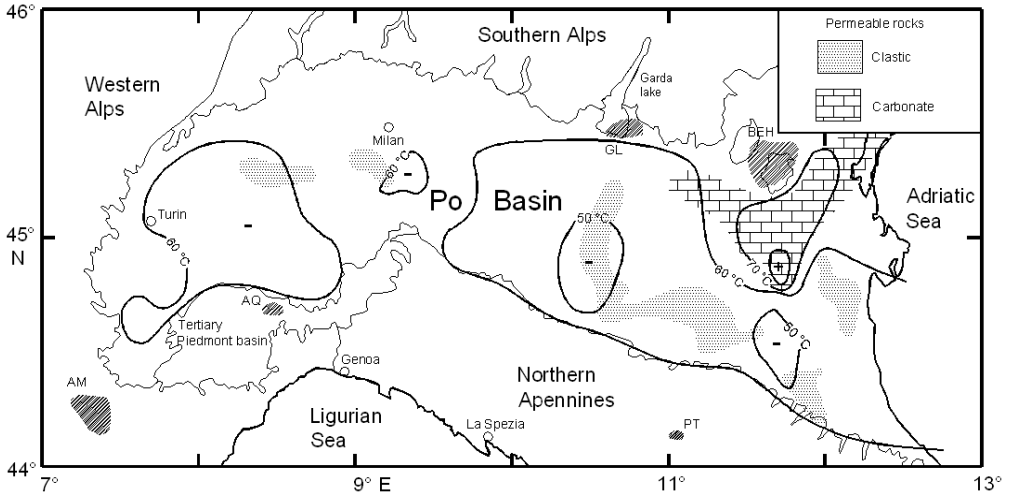


Figure 3: Contour map of temperatures in the Po Plain, as obtained from petroleum well data (see Figure 1), and permeable rocks at 2000 m depth. Main hydrothermal districts: GL - Garda Lake; BEH - Berici Euganei Hills; AQ - Acqui Terme; AM - Argentera Massif; PT - Porretta Terme.

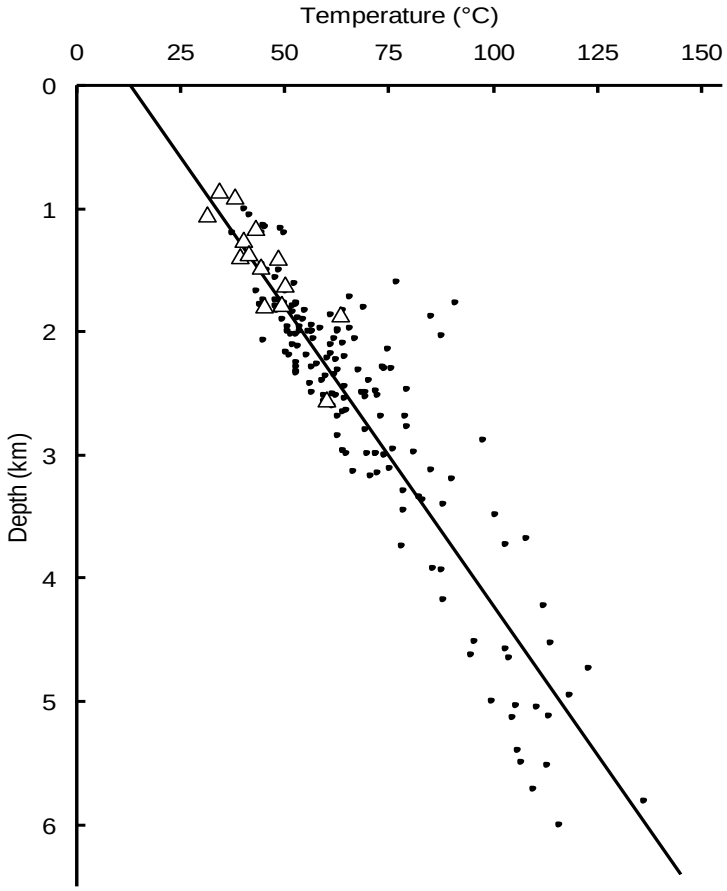


Figure 4a: Temperature data (triangles are DSTs) from the oil wells of the Po Plain (After Paquale et al., 2013).

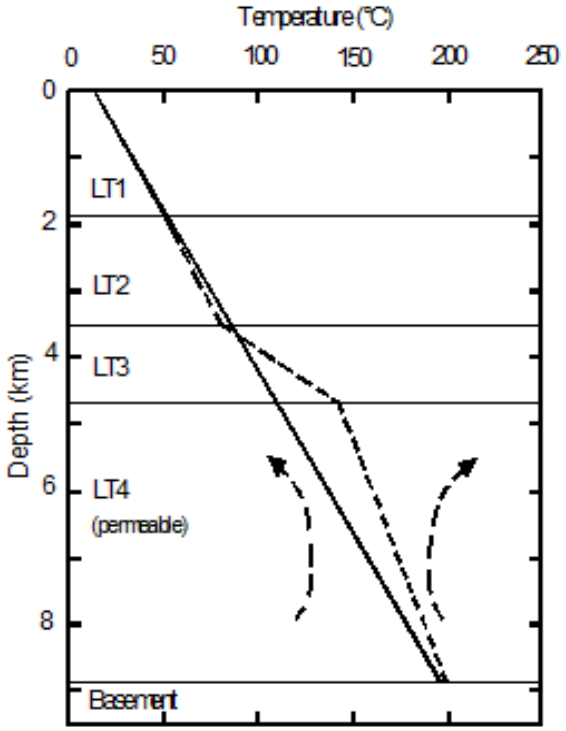


Figure 4b Temperature versus in the four main sedimentary layers (LT-1-LT4) depth as inferred from the thermal gradient (after Pasquale et al., 2013) estimated with inversion (broken line) and by extrapolating the regional thermal gradient of 20.6 mK m^{-1} (continuous line). Arrows indicate likely thermal convection in the deep carbonate unit (LT4).

A modern picture of the terrestrial heat flow and thermal regime of the region was recently proposed by Pasquale et al. (2013 and 2014). Figure 3 shows a map of the temperature expected at 2000 m depth as inferred from the available borehole thermal data. Information on the subsurface thermal state of the Po Plain were derived from temperatures recorded at the bottom (BHTs) and measured during drill stem tests (DST) in oil and gas wells.

All data were processed to obtain the unperturbed temperature of the formation. The corrected BHTs and DST temperatures plotted as a function of depth and constrained with a mean annual surface temperature of 13 °C, yielded an average thermal gradient of 20.6 mK m^{-1} (Figure 4a,b). Data deviation from the best fitting curve is large, with a maximum of about 40 °C at 2 km depth.

GEOTHERMAL RESOURCES

Advective systems

Figure 3 also shows the location of the main geothermal districts scattered in northern Italy. A detailed description of them description is given by Pasquale et al. (2014). The Argentera Massif geothermal district (AM) is the zone of the Western Alps with the highest concentration of thermal discharges, the most important of which are the springs of Vinadio and Valdieri (Michard et al., 1989; Guglielmetti et al., 2010). These springs, which gush out within small areas (as a whole about 10000 m2), show the highest flow rates and temperatures of the entire Alpine chain. Besides, a few shallow wells (about 80 m deep) were also drilled at Vinadio to catch thermal waters. The descending meteoric waters enter a granitic-migmatitic reservoir, and discharge at a total rate of 0.007 m^3 s^{-1} with an average temperature of about 60 °C. The final upward flow of the thermal waters is strictly related to sets of minor fractures, which are connected at depth to the major fault zones. For a surface average temperature of 5 °C, the total thermal yield of the AM springs is about 1.6 MW. According to mass balance calculations performed by Baietto et al. (2008), the total discharge rate might be, instead as large as 0.05 m^3 s^{-1}. In this case, the total thermal power should amount to about 12 MW.

The Sirmione hot springs, which are situated off the Garda Lake southern coast, are the main thermal manifestation of the Garda Lake (GL) geothermal district. According to Balderer et al. (2007) water flows out at the crossing of a NE-SE trending fault line affecting the carbonate bedrock. From the hydrogeological point of view, the Sirmione thermal waters belong to a wide circuit developed within the carbonate formations cropping out between Southern Alps and the exposed Adriatic foreland area, and the recharge area is common to that of Berici-Euganei Hills geothermal district. At present, the flow rate at the main spring is 0.004 m^3 s^{-1} and the temperature is 69 ºC (Castellaccio and Zorzin, 2012). Other unexploited thermal springs occur at both sides of the main water discharge. Moreover, three boreholes, ranging in depth from 400 to 630 m and all reaching the carbonate bedrock, produce thermal water for a total discharge of 0.039 m^3 s^{-1} and an average temperature of 64 °C. The total thermal discharge at Sirmione is thus about 10 MW.

The Berici-Euganei Hills (BEH) geothermal district extends over an area of about 23 km^2 in the northern part of UPF. In this district, several hot springs naturally flowed out in the past, but at present, due to the intensive exploitation, thermal water is by far extracted from more than 250 wells, most of which drilled for several hundred meters as far as the carbonate reservoir. The ground water isotopic and chemical composition led to postulate a meteoric origin of the discharged fluids (Gherardi et al., 2000). Water leaks in the Pre-Alps, at an elevation of about 1500 m, in correspondence of the exposed carbonate formations of the Adriatic foreland), and its deep circulation is controlled by regional faults. The water temperature at the discharge areas ranges from 60 to 86 °C and is very close to the rock-water equilibrium temperature. Therefore, if water warms up due to the geothermal gradient of the UPF unit it is possible to estimate a maximum circulation depth of at least 2000-3000 m. The annual total flow rate extracted in BEH is about 14.4 10^6 m^3 yr^{-1} (Fabbri and Trevisani, 2005). By assuming an average temperature of the thermal water of about 70 °C and a surface temperature of 13 °C, we obtain for BEH a total thermal power extracted of 110 MW.

The Porretta geothermal district (PT), located in the Northern Apennines in an area of less than 1 km^2, consists of several springs whose water temperature ranges from 20 to to 37 °C (Francavilla et al., 1982; Ciancabilla et al., 2007). The geological setting is characterized by two main hydrogeological units, i.e. shales, forming the low-permeability unit, and a marly-arenaceous-silty turbidite with larger permeability, which acts as both the reservoir and the recharge plain of the geothermal system. In PT, the water discharge takes place through a deep regional tectonic fault that connects the reservoir to the surface also displacing the permeable unit. The fault permits the rise of the overpressure warm waters accumulated in depth. No clear information is available about the rock water equilibrium temperature. The total discharge for all the PT springs is 0.006 m^3 s^{-1} and the weighted average temperature is 32 °C. This leads to an estimated total thermal discharge of only 0.5 MW.

The hydrothermal system of Acqui Terme (AQ) is the only geothermal system of northern Italy where

systematic geophysical measurements (borehole temperature logs and thermal conductivity measurements) have been carried out and a remarkable number of thermal data is therefore available (see e.g. Pasquale et al., 1986b; Chiozzi et al., 1998; Verdoya et al., 2008). AQ is located in the Tertiary Piedmont Basin, in the suture zone between the Western Alps and the Northern Apennines. This basin consists of a thick Oligo-Miocenic sedimentary cover of marls and embedded sandstone layers overlying a crystalline metamorphic basement. Over an area of a few square kilometres, numerous thermal springs occurs with a total, natural flow rate of more than 0.015 $m^3 s^{-1}$ and a thermal yield of 3 MW. The main hot spring has the temperature of 70 °C.

South of AQ, thermal data from the metamorphic basement of the Alps indicate that surface heat flow is 76±5 mW m^{-2} (Pasquale et al., 2001). This value can be assumed as the background heat flow of the Tertiary Piedmont Basin. If an average bulk thermal conductivity of 2.2 W m^{-1} K^{-1} is assumed for the cover and the basement, it follows that the regional thermal gradient is 34.5 mK m^{-1}. Geochemical data of the main hot spring argue for a rock–water equilibrium temperature of 108±6 °C. Therefore, we can estimate that the maximum circulation depth of groundwater should be about 2800 m.

On the other hand, temperature logs in boreholes located within the thermal area show an enhanced thermal gradient that appears to occur within a radius of 3-4 km around the thermal manifestations (Chiozzi et al., 1998; Verdoya et al., 2008). This enhanced gradient can be accounted for by water heating at depth because of the regional (background) heat flow and subsequently accumulating at shallower levels within a geothermal reservoir. The water flow path, the heating mechanism and the structure of the AQ hydrothermal system was quantitatively investigated by Pasquale et al. (2011) by means of an analytical model of advective heat transfer within a fractured, water-saturated aquifer.

Deep thermal convection

The oil wells located at Ferrara High and its surroundings, located in the eastern part of the Po Plain (Figure 2), exhibits temperatures that might indicate strong thermal convection. This also appears from the map of the temperatures recorded at 2000 m, which in the Ferrara carbonate structural high can exceed 80 °C (Figure 2). Indeed the Ferrara geothermal system is perhaps the best example of low-enthalpy district heating in northern Italy. Ferrara's district heating system was set up to exploit a ~100 °C-hot saline ground water located at a depth of 2000 m, which was discovered when the potential for oil extraction was investigated in the region.

Pasquale et al., 2013 analysed the regional thermal regime of the sedimentary sequence of the Po Plain and found that there is a vertical variation of thermal gradient. By applying an inversion technique (Speece et al., 1985), based on the lateral constant thermal gradient model, they demonstrated that this cannot be due to variation in thermal conductivity of the sedimentary layers and argued that a possible explanation could lie in the heat transported by water flow in the deep carbonate unit.

Thermal convection in an aquifer heated from below may occur if appropriate heat sources and permeability occur. Water flow can cause a decrease of thermal gradient in the carbonate unit (LT4) and a significant increase in the overlying impermeable unit (Figure 4). Since LT4 is hydraulically insulated, thermal convection might be the driving mechanism. Conditions for thermal convection in LT4, can be analyzed with the Rayleigh number, Ra, defined as (Horton and Rogers, 1945; Lapwood, 1948).

$$Ra = \frac{g\,\alpha_w\,(\rho c_p)_w\,k\,h\,\Delta T}{\nu_w\,k_{in}} \qquad (1)$$

where g is acceleration due to gravity, α_w, ν_w and $(\rho c_p)_w$ is thermal expansion coefficient, kinematic viscosity and volumetric heat capacity, respectively, of the saturating water, h is length over which convection occurs, ΔT is the temperature difference between the top and bottom of this length interval, k and k_{in} are the permeability and the thermal conductivity of the unit.

When the Rayleigh number exceeds the critical value of $4\pi^2$, convection starts and water flow forms convective cells. The potential for thermal convection to take place within LT4 can be quantified with eq. (1). The thickness of the carbonate layer was regarded as the length h of convection and the temperature at the bottom and top was estimated by means of the thermal gradient, representing steady–state thermal conditions.

By taking $Ra=4\pi^2$, g= 9.8 m s^{-2}, average values of $(\rho c_p)_w$, ν_w, α_w k and k_{in} after Paquale et al. (2013) eq. (1) can be rewritten as

$$\left(\frac{dT}{dz}\right)_{min} = \frac{10.0\,10^{-10}}{k\,h^2} \qquad (2)$$

In which $(dT/dz)_{min}$ is the minimum thermal gradient required for convection to occur in LT4. By considering the average values of thermal gradient (13.5 mK m^{-1}) and the thickness h of the carbonate unit (about 5 km), a permeability $k > 3.0\ 10^{-15}$ m^2 is required for thermal convection.

Permeability depends on several parameters, such as the aspect ratio of the flow domain (aquifer depth respect to width) and presence of faults or other discontinuities (Smith and Chapman, 1983, Clauser and Villinger, 1990). Compared with the other sedimentary rocks, carbonates exhibit a wide variety of vertical and horizontal heterogeneities. In general, pores of the carbonates can be affected by mineral dissolution, replacement by other minerals and re-crystallization, which take place during post-depositional processes. Porosity being equal, the permeability can show a wide variation. However, primary porosity is often poor and secondary porosity (e.g. by fissure/fracture) of tectonic origin or related to unloading processes is more important. In the analyzed reservoir, water flow might occur through micro- and macro-fractures, which might have been broadened by karst phenomena. At the Ferrara High and its surroundings (Figure 2 and 3), the larger temperatures observed indicate strong thermal convection. This can be due to increased permeability caused by tectonism yielding enhanced water circulation.

DISCUSSION AND CONCLUSIONS

In the light of the underground thermal state and the hydrogeological setting, conduction appears to be the dominant mechanism of heat transfer of the norther Italy, and advection is restricted to particular hydrogeological systems. These systems are characterized by low-medium enthalpy fluids. Next to the mountain chains groundwater flows by forced convention, whereas in wide sectors of the plain, corresponding to the carbonate basement, thermal convection may take place.

In the Apennines, due to the generally low permeability of the rocks cropping out, water cannot penetrate to large depth and only a small number of thermal springs occur (e.g. Duchi et al., 2005). In the Alps, deep ground water systems can be instead encountered in all major geological and tectonic units. Fractured crystalline rocks (granite, gneiss), karstified formations, or porous sediments (sandstones, fluvio-alluvial deposits) may form geothermal aquifers.

The location and limits of the aquifers are highly dependent on local tectonic features (Sonney and Vuataz, 2010). Deep flow systems reaching 1 to 4 km depth mostly occur due to the presence of thrusts and subvertical faults having higher hydraulic conductivities. These fractures support the rise of deep fluids along the glacial and alluvial valleys, and complex mixing processes with shallow ground water occur (Vuataz, 1997). The outflow of thermal water can differ from one site to another: in some cases, only one large thermal spring occurs whereas in other cases, more than ten springs with different composition and discharge temperature can be present (e.g. Argentera Massif, Berici-Euganei Hills and Acqui Terme geothermal districts).

In the low Po Plain, at intermediate depth beneath the thick and impermeable sediments, a very slow groundwater flow may occur, due to mixing of water of shallow origin with deeper brackish water (e.g. Conti et al., 2000). At larger depth, the carbonate unit plays a major hydrothermal role. There is evidence that in the Pedeappennic zone the carbonate unit hosts a confined and salty aquifer, whose top can be as shallow as about one kilometer. Water in these reservoirs, is related to regional flow systems characterized by cross-formational hydraulic continuity. The groundwater flow is caused not only by topographic gradient, but other phenomena, such as density differences in the fluids permeating rocks and thermal convection may act as additional driving forces (Pasquale et al. 2013).

In conclusions, geothermal resources in northern Italy mainly consist of thermal springs and deep aquifers, suitable for direct-use applications. Minor springs occurring where lower temperatures and water flow rates are recorded, are likely connected with shallow water flow moving through the sedimentary cover that could be partially mixed with deeper hydrothermal water rising from the basement. Under favorable geological and structural conditions, heated water moving towards the surface can produce thermal anomalies, which can be revealed by means of appropriate treatment of temperatures recorded in deep wells. The subsurface temperatures presented in this study form a basic constraint to localize low-enthalpy, confined, deep aquifers occurring beneath the relatively impermeable, low-thermal conductivity cover of sediments. The thermal and hydraulic properties of the sediment cover enhance the deep groundwater temperature and areas with geothermal conditions potentially suitable for the settlement of heat extraction (district heating) can be identified. Such a kind of aquifers is heated at depth by the background regional geothermal flow and transports heat by convection. The sedimentary cover appears to act as a confining layer, characterized by low groundwater flow, except in the presence of faults where thermal water discharge can take place.

REFERENCES

Allegrini, G., Cappetti, G., Sabatelli, F., (1995). “Geothermal development in Italy: country update report”, Proc. World Geotherm. Cong., 1995, Florence, Italy, 1, 201-208.

Baietto, A., Cadoppi P., Martinotti G., Perello P., Perrochet P., Vuataz F.D. (2008). “Assessment of thermal circulations in strike-slip faults systems: the Terme di Valdieri case (Italian western Alps)”. In: Wibberley C.A.J., Kurz W., Imber J., Holdsworth R.E., Collettini C. (eds), The internal structure of fault zones:

implications for mechanical and fluid-flow properties. The Geological Society of London 209, 317-339.

Balderer, W., Leuenberger F., Frei Ch., Surbeck H., Synal H.A. (2007). "Advances in isotope hydrology and its role in sustainable water resources management (HIS-2007)". Proceedings of an International symposium on advances in isotope hydrology and its role in sustainable water resources management. International Atomic Energy Agency Vienna 21-25 May 2007 Vol 2.

Bertani, R., (2010). "Geothermal Power Generation in the World 2005-2010 Update Report". Proceedings World Geothermal Congress 2010 Bali, Indonesia, 25-29.

Carella, R., Sommaruga, C., (2000). "Geothermal space and agribusiness heating in Italy". Proceedings World Geothermal Congress 2000, Kyushu-Tohoku, Japan., 117-122.

Cassano, E., Anelli, L., Fichera, R., Cappelli, V., (1986). "Pianura Padana, interpretazione integrata di dati geofisici e geologici". AGIP, Metod. Appl. Geofisiche, Milano, pp. 28.

Cassano, E., Anelli, L., Fichera, R., (1990). "Geophysical data along the northern Italian sector of the European Geotraverse". Tectonophysics 176, 167-182.

Costa, M., (2003). "The buried, Apenninic arcs of the Po Plain and northern Adriatic Sea (Italy): a new model". Boll. Soc. Geol. It. 122, 3-23.

Castellaccio, E., Zorzin R. (2012). "Acque calde e geotermia della provincia di Verona. Aspetti geologici e applicazioni". Memorie del Museo Civico di Storia Naturale di Verona - 2. Serie. Sezione Scienze della Terra, 8.

Chiozzi, P., Pasquale V., Verdoya M. (1998). "Heat flow anomaly in the Piedmont Tertiary Basin (NW Italy)". Intern. Conf. "The Earth's thermal field and related research methods", Moscow, Russia, May 19-21, 1998, pp. 59-62.

Ciancabilla, N., Ditta M., Italiano F., Martinelli G. (2007). "The Porretta thermal springs (Northern Apennines): seismogenic structures and long-term geochemical monitoring". Ann. of Gephys., 50, 513-526.

Clauser, C., Villinger, H., (1990). "Analysis of conductive and convective heat transfer in a sedimentary basin, demonstrated for the Rheingraben". Geophys. J. Int. 100, 393-414.

Conti, A., Sacchi, E., Chiarle, M., Martinelli, G., Zuppi, G.M., (2000). "Geochemistry of the formation waters in the Po plain (Northern Italy): an overview". Applied Geochemistry 15, 56-65.

Dondi, L., (1985). "Pianura Padana: paleogeografia dall'Oligocene superiore al Pleistocene". Atti del Seminario Progetto Cartografia Geologica, Regione Emilia Romagna, Bologna, 76-101.

Duchi, V., Venturelli, G., Boccasavia, I., Bonicoli, F., Ferrari, C., Poli, D., (2005). "Studio geochimico dei fluidi dell'Appennino Tosco-Emiliano-Romagnolo". Boll. Soc. Geol. It. 124, 475-491.

Fabbri, P., Trevisani S. (2005). "Spatial distribution of temperature in the geothermal Euganeanfield (NE Italy): a simulated annealing approach". Geothermics 34, 617-631.

Francavilla, F., Gorgoni C., G. Magoni G., Martinelli G., Sighinolfi P., Zecchi R. (1982). "Caratteri geologici e geotermici di alcune aree appenniniche". In: Caratteri geoidrologici e geotermici dell'Emilia Romagna. Piagora editrice, Bologna.

Gherardi, F., Panichia C., Caliroa S., Magrob G., Pennisib M. (2000). "Water and gas geochemistry of the Euganean and Berician thermal district (Italy)". Applied Geochemistry 15, 455-474.

Gianelli, G., Puxeddu, M., Batini, F., Bertini, G., Dini, I., Panderi, E., Nicolich, R., (1988). "Geological model of a young volcano□plutonic system: the geothermal region of Monte Amiata (Tuscany, Italy)". Geothermics 17, 27-36.

Guglielmetti, L., (2010). "Multidisciplinary Approach of Geothermal Prospection in the Argentera Massif (South-Western Alps)". PhD thesis, University of Neuchatel, Switzerland, 2012, 215 pp.

Horton, C. W., Rogers Jr., F.T, (1945). "Convection currents in a porous medium". J. Applied Physics 16, 367-370.

Lapwood, E. R., (1948). "Convection of a fluid in a porous medium". Proc. Cambridge Phil. Soc. 44, 508-521.

Michard, G. Grimaud, D., D'Amore, F., and Fancelli, R. (1989). "Influence of mobile ion concentrations on the chemical composition of geothermal waters in granitic areas, example of hot springs from Piemonte (Italy)". Geothermics, 18 (5/6), 729-741.

Pasquale, V., Salvatore F., Montanari F. (1986a). "Mappa preliminare del flusso geotermico nella pianura padana emiliano romagnola". Atti 5° Conv. GNGTS-CNR, Rome, 1129-1140.

Pasquale V., Balbi A., Casale G., Salvatore F. (1986b). "Indagine geotermica sul settore sud-occidentale della Pianura Padana", Atti 5° Conv. GNGTS-CNR, Rome, 1177-1187.

Pasquale V., Verdoya M. (1990). “Geothermal regime of the Po Basin, Italy”. Vol. Spec. Soc. Geol. It. 1, 135-144.

Pasquale, V., Verdoya, M., Chiozzi, P., (1993). “Thermal effects of the dynamic activity from the Ligurian Sea to the Eastern Alps”. Annals Geophys. 36, 91-104.

Pasquale V., Verdoya M., Chiozzi P., (2001). “Radioactive heat generation and its thermal effects in the Alps-Apennines boundary zone”. Tectonophysics 331, 269-283.

Pasquale, V., Verdoya, M., Chiozzi, P., (2003). “Heat-flux budget in the southeastern continental margin of the Tyrrhenian basin”. Physics and Chemistry of the Earth 28, 407-420.

Pasquale, V., Chiozzi, P., Gola, G., Verdoya, M., (2008). “Depth-time correction of petroleum bottom-hole temperatures in the Po Plain, Italy”. Geophysics 6, E187-E197.

Pasquale, V., Chiozzi, P., Verdoya, M., (2010). “Tectonothermal processes and mechanical strength in a recent orogenic belt: Northern Apennines”. J. Geophys. Res. 115, 147-163.

Pasquale, V., Gola, G., Chiozzi, P., Verdoya, M., (2011). “Thermophysical properties of the Po Basin rocks”. Geophys. J. Int. 186, 69-81.

Pasquale, V., Chiozzi, P., Verdoya, M., Gola, G., (2012). “Heat flow in the Western Po Basin and surrounding orogenis belts”. Geophys. J. Int. 190, 8-22.

Pasquale, V., Chiozzi P., Verdoya M., (2013). “Evidence for convention in the deep carbonate aquifer of the eastern sector of the Po Plain, Italy”. Tectonophysics, 594, pp. 1-12.

Pasquale, V. Verdoya, M., Chiozzi, P., (2014). “Heat flow and geothermal resources in northern Italy”. Renewable and Sustainable Energy Reviews, 362, 77-285.

Pieri, M., Groppi, G., (1981). “Subsurface geological structure of the Po Plain, Italy”. Consiglio Nazionale delle Ricerche, Progetto Finalizzato Geodinamica Sottoprogetto “Modello strutturale”, Pubbl. n. 414 del Progetto Finalizzato Geodinamica, CNR, Roma, pp. 32.

Smith, L., Chapman, D.S., (1983). “On the thermal effects of groundwater flow 1: regional scale systems”. J. Geophys. Res. 88, 593-608.

Sommaruga, C., Verdiani, G., (1991). “Elementi di Geotermia, Cooperativa Universitaria Studio Lavoro, Milano”.

Sommaruga, C., Verdiani, G., (1995). “Geotermia - Principi, ricerca, produzione”, La Nuova Italia Scientifica, Roma.

Sonney, R., Vuataz, D., (2010). “Use of Cl/Br ratio to decipher the origin of dissolved mineral components in deep fluids from the Alps range and neighbouring areas”. Proceedings World Geothermal Congress 2010 Bali, Indonesia, 25-29 April 2010.

Speece, M., A., Bowen, T., D., Folcik, J., L., Pollack, H., N., (1985). “Analysis of temperatures in sedimentary basins: the Michigan Basin”. Geophysics 50, 1318-1334.

Verdoya, M., Pasquale, V., Chiozzi, P., (2005). “Thermo-mechanical evolution and rheology of the northern sector of the Tyrrhenian-Apennines system”. J. Volcan. Geoth. Res. 148, 20-30.

Verdoya, M., Pasquale V., Chiozzi P., (2008). “Inferring hydro-geothermal parameters from advectively perturbed thermal logs”. Int. J Earth Sci (Geol Rundsch) 97, 333-344.

Vuataz, F., D., (1997). “Natural variations and human influences on thermal water resources in the Alpine environment”, 33e Conf. Soc. Int. Tech. Hydroth., December 1997, Hakone, Japan.

A CORRELATION OF MERCURY (HG) AND HYDROGEN SULFIDE (H2S) GAS DISTRIBUTION WITH A FAULT STRUCTURE ON ULUBELU GEOTHERMAL SYSTEM

Taufiq[1], Atmojo J. P.[1], Yunis[1], Budiraharjo S.[1], Mujihardi B.[1], Rozaq K.[1], Maharani[2], and Saputra D. D.[2]

[1]Research & Technology Center (RTC) of Pertamina
[2]University of Lampung
Medan Merdeka Timur Street No.6, Jakarta
Email: taufiqgeophysics76@gmail.com

ABSTRACT

Ulubelu Geothermal Field is one of the biggest geothermal energy and production in Sumatera which have a complex geology in subsurface. It caused Ulubelu is located on Great Sumatera Fault (GSF) especially in Semangko Fault. In this study, we investigated a fault structure in this area based on Mercury Gas (Hg) and Hydrogen Sulfide (H_2S) Gas distribution. Mercury and Hydrogen Sulfide Gases is associated with subsurface structure, it's because the gases are distributed from the magmatic rock and moving up to surface with fracture and structure on subsurface. Based on geology, we determine the structure is controlled by graben structure with lineament on northwest to southeast (same as lineament on Sumatera Fault). Based on geochemistry acquisition, on Hg survey, a high value (50-500 ng Hg) is indicated a fault structure (if we made a strike-line), it's same as H_2S value (6-50 ng H_2S), is indicated a deep structure in research area. Based on Geochemistry Map (Hg and H_2S) and Geological Structure Map, its show a positive correlation to determine a fault structure or weakness zone, so we can conclude the mercury (Hg) and hydrogen sulfide (H_2S) gases distribution can help the preliminary surveys to determine a fault structure or weakness zone in the subsurface on geothermal area or hidden geothermal area.

Keywords: Structure distribution, Ulubelu geothermal field

INTRODUCTION

Geothermal System is a system that formed due to geological processed, is the movement of earth's crust, so that the heat produced is delivered from medium called heat source to another medium (rocks above it). To form a geothermal system as a source of geothermal energy, several important components are needed, such as heat source, reservoir rock (permeable), flowing fluid (circulation), geological structure, cap rock, and recharge area.

The Geological structure such as faults and fractures are one of the important elements in determining the prospect of reserves and the source of geothermal energy in the area.

In this research, we would like to analysis a result of Mercury (Hg) and Hydrogen Sulfide (H_2S) gases.

Distribution to identify a fault structure zone in Ulubelu Geothermal Area. It caused Mercury and Hydrogen Sulfide Gases is associated with subsurface structure, it's because the gases are distributed from the magmatic rock and moving up to surface with fracture and structure on subsurface.

THEORY

Regional Geology

The condition of the surface geology at Ulubelu Geothermal Area (Figure 1) is dominated by volcanic rock, it's composed by the complex of granodiorite (Tmg), the older andesites (Tmat) and the Mt. Kabawok pyroclastic (Qpkb) are located in the southeastern part of the field. The Mt. Kurupan pyroclastic (Qpkl) are in the northeast. The Mt. Rindingan complex (Qprl, Qprd) occurs in the west and southwest and the Mt. Kukusan basaltic lava (Tpl) complex is in the south. Between the Mt. Kukusan basaltic andesite lavas and the Mt. Sula andesite lavas (Tps) are pumice tuffs. The Lake Ulubelu and the Mt. Duduk dacite lava (Tpd) complexes are seated in the middle of the area (Masdjuk, 1990).

Geothermal Energy

Geothermal energy is the heat stored in the rock beneath on the earth's surface and the fluid contained therein. Geothermal system consists of elements that made up the system. Essential elements of constituent geothermal system are separated in three aspects, contained a heat source, a permeable reservoir rock, and fluid that bring the heat flow, the illustration of geothermal system can be seen on Figure 2 (Goff and Cathy, 2000).

Mercury (Hg) and Hydrogen Sulfide (H2S) Gases

Geothermal Gases can be divided into two types, condensable and non-condensable gases (reacted with NaOH). Condensable gases such as CO_2 and H_2S can be analyzed using a titration method, while non-condensable gases such as He, H_2, N_2, O_2, Ar, and CH_4 can be analyzed using the chromatography gas method. The results of the gas analysis can show the gases is dominant in the geothermal field, so that it can be applied to calculate the temperature of geothermal area, (Laksminingpuri, 2013).

Mercury (Hg) is one of the metal elements found in the earth's crust, is liquid at room temperature and volatile element. Mercury gas can be found in volcanic activities because it expands at temperature 396 ºC. Hydrogen Sulfide (H_2S) is a colorless, toxic, and flammable gas. This gas can be formed from activity of decomposing bacteria to organic material without oxygen and also formed due to volcanic activity.

RESULT AND DISCUSSION

This research is located in Ulubelu Geothermal Area, 120 km from the capital city of Lampung Province, we need approximately four hours to go to research location (see on the black box on Figure 3). Based on geological map (see on Figure 1), it's indicated a several structure on the research area, we Have a major fault structure such as Ngarip Fault in the West Area, Gunung Tiga (1) Fault in the South, Talang Marsum Fault in the East, Karang Rejo with Datarajan in the Middle and Rindingan Fault in the North of research Area. Overall the fault structure of Ulubelu Geothermal Area controlled by graben structure with northwest to southeast direction of lineament (same as Semangko Fault). With this major fault information, we will spread the geochemistry point acquisition to get a mercury and hydrogen sulfide gas distribution.

In this research, we spread 300 point of geochemistry acquisition with distance per point is 500 meters (gridding point). It covered 9 km in vertically and 10 km horizontally, with total area is 90 km2 (see Figure 1), the acquisition takes 14 days of measurement, so with this value, we hope can recover the area Ulubelu Geothermal System (Fault Structure, Production Wells, and Injection Wells).

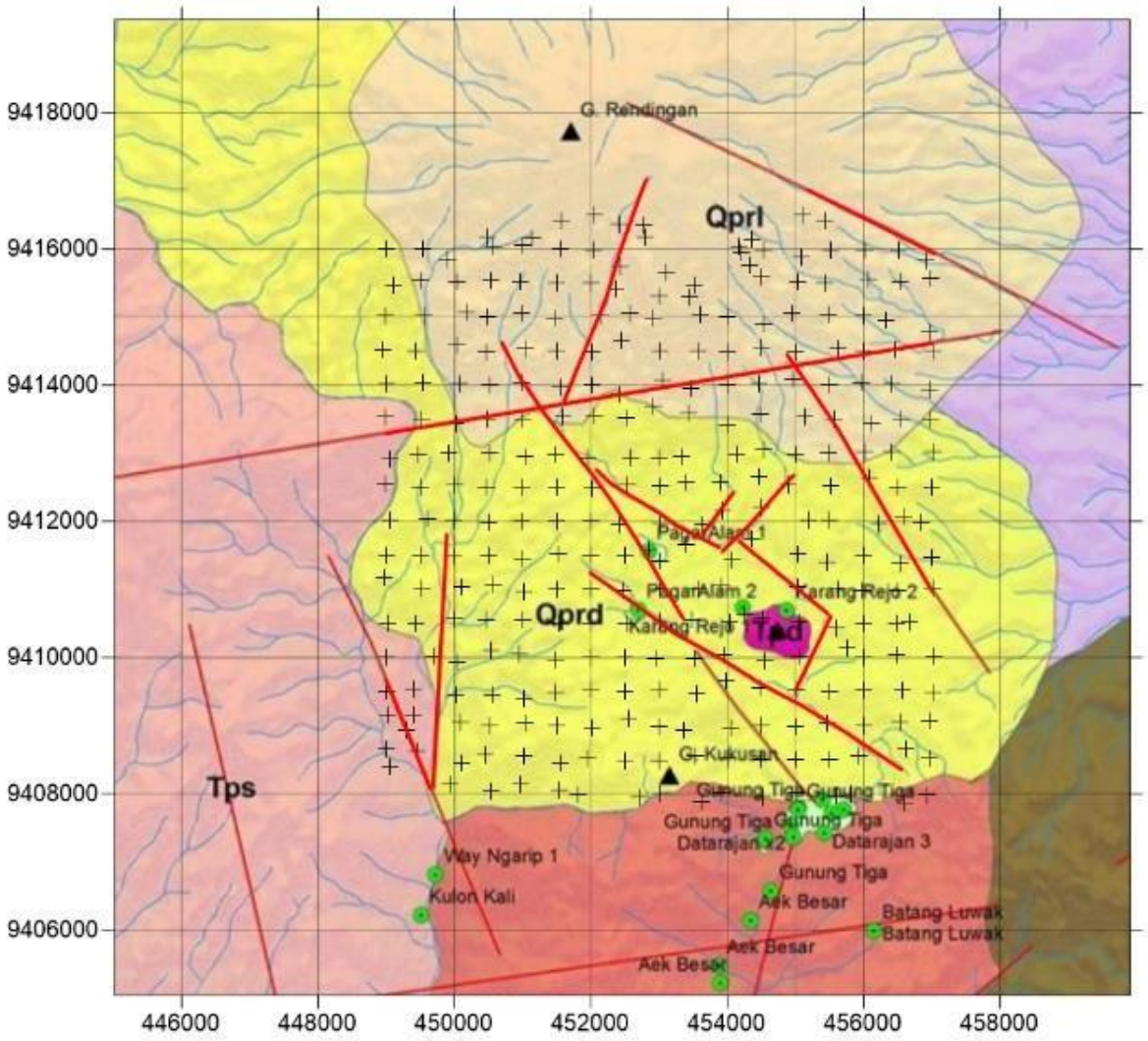


Figure 1: The Geology of Ulubelu Geothermal Area with geochemistry acquisition point (modified from Masdjuk, 1990 & PGE, 2014).

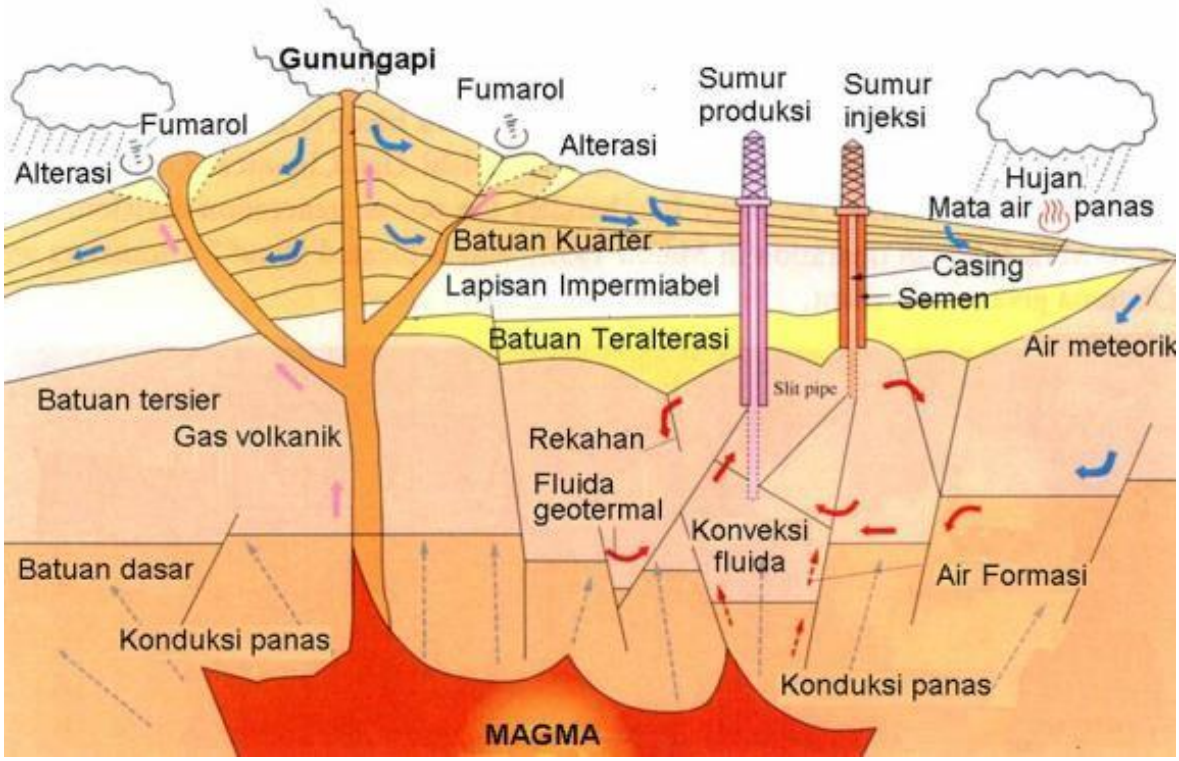


Figure 2: Geothermal System (Putohari, 2009).

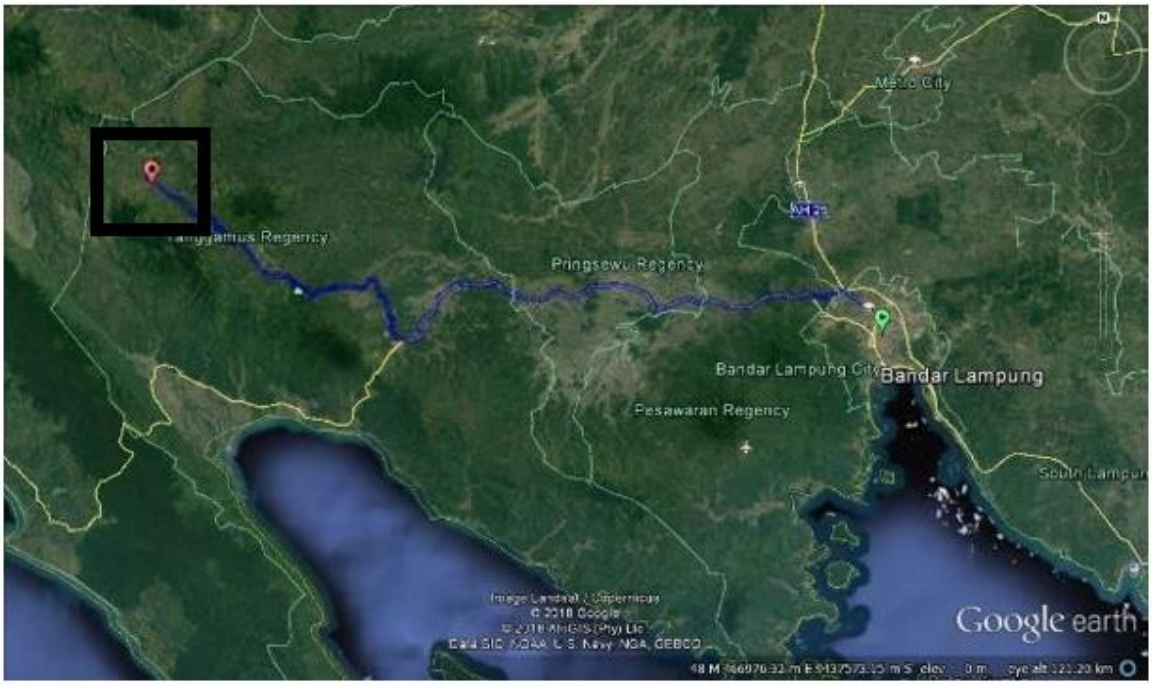


Figure 3: The Location of Ulubelu Geothermal.

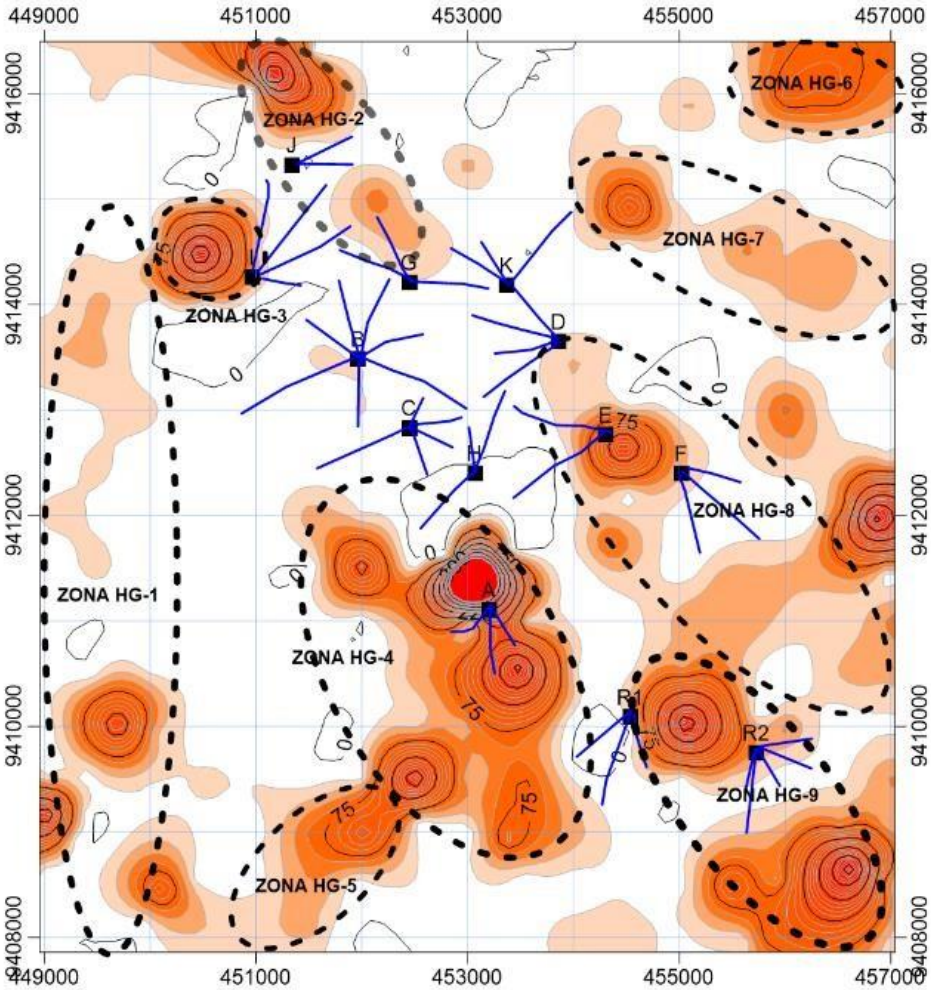


Figure 4: The Result of Hg gas distribution on Ulubelu Geothermal Area.

After the acquisition (14 days), sample of Hg and H_2S is analyzed on Gases Laboratory to get a value of contain. The result of Hg survey is a high value (>50 ng Hg) is indicated the weakness zone or the area with fault structure zone (see Figure 4). The high value we will divide on the 9 zone (with assumption the flow of gases is make a shape of the contour map) spreading on this research area.

The result of H_2S survey is a high value (6-50 ng Hg) is indicated the weakness zone with deeper fault structure zone (see Figure 5). The high value we will divide on the 7 zone (with assumption the flow of gases is make a shape of the contour map) spreading on this research area.

The difference of Hg and H_2S gas distribution is at the depth range of the fault but if seen from the both of map result has a same fracture pattern distribution.

The result of Hg and H_2S surveys then validated with fault or regional structure (with updated data source information). After validating with regional structure map in this area, its show a positive correlation at some fault structure (see Figure 6) such as Ngarip Fault with Zone HG-01, Rindingan (2) Fault with Zone HG-02, Datarajan (1) Fault with Zone HG-04, Gunung Tiga Fault with Zone HG-05, Talang Marsum and Karang Rejo Fault with Zone HG-07 and HG-08. The correlation of H2S map with fault structure map (see Figure 7) show a positive correlation (same as Hg Map) with a deeper fault. If we calculated a correlation between geochemistry maps with a valid fault structure map, we can conclude the value of correlation is higher than 90%.

In the next research, we can validate (phase II), in the different area to determine a fault structure, so if this successful, we can apply this method to help a preliminary survey in a hidden geothermal prospect.

CONCLUSION

The conclusions derived from this paper are:

1. Based on Geochemistry Acquisition, the value of Hg gases with range 40-500 ng Hg is indicated a fault structure or a fracturing zone, it's same as H_2S acquisition (with value 6-50 ng H_2S), but the hydrogen sulfide gases can determine a deep structure in this area.

2. If we validate with regional structure map in this area, its show a positive correlation (higher than 90%) with same fault in the area (if we overlay in the map).
3. In the next research, we can validate (phase II), in the different area to determine a fault structure, so if this successful, we can apply this method to help a preliminary survey in a hidden geothermal prospect.

ACKNOWLEDGEMENT

We would like to thank Research and Technology Center (RTC) of Pertamina to permit a geothermal research team to publish this paper and thanks to University Lampung to join exploration team at Ulubelu Geothermal Area.

REFERENCES

Christenson, B.W., Mroczek, E.K., and Taguchi S., (2002), "The behaviour of Hg in some New Zealand geothermal reservoir and production environments." GRC Transactions, 26, 335-340.

Goff, F. and Cathy J.J., (2000), "Encyclopedia of Volcanoes: Geothermal System", Academic Press, 817-834 pp.

Hochstein, M.P. and Sudarman, S., (2008), "History of Geothermal Exploration in Indonesia from 1970 until 2000", Geothermics, Vol. 37, p.220-266.

Laksminingpuri, N. and Martinus, A, (2013), "The Study of content and temperature of geothermal gases at Kamojang with Diagram grid", Beta Gamma, vol.4 No.2, 69-79.

Masdjuk and Muchsim, (1990), "The Geology of Ulubelu Geothermal Area", Unpublished Internal Report, Geothermal Div., Pertamina.

Mroczek, E. and Graham, D. (2005). "Sampling and Analysis for Mercury in Steam Collected from Geothermal Wells and Fumaroles". Proceeding World Geothermal Congress 2005.

Panjaitan, S., (2010), "Geology of Ulubelu Geothermal Area Based on Magneto telluric Data", Geo-Resources, JSDG, p.69-91.

Putohari, D.R., (2009), "Geothermal waste contains a gold", WordPress.

Simmons, S.F. and Graham, I., (2003), "Volcanic, Geothermal, and Ore-Forming Fluids: Rulers and Witnesses of Processes within the Earth", Society of Economic Geologist, Special Publication No.10, p.111-133.

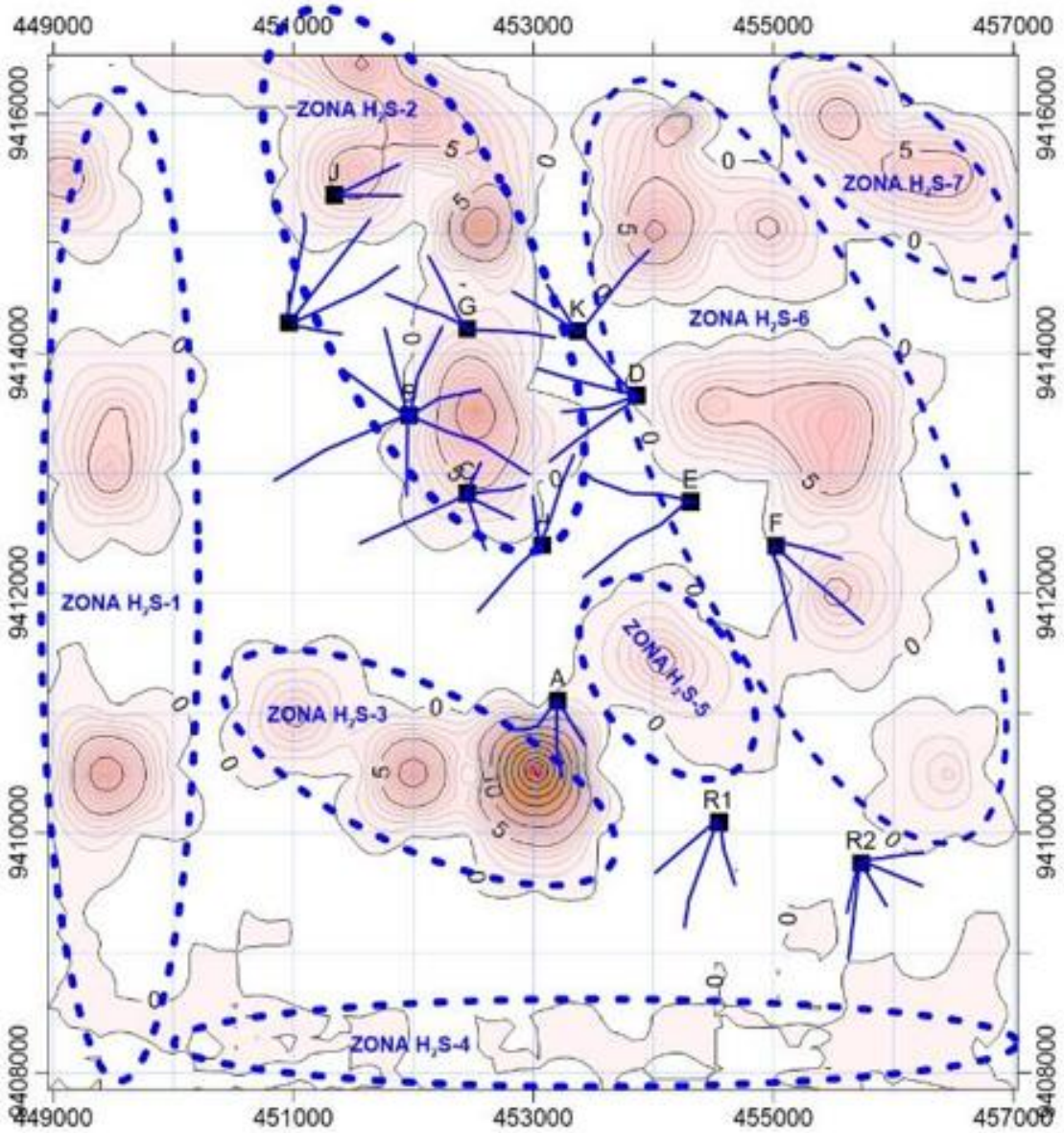


Figure 5: The Result of H2S gas distribution on Ulubelu Geothermal Area.

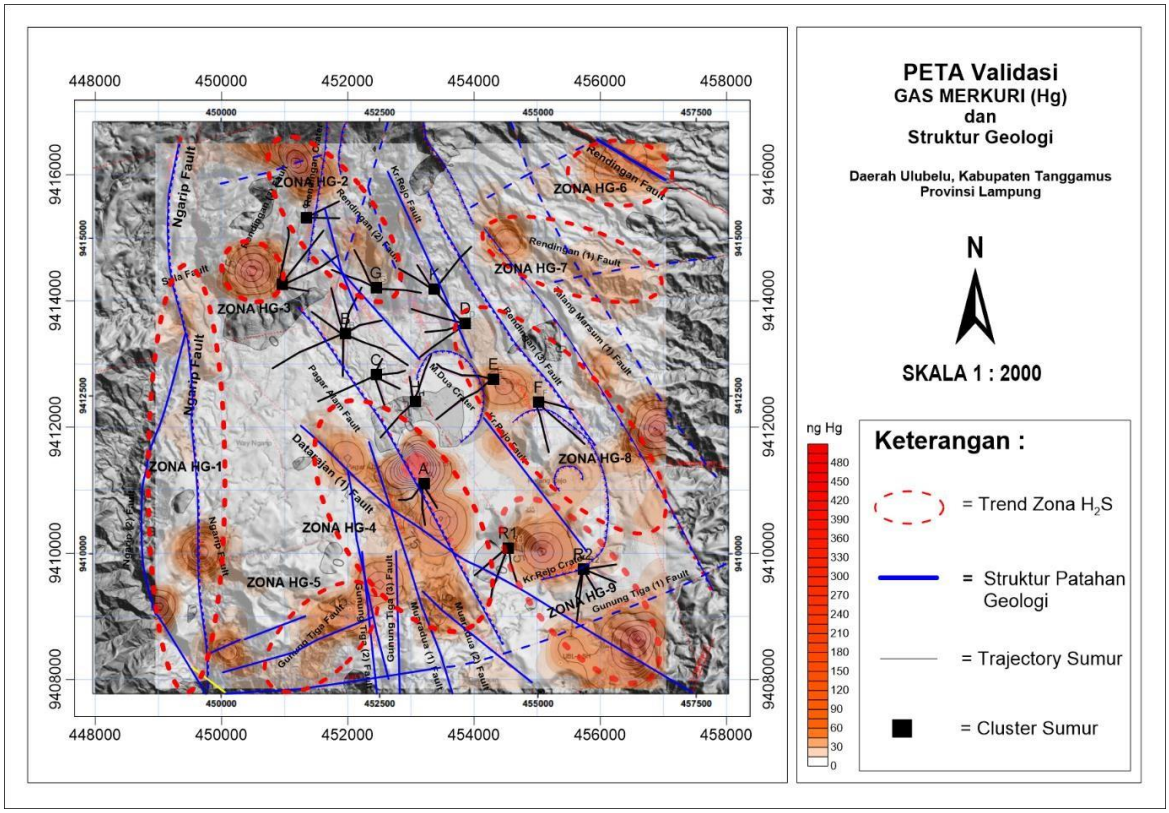


Figure 6: The Validation of mercury gas distribution with a fault structure (PGE) on Ulubelu Geothermal Area.

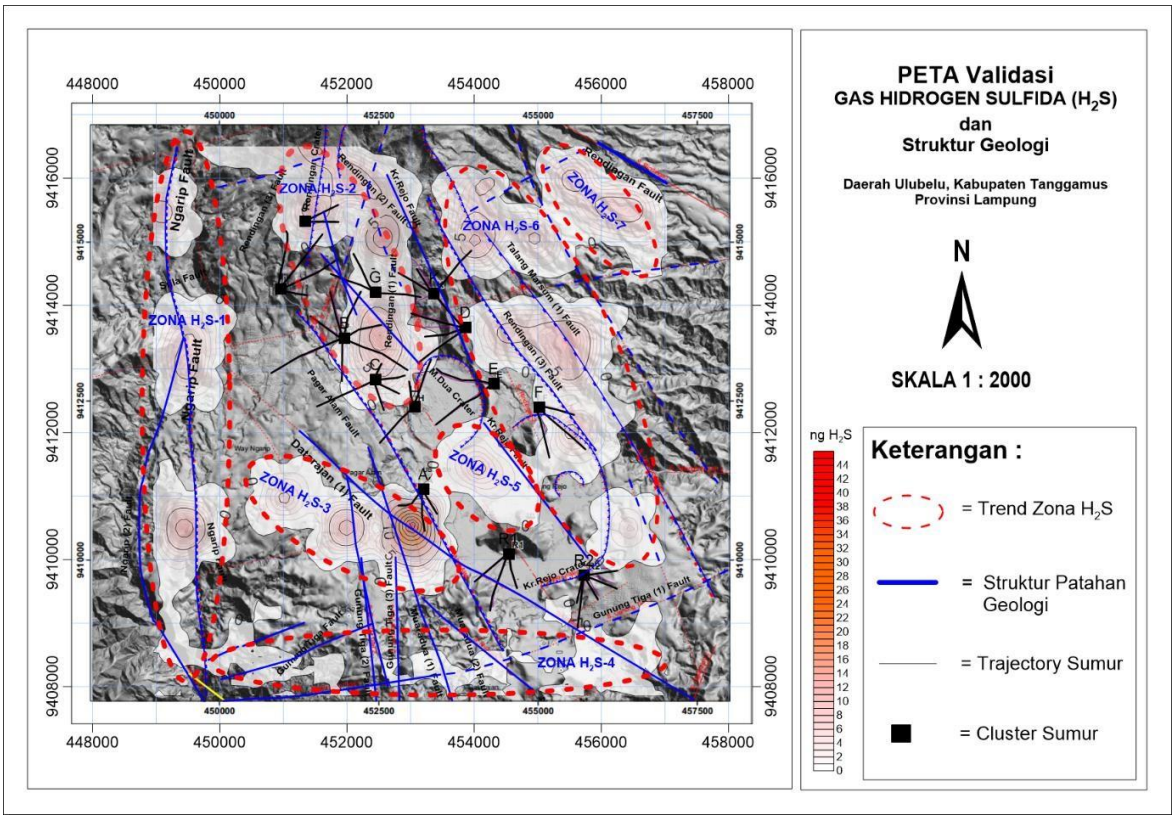


Figure 7: The Validation of H_2S gas distribution with a fault structure (PGE) on Ulubelu Geothermal Area.

A CORRELATION OF ARSENIC (AS) GAS DISTRIBUTION WITH SUBSURFACE TEMPERATURE LOG TO DETERMINE A HIGH TEMPERATURE ROCK OR STEAM ZONE ON ULUBELU GEOTHERMAL SYSTEM

Atmojo, J. P.[1], Budiraharjo, S.[1], Yunis[1], Taufiq[1], Mujihardi, B.[1], Rozaq, K.[1], Maharani[2], and Saputra, D. D.[2]

[1]Research & Technology Center (RTC) of Pertamina
[2]University of Lampung
Medan Merdeka Timur No.6, Jakarta
Email: jatmiko.atmojo@pertamina.com

ABSTRACT

Geothermal System is a heat energy that contain in subsurface can be utilized either directly or indirectly. The conditions for the occurrence of geothermal systems are influenced by several factors like a heat source, reservoir, a fluid on permeable rock, caprock, structure, and recharge area. To determining the existence of a reservoir system we need a geological, geophysical and geochemical studies. In this study, we investigated a high temperature rock or steam zone in this area based on Arsenic (As) Gas distribution and Subsurface Temperature (based on log or proven data). Arsenic (As) Gases is associated with temperature of rock, a volatile element, which only release on high temperature. Based on Arsenic (As) Gas Acquisition on Ulubelu Geothermal Field, we determine a high arsenic gas pattern (with value 75-300 ng As) is indicated a high temperature rock or steam zone. If we overlay with subsurface temperature map on research area, we can see a high As distribution is directly proportional with high temperature (with value 225 until 275ºC), so that it shows a positive correlation with the existence of high temperature rock or steam zone in the research area. Based on this research, we can conclude the Arsenic (As) gases distribution can help the preliminary surveys to determine a high temperature rock or steam zone in the geothermal area or hidden geothermal area.

Keywords: Steam zone determination, Ulubelu geothermal field

INTRODUCTION

Geothermal System is a system that formed due to geological processed, is the movement of earth's crust, so that the heat produced is delivered from medium called heat source to another medium (rocks above it). To form a geothermal system as a source of geothermal energy, several important components are needed, such as heat source, reservoir rock (permeable), flowing fluid (circulation), geological structure, cap rock, and recharge area. Heat Source is one of the important elements in determining the prospect of reserves and the source of geothermal energy in the area.

In this research, we would like to analysis a result of Arsenic (As) gas distribution to identify a high temperature rock or steam zone in Ulubelu Geothermal Area. It caused Arsenic Gases is associated with heat source, it's because the gases is volatile element, it only can be distributed from the magmatic rock and moving up to surface with high temperature.

THEORY

Regional Geology

The condition of the surface geology at Ulubelu Geothermal Area (Figure 1) is dominated by volcanic rock, it's composed by the complex of granodiorite (Tmg), the older andesites (Tmat) and the Mt. Kabawok pyroclastic (Qpkb) are located in the southeastern part of the field. The Mt. Kurupan pyroclastic (Qpkl) are in the northeast. The Mt. Rindingan complex (Qprl, Qprd) occurs in the west and southwest and the Mt. Kukusan basaltic lava (Tpl) complex is in the south, between the Mt. Kukusan basaltic andesite lavas and the Mt. Sula andesite lavas (Tps) are pumice tuffs. The Lake Ulubelu and the Mt. Duduk dacite lava (Tpd) complexes are seated in the middle of the area (Masdjuk, 1990).

Geothermal Energy

Geothermal energy is the heat stored in the rock beneath on the earth's surface and the fluid contained therein. Geothermal system consists of elements that made up the system. Essential elements of constituent geothermal system are separated in three aspects, contained a heat source, a permeable reservoir rock, and fluid that bring the heat flow, the illustration of geothermal system can be seen on Figure 2 (Goff and Cathy, 2000).

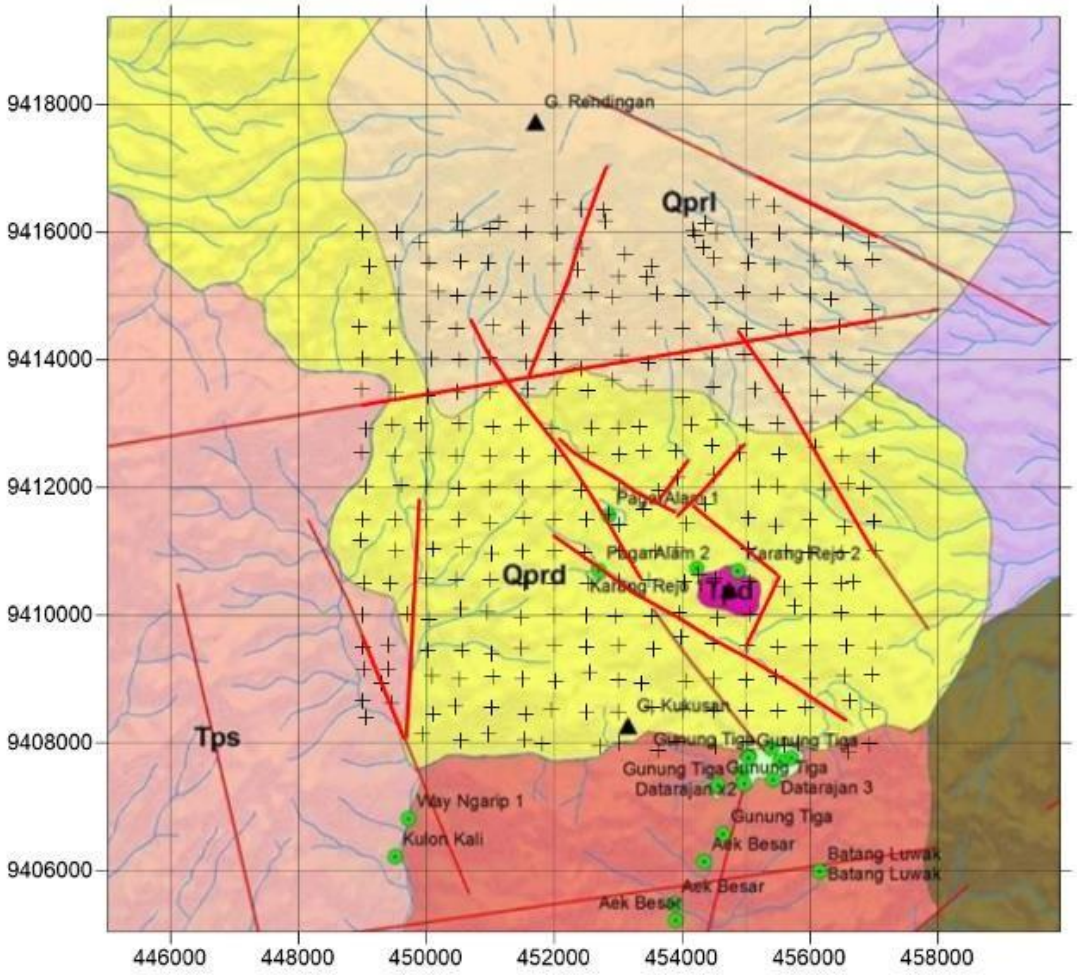


Figure 1: The Geology of Ulubelu Geothermal Area with geochemistry acquisition point (modified from Masdjuk, 1990 & PGE, 2014).

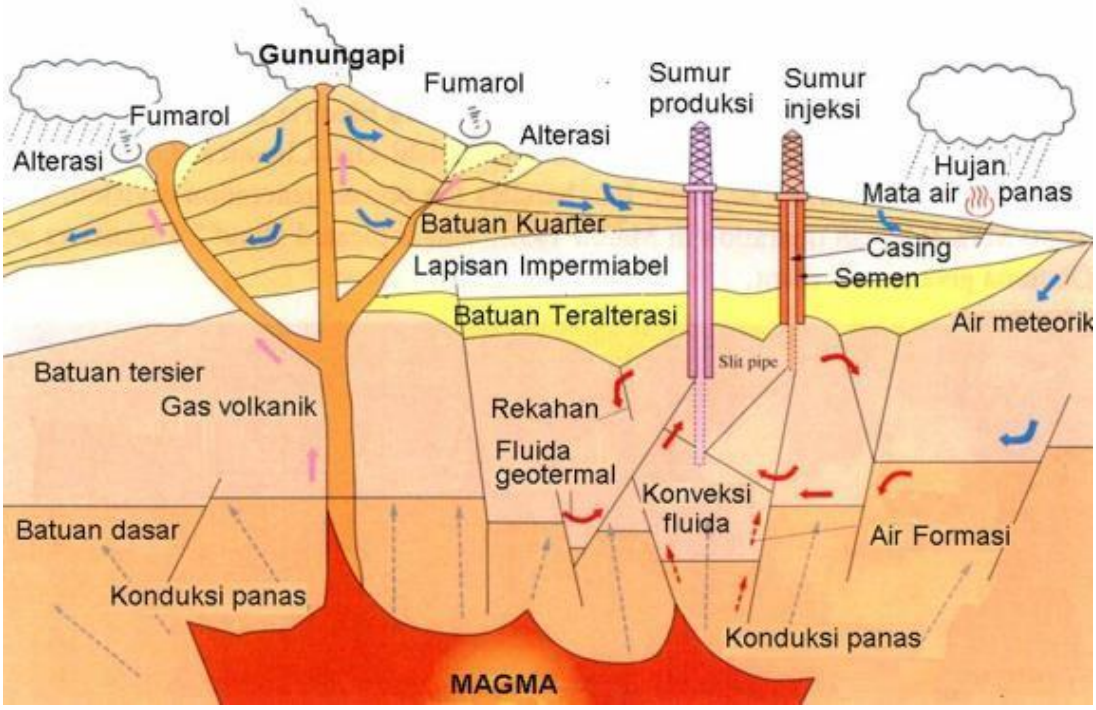


Figure 2: Geothermal System (Putohari, 2009).

Arsenic (As) Gases

Geothermal fluid carries heavy metal elements to the surface, one of which is arsenic (As). Arsenic gases is associated with temperature of rock, a volatile element, which only release on high temperature.

Purnomo and Pichler (2014) conclude in java island was found that the active volcano and geothermal area contain a high concentration of Arsenic gases.

There are three schemes for the existence of Arsenic on the surface. First, the arsenic appears to the surface carried by magmatic fluid which reaches the surface through a fault so that there is no intensive interaction with the side rocks. Second, Arsenic is carried by hydrothermal fluid which interacts with igneous rock as a host-rock that is rich in Arsenic elements. Third, Arsenic is carried by chemical compounds pesticides used by humans in agricultural activities (Purnomo, 2014).

Webster (2005) examined that Arsenic in solution can move to ground water to surface water and then adsorb to surrounding sediments. Not only in sediments, Mohapatra (2007) also tested clay minerals and showed that clay minerals could adsorb Arsenic. Arsenic in sediments and soil is then adsorbed by plant roots and consumed by humans.

RESULT AND DISCUSSION

This research is located in Ulubelu Geothermal Area, 120 km from the capital city of Lampung Province, we need approximately four hours to go to research location (see on the black box on Figure 3).

In this research, we spread 300 point of geochemistry acquisition with distance per point is 500 meters (gridding point). It covered 9 km in vertically and 10 km horizontally, with total area is 90 km2 (see Figure 1), the acquisition takes 14 days of measurement, so with this value, we hope can recover the area of Ulubelu Geothermal System (Production Wells and Injection Wells).

After the acquisition (14 days), sample of Arsenic (As) is analyzed on Gases Laboratory to get a value of contain. The result of Arsenic survey is a high value (75-300 ng As) is indicated the area with high temperature zone or steam zone (see Figure 4). The high value we will divide on the 6 zone (with assumption the flow of gases is make a shape of the contour map) spreading on this research area.

The result of Arsenic surveys then validated with subsurface temperature (based on updated logging data source information) on the area. Overlay both of the data (Arsenic contour map with subsurface temperature data) show a positive correlation between high values of Arsenic (75-300 ng As) with a high subsurface temperature (225-275ºC) (see on Figure 5).

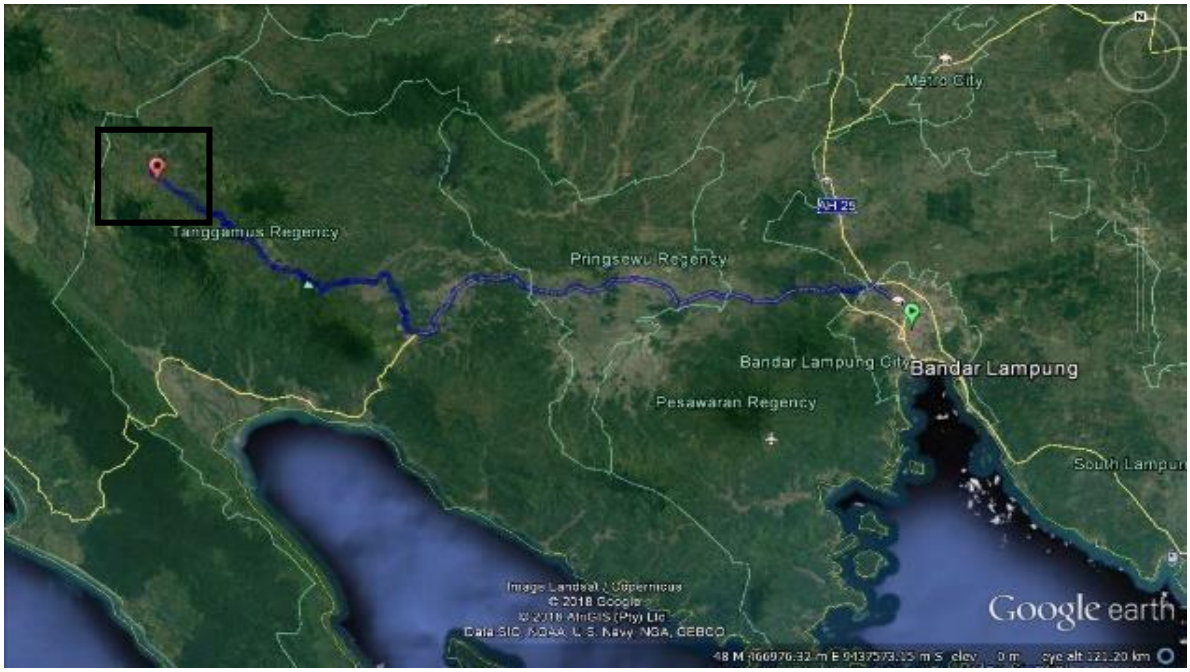


Figure 3: The Location of Ulubelu Geothermal.

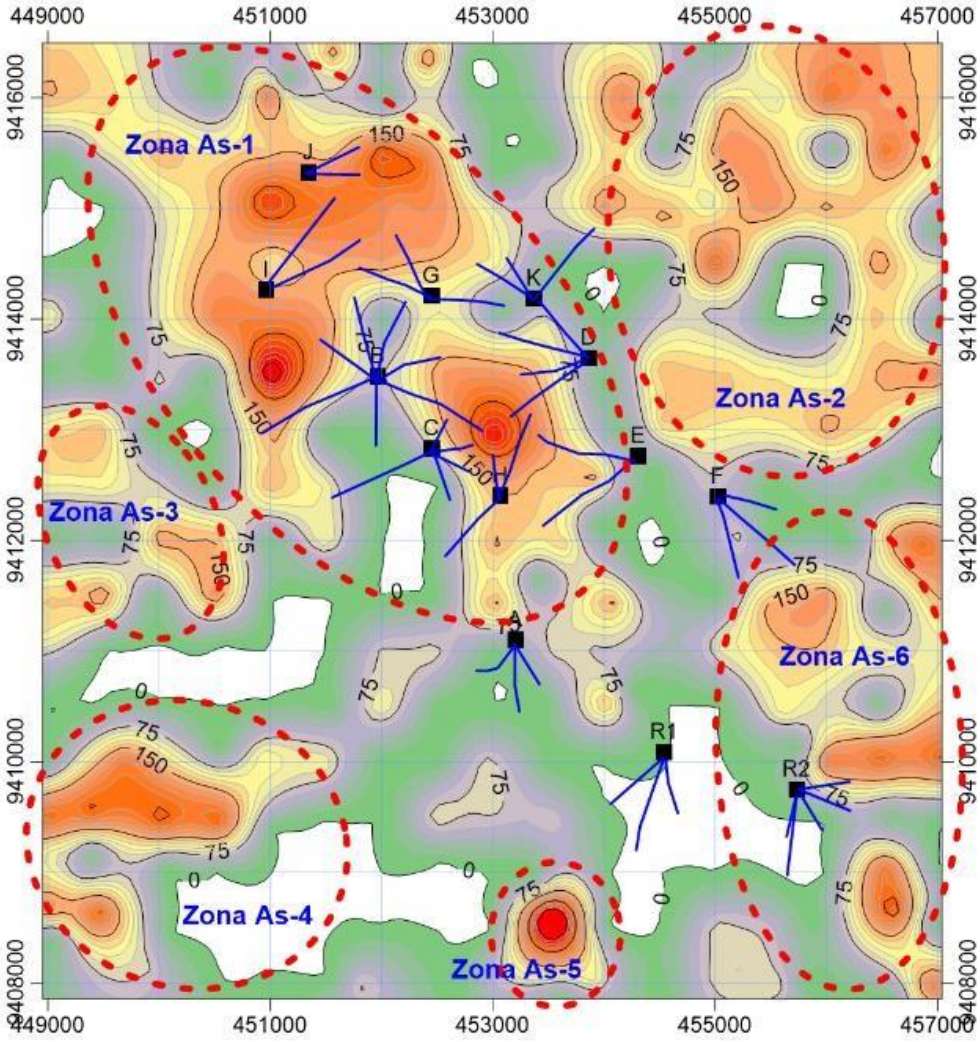


Figure 4: The Result of Hg gas distribution on Ulubelu Geothermal Area.

Overall, we look a correlation of Arsenic contour map with subsurface temperature map show a positive correlation. So, in the next research, we can validate (phase II), in the different area to determine a prospect zone based on temperature map and arsenic contour map, so if this successful, we can apply this method to help a preliminary survey in a hidden geothermal prospect.

CONCLUSION

The conclusions derived from this paper are:

1. Based on Geochemistry Acquisition, the value of Arsenic gases with range 75-300 ng As (on arsenic contour map) is indicated a high temperature rock or a steam zone.
2. If we validate with subsurface temperature map in this area, its show a positive correlation between high arsenic gases pattern with high temperature map (its covered injection and production well on the area).
3. In the next research, we can validate (phase II), in the different area to determine a subsurface temperature based on arsenic gases, so if this successful, we can apply this method to help a preliminary survey in a hidden geothermal prospect.

ACKNOWLEDGEMENT

We would like to thank Research and Technology Center (RTC) of Pertamina to permit a geothermal research team to publish this paper and thanks to University Lampung to join exploration team at Ulubelu Geothermal Area.

REFERENCES

Bundschuh, J., Maity, J., P., (2015), "Geothermal Arsenic: Occurrence, mobility, and environmental implications", Renewable and Sustainable Energy Reviews, vol.42, p.1214-1222.

Giriarso, J., P., Puspadianti, A., Mulyanto, Hartanto, D.B., Siahaan, E.E., (2015), "Initial Geochemical Monitoring on Ulubelu Geothermal Field", Proceedings World Geothermal Congress 2015.

Goff, F., Cathy J., J., (2000), "Encyclopedia of Volcanoes: Geothermal System", Academic Press, 817-834 pp.

Herath, I., Bundschuh, J., Vithanage, M., Bhattacharya, P., (2016), "Geochemical Processes for Mobilization of Arsenic in groundwater", Arsenic Research and Global Sustainability, pp.23-24.

Hochstein, M., P., Sudarman, S., (2008), "History of Geothermal Exploration in Indonesia from 1970 until 2000", Geothermics, Vol. 37, p.220-266.

Masdjuk, Muchsim, (1990), "The Geology of Ulubelu Geothermal Area", Unpublished Internal Report, Geothermal Div., Pertamina.

Panjaitan, S., (2010), "Geology of Ulubelu Geothermal Area Based on Magneto telluric Data", Geo-Resources, JSDG, p.69-91.

Purnomo, B.J., and Pichler, T, (2014), "Arsenic Contamination on Geothermal", Geology.

Putohari, D.R., (2009), "Geothermal waste contains a gold", WordPress.

Wrage, J., Tardani, D., Reich, M, Daniele, L., (2017), "Geochemistry of thermal waters in the Southern Volcanic Zone, Chile – Implications for structural controls on geothermal fluid composition", Chemical Geology, Vol. 466, p.448.

Webster-Brown, J., G., Lane, V., (2005), "The Environmental Fate of Geothermal Arsenic in a Major River System, New Zealand", Proceeding World Geothermal Congress 2005.

THE GEOTHERMAL EXPLORATION OF THE EAST AFRICAN RIFT SYSTEM: RECENT ADVANCES

C. Pasqua[1,2], M. Verdoya[2], and P. Chiozzi[2]

[1]ELC Electroconsult S.p.A., Via Marostica 1, I-20146 Milan, Italy
[2]DISTAV Università di Genova, Viale Benedetto XV 5, I-16132 Genoa, Italy
Email: claudio.pasqua@elc-electroconsult.com

ABSTRACT

The East African Rift System (EARS) is the longest continental rifting in the world (>5000 km long). At regional scale, the most characteristic structural features of EARS are narrow elongated zones of thinned continental lithosphere, which are likely related to asthenospheric intrusions in the upper mantle. At surface, EARS shows up as a series of several thousand kilometers long aligned successions of adjacent individual extensional (rifted) basins, which can be grouped into several segments. Rift basins occur from the Afar region in Eritrea, Ethiopia and Djibouti in the north (Eastern Branch) and continue all the way up to Mozambique (South-eastern Branch) and Botswana (Western Branch). In the Eastern Branch, a number of Quaternary volcanoes occur and superimpose older (Mio-Pliocene) magmatic products. Volcanism is sparser south and west. These volcanological and structural features, together with the high heat flow associated with magmatic activity and hydrothermal circulation, make EARS Africa's largest geothermal potential area. In this paper, new results of recent explorations of geothermal resources in EARS are presented, as obtained from studies carried out in some of the most important geothermal fields of the eastern and western branches of EARS. Geological, geochemical and geophysical (gravity, magnetotelluric and seismic) investigations were carried out in the geothermal prospects of Alalobeda (Ethiopia), Menengai (Kenya), Kiejo-Mbaka and Luhoi (Tanzania), which represent well the different geothermal play types of the region. Our study also supplies an example of guidelines for the optimum procedures of geothermal resource exploration in EARS.

Keywords: Exploration, East African rift

INTRODUCTION

The East African Rift System (EARS) is the most extensive, currently active zone of continental rifting. It is an intracontinental divergent plate boundary at which the African plate is splitting into the Nubian and Somali plates (Figure 1). It can be divided into an Eastern and a Western Branch. To the north, the Eastern Branch includes the Afar region, the Main Ethiopian Rift (MER) and the Kenya Rift. South of the Aswa shear zone, the Western Branch starts, and the Eastern Branch tends to be less well defined. The development of the rift system largely occurred within the Proterozoic basement, at the margins of the Archean cratons of central Africa (Chorowicz, 2005).

Within each rift segment, N-S extensional faulting dominates. Extension in other orientations (NNE-SSW) is occasionally seen along some of the minor rifts distributing deformation away from the main rift branches, like e.g. at the Mweru and Kariba rifts. The Western Branch is seismically active along its entire length. Earthquakes along the Eastern Branch are less frequent than along the Western Branch (Craig et al., 2011).

Abundant Cenozoic volcanism in EARS is widespread in the north, especially in the Eastern Branch, but sparse in the south (Figure 1). Volcanic activity started in the northern part of the Eastern Branch about 30 Ma ago with uplift, whereas in the Western Branch commenced about 12 Ma ago near the Albert Rift and about 7 Ma ago in the Tanganyika Rift (Keller et al., 1994). Most volcanoes are located along the central axis of EARS branches. Off-axis volcanoes are explained with the opening of large tension fractures caused by reactivation of Precambrian zones of weakness (Bosworth, 1987).

In the rift axis of the Eastern Branch, numerous volcanoes of Quaternary age occur, overlying products of Miocene and Pliocene volcanism. The shield volcanoes are built largely of intermediate lavas and associated pyroclastics, thus indicating the presence of shallow, hot bodies (magma chambers). In the Western Branch, there is paucity of volcanism along the entire length of the rift with the main volcanic areas near Kivu Rift (Virunga volcanic province) and between Rukwa and Malawi rifts, in the Rungwe volcanic province (Ebinger et al., 1989; Omenda, 2009). The Western Branch is mostly characterized by the abundance of potassic alkaline rocks that consist of carbonatites, ultrapotassic mafic rocks and potassic mafic-felsic lavas.

These volcanological and structural features, together with the high heat flow associated with magmatic activity and hydrothermal circulation, make EARS Africa's largest geothermal potential area. Hot springs, fumaroles, and steaming grounds are more abundant in the Eastern Branch (Afar Region, MER and Kenya Rift), where shallow magma bodies are the most likely heat sources for

volcano-hosted high-temperature geothermal systems. In the Western Branch, outside of the sparse Quaternary volcanic centers, deep circulation of ground water through the rift master faults, coupled with heating by young dike intrusions or plutons, is the most likely mechanism for explaining some of the geothermal systems (Omenda, 2013).

In view of the structural and volcanological differences between the two branches of the rift system, a classification of EARS geothermal plays according to conventional schemes can be hardly applied, as the geothermal systems often exhibit hybrid characteristics (Moeck, 2014).

In this paper, we review geological, geochemical and geophysical results and present new data and interpretations of recent programs of exploration of geothermal resources in EARS. In particular, we focus on three of the most important geothermal fields (Alalobeda, Menengai and Kiejo-Mbaka) located in the Eastern and Western branches (Figure 1). These fields well represent the different structural, volcanological and hydrogeological realms that may be encountered in EARS.

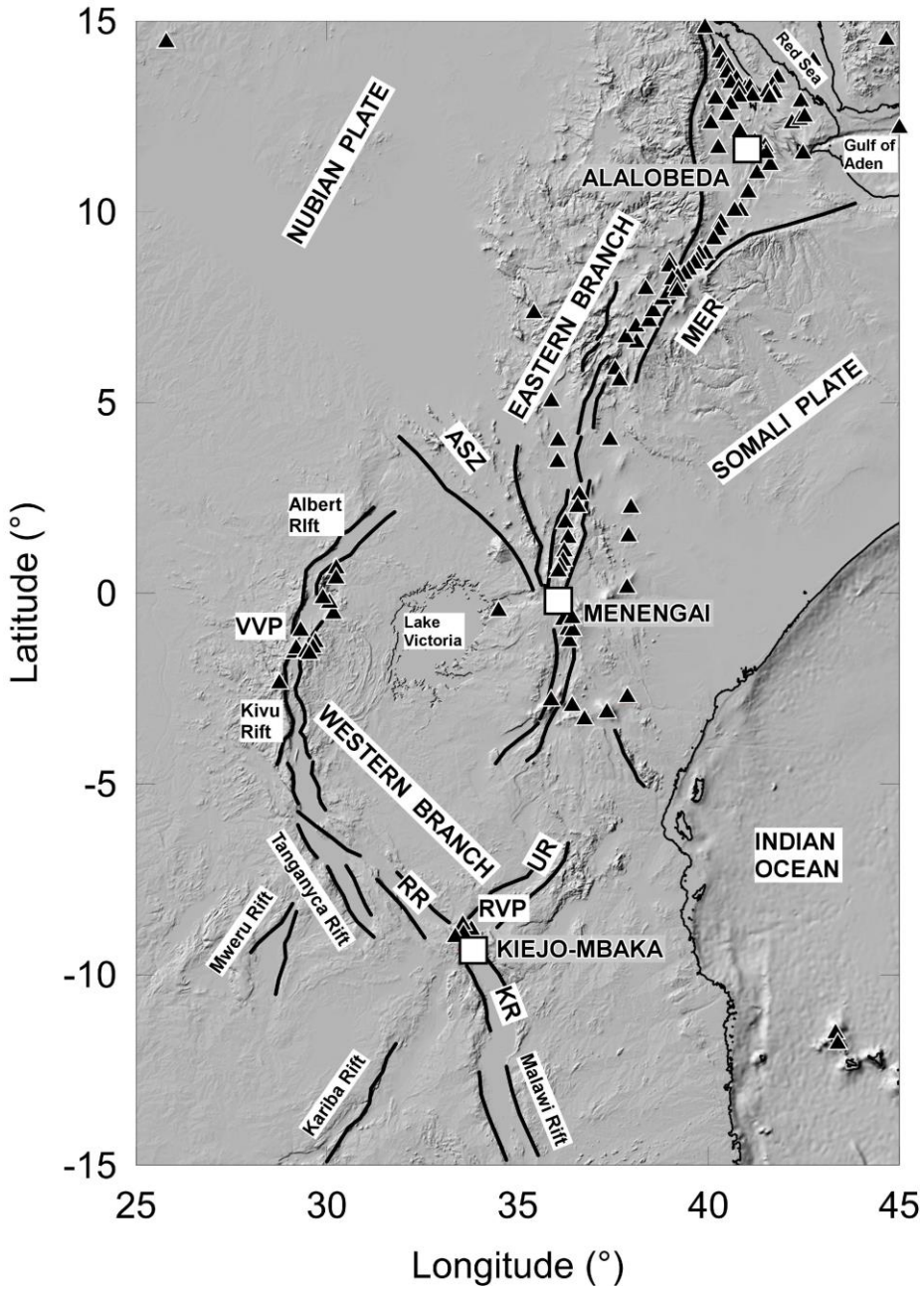


Figure 1: Structural sketch of the East African Rift System and location of the investigated geothermal fields (white squares): MER, Main Ethiopian Rift; ASZ, Aswa shear zone; RR, Rukwa Rift; UR, Usangu Rift; KR, Karonga Rift; VVP, Virunga volcanic province; RVP, Rungwe volcanic province. Major active faults (black lines) and volcanoes (black triangles) are also shown.

The geothermal field of Alalobeda (Ethiopia) is located in the neighborhood of the Afar triple junction. Geoscientific exploration was recently carried out in the framework of a project of evaluation of the geothermal resources of the country (ELC-GSE, 2016). The Menengai geothermal field (Kenya) is located in a young caldera, resulting from the intersection of minor rifts with the Kenya Rift (Omenda, 2009). A series of investigations was carried out to evaluate the potential and the possible development of this geothermal prospect (ELC-GDC, 2015). The Kiejo-Mbaka geothermal area (Tanzania) is located along a NW-SE trending fault system in the Rungwe Volcanic Province (RVP). In view of the national interest in the use and development of geothermal energy, a project was implemented aimed at increasing the knowledge of this geothermal field (ELC-TGDC, 2017).

The data collected within the several surveys allow us to propose conceptual models of each field that give an insight into of the variability of geothermal plays occurring in the different parts of EARS. This can be of help in planning future studies and define optimal procedures of geothermal resource exploration in EARS.

ALALOBEDA

This geothermal prospect is either a fault/fault-leakage controlled or a magmatic geothermal system, occurring in a region of three superimposed rift zones (Figure 2): the Red Sea (NW-SE), the Main Ethiopian Rift (NNE-SSW) and, partly, the Gulf of Aden (ENE-WSW). It is located in the Tendaho graben which the main fault systems are clearly revealed by gravity anomalies and magnetic anomalies recorded by the basalts of the Afar Stratoid Series. Geochemical analyses of water samples identified two water types: i) Sodium-chloride (Alalobeda hot springs and the reservoir liquids encountered in the Dubti prospect); ii) Sodium-bicarbonate type (natural steam condensate, possibly affected by mixing with local rainwaters). Based on the Na-K and K-Mg geothermometers of Giggenbach (1988), all the samples from the Alalobeda thermal springs collected during this work indicate that the reservoir liquid (Figure 3) is close to equilibrium with albite, K-feldspar, chlorite, illite and a silica mineral at ~200-220 °C. Such temperatures are substantially consistent with those (on average 185-225 °C) inferred from fumaroles gases. The western highlands of Ethiopia could act as the main groundwater recharge zone of the geothermal field. However, both the present-day precipitations regime and isotopic data suggest that the Alalobeda geothermal reservoir hosts paleo-water seeped in early times. Groundwater is expected to flow mostly in the Afar Stratoid Series, reaching a depth of 1500-2500 m.

The Alalobeda geothermal field is characterized by a quite continuous seismic activity of low magnitude (<4.0), consistently with the regional pattern. The seismicity cutoff-depth occurs at 3.5-5 km depth. The results of the MT survey showed extremely low resistivity values for the basaltic rocks of the Afar Stratoid Series registered outside of the Tendaho Graben. This is likely due to intense alteration phenomena, which accompany hydrothermal circulation. Along the SW shoulder of the Tendaho Graben, a very thick horizon of low-medium conductivity was detected (Figure 4), which can be at least partly interpreted as the cap-rock formation. Southwards, an increase in resistivity (from 5 to 10 Ω m) of this horizon seems to indicate the end of the cap-rock and consequently could mark the limit of the geothermal system. Below the high-conductivity cap-rock, the more resistive basement (often in excess of 100 Ω m) can act as the reservoir formation, although its resistivity is somewhat higher than that commonly recorded in other geothermal fields.

MENENGAI

This field, occurring in a 12 km-wide caldera (Figure 5), can be classified as convection-dominated magmatic play type. It was recognized as a promising geothermal prospect among the many existing along the Rift Valley in Kenya. After a series of geophysical investigations (micro-seismic monitoring, gravity and MT surveys), geological surveys, geochemical surveys (fumaroles sampling, soil gas surveys) and a soil temperature survey, a first exploratory well MW-01 intercepted a deep reservoir with temperatures exceeding 300 °C. The deep reservoir extends beneath a shallower liquid-dominated reservoir at temperature of 190-200 °C. Irrespective of the provenance, all reservoir liquids belong to the Na-HCO_3 facies. However, no presence of a clear cap-rock was identified; therefore, self-sealing processes were invoked in order to explain the existence of two distinct reservoirs. Following the successful results of MW-01, an exploratory and development campaign started with the drilling of about twenty deep wells aimed at characterizing the deep reservoir properties, delineate the field extension and provide additional steam for power development.

On the basis of available data, a conceptual model of the Menengai geothermal system was obtained (Figure 6). The system is characterized by a liquid dominated shallow reservoir at temperature ranging from 130 to 210 °C, which overlays a deeper high temperature, two-phase or vapour-dominated reservoir, with temperatures reaching 330 °C. Figure 6 shows a conceptual model of the entire system incorporating surface exploration surveys and the findings derived from drilling, logging and testing of geothermal wells.

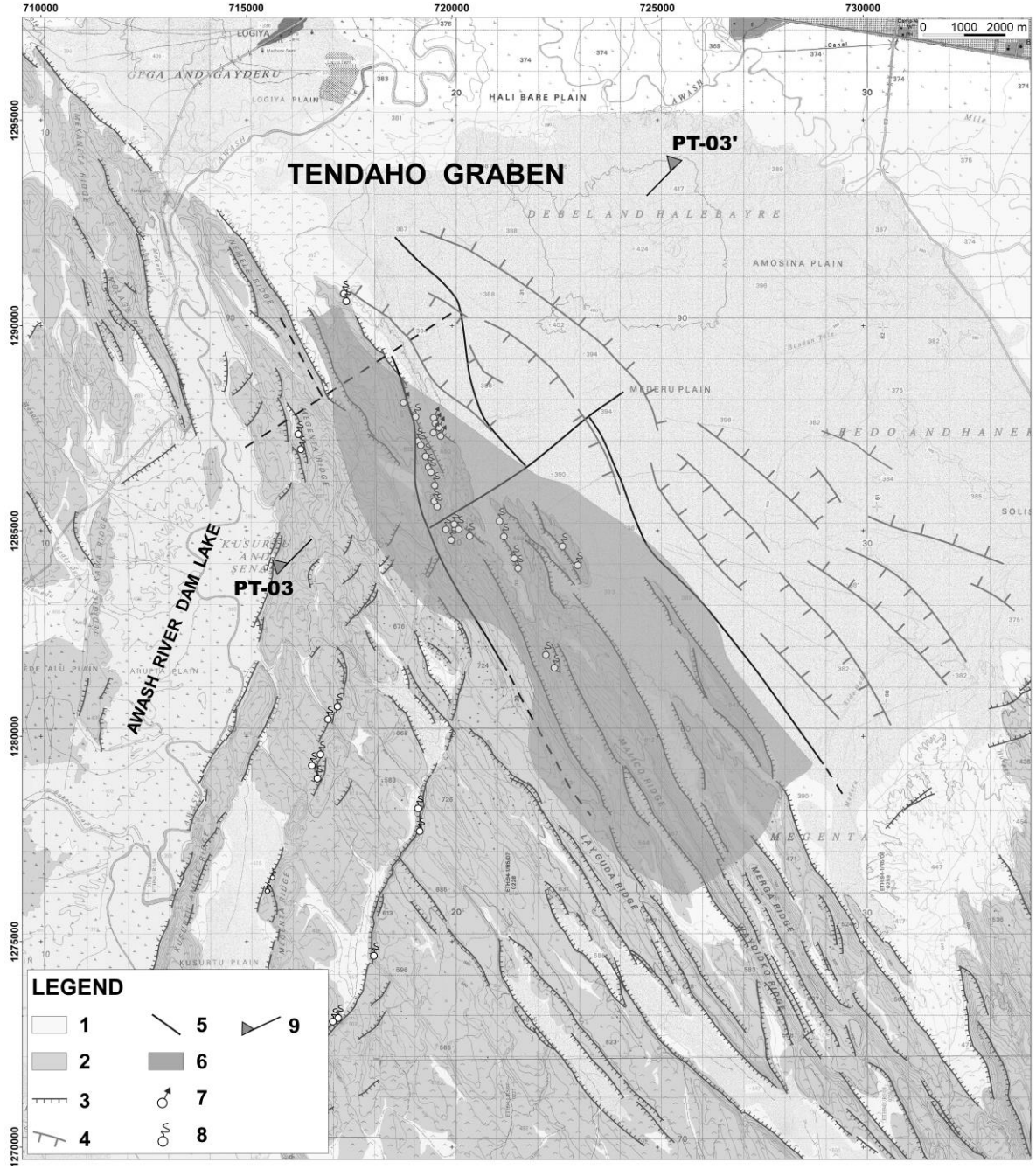


Figure 2: Geological map of the Alalobeda geothermal field. Young sedimentary deposits (1); basaltic rocks of the Afar Stratoid Series (2); main faults inferred from the geological survey (3); faults inferred from the gravity survey (4); faults inferred from the magnetotelluric survey (5); positive Bouguer anomaly (6); hot spring (7); fumarole/steaming ground (8); cross-section of Figure 4 (9).

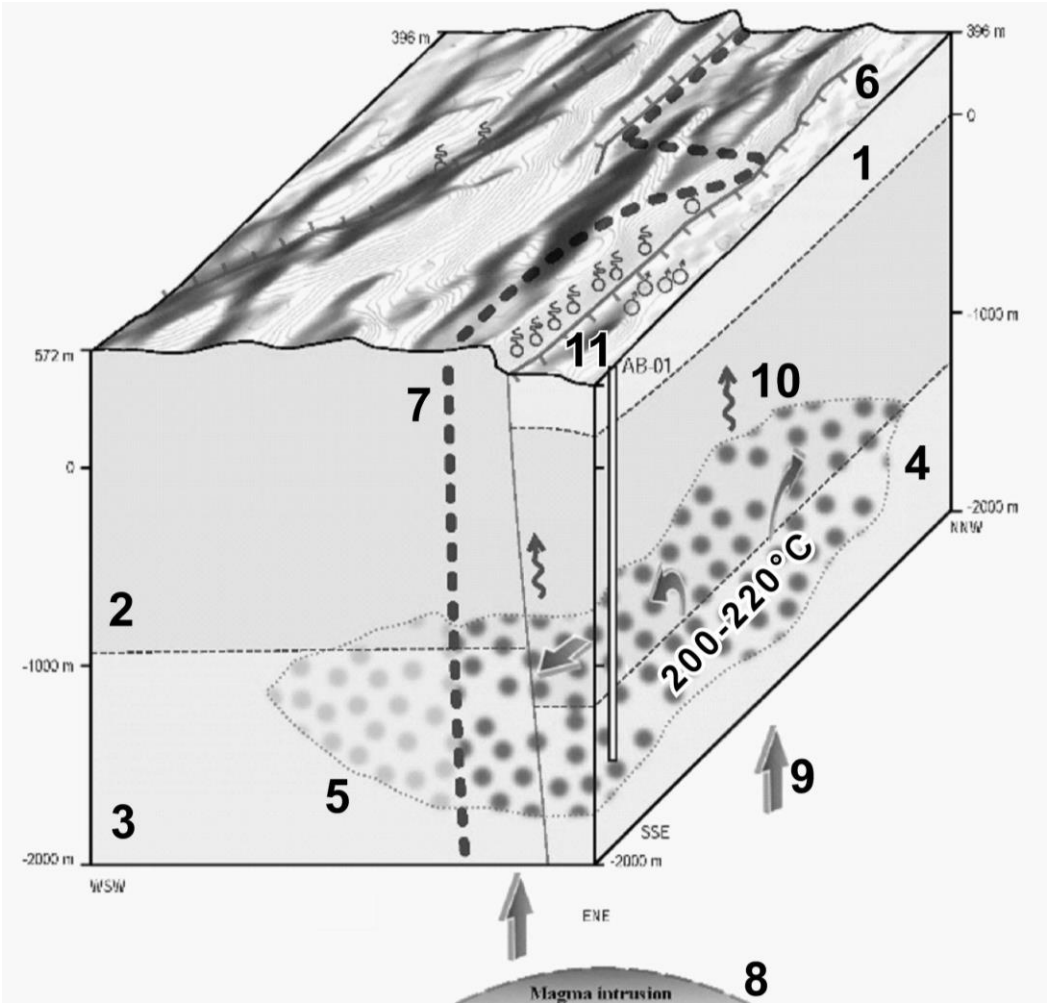


Figure 3: Conceptual Model of the Alalobeda geothermal field. Young sedimentary deposits (1); basaltic rocks of the ASS (2); Dahla basalts fm. (3); probable reservoir (4); possible reservoir (5); main fault (6); geoelectrical discontinuity (7); heat source (8); upflow (9); fluid escape (10); main geothermal manifestations (11).

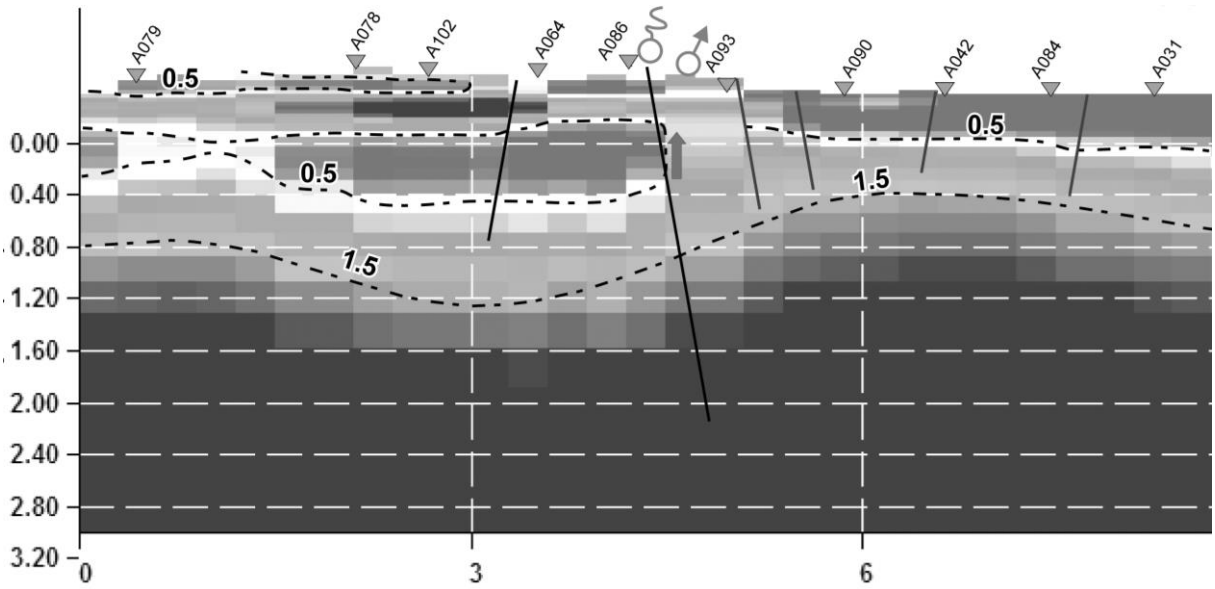


Figure 4: PT-03 3D longitudinal profile. Scale color in Log10 [Resistivity (Ω m)]. Distance/depth scale in km.

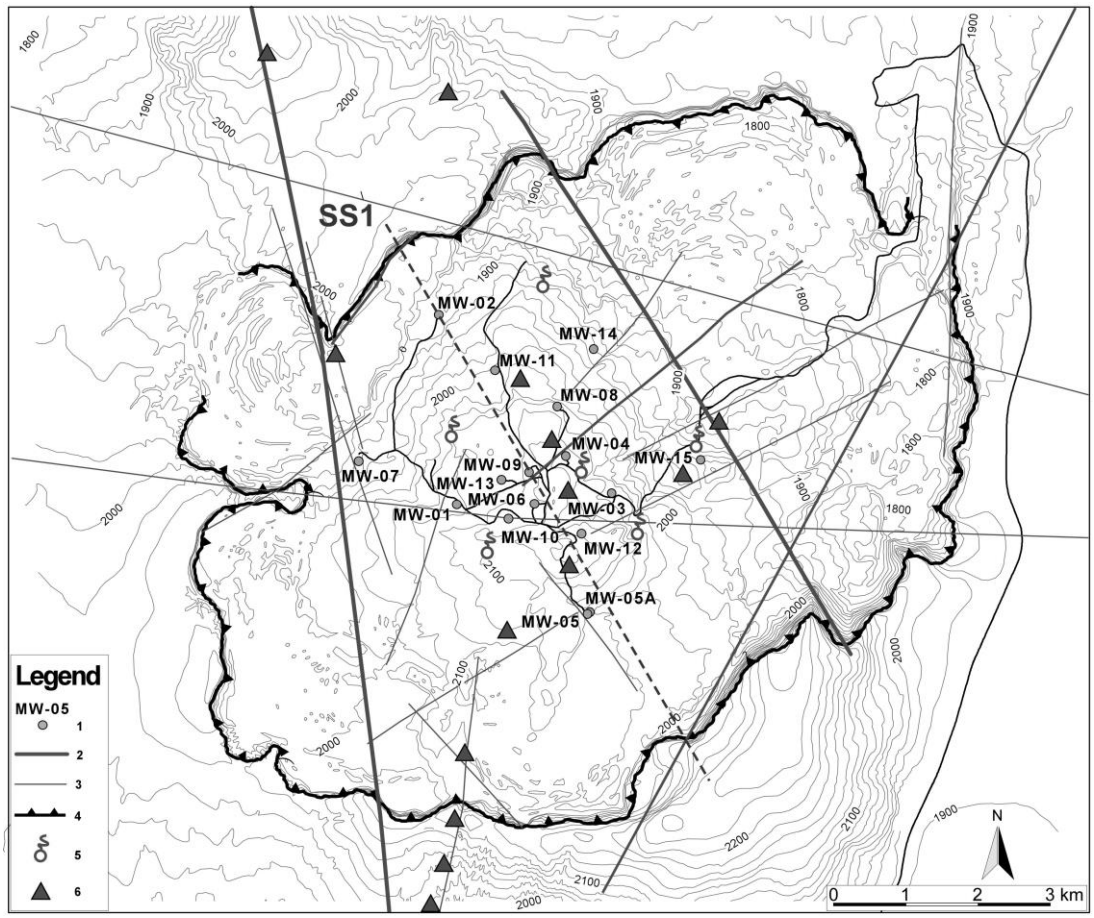


Figure 5: Geological sketch of the Menengai caldera. Drilled wells (1); major fault (2); lineament and fault (3); caldera rim (4); fumarole (5); eruption center (6). The trace of section SS1 (see Figure 6) is shown.

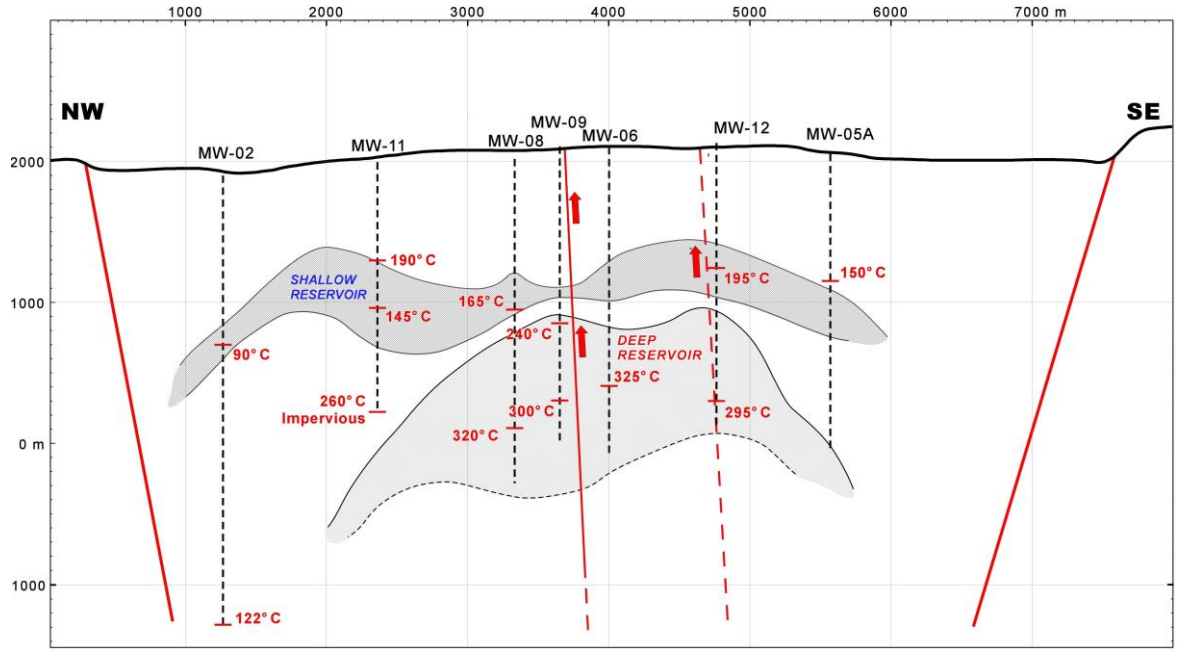


Figure 6: Conceptual model of the Menengai geothermal field along cross-section SS1 (see Figure 5). Dark hatched lines are existing wells; values of the measured temperatures are indicated. The red arrow is the upward flow along the main faults (red line).

The conceptual model, integrated with production testing results, was used to build a 3D numerical model of the geothermal system in order to simulate its thermal structure, check the consistency of

acquired data, and set up the tool for the subsequent modeling of exploitation scenarios (ELC-GDC, 2015). The modeling of the natural state was intended to provide a better picture of the reservoir thermodynamic conditions and simulate the mass and heat flows through the system. A steady-state condition modeling was at first carried out and calibrated against data obtained from geochemical investigations, well pressure and temperature profiles recorded under warm-up and flowing conditions, as well as available production tests results. The 3D natural state reasonably reproduces the liquid dominated shallow reservoir just on top of the deeper, vapour-dominated high temperature reservoir which is feeding the dry steam wells drilled in the central area of the prospect. The deep reservoir is recharged by the upflow of a high temperature mixture of steam and CO_2. The latter accumulates at the culminations of the deep reservoir due to the boiling and condensation processes associated to the heat pipe mechanism supported by the strong heat flow. The gas phase saturation declines, moving from the central vapour-dominated area towards the periphery of the deep reservoir, where the aqueous phase becomes strongly mobile. The thermodynamic conditions and rock properties of the lateral extension of the deep reservoir are poorly constrained by present drilled wells and need to be better characterized in the future, as they are fundamental for the reliable assessment of overall prospect potential and subsequent exploitation of the resources.

KIEJO-MBAKA

This prospect can be classified as a fault-leakage controlled play (extensional domain play), in which convection takes place mostly along the major fault/s and the fluids can leak from the fault/s into permeable layers expanding laterally. It falls within the Rungwe Volcanic Province (RVP), which is situated in the East Africa Rift System at the triple junction of the Rukwa, Usangu and Karonga rift basins (Figure 1). Recent volcanism in the geothermal area is concentrated in the southern sector of the RVP and it is expressed by eruptions of very limited volume and derived from deep sources, which can hardly contribute to the thermal anomaly. Kiejo-Mbaka is underlain by Pre-Cambrian rocks of the metamorphic-intrusive complex, consisting mostly of biotitic gneisses and schists, amphibolites and metagabbroid bodies. The complex is sub-outcropping in the central portion of the focal area (Mbaka ridge) and is covered by a thick sequence of clastic sediments westwards and eastwards. Volcanic products (basalts and ignimbrites) derived from Pleistocene eruptions cover the area with a thickness never exceeding 200 m. Several fault systems were recognized (Figure 7), among which the most important ones are NW-SE and N-S. The Mbaka fault, which controls the hot waters emergences and delimits to the west the Mbaka ridge, belongs to the NW-SE system and is associated with a series of vicariate parallel structures extending in the plain. The Kisyelo fault, which delimits to the east the Mbaka ridge, trends N-S to NNW-SSE.

Three groups of hot springs (Ilwalilo, Kilambo, and Kajala) are found along the Mbaka fault, with a maximum discharge temperature of 64 °C. Geothermometric determinations over these waters indicate a deep temperature of about 140 °C in Kilambo-Kajala and of about 115 °C in Ilwalilo. The reservoir fluid has a Na-HCO_3 chemical composition. The main zone of recharge of the system corresponds to the Elton plateau, which extend to the NE of the Livingstone fault, a major NNW - SSE structure delimiting eastwards the East Africa Rift.

The gravimetric and the magnetotelluric surveys concurred to identify an area characterized by a pronounced positive Bouguer anomaly and high resistivity. Such a block corresponds to the Mbaka ridge, where the basement is either outcropping or sub-outcropping. In the plain which extends west of the Mbaka fault a conductive unit with an average thickness of 1,000 m, a resistivity as low as 0.5 Ω m and a tendency to get thicker moving westward and southward was recognized. In the sector that extends east of the Kisyelo fault, two discontinuous conductive units were identified at shallow and intermediate depth. In both cases, these anomalies were referred to the sequence of clastic sediments and attributed to either primary (fine grained composition) or secondary (moderate temperature hydrothermal alteration) causes.

The reconstruction of the geometry of the reservoir was based on the hypothesis of a fault-leakage controlled play, assuming that the Mbaka fault represents a hydrogeological boundary to the eastern expansion of the heated fluids and taking into consideration the configuration of the conductive unit, interpreted as reflecting the cap-rock of the system (Figure 8). The SW limit of the reservoir is likely to correspond to a long-liner fault which runs about 2 km west of the Mbaka fault and the NW and SE limits have been conventionally set 2 km NW and 3 km SE of the Kilambo manifestations, respectively.

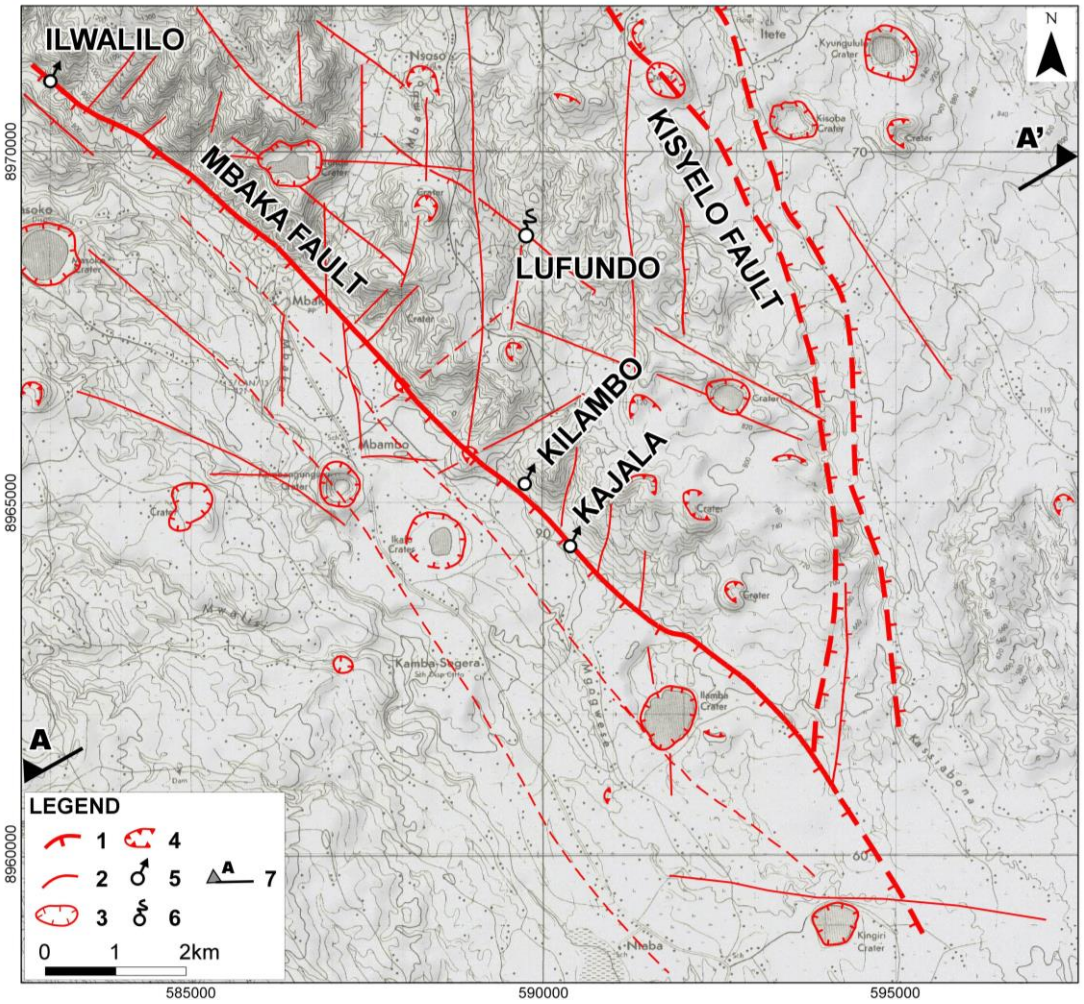


Figure 7: Structural map of the Kiejo-Mbaka geothermal area. Major fault -dashed when inferred from geophysical data- with indication of downthrown side (1); minor fault -dashed when inferred- with no clear indication of downthrown side (2); maar crater rim (3); cinder cone crater rim (4); hot spring (5); fumarole (6); trace of cross-section of Fig. 8 (7).

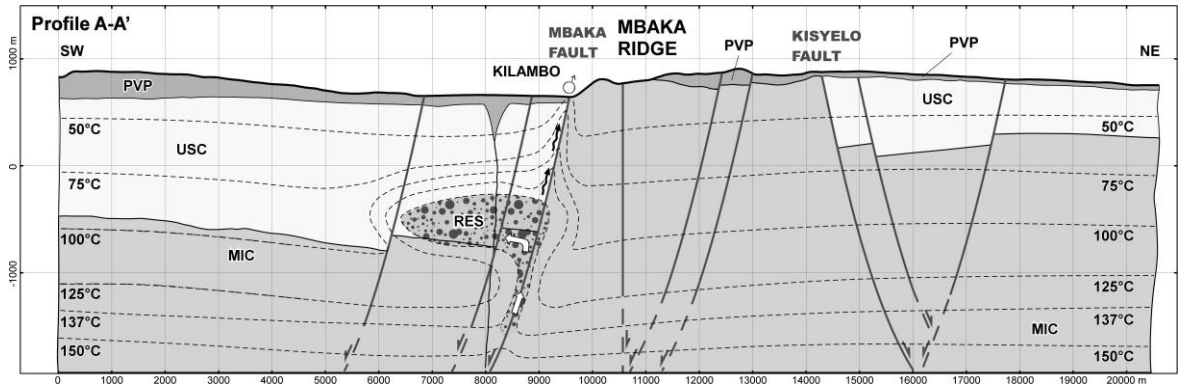


Figure 8: Conceptual model of the Kiejo-Mbaka geothermal field. Neogene-Recent volcanics (PVP); undifferentiated sedimentary complex (USC); metamorphic basement (MIC); geothermal reservoir (RES); dark lines are main fault; dashed lines are isotherms; white arrows indicate upflow; dark arrows indicate escape fluids from the reservoir.

DISCUSSION AND CONCLUSIONS

The comparison of the geothermal plays of EARS with others investigated in the frame of other international geothermal projects in South-East Asia and Central America (see Pasqua, 2019), lead to some final remarks (Pasqua, 2019):

a. *The same geothermal play-types can be found in both compressive (subduction zone) and extensional (rifting) stress conditions, although their characteristics could be partially different.* The plutonic play-type is one typical example. In fore- or back-arc regions of fold-thrust belts along subduction zones (like e.g. the Mataloko geothermal field, Indonesia), a well-developed thick and continuous cap rock mainly formed by clay minerals (illite, smectite, chlorite) is present. On the contrary, in a rifting region (EARS), the "classic" cap rock can be missing, like in the plutonic play of Menengai, where, both from geophysical results and direct information deriving from the drilled wells, the presence of any particular clay-rich layer was not detected. The definition of cap rocks geometry (top/bottom) was inferred analyzing the thermodynamic conditions (pressure and temperature distribution) recorded during the well testing activities.

b. *In a given geodynamic context a "zonation" of the play-types can be recognized*; this is well evident in the EARS. The Western Branch is dominated by the presence of fault/fault leakage controlled types. The presence of persistent volcanic activities is limited to two cases, namely: Virunga (DRC and Uganda) and Rungwe (Tanzania) Volcanic Provinces. On the other hand, in the Eastern Branch the volcanic activities are well represented by the presence of tens of volcanic edifices (considering Eritrea, Djibouti, Ethiopia and Kenya). In these countries, magmatic and plutonic play-types are common. However, fault controlled geothermal systems may be also present, although to date they have not been studied in detail, due to their low temperature which renders these geothermal prospects of relatively low commercial interest.

c. *A different approach should be followed in order to characterize properly the geothermal fields present in the EARS;* we have to note that the common approach to investigate and study a geothermal prospect is to conduct geoscientific investigations, namely: geological, geochemical and geophysical (MT/TEM, gravity and seismic) surveys. In a subduction context the experts tend to believe primarily in the geophysical model derived from the resistivity survey, even because the values of ρ (Ω m), reported in literature, were calibrated in such environment. As mentioned in the Alalobeda (as well as in the Aluto-Langano) case study, unexpectedly low resistivity values were encountered in the basaltic rocks of the Afar Stratoid Series. Then, if the interpreted values of resistivity are simply associated with the standard values of cap rock and reservoir formations, the inferred geophysical conceptual model may be grossly incorrect. Therefore, it is essential to perform an accurate integrated interpretation of all the geoscientific results.

d. *A detailed structural survey is of primary importance especially in the fault-controlled plays, whereas its importance is often under-estimated*; it is important to stress that in the EARS, and especially in the case of fault-controlled play-types, more attention should be focused on the distribution and type of lineaments and faults systems. A high-resolution structural survey allows to define a detailed configuration of fractures and faults that may control the fluid upflow from the reservoir. This information collected at surface may then be linked to the information at depth derived from the geophysical models, strongly reducing the ambiguities of the geophysical interpretation.

e. *The geochemical features of thermal waters of EARS are often quite different from those of most of geothermal systems in subduction-related realms.* In subduction-related systems, mature chloride waters are generally hosted in geothermal reservoirs and migrate laterally discharging at the surface in correspondence of the OUTFLOW zone, while fumarolic activity and steam-heated acid-sulfate waters mark the UPFLOW zone.
The high-temperature geothermal reservoirs of the Eastern branch of the EARS host not only mature chloride waters (e.g., Tendaho and Asal in the Afar), but also mature bicarbonate-chloride and mature bicarbonate waters (e.g., Olkaria and Menengai in Kenya, and Aluto-Langano in Ethiopia - Pasqua, 2019).

f. *Differences in the geochemical signature of hot-spot/ divergent-plate (rift) systems and volcanic subduction zones are also confirmed by available data on volcanic gas*, pointing that subduction zones are enriched in Cl gases (e.g. Symonds et al., 1994; Sawyer et al., 2008). In the Eastern EARS geothermal systems, a lower contribution from Cl-bearing magmatic gas species (chiefly HCl) might be responsible of the lower Cl contents of the geothermal waters (Marini and Pasqua, 2014)

g. *Furthermore, the geothermal systems of the Eastern EARS differ from those of other extensional realms (e.g. Iceland) for the absence of mature sulfate waters.* This difference might be related to the different chemical characters of magmatic gases in these

two extensional realms. Although *Further data are needed*, the chemical features of gases might be controlled by the degree of partial melting in the mantle, which is higher in Iceland compared to the EARS, as indicated by the different volcanic products, i.e. presence of carbonatites in the EARS.

In view of points A-G, the main aspects to be considered in exploration and development of geothermal resources within the EARS, in comparison with the systems hosted in subduction zone environments, can be summarized, as follows:

- ✓ Hundreds of thermal manifestations occur within the EARS, which extends over a length of some 5000 km.
- ✓ In spite of such widespread and intense evidence of thermal anomaly, the present exploitation of geothermal resources for power generation is quite limited, if compared, for example, with the production registered along the Belt of Fire of Indonesia.
- ✓ Such a surprising result can be related to two different causes: (1) Thermal manifestations are often not due to the presence of a hot magmatic source, but rather to the thinning of the Earth's crust, which determines a thermal anomaly of moderate intensity; (2) Numerous and extensive geoscientific investigations have been conducted, but only very few prospects have been directly tested so far through deep drilling.
- ✓ The planned program of drilling in several prospects of Ethiopia and Tanzania, to be carried out in the next few years, from the hand might enhance the "geothermal performance" and on the other provides basic information which can improve the overall understanding of the EARS characteristics.
- ✓ It is in particular very important to define the reasons why, in many instances, favorable thermal conditions are not accompanied by an adequate hydrogeological setting: it is in fact surprising that lithological units with brittle behavior (e.g. basalts) result to be almost impervious in an extensional environment characterized by neo-tectonic activity.
- ✓ Under this situation, it is essential to pay specific attention to the structural setting, in order to design the wells in such a way as to increase the chances of intersecting tectonic features. In fact, it is worth reminding that, while in most Indonesian field permeability tends to be widespread throughout extensive structural blocks (ELC, 2018), in the EARS permeability appears in many cases to be controlled by major faults.
- ✓ As refers to extensional plays, which represent the most common type especially in the western branch of the EARS, the geothermal system tend to be partly overlooked from the commercial point of view, due to their relatively low temperature (in principle in the order of 130-180 °C).

The results of geothermal exploitation in the Great Basin of Western USA and in Turkey show that medium enthalpy resources tend to be more and more technically usable and economically convenient, being now about 10% of the global geothermoelectric generation in the world, thanks to the progress in the combined cycle systems.

REFERENCES

Bosworth, W. (1987), "Off-axis volcanism in the Gregory rift, east Africa: implications for models of continental rifting". Geology, 15, 397-400.

Chorowicz, J. (2005), "The East African rift system", J. Afr. Earth Sci., 43, 379-410.

Craig, T. J., Jackson, J. A., Priestley K., and McKenzie D. (2011), "Earthquake distribution patterns in Africa: their relationship to variations in lithospheric and geological structure, and their rheological implications", Geophys. J. Int., 185, 403-434.

Ebinger, C. J., Deco, A. L., Drake, R. E., and Tesha, A. L. (1989), "Chronology of Volcanism and Rift Basin Propagation: Rungwe Volcanic Province, East Africa", J. Geophys. Res., 94, 15785-15803.

ELC (2018), "Consulting Services for Feasibility Study of Ulumbu and Mataloko Geothermal Power Plant Project". Unpublished.

ELC-GDC (2015), "Updated Reservoir Capacity Report. Under Consultancy Services for the Update of the Feasibility Study for 105 MW Menengai Geothermal Project". June. Unpublished.

ELC-GSE (2016), "Conceptual Model Report. Prepared for GSE under Consultancy Services for Geothermal Surface Exploration in Tendaho Alalobeda, Ethiopia", February. Unpublished.

ELC-TGDC (2017), "Kiejo-Mbaka Final Report. Prepared for TGDC under Surface Exploration and Training in Luhoi and Kiejo-Mbaka Geothermal Areas, project". October. Unpublished.

Giggenbach, W. F. (1988), "Geothermal solute equilibria. Derivation of Na-K-Mg-Ca geoindicators", Geochim. Cosmochim. Acta, 52, 2749-2765.

Keller, G. R., Prodehl, C., Mechie, J., Fuchs, K., Khan, M. A., Maguire, P. K. H., Mooney, W. D., Achauer, U., Davies, P. M., Meyer, R. P., Braile, L. W., Nyambok, I. O., and Thompson, G. A. (1994), "The East African rift system in

the light of KRISP 90", Tectonophysics, 236, 465-483.

Marini L. and Pasqua C. (2014). "Geochemical modeling of water-rock interaction processes in the geothermal systems of the continental rift zone of East Africa and related implications". Proceedings, 5TH African Rift Geothermal Conference (ARGeo-C5) - Arusha International Convention Center (AICC) 27 - 31 October 2014

Moeck, I. S. (2014), "Catalog of geothermal play types based on geologic controls", Renewable and Sustainable Energy Reviews, 37, 867-882

Omenda, P. A. (2009), "The geothermal activity of the East African Rift", Presented at Short Course IV on Exploration for Geothermal Resources, organized by UNU-GTP, KenGen and GDC, at Lake Naivasha, Kenya, November 1-22.

Omenda, P. A. (2013), "The geology and geothermal activity of the East African Rift", Short Course VII on Exploration for Geothermal Resources, organized by UNU-GTP, GDC and KenGen, in Naivasha, Kenya, 31st October - 23rd November.

Pasqua C. (2019), "Advances in the Exploration of Geothermal Resources of the East Africa Rift System (EARS)", Ph.D. Thesis, Doctoral Research of Science and Technology for Environment and Territory, Italy.

Sawyer G. M., Carn S. A., Tsanev V. I., Oppenheimer C., Burton M., (2008). "Investigation into magma degassing at Nyiragongo volcano, Democratic Republic of the Congo". Geochem. Geophys. Geosyst., 9, Q02017, doi:10.1029/2007GC001829.

Symonds R. B., Rose W. I., Bluth G. J. S., Gerlach T. M., (1994). "Volcanic-gas studies: methods, results, and applications. In: "Volatiles in Magmas", M.R. Carroll and J.R. Holloway (Eds.)", Mineralogical Society of America, Reviews in Mineralogy, 30, 1-66

ABSOLUTE DATING OF THERMAL HISTORY USING THERMOLUMINESCENCE

Stephen Simamora, Dikdik Risdianto, and Nizar Muhamad Nurdin

Central for Mineral Coal and Geothermal Resources, Geological Agency of Indonesia, Ministry of Energy and Mineral Resouces
Soekarno-Hatta St No.444, Pasirluyu, Regol, Bandung City, West Java 40254
Email: stephensimamo@gmail.com

ABSTRACT

Thermoluminescence (TL) technique nowadays is widely recognized as dating technique for geothermal exploration such as determining geothermal volcanic material dating and reconstructing thermal history. Although actually it can be applied too for natural geothermal evaluation such as surface manifestation, geothermometry, and subterranean heatflow. TL dating itself is more precise than K/Ar and C-14. This research aim to determine one of geotherma006C heat source at Soppeng District, South Sulawesi. Single-aliquot additive dose protocol is performed to determine equivalent dose, due to the scarcity of prepared sample. Two artificial dose irradiation is given to the sample, which is 10 Gray (Gy) and 30 Gy. Annual dose determined by analyzing the concentration of uranium, thorium, and potassium using X-ray Fluorescence (XRF) method. Two trend line is made to determine both minimum and maximum linear equation. Natural TL intensity shows 14380 arbitrary unit (a.u) and 14430 a.u as the minimum and maximum peak. Irradiated sample with 10 Gy dose shows peak at 1883–1947 a.u, and 30 Gy dose shows peak at 2733-2763 a.u. Regression trend line made by artificial dose show that natural TL intensity equivalent with 304.05-315.96 Gy. Calculation of uranium, thorium, potassium, water content, and beta factor produce annual dose in the amount of 0.5408 Gy. Through TL method, it is known that the absolute age of heat source at soppeng is 573 ± 11 kilo age years old.

Keywords: thermoluminescence, geological dating, thermal history, geothermal

INTRODUCTION

Thermoluminescence can be defined into two perspective: microscopic and macroscopic. Microscopically, thermoluminescence phenomenon start when a material changes from a state of thermodynamic equilibrium into a metastable state, caused by the absorption of external energy that produced by an ionizing radiation. Then when the material heated, ionizing radiation will be released and causing a light emission. Therefore, the material back to its equilibrium condition. Macroscopically, thermoluminescence is a phosphorescence that observed under condition of steadily increasing temperature (Furetta, 2010). Thermoluminescence is applicable for material with crystalline structure or with spurious crystalline content. The material must be insulating material or semiconductor material. A metallic material can't be used for thermoluminescence analysis.

In natural occurrence, a mineral steadily receive radiation exposure from its surrounding. It has been repeatedly proved that the cause of the thermoluminescence is the presence of traces of radioactive elements contained in the rocks as impurities. In the equation of Aitken (1985), the radioactive elements used to determine the age of thermoluminescence is uranium, thorium, and potassium. The relation between thermoluminescence intensity and radiation dose preserved at mineral has been established (Daniels et al., 1953).

As thermoluminescence phenomenon occur by the stimulation of temperature, all the radiation will be released after a heating event and cause the thermoluminescence age to be reset. When cooling happen, steadily mineral will start to absorb radiation. So, it has to be highlighted that thermoluminescence age not always represent the age of a rock. However, thermoluminescence age represent the age of the last heating-event that occur at the mineral. The heating itself can be caused by hydrothermal alteration, tectonic activity, volcanic eruption, magma intrusion, and other phenomenon that involves heating.

Thermoluminescence generally applied for archeology, anthropology, and geology research tool. In archeology TL is mainly used for dating of old pottery, whereas in anthropology TL is used for flint stone. In geology, thermoluminescence has been applied to determine the age of volcanic rock and alteration event (Takashima, 2005), dating of fault or geological structure (Yincan, 2017; McCalpin, 1991), estimates the age of volcanic eruption (Schmidt, 2017; Rufer, 2012; Preusser, 2011), as well to evaluate cooling history, surface thermal manifestation and subterranean heatflow of geothermal field (Tsuchiya, 2000).

METHODOLOGY

One sample was acquired from an andesitic rock that represent the last heating event which assumed to be the heat source of recent geothermal activity. A sample of approximately 500 gram was immediately

wrapped with aluminium foil after sampled to keep the humidity of sample.

The sample then moved into mineral physic laboratory to be prepared. Hard rock sample broke into smaller fragments with a jaw crusher. Those fragments are separated into two groups. A group of 100 gram for Annual Dose (AD) analysis and a group of 300 gram for Equivalent Dose (ED) analysis. The sample fragments for AD is weighted and then roasted in an oven. Dry sample then weighted again, so the water content can be calculated. The dried sample then pulverized to powder using automatic grinder. The powder then analyzed with XRF method to acquire uranium, potassium, and thorium content on the sample.

ED sample fragments crushed with manual mortar into smaller size. Water is added to the manual mortar to keep the fragments cold, because the friction between mortar and rock fragments can inflict heat. The sample then crushed with an agate grinding machine into grains smaller than 1 mm in diameter. Water still added to the grinding machine to avoid heat caused by friction. ED sample than sieved using four kind of sieve size: 10 mesh, 18 mesh, 35 mesh, and 60 mesh. Still, water used in the sieving process. Grain size of 0.25 mm to 1 mm than acquired after the sieving process. ED sample then put in an oven and dried at a temperature of 60 ^{o}C. After the sample have been dried, magnetic mineral separated using a hand magnet. Light colour mineral then acquired after the magnetic treatment. Plagioclase and quartz then picked under binocular microscope, a total of a hundred minerals with size of 0.25 - 1 millimeter was acquired. Minerals then put on a plastic container. Solution of 24% HF then poured into the plastic container to dissolve the outer surface of mineral. The reaction take over 30 minutes. HF solution then removed from the plastic container with tissue. There will be clayey remnants on the mineral's surface after the chemical reaction. HCl solution then added to the plastic container for 30 minutes to remove clayey remnant on the mineral's surface. After that, HCl removed and the minerals dried with temperature room for one night.

Seven grain of quartz then picked under binocular microscope for the natural thermoluminescence (NTL) measurement. The rest of minerals then packed into zip lock plastic to be irradiated. Irradiation process took place in National Nuclear energy Agency (BATAN). Cobalt-60 radioactive isotope is used to irradiate the mineral sample. Irradiated sample divided into 2 dose: 10 Gray and 30 Gray. The thermoluminescence produce by heating of irradiated sample is called artificial thermoluminescence (ATL). Seven grains of quartz picked from each irradiated sample of each dose. The picked quartz has the same grain size, about 5 mm in diameter. Value of beta-factor acquired by inputing mineral size to Mejdahl's Formula (1979).

$$B = e^{-0.445D}$$

B = beta factor
e = Euler's number, approximately equal to 2.718
D = diameter of mineral grain

All the picked quartz put on mini metal container for each of: NTL sample, ATL sample of 10 Gy, and ATL sample of 30 Gy. Single-aliquot is used in this research due to the scarcity of quartz in rock sample. Each sample then measured with TL-2000. Heating rate of TL-2000 set to 2^{o}C/second. Heating start from 50 ^{o}C until 400 ^{o}C. Room temperature set to 20 ^{o}C to keep the instrument cold, cause environment's temperature affect the performance of instrument. Thermoluminescence data set acquired and processed using worksheet, so the graphic of NTL and ATL can be produced. Graphic of NTL and ATL contain temperature as the x-axis and thermoluminescence intensity as the y-axis. Then, the peak value of each graphic obtained and recorded. Those peak value then plotted into graphic of dose versus TL intensity. Through the trend line, a formula is obtained to determine the equivalent dose of NTL. Figure 1 shows the equivalent dose determination.

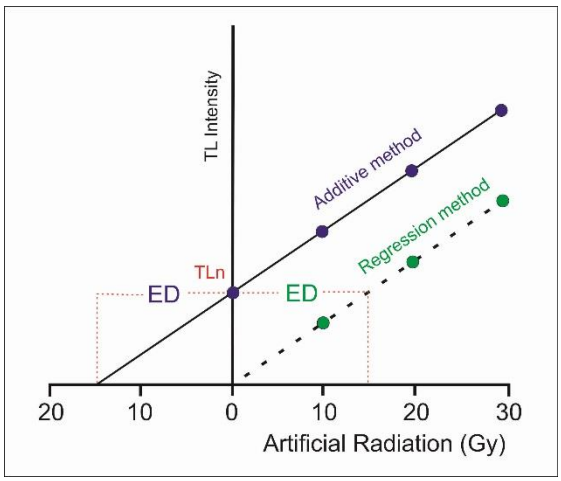


Figure 1: Scheme of equivalent dose determination (Modified from JICA, 2016).

To determine an equivalent dose or paleo dose, there are two method: regression method and additive method. Regression method done by heating the mineral until all the natural radiation in the mineral released, so the thermoluminescence signal reset to zero intensity. Mineral sample then irradiated using artificial radiation to acquire the relation between dose and TL intensity. However, additive method does not need the natural radiation to be reset. So, the radiation inside the mineral is paleo dose plus artificial dose. This research used additive method to determine the equivalent dose.

Age of thermoluminescence than obtained by dividing the paleo dose or equivalent dose with annual dose. Annual dose itself determined by

applying uranium concentration, potassium concentration, thorium concentration, water content, and beta-factor to Aitken's Formula. The represented age of thermoluminescence dating can be known by referencing geological map of sampling spot. Below is the formula of annual dose:

$$AD\ (mGy) = \frac{(0.1148\ \mathrm{U} + 0.0514\ \mathrm{T} + 0.2609\ \mathrm{K})}{(1 + 1.14\ \mathrm{W})} + \frac{(0.1462\ \mathrm{U} + 0.0286\ \mathrm{T} + 0.6893\ \mathrm{K})\ \mathrm{B}}{(1 + 1.25\ \mathrm{W})}$$

U = uranium content (ppm)
T = thorium content (ppm)
K = potassium content (K_2O%)
W = water ratio (H_2O%/ 100)
B = beta-factor (Mejdahl, 1979)

Below is the formula to obtain thermoluminescence age:

$$Age\ (kiloyear) = {ED\ (Gray)}\Big/{AD\ (miliGray)}$$

ED = equivalent dose
AD = annual dose

STUDY CASE

This research undergone to a rock that sampled from Lejja, Soppeng District, South Celebes (Figure 2). There are 14 lithology unit in the research area. These are the lithological unit mentioned sequentially according to the relative age: Volcanic Breccia (Tmbv), Tampaning Andesite Lava (Tmat), Manredareda Andesite Lava (Tmam), Corawali Andesite Lava (Tmac), Bukuere Andesite Lava (Tmab), Soloang Basalt Lava (Tmbs), Lajellu Andesite-Basalt Lava (Tmal), Ladange Andesite Lava (Tmad), Limestone (Tmbg), Diorite Intrusion (Tpd), Padali Rhyolite Lava (Tprp), Latorang Lava Dome (Qpll), Lake Sediment (Qd), and Surface Sediment (Qa). Rock sample that used for this thermoluminescence research is taken from Latorang Lava Dome, which is the youngest volcanic product in Lejja. Therefore, it can be assumed that the age of heat source equivalent with the age of Latorang Lava Dome's age acquired by TL-dating.

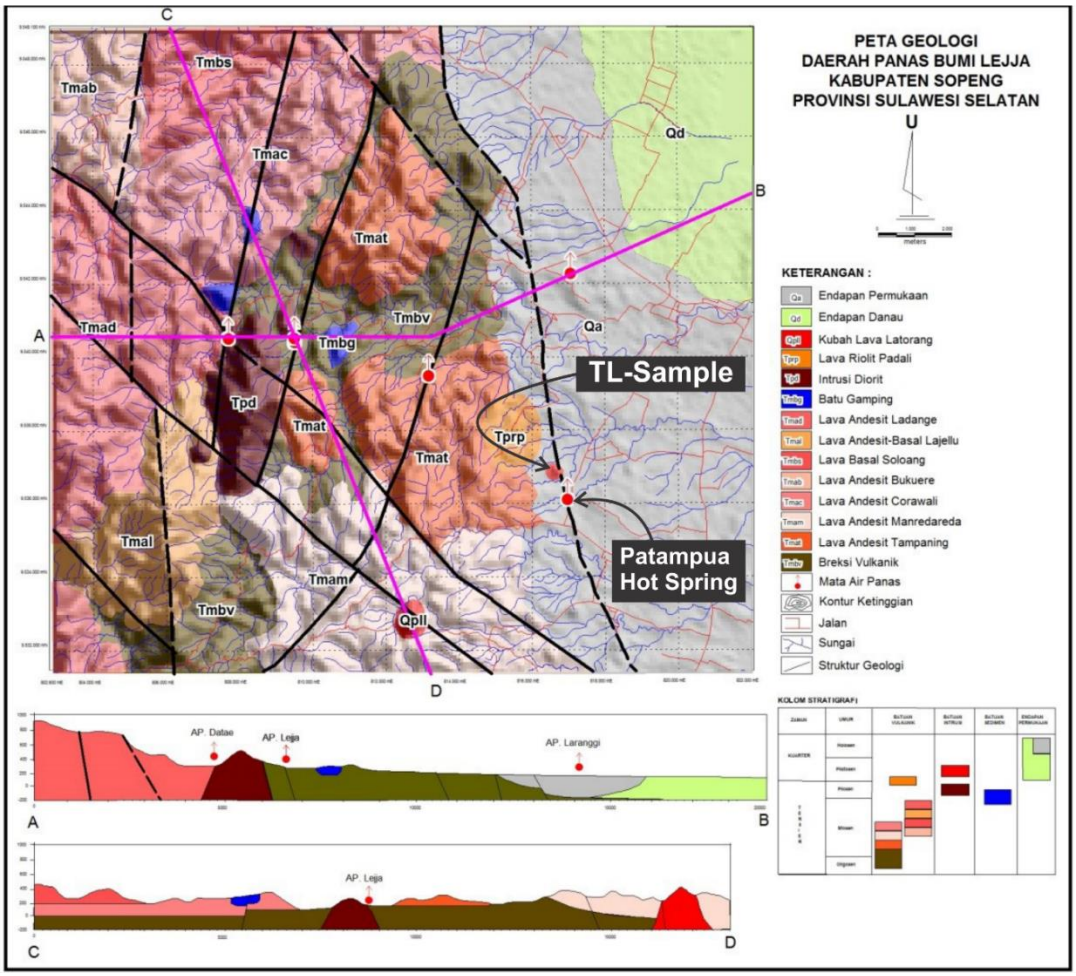


Figure 2: Geology Map of Lejja, Soppeng, South Celebes (Modified form Nurdin, 2018).

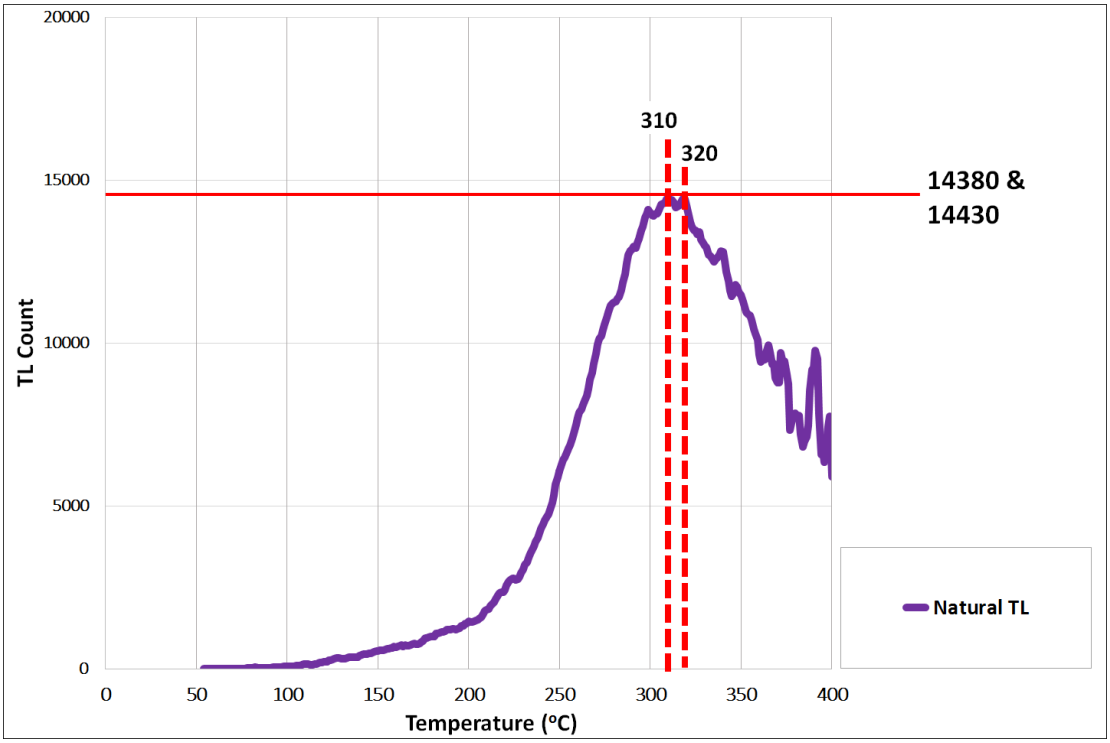


Figure 3: Natural thermoluminescence graphic, TL count in arbitrary unit.

Nine hot spring manifestation found in the research area. One of the manifestations, Patampua Hot Spring, placed about a kilometer from TL-sample. The temperature of the hot spring is 46.02 ^{0}C, while the ambient temperature is 29.42 ^{0}C. However, the ambient temperature at sampling spot is below 28 ^{0}C. So, it can be assumed that Latorang Lava Dome natural thermoluminescence does not affected by Patampua Hot Spring and still preserved the natural radiation obtained from its surrounding. There are two pattern of fault that mostly found in Lejja, North-South direction and Northwest-Southeast direction.

RESULT

ED Determination

Natural thermoluminescence

Two peaks are picked, mentioned as minimum NTL and maximum NTL. Minimum NTL has a value of 14380 arbitrary unit TL intensity and appear at the temperature of 310 ^{0}C. Maximum NTL has a value of 14430 arbitrary unit TL intensity and appear at the temperature of 320 ^{0}C.

Artificial thermoluminescence

Two artificial irradiations of 10 Gray and 30 Gray are used to obtain the ATL graphic. The 10 Gray sample has the minimum peak value of 1883 arbitrary unit and maximum peak value of 1947 arbitrary unit. The 30 Gray sample has the minimum peak value of 2733 arbitrary unit and maximum value of 2763 arbitrary unit. Those peaks appear at the temperature range of 250 – 265 ^{0}C. The figure shows that graphic of 30 Gy irradiated sample is similar to graphic of 10 Gy irradiated sample. Figure 3 shows the natural, while Figure 4 shows the artificial thermoluminescence graphic.

Equivalent dose

Minimum and maximum peak of each irradiated sample is plotted into the graphic. The formula of minimum and maximum equivalent dose then acquired. Formula of minimum and maximum equivalent dose sequentially written below:

$$y = 42.5x + 1458$$
$$y = 40.8x + 1539$$

y is the value of TL count, while x is the value of radiation dose. If the trend line extended, then it will intersect the y-axis. This confirm that the treatment of additive method is well implemented. Minimum and maximum peak value of NTL then inputted to the x-values of each formula, so the equivalent dose can be acquired. The minimum equivalent dose is 304.047 Gray, while the maximum equivalent dose is 315.956 Gray.

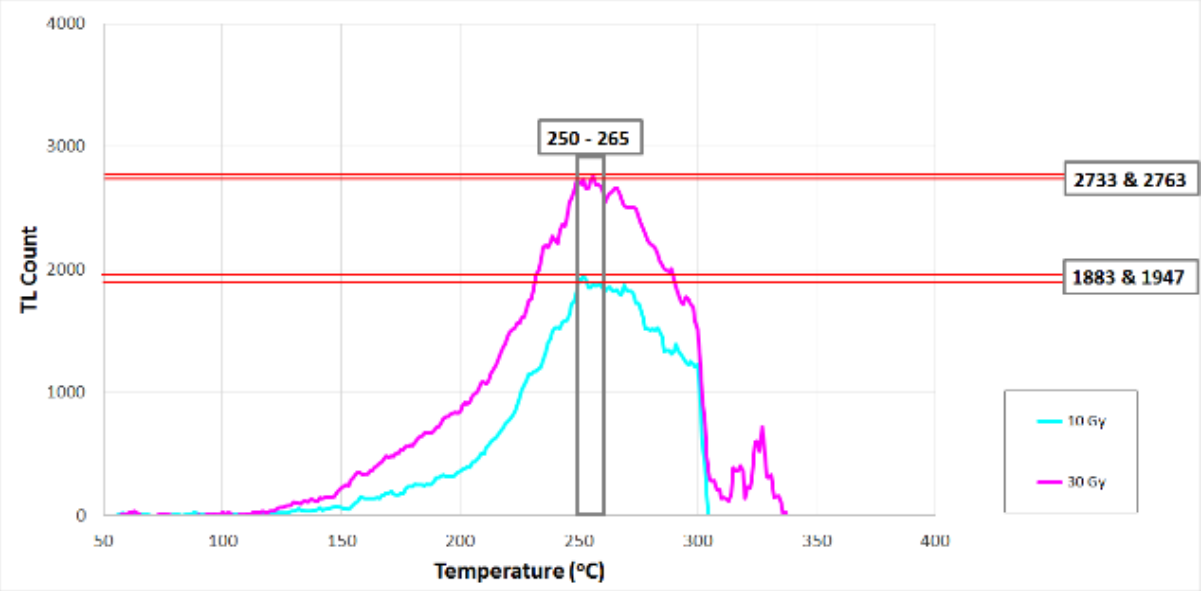


Figure 4: Artificial thermoluminescence graphic, TL count in arbitrary unit.

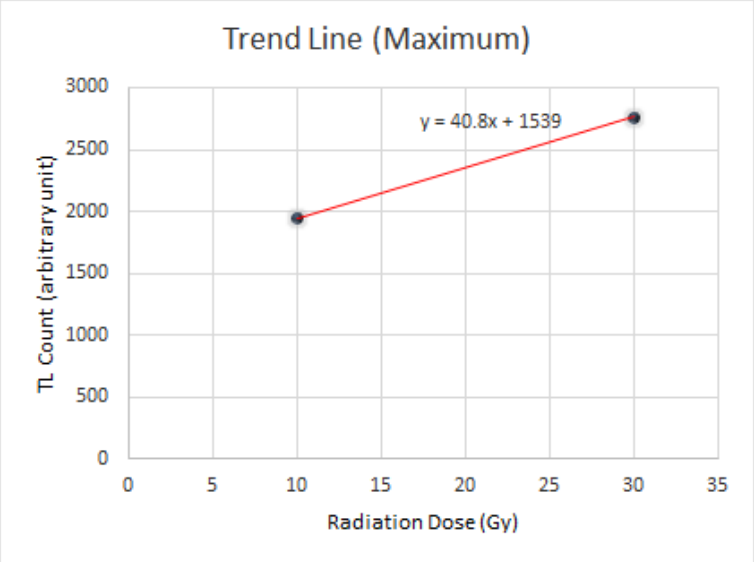


Figure 5: Maximum Trend line.

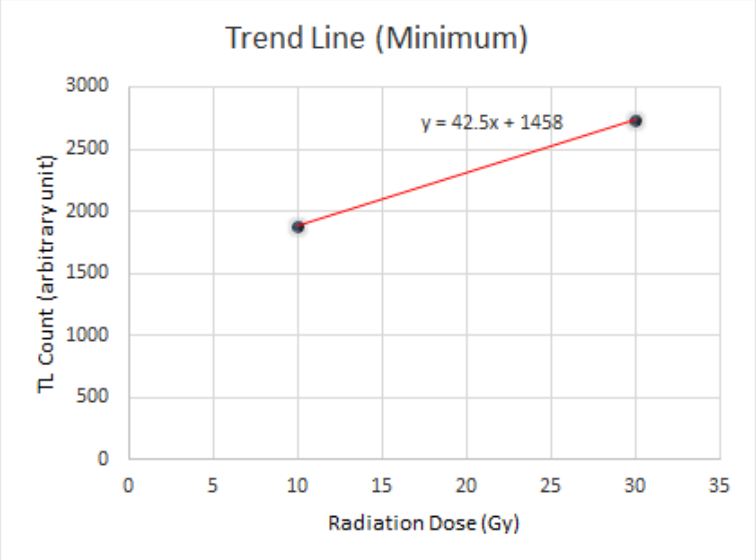


Figure 6: Maximum Trend Line.

AD Determination

Radiation content

Uranium, thorium, and potassium content acquired by X-Ray Fluorescence analysis. Uranium content in the sample is below the detection limit so that uranium content written to be zero. An amount of 34 part per million (ppm) of Thorium is detected in the sample, while there is 0.38% of potassium in the sample. Figure 5 shows the minimum trend line, while Figure 6 shows the maximum trend line.

Water content

Sample has a wet mass of 110.91 gram. The sample then dried in an oven with 60 ^{0}C of temperature for approximately a day. After the sample dried, the mass become 106.91 gram.

Beta-factor

The diameter of quartz grain is about 0.5 mm. Using Mejdahl's formula (1979), beta-factor is acquired. The value of beta-factor after calculation is 0.801.

Annual dose

Using annual dose formula (Aitken, 1985), it is known that every thousand year the sample absorbed an amount of 0.540793 miligray (mGy) dose (Table 1).

Thermoluminescence Age

After these data inputted to Aitken's Formula (1985), the thermoluminescence age result is obtained, which is 573.2338 ± 11.0097 kiloannum. The unit of kiloannum is equal with a thousand of year (Table 2).

DISCUSSION AND CONCLUSION

Thermoluminescence analysis is conducted to the sample of rock which is taken from Latorang Lava Dome. Using single-aliquot and additive dose method, the minimum and maximum equivalent dose acquired. As the artificial dose inputted to the 'Dose vs TL Intensity', the formula for minimum and maximum equivalent dose obtained and applied to get the natural dose. A total of 304.047-315.956 Gy is accumulated at quartz grain of the rock sample from the forming of Latorang Lava Dome. Annual dose acquired by XRF analysis, roasting process, and mineral diameter measurement. The content of uranium at sample is mentioned as zero, cause it below the detection limit of the instrument. Every thousand year, the quartz grain absorbed 0.5408 mGy from the radiation of uranium, thorium and potassium element at its surrounding. The water content also affects the amount of absorbed radiation dose, as high-water content will cause the reduction of radiation absorption.

After ED analysis and AD analysis finished, it just needs a simple equation to obtain the thermoluminescence age. From the calculation, it is known that the thermoluminescence age of sample is 573 ± 11 thousand years ago. This means that Latorang Lava Dome experienced the last heating event at 573 ± 11 thousand years ago. It is known that the natural radiation of Latorang Lava Dome does not affected by the hot spring that placed about 1 kilometer from the sample coordinate. So, the last heating represents the formation of Latorang Lava Dome itself. Because Latorang Lava Dome is the youngest volcanic product at Lejja, it can be assumed that Latorang Lava Dome is the heat source for geothermal system in the research area. Good geothermal potential is a geothermal field that has the most recent eruption that occurred less than 500.000 years ago (Stelling, 2016). But a number of surface manifestation still occur in the research area, it means that there is still geothermal activity. So, this research area has potential and can be utilized.

Table 1: Data for annual dose calculation.

Wet mass (gram)	Dry mass (gram)	U (ppm)	Th (ppm)	K (%)	W (%)	B
110.91	106.91	0	34	0.38	3.6065	0.801

Table 2: Data for thermoluminescence age calculation.

Equivalent Dose (Gy)		Annual Dose (mGy)	TL Age (ka)	
Minimum	Maximum		Maximum	Minimum
304.047	315.955	0.540793	562.224	584.244

REFERENCE

Aitken, M., J., (1985), "Thermoluminescence Dating". Academic Press, New York, p. 359

Furetta, C., (2010), "Handbook of Thermoluminescence (2nd Edition)", World Scientific Publishing Co. Pte. Ltd., Singapore.

Yincan et al, Y., (2017), "Active Faults of Sea Area, Marine Geo-Hazards in Chine", Elsevier, 89–128.

Nurdin et al, N., (2018), "Survei Rinci Panas Bumi dengan Metode Geologi, Geokimia, dan Geofisika Daerah Lejja, Kabupaten Soppeng, Provinsi Sulawesi Selatan", Pusat Sumber Daya Mineral, Batubara, dan Panas Bumi, Bandung

Takashima et al, I., (2005), "Precise Thermoluminescence Dating for Heat Source Volcanic Rocks and Alteration Products at the Tawau Geothermal Area, Sabah, Malaysia", Proceedings World Geothermal Congress, Antalya, Turkey.

Tsuchiya et al, N., (2000), "Thermoluminescence as a new research tool for the evaluation of geothermal activity of the Kakkonda geothermal system, northeast Japan", Geothermics 29, 27-50.

Schmidt et al, C., (2017), "New thermoluminescence age estimates for the Nyos maar eruption (Cameroon Volcanic Line)", PLoS ONE 12(5): e0178545.

Stelling et al, P., (2016), "Geothermal systems in volcanic arcs: Volcanic characteristics and surface manifestations as indicators of geothermal potential and favorability worldwide", Journal of Volcanology and Geothermal Research 324, page 57-72.

Mejdahl, V., (1979), "Thermoluminescence Dating: Beta-Dose Attenuation in Quartz Grains", Archaeometry 21, page 61-72, Great Britain.

McCalpin, J., Forman, S., L., (1991), "Late Quaternary Faulting and Thermoluminescence Dating of the East Cache Fault zone, North-Central Utah", Bulletin of the Seismological Society of America, vol 81, no 1, pp. 139-161.

Daniels et al., F., (1953), "Thermoluminescence as a Research Tool", Department of Chemistry, University of Wisconsin, Madison.

Preusser et al., F., (2011), "Direct dating of Quaternary phreatic maar eruptions by luminescence methods", GSA Data Repository 2011337.

Rufer et al., D., (2012), "Proposing New Approaches for Dating Young Volcanic Eruptions by Luminescence Methods", Geochromonometria 39, page 48-56.

JICA (2016), "Thermoluminescence Dating of Quartz in Rocks", Internal Manual Book.

INTEGRATING OF GEOMAGNETIC DATA AND VERTICAL ELECTRICAL SOUNDING FOR IDENTIFICATION OF RESERVOIR AND GEOTHERMAL FLUIDS IN GEOTHERMAL PROSPECTS RAJABASA MOUNTAIN

Syamsurijal Rasimeng, Jakasura Leandro Tarigan, Ditha Arlinsky. Ar, and M. Ikhsan Fadhillah

Geophysical Engineering, Engineering Faculty, University of Lampung, Indonesia
Jl.Prof. Sumantri Brojonegoro No. 1, Bandar Lampung
Email: syamsurijal.rasimeng@eng.unila.ac.id

ABSTRACT

This study has been done to determine the spread of reservoir rocks and geothermal fluids that are beneath the surface of the geothermal prospect of Mount Rajabasa, South Lampung Regency, Lampung Province. The stages of study carried out in the form of (i) measurement of geomagnetic data and vertical electrical sounding AB/2 150, 300, 450 and 600 meters; (ii) magnetic anomaly data processing consisting of diurnal and IGRF correction, reduction of the surface, upward continuation, separation of regional-residual anomalies, reduction to the pole, and 3D residual anomalies modeling from reduction to the pole; (iii) determining the value of resistivity every depth. The range of geomagnetic anomalies obtained is -419.404 nT to 1429.022 nT. Based on the results of 3D residual anomalies from reduction to the pole process can be estimated that the geothermal reservoir has a susceptibility value of 0.0022 cgs (10^3 SI) to 0.289 cgs (10^3 SI) estimated as intermediate (andesitic-basaltic) rocks. The position of the reservoir is located southwest of the peak of Mount Rajabasa at a depth of 1300 meters below the mean sea level. The results of resistivity analysis showed that the capillary rock was characterized by a low resistivity value (10 - 60 Ωm) and a geothermal reservoir characterized by a high resistivity value (> 210 Ωm). Based on the profile of resistivity anomaly there is a distribution of geothermal fluid from the Northwest and extends with increasing depth. The cross section of the geomagnetic anomaly shows that the geological structure that traverses Northeast - Southwest and North-South is a fluid control factor in the area of the prospect of the Gunung Rajabasa geothermal, South Lampung Regency, Lampung Province.

Keywords: Geothermal, magnetic, Villamasin.

INTRODUCTION

Rajabasa Mountain is located in the south of Sumatra Island, precisely in Kalianda, South Lampung Regency. The presence of several geothermal manifestations on Mount Rajabasa is an indication of the potential for geothermal energy. Based on the interpretation of satellite imagery there are several lithological units produced from three volcanic cones that are interpreted as the old Mount Rajabasa, Mount Balerang, and the young Mount Rajabasa. This result is confirmed by the petrographic results in the field data in the form of fresh rock samples. Some alterations are also found in geothermal manifestations located in the north and south of Mount Rajabasa. Therefore, it is necessary to do research on geological conditions in the geothermal prospect area of Mount Rajabasa (Darmawan et al., 2013).

In this study several geophysical methods were used, namely the magnetic method and the vertical electrical sounding (VES) method. In geothermal exploration, magnetic methods are useful for knowing magnetic field variations in the study area. The variation of magnetism is caused by nonhomogeneous magnetic properties of the earth's crust. Where rocks in geothermal systems generally have low magnetization compared to surrounding rocks. This is due to the demagnetization process by hydrothermal alteration processes, the process of converting existing minerals into paramagnetic or even diamagnetic minerals. The low magnetic value can interpret potential zones as reservoirs and heat sources (Sumintadirejo, 2005). Whereas, the VES method itself is one of the more effective types of resistance methods when used for shallow exploration, rarely providing layer information at depths greater than 1000 or 1500 feet. Therefore this method is rarely used for oil exploration but is more widely used in the field of geological engineering such as determination of bedrock depth, search for water reservoirs, also used in geothermal exploration. Excellence in general is the price of equipment is relatively cheap, survey costs are relatively cheap, the time needed is relatively very fast, can reach 4 measurement points or more per day, workload; small and light equipment so easy to mobilize, the personal needs of around 5 people, especially for Schlumberger configuration and data analysis globally can be directly predicted when on the ground.

METHODS

The study using the geomagnetic method and Vertical Electrical Sounding was carried out in the Rajabasa Mountain, South Lampung Regency, Lampung Province. Figure 1 is a topographical modeling image of the research area accompanied by measurement points carried out in the area.

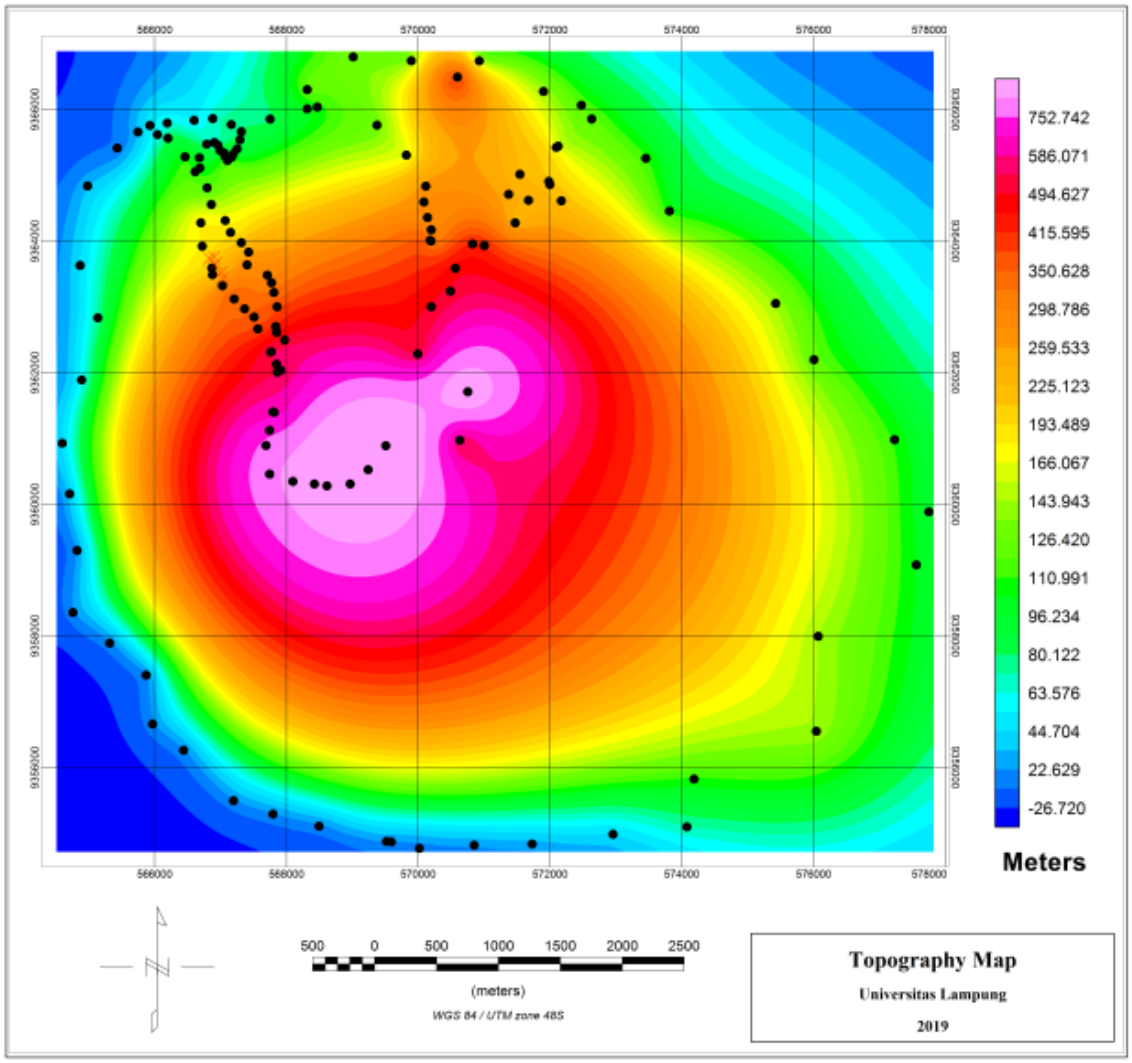


Figure 1: Topography map.

The highest topography of Mount Rajabasa is at a value of 1200 meters above sea level. The point of magnetic measurement is spread from the northwest to the Northeast and around the foot of the mountain. Then for the vertical electrical sounding point of measurement there is an altitude of 200 to 300 meters above the surface of the earth which lies on the Northwest of the mountain area of Rajabasa.

The principle of the magnetic method is to utilize magnetic susceptibility variations found in subsurface rocks. Magnetic method surveys have the benefit of knowing geological structures, such as faults, folds, igneous intrusions, geothermal reservoirs, groundwater aquifers, metal mineral deposits, and others (Lukhvich et al, 2003).

Basically, the data from the measurement of magnetic fields is the contribution of three basic components, namely the main magnetic field of the earth, the outer magnetic field and the anomalous field. The main magnetic field value is the IGRF value. If the value of this main magnetic field is eliminated by diurnal correction, then the contribution of the main magnetic field is eliminated by IGRF correction. IGRF correction can be done by subtracting the IGRF value from the diurnal corrected total magnetic field at each measurement point in the appropriate geographical position. The correction equation (after diurnal correction) can be written as follows:

$$\Delta H = Htotal \pm \Delta Hharian \qquad (1)$$

Basically, the data from the measurement of magnetic fields is the contribution of three basic components, namely the main magnetic field of the earth, the outer magnetic field and the anomalous field. The main magnetic field value is the IGRF value. If the value of this main magnetic field is eliminated by diurnal correction, then the contribution of the main magnetic field is eliminated by IGRF correction. IGRF correction can be done by subtracting the IGRF value from the diurnal corrected total magnetic field at each measurement point in the appropriate geographical position. The correction equation (after diurnal correction) can be written as follows:

$$\Delta H = Htotal \pm \Delta Hharian \pm H_0 \qquad (2)$$

Where H_0 is IGRF

To simplify the processing and interpretation of magnetic data, the anomalous data of the total magnetic field that is still scattered in the topography must be reduced to a flat surface. This transformation must be done, because the data processing process further requires that the magnetic field input be distributed to the flat surface. This reduction uses Taylor series revisions written in equations (Blakely, 1995):

$$\Delta H_{(x,y,z_0)} = \Delta H_{(x,y,z)} - \sum_{n=1}^{n} \frac{z - z_0}{n!} \frac{\partial^n}{\partial x^n} \Delta H_{(x,y,z_0)} \quad (3)$$

Then, an upward continuation process is carried out. upward continuation is performed to reveal anomalies caused by deeper sources or eliminate anomalies caused by superficial sources (Blakely, 1995). upward continuation is carried out on the total magnetic field anomaly map. Determination of regional anomalies is carried out by an upward continuation process on total magnetic field anomalies. The use of upward continuation is expected to help to separate regional anomalies from local anomalies. Continuation process with trial and error test is done by looking at the tendency of contour patterns of the results of continuation at a certain height (Indratmoko et al., 2009). The higher the data continuity, the more local information is lost and the regional information becomes clearer.

After the upward continuation process, a reduction to the pole is carried out. At low geomagnetic latitude magnetic data interpretation is more difficult than at high geomagnetic latitudes since anomaly maxima are not located directly over the causative bodies. This interpretation technique reduce dipole field to monopole field, the anomaly is directly above the causative body as like gravity anomaly, since it assume the perfect induction for simplicity. Reduction to the pole is done by making the object's inclination angle to 90º and its declination 0º. With the reduction to the poles, it is expected to produce a magnetic anomaly pattern that is monopolistic in nature, thus facilitating qualitative interpretation (Yaoguo and Oldenburg, 2001).

After the reduction to pole stage is completed, 3D inversion modeling of residual rock geomagnetic anomalies below the surface. Model parameters from inversion modeling are obtained directly from the data. 3D inversion modeling provides an overview of susceptibility distribution.

If a 3-D subsurface model is built from a set of upright prisms with the intensity of magnetization or homogeneous susceptibility then the vector of magnetic data d (di, i = 1,2, ..., N) is a linear transformation between the intensity of magnetization of each prism (mi, i = 1,2, ..., M) with the kernel matrix (Grandis and Yudistira, 2001) sized (N X M) as follows :

$$d = G\,m \quad (4)$$

where,
G = matrix kernel
m = model parameter
d = data

The kernel matrix is an expression or elaboration of the geometry of an anomalous model built from a collection of prisms. Data (d) is magnetic anomaly data, while the model (m) parameter is the susceptibility of each prism and is the parameter sought. Combined data on the surface (z = 0) and the results of upward continuation (z > 0) produce data with a number greater than the number of model parameters (N> m so that the inversion solution is over-determined (Kusnida et al., 2009)

$$m = [G^T G]^{-1} G^T d \quad (5)$$

Besides using the magnetic method, the VES (Vertical Electrical Sounding) method is also used. According to Loke (2000), in this technique the measurement is the arrangement of the electrodes with the distance of the electrode spacing graduated arbitrarily for the observed point, while the potential electrodes (M and N) are fixed. In this case, the greater the distance of the electrode, the more injected current will be until the measurement location is covered. Where the type of resistance is given by Equations:

$$\rho = K \frac{\Delta V}{I} \quad (6)$$

where,
ρ = apparent resistivity
K = geometric factors
ΔV = potential difference
I = electric current

Based on geoelectric measurement techniques, there are two measurement techniques, namely the geoelectric method of resistivity mapping and sounding. Resistivity mapping geoelectric method is a resistivity method which aims to study the subsurface resistivity variations horizontally. Therefore, in this method the electrode spacing is fixed for all sounding points on the earth's surface. The resistivity sounding geoelectric method aims to study the resistivity variations of rock beneath the earth's surface vertically. In this method, measurements at a sounding point are carried out by changing the distance of the electrode. Changing the distance of the electrode is done from the distance of the small electrode then enlarges gradually. This electrode distance is proportional to the depth of the rock layers detected. The greater the electrode

distance, the deeper the rock layers are detected (Menke, 1984).

The resistivity geoelectric method is one of the common geophysical methods used in geoelectric exploration. Geoelectric resistivity methods can be used to provide subsurface information by utilizing the electrical resistivity properties found in rock layers, where the earth is composed of rocks that have different electrical conductivity. The principle of the resistivity geoelectric method is the electric current is flowed into the earth layer by using two potential electrodes so that the potential current price can be known and the subsurface resistivity value can be determined. The data obtained in the field is the subsurface resistivity value data so that inversion calculations can be performed and resistivity variations obtained from a soil layer system associated with subsurface geological structures (Looke, 1995).

Based on the electrode configuration, a type of configuration is known, namely Schlumberger Configuration. In the Schlumberger configuration current electrodes and potential electrodes are placed as shown in *Figure 2*. This configuration is used to probe changes in subsurface resistivity vertically. At a fixed measuring point, the distance of the current and voltage electrodes is changed. Commonly used methods include Vertical Electrical Sounding (VES). According to Loke (2000), in this technique the measurement is the arrangement of the electrodes with the distance of the electrode spacing graduated arbitrarily for the observed point, while the potential electrodes (M and N) are fixed. In this case, the greater the distance of the electrode, the more injected current will be until the measurement location is covered. Where the type of resistance is given by Equations:

$$\rho = \frac{\pi\,(L^2 - I^2)}{2I}\,\frac{\Delta V}{I} = K\frac{\Delta V}{I} \qquad (7)$$

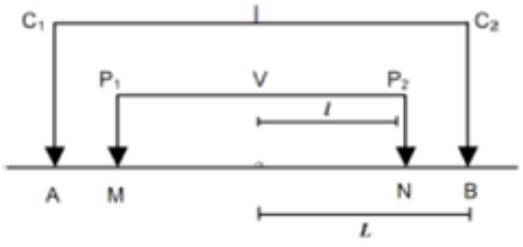


Figure 2: Schlumberger Configuration.

RESULTS AND DISCUSSIONS

Vertical Electrical Sounding

The results of vertical electrical sounding analysis (*Figure* 3) showed that the capillary rock was characterized by a low resistivity value (10 - 60 μm) and a geothermal reservoir characterized by a high resistivity value (> 210 μm). Based on the profile of resistivity anomaly there is a distribution of geothermal fluid from the Northwest and extends with increasing depth. The cross section of the geomagnetic anomaly shows that the geological structure of the Northeast and North-South is a fluid control factor in the area of the prospect of the Gunung Rajabasa geothermal, South Lampung Regency, Lampung Province.

Magnetic Method

Based on *Figure 4*, positive and negative anomalies that show a response to the surface anomaly magnetic surface. The value of the magnetic area is in the range of -419.404 nT to 1429.022 nT. When viewed from the total magnetic field anomaly data, there are considerations with the magnetic anomaly response caused by rocks below the surface. The response was indicated by the closure pair in the south, southeast, northwest, north and central parts of the study area.

On the contour map the results of the reduction to level sufrace do not have a significant difference in the anomalous value when compared with the anomalous value on the total anomaly contour map (*Figure 5*). Qualitative interpretations of the regional anomaly maps obtained are obtained from the upward continuation process (*Figure 6*). Contour maps of regional geomagnetic anomalies determine the high value distribution in the range 622-903.822 nT which extends from the Southwest to the North.

After obtaining regional anomalies, the reduction process is then carried out to obtain residual anomaly values. After obtaining residual anomalies, then interpretations are carried out. Based on *Figure 7*, a residual anomaly map can be interpreted which shows a high anomaly value with a range of values of 751 to 1429 nT which is in the middle of the research area that stretches west and northwest of the study area. Based on these interpretations, that pattern of anomalies can indicate the existence of a geothermal reservoir. After obtaining the remaining anomalies, then the remainder of the anomaly is used for the process of reduction to the poles to eliminate ambiguity in interpretation because of the magnetic nature of the two poles (Yaoguo and Oldenburg, 2001). The results of the reduction to pole process are shown in *Figure 8*. Based on the results of the process of reduction to the poles found in positive and negative patterns of magnetic anomalies. The reduced contours to the poles indicate areas that have high magnetic values produced by subsurface rock responses. The high values on the contours of the reduction to the poles are in the range 2020-6480. Where the high value stretches from North to South, then in the Northeast. Positive and negative anomalous patterns show manifestations. This anomaly shows the demagnetization process occurs below the surface.

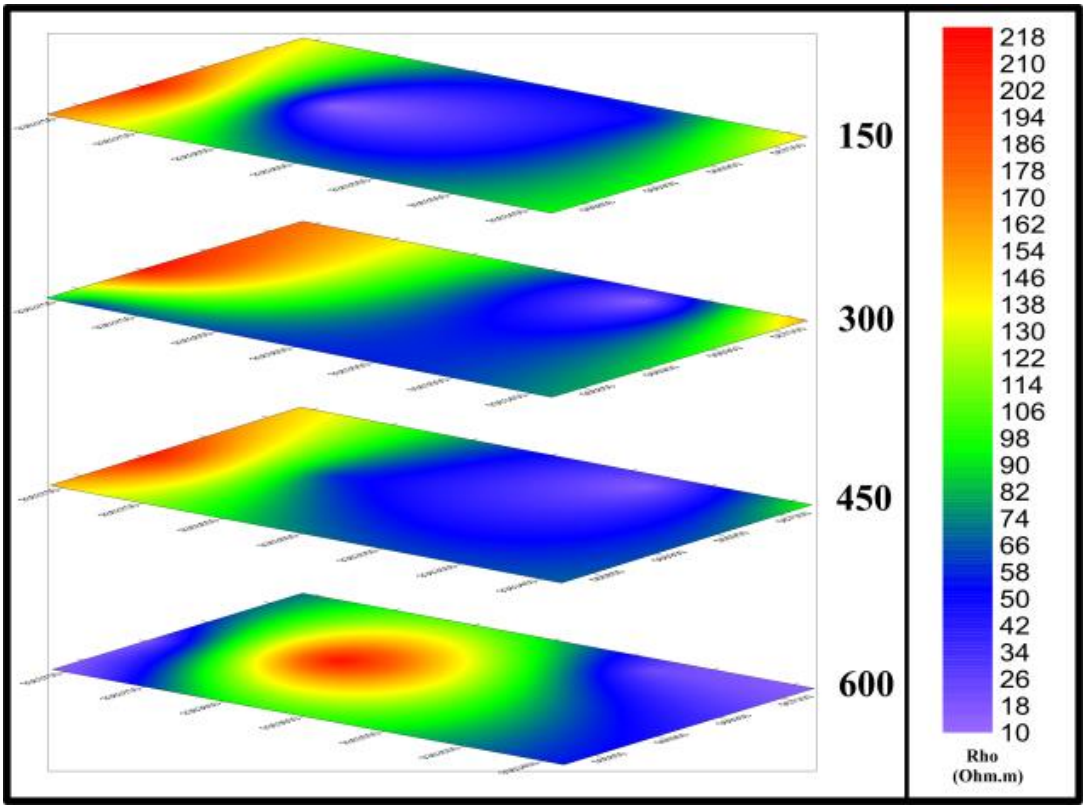


Figure 3: Reduce to level surface anomaly.

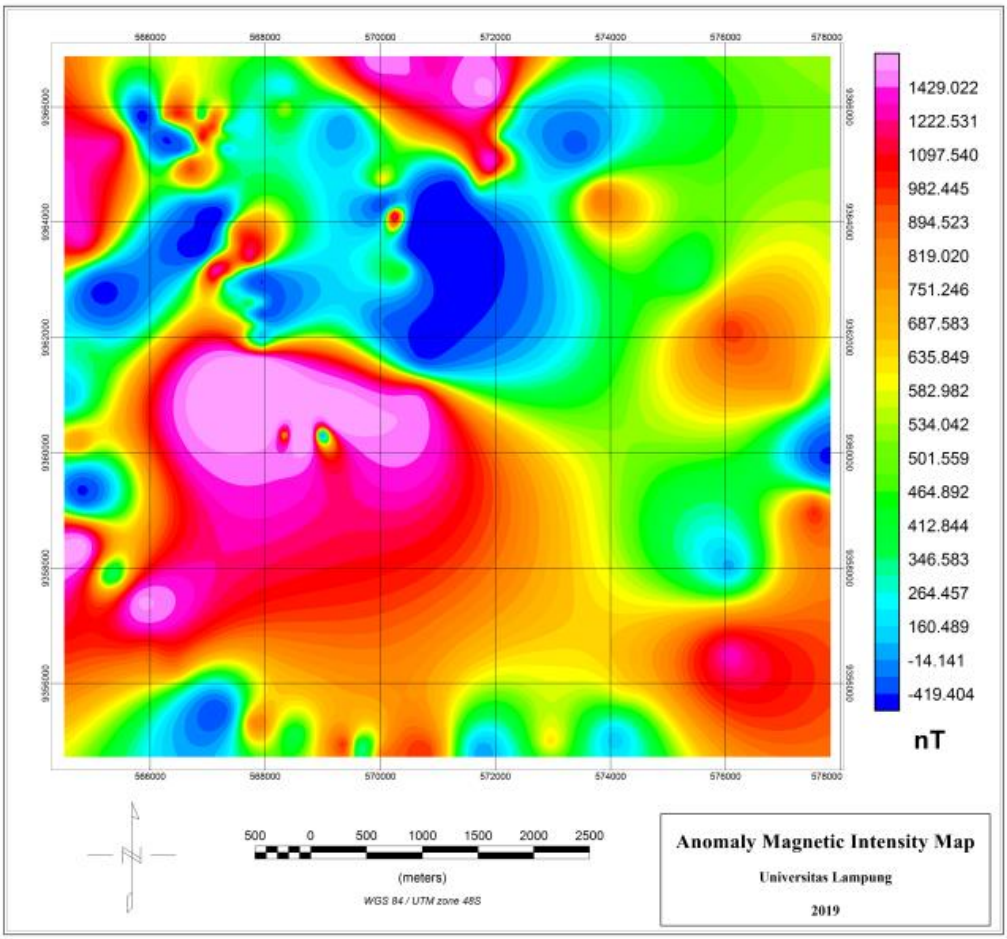


Figure 4: Total magnetic field anomaly.

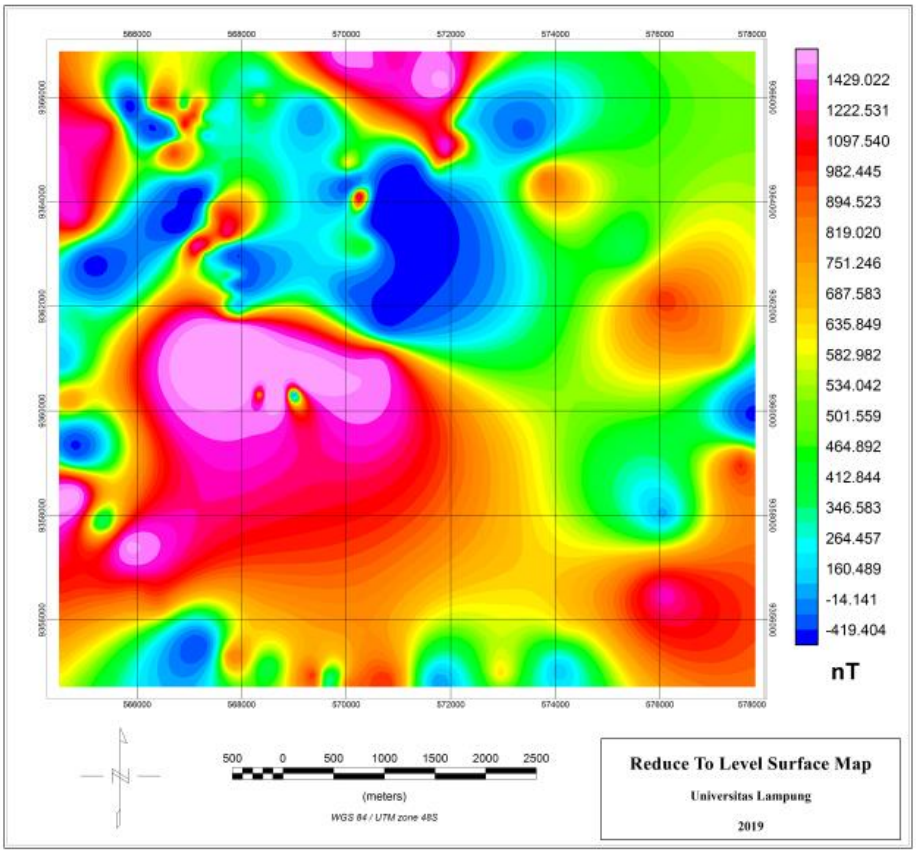


Figure 5: Reduce to level surface anomaly.

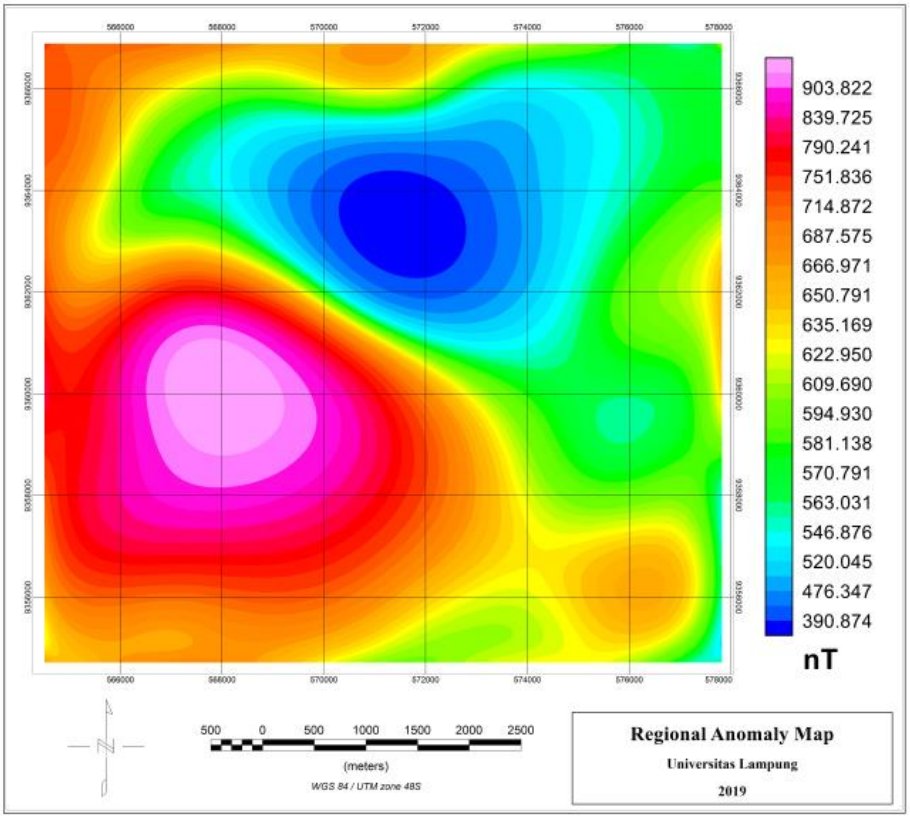


Figure 6: Regional anomaly.

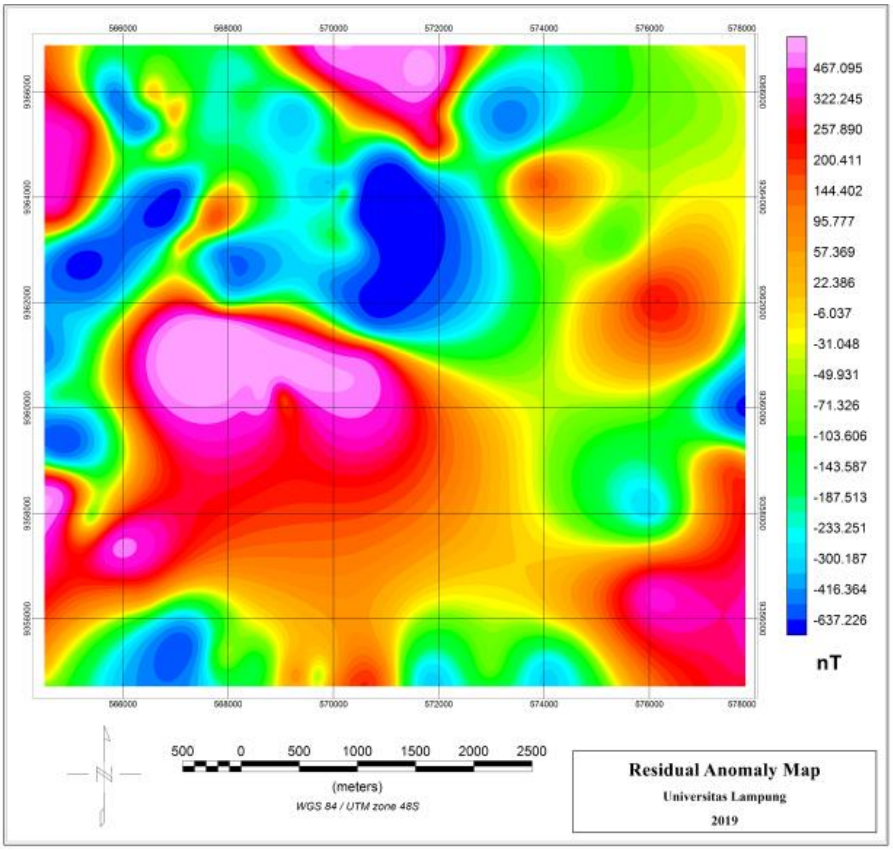


Figure 7: Residual anomaly.

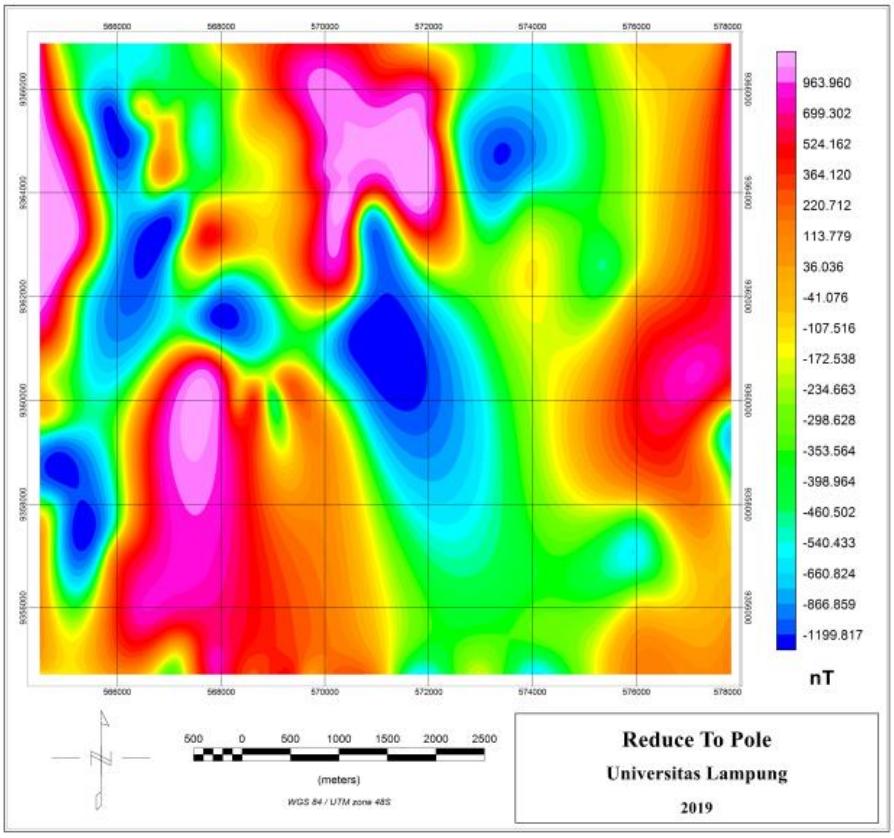


Figure 8: Reduction to pole anomaly.

Then the modeling process is carried out, in this study a 3D modeling process is carried out. Modeling is done to get the distribution and move the rock based on the required surface into a geothermal reservoir. 3D modeling uses anomalous data from the results of reduction to the poles. The results of 3D reduction to polar modeling can be seen in *Figure 9*. Based on the modeling results explain what is meant by the rock released into a geothermal reservoir that has a geometry consisting of a batholite with a type of stone made of igneous rock.

The 3D model (*Figure 10*), the high susceptibility value is found in the part that has a high magnetic anomaly which is indicated by the polar reduction anomaly contour map that is contained in the 3D model. If viewed from the topographic contour map in the 3D model, the high anomaly is found at an altitude of 800 to 1000 meters which is located on the back of Mount Rajabasa. Based on the susceptibility model in the 3D model, the anomaly has a geometry that extends from Northeast to Southwest in the study area. The rock geometry has batholite characteristics, wherein the batholite is an igneous rock that tries to rise to the surface and undergoes hardening and freezing so as to form a large and wide geometry. The susceptibility model has a high value with a range of values of 0.0022 cgs (103 SI) to 0.289 cgs (103 SI) with rock lithology, which is basaltic andesite located at a depth of 1300 meters below mean sea level. Based on this interpretation that the rock is a rock that has the potential to become a geothermal reservoir because it is seen from its very large geometry.

Based on the 3D section model (*Figure 11)*, it can be seen that the high susceptibility value is formed from rocks produced by the intrusion process because it has a geometry that extends from beneath the surface of the earth and then widens when rising to the surface of the earth.

The appearance of the manifestation or crater on Mount Rajabasa is caused by a fairly large fault, so the hydrothermal fluid can come out to the surface through the formed fault field (Rasimeng, 2008). This can be seen with the emergence of manifestations with the northwest-southeast relative direction, namely the manifestation of the Way Sulfur-dry sulfur field-the crater of the peak of Rajabasa-manifestation Simpur. Based on the geological map of the Rajabasa Mountain region consisting of volcanic rocks in the form of lava and breccia, pleistocene volcanic rock in the form of andesite lava and breccia and andesite in the form of andesite lava rock (Mango, et al, 1993).

So, if it is correlated with the magnetic field anomaly that is reduced to the pole, there is a correlation with the magnetic anomaly response caused by the rock below the surface.

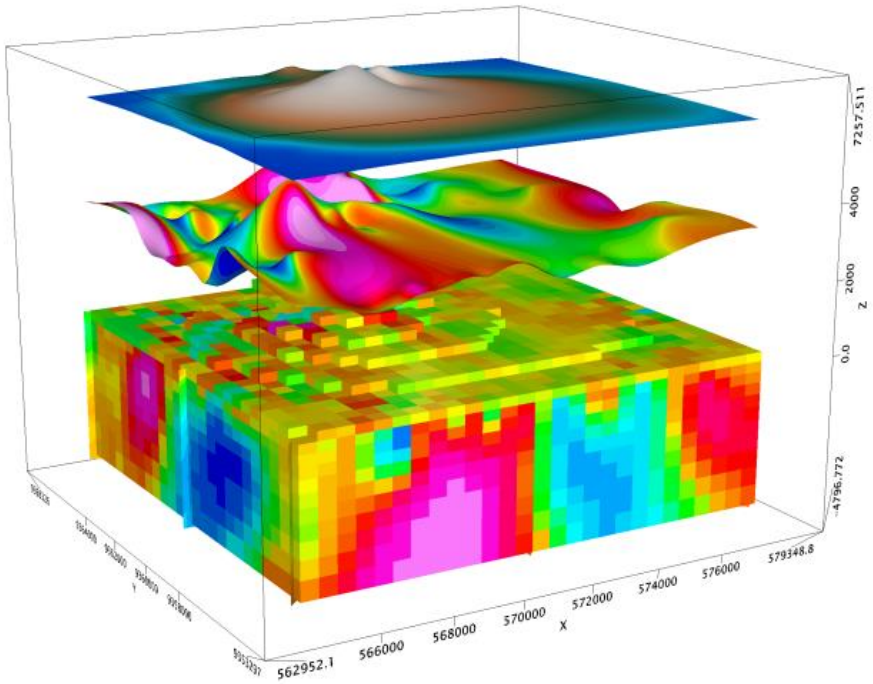


Figure 9: The susceptibility model from the inversion of the reduction to pole residual anomaly in the Rajabasa Mountain region.

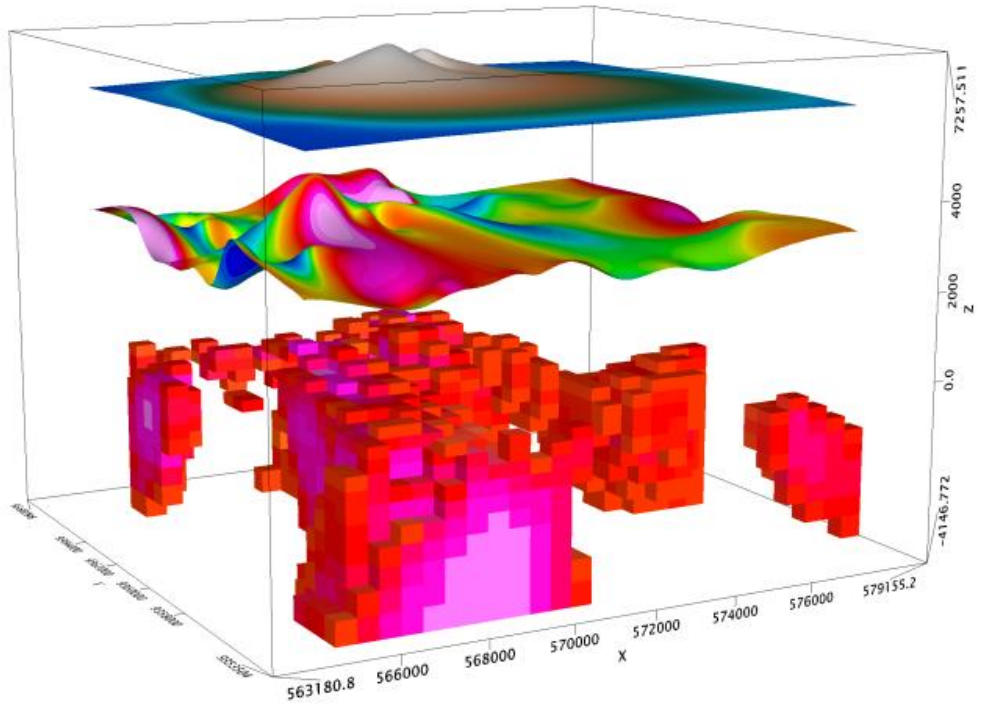


Figure 10: The Susceptibility model from the inversion of the reduction to pole residual anomaly with the highest susceptibility value in the Rajabasa Mountain region.

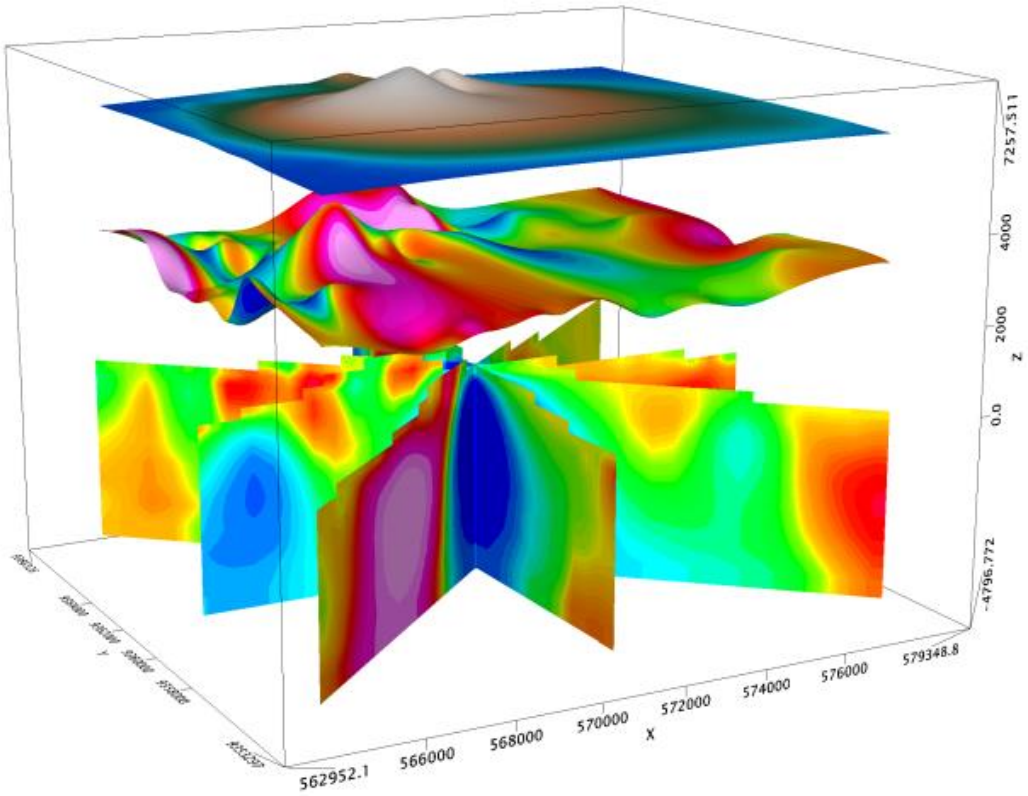


Figure 11: The Susceptibility sections model from the inversion of the reduction to pole residual anomaly in the Rajabasa Mountain region.

CONCLUSION

Based on the results of vertical electrical sounding and magnetic method data processing, the results of vertical electrical sounding analysis indicate that capillary rocks are characterized by low resistivity values (10 - 60 μm) and geothermal reservoirs that are characterized by high resistivity values (> 210 μm). Based on qualitative analysis of magnetic field data from the reduction to pole process at Mount Rajabasa, we can estimate the existence of geothermal reservoirs in the Northeast to Southwest modeling area and also in the study area. Based on 3D modeling, where the susceptibility value generated by the rock response below the surface is in the value range of 0.0022 cgs (103 SI) to 0.289 cgs (103 SI). The subsurface rock geometry is formed by intrusive rocks with basal andesitic lithology and rocks with a combination of tuff and breccia which are used as reservoirs in geothermal systems

REFERENCES

Blakely, R. J. (1995). "Potential Theory in Gravity and Magnetic Applications". Cambridge University Press. Australia.

Darmawan, Lucas, Djoko, I Gede Boy, (2013). "Interpretasi Geologi Gunung Rajabasa Berdasarkan Integrasi Citra Aster, Dem Dan Geologi Permukaan". Prosiding Seminar Nasional Kebumian Ke-6, 11-12 Desember 2013, hlm 285.

Grandis, H. and Yudistira, T., (2001), "Inversi Data Magnetik 3-D (Inversion of 3-D Magnetic Data)", Pertemuan Ilmiah Tahunan HAGI ke-26, Jakarta.

Indratmoko, Putu., Nurwidyanto, M irham., Yulianto, Tony, (2009). "Interpretasi Bawah Permukaan Daerah Manivestasi Panas Bumi Parang Tritis Kabupaten Bantul DIY dengan Metode Magnetik". Jurnal Berkala Fisika, Vol.12, No.4; Oktober 2009, ISSM: 1410-9662. Universitas Diponegoro.

Kusnida, D., Subarsyah and B. Nirwana, (2009). "Basement Configuration of the Tomini Basin deducated from Marine Magetic Interpretation", Indonesia Journal of Geology, Vol. 4, No. 4, Dec., p:269-274.

Loke, M. H, (2000), "Electrical Imaging Surveys for Enviromental and Engineering Studies: A Partical Guide to 2-D and 3-D Surveys". Geophysic, Vol.60, No.6, pp 1682-1690.

Loke, M.H. (1995). "Least Squares Deconvolution of Apparent Resistivity Pseudosection". Geophysics, Vol 60, No.6, pp 1682-1690. Malaysia.

Lukhvich, A.A., A.K Shukevich, I.M. Morozov, N.V. Kremen'kova, V.I. Sharando, and O.V. Bulatov, (2003), "Magnetic Method of Testing the Distribution of Properties over the Depth". Russian Journal of Nondestructive Testing, Vol. 39, No. 9, pp. 665 – 669.

Menke, W., (1984), "Geophysical Data Analysis: Discrete Inverse Theory", Academic Press. Inc: Orlando-Florida.

Rasimeng, S. (2008). "Analisis Sesar Gunung Rajabasa Lampung Selatan sebagai Daerah Prospek Geothermal Berdasarkan Data Anomali Medan Magnet Total". Jurnal Sains MIPA Vol 14 No 1, April 2008

Sumintadirejo, P., (2005), "Vulkanologi dan geothermal. Diktat kuliah vulkanologi dan geothermal", Penerbit ITB.

Yaoguo, L., and Oldenburg, D.W., (2001). "Stable reduction to the pole at the magnetic equator". Geophysics, Vol.66, No.2, pp.571-578.

THE APPLICATION OF EXPERIMENTAL DESIGN USING THREE-LEVEL FULL FACTORIAL DESIGN FOR PROBABILISTIC RESOURCE ASSESSMENT IN ATADEI GEOTHERMAL FIELD, INDONESIA

Marchel Christian Supijo, Heru Berian Pratama, and Sutopo

Geothermal Master Program, Institute Technology of Bandung, Indonesia
Jl. Ganesha No. 10 Bandung
Email: marchelbinsus@gmail.com

ABSTRACT

Energy reserve is the most essential aspect of geothermal development. Resource assessment in the geothermal green field will most likely encounter some difficulties due to the limited initial data and directly impact the accuracy of the estimated resources. Proper electricity potential based on resource assessment affects the development scenario in order to determine optimum capacity to be installed. Therefore, this paper applied the experimental design approach using Full Factorial Design (FFD) 3-level to the TOUGH2 numerical model of Atadei geothermal field to generate probabilistic resource assessment results. This study aimed to perform the Experimental Design (ED) using Full Factorial Design 3-level for probabilistic resource assessment in Atadei geothermal field. A Full Factorial Design 3-level were used to build 81 experiments and investigated four parameters (permeability, porosity, liquid saturation, and feed zone location) at three levels (minimum, most likely, and maximum). The results from multiple model runs were used to create a regression equation (proxy model) and then applied to Monte Carlo simulation to generate a probabilistic distribution of the potential power output. This method had been successfully estimated a more robust electricity potential covering the entire range of possible values of important reservoir parameters. The probabilistic electricity using Monte Carlo based on Full Factorial Design 3-level for 30 years production for P10, P50, and P90 are 11.7 MW, 18.2 MW, and 25.6 MW respectively.

Keywords: resource assessment, experimental design, full factorial design 3-level, TOUGH2, numerical simulation, Atadei geothermal field, Monte Carlo simulation.

INTRODUCTION

To meet Indonesian geothermal target by 2025, which is 7242 MW stated by ESDM (2017), the Indonesian government has committed conducting development in geothermal prospect, including the prospected areas in East Indonesia. One of the prospect areas in Eastern Indonesia, which currently under development is Atadei geothermal prospect area. Atadei is situated in Lembata Regency, East Nusa Tenggara, Indonesia. The location of Atadei geothermal field is shown in Figure 1, and the prospect area is considered as located in a remote area. To reach Atadei from Jakarta would take around two consecutive days, and this is counted as one of the challenges found in developing this field. PT. PLN (a state-owned company), since April 2017 has been the concession owner of this field based on SK-permits No. 1894 K/30/MEM/2017.

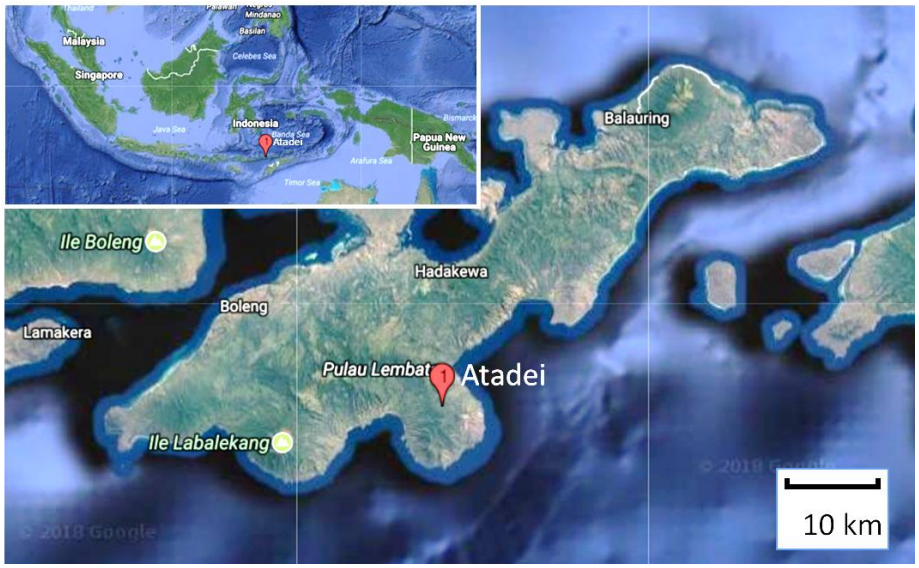


Figure 1: Atadei geothermal greenfield prospect area (Supijo et al.,, 2018).

Nowadays, it is necessary to do probabilistic resource potential assessments that consider the uncertainty of the data. Probabilistic resource assessment is the practice of generating the probability distribution function of a geothermal systems' resource size or resource potential based on the uncertainties of the available reservoir information. The uncertainties in both subsurface parameters and the development to implement in Atadei geothermal greenfield resources can be accommodate used probabilistic assessment. The most common application of probabilistic resource assessment is carried out with the heat stored method. Experimental design (ED) is a systematic way of simultaneously testing multiple variables that affect the response. This study aimed to build a numerical simulation of Atadei geothermal greenfield and to perform the response surface method (RSM) based on Box-Behnken design (BBD) for probabilistic resource assessment.

EXPERIMENTAL DESIGN IN RESERVOIR SIMULATION

The main objectives of experimental design when using reservoir simulations are the following (Quinao & Zarrouk, 2015):

- To systematically design and perform simulation experiments on the reservoir model in order to understand the relationship between uncertain parameters and performance- related responses, and
- To fit a response surface (proxy polynomial) on the simulation experiment result in order to describe the performance-related responses as a polynomial function of the uncertain parameters.

If all parameters are assumed to be measurable, the response surface can be expressed as follows:

$$Y = f\,(x_1, x_2, x_3, \ldots, x_k) \qquad (1)$$

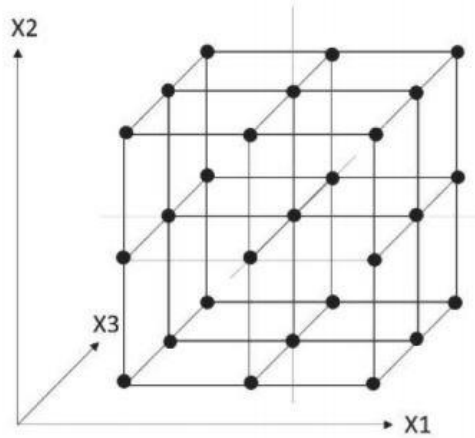


Figure 2: The geometry for Full Factorial Design 3-level (Fukuda et al., 2018).

Where Y is the answer of the system, and x_i the parameters of action called factors (Aslan & Cebeci, 2007).

The parameters that have high uncertainty are porosity, permeability, liquid saturation, and the location of feed zone. With four parameters at three levels, a Full Factorial Design 3-level will be 81 experiments.

INTEGRATED GEOSCIENCE AND WELL DATA REVIEW

Geology review

During May 2000, the explorations that covered around 100 km^2 in the vicinity of Atadei geothermal field produced a geological map that represents the study area, as shown in Figure 3. Based on volcano-stratigraphy, in general, the volcanic products and deposits in Atadei area are divided into two groups. The old volcanic crops out in the northern and southwest part of the study area, the young volcanic product is found in the eastern part of the study area. Aswin, *et al*. (2001), mentioned the cones of young volcanic were formed along with the main lineament which direction is almost N-S. The cones consist mostly of andesite pyroxene lava, and pyroclastic (flow and fall) with two NE-SW (Lewo Kebingin and Mauraja) faults control the geothermal surface manifestation in this study area.

Geochemistry review

According to the previous study of geochemistry survey and analysis conducted by Nanlohy et al., (2003), most of surface thermal features are found at the vicinity of the three SW-NE main faults in Atadei geothermal prospect.

Those main faults are Watuwawer Fault which controls the typical upflow features such as fumaroles and acid hot springs in Watuwawer and Lewokeba; Lewo Kebingin Fault which rules the typical mixture manifestation where fumaroles, acid sulfate and bicarbonate springs were found in just close proximities to the Lewo Kebingin, Wae Mata, and Wae Kowan; Mauraja Fault solely controlling the outflow type of manifestation (bicarbonate waters or dilute chloride-bicarbonate water) in Wai Keti and Wai Tupat. The figure of the ternary plot of water types "Cl-SO_4-HCO3" and ternary plot of ion alkali geothermometer "Na-K-Mg" proposed by Giggenbach (1988) is shown in Figure 4 and Figure 5.

Since there are no springs were classified as partial equilibrium which made the geothermometer "Na-K-Mg" is not applicable. Thus, the reservoir temperature is estimated using geothermal-gases. Based on ammonia geothermometer calculation, the reservoir temperature is 221°C.

The calculated reservoir temperature, then, to be used to estimate the depth of top reservoir (TOR) during the early stage of geothermal exploration by using the method proposed by Saputra et al. (2016). The procedure for estimating the depth of the top reservoir is illustrated in Figure 6. Assuming that the temperature in the interval is conductive and is dominated by a clay cap, thus, the gradient is considered linear.

The result of the early estimated top reservoir in depth is illustrated in Figure 7. It states that the calculated temperature reservoir of 220°C present in the depth of -800 masl, later it is estimated as the top of the reservoir.

Geophysics review

The magnetotelluric survey has been notably indicated the low resistivity layers beneath the Watuwawer manifestation at the near surface of about 200 meters. It extends at the greater depth around 400 meters to the East and the West of Atadei geothermal prospect area. At below 1400 m depth or -800 masl, the contrast of higher resistivity occurred and thickened which is later suggested as a reservoir rock. The exception applied for Watuwawer doming which is attained the contrast resistivity at a relatively shallower depth around 1200 m depth or around -700 masl. It is necessarily agreed with the estimated depth of top reservoir using method proposed by Saputra et,.al (2016) in the earlier exploration stage. Therefore, the authors have adequate confidence in determining the depth of the top reservoir at 1400 m depth and 1200 m depth only for doming/upflow area to be assigned in the numerical model. The result of 3D MT inversion by PSDMBP (2017) is shown in Figure 8, which illustrate the NW-SE cross-section of Atadei.

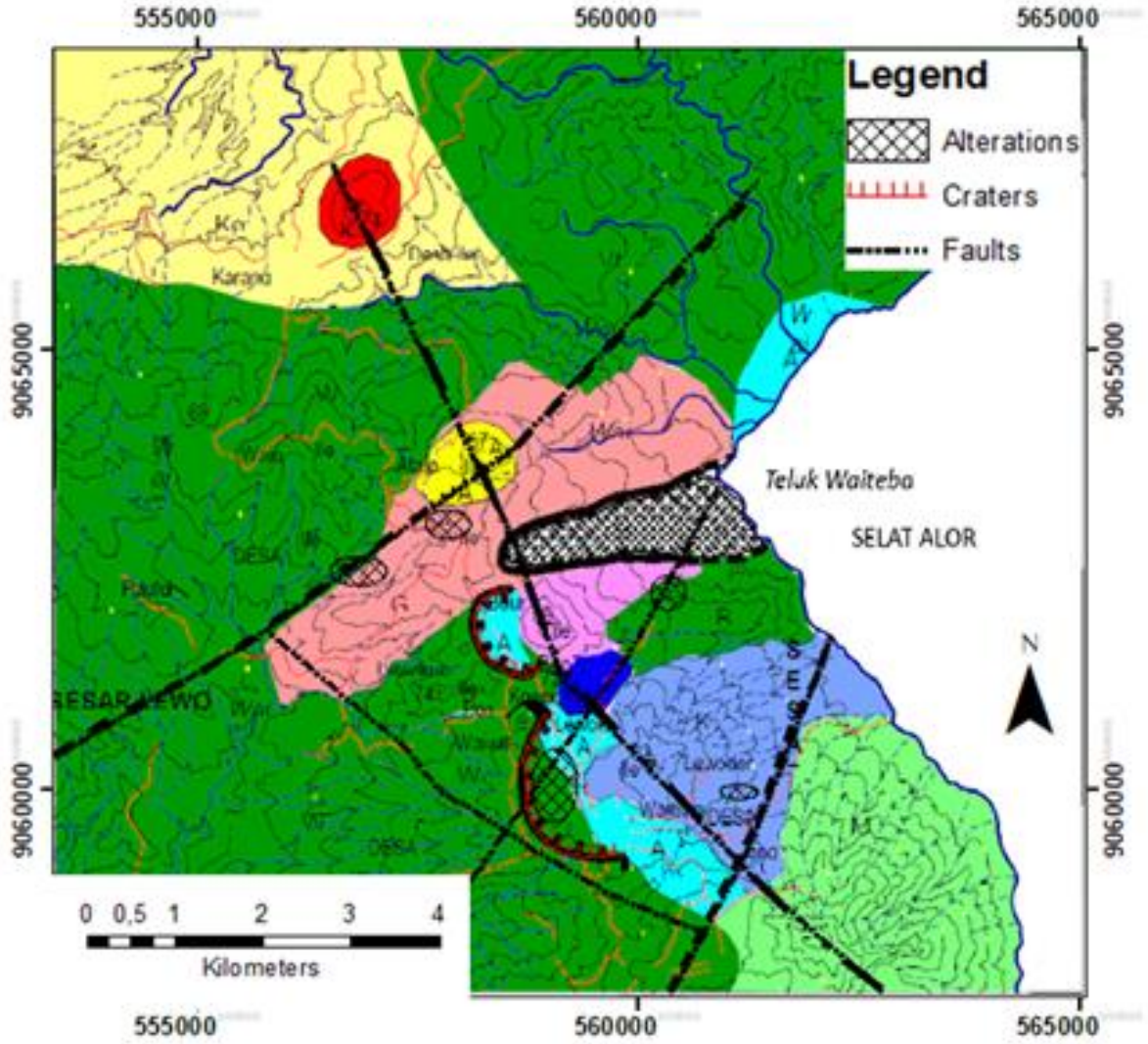


Figure 3: Geological Map of Atadei (after-PSDMBP, 2017).

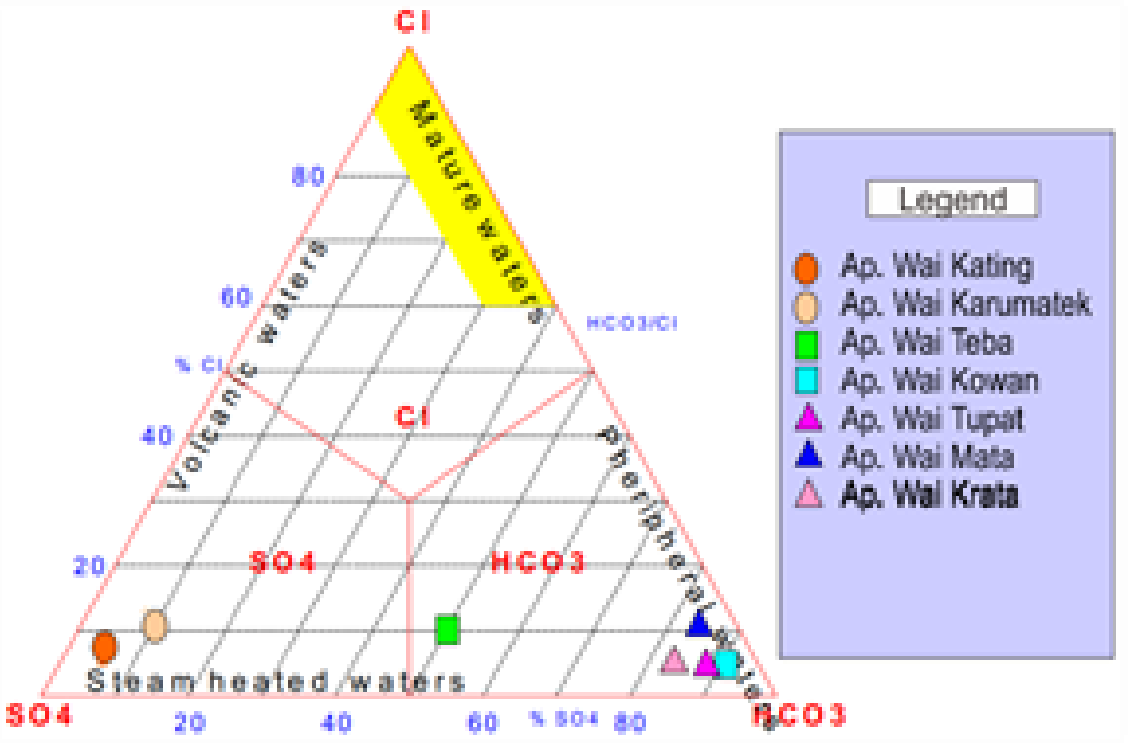


Figure 4: The ternary plot of water types "Cl-SO4-HCO3" (Nanlohy at. al, 2003).

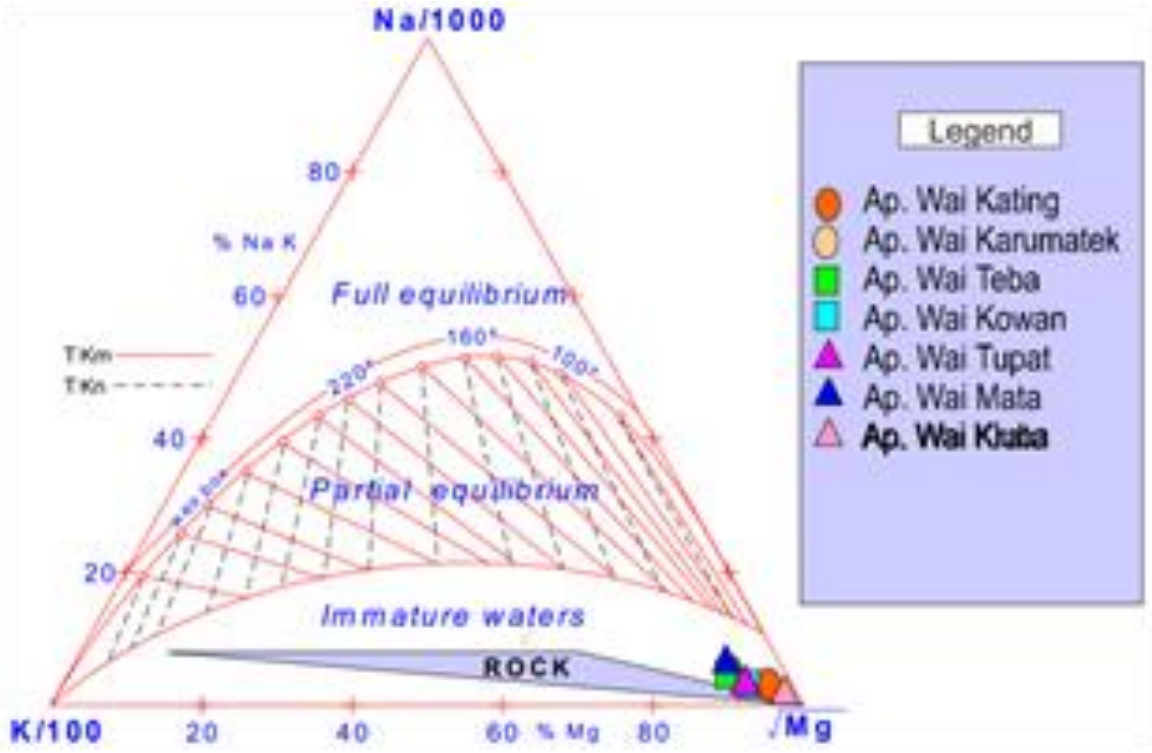


Figure 5: Ternary plot of ion alkali geothermometer "Na-K-Mg" (Nanlohy at. al, 2003).

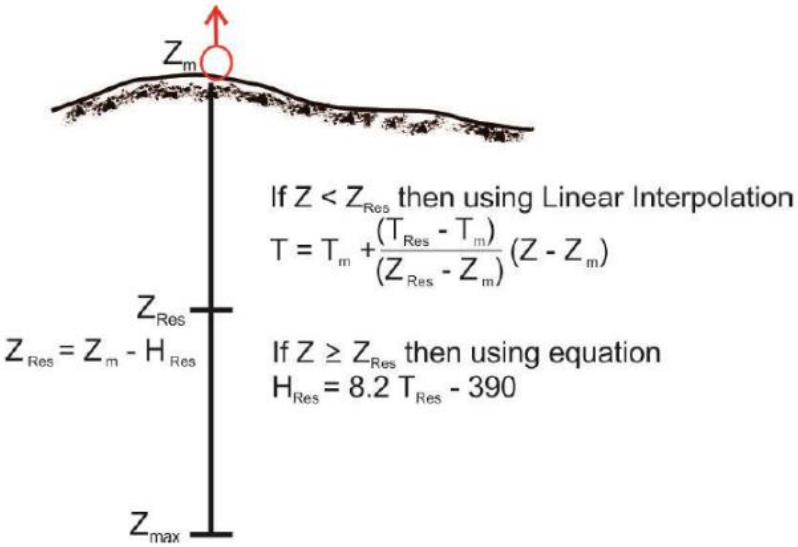


Figure 6: Illustration of the determination of subsurface temperature using temperature from surface manifestation (Saputra et al., 2016).

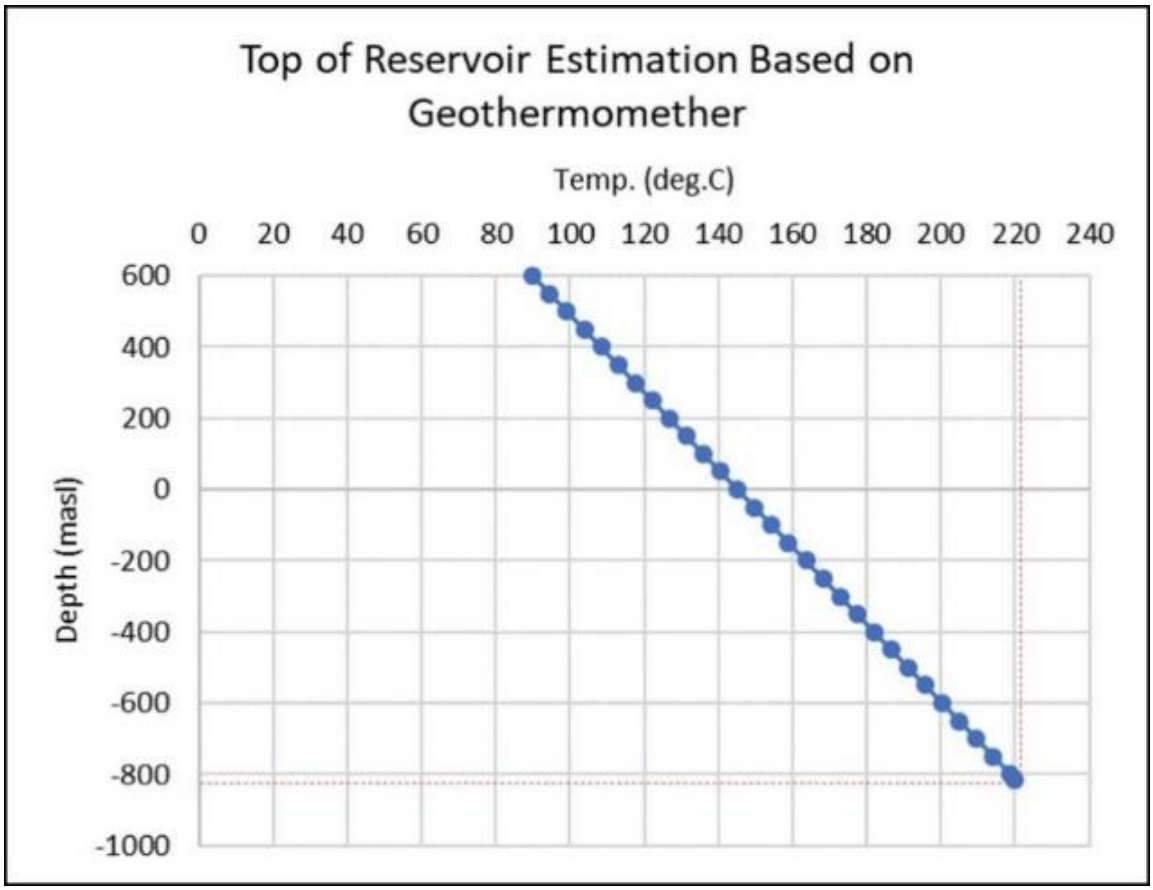


Figure 7: The result of the early estimated top of the reservoir using the method proposed by Saputra et al. (2016).

The resistivity data showed that the low resistivity zone beneath the Watu-wawer caldera relatively occurred at the shallower depth than in any others locations. Being consistent with the presence of fumaroles in the Watuwawer caldera, it strongly suggests that small steam cap has developed naturally in that particular area. The sounding resistivity also indicated another small dooming of suggested steam caps present at Lewo Kebingin and Lewokeba.

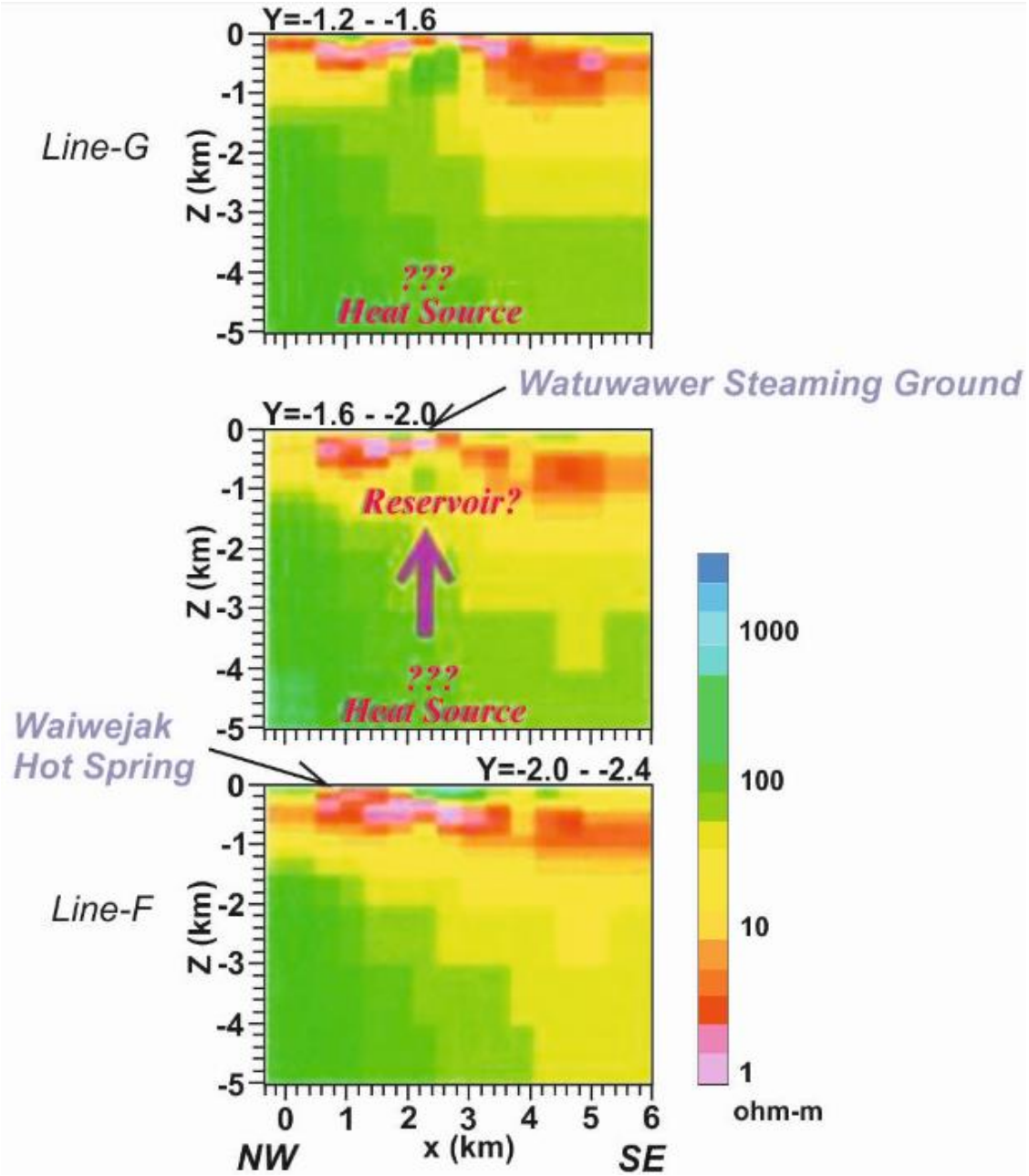


Figure 8: NW-SE cross-section of 3D MT Inversion of Atadei Geothermal Prospect Area.

Well Data

Two gradient temperature wells namely ATD-1 and ATD-2 were drilled to reach a depth of 250 meters, and these wells were drilled to get a better understanding of temperature gradient especially in upflow zone and to delineate the extent of the reservoir at the boundary of the Atadei geothermal field. ATD-1 is situated in the Watuwawer caldera representing temperature gradient in upflow area, meanwhile, ATD-2 is situated in Mauraja nearly intersected with Mauraja Fault in which representing the temperature distribution in the boundary or outflow area (Soetoyo, 2008).

Two years later in 2004, two exploration wells were drilled around the prospect areas of Watuwawer caldera and Bauraja crater, namely AT-1 and AT-2. It is aimed to get a better understanding of temperature distribution, particularly in upflow zone. AT-1 was drilled to the depth of 830.5 m and AT-2 was drilled to the depth of 750 m.

The result of well testing shows AT-1 had wellhead pressure at 7 kscg and AT-2 had wellhead pressure at 0 kscg. However, the temperature of both wells at the wellhead is relatively similar to the environment temperature. Thus the pressure measured at AT-1 wellhead is principally not come from the geothermal fluid. Logging temperature is applied to AT-1 until to the depth of 450 m and found the temperature was at 96.5°C (Sitorus et al., 2005). The

temperature profile from AT-1 well is shown in Figure 9.

Conceptual Model

The conceptual model was updated by Supijo et al. (2018) shown in Figure 10. The conceptual model designed based on comprehensive geoscience reviews and numerical model approach. It appears that hot geothermal fluid is upwelling from the deep part of the Watuwawer caldera. The deep leakage of fracture permeability from WatuWawer Fault and Lewo-Kebingin Fault control the flows of hot fluids in which it ascends through the given vertical permeability-with some fluids flow laterally to the Southeast until rising to the surface through Mauraja Fault as outflow. In contrary to the initial model, there is a change in determining the depth of top reservoir as the updated model has followed the interpretation of Magnetotelluric data rather than DC-Resistivity in which Nanlohy et. al (2003) had followed. It stated that in general top of a reservoir of Atadei geothermal area is situated around the depth of -800 masl, the only exception applied for Watuwawer area in which the reservoir reached the depth of -700 masl.

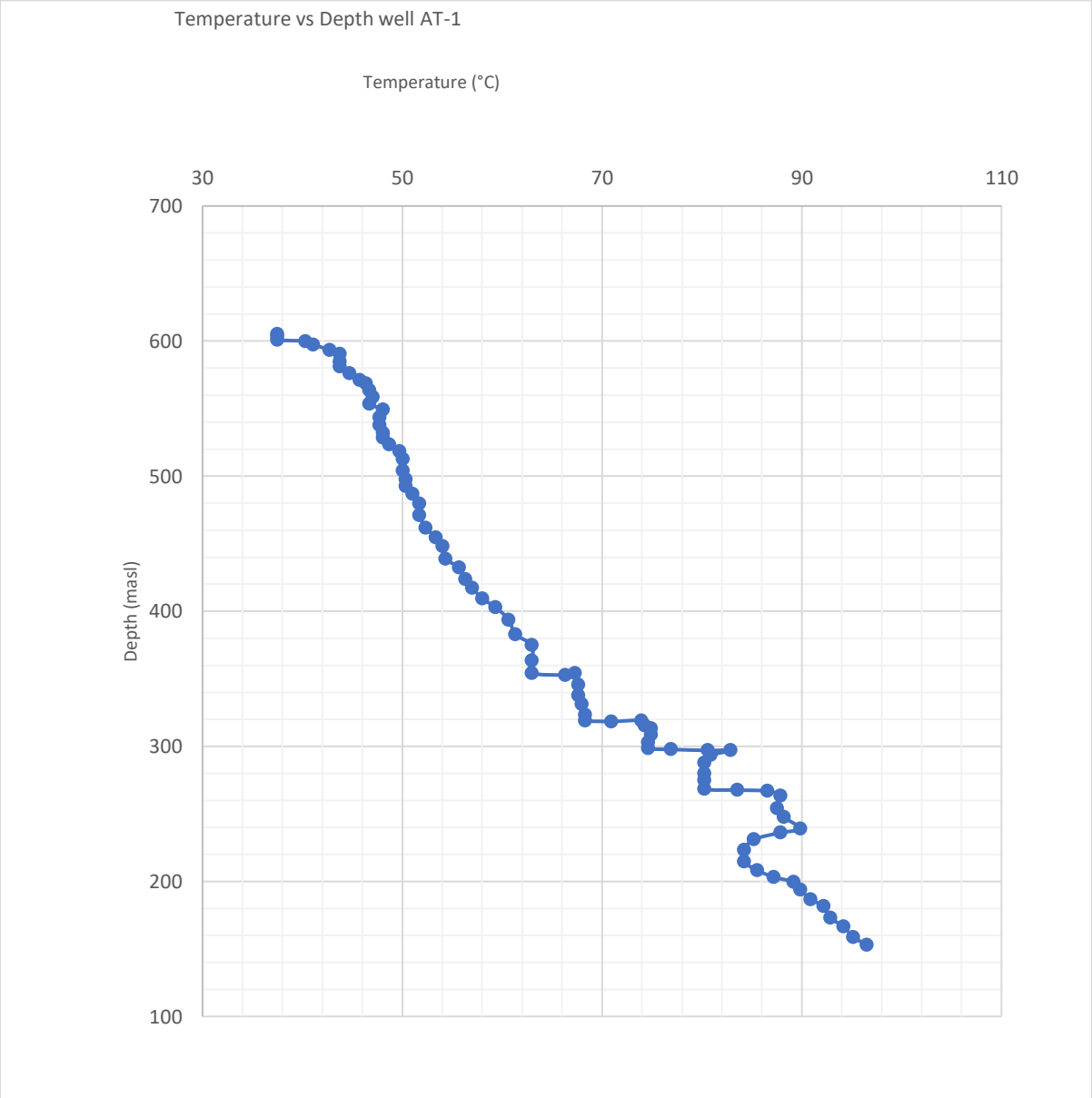


Figure 9: The temperature profile of well AT-1 (Sitorus & Munandar, 2005).

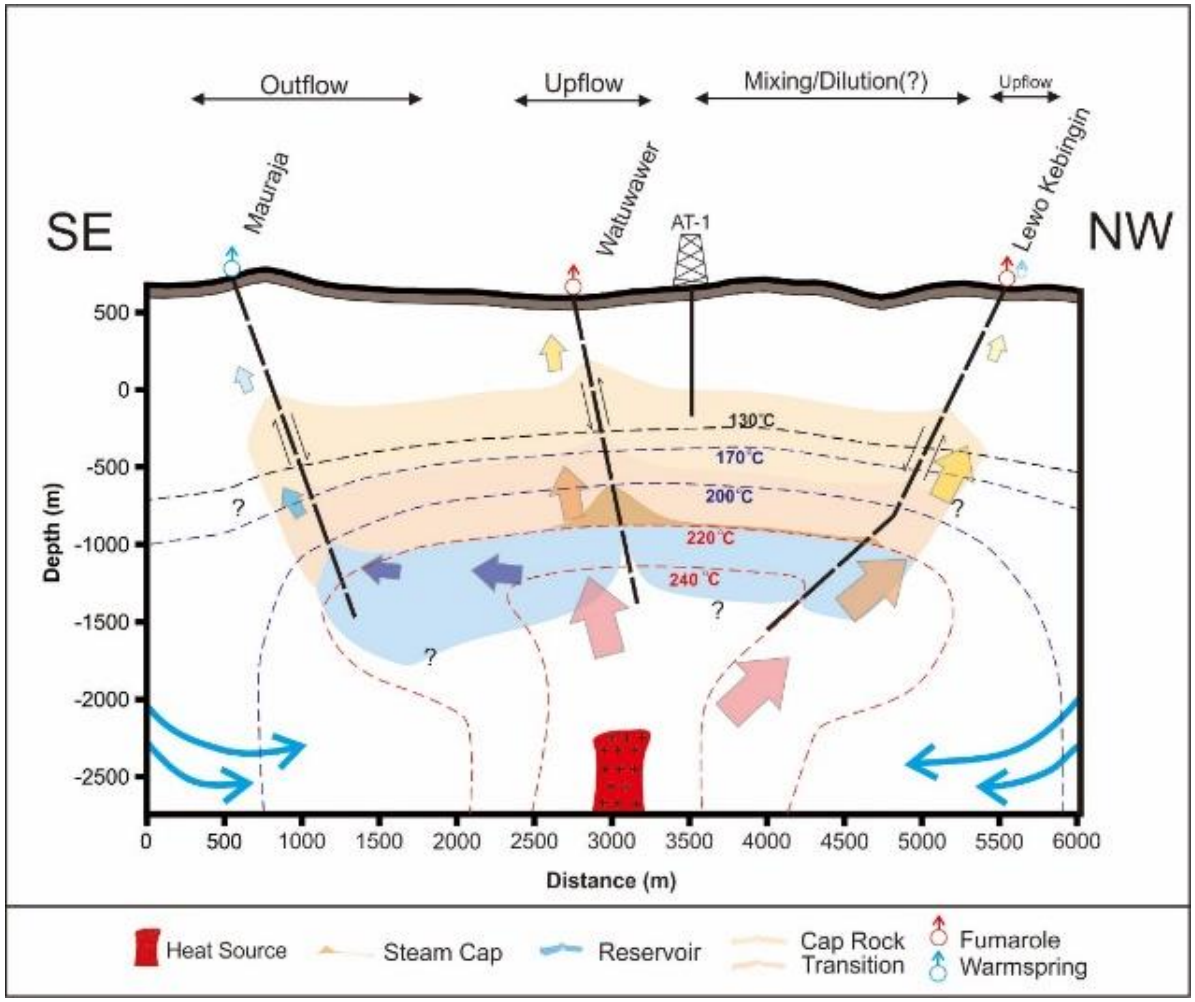


Figure 10: Conceptual model of Atadei geothermal system (Supijo et al., 2018)

ATADEI NUMERICAL MODEL

Gridding and layering

The grid of the model is rotated at 127° to the East to accommodate the material assignment to be necessary for an arrangement with the alignment of the conceptual model. It is covering a total area of 6.4 km x 5 km or equal to 32 km^2 and a total thickness of 3.45 km (i.e. from 950 masl to -2500 masl)-which is demonstrated in Figure 13. The horizontal dimension of grid blocks varies from the smallest 100 m x 100 m to the most significant 500 m x 500 m, the smallest grid blocks are used near the reservoir area, wells, and faults to increase the modeling accuracy on that area. The model is divided into 13 layers with some of the top layers follow the real topographical condition. The total number of grid blocks is 22,560 by using a rectangular grid type. This model used EOS1 for water and water for tracer because of data limitation and to simplify the modeling process.

Initial and boundary condition

The initial condition is needed to input the initial temperature and pressure for each grid-block on the model to fasten the process of running the model. At the initial condition, the normal gradient is used for both temperature and pressure. Meanwhile, the top layer is set to constant at the atmospheric conditions with the pressure is set at 1E-05 Pa, and the temperature is at 25ºC.

Rock properties (assign material)

During the numerical modelling, determining the permeability structure is the most essential step to be iteratively adjusted until the natural state condition was achieved. The iterative process is done by several trial and errors. The permeability structure used in the final modelling is shown in Table 1 and its distribution to the grid model, also shown in Figure 11.

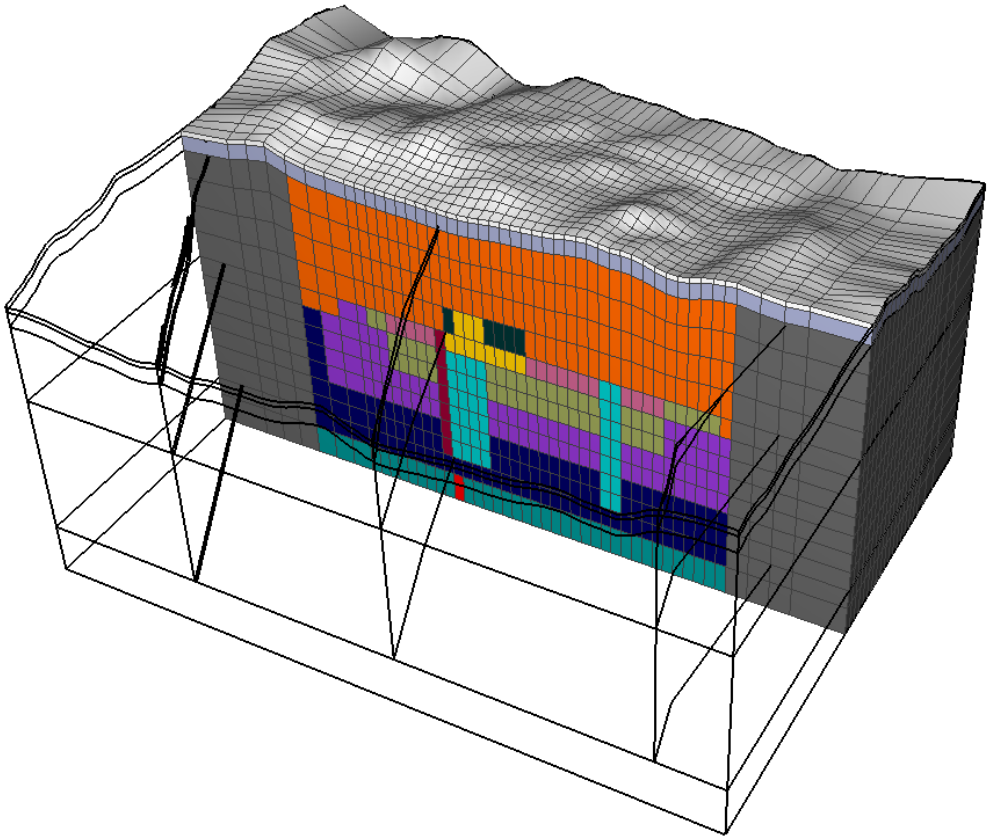


Figure 11: Material assignment to the gridding model.

Table 1: Material properties.

Material	K_{xy} (mD)	K_z (mD)	Color
ATM	10	10	
GW	0.002	0.002	
CAPR	0.00001	0.00001	
BOUND	0.00005	0.00001	
HEAT	100	100	
RES1	60	30	
RES2	40	30	
RES3	20	20	
RES4	10	10	
RES5	70	70	
RESMT	60	30	
FAULT	30	30	
BASE	3	3	
FAUL1	30	20	
TRNS	0.001	0.001	

Numerical modelling result

During the initial state calibration, also called natural state modeling, the computer model was run until natural steady state conditions were reached. The results were then compared against actual wells temperatures and reservoir temperature estimation obtain from geothermometer. To obtain a good fit between model results and field observation data, the permeability structures was adjusted in an iterative process.

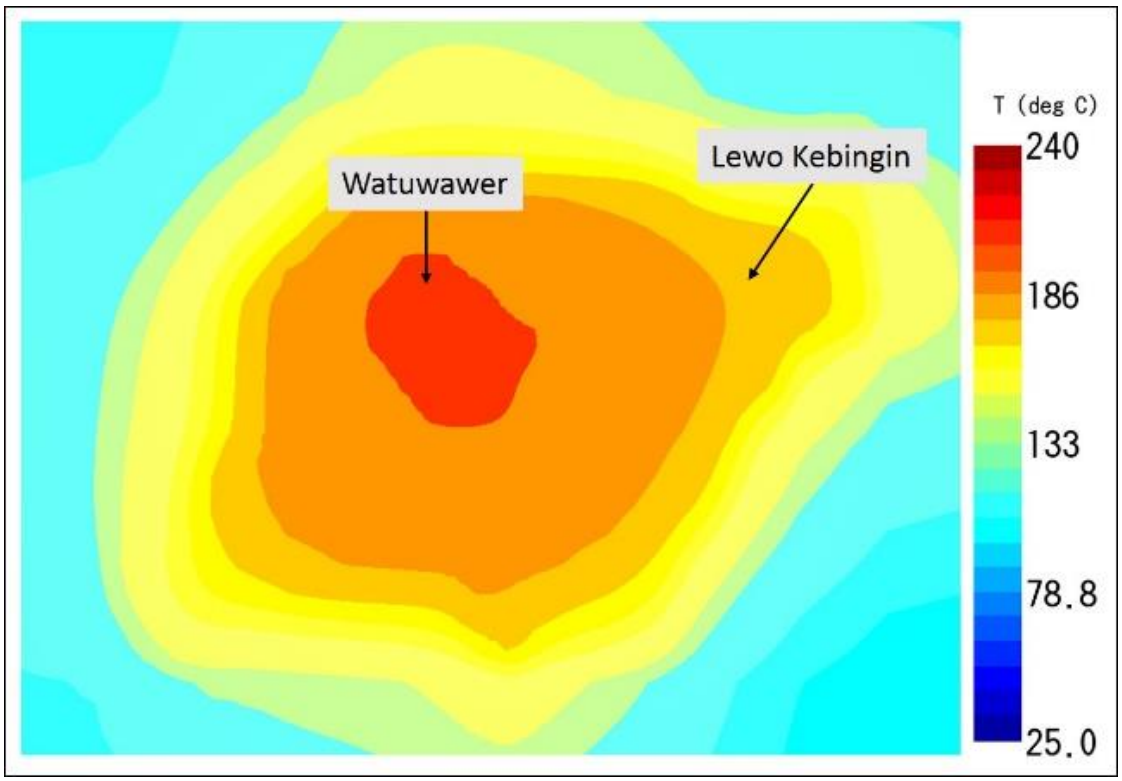


Figure 12: Temperature distribution of the model in the top reservoir.

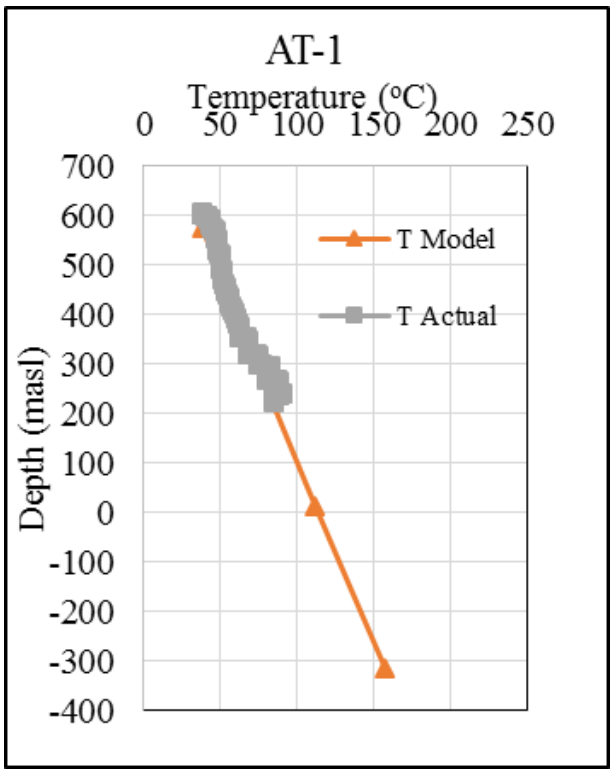


Figure 13: AT-1 temperature matching.

There is only one observation well available to match the model, it is obtained from AT-1. The dummy wells in Atadei area were also used to match the reservoir temperature by comparing with the temperature estimation obtained from the ammonia geothermometer, considering well AT-1 was not reached the depth of the reservoir. The modeling process was carried out by using a pre- and post-processor of TOUGH2. The temperature distribution in top of the reservoir is also shown in Figure 12. Figure 13 indicates the temperature matching of AT-01. It shows a good alignment between the actual and the modeled temperature.

Meanwhile, the distribution of gas saturation in the reservoir which indicated as steam caps is found a relatively further steam formation in Watuwawer and most likely thin steam cap present in Lewo Kebingin as illustrated in Figure 14.

One of the crucial driver outcomes of the reservoir numerical modelling is the simulation of heat and mass flow within the system, as illustrated in Figure 15. It concludes the whole fluid flow process from the upwelling geothermal heat flow beneath the Watuwawer caldera in which the hot fluids ascends directly through the given vertical fracture permeability later emerge as upflow manifestation in Watuwawer, Lewo Keba and Lewo Kebingin. The residual fluids circulate within permeable zones as the hot fluid with lighter in density ascends until it reaches the impermeable layers where heat losses occur resulting in some cooling fluids descending back to the reservoir and some other flow laterally until it emerges as outflow manifestation in the surface in Mauraja and Lewo Kebingin.

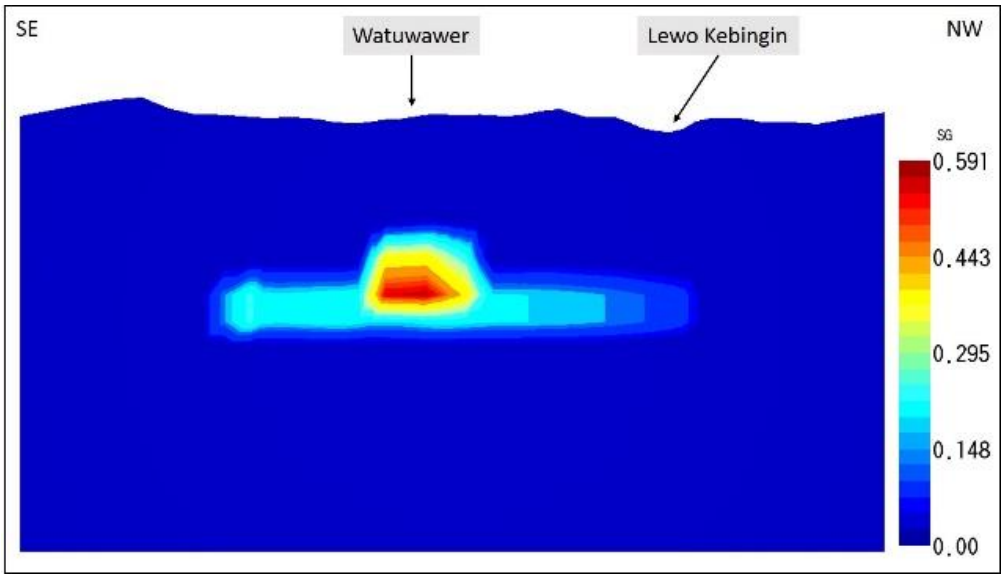


Figure 14: Temperature distribution of the model in the top reservoir.

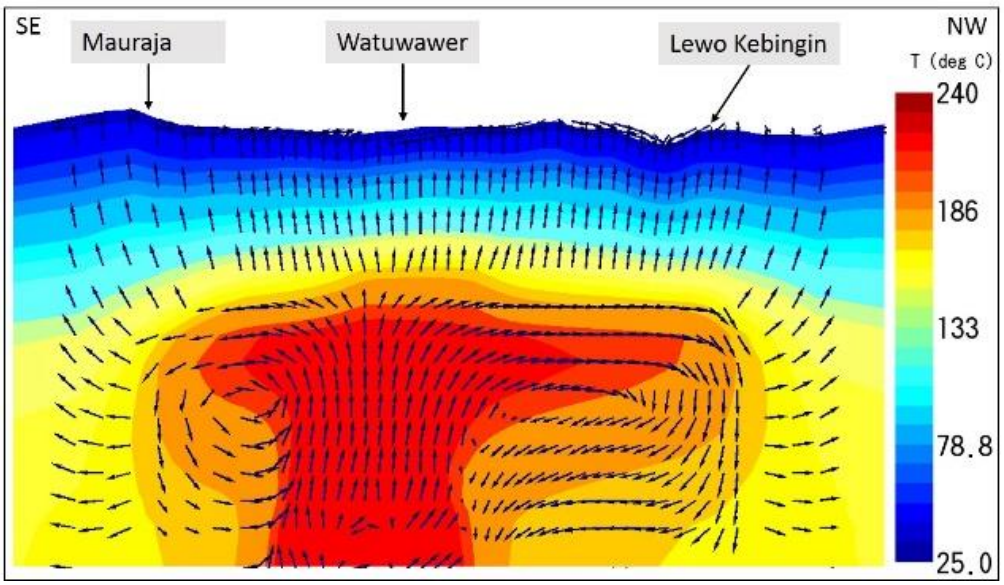


Figure 15: The heat transfer in a vertical slice of the numerical model.

EXPERIMENTAL DESIGN ON THE ATADEI MODEL

The experimental design (ED) concept was applied in Atadei reservoir model in order to analyze the dependency from uncertain reservoir parameters to obtain the amount of production (MW) for 30 years. Furthermore, it also has a purpose to construct polynomial functions (proxy equations) to the reservoir simulation in the probabilistic Monte Carlo simulation. The simulation experiment requires choosing the parameters that will be included in the investigation. The following parameters are deemed sufficient for the current study are porosity, permeability, liquid saturation, and the location of feed zone. The sensitivity for each parameter is shown in Table 2.

A three-level of Full Factorial Design namely minimum, most likely, and maximum with four factors for response surface method was implemented. The required number of runs will be determined based on the Full Factorial Design 3-level. The total run for this study is 81 runs for 30 years of production. Table 3 summarized the entire Full Factorial Design 3-level with four factors.

Table 2: Parameter of response surface method with box-behnken design.

Parameter	Minimum (-1)	Most likely (0)	Maximum (+1)
Porosity (POR)	-20%	Initial Condition	20%
Permeability (PERM)	-20%	Initial Condition	20%
Liquid Saturation (SW)	0.3	0.4	0.5
Feed Zone (FZ)	-600 s/d -800 masl	-800 s/d -1000 masl	-800 s/d -1200 masl

Table 3: Full Factorial Design 3-level combination.

RunOrder	POR	PERM	SW	FZ
1	0	1	0	-1
2	1	0	1	0
3	0	0	0	0
4	0	-1	1	0
5	0	-1	0	-1
6	0	1	-1	0
7	1	0	-1	0
8	0	0	0	0
9	0	0	1	1
10	0	0	0	0
72	-1	0	-1	0
73	-1	0	1	0
74	0	-1	0	1
75	-1	-1	0	0
76	1	1	0	0
77	-1	0	0	-1
78	-1	0	0	1
79	0	1	0	1
80	1	-1	0	0
81	1	0	0	1

The reservoir simulation was run equally distributing using well on deliverability method with PI 1.0E-12 m^3 and WHP 10 bar. The total production into 143 wells with targeting the steam zone and two-phase zone with temperature more than 200°C in the reservoir, as illustrated in Figure 16.

To calculate the electricity potential in MW, the following equation was used:

$$MW_e = \frac{\sum_{m=1}^{L} m \times \Delta t}{L \times SSC} \quad (2)$$

Where MWe is the power capacity in MW, m is the produced steam (kg/s), Δt is the delta time at the simulation (years), L is the project time (years), and SSC is the specific steam consumption (kg/s/MW). The results of Atadei probabilistic resource assessment for 30 years of steam production with 2 kg/s/MW of SSC shown in Table 4.

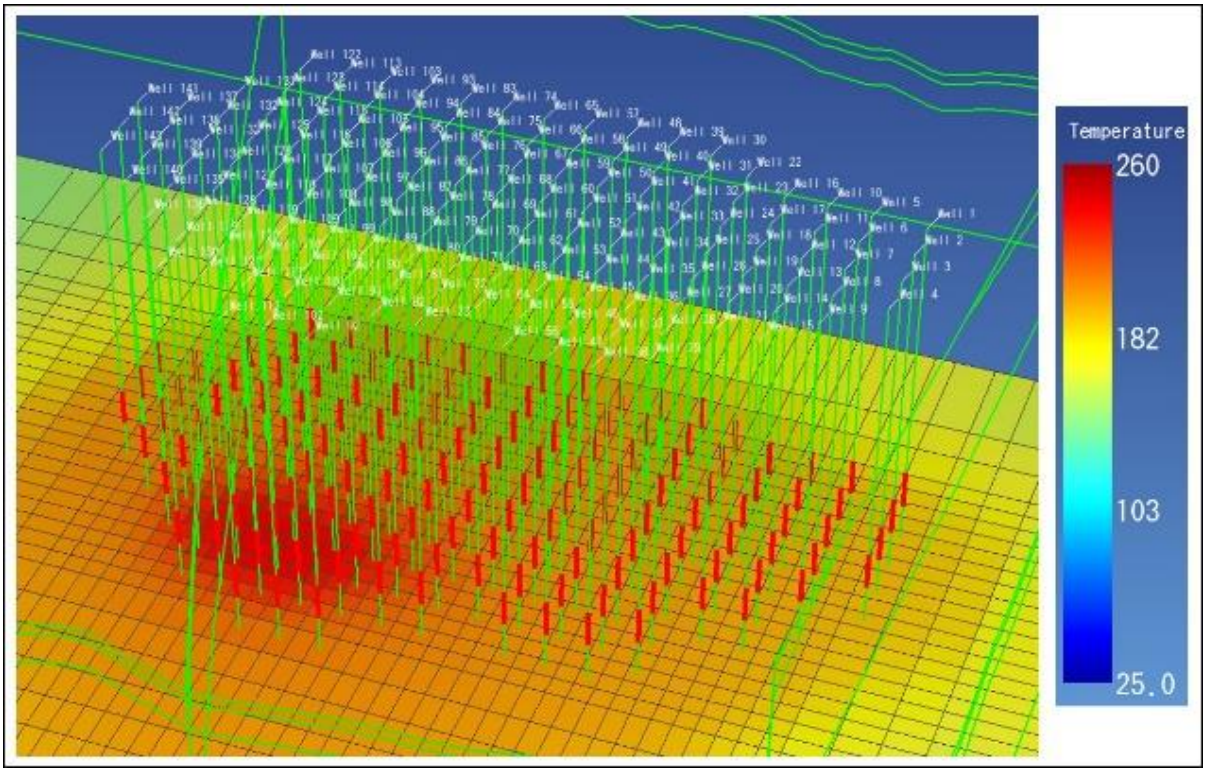


Figure 16: The location of a dummy production well.

Table 4: Results MWe for all combination.

RunOrder	MWe
1	36
2	7
3	21
4	8
5	28
6	34
7	21
8	9
9	36
10	9
72	18
73	9
74	19
75	20
76	35
77	29
78	29
79	19
80	20

Based on a fitted line plot and surface plot carried out on the Full Factorial design 3-level results, the only location of feed zone (FZ) among the parameters tested have a significant effect on the 30 years power capacity of the Atadei geothermal greenfield. These results are shown in Figure 17.

The Atadei numerical simulation is approximated by the polynomial equation to generate the power capacity (MW). The polynomial equation of power capacity as a function of four independent parameters are the results in this study. A three-level proxy model using -1, 0, and +1 parameters to generate the power capacity responses for an Atadei model shown in Equation 3.

MONTE CARLO SIMULATION FOR PROBABILISTIC DISTRIBUTION OF POWER CAPACITY

Monte Carlo simulation with 60,000 random number was carried out on the proxy model, using the probability distributions of the individual parameter as described in Figure 2. The result is a probability distribution function of the power capacity covering the full range of possible outcomes. The proxy model was then applied to calculate the range of possible values for P10, P50, and P90 of MWe. The cumulative distribution for 30 years of steam production of the power capacity shown in Figure 18. The P10, P50, and P90 are 12 MW, 18.5 MW, and 25.8 MW respectively.

$$MWe = 19.270 + 0.291 \times POR + 1.702 \times PERM - 0.046 \times SW + 12.350 \times FZ - 0.005 \times POR \times POR - 0.013 \times PERM \times PERM + 0.052 \times SW \times SW + 1.177 \times FZ \times FZ \quad (V.3)$$

CONCLUSION

From the result of the study based on the integrated geoscience reviews collected from several published scientific papers and field reports, we conclude that:

1. The model of Atadei geothermal greenfield with 6.4 km x 5 km area has successfully developed, and it showed a good match with actual AT-1 well and conceptual model.
2. The numerical simulation with experimental design (ED) based on full factorial design 3-level has successfully applied for Atadei geothermal greenfield.
3. The probabilistic power capacity using Monte Carlo based on Box-Behnken design for 30 years production for P10, P50, and P90 are 12 MW, 18.5 MW, and 25.8 MW respectively.

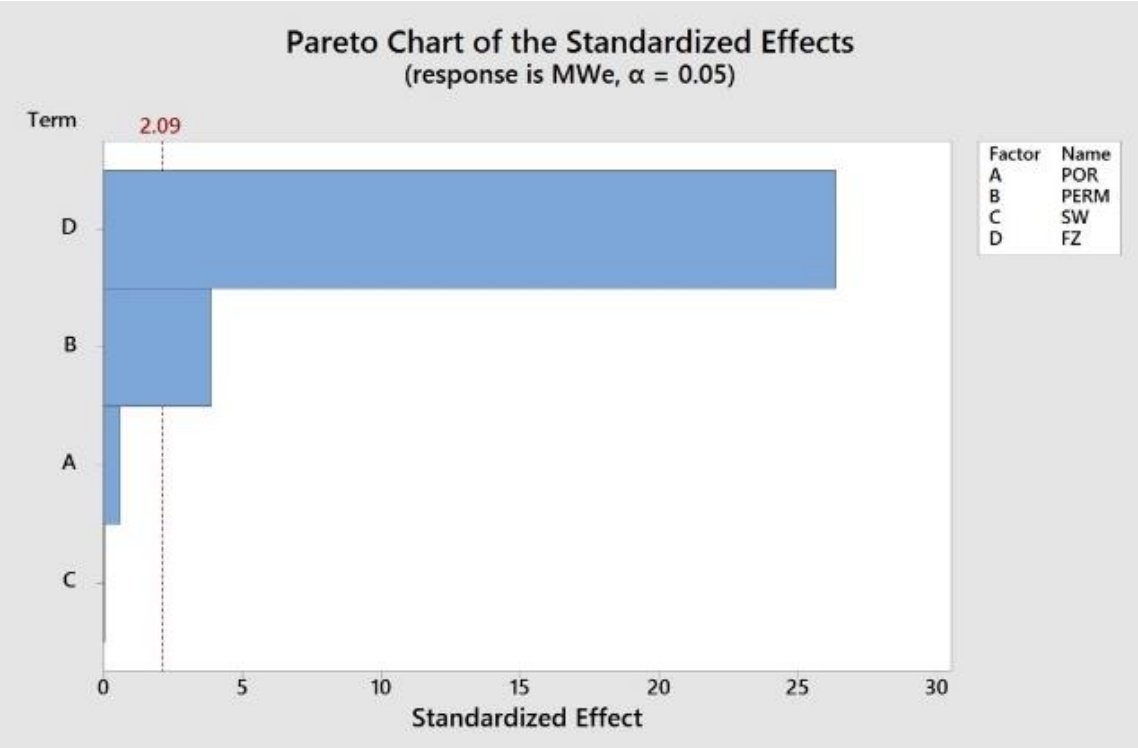


Figure 17: Pareto Chart of Full factorial design 3-level results.

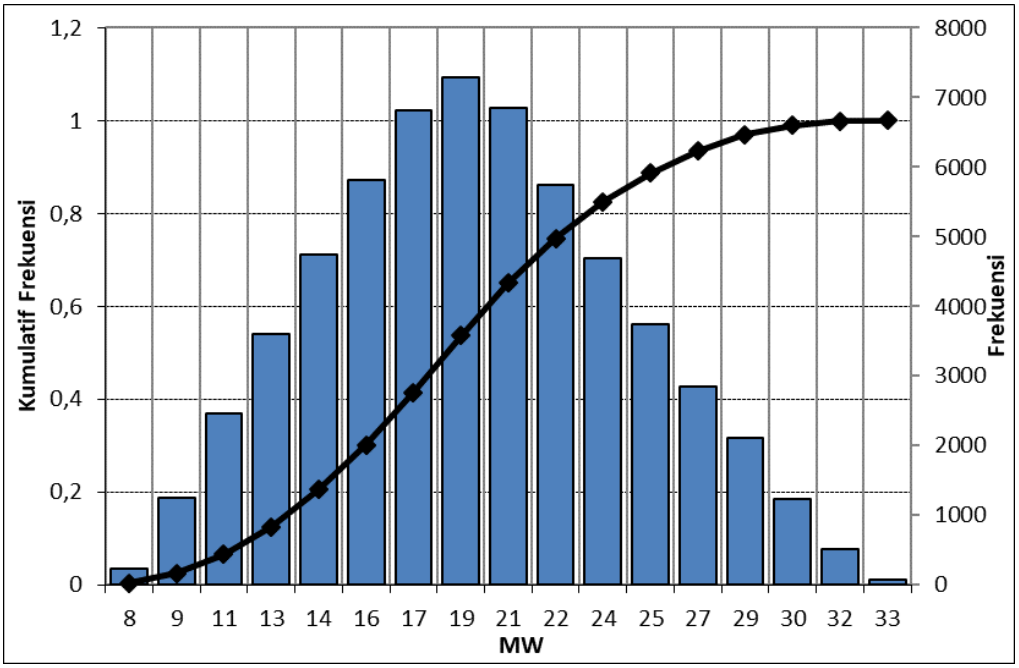


Figure 18: Monte Carlo simulation results with histogram and cumulative distribution functions.

REFERENCES

Aslan, N., & Cebeci, Y. (2007). "Application of Box-Behnken design and response surface methodology for modeling of some Turkish coals". *Fuel*, *86*(1–2), 90–97. https://doi.org/10.1016/j.fuel.2006.06.010

Aswin, D., Sundhoro, H., Munandar, A., Suparman, & Sulaeman, B. (2001). "The Potential of Atedai Geothermal Field Based on Geological, Geochemical and Geophysical Studies, Lomblen Island-East Nusatenggara".

Fukuda, I. M., Pinto, C. F. F., Moreira, C. D. S., Saviano, A. M., & Lourenço, F. R. (2018). "Design of experiments (DoE) applied to pharmaceutical and analytical quality by design (QbD)". *Brazilian Journal of Pharmaceutical Sciences*,

Giggenbach, W.F., (1988). "Geothermal Solute Equilibria – Derivation of Na-K-Mg-Ca geoindicators", *Geochim, Cosmochim, Acta, 52, 2749-2765.*

Nanlohy, F., Kusnadi, D., & Sundhoro, H. (2003). "Program Pengembangan Lapangan Panas Bumi Atadei Kabupaten Lembata – Nusa Tenggara Timur", *1–10.*

Quinao, J. J., & Zarrouk, S. J. (2015). "Probabilistic resource assessment using the Ngatamariki numerical model through experimental design and response surface methods (ED and RSM)". *Proceedings New Zealand Geothermal Workshop, Taupo, New Zealand*, (November).

Saputra, M. P., Suryantini, Catigtig, D., Regandara, R., Asnin, S. N., & Pratama, A. B. (2016). "Geological, isothermal, and isobaric 3-D model construction in early stage of geothermal exploration". *IOP Conference Series: Earth and Environmental Science*, *42*(1).

Sitorus, K., & Munandar, A. (2005). "Karakteristik Geotermal Sumur Eksplorasi At-1, Lapangan Panas Bumi Atadei, Kabupaten Lembata – NTT". *Subdit Panas Bumi, 2, 1–7.*

Soetoyo. (2008). "Kondisi Lingkungan Pasca Pengeboran Sumur Ekplorasi AT-1 dan AT-2 di Lapangan Panas Bumi Atadei, Lembata, Nusa Tenggara Timur", *(Gambar 2), 1–7.*

Supijo, M. C., Wahyono, A. D., Lesmana, A., Harahap, A. H., & Berian, H. (2018). "Updating Conceptual Model Using Numerical Modelling for Geothermal Green Field Prospect Area in Atadei , East Nusa Tenggara , Indonesia". *6th Indonesia International Geothermal Convention & Exhibition 2018.*

POWER DENSITY UPDATE OF INDONESIAN FIELDS

Maxwell Wilmarth, James Stimac, and Gugi Ganefianto

PT Jacobs
15th Floor, Talavera Tower, West Cilandak, South Jakarta 12430
Email: max.wilmarth@jacobs.com

ABSTRACT

This paper updates the power density numbers for operating geothermal fields in Indonesia, including those that have been commissioned since 2010. 12 fields have been updated with production information since 2015. Most of the 12 fields (8 out of 12) fall on the "Main Sequence", a trend of increasing power density with increasing reservoir temperature. An additional two fields fall within the volcanic arcs tectonic group previously identified, making 10 out of 12 fields in Indonesia fall within the previously identified groups of power density pattern. One new high-temperature field is significantly above the curve of the main sequence due to its small production area. While one field lies below the typical power density range for volcanic arc systems.

Keywords: Resource assessment, power density

INTRODUCTION

Resource Capacity Estimates

Resource capacity estimates are commonly made using power density, natural heat loss, stored heat, and numerical modeling (Benoit, 2013; Grant and Bixley, 2011). Quite often, geothermal professionals use power density for first-order estimates of resource capacity, usually expressed in terms of MW/km2. The benefit of an estimate using power density is that it quickly returns a reasonable value, while stored heat estimates may be in error by orders of magnitude, and numerical models require significant time and effort to build but may not be any more accurate than power density unless well calibrated.

Grant (2000) suggested that power density increases with reservoir temperature, indicated 10-20 MW/km2 was a suitable range in early exploration and observed that "…power density for most fields ranges from 8 MW/km2 at 230°C to up to 30 MW/km2 at 300°C". Grant and Bixley (2011) suggested that typical power density estimates used during exploration are 10-15 MW/km2. Power density was discussed as a metric for calculating reserves by Atkinson (2012) with the additional suggestion that an analogue field should be chosen first based on reservoir temperature and production characteristics. Bertani (2005) calculated power density for 69 geothermal fields and found an average value of 7.4 ± 6.0 MW/km2. Sarmiento and Björnsson (2007) quoted power density for some of the geothermal fields in the Philippines. Benoit (2013) presented linear power density for a number of structurally-controlled Basin and Range systems as MW/mile of fault length.

Wilmarth and Stimac (2014) surveyed power density of 53 high-temperature (>200°C) geothermal fields around the world with more than 15 MWnet output and at least 10 years of production history and concluded that power density increases with average reservoir temperature in a manner similar to that proposed by Grant (2000), but that tectonic setting also plays an important role, especially in the power densities of very high-temperature volcanic arc systems (>270°C), which are not correlated with increasing temperature. More purely compressional volcanic arc systems have a negative correlation with temperature, attributed to the closing of permeability structures, as oppose to the more complex structural settings which follows the positive correlation. Wilmarth and Stimac (2015) expanded the study to lower temperature systems (>130°C), to smaller fields with more than 10 MWnet output, and to newer fields with at least 5 years of production history.

METHODOLOGY OF THIS STUDY

This study of power density examined the published literature and surveyed operating companies of Indonesian geothermal fields. To be included in the study the field must have recent reliable data on production well locations and power output.

Power Estimate

Net power output was estimated for each field. In many cases there were recent published values available, but in some cases the estimates were old or it was unclear if the quoted value was net or gross. In fields with long histories, recent estimates were used. This was considered more practical than estimating the lifetime-average power output because the current output can be readily paired with the current wellfield configuration. Figure 1 shows the histogram of MW in 12 Indonesia field, Figure 2 shows the histogram average reservoir temperature in 12 Indonesia field, Figure 3 shows the histogram of production area of 12 Indonesia field, and Figure 4 shows the histogram of power density of 12 Indonesia field.

AREA ESTIMATE

Production area was estimated as a merged 500 m buffer around all current production well tracks. This is the method used in previous papers. The methodology used in this review makes no allowances for isolated, extended-reach deviated production wells which may have dead legs. In some cases of production well locations were ascertained by analysis of publicly available air photos (e.g. Google Earth).

Our methodology pairs a net power output directly with the wells that are producing that output. Injection areas are explicitly excluded, because they can both help (e.g. pressure support) and hurt (e.g. thermal breakthrough) production, and sometimes have no effect (e.g. not connected to main reservoir). We feel that it is more straight-forward to use only the production area for the purpose of calculating power density.

TEMPERATURE ESTIMATE

Average reservoir temperature was the most difficult parameter to estimate. Some fields have consistent, authoritative published values for reservoir temperature. However, all fields have a range of reservoir temperatures and many fields have a very wide range of exploited temperatures corresponding to reservoir compartmentalization or the existence of multiple vertically separated reservoirs. Most fields experience temperature declines over time and so recent values were used. The best estimates were made based on the available published data.

OTHER SOURCES OF UNCERTAINTY

There are many other sources of uncertainty in this methodology. Net output was used rather than gross because these values are much more commonly available, but this means power plant efficiencies are not considered. Wells that are labeled as producers on maps and located on the edge of reservoirs, but are not actually currently producing to the station, could significantly alter the area estimate. Fields that have been producing for more than 5 years but have only recently expanded may have an unsustainable power output. Some fields could expand their production area by moving injection from zones of possible production, or through step-out exploration into higher-power density areas of reservoir. Some fields have wells that produce acid fluids or high gas in otherwise good reservoir area which limits power output.

RESULTS

Operating Indonesian geothermal fields tend to be high temperature and relatively large. This may be a selection bias due to the inherently better economics of larger fields, but there is no doubt that Indonesia is blessed with some of the best geothermal fields in the world.

Most of the 12 fields (8 out of 12) fall on the “Main Sequence”, a trend of increasing power density with increasing reservoir temperature (Figure 5). An additional two fields fall within the volcanic arcs tectonic group identified in Wilmarth and Stimac (2015), making 10 out of 12 fields in Indonesia fall within the previously identified groups of power density pattern. One new high-temperature field (Silangkitang, online in 2017) is significantly above the curve of the main sequence due to its small production area. While one field lies below the typical power density range for volcanic arc systems.

It is probable that as more geothermal fields in Indonesia come online in the coming years that they will fall on different areas of the power density vs. average reservoir temperature plot. In particular, there are many low to moderate temperature geothermal prospects throughout Indonesia which are likely to be developed. Additionally, some of the best geothermal fields to yet be developed worldwide are in Indonesia, and some of these will be high-temperature, higher than the typical range of currently operating geothermal reservoirs in Indonesia (typically 240-290°C).

REFERENCES

Atkinson, P. (2012). “Proved Geothermal Reserves - Framework and Methodology”, New Zealand Geothermal Workshop 2012 Proceedings, Auckland, New Zealand, 34.

Bertani, R. (2005). “World geothermal power generation in the period 2001–2005”, Geothermics 34, 651–690.

Benoit, D. (2013). “An Empirical Injection Limitation in Fault-Hosted Basin and Range Geothermal Systems”, Geothermal Resource Council Transactions, 37, 887-894.

Grant, M. A. (2000). “Geothermal Resource Management”, Proceedings, World Geothermal Congress 2000, Kyushu-Tohoku, Japan.

Grant, M. A., and Bixley, P.F. (2011). “Geothermal Reservoir Engineering 2nd Edition”, Elsevier, Amsterdam, 359.

Sarmiento, Z.F., and Björnsson, G. (2007). “Reliability of early modeling studies for high-temperature reservoirs in Iceland and the Philippines”. Proceedings, Thirty-Second Workshop on Geothermal Reservoir Engineering, 221-232.

Wilmarth, M. and Stimac, J. (2014). "Worldwide Power Density Review", Proceedings, Stanford Geothermal Workshop.

Wilmarth, M. and Stimac, J. (2015). "Power Density in Geothermal Fields", Proceedings, World Geothermal Congress.

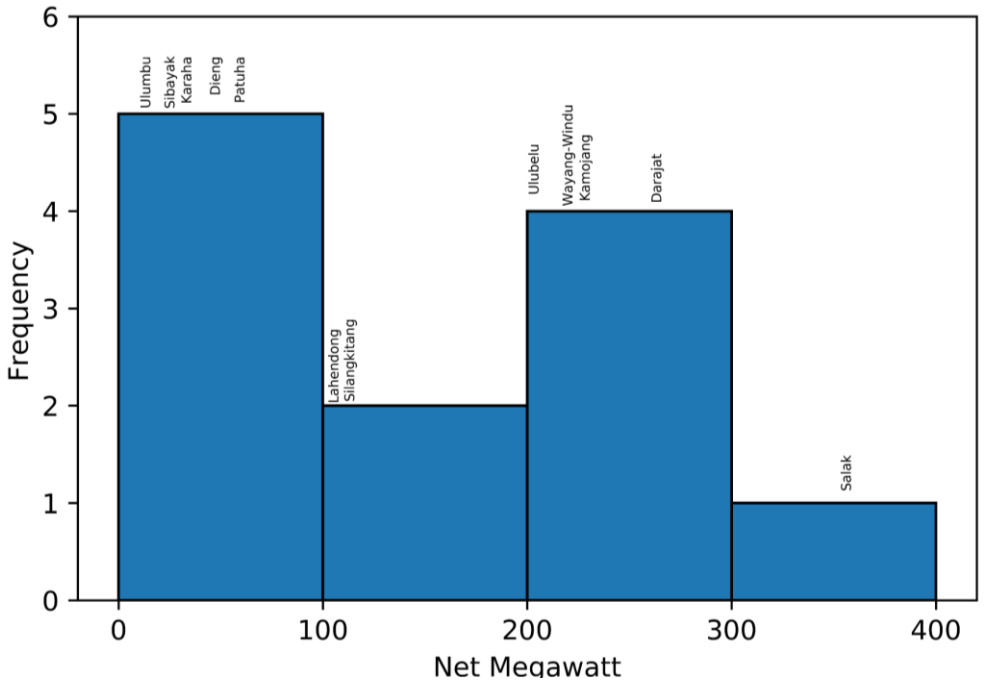


Figure 1: Histogram of MW_{net} for 12 Indonesian geothermal fields.

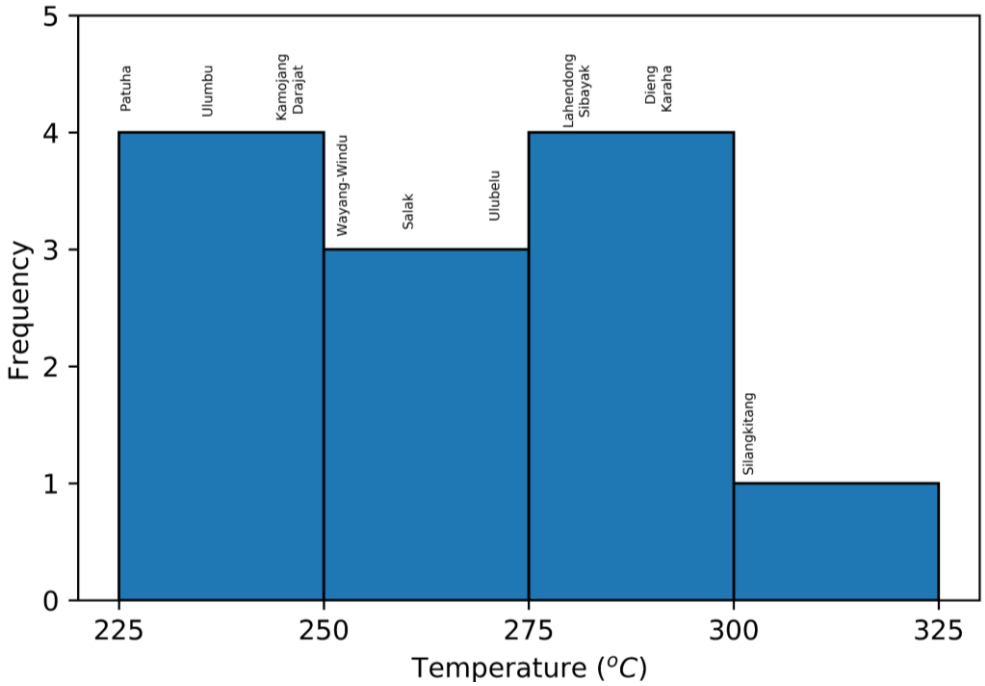


Figure 2: Histogram of Average Reservoir Temperature for 12 Indonesian geothermal fields.

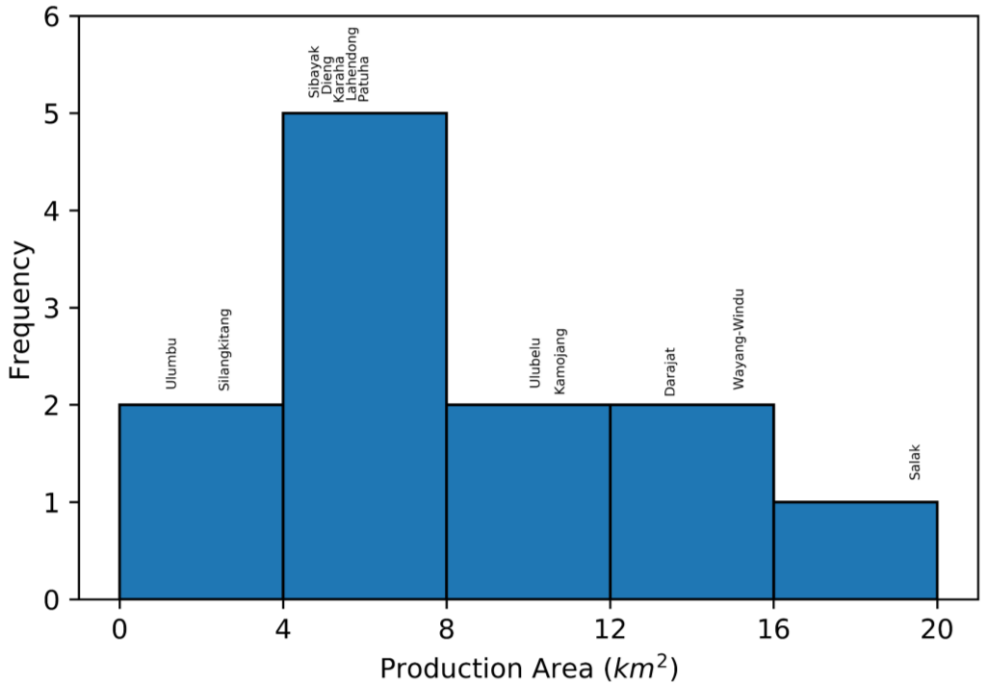


Figure 3: Histogram of Production Area for 12 Indonesian geothermal fields.

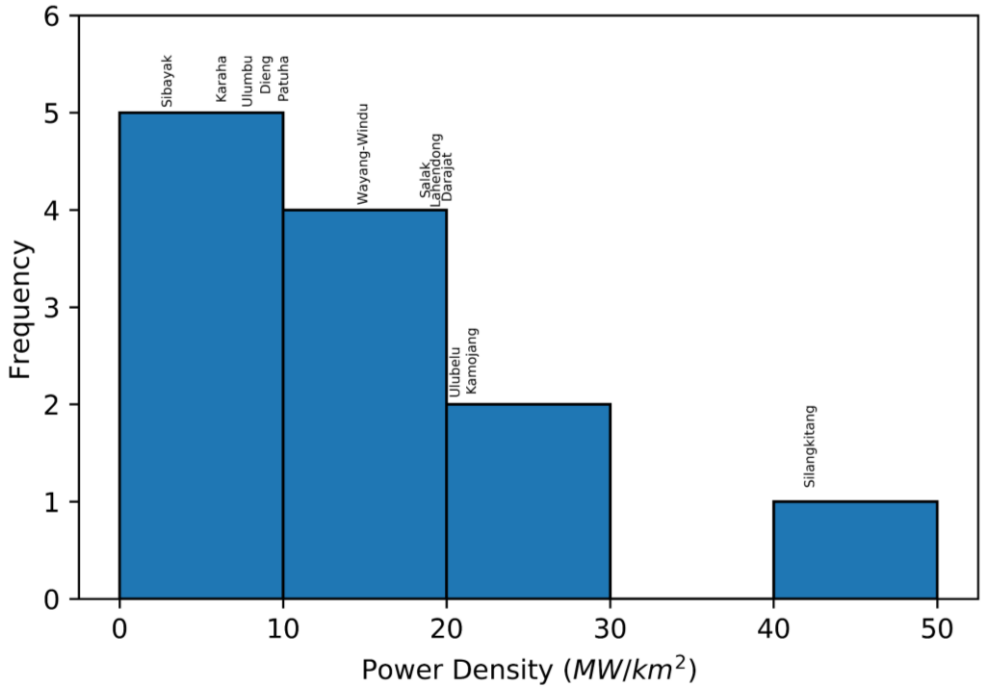


Figure 4: Histogram of Power Density for 12 Indonesian geothermal fields.

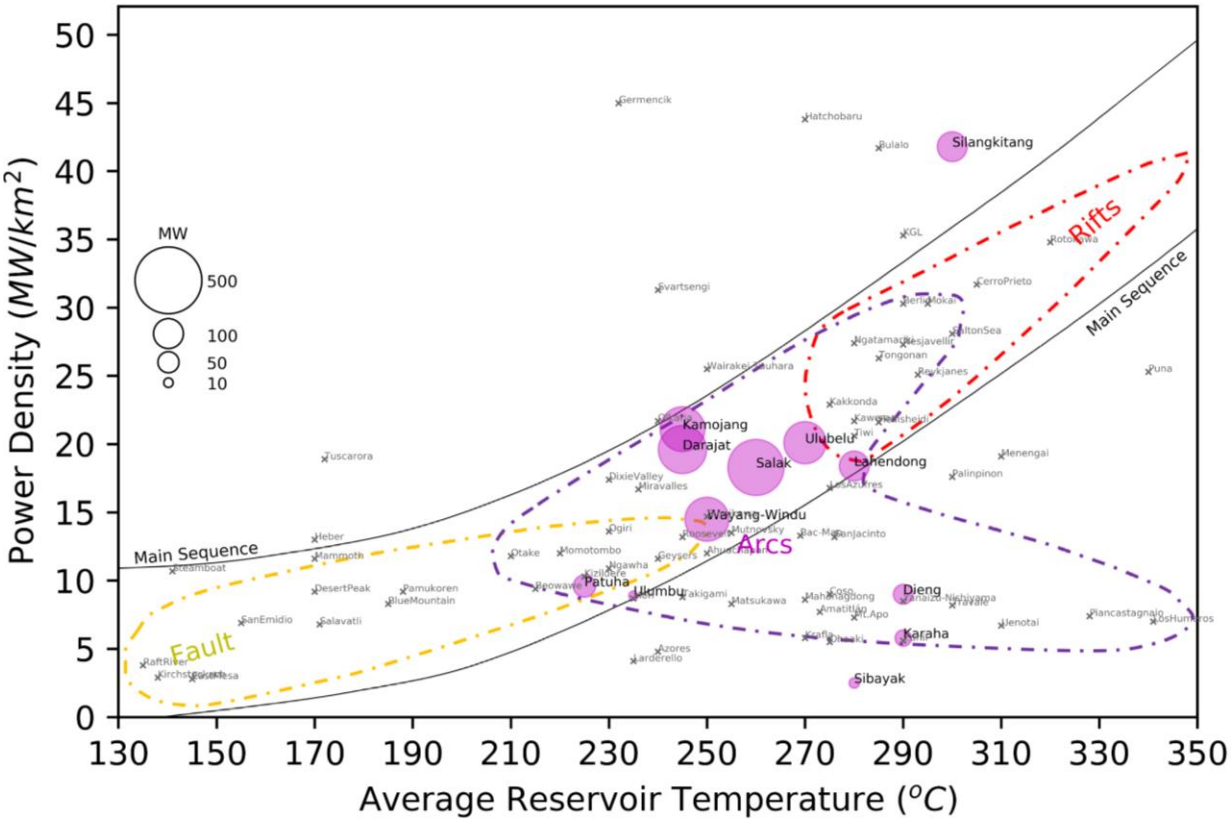


Figure 5: Plot of Power Density vs Average Reservoir Temperature for 12 geothermal fields, updated for 2019. Background data is 2015 data for worldwide fields after Wilmarth and Stimac (2015).

INTEGRATED ADVANCE FRACTURE ANALYSIS: A CASE STUDY FROM FALLON FORGE WELL 21-31, NEVADA, USA

Pasca Siburian[1], Tito Perdana[2], Heri Tanjung[1], Merza Adeyosfi[1], Leonora Lilasari[1], and Sonny Wiyoga[1]

[1]PT Schlumberger Geophysics Nusantara, Jakarta, Indonesia
[2] GeothermEx, A Schlumberger Company, Richmond, California, USA
Email: psiburian@slb.com

ABSTRACT

Targeting structurally controlled permeability remains a challenge in geothermal fields, because of the difficulties in characterizing subsurface structures (faults and fractures) and their behavior within the reservoir. The acquisition of electrical borehole images along with GR, resistivity, sonic, and pressure-temperature data is considered as the best combination for detecting subsurface structures from within the borehole. A total of 651 meters of the aforementioned dataset were acquired, processed and interpreted to provide detailed analysis of subsurface structures, including fracture classification, orientation, and zone.

The conventional fracture analysis using borehole images requires manual dip picking of the fractures as major part of the workflow. Although this method is superior in determining fracture orientation, it was time consuming. The conventional fracture analysis also produces a less detailed, less continuous, and more pessimistic fracture computation results due to the nature of the fractures encountered. For this reason, we performed a new approach of fracture computation to improve the fracture computation results. This new approach includes image calibration, segment extraction, filtering, fracture classification and grouping, and fracture computation. The segment extraction is performed to extract the heterogeneity in the borehole which could represent natural fractures. Whereas, low apparent dips extraction and segment length filters were conducted to filter out features that are non-natural fractures.

The computation of this new approach has produced more reliable and optimistic results of fracture density, aperture and porosity. This new method has also produced more continuous fracture aperture data points compared to the conventional method. The results of this new approach also have a good correlation with the results of sonic fracture analysis.

Keywords: Fracture analysis

INTRODUCTION

Subsurface fluid flow in geothermal reservoirs is controlled mainly by permeable structure (fractures and faults) in the subsurface. Therefore, examining the location and characterization of permeable structures is an important step towards estimating the ultimate productivity of a geothermal reservoir.

Targeting structurally controlled permeability remains a challenge in geothermal fields, because of the difficulties in characterizing subsurface structures and their behavior within the reservoir. Sensitivity of measurement in combination with approximately 80% circumferential coverage (in 8.5-inch borehole) makes Schlumberger's Fullbore Formation MicroImager (FMI) useful for detecting subsurface structures from within the borehole. The accuracy of the borehole images paired with skilled image interpretation and supported by other data such as gamma ray (GR) log, resistivity log, density log, neutron log, sonic log, and pressure-temperature logs helps to understand if fractures or faults are open or healed, which leads to optimized subsurface structure characterization for enhanced well testing and production.

Well 21-31 was logged by Schlumberger on behalf of Sandia National Laboratories (Sandia) using FMI, Platform Express Triple Combo, Sonic Scanner, and Temperature and Pressure Survey tools. The well is located in the Frontier Observatory for Research in Geothermal Energy (FORGE) Fallon Enhanced Geothermal System (EGS) Site, west-central Nevada, United States of America. FORGE is an initiative funded by the US Department of Energy (DOE) that aims to develop the technologies, techniques, and knowledge needed to make EGS in "hot dry rocks" a commercially viable electricity generation option for the US. The FORGE initiative evaluated several potential sites to host the subsurface FORGE laboratory to test various stimulation approaches in crystalline basement rock formation. The parameters required were a hot impermeable reservoir at depths between 1.5 to 4 km, with temperature between 175 and 225°C in crystalline basement rocks. During Phase 1 and Phase 2 of the FORGE project, the Fallon EGS site went through extensive geoscientific characterization to evaluate its suitability as a possible FORGE test site. This research culminated in the drilling of a 2,460 meters Measured Depth (mMD) well, 21-31, in February 2018 (Kraal and Ayling, 2019). The aforementioned logging tools were logged within the 8.5-inch section of the well, from 1,829 to 2,480 mMD, which pass through igneous and metamorphic formations.

The igneous and metamorphic rocks generally undergo brittle deformation compared to most of the sedimentary rocks. This type of deformation potentially produces complexity of fracture networks formed by the tectonic deformation. The complexity of the fracture networks will lead to some difficulties in fracture characterization.

The "conventional" fracture analysis using borehole images requires manual dip picking of the fractures as major part of the workflow. Although this method is superior in determining fracture orientation, it was time consuming. The uncertainty related to the fracture characterization also comes from the subjective point of view of the log analyst or interpreter. The "conventional" fracture analysis also produce a less detailed, less continuous and more pessimistic fracture computation results due to the nature of the fractures encountered. Most of the time, with the limited time of log processing and interpretation, the results of "conventional" fracture characterization have never been accurately revealing the true condition of a fractured reservoir.

In order to overcome these issues, Schlumberger has developed "semi-automatic fracture extraction and characterization" methods, enabling a much faster and more reliable analysis. In the early 2000s, Schlumberger's GeoFrame platform was equipped with a module to pick partial sinusoid manually over the fractures and to perform an automatic fracture counting and density calculation. The fracture aperture computation method for FMI, also known as Luthi- Souhaité method (Luthi and Souhaité, 1990) was also available in the software at that time. The latest development in the GeoFrame BorView module (Kherroubi, 2008), integrated a semi-automatic method (supervised by the interpreter) to extract the fracture traces. The statistics part was also enriched with more meaningful curve computations, such as fracture surface per unit borehole volume (P32), and the fracture volume per unit rock volume (P33). The "Fracture Analysis" plug-in for Schlumberger's Techlog inherits these developments. It is designed to enable fast and easy fracture characterization in a very similar way to the module in GeoFrame (Schlumberger, 2019). The "Fracture Analysis" module automatically extracts fractures present in a borehole image, allows classification into subsets and computes their properties (e.g., aperture, hydraulic aperture) and the associated statistic curves along depth. These "semi-automatic fracture extraction and characterization" methods include image calibration, segment extraction, segment filtering, and fracture computation. The segment extraction is performed to extract the heterogeneity in the borehole which could represent the natural fractures. Whereas, low apparent dips extraction and segment length filters were conducted to filter out non-natural fractures (drilling induced and drilling enhanced fractures).

In this study, we conducted both "conventional" fracture analysis and "semi-automatic fracture extraction and characterization". The objectives of this study are to demonstrate an integrated workflow for highly fractured geothermal reservoir permeability characterization using combination of "conventional" and "semi-automatic fracture extraction" methods from borehole image log to accurately define fracture orientation and compute fracture density, aperture and porosity. The results of fracture pickings and computation will be integrated to the results of the sonic fracture analysis to determine permeable fractures.

GEOLOGIC SETTING

The Fallon site is located in the Carson Sink, a large composite basin in the Basin and Range Province. The general stratigraphy of the area is Late-Miocene to Quaternary basin fill sediments (<1,500 m thick) overlying Miocene volcanic rocks (700-1,300 m thick), and Mesozoic basement consisting of meta-volcanic and meta-sedimentary rocks that are intruded by felsic plutons (Kraal and Ayling, 2019). The site is situated in a west-tilted half graben cut by widely spaced N-S to NNE-SSW striking normal faults with approximately 200 m of displacement (Kraal and Ayling, 2019 [citing Siler, et al., 2018]; Figure 1). Dip magnitudes of these normal faults vary from approximately 50° to 70°.

Quaternary faults have not been observed within the Fallon site, and only a few small (< M.2.0 historic earthquakes have occurred at the site. The Rainbow Mountains fault (approximately 10-15 km east of the Fallon site) ruptured in M 6.9 earthquake in 1954, accommodating oblique normal-dextral motion (Caskey et al., 2004). The Rainbow Mountains fault terminates southward in the vicinity of the Salt Wells geothermal field, 15 km to the southeast of the FORGE site. Increased permeability associated with the horse-tailing southern end of this fault corresponds with the production well field at Salt Sites (Hinz et al., 2014). It is notable that most geothermal systems in the Great Basin region are proximal to recent faults (Bell and Ramelli, 2007; Faulds et al., 2015). The absence of Quaternary faulting at the Fallon site may explain the lack of sufficient permeability in the area (Hinz et al., 2016).

The primary lithologies encountered at the Fallon site in the basin fill are: a) Quaternary sediments, b) Quaternary – Tertiary sediments, c) Miocene mafic volcanic rocks primarily basaltic andesite, but also lithic tuff, andesite, rhyodacite, and volcanic breccia. The basin fill lithologies lie unconformably on top of Mesozoic basement consisting of: a) Mesozoic quartz monzonite, b) Mesozoic meta-

basalt and meta-basaltic-andesite, c) Mesozoic quartzite with to a less extent phyllite, meta-basalt, and marble, d) Mesozoic meta-rhyolite with lesser meta-basalt (Kraal and Ayling, 2019, Figure 1). Proposed formations for EGS stimulation include the quartz monzonite, quartzite, or meta-rhyolite. The deepest wells in the Fallon site that terminate in Mesozoic basement at 2,112-2,886 mMD depth record maximum bottom hole temperatures of 194 to 214°C (Kraal and Ayling, 2019 [citing Blankenship, 2016 and Siler et al., 2016]).

METHODS AND RESULTS

Data

The wireline log data used in this study can be accessed at the Geothermal Data Repository (Fallon, Nevada FORGE Well 21-31 Wireline Logs [data set] from: http://gdr.openei.org/submissions/1068. On 20 March 2018, 24 March 2018, 26 March 2018, and 27 March 2018 FMI log, pressure and temperature logs, sonic logs (i.e., compressional, shear, Stoneley slownesses and raw waveform data), and triple combo logs (i.e., GR, resistivity, neutron porosity, and density data) were collected within the 8.5-inch section of the well, from 1,829 to 2,480 mMD.

FMI image processing and data interpretation were carried out using the Schlumberger's Techlog wellbore software platform (version 2017.2) (Figure 9).

Workflow and Results

The processed-borehole-image was used directly for "manual" lithotype characterization and fracture picking. The manual lithotype characterization was made using a combination of visual investigation of borehole image log textures, along with GR and density (RHOM) logs (Figure 2). The results of the manual lithotype characterization were then compared and crosschecked with the results of cutting analysis. According to the results of cutting analysis, well 21-31 is comprised of Quaternary-Tertiary sediments, Tertiary basaltic-andesite, Tertiary rhyodacite, Mesozoic meta-basalt, Mesozoic quartz monzonite, Mesozoic quartzite, Mesozoic phyllite, and Mesozoic meta-rhyolite (Kraal and Ayling, 2019). Based on this analysis, it could be inferred that this well penetrated three main lithologic types.

Igneous Rock

This lithologic type is interpreted as relatively "fresh" (unaltered) igneous rock. The borehole static image shows a highly resistive contrast (very bright and clean), and mostly associated with low GR reading (although in few intervals show increase in GR reading) and high density (RHOM) reading (Figure 3). According to the results of cutting analysis (Kraal and Ayling, 2019), this "igneous rock" lithologic type may represent Mesozoic quartz monzonite. Fractures are well developed in this lithologic type, and "visually" they show small to large fracture aperture.

Altered Igneous Rock or Altered Metamorphic Rock

The results of alteration process could be interpreted using borehole images. Showing different characteristics than fresh body above, altered igneous rock usually demonstrates more conductive appearance in the borehole static image. This lithologic type is also associated (mostly) with high GR and low density (RHOM) readings (Figure 4). According to the results of cutting analysis (Kraal and Ayling, 2019), this "altered igneous or altered metamorphic rock" lithotype may represent Mesozoic quartz monzonite, Mesozoic meta-basalt, and Mesozoic quartzite. The majority of the aforementioned lithologies are altered. Kraal and Ayling, 2019) reported significant developments of altered minerals such as smectite, chlorite, and illite in these lithologies. In general, altered igneous rocks and altered metamorphic rocks tend to have lower fracture intensity compared to the fresh igneous rock.

Metamorphic Rock

Metamorphic rock demonstrates similar response with the altered igneous rock. It mostly appears conductive with high GR and low density (RHOM) readings. Therefore, mineralogical information from cuttings or well correlation was used to determine the intervals of metamorphic rocks in this well (Figure 5). This metamorphic rock only occupies short intervals compared to the other lithotypes. According to the results of cutting analysis (Kraal and Ayling, 2019), this "metamorphic rock" lithotype may represent Mesozoic meta-rhyolite. Natural fractures are not well developed in this lithotype.

Manual Fracture Characterization

Fractures were picked manually from the borehole image using a sine wave, with its amplitude and azimuth fitted to planar feature on the image. The lowest point of the sinusoid trough defines the dip azimuth, and the amplitude of the sinusoid defines the dip magnitude. The manually interpreted fractures were then classified further based on their orientation (Figure 2).

In this study, we mainly focused on determining the potentially permeable fractures; thus, only those which have conductive traces were picked and classified (Figure 6).
Conductive (open) fractures are well developed over almost entire logged interval (1,829-2,480 mMD). A total of 1,000 conductive (open) fractures were identified; they show dominant strike orientation of NE-SW with minor ESE-WNW, with dip

magnitudes vary from nearly horizontal to nearly vertical (Figure 7). These fracture orientations, however, do not represent the major structural/tectonic trend in the area (N-S to NNE-SSW) as discussed in the Geologic Setting section.

Sandia has conducted a study of geologic structure in the Fallon EGS site. The interpreted geologic structures around 5,000 meters radius proximity from well 21-31 are mainly comprised of NNE-SSW and N-S striking normal faults, with subordinate NNW-SSE striking normal faults, and minor E-W striking normal faults. Dip magnitudes of these normal faults vary from approximately 50° to 70°. Amongst these normal faults, only two (2) faults (NNE-SSW striking Fault X and Fault Y) were expected to be encountered by Well 21-31 (Figure 8). However, none of these faults were encountered in the logged interval (1,829-2,480 mMD). Thus, this might explain that the orientation of conductive (open) fractures in the logged interval do not really represent the major structural / tectonic trend in the area.

Semi-Automatic Fracture Extraction

The "semi-automatic fracture extraction" method was also conducted in this study using Techlog's "Fracture Analysis" module. This workflow requires calibrated borehole image as an input (Figures 2 and 8). First, conductive segments were extracted based on its apparent dip angle. This method, based on the mathematical morphology theory, allows the separate extraction of low apparent dip fracture segments (i.e., apparent dip below 45°) and high apparent dip fracture segments (i.e., apparent dip above 45°). In this framework the initial image is seen as a topographic surface, with crests and troughs (Schlumberger, 2019). It is observed that most of the conductive fractures in well 21-31 have low apparent dip, thus only conductive segments with low apparent dip were extracted. A total of 82,917 of such segments were extracted (Figure 10A).

After completing the extraction process above, we noticed that some segments were found on shapes that do not represent conductive fractures; which mainly are image artifacts. These non-conductive-fracture features were then removed / filtered out using the segment group filtering (Figure 2). This process was performed with respect to two different characteristics: segment length and contrast. The conductive segments that have segment length less than 1.08 inch and contrast less than 2.57 were filtered out in this process and considered as image artifacts. A total of 44,184 non-conductive-fracture features segments were removed in this process (Figure 10B).

Fracture Set Classification

All conductive fractures from Manual Fracture Characterization were classified into six (6) fractures sets based on their strike orientation (with angular difference between each fracture set is 30°; Figure 11). The results of this process were then used to guide Semi-Automatic Fracture Extraction's segments set classification and grouping (Figures 2 and 12). The results of fracture set classification from "Manual Fracture Classification" and "Semi-Automatic Fracture Extraction" are found identical as shown in Figure 13.

Fracture Computation

The fracture computation was performed to calculate P32 (fracture surface per unit borehole volume, also known as 'fracture density'), P33 (fracture volume per unit rock volume, also known as 'fracture porosity), and fracture aperture (FVAH). The fracture computation was performed on both non-classified and classified fractures from Manual Fracture Characterization and Semi-Automatic Fracture Extraction.

Fracture Computation – Non-Classified Fractures

The results of fracture computation of the non-classified fractures show that computed P32, P33, and FVAH from manual fracture characterization and semi-automatic fracture extraction have similar trends. The results of P32 and P33 computations from Manual Fracture Characterization, however, show smaller values compared to the results of P32 and P33 computations from Semi-Automatic Fracture Extraction, by a factor of 4 and 10 respectively. Furthermore, the results of FVAH computation from Semi-Automatic Fracture Extraction demonstrate more continuous and denser fracture aperture points compared to the results of FVAH computation from manual fracture characterization (Figure 14).

Fracture Computation – Classified Fractures

The results of fracture computation of the classified fractures from both Manual Fracture Characterization (Figure 16) and Semi-Automatic Fracture Extraction demonstrate that computed P32 (Figure 15) of each fracture set have an overall similar trend. The results of P32 and P33 (Figure 17) computations of classified fracture from Manual Fracture Characterization, however, show smaller values compared to the results of P32 and P33 computations of classified fractures from Semi-Automatic Fracture Extraction, by a factor of 4 and 5 respectively (Figures 15, 16, 17, and 18).

Sonic Fracture Analysis

The "Stoneley Fracture Analysis" was performed to distinguish open (permeable) fractures and closed fractures, meanwhile the "Fast Stoneley Modelling (Tezuka Modelling)" was conducted to differentiate

Stoneley wave chevron pattern from washout/ bed boundary with open fracture (Figure 2). Based on the Stoneley fracture analysis, there are two (2) intervals with indication of possible permeable fractures: 2,220-2,259 mMD and 1,920-1,940 mMD.

Interval 2,220-2,259 mMD has some open (permeable) fractures based on qualitative FPERM curve and chevron pattern (Figure 19). However, the dipole attenuation in this interval is relatively low, indicating the fractures in this interval are open but do not have deep penetration away from the borehole wall. Interval 1,920-1,940 mMD has open (permeable) fractures as well, but the dipole attenuation is relatively higher compared to interval 2,220-2,259 mMD. It can be concluded that based on Stoneley fracture analysis, the fractures at interval 1,920-1,940 mMD tend to have deeper penetration away from the borehole compared to the fractures at interval 2,220-2,259 mMD, though both are possibly permeable. In most cases, the open fractures with deeper penetration will have better permeability compared to open fracture with low penetration. The dipole attenuation is also used to discriminate between minor and major open fractures.

In agreement with the results of Sonic Fracture Analysis, both borehole image Manual Fracture Characterization and Semi-Automatic Fracture Extraction methods indicate good fracture developments in the intervals of 1,920-1,940 mMD and 2,220-2,259 mMD. Though, semi-automatic fracture extraction method produced more optimistic results of fracture density (P32), aperture (FVAH), and porosity (P33) computations in the aforementioned intervals. Pressure and temperature data demonstrate a 'positive' deflection (to the higher readings) at 2,220-2,259 mMD, which might be associated with permeable fractures and/or fracture network. The highest fracture density (P32) and fracture porosity (P33) are also observed at this interval (2,220-2,259 mMD).

Integrated Fracture Characterization

Integrated Fracture Characterization was performed in order to evaluate the fracture development and productivity of well 21-31. First, the logged interval were subdivided into several discrete zones based on fracture intensity and fracture strike orientation. Each of these discrete zones was then evaluated and analyzed based on borehole image data, sonic data, and pressure-temperature data. The results of this Integrated Fracture Characterization are discussed below.

Fracture Zone 1 (1,829-2,045 mMD)

According to the results of Lithotype Analysis, this interval is comprised of igneous rocks and altered igneous / altered metamorphic rocks. Based on the borehole images, open fractures are well developed in this zone. These open fractures demonstrate a dominant strike orientation of NE-SW with minor ESE-WSW (Figure 20). Potential permeable open fractures are observed in the upper part of this fracture zone (1,920-1,940 mMD). This interpretation is supported by the 'positive' deflection (to the higher readings) of fracture aperture (FVAH) and fracture porosity (P33). In addition, the results of sonic fracture analysis also show a good result in this interval. FPERM and dipole attenuation show moderate to high reading, which may indicate that the fractures in this interval are deeply propagated from borehole wall.

Fracture Zone 2 (2,045-2,135 mMD)

According to the results of Lithotype Analysis, this interval is comprised of igneous rocks and altered igneous / altered metamorphic rocks. Based on the borehole images, open fractures are well developed in this zone. Similar to Fracture Zone 1, the open fractures in this zone demonstrate a dominant strike orientation of NE-SW with minor ESE-WSW (Figure 20). However, it can be observed that this zone does not have a good fracture productivity. Fracture aperture (FVAH) and porosity (P33) demonstrate very low to negligible values. In addition, FPERM and dipole attenuation from Sonic Fracture Analysis show low reading, which may indicate that fractures in this fracture zone are open but do not have deep penetration away from the borehole wall.

Fracture Zone 3 (2,135-2,260 mMD)

According to the results of Lithotype Analysis, this interval is comprised of igneous rocks and altered igneous / altered metamorphic rocks. Based on the borehole images, open fractures are well developed in this zone. The open fractures in this fracture zone demonstrate dominant strike orientations of ENE-WSW and ESE-WNW (Figure 20). Although showing different fracture trends compared to other fracture zones, the Fracture Zone 3 is likely to be the most productive zone in the entire logged interval. This interpretation is supported by high readings of fracture aperture (FVAH) and porosity (P33). The highest fracture density (P32) is also observed in this interval. FPERM from Sonic Fracture Analysis also shows moderate to high readings. Pressure and temperature data also demonstrate a 'positive' deflection (to the higher readings) at this Fracture Zone, which may be associated with permeable fractures and/or fracture network.

Fracture Zone 4 (2,260-2,480 mMD)

According to the results of Lithotype Analysis, this interval is comprised of igneous rocks, altered igneous/altered metamorphic rocks, and metamorphic rocks. Based on the borehole images, open fractures are well developed in this zone. The natural fractures in this zone demonstrate a

dominant strike orientation of NE-SW (Figure 20). However, it can be observed that this zone does not have a good fracture productivity. Similar to Fracture Zone 2, Fracture aperture and porosity in this fracture zone demonstrate low to almost negligible values. In addition, FPERM and dipole attenuation from Sonic Fracture Analysis show low readings, which may indicate that fractures in this fracture zone are open but do not have deep penetration away from the borehole wall.

CONCLUSIONS

This study has demonstrated the values of Semi-Automatic Fracture Extraction for fracture characterization in highly fractured geothermal reservoir:

- The Manual Fracture (Figure 12) Characterization method requires manual dip picking of the fractures as major part of the workflow. Although this method is superior in determining fracture orientation, it is time consuming (picking thousands of fractures over 650 meters in highly fractured geothermal reservoir took a few days), and the results are interpreter-dependent. The conventional fracture analysis also produces a less detailed, less continuous, and more pessimistic fracture computation results due to the nature of the fractures encountered.
- Semi-Automatic Fracture Extraction has enabled a much faster and more reliable (less interpreter-dependent) fracture analysis compared to Manual Fracture Characterization method.
- Semi-Automatic Fracture Extraction method has produced more continuous fracture aperture data points compared to the Manual Fracture Characterization Method.
- The results of fracture computation from Manual Fracture Characterization and Semi-Automatic Fracture extraction have demonstrated similar trend. The results of P32 and P33 computations from Manual Fracture Characterization, however, show smaller values (more pessimistic results) compared to the results of P32 and P33 computations from Semi-Automatic Fracture Extraction. The results of fracture computation are highly dependent on the number of interpreted fracture dips as the main input. Thus, the fracture computation results using Manual Fracture Characterization (Figure 18) will generally yield more pessimistic fracture density and porosity values compared to the semi-automatic fracture analysis.
- The results of Manual Fracture Characterization and Semi-Automatic Fracture Extraction (Figure 15) show good correlations with the results of the Sonic Fracture Analysis.

ACKNOWLEDGEMENT

The data used for this paper were collected and evaluated as part of the Fallon FORGE project, which is funded by the United States Department of Energy (USDOE) under grant EE0007160 to Sandia National Laboratories (the lead organization for the Fallon FORGE project). The authors are grateful for USDOE's support and permission to publish this work.

REFERENCES

Bell, J., Ramelli, A., (2007), "Active Faults and Neotectonics at Geothermal Sites in the Western Basin and Range: Preliminary Results", Geothermal Resources Council Transaction, v. 31, p 375-378.

Caskey, S., Bell, J., Ramelli, A., Wesnousky, S., (2004), "Historical Surface Faulting and Paleoseismicity in the Area of the 1954 Rainbow Mountain-Stillwater Earthquake Sequence, Central Nevada", Bulletin of the Seismological Society of America, v.94, no. 4, p. 1255-1275.

Faulds, J., Hinz, N., (2015), "Favorable Tectonics and Structural Settings of Geothermal Settings in the Great Basin region, western USA: Proxies for Discovering Blind Geothermal Systems", Proceedings, World Geothermal Congress 2015, Melbourne, Australia, 6p.

Hinz, N., Faulds, J., Coolbaugh, M., (2014), "Association Fault Terminations with Fluid Flow in the Salt Wells Geothermal Field, Nevada, USA", Geothermal Resources Council Transaction, v. 38, p. 3-9.

Hinz, N., Faulds, J., Siler, D., Tobin, B., Blake, K., Tiedeman, A., Sabin, A., Blankenship, D., Kennedy, M., Rhodes, G., Nordquist, J., Hickman, S., Glen, J. (2016), "Stratigraphic and Structural Framework of the Proposed Fallon FORGE Site, Nevada", PROCEEDINGS, 41st Workshop on Geothermal Reservoir Engineering Stanford University, Stanford, California, February 22-24, 2016.

Kherroubi, J., (2008), "Automatic Extraction of Natural Fracture Traces from Borehole Images", 19th International Conference on Pattern Recognition (ICPR 2008), IEEE, Tampa, Florida, USA, pp. 1–4.

Kraal, K., Ayling, B., (2019), "Hyperspectral Characterization of Fallon FORGE Well 21-31: New Data and technology Applications",

PROCEEDINGS, 44th Workshop on Geothermal Reservoir Engineering Stanford University, Stanford, California, February 11-13, 2019.

Luthi, S.M., and Souhaite, P., (1990), "Fracture Apertures from Electrical Borehole Scans"; Geophysics, 55, 821 – 833.

Schlumberger, (2019), "Fracture Analysis", Techlog User Guide, March 2019.

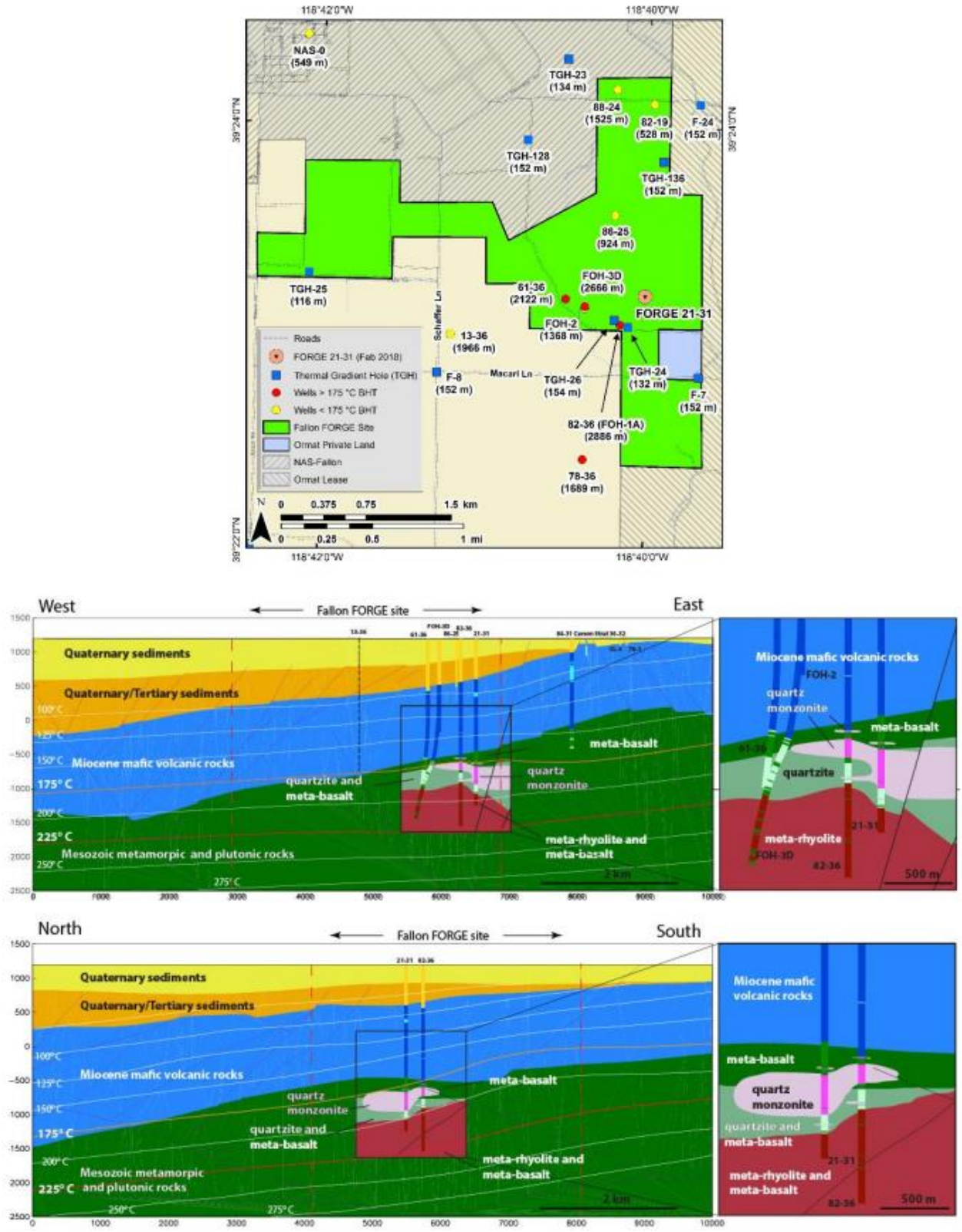


Figure 1: Well locations of the Fallon Forger EGS site (top) and cross sections from site geologic model (bottom; sourced from Kraal and Ayling, 2019).

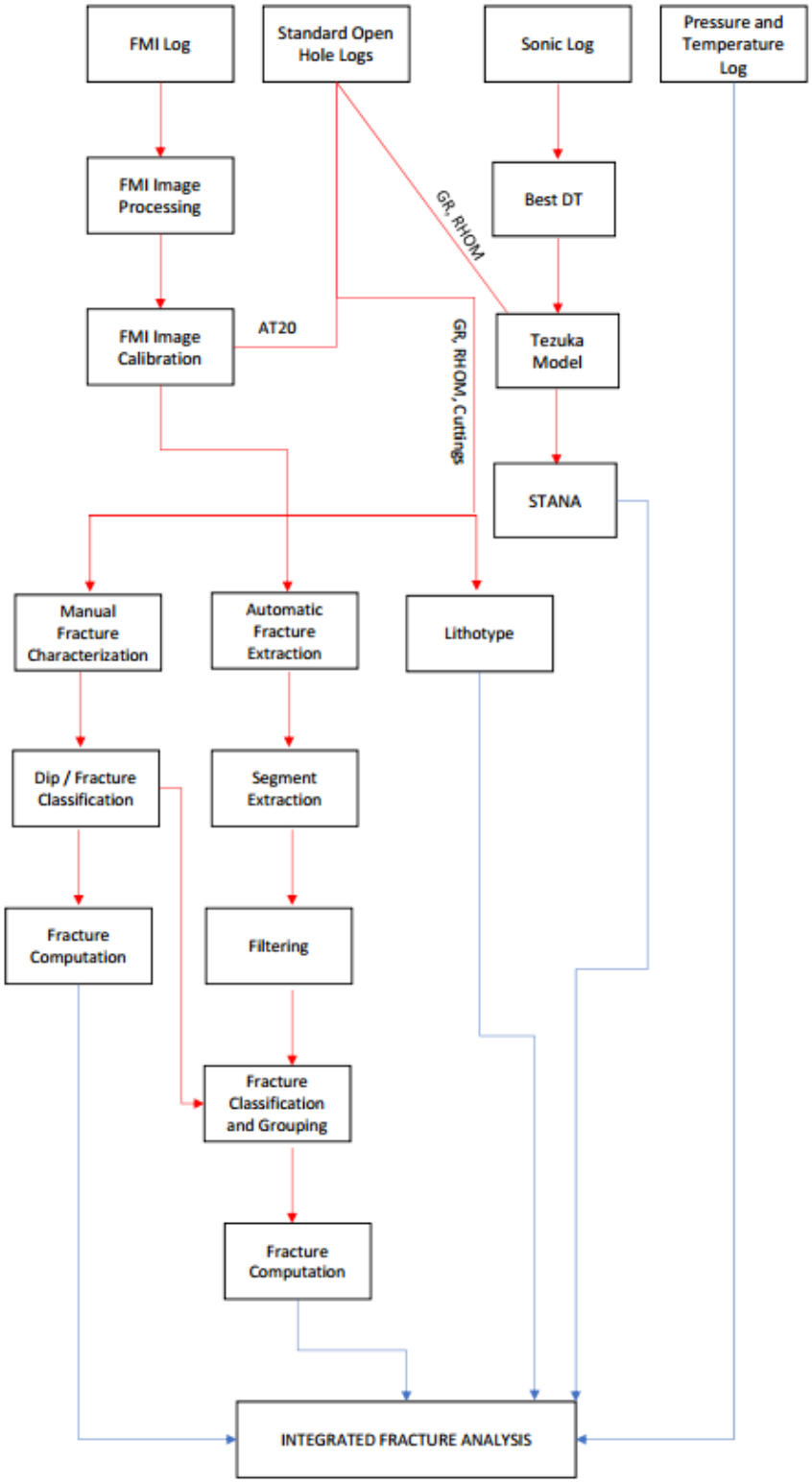


Figure 2: Workflow of Integrated Fracture Analysis using wireline log data from Nevada FORGE Well 21-31. FMI image and sonic data processing and data interpretation were carried out using the Schlumberger's Techlog wellbore software platform (version 2017.2).

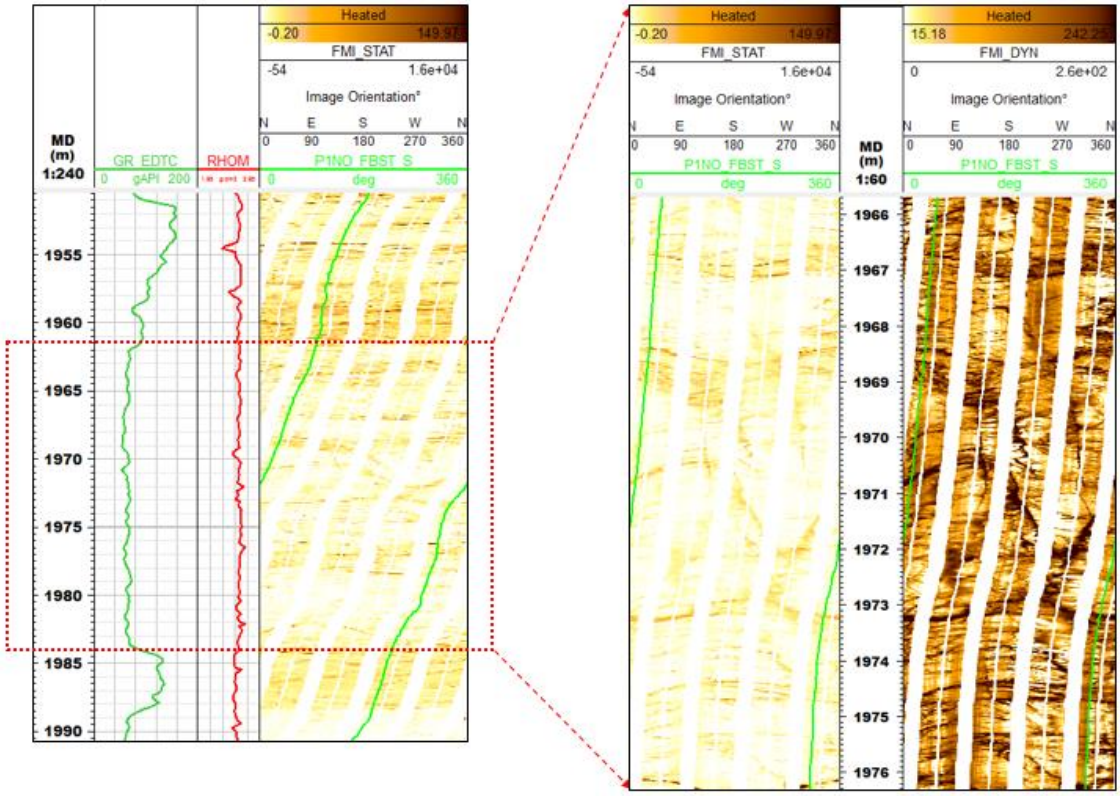


Figure 3: FMI image example of igneous rock lithotype. As seen in the static image, this lithotype demonstrates a highly resistive contrast (very bright and clean), associated with low GR and high density (RHOM) readings. Natural open fractures are well developed in this lithology.

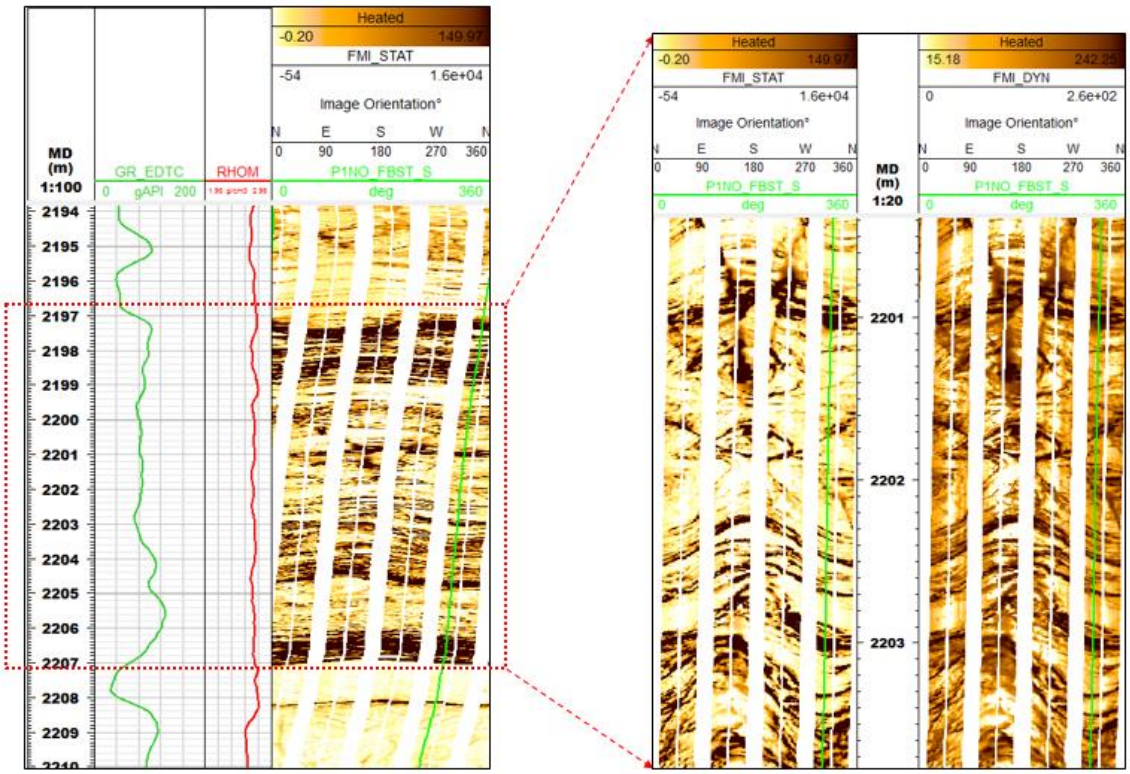


Figure 4: FMI image example of altered Igneous rock lithotype. This interval demonstrates conductive appearance in the static image and generally associated with high GR readings. It is observed that this lithotype has lower fracture intensity compared to the fresh igneous rock intervals.

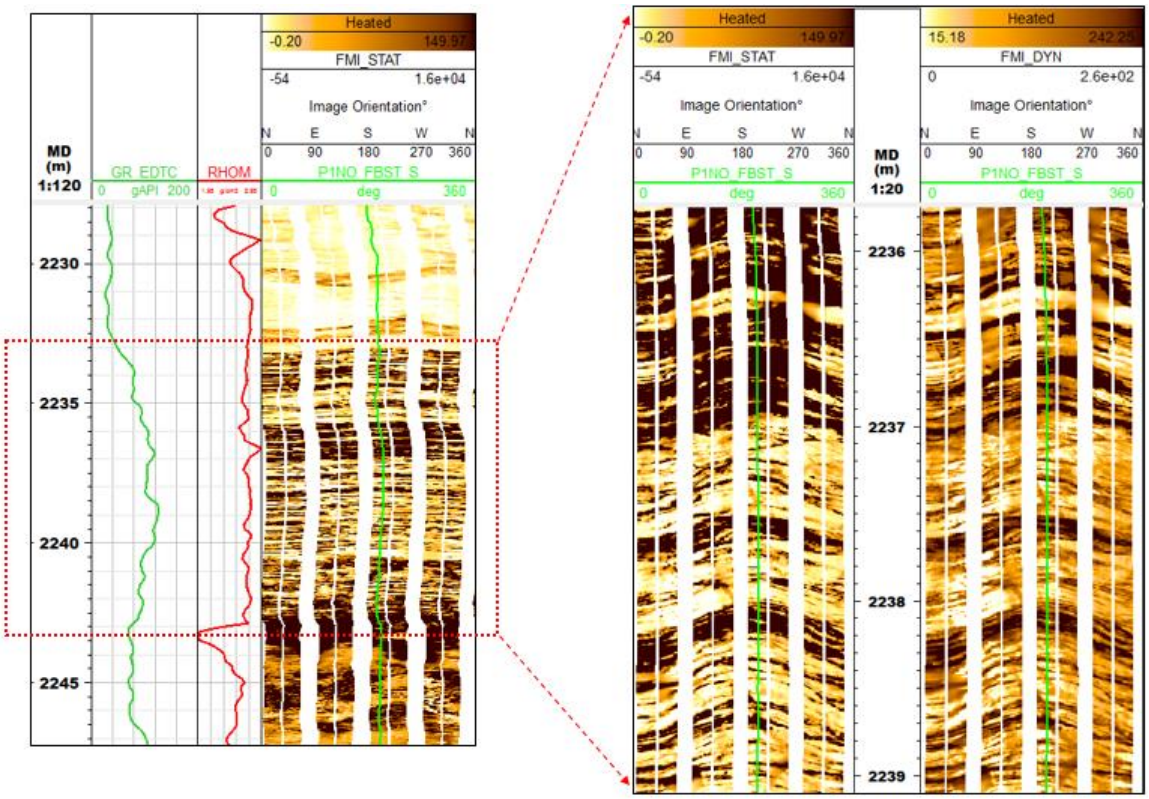


Figure 5: FMI image example of possible metamorphic rock lithotype. Metamorphic rock demonstrates similar response with the altered igneous rocks. Hence further detailed mineralogical analysis needs to be performed to validate this lithotype interpretation.

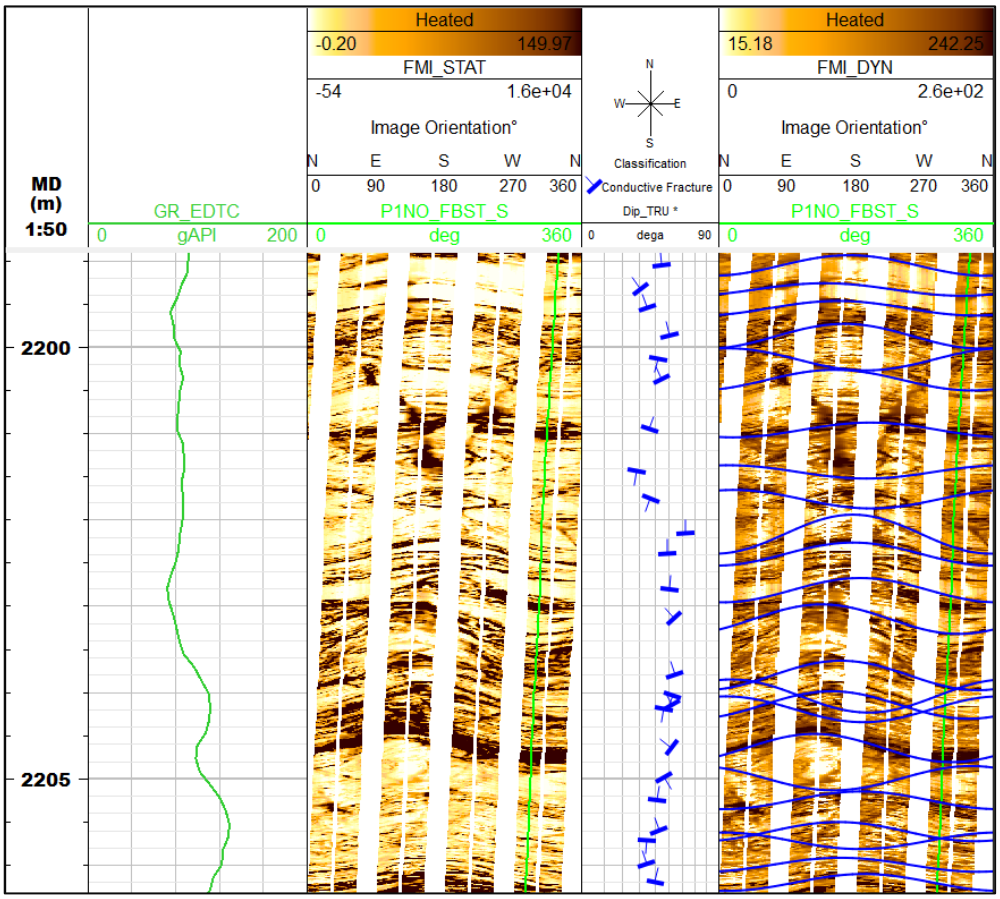


Figure 6: An example of manual dip picking results of conductive (open) fracture in well 21-31.

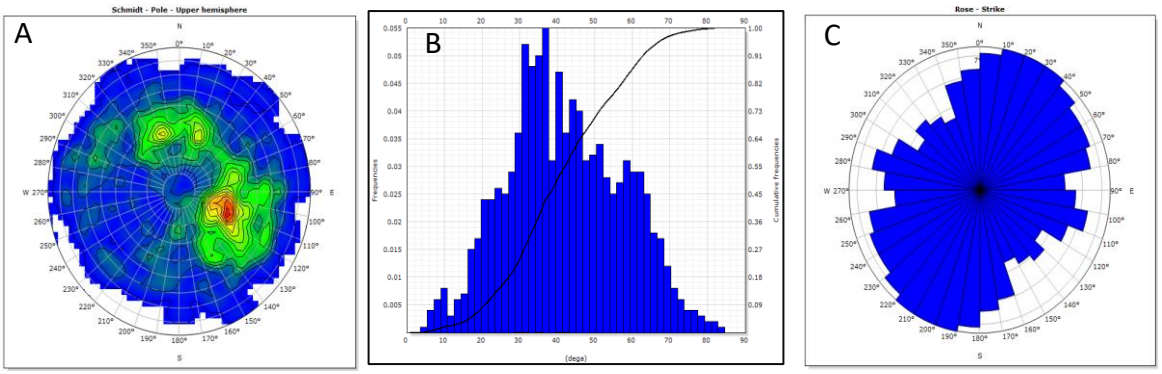


Figure 7: (A)The upper hemisphere Schmidt polar plot demonstrate dominant poles were gathered around 30-40° ESE. (B) The histogram of conductive fractures indicates that conductive fractures' dip magnitudes vary from nearly horizontal to nearly vertical. (C) The strike fan-plot demonstrates a dominant NE-SW with minor ESE-WNW strike orientations of conductive (open) fractures.

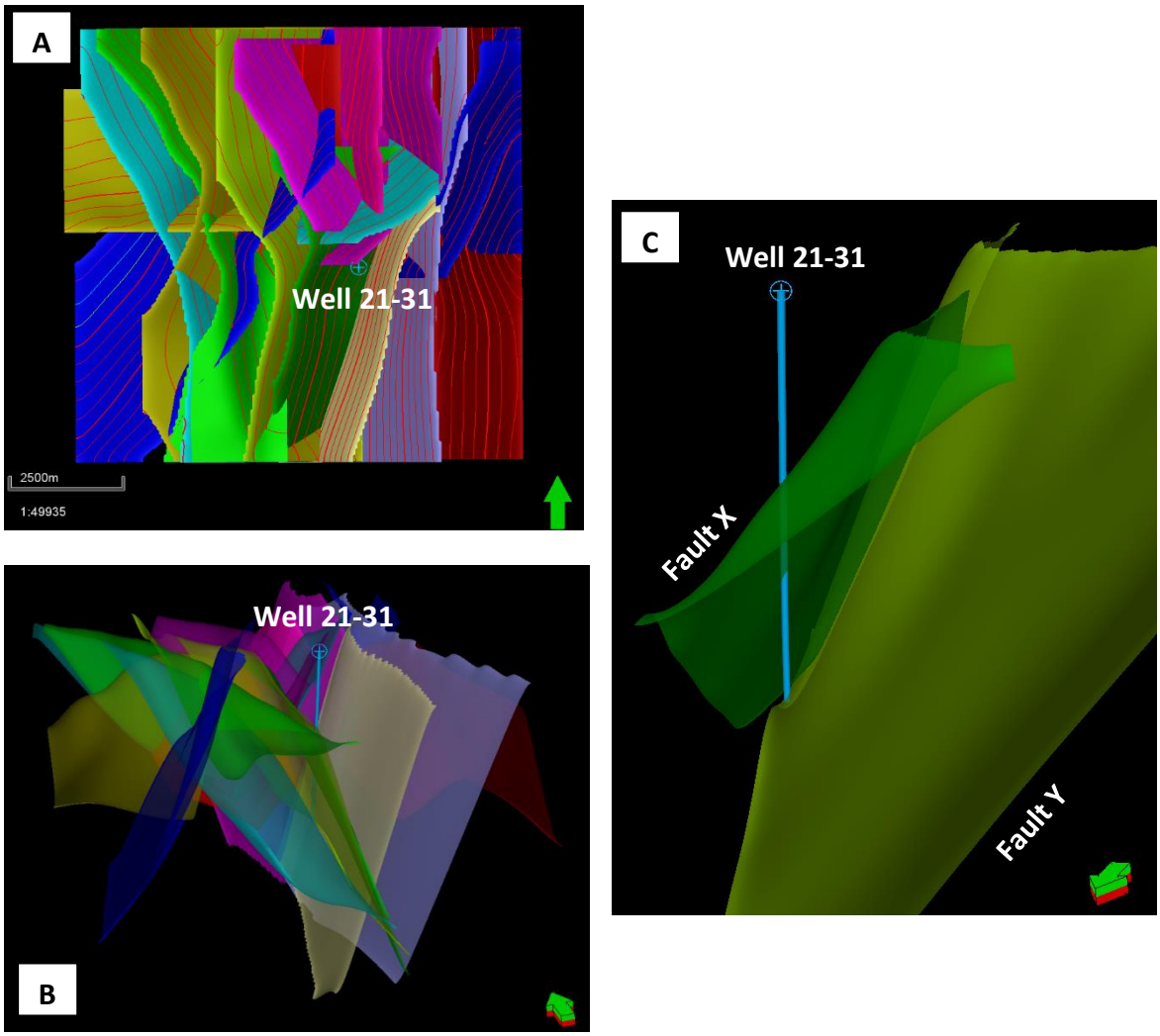


Figure 8: (A). The interpreted fault structures around 5 km radius proximity to the well 21-31. (B). The interpreted faults around 5 km proximity to well 21-31 demonstrate a relatively high angle dip magnitude (around 50-70 degree). (C). Well A was expected to penetrate Fault X and Fault Y; however, none of these faults were encountered in the logged interval (1,829-2,480 mMD).

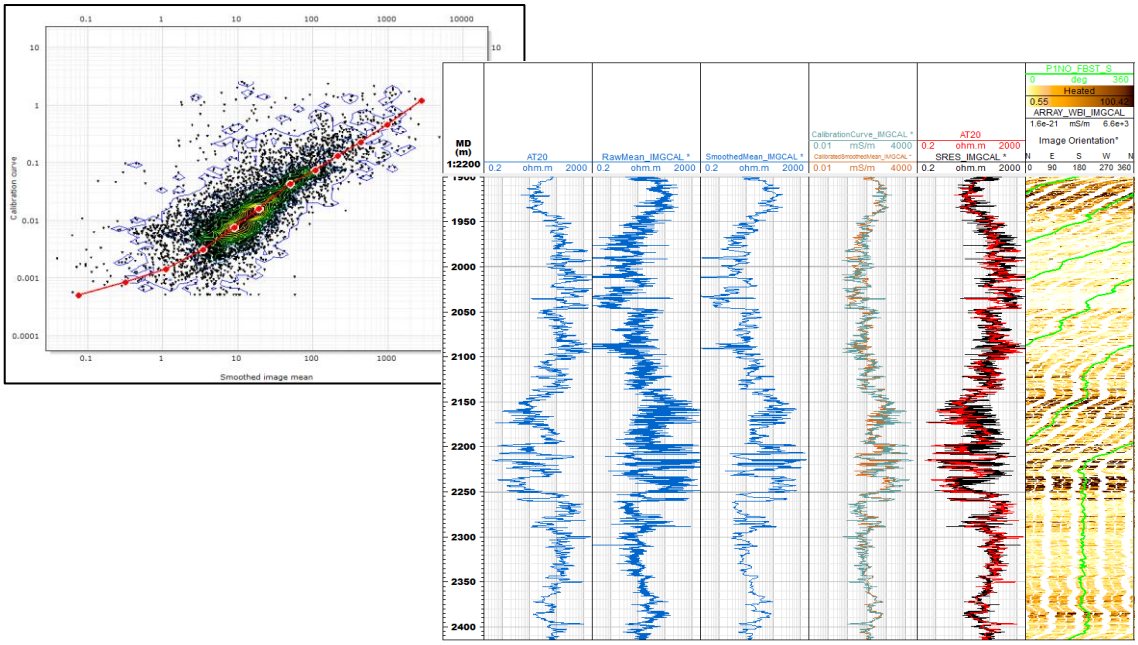


Figure 9: The image calibration process and results in Well 21-31 section 8.5 inch. The produced synthetic resistivity curves from borehole image log (SRES_IMGCAL) matched with the shallow resistivity calibration curves (AT20).

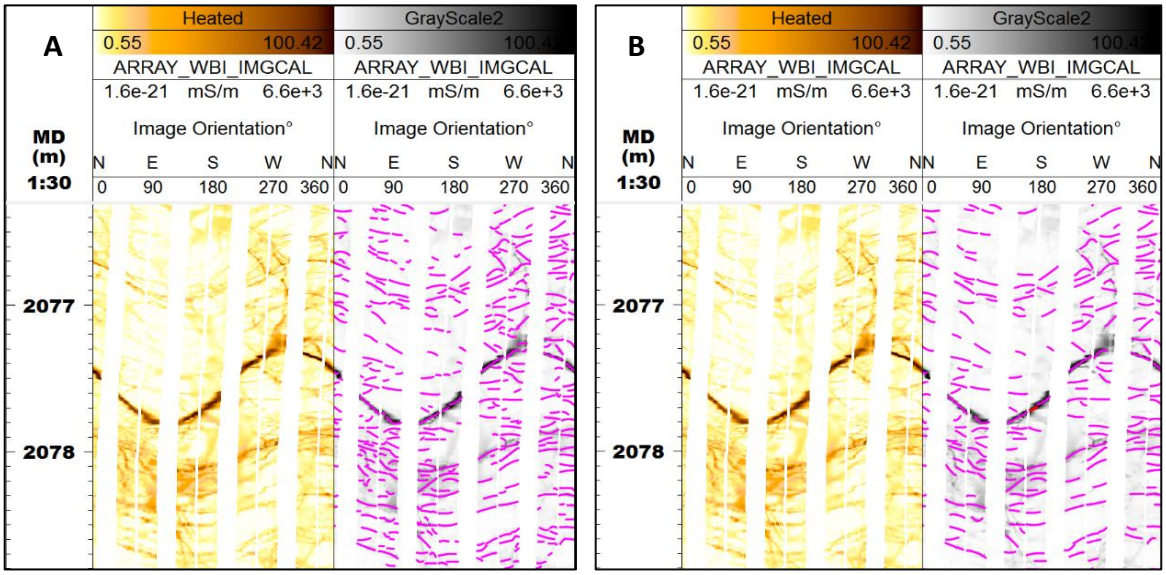


Figure 10: The comparison between initial conductive segment extraction results (A), and the filtered conductive segment extraction results (B) in semi-automatic fracture extraction workflow.

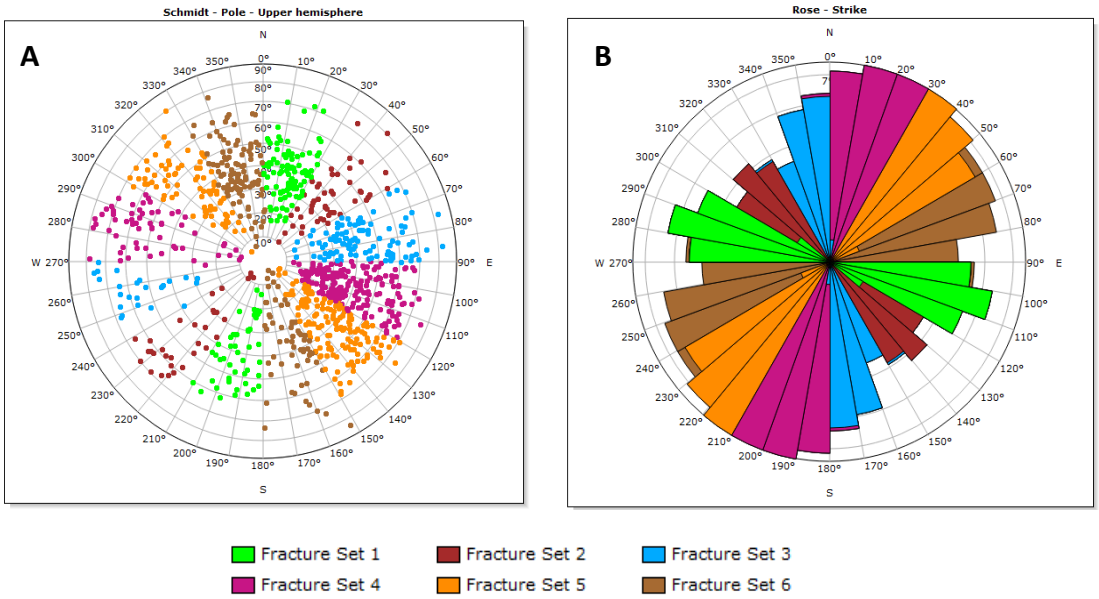


Figure 11: The fracture set subdivision in the upper hemisphere Schmidt polar plot (A) and strike fan-plot (B).

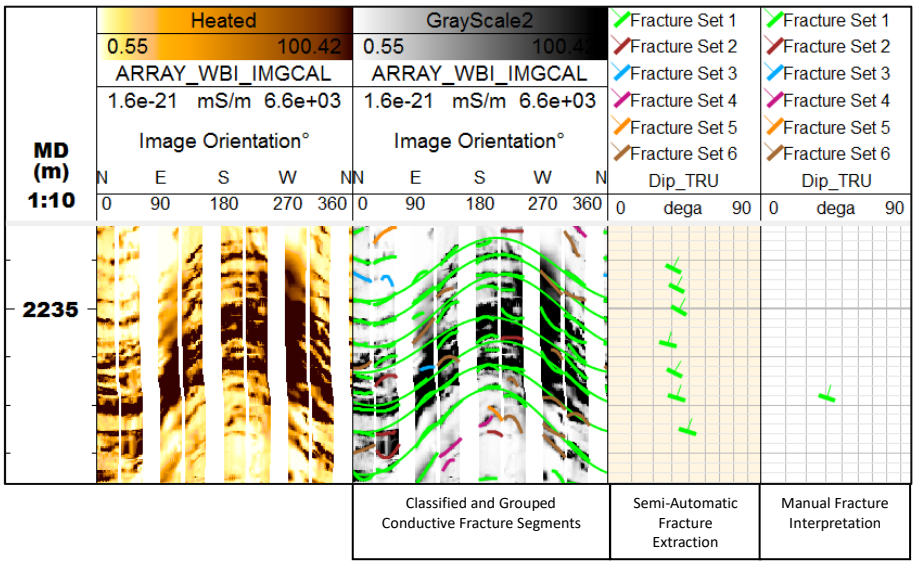


Figure 12: The classification and grouping of conductive segments (track 4) guided by classified manual fracture interpretation results (track 5).

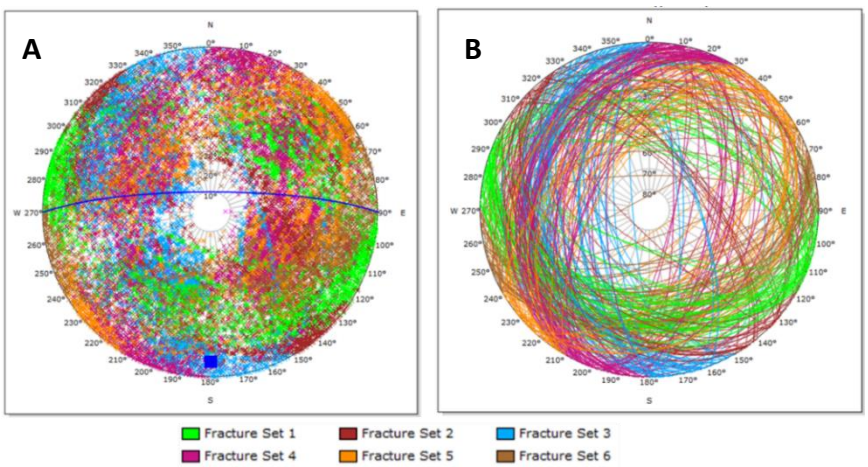


Figure 13: The comparison of fracture set classification between semi-automatic (A) and manual fracture planes (B).

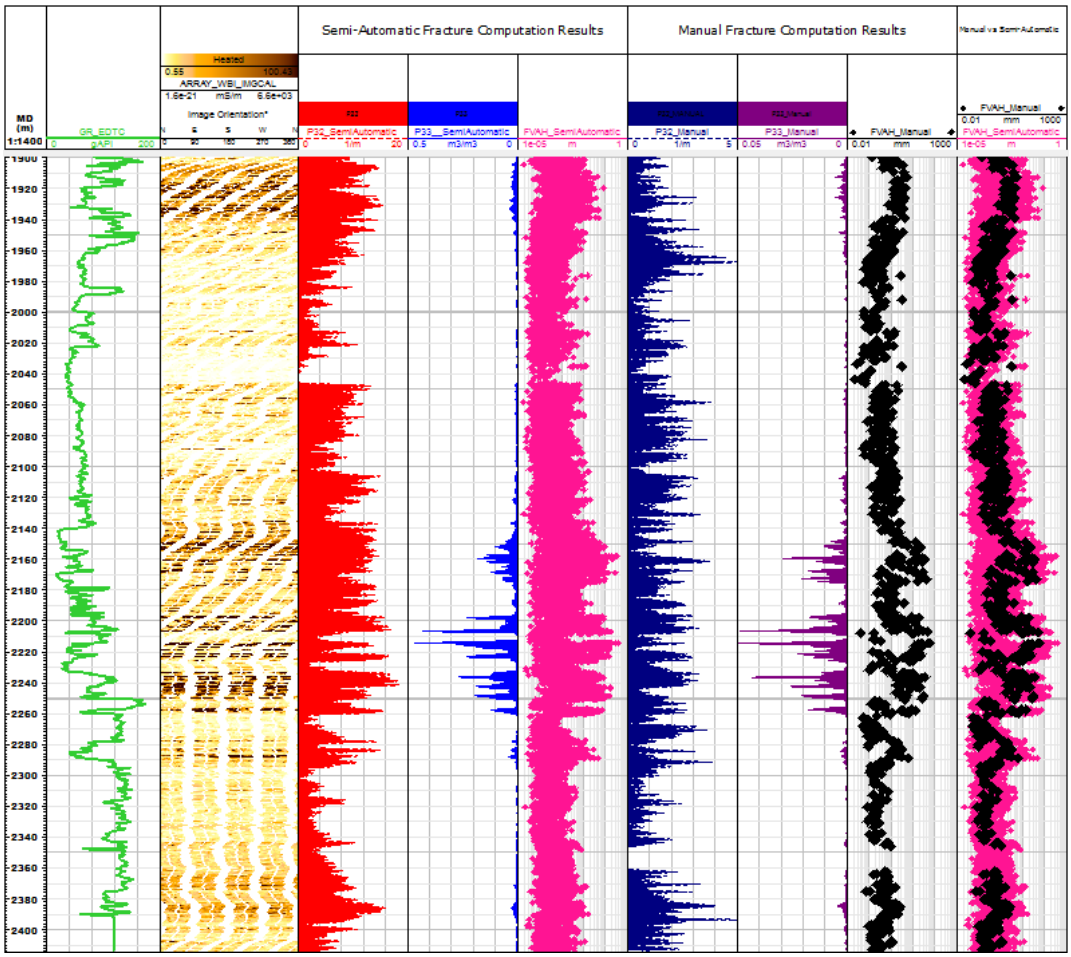


Figure 14: Non-classified fracture density (P32), fracture porosity (P33) and fracture aperture (FVAH) comparison between manual and semi-automatic fracture characterization.

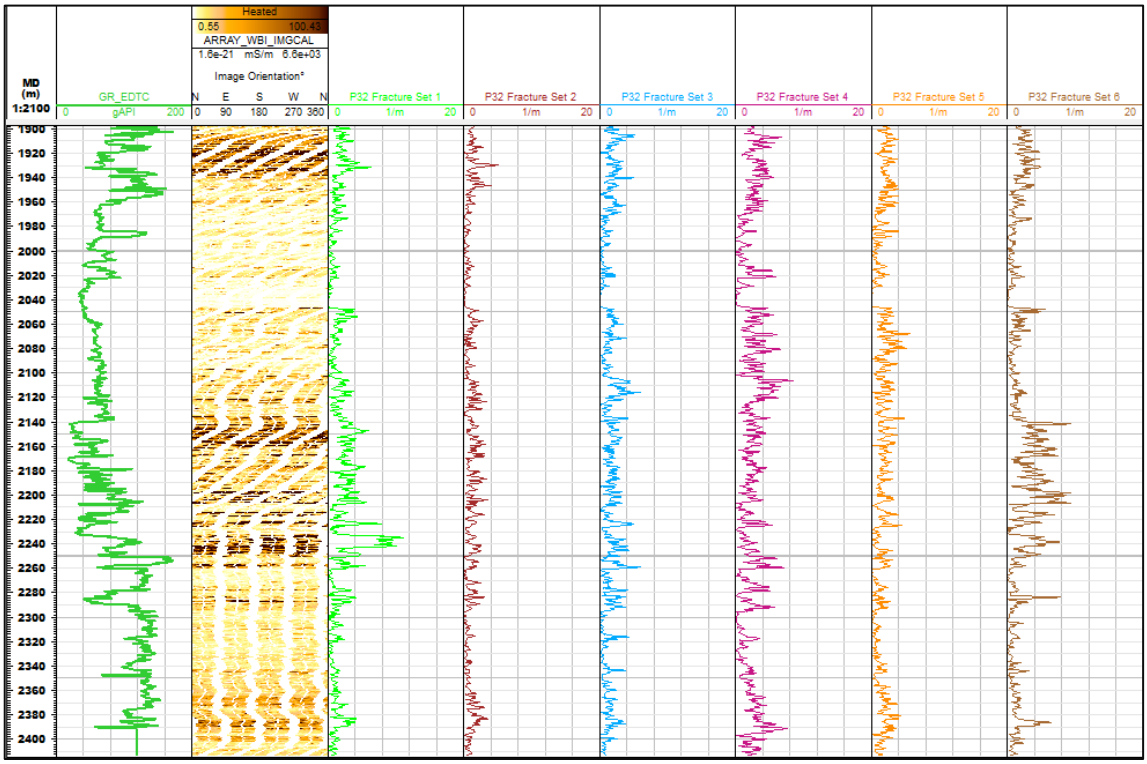


Figure 15: Classified fracture density (P32) computation results of semi-automatic fracture extraction.

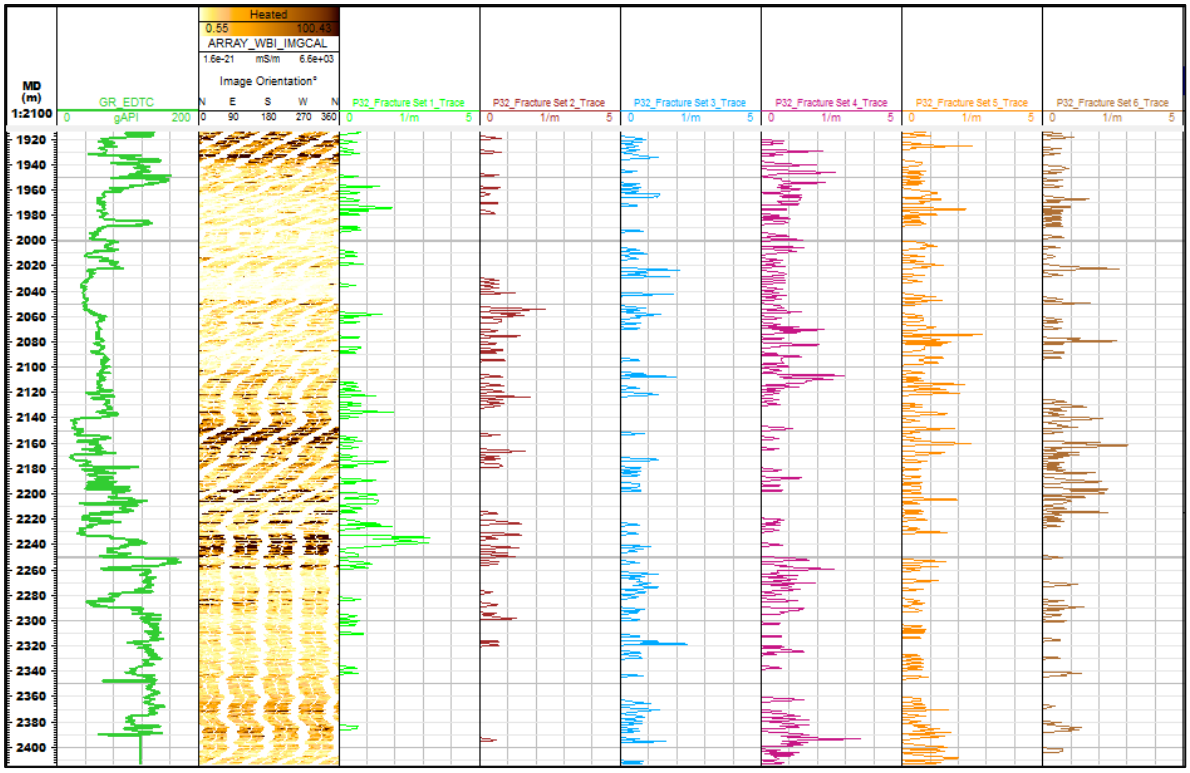


Figure 16: Classified fracture density (P32) computation results of manual fracture characterization.

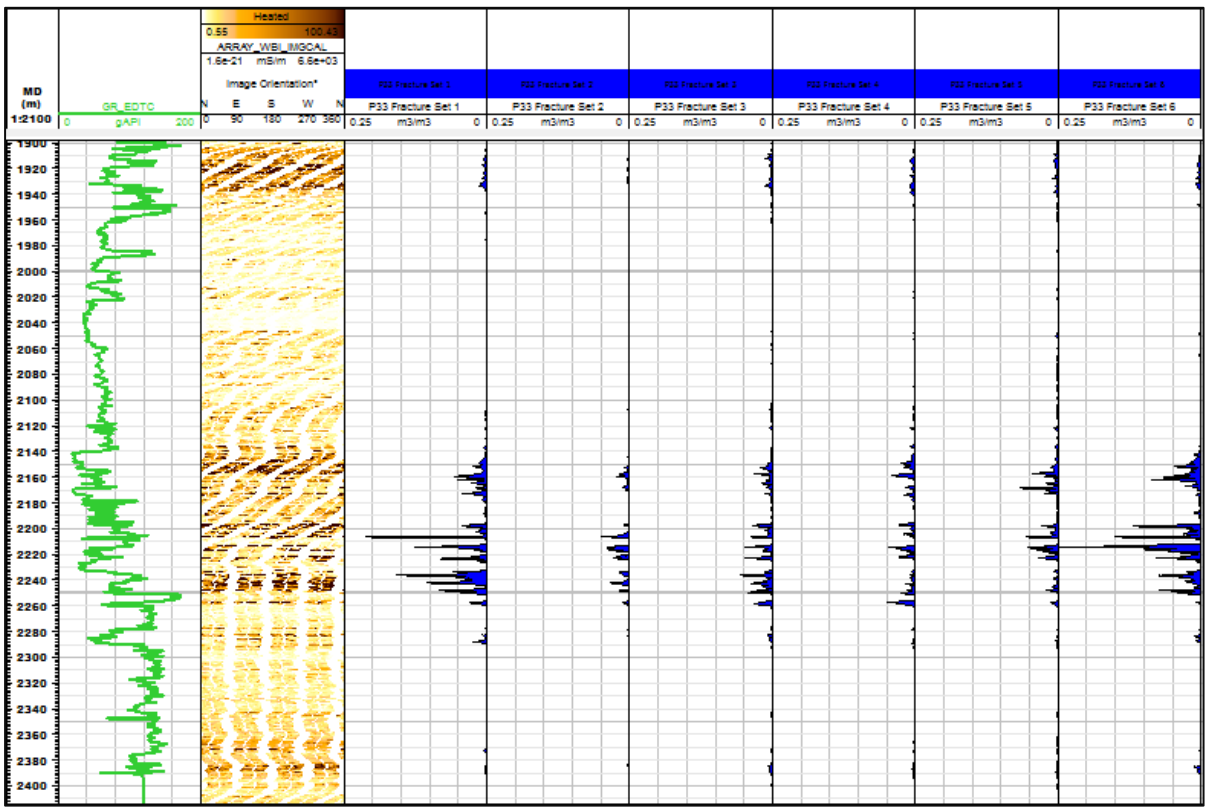


Figure 17: Fracture-set classified fracture porosity (P33) computation results of semi-automatic fracture extraction.

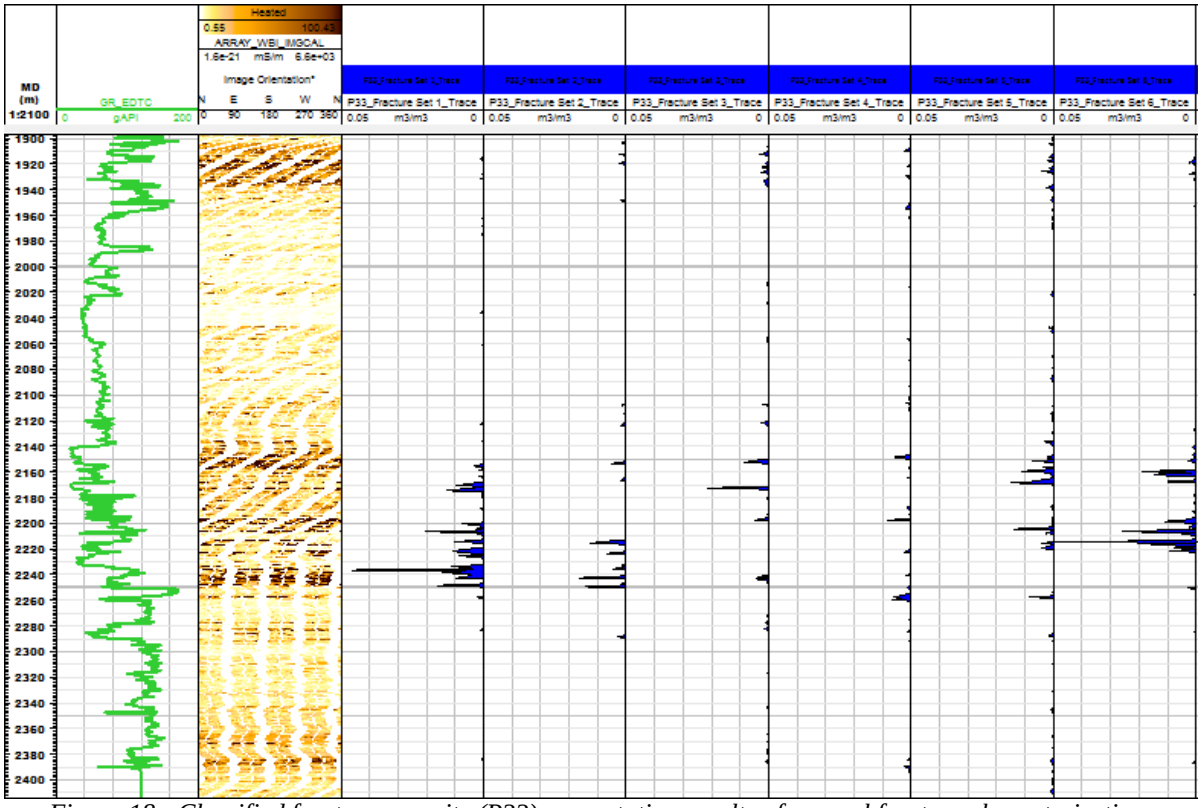


Figure 18: Classified fracture porosity (P33) computation results of manual fracture characterization.

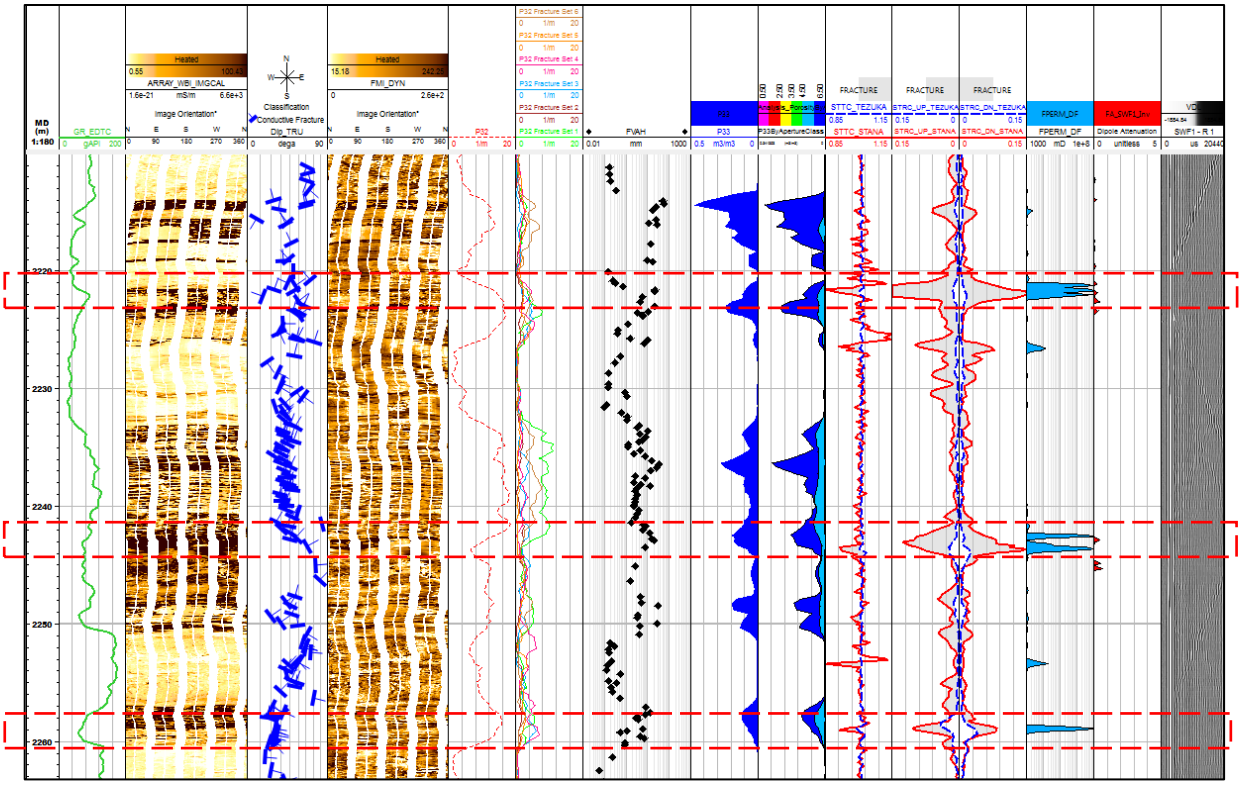


Figure 19: Interval 2,259-2,220 mMD has some open fractures based on qualitative FPERM curve and chevron pattern. However, the dipole attenuation in this interval is relatively low, indicating the fractures in this interval are open but does not have deep penetration away from the borehole.

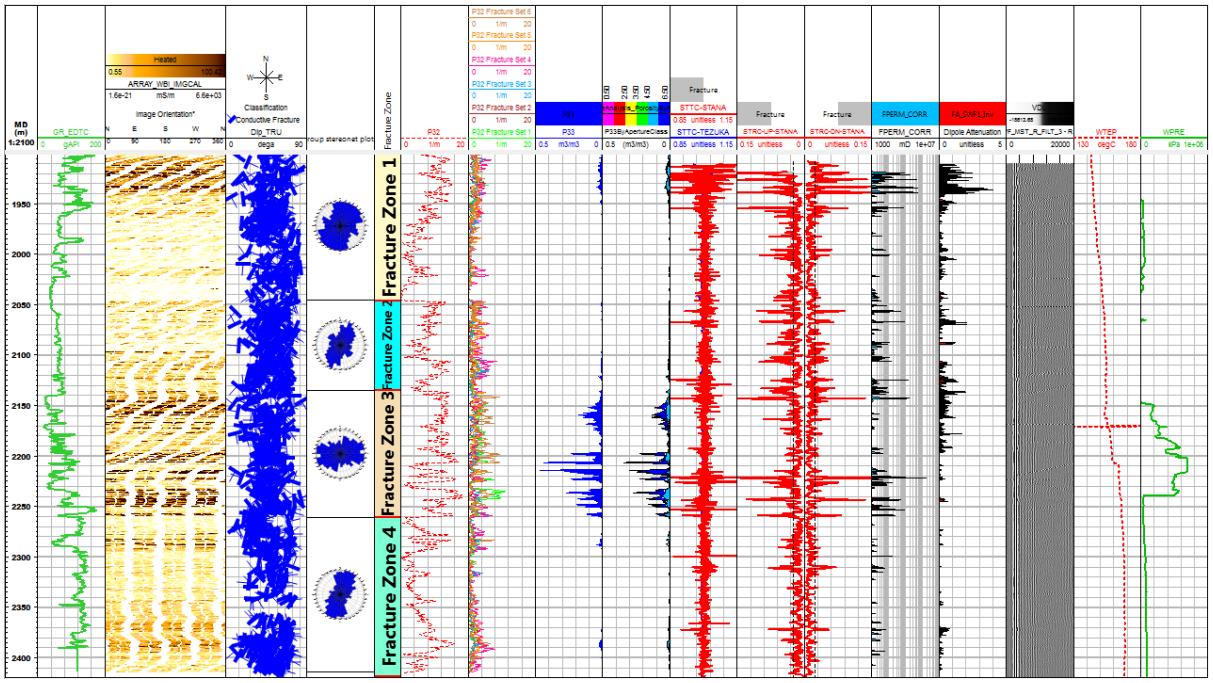


Figure 20: The integration of fracture characterization and computation using borehole image log, open/ permeable fracture determination using Sonic Stoneley Fracture Analysis and Wellbore Pressure-Temperature data.

GEOTHERMAL ACTIVE MANIFESTATIONS IN NON-VOLCANIC AREA OF SOUTH EAST SULAWESI, INDONESIA

Anna Yushantarti and Dudi Hermawan

Center For Mineral, Coal, and Geothermal Resources, MEMR
Jl Soekarno Hatta 444, Bandung, Indonesia
Email: untuk.anna@gmail.com

ABSTRACT

Geothermal manifestations are the first clue for identified a green geothermal areas. Indonesia has about 349 geothermal areas based on Map of Geothermal Areas Distribution and Its Potential in Indonesia 2018. There are many geothermal areas which are not associated with the volcanoes. One of this group is at south east sulawesi area, sulawesi island. To find the geothermal area, firstly is identifying the Surface thermal manifestation, then measuring the physical properties such as temperature, pH, conductivity, etc, and analysing the water samples to cluster the type of surface thermal manifestations. Based on literature data and identifying surface thermal manifestation in 2011, South East Sulawesi province has 16 geothermal areas and a numerous active geothermal manifestations there. Geologically, south east Sulawesi is associated with non-volcanic environment with metamorphic and sedimentary rocks mostly. The geothermal manifestations commonly only warm springs, hot springs, and alteration with temperature about 32 – 80 °C and neutral pH (6-8). Mostly they are bicarbonate and chloride type. This paper only discuss about various inventory of geothermal surface features at geothermal areas of south East Sulawesi.

Keywords: Geothermal Manifestations, South East Sulawesi, Non-Volcanic

INTRODUCTION

The Geological setting of Indonesia gives bless a lot of geological resources for Indonesia such as abundant geothermal potency. Indonesia Geothermal location has been identified about 349 locations by December 2018, with total potency about 25.5 GWe, consisted of 6,407 MWe speculative potency; 3,907 hypothetic potency; 10,160 possible potency; 2,016 probable potency; and 3,062.5 proven potency. The installed capacity by December 2018 reach about 1,948.5 MWe.

Mostly they are associated with quaternary volcanic area with distributed along Sumatera, Java, Bali, East Nusa Tenggara, Banda island, until North Sulawesi. The non-volcanic associated also richest the Indonesia geothermal system, at least about 70 locations or 20% distributed around Sulawesi island, Kalimantan, and Papua with total potency about 1 GWe. This non volcanic-term are characterized by: geothermal system is not correlated with quarter volcanic activity, manifested at sedimentary, plutonic, and metamorphic environment, and also correlated with tectonic processes.

There are 13 geothermal areas have been identified in South East Sulawesi (Geological Agency, 2018). South East Sulawesi is consisted of southeast Sulawesi land and Buton island, with geologically is formed of Triassic metamorphic rock and tertiary sedimentary rock. Data geothermal surface features shows about 15 (fifteen) warmsprings and hotsprings has been identified at leg of southeast Sulawesi. This paper only presents about various surface thermal features at southeast Sulawesi, so this could be a reference to them who will develop geothermal in this area.

METHODS

To find the geothermal area, firstly is identifying the Surface thermal manifestation, then measuring the physical properties such as temperature, pH, conductivity, etc, and analysing the water samples to cluster the type of surface thermal manifestations.

REGIONAL GEOLOGY OF SOUTH EAST SULAWESI LEG

Geologically, South East Sulawesi leg is having metamorphic rock as the basement (Hermawan et al., 2011). The movement of Australia continent to the west which is collision with Asia continent at east side and Pacific continent resulting tectonic movement which is tend to northwest-southeast. This tectonic activity resulting new basins which is filled with sedimentary deposition especially tertiary sedimentary carbonate rocks. The next phase is exogenous process, resulted sedimentation product from metamorphic rock and sedimentary rock which is grouped into conglomerate rock of pre quaternary. Sedimentation activity is still formed until now formed surface deposition: river alluvium and coastal alluvium.

Structure geology patterns at land of south east Sulawesi is dominated with same pattern with Palu-Koro structure which is northwest-southeast. This pattern because of the moving of Banggai Sula continent to the west. The big structures type of strike slip sinistral fault which is still correlated with Palu-Koro structure are Kolaka, Matano, and

Lawanopo fault. They are locally Normal faults which have possibility formed of depression zone which could be formed the secondary permeability at depth. This permeability may form geothermal reservoir at south east Sulawesi arm. The thermal surface features are commonly controlled by this northwest-southeast structures. Figure 1 shows the location of South East Sulawesi, Indonesia. Figure 2 shows the regional geology of South East Sulawesi.

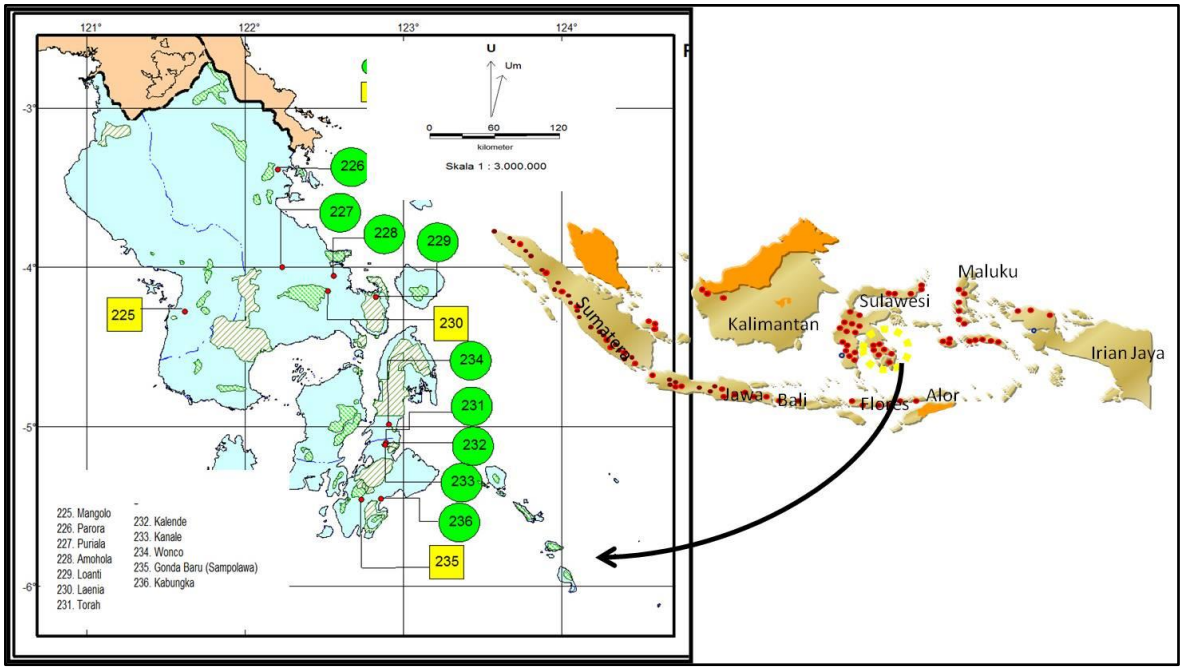


Figure 1: Map Location of South East Sulawesi, Indonesia.

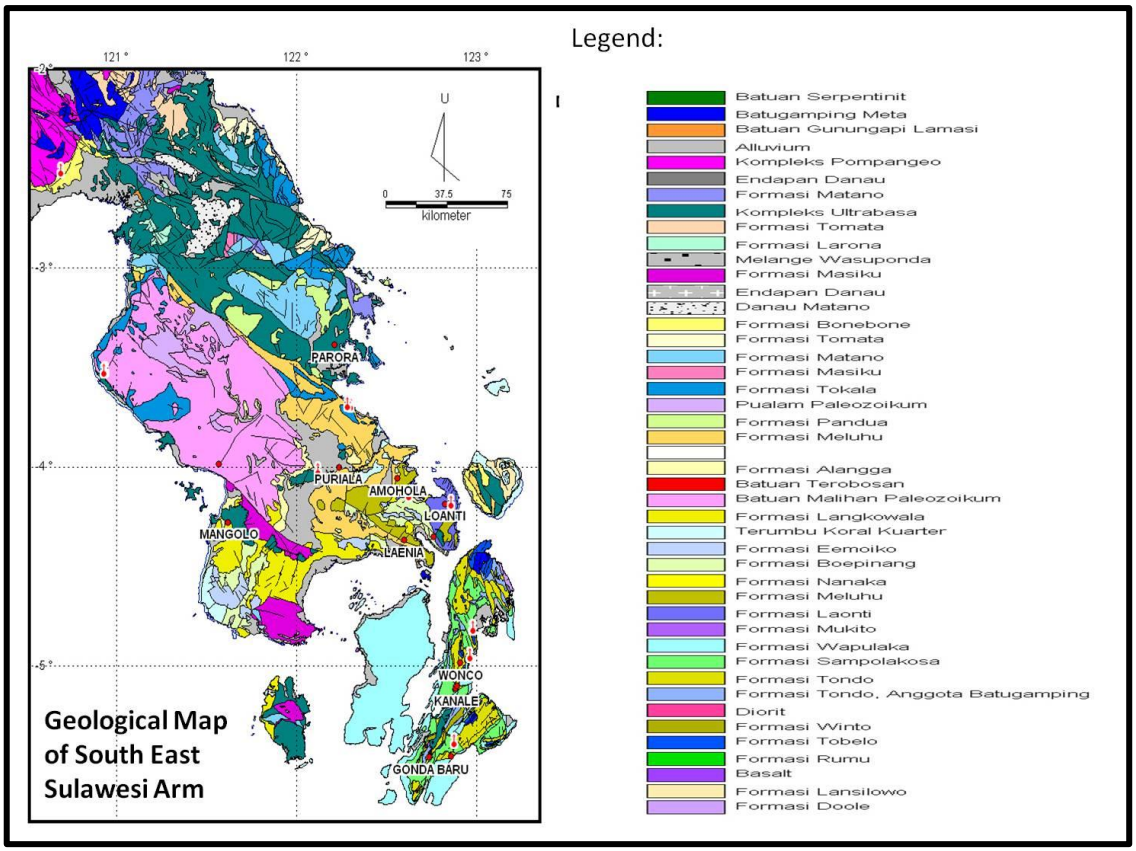


Figure 2: Regional Geology of South East Sulawesi Leg, compiled with several thermal geothermal surfaces areas (modified from Rusmana et al, 1993).

Structures geology at Buton island is different with at south east Sulawesi land. This island is dominated by North-South structures and northeast-southwest structures. The thermal features could be controlled by this thrust faults. Buton island has this characteristic because of the location is at collision zone between Anjungan Tukangbesi-Buton with South East Sulawesi continent.

The geothermal system could be divided by two types: firstly, is at South East Sulawesi land which is mostly probably influenced between geological structures pattern and remain magmatic activity at depth; secondly is at Buton island, probably influenced from mostly combined of geological structures and sedimentary basin as the basement.

GEOTHERMAL SURFACE THERMAL FEATURES AT BUTON ISLAND

Buton island has 6 (six) geothermal areas based on Geothermal distribution map (Geological Agency, 2018), i.e.: Torah (231), Kalende (232), Kanale (233), Wonco (234), Gonda Baru/ Sampolawa (235), and Kabungka (236). The thermal features literature of Torah, Kalende, Kanale, and Wonco unfortunately could not be traced when this paper is being written, so these areas are not included.

Based on the data of geothermal areas at Buton, the thermal geothermal features at Buton island could be clustered into 4 (four) groups (Pusat Sumber Daya Geologi, 2011; DIM, 2002) (Tabel 1), i.e.: Gonda Baru/ Sampolawa, Kabungka/Wening, Buranga, and Bubu (Figure 4).

1) Gonda Baru/Sampolawa thermal features are only warm springs (DIM, 2002), i.e.: Kaongke-Ongkea (36^{o}C, Napal) and Gondabaru (33^{o}C, conglomerate). They are bicarbonate-chloride type, manifested at elevation of about 230 m, neutral pH (7,21), and bubbling gas at the warm springs. It is located at coordinates 05° 28’ 24” S and 122° 44’ 30” E, altitude of 231 m above sea level.

2) Kabunga/ Wening thermal features is Laballe warm springs (38^{o}C), at elevation of 236 m, discharged on conglomerate, bicarbonate-chloride type, neutral pH (7,72), having conductivity of 1.760 µS/cm, and having flow rate about 5 l/s. It is located at coordinates 5° 23' 9" S and 122° 52' 49" E, altitude of 236 m above sea level.

3) Buranga thermal features are Buranga-1 (41,7^{o}C) and Buranga-2 (34,7^{o}C) warm springs. They are bicarbonate type, manifested on limestone, at elevation of 14-28 m, having conductivity of 2.600-3.800 µS/cm, neutral pH (7,02), and having flow rate of 5 l/s buranga-1). It is located at coordinates 4° 48' 52" S and 122° 58' 52" E, altitude of 14 m above sea level.

4) Bubu thermal features are warm springs and it could not be measured because of discharging at the coastal line and closing by the sea water. It is located at coordinates 4° 57' 11" S and 122° 58' 6" E, altitude of 1 m above sea level.

Hall (2002) showed based on heat flow map at Sundaland region, Buton island geothermal areas are having more lower of heat flow rather than average continental value, about < 60 mWm^2 compared to the others area (Figure 3). So, this region has a low to moderate favorable heat source to build a geothermal system. This could be affecting the expression of surface thermal surface at Buton island.

Thermal features of geothermal areas at Buton island are only warm springs (less than 50^{o}C, <50^{o}C), neutral pH, at low terrain, clear, and no deposition at the surface or near warm springs (Table 1). They are bicarbonate-chloride and bicarbonate waters type (Pusat Sumber Daya Geologi, 2011). The mode of heat discharge at Buton area could be distiquished as heat discharge associated with seepage (Hochstein, M. and Browne, P., 2000). This type is describing the discharge of subsurface thermal fluids at both shallow levels and deep levels. Shallow seepage can occur if hot water from a geothermal reservoir discharges by concealed springs at the bottom of a river, a lake, or into shallow groundwater. It is dominant results in low or medium temperature of geothermal system.

Hochstein and Browne (2000) explained that each of geothermal systems are dynamic phenomena. Their surface manifestations are often beautiful and expressions of visible transfer heat energy from subsurface. Each manifestation comes from unique systems. The “true” low-temperature systems are rare in volcanic arc settings, whereas they are common where topography and tectonics allow small heat-sweep systems to develop. A large number of convective low-temperature systems occur in geological settings that favour the development of structurally controlled, smaller heat sweep systems. Most discharge warm water (i.e, <40^o C) are from a network fractures that constitute their reservoir.

Hermawan et al. (2011) explained that the heat source of geothermal systems at Buton island probably correlated with tectonic activity such as geopressure and carbonate rocks dissolution. The geothermal systems at Buton are more combination from geology structures and sediment basin as the basement.
So, surface thermal features at Buton island is only characterized by warm springs (less than 50^{o}C), the

environment geology is a non-volcanic area with sediment basin. The geothermal systems at Buton are more combination from geology structures and sediment basin as the basement.

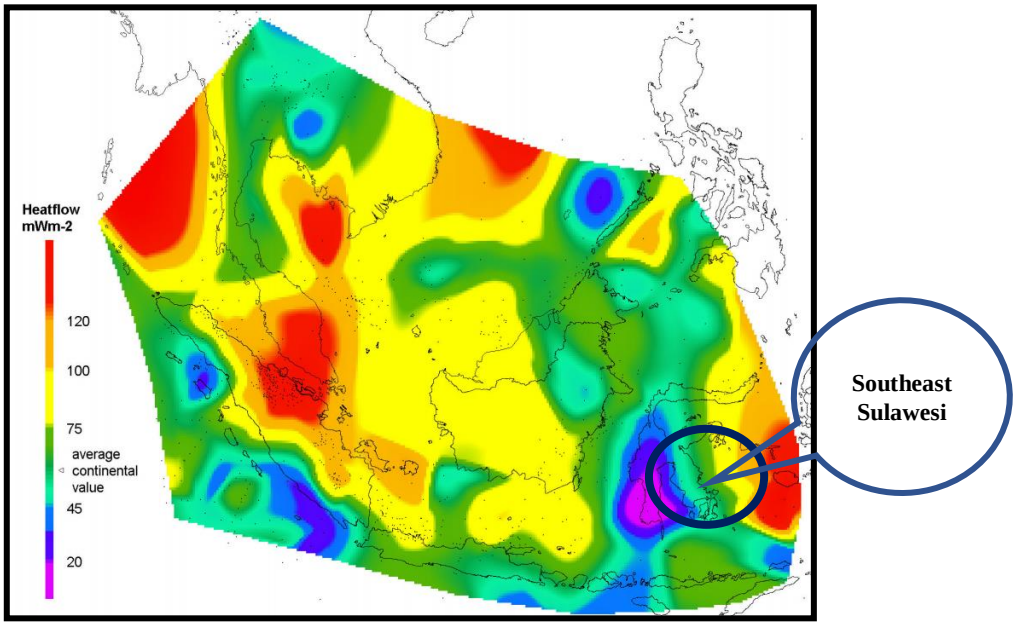


Figure 3: Map of Heat Flow for Sundaland Region (Hall, 2002).

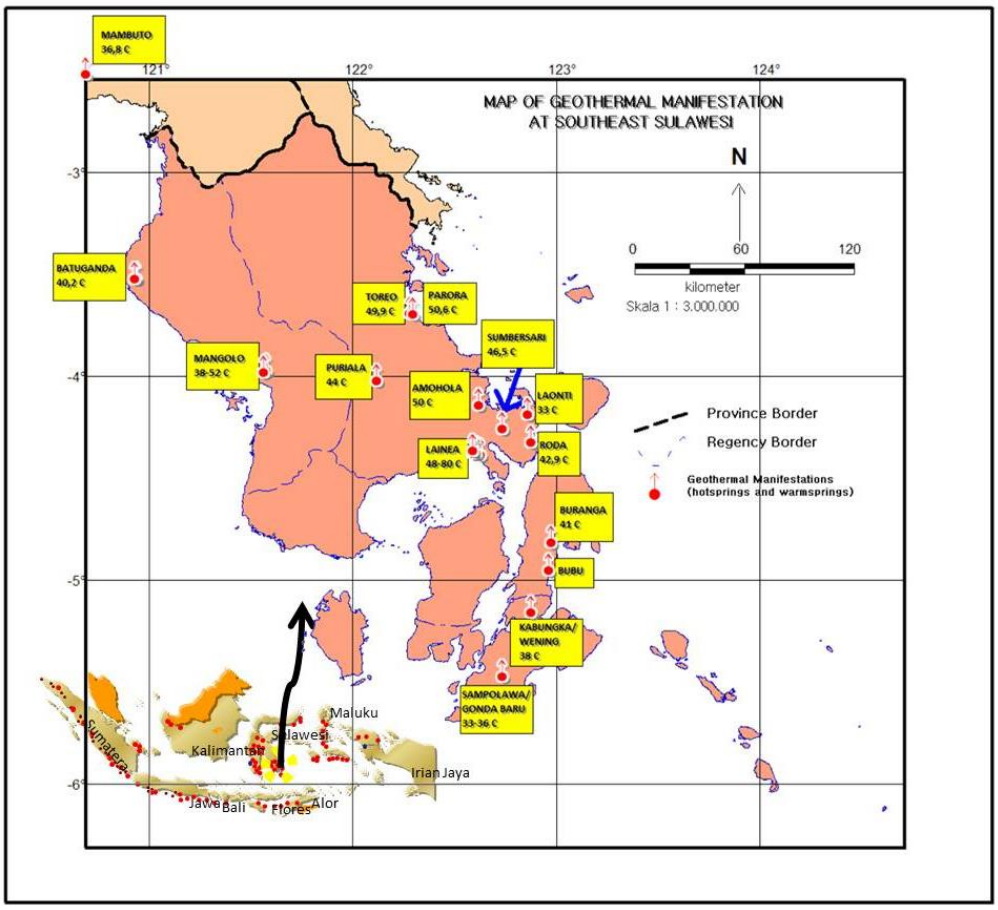


Figure 4: Map of Geothermal Manifestation at Southeast Sulawesi.

Table 1: Surface Thermal Features of Buton island, Southeast Sulawesi, Indonesia.

No.	Thermal Surface Features, Location, (Number in Geothermal Map, Potency)	Coordinate			Temperature (°C)		pH	Debit (l/s)	Conductivity (µS/cm)	Lithology	Type of The Water	Photo and additional description
		Latitude	Longitude	Elevation (m)	Thermal features	Air						
	BUTON ISLAND											
A	**Sampolawa/ Gonda Baru geothermal area (Number 235, possible potency of 1 MWe)**											
1	Kaongke-Ongkea warm springs	05° 28' 24" S	122° 44' 30" E	231	36	27	7.21	5	n.a	Napal	Bicarbonate-chloride	bubling gas at the warm springs
2	Gondabaru warm springs	05° 27' 36 " S	122° 44' 08" E	256	33	27.5	7.06	2	n.a	conglomerate	Bicarbonate-chloride	bubbling gas
B	**Kabungka/Wening geothermal area (236, speculative potency of 25 MWe)**											
1	Laballe warm springs, Winning village, Kec.Pasarwajo, Buton Regency	5° 23' 9" S	122° 52' 49" E	236	38	25.6	7.72	5	1760	conglomerate	Bicarbonate-chloride	 The colour is clear, no smell, no deposition bubble at the warm springs
C	**Buranga geothermal area**											
1	Buranga-1 warm springs, Buranga village, Kecamatan Botunungu, Buton Utara Regency	4° 48' 52" S	122° 58' 52" E	14	41.7	27.9	7.02	5	3800	limestone	Bicarbonate	 The colour is clear, no smell, no deposition bubble at the warm springs
2	Buranga-2 warm springs, Buranga village, Kecamatan Botunungu, Buton Utara Regency	4° 48' 53" S	122° 59' 0" E.	28	34.7	23.6	7.20	0.1	2600	Limestone	Bicarbonate	 The colour is clear, no smell, no deposition bubble at the warm springs
D	**Bubu geothermal area**											
1	Bubu warm springs	4° 57' 11"S	122° 58' 6" E	1	n.a	n.a	n.a	n.a	n.a	n.a	n.a	At border of the coastal line, could not being measured because it is closed with the sea water
E	**Torah (231), Kalende (232), Kanale (234), and Wonco (235) are not available data of the thermal features**											

GEOTHERMAL SURFACE THERMAL FEATURES AT SOUTHEAST SULAWESI LAND

The leg of Southeast Sulawesi Land has 7 (seven) geothermal areas based on Geothermal distribution map (Geological Agency, 2018), i.e.: Mangolo (225), Parora (226), Puriala (227), Amohola (228), Laonti (229), Laenia (230), and Sumbersari (319). But involving with based on the inventory data of thermal manifestations, there are about 11 (eleven) geothermal manifestations (Pusat Sumber Daya Geologi, 2011).

The geothermal manifestations that have been inventory at southeast Sulawesi land could be clustered about 11 (eleven) thermal manifestations areas. They are : (1) Toreo, (2) Parora, (3) Puriala, (4) Amohola, (5) Sumbersari, (6) Roda, (7) Laonti, (8) Lainea, (9) Mangolo, (10) Batuganda, and (11) Mambotu. They are mostly only hot springs and alteration.Toreo, Parora, Puriala, Amohola, Sumbersari, Roda, Laonti, and Lainea are at Konawe Regency-southeast Sulawesi province; Batuganda is at North Kolaka-southeast Sulawesi province, and Mambotu is at North Luwu-South Sulawesi province.

The thermal geothermal features that mention above (Tabel 2,3,4,5), could be described:

1) Toreo
   Toreo hot springs is located at 3º 41' 33,5" S and 122º 17' 5,8" E, altitude of 25 m above sea level, Toreo village, Losalo sub-district, North Konawe regency, Southeast Sulawesi province. It has temperature of 49,9ºC at air temperature of 25,7ºC, electrical conductivity of 1.256 µS/cm, pH of 7,42, flow rate of 5 l/s, area of 5 x 5 m, appeared at two points, clearly color, salty, air bubbles, coming out on alluvium rocks, and chloride type. Based on the regional geological map of Lembar Lasusua-Kendari, Sulawesi (E. Rusmana, et al., 1993), it is in the Meluhu Formation which consists of Sandstone, quartzite, black shale, red shale, filit, batusabak, limestone and siltstone, which aged Trias-Jura (Table 2).

2) Parora
   Parora hot springs is located at 3º41'49" S and 122º37' 31.5" E, altitude of 11 m above sea level, Woi Makula village, Lasola District, North Konawe Regency, Southeast Sulawesi Province. It has temperature of 50,6 ºC at air temperature of 27,5 ºC, electrical conductivity of 26.500 µS/cm, pH 6,13, flow rate of 5 l/s, area of 50x50 m, clearly color, salty, air bubbles, H_2S odor, thick and terraced carbonate sinter, located near the sea, and chloride type. Based on the regional geological map of Lembar Lasusua-Kendari, Sulawesi (E. Rusmana, et al., 1993), it is in the Meluhu Formation which consists of Sandstone, quartzite, black shale, red shale, phylite, coconut shells, limestone and siltstone, which Trias-Jura age (Table 2).

3) Puriala
   Puriala hot springs is located at coordinates 4º1'16,4" S and 122º 7' 19,8" E, altitude of 29 m above sea level, Sonai village, Puriala District, Konawe Regency, Southeast Sulawesi Province. It has temperature of 44ºC at air temperature 29ºC, electrical conductivity of 382 µS/cm, pH 8,72, flow rate of 5 l/s, area 50x30 m, clearly color, tasteless, air bubbles, and bicarbonate type. Based on the regional geological map of Lembar Lasusua-Kendari, Sulawesi (E. Rusmana, et al., 1993), it is in alluvium rocks, which consist of gravel, gluttony, sand and clay, which are Holocene aged.

4) Amohola
   Amohola hot springs is located at coordinates 4º 8'31,3" S and 122º 37' 31,5" E, altitude of 28 m asl, Selabangka village, Moramo District, South Konawe District, Southeast Sulawesi Province. It has temperature of 50ºC at air temperature of 28ºC, electrical conductivity of 8.060 µS/cm, pH 6,82, flow rate of 0,5 l/s, area of 50x30 m, clearly color, salty, air bubbles, thick and wide of carbonate sintered, located near the sea, chloride type, and manifested about 4 hot springs at the surface. Based on the regional geological map of Lembar Lasusua-Kendari, Sulawesi (E. Rusmana, et al., 1993), It appears on the Laonti Formation rocks, which consist of metamorph, marble and filite limestones, which are Trias-Jura (Table 3).

5) Sumbersari
   Sumbersari hot springs is located at coordinates 4º 15' 25,6" S and 122º 44' 26,5" E, altitude of 105 m asl, Sumbersari village, Moramo district, South Konawe Regency, Southeast Sulawesi Province. It has temperature of 46,5ºC at air temperature of 28,3ºC, electrical conductivity of 970 µS/cm, pH 6,65, flow rate of 0,3 l/s, area of 50x30 m, bicarbonate type, and manifested about 8 hot springs at the surface. Warm springs are on the limestone, clear, odorless, tasteless, and having bubbles but not continuous, low-level alteration, and contaminated by river water at the surface (Table 3).

6) Laonti
   Laonti hot water is located at 4º 11'16,4"S and 122º 51' 51" E, altitude of 14 m above sea level, Pondirangga village, Laonti District, South Konawe District, Southeast Sulawesi Province. It has a temperature of 33º C at air temperature

of 25,7 º C, electrical conductivity of 942 µS/cm, pH 7,42, flow rate of 0,5 l/s, area 3X3 m, clearly color, tasteless, air bubbles, oxides iron deposition, bicarbonate type. Based on the regional geological map of Lasusua-Kendari sheet, Sulawesi (E. Rusmana, et al., 1993), it is on the Laonti Formation rocks, which consist of Malih, marble and filite limestones, which are Trias-Jura (Table 3).

7) Roda
Roda hot springs is located at 4^0 18' 38,5" S and 118^0 30' 10,3" E, altitude of 60 m asl, Roda River, Roda Village, South Konawe, It has temperature of 42,9ºC at air temperature of 25,6ºC, electrical conductivity of 1.125µS/cm, pH 6,3, flow rate of 1 l/s, bicarbonate type which consists of the appearance of hot springs and carbonate sintered and hydrothermal breccias (Pusat Sumber Daya Geologi, 2010) (Table 3).

8) Lainea
It consists of 4 (four) groups: Lainea, Landai, Amolowo, and Kaendi (Pusat Sumber Daya Geologi, 2010). The coordinate is at 4^0 21' 56,8" S- 4^0 23' 4,6" S and 122^0 36'41,8" E-122^0 37'55,3" E and all are bicarbonate type (Table 4). They are:

i) Lainea group
It is at Lainea/ Pambuanga river, Lainea village, consist of hot springs and alteration, temperature of 58,2ºC - 80ºC, at an air temperature of 30,1 º C, electrical conductivity 1.300 µS / cm, pH 5,8-6,3, flow rate of 0,5 l/s, appear around the crevices of filite and conglomerates around the Lainea river.

ii) Landai group
It is at Landai river, Kaendi village, and consisted of hot springs and alteration. temperature of 52,8ºC–67,7ºC, at an air temperature of 19,9 º C, electrical conductivity 1.100-1.300 µS/cm, pH 6,52-6,90, flow rate of 0,5-5 l/s, appear at limestone.

iii) Amowolo group
It is at Molowo river, Kaendi village, and consisted of hot springs and alteration. temperature of 48,2ºC–68,7ºC, at an air temperature of 30 º C, electrical conductivity 1.130-1.450 µS/cm, pH 6,30-6,90, flow rate of 0,5-1 l/s, appear at limestone. There is a 10 m thick of carbonate sinter forming stalagmite and stalagtite.

iv) Kaendi group
It is at Kaendi river, Pamandati village, and consisted of hot springs and alteration. temperature of 53,5ºC–73ºC, at air temperature of 26ºC, electrical conductivity 845-1.500 µS/cm, pH 6,35, flow rate of 0,5-20 l/s, appear at limestone.

9) Mangolo
Mangolo hot springs is located at 3^0 58' 19,5" S and 121^0 34' 51,8" E, It has temperature of 38-52ºC, pH 7,5, flow rate of 10 l/s, bicarbonate, and gas bubbles that emerge through malleable limestone slits, which are called local names, namely the Campground and Goa Group (DIM, 2001). This area is dominated by metamorphic rock (Table 4).

10) Batuganda-North Kolaka
Batuganda hot springs is located at 3^0 31' 13" S and 120^0 56' 27" E, altitude of 99-106 m asl, Batuganda Village, Lasusua district, North Kolaka regency, Southeast province (Pusat Sumber Daya Geologi, 2011). It has temperature of 36,1-40,5ºC at air temperature of 24,5ºC, pH 5,78-7,3, flow rate of 0,1 l/s, bicarbonate type, manifested 2 hotsprings, and carbonate sintered. Based on regional geological map of Lembar Lasusua-Kendari, Sulawesi (E.Rusmana, et sl.,1993), it is in Tokala formation, Trias age, which are consisted of calsilutit, limestone, sandstone, napal, and slate, and in Perm-Carbon age Paleozoic igneous rocks consisting of genes, filite, quartzite, slate, and a little marble (Table 5).

11) Mambotu-Luwu Timur
Mambotu hotsprings is located at 2^0 3' 2,4" S and 120^0 41' 39" E, altitude of 187 m asl, Cendana village, Burau district, East Luwu regency, South Sulawesi province, It has temperature of 36,8ºC at air temperature of 29,1ºC, pH 6,7, flow rate of 0,2 l/s, bicarbonate type which consists of the appearance of hot springs and carbonate sintered and hydrothermal breccias (Pusat Sumber Daya Geologi, 2011) (Table 5).

Based on the Regional Geological Map of Lembar Malili, Sulawesi (TO Simandjuntak, et al., 1991), it is at the boundary between the Tertiary Bone-Bone Formation which consists of intersections of sandstones, conglomerates, marl, and tuffaceous clay with Pompangeo Complex Cretaceous- Paleocene aged which consists of schist, genes, marble, serpentine, quartzite, slate, filit, and local breccia.

Hall (2002) showed based on heat flow map at Sundaland region, leg of southeast Sulawesi land are having more lower of heat flow rather than average continental value, about < 60 mWm^2 compared to the others area. This is similar with Buton island (Figure 3). So, this region has a low to

moderate favorable heat source to build a geothermal system. This could be probably affecting also on surface thermal features at leg of southeast Sulawesi leg.

Thermal features of geothermal area at leg of Southeast Land are only warm springs, hot springs, and alteration (less than 50^{o}C and the highest of 80^{o}C), near neutral pH, at low terrain, and clearly colour, low velocity gas seepage. They are chloride and bicarbonate type of waters (Pusat Sumber Daya Geologi, 2011).

Hermawan et al. (2011) explained that the heat source of the leg of southeast Sulawesi land probably from remnant young magmatic activity as intrusion rock. This is supported by gravity data which show the existence of igneous rock at the depth around Lainea hot springs. The geothermal systems at these areas are more combination from geology structures and remnant young magmatic activity at depth.

So, the heat source of southeast Sulawesi land more Favorable than Buron island. This are resulting that it has surface thermal features until 80^{o}C. The character of surface thermal features only warm springs, hot springs, and alteration (less than 50^{o}C and the highest of 80^{o}C), near neutral pH, at low terrain, and clearly colour, low velocity gas seepage. The environment geology is a non-volcanic area with metamorphic mostly.

CONCLUSION

The heat flow pattern on a region could affect the favorable heat source for a geothermal system. Surface thermal springs are extracting the heat from the depth. Leg of southeast Sulawesi land and Buton island are having more lower of heat flow rather than average continental value, about < 60 mWm^{2} compared to the others area.So, this region probably has a low to moderate favorable heat source.

Buton island has surface thermal features only characterized by warm springs (less than 50^{o}C), the environment geology is a non-volcanic area with sediment basin. They are chlorise-bicarbonate and bicarbonate water types.The geothermal systems at Buton are more combination from geology structures and sediment basin as the basement.

Leg of southeast Sulawesi land has the heat source more Favorable than Buron island. This result that it has surface thermal features until 80^{o}C. The character of surface thermal features only warm springs, hot springs, and alteration (less than 50^{o}C and the highest of 80^{o}C), near neutral pH, at low terrain, and clearly colour, low velocity gas seepage. They are chloride and bicarbonate water types. The environment geology is a non-volcanic area with metamorphic mostly. The geothermal systems at this area are more combination from geology structures and remnant young magmatic activity at depth.

REFERENCES

Direktorat Inventarisasi Sumber Daya Mineral (DIM). (2001), “Laporan Penyelidikan Geologi, Geokimia Dan Geofisika Terpadu Daerah Panas Bumi Mangolo, Kabupaten Kolaka, Sulawesi Tenggara”, unpublished Reports of Direktorat Jenderal Geologi dan Sumber Daya Mineral, Departemen Energi dan Sumber Daya Mineral, Indonesia

Direktorat Inventarisasi Sumber Daya Mineral (DIM). (2002), “Laporan Penyelidikan Geologi, Geokimia Dan Geofisika Terpadu Daerah Panas Bumi Gondabaru-Sampolawa, Pulau Buton, Sulawesi Tenggara”, unpublished Reports of Direktorat Jenderal Geologi dan Sumber Daya Mineral, Departemen Energi dan Sumber Daya Mineral, Indonesia

Rusmana, E., Sukido, Sukarna, D., Haryono, E., Simandjuntak, T., O., (1993), “Peta Geologi Lembar Lasusua-Kendari, Sulawesi Skala 1:250.000”. Pusat Penelitian dan Pengembangan Geologi, Bandung, Indonesia.

Geological Agency, Center for Mineral, Coal, and Geothermal Resources (2018), "Geothermal Area Distribution Map and Its Potential in Indonesia December 2018", Bandung

Hall, R., SE Asian Heatflow: call for new data, SE Asia Research Group, Department of Geology Royal Holloway University of London, Egham, Surrey TW20 0EX, UK. (2002)

Hermawan, D., Sugianto, A., Yushantarti, A., Dahlan, Munandar, A., Widodo, S. (2011), “Kajian Panas Bumi Non Vulkanik Daerah Sulawesi Bagian Tenggara”, Prosiding Hasil Kegiatan Pusat Sumber Daya Geologi Tahun 2011, I.3, Pusat Sumber Daya Geologi, Bandung

Hochstein, M. and Browne, P. (2000), "Surface Manifestations of Geothermal Systems with Volcanic Heat Sources", Encyclopedia of Volcanoes, Academic Press, p.835-855

Nicholson, K. (1993), “Geothermal Fluids Chemistry and Exploration Technique”. Springer Verlag,Inc. Berlin.

Sikumbang, N., Sanyoto, P., Supandjono, R., J., B., Gafoer, S., (1995), “Peta Geologi Lembar Buton, Sulawesi Tenggara Skala 1:250.000”. Pusat Penelitian dan Pengembangan Geologi, Bandung, Indonesia.

Pusat Sumber Daya Geologi. (2011), “Laporan Kajian Panas Bumi Non Vulkanik Daerah Sulawesi Bagian Tenggara, Bandung”, unpublished Reports

Simanjuntak, T., O., Surono, Sukido. (1993), “Peta Geologi Lembar Kolaka, Sulawesi Skala 1:250.000”. Pusat Penelitian dan Pengembangan Geologi, Bandung, Indonesia.

Pusat Sumber Daya Geologi. (2010), “Survei Terpadu Geologi dan Geokimia Daerah Panas Bumi Lainea, Kabupaten Konawe Selatan, Provinsi Sulawesi Tenggara”. Pusat Sumber Daya Geologi.

Table 2: Surface Thermal Features of Toreo, Parora, and Puriala, Southeast Sulawesi, Indonesia.

No.	Thermal Surface Features, Location (Number in Geothermal Map, Potency)	Coordinate			Temperature Thermal Features ^{0}C	Temperature Air ^{0}C	pH	Debit l/s.	Conductivity (µS/cm)	Lithology	Type of The Water	Photo and additional description
		Latitude	Longitude	Elevation (m)								
1.	TOREO hotsprings, Toreo village, Losalo District, North Konawe Regency	3^0 41' 33,5" S	122^0 17' 5,8" E	25	49,9	25,7	7,42	5	1256	Alluvium	Chloride	 Size of 5m x 5 m, there are two hotsprings in this area, clear, salty, buble, manifested at alluvial which is consisted of sandstone, etc Trias-Yura age
2	PARORA hotsprings, Woi Makula village, Lasola district, North Konawe Regency (226)	3^0 41' 49" S	122^0 18' 8,6" E	11	50,6	27,5	6,13	5	26500	Alluvium	Chloride	 Size about 50x50m, clear, salty, bubble, H_2S odour, sinter carbonate thick and terrace, near the sea, based on Regional Geology map of Lasusua-Kendari, Sulawesi (E.Rusmana, et al, 1993), it is manifested at Meluhu Formation
3	PURIALA hotsprings, Sonai village, Puriala district, Konawe Regency (227)	4^0 1' 16,4" S	122^0 7' 19,8" E	29	44	29	8,72	5	382	alluvium	bicarbonate	 area 50x30 m, clear, tasteless, air bubbles

Table 3: Surface Thermal Features of Amohola, Sumbersari, Laonti, and Roda, Southeast Sulawesi, Indonesia.

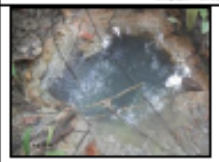
No.	Thermal Surface Features, Location (Number in Geothermal Map, Potency)	Coordinate			Temperature Thermal Features ^{0}C	Temperature Air ^{0}C	pH	Debit l/s.	Conductivity (µS/cm)	Lithology	Type of The Water	Photo and additional description
		Latitude	Longitude	Elevation (m)								
4	AMOHOLA hotsprings (4 hotsprings) Selabangga village, Moramo district, South Konawe regency (228)	4^0 8' 31,3" S	122^{0}37'31,5" E	11	37,2	28	6,82	5	8060	Limestone	chloride	 Size of 50x50m,clear, salty, bubble, H_2S odour, thick nd terracing of sinter carbonate, near the sea
5	SUMBERSARI hotsprings (8 hotsprings) Sumbersari village, Moramo district, South Konawe Regency (319)	4^0 15' 25,6" S	122^{0}44'26,5" E	105	46,5	28,3	6,65	0,3	970	limestone	bicarbonate	 The warm water is clear, odorless, tasteless, and there are bubbles but not continuous, appearing sedimentary surface sediments undergoing low-level alteration,
6	LAONTI hotsprings Pondirangga village, Laonti district, South Konawe regency (229)	4^0 11' 16,4" S	122^0 51' 51" E	14	33	25,7	7.42	0,5	942	limestone	bicarbonate	clearly color, tasteless, air bubbles, oxides iron deposition. Based on the regional geological map of Lembar Lasusua-Kendari, Sulawesi (E. Rusmana, et al., 1993), it is on the Laonti Formation rocks, which consist of Malih, marble and filite limestones, which are Trias-Jura
7	RODA hotsprings Roda village, South Konawe regency	4^0 18' 38,5" S	118^{0}30'10,3" E	60	42,9	25.6	6.3	1	1125	hydrothermal breccias.	bicarbonate	carbonate sintered and hydrothermal breccias. -

Table 4: Surface Thermal Features of Lainea and Mangolo, Southeast Sulawesi, Indonesia.

No.	Thermal Surface Features, Location (Number in Geothermal Map, Potency)	Coordinate			Temperature Thermal Features °C	Temperature Air °C	pH	Debit l/s.	Conductivity (µS/cm)	Lithology	Type of The Water	Photo and additional description
		Latitude	Longitude	Elevation (m)								
8	LAINEA geothermal area (230)				°C	°C		l/s.				
	Lainea Hotsprings (3 (three) hotsprings at the surface) and alteration	4° 23' 4,6" S	122° 37' 55,3" E	71	58.2-80	20.1-30.1	5.8-6.3	0.5	1200-1350	Filitic rocks and conglomerat	bicarbonate	appear around the crevices of filite and conglomerates around the Lainea river
	Landai hotsprings (3 (three) hotsprings at the surface) and alteration	4° 22' 33,1" S	122° 36' 41,8" E	128	52,8-67,7	19.9-30	6.52-6.9	0.5-5	1100-1300	limestone	bicarbonate	Clear and odorless
	Amowolo hotsprings (2 (two) hotsprings at the surface) and alteration	4° 22' 31,8" S	122° 35' 50" E	81	48.2-68.7	30	6.3-6.9	0.5-1	1130-1450	Metamor-phic (Filitic)	bicarbonate	There is a 10 m thick of carbonate sinter forming stalagmite and stalagtite.
	Kaendi hotsprings (4 (four) hotsprings at the surface) and alteration	4° 21' 56,8" S	122° 35' 49,5" E	110	53.5-73	26-29.7	6.25 - 6.56	0.5-20	845-1500	Metamor-phic (Filitic)	bicarbonate	

No.	Thermal Surface Features, Location (Number in Geothermal Map, Potency)	Coordinate			Temperature Thermal Features	Temperature Air	pH	Debit	Conductivity	Lithology	Type of The Water	Photo and additional description
		Latitude	Longitude	Elevation (m)								
9	MANGOLO (225)				°C	°C		l/s.				
	Hotspring Pramuka	3° 58' 19,5" S	121° 34' 51,8" E		52		7.5	10		limestone	Bicarbonate	
	Ulunggolaka				38		7.4				Bicarbonate	
	Telaga Nur	3° 58' 49" S	121° 34' 1,7" E		38		7.5	0.01			bicarbonate	

Table 5: Surface Thermal Features of North Kolaka and East Luwu, Southeast Sulawesi, Indonesia.

No.	Thermal Surface Features, Location (Number in Geothermal Map, Potency)	Coordinate			Temperature Thermal Features	Temperature Air	pH	Debit	Conductivity	Lithology	Type of The Water	Photo and additional description
10	KOLAKA	Latitude	Longitude	Elevation (m)	°C	°C		l/s.				
	BATUGANDA-1 Hotspring Batuganda village, Lasusua district,North .Kolaka Regency	3° 31' 13" S	120° 56' 27" E	99	40,2	27,6	7,3	0,1	n/a	limestone	bicarbonate	Clear and sinter carbonate
	BATUGANDA-2 hotsprings	3° 31' 15" S	120° 55' 54" E	106	36,1-40,5	24,5	5,78	0,2	n/a		bicarbonate	Clear and sinter carbonate

No.	Thermal Surface Features, Location (Number in Geothermal Map, Potency)	Coordinate			Temperature Thermal Features	Temperature Air	pH	Debit	Conductivity	Lithology	Type of The Water	Photo and additional description
	EAST LUWU	Latitude	Longitude	Elevation (m)	°C	°C		l/s.				
11	MAMBUTO Hotsprings Cendana village,.Burau district,.Luwu Timur regency, South Sulawesi province,	2° 31' 2,4" S	120° 41' 39" E	187	36,8	29,1	6,7	0,2	n/a	Napal rocks	bicarbonate	Clear, on lithology margin between metamorphic and napal.

COMPREHENSIVE STUDY OF HOT SPRINGS POTENTIALS IN LOJING GEOTHERMAL COMPLEX, MALAYSIA

Mohammad Noor Akmal Anuar[1], Mohd Hariri Arifin[1], Hassan Baioumy[2], Che Aziz Ali[1], Kamal Roslan[1], Akma Din[3], Norsafina[1], and M. Hasiib Mansor[1]

[1]Center for Earth Sciences and Environment, Faculty of Science and Technology, Universiti Kebangsaan Malaysia, 43600 Bangi, Selangor, Malaysia
[2]Geosciences Department, Faculty of Geosciences and Petroleum Engineering, Universiti Teknologi PETRONAS, 31750 Tronoh, Perak, Malaysia
[3]Bahagian Perkhidmatan Teknikal Jabatan Mineral dan Geosains Malaysia, Ipoh, Malaysia
Email: akmalanuar360@gmail.com

ABSTRACT

Lojing Geothermal Complex is located at Kelantan, Northeast of Peninsular Malaysia. In recent discovery, there are indications of more than fifteen areas of active hot spring sources within the Main Range granite complex. In terms of geothermal power prospect based on thermal activities, the complex is ranked on the top five among eighty locations in Malaysia. This study investigates the hot spring sources and circulation through 2-D electrical resistivity subsurface mapping and induced polarisation method. Correspondingly, balneotheraphy and geotourism have led progressive studies on the area due to an increase of attention among investors towards Lojing Geothermal Complex for recreational developments. Geologically the Lojing Geothermal Complex is cover by Late Triassic granite intrusion with porphyritic texture by feldspar act as its phenocryst, while the hot springs are induced by granite fractures nearby Sungai Ber. Four successive exploration wells were drilled within the studied area where the deepest depth is recorded up to 138 metre with 71.3 ˚C of water surface temperature whereas the rate of hot spring flows was in the range of 15241.82 gal/hour in accordance with V-notch reading. In order to increase geothermal gradient functions, the drilling process was enhanced up to 300 metres in depth for further exploration. High pH alkaline in the range of 9.02 to 9.22 suggested that there is an interaction of host rock within the hydrothermal system. The high amount of Na-bicarbonate and low sulphate concentrations from hydrochemistry analysis proposed that the non-volcanic origin of the complex is identical to other hot spring existences. A lineament study by using the rose diagram indicated that there are two major faults trending in NE-SW and NW-SE directions. The main affecting trends of the hot spring recharge source movements are 220˚ and 138˚ in directions. Comparatively, the structural geological mapping throughout Lojing Geothermal Complex found that there is a river situated about 7 km from the main source of hot springs. It is propounded that the river might act as the hydrothermal system recharge source since it flows in trend with the 220˚ fault line. In addition, a geothermometry study suggested that the reservoir temperature of the hot springs at Sungai Ber is up to 154˚C. Ten survey lines by using pole-dipole array were designed across the existing hot springs. The 2-D electrical resistivity inversion model has shown that the studied area is consisted of granite body fractures with funnel-shaped hot spring channels inside the fault trend. Highly fractured host rock as implication of tectonic activities increase the potentials for hydrothermal exploitation and well excavations. Accordingly, the binary cycle system technology is suitable for a potential geothermal electric power plant development.

Keywords: exploration, Lojing geothermal, hot springs

INTRODUCTION

Arose of geothermal potential interest in Malaysia has attract few investors to look upon its important and usage. Latest exploration has unleased more hot springs source for the need of Malaysia's energy and water supply demand. Malaysia growing rate of geotourism especially in recreational hub has make the construction upon hot springs theme park had increase the demand for new source and strategic area. This study introduces new area which could increase the harvesting geothermal potential in Malaysia. Lojing area is one of the most promising localities out of 80 hot springs source. Lojing Geothermal Complex consists of several clusters randomly distribute hot springs. There are two main localities of Lojing hot springs that are Sungai Ber recreational area located aside of main road and Sungai Mering only accessible 30 km via off road. Lojing is an area located at Main Range where the area is comprised of mainly igneous rocks and other lithology which are sediment and metamorphic rocks. According to Rahman and Mohamed (2001), major trend of the distribution of the rocks is in North – South direction. Igneous rocks can be found distributed at west and east flank of Kelantan at Main Range and Boundary Range respectively and also can be observed at the centre of the state as highlands. Nazaruddin et al, 2014 classified geology of Kelantan into 4 main groups. Two groups are from igneous which are extrusive (volcanic) rock and granitic rocks. The granitic rocks in Lojing

Highland is part of Main Range granite body. This granite body can be found scattered at the west side of Kelantan, Perak and Pahang. Raj (2009) mentioned that several enclaves of metasedimentary rocks are within the granitic body. The size of the xenolith is more than 10 cm. According to Ghani et al, 2013, the main rock type of the Main Range Granite Province is coarse to very coarse grained megacrystic biotite granite. Large sizes of K-feldspar phenocrysts up to 7 cm long are common and often show a distinctly megacrystic appearance in hand specimen.

METHOD

Hydrogeochemistry

Nine water samples are collected from randomly distribute hot springs along with three cold springs water in Lojing geothermal complex. Table 2 shows the code of water samples and its localities along with surface temperature and pH value reading that measured using multimeter at each sampling points. The sampled water was analyzed for major trace elements of SiO_2, Mg, Ca, Na, F, Fe, SO_4, HO_3, Cl and F at the Environmental Science (ES) Laboratories (M) Sdn. Bhd., Kuala Lumpur Malaysia. The elements of SiO_2, Ca, Mg, K, Na and Fe were analyzed by inductively coupled plasma (ICP), while dissolved Cl, and F were analyzed using UV spectrophotometer. Method analysis and detection limits used in this study are summarized in Table 1.

Table 1: The method used and its detection limits of cations and anions analysis for Lojing Geothermal Complex.

Parameters	Method Used	Detection Limit (ppm)
pH	APHA 3120B, 2005	
SiO_2	APHA 3120B, 2005	1
Ca	APHA 3120B, 2005	0.01
Mg	APHA 3120B, 2005	0.01
K	APHA 3120B, 2005	0.01
Na	APHA 3120B, 2005	0.005
Fe	APHA 3120B, 2005	0.005
HO_3	APHA 3120B, 2005	1
SO_4^{2-}	APHA 4500 SO_4^{2-}E, 2005	1
Cl	ASTM D 512, 1981	0.1
F	APHA 3120B, 2005	0.1

Geothermometry

Determination of hot spring water temperature of hot water component can be calculated using dissolve silica. This method is relevant towards warm springs water that either have lost heat by separation of steam or not lost heat before mixing. Truesdell and Fournier, 1977 has outline the analytical and graphical for estimating the temperature proportion of a hot water component mixing with cold water. Using the formulas (1), Fournier (1977) and (2) Arnorsson et al. (1983), the reservoir temperature could be estimate by silica geothermometry.

$$T = \frac{1309}{5.19 - \log [SiO2]} - 273.15 \quad \text{(quartz)} \qquad (1)$$

$$T = \frac{1112}{4.91 - \log [SiO2]} - 273.15 \quad \text{(chalcedony)} \qquad (2)$$

Geophysical survey

Electrical Resistivity Tomography, ERT and Induced Polarization, IP surveys were carried on Lojing geothermal complex. The resistivity and chargeability data are obtained using pole dipole protocol from SAS4000 resistivity meter and ABEM LUND ES10-64C electrode selector system. A total of 15 survey lines varies distance of 400m and 800m with electrodes spacing of 5m and 10m respectively. The measured resistivity survey data were interpreted using RES2DINV inversion software. The inversion method is based on smoothness constrained least-square method (Gauss Newton method). The ERT and IP modeling were optimized by an iterative method, which obtained through low root means square RMS, it reflects good geological correlation.

Lineament

Photo lineament study was carried out by utilizing the terrain map of Google Earth, SRTM (hill shade) and TIN. The focus of this study is on the mapping of negative lineaments, notably those which are directly or likely corresponding to the known/interpreted faults and fault zones or other basement fractures.

SRTM Image using the *Synthetic Aperture Radar (SAR)* technology consist of cells with each elevation. SRTM Image has to be convert into *Digital Elevation Model (DEM)* using ArcGIS software to visualize the negative lineaments. DEM image is generated at the higher topography with no lineament traces and the flat area. TIN Map (*Triangulated Irregular Network*) has been constructed from the contour of Sg. Ber Hot Spring topography base map.

Drilling exploration well

Field exploration was carried out using multi-speed rotary spindle type boring machine and accessories. Steel casting HW size 114.3 mm O.D. and NW 88.9 mm O.D. were used to prevent the collapse of the borehole walls. The boreholes were washed by circulating water from drilling pump and soil samples were collected for visual examination and laboratory testing.

Drilling has been carried out in accordance with good practice as detailed in ASTM D 2113. Drilling consists of obtaining core samples of the full depth of the strata being penetrated. Drilling competent and relatively un-weathered rock, conventional triple and double tube barrels were used. The letter type is confined to good rock without the significant presence of fractures and only swivel-type design is accepted. Non-retractable core barrels with 54.0 mm (N size) of core diameter was used. The core barrel is withdrawn and the core removed as often as may be necessary to secure the maximum possible amount of core. Coring runs are limited to a maximum length of 1.5 m. When less than 95% of the core is recovered from a run, the length of the following run is reduced by 50% recovery is achieved from two consecutive runs.

RESULTS AND DISCUSSIONS

Geological settings

Several hot springs in trend of cluster has been discovered within Lojing area of 64km^2 square area. Figure 1 shows the general geology map of Lojing Geothermal Complex. With two main group located nearby river valley of Sg. Ber and Sg. Mering area. Up to 2016, ten recognized and well-known hot springs source has been recorded by previous study. Newly discovered of three hot springs has merge Lojing area as wide geothermal complex make it already now has 13 out flow of natural hot springs with four artificial exploration wells. Besides, recently cold springs also discovered within this area. All hot springs found to be flowing out of exposed granodiorite outcrop and the cold, warm springs came out from laterite which has make an overburden layer throughout the mountain ranges. Highly fracture and numerous fault line within the main range and river channels of granite batholith seems to trigger the hydrothermal cycle of Lojing geothermal complex.

Lineament study

These lineaments were interpreted to represent discontinuities, such as faults, shear zones or major joints in the bedrock. The thick lines are interpreted as major faults or shear zones, and they are generally traceable for more than 2 km in length. Some of them are traceable continuously for up to 25 km long, notably those which strike almost N-S, NW-SE and NE-SW. The thinner lines are likely representing localized or minor faults and/or major joints. They are generally traceable in the order of 2 km long or less, refer (Figure 2).

Major and minor orientation of these lineament is measured and plotted on rose diagram as shown in Figure 3. Three set of prominent lineaments can be seen from Figure 3 that are, N-S (350-101 – 170-190), NE-SW (040-050 – 220-230) and NW-SE (140-160 – 320-340) lineaments.

Based on SRTM image the major lineament clearly conforms to terrain map from Google Earth image (Figure 4). Where it shows a group of three prominent lineaments are NE-SW (N220E), N-S (N358E) and NW-SE (N150E) lineaments.

From TIN map of Lojing Geothermal Complex reflect relatively consistence results compared to Google Earth and SRTM image, where two sets of lineament pattern exist. N-S (350-010 – 170-190) and NE-SW (040-050 – 220-230) lineaments (Figure 5).

The location of Sg. Ber hot springs HS 10, is found to be related and influenced to NS and NE-SW lineament precluded the NW-SE lineament as it is found to be dissecting not far from location of hot springs. The N-S lineament is prominent and notably between the eastern and central part of the map, (Figure 1). This refer to major basement fracture in Bentong-Raub suture line. Which prominently fractures of deep-seated major fault zone represent the subduction zone between Eastern and Western Belts of Malay Peninsula. While NW-SE lineament is an extension and correlated to regional structure of Bok-Bak Fault line.

Hydrogeochemistry

Physic-chemical analyses of the nine water samples from Lojing hot springs are given in Table 2. The temperatures of the springs vary from 48 to 73 °C and pH values vary between 7.1 and 9.3. The cation contents obtained from the analyzed water samples indicate that SiO_2 contents range from the lowest value of 57 to the highest value of 135 ppm with an average of 100 ppm. Na cation concentrations come as second highest cations with lowest value of 26 to the highest value of 54 ppm with an average of 42 ppm. Other cations such as Ca, K and Fe present in low concentrations with averages of 2.1, 2.3 and 0.71 ppm, respectively. For the anion concentrations, HCO_3 exhibits the highest contents ranging between 41 ppm and 100 ppm with an average of 67.5 ppm followed by SO_4 with concentrations vary between 6 and 22 ppm with an average of 15 ppm. Cl and F occur in very low concentrations with averages of 2.6 and 3.9 ppm, respectively.

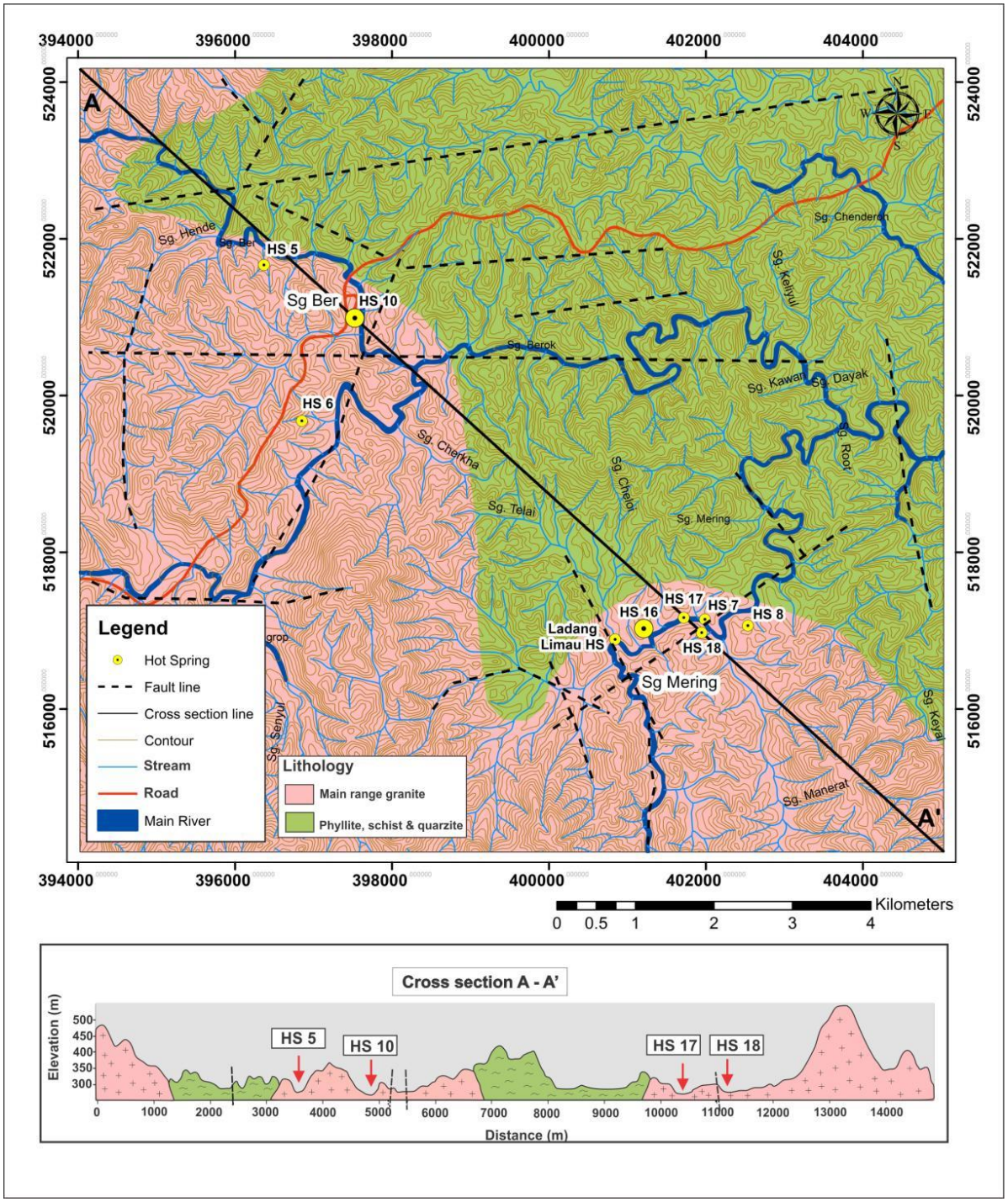


Figure 1: Geological map of Lojing Geothermal Complex area note that the yellow point is hot springs sources.

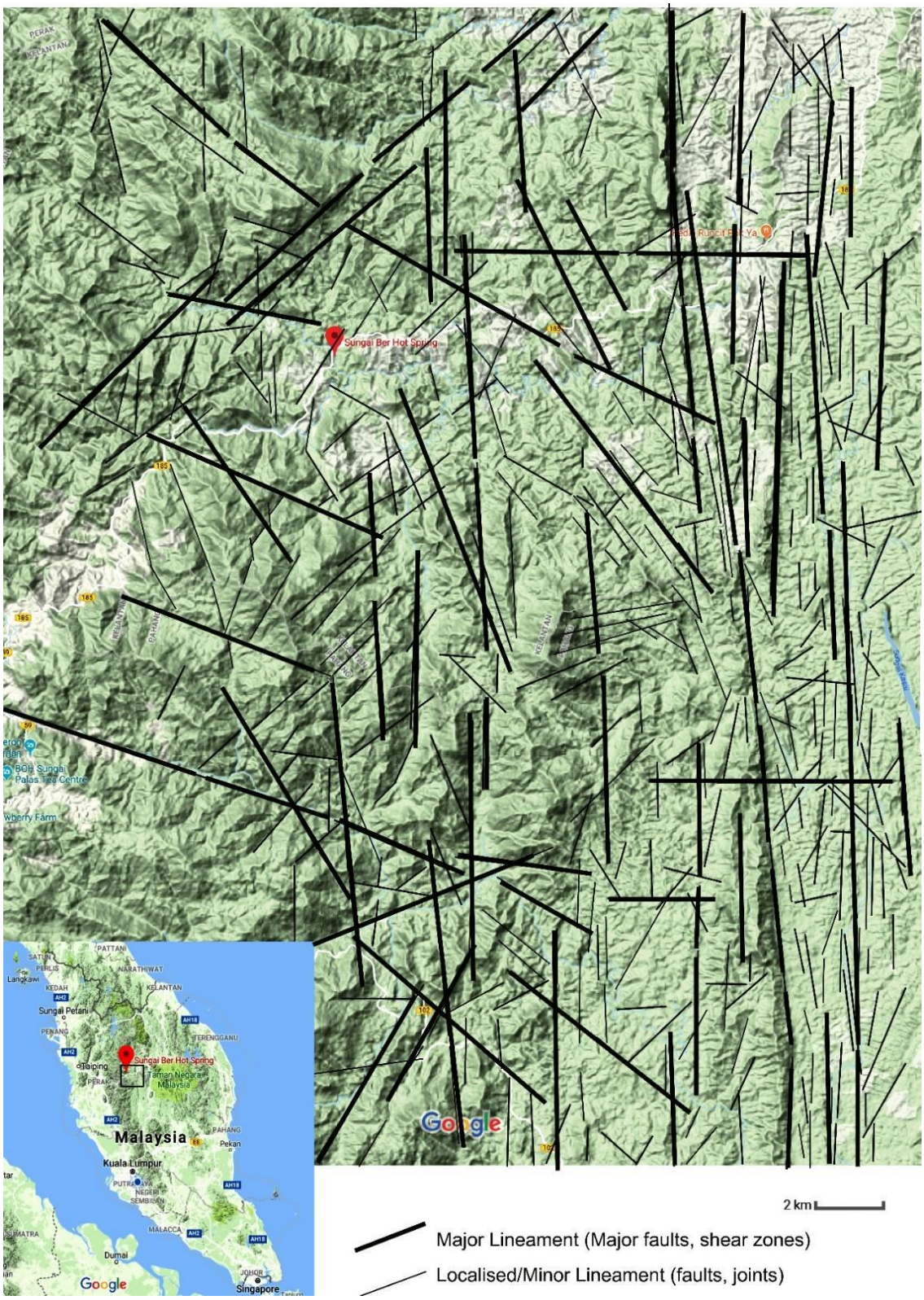


Figure 2: Regional lineament map of Lojing Geothermal Complex area note that the red pin point is Sg Ber hot springs.

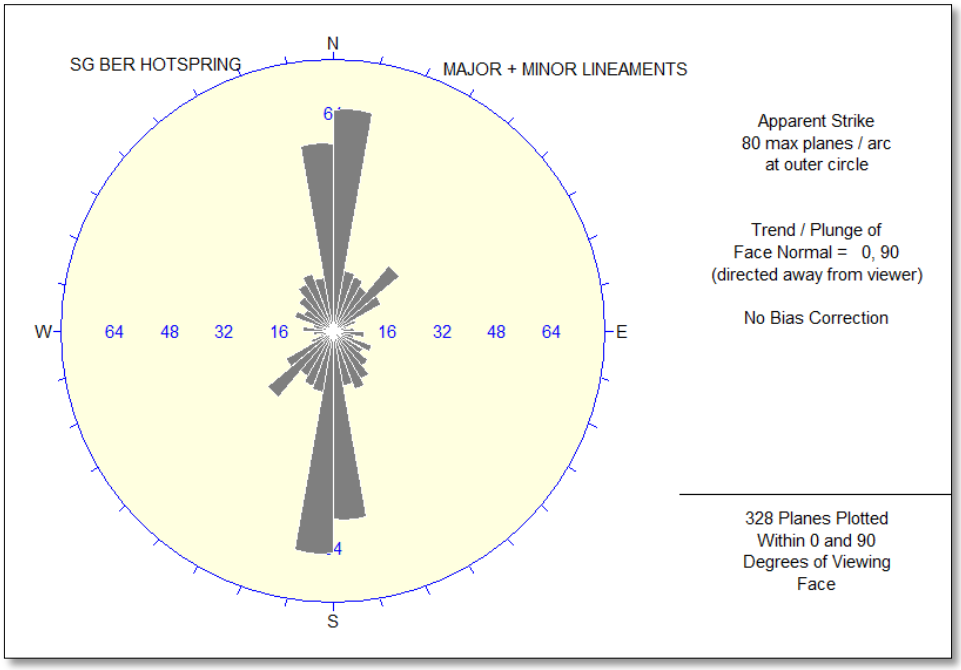


Figure 3: Rose diagram for all traceable lineament from regional Lojing lineament map.

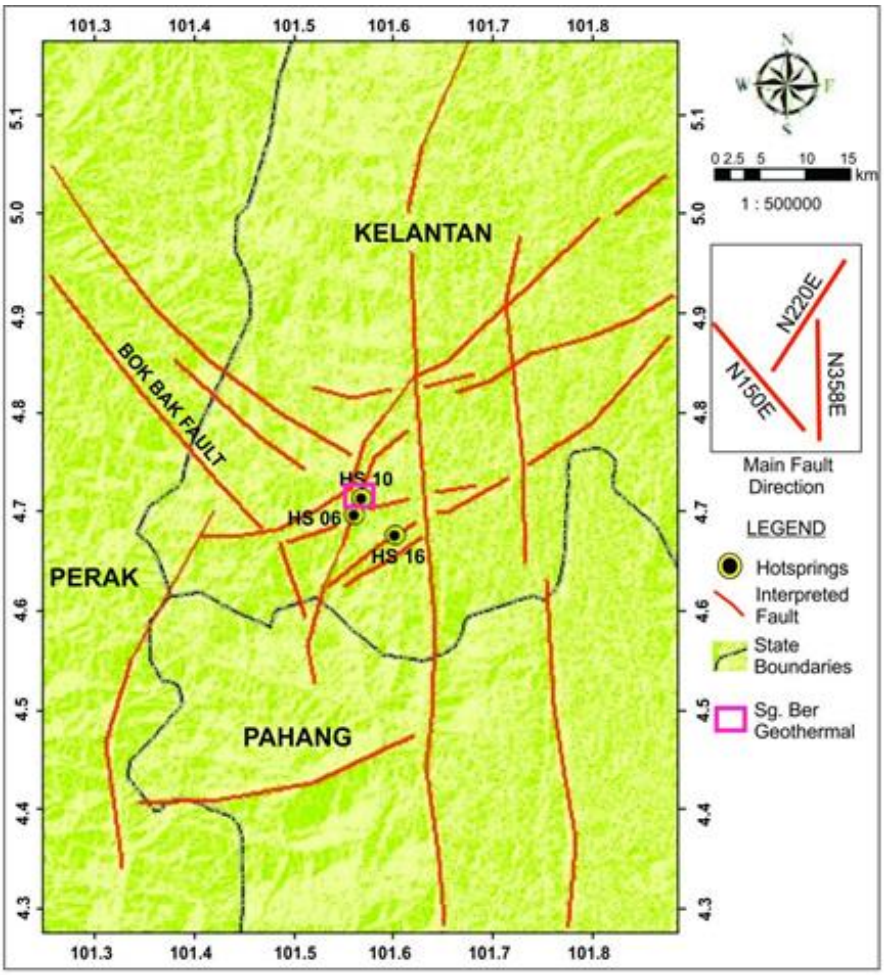


Figure 4: Filtered after raw interpretation for major lineament of STRM image, note that purple box is Sg. Ber hot springs.

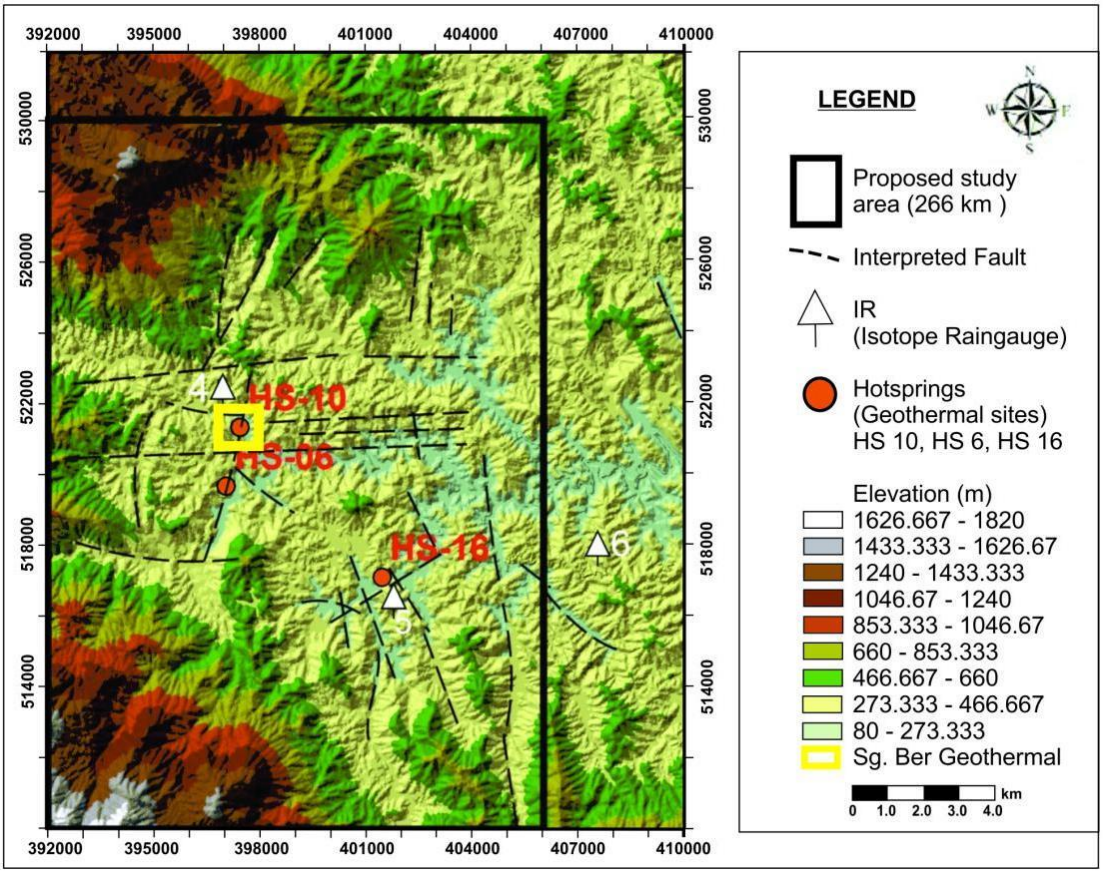


Figure 5: Lineament map from TIN (contour elevation) of Lojing Geothermal Complex.

Table 2: The cations and anions analysis of nine hot springs water samples in Lojing Geothermal Complex.

Hot springs	HS 70	HS 48	HS 45	HS 10	HS 11	HS 6	HS 16	HS 7	HS 8
S.T˚C	71	48	45.4	72	68	63	57	60	70
pH	9.2	9.2	7.13	9.2	9.1	7.5	9.3	8.4	8.5
Ca	1.9	2.1	3.53	1.5	2.2	1.6	2	1.9	2.3
Mg	0.1	0.1	0.37	0.1	0.2	0.1	0.1	0.1	0.1
Na	26	34	23.9	53	54	51	48	47	44
K	2.8	3.2	2.66	2.5	1.5	2.3	2.1	1.9	1.5
Fe	<0.05	0.2	5.58	<0.1	<0.1	<0.1	<0.1	<0.1	<0.1
HO_3	42	42	41	66	68	57	100	100	92
Cl	3.4	5.1	2.6	3	2	2	2	2	1.9
SO_4	9	18	6	20	22	20	15	14	12
F	3.5	3.2	3.4	5.4	5.4	5	3.6	3.1	2.5
SiO_4	135	125	112	134	63	125	57	75	70

Geothermometry

Values from quartz geothermometry ranges from 108˚C to 154˚C. Besides, temperature calculated from chalcedony are lower than quartz geothermometer. Chalcedony geothermometer range from 79˚C to 127˚C, (Table 3).

Table 3: Estimated reservoir temperature calculated from SiO_2 (quartz and chalcedony) from Lojing Geothermal Complex

Hot springs	T (Quartz)	T (Chalcedony)
HS 70 (new)	154.3244	126.898
HS 48 (new)	149.7014	122.1449
HS 45 (new)	143.2752	115.5549
HS 10	153.8734	126.4339
HS 11	112.5606	84.33047
HS 6	149.7014	122.1449
HS16	107.6742	79.40418
HS 7	121.3791	93.24949
HS 8	117.8418	89.66748

Geophysical survey

Three main resistivity and induced polarized IP pseudo profile has been selected out of 15 conducted survey lines. Four main resistivity survey lines has been conducted at well-known Sg. Ber recreational hot springs area. One survey line from well-known Sg. Ber area taken resembling those four survey lines. While another two resemble Sg. Mering and newly discovered Sg. Ber hot springs area. As their pseudo profile of subsurface mapping are interconnected to the geological structure exists at the field.

The inversion model shows that Survey line 1 (HSB2) in Figure 6, has high resistivity anomaly with resistivity values more than 800 Ωm. It indicates the granite bedrock with depth ranging from approximately 10 to 20 m. While, low resistivity zone with values less than 250 Ωm. This feature is located from 230m to 380m with depth in ranging 50m to 125m. This reflect the presence of highly conductive material, which, in this case by the presence of water in the fractured zone. Based to borehole data of tube well at 270m, the lithology of this area consists of unconsolidated sediments made up of loose to dense silty sand up to 14m, then followed by moderated fractured granite up to 108m.

Four survey lines were conducted in parallel towards each other in northeast to southwest direction. In order to see the fault trend and its relationship, hence fence diagram is used. Through structural correlation, the fractured zone is suggested to be aligned in the NE– SE direction. Figure 7 show a fence diagram of four survey lines that has been arranged to determine the correlation of fractured zone of each survey line. The hot spring aquifer is located within the fractured zone and dimensionally wider towards HSB5 (approximately 80 – 130m).

Based on the resistivity and induced polarization (I.P) profile as shown in Figure 8, low resistivity and chargeability values (0 Ωm - 400 Ωm and 0 ms - 7 ms) are interpreted as fractured zone that can be seen from 210m to 410m and 450m to 520m at the depth of 50m to 150m. The low values are due to infiltration of ground water into the fractured zones and can be clearly indicated by the present of hot spring at the center of the survey line. The red dash line illustrates the fracture orientation. High resistivity and induced polarization (I.P) values (900 Ωm - 100000 Ωm and 7 ms - 200 ms) are interpreted as granite bedrock. From field observation, massive granite outcrop is exposed within the Sg. Mering Hot spring area with several sets of fracture pattern. The intermediate resistivity value (400 Ωm - 4000 Ωm) is interpreted as weathered granite bedrock. A proposed drilling location has been proposed for hot water sampling and monitoring purpose at 230m labelled as PDL2. The minimum depth of drilling is 150m.

Newly discovered hot springs in Sg. Ber area are adjacent to the Sg. Ber recreational park just around 400 m towards west deep inside the jungle. This discovery was led by elephant trails, where the warm springs of HS 48 is seen to be as elephant mud pool and bath area. Figure 9 shows the connection of fracture system for HS 70 and HS 48. Where by elevation HS 70 located higher 20 meters on the hill slope. High resistivity and induced polarization (I.P) values (800 Ωm - 3000 Ωm and 1.6 ms – 2.0 ms) are interpreted as granite bedrock. The black dashed line indicates the fracture zone orientations. Low resistivity value from 0 Ωm to 250 Ωm at the depth of 100 m at HS 48 and 75 at HS 70 interpreted as the hot springs channel through fracture system inside granite body. Hot springs HS 70 at 190 m survey line SBR 1, shows distinctive granite outcrop boulder size, where the hot springs escape through side of the boulder. Two proposed drilling location has been proposed for hot water usage for new recreational theme park purpose at 135m and 250m labelled as PDL 1 and PDL 2 respectively.

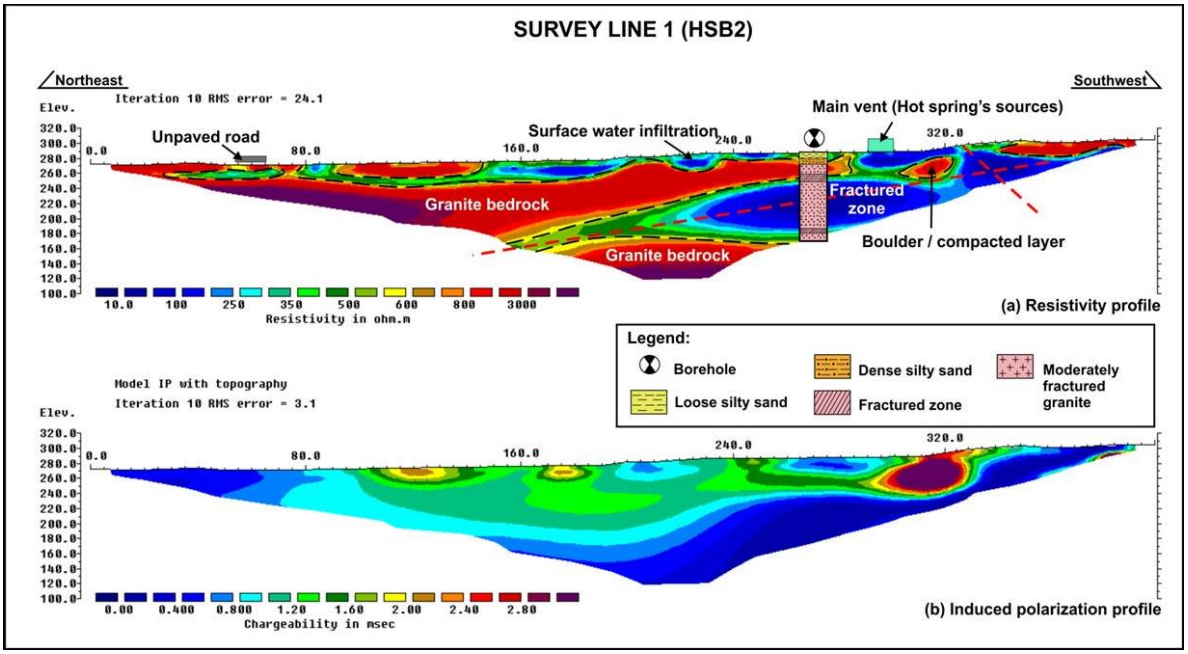


Figure 6: Pseudo profile of resistivity and IP for survey line 1 in Sg. Ber, note that this survey line cross on 100m well and hot springs source.

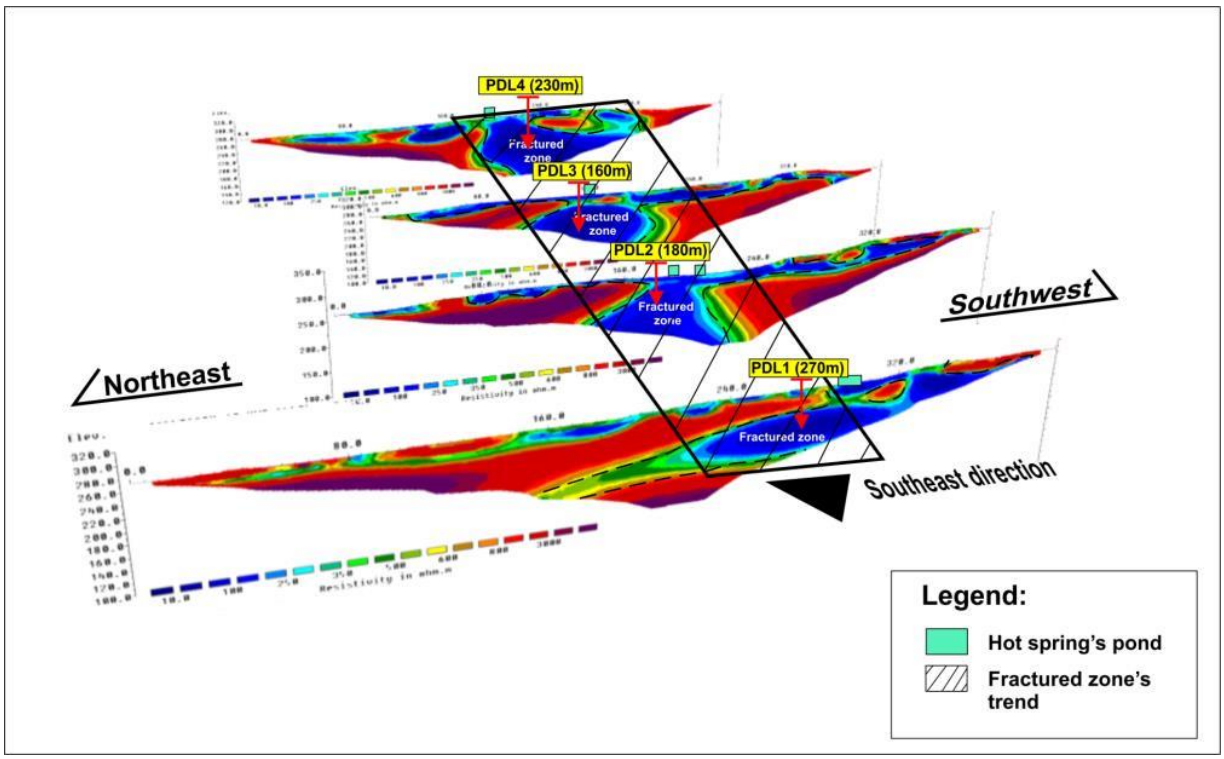


Figure 7: Fence diagram made up of four perpendicular resistivity survey lines at Sg. Ber recreational area. The black box label shows the connected direction of fracture zone in Sg. Ber area toward Southeast direction.

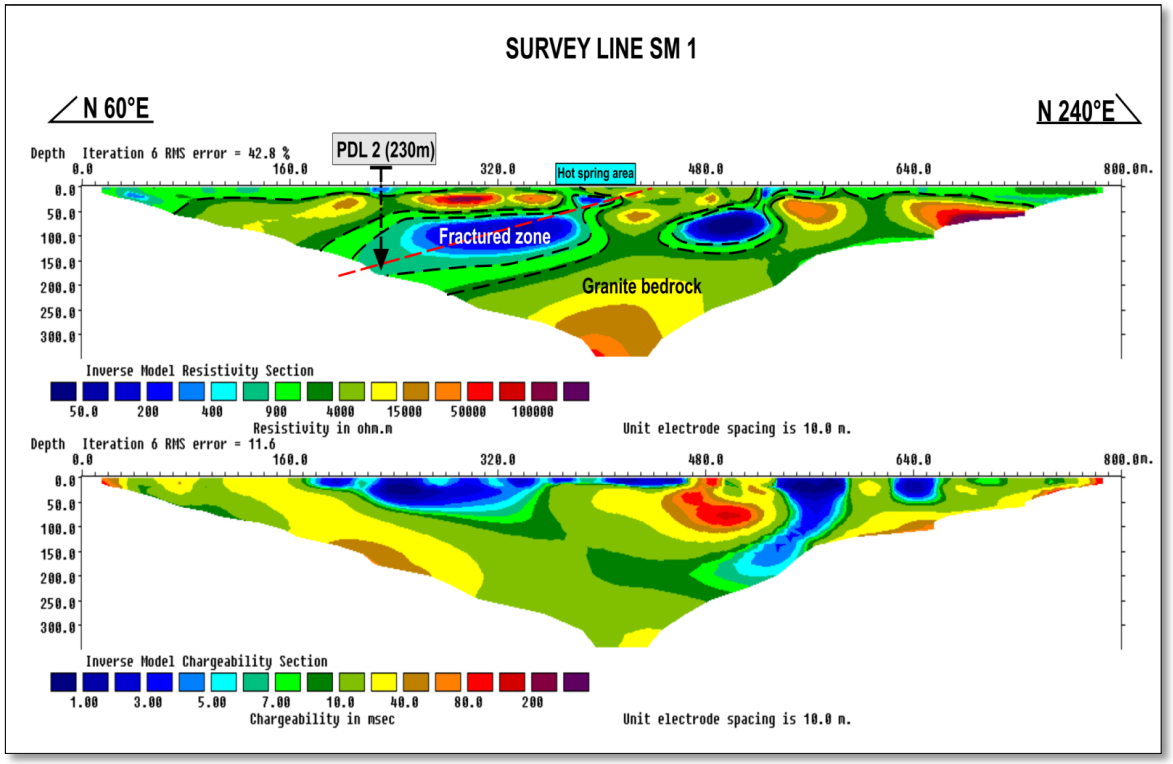


Figure 8: Pseudo profile of resistivity and IP for survey line 1 in Sg. Mering with PDL 2 at 230m of the survey line.

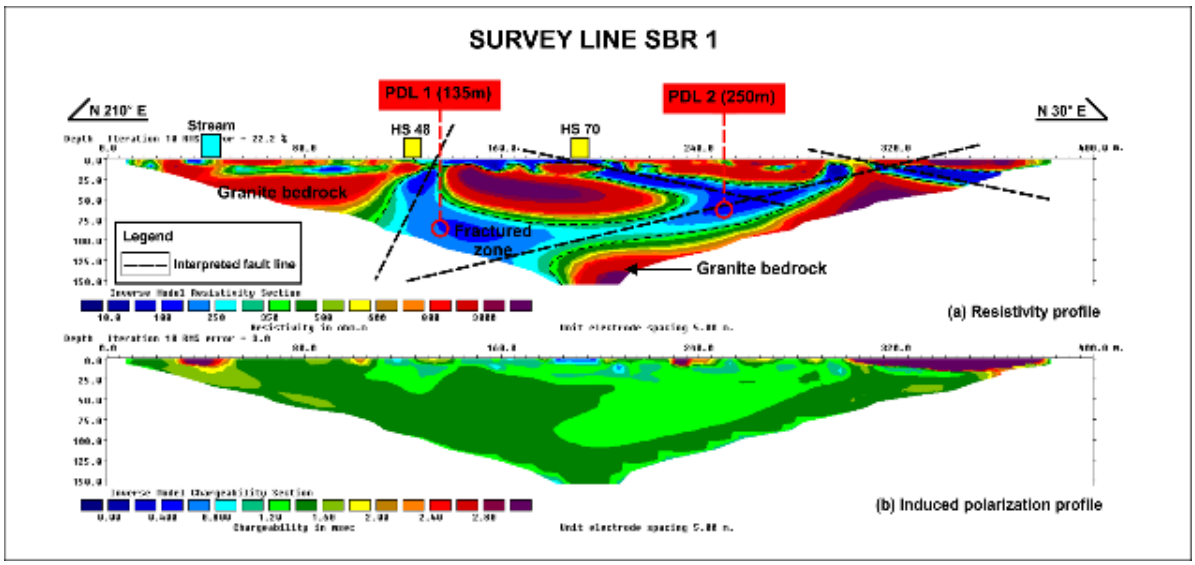


Figure 9: Pseudo profile of resistivity and IP for survey line 1 in Sg. Ber adjacent to Sg. Ber recreational (HSB survey line) area conducted through hot springs of HS 70 and HS 48

Drilling exploration well

Four exploration well managed to be drilled within one year around start form 2018. The exploration mainly focusses on one km^2 square area nearby main source of Sg. Ber natural hot springs recreational area. Two drilled holes at depth of 10 and 30 meters were mainly focus on coring for petrographic analysis, while another two at 100 and 138 meters for tube well. These four drilled holes turned out to be artificial hot springs well as the pin point location are suggested based on geophysical survey at fault lines. The wells are still under monitoring and its aim to fulfill the need of local electricity needs of rural area. Two exploration well best present these project that is the 30 m and 138 m well.

For 30 meters sampling well, the coring process managed to obtain granite specimens. It consists of accessories minerals such as biotite, muscovite and calcite veins. The percentage of biotite is quite high. Hence, the name of the granite is Granite Biotite.

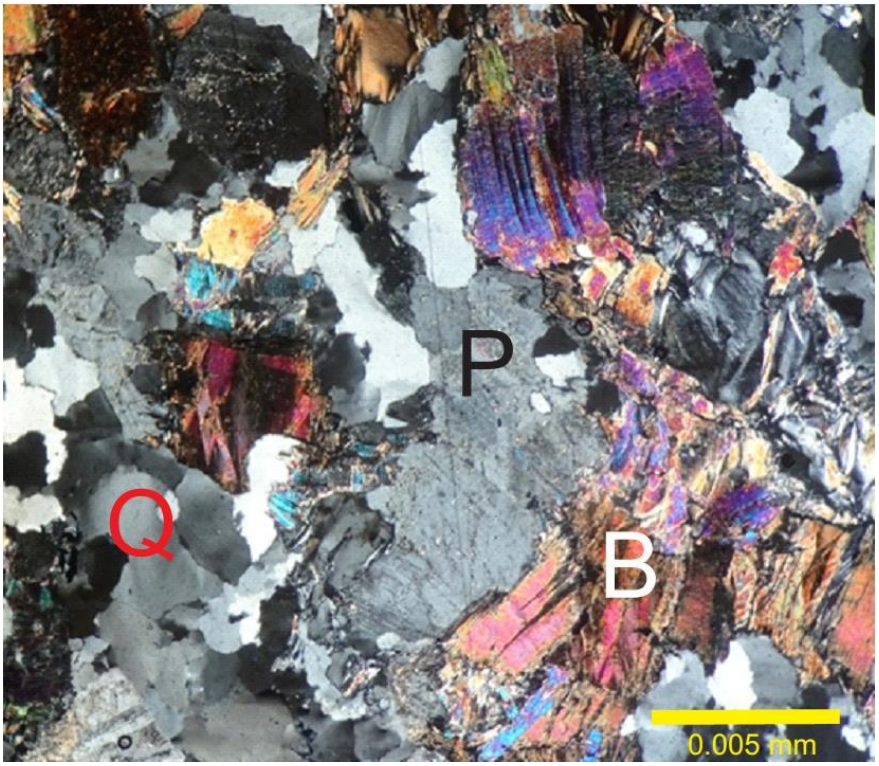


Figure 10: Photomicrograph of core sample from Sg. Ber showing grains of quartz (Q), plagioclase (P) and biotite (B) that made up this Biotite Granite.

This granite biotite is slightly weathered. This granite biotite has highly fractured at the depth of 10.5 meters to 15 meters. At this highly fractured part is where hot water can be found.

Petrography study for Sg. Ber granite biotite selected among the best less altered and fresh samples out of three core samples. It consists of medium grained quartz, plagioclase, and alkali feldspar with holocrystalline phaneritic equi-granular texture (Figure 10). Other minerals present are biotite and hornblende which made up about 15 % of the rock mass by volume. The grains are tightly interlocking with each other and it seems that the sample was not affected by any tectonic process as there is no fracture detected in this sample. Its mineral composition suggests that this rock is biotite granite.

For 138 m exploration well, chunk of samples is obtained as the drilling bid is used. The lithological profile of 138 m well is made up of loose, dark grey, silty sand with some of gravels sand is fine to medium at depth of 0 m - 5 m. Then dense, dark grey, gravelly compounds of sand with medium to coarse sizes at depth of 5 m - 9 m. Depth further, contact of poor, dark grey to pale grey, moderately fractured and moderately weathered granite at depth of 9 m - 14 m. Next, the lithology changed from poor to moderate, dark to light grey, moderately fractured and moderately weathered schist at depth of 14 m - 30 m. Then it is continuously, consist of medium grey, slightly to moderately fractured granite from depth of 30.0 to 138.0 m.

Two interconnected and related fractured zone has been obtained from drilling process as the 100m and 138m well as it is just adjacently 10-meter distance of separation. Where physically huge outburst of hot springs water was observed, and this can also be seen from the pattern of surface temperature monitored during the process in Table 4.

Table 4: The average surface temperature reading during drilling process for two exploration wells in Sg. Ber, Lojing Geothermal Complex.

Exploration Depth (m)	100m well S.T (°C)	138m well S.T (°C)
24	47	45
40	51	60
50	56	51
60	59	40
70	69	42
80	67	53
90	65	56
100	66	65
120		68
138	Nil	71

For both 100 m and 138 m well by comparison, fractured zone contact at depth of 32 meters with rate of water flow, Q=4449.72 Gal/h for 138 m well, while fractured zone contact at 16-meter depth for

100 m well with rate of water flow Q=619.52. Gal/h. Next come the second contact of hot springs water bearing fracture within the 138 m well the fractured zone is at 118 meters depth with rate of water flow Q=15241.82 Gal/h, while the fracture zone in contact at 90m depth with rate of water flow of Q=9662.40 Gal/h for 100 m well. The maximum temperature of groundwater achieved at 138m depth, which is 71°C.

Geothermal potential

Based on the temperature, volume and reservoir parameter, energy capacity of geothermal for electricity in Sungai Ber, Kelantan was estimated using volumetric method. For comparing the result, potential energy calculation based on volumetric method also included. This volumetric method uses one phase of model extraction. Thermal energy that content by rock and water were calculated. Recovery factor represent the small part of the total heat content that can be utilized back from the water and rock. Thermal energy obtained is convert into electricity potential using conversion, function from temperature. The plant life is the result of how long the field potential can be converted. The formulae used to calculate the power capacity is formulae (3).

Power Capacity = (Tr-Ta) x {(1-f) Cprρr + f Cpwρw} x V x RF x CE / (LF x PL) (3)

where,

ρr, ρw	: rock density and fluid density (kg/m3)
Cpr, Cpw	: rock specific and fluid specific heat (kJ/kg-0C)
Tr, Ta	: reservoir temperature and abandonment temperature (0C)
f	: porosity (%)
V	: reservoir volume (km3)
RF	: recovery factor (%)
CE	: conversion efficiency (%)
PL	: plant life (year)
LF	: load factor (%)

Reservoir volume is estimated by identifying the size of the catchment and reservoir area by aerial imaginary and the depth of the reservoir is set at 1000 m depth. Reservoir average temperature and abandonment temperature is based on geothermometer. The resources are a low enthalpy geothermal, the subsurface temperature is estimated as the minimum temperature and 140ºC as the maximum temperature. Rock density that is used as an input is 2750 kg/m^3 that is the experimental density of the granite collected from the Sungai Ber geothermal field. The minimum rock specific heat is set at 0.8 kJ/kg ºC and the maximum is about 1.0 kJ/kg ºC. The rock specific heat is taken base from Standard National Indonesia (SNI 13-6482-2000). The porosity of the rock is 0.15 based on the experimental porosity of the Sungai Ber geothermal field granite. The recovery factor of the geothermal binary plant is set at 25% with the efficiency of the plant to generate and convert energy from the geothermal source is set at 10. The life time of the plant is set at 30 years with the load factor is around 90%. The average power that can be produce by a single well in the area is in the range of 3.14 – 3.25 MWe. Assuming the 3 artisan well-constructed is use as a production well, the total power produce by the three wells are in the range of 9.42 - 9.75 MWe.

Geotourism aspect

As for geotourism aspect, the three newly discovered Sg. Ber hot and warm springs are easily accessible through main road from Cameron Highland to Gua Musang road. Where it just 50 km away from Cameron Highland that is main tourism attraction for coldness of high-altitude weather. The warm springs of HS 45 and HS 48 is recommended for future well exploration to harness the natural pH and favorable temperature for balneotheraphy. Where the hot springs of HS 70 with granite outcrop is proposed for geoheritage site and tourist attraction point. Where usually local society would use it to cook and boil their food by wrapping it with plastic bag. Besides, the Lojing Geothermal Complex is the widest hot springs source in central belt of Malaysia, and there is rarely found hot spring at this region. With lush green preserved tropical jungle and rivers, it surely attracts more tourist to pass by and take a rest for a tranquil vacation. A private investor had an interest in future project that would focus on the infrastructure within the new discovered hot springs park, where chalet and pools will be built for geotourism.

Overview

The distribution pattern of hot springs in Lojing Geothermal Complex can be correlate with lineament patterns from Google Earth, STRM and TIN mapping images. Besides, resistivity survey of resistivity and induced polarization analysis shows the hot springs sources has channel up via highly fracture zones within granite body. The newly discovered hot springs HS 70 and warm springs HS 48 are interconnected via fractured system as shown in resistivity analysis. Yet the temperature different might has relationship with the flow of river water throughout the valley. Where HS 48 is just 80 meters away from the river. Mixing and infiltration of river water and water table within the valley has affected the geochemistry of this warm springs. Although slightly different in minerals content such as SO_4, Na, K, Fe and Cl can be seen by comparing this both hot springs. Yet high amount of dissolve SiO_4 with 125-135 ppm shows significant similarity. In hypothesis both hot springs water came from the same reservoir and interconnected with each other. High pressurize hot springs of HS 70 with higher elevation make it intrude as less mixed hot springs water. Whereas HS 48 temperature has almost

similar elevation with the river and high pressurize upcoming pressure of HS 70 has make HS 48 pressure lower and catalyst the infiltration of river water into its cycle (Sasaki et. al, 2013). Physically the higher rate of flow at HS 70 is observed with vigorous bubbling effect.

Two interconnected horizontal fracture zones have been detected by drilling process of 100 m and 138 m well. The well is categorized as artesian well.

The hydrothermal water cycle within Lojing Geothermal Complex has been influence by meteoric water from surrounding surface as its recharge in low amount of Cl^- ions as it categorized as Na-HCO_3 and Na-Ca- HCO_3 types (Sasaki et. al, 2013). Deep seated fault and highly fracture granitic body nearby to the contact of metamorphic rocks has made up this geothermal complex as randomly distributed over huge area (Purnomo & Pichler, 2014)(Qi et al., 2017). Low amount of sulphurous mineral inside Lojing Geothermal Complex indicated it is a non-volcanic sources and the reservoir is not related to volcanism (Baioumy et. al, 2015). High amount of Na^+, K^+, Ca^{2+}, S, SO_4^{2-} and Cl^- ions within the geochemistry of water promote high health benefits and qualified as for balneotheraphy purposes (Hamzah et. al, 2013).

CONCLUSION

Newly discovered three hot springs in Sg. Ber of Lojing Geothermal Complex area are highly recommended for geothermal exploration and exploitation. These hot springs are classified as non-volcanic origin and Na-HCO_3 type hot springs. Highly fracture granite within mountain ranges has sustained its hydrothermal cycle within deep seated faulted system.

REFERENCES

Abdul Rahim Samsudin, U. H. (1997). “Thermal Springs of Malaysia and their potential development”. Journal of Asian Earth sciences, Vol. 15, 275-284.

Baioumy, H., Nawawi, M., Wagner, K., & Arifin, M. H. (2015). "Geochemistry and geothermometry of non-volcanic hot springs in West Malaysia". Journal of Volcanology and Geothermal Research, 290(December), 12–22.

Arnórsson, S., (1983). "Chemical equilibria in icelandic geothermal systems—Implications for chemical geothermometry investigations". Geothermics 2, 1983, 119-128.

Ghani, A. A., Searle, M., Robb, L., & Chung, S. L. (2013). "Transitional I S type characteristic in the Main Range Granite, Peninsular Malaysia". Journal of Asian Earth Sciences, 76.

Hamzah, Z., Abd Rani, H. L., Saat, A. and Wood, K. (2013). "Determination of Hot Springs Physico-Chemical Water Quality Potentially Use for Balneotherapy". Malaysian Journal of Analytical Sciences, 17(January 2018), 436–444.

Nazaruddin, D. A., Fadilah, N. S., & Zulkarnain, Z. (2014). "Geological Studies to Support the Tourism Site: A Case Study in the Rafflesia Trail, Near Kampung Jedip, Lojing Highlands, Kelantan", Journal of Tropical Resources and Sustainable Science 2014 (July), 835–851.

Purnomo, B. J., & Pichler, T. (2014). "Geothermal systems on the island of Java, Indonesia". Journal of Volcanology and Geothermal Research.

Qi, J., Xua, An, Wu, Zhang, Li, Lu, G. (2017). "Characterizations of Geothermal Springs along the Moxi Deep Fault in the Characterizations of Geothermal Springs along the Moxi Deep Fault in the Western Sichuan Plateau, China". Physics of the Earth and Planetary Interiors, 263(January), 10–22.

Sasaki, K., Ueda, A., & Zhang, J. (2013). "Geochemical Study of Hot Springs Associated with New Geothermal Exploration in the Eastern Part of Toyama Prefecture, Japan". Procedia Earth and Planetary Science, 7(December 2015), 766–769.

CHARACTERIZATION OF CHANGING SURFACE MANIFESTATIONS IN AN EXPLOITED GEOTHERMAL FIELD - HIGH ENTHALPY SYSTEM IN INDONESIA

Lily Suherlina[1], Maren Brehme[2], Juliet Newson[1], and M. Yustin Kamah[3]

[1]Iceland School of Energy, Reykjavik University, Menntavegur 1, 101 Reykjavík, Iceland.
[2]GFZ, Germany, Telegrafenberg, 14473 Potsdam.
[3]PT. Pertamina UTC, Jl. Medan Merdeka Tim. No.6, RT.2/RW.1, Gambir, Kota Jakarta Pusat, Daerah Khusus Ibukota Jakarta 10110, Indonesia
Email: lilyahmad79@gmail.com

ABSTRACT

The test ground for this study is a high-enthalpy geothermal field, in eastern region of Indonesia which has been producing 80 MW and 120 MW respectively from two different geothermal systems. Prominent surface manifestations around the field are hot springs and steam-heated ground. Changes appear in the manifestations probably related to the geothermal activity. A combination between water chemical analysis and field measurements are used to document surface manifestation changes in 2010, 2011, 2012 and 2018. The water analysis includes fluid composition and physicochemical parameters of spring waters. The field visits focused on recording physical changes in the manifestations. The results show the spring waters are evolving toward lower pH and saline. High metal cation concentrations observed in the water. Outcrops and rock samples show acid alteration minerals. Increasing ebullition and changes in size, and water color are obvious in most springs. The changes overtime in surface manifestations may be associated with exploitation activity of the geothermal system and reactivating of tectonic-volcanism activity. The combination of both activities triggers changes of the hydrothermal system and influences the characteristics of the hot springs at the surface.

Keywords: Surface manifestation, monitoring, Lahendong geothermal field

INTRODUCTION

Geothermal surface manifestations are expressions of conditions in the subsurface. Production from geothermal reservoirs can induce changes in surface geothermal features. In boiling systems, drawdown and boiling can be followed by increased activity of surface manifestations leading to increased surface heat flow (Scott, 2012).

QUANTITATIVE CHANGES IN HOT SPRINGS

To investigate temporal changes of spring waters in this geothermal field, water chemistry was analyzed in October 2010, October 2011, March 2012, November 2012 and April 2018. The data from each spring is plotted over time to show chemical changes of the waters. Figure 1 and Figure 2 respectively show two periodical changes of the spring water with respect to Electrical Conductivity (EC) and acidity (pH).

In general, according to Figure 1, the electrical conductivity, as an indicator for salinity, mostly increased during 2010-2012, with a significant increase in M4 and M9. Between 2012-2018, most of the values increase although two springs (M9, M4) decrease to less than original value.

The temporal changes in pH (Figure 2 2) shows the values below four during the surveyed years reflecting the high acidity of spring waters. There are two values (M11, M13) that have pH values higher than 5 throughout 2011-2012, then recently becoming strongly acidic. The steepest decline occurs in M11 and M3.

There is a contradictive trend between temporal charts of EC and pH that indicates the parameters can be associated. For example, the upward trend of EC (Figure 2 2) in hot spring relates to the downward trend in pH and vice versa. A clear example can be seen in orange line (M4) which has low pH below 2 (March 2012 - November 2012) and has high EC; in 2018 EC decreases and the pH increases. This can be related to extensive leaching of surrounding rocks as a result of aggressive pH in the water. The dissolved minerals provide the constituents that increase the conductivity.

The general trend for pH and EC in April 2018 shows the waters to have more dissolved constituents be more acid. In general, the acid waters could be due to increasing volcanic degassing H_2S and reservoir boiling. H_2S is acidic volcanic gas (Lee et al., 2018) and is abundantly p resent in the field and confirmed by the previous gas analysis (Brehme et al., 2015).

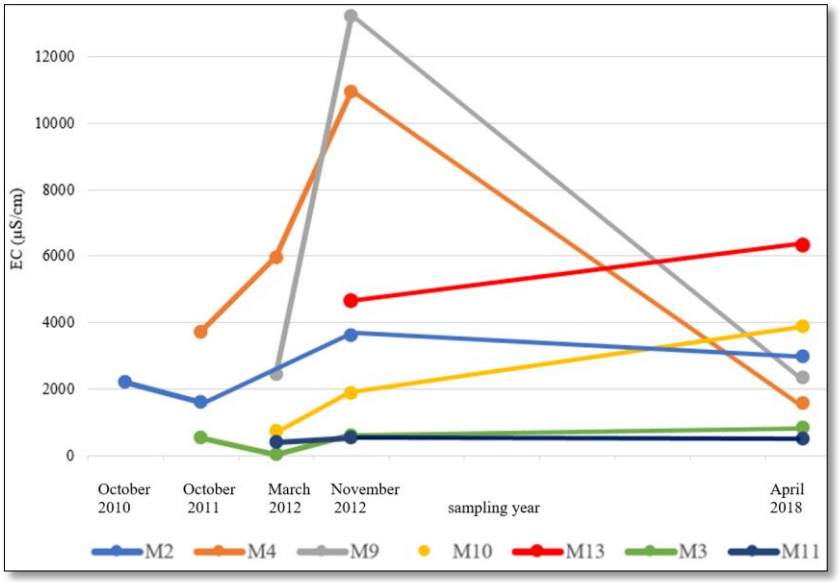


Figure 1: Temporal changes of Electrical conductivity at hot springs during 2010-2011, 2012 and in 2018.

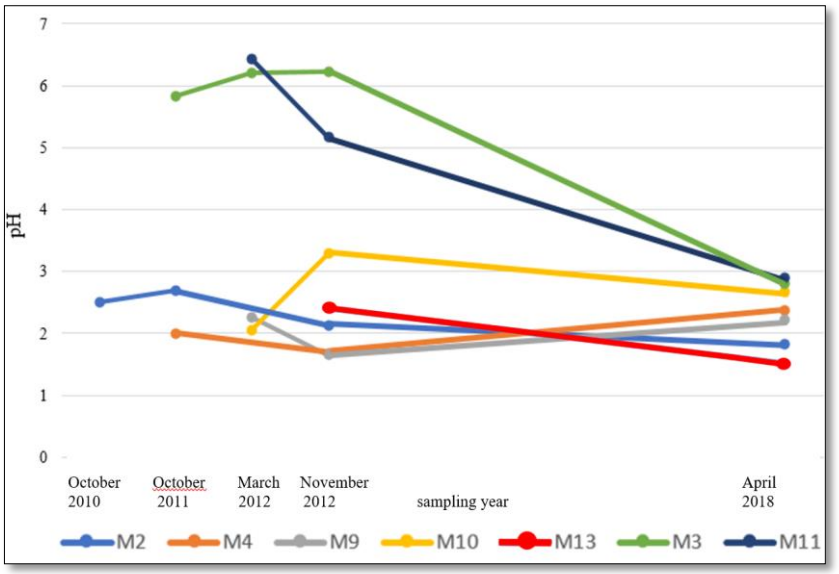


Figure 2: Changes of acidity (pH) for hot springs during 2010-2012, and in 2018.

The study area is surrounded by active volcanoes in the north and south (Surachman et al., 1987) which potentially are major sources of H_2S. H_2S at the surface in 2018 may be triggered by increasing volcanic activity of Mt. Lokon (sources: personal communication; online newspaper of Indonesia (Kumparan)) which is close to the area. Reservoir boiling, at one hand, can contribute to creating steam which will also contain H_2S. This appears to be happening because some wells are showing a trend of increasing steam content.

In regards to increasing salinity, oxidation of hydrogen sulfide (as shown by Equation 1) produces acid sulfate waters which are very reactive to leach out silica and metal cations (Nicholson, 1993). The leaching will eventually generate high concentrations of the dissolved elements in the water and raise the EC.

$$H_2S_{(g)} + 2O_{2(aq)} = 2H^+_{(aq)} + SO_4^{2-}{}_{(aq)} \quad (1)$$

QUALITATIVE CHANGES IN HOT SPRINGS

A primary objective of qualitative temporal analysis is to observe physical changes in hot springs. Three hot springs (M11, M10, M2) are used here to provide comparisons for 2012 and 2018. Their location is shown in Figure 3. The comparisons focus on 2012 and 2018 based on data availability. Two field visits were carried out during 2018 (April and November). The physical changes considered in hot springs include water clarity and color,

ebullition and gas discharged, size, pH and temperature. The changes are described as follows:

M11

This hot spring is within a local farm and lies adjacent to a creek. The bare rock is altered, and the area is surrounded with abundant grasses. Access is relatively difficult. There are two active bubbling spring pools, one small and one large size. Only the large pool will be discussed here as the most significant feature. The bubbles and diameter of pools could not be photographed due to heavy steam, very active boiling and geyser-like activity in the pool. Hence the access for taking photo was very limited (Table 1).

M10

Access to reach M10 is easier than M11 as it is in the bathing area. The prominent feature of activity is an area of steaming ground and intensity of the diffuse steam discharge. It can be categorized as steaming ground (Table 2).

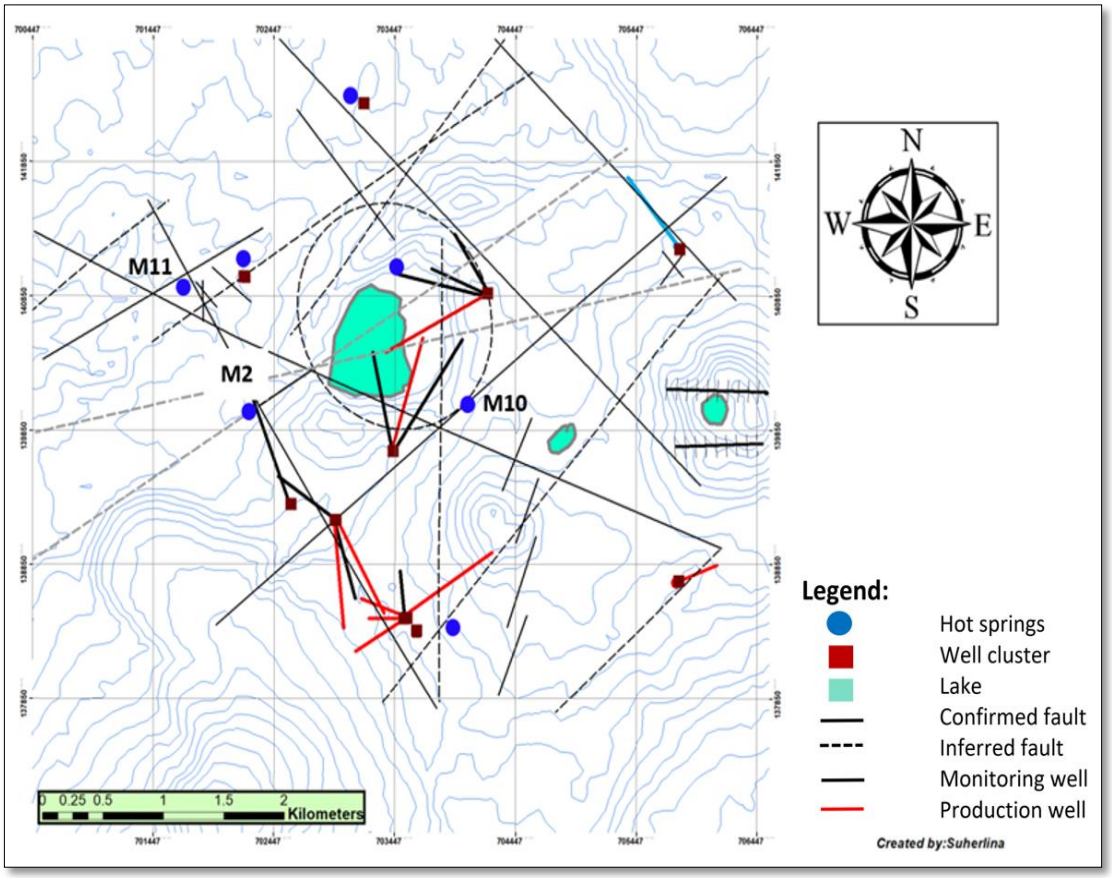


Figure 3: Location of hot springs in M11, M10 and M2.

Table 1: Observed parameters toward changes in M11.

Date	Color	Ebullition	Area	pH	T (°C)
November 2012	Blue-green, slightly cloudy	Minor gas discharge	Pool was not formed	5.16	36.3
April 2018	Blue-green, slightly cloudy	Major gas discharge and bubbling, geyser like eruptions	Pool was approximately 70 cm	2.89	67
November 2018	Blue-green, slightly cloudy	Increased gas discharge and more bubbling, geyser like eruptions	Pool was approximately 1.20 m	2.74	62



Figure 4: Visual features in M11.

Table 2: Observed parameters toward changes in M10.

Date	Color	Ebullition	Area	pH	T (°C)
November 2012	-	Weak steam discharge	-	3.29	72
April 2018	-	Strong steam discharge	-	2.67	24.9
November 2018	-	Very intense steam discharge	-	2.52	66.1



Figure 5: Visual features in M10.

M2

M2 is very easy to reach because it is located in open space and strong smell H_2S guides one to the place (Figure 6). Color is the most obvious physical change observed in M2, as well as bubbling activity in the pool. The water level also changes moderately during the years of observation (Table 3).

Changes in hot springs can inform permeability distribution and reservoir dynamics. First indications are that a reactivation structure currently occurs near M11 (Figure 4) and M10 (Figure 5). This is very likely related to an opening of sealed structures. In M11, for example, there is the new formation of large active pool which previously did not exist. Other evidence is at M10 which now has more abundant gas discharge through small fractures than previously noted. In 2012, there was a very minor gas discharged compared to 2018. Moreover, active ebullition in form of bubbling was observed in hot springs in November 2018.

There are several possible reasons for an increase in heat discharge at the surface. One explanation is that reservoir boiling has increased the steam flow to the surface. The other possibility is there have been changes in permeability due to tectonic strains (opening of new fractures) as the result of an earthquake, or mineral dissolution. There has been a major earthquake (7.5 Mw) in Sulawesi in 2018 (Joint Research Centre EU, 2018) and this may have been a trigger for the permeability changes. It is possible that both of the above effects are acting concurrently, whereby a permeability change caused by seismic activity causes a pressure drop and boiling.

Another change found in surface manifestations is M2 which experiences decreasing water level and color changes. Possible reasons for the water level change are the influence of rainfall, which affects groundwater levels, and the amount of steam condensate. The spring was clear green, turning into green-milky color in 2018. There is possibly more condensed steam and relatively less groundwater in the spring, leading a drop in pH and hence increasing rock dissolution.

Table 3: Observed parameters toward changes in M2.

Date	Color	Ebullition	area	pH	T (°C)
November 2012	Green-clear	Calm	Water level parallels to rim, 15 m diameter	3.29	72
April 2018	Green- milky	Moderate bubbles	Water level below to rim, 9 m diameter	2.67	24.9
November 2018	Green-milky	Strong bubbles	Water level below to rim, 9 m diameter	1.11	62



Figure 6: Visual features in M2.

RELATIONSHIP OF PH, EC AND XRD ANALYSIS OF HOT SPRINGS

This section discusses analysis of the relationship (quantitative, qualitative) of hydrochemical parameters and XRD investigation to verify existence of primary and alteration minerals in rocks.

Qualitative relationship analysis

The analysis shows relationship among geochemical parameters or elements in a scatter plot. The relationship can be positive or inverse depending on how the elements influence each other. The objective of doing qualitative relationship is to show the trend between the elements. One interesting relationship to discuss here is Figure 7 shows an inverse relationship between pH and EC (Electrical Conductivity).

In general, the trend is inverse for all hot springs (Figure 8), referring to an increasing value of EC is followed by a decreasing pH. The lowest acidity (around 1.5) and highest EC (around 6200 µS/cm) is in M13. M11, on the other hand, has the highest pH (2.89) and the lowest EC (400 µS/cm) compared to other hot springs.

The inverse relationship on Figure 7 indicates low pH in the waters lead to increased EC value. This suggests strongly acidic waters aggressively dissolve the minerals from rocks. The high dissolution increases the concentration of dissolved ions in water, therefore the conductivity increases. The outlier trend of M10 in the figure can be explained by the different fluid evolution in this spring. This relationship also explains the trend between EC and pH in the previous temporal plots (Figure 1, Figure 2).

XRD study

The rocks study was carried out using the XRD (XRay Diffraction) method to identify minerals in rocks and solid samples. XRD patterns are directly related to crystal structures. XRD analysis provides information on dominant minerals in the rocks. The measured samples have been taken from the near vicinity of hot springs to analyse hydrothermal alteration assemblages. Reservoir rocks in Lahendong are andesite and volcanic breccias (Koestono, 2010). Typical minerals in the altered rock samples include kaolinite, sulphur, quartz, silica, hematite, cristobalite, pyrite, hematite, goethite and alunite (Brehme, 2015). There are four hot spring samples used XRD investigation M9, M13, M10 and M4 as shown on Figure 8. In general, the predominant alteration minerals from the vicinity of M9, M10, M13 and M4 are cristobalite, sulfur, goethite, hematite, and anhydrite. Some primary minerals including pyroxene, olivine, biotite and muscovite. The dominant clay minerals are illite and epidote. The above minerals are relief high temperature alteration. Condensate apparently compose the spring waters in the Lahendong vicinity. This is a result from boiling of hydrothermal waters which circulate to upper part of the system and reach to the surface waters (Moore et al., 2002). Characteristics of the water typically contains high SO_4 produced by oxidation ascending H_2S and there is no chloride present (Mahon, et al., 2000). Therefore, the spring water is highly acid and very reactive which alters or dissolves the rock-forming minerals. Some of the common hydrothermal minerals formed by this acid-sulfate water are illite, sulfur, anhydrite (Reyes, 1998), hematite, and goethite (Nicholson, 1993). Most of these elements are present in the XRD (Figure 8)

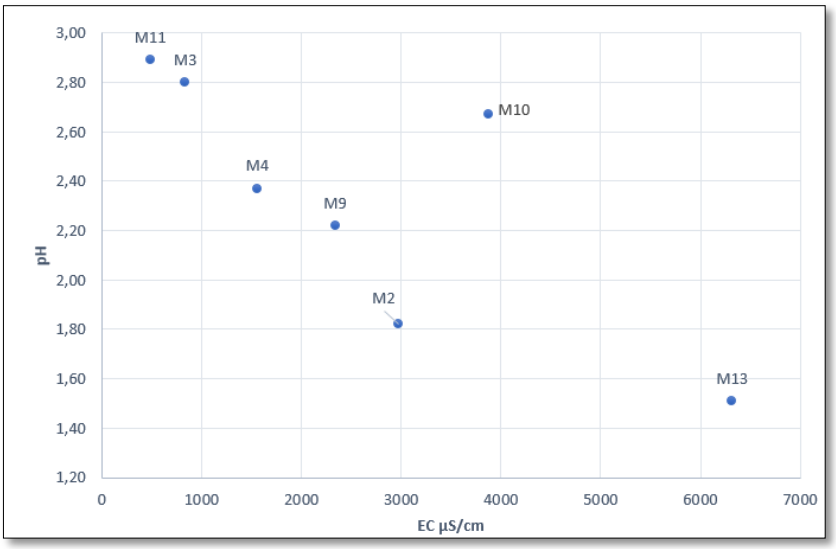


Figure 7: inverse relationship trend for EC and pH in hot springs.

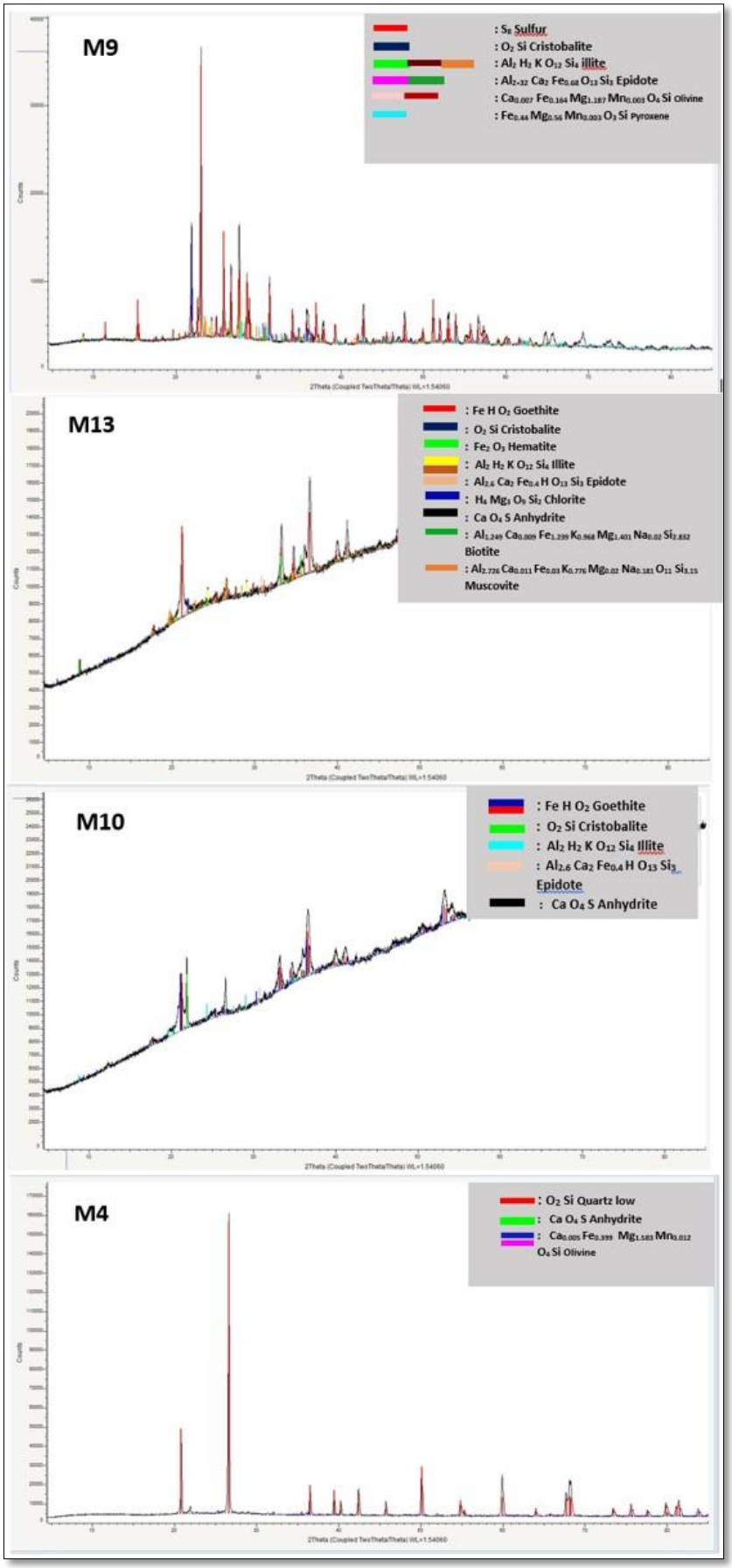


Figure 8: XRD Chart for the springs rock sample.

CONCLUSION

The monitoring of surface manifestations around Field A shows the spring waters have changed over time with recent increases in acidity and EC. The increased pH of the spring could be due to increasing volcanic degassing or reservoir boiling. The waters become more conductive due to extensive leaching as result of aggressive pH in the water, whereby the dissolved minerals provide the constituents that increase the conductivity.

Physical changes in hot springs indicate reactivation structures occur near to M11 and M10. More abundant gas discharge and the new formation of a pool like geyser is found. An increase in heat discharged at the surface can be due to reservoir boiling increasing the steam flow to the surface. The other possibility is there have been changes in permeability due to tectonic strains as the result of an earthquake or mineral dissolution. The decreasing water level and color might also due to an increased proportion of steam condensate and concurrent mineral dissolution/alteration.

The XRD study shows cristobalite, goethite, and anhydrite are found as the acid altered minerals. Illite, epidote and chlorite mostly are indicators of cooled propylitic alteration. The minerals give indicators of temperature higher than 250 ^{o}C (Reyes, 1998).

REFERENCES

Brehme, et al., (2015). “Structurally controlled fluid flow in a high-enthalpy geothermal system – case study Lahendong, Sulawesi (Indonesia) 1–6”. Proceedings World Geothermal Congress. Melbourne, Australia.

Joint Research Centre, (2018). “Executive Summary 2 Situation Overview 7.5 Mw Earthquake in Indonesia”. European Commission.

Kumparan (Indonesian newspaper), (2018): https://kumparan.com/@kumparannews/aktivitas- gunung-lokon-meningkat, accessed by 5 March 2019 at 2 pm.

Koestono, H., (2010). “Lahendong Geothermal Field, Indonesia: Geothermal model based on wells LHD-23 and LHD-28”. Master -Thesis at University of Iceland, p.123.

Lee, et al., (2018) “A review on volcanic gas compositions related to volcanic activities and non-volcanological effects”. Geosciences Journal vol 22, No.1. p.183-197.

Mahon, et al., (2000). “The Chemistry of geothermal fluids in Indonesia and their relationship to water and vapour dominated system”. Proceedings World Geothermal Congress. Kyushu, Japan.

Moore, et al., (2002). “The mineralogic consequences and behavior of descending acid-sulfate waters: an example from the Karaha-Telaga Bodas, Goethermal System, Indonesia”. Proceedings Twenty-Seventh Workshop on Geothermal Reservoir Engineering. Stanford University, California, SGP-TR-171.

Nicholson, (1993). “Geothermal Fluids Chemistry and Exploration Techniques”. School of Applied Sciences. Scotland, United Kingdom.

Reyes, (1998). “Petrology and mineral alteration in hydrothermal systems: From diagenesis to volcanic catastrophes”. United Nations University, Geothermal Training Programme (UNU-GTP), Reykjavik, Iceland.

Scott, (2012). “Guideline for mapping and monitoring geothermal features 9595”. GNS Science, New Zealand.

Surachman, S., Tandirerung, S.A., Buntaran, T., Robert, D., (1987). “Assessment of the Lahendong geothermal field, North Sulawesi, Indonesia”. Proceeding Indonesian Petroleum Association, Sixteenth Annual Convention, October 1987. pp. 385–398.

EVOLUTION OF BEUNGGA GEOTHERMAL SYSTEM REVEALED FROM SURFACE MANIFESTATION

Aidina Anisa[1], Niniek Rina Herdianita[1,2], and Dede Iim Setiawan[3]

[1]Department of Geology, Faculty of Earth Science and Technology (FITB),
Bandung Institute of Technology (ITB)
[2] Petrology, Volcanology and Geochemistry Research Group, Faculty of Earth Science and Technology (FITB),
Bandung Institute of Technology (ITB)
[3] Geothermal Research Group, Center for Geological Resources, Geological Agency
Email: aidinaanisa@gmail.com; herdianita@gl.itb.ac.id; keiimsaja@gmail.com

ABSTRACT

Beungga geothermal field is located at Tangse, Pidie Regency, Aceh Province; it lies at a depression area of pull apart basin within the Sumatera Fault System. Geothermal surface manifestations occur as warm to hot springs and propylitic alteration.

Warm springs having temperatures between 50° and 63°C appear at Beungga as immature, Cl-HCO3 water. Hot springs having temperatures between 77° and 82°C appear at Alue as immature, Cl-HCO3-SO4 water. Beungga and Alue springs discharge from two different reservoirs, i.e. Beungga and Alue reservoirs. The Beungga reservoir is fractured andesite and slate rocks and its fluid has temperature of 110-130°C (from Na/K geothermometer), while the Alue reservoir is associated with fractured slate rocks and filled by 150-170°C (from Na/K geothermometer) thermal fluids. The thermal reservoir fluid is meteoric water origin.

Propylitic alteration, indicated by the presence of epidote, illite, pyrite, and chlorite, is found locally along NW-SE faults. The alteration style indicates that the reservoir was in place and filled by thermal fluid of having normal pH and temperatures of above 220°C.

The occurrence of geothermal surface manifestations shows the evolution of Beungga-Pidie geothermal system. The system has changed from high enthalpy to medium enthalpy, possibly due to a change in heat sources. The past reservoir now exposes to the surface due to erosion and/or fault movement.

Keywords: Geothermal system, surface manifestation

INTRODUCTION

Beungga field is one of the geothermal prospects in Aceh. It is located in Tangse District, Pidie Regency about 40 km southeast from Seulawah AgamVulcano Mountain and 125 km from Banda. Aceh (Figure 1). This area has surface manifestations around Beungga valley. Beungga valley is an NW-SE trending longitudinal shape along 6 km which is limited by the height of the Barisan Mountains. Beungga geothermal system covers the prospect area around 2 km^2. That prospect area is determined based on the location of geothermal manifestations. Geothermal manifestations occur at five locations as warm and hot springs that is utilized directly as a public bathing place. Alteration is found locally along NW-SE fault alignment and fractured rocks. Identification on the characteristics of active and fossil manifestations can conceive the evolution of the geothermal system and geological conditions which influence them.

GEOLOGY

The morphology of the research area is divided into ridges, hills, and valley. The ridges extend from northwest to southeast across the center of the research area. Its elevations about 250 - 650 m with steep slopes between 19° - 45°. In the southwest, the hills with elevations between 300 - 1000 m and slopes of 11° - 26° have disorder alignment. The valley morphology with elevations between 100 - 300 m lies in the center of the research area, also parallel and limited by the ridges. Regional geology of the research area is shown at Banda Aceh Quadrangle Map (Bannett et al., 1981). There are Pre-Tertiary rocks as Slate Unit and Andesite Unit. The Slate Unit in the southwestern part of the research area consists of slate and schist. The Andesite Unit that consists of andesite and basalt overlie the Slate Unit with structural contact. The Slate Unit is equalized with Lam Minet Formation (Mum) while Andesite Unit with Geumpang Formation (Mug) (Bennett et al., 1981). Both of those formations are Late Jurassic – Early Cretaceous in age. Then, they are intruded by grano-diorite batholiths of Gle Seukeun Complex (Barber, 2005). K-Ar methods dating by Van Leuween in Barber (2005) resulted Paleosen - Eosen age for granodiorite intrusion. Sedimentary rocks found in the northwestern part of the research area which is part of the Kotabakti Formation (Bannett et al., 1981). In the research area, these sedimentary rocks consist of sandstone and conglomerates that is formed in Middle-Miocene (Barber, 2005). Alluvial deposits become the youngest deposits.

An NW - SE trending strike-slip fault dominate the geological structures in the research area. It's part of the Sumatera Fault System (SFS) segments that has been active since the Middle Miocene (Barber, 2005). Movements between active parallel fault segments can trigger the step-over process. According to Cunningham and Mann (2007), step-over process accommodates a releasing bend that makes normal faults, then forms depression topography called pull-apart basin. The model of pull apart basin formation is conceived by McClay and Bonora (2001) in Figure 2. Beungga valley of the research area is one of pull-apart basin resulting from these process.

MANIFESTATION

Thermal fluid manifestations

Thermal fluids manifestations were found as warm and hot springs in five locations (Figure 3). There are three warm springs i.e. BG-1, BG-2, and BG-3 at Beungga with temperatures of 50° - 60° C and pH 9-9,3. BG-1 discharge from fractured rocks near the river-edge and collected in a pool for a public bathing place. BG-2 and BG-3 occur at river cliffs. Then, 2 hot springs manifestation i.e. BG-4 and BG-5 are located in Alue, 4 km to the southwest from Beungga. Alue's hot springs is appeared at alluvial near the residential housing with temperature 77° - 83° C and pH 8.3 - 8.7. These hot springs are accommodated in a small tub and used by local people for general purposes. The thermal water manifestations discharging continuously with low average discharge <1 L /s. Thermal water have relatively same characteristics in odorless, tasteless, and occasionally emit low-pressure of gas bubbles.

Figure 3 shows the chemical composition of Beungga thermal water is classified as immature with a balanced combination of Cl-HCO3-SO4 content. It takes a role for the thermal water position in the center of Cl-HCO3-SO4 triangle diagram (Figure 3). The Alue thermal water has a relatively immature chloride sulfate water type. All thermal water shows domination cations of Na and quite high of Cl content that comes from the reservoir, reflected by low K, Mg, and Ca.

The high SO4 concentration in Alue thermal water is affected by sulfate water from magmatic gas condensation. Nicholson (1993) explained that chloride sulfate water comes from mixing geothermal reservoir water with sulfate water at a certain depth. Chloride sulfate water is mixed with groundwater resulted high HCO3 content so that the pH rises to 9 in the Beungga thermal water. Besides, rising of pH is caused by shallow neutralization that may occur from interactions between thermal water with rocks near the surface. Compare with the Beungga manifestations, Alue has higher amount of DHL, SIO2, Cl, F, Na and more neutral pH.

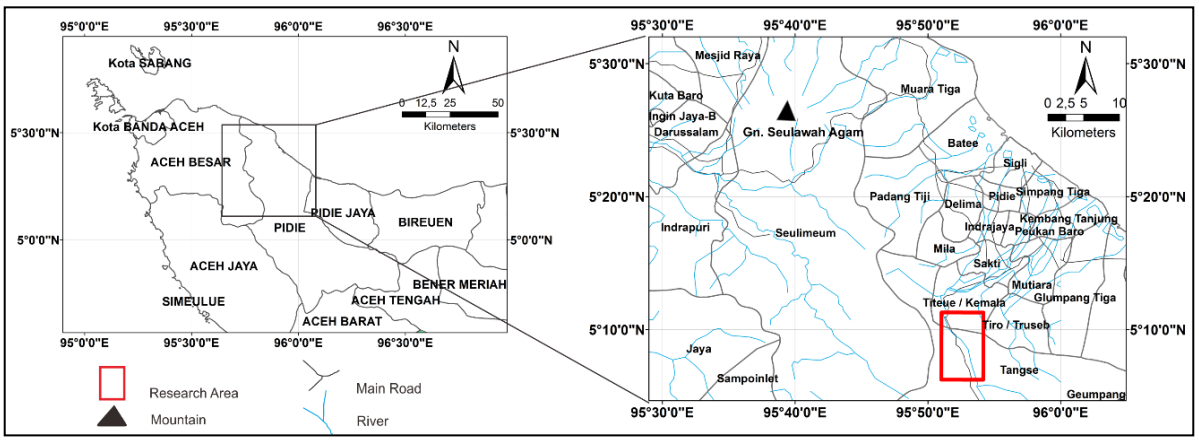


Figure 1: Map of Aceh showing geographic locations of research area.

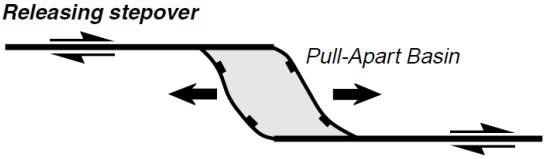


Figure 2: Stepovers model between two offset fault systems produce either pull-apart basins for releasing stepovers (McClay and Bonora, 2001).

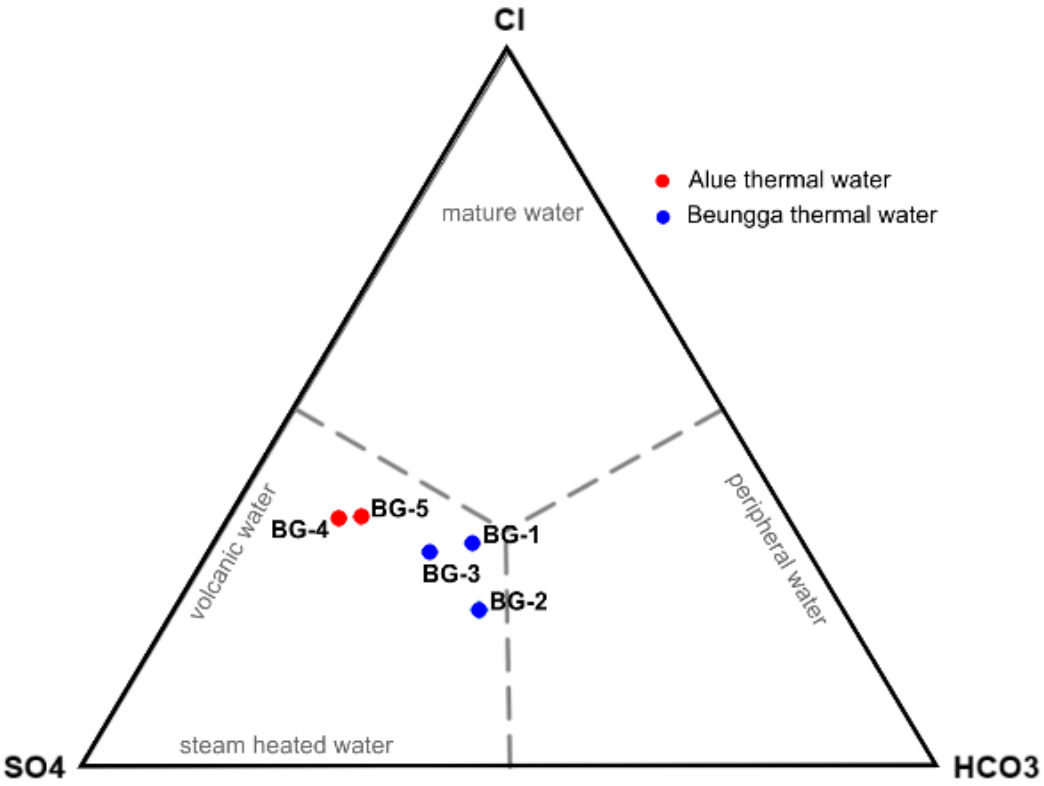


Figure 3: Relative Cl-S04-HCO3 content in triangle diagrams. Blue point for manifestations for Beungga, and red point for Alue.

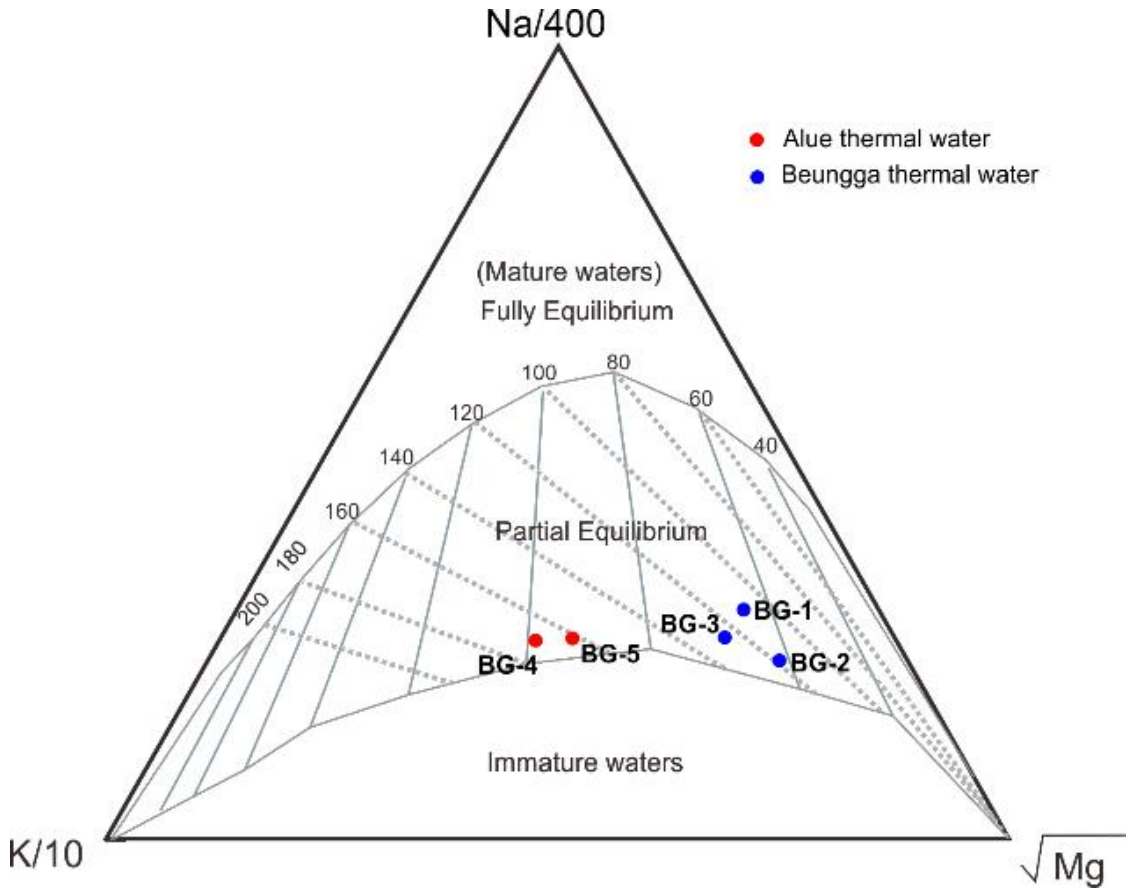


Figure 4: Relative Na-K-Mg concentrations in triangle diagram. Blue point for manifestations for Beungga, and red point for Alue.

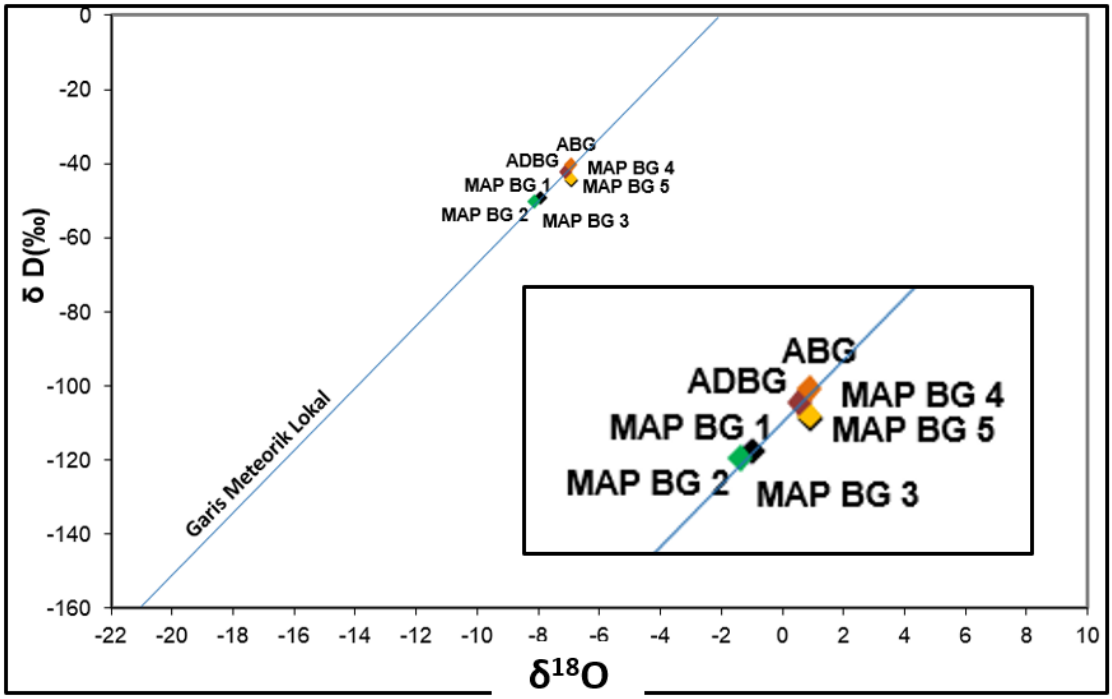


Figure 5: δD - δ18O graphics shows thermal waters origin from meteoric water.

Based on Na-K-Mg diagram for medium enthalpy, Alue and Beungga thermal water are in partial equilibrium with the highest equilibrium on BG-1 (Figure 4). All thermal water are derived from meteoric water that can be seen from isotope trends following local meteoric line (Figure 5).

Surface Alteration

Fossil manifestations are found as propylitic surface alteration that replaced primary minerals with medium intensity. Propylitic alteration with chlorite-epidote-illite-pyrite alteration minerals including quartzite-calcite are found locally in andesite rocks. The alteration has NW-SE trending controlled by fault structures alignment. The pseudomorph texture is seen as primary pyroxene is substituted by chlorite. Dissemination texture in plagioclase is replaced by illite mineral (Figure 6A). The veins are filled with calcite. The association of propylitic minerals on surface alteration indicates the position of the past hydrothermal reservoir.

In the manifestations of BG-2 and BG-3, hot springs discharge out from rock fractures in the river cliff. The rocks around those manifestations are altered totally by quartz mineral, then are filled by calcite mineral on its veins (Figure 6B). This alteration style can be called as silicification.

EVOLUTION OF GEOTHERMAL SYSTEM

Based on the B/Cl ratio on the Cl-Li-B diagram, five thermal waters coming from 2 reservoir groups i.e. Beungga and Alue (Figure 7). BG-1 has relatively difference in the B content comparing to BG-2 and BG-3 (Table 1). However, BG-1 is still grouped into Beungga reservoir because of the geographic location that is near BG-2 and BG-3. The relatively high content of B in BG-1, BG-4, and BG-5, is interpreted by the change of reservoir lithology that is form of fractured slate rocks. Whereas in BG-2 and BG-3, the reservoir is in fractured andesite rocks with a relatively lower B content. The change of chemical water composition while moving from reservoir to the surface is due to water-rock interaction.

Calculation of Na-K Giggenbach and Fournier geothermometers in Nicholson (1993), by using five thermal waters samples, shows that temperature of Alue reservoir is between 150° - 170°C, while Beungga reservoir is 110° - 130°C. Both reservoirs are classified into medium enthalpy reservoir.

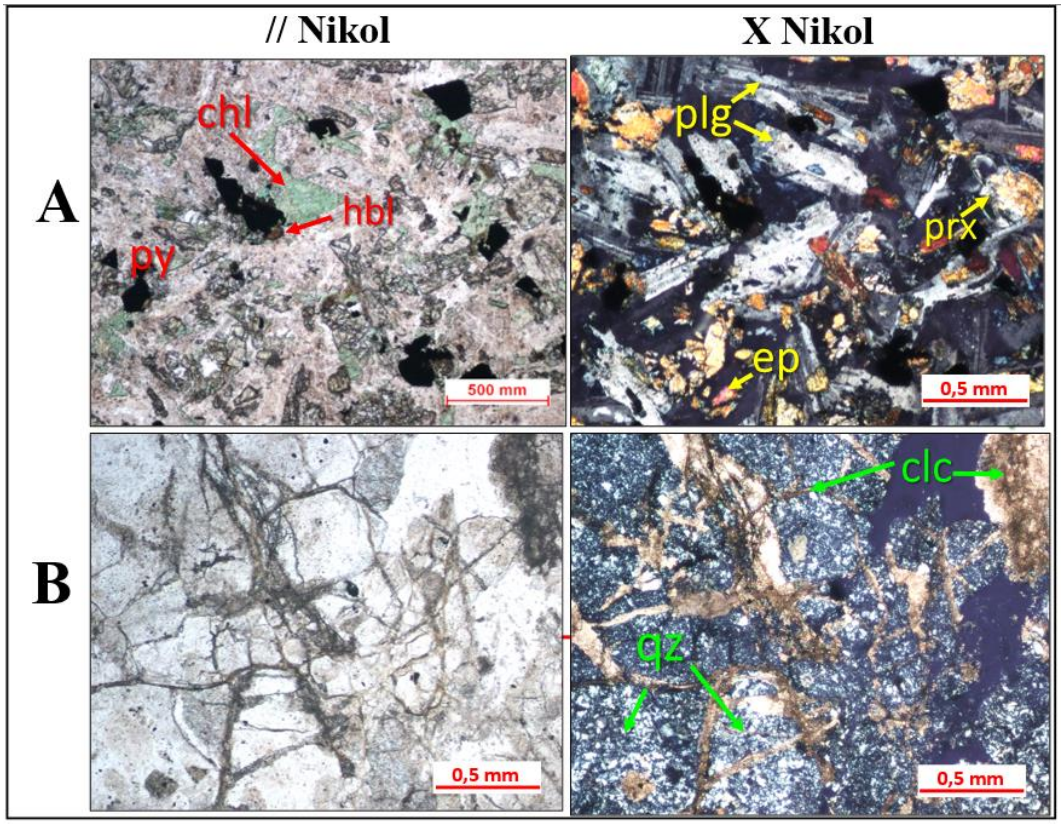


Figure 6: Thin section of andesite altered rocks. (A) Altered by chlorite-epidote-illite-pyrite mineral. (B) Altered by quartz with intensive calcite vein.

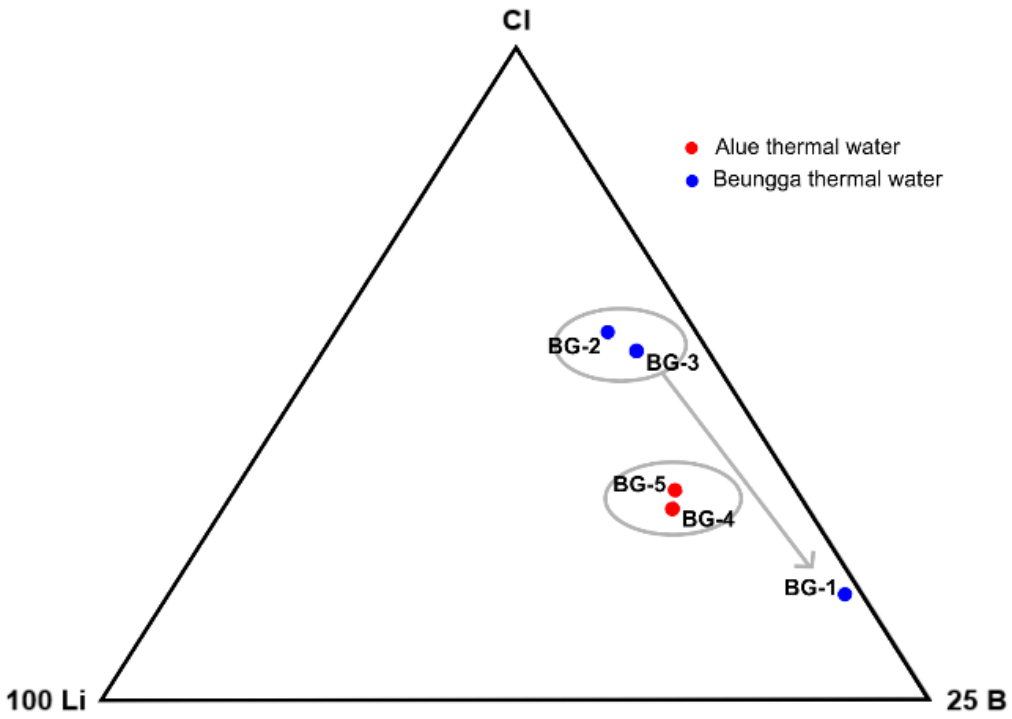


Figure 7: Relative Cl-Li-B concentration in diagram showing trend of reservoir grup.

Alteration patterns that occur in the research area are indicated by the presence of propylitic alteration in the surface rocks. The propylitic mineral association i.e. epidote and illite, reflect neutral pH and high enthalpy of thermal fluids with temperatures above 220°C. Those alteration characteristic interpreted as a past hydrothermal reservoir. It means when propylitic alteration occurred, the research area was below the surface.

The movement of the Sumatran fault segments form strike-slip fault system. The fault segments are step-

over through releasing bends between each other, then produced pull-apart basin that comprised the lowest topography (Cunningham and Man, 2007). In the research area, these process accommodated Beungga valley formation. Therefore, propylitic alteration of the past reservoir rocks in the research area has been exposed to the surface by the structures activity and followed by surface erosion. Figure 8 shows the thermal waters and alteration manifestations in the research area are overlay with fault structures from geological mapping. The alteration pattern can be seen following the fault structures alignment. So then, these strike-slip fault has affected the permeability zone of the past geothermal reservoir. We can conclude that the past reservoir has been formed since the Middle-Miocene due to the activated age of the Sumatera Fault System.

The process of past reservoir rock exposing in the research area is accompanied by a decreasing in groundwater level. After that, the latest geothermal are formed and estimated to have a reservoir at 500 - 700 m depth below the thermal water manifestations. The latest geothermal reservoir has medium enthalpy that might be affected by changes in the heat source condition.

CONCLUSION

The research area is classified as flat terrain topography geothermal system as valley plain shape which is limited by ridges. These valley has longitudinal NW-SE trending. These valley is formed by the role of normal fault in the strike-slip fault system and followed by erosion process. So then, Beungga valley is one of pull-apart basin that is found in Sumatera Fault System.

The thermal water manifestations of hot and warm springs in Beungga and Alue as an existence sign of the latest active geothermal system. The thermal waters come directly from the reservoirs through the upflow zone. The geothermal reservoirs lies in fractured rocks that formed due to the active structures zone. Beungga reservoir occurs in fractured andesite and slate rocks with temperatures ranging from 110° - 130°C, while Alue reservoir has temperatures of 150° - 170°C occurs in fractured slate rocks. The occurence of past geothermal system indicated from the surface alteration in the research area which is found propylitic alteration i.e. epidote-chlorite-illite-pyrite. The past geothermal reservoir had been formed at temperatures above 220°C by those mineral association. Quartz-calcite alteration is found around thermal water manifestations BG-2 and BG-3. This alteration has a formation temperatures of >160°C.

We can conclude that past reservoir rocks has been exposed to the surface influenced by fault activity which is formed pull-apart basin. The geothermal system changes from high enthalpy in the past reservoir (> 220°C) to medium enthalpy (110° - 170°C) in latest reservoir. These evolution occur gradually which is proved by quartz-calcite alteration formed at temperatures >160°C.

Geothermal Beungga has a potential economy to utilize directly as hot water tourism because the manifestation output is in the plain and near the residents' housing. Furthermore, the detailed study is needed for an indirect use plan regarding to economic prospects. However, these geothermal energy has a hypothetical resource potential of 17 MW.

REFERENCES

Barber, A., J., Crow, M., J., and Milsom, J., S., (2005), “Sumatra: Geology, Resources and Tectonic Evolution”, Geological Society, London, Memoirs, 31, 282 pg.

Bennett, J., D., Bridge, D., McC., Cameron, N., R., Djunuddin, Ghazali, S.A., Jeffery, D.H., Kartawa, W., Keats, W., Rock, N.M.S., Thomson, S.J., and Whandoyo, R. (1981), “Geological Map of The Banda Aceh Quadrangle, Sumatera Utara, Skale 1:250.000”, Report of Center for Geological Resources, Geological Agency.

Center for Geological Resources, Geological Agency (2018), “Integrated Survey for Geology, Geochemistry, and Geophysics of Alue Calong Geothermal, Pidie, Aceh Province”, Report of Center for Geological Resources, Geological Agency.

Cunningham, W., D., and Mann, P., (2007), “Tectonics of Strike-Slip Restraining and Releasing bends”, Geological Society Special Publication, 290, 1–12.

McClay, B., and Bonora, M., (2001), “Analog Models of Restraining Stepovers in Strike-Slip”, AAPG Bulletin, 85, 233-260.

Nicholson, K., (1993), “Geothermal Fluids: Chemistry and Exploration Techniques”, Springer-Verlag Heidelberg, Berlin, 263 pg.

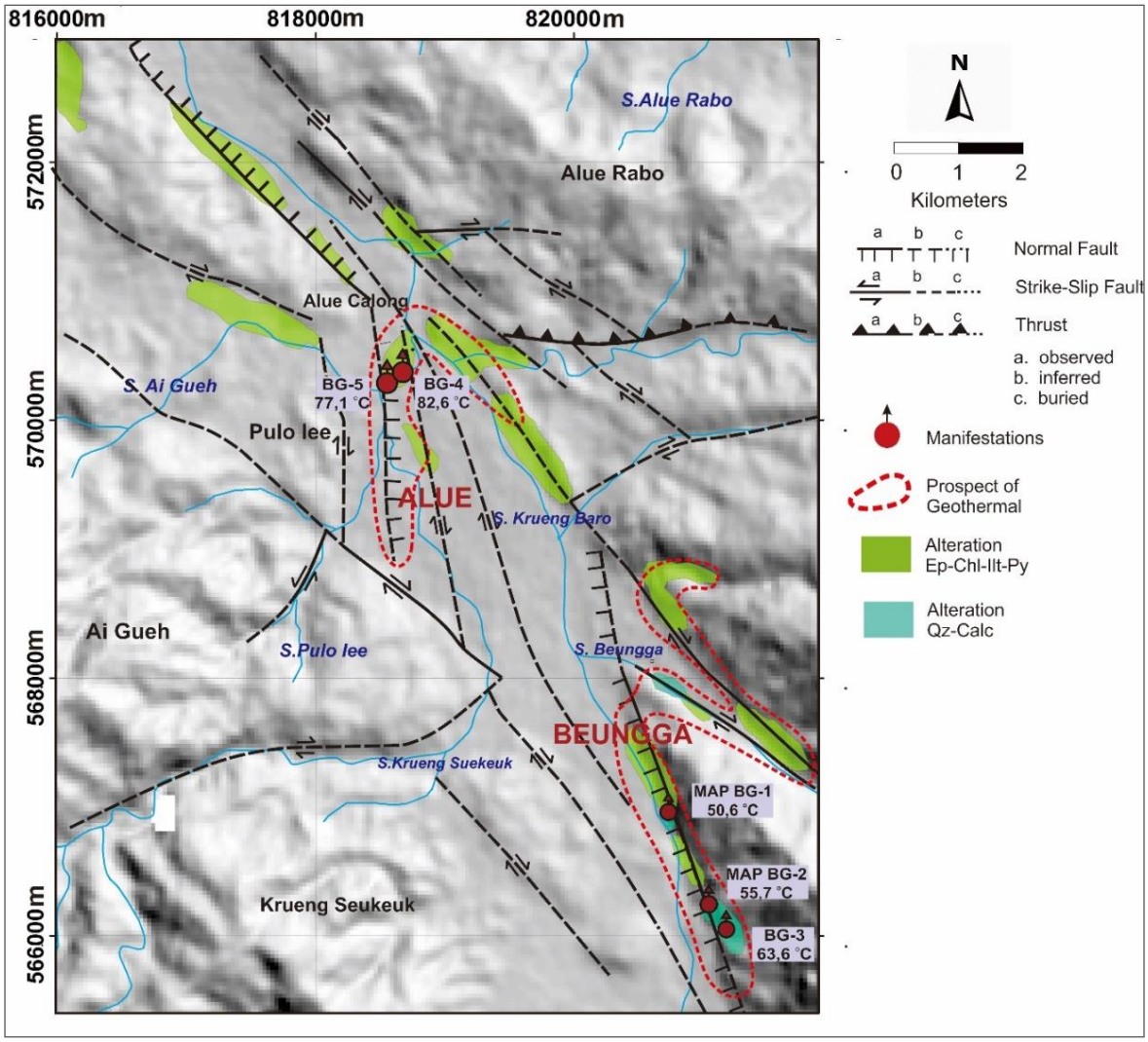


Figure 8: Researh area topography overlay with thermal water manifestations location, alteration, and fault structures.

GEOLOGY OF MT. RATAI-PESAWARAN HYDROTHERMAL SYSTEM, LAMPUNG, INDONESIA

Tri Bagus Prabaswara[1] and Niniek Rina Herdianita[1,2]

[1]Department of Geology, Faculty of Earth Science and Technology (FITB), ITB
[2]Petrology, Volcanology and Geochemistry Research Group, FITB, ITB
Email: bagus_tri@hotmail.com

ABSTRACT

Mt. Ratai-Pesawaran hydrothermal system is associated with a volcanic cone and old caldera structure. The system is located about 25 km southwest Bandar Lampung, South Sumatera. Surface manifestations of the system include Way Cempaka and Penaga hot springs, Margodadi hot pools and geyser at southeast Mt. Ratai-Pesawaran. Siliceous sinter deposit is present at Margodadi and travertine is found at Way Cempaka. The surface manifestations indicate that the hydrothermal reservoir has temperatures of more than 208-220°C.

Lithology of Mt. Ratai-Pesawaran and surrounding is dominated by Tertiary to Quaternary andesitic volcanic rocks. Heat source of the Mt. Ratai-Pesawaran hydrothermal system seems to have evolved during Quaternary from hornblende and biotite andesite to pyroxene andesite. The rock chemistry indicates that the andesitic is potassic calc-alkaline rock produced from partially-melting magma in a subduction zone. Reservoir rock seems to be andesitic volcanic rock which were fractured by the Great Sumatra Fault System.

Keywords: Hydrothermal systems, Mt. Ratai geothermal

INTRODUCTION

Sumatra Island which is located in the southeastern part of the Eurasian Continent Plate and is also part of the convergence between the Indian Ocean plate and the Eurasian Continental Plate. The convergence between the two plates results in subduction along the Sunda Trench and is characterized by a series of volcanic mountains extending from the northwest to southeast called the Barisan Range. The research area (Figure 1) is located in the southeastern part of the Barisan Range which lies in the Quaternary volcanic Mt. Ratai-Pesawaran and the Gebang Tertiary Caldera which is located in the Padang Cermin, Pesawaran District. Several manifestations are found in southeast flanks of Mt. Ratai-Pesawaran such as geyser springs and silica and travertine sinters. An abundant indication of hot springs indicates a large geothermal potential. Therefore, geology and geothermal research is needed in this area.



Figure 1: Research area of Mt. Ratai-Pesawaran, Lampung.

Previous research has been carried out by Mangga et al. (1993) on a regional scale, namely the geological map of Tanjungkarang. In addition, Herdianita et al. (2018) also has conducted a specific study on the geochemistry of geothermal manifestations in the Way Ratai Geothermal Field. The purpose of research and mapping in this area is to be able to update the existing data and provide a second opinion related to Way Ratai geothermal field.

This research is conducted by analyzing the geology and geothermal system in Mt. Ratai-Pesawaran based on geological studies and geochemical studies of geothermal fluids manifestations. Geological studies were carried out by field observations and rock sampling, which are then taken to the laboratory for petrographic analysis to classify the rock types. The XRF method is also used to determine the type of rock based on chemical composition that describes the genesis of the rock. These results will provide an overview of the composition and distribution of lithology and the indication of the geological structure in research area. On the other hand, geochemical studies were conducted by analyzing the chemical composition of geothermal fluid manifestation to comprehend process that occur in geothermal fluids as well as geothermal system in research area. Both of these aspects will provide a better understanding about geology background and geothermal system in Way Ratai Geothermal Field.

GEOLOGY SETTING

Regional Geology

Pre-Tertiary rocks

The oldest rocks in the research area are composed of medium-grade to high-grade metamorphic rocks, namely Undifferentiated G. Kasih Complex and were formed during the Paleozoic era. According to Manga et al. (1994), this unit has been undergone regional scale metamorphism and is considered as a part of the core of Sumatra metamorphic rocks.

The Menanga Formation is a pre-tertiary rock that originate from sedimentation process which were formed during the Early Cretaceous Period. Also, this unit was deposited in the shallow marine environment which is being associated with volcanic arc environment alongside with seaside reefs (Mangga et al., 1994).

Tertiary rocks

Tertiary rocks were composed of rocks that formed due to the process of volcanism and the process of sedimentation that occurs around the Sumatran volcanic arc. At this time, Tarahan and Sabu Formation formed in the Late Eocene - Mid Oligocene epoch and unconformity occured between both of these formations with Menanga Formation. Tarahan Formation is composed of volcanic rocks which were deposited in the continental environment. On the other hand, Sabu Formation consist of sedimentary rocks that were formed by fluvial process around volcanic area. The Hulusimpang Formation is composed by volcanic rocks which were deposited in the late Oligocene - early Miocene. Small intrusions rock was found on the research area, namely Piabung Dacite, which intruded Hulusimpang Formation and interpreted to form during Middle Miocene period.

Quaternary rocks

Quaternary rocks in the study area consist of young volcanic deposits which were deposited in Pleistocene - Holocene composed of andesite basalt lava, volcanic breccia, and tuff along with alluvium sediment Holocene.

Structural Geology

Sumatra Island located at the active southwestern margin of the Sundaland, the southeastern part of the Eurasian Continental Plate and is part of the convergence between the Indian Ocean plate and the Eurasian Continental Plate. Regionally, the geological structures formed in the research area have northwest-southeast lineament direction with minor north-south and northeast-southwest lineament direction.

According to Pulunggono et al. (1992), there are three main tectonic phases in Sumatra and thus formed structural patterns in the southern part of Sumatra. These three main tectonic phases are:

1. First phase: Compression phase (Late Jurassic - Early Cretaceous), which generally formed NE-SW, WNW-ESE, and N-S lineaments. These structures were interpreted as structure formed in the Pre-Tertiary basement.
2. Second phase: Extensional phase (Late Cretaceous – Early Tertiary), which produced normal fault and growth fault with N-S and WNW-ESE orientations. According to Pulunggono et al. (1992) in Barber et al. (2005), then Pre-Tertiary basement structures were reactivated as normal faults during this extension phase in Paleogene.
3. Third phase: Compression phase (Mid-Miocene - recent) produced a NW-SE trending structures and inversion and formed oblique and compression faults. This compressive phase reaches its peak in the Pliocene - Pleistocene period. This tectonic phase, has resulted the occurrence of tectonic inversion on the existing structures.

DATA AND METHODOLOGY

Field observation was carried out in accordance with the geological mapping procedure. Literature studies, satellite imagery and digital elevation model analyses were conducted first before conducting field observation. National digital elevation model (DEMNAS) was used to derive temporary geology structural map and lineament map. Objects need to be considered in conducting lineament analysis were elongated river features, scarp slope, elongated valley features, and ridge discontinuities. As an assumption, those objects are indeed a location of concentrated erosion controlled by the presence of geological structures.

Field observation was conducted to obtain primary data, including lithologic distribution, structural data, surface thermal manifestations, along with water and rock sampling. Rock samples are then taken to the laboratory forpetrographic analysis to classify types of rocks based on mineralogy composition. Some of the rock samples were analyzed using the XRF method and it is intended to determine the composition of rock based on chemical composition.

Water geochemical analysis performed by using primary data and secondary data. Primary data obtained from geothermal manifestation fluid sampling while secondary data was from the previous study by Herdianita et al. (2018).

RESULT AND DISCUSSION

The study area is situated in a Quaternary active volcano overlying Tertiary volcanic products. Rock distribution is depicted in Figure 2, and their vertical relationship were interpreted in geologic cross-section. Lithologic units are divided according to physical and mineral characteristics along with their volcanic origin.

Rhyolite tuff and pyroclastic breccia of Miwang (MTBr)

This unit consist of two lithology, pyroclastic breccia and tuff. Pyroclastic breccia was grayish, with grains size range from coarse ash to block, poorly-sorted, grain-supported, fragments were angular – subangular, and composed of porphyritic andesite lithic fragments and schist lithic fragments, plagioclase, quartz, and magnetite, with groundmass of devitrified. It was slightly altered to clay minerals, epidote, hematite, and chlorite. Schist present as an accidental lithic fragment (McPhie et al., 1993), in which bedrock fragments were eroded by pyroclastic flow. Tuff was grayish, with grain size of fine ash – lapilli, well-sorted, locally welded, has fiamme and eutaxitic texture, and composed of porphyritic andesite lithic fragments, plagioclase, biotite, quartz, and magnetite, with groundmass of devitrified glass. Clay mineral and secondary quartz occur as alterated minerals in these rocks. Mangga et al. (1994) named this unit as Tarahan Formation (Late Eocene – Mid. Oligocene) and radiometric dating (Bellon et al., 2004) indicated an age of 19.7 Ma. Based on the characteristics of outcrops and rocks, the deposition mechanism is interpreted to be pyroclastic flow.

Biotite – Hornblende Andesite of Miwang (MAbh)

This unit consists of biotite-hornblende andesite lava. The andesite is gray with porphyritic texture, hypohyalin, trachytic texture was present, and phenocrysts consist of plagioclase, hypersthene, hornblende, and magnetite. This rock unit moderately altered to clay and hematite. Based on radiometric dating by Bellon et al. (2004), the age of this unit is 16.9 Ma. Based on Mangga et al. (1994), this unit was part of Hulusimpang Formation (Late Oligocene – Early Miocene).

Andesite tuff and pyroclastic breccia of Miwang (MTBa)

This unit consist of two lithology units, pyroclastic breccia and tuff. Pyroclastic breccia is grayish, with grains size ranges from coarse ash to block, poorly-sorted, matrix-supported. Fragments were angular to subangular, and composed of porphyritic andesite lithic fragments, plagioclase, hornblende, biotite, and magnetite, with groundmass of devitrified glass. It was moderately altered to clay minerals and limonite. The tuff was grayish, with grain size of fine ash – lapilli, well-sorted, and composed of porphyritic andesite lithic fragments, plagioclase, biotite, hornblende, and magnetite, with groundmass of devitrified glass. Mangga et al. (1994) named this unit as Hulusimpang Formation (Late Oligocene – Early Miocene) and radiometric dating (Bellon et al., 2004) indicated the age is 16.9 Ma. Based on the characteristics of outcrops and rocks, the deposition mechanism is pyroclastic flow.

Andesite Intrusion (AI)

The andesite is gray in color with porphyritic texture, hypocrystalline, trachytic texture was present. The phenocrysts of this andesite consist of plagioclase, quartz, hornblende, and magnetite. Highly altered to chlorite and calcite. Based on XRF method result, rock chemistry classified this samples as andesite. Thus, this unit is named differently from regional geological unit which this unit is composed of dacite. According to Bellon et al. (2004) the age of this unit is 14.4 Ma (Mid. Miocene). Based on outcrop observation, this geological unit show a discordant contact with andesite tuff and pyroclastic breccia of Miwang (MTBa). Interpretation using outcrops and satellite imagery based on geometry and morphology appearance show that this unit is a stock intrusion.

Hornblende-biotite Andesite of Ratai (RAhb)

This unit consists of hornblende-biotite andesite lava. The andesite is gray with columnar joint presents in the outcrop, porphyritic, hypohyalin, inequigranular, hipidiomorphic, phenocrysts consist of plagioclase, hornblende, biotite, and magnetite. Slightly altered to clay and hematite. Based on XRF method result, rock chemistry indicates that the andesitic is potassic calc-alkaline rock produced from partially-melting magma in a subduction zone. According to field observation and supported by satellite imagery analysis, this unit is lava and younger than andesite tuff and pyroclastic breccia of Miwang. Based on Mangga et al. (1994), this unit is part of Ratai Young Quaternary Volcanics.

Rhyolite lapilli tuff of Ratai (RTLr)

Tuff is grayish in color, grain size of fine ash – lapilli, well-sorted, locally welded, has fiamme and eutaxitic texture, and composed of porphyritic andesite lithic fragments, plagioclase, biotite, hornblende, and magnetite, with groundmass of volcanic glass. Based on the characteristics of outcrops and rocks, the deposition mechanism is pyroclastic flow. Field observation and satellite imagery analysis show this unit was younger than hornblende-biotite Andesite of Ratai (RAhb). Based on Mangga et al. (1998), this unit is part of Ratai Young Quaternary Volcanic.

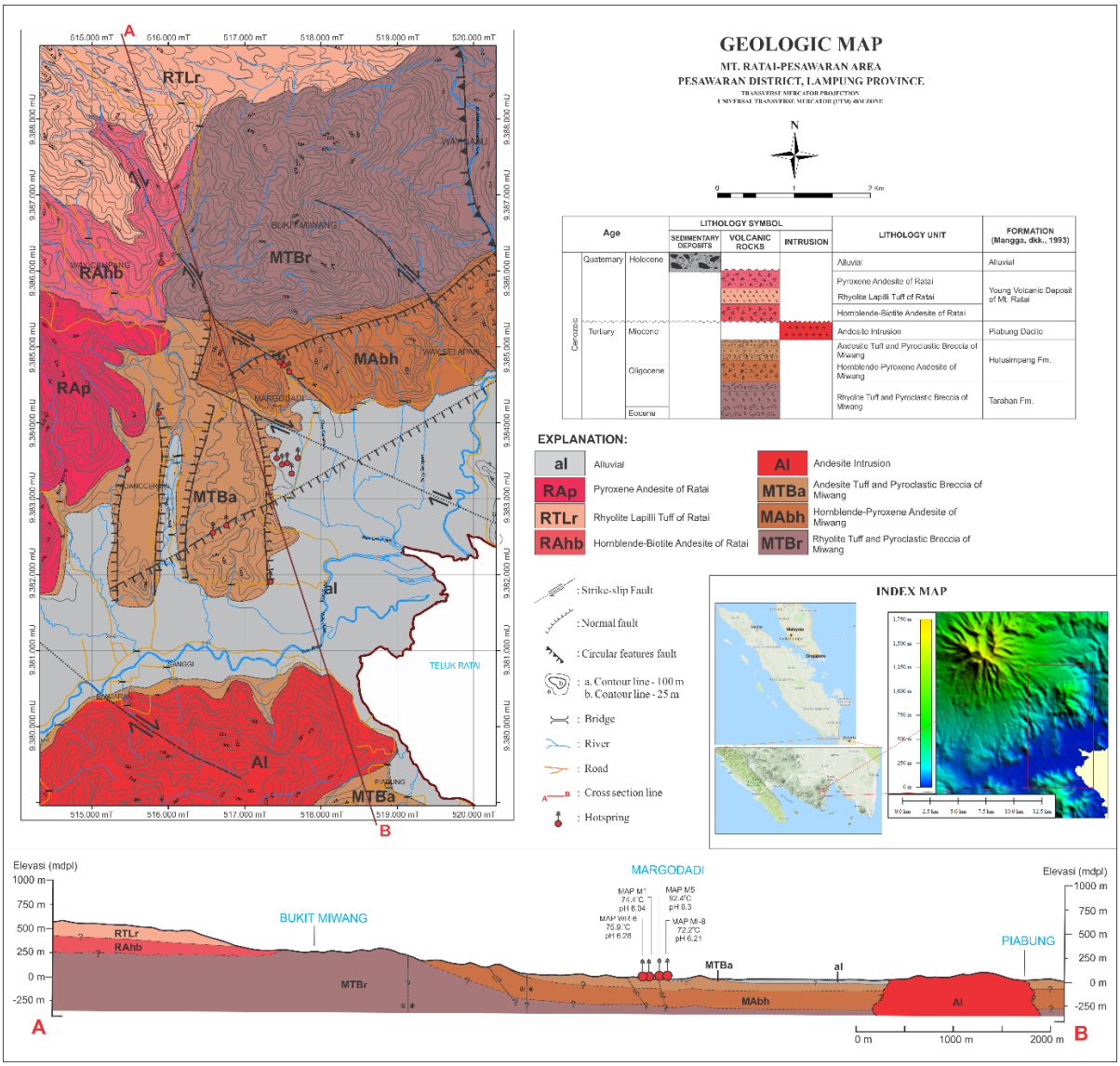


Figure 2: Geology map of Mt. Ratai-Pesawaran area.

Pyroxene Andesite of Ratai (RAp)

This unit consist of pyroxene andesite lava. The andesite is gray with columnar joint and autobreccia presents in the outcrop, porphyritic, hypohyalin, trachytic texture was observed. Phenocrysts consist of plagioclase, augite, hypersthene, magnetite, and volcanic glass. Based on field observation and satellite imagery analysis, this unit is lava and younger than rhyolite lapilli tuff of Ratai (RTLr). In reference of Mangga et al. (1998), this unit is part of Ratai Young Quaternary Volcanics.

Alluvial deposit (al)

This unit is deposited in the east-western part of study area, in Holocene. It was the youngest stratigraphic unit of study area, composed of gravel, sand, and mud, that being deposited as flood plain by fluvial processes of Ratai River and Way Campang River.

Structural geology

The initial identification of the presence of geological structures in Way Ratai Geothermal Field was carried out by analyzing the lineaments using digital elevation model (DEMNAS) as well as satellite imagery, which was further strengthened field observations. As stated early on that the lineament analysis considers several objects to help determine the existence of geological structures, which one of them is plotting the presence of hot springs in the Way Ratai area to observe any alignment of these springs. Result of lineament analysis concluded that there are three mains structural lineamentsand one circular feature in this research area.

Northwest-Southeast Fault

Indication of this fault can be seen through DEMNAS imagery by looking at elongated valley depression and discontinuity between ridges. The presence of thermal manifestation can also indicate that this structure may act as permeable path way. This structural feature observed both in the Tertiary volcanic rocks' unit and the Quaternary volcanic rocks unit. Based on ellipsoid model by Pulunggono et al. (1992), this NW-SE trending fault can be interpreted as right-lateral fault andmay represent shear failure associated with Sumatra Fault System which was initiated in mid-Miocene.

North-South Fault

Indication of this fault direction can be seen from elongated valley depression, scarp slope, and thermal manifestation occurance. Fault with N-S direction occur in Tertiary volcanic rocks unit. Based on Pulunggono et al. (1992), the N-S fault is formed during extensional phase of Early Tertiary.

Northeast-Southwest Fault

Indication of this fault can be seen from elongated valley depression and discontinuity between ridges. Few thermal manifestations also occured in this direction although the presence of thermal manifestation occur just in one local area. Fault with NE-SW direction are cut by the NW-SE and N-S faults and only occur in Tertiary volcanic rocks unit. Therefore, these faults may be considered older than the other two of faults orientations mentioned above. Based on Pulunggono et al. (1992) as cited in Barber et al. (2005), the NE-SW is formed in Pre-Tertiary which reactivated as normal fault in Paleogene.

Circular Features Fault

Indication of this fault can be seen from circular features of ridge or valley depression and the presence of thermal manifestation, associated with epidote minerals close to fault. This fault is cut by NE-SW direction and only observed in rhyolite tuff and pyroclastic breccia of Miwang (MTBr). In summary, this structural fault is interpreted as Gebang caldera collapse which approximately occured in Mid-Oligocene.

Geochemistry of Surface Manifestations

Geochemistry study was carried out by observing and sampling geothermal manifestations at the surface and then followed by laboratorium analysis for its chemical composition. Surface manifestations identified in Mt. Ratai-Pesawaran are geyser, hot spring pool, travertine, silica sinter deposits, and steaming ground. These variations in surface manifestations and their chemical compositions can help to understand the characteristic of the reservoir fluid and geothermal system at Mt. Ratai-Pesawaran. Geochemical analysis was performed using spreadsheets plotting chemistry Liquid v.3 by Powell and Cumming (2010).

Surface Thermal Manifestations

Margodadi area consists of plenty hot spring pools and other different type of manifestations (Figure 3). Based on geochemical analysis, chloride water appears in both of Margodadi hot springs location of M1 and M5, as indicated by high chloride (Cl^-) concentration. The presence of thick silica sinter deposit marks area of chloride water discharge (Nicholson, 1993). The silica sinter also showed layered structures, which shows several deposition periods. Geysers found in Margodadi were discharging intermittently mixture of boiling water, gas, and steam, which require fractured rocks filled with hot water at boiling temperature at shallow depth (Hochstein and Browne, 2000). Steaming ground is also found in Margodadi area (M5), which steam produces by underground boiling of geothermal water reservoir migrates to the surface of independent liquid phase (Nicholson, 1993). Although steaming ground is usually associated with sulphate (SO_4^{2-}) water, this steaming ground

fluid mostly contain chloride (Cl^-). Travertine is identified in Way Cempaka area, which was formed by precipitation of carbonate minerals from bicarbonate hot spring.

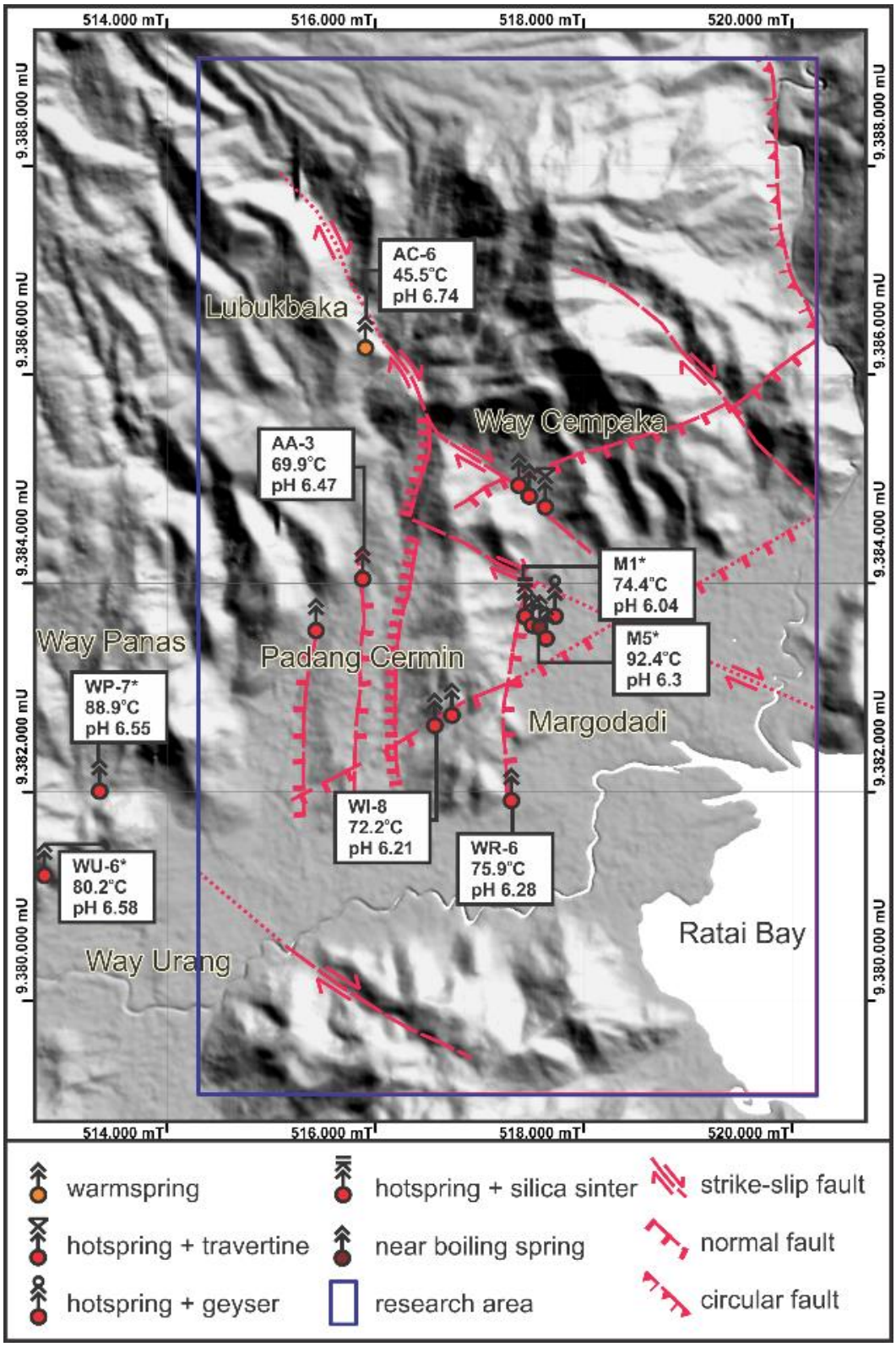


Figure 3: Surface manifestation map. Secondary data from Herdianita et al. (2018) are shown with asterisk symbol (*).

Types of geothermal water

Anion Ternary Diagram (Figure 4) shows several types of geothermal water based on Cl^--HCO_3^--SO_4^{2-} composition. The chloride type water is found in all manifestations in the study area, except Lubukbaka manifestation. Chloride hot springs found associated with silica sinter deposit is showingnear neutral pH and interpreted to originate from reservoir fluid. This statement is supported by high Cl and Na content along with low content of Mg and SO_4^{2-}.

Bicarbonate (HCO_3^-) water appears on Lubukbaka manifestations (AC-6) as indicated by the high HCO_3^- content. Based on Nicholson (1993), bicarbonate water are the product of steam and CO_2 gas condensation into poorly oxygenated sub-surface groundwater. In addition, this statement supported by high Mg content in Lubukbaka sample which indicates ground water mixing.

Cation ternary diagram of Na-K-Mg (Figure 5) used to determine the water equilibration as well as the processes that affect it. It is also used to estimate reservoir temperature based on Na/K Giggenbach (1988) geothermometer. Only one sample of Margodadi manifestation (M1) is fully equilibration water with an estimation of reservoir temperature of approximately 208ºC. Another interesting manifestation sample is Margodadi (M5) which has partially equilibration water with geothermometer temperature of approximately 220ºC.

Almost all of surface manifestations are partially equilibration water except for Lubukbaka manifestation (AC-6) which has immature water equilibration. High Mg content in Lubukbaka manifestation indicated a fluid mixing process between geothermal fluids with groundwater.

Cl-Li-B ternary diagram can be used to determine the source of hot reservoir fluid. Reservoir fluid is characterized by high Cl content and low ratio of B/Cl. The Cl/B ratio is also used to interpret manifestation fluid coming from the same reservoir. Based on Cl-Li-B Ternary diagram (Figure 6), high Cl content are mark with orange circle and it is interpreted as reservoir fluid. Moreover, all surface manifestation has same Cl/B ratio and thus interpreted come from the same reservoir.

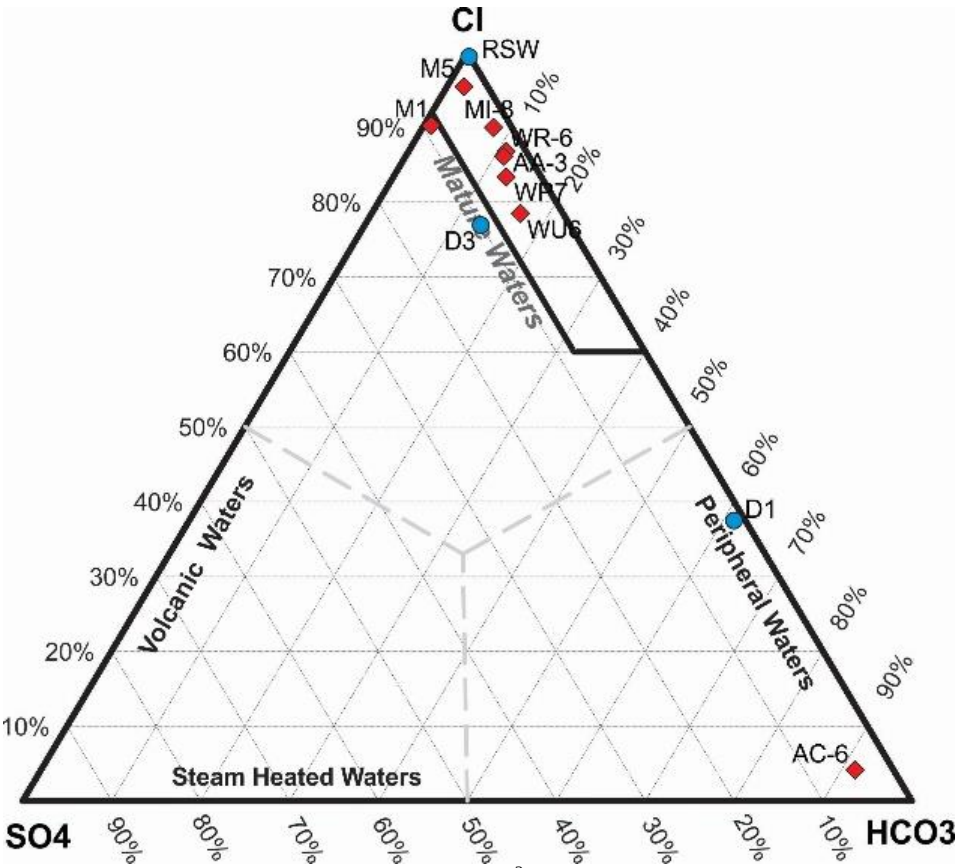


Figure 4: Anion ternary diagram consist of Cl^--HCO_3^--SO_4^{2-} (Giggenbach, 1991) composition used to classified types of geothermal water. Hot springs samples marked by red marker while cold springs samples marked by blue marker.

Enthalpy-Cl diagram (Figure 7) were used to interpret process that occur from reservoir to the surface. This diagram can effectively define trends in subsurface processes and interrelationships between groups of springs or wells within a field (Nicholson, 1993). Note that in enthalpy-Cl diagram (Figure 7), the parent fluid is determined from highest chloride content (Margodadi M1) in surface manifestation and then enthalpy and chloride content were reversed to reservoir conditions. As shown as in Figure 5, boiling process occur between M1 (reservoir) and M1 (manifestation). Boiling process (steam loss) from reservoir to manifestation marked with an increase value in Cl content and decrease value of enthalpy. Process that occur in manifestation AC-6 and AA-3 are dilution by groundwater. Groundwater have cooler water temperature and lower chloride content thus dilution (mixing with groundwater) are marked by decreasing value in enthalpy and Cl content. Finally, process that occurs in other manifestations is boiling process followed by dilution by groundwater, which begins with increasing in Cl value and decreasing in enthalpy value and then followed by decreasing in both of Cl and enthalpy value.

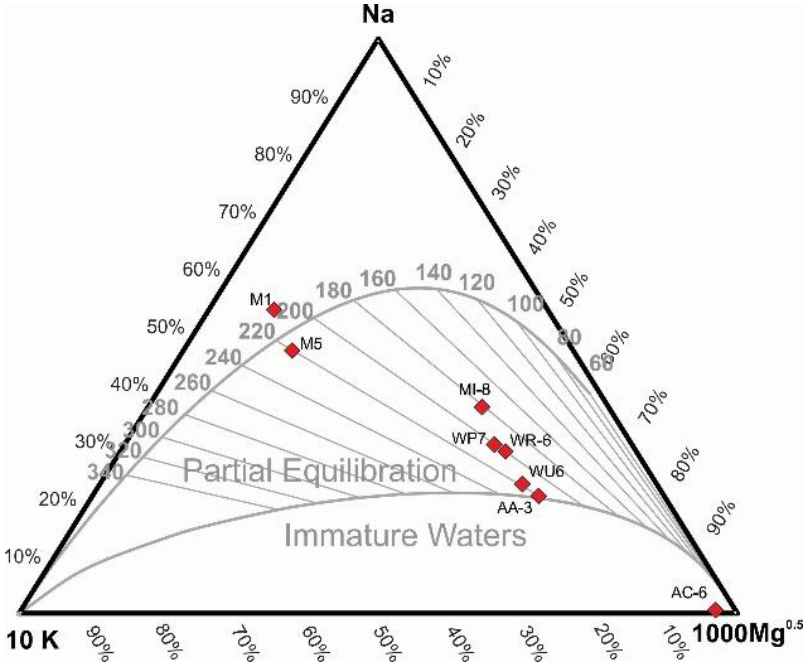


Figure 5: Cation ternary diagram consist of Na-K-Mg composition shows water from manifestation is immature water – fully equilibration.

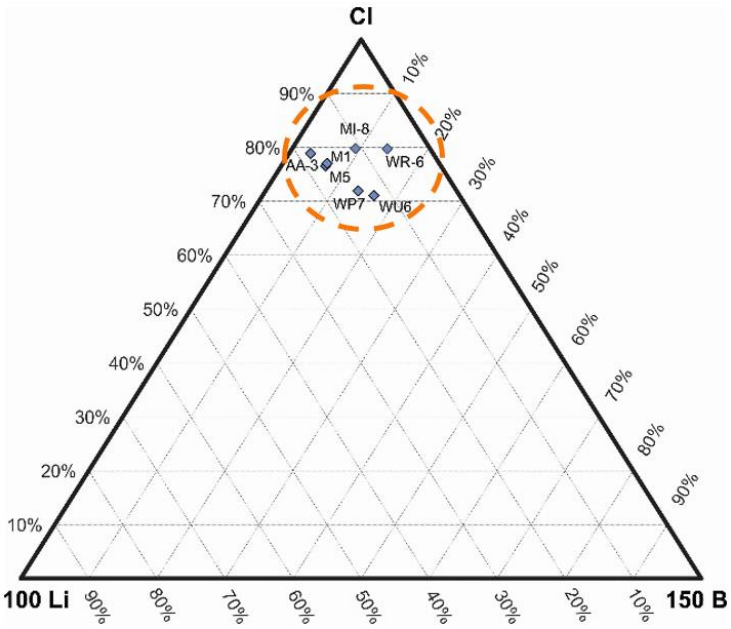


Figure 6: Cl-Li-B ternary diagram shows one reservoir in research area (encircled by orange circle).

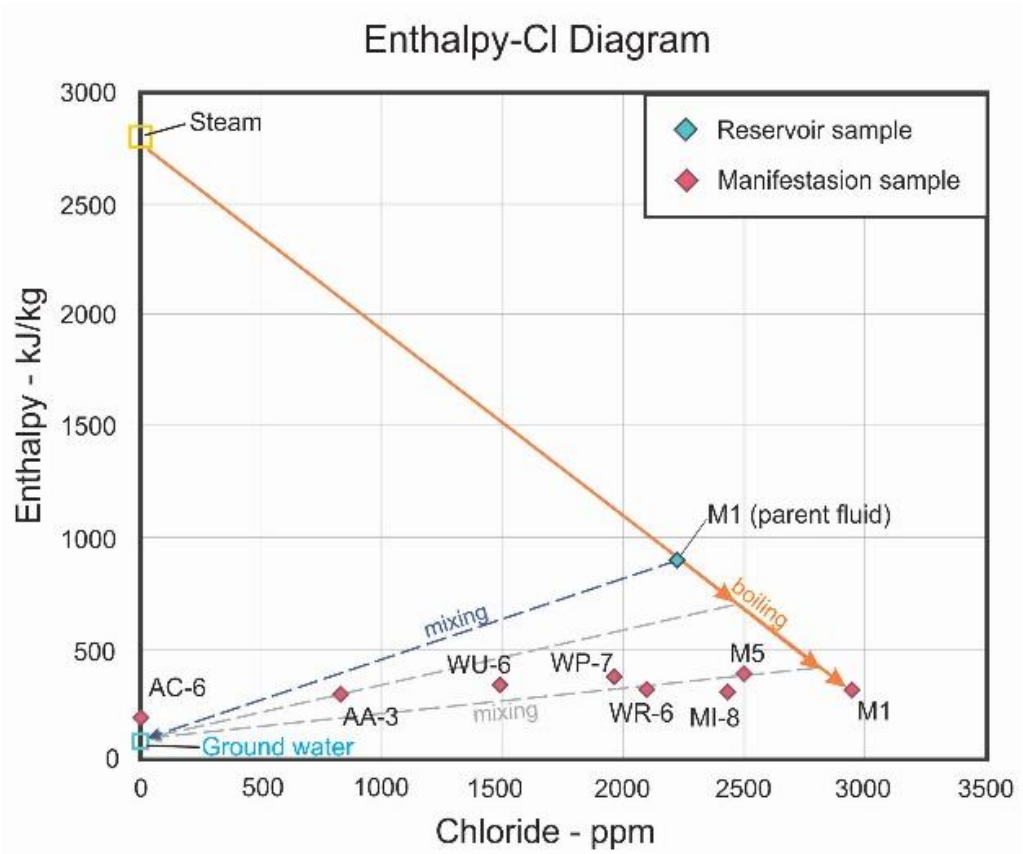


Figure 7: Enthalpy-Cl diagram. Reservoir sample is marked by blue dot marker and manifestation samples are marked by green dot marker.

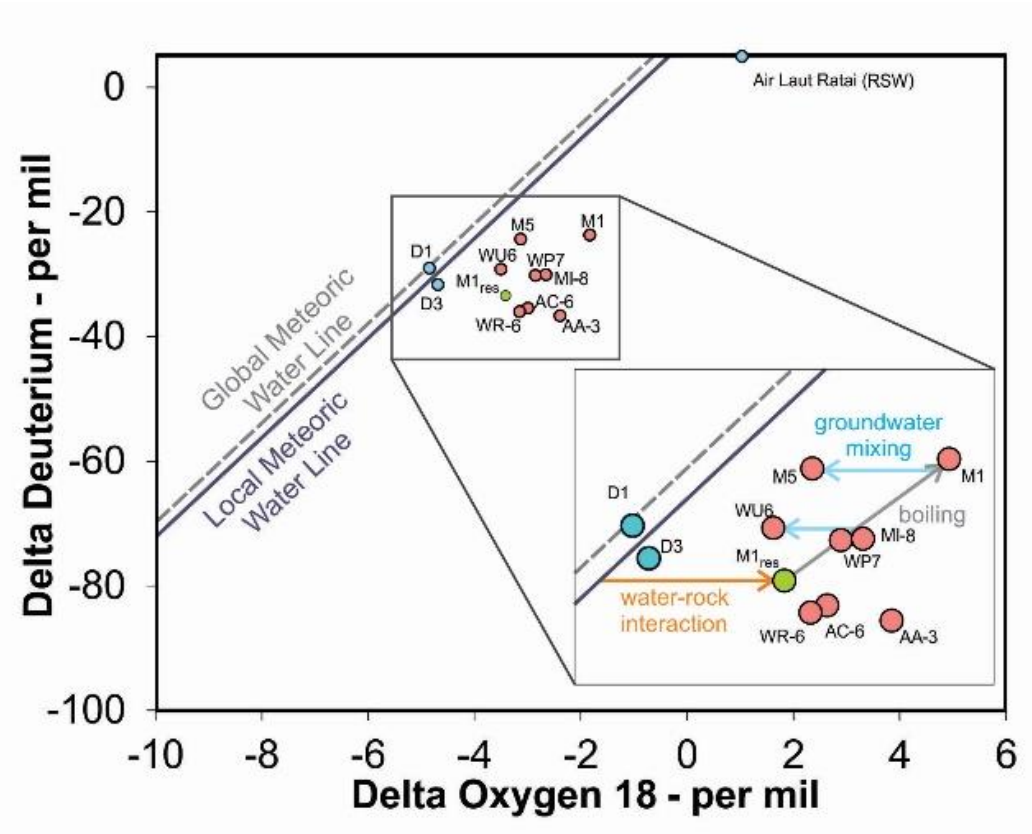


Figure 8: stable isotope oxygen-18 and deuterium shows process of water-rock interaction.

Origin of Geothermal Fluids

The result of stable isotope (δD- $\delta^{18}O$) (Figure 8) is used to recognize the origin and process of water and gasses. According to stable isotope diagram, hot spring manifestation samples are plotted with red marker, reservoir fluid is plotted with green marker, while cold water samples are plot with blue marker. Ratai sea water (RSW) sample were taken from Ratai Bay and was used as marker for mixing with sea water. Cold water samples as D1 and D2 represent meteoric water samples. Stable isotope variation δD and $\delta^{18}O$ local meteoric water follow a linear equation which is calculated based on 2 samples of cold water taken in research area, that is:

$$\delta D = 8\delta^{18}O + 8$$

The diagram shows geothermal fluid on research area has content of $\delta^{18}O$ and δD which is not much different from local meteoric water line (LMWL). Therefore, geothermal fluids in research area derived from meteoric water. Enrichment of $\delta^{18}O$ and no change of δD (LMWL – $M1_{res}$) resulted from water-rock interaction process that involves exchange of oxygen with heavier isotope. Boiling process is occurred on Margodadi M1 which marked by enrichment in both of δD and $\delta^{18}O$. Diminishment of $\delta^{18}O$ and no changes in δD (plotted data move closer to local meteoric water line) resulted from groundwater mixing. Stable isotope diagram also shows, all geothermal fluids have very different δD- $\delta^{18}O$ content with Ratai Sea Water thus geothermal fluids on research area are not related with seawater.

Geothermometer

Geothermometer is an approach which is used to estimate reservoir's temperature based on chemical composition on surface manifestation. In this research, geothermometer uses the Na-K geotermometer of Giggenbach (1988). Surface manifestation samples used for geothermometer are Margodadi manifestation (M1 and M5) due to high chloride content, good ion balance, and partially to fully equilibration water. The result of geothermometer measurement indicate reservoir temperature is around 208-220ºC.

Geothermal System of Way Ratai

Geothermal system indicated that the heat source of Mt. Ratai-Pesawaran geothermal system derived from the intrusion of magma which is the remnant of a remaining volcano. Meteoric water that reaches the heat source is then heated and flow to the surface through the area that has sufficient permeability which estimated as fracture zones caused by the fault system that developed in the study area. Based on Ministry of Energy and Mineral Resources (2017), depth of Way Ratai reservoir is at 750m below the surface. Thus, the reservoir area of research area occurs in Rhyolite tuff and pyroclastic breccia of Miwang (MTBd). Reservoir area is interpreted as liquid dominated system with estimated reservoir temperatures between 208-220°C. Fluid is then accumulated as a result of impermeable rocks form cap rock. Through the permeability zone, reservoir fluids flow to the surface and form neutral chloride hot spring and silica sinter in upflow zone.

CONCLUSION

Geological of research area consist of 8 lithology units which dominated by volcanic rocks. Lithology of Tertiary Period consist of 4 unit which Rhyolite Tuff and Pyroclastic Breccia of Miwang unit is the oldest lithology in this research area and originates from volcanic activity in Late Eocene – Mid. Oligocene. This lithology unit more and less formed at the same time with Gebang Caldera. Biotite – Hornblende Andesite of Miwang and Andesite tuff and pyroclastic breccia of Miwang were deposited in sequence and above rhyolite tuff and pyroclastic breccia of Miwang which formed by volcanic activity on volcanic terranes in Late Oligocene-Early Miocene. During Paleogene (Paleocene-Oligocene), reactivation fault from Pre-Tertiary faults occurred which is marked by faults with NW-SE direction cut Biotite – Hornblende Andesite of Miwang and Andesite tuff and pyroclastic breccia of Miwang unit. Andesite Intrusion intrudes all previous unit in Middle Miocene and interpreted as stock intrusion. Sumatra Faults System were initiated Middle Miocene and continues until Holocene which is marked by fault with NW-SE and N-S direction cut Tertiary rock units. Next, hornblende-biotite andesite of Ratai, rhyolite lapilli tuff of Ratai, and pyroxene andesite of Ratai were deposited sequentially and were formed during Pleistocene – Holocene. Unconformity occurs between hornblende-biotite andesite of Ratai and Andesite tuff and pyroclastic breccia of Miwang thus time gap occurs between Quaternary rocks unit and Tertiary rocks unit. Alluvial deposit was deposited in Holocene and was the youngest unit in research area.

Geochemistry analysis showed that geothermal of research area is dominated by chloride hot spring with near neutral pH and are located in upflow zone. Moreover, geochemistry analysis shows one reservoir with estimated reservoir temperature of 208-220ºC and depth of reservoir 750 m. The isotope data and mixing model diagram shows that reservoir originates from meteoric water that undergoes water-rock interaction. Furthermore, boiling and groundwater mixing process occur and water from reservoir emerge rise to the surface through fractured rocks. Heat source of Mt. Ratai-Pesawaran geothermal system derived from the intrusion of magma which was the remnant of a remaining volcano. Reservoir area occurs in Rhyolite tuff and pyroclastic breccia of Miwang

(MTBr) which were fractured by various faults with N-S, NW-SE, and NE-SW direction.

ACKNOWLEDGEMENT

The authors are grateful to Riset Program Penelitian, Pengabdian kepada Masyarakat dan Inovasi ITB (P3MI-ITB) 2018 for supporting this research.

REFERENCES

Barber, A. J., Crow, M. J., and Milsom, J. S. (2005), "Sumatra: Geology, Resources and Tectonic Evolution," Geological Society, London, Memoirs, 31.

Bellon, H., Maury, R. C., Sutanto, Soeria-Atmadja, R., Gotten, J., and Polvè, M. (2004), "65 m.y.-long magmatic activity in Sumatra (Indonesia) from Palaeocene to Recent," Bulletin de a Society Geologique de France, 175, 61-72.

Giggenbach, W. F. (1988), "Geothermal Solute Equilibria. Derivation of Na-K-Mg-Ca Indicator" Geochimica et Cosmochimica Acta, 52, 2749-2765

Herdianita, N. R., Sucipta, I. G. B. E., Basuki, N. I., and Saepuloh, A. (2018), "Aliran Fluida Hidrotermal dan Evolusi Magmatik Sumber Panas Magmatik di Sistem Geotermal Way Ratai, Lampung, Indonesia," 3rd International Conference of the TREPSEA.

Hochstein, M. P., and Browne, P. R. L., (2000), "Surface Manifestations of Geothermal System with Volcanic Heat Sources," Encyclopedia of Volcanoes, 1, 835-855.

Mangga, S. A., Amirrudin, Suwarti, T., Gafoer, S., and Sidarto (1994), "Geology of the Tanjungkarang Quadrangle, Sumatra," Geological Research and Development Centre.

McPhie, J., Doyle, M., and Allen, R. (1993), "Volcanic Texture: A Guide to The Interpretation of Texture in Volcanic Rocks," Centre of Ore Deposit and Exploration Studies, University of Tasmania.

Ministry of Energy and Mineral Resources (2017), "Potensi Panas Bumi Indonesia," Ministry of Energy and Mineral Resources, 1, 391-397.

Nicholson, K. (1993), "Geothermal Fluids: Chemistry and Exploration Techniques," Springer-Verlag, Berlin Heidelberg.

Powell, T., and Cumming, W. (2010), "Spreadsheet for Geothermal Water and Gas Geochemistry," Proceeding Thirty-Fifth Workshop on Geothermal Reservoir Engineering, Stanford University.

Pulunggono, A., Haryo S., A., and Kosuma, C.G. (1992), "Pre-Tertiary and Tertiary Fault Systems as a Framework of the South Sumatra Basin; a Study Of SAR-Maps," 21stAnnual Convention Proceeding Indonesian Petroleum Association, 1, 339-360.

IDENTIFYING OF GEOTHERMAL MANIFESTATION EXISTENCE AND CHARACTERIZATION OF SULPHIDATION TYPE USING LANDSAT-8 IMAGE PROCESSING RESULTS: CASE STUDY OF MOUNT PAPANDAYAN AREA, GARUT REGENCY, WEST JAVA PROVINCE

Sinatrya Diko Prayudi[1,2], Daffa Arrofi[1], and Rinal Khaidar Ali[1]

[1]Departement of Geological Engineering, Diponegoro University, Semarang, Indonesia
[2]North East Java Research Section, Diponegoro University, Semarang, Indonesia
Email: sinatrya.diko@gmail.com

ABSTRACT

Papandayan Volcano is one of the high potential geothermal fields which is estimated to be developed as a potential electricity supplier in Java-Bali, in terms of the number of geothermal manifestations ejected from the mountain's body. In the geothermal field itself there is a role from hydrothermal solutions as the main component in triggering alteration processes in the surrounding rocks. The alteration process in rocks that occur created several alteration minerals that can be used as an indicator of sulphidation type in research areas, especially around the presence of geothermal manifestations which are generally characterized by high surface temperatures. Determination of sulphidation types is generally based on grouping of characteristic minerals, both characterizing minerals which tend to be acidic (high sulphidation) or neutral (low sulphidation). Determining the presence of alteration minerals found in active geothermal fields can be carried out widely using several methods, one of which uses remote sensing. By using remote sensing analysis, this study focuses on the detection of related alteration minerals to active geothermal fields on Papandayan Volcano, both in the crater and surrounding areas. Processing data from Landsat 8 focused on four main results: surface normalize difference index (NDVI - NDWI) and anomalies in land surface temperature using Land Surface Temperature (LST) to identify the presence of geothermal manifestations, determination of mineral group alteration results using Band Ratio, and determination of sulphidation type by reference to mineral that characterize each type using the Spectral Angle Mapper (SAM). The results obtained show potential geothermal manifestation in regions through the surface temperature, the lateral distribution of the alteration minerals obtained, and the result of overlaying the characteristic mineral data from Landsat data 8. The three results obtained can be used as a reference in the determination of geothermal fields, both known and unknown.

Keywords: Remote sensing, landsat-8, Mt. Papandayan, geothermal

INTRODUCTION

In order to understanding the potential of a geothermal field, the most common thing is to identify the presence of geothermal manifestations on the surface. Generally, in the case of geothermal manifestations that can be exposed to the surface in a fluid phase, the main controller to be able to migrate to the surface is the existence of a path or exit in the form of a fracture. The existence of these pathways, which are generally in the form of permeable zones, usually has a fracture effect that develops in the geothermal region (Soengkono, 1999; Nurohman, 2016). The more fluid outflows, the more existence of surface manifestations is found.

Many studies have been developed to examine the existence of permeable zones in the form of faults that creating the pathway of hydrothermal fluid using geochemical and geophysical data, both case studies in Papandayan Volcano and other geothermal potential areas (Nasution et al., 2008; Nuha et al., 2014; Nurohman et al. 2016; Byrdina et al., 2018). Broadly speaking, research with the data above requires substantial funds and not a short time. Regardless of the accuracy of the data obtained, there is one methodology that has the potential to map geothermal potential areas on a wide scale and relatively faster time, namely as remote estimation approach. This approach involves processing data both image and non-imagery in a study that is tailored to the needs, in this case geothermal exploration. In the Indonesian territory itself, this approach is often reviewed and applied to several geothermal potential areas. On this occasion, the author will examine the method of remote sensing approach for exploration of potential geothermal areas that are quite well known but not yet fully utilized, namely Papandayan Volcano.

Remote sensing itself is often used enough to analyze the geological conditions of a region. Some of those that have been successfully assessed are identification of potential mineral mines (Abhary and Hassani, 2016; Julzarika, 2018), altered rock mapping (Mia and Fujimitsu, 2012), and so on. The remote sensing approach carried out in the Papandayan Volcano case study itself uses the main Landsat-8 OLI/TIRS imagery obtained from the

USGS Earthexplorer image data provider site. The main target of image data processing carried out includes the aspects: mapping the occurrence of other manifestations around Papandayan Volcano and mapping the presence of alteration minerals in the area affected by hydrothermal fluid as a reference to determine the sulphidation type of the target area. Data processing carried out including several GIS-based software and a series of satellite image data processing stages.

Referring to the study conducted by Mazot et al (2008) regarding the distribution of surface manifestations in Papandayan Volcano, there are several locations around the main crater. Geothermal manifestations found in the form of altered rocks, fumaroles, and hot springs. Volcanism activity that occurred in 2002 also provided additional fluid output gaps as successfully mapped by Mazot et al (2007) with the distribution presented in Figure 1.

When referring to the geological map of the Papandayan Volcano area, there are controls for two main geological structure units and several minor geological structures around the volcanic body (Figure 2). This gives an indication of the potential point of emergence of other manifestations and areas that may be affected by hydrothermal alteration in addition to the center of the Papandayan Volcano crater.

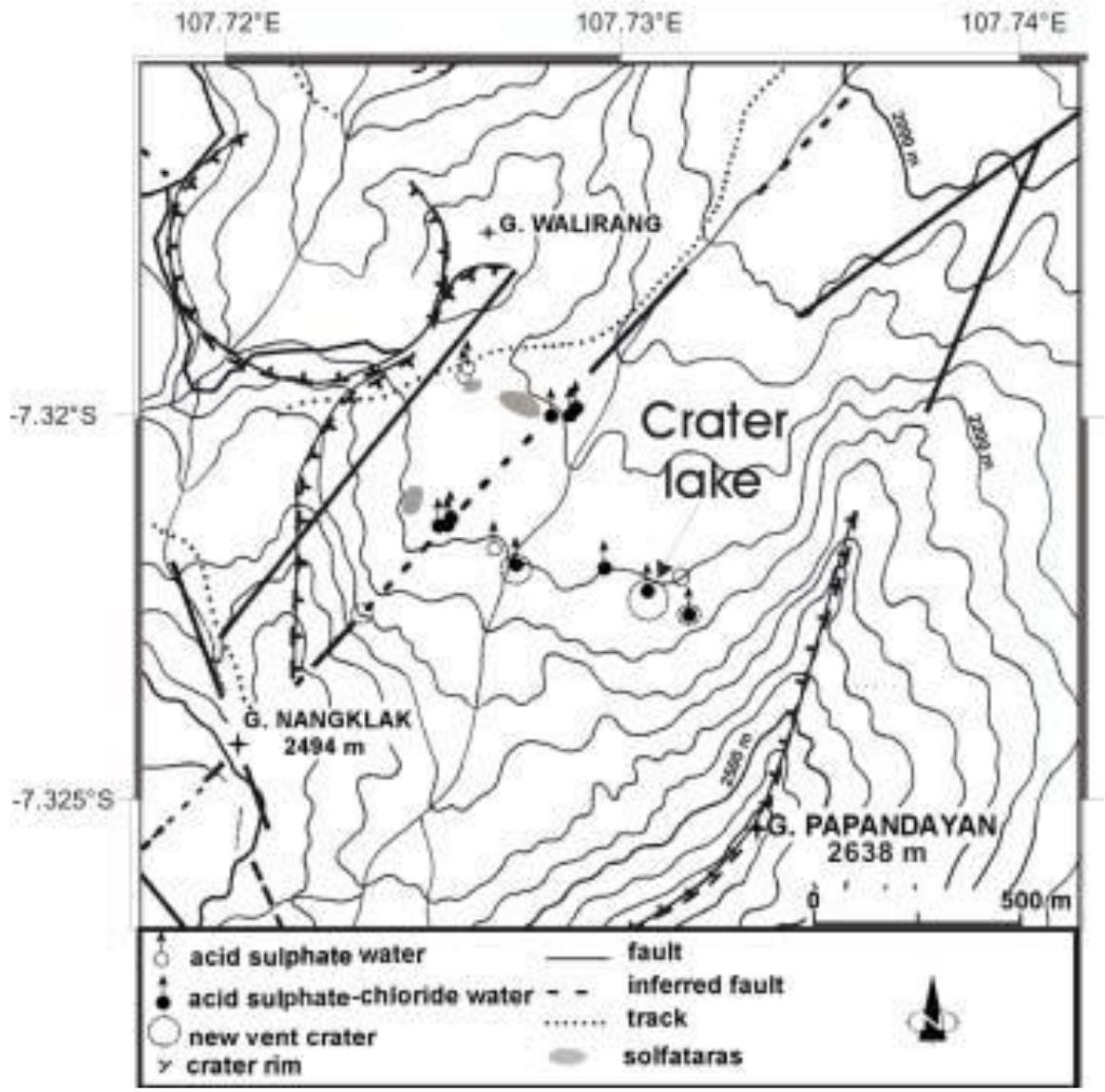


Figure 1: Distribution of morphological, structural and manifestation feature in Papandayan Volcano (Masot et al, 2007).

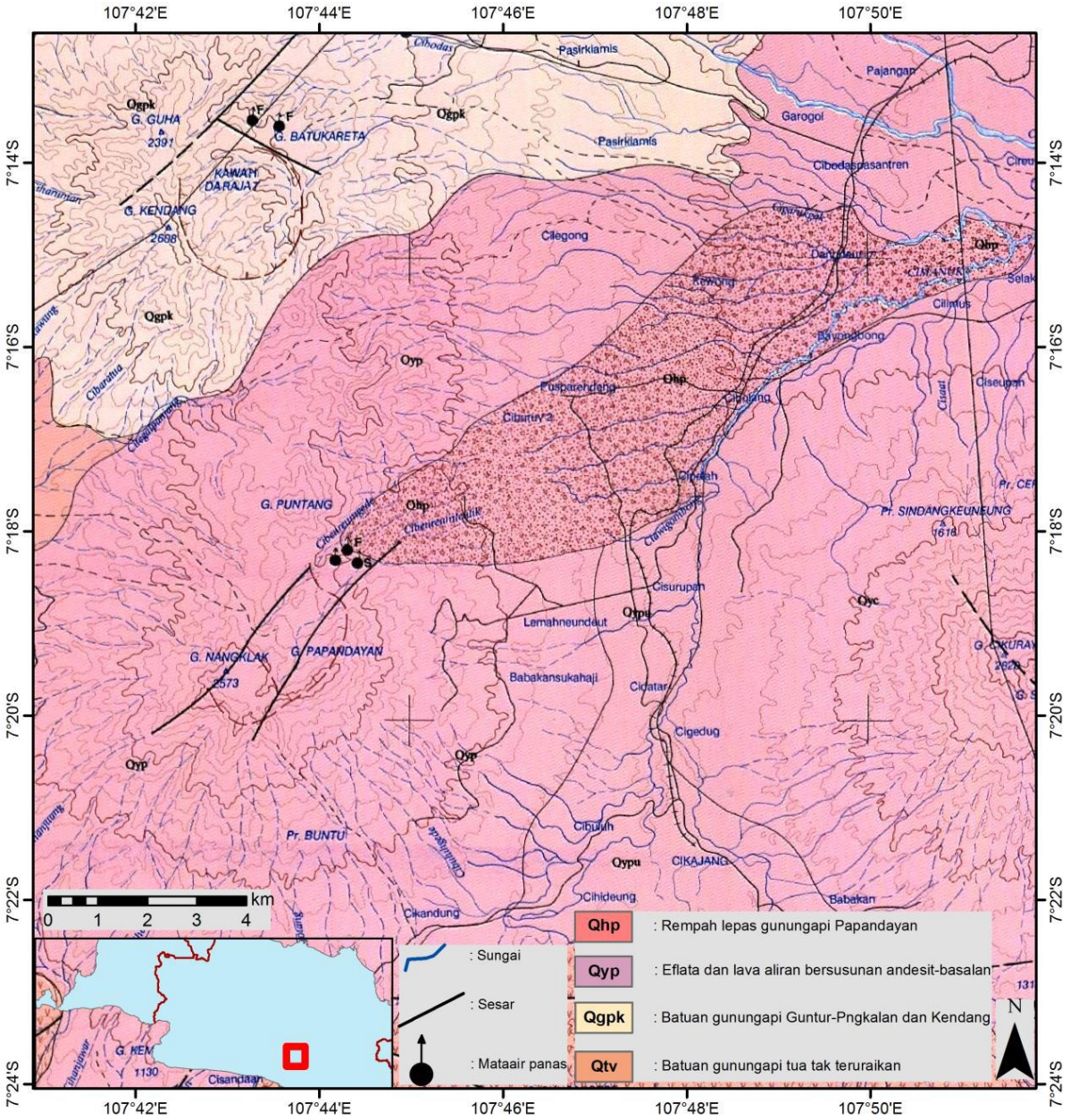


Figure 2: Regional geological map of Papandayan Volcano (Alzwar et al, 1992).

RESEARCH STUDY LOCATION

Papandayan Volcano is one of the few active volcanoes in the West Java region, precisely in the area between Bandung and Garut Regencies. The location is astronomically located at 7 ° 32 ', 107 ° 73' E and has a measured topographic height of 2.665 meters above sea level. According to Fauzi (2015), the position of Papandayan Volcano itself is in the outer circle part which is composed of an active volcanic range in the eastern part of West Java such as Gede, Patuha, Cikuray, Galunggung, Karaha, and Tangkuban Parahu. In the inner part of the circular pattern, there are several volcanoes with proven geothermal potential and are utilized, such as Wayang Windu, Kamojang, Darajat, and Guntur (Figure 3).

Suspecting from the rock stratigraphy conditions in Papandayan Volcano generally composed of two formations types, namely the Papandayan Volcano crumbles part unit (Qhp) and the Papandayan young volcanic rock unit (Qyp). The loose spice unit itself contains volcanic ash left over from past eruptions of Papandayan Volcano and lumps - blocks that were thrown out during volcanic eruptions similar from 2002 event. Whereas the second unit (young volcanic rock) contains eflata and andesite-basaltic flow lava which is rocky older than the previous unit.

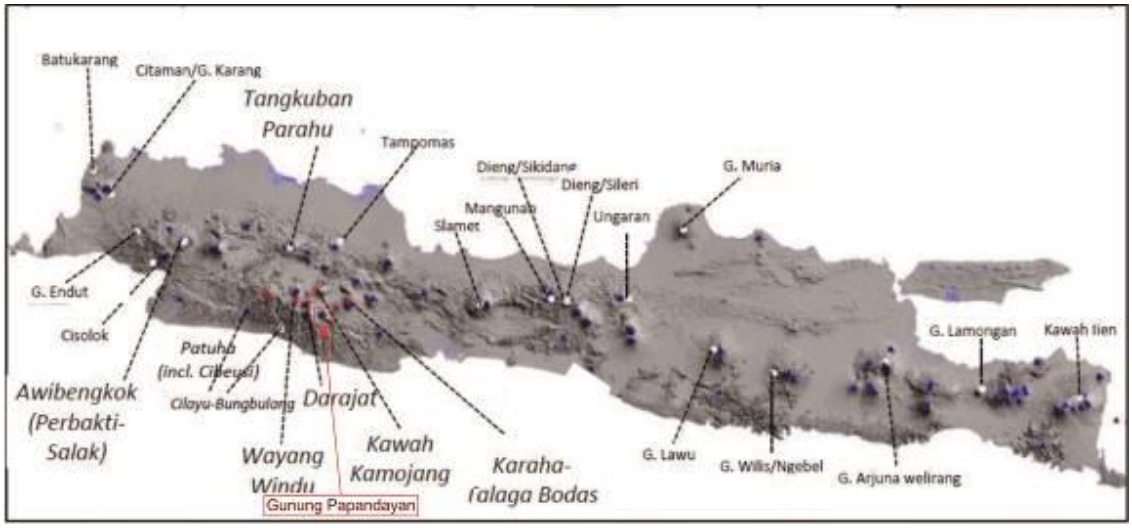


Figure 3: Distribution of active and geothermal-potential site volcano in Java (Hochstein and Crosetti, 2012; Setiawan et al., 2018).

METHOD

Remote sensing carried out in relation to the exploration study of geothermal potential areas in this study is part of the main data analysis. This method can relatively provide information to users without the need for direct contact with objects studied in the field (Lillesand and Kiefer, 1979). Data processing focuses on the main remote sensing image data with easy access: Landsat-8 OLI/TIRS.

Processing data involving Landsat-8 images through several systematic sequences, starting from the initial stage of processing (Pre-Processing), delineating the target area (Region of Interest), directing the classification stage and interpreting image data. The pre-processing phase that is performed using ENVI 5.1 software includes a radiometric calibration mechanism to eliminate any interference that causes image data to be bad. In addition, this process also changes the image's original data value (Digital Number/DN) to the reflectance value that is suitable for directed classification processing. Radiometric correction is done because it has a role to eliminate radiometric distortion that decreases image quality when satellites record earth due to the distance between different satellites in space with a very far surface of the earth, thus affecting the ability of satellite sensors to record the reflectivity of earth objects or called reflectance (Utami, 2015).

Specifically, the use of Landsat-8 imagery focused on the spectral analysis mechanism, which is processing and interpreting spectral data contained in each band. The types of Landsat-8 OLI/TIRS image data used include multispectral bands (1 to 7) and thermal bands (10 and 11). To identify the existence of other sources of manifestations in the Papandayan Volcano region, both types of bands are used intensively. The multispectral band plays a role for processing vegetation index (NDVI) and water (NDWI) which gives an idea of the existence of these manifestation points, while the thermal band to obtain anomalous values of land surface temperature (LST) as an indicator of the hot spot presence of surface manifestations. In an effort to get the final value of LST, according to Anandababu et al (2018) it is necessary to process the thermal band data to obtain a value Thermal of Atmosphere (TOA) Radiance, Brightness Temperature (BT), dan Land Surface Emissivity (LSE or E). Related calculation shows in Equation 1 to 7.

$$NDVI = \frac{Band\ 5\ (NIR) - Band\ 4\ (Red)}{Band\ 5\ (NIR) + Band\ 4\ (Red)} \quad \text{..... (1)}$$

$$NDWI = \frac{Band\ 3\ (Green) - Band\ 5\ (NIR)}{Band\ 3\ (Green) + Band\ 5\ (NIR)} \quad \text{..... (2)}$$

$$L\lambda\ (Radiance/W) = ML * Qcal + AL \quad \text{..... (3)}$$

$$BT = K2/\ln (k1/L\lambda + 1) - 272.15 \quad \text{..... (4)}$$

$$PV = [(NDVI - NDVI\ min)/(NDVI\ max + NDVI\ min)]^2 \quad \text{..... (5)}$$

$$LSE = 0{,}004 * PV + 0{,}986 \quad \text{..... (6)}$$

$$LST = (BT/1) + * (BT/14380) * \ln(E) \quad \text{..... (7)}$$

Where:

- $L\lambda$ = TOA spectral radiance (Watts/ (m^2 * sr * µm))
- ML = Radiance multiaplicative Band (No.)
- AL = Radiance Add Band (No.)
- Qcal = Quantized and calibrated standard product pixel value (DN)
- K1 = K1 Constant Band (No.)
- K2 = K2 Constant Band (No.)
- PV = Proportion of Vegetation

Spectral analysis carried out aside from NDVI processing - NDWI - LST is processing composite band data, band ratio, and processing Spectral Angle Mapper directional classification data. For the concept of using composite band and band ratio is the merging of a number of bands on Landsat 8 image data (three bands with RGB arrangement) into a single data display. Band ratios generally use two sets of bands, where in one collection there are two bands that are compared to the appearance of their reflections. The mechanism of the results of the band ratio itself is an increase in spectral contrast of each band (Segal, 1983) and displays unique information that is not obtained from composites per ordinary band unit (Jensen, 1996). The Directional Spectral Angle Mapper (SAM) classification method is an angle comparison algorithm between vector endmembers and each pixel vector in n-dimensional space (ENVI, 2001). SAM classification recognizes objects based on two things, namely the average spectrum and the spectrum of object classes (specific). If the pixels to be identified have a spectral angle with a degree value that is less than the average spectrum then the pixels enter into the class that has been determined (Figure 4). But on the contrary, if the pixel has a spectral angle with a greater value then the pixel becomes a non-target class (Danoedoro, 2015).

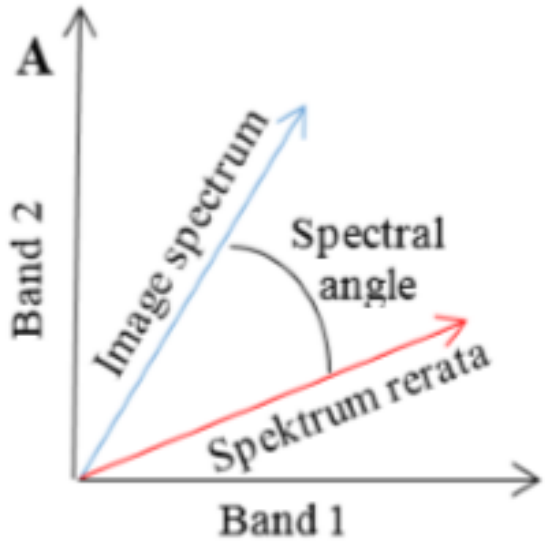


Figure 4: Conceptual model of Spectral Angle Mapper analysis for remote sensing

RESULT AND DISCUSSION

Preprocessing Data

The preparation phase for preprocessing data image data is carried out in accordance with the methodology to improve display quality and image data values. The twofold mechanism is carried out: atmospheric and radiometric correction; where the first type to improving quality becomes cleaner and second aspect to converting value (DN to Reflectance). The results of the atmospheric image correction can be seen in Figures 6A and 6B as well as for radiometric correction results in Tables 1 and 2.

Spectral Analysis: NDVI and NDWI

The first multispectral band analysis in Landsat 8 data is intended to analyze the difference in normalization index of the surface in the study area. The processing results obtained are in the form of surface index of vegetation (NDVI) and water (NDWI) on the surface. Processing data from each index utilizes the reflectance value of each band for objects that are on the surface of the earth. NDVI processing itself uses band number 4 (red) and 5 (near infrared/NIR) multispectral bands. This band plays a role in identifying vegetation because related objects will show high reflectance values compared to other bands, especially NIR bands (Price, 2010). Limits in classification are reflectance values where the vegetation value that is read in the results theoretically is in the range of 0,25 or 0,33 while the non-vegetation object is worth below 0,25. Based on these references, the processing of NDVI data in the Papandayan Volcano area produces the highest range of values of 0,875482 and the lowest of -0,285714. When referring to the parameters above (vegetation and non-vegetation values), the results obtained can be seen in Figure 6A.

For NDWI processing itself targeting occurred water objects using band 3 (green) and 5 (near infrared/NIR). According to Mc Feeters (1996), this processing can map accurately enough the presence of fluid in the form of surface water, such as rivers, lakes, ponds, reservoirs and other bodies of water. The parameter of assessment that distinguishes the body of water from other than water is determined by the limit value >0 (Figure 6B). The result of this spectral analysis ranging from -0,88 to 0,477; separating into three class based on each value range.

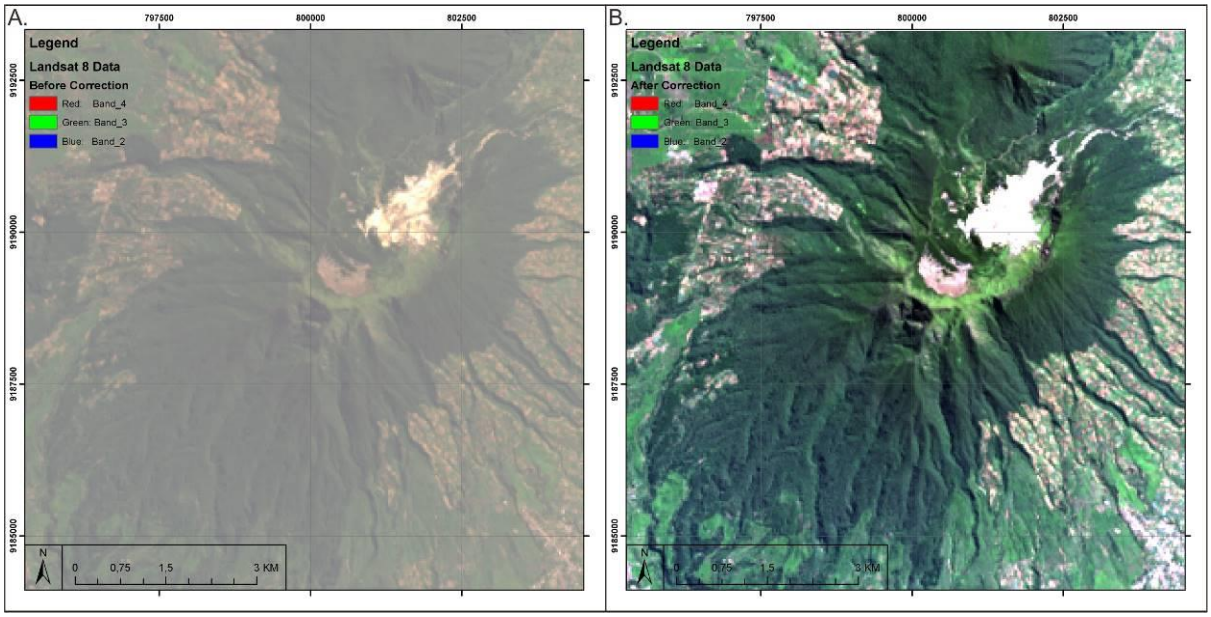


Figure 5: Comparison of uncorrected Landsat 8 data (A) and atmospheric correction result (B) in Papandayan Volcano.

Table 2: Value of Landsat 8 data from 2018 before radiometric correction.

Band Number	Min	Max
Band 1	7776	14093
Band 2	7005	14637
Band 3	6068	15483
Band 4	5575	17065
Band 5	5455	25036
Band 6	5137	20439
Band 7	5070	15803

Table 2: Value of Landsat 8 data from 2018 before radiometric correction.

Band Number	Min	Max
Band 1	0,1404	0,4218
Band 2	0,01	0,3007
Band 3	0,0476	0,3779
Band 4	0,0247	0,3948
Band 5	0,014	0,5727
Band 6	0,0042	0,4385
Band 7	0,0022	0,3274

Spectral Analysis: LST

Processing image data to obtain land surface temperature data (LST) as described in the previous section using thermal bands (10 and 11). Additional data that helps increase the accuracy of results also involves multispectral bands (1 to 7). The utilization of these bands plays a role in the systematic processing of LST data, namely: the acquisition of radiance and brightness temperature data from thermal bands and the acquisition of emissivity data involving the influence of vegetation control which is read by multispectral bands. The formulation of the reference values is a reference calculation as in the methodology section above. The processing results obtained a range of surface temperature values ranging from the lowest value of 12,09ºC and the highest of 35,23ºC. The dominance of values in the study location is the area with a low surface temperature (<30oC) or indicated in yellow to green. The distribution of the resulting temperature value can be seen in Figure 6C.

Interpretation of NDVI – NDWI – LST Overlay Result

The process of overlaying data plays an important role in knowing the distribution of regions and the point of existence of manifestations in the study area. Each of the data raised has different roles and weights at this stage. For NDVI data, regions that show non-vegetation areas increasingly indicate the existence of areas that have the potential for geothermal manifestations. For NDWI data, areas with the presence of water or fluid on the surface of the active volcano region provide an indication of the area of fluid output from the volcano to the surface, so that the water markers play a major role. For LST data, the region with a difference in the average temperature of the earth's surface (20^o - 23ºC).

From each of these data, the data overlay process is done by making each data sorted into 3 potential categories: low potential (1), medium potential (2), and high potential (3). The final results were obtained with range values divided into 3 types: low potential areas (1 - 3), medium (3,1 - 6), and high (6,1 - 9). The results of the overlay process can be seen in Figure 5D.

The results of the overlay of the data provided provide a relative picture of the distribution of regions that are possible for geothermal manifestations. The main region that has geothermal manifestations based on the data overlay above is the crater section of the Papandayan Volcano itself. Other regions indicated there are geothermal manifestations in the area outside the crater located on the northwest and southeast side of the center of the volcano.

Spectral Analysis: Band Composite and Ratio

The concept of using a composite band and band ratio is to combine several bands from Landsat-8 images that have high reflectance values for alteration minerals, especially infrared bands (SWIR and NIR). Some band composites used in the detection of the presence of alteration minerals or rocks that affected hydrothermal alteration processes include: RGB 432, RGB 573, RGB 576, RGB 752, and RGB 567 (Mia and Fujimitsu, 2012). While some types of band ratio methods that play a role in mapping the existence of textures on the surface include: Chica Olma method, Segal method, Kaufmann method, and Abrams method (Zhou et al, 2013). The second analysis method in this section is the use of composite bands for identifying the distribution of hydrothermal altered rocks. The first band composite (RGB 432) illustrates the original color appearance of the area carried out by the study. The secondary band composite (RGB 573) produces a distribution area indicative of the rock outcrops affected by hydrothermal fluid in areas with dark green and increasingly towards blue in strongly altered rocks or geothermal manifestation areas such as fumaroles. For the third composite (RGB 576) it describes altered rocks as a green color to dark green. For the fourth composite (RGB 567) it describes the distribution of rocks exposed in light blue and those with high alterations in dark blue. For the fifth composite (RGB 752) it describes the distribution of fluid on the surface in blue as an indication of geothermal manifestations and rock outcrops in orange to pink. Each of the composites made (Figures 7A to 7E) shows the distribution pattern of the altered rocks located on the inside of the Papandayan Volcano crater and some on the outside of the crater as on the southwest and west sides. The next method used was a band ratio consisting of 4 types analyzed. For the first type, Chica Olma Ratio (6/7: 6/5: 4/2) illustrates the distribution of alteration minerals rich in iron ions in green and iron oxide in blue. For the second type, Segal Ratio (4/2: 6/7: 6/5) describes blue ion-enriched iron and iron oxide with red to pink. For the third type, Kaufmann Ratio (7/5: 5/4: 6/7) describes the distribution of minerals containing iron ions in red and hydroxyl minerals in dark blue. For the last type, Abrams Ratio (6/7: 4/3: 5/6), it describes relatively altered rocks forming iron oxides with a composition of light green to old colors. For the results of each band ratio the outline approaches the similarity with the composite band results, namely the distribution of alteration minerals and hydrothermal altered rocks located in the interior of the crater and some around the Papandayan Volcano crater (Figures 8A to 8D).

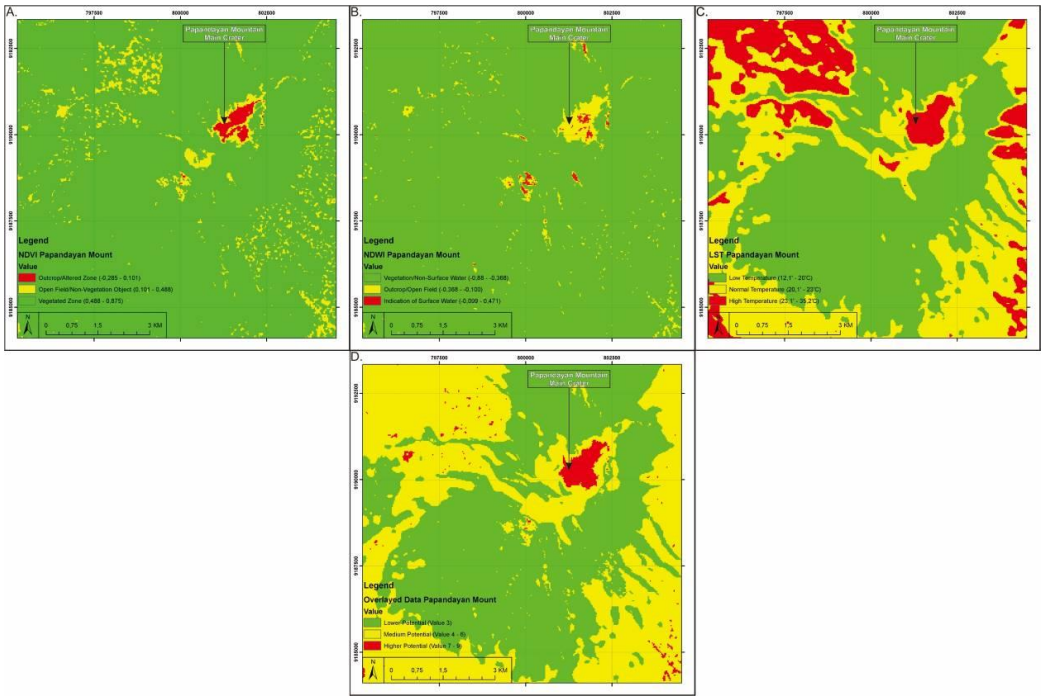


Figure 6: Spectral analysis result in NDVI (A), NDWI (B), LST (C), and overlying map (D) to result geothermal distribution potentially area.

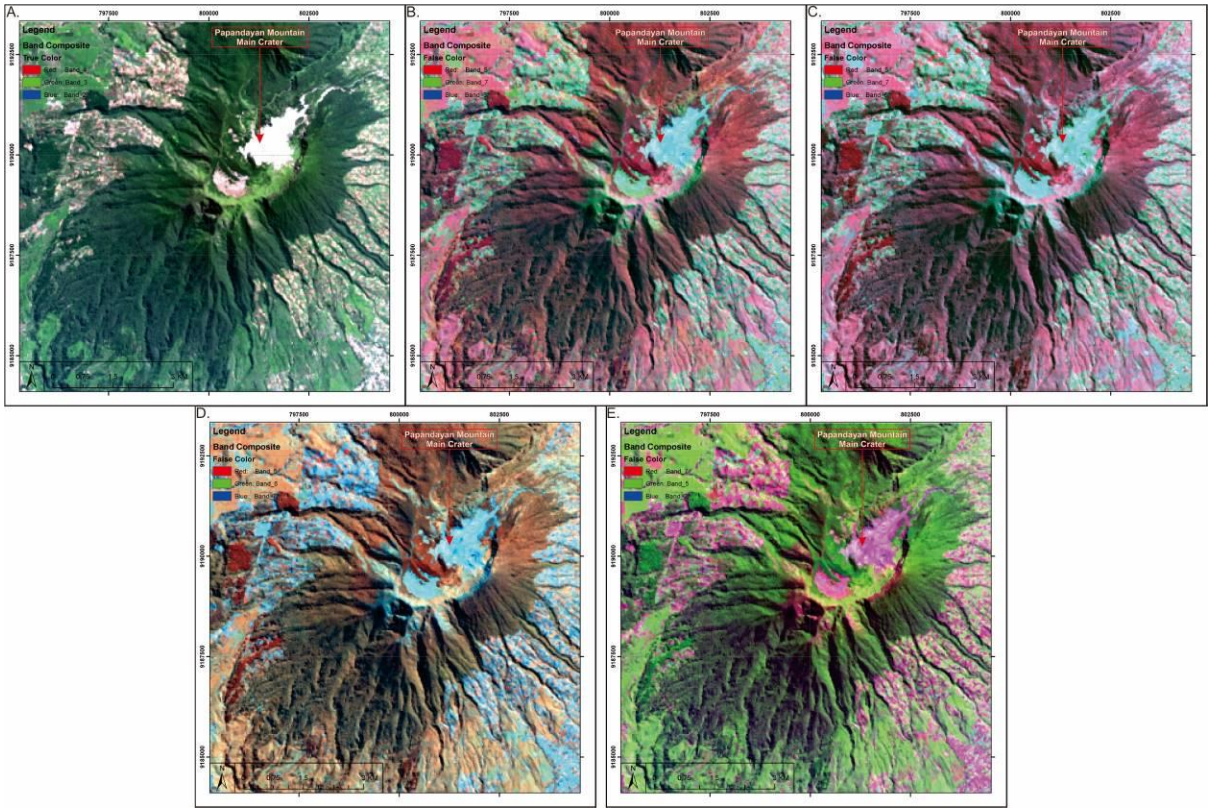


Figure 7: Spectral analysis map from Papandayan Volcano Landsat 8 band composite method in band composition RGB 432 (A), 573 (B), 576 (C), 567 (D), and 752 (E).

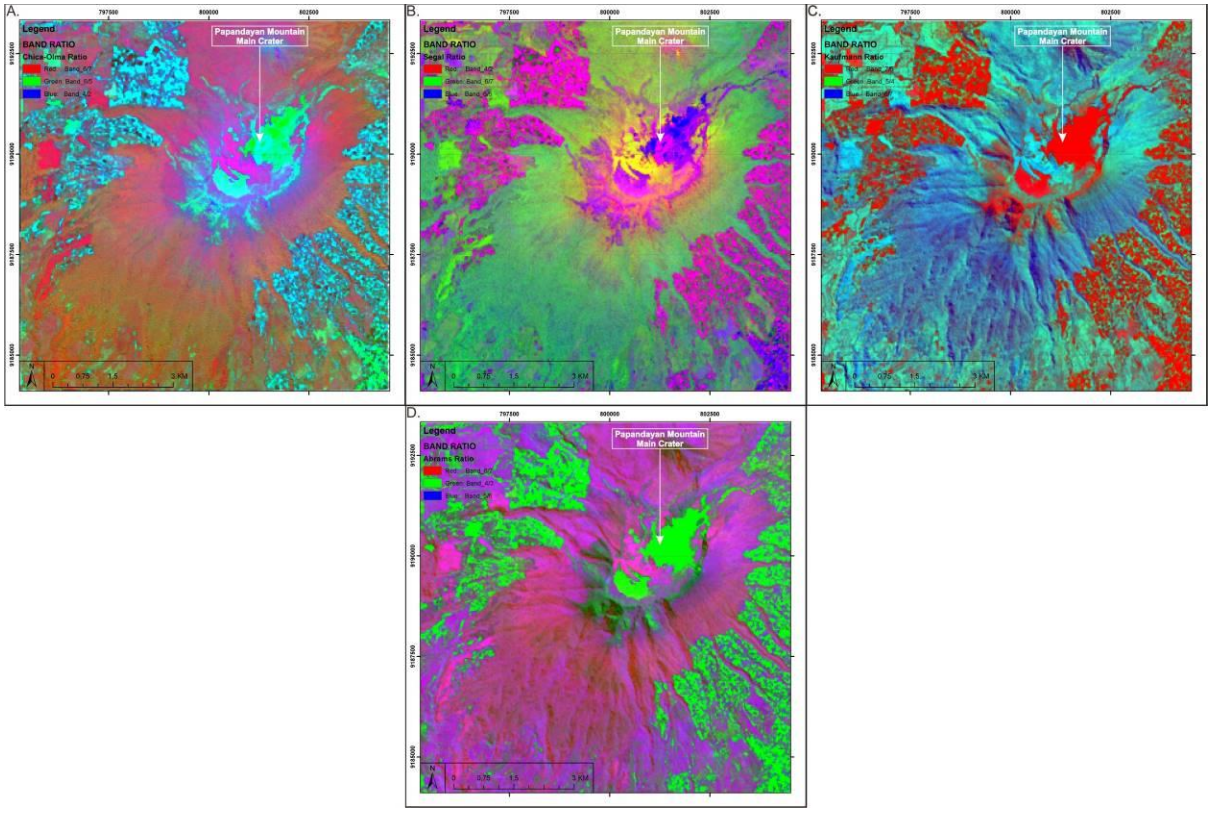


Figure 8: Spectral analysis map result from Papandayan Volcano Landsat 8 band ratio method in Chica Olma (A), Segal (B), Kaufmann (C), and Abrams (D).

Spectral Analysis: Spectral Angle Mapper

The use of Landsat-8 image data that has been radiometrically calibrated from the data digital number to reflectance value can be used further to map the presence of certain minerals on the earth's surface. The utilization of this method through ENVI 5.1 software uses the assumption of the data reflectance value possessed compared to the reflectance of the targeted object (mineral) so that it forms a certain angle. The angle containing the range of reflectance values is a sign of the presence of the object to be searched by the author. Referring to previous research conducted by Mazot et al. (2007) regarding the presence of alteration minerals in Papandayan Volcano, there are several types of minerals through the XRD data found by the researcher. Minerals intended include: native sulfur, christobalite, quartz, pyrite, marcasite, pyrophyllite, alunite, anhydrite, gypsum, kaolinite, enargite, rutile, and anatase.

The collection of minerals referred to in this study is not just a random mineral but refers to certain alteration minerals that characterize the sulphidation type of an active geothermal field. The main reference when examining the problem of hydrothermal and sulphidation processes is the accumulation of sulfur in the study area. The next reference taken comes from the classification of alteration minerals by Morisson (1997). The first collection of minerals, namely high sulphidation with fluids tends to be acidic which can be raised including: alunite, jarosite, halloysite, kaolinite, dickite, pyrophyllite, diaspore, topaz, and rutile. Whereas the second collection of low sulphidation with a fluid composition that tends to be neutral to alkali includes: quartz, pyrite, smectite, illite, chlorite, epidote, biotite, adularia, calcite, mordenite, and laumontite. The collection of minerals above cannot all be displayed in accordance with what stated in the previous explanation due to differences in the reference composition of the Spectral Angle Mapper method, especially Spectral Library (Spec_Lib).

The presence of sulfur in a geothermal region is generally around the area of the discharge of hydrothermal fluid, both fractures and gas holes. Specifically, the output of sulfur is generally known as a fumarole. To find out the distribution of sulfur accumulation as one of the main characteristics of active geothermal areas in the study area, the SAM method was applied at the earliest session. The distribution of sulfur can be seen in Figure 9.

For alteration minerals with acidic fluid associations according to the preceding explanation, each type and distribution raised from the results of the Spectral Angle Mapper method can be seen in Figure. The results of the accumulation of these mineral assemblies totaling 9 types for the type of acidic fluid and 11 types for the neutral fluid to the alkali produced a significant accumulation of distribution when overlaid each of the minerals into one overlay which can be seen further in Figure. From the results of the overlay performed, there is a large accumulation of minerals (patches of each mineral) in the central part of the Papandayan Volcano crater. The boundary value of the assumptions given to each mineral that is raised is that each unit that appears is worth 1 and the one that does not appear is 0, Value which is 9 or close to 9 indicates an intensive hydrothermal alteration that produces alteration minerals from acidic fluids.

From the value of mineral overlay from acidic fluid, the lowest values of 0 and 7 were obtained. This indicates that not all of these mineral collections overlapped, only 7 of the total minerals (Figure 10). On the other hand, those minerals that characterize the fluid type is neutral to alkali, out of a total of 11 minerals that appear there are 10 minerals as the highest yield value and 0 as the lowest (Figure 11). This meaning there are 2 acidic mineral minerals which are mutually incompatible in overlay result, but for minerals related to neutral – alkaline fluid type only one type that not synchronize each other.

Relationship with Sulphidation Type Based on Remote Sensing Result

The types of alteration minerals that can be identified using the SAM method. This method plays a promising role in order to providing information on mineral collections that are most likely to be found in the study area. The tendency for domination or similarity in the distribution of minerals of different types of fluid forming can indicate the type of sulphidation from the geothermal field. Previous research data shows that the dominance of the emergence of high degree alteration minerals and the appearance of hot gases (solfatara) which contain strong acids (H2S - SO2 - HCl).

Referring to the results of mineral, map overlay, it is known that the distribution of associated minerals which characterizes the effect of acidic hydrothermal fluid is 0,404 km2 or 0,481% of the area of 84 km2. For regions with asphyxiation of neutral to alkali fluid minerals, the area is 0,568 km2 or 0,676% of the same area. Comparison of the area of 0,164 km2 or 0,195% is a significant value in an active geothermal region. Broader distribution can be an indication of the dominant process which has an increasingly high influence. Referring to the display of these values (Figure 12), it gives a large indication that the type of fluid that affects the Papandayan Volcano area is neutral to alkaline or tends to be of low sulphidation type.

In the research conducted, in addition to referring the distribution and the abundance of at least overlapping minerals, the most characteristic minerals from sulphidation typical are also the most important points. For a typical type of fluid with an acid, the mineral reference that is the basis of the determinant is the presence of alunite, while for the typical which tends to be neutral to alkali is adularia. Based on mineral characteristics that can appear from the SAM method, it is known that the minerals associated with the type of acid fluid (alunite) are larger than the neutral - alkali (adularia) type. The mineral distribution also does not only focus on the central area of fluid output (volcanic craters), but also on the area around the crater and also the volcanic slopes. Comparison of the distribution of those two minerals presented in Figure 13 gives strong assumption that the type of mineral with acidic fluid characteristics is greater than that. Comparison of the two values according to those described in the pie diagram is 0,319% for alunite minerals compared to 0,074% of the area of 84 km2. The strong distribution of alunite was also explained by Mazot et al (2007) compared to adularia which indirectly did not explain its presence in the Papandayan Volcano region. This indicates strongly that the sulphidation type of the Papandayan Volcano region is classified as high sulphidation.

CONCLUSION

Papandayan volcano located in the border region between Garut Regency and Bandung in general has a high potential for geothermal development. This is evidenced by the number of potential areas as a point of surface manifestation that illustrates the high heat activity under the surface of the earth or inside the body of the Papandayan Volcano. The distribution obtained from the results of the overlay of NDVI data, NDWI and LST shows in general the distribution of potential areas in the craters of the Papandayan Volcano and other regions in the northwest and southeast. In addition to the presence of manifestation points, the main characteristic of high volcanic activity is the presence of alteration minerals as a result of a process of alteration by hydrothermal fluid. The existence of a certain family of alteration minerals also plays a role in determining the type of sulphidation from a geothermal field studied. Based on the band composite and band ratio results, it gives a strong indication of the Papandayan Volcano crater area as an area of intensive alteration. Referring to the mineral distribution of SAM results that have been overlying with each set of characterizing minerals, neutral to alkaline fluid types are the most dominant type of distribution (comparison of values of 0,481% with 0,676%). Whereas if examined from SAM results related to the main mineral sulphidation, the type of high sulphidation affected by acidic fluid, in this case the alunite mineral has a higher distribution than the neutral to alkali type characterized in the form of adularia (comparison value of 0,319% with 0,074%). By knowing the two things above, special treatment that must be applied if some stakeholder or government wanted to develop the Papandayan Volcano area will be more directed and planned.

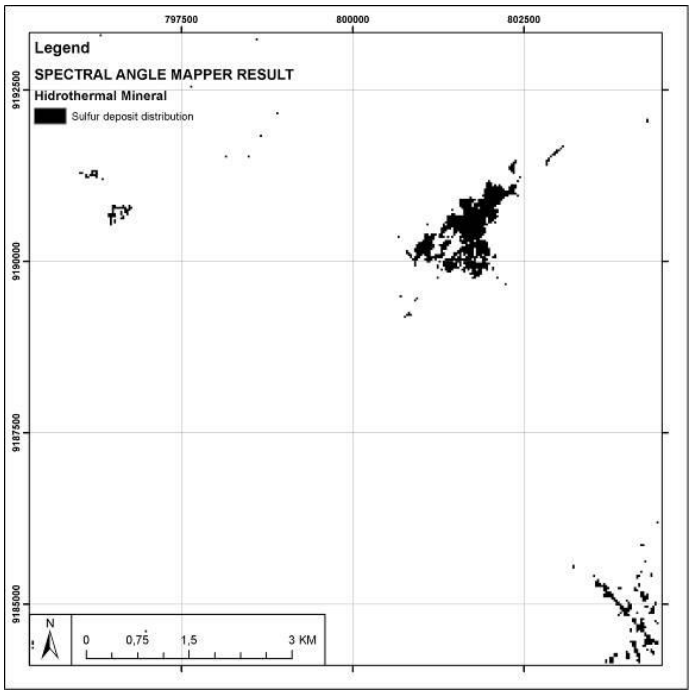


Figure 9: Sulphur distribution in research area based on SAM method

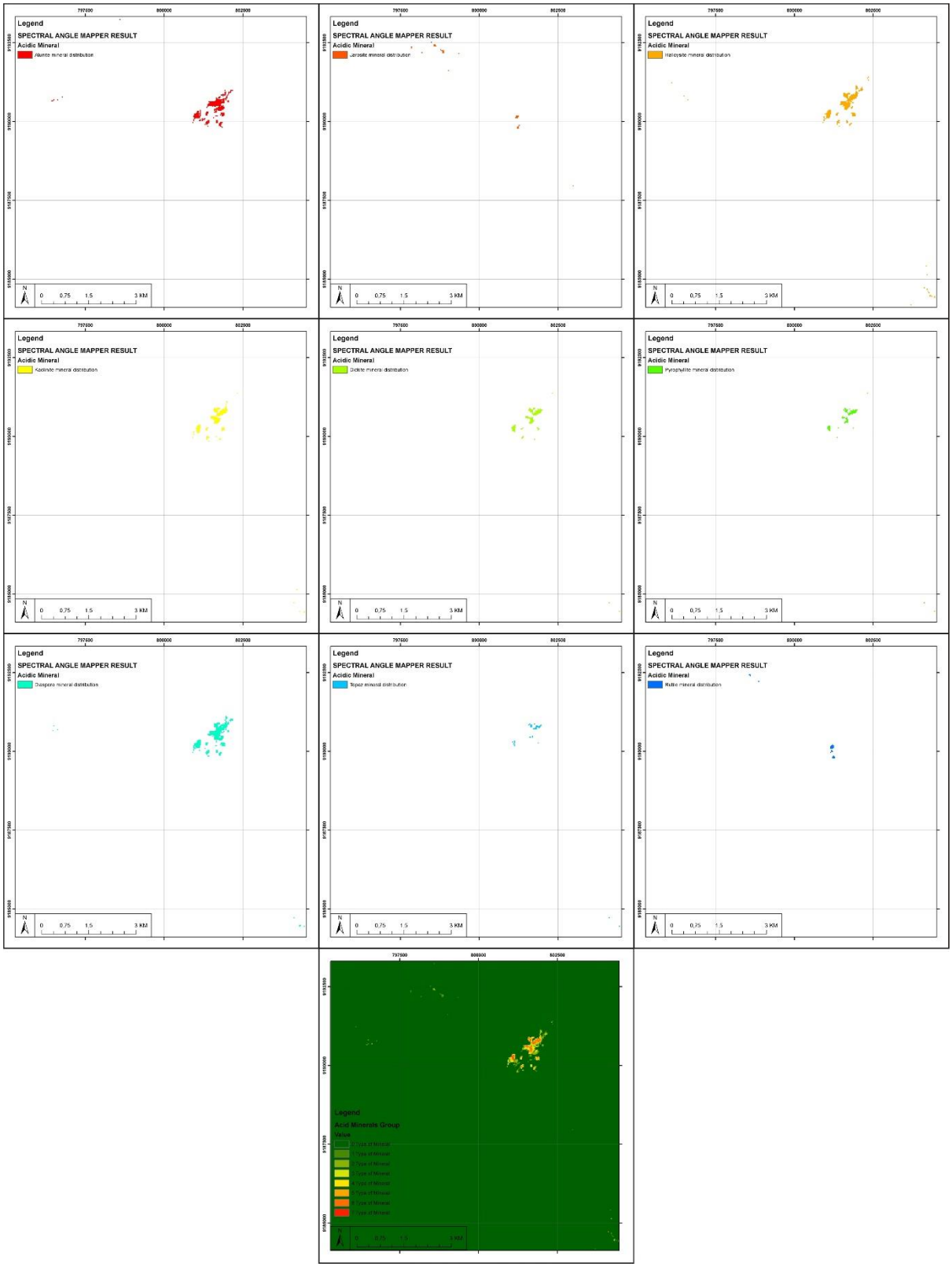


Figure 10: Acidic alteration mineral group distribution in Papandayan Volcano using SAM method.



Figure 11: Neutral - alkaline alteration mineral group distribution in Papandayan Volcano using SAM method.

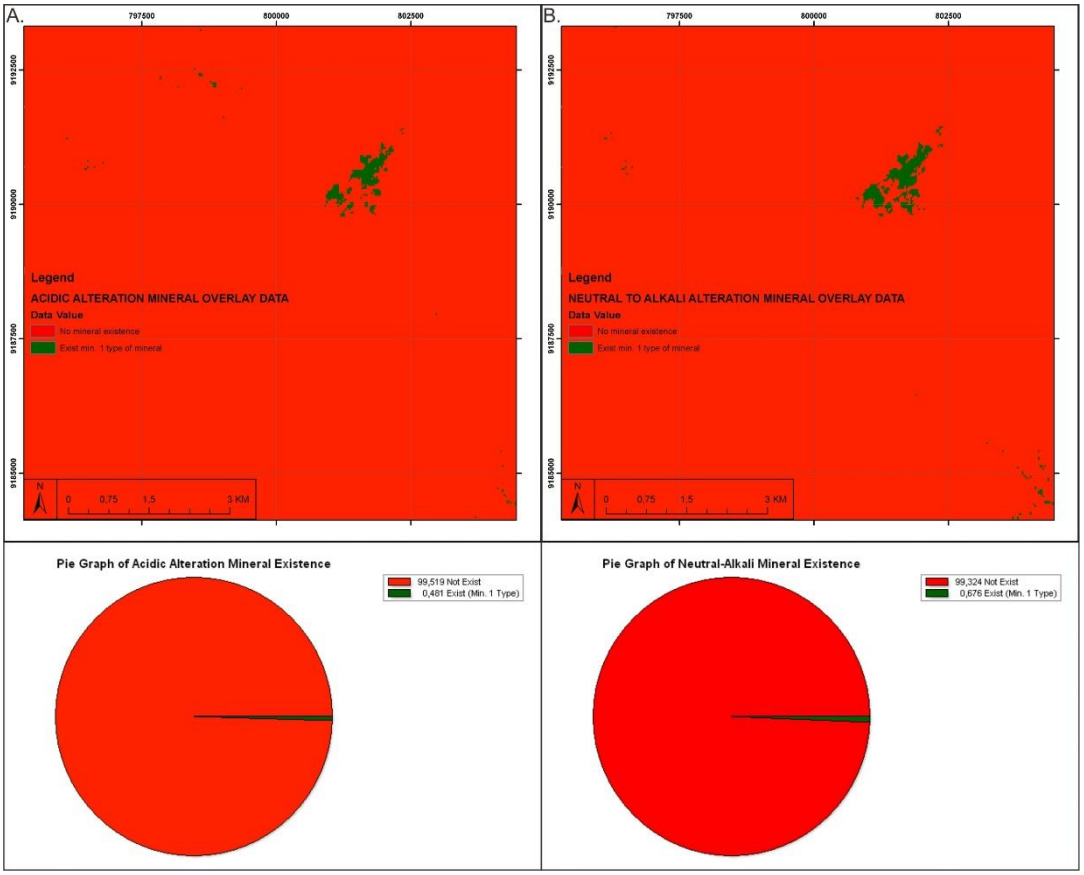


Figure 12: Comparison of acidic (A) and neutral – alkaline alteration mineral distribution in Papandayan Volcano.

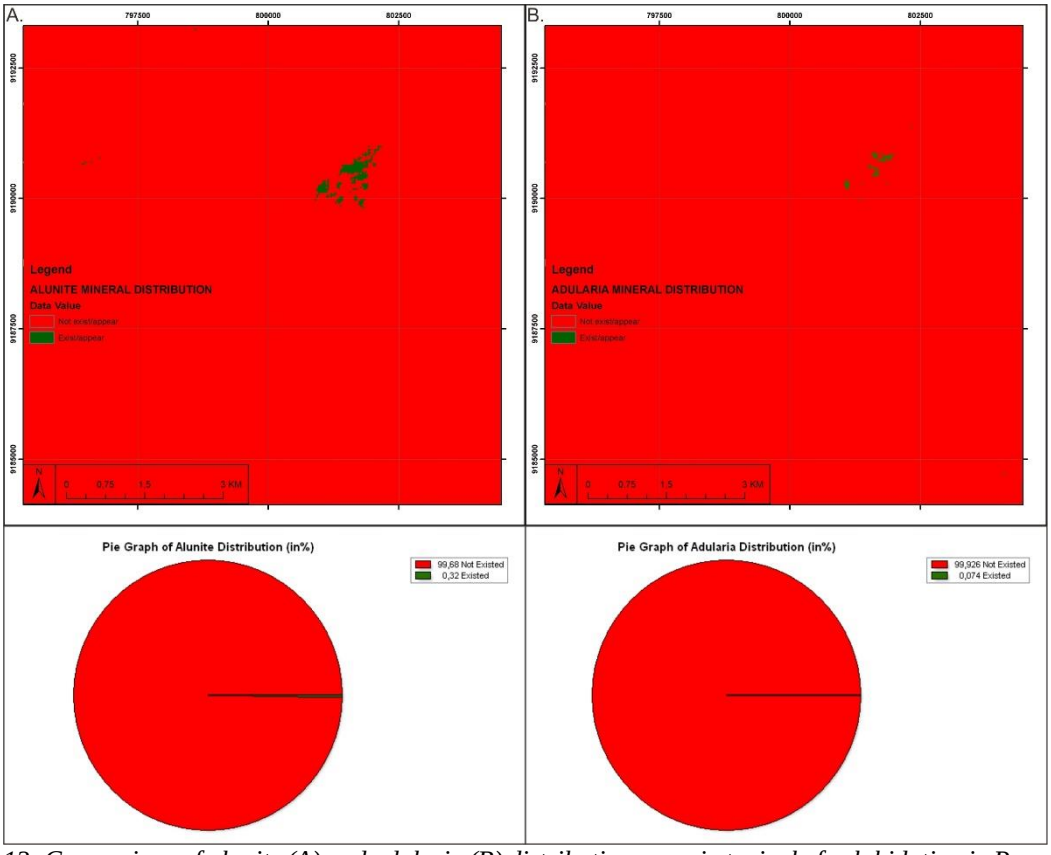


Figure 13: Comparison of alunite (A) and adularia (B) distribution as main typical of sulphidation in Papandayan Volcano.

REFERENCES

Abhary, A., and Hassani, H. (2016), "Mapping Hydrothermal Mineral Deposits Using PCA and BR Methods in Baft 1:100000 Geological Sheet, Iran," International Journal of Advanced Engineering, Management and Science (IJAEMS), 2, 1433-1438.

Alzwar, M., Akbar, N., and Bachri, S. (1992), "Peta Geologi Lembar Garut dan Pamengpeuk, Jawa," Pusat Penelitian dan Pengembangan Geologi. Bandung.

Anandababu, D., Purushothaman, B.M., and Babu, S.S. (2018), "Estimation of Land Surface Temperature using Landsat 9 Data," International Journal of Advance Research, Ideas, and Innovation in Technology (IJARIIT), 4, 177-186.

Byrdina, S., Grandis, H., Sumintareja, P., Caudron, C., Syahbana, D.K., Naffrechoux, H., Gunawan, H., Suantika, G., Vandemeulebrouck, J. (2018), "Structure of the acid hydrothermal system of Papandayan volcano, Indonesia, investigated by geophysical methods," Journal of Volcanology and Geothermal Research, 1-26.

ENVI. (2001). "Atmospheric Correction Module: QUAC and FLAAS User's Guide", ITT Visual Information Solutions.

Fauzi, A., et al., (2015), "Regional Structure Control on Geothermal Systems in West Java, Indonesia," Proc. World Geothermal Congress 2015 (Melbourne, Australia).

Hochstein, M. P., and Crosetti, M. (2012), "Ranking of Indonesia Geothermal Prospect (Known Reserves)," New Zealand Geothermal Workshop 2012.

Jensen, J.R., (1996). "Introductory digital image processing: A remote sensing perspective; 2nd ed", Prentice Hall Series in Geographic Information Science; 318p.

Julzarika, A. (2018), "Penginderaan Jauh untuk Pendeteksian Awal Potensi Tembaga di Sumbawa," Ris.Geo.Tam, 28, 75-89.

Lillesand, T.M., dan Kiefer, R.W. (1987), "Remote Sensing and Image Interpretation." New York: John Wiley & Sons, Inc.

Mazot, A., Bernard, A., and Sutawidjaja, I. S. (2007), "Hydrothermal system of the Papandayan Volcano, West Java, Indonesia and its geochemistry evolution of thermal water after the November 2002 eruption," Jurnal Geologi Indonesia, 2, 15-29.

Mazot, A., Bernard, A., Fischer, T., Inguaggiato, S., dan Sutawijaya, I.S. (2008), "Chemical Evolution of Thermal Waters and Changes in The Hydrothermal System of Papandayan Volcano (West Java, Indonesia) After the November 2002 Eruption," Journal of Volcanology and Geothermal Research, 178, 276–286.

Mc Feeters, S., K., (1996), "The use of the Normalized Difference Water Index (NDWI) in the delineation of open water features," Int. J. Remote Sens, 17, 1425-1432.

Mia, M., B., and Fujimitsu, Y. (2012), "Mapping hydrothermal altered mineral deposits using Landsat 7 ETM+ image in and around Kuju volcano, Kyushu, Japan," J. Earth Syst. Sci., 121, 1049-1057.

Morisson, K., (1997), "Important Hydrothermal Minerals and Their Significance", Geothermal and Mineral Service Division, New Zealand.

Nasution, A., Widarto, D.S., Hutasoit, L., Yuliani, D., and Hadisoemarto, S. (2008), "Geothermal Geophysical Study of Mt. Papandayan, Garut District, West Java Indonesia," Proceedings of the 8th Asian Geothermal Symposium, 8, 47-54.

Nuha, M.U., Yulianto, T., dan Harmoko, U., (2014), "Intepretasi Data Bawah Permukaan Daerah Sumber Air panas Derekan Berdasarkan Data Magnetic," Youngster Physic Journal, 3, .129-134.

Nurohman, H., Bakti, H., Indarto, S., Yulianti, A., Abdulah, A. A., Permana, H., and Gaffar, E. Z. (2016), "Zona Permeabel di Kawah Gunungapi Papandayan Berdasarkan Gas Radon dan Thoron," Ris.Geo.Tam, 26, 131-140,

Price, P., E., (2010), "Image Analysis with ArcGIS 10," US: Terra View.

Segal, D.B., (1983). "Use of Landsat multispectral scanner data for definition of Limonitic exposures in heavily vegetated areas, EL Paso, Texas"; Econ. Geol. 78 711–722.

Setiawan, I., Indarto, S., Sudarsono., Fauzi, A., Yulianti, A., Lintjewas, L., Alkausar, A., and Jakah. (2018), "Geothermal and volcanism in west Java," Earth and Environmental Science, 118, 1-5.

Soengkono, S. (1999), "Te Kopia geothermal system (New Zealand) - the relationship between its structure and Extent," Geothermics, 28, 767-784.

Utami, F., P., (2015). "Analisis Spasial Perubahan Luasan Mangrove Akibat Pengaruh Limpasan Sedimentasi Tersuspensi Dengan Metode Penginderaan Jauh (Studi Kasus : Segara Anakan Kabupaten Cilacap, Jawa Tengah)". Teknik Geodesi, Universitas Diponegoro. Semarang.

Zhou, J., Liu, L., Jiang, D.,Zhuang, D., Mansaray L.R., Zhang B., (2013), "Targeting Mineral Resources with Remote Sensing and Field Data in the Xiemisitai Area, West Junggar, Xinjiang, China." Journal Remote Sensing, 5, 7, pp. 3156-3171.

AN OVERVIEW GEOCHEMISTRY IN SORIK MARAPI GEOTHERMAL FIELD

Ryan Hidayat, Ridha Hendri, and Vicky Chandra

PT. Sorik Marapi Geothermal Power
Recapital Building 5th floor, Jalan Adithiawarman no 55, Jakarta, Indonesia
Email: ryan.hidayat@ksorka.com, ridha.hendri@ksorka.com, vicky.chandra@ksorka.com

ABSTRACT

The thermal manifestation in the Sorik Marapi consists of fumaroles, hot springs, and steaming ground. The water chemistry revealed four types of waters, they are: acid-sulfate waters, acid chloride-sulfate waters, sodium-bicarbonate waters and sodium-chloride.

Based on Trilinear diagram Cl-Li-B wells in PAD A and PAD C shows that the fluid comes from same reservoir. Mixing calculation produced a parent fluid is from well A-107 with chlorite containing 573 ppm and enthalpy 1254 J/gm, while well the C-109 indicated mixing with meteoric water and well A-104 occurred boiling. Stable isotopes analysis also supports that the reservoir fluid is coming from meteoric water and has undergone various amounts of high-temperature water-rock interactions, resulting in a positive δ18O shifting and the isotope results of the manifestations indicate the origin of the fluid originating from meteoric water.

The NCG from wells are primarily composed of carbon dioxide (CO2) and not indicated magmatic influence. Gas geothermometer based on (H2/Ar) and (CO2/Ar) resulted temperature between 175-230°C that lower than wells measurement. Silica calculation of the water sample in wellhead shows that Sorik Merapi wells generally doesn't have silica scaling potential.

Keyword: Sorik Marapi, geochemistry, Manifestation, wells chemistry, silica scaling.

INTRODUCTION

The Sorik Marapi Geothermal Field is located about 650 km south-southeast of Medan, the capital city of North Sumatra province (Figure 1) and situated within the administrative area of Mandailing Natal district. Sorik Marapi Geothermal Power (PT. SMGP) was awarded with the geothermal concession that covers an area of approximately 629 $km^{2.}$ The Sorik Marapi geothermal area is recognized through the existence of surface manifestations such as fumaroles and hot springs. The thermal area lies within a depression zone which is a part of pull-apart basin caused by the displacement of Sumatran Fault Zone. The presence of this range of features and the high magnitude of heat and mass discharged on these features is a strong indication of a high temperature resource (Figure 1).

Sample Geothermal fluids from wells been sampled and analyzed to understanding reservoir conditions such as temperature, mixing or variation to estimate reservoir conditions. The purpose of this paper is to describe the characteristics of geochemical aspect for geothermal power development and monitoring in Sorik Marapi geothermal fields.

THERMAL MANIFESTATION

Surface thermal activity in the Sorik Marapi area covers the full range of features found in high temperature systems and includes: fumaroles, solfataras (steam vents with Sulphur deposition) and hot springs.

The geochemical data indicate that the Sorik Marapi area has two broad types of deep geothermal activity: (1) an acid-magmatic system under the summit of Gunung Sorik Marapi, and (2) mature high temperature system hosted along the broad graben occupying the lower flanks of the volcano (Figure 2).

The Sorik Marapi Volcanic System

The Sorik Marapi volcano is active and much of the surface activity within and around the crater is produced by magmatic steam containing acidic gases HCl and SO2 (in addition to CO2 and H2S), derived directly from a deep magma body. The presence of HCl and SO2 indicates that the upflowing steam is superheated, since these gases are highly soluble and are scrubbed out with any condensation. The acidic gases produce the heavy Sulphur deposition and the saline, acid-chloride crater lake. Acid chloride-sulphate waters on the lower slopes of Sorik Marapi (Siambang spring, Sibanggor Julu, Purba Julu) are believed to mixing reservoir fluid and condensation fluid.

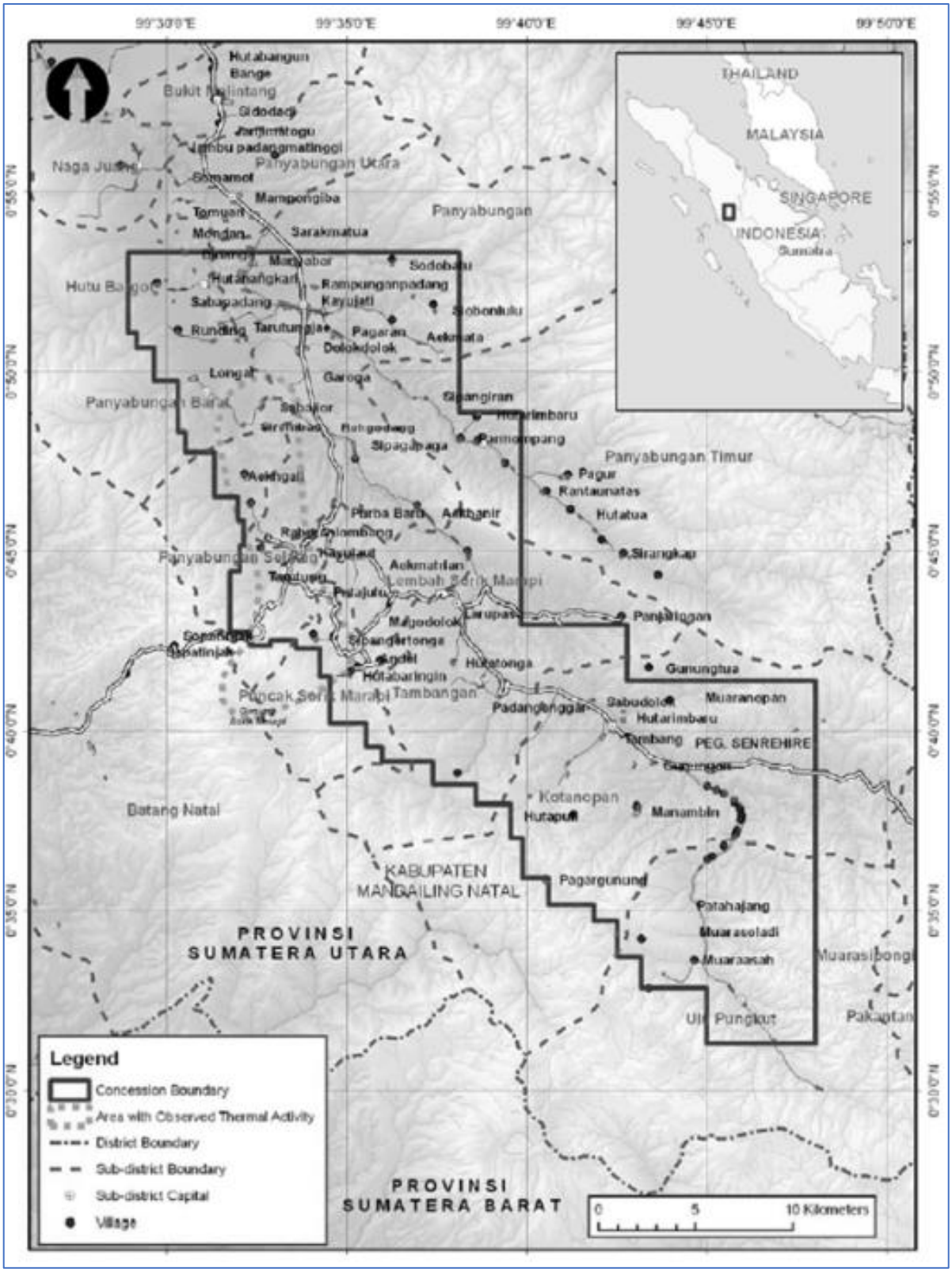


Figure 1: Concession Boundary area of Sorik Marapi Geothermal Project.

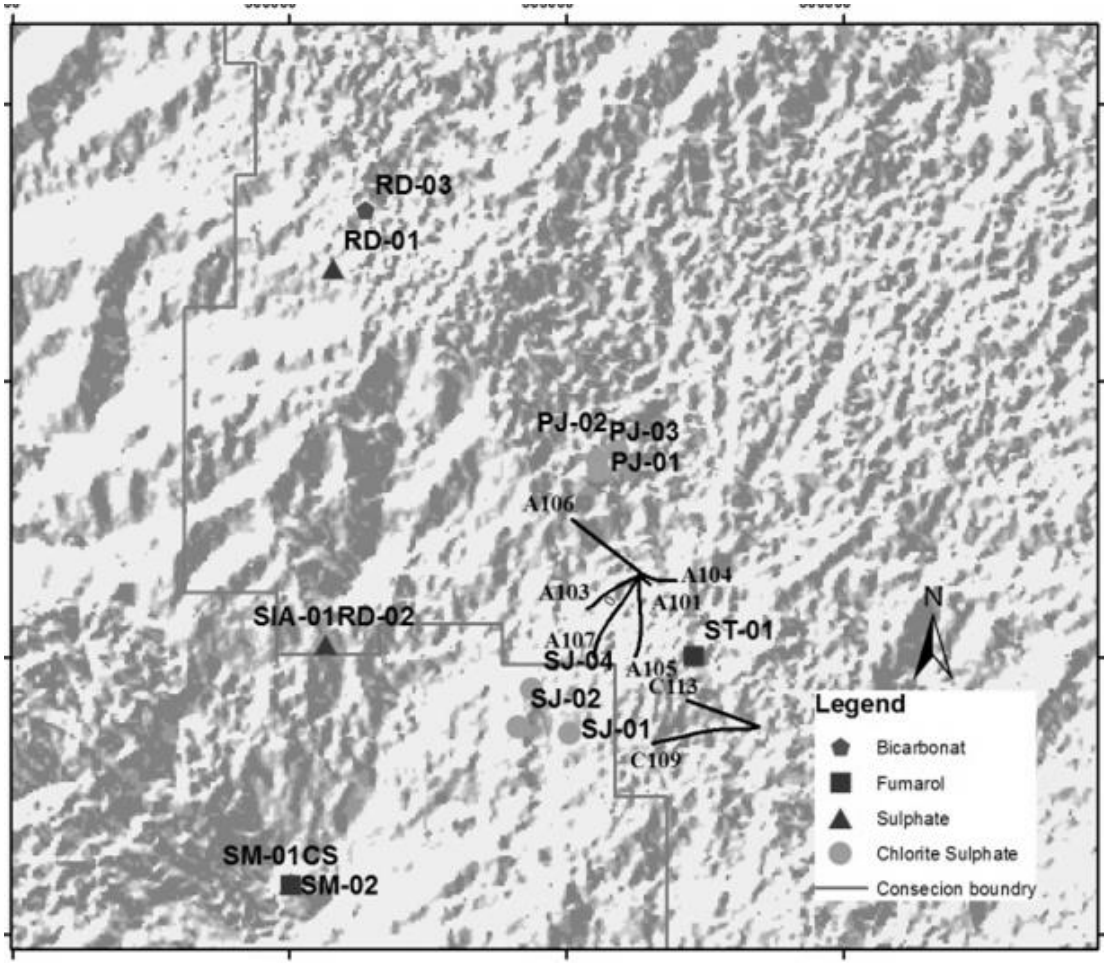


Figure 2: Sorik Marapi manifestation and well trajectory map.

Mature High Temperature Systems

In contrast to those at G. Sorik Marapi, the fumaroles at lower-elevation at Sibanggor Tonga and Roburan Dolok have a chemistry characteristic of steam derived from a mature, non-acidic reservoir. No HCl or SO2 is present and the steam has typical proportions of CO2, H2S and minor gases. The reservoir at these locations is inferred to be high-temperature (more than 270°C based on gas geothermometry, which may indicate conditions in the deeper part of the reservoir) and liquid dominated.

These conditions are likely to be suitable for a single or multiple flash geothermal power plant. There are no direct liquid discharges at the surface from these reservoirs, so there is no definitive confirmation of reservoir chemistry or geothermometry for the upper parts of the liquid reservoir. Some dilute springs near Roburan Lombang indicate mixed chloride from deep reservoir and also bicarbonate that could indicate some two-phase conditions in the shallower reservoirs.

WELL GEOCHEMISTRY

Geothermal fluids from eight wells from pad A and Pad C have been sampled and analyzed with the objectives of 1) understanding reservoir conditions such as temperature, mixing or variation when compared to other Pad A wells, and 2) forecasting potential geochemical-related production issues such as scaling (Table 1).

Table 1: Brine Data from wells.

Sample Name	A101	A 103	A 104	A 105	A 106	A 107	C 109	C 113
Temp C	155	161.6	155.9	197.5	116.3	218.2	154.8	151.6
pH	8.4	8.6	8.51	8.37	8.74	7.2	8.78	8.53
Li	2.4	3.1	3.01	2.66	2.63	2.51	1.86	2.06
Na	340	495	568	438	490	443	393	478
K	74	117	118	79.3	114	83.2	75.9	87.3
Ca	5.9	4.3	5.72	6.28	9.46	3.43	11.7	9.52
Mg	0.01	0.01	0.01	0.01	0.01	0.01	0.01	0.01
SiO2	424	706	686	537	706	701	513	539
B	24	29	34.9	28.6	35	30.3	25.5	29.1
Cl	451	738	860	698	796	690	570	680
SO4	106	58	62.8	72.4	44.6	53.7	99.9	84.2
HCO3	12	29	71.2	71.3	111	53.4	97.7	106
del ^{18}O			-57.6	-60	-56.6	-61.2	-61.2	-60.3
del D			-7.31	-7.71	-7.02	-8	-8	-7.58

Two two-phase (liquid (brine) and vapor (steam + gas)) geochemical samples were collected during well flow test, the approximate flow rate at the time of sampling, the measured chemistry shown in the tables below.

Reservoir Geochemistry

Chemical analysis demonstrates that wells in Sorik Marapi from Pad A and Pad C intercepting a neutral chloride (Cl) type reservoir (Figure 3), Relative ratios of major cations and anions show that all wells have fluid with a similar origin. Base on plotting in Trilinear Diagram Na-K-Mg indicate all wells in Sorik Marapi already equilibrium (Figure 4).

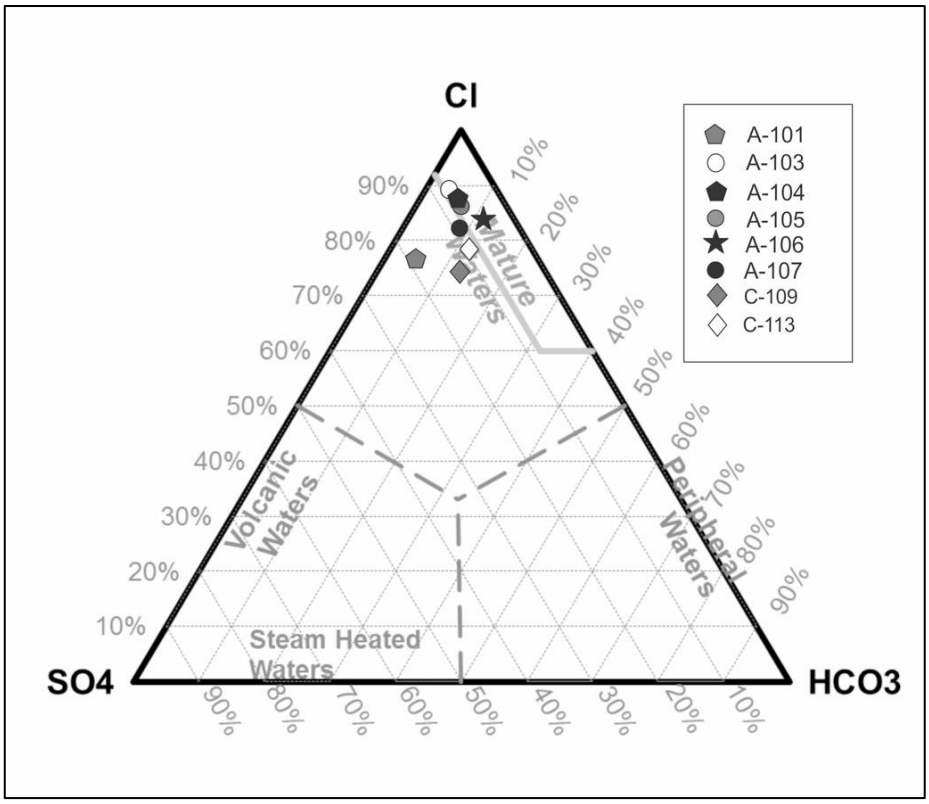


Figure 3: Wells Cl-HCO3-SO4 plot, using Powell & Cumming (2010) format.

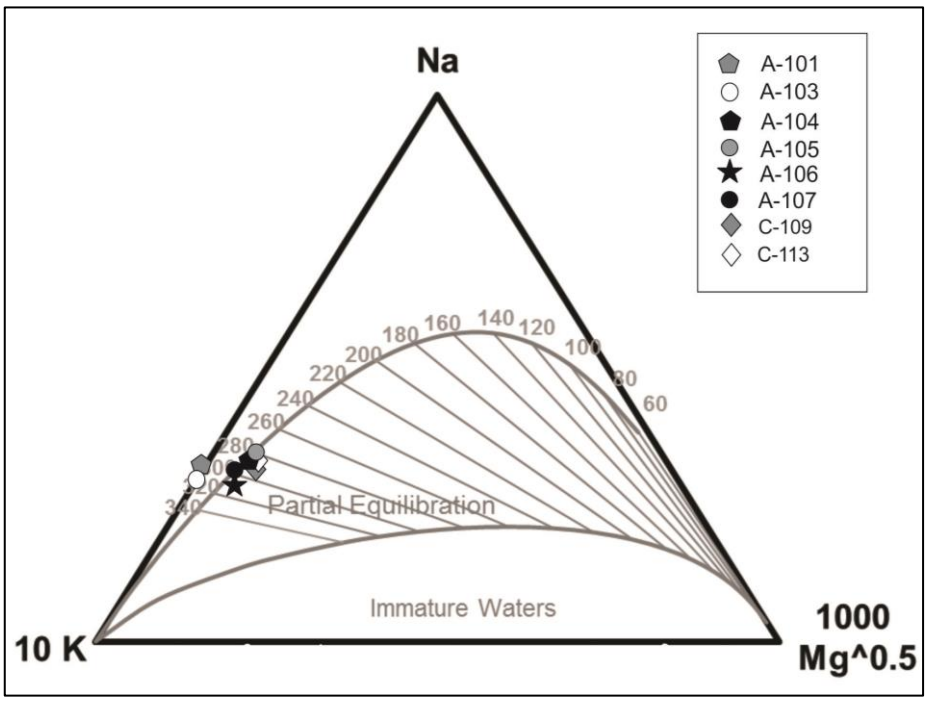


Figure 4: Wells Giggenbach (1988) Na-K-Mg plot, using Powell & Cumming (2010) format.

Non-Condensable Gas

Reservoir fluids produced from wells have relatively low concentration of non-condensable gas (Table 2). The NCG is primarily composed of carbon dioxide (CO2). CO2 comprises an average of ~0.05% of reservoir brine by weight (wt%), and ~70% of dry gas by mole (m%). Hydrogen sulfide (H2S) concentrations range from ~0.006-0.015 wt% and ~15-25 m%.

The Pad A well gas samples suggest that the source of CO2, N2 and Ar gas in reservoir liquid is similar to air-saturated water and no significant magmatic influenced is observed (Figure 5).

Table 2: NCG Data from wells.

Sample Name	A 101	A 103	A 104	A 105	A 106	A 107	C 109	C-113
CO2	23.7	69.8	59.4	62.5	62.5	69.0	42.6	59.0
H2S	3.21	15.43	28.80	23.30	25.30	24.40	9.02	17.60
NH3	0.20	0.26	0.64	0.26	0.39	0.16	0.27	0.45
Ar	0.03	0.08	0.16	0.17	0.15	0.07	0.58	0.29
N2	72.62	13.74	10.40	12.90	10.40	5.33	47.00	22.00
CH4	0.20	0.55	0.43	0.22	0.42	0.46	0.16	0.19
H2	0.08	0.15	0.36	0.59	0.84	0.62	0.44	0.53

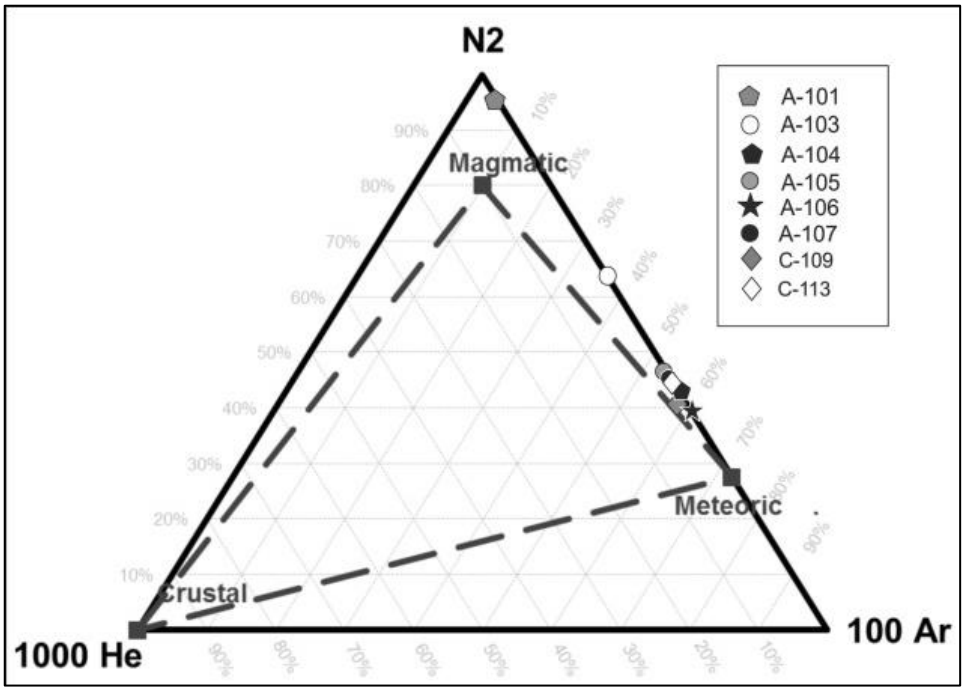


Figure 5: Wells N2, CO2, and Ar plot, using (Giggenbach & Goguel, 1989) format.

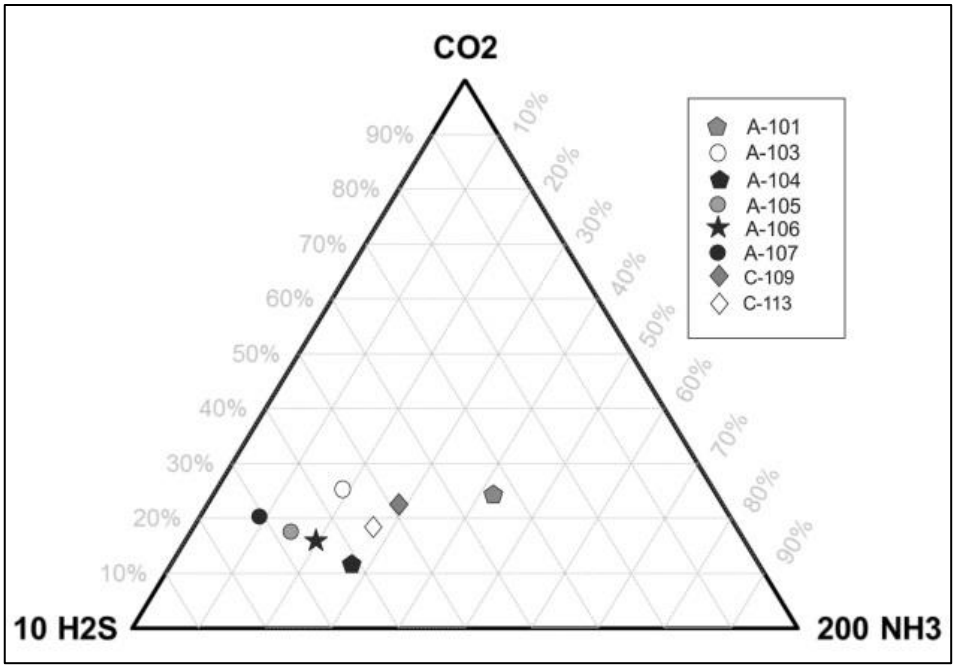


Figure 6: Wells CO2-H2S-NH3 well gas ratio plot (Powell and Cumming 2010, format).

The trilinear for CO2-H2S-NH3 plot for wells samples is shown in Figure 6. The mixing trends observed suggest that the reservoir liquid is a mixture of hot (~260°C) fluids and cooler fluids. A-101, A-104, C-109 and C-113 appear to have a higher proportion of cooler fluids, while A-105, A-106 and A-107 fluids are both hotter and appear to have less mixing.

Gas and Liquid Geothermometers

Using gas geothermometers based on the ratios of hydrogen and argon (H2/Ar) and carbon dioxide and argon (CO2/Ar), the temperature of the reservoir and the liquid saturation can be estimated (Giggenbach & Goguel, 1989). Using recent samples with very little to no air contamination and reliable results samples from regional fumaroles, analysis indicates that the reservoir is liquid saturated, and is equilibrated at a temperature between 200-230°C (Figure 7) This temperature is well below measured temperatures, suggesting that H2 may have re-equilibrated.

Silica (SiO2) geothermometers are calculated from the concentration of dissolved SiO2 in the brine and are rapidly equilibrating, typically indicating near well temperatures. Cation geothermometers are based on the ratios between cations, and function independently of absolute concentrations. Cation geothermometers equilibrate slowly and typically indicate temperatures further from the well. Samples that are likely affect by steam condensate dilution are A-101 samples 1-2, A-103 samples 1-3, A-104 samples 1-4, and A-107 sample 1. Silica temperature estimates for these samples have been omitted from geothermometer plots and tables. Estimated reservoir temperatures were calculated from selected geothermometers (Table 3). Liquid geothermometers based on silica and cations indicate a reservoir temperature of 237-330°C, compared to the measured flowing feed zone temperature of 240-283 °C. Geothermometer except for Na/K which shows the temperature more than 300°C is already equal to the measured temperature, this confirms the well conditions that have equilibrium.

Mixing Calculation

Mixing calculation using wells measurement temperature and chlorite data (Table 4) indicated parent fluid come from well A-107 with chlorite contain around 573 ppm and enthalpy 1254 J/gm (Figure 8). A 101 interpreted that wells have not been in a state of equilibrium, it makes the results of plotting not representative. Wells A-104 are in the boiling zone, evidenced by the higher value of chloride compare to other sample, while wells C-113 slightly conductive cooling. C-109 plotting shows a mixing condition with ground water.

Stable Isotopes

Isotopes of the reservoir fluid from Sorik Marapi fields indicate that the reservoir fluid originates as meteoric water and has undergone various amounts of high-temperature water-rock interaction, resulting in a positive $\delta 18O$ shift of 1 to 2 per mil. Fluids from wells A-104 and A-106 have slightly heavier $\delta 18O$ shift than other wells. This could be the result of longer high-temperature rock interaction, indicating wells A-104 and A-106 may be down gradient to or have higher rock/water ratios than other wells (Figure 9).

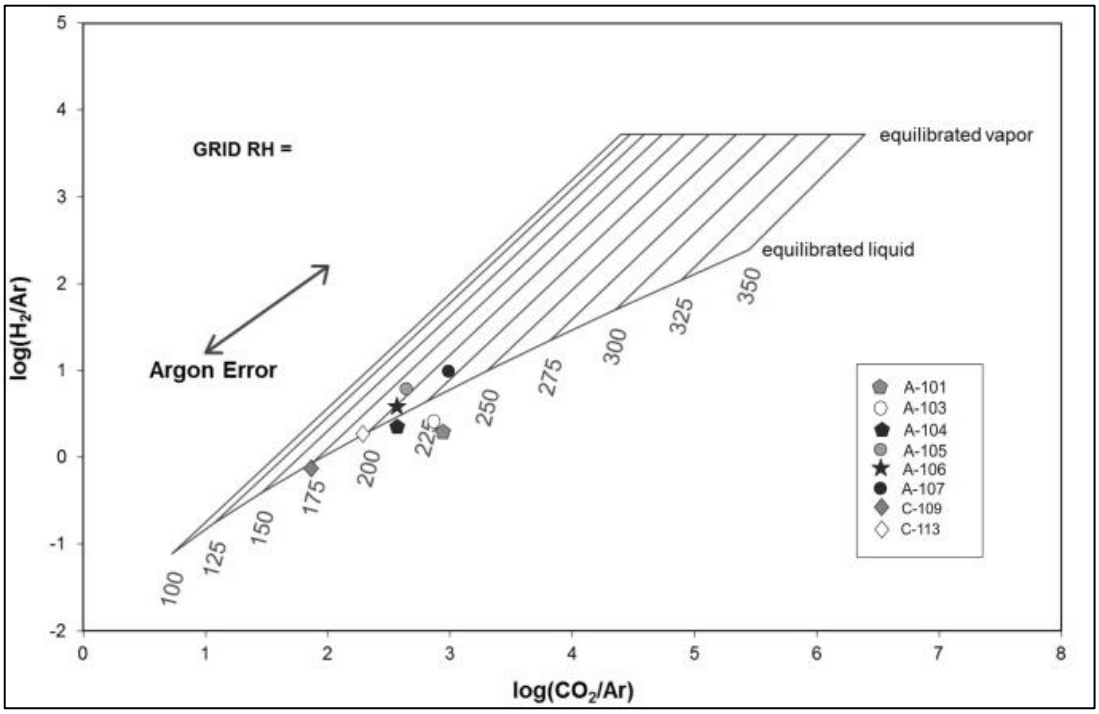


Figure 7: Wells CAR-HAR well gas ratio plot (Powell and Cumming 2010, format).

Table 3: Wells reduced data with selected geothermometers.

Sample Name	Quartz adiabatic	Na-K-Ca	Na/K Fournier 1979	K/Mg Giggenbach 1986	Measured Temperature
A101	238	253	319	261	261
A 103	252	278	330	288	277
A 104	283	267	314	288	262
A 105	259	250	298	265	268
A 106	286	266	328	286	281
A 107	285	260	302	267	283
C 109	255	244	305	262	242
C 113	259	247	299	270	248

SILICA SCALING

Scaling silica is one of problems that occur in the geothermal field, scaling silica is controlled by the chemical and thermodynamic properties of amorphous silica. Silica solubility index (SSI) is a calculation used for determination occurrence of scaling silica, scaling will be formed if SSI has a value above 1. Calculation of the water sample in wellhead shows that Sorik Marapi wells generally doesn't have silica scaling potential, except sample A-106 with a value of 1.61 (Table 5).

Table 4: Well Chlorite contain and enthalpy.

Name	Temp Reservoir (ºC)	CL Reservoir (ppm)	Entalpy (J/gm)
A101	261	346	1142
A 103	277	547	1220
A 104	262	661	1142
A 105	268	578	1175
A 106	281	525	1242
A 107	283	572	1254
C 109	242	463	1047
C 113	248	539	1077

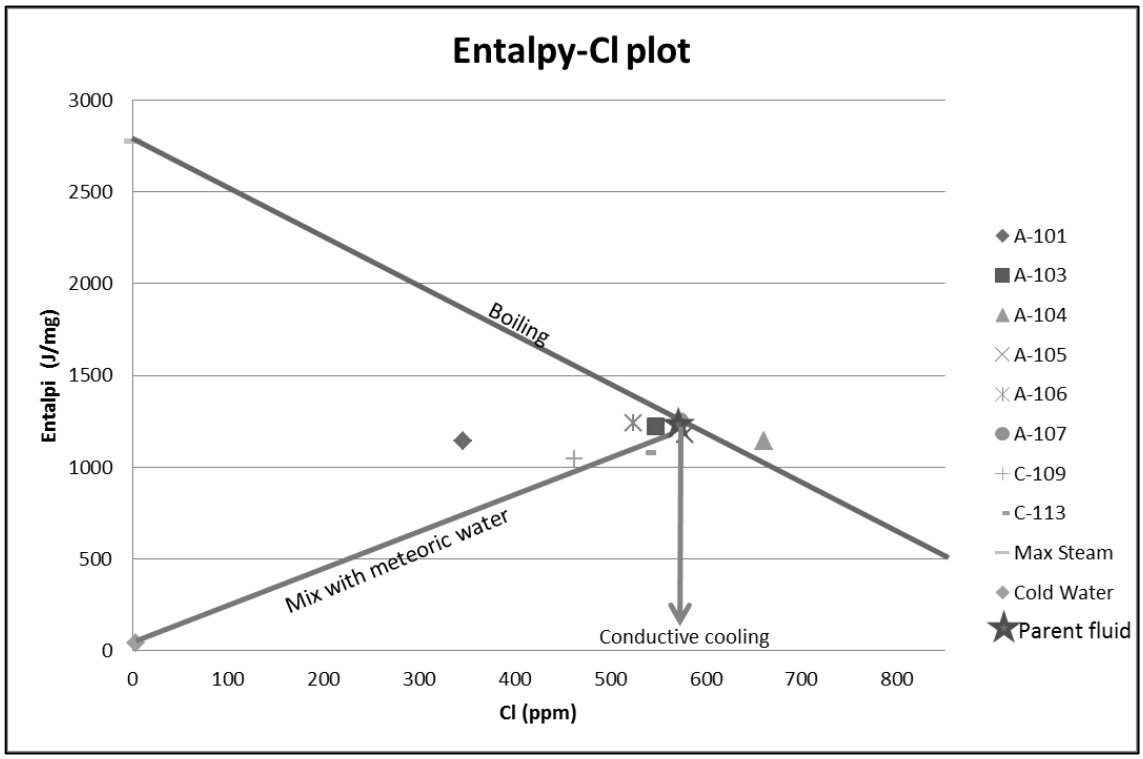


Figure 8: Sorik Marapi Wells mixing calculation.

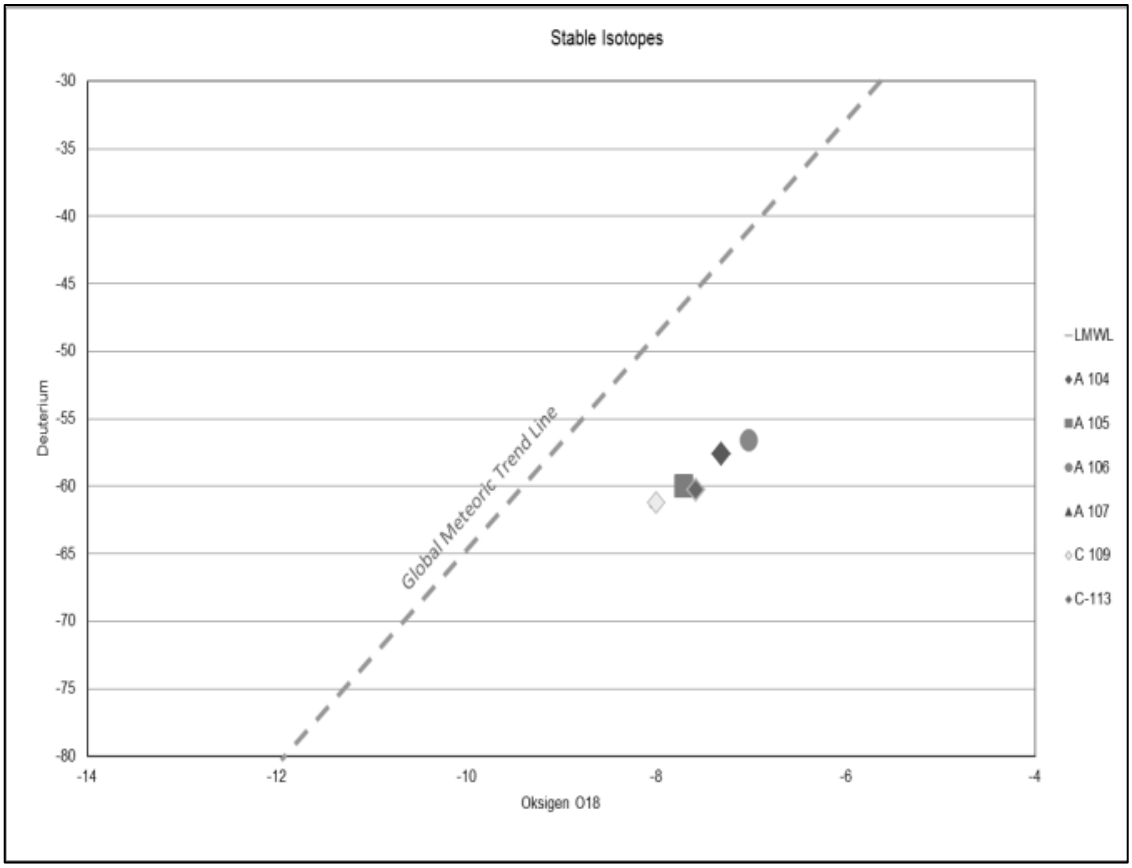


Figure 9: Stable Isotope from Sorik Wells.

Table 5: Silica scaling calculation.

Well	P (bara)	T (°C)	SiO2 (ppm)	SSI
A 101	8.3	155	244	0.38
A 103	12.4	189.4	493	0.42
A 104	13.8	198.2	628	0.68
A 105	13.8	197.5	537	0.58
A 106	1	116.3	706	1.61
A 107	21.4	218.2	701	0.65
C 109	4.26	154.8	513	0.79
C 113	4.02	151.6	539	0.86

CONCLUSION

- Sorik Marapi produces neutral chloride geothermal brines which originated as meteoric water without clear influence of magmatic influx.
- Liquid geothermometer calculation, except Na/K have the same temperature with well measurements, this indicates that the wells are in equilibrium condition, while the gas geothermometer shows a smaller value suggesting that H2 may have re-equilibrated.
- Mixing calculation shows that the fluid parent comes from well A-107, whereas mixing with meteoric water occurs in A109 wells and boiling occurs in well A104.
- Scaling calculation from water sample in wellhead shows that Sorik Marapi wells generally doesn't have silica scaling potential.

REFERENCES

Arnorsson, S., Sigurdsson, S. and Svavarsson, H. (1982). "The chemistry of geothermal waters in Iceland I. Calculation of aqueous speciation from 0° to 370°C". *Geochim. Cosmochim. Acta, 46, 1513-1532.*

Brown, K., (2011). "Thermodynamics and Kinetics of Silica Scaling", *Proceeding International Workshop on Mineral Scaling, Manila.*

D'Amore, F. and Panichi, C. (1980). "Evaluation of deep temperatures by a new gas geothermometer". *Geochim Cosmochim Acta. Vol 44, 549-556.*

Fournier, R.O. and Potter, R.W. II (1982). "A revised and expanded silica (quartz) geothermometer". *Geoth Resources Council Bulletin, 11, 3-12.*

Fournier, R.O. and Truesdell, A.H. (1973). "An empirical Na-K-Ca geothermometer for natural waters". *Geochim. Cosmochim Acta. Vol 37, 1255-1275.*

Fournier R. O. (1989). "Lectures on Geochemical Interpretation of Hydrothermal Waters". *Geothermal Training Programme, Orkustofnun, Grensasvegur, IS-108, Reykjavik, Iceland.*

Geologica. (2017), "A-117 Well Test Result and Analysis,". *PT Sorik Marapi Geothermal Power Assessment Report.*

Giggenbach, W.F. (1988). "Geothermal solute equilibria: derivation of Na-K-Mg-Ca geoindicators". *Geochim. Cosmochim Acta. Vol 52, 2749-2765.*

Giggenbach, W.F. (1991). "Chemical techniques in geothermal exploration. In application of geochemistry in geothermal reservoir development". *(Editor: D'Amore, F.) UNITAR/UNDP Centre on Small Energy Resources, Rome.*

Nicholson, K., (1993), "Geothermal Fluids.Chemistry and Exploration techniques", *Springer- Verlag, Berlin, Heildelberg.*

Powell, T. and Cumming, W. (2010). "Spreadsheets for geothermal water and gas geochemistry". *Stanford University Geothermal Workshop*

SKM, (2011). "Preliminary Resource Assessment Report. Sorik Marapi Geothermal Project, Indonesia". *Prepared for OTP Geothermal. Final Rev.1. 15 Nov. 2011*

IDENTIFICATION OF HEAT SOURCE AND STRUCTURE USING GRAVITY AND MAGNETIC DATA INTEGRATION ON NON-VOLCANIC GEOTHERMAL SYSTEM OF PARANG WEDANG

Muhammad Zaki and Nadya Noorvita

Geophysical Engineering, University of Pembangunan Nasional "Veteran" Yogyakarta
Jl. SWK 104 Lingkar Utara, Yogyakarta, 55283
Email: muhammadzaki3011@gmail.com, nadya_noorvita@yahoo.co.id

ABSTRACT

In the Special Region of Yogyakarta, precisely in the area Parang Wedang, Parangtritis, Bantul were found geothermal manifestations in the form of hot springs. This field was classified as a non-volcanic geothermal system because it is not associated with any active volcano. The research area mostly into Nglanggeran Formation which has the lithology of andesite breccia and lava andesite. This research aims to identify where is the heat source location, the quality of the reservoir and the structure that develops geothermal Parang Wedang system using an integration of gravity and magnetic method and geochemical analysis based on the sample of hot water. Complete Bouguer Anomaly (CBA) map shows on the middle of research, there is a high anomaly value (141 – 138 mGal) that indicated as heat source. That high anomaly value is indicated as a heat source due to andesite intrusive rocks which have a very high density than others. While on the Total Magnetic Intensity (TMI) map shows the low anomaly (-372 to -436 nT) in the same area of CBA's high anomaly value that also could be identified as a heat source. A low anomaly value that causes magnetic intensity value decreasing (demagnetization) due to the high temperature of the heat source. From the Total Horizontal Derivative (THD) map analysis shows a fault with the SW-NE direction. This structure controls the presence of the hot spring on the research area. From the Ternary Diagram Cl-HCO3-SO4 shows that the sample of geothermal fluid on the research area contains high enough chloride. From the calculation of temperature using geothermometer, the reservoir of Parang Wedang geothermal system has a temperature between 63ºC until 133ºC (Juliarta, 2016). Based on the geothermal classification (Hochstein, 1990), the geothermal of Parang Wedang was included in the low to moderate geothermal system.

Keywords: THD, Structure, Heat Source, Gravity, Magnetic

INTRODUCTION

Geothermal energy is a relatively renewable that will not run out. This energy source is constantly active due to radioactive decay of minerals (Supranto, 2008). This energy is also much more environmentally friendly compared to fossil energy. At the moment used as this energy power plants do not need to do the process of burning so that the resulting pollution will be very little.

In the Special Region of Yogyakarta, precisely on area Parang Wedang, Parangtritis, Bantul were found geothermal manifestations in the form of hot springs and travertine. These manifestations indicate the existence of a geothermal system in the Parang Wedang area. This field is classified as a non-volcanic geothermal system, because it is not associated with any active volcano.

Geological, geophysical, and geochemistry research is necessary to done to know the condition of the subsurface and to find out the potential of geothermal in this area. This study aims to identify heat source zones, fault zones, and hot spring analysis. Heat source zones can be analyzed by using integration data of magnetic and gravity method data. The magnetic intensity value is influenced by several things such as minerals, temperature, anisotropic. Meanwhile, the gravitational acceleration value is influenced by rock density on subsurface (Telford, 1990).

Identification of fault zones in a geothermal system is very important, especially for reconstructing the geothermal system model. Deep structure such as fault/fractures can be analyzed by using gradient analysis techniques in order to estimate the relationships between structure and geothermal manifestations on the surface area.

METHOD AND THEORY

Regional Geology

Stratigraphy

The stratigraphy of Parangtritis and its surrounding areas is composed by Tertiary rocks such as volcanic clastic sedimentary rocks, volcanic rocks, clastic carbonate sediments, and Quaternary sediments (Idral et al., 2003). Clastic volcanic sedimentary rocks composed of tufa ash-sized to lapilli which is included in the Miocene Semilir Formation. The thickness of the tuff coating is exposed in Sindet area with a thickness of 75 meters.

Volcanic rock consists of Parangkusumo Lava Unit (Tmlp), Andesite Breccia Unit (Tomb), and Andesite Unit (Toma), which are included in the Nglanggeran Formation. Andesite breccia are interspersed by the lava-andesite lava flows that have a plate structure and have been weathered, and changed by the discovery of chlorite and sericite minerals. Andesite breccia is spread in the northern part of research area with a general slope of the southeast-south layer. Andesite unit in the form of lava which shows the columnar joint, has been altered by the discovery of chlorite minerals. Unit Parangkusumo Lava (Tmlp) in the form Lava Basalt which shows the structure of a lava flow.

Clastic carbonate sedimentary rocks consisting of reef limestone (Tmlc) and sandstone limestone (Tmls) which are included in Middle Miocene to the Lower Pleistocene Wonosari Formation (Wartono et al, 1977). This clastic carbonate sedimentary rocks are found in the east and west of the research area with the appearance of karst.

The sediment surface that can be referred to as Alluvium Unit (Qa). This sediment consists of the results of scraps, weathering, and leaching of surrounding rocks and coastal deposits, consisting of fine-sized sand until coarse-grained. These sediments form sand dunes which are type of barchan dune along the coast of Parangtritis Beach to Depok. The height of the sand dune reached 21 meters above sea level.

Geological Structures

The pattern of geological structure in the research area is mostly related to tectonic symptoms that have occurred in the Java Trench and the formation of the southern mountainous system of Java. The structures in the Parangtritis area are Normal Faults (Bantul, Bambang Lipuro and Mudal), Strike-Slip Faults (Parangkusumo, Soka Nambangngan and Siluk) and fracturing. In general, the Southeast-Northwest fault orientation ranges from N275°W to N310°W and Northeast-Southwest ranges between N20°E to N50°E. Figure 1 shows the geological maps of research area.

Total Horizontal Derivative (THD)

The Total Horizontal Derivatives (THD) or Horizontal Gradient Magnitude (HGM) is commonly used to enhance the anomalous source's boundaries (Grandis, 2017). The greatest advantage of the horizontal gradient method is that it is least susceptible to noise in the data (Setyawan et al., 2015). The horizontal gradient method is used to locate the boundaries of density contrast from gravity data. Lateral density contrast will give rise to a horizontal gradient of gravity anomalies (Blakely, 1996). Characteristics of gravity anomalies that show the presence of lateral changes can be extracted directly from gravity measurement data by determining the horizontal gradient amplitude of the gravity anomaly that can be expressed by the equation (Cordell and Grauch, 1985):

$$\mathrm{HG}\,(x, y) = \left[\left(\frac{\partial g}{\partial x}\right)^2 + \left(\frac{\partial g}{\partial y}\right)^2\right]^{\frac{1}{2}} \qquad (1)$$

where $\left(\frac{\partial g}{\partial x}\right)$ and $\left(\frac{\partial g}{\partial y}\right)$ are the horizontal derivatives of gravity field in the x and y directions.

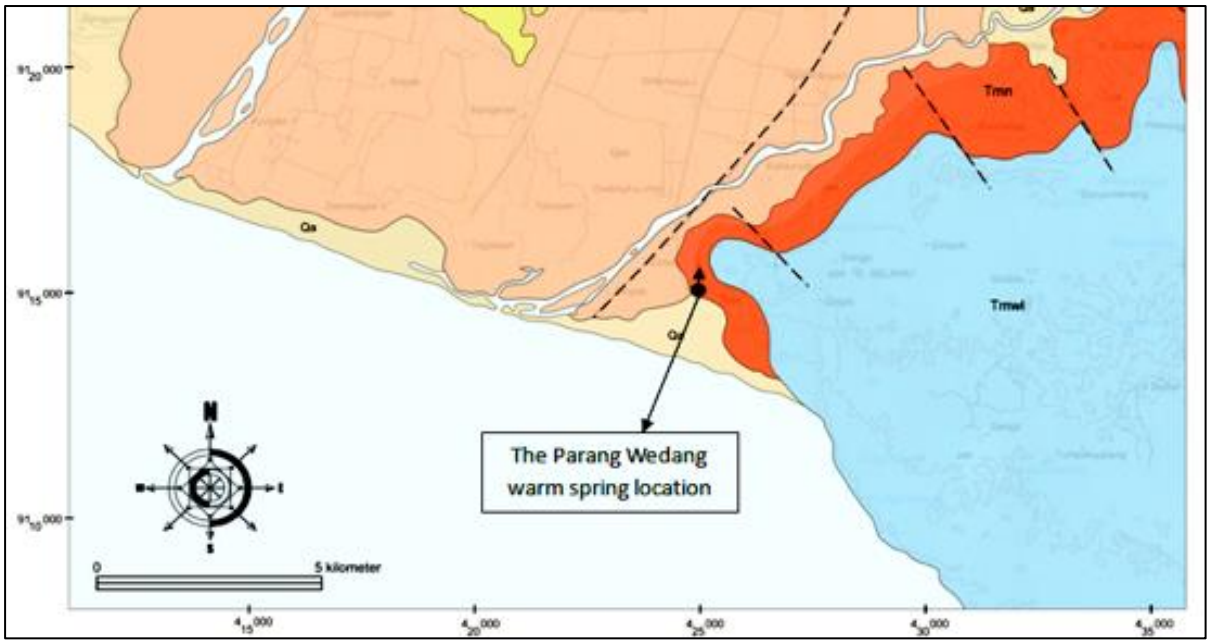


Figure 1: Geological Maps of Research Areas (Juliarka, 2016).

RESEARCH METHODS

Figure 2 is a survey design map of the research area which covers 1.7 x 1.5 km. The blue dot is the measurement point of magnetic method, while the red dot is the measurement point of gravity method. The data were taken during two periods: 29th of April to 2nd of May, 2017 for the gravity method measurement and 15th to 20th of January, 2017 for the magnetic method measurement.

Data consists of 188 gravity stations and 158 magnetic measurement point with the distance between the measurement points is 50 meters. Determining the location of research area is based on the discovery of geothermal manifestations, such as hot springs and travertine. The topography of research area is hills in northern to northeast and plains in southern.

RESULT AND DISCUSSION

Heat source

Figure 3 is a map of Complete Bouguer Anomaly (CBA) that has been carried out upward continuation 50. The process of upward continuation on CBA maps is used to clarify the distribution of lithology on subsurface by removing high-frequency noise. The gravitational acceleration value in this research area generally has a small range (141 to 136 mGal) which means that lithology variations on subsurface are not too heterogeneous. High gravity anomalies (141 to 138 mGal) which dominate the northern of the research area is interpreted as volcanic rocks of the Nglanggeran Formation. This is also supported by the discovery of andesite rock outcrops at several points in research area (Figure 4). Volcanic rock has a greater density value compared to the surrounding rocks that shown by high gravity anomalies. Based on the geology regional data, the research area mostly into Nglanggeran Formation which is consisting of andesite breccia and lava andesite and Quaternary sediments as Alluvium Unit (Qa). Thus, the response to the gravity method in the Nglanggeran Formation tends to be greater than the Quaternary sediments.

A low gravity anomaly (137 to 136 mGal) was found in the south of the research area. This low anomaly is interpreted as Quaternary sediments. However, if we observe to Total Magnetic Intensity (TMI) Upward Continuation 70 map (Figure 5), the southern part of research area has a high magnetic intensity anomaly. Based on geological information, high magnetic anomaly correlates with sand dune which contains a lot of iron sand (Figure 6). This sand dune comes from the eruption of Mount Merapi, which sediment is transported by Opak River and Progo River which disembogue to Southern Coastal.

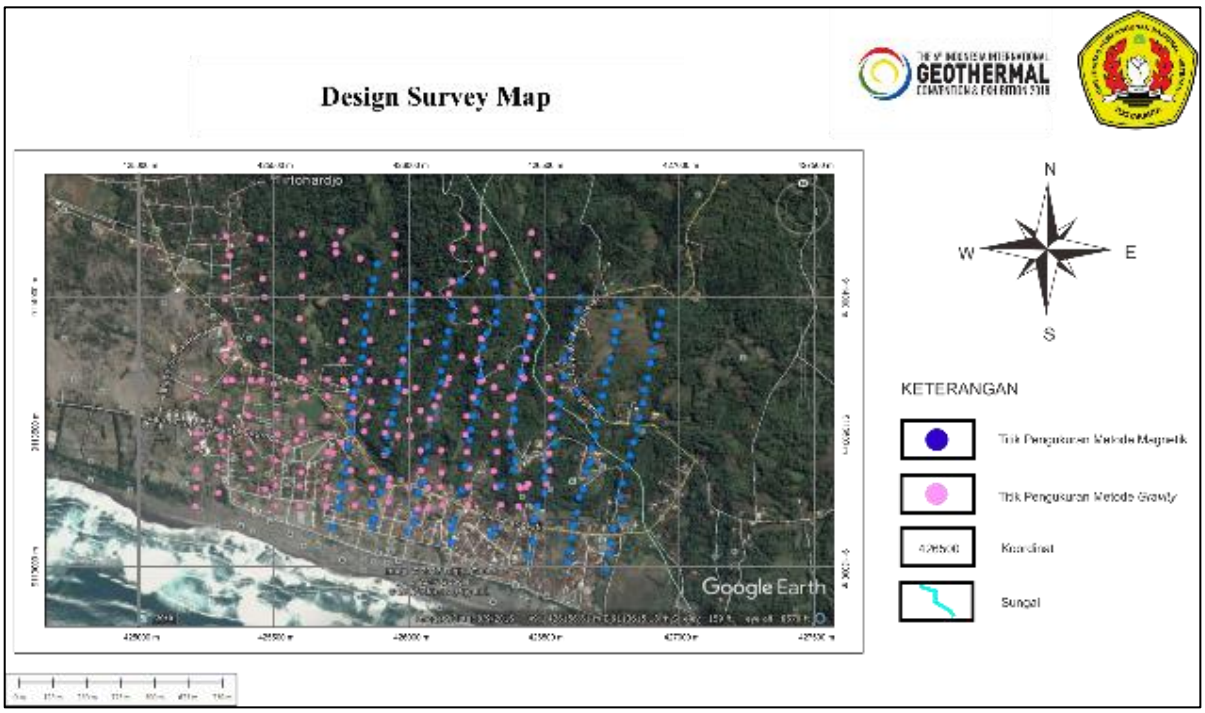


Figure 2: Design Survey Map of Research Areas Using Gravity and Magnetic Methods.

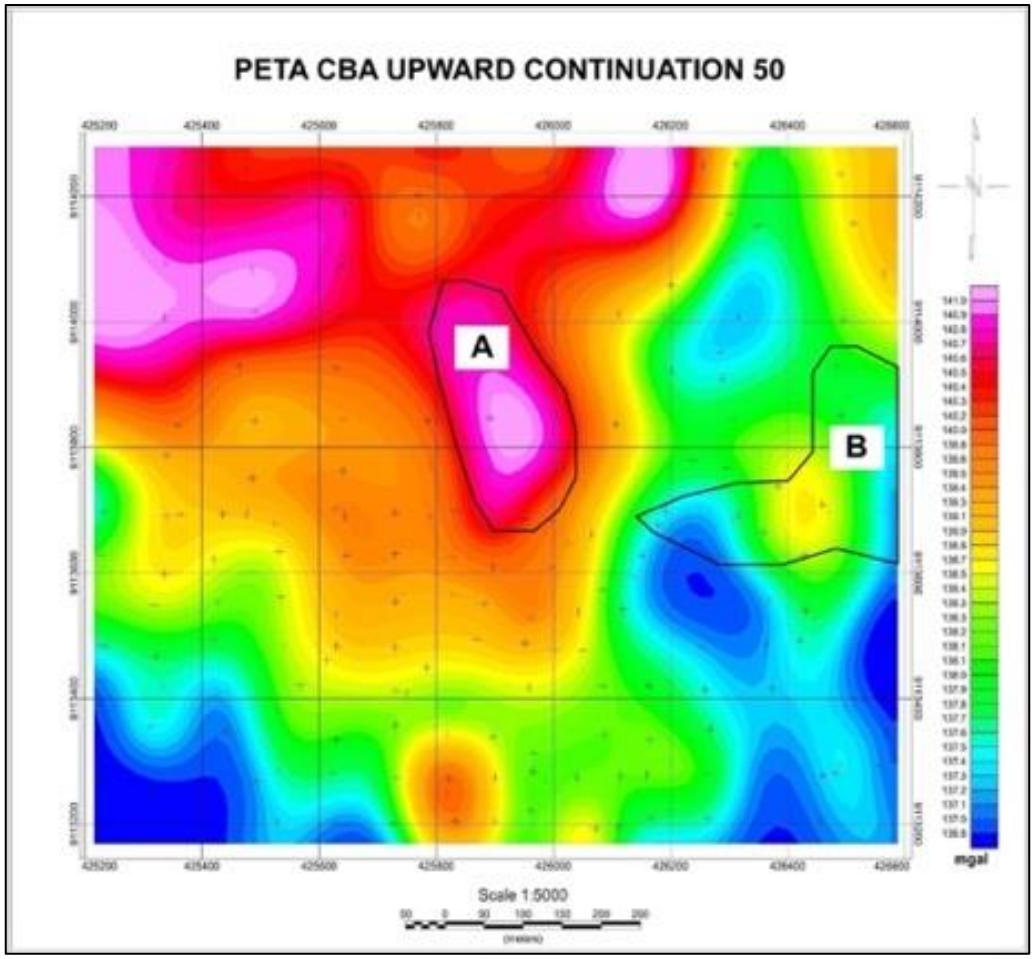


Figure 3: Map of Complete Bouguer Anomaly (CBA) Upward Continuation 50.



Figure 4: The Andesite Rocks Outcrop in Parang Wedang Field.

After integrating magnetic and gravity method results, a heat source is analyzed as in Zone A. Zone A has a high gravitational acceleration value range (141 to 138 mGal) and a low magnetic intensity value (-372 to -436 nT). The magnetic intensity value from the heat source zone will be lower than the surrounding area even in the same lithology. The high temperature in the heat source will randomize the direction of magnetic moment so that the magnetic intensity value is decreasing (demagnetization). It is estimated that the heat sources in Parang Wedang geothermal system is volcanic or intrusion (andesite) rocks that are still uncovered on the surface. Idral, et al (2003) estimated that these rocks were residual magma rocks due to subduction zones in Southern Java.

Zone B is interpreted as a reservoir of volcanic rocks (andesite breccia) that have been altered. In the zone B, there are many structures that are estimated to have high permeability and low density as indicated by low gravity anomalies compared to the western area of zone B which has no structure. Alteration of volcanic rocks can be analyzed by the low magnetic intensity value on the Total Magnetic Intensity (TMI) map. The high temperature factor in hydrothermal causes altered rocks as indicated by a low magnetic anomaly. Estimation of altered andesite rocks are supported by the discovery of chlorite and sericite minerals on the surface by Idral et al (2003) as an indication of hydrothermal process.

Structures

Fault structures characterized by the contrast of rock densities will generally have a maximum horizontal gradient. However, the horizontal gradient magnitude for gravity data still have a limitation. Grauch and Cordell (1987) concluded the maximum horizontal gradient magnitude can be offside from its actual position if the boundaries are not near-vertical and close to each other. There are two possibilities of interpretation of the maximum gradient; whether is correlated with the edge of the mountain body or intrusive of rock or is correlated with the fault structure (Setyawan et al., 2015).

Figure 7 is the result of an overlay between satellite imagery maps with total horizontal derivative (THD) map. There are some maximum magnitudes associated with the location of the travertine and hot springs. These maximum magnitudes are in the same area as zone B which is interpreted as the reservoir zone. Line A, B, C is interpreted as a fault from horizontal gradient magnitude or THD. Line A which has a maximum magnitude value of 0.010 to 0.019 mGal/m is interpreted as a SW-NE fault. The maximum magnitude of line A is associated with the location of the hot spring. This fault is indicated as a water discharge path from the reservoir so that it forms hot springs on surface.

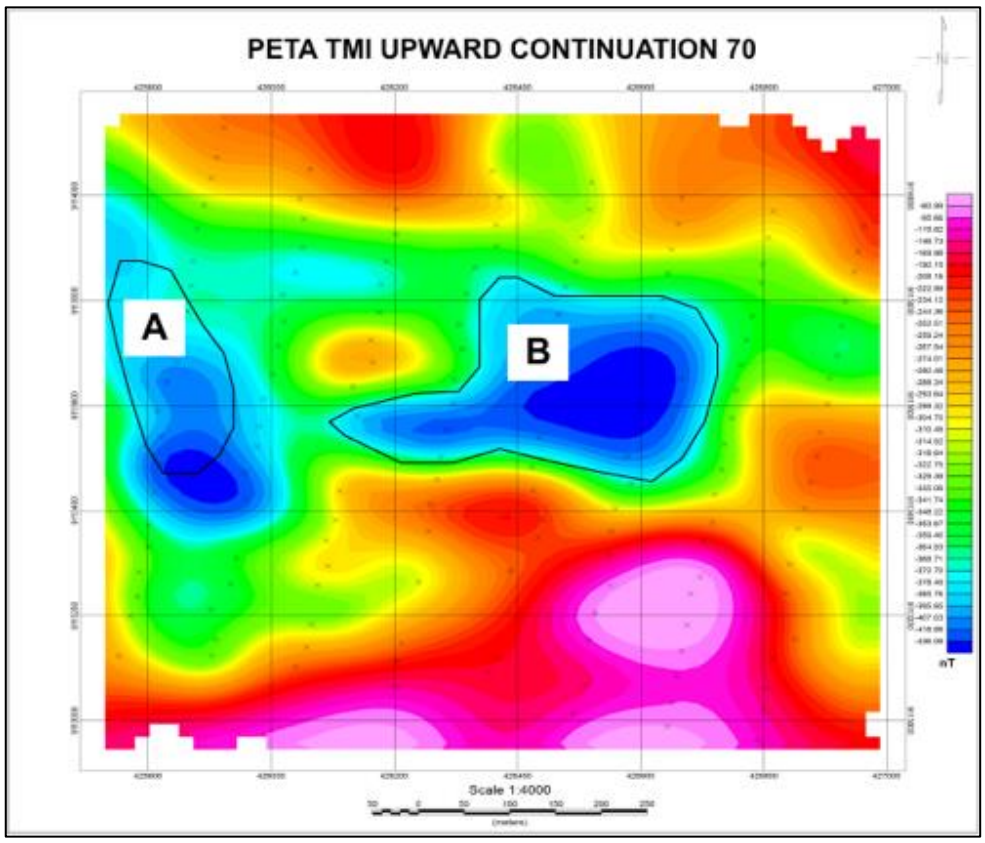


Figure 5: Total Magnetic Intensity (TMI) Upward Continuation 70 Map.



Figure 6: Sand dune along the coast of Parangtritis Beach.

Line B and C which have a maximum magnitude value of 0.010 to 0.019 mGal/m is interpreted as a NW-SE fault. The maximum magnitude of line B is associated with the location of the travertine. This fault is indicated as a water discharge path from reservoir that evidenced by the appearance of travertine. This Travertine looks inactive because there is no hot water around the location (Figure 8).

Parang Wedang hot spring has a temperature of 43 ^{o}C with an air temperature of 25.6 ^{o}C, pH 7.5-7.7, feels salty, odorless, and accumulates in a hot pool (Figure 9) (Idral et al., 2003). Based on the analysis of the Cl-SO4-HCO3 diagram (Figure 10), the Parang Wedang hot spring is located in the chloride position. Based on the calculation of Na+ and Cl- values and ratios, hot springs had a Na/Cl ratio between 0.05 and 0.18. This value confirms that the water from the Parang Wedang hot springs was not mixed with sea water (Juliarka, 2016).

Based on temperature calculations using a geothermometer Na-K, the Parang Wedang geothermal reservoir has a temperature between 63°C and 133°C (Juliarka, 2016). And Based on the geothermal classification (Hochstein, 1990), the geothermal of Parang Wedang is included in the low to moderate geothermal system.

Based on the geophysics data, combining with all existing geological and geochemical data, a model of Parang Wedang geothermal system can be reconstructed. First, meteoric waters flow into underground. Simultaneously, magmatic water flow upward from the subsurface and mix with meteoric water in the reservoir (Juliarka, 2016). Water from the reservoir (Zone B) flow upward to surface through the SW-NE fault (line A) then forms the Parang Wedang hot spring and through the NW-SE fault (line B) then forms travertine.

CONCLUSIONS

Based on discussions and results that mentioned above, the location of the heat source is in zone A which is in the center part of research area. Zone A has a high gravitational acceleration value (141 to 138 mGal) and has a low magnetic intensity value (-372 to -436 nT). The heat sources in Parang Wedang geothermal system are volcanic or intrusion (andesite) rocks that are still uncovered on the surface.

From horizontal gradient magnitude or THD map, it is interpreted that in the east of research area there are faults that have maximum magnitude value of 0.010 to 0.019 mGal/m. These maximum magnitudes associated with the location of the travertine and hot springs. These faults are indicated as a water discharge path from reservoir. Based on geochemical analysis, the Parang Wedang hot spring is located in the chloride position and Parang Wedang geothermal reservoir has a temperature between 63°C and 133°C (Juliarka, 2016), which means Parang Wedang geothermal system is included in low to moderate geothermal system.

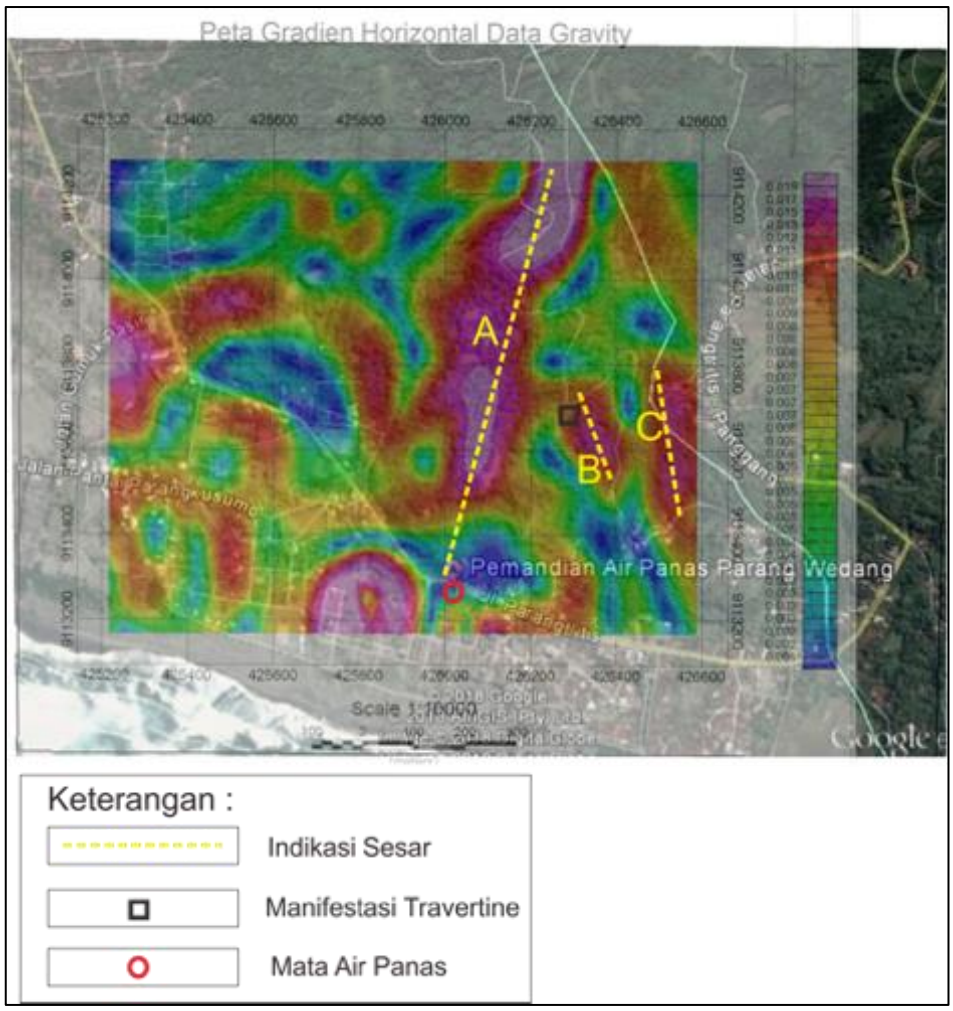


Figure 7: Overlay of Satellite Imagery Map with Total Horizontal Derivative Map.



Figure 8: Parang Wedang Geothermal System Manifestation (Hot Springs and Travertine).



Figure 9: Parang Wedang hot spring accumulates in a hot pool.

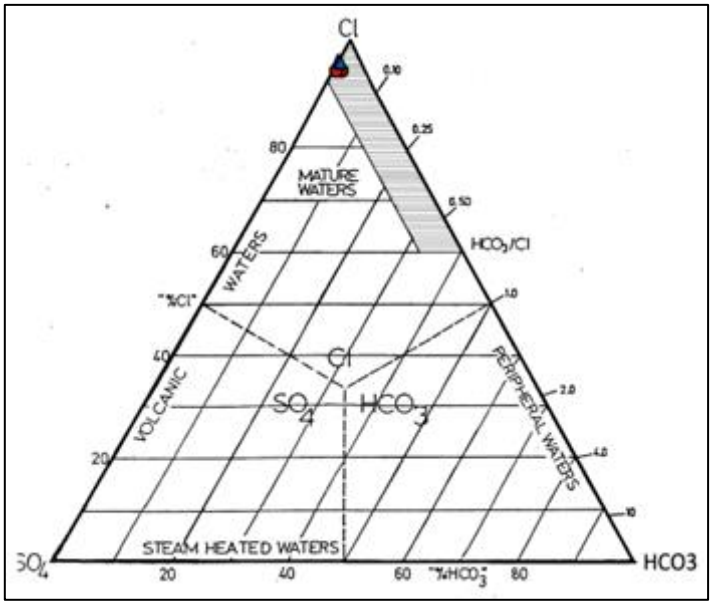


Figure 10: Ternary plot of major anions Cl-, SO4-, HCO3- (where the scale is relative % of anion. The fluid samples in Parang Wedang indicate mature water with chloride dominance (Juliarka, 2016)

REFERENCES

Blakely, R. J. (1996), "Potential Theory in Gravity and Magnetic Application", *Cambridge University Press.*

Cordell, L., and Grauch, V. J. S., (1985), "Mapping Basement Magnetization Zones from Aeromagnetic Data in the San Juan Basin, New Mexico", *Sot. Explor. Geophys,* pp.181-197.

Grandis, H., Dahrin, D., (2017), "The Utility of Free Software for Gravity and Magnetic Advanced Data Processing", *Southeast Asian Conference on Geophysics. IOP Conf. Series: Earth and Environmental Science.*

Grauch, V., S., J., Cordell L. (1987), "Limitations of determining density or magnetic boundaries from the horizontal gradient of gravity or pseudogravity data" *Geophysics, Vol.52, No.1, pp.118–121.*

Hochstein, M., P., (1990), "Classification and Assessment of Geothermal Resources", In: Dickson MH and Fanelli M (eds) Small geothermal resources, *UNITAR/UNDP Centre for Small Energy Resources,* Rome, Italy, 31-59.

Idral, A., Suhanto, E, Sumardi, Kusnadi, D., and Situmorang, T. (2003), "Penyelidikan Terpadu Geologi, Geokima dan Geofisika Daerah Panas Bumi Parangtritis, Yogyakarta," *Kolokium Hasil Kegiatan Inventarisasi Sumber Daya Mineral-DIM, TA. 2003,* **35**, 1-10.

Juliarka, B. R., Niasari S. W. (2016), "Geothermal Exploration Using Geochemical Data; Study Case: Parang Wedang Geothermal Field, Indonesia*" AIP conference Proceedings*, doi: 10.1063/1.4958532.

Setyawan, A., Yudianto, H., Nishijima, J., Hakim, S. (2015), "Horizontal Gradient for Gravity and Magnetic Data Beneath Gedongsongo Geothermal Manifestations, Ungaran, Indonesia", *Proceeding World Geothermal Congress 2015*. Melbourne, Australia.

Supranto. (2008), "Konservasi Energi*". UPN Veteran Yogyakarta Press.*

Telford, W.M., Goldrat, L.P., dan Sherif, R.P., (1990), "Applied Geophysics 2nd Edition", *Cambridge University Press*.

Wartono, R., Sukandar, R., and Rosidi. (1977), "Peta Geologi Lembar Yogyakarta, Jawa,", *Direktorat Geologi*.

PRECISION GRAVITY MONITORING OF SALAK GEOTHERMAL FIELD: INSIGHT AND CONSTRAINTS FOR NUMERICAL SIMULATION

M. Wildan Perdana[1], Fikri Rahmansyah[1], and Gregg Nordquist[2]

[1]Star Energy Geothermal Salak, Sentral Senayan II Office Tower 26th floor,
Jalan Asia Afrika no.8, Jakarta, 10270, Indonesia
[2]Independent Consultant
Email: wildan.perdana@starenergy.co.id

ABSTRACT

The Salak field is a 377 MWe liquid dominated geothermal field, located in West Java province, Indonesia and operated by Star Energy Geothermal. Precision gravity surveys have been conducted eleven times since the first 110MW were commissioned in 1994 using the same gravimeter LaCoste & Romberg (D-117). The latest survey was conducted in mid-2017. An interesting phenomenon is shown in 2017 precision gravity survey result where there was a significant increase of gravity & elevation rates changes. The location and timing of these changes are pointing to the stopping of injection in the southeastern portion of the field.

As a standard practice Star Energy compares the observed gravity with the simulated gravity calculated based on the saturation and mass changes predicted by numerical model. This provides an independent check on mass balance for the numerical model and a quantitative estimate of external recharge into the geothermal system. A mismatch between those two products is observed and is located in northern portion where high-pressure steam cap has been continuously developed. Previous works in 2015 showed too large of a change in the simulated gravity when compared to the observed with a maximum mismatch of about 200 µGals. The 2017 precision gravity data shows a better match with a maximum of about 150 µGals. The mismatch is an indication that the mass balance between natural recharge and the pressure support from injection and from the matrix in the steam cap is not being correctly accounted for in the numerical model. To address this issue is requiring an iterative approach between the reservoir engineers and earth scientists to fine-tune the conceptual model. This is leading to an improved match between observed and simulated gravity data.

*Keywords: G*ravity, numerical model, geophysics, geothermal monitoring

INTRODUCTION

Star Energy Geothermal (SEG) operates Salak (aka Awibengkok) geothermal field located in West Java province, Indonesia with 377 MWe installed capacity. Currently, Salak operates 74 production wells and 22 injection wells with separated condensate and brine injection lines (Figure 1).

Precision gravity monitoring has been implemented in Salak since its initial production period. First precision gravity measurements were conducted in 1994, coincident with the commissioning of the first two 55 MWe power plants. The gravity surveys are collected in conjunction with precision leveling surveys. The purpose of conducting leveling survey parallel to gravity survey is primarily to provide precise elevation data for gravity data reduction to account for the Free Air Gravity (FAG) resulting from changes in the BM elevation with time. In addition, the repeat precision elevation surveys can be used to monitor the land subsidence due to field production. However, the subsidence in Salak is a minor concern since the maximum elevation changes for almost 24 years has been only about 62 cm or with maximum rates of 2.5 cm/ year. The current gravity benchmark (BM) network consist of 72 measurement locations (Figure 2).

At Salak, precision gravity data is used to provide an independent constraint on numerical simulation model. Several publications related to the study on gravity-simulation model comparison has been produced since early 2000'. Nelson (2012) and Nordquist (2010) published papers elaborating how the gravity data provided important insight on numerical model fine-tuning. One of the most prominent issue in Salak was the presence of large gravity mismatch. Hypothesis on the source of mismatch evolved over time which also providing more understanding on reservoir behavior.

As the continuation of the precision gravity and leveling sequential surveys, new gravity data have been obtained. The most recent survey of precision gravity and leveling in Salak was conducted in 2017. In line with that, the gravity and numerical model matching process has been continued. This paper will summarize the recent status of Salak gravity comparison to simulation model.

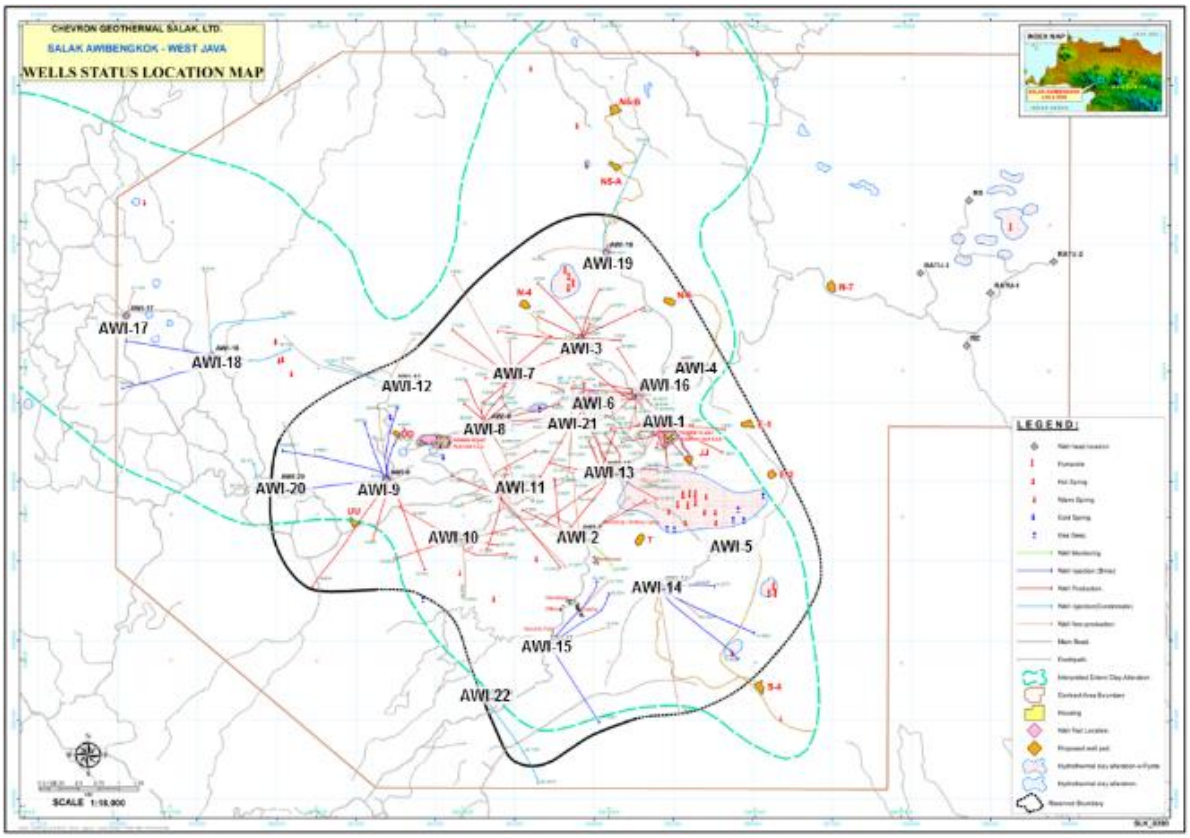


Figure 1: Salak production & injection wells and proven reservoir area.

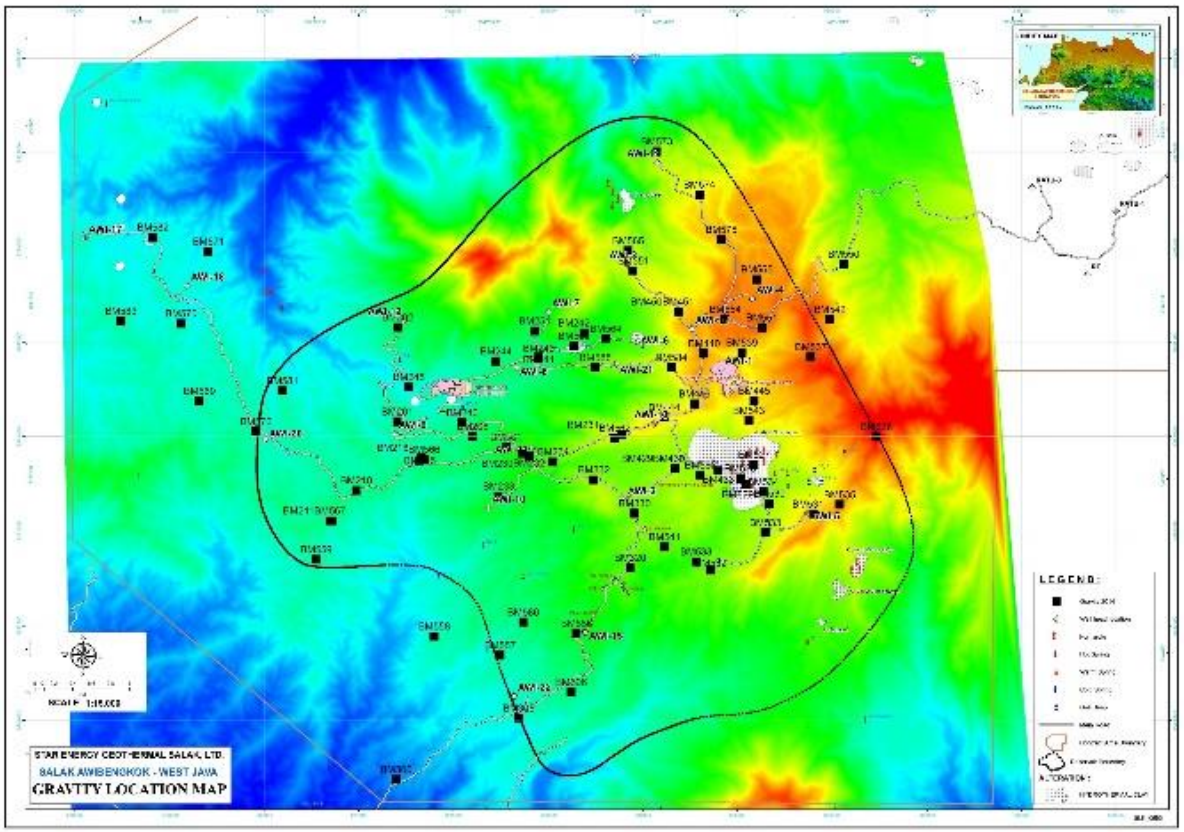


Figure 2: Distributions of gravity benchmark (BM) around Salak field. In total, there are 72 gravity BM in Salak which cover the production area and Cianten caldera. Reference BM (BM300) located away from the reservoir in southwest of Salak field.

GEOLOGICAL & CONCEPTUAL MODEL OVERVIEW

The Salak geothermal system is a liquid-dominated, fracture-controlled reservoir with benign chemistry and low-to-moderate non-condensable gas content. The geothermal system is hosted mainly by andesitic-to-rhyodacitic rocks and floored by Miocene marine sedimentary rocks cut by igneous intrusions (Stimac, 2008).

The commercial Salak reservoir is a moderate-to-high temperature (240–312 ◦C) geothermal resource with high fracture permeability, moderate porosity (mean = 10.6%) and moderate-to-low matrix permeability (geometric mean = 0.026 md). The principal deep upflow zone, with fluid temperatures in the 275–312ºC range, is located in the western part of the field near Awi 9 well pad (Figure 3).

From reservoir pressure, temperature, and geochemical monitoring, the Salak reservoir is subdivided into the west, central, east, and far-east production cells.

Like most volcanic-hosted geothermal systems, permeability at Awibengkok is controlled mainly by the presence of a highly interconnected network of open to partially sealed fractures. Although of secondary importance to well permeability, the amount of fluid stored within microfractures and pores is a significant factor in overall reservoir performance and how much heat can be extracted commercially from the subsurface (Stimac, 2008).

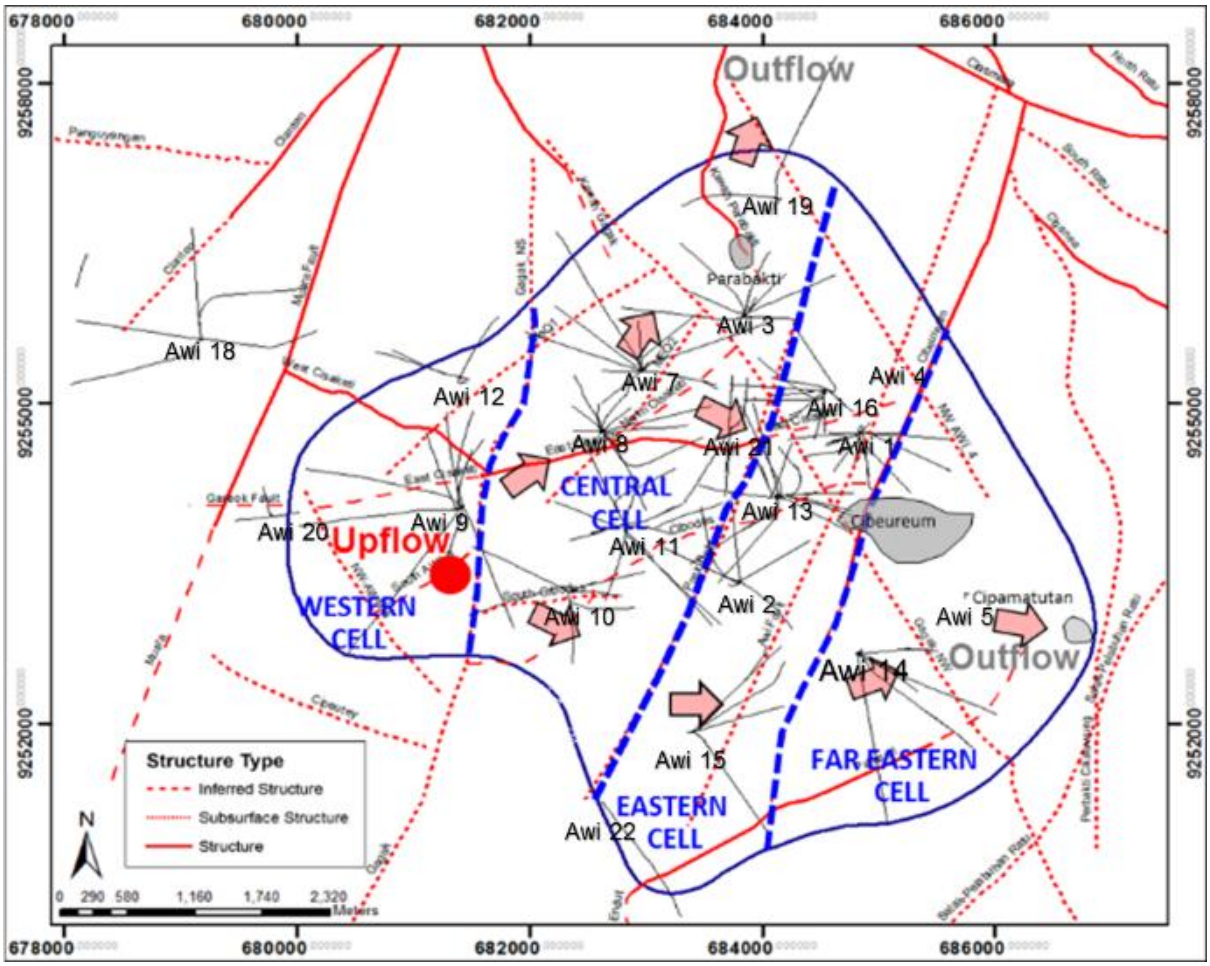


Figure 3: Major upflow in the southwest (or south of Pad 9) and minor upflows (or "hot spots") in the Awi 1, 10, and 15 areas, and preferentially move north-northeast, and outflow at Kawah. Parabakti and Sarimaya hot spring.

PRECISION GRAVITY & LEVELING

The first (base line) precision gravity and leveling surveys were conducted in 1994, coincident with the startup of Salak Units 1 and 2. Through 1999, the surveys were conducted in a yearly basis, except in 1996 where there was no survey. After 1999, the survey interval was changed to every 3 years. In total, there are 11 precision gravity and leveling surveys that have been conducted in Salak in period of 1994 – 2017. The same gravimeter LaCoste & Romberg type D-117 has been utilized consistently in every survey.

The main purpose of precision gravity survey is to monitor reservoir net mass changes, which are detectable by the changes of gravity values measured on the surface during sequential surveys. A standard practice by Star Energy is to compare the observed gravity with the simulated gravity calculated based on the saturation changes and mass changes predicted by the numerical model. This provides an independent check on the mass balance for the numerical model and a quantitative estimate of the amount of external recharge into the geothermal system. A history match of pressure and enthalpy that is consistent with the gravity data provides further confidence that the simulation model is correctly representing the key features of the reservoir and its response to production and injection (Atkinson and Pedersen, 1988).

Precision Gravity: Survey Design, Acquisition, and Data QC

The gravity measurement locations are defined as Primary and Detail benchmark (Wibowo, 2009). The primary BMs are the foundation of the survey and measured multiple times to obtain several independent leg observations between BMs. Primary benchmarks are used as base stations for the measurement of the Detail BMs. The Primary BM locations are selected based on the criteria that they should be low noise and stable, well distributed to allow loop measurement to detail BMs within 3 hours, and easy and not time consuming to access since they are going to be measured frequently. During the field measurements, the data are input into a laptop using an in-house developed program called PGravQC. This program stores the data and provides the operator with a first pass check of how well the meter is performing and check on the consistency of the measurements. Earth tide corrections are applied automatically to ensure that three minimum stable readings of the BM are obtained. The average duration on each particular BM measurement is about 30 minutes. Gravity differences between benchmarks from several measurements (e.g. in primary loop network measurements) are shown in the form of loop misclosures. In an ideal condition, loop misclosures should be zero, however in practice, it is difficult to achieve. This occurs due to noise and other random errors that is included in meter reading value. There are many sources of error on a single gravity measurement that can be divided into external, reader, and instrumental effects (Rymer, 1989).

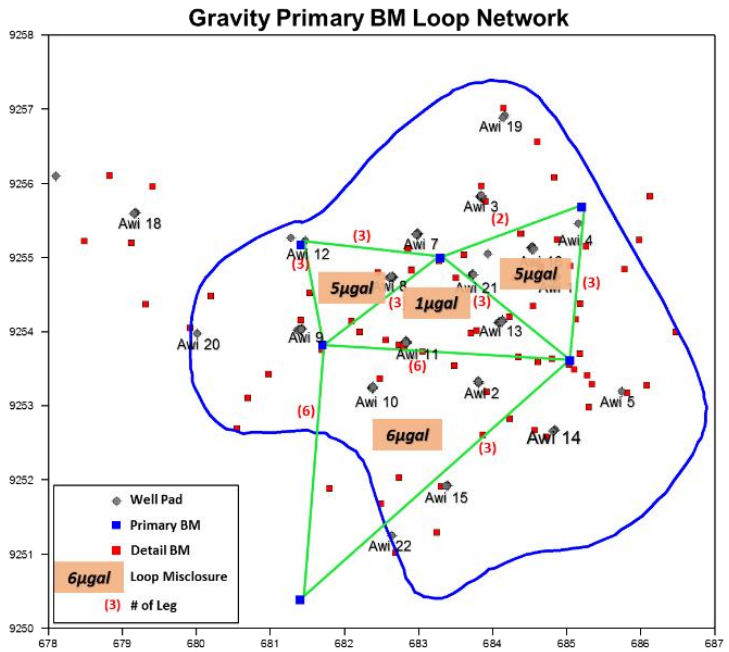


Figure 4: Primary and detail benchmarks network occupied in 2017 Salak survey. All loop misclosures on the primary network are less than 10 µGal. 2 - 6 leg measurements were conducted on each respective primary BM.

Although that it is hard to obtain a zero loop misclosure, a good and reliable primary network should have network loop misclosure less than 10 µGal. As shown on Figure 4, this was achieved for the primary BM network during 2017 precision gravity survey with maximum misclosures of just 6 µGal.

For measurement of the detailed BMs, the procedure is to tie each of them to two different primary BMs. The ties to the respective primary BM are measured on different days and the results are then fully independent. These are then combined to check the loop closure.

All of the data processing is conducted in GRAVPC application, an in-house developed software. It is in GRAVPC that drift, tide, and free-air corrections for the observed gravity data are made followed by a network adjustment. The network adjustment is a least square method that is implemented to distribute the random error value so that all network misclosures are reduced to zero (Pedersen, 1986). As a result, final observed gravity value on each BM posted after implementation of the standard gravity corrections and network adjustment.

Precision Leveling

For the acquisition of precision leveling surveys, two fully automated digital levels instruments were utilized. This is found to improve data quality and shorten survey time due to reduced measuring times and lowering the cases of operator errors. In the latest survey took part in 2017, a total of about 60 km of double run precision leveling was completed, occupying 72 gravity BMs and other secondary leveling measurement points between each gravity BM.

Daily data reductions are conducted to ensure data quality control. The leveling data is processed by a least square adjustment for all survey observations. Least square adjustment eliminates blunder or gross errors from the field data, computes the best fit adjustment for all observations simultaneously and evaluates the accuracy of adjusted final elevations. A 5% chi square test and standard deviation are also performed during the leveling data processing after the least square adjustment is completed. Any incorrect elevation data will fail the chi square test. Standard deviation shows how well the observations have fitted into the adjusted network (Nelson, 2012).

2017 GRAVITY & LEVELING RESULTS

Analysis of the precision gravity is conducted by calculating the difference of the free-air gravity in a certain period. While the Salak precision gravity & leveling surveys have been conducted since 1994 this survey is not used as the baseline. The reason for this is that there was not a detectable change in the gravity in the 1994 – 1998 period (Figure 5). A noticeable gravity decrease started to occur only after the commencement of Salak Units 3, 4, 5, and 6 in 1998. Also, by 1998 there were more BM's that had been installed across the field providing a significantly better areal coverage for the comparison of the observed and simulated gravity changes. Thus, when comparing the observed and simulated gravity they are referenced to 1998.

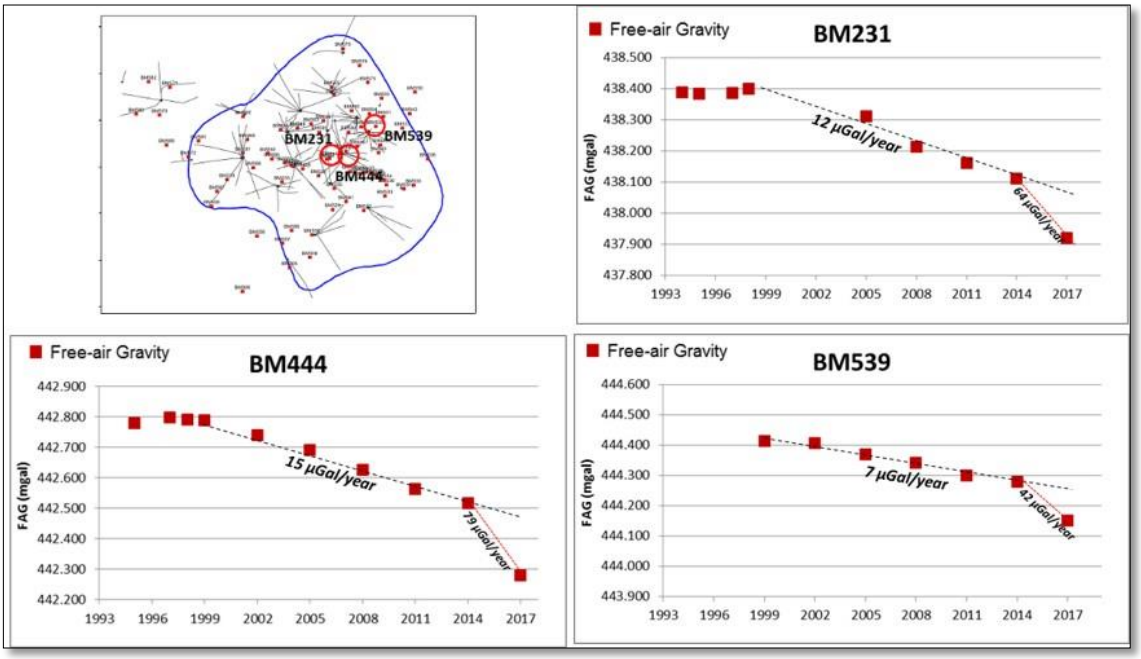


Figure 5: Three BMs located in central part of reservoir area where the biggest gravity changes are occurring. In period of 2014 to 2017, BM231 experienced the most changes of gravity of about -266 µGal

More Rapid Gravity & Elevation Decreases

The 2017 precision gravity and leveling surveys showed that in the eastern portion of the field there was significant increase of gravity and elevation changes compared to previous years. Figure 5 shows that until 2014 the FAG showed constant decrease rates in most areas. For example, the benchmark BM444 where the largest FAG occurred shows yearly rates of about 15 µGal up to 2014. This rate increased significantly between 2014 to 2017 survey where the FAG changes rates increased to 79 µGal/year (Figure 5). The second largest FAG changes on benchmark BM231 has the rates of 12 µGal/year in 1998 to 2014, while for the period of 2014 to 2017 the rates are about 64 µGal/year. The other example is the benchmark BM539 located near Awi 1 where the previous rates of about 7 µGal/year in 1998 to 2014 changed to 42 µGal/year in 2014 to 2017. This behavior occurred consistently in other BMs.

The 2017 precision leveling results also show that the elevation rates of subsidence increased significantly. Examples are shown for BM231 and BM444, where the largest elevation changes have occurred over time (Figure 6). Until 2014, the average of yearly land subsidence rates in those two BMs was about 2.1 cm/year for BM231 and 2.2 cm/year for BM444. The elevation difference between 2014 and 2017 increased from these rates to 6.8 and 6.3, respectively. Similar increases in the subsidence rates are observed for BMs located in south, central, north and eastern portions of the field.

Gravity & Elevation off-trend value

To investigate the pattern of the gravity elevation changes, an "off-trend" value is calculated. Off-trend value is an approximate number of the discrepancy between the 2017 gravity and elevation results compared with the expected values based on the change rates observed through 2014. Figure 6 above shows an example using the elevation data for BM231 and BM444 located in the central portion of the field. These have "off-trend" values of 12 cm and 11 cm, respectively. Figure 7 shows an off-trend value gravity change value calculated for BM444. These "off-trend" values are calculated for all BMs and then contoured to determine where the most significant changes in gravity and subsidence change rates have occurred.

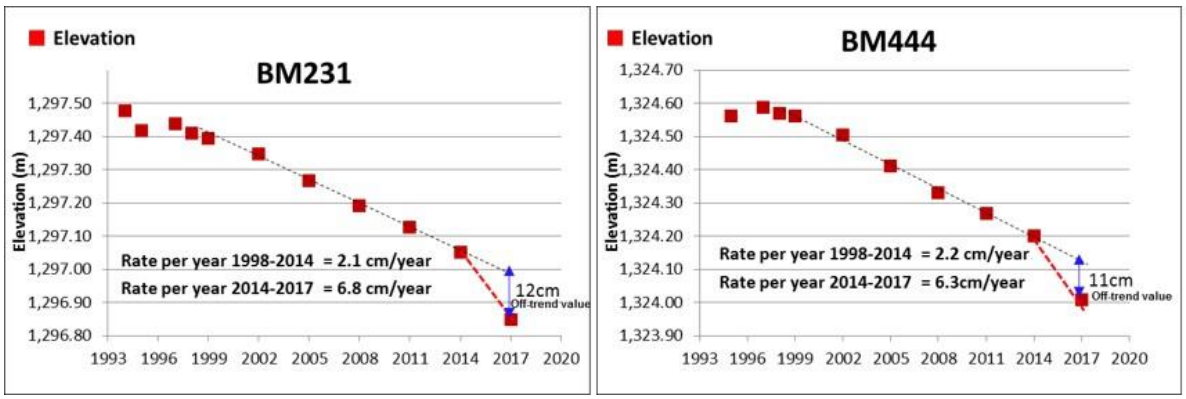


Figure 6: Plot of elevation on BM231 and BM444 where the largest subsidence occurred. The subsidence rates in recent three years on both BMs are much higher compared to the historical trend.

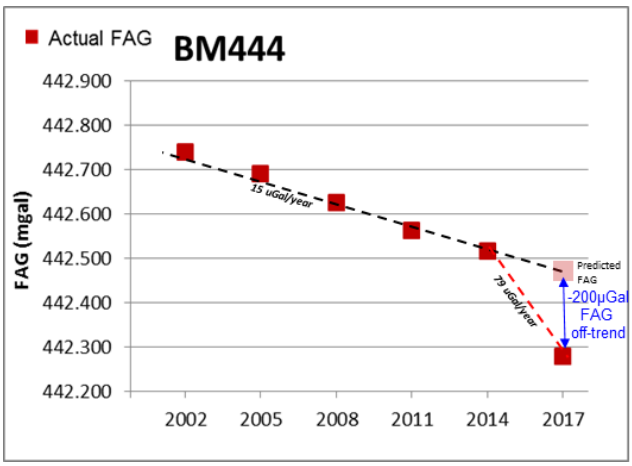


Figure 7: Off-trend value represented the discrepancy between the actual measurement and predicted value. For instance, BM444 has gravity off-trend value as high as -200 µGal.

Figure 8 shows the contoured results for the gravity (colored – microgal) and elevation (black lines – cm). The maximum gravity off-trend are located in the eastern BMs near Awi 1, Awi 13, and Awi 16 with maximum value of about -200 µGal. For the case of subsidence, the largest discrepancy in the subsidence rates are also located in east and southeastern portions of the field in surrounding of Awi 1, Awi 13, and Awi 16 pads. Also shown on the figure are tracer tests results from the Awi 14 injector (thick arrows – from Figure 8). The areas of gravity and elevation off-trend is systematic for both with maximum values located in the eastern portion of the field within the steam cap area and in line with where pressure support is expected due to injection into Awi 14.

Injection Stop at Awi 14

Since the startup of Units 3, 4, 5 and 6 in late 1997, wells on the Awi 14 pad have been utilized for brine injection in the southeast proximal area. In the last 10 years, Awi 14-2 and 14-3 were the two main brine injectors; these wells were re-drilled deeper and away from the production area in 2009 because earlier tracer tests, geochemistry, and production monitoring indicated a direct connection to Awi 1, 13 and 16 production wells. An additional injector, Awi 14-4, was also drilled in 1997 to enable more brine injection at this pad (Abdurachman et al., 2014).

Injection into the Awi 14 area is known to have been providing pressure support to the reservoir especially to the eastern part of Awi 1 and SE part of Awi 13 and Awi 16 where the steam cap is being developed. Results from tracer test in 2002 and 2009 (Figure 9) show that there is distinct connection from Awi 14 area to the North in surrounding of Awi 1, Awi 13, and Awi 16.

In December 2012, all brine injection into Awi 14 was stopped due to landslides near the Awi 14 area which started in 2005 and by 2012 were deemed to pose a significant safety hazard. This resulted in about 30,000,000 Klb per year being moved to Awi 15 (Abdurachman et al., 2014).

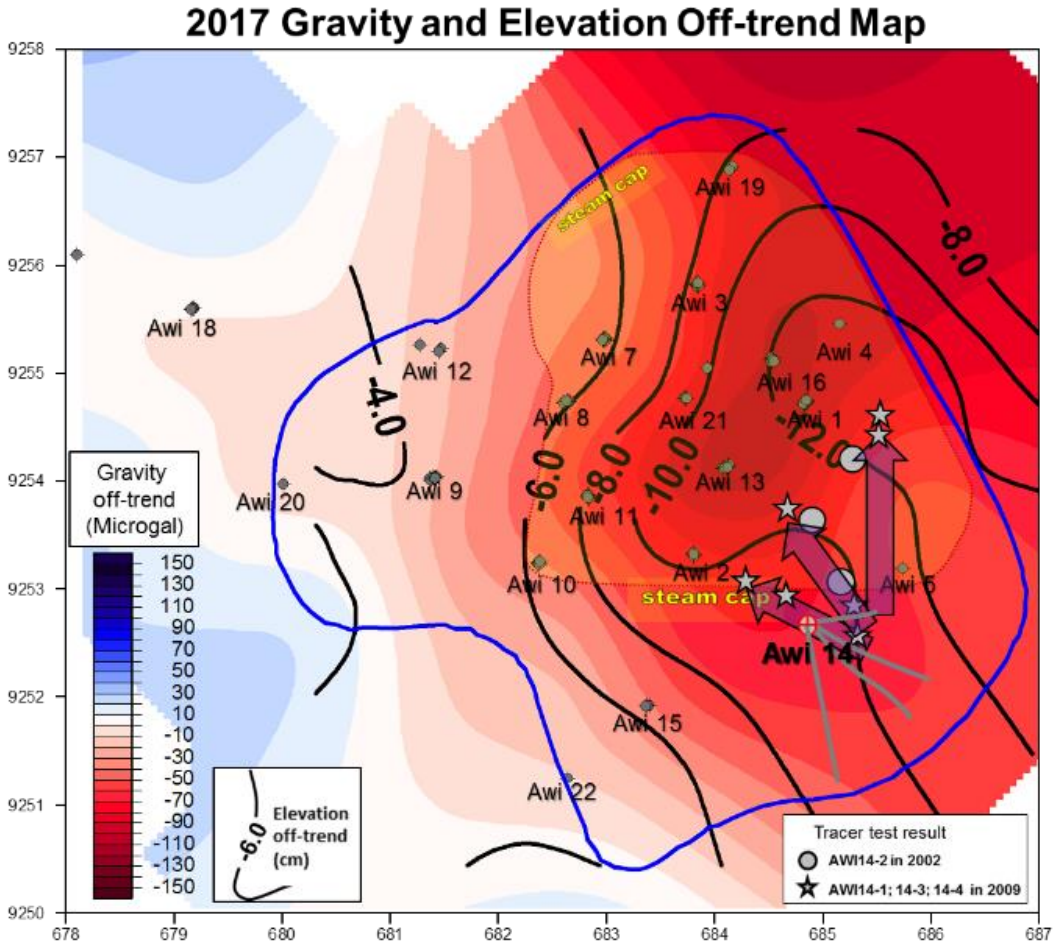


Figure 8: The distribution of the largest area of FAG changes and the maximum elevation discrepancy (black line contour) and FAG off-trend (colored contour) resulted in 2017 gravity & leveling survey. The connectivity between Awi 14 and Awi 1-Awi 13 – Awi 16 emphasize that Awi 14 provides important pressure contribution to Awibengkok reservoir.

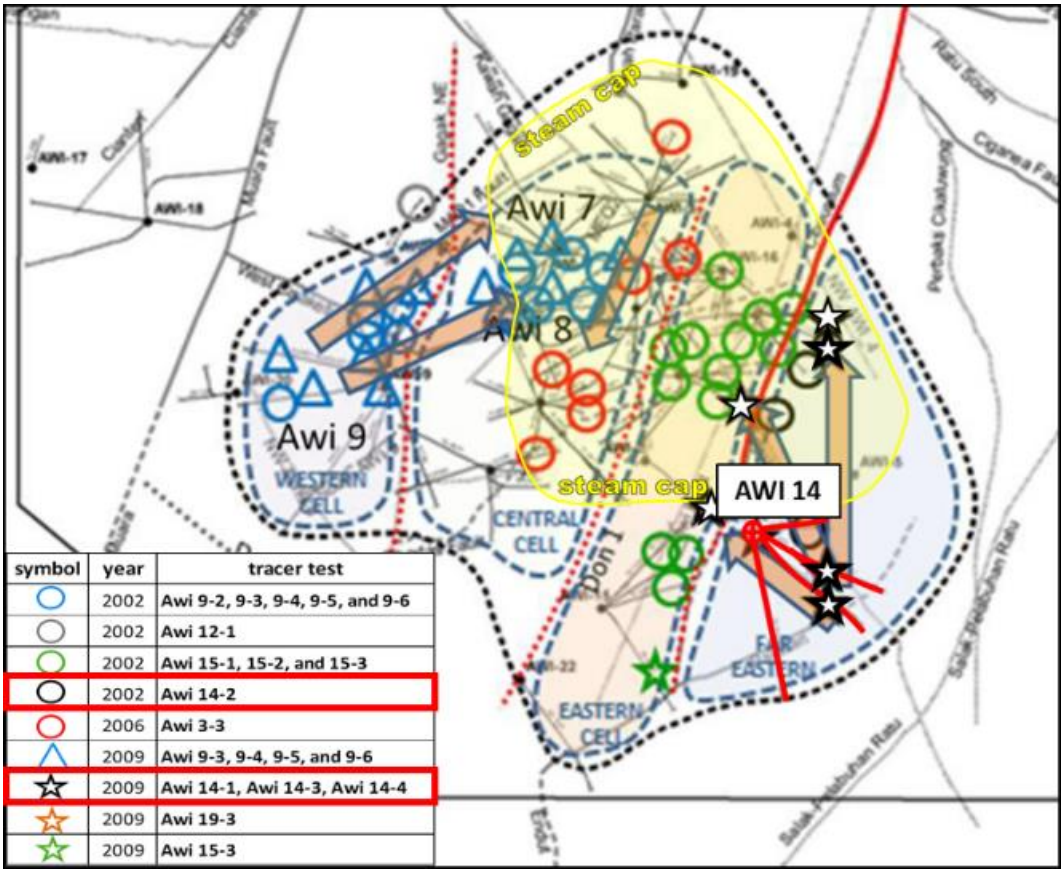


Figure 9: Tracer test result in 2002 to 2009. Two tracer tests in 2002 to 2009 in Awi 14

Impact from Injection and Productions

The rapid increases in the rates of changes for the subsidence and of the free-air gravity observed in 2017 is interpreted to be the result of the changes in the injection and production. The increased rates of change is an indication that the combined impact of stopping brine injection into the Awi 14 wells in late 2012 and more steam production from the steam cap area have resulted in increase rates of saturation changes in the fractures and matrix of the steam cap. These hypothesized increased changes in the saturation would result in larger net mass changes in the steam cap and lowered pore pressures. These would translate to increase FAG and subsidence rates. As the result, in period of 2014 to 2017, large free-air gravity changes in the range of about -100 to -200 µGal were detected in some areas including the central, north, and southeastern portions (Figure 10). The impact of the stoppage of injection was not immediately evident. The 2014 surveys did not show a deviation from the previous gravity and elevation change rates (Perdana, 2018). In 2014, the rates of FAG changes mostly were following the historical trend of gravity decrease (see Figure 5). Comparison between the FAG changes in period of 2011 to 2014 and 2014 to 2017 is shown on Figure 10. This highlights the area of most affected and is centered over the main steam cap

Thus, there was a delay between this significant change in the field's injection in the east and when there was a detectable impact on the gravity and elevation data. By the 2014 survey, the injection at Awi 14 had been stopped for 1.5 years. By the time the next precision gravity and elevation surveys are conducted in 2020 injection into Awi 14 will again be underway.

In term of steam extraction, in 2014 to 2016, the eastern well productions such as Awi 2, Awi 13, and Awi 16 showed increase of excess steam production. Generally, the eastern production area (steam cap) mostly consists of steam producers although there are few numbers of two-phase wells. However, it is obvious that several two-phase wells in eastern production area turned into dry wells (100% steam production) as it can be seen in Table 1 below.

This condition suggests that the steam cap area in Salak reservoir is continuously developed. The concurrent increase of FAG changes and land subsidence rates in recent years indicate that the Awi 14 injectors have played on important role in Awibengkok reservoir pressure regime (Perdana, 2018).

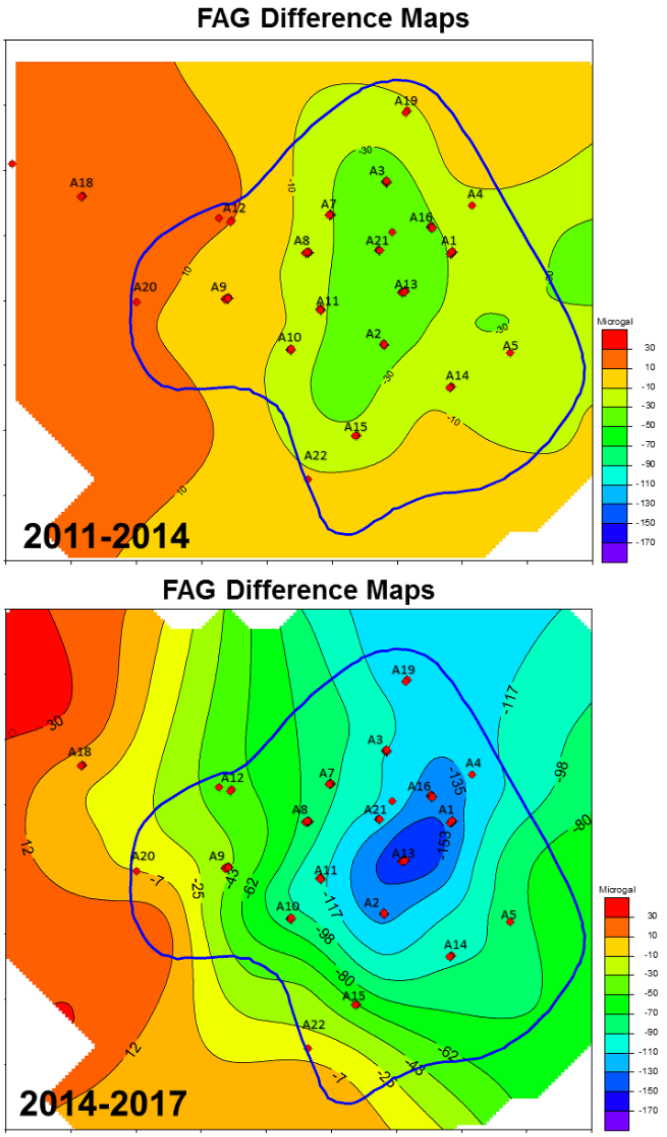


Figure 10: Comparison of FAG changes map between 2011-2014 and 2014-2017 gravity measurement. The rates of FAG decrease in 2014-2017 were much higher compared to 2011-2014 FAG changes.

Table 1: Eastern production experienced increase of the excess steam since 2014. Awi 13 and Awi 16 currently turned into dry wells (100% steam production).

No	Location	2014		2015		2016	
		Steam Extraction Rate (kph)	Excess Steam (%)	Steam Extraction Rate (kph)	Excess Steam (%)	Steam Extraction Rate (kph)	Excess Steam (%)
1	AWI 1	628	99.45%	607	98.63%	636	99.45%
2	AWI 2			216	100.00%	584	100.00%
3	AWI 3	1212	100.00%	1410	100.00%	1325	100.00%
4	AWI 13	527	80.98%	478	100.00%	440	100.00%
5	AWI 16	862	95.53%	834	97.07%	849	100.00%
East		3228	95.60%	3545	99.08%	3834	99.91%
6	AWI 7	471	40.07%	341	28.19%	382	15.54%
7	AWI 8	1108	13.21%	922	6.80%	796	5.90%
8	AWI 9	361	0.00%	328	0.00%	588	0.00%
9	AWI 10	105	0.00%	417	0.00%	352	47.40%
10	AWI 11	313	48.95%	280	58.17%	295	23.73%
11	AWI 21	510	100.00%	515	100.00%	450	100.00%
West		2867	34.81%	2804	35.06%	2863	26.41%

COMPARISON TO SIMULATION MODEL

Since 1999, gravity data have been used as a check and constraints for numerical reservoir models in Salak. Comparison between observed and simulated gravity is conducted to match the trend, magnitude and influenced area of both values over a given period. Simulated gravity is gravity simulation model calculated by internal developed software named GMAP. The GMAP software is used to calculate the simulated gravity based on numerical model output files containing the 3-dimensional array of the model block dimensions and location, matrix & fracture porosity, and matrix & fracture fluid density. Changes in saturation result in a change of the density and, in the case of increased steam saturation, an associated gravity decrease. The simulated gravity change at the surface is calculated by associating this mass change in the block and Newton's law on gravitational force using the method of point mass calculation (Nettleton, 1976). This approach approximates the complex 3D body with a distribution of point masses. Each single block in the model is represented by the point mass at the center of gravity. The gravitational attraction at the surface is the sum of the calculated gravity from all of the blocks center of gravity (Nelson, 2013).

The comparison is conducted between the simulated gravity changes determined by GMAP application and the observed gravity changes based on actual measurement. The simulated gravity is calculated in a certain period e.g. from a base line to recent survey. Using similar period, observed gravity changes are calculated and both data are compared in time series plot and map. The difference between simulated gravity changes and observed gravity changes are calculated and then contoured. The contour map of the observed-simulated discrepancy is called mismatch map. In precision gravity & leveling standard practice, a good match between observed and simulated gravity is usually possible (Perdana, 2018). An example is shown from the Bulalo geothermal field in the Philippines where initially the simulated gravity showed too large a gravity decrease compared to what was observed. This indicated a mismatch in the net mass as a result of not enough external recharge. Changes were applied to the permeability distribution and recharge locations and volumes that eventually resulted in accurate match between the simulated and observed gravity, Figure 11 (Nordquist et al., 2004).

Recent Observed-Simulated Gravity Comparison

The observed-simulated gravity comparison continued after the completion of the most recent precision gravity and leveling survey in September 2017. First attempt of this matching process was to conduct comparison of observed free-air gravity (FAG) changes in period of 1998 – 2017 with the simulated gravity in the same period. During this stage, the simulated model determined from reservoir model v1.2018 which using reference model 2015v14k. Comparison between observed and simulated FAG for the period of 1998 – 2017 are shown on Figure 12.

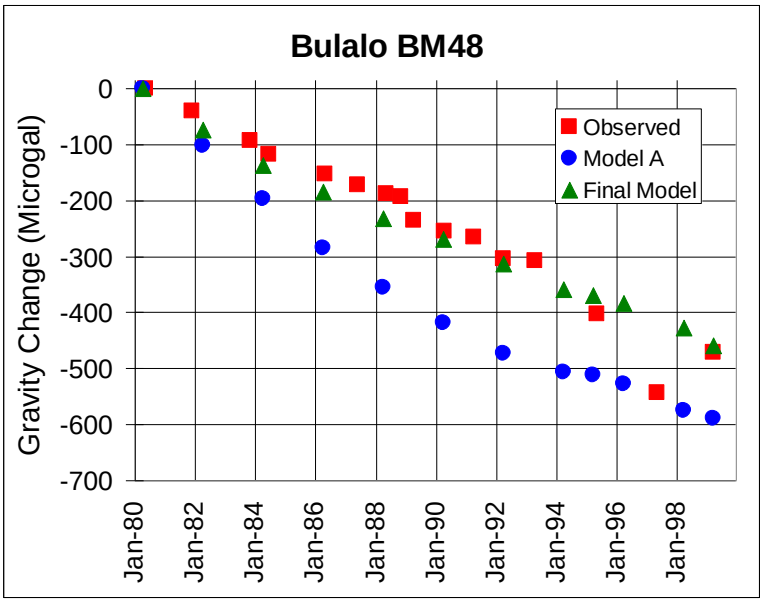


Figure 11: Observed vs simulated gravity trends for the period 1980 to 1999 at BM 48 at Bulalo geothermal field, Philippines. It is shown that there is a different trend between simulated gravity based on Model A (an early version of the numerical model) and the observed gravity trend (red rectangle). After changes applied to the permeability and recharge area & volume, the Final model (green triangle) shows better match with the Observed gravity model.

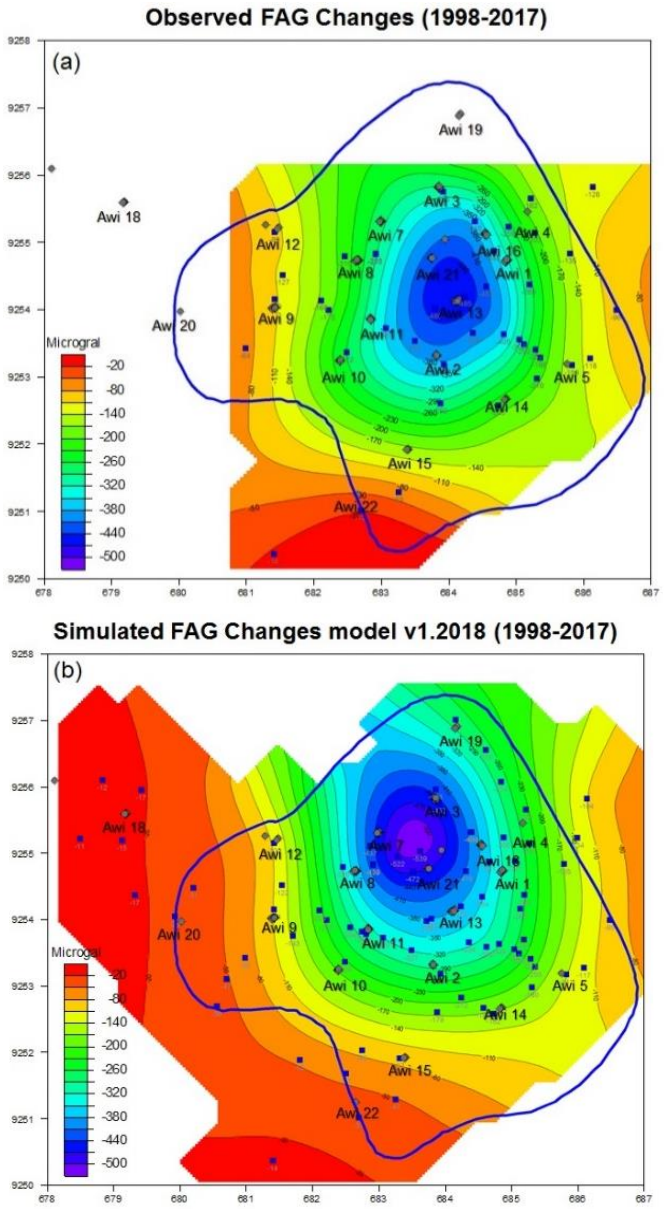


Figure 12: Map of free-air gravity changes in period of 1998 to 2017. Upper figure (a) is showing the observed while the lower figure (b) is the simulated. The largest FAG changes occurred in the central part for both models, however the location is shifted, and the range of FAG changes is slightly higher for simulated model.

The observed model shows that the maximum FAG changes were centralized in the middle part of the field near Awi 13 and Awi 21. The largest change represented by BM444 with value of -485 µGal. While the simulated model v1.2018 the maximum FAG changes are greater (-539 µGal) and shifted to the north.

The next step is to calculate the mismatch value by subtracting observed FAG from the simulated FAG. Figure 13 below is showing the mismatch map (observed-simulated). The result shows that the north & west sectors of the field near Awi 8, Awi 7, Awi 3, and Awi 19 still shows large mismatch with the value about 111 to 146 µGal. Furthermore, the mismatch in southern area of Salak is higher compared to what have been observed prior to 2017 survey. The current mismatch degree in southern portion is about -60 to -110 µGal. Positive value of mismatch means the simulated model decreased faster than observed model and vice versa.

BM in north sector experienced better match due to the end point of the 2017 observed FAG is getting closer to the simulator (BM554), while in the south, BM330 historically shows a good match (up to 2014) and then mismatch arises when the calculation includes the 2017 observed FAG. The Figure 14 below illustrates the importance of matching not just the total gravity changes, but to also take into account the trends and rates of changes in the gravity signature.

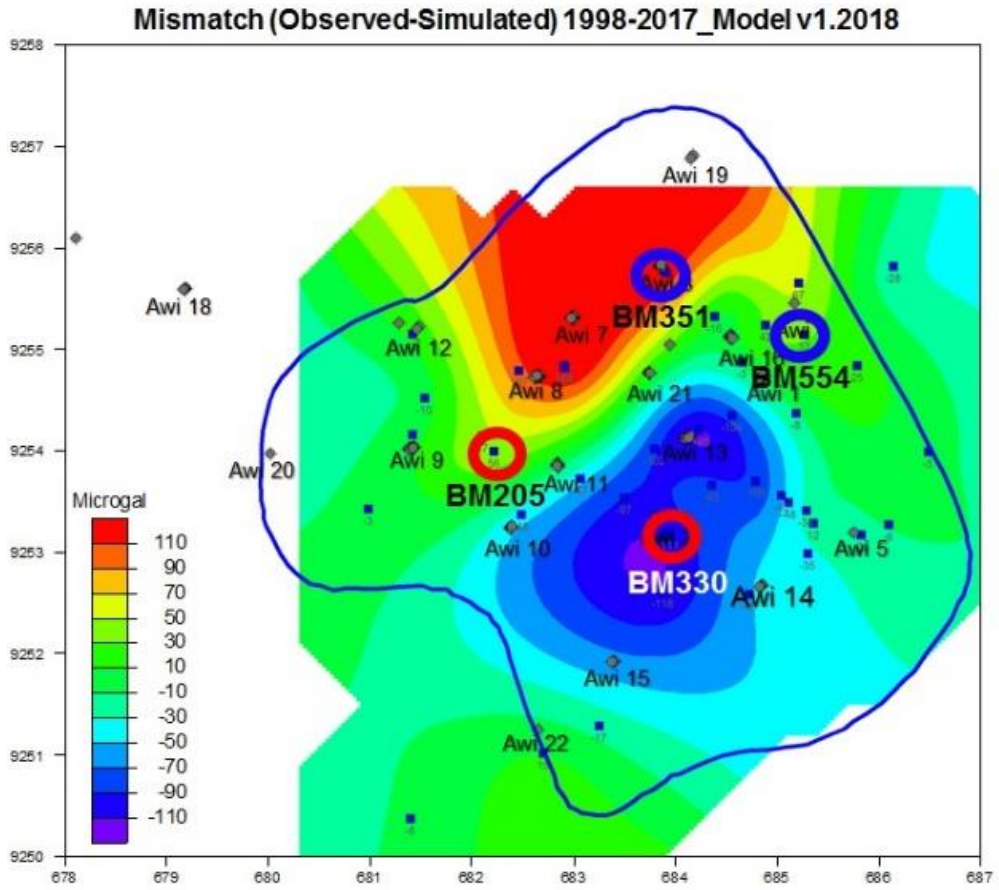


Figure 13: Mismatch between observed gravity and simulated model version v1.2018 in period of 1998-2017. Large mismatch occurred in North (red closures) and South (blue closures).

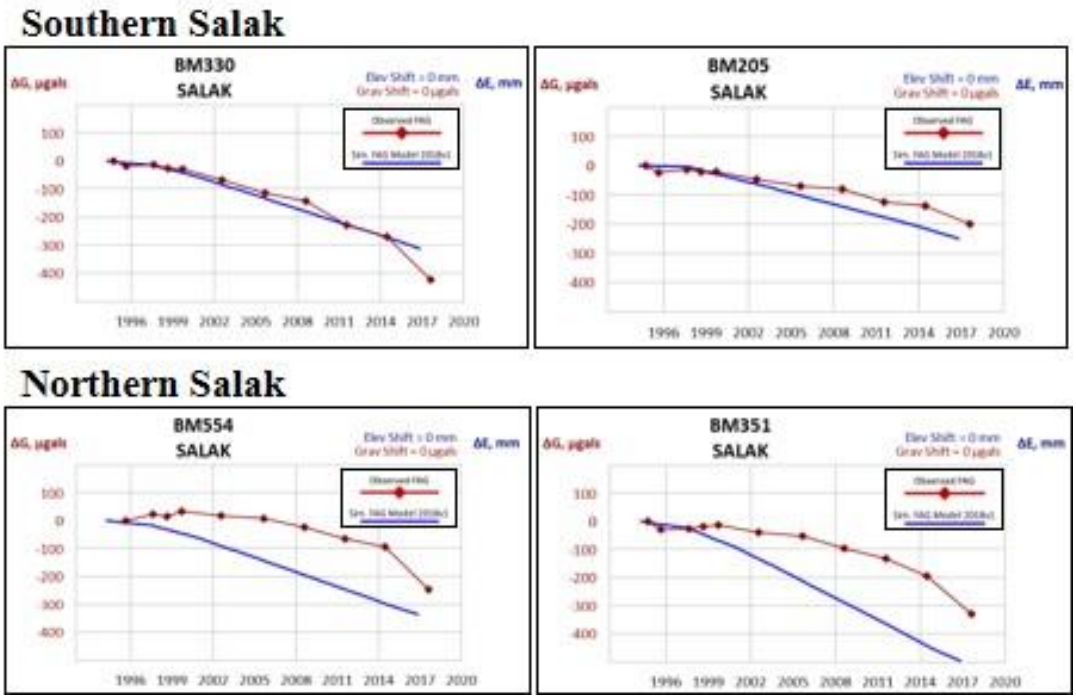


Figure 14: Plot of observed and simulated gravity in northern and southern BMs. In south BM (BM330) mismatch occurred due to large observed FAG decrease in 2017 survey. While in the north (BM351 & BM554), the large drop of observed FAG caused lower mismatch in northern area.

Possible Source of Mismatch Pre-2017

As evident on Figure 14, the occurrence of a gravity mismatch in Salak has been emerged since initial phase of gravity observed-simulated comparison process (Perdana, 2018). Extensive efforts have been made to reduce the mismatch. In 2004, it was decided to implement the Multiple Interacting Continua (MINC) formulation (Pruess, 1991). The MINC formulation allows a discretization of the matrix block into several concentric shells, which can have gradation of pressure, temperature and saturations. This intra-matrix discretization makes possible the existence of a steam saturation gradient inside the matrix blocks. Thus, the matrix tends to release liquid (pressure support) into the system slower. With MINC implemented, fluid from the outermost matrix shell is more easily available to fractures as compared to single matrix block while the innermost shell will be exposed to less drainage and remains at larger liquid saturation. These changes result in less sensitivity of the gravity change to matrix permeability and more reasonable external recharge rates. The application of MINC significantly improved the gravity match (Acuna 2005). However, as shown in Figure 14, it did not "fix" the entire problem.

This led to looking at another potential source for the mismatch. Nordquist, (2010) suggests the mismatch was caused by the presence of a re-saturating shallow aquifer above the reservoir. It was hypothesized that the shallow aquifer caused excess mass reflected in the observed gravity changes. However, subsequent surveys in 2014 and 2017 showed the mismatch continued to worsen, thus leading to a conclusion that this hypothesis is seemingly not the case for answering the mismatch presence.

Recent Attempts to Reduce Gravity Mismatch

With the hypothesis of a re-saturating shallow aquifer unlikely, the efforts to improve the gravity match have shifted to the reservoir parameters. Modifications have been implemented to the TOUGH2 simulator model including the change of matrix permeability, fracture permeability, fracture spacing, and increasing the upflow enthalpy. During 2017-2018, at least ten simulated models have been built as effort to match the gravity (Figure 15).

For each particular process, simulated gravity is determined based on each modified model. Then, gravity mismatch for same period (1998-2017) is calculated based on each model. Modifications on each numerical model resulted specific gravity mismatch results. One example of updated mismatch map determined from model v2a.2018 during the matching process is shown on Figure 16.

In this model, the average matrix permeability was decreased from 15 microdarcy to 2.5 microdarcy for all layers in TOUGH2 simulator. The lower matrix permeability expected to retard the fluid flow from matrix to fracture. As is shown on mismatch in model v1.2018 (Figure 13) the northern sector simulated model decreased more rapidly compared to what was observed. The result shows that there was improvement of the gravity match but only for small amount. Comparison of both models can be seen in the following Figure 17.

Simulated Model	Reference Model	Changelog
v11	v2a	perm matrix times 1.33 for i=1-rna, j=1-12, k=1-12
v16	v10	change permzfr in z=12 and 13 times 3 (brown box)
v30	v16	extend permzfr (value = layer 13) layer 14 - 15
v32	v31	frac spacing in brown box increased up to 500 layer 1 - 10
v33	v32	Improve porosity layer k =5-12 impose porosity from layer 4
v35	v33	Decrease permxma, permyma, permzma to 2.5 microD dari layer 1 - 12. i and j all
v41	v40	increase upflow enthalpy to 10degF; Decrease permxma, permyma, permzma to 5 microD dari layer 1 -12. i and j all; Local adjustment di i= 23, j=15, k=6 5 surrounding block for permzfr 100
v43	v41	
v44	v41	
v2a.2018	v1.2018	Change Permeability Matrix (PERMXMA, PERMYMA, PERMZMA) to 2.5 microdarcy for: i = 14 - 29; j = 4 - 12; k = 2 - 12 Permeability Matrix value for All layers will be the same

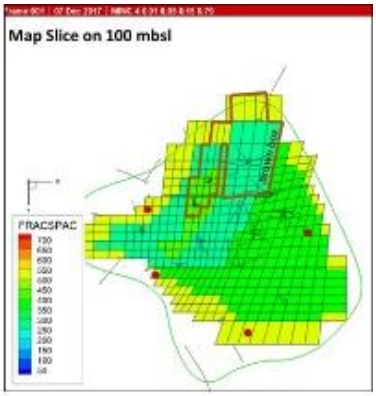


Figure 15: Model variations during gravity matching process. Nine models have been built to match observed gravity. Right figure is showing one example of map slice of fracture spacing in TOUGH2 simulator on 100 mbsl from model v.33.

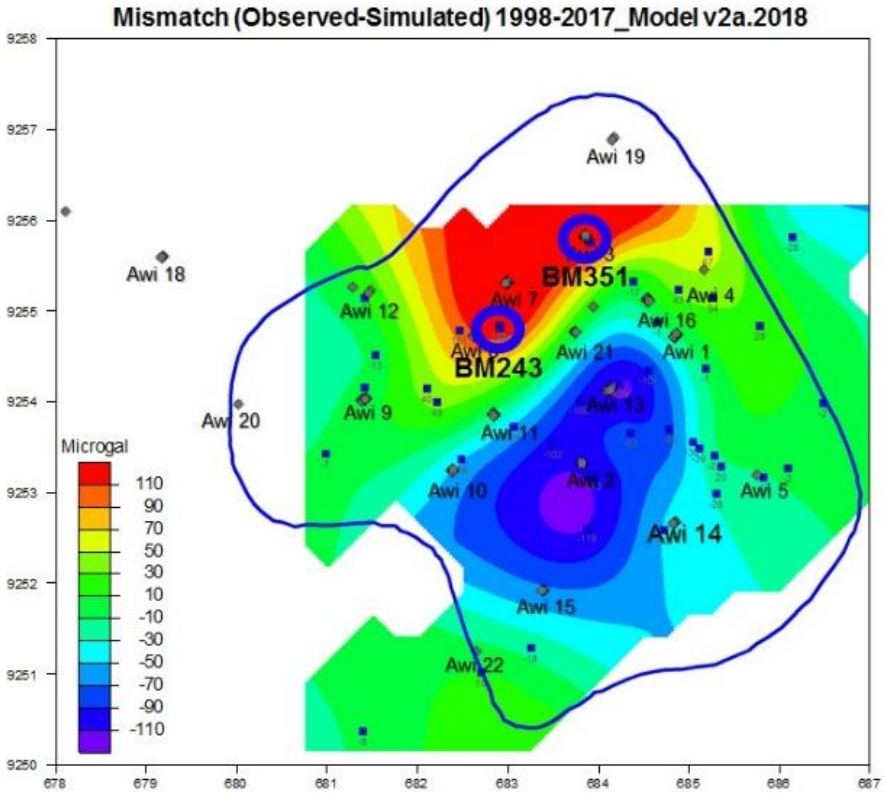


Figure 16: Mismatch resulted from model v2a.2018; modifications on that model only reduced the mismatch in small amount compared to the original model of v1.2018. Large mismatch still emerged in northern portion near Awi 3 and Awi 7. Similar thing occurred for central and southern portion. In general, the updated model only decreased the mismatch of about 20 – 60 µGal.

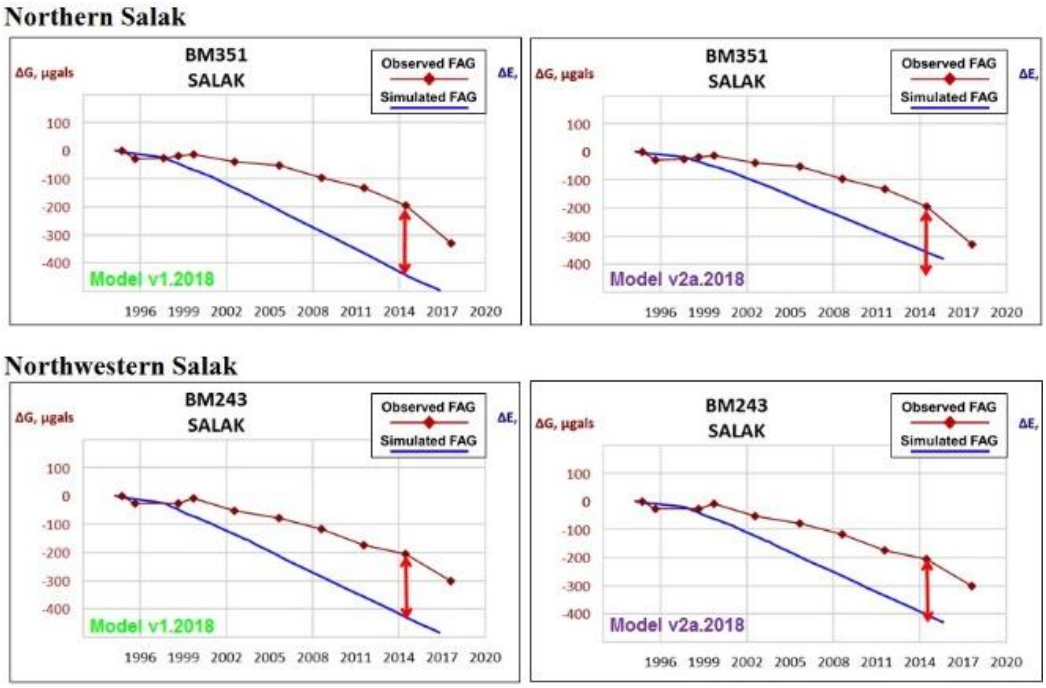


Figure 17: Comparison between original model v1.2018 and modified model v2a.2018 for BM351 in north and BM243 in northwest Salak. The simulated gravity determined from model v2a.2018 shows slower rates of mass extraction compared to the original model. However, the rates are still faster than what is shown by observed gravity.

The recent observation shows that mismatch is still high in northern portion. Moreover, the faster decrease of FAG changes based on 2017 survey even made larger mismatch in central and southern area. The new information from the 2017 survey, which shows more rapid decrease of FAG and land subsidence rates, and the strong link with the injection stoppage at Awi 14 provides new insight of what might be occurring in the reservoir. Pointing to a reservoir process and/or conceptual element that has not been incorporated in current reservoir model. In addition, key will be the full integration of the updated earth model. For example, the new earth model shows a significant difference in the distribution of matrix permeability than is currently in the simulation model. Figure 18 shows the comparison of matrix permeability distribution between current numerical model and new earth model.

Noting that the most significant mismatch in located over the area that currently has relatively high matrix permeability. The area of high matrix permeability was incorporated by the reservoir modeler to match the high-pressure steam cap in that area of the field. But the new earth model does not support having that variation in the matrix permeability, so there must be something else that is driving the simulated dynamic model and it reaction to natural recharge, pressure support from the matrix and injection.

For the planned update for the simulation model, the new workflow for numerical modeling is being prepared to better incorporate the static data as part of the modeling process. This will provide the most up to date geological constraints into the reservoir model. Once completed, the new numerical model is expected to produce better history match of pressure, temperature, enthalpy, and gravity.

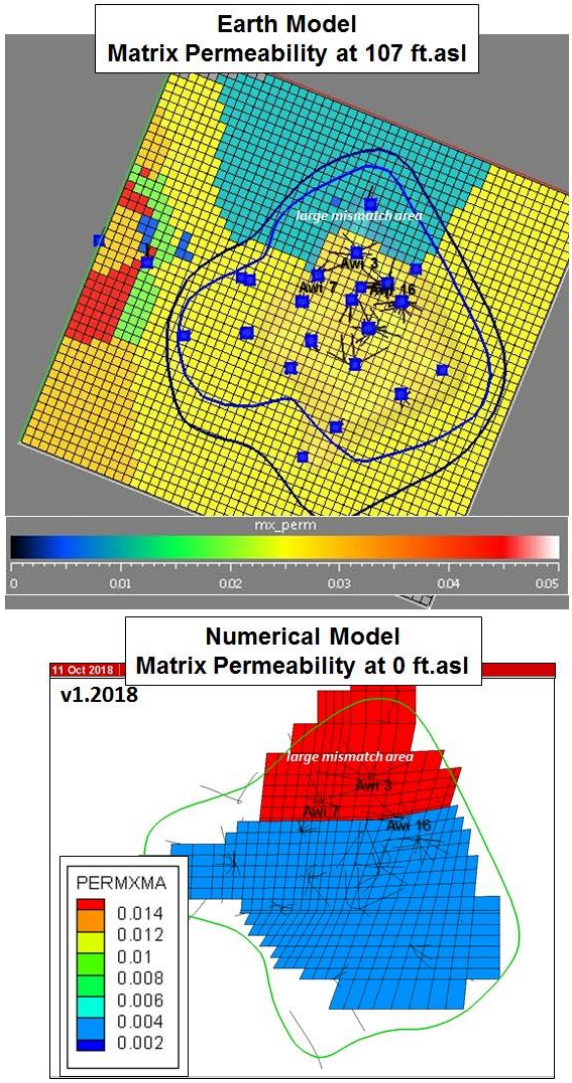


Figure 18: Comparison of matrix permeability distribution at nearly mean sea level between earth model (upper figure) and numerical model v1.2018. The earth model shows equal matrix permeability distribution in central to north Salak near Awi 3, Awi 7, and Awi 16, while the numerical model (lower figure) has higher matrix permeability in that area. The area of matrix permeability difference coincident with the location of the largest mismatch occurrence for Salak gravity-simulation matching.

CONCLUSION

Precision gravity and precision leveling data provide important insight for the reservoir characterization. The faster decrease of gravity and higher rates of land subsidence occurred in recent years may indicate that there is something more interesting in Salak reservoir behaviour.

Result of the analysis on free-air gravity changes provides an important data point and trends that can be used to calibrate reservoir mass balance. Although the current state is still showing large discrepancy between observed gravity and simulation model, the more obtained gravity data, and continuous work on gravity-simulation matching will potentially provide new insight on the understanding of the reservoir character. Continuous attempts on gravity matching process will be performed parallel to the construction of new reservoir model with integration to earth model.

REFERENCES

Abdurachman, F., et al., (2014), "2014 Salak State of the Reservoir," Chevron Geothermal Salak Internal Report.

Acuna, J., (2005), "Salak Engineering Studies Part I. Awibengkok External Recharge and Microgravity," Unpublished Chevron Report.

Atkinson, P.G., Pedersen, J.R., (1988), "Using Precision Gravity Data in Geothermal Reservoir Engineering Modeling Studies," Proceeding of 13th Stanford Workshop on Geothermal Reservoir Engineering, 35-40.

Nelson, C., (2012), "2011 Precision Gravity Result and Model Update in Awibengkok Geothermal Field," Proceedings the 12th Annual Indonesian Geothermal Association Meeting & Conference.

Nelson, C., (2013), "Precision Gravity Monitoring of Salak Geothermal Field: Independent Check on Numerical Simulation," Chevron Geothermal Salak Internal Report.

Nettleton, L. L., (1976), "Gravity and Magnetics in Oil Prospecting," International Series in the Earth and Planetary Sciences.

Nordquist, G.A., Protacio, J.A., Acuna, J., (2004), "Precision Gravity Monitoring of the Bulalo Geothermal Field, Philippines: Independent Checks and Constrains on Numerical Simulation," Geothermics, 33, 37-56.

Nordquist, G.A, Acuna, J., Stimac, J.A., (2010), "Precision Gravity Modeling and Interpretation at the Salak Geothermal Field, Indonesia," Proceeding World Geothermal Congress.

Perdana, M. W., (2018), "2017 Salak Precision Gravity & Leveling Survey Operation Report," Star Energy Geothermal Salak Internal Report.

Perdana, M. W., (2018), "Salak Precision Gravity: Current Status on Comparison to Numerical Simulation," Star Energy Geothermal Salak Internal Report.

Pruess, K., (1991), "TOUGH2-A General Purpose Numerical Simulator for Multiphase Fluid and Heat Flow," Report LBL-29400, Lawrence Berkeley Lab.

Tanuwidjaja, R. et al., (2015), "Salak Shallow Aquifer Study," Chevron Geothermal Salak Internal Presentation.

Wibowo, D., (2009), "Precision Gravity and Leveling Surveys Awibengkok 2008 – Operations Summary," Chevron Geothermal Salak Internal Report.

ANALYSIS OF OPTIMUM STATION SPACING IN MAGNETOTELLURIC DATA ACQUISITION BY USING 3-DIMENSIONAL FORWARD AND INVERSE MODELLING FOR GEOTHERMAL EXPLORATION

Dhara Adhnandya Kumara[1], Yunus Daud[2], Rifqa Agung Wicaksono[3], Wahyu Noor Iqwan[2], Fikri Fahmi[2], and Ewin Rahman Dzuhri[1]

[1]Study Program of Geophysics Universitas Indonesia,
[2]Geothermal Research Center Universitas Indonesia,
[3]Star Energy Geothermal (Wayang Windu) Ltd
Depok, West Javaa
Email: dhara.adhnandyak@gmail.com

ABSTRACT

Magnetotelluric (MT) method is one of geophysical method which commonly used in geothermal exploration. This method is capable to map the clay cap, reservoir zone, and usually the source rock, also the boundary of the prospect zone through the resistivity map interpretation obtained from the data processing. Combined with geology and geochemistry survey (all three called as 3G surveys) would be helpful to identify the geothermal prospect zone. However, how does the survey design is managed would affect the model and interpretation result. Important parameters to provide the best sub-surface image in the MT data acquisition are deciding the number and spacing distance for each station also how does it arranged. The distance between stations should not be too large, it would cause the resolution obtained will be too low and extrapolation also occurs. However, if the distance is too dense it will cost a lot of money and time consuming during the acquisition. Especially in MT surveys, to obtain deeper depth requires a longer measurement time. Usually in geothermal exploration, measurement of MT data can be done up to 24 hours. Thus, when more points are measured the longer the time needed to measure, and the higher the prices should be paid. The use of distance between stations in previous studies are highly varied. This certainly affects the imaging of the geothermal system resulting from the processing of the MT data. This study aims to determine the optimum station spacing and the design survey of MT method for exploration on geothermal fields. Where this research will be carried out by doing 3-Dimensional forward modeling and inverse modelling. By building several models and varied the station spacing, optimum spacing in geothermal area could be concluded.

Keywords: Magnetotelluric, inverse modelling, exploration, geothermal

INTRODUCTION

Currently, Indonesia is trying to meet energy needs for national energy security goals. One of the energies being considered is new and renewable energy, one of which is geothermal energy. To meet this goal, exploration for geothermal energy need to be intensified. Several technologies used to help the exploration and development of this energy, one of them is geophysics method which useful for geothermal energy exploration.

The geophysics method which usually used for geothermal energy exploration is the magnetotelluric method. This method is still the most effective method in geothermal exploration. When conducting magnetotelluric survey, many things need to be considered, especially when making a survey design. One of the important parameters in the data acquisition is deciding the number and spacing for each station to provide the best sub-surface image.

The distance between stations should not be too large, that caused the resolution obtained will be too low and extrapolation also occurs when the data processing obtained. However, if the distance too dense it will also drain the cost and time during the measurement. Especially in magnetotelluric surveys, to obtain deep depth requires a longer measurement time. Usually in geothermal exploration, measurement of magnetotelluric data can be done up to 24 hours. Thus, when more points are measured the longer the time needed to measure.

At present, there is no research that discusses the optimum distance in magnetotelluric data acquisition for geothermal exploration. Based on the literature study, several research for geothermal exploration by using MT method used the station spacing between 1 – 4 km. For example from this research, at Darajat the station spacing used is 1 km with random station plot (Soyer et al., 2018); research at Ulubelu used station spacing between 1 – 2 km (Panjaitan, 2010); meanwhile at Sibayak area 1 – 2 km spacing is used with the total number of station 31 stations (Suparno & Daud, 2005); and at Dieng 2 – 4 km station spacing is used (Gaffar, Permana, Indarto, & Sudrajat., 2014).

The use of distance between stations in previous studies is highly varied. This certainly affects the imaging of the geothermal system resulting from the

processing of the magnetotelluric data. This study aims to determine the most optimum distance between stations for exploration on geothermal fields. Where this research will be carried out by doing forward modeling and inverse modelling. By building several models and varied the station spacing, optimum spacing in geothermal area could be concluded. are free to exceed the target length of eight pages.

METHODOLOGY

The aim of this paper is to analyze the optimum station spacing for geothermal exploration. To achieve that goal, the study used 3-Dimensional forward modelling, also 2D and 3D inverse modeling. Several model with different station spacing is build and then forward calculation is run to obtain the MT curve (apparent resistivity vs phase) for each station. The data that has been obtain will be invert and compared with the model to find the best inverse result that look like the initial model. To understand the flow chart easily, Figure 1 shown the chart flow of the study.

3D Forward Modelling runs by using WinGlink 3D Modelling *software*. Important parameter before building a model is determined the grid size which consist of number of cells at x, y, and z direction. Each cell will have a resistivity value. To run the forward calculation and obtained the MT curve from the model, stations must be provided. After the data obtained, 2D and 3D inversion will be applied. The 2D inversion used WinGlink software provided by Star Energy Geothermal (Wayang Windu) Ltd., while the 3D inversion runs by using MT-3DInvX provided by PT. NewQuest Geotechnology.

The 2D inversion software work in Non-linear conjugate gradient (NLCG) algorithm, while the 3D inversion work in Data space occam algorithm (Siripunvaraporn W., 2005).

BASIC THEORY

2-D Model

The 2D model assumed that resistivity varies laterally in one direction and vertically, while in the other lateral direction homogenous. The direction where resistivity doesn't change (homogenous) called geoelectrical strike.

In 2D case if the measurement of MT Data is parallel with the strike for x direction, the on-diagonal impedance component will be equal zero ($Z_{xx} = Z_{yy} = 0$), while the Z_{xy} and Z_{yx}. Thus, the impedance tensor will be written as:

$$\begin{pmatrix} E_x \\ E_y \end{pmatrix} = \begin{pmatrix} 0 & Z_{xy} \\ Z_{yx} & 0 \end{pmatrix} \begin{pmatrix} H_x \\ H_y \end{pmatrix} \quad (1)$$

In 2D model, there are two independent modes for MT method which is TE mode (E-polarization) and TM mode (B polarization). The TE mode measures electric field that is parallel to the geoelectrical strike. This configuration can be seen on Figure 2.

3-D Model

The 3D Model assume that resistivity values varies in all direction, whether vertical or horizontal. Thus, the Maxwell equation can't be separated in two mode. In 3D model, generally the MT transfer function has non zero value for all component. The impedance tensor can be written as (Teklesenbet, 2012):

$$Z_{3D} = \begin{pmatrix} Z_{xx} & Z_{xy} \\ Z_{yx} & Z_{yy} \end{pmatrix} \quad (2)$$

SYNTHETIC MODEL

Resistivity Model Block

Before forward calculation conducted, a resistivity model should be made. This study uses a simple buried conductive block with the resistivity of 5 Ωm. The block is buried at the depth of 500 m and extend up to 2000 m, so the total thickness of the anomaly object is 1500 m. The dimension of this object is 3 km x 3 km x 1.5 km and buried 500 m from the surface. The surrounding resistivity is 100 Ωm. The model is discretized on a 47 x 47 x 29 layers grid without any air layer. The model can be seen in Figure 1 and Figure 2. T profile is shown in red line (line 01) will be used to analyze each model result (Figure 3).

Station Arrangement Variation

For the forward model the number of station and station spacing will be varied which will affect the design survey used. The aim of this variation is to understand the optimum station spacing and the number of stations in MT data acquisition for geothermal exploration.

The station arrangement can be seen in Figure 4, Figure 5, and Figure 6. At the interest area (marked with red square) which represent up-flow zone in geothermal prospect area, the station spacing will be varied from 250 meters, 500 meters, and 1000 meters. While out of the interest zone the station spacing will be fixed at 1000 meter. The number of stations used for 1000 meters, 500 meters, and 250 meters respectively is 64, 97, and 217 station. While the size of study area is 9 km x 9 km and the interest zone size are 3 km x 3 km.

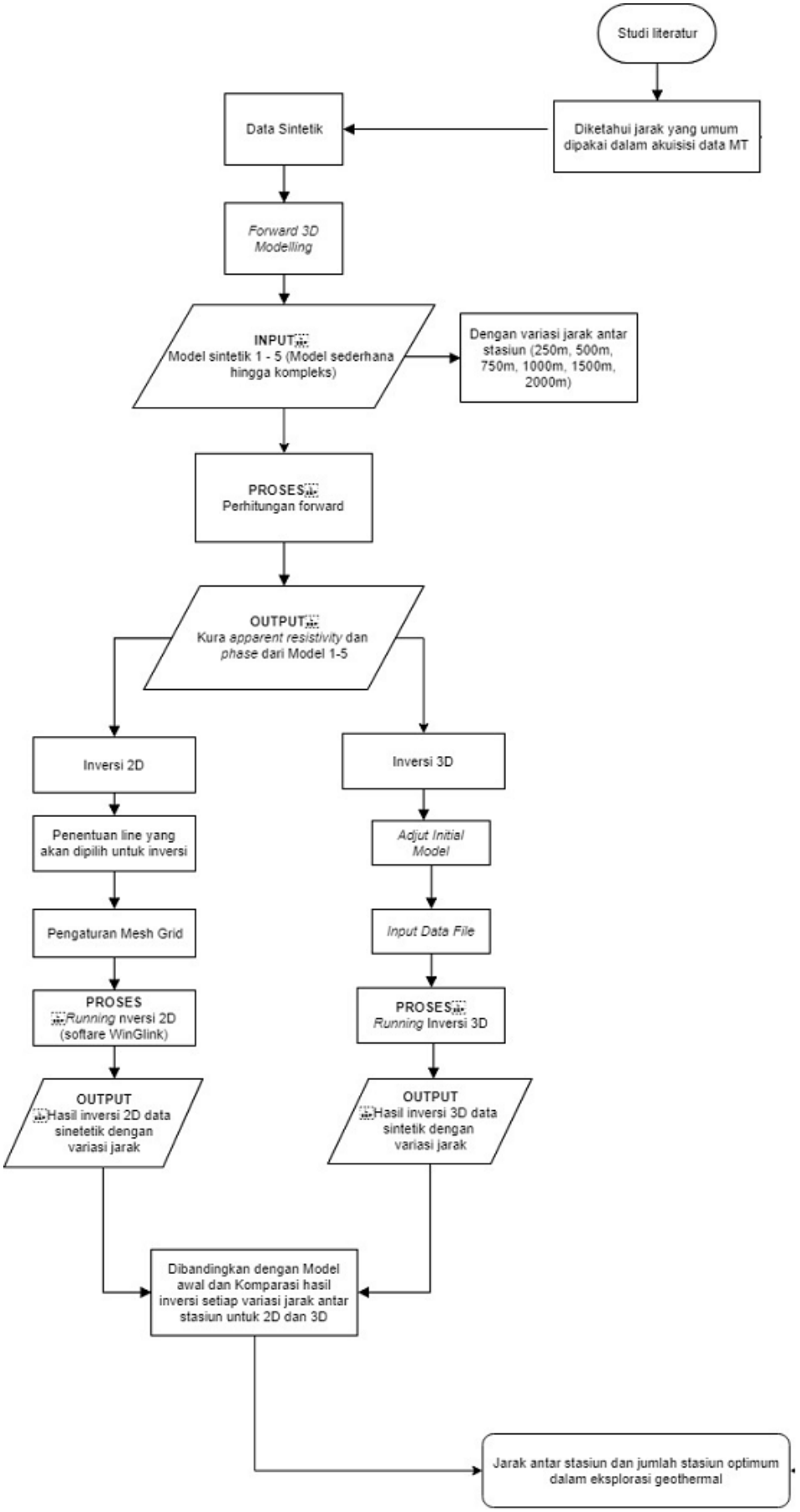


Figure 1: Flow chart.

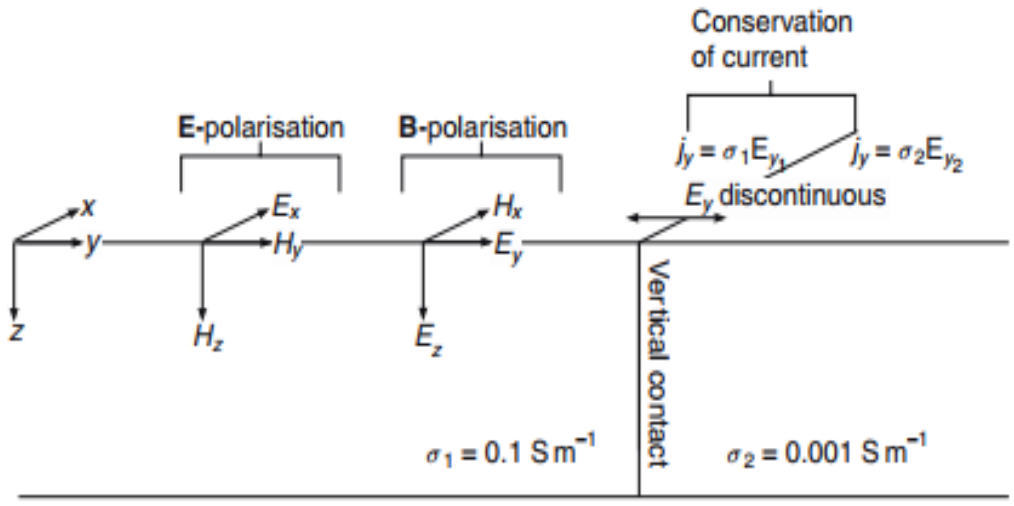


Figure 2: TE mode and TM mode (Simpson & Bhar, 2015).

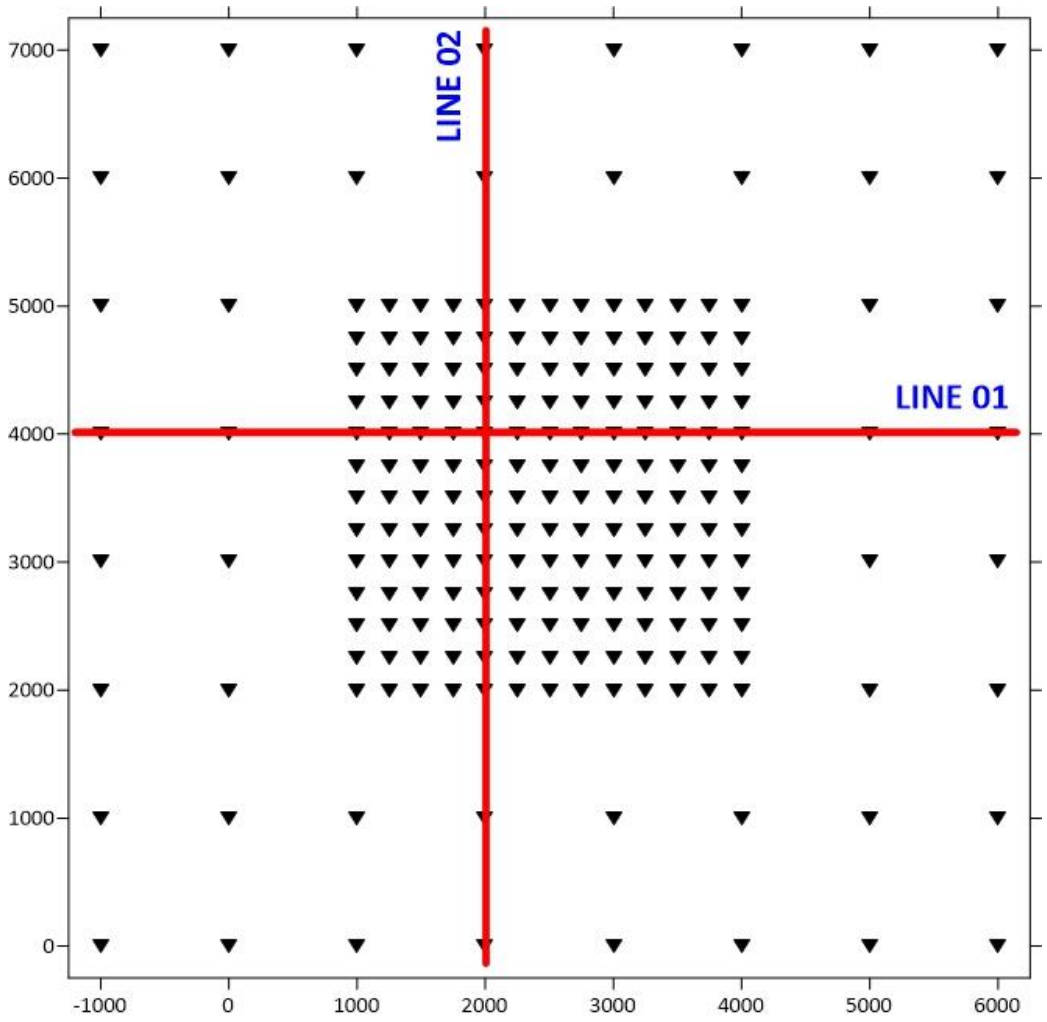


Figure 3: Profile used to analyse the inversion result.

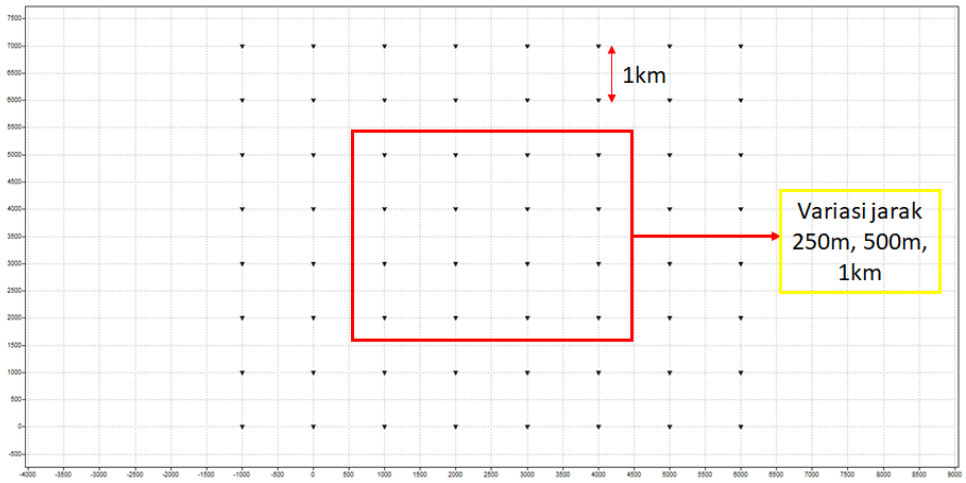


Figure 4: Station variation of 1 km spacing in interest area.

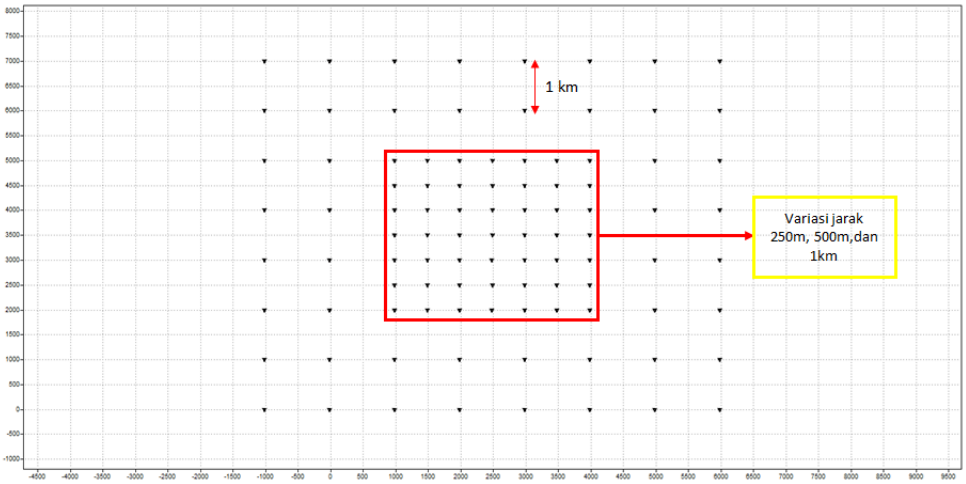


Figure 5: Station variation of 500 meters spacing in interest area.

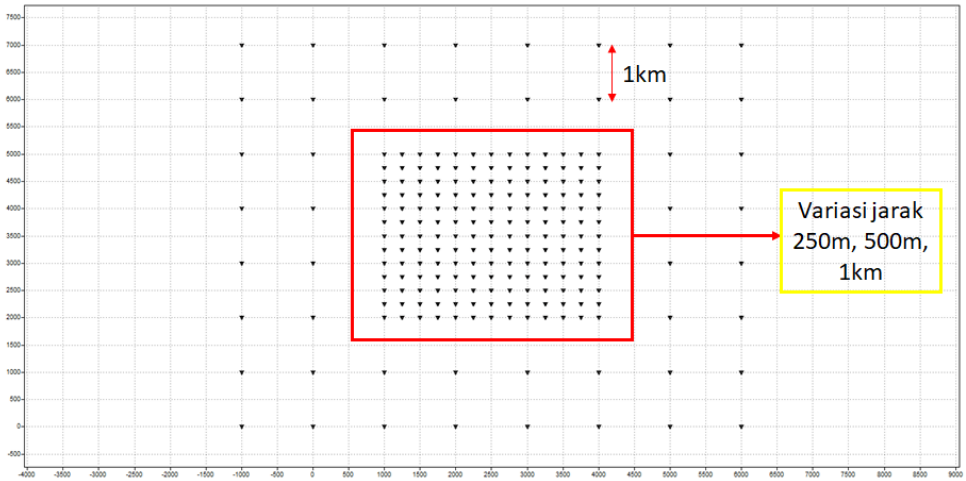


Figure 6: Station variation of 250 meters spacing in interest area.

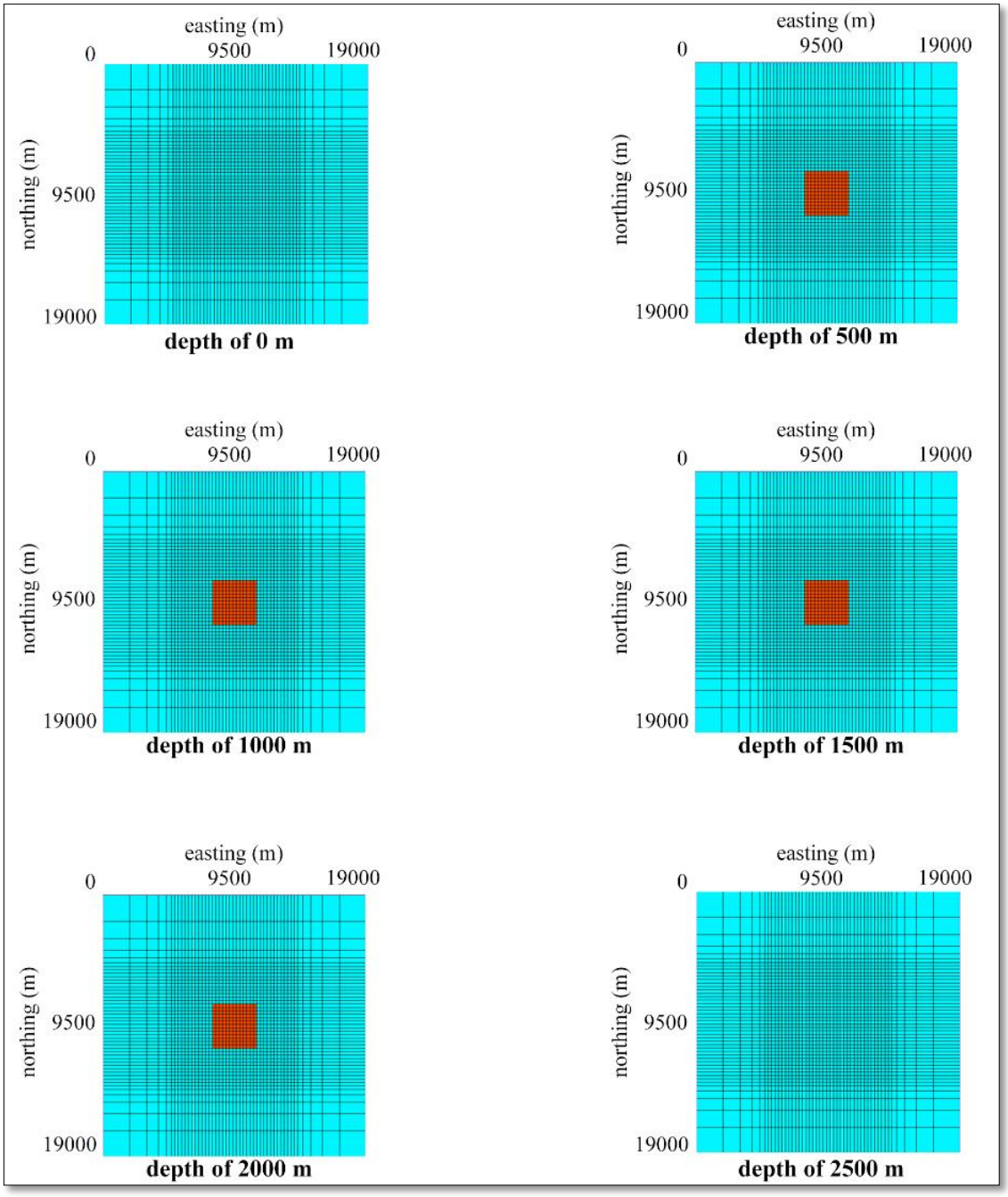


Figure 7: Synthetic model shown from map view (slicing for each depth).

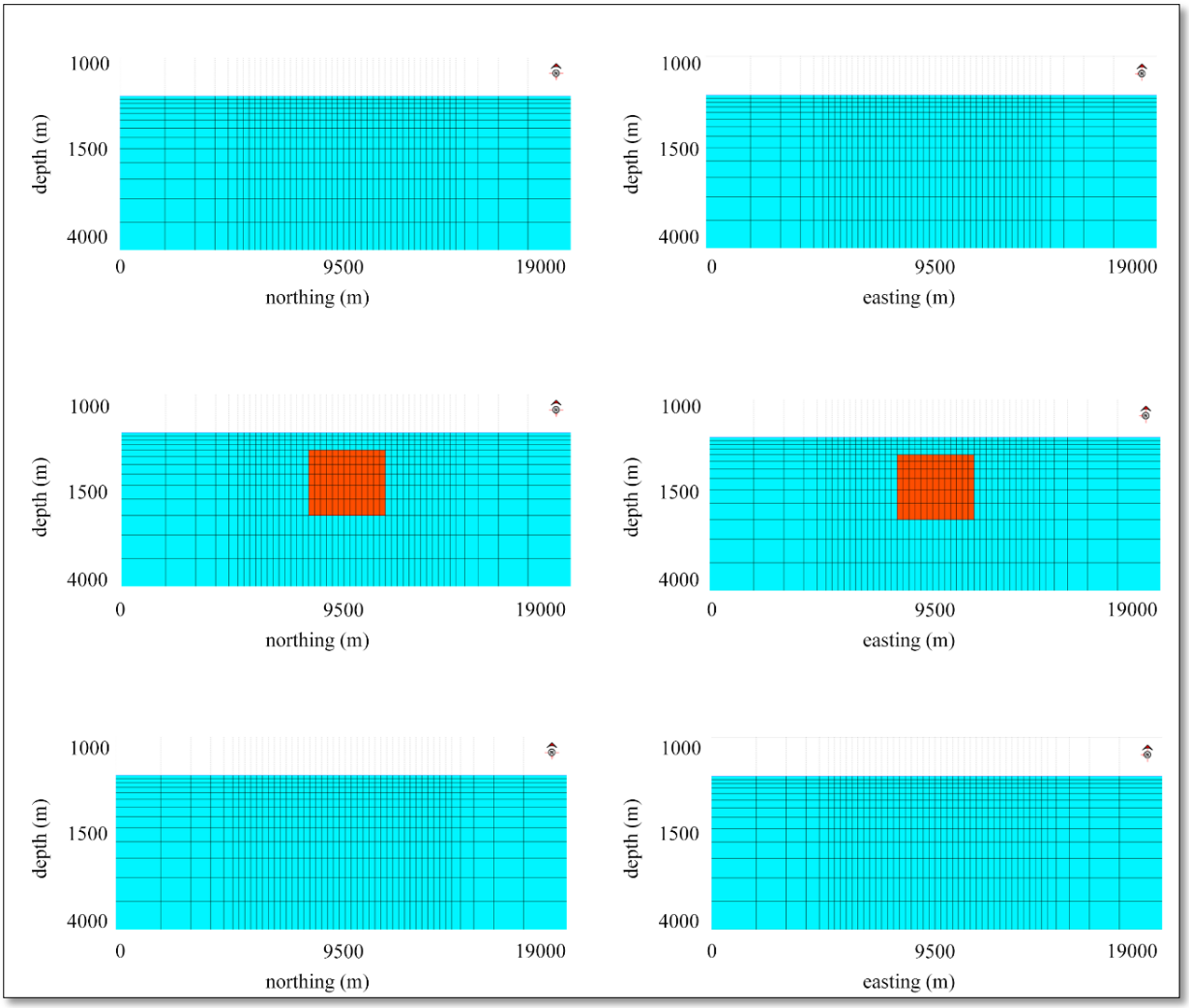


Figure 8: Synthetic model shown from x and y view.

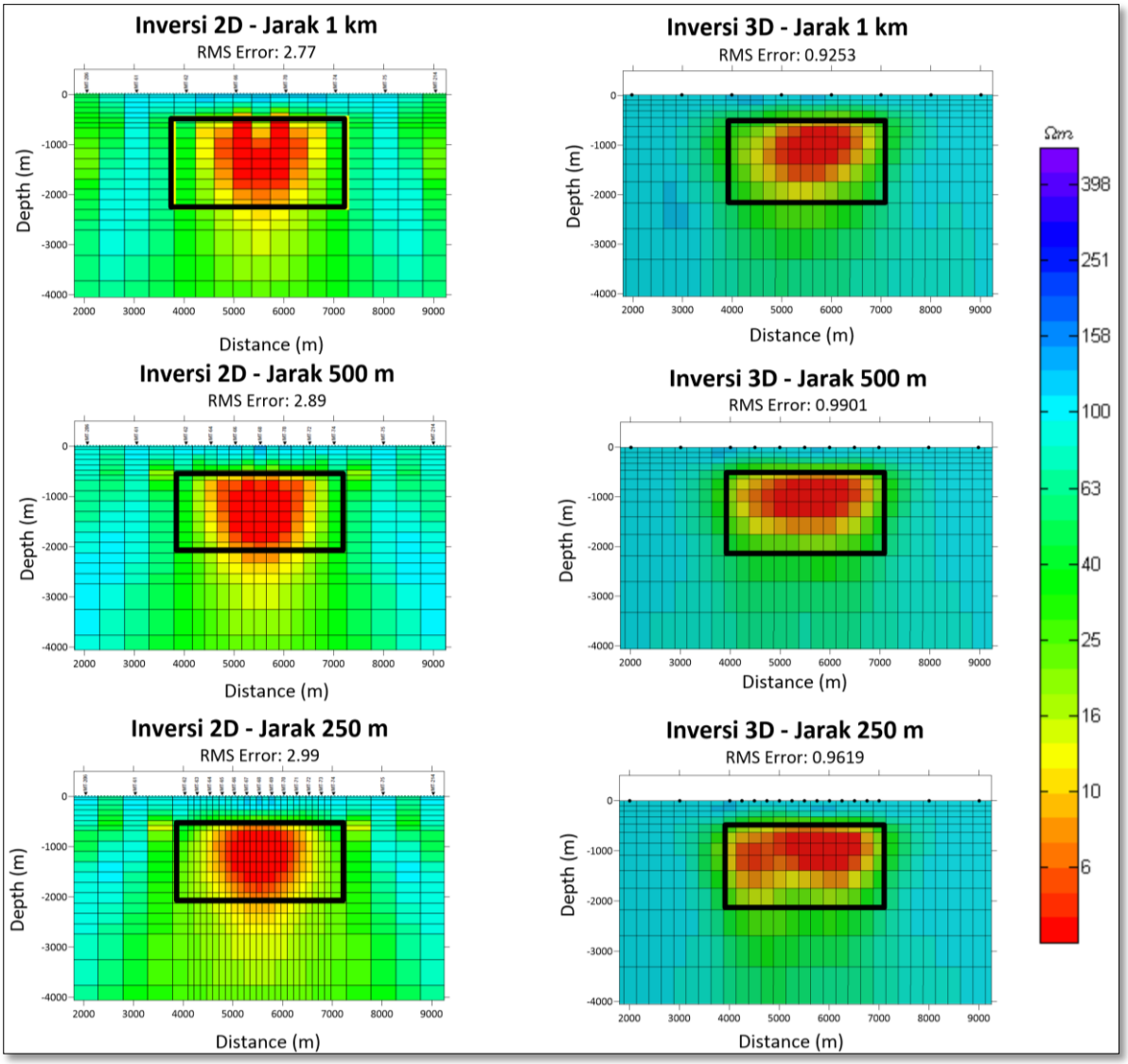


Figure 9: 2D and 3D inversion result for line 01.

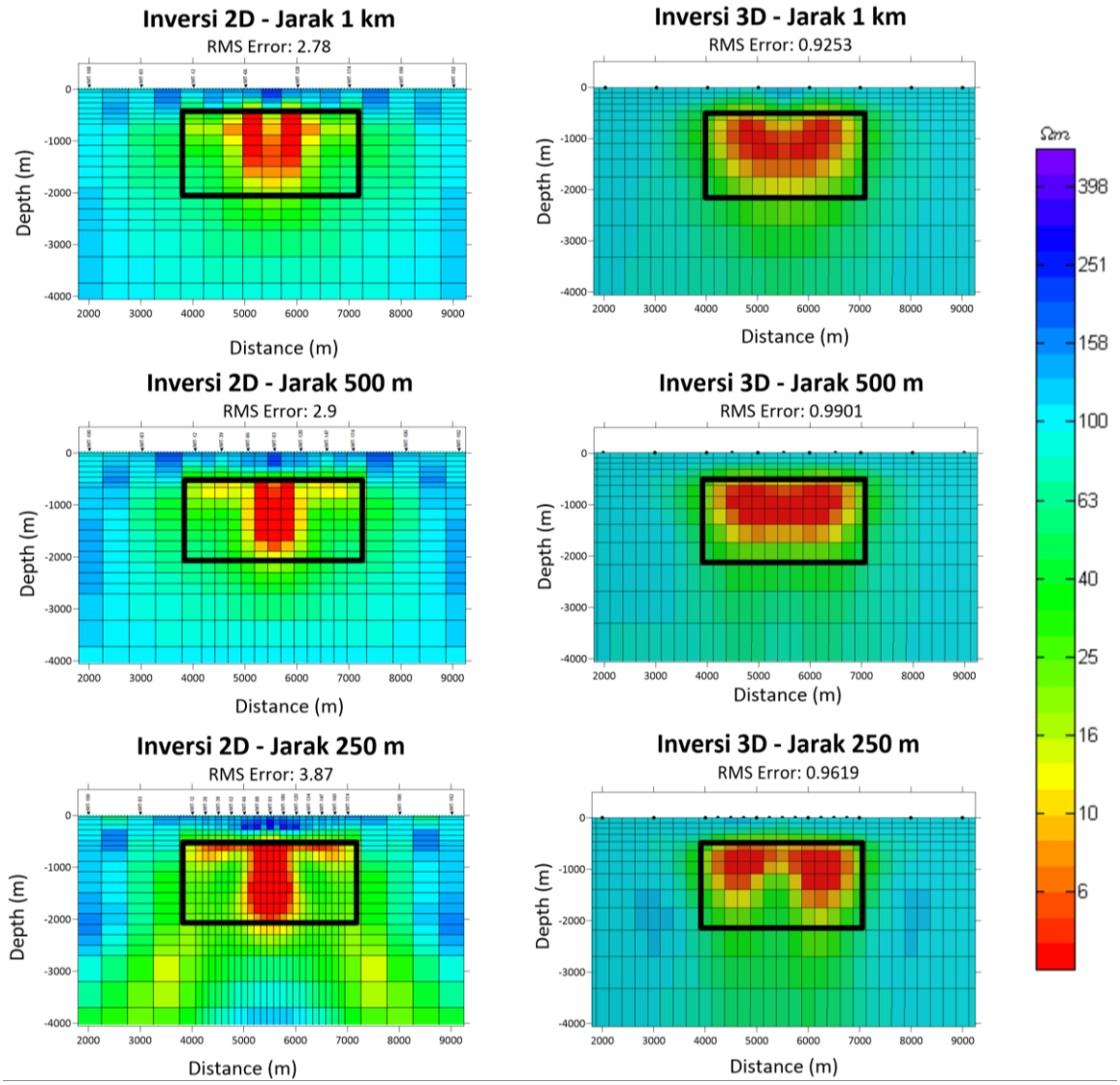


Figure 10: 2D and 3D inversion result for line 02.

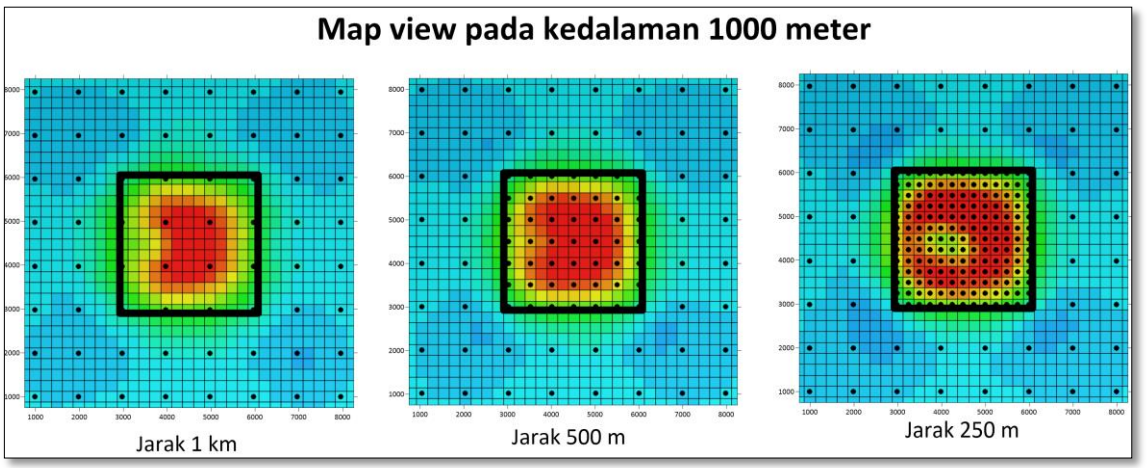


Figure 7: Map view at depth of 1000 meters for 3D inversion.

RESULT AND ANALYSIS

Based on the analysis of synthetic model (Figure 7 and 8), the optimum station spacing could be inferred. The 3D inversion quality for each station spacing shown in table 1. Compared between 500 meters and 250 meters the ability of delineating the vertical and horizontal boundary is similar. Both able to map the conductive body with the size of 3km x 3km for the horizontal side, and around 1.4 km for the thickness

which almost exactly like the initial model. However, the 250 meters shown an up-doming shape which might be cause by the lower iteration chosen to show the inversion result. As the number of stations increase, the longer the time to complete one iteration is needed.

The inversion result (Figure 9 and 10) of 250 m and 500 m looks similar though there is a big difference between the number of stations used. For 250 m variation it needs 217 stations, while for 500 m only needs 97 stations for the same study area. Meanwhile, the 1km 3D inversion result (Figure 11) shows that it is capable on mapping the conductive body likely almost like the initial model. The optimum conclusion is concluded by considering the number of stations used, the time and the cost need to acquire the data. Based on this result, the optimum station spacing for geothermal area exploration concluded to be 500 m - 1km. Where, 1 km could be used for preliminary study and then several stations could be infilled between those station up to 500 m.

Table 1: Quality for each model.

Parameter	Grid 1km		
	1km	**500m**	**250m**
Conductive body	< 5Ωm	< 5Ωm	< 5Ωm
Lateral geometry	2500 meter	2800 meter	3000 meter
Vertical geometry	500 - 2000 meter	500 - 1800 meter	500 - 1800 meter
Background resistivity	Very good	Very good	Very good

CONCLUSION

From this study several things could be concluded, they are:

1. The narrower the station spacing the result shown a good inversion result which almost exactly fit like the model
2. Compared with the 500 m model, the 250 m model doesn't show significant change in the both horizontal and vertical boundary. While, it needs more than 100 station in addition to build the 250 m station model for the same area.
3. For preliminary study, 1 km of station spacing is enough because it could delineate the shape of the object
4. The optimum station spacing for the interest area is 500 m - 1 km. Thought bellow 500 m gives a good result, however considering the time and cost expense to conduct the acquisition it will be not effective and efficient.

REFERENCES

Bronto, S. (2014). "Gunung Api purba Watuadeg: Sumber erupsi dan posisi stratigrafi". Indonesian Journal on Geoscience, 3(3), 117–128. https://doi.org/10.17014/ijog.vol3no3.20081

Exploration. Depok: Diktat Kuliah Universitas Indonesia.

Daud, Y. (2018). "Eksplorasi Geotermal. Depok". Diktat Kuliah.

ESDM. (2017). "Buku Potensi Panas Bumi Indonesia (Vol. 3)". Jakarta: Direktorat Panas Bumi, Kementrian ESDM.

Irfan, R., & Primasatya, S. (2018). "Magnetotellurics Survey Design and it is Implication to Geothermal Exploration. Case Study: Geothermal Area "X" on Indonesia". 7th ITB International Geothermal Workshop.

Jiracek, G. R. (1990). "Near-surface and topographic distortions in electromagnetic induction", (1970), 163–203.

Panjaitan, S. (2010). "Geologi Daerah Panas Bumi Ulubelu Tanggamus, Lampung Utara Berdasarkan Analisis Metode Magnetotellurik (Mt)". Jurnal Geologi Dan Sumberdaya Mineral, 20(2), 69–91.

Simpson, F., & Bahr, K. (2005). "Practical Magnetotelluric". Cambridge: Cambridge University Press.

Siripunvaraporn, W. (2012). "Three-Dimensional Magnetotelluric Inversion: An Introductory Guide for Developers and Users". Surveys in Geophysics, 33(1), 5–27. https://doi.org/10.1007/s10712-011-9122-6

Soyer, W., Mackie, R., Hallinan, S., Pavesi, A., Nordquist, G., Suminar, A., … Nelson, C. (2018). "Geologically consistent multiphysics imaging of the Darajat geothermal steam field". First Break Volume 36, 36(6), 77–83.

Suparno, S., & Daud, Y. (2005). "MAM and MT exploration in the Sibayak Geothermal Field". SEG Houston Annual Meeting, 1728–1732.

Supriyanto. (2007). "Analisis Data Geofisika : Memahami Teori Inversi. Universitas Indonesia". Depok: Universitas Indonesia.

Teklesenbet, A. (2012). "Multidimensional Inversion of MT Data From Geothermal Area, Eritrea; Comparison with Geological Structures and Identification of A Geothermal Reservoir". Iceland: United Nations University.

Unsworth, M. (2008). "Electromagnetic Exploration Methods". Canada.

Vozoff, K. (2011). "The Magnetotelluric Method". Electromagnetic Methods in Applied Geophysics, 641–712.

IDENTIFICATION OF GUCI, TEGAL, CENTRAL JAVA GEOTHERMAL MANIFESTATION BASED ON GEOLOGICAL GUIDE

Arhananta Anggita Mahyudani, Antu Ridha Falkhan Barizi, Riko Dwi Kurniawan, Oscarino Hunaifi Ahmad, and Agus Harjanto

Geological Engineering, University of Pembangunan Nasional "Veteran" Yogyakarta
Jl. SWK No.104, Condongcatur, Depok, Sleman, Special Region of Yogyakarta 55283
Email: arhananta@gmail.com

ABSTRACT

Research on the geothermal, geochemical and geophysical survey of Mount Slamet in the range of 2006-2018 only discussed on a regional scale, but no one has discussed in detail how the geothermal manifestation of the Guci area, Tegal, Central Java. The research method consists of imagery interpretation, secondary geophysical data including data on resistivity, magnetotelluric, and tremor, radon geochemical data, and hot water, then continued with a field check covering measuring section and sampling. A three-dimensional and spatial kriging model of manifestation was made after that. Volcanic rocks found in Guci and its surrounding are altered between lava and altered lahar breccia. These rocks are classified into the products of Mount Slamet if compared to the volcanic rock units that are on the geological map of the sheets of Purwokerto and Tegal which most of them is old lava and a small portion of young lava that generally extends on the river. The types of manifestation that appear on the surface are alteration and hot water. Based on imagery observation, the manifestation are located in Old Slamet Volcano, forming a volcanic texture with a rough texture, and there is a certain fault pattern that traverses Northwest-Southeast trending which cut the body of Old Slamet Mountain. The lineament of the Northwest-Southeast trending structure generally control the activity of the Old Slamet Mountain or the Mingkrik Complex (Figure 5). Based on the interpretation of Radon secondary data, it is interpreted that the Guci area has high permeability. The high concentration of Radon gas indicates the presence of Radon gas migration media to the surface. Hot water manifestation of Guci lies in the lineament of the Northwest-Southeast trending structure according to resistivity and magnetotelluric data which is interpreted as a normal fault.

Keywords: Guci, Geological Guide, Identification, Manifestation.

INTRODUCTON

Background

In Indonesia, Geothermal has 312 potential points, 67 work areas, with total electricity generated 28,910 MWe. (EBTKE, 2016). Mount Slamet is one of the possible volcanoes as geothermal power plants (PLTG) (Widagdo et al., 2013). Geothermal is controlled by the presence of heat sources, rock nests (reservoirs) and cap rocks, and the presence of meteoric water and permeability of primary and secondary rocks such as fractures and faults (Wardhana et al., 2017). Light hot water or mild steam will move up to the surface of the earth through a faulty or rigid path which is a water pass zone in the form of hot springs, fumaroles and solfatara (Indarto et al., 2017). The geological structure that develops in the Mount Slamet complex which is relatively NW-SE, and N-S intersects the Guci area (Permana et al, 2014). The line was strengthened by Nurohman's (2014) study, which said the radon content (Rn) measured in the Guci and Kalipedes areas was of high value - quite high, showed high permeability - was quite high, ie> 40 dpm / L. The instructions for the existence of a geological control structure are also strengthened by Wardhana (2017) and Gaffar (2018) research through geophysical methods. In fact, there are still two controls in geology, that is geomorphology and lithology-stratigraphy, therefore the authors conducted this study in identifying the manifestations of hot water in the Guci region. The research location is located in Guci, Tegal, Central Java, Indonesia (Figure 1).

Method

The research method consisted of image interpretation including the SRTM DEM map and Google Earth, secondary geophysical data including data on resistivity, magnetotelluric, tremor data, radon geochemical data, and hot water, then continued with a field check. Finally, a three-dimensional and spatial kriging model of manifestation is made.



Figure 1: Study Area.

GEOLOGY

Geomorphology

Based on topography and flow patterns, the morphology of Mount Slamet is divided into 2 main parts, namely the morphology of the old Slamet mountain and the young Slamet mountain. The old Slamet Mountain composes the western part and the young Slamet Mountain composes the eastern part of the map. Old Slamet Mountain forms the slope morphology and volcanic foot by showing irregular morphological shapes with rough reliefs and developing dendritic flow patterns with river stadia on young stadia, river valleys in the form of letters "V" with steep slopes. Young Slamet Mountain consists of conical morphology, mountain body, mountain foot, and cinder cone. The cone morphology is the peak of a young volcano, the mountain body occupies the south - east and north side, at the bottom of the cone section. The foot of the mountain, extending from the south - east and north, the cinder cone, develops in the east of the map with the form of regular slopes and fine reliefs. In the eastern part of the young Slamet Mountain peak, there is a volcanic cone peak which is the highest point of Slamet Mountain which is 3432 masl. The flow pattern that develops on this young Slamet body is radial which centers on the Slamet Mountain peak.

Stratigraphy

The lithology found on the Slamet slope is composed of Slamet mountain lava (Qvls), unraveled Slamet volcanic rocks (Qvs) and Slamet mountain lava deposits (Qls). Slamet Mountain Lava (Qvls) consists of andesite lava, young volcanic breccia (eastern part), unregulated Slamet volcanic rock (Qvs) consisting of volcanic breccia, lava, old volcanic tuff (western part) and Slamet mountain lava (Qls) consists of lava, andesite-basalt which is a distribution of young and old volcanic materials and Linggodopo (Qpl) formations composed of volcanic breccia, old volcanic tuff and lava and G. Copet. The lithology that surrounds the slopes of the Islamet is thought to be a scattered basement of various rock formations, such as the Pemali Formation (Tmp), Beetle Formation, Kaliglagah Formation (Tpk), Tread Formation (Tpt), Tract Formation (Tmr), Halang Formation (Tmph).

The Pemali Formation (Tmp) consists of globigerina marl with light gray and greenish gray color, inserts with sandstone limestone, tuffaceous sandstones and coarse sandstones. Generally, a monotonous gray claystone, the bottom is not exposed. Thickness more than 900 m.

The Kumbang Formation (Tmpk) consists of breccia, andesite and tuff lava, in some places there are pumice breccia and passive tuffs, revealed both in G.Kumbang, 2,000 m thick. The Rambat Formation (Tmr), consisting of side sandstones and conglomerates that intersect with several thin layers of napal and shale at the bottom of this formation. Whereas at the top, this formation consists of side grains of light gray to grayish blue, the thickness of this layer is about 300 meters. This formation is Lower Miocene (Van Bemmelen, 1949) and overlaps the Pemali Formation in harmony. The Halang Formation (Tmph) consists of turbidite sedimentary rocks with sedimentary structures such as coating, convolute lamination, flutecast, etc. which are clearly visible. In some locations found coral limestone at the top of this formation which is a member of the limestone (Tmhl). This formation was formed in the Middle Miocene (Van Bemmelen, 1949) with an estimated thickness of 2,400 meters.

The Tapak Formation is composed of graded greenish coarse sandstones to greenish sandstones at the top with a few inserts of gray sand to yellowish gray. At the top there are coral limestones as members of the Tread Formation (Tptl). This formation is Pliocene with a maximum thickness of 500 meters. The Kaliglagah (TPp) Formation is composed of claystone, marl, sandstones and conglomerates in several places where the lignite lens is 10-100cm thick. Figure 2 shows the geological map of study area.

Geological Structure

The main structures that develop in the study area are divided into the northeast, north and southwest of the map. In the northeastern part there is a main structure, namely horizontal faults and drifting with a relative northeast orientation - southwest, a northern part in the form of a horizontal fault with a northwest - southeast orientation which cuts syncline oriented northeast-southeast, the northwest-southeast line is interpreted as (horizontal drift fault), the alignment of the northeast-southwest orientation is interpreted as a horizontal fault fault and the upward fault as the accompanying structure of horizontal drift fault, and the southwest part is northeast oriented - southwest (fault fault) which cuts old Slamet mountain and straightness north-west orientation (drifting fault).

RESULT

Geomorphological Control

Based on Google Earth's interpretation and referring to Widagdo (2013) The morphology of Slamet Mountain volcano can be divided into two main morphological groups (Figure 3). These two main morphologies are:

1. Morphology of Old Slamet Mountain; compose the west part of Mount Slamet.
2. Morphology of Young Mount Slamet; occupying the east part of Mount Slamet.

This geomorphology unit of the young Mount Slamet can be subdivided into:

1. Morphology Cone is the peak of a young volcano.
2. Morphology The body of a mountain, occupying the south-east and north sides, is at the bottom of the conical bag.
3. Morphology Mountain feet, stretching on the south-east and north sides.
4. Cinder's Cone Morphology especially developed in the east of Mount Slamet.

The appearance of the Old Slamet Mountain in the west shows an irregularly morphological form with coarse relief (Figure 3). The flow pattern that develops in the body of this Slamet Ancient Mountain is dendritic with the river stadia on the

young stadia, the valley of the river shaped "V" which with a steep slope. The east part of young Mount Slamet in is a volcanic cone morphology with a regular slope shape with a smooth relief. Peak volcanic cone which is the highest point in Mount Slamet at an altitude of 3432 masl located on the east side of the peak of Mount Young Slamet. The drainage pattern on the body of the Young Slamet Volcano is a radial centered on the summit of Mount Slamet.

Lithology-Stratigraphic Control

The hot springs in the research area appear on the contact between the volcanic breccia and the underlying lava and controlled by the structural geology with the lineament of the northwest-southeast (N130^{o}E) directed structure at the Baturaden and Guci area (Indarto, 2017).

Geological Structure Control

This map is derived from drawing a straightness on a topographic map based on its morphological alignment. From the map we can see that in Guci area there are many straightness as identification of cesarean structure that developed there quite a lot.

The result of DEM SRTM (Figure 6) Mount Slamet morphostructure analysis (Figure 4) shows that the structure of Mount Slamet Complex is controlled by: The northwest-southeast and west-east structures lineament was thought to play a role in controlling the activities of the old Mount Slamet or the Mingkrik Mountain Complex, the northwest-southeast. Which controls the activity of young volcanic the hot spring Guci appears to the surface in a region that is controlled by the north-west direction. The Guci area which lies to the northwest of G. Slamet's body has undergone a volcano-tectonic deformation that forms a depression (graben) (Pratomo et al., 2012), and based on geological data was filled by the Young Mount Slamet deposit. (Bronto et al., 2010, vide Pratomo & Hendrasto, 2012; Djuri et al., 1996).

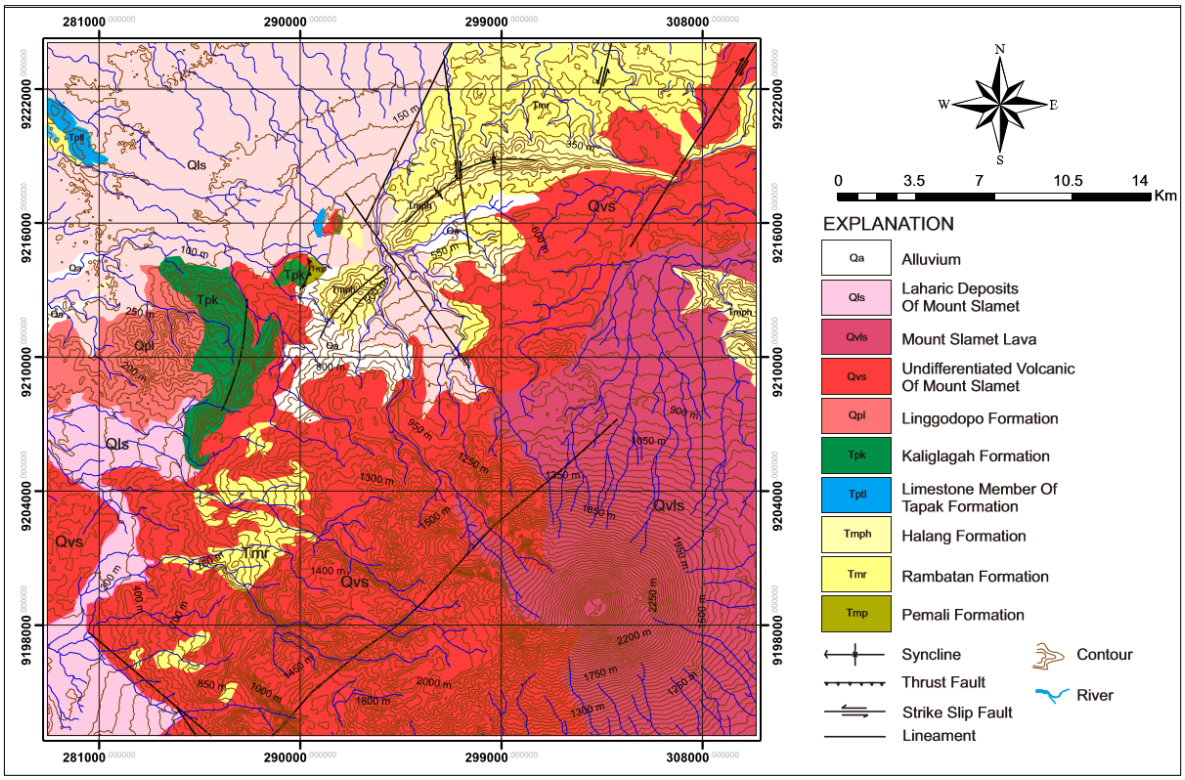


Figure 2: Geological map of study area (Djuri et al, 1996).

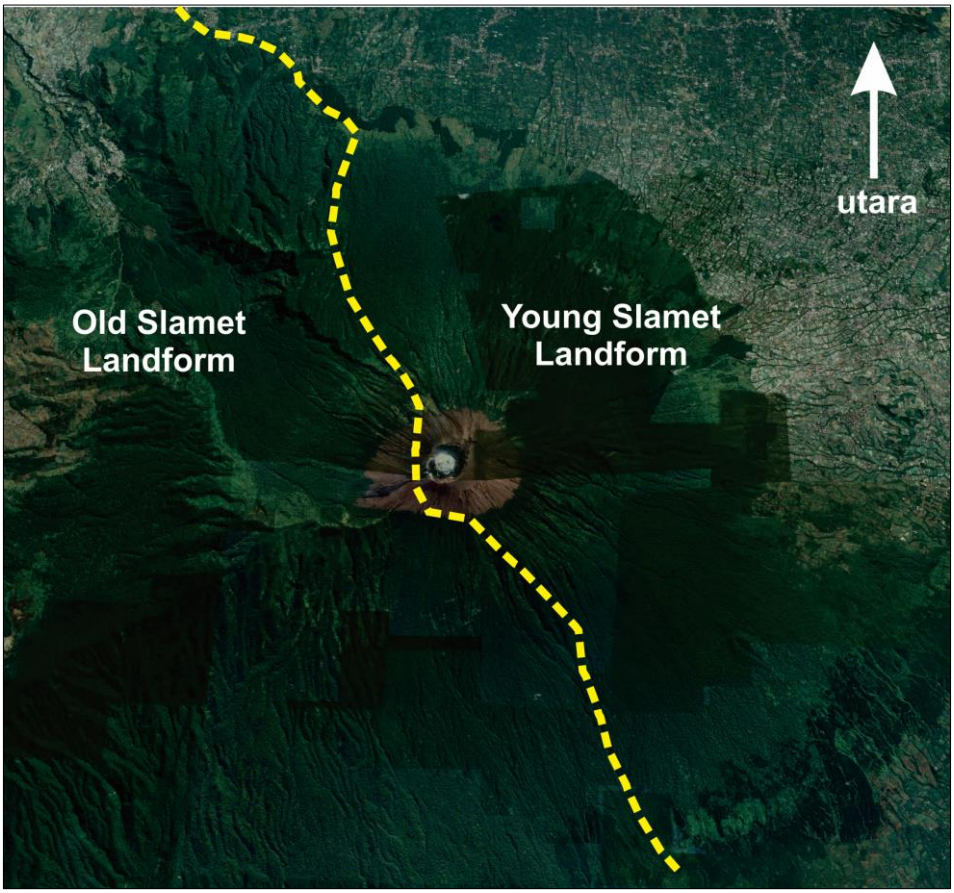


Figure 3: Geomorphology of study area.

Figure 4: 2D MT Section Model (Wardhana, 2017).

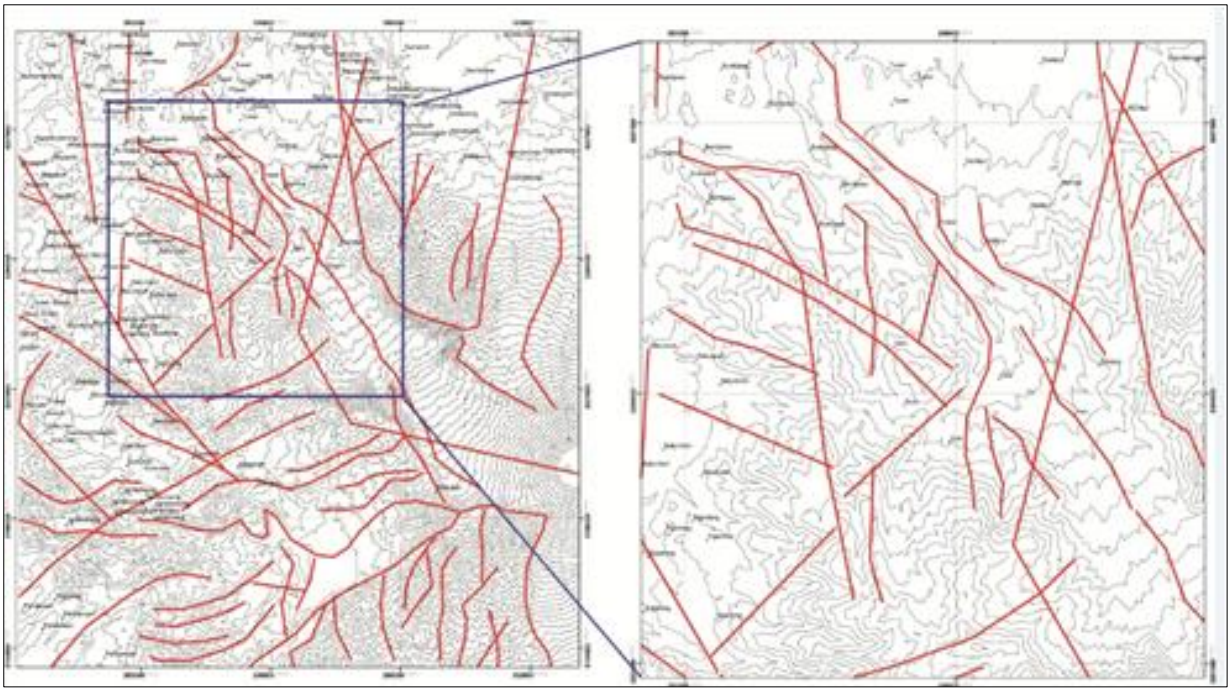


Figure 5: Linement Map of Guci.

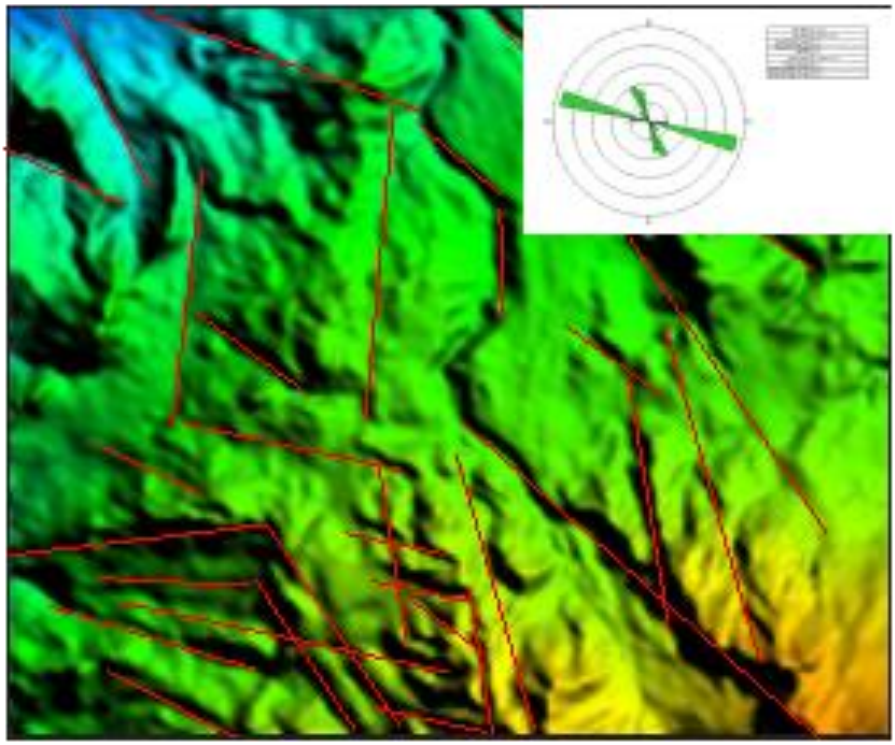


Figure 6: Structural lineament interpretation based on DEM SRTM.

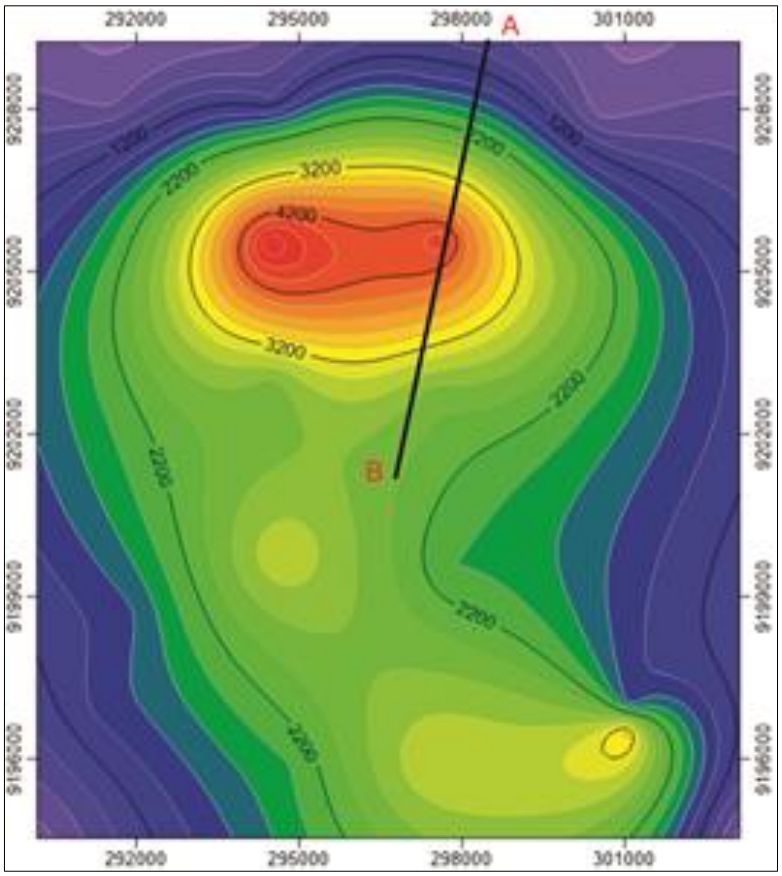


Figure 7: Lineament Density Map of Mount Slamet.

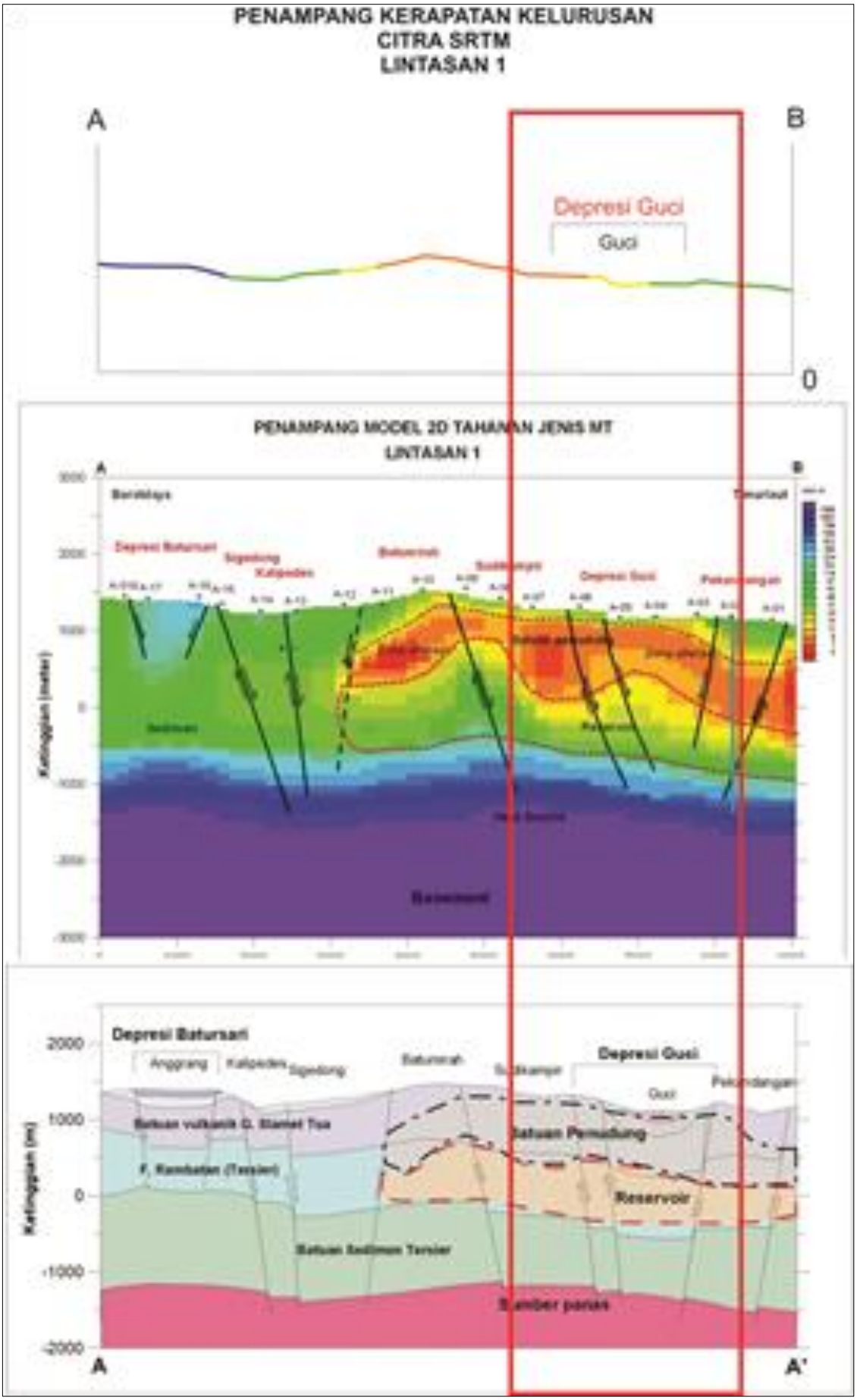


Figure 8: Magnetotelluric data interpretation (Modified by Wardhana, 2017).

This map is a lineament density map obtained based on the dataset data sheets on Mount Slamet. Viewed from the color on the contour where the green color is an area with a small density, while the red color indicates the density of many structural straightness. Can be seen on the map of the north precisely on the area Guci has a high straightness density and become one of the geothermal manifestations in the area. As has been explained in previous research that Trap on Mount Slamet area is Normal Fault.

From the interpretation of the magnetotelluric data, it is found that from the line of the north-east-southeast lineament it is found that the normal faults have Northeast to the Southwest lineament of the cross-cut path to the source of heat where the fault cuts to the source rock.

CONCLUSSION

The distribution of the geomorphological landform of Mount Slamet is controlled by lithology and geological structures. The geological structure with NW-SE direction controls the pattern of distribution of lithology, manifestations, and the form of origin of young and old Slamet. The form of old Slamet volcanic origin controls the manifestation of Guci hot water. Volcanoclastic rocks become reservoirs and caprock, while igneous rocks become a source of heat

REFERENCES

Al Kausar Andrie (2014). “Batuan Volkanik Kaitannya Dengan Terjadinya Manifestasi Panas Bumi Di Permukaan, Daerah Guci, Tegal, Jawa Tengah”. Prosiding Pemaparan Hasil Penelitian Pusat Penelitian Geoteknologi LIPI: 2014

Djuri, M., Samodra, H., Amin, T., C., Gafoer, S., (1996). “Peta Geologi Lembar Purwokerto dan Tegal, Jawa. Skala 1:100.000”. Pusat Survei Geologi. Bandung.

Indarto sri et al (2017). “Struktur Geologi dan Litologi sebagai Kontrol Munculnya Mataair Panas Guci dan Baturaden, Jawa Tengah”. Jurnal RISET Geologi dan Pertambangan, Vol.27, No.1, Juni 2017,97-109

Nurohman, H., et al. (2014). “Konsentrasi Radon di Sekitar Manifestasi Panasbumi Gunung Slamet, Jawa Tengah”. Prosiding Pemaparan Hasil Penelitian Pusat Penelitian Geoteknologi LIPI.

Permana, H., Sudarsono, Sri Indarto, (2014) “Studi Morfostratigrafi Dan Morfostruktur: Studi Kasus Prospek Lapangan Panasbumi Guci, Tegal, Jawa Tengah”. Prosiding Pemaparan Hasil Penelitian Pusat Penelitian Geoteknologi Lipi Tahun 2014.

Situmorang, T., (2008). “Laporan Pekerjaan: Interpretasi Foto Udara dan Landsat, WKP Panasbumi Guci”. Jawa Tengah (non-publikasi).

Wardhana, D., et al, (2017). “Pencitraan Tahanan Jenis Bawah Permukaan Di Area Prospek Panas Bumi Gunung Slamet Berdasarkan Data Magnetotelurik”. Jurnal RISET Geologi dan Pertambangan, Vol.27, No.1, Juni 2017, 111 – 121.

Widagdo, A., et al. (2013). “Pengaruh Struktur Geologi Gunung Slamet Muda dan Tua Terhadap Pola Sebaran Panas Bumi”. Bandung: IRWNS.

DETERMINATION OF GEOTHERMAL RESERVOIR CHARACTERISTIC AND HYDROTHERMAL ALTERATION MODEL BASED ON COMPREHENSIVE SURFACE MAPPING, GEOCHEMICAL, AND XRD ANALYSIS: CASE STUDY OF WIROGOMO AREA

Saifullah Fatah Al-Ayyubi, Garindra Yogiswara, Nabilah Afifah Habni Harahap, Arief Budiman Ustiawan, and Navendra Chista Yogatama

Geological Engineering Department Universitas Diponegoro
Prof. H. Soedarto, SH. Street, Tembalang, Semarang, Central Java, 50275
Email: saifullahfatah1505@gmail.com

ABSTRACT

Indonesia with its large, but partially unexplored geothermal potential is one of the most interesting and suitable places in the world to conduct geothermal exploration research. The manifestation of warm pool and altered rocks on surface indicates the existence of potential geothermal systems in Telomoyo volcanic complex. The study focusses on hydrothermal alteration model and geothermal reservoir characteristic of Telomoyo volcanic rocks administratively located in Wirogomo Area, Semarang Regency. The research was analyzed by surface mapping, geochemical, and XRD analysis. The petrographic analysis was performed to identify lithology, porosity, and mineral alteration formed as a replacement or direct deposition. XRD was running by bulk powder and clay treatment which consisted of air-dried clay, ethylene glycol, and heating treatment, used to determine clay mineral content in rocks. This volcanic area consists of several eruption centers with rocks dominated by basaltic andesite lava and local pyroclastic flows. Based on petrographic data, altered rocks contain minerals which are: plagioclase, pyroxene, secondary quartz, sericite, anhydrite, calcite, and clay mineral. Based on XRD data, altered rocks contain clay minerals which are quartz, albite, illite, sanidine, and magnetite. The result of study showed association of mineral alteration is divided into one zone: smectite-chlorite zone (argillic). This zone consists of low temperature minerals, formed at around 200-250°C on acid environmental condition. Based on fluid geochemical analysis of two warm pool manifestations at research area, the fluid included in type of bicarbonate-chloride acid with equilibrium is included in immature water with an estimated reservoir temperature based on silica geothermometer (Fournier, 1982) is 167°C and Na/K geothermometer (Giggenbach, 1988) is 278°C. This research provides new insight into industrial minerals and develop geothermal potential for alternative energy supply that is environmentally friendly and renewable.

Keywords: Alteration Zone, Surface Mapping, Wirogomo, XRD

INTRODUCTION

Electricity supply-demand tends to increase as the population increases while the supply is not balanced with demand growth, so it is necessary to develop new sources of electrical energy. In Indonesia, the utilization of geothermal as one of renewable energy in order to fulfil the growing need for electricity supply that continues to increase has been developed. Geothermal energy is the energy naturally present inside the earth crust. When a large volume of hot water and steam is trapped in subsurface porous and permeable rock structure and a convective circulating current is set up, it forms a geothermal reservoir. The reason behind this is the existence of several benefits like clean and renewable source of energy which has considerable environmental advantage, with no chemical pollutants or wastes are generated due to geothermal emissions, and the reliability of the power resource. Indonesia has a lot of geothermal potential, but it has not been developed. So that research is carried out on areas that have the potential as geothermal areas, namely in the Wirogomo area, Central Java. Where the Wirogomo area is part of the Telomoyo volcanic rocks. In the preliminary exploration activities and geothermal field development process, the characteristics of a geothermal reservoir are needed to determine the temperature of geothermal fluid using a geothermometer. Determination of reservoir characteristics in the geothermal area of Wirogomo uses geological mapping method, geochemical analysis, and XRD analysis which aims to determine the potential of geothermal energy in the Wirogomo area, and to do detailed mapping if the Wirigomo area is a prospect for PLTP in Central Java. From this research, a new geothermal field area will be obtained to be further developed as a reserve for renewable energy.

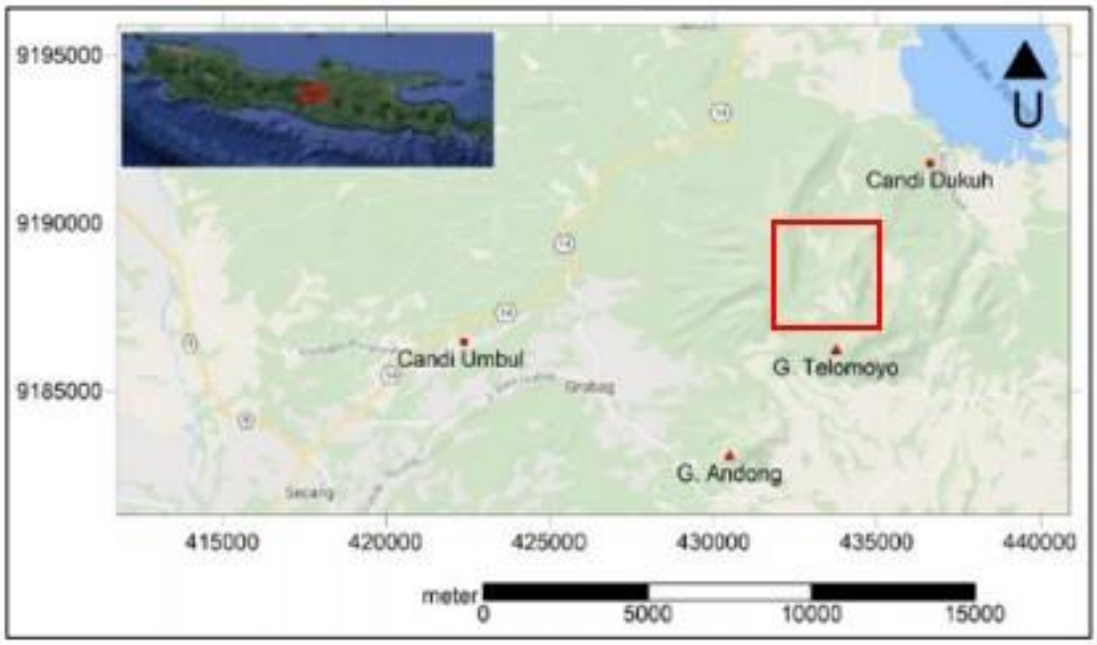


Figure 1: Research Location.

METHODOLOGY

The method used in this research is geological mapping in 3x3 km area that located in Telomoyo, Semarang. The research was analyzed by petrology, petrographic, geochemistry and XRD samples which located vertically until 1512,5 masl. Several samples are used to know the types of lithology, mineral composition, porosity, mineral alteration by Petrology and petrographic analysis. We use XRD method to know an determine clay mineral content in samples of rocks. The Petrology analysis by megascopic description that used to several samples was performed to identify type of lithology and mineral that formed lithology's samples. Petrographic analysis by microscopic description was performed to identified lithology by porosity and any others, also alteration mineral formed as a replacement or direct deposition. XRD analysis was running by bulk powder and clay treatment which consisted of air-dried clay for determine clay mineral content in rocks. Geochemical analysis was carried out to determine the type and type of fluid in research area. That analysis showing about the result about interpretation of mineral association, alteration mineral, temperature and environmental condition, also hydrothermal alteration model.

REGIONAL GEOLOGY

The Telomoyo geothermal system is in a volcanic complex. In the southern part of the study area there is a flow pattern originating from the northeast, located west of Andong Volcano (Figure 1). In the field, this section is an andesite breccia that has undergone compacting. Andesite breccia is classified as an andesite breccia unit as the oldest unit in this area. Andong volcano was formed which produced two eruption products, namely Pagergunung andesite lava flow and Andong pyroclastic breccia. This andesite lava has porphyroafanitic texture, vesicular structure with plagioclase composition.

Suropati volcano product flow that appears in the dominant image flows westward. While Kendil Volcano flows east, west and south. The image shows a rougher texture over a finer textured unit. So that it is estimated that the first eruption unit from Suropati is heading northwest. Suropati-1 andesite lava unit produces a product in the form of andesite lava. The image texture in Suropati Volcano which leads to the southwest is rough. In the field, this flow is andesite lava flow. This flow is included in the Suropati-2 andesite lava unit. Both of these eruption units are basaltic which are seen from the composition of rocks in the form of plagioclase and pyroxene. Along with this volcanic eruption, an Elephant volcanic rock unit was formed to the east of Telomoyo Volcano. This unit produces andesite rocks. The next eruption occurred around Kendil Volcano. In the andesite lava unit, the Kendil eruption is formed in the form of tuff, polymic breccia and andesite lava. This eruption is basaltic with a composition in the form of plagioclase and pyroxene with variations in hornblend content. Along with the Kendil eruption, the Gunung Dukuh volcanic rock unit was formed. The rock is in the form of vesicular andesite with the dominant composition of plagioclase and pyroxene which is not abundant.

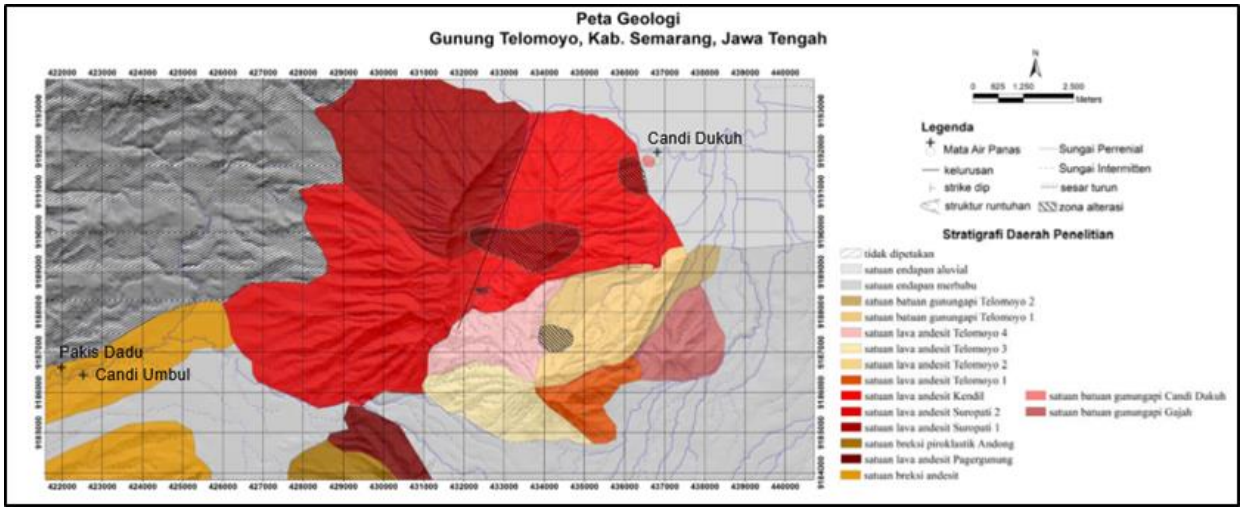


Figure 2: Geological Map of the Research and Surroundings Area (Hutami, et.al. 2014).

The next eruption was formed in south of Kendil Volcano. The first product from Telomoyo, which is called the Telomoyo-1 andesite lava unit, flows eastward. The product produced pyroclastic breccia and andesite lava. Then the next eruption unit, andesite lava unit Telomoyo-2, flows northeastward to Kebumen Village. The next eruption unit is the andesite lava unit Telomoyo-3 which flows on the slopes of the southern side of the Telomoyo Volcano. The fourth eruption unit from Mount Telomoyo flows west and northwest in the form of andesite lava. Andesite lava flow from Telomoyo has a general composition that is basaltic characterized by plagioclase and pyroxene and hornblende. The last phase of this eruption formed an eruption which made the northern part of the slopes of the Telomoyo Volcano collapse to form the Telomoyo-1 volcanic rock unit in the village of Sepakung. These deposits are characterized by the number of andesite blocks on the surface.

During the eruption of Telomoyo Volcano, a downward fault was formed which separated the flow of Telomoyo-1 andesite lava units with Elephant Volcanic rock units. This part of the valley forms the Telomoyo Volcanic rock unit 2. The next phase is the formation of Merbabu Volcano south of the research area. This Merbabu Volcano deposit reaches the edge of the Rawa Pening in the Muncul area and also flows westward to the research area in the Grabag area. Deposits from Merbabu and Suropati Telomoyo influence the sedimentation of Rawa Pening through the main rivers that flow and flow in Rawa Pening. These deposits form an alluvial deposit unit.

The Telomoyo geothermal area is located in the North Serayu Mountains zone, with the oldest rocks of Middle Miocene sedimentary rocks with turbidite deposition mechanisms in the neritic environment. In the Upper Pliocene, the removal process was followed by an effusive eruption of Old Ungaran in the Early Pleistocene which produced the Ungaran lava unit. In addition, in the southeast of Ungaran, Telomoyo volcanic activity occurred which produced lava and pyroclastic deposits. The large eruption of Telomoyo-1 caused collapse and produced a caldera structure followed by the reappearance of Telomoyo's post-caldera volcanic activity which produced lava and pyroclastic deposits.

Volcanic activity continues to form the Telomoyo cone which has an andesitic composition - basaltic and Andong cones. The final phase of Telomoyo's volcanic activity is reflected by scaling cone (scoria cone). At that time in the north (Mount Ungaran) and to the south (Mount Merbabu) there was also volcanic activity which produced lava and pyroclastic deposits. Lava and alluvium deposits are formed along large plains and rivers (Figure 2). The developing geological structure consists of a caldera structure and normal faults trending southwest-northeast that are formed due to the activity of Mount Telomoyo, as well as relatively horizontal-oriented faults north-south and northwest-southeast which are regional structures, and some have been covered by younger rock.

The area estimated to have a high density of geological structure and is estimated to have a high permeability zone located in the northern part of the young cone Telomoyo which is from the northwest slope of the young cone Telomoyo extends north-northeast to the Keningar and Dukuh temples.

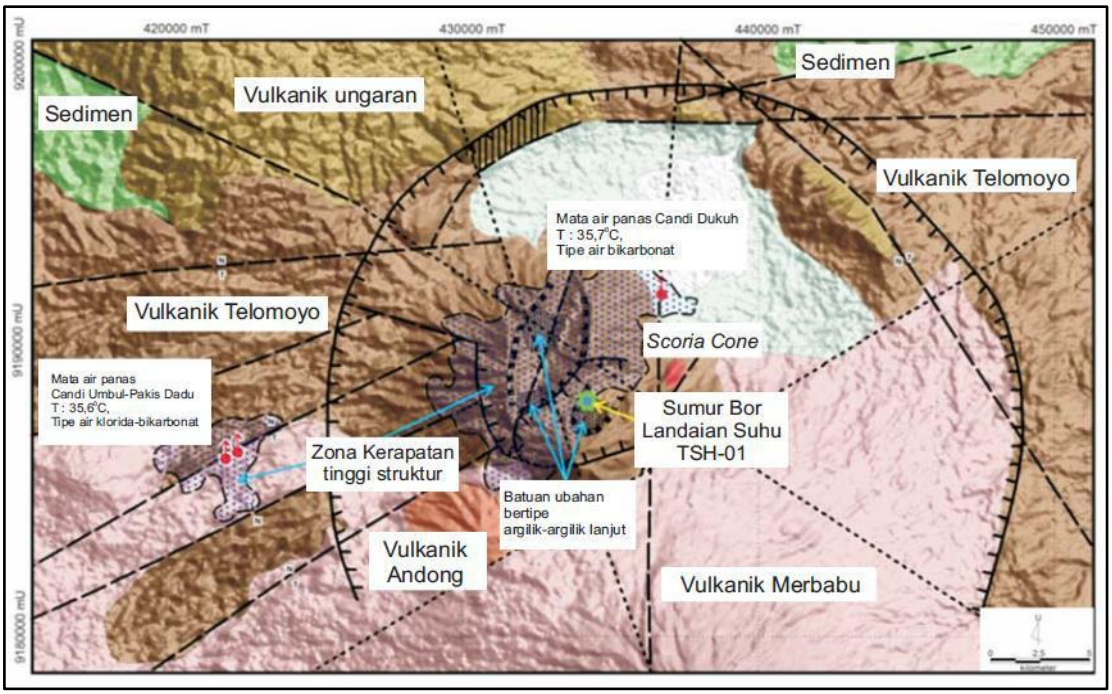


Figure 3: Geological map of the geothermal area of Telomoyo, Central Java Province (Modification of the Geological Map of the Geothermal Integrated Survey Team, PSDG, 2010) 1: 500000 scale.

Geomorphology

The Telomoyo volcanic geomorphology occupies the middle section extending to the east-west of the survey area which covers about 45% of the survey area, slope between 20º-85º. The river pattern is radial, sub-dendritic to sub-parallel. This unit is a morphological form the Mount Telomoyo. These are volcanic rocks such as lava and pyroclastic. The elevation of this morphology unit ranges from 200 - 1850 meter above sea level (masl).

Stratigraphy

Based on the results of the investigation of rock types in the investigation area can be grouped into 18 rock units, which consist of one unit of sedimentary rock, 16 units of volcanic rock, and one unit of surface deposits. Sequences of rock units or stratigraphy from old to young are sedimentary units (Ts), Lava Ungaran-1 (QUv-1), Lava Telomoyo-1 (QTl-1), Pyroclastic Flow Telomoyo-1 (QTap-1), Lava Telomoyo- 2 (QTl-2), Telomoyo-2 (QTap-2) Pyroclastic Flow, Telomoyo (QTjp) Pyroclastic Drop, Andong (Qal) Lava, Lava Telomoyo- (QTl-3), Lava Ungaran-2 (QUv-2), Merbabu-1 (QMl-1) Lava, Merbabu Pyroclastic Flow (QMap), Coluvium Telomoyo (QTk), Pyroclastic Cone (QKp-5), Merbabu-2 (QMl-2) Lava, Merbabu Pyroclastic Fall (QMjp), Merbabu Lahar (QMlh), and Aluvium (Qal). Sediment Unit (TS), is the oldest unit revealed in the northeast and northwest of the survey area with a spread area of 3% of the survey area. This rock unit consists of tuffs which are megascopically grayish-white in color. This rock is the result of other older rock erosion that was not revealed in the survey area. According to the comparison with regional geological maps this rock is part of the Middle Miocene Kerek Formation which is a turbidite sedimentary rock and deposited in the Neritic environment.

Structural Geology

Based on the results of an analysis of DEM maps (digital elevation mode) and topographic maps, as well as structural symptoms on the surface such as the appearance of hot springs, valley and ridge alignment, rigid, fault fields, and rock destruction zones, observable areas of the investigation some geological structures, namely: Rim caldera, there are three reams of caldera formed, namely the first Telomoyo-1 eruption caldera located on the southern slope of the Telomoyo complex opens to the north. Then the second caldera is in the middle of the survey area with a diameter of about 22 km. The structure of the second caldera is estimated to be formed by the presence of vacancies inside the earth due to the eruption of Telomoyo-1 which resulted in subsidence that formed the depression zone in the survey area. While the third caldera is the Telomoyo-2 eruption caldera found on the southeast slope of the Telomoyo complex opening to the northeast.

Volcanic structures in the form of normal faults trending southwest-northeast are formed due to the activity of Mount Telomoyo. This structure also facilitates the emergence of geothermal manifestation of Candi Umbul.

Tectonic structures in the form of horizontal directional faults are relatively north-south and northwest-southeast which are regional structures and some have been covered by younger rock products. Some of these structures are reactivated so that they can facilitate the emergence of the Dukuh Temple geothermal manifestations.

RESULT AND DISCUSSION

Petrology

Andesite Lava Lithology Unit

In regional geology, the research area is included in three formations in the regional geological maps of Magelang-Semarang (Figure 3), namely the volcanic rock units of Gilipetung (Qg), Mount Telomoyo (Qte), and Mount Kendil (Qak). Where constituent lithology in the research area is the rock resulting from volcanic activity. This lithology unit is included in the volcanic rock units of Mount Telomoyo and Mount Gilipetung. Where the appearance of megascopic there is a color difference in andesite lava units formed. In the Telomoyo Mountain unit the color of andesite lava units found has gray color, massive structure, holocrystalline, subhedral texture and mineral composition, namely plagioclase and hornblende, whereas in the andesite lava unit of Mount Gilipetung has a gray megascopic appearance which tends to be dark, structural the composition of the mineral composition is finer. The most dominant distribution of andesite lava lithology units in mapping plots is around 90%, where in the straightness of the valleys in the Wirogomo area there are altered rocks but with low intensity.

This lithology unit is formed from volcanic eruptions that produce lava where lava in this area is intermediate with a silica content of 45-50%. Lava flowing from the top of the volcano will move down the contour to follow the shape of the earth's morphology and the longer it will experience cooling due to a decrease in temperature. The structure formed in the research area is because the movement of the lava is Sheeting Joint (Figure 4).

Autoclastic Lava Lithology Unit

This lithology unit is included in the unit of Mount Gilipetung which is found in outcrops of contact with andesite lava lithology units at STA 1 (Figure 5). The distribution of this unit in the mapping plots is only a little, which is around 10% in the central and northern plots. The autoclastic lava (Figure 6) unit megascopically has a brownish gray color with massive structure, holocrystalline texture and mineral composition, namely plagioclase and hornblende in which the lithology unit has a characteristic that is a composition of the same fragment and matrix.

In general, the formation of autoclastic lava and andesite lava is the same where lava from the earth comes out and flows from the volcanic peak when volcanic eruptions occur, then lava flowing down the contour to follow the morphology will cool down due to a decrease in temperature where andesite lava generally freezes while on lava autoclastic cooling occurs on the surface first and on the inside is still moving so that the outer part that has frozen will go back inside and move so that after cooling it will resemble the appearance of the breccia which has fragments and matrices even though the composition that composes fragments and matrix is the same.



Figure 4: Regional Stratigraphy of Research Area (Thanden, et.al. 1996).



Figure 5: Sitting Joint in Research Area.



Figure 6: Autoclastic Lava.

Based on Geological Mapping (Figure 7), there are 15 observation points (STA), there are 3 STA that are used to take petrographic samples and there is several STA which show alteration where the alteration causes changes in physical, chemical, and composition of rocks. The physical appearance of an altered rock has a lower level of compactness and in the petrographic incision there is an altered mineral composition, where secondary minerals formed tend to be formed due to replacement.

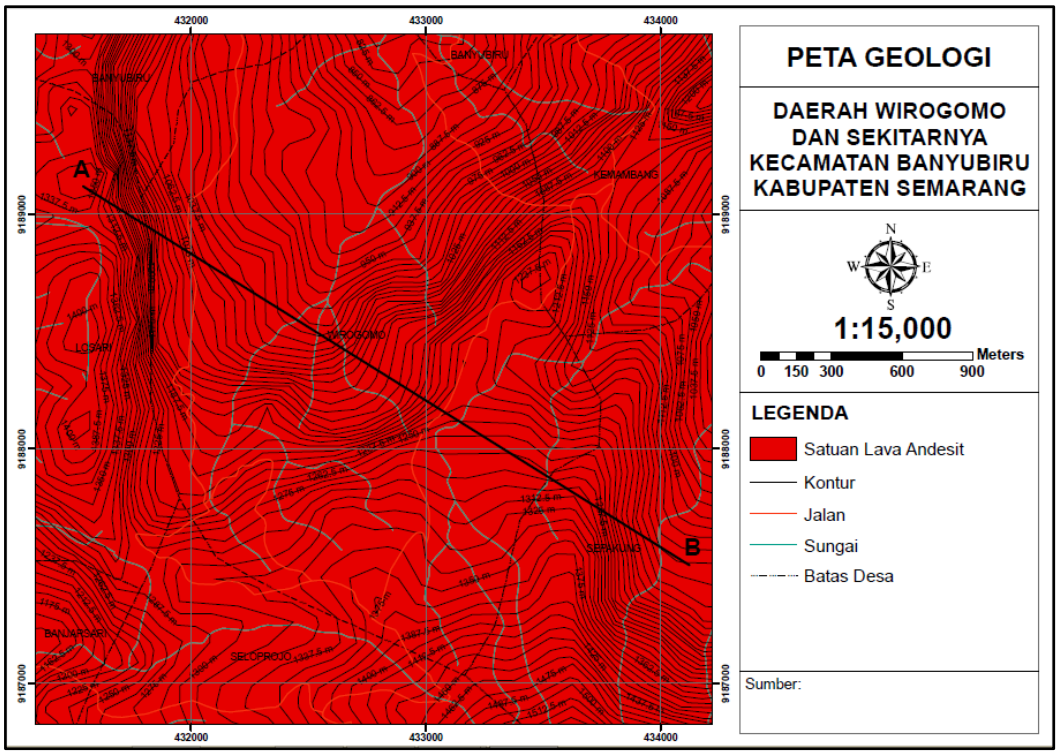


Figure 7: Geological Map of Research Area.

Structural Geology

In regional geology, the geological structure in the study area is the rim of the caldera, normal faults which have a southwest-east direction and horizontal faults that have a relative direction north-south and northwest-southeast. Based on remote sensing analysis using satellite imagery and direct observations in the field such as valley and ridge alignment, stocky in rocks and the presence of waterfalls indicate indications of geological structure in the mapping area.

The geological structure that developed in the study area is the caldera structure which is formed due to intensive volcanic activity. The caldera is formed because of the emptiness in the earth because of the eruption so that it experiences subsidence and forms depression. The diameter of this caldera is around 22 km. In addition, there are indications of normal faults which are indicated by valley and ridge alignments which have a slope of 70-80 ° and the presence of several waterfalls in the study area. Which of these structures is included in the structure formed by volcanic activity.

Petrography

In the research area there were 2 STA which characterized that the rocks experienced alteration processes. Where alteration process is an isochemical process of rock changes by the influence of hydrothermal fluid that changes the composition of the initial mineral or the primary mineral of the rock. As for the rocks that are altered at the station there are rocks that are altered by petrological and physical properties which are brown with massive structures and possess inequigranular granularity (Afanitic porphyry) with holocrystalline crystallinity with prismatic - tabular minerals which have a relationship between minerals is subhedral and the composition that is present is plagioclase which dominates biotite, quartz and amphibole and additional afanitic minerals. In Russel B Travis 1955 classification is called Porphyry Andesite in observations by Petrology of these rocks does not show any secondary minerals or alteration minerals. And petrographically observed mineral composition in the form of plagioclase, quartz, sericite, pyroxene, clay minerals and anhydrite minerals and secondary quartz. In this petrographic alteration type minerals appear to have not experienced high alteration intensity and are identified by rocks undergoing a process alteration replacement of primary minerals. But to identify the type of clay minerals can only use SEM (Scanning Electron Microscope) and XRD (X-Ray Diffraction) analysis.

As for the rocks that are altered at STA 13 (Figure 8 and 9), there are rocks that are altered by petrological and physical properties. They are yellow with massive structure and possess equigranular (afanitic) granularity with hypocrystalline crystallinity with prismatic - tabular minerals which have a relationship between minerals is subhedral and the composition there are predominant plagioclases, quartz and amphibole and additional afanitic minerals. The Russel B Travis 1955 classification was named Andesite in

observations by Petrology. This rock showed no secondary minerals or alteration minerals. And petrographically observed mineral compositions in the form of plagioclase, quartz, clay minerals and sericite and anhydrite minerals and secondary quartz. As well as the incisions are also identified the presence of veins in these rocks where the veins are deposited directly in the form of secondary urate mineral fillers. In this petrographic alteration type, it appears that minerals have undergone considerable alteration intensity and are identified that rocks undergo an alteration process of replacement and direct depositional from their primary minerals.

X-Ray Diffraction (XRD) Analysis

Analysis using XRD data is used to determine the clay mineral content that exists in a rock, because in petrographic analysis the types of clay minerals cannot be identified in detail. The result is that there are minerals such as illite, magnetite, albite, sanidine, and quartz (Figure 10).

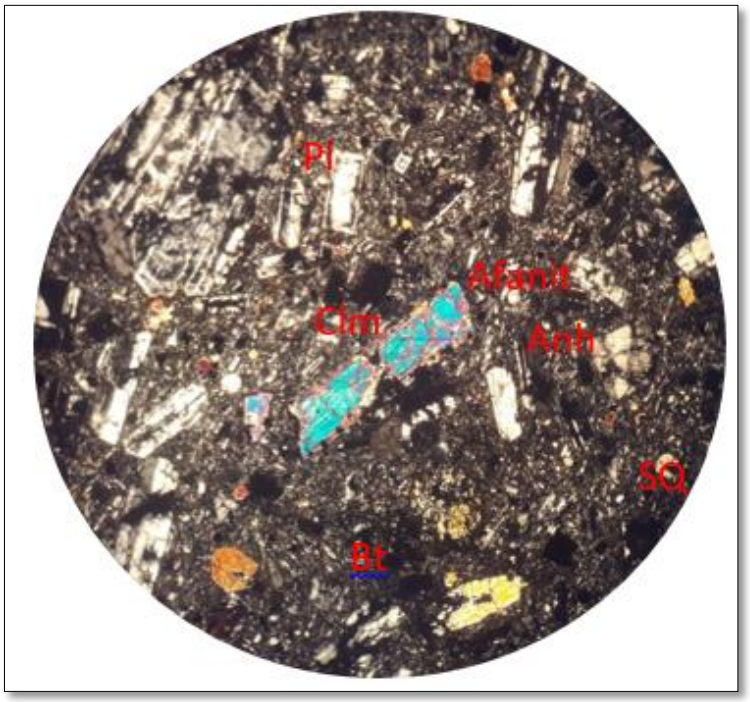


Figure 8: Petrographic Analysis of STA 1.

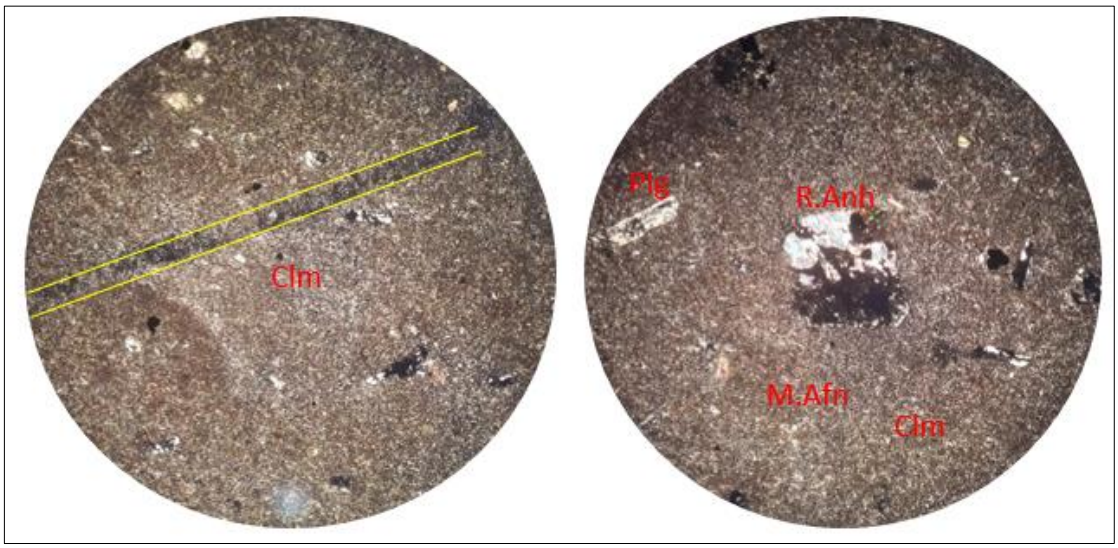


Figure 9: Petrographic Analysis of STA 13.

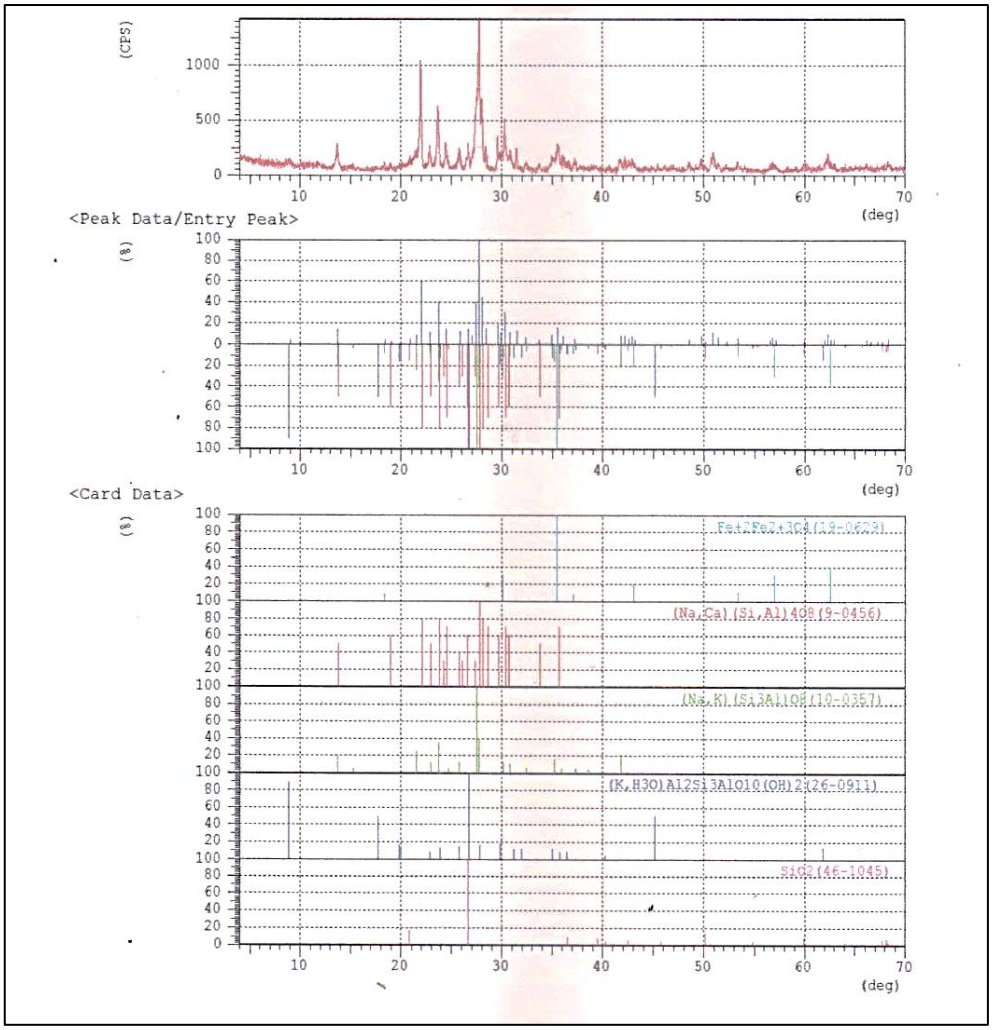


Figure 10: XRD Analysis of Rock Sample.

Geochemistry

Distribution of geothermal manifestations around research area in the form of warm springs in Dukuh Temple and Umbul Temple. The two springs have a temperature that is almost same, around 36 ° C with a neutral pH around 7.3. Analysis of fluid chemistry carried out on water samples manifestations in warm springs can be seen in table 1.

Geothermal fluid type can be known by comparing the concentration of Cl-SO_4-HCO_3 anion using the ternary diagram (Giggenbach, 1991) in Figure 11. Results from the diagram above show the warm spring of the temple Umbul (TL-1) and Candi Dukuh (TL-2) included in water type Chloride - Bicarbonate, where this water is formed because of its dilution of chloride by meteoric water during flowing to surface.

The presence of bicarbonate elements in water is the result of condensation steam under groundwater, where will move to follow the gradient groundwater, further away than the influence of groundwater will be even greater. Both springs are indicated is the system outflow zone Telomoyo geothermal based on type the fluid is chloride-bicarbonate and where is the immature water reservoir fluid has experienced mixing with more water shallow with lowest silica concentration. This is known by plotting of Na - K - Mg elements on Giggenbach ternary diagram (1988) in Figure 12.

Table 1: Results and Analysis of Chemical Characteristics in Warm Springs.

No	Parameter (mg/L)	MAH Candi Umbul (mg/L)	MAH Candi Dukuh (mg/L)
1	SiO2	0.02	0.13
2	Al	0.006	1.014
3	Fe	0.23	1.54
4	Ca	24.567	68.05
5	Mg	3.23	36.53
6	Na	20.305	27.676
7	K	3.45	7.45
8	Cl	17.43	40.13
9	SO4	26.755	43.198
10	HCO3	21.077	36.34
11	CO3	0.009	0.46

In Figure 12. warm springs Dukuh temple and Umbul temple are located at the angle of Mg, but the springs are warm Candi Dukuh is in the corner of the Mg deeper than Umbul Temple. Can be indicated by

the warm spring of the temple Umbul and Candi Dukuh reacts dissolution of the rocks it passes near the surface or dilution by groundwater have high Mg concentration with the level of dissolution at the Temple Hamlet is more intensive than the temple Umbul.

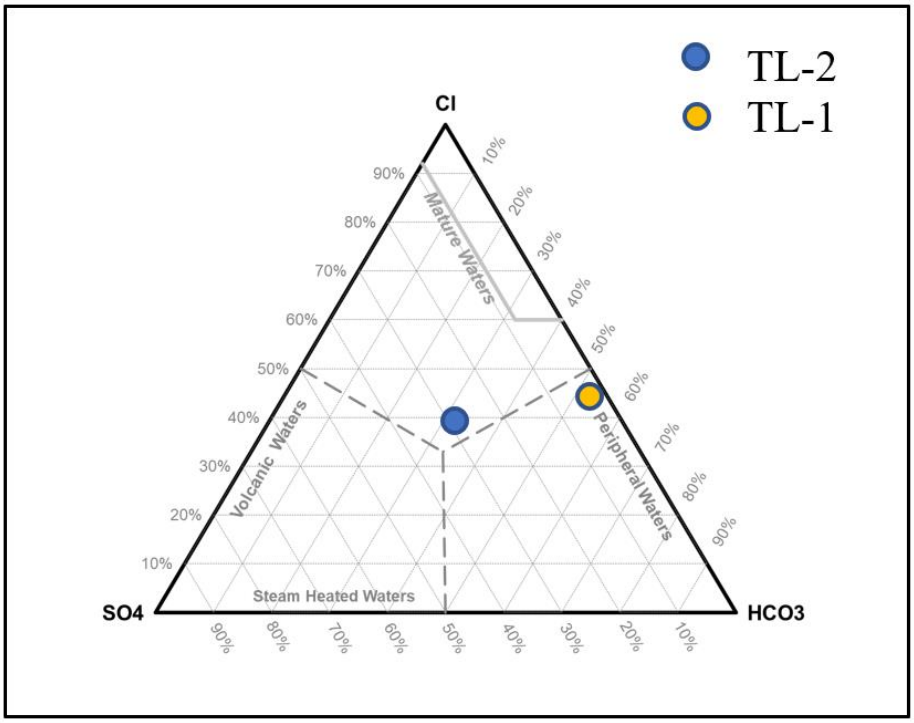


Figure 11: Ternary Diagram Cl-SO_4-HCO_3.

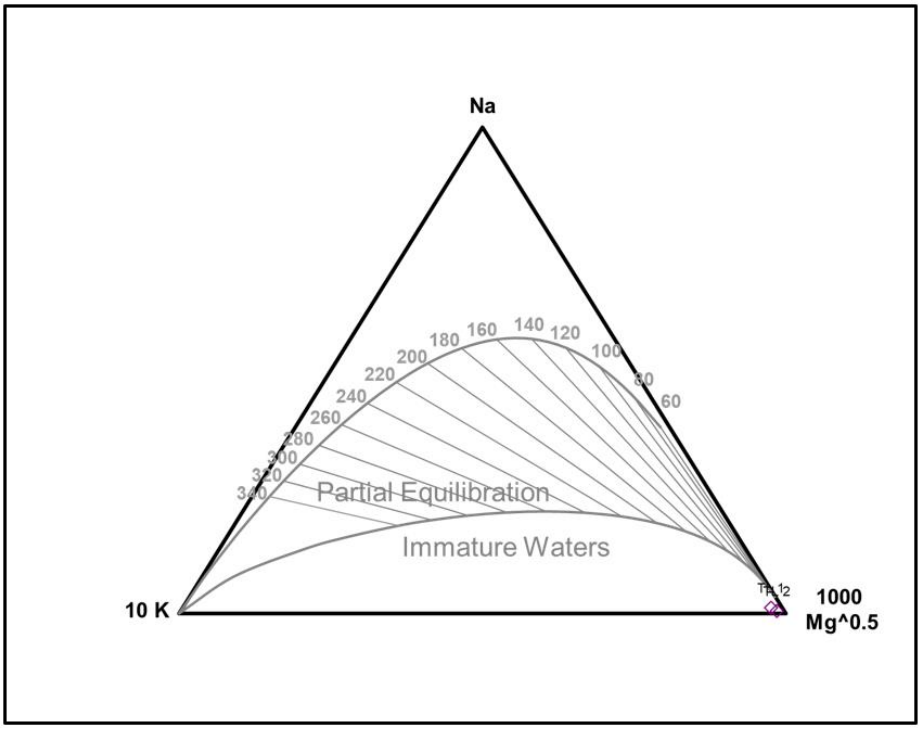


Figure 12: Ternary Diagram Na-K-Mg.

Hydrothermal Alteration Model

Based on the characteristics of the alteration minerals found in Wirogomo village, Kerambang and Seloprojo villages, the secondary mineral assemblages present in the study area are grouped into argillic zones (Figure 13) and based on the classification of Corbett and Leach (1998) with the following explanation:

- The argillic zone found in STA 1 in the village of Wirogomo is characterized by minerals that appear, namely secondary quartz, clay minerals, anhydrite. The temperature range of the association of minerals found ranges from 150-300 ° C based on the table of mineral formation temperature range of Reyes (1990). And according to Corbett and Leach (1998) alteration intensity in these rocks including the medium level.
- The argillic zone is also found in STA 13 in Selogrojo Village with characteristic minerals found namely secondary quartz, sericite, clay minerals and secondary biotite. The temperature
- Range of this mineral association is 210°C - 230°C based on the table of mineral formation temperature range of Reyes (1990). And according to Corbett and Leach (1998). Alteration intensity in these rocks is of moderate level.

Model of the geothermal system in Telomoyo Mountain Complex (Figure 14). is made based on location distribution and manifestation characteristics the existence of rock alteration manifestations that indicate upflow zones indicates a boiling process in the reservoir that produces steam condensate acid. The results of fluid geochemical analysis obtained a type of fluid that appears to the chloride-bicarbonate type surface which is the lateral outflow zone of the system. The reservoir temperature based on the presence of argillic-type alteration also shows a temperature range of 230°C - 260°C. The argillic zone indicates the presence of water vapor that flows directly to the surface to experience condensation with ground water and surface water which causes an oxidation process that converts H_2S to H_2SO_4. Argillic alteration in the upflow zone indicates that far below it there is a reservoir zone which experiences boiling so that the fluid becomes two phases namely steam and water, water vapor rises to the surface. The formation of clay mineral minerals due to hydrothermal alteration results in lower rock permeability (Ramadhan, et.al, 2014). This rock that is altered in the advanced argillic-argillic zone can become a clay cap and become a reservoir hood zone. Composite lithology in the form of thick andesite lava has poor permeability and is a good veil for the Telomoyo Complex geothermal system. Pyroclastic rock found under thick andesite lava is possible to become a potential reservoir in the geothermal system of the Telomoyo complex.

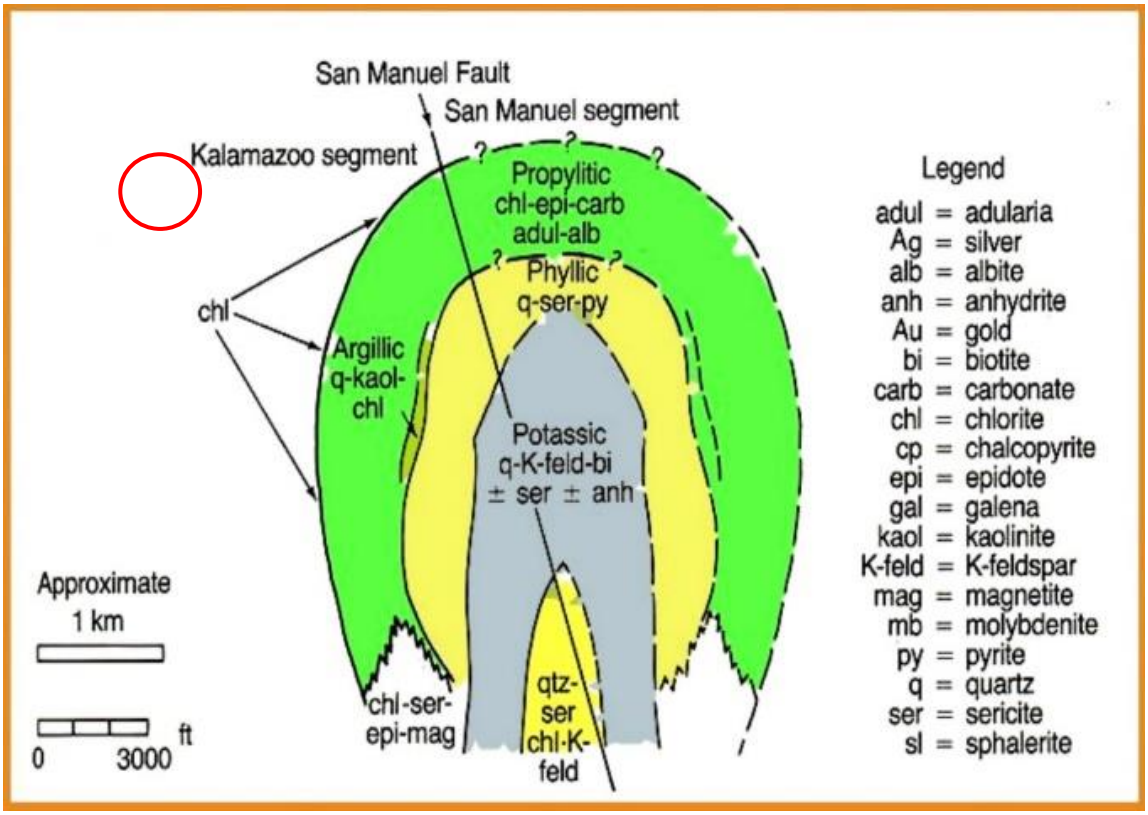


Figure 13: Hydrothermal Alteration Zoning.

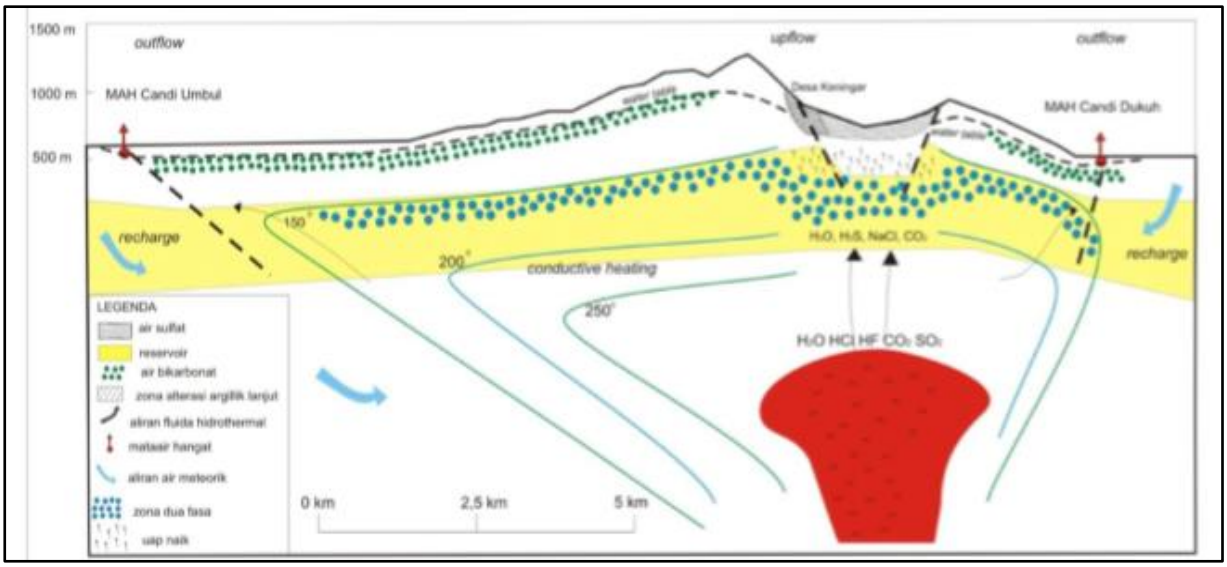


Figure 14: Geothermal Conceptual model of Mt. Telomoyo and its surroundings (Putriutami, et al. 2014).

CONCLUSION

- Geothermal manifestation that found in research area are altered rocks and hot spring, that can be found in Candi Umbul.
- Based on geological mapping, lithology unit in research area are andesitic lava and autoclastic lava.
- The geological structure found in the study area is sheeting joint.
- Petrography analysis shows that mineral content in rocks samples are: plagioclase, quartz, sericite, pyroxene, anhydrite, and clay minerals.
- X-Ray Diffraction analysis used to identify clay minerals shows the content of minerals are: quartz, albite, magnetite, illite, and sanidine.
- Based on fluid geochemical analysis of two warm pool manifestations at research area, the fluid included in type of bicarbonate-chloride acid with equilibrium is included in immature water with an estimated reservoir temperature based on silica geothermometer (Fournier, 1982) is 167 ° C and Na / K geothermometer (Giggenbach, 1988) is 278 ° C.
- Based by petrology, petrography, and xrd analysis shows that alteration zoning of Telomoyo volcanic rock complex is in Argilic zone (Corbett and Leach, 1998).

REFERENCES

Hutami, T., R., Aribowo, Y., et.al. (2014). "Preliminary Study of Geothermal Prospects based on Geothermal, Geochemical, and Isotopic Manifestations of Geothermal Fluids in the Telomoyo Mountain Complex, Semarang Regency, Central Java Province". Semarang: Department of Geological Engineering, Diponegoro University.

Putriutami, Elida, S., et Al. (2014). "Interpretation of the Surface Layer in the Telomoyo Mountain geothermal area, Semarang Regency uses the geoelectric schlumberger configuration resistivity method". Semarang: Department of Physics, Faculty of Science and Mathematics, Diponegoro University, Department of Marine Affairs, Faculty of Fisheries and Marine Sciences, Diponegoro University. 10, 5-17.

Ramadhan, N., Prameswari, M., et.al. (2014). "Evaluation of the Geological and Geochemical Conditions of the Telomoyo Volcanic Geothermal Potential". Yogyakarta: Geological Engineering of Gadjah Mada University. Proceedings of the 7th Earth Science National Seminar. 26:165–188.

Thanden, R., E., Sumadirdja, H., et Al. (1996). "Regional Geology Map of Semarang-Magelang". Lembar: 1408-5, 1409-2. Center for Geological Research and Development.

SEA EFFECT ANALYSIS IN MAGNETOTELLURIC DATA USING FORWARD AND INVERSE 3-D MODELING FOR GEOTHERMAL EXPLORATION

Ewin Rahman Dzuhri[1], Yunus Daud[2], Fikri Fahmi[3], Wahyu Noor Ikhwan[3], and Dhara Adhnandya Kumara[1]

[1]Geophysics Graduate Program, Universitas Indonesia
[2]Master Program in Geothermal Exploration, Graduate Program of Physical Science, Universitas Indonesia
[3]PT. NewQuest Geotechnology
Email: rahmanewin@gmail.com, ydaud@sci.ui.ac.id, fikri.fahmi@newquest-geotechnology.com, wahyu.noor@ui.ac.id, dharaadhnandyak@gmail.com

ABSTRACT

Magnetotelluric (MT) is a geophysical method commonly used in the geothermal survey. MT method can image the resistivity of earth from a few tens of meters to several hundred kilometers depending on the measurement periods. With geology and geochemistry as supporting data (3G), integrated 3G data can be very powerful to delineate geothermal system which is clay cap, reservoir, and heat source. However, in MT data acquisition we have to pay attention to the surroundings of the survey area because there are noises that will affect MT data. One of the noises from the surrounding area is noise from the sea or it is also called coast effect. In order to reduce the noise from MT data acquisition, especially noise from the sea, and miss interpretation of MT data after processing, we have to study the impact of coast effect on MT data during the acquisition and even when inversion. The method of this study is using forward modeling and 3-D inversion using synthetic MT data. The aim of this study is to conclude what causes showed up from MT data affected by the coast effect noise. This sea effect could lead to magnetotelluric data miss interpretation. Thus, by understanding the sea effect on magnetotelluric data and correct it, could improve the quality of subsurface image and lower the geothermal exploration risks.

Keywords: Magnetotelluric, 3-D modelling, exploration

INTRODUCTION

Magnetotelluric (MT) method is a passive electromagnetic method which commonly used to delineate subsurface structure especially in geothermal exploration. The variation of EM signal coming from the sun solar wind is recorded for several hours for each MT stations on the surface. The variation of subsurface resistivity can be measured by applying several steps of data processing and various schemes in inversion modeling process.

In the real condition, the earth has a complex subsurface resistivity variations, both in vertical and lateral, especially in geothermal systems. Several factors that affect the value of resistivity in geothermal system are minerals alteration, fluid content, and temperature (usher et al, 2000). Lateral resistivity variation in earth subsurface affected the MT data is called 3-D effect. Due to this effect, the MT curve, both TE and TM, will give different response. Because of earth complex subsurface structure, 1-D and 2-D modeling are not performed. Thus, several 3-D forward modeling including the sea with distance variation to measured area are performed to obtain synthetic data that have similar condition to the real earth. This paper mostly discusses about the simulation of 3-D effect in MT data using 3-D MT forward and inverse modeling. The MT response represented by apparent resistivity and phase curve in frequency domain was calculated and analyzed in every station for each model. The MT response from each model showed the effect form 3-D effect, which is caused by the sea. Then from each model MT response, further analysis is done to see the influence of 3-D effect using inversion modeling. The inversion method has been studied by Siripunvaraporn et al (2005), and daud et al (2015).

MT CONCEPT

MT method use electromagnetic wave variation as the source to obtain the subsurface resistivity imaging. Electromagnetic waves consist of E (electric) field which varies along lateral direction and H (magnetic) field which varies along lateral and vertical direction. H field in electromagnetic waves come from the earth atmosphere and penetrate through earth layer. Because of H field penetration into earth layer, E field emerges from earth layer.

Impedance (Z) measure the value the ratio of horizontal E field to the orthogonal horizontal magnetic field at a number of frequencies Equation 1, gives earth resistivity (called apparent resistivity) as a function of frequency or period, resulting in a form of depth sounding.

$$Z_{xy} = \frac{E_x}{H_y} \quad (1)$$

Apparent resistivity is an average resistivity for the volume of earth sounded MT stations sounding in a period of time. Apparent resistivity related to

impedance showed in Equation 2. If the earth assumed as a homogenous uniform half space, then the apparent resistivity value is the actual resistivity because there is no other resistivity value (Simpson & Bahr, 2005).

$$\rho_{xy} = \frac{1}{\omega\mu}\left|\frac{E_x}{H_y}\right| \quad (2)$$

Where ω is angular frequency and μ is magnetic permeability which in earth studies the value of μ = $4\pi\ x\ 10^{-7}$ H m^{-1}. The phase differences between the electric and magnetic field can be calculated by using Equation 3.

$$\emptyset_{xy} = \boldsymbol{tan}^{-1}(\boldsymbol{z_{xy}}) \quad (3)$$

Lateral resistivity variation can affect the MT data even though the boundary of resistivity variation boundary located far away from MT acquisition area. Resistivity anomalies affect the MT data from 2-3 times distance from sounding penetration depth (Simpson & Bahr, 2005). An example of lateral resistivity variations that have long distance disturb the sounding volume of the ideal layered earth model showed in Figure 1.

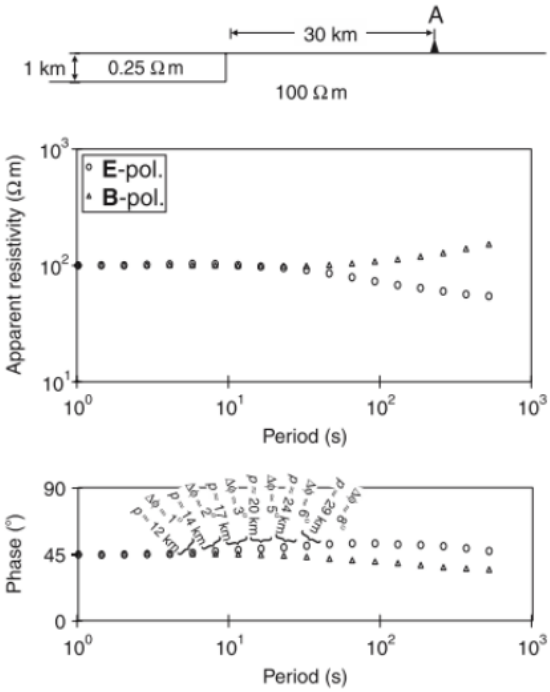


Figure 1: Conductivity body affect the MT data in stations 30 km apart.

IMPEDANCE TENSOR

3-D Model

The impedance tensors in 3-D model assume that resistivity values vary in all direction, vertically and laterally. Because all direction is considered then 3-D tensor impedance is called non-zero element which all the impedance tensor components have value. Thus, the 3-D impedance tensor is given in Equation 4.

$$Z_{3D} = \begin{bmatrix} Z_{xx} & Z_{yx} \\ Z_{xy} & Z_{yy} \end{bmatrix} \quad (4)$$

3-D EFFECT SIMULATION

Several synthetic models were built for performing a simulation of 3-D effect in MT data. The models represent the 3-D earth model. The synthetic model is consist of several cell with certain resistivity value in a 3-D mesh grid. The mesh grid and parameter forward used in this simulation are described in Table 1.

Table 1: Mesh grid and forward parameter for 3-D modeling.

MESH GRID PARAMETER	
Cell Size	250 x 250 x 100
Padding factor	5 / 1.2
Number of Block Model 1	35 x 47 x19
Number of Block Model 2	35 x 35 x 19
FORWARD PARAMETER	
Number of Station	36 / 1000 m
Freq. Range / Point Per Decade	1000 – 0.01 Hz / 8

3-D Model 1

Model 1 is made assumed there is a block shaped anomaly body with geometry 9 km2 (3 x 3 km) starting from depth 600 meter to 2000 meter with resistivity value 5 Ω.m. The resistivity value of surrounding area is 100 Ω.m. An oceanic area with depth 1km and resistivity value 0.3 Ω.m from east part of station area was made with distance 1 km to analyze the effect of ocean affect the MT data Acquisition. Model 1 is shown in Figure 2.

3-D Model 2

Model 2 is made similar to model 1. Model 2 assumed there is a block shaped anomaly body with geometry 9 km2 (3 x 3 km) starting from depth 600 meter to 2000 meter with depth 1km and resistivity value 5 Ω.m. The resistivity value of surrounding area is 100 Ω.m. The difference of model 2 and model 1 is the distance of ocean to MT area which is 4 km. Model 2 is shown in Figure 3. A profile is shown in Figure 4 is used to analyze the sea effect in MT curve and 3-D inversion.

3-D FORWARD MODELING RESULT

The forward modeling performed in model 1 showed in figure 5a and model 2 showed in Figure 5b.

OCEANIC MODELING IN INVERSION MODELING

Inversion process can be done using constrain inversion where specified cell is constant and not changing in every iteration when inversion process is running. The initial model in constrain inversion to reduce the effect of sea is performed using oceanic model. The oceanic model in inversion are represent the ocean in real condition. Oceanic model is shown in Figure 6.

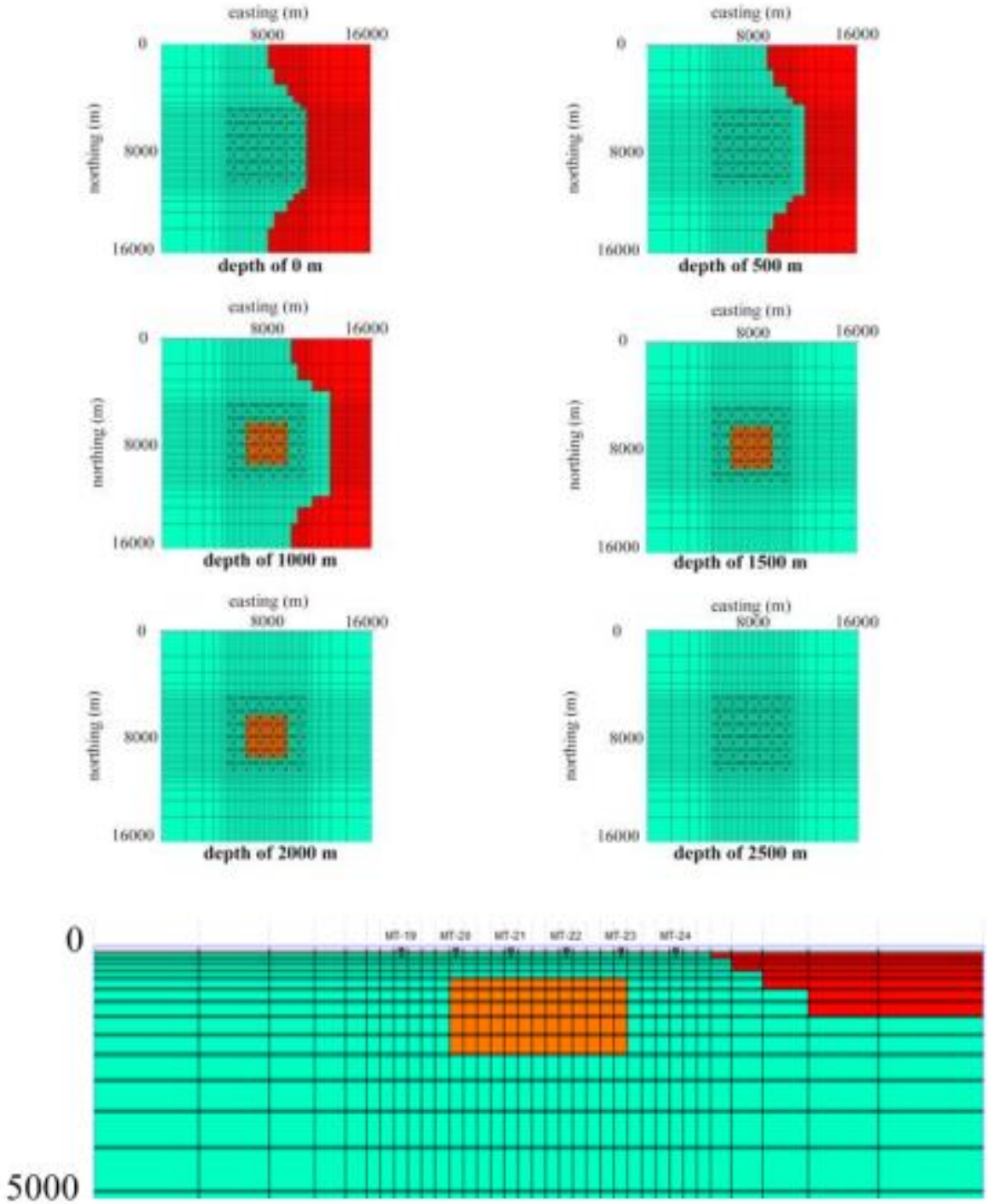


Figure 2: z depth slice and y section of 3-D model 1.

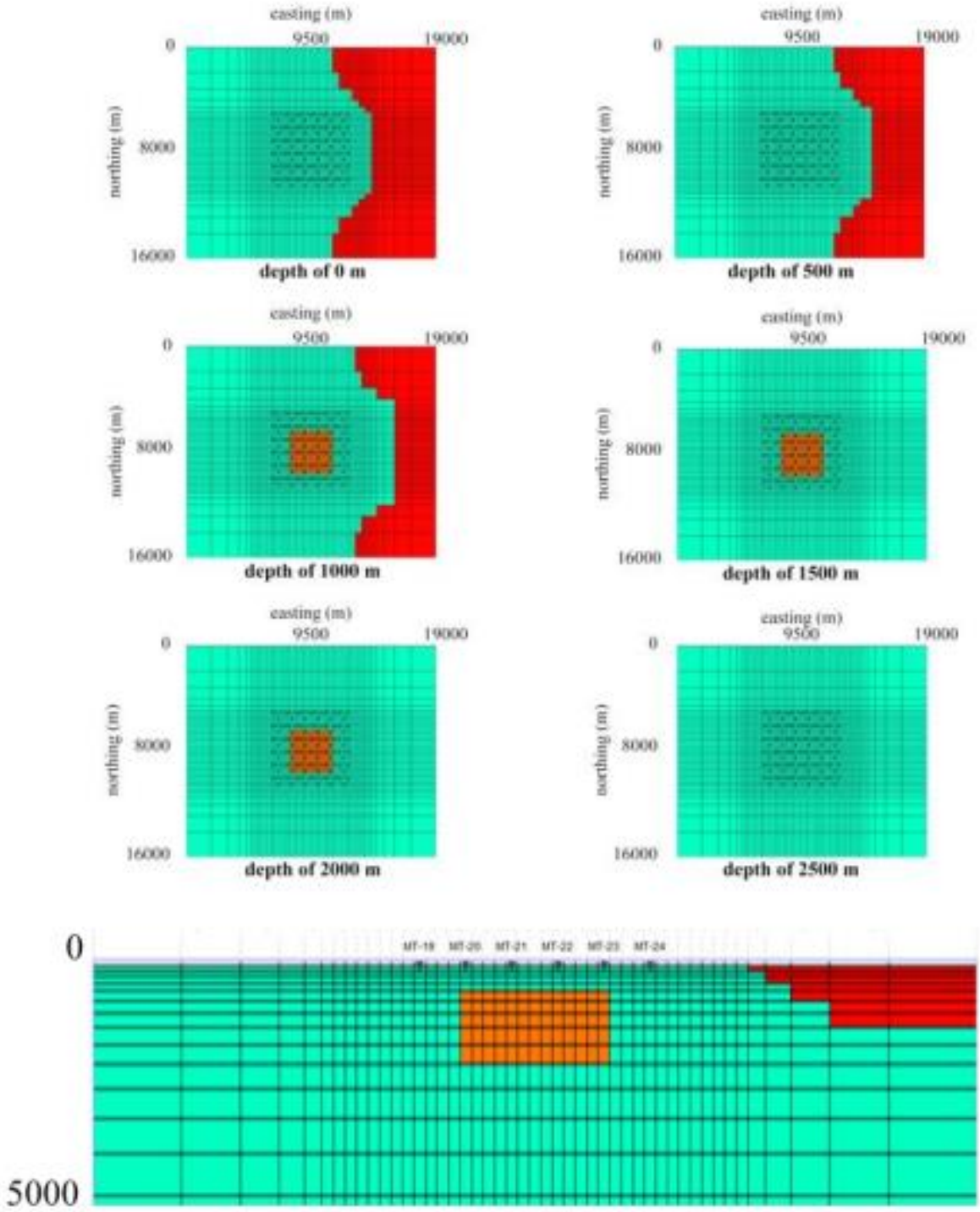


Figure 3: z depth slice and y section of 3-D model 2.



Figure 4: Line profile used to analyze sea effect.

3-D INVERSION MODELING RESULT

The inversion process is performed using MT3DInv-X software (Daud et al, 2012) developed by PT. NewQuest Geotechnology which use Data Space Occam's inversion algorithm introduced by Siripunvaraporn et al. (2005).

Model 1 3-D Inversion

3-D inversion performed with model 1 synthetic data. The results for 3-D inversion using unconstrain inversion are shown in Figure 7a and 3-D inversion using constrain inversion are shown in Figure 7b.

Model 2 3-D Inversion

3-D inversion performed with model 1 synthetic data. The results for 3-D inversion using unconstrain inversion are shown in Figure 8a and 3-D inversion using constrain inversion are shown in Figure 8b.

From 3-D inversion results in model 1 and model 2, can be seen that constrain inversions are more likely close to the initial model in forward modeling.

CONCLUSION

From this simulation, several things can be concluded, they are:

1. The closer the MT station to ocean, the MT curve, TE and TM, will split from higher frequency.
2. Frequency affected from ocean occur in low frequency depends on the distance.
3. 3-D inversion for MT data close to ocean must be performed using constrain inversion.

REFERENCES

Daud, Y., Heditama, D. M., Aswo, W., Pratama, S. A., Agung, L., Amryiah, Q., & Saputra, R. (2012). "3-D Inversion of MT Data Using MT3DINV-X Software". In The 12th Annual Indonesian Geothermal Association Meeting & Conference. Bandung.

Fahmi, F. (2018). "Pengaruh Oceanic Model Dalam Pemodelan Inversi 3-Dimensi Data Magnetotellurik Di Daerah Geotermal "X"". Universitas Indonesia

Simpson, F., & Karsten, B. (2005). "Practical Magnetotelluric". Cambridge: Cambridge University Press.

Siripunvaraporn, W., Egbert, G., & Lenbury, Y. (2005). "Three-dimensional magnetotelluric inversion: data-space method", 150, 3–14.

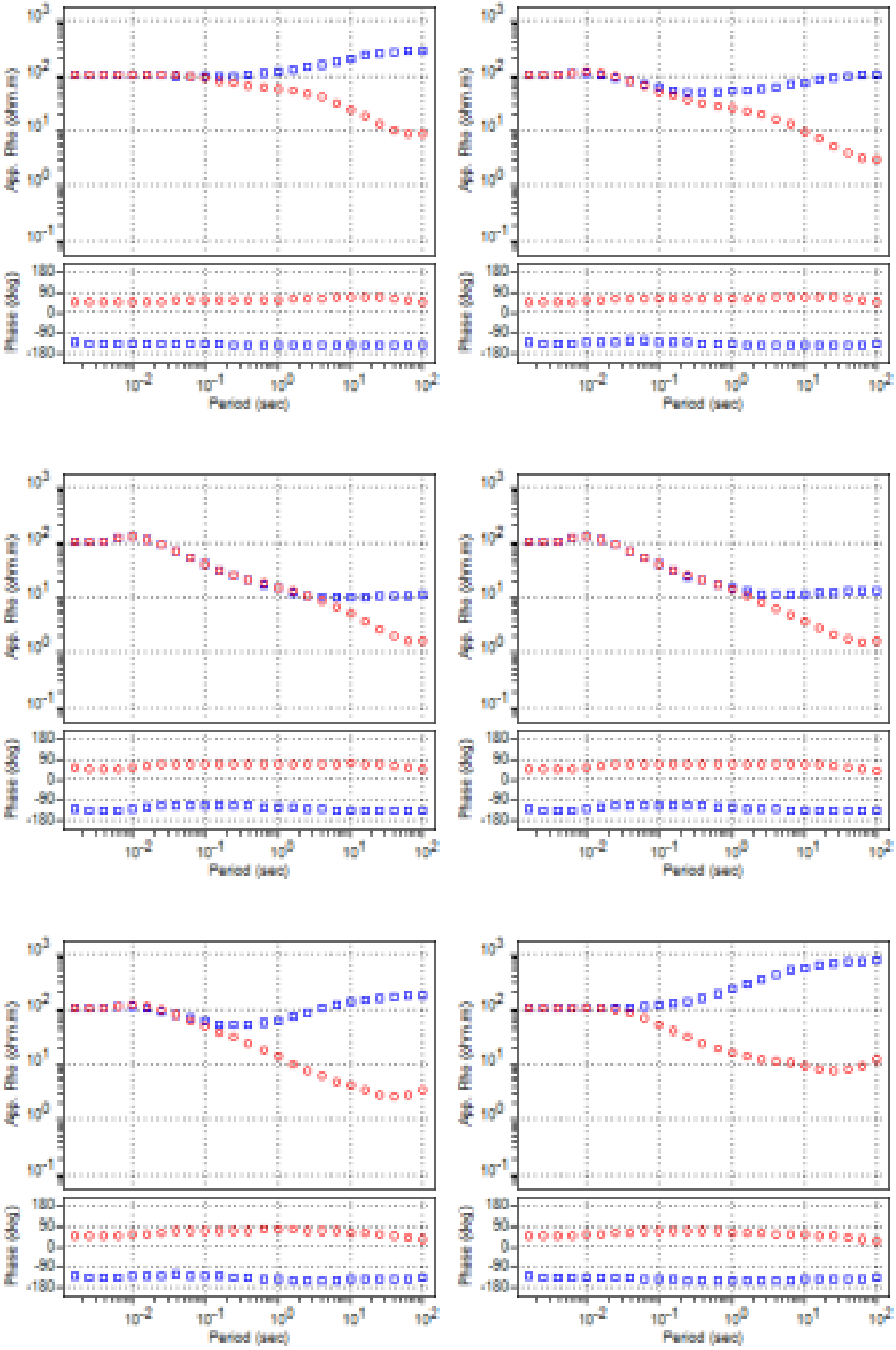


Figure 5a: TE and TM curve from forward modeling model 1, from MT-19 to MT-25 respectively.

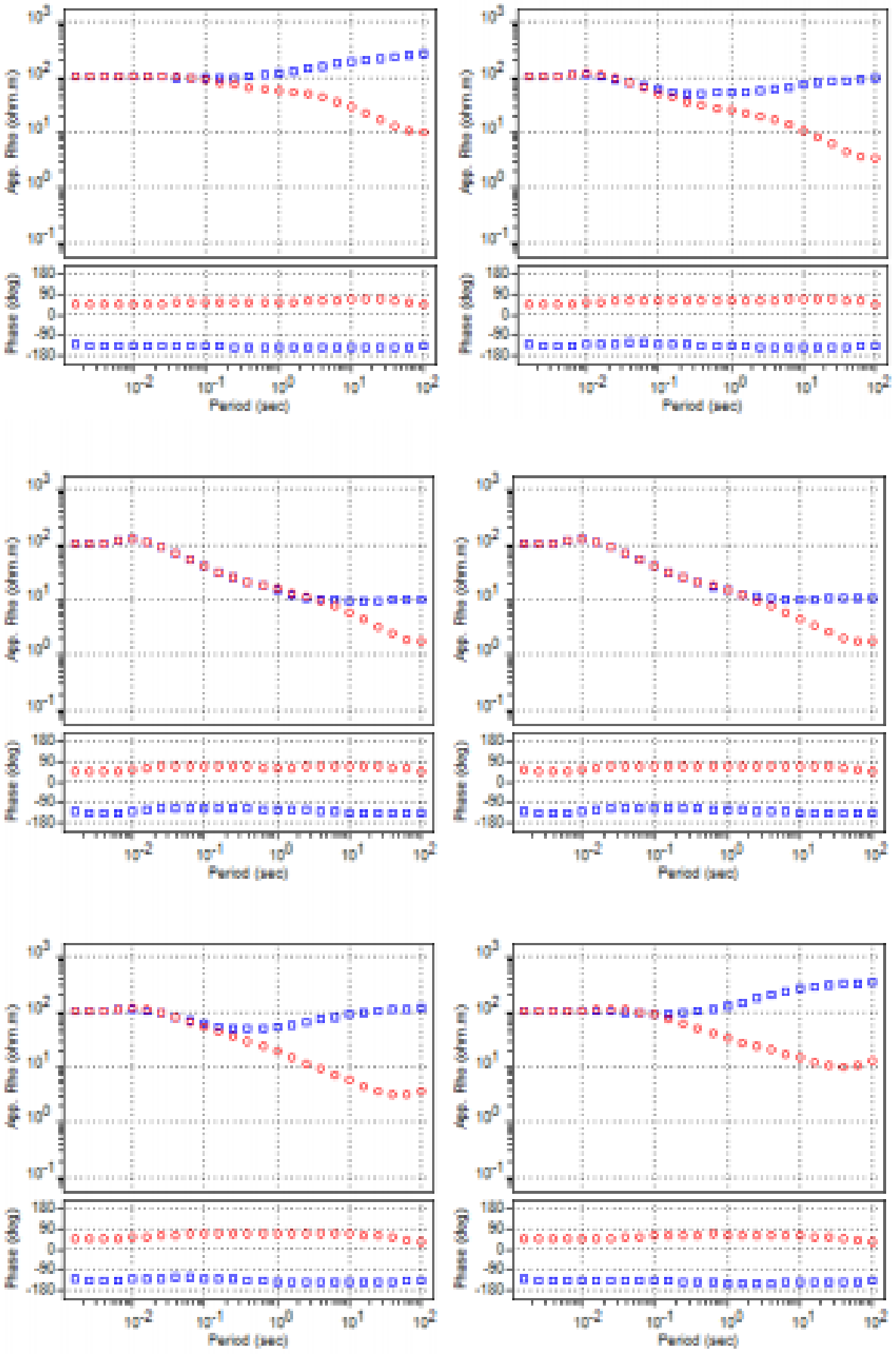


Figure 5b: TE and TM curve from forward modeling model 2, from MT-19 to MT-25 respectively.



Figure 6: Oceanic model scheme as initial model for inversion process.

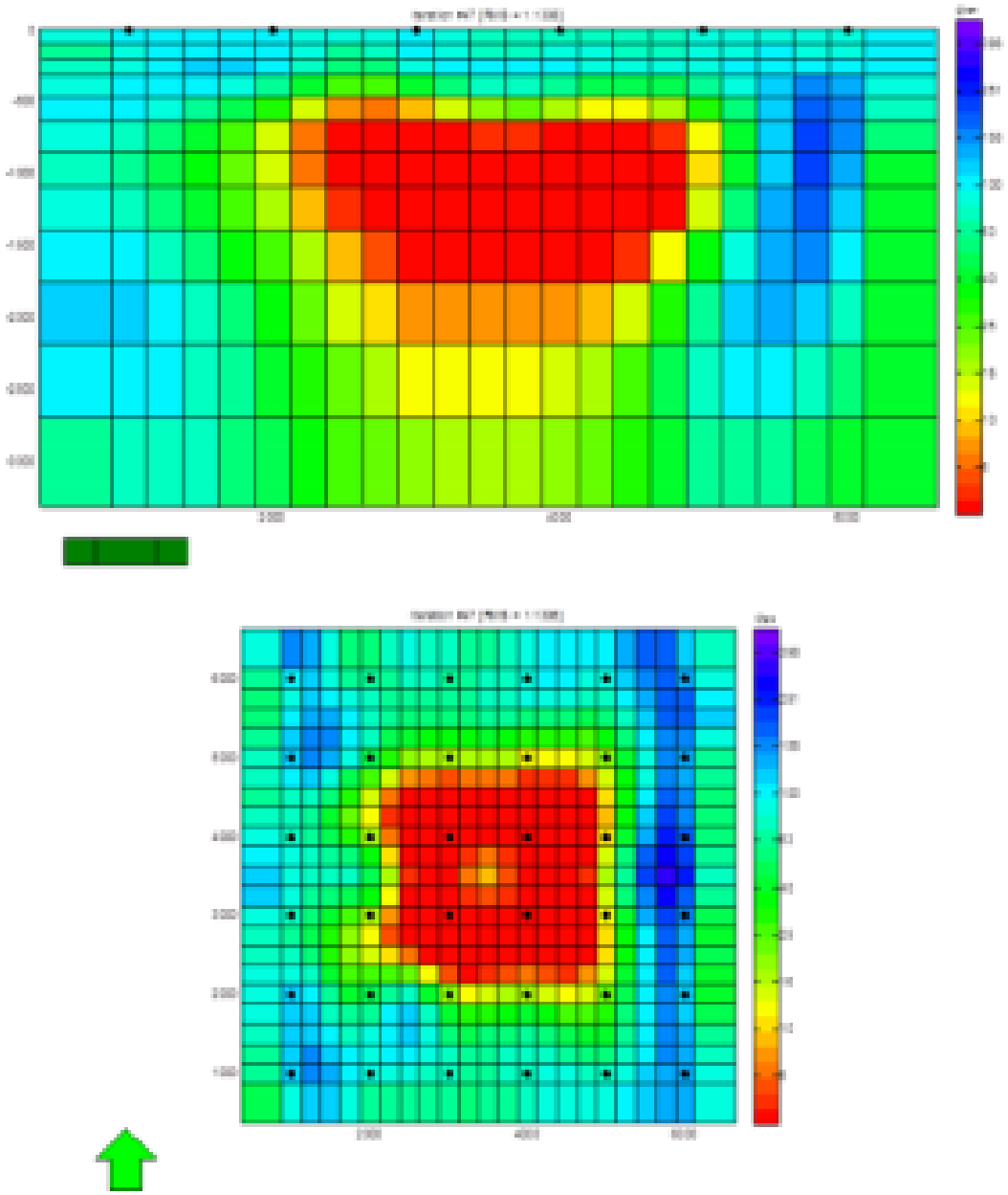


Figure 7a: z view at depth -800 m and y section using un-constrain inversion.

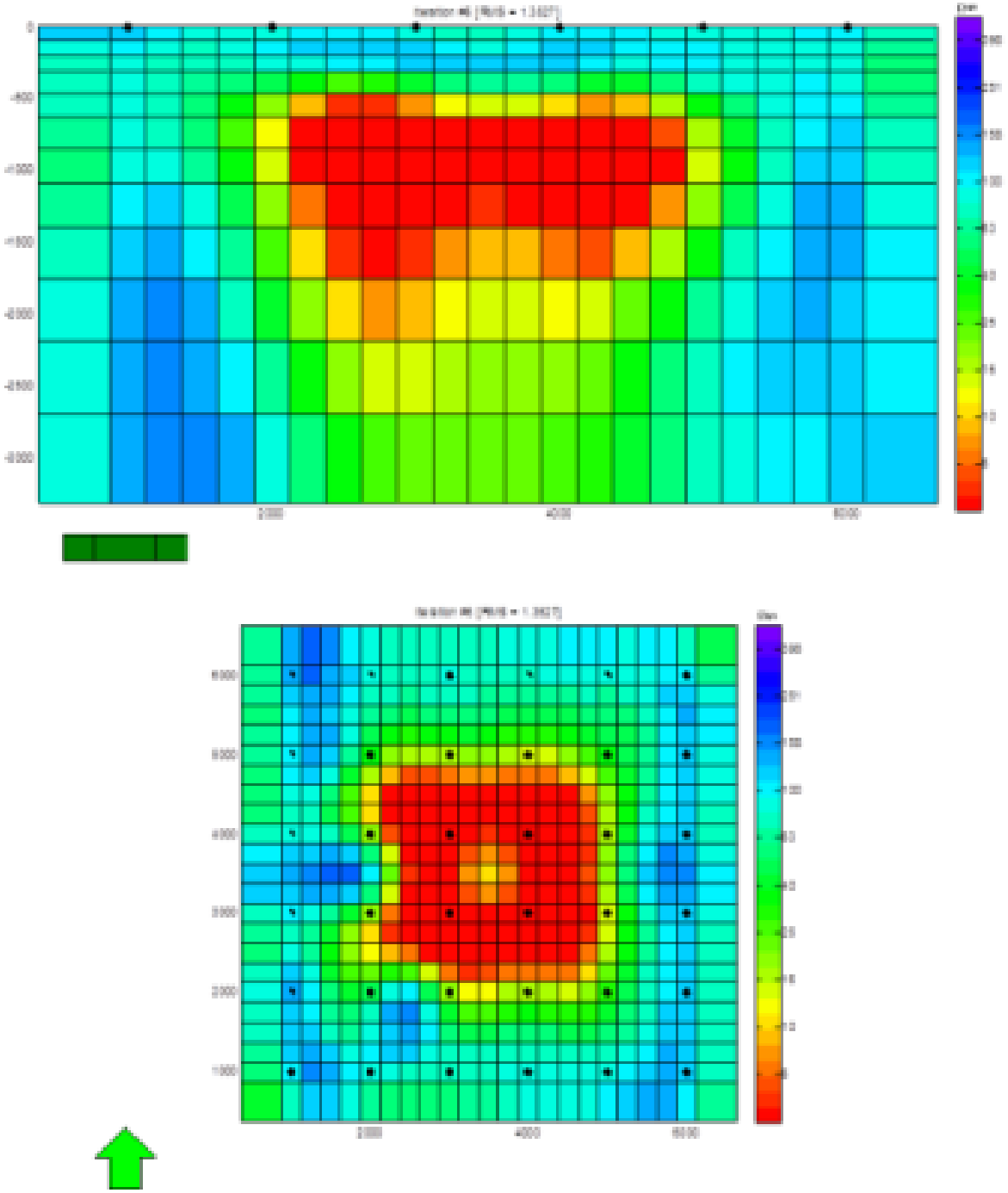


Figure 7b: z view at depth -800 m and y section using constrain inversion.

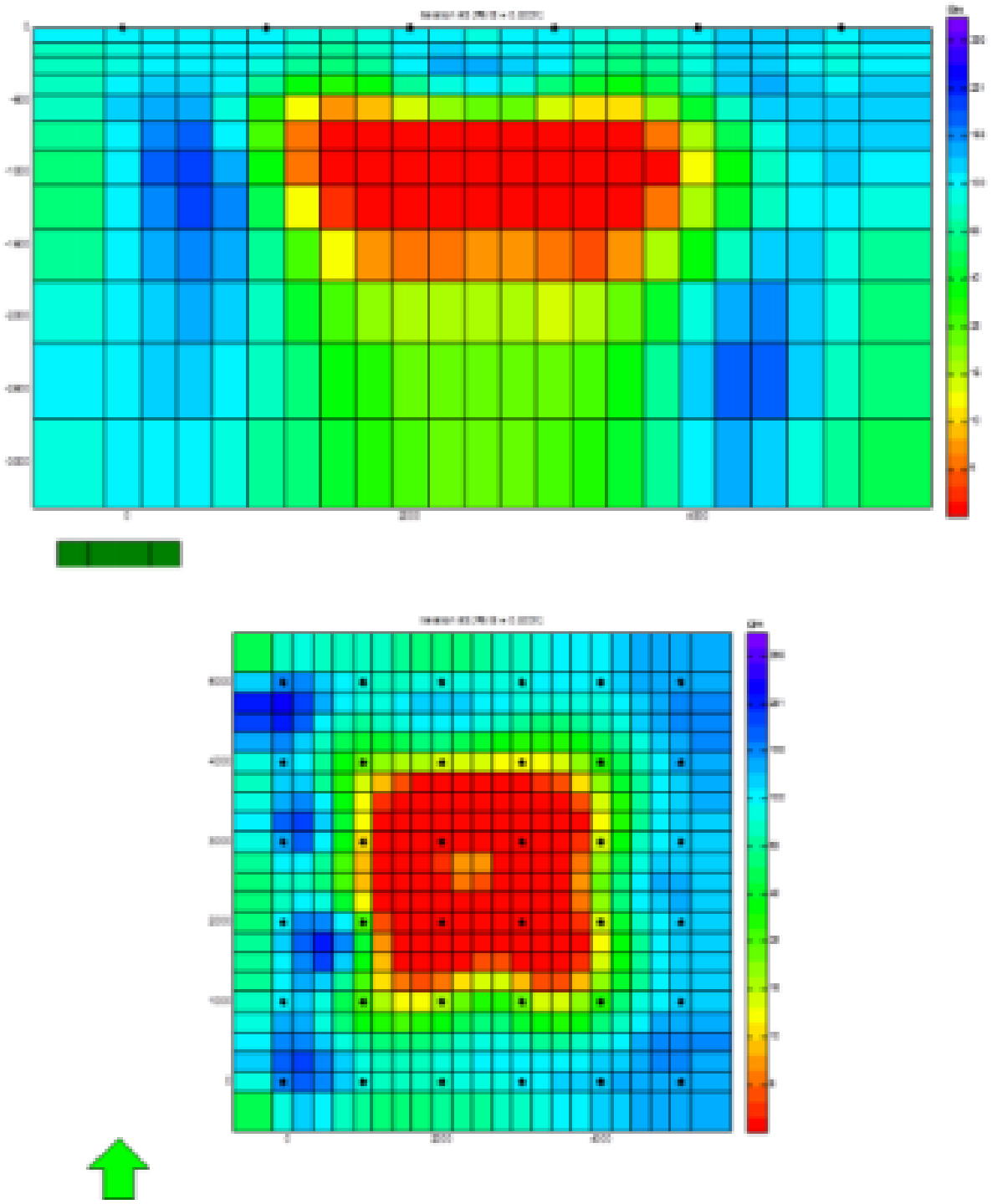


Figure 8a: z view at depth -800 m and y section using un-constrain inversion.

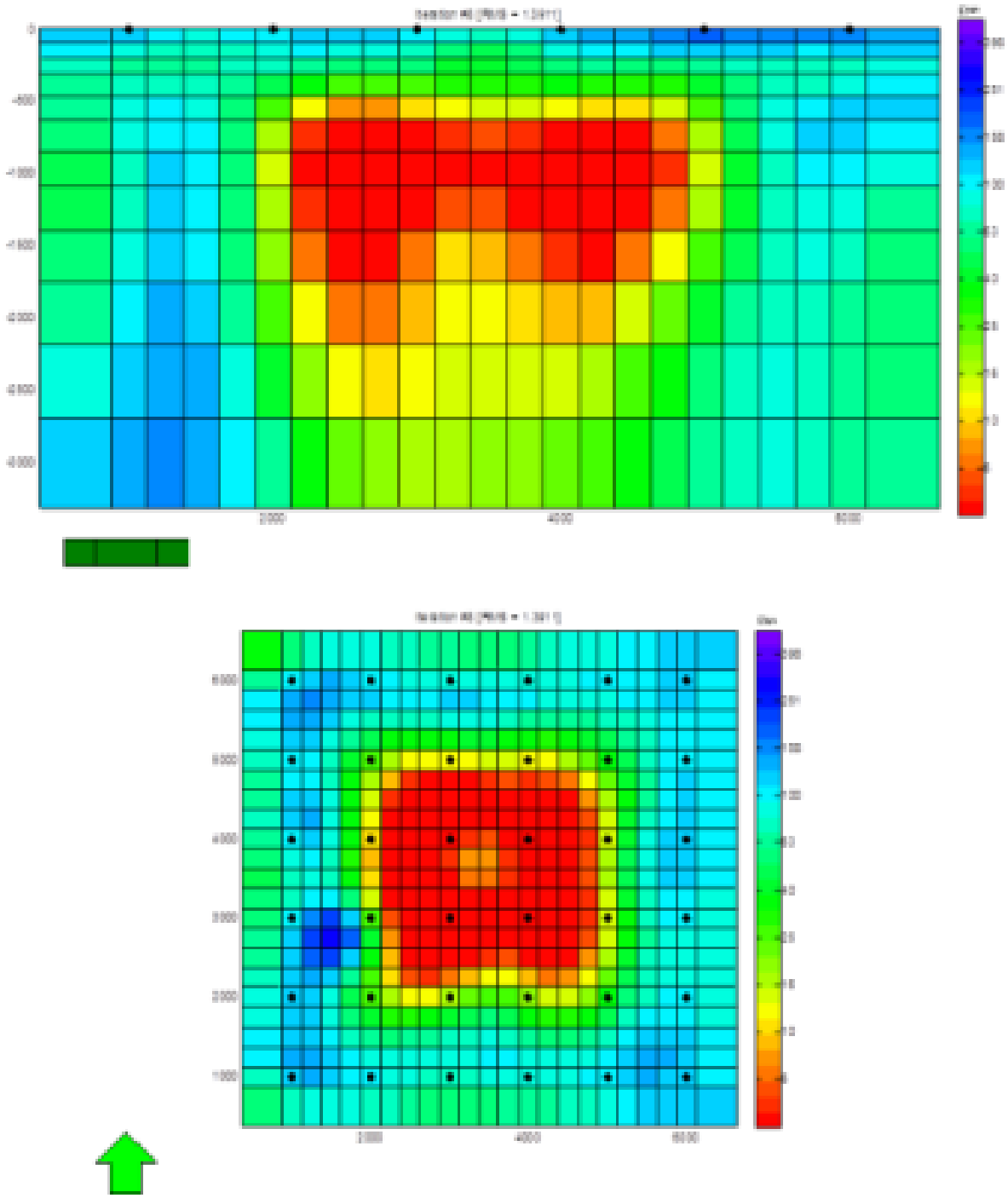


Figure 8b: z view at depth -800 m and y section using constrain inversion.

FAULT FRACTURE DENSITY (FFD) AND ALTERATION ZONE ANALYSIS TO DETERMINE FLUID-ROCK INTERACTIONS TO ENSURE EFFECTIVE DECISION MAKING OF PROSPECTIVE FIELDS IN MOUNT TELOMOYO, SEMARANG

Astri Yunita, Muhammad Ali Akbar, and Velayati Salim

Universitas Diponegoro
Email: astriyunita26@gmail.com, research.aliakbar@gmail.com

ABSTRACT

The Telomoyo geothermal prospect is regionally included in the solo zone which is a quaternary geological environment. The products of Telomoyo volcano are andesite-basaltic lava and pyroclastic rocks. The structure found in the study area is a result of volcanic activity and tectonism, namely in the form of a caldera and normal faults with southwest-northeast trend. The structure and fracture are the initial indications of fluid-rock interactions. This study aims to determine the interaction between fluid and rocks by conducting Fault Fracture Density (FFD) and rock alteration analysis. This study is conducted methodically by field observation, software data processing, and literature from previous studies. The data obtained are FFD data on Telomoyo complex and alteration data in the north area of Mount Telomoyo. The structural analysis shows the direction of the dominant structure is WNW-ESE. Areas with high structural density developed on the north of the young cone of Mount Telomoyo. Alteration data shows that there are two zones, the argillic - advanced argillic alteration zone and the propylitic zone. The former is characterized by the mineral association of alunite, kaolinite, smectite, illite, formed at the temperature of 100°C – 200°C with acidic to almost neutral pH. The latter is characterized by epidote minerals, chlorite, illite formed at the temperature of 230°C – 260°C and neutral pH. Argillic alteration zones are interpreted as cap rock zones. In conclusion, Acidic advanced argillic alteration zones show that in Kemambang Village, Banyubiru Subdistrict, Semarang Regency is located in the upflow zone with the epidote-chlorite zone below as a reservoir. The Mount Telomoyo area is interpreted as a potential geothermal prospect supported by the existence of hot spring manifestations and the distribution of altered rocks as a result of the interaction of hydrothermal fluid with surrounding rocks through rock fractures and permeability.

Keyword: Alteration zone, Fault Fracture Density (FFD), fluid-rock interaction, Telomoyo.

INTRODUCTION

Increasing demand for energy and rising oil prices, especially in the new millenium, have spurred numerous countries to reduce their dependence on oil by utilizing geothermal energy. Currently geothermal energy has been utilized for electricity generation in 24 countries, including Indonesia. Besides that, geothermal fluid is also used for the non-electricity sector in 72 countries, including heating the room, heating water, et cetera.

Identification of geothermal potential can be done directly, if there are no surface signs, literature studies and field surveys can be carried out. In plain view, geothermal potential is seen through hot springs, warm ground, and fumaroles. While for data collection, the steps taken are collecting maps and data from reports and surveys that have been previously carried out in the area to be investigated, in order to get an overview of geological setting, location of areas where surface manifestations, volcanic phenomena, geology and hydrology in the area are being investigated and then determining the places of survey. The time needed for data collection is very dependent on the ease of obtaining maps and reports on the results of surveys that have been carried out previously, but it is estimated that it usually takes about 1 month. The field survey consists of geological, geophysical, hydrological and geochemical surveys.

Nowadays, with the advancements in technology and exploration efforts, companies are able to more effectively and accurately discover new exploration & exploitation opportunities. The methods in this research includes FFD (Fault Fracture Density) and rock alteration analysis. Faults and fractures on the surface are assumed to be weak areas that turns into thermal fluid flow paths so that they become indicator to the location of the reservoir or reservoir steam zone (Suryantini and Wibowo, 2010).

The Telomoyo geothermal prospect is regionally included in the solo zone which is a quaternary geological environment. The products of Telomoyo volcano are andesite-basaltic lava and pyroclastic rocks. The structure found in the study area is a result of volcanic activity and tectonism, namely in the form of a caldera and normal faults with southwest-northeast trend. The structure and fracture are the initial indications of fluid-rock interactions. This study aims to determine the interaction between fluid and rocks by conducting Fault Fracture Density (FFD) and rock alteration analysis.

METHODOLOGY

This research is conducted by field observation, data collection obtained from previous studies, software processing and literature studies. Data were obtained from previous literature and researches with topics related to Fault Fracture Density (FFD) and alteration zone. The data that has been collected is then processed so that it can be developed to the next phase. In order to create research works that can be utilized widely it is required to do the following stages of data processing which includes: a) Examination of data, Data that has been collected is then checked whether it is complete in order to support the hypothesis to be presented in this study. b) Data analysis, Data obtained is then analysed quantitatively or mathematically using software data processing so as to obtain an objective result which is then continued with a qualitative analysis or conveying interpretation based on data that has been obtained. c) Conclusion and further project development, Data that has been analyzed is then drawn conclusions that can generate a new innovation that may be applied or researched further.

GEOLOGICAL SETTING

Based on the physiography, Telomoyo Mountain Complex is included in the Solo Zone. Rows of Merapi-Telomoyo Volcano occupies the western end of the Solo Zone (Bemmelen, 1949). This zone is formed on a volcanic complex that extends northwest-southeast direction, namely the series of Mount Ungaran - Mount Telomoyo - Mount Merbabu - Mount Merapi which is in the environment of Quaternary volcanic geology.

Mount Telomoyo is formed above the ruins of the slopes of Mount Soropati (1300 meters). Gunung Soropati is volcano in the Ungaran Soropati-Merbabu-Merapi row, according to Bemmelen (1941), was active in the Middle-Upper Pleistocene era which later collapsed due to eruption and collapse on the eastern slope and left a U-shaped depression. Mount Soropati is currently only a wall of the caldera, then before the Holocene, Mount Telomoyo (1894 masl) was formed in Soropati's ruined wall. According to Bemmelen, in 1949 the origin of magma from Mount Soropati was olivine basaltic, whereas in Telomoyo it had been differentiated to become more acidic (augite-hypersthene-hornblende andesites).

From the regional stratigraphic and tectonic point of view, it shows that Meratus pattern is the oldest pattern. The faults included in this pattern are Cretaceous to Paleocene and are scattered in the Karimun Jawa Tinggian through Karang Sambung to the Cimandiri area of West Java. This fault is reactivated by younger tectonic activity. The Sundanese pattern is younger than the Meratus pattern. Seismic data shows the Sunda Pattern has reactivated Meratus patterned faults in the Late Eocene to the Late Oligocene. The Javanese pattern shows the youngest pattern and reactivates all existing patterns (Pulunggono, 1994). Seismic data shows that the upward fault pattern with the west-east direction is still active today.

DATA AND RESULTS

Structure Analysis

Based on lineament analysis, four main structures were found, namely in the direction of N270-290°E, N70-90°E, N25-40°E, and N330-350°E. Lineament analysis shows the dominant structure trend in WNW-ESE. The FFD analysis map is a composite map of fault, fracture densities and fracture pieces density maps. From this map it can be delineated to areas with high fracture densities. The area can be used as a basis for determining prospect areas or geothermal manifestations. After delineating, result was found for areas with high fracture density, which is the area located on the NE and NW of Mount Telomoyo and in the SW area of Dukuh Temple. Areas with high density are interpreted to have high permeability. In Dukuh temple area, there were hot spring manifestations with temperatures around 35-36 °C. Figure 1 shows the FFD result.

Alteration Analysis

In addition to geothermal manifestations in the surrounding area of Mount Telomoyo, it was found that there were altered rocks, namely in the sub-district of Banyubiru which is the prospect of geothermal at Mount Telomoyo. In this area, two alteration zones were identified, namely argillic alteration - advanced argillic alteration and propitious alteration. Argillic-argillic alteration is further characterized by the presence of alunite, kaolinite, smectite, illite with a formation temperature of 150-200°C (Table 1 and 2) and acidic pH conditions ranging from acidic - slightly acidic. Figure 2 shows the Further altered argillic-argillic alteration with altered clay minerals. Figure 3 shows the Propylitic alteration with epidote minerals and chlorite changes from olivine and pyroxene and there are altered clay minerals from plagioclase.

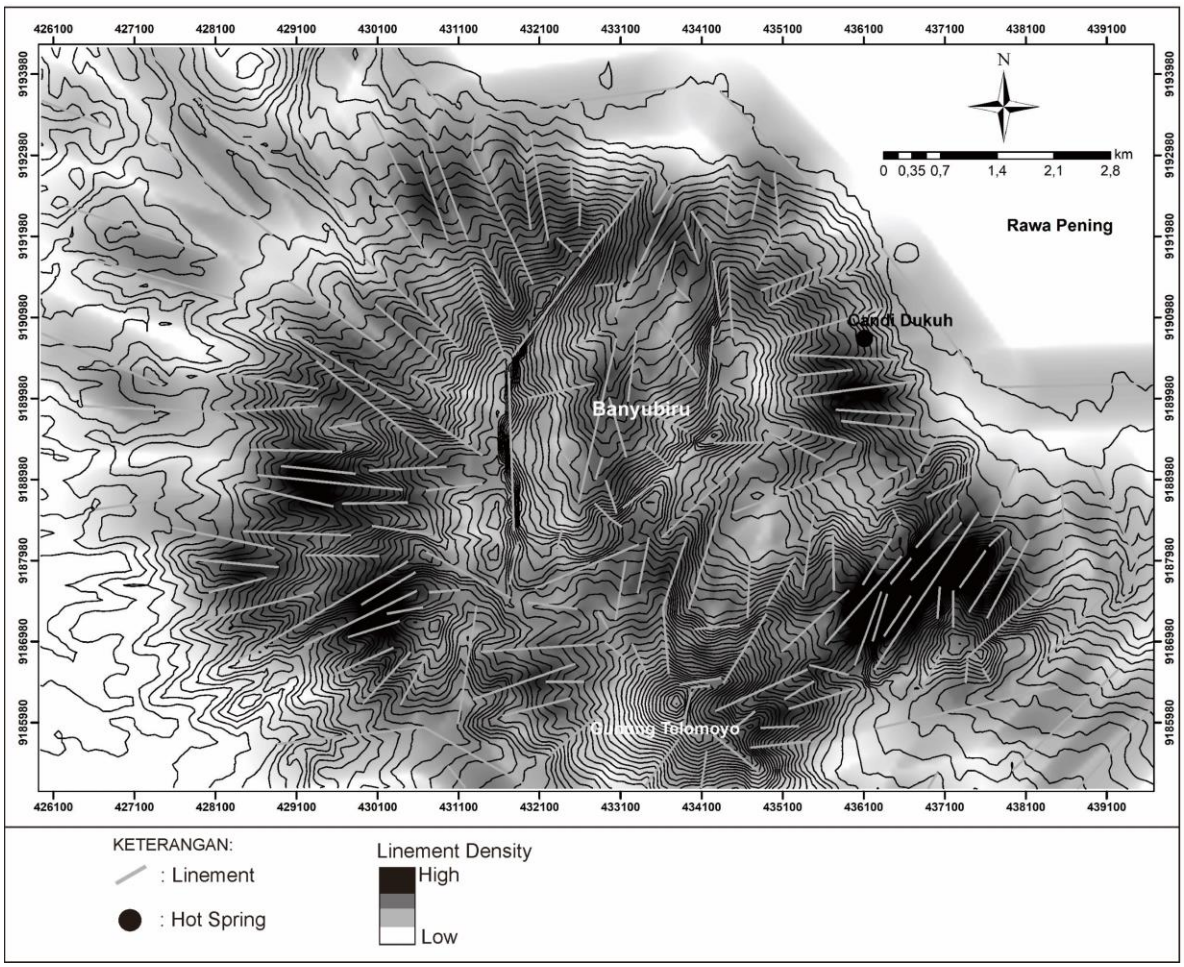


Figure 1: FFD result after post-processing in software.

Table 1: Genesis temperature of kaolinite, alunite, anhydrite.

Suhu Pembentukan (oC)						
	50	100	150	200	250	300
Kaolinit	←	—	—	—	- - -	
Alunit	←	—	—	—	—	—
Ilit			- - -	- - -	- - -	—
Smektit				- - -	- - -	
Anhidrit				←	—	—

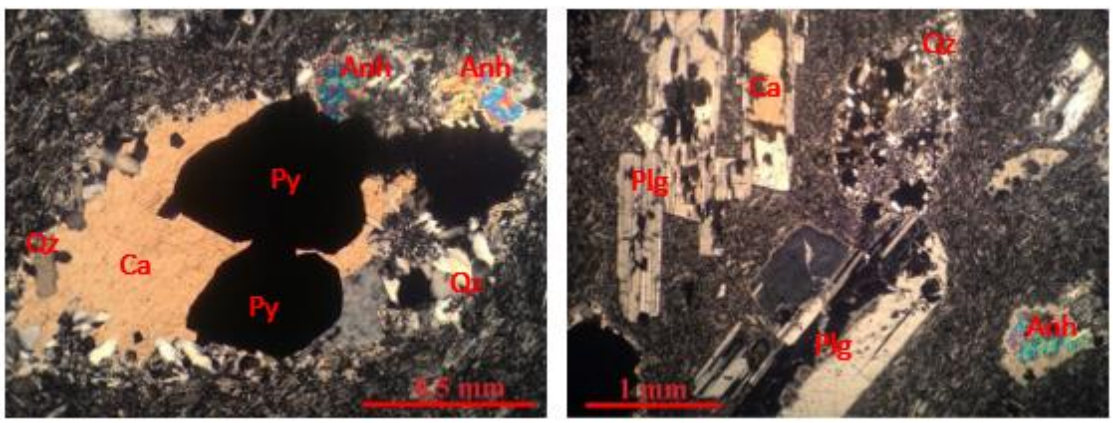


Figure 2: Further altered argillic-argillic alteration with altered clay minerals from plagioclase and anhydrite.

Table 2: Propylitic alteration is characterized by epidote, chlorite and illite minerals with a formation temperature of 230°C - 260°C and neutral pH.

Suhu Pembentukan (oC)						
	50	100	150	200	250	300
Epidot						
Klorit						
Ilit						

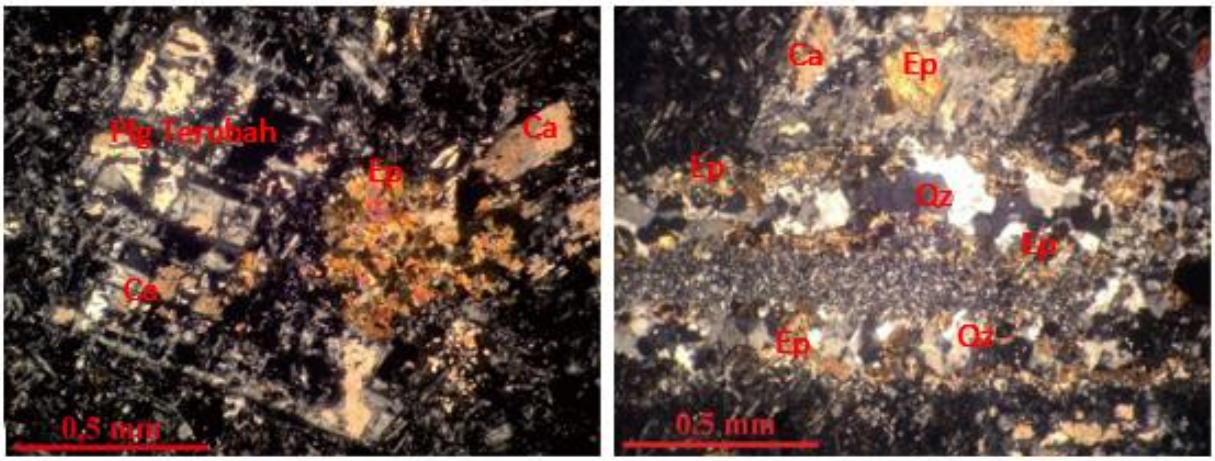


Figure 3: Propylitic alteration with epidote minerals and chlorite changes from olivine and pyroxene and there are altered clay minerals from plagioclase.

DISCUSSION

Further altered argillic - argillic alteration shows the dominant composition of kaolinite and smectite clay minerals. Impermeable clay minerals are interpreted as veil rocks in geothermal systems. Whereas propylitic alterations have high temperatures and there are epidote minerals as a characteristic of reservoirs in geothermal systems. The Mount Telomoyo area is interpreted as a geothermal potential supported by rock fractures and permeability.

CONCLUSION

Mount Telomoyo which consists of telomoyo volcanic rocks has undergone alterations to form advanced argillic-argillic alteration zones and propylitic alteration. Based on the results of FFD analysis, it shows that high density areas in the NE area from the slopes of the Telomoyo Mountain reach Dukuh Temple area and there are also in the NW area of the slopes of Mount Telomoyo. This shows that Mount Telomoyo area has a geothermal prospect and the FFD method is effectively used in the initial stages of exploration after a field survey.

REFERENCES

Browne, P., R., L., (1978). "Hydrothermal Alteration in Active Geothermal Fields". Annual Reviews Incorporated. Earth Planet Sci. Vol. 6: 229-50. www.annualreviews.org

Hermawan, D., Kholid, M., 2010. "Penyelidikan Terpadu Daerah Panas Bumi Candi Umbul-Telomoyo, Provinsi Jawa Tengah". Prosiding Hasil Kegiatan Pusat Sumber Daya Geologi, Buku 1: Bidang Energi.

Hermawan, D., Rezky, Y., (2011). "Deliniasi Daerah Prospek Panas Bumi Berdasarkan Analisis Kelurusan Citra Landsat di Candi Umbul-Telomoyo, Provinsi Jawa Tengah". Buletin Pusat Sumber Daya Geologi, Vol. 6, No.1.

Hutami, R., T., Aribowo, Y., Widiarso, D., A., (2014). "Studi Pendahuluan Daerah Prospek Panasbumi Berdasarkan Data Manifestasi Panasbumi, Geokimia, dan Isotop Fluida Panasbumi Komplek Gunung Telomoyo, Kabupaten Semarang, Jawa Tengah". Geological Engineering E-Journal Vol. 6, No. 1.

Hochstein, M., P., Browne, P., R., L., (2000). "Surface Manifestations of Geothermal System with Volcanic Heat Sources". dalam Sigurdsson, H., ed., Encyclopedia of Volcanoes. 835-855. Academic Press: USA

Lagat, J., (2007). "Hydrothermal Alteration Mineralogy in Geothermal Fields with Case Examples from Olkaria Domes Geothermal Field, Kenya". Presented at Short Course II on Surface Exploration for Geothermal Resources, organized by UNU-GTP and KenGen, at Lake

Naivasha, Kenya (United Nation University-Geothermal Training Programme)

Reyes, A., G., (2000). "Petrology and Mineral Alteration in Hydrothermal Systems: from Diagenesis to Volcanic Catastrophes". ISBN: 9979-68-048-2. United Nations University, Geothermal Training Programme: New Zealand.

Saptadji, N., M., (2001). "Teknik Panasbumi". Bandung: ITB Press.

Thompson, A., J., B., Thompson, J., F., H., (1996). "Atlas of Alteration: A Field and Petrographic Guide to Hydrothermal Alteration Minerals". ISBN: 0-919216-59-5. Mineral Deposits Divison, Geological Association of Canada: Canada.

Budiardjo. (1997). "Resource Characteristic of the Ungaran Field, Central Java Indonesia". Geological Engineering Mineral Technology Faculty, UPN "Veteran", Yogyakarta.

Pulunggono, A., Martodjojo, S., (1994). "Perubahan tektonik Paleogen – Neogen merupakan peristiwa terpenting di Jawa". Proceedings Geologi dan Geotektonik Pulau Jawa.

Bemmelen, R., W., Van. (1949). "The Geology of Indonesia". Vol. 1 A, Government Printing Office, The Hauge.

Suryantini, Wibowo, H., (2010). "Application of Fault and Fracture Density (FFD) Method for Geothermal Exploration in Non-Volcanic Geothermal System; a Case Study in Sulawesi-Indonesia". Proceedings World Geothermal Congress 2010, Bali.

NEW GEOTHERMAL EXPLORATION CONCEPT BASED ON CIRCULAR FEATURE OF LOW BOUGUER ANOMALY: MAGNETOTELLURIC DATA OF WEST JAVA GEOTHERMAL PROSPECT AREA AS THE EVIDENT OF NEW GEOTHERMAL EXPLORATION

Eddy Gaffar, Yayat Sudrajat, and Haryadi Permana

Research Center for Geotechnology, Indonesian Institute of Sciences (LIPI)
Email: Eddy_gaffar@yahoo.com

ABSTRACT

Indonesia has the largest geothermal prospect in the world. It was about 285 geothermal potential locations and 28.000 MW. The current installed capacity is 1,341 MW which put Indonesia in the third position in the world after the US (3,039 MW installed capacity) and the Philippines (1,904 MW). Most of them are concentrated in Java and Sumatera. Geothermal in Java is still influenced by the subduction of oceanic plates from the south of Java island that forms the southern mountains. From a geophysical point of view there is still no new concept that accelerates the process of geothermal exploration. Problem of geothermal exploration was long time to search the prospect area like to search manifestation area from local people, Geological Survey, Geochemical Survey, Geophysical Survey from very regional area that be expected become the prospect area. The new concept is from gravity analysis which is from Bouguer anomaly data from Java Island show circular feature that supposed to be "ancient crater" or hidden caldera. By this geophysical method, it could be simpler to explore geothermal prospect in West Java. Around the small circular feature, there are some large geothermal prospect area such as Guntur, Kamojang, Darajat, Papandayan, Karaha Bodas, Patuha. This concept will try to apply to explore geothermal in Java Island for next future work.

West Java has the largest potential area in Indonesia where approximately 21.7% are located in West Java, spread over 44 locations 11 districts. Geothermal is a reliable energy for West Java. In 2004, the contribution of West Java geothermal energy to the national of 749 MW from the total 807 MW (92.81%), came from 4 PLTP namely Kamojang (140 MW), Awibengkok G. Salak (installed 6 x 55, raised 354 MW), Darajat (145 MW) and Wayang Windu (110 MW).

From the result of this low Bouguer gravity anomaly in central part of West Java shown two circular feature which is big and small circles in the rim of big circle, there are some geothermal prospect areas like Tangkuban Perahu, Ciater, Kamojang (235 MW), Wayang Windu (400 MW), Papandayan, Karaha (70 MW) Talaga Bodas (120 MW), Cikuray, Guntur-Masigit (70 MW), Patuha (190 MW), Ciwidey (140 MW), while in the rim of small circle, also there are some geothermal prospect areas like Kamojang, Darajat, Guntur Masigit, Papandayan, Cikuray, Tampomas, Ciarinem, Cilay, Cibuni, Galunggung, Papandayan.

Keywords: Geothermal, magnetotelluric, gravity, West Java.

INTRODUCTION

Indonesia has largest geothermal prospect in the world (Poernomo, 2015). Indonesia has many resources of geothermal energy derived from volcanic and non-volcanic rock. Indonesia has 285 Geothermal locations with a potential total output of 28 GW of electrical energy, one of the biggest in the world. The current installed capacity is 1,341 MW which put Indonesia in the third position in the world after the US (3,039 MW installed capacity) and the Philippines (1,904 MW). Therefore, to develop the energy potential that can be used as an alternative energy besides oil and gas, more detailed research is required. Referring to the National Energy Road Map, the Indonesian government is targeting that use of geothermal energy should be increased from 807 in 2005 MWe to 9,500 MWe by the year 2025. This target is part of new and renewable energy targets. The development of geothermal projects in Indonesia had been a challenge but with the new Law on Geothermal Energy, it is estimated that the geothermal project progress will also be accelerated.

Indonesia's geothermal is concentrated in Java and Sumatera (Hochstein and Sudarman 2008, Mansoer and Idral, 2008, Nasution and Supriyanto, 2011). Geothermal on Sumatra island is generally controlled by Sumatera fault either the main fault or second or third order fault (Hermawan and Kholid 2010, Gentana et al., 2017, Nukman 2014, Ganefianto et al. 2015). Geothermal in Java is still influenced by the subduction of oceanic plates from the south of Java island that forms the southern mountains extending from West Java to East Java. From a geophysical point of view there is still no new concept that accelerates the process of geothermal exploration. The usual exploration concept is that geothermal is located around the volcano (referred to as the volcano as host) and is located around the fault (fault as host) Purnomo et al., 2014). There is another exploration concept that is from remote sensing analysis (Gaffar and Ismayanto, 2010).

West Java has the largest potential area in Indonesia where approximately 21.7% are located in West Java, spread over 44 locations 11 districts. Geothermal is a reliable energy for West Java. In 2004, the contribution of West Java geothermal energy to the national of 749 MW from the total 807 MW (92.81%), came from 4 geothermal area namely Kamojang (140 MW), Awibengkok G. Salak (installed 6 x 55, raised 354MW), Darajat (145MW) and Wayang Windu (110MW) (West Java Province Book of Geothermal and Mineral, 2010).

Problem of geothermal exploration was long time to search the prospect area like to search manifestation area from local people, geological, geochemical and geophysical survey from very regional area. With the concept of circular feature of low anomaly gravity, it will be cutting the series of geothermal exploration that should be done.

MAGNETOTELLURIC (MT) DATA OF WEST JAVA GEOTHERMAL PROSPECT AREA

For the purpose of geothermal potential, the two-dimensional cross-sectional type of measurement using the MT means that in general the resistance type value can be divided into three parts, low resistance (below 30 Ohm-m), medium resistance (30 - 300 Ohm-m) and high resistance (greater than 300 Ohm-m). The cross section of four geothermal prospect areas in West Jawa, we can see on Figure 1.

Darajat Geothermal

Transformation of smectite to illite at shallow depths and the occurrence of amphibole in thin section (both in disagreement with down hole temperature) reveal the presence of multiple geothermal events in the history of the Darajat field associated with a heat source of more than 280°C (Hadi, 2001).

Integrated geology, geochemistry and geophysics data show numerous similarities in the characteristics between Darajat and the other known geothermal system. Similar to the Geysers, the Darajat vapor system evolved from a liquid dominated environment with a heat source of more than 280° Celsius and has cool to the present temperature of 240° Celsius. Petrography work showed that alteration clays and minerals deposited by the up flowing fluids from the past liquid system have significant control on the plumbing and fluid paths of the vapor system (Nasution et al., 2004).

Karaha - Talaga Bodas Geothermal

The results of magnetotelluric data processing and interpretation indicate that the geothermal system in the research area is composed of shielding layer zone (≤30 Ωm), reservoir zone (>30 Ωm - ≤300 Ωm) and heat source zone (>300 Ωm) and supported by the fracture. The subsurface model has a complete geothermal system component that has a shielding zone, a reservoir zone, a heat source zone and several fractures. Karaha - Talaga Bodas area can be divided into two geothermal system that is geothermal system of Karaha and geothermal system Telaga Bodas.

Karaha Bodas area needs more detailed research to get high resolution from the analysis. Around the prospect area Karaha- Talaga Bodas is still there are some other prospect areas so it should also be examined fluid flow so as not to affect each other's reservoir with each other.

Papandayan – Guntur Geothermal

From the 2D model the magnetotelluric resistivity of the Leles-Papandayan trajectory shows that on the northern part (Leles) near the surface of the high enough resistance type (500 Ohm-m) which is lava while below it to 0 m is a rock with moderate resistance (50-350 Ohm-m), underneath there are rocks with lower resistivity at altitudes of 0 to 1000 m asl with magnitude resistance type 20 - 30 Ohm-m. Starting from the depth of -2000 m above sea level there are rocks with high type resistance up to 5000 Ohm-m. The high type of resistance is interpreted as a heat-containing rock such as volcanic rock which is a source of heat. Rocks with low resistance as seen at cross-sections below GRT-03 and GRT-04 measurements from surface to altitude of -700m above sea level with a resistance value of between 0 and 20 Ohm-m are interpreted as cover rocks such as impermeable alteration rocks. GRT-03 and 04 measurement areas are very close to Guntur and Cipanas mountains where there is hot water location as one of the geothermal manifestations. Similarly, in the southern part (Papandayan) there are rocks with low type resistance (0 - 20 Ohm-m) from the surface to a height of -1000 masl which is interpreted as a teratterated rock area. While rocks with high type resistance up to 5000 Ohm-m exist at altitudes of -1000 to -1500 m which are interpreted as heat-producing rocks. In this area it is in fact an area where there are small craters in the west from the point of measurement of GRT-10 with the manifestations of hot water, solfatar and sulfur. So, the heat source in the Papandayan area is shallower than the heat source in the geothermal prospect area Guntur - Masigit.

CONCLUSION

From the Gravity Bouguer Anomaly of West Java, it seems the Circular Feature low gravity anomaly which is supposed to be "ancient crater". Ancient crater means not always identical to the volcanic crater as it exists today, but sometimes it is a hidden caldera. From the rim of the circular feature, there are some area of high potential of geothermal energy.

In West Java area, there are some potential area that come from small and big circular feature i.e., Tampomas, Tangkuban Perahu, Darajat, Kamojang, Wayang Windu, Patuha, Guntur, Karaha Bodas, Papandayan, Cilayu and Ciarinem.

This circular feature of low anomaly Bouguer gravity, could become the way how to explore geothermal with geophysics methods, and should be check for another area in Java Island for the future research.

ACKNOWLEDGEMENTS

The research was conducted by the Research Center for Geotechnology, Indonesian Institute of Sciences (LIPI). The researcher would like to thank to Ministry of Research Technology and Higher Education Republic of Indonesia for the cost of the seminar. Therefore, the researcher would like to thank PT Geodipa Energy for the permission to get MT acquisition in the PT Geodipa Energy area. Likewise, he would like to thank his colleagues who have helped in field data collection and processing, among others, Mr. Yayat Sudrajat and Sunardi.

REFERENCES

Poernomo, A., Satar, S., Effendi, P., Kusuma, A., Azimudin, T., Sudarwo, S., (2015), "An Overview of Indonesia Geothermal Development – Current Status and Its Challenges", Proceedings World Geothermal Congress 2015 Melbourne, Australia, 19-25 April 2015.

Hochstein, M., P., Sudarman, S., (2008). "History of geothermal exploration in Indonesia from 1970 to 2000". Geothermics 37(3): 220-266.

Mansoer, W., R., Idral, A., (2015), "Geothermal Resources Development in Indonesia: A History", Proc. World Geothermal Congress 2015, Melbourne.

Nasution, A., Supriyanto, E., (2011), "Current Status and New Geothermal Development Areas in Indonesia", Proceedings of the 9th Asian Geothermal Symposium, 7-9 November 2011.

Hermawan, D., Kholid, M., (2010), "Penyelidikan Terpadu Daerah Panas Bumi Candi Umbul-Telomoyo, Provinsi Jawa Tengah". Prosiding Hasil Kegiatan Pusat Sumber Daya Geologi, Buku 1: Bidang Energi.

Gentana, D., Sukiyah, E., Sulaksana, N., Yuningsih, E., T., Balia, L., (2017), "Determination of Tanggamus Geothermal Prospect Area, Lampung Province, South Sumatra Based on Remote Sensing and 3D Micromine Software", FIG Working Week 2017 Surveying the world of tomorrow - From digitalisation to augmented reality Helsinki, Finland, May 29–June 2, 2017.

Nukman, M., (2014), "Geothermal exploration involving structural geology and hydrochemistry in the Tarutung Basin, Northern Central Sumatra (Indonesia)", desertation on der Technischen Universität Berlin zur Erlangung des akademischen Grades Doktor der Naturwissenschaften.

Ganefianto, N., von Hirtz, P., Easley, E., (2015), "A Brief History of the Sarulla Geothermal Field Development", GRC Bulletin March/April 2015.

Purnomo, B., J., Pichler, T., (2014), "Geothermal systems on the island of Java, Indonesia", Journal of Volcanology and Geothermal Research 285, 47–59.

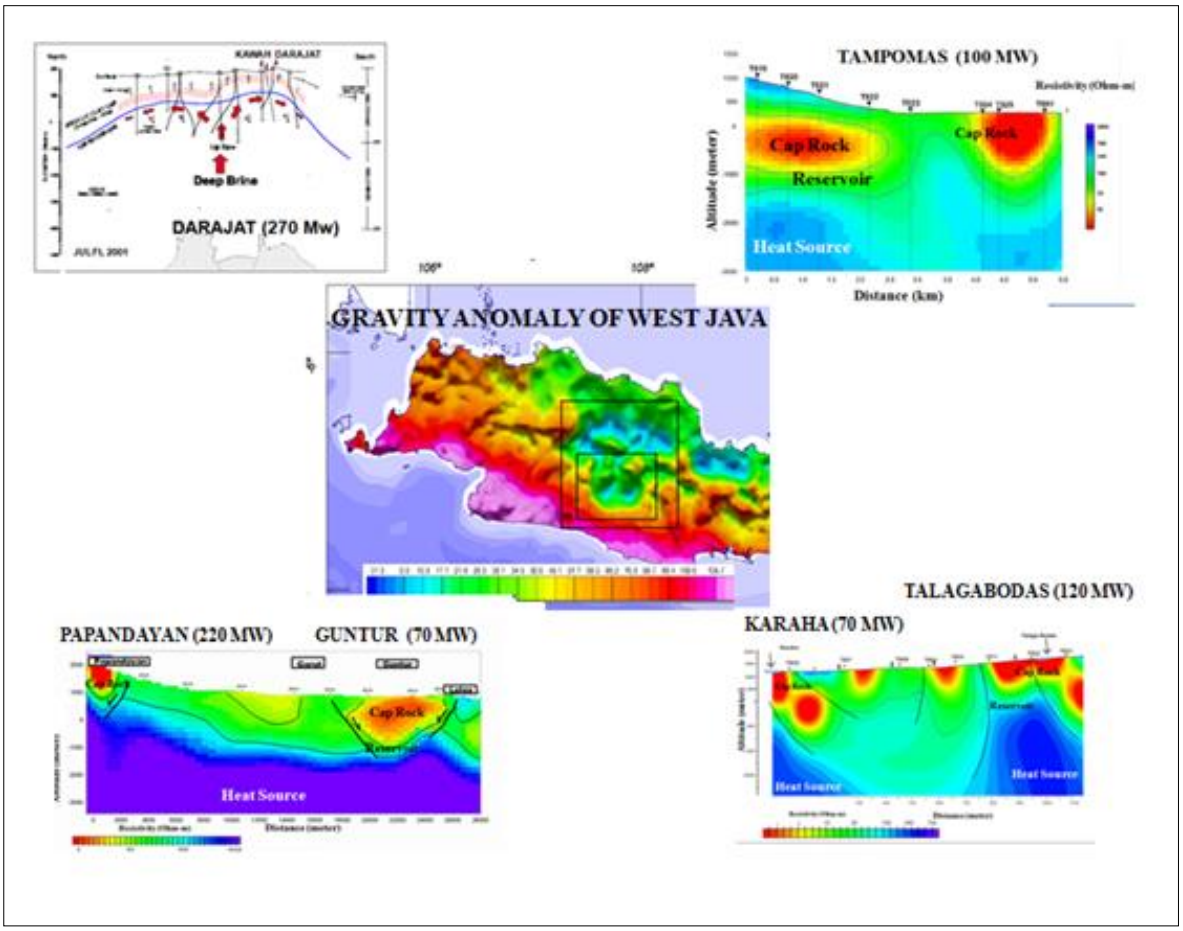


Figure 1: The cross section of four geothermal prospect areas in West Java.

KEPAHIANG GEOTHERMAL VOLUMETRIC POTENTIAL USING MONTE CARLO SIMULATION

Wisnu Ardhi Nugroho, Arino Mangihut Tua Sitanggang, and Daniel Marpaung, Ivan

UPN "Veteran" Yogyakarta
Jl. SWK 104 (North Ring Road) Condongcatur, Yogyakarta
Email: wisnuardhinugroho@gmail.com

ABSTRACT

Kepahiang geothermal working area is one of Indonesia's geothermal prospects located in Bengkulu province with tender preparation or assignment status. Based on various exploration and investigation activities have been conducted, this field is estimated to have great potential. In each geothermal field development, potential assessment is a very important activity. In the early phase, volumetric methods is preferred and widely used in calculating geothermal potential. However, this method has a low accuracy as it applies a single value number in the calculations. Due to data limitations and high uncertainty, the calculation of the geothermal potential of the Kepahiang working area using Monte Carlo simulation to solve the problem. All the parameter input for the simulation obtained from exploration survey that were supported by several correlations and closest reference fields within the span of minimum, most likely, and maximum triangular or rectangular distribution. The simulation will show a number of results from each distributed parameter with the values of P10, P50, and P90 those are 58.73 Mwe, 165.26 MWe, and 384.03. The P50 value is assumed as the representing value of Kepahiang geothermal field potential as the most likely resource capacity. This result is close to the calculation of the potential that has been done which is stated in the book of potential volume I (2017) geothermal potential of 180 MWe.

Keywords: Resource assessment, heat stored method, Kepahiang geothermal field, Monte Carlo simulation

INTRODUCTION

Geothermal Energy is one of the new and renewable energy potentials to be developed. According to Badan Geologi (2017), Indonesia's geothermal resources estimated have a potential of 11.073 GW with reserves of 17.435 GW spread across 342 locations. The utilization of geothermal energy in Indonesia began 35 years ago with the operated of the Kamojang PLTP in 1983. Until now, there are

13 PLTP was operating with a total capacity of 1948.5 MWe or around 7% of the potential.

Geothermal energy is environmentally friendly energy. The utilization of geothermal energy expected to reduce greenhouse gas emissions. Therefore, geothermal energy utilization targeted to reach 7,241 MWe in 2025 and 17,546 MWe by 2050.

The development of geothermal industry requires a continuous process and large investment. Before it can be used commercially, a comprehensive study needed to assess whether the field is prospect. This is done through exploration activities which are integration of various surveys includes geology, geochemistry, geophysics and hydrology.

The purpose of this paper is to estimate the potential of geothermal energy in Kepahiang Bengkulu Field volumetric potential using Monte Carlo Simulation.

GEOLOGICAL FINDING AND REVIEW

The Kepahiang area is located on the subduction lane in the western Sumatra magmatic arc region of the tectonic order of Western Indonesia.

The morphology of the investigation area is grouped into four geomorphological units, consisting of: Puncak Kaba geomorphology unit, Body geomorphology unit (Taba Penanjung, Malintang and Kaba), Kaki Kaba geomorphology units and plain geomorphological units.

The stratigraphy of the investigation area was compiled by the results of four eruption source centers consisting of G. Taba Penanjung, G. Malintang, G. Danau Mas consisting of Komplek G. Kaba having at least eight eruption centers (eruption points), from old to young consisting of G Kaba Tua, Sinder Cones, G. Biring, Mount Bukit Itam, Mount G. 1960, G. Salojuang, G. Penyeluan, and G. Kaba Muda. The rock unit consists of dense, andesitic and basaltic andesitic lavas, pyroclastic fall and flow, lava and surface deposits.

The age of the yield of rocks in young Kaba lava is ± 500,000 years ago (Lab. PSG, 2010). Structure that develops in the area of investigation was Ring fracture, the fault trending northwest - southeast, the fault trending southwest - northeast and the fault trending north - south. The cesarean fault is related to the appearance of geothermal manifestations.

HEAT STORED METHOD

The heat stored method is also called volumetric method is the most commonly used method in estimating the potential of a geothermal field in the early exploratory stage of geothermal development. This method is used to estimate the static energy of the reservoir and provide an initial indication of how much energy can be obtained on the surface and converted to electricity. The potential is estimated based on the heat content stored in reservoir rocks and fluid while excludes all dynamic changes during production, mass balance, permeability, reinjection, injection, pressure change, enthalpy increase or other dynamic conditions (Navas & Pipan, 2015). There are two methods to determine volumetric potential of geothermal fields, i.e. using lumped parameter model and Monte Carlo method. The lumped parameter model assumes that the reservoir has box-shaped with a certain area and thickness and homogeneous which only has one single value parameter (Supriyadi, Srigutomo, & Munandar, 2012). While Monte Carlo method considers the heterogeneity of reservoir parameters.

The general equation used to determine the volumetric potential (in MWe) of a geothermal reservoir produced for t years is given by:

$$H_{el}= \frac{Ah\{(1-\phi)\rho_r C_r+\phi\rho_L C_L\}(T_i-T_f)R_{fn}\eta}{t \times 365 \times 24 \times 3600 \times 1000} \quad \ldots\ldots\ldots\ldots (1)$$

where:

H_{el} = Resource capacity (MWe)
A = Reservoir area (m2)
H = Reservoir thickness (m)
ϕ = Porosity
ρ_r = Rock density (kg/m3)
ρ_L = Fluid density (kg/m3)
C_r = Rock specific heat (kJ/kg^{o}C)
C_L = Fluid specific heat (kJ/kg^{o}C)
T_i = Reservoir average temperature, (^{o}C)
T_f = Reservoir abandon temperature (^{o}C)
R_f = Recovery factor
η = Conversion efficiecy
t = Plant life (year)

MONTE CARLO METHOD

It is a method for calculating volumetric geothermal energy reserves that has been proposed in the middle of the 20th (Metropolis & Ulam, 1949). The Monte Carlo method is growing rapidly and is popular in assessing geothermal potential at the exploration stage because it considers reservoir heterogeneity compared to descriptive methods that only use a single value parameter number to represent the entire reservoir. Reservoir heterogeneity is estimated by using a random number from the model input parameters to solve the problem based on a particular mathematical equation. The random number can be obtained using formula = RAND () in Ms Excel (Utami, 2015). This formula will get a random number as many as the desired iteration.

Monte Carlo simulation consists of several stages. It starts with determining input parameters as maximum, minimum, and most likely values (Table 1). After obtaining all the parameters needed for the calculation, specify the type of distribution for each parameter. The types of distribution commonly used are rectangular and triangular distribution.

Rectangular distribution is used when there are 2 input parameter variables. The parameter values for each iteration use the following equation:

$$X_{@Rn}=X_{min}+Rn\ (X_{max}-X_{min}) \quad \ldots\ldots\ldots\ldots\ldots\ldots (2)$$

Triangle distribution is used when there are 3 input parameter variables. The parameter value for each iteration is using the following equation:

$$X_{@Rn}=X_{min}+\sqrt{Rn\ (X_{max}-X_{min})(X_{most}-X_{min})} \ldots (3)$$

if the random number value is lower than the median value and,

$$X_{@Rn}=X_{max}-\sqrt{(1-Rn)\ (X_{max}-X_{min})(X_{max}-X_{most})} (4)$$

if the random number value is higher than the median value.

Median value can be find using the following equation:

$$Median=\frac{X_{most}-X_{min}}{X_{max}-X_{min}} \quad \ldots\ldots\ldots\ldots\ldots\ldots\ldots\ldots (5)$$

Median value above is not the actual median of uncertain parameter. It is actually the random number that will generate median of the parameter as the equation above is being calculated.

where:

$X_{@Rn}$ = Value of parameter at random number
X_{min} = Minimum value of parameter
X_{max} = Maximum value of parameter
X_{most} = Most likely value of parameter
Rn = random number

Each set of parameter values obtained from a number of simulations were run repeatedly and analyzed statistically. The distribution of simulation output is presented in histogram that describes the frequency distribution and cumulative frequency distribution. Distribution frequency graphs will provide information about the relative probability value, most likely value, and distribution form. While the cumulative frequency graph can give a probability of a certain value. The analysis results can provide an overview of the potential of geothermal field.

INPUT PARAMETERS

Prospect Area

The prospect area of the Kepahiang geothermal field based on the results of the geoscience survey compilation is 32 km^2 (Sugianto & Kristianto A.W., 2011). Whereas based on survey gravity sounding and interpretation of the geological structure as shown in Figure 1, the prospect zone has an area of 22 km^2 which is indicated by a resistivity value of <10 ohms-m as cap rock response.

Reservoir Thickness

By determining economic drilling depth of 3000 m, the distribution of reservoir thickness is seen from the analysis of the magnetotelluric survey map (Figure 2) for the minimum, most likely, and maximum values those are 500 m (line A), 1000 m, and 1250 m (line B).

Temperature Reservoir

Based on the gas geothermometer method using Diagram CAR-HAR (Ulfa, Hutabarat, Firmansyah, & Patonah, 2016) as shown in Figure 3, reservoir temperature of Kepahiang geothermal field is 250ºC. While according to the survey of temperature slope that has been carried out, the reservoir temperature is 306ºC (Rezky & S.L.Simarmata, 2013). Then, based on the graph of the trendline for evaluating the average temperature reservoir of geothermal fields in Indonesia at the exploration stage (Hochstein & Sudarman, 2008) as shown in Figure 4, the reservoir temperature of the Kepahiang geothermal field is 273ºC.

Porosity (ϕ)

The geothermal reservoir rock porosity is assumed from the nearest geothermal exploitation field which has the same reservoir rock type which is andesite. The porosity of the Hululais geothermal working area located 41 km from Kepahiang geothermal field is 5-12% (Kamah et al., 2015) and Lumut balai geothermal working area with a distance of 71 km is 8% (Atmojo, 2017).

Density and Capacity of Hot Rock Reservoir

The heat density and capacity of the Kepahiang geothermal field reservoir is 2500 kg / m3 and 1.1 kJ/kgºC which is determined based on the nearest field (Lumut Balai) which has the same reservoir rock type. (Atmojo, 2017)

Recovery Factor (RF)

RF values are determined based on Correlation between recovery factor and porosity by Muffler (1978) (Figure 5) as a function of reservoir rock porosity (Sarmiento & Steingrimsson, 2008). Those are 12.5%, 20%, and 30%.

Electricity Conversion Efficiency (η)

It is obtained from Correlation between thermal conversion efficiency and reservoir temperatures by Nathenson (1975) and Bodvarsson, (1974) as reservoir temperature function (Sarmiento & Steingrimsson, 2008). The plot results show that the value of the electricity conversion efficiency of 11.75%, 12.67% and 14.09% as shown in Figure 6.

Initial and Final Saturation

It is obtained from the nearest field (Lumut Balai geothermal working area) with initial water saturation is 0.8 and final water saturation is 0.3. (Atmojo, 2017)

Plant Life

Determination of plant life based on SNI 6482: 2018 which is targeted to operate for 30 years. ([BSN] Badan Standarisasi Nasional, 2018)

RESULT AND DISCUSSION

Determination of the static potential of a geothermal field has been conducted by considering the input parameter calculation from the exploration survey that has been previously identified. potential calculations using volumetric methods combined with Monte Carlo simulations where the uncertainty of input parameters is statistically evaluated produces satisfactory output.

Montecarlo simulation is run 5000 times and produce a set of values for each parameter with varying distribution parameters. By simulating the defined input parameters (Table 2) the results of the analysis are obtained as frequency distribution graph and cumulative frequency distribution graph as shown in Figure 7. It can be seen that the potential generated has a range of 58.73 MW to 384.03 MWe with the highest value / most likely parameters appears at 165.26 MWe. These results refer to the cumulative frequency calculated at 10%, 50%, and 90%. By using the values that most likely value for each parameter as input parameters in the volumetric method, the static potential of the Kepahiang geothermal field is 165.26 MWe. Whereas in volume I (2017) the geothermal potential book is 180 MW.

CONCLUSION

Based on the calculations and analyzes that have been carried out, the most likely geothermal potential is 165.26 MWe. This results is close to the calculation of the potential that has been done which is stated in the book of potential volume I (2017) geothermal potential of 180 MW. The results of this potential assessment are considered satisfactory by the author.

REFERENCES

[BSN] Badan Standarisasi Nasional. (2018). "SNI 6482:2018 Parameter dalam estimasi potensi energi panas bumi". Serpong: BSN.

Atmojo, J. P. (2017). "Thermodynamic Model of Geothermal Reservoir at Lumut Balai Field, Sumatera, Indonesia". 3rd International Exchange and Innovation Conference on Engineering & Sciences (IEICES), 173. Fukuoka.

Hochstein, M. P., & Sudarman, S. (2008). "History of geothermal exploration in Indonesia from 1970 to 2000". Elsevier, 37, 257. https://doi.org/10.1016/j.geothermics.2008.01.001

Kamah, M. Y., Palmelay, A. C., Rahardjo, I. B., Thamrin, M. H., Hartanto, D. B., Silaban, M. S., & Sasradipoera, S. D. (2015). "Successful Exploration Campaign and to be Developed in Hululais Geothermal Field, Bengkulu Indonesia". Proceedings World Geothermal Congress 2015, 7. Melbourne.

Metropolis, N., & Ulam, S. (1949). "The Monte Carlo Method". Journal of The American Statistical Association, 44(247), 335.

Navas, H. F., & Pipan, M. (2015). "Methods of Early Geothermal Energy Resource Assessment – A Modern Conceptual and Mathematical Model". Proceedings World Geothermal Congress 2015, (April), 1. Melbourne.

Rezky, Y., & S.L.Simarmata, R. (2013). "Landaian Suhu Daerah Panas Bumi Kepahiang Provinsi Bengkulu". Buletin Sumber Daya Geologi, 8, 127.

Sarmiento, Z. F., & Steingrimsson, B. (2008). "Computer Programme for Resource Assessment and Risk Evaluation Using Monte Carlo Simulation". Short Course on Geothermal Project Management and Development, Organized by UNU-GTP, KenGen and MEMD-DGSM, 7–8. Entebbe, Uganda.

Sugianto, A., & Kristianto A.W., A. (2011). "Survei Magnetotellurik Daerah Panas Bumi Kepahiang, Kabupaten Kepahiang, Bengkulu". Prosiding Hasil Kegiatan Pusat Sumber Daya Geologi, 5.

Supriyadi, Srigutomo, W., & Munandar, A. (2012). "Application Analysis of Monte Carlo to Estimate the Capacity of Geothermal Resources in Lawu Mount". 4th International Conference on Mathematics and Natural Sciences (ICMNS 2012), 1–2. https://doi.org/10.1063/1.4868761

Ulfa, N. Z., Hutabarat, J., Firmansyah, W., & Patonah, A. (2016). "Karakterisasi Temperatur Bawah Permukaan Daerah "NZU": Integrasi Data Geotermometer, Mineral Alterasi dan Data Pengukuran Temperatur Bawah Permukaan". Bandung.

Utami, A. A. (2015). "Penentuan Parameter dan Perhitungan Cadangan Panas Bumi Lapangan "AST" dengan Metode Simulasi Monte Carlo". Seminar Nasional Cendekiawan 2015, 243–244.

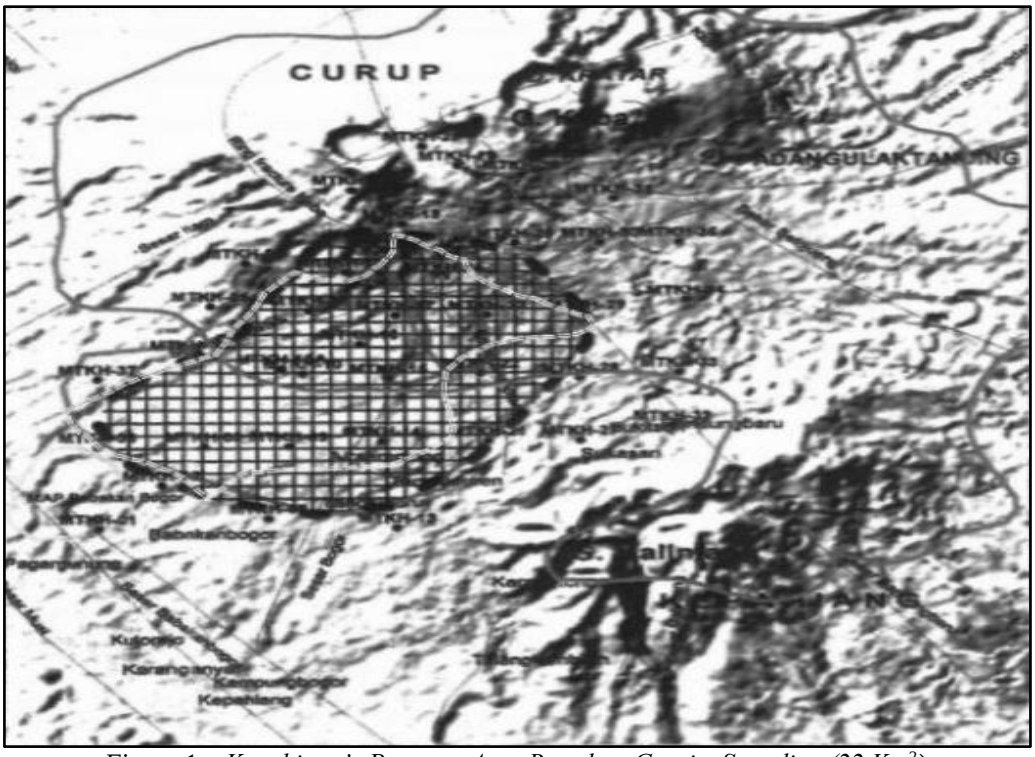


Figure 1: Kepahiang's Prospect Area Based on Gravity Sounding (22 Km^2).

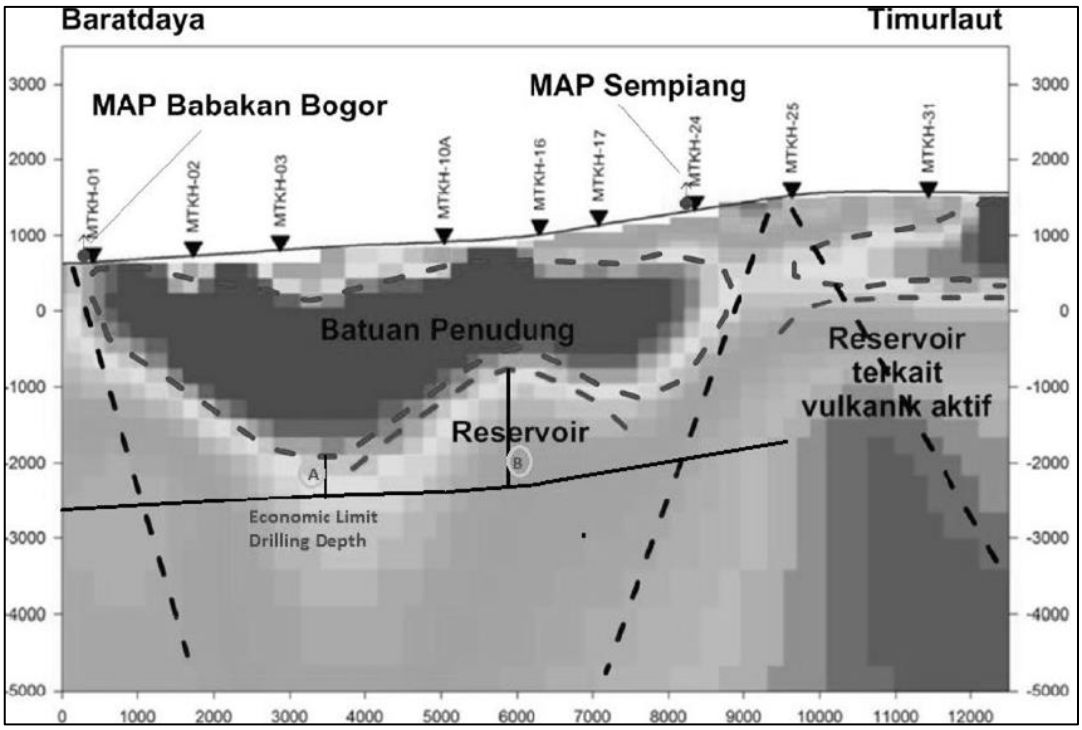


Figure 2: Kepahiang's Reservoir Thickness Based on Magnetotelluric Survey.

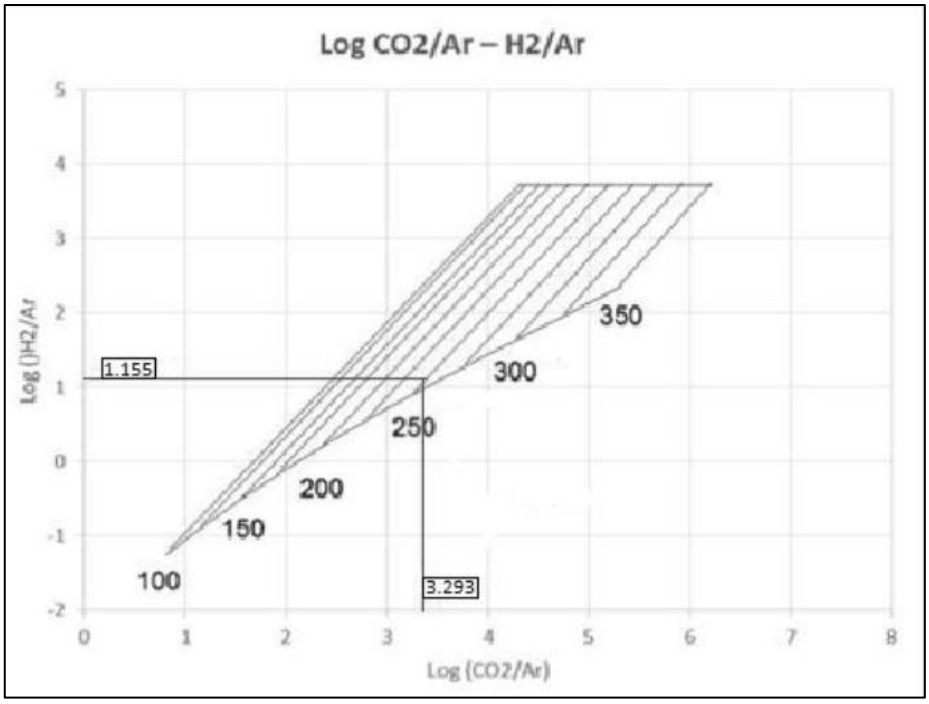


Figure 3: Kepahiang's Reservoir Temperature Based on CAR-HAR Diagram.

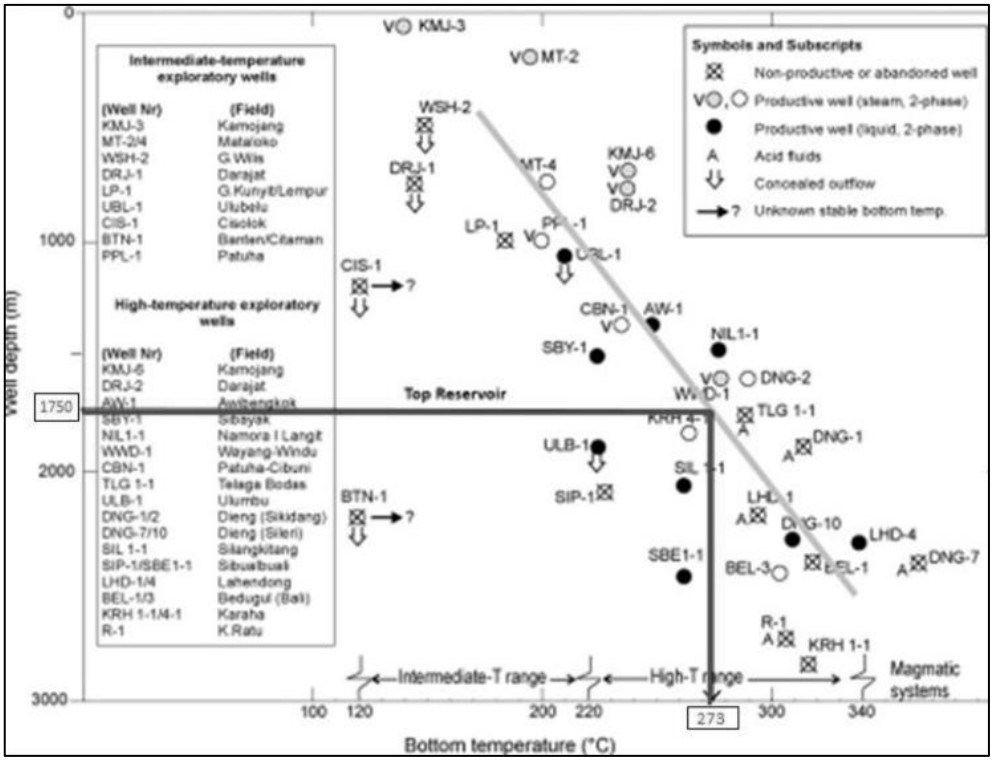


Figure 4: Kepahiang's Reservoir Temperature Based on Average Temperature Reservoir of Geothermal Fields in Indonesia at the Exploration Stage (Hochstein & Sudarman, 2008).

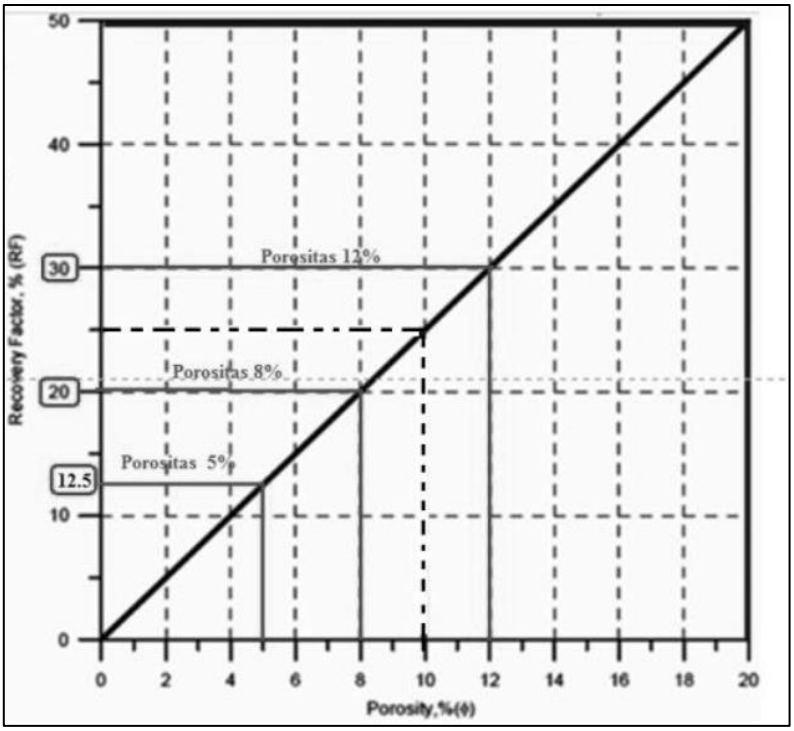


Figure 5: Kepahiang's Recovery Factor Based on Correlation Between Recovery Factor and Porosity (Muffler, 1978).

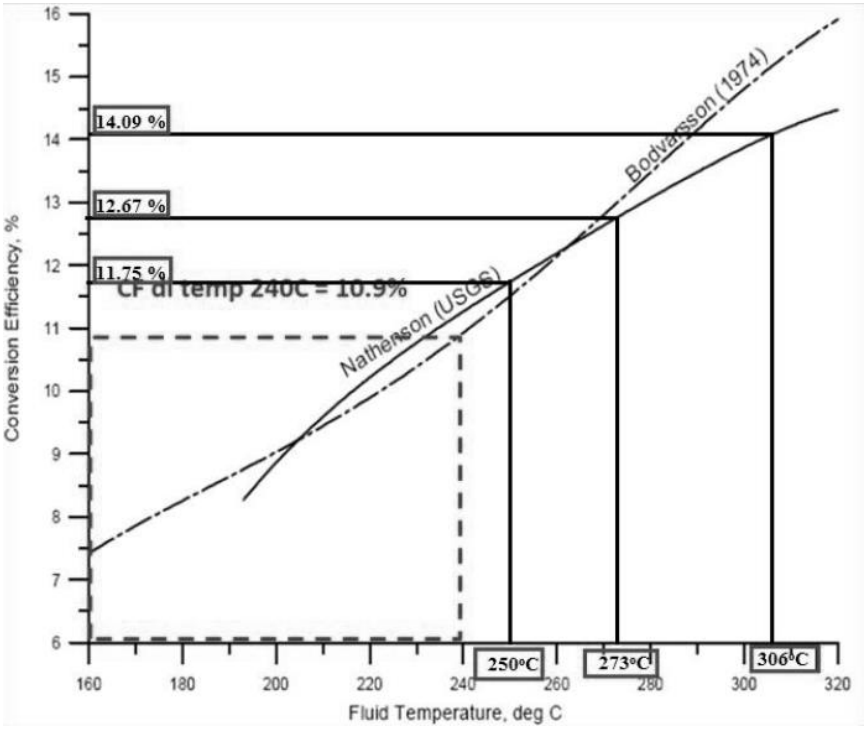


Figure 6: Kepahiang's Thermal Conversion Efficiency Based on Correlation between thermal conversion efficiency and reservoir temperatures by Nathenson (1975) and Bodvarsson, (1974).

Table 1: Input Parameters for Monte Carlo Simulation

Parameter	Min	Most	Max
Luas (km2)	22		32
Ketebalan (m)	500	1000	1250
Porositas	0.05	0.08	0.12
Rock Heat Capacity (kJ/kg C)	1.1	1.1	1.1
Densitas Batuan (kg/m3)	2500	2500	2500
Temperatur Awal (dg C)	250	273	306
Temperatur Akhir (deg C)	180	180	180
Saturasi Air Awal	0.8	0.8	0.8
Saturasi Air Akhir	0.3	0.3	0.3
Electtic Convertion Factor	0.1175	0.1267	0.1409
Recovery Factor	0.125	0.2	0.3
Life Time (years)	30	30	30

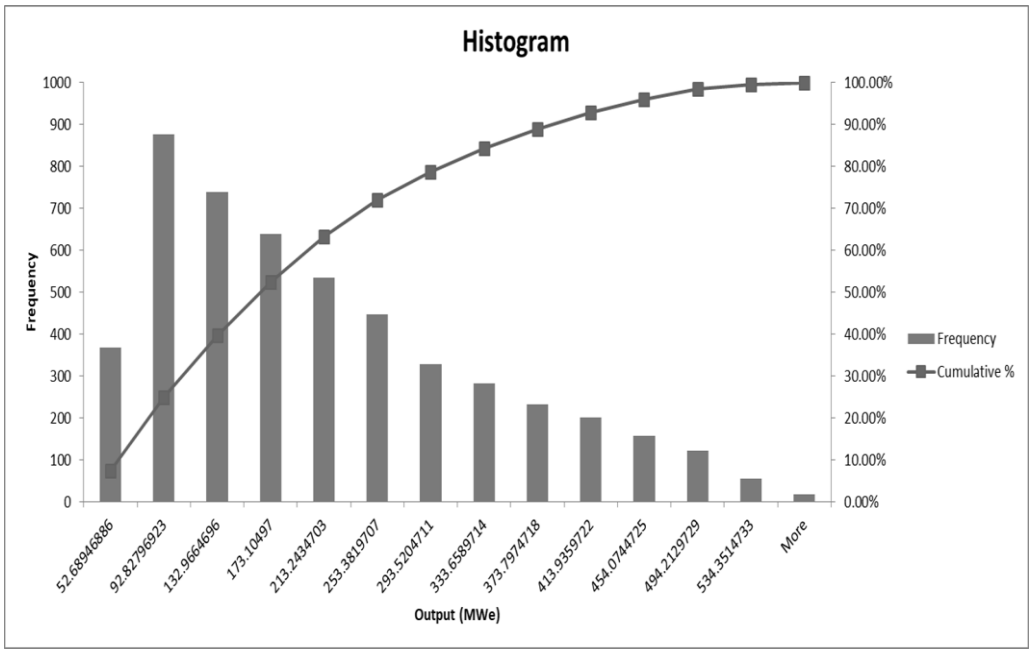


Figure 7: Histogram Output of Monte Carlo Simulation.

Table 2: Potential Output.

Final Result		
P10	58.73084	Mwe
P50	165.2654	Mwe
P80	302.7723	Mwe

COMPARING HORNER & WAPLES IN TEMPERATURE PREDICTION

Muhammad Syarif Fadhlurrahman and Kris Pudyastuti

Trisakti University
Jl. Kyai Tapa no. 1, Jakarta, Indonesia
Email: m.syarif171011710006@std.trisakti.ac.id, krispudyastuti@trisakti.ac.id

ABSTRACT

This study compares two methods of predicting true formation temperature from early post-drilling temperature surveys which rely on different principles: Roux's Horner method (1980) uses extrapolation from data points along Horner-Time with a correction factor from thermal physical properties of the lithology while Waples (2004) relies on the time-since-circulation (Tsc) and formation temperature relative to surface as the correction. The calculated predictions are compared with measured data from when the wells have reached stable temperature. The Waples Method compares less favorably against Roux. However, it has the advantage of needing only one measurement instead of series of measurements as used in Roux's. Both methods suffer from overestimation at feedzone where hot fluid from permeable formation enters the wellbore since both methods presuppose conduction-dominant heat transfer. Waples also fails at correction factor (fs) value at less than 0.97 and performs poorly in vapor-saturated well column environment.

Keywords: Horner method, Waples method, temperature determination

INTRODUCTION

Exploratory drilling is an important phase in the characterization and modeling of geothermal resources. Exploration wells provide direct information of subsurface temperatures which are useful for drawing isotherms, delineating reservoir extent and capacity as well as determining upflow and outflow patterns which also serve as indicators of heat source location. Due to the nature of deep geological drilling, usage of drilling fluids/muds is inevitable which has the side-effect of distorting wellbore temperature downwards (i.e. cooling effect). This is why methods are developed to correct those distortions. Comparisons between different methods have been done in the past such as by Espinosa-Paredes & Garcia-Gutierrez (2003), Eppelbaum & Kutasov (2006), Goutorbe et al. (2007) and Liu et al. (2016).

In this paper, two methods are chosen for analysis and comparison: the well-known Horner Method – in this case based on Roux et al. (1980) work as presented in a textbook by Grant and Bixley (2011) – and the relatively less used Waples et al. (2004) Method. These methods are chosen for their differing methods of correction. Roux's Horner method uses extrapolated heat-up pattern along Horner Time and further corrected with thermophysical properties of the formation. The Waples Method on the other hand uses only the surface temperature, depth relative to surface and time-since-circulation. These two methods are also chosen because a 2016 Egyptian study in the Sinai Peninsula using data from old oil wells employed both methods and yielded similar results. This study thus aims to test their success in a different geological context – namely Sumatra, Indonesia – using data from conventional geothermal wells from a conventional high-enthalpy geothermal resource.

In past comparisons, validation is arrived either via numerical simulation, empirical measurement at a sufficiently distant time or drill stem test. This paper follows the example of Eppelbaum & Kutasov in using long-term temperature surveys as source of validation.

METHOD

Heatup data of two wells (each anonymized as A and B) from Sumatra are treated with the two differing methods. Each measurement is corrected using both methods. Due to its extrapolative method, Roux uses a range of measurement over time for one correction while Waples needs only one measurement for one correction. However, each measurement is treated with Waples for the sake of comparison. Results from both methods are then compared with an empirical data deemed to be close to the reservoir's stable temperature which is judged by the lack of (or close to no) further heatup at that measurement date – this shall be termed 'Measured Temperature'. In a three-way comparison between the Roux Method, the Waples Method and the Measured Temperature, a pattern is expected to be seen which shall serve as basis for analysis.

The Waples corrected temperature is given by the following equation:

$$T_{true} = T_{surface} + f_s \cdot \left(T_{measured} - T_{surface}\right) - 0.001391(Z - 4498) \quad (1)$$

where Z is the depth relative to the surface, True Vertical Depth in meter.

The correction factor f_s is as follows:

$$f_s = (-0.1462 * \ln(T_{sc}) + 1.699)/(0.572 * Z^{0.075}) \quad (2)$$

where T_{sc} is time-since-circulation or the Δt in Horner Time. The Roux Method takes the form

$$T_{true} = T^*_{ws} + mT_{DB}(t_{PD}) \quad (3)$$

It uses a semi-log plot of temperature data (y-axis) versus Horner Time (log x-axis). T*ws is the trend extrapolated to x=0 from the slope *m* of the semi-log plot's heat-up pattern. T_{DB} is the dimensionless correction term which is a function of T_{PD}, the dimensionless circulation time. Respectively, the dimensionless terms take the following forms:

$$T_{DB} = 0.03\Theta^{1.678} t_{PD}^{-0.373} \quad (4)$$

where Θ is the mid-value of the range of Horner times that form the slope, and

$$t_{PD} = \left(\frac{K}{C\rho r_w^2}\right) t_c \quad (5)$$

where K is the thermal conductivity, C is the thermal capacity/specific heat, ρ is the formation density and r_w is the wellbore radius.

A comparison of the different parameters used in the two methods are given in the table below. It can be seen here that Roux's Horner uses more parameters including the thermophysical properties of the formation.

Table 1: Waples vs Horner Parameters.

Waples	Roux's Horner
$T_{surface}$, $T_{measured}$ (°C)	T, (°C)
T_{sc} (days)	t_c, Δt (days)
Z, (m)	r_w (m)
	K (W/mK)
	C (J/kgK)
	ρ (kg/m^3)

RESULTS AND DISCUSSION

Comments On Data

After drilling and completion, each well underwent a series of temperature measurements. These measurements record temperatures at roughly regular intervals of depth and are organized chronologically. Chronological data sets for A and B are presented in Table 1. They are measured relative to the time the drilling operation stopped.

Table 2: Heatup Measurement Dates Post-Drilling

A	17 hours	3 days	6 days	9 days	-
B	13.5 hours	3 days	7 days	10 days	14 days

It should be noted that well B encounters extrapolation problems due to extreme heating and cooling in its early measurements. This might be attributed to instrument error or fluid fluctuations inside the wellbore. Therefore, the problematic data are cut off and the ones used to obtain *m* for Roux are the 7th and 10th days which yield reasonable values.

The Measured Temperatures for A are measurement at 1172 days of heat-up (measured during bleeding) and for B are at 341 days.

Corrected Heatup Patterns

For well A, the extrapolated heatup using Roux's Method shows a significant exaggeration at 673-963 m TVD which roughly corresponds to a permeable zone. Waples's Method shows these same exaggerations although not as pronounced. The Roux method shows better correlation with Measured Temperature than the Waples below the 963 m TVD point. Figure 1 shows the temperature of Waples and Horner method in Well A.

For well B, there is exaggeration for both Roux and Waples at 1400 m TVD and under. It seems to be caused by a permeable zone. Interestingly, this exaggeration causes the Roux extrapolation at that section to match quite well with the Measured Temperature. The Waples Method produces a retrogressive trend at depths lower than 800 m TVD instead of the expected trend approaching the Measured Temperature as the heat-up time increases. This seems to be a feature of the correction factor, f_s. When f_s < 0.97, it produces corrected temperatures lower than recorded temperatures. Figure 2 shows the temperature of Waples and Horner method in Well B.

Discussion

Waples correction factor fails to get the early recorded temperatures closer to the Measured Temperatures at Well "B". This is due to the reduction of the correction factor below 0.97. This reduction happens also at Well "A" but not severe enough to retrogress. The correction factor tends towards reduction the higher the Tsc and the deeper the well depth. This seems to be an inbuilt feature of its mathematical formulation. Across all data sets, it seems that Waples is best used with data from before 8-day Tsc where f_s at all depths stay above 0.97 and thus produce corrected temperatures trending

upwards approaching Measured Temperatures. Despite this, Roux's Method still seems to be the better method as it has sections that overlap with the Measured Temperatures. A potential reason for Waples failure is that it was created and calibrated for off-shore oil wells, hence the lack of failure vis a vis Horner in the Sinai context.

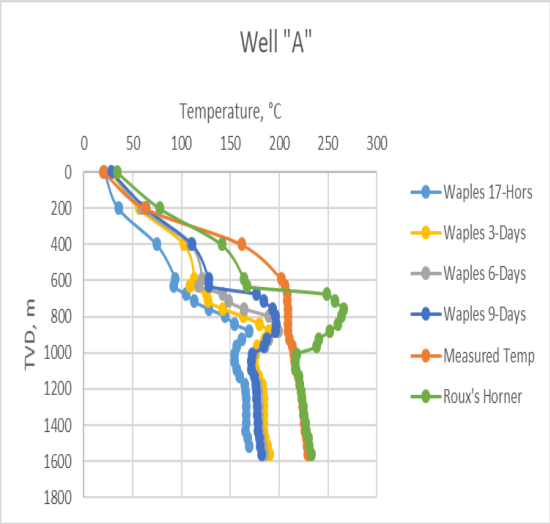


Figure 1: Well "A" with the Two Methods and Actual Temperature.

Discussion

Waples correction factor fails to get the early recorded temperatures closer to the Measured Temperatures at Well "B". This is due to the reduction of the correction factor below 0.97. This reduction happens also at Well "A" but not severe enough to retrogress. The correction factor tends towards reduction the higher the Tsc and the deeper the well depth. This seems to be an inbuilt feature of its mathematical formulation. Across all data sets, it seems that Waples is best used with data from before 8-day Tsc where f_s at all depths stay above 0.97 and thus produce corrected temperatures trending upwards approaching Measured Temperatures. Despite this, Roux's Method still seems to be the better method as it has sections that overlap with the Measured Temperatures. A potential reason for Waples failure is that it was created and calibrated for off-shore oil wells, hence the lack of failure vis a vis Horner in the Sinai context.

Both Waples and Roux's Horner feature exaggerated predictions marked by temperatures significantly higher than Measured Temperatures. This is expected since it is an artifact of the original data. Well test analyses indicate that those areas correlate with high permeability zones. This raises a question on whether a new correction factor should be developed to take account of mass flow, and thus temperature distortions, within wellbores. A more accurate early temperature prediction that better reflects the static formation temperature (i.e. formation temperature at natural state without the disturbances introduced by drilling and exploitation) would make better representative isotherms in geological models.

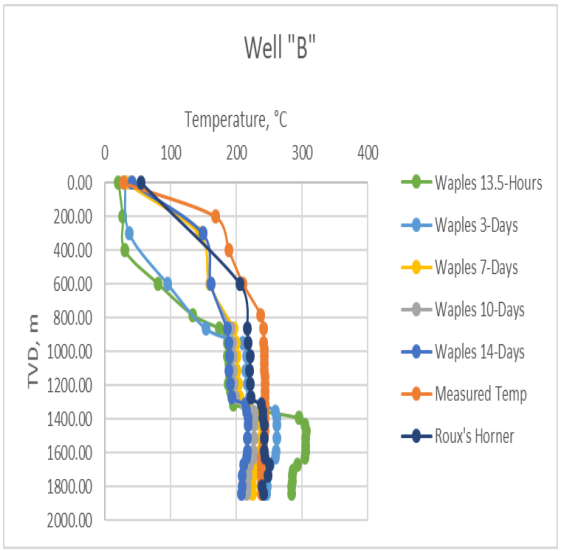


Figure 2: Well "B" with the Two Methods and Actual Temperature.

CONCLUSION

Waples Method is best applied with data at or before 7 days Tsc to avoid retrogression; an artifact of its correction factor's mathematical formulation. Between the two, Roux seems to be the more representative method. In case of hot fluid inflow to the wellbore, well temperature data skews higher and it shows even in the corrected temperatures of both Roux and Waples Methods. It might be of value to invent a correction factor that normalizes these artifacts to better represent the geothermal system's isotherms.

ACKNOWLEDGEMENTS

We are indebted to Pertamina UTC for providing us with field data. Special thanks to Dr. Jatmiko Atmodjo for guidance at Pertamina UTC.

REFERENCES

Atef, H., Abd El-Gawad, A. M. S., Abdel Zaher, M., Farag, K. S. I., (2016), "The contribution of gravity method in geothermal exploration of southern part of the Gulf of Suez–Sinai region, Egypt," NRIAG Journal of Astronomy and Geophysics, 5, 173–185.

Eppelbaum, L. V., & Kutasov, I. M. (2006). "Determination of formation temperatures from temperature logs in deep boreholes: comparison of three methods." Journal of Geophysics and Engineering, 3(4), 348–355.

Espinosa-Paredes, G., & Garcia-Gutierrez, A. (2003). "Estimation of static formation temperatures in geothermal wells." Energy Conversion and Management, 44(8), 1343–1355.

Goutorbe, B., Lucazeau, F., & Bonneville, A. (2007), "Comparison of several BHT correction methods: a case study on an Australian data set." Geophysical Journal International, 170(2), 913–922.

Grant, M. & Bixley, P., (2011), "Geothermal reservoir engineering." Burlington, MA: Academic Press, 305.

Liu, C., Li, K., Chen, Y., Jia, L., & Ma, D. (2016), "Static formation temperature prediction based on bottom hole temperature." Energies, 9(8), 646.

Roux, B., Sanyal, S. K. & Brown, S. L., (1980), "An Improved Approach to Estimating True Reservoir Temperature from Transient Temperature Data." in SPE California Regional Meeting. Society of Petroleum Engineers.

Waples, D. W., Pacheco, J. and Vera, A. (2008), "A method for correcting log-derived temperatures in deep wells, calibrated in the Gulf of Mexico," Petroleum Geoscience, 10, 23.

REMOTE SENSING AND GEOLOGICAL MAPPING METHOD FOR GEOTHERMAL PROSPECT ANALYSIS: CASE STUDY OF TELOMOYO GEOTHERMAL SYSTEM, CENTRAL JAVA

Lestari Butarbutar, Kristina Sarah Yuliana, and Elena Sekar Rahayu

Geological Engineering Department, Diponegoro University
Tembalang, Central Java
Email: lestaributar123@gmail.com, kristinasarahy@gmail.com, elenarahayu04@gmail.com

ABSTRACT

The depletion of fossil fuel in modern era has led to develop another resources that can meet energy needs such as electricity, and one of the energies is geothermal systems. This research located in Telomoyo mount, Central Java. This research is conducted by using primary data that is geological surface mapping, supported by secondary data through literature, and remote sensing method to analize fault fracture density by using arcgis and rockwork software. The study area has morphology in the form of hills or elevations with lithology in the form of igneous rocks. The lithology that found in the study area are Andesite lava and breccia. From the morphology and lithology that found in the study area, it can be interpreted that the study area are controlled by volcanism process. In the petrographic description, several mineral features are formed as a result of hydrothermal alteration processes. Which mineral can also be used as an indicator of an alteration zone. The minerals are Calcite, Quartz, Sericite, Epidote, and Clay minerals, and Opaque minerals. Then clay minerals were analyzed to obtain the types of alunit-kaolinite, montmorillonite, and halloysite. From XRD analysis, there are some type of minerals such as ortoklas, sanidine, augite, gypsum, and surite from the minerals, it can be interpreted that the alteration zone in the Telomoyo area is the Argillic zone. In the study area there was a shear fracture which the main stress was directed NE - SW. The structure in the form of a shear fault at north-south relatively and southeast-southwest that has been reactivated and cause of the manifestations of Candi Dukuh hot springs appeared. Candi Dukuh area are included in the type of bicarbonate-chloride water and in Candi Umbul and Pakis Dadu area are included in the type of chloride bicarbonate water (Giggenbach triangle, 1988). Based on the data is known that geothermal manifestations in the study area are alteration rocks and hot springs.

Keywords: Telomoyo, geothermal system, volcanism, argilic zone, alteration rock, hot spring.

INTRODUCTION

Energy is one of the vital needs for humans. The existence of energy is very closely related to people's welfare. Until now, oil and gas are still the main energy sources for humans, one of them in Indonesia. The existence and affordable prices make people still not switch to using other energy. When viewed from the existence of energy sources, Indonesia is one country with a considerable amount of energy. Ranging from conventional sources such as oil and gas to renewable alternative energy sources, one of them is geothermal. As one of the countries located in the ring of fire in the world, Indonesia has many active volcanoes. The existence of volcanoes is one form of volcanism which is the process of the release of magma from the earth to the surface. The magma that comes out to the surface has an effect on the rock that is skipped during the process to the surface. The effect will provide energy in the form of heat energy that comes from inside the magma. Heat energy that arises can be used as an energy source that can be used for human needs. However, not all volcanoes can be used as an area of geothermal energy utilization. Further research is needed that allows for a volcano to be used as an area for geothermal prospects. One area of the geothermal prospect is Mount Telomoyo in Central Java. In this research we will explain the characteristics of Mount Telomoyo in terms of geology and geochemistry so that it can be said to be one of the locations that has geothermal potential.

METHODS AND DATA

This paper is based on remote sensing method, regional geological data, geological mapping, alteration zone mapping, measurement of geological structures, observation of petrographic incisions, and secondary data assessment.

Remote Sensing

To know about the topography of the area. The result from the density map, and fault fracture density map are there is a main stress was NE-SW. This structure indicate there are tectonic that work on this area and the geothermal manifestation can appears up (Figure 1and 2).

Geomorphology

Physiographically the Telomoyo Mountain Complex is included in the Solo Zone. Rows of Merapi Volcano - Telomoyo occupies the western end of the Solo Zone (Bemmelen, 1949). This zone is formed on a volcanic complex that extends northwest-southeast direction, namely the series of Mount Ungaran - Mount Telomoyo - Mount

Merbabu - Mount Merapi which is in the environment of Quaternary volcanic geology.

Geological Structure

Geological structure analysis in the form of a shear fracture using the Dips software, showed that the main stress was NE-SW directed at 150, N 2090E. The medium level has a direction of 520, N 1000 E. The minimum stress has a direction of 350, N 3100 E (Figure 3).

Geology

- ***Andesite breccia***
  Blackish gray with massive structure (Figure 1). This rock has an average grain size of 4-64 mm with angular grain shape. The constituent material has poor sorting with open packaging. This rock is composed of andesite fragments, a matrix in the form of sand, with non-carbonate cement. (Figure 4)
- ***Andesite lava***
  Brownish gray with a massive structure (Figure 2). This rock has a hypocrystalline type of crystallinity with inequigranular porphyroafanitic of granularity type. The crystalline constituents of this rock have an afanitic size with subhedral crystalline relationships. This rock is composed of afanitic minerals (77%), quartz (5%), plagioclase (10%), biotite (3%), and hornblend (5%) (Figure 5).

Petrographic Analysis

Petrographic analysis was carried out on 2 altered rock samples.

• ***Sample 1***
This rock incision has a holocrystalline type of crystallinity with granularity of afanitic equigranular types. These rocks are composed of the composition of primary minerals namely Opak Minerals (5%), and Afanit Minerals (10%), as well as secondary minerals namely Anhydrite (15%), Secondary Quartz (50%), and Mineral Minerals (20%) (Figure 7) This rock is altered 85% (high) and has the name Andesite Porphyry (Russell B. Travis, 1955) (Figure 6).

• ***Sample 2***
This rock incision has a hypocrystalline type of crystallinity with inequigranular porphyroanranic type of granularity. These rocks are composed of the composition of primary minerals namely Plagioclase (20%), Opak Minerals (5%), and Afanit Minerals (15%), and secondary minerals namely secondary quartz (25%), Sericite (5%), Mineral Clay (25 %), and Calcite (5%) (Figure 8). This rock is altered 60% (high) and has the name Andesite Porphyry (Russell B. Travis, 1955). (Figure 7)

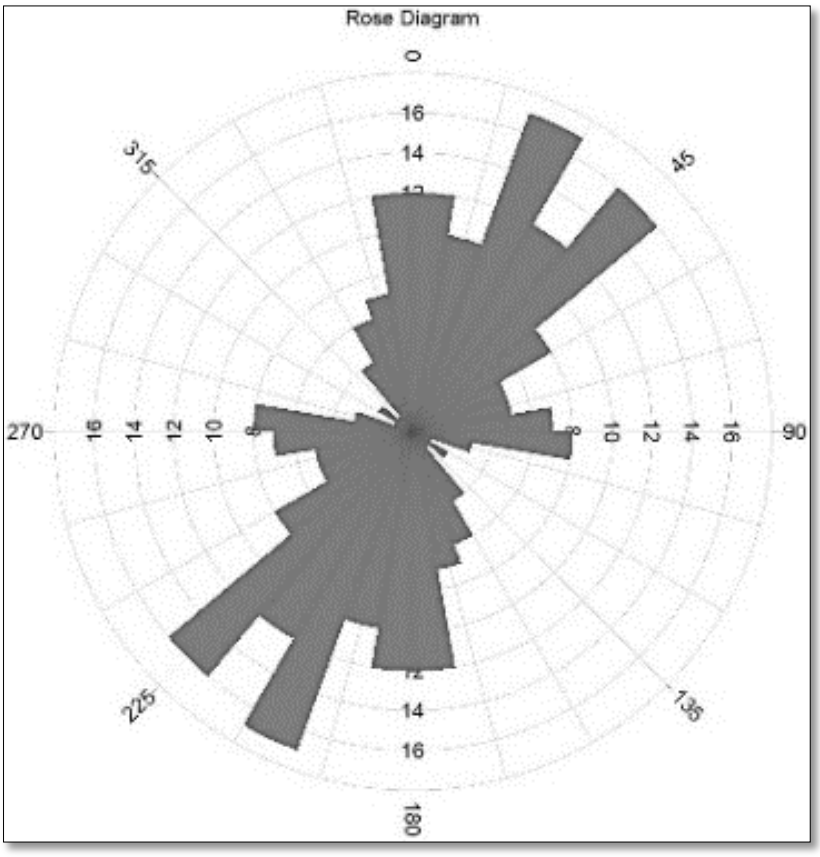


Figure 1: Figure of chemical composition changes.

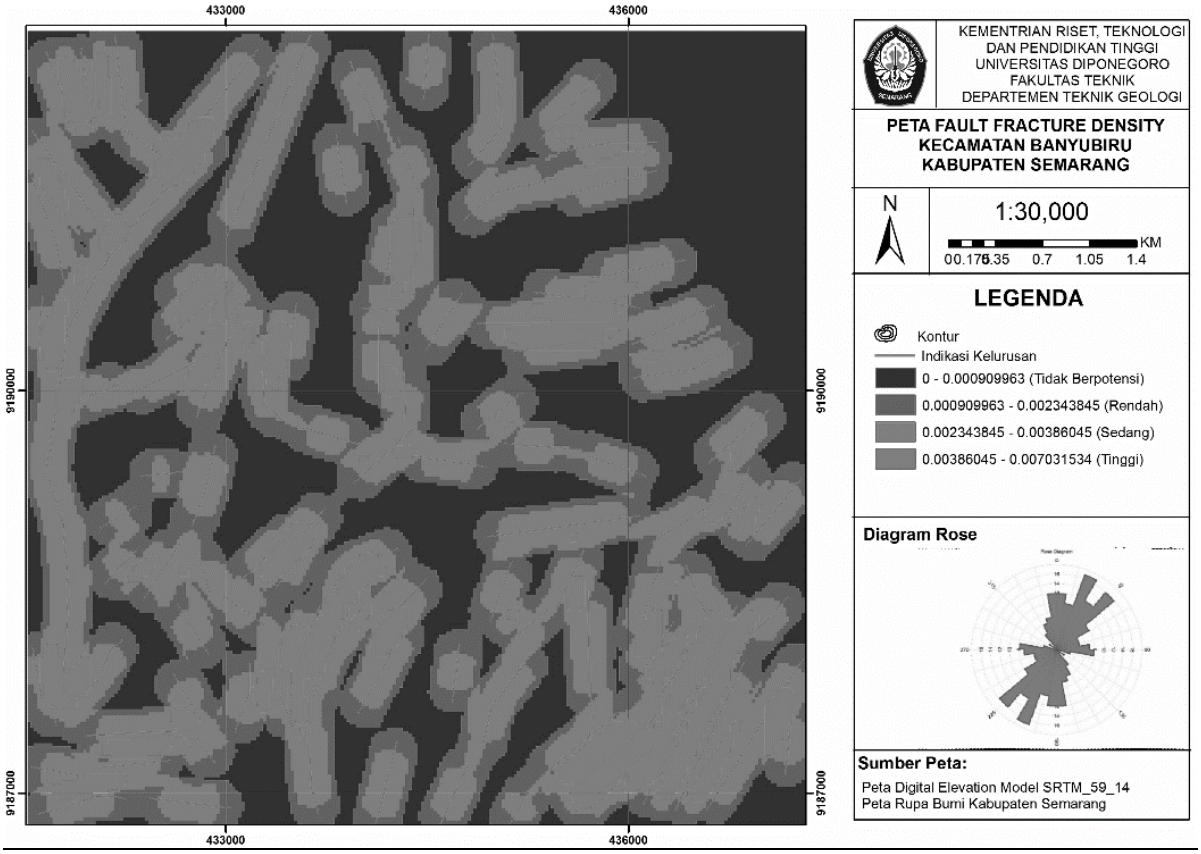


Figure 2: Fault Fracture Density.

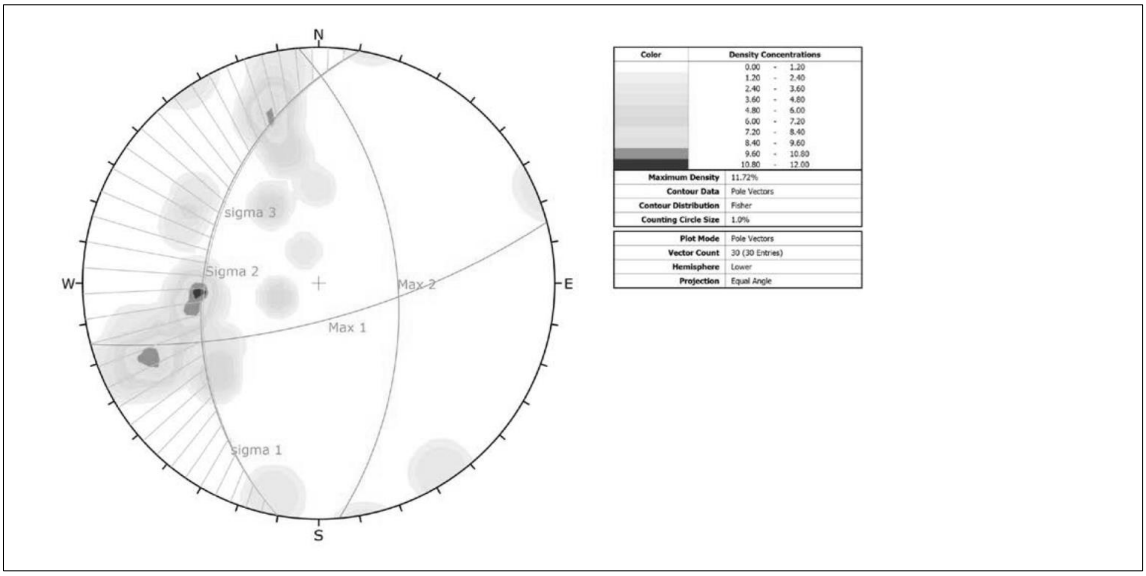


Figure 3: Geological structure analysis.

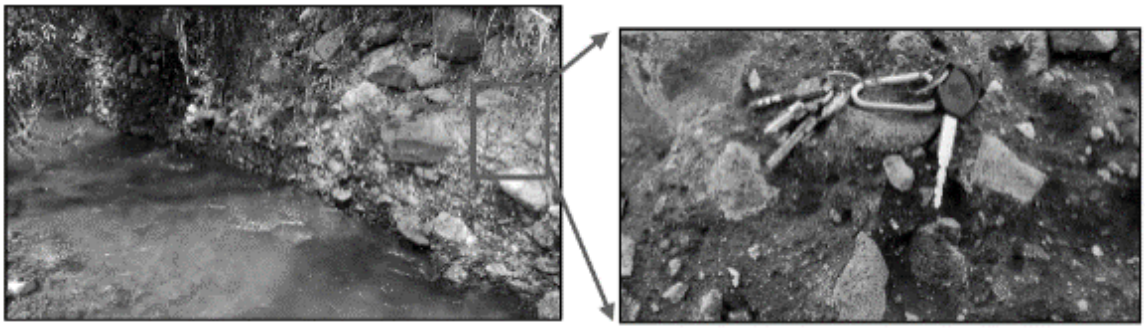


Figure 4: Figure of Andesite Breccia.

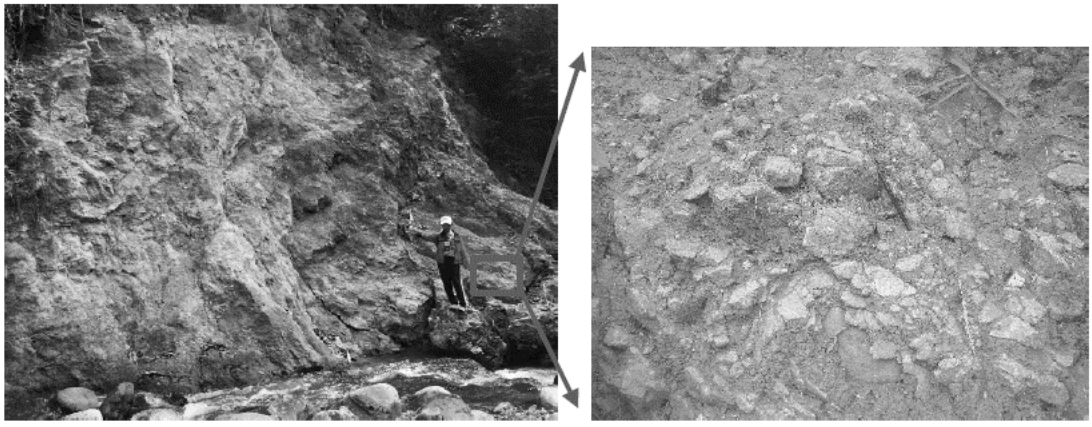


Figure 5: Figure of Andesite Lava.

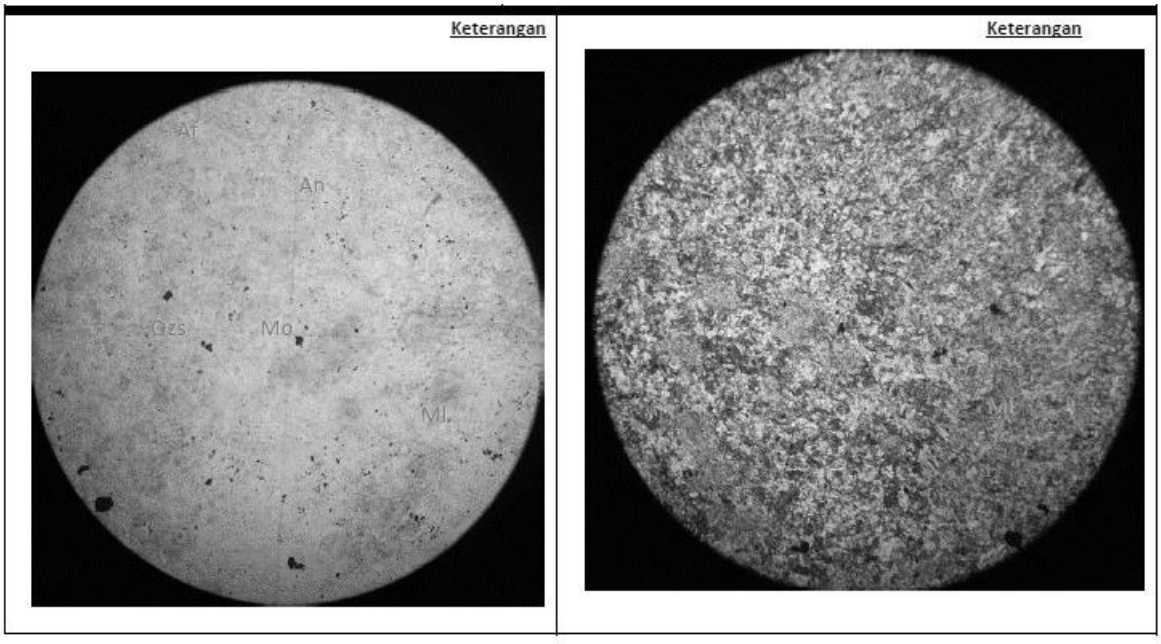


Figure 6: The rock incision of sample 1.

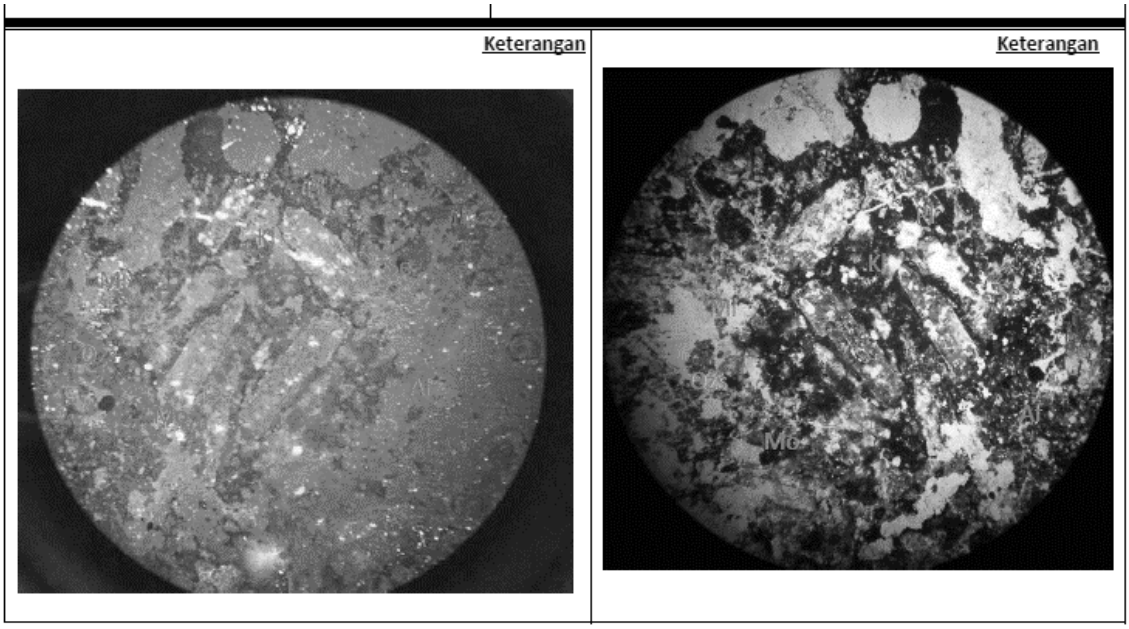


Figure 7: The rock incision of sample 2.

X- Ray Diffraction XRD Analysis

To know about the zone and alteration type of the clay minerals. From the X-Ray Diffraction XRD Analysis, there are many minerals inside, like orthoclas, sanidine, augite, gypsum, and surite (Figure 8).

Alteration Zone

In the study area there were geothermal manifestations that caused changes in the structure and chemical composition of rocks in the area. Alteration in these rocks is affected by hydrothermal fluid. Based on the analysis of megascopically and microscopically terrestrial rock samples, these altered rocks have mineral compositions of Calcite, Quartz, Sericite, Mineral Clay, and Opak Minerals. The composition of alteration minerals can indicate the temperature of formation of an altered rock, based on the classification of Hadenquist (1985) and Reyes (2000). These rocks are altered at a temperature of 220-2700C (Table 1). Based on the classification of Corbeth and Leach (1997), the study area was included in the Argillary Alteration Zone (Figure 10). The distribution of the zone of altered rocks in the study area is shown in Figure 9.

RESULT AND DISCUSSION

Petrology

In the area of mapping lots found several different types of lithology, one of which is:

Andesite breccia unit

In the plots area there are outcrops (Figure 1) which have a blackish gray color, with a size of 4-64 cm which are generally gravel sized, the shape of the grain which has tapered edges or edges so that it can be interpreted that the item has an angular shape. Have a grain size that is not uniform, so it has bad sorting, so that there is a gap between the fragments or, fragments do not close each other, so that it can be interpreted that it has a closed container. There is a composition in the form of andesite fragments, with a matrix of sand and cement-sized material when HCL is not bubbly so that it can be interpreted that the rock has non-carbonate cement. So, based on the composition and texture that the rock is andesite breccia.

Andesite lava

In the plots area there are outcrops (Figure 2) in brownish gray, with the crystallinity texture identified that the rocks are not completely composed of minerals, but there are several glasses. so that it can be interpreted to have hypocrystalline crystallinity. on granularity there are small uniformities and small grain sizes so that it can be interpreted that these rocks have granularity porphyroafanitic inequigranuity. From the appearance that has a very small grain size it can be interpreted that this rock has an afanitic grain value, due to the size of the grain so that the relationship between the grains is less to be seen, so that the relationship between the subhedral items can be interpreted.

In these rocks there are compositions in the form of Afanitic Minerals (77%), Quartz (5%), Plagioclase (10%), Biotite (3%), Amphibole (5%). So, the name of the rock can be interpreted andesite lava based on composition and texture.

Geological Structure

From the results of the analysis of the geological structure in the mapping area, namely the analysis of the geological structure in the form of a shear

fracture, it can be seen that the main stress is NE-SW directed at 15^0, N 209^0E (Figure 3). The medium stress has a direction of 52^0, N 100^0 E. The minimum stress has a direction of 35^0, N 310^0 E. The structure in the form of Shear fault that is relative from north-south and southeast-southwest leads to reactiveation and emergence of the manifestations of Candi Dukuh (Buku Potensi panasbumi jilid 1, 2017).

Geothermal Manifestations

Based on the data obtained, it is known that surface geothermal manifestations in the study area are alteration rocks (Figure 4). Alteration occurs in this area, seen from the high level of weathering. And other manifestations are also found in hot springs in several places (Buku Potensi panasbumi jilid 1, 2017).

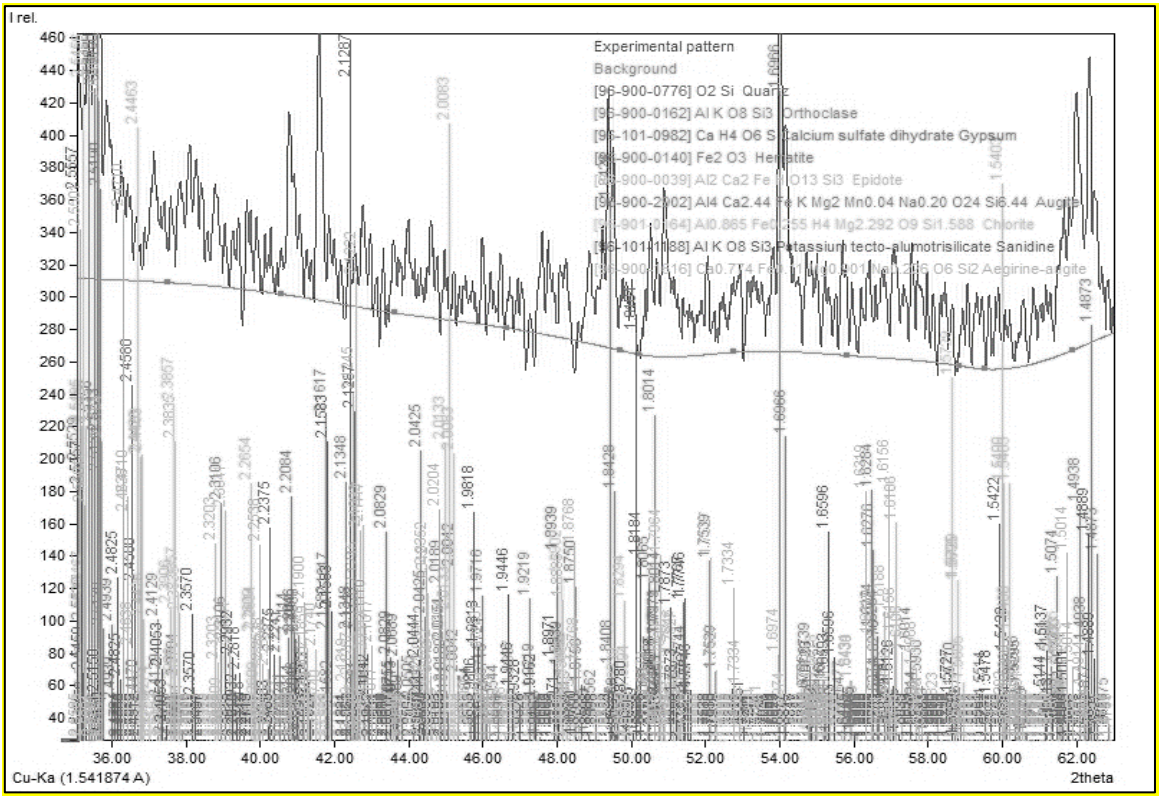


Figure 8: Figure of chemical composition changes.

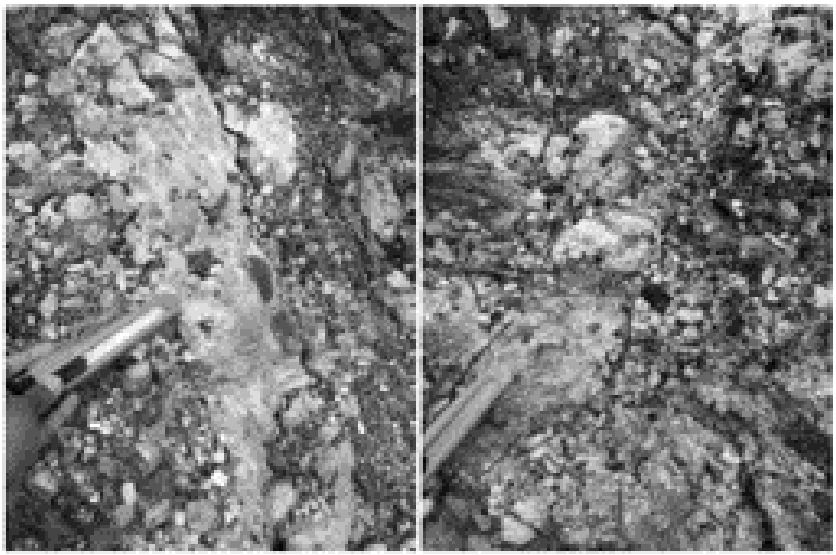


Figure 9: Figure of chemical composition changes.

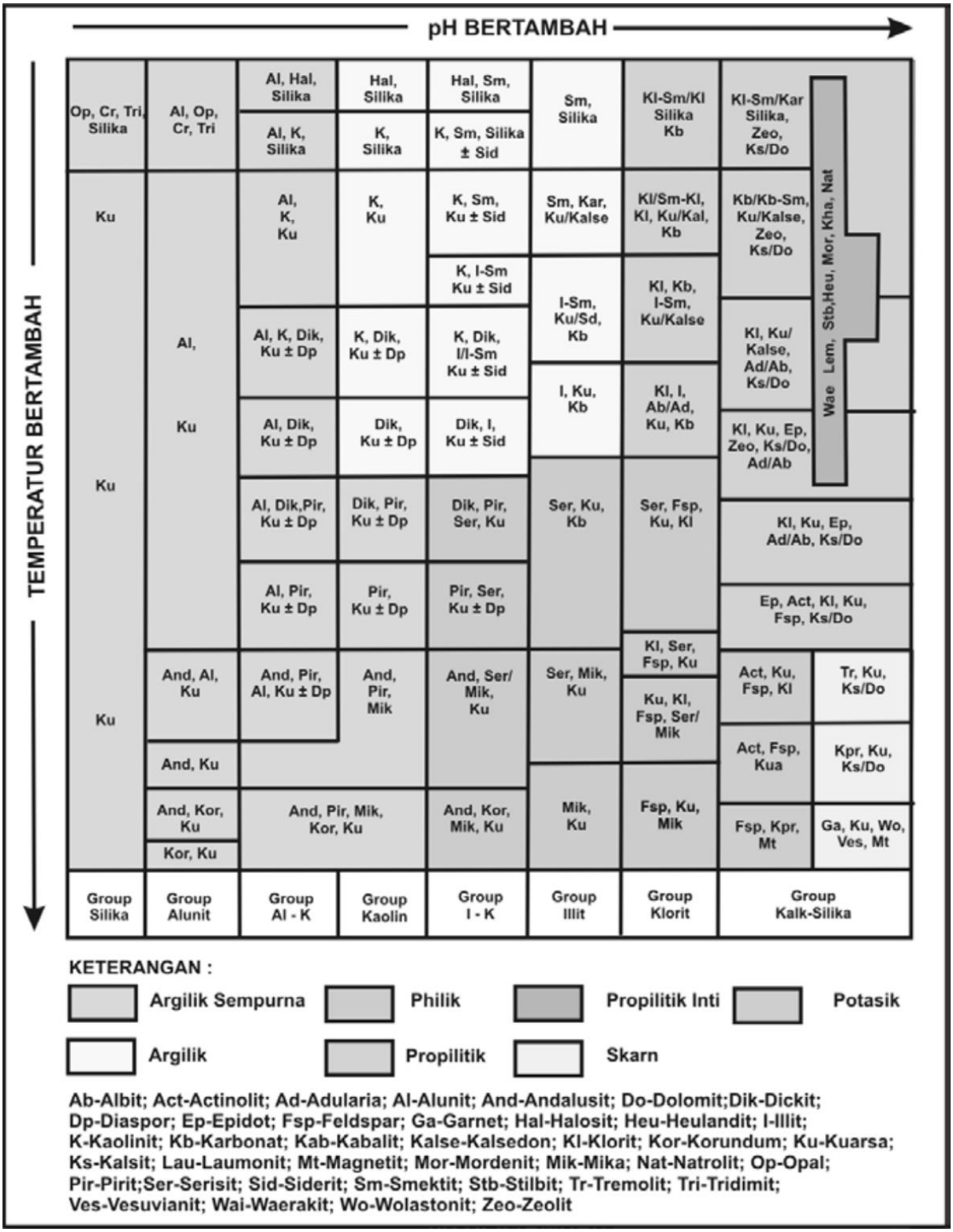


Figure 10: Argillary Alteration Zone.

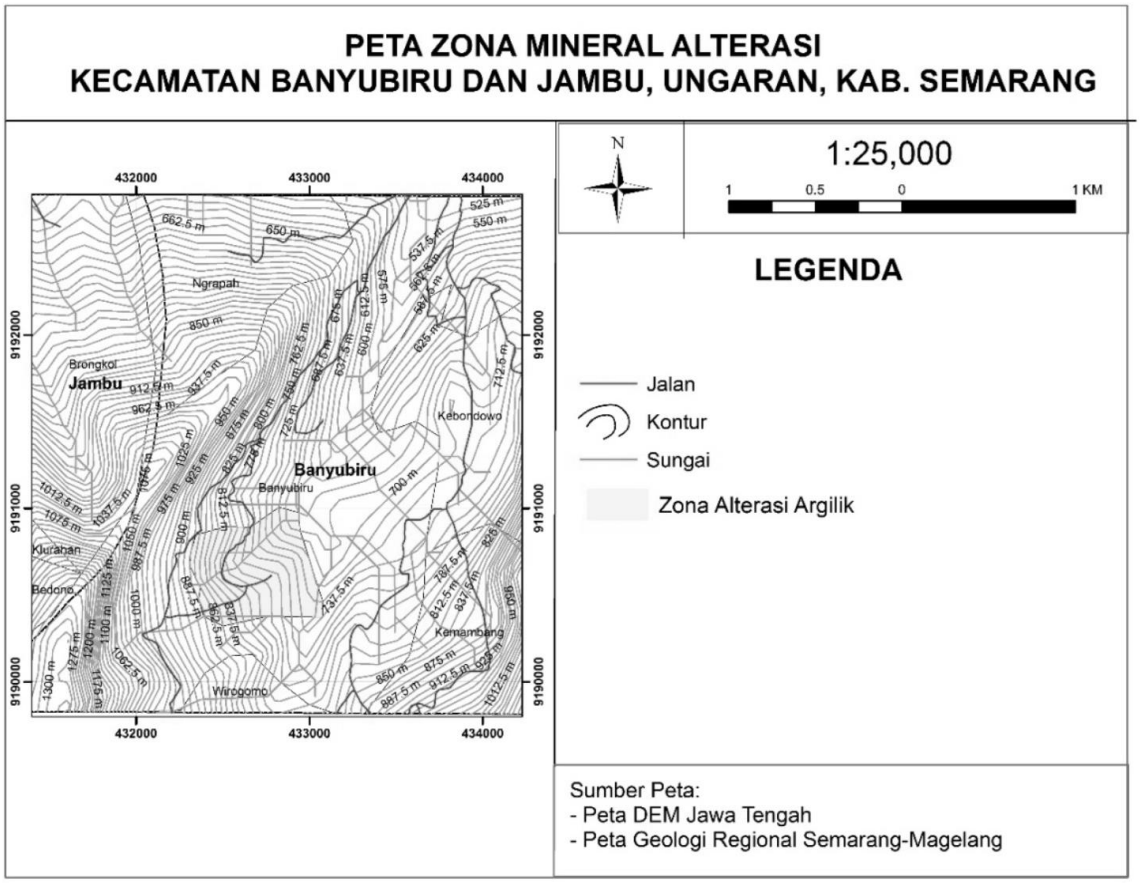


Figure 11: The distribution of alterated rock zone.

Petrographic of Altered Rocks

Based on the results of the mapping that has been done, obtained rocks that have undergone treatment due to the influence of hydrothermal fluid, so that it is interpreted as an altered rock. Alterated rock is one manifestation of the existence of geothermal systems in the area.

Samples were then taken under observation of a polarizing microscope. Observations were carried out at the same time as parallel nicotine (Plane Polarized light / PPL), Cross Polarized Light (XPL) and quartz wedge. Petrographic observations on sample 1 (Figure 5) contained primary minerals and secondary minerals with 4 times magnification. There are Primary minerals in the form of opaque minerals and afanite minerals. Opaq mineral (5%) with a size of 1 mm, black color on the observation of PPL, XPL, and Quartz Wedge. Afanite mineral (10%) with size <1 mm, colorless PPL color, black-red color XPL. There are secondary minerals in the form of anhydrite, secondary quartz, clay minerals and epidote. Anhydrite (20%) (Replacement) with a size of 2 mm, prismatic shape, low-moderate relief, having cleavage, weak pleocroism, colorless PPL color, XPL red to blue, having darkness, strong interference color, positive optical range sign. Secondary Quartz (20%) with 2 mm size, prismatic shape, colorless on PPL and white to black on XPL, has low relief, has no cleavage, has no fractions, does not have pleocroism, has a wavy / polycrystalline dark. Epidote minerals (15%) with a size of 1 mm in the observation PPL has a brown color, with moderate relief and on XPL observations have red to yellow. Mineral clay (30%) with a size of 1 mm, shape like clay granules, PPL and XPL brown color, very fine size, no darkness. From the comparison of secondary minerals to the total amount of all primary minerals with secondary minerals, the levels obtained its alteration is 85% which includes high alteration rates. The name of the rock at the time of the petrographic observation is Andesite Porphyry (Russell B. Travis, 1955).

In sample 2 (Figure 6) petrographic observations were made of primary minerals and secondary minerals with 4 times magnification. Primary minerals include plagioclase minerals, opaque minerals, and afanite minerals. Plagioclase (20%) with a size of <2 mm, prismatic shape, colorless PPL colors, black and white XPL colors, carsbalt-albit twins, low reliefs. Mineral opaq (5%) with a size of 1 mm, color in PPL, XPL, and Quartz Wedge is black. Afanite mineral (15%) with size <1 mm, colorless PPL color, black-red color XPL. There are secondary minerals are secondary quartz sericite, clay minerals and calcite. Secondary Quartz (20%) with 2 mm size, prismatic shape, colorless on PPL

and white to black on XPL, has low relief, has no cleavage, has no fractions, does not have pleocroism, has a wavy / polycrystalline dark. Sericite (10%) (Replacement) with a size of 2 mm, saccharoidal form (such as granulated sugar), colorless to pale gray or pale brown in PPL and white to reddish yellow on the XPL, having darkness and quadrant interference colors on the order II-III. Mineral Clay (25%) (Replacement) with a size of 1 mm, shape like clay granules, PPL and XPL brown color, very fine size, no darkness. Calcite (5%) (Vein) with 2 mm size, prismatic shape, low relief, 2 directional cleavage, colorless on PPL, white to yellow on XPL, strong interference color, negative optical range sign. From the comparison of secondary minerals with the total amount of all primary minerals with secondary minerals, the Alteration rate of 60% (high) was obtained. The name of the rock at the time of the petrographic observation was Andesite Porphyry (Russell B. Travis, 1955).

Temperature and Alteration Zoning

Based on the results of the mapping and also petrographic observations, it was found several mineral features formed as a result of hydrothermal alteration processes. Some alteration minerals found include Calcite, Sericite, Mineral Clay, secondary quartz, epidote and anhydrite. Then clay minerals were analyzed to obtain the types of alunit-kaolinite clay minerals, montmorillonite and halloysite minerals (Buku Potensi panasbumi jilid 1, 2017). These minerals can be used as geotemperature and to determine alteration zoning. The classification of mineral formation temperature is based on the classification of mineral formation temperature in alteration zones according to Hadenquist (1985) and Reyes (2000). Then an approximate temperature of 200 - 300 ^{0}C is obtained (table 1). Of the minerals found with the presence of the percentage of clay minerals namely alunit-kaolinit, montmorillonite, and halloysite minerals (Buku Potensi Panasbumi Jilid 1, 2017). High the secondary quartz minerals as minerals containing a lot of silica and the presence of anhydrite minerals in rocks that have been observed, it can be classified that alteration in the telomoyo region belongs to the argillic zone (According to Corbett and Leach (1997)) (Figure 7).

Geochemistry

The manifestations of the umbul temple-telomoyo are alteration rocks and hot springs and temperatures around 34 - 36 ^{0}C. As for plotting on the Gigenbach triangle, 1988 (Figure 8) it is known that in the dukuh temple area are included in the type of bicarbonate-chloride water and in the umbul temple and pakis dadu are included in the type of chloride bicarbonate water (Buku Potensi Panasbumi Jilid 1, 2017). The type of hot water in dukuh temple which are included in bicarbonate-cloride is interpreted to be formed because of the interaction between water originating from the inner layer and meteoric water originating from the surface.

CONCLUSION

Mount Telomoyo is located in three cities namely Magelang, Temanggung, and Semarang, Central Java Province and includes a solo zone (Bemmelen, 1949). From remote sensing analysis, the main stress from Telomoyo and the area around was NE-SW. The research areas include lithology of andesite lava units and andesite breccia, with rock conditions undergoing changes due to hydrothermal influences. Based on secondary minerals in the results of alteration, it is estimated to have a temperature 220^o-270^{o}C and including the argillic zone (Figure 11). The manifestations of the umbul temple-telomoyo are alteration rocks and hot springs and temperatures around 34 - 36 ^{0}C. As for plotting on the Gigenbach triangle, 1988 (Figure 8) it is known that in the dukuh temple area are included in the type of bicarbonate-chloride water and in the umbul temple and pakis dadu are included in the type of chloride bicarbonate water (Buku Potensi Panasbumi Jilid 1, 2017)

REFERENCES

Bemmelen, R. W. Van., (1949). "The Geology of Indonesia", Vol. 1 A, Government Printing Office, The Hauge.

Corbett, G. J., Leach, T. M., (1997), "SW Pasific Rim Gold and Cooper System (Structure, Alteration, and Mineralization)". Society of Economic Geologists Special Publication 6, 237p.

Hedenquist, J. W., (l987). "Mineralization associated with volcanic-related hydrothermal systems in the Circum-Pacific Basin". in Horn, M.K., ed., Circum Pacific Energy and Mineral Resources Conference, 4th, Singapore, l986, Transactions: American Association of Petroleum Geologists, p. 5l3 – 524.

Nugroho, A., (2013). "Studi Geokimia Fluida Daerah Prospek Panasbumi Gunung Ungaran, Kabupaten Semarang, Jawa Tengah".

Reyes, A. G., Giggenbach, W. F., (1992). "Petrology and fluid chemistry of Magmatic hidrothermal system in the Philipines". In: Y.K. Kharaka dan A. S. Maest 110 (Editors) Water rock Interaction. Proceedings of the 7th International Sympossium on Water rock Interaction, Park City, USA, Balkema, Rotterdam, pp, 1341-1344.

GEOTHERMAL EXPLORATION USING APPLICATIONS GEOLOGICAL MAPPING, FFD SRTM, MODELLING CONCEPT OF STRUCTURAL CONTROL, PETROGRAPHY AND HOT WATER GEOTHERMOMETER ANALYSIS TO IDENTIFICATION AND EVALUATION POTENTIAL OF VOLCANO GEOTHERMAL ENERGY AT CANGAR, EAST JAVA

Yoyok Ragowo Siswomiharjo, Desi Kiswiranti, Venny Ayu Syafriani, Pamela Felita Adibrata, Agung Candra Setiawan, and Dessensa

Geological Engineering, Faculty of Mineral Technology,
AKPRIND Institute of Science & Technology
Jln. Kalisahak No. 28 Yogyakarta
Email: yoyokraider502@gmail.com

ABSTRACT

Geothermal is a type of renewable energy can be used for various needs, including electricity generation and developed as a tourism area such as in Cangar, East Java. Geothermal manifestations of Cangar area in the form of hot springs that appear in two locations along the Cangar river, identified as the heat energy of Mount Volcano Arjuno-Welirang complex. This study aims to identify and evaluate the effective utilization potential of geothermal research areas. The research area is composed of volcanic lithology based on petrographic analysis results known as andesite-basaltic lava, tuff breccia, travertine and sulfide deposits which are the source of their manifestations. Based on geological mapping analysis, modeling concept and FFD (Fault Fracture Density) analysis using lineaments structural analysis from SRTM data, the emergence of geothermal manifestations is controlled by geological structure in the form a normal left slip fault as oblique fault with the southwest-northeast and left slip fault structure with the northwest-southeast and radial structure pattern controlled by volcanic and tectonic processes. Based on geochemistry analysis, the surface water temperature at these two locations ranges from 58^0C-60^0C and by geothermometer and ternary diagram method it is known that the type of fluid is bicarbonate (HCO_3) classified as immature type peripheral zone which caused side rock assimilation and water table contact, the temperature of the reservoir ranges from $94{,}38^0$C-$108{,}70^0$C and it can be interpreted that bedrock in the form of intermediate-acid rock, are present as intrusion and potential range of 4.78-20.4 MWe/Km^2. Based on the results of the SWOT analysis it was concluded that the Cangar area produced effective geothermal manifestations to be used as geotourism areas compared to power plants.

Keyword: Geothermal Potential Manifestation, Exploration, FFD-SRTM, Geological-Mapping, Geothermometer, Cangar-Arjuna-Welirang

INTRODUCTION

Availability of petroleum fuel energy will be increasingly depleted with time travel, one of the potential natural resources that can answer the above-mentioned problems are volcano-geothermal energy. The government of Indonesia has long developed the country, including increasing electric power generation. With the decrease of hydrocarbon reserve, geothermal is a potential resource of a relatively renewable energy resource. Geothermal electric generation has actually long been developed due to the fact about the potential geothermal prospect in Indonesia islands as of the intensive volcanic activities. Indonesia is located on the ring of fire area. There are around 120 active volcanoes which spread from Sabang to Merauke. With a large number of active volcanoes in Indonesia made Indonesia as the country with the largest number of active volcanoes and most active in the world. Indonesia has potential geothermal energy resource with respect to significant volcanic activities. Geothermal energy is a natural resource of new renewable energy and is quite promising as an energy solution in the future, this effort continues to be carried out due to the depletion of fossil energy reserves of petroleum. In general, geothermal energy is in a volcanic area and there are indications of surface manifestations (geothermal surface manifestations) that appear around potential areas such as hot springs, fumaroles, hot mud pools (mud pools), geysers and other types of manifestations. Surface manifestations are estimated to occur because there is heat propagation from the subsurface or because there are fractures that allow geothermal fluid (steam and hot water) geothermal flows to the surface. The distribution of geothermal potential areas in Indonesia based on data from the Ministry of Energy and Mineral Resources in 2014 is located 299 geothermal locations, according to research and development that has been performed, it is known that geothermal resource potential in Indonesia reaches approximately 27,791 MWe. One of which is in Cangar, East Java, namely in the Arjuno-Welirang Mountain Complex. Geothermal potential approved by hot spring approval. Exploration activities have been carried out.

Geochemical surveys and data analysis have been combined with geophysical data from researchers launched for geothermal models in the area. This research aims to utilize and utilize the effective potential of the geothermal research area.

The study was conducted in the Cangar area, East Java, located 20 km from Batu city and included in the Arjuno-Welirang volcano, which is located in geographical coordinates (-7º44'00 "; - 7º45'00") via (112º31'30 "; 112º32 '30 ") or covers an area of 2 km x 2 km = 4 km2, and the Arjuno-Welirang complex is located in the eastern area. Arjuno-Welirang volcano is part of the B/C volcano. The physiographic section of the Solo volcano is Mount the volcano was signed on the quarter volcanic group, which opened up volcanic pathways, both active (type A), or inactive, both type B/C and historical types, which had no activity at all, such as the Kawi-Butak volcano (Sunaryo, 2012).

Geothermal exploration is needed to know and evaluate a geothermal potential to be utilized effectively. For this reason, initial exploration is needed in the form of exploration of geology, geochemistry, and geophysics to provide data used for further exploration (detail). Overall exploration of volcanic geothermal volcanoes has been carried out previously by several researcher's team Survey Terpadu Geologi dan Geokimia, PSDG Bandung in 2010 who carried out initial geological and geochemical exploration, and several exploratory researchers. early geophysics with a large area covering the entire Arjuno-Welirang volcano complex so that it cannot provide a detailed model of an existing geothermal system, so based on this it is necessary to explore geology and geochemistry early again and then detail and combine with previous geophysical data with focus on hot springs that appear in the cangar area, detail exploration by means of cangar geothermal exploration of an area of 4 km^2 with a scale of 12,500 and modeling it so that the data is useful to determine the cangar geothermal systems and models (lithology, cap rock, reservoir, and rock heaters) and potential details to evaluate so that they can be used effectively and can also be used as data for determining the location of drill points. Figure 1 shows the location of potential geothermal in Cangar area.

METHOD

The method of this research is literature study, using geophysical exploration methods with previous research geophysical data models and processing the latest geophysical data with the gravity data method from topex data. then processing srtm-dem (digital elevation model) data with the ffd method or straightness structure. next is field data retrieval with exploration methods of geological and geochemical mapping. analysis of geological data with petrography, geological structure modeling, and geological cross-section analysis and geochemical analysis with laboratory tests and geothermometer analysis (tennary diagram). then swot analysis to evaluate effective use. the literature study is collecting data from previous research, field mapping data are descriptions of rocks and geological structures in the field, measurement of the surface temperature using a geothermometer that processes data using a diagram Na-K-Mg, diagram SO_4-HCO_3-Cl^-. and analysis of diagram Li-B-Cl.

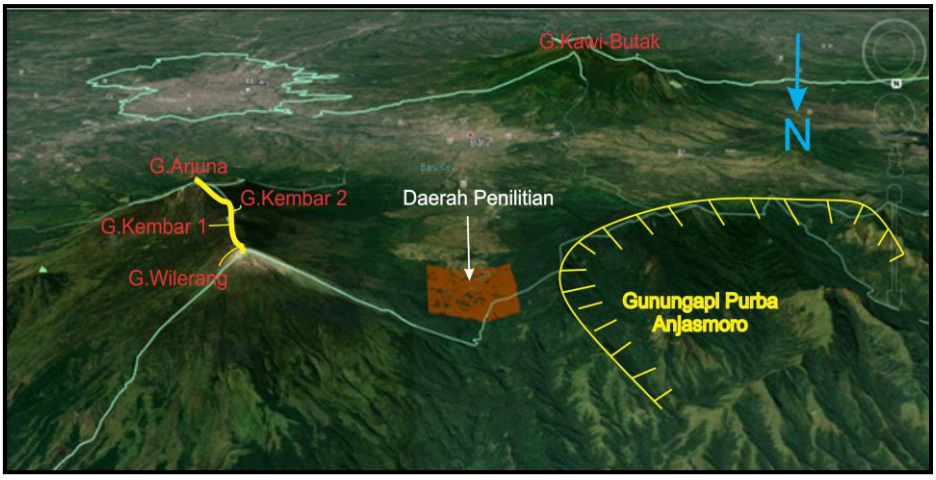


Figure 1: Location of potential geothermal Cangar area in complex of Arjuno-Welirang Volcano.

RESULT & DISCUSSION

Exploration survey has been performed in the area in early March 2019, starting with a literature study of the Arjuno - Welirang (AW) geothermal and specifically about the cangar area. After obtaining secondary data from the initial researcher in the form of geophysical data then analyzing and modeling it to determine the state of the area based on geophysical data. To find out the physical characteristics of the Arjuno-Welirang geothermal system, several experts have conducted geophysical surveys and research in the Arjuno-Welirang area. Figure 2 shows the horizontal gradient of the total residual Arjuno-Welirang geothermal anomaly map showing the use of heat sources.

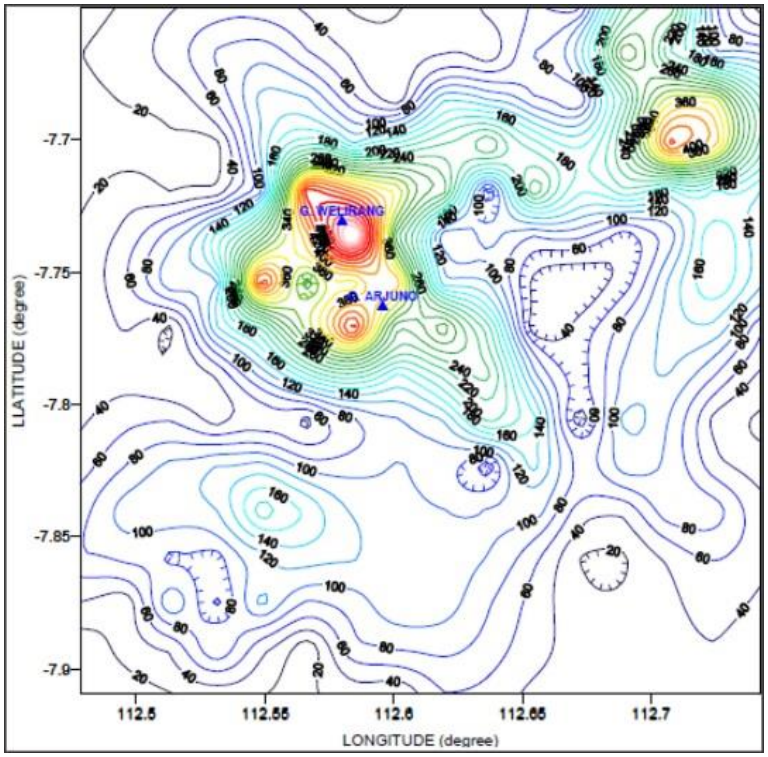


Figure 2: Horizontal gradients residual total magnetic anomaly in Arjuno-Welirang geothermal area (Sunaryo, 2012).

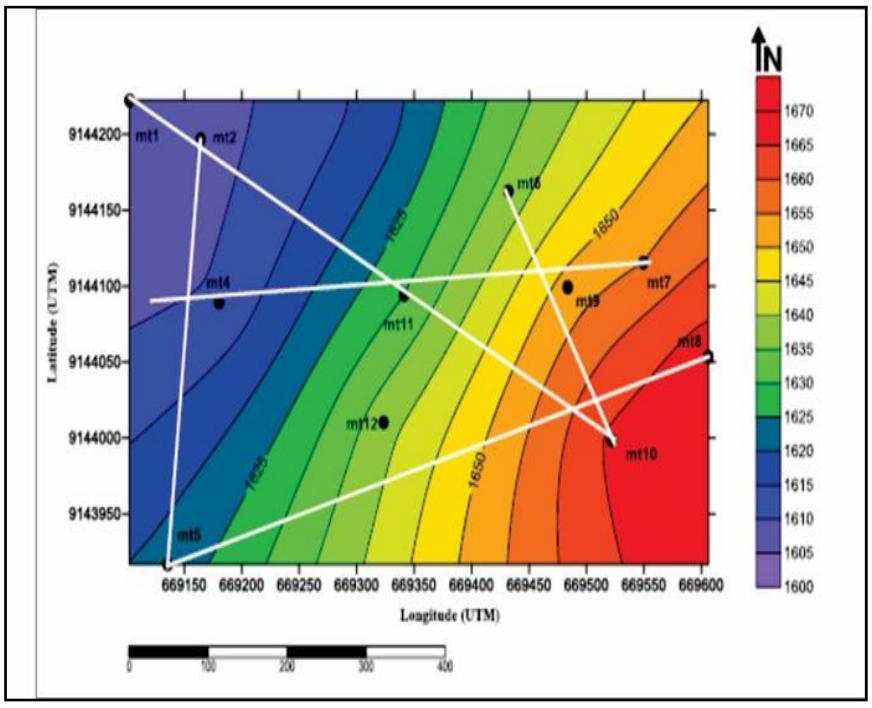


Figure 3: Contour of magnetotelluric elevation in the study area (Rahmawati et al, 2018).

Based on the magnetic anomaly data, the cangar region shows a yellow to red contour with a value of 350 which indicates the magnitude of a magnetic anomaly which can mean that the rock area is composed of lithologies rich in Fe, namely igneous or volcanic rocks and shows a source of heat.

Based on research by Rahmawati et al. 2018 (Figure 3) which acquired magnetotelluric data around the Cangar hot spring, Bumiaji District, Batu City. Data acquisition was carried out in July 2017 with the Metronix ADU-07e magnetotelluric device producing contour data from the study area at an elevation of 1600 – 1670 masl. Figure 4 shows the cross-section 1 model is identified by a layer that has a low resistivity value (≤21 Ω.m) which is on the surface to a depth of 1300 meters. Layers with resistivity values are marked with a red layer. Cross section 2 is in line with the Cangar fault. The results of the cross-section model on line 2 also obtained a layer that has a low resistivity value (≤21 Ω.m) which is on the surface to a depth of 400 meters. This layer with a low resistivity value is thicker than on track 1. In cross-section 3, the layer is identified which has a low resistivity value (≤21 Ω.m) which is only in the southwest and northeast. This layer appears on the surface to a depth of 1000 meters, the thickness of which is quite thin compared to the previous track. Track 3 also intersects line 2 at the point MT5. The result has suitability, namely, there is a breakthrough in the medium resistivity value (21 Ω.m – 167 Ω.m) at the MT5 point, where it is known that around this MT5 point there are manifestations of hot water which are thought to originate from rock cracks caused by Cangar faults. The point of MT5 and MT12 is the dominating rock, which is an igneous rock. The frozen rock comes from freezing from Mount Arjuno-Welirang. The result of cross section 4 is a layer with a low resistivity value (≤21 Ω.m) which appears on the surface to a depth of 600 meters in the west and also in the east. In cross-section 5, a layer which has a low resistivity value (≤21 Ω.m) is spread out evenly at all measurement points. A low resistivity layer appears on the surface to a depth of 1000 meters. Right below the low resistivity layer there is a medium resistance layer and is followed by a high resistance layer (Rahmawati et al, 2018).

So, from the total magnetic gradients residual data of anomaly and magnetotelluric, it is explained that the hot anomalies that occur there occur in igneous lithology due to the formation of Arjuno volcanoes, namely lava. So, the researchers made anomaly geophysical gravity contours based on TOPEX data processing using surfer software (Figure 5). The anomaly geophysical gravity contour map was used to see the basin contact limits of rock contact models in the study area to be used as preliminary data prior to the field by researchers in exploration advanced geological mapping.

Based on data from the geophysical gravity contour map anomaly indicates the existence of a contact limit between rocks that are clearly marked with a significant color change to the southeast which is getting higher with contour values range 261-286. After analyzing the geophysical data then SRTM-DEM data analysis to see the pattern of structural alignment to be used during exploration.

Fault and Fracture Density (FFD) SRTM-DEM Data Analysis

Digital elevation model (DEM) data analysis is the result of contour interpolation from a digital topographic map of a scale of 1: 25,000 with an area of 63 km2 (Figure 6). Interpretation of DEM imagery is carried out by the structure of line alignment patterns in the research field. From the DEM data showing the surface texture of the research area, it can be done with the geological structure of the pattern of withdrawal alignment dominant northwest-southeast and northeast-southwest in the Cangar area. Alignment of several forms of radial patterns against Ridge, river valleys, and reports of volcanic activity. Radial patterns in volcanoes indicate that there is an active volcano in the study area. The area of alignment geological conditions reflected in the observation image of the DEM reflects the relationship between volcanism and geological structure to the emergence of geothermal manifestations.

The conceptual model is based on a generic conceptual model of a volcanic geothermal system, which is appropriate because Arjuno-Welirang is a type of Strato volcano with age at Quaternary and still active. Then the emergence of geothermal manifestations in the Cangar area was formed due to geological structures that trended northwest-southeast and northeast-southwest and associated with the Arjuno-Welirang volcano complex. The SRTM-DEM map FFD data shows the pattern of structures formed and contained in the field. After analyzing the Geophysical data and the SRTM-DEM FFD, the next step is to carry out advanced geological and geochemical explorations to conceptualize the geological structure model and geological cross-sectional model to make the geothermal system model area in detail and evaluate it.

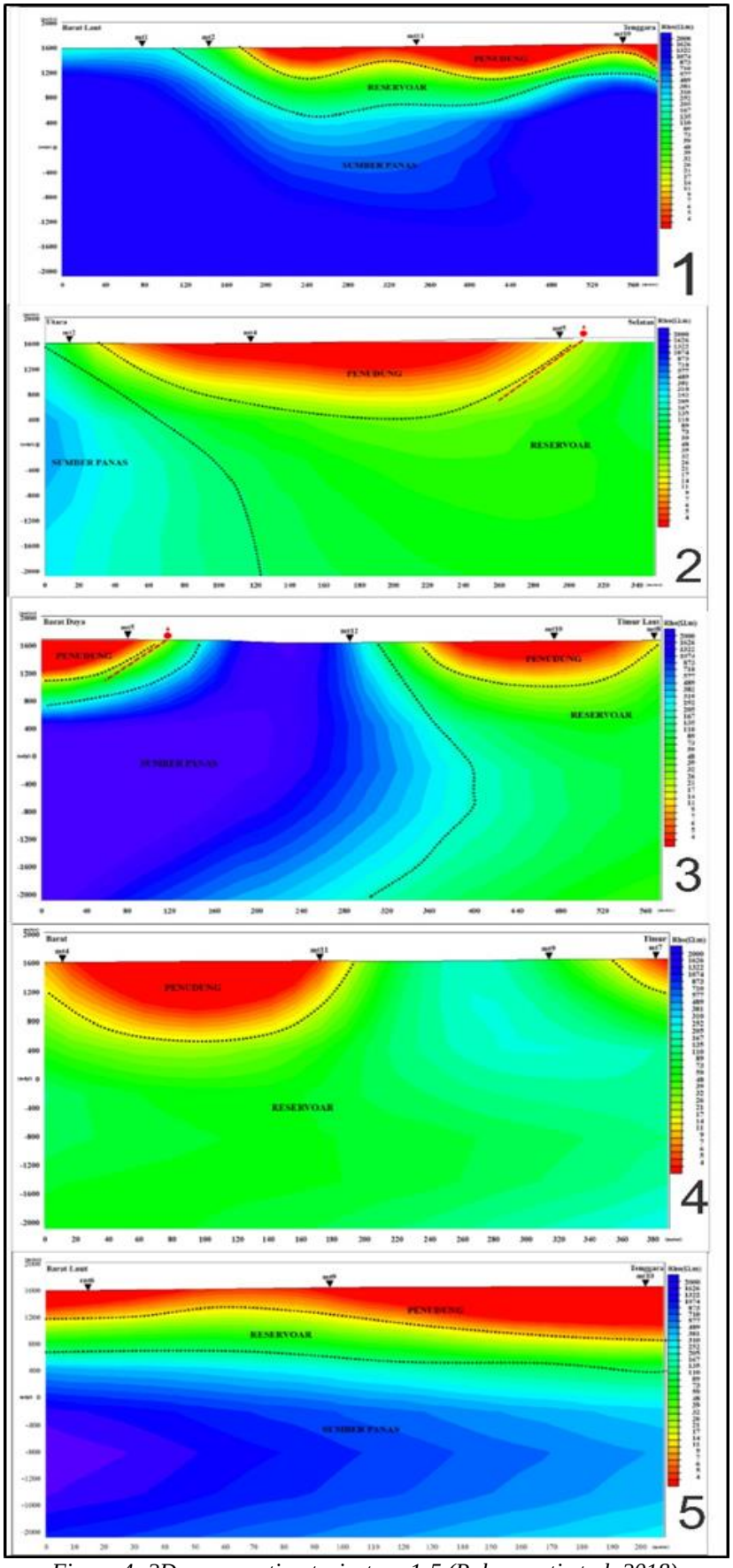


Figure 4: 2D cross section trajectory 1-5 (Rahmawati et al, 2018).

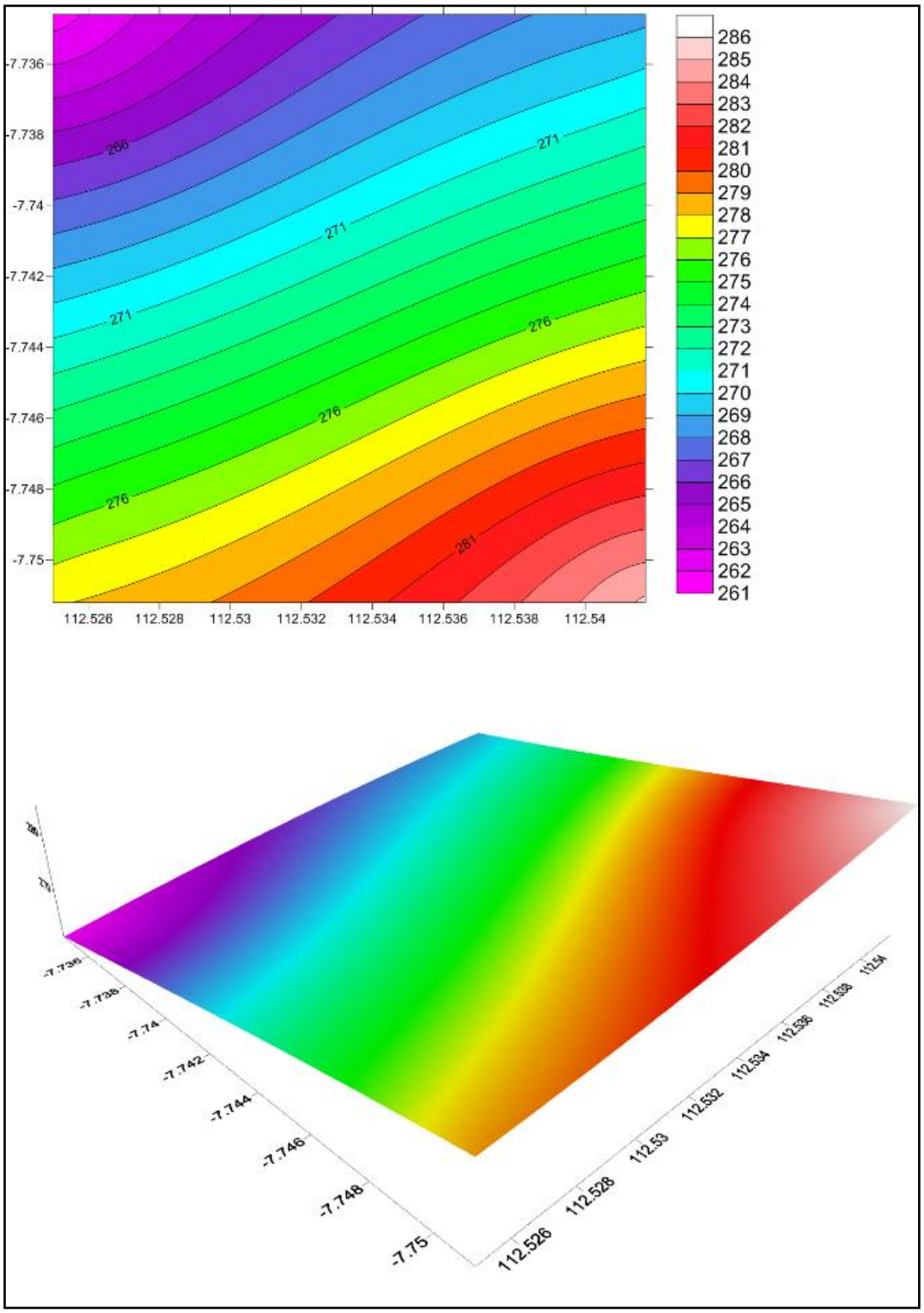


Figure 5: Map of geophysical gravity contour anomaly from TOPEX data.

Geological Data Analysis

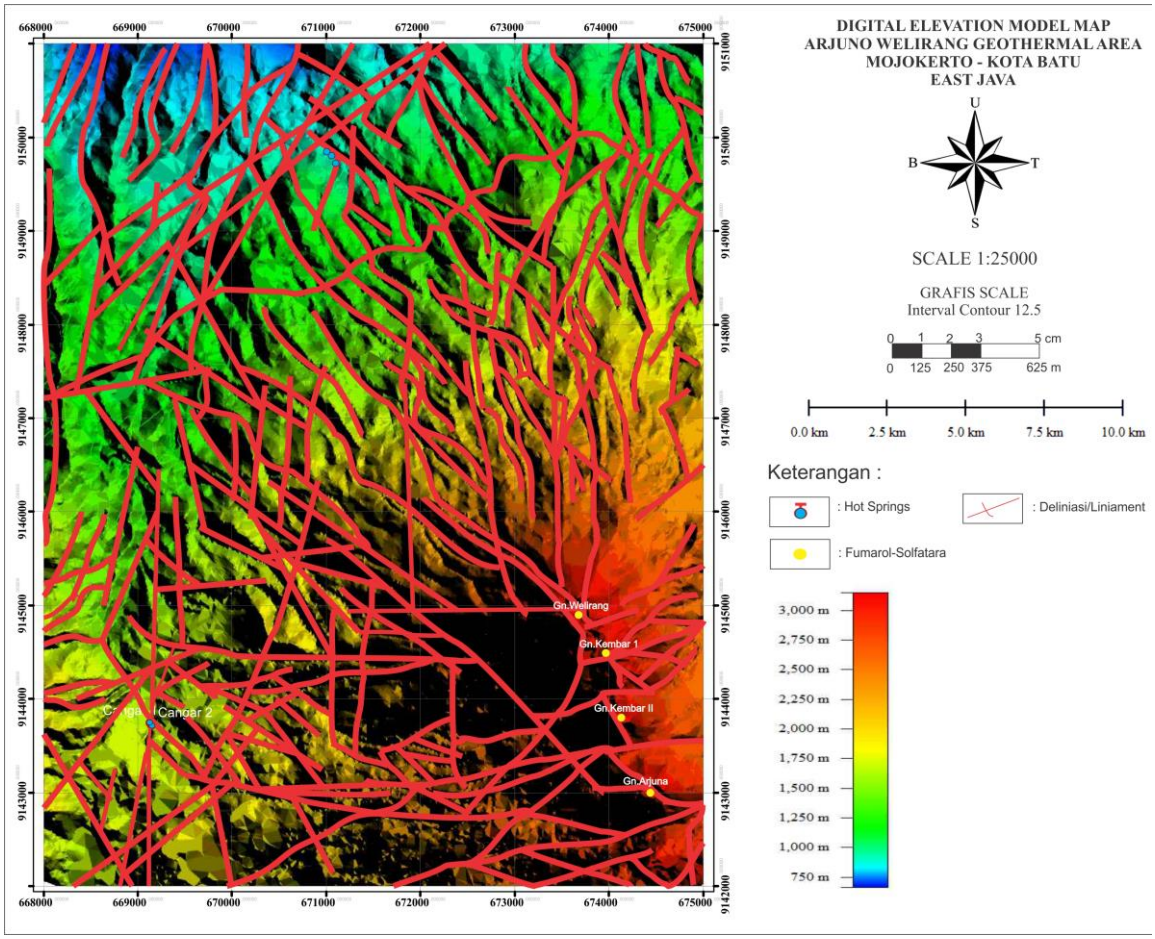
Based on geological mapping, the Cangar area has physiography with volcanic slope morphology and is located in the Arjuno-Welirang volcano complex and is located between Arjuno volcano and Anjasmoro ancient volcano, the flow pattern shows a radial pattern that is formed due to destructive volcanic activity and forms radial fractures. This radial flow pattern is a typical pattern of volcanoes. In regional geology, the Cangar region is composed of the upper Anjasmoro formation (QPVA) and is directly overlapped by the Arjuno-Welirang (QVAW) formation composed of four rock units that originate from volcanic activity. Stratigraphically, the research area is composed of four units of rock from the old to the young, namely

units of Anjasmoro andesite-basaltic rock, Anjasmoro tuff breccia, which is part of the QPVA formation, an old unit of Arjuno andesite-basaltic rock, which are part of the QVA formation, and oppressed by the Arjuno volcanic sediment unit which is part of the QVAW formation that hitches over a unit of old Arjuno andesite-basaltic. Based on geological data of lava andesite-basaltic Anjasmoro QPVA formations of middle Pleistocene quarter formed by magmatic eruption of Anjasmoro ancient volcano and deposited tuff breccia on top in suitability, breccia resulting from lava and tuff avalanches resulting from eruption then settling and undergoing a process of rocking to the northeast, this product from Anjasmoro ancient volcano was deposited in the Cangar and Sumberbrantas hamlet in the study area. Then the old Arjuno lava andesite-basaltic rock was deposited, this unit was formed in the middle Pleistocene quarter due to the magmatic eruption of the old Arjuno volcano which was deposited towards the northwest in the research area after which Arjuno volcanic deposits were deposited now which were deposited in almost all research areas.

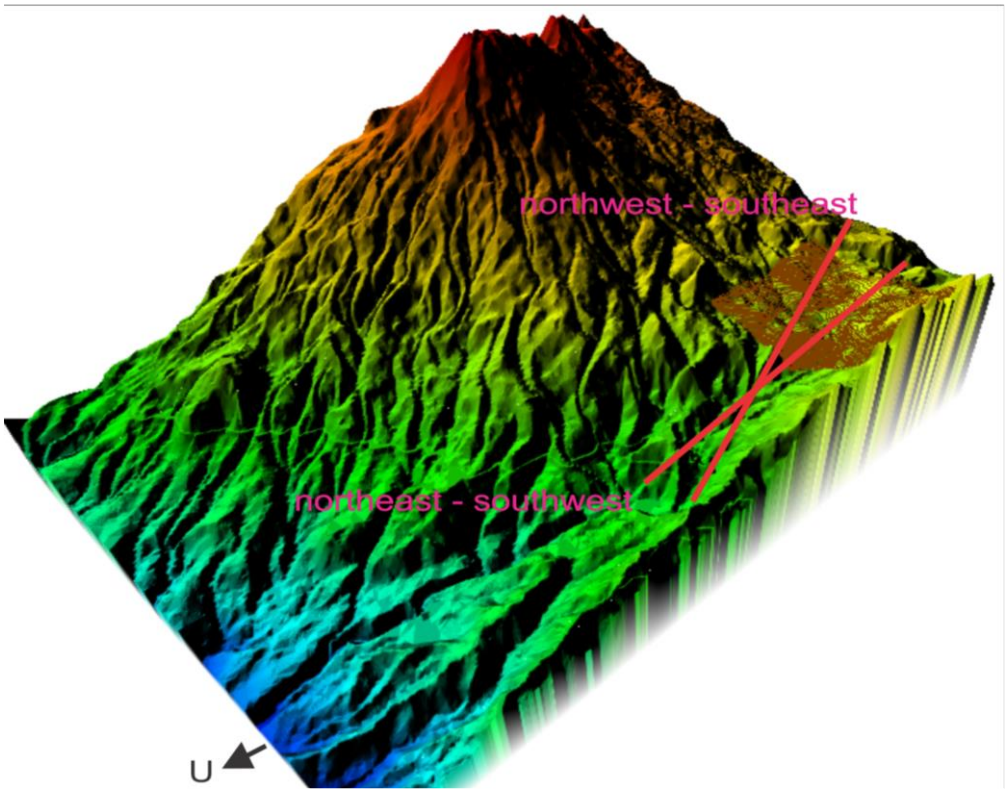
Geological Structure Analysis

Based on field data, there are two geological structures, namely the normal left slip fault direction structure of the northeast and the left slip fault structure direction northwest-southeast (Figure 7 and 8). This structure appears from volcanic processes which are characterized by normal faults and tectonic activities which are characterized by left slip fault.

Geothermal manifestations appear in the form of hot springs and are located in two locations in the research area along the Cangar River (Figure 9 and 10), precisely on the surface in the old Arjuno lava andesite-basalt which is a rock unit of QVA formation that arises due to the normal left slip fault structure southwest-northeast and left slip fault structure trending northwest-southeast.



(a)



(b)

Figure 6: (a) and (b) SRTM-DEM FFD Arjuno-Welirang map.

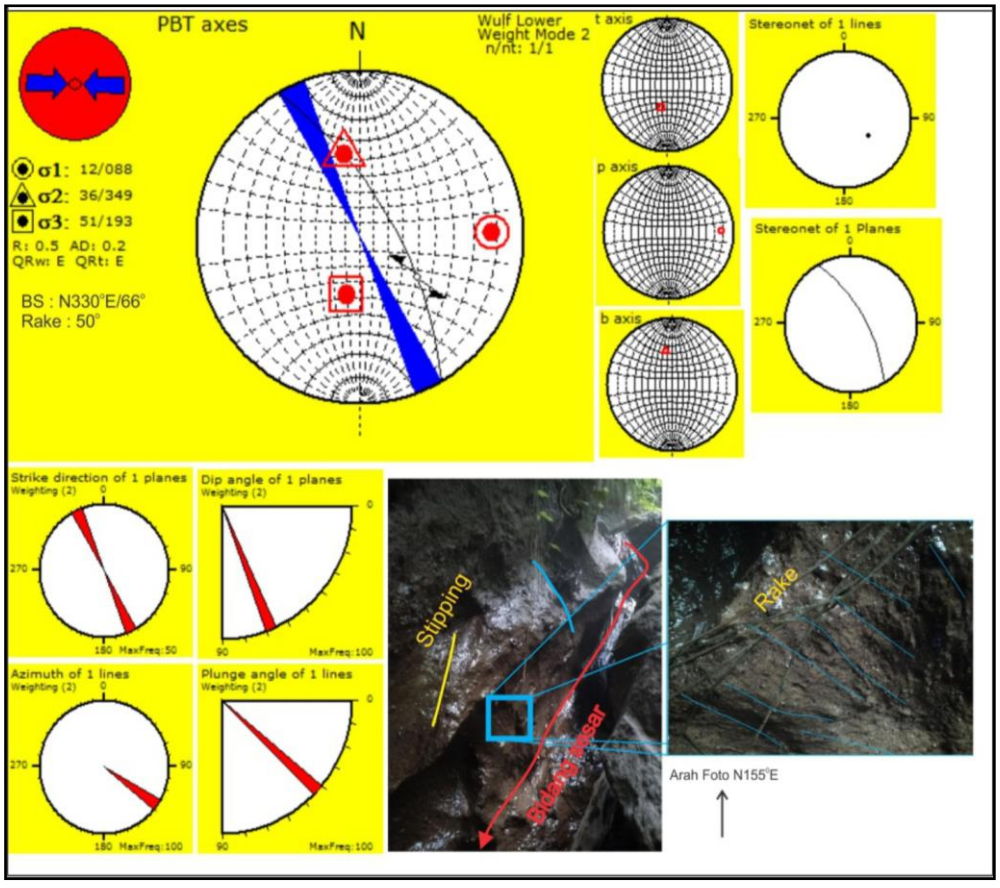


Figure 7: Structure 1(left slip fault) analysis.

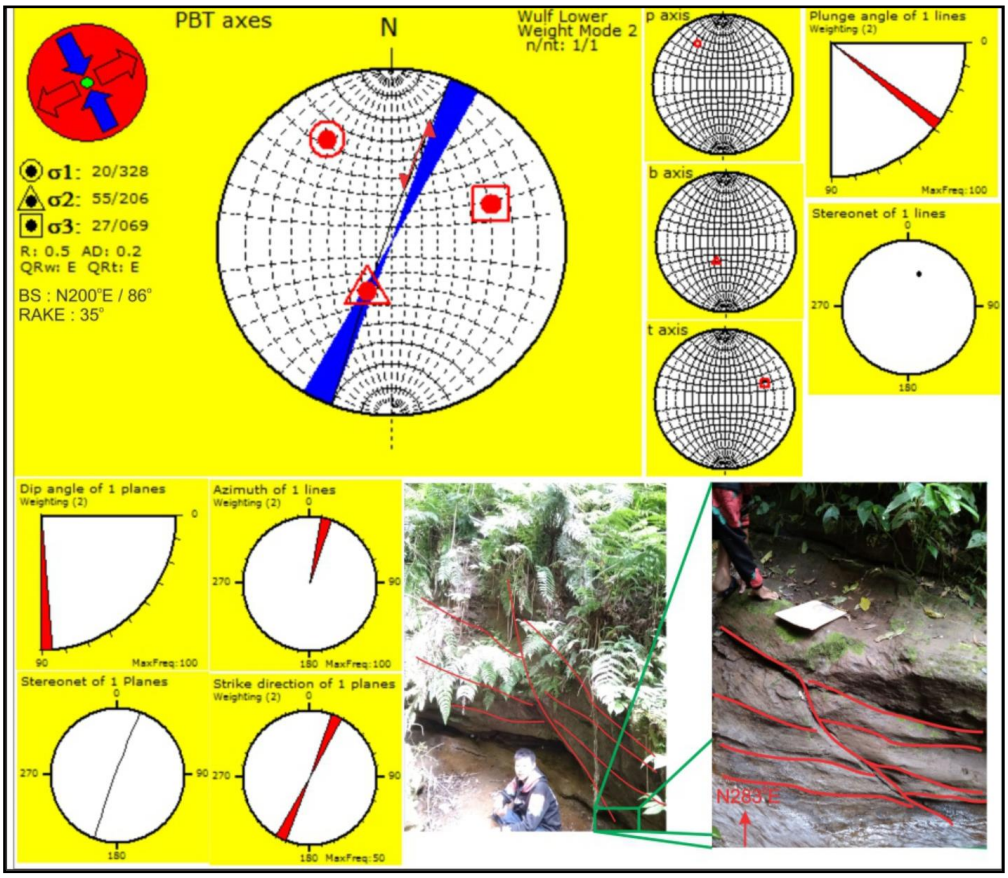


Figure 8: Structure 2 (normal left slip fault) analysis.

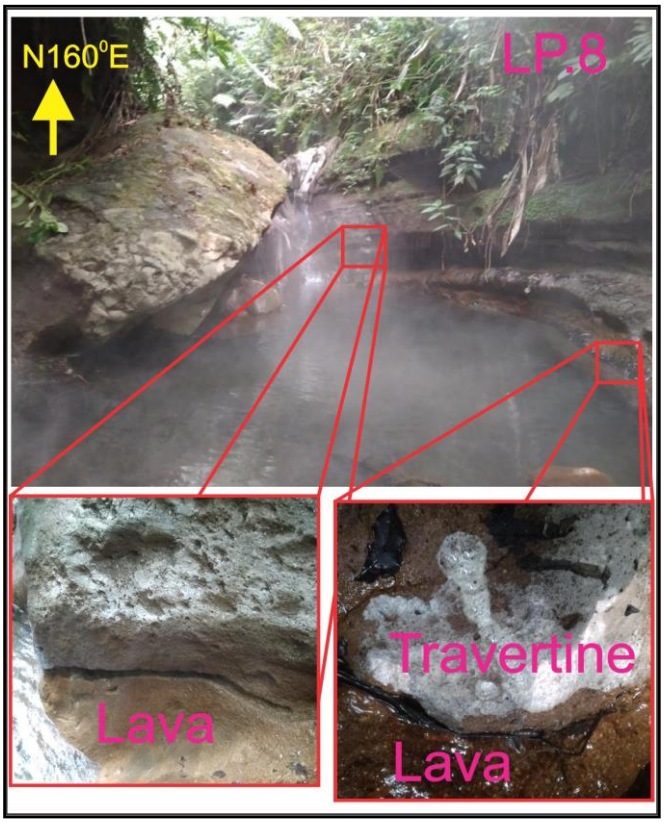


Figure 9: Cangar 1 Geothermal manifestation in LP.8.

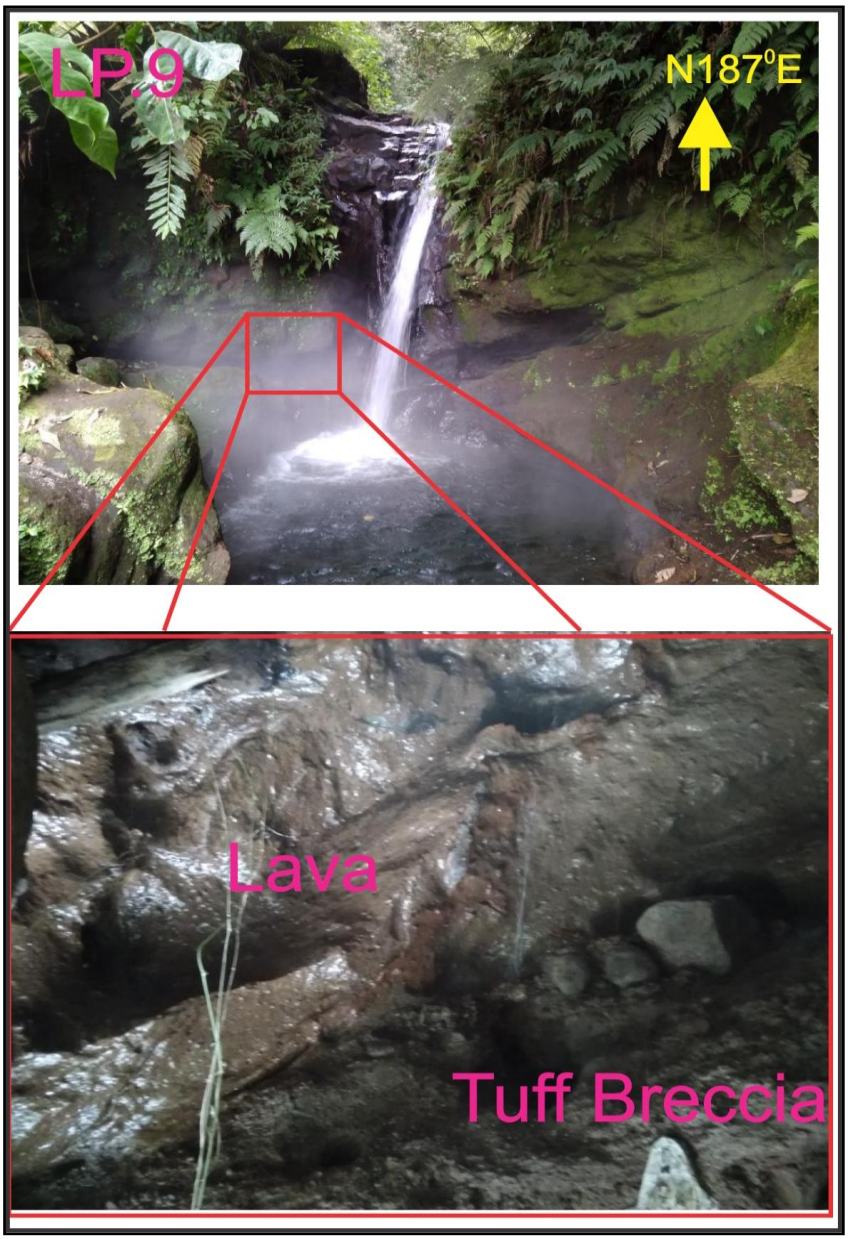


Figure 10: Cangar 2 Geothermal manifestation in LP.9.

Petrology and Petrography Analysis

Based on petrographic analysis of old Arjuno andesite-basaltic lava rock (Figure 11), has a characteristic pilotacytic structure, and texture hypocrystalline, subhedral, inequegranural with a plagioclase composition of 60% (labradorite (An68), bytownite (An42), pyroxene 10%, hornblende 20%, 2% opaque, 7% glass. Megascopic characteristics are grayish gray with greenish chlorite, flow structure and outcrop form a columnar joint.

Travertine is mudstone with calcite (Caco3) composition 80% and 20% mud (Figure 12). Travertine is formed due to the dissolution of Ca plagioclase namely bytownite and labradorite to form travertine deposits on the surface. While Anjasmoro andesite-basaltic lava rock has a characteristic reddish black color with vesicular structure joint setting, and texture porphyritic, subhedral-euhedral, inequigranural, and composition of quartz, feldspar, pyroxene, hornblende and plagioclase (Figure 13). Whereas argillic alteration found in Anjasmoro's andesite-basaltic lava rock body is clay alteration which is formed from feldspar and plagioclase changes and the presence of Sulfur (Figure 14).

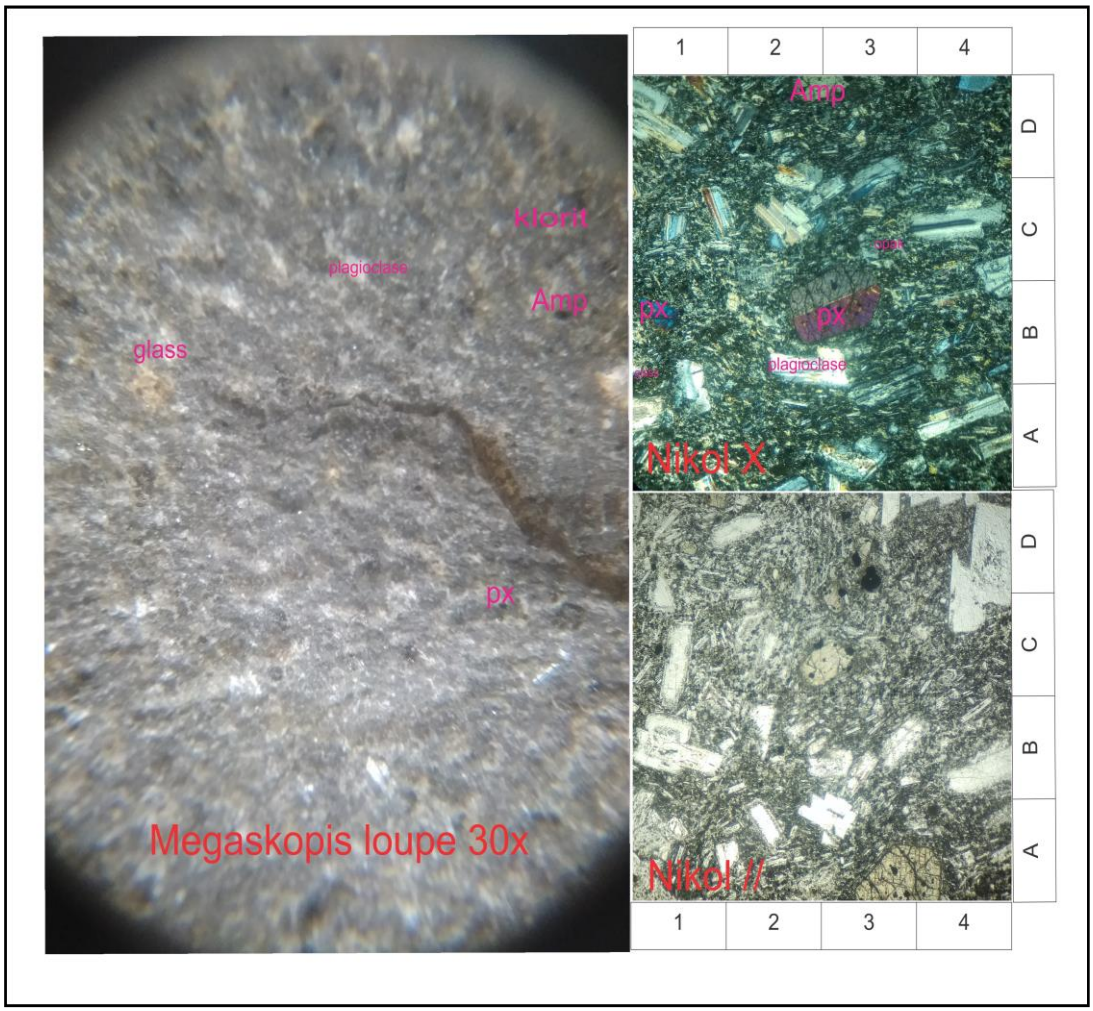


Figure 11: Old Arjuno andesite-basaltic lava rock.

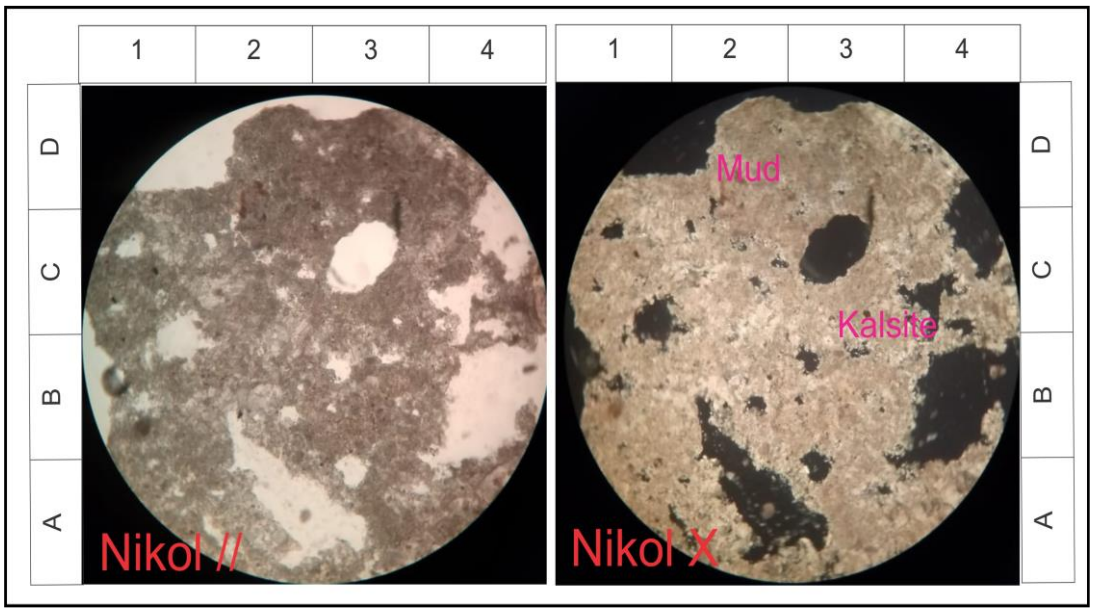


Figure 12: Travertine rock.

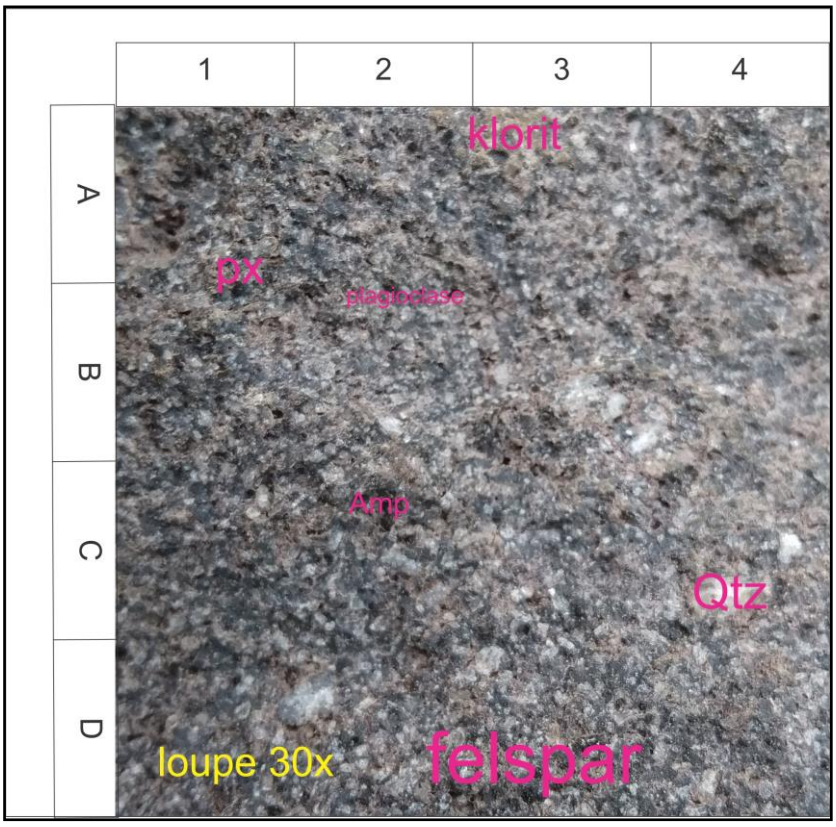


Figure 13: Anjasmoro andesite-basaltic lava rock.

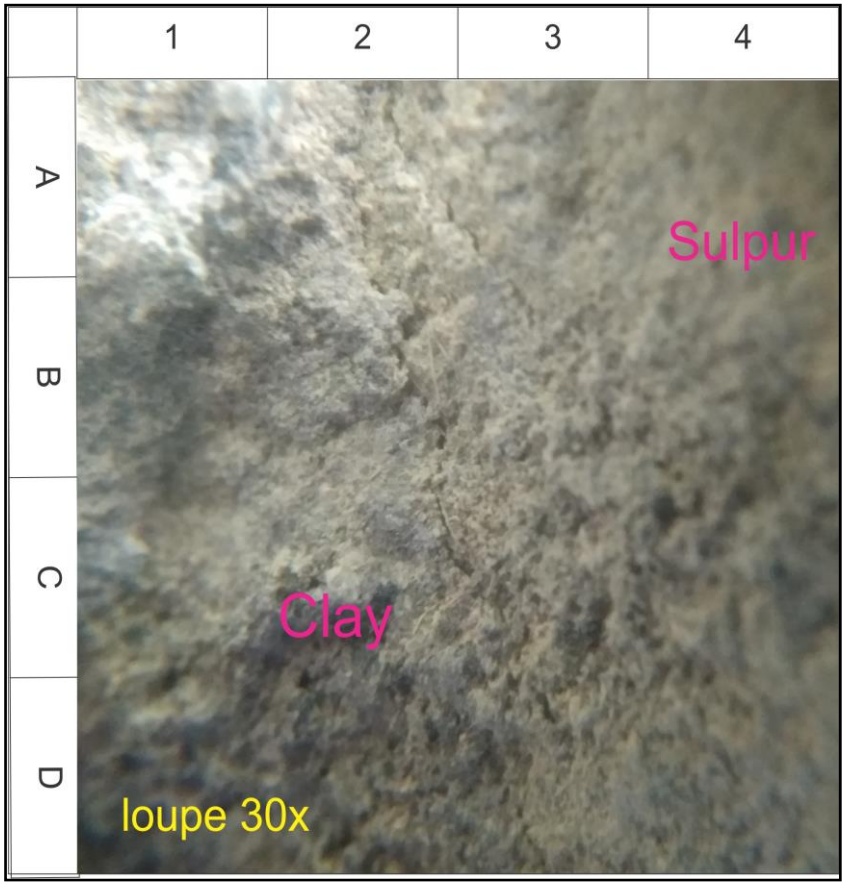


Figure 14: argillic alteration rock.

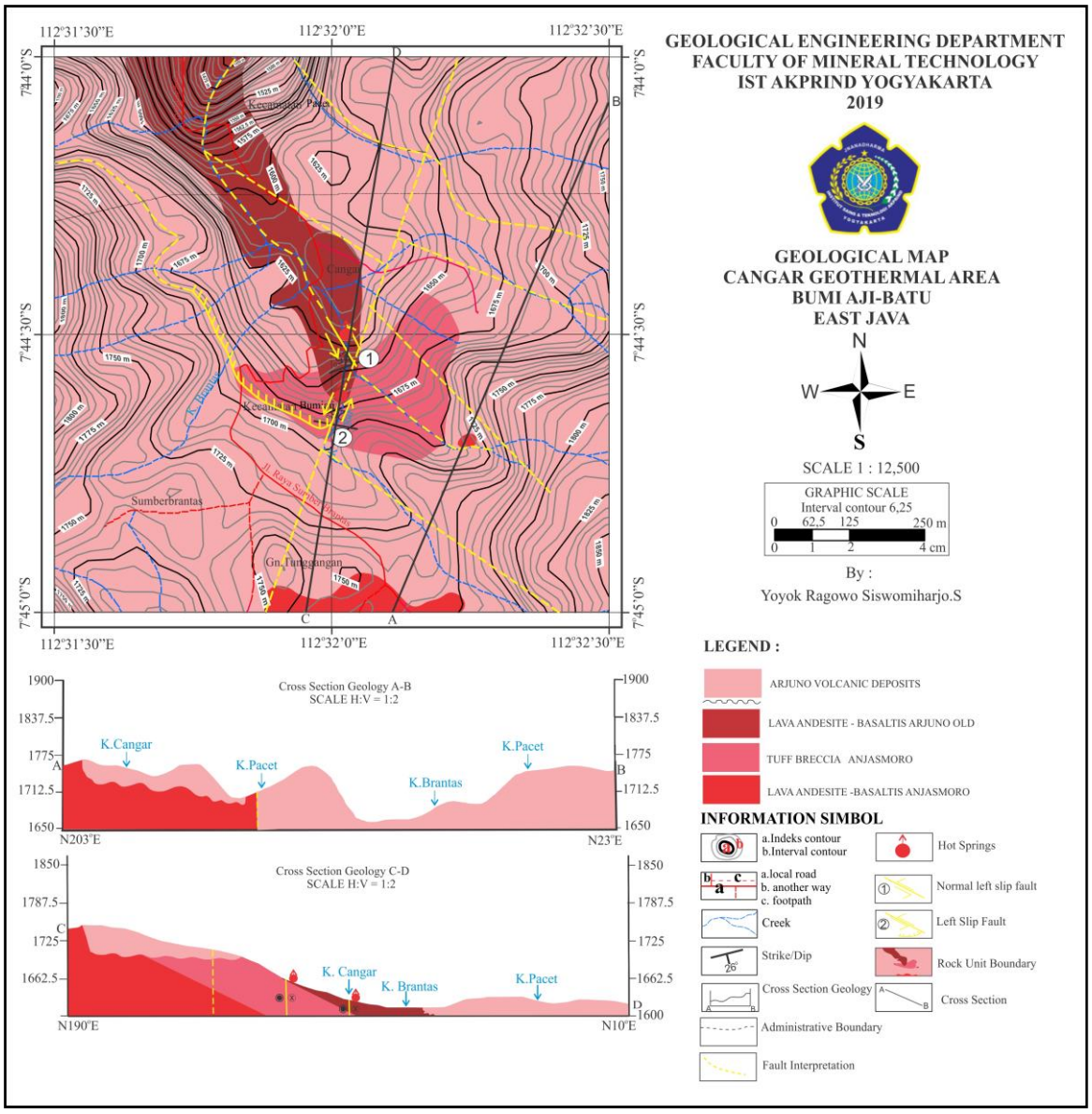


Figure 15: Geological map of Cangar geothermal area.

Geological map that was made from the geological mapping data contains data based on petrology data, petrography, and structural models, so that can be made for geothermal model systems in geology. Based on the geological cross-section (Figure 15) of the appearance of these manifestations due to fractures and geological structure of the caprock, rocks that become caprock of geothermal manifestations of the research area is Anjasmoro andesite-basalt lava QPVA formation, then tuff breccia Anjasmoro is a depressed aquifer type of groundwater reservoir. However due to a normal fault structure this aquifer leaking and mixing with hydrothermal water coming out of the caprock and appearing on the surface through the structure of old Arjuno lava andesite-basaltic rocks QVA formation. This mixing of hydrothermal and water table water dissolves and produces sulfur manifestations on the surface and makes pH close to neutral and forms travertine deposits on the surface exposed to settle on old Arjuno lava andesite basaltic. This Travertine is formed due to the dissolution of the element Ca in the plagioclase mineral and deposited to form mud which forms at temperatures of 300-430C, this travertine is one of the characteristics of the type of bicarbonate water (HCO3). On Anjasmoro lava andesite-basaltic QPVA formations are also deposited by clay as a result of argillic alteration, namely contact between hydrothermal or steam water with water table which occurs due to Igneous breccia cavities that occur in the rock above the tuff breccia and due to fractures and fractures then converts feldspar and plagioclase minerals into clay with formation temperatures below 2000C and neutral pH. Alteration of the Anjasmoro andesite-basaltic lava formation of QPVA was revealed on the surface because of a normal fault that caused the unit above to descend and erode so that it was

exposed on the surface and underwent weathering due to H20 which made the granular alteration clay granularly. Whereas the old Arjuno andesite-basaltic lava rock is a caprock of groundwater. So that in geology, reservoir and heating rocks of the geothermal system the Cangar area is not revealed and is still far below the surface of the study area, researchers interpreted that reservoirs and heating rocks came from old Arjuno volcanoes and Anjasmoro although the exposed caprock was part of Anjasmoro's ancient volcanic rocks because the formation of these two volcanoes in one fracture or crater hole and one time formation formed from volcanic fissures that are older and volcanic type. So, the researcher interpreted the heating rock and reservoir as part of the old Anjasmara ancient volcano which was formed in the lower Pleistocene quarter which is Strato type so that the heating rock and reservoir are very far below the surface. The geological data is then modeled so as to produce a geothermal system model in geological (Figure 16).

Geothermal systems that occur in the Cangar area are complex, volcanically active magmatic systems, namely geothermal systems associated with Quaternary volcanoes which are generally located in high-relief volcanic arcs and are volcanogenic, heat sources come from magma and are of type volcanic found in andesitic volcanoes with steep topography. This system appears outflow in the form of hot water systems with neutral pH or far from the source, namely the reservoir fluid moves upward with manifestations in the form of bicarbonate springs formed from carbon dioxide condensation with groundwater, travertine deposits and clay argillic alterations found at the edges of the geothermal system and the Cangar area is an infiltration area.

Geochemical Analysis

The results of geological data analysis carried out in suitability with the previous results of geophysical analysis and proven based on field mapping data. Then a geochemical analysis is needed to know and evaluate the potential and support the previous data (Table 1).

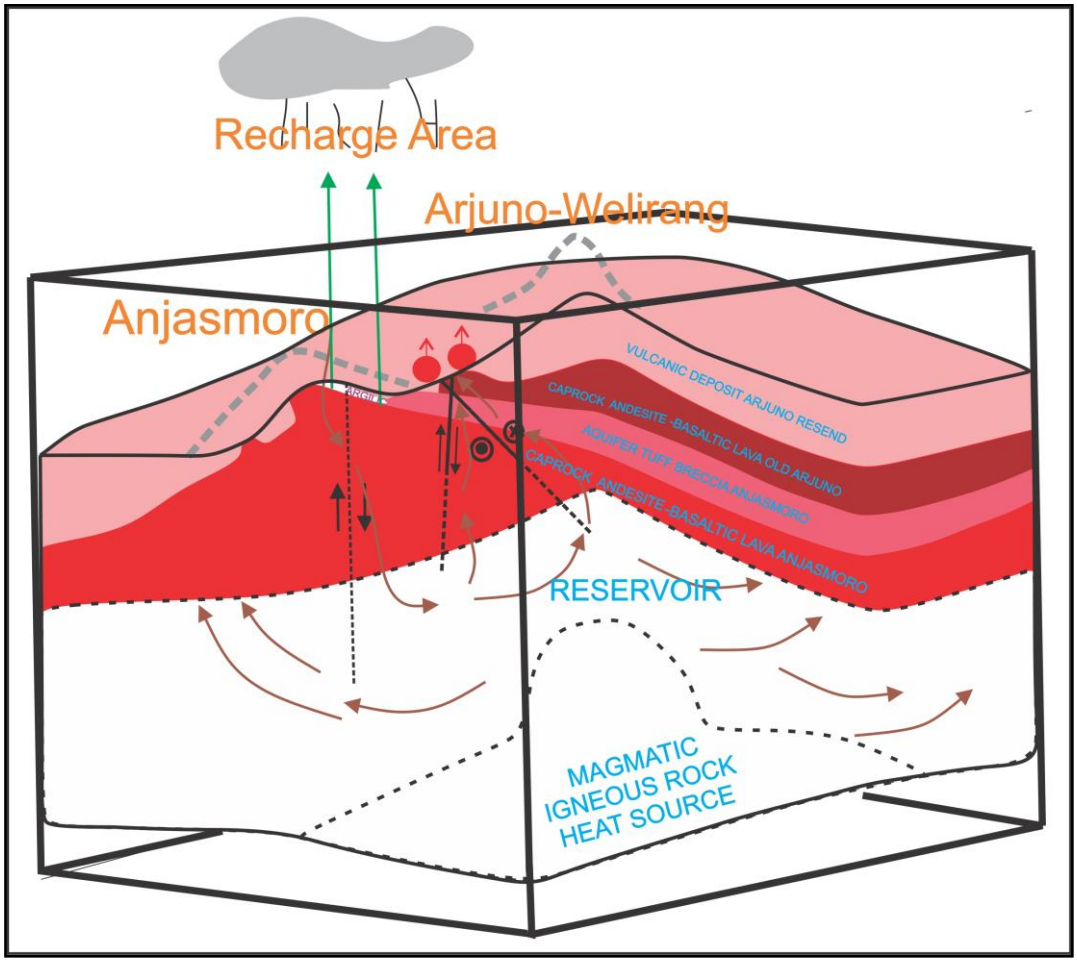


Figure 16: Geothermal system model in geological.

Table 1: Geochemical elements of water samples of Cangar geothermal area.

Sample	D.H.	PH	CL^-	$SO4^-$
Cangar 1	450	6,51	29,52	57
	B	K^+	Li^+	Mg^{++}
	1,53	17,36	0,50	34,22
	HCO_3^-	NA^+	Suhu	
	261,15	59	60	
Cangar 2	D.H.	PH	CL^-	$SO4^-$
	808	6,5	30,2	22,18
	B	K^+	Li^+	Mg^{++}
	1,53	17,36	0,50	34,22
	HCO_3^-	NA^+	Suhu	
	72,47	0,9725	58	

Based on the geothermometer analysis using Ternary SO4-Cl-HCO3 diagram (Figure 17), the results obtained were Cangar 1 SO4 18.89%, CL 13.17%, HOC3 67.94%. Whereas Cangar 2 SO4 17.76%, CL 24.19%, HOC3 58.05%, the plotting results from ternary SO4-Cl-HCO3 diagrams, namely the type of bicarbonate water with a Peripheral water system, were obtained.

Based on the geothermometer analysis using Ternary Na-Mg-K diagram (Figure 18), the results obtained were Cangar 1 Na 8.93%, Mg 88.50%, K 2.57%. Whereas Cangar 2 Na 0.08%, Mg 98.39%, K 1.61%, then get the plotting result from ternary Na-Mg-K diagram, which is the depth of immature waters.

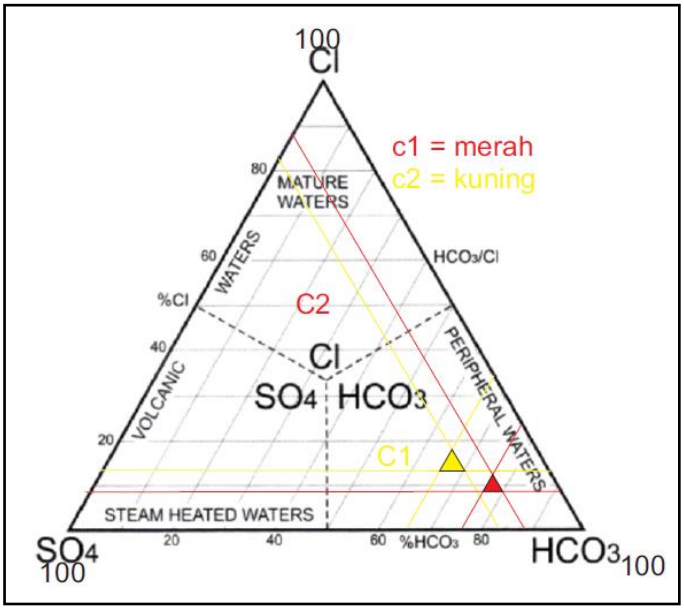


Figure 17: Ternary SO4-Cl-HCO3 diagram.

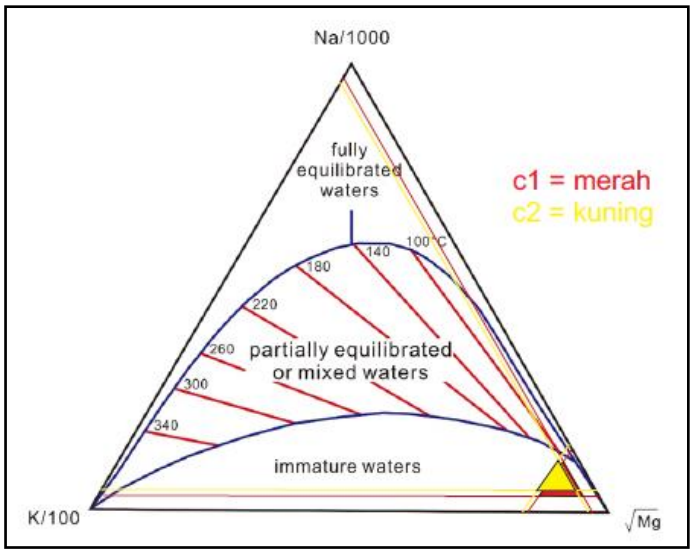


Figure 18: Ternary Na-Mg-K diagram.

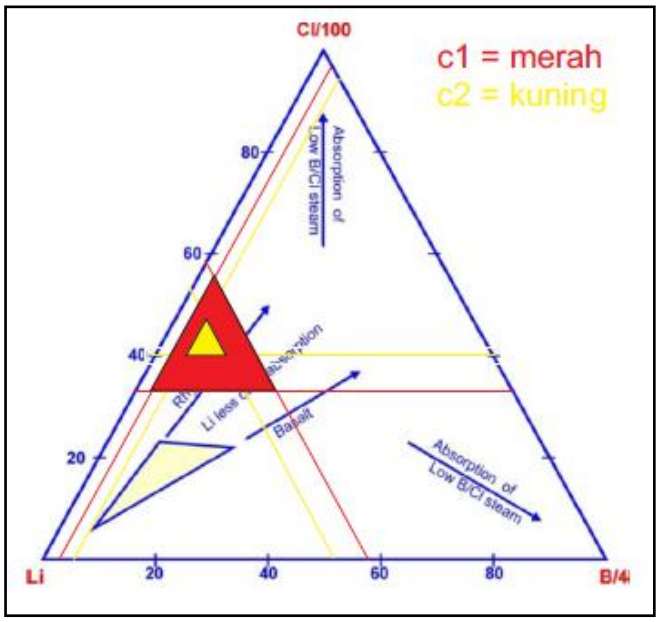


Figure 19: Ternary CL-B-Li diagram.

Based on the geothermometer analysis using Ternary CL-B-Li diagram (Figure 19), the results obtained were Cangar 1 Cl 35.71%, B 4.76%, Li 59.52%. Whereas Cangar 2 Cl is 0.99%, B is 6.06%, Li is 53.54%, so the plotting results from the ternary diagram Cl-B-Li are bedrock or heating rocks are intermediate-acid rocks, are present as intrusions. While the reservoir temperature based on density is obtained from ranges from $94,38^0$C-$108,70^0$C.

Based on the results of the geothermal analysis of Cangar geothermal water type area is bicarbonate (HCO_3) with emergence in the zone of peripheral which side rock assimilation and water table contact and immature maturity or shallow water depth with heating rock or bedrock very far from surface and bedrock rock type is intermediate -acid rocks, are present as intrusions. This indicates that the geothermal fluid has been mixed with surface water. It also indicates that the hot springs are an outflow of the geothermal system. The results of the analysis of geochemical data are the same as the results of geological and geophysical analysis, then further evaluate the potential for effective use of the geothermal research area.

Evaluation Potential

Based on the analysis of FFD-SRTM, gravity, geology and geothermometer data, the similarity of concepts is found, namely hot water coming out through cesarean which is caused by volcanic and tectonic processes and exiting the outflow zone. Then it is proven by geothermometer data and the geological concept of hot water types in the form of bicarbonate according to the manifestations in the field. Conceptually the geochemistry of hot water bicarbonate is formed in the zone of peripheral side rock assimilation and water table contact and immature maturity with heating rock or very far bedrock from surface and bedrock rock type is intermediate -acid rocks In accordance with the geological concept namely system appears outflow in the form of hot water, the reservoir fluid manifestations in the form of bicarbonate springs formed from carbon dioxide condensation with groundwater, travertine deposits and clay argillic alterations found at the edges of the geothermal system and the Cangar area is an infiltration area. This geological data is also proven by geophysical data and the gravity contour map anomaly shows the contact limit between rocks that are clearly marked to the southeast which is getting higher. With contour values 261-286. The results of the combination of the data (Figure 20), interpreted the potential area of the Cangar geothermal reservoir which is 4 Km^2 with reservoir temperature range 94,38ºC-108,70ºC as evidenced by the morphological conditions that form valleys with steep cliffs due to the influence of geological structures and basin boundaries. very clearly indicated by the contour gravity data and can be seen the contact rock on the geological map. The extent of the Cangar geothermal reservoir of 4 Km^2 is also based on the geological cross section that the reservoir is continuous throughout the study area and is still found in the flow of hot water along the Cangar river, this also occurs due to the complex geological structure of the research area. The surface water temperature in the study area can change due to the influence of the infiltration of surface water and contact with hydrothermal water.

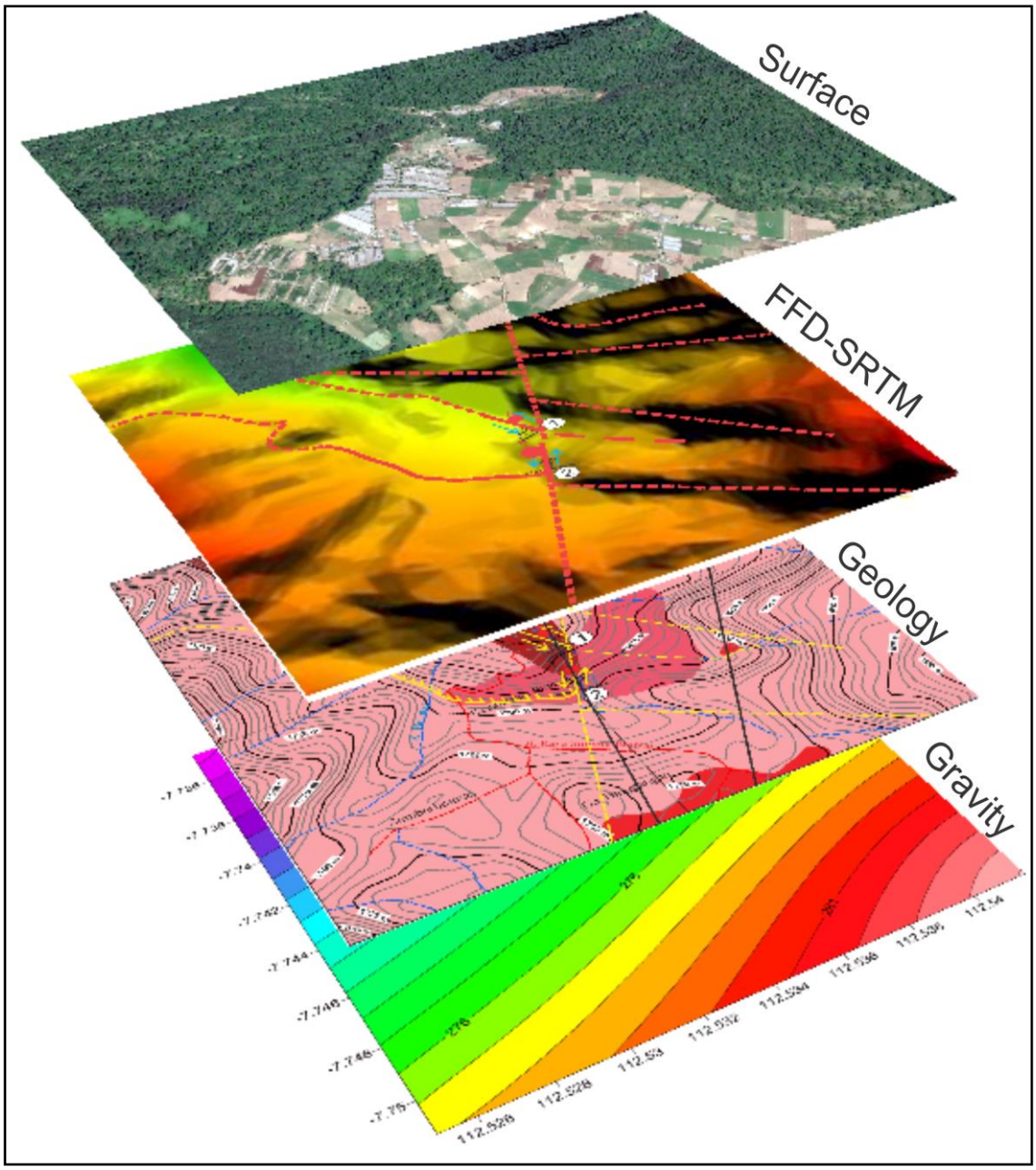


Figure 20: Combination of geophysical data, geology, FFD-SRM and surface appearance.

So, based on the above data the researcher evaluates the potential of the Cangar area geothermal resources based on speculative methods based on the initial estimates of a prospect analogous to the fields that have been developed so that it is generally formulated as:

$$P = 0{,}273 \text{ X } A \text{ (Tr-Tcut off)}$$

P = Potential
A = Reservoir area which is 4 Km^2
Tr = OC reservoir temperature 94,38^{0}C-108,70^{0}C
$T_{Cut\ off}$ = 90^{0}C due to low temperature <125^{0}C

Cangar 1 potential:

P = 0,273 X 4 (94,38-90)
P = 4,78 MWe/Km^2

Cangar 2 potential:

P = 0,273 X 2 (108,70-90)
P = 20,4 MWe/Km^2

So, the geothermal potential of cangar area is range of 4.78-20.4 MWe/Km^2.

Then further evaluate the effective use of the SWOT method (table 2 and 3). Based on the results of SWOT analysis it was concluded that the Cangar area produced effective geothermal manifestations

to be used as geotourism areas compared to power plants.

Table 2: Swot analysis for effective use as geotourism.

STRENGTH (S)	a. As a tourist hot spring bathing place b. Hot water in the research area is effective in improving blood circulation c. Improve the potential economics of the surrounding community d. Around the location offers its own charm
WEAKNESS (W)	a. the route taken is rather difficult.
OPPORTUNITIES (O)	a. Can increase employment and increase revenue for the government b. in the future the place can be a favorite place for visiting the area
THREATS (T)	a. some points are believed to be prone to landslides

Table 3: Swot analysis for effective use as power plants

STRENGTH (S)	a. The Potential of Geothermal Energy b. Increased Electricity Sellin Tariff Commitments c. Increasing the economic potential of the surrounding community d. Increased Infrastructure related to Geothermal Energy e. Mix energy fulfillment f. Potensial 4.78-20.4 MWe / km2
WEAKNESS (W)	a. Expensive costs b. type of bicarbonate water with low temperature > 125^0C c. deep reservoir d. associated with the active volcano Arjuno-Welirang e. The geological structure is complex and can cause drilling failures f. permits that are already due to enter the forest
OPPORTUNITIES (O)	c. Can increase employment and increase revenue for the government d. Can be geowisata
THREATS (T)	a. protected forest land thus increasing costs b. high earthquake potential c. high volcanic eruption potential d. potential for high structural movements

CONCLUSIONS

1. Based on geophysical data from gravity contour map anomaly indicates the existence of a contact limit between rocks that are clearly marked with a significant color change to the southeast which is getting higher with contour values range 261-286.
2. Base on FFD-SRTM analysis geothermal manifestations appear in the Cangar area was formed due to geological structures that trended northwest-southeast and northeast-southwest and associated with the Arjuno-Welirang volcano complex.
3. Based on geological mapping, the Cangar area has physiography with volcanic slope morphology and located in the Arjuno-Welirang volcano complex and is located between Arjuno volcano and Anjasmoro ancient volcano, the flow pattern shows a radial pattern that is formed due to destructive volcanic activity and forms radial fractures. This radial flow pattern is a typical pattern of volcanoes. Stratigraphically, the research area is composed of four units of rock from the old to the young, namely units of Anjasmoro andesite-basaltic rock, Anjasmoro tuff breccia, which is part of the QPVA formation, an old unit of Arjuno andesite-basaltic rock, which are part of the QVA formation, and oppressed by the Arjuno volcanic sediment unit which is part of the QVAW formation that hitches over a unit of old Arjuno andesite-basaltic. Based on geological structure analysis, geothermal manifestations appear in the form of hot springs and are located in two locations in the research area along the Cangar River, precisely on the surface in the old Arjuno lava andesite-basalt which is a rock unit of QVA formation that arises due to the normal left slip fault structure southwest-northeast and left slip fault structure trending northwest-southeast.
4. Based on the geological cross-section of the appearance of these manifestations due to fractures and geological structure of the caprock, rocks that become caprock of geothermal manifestations of the research area is Anjasmoro andesite-basalt lava QPVA formation, then tuff breccia Anjasmoro is a depressed aquifer type of groundwater reservoir. However due to a normal fault

structure this aquifer leaking and mixing with hydrothermal water coming out of the caprock and appearing on the surface through the structure of old Arjuno lava andesite-basaltic rocks QVA formation.

5. Geothermal systems that occur in the Cangar area are complex volcanically active magmatic systems, namely geothermal systems associated with Quaternary volcanoes which are generally located in high-relief volcanic arcs and are volcanogenic, heat sources come from magma and are of type volcanic found in andesitic volcanoes with steep topography. This system appears outflow in the form of hot water systems with neutral pH or far from the source, namely the reservoir fluid moves upward with manifestations in the form of bicarbonate springs formed from carbon dioxide condensation with groundwater, travertine deposits and clay argillic alterations found at the edges of the geothermal system and the Cangar area is an infiltration area.
6. Based on the geothermometer analysis results from ternary SO4-Cl-HCO3 diagrams, namely the type of bicarbonate water with a Peripheral water system, were obtained. The result from ternary Na-Mg-K diagram, which is the depth of immature waters. The results from the ternary diagram Cl-B-Li are bedrock or heating rocks are intermediate-acid rocks, are present as intrusions. While the reservoir temperature based on density is obtained from ranges from 94,38ºC-108,70ºC.
7. Base on speculative methods analysis potential resources of geothermal Cangar area is range of 4.78-20.4 MWe / Km^2.
8. Based on the results of the SWOT analysis it was concluded that the Cangar area produced effective geothermal manifestations to be used as geotourism areas compared to power plants.

ACKNOWLEDGMENT

We would like to thank the IIGCE committee for giving us the opportunity to publish our research. Thank to Laboratory of water quality test Perum Jasa Tirta, HMTG "GAIA", AAPG ISTA SC, SM-IAGI ISTA SC and we would special thanks to MGEI Research Group (MRG) Student Chapter IST AKPRIND Yogyakarta and YPPP for support.

REFERENCES

Wardana, A., O'Sullivan, J., and O'Sullivan, M., (2016), "Natural State and Future Production Modelling of Arjuno-Welirang Geothermal Field, Indonesia". Proceedings 38th New Zealand Geothermal Workshop Auckland, New Zealand, 23 - 25 November 2016.

Bakruddin., Widya Utama., and Dwa Desa Warnana., (2017), "Analisa Batuan Alterasi Panas Bumi Arjuno-Welirang Berdasarkan Sifat Mineraloginya". Journal Inotera. 2. 67-70.

Daud, Y., Fahmi, F., Nuqramadha, W. A., Heditama, D. M., Pratama, S. A. & Suhanto, E. (2015), "3-Dimensional Inversion of MT Data over the Arjuno-Welirang Volcanic Geothermal System, East Java (Indonesia)". Proc. World Geothermal Congress 2015, 1-6.

Hadi, M. N., Kusnadi, D., Rezky, Y. (2010), "Penyelidikan Terpadu Geologi dan Geokimia Daerah Panas Bumi Arjuno-Welirang, Kabupaten Mojokerto dan Malang, Provinsi Jawa Timur". Pusat Sumber Daya Geologi Kementerian Energi dan Sumber Daya Mineral, pp. 405 – 412.

Hamilton, W. (1979), "Tectonic of Indonesian Region ". U.S. Geological Survey Professional Paper. 1078, United States Government Printing Office, Washington, USA, pp. 345.

Rahmawati, Maryanto. S., and Susilo A., (2018), "Identifikasi Sistem Panas Bumi Daerah Cangar, Jawa Timur menggunakan Metode Magnetotelurik". Journal of Physical Science and Engineering. 2. 72– 82.

Santosa, S. and Suwarti, T. (1992), "Peta Geologi Lembar Malang, Jawa Timur, skala 1: 100.000". Pusat Penelitian dan Pengembangan Geologi, Bandung.

Sunaryo, (2012), "Identification of Arjuno-Welirang Volcano-Geothermal Energy Zone by Means of Density and Susceptibility Contrast Parameters". International Journal of Civil & Environmental Engineering IJCEE-IJENS, 12, 9-20.

Tim survey geology dan geokimia PSDG. (2010) "Geological Map Arjuno-Welirang Geothermal Area Mojokerto-Malang-Pasuruan East Java". Badan Geologi, Bandung.

Sumotarto. U., (2018), "Geothermal Energy Potential of Arjuno and Welirang Volcanoes Area, East Java, Indonesia". International Journal of Renewable Energy Research, 8, 614-624.

Williams, H., Turner F. J., and Gilbert C. M. (1982), "Petrography, An Introduction to Study of Rock in Thin Section", University of California, Barkeley, W.H, Freeman and Company, San Fransisco, pp. 406.

DETECTING THE EXISTENCE OF ALTERATION MINERALS IN THE ACTIVE GEOTHERMAL AREA OF TANGKUBAN PERAHU MOUNTAIN AND SURROUNDING AREAS USING RESULTS OF LANDSAT-8 PROCESSING TO IDENTIFY DISTRIBUTION OF SURFACE CONDITION CHANGES FROM THE HYDROTHERMAL PROCESS

Sinatrya Diko Prayudi[1,2], Daffa Arrofi[1], and Rinal Khaidar Ali[1]

[1]Departement of Geological Engineering, Diponegoro University, Semarang, Indonesia
[2]North East Java Research Section, Diponegoro University, Semarang, Indonesia
Email: sinatrya.diko@gmail.com

ABSTRACT

Tangkuban Perahu Mountain is one of the many active volcanoes on Java Island that holds the potential for geothermal development. Some of the evidence shows geothermal manifestations are in several areas which include the presence of deep upflow located nearby it crater and outflow in the Kancah, Cimangu, Maribaya, Ciater, Batugede, Ciracas, and Batukapur regions. The existence of geothermal manifestations on the surface is generally related with the presence of alteration or secondary minerals and clay minerals resulting from alteration processes in the surrounding rocks. Identifying the presence of geothermal minerals plays an important role to undestanding the distribution of areas that have been altered by hydrothermal fluids to strengthen the presence of large reserves of potential within them. By using Landsat-8 image data from 2015 and 2018, the determination of the existence of alteration minerals such as clay minerals and secondary minerals can be relatively mapped in a large area and compared to understand the distribution of altered surface. Processing carried out on Landsat-8 data refers to several methods: band composite, band ratio, and Spectral Angle Mapper (SAM) between 2015 and 2018. The processing results shows the possibility of geothermal manifestations is not only concentrated in areas previously known, but in other areas around the body of Tangkuban Perahu Volcano, relative distribution of alteration minerals, and decreasing of alteration mineral distribution on in 2018 compared to 2015 result.

Keywords: Remote sensing, landsat-8, Mt. Tangkuban Perahu

INTRODUCTION

Identifying the existence of a geothermal potential in an active or dormant volcano is one of the efforts to expanding the development of geothermal renewable energy in Indonesia. The geological setting of Indonesia which is in the part of the world's ring of fire provides many potential locations for the development of alternative energy sources in the future, in this case geothermal energy. To find out whether the geothermal source in the mountain body still holds potential or not, one of the efforts to find out is to identify the process of heat output from underneath the earth to the surface. The process commonly known as heat release in the mountain body, usually raises several as hotspots forming geothermal manifestations. This manifestation generally arises due to the control of geological structures that trigger the emergence of fractures as fluid discharge paths (Soengkono, 1999; Nurohman, 2016).

Some areas that are generally the exit point for manifestations are directly in contact with hydrothermal fluid that triggered alteration processes, namely alteration of side rocks or previously existing ones, especially the rock mineralogy which changes both physically and chemically due to this fluid (Beane, 1982). The focus of the study area which is a key target in the identification of altered areas in this study is the potential geothermal area which is famous for the beauty of natural landscapes and potential geothermal reserve reaching of 90 MWe (Kementrian ESDM, 2017), namely Tangkuban Perahu Volcano.

Tangkuban Perahu Mountain itself become a part of Sunda – Tangkuban Perahu Volcano Complex with evolutionary dynamics tracing the tephrachronology that has changed in at least 4 times in the phase of volcanism (Kartadinata, 2005). For Tangkuban Perahu Volcano itself, volcanism began in 90,000 years ago, with two systems of volcanism: Old Tangkuban Perahu or TPT (> 10,000 years ago) and Young Tangkuban Perahu or TPM (<10,000 years to date). Each volcanism unit produces a distinctive type, where TPT units are phreatomagmatic and magmatic whereas TPM is predominantly phreatic and few magmatic types. The phreatic activity of TPM phase occurs in a short duration but intensively in rapid repetition pattern which is an indicator of active rock alteration processes on the surface and subsurface in the area around the body of Tangkuban Perahu Volcano (Surmayadi, 2011).

In identifying the distribution of hydrothermal minerals and rocks presence, conventional methods such as geophysics and geochemistry are common in several potential geothermal regions in Indonesia (Nuha et al., 2014; Mustopa et al., 2017; Byrdina et al., 2018). Besides the geoscience approach above,

there are other methods by utilizing more easier data access with inexpensive costs. The method is to use remote sensing imagery data. The use of remote sensing for minerals identification, in this case alteration minerals are often used by many researchers, especially in the identification of economical minerals (Julzarika, 2018).

The processing of remote sensing image data in the target area of Tangkuban Perahu Volcano in this study uses single image data: Landsat 8 OLI/TIRS. Processing of image data carried out includes three main points: mapping areas that related to alteration processes, comparing the distribution of minerals and rocks affected by alteration processes on the surface, and identifying the alteration pattern in this location. Data processing carried out involves several GIS-based software and a series processing satellite imagery data derived from two different Landsat image data for years. The simplest methodology for sensory-based identification is as exemplified by Mia and Fujimitsu (2012) and Julzarika (2018) using technical band ratios, composite bands, and several other spectral analysis methods.

Based on research conducted by Achmad et al. (2015), relating to the distribution of surface manifestations in Tangkuban Perahu Volcano, surface manifestations in this area are widely distributed both within the crater body totaling 6 units (New, Upas, Ratu, Jurig, Domas, and Jarian) and some areas outside the crater such as Cimangu, Batu Kapur, Batu Gede, Ciracas, and Batu Gede (see Figure 1). Typical geothermal manifestations are found in the form of altered rocks, solfatara, fumaroles, heated pools, boiling pools, and mud pools (Figure 2).

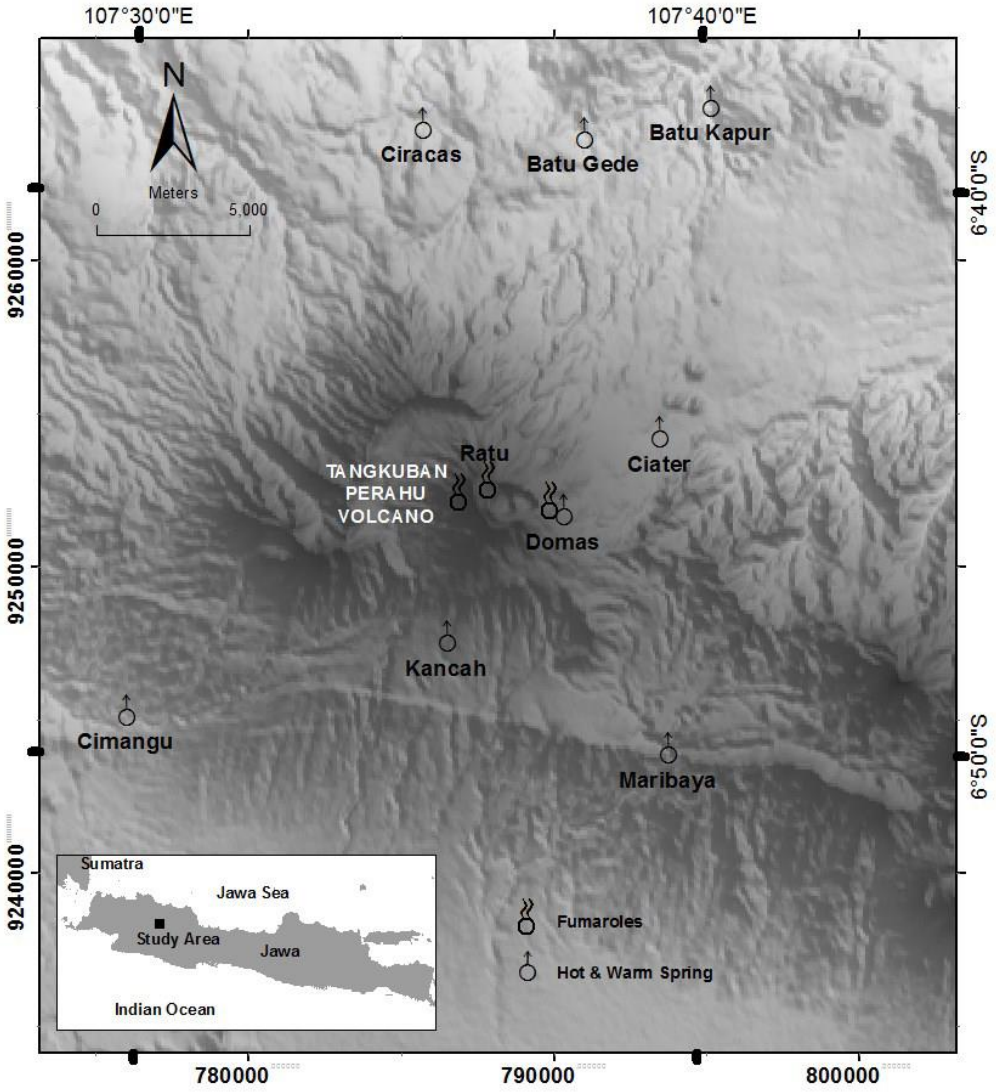


Figure 1: Location of Tangkuban Perahu Volcano and general distribution of geothermal manifestation inside and outside crater (Saputra and Suryantini, 2015).

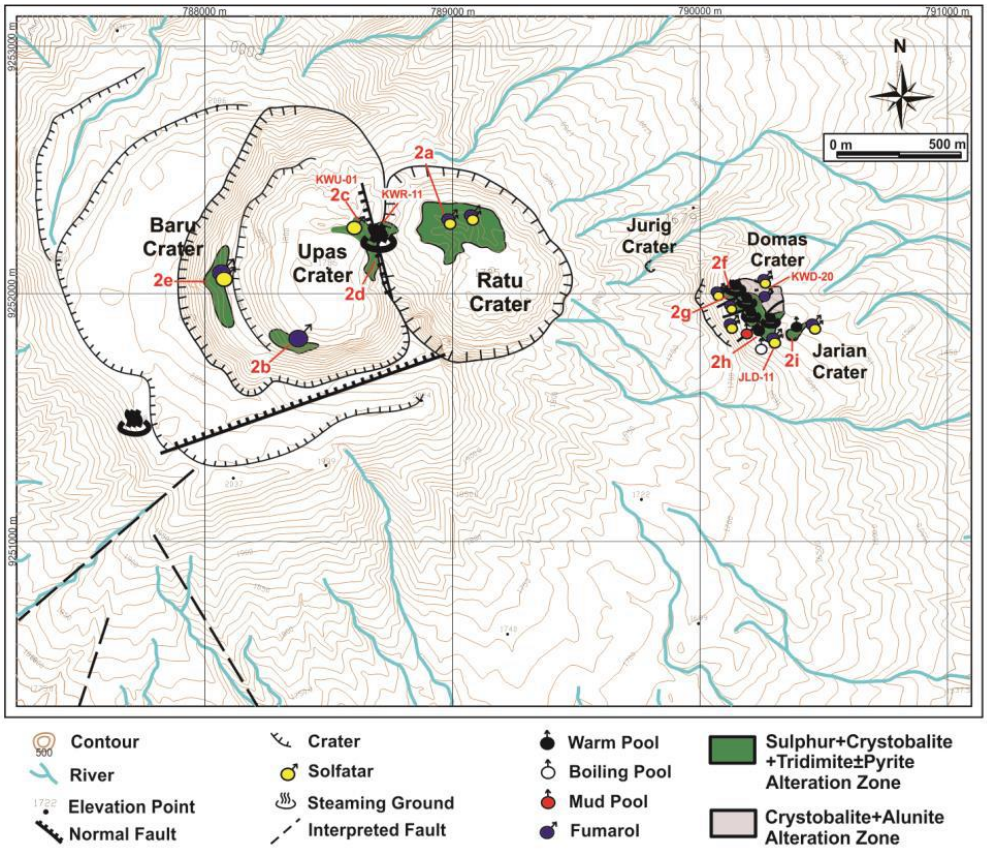


Figure 2: Specific distribution of geothermal manifestation inside crater of Tangkuban Perahu Volcano (Achmad et al, 2015).

The features of the Tangkuban Perahu Mountain geothermal system itself are influenced by two aspects beyond the presence of sub-surface heat activity. The first aspect is the development of two alignments indicated by major faults in the north and south of the mountain which affect the presence of fracture that become manifestations opening for fluid pathways (van Bemmelen, 1949; Nasution, 2004; Hendri et al, 2012). The second aspect is the presence of a cap rock which acts as a barrier to the rate of discharge of the fluid and triggers the concentration of the presence of geothermal manifestations in areas that not have (Nicholson, 1993; Achmad et al., 2015).

RESEARCH LOCATION

Tangkuban Perahu Volcano is one of the active volcanoes in the West Java region, precisely in the Bandung area. Astronomically located at 6º7'17 "- 6º7'17" LS, 107º36'12 "- 107º40'16" BT and has elevation variety of 800 to 2220 meters above sea level. Referring to the research conducted by Fauzi (2015), the location of Tangkuban Perahu Volcano is located on the outermost side of the circular volcanic structure in West Java. The circular structure consists of other volcanoes such as Gede, Patuha, Papandayan, Cikuray; which surround potential active geothermal areas such as Kamojang, Wayang Windu, and Darajat (Figure 3).

Referring to the geological characteristics of the Tangkuban Perahu Volcano area in the previous explanation it is divided into two phases, the Old and Young Tangkuban Perahu. The old phase is dominated by phreatomagmatic deposits characterized by volcanic ash and lapilli, while magmatic deposits are in the form of scoria and volcanic ash. For a typical phreatic type predominantly young phase, deposits are found in the form of tephra with a typical base surge, clay, and altered rocks (Surmayadi, 2011).

METHOD

In the research conducted, the basic methodology used is the analysis of remote sensing images. This method can relatively provide information to users without direct contact with objects studied in the field (Lillesand and Kiefer, 1979). Remote sensing is carried out in relation to an exploration study of geothermal potential areas, especially areas affected by hydrothermal alteration as an output product of intensive geothermal activity. The processing of remote sensing image data carried out involves one type of Landsat 8 OLI/TIRS data from two different years: 2015 data and 2018 with a target area of 50,85 km2 added with comparative study from previous studies as a optimize research material assumption.

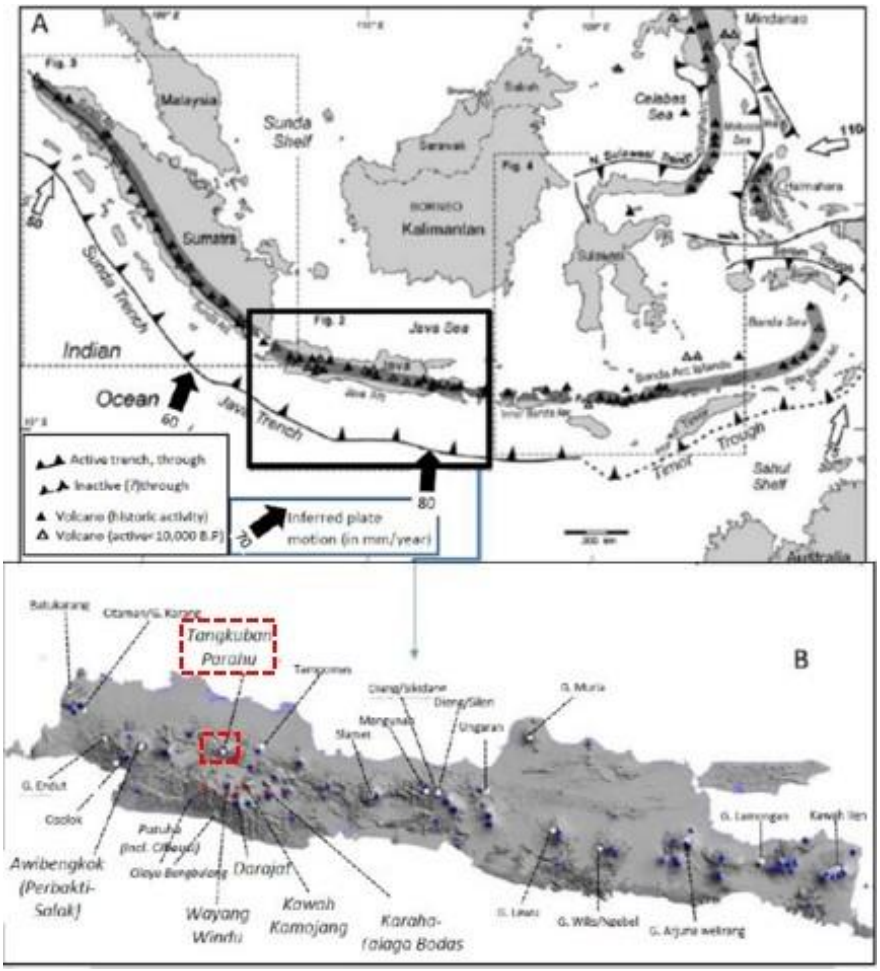


Figure 3: Distribution of active and geothermal-potential site volcano in Java (Hochstein dan Crosetti, 2012; Setiawan dkk, 2018), boxed area determined location of Tangkuban Perahu Volcano.

Processing data involving Landsat-8 images through several systematic sequences, starting from the initial stages of processing (Pre-Processing), delineating the target area (Region of Interest), spectral analysis of images and interpretation of image data. The pre-processing phase carried out using ENVI software 5.1 includes an atmospheric calibration mechanism to eliminate atmospheric and radiometric scattering potential to eliminate radiometric distortions on the surface of the earth or objects that cause image data to be poor (USGS, 2006) and ArcMap 10.3 to map layouting. In addition, this process also changes the value of the original image data (Digital Number / DN) to the reflectance value that is suitable for processing spectral analysis of image data (Utami, 2015).

Broadly speaking, the use of Landsat-8 imagery is focused on the spectral analysis mechanism according to the previous exposure, namely processing and interpretation of spectral data contained in each band. The types of Landsat-8 OLI/TIRS image data used are multispectral bands (1 to 7). The processing mechanism of image data is carried out in the form of Landsat 8 spectral data analysis by making composite band, band ratio, and data processing on Spectral Angle Mapper (SAM) classification. For additional, overlay data in SAM result used to identifying distribution and pattern of alteration process between 2015 and 2018.

For the concept of using composite band and band ratio is the merging of a number of bands on Landsat 8 image data (three bands) into a single data display. Band ratios generally use two sets of bands, where in one collection there are two bands that are compared to the appearance of their reflections. The Spectral Angle Mapper (SAM) classification method is an angle comparison algorithm between vector endmembers and each pixel vector in n-dimensional space (ENVI, 2001). SAM classification recognizes objects based on two things, namely the average spectrum and the spectrum of object classes (specific). If the pixel to be identified has a spectral angle with a degree value of less than the average spectrum, then the pixel enters the specified class and vice versa (Danoedoro, 2015) as shown in Figure 4.

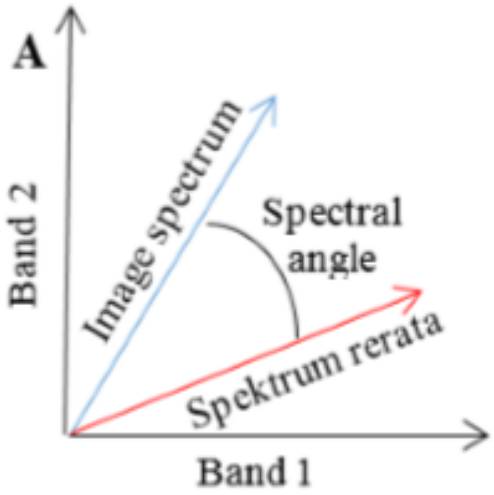


Figure 4: Spectral Angle Mapper conceptual model.

For processing with the SAM method, the processing uses the canal composition Red - Green - Blue or a wavelength of 0.4826 to 6.546 µm. This is because the reference spectrum based on the spectral library (Spec_Lib) of the GIS software used appears in that range. In addition, the wavelength range can characterize the original appearance of the object (target rock or mineral) so as to obtain a distribution that is close to the actual condition.

RESULT AND DISCUSSION

Preprocessing Data

The preparation phase of image data or known as preprocessing is important to do in the starting point of the image processing, especially Landsat 8 OLI/TIRS. Referring from USGS (2006) that Landsat 8 data obtained from original sources, especially Landsat Level 1 (L1), it is necessary to apply image correction, both atmospheric and radiometric. To provide a comparison between uncorrected and corrected images can be observed in Figure 5 below.

Corrections made in addition to generally improving the quality of image display, are also used to obtain data values that ready to be processed. Unprocessed image data has data called digital number (DN) while the data used for the spectral analysis process is reflectance. In a comparison of data, Tables 1 and 2 are Landsat 8 statistical data before being corrected and Tables 3 and 4 for those that have been corrected radiometrically.

Spectral Analysis: Band Composite and Ratio

Some canal composites used in the detection that are adapted for this study are identification of the presence of alteration minerals or rocks that undergo hydrothermal alteration processes, among others: RGB 432, RGB 543, RGB 567, and RGB 752 (Mia and Fujimitsu, 2012). In addition to composite bands, another method that can play a role in identifying the distribution of alteration minerals is the band ratio. The band ratio types that can be used include: the Chica-Olma method, the Segal method, the Kaufmann method, and the Abrams method (Zhou et al, 2013). The result of band ratio itself showing an increase in spectral contrast of each band (Segal, 1983) and displays unique information that is not obtained from composites per ordinary canal unit (Jensen, 1996).

The second analysis method in spectral analysis is composite bands for the identification of hydrothermal altered rocks distribution. The first band composite, RGB 432, illustrates the original color appearance of the area carried out by the research area (true color). The second composite is RGB 543 resulting in the appearance of differences in the distribution area of outcrop (blue) and vegetation (red). The third composite, RGB 567, describes the distribution of vegetation (orange), outcrops of rock (light blue), body of water (black), and high altered rocks (dark blue). The fourth composite, RGB 752, describes the distribution of exposed or exposed rocks (orange to red), vegetation (light green), and body waters (dark blue to black). Each of the composites made can be seen in Figures 6A to 6D for composites for 2015 and 6E to 6H for 2018.

The third method in spectral analysis is a band ratio consisting of 4 types analyzed. The first type, Abrams Ratio (6/7:4/3:5/6) describes relatively rocks that are altered to form iron oxide (light green to old) and clay (reddish). The second type, Chica-Olma Ratio (6/7:6/5:4/2) describes the spread of clay minerals (red), alteration minerals rich in iron ions (green) and iron oxide (blue). The third type, the Kaufmann Ratio (7/5:5/4:6/7) describes the distribution of minerals containing iron ions (red) and hydroxyl minerals (dark blue). The last type, Segal Ratio (4/2:6/7:6/5) describes enriched rocks of iron (blue) and iron oxide (red to pink). The appearance of the distribution of results can be seen in Figures 7A to 7D for 2015 and Figures 7E to 7H for 2018.

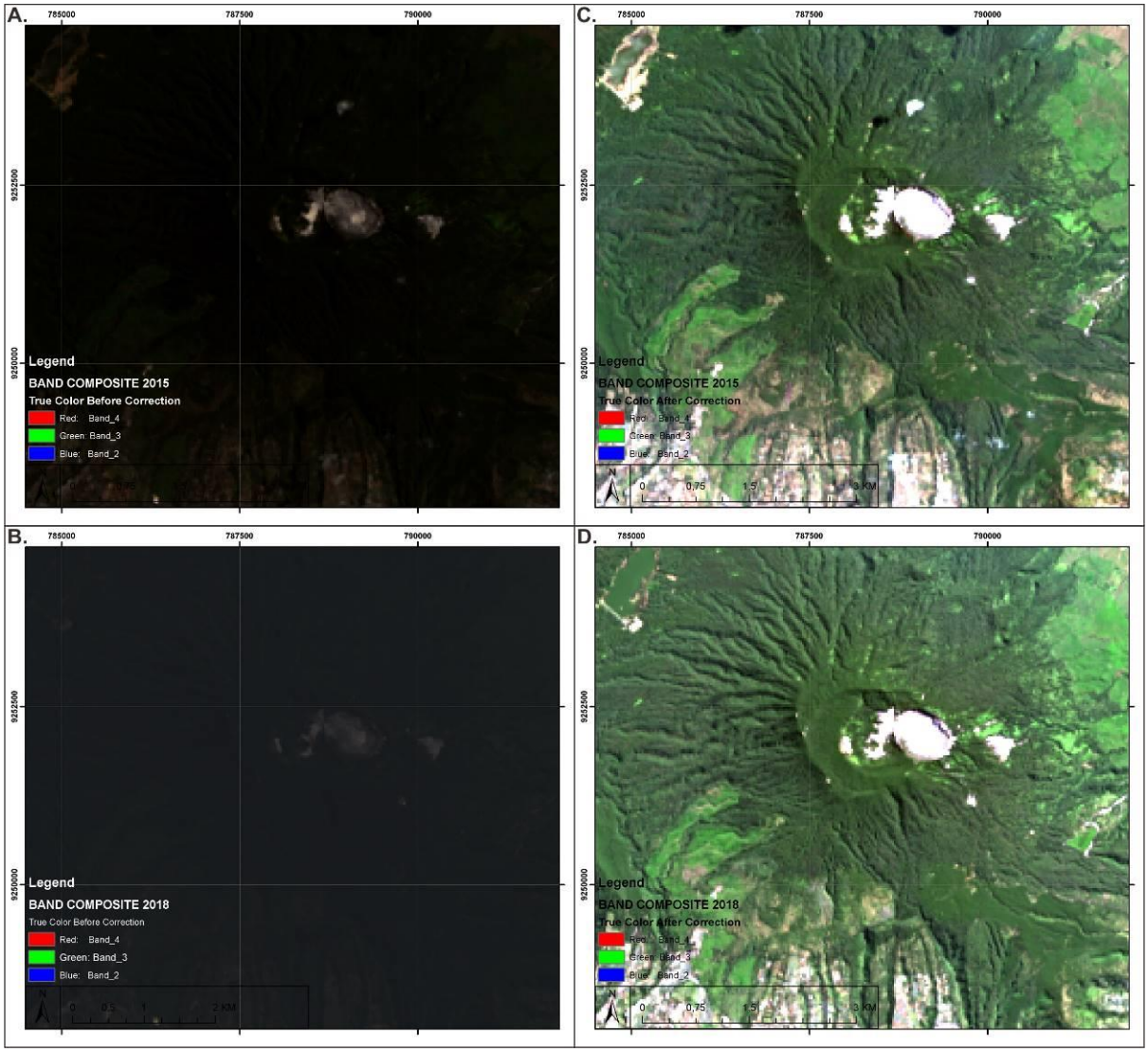


Figure 5: Uncorrected Landsat 8 image from 2015 (A) and 2018 (B) compared with atmospheric correction result from 2015 (C) and 2018 (D).

Table 1: Value of Landsat 8 data from 2015 before radiometric correction.

Band Type	**Min**	**Max**
Band 1 (Coastal)	8587	17635
Band 2 (Blue)	7624	18471
Band 4 (Red)	5678	24693
Band 5 (NIR)	5281	30213
Band 6 (SWIR 1)	5009	42464
Band 7 (SWIR 2)	5007	44142

Table 2: Value of Landsat 8 data from 2018 before radiometric correction.

Band Type	Min	Max
Band 1 (Coastal)	8044	18405
Band 2 (Blue)	7210	18867
Band 3 (Green)	6211	23028
Band 4 (Red)	5864	25373
Band 5 (NIR)	5698	29727
Band 6 (SWIR 1)	5093	38876
Band 7 (SWIR 2)	5068	44142

Table 3: Value of Landsat 8 data from 2015 after radiometric correction.

Band Type	Min	Max
Band 1 (Coastal)	0.000	0.359
Band 2 (Blue)	0.000	0.369
Band 3 (Green)	0.000	0.506
Band 4 (Red)	0.000	0.560
Band 5 (NIR)	0.000	0.611
Band 6 (SWIR 1)	0.000	0.848
Band 7 (SWIR 2)	0.000	0.838

Table 4: Value of Landsat 8 data from 2018 after radiometric correction.

Band Type	Min	Max
Band 1 (Coastal)	0.000	0.465
Band 2 (Blue)	0.000	0.448
Band 3 (Green)	0.000	0.598
Band 4 (Red)	0.000	0.619
Band 5 (NIR)	0.000	0.711
Band 6 (SWIR 1)	0.000	1.000
Band 7 (SWIR 2)	0.000	1.000

Spectral Analysis: Spectral Angle Mapper

The use of Landsat-8 image data that has been radiometrically calibrated from digital number data to reflectance value can be used further to map the presence of certain minerals on the earth's surface. The use of the Spectral Angle Mapper (SAM) method through ENVI 5.1 software uses the assumption of the reflectance value of the data it has compared to the reflectance of the targeted object (mineral) so that it forms a certain angle. That angle contains the range of reflectance values is a sign of the presence of objects to be searched by authors. Referring to previous research conducted by Achmad et al. (2015) about the presence of alteration minerals in Tangkuban Perahu Volcano, there are several types of minerals which through XRD data were discovered by researchers, forming two alteration zones: Sulfur + Crytobalite + Tridimite + Pyrite Alteration Zone and Crystobalite + Alunite Alteration zone. In addition to these minerals, other minerals are also found in the form of secondary quarzt. A typical mineral that can be displayed in the SAM method follows the database from the spectral library (Spec_Lib), where only a portion can be applied. From6 minerals in total refer to previous studies, only 4 types of minerals can be shows in the SAM method: Sulfur, quartz, pyrite, and alunite. Each processing was applied to two Landsat 8 data with different recording years, namely 2015 and 2018. The figure shows the

distribution of the presence of each mineral that was successfully raised through the SAM method in the area of Tangkuban Perahu Volcano both in 2015 on the left side (Figure 6A - 8D) and 2018 on the right side (8E - 8H).

Intepretation Based on Spectral Analysis

Remote sensing methods in related research studies generally need to be proven to strengthen the assumptions given. The distribution of minerals in a geothermal potential area needs to be known precisely to understand the typical and the distribution of areas affected by the process. In research carried out completely refers to the results of remote sensing processing for the distribution of areas undergoing hydrothermal alteration processes in the Tangkuban Perahu Volcanic. Therefore, to provide evidences regarding data validation, a comparative study was conducted with research conducted by Achmad et al (2015) regarding the distribution of alteration zones referring to the presence of its alteration minerals.

Before examining the specific distribution of mineral names found in the study area, there are spectral analysis results which can also be indicators of the distribution of regions affected by alteration processes on the surface. First, the results of the band composite process, especially for RGB composites that characterize high-intensity terrestrial rocks (RGB 567) and terterated rocks from open regions (RGB 752). The color gradation that characterizes the spectral appearance of alteration rocks from each year has decreased color intensity, from 2015 compared to 2018. The color composition that characterizes areas affected by hydrothermal alteration in 2015 processing results is wider and clearer than the results in 2018. Appearance of contrast in color between the results of the relevant year is seen in the northwest, northeast, and southwest of the study area. If it can be studied further, on the results of the composite true color band (RGB 432), the area which is the result of 2018 has wider distribution of vegetation compared to 2015. In addition, in the northwest there are appearance changes in the form of loss the area that was originally exposed (white) is replaced by a bluish-colored object that is indicated as water. From both processing data above, the assumption given is that there is a decrease in the distribution of areas affected by alteration processes because the area is covered by vegetation or submerged by water bodies.

Type of alteration mineral and distribution in the year compared in different distributions. Decreased distribution appears in the results of the Abrams, Chica-Olma, and Kaufmann methods, where colors that characterize the dominant alteration minerals are replaced with other colors that are neither characteristic nor the color intensity decreases. The colors change distribution in comparison between 2015 and 2018 shows in the northwest, northeast and south of research area. For the results of the Segal, there is drastic color change from blue to red in the Tangkuban Perahu Volcano crater. The indications given are similar to the results of the composite band, where the area may have been overgrown with vegetation within a period of 3 years or a filling of the surface by certain objects. The results of the next spectral analysis are band ratios, where each type gives a different The most important in thus section (Spectral Analysis) is the result of processing the Spectral Angle Mapper (SAM) method whose aspects refer to comparative studies of previous studies. As described in the previous section, the types of alteration minerals found by Achmad et al (2015) through XRD analysis in the Tangkuban Perahu Volcano area are native sulfur, crystobalite, tridimite, pyrite, and alunite. Some of the points studied also showed the presence of vuggy quartz textures, anatase minerals, glassy and the presence of secondary quartz in the rock found. The presence of these minerals characterizes the presence of active hydrothermal alteration processes on the surface.

Referring to this research, the Spectral Angle Mapper method cannot bring up all types of minerals according to the total amount of the alteration mineral. This depends on the availability of the reference spectrum in the spectral library from the ENVI software database. The alteration minerals that can be raised from the results of processing SAM above include: alunite, quartz, pyrite, and sulfur. The results of the data processing showed a similar pattern: a decrease in distribution in 2015 with 2018. To understand the distribution comparison, the data overlay process was carried out by combining all the minerals that appeared in each year. The following is a display of the distribution of the alteration minerals that overlap each other in each year compared to the pie chart (Figures 9A and B). The results of the data overlay method obtained two aspects: the wide comparison of altered area and the percentage distribution of areas affected by alteration and the presence of each mineral unit that appears in the same location. Comparison of the distribution value of the altered area from an area of 50.85 km2: the area affected by alteration with an indication of the availability of alteration minerals in 2015 was 8,38 km2 while in 2018 it was 2,45 km2. There is a difference in the value of difference of 5,93 km2 which gives an indication of a reduction in the area that is read as the presence of alteration minerals. This aspect being strengthened by the percentage of the presence of each mineral that overlaps each other in one area from the data overlay showed in pie chart (Figure 7A and 7B).

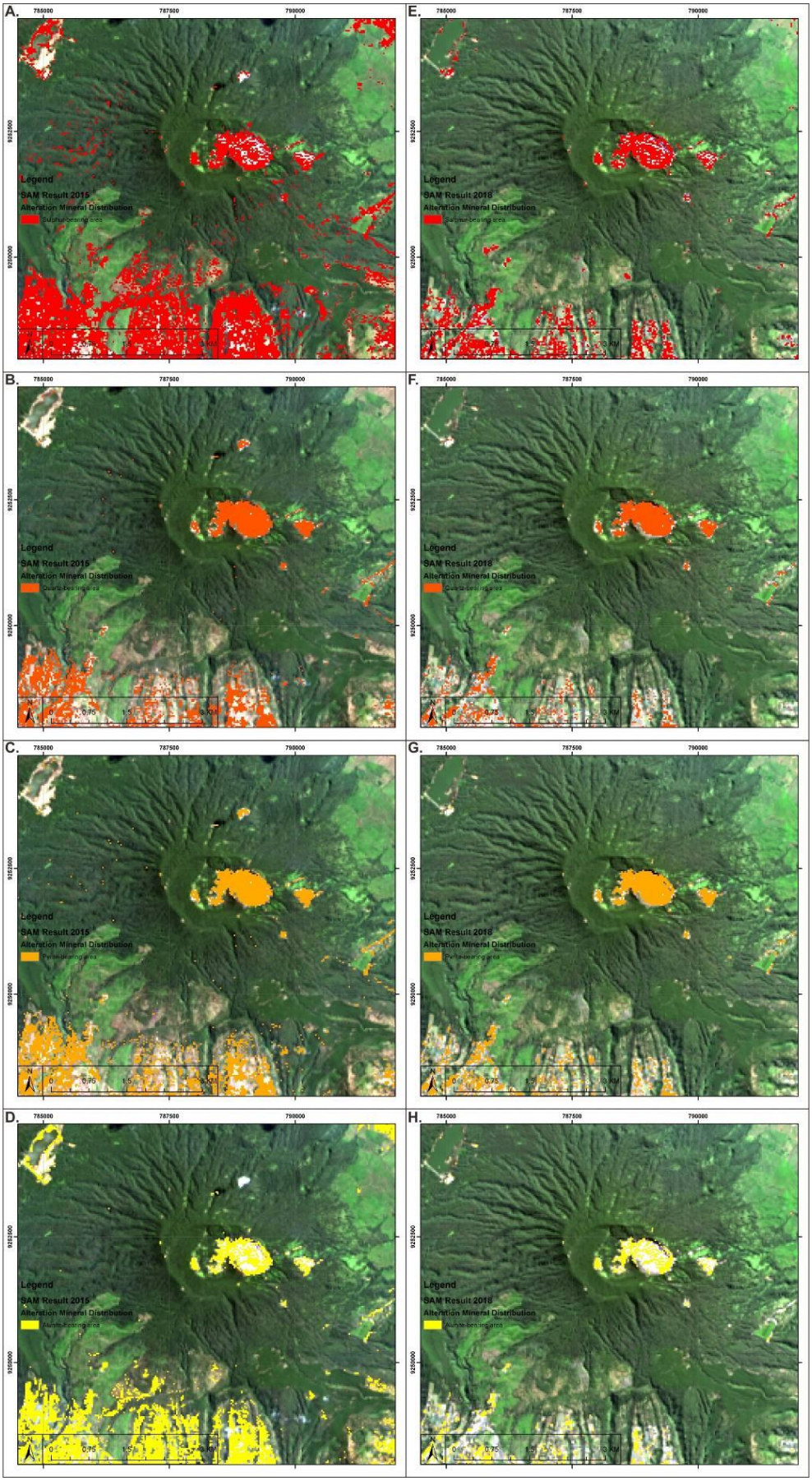


Figure 6: Distribution of several alteration mineral existence in Tangkuban Perahu Volcano processed from Landsat 8 using SAM method, in specific order: sulphur, quartz, pyrite, and alunite (A to D for 2015 data and, E to H for 2018 data).

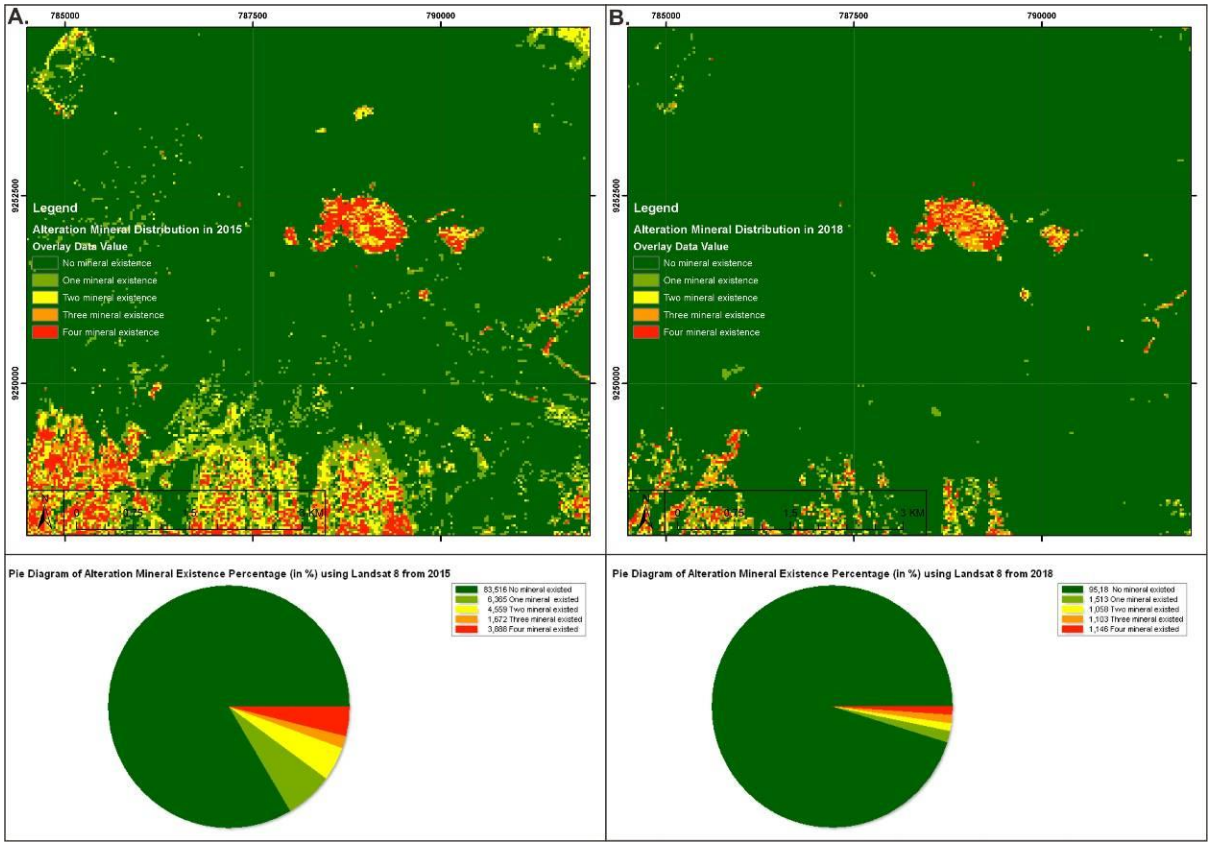


Figure 7: Comparison of several mineral existence and percentage value from overlay SAM mineral result data between 2015 (A) and 2018 (B).

The results of the data overlay showed giving main indication that the regions with abundant alteration minerals in two regions: around the main crater of Tangkuban Perahu Volcano and the area at the bottom (south, southwest, and southeast). For the area around the crater, the correctness of distribution has been proven in the research conducted by Achmad et al. (2015), while the regions other than the surrounding craters, on the lower side, have indications related to the presence of geothermal manifestations in the south, southwest and southeast. (Maribaya) and the northeast part (Ciater) according to the distribution of geothermal manifestation areas studied by Saputra and Suryantini (2015).

In addition to the areas indicated by alteration influences, the results of the overlay above can illustrate that affected area by alteration process is reduced significantly. Areas undergoing change have a distribution pattern with other spectral analysis results, namely in the northwest, northeast, south, and some small changes in distribution in other parts. The effect that is suspected of the related occurrence is the growth of vegetation in the comparison period that can trigger some area cannot be read by the processing of the data (Spectral Angle Mapper). An indication of the loss of the area which is spectrally the area affected by alteration is the appearance of a water body due to filling both naturally and artificially. This can be seen on the northwest side of the Tangkuban Perahu Mountain area in the form of Situ Lembang.

CONCLUSION

Tangkuban Perahu Volcano which is located in the Bandung Regency area in general has a fairly high geothermal potential. This is evidenced by the discovery of many manifestation points and the extent of the area affected by alteration processes; which illustrates the high heat activity under the surface of the earth or inside the body of Tangkuban Perahu Volcano. The distribution of areas affected by hydrothermal alteration is indicated by spectral analysis, especially composite band results, band ratios, and Spectral Angle Mapper. Areas that were found giving some indications of alteration processes generally in the area around the main crater of Tangkuban Perahu Mountain (Domas, Baru, Ratu, etc.) and several areas in the northeast, south, southwest, northwest, south and southeast. This is reinforced by the presence of alteration minerals from the processing of Spectral Angle Mapper such as alunite, pyrite, quartz, and sulfur as indicators of intensive alteration processes. In addition to the distribution of regions affected by alteration processes, through the comparison of the results of different Landsat 8 processing times (2015 and 2018), indications of a change in the value of the area that is read as an area affected by alteration are indicated. Changes in the distribution value from the value of 8.38 km2 to 2.45 km2 give an indication of

the factors that trigger the loss of the area that was originally read by the results of spectral analysis as the area affected by hydrothermal alteration. In addition to the area, the percentage of the presence of overlapping minerals from the mineral overlay process also showed a significant decrease in value. An indication that might appear is the presence of vegetation and other objects that cover the surface of the altered area so that object misreading by spectral analysis.

REFERENCES

Abhary, A., and Hassani, H. (2016), "Mapping Hydrothermal Mineral Deposits Using PCA and BR Methods in Baft 1:100000 Geological Sheet, Iran," *International Journal of Advanced Engineering, Management and Science (IJAEMS)*, 2, 1433-1438.

Achmad, A. S., Suryantini, Susanto, A., Nurdiana, A. (2015), "Hidrothermal Alteration Study of Tangkuban Perahu Craters, and Its Implication to Geothermal Conceptual Model," *Proceedings Indonesia International Geothermal Convention & Exhibition*, 3, pp. 1-6.

Beane, R. E. (1982), "Hydrothermal alteration in silicate rocks, southwestern North America; In," *Advances in Geology of the Porphyry Copper Deposits, Southwestern North America:* Tucson (ed.) Titley S R, Univ. Ariz. Press, 6, pp. 117–137.

Byrdina, S., Grandis, H., Sumintareja, P., Caudron, C., Syahbana, D.K., Naffrechoux, H., Gunawan, H., Suantika, G., Vandemeulebrouck, J. (2018), "Structure of the acid hydrothermal system of Papandayan volcano, Indonesia, investigated by geophysical methods," *Journal of Volcanology and Geothermal Research*, 1-26.

Danoedoro, P. (2015). "Penginderaan Jauh Digital*"*. Yogyakarta: Andi.

ENVI. (2001). "Atmospheric Correction Module: QUAC and FLAAS User's Guide", *ITT Visual Information Solutions.*

Fauzi, A et al., (2015), "Regional Structure Control on Geothermal Systems in West Java, Indonesia," *Proc. World Geothermal Congress 2015* (Melbourne, Australia).

Hendri, R., Prabowo, B. S., Perdana, M. (2012), "Korelasi Intensitas Pola Kelurusan Tangkuban Perahu terhadap Keberadaan Lokasi Manifestasi di Permukaan," *Proceedings the 12th Annual Indonesian Geothermal Association Meeting & Conference*, Bandung.

Hochstein, M. P., and Crosetti, M. (2012), "Ranking of Indonesia Geothermal Prospect (Known Reserves)," *New Zealand Geothermal Workshop 2012*.

Jensen, J. R., (1996). "Introductory digital image processing: A remote sensing perspective; 2nd edn", *Prentice Hall Series in Geographic Information Science*; 318p.

Julzarika, A. (2018), "Penginderaan Jauh untuk Pendeteksian Awal Potensi Tembaga di Sumbawa," *Ris.Geo.Tam*, 28, 75-89.

KESDM. (2017), "Potensi Panasbumi Indonesia Jilid 1," *Jakarta: Kementrian ESDM.*

Kartadinata, M. N., (2005), "Tephrochronological Study on Eruptive History of Sunda-Tangkuban Parahu Volcanic Complex, West Java, Indonesia," Desertasi Doktor, *Nature System Science, Graduate School of Science and Engineering*, Kagoshima University, Japan.

Lillesand, T. M., dan Kiefer, R. W. (1987), "Remote Sensing and Image Interpretation." *New York: John Wiley & Sons, Inc.*

Mia, M. B., and Fujimitsu, Y. (2012), "Mapping hydrothermal altered mineral deposits using Landsat 7 ETM+ image in and around Kuju volcano, Kyushu, Japan," *J. Earth Syst. Sci.*, 121, 1049-1057.

Mustopa, E. J., Nurhasan., Srigutomo, W., Sutarno, D. (2017), "Resistivtiy Structure in Tangkuban Parahu Area Drived from CSAMT Data," *Journal of Physics: Conference Series*, 877, pp. 1-6.

Nasution, A., Kartadinata, M. N., Kobayashi, T., Siregar, D., Sutaningsih, E., Hadisantono, R., Kadarstia, E. (2004) "Geology, Age Dating and Geochemistry of the Tangkuban Perahu Geothermal Area, West Java, Indonesia," J Geotherm. Res. Soc. Japan, 26, No. 3, 285-303.

Nuha, M. U., Yulianto, T., dan Harmoko, U., (2014), "Intepretasi Data Bawah Permukaan Daerah Sumber Air panas Derekan Berdasarkan Data Magnetic*," Youngster Physic Journal, 3*, .129-134.

Nurohman, H., Bakti, H., Indarto, S., Yulianti, A., Abdulah, A. A., Permana, H., and Gaffar, E. Z. (2016), "Zona Permeabel di Kawah Gunungapi Papandayan Berdasarkan Gas Radon dan Thoron," *Ris.Geo.Tam*, 26, 131-140.

Saputra, M. P., Suryantini. (2015), "A Correlation Study between Volcanic Activities and Thermal Water Changes in Tangkuban Perahu Hydrothermal Prospect Jawa Barat, Indonesia." *Proceedings World Geothermal Congress 2015*, pp. 1-5.

Segal, D. B., (1983). "Use of Landsat multispectral scanner data for definition of Limonitic exposures in heavily vegetated areas, EL Paso, Texas". *Econ. Geol.* 78 711–722.

Setiawan, I., Indarto, S., Sudarsono., Fauzi, A., Yulianti, A., Lintjewas, L., Alkausar, A., and Jakah. (2018), "Geothermal and volcanism in west Java," *Earth and Environmental Science*, 118, 1-5.

Soengkono, S. (1999), "Te Kopia geothermal system (New Zealand) - the relationship between its structure and Extent," *Geothermics*, 28, 767-784.

Sumaryadi, M., Sumintadireja, P., Irawan, D., Arisbaya, I. (2011), "Dinamika Vulkanisme Gunungapi Tangkuban Parahu Jawa Barat," *Joint Convention Malang Makasar 2011 The 26th HAGI and 40th IAGI Annual Convention Exhibition*, pp. 1-20.

United States of Geological Survey (USGS). (2006). "Landsat 8 (L8) Data Users Handbook". *Departement of the Interior U.S Geological Survey.*

Utami, F. P. (2015). "Analisis Spasial Perubahan Luasan Mangrove Akibat Pengaruh Limpasan Sedimentasi Tersuspensi Dengan Metode Penginderaan Jauh (Studi Kasus: Segara Anakan Kabupaten Cilacap, Jawa Tengah)." *Teknik Geodesi, Universitas Diponegoro. Semarang.*

Zhou, J., Liu, L., Jiang, D., Zhuang, D., Mansaray L.R., Zhang B., (2013), "Targeting Mineral Resources with Remote Sensing and Field Data in the Xiemisitai Area, West Junggar, Xinjiang, China." *Journal Remote Sensing*, 5, 7, pp. 3156-3171.

Van Bemmelen, R. W. (1949). "The Geology of Indonesia 2 edition," *Martinus Nijhoff, Vol. 1.*

INVESTIGATION OF GEOTHERMAL POTENTIALS OF MOUNTAIN LAMONGAN BASED ON MORPHOSTRUCTURE AND GEOCHEMICAL ANALYSIS

Arhananta[1], Kenny Lekatompessy[1], M. Alhafiq Wahyu Nabillah[1],
Nazwa Khoiratun Hisan[1], and Agus Harjanto[2]

[1]Undergraduated Student of Geological Engineering, UPN "Veteran" Yogyakarta
[2]Lecture of Geological Engineering, UPN "Veteran" Yogyakarta
Jl. SWK 104 (Lingkar Utara), Condongcatur, Yogyakarta 55283
Email: arhananta@gmail.com, kennyleka72@gmail.com, alhafiqmuhammad@gmail.com,
nazwakhoiratunhisan@gmail.com

ABSTRACT

Geothermal energy is one of the renewable energies generated from the process of volcanism. With more than 100 volcanoes, Indonesia is one of the largest geothermal energy producing countries in the world. One of these volcanoes is Gunung Lamongan, East Java. The method used is the method of image interpretation and geochemical methods in the form of: macro straightness analysis, meso straightness, and micro straightness, taking water samples in the form of cations and anions. The research area is included in 3 formations in the East Java stratigraphic order from the oldest to the youngest, namely Argopuro Volcano Rocks, Lamongan Lava, and Lamongan Volcano Rocks. There are 3 lines of geological structure in the form of faults with the East-West orientation on macro straightness that cut Argopuro Volcano Rocks, Lamongan Lava, and Lamongan Volcano Rocks, West-East orientation on meso straightness that cut Argopuro Volcano, Lamongan Lava, and Batuan Lamongan Volcano, as well as the Northwest-Southeast orientation of the micro straightness that cuts Argopuro Volcano Rocks. The constituent rocks are andesite-basal lava, fine-lapilli tuff, lava and volcanic breccia. Geochemical analysis was carried out on 2 samples namely WP 17 and WP 7 through 3 plots in the Ternary Diagram. The first plot in the Ternary Diagram Cl-SO4-HCO3 is interpreted that the sample WP 17 and WP 7 is bicarbonate water. The second plot in the Ternary Diagram Na-K-Mg is interpreted that the samples of WP 17 and WP 7 do not originate from the reservoir and have been influenced by meteoric water. The third plot in the Ternary Diagram Cl-100 / Li-25 / B is interpreted that the B content that is high enough in the study area is affected by the side rocks where the fluid flows.

Keyword: Geochemistry, Lamongan Mountain, Morphostructure

INTRODUCTION

Background

Geothermal energy is one of the renewable energies generated from the process of volcanism. With more than 100 volcanoes, Indonesia is one of the largest geothermal energy producing countries in the world. In Indonesia, Geothermal has 312 potential points, 67 work areas, with total electricity generated 28,910 MWe. (EBTKE, 2016). Lamongan Mountain is one of the possible volcanoes as geothermal power plants (PLTG). One of geological control in geothermal area is geomorphology therefore the authors conducted this study in identifying the manifestations of hot water in the Lamongan region. This study was conducted on Mount Lamongan which is administratively located in Lumajang Regency, East Java Province. Figure 1 shows the study area.

Method

The method used is the method of image interpretation and geochemical methods in the form of: macro straightness analysis, meso straightness, and micro straightness, taking water samples in the form of cations and anions.

GEOLOGY

Regional Stratigraphy

From the map of regional geology of Probolinggo, Java (Suharsono and T. Suharti, 1992) research areas are included in 3 formations in the order of East Java stratigraphy from the oldest to the youngest, namely Argopuro Volcanic Rocks, Lamongan Lavas, and Lamongan Volcanic Rocks.

In general, the Argopuro Volcanic Rocks is composed of andesite-basalt lava, volcanic breksi, and tuff (Suharsono and T. Suharti, 1992). Later, Lamongan Lavas was composed of the basal lava-andesite (Suharsono and T. Suharti, 1992). Lastly, the Lamongan Volcanic Rocks is composed of lava, fine tuff-lapili, and volcanic breksi (Suharsono and T. Suharti, 1992) (Figure2).

Regional Geological Structure

From the map of regional geology of Probolinggo, Java (Suharsono and T. Suharti, 1992) there are 3 lines of geological structures in the research area in the form of macro straightness, meso straightness, and micro straightness. East-West orientation on macro straightness cutting of Argopuro Volcanic Rocks, Lamongan Lavas, and Lamongan Volcanic Rocks, West-East orientation on Meso straightness that cuts Argopuro Volcanic Rocks, Lamongan Lavas, and Lamongan Volcanic Rocks, as well as the Northwest-Southeast orientation of the micro straightness that cuts the Argopuro Volcanic Rocks (Figure 2).

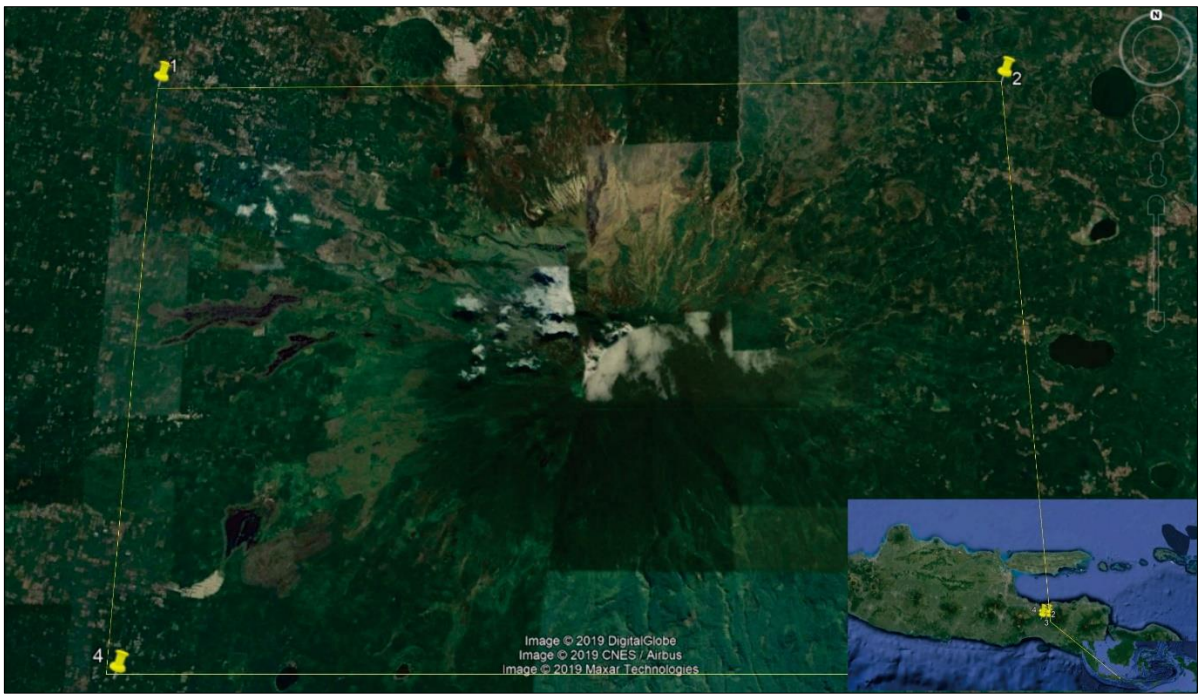


Figure 1: Study Area.

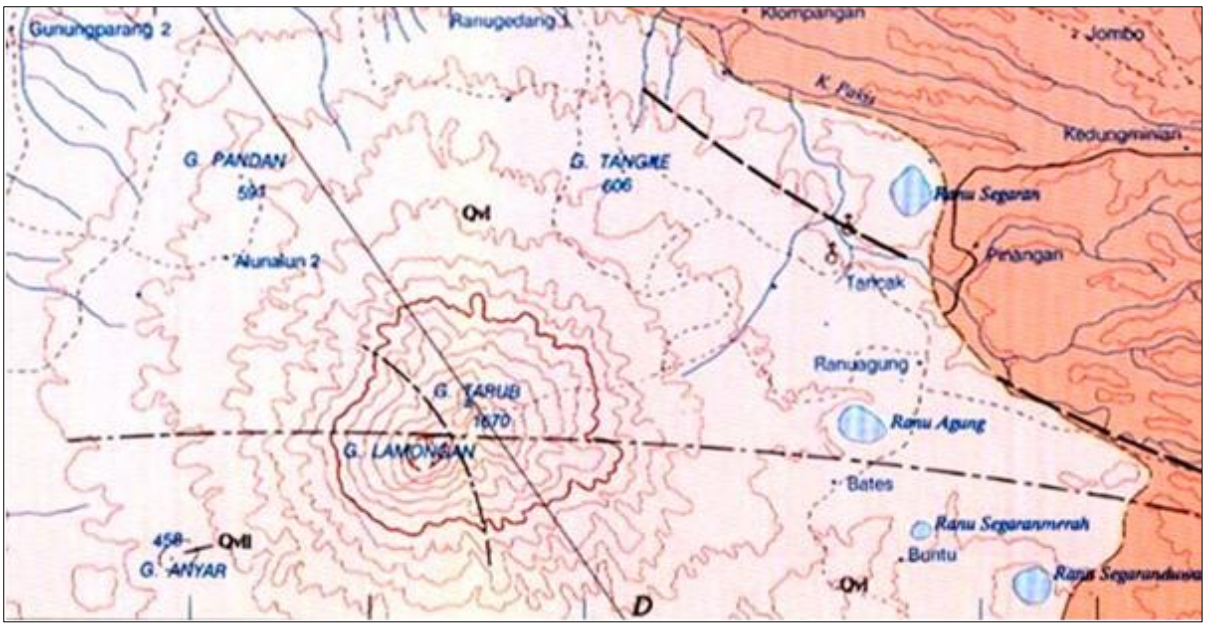


Figure 2: Geological Map of Study Area (Suharsono, 1992).

RESULT

Hot Water Geochemistry

In the geochemical analysis of water in the study area, data obtained in the form of water samples in the form of cation elements and anion elements in samples WP-17 and WP-7 (Tabel 1).

From the first pressing result of water chemical data into a terniary diagram (Giggenbach, 1988) Cl-SO4-HCO3 to know the type of geothermal fluid on the sample WP-17 in the form of a spring water peripheral waters. In the WP-17 sample It can be seen that the clen composition in this diagram is 42%, while the SO4 composition of this diagram is 40%, and the HCO3 composition is 12% in this diagram. In the Terniary diagram (Giggenbach, 1988) The sample WP-17 has a more HCO3 composition than the SO4 and also clen so that it can be interpreted that the type of water in the sample WP-17 is bicarbonate water.

From the first pressing result of water chemical data into terniary diagram (Figure 3) (Giggenbach, 1988) Cl-SO4-HCO3 to know the type of geothermal fluid on the sample WP-7 in the form of river peripheral water. In the WP-7 sample It can be seen that the clen composition in this diagram is 3%, while the SO4 composition of this diagram is < 10%, and the HCO3 composition is 97% in this diagram. In the Terniary diagram (Giggenbach, 1988) The sample WP-7 has a more HCO3 composition than the SO4 and also clen so that it can be interinterpreted that the type of water on the sample WP-7 is bicarbonate water.

Water data analysis samples of the WP-17 and WP-7 were then plotled again into the Na-K – Mg Diagram Ternary diagram (Giggenbach, 1988) to determine the temperature on the WP-17 and WP-7 reservoirs. In the samples of WP-17 and WP-7 after being plotkan into the diagram Na-K-Mg entered into immature water zones. The Data analysed Na-K-Mg terniary diagram (Figure 4) can know the condition below the surface temperature shown in immature water zone, with this result can be said that the samples water WP-17 and WP-7 does not come from reservoar and already influenced by meteoric water.

The third analysis is in the form of chemical water data of WP17 and WP-7 samples and then plotted again into the Ternary Diagram Cl-100 / Li-25 / B diagram (Giggenbach, 1988) (Figure 5.) to determine the water formation environment in the WP-17 sample and WP-7. The data plotted were Cl, Li, and B. After the data were analyzed using a Cl-100 / Li-25 / B terniary diagram (Figure 5), the composition of Cl was 49%, Li was 3%, and B was 48%. With the results of the analysis in the form of high Li content, it was interpreted that the side rocks in the WP-17
sample. In the WP-7 sample the composition of Cl was 13%, Li was <10%, and B was 87%, it can be concluded that in general hot water directly from the reservoir contains marine clastic sediments, such as shale, or like formation water having concentrations Cl, B and CO2 are high. Nicholson (1993) ,. But the B content which is quite high in the study area is influenced by the side rocks where the fuides flow also refers to Nicholson (1993), who also stated that, water from andesitic rocks has a higher boron content than water from other volcanic rocks. Nicholson (1993).

MOFOSTRUCTURE

Macro Lineament

The position of Gunung Lamongan follows a pattern of volcanic distribution on the west-east-oriented Java island parallel to the subduction line in the south of Java island.

Meso Lineament

West-East straightness with volcano complex Bromo-Tengger-Semeru in the west and Iyang Mountains with Gunun Argopuro as the highest and continuous peak to the east to Mount Raung and Ijen.

Table 1: Gochemisty of Hotspring Data (Deon, 2015).

Sample		Ca	Mg	K	Na	Fe	Li	Rb	Si	B	Cl⁻	HCO_3^-	SO_4^{2-}	Ionic balance
WP17 Oct 2012	Spring NE	33.5	37.4	44.1	249	0.0	0.0	0.2	26.1	4.9	330	632	0.0	−19[a]
Tiris 1 June 2012	Spring E	63.9	159	49.0	273	n.d.	0.29	0.17	68	14	355	1280	23.8	−3
Tiris 2 June 2012	Spring E	93.5	227	76.5	406	n.d.	0.39	0.28	83	21	521	2100	23.1	6
Tiris 3 June 2012	Spring E	86.1	201	69.1	370	n.d.	0.35	0.26	77.6	20	465	1650	23.2	−2
Tiris December 2011	Spring E	80.3	168	67.1	353	1.30	0.47	0.28	65.0	13.2	441	1340	n.d.	1
Tiris 5 June 2012	Spring E	61.9	222	45.7	268	n.d.	0.22	0.16	70.4	14	130	1680	4.63	4
Tiris 6 December 2012	Spring E	54.3	192	43.9	254	n.d.	0.3	0.2	57.8	10.3	348	1400	n.d.	−3
WP7 Lad June 2012	Lake	39.7	34.0	8.0	33.3	n.d.	0.0	0.0	20.4	2.0	8.1	427	15.0	−8
WP18 June 2012	River	29.1	17.1	4.7	17.4	n.d.	0.0	0.0	32.5	0.0	11.9	323	11.0	−12
WP 5 June 2012	Diluted and contaminated seawater	257	963	282	773	n.d.	0.0	0.2	4.2	2.0	12,800	610	2450	1

[a] Sampling of WP17 was additionally conducted by the Indonesian project partners. Their sampling yielded similarly poor ionic balances, with the value scattering between −19 and + balance is due to anthropogenic activities of a nearby village (approximately 1 km)

Micro Lineament

The straightness of Mount Lamongan in general can be divided into two, namely the radiary straightaway to the peak and the straightness that cuts the body. The straightness that cuts the body of the mountain in Lamongan to the northwest-southeast that separates the peak of Tarub in the northeast and the peak is still active until now which is in the southwest. The straightness of the west to the northwest, with a good former maar filled with water (Ranu) and dry. This straightness is the most striking and thought to be the central displacement control of the volcano.

In addition, around Mount Lamongan also found many former maars. In the northern part of the relative oriented northeast-southwest. The western and eastern parts are relatively north-south oriented. While in the southern part is oriented relatively northeast-southwest.

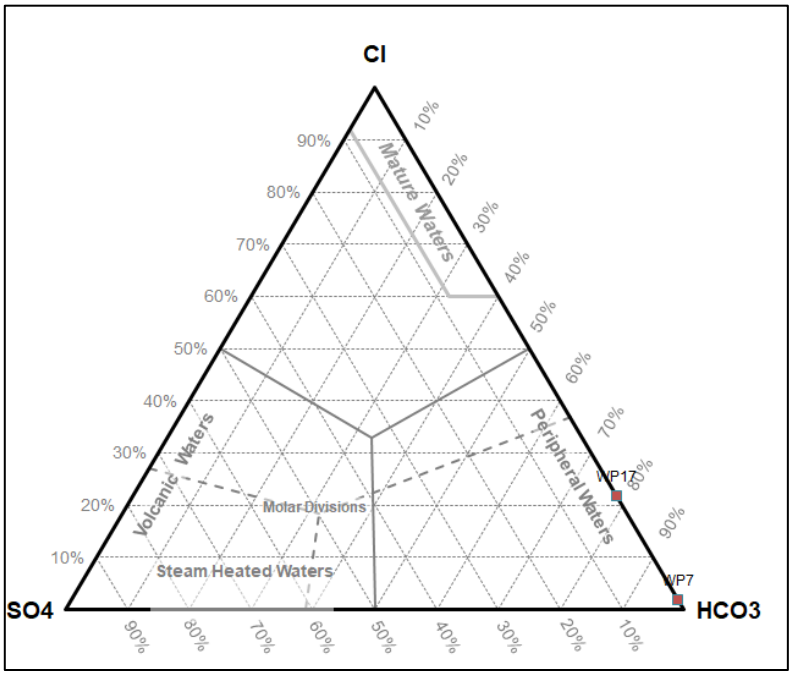


Figure 3: Terniary diagram (Giggenbach, 1988) Cl-SO_4-HCO_3.

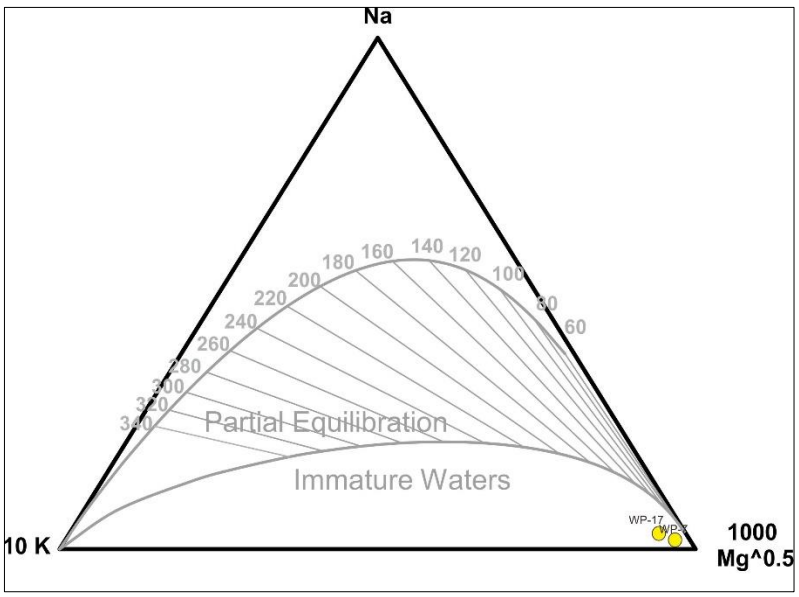


Figure 4: Diagram Na-K-Mg.

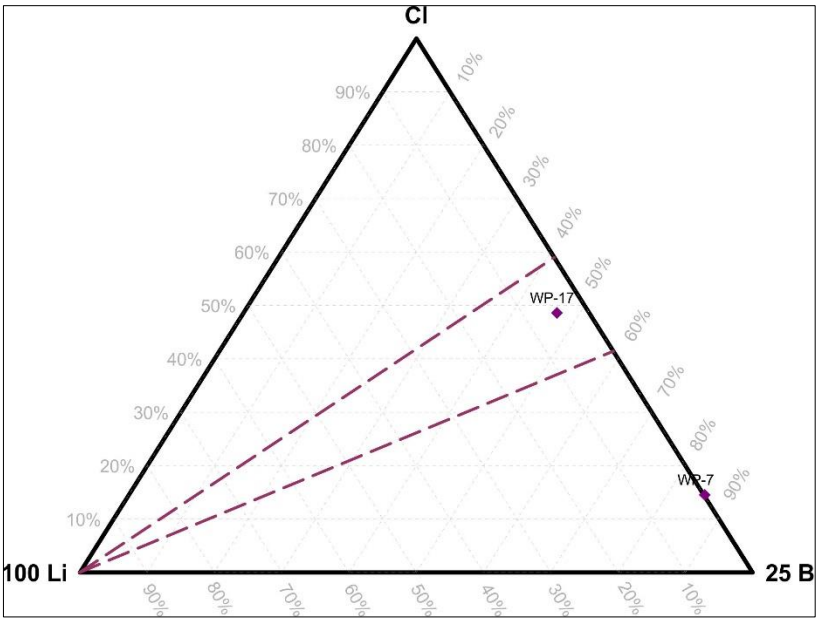


Figure 5: diagram Ternary Diagram Cl- 100/Li-25/B (Giggenbach, 1988).

CONCLUSION

The research area is included in 3 formations in the East Java stratigraphic order from the oldest to the youngest, namely Argopuro Volcano Rocks, Lamongan Lava, and Lamongan Volcano Rocks. There are 3 lines of geological structure in the form of faults with the East-West orientation on macro straightness that cut Argopuro Volcano Rocks, Lamongan Lava, and Lamongan Volcano Rocks, West-East orientation on meso straightness that cut Argopuro Volcano, Lamongan Lava, and Batuan Lamongan Volcano, as well as the Northwest-Southeast orientation of the micro straightness that cuts Argopuro Volcano Rocks. The constituent rocks are andesite-basal lava, fine-lapilli tuff, lava and volcanic breccia. Geochemical analysis was carried out on 2 samples namely WP 17 and WP 7 through 3 plots in the Ternary Diagram. The first plot in the Ternary Diagram Cl-SO4-HCO3 is interpreted that the sample WP 17 and WP 7 is bicarbonate water. The second plot in the Ternary Diagram Na-K-Mg is interpreted that the samples of WP 17 and WP 7 do not originate from the reservoir and have been influenced by meteoric water. The third plot in the Ternary Diagram Cl-100 / Li-25 / B is interpreted that the B content that is high enough in the study area is affected by the side rocks where the fluid flows.

REFERENCES

Deon, Fiorenza et al. (2015). "Geochemical/hydrochemical evaluation of the geothermal potential of the Lamongan volcanic field (Eastern Java, Indonesia)". Geothermal Energy Springer Open Journal (2015) 3:20. DOI 10.1186/s40517-015-0040-6

Hochstein, M., P., Browne, P., R., L., (2000). "Surface manifestations of geothermal systems with volcanic heat sources". In: Sigurdsson H, editor. Encyclopedia of volcanoes. New York: Academic. p. 835–55.

Hochstein, M., P., Sudarman, S., (2008). "History of geothermal exploration in Indonesia from 1970 to 2000". Geothermics; 37:220–66.

Giggenbach, W., F., Goguel, R., L., (1988). "Collection and analysis of geothermal and volcanic waters and gas discharges". DSIR Report CD 2401, 4th edition, Pertone, New Zealand.

Suharsono, et al. (1992). "Peta Geologi Lembar Lumajang". P3G: Bandung.

Verstappen, T., H., (1977). "Remote Sensing in Geomorphology". Amsterdam: Elsevier.

Zuidam, V., (1985). "Terrain Analysis and Classification using Aerial Photographs a Geomorphological Approach".

GEOELECTRICAL STRIKE VS GEOLOGICAL STRIKE TENSOR ROTATION IN 2-D MODELLING OF MAGNETOTELLURIC DATA. STUDY CASE: BONJOL GEOTHERMAL AREA, WEST SUMATERA

Paulus Febrianto Pandu Wibowo[1], Wiwid Joni[2], and Hafiz Hamdalah[1]

[1]Pembangunan Nasional University "Veteran" Yogyakarta
[2]Center for Mineral, Coal and Geothermal Resources - Geological Agency Bandung
Jl. SWK No. 104, Ngropoh, Condong Catur, Daerah Istimewa Yogyakarta
Email: pandupaulus@gmail.com

ABSTRACT

Magnetotelluric is a powerful geophysical method for determining the earth's conductivity structure at depth especially in geothermal area. In processing MT data, we do 2-D inversion modelling to create model of Bonjol geothermal system. But there is a problem in 2-D modelling. The differences of measurement orientation and geoelectrical strike orientation will produce a different subsurface resistivity variation distribution from the real condition and caused a misleading interpretation. By using 13 MT stations in Bonjol geothermal area, MT data need to be rotated to its strongest conductivity variation direction. In order to confirm where MT data should be rotated, we apply two rotation angles to the geoelectrical strike and geological strike. To utilize a major geoelectrical strike, we make use of Weaver et. al. (2000) and Bahr (1988) directionality tools. The analysis result shows that by applying geoelectrical strike obtain reasonable models rather than geological strike. The implication of this study is a better understanding of using the geoelectrical strike as a reliable rotation angle compared to the geological strike.

Keywords: Magnetotelluric, resistivity, inversion modelling, Bonjol

INTRODUCTION

Magnetotelluric (MT) is a passive electromagnetic method that measures changes in the electric and perpendicular magnetic fields to the earth's surface to determine the distribution of the earth's conductivity to depths from tens of meters to several hundred kilometers (Simpson and Bahr, 2005).

According to Hochstein and Browne (2000) and Goff and Janik (2000), geothermal systems consist of several components namely reservoir (permeable), fluid to carry heat from the reservoir to the surface of the earth, impermeable rock, and heat source (Goff and Janik, 2000). The presence of structures as the boundaries of the prospect of geothermal systems, recharge zones and discharge zones depicted as contrast resistivity values is also the target of geothermal exploration.

Analysis of tensor rotation on MT data also needs to be done in 2D modelling to adjust the concept of 2D earth models (TE and TM). The direction of conductivity contrast (rotation angle) is obtained based on the analysis of geoelectrical strike and geological strike on the surface. The direction of geoelectrical strike is generated through Bahr correction method analysis (Pracser et al., 1999) and the WAL method (Weaver et al., 2000). The value of the geoelectrical strike angle of an area may differ from other regions, either in the direction of the geological strike in the study area or different from the geological strike, even worth 0^o (without rotation).

BASIC THEORY

Tensor Rotation

Electromagnetic waves are considered to propagate vertically, then the E and H components used are horizontal components (Simpson and Bahr, 2005). The subsurface conditions will be portrayed more effectively and representative by adjusting measurements to the assumptions of the 2D model. Medium type resistances do not vary toward *x* axis direction which is the strike of the MT (geoelectrical strike) (Xiao, 2004). The strike coordinate system of the impedance tensor has a simple direction that matches the TE (Transverse Electric) and TM (Transverse Magnetic) modes and is used to determine the 2D impedance tensor, with the equation:

$$Z = \begin{bmatrix} 0 & Z_{xy} \\ -Z_{yx} & 0 \end{bmatrix}, |Z_{xy}| \neq |Z_{yx}| \quad (1)$$

In the 2-D model, the values of Z_{xy} and Z_{yx} are not the same. Impedance rotation decomposes electric field (E) and magnetic field (H) into TE and TM modes (Khyzhnyak, 2014) as in Figure 1.

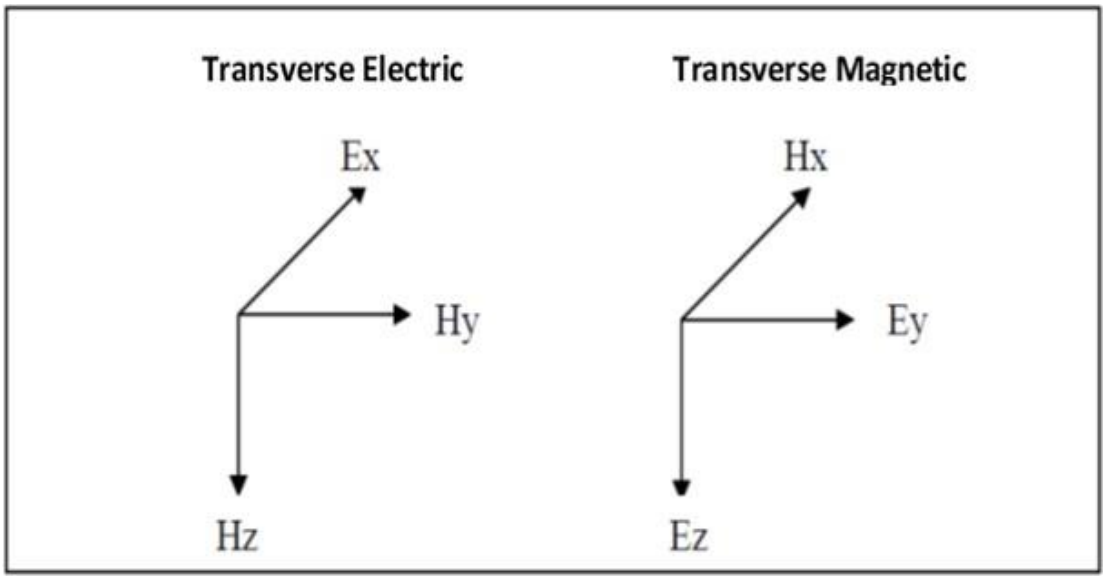


Figure 1: Electric field and magnetic field component on TE and TM polarization in 2D model (Unsworth, 2007).

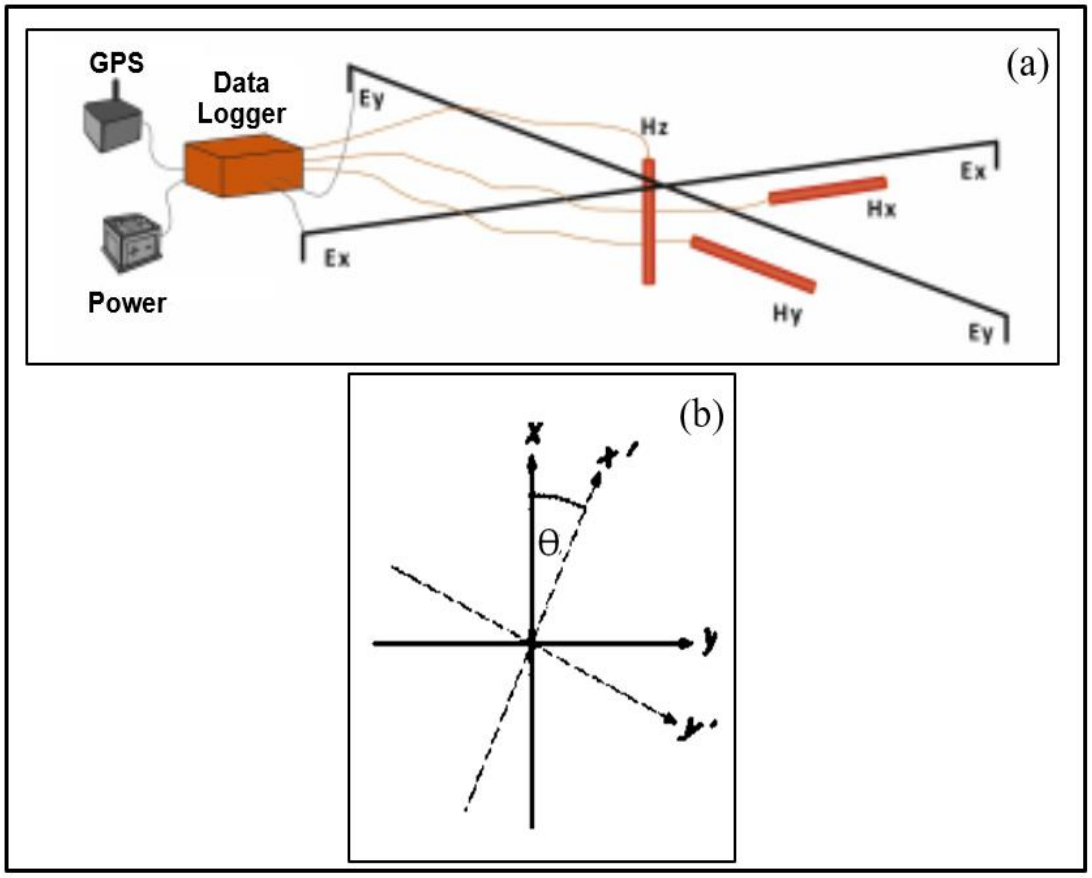


Figure 2: (a) Field set up MT (Khyznyak, 2014) and (b) A rotation through angle (Θ) maps x to x' and y to y' (Simpson and Bahr, 2005).

The varies direction of the structure both on and below the surface causes the actual strike direction to be difficult to know. The impedance matrix (Z_{xx}, Z_{yy}, Z_{xy}, Z_{yx}) can be rotated numerically, so that the measurement direction is made parallel to strike. The coordinate axis of the system from the field layout does not coincide with the strike direction (Figure 2), so measurements in the field do not necessarily correspond to parallel directions or perpendicular strikes.

Figure 2 (b) shows the rotational tensor coordinate system data frame, y represents Ex on TE or Hx on TM, while x describes Hy on TE or Ey on TM. While x' and y' are the results of rotation of x and y of Θ (strike direction angle). Figure 2 (a) shows the set-up measurements in the

field. Clockwise rotation (θ) is explained in the following equation (Jiracek, 2016):

$$\begin{bmatrix} E_x' \\ E_y' \end{bmatrix} = [\mathbf{R}] \begin{bmatrix} E_x \\ E_y \end{bmatrix}. \quad (2)$$

$$\text{with } \mathbf{R} = \begin{bmatrix} cos\,\theta & sin\,\theta \\ -sin\,\theta & cos\,\theta \end{bmatrix} \quad (3)$$

Bahr (1988) and Weaver et al. (2000) provide the equation for obtaining geoelectrical strike values in the following formula:

$$\tan(2\Theta_B) = \frac{[S_1,S_2] - [D_1,D_2]}{[S_1,D_1] + [S_2,D_2]} = \tan(2\Theta_W) \quad (4)$$

with Θ = rotation angle or strike direction
R = rotation matrix
θ_B = rotation angle (Weaver et al., 2000)
θ_W = rotation angle (Bahr, 1988)
$S_1 = Z_{xx} + Z_{yy}$ $S_2 = Z_{xy} + Z_{yx}$
$D_1 = Z_{xx} - Z_{yy}$ $D_2 = Z_{xy} - Z_{yx}$

METHODOLOGY

Research Survey Design

The distribution of measurement points is divided into two modeling trajectories with northeast-southwest direction as shown in Figure 3. Some measurement points are nearby the manifestation of geothermal systems in the form of hot springs. Track 1 has seven MT sounding points that cross two MAPS (hot springs), namely MAP-01 and MAP-02, while track 2 has six MT sounding points that cross one MAP, namely MAP-04.

Data Availability

The MT sounding data used in this study amounted to thirteen points which then the crosspower edited and geoelectrical strike angle determined. Data used in geoelectrical strike analysis is Z_{xx}, Z_{xy}, Z_{yx}, Z_{yy} impedance data at each frequency with each real and imaginary component.

Research Workflow

The processing and analysis of magnetotelluric data starts from the data in the time series and then fourier transforms are carried out, to obtain a cross section of subsurface resistivity.

Figure 4 is the workflow carried out in this study. The following explanation shows steps for processing and analyzing magnetotelluric data. Determination of angles for impedance rotation tensor is obtained from the direction of geoelectrical strike based on the calculation of WAL-Bahr. Geoelectrical strike is the direction of higher conductivty in a 2D or anisotropic medium also the direction of conductive lineament intersecting a horizontal plane (Simpson and Bahr, 2005).

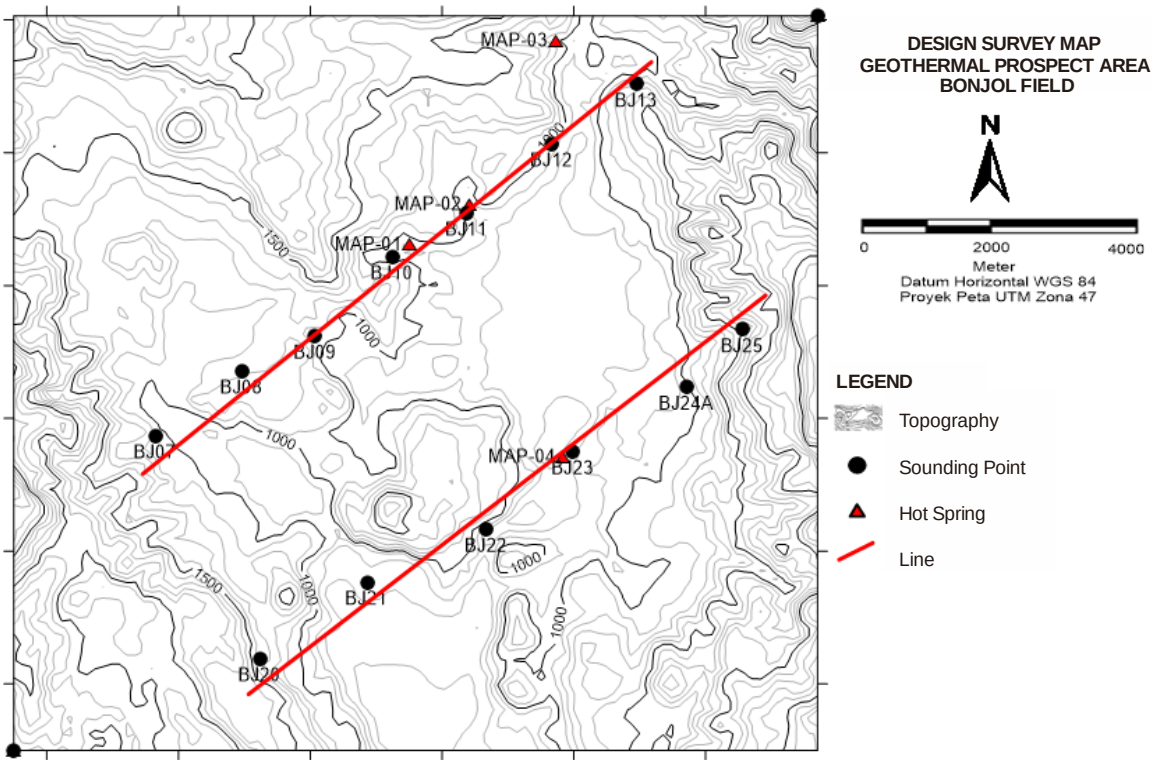


Figure 3: Research survey design map.

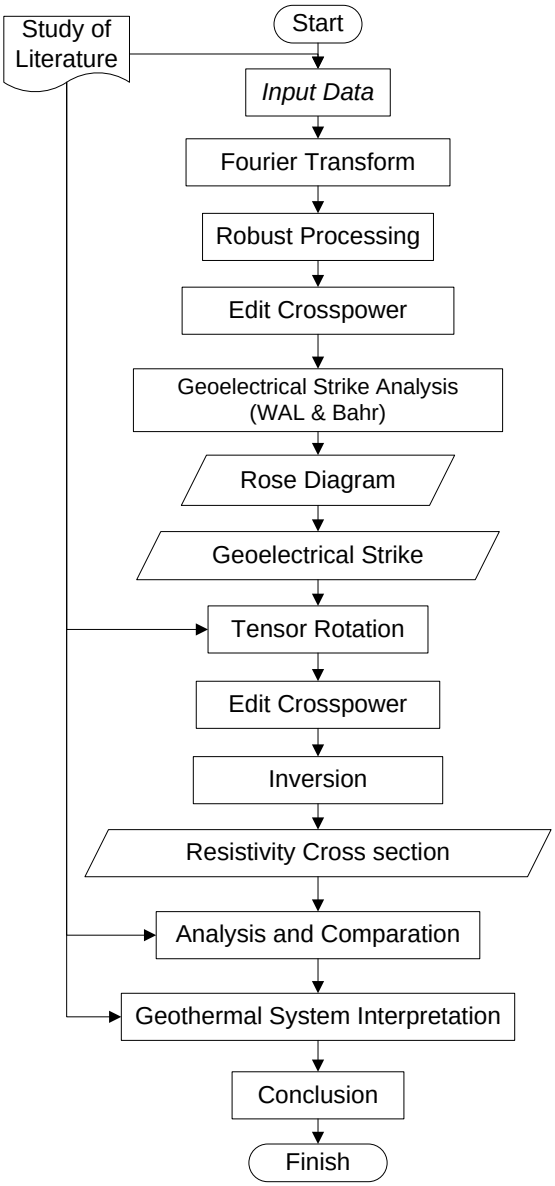


Figure 4: Research workflow diagram.

Angle will be obtained at each frequency which is then plotted in the rose diagram to obtain the dominant angle. The rose diagram is attached in appendix E. The angle is the geoelectric strike that forms the basis of the tensor rotation. The results of crosspower selection were then rotated based on geoelectrical strike and repeated crosspower selection to obtain a trend of resistivity and minimum interference phase.

Rotation results model of geological strike and geoelectrical strike analyzed by adjusting the location of where the geological structure shown in Figure 5 and resistivity contrast to the cross-section is considered as the structure identifier. In this study, geological structure data and manifestations became controls in determining the most appropriate model. To adjust the concept of 2D earth model described by Simpson and Bahr (2005), the measurement data needs to be directed in the direction of resistivity contrast. The geological strike direction is used in the direction of the Semangko fault (N 135 ^{o}E) while the geoelectrical strike is the result of the rose diagram. The selection of the most appropriate model is based on the compatibility of the location of resistivity contrast with the location of the fault in terms of the geological map of the study area and the MT station point. After obtaining a representative model of subsurface conditions reinforced by its geological data, the model is interpreted as a component of the geothermal (fault, cap rock, and reservoir) system in the area based on resistivity contrast values. The resistivity values of each component of the geothermal system are obtained from previous studies considering the local geological conditions of the study area which affected the resistivity value. Previous research (Mustang et al., 2007; Noor, 2012; Cumming, 2000; Palacky, 1988) also became one of the aspects considered in interpretation.

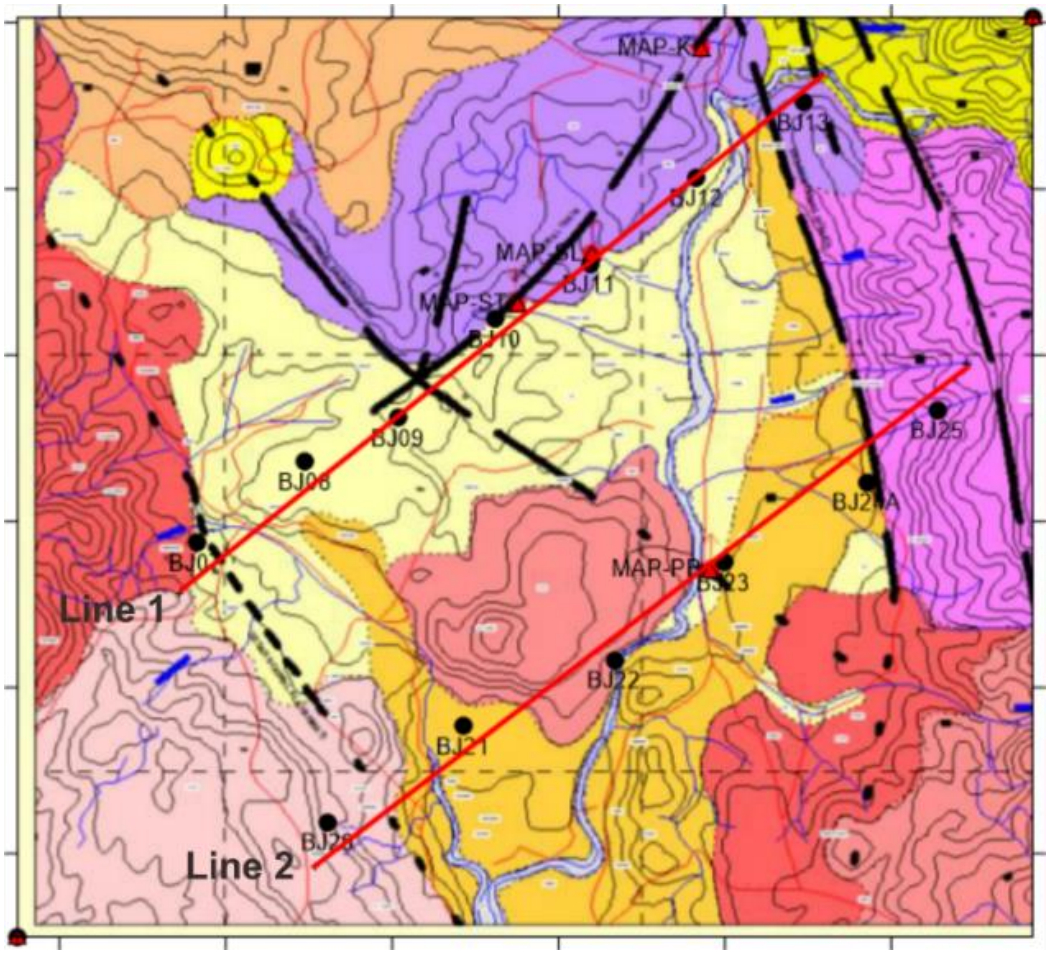


Figure 5: Geological map and MT sounding points.

RESULTS AND DISCUSSION

Geoelectrical Strike and Tensor Rotation

Geoelectrical strike is used as one of the MT 2D tensor rotation reference points. Geoelectrical strike value obtained through equation according to the impedance calculation of Bahr (1988) and Weaver et al. (2000). The analysis will produce angular values at each frequency in each MT station, then the angular values are plotted on the rose diagram to get a general geoelectrical strike direction that works on the track.

Figure 6 is a rose diagram that shows geoelectrical strike on the data station of MT Bonjol field with direction N 0° E. This can occur due to the complexity of the structure and other geological objects that affected the direction of geoelectrical strike. For the purposes of analysis, a comparison between the rotation of the geoelectrical strike angle (N 0° E) and the geological strike in general is carried out as the direction of the Semanko fault NW-SE (N 135° E).

2D Modelling

Figure 7 is the result of track 1 of 2D model for (a) geological strike rotation and (b) geoelectrical strike rotation. If observed on the geological map, there are three structures that are passed by path 1, namely D fault, E fault, and C fault. D fault passes path 1 in the eastern part of station BJ-07, D fault between BJ-09 and BJ-10 while D fault between BJ-12 and BJ-13. The existence of cesarean causes a resistivity contrast value below the surface, especially in geothermal systems, faults generally become the prospect boundary or either the cap rock distribution limit or as a discharge area for the release of geothermal manifestations pathway.

In the 2D model of track 1 geological strike rotation, the location of the geological structure on the surface (dashed black line) is not in accordance with the resistivity contrast position in the 2D model especially for E and C faults. Unlike 2D model of track 1 of geoelectrical strike rotation, geological structure location (D fault, E fault, and C fault) on the surface are between resistivity contrasts. This explains that 2D rotation modeling of geoelectrical strike produces a model that is more in line with the geological conditions in the study area.

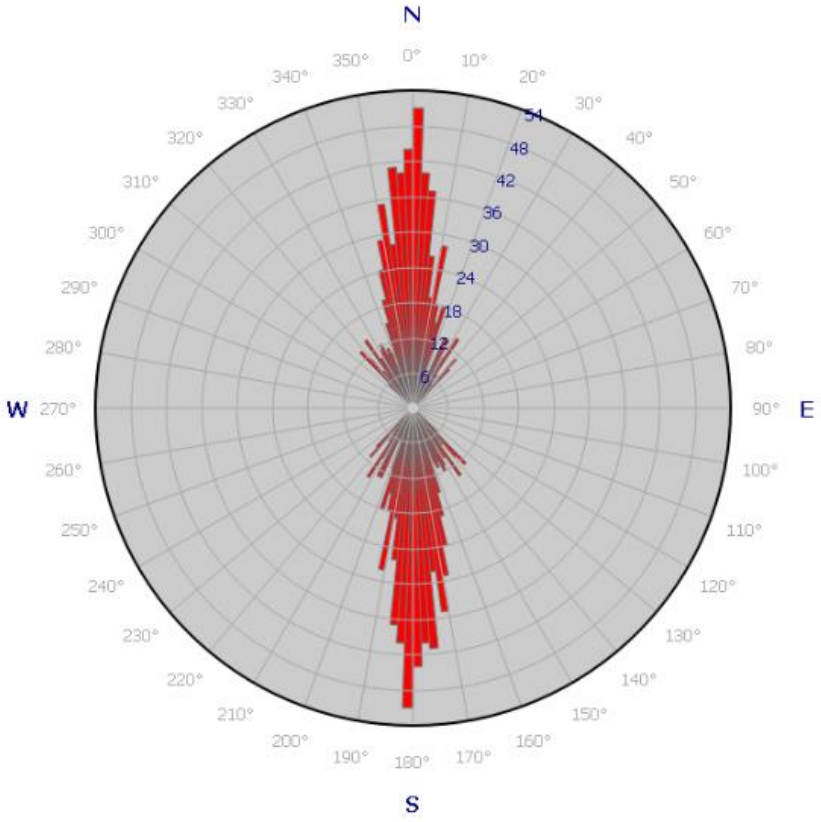


Figure 6: Geoelectrical strike rose diagram line 1 and line 2.

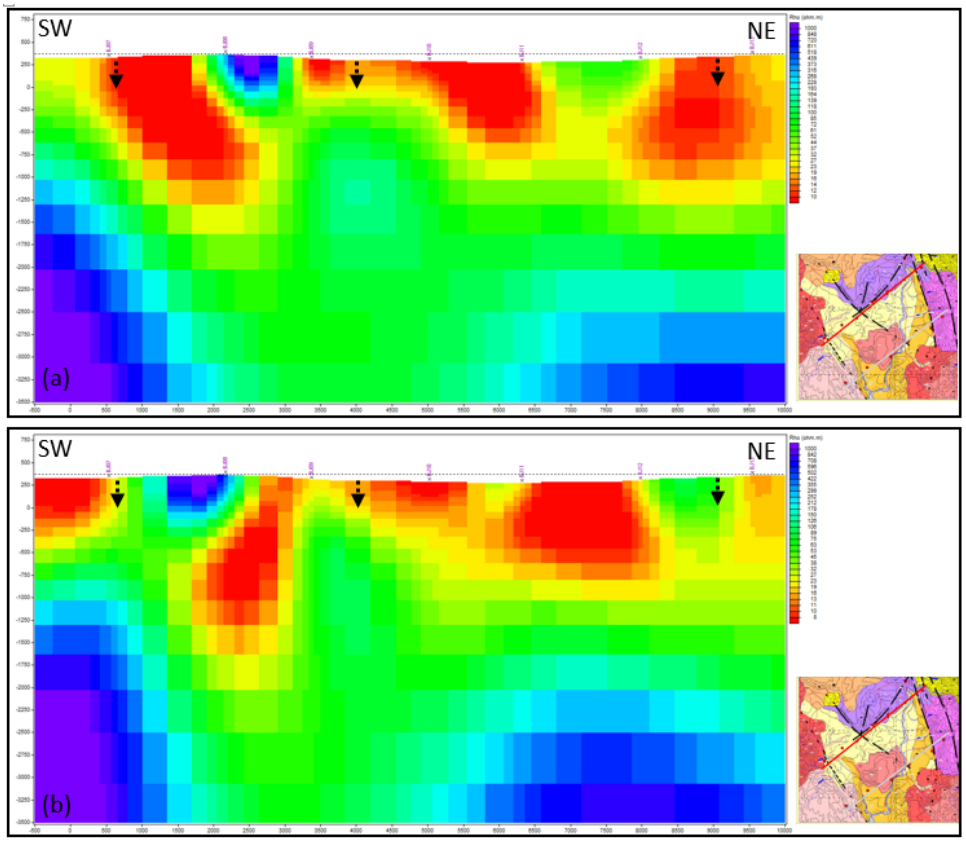


Figure 7: 2D model line 1 (a) geological strike and (b) geoelectrical strike.

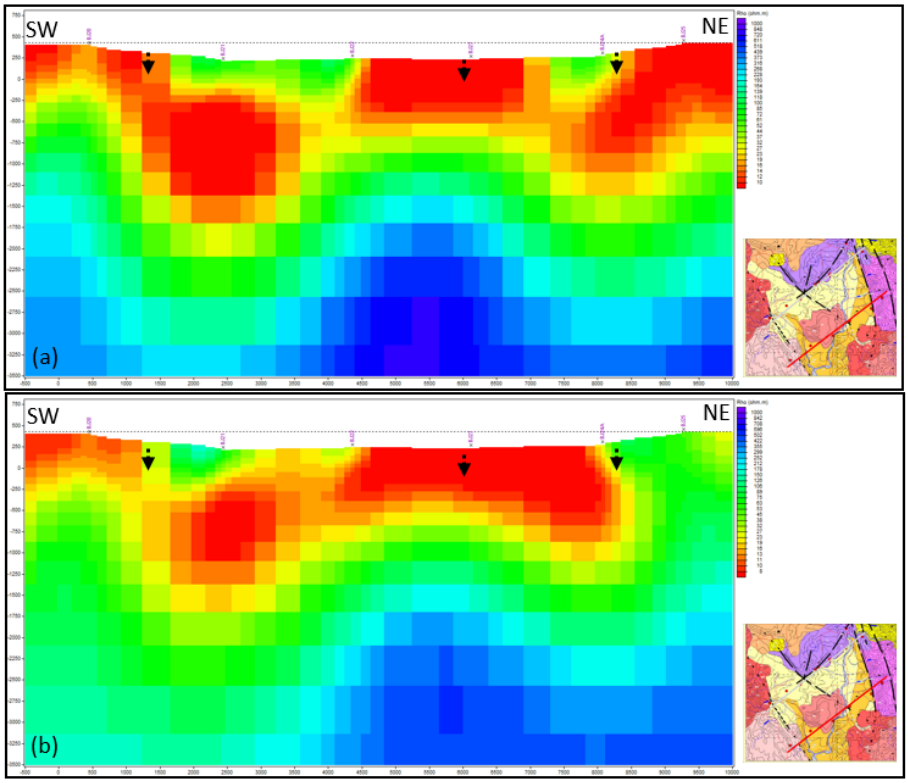


Figure 8: 2D model line 2 (a) geological strike and (b) geoelectrical strike.

2D model track 2 (Figure 8) crosses three faults that are equal to track 1 (D fault, E fault, and C fault). D fault is between BJ-20 and BJ-21, E fault is exact on BJ-23, while C fault is on BJ-24. In the results of 2D modeling of geological strike rotation, the position of the fault (dashed black line) is not exactly in resistivity contrast. Whereas, in 2D modeling of geoelectrical strike rotation, the location of the geological structure on the surface is right in resistivity contrast. However, the E fault that was supposed to be in station BJ-23 was not represented by resistivity contrast either on the results of modeling geoelectrical strike or geological strike. This fault is then considered a discharge area where the cap rock passes hot fluid and gives rise to geothermal manifestations in the form of MAP-04 on the surface.

The results of the tensor rotation influence analysis explain that the results of geoelectrical strike rotation provides a more representative image of the subsurface compared to the results of geological rotation strike modeling on the surface. Interpretation of the Bonjol field geothermal system uses 2D modeling of geoelectrical strike.

Interpretation of Geothermal System

Figure 9 is the result of the interpretation of the geothermal system in the Bonjol field. The interpretation of the magnetotelluric 2D model can illustrate the condition of the geothermal system on place. According to Cumming et al. (2000), resistivity values <10 Ohm.m are in the argillic zone and resistivity values >10 Ohm.m are in the propylitic zone with high temperatures. The low resistivity value (<10 Ohm.m) is considered a cap rock (impermeable) because alteration formed in the area is conductive. The lower part of the cap rock (bottom of clay) borders with the reservoir. Moderate resistivity values (10-120 Ohm.m) are considered as high-temperature reservoirs with permeable propyllic alteration. High resistivity values (>120 Ohm.m) are interpreted as heat sources referring to Palacky (1988) assuming fresh igneous rocks. The geometry of the components of the Bonjol field geothermal system can be estimated from the results of 2D modeling. The thickness of the cap rock varies around 750m with the distribution starting from nearby the surface. The thickness of the reservoir varies around 1000m with depths varying from 750m – 1500m below sea level. And heat source is estimated to be at a depth of more than 1500m below sea level. On geothermal fields, lateral resistivity contrast is considered a structure in the form of a fault. Fault or continuity of a layer will be the limit of the alteration zones distribution on geothermal fields. So that the alteration of the clay on the cap rock will be limited to the fault and cause differences in resistivity values on the hanging wall and foot wall fault. Fault plan can also be a geothermal fluid track and cause the fault field to have a resistivity value with a certain directional direction. Fault in the model is described from the contrast resistivity or not continuing the low resistivity value on the cap rock.

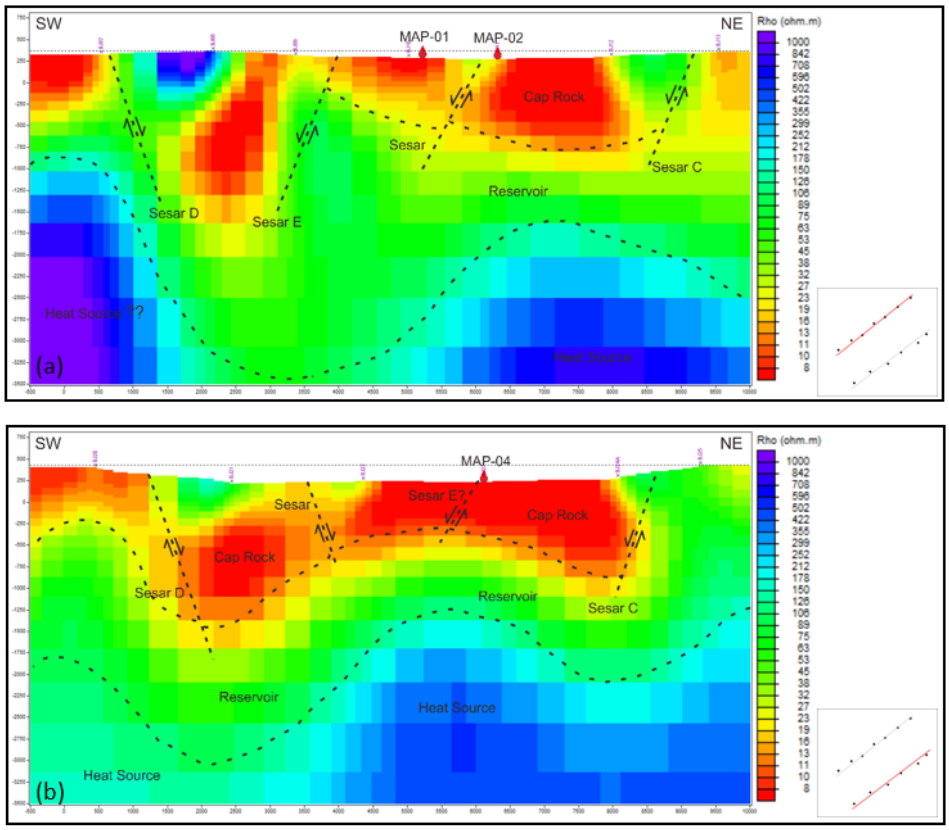


Figure 9: Geothermal system interpretation (a) line 1 and (b) line 2.

Track 1 is interpreted as there are C fault, D fault, and E fault based on resistivity contrast values in 2D modeling as well as one fault indication which is indicated by resistivity contrast values but not revealed on the surface. The interpretation of this fault indication is reinforced by the emergence of 02 hot springs as a manifestation that requires the escape route of the hot fluid contained. On track 2, there are C fault and D fault as a result of the resistivity contrast value interpretation. As well as two fault indications, one of the faults is indicated because there is resistivity contrast in 2D modeling, while the E fault indication is interpreted based on the appearance of hot springs on the surface that flow through geological structures such as faults.

The direction of fault interpretation is adjusted to the type of fault in the geological data and the block description that is relatively moving down. The appearance of hot springs also strengthens the presence of hot fluids below the surface. There are several anomalies which are some indications of a geothermal system such as the presence of a heat source on the track 1 of the SW section. This indication can be ascertained by adding the MT sounding point to the space between the two MT measurement points or at the ends of the modeling track.

The Bonjol geothermal field is included in the classification of volcanic geothermal systems if viewed from the lithological component of the research area and the heat source described in the subsurface model. By observing the resistivity vs. frequency curves at each MT sounding point, it is estimated that the Bonjol field geothermal system is included in the liquid dominated system due to gradual changes and consistent values of frequency resistance. To determine the enthalpy of the Bonjol field geothermal system, it is necessary to do geothermal fluid geochemical analysis and geothermometer studies on the research area.

CONCLUSION

Based on the analysis of magnetotelluric impedance tensor rotation at the Bonjol geothermal field, it can be concluded:

Based on WAL and Bahr analysis, the direction of the geoelectrical strike angle is N 0^{o} E for all data in the study area.

Two types of impedance tensor rotations produce different 2D models. Geoelectrical strike rotation produce 2D models that are more representative (5 appropriate structures) than the strike rotation of surface geology (2 appropriate structures).

There are geothermal system components, namely cap rock (<10 Ohm.m), reservoir (10-120 Ohm.m), heat source (> 120 Ohm.m), and faults which needed to determine the prospect of geothermal energy based on the results of interpretation and 2D model analysis.

ACKNOWLEDGEMENT

Author express special thanks to Center for Mineral, Coal and Geothermal Resources - Geological Agency Bandung who gave the permit to use the Bonjol geothermal area magnetotelluric data. Also special thanks to Maria Gracesica for the help.

REFERENCES

Bahr, Karsten. (1988), "Interpretation of The Magnetotelluric Impedance Tensor Regional Induction and Local Telluric Distortion". Journal Geophysics 62, 119–127.

Cumming, W., Gregg Nordquist and Doddy Astra. (2000), "Geophysical Exploration for Geothermal Resources: An Application for Combined MT-TDEM". SEG 2000 Expanded Abstracts.

Goff, Fraser and Cathy J. Janik. (2000), "Geothermal Systems", Sigurdson Encyclopedia of Volcanoes, Academic Press.

Hochstein, Manfred P. and Patrick R. I. Browne. (2000), "Surface Manifestations of Geothermal Systems with Volcanic Heat Sources", Encyclopedia of Volcanoes, Academic Press.

Khyzhnyak, M., (2014), "Geoelectric Strike and Its Application in Magnetotellurics", Faculty of Earth Science School of Engineering and Natural Sciences University of Iceland, Reykjavik Iceland.

Mustang, Ario, Dendi S. and Timoer S. (2007), "Penyelidikan Gayaberat and Geomagnet Di Daerah Panas Bumi Bonjol, Kabupaten Pasaman Propinsi Sumatera Barat", Bandung: Pusat Sumber Daya Mineral Batubara and Panas Bumi

Noor, Yussuf, Janet Suwai and Deflorah Kangofo. (2012), "Correlating Resistivity with Temperature and Alteration Mineralogy in Menegai Geothermal Field: Case Study of Menengai Exploration Well (MW-01)". GRC Transactions 36.

Palacky, G. J. (1988), "Resistivity Characteristics of Geologic Targets", Electromagnetic Methods in Applied Geophysics. 52-129.

Pracser, E. and L. Szarka. (1999), "A Correction to Bahr's Phase Deviation Method for Tensor Decomposition", Earth Planets Space 51. 1019–1022.

Simpson, Fiona and Karsten Bahr. (2005), "Practical Magnetotellurics", Cambridge: Cambridge University Press.

Unsworth. (2007), "Electromagnetic Exploration Methods", University of Alberta, Canada.

Weaver, J. T., A. K. Agarwal and F. E. M. Lilley. (2000), "Characterization of the Magnetotelluric Tensor in Terms of Its Invariants". Geophysics Journal International 141(2). 321–336.

Xiao, Wen. (2004), "Magnetotelluric Exploration in The Rocky Mountain Foothills", Department of Physics University, Alberta.

HYDROTHERMAL CYCLE ESTIMATION BASED ON RECHARGE AND DISCHARGE ZONE IDENTIFICATION USING GRAVITY METHOD AND GEOCHEMISTRY FLUID ON ARJUNO–WELIRANG COMPLEX, EAST JAVA

Bramasta Adya Dewanta, Ibanes Pramitasari, Tria Ainur Rokhis, Novia Dwi Rantikasari, and Cholisina Anik Perwita

Geophysical Engineering Study Program, Departement of Physics, Mathematics and Science Faculty, Brawijaya University, Indonesia Short address
Email: bramastadya@gmail.com

ABSTRACT

Arjuno-Welirang are volcanic complex that have geothermal potential, indicated by several manifestation in several areas such as hot spring. The hot spring can become the recharge zone, which associated by the existence of the recharge zone. Therefore, identification is carried out to determine both zones, using gravity method. 144 data points are retrieved from satellite data in 7°40'55.10"-7°51'28.12" south hemisphere and 112°27'2.36" - 112°39'17.58" north hemisphere. Data analysis is carried out until complete Bouguer anomaly are obtained, then regional and residual anomaly separation are done using upward continuation method. 2D forward modelling and 3D inverse modelling are done by using M-sys and VOXI software respectively. For geochemical identification, manifestation fluid chemical content information is obtained from open source data.

Keywords: Hydrothermal system, recharge, discharge, Arjuno-Welirang geothermal system

INTRODUCTION

The Indonesian archipelago is located at the confluence of three large plates, there are Eurasia-Australia-India-Pacific so that Indonesia has a complex tectonic order. Subduction between continental plates and oceans results in a melting process of magma in the form of partial melting which means that the components of the collision process and the protective layer of magma (silica / basaltic)) are known as fire rings. The emergence of leases out of the Indonesian market through its technical model is used for Indonesia's geothermal systems (Kasbani, 2009).

The Indonesian geothermal system is generally a hydrothermal system that has a high temperature (> 225°C), only a few of which have moderate temperatures (150 - 225°C). Basically, a hydrothermal type geothermal system is formed as a result of heat transfer from a heat source to its surroundings which occurs by conduction and convection. Conduction heat transfer occurs through rocks, while convection displacement occurs because of contact between water and a heat source. Convection heat transfer basically occurs due to buoyancy. Because the gravitational force of water has a tendency to move downward, but if the water is exposed to the temperature by a heat source, heat transfer will occur so that the water temperature is higher, and the water becomes lighter. This situation causes hotter water to move upward and lighter water to move downwards so that convection occurs (Saptadji, 2000).

One component that plays an important role in geothermal energy is hydrothermal flow. The interaction of heat source, fluid, and permeable components is an important factor in the hydrothermal activity. The fault is control of geothermal energy which is directly related to hydrothermal activity. At certain scale faults also play a major role in determining the limits and evolution of hydrothermal flow (Curewitz and Karson, 1997; Setyawan et al., 2015).

The Arjuno-Welirang Mountain Complex is a stratovolcano type volcano complex. Mount Arjuno is an altitude of 3,339 m (10,955 ft) and Mount Welirang is an altitude of 3,156 m. Almost all of Mount Arjuno-Welirang are Quaternary volcanic rock products. Some volcanic products in this area consist of lava and pyroclastic flows. The stratigraphic component and geological structure are shown in Figure 1. Geological structures that develop in this area are quite complex including normal faults, horizontal faults, rim caldera, and ambles. These faults generally cut the Gunung Arjuno-Welirang complex and trending south, northwest-southeast, southwestern northeast, and west-east. Rim caldera - located in the middle part of the Arjuno-Welirang Mountain complex, while the assemblage sector is in the southern part of the peak of Mount Arjuno-Welirang with openings to the southeast and northeast.

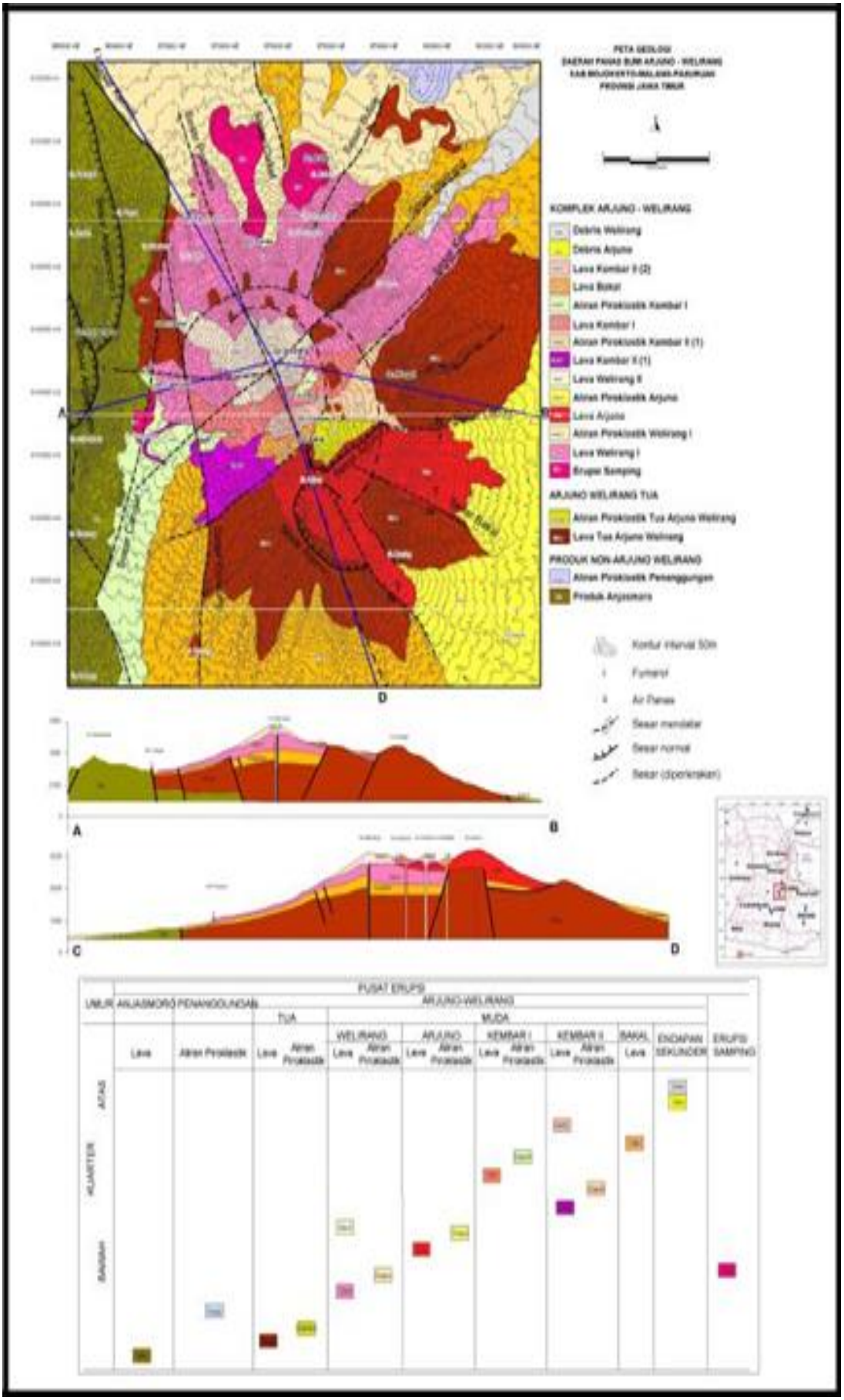


Figure 1: Geological map of the geothermal area of the Arjuno-Welirang mountain complex (PSDG Geological Survey Team, 2010).

Gravity Method

The gravity method is an exploratory method that measures the gravitational field at different points in a certain area. The principle of this method is to distinguish the mass density of the material from the surrounding environment. Gravity intensity is influenced by rock density below the surface. The gravity method works based on the basic principle of Newton's law of gravity, ie the magnitude of the gravitational value between two objects is proportional to the product of the mass of both objects and is inversely proportional to the square of the distance. Newton's Gravity Law can be written in Equation 1:

$$F = G\frac{m1 \cdot m2}{r^2} \qquad (1)$$

Where:

F = the force between two objects (N)
G = gravity constant (6.67×10^{-11} Nm^2/kg^2)
m1, m2 = mass of object 1, mass of object 2 (kg)
r = distance between m1 and m2 (m)

Measurement values on the earth's surface vary. This is caused by many factors, both inside and outside the earth. To eliminate this effect, corrections to the measurement data need to be done (Jumransyah, Sunaryo, and Wasis, 1995).

Bouguer Correction

Bouguer correction needs to be done because of the mass located between the datum and the measurement point with the density ρ (gr/cm) and thickness h (m). Mathematically the Bouguer correction value is written in equation 2 (Lowrie, 2007).

$$BC = 0.1491\ x\ p\ x\ h \qquad (2)$$

Terrain Correction

Topographic conditions around the measurement point. Gravity values can increase due to reduced topography. For example, if there are hills around the location of the measurement point, the hill has a field that can cause the Gravimeter to increase acceleration, on the contrary if around the measurement site contains a valley then can cause the gravimeter to decrease acceleration. Therefore, field correction is needed to eliminate the topography (Jumransyah, Sunaryo and Wasis, 1995), using the Hammer Chart, field correction can be obtained by equation 3 (Ferdiandi, 2014).

$$TC = \frac{2\pi G\rho}{n}\left[RL - RD + \sqrt{R_D^2 - z^2} - \sqrt{R_l^2 - z^2}\right] \qquad (3)$$

Where:

TC = terrain correction
ρ = density (Kg/m^3)
R_L = outer radial
R_D = inner radial
z = height (m)
n = zone length (m)

Forward Modelling

Forward modeling is a method of interpretation that estimates subsurface density by first making subsurface geological objects. The anomalous calculation of the model that was made then compared with Bouguer anomaly which was obtained from the gravity survey. The general principle of this modeling is to minimize the difference in observation anomalies to reduce ambiguity. The meaning of two-dimensional objects here are three-dimensional objects that have the same cross-section anywhere as long as they do not stop at one coordinate. In some cases, the Bouguer anomaly contour pattern is a lined shape that identifies the cause of the anomaly as an elongated object. Modeling is expressed in two-dimensional form because the two-dimensional gravity effects can be displayed in a single profile form. Future modeling for calculating the gravity effect models of subsurface objects with arbitrary cross-sections that can be represented by a polygon containing is expressed as line integrals along the polygon sides (Talwani, et al., 1959).

Forward Modeling is the process of calculating data from theoretical results that will be observed on the earth's surface if the model parameters are known. When making an interpretation, look for a model that produces a suitable and fit response with observational data or field data. So, it is expected that the condition of the model can represent or approach the real situation Often the term forward modeling is used for the trial and error process. Trial and error is a trial and error process to obtain compatibility between theoretical data and field data. It is expected that from this trial and error process a model that matches its response to the data is obtained (Grandis, 2009).

Invers Modelling

This is done after the gravity data has been corrected and separated between local anomalies and regional anomalies. At the modeling stage, gravity data is interpreted to get an idea of the subsurface structure based on the distribution of rock density. Technically the modeling is done by modeling in this study using a prism-shaped 3D object model. If a 3-dimensional mass of an arbitrary shape is

continuously distributed with mass density Dr (a, b, g) as shown in Figure 2, the gravity potential at the point P (x, y, x) above and beyond the distribution of the mass meeting is given by (Kadir, 1996).

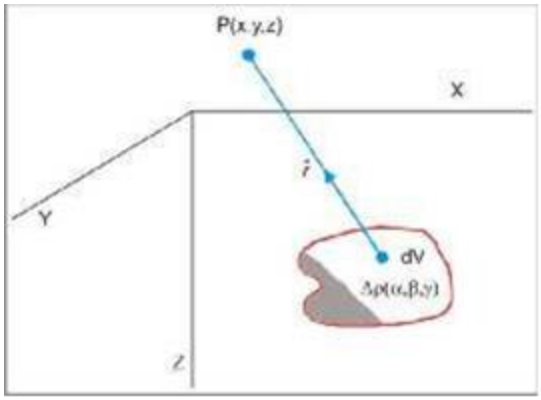


Figure 2: (a) The Potential Effects of Gravity at Point P (b) Upright Prism Objects.

Geochemistry Fluid Type

Nicholson (1993) divide hot spring into some type based on the anion Cl-SO_4-HCO_3:

Chloride Hot Water

This type of water is characteristic of deep geothermal fluid and is included in a high temperature geothermal system. Chloride hot water has a high content of Cl, Na, and K, Ca is often low, SiO2 is quite high (depending on temperature).

Sulfate Hot Water

Hot sulfate water usually occurs in geothermal areas that controlled by active volcanic activity where steam is condensed to surface water. This type of hot water has high SO4 ions, Cl and HCO3 are very low (sometimes 0), containing Na, K, Ca, Mg, Fe, and low pH (<2 – 3).

Bicarbonate Hot Water

Bicarbonate hot water is the result of condensation of water and gas vapor into oxygen-poor subsurface water, found in non-volcanic areas with high-temperature systems. The main ion content is HCO3 and has a pH close to neutral as a result of the reaction of water with local rocks. On the surface, this type of hot water is characterized by the presence of carbonate or travertine sintered deposits.

Chloride – Sulfate Hot Water

The type of hot water mixing water chloride-sulfate can be formed through the process of mixing water chloride with sulfate water at a certain depth; water near the surface discharges with chloride water; condensation of volcanic gas into meteoric water; condensation of a magmatic vapor or flowing fluid containing chloride.

Dilute Chloride-Bicarbonate Hot Water

This type of hot water is formed by the interaction of water chloride with groundwater or bicarbonate water during its lateral flow. This hot water may be in the boundary area (margin) of a high-temperature geothermal system. The ion composition of hot water is dominated by chloride and bicarbonate ions in varying amounts and has a pH of 6-8. To determine the type of geothermal fluid, a ternary plotting diagram can be performed.

METHODOLOGY

This research was conducted in the Arjuno-Welirang Mountain complex, Malang, East Java, with coordinates 7 ° 40'55.10 "-7 ° 51'28.12" LS and 112 ° 27'2.36 "- 112 ° 39'17.58" BT. Gravitational data obtained comes from TOPEX UCSD satellite imagery that has precision per the second unit with a distance of 30-40mm with 4-6 mGal gravitational field resolution. The data collection point is 144 points in the form of gravity anomalies and topographic values, which are then processed by data correction with field correction and Bouguer correction to produce a cross-section in the form of separation of regional anomalies and residual anomalies using the upward continuation method. Advanced data processing is done by 2D modelling in the form of forward modelling in GM-sys software and 3D inversion modelling in VOXI software to identify subsurface structures. For geochemical identification, the data used is open source data in the form of information on fluid chemical content in manifestations in the Padusan and Cangar regions. The analysis is done by plotting a diagram CL - SO4 - HCO3 using the Ternary Diagram (Nicholson, 1993) to determine the type of fluid in the study area as a reference in determining the type of hydrothermal fluid. The interpretation was carried out by correlating the results of the identification of recharge-discharge zones and fluid geochemistry so that the estimation of the hydrothermal cycle in the Arjuno-Welirang area was produced.

RESULT

Based on the fluid geochemical analysis on the ternary diagram of the CL - SO4 - HCO3 type fluid bicarbonate (Table 1 and 2). This is because it is known that the HCO3 (bicarbonate) element is the most dominant element in the ternary diagram (Figure 3) which shows that in 4 hot water samples in the area have the same hot water type namely carbonate water with HCO3 concentration - which is due to adsorption of CO2 and steam condensation into water, thus indicating that the fluid originates from meteoric water that is the soil due to percolation. And with the presence of Cl-SO4 content, the SO4 has been derived from the volatile water-SO4 derived from volatile magma.

Table 1: Calculation Results of Ternary Diagram Concentration Cl - SO4 - HCO3 in the Padusan area.

Sample Location	Concretation (%)		
	Cl^+	SO_4	HCO_3
Padusan 1	20.3482	14.085453	65.5664
Padusan 2	24.2747	7.2698193	68.4555
Padusan 3	21.8449	4.9708848	73.1842
Padusan 4	20.2167	4.5593238	75.2239

Table 2: Calculation Results of Ternary Diagram Concentration Cl - SO_4 - HCO_3.

Sample Location	Concretation (%)		
	Cl^+	SO_4	HCO_3
Cangar 1	20.3482	14.085453	65.5664
Cangar 2	24.2747	7.2698193	68.4555

In determining the type of water fluid in each sample can use Clary SO4 – HCO3 ternary plot diagram. The ternary diagram results in (Figure 4) show that in 2 samples of hot water in the Cangar area have the same type of hot water, that is, bicarbonate water, with a high concentration of HCO3 - which is thought to be due to adsorption of CO2 gas and condensation of steam into water, this is similar with the results of identification of the manifestations of the Padusan region which shows that the fluid comes from meteoric water that enters the soil due to the percolation process. And with the presence of Cl - SO4 content, the meteoric water that has been assimilated with magmatic water is due to Cl - SO4 derived from volatile magma.

Referring to the geochemical analysis of ternary diagrams in the two study areas, namely the Padusan and Cangar regions, it is indicated that fluid flow away from the upflow zone is based on an increase in HCO3 due to fluid flow that interacts with the rock being passed or because of the mixture of infiltrated surface water. Meanwhile, the higher the percentage of SO4 content in the sample indicates that the fluid is close to the upflow zone. So that it can be interpreted that the samples obtained from this study area are in the outflow zone with the main fluid from meteoric water which is assimilated with magmatic water. This is also reinforced by the presence of carbonate deposits (travertine) formed in geothermal manifestations in the Cangar and Padusan regions. From the results of the gravity method data processing in the Arjuno - Welirang Mountain complex area, the author uses a regional anomaly cross section for further processing because the regional anomaly cross section is considered the most representative cross-section in this study. Based on the cross section of regional anomalies the distribution of low to high anomalies is in the orientation of the power directly to the northeast with the lowest anomaly of -2.1 mGal and the highest is 101.2 mGal. In (Figure 5) there is a low anomaly of -2.1 mGal up to 20.6 mGal, shown in dark blue indicating the presence of a crater in the area. In doing the modeling, slicing is carried out in two regions, the first in areas A to A 'through the Padusan manifestation complex which is marked by white dots to the crater. Then slicing the second one is done in area B to B 'through the Cangar manifestation complex to the crater which is marked with a white point from the results of 2D modeling ahead of AA 'incisions and BB incisions' on regional anomalous maps, the image taking structure was obtained in (Figure 6 and 8), where caprock zones were found on the surface 00 1500 m to ≥ 2000 m with a density value of 2,5 gr/cm^3 up to 2.7 gr/cm^3 with type material namely mineral clay and reservoir at depths of ≥2000 m to ≥3000 with density values ≥2.7 gr/cm^3 up to ≥3 gr/cm^3 with the type of material pyroclastic (permeable) deposits which are removed as reservoirs. By looking at changes in contrast anomaly values in the cross-section it can reflect the supporting structure that has control of the hydrothermal flow with the fluid obtained from percolating meteoric air. This interpretation supports the similarity of the results of 2D forward modeling with 3D inverse modeling (Figures 7 and 9).

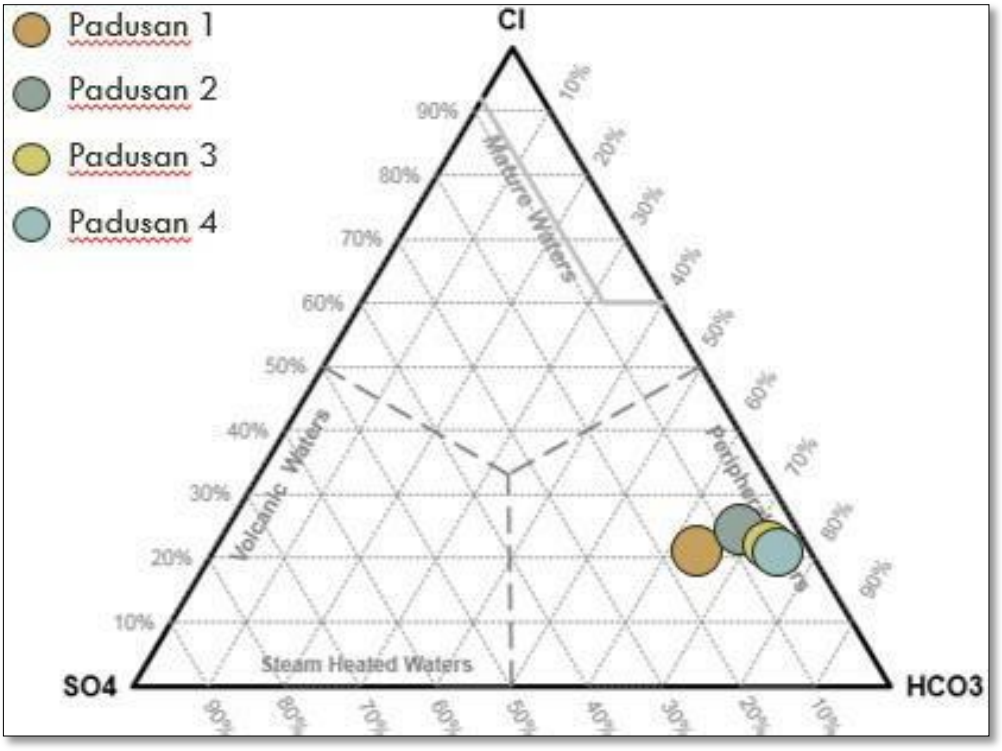


Figure 3: Diagram of Ternary Cl - So4 - HCO3 in the Padusan area.

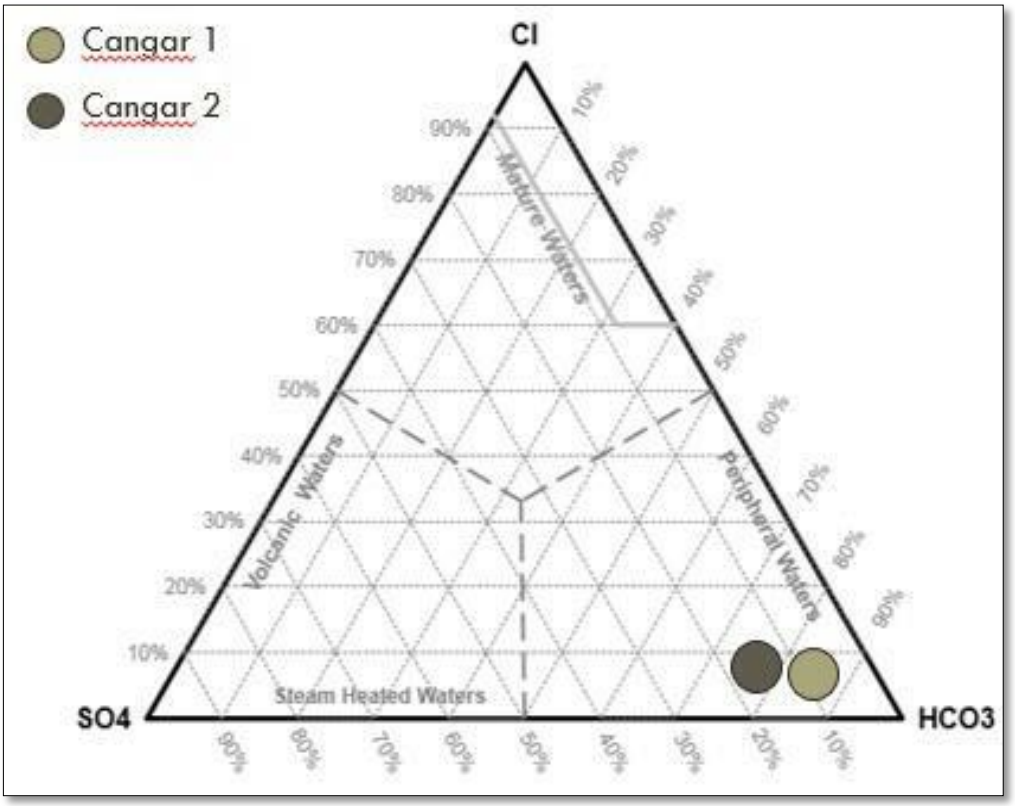


Figure 4: Diagram of Ternary Cl - So4 - HCO3 in the Cangar area.

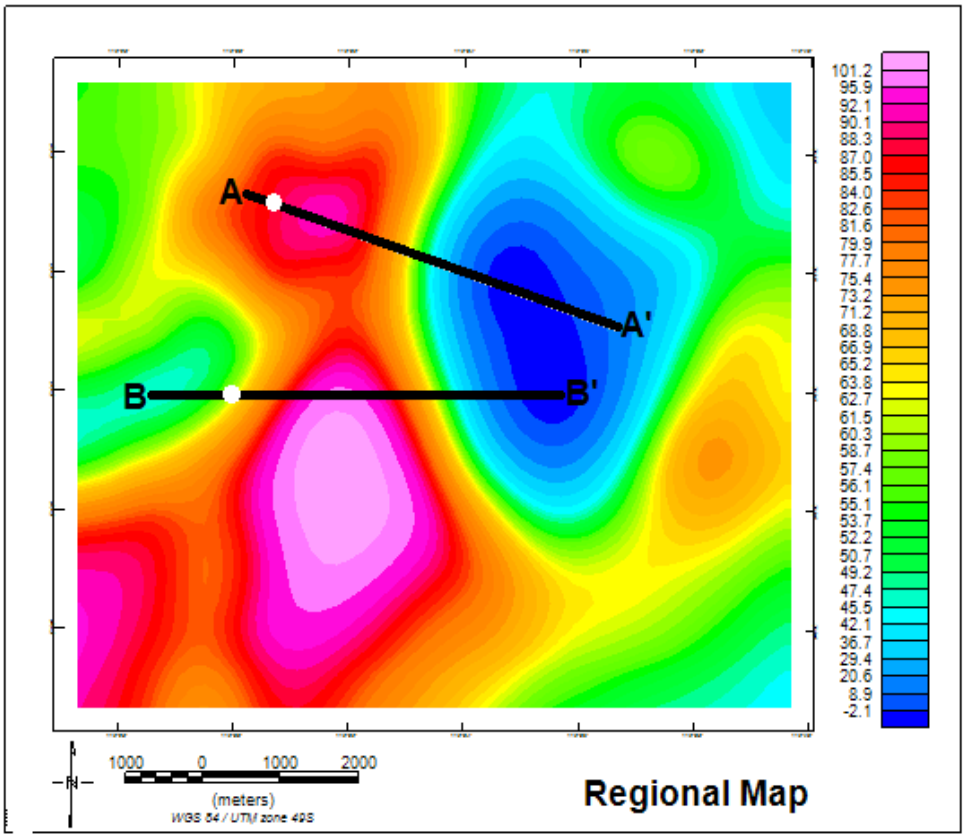


Figure 5: Regional Anomaly Map.

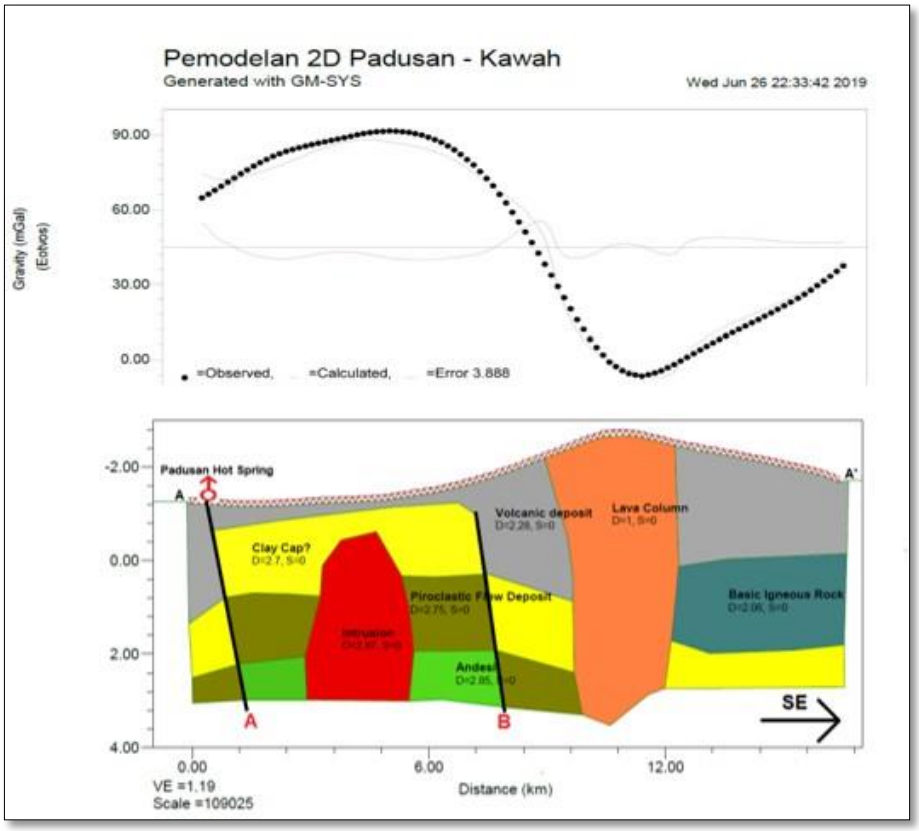


Figure 6: Forward Modelling 2D Padusan – Kawah.

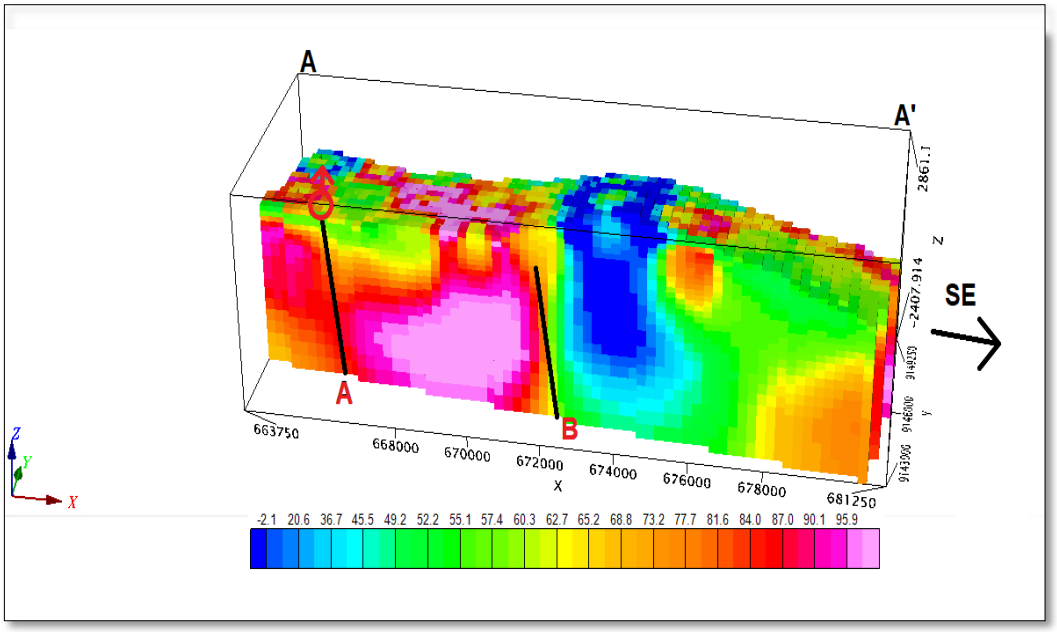


Figure 7: Invers Modelling 3D Padusan – Kawah.

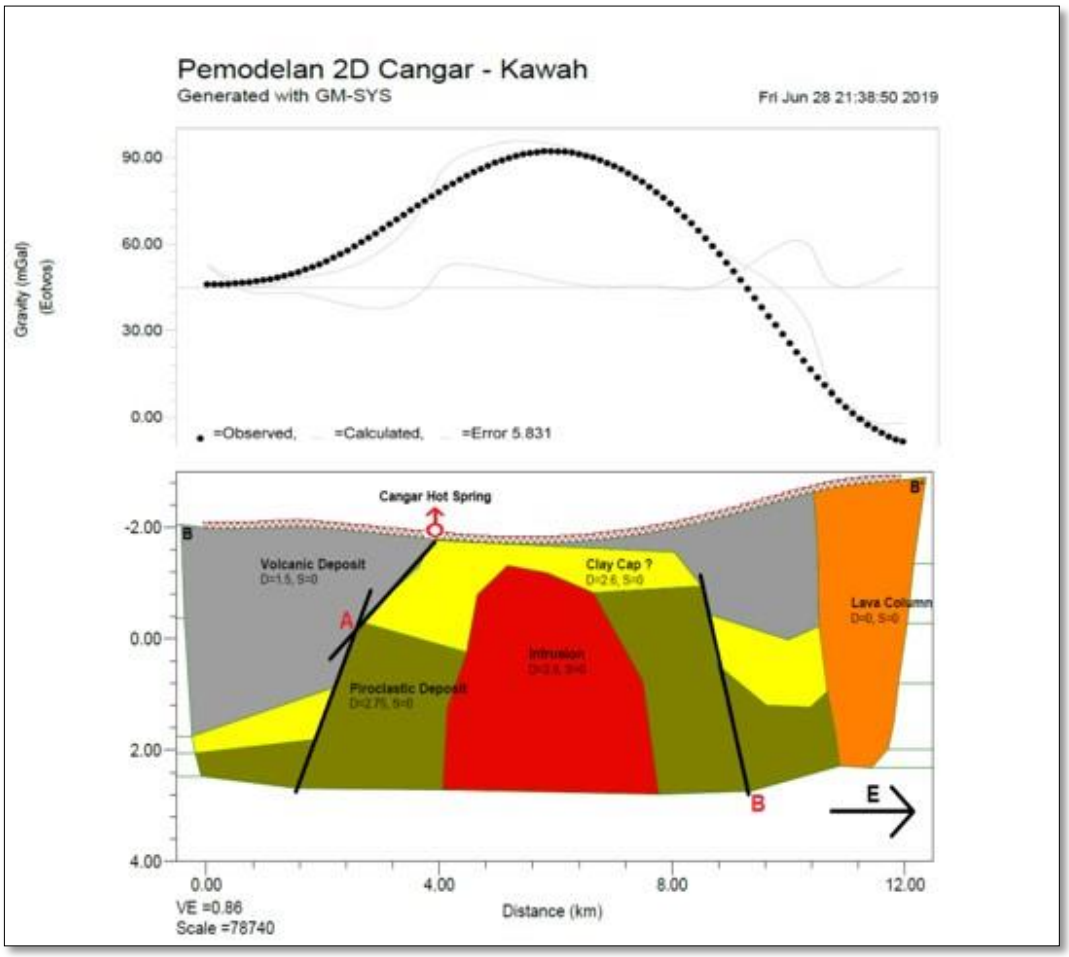


Figure 8: Forward Modelling 2D Cangar – Kawah.

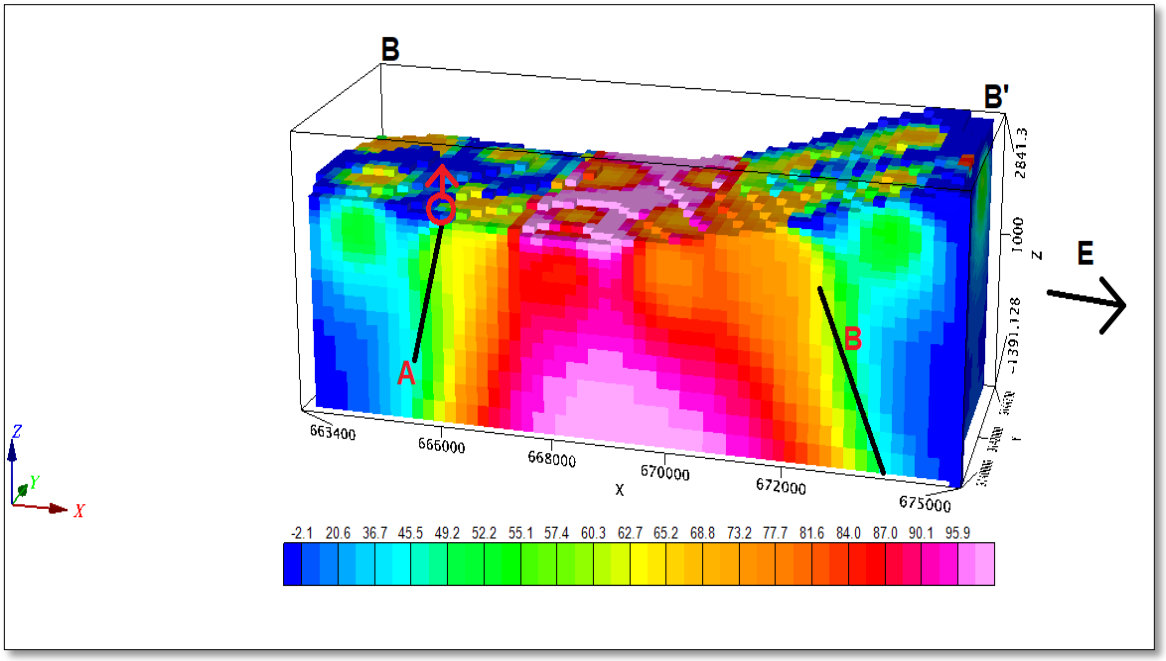


Figure 9: Inversion Modelling 3D Cangar – Kawah.

The recharge zone in mountainous areas is generally located on the slope area, so the meteoric water flowing through the slope will flow to lower elevations according to the nature of the water, then the water will insert at the sloped boundary due to percolation through the volcanic deposit layer which has sufficient cavity both as a fluid entry gap below the surface. The incoming fluid then accumulates and heats up in the reservoir so that it produces high pressure and forces the fluid to exit. The movement of fluid coming out to the surface is supported by the presence of a secondary structure (which is marked by the letter B) which is formed due to intrusion. The structure formed is about clay cap (impermeable) and reservoir. Furthermore, fluid flows with the help of secondary structures formed to the surface (which are marked with letter A) and makes the hydrothermal flow go to the surface to form a discharge zone in the form of hot water manifestation.

Based on the analysis of the hydrothermal flow cycle scheme on each subsurface model of the Padusan and Cangar manifestation complex, a concept model for the hydrothermal cycle on the Mount Arjuno - Welirang geothermal system was carried out. The hydrothermal cycle (Figure 10) is described by fluid originating from meteoric water flowing on the mountain slope which is indicated as the main recharge zone in this cycle model, then water enters the soil due to percolation process which then accumulates in the permeable pyroclastic deposit which is thought to be a reservoir, in the reservoir this happens the assimilation process between meteoric water and magmatic water. With the influence of temperature and pressure which is strong enough to make the fluid move through a supporting structure that controls the direction of the fluid until it finally comes out to the surface forming a manifestation. In this study, the manifestations are in the Padusan and Cangar hot water complex, which is the zone of Mount Arjuno - Welirang geothermal system outflow as well as the discharge zone in the hydrothermal fluid flow cycle model.

CONCLUSION

Based on the results of the data in the study area of the Padusan and Cangar manifestation complex that has been obtained, it can be concluded that in the Arjuno - Welirang geothermal system has the main fluid in the form of meteoric water based on the HCO3 content where the meteoric water is assimilated with magmatic water based on the Cl - SO4 element in it, so that it can be indicated that the research area is in the outflow zone. The meteoric water flows through the slope which is the main recharge zone in this fluid flow cycle scheme. At the boundary of the slope with the layer below, meteoric water percolation occurs because the influence of gravity and elevation gradients that occur makes the water insert below the surface and into the pyroclastic deposits which is indicated as a reservoir on the Arjuno - Welirang geothermal system. From the 2D cross-section model it is indicated that near the study area there is an intrusion that creates a secondary structure in the impermeable layer (clay cap) as a structure that helps control the direction of the fluid flow rate. With enough heat and pressure make the hydrothermal fluid move through the supporting structure until it finally comes out to the surface and make the manifestation as a discharge

zone in the fluid flow cycle scheme with deposits formed in the manifestation complex of the research area in the form of travertine deposits thereby strengthening indications that the hydrothermal fluid originates from meteoric water. However, further identification is needed with other methods to further strengthen the hydrothermal fluid flow cycle scheme of the Arjuno - Welirang geothermal system in the advanced exploration stage.

REFERENCES

Curewitz, D. and Karson, J. A. (1997). "Structural settings of hydrothermal outflow: Fracture permeability maintained by fault propagation and interaction", Journal of Volcanology and Geothermal Research, 79(3–4), pp. 149–168. doi: 10.1016/S0377-0273(97)00027-9.

Grandis, H. (2009), "Pengantar Pemodelan Inversi Geofisika", Bandung: Himpunan Ahli Geofisika Indonesia (HAGI)

Jumransyah, Sunaryo and Wasis, M. A. (1995) "Pendugaan Struktur Bawah Permukaan Gunungapi Kelud Berdasarkan Survei Gayaberat", (September 1995), pp. 1–5. doi: 10.1598/RT.58.7.8.

Nicholson, K. (1993). "Geothermal fluids: Chemistry and exploration techniques". Springer – Verleg, Berlin Heldederbeg

Talwani, M., Worzel, J. L. and Ladisman, M., (1959). "Rapid Gravity Computation for Two Dimensional Bodies with Application to The Medicino Submarine Fractures Zone". Journal of Geophysics Research., Vol. 64 No.1

Kasbani, (2009). "Tipe Sistem Panas Bumi Di Indonesia Dan Estimasi Potensi Energinya", Kelompok Program Penelian Panas Bumi, PMG –Badan Geologi, pp. 64–73.

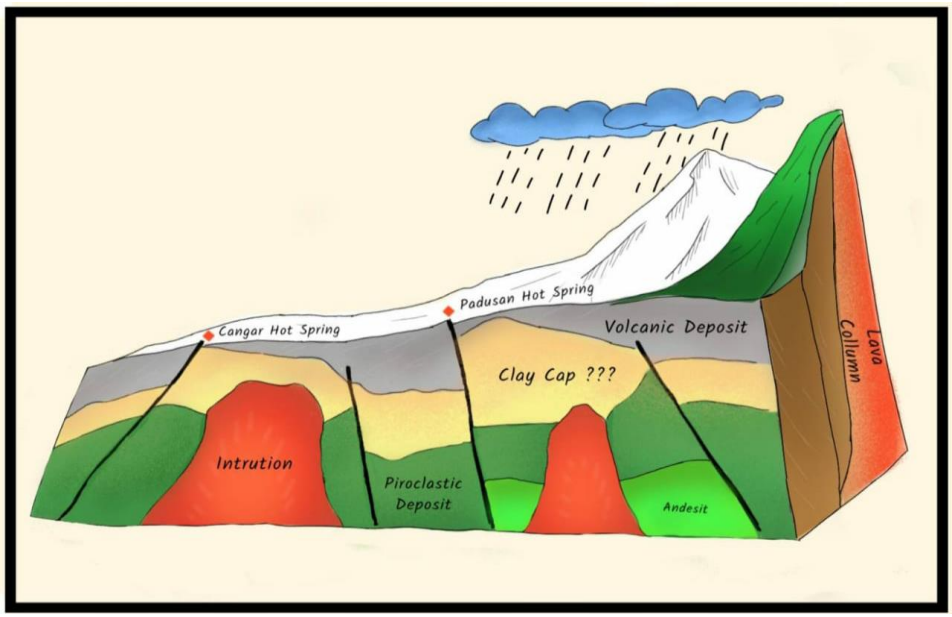


Figure 10: Hydrothermal Cycle Estimation on Arjuno – Welirang Complex.

ANALYSIS OF FAULT AND DISTRIBUTION FLUID GEOTHERMAL USING DEM SATELLITE IMAGE DATA, LANDSAT 8 OLI/TIRS AND SATELLITE GRAVITY IN THE VILLAMASIN GEOTHERMAL PROSPECT AREA, JAYAPURA DISTRICT, EAST OKU REGENCY

Jakasura Leonardo Tarigan[1] and Elsadella Nindya Putri[2]

[1]University of Lampung
[2]Universitas Indonesia
Email: jakasura.tarigan@gmail.com

ABSTRACT

This study has been conducted to identify geothermal potential in the Villamasin geothermal prospect, Jayapura District, East OKU Regency. In this study analysis of geothermal manifestations using DEM and Landsat 8 OLI/TIRS satellite imagery. From the analysis of DEM images, it can be seen the morphological model of the study area which is recognized as the presence of faults, which are marked by contour elevation lines. Through Landsat 8 OLI/TIRS imagery, satellite image analysis is conducted to determine the distribution of vegetation. Related to data analysis, it can be used as additional data to estimate the local allocation of geothermal manifestations. The pattern of fracture morphology, distribution of earth surface temperature and land cover by plants is used as an indication of the location and distribution patterns of manifestations of geothermal potential. Geothermal manifestations generally appear in fault zones around recharge areas. To be able to check fluid distribution, research is done with gravity data on satellite imagery. The results showed the fact that there were significant anomalous changes in the northwest region to the southeast of the study area which could test the reservoir area.

Keywords: Remote sensing, DEM, Landsat-8, geothermal

INTRODUCTION

The research area located in Villamasin is a village located in Jayapura District, Ogan Komering Ulu (OKU) Timur District, South Sumatra. This area is interesting because it has an indication of the potential for geothermal energy which is indicated by several manifestations in the form of altered rocks and hot springs. This manifestation appears in the area around the fault zone. To follow up on this potential, a preliminary survey is needed. In geophysics, preliminary surveys can be carried out by remote sensing by utilizing satellite data such as processing of DEM and Landsat 8 OLI / TIRS satellite images to identify morphological models from the study area, vegetation distribution and estimating the allocation of geothermal manifestations, and processing data satellite gravity to indicate the distribution of geothermal fluids. Where, from the processing of this data an integrated analysis will be carried out to determine the potential of geothermal resources in the research area and as a reference for further research.

THEORY

Remote sensing acts as one of the initial methods used in conducting mapping in diverse needs, especially exploration, this is done because remote sensing can provide a comprehensive initial picture of geological, geomorphological, and other conditions that you want to know (Putra et. Al, 2017). Remote sensing methods that can be done include satellite image processing DEM, Landsat 8 OLI / TIRS, and processing of satellite gravity data. Satellite imagery (Digital Elevation Model) DEM is an image obtained from the extraction of Pleiades satellite images. In general, this image is used to get a picture of the topography and morphology in an area where the image can also show faults. Topographic information sourced from DEM data can be generated using stereo satellite imagery (Trisakti, 2007). Where this stereo is two or more images taken from different recording angles for the same location in the area on the earth. This combination of stereo image is then used to produce DEM with good harmony.

Landsat 8 Operation Land Imager / Thermal Infrared Sensor (OLI / TIRS) is an image launched by the American state on XYZ, and has 11 types of channels with spatial resolutions ranging from 15x15 meters to 100x100 meters (United States Geological Survey, 2016). This analysis of Landsat imagery is used to determine the conditions on the surface of the earth by looking at the reflectance character and the adsorbs of electromagnetic waves from objects on the surface of the earth. And one application is knowing the presence of hydrothermal alteration on a regional scale.

Band ratioing is a technique where digital numbers (brightness values) of one band are divided by that of another band. This corresponds to the peaks of high and low reflectance curve (Pour et al., 2015). This technique improve the contrast and enhances compositional information while suppressing useless information, like earth's surface and shadowing caused by topography surface shadow, allowing highlight some features that cannot be seen

in raw data (Sabins, 1997; Van der Meer, 2012; Ali & Pour 2014).

The gravity method is one of the geophysical methods that measures variations in the Earth's gravitational field. In addition to direct measurements, the current measurement of the gravitational field of the satellite has been developed, namely Geodetic Satellite (GeoSat) and European Remote Sensing-1 (ERS-1) Satellite. This data can be used to map the global gravitational field anomalies on the surface of the earth. Through the processing of gravity data, the distribution of regional and residual anomalies can be mapped in the Villamasin research area which can then be interpreted to find out which control faults or rock contact zones in the study area.

METHODS

The method of this research is processors of satellite image data DEM, Landsat 8 OLI/TIRS, and satellite gravity to identify geothermal potential in the Villamasin research area, Jayapura District, OKU Timur Regency, South Sumatra. The workflow diagram could be seen in Figure 1.

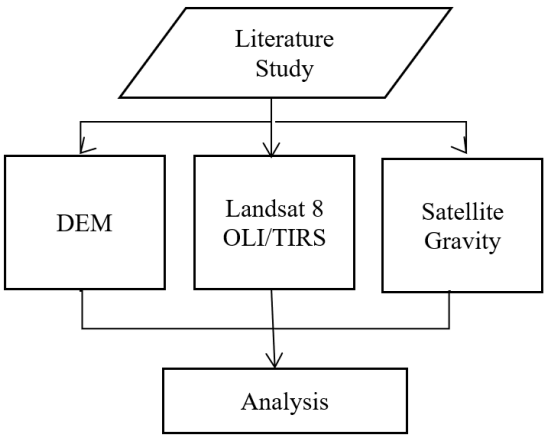


Figure 1: Research Workflow Diagram.

RESULTS AND ANALYSIS

Remote Sensing Method

Morphology and indications of the fault structure of the study area can be identified through the DEM-SRTM (Pradnya et. Al., 2016) Based on the DEM-SRTM map (Figure 2) that the study area is dominated by hills extending in the middle to the south which are produced by ancient volcanoes. The existence of a fault structure can be identified through the initial indication of lineament. The main alignment pattern of the study area goes northwest to southeast and northeast to the southwest. This pattern of structure shows a close relationship to the formation of geothermal manifestations.

Using Landsat 8 OLI imagery, there are six bands (B2, B3, B4, B5, B6 and B7) to make different band combinations. True color image found on Landsat 8 bands 4 (Red), 3 (Green) and 2 (Blue) (Figure 3) (Pour & Hashim, 2014). With a combination of these bands it can be identified vegetations are characterized by dark blue and pink as characterized rivers and lakes and urban areas in addition, some geological structures such as faults can be identified.

The combination of bands with the NIR band (band 5) and two SWIR bands (band 6 and band 7) allows identification of regional scale geological features such as faults, and differentiation of rock outcrops from vegetation (Figure 4). In this picture, the rock protrusion shows dark blue and black water. Some hydrothermal alteration in outcrops areas can be identified as yellow.

Altered rocks are directly related to minerals and changes. Thus, this is applied to the ratio of Landsat 8 OLI 4 band over band 2, to identify areas with abundant iron oxide minerals, as bright tones (Figure 5 (a)). The band 6 ratio over band 5 distinguishes ferro minerals in blue (Figure 5 (b)). Clay minerals are distinguished by images of the band 7 ratio over band 5 with brown color (Figure 5 (c)). The ratio of band 6 over band 7 distinguishes the altered rock containing clay and alunite from unchanging rock, bright tones (Figure 5(d)).

An additional RGB composites was created with bands 4/2, 6/7, 5, and allows identification of outcrops as strong yellow, altered rocks as strong blue and vegetation areas of light green (Figure 6).

Also, the other composite bands, the Kaufmann ratio (7/5; 5/4; 6/7) (Figure 7), which is a good combination for geological purposes. In this picture (Figure 7),This combination ratio ratio is shown as vegetation as purple and water as blue. Some areas of light green can be associated with hydrothermal altered rocks. From the results of regional maps (Figure 8) in the study area, there is a body anomaly which indicates the presence north-south trending fault that can be a hydrothermal pathway.

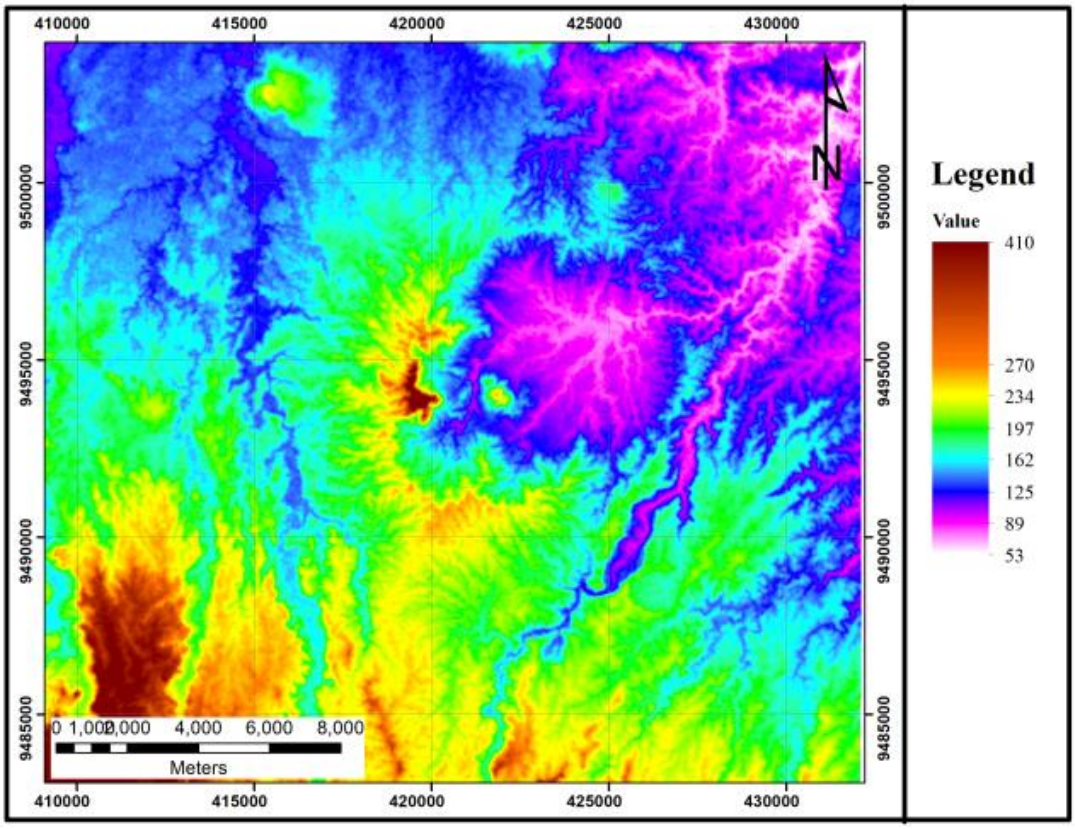


Figure 2: DEM-SRTM which shows the fault structure.

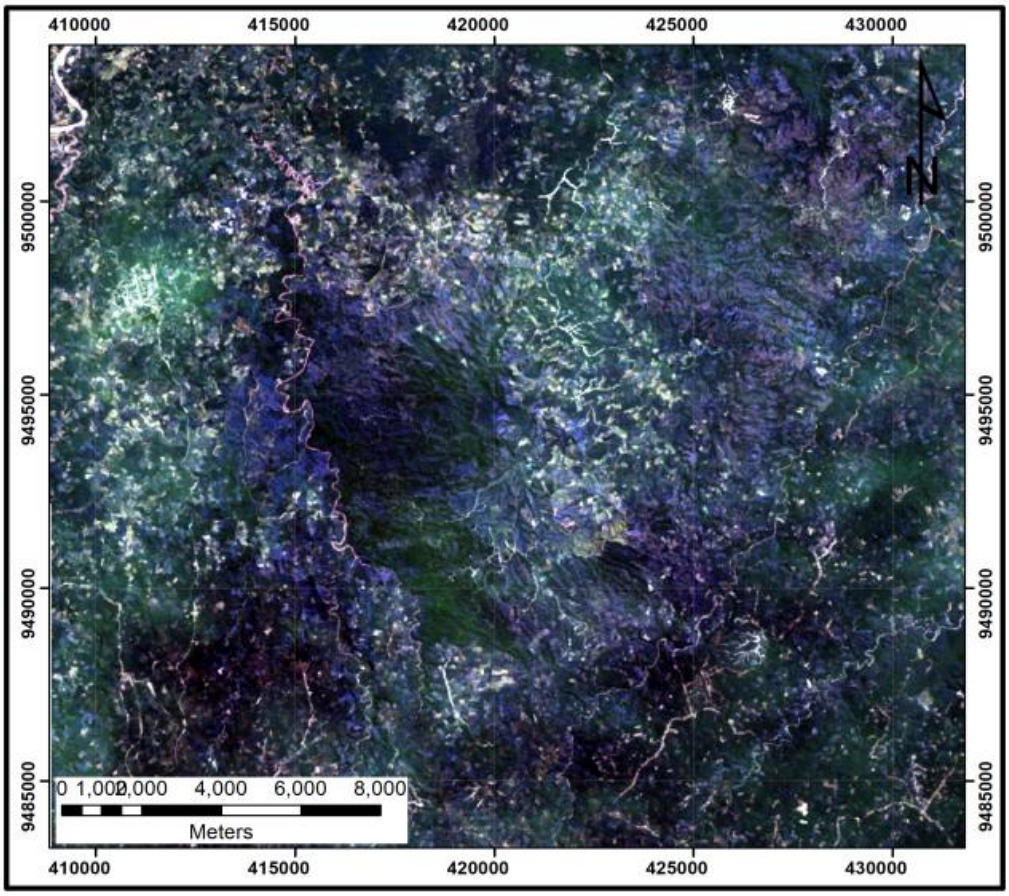


Figure 3: RGB combination of bands 4, 3, 2. Dark blue colour represent vegetation.

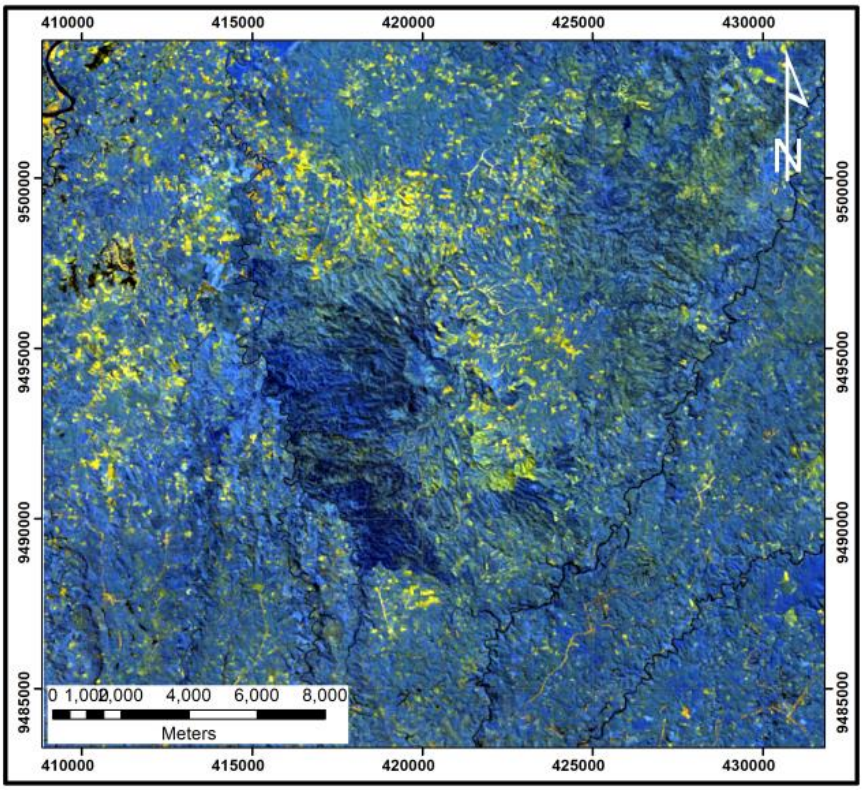


Figure 4: RGB combination for bands 5, 6, 7. This image is a vegetated area appear in dark blue, outcrops are light blue, and water is black. Some altered hydrothermal rocks can be identified as yellow.

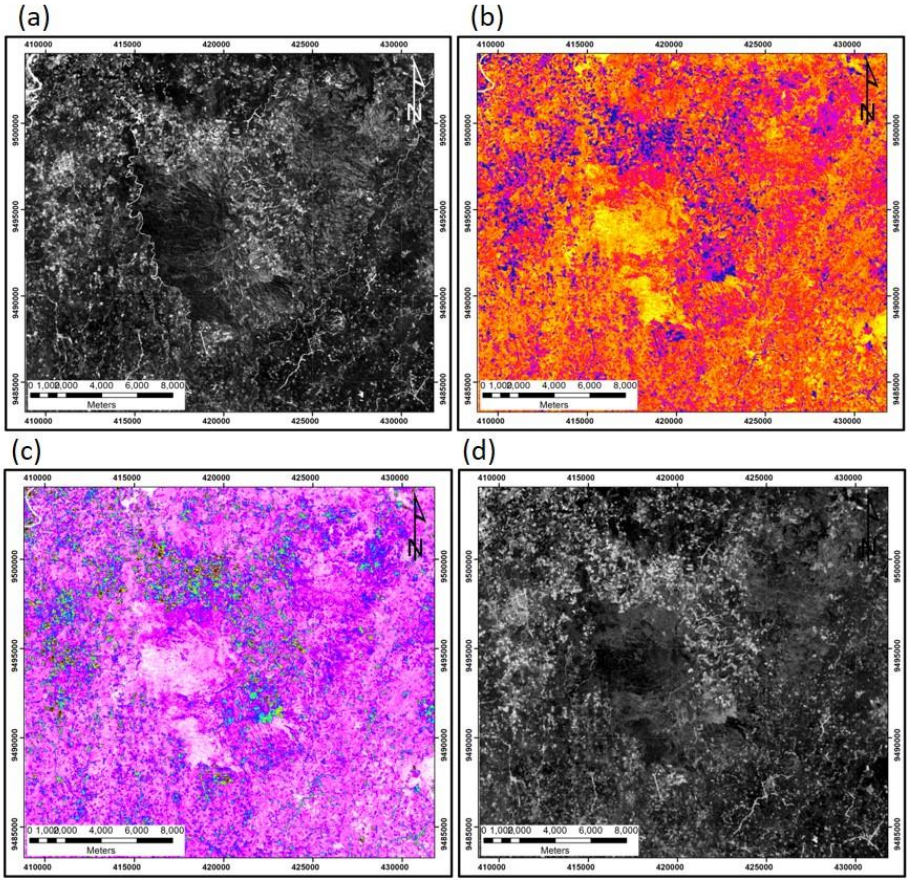


Figure 5: (a) Landsat 8 band ratio 4/2 image reveals areas where iron minerals are shown in bright tones; (b) Landsat 8 band ratio 6/5 image discriminates ferrous minerals with blue color. (c) Landsat 8 band ratio (7/5) image reveals clay minerals, in brown color. (d) Landsat 8 band ratio 6/7 image shows alunite and hydrothermal clay minerals in bright tones.

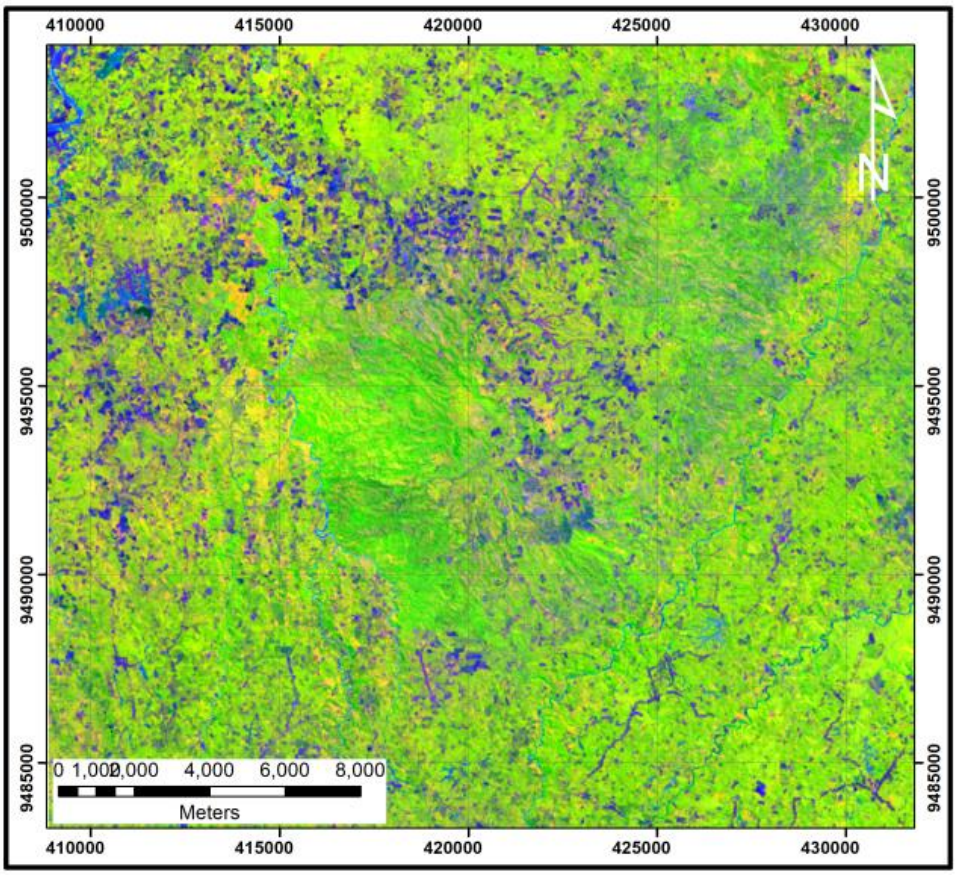


Figure 6: Band ratio of 4/2, 6/7, 5, in RGB. Outcrops are identified as strong yellow, vegetation as light green and water as light blue. Urbanized areas as purple.

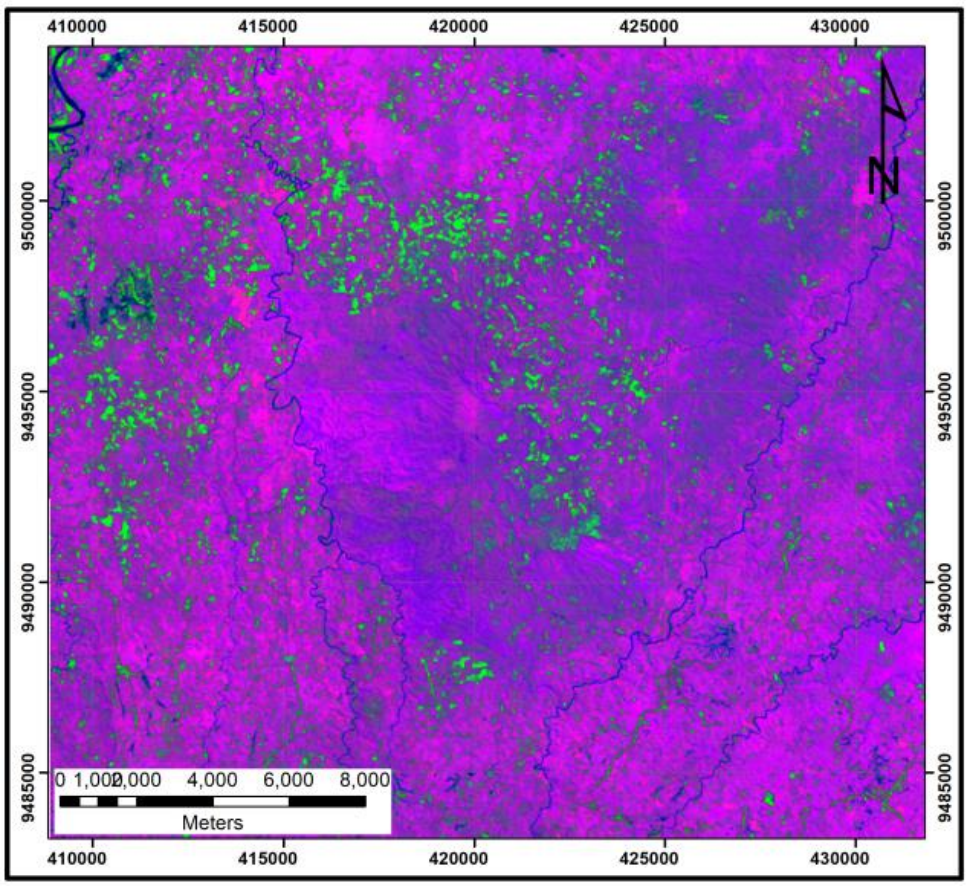


Figure 7: Band ratio of 7/5, 5/4, 6/7, in RGB. This band ratio combination shown vegetation as purple and water as blue. Some light green areas can be related to the hydrothermal alteration.

GRAVITY METHOD

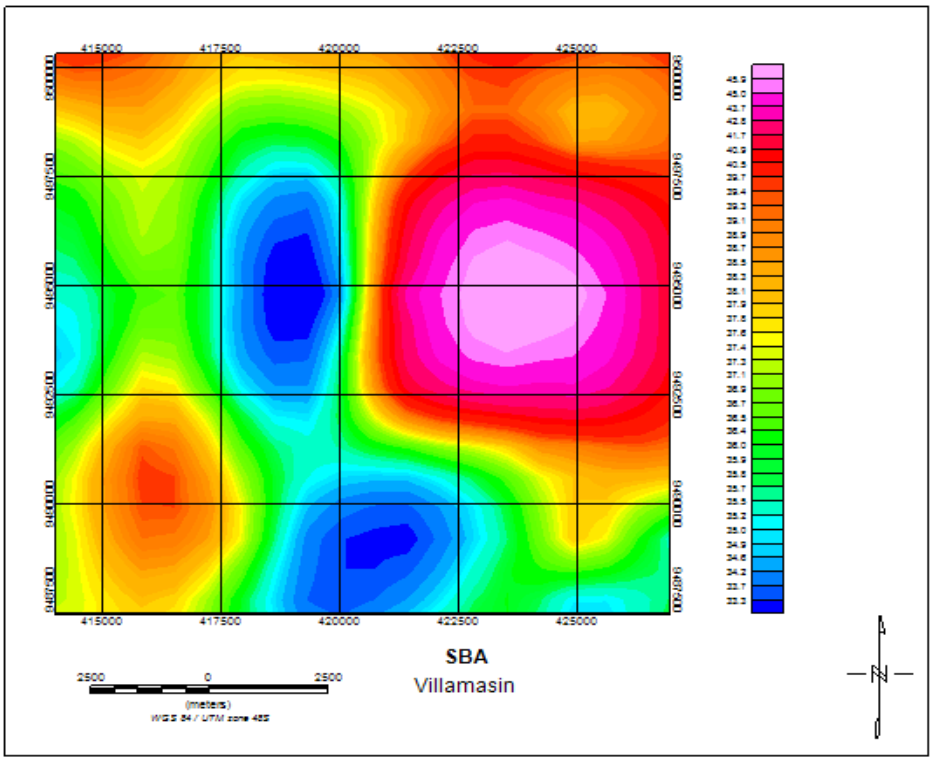


Figure 8: Bouguer Anomaly Map.

CONCLUSIONS

Analysis of Landsat 8 imagery in this study shows that it is effective in data extraction for lithology hydrothermal changes. Target exploration maps are obtained from remote sensing information and other geological data that can be used in future work exploration through the region to find new information, structural patterns and highlights anomalous zones. From the results of regional maps in the study area, there is a body anomaly which indicates the presence north-south trending fault that can be a hydrothermal pathway.

REFERENCES

Ali, A., and Pour, A., (2014). "Lithological mapping and hydrothermal alteration using Landsat 8 data: a case study in ariab mining district, red sea hills, Sudan". International Journal of Basic and Applied Sciences, 3(3), 199–208.

Rui, Mateus. da Cunha Frutuoso (2015). "Mapping hydrothermal gold mineralization using Landsat 8 data". A case of study in Chaves license, Portugal. Universidade do Porto.

Pour, A., & Hashim, M., (2015). "Hydrothermal alteration mapping from Landsat-8 data, Sar Chesmeh copper mining district, south-eastern Islamic Republic of Iran". Journal of Taibah University for Science, 9, 155-166.

Putra, I. D., Nasution, R. A. F., & Harijoko, A. (2017). "Aplikasi Landsat 8 OLI/TIRS dalam Mengidentifikasi Alterasi Hidrotermal Skala Regional: Studi Kasus Daerah Rejang Lebong dan Sekitarnya, Provinsi Bengkulu". Proceeding, Seminar Nasional Kebumian Ke-10.

Pradnya, P., Rendra, R., Sulaksana, N., and Sukiyah, E., (2016). "Interpretasi Keberadaan Struktur Patahan Berdasarkan Analisis Geomorfologi Kuantitatif Sebagai Upaya Awal Penanggulangan Gerakan Tanah di Daerah Baleendah-Ciparay, Bandung, Jawa Barat". Proceeding, Seminar Nasional Ke-III,. Universitas Padjadjaran.

Sabins, F., F., (1999). "Remote sensing for mineral exploration". Ore GeologyReviews 14, 157–183.

Trisakti, B., (2007). "Ekstraksi Otomatis Informasi DEM Dari Citra Stereo PRISM-ALOS". Jakarta. LAPAN.

United States Geological Survey. (2016). "Landsat 8 (L8) Data Users Handbook", United States of America. 106p.

van der Meer, D. F. (2004). "Analysis of spectral absorption features in hyperspectral imagery". International Journal of Applied Earth Observation and Geoinformation, 5, 55 – 68.

SEA WATER DESALINATION USING DISTILLATION METHOD BY UTILIZING THE GEOTHERMAL POTENTIAL OF TEMBOKO LEHI BEACH AS A SOLUTION OF DROUGHT IN SIAU TAGULANDANG BIARO DISTRICT, NORTH SULAWESI

Nikita Christina, Ratna Pertiwi, Muhammad Rizqy Septyandy, and Nurchasanah Ananda Sari

Universitas Indonesia
Jalan Margonda Raya, Depok 16424
Email: nikita.christina@ui.ac.id, ratna.pertiwi61@ui.ac.id,
m.rizqy@sci.ui.ac.id, nurchasanah.ananda@ui.ac.id

ABSTRACT

Desalination is a process of separating salt from sea water which is commonly practiced in coastal area that have limited fresh water. Distillation as one of various methods of desalination is a process of separating the components or substances based on differences in the conditions required to change the phase of the components of the mixture by using selective boiling and condensation. This method offers better and more effective result of sea water desalination due to its ability to massively purify not only the salt from the water but also other contaminants. Temboko Lehi Beach in West Siau District, North Sulawesi lays over geothermal area of Mount Karangetang. High temperature (60 - 80° C) of the sea water in Temboko Lehi Beach which is the only hot sea water in Indonesia proves a great potential of geothermal in Temboko Lehi Beach. Siau Tagulandang Biaro District which is located on a small and isolated island in North Sulawesi makes its people have limited access to clean water and suffer drought. One of efforts to get affordable and sustainable heat source of distillation method to get fresh water is by utilizing the heat vapor of Temboko Lehi Beach that is manifested on its sand. High temperature vapor in Temboko Lehi Beach is compatible to be used as a heat source of distillation method to produce fresh water in order to overcome the lack of clean water in Siau Tagulandang Biaro, North Sulawesi.

Keywords: desalination, distilation, drought, geothermal

INTRODUCTION

Temboko Lehi Beach is located at the foot of Mount Karangetang, which is an active volcanic mountain. Along its coastline, the sea water is high temperature (60 – 80°C) which causes there are no living ecosystem around the beach. Sea water in Temboko Lehi Beach also has less salt content (less than 3,5 %). Beside the high temperature of the sea water, the potential of geothermal under Temboko Lehi Beach can be proved by other surface manifestations such as hot water pond and hot vapor bursting out of the beach sand. Although there is still no further research about the geothermal system under Temboko Lehi beach but based on its surface manifestations it can be estimated that it has great potential of geothermal. The heat in Temboko Lehi Beach is from Mount Karangetang which is formed by the subduction of the Molluca oceanic plate and Eurasia plate. Molluca oceanic plate is subducted to the west under the Eurasian plate and to the east under the Philipphine oceanic plate. The subduction causes Sangihe volcanic arc and Halmahera volcanic arc which are well-known as double volcanic chain. Beside Mount Karangetang, the volcanic chain also formed other volcanic mountains such as Mt. Tongkoko, Mt. Batuangus, and Mt. Tumpa. Mount Karangetang is included in trench-side rocks group, which has compositions basalt to dacite (50,25% - 63,08% SiO_2, low Ba, Rb, Nb, Sr, K). Located in a small island and 137 kilometers apart from the city center, Manado, people in Siau Tagulandang Biaro District have limited access to clean water. Due to the low average rainfall, on April to March with average rainfall is 50-60 mm^3, Siau Tagulandang Biaro District often experiences droughts without clean water resources and causes noxiousness to its people. Desalination has been used for many purposes and the most pronounces benefits being freshwater provision in times of extreme and unexpected weather events like drought. Desalination describes processes used to reduce or remove the concentration of dissolved solids in water such as salt or other minerals to obtain freshwater. The desalination process may include several steps, such as multistage flash distillation (MFD) or reverse osmosis (RO). MFD involves heating saline water to produce water vapor and the condensing the vapor to give pure water. The combination of renewable energy, such as geothermal, with MFD system is very promising to increase fresh water supplies in arid regions. The heat from geothermal can be used to generate electricity for the distillation process itself or utilized directly as a heat source in evaporation stages. Direct use of geothermal energy for heating is also reduce the CO_2 emission by at least 50% compared with fossil fuel fired boilers. Figure 1 shows the tectonic map of Sanghie.

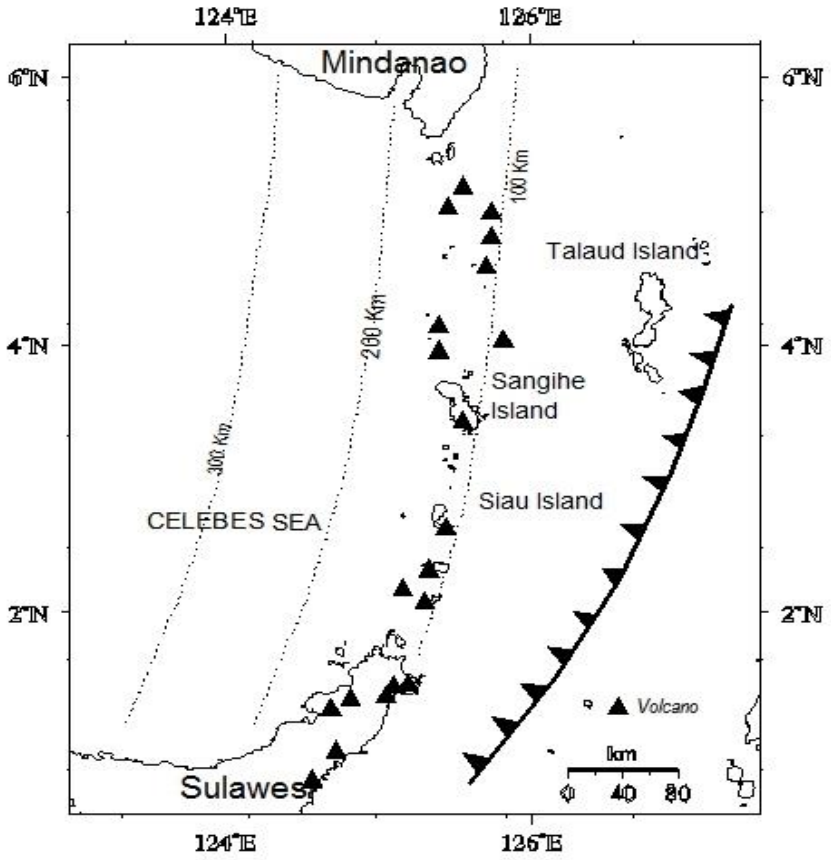


Figure 1: Tectonic map of the Sangihe volcanic arc consisting of two volcanic chains that distributed from around Manado city in the northern peninsula of Sulawesi to the north near Mindanao in Philippine (Iskandar Zulkarnain, 2001).

Table 1: Comparison of CO2, SO2, H2S emissions from electricity generation (MWh) from different energy sources (adapted in part from Fridleifsson, et al., 2008).

Energy Source	Coal	Oil (and gas)	Geothermal
CO_2 (Kg/MWh)	994	839 (599)	40-120
SO_2 (Kg/MWh)	4.71	-	0.16
H_2S (Kg/MWh	-	814 (550)	0.08

DESALINATION USING DISTILLATION METHOD

Desalination is a process of separating salt from saline water to get fresh water from seawater or brackish water. The quality of desalination water determined by the content of Total Dissolved Solid (TDS) in part per million (ppm). Seawater and brackish water have Total Dissolved Solid (TDS) content more than 3000 ppm. Fresh water has maximum Total Dissolved Solid (TDS) content of 500 ppm to be able to be consumed by human. The less amount of Total Dissolved Solid (TDS), the better quality of the water. In thermal desalination, a distillation process occurs and produces fresh water with very low salt content, about 10 ppm. While membrane semipermeable process produces fresh water with salt content about 350 – 500 ppm. Therefore, most existing desalination plants use the distillation method and has been used for the last three decades.

Distillation is a separation process of liquid mixtures based on their boiling points or relative volatility (Cseri, 2018). Commonly, distillation used to purify compounds in solution or to separate mixture of solutes. In a simple distillation, liquid mixtures put into heated container. When it reaches the boiling point of pure water (e.g. the liquid mixture is saltwater), it forms water vapor that moves upwards. Suspending a thermometer above this solution will record the temperature of the escaping vapor. Water vapor will find an empty gap (into the cooling pipe) because it has a high temperature and pressure. The condenser works as a cooling water vapor so the temperature drops, then most of the water vapor will condense and form pure water liquid. The liquid will accumulate as a result of the distillation process. Figure 2 shows the apparatus used in a simple distillation. General equipment that is normally used in installation of seawater desalination is seawater suction system (such as water pump, screen and filter), water pipe network for desalination product, storage tank, receiving equipment, and panel

distribution box. Common problem that appears in distillation process is scaling and corrosion on the evaporator pipes that causes heat transfer ability decreases. Then, the amount of fresh water produced decreases too. Therefore, chemical cleaning regularly and proper material selection are important.

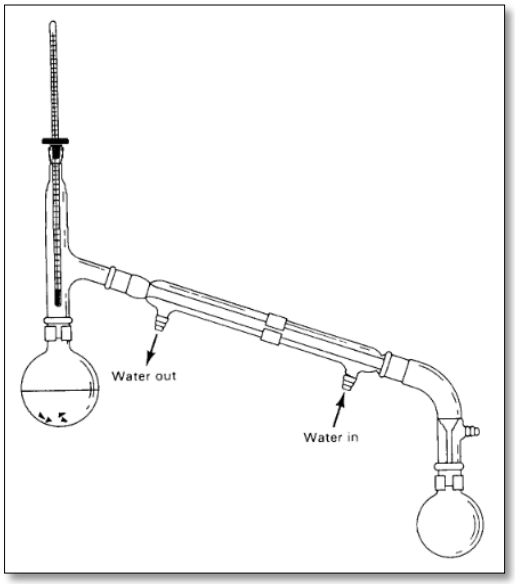


Figure 2: The apparatus used in a simple distillation (source: umsl.edu).

UTILIZING GEOTHERMAL POTENTIAL FOR DISTILLATION METHOD

Due to the increasing population, the need of clean water and energy also increases. Based on Nuclear Technology Review (IAEA, 2004), of all the earth's water only 2.5% is freshwater and 70% of the freshwater is frozen in the icecaps of the Antarctica and Greenland, and most of the remaining freshwater is found in the form of soil moisture or deep within inaccessible aquifers, that are difficult to exploit. This leaves very little, less than 0.08%, of the earth's fresh water available for human consumption. There are currently about 2.3 billion people living worldwide in water-stressed or water-scarce areas. By the year 2025 it is foreseen that the number of people suffering from water stress or scarcity will increase to 3.5 billion. Therefore, the demand for the desalination of seawater in on the rise, along with the energy to the desalination process itself. Indonesia, as the top ten country which utilizes geothermal to generate electricity, has a big potential to use it as an energy source to desalination process to produce fresh water. Figure 3 shows the total electricity generation from geothermal.

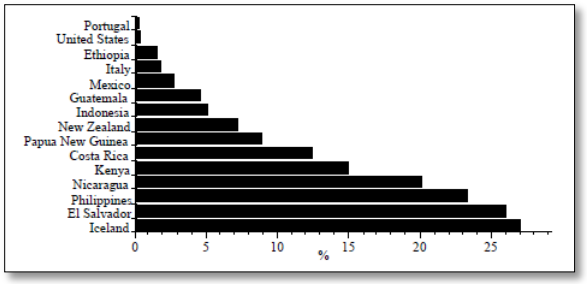


Figure 3: Share of total electricity generation from geothermal resources in the top 15 countries (Dorn, J.G, 2010).

Geothermal energy is energy derived from natural heat beneath the earth's surface. The energy from geothermal is generally stable because the subsurface temperature relatively constant throughout the year and is not influenced by any external conditions, so this energy can be said to be sustainable. Since the only cost needed for direct use of geothermal manifestations is for the installation of the desalination utensils, the costs needed is also smaller than other methods.

In this case, the heat of geothermal manifestations in the sand of Temboko Lehi Beach is used directly to heat the flowing seawater in the pipe. For distillation process, the sufficient temperature to effectively heat the seawater is in the range of 50° C - 150° C. The surface temperature of seawater and the sand in Temboko Lehi reaches 80°C and will be greater in depth, makes Temboko Lehi Beach in the perfect condition to be the heat source in the distillation method. Evaporated seawater will change phase into vapor with very low salinity and will be condensed to be fresh water.

In Figure 4, the seawater pumped from the sea will be filtered to prevent bigger contaminants, such as germs, sea animals and plants, to enter the pipe. The seawater enters the wider pipe and will be forwarded to smaller diameter pipes in the evaporation stage to make the surface area become larger and the sea water can optimally evaporated. The steam from evaporation stage will moves upwards to the titanium alloys condenser and will be condensed into fresh water. The fresh water from the condensation zone will be filtered again to ensure its cleanliness, and then will be accommodated at the storage tank to be pumped up. The residue from the process will be returned to the sea. This method uses geothermal as main source energy and fossil fuel as additional source energy to operate the pump and condenser. Figure 4 shows the overview distillation method to obtain fresh water utilizing heat from geothermal.

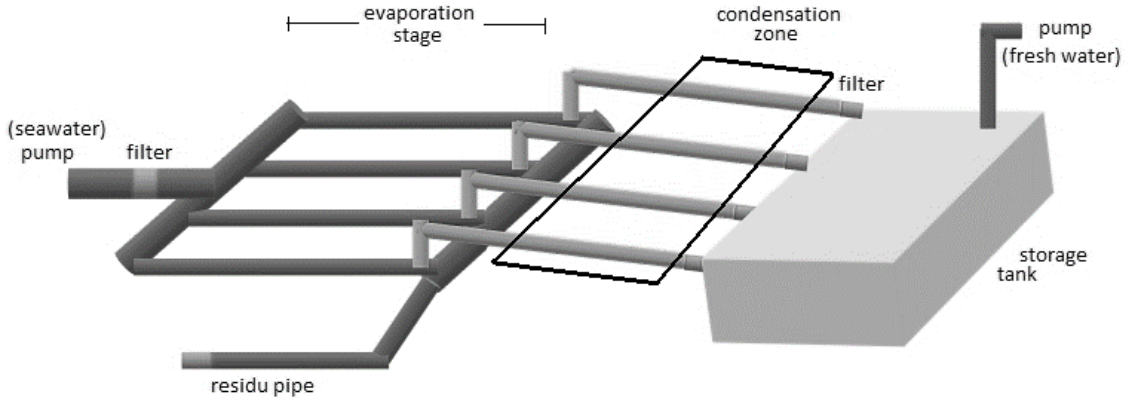


Figure 4: Overview of distillation method to obtain fresh water utilizing heat from geothermal in Temboko Lehi Beach.

CONCLUSION

Seawater desalination using distillation method can be used as a drought solution in Siau Tagulandang Biaro District, North Sulawesi. By utilizing the heat from geothermal manifested in the sand of the beach to be the heat source for evaporation, it can be used to produces fresh water. This process will be sustainable since the main energy source is geothermal. This process produces low salt water content (about 10 ppm) that can be used for daily needs and reduces 50% carbondioxide emission. Since the only cost needed for direct use of geothermal manifestations is for the installation of the desalination utensils, the costs needed is also smaller than other methods. This method is good to be implemented because all of the advantages.

REFERENCES

Abdulloh, S.H. (2015). "Desalinasi Air dengan Memanfaatkan Energi Terbarukan". Bandung: Institut Teknologi Bandung

Badan Pusat Statistik Kab. Kep Siau Tagulandang Biaro. (2018). "Rata-Rata Curah Hujan Setiap Bulan di Kabupaten Kep.Siau Tagula".

Chickos, Garin, & D'Souza. (n.d.). "Distillation. Missouri", U.S.: University of Missouri-St. Louis.

Cseri, L., Razali, M., Pogany, P., & Szekely, G. (2018). "Green Chemistry". Cambridge: Elsevier.

Fridleifsson, I.B.; Bertani, R.; Huenges, E.; Lund, J.W.; Ragnarsson, A.; Rybach, L. (2008). "The possible role and contribution of geothermal energy to the mitigation of climate change". In Proceedings of IPCC Scoping Meeting on Renewable Energy Sources, Luebeck, Germany, 20–25 January.

Goosen, M., Ghaffour, N., Mahmoudi, H. (2010). "Water Desalination Using Geothermal Energy". Energies, Vol. 3 page 1423-1442.

Nugroho, A. (2004). "Uraian Umum Tentang Teknologi Desalinasi". Jurnal Pengembangan Energi Nuklir, Vol. 6 No. 3 & 4.

Parise, T. (2012). "Water Desalination". California: Stanford University.

Walangare, K. B., Lumenta, A., Wuwung, J., & Sugiarso, B. (2013). "Rancang Bangun Alat Konversi Air Laut Menjadi Air Minum Dengan Proses Destilasi Sederhana Menggunakan Pemanas Elektrik. e-Jurnal Teknik Elektro dan Komputer".

Zulkarnain, I. (2001). "Rock Chemistry of Quaternary Volcanics around Manado and Siau Island, North Sulawesi". Jurnal Teknologi Mineral.

FAULT STRUCTURE AND GEOTHERMAL SYSTEM ANALYSIS BASED ON GRAVITY INVERSION MODEL, MAGNETOTELLURIC AND GEOCHEMISTRY OF GEOTHERMAL PROSPECTING FIELD WAI SELABUNG SOUTH SUMATERA

Clara Armiliany, David Suganda Putra Manurung, Davit Manalu, Suharno, and Karyanto

Geophysical Engineering Department, Universitas Lampung
Bandar Lampung, Indonesia
Email: clara.armiliany6@gmail.com

ABSTRACT

Increased global energy consumption and decreased of fosil fuel stocks provides us to find a renewable and green energy, and geothermal energy is one of them. One of indonesian regions that has geothermal prospect fields is Wai Selabung, Oku Selatan residence, South Sumatera province with 15 km2 abroad. Gravity, Magneotelluric, and Geochemistry surveys are intended to observe fault structure and geothermal system to see a global picture of energy on that areas. Formation of geothermal system on Wai Selabung were influenced by vulcanic environment and tectonic with same direction as Sumateras fault. Results of SVD Bouguer anomaly residual analisys shows two normal fault and one thrust fault directing NW-SE on Kota dalam and Teluk Agung, and one thrust fault in Sinarmarga. Based on 3D Bouguer anomaly inversion model, we were obtained two reservoar with densities 1.4-1.7 gr/cm3 and total volume 15.7 km3, Cap rock with densities 2-2.4 gr/cm3 and resestivities <20 ohm as a vulcanic alteration, and Heat source with densities 2.4-2.9 gr/cm3 as a intrution lava Tebat gayat. Integrated compilation shows reservoar temperature based on geotermometer Na-K-Mg was 170oC, so hipotesis potential energy classes on prospecting field is 182 MWe.

Keywords: Geothermal, Faults, Gravity, Geochemistry

INTRODUCTION

Indonesia is rich in the potential of geothermal dry-steam and hot-water to connect with a number of 7,000 km of volcanoes bordered by Indo-Australian plate southwards. Convergence and strike-slip movements The plate boundaries are believed to result in large concentrations of High-temperature geothermal systems close to the plate edges in Sumatra, Java, Nusa Tenggara, and Halmahera.

In the previous research, a complete 2D Bouguer anomaly and residual Bouguer anomaly have been obtained. Modeling is associated with geological information in the area so information on the subsurface structure of the research area can be obtained. At this time a 3D model of the Wai Selabung geothermal system is needed to accurately analyze the geothermal system of the area. In this study a complete Bouguer anomaly 3D inversion modeling and filtering of complete Second Vertical Derivative Bouguer anomalies, regional and residual Bouguer anomalies are correlated with the data Magnetotelluric resistivity and geochemical data of the study area. This is done to determine the fault structure and 3D models of geothermal systems along with the characteristics of the geothermal system in the Wai Selabung area.

Then, in exploration activities, geophysical surveys produce estimates and mapping of geothermal system components based on rock physical properties so that an estimate of the subsurface geothermal system can be obtained. The application of rock physical properties to mapping the presence of geothermal components such as the nature of rock density is used to determine the subsurface structure which generally helps as a fluid circulation control area and estimation of geothermal reservoirs (Hidayat and Basid, 2011).

REGIONAL GEOLOGY

The grouping of rock units is based on the results of observations and analyzes in the field and in the laboratory. In general the constituent rocks in the investigation area are dominated by volcanic rocks, based on the physical characteristics and age of the rocks, and are compared with the regional geology of the local area, then the rock units are obtained in the order from old to young as follows (Figure 3): Jangkang Root, Sandstone, Lava Asadimana Lava Unit, Pematang Gong Lava, Old Breccia, Pyrolastic Ranau Flow, Sapatuhu Pyroclastic Flow, Fall of Pyroclastic Ranau, Lava Laai, Crooked Lava, Lava Pandan, Lava Gedang, Perean Lava, Lord Lava Tebat Gayat, and Alluvium deposits. The geological structure pattern is dominated by the northwest-southeast direction which is truncated by a fault with the southwest-northeast and north-south direction. Manifestations appear on the surface as an effect of the meeting between the Sumatran fault and its antithetic, so that produces an excellent permeable zone for passing fluid to the surface. Tentative geothermal model can be seen in Figure 1.

Faults in the Wai Selabung area are grouped into three main directional patterns namely northwest-southeast, north-south, and southwest-northeast. Besides this pattern, we can recognize the formation of crater structures that appear in volcanic rocks.

The northwest-southeast fault pattern is indicated by the Asadimana fault, Kayumanis fault, Telukagung fault, Kotadalam fault, and Wai Selabung fault which fills the middle part of the Depression, possibly this Pre-Tertiary fault and is still active today. This fault is cut by other faults that are patterned north-south and southwest-northeast which are thought to be younger. Wai Selabung Fault and Kotadalam fault are estimated controls the appearance of hot Dumping Tubes that appear on the Wai Selabung river wall.

The north-south fault pattern is represented by Pematangbuluh fault, Perean fault, Sinarmarga fault, and Akarjangkang fault. The fault follows the Sundanese pattern formed in the Eocene and is thought to be an old fault, indicated by changes in the flow of the river flow and also topography. Some faults cut the depression formed by the Sumatran fault which traverses northwest-southeast around Sinarmarga and Talanan. The rootjangkang fault is thought to be one of the faults that control the emergence of Wai Selabung 1-2 hot water and possibly as forming a permeable zone for the Wai Selabung reservoir area.

The southwest fault pattern - northeast, in contrast to the direction of the Sumatra fault and, is estimated to be antithetic. Some faults that have this pattern are the Pematanggong fault and the Gistong fault. Gistong Fault is estimated as a control structure that facilitates the emergence of Lubuk Suban hot water which is in the old andesite lava rock of Akarjangkang.

BASIC THEORY

Gravity Method

Bouguer Anomaly

The gravity method emphasizes the change in the value of gravity caused by variations in the mass of the subsurface by applying the concept of anomaly gravity (Bouguer Anomaly) which is from the difference in measured gravity values with reference gravity (theoretical gravity values for a theoretical model of the earth). These differences reflect variations in mass that occur in an area with the surrounding area towards the lateral and vertical direction which is then used to get a picture of subsurface structures. Therefore, gravity anomalies must be calculated in such a way as to avoid the gravitational effects of unwanted components by applying corrections.

a. Drift Correction

Drift correction is done by designing a closed acquisition design so that differences in reading deviations can be calculated in a certain time which is assumed to be linear. After drift correction the difference in the value between the observation point and base is determined by multiplying the reading value and the calibration factor of the gravimeter device.

b. Tide Correction

Measurements of gravity vary with time due to periodic variations in the gravitational effects of the sun and moon in relation to the movement of the two orbitals.

c. Lattitude Correction

The shape of the earth that is not round, there are differences in the radius of the earth at the pole with the equator. This makes a difference in the value of gravity due to the influence of latitude of the earth. The value of the theoretical gravitational acceleration determined is the gravitational acceleration located in the datum plane (height z = 0) as a geodesic reference point (Sarkowi, 2014).

d. Free Air Correction

The gravitational value of observation is influenced by the height of the point from the surface of the earth, the higher the point is so the gravitational value of observation will decrease and the lower the point is the greater the value of gravity will increase.

e. Bouguer Correction

Bouguer correction is calculated because of the pulling effect of the material or mass that is between the measurement point and the datum field that has not been calculated in the correction of free air (Reynolds, 1997).

Interpretation Method

a. Spectrum Analysis

Spectrum analysis is performed to estimate the width of the window and depth of gravity anomaly. In addition, spectrum analysis can also be used to compare spectrum responses from various filtering methods. Spectrum analysis is done by transforming Fourier predetermined trajectories. The spectrum is derived from the gravitational potential observed in a horizontal plane where the Fourier transformation is as follows (Blakely, 1996).

b. Moving Average Method

Moving the average method is done by an averaging values gravity anomaly. The results of the moving average method are regional anomalies. The residual anomaly value is obtained by subtracting the total anomaly from the regional anomaly.

c. Second Vertical Derivative (SVD)

Second vertical derivatives are one of the filtering techniques that can give rise to residual anomalies (superficial effects) of the presence of fault structures in an area that can be well known using this technique. SVD is a high pass filter or increases the value of anomalies with short wavelengths.

RESEARCH METHODOLOGY

Data and Softwares

1. Geochemical and magnetotelluric data in the Wai Selabung area, Kab. South Oku Prov. South Sumatra,
2. Complete Bouguer Anomaly Map and Geological Map of Wai Selabung geothermal area, South Oku District, South Sumatra Province,
3. Software.

Procedure of Research

In this research, several stages of research were carried out which were explained as follows:

1. The gravity data that is processed is secondary gravity data in the form of a complete Bouguer anomaly map.
2. Then, collect all the coordinate values and AB values in the input to Microsoft Excel. Then do a grid of data from the Excel data and then on the grid menu, set the space, then click OK.
3. Furthermore, the gravity anomaly is filtered using the moving average method to obtain regional anomalous values, the residual anomaly value is obtained by reducing the total anomaly value with the value of 47 regional anomalies. The complete Bouguer anomaly map, regional anomaly map, and the residual anomaly map are then filtered using the elkins filter (Elkins, 1951) so that the second vertical derivative anomaly contour value is obtained to obtain the shallow fault information of the surrounding area. From the complete Bouguer anomaly map, a 3-dimensional modeling path is determined using the modeling inverse method.

After obtaining a 3-dimensional model from Bouguer anomalies, a 3-dimensional model of geothermal dimension based on the geothermal system reference model of the study was correlated with magnetotelluric data and the geochemical data of the study area.

RESULT AND DISCUSSION

Bouguer Anomaly of Research Area

Measurements were made with a number of points, namely 290 measuring points as given in Figure 2. Bouguer anomaly map and distribution of gravity measurement points in Figure 2 show that the study area has varying anomalous values which are 8 mGal to 48 mGal. Where is the anomaly value High Bouguer has a value range of 36 mGal up to 48 mGal located in the northwest, middle and northeast regions of the research area. Positive value gravity anomaly (compared to the surroundings) is related to high-density value. That can show something interesting for geothermal exploration.

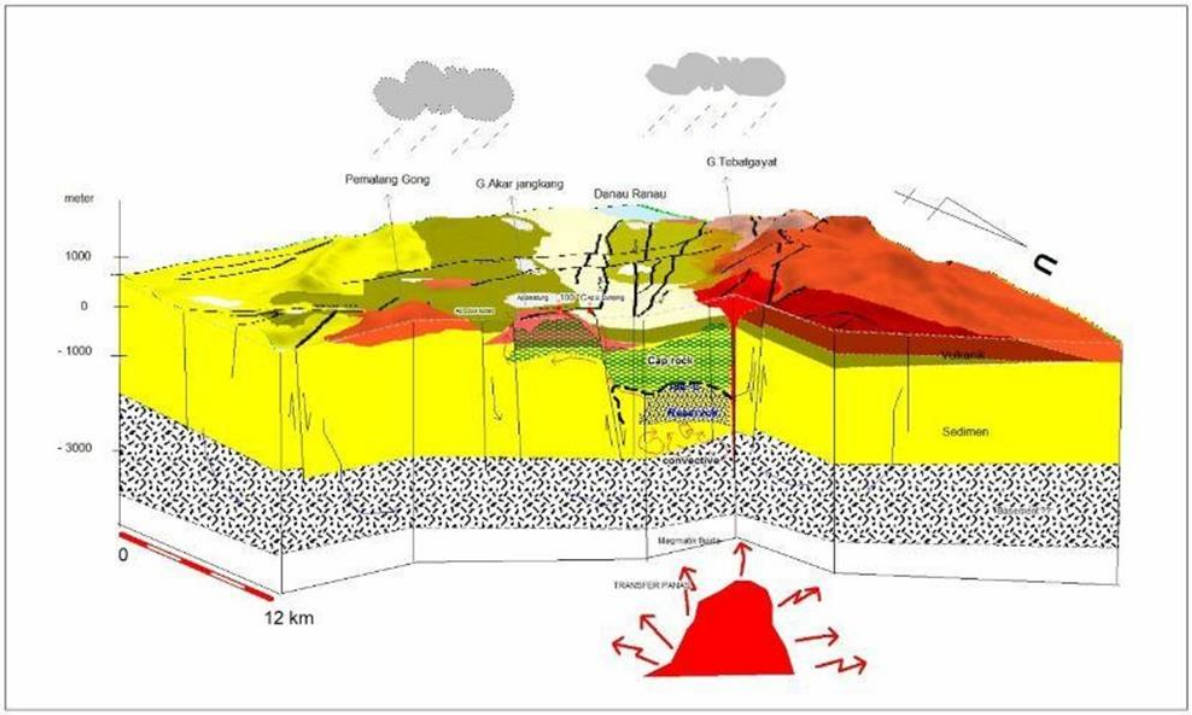


Figure 1: Tentative geothermal model in Wai Selabung area (PSDG, 2011).

The low Bouguer anomaly value has a range of values of 8 mGal to 22 mGal which is in the middle of the study area flanked by medium gravity values with contour values ranging from 22 mGal to 36 mGal in the Sinarmarga and Kotadalam regions. This low anomaly is suspected because of the presence of a collapse zone in an area that coincides with the area where manifestations of hot water and alteration rock. Manifestations appear on the surface as a result of the meeting between the Sumatran fault and its antithetic, resulting in an excellent permeable zone for passing fluid to the surface.

Spectrum Analysis

Figure 3 shows a graph of spectrum analysis on line A-A 'where the boundary zone between regional and residuals is at Kc = 0.001375 with a grid space of 200 meters. Based on the first-order and second-order straight line equations, the depth of the regional anomaly is 1919 meters, and the residual anomaly is at a depth of 570 meters. From the Blakely equation, the width of the 23 x 23 window is obtained.

Figure 4 shows a graph of spectrum analysis on line B-B 'where the boundary zone between regional and residuals is at Kc = 0.001507 with a grid space of 200 meters. Regional anomaly depth of 2548 meters was obtained and the residual anomaly depth of 193 meters with a window width of 21 x 21.

Figure 5 shows a graph of spectrum analysis on line C-C 'where the boundary zone between regional and residuals is at Kc = 0.001656 with a grid space of 200 meters. Obtained regional anomaly depth value of 2519 meters and residual anomaly depth of 173 meters with a width of 19 x 19 windows.

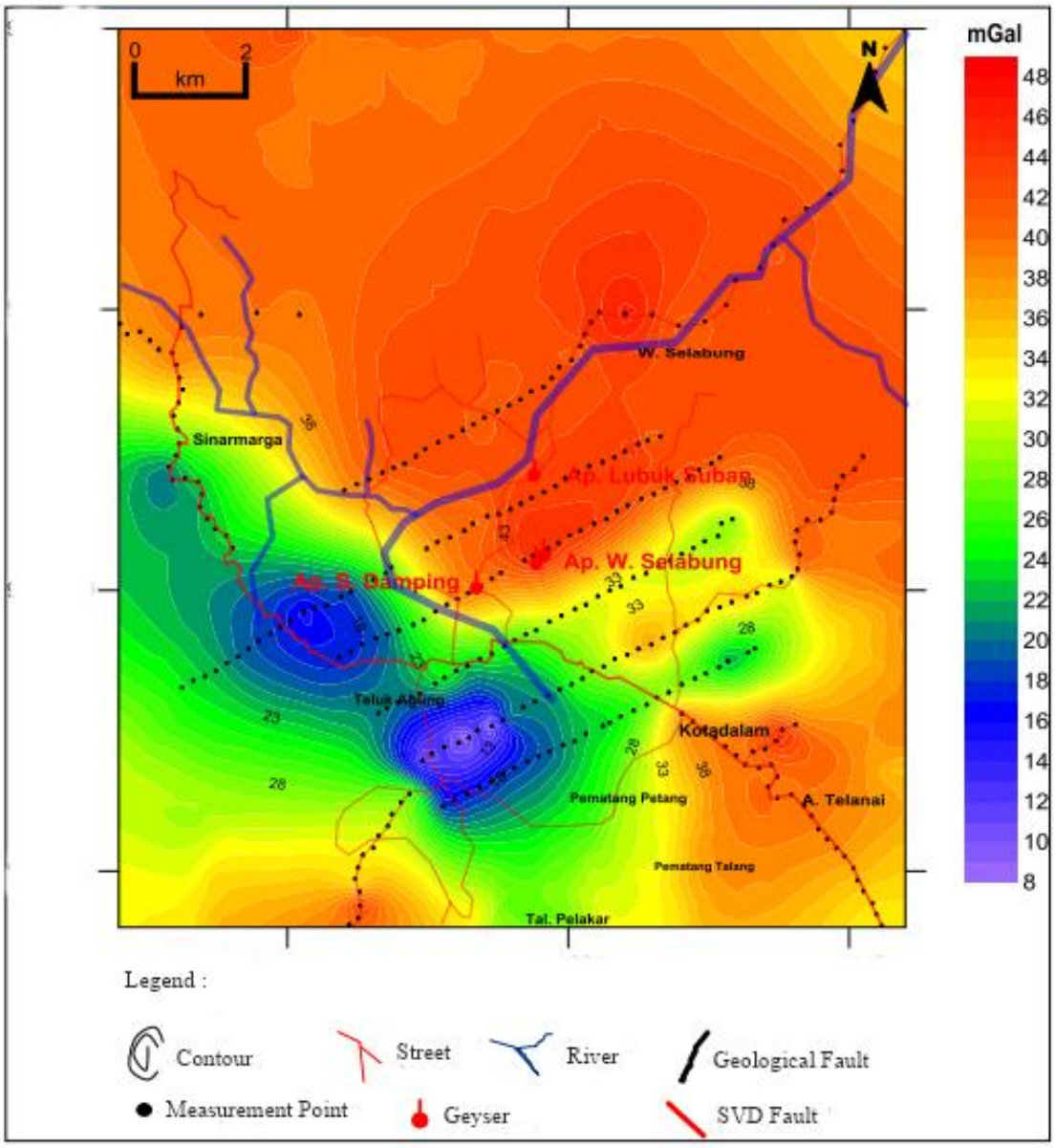


Figure 2: Map of Bouguer Anomaly Research Area.

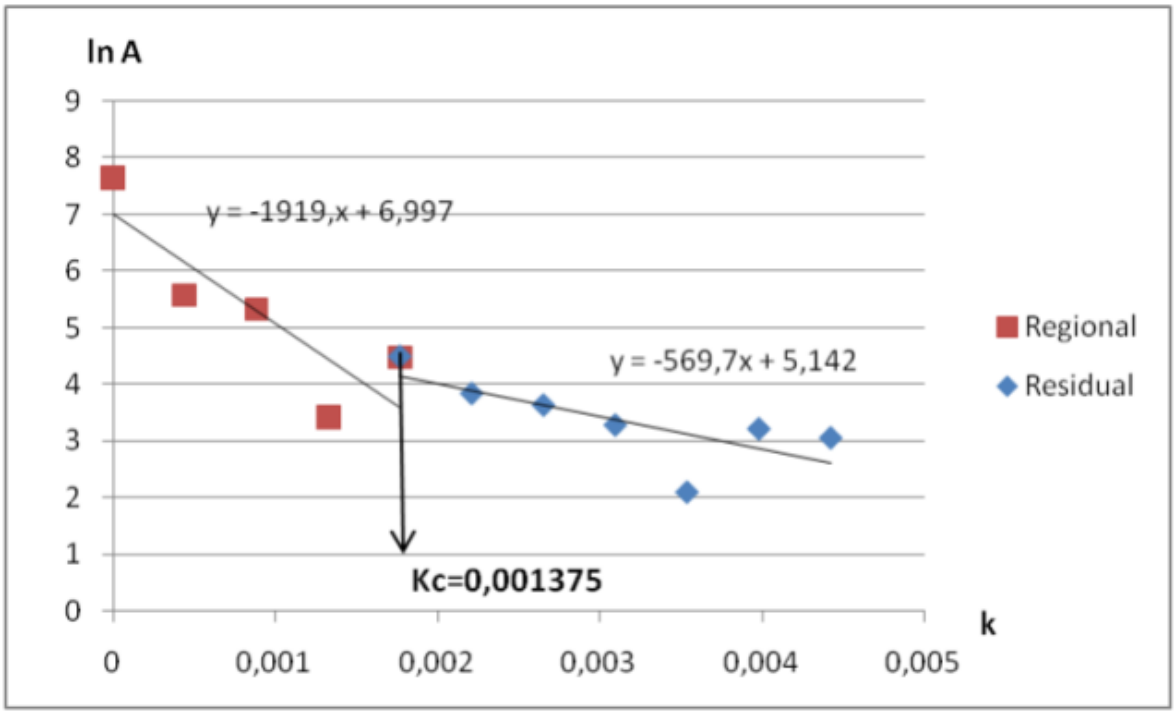


Figure 3: Spectrum Analysis Chart of A-A cross-section profiles.

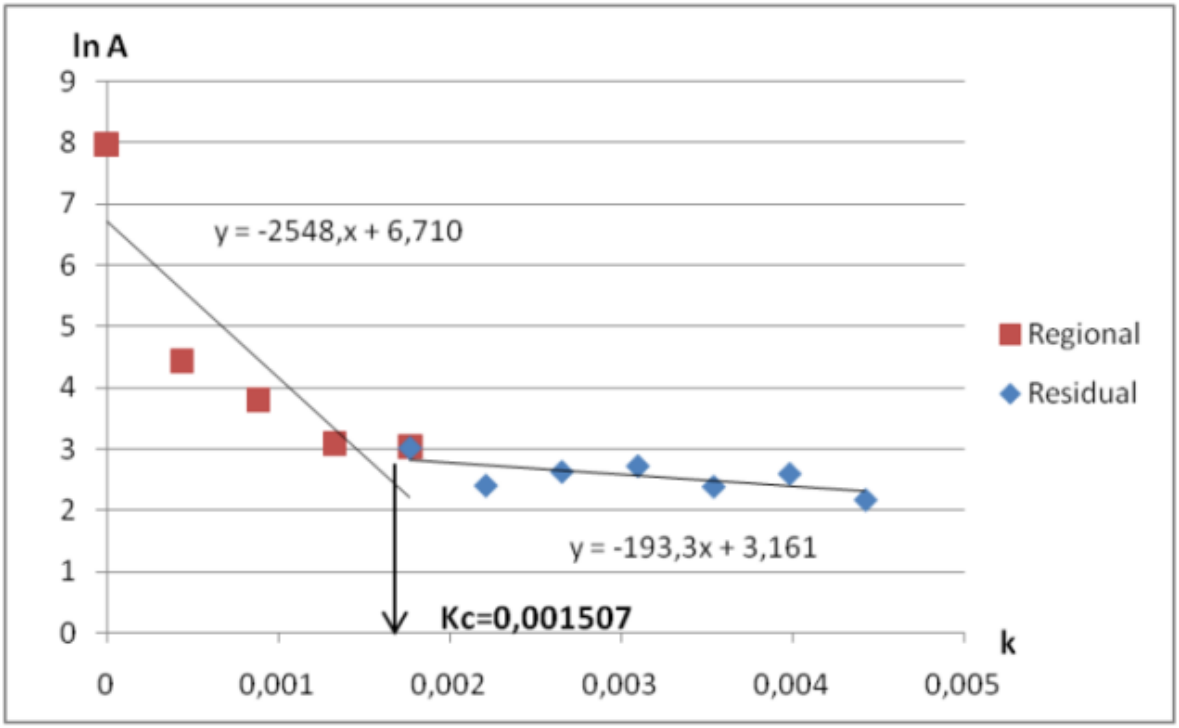


Figure 4: Spectrum analysis chart of B-B cross section profiles.

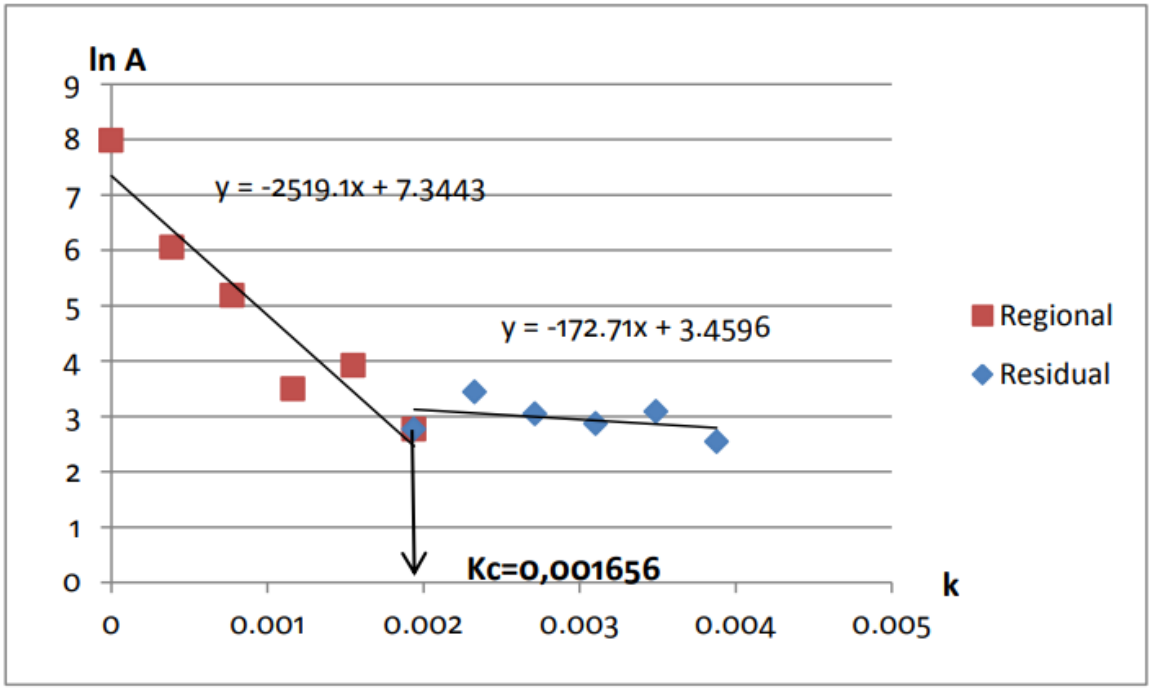


Figure 5: Spectrum analysis graph of C-C cross section profile.

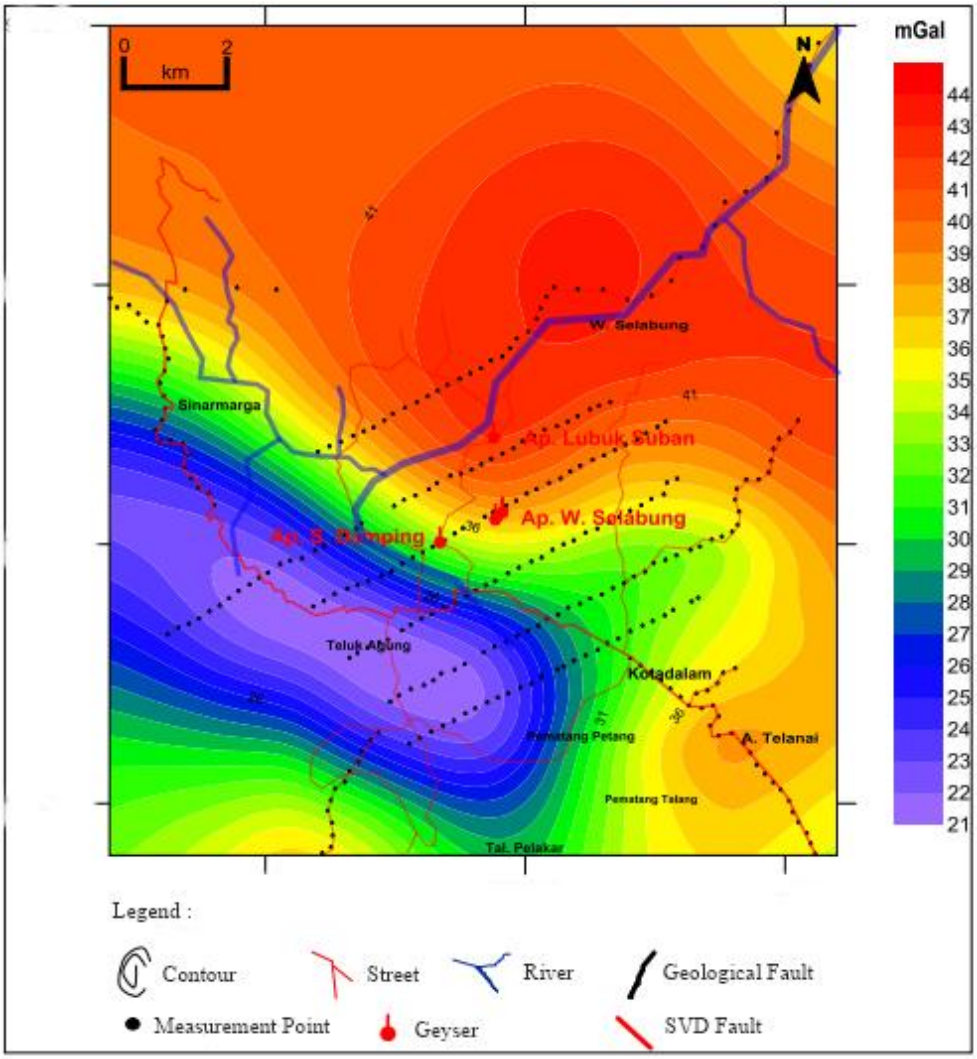


Figure 6: Regional Regional Anomaly Map of Research.

Regional Anomaly

Map of regional gravity anomalies (Figure 6) grouped the distribution of low regional gravity (21 to 29 mGal) in the southwest to the south is shown by purple to dark blue. The distribution of moderate regional gravity (30 to 37 mGal) in the southeast, east, and slightly in the west is indicated by green to yellow around the low anomaly area. And the distribution of regional gravity is high (> 38mGal) in the north to east direction indicated by orange to red. This regional anomaly shows a lineation pattern that traverses the north south with a value that decreases in the south and enlarges to the north.

Residual Anomaly

The low residual anomaly value has a negative value range of -13 mGal up to -5 mGal forming poles in the area around Inner City, Agung Bay, and Pematang Gong (Figure 7). Moderate residual gravity values with a range of values of -4 mGal to 3 mGal dominate the investigation area in the north, south, east and west. The value of high residual gravity with a value of> 4 mGal points in the middle of the study area between the gong and Agung bay where geothermal manifestations are found and at the end of the area to the southeast of the study area.

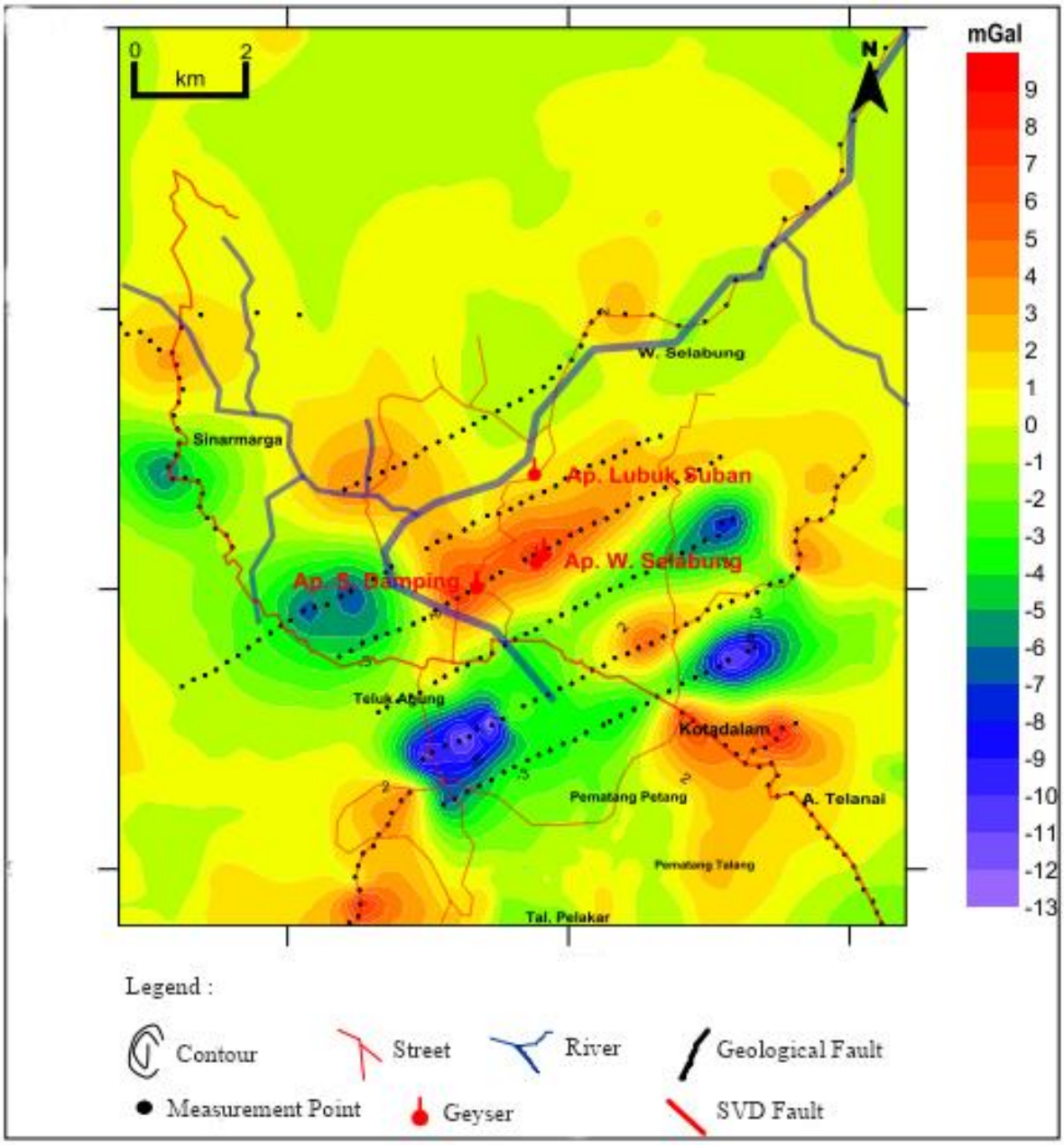


Figure 7: Research Area Residual Anomaly Map.

Second Vertical Derivative (SVD)

Figure 8 shows the contour map of the Second Vertical Derivative Bouguer anomaly in the study area. Bouguer anomaly values that have been filtered SVD are divided into 3 parts, namely low anomaly values (-6.5 to -3 mGal), moderate gravity values (-3 to 2 mGal) and high gravity values (> 2 mGal). The zero contour (indicated by the black contour line) flanked by high and low anomalies indicates the shallow fault structure of the study area. There are 6 areas where zero contours are flanked by high and low anomalies which are directed east around the Inner City, in the south in the vicinity of Pematang Petang and also around hot water manifestations. Structural patterns that can be drawn based on the SVD anomaly contour map shows northwest-southeast, and southwest-east.

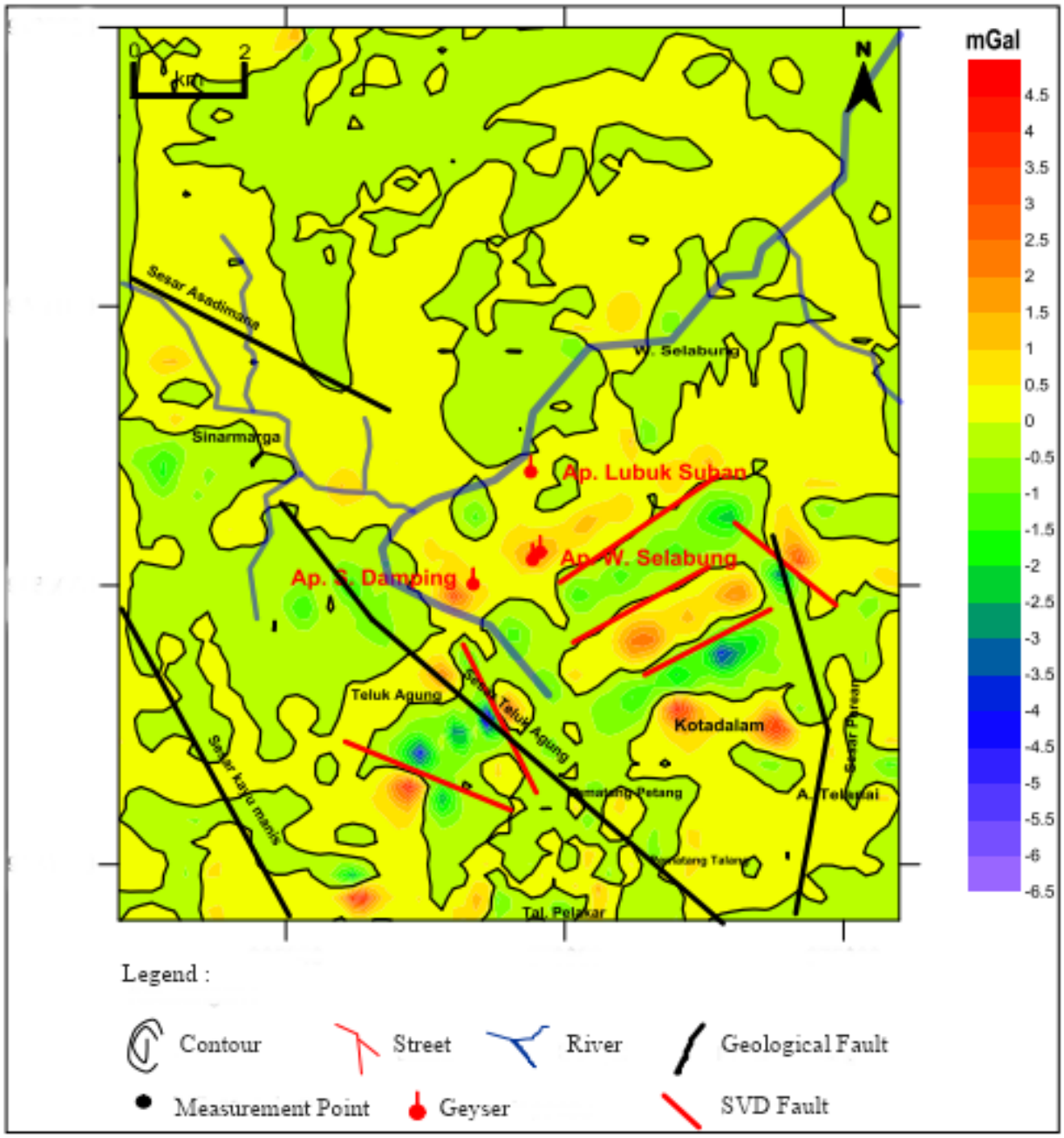


Figure 8: SVD contour map Bouguer Anomaly Research Area.

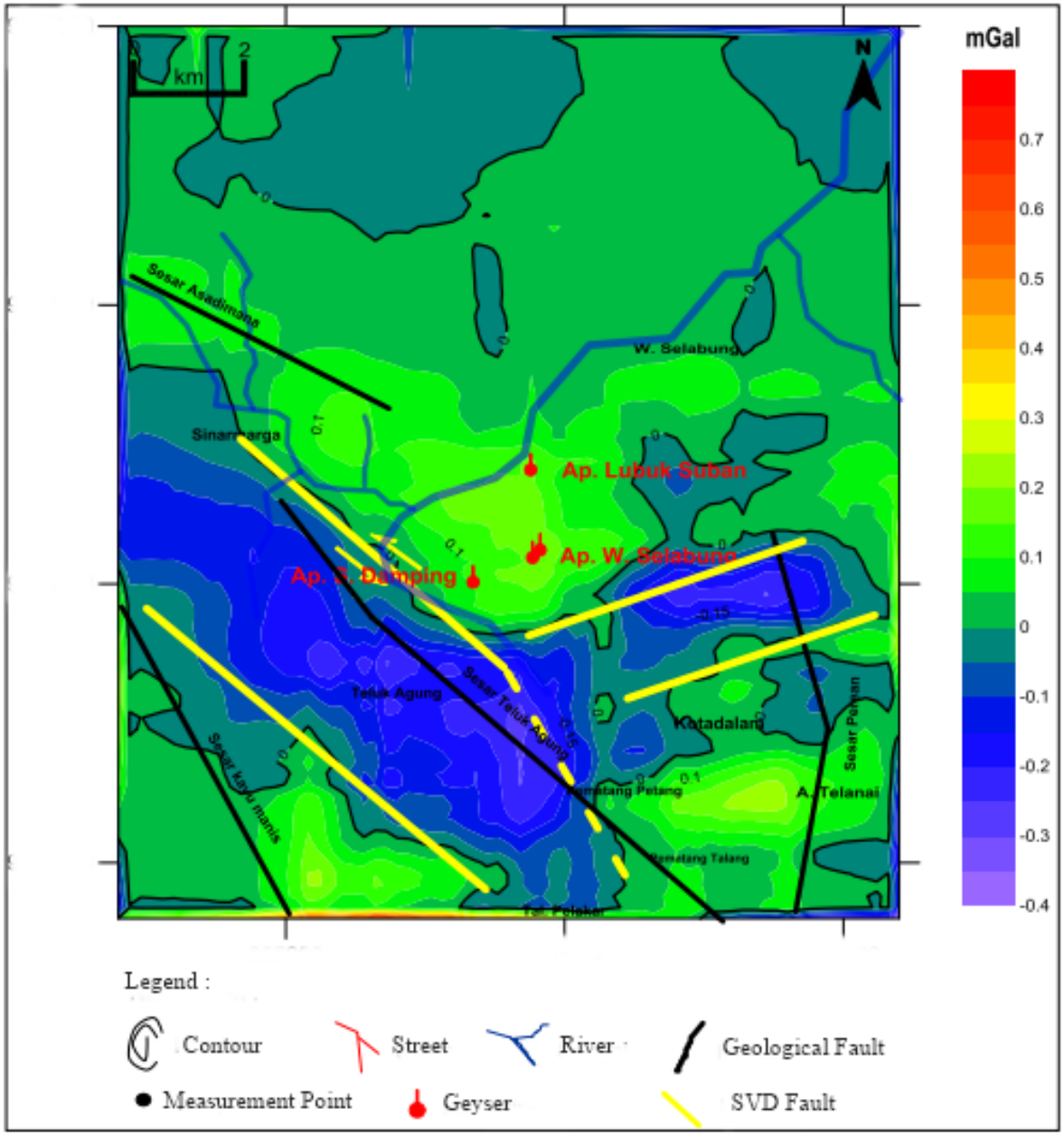


Figure 9: Map of Regional SVD Contour of Research Areas.

Figure 9 shows the SVD contour map of the regional anomalies of the study area. The anomalous contour on this regional contour map has a range of -0.4 to 0.7 mGal. The structure pattern that can be drawn based on this contour map is illustrated by the yellow line, the dotted yellow line shows the possible continuity of the regional SVD fault.

Figure 8 shows the SVD contour map of residual anomalies. This map has a similar picture to the SVD map of Bouguer anomalies with a range of values of -6 to 4.5 mGal. The difference from the SVD map of residual anomalies with SVD maps of Bouguer anomalies is that the anomaly values indicated are more superficial anomalous values. The fault that can be drawn based on SVD maps is that the residual anomaly is the same as the fault on the SVD map. Bouguer anomalies are the west-southeast and west direction. Figure 10 shows the contour map of residual anomalies overlaid with the geological map of the study area. The red and yellow lines show the SVD fault, the black contour line shows the zero SVD value and the blue line shows the slice on the 5 faults. It can be seen on the SVD map that 4 SVD faults are flanked by 2 different strata and only SVD 2 faults are not. Figure 11 shows a graph of slicing out of five faults. Slice 1 and 4 graphs show a graph of the maximum SVD value that is higher than the minimum value, this indicates that the slice 1 and 4 faults are broken down. While slice graphs 2.3, and 5 show a graph of the minimum SVD value that is greater than the graph of the maximum SVD value, this indicates that the faults at slices 2.3 and 5 are upward faults.

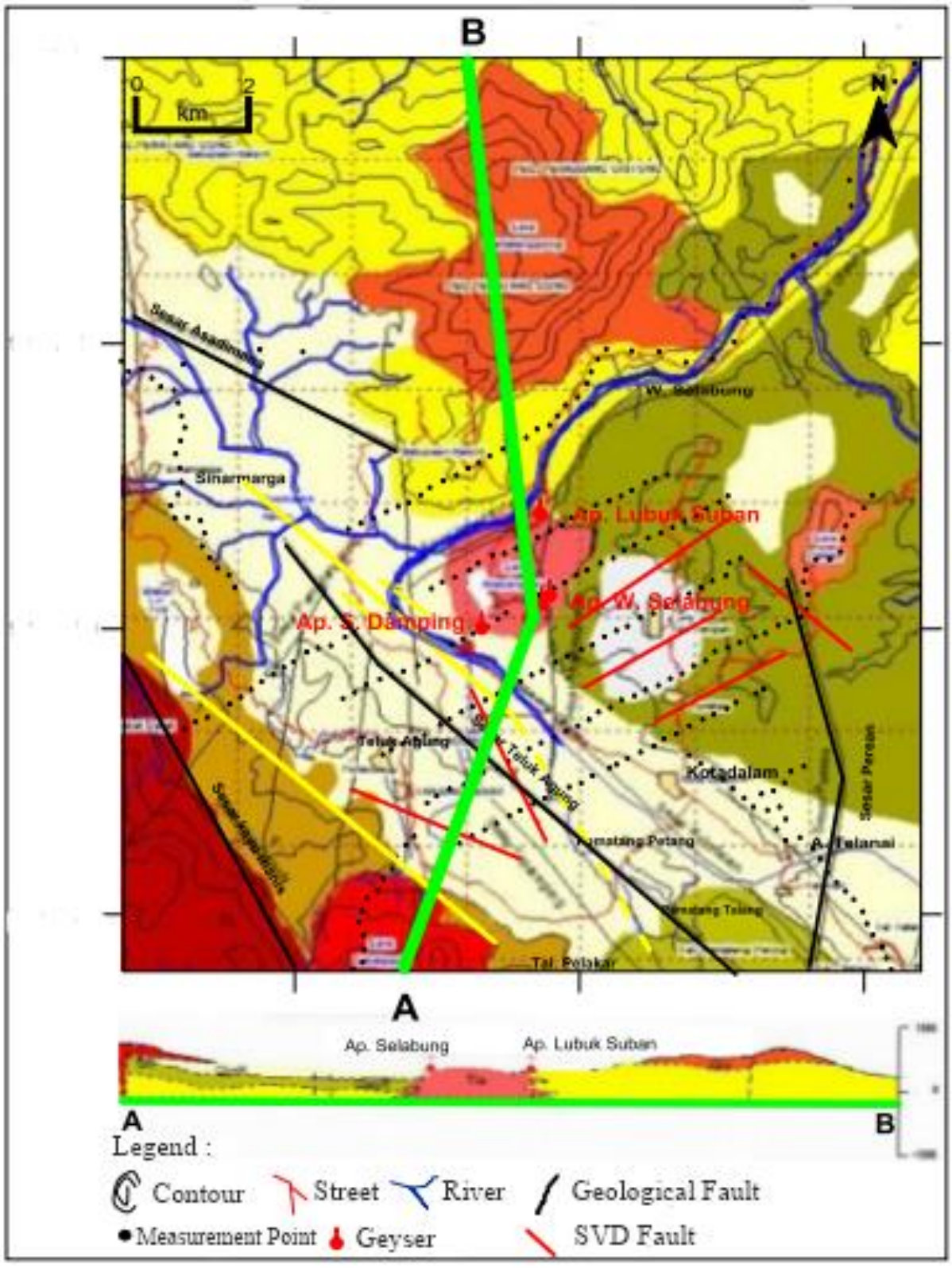


Figure 10: Map of residual anomaly contours of geological overlay with slicing on SVD fault.

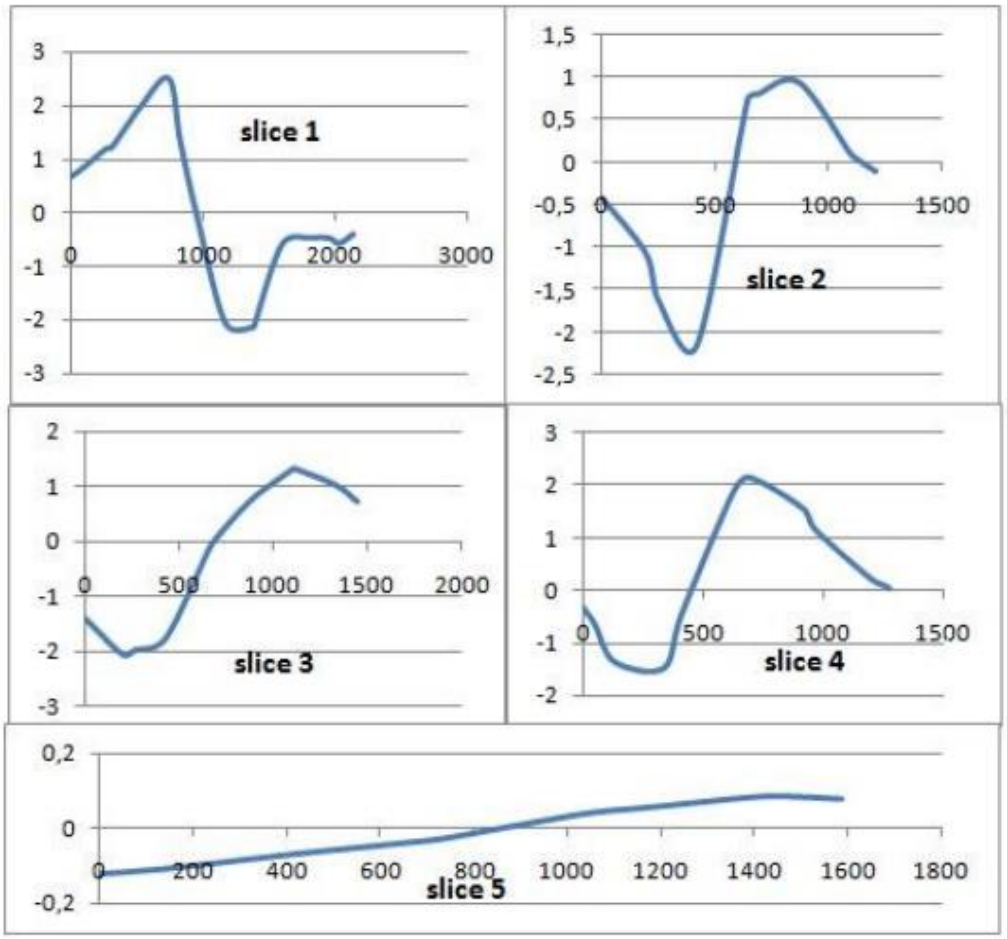


Figure 11: Determination of surface density of the research area.

Bouguer Anomaly of 3D Inversion Modelling

The inversion results from the Bouguer anomaly (seen from the south) produce density distribution as shown in Figure 12 with a range of values of 1.4 to 2.9 gr / cm3 with a maximum depth of 5989 meters and a maximum topographic height of 1011 meters. The value of low surface density distribution is indicated by dark blue in the west to south with a density value of 1.4 to 1.7 gr/cm^3.

This area is in the geological order of the old breccia, which is in the Miocene age which is abundant by the pleistocene gayat lava. Medium density values ranging from 2 to 2.4 gr/cm^3 are marked with light blue to yellow. Medium density distribution is at the end of the study areas directed northwest, northeast and southeast and most are at a depth of 700 meters. The medium density value is probably tertiary-aged sandstone sediment deposits. The value of the distribution of high-density ranges from 2.4 to 2.9 gr / cm3 indicated by yellow to pink. High density distribution values are spread at a depth of 700 meters down, high density values are interesting in gravity surveys because they indicate the potential of the heat source and the possibility of hydrothermal silicate deposits.

Figure 13 shows slicing A on fault 1, 2, and 4 SVD maps of Bouguer anomalies. Then slicing in the 3 dimensional model of density distribution with the same cutting point is obtained as shown in Figure 35. Based on the geological map of this area there is a cinnamon fault with a northwest-southeast direction that is in accordance with fault direction 1 and 2. To find out the type of fault in this area we use the maximum and minimum SVD graph analysis of Bouguer anomalies in fault 1 it indicates that the fault is a broken down while in fracture 2 it is described as an upward fracture. Fault 1 has a very noticeable density change at a depth of 700 meters with a density of 2.4 gr/cm^3 from the southwest (shown by yellow) down to less than 1.7 gr/cm^3 (indicated by blue), possibly this caused by changes in the young to old layer. In fracture 2 the change in density is not too striking from the southwest to the east, the changes range from 1.7 gr/cm^3 to 2 gr/cm^3, the stratigraphy that is crossed by this fault is the fall of the silt pyroclastic. At fault 4 the change in density is also not too large ranging from 2 gr/cm^3 to 2.4 gr/cm^3 with the stratigraphy being passed is the sapatuhu pyroclastic flow.

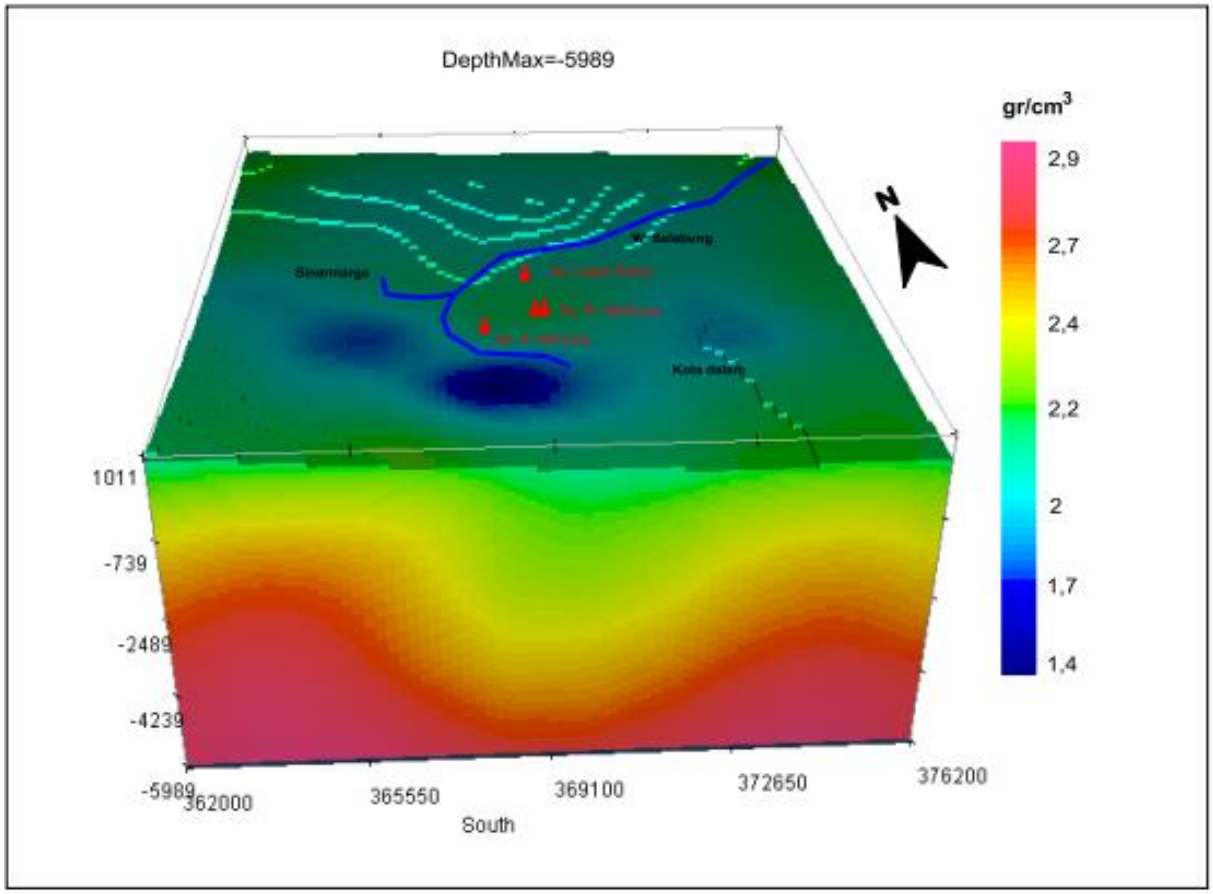


Figure 12: The 3D inversion anomaly Bouguer density distribution model with maximum depth of 5989 meters below the Mean Sea Level.

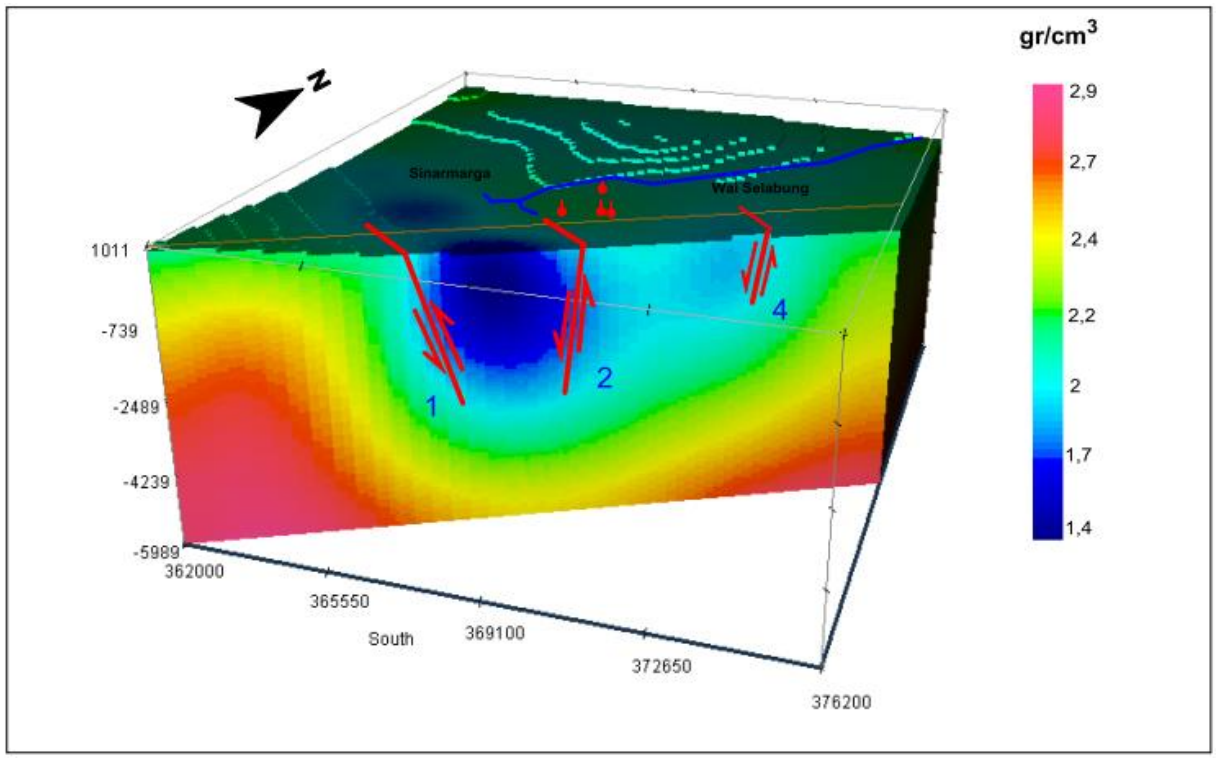


Figure 13: The density distribution result of 3D inversion Bouguer anomaly SE trending cross section with plot A slice fault.

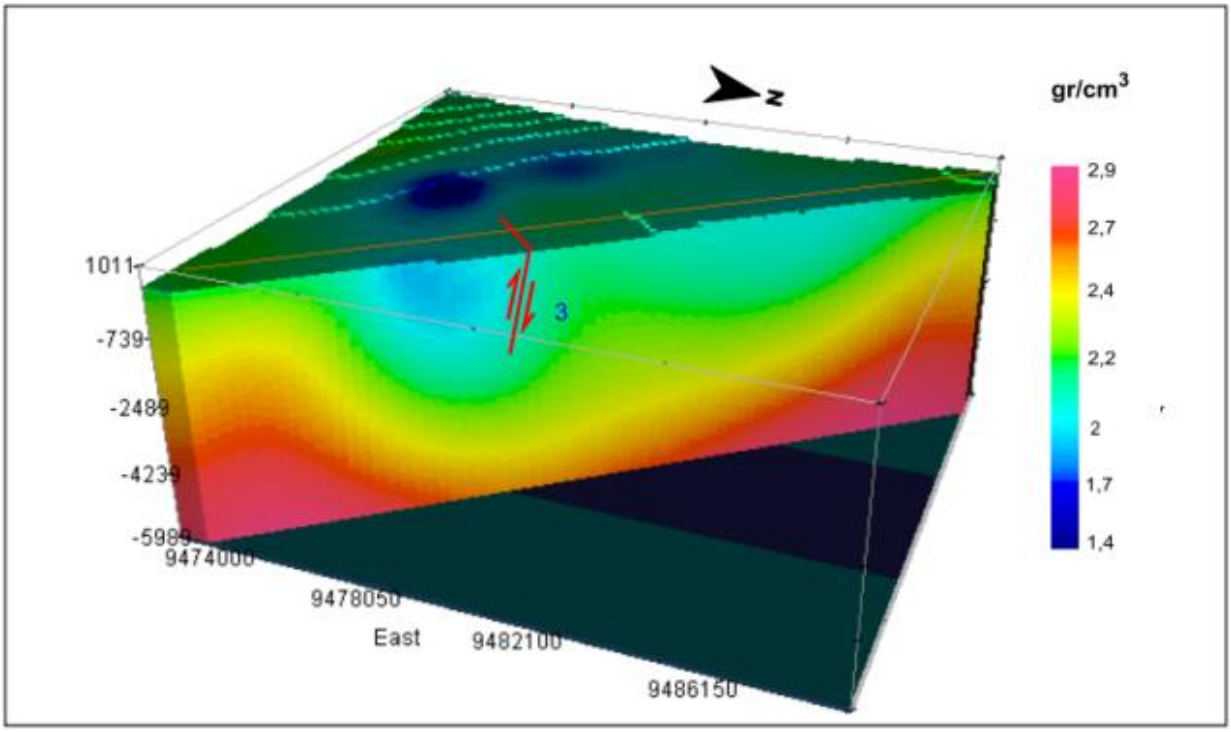


Figure 14: The density distribution result of 3D inversion Bouguer anomaly WE trending cross section with B slice fault plot.

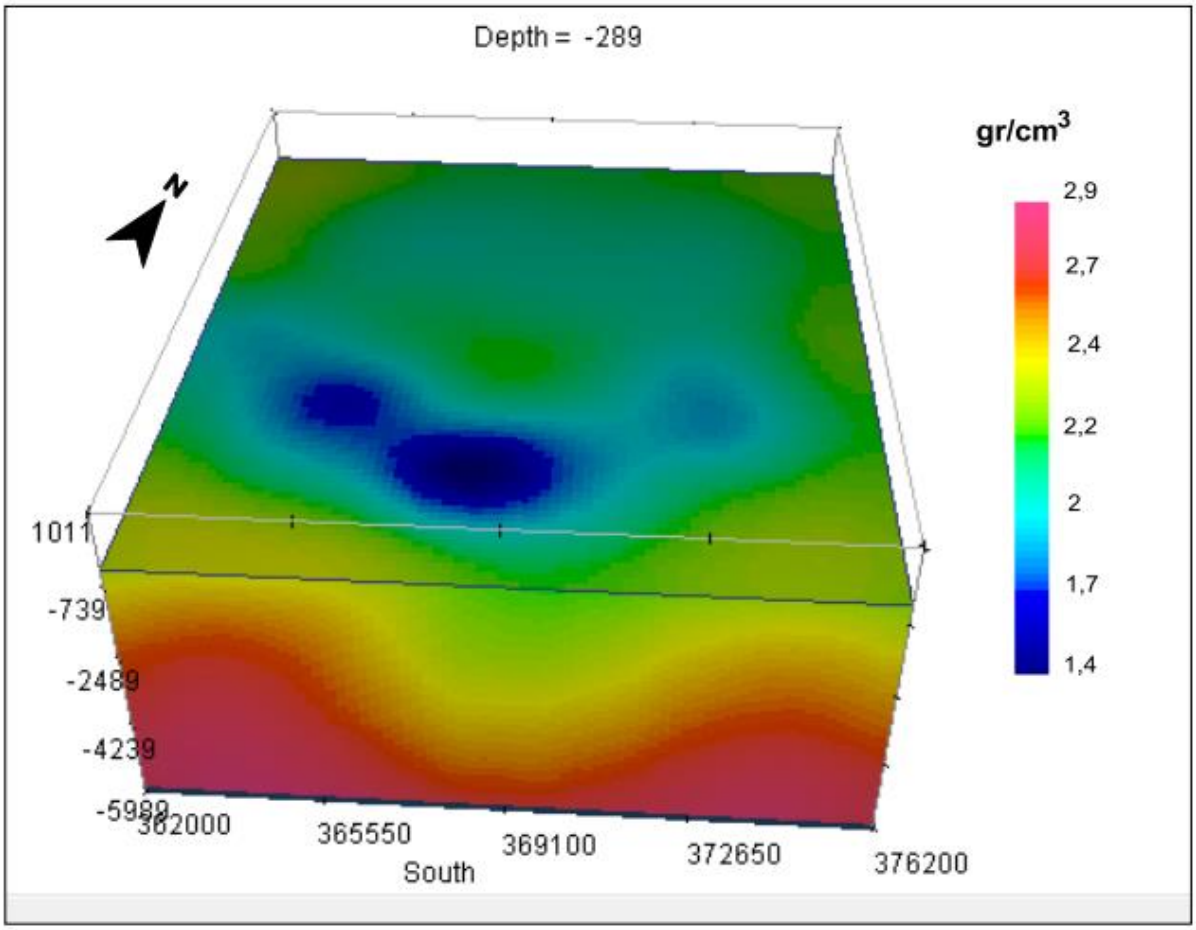


Figure 15: The first discontinuity field in the yield density distribution model 3D inversion Bouguer anomaly at a depth of 289 meters Mean Sea Level.

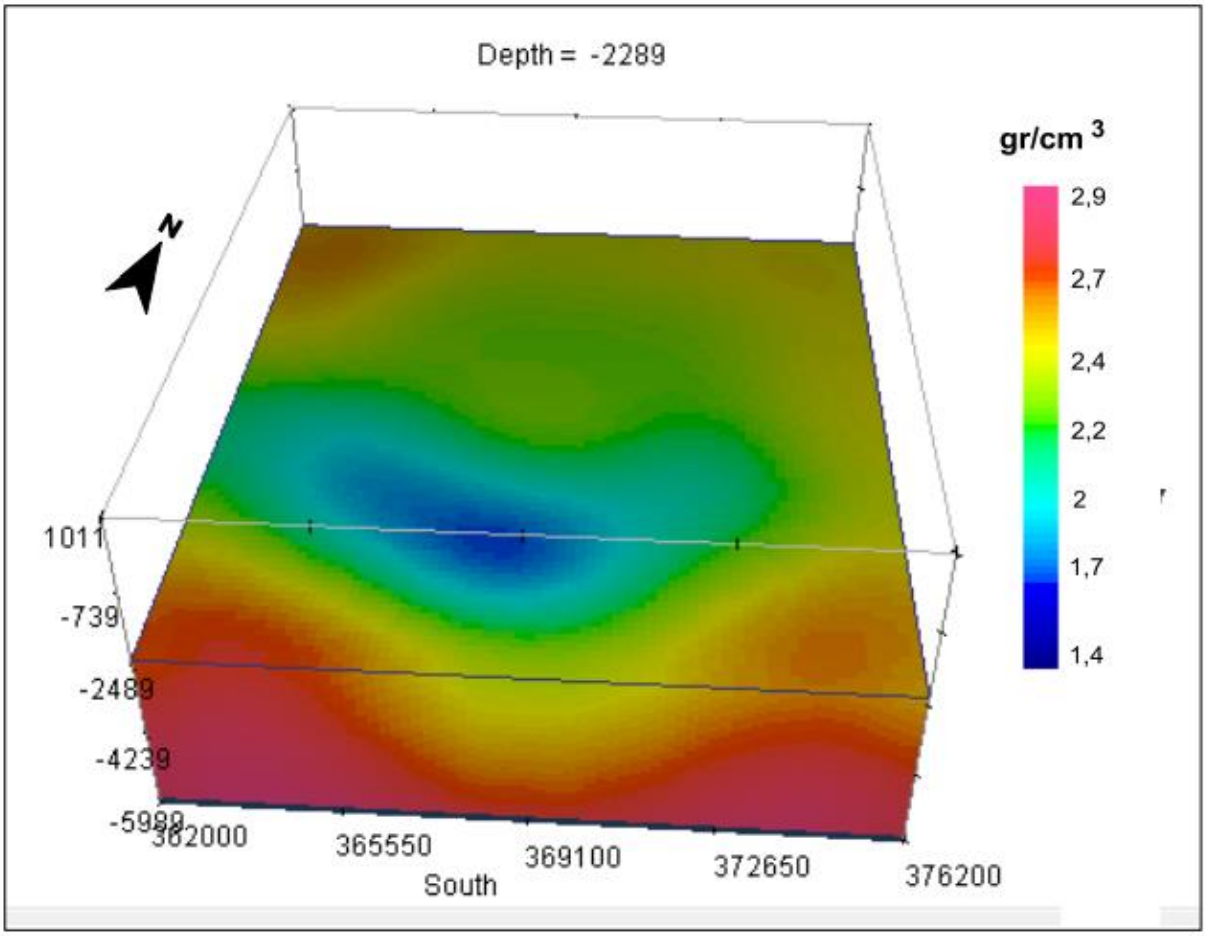


Figure 16: The second discontinuity field in the yield density distribution model 3D inversion Bouguer anomaly at a depth of 2289 meters Mean Sea Level.

In Figure 14 it also shows slicing B which cuts the fault 3 of the SVD map of Bouguer anomalies. Geologically this fault passes through two different geological strata, namely the pyroclastic flow of temperature and the fall of the pyroclastic shutter which is equally late tertiary. At a depth of 700 meters the density value is seen from the southeast to the northwest by 2.4 gr/cm^3 at the beginning and in the middle to the end the value tends to be stable around 2 gr/cm^3.

By using the average depth of fields 1 and 2 discontinuities in model 3 the dimensions of the distribution of the study area density. Figure 15 shows the 3-dimensional model of the distribution of density which shows the first discontinuity field, this also shows a picture of the residual anomaly value of the study area. On the surface to a depth of 289 meters below the surface of the study area with densities ranging from 1.4 to 2.4 gr/cm^3, it is likely to be a tertiary-aged sandstone sediment coating area.

Figure 16 shows the 3-dimensional model of density distribution at a depth of 2289 meters, this model shows the second discontinuity field which also shows a description of the regional anomalous value of the study area. Based on the value of the density and geological data of the study area at a depth of 2289 meters to a depth of 5989 meters below the surface, the value of its density ranges from 1.4 to 2.9 gr/cm^3 the possibility of this area is a basement.

GeochemistryAnalysis

Geochemical analysis was carried out on Wai Selabung hot water and geothermal water from 6 water samples (Wai Selabung 1 hot water, Wai Selabung 2, Wai Selabung 3, Lubuk Suban, Damping Savings, and Pematang Tiga cold water), and hot water outside location map of the investigation (Arumantai hot water and hot water Batu City). The concentration of silica in the study area showed values of less than 90 mg/l except for the hot springs of Selabung Damping, Arumantai and Kota Batu, which were higher at 167, 204 and 126 mg/l. The high Ca and Mg concentrations are found in Wai Selabung 3, Dabung, Batu and Arumantai hotspots, indicating high mixing with surface water. Large Ca concentrations (> 50 ppm) and Mg indicate the reservoir has a temperature that is not too high. The upflow zone usually has a high temperature, proven by the manifestations of Wai Selabung 1 and 2 hot water which have temperatures ranging from 900ºC. The outflow zone has a lower

temperature value found in Lubuk Suban hot water manifestations which have a temperature of 680ºC.

The relatively low temperature hot springs (hot water Wai 3, Damping and Arumantai) are included in the type of bicarbonate (HCO_3), while the hot springs are high (Wai Selabung 1 and Wai 2) type chloride sulfate ($ClSO_4$) and bicarbonate chloride ($Cl\text{-}HCO_3$). Lubuk Suban hot spring and Batu City are chloride bicarbonate and chloride sulfate types. Water pH on geothermal manifestations in Wai Selabung area has an average pH neutral. To determine the origin of our reservoir recharge water using stable D-deutrium and 18O isotopes. Plotting isotope analysis in the δD graph with δ18O (Figure 52), shows that Wai Selabung 2 and Wai Selabung 3 hot water are located very close to the Meteoric Water Line (MWL), indicating the magnitude of the effect of meteoric water or surface water. While other hot water, namely hot water Wai Selabung 1, Lubuk Suban, Selabung Damping, Arumatai, and Kota Batu showed that oxygen enrichment ranged from 1.14 - 1.84% so that the position in the graph is on the right side of the MWL line, indications for the formation of hot springs are related to the interaction between hot fluids in geothermal systems and rocks that cause 18O enrichment. This indication shows that Wai Selabung 1 hot water, Lubuk Suban, Selabung Damping, Arumatai, and Batu City are more influenced by magmatic fluid.

After obtaining and analyzing the geoscience, geochemical and topographic data of the research area we can illustrate in a compilation map that shows the prospect area, manifestation, type resistivity distribution and residual anomaly. Referring to the volume of the first reservoir in the west of the study area of 2.5 Km^3, the estimation of temperature based on the Na-K-Mg and silica method gets a price of 1700ºC, then the 1200ºC cutoff assumes an assumption of potential resource class of the first reserve Wai Selabung area of 29 MWe. In the second reservoir south of the study area with a volume of 13.2 Km^3, the estimated potential reserve class resources of 153 MWe were obtained. So that the total potential resource of the unexpected reserve area in the Wai Selabung geothermal prospect area is 182 MWe.

CONCLUSION

From the results of the research in Wai Selabung district. South Oku Prov. South Sumatra, the following conclusions are obtained:

1. The Bouguer anomaly in the study area has a value of 36 mGal up to 48 mGal with a high anomaly (> 36 mGal) next to north and east of the research area in the Wai Selabung area, whereas low anomalies (8-22 mGal) south and west occupy the area Agung Bay.
2. Second vertical derivative analysis of Bouguer anomalies and anomalies Bouguer Residual shows that there are two patterns of broken down structures and an upward fracture direction northwest-southeast which is in the same direction as the main fault in the Inner City and Agung Bay, also a fault pattern rises trending southwest-east in the Kota Dalam area, while map analysis Regional SVD of Bouguer anomalies shows that the main fault is directed northwest southeast in the Sinarmarga area until Agung Bay is a rising fault.
3. The field of discontinuity in the research area is based on analysis the spectrum produces two discontinuities representing residual and regional anomalies. The first discontinuity field has 300 meter depth represents noise and the discontinuity field the second has a depth of 2300 meter representing regional anomalies.
4. Bouguer's anomaly 3D inversion modeling results show that prospects for geothermal reservoirs in the Teluk Agung area on 900 meter below the MSL with a total volume of 15.7 km^2. Heat source geothermal in the form of intrusion of plistocene-aged gayat lava basalt which penetrates older sandstone sediments. Based on density and magnetotelluric distribution data analysis, Cap Rock from the system. Geothermal research area has a density value of <2 gr/cm^3 and value <20 ohms in the form of volcanic alteration.
5. Based on the results of geochemical analysis of geothermal fluids, the type of geothermal fluid Wai 3 is obtained, S. Damping and Arumantai falls into the type of bicarbonate (HCO_3), while hot springs W. Savings 1 and 2 are of type chloride sulfate ($Cl\text{-}SO_4$) and chloride bicarbonate ($Cl\text{-}HCO_3$). The flow zone is in the Teluk Agung area and the outflow zone is in the area near the river in the Lubuk Suban hot spring. Based on the Na-K-Mg and silica methods, the temperature value of 170 is a medium temperature geothermal system. Based on D-deuterium and 18O isotope data, it is known that manifestations W. Savings 2 and 3 are from meteoric water, while manifest W. Selabung 1, Lubuk Suban, S. Damping, Batu City, Arumantai indicate enrichment of Oxygen which shows the origin of fluid coming from fluid magmatic.
6. Based on the temperature estimation method Na-K-Mg and silica get the price of 1700ºC with a 1200ºC cutoff, then the estimated energy potential of the estimated reserve class resource in the reservoir in the west of the research area with a volume of 2.5 Km^3 was obtained at 29 MWe. In the second reservoir in the south of the research area with a volume of 13.2 Km^3, the potential energy source of the estimated reserve class was 152 MWe so that the total estimated potential energy resources for the class of

reserves of the Wai Selabung area were 182 MWe.

REFERENCES

Elkins, T., A., (1951), "The Second Derivative Method of Gravity" *Interpretation Geophysics. Bab XVI. Hal 29-50 dan V.23, 97-127.*

Harsh, G., and Sukanta, R., (2007), "Geothermal Energy: An Alternative Resource for the 21st Century". *Elsevier B.V. Amsterdam.*

Huenges, E., (2010), "Geothermal Energy System: Exploration, Development, Utilization". *Wiley Vch. Germany.*

Kearey, P., (2002), "An Introduction to Geophysical Exploration 3rd Edition". *Blackwell ltd. London.*

Nettleton, L., L., (1939), "Determination of Density for Reduction of Gravimeter Observation". *Geophysics. 183.*

Pedro, A., S., and Jose, A., R., (2009), "Gravity Surveys Contribution to Geothermal Exploration in El Salvador: The Cases of Berlin, Ahuchapan and San Vicente Areas". *LaGeo. El Salvador.*

Pusat Sumber Daya Geologi, (2011), "Integrated Survey of Geology, Geochemistry and Geophysics of the Wai Selabung Geothermal Area, South Oku District, South Sumatra Province". *PSDG. Bandung.*

Reynolds, J., M., (1997), "An Introduction to Applied and Environment Geophysics". *John Wiley and Sons ltd. England.*

Sarkowi, M., (2014), "Eksplorasi Gayaberat". *Lembaga Penelitian Universitas Lampung. Lampung.*

Suharno, (2010), "Pengembangan Prospek Panas Bumi". *Unila. Bandar Lampung.*

Telford, W., M., (1990), "Applied Geophysics 2nd ed". *Cambridge University Press. Cambridge.*

UBC-Geophysical Inversion Facility, (2001), "A Program Library for Forward Modelling and Inversion of Gravity Data over 3D Structures". *Department of Earth and Ocean Sciences University of British Columbia. Vancouver.*

GEOLOGY AND THE RELATIONSHIP OF LINEAMENT DENSITY WITH GEOTHERMAL MANIFESTATION DISTRIBUTION IN NORTHERN BAJAWA AREA, NGADA DISTRIC, EAST NUSA TENGGARA PROVINCE, INDONESIA

Astri Indra Mustika, Agung Setianto, and Agung Harijoko

Geological Engineering Department, Faculty of Engineering, Universitas Gadjah Mada
Senolowo, Sinduadi, Mlati, Sleman Regency, Special Region of Yogyakarta 55284
Email: astriindraa@live.com

ABSTRACT

Flores Island has been declared by the Ministry Energy and Mineral Resource of Indonesia as The Geothermal Island. One of the areas that have geothermal potential in Flores is Northern Bajawa part of Ngada regency, East Nusa Tenggara province. The northern Bajawa area has a unique morphological condition that consist of volcanic cinder cone complex and there are some indications that in this area is a highly potential in geothermal. The indication of highly potential geothermal is the presence of geothermal manifestation in northern Bajawa area. Geothermal manifestation that found in the surface can be distinguished by remote sensing method. This study aims to identify the geologic condition, distribution of geothermal manifestations, and the relationship between lineament density and geothermal manifestation in northern Bajawa area. This study using integration of ASTER imaginary to discover the distribution of geothermal manifestation, DEM to recognize the lineament and satellite gravity data to determine the gravity anomalies. The research is using DEM with 8m resolution and the ASTER imaginary that have 3 sub-systems; each of system has the resolution such as VNIR 15m, SWIR 30 m and TIR 90 m.

The result of remote sensing data analysis integrated with surface field data showed that the study area is composed of lithology from volcanic product such as lava and pyroclastic. Geothermal manifestations that have been discovered in the study area are hot spring and altered rock located in Bajawa and Mengeruda regions. Geothermal manifestation lies in the high density of geologic lineament. This proves that geothermal manifestations in the study area are associated with geologic structure.

Keywords: lineament, geothermal manifestation, ASTER, DEM

INTRODUCTION

Since 2017 Flores has been declared by Ministry Energy and mineral Resource of Indonesia as The Geothermal Island. According to Sitorus and Aswin (2002) the result of Sub Directorate of Geothermal survey there were 18 locations of geothermal manifestations in East Nusa Tenggara regions, spread in six districts. Six locations are still in preliminary investigation, while 10 locations are already in detailed investigation stage. The rest of 2 locations already in drilling process. Based on the results of the East Nusa Tenggara regional inventory and exploration reaching 1055 MW consisting of 125 MW of Speculative Resources, 374 MW of Hypothesis Resources and 542 MW of suspected reserves and 14 MW of proven reserves.

Bajawa is located in Flores part of East Nusa Tenggara province, Indonesia as showed in Figure 1. Based on the regional geological map of the Ruteng by Koesoemadinata et al (1994) hot springs which is one of the geothermal manifestations were found. Muraoka, et al. (1999) stated that from the results of the analysis of ASTER VNIR and TIR previously there was a volcanic cone complex in the Bajawa area with a North South direction that might have an association with the presence of heat anomalies in the study area. This volcanic cone complex in the Bajawa area can be an indication of the heat source of the geothermal system in the research area. All geothermal manifestations such as steaming ground and hot springs that have been observed are associated with a volcanic cone complex in Bajawa.

The method that can be used in exploration of geothermal potential in remote area is using remote sensing methods which are also supported by field data collection. The advantage of using the remote sensing method itself besides being able to save time can also save costs and make geological mapping and surface data retrieval more effective and efficient.

The remote sensing method using ASTER imaginary and DEM data. ASTER imaginary is using to discover the surface kinetic temperature anomalies. Aside from DEM data is to analyze the lineament density in the research area. After ASTER image processing then based on the result then the ground check is done to ensure the anomalies on the field. The final method is integrate the result of remote sensing method and the field data to find the relationship between geothermal manifestation and lineament density in the research area.

This study aims to identify the geologic condition, distribution of geothermal manifestations, and the relationship between lineament density and

geothermal manifestation in northern Bajawa area. This study using integration of ASTER imaginary to discover the distribution of geothermal manifestation, DEM to recognize the lineament and satellite gravity data to determine the gravity anomalies. The field data has been collected in April 2018.

RESEARCH METHOD

The method of research is divided into 4 steps; perliminary, field data collection, laboratory analysis, data integration and intepretation. Perliminary step started with literature study, data collection and processing DEM, ASTER imaginary and satellite gravity data. ASTER imaginary can be download at https://asterweb.jpl.nasa.gov/. This research is using ASTER imaginary data level 2 from VNIR,SWIR and TIR band, DEMNAS 8 meter resolution that can be downloaded at http://tides.big.go.id/DEMNAS/ and global gravity anomaly that can be downloaded at https://topex.ucsd.edu/cgi-bin/get_data.cgi. The perliminary step also includes studio work where at this stage making tentative geological map, alteration map, thermal anomaly map, and gravity anomaly map and lineament distribution.

Field data collection consist of field observising, lithology description, rock sampling and temperature measurement in geothermal manifestation. The next step is laboratory analysis step including petrography and XRD analysis of rock sampling from the field. The last step is integraton and intepretation data from field work and studio work. Integration of research results, interpretations and secondary data and literature studies, is used to explain the geological conditions in the study area and the geothermal manifestation in the study area.

RESULT AND DISCUSSION

Geology

Based of the ASTER, DEM analysis, field observation and the result of laboratory analysis using XRD and thin section; The study area is divided into 3 lithology units. Lithology unit that exist in this area namely from the youngest to the older; Inelika Lava and Phyroclastic unit, Golewa Lava and Phyroclastic Unit, and Soa Lava and Phyroclastic unit.

The boundary between each lithology unit is based on the integration of DEM imaginary analysis, field data and previous research. The unit name is based on the dominant rock group in that area also the name of the area itself. DEM analysis to create the boundary is using ridge line tools which the result can determine the flow of the eruption product from the source based on the cross-cutting relationship. The result of the ridge line map shown in the Figure 2.

Inelika lava and phyroclastic unit located in west of research area extending from north to south. Acording to Koesoemadinata (1994) lava and phyroclastic unit are part of the Young Volcanic Unit (Qhv) and based on Muraoka et al. (2002) this lithology unit consisted of material resulting from Pleistocene volcanic eruptions. This lithology unit consists of lava deposits and andesite lava. There are several areas that have a thickness of lava deposits up to 10 meters. In this unit there are volcanic cone complexes extending from north to south. The Inelika pyroclastic and lava lithology units are derived from these volcanic cone products. The outcrop of this unit can as shown in Figure 3.

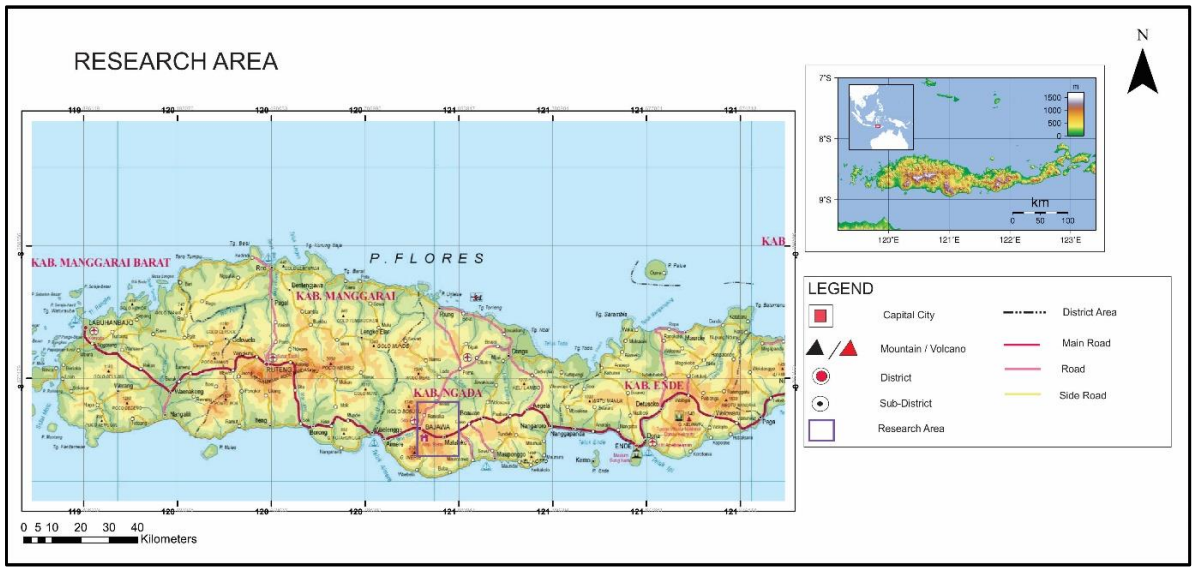


Figure 1: Research Area.

Golewa Lava and Phyroclastic Unit are located in east of the study area. This lithology unit also extending from north to south. According to Muraoka et al (2002) this unit has a Pleistocene age. In units there are no volcanic cone complexes like in Inelika. There are geothermal manifestations such as hot springs and altered rock in this area. The outcrop of this unit shows in Figure 4.

The lava and pyroclastic Soa units are the oldest aged units in the study area. According to Muraoka et al. (2002) this unit has a Pleistocene age which is located under the Inelika lava and pyroclastic lithology units. This lithology unit is located in the northern part of the research area to the middle. The outcrops found in this area are more weathered compared to other lithological units.

Most areas in the lithology unit of lava and pyroclastic Soa are residential areas. This lithology unit also consists of products from volcanic eruptions in the form of lava and pyroclastic. In Figure 5 there are several observation locations in this lithology unit.

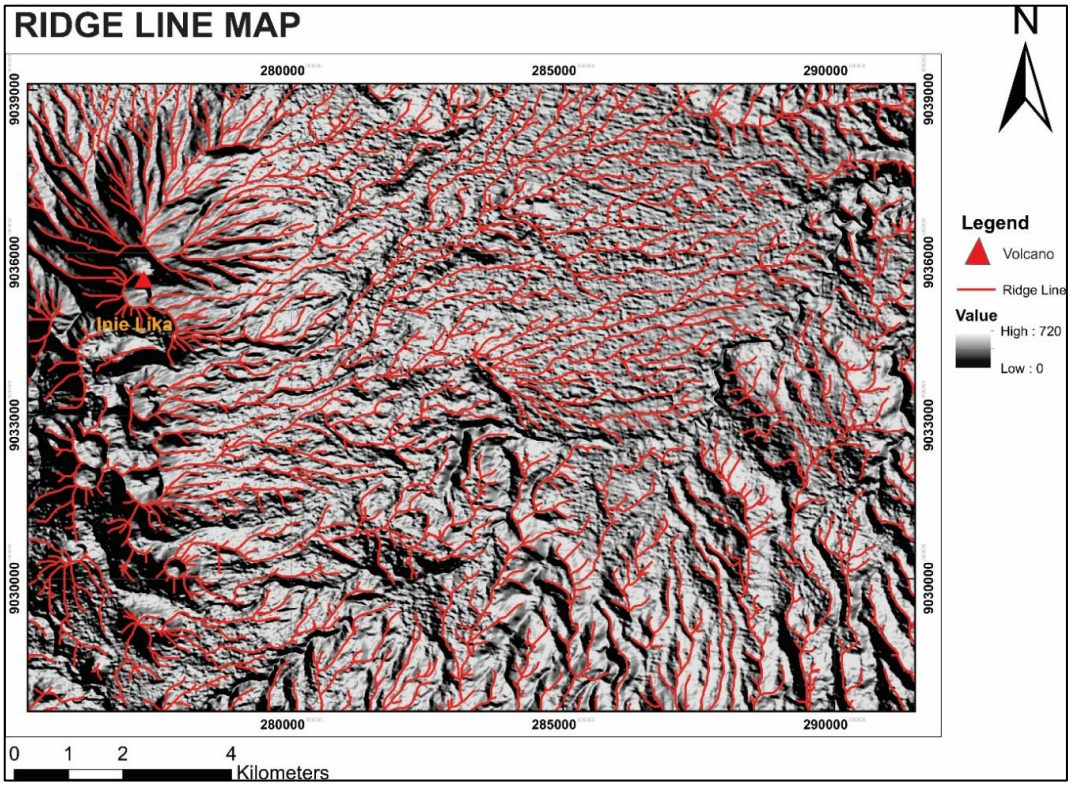


Figure 2: Ridge Line Map.



Figure 3: Outcrop in Inelika Lava and Phyroclastic Unit.



Figure 4: Outcrop in Golewa Lava and Phyroclastic Unit.



Figure 5: Outcrop in Soa Lava and Phyroclastic Unit.

Based on the integration of DEM analysis, field work and previous study in Bajawa area, the Geology map of the Northern Part Bajawa area can be can be made as shown in Figure 6. The geology map also has two cross section to get a better picture of relationship between lithology units.

The results of the XRD analysis carried out at the two manifestation locations also showed that at that location alteration minerals were found.

Heat Anomaly

Heat anomaly using ASTER imaginary in study area which is generated from TIR band and also integrated with other map to minimized the presence of false anomalies caused by other factors beside geothermal manifestation. The other factor that can caused false anomalies such as human activities or the existence of a volcanic body which causes the temperature to be higher than the surroundings.

Figure 7 show the kinetic linear map show the temperature map in research area. The area with heat anomaly show in red color which has temperature more than 35ºC. Based on the field data, the average temperature in research area is between 22.5ºC – 22.7ºC.

One of the weaknesses in using the ASTER image aside from limited resolution and also the existence of clouds that cover the area at the time of retrieval of the data that the heat anomaly data generated in the cloud-covered area will not be representative of that area. To overcome this, a ground check is needed so that field data and studio work maps can be integrated for analysis with other parameters.

Figure 7 shows that geothermal manifestations in Bajawa Utara are at low temperatures. This is possible because considering the image resolution used in making this temperature anomaly map is 90m which the real dimention of geothermal manifestation is less than 90 m. Contrary in Soa area, the geothermal manifestation lay on the high temperature area which has temperature more than 35ºC.

Lineament Density

Lineament analysis is done by 2 methods, namely manually and automatically using PCI Geomatica software. Manually pulling Lineament is done with

a qualitative method by pulling Lineament into the valley. In the analysis of Lineament with software PCI Geomatica, the Lineament that is detect by the software is on both the ridge and valley.

The results of Lineament analysis both manually and automatically using software can be seen in Figure 8 based on the Lineament that has been obtained, an analysis is carried out to determine the direction of the main stresses based on the existing line. The results of manual Lineament analysis show that the main direction of lineaments in the study area is NW-SE (Northwest - Southeast), while the results of Lineament analysis conducted with software show a different direction, W-E (West-East). In addition, continuation carried out manually has better results and is also better than the analysis carried out automatically using PCI Geomatica software. Figure 8 show the result of lieament map.

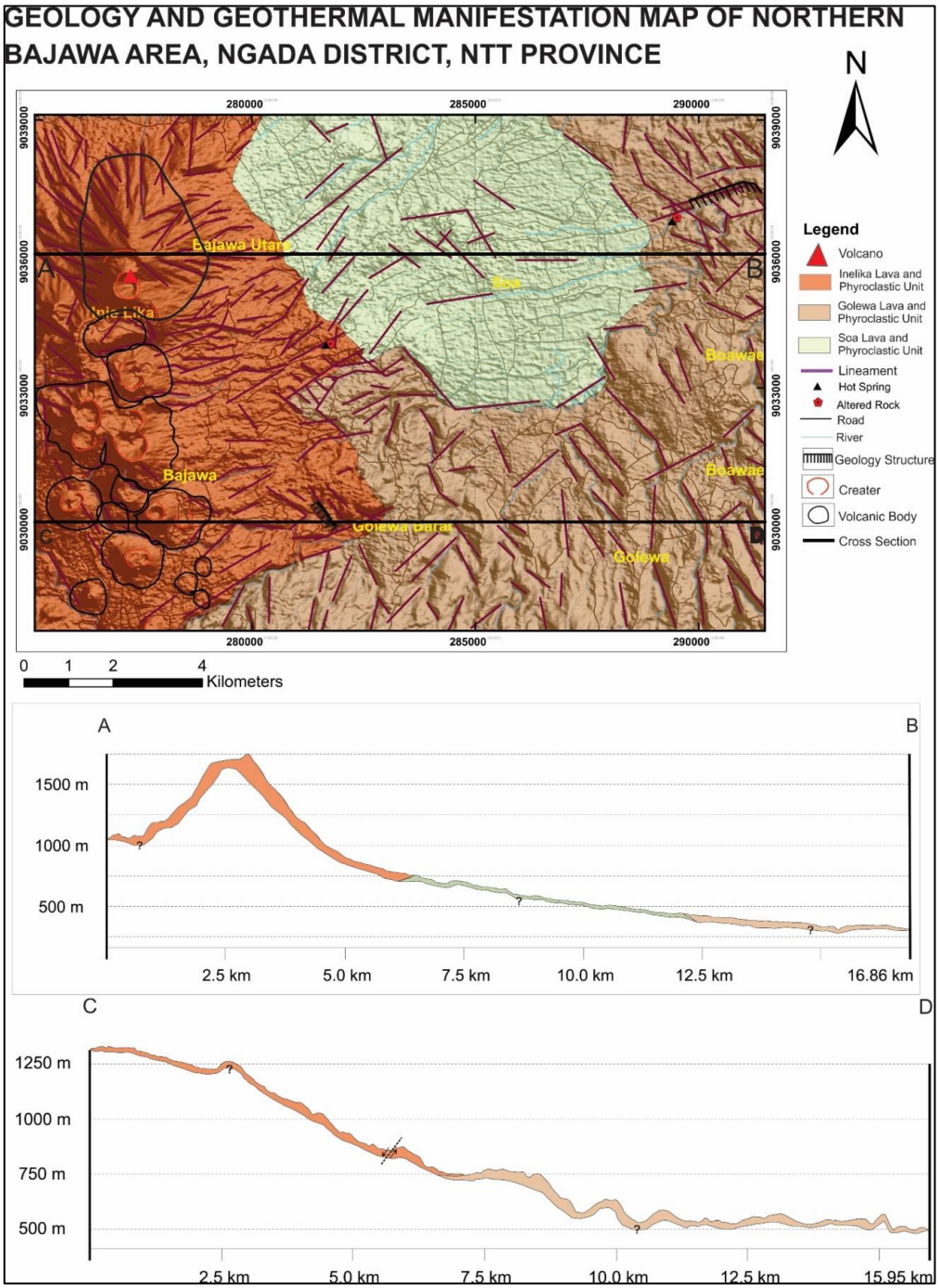


Figure 6: Geologic Map of research area.

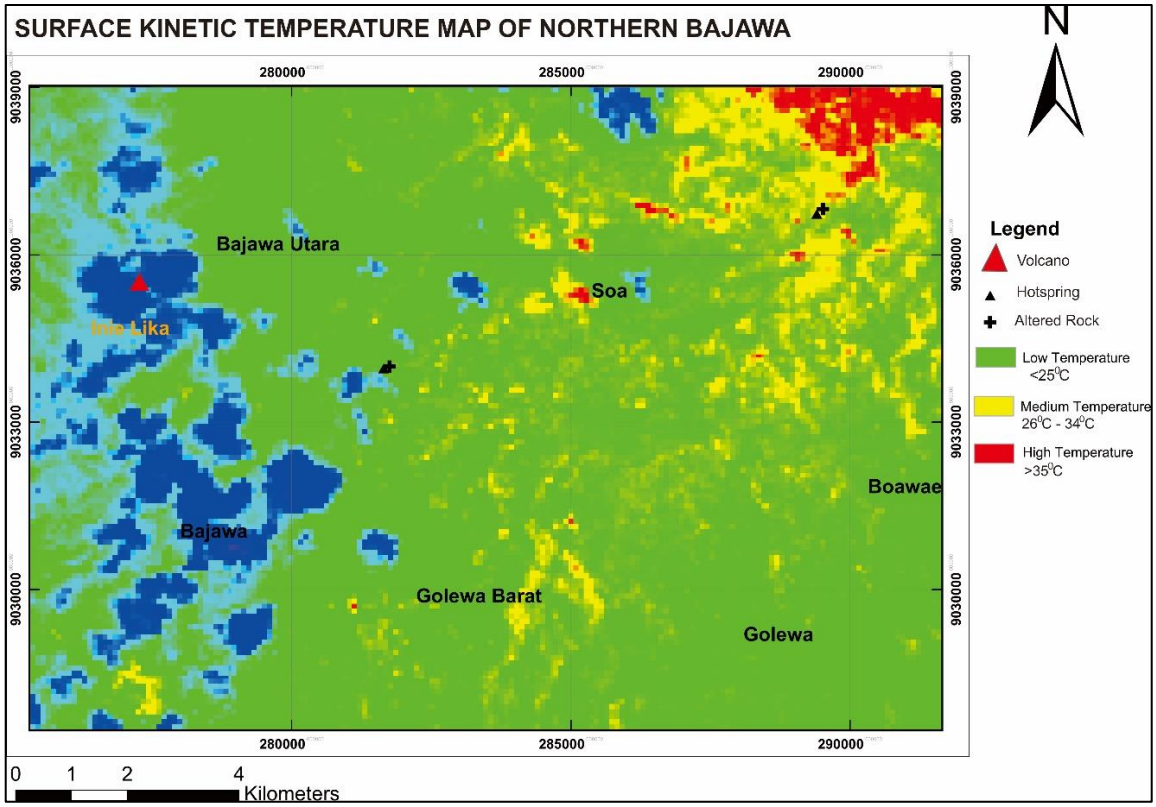


Figure 7: Surface Kinetic Temperature.

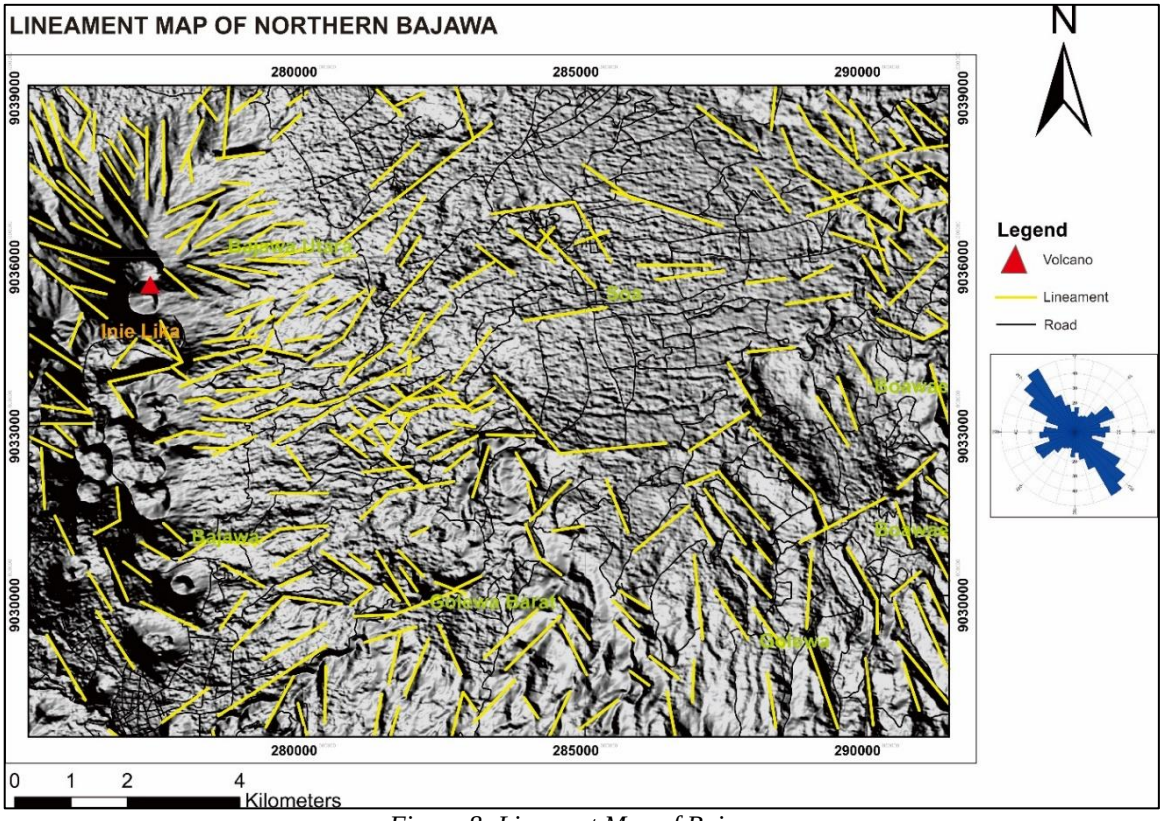


Figure 8: Linement Map of Bajawa.

Based on Muroka et al (2000) the dominant direction of lineament in the Bajawa area is NW-SE (Northwest - Southeast), where from this line there are only faults in the Mengeruda area which can be found in the field. The fracture found in Mengeruda has to do with the presence of geothermal manifestations in the area in the form of hot springs and terrestrial rocks found in the Mengeruda area.

Based on the lineament map in the research area which is done manually because the lineament is in the field, which means weak zones associated with the presence of geological structures, a lineament density map is created at the study site. Lineament density is divided into 3 classifications based on Soengkono (1999), namely low, medium and high. The green color on the lineament density map shows a low intensity which has a length of lineament between 0 to 1.5 km/km^2, for yellow indicates that the intensity is moderate 1.51 - 3 km/km^2 while for red indicates the area has a high intensity is has a length of more than 3 km/km^2.

Figure 9 shows the results of a straightness density map made based on the alignment maps in the study area. Areas that have high straightness intensity are in the northern region. Areas that have densities that are currently in Bajawa and West Golewa. The intensity of this straightness is strongly influenced by the morphology of the research area which is a volcanic area. The results of the lineament density map in the study area indicate that the geothermal manifestations in the Bajawa and Soa regions are in areas that have high density, which have a lineament length of more than 3km/km^2.

DISCUSSION

Based on field data and integration of the image analysis that has been carried out that the study area has 2 geothermal manifestation locations, namely the Mengeruda area in the northern part of Soa and the Bajawa area. Figure 10 is a comparison of line density compared to gravity data in the study area.

The results of the analysis conducted by comparing the map of lineament density with the gravity data in the study location can be seen that the geothermal manifestations in Mengeruda, the northern Soa region are in areas that have high lineament density and have low gravity values. The results of this comparison analysis show inverse comparisons where areas with high lineament density have low gravity anomalies. The comparison between lineament density map and gravity data can be shown in Figure 10.

Areas that have high lineament density do not always have geothermal manifestations, but the geothermal manifestations in the study area are found in areas that have high lineament density. Lineament density in the area of geothermal potential can be a reference for indications of geothermal manifestations in an area, where the density of lineament is in the presence of geological structures.

This low gravity value indicates that the region has a low rock density value. Rock density which is low associated with these rocks has a good porosity hole where in the volcanic region porosity is related to the presence of fractures or fractures found in these rocks due to the presence of geological structures. Geothermal manifestations in the Bajawa area, are located in areas that have high lineament density and also areas that have moderate gravity values. This indicates that this manifestation is associated with the existence of geological structures in the research area.

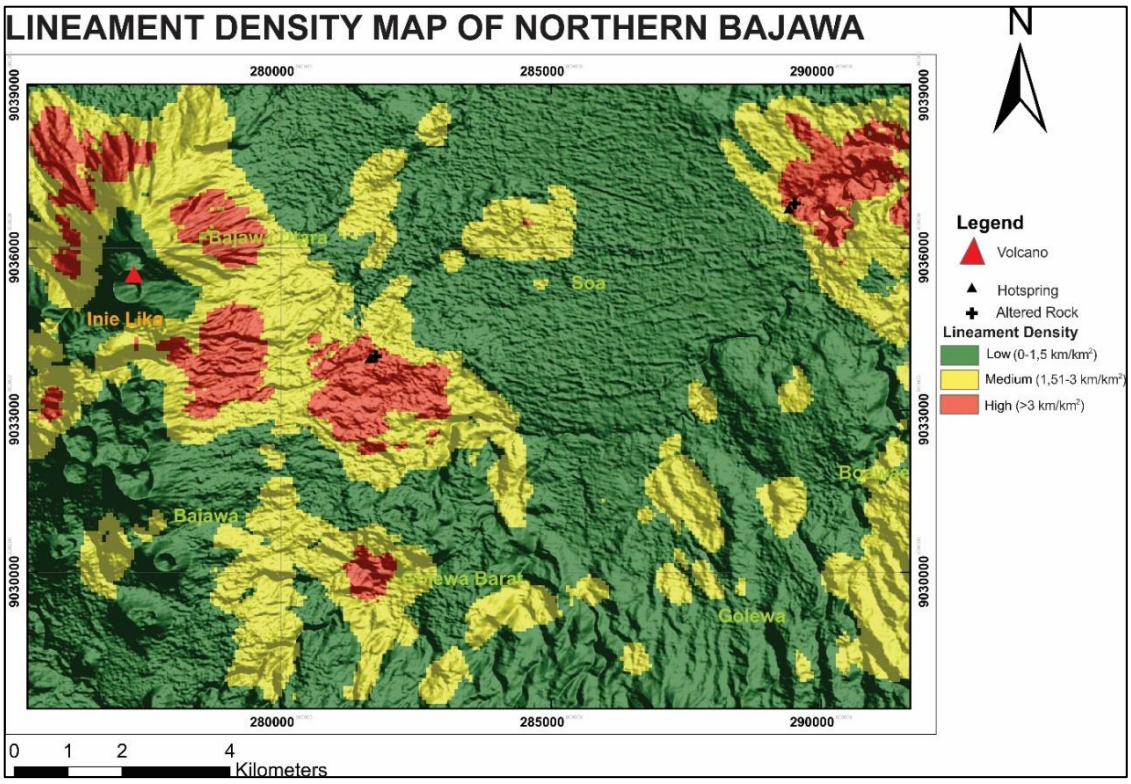


Figure 9: Lineament Density Map of Bajawa.

Based on all analyzes that have been carried out, all geothermal manifestations are associated with the high intensity of lineament in the area. The high intensity of lineament indicates an association with the existence of geological structures that can cause fractures in volcanic lithology. The existence of this geological structure can affect secondary permeability in volcanic rocks so that these rocks can drain fluid that is present in the geothermal system to the surface and become a geothermal manifestation.

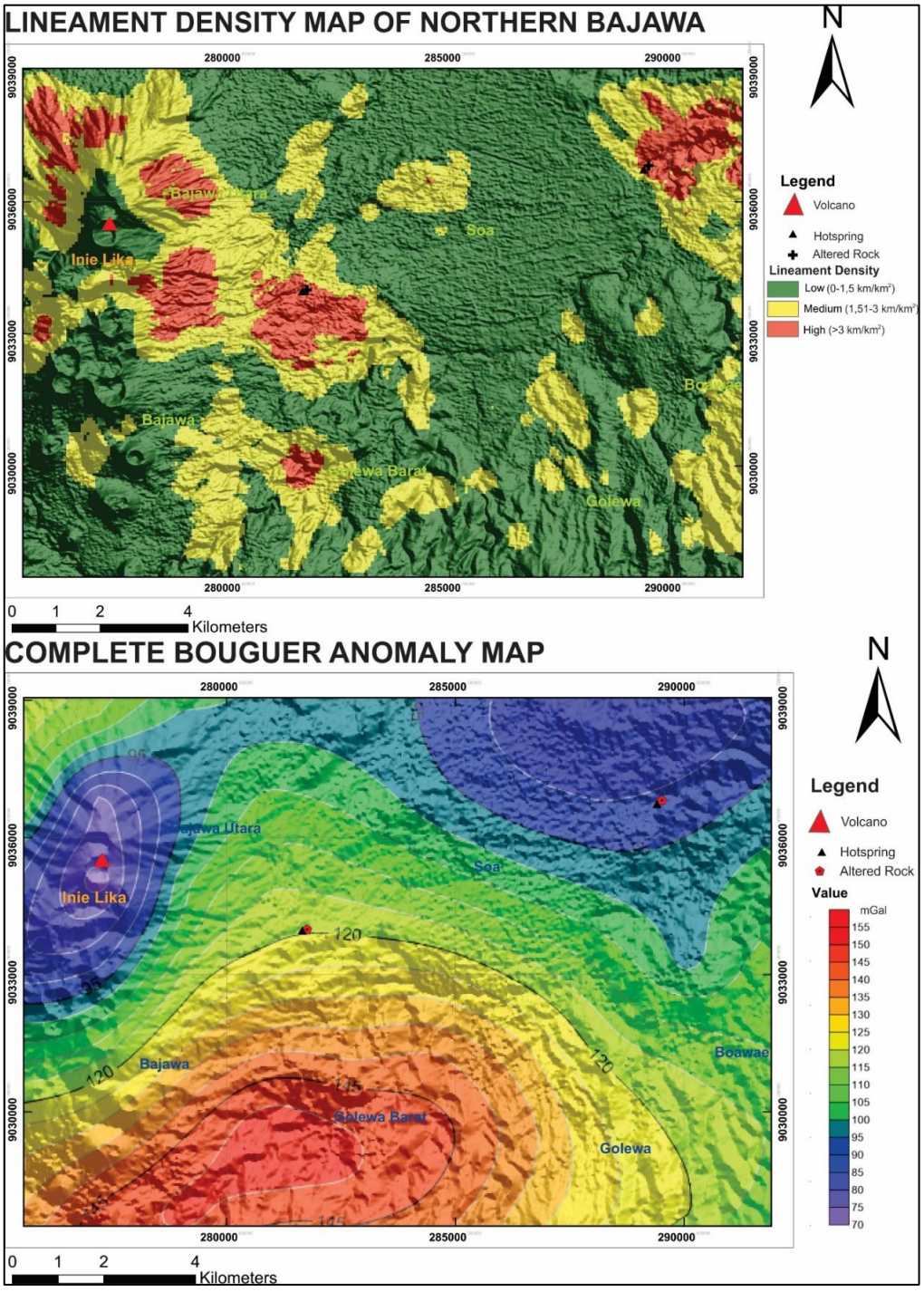


Figure 10: Comparison Linement Density Map and Gravity Map of Bajawa.

CONCLUSION

Based on the results of the analysis and interpretation carried out in the research area, conclusions can be taken as follows:

1. Geological conditions in the study area are volcanic cone complex regions composed of lithology originating from volcanic eruptions which can be divided into 3 units, namely Inelika lava and pyroclastic units, Golewa lava and pyroclastic units and Soa Lava and pyroclastic units.
2. Geothermal manifestations found in the study area in the form of hot springs and rocks that have undergone alterations in the Bajawa and Mengeruda regions, and the northern part of Soa.
3. The density of line density at the study site can be divided into 3, namely low, medium and high density where the highest density is in the northern part of Mengeruda and Soa areas where the area also has a low gravity anomaly.
4. Geothermal manifestations in the research location are in areas that have high straightness density so that it can be concluded that geothermal manifestations at the study site are associated with geological structure.

REFERENCE

Abrams, M., Hook, S., and Ramachandran, B, (2002), "ASTER User Handbook: Version 2". *Jet Propulsion Laboratory/California Institute of Technology.*

Cires, J., Marturia, J., De Paz, A., Casanovas, J., and Lleopart, A., (1997), "Digital Elevation Model, a Useful Tool for Geological Mapping, Some Examples from Catalonia, Servei Geologic de Catalunya", *Institut Cartographic de Catalunya.*

Hewson, R., Cudahy, T., and Shoji, M., (2003), "Evaluation and Processing of Satellite ASTER Image Data to Generate Accurate, Seamless Geological Maps for Regional Surveys". *CSIRO Exploration and Mining, ARRC, Western Australia.*

Kalinowski, A., and Oliver, S., (2004), "ASTER Mineral Index Processing Manual". *Remote Sensing Applications Geoscience, Australia.*

Koesoemadinata, S. Noya, Y. and Kadarisman, D., (1994), "Peta Geologi Lembar Ruteng, Nusa Tenggara, Skala 1:250.000", *Pusat Penelitan dan Pengembangan Geologi, Bandung*

Muraoka, H., Nasution, A., Urai, M., Takahashi, M., and Takashima, I., (1999), "A geothermal regime constrained by dike-shaped magma in Bajawa, Flores, Indonesia". *In: Abstract of 1999 Annual Meeting of Geothermal Research Society of Japan.*

Sulaeman, B., and Nasution, (2002), "Geochemical characteristics of hot spring water at Bajawa area, central Flores, Indonesia". *Special Publication: Indonesia-Japan Geothermal Exploration Project in Flores Island, p.153-171*

Sehah, F., A., K., (2012), "Pemanfaatan Data Anomali Gravitasi Citra GEOSAT dan ERS-1 Satellite untuk Memodelkan Struktur Geologi Cekungan Bentasari Brebes". *Indonesian Journal of Applied Physics Vol. 2 No. 2 halaman 184.*

Soengkono, S., (1999), "Te Kopia Geothermal System (New Zealand) – The Relationship between its Structure and Extent". *Geothermal Institute the University of Auckland.*

Yamaguchi, Y., and Naito, C., (2003), "Spectral Indices for Lithologic Discrimination and Mapping by Using the ASTER SWIR Bands". *International Journal Remote Sensing*, Vol. 24, No. 22, 4311-4323.

Engineering



This page is intentionally left blank



REPRESENTATIVE RESULTS AND COSTS SAVED: SLIM HOLE

Ingo P.C. Rott

PRAKLA Bohrtechnik GmbH
PT. BAUER Equipment Indonesia
Moorbeerenweg 3, D-31228 Peine, Germany
Email: ingo.rott@prakla.de

ABSTRACT

Slim Hole drilling for geothermal exploration does not have enthusiastic followers, partially due to the very slim approach (coring HQ and NQ) leaving little room to meet unexpected geological and technical challenges. In general, this means mobilizing a smaller core drilling rig first, and a larger production drilling rig later (driving costs).

Also, much criticized is that production testing results are not representative when produced from a very narrow well, mainly due to high drag and pressure losses of the steam on the upward flow, resulting in the necessity to ream the hole prior to production testing.

The solution could be to drill the coring section in a slightly larger diameter (e.g. SQ, i.e. a max. 102 mm core diameter with a max. drilling diameter of 6.1/2"). This would allow for larger final diameter completion, with reproducible production flow results (due to less pressure losses), as a 5" liner could be installed without having to ream the hole after coring! A larger liner size would also increase capability to perform downhole wireline logging for well characterization. Similar projects have shown possible cost reductions of approx. 30%. Furthermore, the core samples obtained by SQ size coring are less exposed to vibrations revealing more and better geological details and delivery more representative cores as to the competency of the rock. Larger pore spaces or even smaller cavities are more likely to be recorded correctly when drilling SQ cores. Nor are the cores influenced by mud ingression as smaller cores.

Modern, fully hydraulically driven drilling rigs today allow for SQ core drilling to 3500 m depths, with a final drilling diameter of 6.1/2", and are also capable of drilling production wells in standard or large completion to at least 2500 m depths. These new generation rigs are essential to further reduce daily operational costs (less fuel consumption, less wear and tear, less crew, etc.).

Keywords: Cost efficiency, drilling, slim hole

SLIM HOLE EXPLORATION

History has a subtle way of repeating itself, especially when it becomes habitual making mistakes due to taking short cuts. The slim hole approach prior to drilling the large diameter geothermal production wells, had been discussed as early as in the 1990's, only to be sacrificed and trash-canned in the 1998 crisis. One of the reasons of doing away with the slim hole approach had been massive idle capacities of large and heavy platform rigs that were desperately looking for new jobs, after the oil market had slumped considerably.

There were, and still are, a number of reasons to conduct slim hole exploration and production testing, before spending huge sums of money in geothermal large diameter production well drilling. The major reason is the apparent lack of detailed steam-pay-zone information.

All preliminary field surveys rely predominantly on surface geological survey, (including potential hot water or steam sources). In addition, geothermal gradient control wells are drilled (maybe as cored wells) and surveyed, and perhaps some seismic exploration was conducted as well. To put it bluntly, nothing more than just a few pokes into the ground. True enough, fast geothermal gradient rises over depth are a good indicator, that a potential heat source is reasonably near. And the geological information obtained from seismic exploration is invaluable as well. But all this information gives no clues as to pay-zone location, porosity, and permeability. Nor any information about how much steam is actually available for power generation.

These remaining question marks require an answer as good as technically possible, to allow for reliable and representative evaluation of the potential geothermal prospect, without which no power plant concept should be initiated.

Exploration Data Required

Ideally, the first source of geological information from the pay-zone would be collected in the form of cores. Cores are columns of rock obtained by cutting the rock with special bits that cut a ring.

If one would drill such a rock column from the start (i.e. from surface), then it is theoretically possible to obtain a continuous rock sample that represent the complete bore hole drilled. This core would be able to provide information about the rock type, the grains or minerals that make up this rock, their color and hardness, if any pore space (i.e. porosity) is available, and whether this pore space in

interconnected (i.e. permeability), allowing fluids or gases to flow through the pores. And ideally, what type of fluid or gas fills this pore space.

Other features that can be depicted from such cores are structural and tectonic geological features such as bedding planes, fault or shear zones, former erosion surface, or even contact zones with respective mineral alterations (or even recrystallizations) due to great heat influence. This list is far from being complete. But it already can provide a good idea how precious good geological information is.

Apart from the geological data required, a future power plant can only be planned when reliable (i.e. reproductive) production data of steam from the well can be obtained:

- How much steam flows from the pay-zone?
- How hot is it?
- At what pressure does this flow originate?
- What is the chemical composition of the steam?

All these above mentioned features, and others, need to be addressed and answers obtained, as they will have massive implications on the design of the complete power plant production cycle later on.

Coring Methodology

Core drilling has always been a somewhat special undertaking, as it always meant retrieving the rock column (at least parts of it) at regular intervals. Also the bits used can differ considerably, depending on the system as well as the rig type used. Conventional platform drilling rigs, being rotary table driven via a Kelly bar, are incapable of providing the fast rotation speeds as required when using diamond coring bits. As a result, roller cone bits were modified to not meet at the center, but rather pulled apart in such a way, that a rock column can be cut (Figure 1) at approx. 150 rpm max.

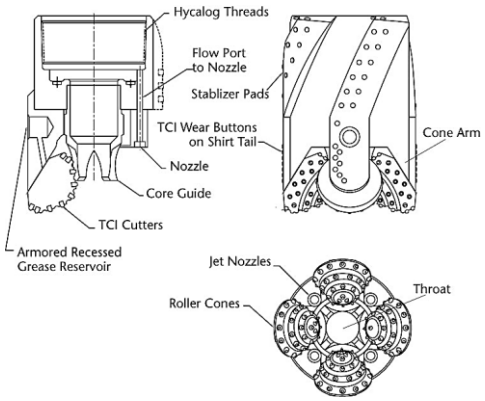


Figure 1. Schematic of the four rollers cone core bit (Graber et al, 2002, doi 10.2973 odp.tn.31.2002)

Alternatively, so-called coring rigs are capable of drilling at much faster rotational speeds, due to being top drive driven. Top drives are capable of rotating up to 1700 rpm and more. These very fast speeds allow the use of special coring bits that are made of diamonds imbedded in special matrixes. In comparison to the cone core bits, these diamond coring bits allow for considerably less thick cutting ration between outer and inner diameters (known as cutting kerf – Figure 2). The faster rotation speeds and the relatively thinner kerfs result in faster rates of penetration (RoP).



Figure 2. Diamond surface set coring bit (picture by the author)

Once the rock column had been cut, it would have been pushed into the respective core barrel. The core barrel would define the maximum length of the core that could be retrieved at one go. It is in this core retrieving method, that currently two different systems are distinguished.

Conventional coring

Conventional coring implies that once the core barrel has been drilled to be full, the complete drill string (consisting of bottom hole assembly – BHA – and all drill rods used) have to be pulled out of hole (POOH – brought back to surface). In deeper drilled wells, such a task can take up to a day. The then emptied core barrel with the complete BHA and drill string would consequently have to be reinserted into the borehole (run in hole – RIH).

The Oil & Gas industry is using this coring method, and it helps explain why coring is restricted to the absolute minimum. It is just too time consuming. In consequence, very long core barrels (up to 18 m in length), are being used, not necessarily implying that all core runs are that long, though.

This coring method is currently considered the only reliably safe way to drill a core when having to use a blow-out-prevention (BOP) system.

In other drilling scenarios, this system is also still employed, e.g. in the mining industry, when drilling

very large diameter cores (of up to more than 12" diameters). But these boreholes are generally not as deep, making round trips (POOH and RIH of the complete drill string), not such a time consuming issue.

Wire-line coring

In this method, as the name implies, cores are retrieved by a wire-line system. The basic requirement for this work, is that the drill rods are internally flush (i.e. there are no internal upsets or restrictions). Thus, it is possible to catch the core barrel with special retrieving systems using latches and overshots, and pull it back to surface by a cable, through the drill rods.

As can be seen, running round trips (POOH and RIH of the complete drill string) have become obsolete. In deep wells, e.g. with 3000 m depth, a core barrel run would be reduced to approx. 1 hour, instead of a complete day (24 hours – on a platform rig).

This system was devised in the mining industry, and exists in various sizes (core diameter and drilling diameter wise – Table. 1)

.

In the mining business, more often than not, time is money, exact geological results not necessarily required, as the deposit evaluation had already been conducted, and coring is then only used to determine the content gradient. In this special case, it is used to help in the decision-making process where to expand the mine next.

The coring diameters used in this case are HQ and NQ sizes. The main drilling parameter of these coring sizes is fast rotation speeds (especially in the context of hard rocks) up to 1400 rpm. Due to these high rotation speeds, and the associated vibrations in the drill string that go along with it, good core sample recovery is often not possible. All the more if the rock column drilled happened to be in a fault or shear zone, as the disintegrated formation will easily break up (caused by the vibrations), and all the fines are washed away by the mud stream.

Drill string weights, on the other hand are small, due to the fact that the drill rods are generally thin walled, and not only internally flush, but also on the on the outside (externally flush). The reduced weight is also an advantage, when drilling at high rotation speeds, but obviously the thin rods cannot take excessive torque, and tensile strain. Wear and tear is also high on the rods with these systems.

The SQ and PQ sizes are more commonly used in in Europe, and there in the geotechnical investigation of large construction sites (e.g. dams and tunnel projects). Obtaining detailed geological information is essential and of upmost importance in this case. Thus larger cores are preferred. The main reasons being better full core recovery, but also less impact of drill mud in the sample obtained.

These larger cores only require 200 to 350 rpm at the most to cut even hard rock. The depth range of the equipment required to drill the cores is also incredible, as it can be used to 2500 m (SK 4.1/4" B) or even 3000 m (SK 5.1/2" B). This is only possible due to the drill rods being externally upset. This means that the pin and box at the tool-joints have larger outer diameters than the external diameter of the drill pipe itself.

This feature results in larger cutting kerfs, as a larger annular space needs to be drilled to accommodate the external upset of the tool-joint. In consequence the RoP is increased slightly. There are more advantages than meets the eye, though.

- The upset tool-joints allow for less drag and wear of the drill rods when drilling inclined well trajectories.

Table 1. Classification of the standard (and not so standard) wire-line coring systems available (by the author)

Wire-Line Coring System	Core-Ø	Core-Ø	Drill-Ø	Drill-Ø
AQ (AWL)	27.0 mm	1.1 inch	48.0 mm	1.9 inch
BQ (BWL)	36.3 mm	1.4 inch	59.7 mm	2.4 inch
NQ (NWL)	47.5 mm	1.9 inch	75.4 mm	3.0 inch
HQ (HWL)	63.5 mm	2.5 inch	95.8 mm	3.8 inch
PQ (PWL)	84.8 mm	3.3 inch	122.3 mm	4.8 inch
SK 4.1/4" B - similar PQ	69,0 mm	2.7 inch	120,6 mm	4,8 inch
SQ (SWL)	102.0 mm	4.0 inch	146.0 mm	5.7 inch
SK 5.1/2" B - similar SQ	101,4 mm	3.9 inch	165 mm	6.5 inch
SQ - CSK146	102.0 mm	4.0 inch	146-165 mm	5.7-6.5 inch
"TQ" - CSK176	132.0 mm	5.2 inch	176-185 mm	6.9-7.3 inch
New, only by PRAKLA: "UQ" - CSK213 - "BCSK"	153.0 mm	6.0 inch	213.0 mm	8.4 inch

- The drill pipe and tool connection can take higher torque and tensile strain, which allows for deeper wells to be drilled.
- As the complete drill string is stiffer than that of the smaller coring sizes, vibrations (with all their consequences) are restricted, core recovery improved.
- Higher torque and more weight on bit can be tolerated by the system, and may be required in certain geological settings.
- The same drill pipe could also be used as directional drilling drill pipe, enabling costs to be saved in that respect.

Problems Encountered While Drilling

Regardless with which coring method the drilling was conducted, drilling a cored hole is always subjected to drilling complications. The first reason is that the drill mud has sufficient time to react with the freshly cut geology of the bore hole wall and at the bottom of the hole.

Especially more so during the long time it takes to retrieve the core sample. Here the conventional coring is even more of a disadvantage, as a round-trip of pulling out and running back in hole with the complete drill string always bears the danger that the bore-hole will collapse or fail due to instable geology, swelling clays or other reasons.

Even if the whole process of retrieving the core and returning the empty core barrel to the bottom of the BHA with wire-line takes only 6 to 8% of the time running a round trip would, the problematics remain the same. But there is one big difference – the mud column is not heaved or moved in such a fashion when running the wire-line coring system as would be when running a round trip. Especially when trying to save time by pulling the drill pipes fast, a surge could be caused by the piston effect of the drill pipes in the mud, and this could cause large portions of a weakened bore-hole wall to collapse.

Another problem encountered while drilling, especially in young volcanic areas, are complete drill mud losses. This can happen any time, regardless which drilling method was currently used. In coring this could be especially drastic, as the drill mud is not only required to move away all the cuttings, but also urgently required to lubricate and cool the drill bit, due to high rotation speeds used to core.

A hot running diamond coring bit will make the bit matrix (in which the diamonds are embedded) hard and brittle, with the result of the cutting kerf of the bit breaking up, and then there are very destructive elements in the hole, that contribute to extreme expensive wear and tear of the BHA.
As long as fresh water can be supplied to a well, this problem of a bit overheating, can be assumed negligible. The other problem remains, though: What to do with the cuttings being generated by the rotating bit? Ideally the continuously fresh water being poured into the well will follow some passage, as after all, there is a complete mud loss. Should this passage be large enough to allow for the cuttings to be carried away in as well, then continued drilling is possible.

The problem is rather when this is not the case. On the one hand, the accumulating cuttings at the bottom of the bore hole could contribute to clogging the passage of mud loss, which would enable mud circulation again. More often than not, this is not the case. Then there is the danger of running the BHA in cuttings-remains and eventually getting the complete tool string stuck, even as far as losing the expensive BHA completely.

The next question would be how could such a hole be saved? By milling? By side tracking? Or must such a well be abandoned completely? None of these answers are satisfactory. So, drilling operations are keen on having NOT to make such a decision, and would rather stop drilling in time when complete mud losses occur.

This would generally call for the cored hole to be cemented (hoping that this measure would clog the loss passage, and/or have the hole reamed (enlarged), so that an intermediate casing could be installed.

The enlarging of a hole sounds easy, but is generally not. For one, it depends a great deal on how big the reaming steps are, and how small the pilot hole is. The problem with having drilled HQ (3.3/4" max. drilling diameter) and NQ (3" max. drilling diameter) coring systems, is that these very small pilot holes may have to be enlarged to as big as 12.1/4" or even 17.1/2" (to allow for installation and cementation of 9.5/8" or 13.3/8" casings respectively).

Due to the mentioned very small pilot holes, the enlarging process will have to be conducted in at least two steps by so-called hole openers (Figure 3). Due to the massive increase of annular space, the mud pump capacities have to be increased as well (generally not the issue on a deep drilling site). The upstream velocity of drill mud should be calculated to be 0.5 to 1 m/s in the larger annular spaces. In the pilot hole this would lead to considerably more than 1.5 m/s, which could cause additional well bore erosion problems, that will eventually lead to wall collapses.

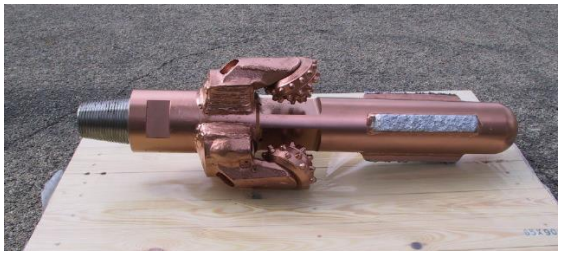


Figure 3. Hole-opener bit with pilot bull-plug (picture by the author)

The hole opener in Figure 3 is not ideal, for one feature: It does not have a proper pilot bit, which could clean out back-fall in the pilot hole, which is sure to happen in a reaming process.

Enlarging a bore hole with hole-openers that are equipped with a pilot bit of respective size (Figure 4) is thus essential. If the enlarging is conducted without any guidance, the pilot hole trajectory will be lost. Drilling a larger hole with a regular type of tricone roller bit (without any pilot as guidance) will lead to a newly drilled hole, with a different well trajectory. This hole could be considered unsafe, as the initially drilled portion was never sealed off properly, and could become a new pathway for gases, that would endanger the safety of the complete well after it goes in production.

Drilling the coring section with the larger diameters of PQ or even SQ would make the enlarging of the bore-hole to 12.1/4" or 17.1/2" indeed easier, and this could be conducted in one step.

Last but not least (and this list is for sure not complete, only having mentioned the most common causes and cures for drilling problems), the unexpected encounter of any type of a gas reservoir. This is a standard situation in volcanic settings, and it is the reason why also top-hole sections are required to be drilled with some sort of BOP protection.



Figure 4. Hole-opener bit with pilot roller bit – rollers and cones can be exchanged when worn down (picture by the author)

PROPOSAL SLIM HOLE APPROACH

Hitting a gas reservoir will automatically call for the installation and cementation of an additional casing. As this may happen in a coring section, the challenge here would be to find a way to still enlarge the hole to allow for further coring down the hole. The smaller the coring system chosen to start off with, the less chances are left to continue coring. This again would sensibly call for a larger coring diameter to start with (i.e. SQ size with SK 5.1/2" B, and max. 165 mm drilling diameter), as then, all smaller sizes could still be used to get to the planned pay-zone depth. Especially, if the gas encounter already happens at 200 m depth, as was the case in Mataloko (NTT).

Taking the options and advantages of the systems mentioned earlier into account, a revised concept of the slim hole approach for geothermal exploration and production test drilling can be considered (Figure 5).

In this concept, the initial well diameters for conductor and surface casing installation and cementation are close to large production well diameters. These were considered only to enable further telescoping of casings further down the well, while ensuring large core drilling abilities in the upper reaches of the well, but also in the lower part with the potential pay-zone interest. A large core drilling diameter in the pay-zone will render any reaming obsolete, as with a maximum possible drilling diameter of 6.1/2" (165 mm) may still allow for the installation of a 5" liner.

The well sketch presented in Figure 5 gives a number of options still allowing for larger core diameters to be drilled as far down as the proposed pay-zone. The open hole diameters presented are the general standard diameters drilled for the installation and cementation of the respective casing sizes.

Two different approaches for conductor casing depths have been presented, to allow for difficult overburden systems to be cased. Also, different drilling methods and the use of different type of drilling rigs (e.g. a piling rig to drill and case the conductor casing down to 80 m in one go, using an extendable, telescopic kelly bar and a cased auger drilling system) can thus be considered. Of course, a deep conductor could be drilled using direct mud circulation method, or even a mud-rotary reverse circulation method (e.g. using air-lift).

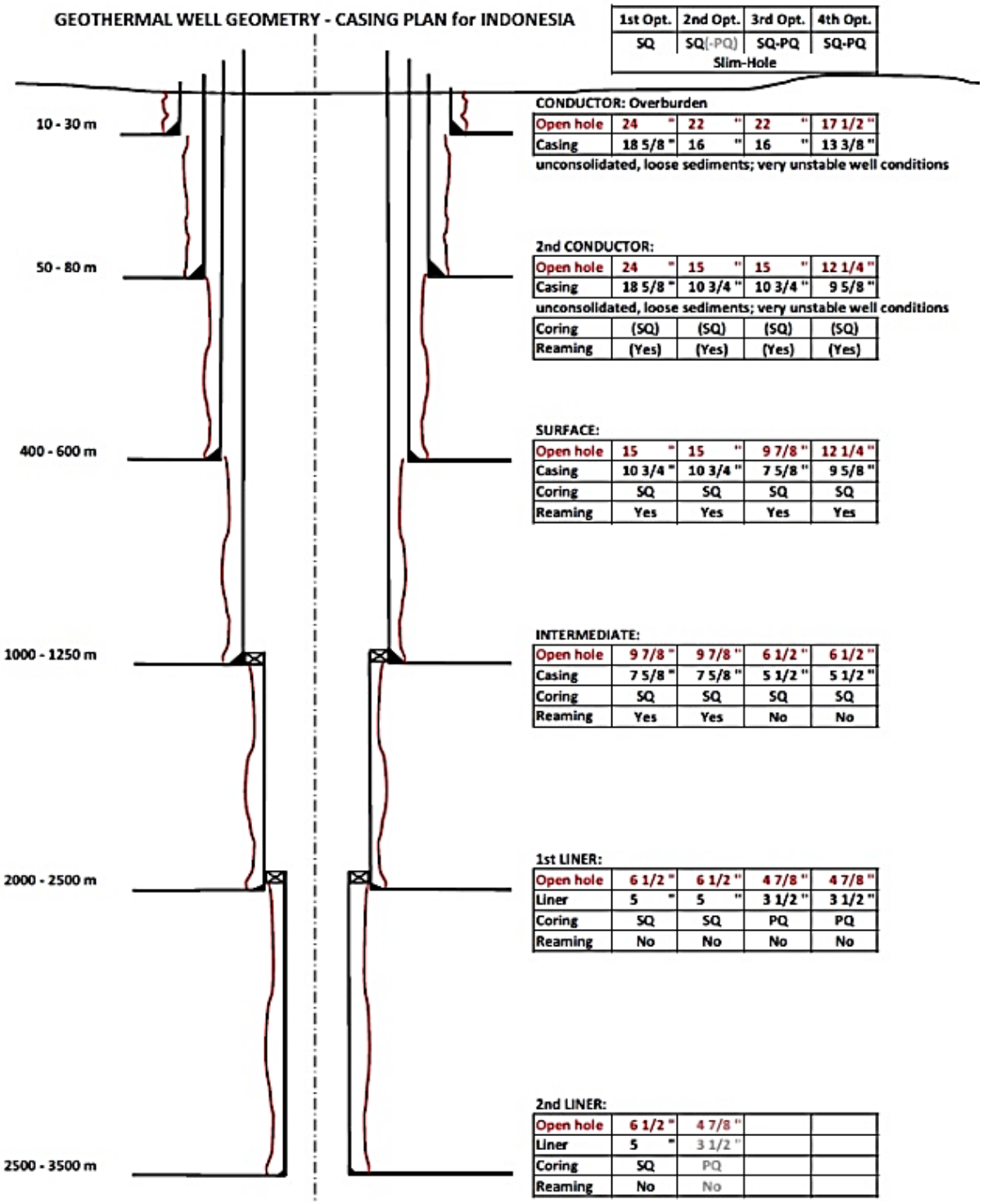


Figure 5. Suggestion for a slim hole using SQ coring (drawing by the author)

In the case of an overburden system being made up of boulders, conventional drilling will be difficult, then down-the-hole hammer drilling systems could be used, that simultaneously pull a casing into the hole along with the bit. Similar approaches can be considered for the drilling of the surface casing and later intermediate casing sections as well, geology and BOP requirements allowing.

Should these upper reaches of the proposed well be cored already as well, then the occurrence of any gas reservoir would be known and thus reaming jobs could be reconsidered in alternative drilling methods.

Especially the enlarging of a SQ core well, to larger diameters such a 17.1/2" would be possible in one step, using multi-staged hole-opener bits together with the mud rotary reverse circulation air-lift

drilling method. This drilling method will be described in the next section.
The coring in large diameters to deep depths, is standard for geotechnical investigations in Europe. There are the number examples where SQ coring sizes have been taken as deep (or long) as 3500 m for the investigation of various Trans-Alpine basis tunnels such as Mont-Cenis, Simplon, Gotthard, Brenner and the Semmering Projects in France, Switzerland, Italy and Austria.

Large diameter cores provide more and better detailed geological information, than smaller core diameters. This is valid as well when drilled in fault or shear zones, or when having to pass through land-slides. The core recovery can be 95% or more, even when drilling through inhomogeneous geology (e.g.: fractures in hard rock filled with clays), with the fracture fillings being documented as well.

The main reasons hereof are slower rotation speeds, lesser vibrations on the drill string, and lesser influence of the drill mud in the core sample.
If a mud can ingress 10 mm deep into the core while drilling (due to geological features such as cracks, cleavage, fractures, pores, etc.), drilling a HQ core, would have only roughly 40 mm of the central core without influence of the mud, of 63.5 mm core diameter (this is roughly 53% of the core cross-sectional area!). Drilling a NQ core would have more than 66% influenced by mud! And a SQ core would only have some 36% influenced by the mud. Should the sample quality be so bad (i.e. weak, unconsolidated, etc.), it is easy to imagine why such smaller core sample get washed away, disintegrated during drilling. The geological information being lost forever.

Good core quality is also of a great advantage when it comes to calibrating circumferential bore-hole imaging logs, so than when later core losses occur, geophysical logs can still provide some of the information lost.

Moving from the geological side to the drilling side, larger drilled coring diameters also lead to the possibility of installing larger production test liners. And this without having to enlarge the existing hole. Again, having a larger hole has advantages for better geophysical logging results (especially if logging is required in a cased hole scenario, i.e. after completion of the well), and of course in obtaining representative and reproductive production test results.

The larger the production test liner can be, the less pressure losses are encountered when conducting production testing. Thus the cored exploration well can be used for production testing and possible costs of a third well saved (i.e. a saving of 33.3% without taking any operational costs saved into account, due to not having to ream the final section).

Nonconventional Drilling Methods

The fact that the first geothermal wells drilled were always drilled by specialists from the Oil & Gas field, quickly explains why the Oil & Gas standards are omnipresent. Due to the partially very hazardous environment in which Oil & Gas but also geothermal well drilling have to be conducted in, it is understandable, why this fact was never challenged. Pressurized gases (Methane, H_2S-gas, CO and CO_2 gas and steam) require special blow out prevention measures. All the more so, as every one of these gases can kill, being prone to ignite easily, being toxic, being pressurized and/or very hot, or due to any combination of these features.

As soon as dangers are involved, that can cause harm to man and equipment, the requirement for strict standards and stringently enforced HSE codes is a prerequisite. But the relative dimensions of the dangers possibly encountered also needs to be respected.
Gas reservoirs encountered at 200 m depth, can be fatal, but are not necessarily large. Production testing of these occurrences could be a thing to consider (especially in the case of methane gas, as this could be a commodity to exploit later on as well).

If coring was conducted from a very early point of the well design, e.g. right after the setting of the conductor casing, then information obtained during coring, can be taken into account and allow for possible changes in the drilling procedures for the next hole-opening stage. Here the context of not having encountered any gas of sorts can be very cost saving, if reacted to.

It also has to be taken into account that the steam (which is the actual target of drilling a geothermal production well) is not exposed to the extreme pressures as is the case in petroleum and natural gas reservoirs. More often than not, a steam reservoir does not have pressures that exceed 3000 psi (206 bar).

These relatively low production pressures also need consideration when killing a well, e.g. for work-over processes. The well activation by swabbing could be ineffective, as the killing process could have clogged the major passages of the steam deep in the formation, and due to the restricted formation pressure, these obstacles will not be mobilized.

Another issue not sufficiently investigated to date are the effects mud additives have when coming in contact with very hot (>200°C) and heavily mineralized steam. Under certain conditions the mud could bake and become an insoluble ceramic sort of clogging agent.

The Oil & Gas drilling experts are familiar with underbalanced drilling methods, such as aerated

services, that are taken into account, when the situation allows for these to be used. Due to the extra equipment and service personnel required, this becomes a cost driving issue.

Changing the approach in such a case to a mining oriented way of drilling (as had been the case in wire-line coring already), more costs could be saved for individual stages of well completion.

Reverse circulation air-lift drilling

One of the drilling methods mentioned in this article demonstrates perfectly the cost-saving issue while being more efficient in large diameter drilling as well, at the same time. This is mud rotary reverse circulation drilling using air-lift.

This drilling method is used in drilling large diameter deep de-watering wells or for bulk-sampling in the mining sector. While it does require specialized equipment, the costs of this can be very moderate, and are required to be purchased only once.

Due to the fact that the Oil & Gas industry is always drilling with BOPs, this drilling method was never on their mind. Reverse circulation implies that the downstream side of the mud is in the annular space, and the upstream side (with the cuttings transport back to surface) is inside the drill string, the mud passing through the drilling bit.

This system can work with negative pressure systems (e.g. suction drilling) but these systems are generally restricted to max. 100 m depth. Conventional pumps cannot be used in this system of drilling, as is the case in direct circulation drilling, due to the downward flow in the annular space not being sufficiently confined.

And it is not required to be so. If air were to be introduced into the system, inside the drill string, then this air would instantaneously alter the density of the drill mud at that point. The less dense drill mud would immediately try to rise fast, to be on top of the heavier mud, that is currently overlaying it. The void generated due to the less dense mud rising, is immediately filled by higher dense mud from below, based on the principle of communicating columns. Continuous influx of air will complete the circulation, without the use of a pump (Figure 6).

This system can work from depths of 30 m to more than 1500 m, and can be used to drill any size, but is most efficient when drilling 12” (300 mm) or larger. There is no real limit. A mining shaft had been sunk in unconsolidated rock with a drilled diameter of 8m using this drilling method.

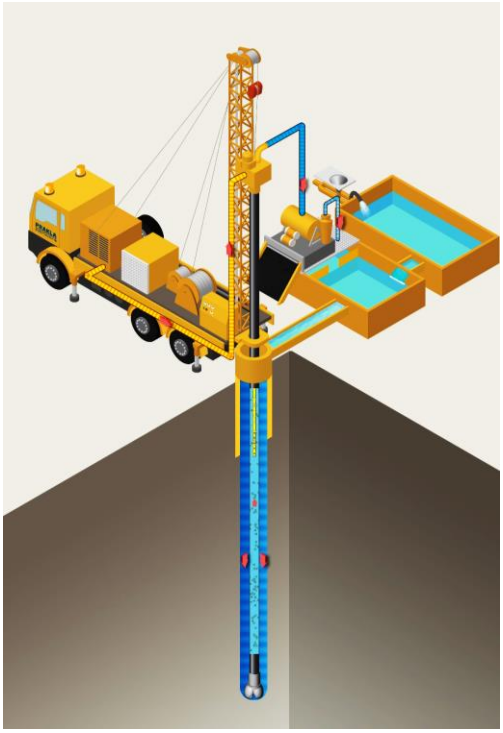


Figure 6. Schematic presentation of Mud Rotary Reverse Circulation Air-Lift Drilling (© by PRAKLA)

Equipment-wise there are two different approaches as how to drill reverse circulation air-lift. The most common method is using respectively dimensioned dual walled drill pipe, whereby the air is passed downwards in the annulus between the two pipes, and injected into the inner pipe by special cross-over- or injection subs. Alternatively single wall internal flush drill pipe can be used as well, but emphasis should be laid on the fact that the internal ID should be a maximum. In this case additional 1” to 2” air inlet pipes are required to get the air to where it is needed. This second method is less expensive in the original purchase and more flexible in how deep the air exit can be placed.

Regardless which method is chosen in the end, the internal free passage of the wash-pipe at the top drive must be as large as possible (where-by an ID of 150 mm is considered as the minimum requirement. If dual walled pie is used, the top drive will require an additional air-supply swivel. In case the air inlet pipe is used, an adjustment of this air-pipe will be required. One solution is to install it by a flange at the discharge bend of the swivel.

Ideally the annular space should be considerably larger than the drill pipe inner cross-section, because in this case the downward flow is relatively slow (less than 0.4 m/s) and laminar, while the upstream flow inside the drill string can be 3-5 m/s of even faster. The flow inside the drill string is turbulent, especially in the aerated part.

The laminar flow in the annular space is good, as it allows for a stable filter cake to establish itself, and there is no erosion of the borehole wall. The situation is quite the contrary inside the drill string, very turbulent, and fast flowing. But as the system is confined, the borehole is not endangered by these turbulences.

The drill mud, including the air and the cuttings are transported through the wash-pipe of the top drive, and further a discharge hose to a pacifier cyclone that empties onto a shale shaker over a mud tank or pit.

This method is most economical, due to the fact that no pump is involved with parts exposed to abrasive cuttings, thus not requiring any replacement of wear and tear parts. The lifetime expectancy of tricone roller bits is increase by up to 10% due to the simple fact that the cuttings are removed immediately after being produced, which in turn is due to the extreme fast acceleration of the drill mud at the bit entering the drill string, caused by the injection of air further up the string.

In conventional direct circulation drilling, especially when drilling large diameters in weak, unstable or unconsolidated geological conditions (often the case in surface casing drilling), the tricone roller bit is exposed to frequent regrinding of the cuttings as the upstream velocity is too slow to allow for sufficient fast upstream transportation of the cuttings to surface. The reason here for can be found in the fear of eroding the borehole wall due to turbulent or too fast flow of mud, or insufficient pump capacities.

The air requirement is a function of the static water-level of the groundwater. If the groundwater level is not deep than 60 m below surface, then a single stage compressor is sufficient, at deeper groundwater levels, a dual stage compressor will be required.

As mud loss zones are frequently associated with zones of high water permeability, this drilling method could actual still work when conventionally there is a mud loss, as the pressure in this system is restricted to the hydrostatic pressure of the column of mud only. Water flowing to the well can be used and lifted as well.

The most drilling problems encountered when drilling through young geological formations, especially in a volcanic surrounding, are encountered within the first 600 - 800 m drilled. This corresponds to the conductor, surface and intermediate casing sections. Reaming or hole-opening jobs in these sections are even more critical. But with this reverse circulation air-lift drilling methods, there is a large chance that these difficult passages can be mastered with ease.

Another reverse circulation method

Reverse circulation (RC) drilling is also possible with down-the-hole (DTH) hammer equipment to enlarge a pilot hole to casing installation diameters. In case it is essential to use dual walled drill pipe, as the air is require to be brought to the tool (i.e. the hammer). While there are reverse circulation hammers available in the market, it is not necessarily required to use these, as due to their design they are prone to have excessive wear and tear internally in the hammer due to the return passage. A more economical solution would be to use a regular DTH hammer (for direct circulation) in connection with a cross-over-reentry sub with a disc-packer over the hammer, to take the cuttings and the return air-stream upwards back into the inner if the dual walled drill pipe.

Operationally, this drilling method allows for considerable reduction of the amount of compressors required to lift the cuttings back to surface. And operation cost wise, the compressors are the most expensive cost driver in DTH operations, due to their extreme high fuel consumption.

Another invaluable advantage of drilling RC DTH hammer is that when returns of cuttings are no longer possible drilling DTH conventionally (due to circulation losses on the way up), RC drilling allows for cuttings to be transported back to surface. This ensures a safe continuation of drilling, without any danger of losing the drilling string with its BHA, caused by re-sedimentation of the cuttings behind the tool.

DTH hammer bits can be obtained as hole openers as well, with a TCI-studded bull-nose to act as guide and still being able to remove filled passages in the pilot hole if required. This ensures that the original well trajectory is maintained during the enlarging process.

CONCLUSIONS AND SUMMARY

Geothermal development projects in the past three decades in Indonesia have shown that the preliminary geological survey have not provided sufficient geological information to enable a reliable prediction of potential production values. Not even the location of the anticipated steam reservoir (pay-zone) could be determined with certainty at all times. In consequence more emphasis needed to be laid in obtaining more detailed geological and production relevant information when starting to develop a new geothermal field.

Wireline diamond coring technologies are the obvious solution to get at invaluable first-hand geological information, directly where the drilling takes place. As exploration coring surveys conducted during the preliminary survey never were

projected to go into the actual steam reservoirs, this missing information needs to be collected urgently, before designing potential production wells and power plant units. Thus, it is essential to obtain high quality geological data, as near complete as possible and in sufficient quantities to enable reliable analysis.

With these pre-requisitions, a larger coring diameter is more likely to provide such cores that allow more detailed analysis. Ideally a SQ coring system designed for deep exploration, even in deviated well trajectories, would be the preferred choice by geologists.

Such a SQ coring system could be the SK 5.1/2" B system introduced, that drills a 101.4 mm (4") core with a 165 mm (6.1/2") OD drilling bit. References made in difficult geological settings, for geotechnical investigations in Europe have already proved the reliability of this system. The advantages of drilling such a large core are as follows:

- Ensured larger proportion of core recovery (exceeding 95%).
- Rock quality designation (RQD) – a measure of degree of jointing or fracturing of a rock – is not lowered artificially due to massive vibration of the drill string disintegrating the core.
- The influence of drill mud on the core is reduced by up to 50% or more (depending on coring diameters compared), thus causing less sample material of core to be lost.
- Open hole geophysical surveys can be conducted with robust Oil & Gas equipment.
- Installation of a 5" production liner for reliable and reproducible production testing analysis is possible without additional enlarging of the core bore.
- Less drag and pressure losses during upstream production testing due to the larger liner ID available.
- Post completion geophysical well characterization logging is possible with proven tools already on the market.
- Redundancy coring systems (such as a PQ system with a 69 mm (nearly 2.3/4") core and a maximum outer drilling diameter of 120.6 mm (4.3/4")) would allow to use the SQ drill string as a temporary casing and continue top core with excellent results.

The costs saved with having taken this approach could amount to more than 30% of the price for drilling a new slim hole production well due to reliable systems being used, and due to reaming jobs becoming obsolete. Especially enlarging of well bores being a very delicate and critical process, resulting in more well losses than drilling the planned final diameter from start.

Modern, fully hydraulically driven drilling rigs today allow for SQ core drilling to 3500 m depths, with a final drilling diameter of 6.1/2", and are also capable of drilling production wells in standard or large completion to at least 2500 m depths. This type of new generation rig (e.g. the PRAKLA RB-T 100 or RB-T 135) is essential to further reduce daily operational costs (less fuel consumption, less wear and tear, less crew, easier and faster mobilization and demobilization, etc).

Together with the possibility of conducting non-conventional reverse circulation drilling methods to ease enlarging well-bore diameters in the top hole section, these new rigs prove daily that they are truly multi-purpose drilling rigs, capable of rigging down, moving location and rigging up ready to spud with a single day-light shift.

REFERENCES

Arnold, W. [Editor] (1993), "Flachbohrtechnik [Translation: Shallow Drilling Technology]", Dt. Verlag f. Grundstoffindustrie, Leipzig, Stuttgart, 968 p., 1st Edition.

Graber, K. K., Pollard, E., Jonasson, B., Schulte, E. (2002), "Overview of Ocean Drilling Program Engineering Tools and Hardware," Technical Notes 31, doi 10.2973 odp.tn.31.2002.

GEOCHEMISTRY ROLE IN GEOTHERMAL BINARY BRINE IN THE FIRST INTEGRATED COMBINE CYCLE POWER PLANT OPERATION IN INDONESIA: SARULLA CASE STUDY

Muhamad Andhika, Mona Natalia Siahaan, Sanif Isa Aritonang, Rizvy Asnin Nasution, Sahat Berutu

Sarulla Operation Ltd.
Jalan Pahae Sipirok Sigurung-gurung Pahae Jae, Tapanuli Utara, Sumatera Utara – Indonesia
Email: muhamad.andhika@sarulla-geothermal.com

ABSTRACT

Integrated geothermal combine cycle unit (IGCCU) powerplant has been installed for over 1 year in Sarulla and it is the first IGCCU that operate commercially in Indonesia. IGCCU in Sarulla consist of one steam turbine generator (STG), 4 units of steam binary (bottoming), and two units of brine binary with net total of generation is 110 MW. Compare to conventional geothermal power plant, which only utilize STG, IGCCU can produce 45% more power. Binary brine, as part of IGCCU, is a game changer since it can be implemented either in high temperature or medium temperature geothermal system thus binary brine has a big opportunity to use widely in Indonesia. To generate additional load, in IGCCU, heat from brine is extracted first before injected to reinjection well and therefor increase silica deposition risk. To overcome this problem, Silica saturation index (SSI) should prevent to exceed 1 and prolong induction time. The effort to hold up SSI bigger than 1, is using 2 ways. First is by applying pH modification method which lower the pH of brine until 5, from 6.7, by adding sulphuric acid (H2SO4) to the brine in Brine binary inlet. To ensure homogenic mix of brine and H2SO4, two static mixers was used. The pH is monitored very closely and online by using pH monitoring system that implanted after static mixer pipe but before entering brine binary. Second effort is mixing output of binary brine, that already cools down at 130 °C, with condensate from bottoming, which has temperature 80 °C. This treatment will be able to dilute dissolve Silica, since condensate only contain less than 0.1 ppm of Silica, and in turn decrease SSI value. As pioneer of IGCCU user, the experience of binary brine operation in Sarulla is very valuable for the development of binary utilization in Indonesia. The technology is adaptable to high temperature type and increase the efficiency of geothermal fluid consumption compare to conventional geothermal power plant.

Keywords: Geochemistry, binary power plant, Sarulla

INTRODUCTION

SIL (Silangkitang) Geothermal Power Plant is one of Sarulla Operations Limited (SOL) Geothermal Working Area, which located in Tapanuli Utara District. It is approximately 300 km southeast of Medan, in North Sumatera (Figure 1). Silangkitang power plant has generation for 110 MW, consisting of 4 production wells and 9 reinjection wells (Figure 2).

Geothermal system is characterized with high temperature neutral chloride system. It has liquid dominated wells, with highest wells is above 300 C. This field is stretching in Sarulla graben along the main trace of the Great Sumatra Fault (GSF). Permeability of the system is strongly controlled by this GSF. The fumaroles and springs are also found throughout GSF around power plant area.

GEOTHERMAL POWER GENERATION SYSTEM

Single Flash

Most of geothermal site that have been used to generate electricity in Indonesia is high enthalpy type since it produces enough steam to fulfil its economic feasibility. Therefore, single flash system is the primary power in Indonesia geothermal industry and all geothermal power plant rely only it to generate power before Sarulla field was operated. Single flash uses only steam and all the brine is reinjected directly after separated from steam. This reinjection type known as hot reinjection system. The benefit of hot reinjection system is it can avoid cooling of the reservoir and reduce the risk of silica scaling.

Geothermal Binary plant

The first commercial Geothermal binary power plant is operated in Kamchatka site, Russia (Dipippo, 2007) and it runs for many years and prove that the binary system is reliable. The most common type of binary is organic Rankine cycle or ORC. It uses organic fluid to as working fluid after extract heat from geothermal fluid. Nowadays, ORC not only make use of brine to extract heat but also use steam. The most common organic fluid that use is pentane. Since Sarula use Ormat ORC, then its units named OEC (Ormat energy converter) bottoming for binary steam and OEC brine for binary brine.

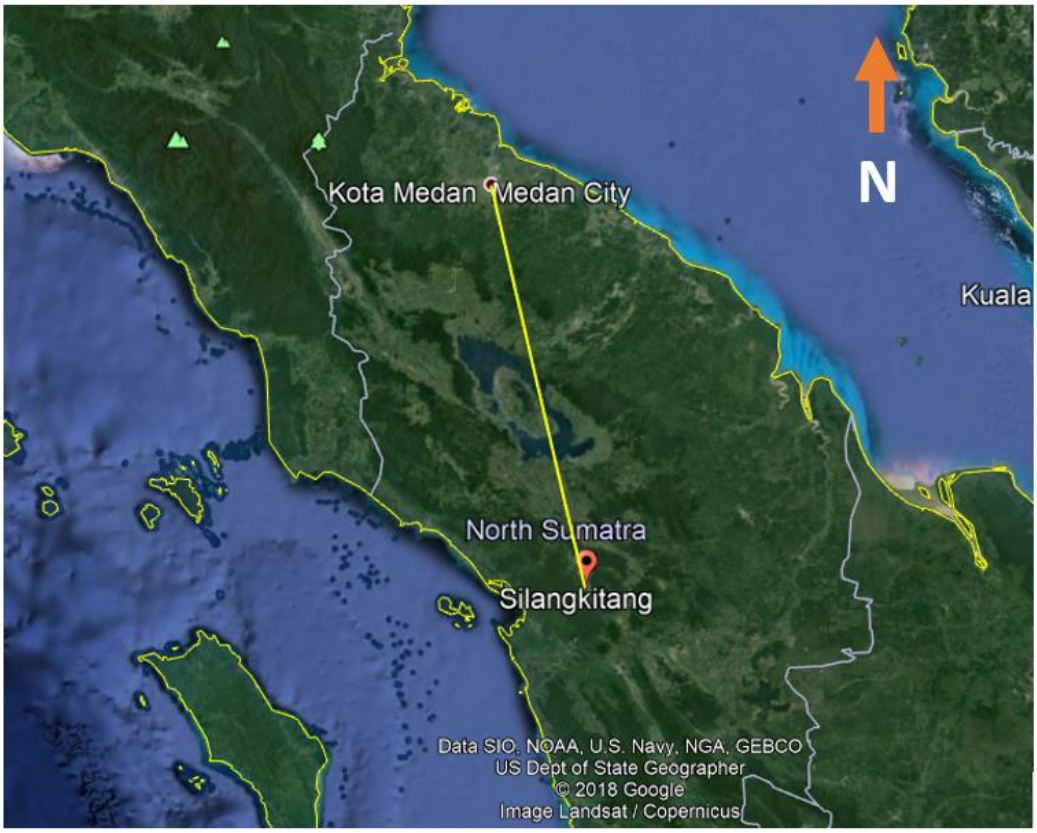


Figure 1: Location of map (source: google earth)

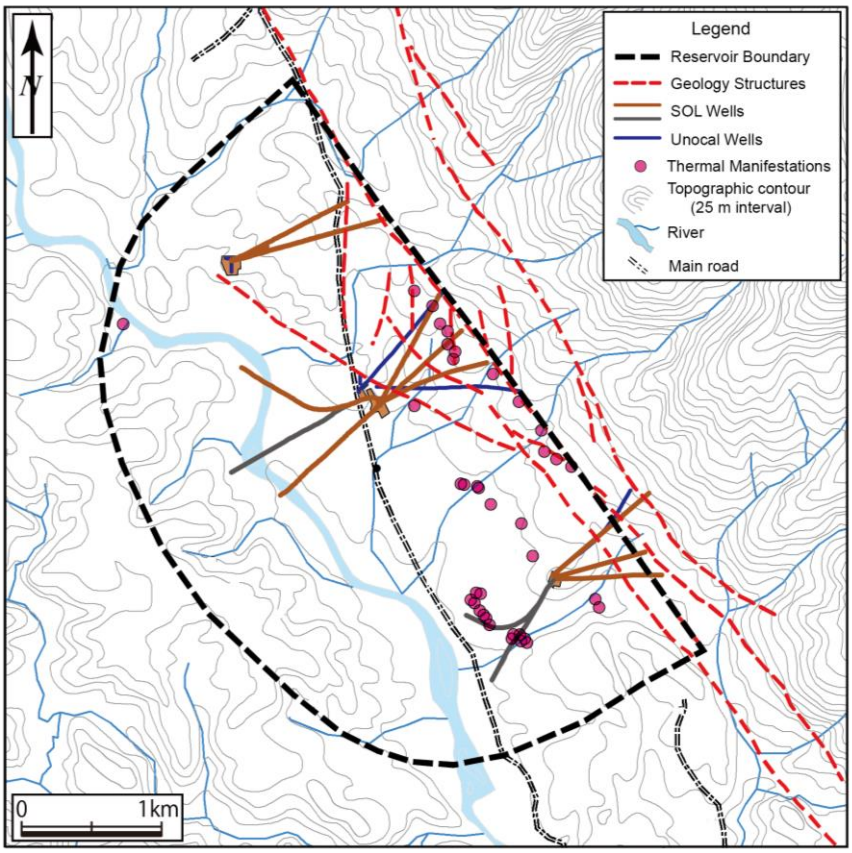


Figure 2: SIL base map with well directions, reservoir boundary and geology structures

Integrated combine cycle unit

To extend efficiency and generate more power, the concept of integrated combine cycle unit (ICCU) was introduced. Sarulla is the first site that installed and operate ICCU consisted of 1 steam turbine generator (STG), 4 OEC bottoming, and 2 OEC brine.

BINARY BRINE IN SARULLA

The application of ICCU in Indonesia open many opportunities including knowledge, best practice operation, and a new level of efficiency. Problems that arise during operation of ICCU bring us closer to better knowledge on handling complicated geothermal operation such as ICCU. One of the prominent problems that should be handle properly is silica scale during heat exchange between brine and pentane in binary brine.

Silica saturation problem at Binary brine

Silica solubility depends very much on temperature. This discussion was stressed up earlier by Fournier & Rowe (1977) as shown in picture below which took from their paper (Figure 3).

From Figure above, we understand that the solubility of silica will increase with increasing temperature and decrease with decreasing temperature. the effect of temperature is vital for silica solubility. When silica concentration beyond its solubility, then silica will become over saturated. Over saturation condition should be avoided otherwise it will lead to silica precipitation.

The main process of binary brine is heat transfer from brine to pentane. After heat transfer process, brine temperature will decrease significantly from 209 °C to 142°C. This situation will definitely give rise to silica over saturation condition (Figure 4).

Over saturation condition certainly will result in higher Silica saturation index (SSI). From Figure 5, we can see that SSI in binary outlet already higher than 1 which can induce the formation of silica scale inside of heat exchanger tubing in binary brine unless no action is being taken. The effect even can be more devastated in reinjection header since cooler condensate waste from binary steam is being added to the brine which decrease the fluid temperature even lower.

pH modification

The opportunity to generate more power with binary brine comes with bigger risk of silica scale inside of heat exchanger, reinjection pipeline, and reinjection well. To overcome this problem, pH modification has been installed in binary brine inlet. Before brine entering heat exchanger, brine pH was modified to 5 by using H2SO4. This is very tricky since we need to be careful with pH value. If we are adding many H_2SO_4 to the brine, then the brine pH will be acid and it can corrode the pipeline and binary brine tubing. If we add it too small and the pH is higher than 5.5 then we increase the possibility of silica scale formation.

Some geothermal expert already tested this method and in general they come up with good results. It is well known that lower pH can inhibit the formation of silica scale even though it cannot increase its solubility as shown in Figure 6 from Kevin Brown paper.

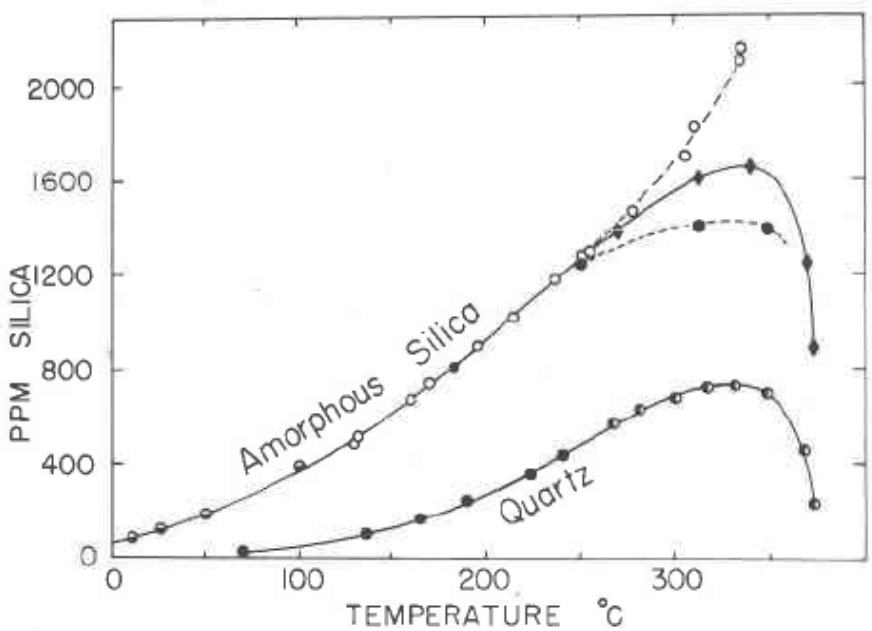


Figure 3: Image copy from Fournier and Rowe paper on Amorphous Silica solubility dependent on temperature

Field experiment from Carlos E. Guerra and Patricia E. Jacobo in Berlin and Ahuacupan field shows that in pH 5, silica precipitation can be delayed for 2 hours (Grassiani, 2000) as shown in Figure 7.

From our monitoring, when brine pH is controlled properly, the fear of silica precipitation can be set aside. The change of silica concentration in Brine during pH modification can be seen in Figure 8.

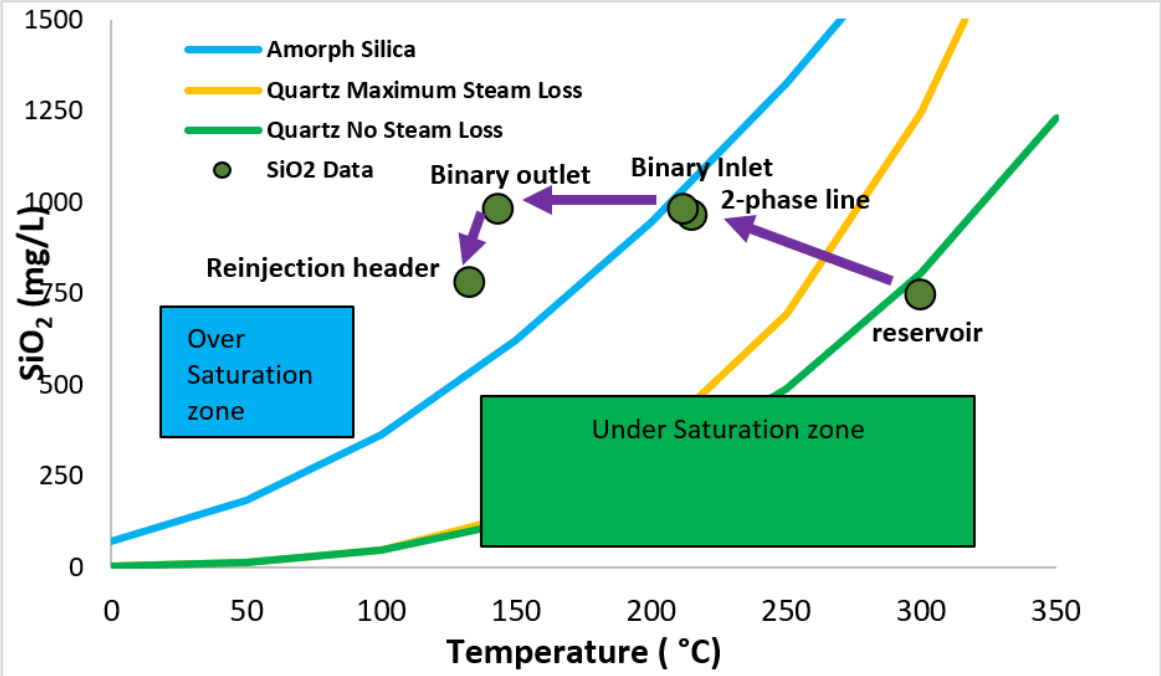


Figure 4: Temperature effect on Silica solubility (modified from (Utami, Herdianita, & Atmaja, 2014)

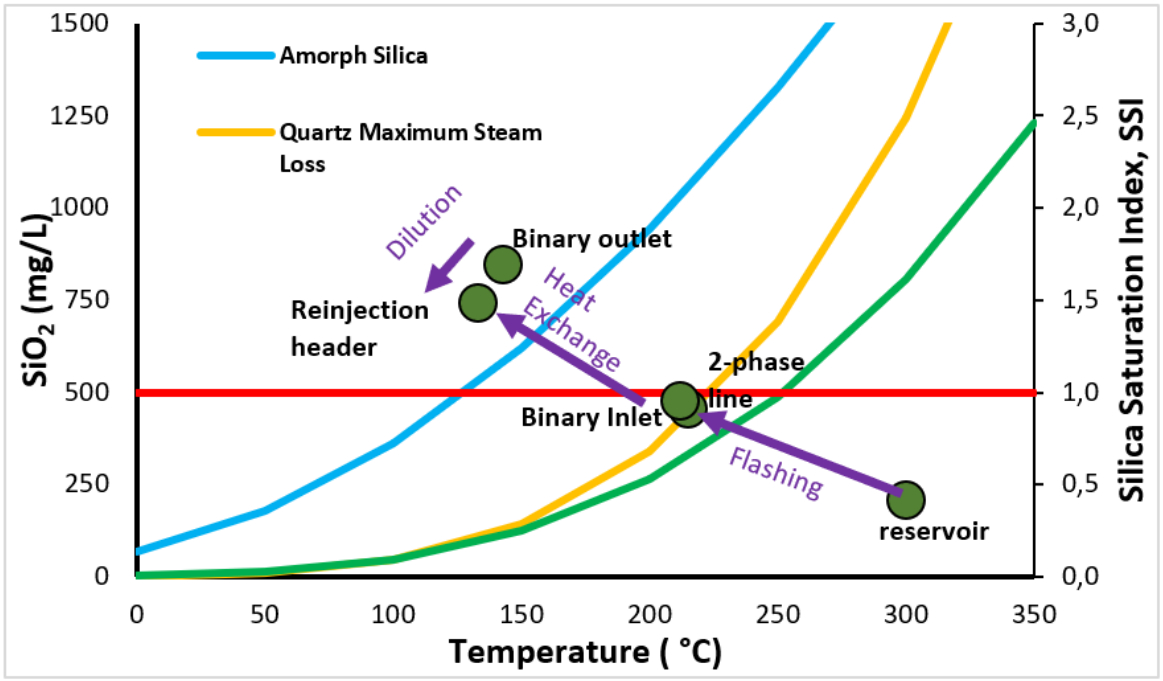


Figure 5: The effect of Temperature on SSI

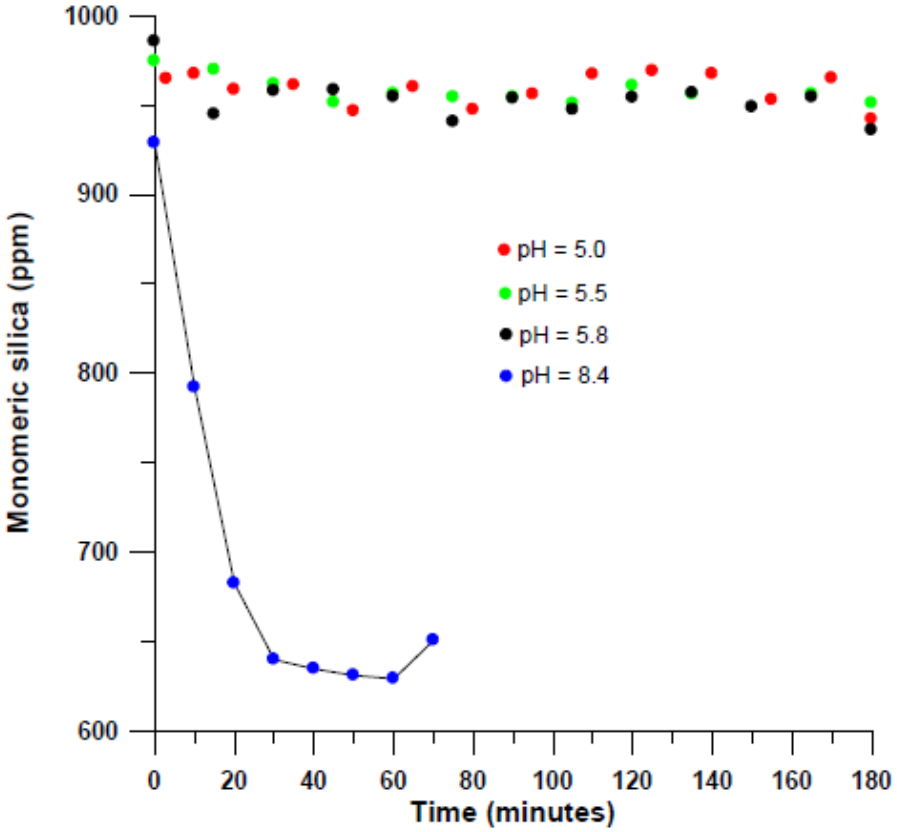


Figure 6: Kinetics of silica scaling in various pH condition (Browne, 2011)

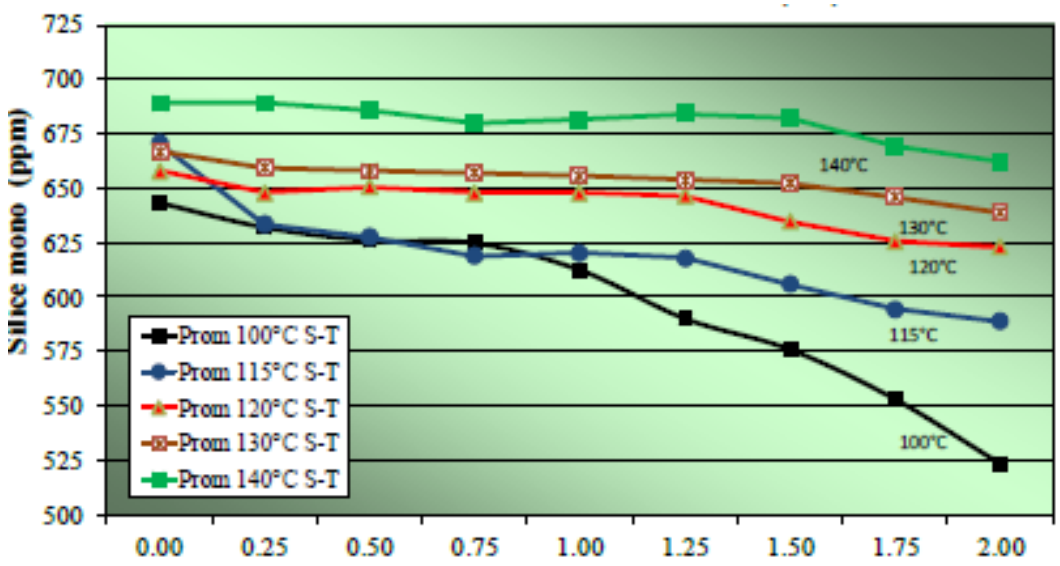


Figure 7: pH Modifications for Silica Control in Geothermal Fluids ((Guerra & Jacobo, 2012)

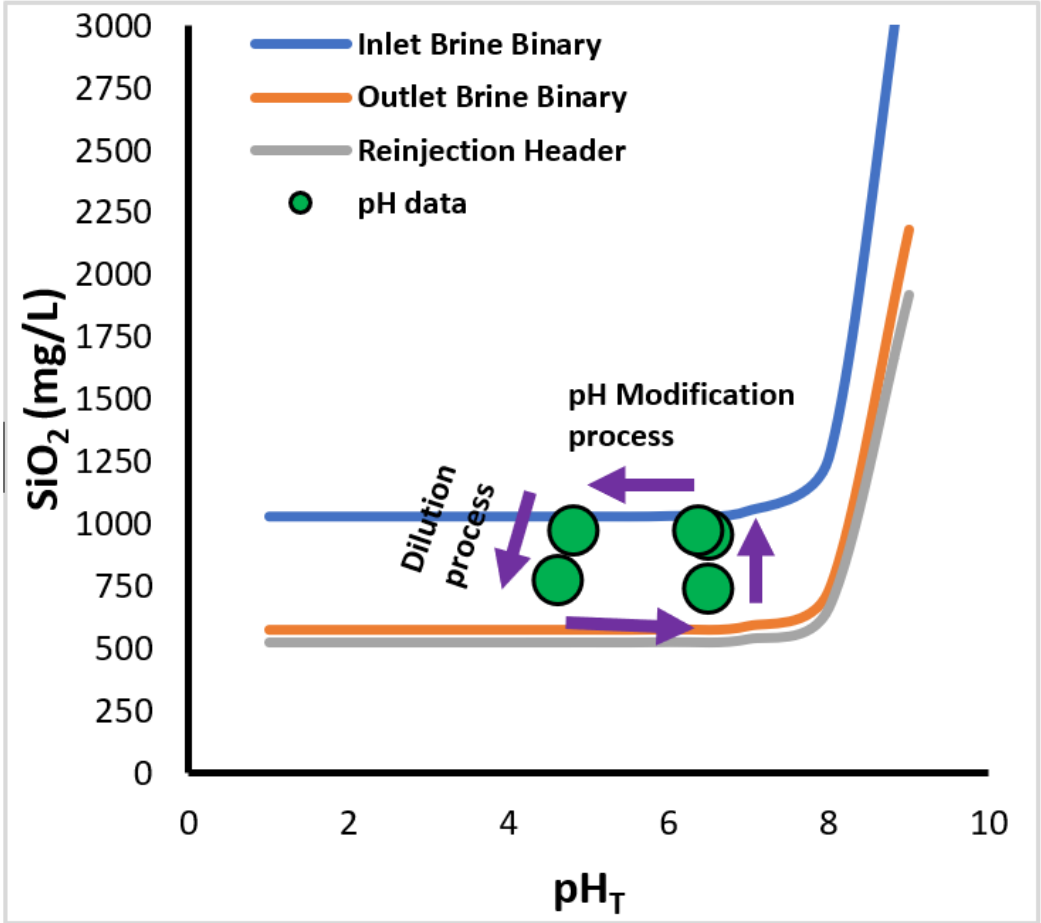


Figure 8: The effect of pH on silica solubility during pH modification process

Increase silica saturation in reinjection process: Dilution

pH modification treatment is not enough to prevent silica precipitation, or at least can only hold silica formation for 2 hours. It means that reinjection well still have big risk from silica scaling issue which can be addressed by decreasing the pH even lower or decreasing the saturation of silica. If we lower the pH, corrosion will be our next big problem. Therefore, decreasing silica saturation is the most possible and cheapest way to overcome silica precipitation in reinjection wellbore. From Figure 6. We can see that silica concentration is reduced from 982 mg/L to 778 mg/L which lead to decreasing silica saturation in brine. The change in concentration is occur due to injection of condensates from binary bottoming outlet. Condensate contain very little silica, around 0.1 mg/L, and that's why adding condensate to brine will lead to dilution process of silica in brine. While mixing cooler condensate to brine in reinjection can decrease brine temperature, SSI of mixing fluid still lower than brine SSI before mixing (Figure 3).

Prevent reservoir cooling: Reinjection well direction

Binary brine operation also has implication in reinjection well design. With lower temperature, reinjected brine can cool down reservoir when reinjection well have direct and close connection to production well. In the other hand, if reinjected brine is not experience breakthrough to production well and causes reservoir has less pressure support that lead to less brine supply and finally affected binary brine operation

ICCU EFFECT TO BINARY BRINE

After 1-year operation of ICCU, we realize that ICCU is more complex than operate only single flash system. To avoid silica scale problem in reinjection pipeline and reinjection well, brine outlet of binary brine depends on condensate flow that produce from binary steam. When binary steam having problem and amount of condensate that needed to dilute brine is not sufficient to decrease silica saturation to a safe value, then the silica formation risk is rise. Other problem is in pH modification system. Our pH modification system uses concentrated H_2SO_4 (98%) and need to be diluted ad we perform dilution by using condensate. When pH modification is not working properly, for

example the dilution fluid is too small, then we will have corrosion issue.

CONCLUSION

As pioneer of ICCU user, the experience of binary brine operation in Sarulla is very valuable for the development of binary utilization in Indonesia. The technology is adaptable to high temperature type and increase the efficiency of geothermal fluid consumption compare to conventional geothermal power plant. Silica is the biggest problem since its solubility depends on temperature. With pH modification and dilution process, Silica scale formation risk can be minimized. Close monitoring system can create higher reliability and prevent loss due to corrosion and or scaling.

REFERENCES

Browne, K. (2011). "Thermodynamics and Kinetics of Silica Scaling". International Workshop on Mineral Scaling . Manila.

Dipippo, R. (2007). "Geothermal Power Plants: Principles, Applications, Case Studies and Enviromental impact". Masschusetts: Butterworth-Heinemann.

Fournier, R. O., & Rowe, J. J. (1977). "The Solubility of Amorphous Silica in Water at High Temperature and High Pressure". Geothermics, 62, 1052-1056.

Grassiani, M. (2000). "Siliceous Scaling Aspects of Geothermal Power Generation Using Binary Cycle Heat Recovery". World Geothermal Congress. Kyushu - Tohoku, Japan.

Guerra , C. E., & Jacobo, P. E. (2012). "pH Modifications for Silica Control in Geothermal Fluids". Short Course on Geothermal Development and Geothermal Wells.

Utami, W. S., Herdianita, N. R., & Atmaja, R. W. (2014). "The Effect of Temperature and pH on the Formation of Silica Scaling of Dieng Geothermal Field, Central Java, Indonesia". Thirty-Ninth Workshop on Geothermal Reservoir Engineering Stanford University. San Fransisco: Stanford University.

THERMO-HYDRO-MECHANICAL MODELING TO SIMULATE LAHENDONG GEOTHERMAL FIELD

Muhammad Qarinur[1], Hideaki Yasuhara[1], Naoki Kinoshita[1], Sho Ogata[2]

[1]Department of Civil and Environmental Engineering, Ehime University
Matsuyama 790-8577, Japan
[2]Department of Urban Management, Kyoto University
Kyoto 615-8540, Japan
Email: mqarinur@gmail.com

ABSTRACT

Thermo-hydro-mechanical (THM) modeling was proposed to simulate natural state condition in Lahendong geothermal field. It is necessary to find out the reservoir characteristics, hydrogeology, location and total energy of the heat source. Based on the basic classifications of geothermal energy, Lahendong geothermal field is a hydrothermal system which has sufficient fluids, high average thermal gradients, high rock permeability, and high porosity. Coupled THM model has been applied to enhanced geothermal systems (EGS), but it has seldom been used in the hydrothermal system. Several conceptual and numerical models have been developed to do such investigation. In this study, we tried to improve the numerical model that was developed by Yani (2006). COMSOL Multiphysics (COMSOL Multiphysics® v. 5.4, 2018) was used for modeling the 3D numerical model to predict the evolution of rock temperature in the Lahendong geothermal reservoir. The reservoir is treated as a fractured porous medium by adopting discrete fractured model (DFM) which uses grid nodes to represent flow relationship among fracture to fracture, fracture to matrix, and matrix to matrix. Based on the results, the natural state conditions have been reached when the reasonable numerical results corresponding to the well pressure and temperature data were obtained. Finally, this model can be used to evaluate the sustainability of the reservoir, improve production performance, and develop a new geothermal resource.

INTRODUCTION

Indonesia is the second largest country in the world in utilizing geothermal energy for electricity. At least 1,948 MWe power generation capacity have been installed until the end of 2018. In order to develop new geothermal sites and improve production performance, further theoretical research and numerical simulation in the geothermal field is still needed. A case study from the Lahendong geothermal field, Indonesia is simulated with three dimensional (3D) numerical model to study the characteristics of fluid flow, heat transfer and solid deformation in the geothermal field.

The Lahendong geothermal field is located in Tomohon, North Sulawesi, Indonesia (Figure 1). Currently, the Lahendong geothermal field has four units with a total production capacity of 80 MWe (Brehme, *et al.*, 2017). The first 20 MWe unit has been producing electricity since June 2001, and unit-2 in 2007, unit-3 and unit-4 in 2009 also have the same capacity as the unit-1. Therefore, it is important to understand the reservoir characteristic to evaluate the sustainability of the reservoir.

There has been some research on the application of the numerical simulation to simulate the Lahendong geothermal system. Yani (2006) has developed a numerical model to simulate the Lahendong geothermal reservoir and validated the model predictions by using the measured temperature and pressure data. Sumantoro *et al*., (2015) improved Yani (2006) numerical model by adding the actual topography, expanding the total area, and modified input parameters. Brehme *et al*., (2016) simulated permeability distribution to determine subsurface fluid flow by using thermal-hydraulic simulation. Prasetyo *et al*., (2016) used inverse modeling technique to achieve the good parameters and natural state model in Lahendong geothermal field. Although similar research has been studied, there is still a challenge to accurately estimate the natural state condition and simulate future production scenarios in this location.

Interactions between heat transfer, fluid flow, deformation, species transport, and chemical reactions become important issues in the geothermal reservoir (Chen et al., 2013). In this study, heat transfer, fluid flow, and solid deformation processes have been considered, which are generally termed as thermal, hydraulic and mechanical (THM) coupling. Adopting a discrete fracture model (DFM), the geothermal reservoir is treated as a fractured porous medium that consists of the rock matrix and discrete fractures.

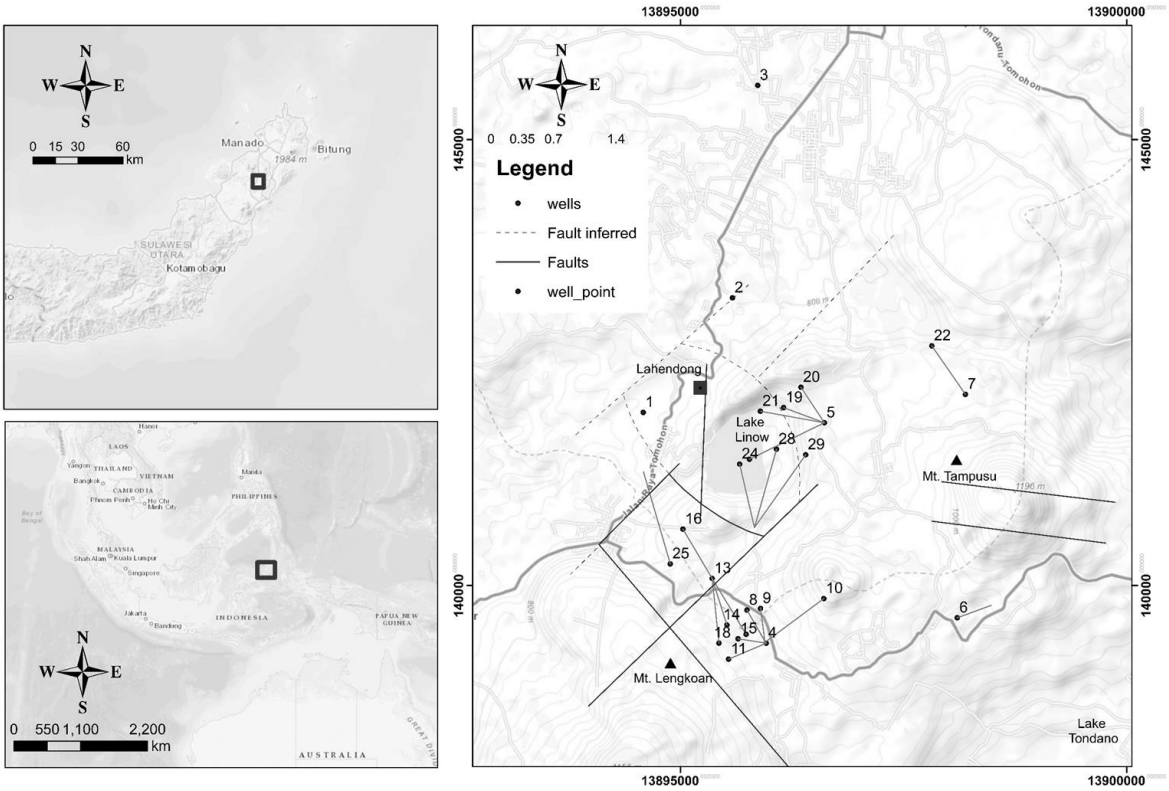


Figure 1: Location of the Lahendong geothermal field (Detailed faults and wells are based on Brehme et al., 2016; Koestono, 2010)

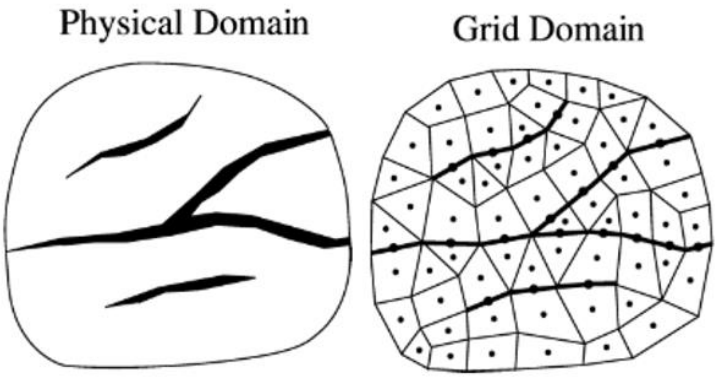


Figure 2: Fracture porous medium (Karimi-Fard et al., 2004)

Finally, the 3D numerical model of the Lahendong geothermal field is created in COMSOL Multiphysics 5.4 to estimate the evolution of reservoir temperature in the Lahendong geothermal field.

METHODOLOGY

Model Overview

The discrete fracture model (DFM) was first used by Karimi-Fard, Durlofsky, & Aziz, (2004) to apply for reservoir simulation. The DFM uses grid nodes to represent flow relationship among fracture to fracture, fracture to matrix, and matrix to matrix. As shown in Figure 2, the physical domain represents the real conditions in the field, and the grid domain is discretization from the physical domain. In the grid domain, the fracture thickness is not represented. However, it is considered in the computational domain for the flow-rate evaluation. This simplification should increase the simulation speed and these grid domains will be implemented by using finite element method.

Governing Equations

In order to describe the coupled THM processes in the geothermal reservoir simulation, COMSOL Multiphysics (COMSOL Multiphysics® v. 5.4, 2018) is used to solve the differential equations among the fluid flow, heat transfer, and geomechanics. These differential equations are divided into the rock matrix and the fractures model.

The governing equations of a coupled THM model are described by Xin *et al.*, (2019) as follows:

Rock mass flow

Due to the permeability in the rock matrix is less than that in the fractures, groundwater flow in the rock matrix is calculated by Darcy's law. Whereas the groundwater flow in the fractures is calculated by modified Darcy's law. The equations for the rock matrix and the fractures flow are expressed by

$$S\frac{\partial p}{\partial t} + \nabla\left(-\frac{\kappa}{\eta}(\nabla p + \rho_w g \nabla z)\right) = -\frac{\partial e}{\partial t} + Q \quad (1)$$

$$d_f S_f \frac{\partial p}{\partial t} + \nabla_\tau\left(-d_f \frac{\kappa_f}{\eta}(\nabla_\tau p + \rho_w g \nabla_\tau z)\right) = -d_f \frac{\partial e_f}{\partial t} + Q_f \quad (2)$$

where S is the rock matrix storage coefficient [1/Pa], p is the hydrostatic pressure [Pa], t is the time [s], κ is the rock matrix permeability [m^2], η is the dynamic fluid viscosity [Pa·s], ρ_w is the fluid density [kg/m^3], g is the gravitation [m/s^2], e is the volumetric strain of rock matrix [-], Q is the source-sink term of the seepage process [s^{-1}], d_f is the fracture thickness [m], S_f is the fracture storage coefficient [1/Pa], ∇_τ is the gradient operator restricted to the fracture's tangential plane, κ_f is the fracture permeability [m^2], e_f is the volumetric strain of fracture [-], Q_f is the flow exchange between rock matrix and fracture [s^{-1}].

Rock mass temperature

The rock mass temperature is energy conservation in the rock matrix is described as

$$\rho C_s \frac{\partial T_s}{\partial t} + \nabla \cdot (-\lambda \nabla T_s) = 0 \quad (3)$$

where ρ is the rock density [kg/m^3], C_s is the specific heat capacity of rock matrix [J/kg/K], T_s is the rock temperature [ºC], λ is the thermal conductivity of rock [W/m/K].

Energy conservation in the discrete fracture is defined as

$$d_f \rho_w C_w \frac{\partial T_f}{\partial t} + d_f \rho_w C_w \cdot u_f \nabla_\tau T_f = \nabla_\tau \cdot \left(d_f \lambda_f \nabla_\tau T_f\right) + h(T_s - T_f) \quad (4)$$

where C_w is the specific heat capacity of fluid [J/kg/K], T_f is the water temperature in the discrete fracture [ºC], u_f is the fluid flow velocity in the discrete fracture, λ_f is the thermal conductivity of fluid [W/m/K], h is the convection efficiency [W/m^2/K].

Rock mass stress field

The equilibrium equation to evaluate the mechanical process in the rock structure given by

$$\sigma_{ij,j} + F_i = 0 \quad (5)$$

where $\sigma_{ij,j}$ is the Cauchy stress tensor, F_i is the body force per unit volume in the x, y, z coordinate in 3D. The deformation equation of the rock matrix is expressed by

$$\frac{E}{2(1+v)}u_{i,jj} + \frac{E}{2(1+v)(1-2v)}u_{j,ji} - \alpha_B p_{,i} - \alpha_T \frac{E}{(1-2v)}T_{s,i} + F_i = 0 \quad (6)$$

where E is the elastic modulus [Pa], v is the Poisson's ratio [-], u is the displacement [mm], α_B is the Biot-Willis coefficient [-], α_T is the thermal expansion coefficient [1/K].

The deformation equation of the fractures given as

$$u_{fn} = \frac{\sigma'_n}{k_n},\ u_{fs1} = \frac{\sigma'_{s1}}{k_s}, u_{fs2} = \frac{\sigma'_{s2}}{k_s} \quad (7)$$

$$\sigma'_n = \sigma_n - \alpha_B p, \sigma'_{s1} = \sigma_{s1}, \sigma'_{s2} = \sigma_{s2} \quad (8)$$

where u_f is the displacement of fracture [mm], σ' is the effective stress of fracture [Pa], k is the fracture stiffness [Pa/m]. The subscripts n and s refer to the normal and tangential directions.

Calibration and validation of the model

Heat transfer in the single fracture

The heat transfer in the single fracture is expected to represent the complex fracture networks in the realistic geothermal reservoir. Lauwerier (1955) created an analytical solution to solve heat transfer in saturated porous media. Lauwerier assumes that heat transfer in the fracture is transported only by convection. Heat transfer by conduction is restrained in Y direction of the rock matrix. Figure 3 shows the schematic of the single fracture model in the Lauwerier problem. The analytical solution to this problem is described as

$$T_f = T_0 + (T_{in} - T_0)\, erfc\left(\frac{\lambda x}{2\rho_w C_w d_f \sqrt{\frac{\lambda}{\rho C_s} V_w (V_w t - x)}}\right) U\left(t - \frac{x}{V_w}\right) \quad (9)$$

where T_0 is the initial temperature [ºC], V_w is the flow rate [m/s], *erfc* is the complementary error function, and U is a unit step function.

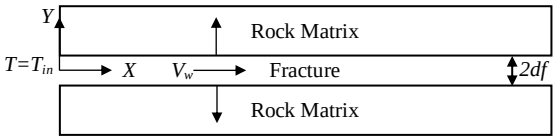


Figure 3: Schematic of the Lauwerier problem in the single fracture model.

In this section, a 2D single fracture numerical model is studied to solving thermo-hydro coupling based on Lauwerier problem. A single fracture with aperture 2 d_f = 1 mm and rock matrix domain in 100 m x 100 m is modeled. The parameters utilized in the calculations are summarized in Table 1.

Table 1: Parameters of the rock matrix and fracture in the single fracture model

Parameter	Unit	Value
T_0	ºC	320
T_{in}	ºC	40
λ	W/m/K	3
ρ_w	kg/m^3	1000
C_w	J/kg/K	4200
ρ	kg/m^3	2500
C_s	J/kg/K	1000
d_f	m	5 x 10^{-4}
V_w	m/s	0.01

Figure 4 shows the temperature distribution along the fracture at different times (t) 10 days, 50 days, and 100 days. The numerical solutions are in very good agreement with the analytical solutions. Figure 5 shows the temperature distribution at three different positions in the fracture (x = 10 m, 20 m, and 50 m). The numerical solutions are a good agreement with the analytical solutions, although there is a slight difference at the point closed to the heat source. The temperature contours distribution with different time is shown in Figure 6. It can be seen that the temperature in the fracture decreases with a time faster than in the rock matrix.

Natural state simulation

The model was calibrated and validated by comparing the simulated results with the measured temperature and pressure data. The location, area and flow rate were adjusted based on the conceptual model and were obtained by a trial-and-error process.

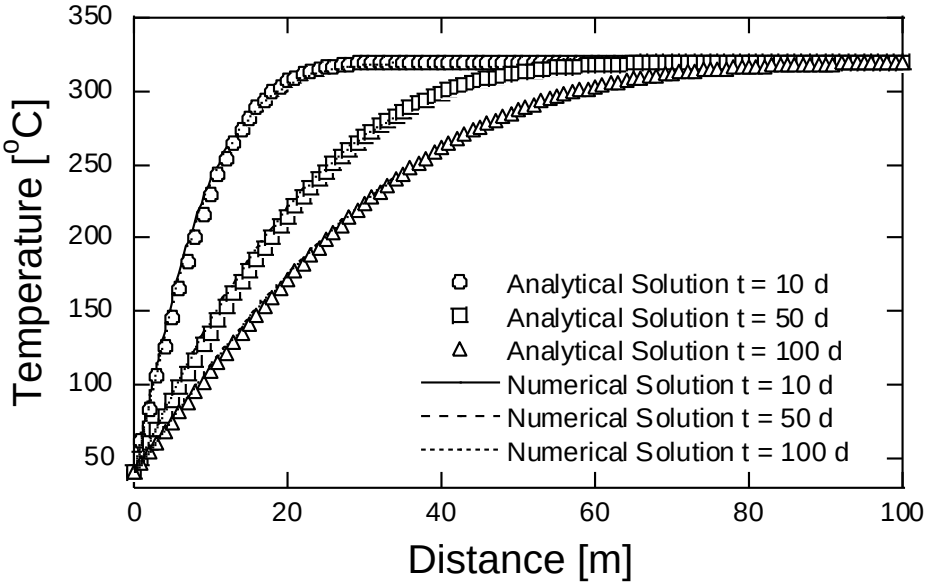


Figure 4: Comparison of temperature distribution with the distance between the analytical solution and numerical solution

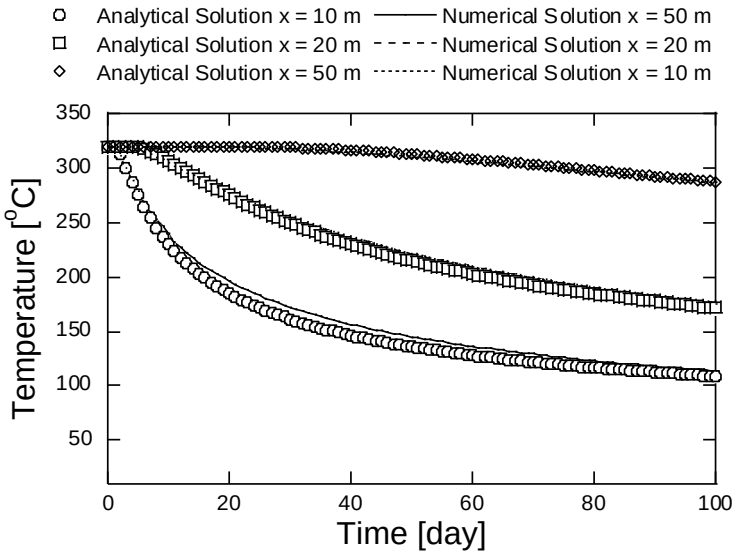


Figure 5: Comparison of temperature distribution with the time between the analytical solution and numerical solution

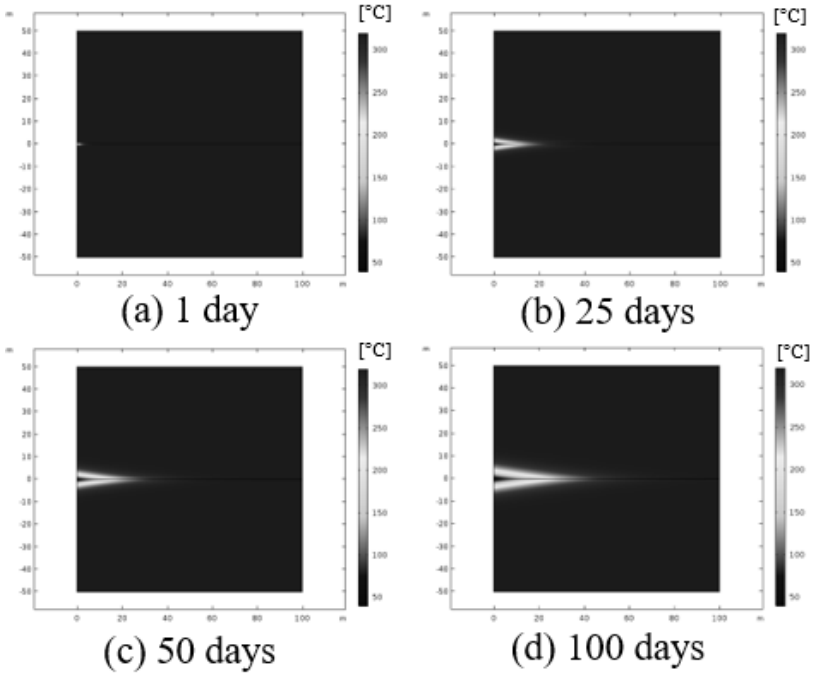


Figure 6: Temperature contours distribution in the single fracture model after 1, 25, 50, and 100 days.

COMPUTATIONAL MODEL

Based on the actual conditions, the locations of the research area are shown in Figure 1. It is assumed that the area is covering 35 km^2 with a domain of 5000 m x 7000 m x 2700 m (Figure 7 and Figure 8). The 3D computational model in the current study is also shown in Figure 7. As reported by Sumintadireja, Sudarman, & Zaini, (2001), the wells in Lahendong are located in each formation, such as the Post-Tondano/Pangolombian unit at the top (0 – 850 m bgl), the Tondano unit at 350 - 1,100 m bgl and the Pre-Tondano unit at the bottom (1,100 - 1,600 m bgl). Based on that study, geological layers are set to be three main layers and the fault zone is assumed as the fracture area. The finite element mesh used in the calculation is shown in Figure 9.

Initial and boundary conditions

In the eastside boundary, there is 25°C heat coming into the reservoir. In the other boundaries, there are no heat or mass coming into the reservoir. The temperature gradient is 0.09 °C/m from the top to the bottom of the layer. The groundwater level follows the water table elevation in the wells, especially the wells located close to the boundary side. The top of model follows the topography based on 1 Arc-second digital elevation model (DEM) United States geological survey (USGS) map. The mass flow from the heat source is located mainly beneath LHD-1

and LHD-4 with the temperature about 300 ºC and 320 ºC, respectively.

Model parameters

The accuracy of obtaining results that match the actual conditions in numerical simulations depends on the selection of computational parameters. Due to lack of several data to perform numerical simulations, several parameters are selected by assumptions and references of the existing numerical simulations. The parameters used in the numerical model are listed in Table 2.

Table 2: Parameters of the rock matrix and fracture properties (Khasani, et al., 2001; Silitonga, Siahaan, & Suroso, 2005; Yani, 2006)

Name	Porosity	Density [kg m^{-3}]	Permeability (m^2)			Heat conductivity [W m^{-1} K^{-1}]	Specific heat [J kg^{-1} K^{-1}]	Elastic modulus [GPa]	Poisson's ratio [-]
			K_x	K_y	K_z				
Pangolombian	0.15	2500	1 x 10^{-15}	1 x 10^{-15}	1 x 10^{-16}	2	1000	10	0.4
Tondano	0.22	2500	5 x 10^{-16}	1 x 10^{-15}	5 x 10^{-17}	2.9	1000	20	0.35
Pre-Tondano	0.1	2500	1 x 10^{-16}	5 x 10^{-16}	1 x 10^{-16}	3.5	1000	30	0.3
Fracture	0.1	2500	7 x 10^{-15}	2 x 10^{-15}	2 x 10^{-15}	2	1000	-	-

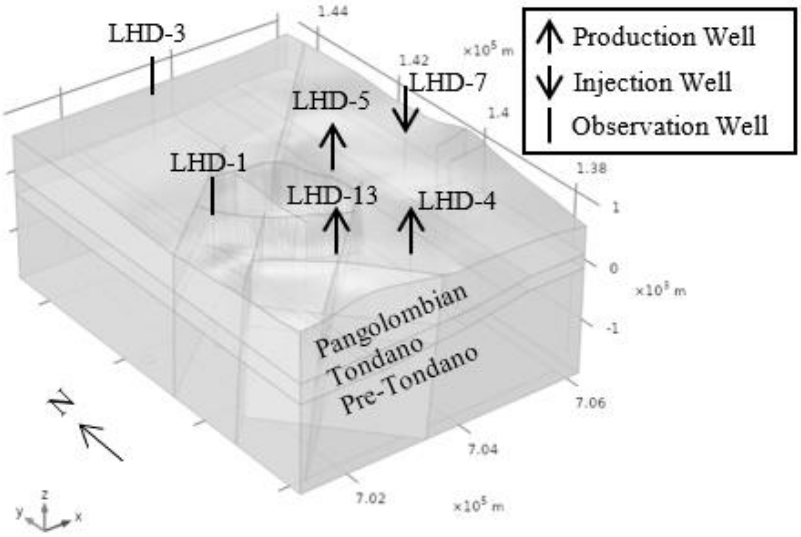


Figure 7: The 3D model geometry of Lahendong geothermal field.

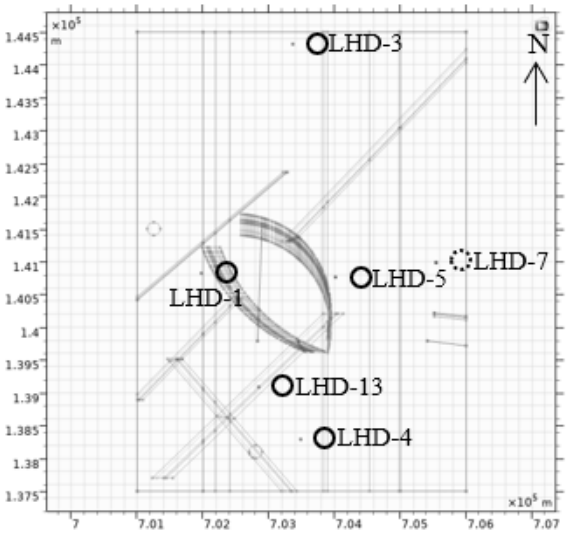


Figure 8: A cut plane at Z = -1130 m

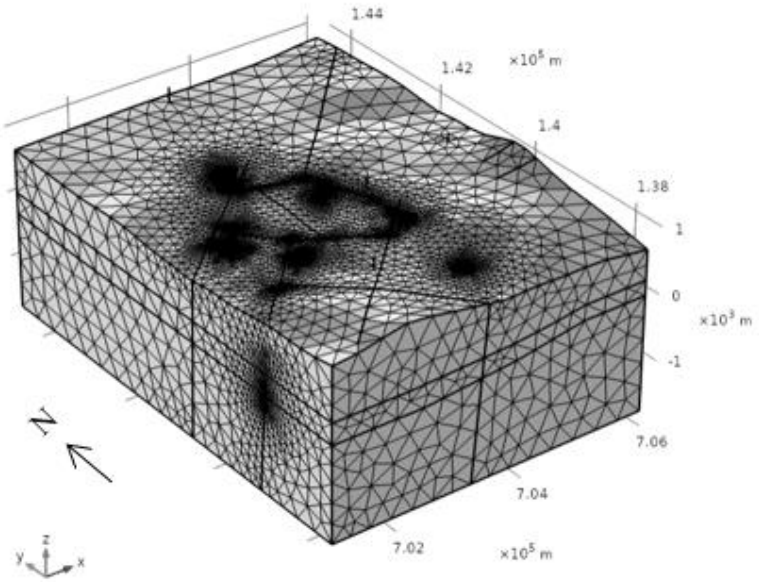


Figure 9: Mesh system of Lahendong geothermal field (elements: tetrahedra 353080, triangles 54860).

RESULTS

Natural State Condition

The rock temperature in natural state condition results is shown in Figure 10. It can be seen that the heat source comes from the southern area towards the northern area. Because of that, the southern area has a higher reservoir temperature than the northern area.

The wells in the southern zone seems more promising as the production wells than wells in the northern zone. It means that the development of this area would be focused in the southern zone. Brine and condensate from production wells are reinjected back into the reservoir in the northern area, such as in the well LHD-7 which has a low temperature as explained by Prabowo *et al.* (2015).

In this research, six of the horizontal wells (LHD-1, LHD-3, LHD-4, LHD-5, LHD-7, and LHD-13) are explained as representative of the other wells. Figure 11 shows our predictions of pore pressure in the natural state condition compared to the actual measurements and model predictions reported by Yani (2006). Based on the results, the initial pressure distribution in this area is hydrostatic. Almost all of the pressure prediction closely matches the measured data. The appropriate groundwater level model became an important issue to make the model more accurately.

As shown in Figure 12, the temperature prediction in natural state condition is compared to the actual temperature data and numerical model. The temperature results in the well LHD-1 at well depth less than 600 m bgl is lower than the well data, and at the well depth more than 600 m bgl, the result is higher than the well data. This might be because the mass heat flow close to the well LHD-1 is slow to flow from the bottom to the top of the model.

Our temperature predictions in the well LHD-3 are close to the measured temperature and the predictions by Yani (2006). This well is located in the outside of main geothermal area. Therefore, the result is similar with the thermal gradient. In the well LHD-4, the well depth less than 700 m bgl is lower than the measured temperature. Based on Yani (2006), wells in pad LHD-4 are affected by lateral cold water flow at sea level depth. It means that this layer may have slightly different characteristics from the others. However, after the well depth more than 700 m bgl, the temperature results from current model more slightly increase with depth and has a similar trend with the measured temperature data. For the well LHD-5, the results gradually increase with depth. This is because the hot water flows from the southwest to northeast mixes with the cool water flows from southeast to northwest (Yani, 2006).

The temperature results in well LHD-7 has a different result from the measured temperature. In the real condition, LHD-7 has the lowest temperature in the field and indicated cold water flow in this part. The temperature for LHD-13 match with the measured temperature until the well depth 1000 m bgl. After that depth, the well temperature is higher than the measured data.

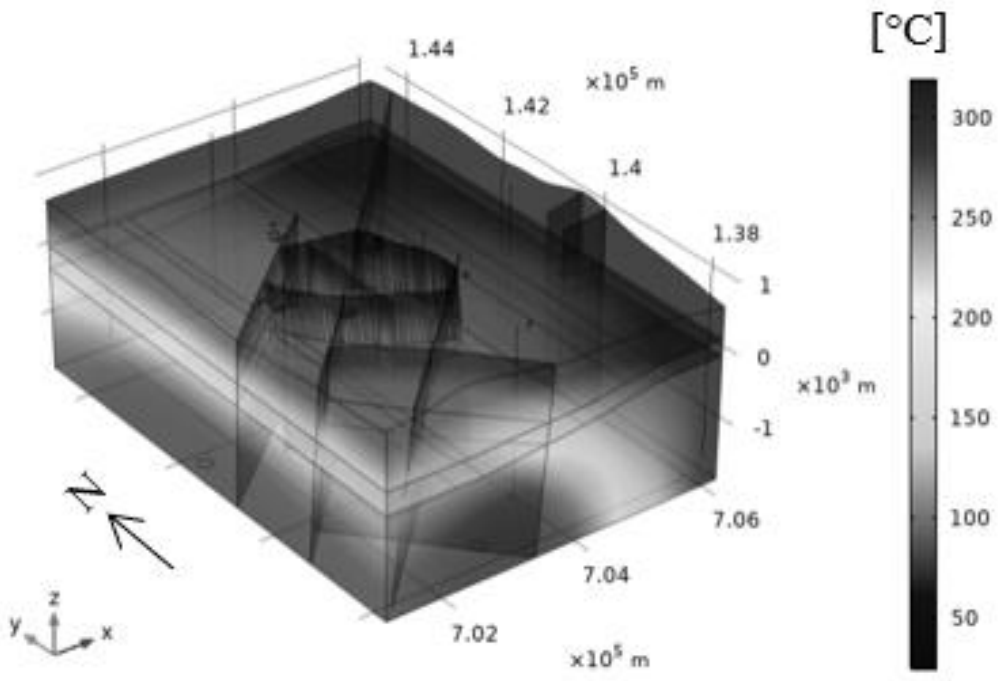


Figure 10: Temperature of natural state simulation

CONCLUSIONS

Thermo-hydro-mechanical (THM) coupling by adopting the discrete fracture model was established to simulate natural state condition in Lahendong geothermal field. The model has been presented based on the conceptual model and numerical simulation reported by Yani (2006). The southern area should be suitable to be production wells because it is close to the heat source, while the northern area should be appropriate as the reinjection locations.

The results obtained in this natural state model are important to further analyze reservoir conditions in terms of development and production enhancement. Therefore, further research is still required. Readjustment of the parameters that affect the results of the modeling must be considered in order to develop an appropriate model. Furthermore, the effects of chemical processes are not considered in this work and should be considered in the future works to obtain more plausible estimations of the energy production.

ACKNOWLEDGMENT

This work was supported by Research Foundation for the Electrotechnology of Chubu, and by Japanese Society for Rock Mechanics. Their support is gratefully acknowledged.

REFERENCES

Brehme, M., Bauer, K., Nukman, M., & Regenspurg, S. (2017). "Self-organizing maps in geothermal exploration–A new approach for understanding geochemical processes and fluid evolution". Journal of Volcanology and Geothermal Research, 336, 19–32.

Brehme, M., Blöcher, G., Cacace, M., Kamah, Y., Sauter, M., & Zimmermann, G. (2016). "Permeability distribution in the Lahendong geothermal field: A blind fault captured by thermal–hydraulic simulation". Environmental Earth Sciences, 75(14), 1088.

Chen, B., Song, E., & Cheng, X. (2013). "Plane-Symmetrical Simulation of Flow and Heat Transport in Fractured Geological Media: A Discrete Fracture Model with Comsol". In Multiphysical Testing of Soils and Shales (pp. 149–154).

COMSOL Multiphysics® v. 5.4. (2018). "COMSOL Multiphysics". Retrieved from www.comsol.com

Karimi-Fard, M., Durlofsky, L. J., & Aziz, K. (2004). "An Efficient Discrete-Fracture Model Applicable for General-Purpose Reservoir Simulators". SPE Journal, 9(02), 227–236.

Khasani, Itoi, R., Fukuda, M., & Sudarman, S. (2001). "Interpretation of well logging data on Lahendong geothermal field, Indonesia". Proceeding of the 5th INAGA Annual Scientific Conference & Exhibitions. Yogyakarta.

Koestono, H. (2010). "Lahendong Geothermal Field, Indonesia : Geothermal model based on wells LHD-23 and LHD-28". United Nations University.

Lauwerier, H. A. (1955). "The transport of heat in an oil layer caused by the injection of hot fluid".

Applied Scientific Research, Section A, 5(2–3), 145–150.

Prabowo, T., Yuniar, D. M., Suryanto, S., & Silaban, M. (2015). "Tracer Test Implementation and Analysis in Order to Evaluate Reinjection Effects in Lahendong Field". World Geothermal Congress 2015, (April), 1–6.

Prasetyo, F., O'Sullivan, J., & O'Sullivan, M. (2016). "Inverse Modelling of Lahendong Geothermal Field". Proceedings 38th New Zealand Geothermal Workshop, (November).

Silitonga, T. H., Siahaan, E. E., & Suroso. (2005). "A Poisson's ratio distribution from Wadati diagram as indicator of fracturing of Lahendong geothermal field, North Sulawesi, Indonesia". World Geotermal Congress 2015, (April).

Sumantoro, Z. Z., Angus, Y., O'Sullivan, J. P., & O'Sullivan, M. J. (2015). "Reservoir Modelling of Lahendong Geothermal Field , Sulawesi - Indonesia". Proceedings 37th New Zealand Geothermal Workshop, (November).

Sumintadireja, P., Sudarman, S., & Zaini, I. (2001). "Lahendong geothermal field boundary based on geological and geophysical data". The 5th Inaga Annual Scientific Conference & Exhibitions. Yogyakarta.

Xin, Y., Sun, Z., Zhuang, L., Yao, J., Zhang, K., Fan, D., … Jiang, C. (2019). "Numerical simulation of fluid flow and heat transfer in EGS with thermal-hydraulic-mechanical coupling method based on a rough fracture model". Energy Procedia, 158, 6038–6045.

Yani, A. (2006). "Numerical modelling of the Lahendong geothermal system, Indonesia". United Nations University, (24), 34.

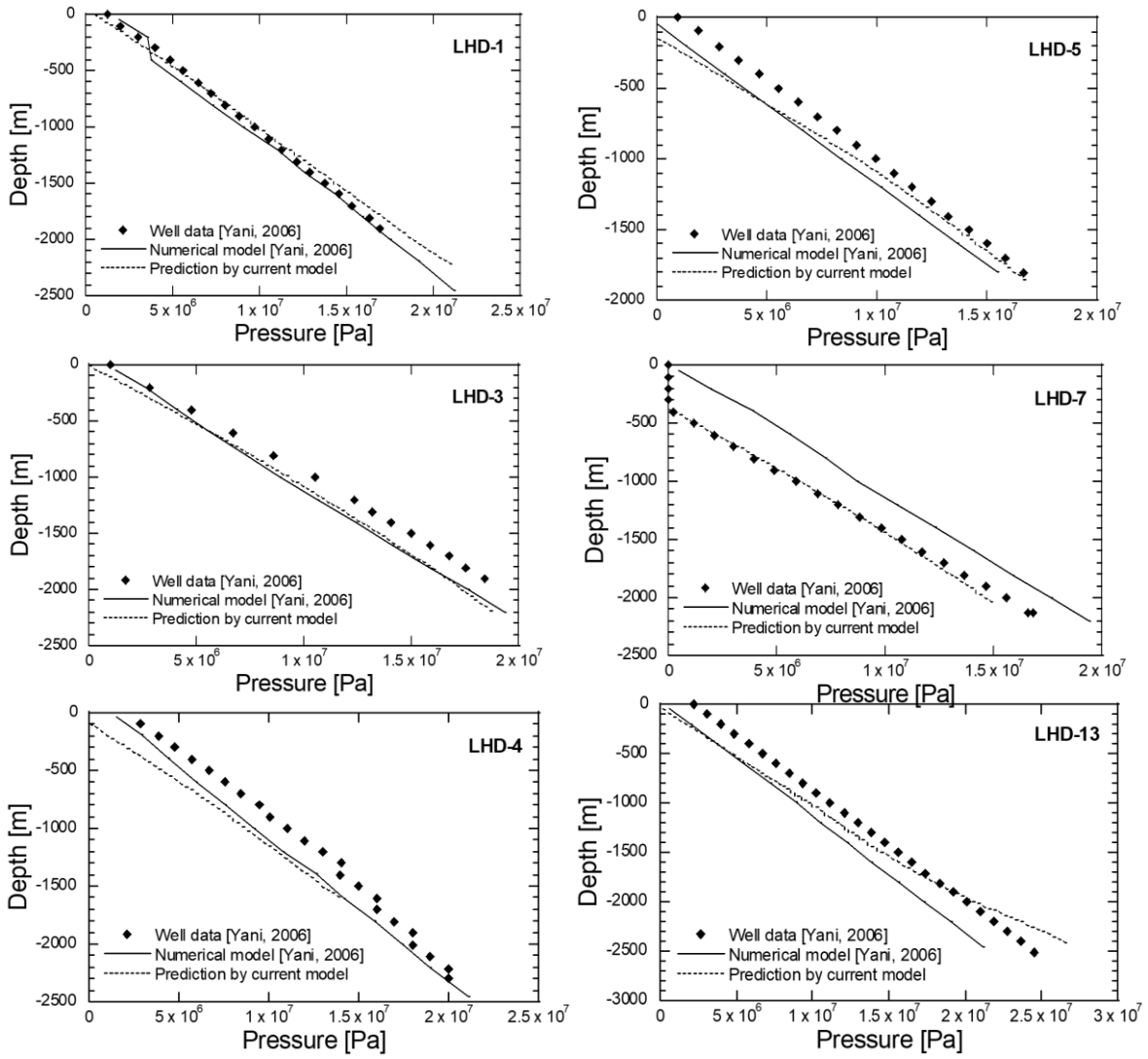


Figure 11: Comparison of pore pressure in natural state condition between measured and simulated.

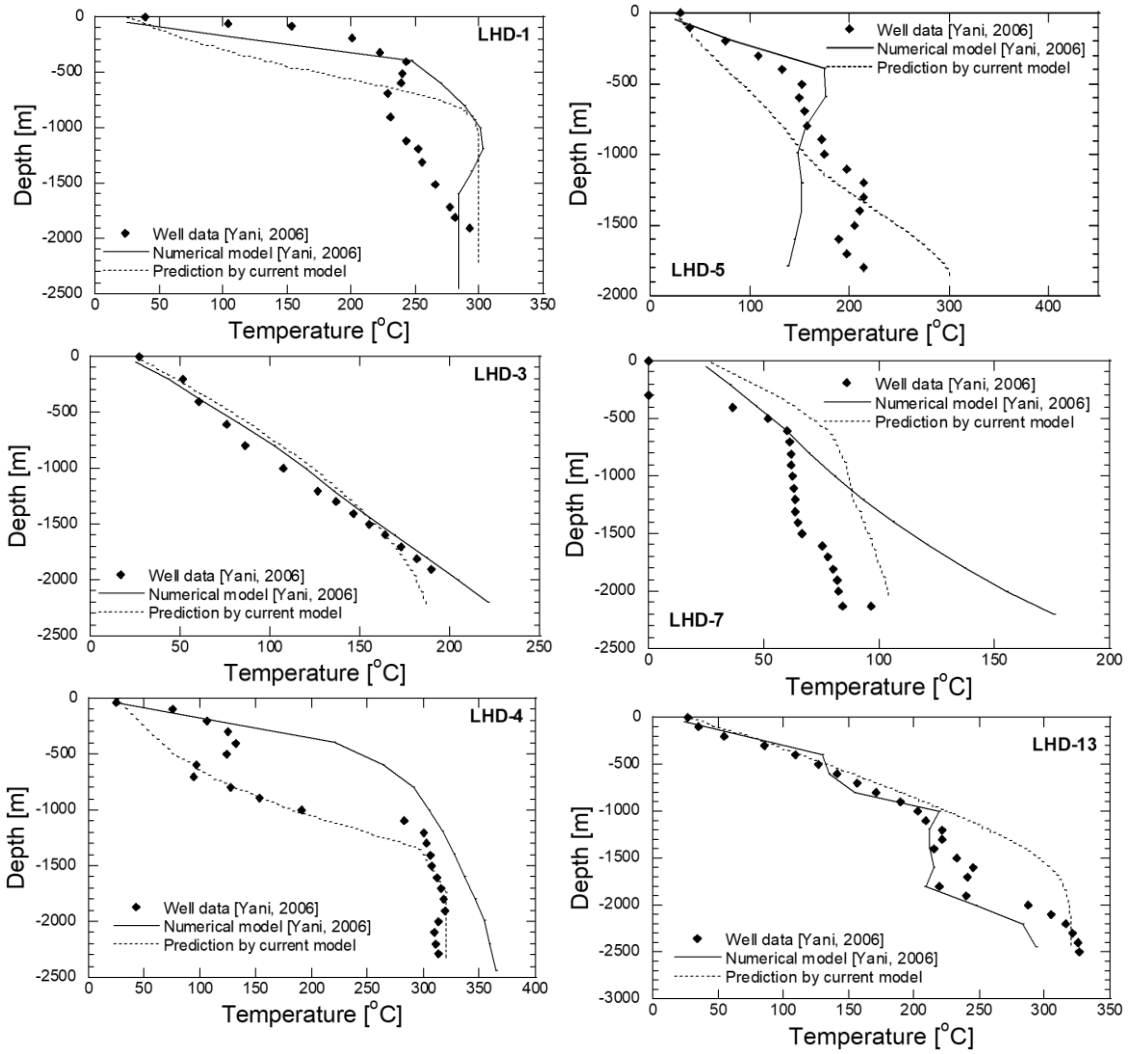


Figure 12: Comparison of temperature in natural state condition between measured and simulate.

THERMODYNAMICS AND PROCUREMENT COST ANALYSIS OF DEVELOPING BINARY CYCLE FROM BACK PRESSURE TURBINE POWER PLANT IN FLORES, INDONESIA

Naufal Nandaliarasyad[1], Dimas Taha Maulana[1], Reza Adiprana[3], Prihadi Setyo Darmanto[2]

[1]Faculty of Mining and Petroleum Engineering, Institut Teknologi Bandung
[2]Faculty of Mechanical and Aerospace Engineering, Institut Teknologi Bandung
[3]PT. Indonesia Power
Email: naufaln28@gmail.com

ABSTRACT

Optimum utilization of energy sources has been a matter of great concern in recent years, including for geothermal energy. Binary cycle can be used as a bottoming unit for the geothermal power plant and thus can optimize energy utilization. A geothermal power plant in Flores, Indonesia is upgradable by using binary cycle as the bottoming unit. There still has a considerable amount of energy from the exhaust steam of the backpressure turbine used in the power plant. More than 62000 kg per hour of steam with 2400 kJ/kg enthalpy can be used as a heating fluid for the binary cycle. Thermodynamic calculation was conducted to find the optimum condition to generate electricity from the binary cycle. Propyne, isopentane, butane, isobutane, and isobutene were selected as a possible working fluid. The optimum working fluid for this binary cycle is Propyne and isopentane with the Thermal efficiency is 10.60% and 10.50% respectively with 2.25 MW and 1.98 MW electricity generated. But, from the Procurement Cost calculation, the ORC model with the working fluid that has the lowest Procurement Cost per kW is isopentane with US$ 1,628 / kW. So based on this study it was concluded that the use of Isopentane is the best choice for use in the ORC Cycle Bottoming unit in this field.

Keywords: Binary cycle, cost analysis

INTRODUCTION

In the past 10 years, the number of research or the development of binary cycle is increasing. It is because binary cycle can provide the energy conversion from low grade or waste heat sources.

Binary cycles are developing technologies to utilize energy derived from heat exhaust or low temperature heat sources. Even in the geothermal world, there is a lot of research on developing binary cycles. Some papers (Ahangar, 2012; Bao & Zhao, 2013; Gitobu, 2016; D. Wang, Ling, Peng, Liu, & Tao, 2013; E. H. Wang et al., 2011) concludes that binary cycles can be used in geothermal power plants to utilize residual heat from flash system generators that are already operating or from geothermal sources with medium or low temperatures.

The research that has been done (Monroy Parada, 2013; Wolf & Gabbay, 2015) has carried out research in developing binary cycles to utilize waste heat from an operating flash system power plant. Some of them use wasted steam from plants that use back pressure turbines. In a back pressure turbine, there is no condenser attached to the outlet side of the turbine. So that the geothermal fluid used to rotate the turbine is immediately released into the environment. The outlet side of this back pressure turbine type turbine follows the value of atmospheric pressure in the environment.

The energy from steam that is wasted into the environment can still be reused by using binary cycles. One of the geothermal power plants in the Flores area, Indonesia uses back pressure turbines in its generating cycle.

In this study, an analysis of the possibility of installing a binary cycle in geothermal power plants in Flores, Indonesia will be conducted. The hope is that by pairing the binary cycle, the efficiency of the plant will generally increase. Because the energy wasted into the environment from the back-pressure turbine can be reused and can produce electrical energy.

ORGANIC RANKINE CYCLE

Binary cycle comes from the word "*binary*" that means two. The binary cycle means there are two different cycles in the whole process cycle. In geothermal, binary cycle is using a working fluid as a main fluid to generate power from the steam turbine and using geothermal fluid as heating fluid. The working fluid gets its energy from the heating fluid by the heat transfer process at the heat exchanger component.

The organic rankine cycle is a binary cycle which using organic fluid as the working fluid. Organic Rankine Cycle (ORC) can use heat sources with a fairly wide temperature range. From low temperatures, around 80ºC to high temperatures or around 500ºC (Bao & Zhao, 2013). The sources of heat used vary, such as from geothermal, solar heat, industrial waste heat, biomass, even from the sea.

The advantage of using ORC is that it can utilize residual heat or heat with low temperatures more

efficiently than using conventional generating cycles. Conventional generating cycles such as flash steam plants in geothermal plants are technically inefficient to utilize geothermal sources with temperatures below 150°C. While the binary cycle, especially ORC can utilize heat with this temperature more efficiently. Some other advantages of using ORC in utilizing low-temperature heat sources are in terms of economics, in terms of practicality (smaller systems) and reduced emissions of CO, CO_2, NO_x and other atmospheric pollutants (Dai, Wang, & Gao, 2009; Dipippo, 2007)

As shown in Figure 1, this binary cycle or organic rankine cycle consists of several stages, which make a closed cycle.

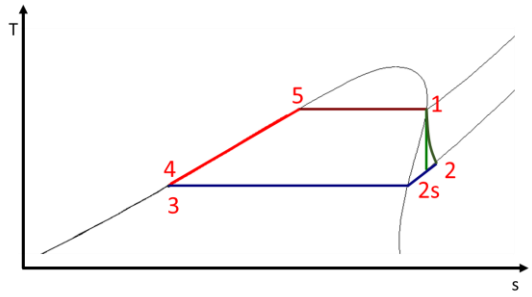


Figure 1: T-s Diagram of Binary cycle

Points 1-2 are the isentropic stages of the turbine. At that stage, the energy in the steam is converted into motion energy in the turbine used to produce electricity in the generator. Point 2-3 is the stage of condensation or phase change from steam to liquid phase. Point 3-4 is a stage of isentropic increase in pressure carried out by the pump. Points 4-5-1 are stages of heat exchange between organic working fluids and heating fluids. Specifically, at Point 4-5 it is heating the working fluid until it reaches the boiling point of the working fluid at the working pressure that has been given by the pump. Next point 5-1 is the stage of working fluid phase change from the liquid phase to the vapor phase and then used to rotate the turbine at Point 2.

In doing the closed cycle, there are several main components in the binary cycle. Component components include Heat Exchanger, Turbine, Pump, and Condenser. The Heat Exchanger is divided into two stages, namely the Pre-Heater and Evaporator.

Turbine

In this component, the organic working fluid entering is in the vapor phase. The energy from the steam is converted into motion energy in the turbine. The motion energy will then be used to rotate the generator to produce electrical energy.
Thermodynamic analysis of a binary cycle turbine is similar to a steam turbine in general. The assumptions used are ignoring potential energy and kinetic energy. Then this process occurs in adiabatic and steady processes. The equation of the process in the turbine can be described as follows

$$\dot{W}_T = \dot{m}_{wf}(h_1 - h_2) = \dot{m}_{wf}\eta_T(h_1 - h_{2s})$$

Turbine efficiency is the characteristic value of the turbine itself, and that value represents the ratio between the actual enthalpy changes in the turbine to its isentropic enthalpy changes. (Gitobu, 2016)

Condenser

In the condenser, the turbine output phase will be condensed or turned into a liquid phase. The energy derived from the working fluid will be absorbed by the cooling fluid. This cooling fluid can be either water or air.

The process of transferring heat from the working fluid to the cooling fluid can be represented by the following equation

$$\dot{Q_{2-3}} = \dot{m}_{wf}(h_2 - h_3) = \dot{m}_{cf}C_{cf}(T_x - T_y)$$

Pump

The working fluid will experience a decrease in pressure when going through the turbine. For the binary cycle to have a closed cycle, the pressure from the working fluid must be returned to the position of the turbine inlet pressure. This is done by the pump.

The work on the pump can be analyzed through the following equation

$$\dot{W}_P = \dot{m}_{wf}(h_4 - h_3) = \frac{\dot{m}_{wf}(h_{4s} - h_3)}{\eta_P}$$
$$= \dot{m}_{wf}.v_f(p_4 - p_3)$$

Heat Exchanger

This heat exchanger serves to move the heat energy that comes from the heating fluid to the working fluid to convert the phase from the working fluid to the vapor phase. There are two processes in this heat exchanger, namely the Pre-Heater and Evaporator process. The process can be separated into two components or fixed on one heat exchanger component. The heat transfer process on a heat exchanger can be seen in Figure 2

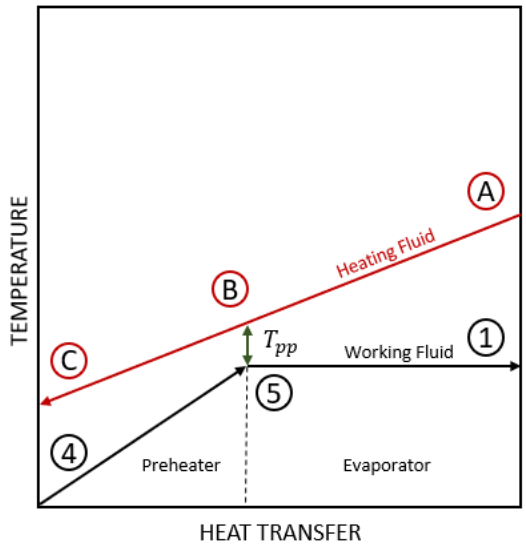


Figure 2: Temperature - Heat transfer diagram for preheater and evaporator

The heat transfer process in the heat exchanger can be reviewed one by one

Pre-heater:

$$\dot{m}_{hf} C_{hf} (T_B - T_C) = \dot{m}_{wf} (h_5 - h_4)$$

Evaporator:

$$\dot{m}_{hf} C_{hf} (T_A - T_B) = \dot{m}_{wf} (h_1 - h_5)$$

BINARY CYCLE MODEL

In this study, a binary cycle model was created that will be used to utilize residual heat from geothermal power plants in the Flores, Indonesia area. The geothermal power plant uses a back pressure turbine which produces residual heat with energy that can still be utilized.

Back pressure turbine is one type of steam turbine besides condensing turbine. In this type of turbine, the turbine output side is not connected to the condenser, so that the pressure parameters on the turbine output side depending on the environmental parameters, and the fluid will be immediately released into the environment.

At one of the power plants located in Flores, Indonesia, the fluid coming out of the back pressure turbine at the plant still has a temperature of 99°C with an enthalpy of 2435 kJ / kg at environmental pressure which is around 0.98 absolute bar.

The model of the binary cycle that will be made in this study is a simple organic rankine cycle consisting of a Preheater, Evaporator, Turbine / Expanders, Condensers, and Pumps. Figure 3 shows the model scheme of organic rankine cycle used in this study.

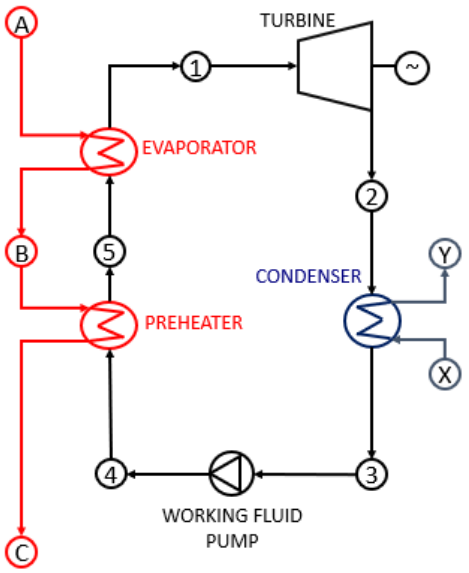


Figure 3: Model scheme of the Organic Rankine Cycle

The working fluid used will be selected based on several consideration factors. Menurut (Bao & Zhao, 2013; Monroy Parada, 2013) considerations in selecting working fluids for binary cycles, especially organic rankine cycles in general, have a low boiling point, and also have a temperature critical point and lower pressure than water. In addition to the critical points, other considerations are specific heat, density, molecular weight, freezing point, conductivity, and viscosity. In addition, according to (Aljundi, 2011), the working fluid to be chosen must also consider other characteristics, such as toxicity, flammability, Global warming potential (GWP), and Ozone Depletion Potential (ODP).

Table 1 shows the list of potential working fluids that can be used in this study. As the boundary, the heat source used in this study has a 98°C of temperature. So that some organic working fluids are chosen which have a critical point not far from the heat source used. Thermodynamics properties of the working fluids are taken from the literature (Aljundi, 2011; Bao & Zhao, 2013; Chen, Goswami, & Stefanakos, 2010; DiPippo, 2008). Temperature parameters such as the boiling point and the critical point of the selected working fluid are shown in Table 2.

Table 1: List of potential working fluids to be used in this study

Working Fluid	**SHRAE number**	**Formula**
Isobutane	R-600a	i-C_4H_{10}
Butane	R-600	C_4H_{10}
Isopentane	R-601a	i-C_5H_{12}
Isobutene		C_4H_8

Propane	R-290	C_3H_8
Propyne		C_3H_4
Neopentane		C_5H_{12}
1,1,1,2-Tetrafluoroethan	R-134a	$C_2H_2F_4$
1,1,1,3,3-Pentafluoropropan	R-245fa	$C_3H_3F_5$
1,1,1,3,3,3-Hexafluoropropan	R-236fa	$C_3H_2F_6$

Table 2: Boiling and Critical Temperature of the working fluids

Working Fluid	Boiling Point	Critical Temperature
Isobutane	-11.7 ºC	
Butane	-0.4 ºC	
Isopentane	27.7 ºC	
Isobutene	-6.9 ºC	
Propane	-42 ºC	
Propyne	-23.2 ºC	
Neopentane	9.5 ºC	
R-134a	-26.3 ºC	
R-245fa	15.3 ºC	
R-236fa	-1.4 ºC	

As previously stated, apart from the technical parameters, environmental parameters need to be taken into account in the selection of working fluids. Table 3 shows the value of Ozone Depletion Potential (ODP) and Global Warming Potential (GWP) of the working fluid.

Table 3: ODP and GWP value for the selected working fluids

Working Fluid	ODP	GWP
Isobutane	0	3
Butane	0	4
Isopentane	0	5
Isobutene	0	3
Propane	0	3
Propyne	0	
Neopentane	0	
R-134a	0	1430
R-245fa	0	1030
R-236fa	0	9810

Some working fluids such as R134a, R245fa, and R236fa have a fairly high GWP value. This means that the working fluid has a high risk of environmental pollution.

Furthermore, the working fluid that is in accordance with the technical and economic criteria will be included in the ORC model that has been made. Thermodynamic calculations are performed using Microsoft Excel software that has been integrated with REFPROP 9.0 software to obtain thermodynamic parameters from its organic working fluid. Several assumptions are used in this study and can be seen in Table 4.

Table 4: Assumptions used in this study

Parameter	Nilai	Sumber
η turbine	90 %	(Astolfi et al., 2019; Baragbah & Darmanto, 2015)
η generator	96%	(Astolfi et al., 2019)
η pump	80%	(Astolfi et al., 2019)
Air Cooled Condenser Fan Power	0,15 kW/kg/s udara	(Toffolo, Lazzaretto, Manente, & Paci, 2014)
Pinch Point	5ºC	(Astolfi et al., 2019; Baragbah & Darmanto, 2015)

Using the pinch point assumption as shown in Table 4, the turbine input pressure value can be searched, that is by using a saturated vapor condition from the working fluid with a temperature difference of 5ºC from the heating fluid temperature. Furthermore, the calculation on the ORC cycle is calculated in stages. In the condenser, the limit of the temperature value of the working fluid is ambient temperature or environmental temperature. The value of ambient temperature in the generator environment according to field data is 27.45ºC. The type of cooler used in the condenser in the ORC cycle is the Air Cooled Condenser, taking into account the amount of air flow needed in the condensation process. The amount of air flow used influences the amount of power used by the fan on the Air-Cooled Condenser (ACC).

RESULT AND DISCUSSION

Based on the thermodynamic calculations that have been carried out using the parameters mentioned earlier, we can obtain the power values that can be produced by this ORC model and also the thermal efficiency value. Figure 4 shows one of the T-s diagrams of the model made in this study. One of the working fluids used for the example of this model is isopentane. Based on Figure 4, we can see the process that occurs in one cycle in the ORC model. Temperature changes occur in the working fluid in the Preheater component, turbine, and condenser. While the evaporator fluid work does not experience changes in temperature, but only undergoes a phase change. Same is the case with heating fluid which does not change temperature significantly, because the initial phase of the heating fluid is steam and when it exits the heat exchanger it turns into a liquid phase.

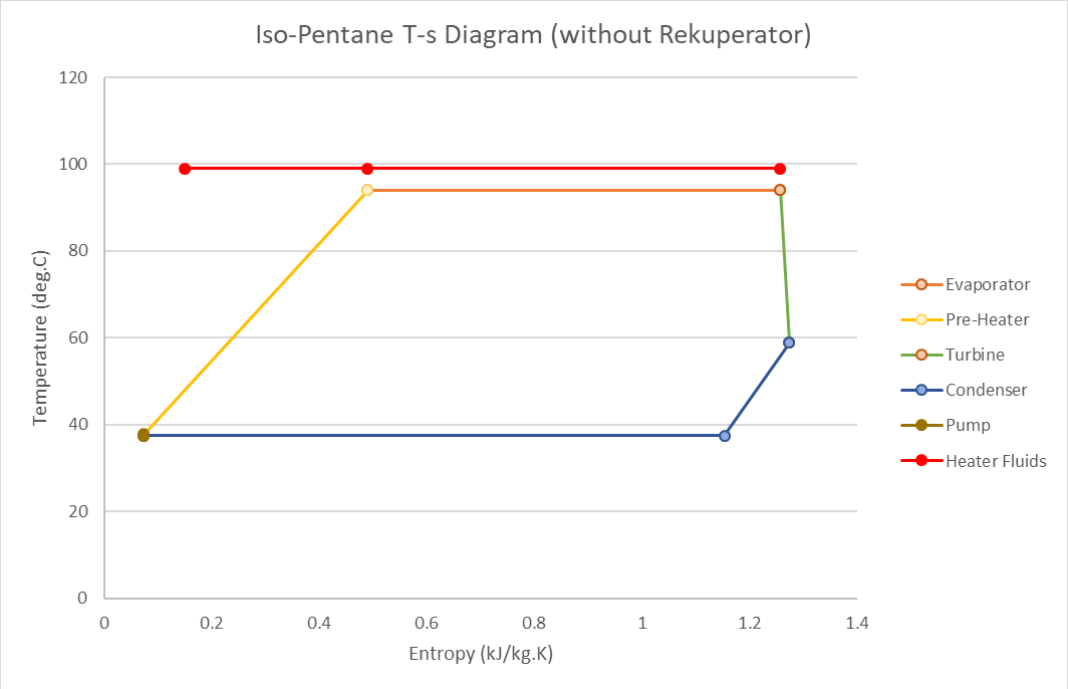


Figure 4: T-s diagram for ORC model using isopentane as working fluid

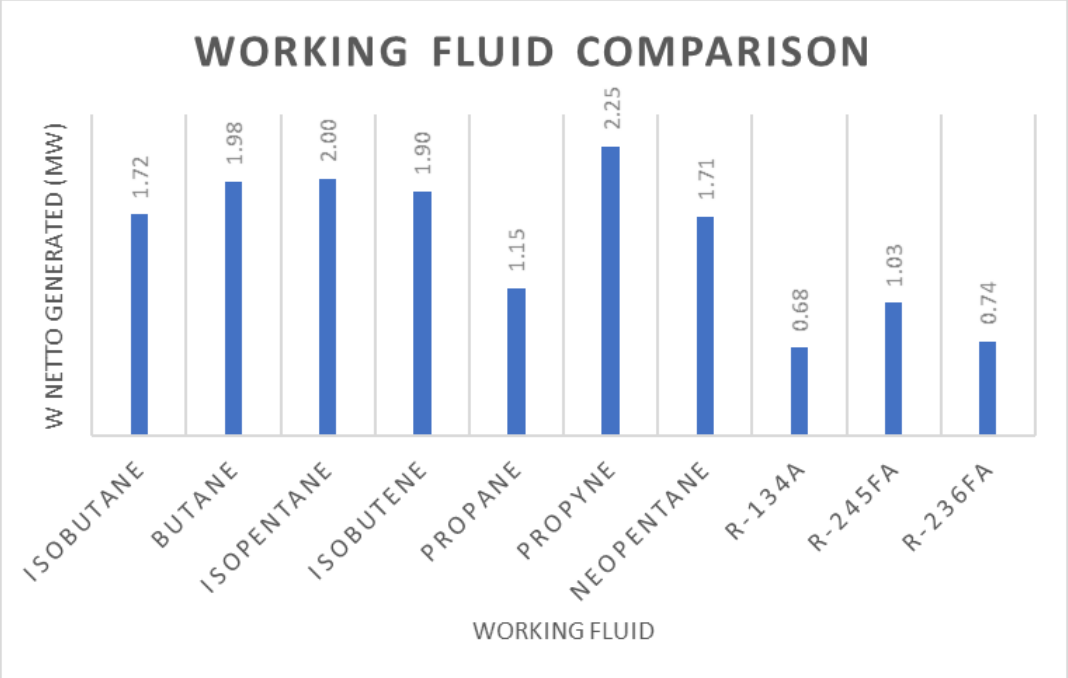


Figure 5: Working fluids comparison by power generated

There are 10 models made in this study. The variation that is changed for each model is the working fluid used in the model. In Figure 5 and Figure 6, a comparison of each model is seen from the net power generated from the ORC model as well as from its thermal efficiency value. Calculation of net power value is to reduce the value of power that can be produced by the generator in the ORC model with the value of pump power and fan power in the water-cooled condenser. While for calculating the value of thermal efficiency is to compare the value of the power produced with the available heating value.

$$W_{net} = W_{gen} - (W_{pump} + W_{ACC})$$

$$\eta_{th} = \frac{W_{net}}{Q_{in}}$$

PROCUREMENT COST ANALYSIS

Another aspect that must be considered in developing ORC is its economic review. In this

study, we will briefly mention the general picture of the economic calculation of the ORC model.

The parameters that will be used for economic calculations in this study are obtained from the literature (Ahangar, 2012; Mwagomba, 2016) as shown from Table 5.

From the ORC model that has been made, then the size of the heat exchanger can be calculated, as well as the power for components such as turbines, fans, and pumps. The calculation for the size of the heat exchanger uses a simple equation as follows

$$Q = UA\ LMTD$$

It can be seen from Table 6 that the average Procurement Cost of each working fluid is equal to US$ 3,074,026.31.

CONCLUSION

The power that can be produced by the ORC model in this study, which is using a heating fluid in the phase of steam, output of the back-pressure turbine with an enthalpy of 2435 kJ / kg at a pressure of 0.98 bar, is in the range of 0.68-2.25 MW. The working fluid with the lowest power generated is R134a. In addition to producing low power, R134a also has a fairly large GWP value which is above 1400, therefore R134a is not recommended for use as a working fluid if ORC will be built on this plant. The working fluids with the highest power generated are Propyne, Isopentane, and Butane with values of 2.25 MW, 1.98 MW, and 1.90 MW respectively. The three working fluids with the highest power generated also have high thermal efficiency, which are 10.60%, 10.50%, and 10.41%.

From an economic standpoint, a brief review of Procurement Cost shows that the highest working fluid with Cost / kW is Propane with $ 2,910 / kW and the lowest is isopentane with $ 1,628 / kW.

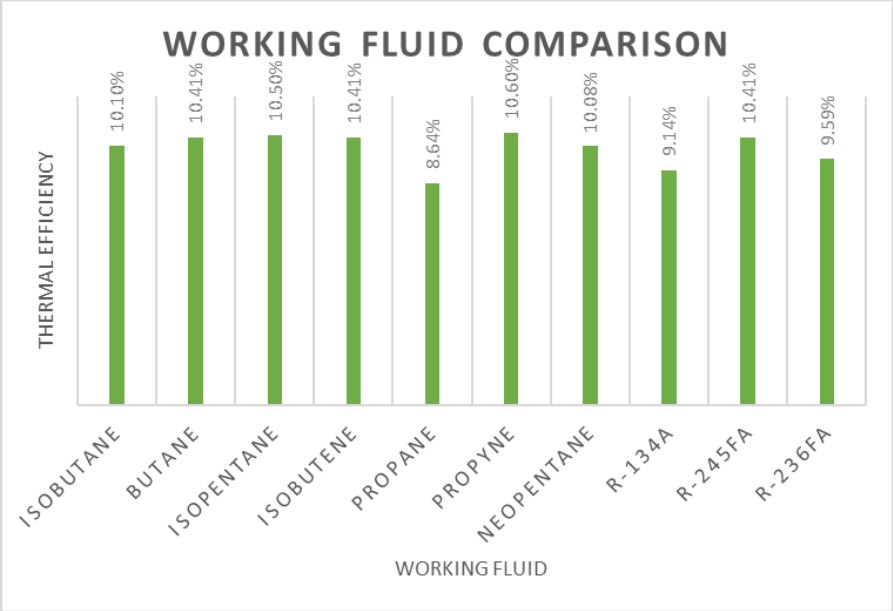


Figure 6: Working fluids comparison by thermal efficiency

Table 5: Unit Cost Parameter for the Economic Calculations

Vaporizer Unit Cost	(US$/m2)	500
Preheater Unit Cost	(US$/m2)	450
Recuperator Unit Cost	(US$/m2)	600
Condenser Unit Cost	(US$/m2)	400
Turbine Unit Cost	(US$/kW)	500
Fan Unit Cost	(US$/kW)	400
Pump Unit Cost	(US$/kW)	450

Table 6: Total Procurement Cost and Procurement Cost per kW for each ORC model

Working Fluids	Net Power (kW)	Procurement Cost (US$)	Cost/kW (US$)
isobutane	1722.67	3,296,708.55	1,913.72
Butane	1975.78	3,598,502.74	1,821.30
isopentane	1999.83	3,257,548.29	1,628.91
isobutene	1904.52	3,825,791.88	2,008.80
Propane	1147.09	3,338,592.56	2,910.48
Propyne	2250.03	5,451,407.52	2,422.82
Neopentane	1708.04	2,826,504.54	1,654.83
R-134a	684.77	1,867,518.55	2,727.22
R-245fa	1034.54	1,881,002.51	1,818.21
R-236fa	736.05	1,396,686.00	1,897.55

REFERENCES

Ahangar, F. A. (2012). "Feasibility Study of Developing a Binary Power Plant in the Low-Temperature Geothermal Field in Puga, Jammu and Kashmir, India". United Nations University, (6).

Aljundi, I. H. (2011). "Effect of dry hydrocarbons and critical point temperature on the efficiencies of organic Rankine cycle". Renewable Energy, 36(4), 1196–1202. https://doi.org/10.1016/j.renene.2010.09.022

Astolfi, M., La, L. N., Romano, M. C., Merlo, U., Filippini, S., & Macchi, E. (2019). "Techno-economic optimization of a geothermal ORC with novel " Emeritus " heat rejection units in hot climates". Renewable Energy, (xxxx). https://doi.org/10.1016/j.renene.2019.01.065

Bao, J., & Zhao, L. (2013). "A review of working fluid and expander selections for organic Rankine cycle". Renewable and Sustainable Energy Reviews, 24, 325–342. https://doi.org/10.1016/j.rser.2013.03.040

Baragbah, F. H., & Darmanto, P. S. (2015). "Effect of Organic Rankine Cycle Modification To System". 37th New Zealand Geothermal Workshop, (10).

Chen, H., Goswami, D. Y., & Stefanakos, E. K. (2010). "A review of thermodynamic cycles and working fluids for the conversion of low-grade heat". Renewable and Sustainable Energy Reviews, 14(9), 3059–3067. https://doi.org/10.1016/j.rser.2010.07.006

Dai, Y., Wang, J., & Gao, L. (2009). "Parametric optimization and comparative study of organic Rankine cycle (ORC) for low grade waste heat recovery". Energy Conversion and Management, 50(3), 576–582. https://doi.org/10.1016/j.enconman.2008.10.018

Dipippo, R. (2007). "Geothermal Power Plants, Principles Applications, Case Studies, and Environmental Impact (2nd Edition)". Massachusetts. https://doi.org/10.1017/CBO9780511613142.001

DiPippo, R. (2008). "Geothermal Power Plants: Principles, Applications, Case Studies and Environmental Impact". Library of Congress Cataloging-in-Publication Data, 490. https://doi.org/10.1016/C2014-0-02885-7

Gitobu, G. G. (2016). "Model Organic Rankine Cycle For Brine at Olkaria Geothermal Field, Kenya", (15).

Monroy Parada, A. F. (2013). "Geothermal Binary Cycle Power Plant Principles , Operation and Maintenance". UNU-GTP-2013-20.

Mwagomba, T. (2016). "Preliminary Technical and Economic Feasibility Study of Binary Power Plant for Chiweta Geothermal Field , Malawi". Geothermal Training Programe, 1(January).

Toffolo, A., Lazzaretto, A., Manente, G., & Paci, M. (2014). "A multi-criteria approach for the optimal selection of working fluid and design parameters in Organic Rankine Cycle systems". Applied Energy, 121, 219–232. https://doi.org/10.1016/j.apenergy.2014.01.089

Wang, D., Ling, X., Peng, H., Liu, L., & Tao, L. L. (2013). "Efficiency and optimal performance evaluation of organic Rankine cycle for low grade waste heat power generation". Energy, 50(1), 343–352. https://doi.org/10.1016/j.energy.2012.11.010

Wang, E. H., Zhang, H. G., Fan, B. Y., Ouyang, M. G., Zhao, Y., & Mu, Q. H. (2011). "Study of working fluid selection of organic Rankine cycle (ORC) for engine waste heat recovery". Energy, 36(5), 3406–3418. https://doi.org/10.1016/j.energy.2011.03.041

Wolf, N., & Gabbay, A. (2015). "Sarulla 330 MW Geothermal Project Key Success Factors in Development". World Geothermal Congress 2015, 39(April), 19–25.

ORC, AN EFFICIENT AND DEPENDABLE SOLUTION FOR MODERN GEOTHERMAL APPLICATIONS, TURBODEN'S EUROPEAN EXPERIENCE

Joseph Bonafin and David Paul

Turboden, via Cernaia 10, 25124 Brescia, Italy
Email: info@turboden.it

ABSTRACT

Turboden is a leader in the Organic Rankine Cycle Technology (ORC) technology and business. The company was established in 1980, so has almost 4 decades of experience behind it. Currently there are already 380 Turboden ORC plants in operation or under construction in 42 countries worldwide, utilizing turbines designed in-house. Turboden has seven geothermal binary plants in operation, and two under construction. The plants are located in Germany, France, Austria and Croatia, supplying base-load power and heat for the local communities. In the last few years, Turboden has successfully implemented 4 geothermal plants in the Molasse basin (Bavaria, south of Munich). One 5 MW geothermal power plant (in Sauerlach), two 5.6 MW plants in the same region (in Dürrnhaar and Kirchstockach), and a 4.1 MW cogen geothermal plant in the city of Traunreut, designed to deliver also up to 12 MW thermal power to the local heating grid (Bonafin, 2015). In August 2017, Turboden won a European tender for a 3.4 MWel plant to be realized in Holzkirchen. This order establishes the Turboden's leadership in the German ORC geothermal market. Turboden's successful experience continues in France, for the Soultz-sous-Forêts plant in operation. Currently Turboden is in the construction phase for another geothermal plant in the Upper Rhyne Valley. In Croatia, Turboden has constructed one of the largest single ORC turbines for the 17.5 MW Velika Ciglena project which has been in operation since December 2018. The technical features and the operational data of these plants will be described in detail, focusing on both the performance figures and availability of the ORC unit and on the overall availability of the projects (including downhole geothermal pumps and balance of plant).

Keywords: Turboden, organic rankine cycle

OVERVIEW OF TURBODEN'S PRESENCE IN EUROPE

Turboden has a growing presence in the European geothermal market, and this has been increasing very by year, buoyed by solid and dependable performances of its existing plants in operation.

Germany, more specifically the Molasse basin, has been an area of focus for Turboden and its efforts have been rewarded with four geothermal plants operating with high availability. Another one, in

Holzkirchen, is currently under construction and will add to the reference list of Turboden once it is commissioned.

Moving away from Germany, other developments include a 17.5 MW plant built in Croatia for the production of electricity. The Velika Ciglena plant hosts one of the biggest turbines ever built for a binary plant. Another plant worth of mentioning is the Soultz-sous-Forêts plant, located in France, in operation since 2016 with continuous operation and good performance figures.

We look at each of these plants in more detail below.

SAUERLACH

Sauerlach geothermal plant has been in operation since the beginning of 2013. It is one of the three geothermal plants operated by the local utility provider StadtWerke München, built by Turboden. Sauerlach plant has a gross power of 5 MW with a water temperature of 140°C. It uses a custom turbo-generator to maximize efficiency, minimize noise emissions and provide maximum usage of the available limited space. The plant is a unique example of architectural integration of a power plant with a building, with a turbogenerator indoor (two turbines coupled to the same double-shaft generator), and a dissipation system (air cooled condensers) placed on the roof. This flexibility in lay out design that Turboden brought to this project is one of the unique features of this plant. Along with the production of electricity, the plant is capable of island mode operation to feed the local municipality with highly available heat. This allows the operation of the unit in the absence of a local utility grid. Figure 1 shows the Sauerlach geothermal plant.

The Sauerlach ORC power plant won the Geothermal Energy Prize of Bavaria mainly due to the outstanding operational data in 2017. During this period the plant reached an overall availability (including balance of plant and ESP pump) of 98%. When reviewed by itself, the ORC availability was a very high 99.5% (Duvia, 2009), which reiterates the high dependability and reliability of Turboden's ORC units. Figure 2 shows the Kirchstockach geothermal plant. Figure 3 shows the Dürrnhaar geothermal plant.



Figure 1: Sauerlach geothermal plant



Figure 2: Kirchstockach geothermal plant



Figure 3: Dürrnhaar geothermal plant

KIRCHSTOCKACH AND DÜRRNHAAR

Kirchstockach and Dürrnhaar plants have followed Sauerlach in Turboden's expansion in the Molasse Basin of Bavaria. They are electric power-only plants with an identical gross power output of 5.6 MW from the generator terminals. Both plants are in operation since 2012 and operated by StadtWerke München since the takeover in 2016. Due to the proximity of the plants to the city of Munich, stringent noise limits are required to allow the units to be located at the current site. Fortunately, with the help of detailed noise reduction engineering efforts, these strict requirements have been successfully achieved and the plant is operating acceptably since the commissioning of the units. Another distinctive feature is that the organic working fluid used in this plant is HFC-245fa, a non-flammable liquid, and this helped to minimize the environmental risk in this area, so that there is no detrimental effect to a forest nearby. Both plants have double-pressure level cycles with a geothermal water temperature of 138°C.

A detailed analysis of availability and performance of the ORC conducted in collaboration with the owner shows the following average performance figures in the period 2015-2017.

Dürrnhaar: Average ORC availability 98.2%; total availability of plant (including ESP pump and balance of plant): 83%.

Kirchstockach: Average ORC availability 9811%; total availability of plant (including ESP pump and balance of plant): 90.1%.

Both plants have exceeded the guaranteed performance for operation by far during the above mentioned 3 years period, despite real world operating conditions (scaling at evaporator inlet, and fouling on air condensers. Turboden implemented the needed O & M activities including removal of the fouling on the air condeners which contributed to the high availability numbers. (Duvia, 2009)

TRAUNREUT

Located in Traunreut, a town in southeastern Bavaria which is located on a deep geothermal reservoir, the Traunreut power plant has been in operation since 2016. GKT (Geothermische Kraftwerkgesellschaft Traunreut GmbH) is operating the plant which produces about 4 MW electric power by using geothermal water at 118 °C and it is coupled with the district heating system of Traunreut.

The plant is able to deliver a peak load of 12 MW thermal power. HFC-134a is the organic working fluid of choice for the operation, while the plant is optimized for highly efficient electricity production at a very low sound level (< 92 dBa PWL).

SOULTZ-SOUS-FORÊTS

The well-known Soultz-sous-Forêts geothermal site, located in Northern Alsace (France) is home to a Turboden ORC unit of 1.7 MWe. The reservoir is a deep fractured granite, thus the type and quality of the brine has high salinity (about 100 g/l of TDS). An enhanced geothermal system has been developed by GEIE to produce geothermal water at 160 °C. Thus, Turboden provided an innovative air-cooled ORC plant to exploit the heat from the geothermal brine and reinject into the source with a temperature of 75 °C. Turboden has the capability to analyse and determine the most suitable working fluid for each geothermal resource and select that fluid to maximize performance, while taking into account the required environmental impact requirements. And in this case, the working fluid selected for the single-pressure level process was isobutane, which has proven to be a good choice, as it has provided excellent performance results. Figure 4 shows the Soultz-sous-Forêts geothermal plant.

A detailed analysis of availability conducted in collaboration with the Owner has shown the following availability figures in the period 2017-2018:
Average ORC availability : 99.9%
Overall plant availability (including line shaft pump and balance of plant) : 91.2% (Duvia, 2009).

HOLZKIRCHEN

The town of Holzkirchen is located in the south of Munich, on the Molasse basin. Turboden is constructing a 3.4 MW to be delivered to its customer, Geothermie Holzkirchen GmbH, in 2019. The aim of the customer is to provide the local grid with electric energy and server the households connected to the district heating network with clean thermal energy. Figure 5 shows the Holzkirchen geothermal plant.

A double-pressure level system is being adopted by Turboden, which utilizes isobutane as the working fluid. The combined heat and power plant will have a geothermal water temperature of 152°C at the inlet and 50 °C at the outlet. This is possible due to the low salinity of the geothermal water. The plant is currently under commissioning, with start-up expected very soon.



Figure 4: Soultz-sous-Forêts geothermal plant



Figure 5: Holzkirchen geothermal plant



Figure 6: Velika Ciglena geothermal plant



Figure 7: Afyon geothermal plant

VELIKA CIGLENA

In Croatia, Turboden designed and constructed one of the largest single ORC turbines, for the 17.5 MW Velika Ciglena project. Figure 6 shows the Velika Ciglena geothermal plant.

The innovation here for this particular ORC is the adoption of the 5 stages large axial ORC turbine for this geothermal application, a first of its kind for this application. The Velika Ciglena project uses steam and hot water at 170 °C to produce electricity to the local power grid. The region of Velika Ciglena is situated in Bjelovar subdepression, the north east of Croatia. The Turboden ORC plant converts the heat harnessed from two geothermal wells into base-load renewable electricity. The ORC process is based on a single turbine, with isobutane as working fluid. The cooling is accomplished by air cooled condensers. As of today, the Velika Ciglena is the largest single turbine installed in a geothermal ORC power plant in Europe. The plant was commissioned in December 2018.

AFYON

Afyon Jeotermal Turizm ve Ticaret A.Ş (AFJET); was established in 1994 with the purpose of installing district heating facilities exploiting geothermal water resources and providing greenhouses with the return water. The company is a municipal enterprise and owns 24 geothermal wells to date and provides heating for 23,900 homes. Figure 7 shows the Afyon geothermal plant.

In addition to electricity production, AFJET also provides heating for homes in the area and water for the greenhouses.

A custom made Turboden ORC solution was designed to address the customer's need and the plant was put into operation in 2017. The unit produces 3 MWe. The geothermal brine is exploited at a temperature of 110°C and a flow rate of 150 kg/s while cooling towers are employed to cool down the condenser of the ORC.

NEW PROJECT IN FRANCE

Turboden has been awarded a new project in the Upper Rhyne Valley in France by Fonroche Geothermie. The projected power output will be 11 MWe exploiting the liquid brine at 200°C from a single deep well in Vendenheim (close to Strasbourg). The project is still under construction with the estimated start-up date is by the end of 2019.

CONCLUSION

Based on the experience and field data from Turboden's geothermal ORC installations in Europe, the following key conclusions can be reached.

First, Turboden's ORC units have very high reliability and availability, achieving in the 99% range provided the heat input is stable and meets the designed conditions.

Secondly, Turboden is growing the market and becoming a leader in Europe for ORC geothermal, particularly in Germany. (Now the company is spreading their products to other parts of the world including Asia, Africa, North, Central and South America).

Finally, Turboden is very flexible and capable in customizing designs to meet the local requirements in terms of space available, maximizing turbine efficiency, meeting stringent noise constraints, using different fluids for different locations and resources to optimize the environmental impact, and a large variation in size from about 1 MW to about 20 MW for a single turbine.

REFERENCES

Bonafin, Del Carria, Gaia, Duvia (2015), "Turboden Geothermal References in Bavaria: Technology, Drivers and Operation," Proceedings World Geothermal Congress, Melbourne.

Duvia (2009), "Updated operational experience of ORC Plants in Europe", Presentation at Geotherm Expo and Congress Offenburg.

.

DRILLING COST REDUCTION INITIATIVES FOR GEOTHERMAL DRILLING

Yudi Hartono, Ashadi, Sentanu W. Reksalegora

PT Sokoria Geothermal Indonesia
Recapital Building, 5th Floor, Jalan Adityawarman No 55, Jakarta Selatan 12160
Email: Yudi.hartono@ksorka.com

ABSTRACT

Indonesia holds the potential to be the largest geothermal energy producer in the world. With exploration and development drilling being one of the major economic consideration in a geothermal project, it is very important for companies to optimize the cost of drilling as efficiently as possible. Various aspects of drilling project and the possible cost saving initiatives are discussed in this paper in order to raise awareness about the importance of cost saving in drilling geothermal wells.

Keywords: Drilling, cost analysis

INTRODUCTION

As of May 2018, Indonesia is the world's second largest geothermal energy producer with 1925 MWe capacity. The Indonesian government aims to make the country the largest geothermal energy producer by 2025 (Apriani, Randle, & Paripurna, 2018). One of the main factors that can really decides whether or not a geothermal project is feasible is its project economics. A geothermal project cost is usually divided into several categories, normally representing the different phase of the project. Two of the main project phases, exploration and development both involves drilling, which holds a significant financial risk and could be allocated up to 40% of the total budget of a geothermal project (Gul & Aslanoglu, 2018). Because drilling operations makes up a large portion of the total budget, planning and budgeting becomes critical. Cost saving initiatives in drilling can come from many various activities. Prior to the start of drilling operations, proper cost saving initiatives and planning must also be done so that future operations can be carried out smoothly. This paper will discuss the various cost saving initiatives that can be taken to optimize cost in geothermal well drilling. The initiatives will be divided into five categories i.e, well design optimization, infrastructure improvement, material selection, contract strategy, and operational efficiency.

DRILLING COST REDUCTION INITIATIVES

Well Design Optimization

No two wells are the same. Each well is drilled differently with different design. Each well has different uncertainty & risk in how much megawatts can actually be produced at its final depth. To optimize the cost of drilling, one of the first steps is to optimize the well design, starting from the target depth, followed by the size of the well.

Target Depth

Various literatures in both oil and gas and geothermal drilling have reviewed that the depth of a well is a main factor in determining cost of well construction. This is mainly due to the fact that drilling cost is a function of time (Kipsang, 2015). The deeper the well, the higher the cost as more time is needed to drill. A study of depth of wells versus cost has been done for geothermal wells in Indonesia as seen in Figure 1. There are two common categorizations of well depth, deep and shallow. The two categories are usually correlated to the reservoir zone and final well purpose, whether it is injection or production. Drilling a shallow well can be 13% relatively cheaper compared to deep well. This may sound as an over-generalization and could be field-specific, however the message is that if we do not really need to drill deep then don't. In order to optimize the well depth or well target, a feed zone study must first be done. Although this may incur extra costs, once the feed zones have been identified, a well can be drilled to hit the targets, ultimately saving time and resources.

Well Sizing

The three common types of well size in geothermal drilling are big bore, standard, and slim sized hole (Figure 2). The different sizes of well has its own advantages and disadvantages. The size selection will determine the rig selection, which will be discussed in a later section. For geothermal drilling, the most common well size is the big hole and the standard hole. The big hole will allow reduced risk at a slightly higher price (Purwanto, Suwarno, Lukman, & Herdiyanto, 2018) compared to a standard/slim hole design. However, this will be beneficial overall, especially in exploration drilling, where data are limited, and risk are significantly higher. The big hole well design will allow drilling to set casing early in the 12-1/4" section if needed then continue to the 9-7/8" hole in case any drilling problems are encountered – hence increasing the chance to reach the target depth. The big bore well also has a bigger annular clearance, allowing better hole cleaning and lower risk of having a stuck pipe caused by hole cleaning problem. Various industrial information has shown that the cost of big hole is not

necessarily higher than the cost of standard hole, at similar depth. Thorough statistic studies have not been done yet, but this could be another interesting subject for future study.

Infrastructure Improvement

Water Supply

After identifying the cost-optimized well design, the infrastructure of the project will need to be established. In all geothermal drilling project, water is and will always be the critical factor. Sufficient water supply is critical in geothermal drilling because, drilling fluid is expected to be lost into the formation when encountering fractures. It is recommended that the water system can deliver approximately 1400 gpm to avoid any cost from rig standby due to water shortage and/or also increasing risk of hole cleaning & well control problem. In order to ensure cost is optimized during the construction of water supply pipeline from the source to the well pad, several alternative selections are available, including choosing the right material for the pipeline, selecting proper pump station, and selecting the right water pump. As for material selection, using galvanized steel pipe or steel pipe line instead of HDPE is preferred. The steel pipe lines allow maximum water pump flow rate and pressure due to the higher burst pressure capacity, which is crucial in total loss condition. Steel pipes typically have a pressure capacity of approximately 1000 psi, compared to the 300 psi HDPE pipes. The pipe type also allow easy repair in case of damage. With the higher capacity of the steel pipe, a few bigger water pump can be deployed instead of a number of small water pumps. This will reduce the number of personnel required to monitor the pump station. Author has not seen thorough study in water system optimization, hence this could also be a good subject for future study, in relation to cost optimization.

Well Pad

In relation to the water supply availability, it is important to choose the location of the well pad that is optimum for water supply. This can reduce the amount of pipeline construction, which may expose the company to a variety of issue such as land clearance and acquisition with the government or the community. Since most geothermal project location in Indonesia is located in places with minimum access, evaluation of existing access roads and facilities in the area to the well pad can reduce cost of infrastructure. Hazard issue such as landslides should also be identified before starting construction of well pad, so that safeguards can be built in place. Well pads that are built at a lower elevation will have lower risk compared to the ones built at higher elevation. The lower elevation well pads also require less time for travel and will most likely have a better well trajectory and shallower well TD as heat source are normally located closer to the base of a mountain. The typical well pad requires 1-1.5 hectares of area for a maximum of three wells. For future cost saving, the well pad should be mapped, and the number of wells should be decided before the well pad is constructed. Future expansions, workovers, or future well test should be considered so that production pipeline design can be planned out beforehand to avoid future delays in the project.

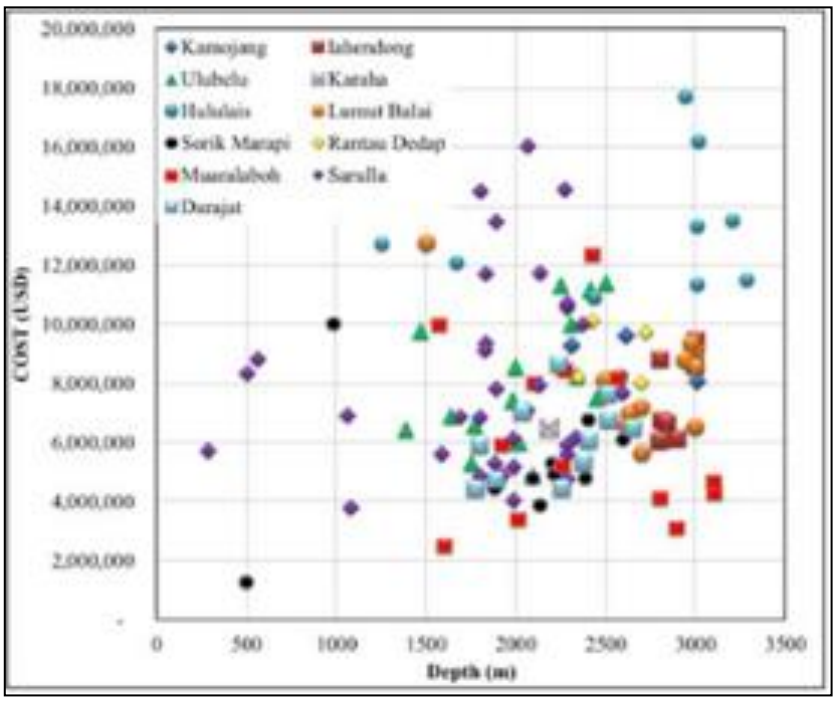


Figure 1: Geothermal well depth versus depth (Purwanto, Suwarno, Lukman, & Herdiyanto, 2018).

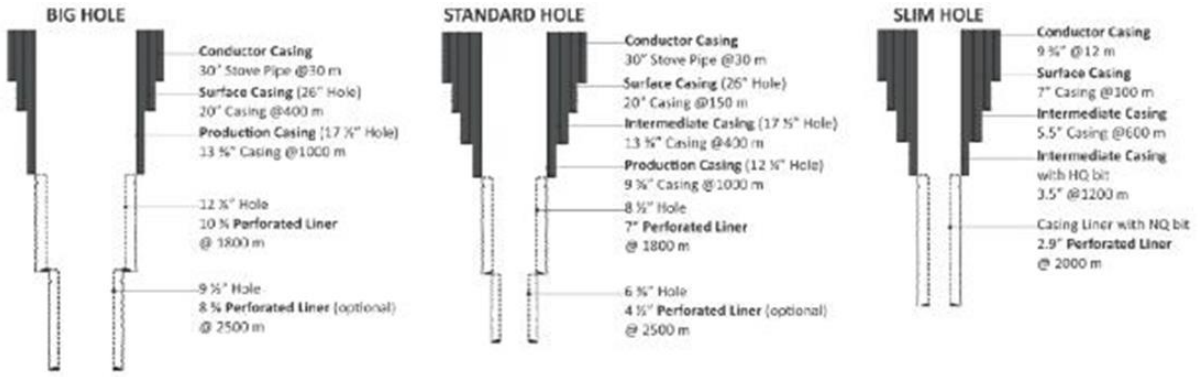


Figure 2: Common well size in geothermal drilling (Purba, Adiyatama, Umam, & Muhammad, 2019).

Community Issue

One of the most crucial part of all operations is the people or the community. In most geothermal drilling project Indonesia, the drilling site is often located near villages far from established facilities. Mobilization through these areas will inevitably force the operation team to involve the people in the area. Negotiations and public awareness have to be made ahead of time before the project starts to avoid any future issue with the community. As discussed in publication, community lands or tanah adat might be hard to acquire from the locals. Furthermore, productive lands that are used as farming lands might require long negotiations before it can actually be acquired (Purba, Adiyatama, Umam, & Muhammad, 2019). Utilizing local water sources may also receive negative feedbacks from the community as it disrupts their normal activities. During all parts of the project, the community has to be involved. Local workers should be hired to avoid issues during operations. Delay in operations will be costly as it stops drilling activity, increasing non-productive time. One of the options to avoid conflict is to involve local police force to help escort truck convoys during mobilizations. Periodic training or CSRs should also be given to empower the locals. Initiatives for the community will need to be done regularly to avoid any hindrance to the operations. It is important to keep in mind that drilling is a function of time, but without the people there will be no operation. In general, approach to the community must not merely be seen as obligation. The company must carry the spirit to develop the social-economy level of the community.

Material Selection

Some of the materials that needs to be selected prior to the start of a drilling project are casing and well head. The idea is we need to purchase material that is suitable for the application, but not to be over-spec. Also, some materials are easier to run hence potential for rig-time saving.

Casing Cost

Various grades of casing exist and serves different purposes in the energy industry. In the geothermal industry, the most important property of the casing is that it has to be able to withstand high temperature. According to various literature and experiences, casing grade L-80 will be the best casing for the production section. Furthermore, to save time, using quick type connection, operation can save up to 15 minutes rig time per joint, which can add up to a net saving of $550/joint (assuming rig cost of $3,000/hr and $200 cost for quick connection). Casing price can also be affected by the origin of the manufacturer. It is often thought that Chinese manufactured casing is cheaper than others. Some operator may be reluctant to use Chinese manufactured casing due to lack of quality, however mitigation such as detailed quality checking can ensure the quality of materials and save the cost of a well in the long run.

Well head

Choosing the right wellhead type can save significant rig time. Two types of well head are the slip-on weld and the pre welded wellhead. From experience, the pre-welded wellhead installation tends to be faster and can save up to one day of rig time.

Table 1: Comparison of different contract types.

Description	Discrete	ISM	SIPM	IPM
Operator Risk	Very Low	Low	Medium	High
Project Manager	Company Rep	Company Rep	Contractor Rep	Contractor Rep
Well Cost	5-6 M	4-5 M	7-8 M	7-10 M
Resources	>10 person	3-8 person	3-5 person	2-3 person
No. of Contract	30-50	<10	2-5	1
Dispute Risk	Very Low	Low	Medium	High
Procurement Time				
Materials	6-9 months	6-9 months	6-12 months	6-12 months
Services	9-12 months	5-8 months	9-18 months	9-15 months
Interface	>15 Reps	3-10 Reps	3-5 Reps	1 Reps
Penalty	Individual	Individual	All Services	All Services
Excess Material	Yes	Yes	Yes	None
Master List Facility	Company to Provide	Company to Provide	Company to Provide	None
Tax Over Tax	None	None-Minimum	Sub Contractors to SIPM	Sub Contractors to IPM
Double Profit	None	None-Minimum	Sub Contractors to SIPM	Sub Contractors to IPM
Mob/Demob	Individual	Individual-Share	Individual-Share	Share
Lesson Learnt	Minimum	Available	Available	Available
Vendor List	Lot	Lot	Adequate	Adequate
Charging Method	Direct to Company	Direct to Company	Direct to Company	To IPM Leader-To Company

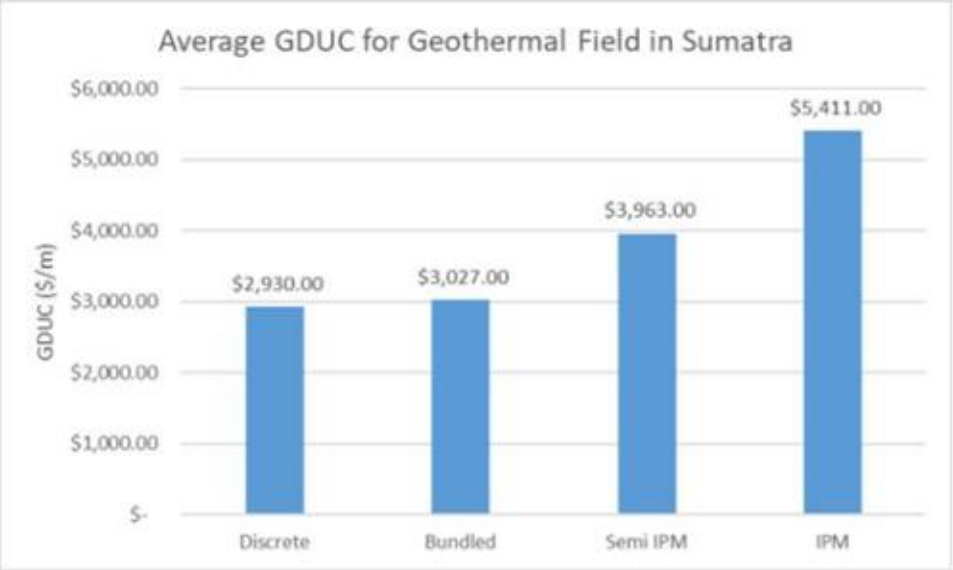


Figure 3: Average geothermal drilling unit cost in Sumatra.

Contract Strategy

Contract is an important part of the project as it defines the scope of work of the contractors. Determining the contract type that aligns with the company's goal, size, and budget will save cost in the long run. Table 1 compares the types of contract found in geothermal industry. One strategy to optimize contract is to use discrete contract to hire third party contractors. This will reduce the operator's risk and be able to obtain the most competitive price for the services are controlled to align with the company's goal and budget. According to published study (Purwanto, Suwarno, Lukman, & Herdiyanto, 2018), the discrete contract is the lowest priced compared to the other contract types (Figure 3).

During daily operation, drilling team will deal with various service contractors. It is best that all of the service contractors have a clear statement on when their charges are applicable. For example, the most cost efficient would be after the well has been spudded or only when instruction to perform has been issued. Standby charges conditions, such as during pad moving should also be clearly defined. Negotiations with the contractors should be done during tender process. In addition, the contracts should also determine the minimum requirement of experience for the personnel working on the project.

Rig Selection

One of the contracts that needs to be critically assessed prior to the start of the project is the rig contract. The rig selection will depend on the size of the well that has been chosen. The two major types

of rigs are the >1000 HP (for big bore and standard hole) and the 150-220 HP (for slim holes). It is important to choose the rig size appropriate for the chosen well design. The rig size will affect the mobilization cost as bigger size requires more loads, time and fuel. Some of the rig criteria that should be taken into consideration in saving cost is shown in Table 2 below.

Operation Efficiency

Cost saving initiatives must also be done to the various parts of the daily drilling operation. Some of the major contractors in operation includes, but not limited to, directional drilling, drilling fluid, cementing, drilling bit, pipe recovery, and fuel consumption.

Directional Drilling

In geothermal drilling, directional drilling will most likely be needed to reach the target heat zone due to the location of geothermal sites previously mentioned in the infrastructure section. Directional drilling cost will also be affected by the location of the site and wellhead as it affects the final well trajectory. One of the cost saving initiatives that can be taken to make sure the directional drilling cost is optimum is making sure the contract explicitly states specific charges that can be applied to the company.

Drilling Bits

In saving cost for drilling bits, the end goal is to save time and number of bits being used. One of the advancement in drilling bit is the Kymera bit, which is a combination of roller cone and PDC bit developed by Baker Hughes. The bit have been proven to save drilling cost by increasing the ROP and total depth per bit run in geothermal wells and ultimately reducing the cost per unit depth when compared to standard roller cone bits (Rickard, Bailey, Pahler, & Cory, 2014). Drilling engineers should consult with geologist to determine what type of formation the bit will have to go through. In the earlier section, an expensive Kymera bit might not be needed if a normal PDC/roller cone bit can do the job. Calculation can also be done to determine when each bit will be more economic for the well based on the length of each hole section.

Cementing Cost

For geothermal well, cementing is normally done from the top section down to the section prior to the production zone (normally 13-3/8" tie-back casing). Similar to drilling fluid, using book price should be avoided and the consumables should be included in the initial contract. Cement recipes and mixture should also be specified beforehand to avoid any new untested recipes being used during actual operation. There has been some engineering improvement in slurry design that is applicable for geothermal lost-circulation situation. In addition, to save time, top job cement or remedial cementing should be done offline or parallel with productive rig time. During wait on cement (WOC), rig offline jobs should be done to be productive. Running BHA during WOC is also an option if it is not too risky.

Table 2: Different rig function applicable for cost saving.

Rig Equipment Capability	Function
Overhead BOP Crane	Reduce flat rig time: faster NU & ND BOP
BOP Test Stump	Reduce flat rig time: Offline BOP pressure test.
Split Type Rotary Table	Capable run pre-welded wellhead with production casing
Rig Skidding Devices	Easier and faster to rig move between well in same well pad.
Rig Skid with DP stands	Reduce rig time to LD and re-MU DP stands
Drill String MU equipment	Faster and saver MU drill string
Offline MU DP stand	Reduce flat rig time: Offline MU stand DP
DP hard banding	Avoid rig time to LD DP and replace.
DP internal coating	Prevent DP washout, avoid extra BHA trip
Complete Fishing Tool and Inspected	Rig to provide complete and detail fishing tool, including capable to fish internal parts of downhole equipment
Sufficient heavy equipment on site	To avoid delays from availability of heavy equipment

Pipe Recovery

With total loss circulation drilling, stuck pipe becomes a common problem in geothermal drilling. Pipe recovery becomes a contingency in case the pipe becomes unable to be freed using conventional means. Since pipe recovery services are not part of the daily operations, it is important to clearly state the standby rate/operating rate in the contract. If explosives are part of the pipe recovery, the cost of permits, bunkers, mobilization, and disposal must be included as part of the pricing. Another option is to use mechanical pipe cutter. The downside is mechanical pipe cutter can only cut drill pipe.

Fuel Consumption

Fuel is a crucial part of operations that also demands cost control. As mentioned in the previous sections, geothermal sites in Indonesia are often far from existing surface facilities and access might be far, if not limited. Therefore, it is very important to manage fuel availability in order to avoid rig standby due to fuel shortage. Supply runs must also be scheduled and organized to avoid delays. The 1500 HP old rig for example, can take up to 12,000 L/day of fuel. In order to save cost and avoid extreme price fluctuation, fuel price handling cost should be stated on the contract. One last note, since the fuel used in Indonesia are mostly biosolar, standard quality of fuel is best to be stated in the contract. From experience, due to the cold weather in the mountain, these fuels tend to form gels, which is detrimental to the efficiency of the equipment on site. If quality control can be maintained and ideal storage condition maintained on site, equipment downtime due to fuel can be avoided.

FUTURE IMPROVEMENT

Accurate drilling planning and costing is an important design step prior and during geothermal drilling operation. Initiatives to reduce cost should always be taken when possible. These initiatives normally come from various experiences of the drilling engineers and management involved. The initiatives discussed in this paper are summarized below (Table 3). Due to various interests, currently there are only a few published data of cost saving initiatives and geothermal well cost in Indonesia. Future improvements such as published documentations of cost savings in geothermal well will help drilling engineers develop a better well economics for the project.

CONCLUSION

Indonesia holds huge potential for future geothermal drilling projects. In order to ensure the projects are economically feasible for companies, one of the most important responsibility that drilling engineers must carry is to optimize the cost of wells. Some of the initiatives that can be taken is optimizing the well design, infrastructure, materials, contract strategy, and operations. Choosing the right equipment, material, contract, and personnel for the operation are some of cost-saving initiatives management can take in these categories. As drilling cost is a function of time, it is crucial to identify time-saving initiatives in the whole drilling operation planning in order to save cost, from the beginning to the end. Some future improvements that can be done regarding cost saving in the geothermal industry is to gather data from various geothermal project about the main cost and problem in cost controlling during drilling. In the future, these data will become valuable towards becoming the largest geothermal energy producer country in the world.

Table 3: Summary of cost-saving initiatives.

Components	Cost Saving Initiatives
Target Depth	Determine feed zones, drill shallow-effective wells if possible
Well Sizing	Well size based on risk factor
Water Supply	Distance, pipe material, number of pump station
Well Pad	Low elevation, existing surface facilities, plan for future operations
Community Issue	Socialization, regular training, development spirit.
Casing Cost	Casing material hi-temp resistance, detailed quality checks, quick connection
Well Head	Quick to install, pre-welded
Rig Selection	Adjust with well size, clear contract with rig contractor
Fuel Consumption	Fuel availability, fuel contract price
Directional Drilling	Clear contract, experienced personnel, smoothest trajectory to target
Drilling Bit	Hybrid bit saves time (need field-specific test)
Cementing Cost	Improved slurry design, additive for lost circulation, simultaneous offline operation
Drilling Fluid	Avoid book price, hi-vis in TLC, water in TLC
Pipe Recovery	Clear standby rate, clear price on explosive requirements

REFERENCES

Apriani, D., Randle, J., & Paripurna, A. (2018). "Government Drilling Program for Geothermal Exploration in Indonesia". 40th New Zealand Geothermal Workshop. Taupo.

Gul, S., & Aslanoglu, V. (2018). “Drilling and Well Completion Cost Analysis of Geothermal Wells in Turkey”. 43rd Workshop on Geothermal Reservoir Engineering. Stanford.

Kipsang, C. (2015). “Cost Models for Geothermal Wells”. World Geothermal Congress. Melbourne.

Purba, D. P., Adiyatama, D. W., Umam, M. F., & Muhammad, F. (2019). “Key Considerations in Developing Strategy for Geothermal Exploration Drilling Project in Indonesia”. 44th Workshop on Geothermal Reservoir Engineering. Stanford.

Purwanto, E. H., Suwarno, E., Lukman, R. F., & Herdiyanto, B. (2018). “Geothermal Drilling in Indonesia: A Review of Drilling Operation, Evaluation of Well Cost and Well Capacity”. The 6th Indonesian Geothermal Convention and Exhibition. Jakarta.

Rickard, W., Bailey, A., Pahler, M., & Cory, S. (2014). “Kymera Hybrid Bit Technology Reduces Drilling Cost”. Thirty-Ninth Workshop on Geothermal Reservoir Engineering. Stanford.

CORROSION PREVENTION OF BURRIED REINJECTION PIPELINE USING GEOTHERMAL-POWERED IMPRESSED CURRENT CATHODIC PROTECTION IN LAHENDONG GEOTHERMAL AREA

Viqar Adly Gani, Achmad Ardialim, Ahmad Indra Sakti, Luhung Pravubinantaka, Albarrosyah Putra

PT. Pertamina Geothermal Energy
Tomohon, North Sulawesi, Indonesia
Email: viqar.gani@pertamina.com

ABSTRACT

A low pH Brine that flows through carbon steel pipe to the reinjection well will expose a rapid rate of pipe corrosion. Moreover, underground installation of pipe will multiply this corrosion effect and lead in environment pollution and financial losses. This issue could be reduced by applying novel method of corrosion prevention named Geothermal-powered Impressed Current Cathodic Protection (GICCP). This system utilizes a geothermal power source from heat of geothermal pipeline and converts to electric power by using thermoelectric device. Then the electric power is used in GICCP to develop a high potential difference between the surface of pipe to be protected and an anode. It is expected that the implementation of GICCP could inhibit the corrosion rate, extend the remaining life of pipeline, and reduce downtime period as well as the possibility of financial losses in geothermal industry.

Keywords: corrosion, geothermal-powered impressed current cathodic protection, brine

INTRODUCTION

The piping system is one of the most important and most widely used fluid distribution facilities in the industrial world. The fluid that is supplied by the pipe usually has its own characteristics so that it can affect the performance or quality of the pipe itself. The influencing characteristics include fluid temperature, fluid pH, fluid content, etc. One of the effects of the characteristics of an adverse fluid is the occurrence of corrosion which can cause failure in a material.

Corrosion is a natural process that cannot be avoided which can reduce the quality and physical properties of a material. One of the causes of the increase in the corrosion rate of a material is the low pH and the high temperature of the fluid flowing in the material. Corrosion is the electrochemical/chemical interaction process between metal materials and the environment that causes changes in metal properties so that there is a significant weakening of the function of metals, environment and systems. The process of corrosion in metals occurs because of the nature of metals that are easily oxidized both at low temperatures and at high temperatures (DIN EN ISO, 2015).

The common methodologies deployed to prevent Corrosion include the use of anodic and cathodic inhibitors, barrier coatings and sacrificial anodic method. However, it has been proven quite extensively in various research studies that the most efficient of these corrosion prevention techniques is Impressed Current Cathodic Protection. This technique involves impressing current over the cathode of the corrosion cell, thereby providing a stream of electrons over the metallic surface. This technique is clearly more preferred than the sacrificial anode system. The voltage differences between anode and cathode are limited in sacrificial anode systems to approximately one volt or less, depending on the anode material and particular environment. Impressed current systems can use larger voltage differences. The larger voltages available with impressed currents allow remote anode locations,producing more efficient current distribution patterns along the protected cathode. These larger voltages are useful in low conductivity environments such as freshwater and concrete (Shankar et al., 2014).

In this proposed system of Impressed Current Cathodic Protection, output power from the heat of geothermal pipeline is converted into electric power by using thermoelectric device. Then it used to charge and recharge the DC battery source enabling continuous current supply to the iron pipelines employed as the cathode. The subject of corrosion has undergone an irreversible transformation from a state of isolation and obscurity to a recognized discipline of engineering, making it a subject of extreme importance that requires attention. In this era of energy and power crisis, renewable energy sources like geothermal energy exhibit their potential to provide a complete solution to various challenges facing mankind, when used in conjunction with existing protection principles available.

CORROSION

Corrosion is an electrochemical oxidation reaction that requires an anode, a cathode, an electron pathway and an electrolyte to take place. The complete system comprising these components is

called a corrosion cell. The process of corrosion is mostly a nuisance since it leads to the damage of metals and must be prevented from taking place. This is often the case in buried metallic structures such as pipelines, oil storage tanks, oil and gas wells, offshore structures, seagoing ship hulls, marine pilings, water tanks and some chemical equipment (Table 1) (Kean and Davies, 1981).

The anode is generally represented as the negative terminal of the electrolytic cell. In Impressed Current Cathodic Protection method, the positive terminal of the battery is connected to the anode. Zinc has been employed as the anode in this model. Zinc is a good conductor of electricity and enhances low current density current discharge. It also offers low resistance to the electrolyte due its high ratio of surface area to weight. The consumption rate of zinc is about 0.25 Kg/A/Year which makes it a favorable and an economical choice, among the different anode materials available (Shankar et al., 2014).

The consideration of using zinc as the anode in this cathodic protection system is because zinc is commonly used in underground pipeline system. Zinc has density of 7.1 g m^{-3}, potential volts of -1.10 Cu/CuSO_4, and Amp-hrs of 780 per kg (Francis,).

The potential required for cathodic protection in this model is -850mV (Table 2). If it meets these criteria, the pipe will be well protected.

The Cathode is generally represented as the positive terminal of the electrolytic cell. In Impressed Current Cathodic Protection method, the negative terminal of the battery is connected to the cathode. An iron pipe has been employed as the cathode in this model and the objective of deploying this method is to protect the iron pipe from Corrosion. The utility of iron pipelines in transporting commercial liquids over long distances is significant and thereby it is chosen as the cathodic material in this model (Shankar et al., 2014).

The electrolyte is the electrically conductive solution that enables the flow of electrons and must be present for corrosion to occur (Table 3). Soil has been utilized as the electrolyte due to its ability to enhance corrosion owing to differences in soil resistivity, oxygen concentrations, moisture content and various ion concentrations. It is a medium that contributes a great deal to the corrosion of underground pipelines when left unprotected (Shankar et al., 2014).

Table 1: Common Reference Electrodes and Their Potentials and Temperature Coefficients (NACE International Standard, 2013).

Reference Electrode	Electrolyte Solution	Potential at 25 °C [77 °F] (V/SHE)	Potential at 25 °C [77 °F] (V/CSE)	Temperature Coefficient mV/°C (mV/°F)	Typical Usage
$Cu/CuSO_4$ (CSE)	Sat. $CuSO_4$	+0.316[76]	0	0.9 (0.5)[76]	soils, fresh water
Ag/AgCl[(A)] (SSC)	0.6 M NaCl (3 ½%)	+0.256[77]	–0.06	– 0.33 (0.18)[77]	seawater, brackish[(B)]
Ag/AgCl[(C)] (SSC)	Sat. KCl	+0.222[78]	–0.094	– 0.70 (0.39)[78]	---
Ag/AgCl[(C)] (SSC)	0.1 N KCl	+0.288[79]	–0.028	– 0.43 (0.24)[79]	---
Sat. Calomel (SCE)	Sat. KCl	+0.244[10]	–0.072	– 0.70 (0.39)[10]	water, laboratory
Zn (ZRE)	Saline Solution	–0.79 ± 0.1[65]	–1.1 ± 0.1[65]	---	seawater
Zn (ZRE)	Soil	–0.80 ± 0.1[65]	–1.1 ± 0.1[65]	---	underground

[(A)]Solid junction.
[(B)]Potential becomes more electropositive with increasing resistivity. See nomograph for correction in waters of varying resistivity in NACE SP0176,[10] or see reference 77.
[(C)]Liquid junction.

Table 2: Potential required for cathodic protection (Francis,).

Metal	Potential (Cu/CuSO_4)
Steel	-850 mV
Steel (sulphate reducing bacteria)	-950 mV
Copper alloys	-500 to -650 mV
Lead	-600 mV
Aluminum	-950 to -1200 mV

Table 3: Current densities required to protect steel (Francis,).

Environment	Current density A m^{-2}
Acidic solutions	350 - 500
Saline solutions	-.3 - 10
Sea water	0.05 – 0.15
Saline mud	0.025 – 0.05

MECHANISM OF CORROSION IN UNDERGROUND PIPELINES

In the case of underground iron pipelines, corrosion is quite significant because corrosion cell components are prevalent inherently and enhance the process of corrosion. These iron pipelines run over long distances without any kind of protection against corrosion. The iron pipelines are subjected to the aggressive action of organic and inorganic anions and the interaction results in the corrosion process. This makes this process an electrochemical or a spontaneous process (Ferraris et al., 2012).
In observing the mechanism of corrosion in iron it is noticed that Fe^{2+} ions are released from the anode by the process of oxidation and OH^- ions from the cathode by reduction on the metal surface. The negative and positive ions combine together to form a white precipitate of solid Iron (II) Hydroxide. The various chemical reactions are as follows: (Shankar et al., 2014)

Oxidation half reaction:
Fe(s)$\rightarrow Fe^{2+}(aq) + 2e^-$ (1)

Reduction half reaction:
O_2 (g) + $2H_2O$ (l) + $4e^- \rightarrow 4OH^-$ (2)

Overall equation:

$Fe^{2+} + 2OH^- \rightarrow FE(OH)_2(s)$ (3)

The rate of anode reaction must equal the rate of cathode reaction in the corrosion cell. The corrosion process is eliminated by inhibiting the occurrence of any one of these reactions from taking place (Ferraris et al., 2012). A soil with lower resistivity is more effective as an electrolyte and a conductive path, facilitating galvanic corrosion (Purwanto, 2010).

Table 4: Soil Resistivity and Corrosivity (Purwanto, 2010)

Field-Measured Soil Resistivity (ohm-cm)	Soil Corrosiveness in Disturbed Soils
<1,000	Severely corrosive
1,000-5,000	Corrosive
5,000-10,000	Moderately corrosive
>10,000	Slightly corrosive

The potential possessed by steel in aerated soil (eg sand) does not differ greatly from steel potential in non-aerated soils (eg clay). However, if there is damage to the cover or pipe lining and contact with different types of soil, there will be potential differences that can cause corrosion currents in the soil. Pipe coating damage in non-aerated (clay) soils, corrosion can occur with a corrosion rate of more than one tenth (0.1) mm per year (Purwanto, 2010). Figure 1 shows the external factors that affecting soil corrosion.

CATHODIC PROTECTION PRINCIPLE

Cathodic protection is an electrical means of mitigating corrosion on buried and submerged structures. Cathodic Protection involves the application of a DC (direct current) onto the surface of a metal structure. Since corrosion only occurs at locations where current discharges from a metal surface, corrosion control may be achieved by applying a net DC current flow onto the entire surface of a structure. In those areas where current collects, corrosion is controlled (1``, 2010).

Two types of cathodic protection systems exist. The first type uses galvanic anodes for protection and the second type of system is an impressed current system. For the impressed current cathodic protection system, this system utilizes an external power source to develop a high potential difference between the surface to be protected and an anode. A series of anodes installed in the ground are referred to as a groundbed. Impressed current type systems are advantageous because high driving voltages can be developed with an external power supply. (Purwanto, 2010)

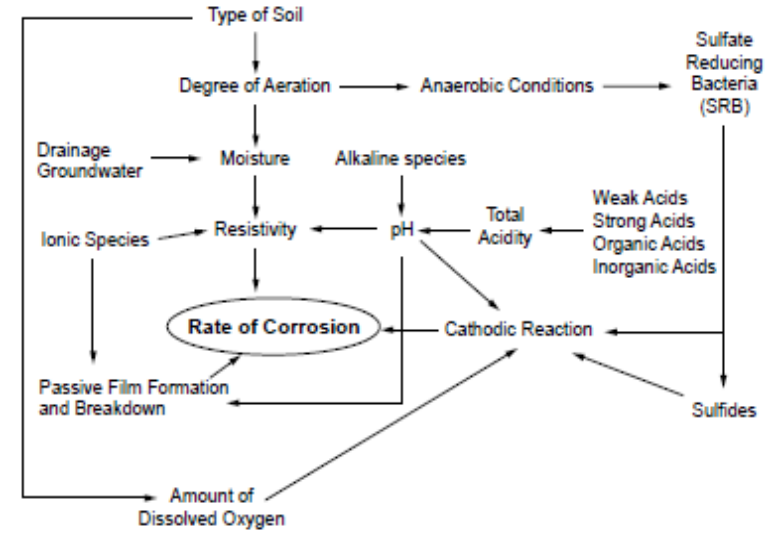


Figure 1: External Factors that Affecting Soil Corrosion (Purwanto, 2010).

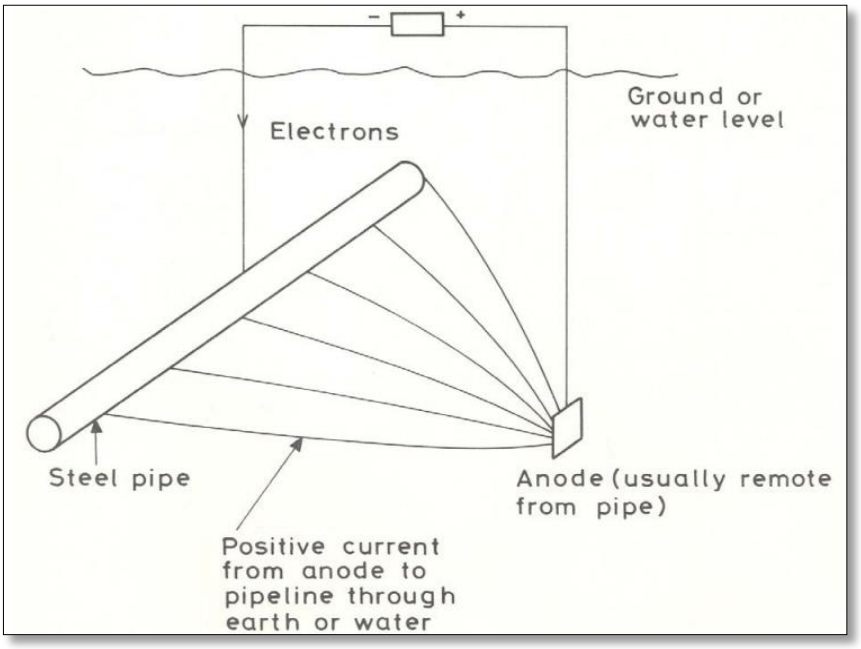


Figure 2: Impressed Current Cathodic Protection principle (Purwanto, 2010).

DESIGNING GEOTHERMAL-POWERED IMPRESSED CURRENT CATHODIC PROTECTION SYSTEM

Geothermal-powered Impressed Current Cathodic Protection system will be used primarily in underground/buried pipeline where the electrolyte resistivity is high and is more economically feasible compared to ordinary sacrificial anodic protection systems. The proposed Geothermal-powered Impressed Current Cathodic Protection experimental set-up consists of a typical electrochemical cell wherein the pipeline acts as the cathode and zinc acts as the anode. Soil is deployed as the electrolyte to ensure current passage. The driving force for this set-up is a 12volts, 20 ampere-hour lead acid battery, which is charged by the thermoelectric setup. The generated output voltage from the thermoelectric system is regulated adequately using LM723 voltage regulator. The LM723 voltage regulator also ensures the battery is prevented from overcharging. Geothermal-powered Impressed Current Cathodic Protection is preferred over sacrificial anode method as it ensures low capital investment is incurred for protection of underground/buried pipeline. Figure 2 shows the impressed current cathodic protection principle.

Impressed current systems typically use a power source known as a rectifier. The rectifier converts ac power to dc power and provides adjustability to the system. The current output may be increased by increasing the voltage. A transformer is used to adjust the output voltage of the rectifier. This is accomplished by adjusting tap bars on the front panel of the unit. A rectifying element, such as a diode bridge circuit, is used to convert AC power to DC power (ripple) (Purwanto, 2010).

Geothermal-powered Impressed Current Cathodic Protection has a clear edge over other methods of corrosion prevention. It makes it possible to adjust the current and voltage, with an ability to provide an unlimited current output. (Shankar et al., 2014) This technique can be adopted over a wide range of resistive environments and works quite well on underground/buried pipeline which are typically employed in most of the geothermal industrial sectors. Figure 3 shows the design of geothermal-powered impressed current cathodic protection. Figure 4 shows the schematic diagram of geothermal-powered impressed current cathodic protection system.

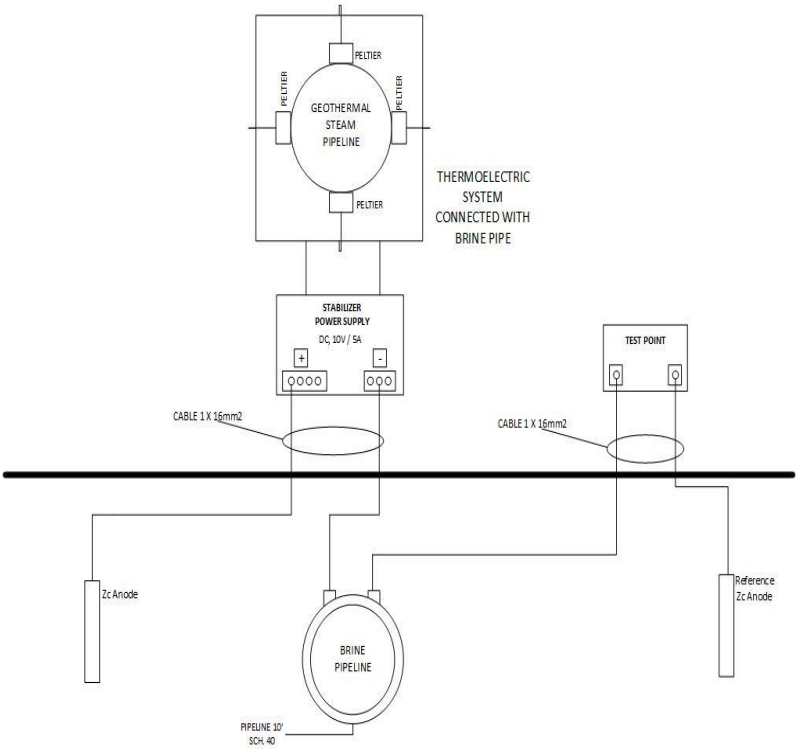


Figure 3: Design of Geothermal-powered Impressed Current Cathodic Protection.

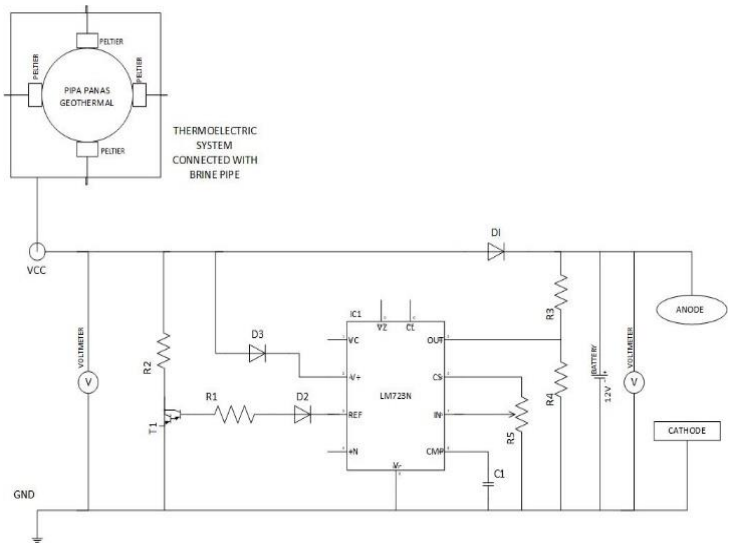


Figure 4: Schematic Diagram of Geothermal-powered Impressed Current Cathodic Protection System.

Material used for this system
- Reducing Volt LM723 Adjustable DC to AC Voltage: 2ea
- Thermal Adhesive Tape 3M Double Side 9448A: 2ea
- Heatsink 40x40x11 mm: 40ea
- Peltier Thermoelectric Module SP1848-27145: 40ea
- DC-DC Boost Converter Digital 400W: 1ea
- Dual Display voltmeter digital: 5ea
- Zinc Anode WW B9 (8.3 Kg): 2ea

The voltage generated from the thermoelectric system is utilized as power source of this system and to charge the battery to its maximum level. By employing the LM723 regulator, current and voltage are sensed using the current meter and voltage meter. The output voltage of the battery is given back to the inverting input of the voltage regulator to obtain a constant output voltage on -850mV. Capacitor C1 is used for frequency compensation and to bypass high frequency noises. Thermoelectric system will charge the battery and also supplies current to the pipeline all day long. In this system, battery is used as a backup energy storage and as the stabilizer when the output current from the thermoelectric system is unstable.

CALCULATION

The pipe that want to be protected is 10-inch SCH 40 carbon steel pipe and have 1500m length. To calculate the surface area to be protected:

SA = π x OD x L …… (1)

Where, OD = outside diameter of pipe (m)
L = length of pipe (m)
π = 3.14519
SA = Area to be protected (m^2)

Based on this equation, the size of the area to be protected is about 1285.83 m^2

Electrical Current Requirement

$$I = \left[\frac{SA \; x \; CD \; x \; CB}{1000} \right] x \; (1+SF_1) \ldots\ldots\ldots\ldots\ldots\ldots (2)$$

Where,
I_t = the total current needed to protect the pipe(A)
SA = surface area to be protected (m^2)
CD = current density in ambient temperature (mA/m^2)
CB = The damage of protected layer
SF_1 = Safety factor

Based on this equation, the total current needed to protect the pipe is 3214.375 mA

Geothermal pipe temperature is about 125° celcius, and the ambient temperature is 25° celcius. Then with temperature difference about 100°Celcius, peltier SP1848-27145SA can produce around 4.8V and 669mA. For supplying the Geothermal-powered Impressed Current Cathodic Protection system, it needs = 3214.375 mA/669mA =4,8= ~5 peltier. The voltage needs 9.5/4.8 = 1,97=~2. Then total peltier needs 5x2 = 10 peltier

CONCLUSION

Based on the obtained discussion and literature review
1. The utilization of heat from geothermal steam pipeline as a source of electrical energy for the impressed current cathodic protection system is a new breakthrough in the process of corrosion prevention that can be applied to underground/buried pipeline system.
2. The success of applying this impressed current cathodic protection can be achieved by maintaining the stability of the energy source which is equal to 10V / 5A and maintaining the potential difference of the anode and cathode by more negative than -850 mV.

REFERENCES

Francis, P., E.,"Cathodic Protection". Cathodic Protection/BM.

DIN EN ISO 8044 (2015), "Corrosion of metals and alloys – Basic terms and definitions".

Durham, M. O. and Durham, R. A., (2005), "Cathodic Protection". IEEE Industry applications Magazine.

Eur Ing R. L. Kean of ARK Corrosion Services and K. G. Davies (1981), "Cathodic Protection", Corrosion Engineer, this is an update of a DTI publication first issued in, pp. 1-8

Ferraris, F., Parvis, M., Angelini, E., Grassini, S., (2012) "Measuring system for enhanced cathodic corrosion protection", Instrumentation and Measurement Technology conference, IEEE International, pp-1583 – 1587.

NACE International Standard (2013), "Control of External Corrosion on Underground or Submerged Metallic Piping System", National Association of Corrosion Engineer, pp 1-60.

Purwanto, T.P. (2010), "Cathodic Protection". Modul 6.

Purwanto, T.P. (2010), "Corrosion Control and Cathodic Protection".

Purwanto, T.P. (2010), "Underground Corrosion". Modul 3.

Sai Shankar B., K P Pranav., Kirain Raj R (2014), "Solar Powered Corrosion Prevention in Iron Pipelines using Impressed Current Cathodic Protection". Sri Sai Ram Engineering College, pp-1-6.

Sulistijono., "Desain sistem proteksi katodik arus paksa (iccp) untuk pipa air didalam tanah". T. Material & Metalurgi FTI-ITS, pp-1-21.

A THERMAL CASING CONNECTION TEST FOR GEOTHERMAL WELLS IN KS ORKA

M. Fahmi.Sungkar[1], Hendra Simanjuntak[1], Boga Isa[2], Ashadi Ashadi[2], and Yudi Hartono[2]

[1]PT. Citra Tubindo Tbk
[2]KS ORKA (PT SMGP and PT SGI)
Email: fahmi.sungkar@citratubindo.com

ABSTRACT

Determining the proper casing and its connection for geothermal wells is very crucial. The casing and its connection experience various loads not only during drilling operations but also during production operations. In order to determine the suitable connections, various loads to the casings and connection during drilling and production are simulated. This paper presents the testing protocol used to qualify the Premium NS-CC connection used by KS ORKA (Sorik Marapi and Sokoria), a geothermal operator in Indonesia on the 13 3/8'' 68# L80 Type 1 production casing. The testing protocol is referred to the ISO/PAS 12835:2013, Thermal Well Casing Connection Evaluation Protocol (TWCCEP), with some abbreviation. The test was conducted using 2+2 casing specimens at PT Citra Tubindo testing facility in Batam, Indonesia. Total of 30 thermal load cycles at temperature range of 35º – 290º C have been used to anticipate geothermal well life time as requested by KS ORKA drilling team. This paper summarizes the testing process from beginning to the end and the successful testing result of the NS-CC Premium casing connection that are used in KS ORKA (Sorik Marapi and Sokoria).

Keywords: Drilling, casing connection test, thermal cycle, production casing, geothermal well, TWCCEP, casing design

INTRODUCTION

KS ORKA is one of the geothermal operators in Indonesia that currently has two concession areas operated by its subsidiaries. The first one is located in Mandailing Natal District, North Sumatra which is operated by PT. Sorik Marapi Geothermal Power (SMGP). The second one is located in Ende, East Nusa Tenggara which is operated by PT. Sokoria Geothermal Indonesia (SGI). Since August 2018, KS ORKA has drilled a total of 24 wells, both in Sorik Marapi and Sokoria. All wells are mostly using NS-CC connection for its Production Casing section (Liner & Tie Back). NS-CC Connection is a Premium Gas Tight Connection that has a same performance as the pipe body, which was considered as a suitable connection to handle KS ORKA well challenges. One of the challenges faced by KS ORKA is the reservoir condition where the steam production temperature could be as high as 280º C during its production activity. The other challenge is the profitability of all of their projects must be maintained for minimum 30 years of production. To provide additional assurance to KS ORKA, PT. Citra Tubindo Tbk (PTCT), a subsidiary of Vallourec Group, has conducted a Thermal Test using 13-3/8" 68# L80 Type 1 NS-CC Premium Connection at CDEC Facility (Connection Development & Evaluation Center), that can mimic the actual wellbore condition especially during the production. CDEC facility is PTCT inhouse tubular testing facility that can simulate a testing protocol based on ISO 13679, API 5C5, or ISO: PAS 12835:2013 TWCCEP. The objective of this technical paper is to report the qualification test conducted to NS-CC Premium Connection from beginning to the end.

WHAT IS TWCCEP?

Casing connections in thermal wells experience extreme loads due to exposure of high temperatures steam between 180ºC-350ºC in cemented condition. Thermal Well Casing Connection Evaluation Protocol (TWCCEP) was published as ISO Publicly Available Specification (PAS) 12835 on 2013–12-15 purposely for oil and gas Industry.

TWCCEP provides procedures for assessing the suitability of threaded connections for service in intermediate or production casing strings of thermal recovery wells initially for Cyclic Steam Stimulation (CSS) and Steam Assisted Gravity Drainage (SAGD). TWCCEP has been developed through a multi-client project (MCP), coordinated by Noetic Engineering 2008 Inc (Noetic) and sponsored by operators and connection manufacturers involved in thermal-well operations in Canada. TWCCEP is intended for connection assessments for strain-based design applications. It is not intended for elastic-design applications addressed by ISO 13679 and API 5C5.

The thermal casing connection test for KS ORKA was conducted as part of assurance drilling program and refer to ISO: PAS 12835:2013 TWCCEP protocol with several abbreviation on Casing 13-3/8" 68# L80 Type 1. 30 thermal load cycles with ASL 290 are chosen to simulate the conditions. Figure 1 shows the geothermal well design.

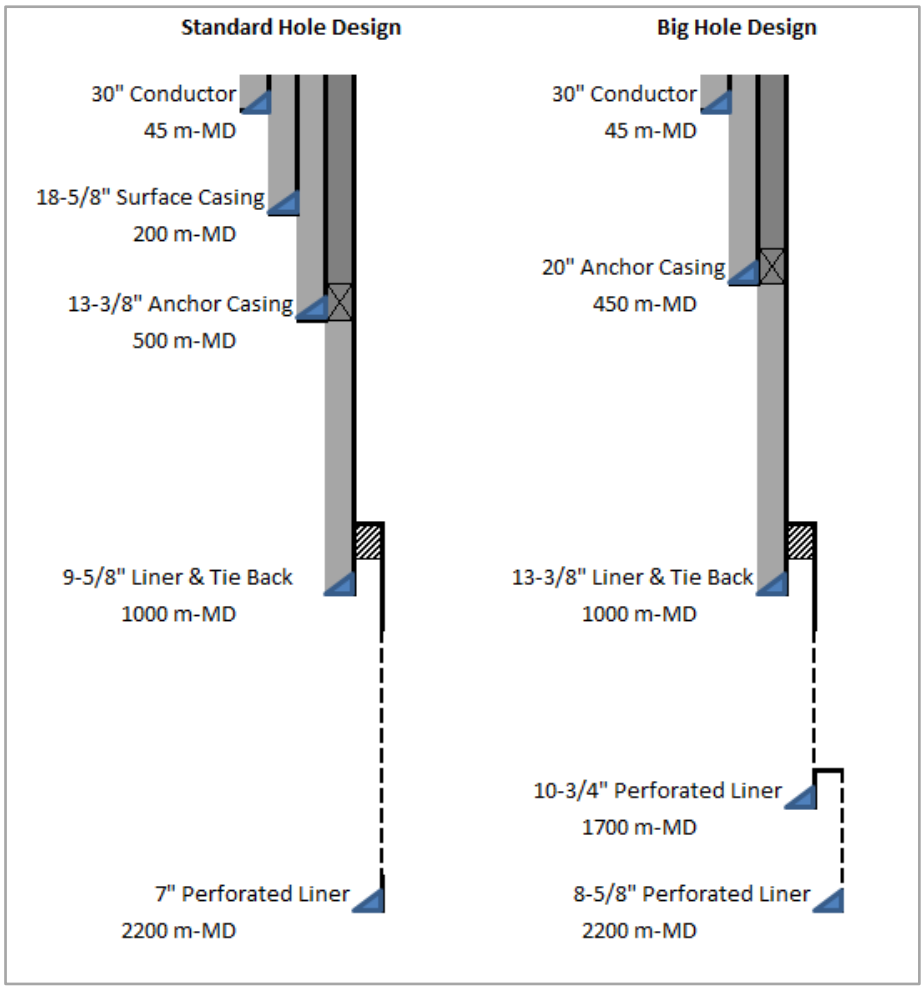


Figure 1: Geothermal Well Design.

GEOTHERMAL WELL DESIGN

There are two wells design in KS ORKA: 1. Standard Well Design and 2. Big Hole Well Design. The well trajectory for both designs are simple 2D model "J" type profile with hole inclination up to 40 deg inclination or 3-5 deg/100ft Dogleg. The anticipated static reservoir temperature is up to 280 deg C with bottom hole pressure not exceeding 1000 psi at the surface. Multiple fractures are anticipated when drilling the reservoir section covered by perforated production casing liner.

The production casing – Liner & Tieback (13-3/8" casing for Big Hole and 9-5/8" casing for Standard Hole) is the casing that experienced the highest load not only during drilling operations but also during production operations. During Production Operations, there are at least three activity that resulting different temperature range: Shut in, Flowing and Injection. This gives an axial load cycling that cause production casing in compression or in tension mode.

Failure in selecting the right type casing connection could cause casing or connection problem that lead to losing the well integrity, hence create catastrophic condition. KS ORKA, since beginning of Drilling Project, has used a NS-CC casing connection for most of its Production Casing, either for Big Hole or Standard Hole wells. There are 24 wells have been drilled up to date and all production casings are mostly using NS-CC premium connection.

QUALIFICATION CONTEXT

Testing Procedure and Reference Documents

The testing procedure was developed by PTCT, reviewed and agreed by KS ORKA. An Official Testing Procedure (OTP) number VRCC 18-0204 that refer to ISO: PAS 12835:2013 TWCCEP protocol with several abbreviation was finalized with highlights as following (Table 1):

1. Two sealability test sampel with 2 spare sample are prepared based on TWCCEP 1.3 Worst Case configuration, WST (Worst Sealability on Tension at low temperature) and WSC (Worst-case for Sealability in Compression at high temperature).
2. Total of 30 Thermal cycle is targeted insted of 10 Thermal Cycle (exceed TWCCEP requirements).

3. Optional Bending Test represented by Task 4.3 of the TWCCEP is not performed, since the 13-3/8" NS-CC Connection has already been evaluated on bending as per ISO 13679.
4. Limit Strain Test to be performed as per Task 4.4
5. Temperature tolerance during hold times is ± 15ºC both on Pipe body and Coupling.
6. A maximum of 6 thermocouples to be placedd on to monitor the temperature. No insulation method is used during testing.
7. No strain gauges to be placed on test samples.
8. Both test sample to be tested separately.

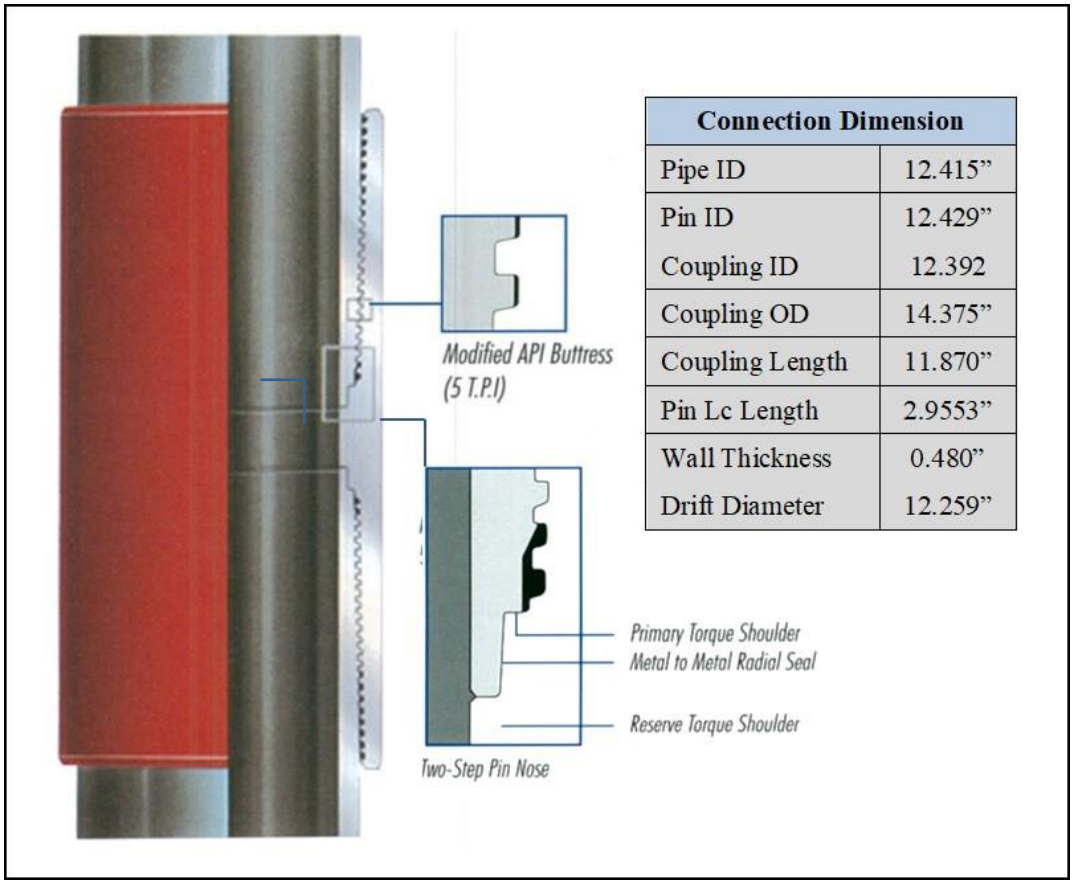
Table 1: Main Conditions of Testing.

Application severity level	ASL 290
Galling resistance test	2x Make & Break
Thermal Cycle (30x)	290ºC, maintain at zero strain
Limit Strain Test	Tension to failure (exceed the tensile strain threshold)

Connection Main Characteristic

NS-CC (NS Connection for Casing) is PTCT Proprietary Thread and Coupled (T&C) Gas Tight Connection providing the most field worthy tubular for oil and gas and geothermal application. KS ORKA drilling team has experience using NS-CC and has selected this casing connection for geothermal Production Casing application. This connection is also interchangeable with API BTC connection which give more flexibility on selecting the casing accessories. On Figure 2 we can found NS-CC Connection Design and Dimension for 13-3/8" pipes with 68 pound per foot (ppf/#).

NS-CC is a high performance gas-tight connection for a critical environments such as high compression, bending, fatigue resistance. The "Two-Step pin nose" allows the metal to metal seal to be protected from running, over torque damage, and also provide a high compression performance. NS-CC connection have a flush ID Design, which very important to prevent localized erosion that could lead to actual destruction of the connection. NS-CC is rated 100% Pipe Body Yield in Tension, Compression, Internal, and External Pressure, making its the best choice for Thermal Well application in KS ORKA fields. NS-CC Performance on 13-3/8" 68# L80 Type 1 could be found on Table 2.



Connection Dimension	
Pipe ID	12.415"
Pin ID	12.429"
Coupling ID	12.392
Coupling OD	14.375"
Coupling Length	11.870"
Pin Lc Length	2.9553"
Wall Thickness	0.480"
Drift Diameter	12.259"

Figure 2: NS-CC Connection Design and Dimension.

Table 2: 13-3/8" 68# L80 Type 1 NS-CC Performance

Connection Performance				Make up Torque		
Tension (klb)	Comp (klb)	Burst (psi)	Collapse (psi)	Min (lb-ft)	Opt (lb-ft)	Max (lb-ft)
1,545	1,545	5,020	2,260	12,300	14,100	15,900

Table 3: L80 Type 1 Chemical Composition

Group	Grade	C	Mn	Mo	Cr	Ni	Cu	P	S	Si
		Max	Max	Max	Max	Max	Max	Max	Max	Max
2	L80 Type 1	0.43	1.9	-	-	0.25	0.35	0.03	0.03	0.45

Table 4: L80 Type 1 Mechanical Properties.

Group	Grade	Elongation (%)	Yield Strength (Ksi)		Tensile Strength (Ksi)	Hardness Max	
			Min	Max	Min	HRC	HBW
2	L80 Type 1	0.5	80	95	95	23	241

Material Main Characteristic

13-3/8" 68# L80 Type 1 Material was used to prepare 2 Test Samples and 2 Spare Sampels addressed for this test. L80 Type 1 material is a Group 2 material based on API 5 CT 9th Edition dedicated for Sour Service (Hydrogen sulfide) Environment. On Table 3 we could found the chemical composition of L80 Type 1 Material based on API 5CT 9th Edition, Table 4.

The green pipe was produced by Anhui Tianda Oil Pipe Co ltd, a Vallourec subsidiary Rolling Mill in China. The green pipe was delivered to PT. Citra Tubindo Tbk in Batam, Indonesia for Heat Treatment and Threading Process. In Batam hardening, quenching, and tempering process has been done to achieve L80 type 1 mechanical properties. The Plain end pipe was inspected based on API 5CT 9th Edition Annex H for Product Specification Level (PSL) 2. On Table 4 below we can find L80 Type 1 Mechanical Properties based on API 5CT 9th Edition, Table 5.

QUALIFICATION PROGRAM AND RESULT

Testing Flow Chart

The scope of the full-scale tests has been structured to reflect the loading encountered by casing and connection systems during assembly and field service. The Galling Resistance Test is conducted to verify that the candidate connection can withstand multiple make-ups and break-outs (M&B) without severe galling of thread surfaces or appreciable deterioration of seal surfaces. Two M&B test will be done with min dope and max torque configuration. One final Make Up will be done with max dope and min torque configuration. A high boiling point running dope such as Topco Greenseal II Thermal has been used for the test. Bending Analysis is recommended for applications in which severe bending is anticipated during installation or during well operation. As this is not anticipated in KS ORKA field case, it was then agreed to skip the Bending Test with the considerations that the typical well design has a low dogleg situation and NS-CC Connection bending performance has already been evaluated based on ISO 13679.

The Thermal Cycle Test assesses NS-CC Connection sealability and structural integrity under combined, thermally- induced cyclic loading. This test includes specimen bake-out and multiple thermal cycles with temperature and pressure changes consistent with ASL 290. Two specimens are cycled individually. Every specimen have to pass an average of 1 ml/min leak rate at 290º C Temperature and 10 ml/min at ambient temperature during the hold time. Upon completion of the Thermal Cycle Test, both of the specimens are subjected to the Limit-Strain Test, in which limits of connection structural integrity and (optionally) sealability are assessed under increasing, tensile axial strain. The test will be on ambient temperature with a leak rate similar to thermal cycle test of 10 ml/min. Figure 3 shows the full-scale test flow chart.



Figure 3: Full-scale Test Flow Chart

Galling resistance, structural strength, and sealability measured in the full-scale tests are the only full-scale test results contribute to the pass-fail assessment. Program reporting is conducted based on TWCCEP Task 5.1 Evaluation Report. The Evaluation Report contains all analytical and test data collected in the Evaluation Program. The Inspection Report is prepared based on Task 5.2 and attached to the Evaluation Report. The Inspection Report where describes on section 13, verifies compliance of the conducted Evaluation Program with TWCCEP's procedures. To maintain the transparency of the full-scale test, we invited Third Party Inspector from Bureau Veritas Indonesia to be present during the test with the activity description as listed in the Table 5.

Table 5: Inspection Activity Description

Operation	Verification
Machining Sample	Monitoring
Visual and Dimensional Inspection	Monitoring / Reporting
Galling resistance test	Witness
Thermal-cycle	Witness & Monitoring
Limit strain test	Witness & Monitoring

Sample Preperation

Mother pipes and coupling material were heatreated in PTCT Heattreatment facility and transefered to CDEC facility on plain end condition. CDEC lead the sample preperation as per TWCCEP Section 11.3. Sample was mapped and cutted before the maschining process beginning. NS-CC Connection was threaded on each Test Pin and Box. And For the Test Caps sides was using VAM® TOP Connection as the default connection for Test Caps in CDEC facility for 13-3/8" pipes. The final samples configuration can be found on the Figure 4 below

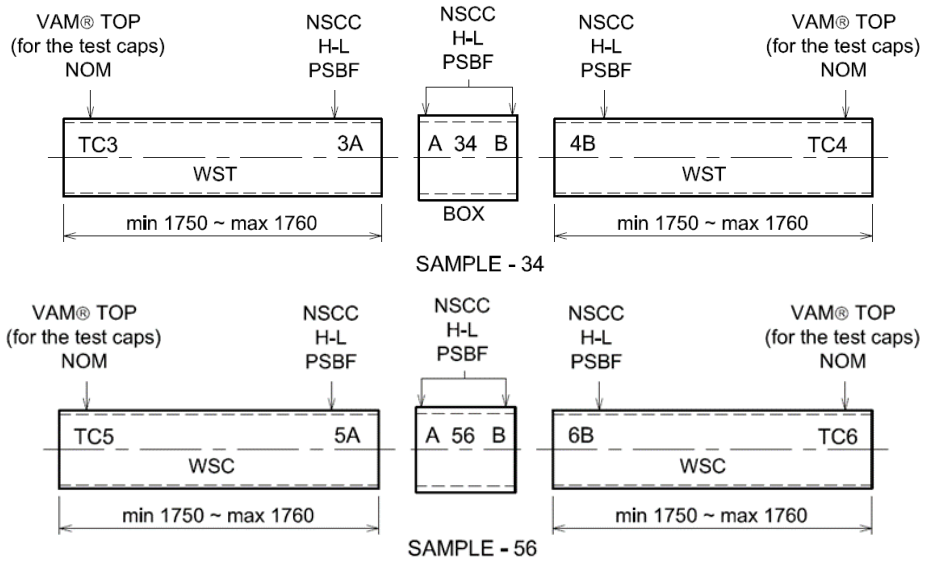


Figure 4: Samples Layout and Marking.

Sample Machining

FEA simulation can identify the worst-case scenarios on metal to metal seal and threads. Mainly the connection taper, threads interferences, and seal interference are the targets. Vallourec R&D departement in France ran a simulation on nominal case and the they ran additional simulations to simulate different taper or interferences configurations and compare them to the reference.

The worst configuration (Table 6) from all 3 aspects will be chosen for the tested specimens. The worst-case specimen configurations are as follows:

1. Worst-case for sealability in tension at low temperature (WST).
2. Worst-case for sealability in compression at high temperature (WSC).

Connection End Finishing

The end finishing for NS-CC Connection has folowed the Surface treatment procedure of TS-06 for Carbon Steel material. NS-CC Pin side was left as machined and the Box side has a Manganese Phosphate treatment to improve its galling resistance .

Port Holes

In order to evaluate the sealability performance of connection metal to metal seal, two port holes were drilled on the coupling of test samples, according to TWCCEP 1.3, Section 12.1.4. The port holes were drilled on the coupling for each pin end. The port holes is connected to a bubble meter device located in the control room.

Test Guidlines and Acceptance Criteria

Make up and Break out Test

Make-up were conducted in the horizontal position with the specified torque and dope application range according to TWCCEP 1.3, Section 12.2.5.2. Dope quantity and make-up torque are calculated within the Official Testing Procedure (OTP), reference number VRCC 18-0204.

Connections shall meet the performance requirements in galling resistance test. Requirements are as follow:

- Each connection must be achieved 2 number of M&B cycles.
- Make-up torques have been within limits specified for this test between a min recommended make up torque of 12.300 ft-lb and max recommended make torque of 15.300 ft-lb.
- No severe galling on seal or threads during testing.

Following each M&B test, the specimens are visually inspected with the following criteria:

- The connection must be free of heavy damage.
- For the threads, it is acceptable to have light damage (scratches, indentations, knocks), provided it can be completely removed with a small file with the original profile. No galling is acceptable.
- For the seals, it is acceptable to have small circumferential scratches, but no repair is allowed.

Sealability Test

Test samples follows Thermal Cycle Tests per TWCCEP 1.3, Section 12.3 with amendments listed in Section 1.1. Detail set-up and instrumentation process as per TWCCEP 1.3 are shown below:

- Controlled Elongation Interval (LCEI):
  Control of a specimen string's elongation within the Controlled Elongation Interval is measured by using LSD (Long Stroke Displacement) transducer. The LSD placed apart from the surface of the specimen string to minimize heats effects on the instruments.The LSD is connected to DAQ (Data Acquisition).
- Axial force:
  Axial force on each specimen string measured and recorded for each thermal cycle test and limit strain test.
- Heating:
  Heating on the specimen string performed by ceramic heater. Rate of temperature increment at any thermocouple location along the specimen string is not exceed 5°C (9°F) per minute.

Table 6: Specimen Worst-case Configuration.

Specimen	Seal Interference	Thread Interference	Taper
WST	Min	Max	Pin Slow / Box Fast (PSBF)
WSC	Min	Max	Pin Slow / Box Fast (PSBF)

- Cooling:
  The cooling system is using pressurized ambient air. Rate of temperature decrement at any thermocouple location along the specimen string is not exceed 5°C (9°F) per minute.
- Temperature measurement:
  At least six thermocouples shall be placed on the samples. During holding times, temperatures tolerances to be ± 15°C on both pipe body and coupling. Ambient temperature selected within the range of 5 °C and 40 °C. The high cycle temperature as close as reasonably possible to 290°C.
- Internal mandrel:
  An internal mandrel made of aluminium shall be used, in order to reduce the volume of gas used to pressurize the test sample.
- Internal pressure:
  Internal pressure applied using Nitrogen with a pressure around 7,4 Mpa (approx 1074 psi) as per TWCCEP ASL 290. The internal pressure in each specimen string measured continously during the test and recorded by the data acquisition system.
- Seepage Detection:
  Seepage detection system is connected to a bubble meter device via ports drilled radially through the coupling wall. The ports diameters roughly 2.4 mm (3/32 in) and enlarged at the outer ends for attachment of seepage monitoring tube. The OD of the tubes is 3.2 mm (1/8 in). The tubes is connecting specimens and the bubble leak trap in the control room.
- Data acquisition (DAQ):
  A computerized data acquisition system is recording continuously for the Temperatures at all thermocouple locations, Elongation of the specimen string within the controlled elongation interval, Axial stroke of the test frame actuator, Axial force imposed on the specimen string, Internal pressure, Date and time.

Connections shall meet the performance requirements in thermal cycle test. Requirements are as follows:

- No structural failure has occurred during the 30 Thermal Cycle operation.
- Per-connection average leak rate at hold time in high temperature cycle does not exceed 1 ml/min.
- Per-connection average leak rate at hold time in low temperature cycle does not exceed 10 ml / min.

Limit Strain Test

Both test specimens follow limit-strain tests as per TWCCEP 1.3 Section 12.5, with amendments as described in Section 1.1 of this document. The Limit-Strain Test can be performed in any test configuration that gradually applies tensile axial strain to the test specimen. Both Localized Strain Seepage and Tension limit tests to be performed. Each test specimen shall be pulled from zero strain to failure. An internal mandrel shall be used to minimize the gas volume and then to reduce energy stored in the compressed gas.

For Localized Strain Seepage, the connections shall meet the performance requirements in limit-strain test. Requirements are as follows:

- No structural failure occurs before average pipe strain equals the localized strain value.
- Average seepage rate is measured and reported for all holds at constant strain less than or equal to the localized strain value for each sample.

For Tension Limit, the Connections shall meet the performance requirements in limit-strain test. Requirements are as follows:

- No structural failure occurs before the average pipe strain in each limit-strain specimen exceeds the tensile strain threshold.
- No decrease in axial force with increase in average pipe strain is observed for two consecutive strain increments before the average pipe strain exceeds the tensile strain threshold.

Test Result

Make and Break Out

The results of two times make-up and break-out applied on the sample 3A with the specified torque and dope are listed in Table 7 below.

Table 7: Make out and Break out Result

Samples			Make-up	Break-out	Result
Pin	Coupling	M&B Sequence	Final Torque (ft.lb)	Torque (ft.lb)	
3A	34A	1	15,307	21,941	ACCEPTED
3A	34A	2	15,478	28,434	ACCEPTED
5A	56A	1	15,285	17,643	ACCEPTED
5A	56A	2	15,207	26,178	ACCEPTED

All final torque values are compliant to NS-CC recomended Torque value. All shouldering Torque are within the acceptance range. No deformation and galling observed.

Thermal Cycles Sealability Test

2 main samples and 2 spare samples has been tested seperatly with 30 Thermal Cycles. The result of all samples with final make up can be found on Table 8 below.

All Samples survived after 30 Thermal Cycle with no structural and sealability failure recorded.

Limit Strain Test

For Localized Strain page, all samples survived the test with no structural failure. All average seepage rate is measured and reported for all holds.
For Tension Limit result, structural failure occured before the axial strain reached the tension strain threshold of 30.000 με. Specimen 3.4 was broken at 28.200 με and axial load at 800 tons. Meanwhile Specimen 5.6 survived the test with no structural failure before the average pipe strain. Figure 5 shows the limit strain test for specimen 5.6.

Table 8: Thermal Cycle Result

Sample	Final MU	Thermal Cycles Test Result
	Max Dope / Min Torque	
3A	OK	OK
4B	OK	OK
5A	OK	OK
6B	OK	OK

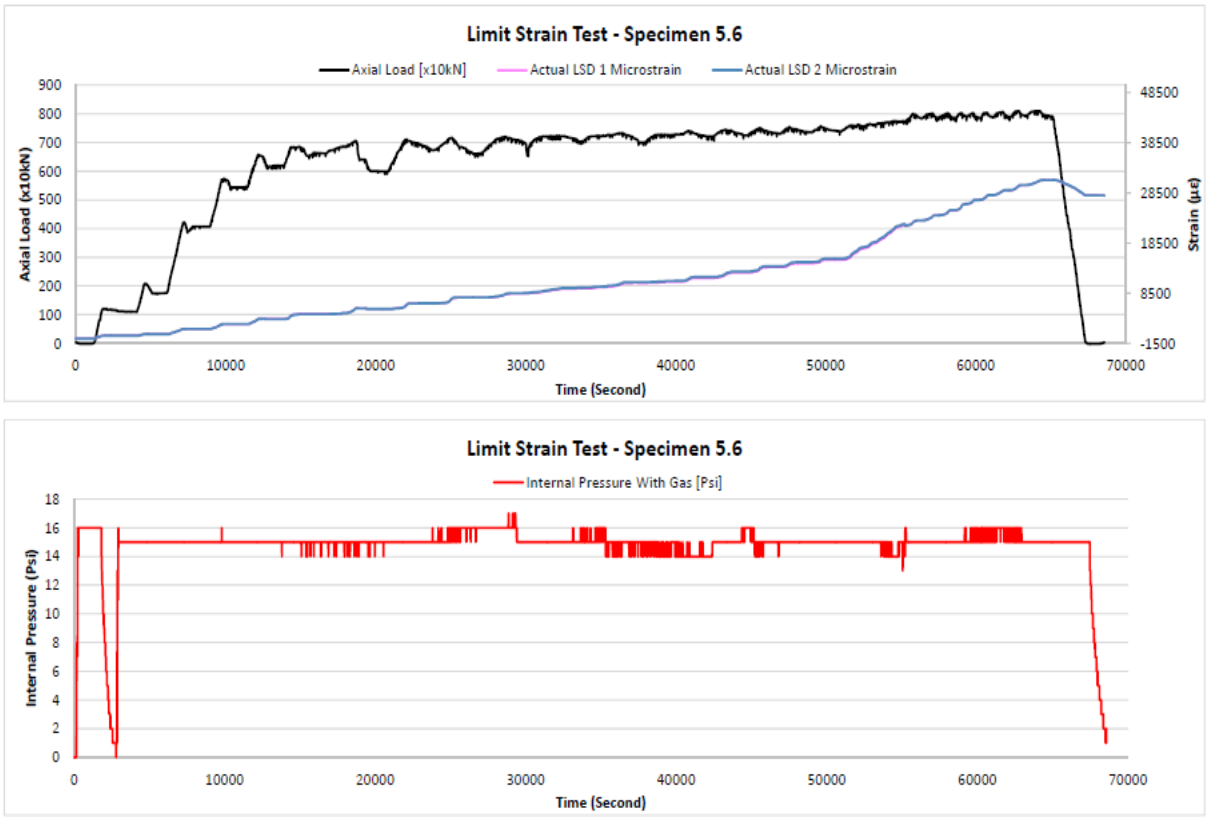


Figure 5: Limit Strain Test for Specimen 5.6.

CONCLUSION

- Selecting a proper production casing and casing connection for geothermal well is very crucial as the production casing and its connection will experience various loads not only during drilling operations but also during its lifetime production operations.
- In geothermal, the thermal load caused by temperature cycle during the production operations could potentially the highest load experienced by the production casing and its connection.
- The NS-CC connection for 13-3/8" 68# L80 Type 1 production casing has passed the TWCCEP for geothermal application with 30 Thermal Cycle. Hence this connection is considered suitable for geothermal operator, and in this case for KS ORKA.

RECOMMENDATION

It is recommended to use proper production casing connection for geothermal wells, especially those that has passed an applicable test. One of the applicable test that can mimic geothermal condition is TWCCEP test protocol. The NS-CC connection for the 13-3/8" 68# L80 Type 1 production casing, which has already passed the TWCCEP test, is one of assured option for geothermal well in Indonesia and worldwide.

ACKNOWLEDGEMENT

We would like to appreciate those who has conducted the entire testing work and who has support the preparation of this paper, both at Vallourec and KS ORKA Drilling Team. The authors would also like to acknowledge Firman Prasongko, Alvaro Rodriguez Martin, Sebastien Cochet, CDEC Batam, and Jakarta Technical Team who gave a full support. Huge appreciation to all CDEC Batam member who has made everything happen from preparation until finish. This is a monumental achievement for all of us as a team.

REFERENCES

American Petroleum Institut. Standards 5CT (2012). "Specification for Casing and Tubing", 9th Edition.

International Organization for Standarization (2002). "Recommended Practice on Procedures for Testing Casing and Tubing Connections". ISO 13679:2002.

Noetic Engineering (2012). "Thermal Well Casing Connection Evaluation Protocol (TWCCEP)". Public Domain Edition 1.3.

Riyanto, N., Napitupulu, G., and Wahyudin, S. S. (2017). "Connection Selection for Tie Back Production Casing in Geothermal Wells".

GEOTHERMAL CEMENTING DESIGN AND METHODOLOGY ENHANCEMENT IN WAYANG WINDU

Eric Tanoto[1], Allam Putra Rachimillah[1], Cinto Azwar[1], Febra Sakti Dewa[1], and Tommy Souvanir[2]

[1]Schlumberger
[2]Star Energy
Email: ETanoto@slb.com

ABSTRACT

Cementing in geothermal well mostly faced great challenge in start-up planning, mobilization, and the technical data such as data of fracture gradient to determine the maximum equivalent circulating density (ECD) and the correct bottom hole circulating temperature (BHCT) to perform cement job. Combining many sources of data needed to determine the right ECD and BHCT which might be differ from the oil and gas well. Besides that, chosen cementing method and design also result in the quality of the cement job itself. Integrated Drilling Services give the benefit on planning, readiness, reviewing, and execution. Project Readiness Assessment (PRA) tool is use the project-readiness of each services. This resulting excellent service quality delivered to the client. Equipment selection and setup is important to ensure the execution run flawlessly. Another consideration, determining the correct bottom hole circulating temperature is critical to get the cement quality as designed in the recipe, this factor affects the option of component chemical in the cement. A software simulation was used to determine the prediction of temperature in geothermal well. Improvement on solid quality shoe track and less wellhead growth are achieved by implementing the cementing design best practices. Stab-in method is mostly used in the surface and tie-back casing cementing due to its advantages time-saving and reduce cement return on surface. However, this method also has some issues such as stinger leak and contamination on shoe track which might affect the quality of cement. Many improvements were made to minimize these disadvantages to achieve zero non-productive time. This paper will discuss the case histories from 3 wells in the west region of Java field where improvement on cementing execution to achieve operational excellence delivered by combining project-readiness assessment, equipment selection and setup, cementing design, and best practices.

Keywords: Cementing design, Geothermal, Wayang Windu

INTRODUCTION

Geothermal that has been proven its reliability in the sector of electricity for instance, still experience constraints in its development. The overlapping between lands and protected forests and conservation areas of forests, and national parks becomes the main problem in its development. Aside from that, several other problems that have been mitigated:

- Lack of geological, geophysical and geochemical data causing the low accuracy in determining the magnitude of potential
- High resource risk (in upstream sector) level
- High investment cost while energy price is less competitive, limited equity funds, and limited mechanism of funding and incentive
- Uncertainty in legal aspects and the lack of cross-sector coordination
- Lack of human resources that have specific competences in geothermal
- Social issues (Poernomo and Satar, 2015).

To drill a geothermal well, there is not only a discussion on technical side but also an extensive effort on the operational side. This paper will discuss on the preparation, execution and evaluation phases of Wayang Windu project.An overview looks on a project was completed by assessing the challenges in order to provide full solution to client.

DESIGN AND PREPARATION

Project-Readiness Assessment

Project Readiness Assessment is a tool designed to assess the project delivery readiness at the various stages or phrases of a project. A single interactive website that allow the users to create projects, perform meeting reviews, and create remedial work plans. This risk management tool will identify as early as possible the areas of concern where on-time project delivery to a customer could be affected and to develop the appropriate action plan to prevent any derailment of the project.

The framework is defined to ensure questions to the key project readiness are answered which divided into 4 large areas/ categories:

- Exposure and Complexity, is used to identify the challenges and the technical complexity that a project will face during execution process. It covers the operational

environment and the service type requirement.

- Process and Procedures, is used to identify whether the location and Product Lines have the compatible and adequate processes and procedures to face the challenges of a new project
- Equipment and Technology, is used to assess whether the location is fully equipped to meet the project specifications and requirements.
- People and Competencies, is used to assess whether the people and proficiency is capable to support the project.

PRA consists of three main areas:

A. Phase 1 Transition and Design & Phase 2 Planning and Resource Demand

During phase 1, a lot of effort was put on the technical cementing design. Extensive experience on this field during last campaign 2015 till 2016 becomes one of the strength points. Lesson-learned and improvement plan were captured after the execution of the nearest well in the planned well. The partial or total losses during cementing job on 13-3/8in liner is the critical face for two reasons. First, the squeeze job is time consuming, the historical wells show 3-5 cement plugs were needed to provide a good sealing between the 13-3/8 in liner and 20 in casing. Second, the quality of cement in the liner lap if the cement able to reach the top of liner would affect the integrity in the overlap of the liner which becomes the base of 13-3/8in casing tieback.

There are 4 main important areas regarding the resources planning which includes knowledge center, people, equipment, and chemical additives.

- Knowledge center is important to involve the person and document which helps giving more understanding regarding the challenges that may be faced in Wayang Windu cementing.
- Second, people aspect covers the technical engineer who plays a focal point as bridge of between two companies. Experience cementing supervisor also essential as a leader in the location. Ensuring every key player has met the requirement competencies.
- Equipment selection covers the specification and maintenance including spare part readiness. Cementing in geothermal often requires a cementing pump with endurance to pump huge volume of cement in short interval. Cementing pump with full redundancies is one of the mitigations to overheat issue in the engine.
- Involving the competent personnel on the cementing project is the step to ensure the quality of the job. High temperature will be experienced by the well once it is on production. The cemented casing strings will be subjected to significant cyclical axial stress caused by changes in temperature due to production of high temperature geothermal fluids that can then be followed by the injection of cold water for well kill operations to perform wellbore maintenance (Torres, A. 2014). It is not only about the casing but also the cement must able to withstand the high temperature during production phase to achieve good well integrity. Silica additive is incorporated to prevent strength retrogression of cement. Typical additives of antifoam, dispersant, accelerator and retarder must be prepared to cover wide variety of temperature range because every chemical has their own limit usage based on the circulating temperature.

B. Phase 3 Sourcing and Allocation and Phase 4 Final Check

To ensure the project is delivered on time, the sourcing and allocation of resources must be monitored. The inspection of the equipment was performed to ensure the expectation of each side.

C. Phase 5 Execute

Execution was performed as per checklist and agreed job procedure. Every job will start by briefing and job risk index. Job risk index is a procedure of discussion between the location team with the line management and engineer to ensure that every risk and preparation was captured. It also ensures that the approval risk of every job was calculated to ensure that the escalation to the right and authorized person is completed.

The score of each assessment topic or category is showed on the Figure 1.

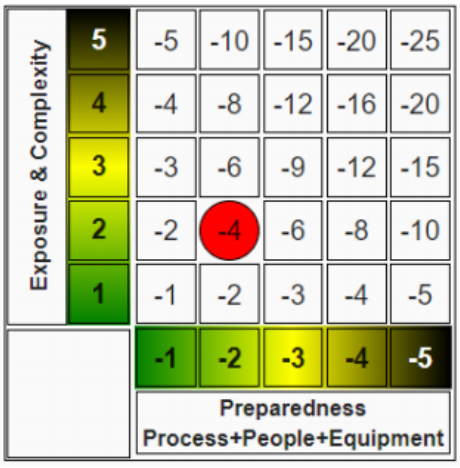


Figure 1: Matrix 5x5.

Equipment Selection

Equipment selection during preparing Wayang Windu well takes into account the amount of volume needed to be pumped and the types of cementing pump. Considering the highest volume of the cement job will be 20in casing cementing, the preparation of silos and water tank is prepared to exceed the 20in casing job requirement. The cementing pump provided for this project has the full redundancy system which means that each engine (front or rear) has the capability to function as the source of rotation for the centrifugal pump and the triplex pump which will act as a low-pressure pump to mix additives with cement blend and high-pressure pump to deliver cement into the well.

The equipment set up depends on the location area and availability, on this project. The proposed equipment layout is as per Figure 2 and Figure 3, are proven to be the suitable solution for the project.

Technical Cementing

The challenges of drilling geothermal wells are the lost circulation and the high temperature of the well. A full length of cement sheath on the annulus of a casing and formation most of the time is difficult to be achieved because the cementing is performed during lost circulation condition. Lost circulation isn't fixed as they are encountered because some lost circulation zones might need 10 to 20 cements plugs to seal them (Finger, 2010). It even hasn't considered the time to wait on cement between each plug. The well is frequently drilled without returns to the next casing point. As the consequences, there is no return on the primary cementing which leads to the need to do a cement job from the annulus of casing or top job. The different types of loss zone are the following unconsolidated sands, cavernous & vugular zones, depleted formations, induced fractures, natural fractures.

The typical losses in the geothermal well is cavernous or large fractures which is indicated by sudden drop of the fluid level without any change of density of drilling fluids or any drilling practices. It happens on the 17-1/2 in of open hole, the consequence is during the cementing job on 13-3/8in liner most of the times there is no returns.

The other aspect of determining the temperatures of cementing job is critical to ensure the thickening time for the job is enough for the total pumping time of a job. Circulating temperature on a cementing job for a full return well and a partial/ total loss well must be simulated on a different consideration. A cementing software is used to predict the circulating temperature for both scenarios. A full return well will have lower circulating temperature because the fluid circulated becomes the media for heat transfer. It will even lower the temperature further if the solid content in the fluid is higher. The simulation showed on Figure 4. Temperature determination is also challenging if the cementing plug is needed to perform near reservoir zone, this is especially happened if the operation requires to do a cement plug or side track near the reservoir area, where expected heating rate is very high.

Cement system applied on geothermal well is also discussed during the initial phase of project because high temperature will be experienced by the well once it is on production. Cement has two important functions: to give the casing mechanical support under its sometimes-intense thermal cycling between production and shut-in, and to protect the outside of the casing from corrosion by in-situ fields (Finger, J. Blankenship D. 2010). In a typical Wayang Windu wells, cement will cover the surface casing, intermediate liner, and the intermediate tieback.

The cemented casing strings will be subjected to significant cyclical axial stress caused by changes in temperature due to production of high temperature geothermal fluids that then be followed by the injection of cold water for well kill operations to perform wellbore maintenance (Torres, A. 2014).

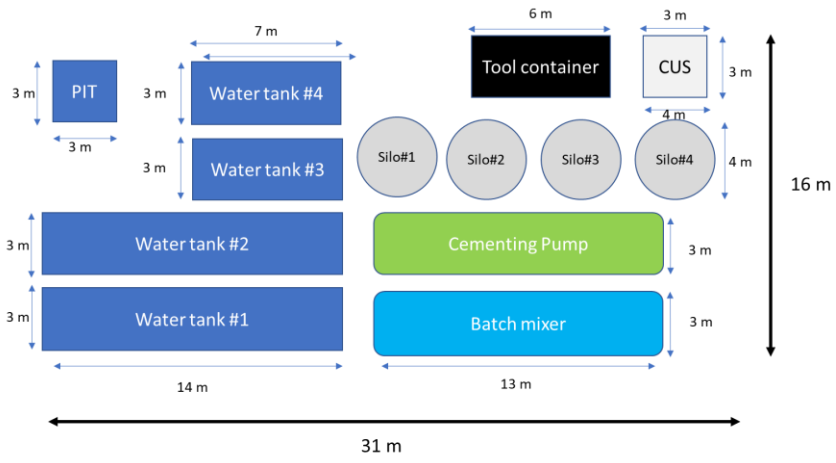


Figure 2: Layout Cementing Set up on Location.

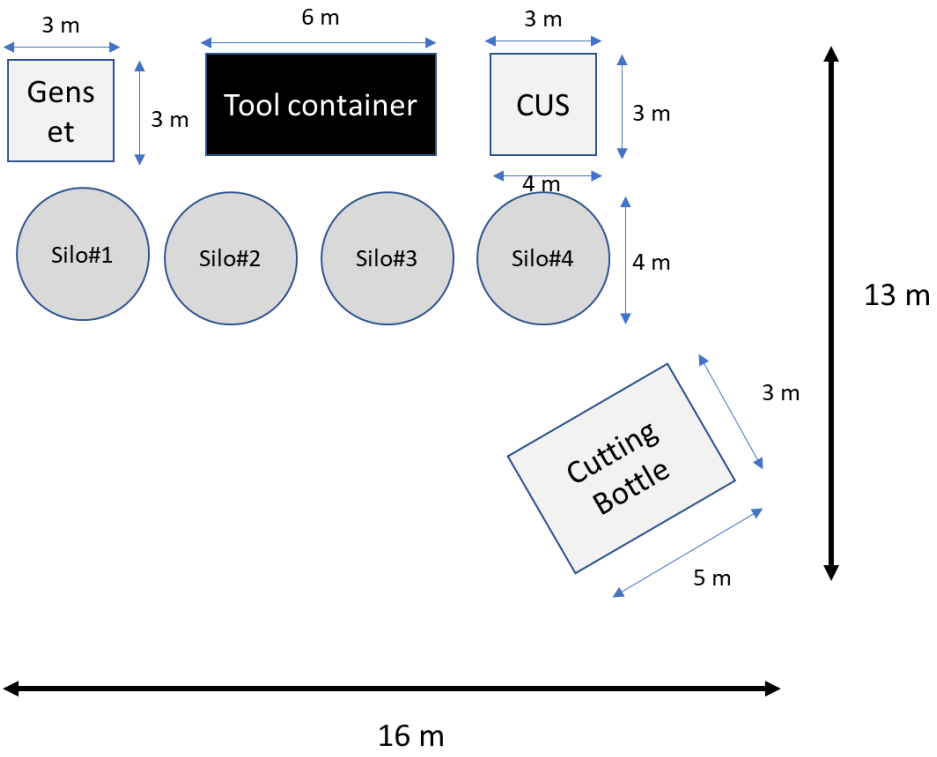


Figure 3: Layout Bulk plant on Location.

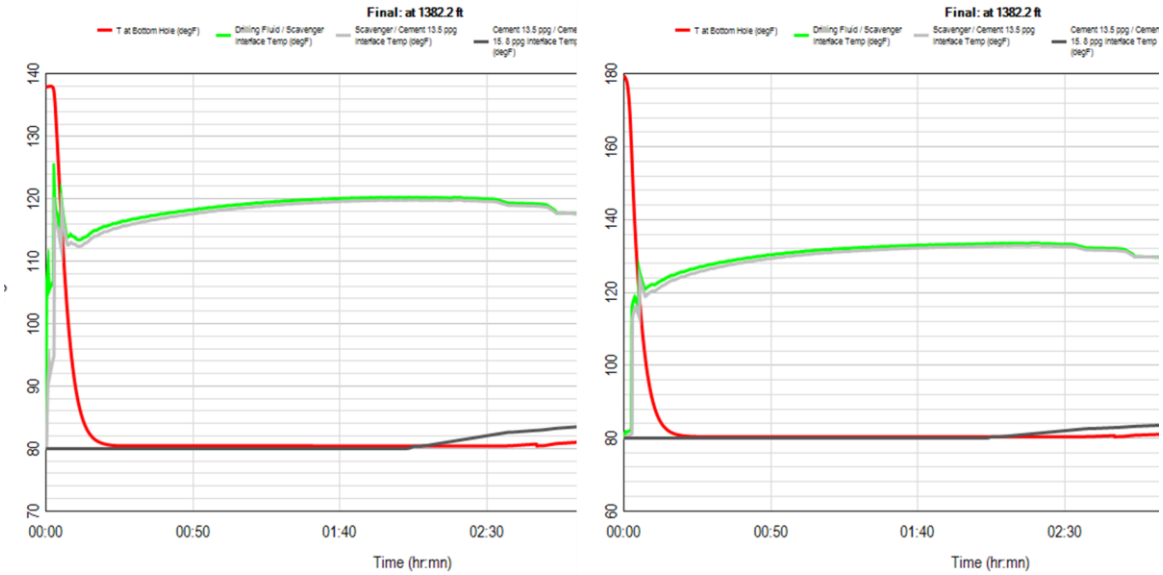


Figure 4: Simulation from cementing software of two modes: (left) with mud circulation mode; (right) with geothermal mode.

EXECUTION AND LESSON LEARNED

Surface Casing

Cement Design on the 20-in surface casing is designed on the 14.0 ppg single slurry. The cement system is cement G with 40% of silica. The addition of silica will act as a prevention of strength retrogression on cement which exposed to temperature more than 230 ^{0}F. The challenge on cementing 20in casing is the low formation strength. The 14.0 ppg is used to lower the ECD during cementing instead of the conventional 15.8 ppg cement slurry. Free water cement must be fulfilled

by the specific cement to prevent any water trap which may cause casing collapse.

On the second well out of 3 wells, it was found out soft cement on shaker during drilling the shoe track. Based on the weight on bit data, it shows variation from 2 Klbs-10 Klbs. The cement was drilled after the cement reach 500 psi on the UCA. Although the Formation Integrity Test showed good integrity of cement around the shoe.

Root cause analysis of this event was created based on two assumptions. First, the dart wipes any mud or cement cake film in the drill pipe which created a contamination on the shoe track. Second, the displacement volume pass through the dart which also strengthened by the additional 1 bbl of displacement pumped because no bump plug was observed. Those two assumptions lead to the contamination of mud and cement in the shoe track.

Later on, the investigation was found that the contamination of 10% of mud leads to deterioration of cement compressive strength. The full cement CS was expected to reach 500 psi on 8 hours but with 10% contamination the final compressive strength is only 276 after 36 hours. The low tolerance of cement to the contamination leads to an idea to change the initial design of single 14.0 ppg cement slurry. A combination of 13.5 ppg cement and 15.8 ppg cement able to create the same ECD but provide advantage on stronger cement near the shoe track. The ECD simulation is shown on Figure 5 and Figure 6. The system of lead and tail slurry enable the cementing company to have lower thickening time on the tail cement slurry due to lower volume to be pumped. Lower thickening time will minimize the usage of retarder or even usage of accelerator which becomes the initiation of early compressive strength on the cement. The result of early compressive strength on cement was observed on Figure 7 in which comparison of weight on bit plotted in graphic to show that combination of 13.5 ppg and 15.8 ppg can be use as alternative to reach two objectives, lowering ECD and get more strength in the shoe track.

Intermediate Liner

Cement Design on the 13-3/8 in liner is designed with 14.0 ppg single slurry. The cement is designed to reach the top of liner which will becomes the base for the next 13-3/8 in tieback cementing. The verification of this base is by pressure test the liner lap before proceeding to the next operation. Squeeze liner lap must be prepared to improve the cement or top up the cement in the annular of liner 13-3/8 and casing 20 in. Two types of cement system must be prepared. First one, the cement slurry with high fluid loss control to encounter the condition with ability to inject fluid into liner lap is low/ difficult. In this case, the cement is expected to be squeezed in small gap. The fluid loss desired is less than 50 mL. The second type is the cement slurry with low fluid loss control to encounter the condition with high injectivity which means the fluid can be injected easily to the liner lap. The fluid loss of the cement is designed to be uncontrolled so that it can bridge the gap in the liner lap.

Cementing on intermediate 13-3/8 in liner in Wayang Windu wells was challenging because there was no return at all during the cementing job. This was happened on the first well where the excess of the cement job was designed on 75% excess but there was no return at all. The best practice on historical wells was to balance plug 100 bbls of 15.8 ppg cement slurry right after the cement job. The losses on liner lap was still unable to be cured. Three times of squeeze cement jobs was performed in order to get a good seal on the liner lap between 13-3/8 in liner and 20 in casing.

As the further design improvement, a mixture of chemical which has ability to create instant gel once activated in contact to each other is prepared to reduce the number of squeeze liner jobs. The system can be used by combination with cement and without cement. For the permanent seal, the combination with cement will provide a stronger and more reliable compressive strength.

Tieback Casing

Cement Design on the 13-3/8 tieback is a special string on the Wayang Windu Geothermal. This string will be exposed to the drastic temperature change. The full sheath of cement covering the casing is needed, good compressive strength of cement is expected on this cement. The design of this cement is 16.5 ppg single slurry cement. The comparison of choosing 16.2 ppg compared to conventional 15.8 ppg is taken based on two considerations. First, the 16.2 ppg will give more compressive strength, tensile strength of the cement which make it better as a cement sheath. Second, the tested liner lap is provided more room to pump high density cement which will give better properties.

Execution of 13-3/8in tieback casing is straightforward especially the squeeze liner lap had been pressure tested as the requirement of solid base for this job. Excess 50% is used as a safety net to ensure 16.2 ppg cement return is reach till the surface. The wellhead growth is reported to be minimum on these three wells.

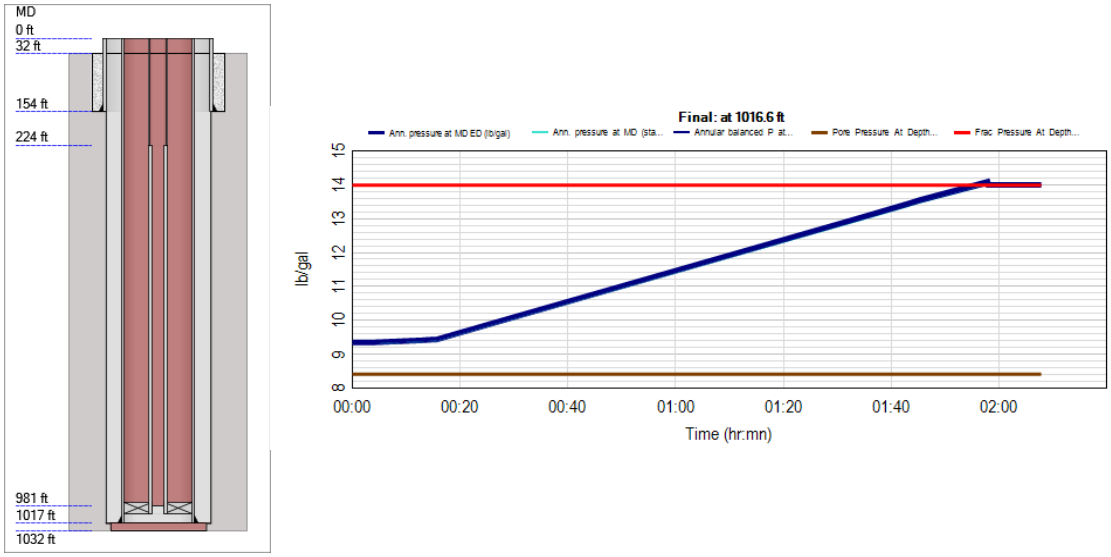


Figure 5: Illustration of Equivalent Circulating Density of single cement slurry 14.0 ppg.

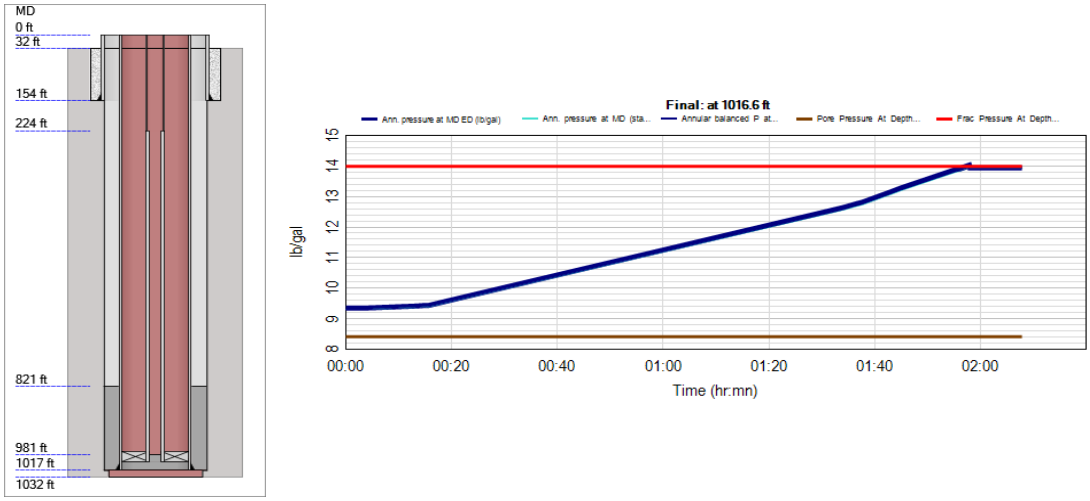


Figure 6: Illustration of Equivalent Circulating Density of combination cement slurry 13.5 ppg and 15.8 ppg.

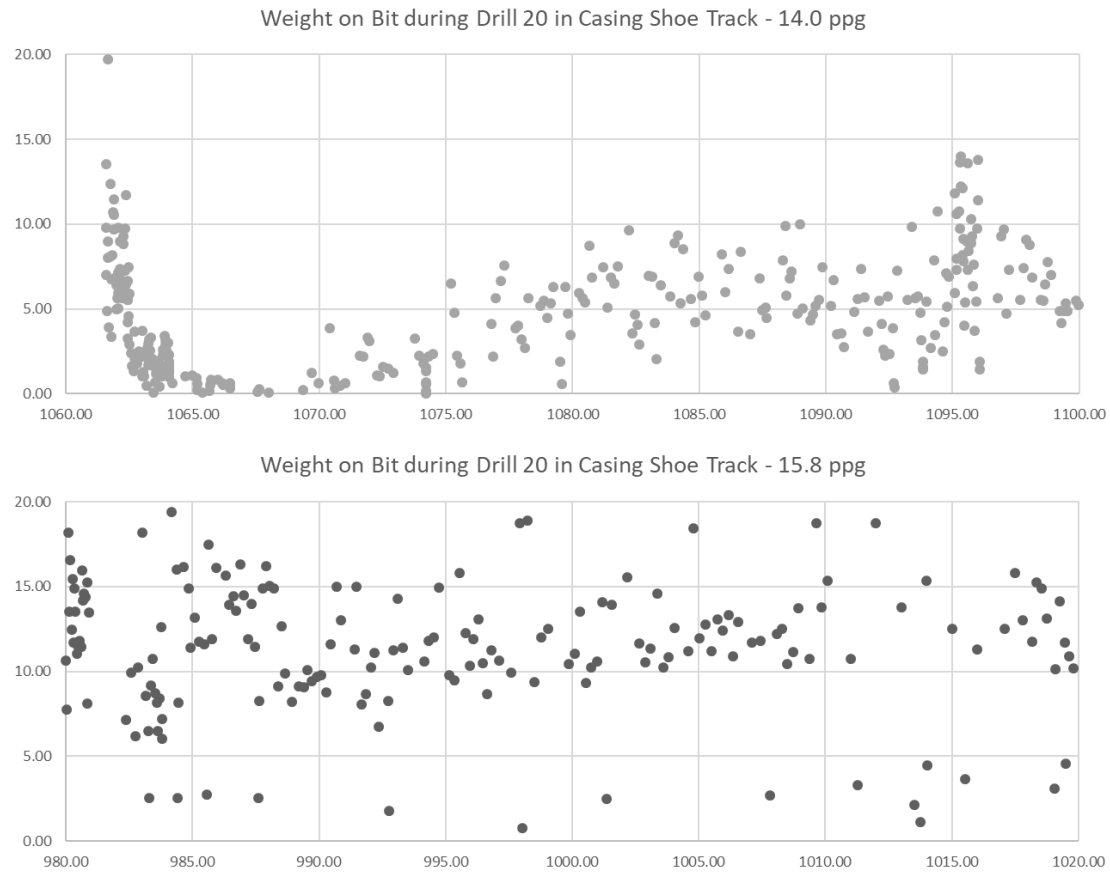


Figure 7: Weight on Bit Comparison during drill 20in casing shoe track. X-Axis in feet; Y-Axis in Klbs.

The only concern for tieback casing is the method of stab-in stinger which has a chance of leaking which has a chance of leaking sealing between stinger and the float collar. There are many factors lead to this event such as an unwanted material located in the sting-in area, worn out stinger O-rings or compatibility issues of stinger and the float collar.

CONCLUSION

Delivering a great cementing operation comes from looking into detail into all constituent components. It comes from identifying the real challenges, preparing the correct procedures and contingencies, sourcing the adequate equipment and technology, and collaborating with the expert and competent personnel.

Proficient equipment with full redundancy engine has a great benefit for delivery cementing job, especially in a size constrained location.

Understanding the circulating temperature with modelling software is crucial for selecting additive and affecting the rheology and mechanical properties of the cement system.

REFERENCES

Finger, J. Blankenship D. (2010). "Handbook of Best Practices for Geothermal Drilling". New Mexico, Sandia National Laboratories.

Poernomo, A., Satar, S. et al. (2015). "An Overview of Indonesia Geothermal Development – Current Status and Its Challenges", Melbourne, 19-25 April.

Torres, A. (2014). "Challenges of Casing Design in Geothermal Wells". Presented at IADC/SPE Asia Pacific Drilling Technology Conference, Bangkok, 25-27 August. SPE-170480-MS.

.

OBTAINING ULTIMATE ZONAL ISOLATION IN GEOTHERMAL WELL: RECOMMENDATION & BEST PRACTICE OF GEOTHERMAL WELL CEMENTING DESIGN & OPERATION

Allam Putra Rachimillah, Eric Tanoto, and Cinto Azwar

Schlumberger
Email: ARachimillah@slb.com, ETanoto@slb.com, CAzwar@slb.com

ABSTRACT

Cementing is one of sequences in drilling operation which is purposed to isolate different zones and provide integrity for longer well life. Different from oil and gas wells, Geothermal wells have unique challenges for the cementing operation. Robust cementing design and correct best practice during cementing operation is needed to achieve the cementing objective in geothermal well. Intermediate section cementing is most critical since this is where the steam will flow to surface. Thus, cement behind the intermediate section must be fully integrated. Several methods for intermediate primary cementing have been introduced to geothermal operation in Indonesia, which are long string method, liner-tieback method, and two stage method. Analysis and the comparison of every method is described in detail to permit readers choose the best method. Primary cement design improvement is needed to have longer well life in geothermal well. With the high heating rate of geothermal well, temperature prediction plays important part in cement design. Free water sensitivity test is needed to be done for primary cementing job to ensure no casing collapse to happen. Centralizer selection also play important part to avoid mud channeling as well as preventing fluid pocket to exist. Massive lost circulation is very common in surface and intermediate section of geothermal wells. Several times, normal LCM could not handle the losses and multiple cement plugs need to be done. An improved lost circulation plugs design and execution is introduced to handle massive losses in geothermal environment. Many geothermal wells are executed in different method by geothermal operators. Analysis of different cementing approach is introduced to ensure having a robust cement design and fit for purpose cementing method. This paper will discuss the cementing design, recommendation, and best practices to achieve the ultimate zonal isolation of geothermal well.

Keywords: zonal isolation, well cementing design and operation.

OVERVIEW OF CEMENTING OPERATION IN GEOTHERMAL WELL

Geothermal energy is thermal energy generated and stored in the Earth. The geothermal energy of the Earth's crust originates from the original formation of the planet. The geothermal gradient, which is the difference in temperature between the core of the planet and its surface, drives a continuous conduction of thermal energy in the form of heat from the core to the surface.

Geothermal wells are drilled to look for fractures, which produce steam (dry/wet) that will energize the turbine and finally generate electricity. Steam/Hot water reservoirs are often identified with high temperature and permeability (fractures/losses).

Since the target formation in a geothermal well is mainly igneous rocks, the challenges are different from oil and gas wells which target sedimentary rock formations.

Cementing operation is one of the important things to be look at in drilling the well. Complete and durable zonal isolation is the foremost goal of the cement job. The quality of the cement job has a direct impact on the economic longevity of the well (Nelson and Guillot, 2006).

In geothermal well, there are two things that is highly related to the cementing operation. The first thing to be look at in the geothermal well is the high temperature steam will flow through the production casing and it will affect the cement condition in long term condition.

When exposed to high temperature (more than 230 deg F), set cement will undergo a phenomenon called strength retrogression. This is where the cement will lose its compressive strength overtime due to the exposure of high temperature. In geothermal well, every casing section has the risk of high temperature steam flow, directly or indirectly (Eilers and Root, 1976). To overcome this challenge, in every cementing job in geothermal well, cement with 35 – 40 % silica content is used to prevent strength retrogression.

In some cases where the temperature from reservoir is believed to be very hot, theoretically it needs a special cement system that can handle expansion of the casing due to extreme temperature cycle. The use of software simulation recommended to evaluate whether the final mechanical properties of cement are enough to handle the impact of pressure and

temperature load cycles from the flow of the steam after drilling to the production phase.

Another thing to be look at in the geothermal well regarding high temperature steam production is the presence of trapped fluid between set cement.

Trapped fluid is dangerous due to its impact when the well heats up during production. The effect is the worst in casing-casing section (i.e. tieback section) due to high possibility of casing collapse. Trapped fluid can also be caused by improper mud removal. Cement slurry design for primary cement jobs also must have zero free fluid. This is to avoid any free water that could become a trapped fluid.

The second thing to be the massive lost circulation in geothermal well. Due to fractures in the volcanic formation, loss circulation is always encountered in geothermal wells. Loss circulation could be due to natural fracture, induced fracture or even cavernous formation.

In most cases, in the event of loss circulation before reaching the reservoir zone, loss circulation plugs are needed to cure the losses before resuming drilling. Remedial cementing is commonly done for borehole stabilization in problematic zones. Unstable zones (like reactive clays or rubble formations) must be cured in order to continue drilling ahead. However, in several cases, drilling might be continued with no returns (blind drilling) with flooding of freshwater from the annulus and string if no problematic zones are encountered.

It is important to note that any cementing job (including remedial cementing) should not be done in the reservoir zone of geothermal well since it will alter steam production. Degradable materials should be considered in this case.

CEMENTING METHOD IN PRODUCTION STRING

To achieve the cementing objective, full cement coverage until surface, especially in casing to casing section is very important. Competent shoe also needed to be achieved to avoid any path for steam or cold water to migrate behind the casing.

In geothermal wells, primary cementing is done only in the surface and intermediate sections. Pumping cement in production/reservoir zone is prohibited since it might alter the steam production.

Intermediate section cementing is most critical since this is where the steam will flow to surface, which is why it is becoming the production string. Thus, cement behind the intermediate section must be fully integrated. Any damage to the cement behind the intermediate section might cause the well to undergo workover jobs.

There several methods to perform the intermediate section cementing which it has its own advantage and disadvantage.

Long String Method

In Long String method, single casing is run from TD to surface. This method is usually chosen when the formation is strong enough to hold the hydrostatic of cement column up to surface.

This method has shorter operating time for the primary job compared to other methods. This is due to its single stage method with no wait on cement time spent between stages.

This method has a risk of having water trapped if loss circulation occurs during cement job or cement slurry is not enough to cover annular volume. If this happens, there is a major possibility of water remaining above cement in the casing-casing section after the cement job is done.

Annular cementing might be required to get cement up to surface after the primary cement job. Macaroni pipes need to be prepared and the ability to run them into the annulus needs to be ensured.

In case volume of cement pumped is not enough, annular cementing is required right after the primary cement job to push out the water in casing-casing section, to avoid trapping water.

Long string method is better executed with stab-in method compared to dual plug method. This allows flexibility to adjust the cement volume pumped. This also helps to avoid insufficient cement volume or excessive cement at surface.

Stab-in method requires extra care since the section might go to more than 1000 m MD and might be deviated. Ample weight is needed to have the stinger kept in place during cementing. Appropriate O-ring rubber temperature rating needs to be ensured prior to RIH stinger.

Liner and Tieback

In this method, liner string is run first from TD to previous casing and then continued with tieback string up to surface. This method is chosen when the formation is not strong enough to hold the hydrostatic of cement column up to surface.

With this method, extra operating time is needed after the liner cement job before tieback string can be run. This includes wait on cement time for cement to set at top of liner and then drilling cement to clean out top of liner and receptacle. In case liner lap is not filled by cement or liner lap is not holding pressure, a liner lap squeeze must need be done before tieback can be run.

However, once the liner is fully cemented, tieback cementing can be done without any concerns of having losses. Thus, this method can optimize well integrity.

In geothermal wells, the liner is usually run without any liner packer. Since packer is normally inflated by fluid (usually mud), this will be a weak point when temperature rises: the packer might burst due to expansion. In the worst case, it might cause a casing collapse.

In liner + tieback method, the space out overlap between liner and tieback is a weak point since there is no metal to metal, only cement. This is usually mitigated by having a longer space out overlap thus create longer cement interval. Figure 1 shows the comparison of cementing method for production string.

Two Stage

In this method, single casing is run from TD to surface. Ported collar is run in the casing string, to enable circulation from inside the string into the annulus for the second stage.

This method allows a single casing to be run and eliminate the risk of losses in the casing-casing section by having a packer set below the ported collar after first stage job.

However, this method is not preferable due to several weak points in dual stage tool, which are:

- Dual stage packer is inflated by fluid (usually mud)
- Port collar has rubber seal which could eventually break when heated

CEMENTING FOR LOST CIRCULATION

In severe lost condition where gaining return is needed to continue drilling ahead, cementing job is becoming one of option to cure the losses. However, special method and approach is needed to have a successful lost circulation plug.

Fit-for-Purpose Lost Circulation Plug

In every lost circulation case, it is very important to understand the characteristic of the losses. Since in fact, different type of losses needs different solution. By understanding the lost circulation characteristic, cement slurry can be designed to achieve better chance to cure the losses.

In total loss condition (Table 1), it is preferred to pump cement with higher density and higher gel up rate. This has been observed to increase the success rate of LCP. In case of partial losses, density should be adjusted in respect to expected frac pressure to avoid increasing the loss rate.

Loss circulation plug in geothermal well is done in the same way as oil and gas wells: normal balance plug method. Most of the cases of losses that in geothermal wells require loss circulation plug. In the event of total losses, bullheading a cement plug with open end positioned above the loss zone is safer and more effective. For stabilization plugs in problematic zones, plug placement is very critical to avoid pipe getting stuck due to formation instability as well.

Long String	Liner + Tieback	Two Stage
Pros ▪ Safe time due to single run of string ▪ Full metal casing from bottom to surface. Eliminate weak point of no gap between casing.	Pros ▪ More assurance in casing to casing section ▪ Less risk of losses due to lower hydrostatic column	Pros ▪ Safe time due to single run of string ▪ More assurance in casing to casing section ▪ Less risk of losses due to lower hydrostatic column
Cons ▪ Higher probability of loss during cementing due to high column of cement ▪ Higher probability to have water trap inside casing	Cons ▪ Additional time spent after liner job before tieback ▪ Weak point of tieback receptacle which has no full metal joint	Cons ▪ Weak point of dual stage packer and port collar seal which could not stand high temperature of steam ▪ Presence of gap between annulus behind port collar and dual stage packer

Figure 1: Comparison of cementing method for production string.

Table 1: Criteria for Lost Circulation Plug Slurry Design.

Properties	Criteria
Density	High density for total loss, Lower density for partial loss
Rheology	Thick slurry for total loss
Thickening Time	Shorten safety time for faster gel up
Cement volume	>200 bbls for surface total losses

Reactive cement

In severe lost circulation condition, cement slurry is expected to set very fast to avoid the migration to the loss zone, thus can decrease or even stop the losses. This special system utilizes specialized silicate solutions. They can be used to effectively seal problem zones of lost circulation.

A solution of sodium silicate and water forms a rigid semi-permanent gel when in contact with a heavy-calcium or sodium brine. When the cement contacts the gel resulting from the sodium chloride and calcium chloride solution, the cement will set very rapidly. This system forms a permanent seal that can only be drilled out.

GEOTHERMAL WORKOVER CEMENTING OPERATION

Leaked casing, liner lap, and tieback receptacle

Casing leaks in geothermal wells are often caused by external factors such as CO2 or H2S attack. In several cases, it might be due to connection failure.

Tieback receptacle leak is caused by tieback to liner overlap not having full cement coverage. To prevent this issue, it is recommended to increase the overlap/tieback stem as well as have excess cement in tieback cementing. It is recommended as well to place hi-vis pill below tieback receptacle to prevent cement from falling into the liner.

In case the condition of the casing is complex, it is common to have another smaller casing size to be run to isolate the problematic casing section.

Casing Collapse

Casing collapse refers to casing damage due to force from behind the casing being higher than the casing collapse rating. This happens due to the presence of water trapped in casing-casing annulus which expands when hot steam flows.

Trapped water cannot be mitigated by increasing the casing grade as it can generate pressures higher than the collapse resistance of usual API casing. A rule of thumb is that for every 1-degree F temperature increase, there is 50 psi pressure increase **(**Torres, 2014).

Cold water intrusion

This is an event when water from intermediate or surface section comes into the borehole from behind casing. This reduces the steam temperature. It happens when cement does not isolate the casing from formation and/or casing is corroded.

Sealing Reservoir Zone

The main challenge for workover operation is how to seal the reservoir zone so that any cementing job will not harm the steam zone

Permanent or retrievable bridge plug is not preferred due to its temperature rating and difficulties to be milled. In most cases, after the workover operation, it was found that the bridge plug fell down since high temperature from below burst the rubber elements.

Bridge plug junk dropped into the reservoir zone poses a risk of reducing the steam flow area. Wooden plug is preferred rather than bridge plug as it is easy to drill. Wooden plug OD is normally equal to casing ID but it can still be pushed down due to its flexibility. Common practice is to drop wooden plug and let it land on top of liner. Cement is dropped on top of it as a temporary barrier. After workover operation has been done cement and the wooden plug are drilled out.

SPECIAL CONSIDERATION IN CEMENTING DESING

Temperature Estimation

Temperature gradient in geothermal wells is different from oil and gas wells. While oil/gas well has a fixed temperature gradient, geothermal well has a changing gradient due to the presence of steam in the reservoir formation. Gradient in surface and intermediate sections is usually very high while after entering reservoir zone, the temperature becomes stable throughout drilling. This is mostly due to rock formation of geothermal wells which is made of igneous rock, not sedimentary rock. In geothermal wells with dry steam reservoir, high heat convection between the layers of formation is sometimes encountered. Even though this is not yet proven, precautions need to be taken when cementing job is done near the reservoir zone. Figure 2 shows the comparison of temperature gradient between geothermal and oil & gas.

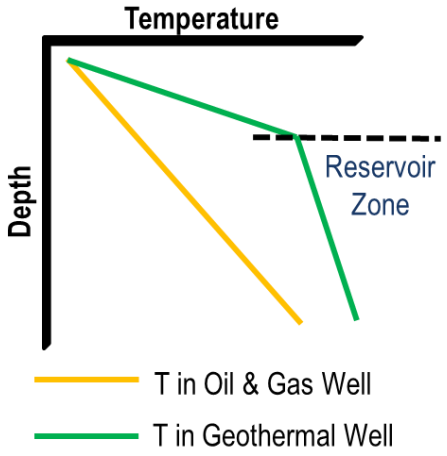


Figure 2: Comparison of temperature gradient between geothermal and oil & gas well.

In several cases in intermediate section, when the zone is closer to reservoir section, heat up rates are higher. In this case, do not idle for a long time without circulation. Once the well heats up, there is a possibility of steam kick to occur.

MWD temperature often gives misleading information when drilling in loss condition (Table 2). Often it gives a lower reading due to flooding of freshwater from the annulus.

Table 2: Defining temperature for cementing job.

Data Used	Remarks
Reference well	Use the temperature at the same TVD as BHST
Software simulation	Use geothermal profile instead of mud circulation for temperature simulation module. Ensure volcanic formation is used.
MWD temperature	Compare temperature from simulation with MWD temperature. Ensure at least minimum +10 deg C margin between MWD and simulation.
Expected reservoir zone	If reservoir depth is close, expected heating rate is very high. Minimum +10 degC margin from software simulation is recommended.

Centralizer Selection

Centralization is a must to achieve good mud removal, especially in casing-casing section, i.e. liner overlap and tieback casing.

Centralizer without full body fins are preferred. This is to avoid poor mud displacement across the centralizer (inside the fin) since the fin area has limited opening.

Most cases of casing collapse and connection failure occur in the shallow section. This may be associated with inefficient displacement of water trapped across centralizers, and viscous fingers. To improve water displacement, consider pumping excess cement to increase the cement contact time **(**Torres, 2014).

GEOTHERMAL CEMENTING EQUIPMENT

Geothermal wells are always associated with a harsh drilling environment with unexpected events always happening during the drilling process. Furthermore, backup requirements are also to be considered as the geothermal location is generally in a tough-to-access remote area.

For locations in high mountain areas, gaining a big enough area for a well site pad is very difficult. While challenging terrain is the main factor, the piping of existing steam production that could not be cut down during the drilling operation adds to the complication. Figure 3 shows the cementing equipment setup.

Commonly, onshore cementing pump units are manufactured with a simple design, in order to achieve higher mobility. It is a common mindset that land operation is always associated with simple and small volume of cementing jobs. However, challenges arise when executing a cementing job in a remote area, which requires not only a mobile unit but also surviving in a harsh drilling environment.

- It is recommended to have cementing pump unit with built in backup as well as high mobility
- Sufficient fluid tanks and cement silos need to be ready for unexpected loss scenarios
- Air dryer is needed as well due to high humidity of air.



Figure 3: Cementing Equipment Setup.

OPERATIONAL BEST PRACTICES

Below are the several operational best practices that is used in Geothermal Cementing Operation in Indonesia:

- Ensure no fluid is dropped into the annulus during WOC for primary casing job, cover the annulus during WOC.
- For surface casing job, set the casing in a c-plate/casing slip. This is to enable pumping top job in parallel when drilling next hole section.
- If feasible, tieback string to be set in vertical section to ensure of having the best standoff.
- Sufficient slurry volume for tieback job – additional 20-30 bbl cement slurry after first cement returns are observed.
- Displace the fluid above liner receptacle after liner is successfully pressure tested to water – this is to enhance mud removal.
- Slow down the pump rate while switching silos to ensure density is not dropped during mixing and pumping on fly operation.
- USIT on the production string job to ensure no pocket of trapped water.
- UCA Equipment to be in the field as a reliable source for WOC for liner job.

CONCLUSION

1. Cementing in geothermal well is important for having zonal isolation between geological layers and to have longer well life
2. Main challenge in geothermal cementing operation is the high steam temperature during production, which cause strength retrogression and casing collapse if any trapped fluid is presence
3. Primary cementing in intermediate section is very important since it is the string for the steam flow (production string). The primary cementing job need to be done in the best method to achieve the cementing objective.
4. Lost circulation is very common to be found in surface and intermediate section in geothermal well. To overcome the losses, fit-for-purpose cement slurry design is needed.
5. Geothermal well has a very high temperature in the surface and the closes it gets to the reservoir zone, the heating rate become very high, thus affecting the cement slurry.

REFERENCES

Nelson E.B., Guillot D. (2006), “Well Cementing, second edition”, Page 14

Eilers L.H., Root R.L. (1976), “Long Term Effect of High Temperature on Strength Retrogression of Cements” Presented on 8-9 April. SPE 5871

Torres, A. (2014). “Challenges of Casing Design in Geothermal Wells”. Presented at IADC/SPE Asia Pacific Drilling Technology Conference, Bangkok, 25-27 August. SPE-170480-MS.

ACHIEVEMENTS AND CHALLENGES TO UTILIZE EXPLORATION WELLS INTO DEVELOPMENT OF COMMERCIAL GEOTHERMAL POWER PLANTS, CASE STUDY ULUMBU 4 X 2.5 MW

Sugeng Triyono, Dwi Handoyo Saputro, and Budi Wibowo

PT. Indonesia Power
Centennial Building Fl.7, Jln. Jendral Gatot Subtoto, Jakarta, Indonesia.
Email: sugeng@indonesiapower.co.id

ABSTRACT

The 3 (three) exploration wells drilled in prospective Ulumbu geothermal field, Flores Island, East Nusa Tenggara Province – Indonesia. After years of silent since 1995, one of those wells is utilized to feed the 4x2.5 MW power generation plants, total accomplishment in 2014. This is achievements to monetize the steam resource, therefore to convert single well pad into power plants food print gives challenges during lifetime of operation power plants. Potential resource of 100 MWe, from this Ulumbu field will be a major role on supplying electricity to the island in the short future time. Those 4 units consist of two different design of power plants, about half of the electricity generated from back pressure turbine. The others are typical condensing steam turbine. In the sense of increasing efficiency, waste steam from back pressure turbine is potentially to generate additional more electricity. Limited space available for expansion, experienced fast declining capacity during operation due to scale deposition on the rotary and stationary turbines blades, heavy corrosion on piping, balance of plants, are among challenges during 8 years operation of power plants. The paper serves description on operation and maintenance of Ulumbu power plants since commercial operation date up to today operation.

Keywords: Operation and maintenance, Ulumbu geothermal field

EXPLORATION PHASE

Geothermal Features on the Project Location

The Ulumbu geothermal field is located on Flores Island in eastern Indonesia (Figure 1). The geothermal field is located about 11 km to the south of Ruteng the regional capital of the Manggarai District of the island, in the southwestern flank of the Poco Leok volcanic complex, about 13 km SW of the active volcano Anak Ranaka.

The heat discharged from the extensive surface manifestations in the Wai Kokor valley at the Ulumbu geothermal field has been estimated at 20 - 100 MWt (Mahon et al., 1992) and at 100 MWt by WestJEC (2008).

The spectacular fumarole field in the Wai Kokor valley (650 m) dominates the thermal activity at Ulumbu and contributes to the dominant proportion of the estimated 100 MW thermal natural surface heat flow from the system (WestJEC, 2008). Scattered over a large area to the east, west and south of the fumaroles are a number of warm bicarbonate type springs with low chloride contents.

Preliminary scientific surveys were mostly conducted by the VSI. Exploration/production drilling was carried out by PT PLN, with assistance from GENZL and the New Zealand Ministry of Foreign Affairs and Trade. Test results suggested that at least 15MWe could be generated by the three wells (Kasbani et al., 1997).

Mains geological features

Flores Island forms part of the Banda Island arc system that comprises Upper Cenozoic volcanic rocks with volcanogenic and carbonate sediments (Hamilton, 1979). The volcanic rocks are dominantly of mafic and intermediate calc-alkaline composition and are unconformably underlain by Tertiary sediments.

The oldest rocks exposed are of Middle Miocene age (Koesoemadinata et al., 1981). The Ulumbu field occurs on the southern flank of the Poco Leok volcanic complex and is about 650 m above sea level (KRTMERT, 1989). The youngest rocks outcrop approximately 7 km north of Poco Leok. These are andesites, basaltic andesites, silicic andesites and dacite domes that overlie rocks of the Poco Rii volcano which erupted lavas and breccias, dominated by andesitic to basaltic andesite lithologies. The most recent volcanic event in the region was the 1987 eruption of a dome of silicic andesite - dacite (Anak Ranakah), about 10 km north east of Poco Leok (Sjarifudin & Rakimin, 1988) (Kasbani, et al., 1997).

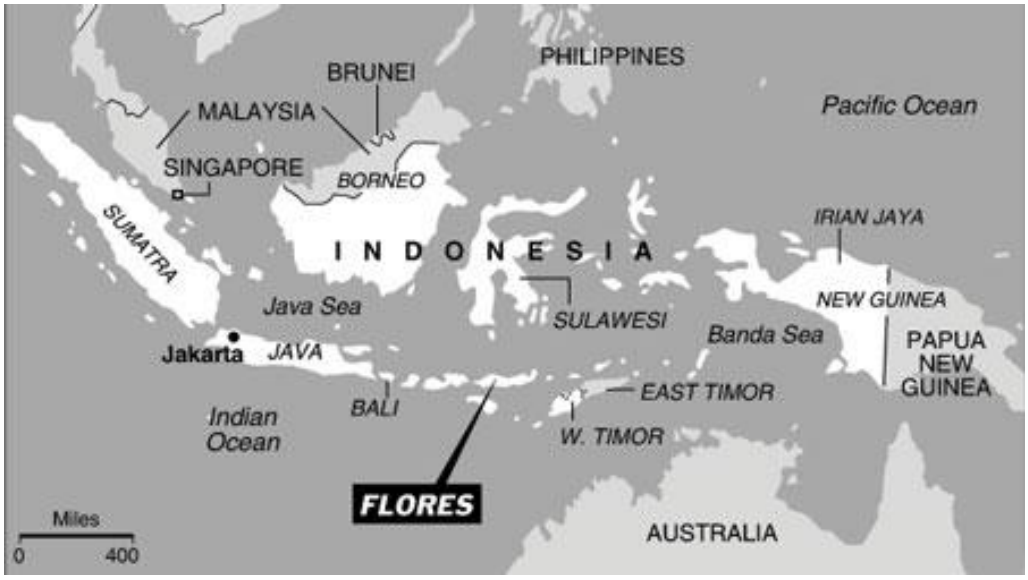


Figure 1: Location map for Flores Island in eastern Indonesia.

Main Geochemistry Features

Most thermal features in the Ulumbu geothermal field occur over an area of about 28 km^2 within the crater and on the western and southwestern flanks of the Poco Leok complex. Features include hot springs, fumaroles, mud pots and steaming ground. The springs are mostly characterized by high concentrations of sulphate, very low chloride content and low pH (3), but some are of neutral pH - bicarbonate type. No chloride waters discharge at the surface.

Mains Geophysics Features

Schlumberger resistivity surveys were carried out over the Ulumbu prospect in 1982 and 1985. (Simanjuntak 1982 and 1985). The survey results are summarized in VSI website as follows.

Most of the Schlumberger measurements were in the form of soundings to AB/2=2000 m, along surveyed lines. The lines were concentrated in a 100 km2 area centered on Wai Kokor, although some additional lines were also measured further north (around Ruteng). The surveys appear to have delineated a potential geothermal reservoir area which includes the Wai Kokor thermal area. Significantly, a survey line which extended further east across the Mesir, or Lunggar, "thermal" area indicated generally higher resistivities at depth (10 ohm-m), but low resistivity near-surface. This may mean the Lunggar area is now almost cool, and there is only an alteration zone near surface which is contributing to the low resistivity. It was not possible to ascertain whether or not there is a surface thermal anomaly in this area. The zone of lowest resistivity appears to be roughly delineated by the 10 ohm-m apparent resistivity contour on the AB/2=1000 m spacing map. The underlying geothermal system probably has a simpler shape than shown by this contour, but the contour may be indicative of the total area of lowest resistivity. This is of the order of 10 km2, but the estimate is clearly poorly controlled in several places, particularly in the region of higher topography to the north. Geographically, the low resistivity anomaly extends to around Wai Mantar in the north, and possibly to Wai Garit in the south. Very low resistivities, which were found at depth 2 km further south, may be influenced by conductive sediments beneath the volcanic pile. The most attractive target area based on geophysical survey results was proposed as the north of the Wai Kokor thermal area, in the region of higher topography. thermal features in the Ulumbu geothermal field occur over an area of about 28 km2 within the crater and on the western and southwestern flanks of the Poco Leok complex, as per shown in Figure 2.

Drilling of Explorations Wells

Three deep exploration wells were drilled from the same drill pad in 1994 – 1995 less than 100 m away from the fumaroles. ULB – 01 is vertical drilling and subsequent drilling of deviated wells to target crater area underneath ULB – 02 and to target perimetric of the reservoir ULB – 03, as per Figure 3.

The measured temperatures are up to 240°C with a productive steam zone at 750 m (Grant el al., 1997; Kasbani et al., 1997). The deepest well (ULB-01) encountered Quaternary volcanics to a depth of 838 m with Tertiary sediments below this to the well bottom, at 1887 m. ULB-02 is directionally drilled to the NE and was the main producer with about 12 MW of dry steam.

GENZL (1996) The first test on ULB – 02 exploration well was done on May 10, 1996, used vertical discharge testing with pipe lip diameter of 10". During test the well produce 140 tones/hour dry steam at well head pressure (WHP) of 4 Barg. In May 1996, after installation of horizontal pipe and

separator and silencer, the well ULB-2 produced dry steam at discharge flow rate of 75 tones/hour, at WHP of 26 barg for about 8 days (GENZL 1996). Figure 4 illustrates geothermal system modelling after 3 exploration drilling wells in Ulumbu area.

When PLN (the Indonesian State Electricity Company), planned to utilize the steam from ULB-2 to generate small steam power plants, PLN requested consultant to do testing on ULB-2 to ascertain the steam available on the well head. The test done during August 1, 2004 – September 26, 2004 with the following data;

- Equivalent MWe output ULB-02 is about 13.0 - 15.6 MWe. Steam is dry superheated, flow rate of 108 – 112 tones/hour, at WHP of 11.0-13.00 barg, enthalpy measured of 2772 - 2788 kJ/kg and steam temperature of 164 – 186.5°C. Shut in pressure is about 30.5 barg.
- Major feed zone of ULB – 2, is in the depth of 650 – 700 m depth, 50 m thick, measured from the surface. Permeability of feed zone is about 296 darcy-meter. Formation pressure is about 32.1 barg, with temperature in the range of 233 – 234 °C.
- Non condensable gas "NCG" is about 2.15% - 2.78% of total weigh or 0.94% - 1.26% mol.

The second well test requested by PLN to different consultant, was 2011. Flow test was done within November 22 – 27, 2011, horizontal test as per the previous existing testing facilities. The test result on ULB – 2 as the following;

- Stabilize flow rate on 117.2 tones/hour with pressure of 10.8 barg WHP, while reduce opening the valve steam flow rate down to 73.3 tones/hour at WHP of 19.6 barg. Fully open valve, produce steam flow rate of 132.5 tones/hour at WHP of 7.45 barg. Orifice diameter is of 200 mm ID.
- Enthalpy of the steam is in the range of 2773 – 2787 KJ/kg, in accordance with steam wetness of 0.01 – 0.53%.
- Hydraulic transmissivity "kh" is 276.2 Darcy-meter, skin coefficient of 19, highly permeable reservoir.
- Chemical analyses shown the Non-Condensable Gas "NCG" of about 2.33% - 2.53% by weight, pH condensate 5.06 – 5.59. The nearest water surface has pH of 5.6 – 6.67.

COMMERCIALIZATION PHASE

Electricity Supply and Demand in Ruteng

Prior developments of Ulumbu Geothermal power plants, electricity productions were depending on the diesel power plants. Back to PLN electricity Planning 2013 – 2022, Ulumbu geothermal is a potential geothermal resource to be utilized to substitute diesel power plants. Ulumbu power plants will feed isolated distribution area of Ruteng, which was still depending on diesel power plants. Electricity is delivered through 20 KV isolated distribution wire, with total installed capacity of 13.1 MW, diesel-based power plants. All diesel combined only able to supply 10 MW during peak time, while electricity peak demand of 7 MW. The later 70 KV transmission line, eventually connected the western part of the island in 2019, further expansion of 70 KV transmission line will connect the island planned by 2019.

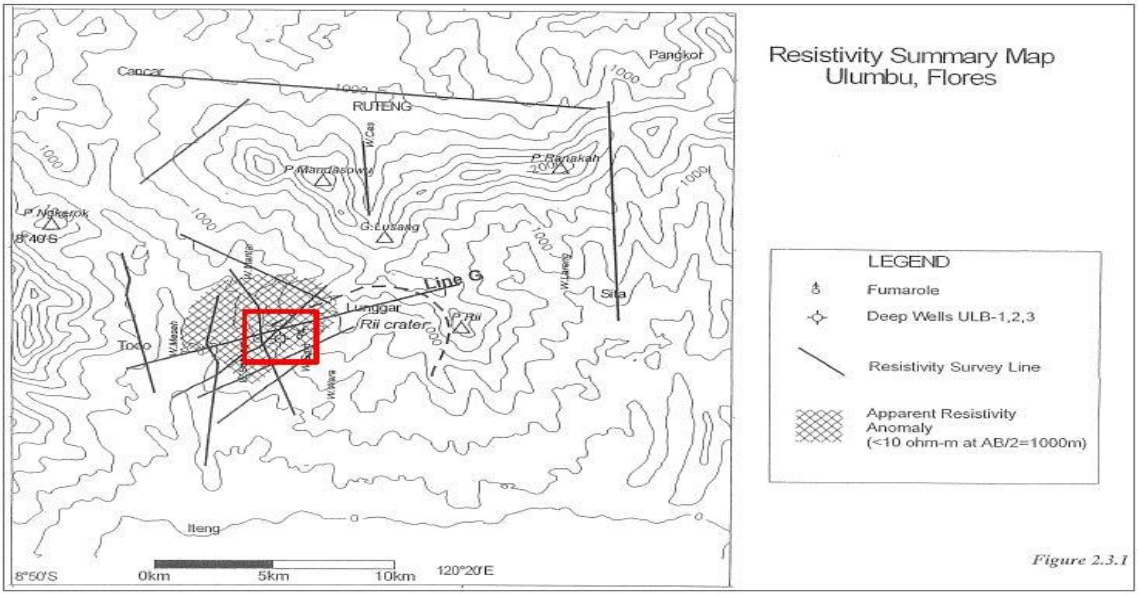


Figure 2: Location map for Flores Island in eastern Indonesia.

Long planning developments of Ulumbu power plants is shown in the Table 1.

The first power plant, a 2 x 2.5 MW condensing unit built and commissioned in 2012 (Unit 1 Reliability Run was completed on 18 June 2012 and Unit 2 Reliability Run completed on 20 February 2012). These new geothermal power plants receive steam from well ULB – 02, which able to produce 13 – 15 MWe, at WHP 8 barg, as per well testing data recorded on 2004 and 2011.

Considering successful operation of 2 x 2500 KW condensing powerplants, the expansion development of power plants was needed, to cater electricity demand increase on the area. The second construction project was new 2 x 2.5 MW back pressure plants designed by Geothermal Development Associates (Reno, Nevada). These power plants were commissioned in October 2014 with PLN accepting the certificate of operation in September 2014. Since then, total 10 MW of 4 units Ulumbu geothermal power plants become backbone to supply electricity in Ruteng Area.

Therefore, as per shown in Table 2, performance parameters of 4 x 2500 KW Ulumbu Power Generation plants far beyond typical performance power plants in comparison with others geothermal power plants such as Kamojang of total install capacity of 340 MW, Gunung Salak 360 MW, and others power plants.

One of the reasons, is before Ulumbu power plants connected to 70 KV transmission line in 2018, operation of powerplants restricted by demand constraint. During peak time, demand load was 7 – 8 MW, considering load factor is about 62%, equivalent with off peak demand capacity of 4 – 5 MW. Peak time is about 4 hours from 18 - 22 pm.

After Ulumbu power plants are connected 70 KV transmission line, operation of power plants restricted by steam supply constraint. After 7 years operation of power plants, production steam from ULB – 02, is no longer enough to feed the power plants at maximum rated capacity, as per shown in Table 2.

Declining ULB – 02 and Scale build up

Steam Production Continuous Decline from ULB – 02 Exploration Well.

ULB – 02 is design for exploration well, even though later on be converted to exploitation wells (Table 3). Response of ULB – 02, after years produce steam for power plants, noticed experience of declining response based on data collected in 2015 – 2017.

Converting exploration wells into exploitation wells, as per Ulumbu case, ULB – 02, experience of reduce reservoir pressure significantly. Since this is the only well available in Ulumbu, other wells ULB – 1, and ULB – 03, are not economically viable to support the production steam to feed power plants. Dynamic changing properties of ULB – 02, may change from dry steam to more wet steam, as well changing NCG in the steam contents in the reservoir.

Further exploitation on a single well, case ULB – 02, may lead to further declining pressure that achieve boiling hot water, leaving behind scale deposition. Initially, scaling located inside the well, therefore, considering further potential drawn down water level, that may touch boiling pressure in the upper part of the reservoir occur in the reservoir, leaving scale deposition in the reservoir, if contaminated with local ground water.

Since, power plants begin in operation, no reinjection well have been drilled to maintain water level in the reservoir. Trial to use ULB – 1, to become reinjection well, experience of well interference with ULB – 02, that indicated to cool down the reservoir, after recorded steam production from ULB – 02, becoming more wet.

Figure 5 and Figure 6 are presenting response of ULB – 02, after producing steam to feed total of 10 MW Ulumbu plants in 2015, 2016 and 2017. Increasing steam flow is required to meet demand production, as a consequence of reducing WHP to give more opening valve for increasing steam flow production.

Noted in the Figure 5 and Figure 6, that total MW deliver to the 20 KV grid was in the maximum rated capacity of 6 MW. This is due demand constraint. After 70 KV has been connected to Ulumbu power plants, the electricity production is also not achieved the maximum rated capacity of 10 MW, as per presented in Table 1, because of limited steam flow from ULB – 02, and at the same time, scale deposition has reduced maximum rated capacity of back pressure turbine quite significant.

Scale Build up in the Turbine Blades of Back Pressure Turbines.

After experiencing years of operation, the back-pressure turbine tends to decrease capacity much faster than condensing turbine, because of scale deposition in turbine blades. The capacity decrease of power plants ADB unit 1 and 2, has more than 50% from installed capacity. Deposit has block severally of steam flow along the gap among turbine blades, as per shown in Figure 7. Deposit is hard solid particles strongly bonded in the contact area where steam is flowing across the area gap. It is believed that scale minerals originally rock mineral that dissolve in to geothermal liquid because of elevated temperature and pressure in the form of dissolved solids in the geothermal fluid. During exploitation of the field, the fluid is brought to the surface and heat is extracted to generated electricity

power. When steam is extracted to become the working fluid, there is the possibility of depositing some of the dissolved species, because of dropping temperature after heat is used. The most common mineral scales encountered in deposition of geothermal fluid are silica (SiO_2) and other silicate mineral.

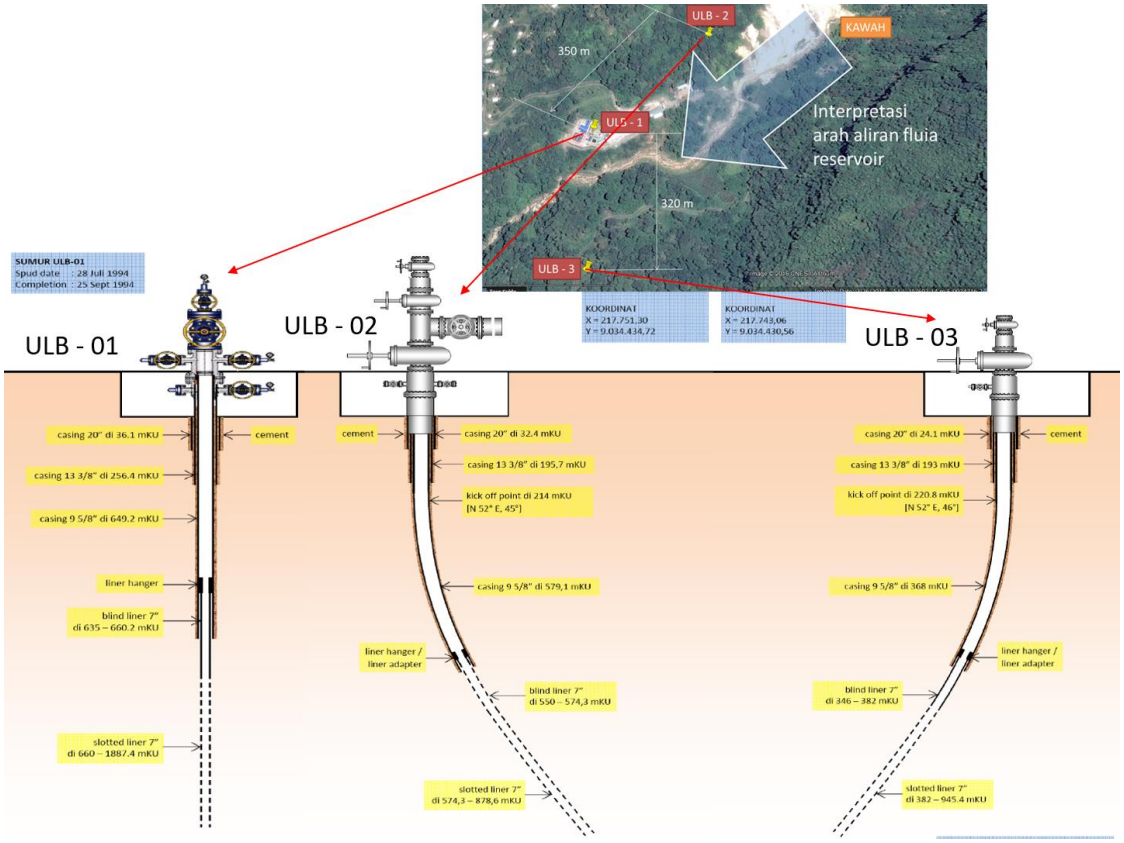


Figure 3: Exploration wells of ULB – 01, ULB – 02, and ULB – 03.

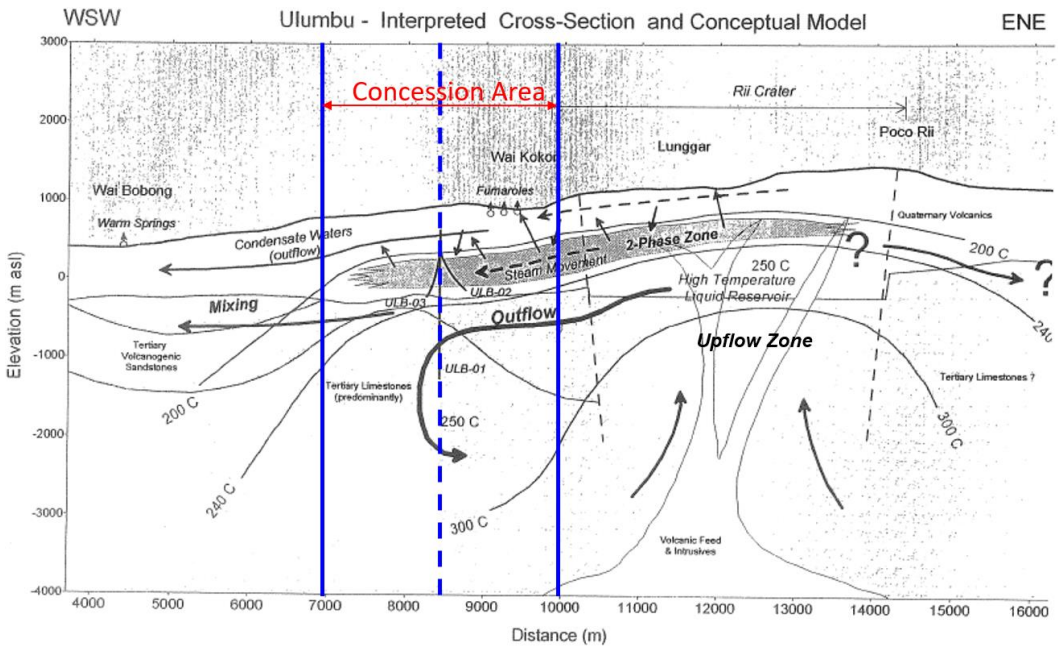


Figure 4: Geothermal system modelling after 3 exploration drilling wells in Ulumbu area.

Table 1:Milestones activities developments of 4 x 2500 KW power plants in Ulumbu.

No.	Date	Activities
1	2001	Asian Development Bank (ADB) give grant as per technical assistance of TA No. 3481-INO for Outer Islands Electrification Project (in this project included development of Ulumbu geothermal concession)
2	11 Feb 2008	Contract signing of ADB 2 x 2.5 MW
3	9 May 2008	Permitted issued for development of Ulumbu power plants with capacity of 2 x 2.5 MW located in District Satamese, - Manggarai
4	18 Oct 2013 to 20 Oct 2014	Preparation for construction included civil works to prepare Iteng temporary jetty for receiving material through shipments.
5	2 Des 2013 to 26 March 2014	Delivery material included mobilization to site ULB
6	17 Feb 2014 to 4 June 2014	*erection period of* mechanical and electrical
7	10 – 11 Jul 2014	*First rolling* turbine U1-2 ADB (speed 1,500 to 5,000 rpm)
8	15 Jul 2014	*First synchronize* U1-2 ADB
9	22 – 26 August 2014	*Load test* U1-2 ADB (110%)
10	22 – 29 August 2014	*Reliability Run test* U1-2 ADB
11	30 – 31 August 2014	*Performance test* U1-2 ADB
12	4 Sep 2014	Taking Over operation power plants (STOP) PLTP Ulumbu 2 x 2.5 MW
13	9 Sep 2014	Certificate of Operation Sertifikat Laik Operasi (SLO) Unit 1-2 ADB
14	9 Sep 2014	*Commercially Operating Date* (COD)
15	11 Sep 2014	*Taking Over Certificate* (TOC) Unit 1-2 ADB

Table 2:Performance parameters of 4 x 2500 KW Ulumbu Power Generation Plants up to February 2019.

No.	Unit	Installed Capacity	Maximum Capacity	Average Load	Reliability Run	Remark
		KW				
1	ADB # 1	2,500	1,900	1,000	Oct' 2014	*)
2	ADB # 2	2,500	2,000	1,319	Oct' 2014	*)
3	APBN # 3	2,500	2,500	2,349	June 2012	**)
4	APBN # 4	2,500	2,500	2,421	Feb ' 2012	**)
	TOTAL	10,000	8,900	7,089		
*). Capacity de-rating due to scale deposition on blades						
**). Steam flow constraint, from ULB - 2.						

Table 3:Performance parameters of 4 x 2500 KW Ulumbu Power Generation Plants as per February 2019 only.

No.	Unit	CF	Electricity Production	EAF	Remark
		%	kWh	%	
1	ADB # 1	10.65	1,743,841	19.9	*)
2	ADB # 2	9.57	1,567,177	100.0	*)
3	APBN # 3	19.93	3,263,946	100.0	*)
4	APBN # 4	17.85	2,922,791	100.0	*)
	TOTAL		9,497,755		
*). CF and kWh production as per up to February - 2019					

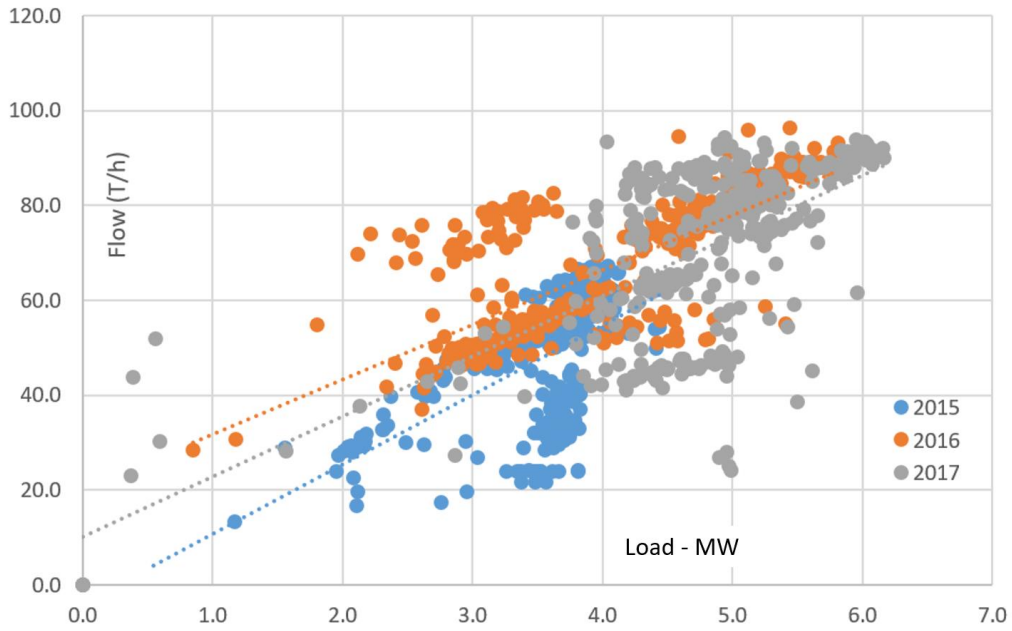


Figure 5: Response of ULB – 02, after feed steam to 10 MW Ulumbu plants in 2015, 2016 and 2017, increasing steam flow to meet demand production.

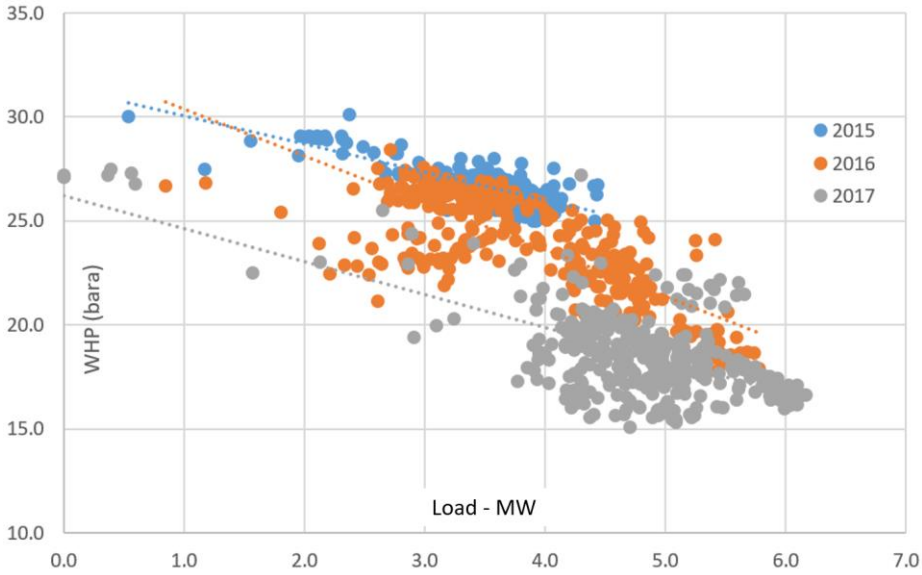


Figure 6: Response of ULB – 02, after feed steam to 10 MW Ulumbu plants in 2015, 2016 and 2017, increasing load demand, and decreasing WHP.

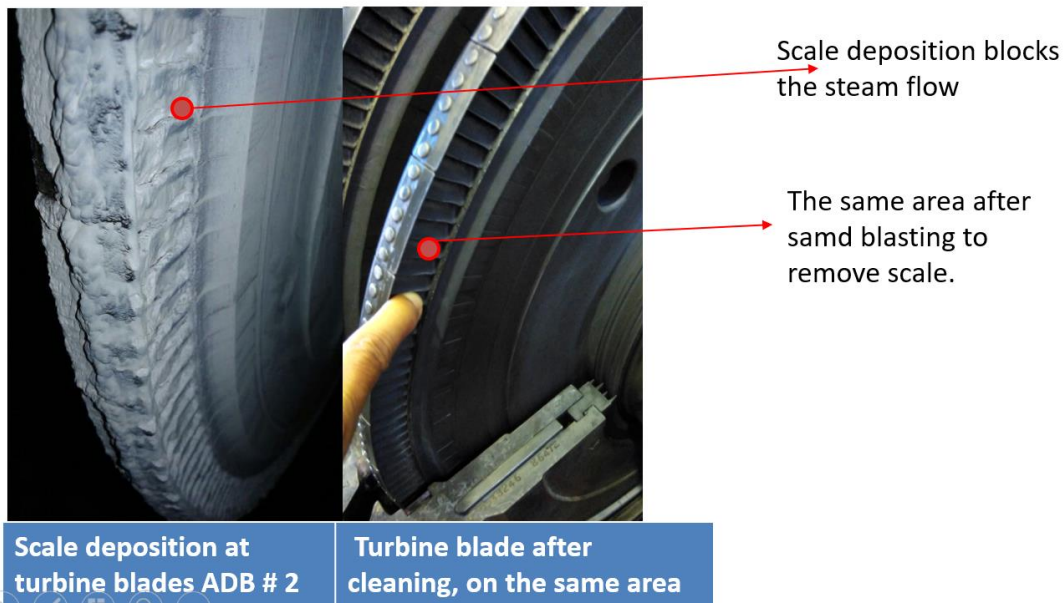


Figure 7: Heavy scale has blocked steam flow among the gap of turbine blades.

During overhaul, cleaning deposition can be done by traditional tools such as sizzle, or mechanical cleaning by sand blasting. As per experienced on Ulumbu ADB plants, sand blasting cleaning has no better scrapping the scale deposit than traditional sizzle cleaning, in term of performance capacity achieved after in operation. Therefore, deposit cleaning with sand blasting has much more fast than traditional blades cleaning.

Experienced of ADB units, the heavy scale deposition phenomenon was much faster when stream strainer in the common header broken. As per Figure 8, design of ADB units have no cyclone separator and demister installed as a part of the steam cleaning system. Steam from ULB – 02, is fed into common header that equipped with with steam strainer, to reduce steam impurities. Then this steam flow directly to spin turbine coupled with generator to generate electricity, as per shown in Figure 8.

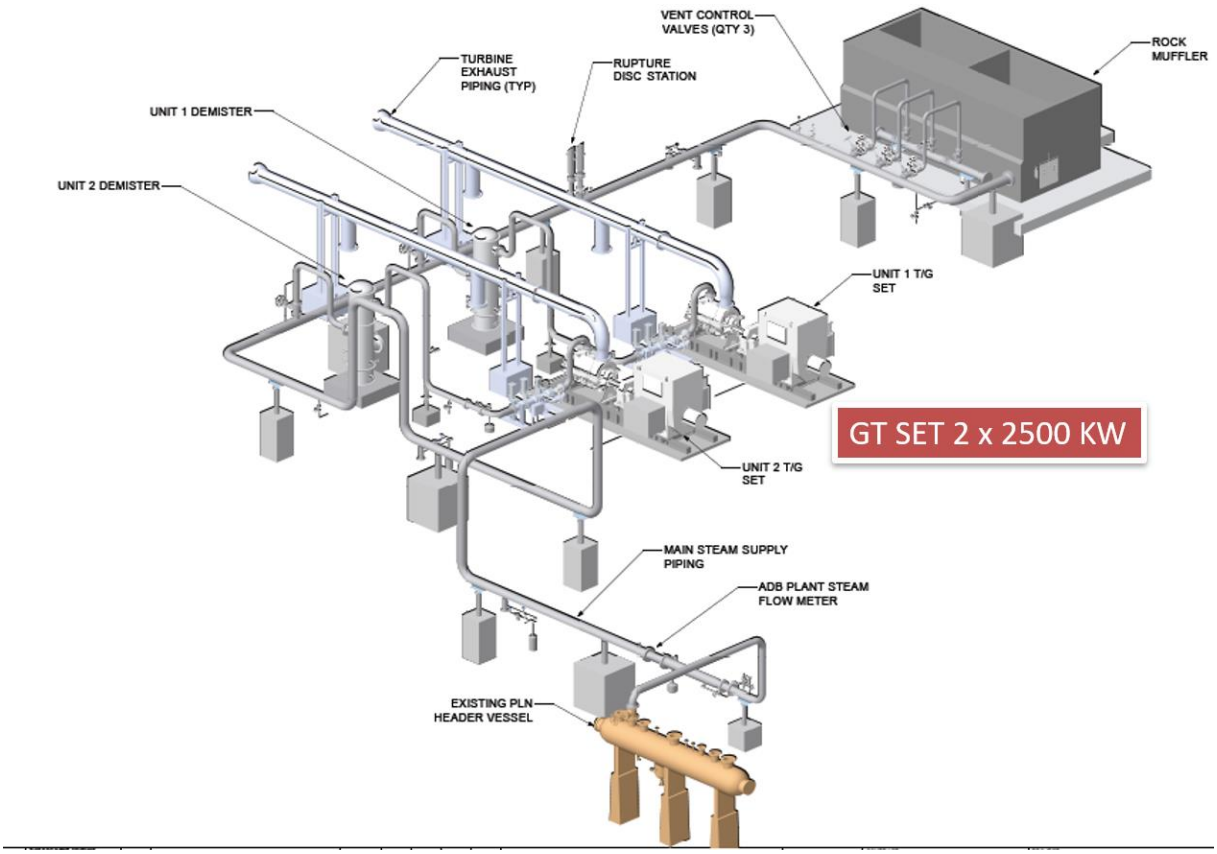


Figure 8: Schematic diagram of steam facility on ADB unit that have no cyclone separator and demister.

PLANNED FOR EXPANSION

Operation Constraint of Existing Power Plants

Other than declining of steam flow from ULB – 02, and scale deposition on ADB power plants, there are others operation constraint for Ulumbu Power plants such difficult maintenance ability and corrosive environments due to disperse sulfur dioxide.

Maintenance Ability of Explorations Wells

These 3 explorations wells are located on the same pad. These 4 units power plants are located very close to the drilling pad, in as such the main steam transmission pipe line, has caused challenge of equipment's such as crane to do well maintenance.

Exposing H2S Lead to Environment Corrosive Area

Typical geothermal area is environment corrosive area because of natural H_2S release from reservoir that considered as non-condensable gas. Sulfur is in contact with mist will form corrosive substance liquid. This H_2S is in contact with water drift from cooling tower unit APBN, to become acid sulfite dropped liquid that trigger heavy corrosion on power plants equipment's such as H-beam, handrail and so on. The presence of H_2S has been becoming accelerated aging solvent of power plant, that will reduce last life for the remaining life time of power plants.

Other than those above problem, elevation of those power plants is located in the valley of the hilly area, close to the existing river. In consequences, plume from cooling tower condensing plants have no chance to disperse to more wide area, falling down to contact with NCG from ADB plants to accelerate corrosion environment on the area.

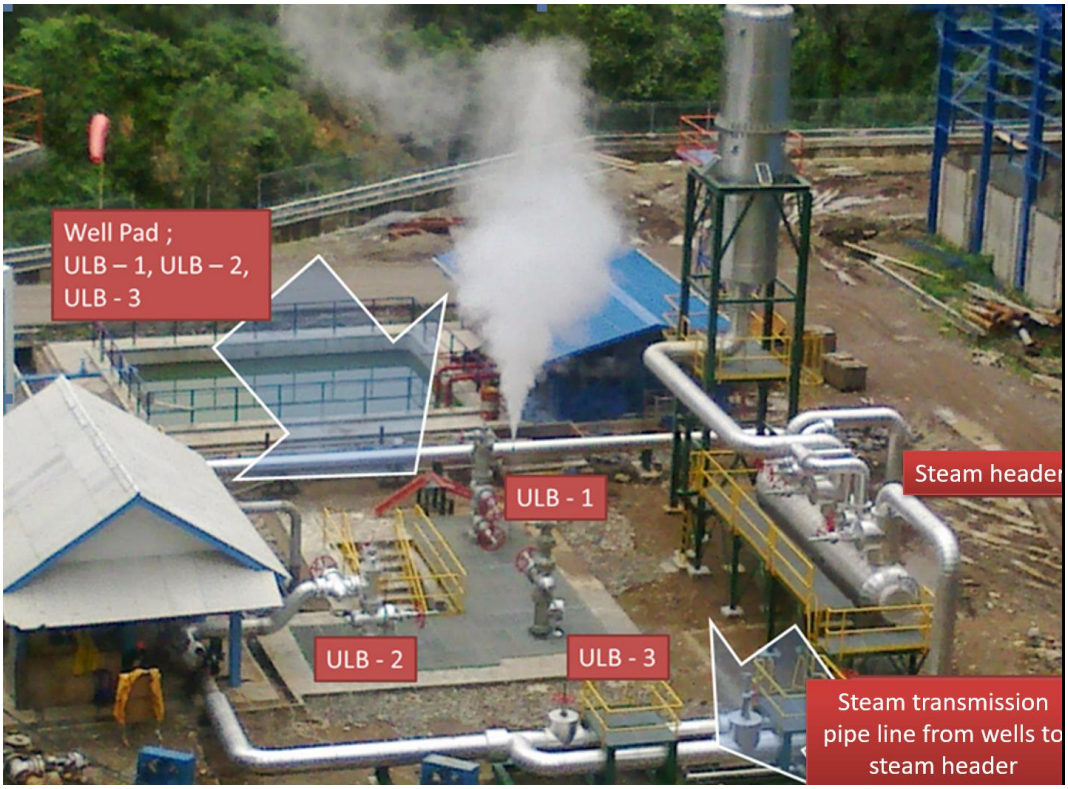


Figure 9: Challenge maintenance ability of ULB exploration wells due surrounded by main steam transmission line.

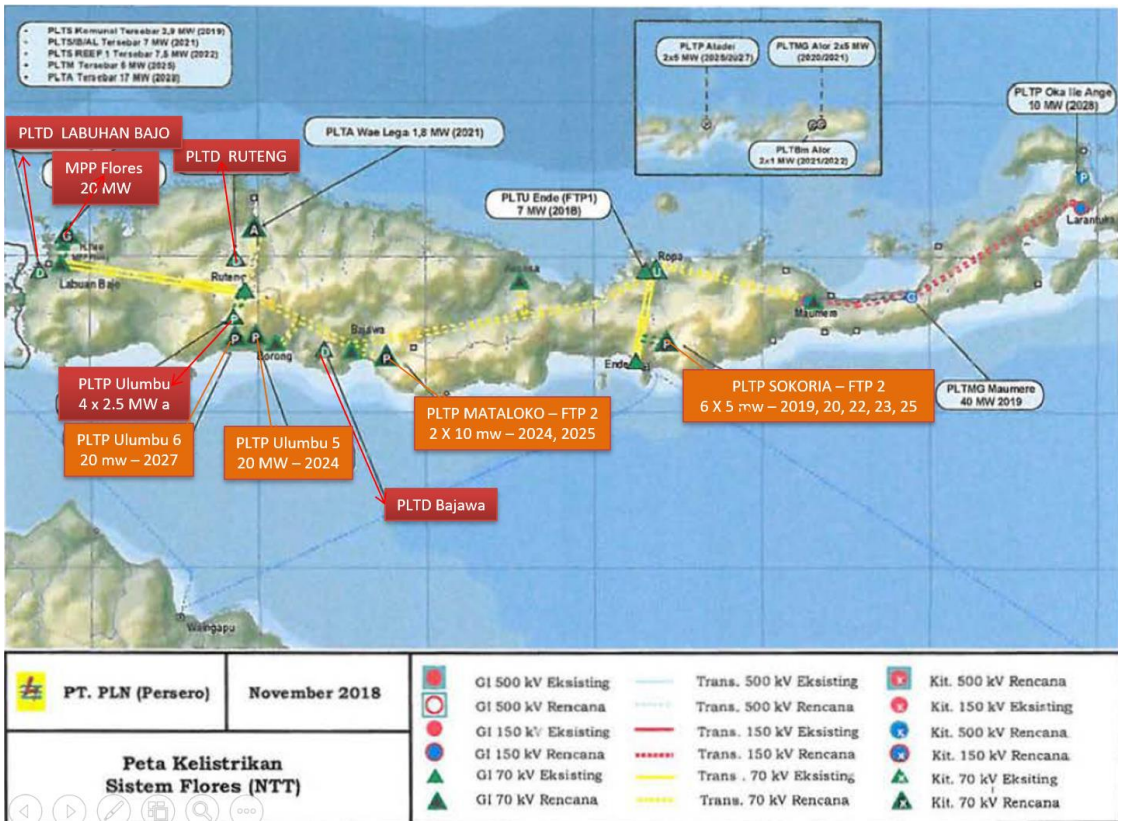


Figure 10: PLN's RUPTL 2019 – 2028 electricity development for Flores Island.

Future Expansion of Ulumbu Geothermal Power Plants

Considering the operation constraints of the existing Ulumbu power plants, and also to do development of MW expansion power generation plants to optimize Ulumbu geothermal field, then the expansion will be as following;

- Installing binary power plants to convert exhaust gas from ADB power plants. This new ORC (Organic Ranking Cycle) can produce electricity of about 3 MW.
- Extension of new unit power generation plants as per issued in the PLN RUPTL, PLN long term planning on development new power generation plants.

As per stated in the PLN's RUPTL 2019 – 2028, the development of electricity in Flores Island will include development of 70 KV transmission line to connect those 2 subsystems, western part of the island consist of subsystem 70 kV Labuan Bajo – Ruteng, and eastern part of the island 70 kV Ende - Ropa Maumere, as per shown in Figure 10 10.

Others geothermal potential that will be developed as per PLN's RUPTL, as the following;

- Ulumbu 5, 20 MW in 2024
- Ulumbu 6, 20 MW in 2026
- Mataloko – FTP 2, 2 X 10 mw – 2024, 2025
- Sokoria – FTP 2, 6 X 5 mw – 2019, 20, 22, 23, 25

As per the RUPTL, to strengthen kWh transfer from western part of Flores and eastern part of Flores, with 150 KV transmission line, and also 70 KV transmission line as per on the Table 4.

REFERENCES

Engineering and Consulting Firms Association, Japan (2008), "Pre-Feasibility Study for Geothermal Power Development Projects in Scattered Islands of East Indonesia"

PT. PLN (Persero) (2019), "Rencana Usaha Penyediaan Tenaga Listrik PT. PLN (Persero) 209 – 2028"

PT. Indonesia Power, Jln. Jendral Gatot Subroto Kav 18 Jakarta (2009), "Laporan Supporting Tahap II" Internal report.

PT. Indoneia Power, Jln. Jendral Gatot Subroto Kav 18 Jakarta (2017), "Proposal Organic Rankine Cycle (ORC) Bottoming Cycle" Internal report.

Table 4:Development of 150 KV and 70 KV transmission line on Flores island

No.	Transmission From	Voltage	Length	COD	Status
		KV	KMS		
1	Maumere - PP Peakers	150 KV	56	2019	Construction
2	Bajawa - Ruteng	70 KV	120	2019	Construction
3	Meumere - Ropa	70 KV	120	2019	Construction
4	PLTP Sokoria - Ende / Ropa	70 KV	20	2019	Planning
5	Ropa - Bajawa	70 KV	190	2019	Construction

FUJI GEOTHERMAL ORC POWER GENERATION SYSTEM

Hiroshi Oyama and Shigeto Yamada

1923/FUJI ELECTRIC CO., LTD., 1-1 Tanabeshinden,
Kawasaki-ku, Kawasaki-city 210-9530, Japan
Email: oyama-hiroshi@fujielectric.com

ABSTRACT

Geothermal energy is recognized as one of the important renewable energy also in Japan, however the current generating capacity is only about 0.2% of total electricity generation. After the Great East Japan Earthquake followed by the Fukushima nuclear power plant accident, Japan's government accelerated various deregulations and incentives to promote usage of the renewable energy. However there still are some difficulties to expand the geothermal energy development in Japan. Large capacity geothermal resource developments are still ongoing, and recent developments are mainly small capacity such as 100kW class "Onsen (hot-spa)" power generation or 2,000-5,000 kW medium size power plants.

Under this situation, Fuji Electric Co., Ltd. (Fuji) had constructed two ORC power plants as the EPC contractor in 2017 and 2018. One is Takigami binary power plant (5,050kW) which Idemitsu Oita Geothermal Co., Ltd. started commercial operation at Oita Japan in March 2017. The other is Yamagawa binary power station (4,990kW) which Kyuden Mirai Energy Co., Inc. started commercial operation at Kagoshima in February 2018. Both power plants generate electricity using reinjection brine of the existing flash system geothermal power plant. On the other hand, there are differences in system such as cooling system, working fluid between these two plants. This paper introduces the overview of these two plants.

Keywords: organic rankine cycle, Fuji geothermal

INTRODUCTION

It is said that Japan has the world third largest potential of geothermal resources. METI, Ministry of Economy, Trade and Industry, has been studying what issues need to be solved to promote more geothermal energy development and the result of the study was reported in 2009. Based on the report, METI started to promote incentives and deregulations. Such promotions were accelerated after the Great East Japan Earthquake in 2011 followed by the Fukushima nuclear power plant accident, and various incentives and deregulations were issued including a feed-in tariff (FIT). The tariff under the Japan's FIT for a newly constructed geothermal energy is 26 yen/kWh for 15,000kW and larger capacity and 40 yen/kWh for less than 15,000kW. However, the installed capacity of the geothermal power plants is just 530MW as of early 2017 and its generation is only about 0.2% of total electricity generation. Most of large capacity geothermal developments are still under exploration or construction stage, on the other hand, small and medium capacity geothermal power plants have been constructed already, utilizing the existing hot-spa hot water or newly drilled production wells. Especially, 37 units of small capacity ORC power generating system were installed from 2011 to 2017, ranging from 20kW to 440kW. Table 1 is the list of geothermal power plants constructed after the Great East Japan Earthquake until March 2017.

FUJI ORC POWER GENERATION SYSTEM

Fuji constructed the 220kW ORC power plant as a pilot unit and operated it from 2006 to 2009 to verify its design, operability and performance. Fuji has supplied 82 units of flash system geothermal power plant and total generation capacity 3,200MW for 35 years. Fuji designs and provides the geothermal ORC system based on the technology of the flash system and experiences of the above pilot plant.

Fuji has two models of ORC turbine named Frame6 and Frame10. Fuji provides any system of over 5,000kW by combining these two models. Fuji optimizes turbine blade design and provides highly efficient turbines although the turbine frame is two models. Table 2 shows typical specification.

Table 2: Typical specification.

Turbine Model		Frame6	Frame10	2xFrame10
Rating	MW	~ 6	~ 10	~ 15
Heat source		Steam / Brine		Brine
Cycle		Single pressure		Dual
Working fluid		Normal pentane / R245fa		

FEATURES OF TAKIGAMI BINARY POWER PLANT

Takigami Binary Power Plant is located at Kokonoe-machi, Oita in Kyushu area, and is operated by Idemitsu Oita Geothermal Co., Ltd. (Idemitsu). Idemitsu has been supplying geothermal steam to Takigami Power Station operated by Kyushu Electric Power Co., Inc. since 1996, and their steam supply business is very successful. There is more than 1,000 t/h separated brine at about 130 ºC being reinjected. The idea is to utilize this separated brine to generate additional electricity, without adding a new production well. The power plant location was selected at a spare space in the existing production well pad area, therefore, additional land development was not required. Idemitsu and Fuji signed an EPC Contract in April 2015, construction completed by the end of February 2017, and the commercial operation commenced on March 1, 2017. This is the first installation of a commercial geothermal ORC power plant by Fuji. The rated generator output is 4,500kW under the average annual ambient wet bulb temperature, and the maximum generator output is 5,050kW at the average winter time ambient wet bulb temperature. The registered output of 5,050 kW is the largest of any geothermal ORC unit in Japan.

Table 1: Geothermal power plants constructed in Japan in 2011 – 2017.

Location	Type	Capacity kW	Completion	Location	Type	Capacity kW	Completion
Oita	ORC	1x72	2013.01	Oita	ORC	1x125	2015.07
Oita	ORC	2x72	2014.01	Oita	ORC	3x20	2015.08
Oita	ORC	2x72	2014.01	Nagasaki	ORC	3x72	2015.09
Nagano	ORC	1x20	2014.04	Oita	ORC	1x20	2015.12
Hyogo	ORC	2x20	2014.04	Oita	ORC	1x125	2016.01
Oita	ORC	1x72	2014.07	Tochigi	ORC	1x20	2016.03
Kumamoto	ORC	3x20	2014.07	Oita	ORC	1x65	2016.04
Oita	ORC	4x125	2014.11	Oita	ORC	1x125	2016.07
Tottori	ORC	1x20	2015.01	Oita	ORC	1x125	2016.07
Oita	--	1x11	2015.02	Oita	ORC	1x72	2016.09
Kagoshima	ORC	1x1,580	2015.02	Hokkaido	ORC	1x125	2016.11
Oita	ORC	1x5,000	2015.06	Fukushima	ORC	1x440	2016.11
Oita	ORC	2x125	2015.06	Hokkaido	ORC	1x72	2017.03
Kumamoto	Flash	1x2,000	2015.06	Oita	ORC	1x5,050	2017.03

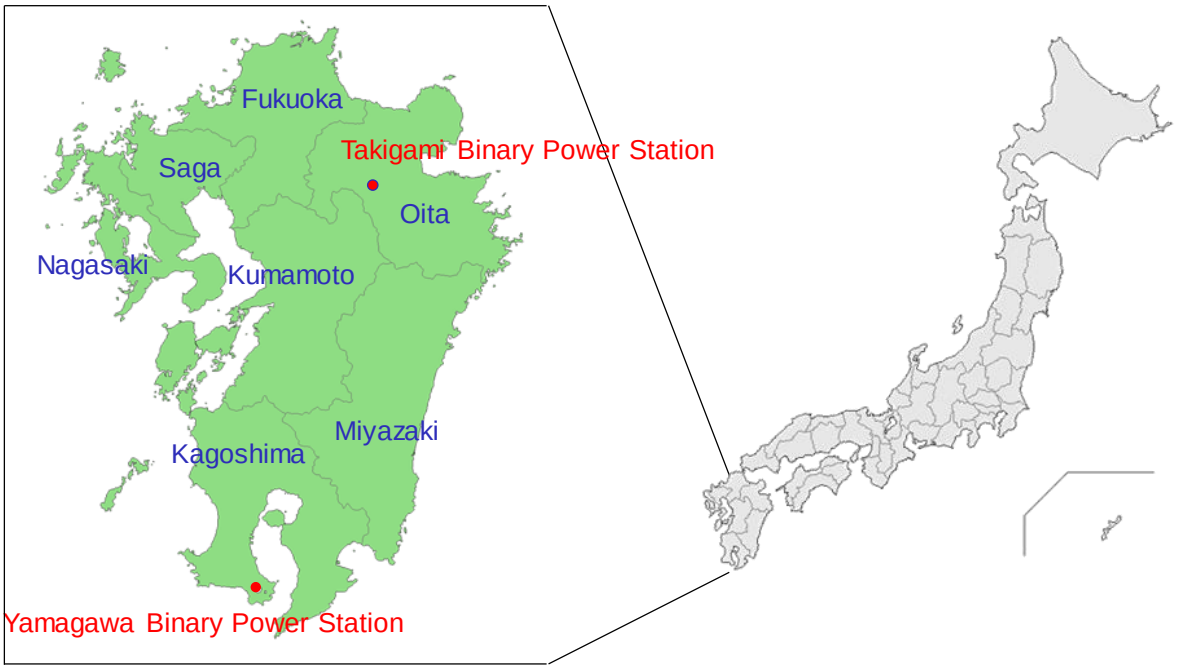


Figure 1: Location of Takigami Binary Power Plant and Yamagawa Binary Power Station.

Overview of Power Plant

Figure 2 shows an overview of the Takigami Binary Power Plant. Figure 3 shows a system flow. The brine branched from the reinjection line is pressurized by two brine supply pumps and goes to one super-heater, two evaporators, one preheater and back to the reinjection line. Due to the restriction of available area, a water-cooled condenser is used, and the cooling tower is constructed for the cooling water supply to two water-cooled condensers. Makeup water to the cooling water circuit is supplied by surplus water from the cooling tower at the existing Takigami Power Plant. R245fa is used as the working fluid to minimize the plot area of the plant, eliminating the additional area that would have been required for the fire-fighting system and fire-fighting area if hydrocarbon had been used as the working fluid.



Figure 2: Overview of the Takigami Binary Power Plant.

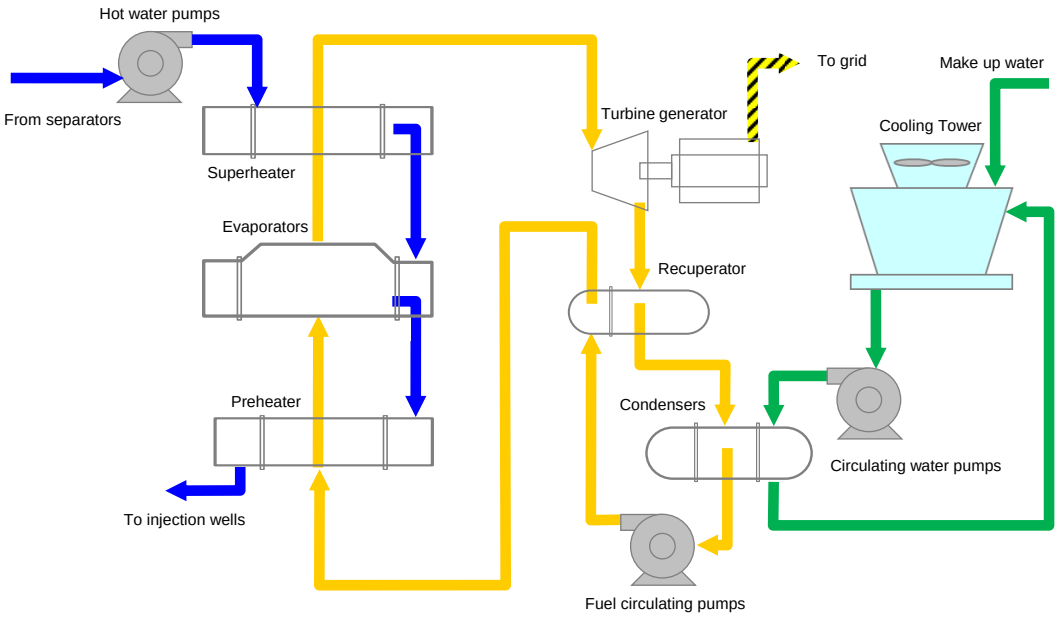


Figure 3: System flow of the Takigami Binary Power Plant.

Features of each equipment

a. Turbine

The turbine was designed and manufactured by Fuji. The turbine uses reaction blades and basically a similar design to Fuji's geothermal steam turbines. The basic difference is the shaft seal type; Fuji's ORC turbine uses double mechanical seals, while the geothermal steam turbines use a steam seal. The turbine rotation speed is 1,800 rpm which is half of Fuji's standard geothermal steam turbines. Table 3 shows the specifications of the ORC turbine.

Table 3: Specifications of Takigami ORC turbine.

Rated inlet vapor pressure	kPaG	1,440
Rated inlet vapor temperature	°C	120
Rated generator output	kW	4,500
Maximum generator output	kW	5,050
Rotating speed	Min^{-1}	1,800

b. Heat exchangers

The heating system consists of one preheater, two evaporators and one super-heater. The material of tubes for all of these heat exchangers is duplex stainless steel, based on the long-term operational experience of the reinjection system by Idemitsu. Figure 4 shows the heating-circuit heat exchangers.



Figure 4: Preheater, evaporators and super-heater.

The cooling system consists of one recuperator and two water-cooled condensers. The condenser tubes are of 316 stainless steel. The condensed working fluid is extracted by the working fluid pumps and pumped to the preheater. Figure 5 shows the cooling-circuit heat exchangers.

Site construction works and commissioning works

Construction of the civil works commenced in April 2016, and construction of the electro-mechanical works commenced in September 2016. All components of the equipment are installed outdoors except for the electrical and control system. The Kyushu area is located the south-west part of Japan; however, the ambient temperature goes down below 0 °C in winter, and snow sometimes fell at the site. The site-testing works commenced in December 2016, therefore the site-testing and commissioning works were sometimes conducted under down to -10 °C ambient temperatures or during snow storms. Even under such severe ambient conditions, the site-testing and commissioning works proceeded on schedule, and the performance test was completed in the middle of February 2017, followed by one week of continuous operation confirmation.



Figure 5: Water cooled condensers and recuperator.

FEATURES OF YAMAGAWA BINARY POWER STATION

The Yamagawa Binary Power Station is located at the Yamagawa Power Station which is the geothermal power plant operated by Kyushu Electric Power Co., Inc. in Ibusuki-City, Kagoshima of Kyushu area, and is operated by Kyuden Mirai Energy Company, Inc. (Kyuden Mirai). The brine from the separator had been directly returned to the reinjection wells at the Yamagawa power station. The brine is more than 600 t/h at about 180 °C. This power station effectively utilizes the heat of this brine (approx. 600t/h) and make generation, without adding a new production well. Kyuden Mirai and Fuji signed an EPC Contract in June 2016, the construction works completed and the commercial operation commenced on February, 2018. The rated and maximum generator output is 4,990kW.

Overview of Power Plant

Figure 6 shows an overview of the Yamagawa Binary Power Station. Figure 7 shows a system flow. The brine branched from the reinjection line is changed to two phase fluid by the separator inlet valve and goes to the separator. The two-phase fluid is separated brine and steam. After that the brine goes to the preheater and the steam goes to the evaporator. Normal pentane (n-pentane) is used as the working fluid. Because n-pentane is flammable fluid, fire-fighting system was supplied and fire-fighting area was laid out around the binary system.

n-pentane is pressurized by the pentane pumps and goes to the recuperator, the preheater and the evaporator. The n-petane is heated by the preheater and vaporized by the evaporator. The vaporized n-pentane rotates the turbine. The type of condenser is air cooled condenser because no available cooling water.



Figure 6: Overview of the Yamagawa Binary Power Station.

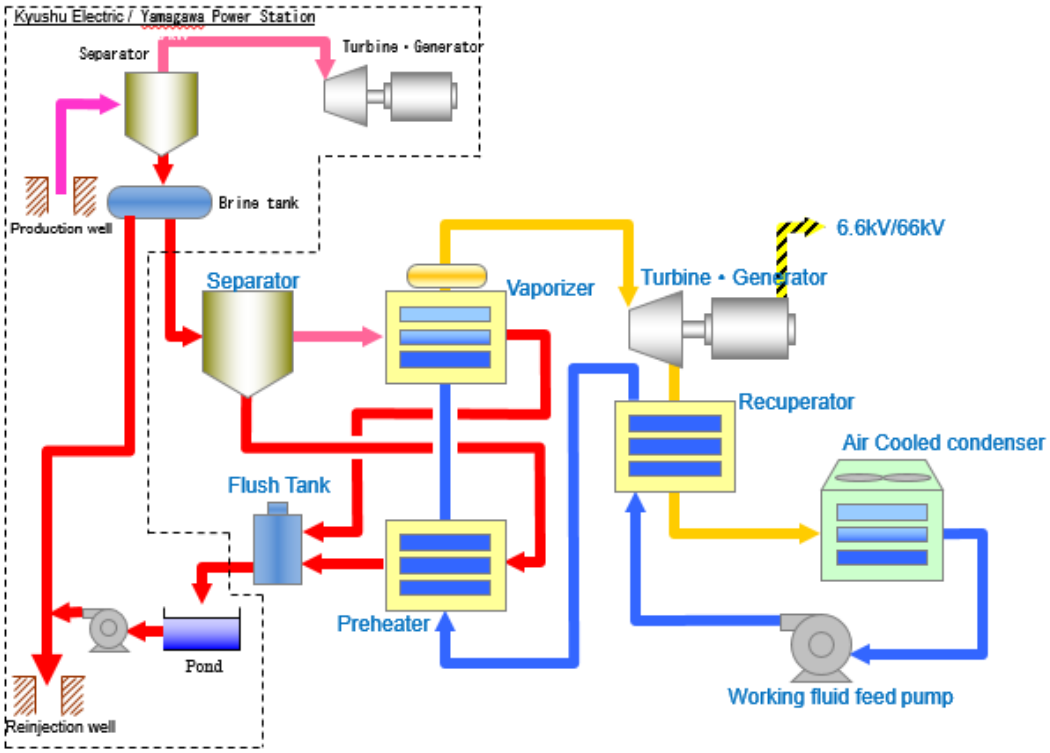


Figure 7: System flow of the Yamagawa Binary Power Station.

Features of each equipment

a. Turbine

The turbine was designed and manufactured by Fuji as well as Takigami Table 4 shows the specifications of the ORC turbine and Figure 8 shows the ORC turbine and the generator.

Table 4 Specifications of Yamagawa ORC turbine.

Rated inlet vapor pressure	kPaG	820
Rated inlet vapor temperature	°C	122.1
Rated generator output	kW	4,990
Maximum generator output	kW	4,990
Rotating speed	min^{-1}	1,800

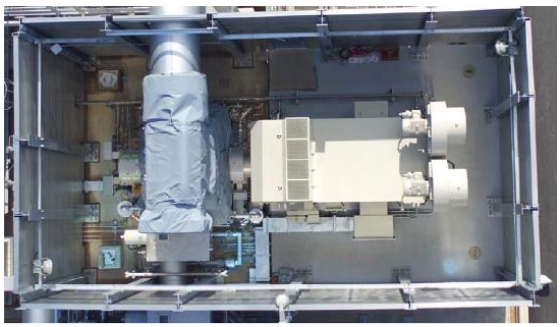


Figure 8: ORC turbine and Generator.

b. Heat exchangers

The heating system consists of one preheater and one evaporator. The material of tubes for all of these heat exchangers is super duplex stainless steel, considering composition in brine which has high chloride ion. The cooling system consists of one recuperator and air-cooled condenser. The fan blades and motors are low noise type considering surrounding environment. The condensed n-pentane is extracted by the pentane pumps and pumped to the preheater. Figure 9 shows the heat exchangers.



Figure 9: Heat exchangers.

Site construction works and commissioning works

Construction of the electro-mechanical works commenced in May 2017. All components of the equipment are installed outdoors except for the electrical and control system. The Kagoshima area is located in typhoon street. The typhoons came four times to the power station area during construction period. Measures to prevent scattering and upset were carried out each time. The site-testing works and commissioning commenced in December, 2017. The all commissioning works and the performance test were completed in February, 2018 and the commercial operation commenced.

CONCLUSIONS

Fuji completed two plants with different type of ORC system Takigami and Yamagawa, as working fluid and cooling system. Fuji will reflect the findings obtained from these plants in the future plant design and will provide total solution for geothermal power generation industry both flash and ORC system.

REFERENCES

Thermal and Nuclear Power Engineering Society: "Current Condition and Trends of Geothermal Power Generation in Japan 2017 (Japanese only)"

UTILIZATION OF SURFACE GEOTHERMAL MANIFESTATION (STEAMING GROUND) AS SMALL-SCALE ELECTRICAL POWER PLANT IN KAWAH MATI KAMOJANG, GARUT REGENCY: THERMOELECTRIC COOLER TECHNOLOGY

Navendra Chista Yogatama, Dani Muhamad Iqbal, Hezron Christian Marbun, Kodrat Cahyo Wicaksono, and Meliana Atmika

Geological Engineering Department, Diponegoro University
Prof.H.Soedarto S.H. Street, Tembalang, Semarang, Central Java
Email: navendra.research@gmail.com

ABSTRACT

Indonesia has the deficit of 1,000 MW power supply in 2018. TEC (Thermoeletric Cooler) technology is an appropriate technological innovation to overcome the deficit, considering Indonesia has 40% of the world's geothermal potential that the energy can be converted. TEC (Thermoelectric Cooler) technology is a renewable energy that suitable to be the solution of energy crisis in Indonesia. One of Indonesia's area that has the potential to be utilized in the development of TEC technology is Kawah Mati Kamojang, Garut. The used methods in this paper are literature study and building a TEC (Thermoeletric Cooler) power plant to obtain comprehensive research results. The TEC powerplant uses a surface geothermal manifestation (steaming ground) to generate electrical energy. The working system is to convert geothermal energy into electrical energy by using peltier on TEC. In TEC powerplant, there are two heatsinks. The first heatsink is placed on top of the steaming ground manifestation temperature of 70.6°C, while the output heatsink is passed by the river water flow around the location of the manifestation at temperatures of 19-30°C. In the middle of warm heatsink and output heatsink put the peltier, so the peltier has difference temperature of about 40°C. This condition will produce the electrical energy. From this research, known that one of TEC technology can produce electrical power of 686.424 KWh. While the average electricity requirement for house/family only 145.408 KWh, then with 686.424 KWh electricity generated from TEC technology can meet the electrical energy needs for about 4 houses/family. Besides that, the cost of making TEC power plant is also quite economical. It is just about 2,400,000 IDR per TEC power plant.

Keywords: Garut, Kawah Mati Kamojang, Steaming ground, Thermoelectric Cooler

INTRODUCTION

Fossil energy is one of the unrenewable energies, so that in the future fossil energy will run out. This condition causes the energy crisis, therefore there needs to be a solution to achieve national energy security. One of the new and renewable energies in accordance with Indonesia's geographical condition is geothermal with Thermoelectric Cooler (TEC) technology. TEC powerplant uses surface geothermal manifestation for building steaming ground to produce electrical energy. The working system of this technology is converting geothermal energy into electrical energy using peltier at TEC. In the TEC series of devices there are two heatsinks.

One of geothermal producing areas in Indonesia that has potential to be utilized in developing TEC technology is dead crater located in Garut, West Java. This crater is located in the southeast part of the Crater. This location was an active crater, but now it is unactive. In this location, sulphur has been crystallized and formed as flower petals. The soil is fairly hot temperature, or can be referred to as steaming ground, which indicates that the lower part of the frozen soil layer still has hydrothermal activity continues until now. Steaming ground measurements showed soil temperature of 70° - 60° C.

The purpose of this paper is to provide information and add insight to readers about the potential of steaming ground as a source of renewable electricity in the Kawah Mati Kamojang, Garut to overcome the national energy crisis.

The benefits that can be obtained after reading this paper are that the reader can find out the right solution to deal with the national energy crisis that will occur in the future, through innovations from new and renewable energy with one of them being steam ground with TEC technology. Where the use of steaming ground with TEC technology has many advantages compared to existing conventional energy and other renewable energy and is very suitable with the geographical conditions of Indonesia which is a country surrounded by volcanic arcs.

LITERATURE REVIEW

Thermoelectric Coolers (TEC) are electronic components that use the Peltier effect to make heat flux at junction between two different types of material. This component works as an active heat pump in the form of a solid which transfers heat from one side to the other side of the opposite, with electrical energy consumption depending on the direction of the flow of electric current. This component is known as the peltier device, peltier heat pump, solid state refrigerator, or Thermoelectric Cooler (TEC).

The principle of Thermoelectric cooling was first discovered in 1834 by Jean Peltier, so the results of this invention are often called "Peltier Coolers" If there is an electric current flow, it will be accompanied by heat from the current (Joule heating). Jean Peltier observes this, that when an electric current pass through the meeting of two different conductors (thermocouple), there will be a heating effect that cannot be explained by Joule heating alone. Even depending on the direction of the current, the effect can be either heating or cooling. Even though it has the name "cooler" or cooler according to its main application, TEC can also be used as a heater by reversing the placement of these electronic components. Thus, TEC can be used as a temperature controller.

The working system of the TEC is when two conductors are connected to an electrical contact, electrons will flow from one conductor which has electrons less bound to a conductor that has more bound electrons. An easy reason for this is the degree of difference between the two conductors. The difference in fermi is the term used to describe the part of a collection of electron energy levels at absolute zero. This concept comes from Fermi-Dirac statistics. The concept of fermi energy is a very important concept for understanding the electrical and thermal properties of solid objects. Both electrical and thermal processes usually involve electron energy. When two conductors with different fermi levels are combined, electrons will flow from a higher-level conductor to a lower level, until the electrostatic potential changes bring the two fermi levels to the same value.

The current that passes through the Junction both forward and backward direction will produce a temperature difference. If the temperature of the heat junction (heatsink) can be kept low by reducing or eliminating the heat generated, then the temperature of the cold part can be maintained as desired and can be several tens of degrees below the zero point. (Nurhadi, 2015).

METODOLOGY

Information Collecting Techniques

This paper is written based on data obtained not by direct observation in the field but obtained from accurate secondary data. making a TEC (Thermoeletric Cooler) tool model to obtain comprehensive research results. Figure 1 shows the research methodology.

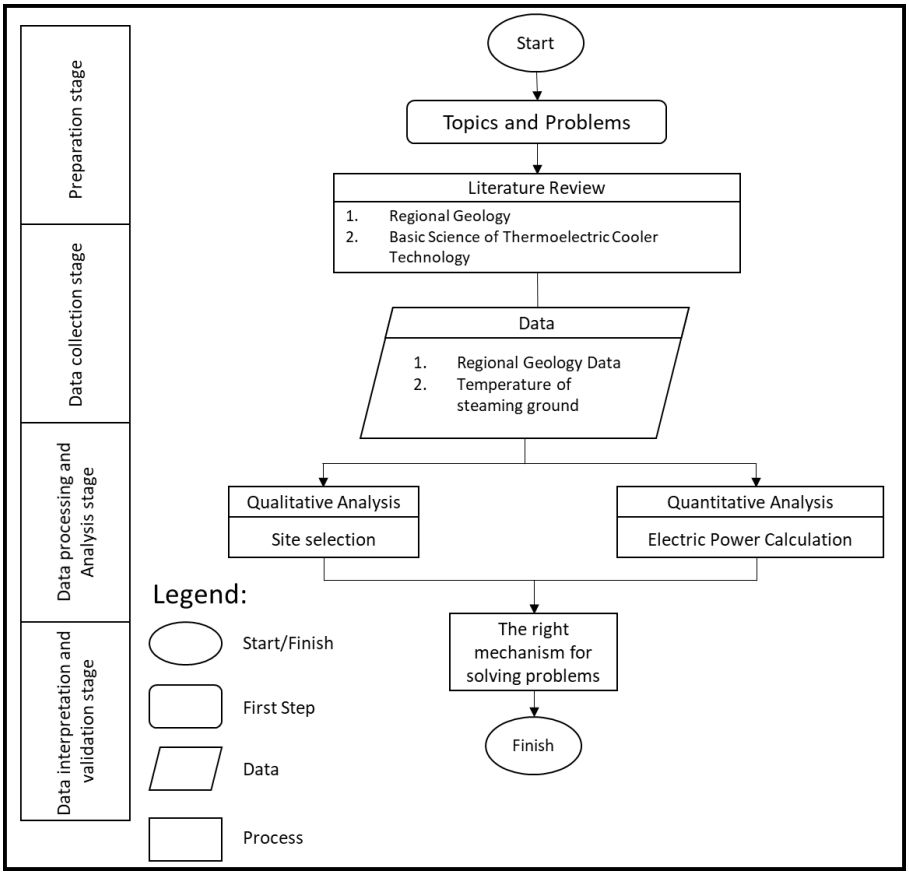


Figure 1: Research Methodology Flowchart.

Data Processing Techniques

Data that has been collected is still raw material or crude data that needs to be processed first so that it can be utilized more. In order for research analysis to produce works that can be widely used, data processing stages are needed, including:

a. Data checking

The data that has been collected will be examined whether it is complete in order to strengthen the opinions that will be conveyed in this paper.

b. Data analyzing

Data that has been obtained will be analyzed quantitatively or mathematically so as to obtain objective results which are then followed by qualitative analysis or conveying personal opinions based on the data that has been obtained.

c. Draw conclusions

The data that has been analyzed is then drawn conclusions so that it can produce a new innovation that might be applied or investigated further.

RESULTS AND DISCUSSIONS

TEC (Thermoelectric Cooler) can work optimally and produce electrical energy if there is a temperature difference between the hot side and the cold side in the constituent part of the device. This tool can work to convert to energy with temperature differences between 0º to 80º. One area that has the potential to be utilized in the development of TEC (Thermoelectrical Cooler) technology is the Kawah Mati Kamojang which has a 70.6º steaming ground temperature. And on the cold side flowed by river water which has a temperature of 19º to 30º, so there is a difference between hot temperatures and cold temperatures around 40º. In addition, the Kawah Mati Kamojang is a place that is no longer used but still has high potential to be used as a producer of geothermal power. So that, in the Kawah Mati Kamojang is suitable for the development of TEC technology. Figure 2 shows the Kawah Mati Kamojang.



Figure 2: Kawah Mati Kamojang.

From the results of research that has been done, it can be seen that the working system of the TEC is by using a peltier effect that is if two different metals are connected then heat is transferred to the connection, then a heat pump phenomenon will occur. This principle is what thermoelectric uses as a coolant / heat pump. From the phenomenon of heat pumps can produce electrical energy from the device. Electricity can be used to meet the electrical energy needs of residents around the Kawah Mati Kamojang. Figure 3 shows the peltier effect.

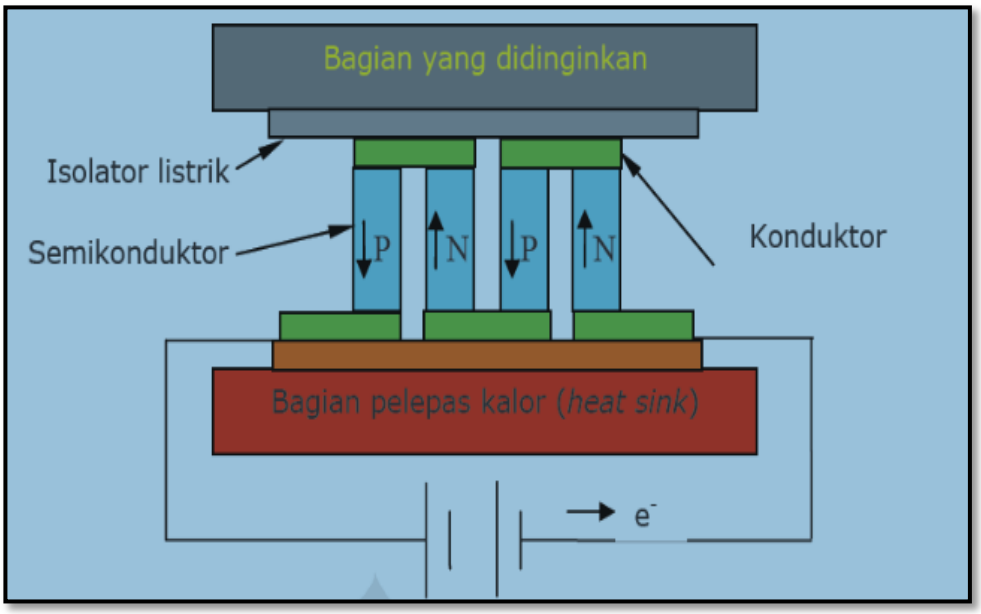


Figure 3: Peltier Effect.

Before testing the tool, various designs were carried out in making this prototype because in this case the consideration was in conducting a prototype test. In testing the prototype, it can be done by means of the first heatsink placed above the ground steaming manifestations at a temperature of 70º - 60º C, while the output heatsink is passed on the river water flow around the location of the manifestation temperature of 19º – 30º C. In the middle between the heat heatsink and the output heat sink is put peltier, so the peltier experiences a difference in temperature difference of 40º C. The data collection technique in this study was carried out by measuring the output voltage and current output produced by the TEC, and at what temperature produced maximum voltage and current. Figure 4 shows the testing of thermoelectric cooler technology in the Kawa Mati Kamojang.

In this test, a TEC tool with an area of 1 m x 1 m 3 cm was used which was placed on the steaming ground of the Kawah Mati Kamojang. The following are the test results from the study (Table 1):

Table 1: Results of Kawah Mati Kamojang Test.

Hot Temperature (ºC)	Cold Temperature (ºC)	Temperature Difference (ºC)	Voltage (V)
50º	19º	31º	1.65
57º	24º	33º	1.70
62º	26º	36º	1.76
70º	30º	40º	1.8

Data obtained in the observation area are then analyzed using equations and mathematical calculations to calculate the potential of electrical energy that can be produced by TEC in the Kawah Mati Kamojang. From the research that has been done, one TEC device measuring 1 m^2 can produce 686.424 KWh of electric power. While the average electricity demand per house/family is 145.408 KWh only, so the electric power of 686.424 KWh generated from the two power plants can meet the electricity needs for around 4 houses/families. Figure 5 shows the thermoelectric cooler power plant technology model. Figure 6 shows the components of thermoelectric.

The following is a detailed calculation to determine the potential for electrical energy produced from TEC in the Kawah Mati Kamojang:

In calculating TEC electric power, the first step is to calculate the electrical resistance generated by this tool with the formula:

$R = (\rho \, . \, l)/ A$
$= 0.029 \times 1/ 1$
$=$ **0.029 ohm**

It is known that the temperature difference in the peltier of 40 0C will produce a voltage of 1.8 V. Where, the calculation of the electrical power produced by the TEC is as follows:

$P = V^2/ R$
$= (1.8)^2/ 0{,}029$
$= 28{,}601.4 \times 1$ KW/ 1000-Watt x 24 hours
$=$ **686.424 KWh**

With the electrical power produced is quite large, namely 686.424 KWh, the making of this tool is quite economical, which is 2,400,000 IDR per tool (Table 2).

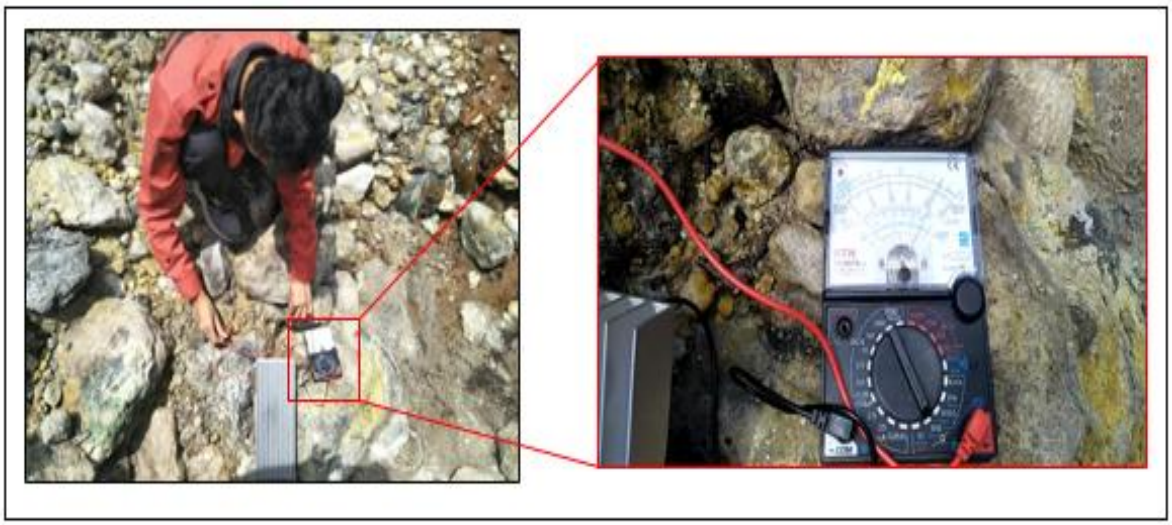


Figure 4: Testing of Thermoelectric Cooler Technology in the Kawah Mati Kamojang.

Table 2: Cost Details of Thermoelectric Cooler Technology.

No.	Tool's name	Unit	Price (Rp)	Total (Rp)
1	TEC1-12706 91.2W TEC Peltier (4 cm x 4 cm)	16	30,200	483,200
2	*Heatsink* (12 cm x 3,5 cm)	30	55,000	1,650,000
3	Cable (1 x 1,5 mm, length 50 m)	2	110,000	220,000
4	*Dextone* Glue	2	23,400	46,800
Total				2,400,000

There are several requirements for a power generation technology feasible to be applied in Indonesia. These conditions include accessibility, availability, acceptability and also marketability. All of these requirements are absolutely fulfilled so that TEC technology can compete with other conventional energy sources which will one day be used up if explored. Efforts to meet these criteria are not impossible, but things that can be learned and adjusted so that their use is effective.

In this case, we see that in terms of accessibility, TEC technology can be accessed in several surface geothermal manifestations in the Indonesian region including the Kawah Mati Kamojang area because it remembers that Indonesia is surrounded by volcanic arcs. In terms of availability, of course, Indonesia has a lot of geothermal potential whose specifications are suitable for the development of TEC technology, while community acceptability will be high considering that TEC technology is clean power and the final question is marketability. Marketability or selling power of TEC technology is high because both of these technologies are very cheap, which only costs around Rp. 2,400,000 per tool. This is certainly cheaper when compared to conventional power generation technology, so it can attract investors to invest.

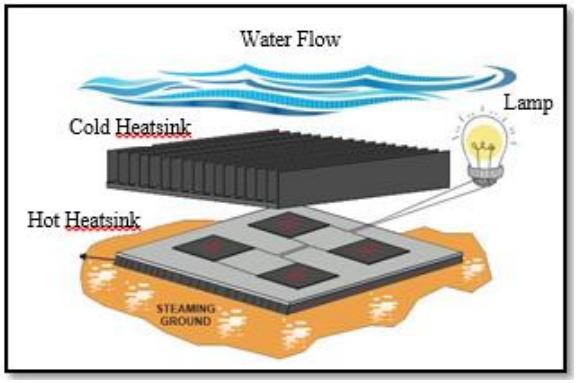


Figure 5: Thermoelectric Cooler Power Plant Technology Model

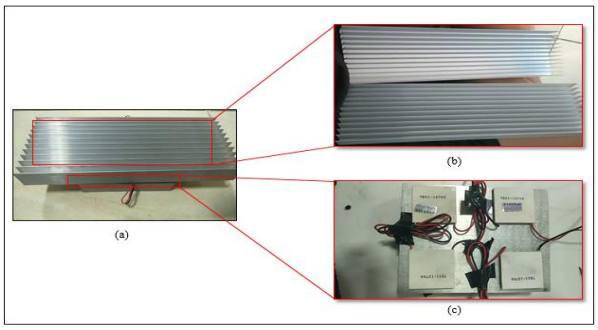


Figure 6: (a) Whole Components of Thermoelectric Cooler Power Generation Technology, (b) Heatsinks, (c) TEC Components.

CONCLUSION

Indonesia has considerable potential to develop TEC technology because Indonesia has the largest geothermal potential in the world at 40%. The application of TEC technology in the Kawah Mati Kamojang can produce 686.424 KWh of electric power. While the average electricity demand per house / family is 145.408 KWh only, then with an electric power of 686.424 KWh it can meet the electricity needs for around 4 houses / families. With the electrical power produced is quite large, namely 686.424 KWh, the making of this tool is quite economical, which is 2,400,000 IDR per tool. Then, locations that have potential energy resources with similar characteristics are suitable locations for the implementation of TEC technology.

ACKNOWLEDGEMENTS

The author would like to thank the Department of Geological Engineering, Diponegoro University in particular Mr. Najib, ST., M. Eng., Ph.D as Head of the Department of Geological Engineering at Diponegoro University and North East Java Research Section who have provided knowledge and human resources for this research, and Indonesia International Geothermal Convention & Exhibition 2019 as the organizer of this competition.

REFERENCES

Alzwar, M S.Bachri, N. Akbar, (1992). "Peta Geologi Lembar Garut dan Pameungpeuk". *Pusat Penelitian dan Pengembangan Geologi (Indonesia).*

Budi Santosa, Nurhadi. (2015). "Mengenal Thermo-Electric (PELTIER)". *Malang: Widyaiswara PTK BOE Malang.*

Djafar, Zuryati. (2011). "Pengaruh Variasi Temperatur Fluida Panas Terhadap Karakteristik Modul Termoelektrik Generator". *Depok: Dept. Teknik Mesin-FT UI.*

Hilyah, Anik. (2010). "Studi Gempa Mikro untuk mendeteksi Rekahan di area Panas bumi Kamojang Kabupaten Garut*". Jurnal Fisika dan Aplikasinya. Volume 6, Nomor 2 Juni, 2010.*

Intan, Dwi Nur Ramdini, dkk. (2014). "Thermoelectric Generator". *Fisika-FST UIN Sunan Gunung Jati: Bandung.*

M. Sugeng Riyadi, Ary Akbar N, dkk. (2016). "Analisis Pembangkit Listrik Sederhana Berbasis Thermoelectric Cooler Dengan Media Batu Andesit*". Universitas Negeri Jakarta: Jurnal RISENOLOGI KPM UNJ Vol. I Edisi 2.*

Poetro. E. J., dan Handoko. R. C. (2013). "Analisis Kinerja Sistem Pendingin Arus Searah Yang Menggunakan Heatsink Jenis Extruded Dibandingkan Dengan Heatsink Jenis Slot". *Jurnal Teknik Mesin, Vol. 2, pp 178-188.*

SALAK TURBINE ROTOR SUSCEPTIBILITY ANALYSIS AGAINST SULFIDE STRESS CRACKING

Diva E. Nataprawira and Adrian Muskan

Star Energy Geothermal Salak, Ltd.
Jayanegara, Kabandungan, Sukabumi 43368
Email: diva.nataprawira@starenergy.co.id

ABSTRACT

Geothermal energy is a clean and renewable source of power. Geothermal power plant also have very limited impact to the environment. Geothermal power plant utilize the thermal energy from geothermal steam and generate the electricity. Geothermal steam that carry out to the surface contains various level of Sulphur together with heavy elements, which are highly corrosive. Sulfide stress cracking (SSC) is a common damage mechanism that occurs at most geothermal steam turbine. SSC is a combined presence of corrosive elements and high stresses in highly loaded locations, blades, discs, rotors, and diaphragms. Star Energy Geothermal Salak, Ltd. (SEGS) operates three typical 65.6 MW Geothermal Steam Turbine. It has been in operation since 1997 and has been exposed by geothermal steam for 20 years. To determine how susceptible Salak turbine rotor against SSC during normal condition and find out the opportunity to avoid the SSC, then further assessment is conducted. The assessment is conducted by analyzing the three factors that contribute to the SCC establishment. The three factors are geothermal steam properties, turbine rotor material and surface hardness. The analysis also uses ANSI/NACE MR0175/ISO 15156-1:2015 as a reference. The analysis show that Salak turbine rotor has low level of susceptibility against SSC based On NACE MR0175. Salak environmental severity regarding the SSC is in region 0.

Keywords: Turbine, rotor, analysis

INTRODUCTION

SEGS field is located along the Sunda Volcanic Arc in West Java Province, Indonesia, about 70 KM south of Jakarta.

SEGS is one of the largest geothermal fields in Indonesia and is categorized as the sixth largest in the world. SEGS power plant operates 3 x 65.6 MW steam turbine to produce electricity and provides the remaining steam to PLN to produce 3 x 60 MW electricity**.**

Salak Operating Condition

Salak steam conditions with generation 65.6 MW are approximately 460 ton/hrs main-steam flow, at temperature of 165-170 ºC and pressure of 6-6.6 Bara. Salak steam that flow to Unit 4,5,6 also consist with 1.3% to 1.8% of Non-Condensable Gas (NCG) and steam pH 5.23. Salak steam condition for Unit 4, 5, 6 can be seen in Table 1.

Salak Unit 4, 5, 6 Turbine Rotor Specification

The turbine is manufactured, supplied and installed by Fuji Electric Company. It is a single cylinder, double flow, and dual entry condensing type unit. The rotating turbine blades are all reaction style. There are nine stages of blade on each end of the turbine. Salak turbine rotor is a “drum” style rotor design. Figure 1 shows a sectional drawing of Unit Turbine Rotor.

SULFIDE STRESS CRACKING

Sulfide Stress Cracking (SSC) is one of Environmentally Assisted Cracking (EAC) mechanism. SSC is the cracking of a metal under the combined action of tensile stress and corrosion in the presence of water and hydrogen sulfide.

Sulfide stress cracking is a form of hydrogen embrittlement that occurs in high-strength steels and in localized hard zones in weldment of susceptible materials when the environment contains wet H_2S.

The mechanism involves hydrogen in the metal diffusing to the points of stress concentration. One can visualize the stress pulling the atomic lattice further apart, making more "room" for hydrogen. Once the hydrogen diffuses into this area, it stiffens the metal by reducing the ability of the metal atoms to move relative to each other. The metal will then tend to crack, rather than stretch by yielding. SSC is generally limited to steels having a hardness of 22 or greater on the Rockwell C scale. Figure 2 shows SSC typical crack damage.

Table 1: Salak Steam Condition.

Description	Unit	SLK-4	SLK-5	SLK-6
Generation (SMPP)	MW	65.6	65.6	65.6
Steam Pressure	Bar	6 - 6.6	6 - 6.6	6 - 6.6
Steam Temperature	^{O}C	165-170	165-170	165-170
Steam pH*		5.23	5.23	5.23
NCG*	% (gas to steam)	1.835	1.432	1.352
H2S***	Ppm by weight	535	508	471

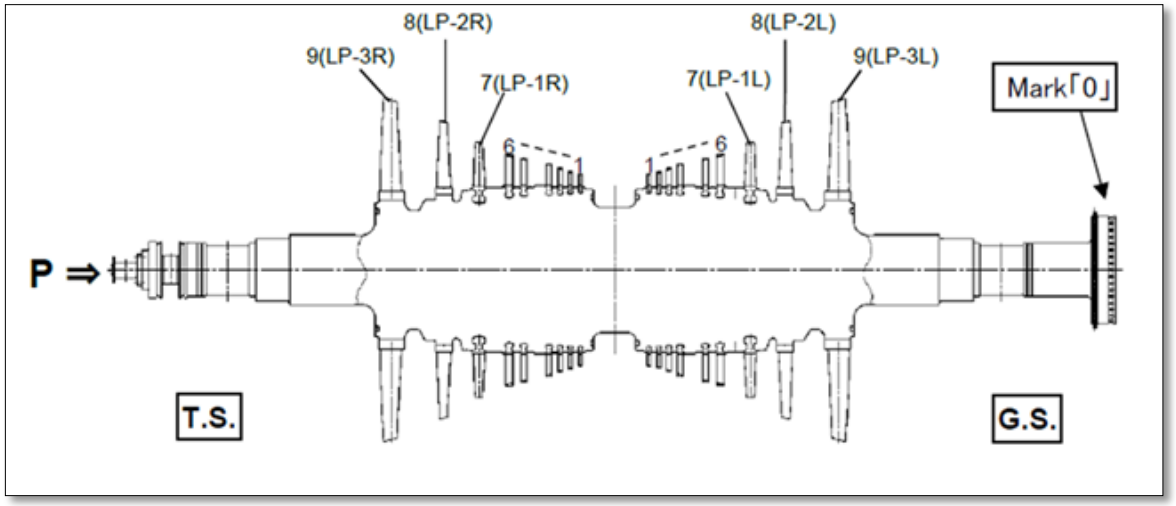


Figure 1: Salak turbine rotor sectional drawing.

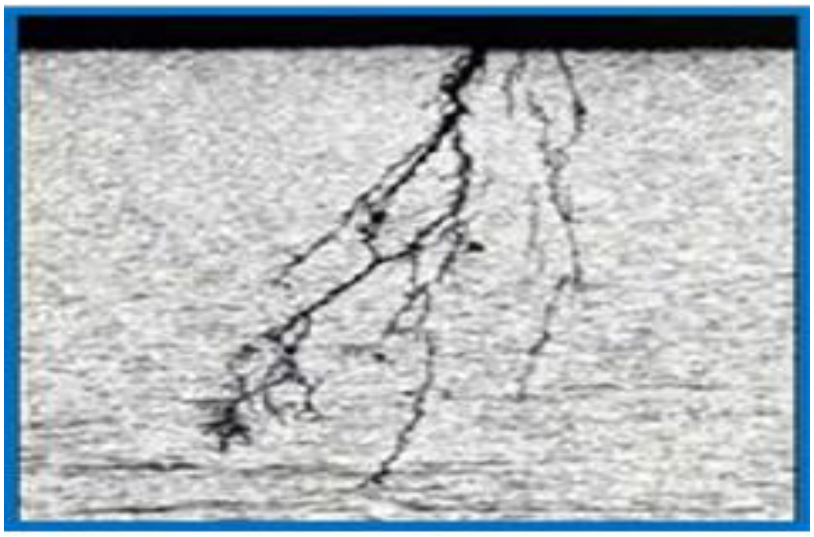


Figure 2: SSC Crack.

Geothermal steam that carry out to the surface contains various level of Sulphur together with heavy elements, which are highly corrosive. Sulfide stress cracking (SSC) is a common damage mechanism that occurs most geothermal steam turbine. SSC is a combined presence of corrosive elements and high stresses in highly loaded locations (blades, discs, rotors, diaphragms, etc.). The three factor that contribute to the SSC establishment are geothermal steam properties, turbine rotor material and surface hardness.

DATA

Susceptibility level of Salak turbine rotor against SSC can be analyzed and determined from three data as follows:

1. Salak Steam Properties

2. Salak Turbine Rotor Material
3. Salak Turbine Rotor Surface Hardness

Salak Steam Properties

To determine Salak steam properties, steam sample has been taken frequently by Salak geoscience team. Sampling location is in Unit 4, 5, 6 steam scrubber before the steam enters the turbine system. For this analysis, steam properties from 2012 to 2018 are used. Salak steam properties can be seen in Table 2.

Salak Turbine Rotor Material

Salak turbine Rotor material 30CrMoNiV 4-11 is a low alloy steel with mist quenched and furnace cooled heat treatment. This material consists of 0.27 % Carbon, 1.2% Cr and others component. Material chemical composition can be seen in Figure 3.

Salak Turbine Rotor Surface Hardness

Salak turbine rotor hardness can be known from OEM Manufacture Data. OEM Manufacture Data shown the rotor hardness is 217-219 HB or equal with 19 HRC. Figure 4 below shown Salak rotor hardness from OEM Manufacture Data.

Actual surface hardness also has been taken by Salak team during rotor refurbishment process. The actual surface hardness can be seen in Figure 5.

Table 2: Salak Steam Properties.

			4645RI (1-5) January 14, 2016	
Descriptor:	AWI-Scrubber U4 Steam 11-09-15 10:47			
Lab Number:	4645RI-1			
Sample Gas/Steam Ratio (ft^3/lb):		0.1597		
Sample Gas/Steam Ratio (moles /10^6 moles H_2O		8148		
Sample Gas/Steam Ratio (ppm by Weight):		18941		
Percent Air[1] in Sample:		0.091		
STP mls of Air[1] in Sample:		2.47		
Total Weight of Condensate (grams):		274		
Initial Headspace Pressure (psia @ STP):		5.37		
Gas		**Dry Gas % by Volume**	**Moles per 10^6 Moles Water**	**Parts per Million by Weight**
Water Vapor		N/A	N/A	9.81E+05
Carbon Dioxide		9.34E+01	7.61E+03	1.82E+04
Hydrogen Sulfide		3.54E+00	2.88E+02	5.35E+02
Ammonia		3.53E-01	2.88E+01	2.67E+01
Argon		8.96E-04	7.30E-02	1.59E-01
Nitrogen		4.32E-01	3.52E+01	5.37E+01
Methane		1.05E+00	8.56E+01	7.48E+01
Hydrogen		1.24E+00	1.01E+02	1.11E+01
1. Air content based on Oxygen determination				

SAMPLE DATE	pH	SILICA	CHLORIDE	SODIUM	IRON	TOTAL SOLID
		(mg/L)	(mg/L)	(mg/L)	(mg/L)	(mg/L)
Limits	N/A	< 1.00	< 1.00	N/A	N/A	N/A
			ND : Not Detactable < 0.01 mg/L (Sodium,Iron, Silica)			
			ND : Not Detactable < 0.015 mg/L (Chloride)			
			ND : Not Detactable < 10 mg/L (Total Solid)			
Control Data (Max)	5.35	0.222	0.421	0.273	0.50	21.00
January 1, 2016	5.19	0.019	ND	ND	0.04	ND
January 2, 2016	4.00	0.019	ND	ND	0.05	12.0
January 3, 2016	5.08	0.023	ND	ND	0.07	12.00
January 4, 2016	5.17	0.023	ND	ND	0.04	12.00
January 5, 2016	5.28	0.011	ND	ND	0.06	ND
January 6, 2016	5.35	0.019	ND	ND	0.03	ND
January 7, 2016	5.15	0.042	ND	ND	0.04	13.00
January 8, 2016	5.23	0.025	ND	ND	0.05	ND
January 9, 2016	5.24	0.011	ND	ND	0.07	ND
January 10, 2016	5.28	0.020	ND	ND	0.07	ND
January 11, 2016	5.14	0.040	ND	ND	0.05	ND
January 12, 2016	5.22	0.017	ND	ND	0.04	ND
January 13, 2016	5.21	0.021	ND	ND	0.04	15.0
January 14, 2016	5.15	ND	ND	ND	0.06	ND

Customer : Fuji Electric Co., Ltd.
P. O. No : K1Z69020G2
Project : FLUOR DANIEL/UNOCAL(Salak)
Article : Turbine Rotor Shaft
Dwg. No : ST214921A
Material : 30CrMoNiV411
KSL. O. No : 95-36B60-0
Heat. No : W50593-1

MECHANICAL PROPERTY TEST REPORT

STEEL CASTING & FORGING PLANT, TAKASAGO KOBE STEEL, LTD.

Date of Test : January 9, 1996

Chemical Composition (wt %)

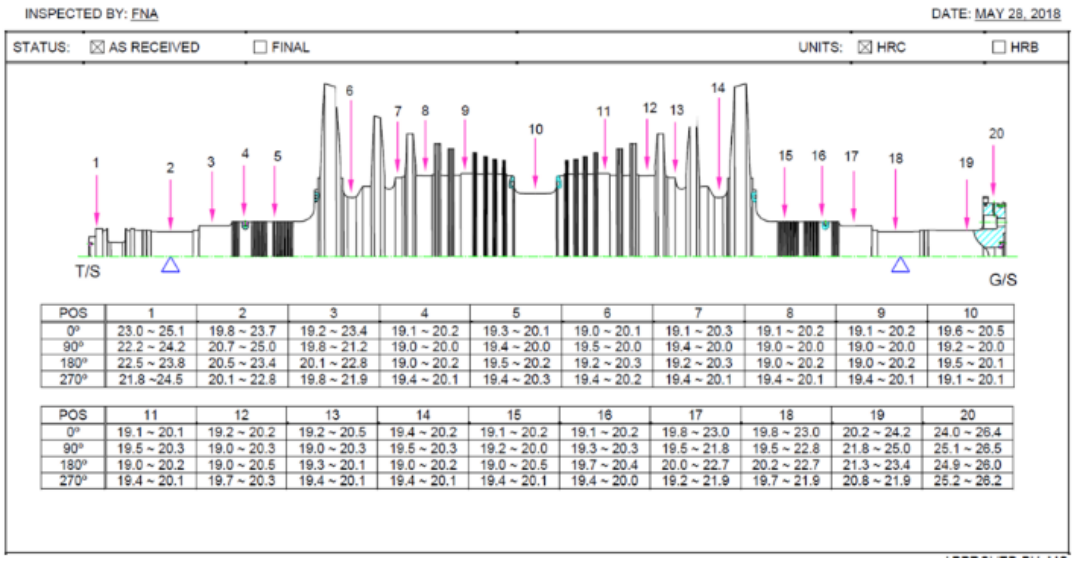
Elements	C	Si	Mn	P	S	Cu	Ni	Cr	Mo	V	Sn	Al	Sb	As	N	P. P. M H	P. P. M O
Speci-fication	.26 -.32	Max. .30	.35 -.85	Max. .015	Max. .015	-	.50 -.75	.90 -1.20	1.00 -1.20	.25 -.35	-	-	-	-	-	-	-
Ladle	.27	.08	.71	.005	.001	.03	.64	1.19	1.04	.27	.003	.001	0005	.002	-	-	-
Product																	

FLUOR DANIEL - BCPT
SALAK GEOTHERMAL POWER PLANT
PURCH ORDER NO.:450941-4-0301-01
CONTRACT NO.:450901
EQUIPMENT TAG NO.:T-500
CLIENT : UNOCAL GEOTHERMAL OF INDONESIA LTD.
PROJECT LOCATION : MOUNT SALAK,WEST JAWA,INDONESIA

Figure 3: Salak turbine rotor material chemical composition.

Tensile Test					Charpy Impact Test	Hardness test	Result
Size of T. P: 12(mm) Dia. 60(mm) G. L					(Notch : 2 mm V.)		
Spec.	Y.S.(0.2%) off set kgf/mm²(N/mm²)	T. S.	E. L (%)	R. A (%)	Unit : +20°C kgf-m(J)	HB	
Tang.	min 56-70 (549-686)	70-85 (686-834)	min 15	min 40	min 2.4 (23.5) *(Mean Value)	REF.	
~~Center Core~~	min	min	min	min	min		
Tangential direction							
T1	60 (587)	73 (717)	20	69	19.1 19.1 19.6 *(19.3) (187.2)(187.2)(192.6)*(189.0)	219 217	Pass
T2	60 (587)	73 (712)	21	72	18.5 18.5 18.3 *(18.4) (181.8)(181.8)(179.1)*(180.9)	217 218	

Figure 4: Salak turbine rotor hardness-based OEM Manufacture Data.



POS	1	2	3	4	5	6	7	8	9	10
0°	23.0 ~ 25.1	19.8 ~ 23.7	19.2 ~ 23.4	19.1 ~ 20.2	19.3 ~ 20.1	19.0 ~ 20.1	19.1 ~ 20.3	19.1 ~ 20.2	19.1 ~ 20.2	19.6 ~ 20.5
90°	22.2 ~ 24.2	20.7 ~ 25.0	19.8 ~ 21.2	19.0 ~ 20.0	19.4 ~ 20.0	19.5 ~ 20.0	19.4 ~ 20.0	19.0 ~ 20.0	19.0 ~ 20.0	19.2 ~ 20.0
180°	22.5 ~ 23.8	20.5 ~ 23.4	20.1 ~ 22.8	19.0 ~ 20.2	19.5 ~ 20.2	19.2 ~ 20.3	19.2 ~ 20.3	19.0 ~ 20.2	19.0 ~ 20.2	19.5 ~ 20.1
270°	21.8 ~24.5	20.1 ~ 22.8	19.8 ~ 21.9	19.4 ~ 20.1	19.4 ~ 20.3	19.4 ~ 20.2	19.4 ~ 20.1	19.4 ~ 20.1	19.4 ~ 20.1	19.1 ~ 20.1

POS	11	12	13	14	15	16	17	18	19	20
0°	19.1 ~ 20.1	19.2 ~ 20.2	19.2 ~ 20.5	19.4 ~ 20.2	19.1 ~ 20.2	19.1 ~ 20.2	19.8 ~ 23.0	19.8 ~ 23.0	20.2 ~ 24.2	24.0 ~ 26.4
90°	19.5 ~ 20.3	19.0 ~ 20.3	19.0 ~ 20.3	19.5 ~ 20.3	19.2 ~ 20.0	19.3 ~ 20.3	19.5 ~ 21.8	19.5 ~ 22.8	21.8 ~ 25.0	25.1 ~ 26.5
180°	19.0 ~ 20.2	19.0 ~ 20.5	19.3 ~ 20.1	19.0 ~ 20.2	19.0 ~ 20.5	19.7 ~ 20.4	20.0 ~ 22.7	20.2 ~ 22.7	21.3 ~ 23.4	24.9 ~ 26.0
270°	19.4 ~ 20.1	19.7 ~ 20.3	19.4 ~ 20.1	19.4 ~ 20.1	19.4 ~ 20.1	19.4 ~ 20.0	19.2 ~ 21.9	19.7 ~ 21.9	20.8 ~ 21.9	25.2 ~ 26.2

Figure 5: Salak turbine rotor hardness based on OEM Manufacture Data.

ANALYSIS

The analysis will start from H2S partial pressure calculation from Salak steam properties data to determine Salak environmental severity against SSC then continue with Salak turbine rotor material and surface hardness.

Regions of Environmental Severity with Respect To the SSC

Based on NACE MR0175 standard, the severity of H_2S-containing environment can be determined by calculate the H2S partial pressure from Salak Steam Properties data and steam pH then plot the calculation result into regions of severity environmental graphic. The graphic can be seen in Figure 6.

X H_2S partial pressure, expressed in kilopascals, Y *in situ* pH, 0 region 0, 1 SSC region 1, 2 SSC region 2 and 3 SSC region 3

The environmental severity with respect to the SSC are divided into four regions. The lowest severity is region 0. The severity region will determine the selected material that suitable with environmental condition.

H_2S partial pressure is calculated from 2012 to 2018 steam properties data. H_2S partial pressure can be determined by multiply H_2S mole percent with steam total pressure. The plotting result of can be seen from Figure 7 to Figure 9 for Salak Unit 4, 5, 6.

It can be seen on the figure above that Salak Unit 4, 5, 6 are in the region 0.

Salak Turbine Rotor Material and Surface Hardness

Based OEM manufacture data, Salak turbine Rotor material is a low alloy steel with mist quenched and furnace cooled heat treatment with surface hardness 19 HRC and 20.5 maximum hardness from actual hardness check.

The surface hardness is less than 22 HRC which is the maximum hardness that acceptable for SSC resistant carbon and low alloy steel based on NACE MR0175 standard

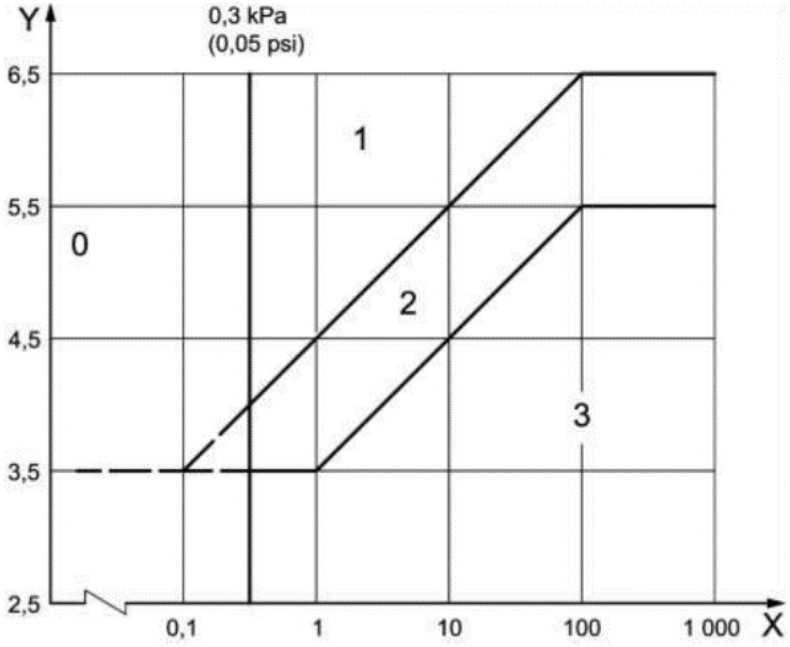


Figure 6: Regions of environmental severity with respect to the SSC of carbon and low-alloy steels.

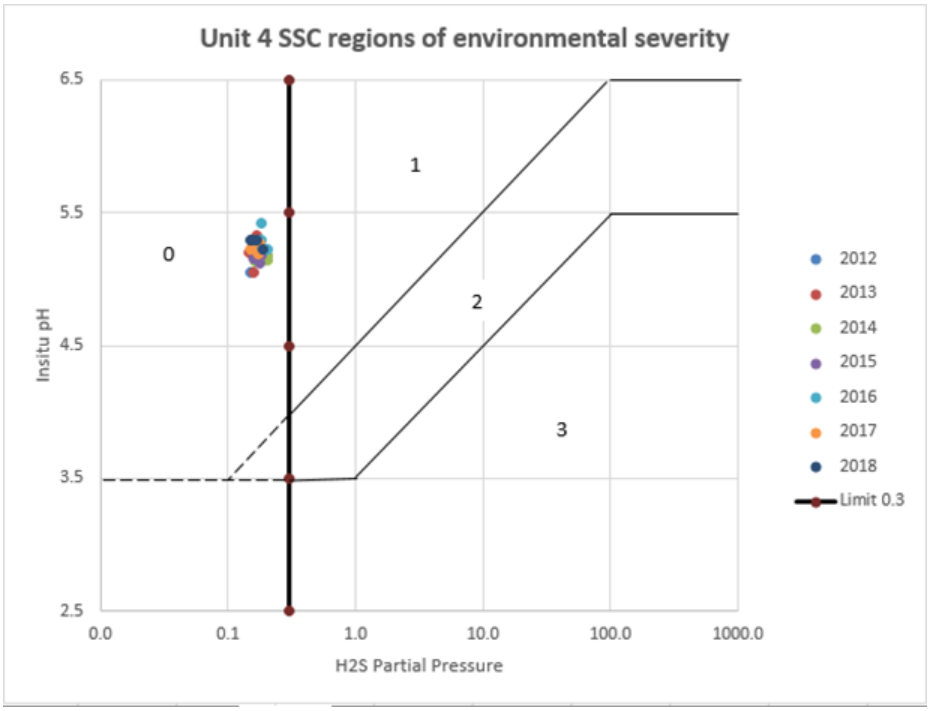


Figure 7: Salak Unit 4 regions of environmental severity with respect to the SSC.

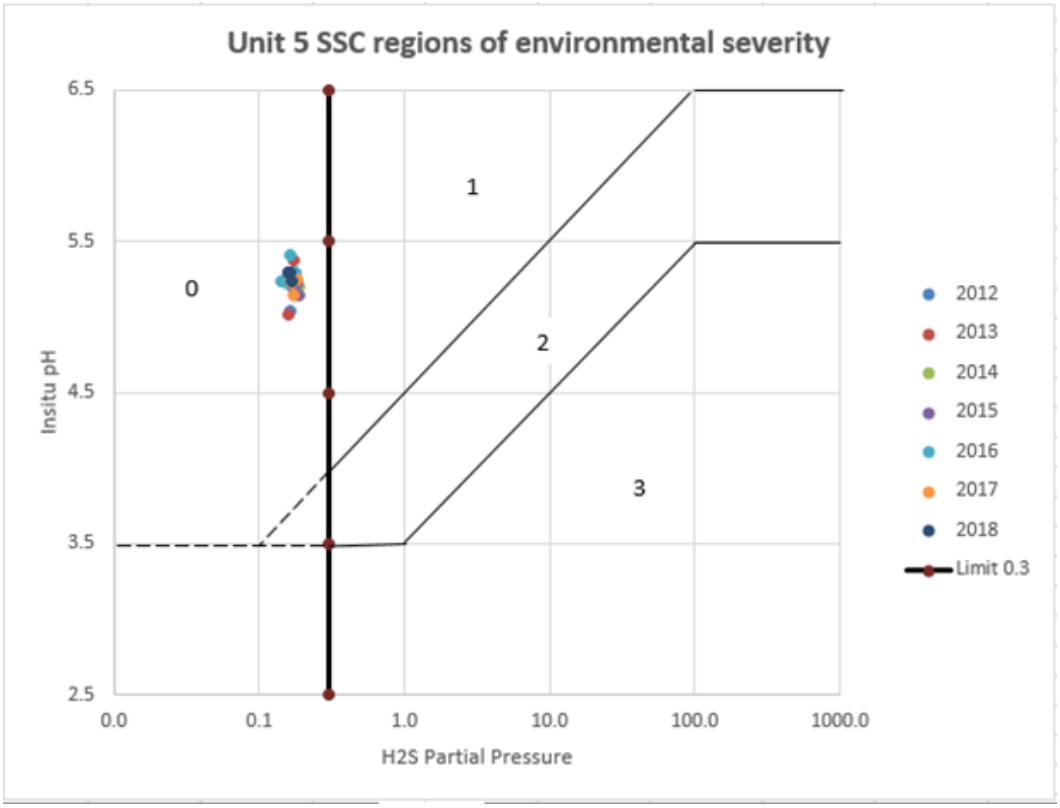


Figure 8: Salak Unit 5 regions of environmental severity with respect to the SSC.

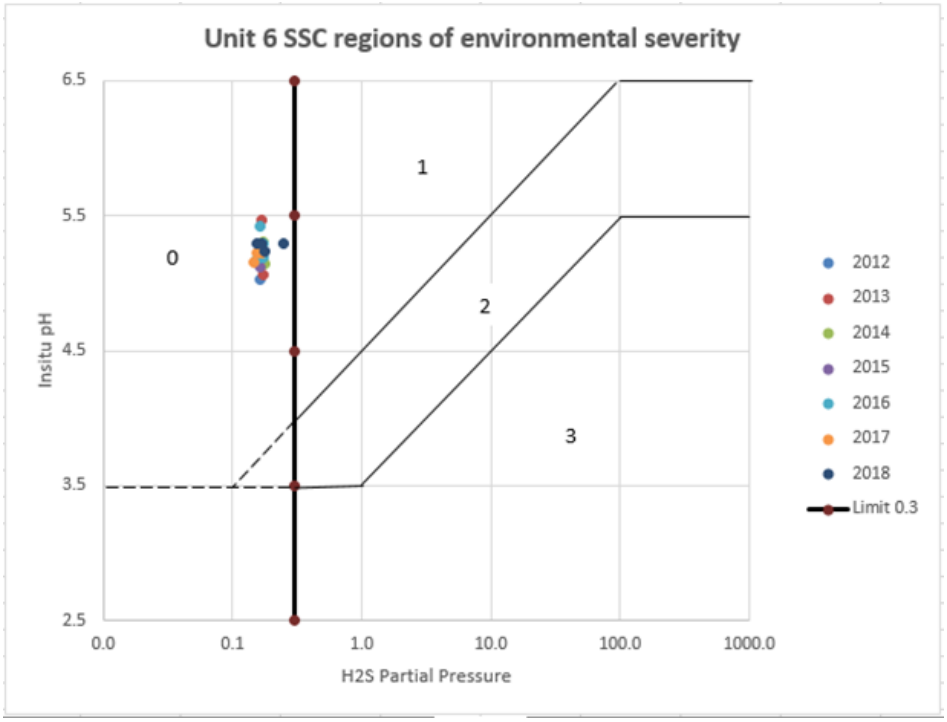


Figure 9: Salak Unit 5 regions of environmental severity with respect to the SSC.

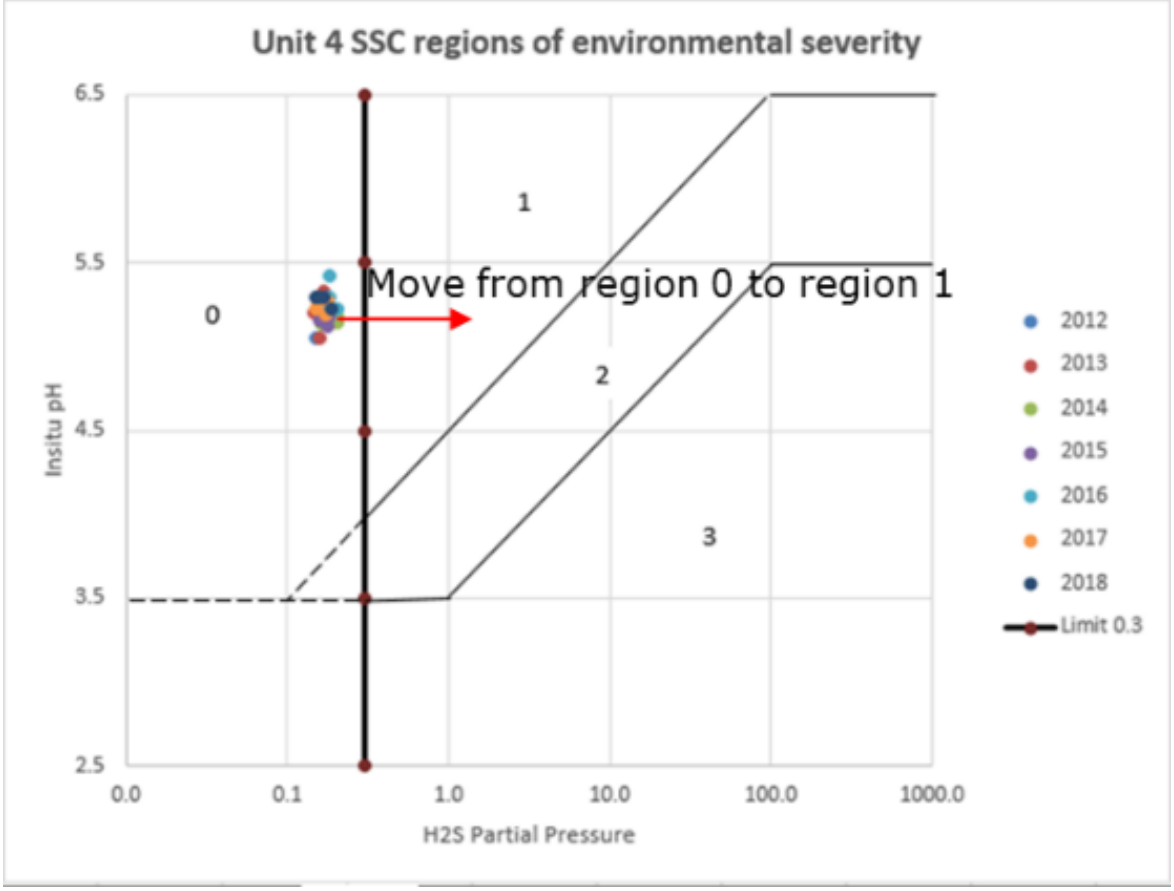


Figure 10: Salak Unit 5 regions of environmental severity with respect to the SSC.

CONCLUSION

From analysis above, it can be concluded as follows:

1. Salak environmental severity regarding the SSC is in region 0. Based on NACE MR0175 "Normally, no precautions are required for the selection of steels for use under these conditions". Nevertheless, steel that have high susceptibility of SSC can crack in this region.
2. Salak turbine rotor material is 30CrMoNiV 4-11 which is a low alloy steel. The actual material hardness is 20.5 HRC maximum hardness. Based on NACE MR0175 A.2.1.2 "Carbon and low-alloy steels are acceptable at 22 HRC maximum hardness provided they contain less than 1 % mass fraction nickel, are not free-machining steels and are used in one of the following heat-treatment: hot rolled, annealed, normalized, normalized and tempered"
3. Salak turbine rotor has a low level of susceptibility against SSC.

FUTURE CHALLENGES

1. Salak team have a plan to utilize high NCG steam into power plant. High NCG steam have high contain of H2S and have possibility to move Salak SSC regions of environmental severity due to higher H2S partial pressure. If the regions move, the existing rotor turbine material has possibility need to be upgraded. Figure 10 shown the region movement due to higher H2S partial pressure Salak turbine rotor already enter the deterioration period, some of erosion has found on critical area. One of alternative is to repair the turbine erosion with welding repair. Welding repair involves thermal input which can result the residual stress in the Heat Affected Zone (HAZ). To release the residual stress, Post-Weld Heat Treatment (PWHT) need to be conducted after welding process. After PWHT process completed, surface hardness of the rotor needs to be checked and recorded to make sure the hardness is not above 22 HRC.

ACKNOWLEDGEMENTS

Many thanks to the following people who assisted the author with technical discussions as well as supported the development of this paper.

1. Budi Hadi Permana – Mechanical Engineer, Star Energy Geothermal Salak.
2. Hernawan Heriyanto – Reliability and Integrity Engineer, Star Energy Geothermal Salak
3. Prayitna – Earth Science Geochemist, Star Energy Geothermal Salak

REFERENCES

ANSI/NACE MR0175/ISO15156-1:2015 (2015). "Materials for use in H2S-containing environments in oil and gas production".

CPM 400 (2006). "Characteristic Corrosion Phenomena".

Fuji Electric Co. Ltd (1996). "Shop Inspection and Test Report".

Salak Repair FUJI 55 MW Steam Turbine Rotor report (2018).

DEVELOPMENT OF THE FIRST DUAL FLASH GEOTHERMAL POWER PLANT IN INDONESIA

Munggang H. Purnanto, Stefanus Wisanto, and Ruswanto bin Nurudin Data

PT. Supreme Energy Muara Laboh, Sentraya Tower 23th Floor,
Jl. Iskandarsyah Raya No. 1A Kebayoran Baru, Jakarta Selatan, Indonesia
Email: munggang-hendro@supreme-energy.com

ABSTRACT

PT. Supreme Energy Muara Laboh (SEML) is currently constructing a 1 x 80 MW geothermal power plant in South Solok Regency, West Sumatera. The plant utilizes dual flash technology and will mark an important milestone since it will become the first dual flash geothermal power plant in Indonesia. The Engineering, Procurement and Construction (EPC) was started in March 2017. The drilling campaign to achieve 100% steam available at the surface was started in parallel with EPC activities. This becomes a challenge for SEML's project team considering that understanding on underground resources evolve over time when more data is obtained. The design of above ground facilities should have some flexibilities to accommodate such change.

The original Muara Laboh above surface facilities was designed for geothermal fluid taken from reservoir with temperature of less than 250 deg. C. However, after the drilling, the new data shows that the more sustained resources should be taken from high temperature reservoir (more than 290 deg. C). Utilizing the original above surface facilities will create silica scaling problem. Thus, new facilities will be added to allow the fluid mixing between the two resources while minimizing the potential silica scaling. The additional facilities should be simple, robust enough, and will not jeopardize the Commercial Operation Date (COD) target of the plant. This paper presents the experience of constructing Muara Laboh Geothermal Power Plant. The original process configuration design is presented, including modification plan to prevent silica scaling problem.

Keywords: Dual flash power plant, geothermal

INTRODUCTION

The presence of geothermal potential in Muara Laboh field is indicated by three principle surface manifestations: Patah Sembilan fumaroles to the south, Idung Mancung fumaroles in the middle and Sapan Malulong springs to the north (Situmorang et al., 2016). The prospect lies along the segment of the Great Sumatera Fault in South Solok Regency of

West Sumatera at elevation ranging from 450 to 2000 masl. Three temperature gradient wells were drilled by Pertamina in 1992 to early 1993, named as MLB-1, MLB-2 and MLB-3, with the depth of 275m, 250m and 225m respectively (Wisnandary and Alamsyah, 2012). Supreme Energy started geoscientific exploration in 2008 after receiving Preliminary Survey Permit from the Minister of Energy and Mineral Resources as administered by the Directorate of Minerals, Coal and Geothermal. This is the first exploration activity after the issuance of UU 27/2013 and PP 59/2007. An initial prefeasibility study based on data from surface manifestations and early Pertamina's gradient wells indicated the occurrence of a liquid dominated reservoir system with a temperature range of 210-320 deg.C at Muara Laboh that could support development of 220MWe power plant for 30 years (Wisnandary and Alamsyah, 2012).

Following the approval of Power Purchase Agreement (PPA) with PLN, Supreme Energy immediately started the construction of access roads, wellpads, service water supply and other supporting infrastructure for drilling. The first full diameter of exploration well was drilled at well ML-A1 in the third quarter of 2012. By end of 2013, total six full diameter exploration wells were drilled: ML-A1, ML-B1, ML-C1, ML-E1, ML-H1 and ML-H2. Situmorang et al., (2016) used the data from these new wells to update the earlier conceptual model and to run reservoir model to forecast future reservoir performance after long term extraction. The model confirmed that the steam supply is sufficient for a 60 MW single flash power unit and can increase to 70 MW using dual flash technology by further flashing the brine from the first flash. During tendering process, optimization in the power plant design has improved the steam rate consumption and increased the power plant capacity significantly to 80 MW with the steam mass flow remains the same. The second amendment of PPA that signed by PLN in Q3 of 2016 allows Muara Laboh field to be developed commercially. With the new tariff, Supreme Energy was able to secure funding for the field development in January 2017. The Engineering, Procurement and Construction (EPC) of Muara Laboh Geothermal Power Plant was started in March 2017 for a capacity of 80 MW based on dual flash technology. The EPC contract was awarded to Consortium of Sumitomo and Rekayasa Industri. Turbine and generator were supplied by Fuji Electric Japan.

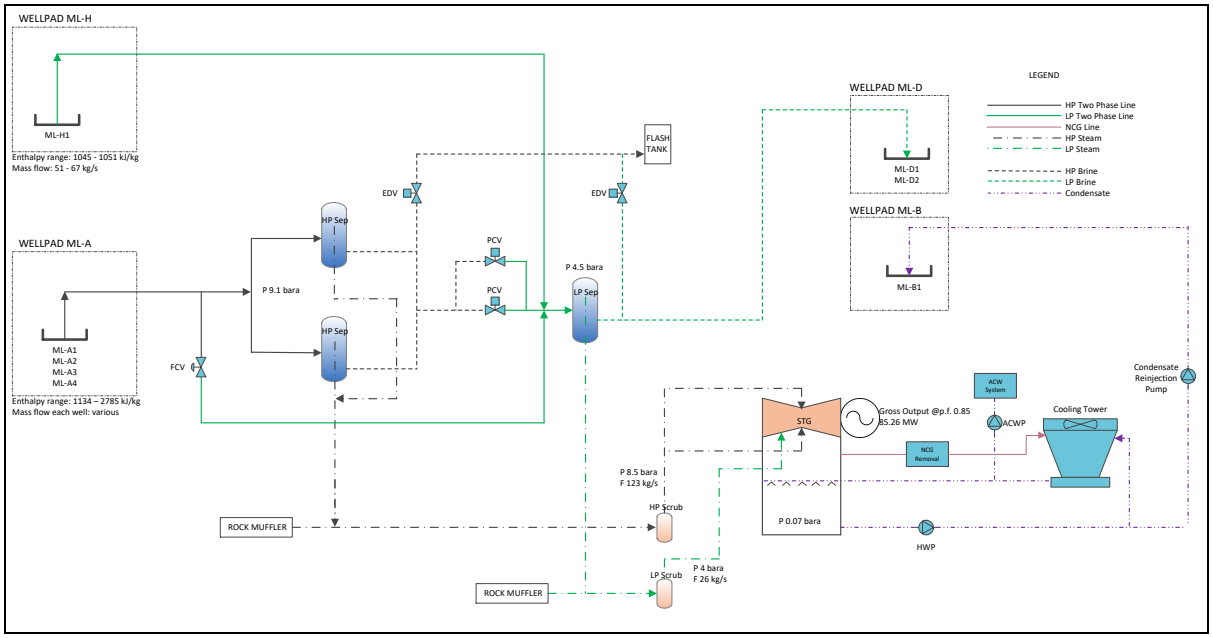


Figure 1: Simplified PFD Muara Laboh Power Plant.

In parallel with EPC works, Supreme Energy conducted drilling campaign from May 2017 to June 2018 to drill 12 new wells, consist of 9 production wells and 3 injection wells. The drilling is succeeded, the production wells are able to provide more than sufficient steam needed to generate 80MW including buffer, while the injection wells meet the injection capacity target.

POWER PLANT DESIGN DESCRIPTION

There is a risk for starting EPC works when the steam is not 100% available yet because the design of above surface facilities of power plant is largely dependent on the geothermal fluid characteristic. When data is not available prior to EPC, assumption is needed and the chosen process design might not be the most efficient one if the actual data is different from assumption. This is the case with Muara Laboh project.

The initial design process of the plant was based on the post-exploration-drilling reservoir model described by Situmorang et al. (2016). The exploration wells provide 40 kg/s of HP steam and 17 kg/s of LP steam available at well head from ML-A1 and ML-H1. The reservoir temperature range is between 235 deg. C to 255 deg.C with enthalpy range from 1014 kJ/kg to 1559 kJ/kg (Situmorang et al., 2016).

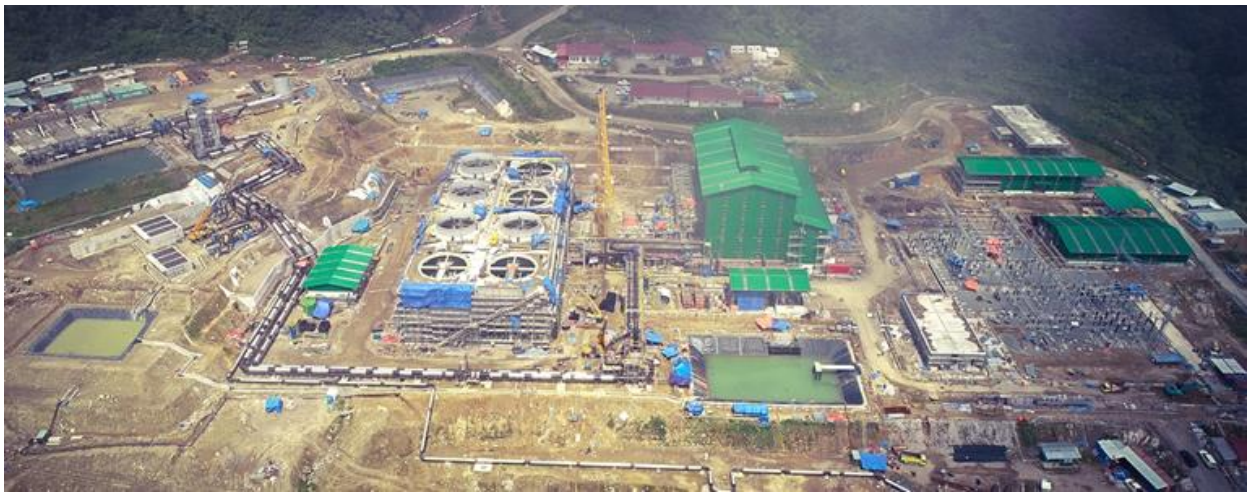
In order to generate 80MW, 9 new production wells are needed to provide 144 kg/s and 29.4 kg/s of HP steam and LP steam respectively including 20% steam buffer to mitigate potential transient decline after COD and to provide operational flexibility. Three new injection wells are needed to reinject all produced brine and condensate from the plant.

A simplified Process Flow Diagram (PFD) of Muara Laboh geothermal power plant is given in Figure 1. The design follows a typical dual flash design. Two separator pressures are selected: 9.1 bara for High Pressure (HP) separator and 4.5 bara for Low Pressure (LP) separator. Two HP separators are provided, each is designed for Total Mass Flow (TMF) of 267 kg/s. Only one LP separator is provided and it is designed for TMF of 503 kg/s. Dimension of all separators design follow Lazalde-Crabtree's approach (1984).

Wellpad ML-A provides the HP two-phase fluid. The separated brine from ML-A is mixed with LP two-phase fluid from ML-H1. In case of lack of LP fluid from ML-H1, a bypass line is installed from ML-A to LP system via Flow Control Valve (FCV) to reduce the pressure and regulate the flow.

The separated HP steam and LP steam then go to the HP scrubber and LP scrubber respectively. The scrubber is from multi-cyclone type. Different from conventional single-cyclone type, the scrubber uses multiple smaller pipes inside the vessel that work on cyclone principle. It is believed that the design will be able to deliver output steam dryness not less than 99.98%. Figure 2 shows the aerial photo of Muarah Laboh power plant.

The steam turbine is from single cylinder and downward double exhaust type. Turbine output design capacity during normal operation is 85.26 MW, the capacity can be increased up to 88.81 MW. The generator is from Totally Enclosed Water to Air Cooled (TEWAC) type. Generator rated speed is 3000 RPM, rated voltage is 11 kV and rated capacity



is 105 MVA. Both steam turbine and generator are manufactured by Fuji Electric Japan.

Figure 2: Aerial Photo Muara Laboh Power Plant (progress June 2019, photo by SEML).

The condenser is from Advanced Direct Contact Condenser (ADCC) type, manufactured by SPX. The internal design uses spray and fill type. Condenser pressure is rated at 0.07 bara.

The Gas Removal Design (GRS) for Non-Condensable Gas (NCG) consists of 3x50% trains: train A, train B, and train C. Each train A and train B consists of 2 stages steam ejector and 1 vacuum pump, while train C consists of 3 stages steam ejectors. During plant normal operation, 2 out of 3 GRS trains can be used to achieve 100% capacity. NCG is discharged to atmosphere via cooling tower.

A simplified single line diagram of Muara Laboh Power Plant is given in Figure 3. For internal power consumption (balance of plant), the plant utilizes voltage level of 6.3kV system (medium voltage) and 400V system (low voltage). There are also 110VDC system and 230VAC UPS system for DCS, protection relay and other critical application. Large electric motors (>200kW) are installed at MV level. There are 6 MV electric motors in Muara Laboh and they contribute to the largest parasitic loads in the power plant.

An emergency diesel generator (EDG) is installed at LV common essential bus with capacity of 800kVA. The EDG is provided to ensure sufficient electric power supply is available to enable the plant to be shutdown safely in the event of loss of transmission grid connection. The EDG is not sized for black start-up of the plant.

Part of SEML's scope under current PPA is to build, own and operate the 150kV switchyard. Point of energy transaction with PLN is at 150kV switchyard incoming line bays. To deliver the energy, PLN is required to build ±90 km transmission line network from power plant to Dharmasraya regency and connect with the existing 275kV Sumatera's grid. The network consists of 292 towers 150 kV, 14 towers 275 kV, 1 HV substation 150kV at Muara Labuh (South Solok Regency) and 1 EHV substation 150kV/275kV at Sungai Rumbai (Dharmasraya Regency). This is the first 150kV transmission line in South Solok and will improve the electricity quality in the area.

POTENTIAL SILICA PROBLEM FROM HIGH TEMPERATURE RESOURCES

The outcomes of development drilling in 2017 – 2018 show different resource characteristics with the initial assumption used to develop Muara Laboh power plant. Some of the new wells from ML-H and ML-F have been found to correspond to high liquid reservoir temperature (>290 deg. C). Mixing the fluids from these new wells with the fluids from ML-A using current design configuration will result in oversaturated silica in brine (Silica Saturation Index or SSI > 1). Silica scaling will likely to occur and will create problem in the plant, particularly in reinjection pipeline.

Connecting the resources from ML-H and ML-F is unavoidable because ML-A alone will not be able to sustain 80MW generation over 30 years of operation. Because of such condition, in the middle of EPC of original development, SEML assessed several modification options to mitigate the potential silica scaling to allow mixing the fluids from high temperature reservoir. The agreed criteria for the modification design are simple, robust and will not jeopardize the Commercial Operation Date (COD) of original schedule. Acid dosing option is not considered for this time due to its complexity and time constraint. Figure 4 shows the simplified SLD of Muarah Laboh power plant.

From assessment, it was concluded that silica scaling can be avoided if two-phase fluid high temperature reservoir is flashed at higher pressure (see Figure 5). New High High Pressure (HHP) separator is required for such flashing process. The

separated HHP steam will be mixed with the HP steam via let down valve (LDV) while the resulted HHP brines will go directly to the injection well. Two scrubbing sections at upstream and downstream of LDV will be installed. Wash water system is required at upstream LDV while de-superheating water system is required at downstream LDV. Several drain pots are installed to remove excess water and scrubbed residue.

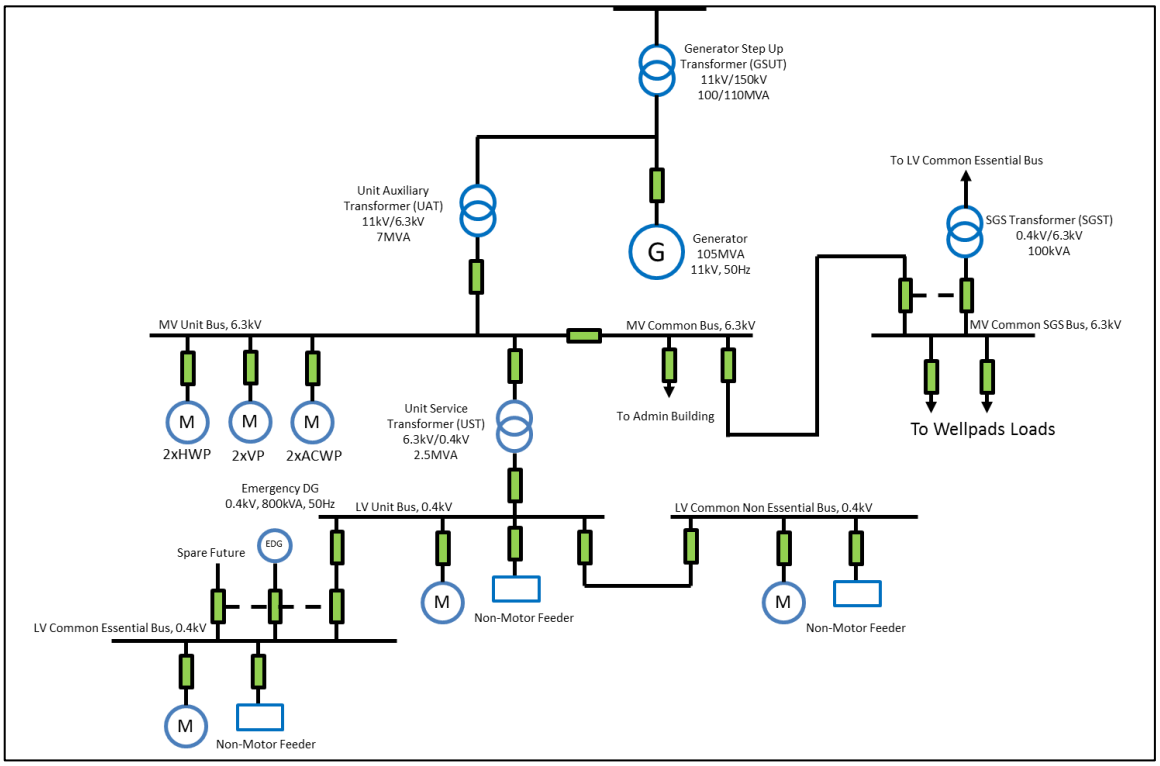


Figure 3: Simplified SLD of Muara Laboh Power Plant (exclude swithcyard).

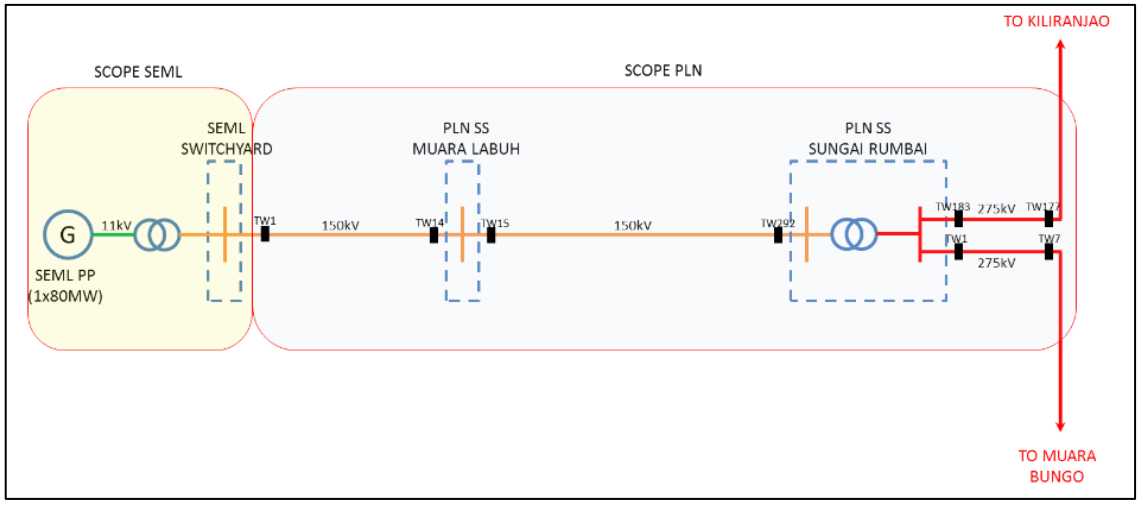


Figure 4: Transmission Line from Muara Laboh Power Plant to PLN's 275kV network.

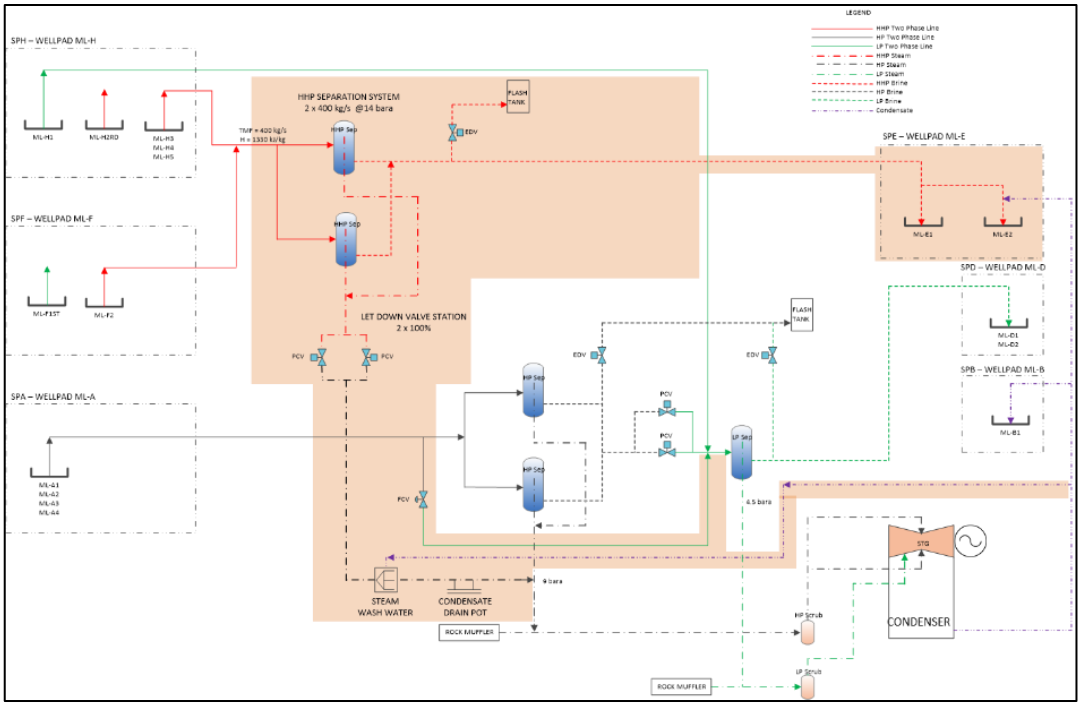


Figure 5: Modification Plan for Silica Scaling Mitigation.

FUTURE PLAN

The construction of Muara Laboh geothermal power plant is now close to completion. Currently, the project is in commissioning phase and it is expected that COD will happen by Q4 of 2019. All involving parties are working together to maintain the schedule. In parallel, EPC Contractor has been starting the design of silica scaling mitigation works to ensure that the system is ready for use within 1 year from the COD.

The high temperature brine from HHP separator still has stored energy from in optimized heat utilization. There is potential to utilize the energy from hot brine for future additional unit.

ACKNOWLEDGEMENT

The authors would like to thank the management of PT. Supreme Energy Muara Laboh for permission to publish this paper.

REFERENCES

Brown, K. (2018), "Scaling Considerations at Muara Laboh", ML-PRD-RPT-0074, Supreme Energy Unpublished Report

Lazalde-Crabtree, H. (1984), "Design Approach of Steam-Water Separators and Steam Dryers for Geothermal Applications", Geothermal Resources Council Bulletin September 1984

Situmorang, J., Martikno, R., Putra, A. P. and Ganefianto, N. (2016), "A Reservoir Simulation of the Muara Laboh Field, Indonesia", Proceedings 41st Workshop on Geothermal Reservoir Engineering Stanford University, Stanford, California

Supreme Energy (2016). "Muara Laboh Geothermal Power Project Stage 1 Development Feasibility Study", ML-PRD-RPT-0018, Unpublished Report

Supreme Energy (2018). "Muara Laboh Stage-1 Development Drilling and Welltesting Report", Unpublished Report

Wisnandary, M. C. and Alamsyah, O. (2012), "Zero Generation of Muara Laboh Numerical Model: Role of Heat Loss and Shallow Wells Data on Preliminary Natural State Modeling", GRC Transactions, Vol. 36

A SIMPLE PREDICTION AND APPROACH TO DETERMINE RESERVOIR PRESSURE

Erwandi Yanto, Gamal Hastriansyah, Ahmad Fahmi Fanani, M. Bayu Saputra, Fadiel Evan Marastio, Fernando Pasaribu, and Marihot S.P. Silaban

PT. Pertamina Geothermal Energy
Skyline Building, 19th Floor, Jakarta Pusat, Daerah Khusus Ibukota Jakarta 10340
Email: erwandi.yanto@pertamina.com

ABSTRACT

In general, determining the productivity and injection capacity of wells requires reservoir pressure parameters. However, on the other hand when the well is warming up very often the determination of the reservoir is still difficult, especially when there is no pressure pivot point that can only be obtained from the measurement of repetitive temperature and pressure on the well. Therefore, alternative and practical steps are needed to determine the reservoir pressure value which can then be used to determine the reservoir depth, calculation of well productivity to well injection capacity. As for the method offered is to cross-plot between reservoir pressure and depth in the nearest wells in one area that has relatively the same geological and reservoir conditions.

Keywords: Reservoir, pressure determination

INTRODUCTION

Reservoir pressure is one of the most critical parameter to determine the potential of geothermal wells. Either production or reinjection wells, reservoir pressure determination must be rapidly known to assess the drilling successibility. Reservoir pressure is characterized by the existing of permeable zone especially as feed zone in geothermal wells. Subsurface formation structure usually contributes any feeding pressure into wellbore.

REGIONAL GEOLOGY

Geologically (Table 1), Sumatra consists of three fault systems:

- Sumatra Subduction System (Collision between Indo Australia Plate and Eurasian Plate)
- Mentawai Fault System
- The Sumatran "Semangko" Fault System (Hamilton 1979)

Based on the analysis of geological structure obtained from surface alignment and fracture analysis or sub surface geological structure of geophysical data and logging data, it can be seen that there is suitability of fracture pattern or geological structure between the wells in this Thermex area with structure pattern regional of Sumatra Island that is south-east-northwest with type of fault movement in the form of strike-slip regime.

This fracture pattern is generally controlled by a subduction zone in the western part of Sumatra that causes the movement of the western Sunda Land plate i.e the Sumatra plate. In addition, tectonic controls associated with volcanic activity result in volcanic arcs extending along the Sumatra fault.

Based on the analysis of geological structure obtained from surface alignment and fracture analysis or sub surface geological structure of geophysical data and logging data, it can be seen that there is suitability of fracture pattern or geological structure between the wells in this Thermex area with structure pattern regional of Sumatra Island that is south-east-northwest with type of fault movement in the form of strike-slip regime. Figure 1 shows the Sumatra tectonic system.

This fracture pattern is generally controlled by a subduction zone in the western part of Sumatra that causes the movement of the western Sunda Land plate ie the Sumatra plate. In addition, tectonic controls associated with volcanic activity result in volcanic arcs extending along the Sumatra fault. Figure 2 shows the stress magnitude of UBL area. Figure 3 shows the Determination of Pivot Point as Reservoir Pressure in 1 well. Figure 4 shows the Compilation of reservoir pressure based on pivot point for each well.

Table 1: Historical Geology of Thermex Area.

Era	Age	Formation
Quartenary		Mt. Tanggamus
		Mt. Kabawok
	1.4 Ma	Mt. Rendingan
		Mt. Argomulyo
		Mt. Tiga
		Mt. Kukusan
		Mt. Mas
		Mt. Duduk
		Mt. Aekabang
		Mt. Waypanas
Tertiary		Mt. Sula Muda
		Mt. Sula

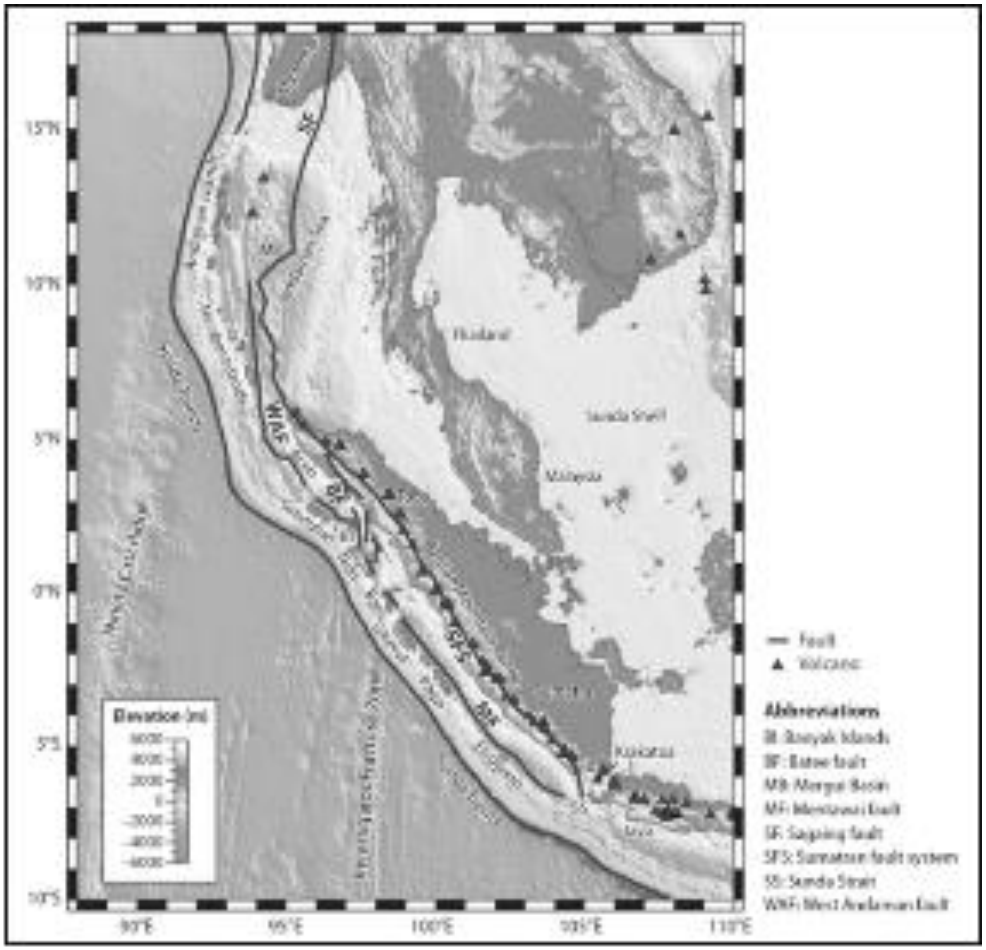


Figure 1: Sumatra Tectonic System, Hamilton 1979 (Global Volcanism Program).

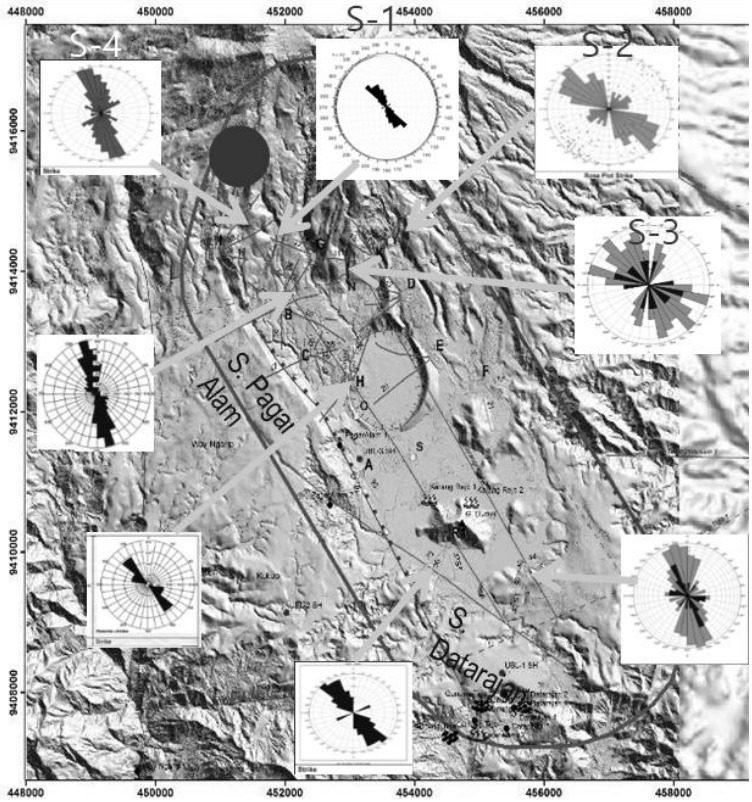


Figure 2: Stress Magnitude of UBL Area.

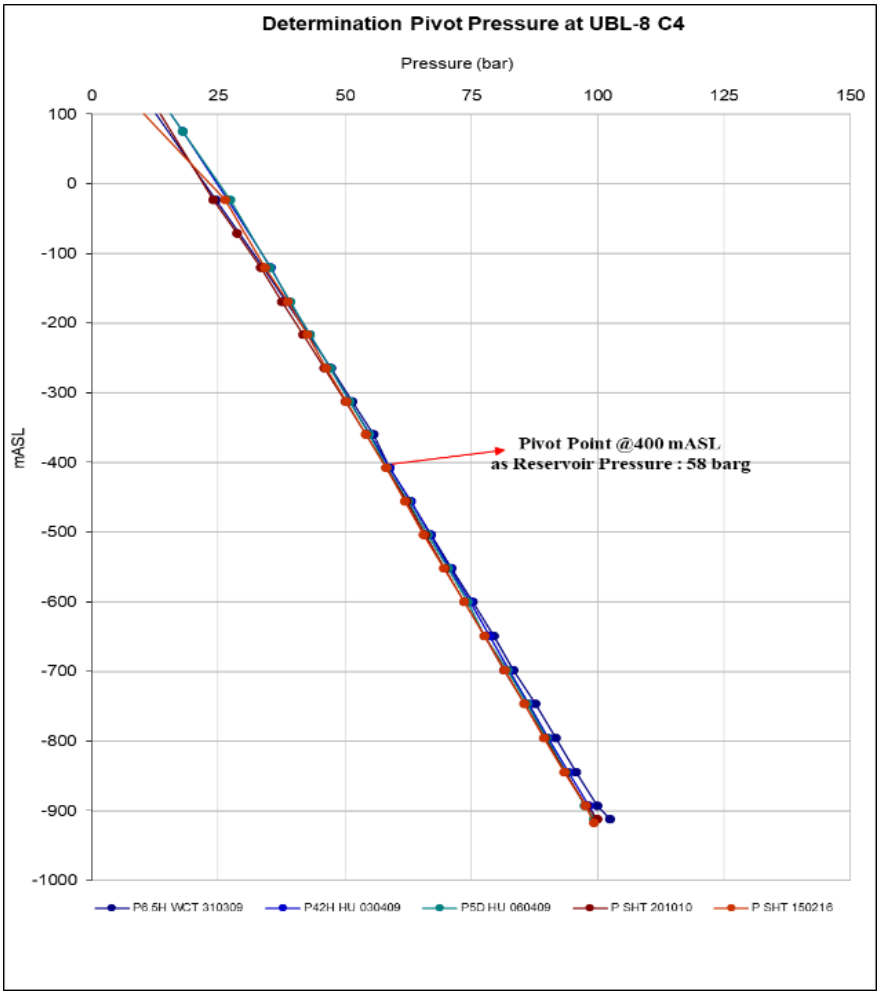


Figure 3: Determination of Pivot Point as Reservoir Pressure in 1 well.

DATA

Table 2: Reservoir Data Recapitulation of Wells in UBL.

Well Name	Reservoir Elevation (mASL)	Reservoir Pressure (barg)	Well Name	Reservoir Elevation (mASL)	Reservoir Pressure (barg)
UBL-1	-950	90	UBL-30	-1327	112
UBL-2	-889	78	UBL-31	-1369	128
UBL-3	-1359	127	UBL-32	-1027	98
UBL-5	-922	91	UBL-33	-1287	107
UBL-6	-67	25	UBL-34	-375	59
UBL-7	-882	93	UBL-35	-853	79
UBL-8	-952	103	UBL-36	-1363	113
UBL-10	-1621	139	UBL-37	-553	58
UBL-11	-1159	107	UBL-38	-1075	90
UBL-12	-1379	118	UBL-39	-1142	110
UBL-13	-1679	130	UBL-40	-738	68
UBL-14	-1379	126	UBL-41	-1033	101
UBL-15	-957	94	UBL-43	-852	84
UBL-16	-697	66	UBL-45	-975	99
UBL-18	-975	87	UBL-46	-1488	146
UBL-19	-1362	117	UBL-47	-1495	125
UBL-20	-1472	110	UBL-48	-1563	137
UBL-22	-919	72	UBL-49	-1225	106
UBL-23	-517	57	UBL-50	-1430	120
UBL-25	-1197	100	UBL-51	-983	79
UBL-26	-1252	121	UBL-52	-1329	103
UBL-27	-822	78	UBL-53	-237	55
UBL-29	-994	105	UBL-54	-1329	103

RESULT

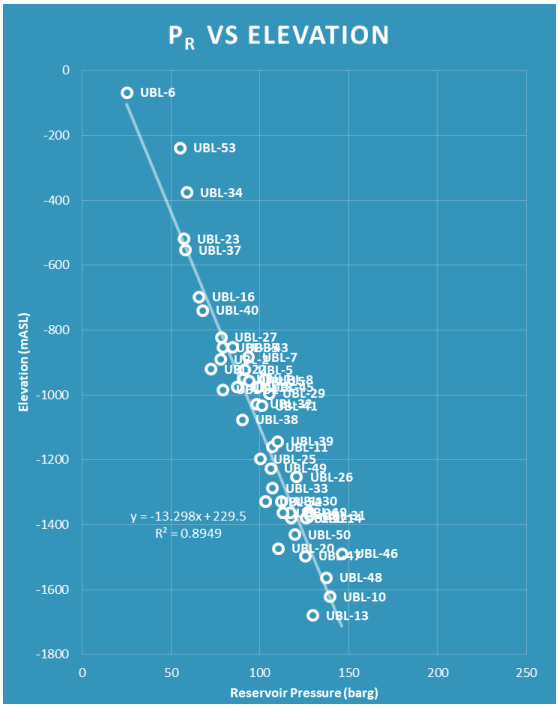


Figure 4: Compilation of reservoir pressure based on pivot point for each well.

$y = -13.298x + 229.5$
$R^2 = 0.8949$

Where:
Y axis : elevation (mASL)
X axis : reservoir pressure

The equation can be used to predict the unknown reservoir pressure in similar area due to late heating up of new well after drilling operation.

Then, after determining the predicted reservoir pressure can be as an input (Table 2) to calculate well productivity or injectivity.

CONCLUSION

- Reservoir pressure is related to permeable zone of a well.
- Permeable zone in each of wells is characterized by fracture or structural geology network beneath.
- Reservoir pressure determination of late heating up well can be predicted from another well in a similar geothermal system.
- Reservoir pressure of well can be showed by pivot point of several pressure measurement when heating up of the well.
- For UBL area, the equation to predict the reservoir pressure could be :

$y = -13.298x + 229.5$
$R^2 = 0.8949$

Where:
Y axis : elevation (mASL)
X axis : reservoir pressure

REFERENCES

Hamilton, W.R., (1979). "Tectonics of The Indonesia Region". United States Geological Survey.

Harding, T. P., and J. D. Lowell, (1979). "Structural styles, their plate-tectonic habitats and hydrocarbon traps in petroleum provinces". AAPG Bulletin, v. 63, p. 1016-1058.

M. J. Heap & J. I. Farquharson & P. Baud & Y. Lavallée & T. Reuschlé, (2015). "Fracture and compaction of andesite in a volcanic". Bull Volcanol (2015) 77: 55

Pertamina Geothermal Energy Database, (2012). "Geoscience Database, Sumatera Region". DKI Jakarta.

Wilson, C.J.N., Houghton, B.F., McWilliams, M.O., Lanphere, M. a., Weaver, S.D., and Briggs, R.M., (1995). "Volcanic and structural evolution of Taupo Volcanic Zone, New Zealand: a review". Journal of Volcanology and Geothermal Research, v. 68, p. 1–28.

NITROGEN LIFTING METHOD TO DISCHARGE GEOTHERMAL WELLS

Erwandi Yanto, Gamal Hastriansyah, Ahmad Fahmi Fanani, M. Bayu Saputra, Fadiel Evan Marastio, Fernando Pasaribu, and Marihot S.P. Silaban

PT. Pertamina Geothermal Energy
Skyline Building, 19th Floor, Jakarta Pusat, Daerah Khusus Ibukota Jakarta 10340
Email: erwandi.yanto@pertamina.com

ABSTRACT

Well X-1 have been drilled to obtain resource confirmation and obtain an overview of the conceptual concept of the Area prospect. Based on exploration data point of view, 5 wells that have been drilled have provided many subsurface data that provide resource confirmation and the Kerinci reservoir conceptual model. However, from the five wells, the X-1 wells cannot be discharged. This causes the potential productivity of the well has not yet been proven which has led to further development plans that cannot be accurately arranged. This also causes the two wells to have no economic value in productivity. Therefore, to achieve the exploration objectives, namely to prepare a development plan, these two wells need to be stimulated through unloading water coloumn and annular velocity so that it reaches a continuous discharge condition. Several studies have been conducted to identify the needs and solutions for the two wells not yet discharged.

Keywords: Well stimulation, nitrogen lifting method

THEORY

Well discharge stimulation methods (Mubarok, et al., 2017):

- Air compression
- Well to well injection
- Nitrogen injection
- Air lifting
- Steam heating by boiler

Nitrogen well injection method used nitrogen gas to decrease the density of water column. Nitrogen is the best gas for discharge stimulating geothermal well because it is chemically stable, non-corrosive, low solubility, inert, and non-toxic (Mubarok and zarrouk, 2017). The nitrogen gas injected through the coil tubing unit through the pipe line, then the nitrogen gas mixes with the water and decreases the density of the cold-water column. Nitrogen injection consider to be the last resort for discharge stimulation. Sometimes if this technique doesn't work then the well will not discharge. Figure 1 shows the Coiled Tubing Schematic for Air Lifting.

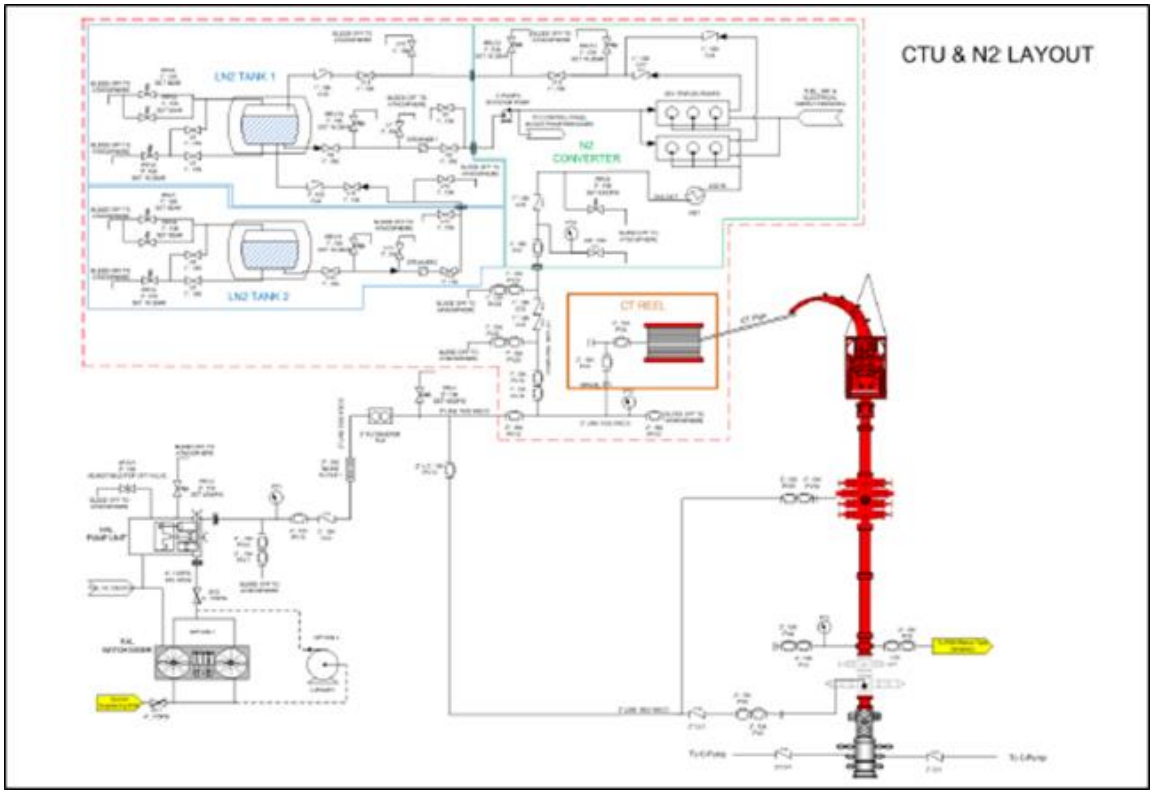


Figure 1: Coiled Tubing Schematic for Air Lifting.

ISSUES

Targeted drilling of these wells has obtained several targets that provide confirmation of the conceptual model. The water column from the permeable zone is as high as ± 1000 m (vertical) equivalent to 100 bar of hydrostatic pressure. The difference in saturation temperature reaches 130ºC. The well can be compressed up to ± 100 bar, which in theory makes the water column reach saturation, however the well has not been able to discharge which is likely due to excessive condensation during the discharge effort. FZ temperature (± 1900 mku) based on correlation may still increase up to ± 260ºC. Well stimulation by reducing hydrostatic pressure above the feedzone so that the reservoir pressure can lift the surface fluid. It is done by injecting air into the water column so that the fluid density in the column drops which results in a downward pressure (Ph = ρgh) (Table 1). Figure 2 shows the well X-1 profile. Figure 3 shows the Layout Air Lifting Equipment. Figure 4 shows the P&T Profile of Well X-1. Figure 5 shows the Schematic Nitrogen Lifting Design.

WELL HISTORY

Well Name	: X-1
Formation Type	: Volcanic
KOP	: 260 mMD
KOP Side Track	: 435 mMD
Max Deviation	: 43.1º
Wellhead Connection	: 12” 900# RTJ R-57 x 4 - 1/16” 10K A

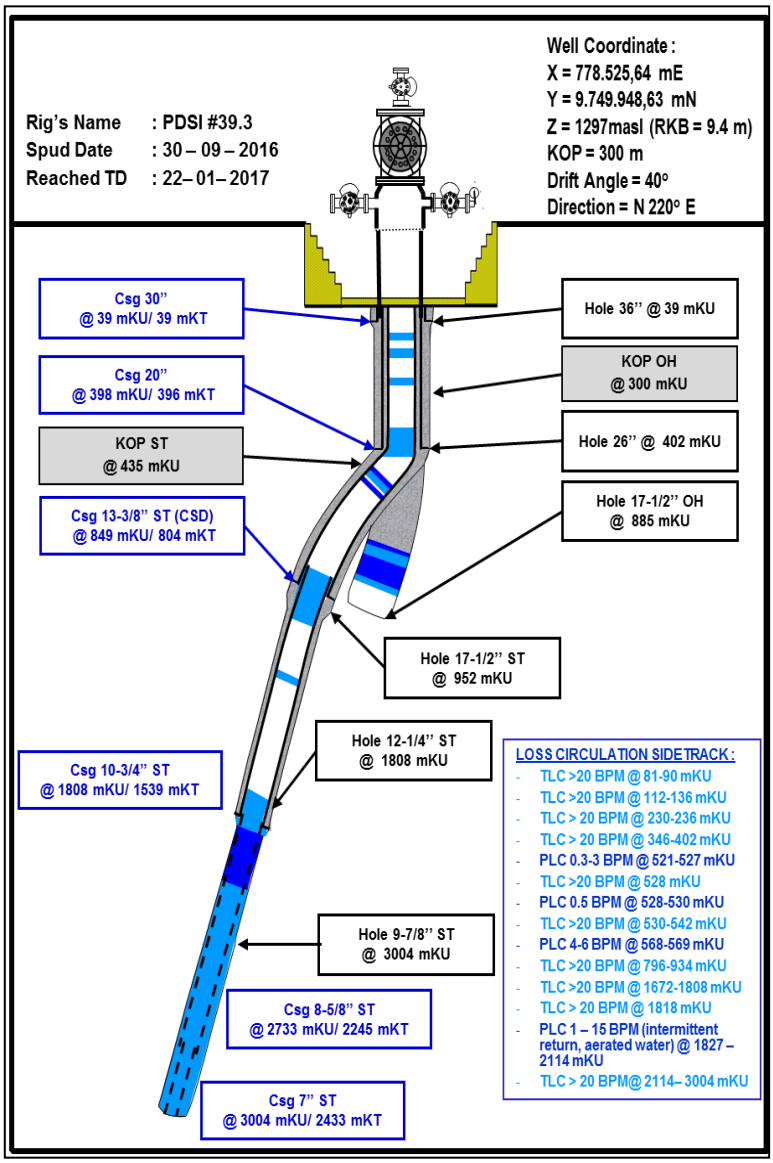


Figure 2: Well X-1 Profile.

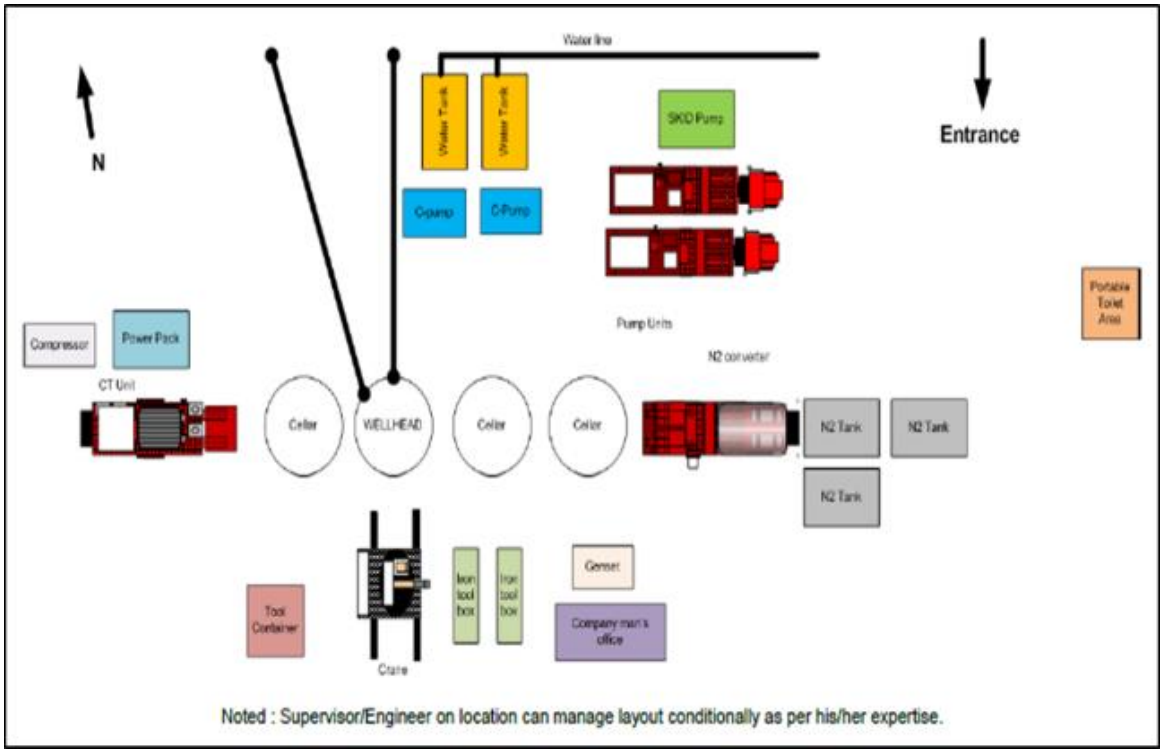


Figure 3: Layout Air Lifting Equipment.

GEOCHEMICAL ANALYSIS

Table 1: Geochemistry Characteristic of Well X-1 and surrounding area.

Aspect		Well **X-1**
NCG		0.6-0.8%
pH		Near Netral 6-7
Salinity		Cl 1200-2000 ppm Na avrg 1000 ppm
Arsenic		1.2-3 (environtmental issue)
Total Disolve Solid		Avrg 3000
WHP		Small
Scalling Potential	**Silica**	<160 degC
	Anhydrit	>170 degC
	Calcite	>90 degC
Temp downhole		220 – 260 degC
Temp Geothermometer Silica		212-280 degC

RESERVOIR SUMMARY

- Major Feed Zone at depth 1850 mMD which contribute until 98 %.
- Flashing Zone at depth ± 650 mMD
- Reservoir Temperature 300ºC, Heating Up ± 10 months.
- Permeable zone at depth ± 1800 mMD.

NITROGEN INJECTION DESIGN

A. Minimum Nitrogen Volume

Lift fluid from 600 m to a level where HP at payzone ~ 1,808 m is at 60 ksc.
P = 60 ksc = 853.4 psi
Top of Fluid Level (ft) = 853.4 psi: (0.052 x 8.6 ppg)
= 1,908.3 ft ~ 581.62 m.

$$N_2 = N_2F \; x \; RIH \; x \; (ID^2 x 0.0009714) \frac{scf}{min}$$

N_2 = Nitrogen Pump Rate (scf/min)
RIH = Run In Hole Speed (ft/min)
N_2F = N_2 / fluid ratio (scf/bbl)
(usually aim for 500)
ID = Wellbore ID (in.)
Wellbore Volume Factor = ID^2 x 0.0009714 (bbl/min)

In this case, used speed 20 ft/min, so:

1. At casing 13-3/8" OD
   N_2 rate = 500 scf/bbls x 20 fpm x (12.615^2) x 0.0009714
   = 1,545.93 scf/min
2. At casing 10-3/4" OD
   N_2 rate = 500 scf/bbls x 20 fpm x (9.95^2) x 0.0009714
   = 961.74 scf/min

- Time Pumping:
  - Time to unload fluid = Length/RIH Speed
  - Unload Length is from 600 m to 1,226.4 m = 626.4 m ~ 2,055.2 ft
  - Time = 2,055.2 ft/20 ft/min = 103 min.

- N_2 Requirement for Unloading
  - Section 13-3/8" casing = 1,545.93 scf/min * 103 min = 159,231 scf
  - Section 10-3/4" casing = 961.74 scf/min * 103 min = 99,060 scf

» Total = 159,231 scf + 99,060 scf
= 258,291 scf = ~2,774 gal.

B. Lifting to Bottom Well

1. At casing 13-3/8" OD
   N_2 rate = 500 scf/bbls x 20 fpm x (12.615^2) x 0.0009714
   = 1,545.93 scf/min
2. At casing 13-3/8" OD
   N_2 rate = 500 scf/bbls x 20 fpm x (9.95^2) x 0.0009714
   = 961.74 scf/min
3. At casing 8-5/8" OD
   N_2 rate = 500 scf/bbls x 20 fpm x (7.625^2) x 0.0009714
   = 564 scf/min
4. At casing 7" OD
   N2 rate = 500 scf/bbls x 20 fpm x (5.376^2) x 0.0009714
   = 280 scf/min

- Time Pumping:
  - Time to unload fluid = Length/RIH Speed
  - Unload Length is from 700 m to 3,004 m = 2,304 m ~ 7,557 ft
  - Time = 7,557 ft/20 ft/min = 377.85 min.

- N_2 Requirement for Unloading
  - Section 13-3/8" casing = 1,545.93 scf/min * (((849 – 700 m) *3.28)/20 fpm) = 37,776 scf
  - Section 10-3/4" casing = 961.74 scf/min * (((1808 – 889 m) *3.28)/20 fpm) = 151,258 scf
  - Section 8-5/8" casing = 564 scf/min * (((2733 – 1808 m) *3.28)/20 fpm) = 85,558 scf
  - Section 7" casing = 280 scf/min * (((3004 – 2733 m) *3.28)/20 fpm) = 12,444 scf

» Total = 37,776 scf + 151,258 scf + 85,558 scf + 12,444 scf = 283,036 scf
= ~3,082 gal.

FIELD OPERATION

The operational of Nitrogen Lifting used Coiled Tubing unit to inject liquid nitrogen into depth target at 1300 mMD. The stimulation only needs 1 day to unload liquid from Well X-1. During this operation, there was an obstacle when the bubble appears in the well which made pressure lose inside tubing so that the liquid nitrogen couldn't be injected to the well (Table 2).

Table 2: Calculation and Estimation of Minimum Nitrogen Volume.

Parameter	Minimum Unloading Volume Case A	Minimum Unloading Volume Case B	Unloading Volume to Bottom Well Case B
Injection Volume (Gallon)	2034 Gal	2774 Gal	3082 Gal
Injection Depth (mMD)	1900 mMD	1226 mMD	3004 mMD

Table 3: Operational of Nitrogen Lifting Parameter in Well X-1.

Parameter	Value
Injection Time	7 hours
Maximum CT Depth	1300 mMD
Volume Nitrogen when Flow Occurred (Operation Only)	1932 Gal
Total Volume Nitrogen (Operation Only)	3277 Gal
Wellhead Pressure @ 22.00	3 bar

RESULT

Due to assess the succesibility of nitrogen lifting operation in well X-1, well discharge test had been conducted after nitrogen lifting (Table 3). The discharge test duration 1 day which is 18 January 2018.

The result is that well X-1 can discharge with increasing wellhead pressure from 3 barg (previously) into 3.7 barg, line pressure 2.5 barg into 3.2 barg, lip pressure from 0.6 barg into 1 barg, whereas the brine level in weirbox relatively constant with height 55 cm from v-notch. Figure 6 shows the parameter data of nitrogen lifting. Figure 7 shows the data monitoring during discharge test after nitrogen lifting operation.

CONCLUSION

- After shut in the well X-1, an attempt to open the well is carried out with maximum pressure 92 bar, tried 10 times to not discharge successfully
- N_2 lifting managed to drain the well at the initial well pressure when it opened 3 barg
- Production test results:
  Increase from 2.22 MW to 3.09 MW The well experienced a decrease in pressure until finally the well stopped discharge
- P&T measurement is done by first making a dummy measurement (tag at 612 mMD)
- There is solids carried to the surface on the dummy and at the well test facility
- XRD results on mineral solid samples in Well X-1 are Calcite ($CaCO_3$)

REFERENCES

Aqui, A.R. (1997): "Well Discharge Stimulation of Some Geothermal Wells in the Philippines by Nitrogen Gas Injection". Proc. 18th PNOC-EDC Geotlieriiial Conference, Makati City, Pliilippines, I1'pp. 101-112.

Kaya. Tevfik, Mertoglu, Orhan (2005). "Engineering Aspect of Geothermal Production Well with Dowa Down Hole pumps". Orme Jeotermal.

Mubarok, Mohamad Husni, Zarrouk. Sadiq (2017). "Discharge Stimulation of Geothermal Wells". University of Auckland.

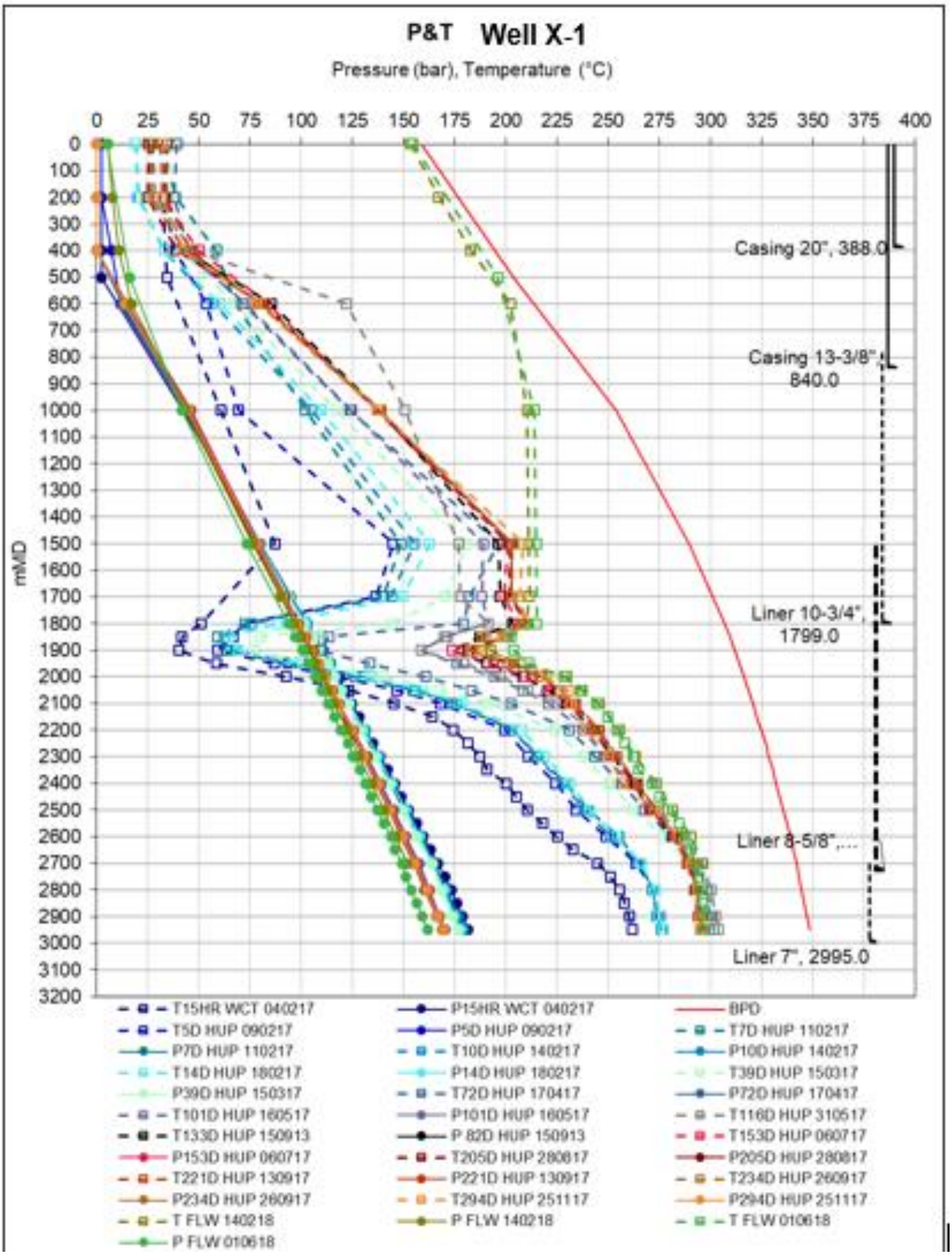


Figure 4.P&T Profile of Well X-1

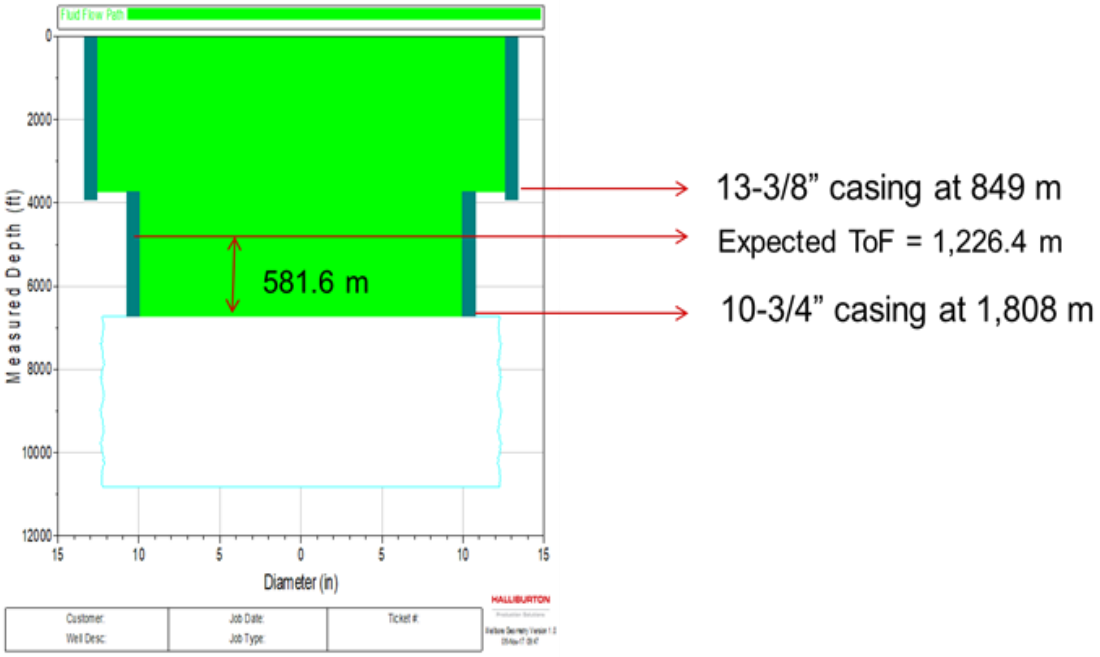


Figure 5: Schematic Nitrogen Lifting Design

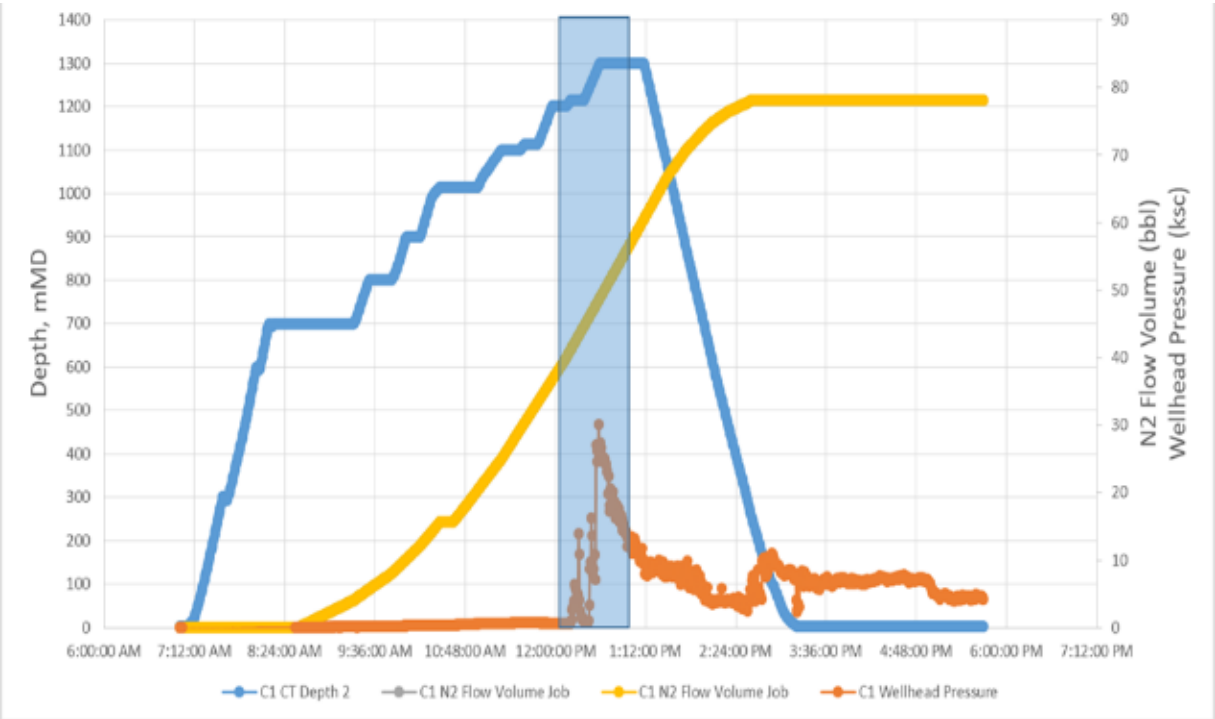


Figure 6. Parameter Data OF Nitrogen Lifting

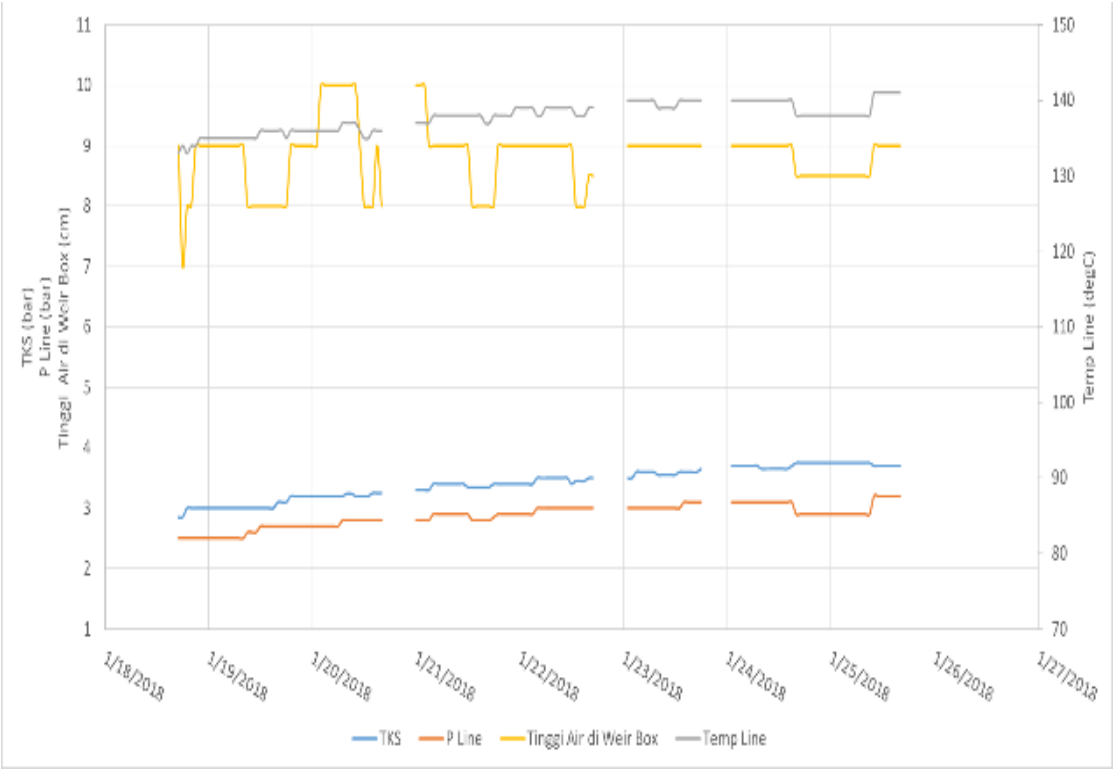


Figure 7. Data monitoring during Discharge test after Nitrogen Lifting Operation

Table 4: Operational of Nitrogen Lifting Parameter in Well X-1

Well	Elevation (m)	WHP (Kscg)	P atm (bara)	P-sep		Entalphy (kJ/kg)				X-Dryness (%)	Flow (Ton/hr)			Note
				barg	bara	H	hf	hg	hfg		Total	Steam	Brine	
X-1	1300	4.08	0.870	2.00	2.87	1027	504	2707	2203	17.17%	204.78	48.65	156.13	Uji Produksi 2018

Table 5: Well X-1 production capacity

Well	"WHP (ksc) "	"Sim Flow (t/hr)"	"Steam Flow (t/hr)"	"brine Flow (t/hr)"	"Sim flowing Enth (kJ/kg)"	Dryness	MW
Original	4.08	203.61	33.33	170.28	982.70	0.16	2.22
2xPI	4.08	283.96	46.35	237.61	980.68	0.16	3.09

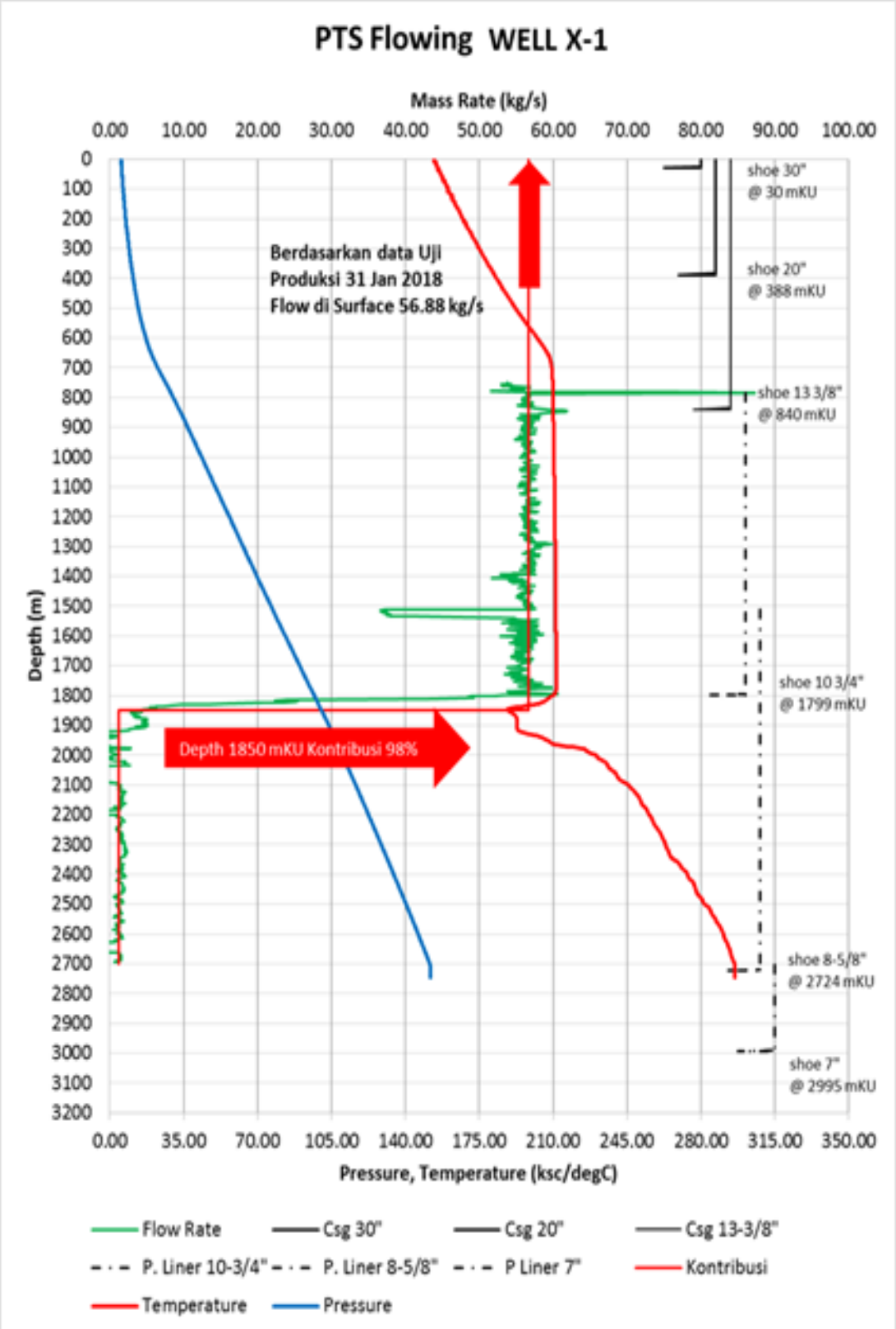


Figure 8. PTS Flowing after Nitrogen Lifting Operation

Enclosure:

Well Name	:	KRC X-1	
Bottom of Liner (BOL)	:	2995	m
Depth of Main Permeable Zone (MPZ)	:	1613	mTVD
Water Level	:	400	mTVD
Measured temperature at MPZ	:	183	°C
Measured pressure at MPZ	:	10.2024	Mpag
Casing Diameter	:	12.41	in
Coil Tube Diameter	:	2	in
Parameter		**Nilai**	**Unit**
$dP=(P_{@surface}-P_{@mpz})$	=	9.230007075	Mpa.a
L	=	1613	m
dp/dL	=	0.005722261	MPa.a/m
	=	5722.261051	Pa.a/m
$\rho_{mix} = (dP/dL)/g$	=	583.3089756	kg/m³
T_1	=	273	K
P_1	=	0.101325	Mpa
V_1	=	0.8	m³/kg
T_2 (Rata-Rata T Kolom Air)	=	315.75	K
P_2	=	9.23	Mpa
$V_2 = (P_1.V_1.T_2)/(T_1.P_2)$ --> V_{gas}	=	0.010157464	m³/kg
$V_{air@T2}$	=	0.001008974	m³/kg
$V_{mixture} = 1/\rho_{mix}$	=	0.001714357	m³/kg
$x = (V_{mixture}-V_{air})/(V_{gas}-V_{air})$	=	0.077103768	
H = (L-water level) --> Total kolam air	=	1213	m
R_1 (jari-jari tubing)	=	0.0254	m
R_0 (jari-jari casing)	=	0.157607	m
$D_{ch} = 3.1416[R_1+((R_0-R_1/2)]$ --> Diameter Karakteristik Pipa	=	0.287467396	m
$v_b = [(0.29352).(2g.D_{ch})^{0.5}]$ --> Kecepatan Bubble	=	0.897078194	m/s
Rise Time = H/v_b	=	1740.12042	s
α (Void Fraction)	=	0.310749992	
A =(luas area casing-luas area tubing) --> luas area anulus	=	0.075971692	m²
$W_{(x)} = A.(1-a).v_b/V_2$ --> Gas flowrate	=	3.593559171	kg/s
$V_{liquid@2}=W(x).$Rise Time	=	6253.225693	kg
	=	**2034**	**gallon**

DESIGN AND APPLICATION OF AERATED AND FOAM DRILLING FLUID, CASE STUDY IN DRILLING OPERATION IN INDONESIA

Wisnu Adi Nugroho, Ali Imran Rangkuti, and Satria Hermawan

Pertamina Drilling Services Indonesia
Jl. Matraman Raya No. 87 Jakarta Timur
Email: wisnu.nugroho@pertamina.com

ABSTRACT

Underbalance drilling is a common application in highly fractured and subnormal pressured formation. Technical reasons such as reservoir damage, drilling in depleted zone and hard drilling lead to more economic value in drilling operation. There are several ways to achieve underbalanced well pressure while drilling. One of the most common technique is air, aerated-mud and foam drilling or commonly known as Aerated Drilling.

Drilling with air, aerated-fluid and foam can lead to numerous advantages. In spite of the advantages, it also brings more challenge in design and operation. Cutting transport should be properly calculated to achieve a clean bottom hole condition. Air and gas parameters should be properly designed to prevent Wellbore wash out and formation collapse. All of them should be properly design while maintaining underbalance condition.

In some cases, improper aerated drilling parameters potentially leads to drilling problems such as lost circulation and stuck pipe. This condition should have been mitigated with the proper design of Air, Gas and Foam injection rate. Guo and Ghalambor in 2002 describe main criterion in aerated drilling design. Guo's technique can be applied in air, foam and aerated-liquid drilling. In 2009 Lyons adds more complicated technique, including calculation of liquid hold up and unstable foam drilling. Calculations in this paper are based on both criterion and technique. On operational side, several key takeaways are drawn based on operational challenges in multiple combination of operational conditions.

This paper proposes comprehensive techniques to design and parameter in operation in aerated drilling. Several cases are presented in this paper and being evaluated using proposed technique. All of the data are taken from real underbalance drilling parameters in Drilling Operation in Indonesia.

Keywords: Aerated, drilling, geothermal

INTRODUCTION

Underbalanced condition is required while drilling trough fractured and low-pressure formation. Common applications to achieve underbalanced conditions are foam mud, aerated fluid and air/mist drilling. There are two parameters as variable to be controlled in those techniques, air rate and liquid rate.

Inadequate air and liquid flow rate combination can lead to another hole problem. Lack of bottomhole pressure below casing shoe can lead to hole instability issue, inadequate cutting carrying capacity can lead to cutting pack off and high velocity air lead to wellbore washout problem. Those problem should be accounted while maintaining underbalanced conditions.

METHOD

This paper uses Guo et al. (2002) criterions for underbalanced drilling with air, foam and aerated drilling. The detailed criterions are minimum velocity, minimum kinetic energy, bottomhole pressureand foam stability. When drilling with mud motor, flow rate shoud be calculated using two phase flow equations.

Air Drilling

Minimum Velocity criteria:

$$V_t = \sqrt{4gd_c \frac{\rho_c - \rho_f}{3C_d \rho_f}} \quad (1)$$

Minimum Kinetic Energy:

$$V_{min} = V_s \sqrt{\frac{P_s}{P_{bh}}} \quad (2)$$

Bottomhole Pressure:

$$P_b = \sqrt{\left(P_s^2 - \frac{abT_s^2}{G-a}\right)\left(\frac{T}{T_s}\right)^{\frac{2a}{G}}} + \frac{abT^2}{G-a} \quad (3)$$

$$\mathrm{T} = T_s + Gh \quad (4)$$

$$\mathrm{a} = \frac{SQ + 28.8\ ROP\ D_h^2}{53.3Q} \quad (5)$$

$$b = \frac{1.625\ x\ 10^{-6} Q^2}{(D_h - D_p)^{1.333}(D_h^2 - D_p^2)^2} \quad (6)$$

Foam Drilling

In foam drilling, the mixture of foam and cuttings cannot be treated as a homogeneous mixture. It

makes the minimum kinetic energy criterion for air drilling cannot be applied in foam drilling. The cutting transport requirements for foam drilling are presented below:

$$V_{si} = 1.56 \frac{D_s(\rho_s - \rho_{fm})^{0.667}}{\rho_{fm}^{0.333} - \mu_e^{0.333}} \quad (7)$$

Foam Stability

Foam are stable when volumetric gas content is 0.55-0.975. When the gas phase is greater than 0.975, the continuous cellular foam structure that entraps gaseous phase become unstable, and the foam turns into mist. When the gas phase is less than 0.55, the foam structure tends to break down.

Foam quality also related to cutting lifting capacity. Figure 1 shows the relation between foam quality and relative lifting force. The lifting capacity starts to increase at foam quality of 0.6. The best lifting capacity achieved with foam quality ranges from 0.72 – 0.97. It declines after reach 0.97 as the foam begin to unstable.

Foam quality index is defined as :

$$\Gamma = \frac{V_g}{V_g + V_l} \quad (8)$$

The pressure ratio between bottom hole pressures to surface pressure should be maintained to keep the foam quality as desired.

$$\frac{P_{bh}}{P_s} = \frac{T_{bh}\Gamma_s(1-\Gamma_{bh})}{T_s\Gamma_{bh}(1-\Gamma_s)} \quad (9)$$

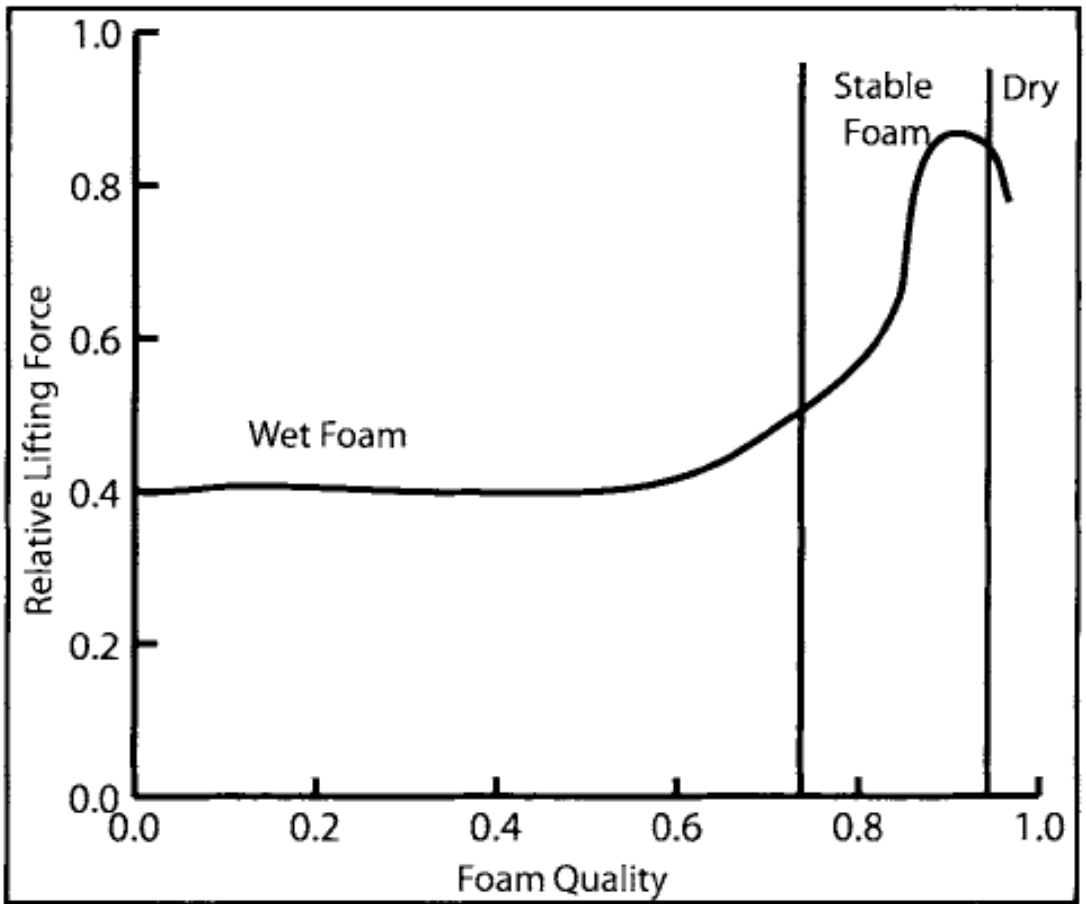


Figure 1: Foam lifting capacity curve from Bayer et al. (1972).

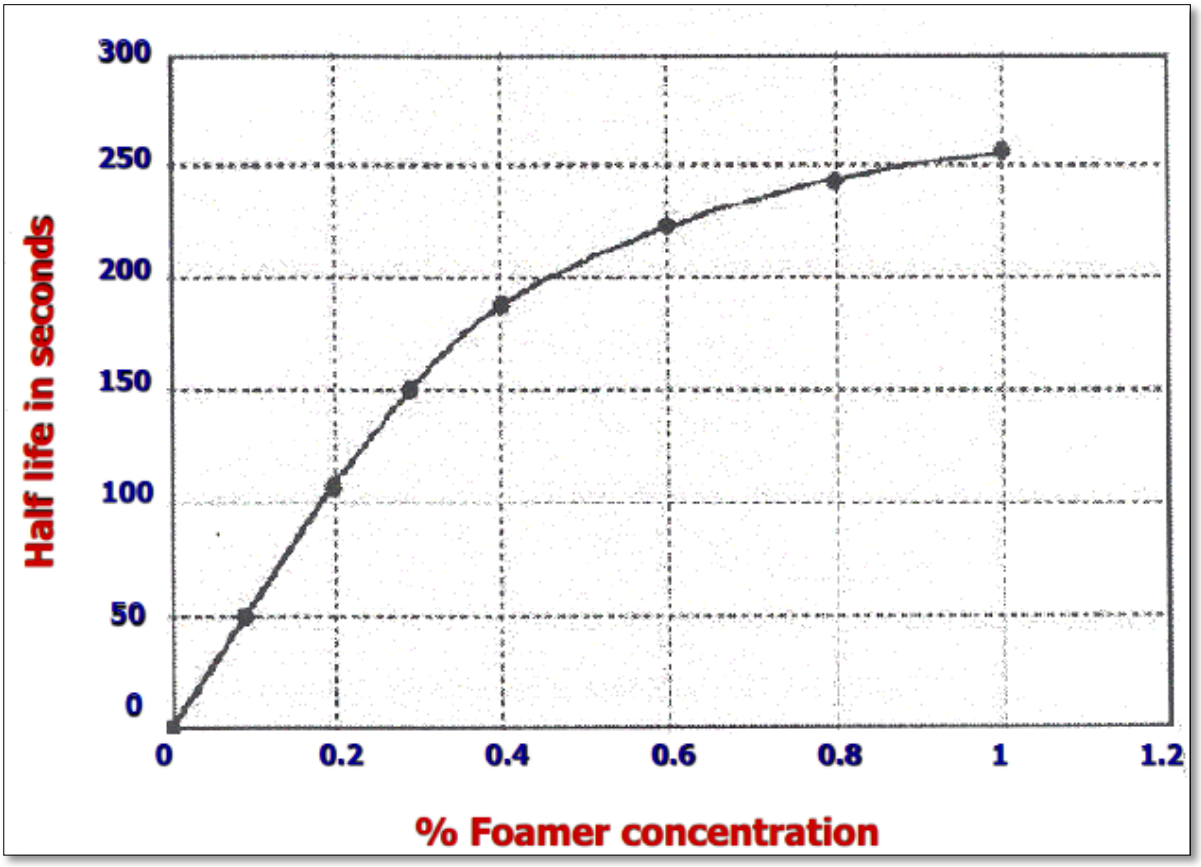


Figure 2: Half-life foam curve from Beyer et al. (1972).

Foamer

Foam is a low density system that has the advantage of having a high lifting and hole cleaning capacity that can be combined with a very low fluid flow. Foam operation has several advantages and common in underbalance drilling operations.

Main objectives when design foam operation are foam quality and stability. Half-life measures the persistence of the foam under athmospheric pressure. Higher value shows higher quality. Foam quality can be achieved with foamer additive. Figure 2 shows optimum foam quality can be achieved with 1 % foamer concentration. After reach optimum concentration, adding more foamer would not affect much on foam quality.

Special considerations should also be accounted when dealing with foam drilling, those are: motor operation, bottom hole temperature and presence of hydrocarbon.

Aerated Drilling Cutting transport

In aerated mud drilling, cuttings are large and move up the annulus at velocities significantly less than the in situ fluid velocity. Generally, flow of aerated water falls into a turbulent flow and flow in oil falls into a transitional regime between turbulent and laminar. It is safe to consider the flow as turbulent flow region. For turbulent flow (Re>2000) the cuttings terminal settling velocity can be estimated using the following equations.

$$v_{sl} = 5.35\sqrt{\frac{D_s(\rho_s - \rho_f)}{\rho_f}} \quad (10)$$

$$v_m = v_{sl} + v_{tr} \quad (11)$$

$$v_{tr} = \frac{\pi d_b^2}{4AC_p}\left(\frac{ROP}{3600}\right) \quad (12)$$

Borehole Pressure Criteria

Flowing bottom hole pressure is an important parameter in aerated drilling. Mixture of air and liquids are generating flowing bottom hole pressure while pressure drop occurs in the annulus. Liquids are combinations of drilling mud and any formation fluid presence.

The flowing borehole pressure can be formulated as follow:

$$\mathrm{dP} = \gamma_m\left(1 + \frac{fv^3}{2gD_h}\right)dh \quad (13)$$

Where

$$\gamma_m = \frac{A+B+C+D}{E[F+1]} \quad (14)$$

Where:

$$A = 9.45 \times 10^{-5} d_b^2 S_s R_p$$
$$B = 1.667 \times 10^{-2} W_m Q_m$$
$$C = 9.7327 \times 10^{-2} S_l Q_f$$
$$D = 1.275 \times 10^{-3} S_g Q_{go} P$$
$$E = 6.7846 \times 10^{-2} T Q_{go}$$
$$F = \frac{2.2283 \times 10^{-3} Q_m + 1.5597 \times 10^{-3} Q_f}{6.7846 \times 10^{-2} T Q_{go}} P$$

$$f = \left[\frac{1}{1.74 - 2log\left(\frac{2e}{d_H}\right)}\right]^2 \quad (15)$$

Liquid-Gas Rate Window

Guo et al., 2002 describe the liquid gas rate window (LGRW) as combinations of liquid flow rate that meets a certain requirements. The gas injection rate should be carefully designed, so the flowing bottom-hole pressure is less than formation pore pressure under drilling condition, and bottom hole pressure is greater than formation collapse pressure. In this paper, the formation collapse pressure is measured at the weakest point of open hole, which is pressure at the casing shoe. Other limits in designing liquid and gas rate include cutting-carrying capacity and wellbore washout or equipment limit.

The right boundary of LGRW is the curve of liquid gas rate combination that yield casing shoe pressure. This pressure should be maintained to be higher than formation collapse pressure. Since both liquid and gas should be constantly pumped into the well during drilling, this boundary counts the limit as circulating pressure. During circulation-break such as during connection, liquid and gas was replaced by high viscosity mud and original mud. Both has higher hydrostatic pressure relative to aerated drilling. Determining formation collapse pressure is complex tasks of geo-mechanics. This paper did not cover this task.

The left boundary of LGWR is determined by the curve of combination of liquid and gas rate that meets the requirements for an underbalanced condition. Both needs to be maintained below formation pressure at the bottom hole. The combination of liquid and gas rate that equal to formation pressure can be determined based on Guo's model. For the same mud rate, higher gas injection rate result in lower bottom hole pressure.

The lower boundary of LGRW can be determined based on carrying capacity of the fluid and gas mixture under bottom hole condition. This can be determined by plot the maximum allowable cutting diameter under certain mud flow rate and air injection rate.

Guo et al. (2003) determined the upper limit as a combination of liquid and gas rate that achieved wellbore washout pressure. The wellbore washout is not a common in geothermal formation. This paper will use equipment's technical limit as the upper limit of LGRW.

Mud Motor Operation

For operating with mud motor, we need to know equivalent flow rate for air injection under bottom hole conditions. Best estimation on two phase flow inside pipe are described as follow:

$$V_{eq} = \frac{\left(\frac{P_s}{P_{bh}}\right)\left(\frac{T_{bh}}{T_s}\right)Q_g + Q_m}{\frac{\pi}{4}D_h^2} \quad (16)$$

As a result of Pressure as function of depth, h. Velocity is also change with depth.

RESULT

Foam Drilling

In foam drilling, foam quality is the most important parameter. To achieve stable foam, foam quality should be maintaining between 0.65-0.97. Foam quality will change as temperature and pressure change. This simulation based on assumption that desired foam quality at the bottom of the hole is 0.65 and foam quality at the surface 0.97. Another parameter that related to foam quality is gas-liquid ratio (GLR). GLR should be maintain at calculated ranges to achieve desired foam quality at certain pressure and temperature. Figure 3shows required GLR vs actual GLR.

As shown in Figure 3. actual GLR are lower than required GLR. This means, foam are not in stable condition and has actual foam quality less than 0.65. Unstable foam quality will result in improper hole cleaning. One of the reasons of foam drilling is to ensure hole cleaning in underbraced condition. The liquid phase of foam in well C-1 is water. Without proper additives, water does not perform good quality hole cleaning.

Guo et al, (2002) describe that under surface conditions GLR should be maintain below 4.32 scfm/gpm. When required GLR for bottomhole condition is higher than 4.32 scfm/gpm, surface backpressure should be applied to the choke. Figure 4 shows required surface back pressure to maintain surface foam quality index above 0.97

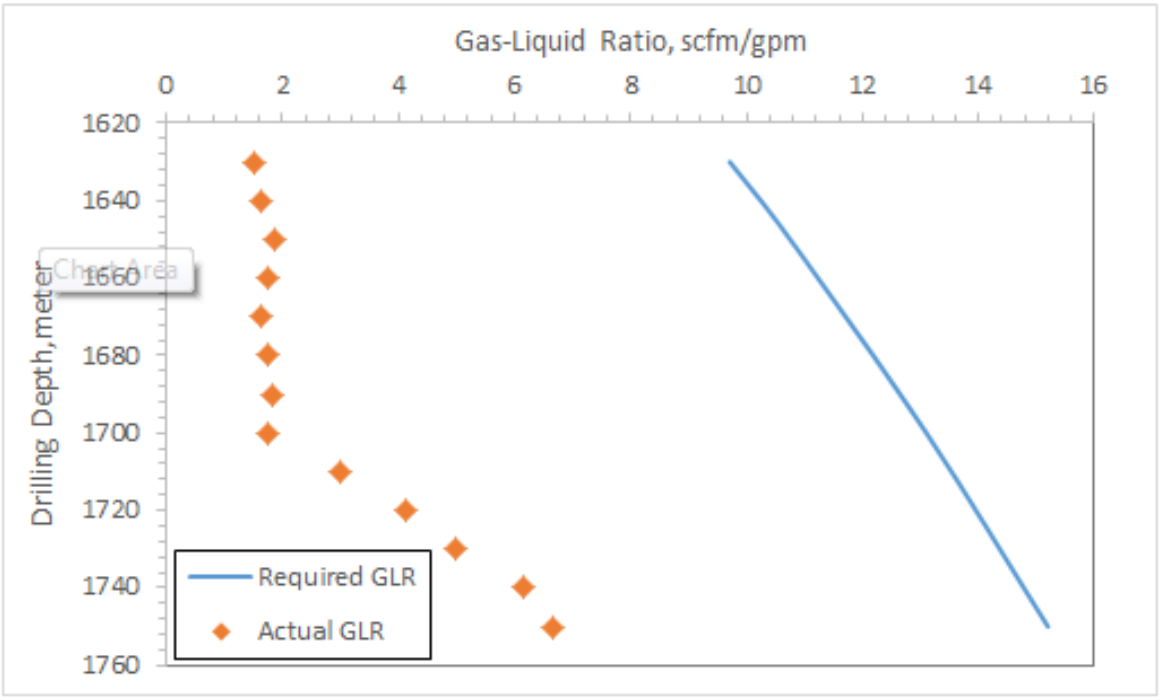


Figure 3: Required gas-liquid ratio vs actual gas-liquid ratio.

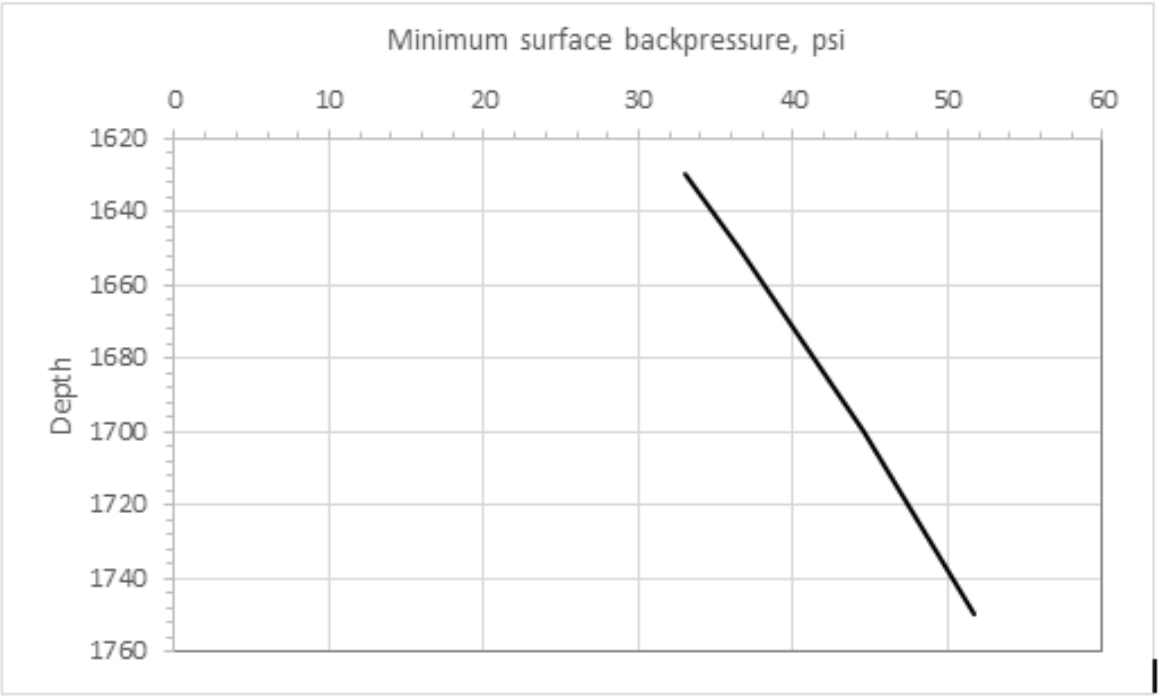


Figure 4: Minimum surface back pressure.

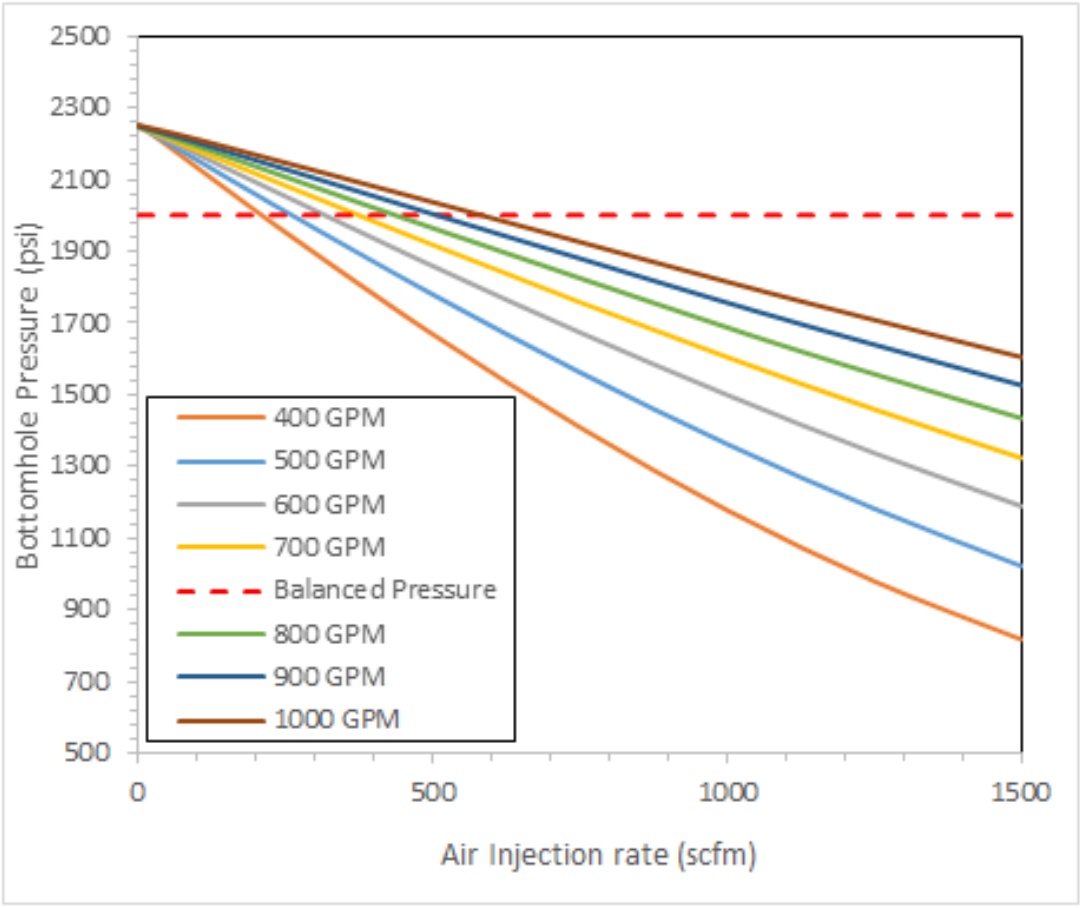


Figure 5: Flow rate combination that will yield balanced bottom hole pressure.

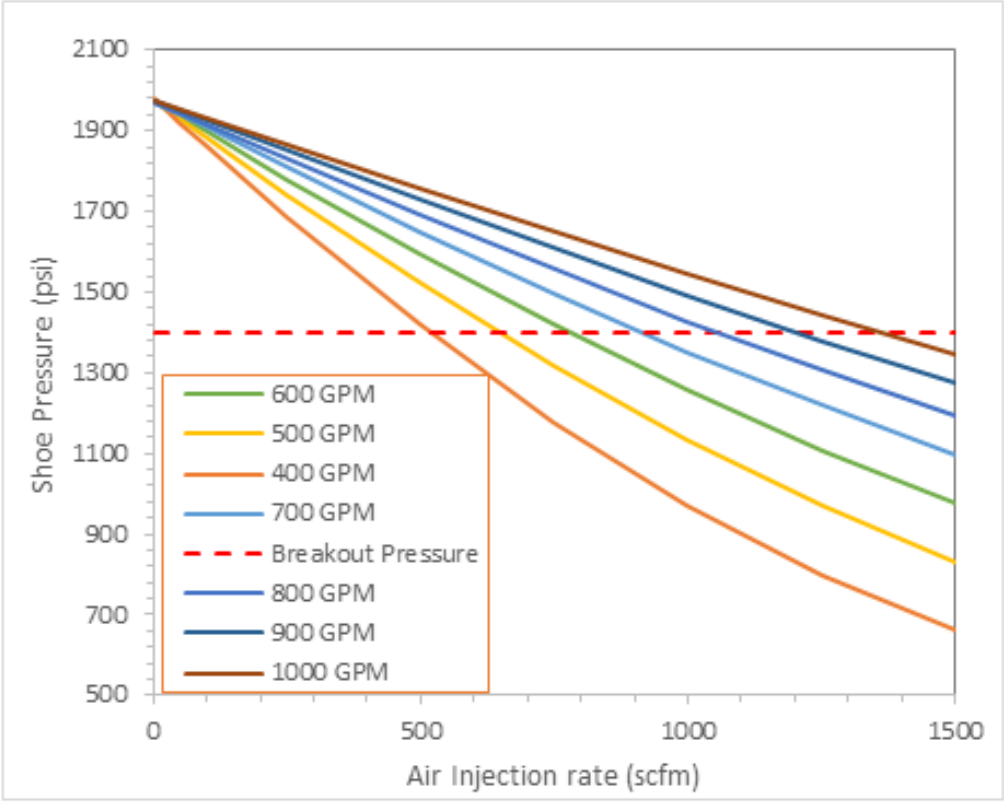


Figure 6: Flow rate combination that will yield to collapse pressure at casing shoe.

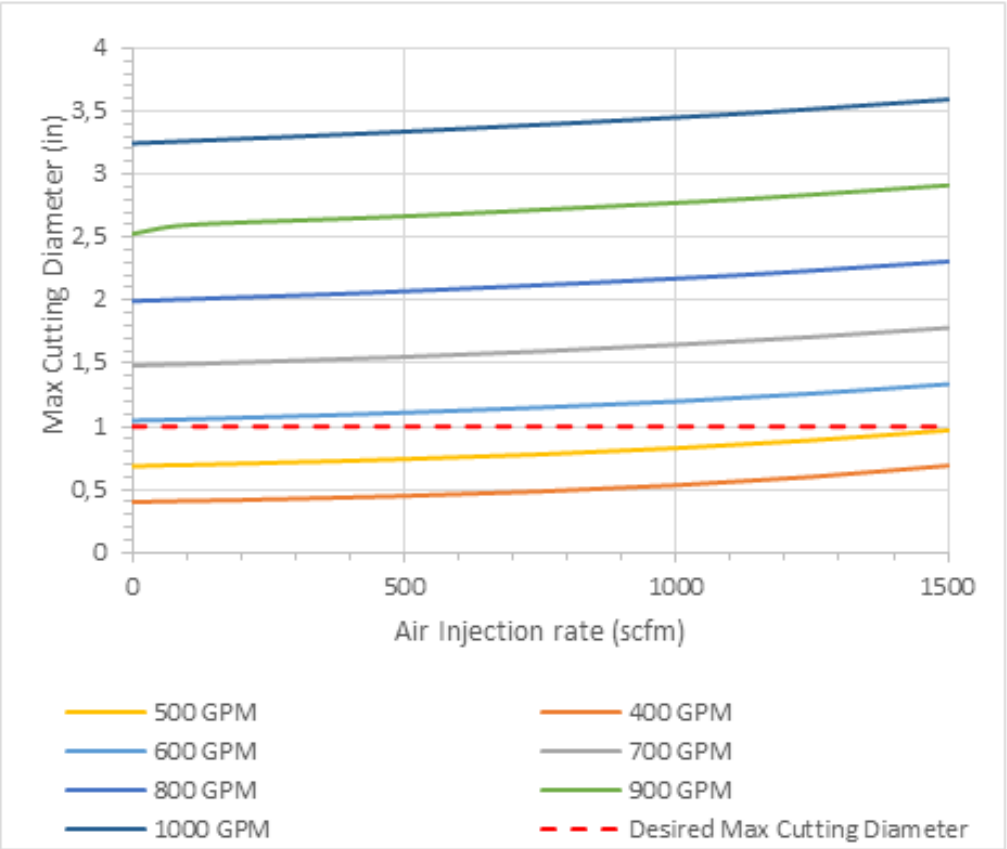


Figure 7: Maximum cutting diameter for combinations of air rate and mudflow.

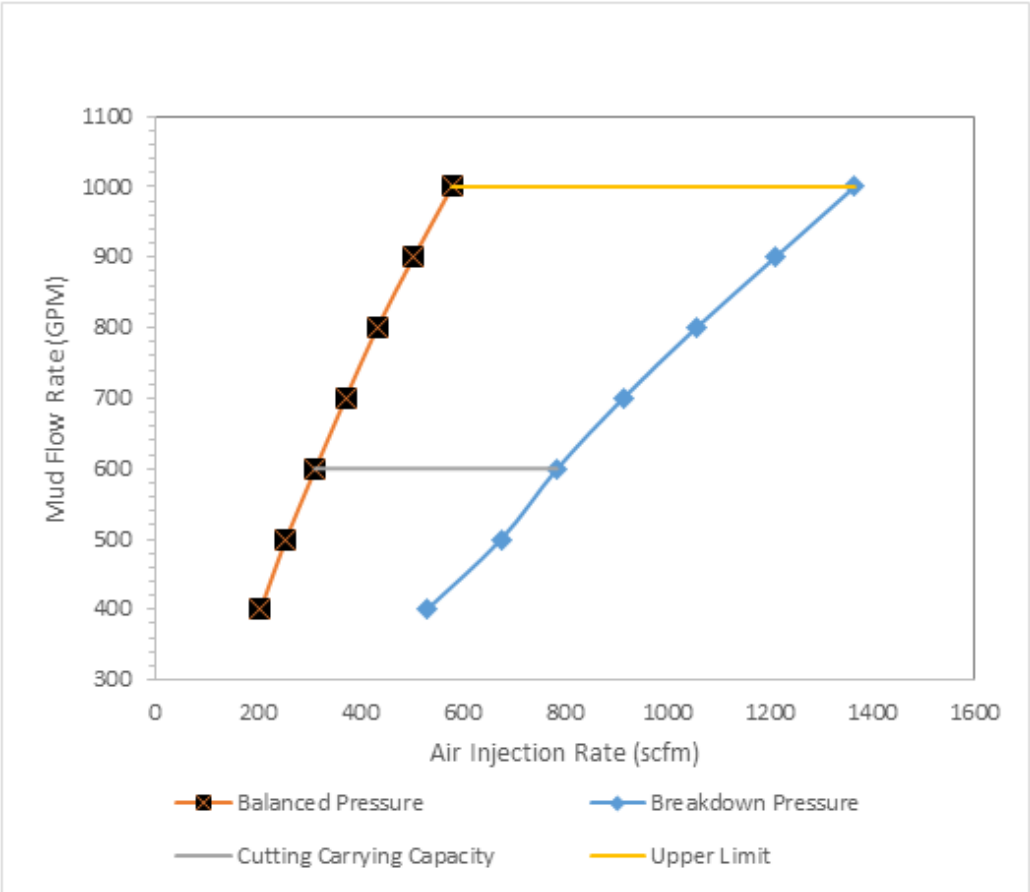


Figure 8: Final result of Liquid – Gas Rate Window.

The gas final result of gas-liquid volume requirements for well C-1 at depth of 1750 mMD, with several assumptions:

Γs : 0.97
Γbh : 0.65
v_f : 2.2 fps

Simulation results:

Q_{go} : 2567 scfm
Q_l : 161 gpm
GLR: 16 scfm/gpm
P_{bh} : 1223 psi

Based on simulations, actual gas and liquid injection rate in well C-1 is not adequate to form stable foam. This simulation is based on Guo's model for foam drilling.

Aerated Drilling

Figure 5 shows combination of air injection and mud rate that balance formation pressure (dashed line). Above the red line, bottomhole pressure will exceed formation pressure. Below the red line, bottomhole pressure will less than formation pressure. The latter is required condition in underbalanced drilling. The combinations then plotted in LGWR chart as left boundary.

Figure 6 shows combination of air injection and mud rate that balance formation collapse pressure at point below casing shoe. Above the red line, pressure at casing shoe will exceed required formation breakout pressure. Below the red line, borehole pressure at casing shoe will less than required formation collapse pressure. Pressure at casing shoe should be maintain above formation collapse pressure. The combinations then plotted in LGWR chart as right boundary.

Figure 7 shows maximum cutting diameter for different combinations of air rate and mud flow rate. The red dashed line is desired maximum cutting diameter (Dc: 1 inch). That value achieved at mud flow rate equals to 600 GPM. This mud flow rate is the bottom limit of LGRW.

Guo et al., 2002 described the upper limit of LGRW as wash out pressure. Since wash out pressure is not determined, this upper limit is determined by the maximum flow rate delivered by mud pump. This limit is equal to mechanical limit of mud pump. There are two National 9P-100 with maximum combined flow rate 1000 gpm.

Figure 8 shows final result of LGRW of Well X. This chart based on previous calculation and determination based on Guo's technique. This LGWR is based on assumption of formation pressure equals 2000 psi, formation collapse pressure 1400 psi and desired cutting diameter 1 inch. Actual combination of air and mud flow rate is inside the window. This means actual flow rate is adequate to overcome formation collapse pressure, to achieve underbalance conditions, adequate to lift 1-inch cuttings, and below maximum capacity of mud pump.

CONCLUSION

Combination of mud and air flow rate is an important parameter for aerated drilling. Operating envelopes needs to be designed prior to operation. In the case shown above, air and liquid flow rate combination in Well X is located inside the LGRW. Thus it is adequate based on Guo's criteria.

For foam drilling, GLR and surface back pressure are important parameters in operation. In the case shown above, GLR in well C-1 is below minimum requirements to form stable foam under bottom hole condition. Surface backpressures are needed to form stable foam in the surface condition.

REFERENCES

Guo B., Ghalambor A. (2002). "Gas Volume Requirements for Underbalanced Drilling-Deviated Holes", *Penn Well Corporation, Tulsa, Oklahoma.*

Guo B., Sun K., Ghalambor A. (2003). "A Closed Form Hydraulic Equation for Predicting Bottomhole Pressure in UBD with Foam", *Proceeding IADC/SPE Underbalanced Technology Conference, Houston, Texas.*

Bayer A.H., Millhone R.S., Foote R.W. (1972). "Flow behavior of Foam as Well Circulating Fluid", *SPE 3986*

NOMENCLATURE

g	Gravitational Acceleration (32,17 ft/sec^2)
d_c	Particle diameter, ft
C_d	Drag coeficient
ρ_c	Density of cutting, lbm/ft^3
ρ_f	Density of fluid, lbm/ft^3
P_s	Surface air pressure, psia
T_s	Surface Temperature, ^oF
G	Annular Temperature Gradient,^oF/100 ft
T	Downhole temperature, ^oF
h	Hole depth,ft
S	Gas Specific Gravity
Q	Gas flow rate, scf/m
ROP	Penetration rate, ft/m
D_h	Hole diameter, ft
D_p	Drill pipe diameter, ft
V_{si}	Slip velocity, ft/s
D_s	Cutting equivalent diameter, ft
ρ_s	Solid density, lb/ft^3
ρ_s	foam density,lb/ft^3
μ_e	effective velocity, lb/ ft s
V_g	gas volume, ft^3

V_l	liquid volume, ft^3
v_{sl}	slip velocity, ft/s (double, previously V_{si})
v_m	mixture velocity, ft/s
v_f	foam velocity, ft/s
v_{tr}	transport velocity, ft/s
d_b	bit diameter, ft
C_p	particle concentration, %
dP	borehole pressure, psi
γm	specific weight of mixture, lb/ft3
f	Moody's friction factor, dimensionless
v	fluid velocity, fps
dh	depth incremental, ft
g	gravity constant, 32.2
d_H	hydraulic diameter, in
db	bit diameter, in
Ss	specific gravity of cuttings relative to water
Wm	mud weight, ppg
Q_m	mud flow, gpm
Sl	specific gravity of mud relative to water
Qf	formation fluid influx rate, bbl/hr
Sg	specific gravity of gas relative to air
Q_g	gas flow rate, sfcm
Ql	liquid/water flow rate
T	average temperature, R
e	material roughness, in
P_{bh}	Bottomhole pressure, psi
P_s	Surface back pressure,psi
T_{bh}	Bottomhole temperature, ^oF
T_s	Surface temperature, ^oF
Γbh	Bottomhole foam quality
Γs	Surface foam quality
V_s	Mixture Velocity at surface, ft/s
V_{min}	Minimum Velocity to achieve Min KE, ft/s
V_{eq}	Equivalent Flow Rate, gpm
GLR	Gas Liquid Ratio
LGRW	Liquid Gas Rate Window

HYBRID DRILL BIT TECHNOLOGY, IMPROVED ROP, DRILLED INTERVAL AND CONTRIBUTED TO 96 HOURS CUMULATIVE SAVING IN ONE GEOTHERMAL WELL IN SOUTH SUMATERA OPERATION

Mohammad Khairanto Nugroho and Son N. Pham

Baker Hughes, a GE Company (BHGE)
Email: Mohammad.KhairantoNugroho@bakerhughes.com,
Son.Pham2@bakerhughes.com

ABSTRACT

Geothermal drilling through long directional intervals of volcanic formations is a challenging operation. Tungsten carbide insert (TCI) Roller-Cone was commonly used in this application, resulting in multiple trips to complete the well. The hybrid bit design, once applied in this high cost and challenging drilling operation, has drilled the section consistently with one bit, improved rate of penetration (ROP), and delivered significant cost savings from reduced hours of drilling time.

The hybrid drill bit, combining roller cone and fixed cutter elements, synergizes the best attributes of both bit types. The combination of the smooth, low torque crushing-action from the rolling cones and the aggressive shearing action of PDC offers the most suitable cutting mechanism for the challenging geothermal application.

A geothermal operator in Sumatera applied the hybrid bit technology in three consecutive hole section of $17^1/_2$-in., $12^1/_4$-in., and $9^7/_8$-in. Outstanding performance improvements in all whole sections were achieved when the hybrid bits consistently delivered significantly longer drilled intervals and higher on-bottom ROP than the offset. Consequently, 96 hours of operation time was saved by employment of the hybrid drill bit technology.

In this paper, the author presents the development of the hybrid bit technology, the results of laboratory tests in company testing facility and the application results in $17^1/_2$-in., $12^1/_4$-in., and $9^7/_8$-in. hole sections. The performance indicators used in the paper are drilled interval, ROP, and day-vs-depth chart comparing plan to actual drilling results. Day-vs-depth chart used for the comparison has been normalized due to the actual well was drilled deeper than the plan.

Keywords: Drill bit, hybrid, geothermal

INTRODUCTION

A client in south Sumatera has a challenging geothermal application requiring the drilling of a long, deviated wellbore through volcanic formation (see Figure 1). Tungsten carbide insert (TCI) Roller-Cone bit commonly used in this application result in multiple trips to complete the well. The hybrid bit design, once applied in this high cost and challenging drilling operation, has drilled the section consistently with one bit, at an improved rate of penetration (ROP), thus delivering significant cost savings from the reduced hours of drilling time.

HYBRID DRILL BIT DESIGN

TCI which implements a crushing rock failure mechanism are commonly used in geothermal drilling for its low and smooth torque. However, they penetrate the rock slowly due to low aggressiveness, and consequently drill short intervals due to bearing revolution limits. In contrast, a PDC bit, has an aggressive shearing cutting mechanism which allows higher ROP. However, this high aggressiveness can lead to unstable tool face and higher torsional vibration causing operational challenges. Additionally, even minor cutter damage can drastically reduce the efficiency of PDC bits in hard rock environments.

The hybrid drill bit design combining roller cone and fixed cutter elements, not only benefits from both types, but also synergizes their best attributes (see Figure 2).

As stated by Pessier et al. (2010) with the combination of the intermittent crushing of roller cones and continuous shearing and scraping of PDC blades as illustrated in Figure 3, the hybrid drill bit delivers several benefits in challenging applications including but not limited to:

1) Low ROP applications with TCI, 2) torque or weight-on-bit limited applications with large diameter PDC or TCI, 3) applications with high torque fluctuation causing premature bit and bottom hole assembly failure, 4) directional applications with adjustable-kick-off motors facing limited drilling parameters, poor tool face control and/or low steerability.

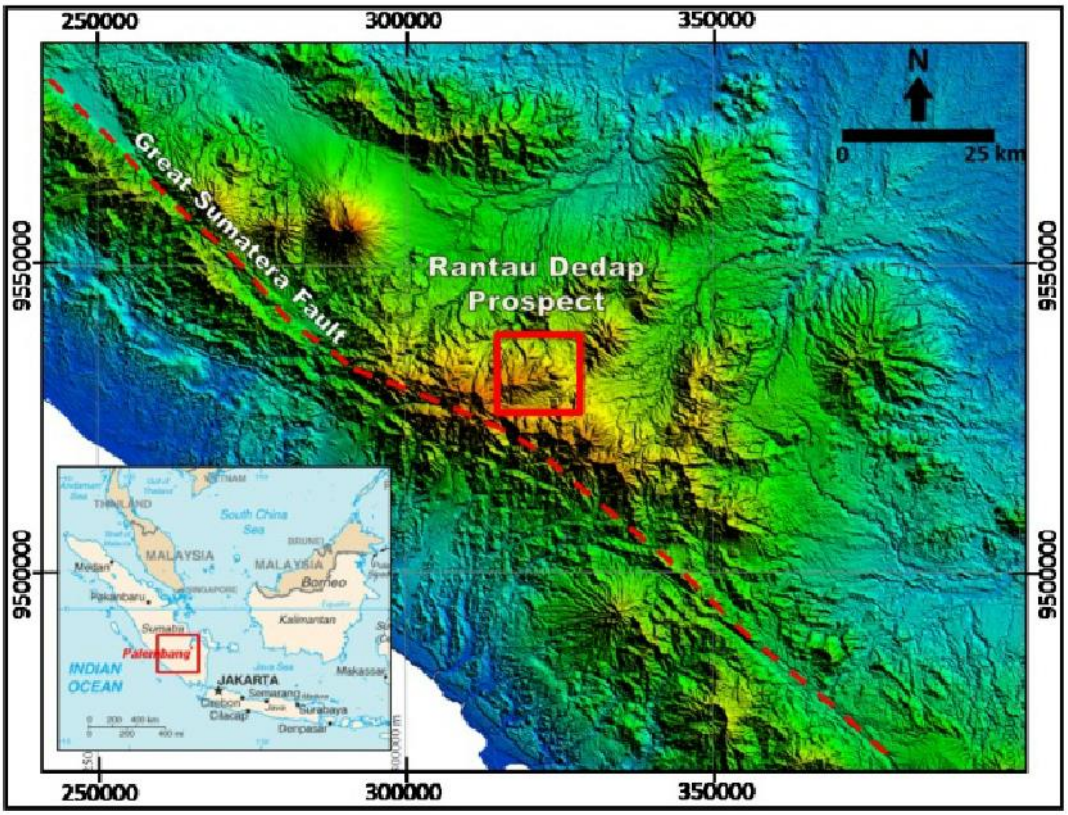


Figure 1: Geothermal field, where the Hybrid bit was utilized.



Figure 2: Top view of one example hybrid drill bit design.

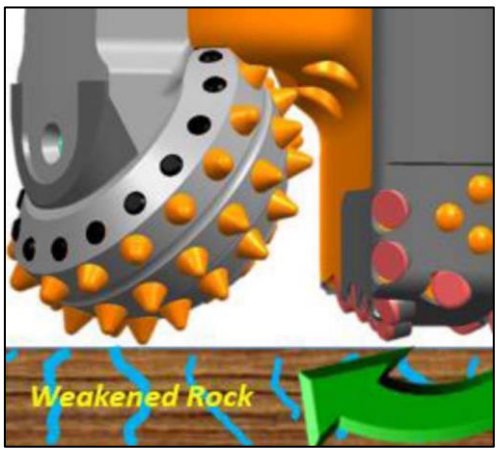


Figure 3: Hybrid drill bit cutting action illustration.

HYBRID DRILL BIT DEVELOPMENT

The first generation of modern hybrid drill bits was introduced to the industry in 2012. Ongoing development since that time has led to continuous improvement of the core hybrid bit technologies.

One of these evolutions, in 2016, changed how the roller cones were designed. Insert density and sharpness of both inner and outer rows were increased to provoke networks of connected mini-fractures, which increase the efficiency and stability of the bit significantly. The advances of carbide grades and PDC technology in terms of both materials and geometry also contributed significantly to the success of this generation in several applications, especially in extreme applications with high vibrations and hard and abrasive formations. The evolution of cone designs in 17-1/2in. hybrid bits were demonstrated in Figure 4 as an example.

The latest generation, introduced in 2018, built off the success from the cone designs with optimized diamond coverage, especially in the critical shoulder and gauge areas. Higher blade counts and novel placement of key cutters in the shoulder of the bit are two examples. These changes allowed increased bit life and provided consistently higher ROP and enabled reaching planned TD in one run.

Figure 5 is the summary of the hybrid bit evolution since its introduction in 2012.

LABORATORY TEST

The efficiency of hybrid bits in hard formations was demonstrated through a laboratory test. The test was conducted in a layered core (see Figure 6) under confining pressure to evaluate performance of different bit types through interbedded formations. The rock included layers of three rock types, Carthage Marble with 15,000 psi unconfined compressive strength (UCS), Jasper Quartzite with 36,000 psi UCS, and Gabbro with 49,000psi UCS. The tests were conducted under 4,000psi bottom hole pressure.

As expected, the TCI bit delivered the lowest ROP in all rock types (Figure 7). PDC showed an ROP advantage in the softest Carthage formation, but its ROP was significantly reduced in harder rocks of Jasper Quartzite and Gabbro. The hybrid bit, despite similar torques, delivered slightly higher ROP than PDC in Carthage due to its higher efficiency. The higher ROP of the hybrid bit compared with other two bits became more significant in the harder rock, which was the result from the more suitable cutting mechanism of the hybrid technology.

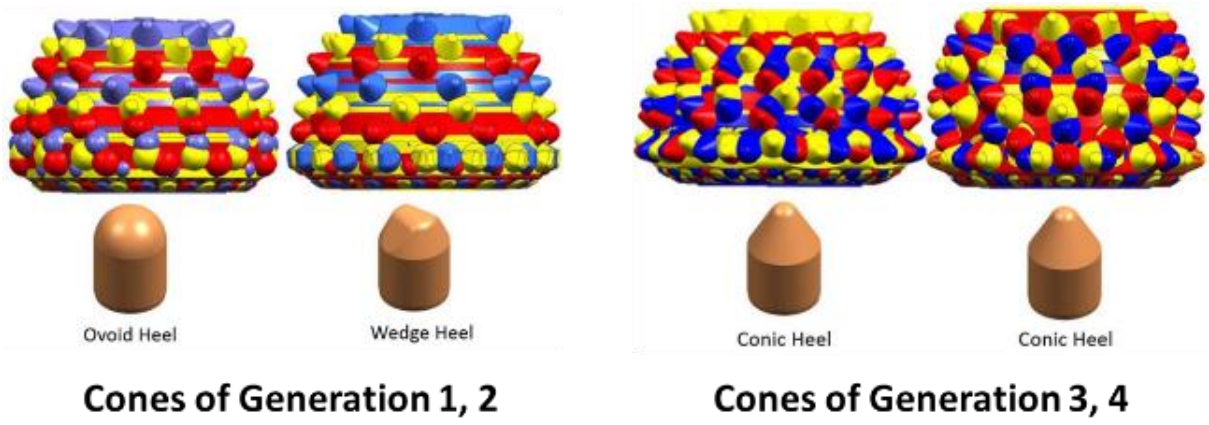


Figure 4: Hybrid bit's cone design evolution.

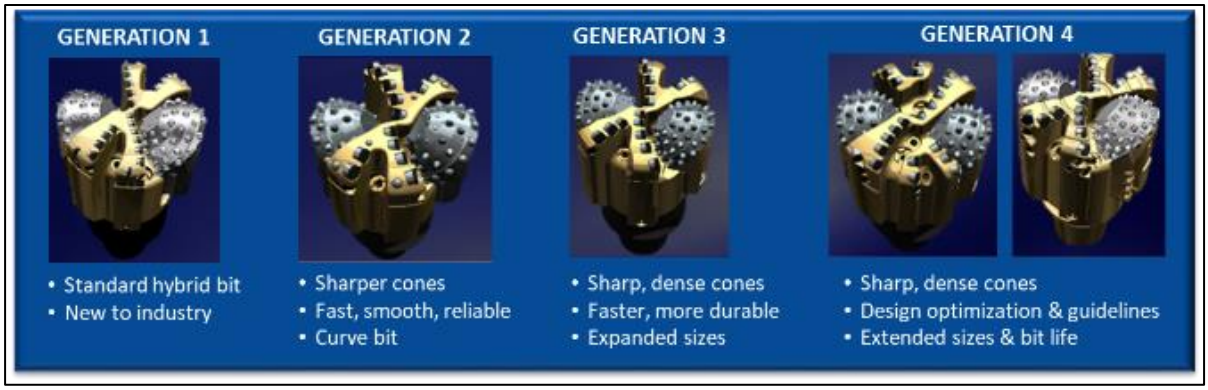


Figure 5: The hybrid drill bit evolution.

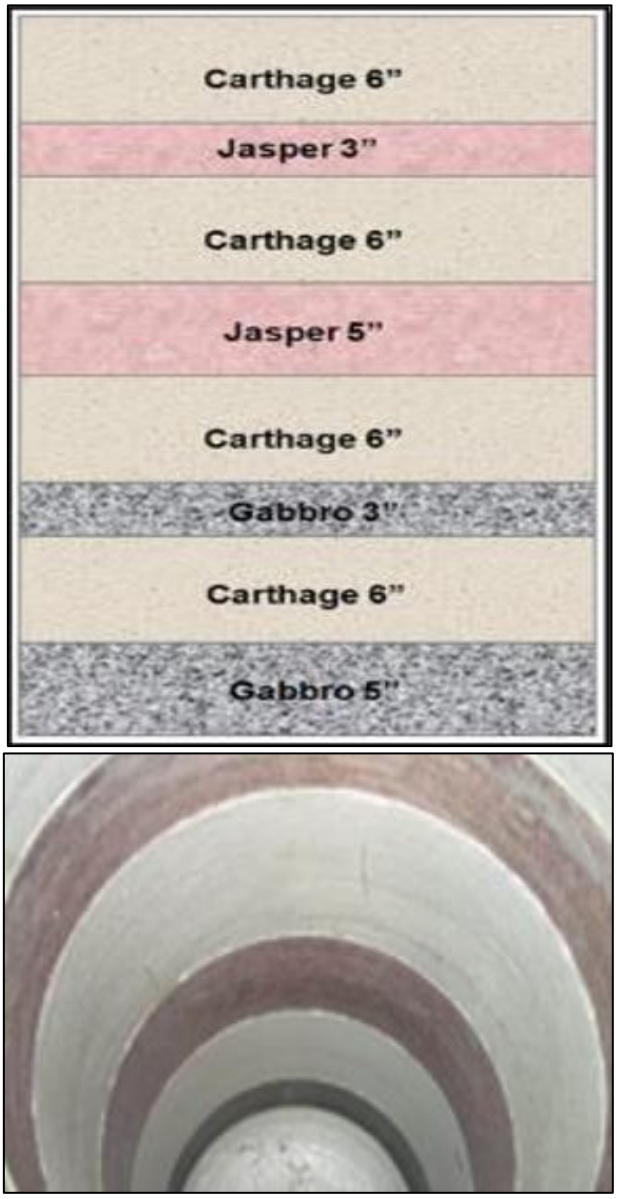


Figure 6: Rock-layered configuration for laboratorial test.

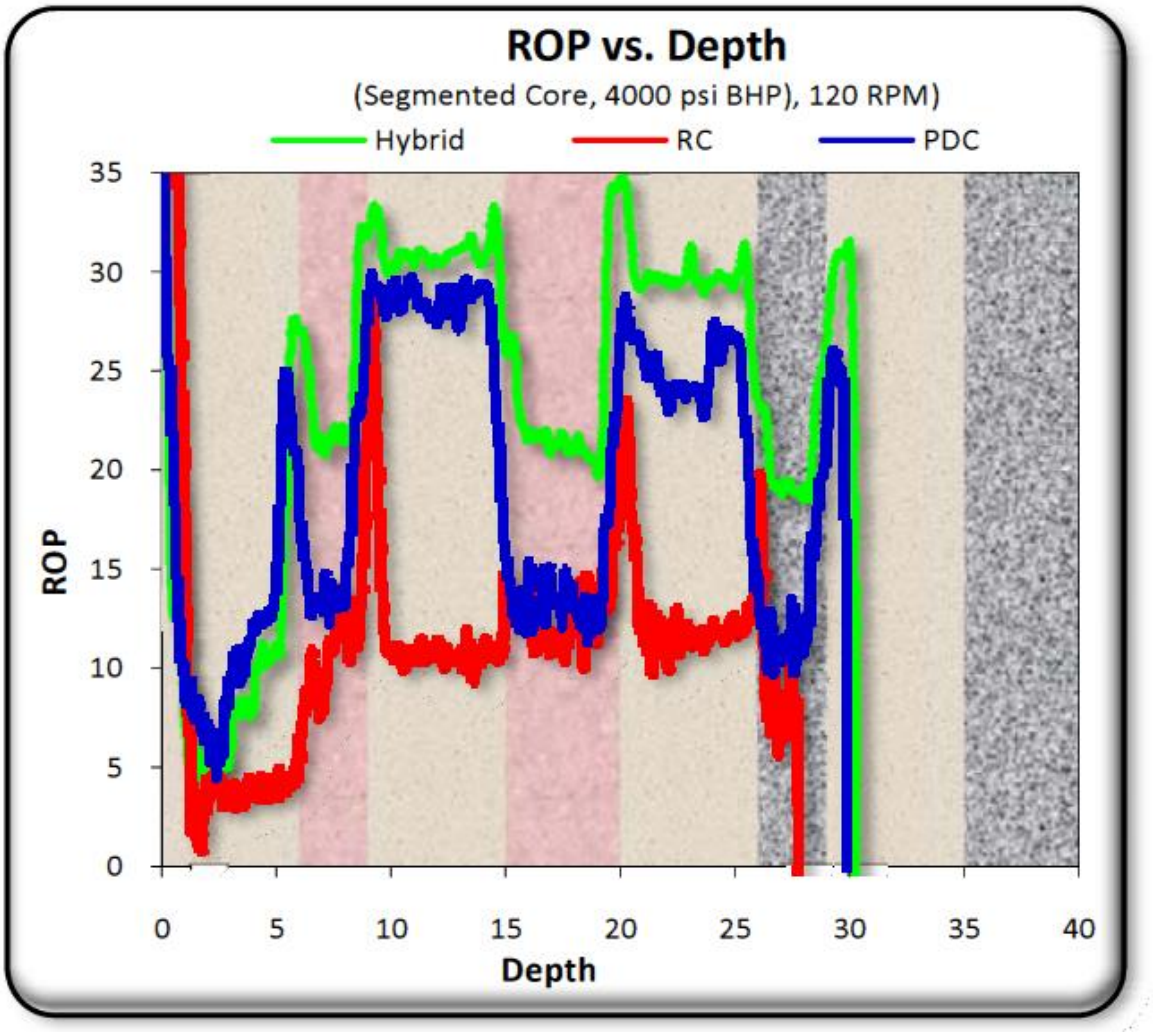


Figure 7: ROP result of different bits.

Figure 8 illustrates the torque results. The PDC experienced very high torque fluctuation when drilling through different rock types, which could cause all types of vibration-related issues including high torsional vibration, poor tool face control and bit whirl. In contrast, the hybrid bit was able to achieve very low torque oscillations, 50-60% lower than PDC. This would result in lower stick-slip at low rpm and reduce the risk of whirl at high rpm.
The torque signatures of these bits are further demonstrated in Figure 9 to reveal their impact on tool face control. In the same range of applied WOB, the hybrid bit generates less torque variation than standard PDC and PDC with depth of cut control (DOCC) feature, thus delivers better tool face control.

APPLICATION

A geothermal operator in south Sumatera applied the hybrid bit technology in three consecutive hole sections of $17^1/_2$-in., $12^1/_4$-in., and $9^7/_8$-in. in Well-7.

The 17-1/2-in. hole section was drilled with a three cone, six bladed hybrid bit with a mud-motor from 400 m measured depth (MD) to 1,228 m MD. The objective of this section was to drill volcanic rocks, maintain a vertical well profile and reach TD in 1 run.

Despite the hard and abrasive formation during drilling, the bit achieved the drilling objective by completed the section with one bit run with 828 meters drilled interval and 9.94 m/hr on-bottom ROP. Compared with the average performance of offset wells in the same field which usually required 1 - 2 bit runs with TCI, the hybrid bit drilled 61% faster and 89% longer. That comparison was plotted in Figure 10.

Compared with the normalized drilling plan for 17-1/2-in. hole section of 140.5 hours, the actual result with the hybrid bit of 111.5 hours, contributed to 29 hours saved drilling time operation for this section.

Figure 11 are pictures of the hybrid bit before and after the run.

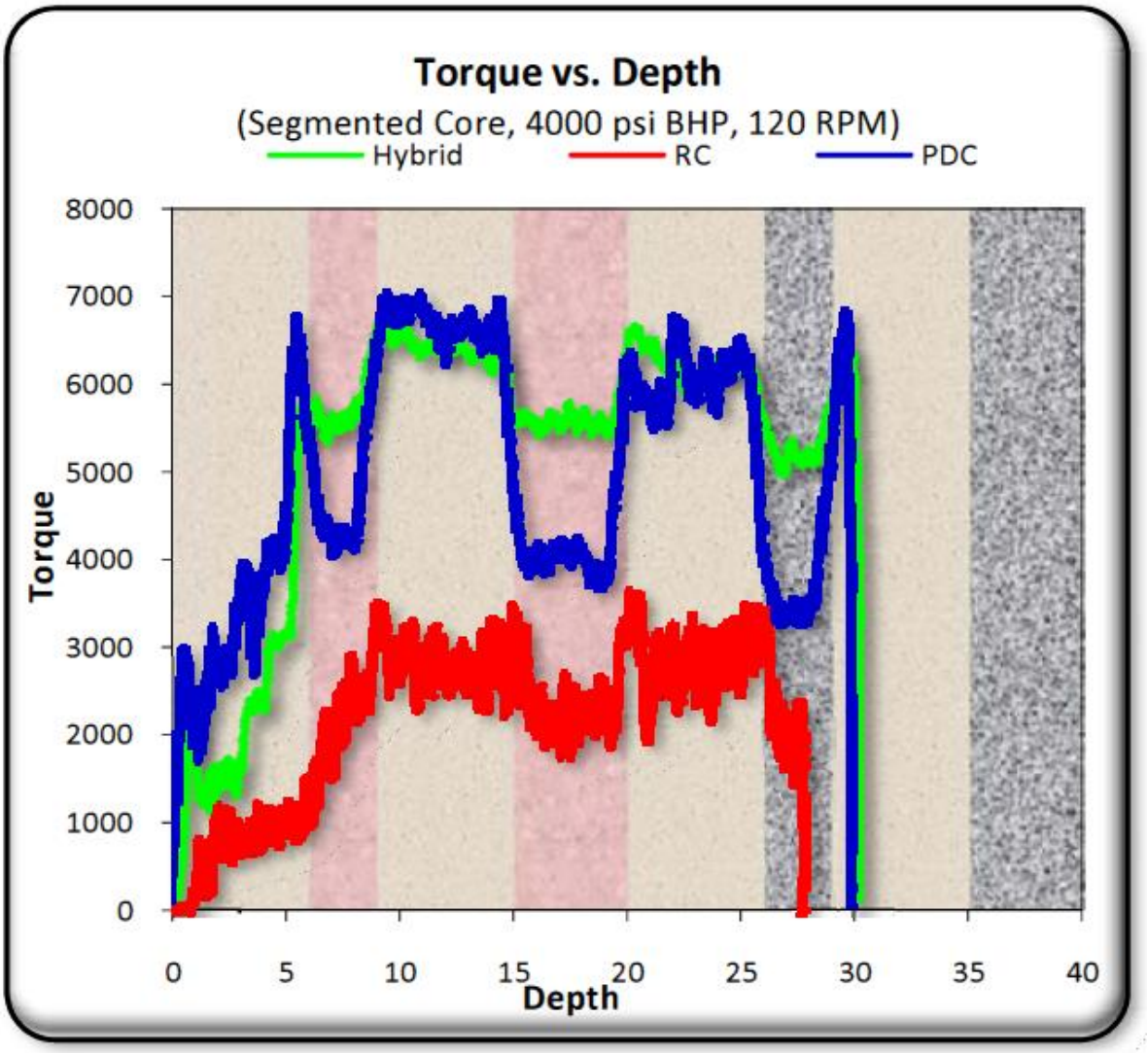


Figure 8: Torque result of different bits.

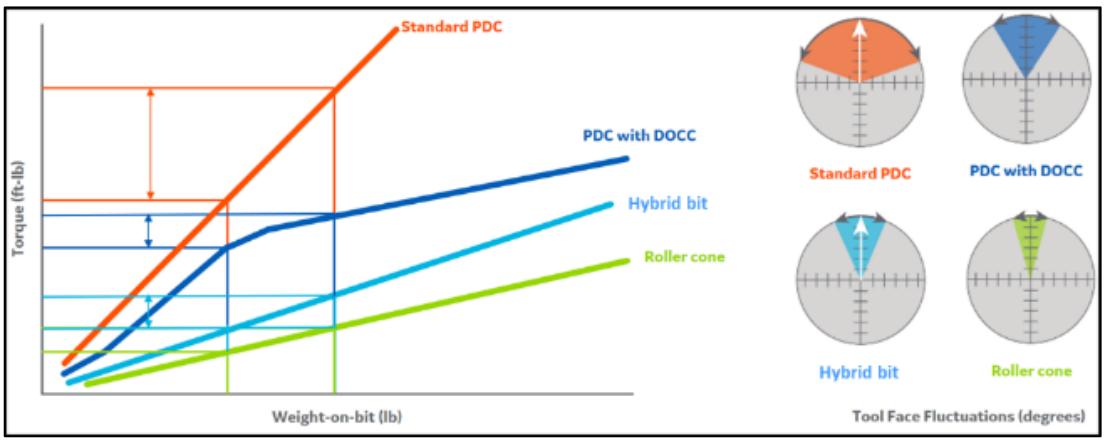


Figure 9: WOB vs Torque chart comparison for TCI, standard PDC, PDC with Depth-of-Cut Control (DOCC), and hybrid bit.

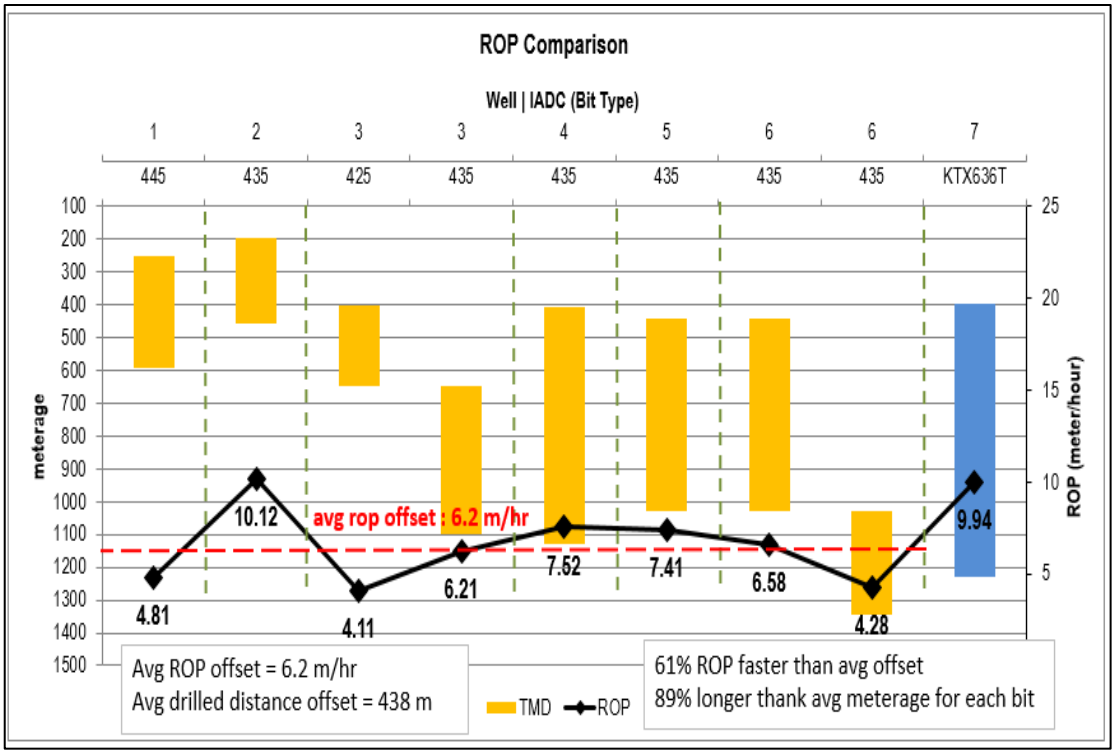


Figure 10: Comparison between 17-1/2-in. hybrid bit and offset wells.

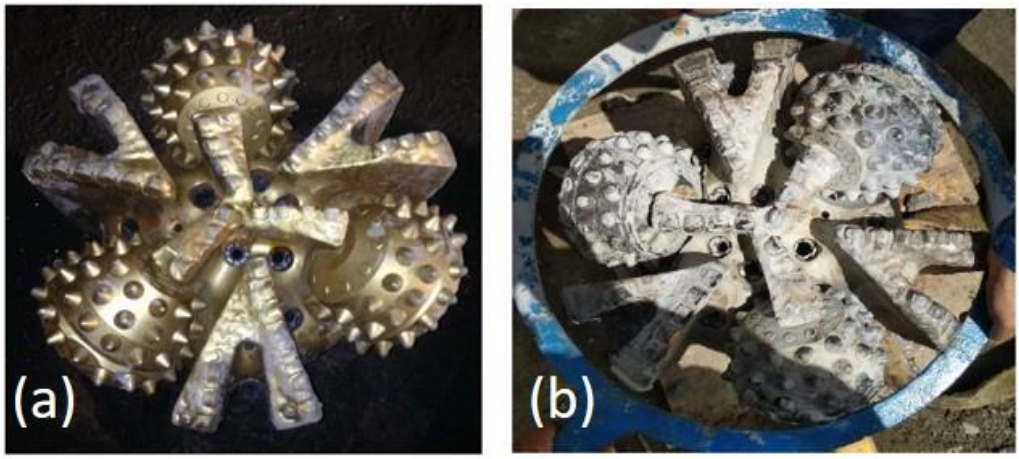


Figure 11: 17-1/2-in. hybrid bit (a) before run, (b) after run.

The 1,500 m-long 12-1/4-in. hole section was planned directionally with a mud motor through thick, hard and abrasive granodiorite formation. In this type of application, TCI bits usually have very low ROP. The section was drilled with 5 bits including 3 hybrid bits, 1 PDC bit, and 1 TCI bit with 647 IADC.

The hybrid bits applied in three intervals of this 12-1/4-in. hole section: The first one was drilled from 1228 m-MD to 1900 m-MD. The second interval was drilled from 2199-m-MD to 2393 m-MD. The last interval was drilled from 2393 m-MD to TD section at 2756 m-MD. The drilling plan for 12-1/4-in hole section in the first, second, and third intervals were 142.5 hours, 41.1 hours, and 77 hours. The actual result with hybrid bits for these intervals were 81.5 hours, 48 hours, and 66.5 hours. For the first and third intervals, 61.1 hours and 10.5 hours drilling operation time were saved. For the second interval, took 6.9 hours longer of drilling operation time compared to the plan. In overall, the hybrid bits used in this section still contributed to 64.6 hours saved operation time.

In term of performance, the hybrid bits used in this section outperformed offset bits, with an average on-bottom ROP of 12.21 m/hr and 410 meters average drilled interval, which is 67% higher and 13% longer than the average on-bottom ROP and drilled interval

of offset performance in this hole section. That comparison can be found in Figure 12 below.

The pictures of a three bladed, three cone hybrid bit and a two cone four blade hybrid deployed in this section can be found below in Figure 13.

The reservoir 9-7/8-in. tangent hole section was to be drilled with a mud motor through thick granodiorite with a deeper measured depth compared to the offset well. The two cone, five blade hybrids with extended cone design was used. This bit was specifically designed for extremely hard and abrasive formations. Unlike other hybrid designs, one cone was extended to the center of the bit, providing crushing and shearing across the full bit diameter, thus increasing the durability and efficiency of the hybrid bit significantly in the extremely hard and abrasive formation. The first run of this new hybrid bit was conservative to understand the bit life and performance; thus the bit was pulled out early to inspect the bit condition. Once on surface, the hybrid bit was found to be in green dull condition, with very light wear or damage. The second hybrid was then run in hole, drilled to section TD and pulled out of hole with a green dull condition.

As Figure 14 shows, the hybrid bits performed well, particularly considering the deeper depths in which they were used. Their average ROP of 10.4 m/h and drilled interval of 222m were 22% higher and 15% longer than those of the offset. Another highlight was the green dull condition of the hybrid bits in (Figure 15) indicated that higher ROP and longer drilled interval could be achieved.

The drilling plan for 9-7/8-in. hole section was 89 hours with 444 meter drilled interval, start from 2756 m-MD to TD well at 3200 m-MD. Compared with the normalized drilling plan for 9-7/8-in. hole section of 89 hours, the actual result with the hybrid bits of 86.5 hours, contributed to 2.5 hours saved operation time.

CONCLUSION

Outstanding performance improvements in all hole sections were achieved when the hybrid bits consistently delivered significantly longer drilling intervals and higher on-bottom penetration rates than the offsets. As a result, drilling operation time saved for the 17-1/2-in., 12-1/4-in., and 9-7/8-in. were 29 hours, 64.6 hours and 2.5 hours.

In summary, the operator and all contractors have successfully performed and worked as an excellent team during the operation. As a result, the overall operation completed earlier than the plan, 159.2 hours was saved. Employment of the hybrid drill bit technology contributed to 96 hours of 159 hours saving in cumulative of drilling operation time for the operator (Figure 16).

After this well, the hybrid technology was also applied in the top hole 26-in. section and delivered outstanding performance. For 9-7/8-in bits used in this well with green dull condition as mentioned before, was applied to drill in other wells and also delivered outstanding performance.

Bit performance and dull conditions are reviewed regularly for continuous optimization with advancement in technologies including PDC cutters, carbide grades, bearing design, PDC cutter layouts and cone designs. Consequently, more consistent performance improvements have been recorded.

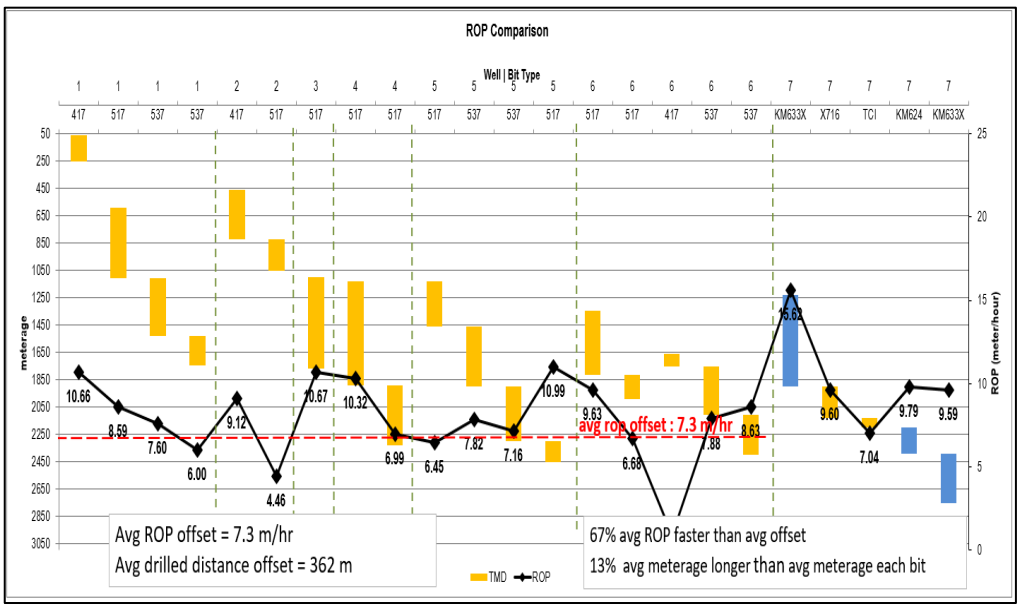


Figure 12: Performance comparison of hybrid bit and Offset in the 12-1/4in section.

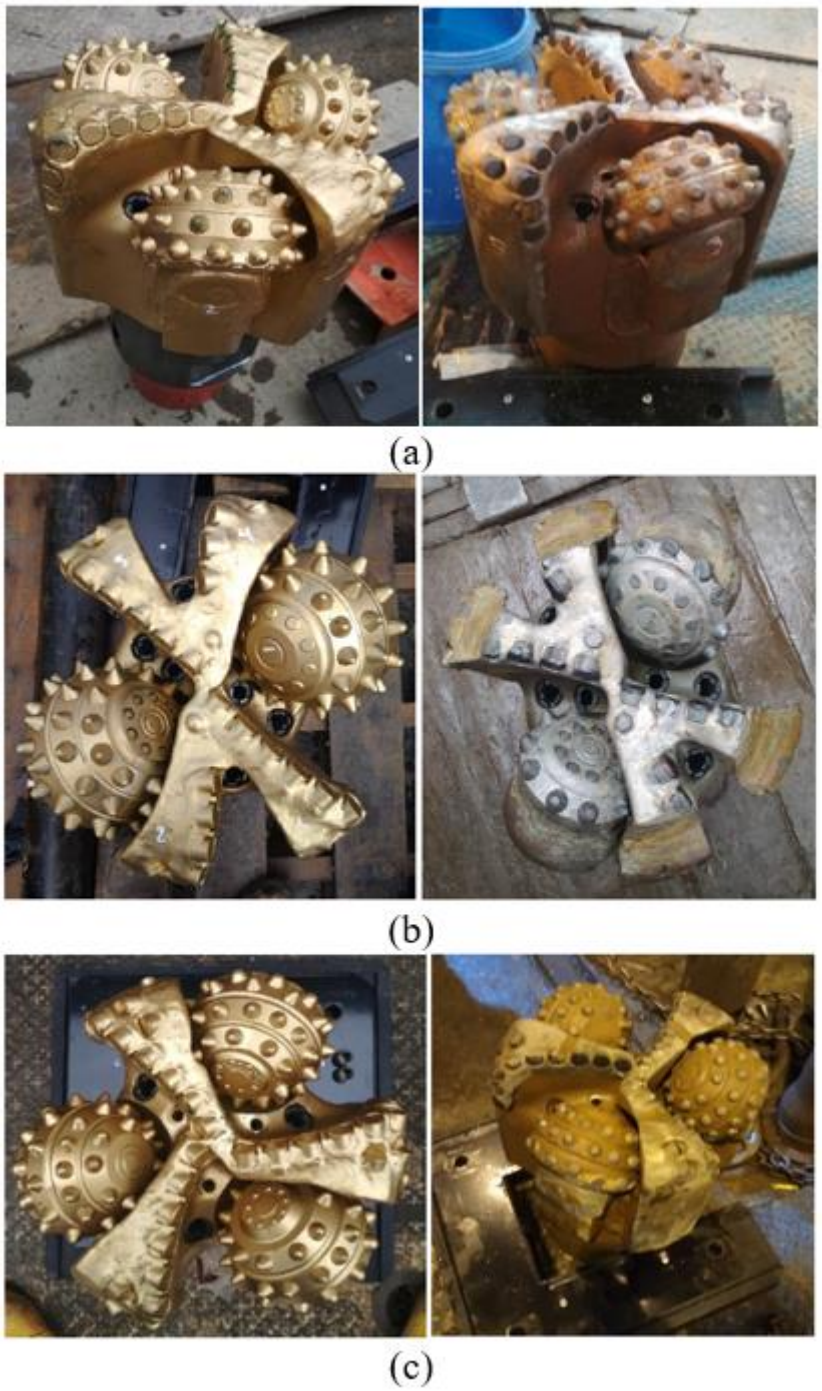


Figure 13: 12-1/4-in. hybrid bits before (left) and after (right) run: (a) three cone-three blade (b) two cone-four blade, (c) three cone-three blade.

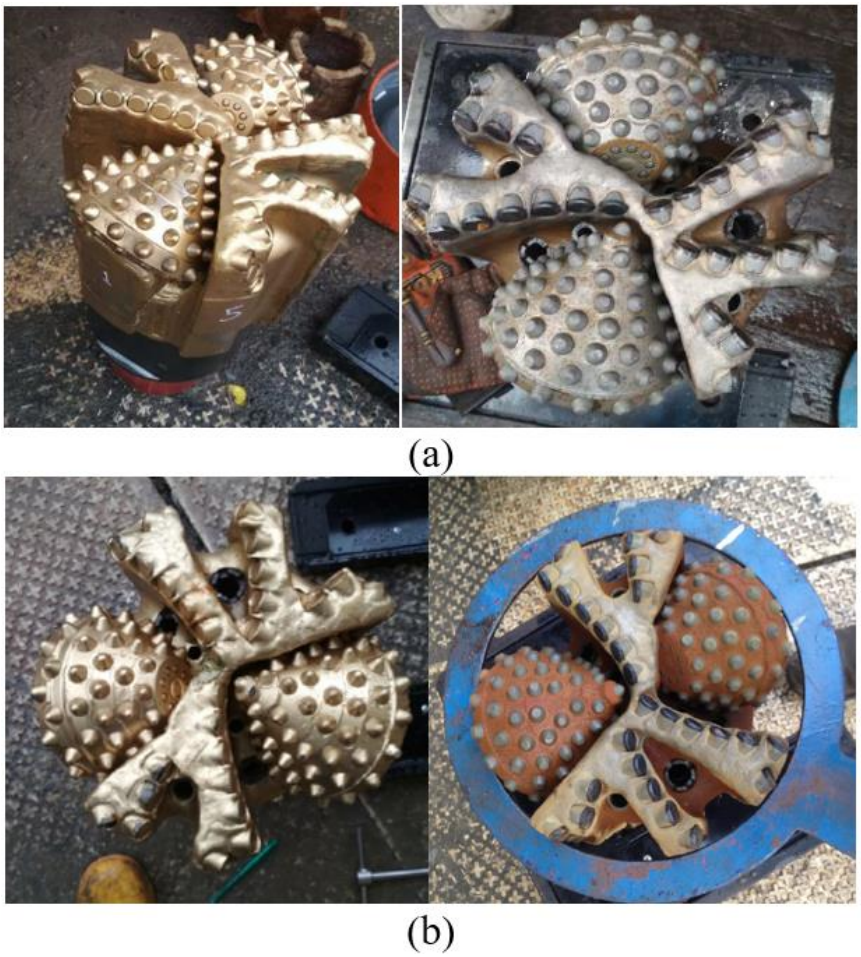


Figure 15: 9-7/8-in. hybrid bits before (left) and after (right) run: (a) first run, (b) second run.

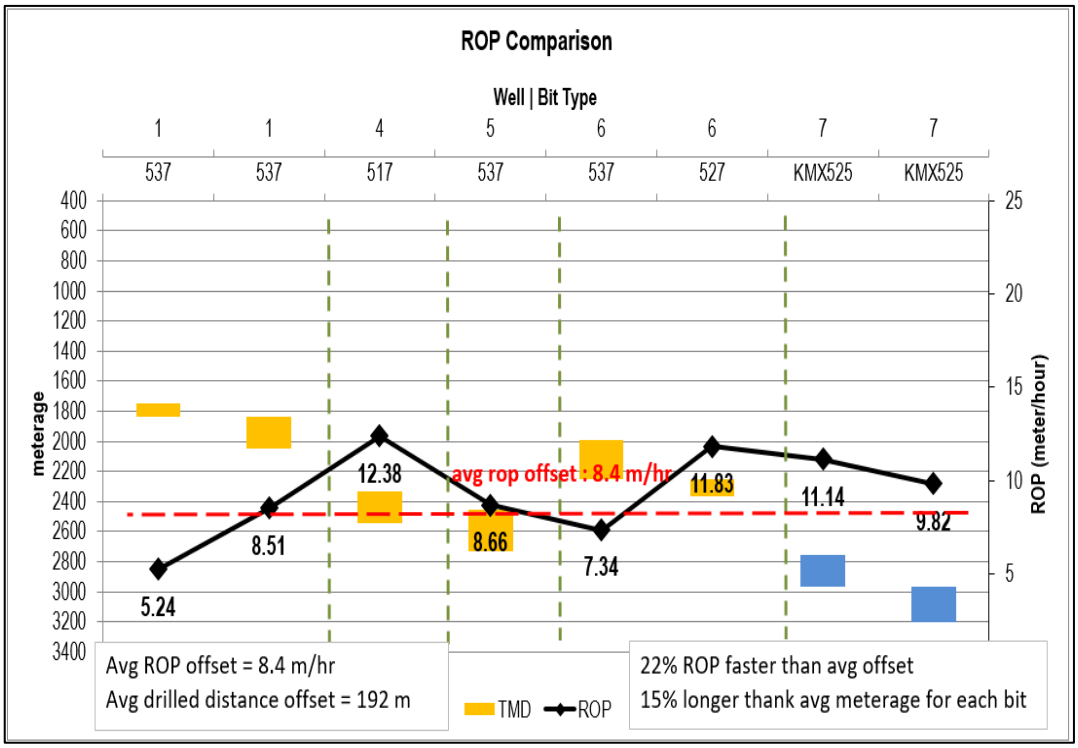


Figure 14: Performance comparison of 9-7/8-in. hybrid bit and offset.

ACKNOWLEDGEMENT

The authors wish to express gratitude to Supreme Energy and Baker Hughes, a GE company for permission to release the field performance, data validation, and bit development process outlined in this paper.

NOMENCLATURE

PDC – Polycrystalline Diamond Compact
ROP – Rate of Penetration
RPM – Rotation per Minute
TCI – Tungsten Carbide Insert
UCS – Unconfined Compressive Strength
WOB – Weight on Bit
DOCC – Depth of Cut Control
MD – Measured Depth

REFERENCES

Pessier, R and Damschen, M. (2010). "Hybrid Bits Offer Advantages in Selected Roller Cone and PDC Bit Applications." Paper SPE 128741 presented at the SPE/IADC Drilling Conference and Exhibition, New Orleans, Louisiana, USA 2-4 February.

Thomson, I; Krasuk, R; Silva, N; and Romero, K. (2011). "Hybrid Drill Bit Improves Drilling Performance in Heterogeneous Formations in Brazil". Paper SPE 143686 presented at the Brazil Offshore Conference and Exhibition, Macae, Brazil, 14-17 June.

Di Pasquale, M; Calvaresi, E; and Pecantet, S. (2013). "A Breakthrough Performance for an Inland Application with a Hybrid Bit Technology". Paper SPE 163436 presented at the SPE/IADC Drilling Conference and Exhibition, Amsterdam, The Netherlands, 5-7 March.

Holub, Chase M; Chiniwala, Barzin; Montgomery, Jonathan; and Buske, Robert J. (2015). "Innovative Hybrid Bit Delivers Breakthrough in a Deepwater Exploration Well on the West Coast of Ireland". Paper SPE 173029 presented at the SPE/IADC Drilling Conference and Exhibition, London, England, UK, 17-19 March.

K. Bone, Baker Hughes, a GE company; Kerimofski and J. Gauld, ConocoPhillips (2018). "Large Diameter Hybrid Bit with Sharp and Dense Inserts Drills Hard Carbonate Formations with Exceptional ROP". OTC-28491-MS presented at the Offshore Technology Conference Asia held in Kuala Lumpur, Malaysia, 20-23 March 2018.

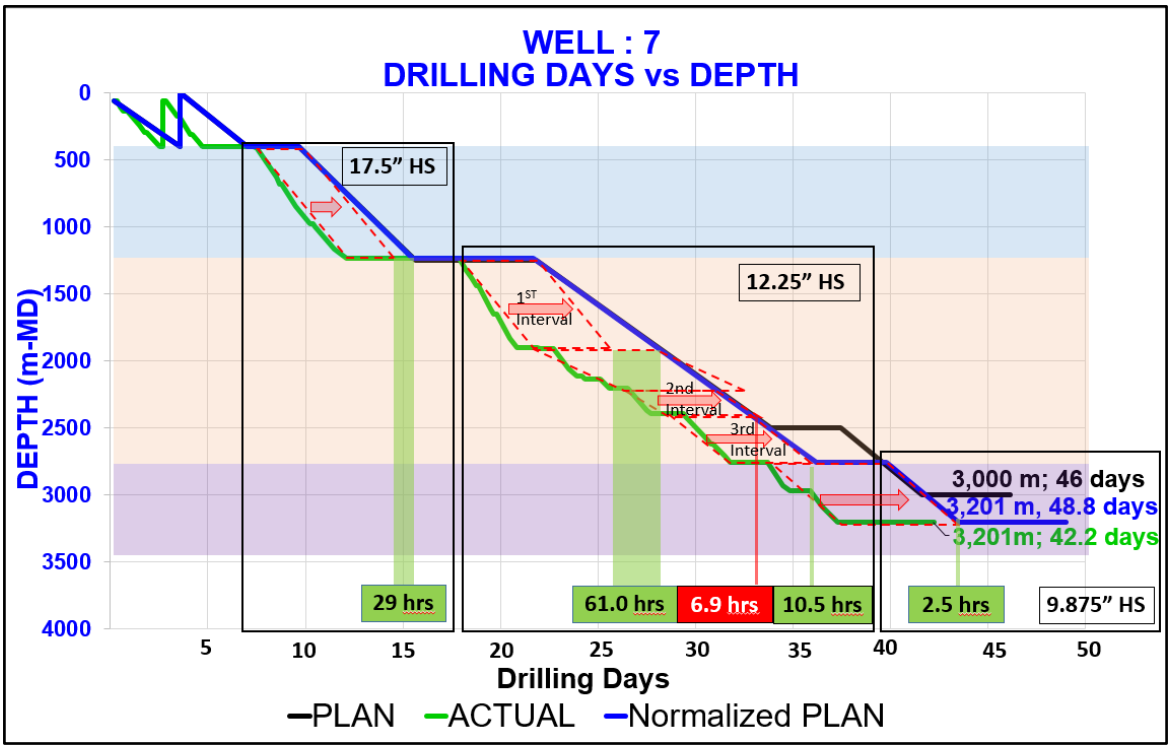


Figure 16: Day vs Depth Chart for Well 7.

SUPERHYDROPHOBIC SELF CLEANING LAYER IN PIPE SCALING

Cynthia Dewi Susanto[1], Jose Prima Boang Manalu[2], Ignatius Bernadi[1], and Roynaldo Lumban Batu[2]

[1]Chemical Engineering Department,
[2]Geological Engineering Department of Diponegoro University
Jl. Prof Soedarto, Semarang, Central Java, Indonesia 50275
Email: cynthiadewi@students.undip.ac.id

ABSTRACT

Silica scaling is a problem that is often found in geothermal power plants, especially those that utilize water dominated (brine) fluid. Silica scaling can be formed due to flashing which causes a decrease in pressure, temperature and increase in pH so that the solubility of the brine changes. This pipe blockage can lead to corrosion and even replace pipes and increase production costs. Therefore, the problem regarding the study of Silica Scaling in the brine injection pathway in a field is very necessary, especially the Dieng geothermal field, Central Java. To prevent this from happening, the superhydrophobic layer made from TMCS - Nanosilica as a cleaning agent itself is coated on the pipe. Nanosilica was synthesized by dry silica reduction using High Energy Milling (HEM) Ellips-3D and filtered through the ASTM E-11 filter, then added with TMCS as a connecting agent. This research method is in the form of laboratory analysis where the coating method used is a plasma spray coating to reach a water contact angle (WCA) higher than 150°. To find the maximum anti-wear capacity of the coating, the optimal pressure is 10 kPa with a composition of 5.5% w/v silica with 13% v/v TMCS using isooctane as solvent. The cleaning itself is based on the Lotus effect which makes contaminants accumulate on the surface due to the impact of air repulsion, then released. With pipe coating in the Geothermal industry, corrosion problems and scaling in pipes can be solved.

Keywords: silica scaling, TMCS–nanosilica, self-cleaning

INTRODUCTION

The Dieng geothermal field is a Java geothermal source with a potential of ± 200 MW managed by PT. Geo Dipa Energi, previously managed by HCE (Himpurna California Energy). In 2011 the company was a state-owned company and had the right to manage two geothermal fields in Java, namely Dieng (Central Java, 60 MW) and Patuha (West Java, 10 MW). The Dieng geothermal system is included in the water dominated category with its production fluid composition of 60% water and 40% steam (Saptadji, 2001). Therefore, before entering the power plant the production fluid must be separated first with the separator so that the liquid fraction (brine) is separated by clean steam so that it does not carry along to the power plant area. The production fluid in Dieng contain ± 900 mg / L silica causing the potential for silica scaling in the Dieng geothermal field to be quite high (Pohan, 2012).

Scaling is a sediment originating from mineral salts in the fluid which results in changes in the surface of the media being traversed. Silica deposition is one of the common problems found in geothermal steam production facilities that can be formed both in the well area (surface area). Silica scaling in the production pipe results in reducing the diameter of the pipe, thereby reducing the flow rate and even the pipe can be clogged so that it must be replaced (Ciptadi, 2001).

The term superhydrophobicity was introduced in 1976 by Reick to describe hydrophobic particle coating made of hydrophobic fumed silicon dioxide, where the shape of water remains almost spherical and the force of adhesion is negligible. The finding of the lotus effect accelerates the wide use of superhydrophobicity, especially in the past decade. Superhydrophobic coatings with water contact angle (WCA) > 150° (Wang et al., 2015) and sliding angle (WSA) lower than 10° have a wide potential application in the fields of self-cleaning, anti-corrosion, anti-icing, water proofing, biomedical instrument, marine antifouling.

The purpose of this study is to implement a concept fabrication of superhydrophobic surface on the pipe as a step to prevent scaling in Dieng geothermal field.

METHODS

The ways to construct superhydrophobic surfaces was prepared in the following three steps: (1) nanometers silica preparation (2) Spraying modified nanometers silica on various substrates.

Nanometers Silica Prepartion

Initially, the nanometers silica with concentration 5.5% w/v dispersed in 20 ml of solvent (n-Hexane, xylene, isooctane). The solution was ultrasonicated for 15 min. In the next step, added TMCS with various concentration slowly to this mixture, which was heating at 50ºC for 2 hours to obtain homogenous solution.

Spraying Modified Nanometers Silica

The formation of the superhydrophobic layer on the surface of the material (bamboo, glass and zinc iron) is carried out by spray method. First, the material is cleaned by dissolving in 98% methanol followed by acetone 98% solution for 15 minutes respectively. After that, dried in the oven at 105ºC for 1 hour then cooled in desiccator. Further, the coatings were prepared using a spray method at room temperature (~27ºC). The superhydrophobic solution was sprayed on the material substances with 90 psi compressed air gas using a spray gun (Minijet 3000 B HVLP) with a nozzle diameter of 1 mm, which was connected to an air compressor. The distance between the spray gun and the substrates was fixed at 20 cm. The same coating procedure was repeated two more times under a fixed condition with the same sample to obtain a uniform and rough-textured silica coating. All the prepared coatings were first kept in room temperature for an hour to enhance the adhesion of the coating material to the substrate, then the coatings material was annealed at 150ºC for 5 h in order to remove trapped residual solvent and improve the bonding strength of materials with substrates. The last step is characterization of the resulting product.

Surface Analysis for Spray Coated

The final material coating will be analyzed using XRF Spectrophotometer (XRF, PW4030/45B), scanning electron microscope (SEM, Zeiss Ultra60 FE-SEM), Brunauer–Emmett–Teller (BET) Model ASAP 2000 made by Micromeritics, X-Ray Diffraction (XRD) Merk PanAnalytica, also contact angle and sliding angle measurement (Canon digital camera (G 15 series) to determine its compositions, surface structure photograph, surface area, silica structure and hydrophobicity. The analysis will be done in the laboratory of Malang University, Indonesia. This Analysis can be easily achieved superhydrophobic property for spray coating.

Durability Test

Two 4x4x1 cm^3 bamboo (coated and uncoated bamboo) from Tembalang, Semarang city were immersed in 70 ºC hot water for 7 h. After that, they were weighed and visually investigated. This acceleration treatment is equivalent to an outdoor exposure of bamboo during a 1 year period

Characterization

The final material coating will be analyzed using XRF Spectrophotometer (XRF, PW4030/45B), scanning electron microscope (SEM, Zeiss Ultra60 FE-SEM), Brunauer–Emmett–Teller (BET) Model ASAP 2000 made by Micromeritics, X-Ray Diffraction (XRD) Merk PanAnalytica, also contact angle and sliding angle measurement (Canon digital camera (G 15 series) to determine its compositions, surface structure photograph, surface area, silica structure and hydrophobicity.

GEOLOGICAL SETTING (JOSE)

Physiographically, the area of Central Java is divided into 4 East-West trending zones (Van Bemmelen, 1949). These 4 zones are the Central Coast of Central Java, the North Serayu, Serayu Selatan Mountains, and the South Coast Plains of Central Java. Meanwhile, the Dieng Plateau itself is included in the North Serayu zone is limited by its western side Karangkobar and its western area bounded by Ungaran (Van Bemmelen, 1949).

According to Pardiyanto (1970), geomorphology and the area surrounding the Dieng Plateau can be divided into two kinds consisting of mountainous areas and the highlands (Plateau). The mountainous area covers almost all parts of the edge consisting of one straightness of volcanoes (Mount Srodja, Mount Kunir, Mount Pakuwadja, Mount Kendil, Mount Butak, Mount Patarangan, Mount Prahu, Mount Patakbanteng, Mount Djurangsawah, Mount Blumbang, and some domes solitary such as Mt. Bisma and Mount Nagasari). Meanwhile, the plateau area itself is located between rows of volcanoes and dome solitary, generally have filled volcanic material consisting of Dieng, Batur Highlands and Highlands Sidongkal).

Regional stratigraphy in the study area according to Condon et al. (1996), consists of eleven lithologies in the order of old to young is Unit Members Breccia Formation Tapak, Unit Members Limestone Formation Tapak, Unit Formation Tapak, Unit Formation Kalibiuk, Unit Members Clay Formation Ligung, Unit Members Breccia Formation Ligung, Unit Stone Mountain fire Jembangan, Lake and Alluvium Sediment Unit, Unit Dieng Volcano rocks, rocks Unit Volcano Sundoro, Alluvium Deposition Unit.

According to Gunawan (1968) op.cit. Zaenudin (2006) The geological structure of Dieng and its surroundings is influenced by tectonic movements of Quaternary which is still active to date. A great fold does not occur, but clearly there are two Quaternary fractures that can be observed. The first fracture was found in the west part in the formation of Ratamba Block accompanied by fracturing. The second fracture is influenced in the eastern region of Sigedang graben from Tlerep-Butak Volcano and Graben Watumbu from Prahu. Meanwhile, the study summarized by Condon et al. (1996) states that the existing geological structures consist of fault, straightness, and fractures involving rocks aged from Cretaceous to Holocene.

RESULTS

Analysis of Superhydrophobic Durability

In practical application, the superhydrophobic surfaces generally need to be stable in the acid−base

circumstance. A carbon nanofiber arrays was prepared through thermal pyrolysis of nanostructured polyacrylonitrile (PAN) film (Feng et al., 2003). The structures of these carbon nanofibers were similar to that of graphite, which is responsible for the durability to the corrosion of acid and base. They have also fabricated stable bioinspired superhydrophobic surfaces by one-step solution-immersion process, and the superhydrophobic coating is very stable upon treatment with various solvents, as mentioned above (Wang et al., 2006).

Qiao et al. (2018) did an alloy coating surface modification using heptadecafluoro1,1,2,2-tetrahydro-decyl-1-trimethoxysilane (FAS17) (97%) to reduce the surface energy on Q235 steel substrate using plasma spray method. The corresponding water contact angle and sliding angle were 154° ± 2° and 4° ± 1°, respectively. They stated that the hydrophobicity decreased when the spray power increased

Fabrication of Superhydrophobic Surface

Self-Cleaning Process

The superhydrophobic coating on metal can inhibit the corrosion by restricting the diffusion of water molecules (Latthe et al., 2019). Meanwhile, the particle removal process by the jumping water condensate was strongly influenced by the wettability. Depending on their wettability, particles have a tendency to either attach to the air–liquid interface or detach into the bulk fluid. As a guideline, the energy required to detach a spherical particle from a flat interface is proportional to

$$(1 - |cos\ \theta_1|)^2 \qquad (1)$$

where θ_1 is the contact angle of water on the particle (Binks, 2006). There are three different process of particle removal, they are floating, lifting, and aggregating.

Silica scaling is considered as aggregating process when a clump of silica particles was subject to condensing vapor, the water condensate formed liquid bridges among neighboring particles. Under the right circumstances as in Figure 1, the immersion

force among neighboring particles (Kralchevsky & Nagayama, 2000) deformed the loosely connected particles into a tighter cluster, and the particle cluster eventually jumped away from the surface.

The aggregation process reduced the overall surface area, releasing surface energy that was converted to kinetic energy of the jumping particle cluster (Wisdom et al., 2013). Based on the experiment of Hu et al. (2011) to demonstrate the self-cleaning capability by the jumping condensate, they used silica particles to represent contamination of inorganic origins in superhydrophobic surface.

The aggregating mechanism of particle removal seems to be unique to the superhydrophobic surface, which among other things minimizes the adhesion between the particle cluster and the surface.

In the latter case, the jumping condensate provides enough momentum for the contaminants to move out of the thin viscous boundary layer for airflow removal to become effective, much like the ballistospore discharge (Pringle et al., 2005 & Noblin et al., 2010). Wisdom et al. (2013) experimentally confirmed that the jumping drops can accomplish self-cleaning regardless of the orientation of the superhydrophobic surface.

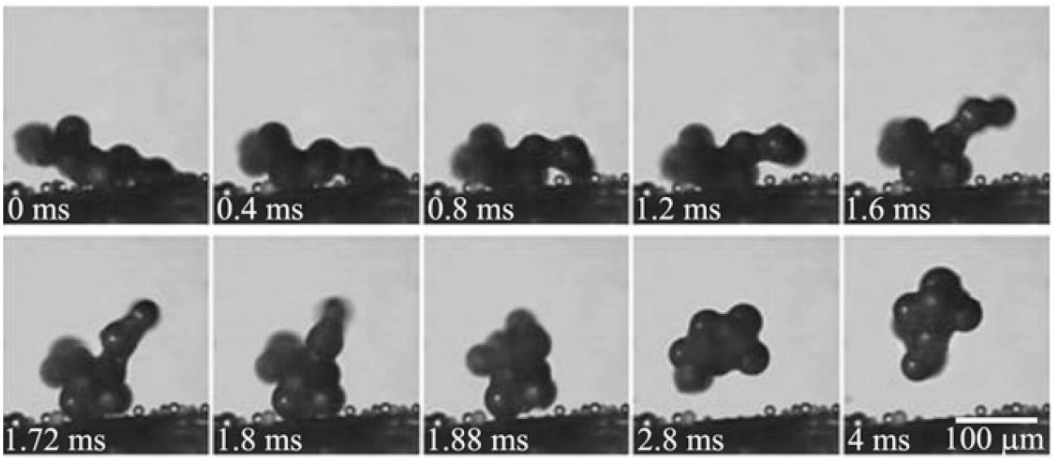


Figure 1: Aggregating removal process: When water vapor condensed on a clump of 50-µm-diameter glass particles, the growing liquid bridge among the neighboring drops led to particle aggregation. The aggregation process caused the particle clump to eventually jump off the surface.

CONCLUSIONS

Silica scaling has the potential to occur along the brine injection pipeline that connects wells to the geothermal field in Dieng. This risks the company in the use of wasteful pipes. The superhydrophobic layer in proven metal can inhibit corrosion by limiting the diffusion of water molecules the techniques which seem to be suitable for the coatings to be used in the plasma treatment techniques, soluble gel methods and some spraying techniques. These coatings function on the basis of micro and nano-level surface roughness which is easily damaged by mechanical stresses. Therefore mechanical stability needs to be ensured. Also the thermal stability of these coatings must be ensured. The coatings are not exposed to very high temperatures. . The aggregation mechanism of particle removal seems unique to supercidrophobic surfaces, which, among other things, minimize adhesion between particle groups and surfaces.

REFERENCES

Binks B, Horozov T, eds. (2006). "Colloidal Particles at Liquid Interfaces". Cambridge Univ Press, Cambridge, UK.

Feng, L.; Yang, Z. L.; Zhai, J.; Song, Y. L.; Liu, B. Q.; Ma, Y. M.; Yang, Z. Z.; Jiang, L.; Zhu, D. B. (2003). "Superhydrophobicity of nanostructured carbon films in a wide range of pH values". Angew. Chem., Int. Ed., 42 (35), 4217−4220.

Hu HM, Watson JA, Cribb BW, Watson GS. (2011). "Fouling of nanostructured insect cuticle: Adhesion of natural and artificial contaminants". Biofouling 27(10):1125–1137.

Kralchevsky PA, Nagayama K. (2000). "Capillary interactions between particles bound to interfaces, liquid films and biomembranes". Adv Colloid Interface Sci, 85(2–3):145–192.

Latthe, S. S., Sutar, R. S., Kodag, V. S., Bhosale, A. K., Kumar, A. M., Sadasivuni, K. K., Xing, R., Liu, S. (2019). "Self–cleaning superhydrophobic coatings: Potential industrial applications". Progress in Organic Coatings, 128, 52–58.

Lian, F., Tan, J. Z., Zhang, H.C. (2014). "Preparation of superhydrophobic titanium alloy surface and its antifouling of halobios". Rare Metal Mater. Eng. 43, 2267–2271.

Purnomo, A., Dalanta, F., Oktaviani, A. D., and Silviana, S. (2018). "Superhydrophobic coatings and self-cleaning through the use of geothermal scaling silica in improvement of material resistance". AIP Conference Proceedings, 2026, 020077.

Qiao, J. H., Jin, X., Qin, J. H., Liu, H. T., Luo, Y., Zhang, D. K. (2018). "A super-hard superhydrophobic Fe-based amorphous alloy coating". Surface & Coatings Technology, 334, 286–291.

Saptadji, N.M. (2001). "Teknik Panas Bumi". Bandung: Bandung Institute of Technology

Wang, S.; Feng, L.; Jiang, L. (2006). "One-Step Solution-Immersion Process for the Fabrication of Stable Bionic Superhydrophobic Surfaces". Adv. Mater., 18, 767−770.

Wang, S.T., Liu, K.S., Yao, X., Jiang, L. (2015). "Bioinspired surfaces with superwettability: new insight on theory, design, and applications". Chem. Rev, 115, 8230–8293.

Wisdom, K. M., Watson, J. A., Qua, X., Liua, F., Watson, G. S., and Chena, C. H. (2013). "Self-cleaning of superhydrophobic surfaces by self-propelled jumping condensate". PNAS, 110, 20.

DARAJAT GEOTHERMAL POWER PLANT PROTECTION SYSTEM IMPROVEMENT

Nixon Manik and Bayu Satmoko

Star Energy Geothermal Darajat II Ltd.
Pasirwangi, Garut, West Java, Indonesia
Email: Nixon.manik@starenergy.co.id, bayu.satmoko@starenergy.co.id

ABSTRACT

A good performance of power system protection is a form of active insurance, designed to maintain a high degree of service continuity and limit the damage of the main equipment's. Assessment on Electrical Protection (EPA) should be taken to improve the performance of power system protection. Some incident investigations related to power system protection that involving electrical subject matter expert has been done and recommend to conduct electrical protection asessment of 150 kV (interconnection with PLN Grid), 13.8kV, 6.3kV, and 380V system.

Darajat Geothermal Power Plant has 3 unit turbine generator. Darajat I was operated by PT IP with power generation 55MW, while Darajat II and Darajat III were operated by Star Energy with power generation 95MW and 121MW. The latest electrical protection study at Darajat II was conducted on 2008 and DRJ III on 2006. Since PLN grid and internal power plant loads are changing, it is required to review all electrical protection system to ensure working properly to protect all electrical equipment.

Darajat electrical protection assesment has some findings and recommendations such as correction for relay general setup, changing the protection scheme for "100% Generator Ground Fault Protection", adding new scheme for (out of step protection) and modification on loss of field relay setting. Some recommendations had been done during Darajat II shutdown and turn around on October 2016, resulting unit faster and more selective protection when fault occurred.

Keywords: Protection systems, power plant

INTRODUCTION

Darajat Geothermal Power Plant is located approximately 150 km southeast of Jakarta, Indonesia and 35 km of Bandung, West Java, Indonesia as shown in Figure 1.

Darajat Geothermal Power Plant consist of three-unit turbine generator. Darajat I with capacity 55MWwas operated by PT. Indonesia Power while the steam supplied by Star energy Geothermal Darajat II (SEGD II). Darajat II and Darajat III with capacity 95MW and 121MW were operated by SEGD II. Figure 2 shows that all three-unit power plant had been connected to 150KV Java-Bali grid system theough 13.8KV generator circuit breaker, 13.8/150KV generator transformer and 150KV line circuit breaker.



Figure 1: Star Energy Geothermal Plant locations at West Java, Indonesia.

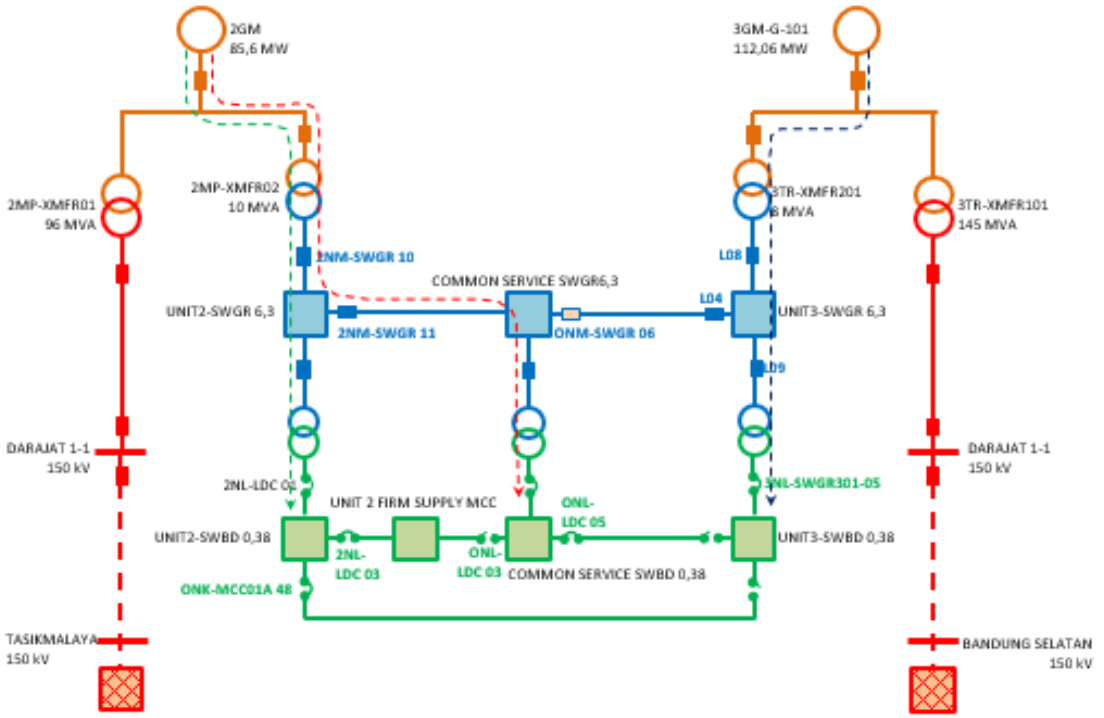


Figure 2: Simplified Darajat Geothermal Power Plant.

Background

There are three black out incidents in between 2013 and 2015. Investigation had been conducted with recommendation to review all electrical protection system for Darajat II and Darajat III. In 2015, Darajat Geothermal Power Plant conducted electrical protection study to fulfill this recommendation.

The latest electrical protection study on Darajat II was conducted in 2008 while on Darajat III was conducted in 2006. Since the load of Java-Bali grid system and internal power plant configuration are changing overtime, an internal engineering standard recommends that the study shall be conducted regularly in every 4 to 5 year. Therefore, it is required to review all electrical protection system to ensure it work properly to protect the equipment properly.

Electrical Protection Assessment (EPA) for Darajat II and Darajat III Power System Protection (PSP) had performed based on the existing relay protection setting and its philosophy background. The other reference for EPA was the Disturbance Fault Recorder (DFR) that recorded performance of the existing power system protection during system faults.

The purpose of this study is to review the existing Darajat II and Darajat III major protective relays setting, protection scheme and fault experiences on the operation system.

POWER SYSTEM PROTECTION (PSP) ASSESSMENT

Relaying Philosophy

Each electrical power system elements or elements connection shall be provided with at least two independent protection systems with redundant configuration. In this context, elements connection is considered as a group of elements connected together whose boundary is defined by circuit breaker(s). Independent protection system means relays hardware which its function is not depending on the performance of other relay. When one system is out of service, then the other one is still active.

1. Redundant protection
   Redundant protection may be formed by the combination of:

   a) Two or more sets of protection system, both as main protections or,
   b) One set as main & one set of non-unit protection function as backup protection or, 3) both is non-unit protections.

   Backup relaying (IEEE Standard Dictionary): “Protection that operates independently of specified components in the primary protective system and that is intended to operate if the primary protection fails or is temporary out of service”.

2. Selectivity
   On the occurrence of a fault on the power system network or in Darajat II and Darajat III system, both high speed discriminating protection shall rapidly detect the fault and initiate the opening of only those circuit breaker(s) which are necessary to disconnect the faulted electrical element from the network. In Darajat II case, major fault within generator or generator transformer initiate the main protection to open generator circuit breaker, field circuit breaker and shutdown the unit.

   Operation of "time graded" back-up protection takes place as a result of the failure of main protection(s) or in case of circuit breaker failing to operate (i.e. circuit breaker failure protection). All backup protection systems shall be able to discriminate with main protection system, circuit breaker failure protection and with other backup protection systems installed on Darajat II, Darajat III and 150 kV grid systems.

3. Reliability
   PSP must either operate in response to trouble/system fault in their assign area (dependability aspect) or block (stable/not operate) if the trouble is "out zone" or outside their design area (security aspect).

   Dependability can be checked during site test for maintenance by simulated test or by fault simulation. Security, on the other hand is much more difficult to check. A true test of system security would have to measure response to almost infinite variety of potential trouble in the power system and its environment.

   DFR, records the performance of PSP for several years' service operation. It will provide valuable information for engineers to evaluate the reliability (dependability and security) of PSP applied at Darajat II and Darajat III.

4. Fault clearing time
   The protection system at Darajat II and Darajat III shall be capable of achieving the discrimination fault clearance times, inclusive of circuit breaker time.

   Fault clearing time for fault at 150 kV line to Darajat I shall be < 90 milliseconds (grid code requirement), but to minimize the risk within Darajat II main equipment's, the faster is better as long as the security aspect is still fulfilled.

   Fault clearing time for fault at Darajat II or Darajat III within main protection zone shall be cleared in basic time (high speed).

   The effect of all points mentioned above is a form of active insurance designed to maintain a high degree of service continuity of Darajat II and Darajat III power plant, and limit the damage of the main equipment's.

Power System Protection Review

The evaluation or review for Darajat II and Darajat III PSP comprises the evaluation of protection system applied for generator, transformer and 150 kV line, 6.3 switchgear and associated MV feeders and Main Line of 380V system.

Fault Records

Below fault records provides data of Darajat II protection relay performance during system faults. The dependability of protection relays is evaluated based on selectivity and fault clearing time. On the other side the security aspect is evaluated based on the relay stability during "out zone fault" or when "non-system fault" occurs (if any). DFR records 10 cases system fault from April 2013 - July 2015. The late response or fail to operate of protection system only found in 15 April 2013 which are neutral overvoltage (59N) and third harmonic neutral under voltage (27TN), while in the other fault records the protection is working properly.

DFR records in 15 April 2013

Figure 3 shows the fault location in single line diagram and three line diagram. Fault had occurred in Darajat II generator stator winding with fault type is Phase B to Ground then Phase C to Ground which develop Phase B – Phase C – Ground. Figure 4 shows the evolution of fault that occurred on 15 April 2013 at Darajat II generator stator.

Analysis & Recommendation

Refer to Figure 3:

1. Fault current level of the first ph-B ground fault is very low, phase current almost no change.
2. When the first fault developed to (ph-B) – (ph-C) – ground fault current is approx. (|Ia|=5.79 kA), (|Ib|=16.9 kA), (|Ic|=21.26 kA). Fault current at fault point is equal to the sum of fault current contribution from system (Ifsys) and from generator (Ifgen).
3. As DFR current measuring channel is connected to CT located between generator and main transformer, fault current recorded by DFR is fault current contribution from system

Refer to Figure 4, fault evolution can be explained:

1. First Fault: Ph-B-to Ground fault for 800 milliseconds, this fault is than developed to Ph-B-Ph-C-to Ground: no record from protective relay nor other monitoring device verify that ground fault protection for Darajat II generator (59N and/or 27TN) is active/ operate.

2. Second Fault: When the first fault develops to become Ph-B-Ph-C-to Ground (the second fault), generator protection function 87responses and release command to clear the fault by opening generator CB. Total fault clearing time for second Fault is 60 milliseconds (3 cycles).
3. During the period of First Fault there is no signature of arc on generator neutral voltage records and record of phase-B generator voltage. The only arc signature is at the transition between First and Second Fault.
4. Simultaneous with the order to open generator CB, order was also sent to shutdown prime mover and open Generator Field Breaker.

From above analysis, it is concluded that the existing protection scheme for "100%generator stator ground fault which consist of 59N and or 27TN" was unable or fail to avoid catastrophic damage which is initiated by stator ground fault.

The study recommends to replace the existing protection scheme of 100% generator stator ground fault protection with other scheme which is faster and selective. The new scheme shall protect generator stator winding, including transformers winding at 13.8 kV side when generator CB is closed.

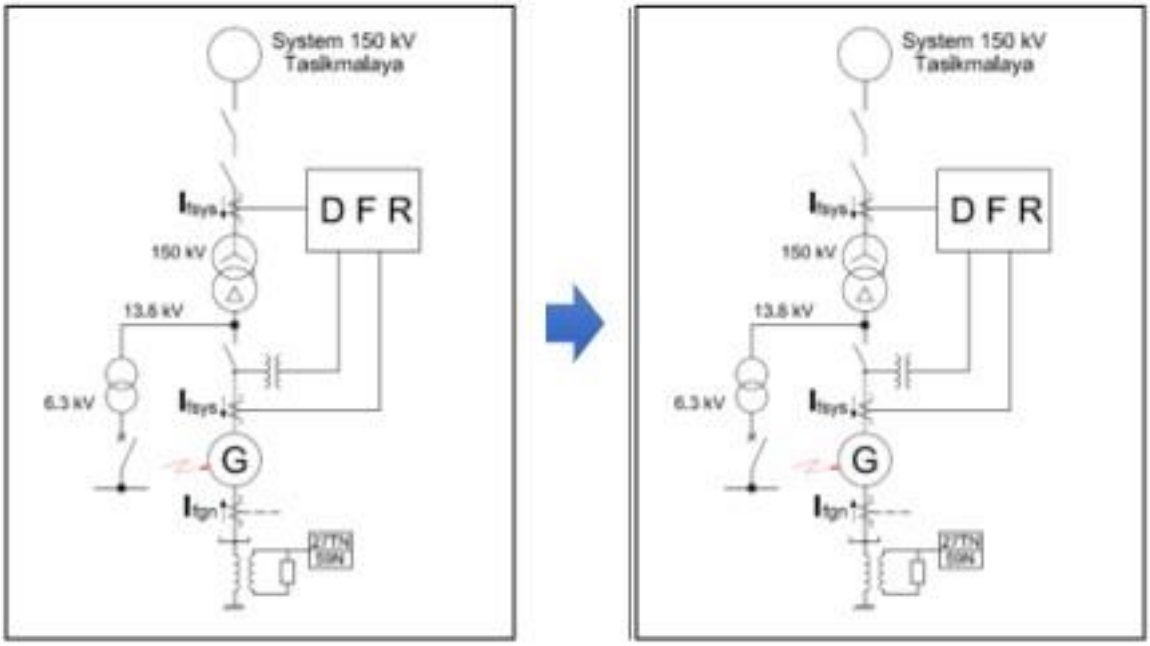


Figure 3: Single Line Diagram and Three Line Diagram of Fault Point.

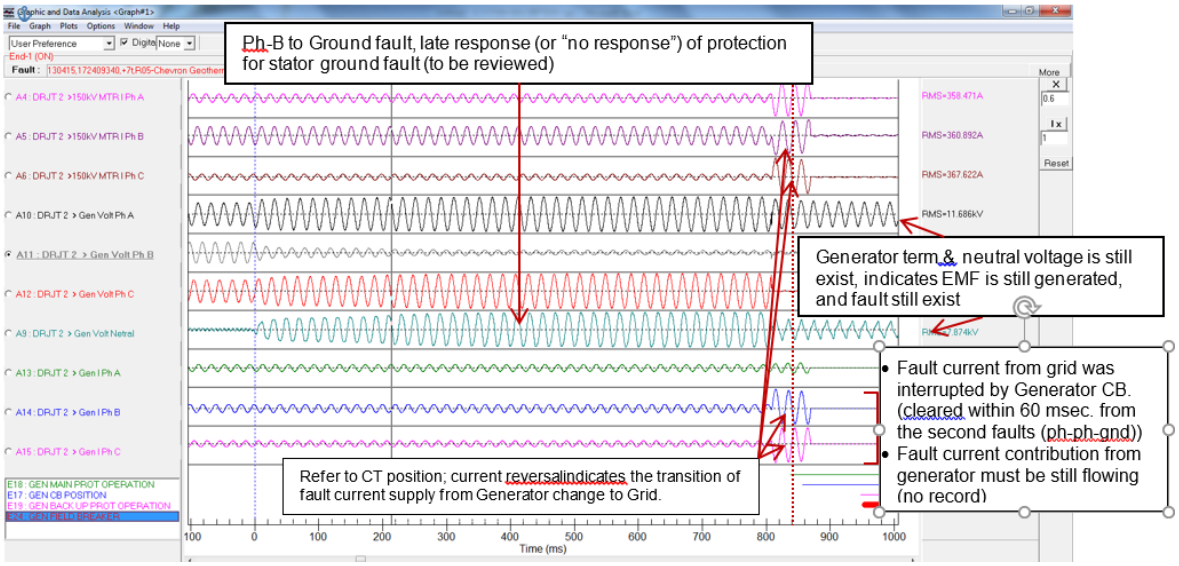


Figure 4: Fault Evolution Record on 15 April 2019.

POWER SYSTEM PROTECTION (PSP) IMPROVEMENT

Based on the study result and recommendation, we do discussion with relay protection OEM and vendors to check new scheme of 100% generator stator ground fault protection system. The scheme protection system using principle of Low frequency or sub harmonic injection is the preference. One of the OEM and vendor which applied this scheme is Beckwith M-3425 series

Sub-harmonic Voltage Injection Scheme

These schemes are widely used in Europe and are just beginning to be used in the U.S. This scheme injected a low frequency sub-harmonic into the generator stator winding. The injected frequency ranges from 15-20 Hz. The signal is injected into the neutral grounding transformer.

Figure 5 illustrates the subharmonic voltage injection scheme. The use of a low frequency sub-harmonic makes the generator and terminal bus capacitive reactance a high impedance. Thus, the KVA size of the injection transformer is reduced over what it would be if fundamental frequency were used.

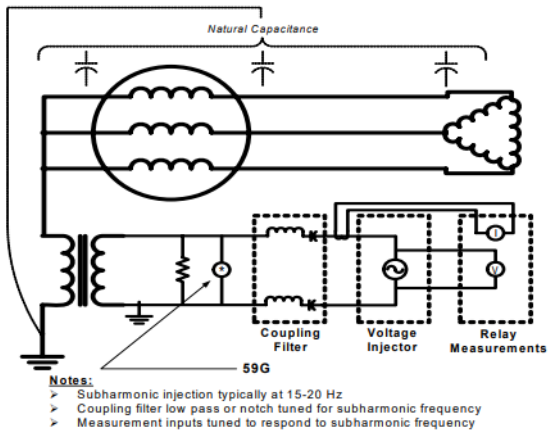


Figure 5: Sub-harmonic Voltage Injection Scheme.

Figure 6 shows the coupling filter and voltage injector that is installed in the secondary of the generator grounding transformer. Typical subharmonic normal capacitive current is in the milliamp range. Under normal conditions, this small level of changing current will flow at the subharmonic frequency.

When a ground fault occurs anywhere in the winding of the generator or its associated bus work, the capacitance is shorted in that phase and a higher current flows which can be detected by an overcurrent relay. The relay portion of the scheme in modern applications is usually in a digital multifunction generator protection package that typically includes all other generator protection functions. Integration of this function within a multifunction relay has reduced the scheme cost over separate relaying that was required in the older electronic versions of this scheme.

The scheme is not affected by generator MW and MVAR loading and will detect ground faults at any location within the generator winding. It will also detect ground faults in both windings of a two-winding generator transformer. Typically, the conventional 59G relay is used with this scheme to provide backup.

Field measurements of the normal sub-harmonic capacitive current are required for commissioning. Digital relays typically measure this value and display it in a metering screen. Perhaps this scheme's major feature can detect stator ground faults when the generator is off-line, allowing the user to detect stator ground prior to putting the generator in-service.



Figure 6: Coupling Filter and Voltage Injector.

Field Installation

The new scheme of 100% generator stator ground fault protection system using Beckwith 3425A – 64S protection function had been installed in Darajat II in 2016 and plan to be installed also in Darajat III.

Performance Review

After installing the new scheme of 100% generator stator ground fault, Darajat II can detect early warning of fault in generator stator. It will give us an alarm if something happen, so we can discuss and decided what we will do for the mitigation.

CONCLUSION

Electrical protection system study shall be conducted regularly in every 4 to 5 year to accommodate the development of grid load and other power plant.

Darajat electrical protection system study recommends to replace the existing protection scheme of 100% generator stator ground fault protection with other scheme which is faster and selective.

REFERENCES

Chevron Geothermal Indonesia Ltd. (2016). "Electrical Protection Assessment". Garut, West Java, Indonesia.

Star Energy Geothermal (2017). "P2RM: 1st Quarter 2017 Report". Jakarta, Indonesia.

Turner, Steve (2011), "Protecting Large Machines for Arcing Faults," Beckwith Electric Company, 1-9.

Hartman, Wayne (2011), "Advanced Generator Ground Fault Protections," Beckwith Electric Company, 12-15.

ANALYSIS OF PRODUCTION TEST BY USING HORIZONTAL LIP PRESSURE TEST METHOD IN Y-WELL OF K-CLUSTER IN PT. PERTAMINA GEOTHERMAL ENERGY AREA OF ULUBELU, LAMPUNG

Audiah Fadhilah, Ubaidillah Anwar Prabu, and Wenny Herlina

Mining Engineering Department, Faculty of Engineering, Sriwijaya University
Jl. Srijaya Negara Bukit Besar, Palembang, Sumatera Selatan, 30139, Indonesia
Email: audiafadilah@gmail.com

ABSTRACT

PT. Pertamina Geothermal Energy is a geothermal energy industry company located in Ulubelu area, Lampung Province . The main objectives of the company are the exploration and exploitation of geothermal energy in the form of geothermal power plants. To obtain a picture of the optimal potential of the well, a production test is carried out. Horizontal lip pressure test method, one of the methods of production test, was chosen as it is very suitable to be applied to new wells in the exploration drilling stage where production facilities are inadequate and not yet available. This method was to know the picture of well productivity, brine, total, Dryness-X, and total enthalpy (H) to obtain the deliverability value of a well. Horizontal lip pressure test is chosen by using parameter of Well Head Pressure (WHP), pipe lip pressure, the height of brine on wear box (h) was 34.5 cm, the height from the base of wear box to v-notch (D) was 40.5 cm, the width of wear box was 1.250m, pipe lip diameter (d) was 10.00 inch, the width of pipe area (A) was 508.7 cm^2, and maximum discharge pressure was 20 ksog. Modificated Russell James equation was used to know the picture of well productivity thus total enthalpy value (H) was obtained for 1256,4171 T/J from which output curve was made, so that deliverability amount was known where optimal condition occured for WHP = 11 kscg with steam rate, brine , total, and dryness fraction respectively were 121,5454 T/J; 372,4338 T/J; 493,9792 T/J; 0,23542592 T/J. After obtaining the deliverability value,, the next step was to determine production capacity using well-generating capacity formula, so that the amount of production of Y-well of K-cluster in PT.Pertamina Geothermal Energy of Ulubelu area was obtained as 15,1 MW.

Keywords: Production test, lip pressure method

INTRODUCTION

Production test is aimed to know the production capability of a well that is the magnitude of the production rate and the enthalpy of fluid at various Well Head pressures (Irsamukhti, 2014).

Horizontal lip production test is one of the appropriate methods to be applied to new wells in exploration drilling stage where adequate production facilities are not yet available (Saptadji, 2001). Errors in horizontal lip production test method is commonly caused by equipments (Suhartono, 2012). A study conducted by Karamaker and Cheng (1980) denoted that the error margin of James Lip Pressure method was 8% (Pawitra, 2014). This method is considered capable of providing accurate estimation results to determine the total enthalpy value and well deliverability. Moreover, this test does not cost too much (Shen, 1981).

The writer is interested to study the problems in Y-well of K-cluster in PT Pertamina Geothermal Energy of Ulubelu, Lampung. Analyses will be done by using horizontal lip pressure test method in Y-well of K-cluster Russell James's contribution so that the optimal potential in the well can be known.

To find out the optimal conditions, several parameters needed as reference calculations are used in this study. The parameters include the Well Head pressure (WHP), Lip Pressure (PC), the hight of brine on wear box (H), the height from the base of wear box to v-notch (B), pipe lip diameter (d), the width of pipe area (A) and maximum discharge pressure and technical data of Y-well of K-cluster (Table 1). The calculation is done by using the Rusel James equation to find out the total enthalpy value (H) in the well.

RESEARCH METHODS

Research methods are carried out to facilitate the writing step so that the research process and problem solving in the research area are more directed.

Data Collection

The steps in data collection methods in this study are as follows: Table 1 shows parameters needed for the next stage, namely the stages of data processing.

Data Processing

The steps in data processing methods in this study are as follows:

Setting parameter

Parameter setting is used to know the production capability of Y-well of K-cluster by getting data from the field or secondary data.

Tabel 1: Horizontal lip pressure test parameters.

No.	PARAMETER DATA OF HORIZONTAL LIP PRESSURE
1	Well Head Pressure (WHP)
2	Lip Pressure (PC)
3	The Height of Brine on Wear Box (H)
4	The Height from the Base of Wear Box to V-Notch (D)
5	The Width of Wear Box (B)
6	Lip Pipe Diameter (d)
7	The Width of Area Pipe(A)
8	Maximum Discharge Pressure

Calculating the total enthalpy value (H) using the Russel james equation:

$W_{atm} = K.\ (001.h_{weir})^{25}.60.\frac{\rho \text{brine.atm}}{1000}$(Ton/jam) (1)

Where K:(1)

$K = 81.2 + \frac{0.24}{0.01.h_{weir}} + \left[8.4 + \frac{12}{\sqrt{0.01.D_{weir}}}\right] . \left[\frac{0.01.h_{weir}}{0.01.B_{weir}} - 0.09\right]$

The Russell James equation is used to find the iterated H value:

$$\frac{W_{atm}}{Area.[P_{lip} + P_{atm}]^{0.96}} = 0.184.3600.\left[\frac{hg_{atm} - H}{hfg_{atm} H^{1.102}}\right] (2)$$

Total Enthalpy Value (H):

$$M_{uap} = W_{atm}\left[\frac{hfg_{atm}}{hg_{atm} - H}\right](ton/Jam) \quad (3)$$

Where:

Area P_{lip} = The width of lip pipe [cm^2]

h_{gatm} = Liquid enthalpy at P separator (KJ/kg.ºC)

h_{fatm} = Liquid enthalpy at P atm (KJ/kg.ºC)

h_{fgatm} =Vapor-liquid enthalpy at P atm (KJ/kg.oC)

$Q_{Electrica}$ = Potential of wells (MW)

M_{uap} = Total mass flow rate (tonnes/hour)

Calculating and creating steam and brine rate curves

The steam rate is calculated by plotting the Well Head Pressure (WHP) and the steam flowrate mass value with the formula $\frac{\text{total}}{x}$ so that the equation of the steam rate y = -0,793x^2 + 18,068x +18,823. By plotting the Well Head Pressure (WHP) and mass of brine flowrate with the formula [total – steam], so the brine rate equation is obtained y = -5,5022x^2 + 148,25x – 592,55.

Creating deliverability curves

This step is done by inputting the results of steam rate, brine rate, total, dryness-x and total enthalpy value (H) and Well Head pressure (WHP) according to the test data that takes place in the field, then selecting all the data using the line with markers curve graph so that the deliverability curve will be obtained.

Determining optimization capacity of well production

After knowing the deliverability value of the well, well capacity is calculated using the equation. Generated potential is:

$$\text{Well Generation Capacity} = \frac{M_{steam}}{Steam\ Consumption} \quad (4)$$

RESULTS AND DISCUSSIONS

Table 2 shows the condition of Well Head pressure when the valve opening is played as much as 100%, 40%, and 35%.

The data of Well Head pressure (WHP) was taken in the field at Y-well of K-cluster. Table 3 is the secondary data taken from measurement results in the field. Table 4 is the result of the calculation of the horizontal lip pressure production test method showing the production value of steam, brine and total production in the well flowrate mass and from the results, the mass value of flowrate and the total enthalpy value (H) in the well obtained using the Russell James equation.

Table 5 is the deliverability value obtained from the y-equation.

Tabel 2: Value of well head pressure (WHP).

Valve Opening	*Well Head Pressure*
100%	*10,4 - 14,1 ksog*
40%	*14,8 - 18,8 ksog*
35%	*19,8 - 20,0 ksog*

Tabel 3: Data on measurement results in the field.

Data	
The height of brine on wear box (h)	34,5cm
The height from the base of wear box to v-notch (d)	40,5 cm
The width of wear box (b)	1,205m
Lip pipe diameter (d)	10 inch
The width of area pipe (A)	508,7cm^2
Maximum discharge press	20 ksog

Tabel 4: Data from the calculation of the lip test method tabel 4. Data from the calculation of the lip test method.

WHP	PC		hV-Notch	T brine	Density	K
(Barg)	(Barg)	(Bara)	(m)	(°C)	(kg/m3)	
14,1	3,1	4,1	0,345	95	962,07	82,95
18,8	1,7	2,6	0,3	95	962,1	82,6
20	1	1,9	0,245	94,5	962,43	82,53

Here are the figures based on the table. Figure 1 is the curve showing steam rate of UBL Y-well of K-cluster based on the output curve, so the equation y= -0,7936x^2+18,068x+18,823 is obtained. Meanwhile, Figure 2 is the curve of steam and brine rate showing that the steam rate is the same as that in Figure 1, and from the brine rate y= -5,5022x^2+148,25x-592,55 is obtained. Figure 3 shows the steam and brine curve.

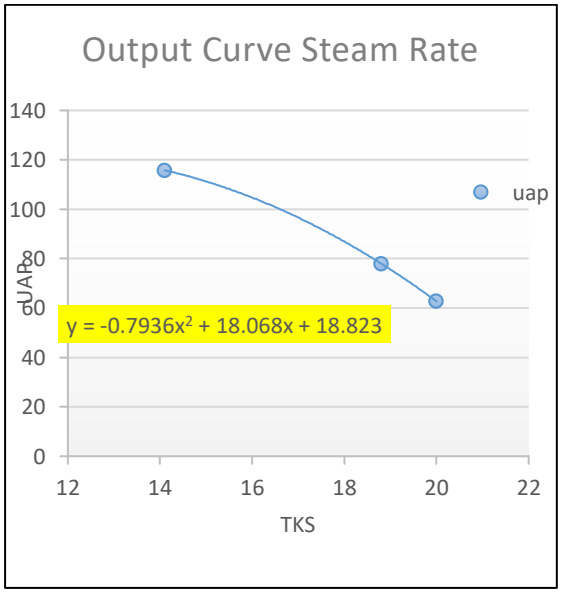


Figure 1: Steam rate curve based on horizontal lip pressure test results.

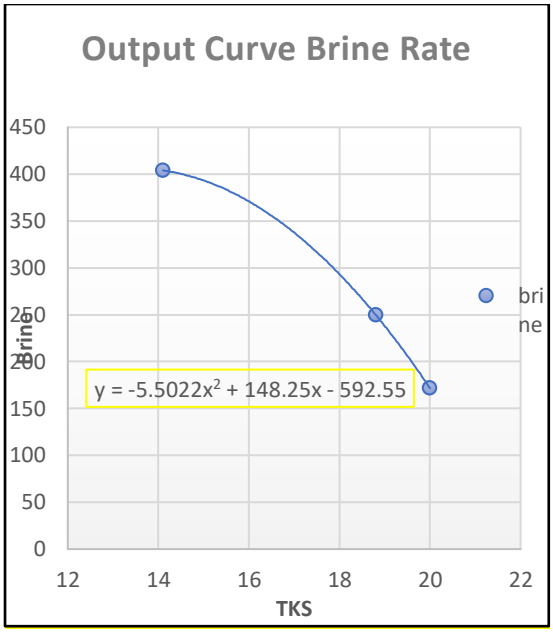


Figure 2: Brine rate curve based on lip flat production test results.

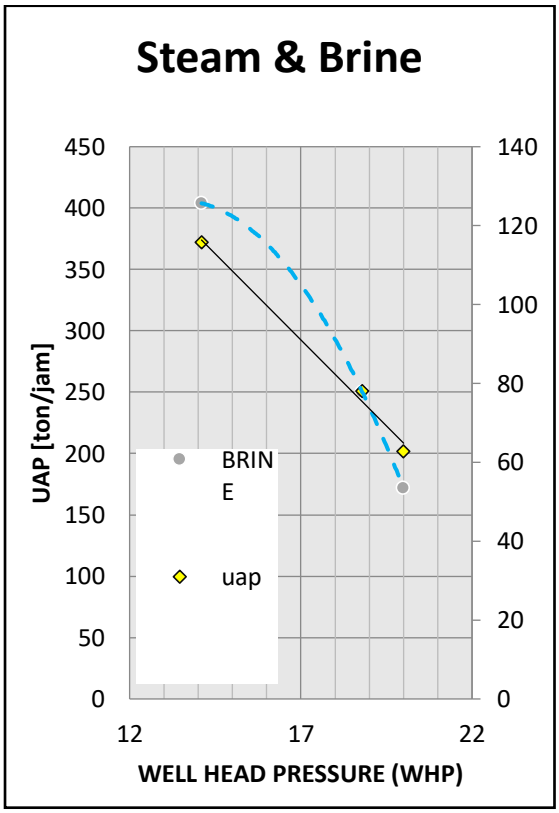


Figure 3: Steam and Brine curve.

Furthermore, he results of deliverability shows as follow.

Table 5: Deliverability.

RESULTS			
WHP	STEAM	BRINE	TOTAL
10	120,143	339,73	459,873
11	121,545	372,4338	493,9792
12	121,361	394,1332	515,4938
13	119,589	404,8282	524,4168
14	116,229	404,5188	520,7482
15	111,283	393,205	504,488
16	104,749	370,8868	475,6362
17	96,6286	337,5642	434,1928
18	86,9206	293,2372	380,1578
19	75,6254	237,9058	313,5312
20	62,743	171,57	234,313

RESULTS	
X	H
0,261252563	1287,0802
0,24605368	1256,41712
0,235425916	1234,9677
0,228041131	1220,06683
0,223196931	1210,29677
0,22058602	1205,02406
0,220230083	1204,30586
0,222547679	1208,98671
0,228643474	1221,28223
0,241205341	1246,62931
0,267774302	1300,23963

Based on the output curve and the analyses conducted at UBL Y-well of K-cluster, the well production capacity generated by UBL Y-well of K-cluster is shown in Figure 4.

Based on output curve in well UBL Y cluster K, well production capacity produced by UBL Center K wells at the highest steam production rate occurs in WHP = 11 kscg with steam, brine, and total rates and successive dryness fractions of 121.5454 T / J; 372,4338 T / J; 493,9792 T / J; 0,23542592 T / J, from the graphs obtained, the power generated at the optimum condition (WHP 11 Kscg) is then calculated using the formula.

$$Well\ generator\ capaci = \frac{Msteam}{steam\ consumption}$$

$$Well\ generator\ capacity = \frac{121{,}5454\ T/J}{8\left(\frac{T}{h}\right)Mwe}$$

Well generator capacity = 15,1 MWe

From the calculation of the capacity of the well generator, the power resulted by Y-well of K-cluster is 15.1 MW.

CONCLUSIONS

1. From the results of horizontal lip pressure production test by contributing Russell James equation, the required parameters consist of the Well Head Pressure (TKS), lip pressure (Pc), The Height from the Base of Wear Box to V-Notch (D), The Width of Wear Box (B), lip pipe diameter (d), area of area pipe (A), Masimum Discharge Press.
2. During the test process, there are 3 openings of the wing valve (throttle valve), namely at openings of 100%, 40%, and 33%. From the test results it is known that the conditions not 100% have the total rate of two-phase fluid in the form of steam and brine and the greatest outgoing power each falls on WHP - = 11 kscg with steam, brine, and total and dryness fractions respectively 121,5454 T / J; 372,4338 T / J; 493,9792 T / J; 0,23542592 T / J,
3. Optimal well capacity obtained from the lip test method conducted at Y-well of K-cluster is 15.1 MW.

REFERENCES

Irsamukhti, Robi; Putra, Alfianto Perdana; Novianto. (2014). "James Lip Pressure Method for Low Flow Rate Geothermal Well: ML-5 Case Study". Proceedings of 14th IIGCE Tahun 2014, Jakarta: Indonesian Geothermal Association.

Saptadji, Nenny M. (2001). "Injectivity and Productivity Estimation in Multiple Feed Geothermal Wells". New Zealand: Department of Petroleum Engineering, Stanford University.

Suhartono, Nur. (2012) . "Pola Sistem Panasbumi dan Jenis Geothermal Dalam Estimasi Cadangan Daerah Kamojang". Tenik Geologi UPN "Veteran" Yogyakarta: Yogyakarta.

Pawitra, B.A. (2014). "Discharge Characteristics Production Test Activities and Comprehensive Well Testing Implementation during Exploration Phase in Ulubelu, Indonesia". Bandung: Institut Teknologi Bandung.

Shen J. (1981). "Horizontal Discharge Characteristics of Triangular-Notch Thin-Plate Weirs". Geological Survey Water-Supply Paper 1617-B, US Department of Interior.

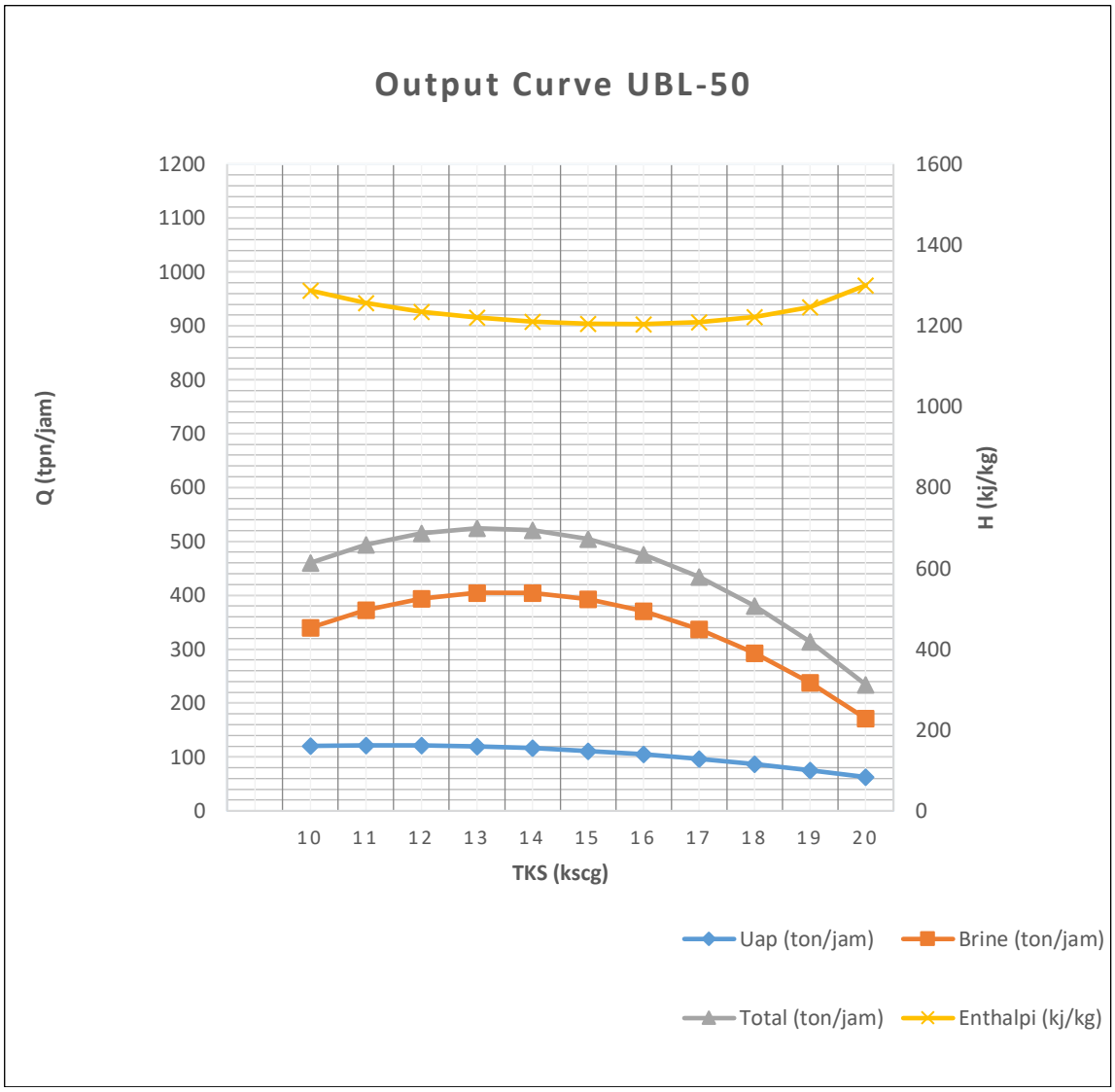


Figure 4: Output Curve of UBL Y-well of K-cluster.

UNIFIED LOGGING UNIT - DIGITALIZING GEOTHERMAL DRILLING IN STAR ENERGY GEOTHERMAL

Febra Sakti Dewa, Sufian Elsaleh, Hulyadi Halim, Mousa Namavar, Charbel Oueis, Tommy Souvanir, and Doddy Darmawan

Schlumberger
Star Energy
Email: FDewa@slb.com

ABSTRACT

Geothermal drilling has always presented a challenge throughout the exploration lifecycle. Not only that it makes up significant portion of the overall project spending, but it also can hugely affect project economics if not managed properly. Making informed decisions and data driven actions is an absolute paramount in driving drilling performance and reducing the risk of budget overruns.

For years the industry has been applying discrete drilling services and relying on incremental enhancements to improve drilling efficiency. While this has produced noteworthy results, performance is still plagued by inefficiencies due to the interfaces between multiple service providers.

Integrated Services contract is the key enabler which provides Schlumberger the platform to unify mudlogging and directional drilling services into a single coherent service providing measurements from both downhole and surface data, breaking the barriers and creating a more collaborative environment.

Mudlogging and Directional services are collocated in one logging unit utilizing integrated data acquisition system to stream realtime surface measurements from every corner of the rig coupled by downhole data. These data then transmitted to 24/7 RTDC (Real Time Decision Centre) established at client office for further processing such as parameters monitoring & optimization, predictive analytics, benchmarking, and reporting.

This setup has benefited both Star Energy and Schlumberger in a lot of different ways such as enhance data quality, seamless data transmission, effective communication, less footprint, less headcount and faster rig up time.

Keywords: Geothermal, IPM, Star Energy

PROJECT OVERVIEW

Schlumberger is providing integrated services to Star Energy Geothermal (SEG) who undertook Make Up Well (MUW) drilling campaign to remedy the steam short and maintain sustainability of steam supply in 3 different fields (Wayang Windu, Darajat and Salak). The drilling phase includes 15 wells in total with the sequence of 4 wells in Wayang Windu, 6 wells in Darajat, and 5 wells in Salak. It will be a one land rig operation in three different fields all in west Java area whilst command centre located in Jakarta.

CONTRACTUAL SETUP

The contract model is bundle service of Schlumberger inhouse services, third party and project management inclusive. Schlumberger Scope of work on this project is to provide services from the following services:

- Directional Drilling (DD) & Measurement While Drilling Services (MWD)
- Mudlogging & Drilling Parameter Monitoring
- Wireline
- Drilling Fluid and Solids Control
- Fishing Services
- Cementing Services
- Liner Adapter
- Air Drilling Services

With all the services under one umbrella, Schlumberger sees the opportunity to further improve efficiency by combining Directional Drilling (DD) & Measurement While Drilling Services (MWD) and Mudlogging & Drilling parameter Monitoring.

Schlumberger product line providing the said services are:

- Drilling & Measurement (D&M) - Directional Drilling (DD) & Measurement While Drilling Services (MWD)
- Geoservices (GSS) - Mudlogging & Drilling parameter Monitoring

EQUIPMENT SETUP

Xem MWD Downhole Tool

In this project, Schlumberger deployed proprietary XEM MWD tool that transmits data uphole through electromagnetic propagation technology.

XEM - Extreme is Measurement While Drilling with electromagnetic (EM) telemetry system offering: Inclination/Azimuth, Full MWD, Gamma-ray

logging, and Bore/ Annular Pressure While Drilling (PWD) - all for over-balanced and under-balanced applications. Figure 1 shows the XEM MWD downhole tool.

Features of Extreme, the next generation EM MWD, including but not limited to:

- Safe – No risk of catastrophic lithium battery failure in dry air applications
- Speed – Up to 12 bits per second telemetry rate
- Efficient – Surveys are taken and transmitted during connections allowing rig crew ability to prepare directional plans prior to back on bottom drilling with zero NPT
- Full Suite – Capable of providing multiple critical measurements on real time
- Robust – Designed and constructed using the most advance engineering, design, and manufacturing processes
- Reliable – Superior performance in air drilling and high LCM environments



Figure 1: XEM MWD Downhole Tool.

Real Time Data Measurement obtained by XEM MWD Tool are:

- DH Temperature
- DH Pressure
- Survey (Azimuth and Inclination)
- Gamma Ray
- Shock & Vibration
- Collar RPM

Combined Services Unit

In Star Energy Geothermal drilling project, Geoservices deployed latest generation acquisition system "GN5" which featured latest hardware and software to support drilling operation. Figure 2 shows the combined services unit, while Figure 3 shows the view from insidue the logging unit.

The acquisition system can connect and process data from up 250 sensors at 1-Hz acquisition frequency and up to 8 sensors at 50 hz.

GSS/D&M Combined Services Unit, a key enabler for the program, was deployed at the wellsite. The unit host both D&M and Geoservices surface system and can accommodate a full set of crew on tour (1 Directional Driller, 1 MWD Engineer, 1 Data Analyst, 1 Geologist, 1 Sample Catcher).



Figure 2: Combined Services Unit.



Figure 3: A view from inside the logging unit.

Mudlogging services acquired below measurements at surface:

- Rate of Penetration
- Hook Loads, Hook Height, Hook Speed
- Bit Time & Revolution
- Stand Pipe Pressure
- Air Booster Pressure (5000 psi)
- Air Flow Rate (Aerated Mud System)
- WOB
- Mud Pit volume
- Pump SPM & Cumulative Stroke Counter Pump
- Drilling Fluid Flow Rate
- Temperature in and out
- Mud density in and out
- Torque
- RPM (TDS, Rotary Table & Downhole)
- Flow line rate. & volume
- Mechanical Specific Energy (MSE, calculated based on Company algorithms)
- Condensate Water or Fresh Water feed to the rig site
- Annulus filling line (desander line) flow rate
- Cementing Pressure
- Standpipe Pressure While Drilling

VSAT – Satellite Data Transmission

A field deployed portable VSAT SCPC (Very Small Apperture Terminal Single Channel Per Carrier) is established to transmit data from the wellsite to InterACT server centralized in Jakarta.

VSAT C-Band 2.4 m fixed antenna was installed and commissioned at remote site and the antenna equipped with C-Band RF unit, SCPC satellite modem, router, switch and out of band management (OBM) device. Asiasat-4 satellite is selected as it covers Indonesia area, especially west Java area.

InterACT* system

Schlumberger InterACT* is a global connectivity, collaboration, and information service which is designed to provide quick access and can serve as data transmission portal.

InterACT service enables remote teams to proactively address their challenges, provides a secure online workspace, and enables collaboration, exploration, and implementation of new ways of working together.

The integrated InterACT Visualization display includes interactive time-depth log viewers for formation evaluation log data, a driller's console, lithology and cuttings data, numerical display, and events that update as they happen. Additionally, testing operations and sampling processes can be witnessed in real time.

Available mobile application for Apple® iPad® and iPhone® offers instant data availability/viewing. HTML5-enabled platform supports mobile data access, regardless of device type.

Data can also be streamed in real time directly from the InterACT database into analytical applications, such as the Petrel* E&P software, Perform Toolkit and TechLog* wellbore software platforms, and any third-party WITSML-compliant products, facilitate model-based surveillance while drilling & analyze, predict, and mitigate drilling risk. Figure 4 shows the network and data transmission diagram from wellsite to town, while Figure 5 shows the interACT device.

24/7 Real Time Decision Center (RTDC)

Real Time Decision Center is one of the innovations which is applied in this campaign to improve communication protocol and operation efficiency. It enables both STAR Energy and Schlumberger in town to continuously monitor critical project to ensure safe operation and quality assurance at all time. The flow of information streamed through InterACT is valuable to support the decision-making process and real time intervention such as wash out detection and T&D monitoring. It becomes even more essential when abnormal situation occurs e.g., stuck pipe and hole stability issue, enabling immediate data analysis and corrective action plan.

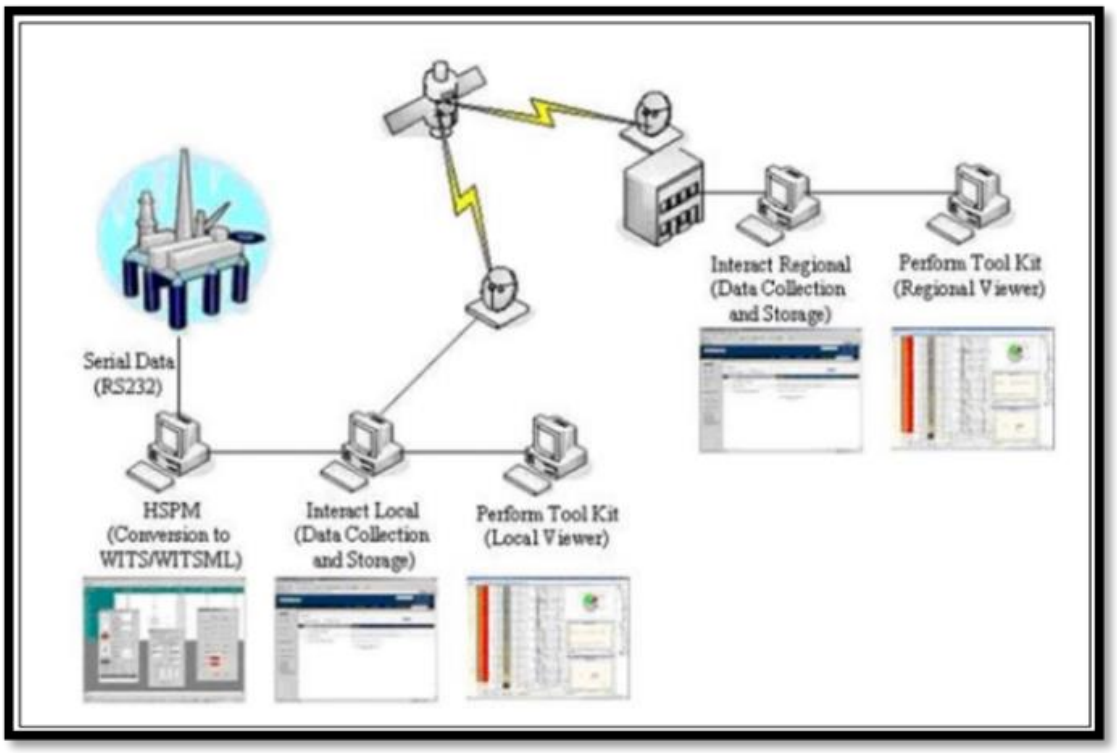


Figure 4: Network & Data Transmission diagram from wellsite to town via VSAT.

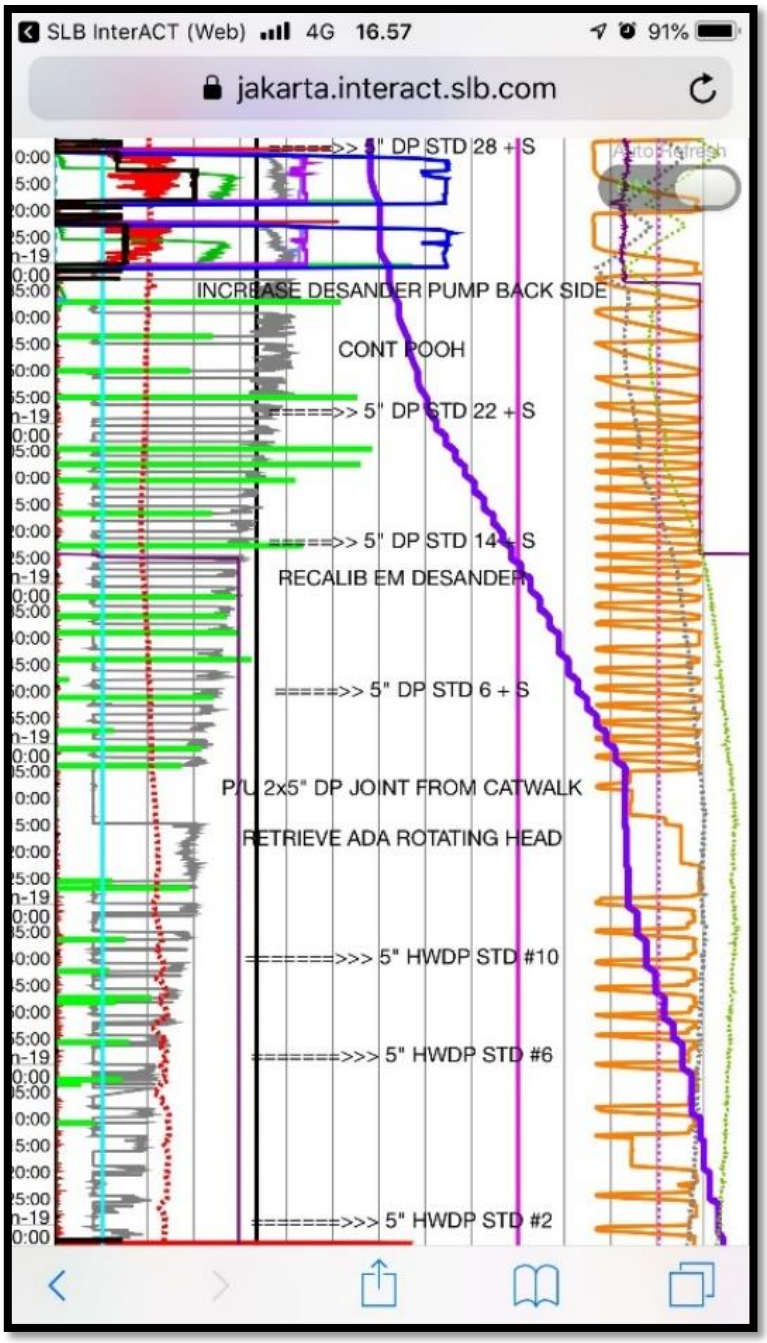


Figure 5: InterACT view from mobile device.

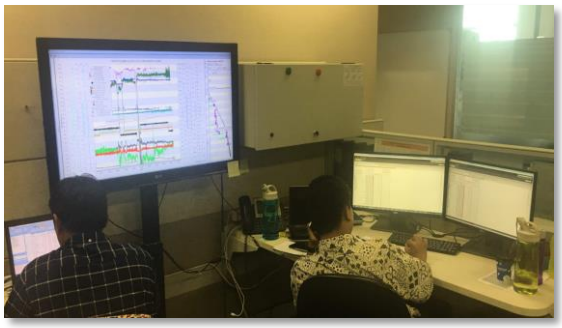


Figure 6: Schlumberger 24/7 Real Time Decision Centre at Star Energy Office.

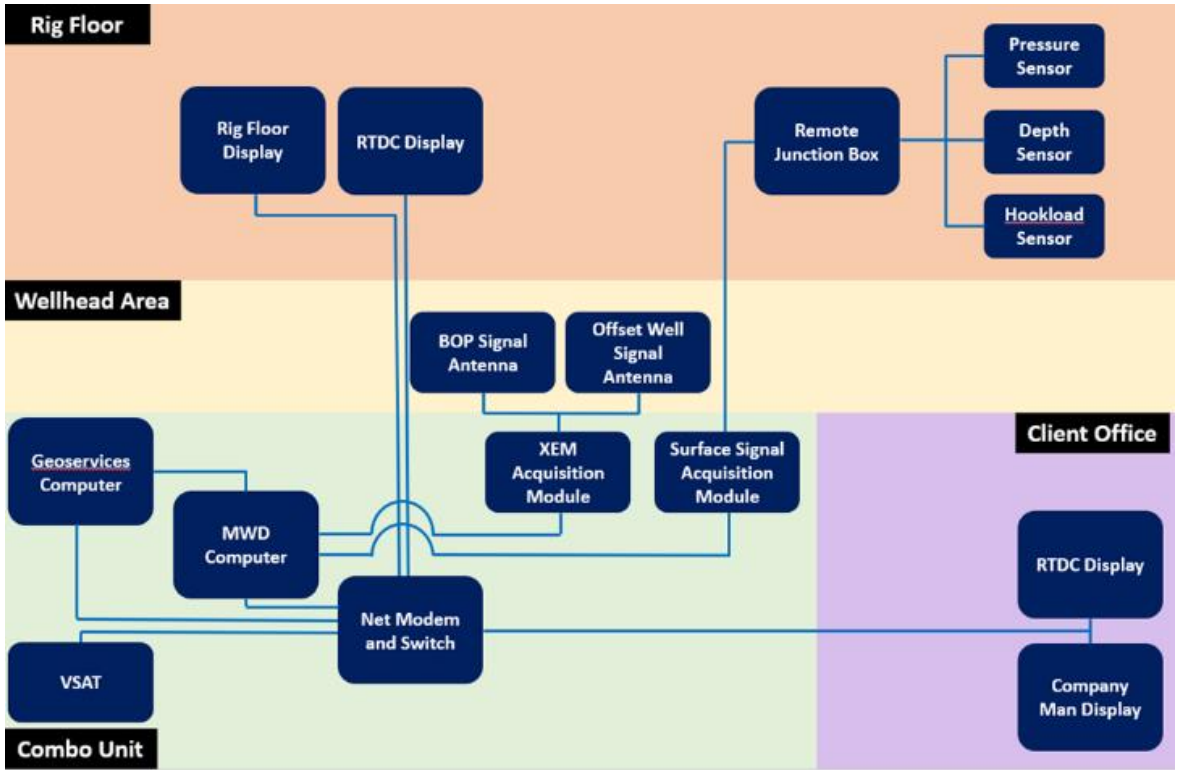


Figure 7: Schlumberger & Star Energy Equipment Setup Diagram.

Overall Equipment Setup

Analogic signal from sensors are sent to field boxes, converted to digital signal and then sent to the Mud logging unit. Those data are then processed and displayed to be monitored and reported. Data are displayed in several screens (ML, Rig floor, client stations) and alarm can be set internal and external (siren, beacon, traffic light). Data recorded by the mud logging acquisition system then sent via WITSML to MWD Maxwell data acquisition system. Maxwell then combines the mudlogging and MWD data together and send it through VSAT to InterACT Real Time Data server to be displayed remotely wherever its required. Figure 6 shows the Schlumberger real time decision centre at Star Energy office. Figure 7 shows the equipment diagram setup.

Equipment Summary of Change Before vs After State:

Before

- Directional Drilling and Measurement While Drilling Services resides in a separate cabin to Mudlogging services.
- A separate acquisition system deployed and no shared sensor/acquisition system between MWD and Mudlogging services
- MWD and Mudlogging Data are independently transmitted to client database through witsml.

After

- MWD services collocated inside Mudlogging Combo Unit
- Acquisition systems are run concurrently, and sensors are shared between MWD and Mudlogging services
- Mudlogging Data and MWD Data are merged through MWD wits server into a single WITSML file and transmitted to InterACT

PERSONNEL SETUP

Data Analyst (Before):
A person who monitors drilling parameters and is responsible for maintaining geological service sensors, gas equipment and data acquisition equipment to aid safe and efficient well operations, as well as the delivery of high-quality drilling and gas data to the customer at the well site.

MWD Engineer (Before):
An engineer who makes use of the Logging/Measurement While Drilling tools such as Mud Pulse and Electromagnetic Measurement while drilling system.

ACE Engineer (After):
The Acquisition & Control Engineer "ACE" is a Field Technical Analyst responsible for delivering high quality Well Monitoring & MWD measurements services to the client at the well site or through Remote Operations in real time. His/her primary responsibility is to acquire, log, analyze and report well behavior and MWD Measurement.Training of ACE engineer involves a

three-week preschool workshop at the wellsite followed by four weeks at a learning center.

The broad ACE competency spectrum, covering surface mud logging and downhole MWD, enables efficient identification of drilling events such as stick slip, vibration and washouts, leading to improved drilling efficiency for clients. The ACE's combined role also helps to streamline wellsite communication with the client. Figure 8 shows the phase of deployment.

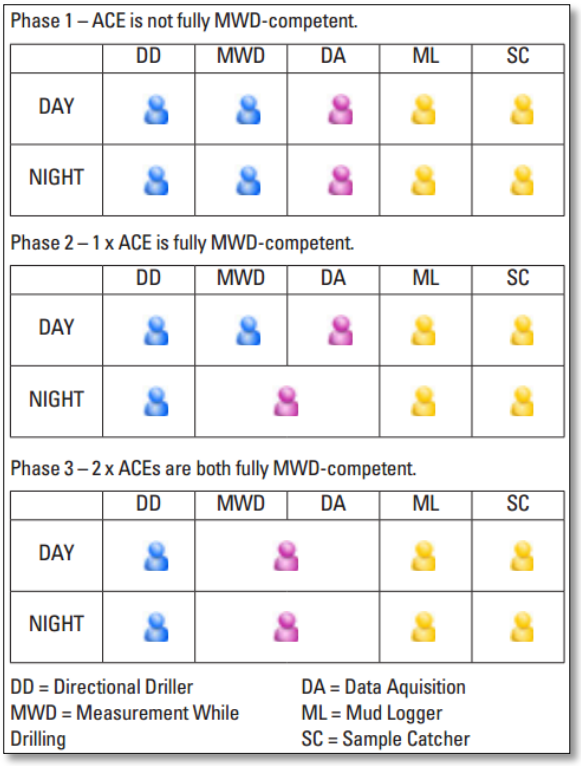


Figure 8: Phase of deployment.

Personnel Summary of Change Before vs After State:

Before

- 2 MWD engineer hand deployed at the wellsite to cover day and night shift
- 2 Data Analyst engineer deployed at the wellsite to cover day and night shift

After

- 1 MWD engineer hand deployed at the wellsite to cover day shift
- 1 ACE Engineer hand deployed at the wellsite to cover night shift
- 1 Data Analyst engineer deployed at the wellsite to cover day shift

*(Schlumberger in Star Energy Project is at **phase 2** of deployment)*

BENEFIT

1. Safe footprint and deck space
   By having MWD acquisition system collocated inside mudlogging unit, deck space will free up. MWD shack normally do not occupy lots of space, but in space constraint environment such as offshore rig and congested wellpad, it is extremely beneficial. In Star Energy Geothermal Make Up Well drilling campaign, SLB had to operate in existing wellpad where there are lots of well already been drilled and producing. Existing steam lines run across wellpad making it less space for the rig and services to settle. By having Mudlogging and MWD in the same cabin, it reduced the need to fit in a 15 ft container.

2. Less assets & resources
   A unified logging unit means that there is less logging unit necessary to deploy. This would bring lots of savings in terms of asset costs and running overhead costs. There are currently measurement/data that are redundantly being measured by both MWD and Mudlogging. This can also be eliminated by having a joint acquisition system between MWD and Mudlogging which result to lesser sensor being rigged up. Less power consumption is another benefit as a result to this unification.

3. Less HSE risk
   Less assets & personnel would mean less exposure to personnel and equipment. Lesser equipment to maintain hence lesser risk/likelihood for something to go wrong. Same goes to personnel, reducing POB count will reduce probability of accident/incident to happen.

4. Easy and fast communication
   Collocating MWD and Mudlogging unit would mean having Directional Drillers, MWD Engineer, Data Analyst and Geologist in the same unit. This reduces the amount of time and effort wasted to communicate between individuals.

5. Reduce Headcount
   ACE engineer is a multiskilled engineer who is capable to do the night hand MWD task along with mudlogging activities. This eliminate requirement to deploy a night hand MWD. As a redundancy system, SLB implement a remote operation system whereby realtime monitoring engineer will be available 24/7 at Jakarta Operation Support Centre to log in through VSAT and do a realtime intervention if necessary.

6. Data Integration

An automatic data integration is a result of a joint acquisition system. Downhole data and surface parameter measurement from every corner of the rig are streamed into a single database before it gets sent through internet via SLB VSAT.

7. Scalability
   Service expansion is possible through the combined services unit. Data acquisition can easily be expanded through other services such as advance LWD services coupled by realtime XRD to obtain comprehensive formation evaluation service. Another example is tapping Air Drilling or Managed Pressure Drilling Service and integrating it with downhole measurement will enable a more comprehensive drilling mechanic analysis.

8. Improved Data Quality
   By having redundant sensors and multiple personnel from different job roles in the same unit, real time data can be QCd from all angle to ensure data accuracy and quality. Data verification can be done as soon as it comes. Any abnormal data can be spotted and correlated against downhole and/or surface event immediately. Troubleshooting and Calibration to rectify measurement can be done on the fly.

9. Comprehensive data analysis resulting into better technical advice and decision making
   Service Company will be more value to customers if capable not only to provide service as required but also to provide technical recommendations supported by valid data/information. Both surface and downhole data can be easily analyzed against each other. Valid technical advice can be given to company, and as a result better decision making for actions/interventions to drilling operation.

10. Career Opportunity and Advancement
    With ACE Engineer position now been implemented, mudlogger will now have opportunity to progress through their career into becoming MWD engineer and further to Directional Drilling. A more complete competency and experience matrix can be obtained through the ACE program.

11. Redundancy (Backup System) – reliability
    In drilling environment where everything is referred to depth, having both mudlogging and MWD acquisition system unified in a single logging cabin create a redundancy system especially for depth measurement. In the case whereby one is down (ie. mudlogging depth sensor failed), acquisition can resume by switching mudlogging depth inputs to MWD. This will also apply vice versa, so the need to stop drilling operation due to failed depth sensor/measurement can be eliminated.

12. Reduced Contracting and Procurement process
    The key enabler for drilling contractor to integrate mudlogging service and directional service is an umbrella contract where mudlogging and directional no longer segregated by a separate contract. With all the benefits listed above it is encouraged for operator to start procuring directional and mudlogging service in a single contract/tender.

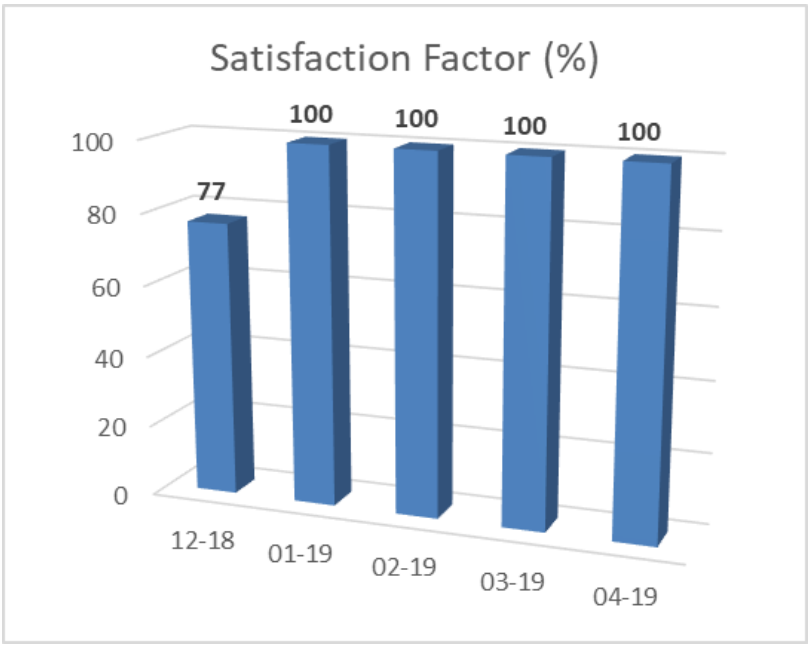
RESULTS

Below statistics obtained from client service quality feedback from the start of drilling campaign. This scoring was done quarterly by drilling representative at the wellsite (lead drilling supervisor and wellsite geologist). At the beginning there was hesitation to change from traditional way of doing things to a new way of working. Complaint such as crowded and less space available in the unit was communicated. However soon after adjustment was made, benefits outweigh the downside and client seen the improvement in service quality. At the end this model was accepted and continued to be implemented to present time. Figure 9 shwos the salinification factor.

CONCLUSION

With all the benefits gained through combining mudlogging and directional service collocated in the same combined services unit, it is highly recommended to implement this initiative in drilling projects. This will break a lot of barrier and drive performance. Not only does this initiative brings efficiency to operation by cutting down resources (assets, spare parts, personnel, maintenance) but it also delivers better performance such as improved data quality, better technical advice, and increased reliability (less NPT). Nonetheless HSE risk also gets reduced by the less exposure to personnel and equipment.

It all should start from going out of the traditional way of contracting where directional drilling and mudlogging are contracted separately and start combining them into a single tender/contract. This will be the first step, key enabler and facilitator for such initiative to materialize.



Performance Efficiency

Depth Drilled (m)	Data Loss (m)	Logging Efficiency	Operating Hours (h)	Non Productive Time (h)	Operating Efficiency
6,639	0	100.00%	4,368	0	100.00%

See more onPerformance Efficiency detail tab

Figure 9: Satisfaction Factor Statistic & Operational Summary.

NOMENCLATURE

SLB - Schlumberger
RTDC – Real Time Decision Centre
SEG – Star Energy Geothermal
MUW – Make Up Well
DD – Directional Drilling
MWD – Measurement While Drilling
D&M – Drilling & Measurement
GSS - Geoservices
XEM – Xtreme Electro Magnetic
EM – Electro Magnetic
PWD – Pressure While Drilling
NPT – Non-Productive Time
LCM – Loss Circulation Material
DH – Down Hole
RPM – Rotation Per Minute
TDS – Top Drive System
MSE – Mechanical Specific Energy
VSAT - Very Small Apperture Terminal
SCPC - Single Channel Per Carrier
OBM – Out of Band Management
WITSML – Wellsite Information Transfer Standard Markup Language
T&D – Torque & Drag
POB – Personnel On Board
XRD – Xray Diffraction
QC – Quality Control
HSE – Health Safety and Environment

REAL TIME DECISION CENTER: DRIVING OPERATIONAL EXCELLENCE IN GEOTHERMAL DRILLING

Gatra Kusuma, Febra Sakti Dewa, Puthut Hadi Surya, Tommy Souvanir, Agus Ziyad Kurnia, and Hulyadi Halim

Star Energy Geothermal and Schlumberger
Email: GKusuma@slb.com, FDewa@slb.com, PSurya@slb.com, tommysouvanir@starenergy.com, akurnia2@slb.com, HHalim@slb.com

ABSTRACT

There has been a steep increased in drilling activity happening over the past years in search of geothermal energy. Geothermal drilling is a unique and risky environment whereby stuck pipe as a result of drilling under loss circulation condition is the main source of non-productive time. Historical statistic indicates 30% - 40% geothermal wells drilled involved a significant amount of time spent to combat stuck pipe and, in most occasion, resulted in lost in hole (LIH). To strive for an efficient and effective geothermal drilling operation, a new approach is needed to be introduced to the industry.

Realtime Decision Centre (RTDC) was introduced in STAR Energy Geothermal Drilling Campaign as a mean to have a dedicated 24/7 real time monitoring center. Data acquired from every corner of the rig is streamed in real time to RTDC, being monitored and analyzed. By gathering real-time data measurements, comparing pre-simulation results with actual measurements, running new simulation to adjust with changing of actual drilling condition enabled well team to make informed of early detection warning, decision and execute data driven action and benchmarked in multiple ways for better visibility of well status. The operation significantly benefited from the continuous flow of reliable and accurate processed information.

This paper will showcase the workflow design of RTDC, drilling monitoring & optimization and the implementation of escalation protocol. After 5 months and 3 wells drilled in the campaign, no stuck pipe which lead to lost in hole had happened.

Keywords: Drilling, geothermal

INTRODUCTION

Star Energy restarted their drilling campaign at the end of 2018 after almost two years. The return of Star Energy to start the drilling campaign is in line with the government's goal of targeting national electricity supply. This drilling campaign will be carried out in several fields and the first field that will be done in WayangWindu Field. Star Energy and Schlumberger have collaborated on several previous drilling campaigns, especially in WayangWindu with quite good results. This achievement will be a trigger for more satisfying results by reducing the risk of getting stuck which is the biggest risk during the drilling process. Thus, preventing and minimizing the occurrence of stuck becomes the main target of increasing service quality.

RTDC come up with the main goal to improve service quality. By providing a real-time operation monitoring for 24/7 connection with the field. Service quality was improved through timely intervention, capture and share the knowledge. Dealing with challenging environments requires real time monitoring that is able to fulfill its objectives. The idea is to improve the decision-making process and increase response time to potential problems before they occur. This must be achieved by defining operational workflows that utilize real-time data to improve plans, execution, evaluation stages. Discussion of the operational framework and background and the role of technology to support operational performance will be described in this paper.

DESIGNING AND PLANNING STAGE

BHA Configuration and tendency

Designing BHA is considered for each need. The need for the capability of the dog leg to catch up the plan, minimize sliding footage when drilling the vertical section, tangent section and also when penetrating the reservoir.

In the building section, sliding strategy need to be conducted prior to proceed drilling process. Correlate with Formation prognosis which formation could deliver DLS as per expected and also optimum ROP. Thus, all of the main objectives are to penetrate the formation until the plan TD and return to the surface safely.

Drilling Office **(**DOX) software are used to configure the BHA as shown in Figure 1. Analyzing the behavior or capability and tendency of BHA must be done prior import the BHA into Perform Tool Kit **(**PTK) software. In PTK, the next process which is monitoring the drilling process will take place.

The results of the capability and tendency of the configured BHA as shown in Figure 2 will be used

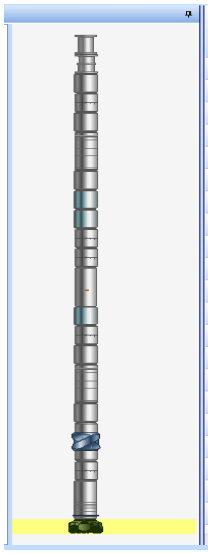
to determine the drilling practices. This BHA capability and tendency will be monitored and adjusted during the drilling process so the optimum drilling parameters will be determined.

Adjusting BHA tendency by the drilling environment shows a significant difference to the previous tendency. By looking at the new tendency of the BHA, the highest of WOB limit need to be applied to get less drop tendency. In more detail Figure 3 can be a reference.

As much as possible the well trajectory shall be as simple as possible to reduce directional work especially in TLC and tuffaceous siltstone one areas It requires to slide when steering with mud motor. The pipe will steady (no rotation) for a period of time. There is a risk that drilled cuttings accumulate around the BHA and could lead to the stuck the pipe event. The risk is increased when sliding in a total loss zone, since the drilled cuttings will not circulate out to surface.

The well trajectory is designed so that the steering work ended prior entering the reservoir. It would then be avoiding steering the well in the total loss zone. Wells were kicked off in either 26" or 17-1/2" and finished the steering prior to enter the reservoir formation.

The well trajectory is also optimized in term of build and turn required. It was preferred to design 2D well trajectory which purely build rather than 3D. It will reduce overall torque and drag at well TD significantly.



	Catalog	Type	Desc.	Manu.	Serial Number	OD (in) / ID (in)	Max OD (in)	Bot Type / Top Type	Bot Gender / Top Gender	FN OD (in) / FN Length (ft)	Length (ft)	Cum. Length (ft)
1		Bit	26" Baker TCI Bit, VG-09 , IADC: 435, New	Baker	5289241	9.75 / 3.75	26	7-5/8 REG	Pin		1.78	1.78
2		Motor	A962M7848GT (25-3/4" Sleeve, 1.15 ABH)	Schlumberger	03362	9.625 / 7.85	25.75	7-5/8 REG / 7-5/8 REG	Box		30.35	32.13
3		Misc. Sub	9-1/2" Catcher Sub w/ NP Plunger Float Sub	Schlumberger	FS96CS042 6	9.5 / 2.813	9.5	7-5/8 REG / 7-5/8 REG	Pin Box		3.75	35.88
4		Stabilizer	24" IBS Stabilizer	Schlumberger	78625 H	9.5 / 3	24	7-5/8 REG / 7-5/8 REG	Pin Box	9.5 / 2.36	7.5	43.38
5		Collar	1 x 9-1/2" Collar	Rig DATI	Rig DATI	9.63 / 3.06	9.63	7-5/8 REG / 7-5/8 REG	Pin Box		30.98	74.36
6		Shock Sub	Shock Sub 9-1/2"	NOV	151-2673996	9.5 / 2.813	9.75	7-5/8 REG / 7-5/8 REG	Pin Box	9.625 / 1.83	12.35	86.71
7		Collar	1 x 9-1/2" Collar	Rig DATI	Rig DATI	9.63 / 3.06	9.63	7-5/8 REG / 7-5/8 REG	Pin Box		30.95	117.66
8		Misc. Sub	Crossover (7-5/8" Reg Pin x 6-5/8" Reg Box)	Rig DATI	Rig DATI	8.25 / 2.81	9.5	7-5/8 REG / 6-5/8 REG	Pin Box	8 / 1.92	3.64	121.3
9		Collar	8" NMDC	Schlumberger	63047	8.25 / 3	8.25	6-5/8 REG / 6-5/8 REG	Pin Box		25.37	146.67
10		MWD	MWD XEM 800	Schlumberger (...	1867	8.5 / 3.5	8.5	6-5/8 REG / 6-5/8 REG	Pin Box		32.95	179.62
11		Misc. Sub	MWD Gap Sub	Schlumberger (...	GSD0160R	8 / 3.5	8	6-5/8 REG / 6-5/8 REG	Pin Box		3.4	183.02
12		Misc. Sub	UBHO sub	Schlumberger	1020294-1-17	8.25 / 3.25	8.25	6-5/8 REG / 6-5/8 REG	Pin Box		3.02	186.04
13		Collar	8" NMDC	Schlumberger	BMS-0057-4-12	7.75 / 2.75	7.75	6-5/8 REG / 6-5/8 REG	Pin Box		27.65	213.69
14		Collar	8.25" Pony NMDC	Schlumberger	63048J-JOP17-02	8.25 / 2.875	8.25	6-5/8 REG / 6-5/8 REG	Pin Box		12.15	225.84
15		Collar	7 x 8" Collar	Rig DATI	Rig DATI	8 / 2.812	8	6-5/8 REG / 6-5/8 REG	Pin Box		215.14	440.98
16		Jar	8" Hydraulic Jar	Smith	41087 J	8 / 3	8	6-5/8 REG / 6-5/8 REG	Pin Box	8 / 2.02	32.35	473.33
17		Collar	4 x 8" Collar	Rig DATI	Rig DATI	8 / 2.812	8	6-5/8 REG / 6-5/8 REG	Pin Box		124.17	597.5
18		Misc. Sub	Crossover (6-5/8" Reg Pin x 4-1/2" IF Box)	Rig DATI	Rig DATI	6.75 / 2.81	8	6-5/8 REG / NC50 (4 1/2...	Pin Box		3.66	601.16
19		Collar	3 x 6-3/4" Collar	Rig DATI	Rig DATI	6.75 / 2.875	6.75	NC50 (4 1/2... / NC50 (4 1/2...	Pin Box		93.23	694.39
20		HWDP	9 x 5" HWDP	Rig DATI	Rig DATI	5 / 3	6.5	NC50 (4 1/2... / NC50 (4 1/2...	Pin Box		277.54	971.93
21		Drill Pipe	5" 19.50 DPS, Premium	Rig DATI	Rig DATI	4.855 / 4.276	6.625	NC50 (4 1/2... / NC50 (4 1/2...	Pin Box		30	1001.93

Figure 1: BHA Configuration.

DWOB	Rotary Build Rate	DLS in sliding	Effective Toolface in sliding	Build Rate at 100% setting	Turn Rate at 100% setting	Solution Converged
1000 lbf	deg/100ft	deg/100ft	deg	deg/100ft	deg/100ft	
0.00	-0.33	3.34	0.00	3.34	0.00	Yes
5.00	-0.38	3.26	0.00	3.26	0.00	Yes
10.00	-0.31	3.41	0.00	3.41	0.00	Yes
15.00	-0.27	3.68	0.00	3.68	0.00	Yes
20.00	-0.18	3.87	0.00	3.87	0.00	Yes
25.00	-0.16	3.89	0.00	3.89	0.00	Yes
30.00	-0.15	3.93	0.00	3.93	0.00	Yes
35.00	-0.17	3.89	0.00	3.89	0.00	Yes
40.00	-0.18	3.89	0.00	3.89	0.00	Yes

Figure 2: BHA Tendency on planning stage.

DWOB (1000 lbf)	Rotary Build Rate (deg/100ft)	DLS in sliding (deg/100ft)	Effective Toolface in sliding (deg)
0.00	-1.27	3.47	0.00
5.00	-1.26	3.49	0.00
10.00	-1.12	3.52	0.00
15.00	-0.94	3.55	0.00
20.00	-0.77	3.57	0.00
25.00	-0.59	3.60	0.00
30.00	-0.43	3.63	0.00
35.00	-0.28	3.66	0.00
40.00	-0.16	3.69	0.00
45.00	-0.03	3.73	0.00

Figure 3: BHA Tendency adjusted on execution stage.

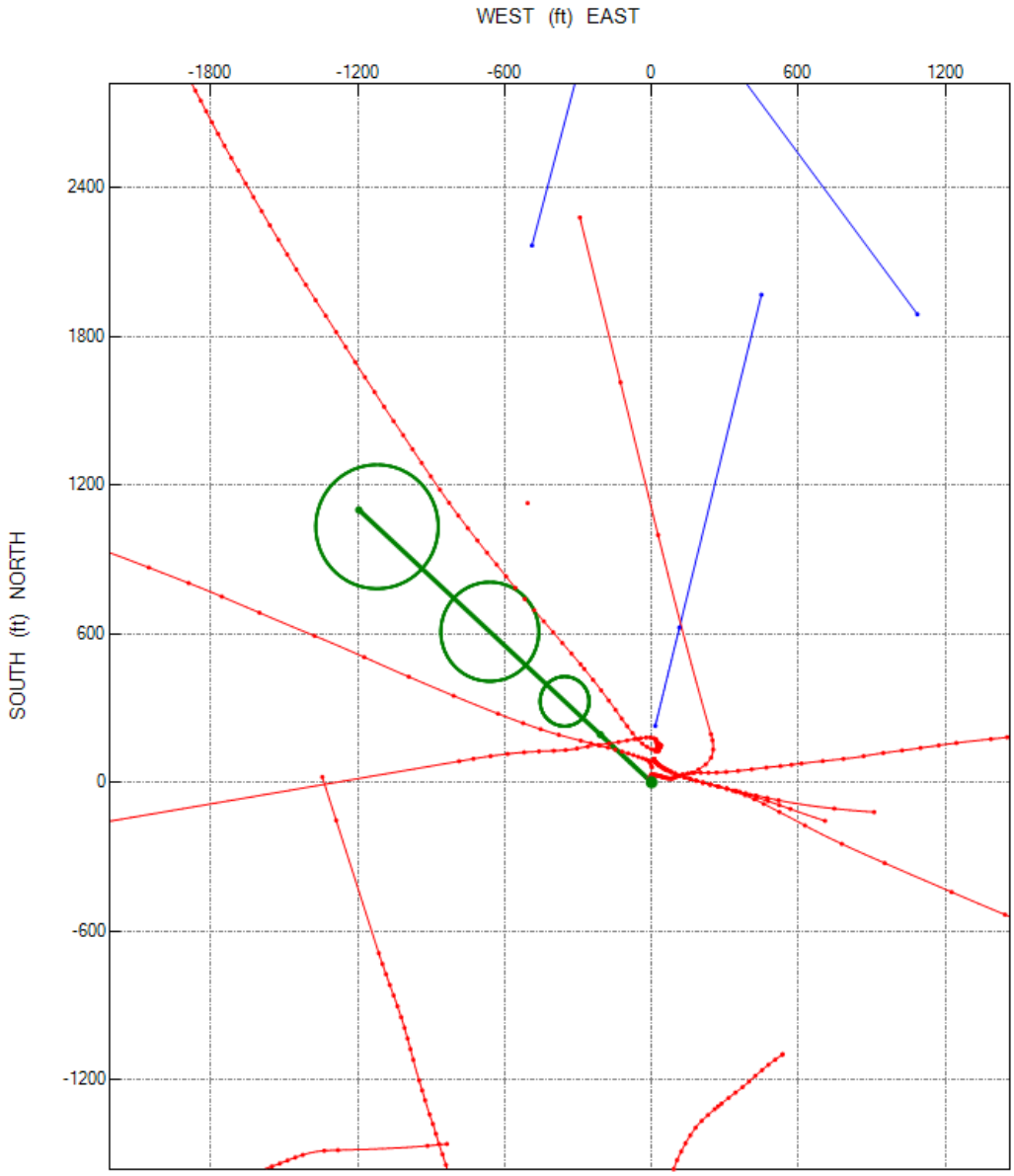


Figure 4: Plan view of subject and offset well.

Anti-collision analysis

It is uncommon that there are more than 6 slots in one well pad in this field. The center-to-center distance between slots are approximately 20ft distance. The well trajectory has to be designed to avoid collision with other wells especially at the shallower section.

Drilling Office (DOX) software are used to simulate the anti-collision. It takes into account the error of uncertainty (EOU) of the survey tools. The oriented separation factor (OSF) between planned well and offset wells are then calculated.

Due to ferro-magnetic property / iron oxide of volcanic formation, the azimuthal magnetic surveys measurement are affected and this resulting a bigger EOU. Since the EOU is bigger, the SF is also bigger and less than 1.5 which is the maximum required by Schlumberger standard.

A prevention plan is developed to avoid collision with other wells. That includes ensuring center-to-center distance between planned wells and offset well as far as possible; and to use the traveling cylinder (TC) plot as guidance for the directional driller when steering the well.

Drilling in this field has risk collision with offset wells. More attention related Anti Collision issues need to be done. To avoid it we have to monitoring actual survey, made projection at least 2 stands ahead and check MWD survey criteria (Field interference) values each survey. Also, we have to see Travelling Cylinder Plot to know the position compare offset wells. Figure 4 shows the plan view of subject and offset well.

The Normal Plane method is used to produce the Traveling Cylinder plot for graphical visualization of the no-go areas that the bit shall not cross, while 3D least distance is used to monitor the Anti-Collision working with the numerical results. The visualization of the Anti-Collision situation using was clearly shown in Figure 5.

By monitoring the Travelling cylinder plots which are undistorted and depict the true 3-D relative position of surrounding wells, these plots are especially useful for forward projections. Scanning down the offset survey ensures that no portion of the offset well is missed. This ability is especially important for detecting close approaches between wells oriented perpendicularly.

Real time data streaming set up

All data from each corner in rig site was sent and combined in mud logger unit. The collected data was transferred to Star Energy folder in InterAct data base via a network of secure VSAT network. By having an access into this folder make the InterAct user easy to monitor the drilling process anytime and anywhere.

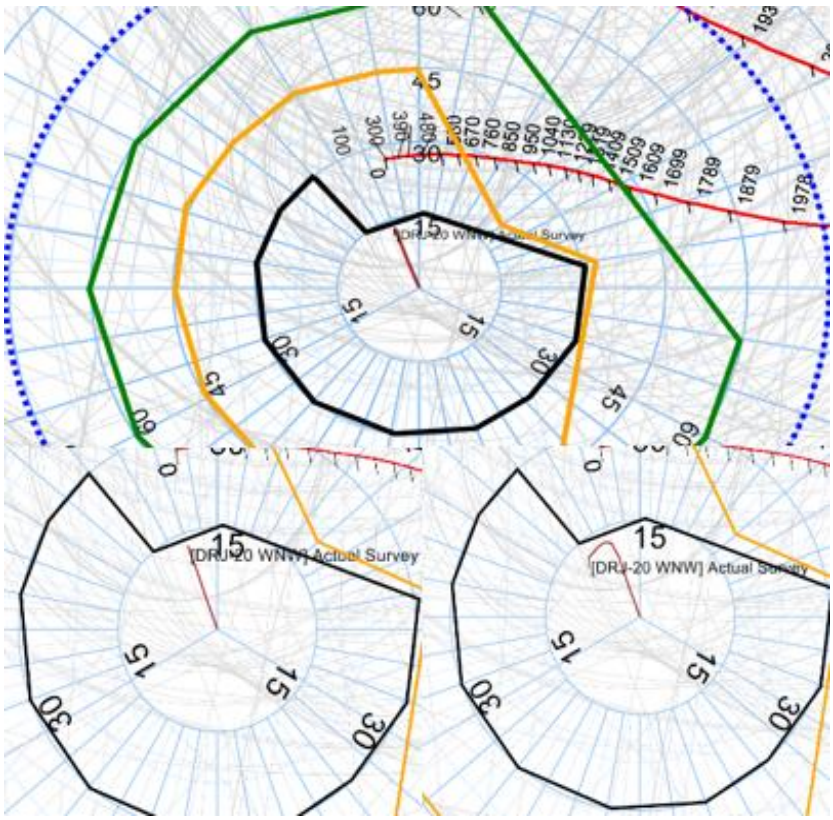


Figure 5: Travelling Cylinder Plot.

DRILLING MONITORING

Drilling analysis

The main challenges while drilling in geothermal are stuck pipe incident and well control events. It can be avoided if the realtime data can be interpreted properly. By displaying drilling parameters in real time such as Pressure, Torque, Hookload, Flowrate, WOB, ROP, ECD, Temperature, Vibration, pump strokes, and also Torque & Drag analysis can give early sign and indication of various event.

Drilling analysis in time base log as shown in Figure 7 which is consist of drilling parameter curve. Any abnormal behavior in one parameter can be clearly understood by looking at another curve/parameter. Hence those unwanted events can be avoided by immediately applying the proper corrective actions.

User with an access possible to monitor drilling activity through mobile phone as shown in Figure 8. Ease in monitoring each drilling activity is very helpful for the decision-making process. RTDC engineer as a key person in the monitor process will discuss with each related party referring to the same drilling log activity page. If each party has the same picture of the conditions of the ongoing drilling, the ease of discussion will help make good decisions.

Directional control

Directional control from MWD can be monitored closely, Realtime Continues Inclination, Azimuth and DLS. The tendency of BHA can be analyzed as shown in Figure 10. The dropping tendency correspond to applied surface weight on bit was clearly present on the log. Adjusted parameter with increasing surface weight on bit to counter the dropping tendency was success to maintain the hole inclination.

When drilling hard andesite formation, a normal stabilizer blade can be easily worn out, and hence reduced the OD. It will then reduce the dog leg capability of this mud motor-stabilizer configuration. Stabilizers that are used in this geothermal drilling campaign has hardfacing HF 6000. This process applies tough molten carbide particles of varying sizes, held in a nickel chrome matrix which provides excellent bonding properties and greater surface wear characteristics are achieved. Figure 9 shows the continuous survey.

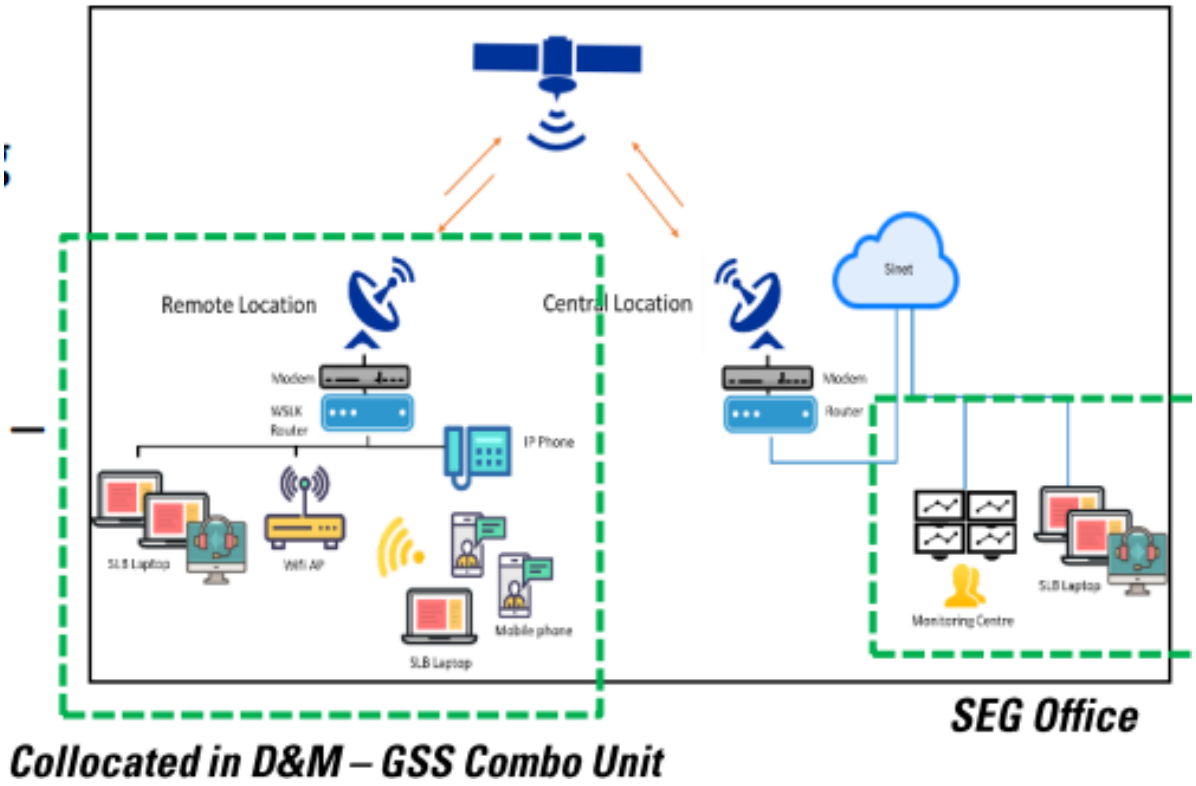


Figure 6: Data stream mapping.

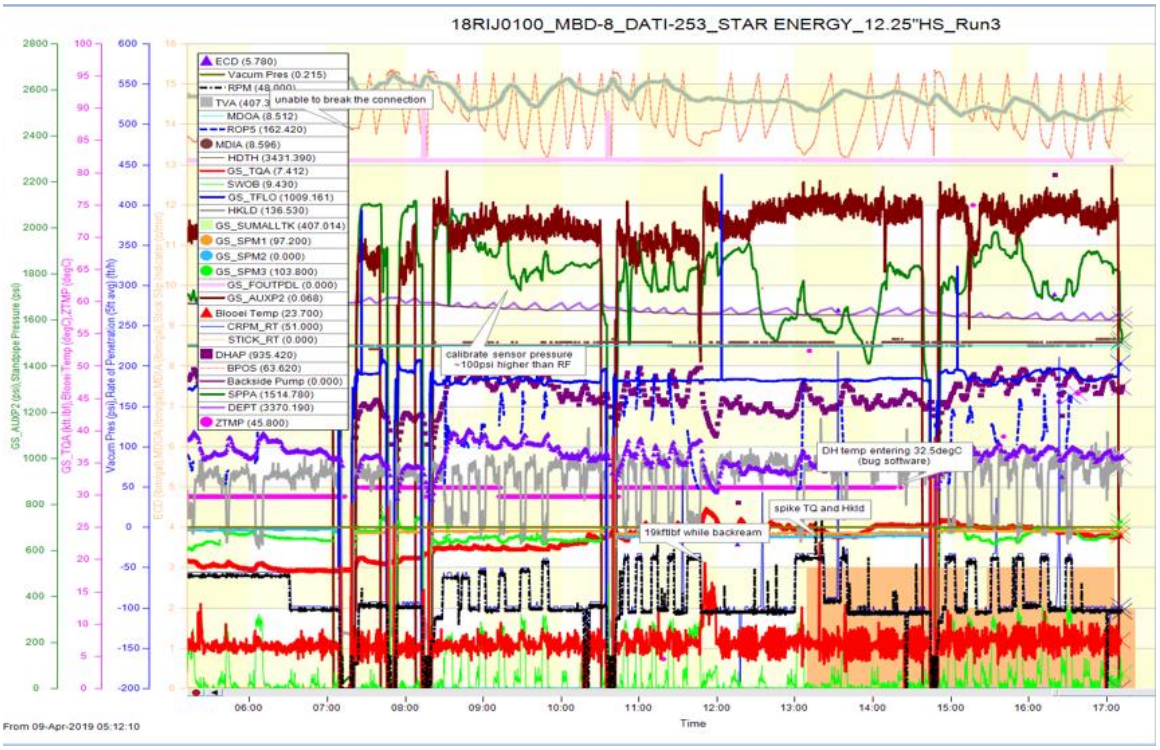


Figure 7: Drilling analysis.

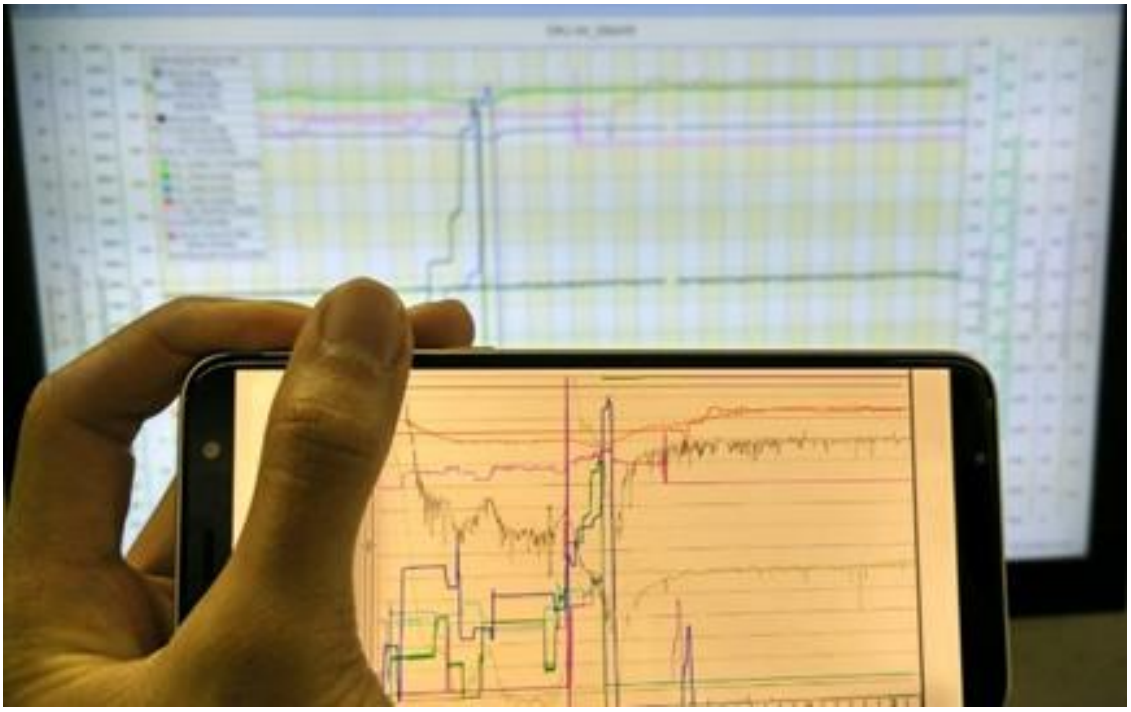


Figure 8: Monitoring through mobile phone.

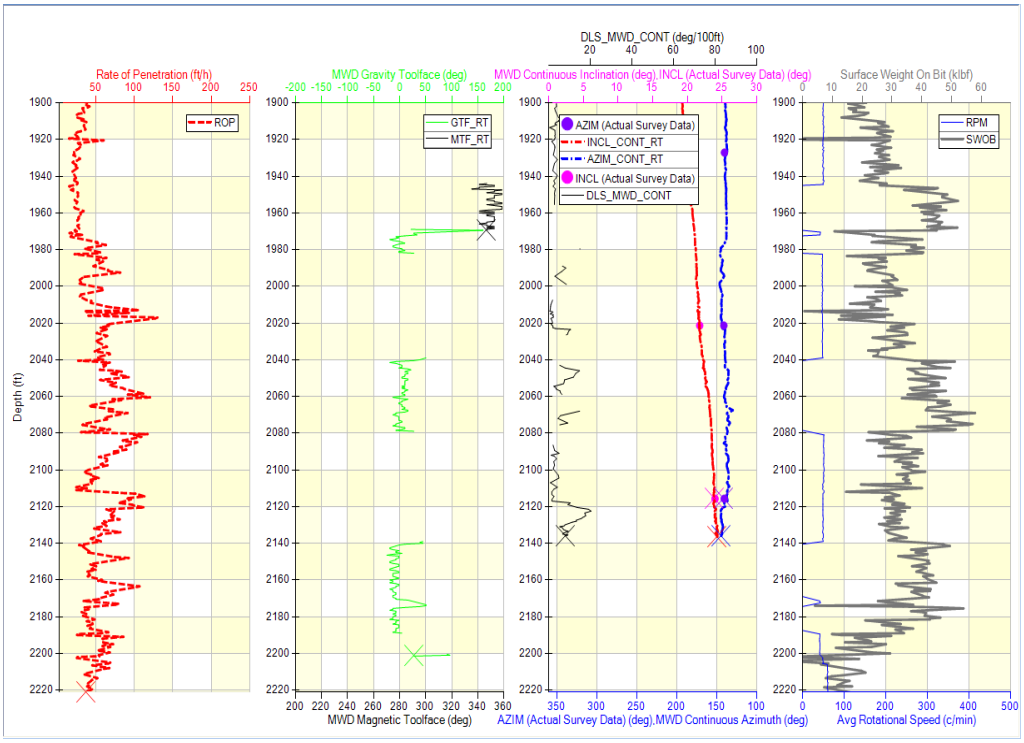


Figure 9: Continuous survey.

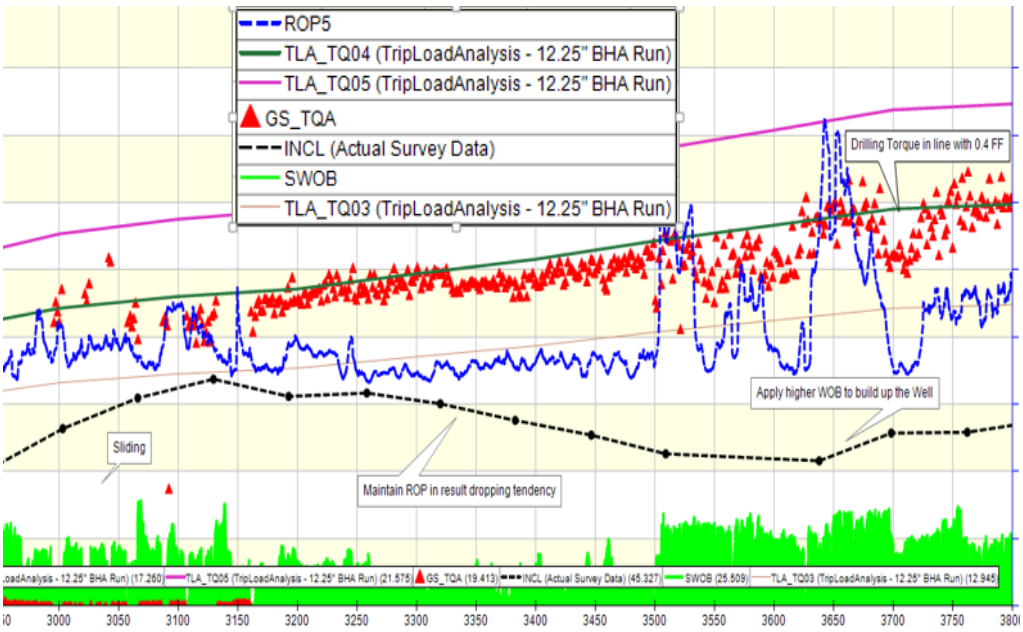


Figure 10: Well inclination tendency.

Realtime comparision VS offset Well

Offset wells data was the most valuable reference data both in designing and executing stage. As reference data, each applied parameter and its behaviour will help to determine drilling condition. Monitoring Plot between Realtime data versus offset wells as a benchmark, it is ease RTDC engineer to determine any abnormaly event at depth based.

Torque and Drag Analysis

Torque and Drag Analysis one of the tools monitoring and surveillance software, it good tools to detect any deviation related hole condition. The input software are BHA component, Block weight, well trajectory, drilling fluids and formation friction factors to get T&D modelling. Real time Data (T&D actual) Drilling Torque, Ream/ Back ream Torque. Also, P/U Weight, Rotating Weight and S/O weight that taken prior connection will be plotted against

T&D Model. In case any variation or deviation from expected trend (FF), it can be indication of hole cleaning issues or formation changes and need to take an appropriate corrective action.

Tripping monitoring

During wiper trips there are a number of considerations to take into account in order to analyze properly the BHA configuration, formation tops, well geometry, log data and more. By looking at the historical drilling parameter on drilling process we can use the tendency of this BHA on drilled Well as references while tripping in/out the hole. Deviation from the trend will recognize clearly by using this plot, shown in Figure 13.

STUCK PIPE PREVENTION AND MITIGATION

As the main objective of the RTDC is to improve service quality, mitigate and prevent stuck pipe event need to be taken into account. Delivering directional service with high risk of getting stuck either drilling in surface section or while penetrating reservoir zone were the challenges during the campaign. Many possible causes could be presnt while drilling, such inability to clean the well, swelling of highly reactive clay i.e. Smectite Clay in water-based drilling fluid, combined with hard and abrasive formation, total loss circulation (TLC) due to fractured formation. Figure 11 shows the current and offset well. Figure 12 shows the torque and drag analysis.

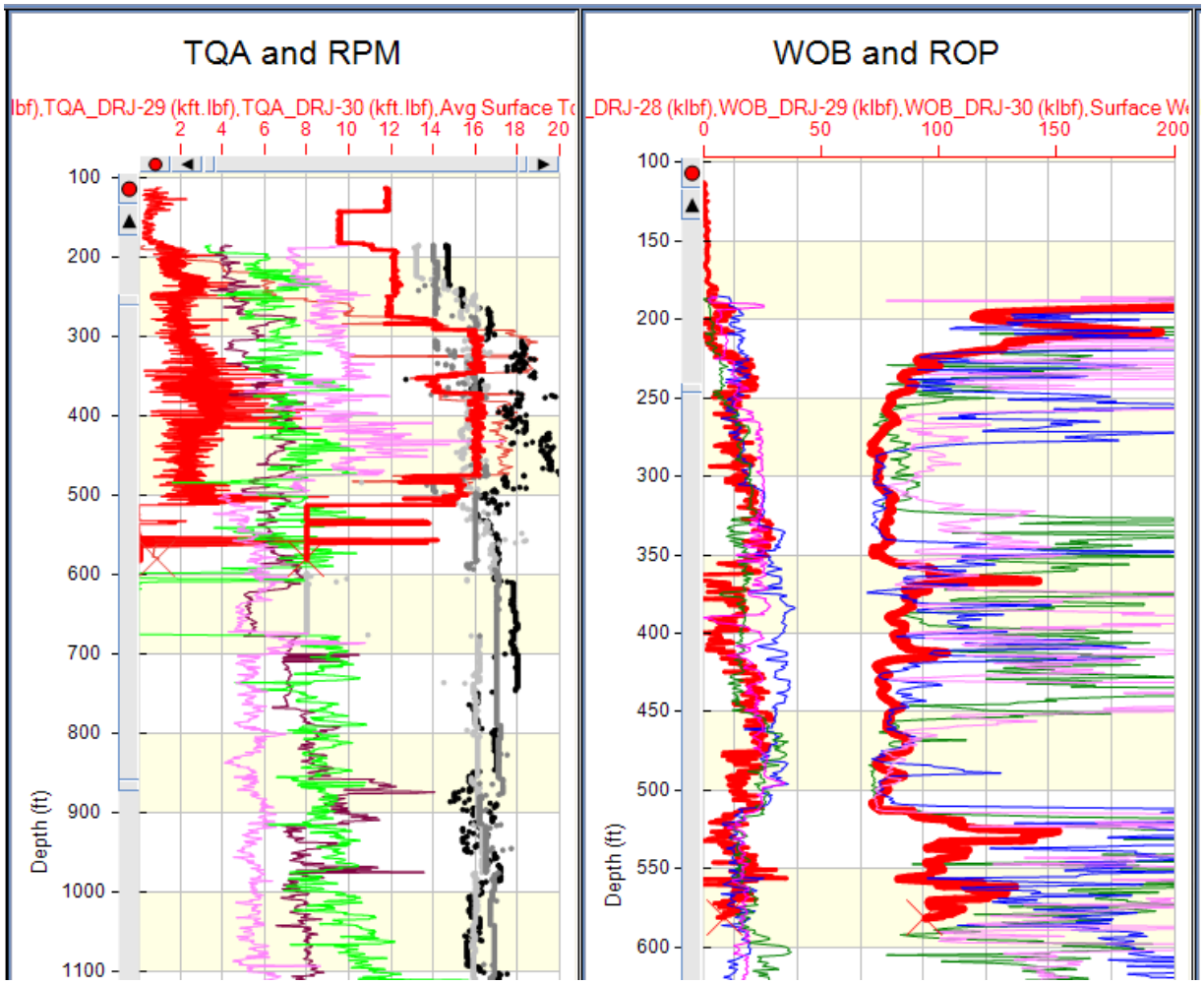


Figure 11: Current and Offset Wells.

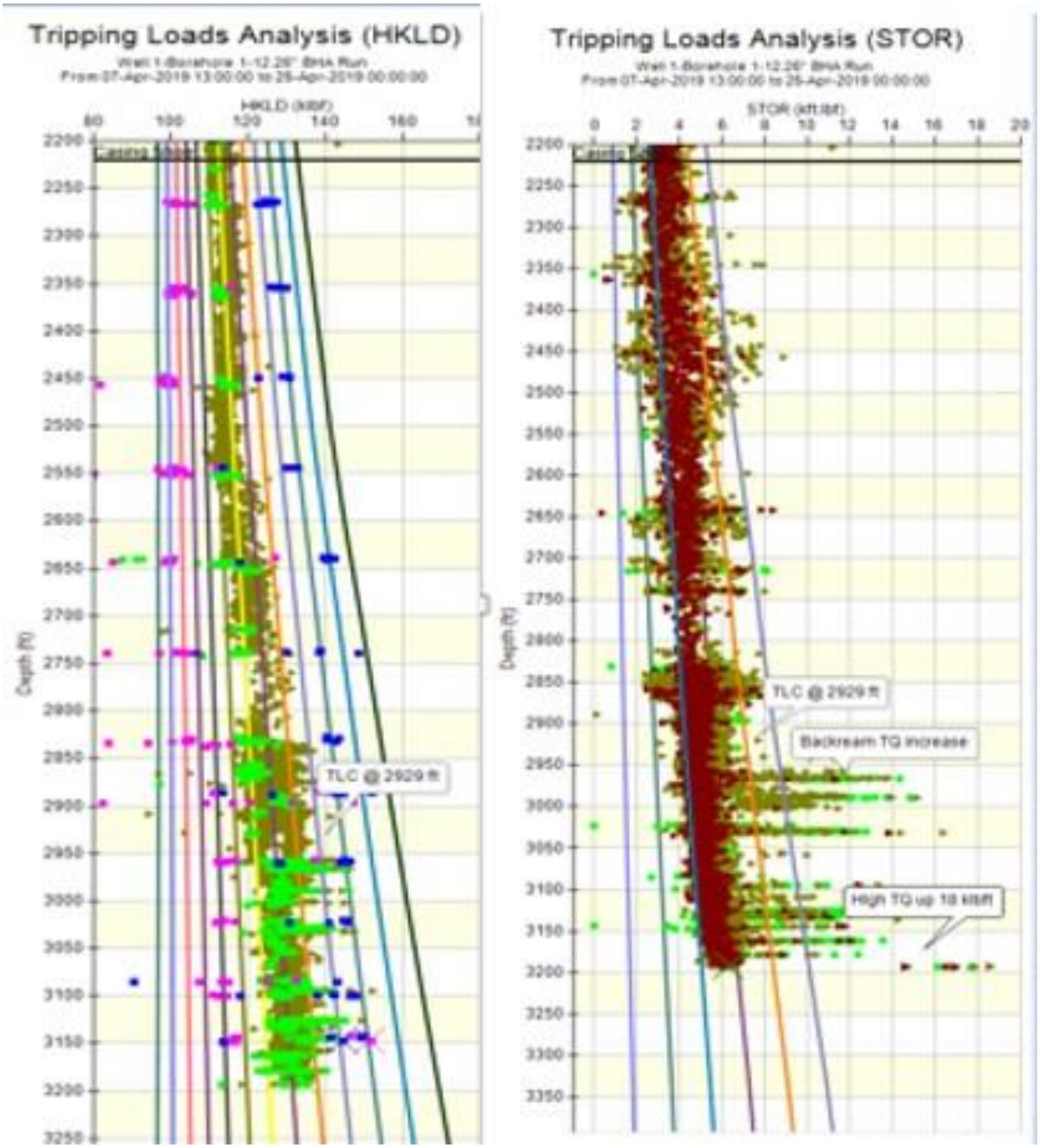


Figure 12: Torque & Drag Analysis.

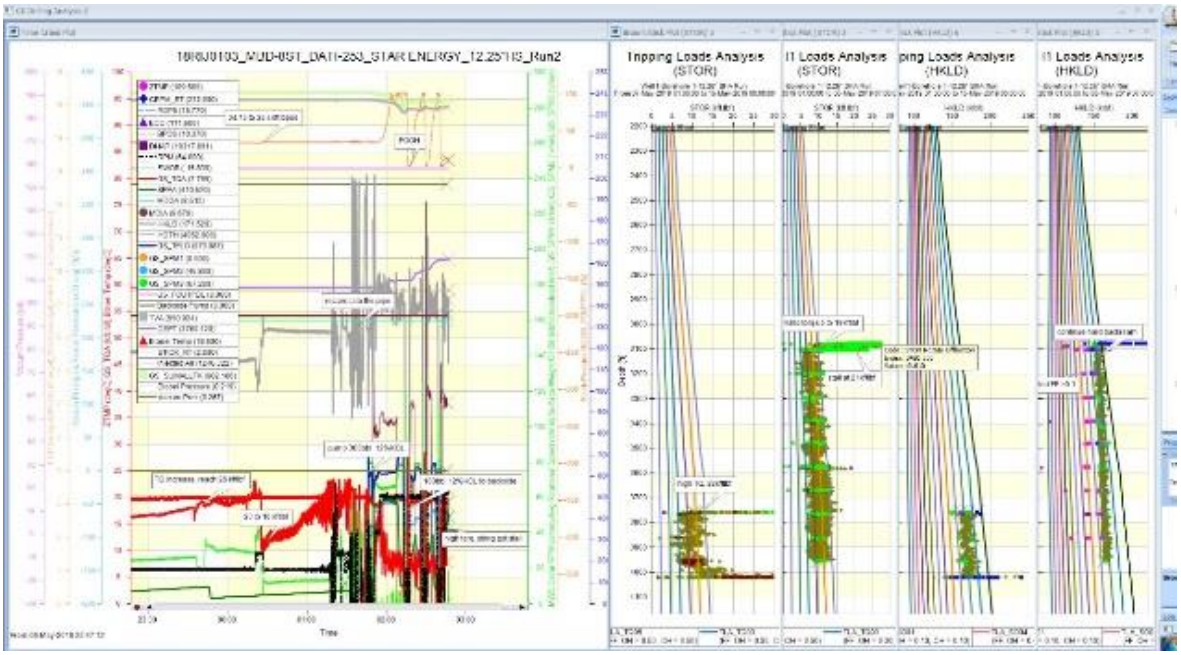


Figure 13: Tripping Analysis.

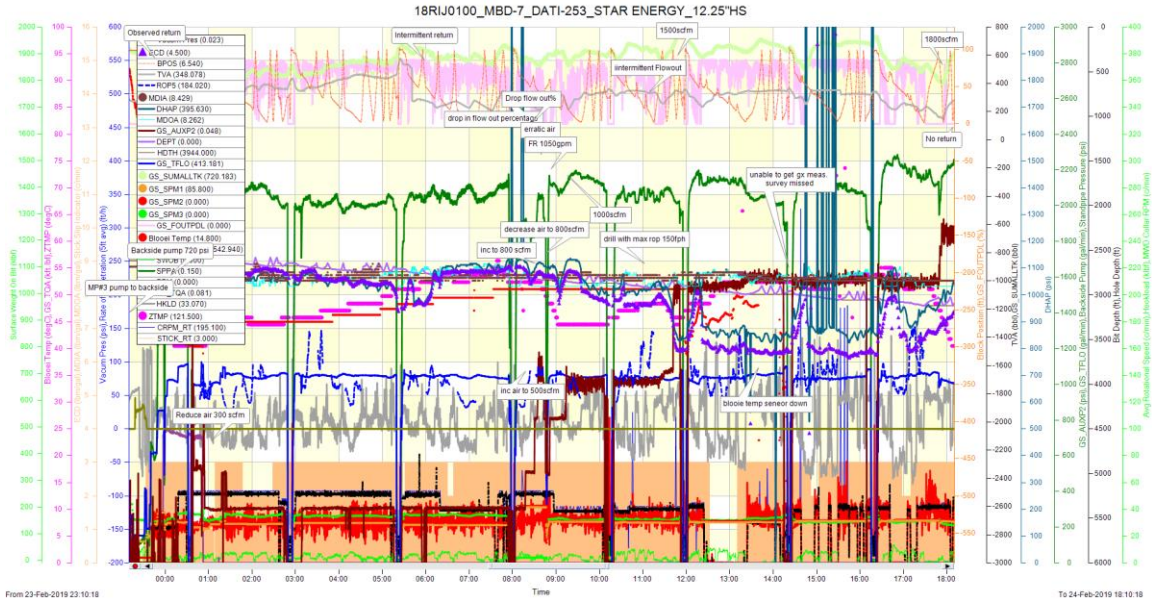


Figure 14: Drilling condition.

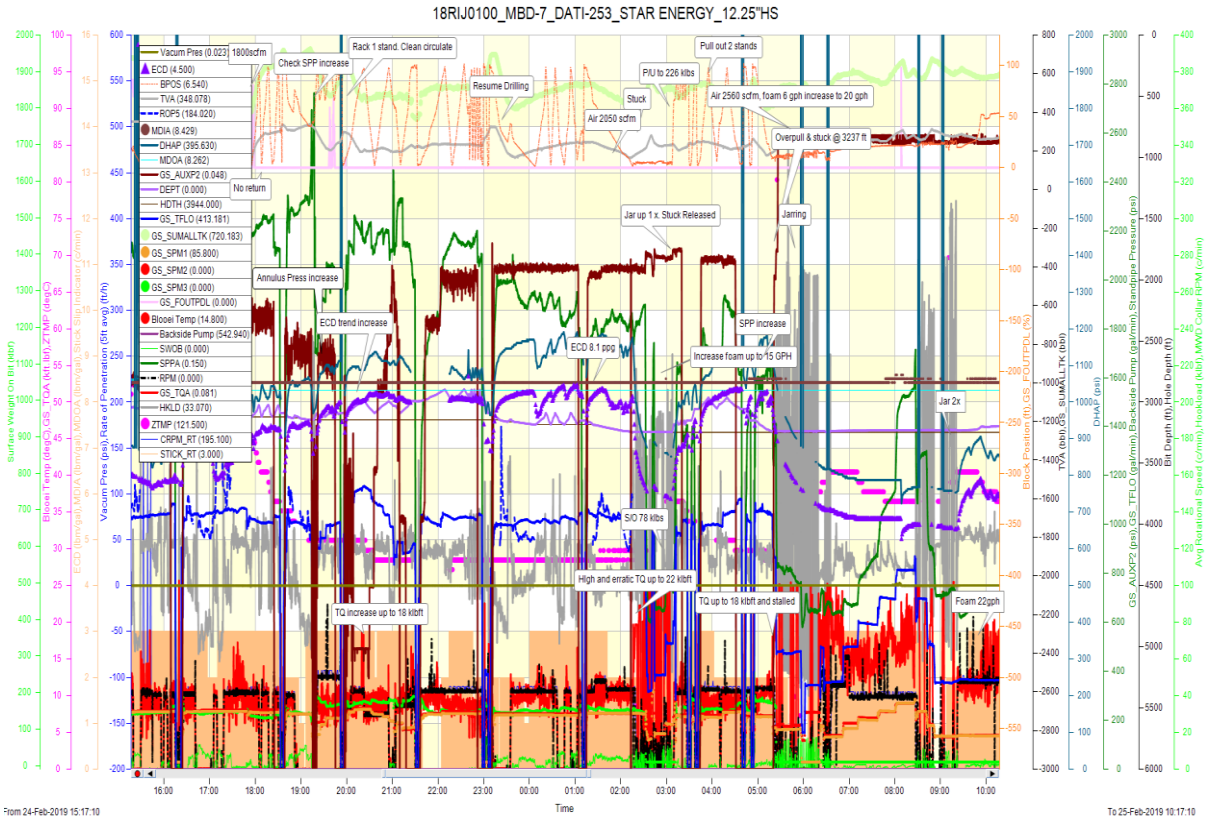


Figure 15: Stuck pipe event.

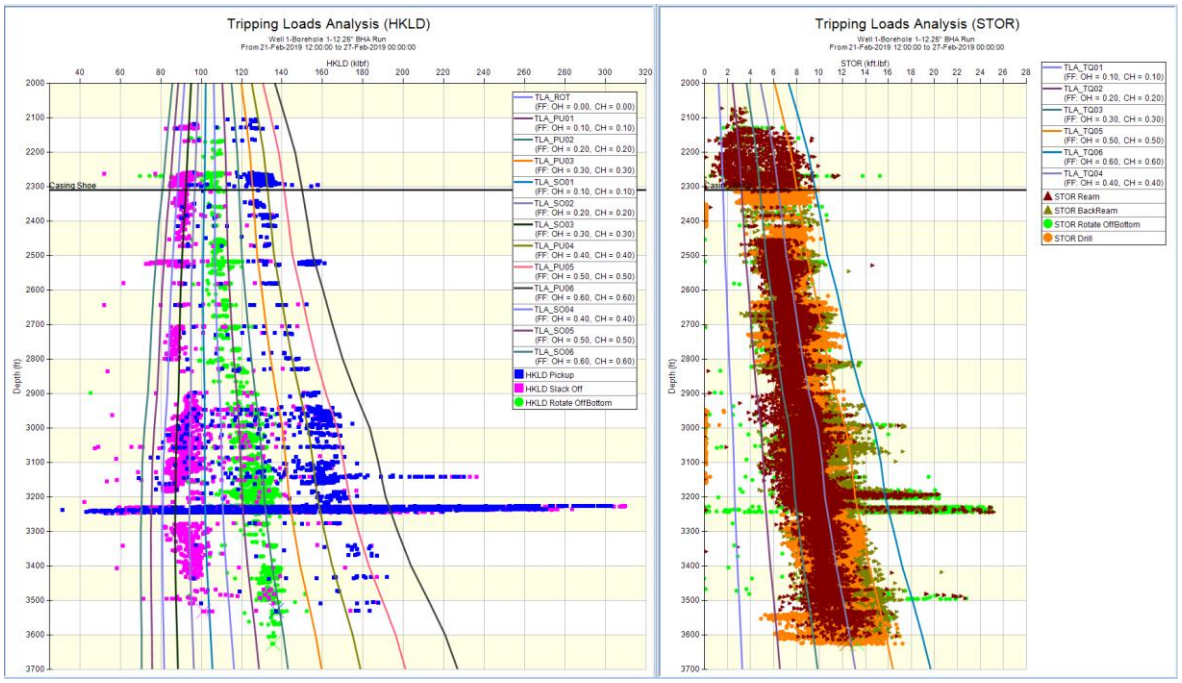


Figure 16: T&D tendency.

Case study At Wayang windu field, experienced stuck pipe and released.

- Drilled 12 ¼" HS from 2130 ft with Full Return
- Got PLC at 2541 ft, Drilled with aerated Mud, combination injected air 300-1000 scfm (intermittent flowout return) Torque reading 5-12 klbft.
- Got TLC at 3120 ft. Circulate hole clean prior continue drilling. Drilling with aerated mud 1800 -2000 scfm + Foam 6 bph, Flowrate 1000 gpm, ECD 8.2 ppg, DH Annulus Pres 1150 psi, TQ 2-12 klbft. After standown at 3238 ft, backream 3 ft pipe got stalled, TQ up to 22 klbft. Pipe got stuck. Released the stuck with Work on pipe, and Jarring 17 times while adjust the air + foam percentage.
- Based on the real time data we can analyze the parameter that ECD suddenly drop from 8.2 ppg to 6 ppg, DHAP drop 1150 to 900 psi. indicated that Flow level suddenly drop that might has a lot of cutting and fall down to BHA.

- Lesson learn and mitigation from this stuck pipe. Prior entering the TLC and resevoir zone, do the clean circulation and make short trip to check the hole condition and to unload the cutting. Drilling with precaution, do the backreaming every 15-20 ft the check the drilling parameter Torque, Annulus Pressure, etc. Check Torque and Drag Analysis if the realtime plot trend deviated from the model can help us to analyze the hole condition not good or formation change.

OPTIMIZATION WORKFLOWS

ROP Optimization

The main contributors to reduction of ROP are Vibrations and Bit Cleaning issue. Vibrations can be induced by external excitations such as bit-formation interactions, or when the frequency of the applied force equals the natural vibration frequency of the drill string and resonance occur. It may also be caused by the dragging forces caused by flow inside and outside of the drill string. Drilling vibrations are extremely complex, because of the random nature of the multiple factor affecting it.

There are a few of optimization workflows which help from Real time data can be implemented to be more proactive when it comes to analyzing trends, anticipating problems and hence making right decisions timely. To optimize drilling operation, at PTK software has discrimination plot that able to find tune the best drilling parameter. Shown at Figure 17 for ROP optimization.

Parameters and rock properties, which in combination will result in rate of penetration. This relationship can be used operationally by observing the ratio of change in MSE while adjusting parameters, or when lithological changes occur and how this affect the energy values.

MSE can be plotted on Real time to show the best possible parameters for efficient drilling and useful to analyze bit condition as shown in Figure 18. Mechanical Specific Energy (MSE) is the energy spent for drilling, and it depends on drilling.

COMMUNICATION PROTOCOL

The Communication Protocol determines the responsible persons of team who will be informed immediately by Phone or mobile group conversation in case of events detections or deviations from planned operations workflow. Realtime PTK monitoring Plot also displaying at the Company Man office, put annotation Regularly for any important event as Level 0. For Level 1, 2, 3 classification events and action to do showing at Figure 19.

CONCLUSION

The real-time data allows professional response as events occur. RTDC provide an advanced visualization and other technologies to drive more efficient and effective collaboration decision-making leading to recognisable value. By using PTK and DOX software as presented to enable expertise in all stages of well planning, execution, and evaluation; improved communication, interpretation, and fast reaction time can be done in real-time. Generally, the collaboating DOX and PTK software in RTDC enable to provide:

- Present and playback the drilled well data at prespud meeting of the new well or post job meeting drilled well to improve the understanding, awareness and corrective action taken and also right decision.
- Monitor the tendency during drilling to determine any abnormaly could be occur while drilling the formation

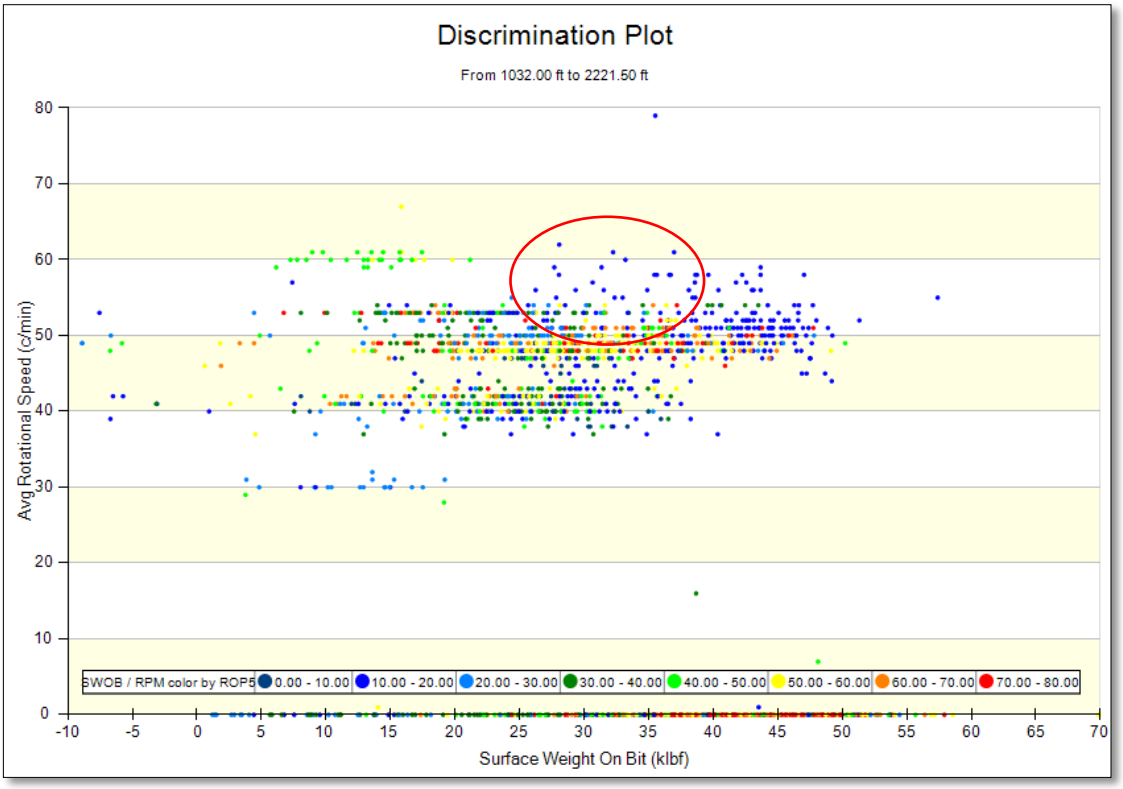


Figure 17: ROP Discrimination Plot.

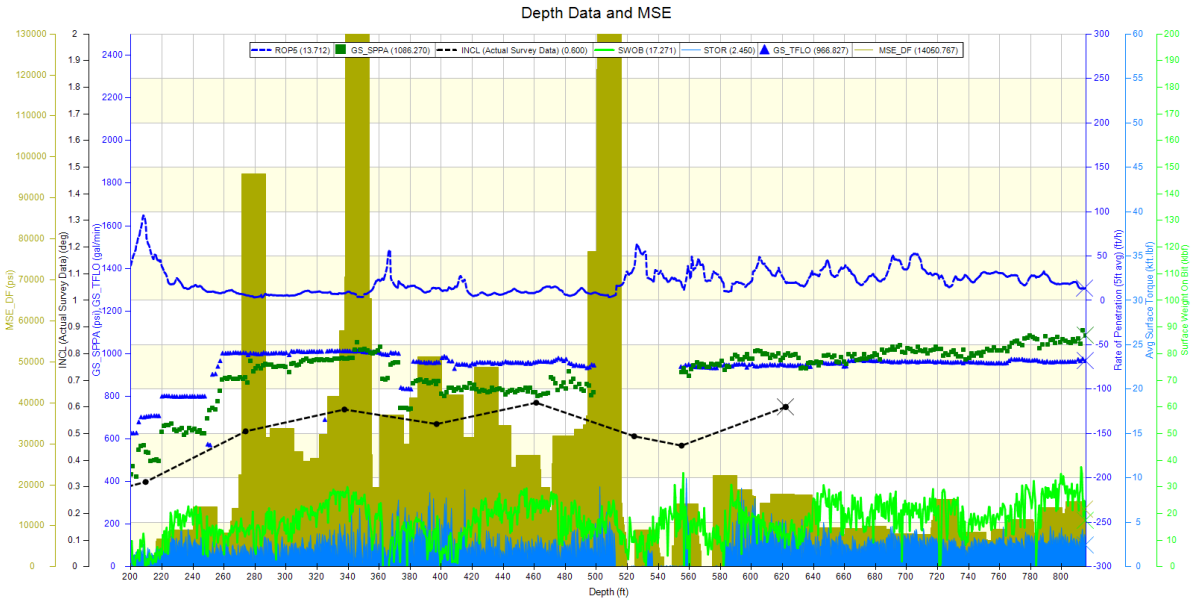


Figure 18: MSE Plot.

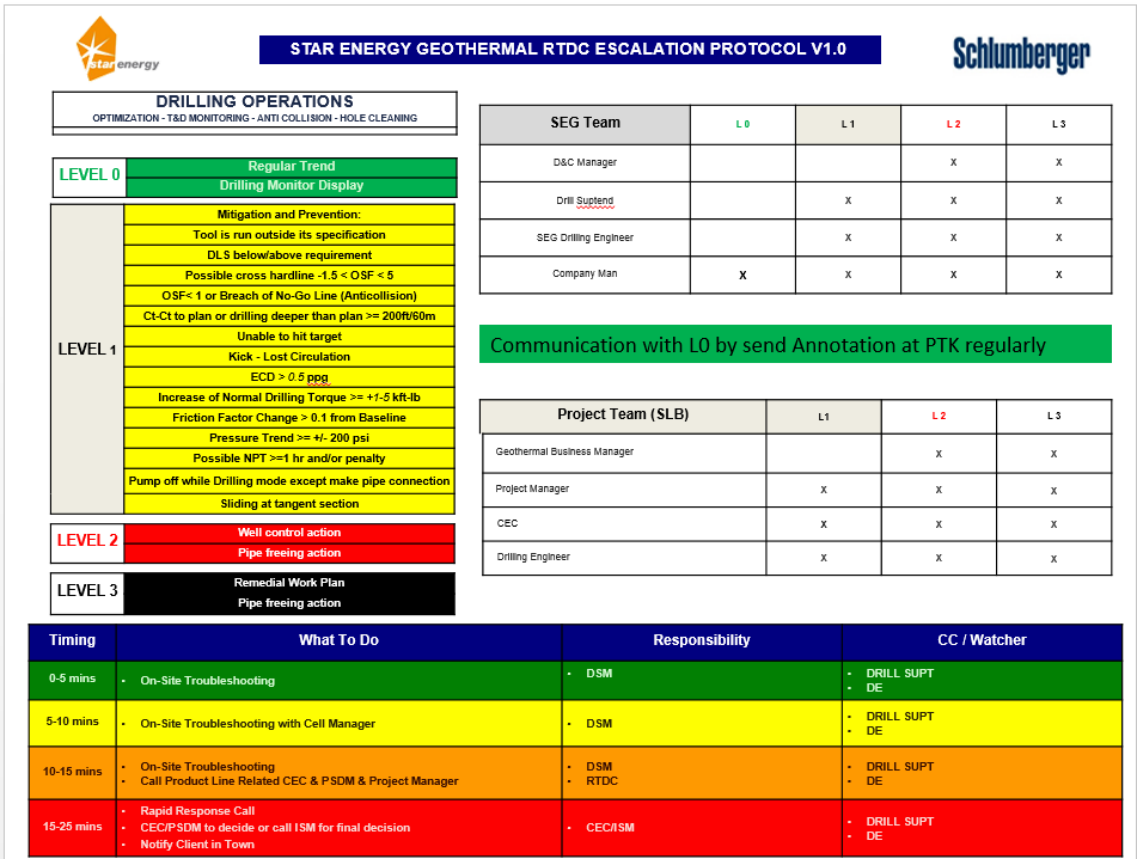


Figure 19: Communication Protocol.

REFERENCES

Schlumberger In Touch Database,

"DOX Single Point Analysis -Torque and Drag BasicConcept in Correlation with API RP 7G" (Content ID6042882).

Nahun Vega, "Drilling Efficiency Through MSE" IPM Project

SPE-110563-PP. Improving the Value of Real-Time Drilling Data to Aid Collaboration, Drilling Optimization, and Decision Making.

SPE-172740. The Implementation Of Real Time Data Drilling Decision Centre (RTTDC) in Kuwait.

COMPREHENSIVE AERATED DIRECTIONAL DRILLING APPLICATION IN WAYANG WINDU GEOTHERMAL PROJECT CAMPAIGN

Agus Ziyad Kurnia[1], Tommy Souvanir[2], and Citra Christina[3]

[1]Schlumberger
[2]PT. Star Energy Geothermal
[3]Aerated Drilling Associates
Email: AKurnia2@slb.com; Tommy.Souvanir@starenergy.co.id; citra@airdrilling.com

ABSTRACT

Aerated Drilling is a common practice in geothermal drilling operations. This method is being utilized mainly in reservoir section in case of losses due to abundant natural fractures with subnormal pore pressure. In PLC or TLC condition, this method is being utilized to maintain fluid level and transporting drilled cuttings to surface or into fractures zone and to avoid differential sticking by reducing the differential pressure. However, it can be applied also when there is no loss circulation, which in this case to improve rate of penetration (ROP).

In the application, air and mud ratio has to be designed and controlled in such way to maintain the wellbore stability. By maintaining the wellbore stability, the objective of using aerated drilling can be achieved. Applying excessive air ratio can lead to underbalance condition that can cause the wellbore instability, or hole collapse. Wellbore collapse creates cuttings caving size which is difficult to circulate out to surface and lead to hole pack off condition and ultimately stuck pipe condition.

This paper discusses on the multiphase flow modelling in aerated drilling in Wayang Windu wells (3 wells) to determine effective operational window considering several factors such as pore pressure, hole cleaning, and Motor limits. By utilizing APWD ECD measurement, the actual ECD can be determined that can be benchmarked against design simulation. The simulation is using both Aerated software and Directional Hydraulics to make it as a complete analysis. By doing this we will have the ability Real time measurement to ensure that actual ECD is not fall below formation pore pressure that can potentially collapsing the wellbore.

Keywords: Aereted drilling, Wayang Windu geothermal

MOTOR AND MWD IN AERATED DIRECTIONAL DRILLING

Motor and MWD in Aerated Condition

If the excessive mixture flowrate of gas and liquid flows through motor, there is potentially occurrence of over speeding will occur and in the other hand, if mixture flow rate is less than minimum, then motor cannot rotate. In this project, we are using mud lubricated type of bearing, thus in order to have proper bearing lubrication need to have minimum 250 psi pressure drop across the bit.

In terms of MWD, in this project MWD XEM with electromagnetic telemetry is being used thus there is no limiter in terms of liquid to gas ratio. Figure 1 is showing aerated directional drilling criteria that need to be met in design and execution phase.

Multi Objective	Multi Constraint
Qmix value as desired by user	Qmix within motor capability
Minimum Qm or Qgo within range	Pressure drop at bit > 250
	ECD within Pore & Fracture Pressure
	Hole Cleaning
	GLR value < 1 (Foam Stability)

Figure 1: Aerated Directional Drilling Design Criteria.

In order to understand the mixture of flow rate output, detailed engineering simulation has been done by ADA and SLB team and since different software is being utilized, thus comparison need to be done rigorously between the software output.

Positive Displacement Motor is chosen as the directional drilling tool for this project due to following reasons:

- Ability to deliver high flow rate
- Adequate flow pressure compatibility with fluid system and rig equipment
- It is simple to monitor running parameter and easily to identify the problem
- Compatible with various drilling fluid
- Superior performance & reliability
- High temperature configuration available
- SLB Motor Include motor catcher that act as a catcher whenever twist off is occurred on motor connection
- Many options on torque capability of the tool

Apart from the tool that being used, in terms of geothermal well design, well trajectory is designed to be as simple as possible to reduce directional work especially in the reservoir section which Total Loss Circulation (TLC) is expected. It requires slide drilling when steering with mud motor. The pipe will steady (no rotation) for a period of time with the risk of drilled cuttings accumulated around the Bottom Hole Assembly (BHA) that could lead to the stuck the pipe event. The risk is increasing when sliding in TLC zone, since the drilled cuttings cannot be circulated out to surface. Aerated in this case will help in moving away the cuttings from the BHA.

The well trajectory is designed so that the steering work ended prior entering the TOR and no steering when drilling with TLC. All directional work will be done at shallow depth either in 26" Hole Section or 17-1/2" Hole Section.

The well trajectory is also optimized in term of build and turns requirement. It is preferred to design 2D well trajectory which purely build rather than 3D well trajectory. The 2D well trajectory gives torque and drag value lesser than 3D Well trajectory at well total depth.

There are target faults to be penetrated at different depths. This involved extensive discussion with Sub Surface and Drilling team to simplify the target and fault intersections. The dog leg is designed to be at maximum 3 deg/30m. The length of steering interval is reduced so that the side force is also kept low. The surface casings then could be run to shoe depth without significant problem.

In order to achieve objective of the well, directional drilling method with aerated need to accommodate mixture of flow rate and pressure drop that within the operating specification of Motor and MWD downhole. Using each of the experience from SE Drilling team, SLB D&M (Drilling & Measurement) and ADA (Air Drilling Associates), the equation that is used to derive this chart will help us to determine the optimum mud flow rate and air flow rate to ensure that our tools are being run within specification.

Figure 2 is showing mixture of flow rate when pumping Air and Water, with boundary limit of Motor flow rate 600-1200 GPM. This is monitored on daily basis during execution and will be a reference for aerated drilling design basics. Figure 3 shows the pressure drop sensitivity when pumping air and water. The project is using mud lubricated motor bearing, hence motor lubrication is required by providing minimum 250 PSI pressure drop at the bit.

BHA Torque and Drag in Geothermal Environment

Torque and Drag Model is one important tool to monitor hole cleaning to prevent stuck pipe incident. Figure 4 shows Torque and Drag Model vs Actual. On the planning stage, 0.35 friction factor was utilized as a basis of torque and drag design.

Through our learning curve in these geothermal practices with total loss, no return, and aerated drilling, resulted in higher friction factor. Below is the geothermal well drilling characteristic that become main consideration for torque and drag design:

- In total loss situation with NO Return, the hole has low fluid level.
- Basically, everything that being pumped from inside the drill string and annulus is goes to formation/ fractures.
- Low Hydrodynamic Pressure / ECD (mix air + mud) that reduces the buoyancy of the string (after turn-on Air Drilling).
- All of above situation are contributing to high friction factor – causing high torque.
- Simplify well design based on given target to reduce the overall surface torque.

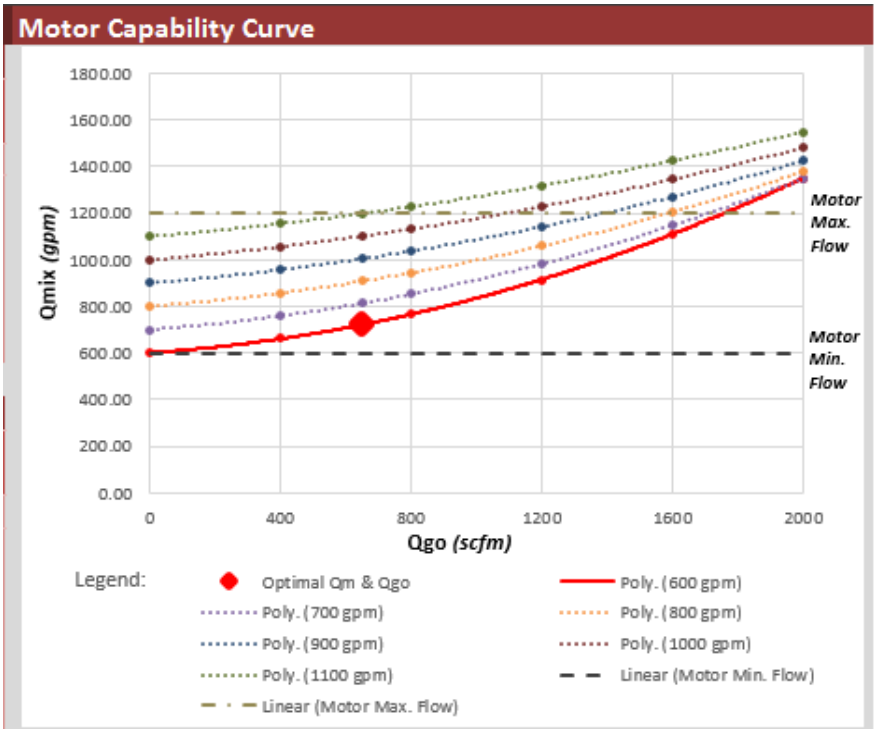


Figure 2: Aerated drilling mixture flow rate sensitivity.

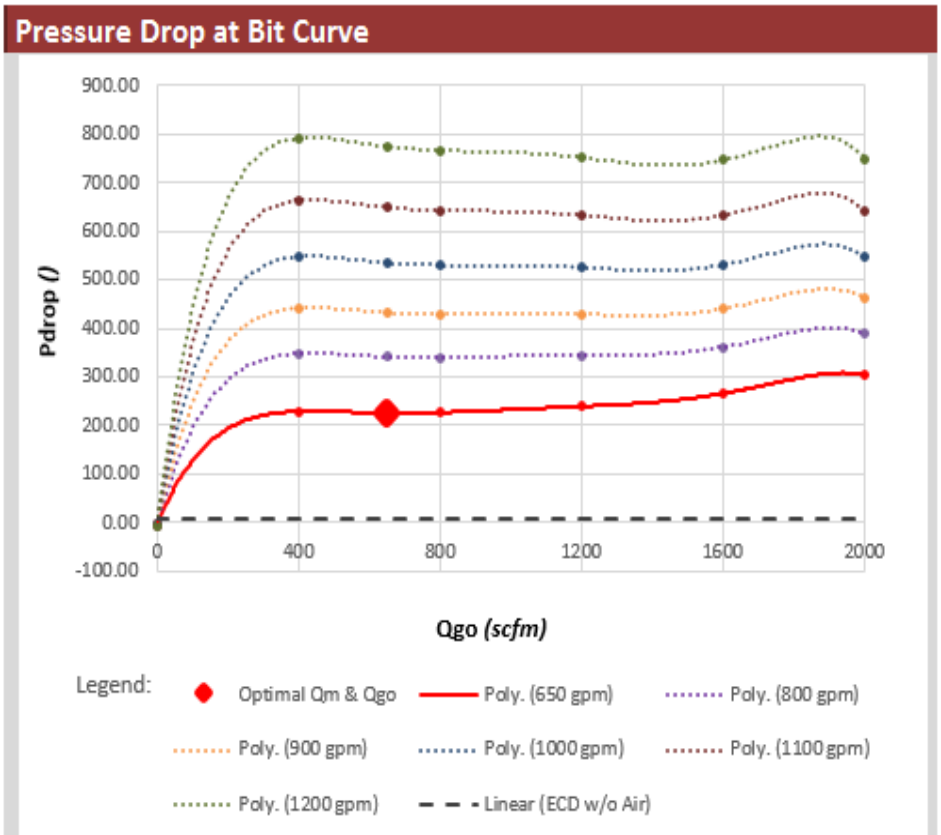


Figure 3: SLB Motor pressure drop sensitivity.

This need to be factored in the future geothermal torque and drag design. Based on the first well experience, the following steps are taken to reduce overall surface torque: Simplify well trajectory to 2D profile, lighten the BHA (used 6 ½ in jar with6 ½ in DC instead of 8 in jar with 8 in DC).

AERATED HYDRAULICS DESIGN AND ACTUAL EXECUTION

Basic Theory of Aerated Application

$$b(P-P_s)+\frac{1-2bM}{2}\ln\left|\frac{(P+M)^2+N}{(P_s+M)^2+N}\right| - \frac{M+bN-bM^2}{\sqrt{N}}\left[\tan^{-1}\left(\frac{P+M}{\sqrt{N}}\right)-\tan^{-1}\left(\frac{P_s+M}{\sqrt{N}}\right)\right] = a(1+d^2e)L \quad (1)$$

Figure 5: Aerated Basic formulation.

$$ECD_{MAXWELL}\,(ppg) = \frac{APRS_c}{0.052 \cdot TVD\,(ft)}$$

Figure 6: Actual ECD formulation from APWD sensor.

Pipe connection is critical phase in the aerated drilling. During this event, friction is not present in contributing the wellbore pressure for wellbore stability, therefore wellbore pressure only exerted by hydrostatic pressure of the mixed fluid.

Therefore, it is a good practice to keep pumping the annulus to maintain the fluid level during the connections in the PLC or TLC zone.

Another reason form annulus pumping is to cool down the wellbore to prevent steam flow. Normal connection time is around 3-5 minutes, with inner string pumping away higher than loss rate (in WW project max 400 gpm loss rate), excess pumping rate still possible to manage the liquid level

On the other hand, annulus pumping has down side to pack off or push down the cutting to large contact area like stabilizer. Thus, extensive precaution and monitoring is paramount on this practice.

In the analysis, we mostly present the static condition as worst-case condition. Boyun Guo & Ali Ghalambor (Figure 5) hydraulic equation for aerated drilling in inclines well is utilized in the analysis. The concept of critical condition during pipe connection also adopted from those both authors. Aerated Drilling Safe Window has to be designed to give the sufficient and safe parameter in order to maintain the wellbore stability.

Figure 6 shows the ECD formulation that derived from actual APWD sensor. The actual result from 3 wells can be seen in later section from this paper.

Determination of Operational Window

Determination of operational parameters, such as ECD, combination gas flow rate and mud rate, downhole tools flow envelope, and pressure drop requirement leads to an outcome referred as operational window. Figure out ECD from combination gas flow rate (scfm) and mud rate (gpm) and figure out the geothermal formation pressure are crucial for the successful aerated drilling. The parameters of aerated drilling are very crucial to be maintained to create a stable circulation. Stable circulation is very essential to reduce risk of stuck pipe and have a drilling efficient and effective.

Figure 7 shows the chart of theoretical combination flow rate vs BHCP vs ECD. The yellow shading is the range of formation pressure (6-8 ppg) and the desired operational window that can be used to determine the parameter air injection and mud rate. There are some asssumptions in this simulation:

- Water level
- ROP – rate of generation of cutting
- Data temperature gradient from offset wells

The left boundary (the blue line) is the mud motor limit. For directional drilling that use mud motor, we have to know the limit of the motor, especially the minimum flow rate in mud motor operation. In this simulation, we calculate equivalent liquid volume (ELV), the combination of mud motor flow rate (gpm) and rate of air (scfm).

The right boundary (the red line) is the minimum velocity. The main objectives of aerated simulation is to calculate BHCP and ECD. Manage ECD by pumping various air/mud ratio and identifying the formation pressure is very essential to achieve continous circulation.

By drilling data, PWD shows that in the feed zone ECD will drop significantly, it show the water level is drop to the certain depth. But, in the simulation we will see the differences; because the simulation assumed that the circulation is full return while the actual data show the water level is drop.

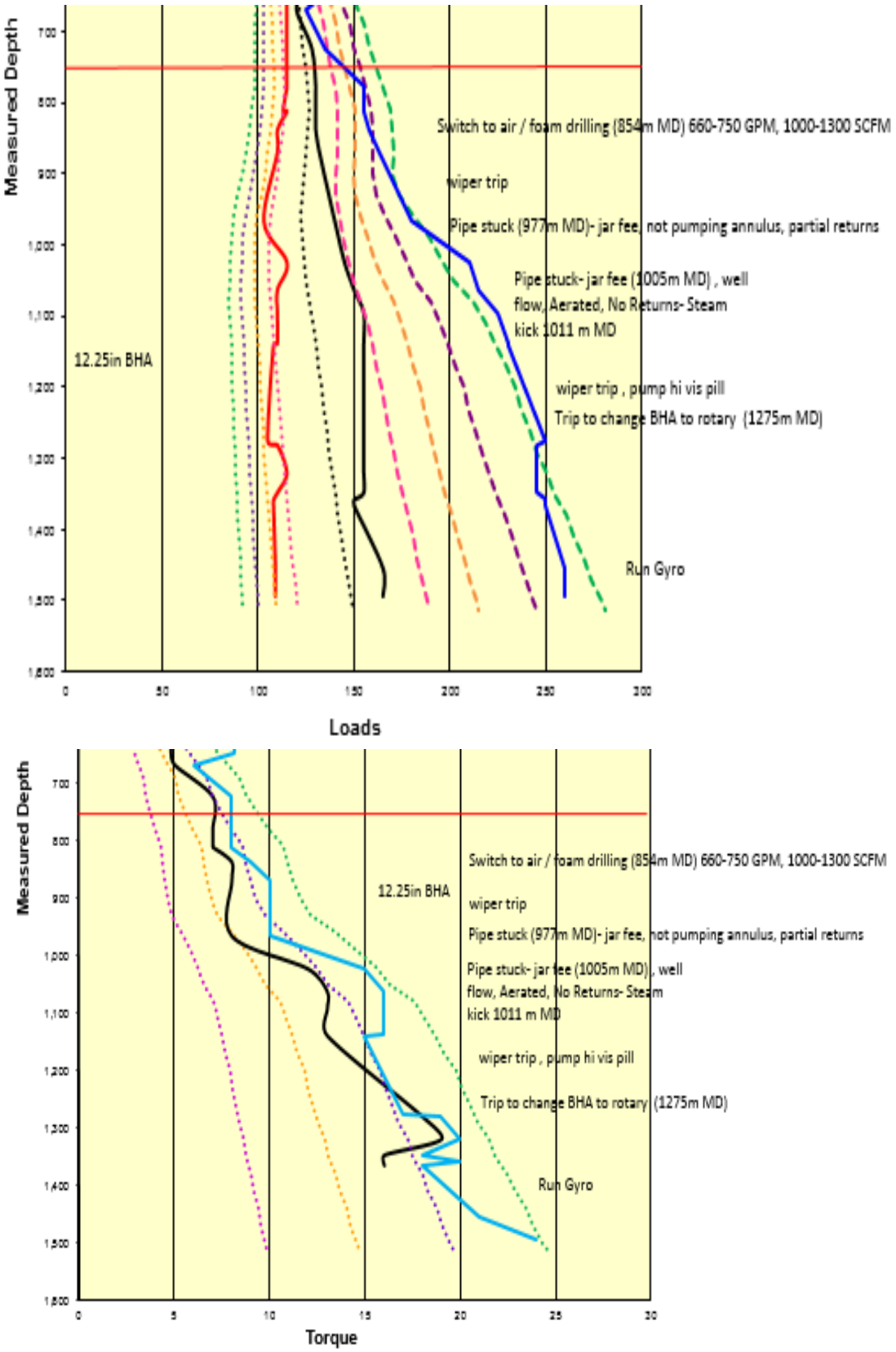


Figure 4: Torque and Drag characteristic in geothermal well.

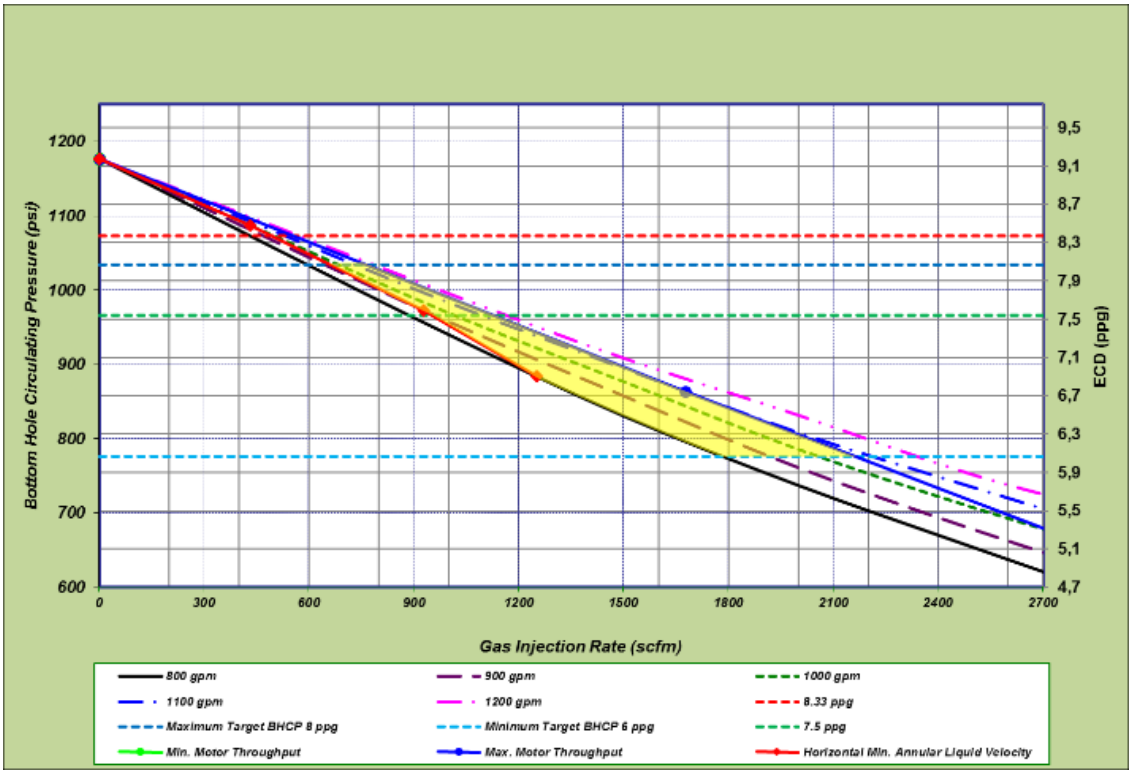


Figure 7: Simulation of Flow Rate Combination vs BHCP vs ECD.

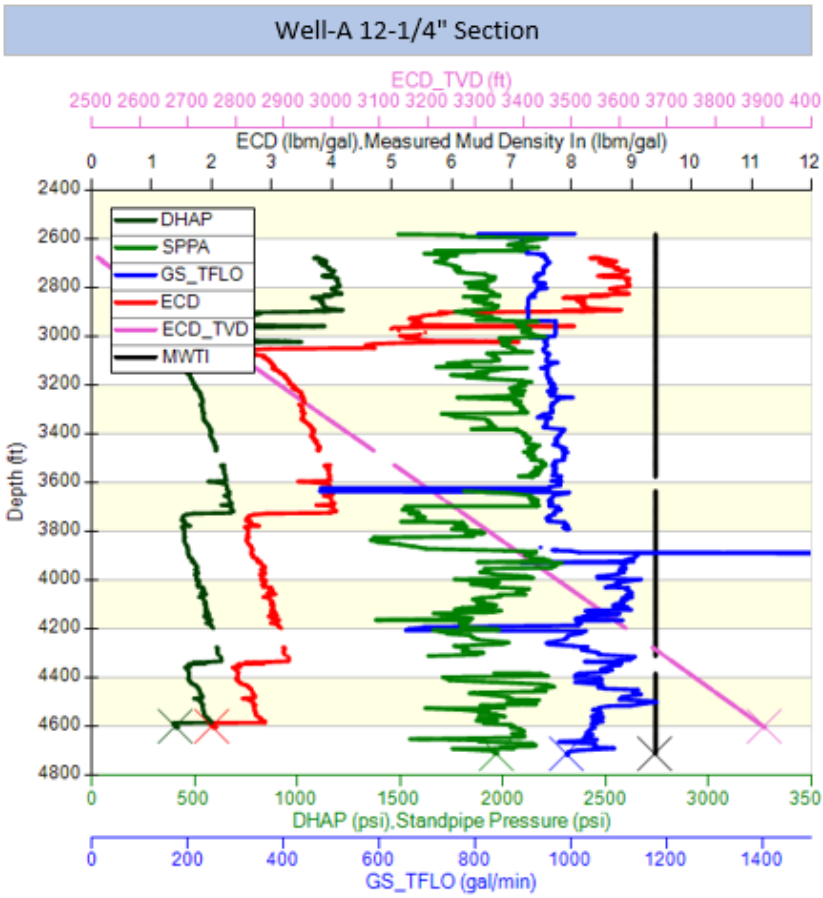


Figure 8: Real Time Actual ECD at Well-A.

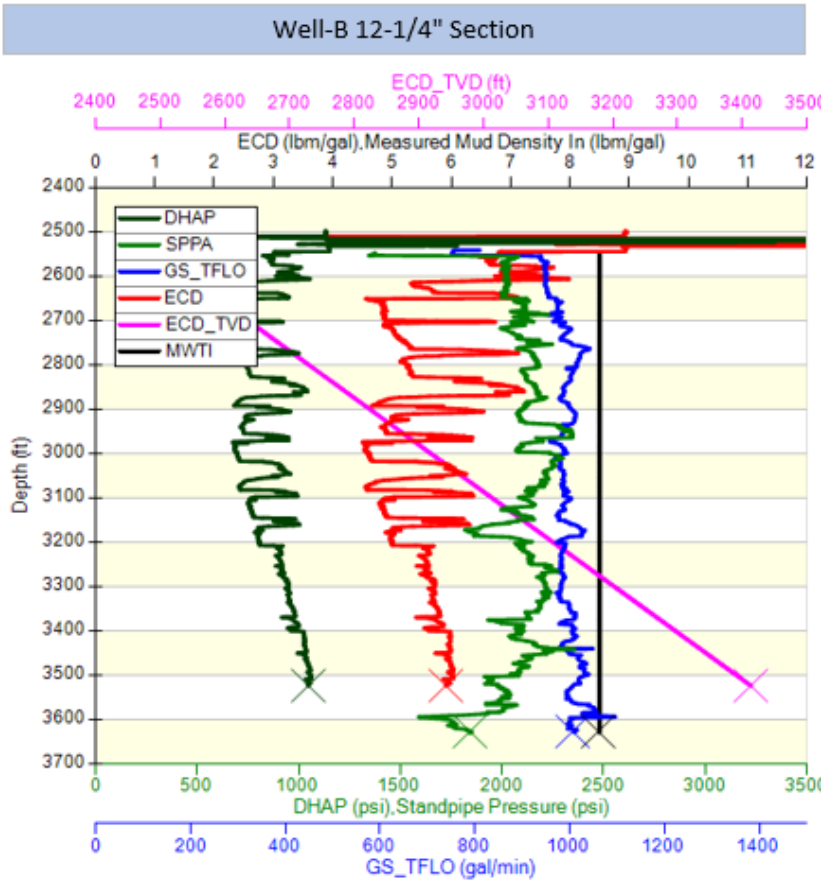


Figure 9: Real Time Actual ECD at Well-B.

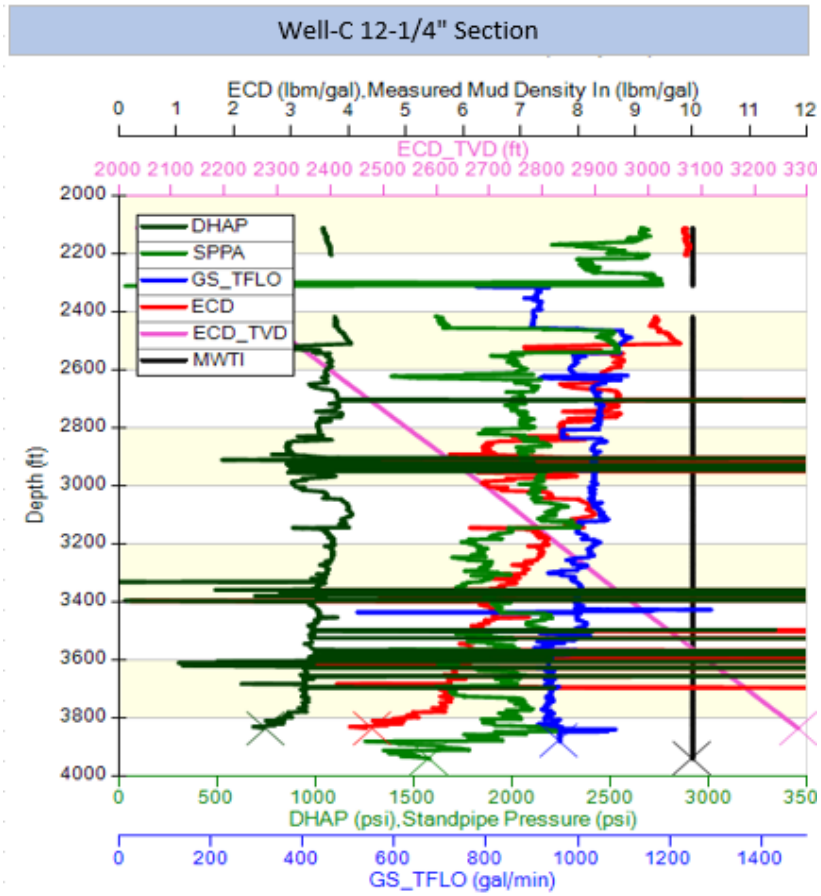


Figure 10: Real Time Actual ECD at Well-C.

CONCLUSION

- The main challenges in geothermal project in terms of directional drilling was clearly identified before the startup of the project and solution is provided.
- In terms of achieving overall well objective in TLC condition, hydraulics between SLB D&M and ADA was thoroughly reviewed for all basis of design.
- Multiphase flow in geothermal drilling was studied to come up in safe operating window in terms of flow rate and pressure drop for motor and MWD operation.
- Torque and drag characteristic of geothermal wells with aerated was analyzed and based calibrated during execution. Found out the best friction factor for translational and rotational motion is 0.5.
- Stable drilling parameters roadmap was executed and proven to be effective during execution.
- Maintain ECD and knowing the formation pressure is very essential to achieve the continous circulation and prevent from drillling problem like stuck pipe.
- PWD will help to provide data pressure profile and help aerated drilling to create ECD desired.

ACKNOWLEDGEMENTS

The authors would like to thank both Star Energy and Schlumberger for permission to publish the data and information contained in this pape

NOMENCLATURE

BHA	: Bottom Hole Assembly
DLS	: Dogleg Severity
FAC	: Field Acceptance Criteria
FEA	: Finite Element Analysis
ID	: Inner Diameter
MWD	: Measurement While Drilling
OD	: Outer Diameter
ROP	: Rate of Penetration
RPM	: Revolutions Per Minute
SRPM	: Surface RPM
LIH	: Lost in Hole

REFERENCES

Schlumberger In Touch Database

"DOX Single Point Analysis -Torque and Drag Basic Concept in Correlation with API RP 7G" (Content ID 6042882)

Aslaksen, H., Annand, M., Duncan, R., Fjaere, A., Paez, L., Tran, U. (2007),

“Integrated FEA Modeling Offers System Approach to Drillstring Optimization”, paper IADC/SPE 99018 presented at the IADC/SPE Drilling Conference, Miami, Florida, 21-23 February 2007.

Global Business Guide (2016)

“Overview of Geothermal Energy in Indonesia” [online], (http://www.gbgindonesia.com/en/energy/article/2011/overview_of_geothermal_energy_in_indonesia.php), accessed on 15 January 2016).

FOCUS IMPROVEMENT: MEASURING LEVEL OF CONDENSATE PUMP TO INCREASE UNIT RELIABILITY UP TO 98%

Richard Alexander, Argy Rigwan, Efrata Meliala, Querubin Wendell, and Kadar Aditama

Sarulla Operation Ltd
Silangkitang (SIL) Power Plant, North Sumatra
Email: richard.alexander@sarulla-geothermal.com, argy.rigwan@sarulla-geothermal.com, efrata.meliala, @sarulla-geothermal.com

ABSTRACT

Sarulla Operation Limited is a geothermal company that recently operates SIL site and NIL site which consisted of STG and binary. The binary consist of bottoming/condensate binary and brine binary.

Bottoming has condensate pump to deliver its fluids to reinjection well. The level transmitter in pump's barrel has to control its pump to maintain the level of heat exchanger in term of generating load. It should be reliable to maintain production activity, therefore engineering design and maintenance strategy are the important things to assess. The existing design, magnetostrictive method has been applied. We conducted assessment about this method and found the failure rate around 1 case/2 month. The possibilities problem are spike signal and static measurement problem which cause by elasticity of rod material and cantilever design. Rod bended and floater sensor problem are the common evidence due to condensate flow in the barrel. That floater can move violently and send the spike signal to control system which can trigger unit partial trip. Moreover, there are many possibilities problem contribute to this case.

Based on that evidence, to overcome this problem we conducted engineering design review and assessment of maintenance strategy, to ensure that problem cannot be occur repeatedly. As the result, we installed the new type of level transmitter by guided wave radar. Nowadays, we have increasing the reliability of bottoming unit up to 98%.

Keywords: Condensate, Bottoming Binary, Magnetostrictive, Guided Radar, Reliability

INTRODUCTION

The potential of geothermal energy in Indonesia is up to 30 to 40% of total geothermal energy available in the world [1]. Sarulla Geothermal Power Plant is the first geothermal that using binary combine cycle system in Indonesia, 110 Mw for each unit with total capacity 330 Mw gross power and which the steam turbine generator (STG) generated 62,8 Mw power and 47,2 Mw power from Brine Binary and Binary Bottoming. The power consumption of the Sarulla 7 Mw is the equals below 10% of the total generation that delivered to PLN grid.

In order to maintain this power plant, 110 Mw that we have been generated since March 2017 to supporting SUMBAGUT (Sumatera Bagian Utara) grid. All the equipment that supported binary combine cycle unit, the equipment should be reliable through the best maintenance strategy and improvement as well.

Bottoming unit is the parts of Sarulla binary combine cycle system, the bottoming unit are generated 8 Mw each unit and total capacity for 4 units is 24 Mw. Outlet steam from steam turbine generator (STG) with 105 ºC flows to the vaporizer of the bottoming unit, to heating up the working fluid pentane liquid (C5H12) up to 5,40 bar and 95,5 ºC temperature to generate 8 Mw by two side of turbine clockwise and counter clockwise turbine 1500 rpm.

In this continue production process, vaporizer pressure and temperature suddenly decreased. It has become a serious matter for Sarulla bottoming unit to sustain and continue its production. From the point of view of power generation, this issue is concerned with several parameter including condensate level control, level transmitter and discharge control valve.

Over the several months after COD on March 2016, bottoming unit production experienced tripped by different pressure low between inlet and outlet turbine. Based on preliminary investigation, the main cause of the tripping problem is coming from condensate level unstable when the unit running full load.

Based on investigation of the failure, the level transmitter bottoming unit used is unstable reading and the Variable Frequency Drive (VFD) of the condensate pump controlling that input feedback is from level transmitter become unstable as well. Therefore level measurement method study is needed to overcome level controlling problem that affected bottoming unit trip.

BOTTOMING ORMAT ENERGY CONVERTER (OEC)

Bottoming unit Ormat Energy Converter (OEC) is a part of Sarulla geothermal combine cycle unit with capacity 8 Mw per each unit. The bottoming OECs (Ormat Energy Converter) heated by the low

pressure steam exiting the topping steam turbine. The steam exits the steam turbine and enters the OEC vaporizer at just above atmospheric pressure.

LEVEL TRANSMITTER MEASUREMENT PROBLEM

Since the Sarulla project started for this set-up used magneto-strictive gauge type level measurement method, it was observed that the rod material exceeded the required length of no more than 3 meter, the rod easy to bend and also the rod can be damaged by turbulence. The sensor cable at the bottom tip was found open which can be caused by vibrating surface and hot temperature at the bottom therefore it opens until resulted to intermittent connection and visible as HMI indicates fluctuating values similar to a loose connection state. Thus, the usual problem displays as fluctuation or spike in the measurement. Figure 1 shows OEC process diagram. The condensate level trending program is shown in Figure 2.

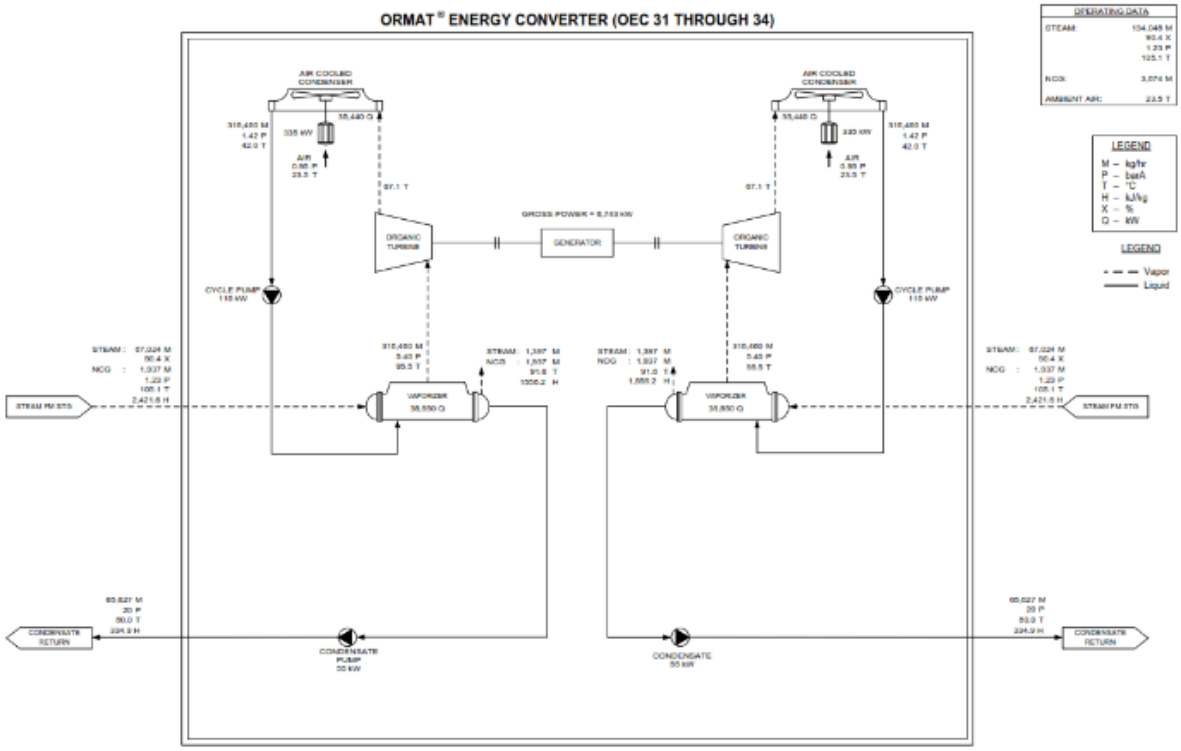


Figure 1: Ormat Energy Converter (OEC) process diagram.

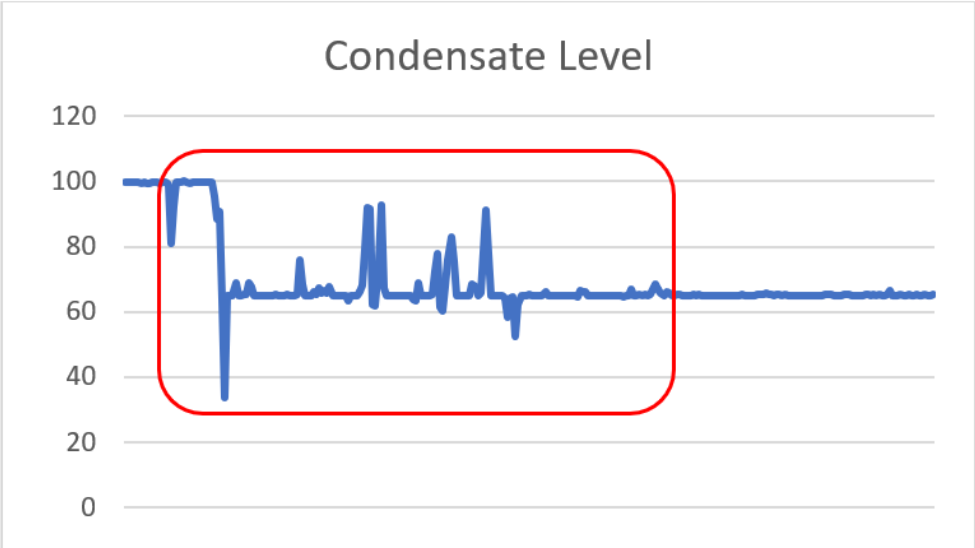


Figure 2: Condensate level trending problem.

Condensate level become fluctuating or stuck up (error reading) and it was become big impact during plant running, because of this the plant will be decreasing the power generation if the condensate level is not controlling very well then, the level increase into the vaporizer. Not only derating effect, this problem will damage our condensate pump as well if the actual level is become low and the level transmitter reading is not correct, the pump will not trip from actual level.

Table 1: Root Cause Failure Analysis.

Problem	Why-1	Why-2
Condensate level transmitter failure	Floater sensor damaged/stuck up	Density fluctuations
	Sensor rod bent	High vibration due to rod length more than 4 meters

The root causes analysis (Table 1) result those causes (Rod sensitive, moving part stuck up, sensor damaged) occurred for the magneto-strictive level transmitter. Those problems can be participated to impact plant problem (OEC). Figure 3 shows the condensate level HMI trending.

MAGNETO-STRICTIVE CASES:

Case 1:
Due to avoid rod sensitive (4 meter of length) rod support for keeping the rod stable is needed, two pcs rod supports were installed in magneto-strictive transmitter and the rod of level transmitter experienced more stable. However, those the rod supports were blocking the floater sensor to sensing full scale (0 to 100%), it is only 50% measuring due to support blocking and was become dangerous for condensate pump operation while the actual level at below than 50%.

Case 2:
Floater sensor is moving part for measuring the actual condensate level, basically the floater sensor can be following the liquid level at normal condition. At the some point the floater does not working properly because of floater stuck up or sensor damage even the liquid is fluctuating in normal condition.

STUDY LEVEL MEASUREMENT METHOD BY FLOATING TRANSMITTER

Based on magneto strictive manual book that the floater level method has some weakness, one of the weakness is density changing effect will make serious problem and the floater will get a permanent damage by high turbulence and change in density can cause measuring error as well.

This matter related with Archimedes principles buoyant force which is the buoyant force is the net upward force on any object in any fluid. If there is any pressure and temperature changing in condensate liquid, the floater of level transmitter will be affected (See the formula below).



Figure 3: Condensate level HMI trending.

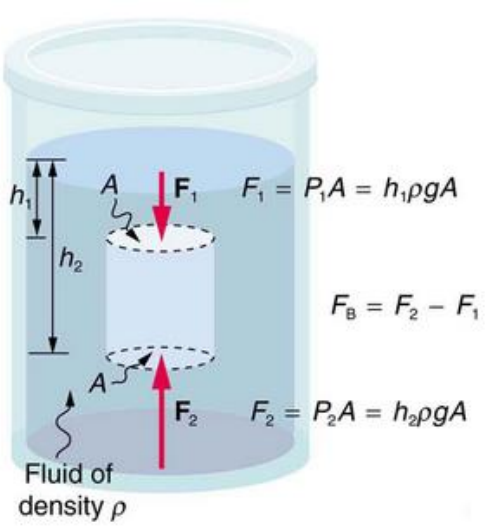


Figure 4: Buoyancy Archimedes principle theory.

Where Fb is the buoyant force and wA is the weight of the fluid displaced by the object. Figure 4 shows the buoyancy Archimedes principle theory. Density is calculated by dividing the mass by the volume (Density = mass/volume). For example, 10 gram of fresh water has a volume of 10 milliliters. This result in a density of one gram per milliliter (10g/10 mL = 1 g/mL). Unlike mass and volume, increasing the amount of material measured does not increase or decrease density. If the density increase or decrease suddenly, the floater of LIT will be floating or drowned even the actual level mostly stable. In this case the level reading suddenly unstable.

IMPROVING LEVEL MEASUREMENT USING GUIDED WAVE (GWR) RADAR METHOD

The fundamentals of guided wave radar measurement come directly from Time Domain Reflectometry (TDR). TDR instruments launch low amplitude, high frequency pulses onto antenna probe and sequentially sample reflected signal amplitudes.

The wave guided is a probe immersed in the liquid (or dry, bulk-media). The high frequency electromagnetic pulses transmitted down the probe are reflected at the point of discontinuity between the air and the process medium. As with other "time of flight" instruments, those reflections are measured by high-speed circuitry in the transmitter, thus establishing the level measurement. The dielectric constant for typical process media can range from 1.4-100. The higher the dielectric constant of the medium being measured, the stronger the reflected signal is. Figure 5 shows the guided wave radar measurement method. The condensate level trending using GWR is shown in Figure 6.

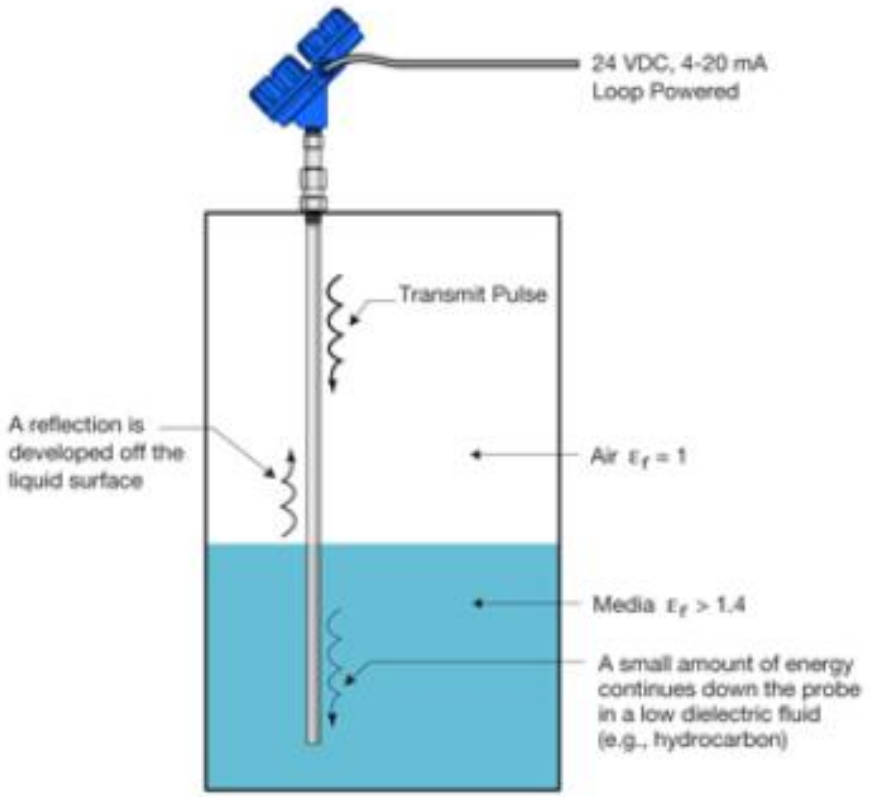


Figure 5: Guided wave radar measurement method.

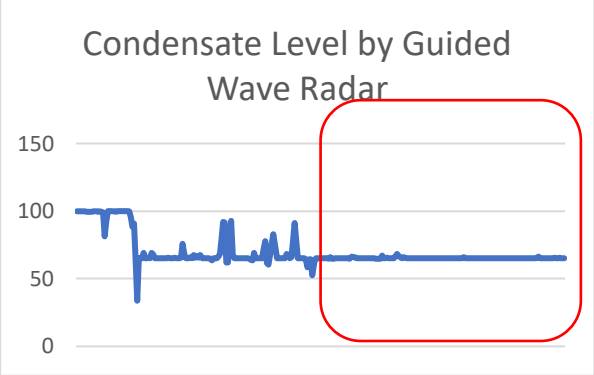


Figure 6: Condensate level trending using Guided Wave Radar (GWR).

The key advantage of guided wave radar level measurement is that no compensation is necessary for change in density, dielectric or conductivity of fluid. Changes in pressure, temperature and most vapor space conditions have no impact on measurement accuracy, GWR is unaffected by high turbulence or vibrations; and build-up has practically no effect, meaning no need for re-calibration.

Density fluctuations, steam generation or strong pressure and temperature fluctuations do not influence the measuring result. Also, buildup on the probe or the vessel wall do not influence the measurement.

CONCLUSIONS

Turbulence process and density fluctuation in condensate level controlling was made floating level transmitter (Magneto-stricitve) damaged and it was disturbing plant process due to inaccurate measurement. Based on density fluctuation study for floater phenomenon if any temperature or pressure change, the floater is not stable and also magneto strictive with length of rod more than 4 meters can get more impact from turbulence process due to elastic material.

Guided Wave Radar (GWR) can overcome condensate level error measurement to increase plant reliability up to 98% with maintenance free and accurate measuring in OEC bottoming. GWR more reliable for high turbulence because the measurement method is non-contact and will not affected by vapor, sludge, buildup, foam generation and condensation contaminated because of GWR system using microwave with high frequency more than 5 GHz. Disturbance from any density fluctuation or high turbulence has eliminated by GWR.

REFFERENCE

Wilkeys. R.J Buoyancy Archimedes principle. http://courses.washington.edu/phy115a/slides/03-115sp13-fluids2.pdf

https://www.kontram.fi/media/mikroaaltotutka-pinnanmittaukset/46597-en-level-and-interface-measurement-in-liquids-vegaflex-81-83-86.pdf

https://sciencing.com/density-mass- volume-related-6399069.html

https://www.flowcontrolnetwork.com/how-guided-wave-radar-level-measurement-works/

OPTIMIZATION OF USING COOLING TOWER FAN IN THE GEOTHERMAL POWER PLANT OF ULUBELU UNIT 4 IN HOUSE LOAD SAVING

Nizar Muslim and Yusup Anwar Ridwan

Pertamina Geothermal Energy - Ulubelu
Ulubelu Street – Muara Dua, Ulubelu District, Lampung 35379
Email: nizar.muslim@pertamina.com, yusup.ridwan@pertamina.com

ABSTRACT

The Geothermal Power Plant of Ulubelu Unit 4 is a plant owned by Pertamina Geothermal Energy with a capacity of 55 MW. In this unit there are problems in the availability of steam supply, so that capacity can be generated only 37 MW. The generated power will be used to supply to the grid (PLN) and house load. Unit 4 is trying to save on its own usage so that can maximize the power to supply to the grid (PLN). One of them is optimizing the usage of cooling tower fans. Unit 4 is equipped with 6 cooling tower fans with a load capacity of 150 kW each. The assumption when the power that can be generated is only 37 MW, then the need for the cooling process does not require 6 cooling tower fans to work simultaneously. The method used to turn off 1 cooling tower fan in a few hours by observing whether there are changes in operating parameters. The operating parameters that we observe include power generated, house load power, turbine inlet pressure, condenser pressure, water cooling temperature, main control valve opening, and steam consumption. If all these parameters are normal, then the next stop the second cooling tower fan and observing the parameters again. From the observations, it was found that if first cooling tower fan is turned off, all parameters that observe are still normal. When stopped the second cooling tower fan, there was a change in the turbine inlet pressure and the cooling temperature was quite significant. So, conclusion that at 37 MW power generated can save the use of cooling tower fans in only one unit. If the savings from 1 cooling tower fan unit are converted into rupiah, it is around IDR 4,634,939.4 per day.

Keywords: Cooling tower, optimization, Ulubelu

INTRODUCTION

Ulubelu unit 4 is a geothermal power plant located in Ulubelu District, Tanggamus District, Lampung Province which is managed by PT. Pertamina Geothermal Energy with a capacity of 55 MW.

Steam turbine main drive is produced by production wells which are then separated by a separator between steam and brine (water). The steam then goes to the scrubber to make sure steam entering the turbine is completely dry. Figure 1 shows the flow process of Ulubelu unit 4.

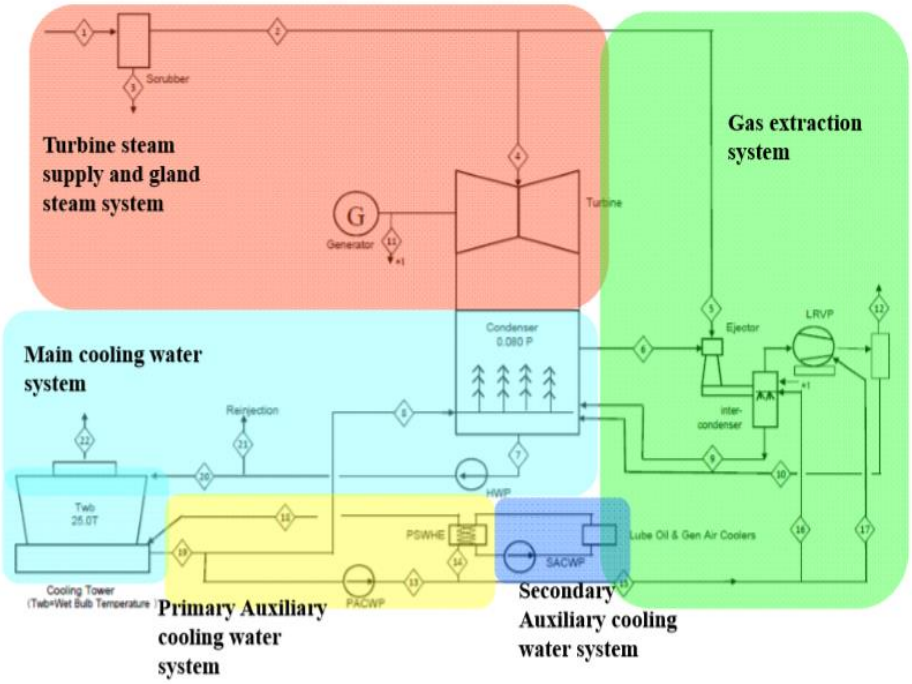


Figure 1: Flow Process Geothermal Power Plant of Ulubelu Unit 4.

Steam enters the turbine with a pressure of 6.5 barg and a temperature of 167ºC. The steam mass flow rate is 350 tons/hour. The turbine will rotate at a speed of 3000 rpm. Down below the turbine, there is a condenser that works in direct contact with a pressure of 0.08 bara. Water coming out of the condenser will be flowed by two hot well pumps to the cooling tower. In cooling tower, water with a mass rate of about 18,000 m3/hour. Water from the cooling tower will be circulated back to the condenser and other cooling systems. Excess water will be channeled to reinjection wells.

Table 1: Specification of Cooling Tower.

	Remark	Unit
Selection	Induced Draft	
Tower Type	Concrete Shell Counterflow Mechanical Draft	
Circulating Water Flow	18000	m3/h
Hot (Inlet) Water Temperatur	38.8	°C
Cold (Outlet) Water Temperatur	28	°C
Wet Bulb Temperatur	25	°C
Power	150	kW
Number of Cells	6	
Fans per Cell	1	
Total Number of Fans	6	
Heat Load	8.12E+05	MJ/h
Design Relative Humidity	90%	
outlet water mass flowrate	14600	m3/h
Air delivery per fan	42863	[m3/min]
motor speed	1475	rpm
fan speed	103.6	rpm
speed reducer number	6	
speed reducer ratio	1 : 13.996	

Ulubelu unit 4 is making efforts to save on its house load. House load is the electrical power consumption needed to supply power for equipment such as motors, lighting, etc in the area of unit 4. The effort is optimizing the use of cooling tower fans. When it is fully operational (power generated by 55 MW), unit 4 requires 6 cooling tower fans that work together with a total power of 900 kW. For now, the power generated by unit 4 only 37 MW due to limited steam availability. With these conditions, some cooling tower fans can be turned off to reduce house load. However, this will affect the temperature of the water coming out of the cooling tower. Then these parameters must be kept according to standard specifications (Table 1). Research and simulations will be conducted to determine the optimum number of cooling tower fans when certain generation power without exceeding the operating standard limit, so that the house load will be more efficient and effective.

METHODOLOGY

The power generated by the power plant is very dependent on the availability of steam, so if there are some problem of steam field facilities, such as decreasing pressure wells, leaking lines, and other problems that will reduce supply and pressure of steam which will be decreasing power that can be generated. When the generated power can't reach maximum capacity, whether the process is still needed on the cooling tower using 6 active fan cooling towers simultaneously or not.

Based on the *Tata Kerja Individu* (Standard Operational Procedure) of the startup unit, three of the six cooling tower fans are turned on before the rolling turbine and the other three are turned on after the unit load reaches 27.5 MW (50%). This is also a consideration if the power generation of 37 MW (67.27%) does not require six fan cooling fans to be ignited simultaneously.

The parameter that becomes a limitation in this research and simulation is exhaust steam pressure high limit curve (Figure 3) which shows the point where the operation is still normal, because the cooling performance of the cooling tower will affect the values of the exhaust steam pressure high limit curve. Figure 2 shows the cooling tower of Ulubelu unit 4.



Figure 2: Cooling Tower of Ulubelu Unit 4.

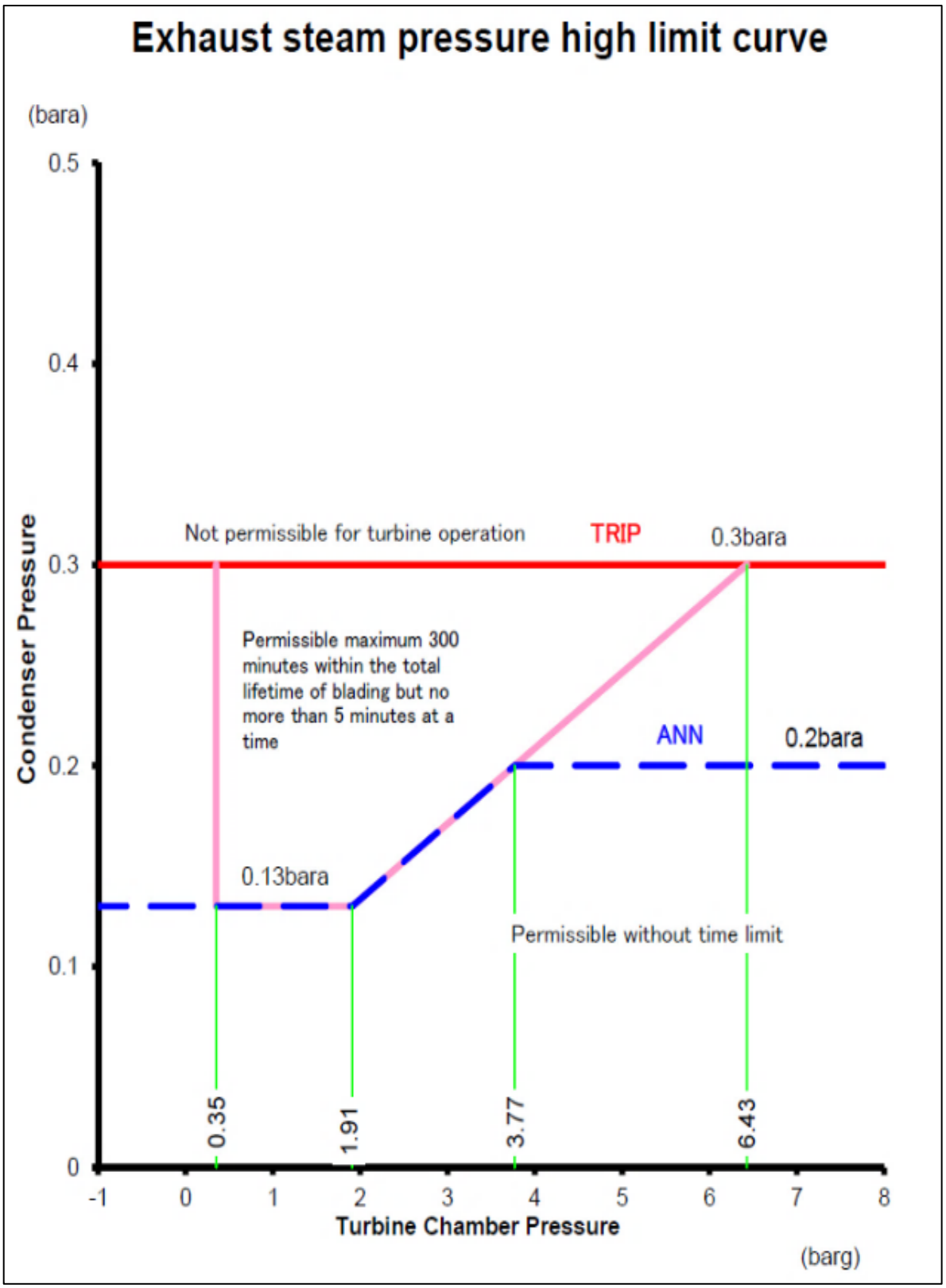


Figure 3: Exhaust Steam Pressure High Limit Curve.

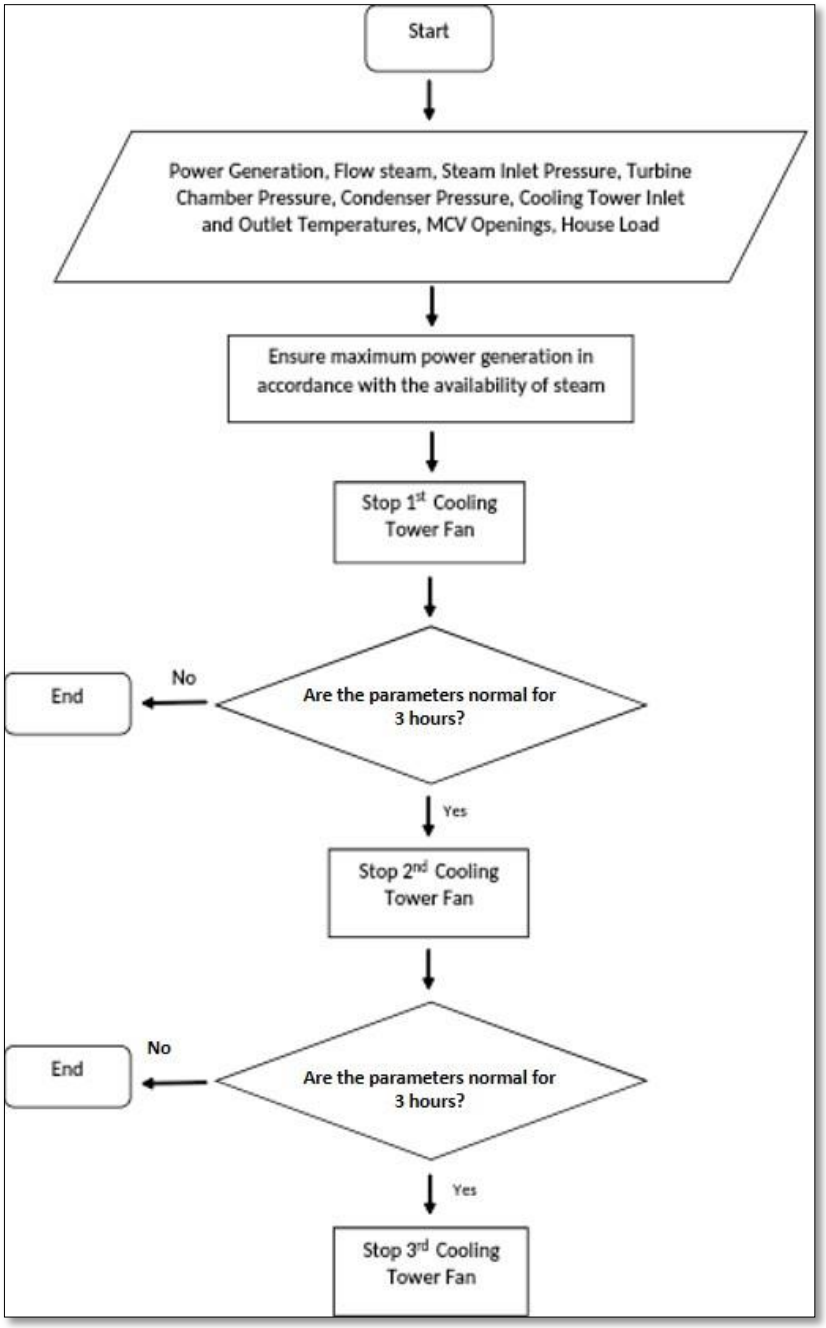


Figure 4: Flowchart of Simulation.

The method used is by retrieving data/trending from several parameters including power generation, flow steam, inlet pressure, turbine chamber pressure, condenser pressure, cooling tower inlet temperature, cooling tower outlet temperature, percentage of MCV openings, and house load. Simulation and data collection are carried out for 24 hours for each process according to the flowchart (Figure 4). Figure 3 shows the Exhaust Steam Pressure High Limit Curve.

RESULT

Results of simulation and data retrieval in unit 4 when power generated by 37 MW, shown that all parameters which become a standard reference for the operation of the power plant are still in normal conditions when first cooling tower fan is turned off for more than 3 hours. It is shown by a trend graph when the simulation is done (Figure 5). But when the second cooling tower fan is turned off, there is a significant increasing value of some parameters such as turbine chamber pressure, condenser pressure, water cooling temperature, MCV opening and flow steam consumption. Parameters were observed for up to 10 minutes, but the value keeps increased. This causes emergency dump valve on the separator dumping continuously because separator level becomes high, and this is an abnormal operation condition. There no sign to be stable, so the second cooling tower fan is turned on again to keep those parameters normal again.

The main purpose of all this is to save house load power in unit 4. The saving house load power is shown by trend graph (Figure 5) and calculate the average of house load based time of each stage of the flowchart (Table 2).

Table 2: The House Load during Simulation

	All Cooling Tower Fan ON	Stop 1st Cooling Tower Fan	Stop 2nd Cooling Tower Fan
House Load (kW)	3252.87	3075.97	2966.19

From the effort to save house load unit 4 at 37 MW power generation, it can save 176.9 kW from only stop one cooling tower fan. So, if it converted into savings per day, the savings are:

Saving = house load saving x 24 h x inflation index x price/kWh
=176.9 kW x 24 h x 1.03043 x 0.0753 USD/kWh
= 329.42 USD (1 USD = IDR 14,070)
= IDR 4,634,939.4 (saving per day)

This house load saving is carried out from April 2019, so that until the end of 2019 the savings made from house load unit 4 are estimated to be around IDR 1,251,433,638.

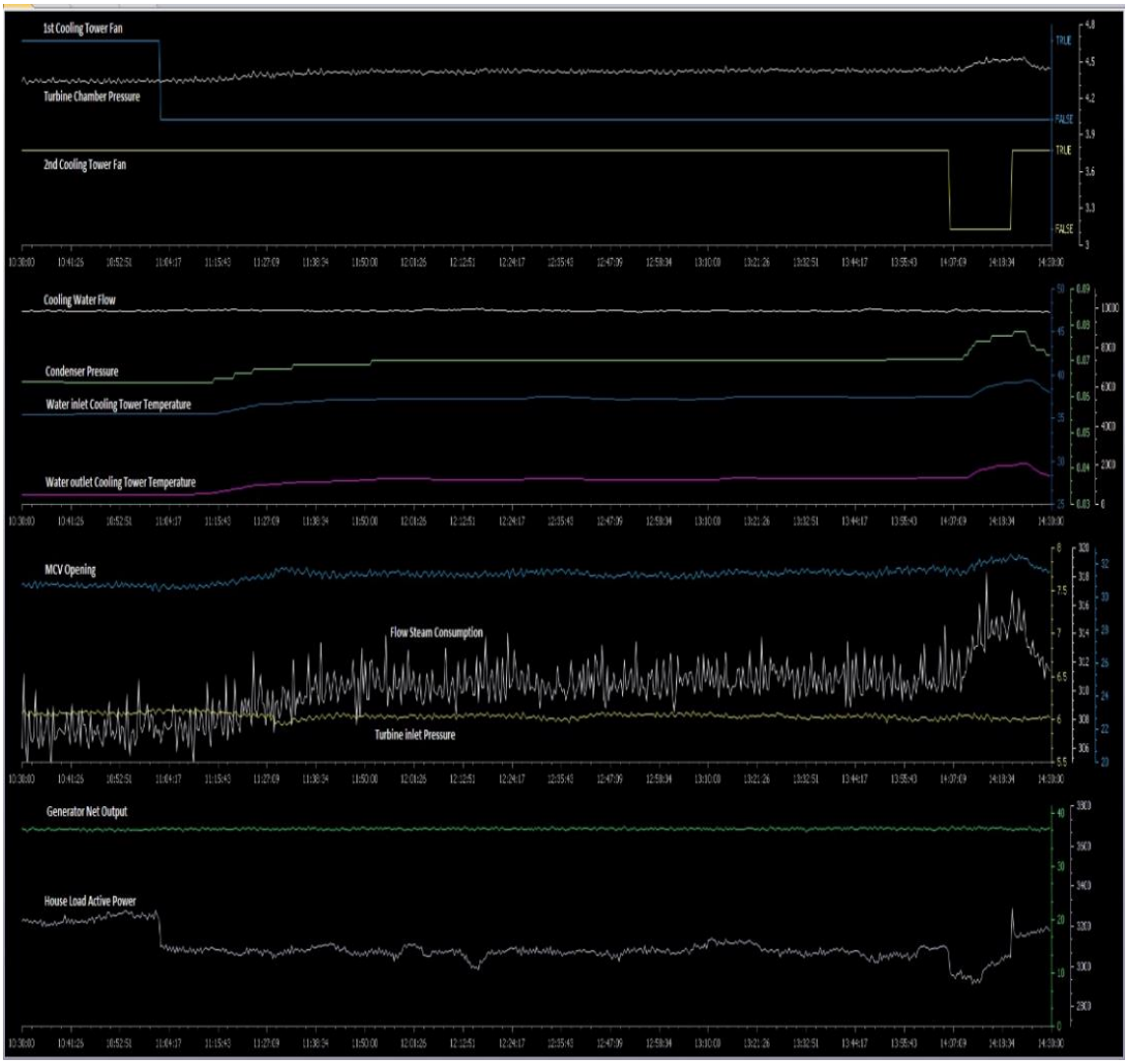


Figure 5: Trend Graph of Simulation.

CONCLUSION

Cooling fan tower is one of the important components in the operation of unit 4 geothermal power plant, especially in the cooling system. However, cooling tower fans have loads of 900 kW total for 6 operating units.

With the condition of power generation that is not optimal, about 37 MW from maximum capacity 55 MW, the house load can be more efficient by knowing the number of cooling towers needed with this condition.

From the results of simulations and data collection, it was produced that the unit 4 with 37 MW power generated could be more efficient using only the five cooling tower fans. So, we can save on the use of 1 cooling tower fan.

The savings made from the results of this are IDR 4,634,939.4 per day.

REFERENCES

Fuji Electric Co.Ltd. (2014). “Vendor Document”. Journal of Fluid Mechanics. 254: 73-79.

Fuji Electric Co.Ltd. (2015). “Operation Manual for Power Plant System”. 65.

Pertamina Geothermal Energy. (2011). “Perjanjian Jual Beli Tenaga Listrik PLTP Ulubelu Unit 3 dan Unit 4”. 36: 16-19.

Pertamina Geothermal Energy. (2017). “Tata Kerja Individu Start Up Unit 4”. Lampung.

INCIDENT INVESTIGATION AND ROOT CAUSE ANALYSIS (RCA) BEST PRACTICES TO IMPROVE SAFE AND RELIABLE GEOTHERMAL PLANT OPERATIONS

U. Anang Ishak and Indra Rahmansyah

Star Energy Geothermal Salak/Darajat
Sentral Senayan Office Tower II - 24th Floor, Jl. Asia Afrika no 8, Jakarta 10270, Indonesia
Email: uaischak@starenergy.co.id, irav@starenergy.co.id

ABSTRACT

Star Energy Geothermal Salak/Darajat implement Integrated Geothermal Operations Management System (IGOMS). One element of IGOMS is Incident Investigation Reporting that uses Root Cause Analysis (RCA) business process to ensure that each incident/near miss is reported and investigated, and root causes shall be identified to reduce or eliminate systemic causes and to prevent future incidents.

Incident investigation and root cause analysis is a systematic and integrated process that drives the team for critical thinking and problem solving. This process consist of ten items that correlated each other: data gathering, team formation, sequence of event, protective systems, root causes, cause verification, recommendations, investigation documentation, reporting and root cause categorization. The input of investigation process normally is data collection from the four P's sources: Position, People, Parts, Paper and other electronic information. While the outputs of incident investigation process are root causes, the category and corrective action complete with person in charge, detailed recommended activities, due date and deliverables. Root Cause Analysis methodology usually works with two different approaches whether Why Tree or Five Why. This Root Cause Analysis methodology can be selected based on the incident complexity or referring to company internal procedure.

By implementing the Incident Investigation process and Root Cause Analysis best practices, SEGS/SEGD take benefits to improve the geothermal plant operations, safety as well as the reliability. Since RCA output touches the root cause, the corrective action will prevent the incident from recurring, reduce the consequences of recurrence or reduce the frequency of recurrence. The recommendations and reporting are important for lesson learnt and lookback session. The root causes categorization are also valuable data to prioritize the improvement program with focusing activities based on data analysis.

Keywords: Root cause analysis, plant operation

INTRODUCTION

Star Energy Geothermal operates three different locations of Geothermal Power Plant at West Java with total capacity 875 MW (see Figure 1). Star Energy Geothermal (Wayang Windu), Ltd generates 227 MW, consist of two units 1 x 110 MW and 1 x 117 MW. Star Energy Geothermal Salak, Ltd (SEGS) generates 377 MW consist of 3 x 65.6 MW and supply steam to PLN to produce 3 x 60 MW electricity. While Star Energy Geothermal Darajat II, Limited (SEGD) generates 271 MW consists of 1 x 95 MW and 1 x 121 MW as well as to supply steam to PLN to produce 1 x 55 MW electricity.



Figure 1: Star Energy Geothermal Plant locations at West Java, Indonesia.

The Star Energy Geothermal continues renewable energy growth by pursuing opportunities to expand and develop geothermal energy. The company focuses to the strategic target to be the world's largest geothermal power producer by generating 1,200 MW in 2028. In parallel to the renewable energy development plan, SEGS/SEGD also pay attention to the safe and reliable operations of existing facilities by implementing Integrated Geothermal Operations Management System (IGOMS).

IGOMS is a systematic management system in the fields of Personal & Process Safety, Health, Environment, Operations Reliability and Efficiency to achieve a world-class geothermal operation that is safe, reliable, efficient, and environmentally friendly. IGOMS consists of 12 Elements and 52 Standards/Expectations. One of the IGOMS elements is the Incident Investigation & Reporting process.

INCIDENT INVESTIGATION

The terms incident investigation and root cause analysis are often used synonymously. In fact, they are two different things. Incident investigation refers to the systematic account and analysis of an incident. Root cause analysis is one part of conducting the incident investigation.

The definition of incident investigation is the systematic account and analysis of an incident based on information gathered by a thorough examination of all root causes involved. The investigation will normally result in the preparation of a logical, sequential report of the events with recommended preventive strategies.

A traditional view of incidents is that they are typically caused by shortcomings in human competence, attention or attitude. However, the recent view changes the incidents cause is no longer human errors or violations. It is not the cause of failure, but a symptom of failure - trouble deeper within the system. Human cause is not random; it is tied to features of the tasks humans perform, equipment, work systems, and processes, and culture of the organization. In this perspective, human cause is not the conclusion but rather the starting point of investigations.

Incidents can be the result of active errors or latent errors. Active errors are the acts or conditions immediately involved in the incident situation. They typically involve the front-line personnel; the consequences are immediate and can often be prevented by well-designed equipment and processes and strong culture. Latent errors are influenced by latent conditions.

Latent conditions include the managerial influences and social pressures that make up the culture ("the way we do things around here") and can influence equipment, work systems, and processes and highlight supervisory inadequacies. They tend to be hidden until triggered by an event. Latent conditions can lead to latent error. Latent error may occur when several latent conditions combine in an unforeseen way. People may make errors irrespective of how much training they have completed, how experienced they are, or how motivated they are to do it right. Latent error provides as great, if not greater, potential danger to safety as active errors. Latent conditions are usually hidden within an organization until it is triggered by an event likely to have serious consequences.

The purpose of an incident investigation is to determine the root causes of an incident or near miss to prevent repeating the event, to reduce the consequences of recurrence or to reduce the frequency of recurrence. The lessons learned from investigations can be leveraged to prevent future incidents.

10-Step Investigation Process

The 10-step investigation process is used to gain an understanding of the incident, its causes and what corrective actions are necessary to prevent recurrence. The line of reasoning in the investigation process is: It begins with the incident and identifies the problem (condition, situation or action that was not wanted and not planned). It outlines what happened step by step in a timeline. Then it determines what protective system could have prevented this occurrence. The next step is to investigate the reasons why this situation happens using the Why Tree or Five Why methodology.

The following are the 10 steps of the incident investigation process.

1. Gather data
2. Form the investigation team
3. Develop the sequence of events
4. Identify protective systems
5. Conduct Root Cause Analysis (RCA) using Why Tree or Five Why methodology
6. Verify potential causes
7. Develop recommendations
8. Document the investigation
9. Review and issue the report
10. Categorize the root causes and the incident

The Figure 2 below describes the steps of incident investigation processes. It starts from the event occurrence, continues to 10-step incident investigation process and it will end with solutions implementation.

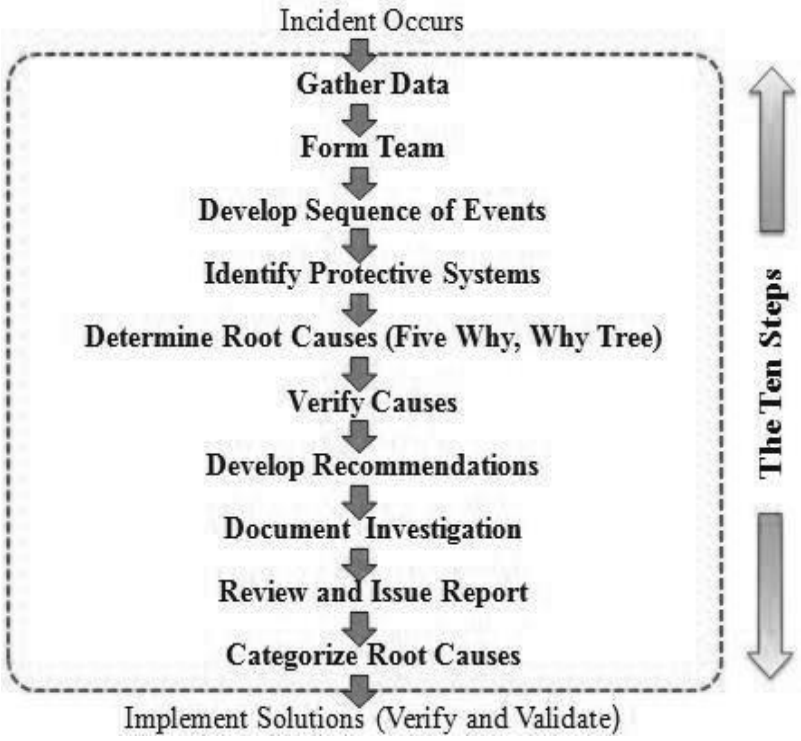


Figure 2: The 10-Step Investigation process.

Incident Investigation Inputs

The important process of incident investigation step is to collect the inputs consist of the facts that are associated with the incident. This data gathering process should be started sooner after or even during the incident occurrence (without compromising safety, security and or recovery activities).

The investigation inputs that should be collected consists of events and conditions before, during and after the occurrence; personnel involvement (including actions taken or not taken); environmental factors; and other information having relevance to the occurrence. A disciplined approach to data gathering is very important. All data need to be properly identified and labeled. Data need to be organized and stored in a secure location until the investigation is completed.

Data collection will be an ongoing step in the investigation process. As the team investigates, additional data may be needed. It is important to try to get as much data as possible during the initial data gathering phase because some data may not be available later. The Four Ps of Data Gathering: People, Position, Paper and Parts.

People

People are important as data sources because they can relay information about everything that they were aware of before and at the time of the incident. Interviews and written signed statements are the two modes for documenting people's recollections of what happened leading up to and after the incident. Often, combining the two is the most effective approach.

The purpose of interviews and written statements is to obtain information that can be used in preparing the sequence of events and determining the root causes. The interview processes need to figure out what happened. Interviewee should focus on what they saw, heard, smelled and experienced.

In incidents in which human performance appears to be an issue, a key approach is determining the situation people found themselves in at the time that may have influenced their decision-making process. It is important to obtain a meaningful understanding of what influenced the individual's actions, including behaviors, motivation, state of mind and the leader's direction, feedback and coaching. Understanding context is the key to a successful human performance investigation and to providing lessons learned for the future.

Position

Position refers to what the status was before the incident occurred. This includes:

- Weather and tide conditions
- Process and equipment status
- Job/work status
- Work going on around the area
- Human factors issues

The interviewer should frame the questions to understand reasoning, and get facts about the ease or difficulty of performing standard job tasks, e.g., complexity, physical limitations to work equipment

and mental limitations (too many things to do with production goals, schedule and other potential issues).

Paper and electronic records/reports

This section refers to the documentation trail both before and after the incident, including:

- Logs, charts and notes that indicate what was going on at the time
- Failure analysis report
- Copies of standing orders or procedures
- Training records
- Electronic records and data in control systems
- Radio recordings
- Vehicle computer records
- Closed Circuit Television (CCTV)

Parts

This section refers to how the incident site looks after the incident occurred and what the physical data are telling us. Examples of physical data to gather are as follows:

- Parts, pieces and other things that can be secured.
- Photographs, videos, sketches or diagrams of the scene; equipment involved; or what was going on at the time.
- Process, equipment, and work systems samples.
- Samples taken on a sample log.

ROOT CAUSE ANALYSIS

Basically Root Cause Analysis is a part of Incident Investigation process. Following the data gathering, team may start the development of sequence of event and protective system as well as to conduct root cause analysis. The goal of incident investigation system is to work through all causes, including physical, human and system to find and eliminate all root causes that result in incidents.

Root Cause Analysis is a methodology used to lead an investigator to the root cause(s) of an incident.

Based on SEGD/SEGS best practices, there are two methods of Root Cause Analysis. The Why Tree method can be used on all levels of events, but primarily on complex events. The Five Why method will only be used on simple events.

Incident Causes

The incident causes consist of physical, human or system causes. These are typically sequential, although not 100 percent of the time. A physical cause is caused by a human cause, which in turn is often caused by a system cause (see Figure 3).

Physical causes

Physical causes are the equipment failures or changes in physical conditions that lead to an incident. Some examples of physical causes are: The piping broke or leaked, the pump was vibrating, the temperature indicator failed, the furnace tubes corroded, the tank was struck by lightning or the electrical circuit was shorted out. Physical causes can be verified with physical evidence: a broken pipe, a failed temperature indicator, presence of corrosion by-products, etc.

Human causes

Majority of human causes are influenced by system failures or systems that failed to support the proper human action or inaction. The influences can be classified as one or more of the following elements:

1. Culture
2. People
3. Equipment, work systems and processes

Many, but not all, of the factors considered under the three elements of human performance listed above can be ultimately attributed to a system-level cause. Human causes are not just limited to the direct actions or inactions of individuals at the end of the chain or who may have been the last to touch or interact with the process.

System causes

System causes are generally management system failures or deficiencies leading to an incident. Management systems constitute a mix of policies, procedures, roles and responsibilities, and work processes that make up the support network for the organization.

Mature incident investigation systems look at all causes to determine root causes in physical, human and management systems. Figure 4 below shows the concepts of root cause.

In addition, root cause is the lowest system-level of cause(s) that:

- It can be reasonably identified.
- If it is corrected, it would prevent the incident from recurring.
- The organization has control to fix.

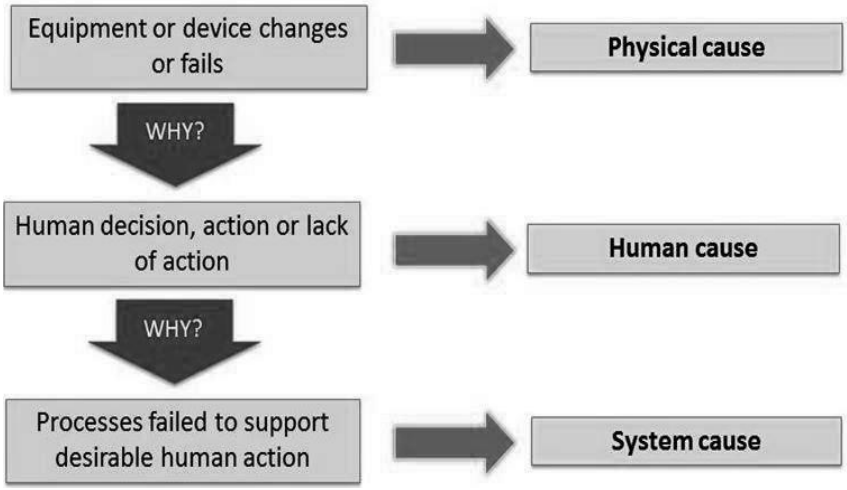


Figure 3: Flow chart of causes.

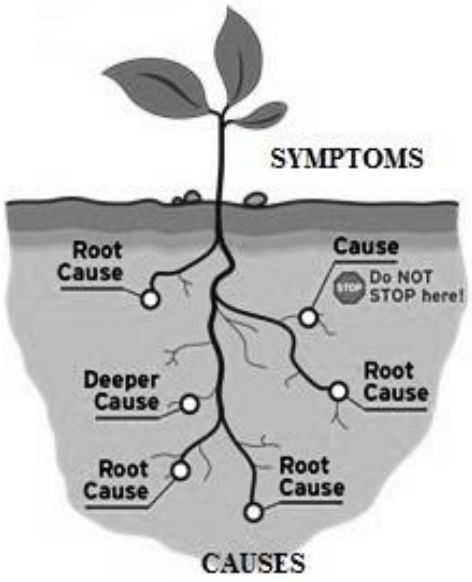


Figure 4: Root causes and symptoms.

Once the root cause is identified, team will develop corrective action recommendation completed with person in charge, detailed recommended activities, due date and deliverables. Recomendation usually refers to SMART concept consist of Specific, Measureable, Accountable, Relevant and Time limit.

Root Causes Categorization

At the conclusion of the root cause analysis, the team is required to categorize each root cause into common categories to identify performance trends. Because there are an infinite number of potential root causes (based on the fact that each incident is unique), a list of standard root cause categories has been established into which the actual root causes will flow. The intent is to capture the conclusion from every branch of the Why Tree, even if that cause is further explored in another branch of the analysis.

The following seventeen general root cause categories have been selected to record and trend incident causes. It is important to note that the investigation may have identified more than one root cause and all of them should be recorded as outcomes of the analysis.

The investigation team is in the best position to select the categories that most closely relate to the actual root causes of the incident. The intent of the categorization process is to capture all root causes determined during the investigation so that the corporation has a way of tracking performance trends. Recording and trending performance in terms of adherence with the tenets gives the company another view of operational performance.

The current list of root cause categories are as follows:

1. Assessments or audits
2. Communications
3. Contractor safety, health, environment management
4. Design
5. Emergency response
6. Human performance
7. Near miss investigation
8. Quality control or acceptance testing
9. Leadership accountability
10. Management of change
11. Natural phenomenon
12. Pre-startup safety reviews
13. Preventive maintenance, inspection, testing, or repair
14. Procedures or safe work practices
15. Risk assessment
16. Supervision/work direction
17. Training/competency

One of the best uses of Root Cause Analysis data is to find repeating causes or common causes of incidents or operability problems. These can be dismissed as one-time, anomalous causes. Keeping root causes data can help to spot trends. The incidents and their root causes can be categorized any number of ways whether by equipment type, time, Organization Capability (OC), Process Safety Management (PSM) element, IGOMS element or Lost Production Opportunity (LPO).

SEGS/SEGD BEST PRACTICES

In order to achieve safe and reliable operations of geothermal plants, SEGS/SEGD have been implementing Incident Investigation and Root Cause Analysis processes. These best practices significantly contribute SEGS/SEGD to achieve asset business plans, maintain safe operation, improve reliability and reduce lost production opportunity.

The following are the benefits of using formalized and systematic Incident Investigation and Root Cause Analysis processes:

- Meet compliance and company regulation.
- Bring together technical expertise, experience and data analysis to find the root causes.
- Use a systematic method to help find all the causes.
- Focus on facts to determine the root causes.
- Identify recommendations to resolve the problem.
- Achieve results that are consistent and supportable.
- Share the lesson learned information to prevent the incident from recurring, reduce the consequences of recurrence or the frequency of recurrence.
- Prioritize the improvement program with focusing activities based on data analysis.

Root Cause Categories 2012-2016

As part of continual improvement, SEGS/SEGD continues to evaluate the reporting data of Incident Investigation and Root Cause Analysis processes. This evaluation data is used to focus on company improvement program, resources and schedule based on the findings. Detail chart of SEGS/SEGS root cause categories during period 2012-2016 is shown in the Figure 5 below.

According to Incident Investigation Reporting data during period 2012-2016, SEGS/SEGD can identify the Top 5 most frequently cited root cause categories as follows:

1. Procedures or Safe Work Practices (24%)
2. Design (15%)
3. Risk Management (13%)
4. Preventive Maintenance, Inspection, Testing or Repair (11%)
5. Training/Competency (9%)

SUMMARY

The following are the summary of Incident Investigation and Root Cause Analysis (RCA) best Practices to SEGS/SEGD geothermal plant:

1. Incident investigation is the systematic account and analysis of an incident or near miss based on information gathered by a thorough examination of all root causes involved.
2. Root Cause Analysis (RCA) is one part of conducting the incident investigation. RCA is a methodology used to lead an investigator to the root cause(s) of an incident. There are two RCA methods usually used Why Tree for mostly complex event and Five Why for simple event.
3. Categorization of root causes data will identify repeating causes or common causes of incidents or operability problems. Evaluation of root causes data can help to spot trends and prepare the solution as well as mitigation plans.
4. SEGS/SEGD has implemented the Incident Investigation and Root Cause Analysis processes since several years ago and it contributes significant benefits to maintain safe operation, improve plant reliability, achieve asset business plans and reduce lost production opportunity.
5. According to Incident Investigation Reporting data during period 2012-2016, SEGS/SEGD can identify the Top 5 root cause categories. Based on these findings, SEGS/SEGD can focus on improvement development plans and prioritize the resources to close the gaps.

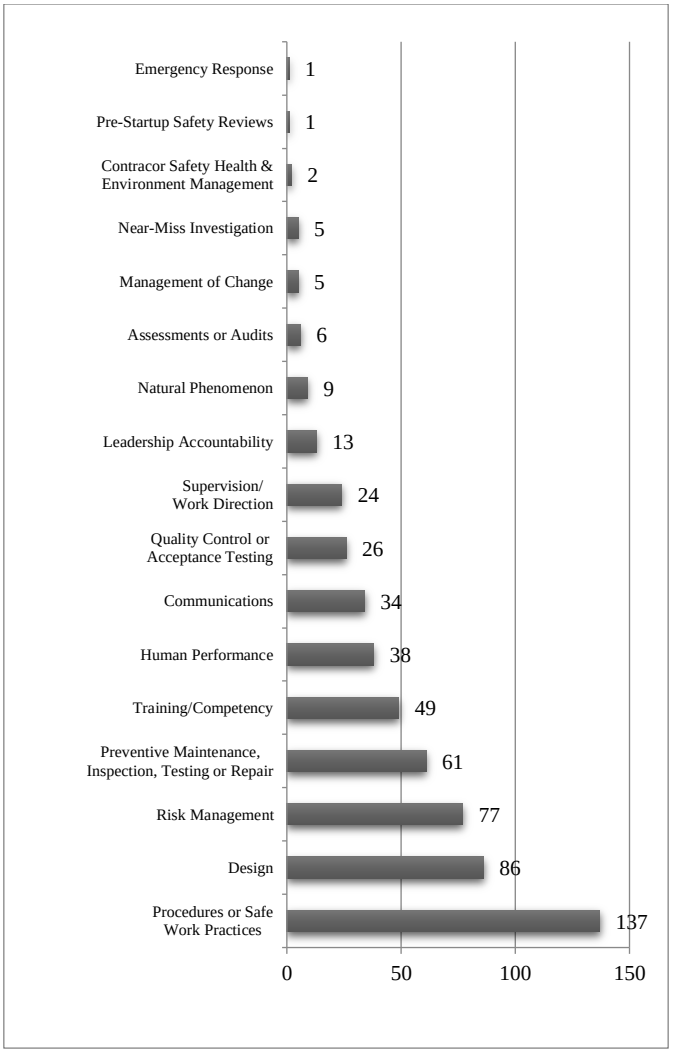


Figure 5: SEGS/SEGS root cause categories during period 2012-2016.

FORWARD PLAN

In order to increase effectiveness of existing Incident Investigation and Root Cause Analysis (RCA) processes, SEGS/SEGD develop several improvements plans such as:

1. Under the IGOMS development plan, continue to integrate Incident Investigation Reporting business process into other management system element.
2. Develop Incident Investigation Reporting online system using IT applications and facilities. This includes the Why Tree Builder software tool development.
3. Maintain the competency of Incident Investigation and Root Cause Analysis facilitator by conducting training, investigation exposure and routine audit process.
4. Share the Incident Investigation and Root Cause Analysis best practices and lesson learned to Wayang Windu.

DEFINITIONS

Active error: An error that has immediate negative consequences.

Condition: Any as-found state, whether or not resulting from an event, that may have compliance, safety, health, quality assurance, security, plant reliability & integrity, operational or environmental implications. Conditions may be supporting information for the event. Conditions may not have a direct (apparent) link to the event. An action not done is a condition.

Cause (causal factor): A condition or an event that results in an effect (anything that shapes or influences the outcome). This may be anything from cavitation in a pump, a pipe break, an operator error or a weakness or deficiency in management or administration. Causal factors are the cause(s) that follow the direct cause(s), ultimately leading to the root cause(s).

Culture: An organization's system of commonly held values and beliefs that influence the attitudes, choices and behaviors of the individuals of the organization.

Direct cause: The cause, or causes, that directly resulted in the occurrence. For example, in the case of a leak, the direct cause could have been the

problem in the component or equipment that leaked. In the case of a system misalignment, the direct cause could have been operator error in the alignment. They are the first-level causes in the Why Tree under the incident.

Event: Events are actions. They describe who did what in the time surrounding the incident. An event is a single action. Events should be able to be directly related to the incident.

Human cause: A human error or violation.

Human error: An action or inaction that unintentionally results in an undesirable outcome or deviates from a set of rules or expectations. Human error can be either active error(s) or latent error.

Incident investigation: The systematic account and analysis of an incident based on information gathered by a thorough examination of all root causes involved. The investigation will normally result in the preparation of a logical, sequential report of the events with recommended preventive strategies.

Latent conditions: Undetected deficiencies in the organization or systems lying dormant that can provoke errors and create gaps in the safeguards.

Latent error: A human error whose effects can lie unnoticed in a system for a long time without apparent outcome. They are then triggered by an event and are likely to result in a serious consequence.

Near miss: An unplanned event having a potential but unrealized consequence of injury or damage to property, the environment, the company's reputation, or financial performance.

Root cause: The lowest level of cause(s) that can reasonably be identified which, if corrected, would prevent the incident from happening and that the organization has control to fix.

Root Cause Analysis (RCA): A technique or methodology used to lead an investigator to the basic or root cause(s) of an incident.

Physical Cause: The equipment failures or changes in physical conditions that lead to an incident.

Protective system: Any management system or hardware that reduces the potential for having the incident (probability) or the consequences of the incident (severity).

System Cause: Generally management system failures or deficiencies leading to an incident. Management systems constitute a mix of policies, procedures, roles and responsibilities, and work processes that make up the support network for the organization.

Violation: action or inaction that intentionally deviates from a set of rules. Violations can also be referred to as non-compliance.

REFERENCES

Ischak, U.A., Kurniawan, I. (2019), "Implementation of Plant Performance & Reliability Monitoring (P2RM) to Darajat and Salak Geothermal Power Plant," 2019 IERE - PLN Bali Workshop

Star Energy Geothermal Salak/Darajat. (2017). "Incident Investigation Facilitator Handbook". SHE Department

Star Energy Geothermal Salak/Darajat. (2017). "Incident Investigation & Reporting (II&R)", SHE Department

Star Energy Geothermal Salak/Darajat. (2019). "Integrated Geothermal Operations Management System (IGOMS) Manual". SHE Department

Star Energy Geothermal Salak/Darajat. (2016). "Incident Investigation List". SHE Department

MAINTAINING THE AVAILABILITY OF STEAM SUPPLY TO GEOTHERMAL POWER PLANT UNIT 1-4 WITH PIPELINE DEBOTTLENECKING PROJECT AT PGE LAHENDONG

Achmad Sani Zahid, Mukhamad Nashir, Viqar Adly Gani, Bagus Reka Susilo, Manda Wijaya Kusumah, and Apriyansah Toni

PT Pertamina Geothermal Energy Area Lahendong
Jl. Raya Tomohon no.420, Tomohon, North Sulawesi
Email: achmad.zahid@pertamina.com

ABSTRACT

Pertamina Geothermal Energy operates steam fields in Lahendong, North Sulawesi to supply steam to PLN's GPP Units 1-4 from 6 clusters. As time went on, the steam production from LHD-23 and LHD-28 is declining after well remedial. Previously, steam supply for Unit 3&4 from LHD-23 was 212 ton/h and LHD-28 was 184 ton/h, after remedial the flow reduced to 20 ton/h from LHD-23 and 109 ton/h from LHD-28. In other side, bottleneck occurs in pipeline from cluster 13B which has only 14" NPS so the maximum steam flow limited to 90 ton/h whereas there are 3 high potential wells in the cluster (approximately total 300-400 ton/h), and the 14" pipeline joins the pipeline of LHD-28 which is 24". This has led to an alternative solution to fulfill the steam supply for GPP Unit 3&4 by developing a new independent pipeline to maximize high potential wells in cluster 13B. However, the NCG of LHD-47 is higher than the other wells, so we did simulation to mix the fluids from those 3 wells and design the pipeline interconnecting between the new and existing line. The new pipeline design is 24" NPS and built in parallel with existing pipeline. This pipeline accommodate the steam produced from all wells at cluster 13B and the NCG value meet the steam supply requirements of GPP Unit 3&4. In other hand, the pipeline is also connecting unit 1&2 and unit 3&4 in the interconnection line at cluster 13.

Keywords: Operaion, Lahendong geothermal field

INTRODUCTION

Pertamina Geothermal Energy Area Lahendong located at Tomohon, North Sulawesi. PGE operates the steam field for GPP unit 1-4 which are PLN possession. PGE should deliver the steam to PLN's turbine to generate total 80 MW for unit 1-4.

There is some condition that PGE should meet for the steam quality, such as the composition of non-condensable gas (NCG), total dissolve solid (TDS), dryness, and the amount of the steam itself.

GPP unit 1&2 is supplied from cluster 4 and 13, while the GPP unit 3&4 is supplied from cluster 5, 13B and 24. Because of the natural production declining from the wells in cluster 5 and 24, there is a potential of fine (DoP) for PGE that cannot meet the requirement of the amount of steam delivered to GPP unit 3&4.

PROBLEM

PGE has 3 potential wells that have not been produced, which are LHD-47 LHD-48 LHD-49 in cluster 13B. The potential steam not only can be used for unit 3&4 but also can be used for unit 1 & 2. LHD-48 is already produced but cannot be maximized because the 'bottleneck' in the existing pipeline. The existing pipeline only has 14in NPS, which approximately limited to 100 ton/h steam flow. Because of this, the flow of LHD-48 is limited and the other two wells cannot be produced.

Not only that, the 14in pipeline is combine with 24in NPS from LHD-28 pipeline in cluster 24 so the maximum flow in the pipeline is reached. The maximum flow from cluster 24 and 13B is limited to approximately 200 ton/h. Steam flow required for GPP unit 3&4 is 400 ton/h to generate 40 MW.

PGE cannot meet the requirement for steam supply and potentially get fined (DoP) from PLN as the owner of the GPP unit 3&4.

This problem has led to an alternative solution to maximize production from cluster 13B and meet the requirement of steam supply GPP unit 3&4.

Operation, Maintenance, and Engineering team did the simulation to get the problem done by construct the new pipeline called 'Debottlenecking Project'.

SOLUTION

The team did the process simulation using HYSYS with the data from previous well testing. Besides that, the piping team using AutoPIPE to simulate the stress analysis.

Wells Data

In 2016, well LHD-47 LHD-48 LHD-49 was tested to know the potential of the wells after drilling. However, because the safety and environment matters the test was postponed. To avoid the loss production, LHD-48 was still flowing but directly into the system. The exact data of the well is still

unknown, but until 2019 well LHD-48 produces more than 100 ton/h steam.

LHD-47 was already tested in 2019 and the data showed that the potential steam flow is 130 ton/h.

For well LHD-49 has not been tested yet, but already flowing to atmospheric flash tank to bleed the well using side valve. From the observation, the flow shows a bigger potential than the previous well testing.

Well LHD-47

To simulate the process, we were using the last production test data as below (Figure 1).

Stream Name	LHD-47
Vapour / Phase Fraction	0,7306
Temperature [C]	263,5
Pressure [bar]	**49,00**
Molar Flow [kgmole/h]	8293
Mass Flow [tonne/h]	**150,0**
Std Ideal Liq Vol Flow [m3/h]	150,5
Molar Enthalpy [kJ/kgmole]	-2,443e+005
Molar Entropy [kJ/kgmole-C]	143,8
Heat Flow [kJ/h]	-2,026e+009
Liq Vol Flow @Std Cond [m3/h]	147,7
Fluid Package	*Basis-1*
Utility Type	

Figure 1: fluid properties in the simulation of LHD-47.

And the composition as shown below (Figure 2).

	Mass Fractions
H2O	**0,9930**
H2S	**0,0010**
CO2	**0,0060**

Figure 2: Composition of fluid used in the simulation of LHD-47.

Well LHD-48

To simulate the process, we were using the last production test data as below (Figure 3).

Stream Name	LHD-48
Vapour / Phase Fraction	0,5015
Temperature [C]	257,9
Pressure [bar]	**45,00**
Molar Flow [kgmole/h]	8283
Mass Flow [tonne/h]	**150,0**
Std Ideal Liq Vol Flow [m3/h]	150,6
Molar Enthalpy [kJ/kgmole]	-2,516e+005
Molar Entropy [kJ/kgmole-C]	130,7
Heat Flow [kJ/h]	-2,084e+009
Liq Vol Flow @Std Cond [m3/h]	147,6
Fluid Package	*Basis-1*
Utility Type	

Figure 3: fluid properties in the simulation of LHD-48.

And the composition as shown below (Figure 4).

	Mass Fractions
H2O	**0,9910**
H2S	**0,0010**
CO2	**0,0080**

Figure 4: Composition of fluid used in the simulation of LHD-48.

Well LHD-49

To simulate the process, we were using the last production test data as below (Figure 5).

Stream Name	LHD-49
Vapour / Phase Fraction	0,7864
Temperature [C]	212,7
Pressure [bar]	**20,00**
Molar Flow [kgmole/h]	5536
Mass Flow [tonne/h]	**100,0**
Std Ideal Liq Vol Flow [m3/h]	100,3
Molar Enthalpy [kJ/kgmole]	-2,439e+005
Molar Entropy [kJ/kgmole-C]	149,2
Heat Flow [kJ/h]	-1,351e+009
Liq Vol Flow @Std Cond [m3/h]	98,48
Fluid Package	*Basis-1*
Utility Type	

Figure 5: fluid properties in the simulation of LHD-49.

And the composition as shown below (Figure 6).

	Mass Fractions
H2O	**0,9954**
H2S	**0,0006**
CO2	**0,0040**

Figure 6: Composition of fluid used in the simulation of LHD-49.

Simulation

The simulation was made with modification of existing line. Originally there is only one line of two-phase fluid for each well. The team simulate using cross-tee flange, so the fluid outlet separates into two lines as seen below.

The existing line from 3 wells combined and mixed in a header and go to separator 47A. The new two-phase line combines in a new header and go to new separator 47B. Simulation (Figure 7 and 8) showed the outlet of separator already meet the steam quality required and the flow required.

The process team calculate the pipe size for the new pipeline. The simulation showed that pipe with 24in NPS is the best and optimum size for the new pipeline. After that we calculate the pressure drop and simulate using HYSYS to get the steam required as shown below. After process simulation, the piping team did the simulation of stress analysis to design the piping and the pipe support.

This project includes civil scope for the construction of the pipe support for the new pipeline.

CONCLUSION

The simulation showed that if the wells in cluster 13B optimized, PGE need to construct the new pipeline to deliver steam to GPP unit 3&4 using 24in pipe with an independent line, not combine with existing line to avoid the bottleneck. The simulation showed that this project already meets the requirement of steam quality and steam (Figure 9 and 10) amount to generate electricity for GPP unit 3&4.

The best practice that used for the well optimizing is summarized by yearly of experience as well with proper engineering justification. Determination on how to solve the problem with no return is not an issue if the indication showing green light to simulate as well to handle the construction safely and effectively (Figure 11). However further study and improvement are required in order to enhance the performance and efficiency of the design and simulation in the future.

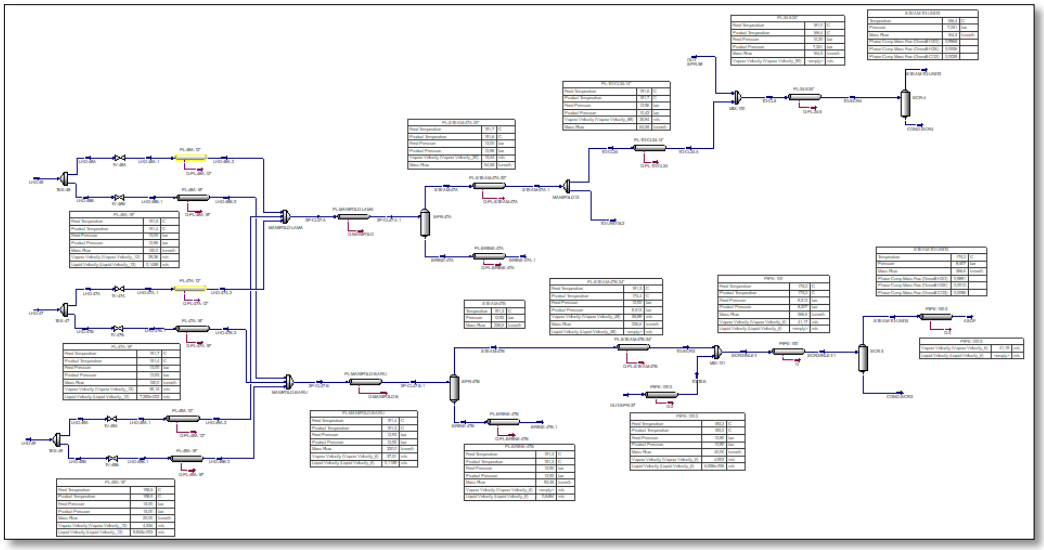


Figure 7: Schematic diagram of steam process simulation from LHD-47, LHD-48, and LHD-49 using HYSYS.

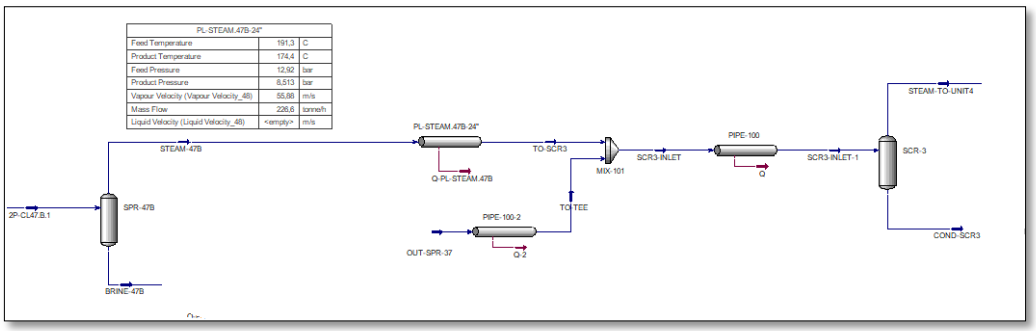


Figure 8: Schematic diagram of steam process simulation from Cluster LHD-47 to Unit 4.

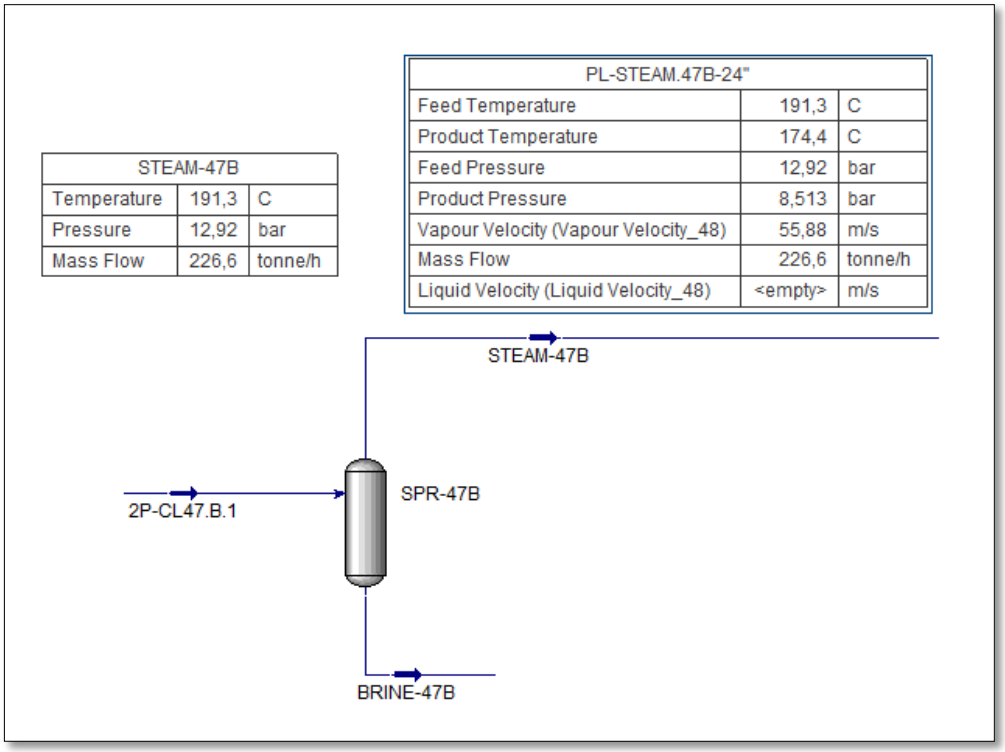


Figure 9: Fluid properties as the result of separation process from cluster LHD-47 to steam pipeline 24 inch.

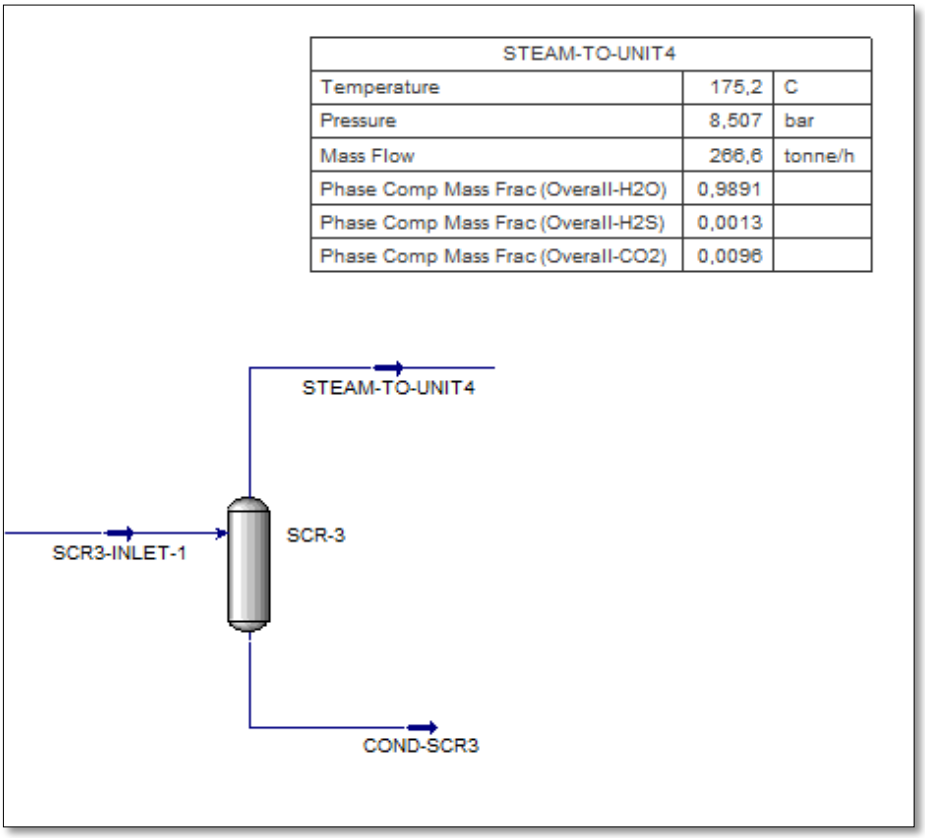


Figure 10: Fluid properties from Scrubber-3 to Unit 4.

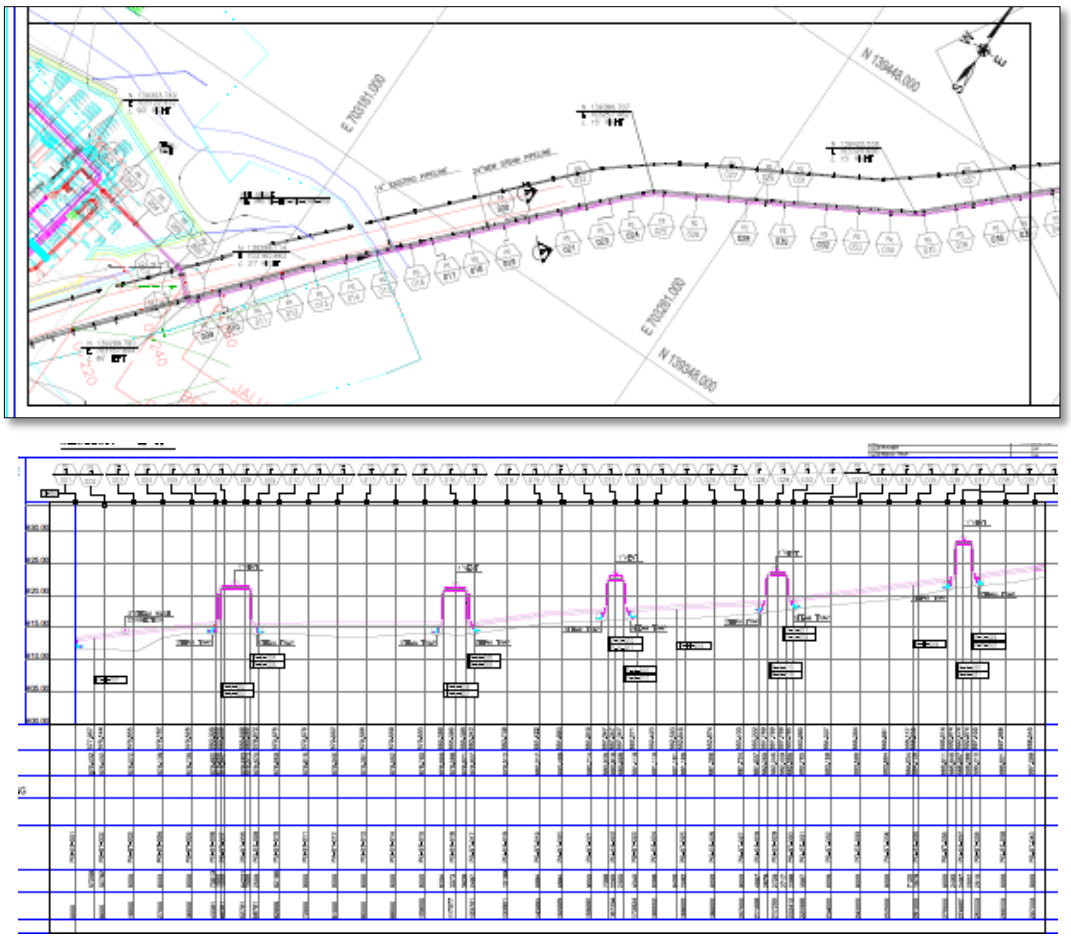


Figure 11. Pipeline design.

MACHINE LEARNING MODEL FOR IMPROVING SINGLE FLASH GEOTHERMAL ENERGY PRODUCTION: A CASE OF INDONESIA

Aldi Cahya Muhammad[1], K. Habibul Kabir[1], and Adam A. Alli[2]

[1] Islamic University of Technology
Board Bazar, Gazipur 1704, Bangladesh
[2]Islamic University in Uganda
Kumi rd, Mbale, Uganda
Email: aldicahya@iut-dhaka.edu

ABSTRACT

Advances in Machine Learning (ML) provide an opportunity to reduce cost in geothermal projects starting from resource exploration to power plant operation. Geothermal energy plays an important function in the generation of clean energy and mitigates global warming. Many countries are looking forward to alternative energy sources to replace unclean energy like fossil, coal, etc. Indonesia has successfully positioned itself second in the top ten countries in the world that produces geothermal renewable energy. In this paper, we are motivated to explore the potential of geothermal energy in Indonesia and provide design strategies to improve the prediction of single flash geothermal power generation using a machine learning approach. In our study, we use machine learning to improve operations in the geothermal single flash process. Specifically, predict the power production, life of well, power requirement on the grid, etc. The study, in the end, provides an efficient prediction mechanism of geothermal energy produced by single flash technology at a given enthalpy in isenthalpic process, where, changes in kinetic and potential energy are negligible. This strategy enables efficient utilization of geothermal energy in developing a green ecosystem in Indonesia.

Keywords: Geothermal energy, Machine learning, Renewable energy, Single flash geothermal power plant

INTRODUCTION

Indonesia has a high energy demand. This is because of its rapid development, industrialization strategy, and high increase in her population (Badan Pusat Statistik Indonesia, 2013). Comparing to other countries, increasing population, and rapid industrialization demands high energy consumption. Thus, high energy demand results in using energy sources that may increase the effect of global warming. To decrease the effect of global warming, finding green energy alternatives become a key role in such countries. Moreover, the use of fossil as a source of power dominates (Maulida et al., 2019). Development of greener sources of energy is likely to bridge the energy gap and preserve the environment. Increasing the trend of renewable energy utilization, for example, geothermal energy, solar, wind, etc. has the capacity to fill the gap of energy consumption in Indonesia.

The development of geothermal energy is improving fast as part of Indonesia's energy development plan (Hasan et al. 2013). One part of the improvement is the development of a geothermal power plant in high enthalpy reservoirs in the country. Being in the ring of fire, Indonesia is surrounded by high enthalpy reservoirs that provide excellent geothermal potential (Prambudi, 2018). In fact, Indonesia is estimated to possess 40% of the world's geothermal potentiall (ADB, 2015). As of current, it is rated as the second biggest user of geothermal energy in the world (Ritcher, 2019).

Most of the power plants are constructed based on either single flash or dry steam power production technology. The nature of the power plant technology used is determined by the type of the well. In cases where the well is water dominated at high temperature, single flash technology is adopted. Otherwise, dry steam technology is used. Other geothermal power plant that may be used include binary and hybrid. In a binary system, the well is water dominated at a lower temperature compared to the geothermal single flash system. Binary system is not used in Indonesia, because most of the wells have high temperatures. Moreover, the hybrid technology of power production may be used. The hybrid may consist of a pipeline of the geothermal system to create a multiple flash system. They may consist of a combination of other green sources of energy e.g. hydro, solar, and wind. Hybrid technologies are used to maximize the production of power. Currently, hybrid technologies are not common in Indonesia.

Using enthalpy potential, the production capacity in a single flash can be estimated. Modeling a single flash environment enables prediction of power output from the well as a source of energy. Further, the utilization of the power output of the plant can be effectively predicted.

Machine learning techniques for supporting green energy production and prediction has been proposed in (Rezvanbehbahani, 2017). Recently, machine learning has been adopted in science and engineering. Machine learning has a dominant power to solve complex problem (Alli and Alam, 2019). For example

in computing, it has been used in image processing and speech recognition, in business it has been used to predict business trends, in government, it has been used for policy improvement, etc (Afouras et al., 2018). In this paper, we use machine learning to improve the single flash geothermal energy prediction of power output using thermodynamic properties of the brine harvested from the well.

Thus, the contribution of this paper is twofold as follows:

i) We developed an artificial neural network model to illustrate the use of machine learning in predicting the power output in a geothermal power plant.
ii) We created a machine learning module for enthalpies and entropies to illustrate the use of machine learning to generate thermodynamic properties of the brine.

The rest of the paper is organized as follows, section 2, introduces the geothermal basics, in section 3, we present geothermal single flash system, in section 4, we present related works, in section 5, we present our model, results are presented in section 6 and the conclusion is drawn in section 7.

GEOTHERMAL BASIC

Geothermal energy is categorized as renewable energy because it is naturally produced. The utilization of geothermal energy is commonly harvested from the underground reservoir which contains hot water or steam. Typically, the hot underground reservoir is located in the active volcanic region. A typical reservoir is either water or steam dominated with hydrothermal characteristics. Unlike other sources of green energy e.g., wind and solar that are dependent on factors such as wind speed or intensity of the sun, geothermal energy are independent and available always. For example, solar power generation depends on the sun strength, when the sun strength is low, energy harvested is low. Ideally when investing in solar, investing in batteries is a requirement. This investment makes solar power plant more expensive than geothermal in the long run. In general, the location of the geothermal well is determined by geothermal surface manifestation. These include the availability of hot springs, hot rocks, scarce vegetation, etc. The indication through the surface might assume the development of geothermal energy for power production. Finding wells is done by drilling process in strategic positions around manifestations. This process is used to discover the initial parameter such as temperature, depth, pressure, etc. that form the basis of the decision to develop a viable geothermal plant.

The most important of geothermal energy sources utilization parameter is the temperature. The availability of temperature varies depending upon the depth of geothermal wells. Generally, the geothermal gradient in the ring of fire is about $0.025^{o}C\ m^{-1}$ to $0.03^{o}C\ m^{-1}$ (Newman, 2017). Therefore, knowing the temperatures allows the feasible design of geothermal power plant system. Moreover, the temperature is an important factor in classifying the use of geothermal energy source. For higher temperatures above $130^{o}C$ and below $180^{o}C$ the source can be used for power production using the single flash system, otherwise, at low temperatures, the source may be used in drying organic material, space heating, animal husbandry, etc (Patsa et al., 2015).

Geothermal for power production basically use the thermodynamic properties of brine. These properties include temperature, enthalpy, concentration, entropy, flow rate, pressure, etc. They are used in combination with the laws of thermodynamics to calculate the ability to do work of the geothermal power plant. The power production potentially predicted along with thermodynamic and chemical properties of the brine in the reservoir allows us to estimate the amount of power that will be produced.

GEOTHERMAL SINGLE FLASH SYSTEM

In this technology, the geothermal fluid is harvested from liquid dominant wells heated earth crust as a result of movement in the tectonic plates. This technology is dominantly applied in geothermal plants in Indonesia (Pambudi et al., 2014).

The components in designing geothermal electricity plant include the geothermal well, flash tank, turbine attached to a generator, condenser, and the pump. The geothermal well is the major source of energy that drives the production of geothermal power. There are two types of wells constructed at the site. The production well which is responsible for the production of brine at high temperatures that is fed into the flash tank. The flash is to stabilize the pressure and temperature through vapor-liquid equilibrium. In this case, the flash tank acts as a separator between vapor and liquid. The liquid is injected back to the well, whereas the vapor is scrubbed before being directed through a jet nozzle, then to the impeller which in turn drives the generator. During operation, the brine from production well enters the flash tank. The pressure causes the liquid to turn into steam (flashing). At vapor-liquid equilibrium (VLE), the inflow brine is separated into two, the steam and the liquid. The steam is harvested at steady temperature and velocity to drive the turbine. At the same time, the liquid residue is pumped back into the well. At the turbine end, the vapor temperature reduces and is converted into steam which is not useful. This steam can be condensed and pumped back into the well or used for other purposes. The liquid in the flash is drained out and pumped to the well if the temperature has dropped below a certain threshold, otherwise, the liquid can be fed in another flash to achieve double

flash technology. The power generated from the turbine end is placed on the grid for transmission. Figure 1 shows the geothermal single flash design model.

OVERVIEW OF THE COMPONENTS OF THE GEOTHERMAL SINGLE FLASH SYSTEM

The Well

The heat source of geothermal energy is well located deep below the earth surface. The center of the earth is very hot. The tectonic activity cause fractures in the earth crust. Because of the high temperature, there is a difference in pressure from the heat source and the surface of the earth. This causes the magma to flow through the cracks, which in turn causes water along the path of the cracks to heat up. The underground contains hot fluid or brine that is collected in a specific pool creating a form of the reservoir. The brine contains hot water and another component of silica in a certain concentration. Normally, the well close to the earth surface is exhibited by existing of hot spring, mud bubbling, and fumarole. The well is characterized into either vapor-dominated or water dominated. The well is a major component of geothermal power production plant (Valdimarsson, 2011).

The Depth of the Well

In the exploration phase of the well, open wells are drilled. From these wells samples of the brine is collected and their concentration measured along with the temperature and pressure. In this process depth of the well is determined. Temperature is one of the major variable used to determine the viability of power generated. As you dig deeper into the well, the temperature continuous increasing that allows for determining the temperature gradient. The temperature gradient is used for predicting the depth of the well (Yang et al., 2019). The depth of the geothermal well is given by the following equation (1).

$$d_m = g_t.T + K \quad \text{.....(1)}$$

where K is a scalar constant (Table 1) reflecting the minimum depth before hitting the surface of the well, g_t is the temperature gradient, T is the temperature at a specific depth, and d_m is the depth of the well.

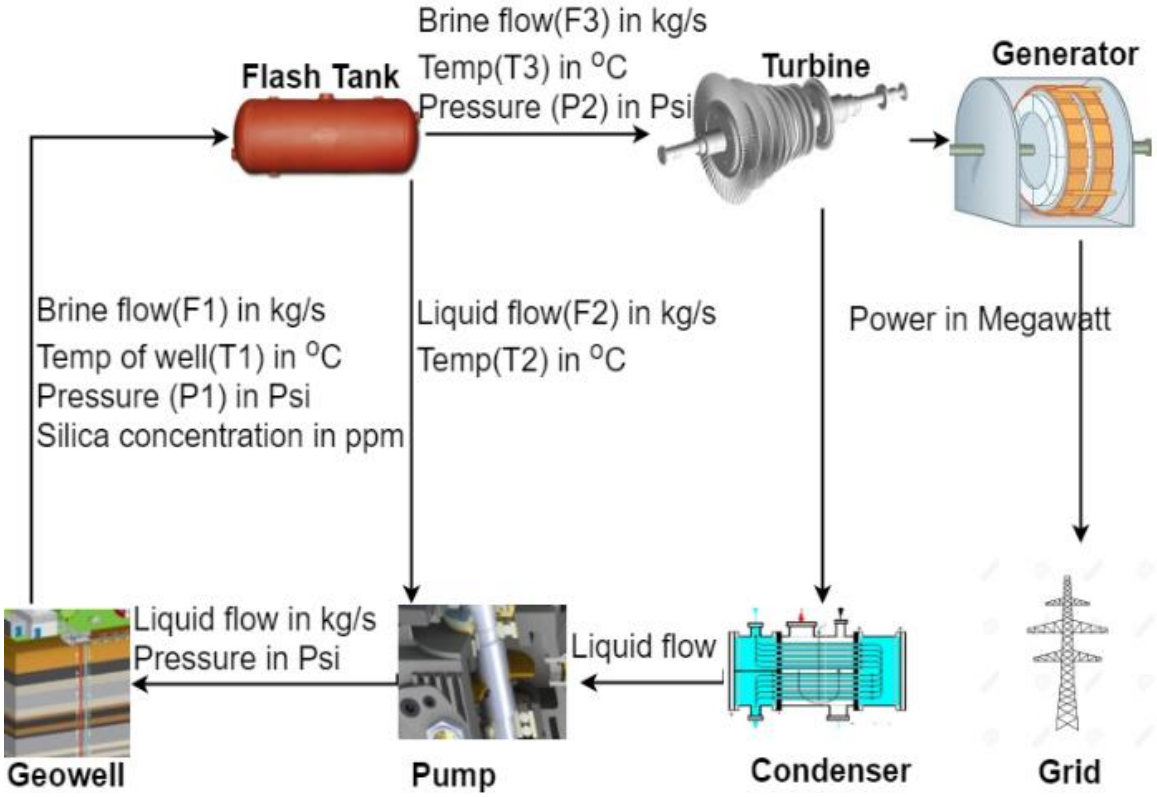


Figure 1: Geothermal Single Flash Design Model.

Table 1: Showing the definition of Constant.

Symbol	Measure	Unit
d_m	Depth of Well	m
g_t	Gradient	$^oC/m$
T	Temperature	^oC
P	Pressure	bar
$\dot{m}$	Flow rate	$kg/_s$
t_a	Lifespan	time
T_o	Original Temperature	^oC
V_o	Volumetric Flow rate	$kg/_s$
$\dot{W}_e$	System Output	kW
$x_{2,3,5}$	Dryness Fraction	-
$h_{1,2,3,4,5,5s,6,7}$	Enthalpies	$kJ/_{kg}$
w_t	Turbine Work	kW
n_t	Turbine Efficiency	-
$\dot{W}_t$	Turbine power	kW
$\dot{m}_s$	Mass flow rate	$kg/_s$
$\dot{m}_t$	Total mass flow rate	$kg/_s$
n_g	Generator efficiency	-
n_{td}	Turbine constant	-
$s_{4,6,7}$	Entropies	$kJ/_{kg.K}$
A	Factor A	-
$\dot{m}_{cw}$	Mass flow rate cooling water	$kg/_s$
c	Constant specific	$4.2kJ/_{kg.K}$
ΔT	Rise temperature	^oC
T_6	Condenser temperature	^oC
T_{cw}	Cooling tower temperature	^oC
P_2	Pressure mass flow	bar

Life of the well

The most promising case for successful geothermal power plant is the availability of geothermal well. Every 1000 meter of the depth the temperature increases by 25-30^{o}C (Dipippo, 2012). The activity of drilling a well cost 45% of the total project of building a geothermal power plant (Hou et al., 2018). Therefore, having a well which will live for a short time is infeasible. In our study, we lay a method to estimate the life of a well-using machine learning. This follows a supervised model in equation (2).

$$t_a = f(T_0, \frac{dT}{dH}, V_0, \dot{W}_e) \quad \text{(Zhao et al., 2015)…(2)}$$

where t_a, is the lifespan of the well, T_0 the original temperature of the well, $\frac{dT}{dH}$ is the geothermal gradient, V_0 is the volume flow rate, and W_e is the system power output.

We assume there exist $n = \{1,2,3 \ldots\}$ wells that power geothermal power plant. From each well, temperature, pressure, flow rate and concentration of the brine can be measured from time to time. Keeping other conditions such as the wear and tire of the pipes in the well, the life of the well mainly depends on temperature. From the time of first utilization, the temperature of the well reduces gradually. The reduction may be so small but after a long period of time the well may cool down, thus the well becomes unusable for power production.

We may find the high pressure, temperature and high flow rate during exploration as well as power generation for some considerable amount of time. Nonetheless, continuous use may result in a decrease in efficiency of the well. When the efficiency reduces below the threshold the well is closed. Authors in (Dipippo, 2012) assert that well may live between 20-30 years. Along with the decreasing temperature, pressure and flow rate, tire and wear of the infrastructure, and environmental factors may cause well to be shut down. As a result of decreasing efficiency of a well, it is important to determine the life of the well before the well is brought to complete shutdown.

At the same vicinity, there are often many wells (production wells and injection wells). Each of these wells may have their own parameter that varies. Every single well has their temperature, pressure, flow rate, etc. therefore, the lifespan of well differ.

The Flash Tank

The device used in geothermal electricity power production to separate a mixture of vapor and liquid is the flash tank. This is achieved by the separation mechanism. The flash tank is one of the unit operations of brine. The brine contains many components which include water, pentane, butane ammonia, etc., (Dipippo, 2012) on entry into the flash tank the saturated liquid is immediately flashed due to pressure drop as a result of passing through a throttling device at some pressure and temperature. Evaporation occurs within the vessel causing the brine to separate into vapor and liquid. The brine may be partially or totally flashed into a vapor.

Flash Process

The brine at temperature (T) enters the inlet of the separator. Flashing occurs at state 1 (as shown in Figure 2 and Figure 3), near to the critical point on the saturation curve. Two phases of brine occur i.e. vapor and liquid form. This process occurs steadily, spontaneously and adiabatically. No work is involved. This allows us to neglect any changes in

kinetic and potential energy, hence the process is isenthalpic. That means enthalpies at point 1 and 2 are same, see Figure 3. Generally, enthalpy is labeled as h_i, where $i = (1,2,3,\dots)$ is points along the enthalpy curve that describes the condition of the brine. During the flashing process $h_1 = h_2$ at constant pressure. The above process allows us to compute the dryness fraction.

The dryness fraction is a ratio of liquid to vapor in the brine. The dryness fraction is given by the following equation (3).

$$x_2 = \frac{h_2 - h_3}{h_4 - h_3} \quad \dots\dots\dots\dots\dots\dots\dots\dots\dots\dots\dots\dots\dots\dots\dots\dots\dots\dots \quad (3)$$

The dryness fraction determines the quality of the mixture after flashing. It is an important factor in predicting the amount of power generated at the turbine. By definition, it is the ratio of evaporating enthalpies $(h_2 - h_3)$ to steam enthalpies $(h_4 - h_3)$. This gives a steam mass fraction of the mixture which flows to the turbine.

The analysis for generating electricity for a single flash geothermal power plant is based on the principle of thermodynamic of the conversion process. The Temperature-entropy diagram Figure 2 and Temperature-enthalpy diagram Figure 3 explain the ideal process of flashing. Authors in (Yunus et al., 2015) provide a comprehensive discussion about the flashing process.

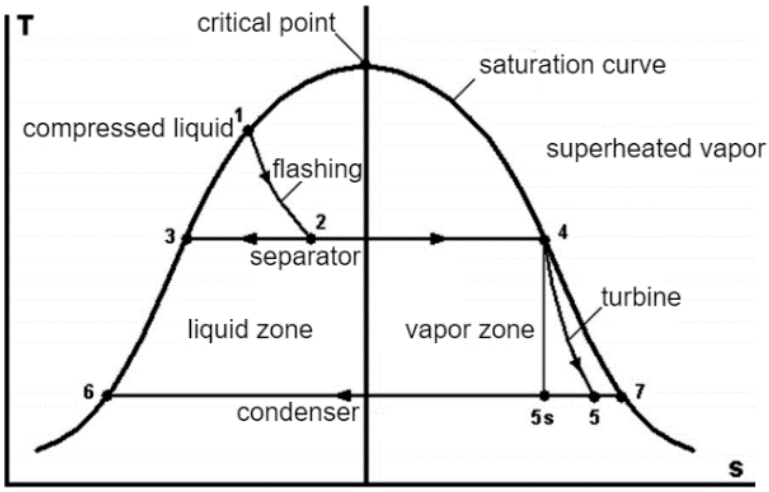


Figure 2: Temperature-entropy diagram.

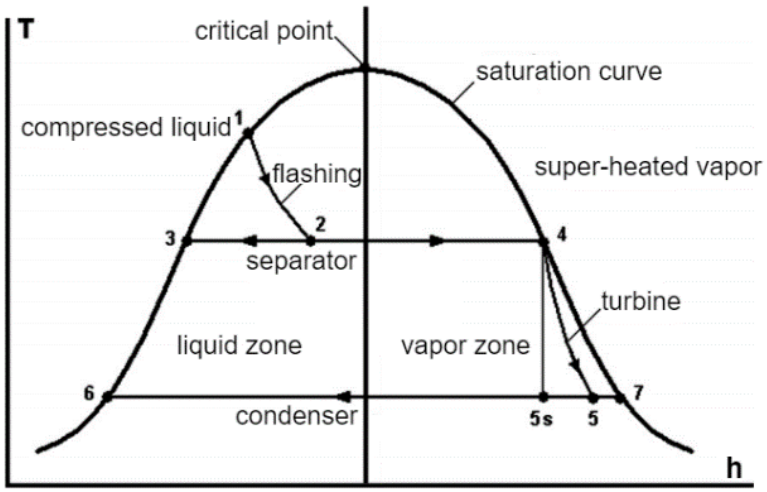


Figure 3: Temperature-enthalpy diagram.

From the diagrams, the left portion from the critical point is a saturated liquid which forms enthalpies and entropies in the liquid condition, whereas the right-side forms enthalpies and entropies in the vapor condition. The intersection of the conditions forms a critical point that occurs at the maximum temperature where liquid starts to turn into vapor. For further explanation refer to the works in (Dipippo, 2012).

Turbine

This component of geothermal system consists of impellers which are rotated by a vapor that comes from the flash tank through jet nozzles directly pointed to them. The turbine is attached to the generator which is responsible for producing power. The power produced by the turbine is critical for determining the capacity of a power plant (Dipippo, 2012). In our study, we modeled this process based on turbine expansion computation.

Turbine expansion process

The turbine expansion process is based on the work done by the turbine (w_t). w_t is the enthalpy difference at the inlet of the turbine (h_4) and the enthalpy at the outlet of the turbine (h_5). Work produced by the turbine is given by the following equation (4)

$$w_t = h_4 - h_5 \quad (4)$$

The ideal process occurs between point 5 and $5s$. To compute the efficiency of the turbine we find the ratio of actual turbine work to ideal turbine work is represented by the following equation (5).

$$n_t = \frac{h_4 - h_5}{h_4 - h_{5s}} \quad (5)$$

The turbine power is expressed by equation (6), which is computed as a product of dryness fraction, total mass flow, and work produced by the turbine. To this end, we can compute the gross electric power as in equation (7), which is the product of generator efficiency and turbine power. In another way, the generator efficiency can be considered as a constant specification of the generator. Otherwise, isentropic efficiency is considered as computed in equation (8).

$$\dot{W}_t = \dot{m}_s - w_t = w_t = x_2 \dot{m}_{total} w_t \quad (6)$$

The gross electrical power equal to generator efficiency and turbine power is expressed as

$$\dot{W}_e = n_g \dot{W}_t \quad (7)$$

Isentropic efficiency is written by

$$n_{tw} = n_{td} \times \left[\frac{x_4 + x_5}{2}\right] \quad (8)$$

Generally speaking, $n_{td} = 0.850$ assume by 85% of dry turbine efficiency, this assumes a threshold of 85% is sufficient.

Enthalpy $h5_S$ can be computed by following equation 9. Enthalpy $h5$ can be computed by the following equation (10). Where factor $A \equiv 0.425(h_4 - h_{5S})$.

$$h_{5s} = h_6 + [h_7 - h_6] \times \left[\frac{s_4 + s_6}{s_7 - s_6}\right] \quad (9)$$

As well as the enthalpy of $5s$ is found by the following equation

$$h_5 = \frac{h_4 - A\left[1 - \frac{h_6}{h_7 - h_6}\right]}{1 + \frac{A}{h_7 - h_6}} \quad (10)$$

When the dryness fraction is 1 double flash technology is appropriate and $h5$ is computed by the following equation (11).

$$h_5 = \frac{h_4 - A\left[x_4 - \frac{h_6}{h_7 - h_6}\right]}{1 + \frac{A}{h_7 - h_6}} \ (for\ x_4 < 1) \quad (11)$$

The comprehensive discussion about turbine expansion process is given in. (Dipippo, 2012)

Condenser

The condenser is a kind of heat exchanger where vapors are converted into liquid. It is the art of removing the heat using a coolant such as water. The cooling is attained from a cooling tower. A condenser is normally used in all geothermal plants. The aim of the condenser is to maximize turbine efficiency. It maintains removing dissolved noncondensable gases from the condensate. Further, the cooling content is re-injected into the well. The processes in the condenser can be modeled using equation (12) and (13). (Najafabadi, 2015)

$$\dot{m}_{cw} = x_2 \dot{m}_{total} \times \left[\frac{h_5 - h_6}{c\Delta T}\right] \quad (12)$$

$$\dot{m}_{cw} = x_2 \dot{m}_{total} \times \left[\frac{h_5 - h_6}{c(T_6 - T_{cw})\Delta T}\right] \quad (13)$$

RELATED WORKS

Moya et. al (2018) explored the aspect of geothermal energy development, geothermal power plant technology, and the common geothermal direct uses. Five power plant technologies are mentioned in this study. They include single-flash, double-flash, and dry-steam technologies for power generation in a geothermal power plant. Other technologies mentioned are binary and hybrid power plants technologies. Single flash is used for electricity conversion when geothermal production wells are producing a mixture of brine. Double flash steam power plants are an improvement on the single-flash. Dry-steam power plants are often used in the most efficient power plant with high enthalpy vapor-dominant wells at high temperatures in hydrothermal reservoirs. Binary power plants configurations are used for low-temperature geothermal resources.

Hybrid may adopt more than one of a single flash, double flash or dry steam configurations for geothermal conversion. The authors mention that geothermal resources are not only used for electricity generation but can also be adopted for direct use. Direct use of geothermal energy ranges from applications that need high temperatures, and those which need moderate temperature. These applications include drying cement blocks, drying agricultural products, and house warming. In this particular study, the state-of-the-art in geothermal energy was given.

Authors in (Binaa et al., 2009) investigated the Indonesian geothermal resources, based on the ability to generate power using Specific Exergy Index (SExI). In this study, the Exergy concept was developed as a geothermal resource classification tool. Exergetic classification of geothermal resources was applied to 11 power plants under operation. The results of SExI values show that nine geothermal fields are classified as having high Exergy resource, whereas the remaining two power plants are classified as medium geothermal resources. According to them, the location of the power plants in different Islands of Indonesia determines their classes. They concluded that the power plants with medium Exergy are located in Sumatra Island, whereas the rest are found in Java, Bali, Nusa Tenggara, and Sulawesi. Geothermal resources in Java Island are ranked first with the highest Exergy resources concentration. Darajat power plant has the highest SExI value of 0.94 amongst all powered investigated in that study.

Authors in (Prambudi, 2018), investigated the geothermal potential in the ring of fire, where Indonesia is located. They mentioned that the location of Indonesia, specifically the Java Island contributes, significantly to Indonesians geothermal potential. The predicted geothermal potential is almost 29 GW in 312 locations spread across most of Java, Sulawesi, Sumatra, Maluku, Bali and Nusa Tenggara. In this paper, the utilization ratio mentioned is about 5%, with power generated being 1533.5 MW of electricity from 11 geothermal power plant. Accordingly, the current power generated as of current is close to 2000 MW making Indonesia the second geothermal biggest user in the world (Ritcher, 2019). The characteristics of most of the geothermal reservoirs are water-dominated. They employ single flash technology for power production (Prambudi, 2018).

Authors in (Pambudi et al., 2014) investigated Exergy analysis and optimization by developing a mathematical model that is applied to the Dieng single-flash geothermal power plant in Indonesia. Calculations were conducted by using EES software using methods based on the laws of thermodynamics. The optimization of the plant is carried out by adjusting the separator pressure. The result of the optimization process shows that the Dieng geothermal power plant operates under close to optimal conditions.

The prediction of geothermal power plant system performance using an artificial neural network (ANN) under a broad range of operating conditions. The applicability and capability of artificial neural network approach were used for predicting geothermal power plant specific steam consumption. They used the data collected from Kamojang geothermal power plant to predict the performance in the first quarter of 2015. From this study, a combination of good sufficient training data, and independent measurement of steam flow for validation using the neural network approaches can be utilized to develop a good performance prediction. It is able to identify the degradation of the plant or instruments. Nonetheless, an independent measurement of steam flow is required to validate the measurement of ANN prediction. The data shift from ANN predicted value can be a good sign to perform comprehensive analysis on the plant to prevent losses, especially in steam sales contract scheme. Plant operator also gets a better perspective on the plant real-time performance by comparing plant real-time data and data prediction from ANN. This study is one of the kinds that make the use of machine learning methodologies useful in geothermal power generation problems.

Maulida et al. (2019), addressed a private sector perspective in rethinking renewable energy targets and electricity sector reform in Indonesia. It discussed Indonesia's current renewable energy policies and future outlook for achieving the targets. It serves as a literature review of Indonesia's changing energy policy landscape as part of research investigating renewable energy targets and the role of the private sector reforms in the renewable energy industry. The changes in Indonesia's policy landscape have been rapid, and the authors have tried to capture the dynamics. It also serves to understand of renewable energy targets in Indonesia and to predict future trends. As the basis of policy and decision-making in renewable energy. This study enrich the existing literature on renewable energy policy which are of the importance of engaging the private sector. The lessons from Indonesia's experience may provide insights for policymakers notably in developing countries. This study calls on means of predicting the different dimensions that could result in policy improvement based on prediction mechanism. Policy issues such as how much power production is sufficient for residences in particular villages without harming the environment can easily be answered by machine learning. Other important issues that can be predicted using machine learning include the life of the well, distribution of power generated, etc. These issues may form important components of contracts between the government and the private’s sectors.

Authors in (Perera, 2014) surveyed different machine learning techniques used to address the issues related to the generation of renewable energy. More

importantly a discussion on the integration of machine learning in the power grid utilization. In this study, they assert that machine learning techniques have been successfully used in the planning of renewable energy plants based on available data with reasonable accuracy. They published literature on location, sizing, and configuration of wind and PV systems based on machine learning techniques. They continued to underline their popularity, particularly in isolated areas. They also indicate that to generalize the machine learning models for each and every aspect of renewable energy generation and integration into the grid is quite difficult. But strong coordination is necessary among the different prediction and decision-making models to better enhance the grid's overall efficiency and effectiveness. This shows the potential of machine learning as a design tool in strategic planning and policy-making in renewable energy environment.

In this paper, therefore, we adopt machine learning strategies in the prediction of power output in a geothermal power plant environment. First, we adopt machine learning in predicting information about the well. Secondly, we use machine learning in predicting how much power can be generated from a power plant based on enthalpies and entropies of the brine.

MACHINE LEARNING APPROACH FOR POWER GENERATION

Advances in Machine Learning (ML) provide an opportunity to reduce cost in geothermal projects starting from resource exploration to power plant operation. Application of machine learning in geothermal exploration is still in its infant stages. Specifically, there are still existing gaps in the use of machine learning strategies in geological, geochemical, borehole, etc. In this study, we illustrate the use of machine learning to predict single flash geothermal energy production using Artificial Neural Network (ANN).

Artificial Neural Networks (ANN) are computational system models that are obtainable as of interconnected neurons. It computes values from inputs by feeding information through the network. An Artificial Neural Network is used for a particular application through a training and learning process. Similar to other machine learning methodologies, neural networks are used to answer a widespread in many hard to solve tasks. ANN is an efficient machine learning mechanism used to predict the state of events from data with acceptable error results. It provides high accuracy and reliability prediction experiments. ANN is used to predict the performance of a specific system (Ruliandi, 2015).

In this paper, we use MATLAB/Simulink for our single flash geothermal model operations. Simulink is one of the common tools for soft computing. Soft computing provides a natural way to argue a complex phenomenon in which computational mechanism based on mathematical modeling. It is a basis of many applications in medical engineering, computer vision, and pattern recognition. Soft computing includes Artificial Neural Network, a method imitated the brain mechanism in solving problems. Secondly, fuzzy logic attempts to solve problems with an open and precise spectrum of data that make it possible to find a list of the precise solution without involving complex math. Lastly, in genetic algorithms have been inspired as a soft computing method that is used to find problems that include natural selection. It is one of the common software to develop machine learning.

In this paper, we are inspired to use Artificial Neural Network to improve the operation of the single flash geothermal plant to model the well depth, flash tank, turbine, the grid and the lifespan of the well.

Experimental setting

Table 2 shows the items and specification of the simulation environment we used to design, develop, and implement the simulation experiment.

Table 2: Showing Items and specification of the Experiment.

Items	Specification
Processor	Intel Core i3-3217U CPU @1.8GHz
Operating System	Windows 10 64 bits O/S
Hard Disk	500 GB
RAM	4.00 GB
Simulation Environment	MATLAB 2015

The Well Machine Learning

The use of the neural network as part of machine learning to predict the desired depth of the well. We measure temperature and depth at different point of well that composes the dataset. The sample of the data used for training to the neural network. The trained neural network is used to predict the depth of the well by capturing the temperature as an input.

The Figure 4 represent the geothermal machine learning well model. In this model, there are two machine learning modules. The first module imputes temperature and output depth, while the second neural network module imputes temperature, gradient, flow rate and power output generated from the turbine. From the presented dataset, we enter the temperature, temperature gradient, volumetric flow rate and power output as inputs. Neural Network module one accepts temperature and outputs depth. The second module accepts all the inputs and outputs the lifespan of the well. Target outputs and the sample used to verify our trained Neural Network is set accordingly. The training function used in here is TRAINLM, the adaption learning function chosen is LEARNGDM, the performance function is MSE. We use 10 layers and the transfer function is PURELIN.

The machine that we develop learns through many times of training. We observed, our results through adjusting temperature different values. For instance, at the temperature 180^{o}C, the depth attained to 570 meters from the surface of the well according to the trained data.

The Flash Machine Learning Model

In this model, machine learning is used to predict the enthalpies in Figure 5 and entropies in Figure 6. We choose to use machine learning to generate the values of enthalpies and entropies at a given temperature. We are inspired to use machine learning to predict the correct value to replace the huge saturated water temperature table (Yunus et al., 2015). The use of the machine learning lifts the burden of lookup for values of enthalpy and entropy of a given temperature in the flash. Using similar neural network setting in section 5.2 and the saturated water temperature table data we train the neural network to predict the entropies and enthalpies with at most accuracy. For enthalpies, we assume temperature at the Vapor-Liquid Equilibrium, where for entropies we assume temperature at condensation point i.e. the point at which vapor ceases to produce efficient work at the turbine. Literature suggests that if the temperature drop by 15% then the vapor is not sufficient for power production. In this case, we adopt this temperature to compute entropies at condensation. Therefore, a drop of 15% is the threshold against with dryness of the steam is acceptable at the turbine. Based on these conditions, the machine learning strategy can be applied to simulate enthalpy and entropy.

Using enthalpy and entropy generated through a machine learning process, the dryness fraction can be computed using equation (3). The dryness fraction is used to determine the quality of steam that goes to the turbine at the isobaric condition. To produce the enthalpy and entropy, the machine learning modules have been trained using data obtained from the property table and charts for saturated water in (Yunus et al., 2015). We observed during simulation, the enthalpies and entropies produced by our system are the same with a very small margin of error. We conclude that the predicted steam quality maintains the turbine efficiency. Therefore, the predictions are used to compute turbine efficiency using equation (4), turbine power using equation (5), power on the grid using equation (6). The characteristics of ANN in determining entropies and enthalpies remain the same as those in section 5.2.

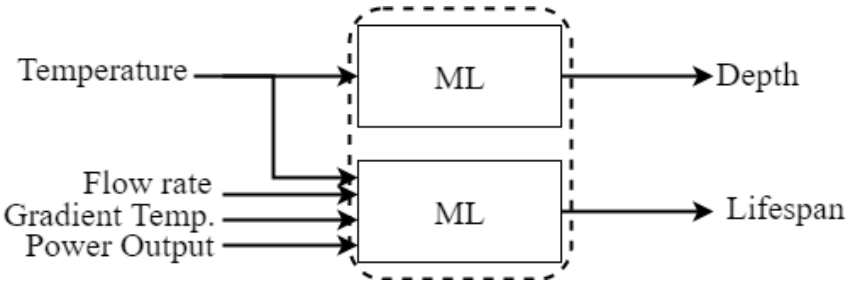


Figure 4: The well machine learning model.

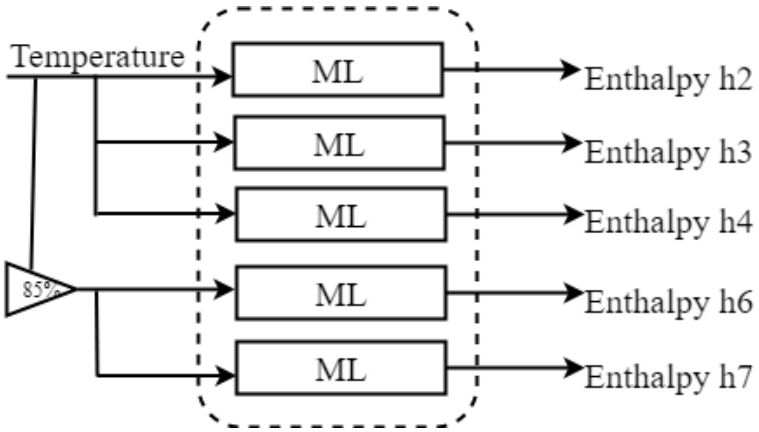


Figure 5: Flash machine learning model.

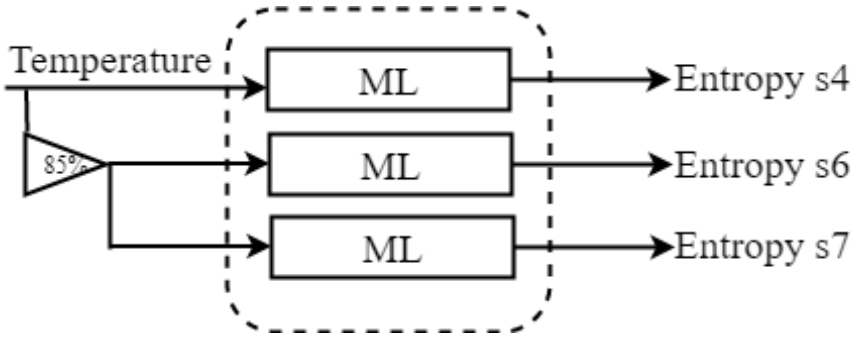


Figure 6: Entropy machine learning model.



Figure 7: Mass flow rate machine learning model.

Predicting the Mass Flow Rate

The flow rate is an important component of determining the power produced by the turbine. According to authors in (Dipippo, 2012), the mass flow rate at a given absolute pressure can be determined by equation (14) for chocked well, moreover, for the non-chocked well equation (15) is used to compute the mass flow rate. We use this equation (14) to generate data that is used to train a NN for determining the mass flow rate. Figure 7 represents the mass flow rate machine learning model.

$$\dot{m}_{total} = 99.6663 - 2.6287P_2 + 0.5802{P^2}_2 - 0.04212{P^3}_2 \quad \text{(14)}$$

$$\dot{m}_{total} = 44.333 - 0.3363P_2 - 0.1357{P^2}_2 \quad \text{(15)}$$

Turbine Module

At the turbine, the work produced is computed by equation (4), turbine efficiency in equation (5), the power produced by the turbine is computed using equation (6) the value of dryness fraction, mass flow rate produced by Figure 7, and the work produced by the turbine is used to determine power produced by the turbine.

The quality of power depends on enthalpies which in turn determine the dryness fraction. The mass flow rate in the non-choked well is determined by using the second order equation (15) which can be modeled using machine learning on its own.

Grid Module

The power estimated at the turbine is gross mechanical power. The gross electric power is estimated by equation (7). The efficiency of the generator should not be less than 85%. Otherwise, the power produced will not be sufficient.

RESULTS AND DISCUSSION

Presentation of Results

In this section, we present the results of the simulation experiment in Table 3.

Table 3: Showing a variation of temperature and geothermal parameters in a single flash.

T	P	x_2	w_t	n_t	$\dot{W}_t$	$\dot{W}_e$
100	1.01	0.81	77.3	0.84	6170	6108
120	1.99	0.77	86.1	0.83	6466	6401
140	3.61	0.72	93.4	0.83	6555	6489
160	6.18	0.66	99.1	0.83	6404	6340
165	7.00	0.66	100.3	0.84	6310	6247
170	7.92	0.65	101.5	0.83	6173	6112
175	8.93	0.64	102.6	0.83	5970	5910
180	10.02	0.62	103.6	0.83	5678	5622
185	11.23	0.60	104.6	0.83	5250	5198
190	12.55	0.59	105.4	0.83	4636	4589
195	13.98	0.57	106.2	0.83	3770	3732
200	15.54	0.56	106.8	0.83	2486	2461
205	17.24	0.54	109.3	0.83	680	673

Discussion of Results

Dryness Fraction

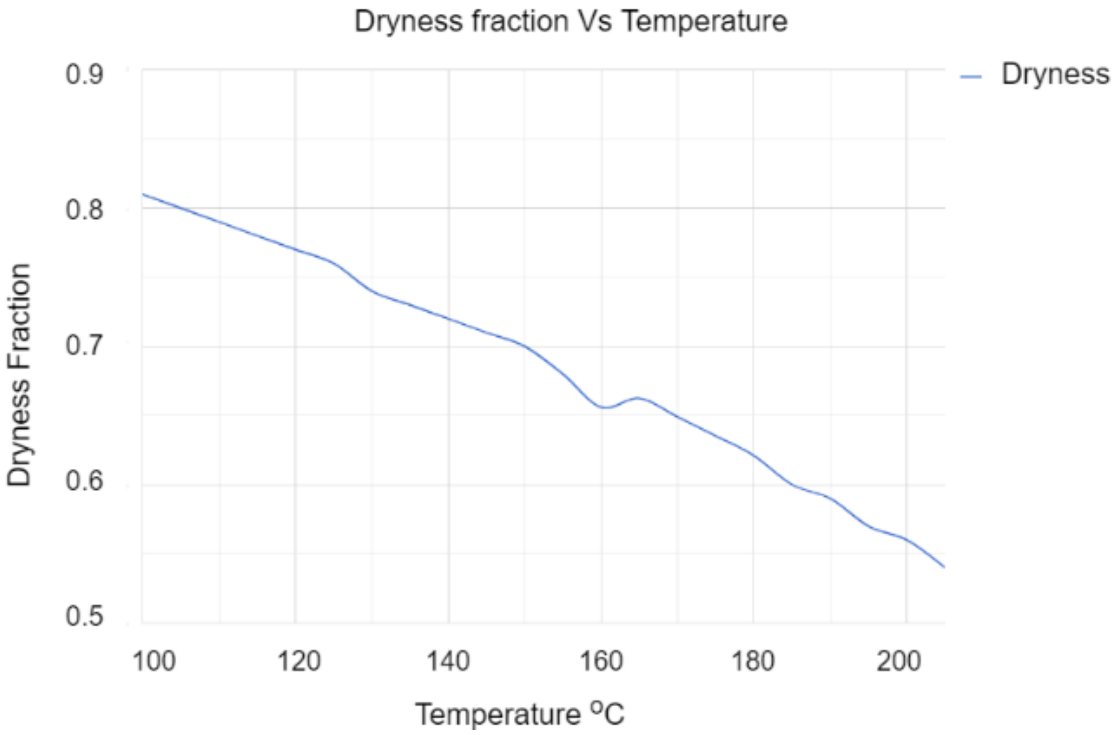


Figure 8: Dryness fraction.

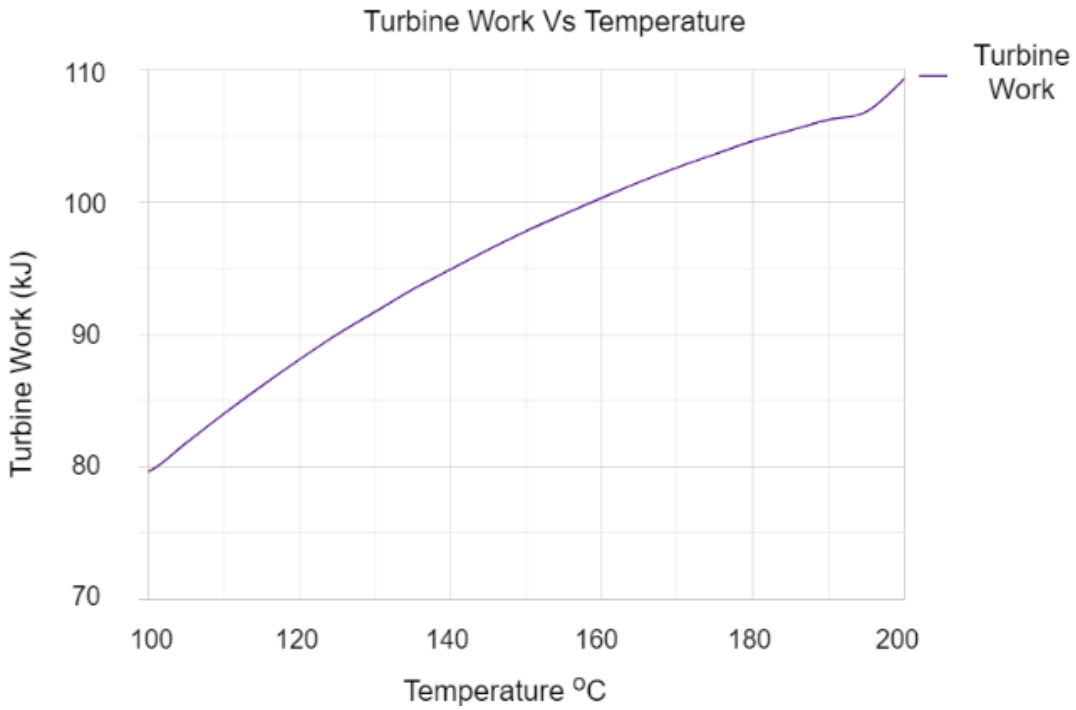


Figure 9: Work turbine.

The graph in Figure 8 shows dryness fraction against temperature. From the graph higher temperatures results in low dryness fraction. As the temperature is increased from 100 towards 205ºC, the dryness fraction drops from 0.81 to 0.54. Consequently, the work done as a result increase from 77.3 to 109.3. Moreover, the pressure is observed to increase with temperature. The dryness fraction at low temperature is high because of the liquid content in brine. As the temperature increase, the liquid content reduces creating low dryness fraction hence increase in work. These results imply that the flash achieved better performance when the dryness fraction is between 0.68 and 0.77 in the temperature range of 120 to 155ºC.

Turbine Work

The graph in Figure 9 shows the effect of temperature on the work done by the turbine. As the temperature increases the work done increases gradually with a low gradient. This implies that at high-temperature work done is high therefore the power output is low. At temperature above 205ºC, the work done is more than 109 beyond which there is no power output at the turbine. At very high temperatures the pressure is very high and the liquid content in the vapor is very low, this is not supported by the single flash technology. For that reason, if the well temperature is found to be beyond 200ºC is better to use other technologies such as dry steam.

Power generated

The graph is shown in Figure 10 shows power produced by the turbine as well as power generated on the grid. From the simulation, maximum power is observed when the temperature is 140ºC, dryness fraction is 0.72, the pressure is 3.61 bar, and generator efficiency of 99% maximum power observed is 6.489 MW per well. From our observation, the power generated at the turbine is parabolic. At low temperatures, power production is low, at moderate temperature especially above 120ºC and below 190ºC power produces is considerably high. At very high temperatures, the power produced is very low using flash technology. For example, at 195 the power produce is 3 MW, at 200 the power reduces by up to 65%, at 205ºC the power reduces to less than 1 MW, beyond 205ºC there is no power produced at the turbine. Therefore, if a well is observed to have initial temperatures exceeding 180ºC it is rational to use other technologies than single flash. The power on the grid follows the same trajectory with the power by turbine, and mainly depend on generator efficiency.

In this section, we have presented the result of our simulation experiment in Table 2. We have presented graphical results specifically on dryness fraction, work produced by a turbine in Figure 8 and Figure 9, which major factors that determine the performance of a geothermal are setting in single flash technology. The results show that machine learning can effectively be used in the operations of a single flash. Generally speaking, embedding machine learning in a geothermal environment can improve operations.

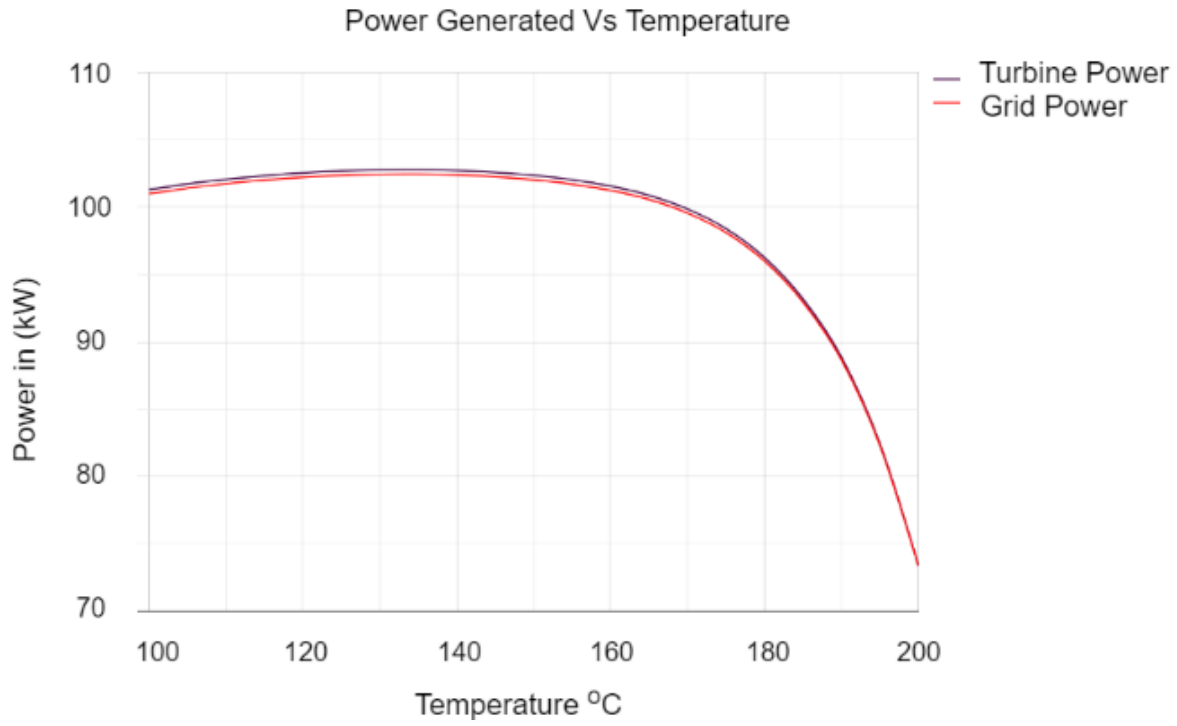


Figure 10: Power by turbine and grid.

CONCLUSION

Our proposed model produces results for the well, flash, and turbine for the isobaric condition. We use machine learning to determine the well life, depth, enthalpies, entropies, and mass flow rate, turbine work, turbine efficiency, dryness fraction, and grid power. This model produces reliable results. Training the neural networks with more data will produce result with at most accuracy.

Conclusively, our result portrays that machine learning can improve performance prediction in a single flash ecosystem. Specifically, to predict, at given Temperature (T) and Pressure (P) we can tell how much power can be produced at both the turbine and the grid. Secondly, it is possible to predict the depth of the well and its life. In the future, we intend to use machine learning to explore other technologies such as double flash. Moreover, geothermal smart grid is a good candidate for application of machine learning.

REFERENCES

Badan Pusat Statistik Indonesia (2013), "Indonesia Population Projection 2010-2035", *no. 6*.

Maulidia, P. Dargusch, P. Ashworth, and F. Ardiansyah (2019), "Rethinking renewable energy targets and electricity sector reform in Indonesia: A private sector perspective," *Renew. Sustain. Energy Rev.*, vol. 101, pp. 231–247, Mar.

Hasan, T. M. I. Mahlia, and H. Nur (2012), "A review on energy scenario and sustainable energy in Indonesia," *Renew. Sustain. Energy Rev.*, vol. 16, no. 4, pp. 2316–2328, May.

Pambudi (2018), "Geothermal power generation in Indonesia, a country within the ring of fire: Current status, future development and policy," *Renew. Sustain. Energy Rev.*, vol. 81, no. April 2016, pp. 2893–2901, Jan.

ADB and W. Bank (2015), "Unlocking Indonesia's Geothermal Potential".

Alexander Ritcher, "The Top 10 Geothermal Countries 2018 - based on installed generation capacity (MWe) | Think GeoEnergy - Geothermal Energy News," 2018. [Online]. Available: http://www.thinkgeoenergy.com/the-top-10-geothermal-countries-2018-based-on-installed-generation-capacity-mwe/. [Accessed: 21-Jun-2019].

Rezvanbehbahani, L. A. Stearns, A. Kadivar, J. D. Walker, and C. J. van der Veen (2017), "Predicting the Geothermal Heat Flux in Greenland: A Machine Learning Approach," *Geophys. Res. Lett.*, vol. 44, no. 24, pp. 12,271-12,279.

Mellit, A and Benghanem, M and Arab, A Hadj and Guessoum (2003), "Modelling of sizing the photovoltaic system parameters using artificial neural network," *Proc. IEEE, CCA*, vol. 1, pp. 353–357.

Malik and S. Mishra (2016), "Artificial neural network and empirical mode decomposition based imbalance fault diagnosis of wind turbine using TurbSim, FAST and Simulink," *IET Renew. Power Gener.*, vol. 11, no. 6, pp. 889–902.

Perera, Z. Aung, and W. L. Woon (2014), "Machine Learning Techniques for Supporting Renewable Energy Generation and Integration: A Survey," *Lect. Notes Comput. Sci. (including Subser. Lect. Notes Artif. Intell. Lect. Notes Bioinformatics)*, vol. 8817, pp. 81–96.

Ruliandi (2015), "Geothermal power plant system performance prediction using artificial neural networks," *2015 IEEE Conf. Technol. Sustain. SusTech 2015*, pp. 216–223.

Alli and M. M. Alam (2019), "SecOFF-FCIoT: Machine learning based secure offloading in Fog-Cloud of things for smart city applications," *Internet of Things*, vol. 7, p. 100070, Sep.

Afouras, J. S. Chung, A. Senior, O. Vinyals, and A. Zisserman (2018), "Deep Audio-visual Speech Recognition," *IEEE Trans. Pattern Anal. Mach. Intell.*, vol. PP, no. c, p. 1.

Mulvey (2017), "Machine Learning and Financial Planning," *IEEE Potentials*, vol. 36, no. 6, pp. 8–13,.

Carbonneau, K. Laframboise, and R. Vahidov (2008), "Application of machine learning techniques for supply chain demand forecasting," *Eur. J. Oper. Res.*, vol. 184, no. 3, pp. 1140–1154,.

Xiao, X. Wan, X. Lu, Y. Zhang, and D. Wu (2018), "IoT Security Techniques Based on Machine Learning," pp. 1–20.

Kourou, T. P. Exarchos, K. P. Exarchos, M. V. Karamouzis, and D. I. Fotiadis (2015), "Machine learning applications in cancer prognosis and prediction," *Comput. Struct. Biotechnol. J.*, vol. 13, pp. 8–17,.

Kotsiantis, I. D. Zaharakis, and P. E. Pintelas (2006), "Paper 1 (20)," *Artif. Intell. Rev.*, vol. 26, pp. 159–190.

Newman, "Geothermal (2017)," *Final Energy Cris.*, pp. 233–238.

Patsa, S. J. Zarrouk, and D. Van Zyl (2015), "The Lindal diagram for mining engineering," *Trans. - Geotherm. Resour. Counc.*, vol. 39, pp. 151–156.

Pambudi, R. Itoi, S. Jalilinasrabady, and K. Jaelani (2014), "Exergy analysis and optimization of

Dieng single-Flash geothermal power plant," *Energy Convers. Manag.*, vol. 78, pp. 405–411.

Valdimarsson (2011), "Geothermal power plant cycles and main components," *Short course Geotherm. drilling, Resour. Dev. power plants*, pp. 16--22.

Yang, D. Tang, Y. Chen, G. Li, X. Zhang, and Y. Meng (2019), "Determining initial formation temperature considering radial temperature gradient and axial thermal conduction of the wellbore fluid," *Appl. Therm. Eng.*, vol. 147, pp. 876–885, Jan.

Dipippo and D. Ph (2012), *Geothermal Power Plants : Principles , Applications , Case Studies and Environmental Impact Third Edition*.

Hou, M. Cao, and P. Liu (2018), "Development and utilization of geothermal energy in China: Current practices and future strategies," *Renew. Energy*, vol. 125, pp. 401–412, Sep..

Zhao, Z. Feng, Z. Feng, D. Yang, and W. Liang (2015), "THM (Thermo-hydro-mechanical) coupled mathematical model of fractured media and numerical simulation of a 3D enhanced geothermal system at 573 K and buried depth 6000 e 7000 M," *Energy*, pp. 1–13.

Yunus, A. Cengel, & Micheal, A. (2015), *Thermodynamics: An Engineering Approach*, 8th ed. New York: McGraw-Hill Education.

Najafabadi (2015), "Geothermal Power Plant Condensers in the World," no. 46, pp. 19–25.

Moya, C. Aldás, and P. Kaparaju (2018), "Geothermal energy: Power plant technology and direct heat applications," *Renew. Sustain. Energy Rev.*, vol. 94, no. May, pp. 889–901, Oct.

Saeid Mohammadzadeh Binaa, Saeid Jalilinasrabadyb, Hikari Fujiic (2009), "Classification of geothermal resources in Indonesia by applying exergy concept," Rev. Sci. Instrum., vol. 80, no. 6, p. 063102, Jun.

STUDY CASE COMPARISON OF LONG STRING AND TIE BACK STRING IN DARAJAT FIELD

Khansa Hanifa Zahra, Suci Nur Hidayah, and Mohammad Fidi Abganis Hermawan

UPN Veteran Yogyakarta
Jl. SWK No.104, Ngropoh, Condongcatur, Kec. Depok, Kabupaten Sleman, Daerah Istimewa Yogyakarta
Email: khansahz1698@gmail.com

ABSTRACT

Cementing is an important process to strengthen the position of casing in the formation. Lots of fracture zones are the major challenges in geothermal drilling which give impact to lose circulation and make the cementing process will be not economical. This paper discusses the configuration of the casing which is compatible to be applied to the Darajat field. On cementing long string consists of a pipe called long string and installed from the wellhead until to the targeted zone. Tie back liner cementing is done on the casing consisting of two pipes with additional insulation on the bottom of the well and extending the top production liner to the wellhead which is also cemented. The advantages of tie back cementing liner are safe to use at high temperatures. There are several parameters that can be taken into consideration when choosing a long string or tie back string. There are many problems in cementing long strings compared to tie back strings, long strings installation is at 2789 - 3998 ft which is more shallow then tie back string is at 2773 – 5460 ft, higher pressure after test in tieback liner, after being operated, it turns out that there are many problems that happen in the tie back liner, one of which is leak on cement so that it creates the potential for water trapped on the casing 13 3/8". By Installing the long string there is no problem with the cementing. When installing a tie back liner, the BOP must be removed, thereby reducing the effectiveness of installation, when compared to long casing that do not need to release BOP. From the supporting data, it can be concluded that the long string cementing is more efficient than tieback liner cementing because the time needed is less, does not cause many problems, and long string installation is cheaper than the tieback liner.

Keywords: Cementing, long string, tie back string, geothermal

INTRODUCTION

Not similar to oil and gas wells, casings design in Geothermal wells are harder, especially in high HPHT (High Pressure and High Temperature). Drilling in HPHT wells will affect drilling fluid rheology, unsuccessful drilling program finally impact to escalate the economic, technical and operational challenges. One of the most important aspects in casing design is the production string which has a function to connect productive formation to the wellhead, Darajat geothermal field is one of the field with HPHT condition, because the field categorized as vapour-dominated system which is the reservoir rock's pore contains hot vapour (Zulfa Rozifah,2013) with the reservoir temperature > 220℃. Based on field data, the Darajat field consists of two types of production string which is long string and tie back string casing. To avoid the problem in HPHT we have to know what is the best design base on the criteria of that well. In this paper, we will discuss the configuration of the casing which is compatible to be applied to the field based on its condition.

FIELD OVERVIEW

The Darajat geothermal field resource since 1984 to generate electricity, It is located about 50 km south-east of Bandung in West Java, Indonesia. The Darajat field is the situation at the eastern side of a range of volcanic centres nearly 30 km and includes as the active volcanoes Gunung Papandayan and Gunung Guntur. On the North-South side, it is located near Gunung Kendang. Darajad is at an elevation of 1750-2000 meters above sea level and lies about 9 km southwest of the producing Kamojang geothermal field and 10 km east of Wayang Windu Geothermal field (Sri Rejeki, 2010). The shape of reservoir in the field is a bowl shape based on geophysics data identification, the reservoir bottom extending to approximately – 3500 meter above sea level.

Andesit lavas and intrusives dominated the reservoir rocks and replied by thin lavas and pyroclastics. The location of permeable zone is located within the lava/ intrusive complex at an elevation of 200-800 m above sea level in the northwestern part of area.

As vapour dominated system Darajad geothermal field mainly producing dry steam at pressure approximately 470 psi and about 1.5% non-condensible gas content. Figure 1 shows the Darajat area, while Figure 2 shows the Darajat location.

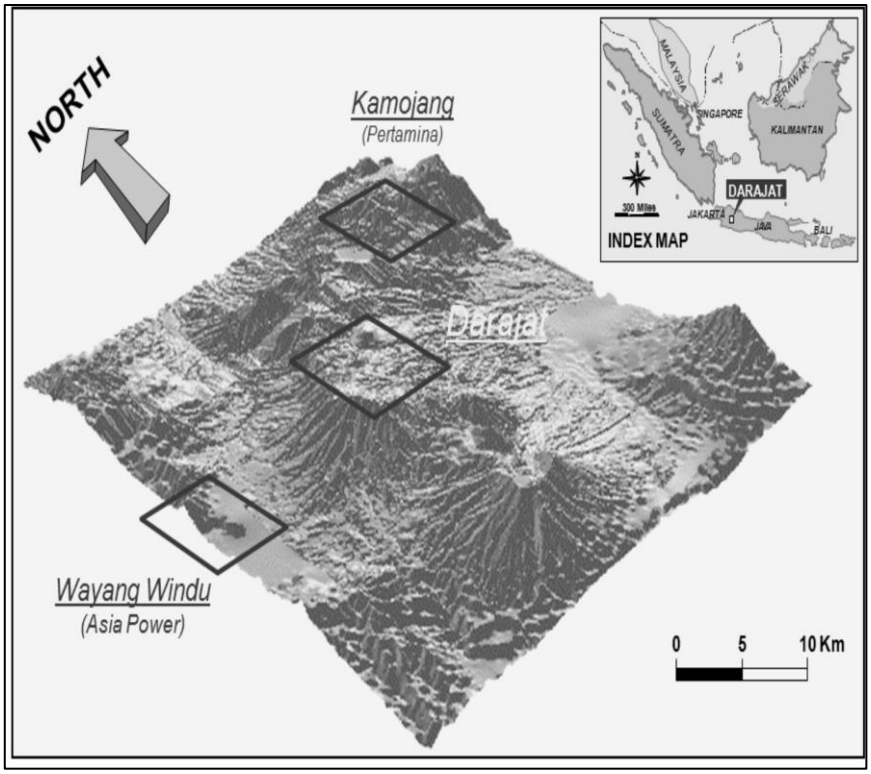


Figure 1: Map of Darajat and Surounding area (Sri Rejeki, 2010).

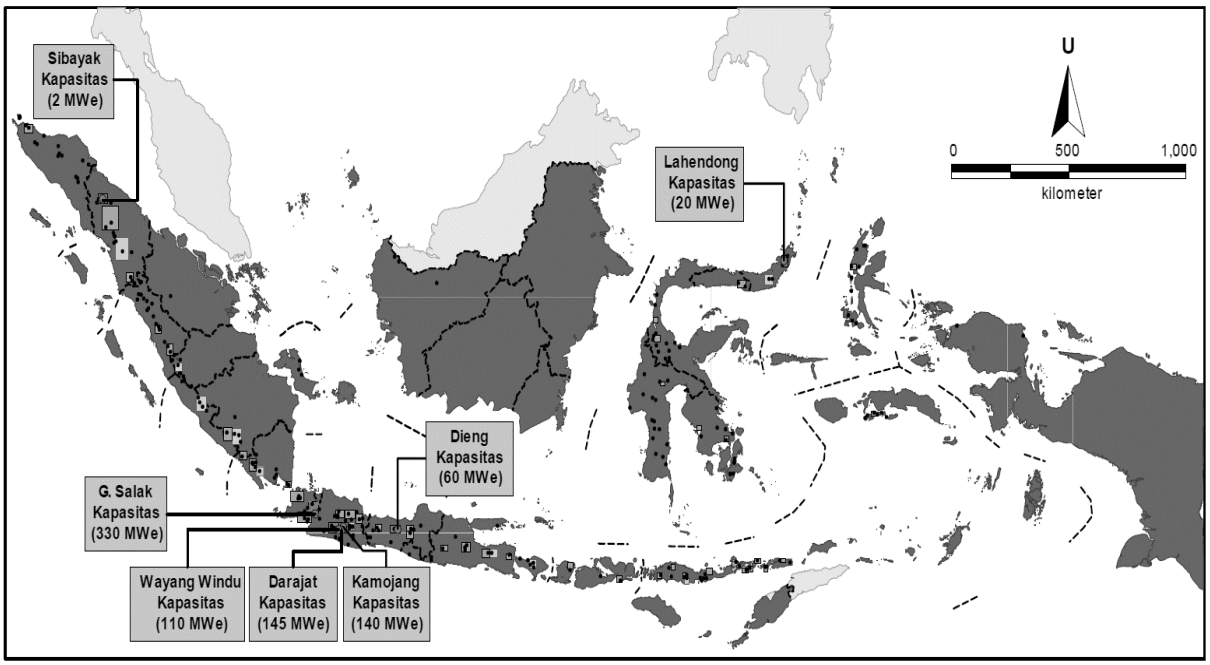


Figure 2: Location of Darajad Field (Rinna Wahyuningsih).

LITERATURE REVIEW

Casing Design

The well design defines the desired final status of the well. Geothermal well designs and drilling practices are similar worldwide (Hossein-Pourazad, 2005). The functions of casing design are similar depending on whether the well is drilled vertically or directionally. The casing is designed to accomplished two different functions, the first which is to allow safe drilling of the well and face up any condition in drilling process and the second is to meet the well's objectives without additional workover during the well's lifetime (Abdirasak Omar Moumin, 2013).

Casing design has several intervals which have a different function in geothermal wells. The type of casings is:

- The conductor casing is the first casing to be installed to seal off the unconsolidated formations at shallow depths to prevent cave-ins.
- The surface casing installed after conductor casing, the function is to support BOP (Blow Out Preventer) equipment and the others casing.
- The anchor casing usually runs in the deeper wells where some condition makes it unsafe to drill from the surface casing to the production casing in the hole section.
- The production casing is to isolate the production zones, to provide reservoir fluid control, and permit selective production in multi-zone production.
- A liner is a casing string which does not reach the surface and is suspended from the inside of the previous casing string by a liner hanger. In liner completion, liner or production casing act like a production string and the liner can be perforated and set in the productive formation session.

Special Casing Tools

Barrier is a fundamental tool to control the subsurface pressure and prevent the flow of hydrocarbon or some fluid which does not have to migrate from the reservoir to the well during drilling, casing, and completion of the well. While barriers become part of well design. The standard state there will use barrier in place if the condition like hydrocarbon-bearing formation and abnormally pressure formation with potential to flow to surface. Barrier can be cement, casing, drilling fluid (mud), metal or plastic mechanical plugs as the sample of primary barrier and BOP as the second barrier if the primary barrier cannot prevent the wellbore unstable condition.

Centralizers are a device which has function to keep the casing or liner in the centre of the casing string and prevent the casing from sticking while running in hole.

Floating Equipment for Inner String Cementing is used after pumping to holding the slurry in place and has the following features like provide casing buoyancy, guides casing into hole, and prevents reentry of cement. The example of floating equipment is float collar, cementing plugs, float shoe and the multiple stage cementer. Figure 3 shows the long string design in Darajat.

Long Casing String

Long casing string is one of types production casing string for geothermal wells, it depends from the wellhead through casing hanger until to the top of productive formation, when we choose long string as production casing, which it must have consideration to install annular barrier too. Based on American Petroleum Institute, 2013) there is some consideration when selecting a long string casing and the following consideration that have relation to be discussed in this paper:

- There are two verifiable physical barriers which are annular cement and casing hanger seal
- Slurry design, placement of cement and verification of cement
- Some of well's experience is losses or have poor mud/cement displacement efficiency, then need to increase levels of evaluation to confirm the cement barrier
- The potential for annular gas migration, which result in additional casing ad wellheads loads.
- Short transition time, anti-gas migration properties, fluid loss and rheology.
- Lost circulation problem happen during cementing from Equivalent Circulating Density (ECD)
- The effect of thermal cooling of the mud. The hydrostatic pressure can change prior to the cement is set.

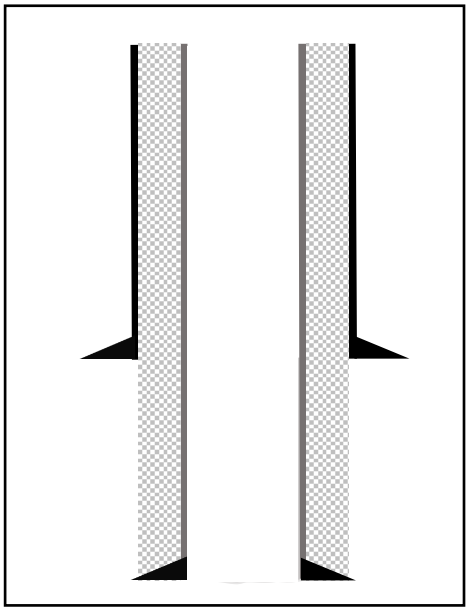


Figure 3: Design of Long string in Darajat field.

Cementing the Long Casing String

Cementing methods for the long string casing are single stage cementing and multi-stages cementing. These methods are selected based on well depth. Single stage cementing is one of the common cementing method applied in geothermal field.

In single stage cementing, at the first put in the casing string with all the required cementing accessories such centralizers, float shoe, and float collar in the well, before cementing process clean the well by circulating drilling fluid, then pump the

cement into the casing, down to the casing shoe then up into the annulus. It is the most common cementing operation in drilling process. In some conditions for the deeper wells with critical fracture gradient, cementing in long casing string cannot be applied because there is a differential of the hydrostatic pressure of the cement column. In this condition, multi-stages cementing usually applied for reducing hydrostatic pressure on weak formations to prevent fracture.

Multi-stages in this paper only discuss two stages cementing. The procedure of two stages cementing is divided into two parts, which is the first part of the cementing job is similar to the single stage cementing but not used the bottom plug or wiper plug.

For the second part, the job needs to use a stage collar or DV (Differential Valve) which can open and close to allows pumping cement from the inner part of the casing string to the annulus. DV is located at the midpoint of the casing or at the place where the upper cementing is performed. At first, the stage collar is sealed off and release the first stage plug following after pumping the spacer and cement slurry by using mud as displacement fluid. When the plug landed onto the float collar the pressure will increase.

Challenges Cementing the Long Casing String

There are some critical factors which must take precedence in long casing cementing:

- Centralization, the centre's position of the casing is important in cementing process. To provide the centre position in the hole and allow cement flow around the casing by using centralizers.
- Mud removal/ pump rate, mud removal can support the success of cementing process, mud column which contaminates cement can damage cement bounding and effect channelling.
- Channelling, if the cement and formation do not have a good bonding condition it will cause a channelling problem.
- Bounding, slurry contamination by drilling fluid can affect cement bonding, increase the quality rheology design for the fluid is important to get the best cementing result.
- Volume, in cementing geothermal there are many fractures which will increase risk of lost circulation and reduce the volume of cement.
- Back-Pressure, according to Schlumberger back pressure is the pressure within a system caused by fluid friction or induced resistance to flow through the system.

Tie Back Liner String

Tieback casing is commonly used for HPHT wells in the geothermal field. The tieback string extends the production liner back to the wellhead. Liner with tieback string provides a pressure-containing system from base of the liner to the top of the tieback casing (Yakely, 2015). Tieback casing is normally included in the casing design with the function to repair damaged, worn, and corroded existing liner or casing and also to provide additional protection against troublesome intervals (e.g., high-pressure layers, sloughing shales). Tieback casing provides extra pressure integrity from top of liner to the wellhead. This combination also installed in the revealed gas interval where there is a big loss circulation problem. When applied to geothermal wells, tieback casing design has advantages, which are:

1. The thin casing can be covered with new tieback casing at the end of drilling well.
2. It provides the chance to have a successful cement job in critical casing to casing section of the well.

In the other hand, tieback casing also has drawbacks, which are:

1. The liner tieback string design provided more barriers against potential gas flow up the annular space.
2. The connection between tieback and liner will eternally leak down the lap during the production of the well.

Tieback string is short and eternally lighter than long casing string. If pre-tensioning is not imparted to the tieback, tie back will yield in compression if the change in temperature (ΔT) is sufficiently large. For tiebacks with buttress threads, this yielding will result in a loss of pressure containment. This yielding can be prevented if the maximum heat-up temperatures are known beforehand and the tieback is pre-tensioned before cement sets. This will necessitate the use of latch down slip assemblies in the tieback receptacle or above the receptacle (Nelson, 1990).

Since liner combined with the tieback string will increase the well construction complexity, thus it must be considered by the following indicators.

- Tieback stem and liner Polished Bore Receptacle (PBR) interface design
- Installation space-out engages the tieback stem seals when casing hanger is landed in the wellhead.
- Tieback anchoring method to limit seal movement during the well’s life cycle.
- An additional trapped annulus subject to APB loads.

Cementing the Tieback String

Placing and cementing can be a difficult operation to perform. Therefore design and planning must be executed to ensure a seal between the liner and the previous casing. The liner is run into the well on the drill pipe and the cementing operation is carried out through the same drill pipe. The liner hanger is the key element when running and cementing liner.

For cementing the tieback, a drillable bridge plug is required to be set in the liner to isolate the newly drilled production hole. The plug should be located immediately below or close to the tie back receptacle to avoid any fluid contamination of the slurry. In at least two tieback failure incidents that have been attributed to trapped fluid expansion, the bridge plug was set at least 117m below the tieback receptacle. In one case, water occupied the space between the bridge plug and the receptacle. A thick gel with a relatively high density should be used to prevent the heavy tieback cement slurry from failing through the liquid column. Other sources of trapped fluid in tieback cement jobs are:

1. The presence of free water in slurry.
2. Insufficient excess slurry column to ensure complete displacement of the pre-flush fluids.

A tieback casing can be run in wells that have already been completed by first using the casing cutter to cut the liners up to just below the cold zone in the well. A drillable bridge plug should be located immediately below or close to the tieback receptacle to avoid any fluid contamination of the slurry.

Commonly overlooked with tieback design, is the quality of cement job in any casing to casing annular space beyond the two inner strings associated with the tieback. If this has trapped fluid in the casing to casing annulus, this may still cause imposition of two inner strings of the casing (Anchor and tieback). A study has shown that this type of two or composite casing string failure is possible when subjected to trapped fluid pressure. A solution to minimize the risk is to run a tieback arrangement for the anchor casing instead of running a single string as is commonly done.

Challenges Cementing the Tieback String

Tieback string requires long column of cement. The cement column is determined by the amount of lateral support required to prevent the casing to buckle. The static temperature at the TOC column and at the bottom of the cement column can be significantly different from each other. During placement, the temperature at TOC can be substantially lower than the bottom hole circulating temperature. The slurry can be difficult due to the temperature differentials. Temperature and pressure variations produce stresses on the casing and cement. The material can exceed the property limits as a result. Figure 4 shows the design of tie back liner string in Darajat.

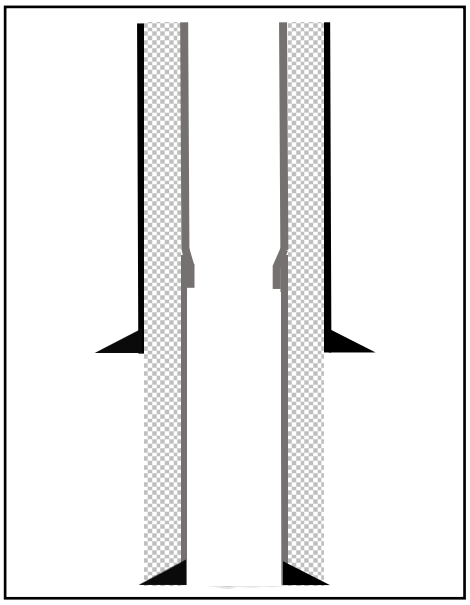


Figure 4: Design of Tie Back Liner String in Darajat field.

RESULT

Long Casing String

In Darajat field long casing string applied to 2789 - 3998 ft in the subsurface condition which is shallower than tie back string is at 2773 – 5460 ft. there are some methods in long casing string cementing process in Darajat field, and only three methods will be discuss here.

The first is *long casing string with single stage* cementing, the simple design can see in Figure 3, which only a long production casing without additional tools, because the model is simple it only takes the shorter time the others method. From Table 1 there are some indicators after installed casing long string with single stage method used 2 barriers which is primary and secondary barrier, from cement quality indicator show that cement mostly no return to surface and it means there are loss circulation indicator while cementing process, pressure test is mostly failed possibility because of HPHT condition in geothermal well, even though pressure test can measure casing pressure to analyze leak of casing. Analysis from long term integrity, there is casing problem was found, and based on leak of test to measure formation fracture pressure in this casing string there is no casing leak, It means the application of this casing string is safe for this field.

In addition to casing frame work for the successfully casing installation, we can also analyze some indicators from the cementing frame work related to Table 2,which are there is no the risk of water

trapped below port and risk of equipment in single stage method, for the secondary barrier in long casing string does not have to remove BOP, so it will increase drilling efficiency. Risk of 13 3/8" leak has potential effect on trapped water which will decrease cement bounding. The time needed to execution it process is lower than the other method, but there are high potential of casing growth and will create the distance from free point. Figure 5 shows the design of long string with DV below 20" shoe in Darajat.

Table 1: Comparison Casing Framework in Darajat field.

BARRIER	TIE-BACK DESIGN		LONG STRING	LONG STRING WITH DV
	LINER	TIE-BACK		
INSTALLATION -Barrier -Operational	2	1	2	2 Several DV failure
CEMENT QUALITY -Return -Pressure Test -Drill Out Cement	-Mostly no return -Mostly failed -Mostly cement not found	-Returns -Liner Lap Test mostly failed -Mostly cement not found	-Mostly no return -Mostly failed -Mostly cement not found	-Mostly no return -Mostly failed -Mostly cement not found
LONG TERM INTEGRITY -Casing Problem -Leak	-Many -Few	-Many -Few	-None -None	-No issue with trapped water -None

Table 2: Comparison Cementing Framework in Darajat field.

DESIGN	TIE-BACK	LONG STRING	LONG STRING WITH DV	LONG STRING WITH DV
Port/ Tie-back Location	Above 20" Shoe	NA	Below 20" Shoe	Above 20" Shoe
CEMENT PLACEMENT				
Upper Part	Confirmed	Unconfirmed	Unconfirmed	Unconfirmed
Lower Part	Unconfirmed	Unconfirmed	Unconfirmed	Unconfirmed
BARRIER DURING INSTALL	2	2	2	2
RISK OF TRAPPED	No	No	Yes	No
RISK OF EQUIPMENT	No	No	Yes	Yes
BOP REMOVAL	Yes	No	No	No
RISK OF 13 3/8" LEAK	Medium	Low	High	Medium
TEMPERATURE LIMIT	NA	NA	400 (DV limit)	400 (DV limit)
TOTAL EXECUTION	Medium	Low	High	High
EFFECT OF CASING GROWTH	Low	High	High	High

The second is *long casing string with DV (Differential Valve) below the 20" shoe,* commonly some of well in geothermal is deeper then oil and gas, it supposed need to use dual stages cementing with additional tool *DV (Differential Valve)* with DV below 20" shoe. Table 1 used to analyze long string with DV above and also below the 20" shoe, which is have 2 barriers and in the operational have several DV failures, in cement quality side cement mostly no return to the surface, then the pressure test mostly failed for the same case in single stage.

There is no casing problem and leak of casing for this casing string. Based on table 2 we will analyze the cementing framework, this casing potential to has water trapped below port and failure of DV collar. For BOP installation is same like single stage method. But the differential are from potential effect on trapped water and total execution time is higher than the long casing string with single stage cementing and the last is *long casing string with DV (Differential Valve) above the 20" shoe.* For analysis is almost same like DV above 20" shoe. The differential only from there is no risk of water trapped below port and potential effect on trapped water is medium. Figure 6 shows the design of long string with DV above 20" in Darajat.

Tie back Liner String

Based on the name of tie back liner string, this string consists of two part which are liner string as the part hang on the production casing and the tie back casing that tie the liner to the surface through casing hanger in wellhead. There are several indicators to analyze success or failure of tie back liner string

application in Darajat field. In this analysis we will be divided into two parts such as liner string and tie back casing.

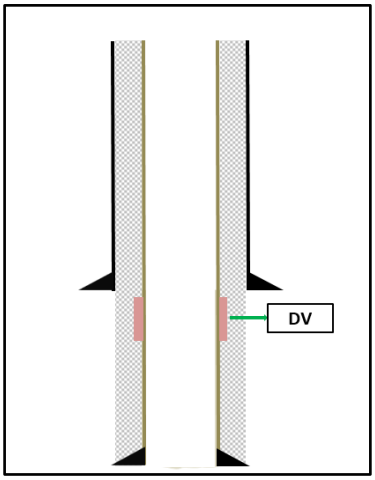


Figure 5: Design of Long string with DV below 20" shoe in Darajat field.

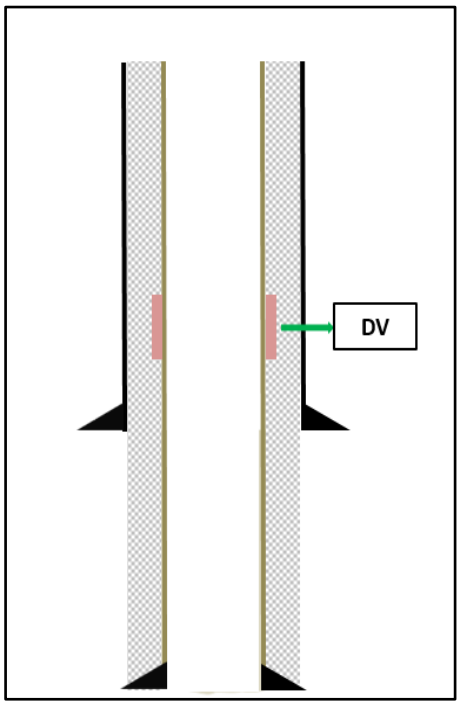


Figure 6: Design of Long string with DV above 20" shoe in Darajat field.

Liner, from table 1 we know that liner use two barriers and there is no failure in the operational. From cement quality, cement mostly no return to surface because the position of liner in the depth condition and has a big potential to loss in the formation fracture, and also in pressure test mostly failed but sometime is success. In long term integrity there are many casing problems and leak of cement. To complete the analysis we can also use table 2 for liner and tie back casing, in the test we know there is no risk of water trapped below tie back and risk of equipment, but in installation tie back liner string BOP must be remove from the wellhead and it will take more long time execution process then long casing string, the effect of casing growth is not high like long casing.

Tie back casing for tie back only use one barrier, for cement quality there are cement returns to surface it is indicate that cementing is complete in tie back session. But for the pressure test mostly failed, for long term integrity there are many casing problem and leak of cement.

DISCUSSION

Comparison of Long String And Tie Back String

The general differences of long casing string and tie-back liner String:

1. Installation of tie-back liner string takes longer time than long casing string
2. Tie back liner string is cheaper then long casing string
3. Tie back string installation process is more expensive
4. Tie back liner string is more safety for HPHT wells, and well which contain gas
5. Installation of tie-back liner string have to remove BOP while long casing string does not.

Production Casing String in Darajat Field

According to Monika Saevareid, 2017, liner tieback string is often selected as a production casing rather than a full string casing in HPHT wells. But in Darajat field with HPHT wells, not all of wells use tie back liner string related to some theories. Darajat field installed some types of production casing such as long casing string, long casing string with DV and also tie back liner string. But in here we will discuss what condition that will make decision to choose long casing string or tie back casing string.

Long string installed at 2789 - 3998 ft which is shallower then tie back liner string is at 2773 – 5460 ft. for this condition we can analyze that tie back is designed for deeper well to avoid HPHT condition to maintain casing strength and stability.

After doing some analysis, the authors know that in Darajat field had installed tie back string which has more problems than long string, because for the installation the conjunction between liner string and tie back casing is easier to be failure affect by HPHT. In science, tie back liner string as a young technology besides long casing string, so there are many problems which can not to dissolve right now. So, in application tie back liner has many problems. Even though the tie back liner can provide less weight suspended from the casing head, because the lower section is suspended from the liner hanger and the upper section hangs from the casing head. Tie

back liner designed as the safer choice in HPHT wells, due to improved drilling hydraulics and also decrease pressure drop. But for right now long string is still the best choice for the field, it because only has the few problems and also cheaper than tie back liner string.

CONCLUSION

1) Darajat geothermal field consist of 3 types of casing design such as long casing string, long casing string with DV, and tie back liner casing
2) Tie back casing string has the most problems when applied in Darajat field
3) For cementing process the cement mostly no return to the surface, both of long casing string and tie back liner
4) Execution time in installation tie back string is more longer then long casing string but shorter then long casing string with DV because have to use dual stages cementing.
5) Long casing string with DV is not effective if we compare with only long casing string because will take a longer time.
6) Until the end of discussion the authors conclude that long casing string is more suitable to applied in Darajat Geothermal field.

REFERENCES

Sri Rejeki (2010). "Geological Conceptual Model Update of the Darajat Geothermal Field Indonesia". Bali, Proceedings World Geothermal Congress 2010

Monika Saevareid (2017). "Selection of Long or Short String Production Casing on HPHT Wells". University of Stavanger.

Douglas P.MacEachem (2003). "Advances in Tieback Cementing, presented at the SPE/IADC Drilling Conference held in Amsterdam the Netherlands". 19-21 February 2003.SPE/IADC 79907

Carlos Emilio Guerra Guerrero (1998). "Cementing of Geothermal Wells". Number 6. Pages 158-172.1998.

Samuel Ikinya Ng'ang'a (2014). "Cementing Processes in Geothermal Well Drilling: Application and Techniques". Number 23. Pages 449.2014.

Abdirasak Omar Moumin (2013) "Geothermal Well Design". Number 28.pages 659-670. Geohermal Training Programme.

Riza and B.R.Berry (1998). "Slimhole Drilling Experience at Darajat Geothermal Field,West Java Indonesia". Proceeding 20th NZ Geothermal Workshop 1998.

Medi Kurnia Putri (2014). "Introdution to Geothermal System of Way Ratai". Proceeding Indonesia International Geothermal Convention & Exhibition 2014. Jakara Convention Center, Indonesia 4-6 June 2014

James N. A. Southon (2005). 'Geothermal Well Design, Construction and Failures". Proceeding World Geothermal Congress 2005. Antalya, Turkey, 24-29 April 2005

Anouar Elhancha (2016). "Deeper Tieback Cementing Design Challenges and Engineering Approach- Gulf of Mexico Case Study". presented at the SPE/IADC Drilling Conference and Exhibition in Fort Worth, Texas. 1- 3 Maret 2016. IADC/SPE-178884-MS.

EFFECTIVENESS OF GEOTHERMAL OPERATOR FOR DELIVERING MAXIMIZE PLANT AVAILABILITY FACTOR

Arnaldo Napitu

PT. Medco Geothermal Sarulla
NIL Power Plant – Simataniari Village – Pahae Julu District
North Tapanuli Regency, North Sumatra Province 22463
Email: arnaldo.napitu@sarulla-geothermal.com

ABSTRACT

Keep the plant on line as long as possible and take it down for as short a time as possible. Get as much power out of the machine as possible when it is on line – generate at or close to full rated output. Thus, more or less expectations of the performance results set forth in the business plan. Of course, in the corridor of work safety is the most priority and also good cooperation from all parties is needed to make it happen.

Operator effectiveness is fundamentals to power plant performance. Daily decisions of control room and field personnel directly impacting safety, production, process availability, and quality. Therefore, establishing a competent operator in accordance with its duties and responsibilities become very important. Effectiveness can be interpreted as something that can achieve the maximum goal as expected, besides that effectiveness can also be interpreted as one business that is never tried before the desired expectations have not been achieved. In other words, make continuous improvement.

Objectively from this paper is how the operators effectiveness can deliver maximize power plant availability and improve reliability of the power plant, with several methods used, among others, are early detect abnormal conditions of an equipment and or system , do small repairs of equipment , perform power plant system integration, identify , and monitor degrading asset performance before failure occurs. By following this the expected results, significant improvement in availability, performance, and product quality will follow.

Keywords: Operation and maintenance, geothermal

INTRODUCTION

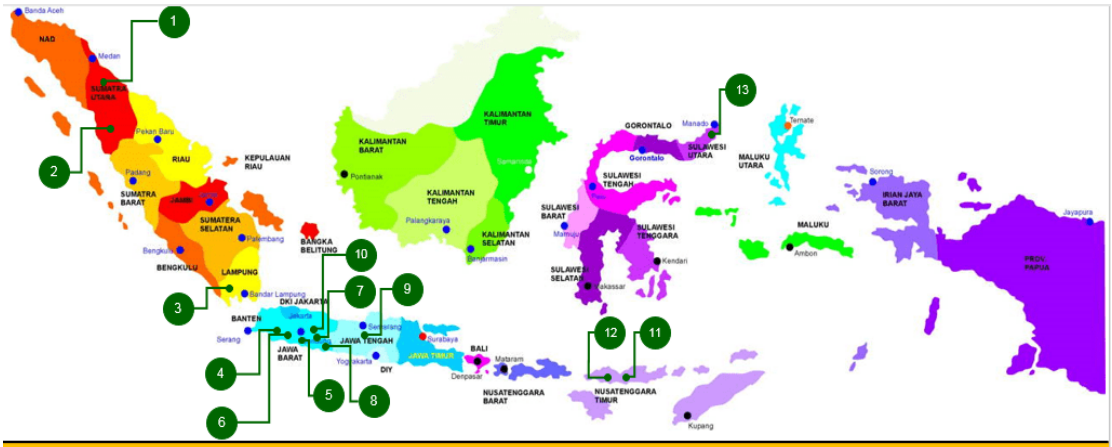
With about 40% of the world's geothermal reserves being located below the surface of Indonesia, the country is estimated to contain huge potential for this renewable energy. It's clear that geothermal become more reliable long-term energy opportunity in the future. Made reference to target in 2025, geothermal can contribution as big as 7200 MW. Now total capacity is more than 1924 MW, this achievement puts Indonesia as the second geothermal power producer in the world after The United States, which was originally occupied by the Philippines. Not only needful finance resource available but also operators who can perform process plant operations in efficient, safe, and reliable. Geothermal power plant operation requires multi skills.

Running the Power Plant safely and in accordance with the functions of its operating conditions is the expectation of each company. That is, if the plant's capacity is 110 MW, it is desirable that the plant works to produce 110 MW. Of course, with certain time intervals to stop operating for maintenance activities. Maximizing Plant Availability. Plant on line brings benefits, Plant shut down show's loss of profit. Maintaining Plant on line as much as possible and reducing plant shut down to a minimum. For the purposes of O & M philosophy in general in the industry. It is important to understand all the power plant and steam field technicians as the main tasks.

Namora I Langit (NIL) Geothermal Field

The NIL geothermal field is located about 300 km southeast of Medan in North Sumatra at an elevation of 800 – 900 meters above sea level. The NIL geothermal field has been operated since October 2017 for Unit 1 and May 2018 for Unit 2 with the support of 11 production wells and 10 injection wells. Most of the production wells are drilled away from the Great Sumatera Fault (GSF) while the injection wells are mostly perpendicular to the GSF. The production wells are drilled towards the hypotechnical up flow zone which located in the eastern area of the prospect. The produced Non-Condensable Gas (NCG) at the wellhead is within 6.0 – 9.0 wt.% with the highest one is shown by the easternmost and the northern wells meanwhile relatively lower gas is demonstrated by the western and southwestern wells. The south and southwest wells show relatively higher H_2S content.

Figure 1 shows the geothermal field located in Indonesia, while Figure 2 shows the location of Namora I Langit geothermal field.



	1	2	3	4	5	6	7	8	9	10	11	12	13
Geothermal power plant name	PLTP Sibayak	PLTP Sarulla	PLTP Ulubelu	PLTP Salak	PLTP Wayang Windu	PLTP Patuha	PLTP Kamojang	PLTP Darajat	PLTP Dieng	PLTP Karaha	PLTP Matalako	PLTP Ulumbu	PLTP Lahendong
Operator	PT Pertamina Geothermal Energy	Sarulla Operation Ltd	PT Pertamina Geothermal Energy	PT Star Energy Salak Geothermal Salak, Ltd	Star Energy Geothermal Wayang Windu	PT Geo Dipa Energy	PT Pertamina Geotherm al Energy	Star Energy Geothermal Darajat	PT Geo Dipa Energy	PT Pertamina Geothermal Energy	PT PLN	PT PLN	PT Pertamina Geothermal Energy
Capacity (MW)	12	330	220	377	227	55	235	270	60	30	2,5	10	120
Operating Area	Sibayak-Sinabung, North Sumatera	Sibual-buali, North Sumatera	Waypanas, Lampung	Cibeureum-Parabakti, West Java	Pangalengan, West Java	Pangalengan, West Java	Kamojang-Darajat, West Java	Kamojang-Darajat, West Java	Dataran Tinggi Dieng, Central Java	Karaha Bodas, West Java	Matalako, NTT	Ulumbu, NTT	Lahendong-Tompaso, North Sulawesi

Figure 1: Geothermal field in Indonesia that already operates (www.geothermalresourcescouncil.blogspot.com).

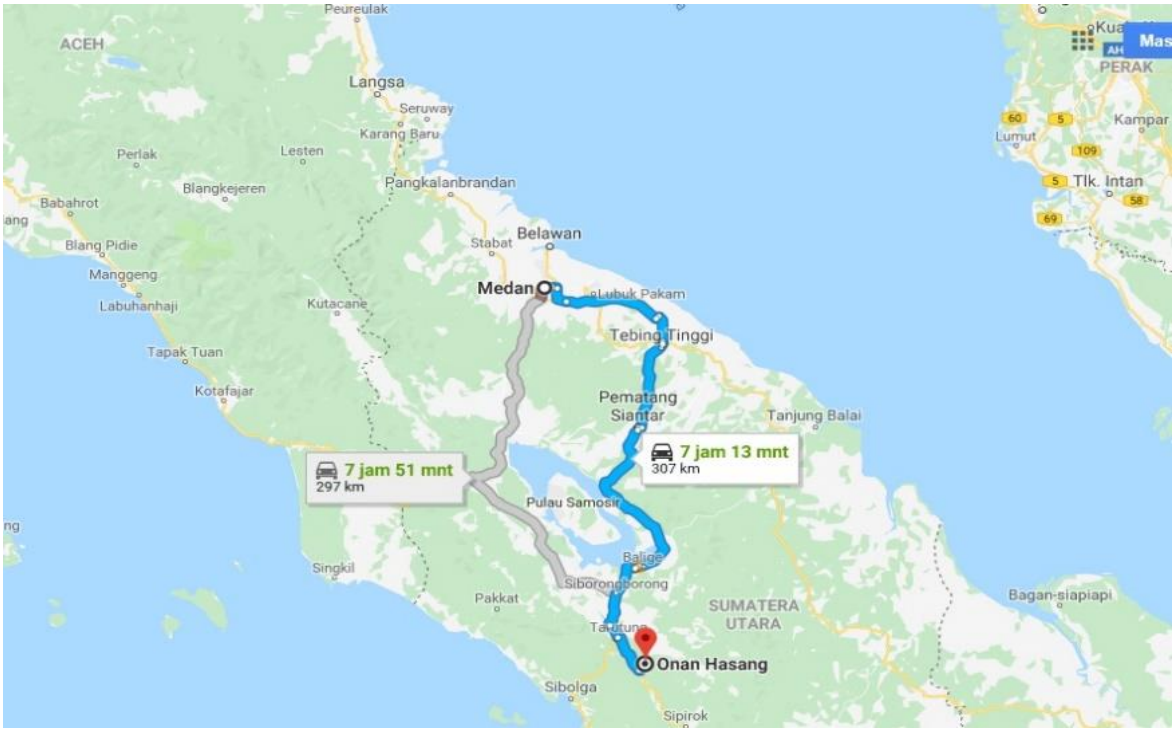


Figure 2: Map of Namora I Langit Geothermal Field (taken form Google map).

Sarulla Geothermal Power Plant – Unit 1 and Unit 2 Namora I Langit

Located in the Sibual-Bualli (Kabupaten Tapanuli Utara – Sumatera Utara) geothermal working area (WKP), the Unit 1 and Unit 2 of NIL geothermal power plant is currently producing 232 MW gross. Using an integrated type of geothermal combination system. Each unit consists of a unit of steam turbine generator – a flash system, two OEC Brine units, and four OEC Bottoming units that utilize the remaining heat from the steam turbine back pressure type – binary cycle system. This system of Integrated Geothermal Combined Cycle Unit is the first time it has been applied in Indonesia. Figure 3 shows the schematic diagram of Integrated Geothermal Combine Cycle Unit.

RESEARCH METHOD

The development of power generation industry now continues to grow and compete. Financial and

technical flexibility generate power quickly, high availability, allows incremental development of large resources to meet rising demand and can use revenue to continue development are several important factors for the future geothermal power industry. Of course, there are many changes that affect power plant operator. Than question and attitude is how to put the operator in the best position to successfully deal with these changes.

The availability factor of a power plant is the amount of time that it is able to produce generation - electricity over a certain period, divided by the amount of the time in the period. Generation (MWh) x Tariff (US $ / MWh) = Revenue (US $). This shows if tariff fixed, any reduction in MW (Generation) or h can lead to lower revenue. And if tariff varies, loss of ability to capture high price events. So, increasing availability is always valuable.

From the description above it is clear that the operator have a role and contribution to achieve maximum availability factor. And to achieve its required for the effectiveness of the operator. There are many ways can be obtained to improve operator effectiveness. Specially, these are:

1. Conduct a plant system integration.
2. Maximum use of HMI performance.
3. Continuous improvement of operator competence.
4. Involvement directly in the process of making Operating Procedure.
5. Human factors and ergomomics.

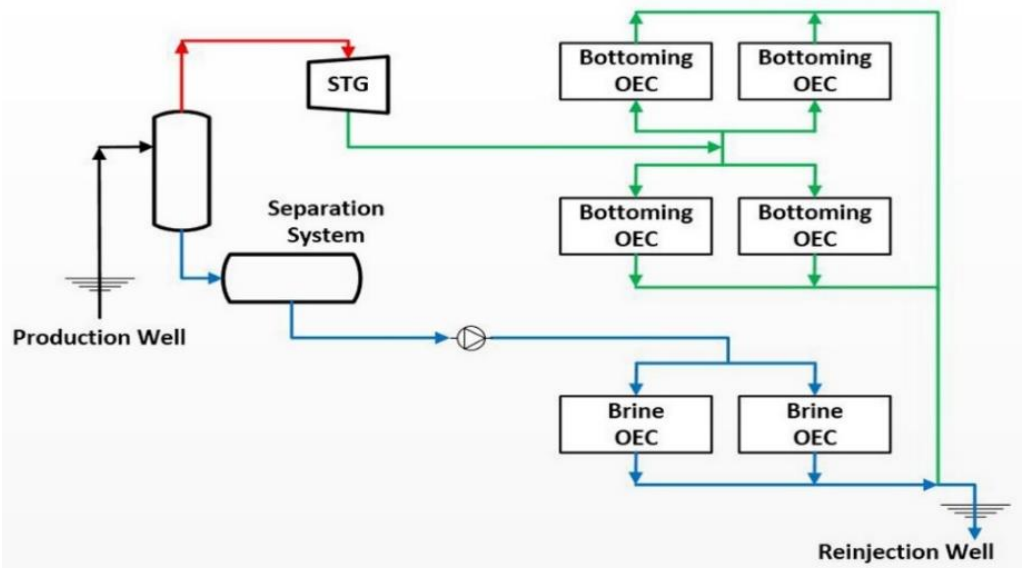


Figure 3: Schematic showing principles of operation of an Integrated Geothermal Combine Cycle Unit.

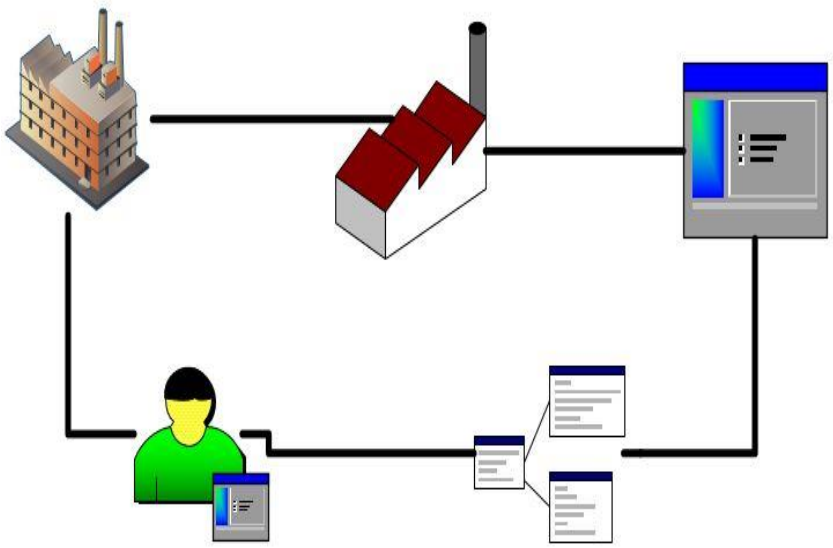


Figure 4: Illustration Plant System Integration.

Conduct a Plant System Integration

In modern operations, decisions are made with data to reduce errors and minimize risk. Common problem in such area is heavy too much data, but not fast enough data processing. Then, unproductive time was spent to derive, process, and selecting the options. For example, for production wells, what is the maximum output, what percentage of steam and brine, how to trend the chemical content, how much pressure is allowed. This is important when starting up, shut down, and other activities that require contain wells to be shut down or on line. By knowing the complete characteristics of each well, we can plan the processing time accurately. Figure 4 shows the illustration plant system integration.

No longer waste time searching for history data or asking other parties. Organize an integration of information data between steam field and power plant**.** With an integration system it makes operator work more efficient. For example , the load regulator (Dispatcher PLN) asks for a 35 MW reduction in load , from operator's power plant data knowing that with a decrease in load of about 35 MW , the steam consumption needed is only 300 ton/hr. Information on steam field data , for example Well 2 in Well Pad B output 200 ton/hr. and Well 3 in Well Pad C output 100 ton/hr. Thus, operator can determine which well will be maneuvered. Or for example there are maintenance activities that requires the well to be shut in then with the integration systems, the amount of steam consumption and others, the operator can quickly, measurably, and accurately determine the replacement well. We can also capture the changing dynamics of the reservoir from well head pressure and output flow rate. Analyze laboratory information about the chemical content of geothermal fluids. Then mapping which wells are the most acidic and if there is a demand for a decrease in load, with this integration system the operator will temporary reduce or close (as needed) the wells that have been mapped. Thus, it can save the use chemical additive to neutralize the acid well. Enhancing mid-term and long-term operational decision to improve generation performance. We can process and improves the ability to address performance degradation before it affects production. With hope to the future companies to move away from reactive or corrective repairs to become best in class predictive procedures. Figure 5 shows the illustration of alarm presentation features.

Maximum Use of HMI Performance

The Operators must have access to all relevant data and tools that help him make decisions and act quickly in relation to a situation in the process. All data must be synchronized and presented in a unified way, in context, and without the need to login and browse in separate systems. It is also important that all screens support transfer of information. Information specifically for alarm system. Once again that the purpose of an alarm system is to direct the operator's attention to plant conditions requiring timely assessment or action. It is important to know what alarms most often appear, distribute the alarms according to the scale of importance, and the operator's action to normalize the alarm. For example, the emergence of an alarm 'warning' for the difference pressure of heat exchangers. With the maximum use of HMI performance, operators can create event frequency alarm, duration alarms, time to acknowledge, and operator actions. So that the introduction of the characteristic of each equipment can be known, the performance of the equipment is measured, and prevention before the equipment is damaged can be prevented. Here are some things that are suggested to be maximizing the usage of HMI.

- Provide the facilities simulator.
- Provide alarm presentation features and advanced alarm analysis.
- Can display the Operating Procedure.
- Reminiscent of work measures, so that when there is miss job steps, operators can immediately know.
- Displays the safe operating parameter limits.
- Information for a system that is currently in the by pass system.

Continuous Improvement of Operator Competence

Geothermal power plant operation requires skills in system design and operation, power plant and steam field chemistry, maintenance of equipment and plant, community liaison, mechanical, environment, and electrical. Why is there enough ability to have? because of that ability to make the correct decision at the right time has a huge impact on plant profitability, safety and reliability. Or in other words, by taking the wrong decision at the wrong time the operator could harm fellow workers, the surrounding community and environment, as well as seriously reduce plant profitability. With this continuous improvement of operator competence, it is expected that operators can make small, safe and temporary small repairs. So that operations continue to run normally. Do not always expect others to improve but play an active role in all their duties. To keep competing, currently some companies try to make a lot of things with a bit of action. Like the principle of economy, with minimal capital gain maximum results. The company is working hard to be able to use its human resources more efficiently. Companies now have fewer people managing larger plant areas. Thus, it is clear that the competence of the operator should keep on the increase. Here are some things in order to increase the competence of operator;

- Performed on the job training.
- Self training and or with e-learning.
- Public training in abroad and domestic.
- Share knowledge with geothermal practitioners.
- Training simulators familiarize operators with their actual work environment.

Involvement Directly in the Process of Making Operating Procedure

Operating Procedures (OP) are different from manual books or practical science that forms the basis of the logic of how a process should be run. OP are rigid in the sense that operators should not maneuver operations beyond what is written in the operating procedure. In OP is no explanation as to why operators should perform operational phases, very practical and to the point. The operator must be able to act quickly, accuratel, validate, fine tune, and practice the OP unlimited improving the Safety of the Operation. So with instructions, steps, and guidelines for OP, every work whether it is start up, monitoring, shut down, and other routine activities becomes measureable. That means if you will shut down unit, estimated processing time can be determined. So that it can also manage manpower effectively, can maximize every activity in the framework of repair and maintenance and if there are questions from other parties can provide accurate information or answers. OP becomes systematic and structured reference for operators in running power plant. Structured meaning easily understood, there is a limit on the information secure operation, the consequence of deviation, and also consider human factors. Basically every operator already understand the cycle of geothermal power plant, started production of the well, energy conversion generates electricity, than get the injection right back to the injection wells. But in fact, a lot of different things on the energy conversion process, such as ranging from equipment limitations, changes in equipment performance, enviromental changes, equipment failure, and other related changes changes with human safety and equipment. Thus operator involvement is needed in making OP, or with the existing OP, the operator conducts comprehensive review that is integrated with the actual conditions in the field and direct experience when operating. Another reason is because operator are parties who interact with systems and equipment every day. So, the latest developments, circumstances, and conditions of equipment that are most aware are operators. Next, together to add on modify the OP and perform OP simulation. So with Operator involvement in making OP, review, modification, and simulation, Operator competencies and effectiveness can be ongoing and ongoing.

Human Factors and Ergonomics

Human factors focus on human beings and their interactions with products, equipment, facilities, procedures, and environments used in work and everyday living. And ergonomics is a body of knowledge about human abilities, human limitations, and other human characteristics that are relevant to design. For operators to be effective, we have to recognize the importance of human factors and the need to make the work environment conducive to efficiency and wellbeing. The best way to do this is to aim for a perfect fit between the operator, desktop equipment and control room environment. Each operator should have their own display to arrange graphics as they want them and to get an optimal view of that part of the process under their control.

Specifically, for two or more units in one power plant. Identification errors often occurs. For example, Unit 1 and Unit 2 are operating normally. And a condensate pump trip in Unit 2. Because of human factors, the control room operator asks the field operator to check and reset the condensate pump in Unit 1. Or in the context of maintenance activities in Unit 1, but the operator releases and isolates energy in Unit 2. Misidentification of systems and equipment. This shows the importance of human factors and ergonomics for the operator's work environment. So that the operator is expected to stay focused both in normal operation or abnormal conditions. Figure shows the key of productive and reliable operations.

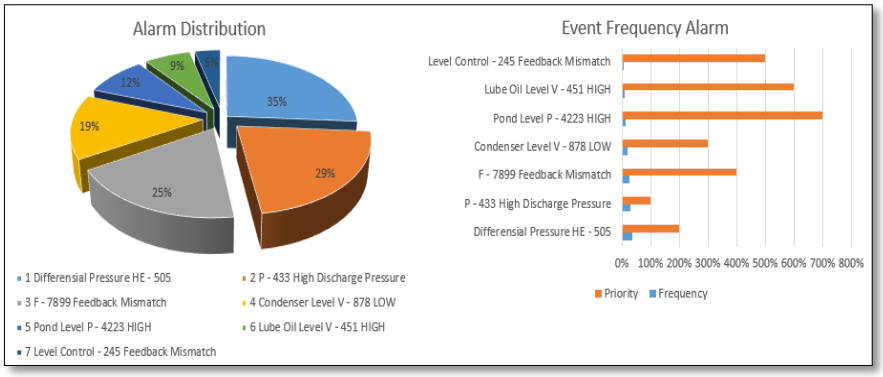


Figure 5: Illustration of Alarm presentation Features.



Figure 6: Operator wellbeing is the key to productive and reliable operations (www.new.abb.com).

RESULT

Here are some actions of operator effectiveness that have been carried out.

Action 1

Figure 7 shows condensate level, discharge pressure pump, and discharge valve opening which is not synchronous. The discharge valve is late and responds too quickly – failed to control, resulting in the condensate level going up and going down. And the condensate pump turns off. Operator does manual / semi tuning, by manually discharging the discharge valve. While monitoring the condensate level and adjusting the discharge valve manually. When the condensate level tends to be stable, return the discharge valve to the AUTO position.

Action 2

The Red line in Figure 8 below shows the condensate flow rate, where the reading is stable high, while the discharge pressure pump, condensate level, and discharge valve opening show stable conditions. This means that there is an abnormal flow rate. And be sure to read local transmitter, find an indication of Bad – Meter body Fault. Operator done a correct reading of the error flow rate on HMI by resetting it as its local transmitter.

For Action 1 and Action 2. No need to create a WO /Service Request for repair. So, the Maintenance Team can be allocated to the task or other more important work. An important operational parameter can be right back in the monitor.

Action 3

On time water overflowed to the floor. After being investigated found a running pump but with very low flow and high-pressure discharge. So that the pump strainer is suspected of being dirty and clogged. Operator then makes minor repairs by removing, cleaning, and replacing the pump strainer.

Action 4

On certain parts the strainer is installed in the pipe line with weld (Figure 9). So that it does not allow the operator to make minor repairs if there is a problem with the strainer. Found that there are two strainers that are problematic so that the pumping of the sump cannot be done. To overcome this problem temporarily, the operator modified the pipeline. Remove the part of the pipe with the strainers and replace it temporarily with a hose.

For Action 3 and Action 4. Same as above, no need to create a WO. Previously, operators use a submersible pump to pump the water right in the pond. Requires more time and energy to take on the pump, installing it in the pond, preparing the line hose from the pond to the gutter, and monitors a decrease in local level periodically. By doing minor repairs, time and effort saving and can be used for other work that matters.

Action 5

In each shift, the operator conducts brine sampling three times. Then the sample is measured by the pH value and compared with the On-line pH monitoring system. Sometimes the tapping point for sampling is clogged, so the sample does not come out. The Operator makes small repairs to smooth the clogged path by removing the tubing from the fixed valve, cleaning the clogged part, and re-installing it.



Figure 7: Trending of Condensate Level, Discharge Opening, and Discharge Pressure.



Figure 8: Trending of Condensate Pump Flow Rate and Transmitter Meter body Fault Indication.



Figure 9: Temporary pipe modification.

Action 6

Operator replaces the broken fuse. Fuse is a safety device that works to break the electric or excessive current. Under certain conditions, midnight and lighting rain can cause fuse to break. Not quite possible if you call Maintenance Team to come to the Power Plant to replace the fuse. It takes time, while the operating parameters are attempted immediately.

For Action 5 and Action 6. All corrective actions by the operator are always recorded and reported to maintenance as equipment history data. Some corrective actions are also temporary while awaiting thorough repairs by maintenance. More about action 6 - fuse replacement. It is known that the control level works to maintain the accumulator level at a certain value. And if the accumulator level is unreadable because the fuse is broken, the input value to the control level is not correct. In this situation, there must be at least 2 operators to replace the task level control. 1 operator monitor level accumulator at local sight glass and 1 operator controls valve opening level control. It can imagine the work and actions taken. In addition to being inefficient and unsafe, a little negligence in monitoring and controlling can cause a high level in the accumulator which can result in unit trips. But with the effectiveness and competence of the operator this can be avoided and success in handling abnormal situations.

Action 7

The red line in Figure 10 shows the trend for the compressor air pressure to one of the binary units. Normal pressure of direct read zero and the corresponding logic, because the compressor air pressure loss then the trip unit. The operator checks the compressor control air pressure and normal readable (the green line). Further checks on the premises, since the main compressor air pressure in HMI read normal then ascertained reading the pressure transmitter problem. Ascertained again by looking at the readings of pressure in air receiver tank-read the same with that of the main compressor. The operator checks the condition of the pressure transmitter and found meter body fault. Next do a small improvement by way of undoing one of the cables and pair it again - reset power. The results on the pressure good, readable transmitter in HMI go back read normal.

Several times the NIL power plant experienced interference from the outside and inside which caused the blackout condition. At the beginning we needed a long time to be able to overcome this emergency and return it to normal conditions. Some things that cause takes a long time such as, ignorance of the operator, inaccuracies in the field, and conditions that have changed. But by holding a black out simulation, reviewing and modifying the Operating Procedure, creating best practices and flow chart actions, now we have been able to reduce loss time - down time due to the condition of outages. Previously it took 2 to 4 hours for the recovery unit, now it only takes 1 hour to return the unit to normal conditions.

CONCLUSION

The data showed that the effectiveness of the operator such as conduct a plant system integration, maximum use of HMI performance, continuous improvement of operator competence, involvement directly in the process of making operating procedure, and human factors ergonomics can have a big impact on plant profitability and the value of plant availability factor. With the effectiveness of the operator, the geothermal power plant operations can be run with safe, reliable, efficient, and increase the competence of the operator. Abnormal situations – upset conditions, spurious trips, and unplanned outages that affect availability can be avoided.

REFERENCES

DiPippo, R. (2005). “Geothermal Power Plants: Principles, Applications and Case Studies”, Elsevier Ltd

Dirjen EBTKE (2017): “Kejar Target 7200 MW tahun 2025 Pemerintah Rencanakan Penetapan 3 WKP Baru”. Jakarta. Diambil dari: www.ebtke.esdm.go.id (28 April 2017)

Hari K, Otto., Yudho Wibowo, Boy (2018): “Operating Procedure in Improving Operator Competencies”. Proceedings The 5th Indonesia International Geothermal Convention & Exhibition 2018, Jakarta, Indonesia, 2-4 August 2018, pp 1-2.

http://new.abb.com

J. B. Hullen and P. M. Wright (Energy & Geoscience Institute at The University of Utah), “Clean Sustainable Energy for The Benefit of Humanity and The Environment”, U.S. Department of Energy Brochure, May 2001.

Saptadji, Nenny (2011). “Penelitian dan Pengembangan SDM Untuk Mendukung Pengusahaan Geothermal di Indonesia”. Disampaikan pada acara National Geothermal Seminar di Universitas Padjajaran Bandung, 19 November 2011.

Sudarman, Sayogi., Heru Triyanto, Roni., Sudiono, Bambang (2013). “Preparation of Qualified Geothermal Technicians”. Proc. 13th Indonesia International GEOTHERMAL Convention & Exhibition 12-14, Jakarta,Indonesia, pp 1-2.

Simatupang, Christovik., Matsuda, Koji., Easley, Elisabeth., Astra, Doddy (2018): “Fluid Chemistry Characteristic of Namora I Langit, A Geothermal System Within the Great Sumatera

Fault", Proceedings The 6th Indonesia International Geothermal Convention & Exhibition 2018, Jakarta, Indonesia, 5-8 September 2018, pp 1-2.

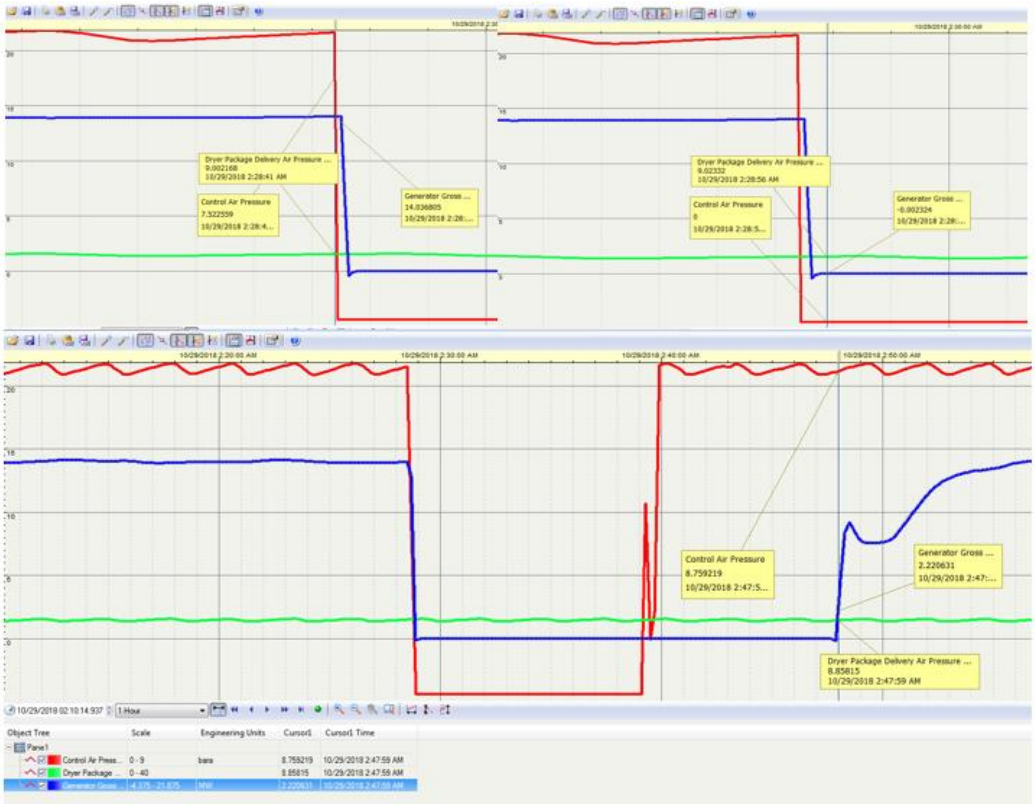


Figure 10: Trending of Air Compressor, Generator Gross Load, and Control Air Compressor.

General



This page is intentionally left blank



LIFE CYCLE ANALYSIS OF GEOTHERMAL POWER PLANT SYSTEM OPERATION IN THE LAHENDONG GEOTHERMAL FIELD

Muhammad Gilang Madiantara, Ahmad Indra Sakti Harahap, Ramadoni Febriandinata

PT. Pertamina Geothermal Energy Area Lahendong
Jalan Raya Tomohon 420, Kota Tomohon, Sulawesi Utara, Indonesia 95431
Email: muhammad.gilang@pertamina.com, ahmad.harahap@pertamina.com,
ramadoni.febriandina@pertamina.com

ABSTRACT

Background, aim, and scope in this study, are to evaluate the environmental impacts from the geothermal power plant system operation in the Lahendong geothermal field using life cycle analysis. Geothermal Energy is one of the largest energy sources in Indonesia compare to other renewable sources. Life cycle inventory of geothermal power plant is constructed based on inflows and outflows from every operational process. All data from life cycle inventory are then gone through classification, characterization, normalization, and weighting to generate a life cycle impact assessment. This study is a useful reference for environmental impact hotspot identification and as a comparison of environmental impacts with another method of electricity generation. Its analysis concludes that geothermal power plant mostly contributes to Climate change 48,78 % of total environmental impact.

Keywords: Geothermal, Energy, Power plant, LCA, Steam, Brine, Lahendong

INTRODUCTION

This paper presents a life cycle analysis (LCA) of geothermal power plant system operation in the Lahendong geothermal field. LCA is a novel method to thoroughly accounts for pollution, waste, and resources related to delivering a specific product or service. LCA identifies environmental hotspots and enables comparison with another way of electricity generation (Solli et al. 2009). LCA defines a "cradle-to-grave" approach to assessing industrial systems. "Cradle-to-grave" starts with the collection of raw materials from the primary sources to create a product and ends at the point when all materials are returned to the earth. There is also another series in between that system, which introduced as “Gate-to-gate” approach. “Gate-to-gate” is a continuous process of raw material that has been transformed from semi-finished materials to other semi-finished materials before it becomes to be the final products.

LCA calculates an estimation of cumulative environmental impacts resulting from all stages in the product life cycle as well as to identify the most significant impact on the environment (Bacon in Putri, et al., 2014). After finding out the critical-environmental impacts of all activities, it will provide several alternatives for improvement at each stage of the supply chain. These improvements are proposed to utilize as a basis to formulate baseline for existing life cycle level so that supply chains obtained forwards are by the green supply chain management concept (Putri, et al., 2014).

Geothermal Energy

In terms of renewable energy in the 21st century, Energy production from biomass, solar, wind energy, hydropower, and geothermal becomes the main concern to foster sustainable development and protect the environment. Thus, the pressure is growing around the globe to speed up its utilization. Whereas geothermal energy has received the least attention and this may have to do with the fact that geothermal energy is available and abundance on specific locations around the globe, mostly near tectonic plate boundaries.

Geothermal is derived from the Greek word; geo means earth and thermal means heat, and it can be interpreted as a geothermal heat or energy produced from the earth. The energy contained in the geothermal fluid is the water of which can be in the vapor phase, liquid, or both as a mixture. The fluid is usually located at a more than 1km depth below the earth's surface. (Nasruddin, Alhamid, et al., 2016).

Geothermal energy is located at a location traversed by a Ring of Fire which spreads in the United States, Canada, Italy, Japan, Indonesia, the Philippines, New Zealand, and some other countries. Heat is generated and stored in the mantle and core of the earth, and deep faults let water to flow to these heat sources, and the rising hot water creates a geothermal reservoir which can reach temperatures of 350 °C or higher and this energy moves to the earth’s surface by conduction and convection. Geothermal energy occurs due to three essential elements in a specific location within the earth: the source of heat, water, and permeable layer (Dickson, Fanell, et al., 2013).

Indonesia is one of the countries that have the chance to implement this promising energy. It has the volcanoes that spread on the island of Sumatra, Jawa, Nusa Tenggara, Maluku, and Sulawesi, where there are 117 active volcanoes. As a result,

Indonesia consists of 256 potential areas of geothermal energy. It draws the fact that Indonesia has the enormous potential of geothermal energy globally, which covers about 40% of the world's potential or at 28,617 MW. The geothermal energy system in this country is generally by a hydrothermal system that having a high temperature that over 225 °C and only a few of hydrothermal systems have a lower temperature about 150–225 °C. The country's geothermal potential and installed capacity status are presented in Table 1 (EBTKE, 2014). Although the sizeable geothermal potential in Indonesia, up to today, the utilization is still not optimal, especially for power generation purposes (Ilyas Z, 2012).

Table 1: Geothermal energy potential in Indonesia.

Island	Potential Energy (MW)			Installed Capacity
	Resources	Reserve	Total	
Sumatera	5516	7244	12760	122
Jawa	3536	6181	9717	1134
Bali, NT	777	1028	1805	7,5
Sulawesi	1442	1602	3044	80
Maluku	642	429	1071	-
Kalimantan	145	-	145	-
Papua	75	-	75	-
Total			28617	1343,5

According to the reservoir fluid temperatures, the geothermal reservoir has been classified as low, medium, and high enthalpy resources. This classification aims to predict its capacity, physical and chemical characteristics, and as a reference to initiate the geothermal power plant design and construction.

Life Cycle Geothermal Energy

The product of this life cycle is to generate electrical current from geothermal energy. The heat deposit in geothermal reservoir appears to the surface in the form of steam and brine and generates to be high voltage electricity. This stage known as "cradle-to-gate" where the electricity is still could be used and transformed into another form in obtaining its final products, e.g., powering the household equipment for lighting, cleaning, etc.

The "cradle-to-grave" process encounters several steps. It starts from the reservoir fluid--at specified temperature and pressure—that flow to the surface. This fluid commonly consists of 2 phase of liquids: steam and brine. Both are flown through the pipeline, separated and purified in a few pressure vessel, and entered the steam turbine to generate electricity.

That process is considered to secure the superheated state of dried steam and ensure the lowest possible NCG and other particles carried before entering the main turbine.

Moreover, the steam that leaves the main turbine will be condensed and goes through a cooling tower to reach ambient temperature and further turned as condensate. Condensate, along with hot brine, will run to the cooling pond, preparing for reinjection, back to geothermal reservoir. This condition circulates under the earth in a certain period until it rises again to the surface.

At the same time, the steam-powered turbine rotates at an adjustable flow rate to produce an electrical current that generating from a coupled generator. Amount of this product to a greater extent will deliver to PLN, and the rest will use for internal equipment.

METHODOLOGY

LCA phase following ISO 14040 is shown in Figure 1 (Marriot, 2007 in Santoso, 2012):

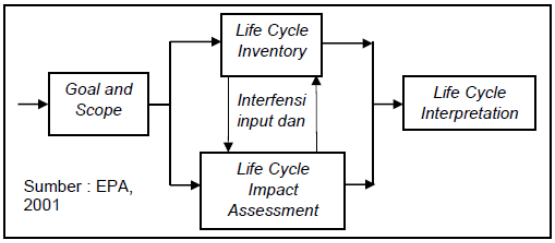


Figure 1: LCA methodology ISO 14040.

Goal and Scope aim to formulate and define objectives of systems that limit by its boundaries, and assumptions related to impacts environmentally throughout the life cycle of the system, as well as the selection of methods in implementing LCA. Data is collecting and exercising through Software OpenLCA 1.8.0.

Life Cycle Inventory (LCI) is conducted by identifying all process involved in the geothermal power plant system, possible impacts, qualitative input and output, emission and waste produced, etc. Analysis method could be used through several methods, as follows (Table 2):

Table 2: LCA methods.

No	Method	Note
1	EPD 2013	The method is used to declare an environmentally friendly product
2	EPS 2000	The method is used to develop an internal company's product. Model and data of product are created from "aimed utilization" point of view
3	Impact 2002+	The method is to assess the impact by implementing

		the midpoint/damage approach that connects to all life cycle inventory.
4	ReCiPe	The method that integrates the problem-oriented and damage-oriented approach.
5	ILCD 2011 Midpoint+	Correction method application
6	Building for Environmental and Economic Sustainability (BEES)	The method that integrates partial life cycle assessment and life cycle cost for construction material and tools. It helps to select a product that has the environment and economic balance.
7	IPCC 2013	The method based on the climate change factor in 20 and 100 years period of time.

LCI includes data collection and calculation of input and output to the environment of the system being evaluated. This phase is an inventory of resource use, energy use, and release to the environment related to the system being assessed.

Life Cycle Impact Assessment (LCIA) is the handling of impacts on the environment; all use impacts of resources and emissions produced are grouped and quantified into a certain number of impact categories which are then weighted according to their level of importance. The stages in LCIA itself consist of Characterization, Normalization, Weighting, and Single score that have an explanation, namely (Sitepu, 2011):

- Characterization is the stage where the overall input and output will be assessed for its contribution by the impact categories specified in the previous step. The results of this stage are a profile of the environmental impact of the system being observed.
- Normalization is a stage where the overall impact that has been assessed and will be compared and simplified is made based on the same size. The purpose of a valuation is to get an equal comparison value for each impact category so that it facilitates further interpretation.
- Weighting is a method that allows the weighting stage in the impact categories. It means that the result of the impact category indicator will be multiplied by the weighting factor, and will be accumulated as the total score.
- The single score shows each production process that has an impact on the environment.

Interpretation is an integration of the results of life-cycle inventory and life-cycle impact assessment, which is then used to review, draw conclusions and recommendations that are consistent with the objectives and scope that have been formulated.

SYSTEM DESCRIPTION

This study evaluates the environmental impacts of the geothermal power plant system operation in the Lahendong geothermal field. This field consists of 6 units of generating unit and capacity of 20 MW, each of which has 120 MW of total capacity. These generating units are located across Tomohon city and Minahasa Regency, North Sulawesi with each having a closed fluid collection and reinjection system (FCRS). For the sake of simplicity, we only evaluate unit 5 & 6 generating unit and fluid collection and reinjection system supporting this unit as PT Pertamina Geothermal Energy Area Lahendong owns these facilities. Figure 2 shows the Lahendong geothermal power plant.



Figure 2: Geothermal power plant in Lahendong geothermal field.

Geothermal energy is a renewable resource. One of its most significant advantages is that it is continuously available. The constant flow of heat from the Earth ensures an inexhaustible and virtually limitless supply of energy for billions of years to come (Geothermal 101: Basics of geothermal energy, 2014). According to Nenny Saptadji in Sekilas tentang Panas Bumi, the type of hydrothermal geothermal system is formed as a result of heat transfer from a heat source to its surroundings which occurs by conduction and by convection. Conduction heat transfer occurs through rocks, while convection heat transfer occurs because of contact between water and a heat source. Convection heat transfer occurs due to buoyancy. The illustration of geothermal power plant systems is shown in Figure 3, While Figure 4 shows the illustration of power plant facilities. Water because gravitational forces always tend to move down, but if the water is in contact with a heat source, heat transfer will occur so that the water temperature becomes higher and the water becomes lighter. This situation causes hotter water to move upward, and colder water moves downward, resulting in water circulation or convection currents.

Usage of Geothermal energy as electricity process begins from heated 2 phase fluid (steam and brine)

from production wells that coming from the geothermal reservoir. Then, this 2 phases fluid is separated using a separator vessel to separate steam and brine content. And then this brine is reinjected through a reinjection well go back to the geothermal reservoir while the wet steam through Scrubber (another vessel like separator) to increase the steam dryness before it goes through to the steam turbine for the electricity generation process. Dry steam kinetic power (heat and pressure) is used to rotate the turbine blade that connected to an electric generator that goes through an electrical induction process to generate electricity. The electricity produced is then transferred to the electrical grid while a small portion is used for household power used. Steam after the turbine is changed to condensate by cooling process and reinjected through reinjection pipeline and mixed with brine (after separator vessel) to the reinjection well. However, Electricity generation process from a geothermal power plant produces environmental green energy but still produced emission along the way. The emission quality standards from geothermal energy process are ruled in Minister of Environmental Republic of Indonesia Regulation No.21/2008, which is NH3 is 0,5 mg/Nm3, and H2S is 35 mg/Nm3 and emission of PT. Pertamina Geothermal Energy Area Lahendong that is produced is bellow than the quality standard.

CALCULATION

The life cycle data inventory of Unit 5 & 6 geothermal power plant system operation is presented in appendix. This data contains 15 processes, 26 products, and seven elementary flows that encompass emissions and resource consumption that are associated with a product's life cycle in term of environmental burdens, human health, and resources. From this life cycle data inventory, we then construct a life cycle model of Unit 5 & 6 geothermal power plant system operation. We construct a life cycle model in openLCA 1.8.0 software as portrayed by Figure 5.

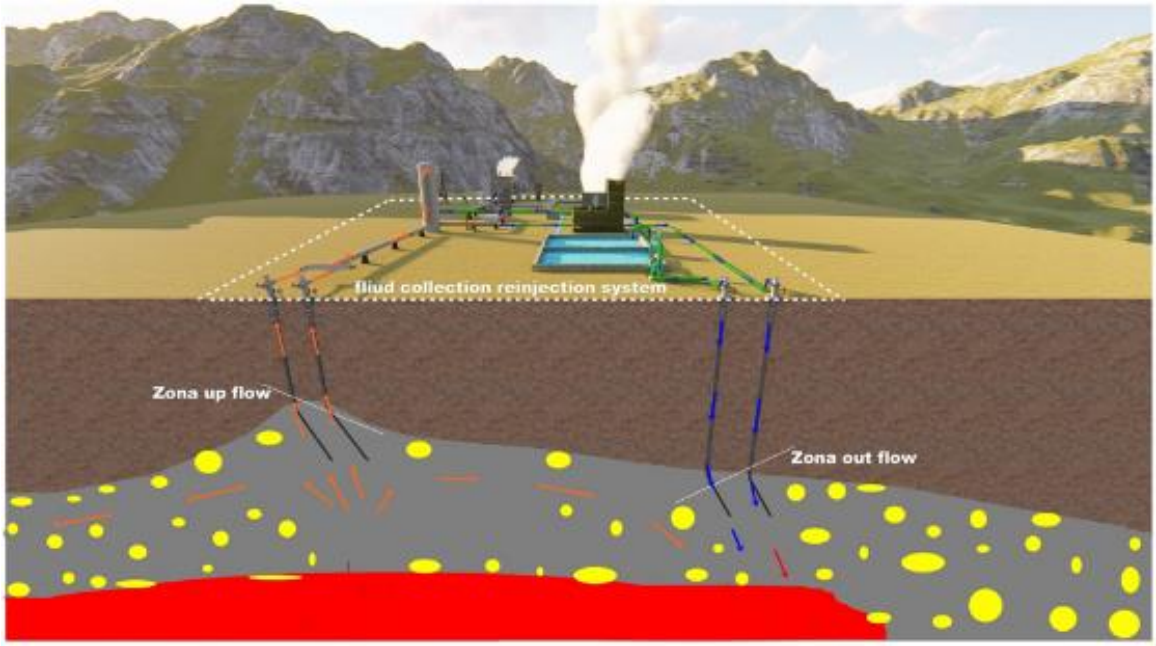


Figure 3: Illustration of geothermal power plant system.

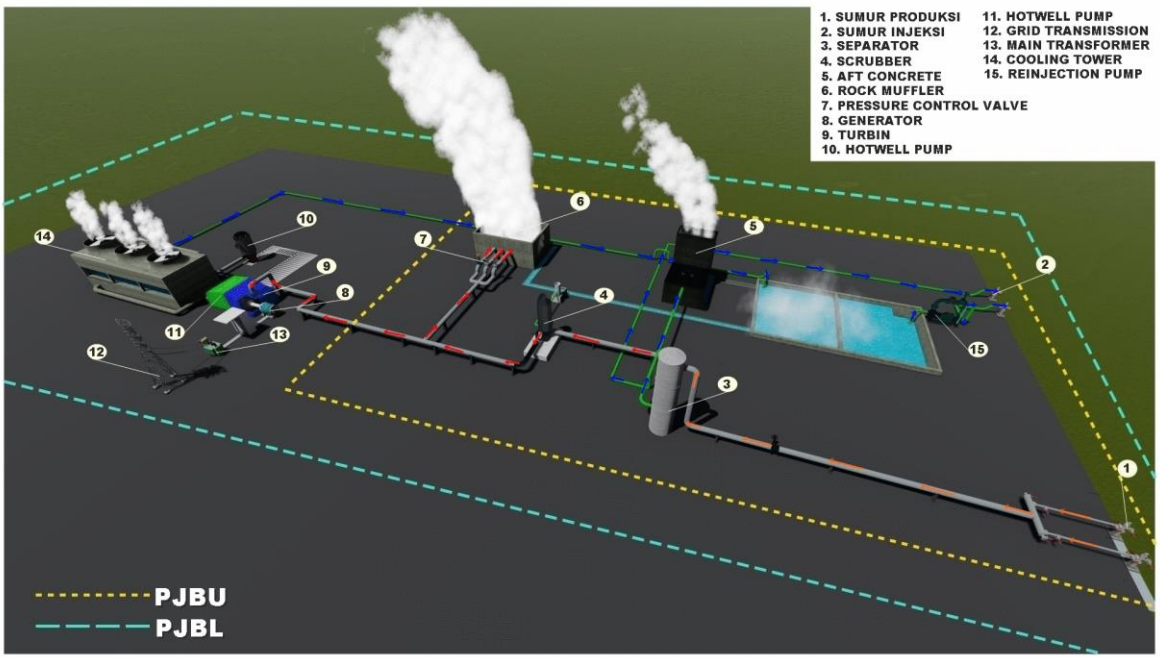


Figure 4: Illustration of geothermal power plant facilities.

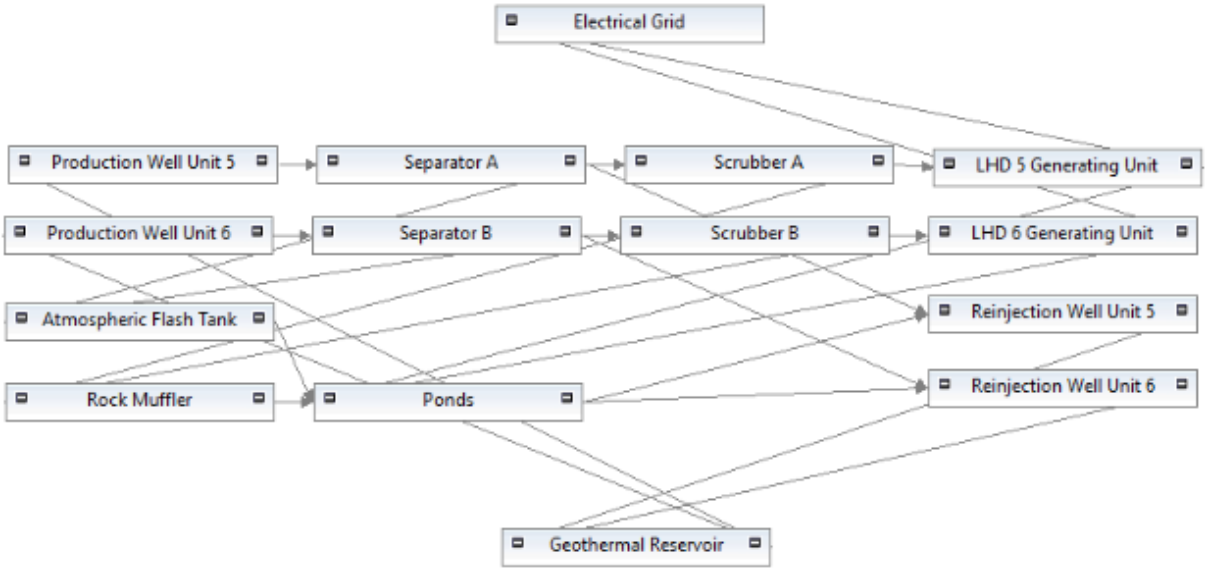


Figure 5: Life cycle model of geothermal power plant.

After all the processes and flows are connected, we then run the environmental impact calculation in openLCA 1.8.0 software using ReCiPe 2008 midpoint impact assessment method to translate emissions and resource extractions into a limited number of environmental impact scores using characterization factors. Using this ReCipE 2008 midpoint impact assessment method, we calculate 18 impact categories of environmental impact assessment to this life cycle model. All list of 18 impact categories is shown in Table 3. To gel equal comparison from all impact categories, we then use the World ReCiPe (person/year) normalization method.

Characterization results from this life cycle model calculation are shown in Table 4. from this result climate change is the biggest weight releases from unit 5 & 6 geothermal power plant system operation in the Lahendong area 4.458.109,73 kg CO2 eq of all weight releases. Followed by terrestrial acidification 16719,01 kg SO2 eq and particulate matter formation 2.183,70 kg PM10 eq.

Normalization results from this life cycle model calculation are shown in Table 5. from this result climate change is the biggest environmental impact by weight from unit 5 & 6 geothermal power plant system operation in the Lahendong area (48,78%) of all environmental impacts. Followed by terrestrial acidification (33,01%) and particulate matter formation (11,71%).

CONCLUSIONS

PT. Pertamina Geothermal Energy Area Lahendong fully owns 2 units of geothermal power plant, which is unit 5 & 6 geothermal power plant. In 2018 unit 5 produces 154.224.870 GWh and unit 6 produces 161.415.220 GWh of electricity. Life cycle model shows that geothermal reservoir is the source of energy to geothermal electricity generation through geothermal fluid. According to Life cycle analysis of geothermal power plant operation system, we can conclude that geothermal operation system contribution to climate change, terrestrial acidification, particulate matter formation, marine eutrophication, photochemical oxidant formation, with climate change as the most significant contributor with 48,78% of total environmental impact.

Table 3: List of impact catergories

Impact category	Reference unit
Agricultural land occupation	m2*a
Climate Change	kg CO2 eq
Fossil depletion	kg oil eq
Freshwater ecotoxicity	kg 1,4-DB eq
Freshwater eutrophication	kg P eq
Human toxicity	kg 1,4-DB eq
Ionising radiation	kg U235 eq
Marine ecotoxicity	kg 1,4-DB eq
Marine eutrophication	kg N eq
Metal depletion	kg Fe eq
Natural land transformation	m2
Ozone depletion	kg CFC-11 eq
Particulate matter formation	kg PM10 eq
Photochemical oxidant formation	kg NMVOC
Terrestrial acidification	kg SO2 eq
Terrestrial ecotoxicity	kg 1,4-DB eq
Urban land occupation	m2*a
Water depletion	m3

Table 4: Result of characterization.

Impact category	Result
Climate Change (kg CO2 eq)	4.458.109,73
Terrestrial acidification (kg SO2 eq)	16.719,01
Particulate matter formation (kg PM10 eq)	2.183,71
Marine eutrophication (kg N eq)	627,82
Photochemical oxidant formation (kg NMVOC)	36,89

Table 5: Result of normalization.

Impact category	Normalization Score	% Overall
Climate Change	646,94	48,78%
Terrestrial acidification	437,82	33,01%
Particulate matter formation	155,33	11,71%
Marine eutrophication	85,54	6,45%
Photochemical oxidant formation	0,65	0,05%

REFERENCES

Dickson MH, Fanelli M., (2013), "Geothermal energy: utilization and technology," Routledge.

Geothermal energy association., (2014), "Geothermal 101: Basics of geothermal energy", 5.

Ilyas Z., (2012), "Pemanfaatan energy geothermal dan dampak perubahan iklim", Seminar Nasional VIII SDM Teknologi Nuklir.

Indonesia DEBTKE, KEDSDM-R, (2014), "Pengembangan panas bumi di Indonesia", Direktorat Energy Baru Terbarukan Dan Konservasi Energi – Kementerian Energi dan Sumber daya Mineral – Republik Indonesia.

Nasruddin, Alhamid I. M., Daud Y., Surachman A., Sugiyono A., Aditya H.B., Mahlia, (2016), "Potential of geothermal energy for electricity generation in Indonesia: A review," Renewable and Sustainable Energy Reviews, 53, 733-740.

Putri et al., (2014), " Evaluasi dampak Lingkungan pada aktivitas Supply Chain Produk Susu KUD Batu dengan Implementasi Life Cycle Assessment (LCA) dan Pendekatan Analytical Network Process (ANP)" Universitas Brawijaya Malang.

Santoso, Haryo, Ronald, (2012), "Rekayasa Nilai dan Analisis daur hidup pada model alat potong kuku dengan limbah kayu di CV Piranti Works" Universitas Diponegoro Semarang.

Saptadji, Nenny., "Sekilas Tentang Panas Bumi", Institut Teknologi Bandung, 3.

Sari A.T, (2017), "Life Cycle Assessment (LCA) emisi pada proses produksi bahan bakar minyak (BBM) jenis solar dengan pendekatan metode Analytical Hierarchy Process (AHP)" Institut Teknik Surabaya.

Solli C, Reenass Marte, Stromman H. A, Hertwich G. E., (2009), "Life cycle assessment of wood-based heating in Norway," International Journal Life Cycle Assessment, 14, 517-528.

APPENDIX

Geothermal Reservoir

Input			Output		
Flow	Unit	Amount	Flow	Unit	Amount
Recharged water unit 5	ton	6.416.528,43	Geothermal 2 phase fluid to production well unit 5	ton	8.363.872,05
Recharged water unit 6	ton	6.229.932,37	Geothermal 2 phase fluid to production well unit 6	ton	8.191.153,55
Energy, Geothermal, Converted	GWh	2.104.267.266,67			
Fresh water	ton	3.908.564,80			

Production Well Unit 5

Input			Output		
Flow	Unit	Amount	Flow	Unit	Amount
Geothermal 2 phase fluid to production well unit 5	ton	8.363.872,05	Geothermal 2 phase fluid to separator A	ton	8.363.872,05

Production Well Unit 6

Input			Output		
Flow	Unit	Amount	Flow	Unit	Amount
Geothermal 2 phase fluid to production well unit 6	ton	8.191.153,55	Geothermal 2 phase fluid to separator B	ton	8.191.153,55

Separator A

Input			Output		
Flow	Unit	Amount	Flow	Unit	Amount
Geothermal 2 phase fluid to separator A	ton	8.363.872,05	Steam to Scrubber A	ton	1.197.681,97
			Brine to AFT (A)	ton	1.081.769,10
			Brine to reinjection well unit 5	ton	6.084.420,98

Separator B

Input			Output		
Flow	Unit	Amount	Flow	Unit	Amount
Geothermal 2 phase fluid to separator B	ton	8.191.153,55	Steam to Scrubber B	ton	1.211.559,53
			Brine to AFT (B)	ton	1.081.769,10
			Brine to reinjection well unit 6	ton	5.897.824,92

Scrubber A

Input			Output		
Flow	Unit	Amount	Flow	Unit	Amount
Steam to Scrubber A	ton	1.197.681,97	Steam to generating unit 5	ton	1.052.623,01
			Steam to rock muffler (A)	ton	145.058,96

Scrubber B

Input			Output		
Flow	Unit	Amount	Flow	Unit	Amount
Steam to Scrubber B	ton	1.211.559,53	Steam to generating unit 6	ton	1.129.195,12
			Steam to rock muffler (B)	ton	82.364,41

Atmospheric Flash Tank

Input			Output		
Flow	Unit	Amount	Flow	Unit	Amount
Brine to AFT (A)	ton	1.081.769,10	Water vapor	ton	1.839.007,47
Brine to AFT (B)	ton	1.081.769,10	Brine to pond	ton	324.530,73

Rock Muffler

Input			Output		
Flow	Unit	Amount	Flow	Unit	Amount
Steam to rock muffler (A)	ton	145.058,96	Water vapor	ton	274.761,07
Steam to rock muffler (B)	ton	145.058,96	CO2	ton	846,29
		290.118	H2S	ton	47,43
			NH3	ton	1,32
			CH4	ton	0,70
			Condensate rock muffler	ton	14.461,11

LHD 5 Generating unit

Input			Output		
Flow	Unit	Amount	Flow	Unit	Amount
Steam to generating unit 5	ton	1.052.623,01	Water vapor	ton	756.157,93
			CO2	ton	3.283,91
			H2S	ton	199,51
			NH3	ton	5,18
			CH4	ton	2,60
			Condensate unit 5	ton	158.860,38
			High voltage electricity unit 5	GWh	154.224.870,00

LHD 6 Generating unit

Input			Output		
Flow	Unit	Amount	Flow	Unit	Amount
Steam to generating unit 6	ton	1.129.195,12	Water vapor	ton	818.763,65
			CO2	ton	3.065,03
			H2S	ton	155,16
			NH3	ton	4,74
			CH4	ton	2,69
			Condensate unit 6	ton	166.362,68
			High voltage electrivity unit 6	GWh	161.415.220,00

Ponds

Input			Output		
Flow	Unit	Amount	Flow	Unit	Amount
Brine to pond	ton	324.530,73	Ponds fluid to reinjection well unit 5	ton	332.107,45
Condensate unit 5	ton	158.860,38	Ponds fluid to reinjection well unit 6	ton	332.107,45
Condensate unit 6	ton	166.362,68			
Condensate rock muffler	ton	14.461,11			

Reinjection Well Unit 5

Input			Output		
Flow	Unit	Amount	Flow	Unit	Amount
Ponds fluid to reinjection well unit 5	ton	332.107,45	Recharged water unit 5	ton	6.416.528,43
Brine to reinjection well unit 5	ton	6.084.420,98			

Reinjection Well Unit 6

Input			Output		
Flow	Unit	Amount	Flow	Unit	Amount
Ponds fluid to reinjection well unit 6	ton	332.107,45	Recharged water unit 6	ton	6.229.932,37
Brine to reinjection well unit 6	ton	5.897.824,92			

Electrical Grid

Input			Output		
Flow	Unit	Amount	Flow	Unit	Amount
High voltage electricity unit 5	GWh	154.224.870,00	Electricity	GWh	315.640.090,00
High voltage electricity unit 6	GWh	161.415.220,00			

THE GEOTHERMAL CAPACITY-BUILDING INITIATIVES BY THE MINISTRY OF ENERGY AND MINERAL RESOURCES

Mukhamad Faeshol Umam[1], Husin Setia Nugraha[2], Ahmad Fathoni[2]

[1]Human Resource Development Agency of MEMR
[2]Directorate General of New, Renewable Energy, and Energy Conservation of MEMR
Jl. Gatot Subroto Kav. 49 Jakarta
Email: mukhamad.umam@esdm.go.id

ABSTRACT

Indonesia targets 23% of renewable energy in the energy mix in 2025. This target includes around 5% energy generated from geothermal or around 7200MW installed capacity. The Indonesian government, through the Ministry of Energy and Mineral Resources (MEMR), oversees this target by issuing regulations as a stimulus to support the achievement of the 2025's goal. The Ministry of Energy and Mineral Resources also conducts various capacity building programs for geothermal human resources through the Directorate General of New, Renewable Energy, and Energy Conservation (Dirjen EBTKE) and Human Resource Development Agency of MEMR (BPSDM ESDM).

This paper discusses the role of these two institutions in geothermal development, focusing on capacity building in recent years and proposes some improvement strategies. This paper will also present several cooperation programs from abroad to develop geothermal human resources in Indonesia. This paper will give special attention to geothermal drilling training and certification programs as an evaluation and input for continuous improvement.

Keywords: Capacity-building, geothermal

INTRODUCTION

The government of Indonesia (GoI) targets the portions of new and renewable energy in the national energy mix to reach 23 percent In 2025. This target is also written in National Energy Policy (KEN) and the General Plan for National Energy (RUEN). This goal is also the GoI's commitment to the Paris Agreement in 2015.

However, until the end of 2018, the total installed capacity of the Renewable Energy Generation is 12.39% with a geothermal generating capacity of 1,948.5 MW (MEMR, 2019). It is estimated that for seven years, geothermal power can add about 2% of the use of renewable energy in a national energy mix followed by a hydroelectric power plant and solar power plant.

A significant increase in human resources is needed to achieve the 2025's geothermal goal. EHE (2015) estimated that to meet the MEMR development plans, Indonesia requires 1,300 to 2,200 additional geothermal trained engineers and scientists by 2020, and a further 500 to 800 by 2025. There is also a need for around 260 central and regional government regulatory staff to be trained in appropriate areas of geothermal expertise, and further staffing resources in training institutions.

The MEMR is a ministry that has the duty and responsibility to regulate and supervise the geothermal industry so that it develops well. Furthermore, the development of geothermal human resources in addition to the task of the ministry of education through formal education is also supported by MEMR through Dirjen EBTKE and BPSDM.

SKILL REQUIREMENTS AT GEOTHERMAL DEVELOPMENT STAGES

Development of a geothermal project according to Gehringer & Loksha (2012) and Hervey et al. (2014) is divided into eight phases, namely preliminary survey, exploration, test drilling, project review and planning, field development, power plant construction, commissioning, and operation and monitoring. Each of these stages requires skilled and competent personnel to perform specific tasks. Campen, O'Sullivan, & Rai-IRENA (2015) identify the typical types of expertise needed for each step of the geothermal project as follows:

- Preliminary survey and exploration phases require geologists, geochemists, geophysicists, hydrologists, and engineers;
- Test drilling phase requires drilling engineers, crew and managers, geologists, reservoir engineers and modelers, heavy transport personnel, and construction personnel;
- Project review and planning, field development, power plant construction, and commissioning phases require drilling engineers, crew and managers, plant and prospect engineers and managers, reservoir engineers and modelers, heavy transport personnel, and construction personnel;
- Operation and monitoring phases require steam field and plant managers and engineers, operators and technicians, reservoir engineers and modelers, geologists, geochemists, geophysicists, and service and maintenance personnel.

In addition to the above roles, every stage of geothermal development also requires enabling personnel such as environmental, regulatory, and investment experts as well as general personnel covering social experts, lawyers, financial analysts, contracting personnel, coordinators, and project managers.

Preliminary survey

At this stage, the geologist is obligated to identify the geological setting, geothermal potential type, and assess the possible geothermal evidence to guide further activities. Surveillance data of existing geothermal areas is also needed to be collected by air imaging or remote sensing of satellites.

Moreover, hydrologists are tasked with identifying water resources and hot springs, while general personnel is required to analyze information from available literature such as any drilling data, petroleum or mineral exploration history, and informal data from residents as a useful background to understanding subsurface conditions.

Exploration

Once the results of the initial survey show satisfactory results and meet the legal requirements, the next stage of surface exploration can commence. Generally, the geoscientists (geologists, geochemists, and geophysicists) should be able to collect geoscientific data with practical surveying of the surface and sub-surface to minimize uncertainty. This activity is mainly related to the approximate main reservoir parameters such as temperature, depth, area, mineralized zone, and permeability to prove resources. They should also provide primary environmental data and assist monitoring throughout the life of the project by integrating all geoscience aspects related to geothermal systems to create conceptual models that guide exploration, drilling and further management of resources.

Test drilling

This stage is a significant step to confirm the existence, precise location, and reservoir potential by involving more engineers than scientists. Predictions about the productivity of the well are rarely accurate before drilling commences. Gehringer & Loksha (2012) and Hervey et al. (2014) estimate that about 10 to 30 percent of drilled production wells are producing remarkably low power or are very weak to harness. Although test drilling usually drills slim holes, the skill required in this stage is identical to drilling for production and drilling of reinjection wells. Figure 1 describes the companies and experts involved in the drilling operation of an oil well. Nonetheless, until recently this scheme is still being applied in geothermal drilling.

Ford (2004) describes the roles and functions of those who manage drilling operations as follows:

- The operating company or operator is the main company that manages drilling and production operations. Operators are tasked to prepare designs, work programs, transportation services, consumable goods, and support for drilling operations. Operators typically employ drilling contractors and service companies to drill a well.
- Drilling contractors are tasked to provide drilling rigs and personnel to drill wells, so they are also responsible for maintaining drill rigs and training personnel required to operate the rigs.
- The service company provides specific specialized skills or equipment such as logging and surveying during drilling so that it is also tasked to develop and maintain the equipment and hire staff as operators.

Furthermore, some of the key personnel involved in a drilling operation are as follows:

1. The company man is a representative of the operators who is placed on the rig to ensure drilling operations run as planned (schedule and budget), make decisions affecting well progress, and manage the availability of drilling equipment and materials (Ford, 2004).
2. The drilling engineer is responsible for designing wells and casing along with the cementing program, drilling rig selection and other drilling support equipment.
3. Geologists are responsible for assisting and supervising drilling, geological logging, analyzing and interpreting drill cuttings and cores, helping to determine the productivity of wells, determining drilling and different depth, and estimating corrosion risk.
4. The rig manager is the highest representative of the rig contracting company whose job it is to ensure the rigs are provided according to the operator's requirements (as per the contract).
5. The tool pusher is responsible for overseeing the daily activities of all rig crews on the rig site, including equipment maintenance.
6. The driller is tasked to prepare drill series such as Bottom Hole Assembly (BHA) and BOP and communicate directly with crews.
7. Drilling crews are working under the direction of the driller and are tasked with performing manual activities related to well drilling which generally comprise of:
   a) Derrickman oversees helping driller running in hole or pull out BHA of the hole (trimming).
   b) Floorman or roughneck unplug the drill pipe circuit, install the sheath, install rig tong, operate spinner, and so forth.
   c) Supporting crews such as mechanics, electricians, tow carriers, roustabouts, and others.

8. The mud engineer is tasked to prepare drilling mud by the drilling program that has been approved.
9. The directional driller is the person responsible for directional drilling by the direction/target set in the drilling program.
10. Heavy transport and construction personnel are assigned for the transportation and construction of drilling rigs.
11. Reservoir engineers and modelers at this stage will update the models that have been made at the exploration stage using data from the geoscientist obtained from drilling.

Project review and planning

This stage usually only involves general staff for data evaluation from the previous stage of the preliminary survey, exploration, and test drilling. They will then conduct a feasibility study covering the financial aspect, risk analysis, construction, and drilling program to determine the amount of investment required for the most effective program. The reservoir modelers will process the data into a numerical reservoir model to estimate the possibility of production per production well.

Field development

This stage begins with the drilling of production wells and injection wells by drilling engineers and crew. This activity involves expertise as described in the test-drilling phase. At this stage, construction personnel builds pipelines to connect wells to a gathering system and a power plant. On the other hand, the reservoir engineer will calculate the exact production wells to produce optimal production. They should also select the location of the reinjection wells to restore the geothermal fluid to the reservoir and support the pressure on the reservoir but should prevent the cooling of the geothermal reservoir. Furthermore, the hydrologist will assist the reservoir engineer in mapping the underground flow pattern from the numerical reservoir analysis based on the conceptual and mathematical model of the reservoir made by the modeler of the reservoir.

Power plant construction

At this stage, plant engineers will plan and design the power plant according to the specifications of successful drilling results. The construction personnel is responsible for installing a steam collection system with one or more separators, turbines, generators, condensers and cooling systems either utilizing water or air. Pipe installation is also carried out for reinjection of the cooled geothermal fluid to the reservoir through reinjection wells. Moreover, civil works and infrastructure such as roads and well pad access are also built at this stage as well as the construction of transmission lines through substations.

Commissioning

This phase mainly involves general personnel, including lawyers, financial analysts, contracting staff, and project managers to solve many technical problems such as contracts with procurement, engineering, and construction contractors of power plants. Furthermore, the power plant engineer is tasked with adjusting the efficiency of the power plant and ensuring its operability satisfies its particular design conditions by testing all the components and related equipment (Gehringer and Loksha, 2012).

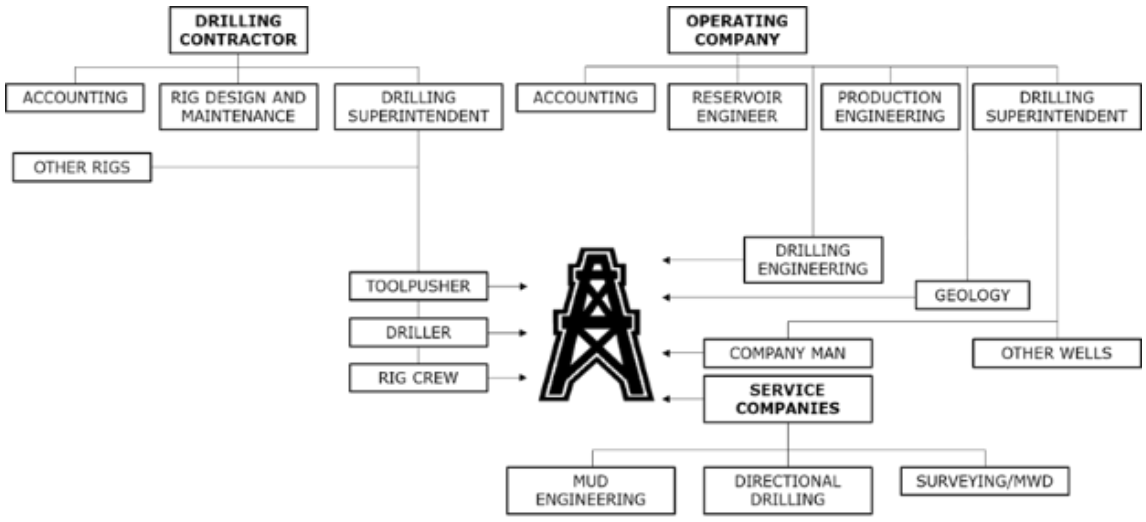


Figure 1: Personnel involved in drilling an oil well (adapted from Ford, 2004).

Operation and maintenance

Here is an outline of the duties of each staff member at this stage:

1. Operators or technicians are tasked with conducting steam operations in steam fields to ensure that a steam supply to the generator remains optimal and operates equipment at power plant installations.
2. Steam field engineers are tasked with designing and executing new production well drilling to increase or maintain production capacity, and drilling of new reinjection wells if necessary.
3. Service and maintenance personnel are tasked with performing routine maintenance to ensure optimum and safe factory performance, and prompt repairs to solve problems such as scaling, and casing failure due to corrosion or collapse.
4. Plant managers and engineers are tasked with improving plant efficiency and solving production or injection problems such as changes in injection strategies from studying reservoir modeling that is continuously updated by reservoir engineers and modelers according to operating conditions, geophysical observations and chemical analysis.
5. Supervisors of production operations are tasked with planning, controlling, supervising, evaluating, and handling the work when there is a problem in the care of the well.
6. Production operators are tasked with preparing activity units and conducting well maintenance, including killing a well.
7. The geoscientist is responsible for monitoring surface activity, potential contaminants (water and gas), down-hole surveys, production well testing and injection wells, geochemical analysis, and geophysical analysis including microseismic to determine the direction of fluid flow. The results of the data are used to establish the baseline data for subsequent monitoring of the geothermal system.

Geothermal development requires many staff and experts at every stage. Therefore, human resource development (HRD) is also an essential aspect in the successful development of geothermal drilling. This study will focus more on the drilling competencies since these are the most expensive and crucial stages of the development. The drilling engineers and crew are also the most prospective target for skill transfers from the oil and gas industries to geothermal business, due to the frequent exchange and sharing of technologies between them.

REGULATION ON GEOTHERMAL HUMAN RESOURCE DEVELOPMENT

President decree No 22 the Year 2017

Indonesia national energy policy is described in the Presidential Regulation of the Republic of Indonesia Number 22 the Year 2017 About the General Plan of National Energy (RUEN). The National Energy Board (DEN) as the drafter of RUEN performs a series of modeling as a reference in energy development in Indonesia until 2050. The result of the modeling of primary energy supply shows that geothermal contribution to new Renewable Energy (EBT) supply is 21.8 MTOE or 23.6% in 2025 and 58.8 MTOE or 18.6% by 2050. While the modeling results of the development of EBT power plants show geothermal generating 7,241.5 MW in 2025 and 17,546 MW in 2050 or 59% of the geothermal potential of 29.5 GW.

However, this RUEN does not specify as much about the development of human resources as a step to achieve the target of geothermal power plant development (PLTP). Strategic actions for the development of PLTP according to RUEN include improving the quality and quantity of potential resources and geothermal resource surveys, preliminary survey and exploration assignments by government agencies or business entities and assignments of State-Owned Enterprises (BUMN) or Public Service Bodies (BLU) to develop PLTP.

2015-2019 MEMR strategic plan

Based on the 2015-2019 MEMR strategic plan stipulated through the Minister of Energy and Mineral Resources Decree No. 13 of 2015, the strategic targets and indicators of MEMR performance in 2015-2019 in terms of EBT development is to increase the installed capacity of EBT power plants to 16,996 MW by 2019 with the target installed capacity of Geothermal Energy being 3195 MW.

On the other hand, the quality of human resources targets includes:

1. Organizing competency-based education and training with the aim of 65% of the total training conducted in 2019.
2. Increased certification of Energy and Mineral Resource personnel
3. Competency enhancement and teaching staff certification
4. Acceleration of the process to implement professional training institutions accreditation by the MEMR Education and Training Agency
5. Increased cooperation with Local government agencies, the private sector, KKS and Stakeholders
6. Optimizing and improving the quality of education and training facilities

7. Acceleration of the Indonesian national competency work standard (SKKNI) in the Energy and Mineral Resource sector
8. Accelerating the preparation of the Polytechnic of Akamigas infrastructure.
9. Organizing activities to improve community competency to fill the opportunities for skilled labor markets at home and abroad by utilizing CSR funds to encourage the acceleration of the supply of prevocational energy in the Energy and Mineral Resource sector

CAPACITY BUILDING PROGRAM BY THE MEMR

Directorate General of New, Renewable Energy, and Energy Conservation

The Geothermal Directorate has designed a master plan for developing human resources in the geothermal sector which can be divided into 3 (three) stages, namely increasing geothermal awareness among campuses, linking & matching steps between research and industry, and building human resource competence.

The stage of increasing geothermal awareness among campuses is an introduction of geothermal activities to colleges. This activity has been started since 2012 through Program Geothermal Going to Campus (GGtC). These activities have been carried out on several universities with the subjects including the linking & matching stage is an effort to bridge industrial and school needs through the application of SKKNI in the world of education and optimization of research and development through cooperation between universities, government, and industry.

Seventeen universities already have involved in the program namely ITS, USU, Trisakti University, UNILA, UNDIP, UNSRI, UNAND, University of Mataram, Institute Technology of Medan, UNSRAT, UPN, UNSYAH, UNSOED, University of Jambi, Nusa Cendana University, UNPAD, and UNHAS.

In the universities have been conducting two activities, the general 649tadium and project case study. The general 649tadium, so-called “Kelas Umum”, is to give general understanding about geothermal in several subjects to the lecturers and students. Whereas, the project case, so-called Kelas Khusus is a days simulation as practitioners, how to evaluate one of the stages to develop geothermal potential. The simulation was starting from subsurface analysis up to project financial analysis. Until 2010, the activities were a building of human resource competence stage. One of the activities is the implementation phase of the SKKNI. The application of research and development is divided into two focuses, namely the development of the core competency focus of the geothermal sector and the focus of competency in supporting the geothermal industry.

As parts of the GGtC program, Directorate of Geothermal, funded by the World Bank grant, will hold a certification for the geothermal geologist in expert level. The certification will involve five universities within the program. Up to now, there are 3 (three) SKKNI. The SKKNI's are for the geothermal geologist, geothermal geochemist and geothermal geophysicist.

Besides SKKNI, in geothermal, there are three Special Competence Standard (Standard Kompetensi Khusus), namely Pengawas Operasional Pertama (POP), Pengawas Operasional Madya (POM), and Pengawas Operasional Utama (POU). There are 1548 experts in total have been certified, 1230 in POP level, 233 in POM level, and 85 in POU level.

Human Resource Development Agency

Supervisor training at PPSDM KEBTKE

The Center for Human Resource Development of Electricity, New, Renewable, and Energy Conservation (PPSDM KEBTKE) is the only training center under the ministry responsible for geothermal fields as part of renewable energy sources. However, due to the vast area of responsibility for this center, training is more devoted to downstream industries or electricity generation. Even though the center provides training for industries and government, geothermal-related training that is conducted mainly for government officials includes technical training for geothermal working area, technical training introduction of a geothermal working budget and expenditure plan, and specialized training of HSE geothermal inspection.

In 2018, the center had organized three geothermal power plant supervision training (POP and POM) and planned to hold a similar training program again this year.

PPSDM KEBTKE has also hosted a New Zealand Support for Training in the Indonesia Geothermal Sector (NZSTIGS) program that has signed on September 5, 2018 by GoI and New Zealand to develop and provide practical training for geothermal technicians and operators for the next five years. The program is called Trains the Trainers (TTT) Mastery Level which was held from October 15, 2018, for four weeks with instructors from the Waikato Institute of Technology (WINTEC) of New Zealand.
The NZSTIGS TTT program has the purpose of building the teaching skills and skills of trainers in

the Indonesian geothermal industry and the education sector to ensure better learning outcomes. These programs will develop the skills of Instructors from MEMR and geothermal companies in Indonesia with pedagogical knowledge to provide ongoing support and effective training.

Exploration training PPSDM Geominerba

The Center for Human Resource Development of Geology, Minerals, and Coal (PPSDM Geominerba) is a merger of geology and mineral training centers in the framework of bureaucratic efficiency. This geological field covers all types of mining, including geothermal. This center has organized training on inventory, auction of geothermal, and exploration work areas in recent years.

Drilling training PPSDM Migas

The center of human resources development for oil and gas (PPSDM Migas) has been in operation for more than half a century under a different name. Currently, PPSDM employs approximately 280 employees, including 59 professional trainers and 70 laboratory staff.

The center offers various training programs which include long term apprentice programs, short courses, basic to advanced levels of training, and in-house training, even though it currently relies more on short-term training programs.

For drilling training, the center delivers around 30 training and drilling certification per year for floorman, derrickmen, drillers, and toolpushers. The training generally covers upstream oil and gas activities, well control techniques, BOP equipment, engineering and drill tools, and safety of drilling. Figure 2 shows the number of trainees in PPSDM Migas since 2010.

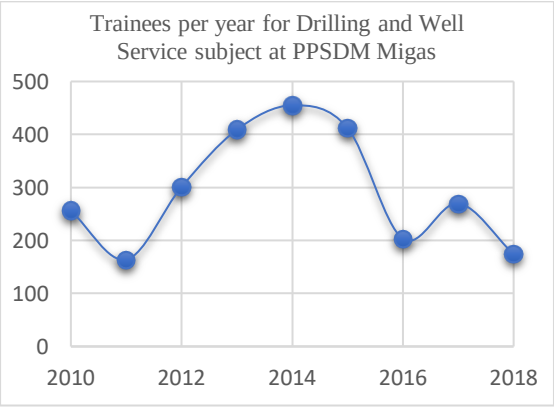


Figure 2: Number of trainees in PPSDM Migas since 2010 (PPSDM Migas, 2018).

PPSDM Migas is accredited by the International Association of Drilling Contractors (IADC) the USA and a member of the IWCF UK. The center is also certified by the National Accreditation Committee (KAN), which is a member of the International Accreditation Forum (IAF).

In addition to regular drilling training for oil and gas and geothermal industries, the center has also undertaken training for a managerial level, which included drilling engineers and supervisors of Geothermal Well Drilling that was delivered in 2017. The training was a pilot course funded through the New Zealand Aid Programme by the Ministry of Foreign Affairs and Trade (MFAT) in cooperation with BPSDM. The aim of the training was to support Indonesia's geothermal sector by increasing the number of geothermal well drilling specialists as well as upgrading their competency.

The center also has its own professional certification body, namely LSP PPT Migas. The LSP began certifying from 1999 with accreditation from the National Accreditation Committee (KAN-BSP) and the National Personal Accreditation Committee (BNSP).

The scope of the certification in PPSDM Migas includes HSE, seismicity, drilling, production, and aviation. Most workers in the oil and gas industry in Indonesia indeed have been certified in PPSDM Migas. The certificate commonly has a valid period of three years and should be renewed by taking a new assessment. Figure 3 shows the certification takers at PPSDM Migas from 2012 to 2018.

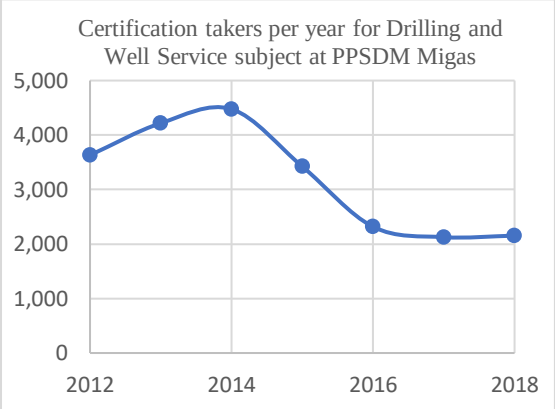


Figure 3: Certification takers at PPSDM Migas from 2012 to 2018 (PPSDM Migas, 2018).

The competency standards for drilling in Indonesia can be implemented for both geothermal, oil and gas industry (Umam et al., 2018). For drilling, certification is available for a floorman (level 2), a derrickman (level 3), a driller (level 4), and supervisor (level 5) which includes a toolpusher, rig superintendent, company man, and rig manager. The requirements for following (level 2-4) certification are a secondary education certificate and two years' experience at a lower level. To be able to take a driller certification, for example, a derrickman requires at least two years' experience as evidenced

by a warrant from the company, while to earn a derrickman certification, two years' experience as a floorman is needed.

This center, in collaboration with a geothermal company, had implemented Operation Maintenance Training with a duration of two and a half months last year. The training was attended by 23 students who were the prospective operators of geothermal power plants in Sumatra, all of which were local residents. This education and training program was a pilot project and is expected to be followed by further education and training with improvements on facilities and trainers.

EDUCATION BY STAKEHOLDERS

Universities

There are five universities currently have a geothermal department or research center as follows:

Institute of Technology Bandung (ITB)

ITB offers a four-semester master's program from 2008 under the Faculty of Mining and Petroleum Technology. The program covers a wide area of geothermal energy exploration, exploitation, utilization, management, economics, and environment.

The university also offers short courses to support the development of geothermal drilling in Indonesia. This course started as early as 1994 when ITB was in collaboration with the Geothermal Institute, University of Auckland to develop and deliver "Geothermal Technology, Teaching the Teachers" (Saptadji, 2010). Currently, there are 3-15 day short courses that are available for the public, which is divided into the engineering and geoscience group.

University of Gadjah Mada (UGM)

UGM, in collaboration with the University of Auckland and GNS Science, has been running geothermal basic and advanced courses since 2010. The five days courses are mainly for the staff of geothermal companies with a focus on geothermal engineering and geoscience.

University of Indonesia (UI)

The UI offers a Master in Geothermal Energy Exploration under the Department of Physics. Unfortunately, currently, there is no training in geothermal development by UI. With the availability of experts and trainers, however, the UI can be utilized for geothermal training in the future.

Institute of Technology Surabaya (ITS)

A Master Program of Geothermal Engineering in the ITS has been offered in the Department of Geomatics Engineering, under the Faculty of Civil, Environmental and Mechanical Engineering from 2009. The institute is located in East Java, which is the province with a potential of around 1300 MW, but currently has no utilization. Hence, it is expected to help geothermal development in eastern Java Island.

University of Diponegoro (Undip)

The Undip has offered a Master of Energy program since 2014 although not specific in geothermal training. The university also has a center for geothermal research under the faculty of Science and Math. Like ITS, the university has an advantage because of its location in Central Java Province, which has about 1800 MW of geothermal potential, but only 60 MW is used (Dieng field). Thus, the university is expected to be utilized for future geothermal training.

Geothermal companies

Some geothermal operator companies have their training centers such as Pertamina and PLN. Within these training centers, prospective employees can be trained by the needs of the company. Unfortunately, since they are not for the public, these centers cannot be utilized for other companies.

International support

From its first commercial utilization, the geothermal industry in Indonesia has been assisted by international aid. The following is a summary of several international institutions that help Indonesia develop geothermal programs:

Netherlands (GEOCAP) geothermal capacity building program

The Geothermal Capacity Building Program Indonesia-Netherlands (GEOCAP) is an international collaboration between Indonesian and Dutch institutions to contribute a National Geothermal Capacity Building Programme (NGCBP). The goal of this program is to develop a close link between geothermal programs for education, training, and research such as universities, scientific institutions, and industrial partners. Further, this program also aims to support the Indonesian government to improve the utilization of geothermal resources by developing a database of subsurface layers.

Several organizations that involved in this program include the University of Twente, INAGA/API, TNO – Netherlands Organization for Applied Scientific Research, ITB, Delft Technical University (TUDelft), UI, UGM, Utrecht University, IF Technology, DNV-GL Energy, and Well Engineering Partners (WEP).

USAID

The Geothermal Education Capacity Building project funded by USAID was a university partnership between the University of Southern California (USC) and the ITB from 2012 to 2015. The program aimed to build the capacity of the geothermal education program at ITB with the support of PT Star Energy, which is an Indonesian geothermal company.

USAID has also been working with the Indonesian Geothermal Association (INAGA) from 2011 to 2014 to deliver a geothermal Human Resource program that covers a master's degree course, training of trainers, and an introductory geothermal program. There was also technician-level training for staff of various geothermal producers including Pertamina Geothermal Energy (PGE), Supreme Energy, Star Energy, and Chevron Geothermal.

New Zealand Ministry of Foreign Affairs and Trade (MFAT)

MFAT regularly gives technical assistance and capacity building to accelerate Indonesia's geothermal development. The aim of the aid is mainly to support the Government of Indonesia's geothermal energy human resources development strategy. Beside NZSTIGS program, MFAT through GNS Science regularly delivers short courses in collaboration with UGM. Further, MFAT has organized some targeted training, which includes geothermal well drilling.

In the higher education level, about 60 post-graduate and 36 short-term training scholarships are offered to Indonesians to study in New Zealand. The majority of the awards are for renewable energy include geothermal followed by agriculture, disaster risk management, public sector leadership, and private sector development.

CONCLUSION AND RECOMMENDATION

This paper is a review of competency needs in the geothermal industry, regulations related to the development of the geothermal human resource, capacity building programs by the MEMR, and support from stakeholders. It can be concluded that to meet geothermal human resource needs, both quality and quantity, all parties, both government, companies, and educational institutions, are needed. The government, through the Director General of EBTKE and the Human Resource Development Agency, has carried out various roles, including the preparation of SKKNI and training in the geothermal field.

However, many tasks must be done in the future, such as synergized policies with other stakeholders. This synergy problem can be seen as the mismatching between formal school graduates and the needs of the geothermal industry. Further, the capacity building program was sporadic, making the measurement of successfulness difficult.

Other stakeholders are also expected to be more proactive in developing geothermal human resources. In addition to increasing knowledge, it must be ensured that the skills acquired by competency development participants will be useful for the community. Beneficiaries are also expected to be more widespread so that the rejection of geothermal projects so far will decrease with the massively spread of information about geothermal energy.

REFERENCES

Campen, B. V., O'Sullivan, J., & Rai-IRENA, K. (2015). "Geothermal Capacity Needs Assessment Methodology (peer reviewed)". University of Auckland Geothermal Institute; IRENA.

East Harbour Energy [EHE] (2015). "Indonesia, Geothermal Energy Human Resource Development Programme – Strategy". A report for Government of Indonesia through the New Zealand Ministry of Foreign Affairs and Trade (MFAT).

Finger, J., & Blankenship, D. (2010). "Handbook of best practices for geothermal drilling". Sandia National Laboratories, Albuquerque.

Ford, J. (2004). "Drilling Engineering". Herriot-Watt University, Department of Petroleum Engineering. 540 pp

Gehringer, M., Loksha, V. (2012). "Geothermal handbook: planning and financing power generation". ESMAP technical report; no. 002/12. Washington, DC: World Bank. Retrieved from

https://www.esmap.org/sites/esmap.org/files/DocumentLibrary/FINAL_Geothermal%20Handbook_TR002-12_Reduced.pdf; http://documents.worldbank.org/curated/en/396091468330258187/Geothermal-handbook-planning-and-financing-power-generation

Hervey, Colin; Beardsmore, Graeme; Moeck, Inga; Ruter, Horst; Bauer, Stefan. (2014). "Best practices guide for geothermal exploration". Washington, D.C.: World Bank Group.

MEMR (2008). "Pemberlakuan Standar Kompetensi Kerja Nasional Indonesia di Bidang Kegiatan Usaha Minyak dan Gas Bumi Secara Wajib" [The enforcement of the Indonesian National Competency Standards in the Field of Oil and Natural Gas Business Activities]. Ministry of Energy and Mineral Resources.

MEMR (2015). “Rencana Strategis KESDM 2015-2019 [Strategic Plan of MEMR 2015-2019]”. Ministry of Energy and Mineral Resources.

MEMR (2017). “Pemerintah optimis capai target kapasitas terpasang panas bumi pada tahun 2017 [Press Release: The government is optimistic to achieve geothermal installed capacity target in 2017]”. Ministry of Energy and Mineral Resource.

MEMR (2019). “Laporan Kinerja Tahun 2018 [2018 Performance Report]”. Ministry of Energy and Mineral Resource.

PPSDM Migas (2017). “Proposal PPK BLU PPSDM Migas [Proposal of Financial Management System of PPSDM Migas Public Service Board]”. Pusat Pengembangan Sumber Daya Manusia Minyak dan Gas Bumi. Cepu, Jawa Tengah.

RUEN (2017). “Rencana Umum Energi Nasional”, An attachment of Presidential Decree Number 22/2017.

Saptadji, N. M. (2010). “Geothermal Education for supporting geothermal development in Indonesia”. In Proceedings World Geothermal Congress.

Umam, M. F., Purba, D., &Adityatama, D. W. (2019). “Drilling Professional Skills Transfer: Petroleum Industry Support to Geothermal Development in Indonesia”. Simposium IATMI 2018. Padang.

THE APPLICATION OF NUMERICAL SIMULATION RESULT FOR GEOTHERMAL FINANCIAL MODEL WITH PROBABILISTIC APPROACH: A COMPREHENSIVE STUDY

Nevi Cahya Winofa[1], Ade Lesmana[2], Heru Berian Pratama[2], Nenny Miryani Saptadji[2], Ali Ashat[3]

[1]Petroleum Engineering Study Program, Institut Teknologi Bandung, Indonesia.
[2]Geothermal Engineering Study Program, Institut Teknologi Bandung, Indonesia.
Jl. Ganesha No.10, Bandung, West Java, Indonesia.
[3]Department of Earth Resources Engineering, Faculty of Engineering,
Kyushu University., Fukuoka 819-0395, Japan.
Email: nevicahyawinofa@gmail.com

ABSTRACT

Feasibility of developing geothermal projects is depend on financial return generated from investment. One of the strategies to achieve optimum return is formulating the economics of geothermal projects in a financial model with a high level of confidence. Technical input parameters in the financial model are determined by the amount of available geothermal reserve in the form of a field development scenario. The best method for predicting geothermal reserve is a numerical simulation. The objective of this study is to determine the electricity tariff to generate 50 MW (stepwise), and 90 MW (stepwise) which meet the 50% of Rate of Return value will be equal or not exceed 16% (P50) for certain geothermal field with probabilistic approach. This study started with determining the technical input parameters: the number of productions; make-up; and injection wells from each development scenarios based on numerical simulation result that have been studied by another researcher. Total investment was calculated to generate 50 MW (stepwise), and 90 MW (stepwise), respectively. The result shows that 50% of the estimates will be equal or less than 4.86, and 4.81 Million USD/MW, respectively. The electricity tariff that meet the P50 of Rate of Return at 16% was also calculated, 14.80, and 15.50 cents/kWh, respectively. Then these tariffs were evaluated based on Average Cost of Electricity Generation (BPP) on relevant local grid. As a result, 50 MW (stepwise), and 90 MW (stepwise) scenario are feasible to be developed.

Keywords: Financial model, numerical model, Monte Carlo simulation

INTRODUCTION

Feasibility of developing a new geothermal power project depends on the financial return that would result from the investment (Quinivan et al., 2015). Financial model is developed to simulate the financial return of a geothermal project. One of the strategies to achieve optimum return is formulating the economics of geothermal projects in a financial model with a high level of confidence. Technical input parameters in the financial model are determined by the amount of available geothermal reserve in the form of a field development scenario. There are several methods in geothermal potential calculation which are volumetric, analytical and numerical (Ketilsson, 2007). Numerical simulation is the best method if there are detailed and comprehensive data. This method can be used to predict reservoir performance in the long period (Axelsson, 2016). The numerical simulation result is very suitable to be used as input parameters of the technical aspects to increase the level of confidence in the financial model. Investment feasibility analysis of numerical simulation result on the Kepahiang, Bengkulu geothermal field has been carried out by Pane (2015). However, the investment feasibility analysis still used a single flow calculation, simulating one fixed value for each parameter. However, in the real conditions of the field are very dynamic, having high risk and uncertainty. This weakness can be overcome by a probabilistic approach.

The probabilistic approach in investment feasibility analysis is very useful in investigating risks that arise in geothermal investment (Fatony et al., 2010). The probabilistic method is not something new in the financial model. Fatony et al. (2010) developed Monte Carlo Simulator to determine Internal Rate of Return (IRR) and cash flow of geothermal projects. Then Quinlivan et al. (2015) used a Monte Carlo simulator to make probabilistic distribution of electricity tariff that meet specific investment criteria (e.g. target of the Internal Rate of Return (IRR) or Net Present Value (NPV) target). However, both studies still did not use numerical simulation results as input parameters.

A geothermal financial model was applied to two different development scenarios, 50 MW (stepwise) and 90 MW (stepwise) in a certain field that have been studied by another researcher. The objectives of this study were first, to assess the amount of investment needed to generate 50 MWe (stepwise) and 90 MWe (stepwise). Second, to determine electricity tariff and economic indicators (e.g., Net Present Value, Profitability Index and Pay Out Time) that meet 50% of Rate of Return value will be

equal or less than 16%. Third, to evaluate the electricity prices based on Average Cost of Electricity Generation (BPP) on relevant local grid. Fourth, to determine sensitive financial parameters to Rate of Return. This model is the first geothermal financial model that uses numerical simulation results and applies a probabilistic approach.

DEVELOPMENT SCENARIO

The technical input parameters in the financial model are determined by the amount of available geothermal reserve in the form of a field development scenario. This study was applied to two different scenarios, 50 MW (stepwise), and 90 MW (stepwise) in Ulumbu Field which had been studied by Kurniawan (2018).

Ulumbu Field Overview

Ulumbu geothermal field is located in Wewo, Manggarai, East Nusa Tenggara, Indonesia. Figure 1 shows location of Ulumbu Field. The geothermal system of this field is the steam cap above the liquid-dominated reservoir with a temperature of 230-240^{0}C. Three wells were drilled in 1994-1996. ULB-01 and ULB-02 are planned as production wells and ULB-03 as injection wells (Nasution et al., 2016).

This field is managed by PT. PLN and has produced in two phases. The first phase began in December 2012 while the second phase started in September 2014. Both phases each produce electricity of 2x2.5 MW through the installation of wellhead generating units so that the total installed capacity in this field is 4x2.5 MW or 10 MW (Adiprana, 2018 in Kurniawan, 2018).

Ulumbu Field Development Scenario

Probabilistic analysis is applied to calculate geothermal reserve. The results of P10, P50, P90 are 83 MWe, 95 MWe, and 109 MWe, respectively. The P10 is the basis for the development stage of the development plan. Kurniawan (2018) proposed the development scenarios of the Ulumbu field based on three periods of reservoir performance forecasting. Figure 2 shows the development strategies of the Ulumbu field. The first period is reservoir performance forecasting from 2018 to 2020, the second period is reservoir performance forecasting from 2020 to 2024, and the third period is reservoir performance forecasting from 2024 to 2050. The three periods each have two development scenarios, namely:

50 MW (stepwise) Development Scenario

The first period was assumed not to require make-up wells and additional power, the second period a new unit of 1x20 MW was added, and the third period a new unit of 1x20 MW was added. This scenario required seven production wells, nine make-up wells, and one injection well. This scenario was following PLN's target to increase electricity production, addition of 2x20 MW, with an operation target in 2020 and 2024, respectively (Adiprana, 2018 in Kurniawan, 2018).

90 MW (stepwise) Development Scenario

The first period was assumed not to require make-up wells and additional power, the second period a new unit of 2x20 MW was added, and the third period a new unit of 2x20 MW was added. This scenario required seven production wells, nine make-up wells, and one injection well.

METHODOLOGY

This study began by determining the technical input parameter in financial model from 50 MW (stepwise) and 90 MW (stepwise) development scenarios in Ulumbu field. The number of productions, make-up, and injection wells from each development scenario are used as a technical input parameter. Total investment was calculated to generate 50 MW (stepwise), and 90 MW (stepwise). Moreover, electricity tariff was also calculated at 50% of Rate of Return value will be equal or less than 16% (P50). These tariffs were evaluated based on Average Cost of Electricity Generation (BPP) on relevant local grid. Figure 3 shown the complete flow chart of this study.

FINANCIAL MODEL

Financial model is everything that is used to calculate, predict or estimate financial numbers (Financewalk, 2014). Financial and/or economic model are needed for several reasons, including (Randle, 2005):

1. Economic analysis of project viability - often from a national economic perspective
2. Evaluation of technical alternatives
3. Tender evaluation
4. Business planning
5. Project financing for both equity and debt participants

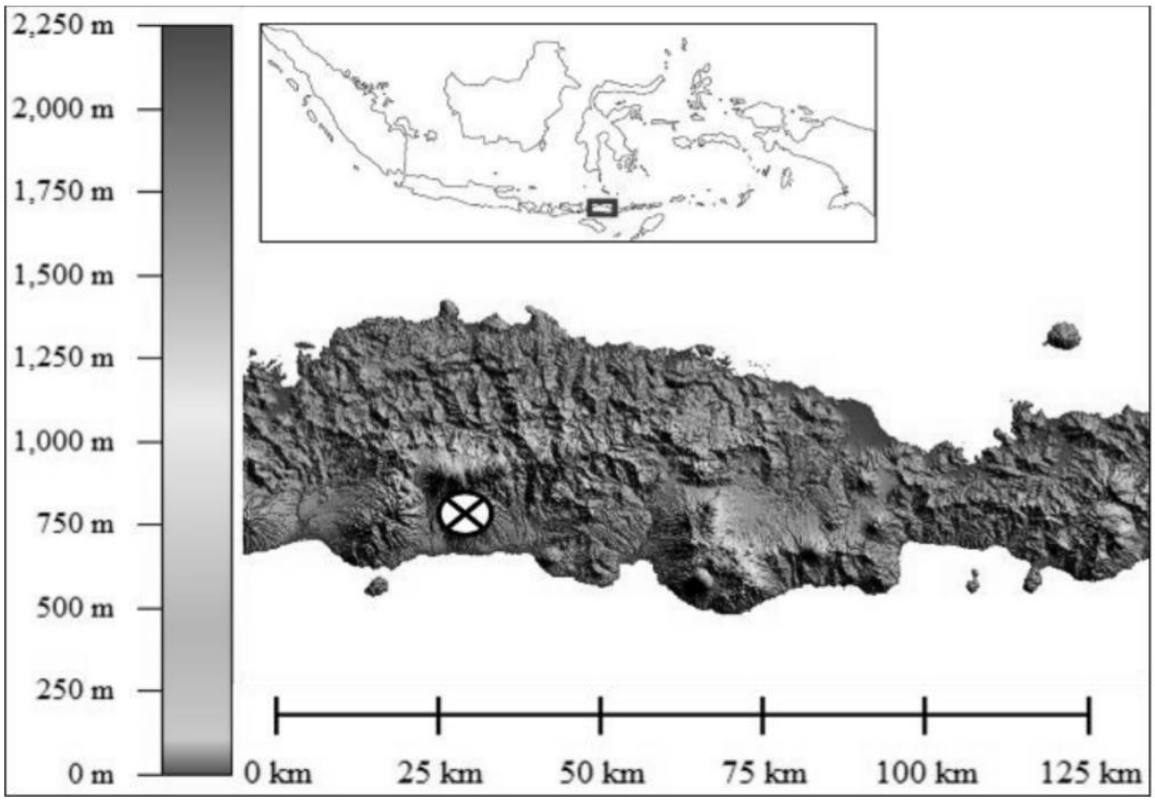


Figure 1: Location of Ulumbu Field (Mendive et al.,2016).

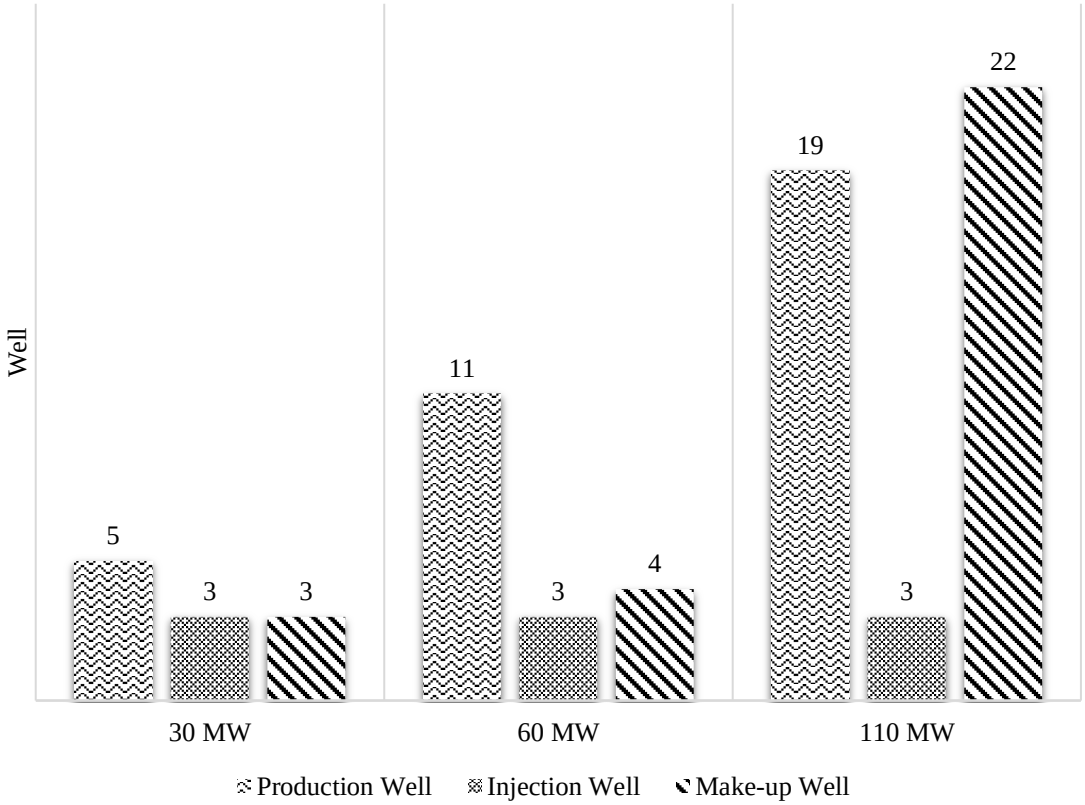


Figure 2: Development Scenario Ulumbu Field (Kurniawan, 2018).

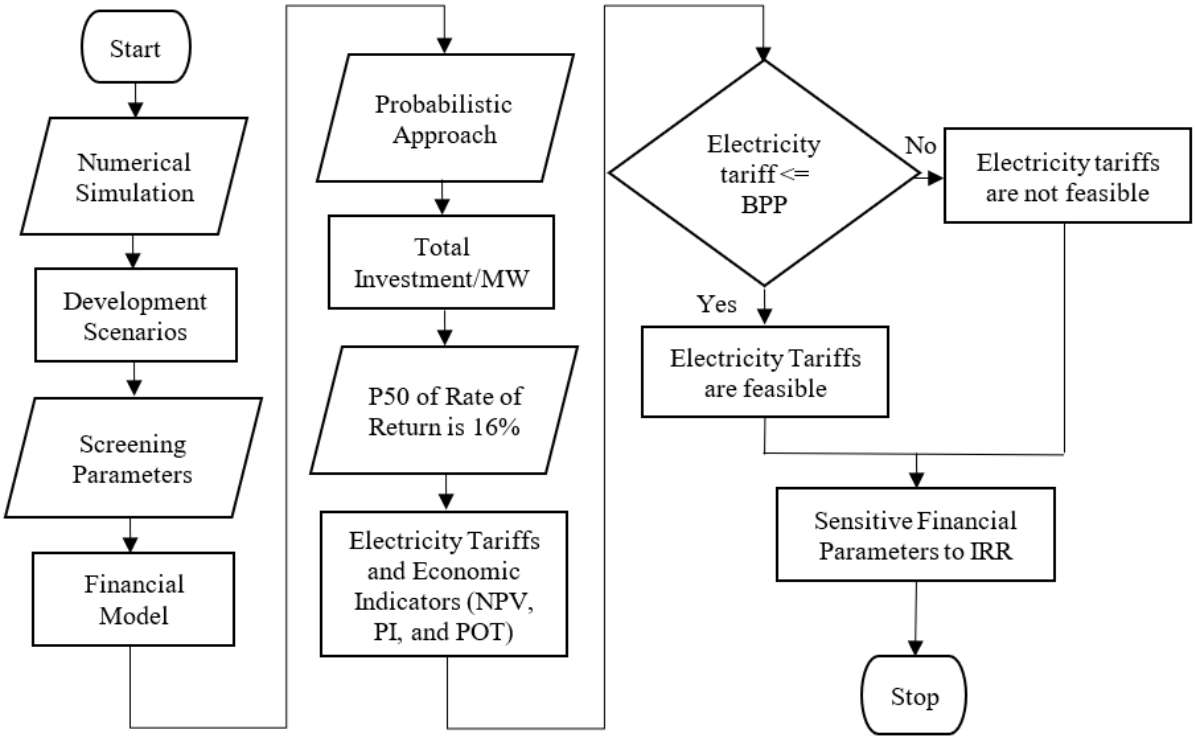


Figure 3: Working flowchart of the study.

In geothermal business activities, the financial model is built through a number of parameters, including (Ashat, 2019):

1. Revenue
2. Tangible and Intangible Capital Investment
3. Expenses
4. Depreciation and Amortization
5. Taxable Income
6. Tax
7. Loan
8. Cash Flow
9. Economic Indicators (e.g. Net Present Value (NPV), Rate of Return, Profitability Index (PI) and Pay Out Time (POT))

Those parameters are interconnected parameters in a financial model. The overall structure and interrelationships are shown in Figure 4.

Geothermal Project Schedule

The activity schedule is made with a factorial approach or the percentage of project achievement per year. The project schedule is modified from geothermal development planning which made by Gehringer & Loksha (2012). Table B.1 shows geothermal project schedule Ulumbu field.

Revenue

Geothermal income comes from the sale of geothermal electricity. The amount of revenue is influenced by the electricity tariff and geothermal capacity factor. The good performance of many geothermal plants around the world places the availability factor to be from 90-97% (Sarmiento et al., 2013).

Tangible and Intangible Capital Investment

A valuable financial geothermal model is one which integrates all the costs through all the phases of development and presents the resulting information in a manner to help various users make the appropriate decision (Ngugi, 2014). Capital investment in the geothermal business is divided into two part, namely upstream and downstream investment capital. Upstream capital investment concerns about steam availability and downstream investments related to electricity generation. The upstream capital investment consists of:

1. Well Cost (Exploration Well, Production Well, and Injection Well).
2. Land, Road Access and Site Work Cost.
3. Steam Gathering System Cost.
4. Piping and Production Facilities/ Steam Field Above Ground System (SAGS) Cost.

Upstream capital investment is divided into two tangible and intangible capital investments. Danar (2010) assumes that intangible investment capital is 30% of wells, land, road access, and site work cost while the remainder is tangible investment capital. Downstream investment capital consists of:

1. Power Plant Detail Engineering Cost,
2. Power Plant Procurement/Construction Cost,
3. Commissioning Cost.

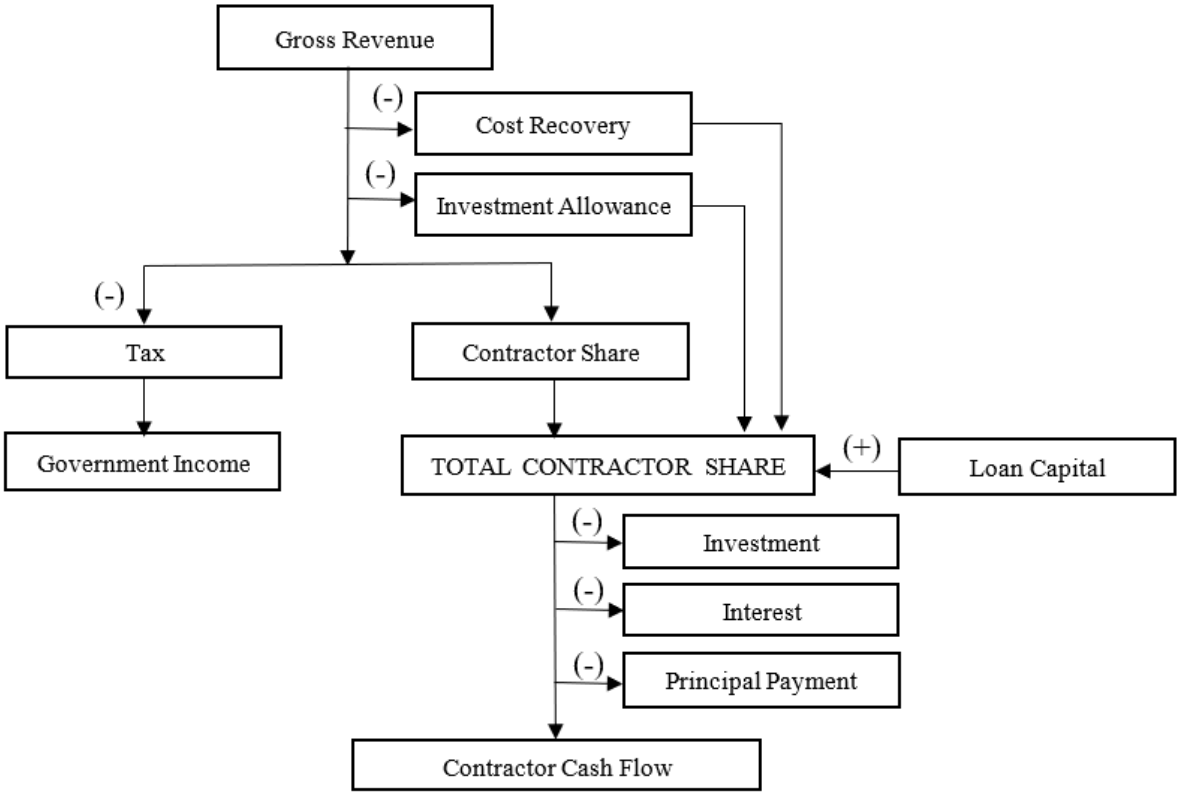


Figure 4: Working flowchart of the financial Model (Modified from Ashat, 2019).

Table B.2 shows shows capital investment cost assumption for Ulumbu Field.

Expense

Likewise, expenses are also divided into upstream and downstream expenses. Upstream expenses consist of:

1. Exploration Survey (Geology, Geochemistry, Geophysics).
2. Core Holes Cost.
3. Resource Study and Modelling Cost.
4. Operation and Maintenance cost.
5. Feasibility Study.

While downstream expenses consist of:

1. Operation and Maintenance Cost
2. Others (Management/Administration Cost)

Table A.2 shows expense assumption for Ulumbu Field.

Incentive Tax

Incentive tax is regulated in the Minister of Finance Regulation No. 21 / PMK.011 / 2010 concerning the provision of tax and customs facilities for activities to utilize renewable energy sources. Incentive tax in the form of income tax reduction include:

Investment Tax Allowance

The reduction tariff in net income is 30% of the total investment, charged for six years each at 5% per year.

Depreciation and Amortization

The depreciation period and rate are divided into four groups based on the type of assets. Group three has a depreciation period of 8 years and a depreciation rate of 25% (decline balance).

Production Bonus

Geothermal permit owner must expend production bonus to the regional government on the relevant work area. Production bonus is regulated in Law No. 21/2014 concerning geothermal energy. The production bonus is charged with a certain percentage of gross revenues since the first unit commercially produced.

The rate of production bonus is regulated in government regulation No. 28/2016. The production bonus is charged at 0.05% of the gross sales revenue of electricity with the provisions is not yet produced at the time Law No. 21/2014 be in force, starting from the first unit is produced commercially.

Taxable Income

The corporate income tax rate in Indonesia is regulated in Law No. 36/2008 concerning the fourth amendment to Law No.7/1983 concerning income

tax. The compatible tariffs for a geothermal corporation are 25% of gross income (after incentive tax reduction), which be in force since the 2010 tax year.

Loan

Debt: Equity can be adjusted by the user, which typical value is 70:30 (Quinlivan et al., 2015). In loans, several things need to be considered, namely the repayment period, Interest During Construction (IDC) and interest. The length of the repayment period will affect the amount of annual payment. The length of the repayment period, IDC and interest depend on the type of bank that provides the loan.

Commercial banks (e.g. HSBC, SCB) may offer interest rates in the range 8%-12%, but they have limited funds and frequently they syndicate together to provide the required debt. Even so, when the total funding requirements for a greenfield geothermal project are in the range US$500Million - US$1Billion even a commercial syndicate may not be able to cover the total debt and, in the case of projects in developing countries, bilateral or multilateral international development investment banks may need to be involved. These banks (such as JBIC, ADB, IADB etc) have greater funds available that commercial banks and can offer lower interest rates in the range 4%-8%. Additionally, in certain circumstances in developing countries, "government to government" cooperation can offer lower interest rates even less than 4% such as World Bank, JICA, KfW etc., with grace periods and much longer repayment periods than commercial or international development banks can offer (Quinlivan et al., 2015). In this study, it is assumed that the development of the Ulumbu field owe from international development banks with an IDC and interest are same, which are 4%, a grace period of 7 years and a repayment period of 20 years.

Cash Flow

Cash flow elements:

1. Loan Capital (cash inflow).
2. Revenue (cash inflow).
3. Total Capital Investment (cash outflow).
4. Total Expenses (cash outflow).
5. IDC/Interest (cash outflow).
6. Income Tax (cash outflow).
7. Principle Payment (cash outflow).

Economic Indicators

Determination of electricity tariff is based on economic indicators. Economic indicators commonly used in evaluating electricity price include:

1) Net Present Value (NPV)

Net Present Value is the discounted net value (present value) of expenditure and income over the project life using a nominated discount rate. If the NPV is greater than zero then the investment is more attractive than the discount rate. Discount rates for geothermal projects are usually set at 10% (Quinlivan et al., 2015).

2) Rate of Return

The discount rate at which the net present is zero. If the IRR is greater than the Required Rate of Return (RRR), then the proposed project is feasible to implement. The ideal IRR desired by the company is 16% regarding the statement of the previous Chairman of the Indonesian Geothermal Association (API), Abadi Poernomo (Beritasatu, 2012).

3) Profitability Index (PI)

PI is the ratio of the amount of present value cash flow in the future to the sum of the present value of initial investment. If the PI is greater than one, then the investment is more attractive than the discount rate. PI greater than 1.2 are more sought in geothermal business (Quinlivan et al., 2015).

4) Pay Out Time (POT)

POT is the length of time needed to recover all costs incurred in a project. POT can be a consideration in investing because longer period usually is not too desirable in geothermal investment.

All variable that affecting financial modelling are summarized in Table. B.3.

PROBABILISTIC APPROACH IN FINANCIAL MODEL

A probabilistic approach is applied with Monte Carlo simulation. Monte Carlo simulation is programmed using Excel® (Microsoft Corporation) spreadsheet. Monte Carlo simulation is implemented to calculate 90%, 50% and 10% of total investment and economic indicators (e.g., NPV, PI, and POT) estimates for 50 MW (stepwise) and 90 MW (stepwise) scenarios in Ulumbu field.

50 MW (stepwise) Development Scenario

Total Investment

Figure 4 and A.1 depict Monte Carlo simulation result of total investment per MW for 50 MW (stepwise) development scenario. The result shows that 10% of total investment per MW value will be equal or not exceed 4.66 Million USD. Meanwhile, 50% of total investment per MW value will be equal or less than 4.86 Million USD. For 90% of estimates, total investment per MW value will be equal or lower than 5.05 Million USD.

This investment is reasonable because Ulumbu unit II was built with an investment of 4.00 Million USD (Kontan.co.id, 2014). Likewise, Sokoria geothermal field in Ende Regency, East Nusa Tenggara developed by PT Sokoria Geothermal Indonesia with an investment of 4.50 Million USD to generate 5 MW (Katadata.co.id, 2018).

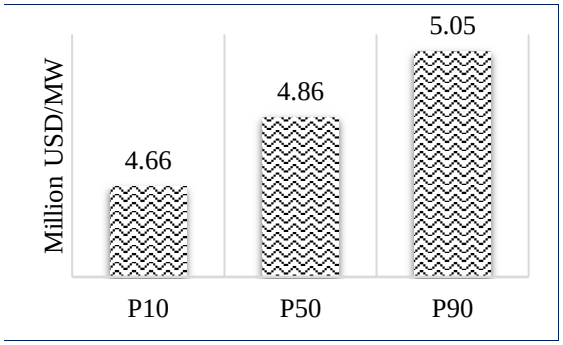


Figure 5: Monte Carlo Simulation Result of total investment/MW for 50 MW (stepwise) development scenario.

Electricity Tariff and Economic Indicators

Electricity tariff that meet 50% of Rate of Return value will be equal or not exceed 16% is 14.8 cents/kWh. Figure 5 and A.2 depict Monte Carlo simulation result of NPV for 50 MW (stepwise) development scenario. The result shows that 10% of NPV gained is equal or less than 39.11 Million USD. Meanwhile, 50% of NPV gained equal or not exceed 41.19 Million USD.

For 90% of estimates, NPV gained equal or not exceed 43.48 Million USD. This development scenario is feasible to be developed based on NPV because P10, P50 and P90 of NPV are positive.

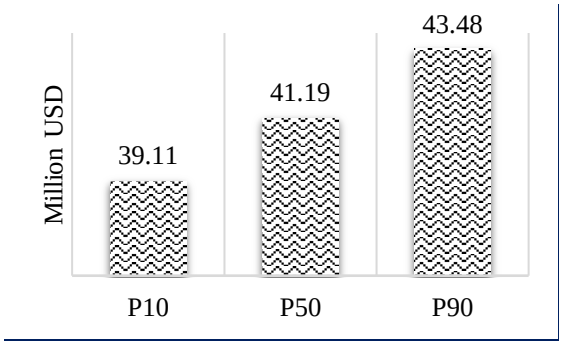


Figure 6: Monte Carlo Simulation Result of NPV for 50 MW (stepwise) development scenario.

PI is also calculated for 50 MW (stepwise) development scenario. Figure 6 and A.3 depict Monte Carlo simulation result of PI calculated for 50 MW (stepwise) development scenario. The result shows that 10% of PI value are equal or less than 1.47. Meanwhile, 50% of PI value are equal or less than 1.52. For 90% of estimates, PI value are equal or less than 1.58. The investment in this development scenario is attractive because the P10, P50 and P90 of PI are greater than 1.2.

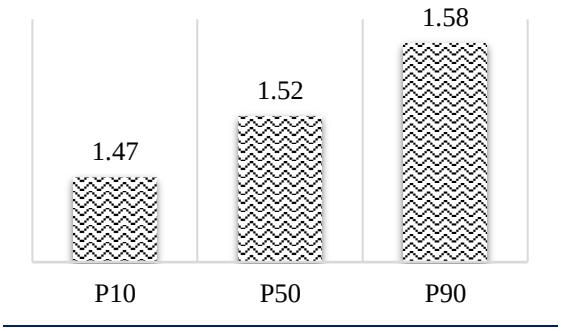


Figure 7: Monte Carlo Simulation Result of PI for 50 MW (stepwise) development scenario.

Based on the results of the geothermal cumulative cash flow projection for the 50 MW (stepwise) development scenario, the developer will gain profit two years after commercial date. Figure A.4 shows cumulative cash flow for 50 MW (stepwise) generation.

90 MW (stepwise) Development Scenario

Total Investment

Figure 7 and A.5 depicts histogram of Monte Carlo simulation result of total investment per MW for 90 MW (stepwise) development scenario. The result shows that 10% of total investment per MW value will be equal or not exceed 4.60 Million USD. Meanwhile, 50% of total investment per MW value will be equal or less than 4.81 Million USD.

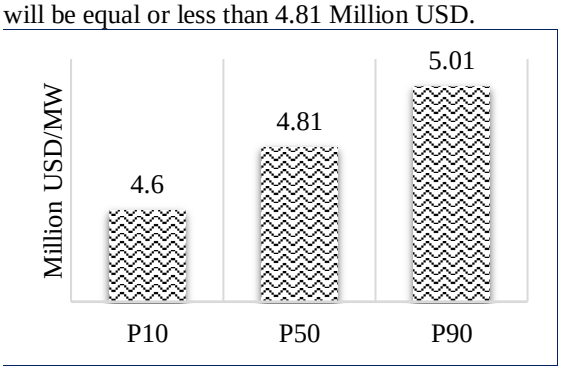


Figure 8: Monte Carlo Simulation Result of total investment/MW for 90 MW (stepwise) development scenario.

For 90% of estimates, total investment per MW value will be equal or lower than 5.01 Million USD.

Electricity tariff and Economic Indicators

Electricity tariff that meet 50% of Rate of Return value will be equal or not exceed 16% is 15.50 cents/kWh. Figure 8 and A.6 depict Monte Carlo

simulation result of NPV for 90 MW (stepwise) development scenario. The result shows that 10% of NPV gained is equal or less than 66.5 Million USD. Meanwhile, 50% of NPV gained equal or not exceed 70.31 Million USD. For 90% of estimates, NPV gained equal or not exceed 74.32 Million USD. This development scenario is feasible to be developed based on NPV because P10, P50 and P90 of NPV are positive.

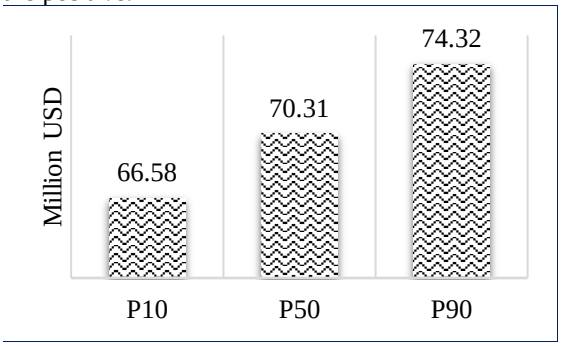


Figure 9: Monte Carlo Simulation Result of NPV for 90 MW (stepwise) development scenario.

PI is also calculated for 90 MW (stepwise) development scenario. Figure 9 and A.7 depict Monte Carlo simulation result of PI calculated for 90 MW (stepwise) development scenario. The result shows that 10% of PI value are equal or less than 1.50. Meanwhile, 50% of PI value are equal or less than 1.54. For 90% of estimates, PI value are equal PI value are equal or less than 1.60. The investment in this development scenario is attractive because the P10, P50 and P90 of PI are greater than 1.2.

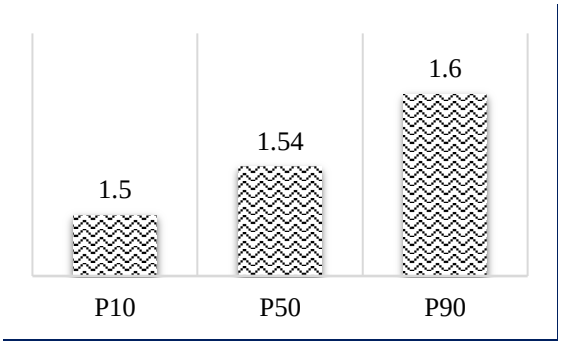


Figure 10: Monte Carlo Simulation Result of PI for 90 MW (stepwise) development scenario.

Based on the results of the geothermal cumulative cash flow projection for the 90 MW (stepwise) development scenario, the developer will gain profit two years after commercial date. Figure A.8 shows cumulative cash flow for 90 MW (stepwise) generation.

AVERAGE COST OF ELECTRICITY GENERATION (BPP)

The average cost of electricity generation (BPP) is calculated by summating the total generation, transmission, and distribution costs for PLN divided by the total sales of electricity produced for each island/(sub) grid (Van B, 2017). According to Ministry of Energy and Mineral Resources Regulation No. 12/2017, renewable energy tariff (including geothermal) negotiated in Power Purchase Agreement (PPA) between developer and buyer must not exceed the existing Average Generation Cost (BPP) on the relevant local grid. If the average local grid generation cost is lower than the average national generation cost, the tariff needs to be negotiated between developer and buyer. Table 6 shows geothermal ceiling price East Nusa Tenggara (West Flores) and national based on MEMR Regulation No.55 K/20/MEM/2019 (Table 1).

Table 1: Geothermal ceiling price in West Java and East Nusa Tenggara (West Flores) based on MEMR Regulation No.55 K/20/MEM/2019.

Region	BPP (US cent/kWh)
East Nusa Tenggara (West Flores)	17.58
National BPP	7.86

Ulumbu field is located in East Nusa Tenggara (West Flores). The average East Nusa Tenggara (West Flores) generation cost is higher than the average national generation cost that means the tariff must not exceed the existing Average Generation Cost (BPP). Financial model result shows that electricity tariff of 50 MW (stepwise) and 90 MW (stepwise) scenario in Ulumbu field are lower than the average East Nusa Tenggara (West Flores) generation cost. Therefore, 50 MW (stepwise) and 90 MW (stepwise) scenario are feasible based on BPP.

SENSITIVITY OF FINANCIAL PARAMETER TO RATE OF RETURN

Sensitivity analysis was conducted to see how the IRR could vary with regards to financial parameters. Figure A.9 illustrates sensitivity result of financial parameters for 50 MW (stepwise) in Ulumbu Field. The result shows that exploration well drilling cost, development well drilling cost, power plant include Engineering, Procurement, Construction, and Commissioning (EPCC) cost, land cost, access, site work and make-up well drilling were the most sensitive parameters, sequentially. Furthermore, Figure A.10 illustrates sensitivity result of financial parameters for 90 MW (stepwise). As a result, exploration well drilling cost, development well drilling cost, and power plant (EPCC), make-up well drilling, and land cost, access, and site work cost mainly affected IRR value, sequentially.

CONCLUSION

According to the financial model, the following main conclusions can be made:

1. Total investment to develop 50 MW (stepwise), was equal or less than 4.86 Million USD/MW. In same way, 90 MW (stepwise) was equal or less 4.81 Million USD/MW.
2. Electricity tariff was calculated to develop 50 MW (stepwise) in Ulumbu field that meet Rate of Return criteria, 50 % of Rate of Return value was equal or not exceed 16%, was 14.80 cents/kWh. Likewise, 90 MW (stepwise) was 15.50 cents/kWh.
3. Based Average Cost of Electricity Generation (BPP) on the relevant local grid, it was obtained that 50 MW (stepwise), and 90 MW (stepwise) scenario in Ulumbu field are feasible to be developed.
4. Sensitivity results show that Rate of Return was strongly affected by exploration well drilling cost, development drilling cost and power plant (EPCC) cost.

RECOMMENDATION

Further improvements are required to make the model better, such improvements include:

1. Investigate numerical simulation result updates. Numerical simulation result will be updated if there are any changes in production data trends and well addition.
2. The model has taken a simplistic approach to representing steam field development and plant development. The modeler needs to break down the cost into a number of small elements to reflect the actual expected cash flow. The modeler also needs to aware for plant degradation.
3. Explore more tariff and non-tariff policy options and their updates especially for income tax, incentive tax and BPP values. Ministry of Energy and Mineral Resources (MEMR) sets the geothermal ceiling tariff based on annual BPP by referring to PLN's proposal.
4. Generate scenario with lower IRR varied to represent the real condition (based on personal communication with expert, IRR of geothermal in Indonesia is ranged from 12% to 14%).
5. Create scenario with vary equity: debt ratio, interest rate and repayment period. It can help investors to assess the feasibility of the investment if the investment costs are not just from one source.

DISCLAIMER

The financial model in this paper is based on numerical simulation results in the form of 50 MW (stepwise) and 90 MW (stepwise) in Ulumbu field that have been studied by Kurniawan (2018). This financial model can be changed according to the amount of available data and the assumptions used.

REFERENCES

Antonaria et al., (2014). "Geothermal Handbook for Indonesia. Jakarta, Indonesia". Directorate for Energy Resource, Mineral and Mining, Ministry of National Development Planning/ National Development Planning Agency (BAPPENAS).

Ashat, Ali. (2019). "Analisa Keekonomian Prospek Panas Bumi. [PowerPoint slides]". Faculty of Mining and Petroleum Engineering. Institut Teknologi Bandung: Bandung.

Axelsson, G., (2016). "Nature and Assessment of Geothermal Resources6555." SDG Short Course I on Sustainability and Enviromental Management of Geothermal Resources Utilization and the Role of Geothermal in Combating Climate Change. Santa Tecla, El Savador. September 4-10, 2016.

Beritasatu. (2012): "23 Proyek Panas Bumi Terancam Merangkak".

Bisnis.com. (2018): "Proyek PLTP Ulumbu & Mataloko: PLN Kantongi pinjaman KfW Rp.2,6 Trilliun."

Law, Indonesia. (2008). "Perubahan Keempat atas Undang-undang Nomor 7 Tahun 1983 Tentang Pajak Penghasilan [Law No.38/2008]"

Law, Indonesia. (2014). "Energi Panas Bumi [Law No.21/2014]"

Danar, Agus and R. Sukyar. (2010). "Energi Panas Bumi di Indonesia: Kebijakan Pengembangan dan Keputusan Investasi". Badan Geologi Kementerian Energi dan Sumber Daya Mineral, Jakarta. ISBN 978-979-18509-8-8.

Fantony, M. Ghadavi et al., (2016). "Application of Monte Carlo Simulation for Determining IRR and Cash flow of a Geothermal Project." Proceedings World Geothermal Congress 2010. Bali, Indonesia. 25-29 April 2010.

Financewalk, 2014: "What is financial modelling?"

Gehringer, Magnus, and Victor Loksha. (2012). "Energy Sector Management Assistance Program (ESMAP): Geothermal Handbook: Planning and Financing Power Generation". Washington DC: The World Bank Group.

Government Regulation, Indonesia. (2016). "Besaran dan Tata Cara Pemberian Bonus Produksi Panas Bumi [Government Regulation No.28/2016]"

Hennerberger, Roger. (2010). "Cost and Financial Risk of Geothermal Project". Istanbul: GeothermEx, Schlumberger.

Katadata.co.id. (2018). “Beroperasi 2019, Empat pembangkit Panas Bumi Alirkan Listrik 180 MW”

Ketilsson, J. (2007). “Production Capacity Assessment of Geothermal Resources by Numerical Modelling”, M.Sc. Thesis, Engineering Department, University of Iceland, Reykjavik.

Kontan.co.id. (2014). “PLN bangun PLTP dan tambah kapasitas”

Kurniawan, Iqbal. (2018). “Field Development Study of Ulumbu Geothermal Field Based on Reservoir Simulation”. Thesis. Faculty of Mining and Petroleum Engineering. Institut Teknologi Bandung: Bandung.

Ministry of Energy and Minerals Resources Regulation, Indonesia. (2017). “Pemanfaatan Sumber Energi Terbarukan untuk Penyediaan Tenaga Listrik [MEMR No.12/2017]”

Ministry of Energy and Minerals Resources Regulation, Indonesia. (2018). “Besaran Biaya Pokok Penyediaan Pembangkitan PT Perusahaan Listrik Negara (Persero) [MEMR No.55 K/20/2019]”

Ministry of Finance. Regulation, Indonesia. (2010). “Pemberian Fasilitas Perpajakan dan Kepabeanan untuk Kegiatan Pemanfaatan Sumber Energi Terbarukan [Ministry of Finance Regulation No. 21/PMK.011/2010]”

Nasution et al., (2010). “The Ulumbu Geothermal Development West Flores, Eastern Indonesia”. Chiangmai: The 11th Asian Geothermal Syposium.

Ngungi, Paul K., (2014). “Financial Modelling of Geothermal Power Project.” Presented at “Short Course VI on Utilization of Low- and Medium-Enthalpy Geothermal Resources and Financial Aspects of Utilization”, organized by UNU-GTP and LaGeo, Santa Tecla, El Salvador, March 23-29, 2014.

Pane, Ilham Akbar., (2015). “Analisis Kelayakan Investasi Pengembangan dengan Variasi Model Numerik Hasil Eksperimental Desain Plackett-Burman pada Lapangan Geothermal Kepahiang, Bengkulu.” Thesis. Faculty of Mining and Petroleum Engineering. Institut Teknologi Bandung: Bandung.

Purwanto, Eko Hari. (2018). “Geothermal Drilling in Indonesia: A Review of Drilling Operation, Evaluation of Well Cost and Well Capacity”. Proceedings, The 6th Indonesia International Geothermal Convention & Exhibition 2018, Cendrawasih Hall- Jakarta Convention Center Indonesia, September 5th -8th ,2018. In press.

Quinlivan, Paul, et al., (2015). “Assessing Geothermal Tariffs in the Face of Uncertainty, a Probabilistic Approach”. Proceedings World Geothermal Congress 2015 Melbourne, Australia, 19-25 April 2015.

Randle, James B., (2005). “Financial Modelling of Geothermal projects.” Proceeding World Geothermal Congress 2005. Abtalya, Turkey. April 24-29, 2005

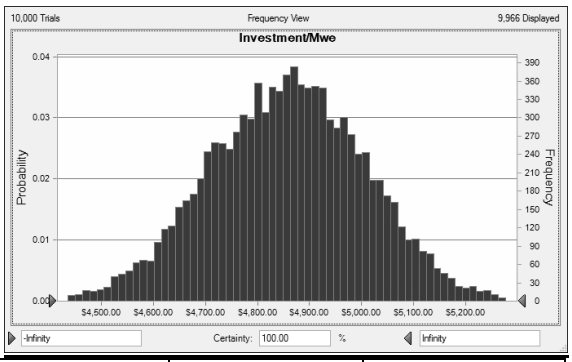
Richter, Alexander. (2017): “Indonesia Plans Auctions for Geothermal projects valued $ 1billion”

Sarmiento, Zosimo F., Benedikt Steingrímsson, and Gudni Axelsson. (2013). “Volumetric Resource Assesment”. Presented at Short Course V on Conceptual Modelling of Geothermal Systems, organized by UNU-GTP and LaGeo, in Santa Tecla, El Salvador, February 24 - March 2, 2013.

Van B, Campen et al., (2017). “Analysis of New Indonesia Geothermal Tariff System and Impact of Feasibility of Geothermal Plants in Eastern Indonesia in the Next Decade”. Proceedings 39th New Zealand Geothermal Workshop. Rotorua, New Zealand. 22-24 November 2017

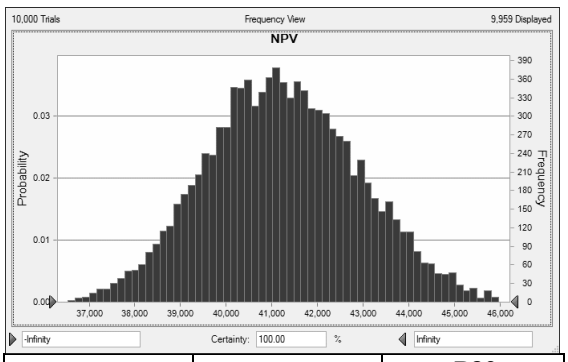
Wahjosoedibjo, Anton S., and Madjedi Hasan. (2018). “Indonesia’s Geothermal Development: Where is it Going?” Proceeding, 43rd Workshop on Geothermal Reservoir Engineering, Stanford University, California, February 12-14, 2018.

APPENDIX A



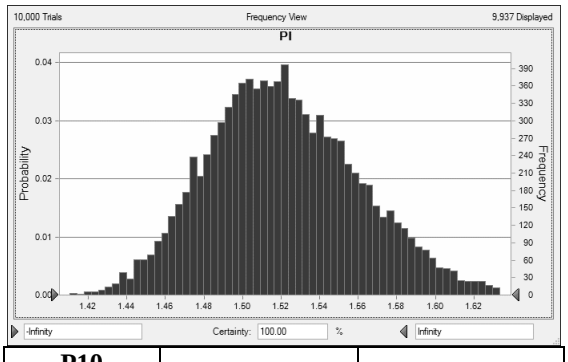
P10	P50	P90
$4,662,440	$4,859,620	$5,047,880

Figure A.1: Histogram of Monte Carlo simulation result of total investment per MW for 50 MW (stepwise) development scenario.



P10	P50	P90
1.47	1.52	1.58

Figure A.2: Histogram of Monte Carlo simulation result of NPV for 50 MW (stepwise) development scenario.



P10	P50	P90
= 1.47	**P50=** 1.52	**P90=** 1.58

Figure A.3: Histogram of Monte Carlo simulation result of PI for 50 MW (stepwise) development scenario.

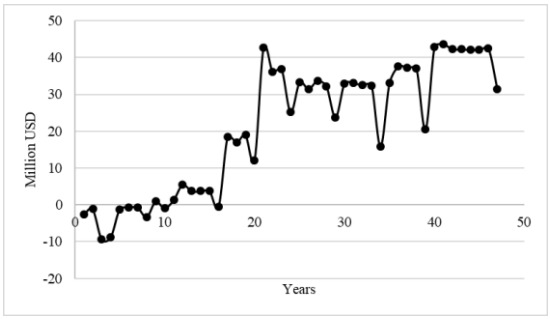
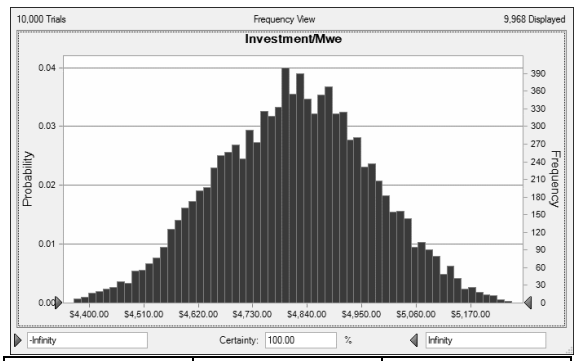
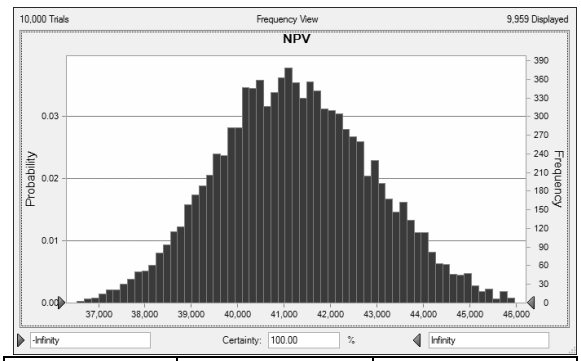


Figure A.4: Cumulative Cash Flow for 50 MW (stepwise) Power Generation Development.



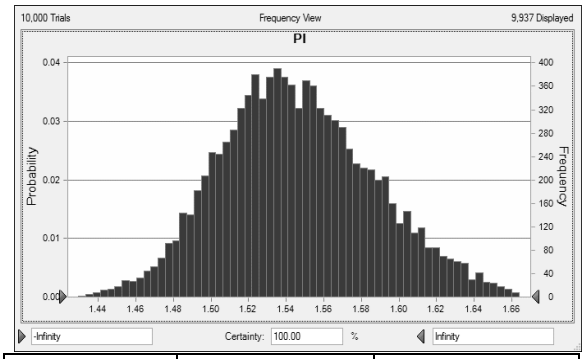
P10	P50	P90
$4,602,580	$4,814,840	$5,013,100

Figure A.5: Histogram of Monte Carlo simulation result of total investment per MW for 90 MW (stepwise) development scenario.



P10	P50	P90
$66,583,000	$70,313,000	$74,323,000

Figure A.6: Histogram of Monte Carlo simulation result of NPV for 90 MW (stepwise) development scenario.



P10	P50	P90
1.50	1.54	1.60

Figure A.7: Histogram of Monte Carlo simulation result of PI for 50 MW (stepwise) development scenario.

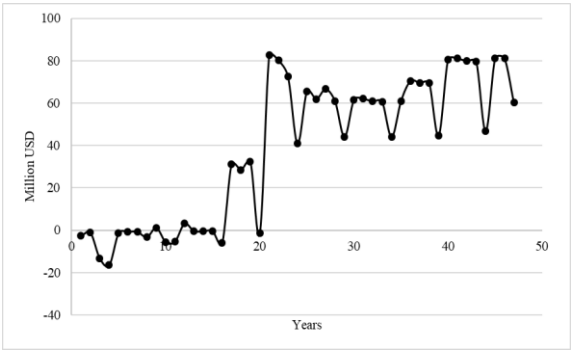


Figure A.8: Cumulative Cash Flow for 50 MW (stepwise) Power Generation Development.

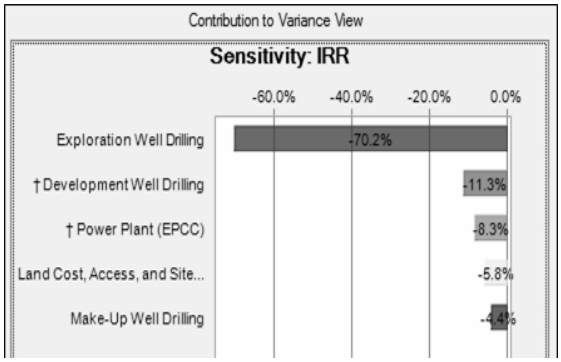


Figure A.9: Sensitivity result of financial parameters to Rate of Return for 50 MW (stepwise) scenario in Ulumbu field.

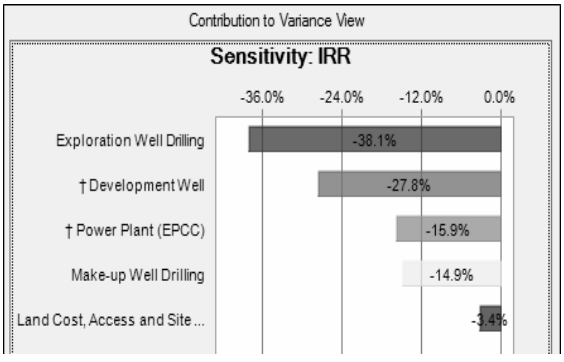


Figure A.10: Sensitivity result of financial parameters to Rate of Return for 90 MW (stepwise) scenario in Ulumbu field.

APPENDIX B

Table B.1: Ulumbu Field Project Schedule.

Parameters								2012	2013	2014	2015	2016	2017	2018	2019	2020	2021	2022	2023	2024
	1	2	3	4	5	6	7	8	9	10	11	12	13	14	15	16	17	18	19	20
STEAM FIELD DEVELOPMENT																				
Capital																				
Exploration drilling			50%	50%																
Development Well										50%	50%					50%	50%			
Injection well										50%	50%					50%	50%			
Make-up Well																				
Land cost, access and site work (included Env. Study and Civil Work)	100%																			
Steam Gathering System and Substation, Connection to Grid (transmission)				50%	50%			50%	50%		50%	50%					50%	50%		
SAGS (Piping and Production Facilities)				50%	50%			50%	50%		50%	50%					50%	50%		
Connection/ Transmission (Swichyard, Grid Connection, Tranmission)						50%	50%													
Expense																				
Detailed G-G-G Survey	50%	50%																		
Core holes			100%																	
Resource study & Modelling			100%																	
Operating cost (Upstream) 1 and 2 unit								25%	100%	100%	100%	100%	100%	100%	100%	100%	100%	100%	100%	100%
Operating cost (Upstream) 3 and 4 unit										25%	100%	100%	100%	100%	100%	100%	100%	100%	100%	100%
Operating cost (Upstream) 5 unit																25%	100%	100%	100%	100%
Operating cost (Upstream) 6 unit																				25%

Feasibility Study				100%															
PLANT DEVELOPMENT																			
Capital																			
Power Plant (Engineering, Procurement, Construction,Comissioning (Condensing Turbine))					33%	33%	33%	50%	50%				33%	33%	33%			50%	50%	
Expense																			
Operating cost (Downstream (Backpressure Turbine)) 1 and 2 unit								25%	100%	100%	100%	100%	100%	100%	100%	100%	100%	100%	100%	100%
Operating cost (Downstream (Condensing Turbine)) 3 and 4 unit										25%	100%	100%	100%	100%	100%	100%	100%	100%	100%	100%
Operating cost (Downstream (Condensing Turbine)) 5 unit																25%	100%	100%	100%	100%
Operating cost (Downstream (Condensing Turbine)) 6 unit																				25%
Other Cost (Administration/Management)	14%	14%	14%	14%	14%	14%	14%	50%	50%	17%	17%	17%	17%	17%	17%	25%	25%	25%	25%	

Table B.2: Summary of Ulumbu Field Cost Components.

Parameters	Unit	Price per unit (Million USD)			References
		Minimum	Most-likely	Maximum	
STEAM FIELD DEVELOPMENT					
Capital					
Exploration drilling	Well	$ 4.00	$ 7.00	$ 8.00	Purwanto et al. (2018); Bisnis.com (2018)
Development drilling	Well	$ 4.00	$ 7.00	$ 8.00	Purwanto et al. (2018); Bisnis.com (2018)
Development makeup	Well	$ 4.00	$ 7.00	$ 8.00	Purwanto et al. (2018); Bisnis.com (2018)
Injection well	Well	$ 4.00	$ 7.00	$ 8.00	Purwanto et al. (2018); Bisnis.com (2018)
Land cost, access and site work (included env. Study and civil work)	Activity /MW	$ 5.00		$ 7.00	Antonaria et al. (2014)
Steam Gathering System and Substation, Connection to Grid (transmission)	Activity /MW	$ 0.24	$ 0.32	$ 0.44	Gehringer & Loksha (2012)
SAGS (Piping and Production Facilities)	Activity	$ 0.33	$ 0.35	$ 0.40	Wahjosoedibjo (2018)
Expense					
Detailed G-G-G Survey	Activity	$ 1.00	$ 2.00	$ 3.00	Antonaria et al. (2014)
Core holes	Activity	$ 1.00		$ 1.20	Antonaria et al. (2014); Escalation 20%
Resource study	Activity	$ 0.1		$ 0.12	Henneberger (2013); Escalation 20%
Operating cost (Upstream)	Activity /MW	$ 0.03		$ 0.036	UNFCC (2012); Escalation 20%
Feasibility Study	Activity /MW	$ 0.10	$ 0.14	$ 0.20	Antonaria et al. (2014)
PLANT DEVELOPMENT					
Capital					
Backpressure power plant equipment construction & Install (Include Design Engineering, Power Plant procurement/Constructions, Testing/ Commissioning).	/MW	$ 1.22		$ 1.35	Sanyal (2004); EPA (2015); Escalation 20%
Condensing power plant equipment construction & Install. (Include Design Engineering, Power Plant procurement/Constructions, Testing/ Commissioning).	/MW	$ 1.90		$ 2.50	Sanyal (2004); Wahjosoedibjo (2018)
Expense					
Operating cost (Backpressure power plant)	/power plant cost	1.5%		2.5%	Gehringer & Loksha (2012)
Operating cost (Condensing power plant)	/power plant cost	1.5%		2.5%	Gehringer & Loksha (2012)
Other Cost (Administration and Management)	Activity /MW	$ 0.25		$ 0.30	Henneberger (2013); Escalation 20%

Table B.3: Variables Affecting Financial Modelling.

Technical Factors		
Parameters	Value	References
Capacity Factor	90%	Sarmiento (2013)
Production Well DSR	80%	Wahjosoedibjo (2018)
Additional Production Factor	25%	Expert Judgement
Financial Factors		
Tangible Cost	30%	Danar (2010)
Depreciation Period	8 Years	Ministry of Finance Regulation No. 21/PMK.011/2010
Depreciation Rate (Decline Balance)	25%	Ministry of Finance Regulation No. 21/PMK.011/2010
Equity : Debt	30 : 70	Quinlivan, et al. (2015)
Loan Period	20 Years	Quinlivan, et al. (2015)
Interest	4%	Quinlivan, et al. (2015)
Interest During Construction	4%	Quinlivan, et al. (2015)
Production Bonus	0.5%	Government Regulation No. 28/2016
Tax Rate	25%	Law No. 36/2008
Investment Tax Allowance (for 6 years)	5%	Ministry of Finance Regulation No. 21/PMK.011/2010
Discount Rate	10%	Quinlivan, et al. (2015)

OPTIMIZING OPERATIONAL EXPENSE BY DEVELOPING A MONITORING AND UPDATING SYSTEM OF OPERATIONAL BUDGET STATUS AT PT PGE KAMOJANG

Raka Kautsar Lahia, Reza Amaludin, Dona Febi Rosalina, A.Novi Purwono

PT Pertamina Geothermal Energy
Jl. Raya Kamojang , Laksana, Ibun, Bandung, Jawa Barat 40384
Email: raka.kautsar@pertamina.com

ABSTRACT

The operating cost budget is the main funding source in carrying out the company's operational activities. Control of the use of operational expenses is needed so that previously planned activities can be realized. The problem faced is the unavailability of detailed, accurate and comprehensive data on the operational cost budget status. Developing a monitoring and updating system of operational expense is a solution to this problem . This system become the main tool in monitoring budget status to obtain accurate, fast and detail data on operational expense. This system also make the budget users easy in monitoring and updating their operational budget status at any time so that the operational budget can be optimized. Using this system, the current operational budget status of PT PGE Kamojang can be seen and updated instantly. This system has proven to be able to support the efficiency of the Kamojang operational expense from 2016 to 2018 and already applied in other PT PGE operational areas.

Keywords: Operation, financial, expense

INTRODUCTION

PT Pertamina Geothermal Energy Area Kamojang (PGE Kamojang) is one of the areas owned by PT Pertamina Geothermal Energy. Located in Bandung Regency, West Java province, PGE Kamojang currently has a generating capacity of 235 Mega Watts (MW) generated by 5 PLTP Units. Unit 1 (30 MW), unit 2 (55 MW), and Unit 3 (55 MW) belonging to Indonesia Power, as well as Unit 4 (60 MW) and Unit 5 (35 MW) belonging to PT Pertamina Geothermal Energy. For units 1,2 and 3 contracts that are owned are Steam Sale and Purchase Agreement, while for units 4 and 5 the contract that is owned is an Electricity Purchase Agreement. PGE Kamojang has been operating since 1980.

In carrying out the company's operational activities, PGE Kamojang uses the Operating Cost Budget (ABO). ABO is a funding resource to run a company's business operations that has been poured into a financial unit that is reflected in the company's profit and loss in one fiscal year.

ABO is proposed one year before the current year budget as one of the proposed documents for the Company's Budget Plan (RKAP). The ABO proposal is a breakdown of activities and its budget. After being proposed by each division, the ABO proposal through the process of a challenge session from the area (bottom level) to the headquartes (top level). Once the ABO proposal was approved then it will be allocated to each division/cost center and can be used in the current year. In PT PGE including PT PGE Kamojang , ABO data and its history can be seen through SAP Software.

The use of ABO in the current year must always be monitored so that the realization is in accordance with the plans that have been submitted and approved before. In the period of 2015 - 2018 there were various problems related to ABO monitoring in the PGE Kamojang.

In 2015, when author joined the Planning & Engineering division at the Budget analyst position the mechanism used to did ABO monitong was very simple. The Budget Analyst opened SAP and then copied the budget status data from SAP into Microsoft Excel on the laptop. Budget analyst then processed the data manually to get a recapitulation of the ABO Kamojang condition.

In 2016, an analysis was conducted and it was found that there was an inaccurate information on available budget data on budget monitoring tool. The deviation was up to 347%. Beside that, the time needed to produce an ABO status recapitulation data was also relatively long, which averages up to 115 minutes.

In 2017 after the problem of accuracy along with the time of recapitulation of ABO data in the Kamojang area was resolved there was a new problem related to the availability of the ABO prognosis which is only 54.5% of the ABO Prognosis data available in 2016.

After the problem of the prognosis data availability was solved, in 2018 a re-analysis was carried out and it was found that the ABO Prognosis data in 2017 on average was 10 % above the target of efficiency.

Author believes that those problems are common problems that could be founded in another company, especially in geothermal companies. Those problem could give a direct impact in the effort of optimizing

the usage of operational expense. In this paper author will explain how to overcome those problems until its resolved and hopefully it can be useful for others.

METHODOLOGY

The methodology used in solving those problems are:

1. Determination of theme.
2. Determination of the root causes (using fish-bone diagrams).
3. Determination of the dominant causes (combination of the delphi method and the pareto diagram).
4. Planning improvements.
5. Implementation of improvement.
6. Evaluation of improvement results.
7. Making new standards.

EXPERIMENTS AND RESULTS

Improving accuracy of budget data

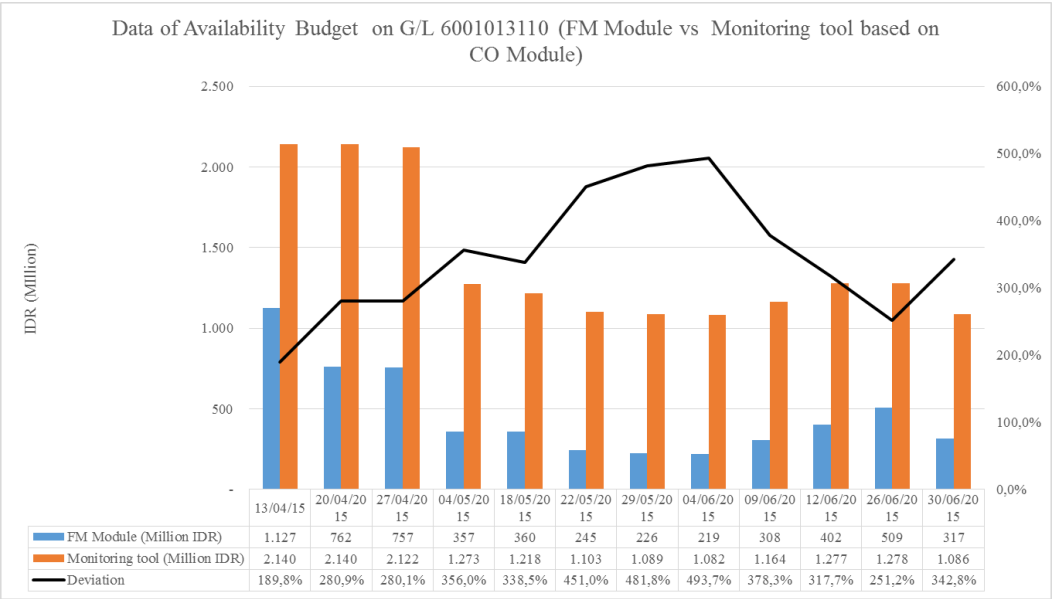
In 2016, an analysis was conducted and it was found that there was an inaccurate information about available budget data that provided on tool of budget monitoring. Tool of budget monitoring is a simple worksheet in Microsoft Excel that used to produce PGE Kamojang's ABO data. Source of this tool was from the Controlling (CO) Module SAP. In that analysis author found that there was a difference between CO Module and FM (Fund Management) Module. The difference between CO and FM Module are up to 347%. Figure 1 shows the deviation of available budget data between monitoring tool and FM Module before improvement.

The interesting fact in this case was CO Module in MySAP (T-code S_ALR_87013620) does not accommodate the transaction made from the SAP PM Module (Plant Maintenance Module).

The root cause of the problem was sought and found that the monitoring tool and it source should be replaced by the new tool and the new resource that valid. Figure 2 shows the display of the monitoring tool that has been re-made. To overcome this accuracy problem, ABO monitoring tool are "remade" by author using FM Module data as a main source. FM module data (code-ZFMBUDCONIDR) is more accurate than the CO Module for displaying available budget data because in FM Module the transactions from PM Modules that were not recorded in the CO module was recorded. Monitoring tools are made using Microsoft Excel as a base with the following steps:

1. Program Preparation.
2. Modification of the ABO monitoring program.
3. Monitoring of the improvement.
4. Development of the improvement.
5. Program implementation.

Repairs are carried out for 3 months at no cost. This Microsoft Excel based monitoring tool was created as a template and calculation tool in which the Index and Match formulas and macros are inputted. Budget analyst only needed to download raw data from SAP through the FM module with the ZFMBUDCONIDR T-code and change the format to .xls then copy it to the monitoring tool. After doing that procedure, the status of the operating budget conditions will be available.

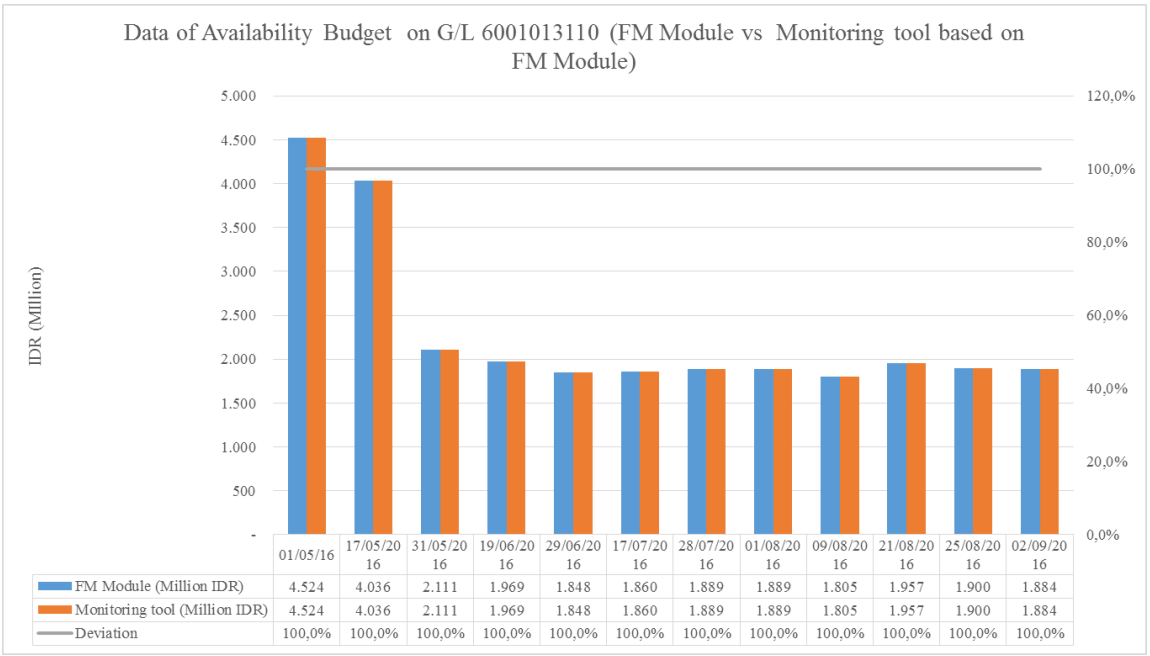


	13/04/15	20/04/2015	27/04/2015	04/05/2015	18/05/2015	22/05/2015	29/05/2015	04/06/2015	09/06/2015	12/06/2015	26/06/2015	30/06/2015
FM Module (Million IDR)	1.127	762	757	357	360	245	226	219	308	402	509	317
Monitoring tool (Million IDR)	2.140	2.140	2.122	1.273	1.218	1.103	1.089	1.082	1.164	1.277	1.278	1.086
Deviation	189,8%	280,9%	280,1%	356,0%	338,5%	451,0%	481,8%	493,7%	378,3%	317,7%	251,2%	342,8%

Figure 1: Deviation of available budget data between monitoring tool and FM Module before improvement.



Figure 2: Display of the monitoring tool that has been re-made.



	01/05/16	17/05/2016	31/05/2016	19/06/2016	29/06/2016	17/07/2016	28/07/2016	01/08/2016	09/08/2016	21/08/2016	25/08/2016	02/09/2016
FM Module (Million IDR)	4.524	4.036	2.111	1.969	1.848	1.860	1.889	1.889	1.805	1.957	1.900	1.884
Monitoring tool (Million IDR)	4.524	4.036	2.111	1.969	1.848	1.860	1.889	1.889	1.805	1.957	1.900	1.884
Deviation	100,0%	100,0%	100,0%	100,0%	100,0%	100,0%	100,0%	100,0%	100,0%	100,0%	100,0%	100,0%

Figure 3: Deviation of available budget data between monitoring tool and FM Module after improvement.

With these new tools and new resource, available budget data was become accurate and the time needed to update the budget status is reduced from 115 minutes to 5 minutes. Figure 3 shows the deviation of available budget data between monitoring tool and FM Module after improvement. Table 1 shows the availability of ABO prognosis data on year 2016.

Improving availability of ABO prognosis data

In 2017, an analysis done by author and found that in 2016 only 54.5% of ABO Prognosis data was available. It means that in certain months the ABO prognosis data was not available while the ABO prognosis data is needed to optimize ABO. Figure 4 shows the root causes of the problems and its solution. Figure 5 shows the improvement design.

Table 1: Availability of ABO prognosis data on year 2016.

Month (2016)	Jan	Feb	Mar	Apr	Mei	Jun	Jul	Agus	Sep	Okt	Nov	Total	% Total
Budget Prognosis data Available	1	-	-	1	-	-	-	1	1	1	1	6	54,5%
Budget Prognosis data Needed	1	1	1	1	1	1	1	1	1	1	1	11	

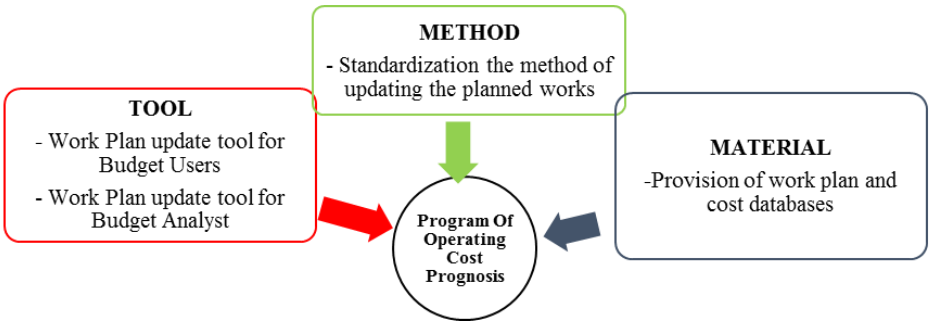


Figure 4: Root causes of the problems and its solusion.

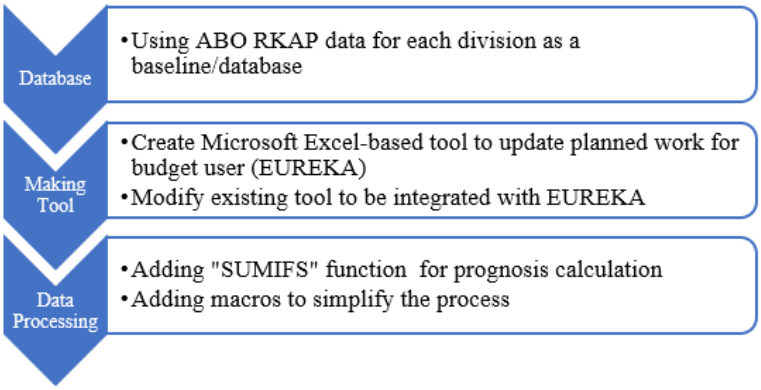


Figure 5: Improvement design.

By this fact, the root causes of the problem were traced and found that the tools, methods and materials were the three contributing factors to the lack availability of ABO prognosis data problem.

After author designed the alternative improvement that have been chosen. Improvement was carried out for 2 months at no cost.

This work plan update tool was based on Microsoft Excel. This tool was used as a standard template that contains a database of work plans for each function that already approved before so that the budget user knew the work plans that have been planned in advance.

After the template created, improvements are made to the ABO status update tool that was created previously. Adding a work plan macrosheet so the file could call the update work plan file.

The improvements was worked very well that prognosis data became available every month. Beside that, the time needed to did a recapitulation data to make a prognosis also reduced, from 45 minute to 4.5 minutes.

Developing web-based sytem to improve the Accuracy of ABO Prognosis data

It was found from the 2017 data that the average ABO Prognosis data was above 10% of the target given by the company. This condition could cause an over budget condition in ABO usage.

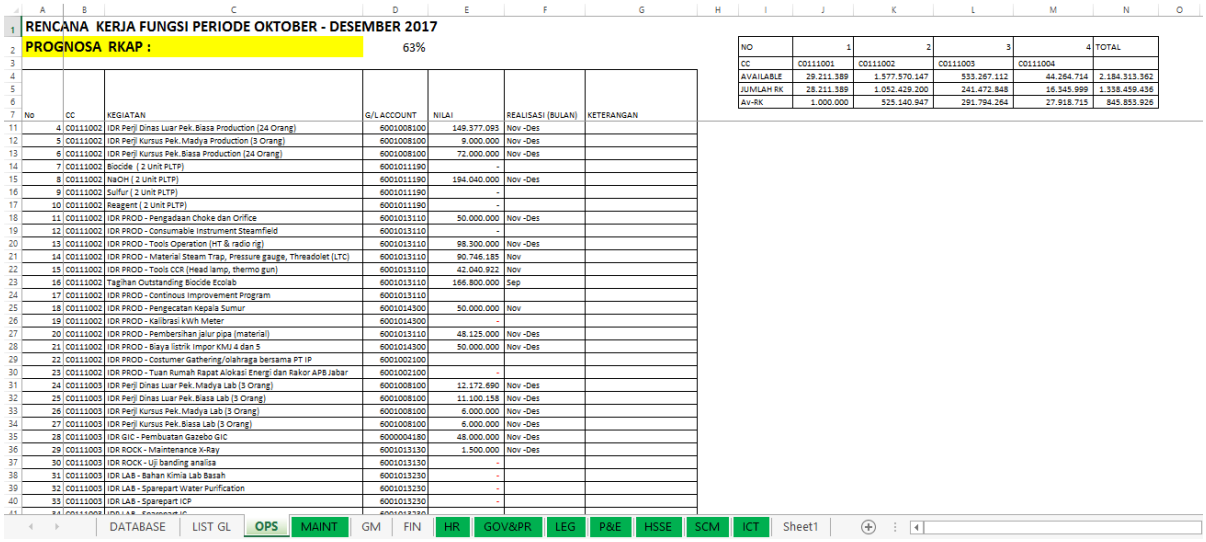
The main cause of this problem is that the existing tools was not accommodated the current or updated status and updated budget requirements of each work plan. The method used was:

1. Budget Analyst sent a Microsoft Excel File that contain the latest work plan and budget to the budget users.
2. Budget users did update the data then sent back the file to Budget Analyst.
3. Budget Analyst did recapitulate the submitted data.
4. Prognosis data obtained.

This kind of process tooked an average of 3-4 days, especially in the process updating data by the budget users. A brand new way of making a prognosis is

needed to shorten the time. Figure 6 shows the standard template of work plan database.

The solution to shorten the time was an integrated web-based system that easy, simple, and also compatible on mobile phones so that it can facilitate budget users in controlling budget usage and speed up the process of making ABO prognosis. Figure 7 shows the additional sheet to compile each workplan from the budget users. Figure 8 shows the availability of budget prognosis data before improvement. Figure 9 shows the availability of budget prognosis data after improvement.



RENCANA KERJA FUNGSI PERIODE OKTOBER - DESEMBER 2017

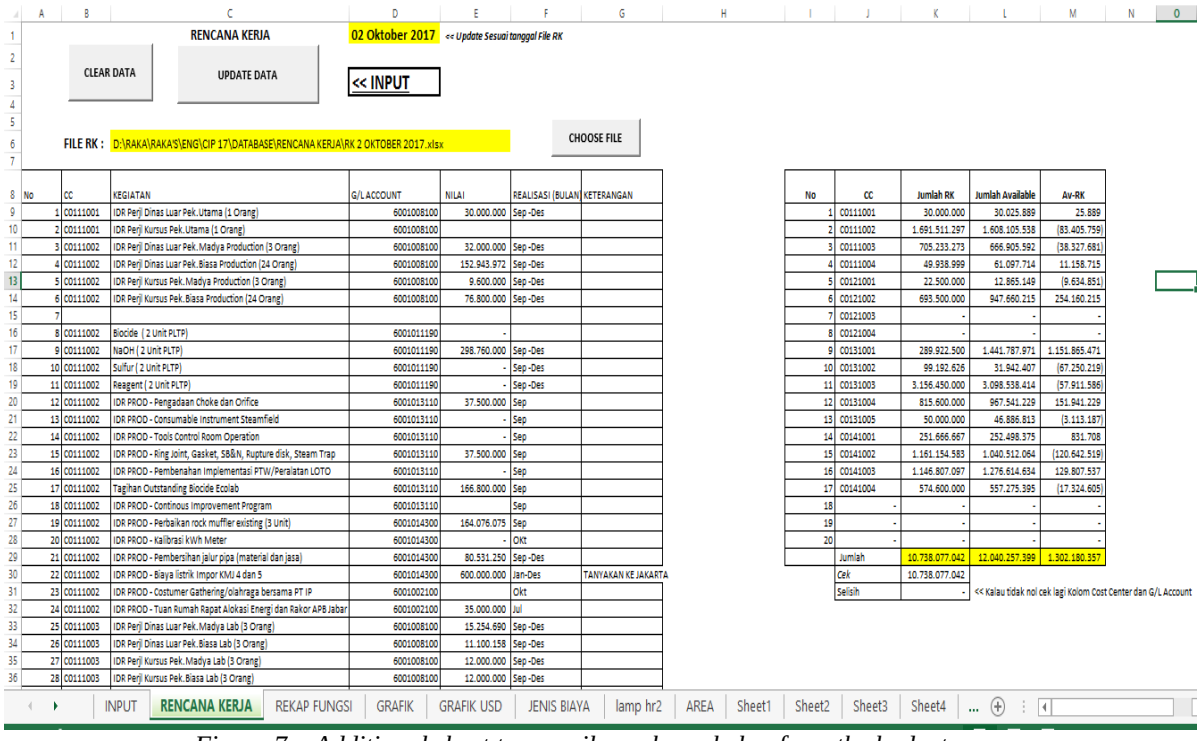
PROGNOSA RKAP : 63%

NO	1	2	3	4	TOTAL
CC	C0111001	C0111002	C0111003	C0111004	
AVAILABLE	29.211.389	1.577.570.147	533.267.112	44.264.714	2.184.313.362
JUMLAH RK	28.211.389	1.052.429.200	241.472.848	16.345.999	1.338.459.436
Av-RK	1.000.000	525.140.947	291.794.264	27.918.715	845.853.926

No	CC	KEGIATAN	G/L ACCOUNT	NILAI	REALISASI (BULAN)	KETERANGAN
4	C0111002	IDR Perjl Dinas Luar Pek.Biasa Production (24 Orang)	6001008100	149.377.093	Nov -Des	
5	C0111002	IDR Perjl Kursus Pek.Madya Production (3 Orang)	6001008100	9.000.000	Nov -Des	
6	C0111002	IDR Perjl Kursus Pek.Biasa Production (24 Orang)	6001008100	72.000.000	Nov -Des	
7	C0111002	Biocide (2 Unit PLTP)	6001011190	-		
8	C0111002	NaOH (2 Unit PLTP)	6001011190	194.040.000	Nov -Des	
9	C0111002	Sulfur (2 Unit PLTP)	6001011190	-		
10	C0111002	Reagent (2 Unit PLTP)	6001011190	-		
11	C0111002	IDR PROD - Pengadaan Choke dan Orifice	6001013110	50.000.000	Nov -Des	
12	C0111002	IDR PROD - Consumable Instrument Steamfield	6001013110	-		
13	C0111002	IDR PROD - Tools Operation (HT & radio rig)	6001013110	98.300.000	Nov -Des	
14	C0111002	IDR PROD - Material Steam Trap, Pressure gauge, Threadolet (LTC)	6001013110	90.746.185	Nov	
15	C0111002	IDR PROD - Tools CCR (Head lamp, thermo gun)	6001013110	42.040.922	Nov	
16	C0111002	Tagihan Outstanding Biocide Ecolab	6001013110	166.800.000	Sep	
17	C0111002	IDR PROD - Continous Improvement Program	6001013110			
18	C0111002	IDR PROD - Pengecatan Kepala Sumur	6001014300	50.000.000	Nov	
19	C0111002	IDR PROD - Kalibrasi kWh Meter	6001014300			
20	C0111002	IDR PROD - Pembersihan jalur pipa (material)	6001013110	48.125.000	Nov -Des	
21	C0111002	IDR PROD - Biaya listrik Impor KMJ 4 dan 5	6001014300	50.000.000	Nov -Des	
22	C0111002	IDR PROD - Costumer Gathering/olahraga bersama PT IP	6001002100	-		
23	C0111002	IDR PROD - Tuan Rumah Rapat Alokasi Energi dan Rakor APB Jabar	6001002100	-		
24	C0111003	IDR Perjl Dinas Luar Pek. Madya Lab (3 Orang)	6001008100	12.172.690	Nov -Des	
25	C0111003	IDR Perjl Dinas Luar Pek.Biasa Lab (3 Orang)	6001008100	11.100.158	Nov -Des	
26	C0111003	IDR Perjl Kursus Pek. Madya Lab (3 Orang)	6001008100	6.000.000	Nov -Des	
27	C0111003	IDR Perjl Kursus Pek.Biasa Lab (3 Orang)	6001008100	6.000.000	Nov -Des	
28	C0111003	IDR GIC - Pembuatan Gazebo GIC	6000004180	48.000.000	Nov -Des	
29	C0111003	IDR ROCK - Maintenance X-Ray	6001013130	1.500.000	Nov -Des	
30	C0111003	IDR ROCK - Uji banding analisa	6001013130	-		
31	C0111003	IDR LAB - Bahan Kimia Lab Basah	6001013230	-		
32	C0111003	IDR LAB - Sparepart Water Purification	6001013230	-		
33	C0111003	IDR LAB - Sparepart ICP	6001013230	-		

DATABASE | LIST GL | OPS | MAINT | GM | FIN | HR | GOV&PR | LEG | P&E | HSSE | SCM | ICT | Sheet1

Figure 6: Standard template of work plan database.



RENCANA KERJA 02 Oktober 2017 << Update Sesuai tanggal File RK

CLEAR DATA | UPDATE DATA | << INPUT

FILE RK : D:\RAKA\RAKA'S\ENG\CIP 17\DATABASE\RENCANA KERJA\RK 2 OKTOBER 2017.xlsx | CHOOSE FILE

No	CC	KEGIATAN	G/L ACCOUNT	NILAI	REALISASI (BULAN)	KETERANGAN
1	C0111001	IDR Perjl Dinas Luar Pek.Utama (1 Orang)	6001008100	30.000.000	Sep -Des	
2	C0111001	IDR Perjl Kursus Pek.Utama (1 Orang)	6001008100			
3	C0111002	IDR Perjl Dinas Luar Pek.Madya Production (3 Orang)	6001008100	32.000.000	Sep -Des	
4	C0111002	IDR Perjl Dinas Luar Pek.Biasa Production (24 Orang)	6001008100	152.943.972	Sep -Des	
5	C0111002	IDR Perjl Kursus Pek.Madya Production (3 Orang)	6001008100	9.600.000	Sep -Des	
6	C0111002	IDR Perjl Kursus Pek.Biasa Production (24 Orang)	6001008100	76.800.000	Sep -Des	
7						
8	C0111002	Biocide (2 Unit PLTP)	6001011190	-		
9	C0111002	NaOH (2 Unit PLTP)	6001011190	298.760.000	Sep -Des	
10	C0111002	Sulfur (2 Unit PLTP)	6001011190	-	Sep -Des	
11	C0111002	Reagent (2 Unit PLTP)	6001011190	-	Sep -Des	
12	C0111002	IDR PROD - Pengadaan Choke dan Orifice	6001013110	37.500.000	Sep	
13	C0111002	IDR PROD - Consumable Instrument Steamfield	6001013110	-	Sep	
14	C0111002	IDR PROD - Tools Control Room Operation	6001013110	-	Sep	
15	C0111002	IDR PROD - Ring joint, Gasket, SB&N, Rupture disk, Steam Trap	6001013110	37.500.000	Sep	
16	C0111002	IDR PROD - Pembenahan Implementasi PTW/Peralatan LOTO	6001013110	-	Sep	
17	C0111002	Tagihan Outstanding Biocide Ecolab	6001013110	166.800.000	Sep	
18	C0111002	IDR PROD - Continous Improvement Program	6001013110		Sep	
19	C0111002	IDR PROD - Perbaikan rock muffler existing (3 Unit)	6001014300	164.076.075	Sep	
20	C0111002	IDR PROD - Kalibrasi kWh Meter	6001014300	-	Okt	
21	C0111002	IDR PROD - Pembersihan jalur pipa (material dan jasa)	6001014300	80.531.250	Sep -Des	
22	C0111002	IDR PROD - Biaya listrik Impor KMJ 4 dan 5	6001014300	600.000.000	Jan-Des	TANYAKAN KE JAKARTA
23	C0111002	IDR PROD - Costumer Gathering/olahraga bersama PT IP	6001002100		Okt	
24	C0111002	IDR PROD - Tuan Rumah Rapat Alokasi Energi dan Rakor APB Jabar	6001002100	35.000.000	Jul	
25	C0111003	IDR Perjl Dinas Luar Pek.Madya Lab (3 Orang)	6001008100	15.254.690	Sep -Des	
26	C0111003	IDR Perjl Dinas Luar Pek.Biasa Lab (3 Orang)	6001008100	11.100.158	Sep -Des	
27	C0111003	IDR Perjl Kursus Pek. Madya Lab (3 Orang)	6001008100	12.000.000	Sep -Des	
28	C0111003	IDR Perjl Kursus Pek.Biasa Lab (3 Orang)	6001008100	12.000.000	Sep -Des	

No	CC	Jumlah RK	Jumlah Available	Av-RK
1	C0111001	30.000.000	30.025.889	25.889
2	C0111002	1.691.511.297	1.608.105.538	(83.405.759)
3	C0111003	705.233.273	666.905.592	(38.327.681)
4	C0111004	49.938.999	61.097.714	11.158.715
5	C0121001	22.500.000	12.865.149	(9.634.851)
6	C0121002	693.500.000	947.660.215	254.160.215
7	C0121003	-	-	-
8	C0121004	-	-	-
9	C0131001	289.922.500	1.441.787.971	1.151.865.471
10	C0131002	99.192.626	31.942.407	(67.250.219)
11	C0131003	3.156.450.000	3.098.538.414	(57.911.586)
12	C0131004	815.600.000	967.541.229	151.941.229
13	C0131005	50.000.000	46.886.813	(3.113.187)
14	C0141001	251.666.667	252.498.375	831.708
15	C0141002	1.161.154.583	1.040.512.064	(120.642.519)
16	C0141003	1.146.807.097	1.276.614.634	129.807.537
17	C0141004	574.600.000	557.275.395	(17.324.605)
18	-	-	-	-
19	-	-	-	-
20	-	-	-	-
	Jumlah	10.738.077.042	12.040.257.399	1.302.180.357
	Cek	10.738.077.042		
	Selisih	-	<< Kalau tidak nol cek lagi Kolom Cost Center dan G/L Account	

INPUT | RENCANA KERJA | REKAP FUNGSI | GRAFIK | GRAFIK USD | JENIS BIAYA | lamp hr2 | AREA | Sheet1 | Sheet2 | Sheet3 | Sheet4 | ...

Figure 7: Additional sheet to compile each workplan from the budget users.

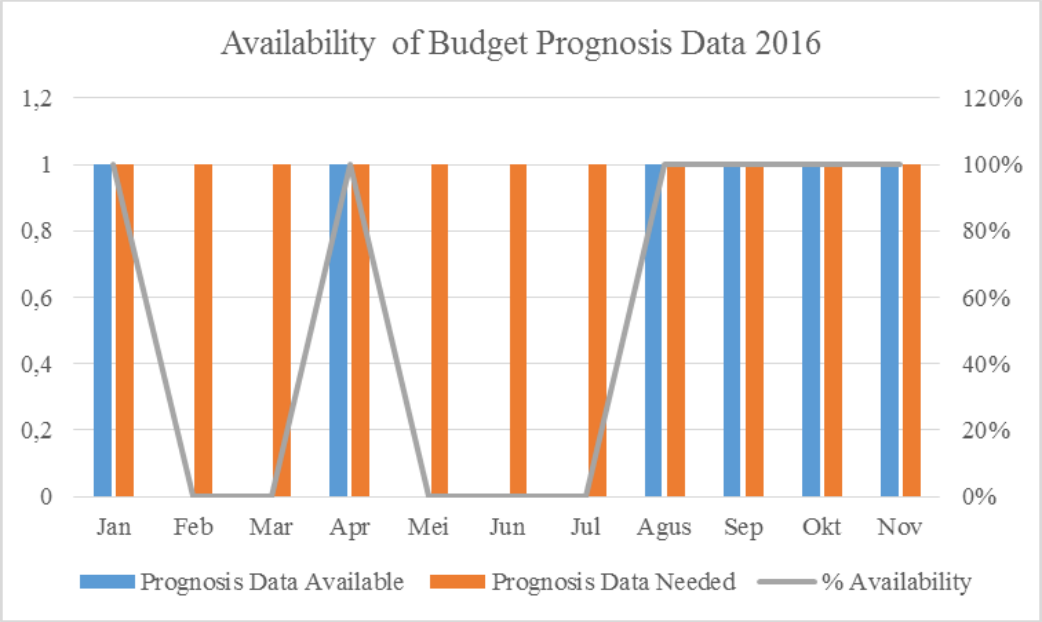


Figure 8: Availability of budget prognosis data before improvement.

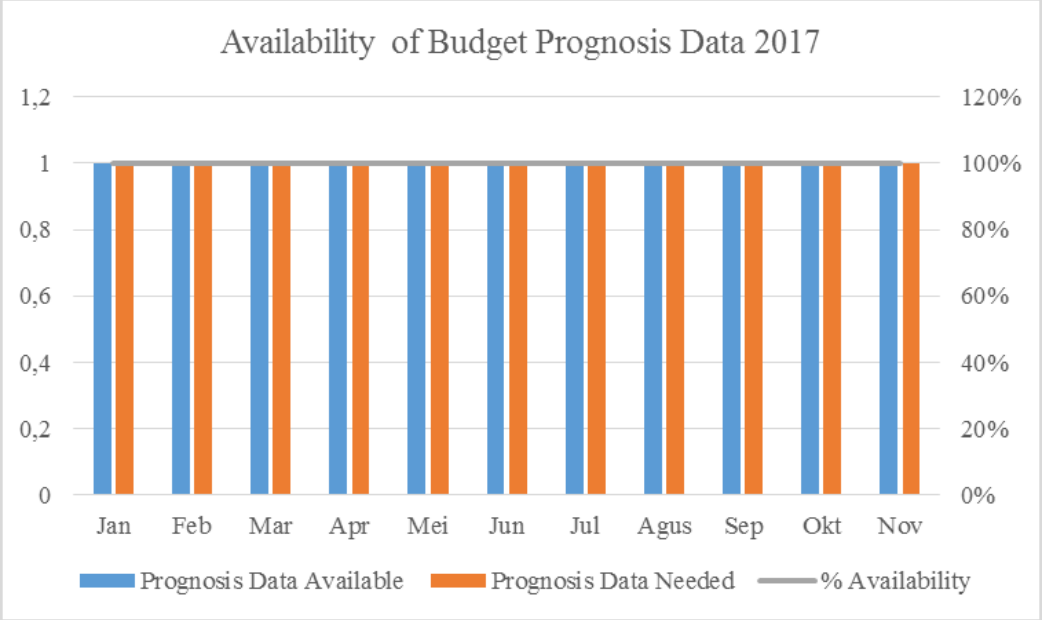


Figure 9: Availability of budget prognosis data after improvement.

Improvements were carried out for 4 months and used the google sheet application as a basis.

The google sheet application was chosen because the application contain facilities that really helpul:

1. Multiple log in
2. Chat room
3. Notification to email

The google sheet also provides a mobile version of the application to facilitate the budget user in updating work plans from their smartphones.

Authors created a new tool, a worksheet contain company's work plan and budget on google sheet then created accounts for budget users. Every budget user could accessed this web-based worksheet by using the accounts created. This tool also equipped with a calculation of prognosis so that every budget user could get information about operating budget prognosis. By using this tool, every budget users could accessed and updated the work plan and budget everytime and everywhere. Figure 10 shows the trend of prognosis data before improvement. Figure 11 shows the beb-based tool to monitor and update status of ABO.

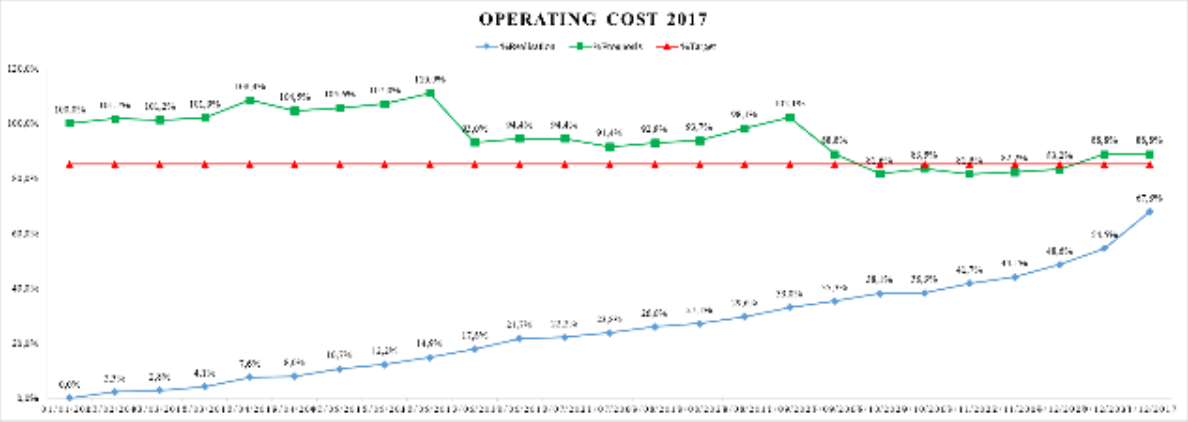


Figure 10: Trend of prognosis data before improvement.

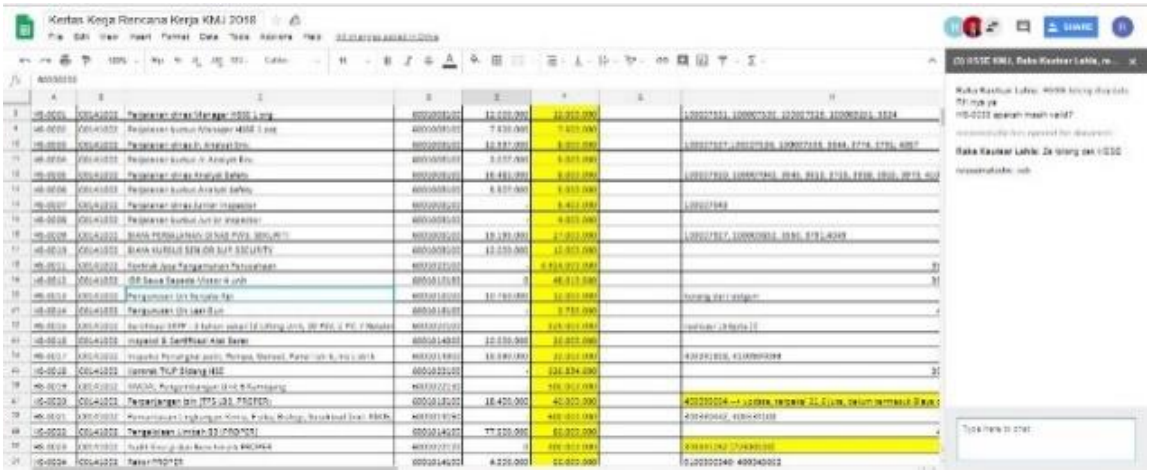


Figure 11: Web-based tool to monitor and update status of ABO.

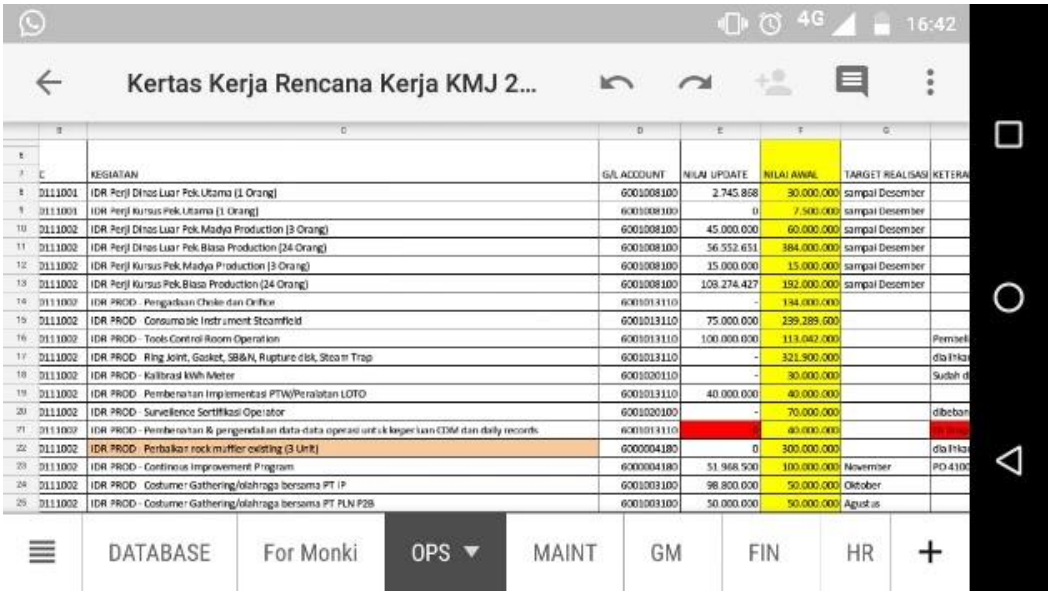


Figure 12: Mobile version of the tool.

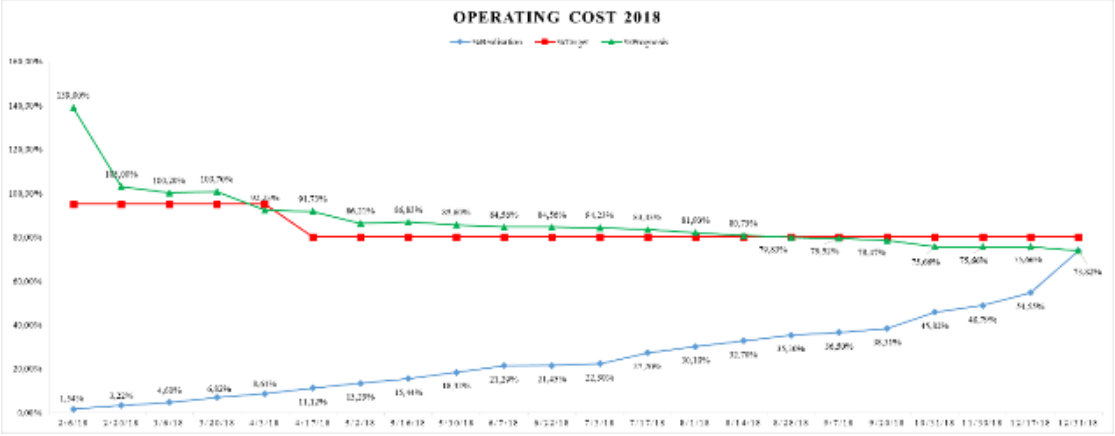


Figure 13: Trend of prognosis data after improvement.

This new tool gave a great impact to absorption of operating costs budget. From the graph, it could be seen that in 2018 the prognosis was close to the target given by the company so that the absorption of the operating budget optimum. Figure 12 shows the mobile version of the tool. Figure 13 shows the trend of prognosis data after improvement.

Table 2: Comparation of 2016-2018 Operating Budget Realisation.

Year	Planned Operating Budget	Realisation target by Company	End Year Realisation	Unutilized Operating Budget
	Percentage	Percentage	Percentage	Percentage
	(a)	(b)	(c)	(d)
2016	100%	80%	62%	18%
2017	100%	85%	68%	17%
2018	100%	80%	74%	6%

It can be seen from the table above that the realisation of ABO from 2016 to 2018 was increased (Table 2). In 2018, 74% of the budget was absorbed, a significant increase compared to the previous 2 years. The unutilized budget was reduced from 18% in 2016 to 6% in 2018. This is an indicator that the optimization of the use of ABO was successful in the midst of the efficiency policies implemented by the company.

CONCLUSION

From the explanation above, it can be concluded that The ABO monitoring process requires three importants things:

1. Accurate ABO condition (actual, commitment, available) data
2. Updated work plan and budget
3. Updated ABO prognosis data

Budget users and Budget analyst currently can obtain those three importants things easily by accessing the web-based ABO monitoring and updating system. This system is the best solution and already proven for helping budget analyst to optimize the operational expense in PT Pertamina Geothermal Energy Kamojang.

THE BENEFIT AND ROLE OF WOMEN IN GEOTHERMAL (WING) INDONESIA ON SUPPORTING RENEWABLE ENERGY INDUSTRY

Ratih Nurruhliati[1,2], Jane Brotheridge[1,3], Jane Bydder[1,3], Pri Utami[1,4], Kris Pudyastuti[1,5]

[1]Women in Geothermal (WING) Indonesia
[2]Geothermal Consultant, Sanur, Bali, Indonesia
[3]Jacobs, New Zealand
[4]Gajah Mada University, Yogyakarta
[5]Trisakti University, Jakarta
Email: wingindonesiainfo@gmail.com

ABSTRACT

On the 11th March 2019, WING Indonesia was launched, as part of the World Network of WING International, with the support from the New Zealand Government and Jacobs. Prior to the launching, in 2018 and in conjunction with International Women's Day (8th March) the WING Movement was introduced to Indonesia. The Indonesian chapter of WING is endorsed by Indonesian Geothermal Association (INAGA).

The mission and vision are aligned with United Nation (UN) Sustainability Development Goals with focus on climate change, gender equality, and ending poverty. Therefore, an effort to participate in addressing the global climate change crisis, reduce carbon emissions and increase the participation of women, WING is embedding itself within the frontline Indonesian geothermal community with the role of women.

The WING Indonesia program is to support women in all areas of Geothermal from social to technical to regulatory. The program will include community education, sharing sessions, and networking in Indonesia as well as International Community.

Keywords: Women in geothermal, Indonesia

WOMEN IN GEOTHERMAL (WING) INDONESIA

The Women in Geothermal (WING) Indonesia was launched in Jakarta on the 11th March 2019. The event was well attended by all geothermal related institute and/organization, government agencies, universities, consultants, private companies, law firms, banks and other associations.

Here is the documentation of the event. Figure 1 shows the participant of WING Indonesia launching. Figure 2 shows the WING Indonesia account in Facebook and Instagram platform.



Figure 1: All participants WING Indonesia Launching, Jakarta, 11th March 2019.



Figure 2: The activities of WING Indonesia can be followed on the platform of Facebook and Instagram, will soon in Twitter and on LinkedIn.

WING Indonesia mission is promoting the Education, Professional Development, and Advancement of Women in Geothermal Community.

WING Indonesia has some program that related to the mission and it is so far run by member activity and volunteer based. One of the direct activities that has been active the social media with IG and FB platform, as a way to be connected to public and Geothermal related like minded people. The 21st way to share any topics direct and indirect on Geothermal.

SUSTAINABLE DEVELOPMENT GOALS

On September 25th, 2015, 193 world leaders have committed to 17 goals to achieve 3 extraordinary things in the next 15 years.

Those goals are to be achieved by 2030:

1. End the extreme poverty
2. Fight inequality and injustice
3. Combat climate change

The Global Goals for sustainable development could get these things done with participation of all people in all countries and for all people. Figure 3 shows the United Nation sustainable development goals illustration. Figure 4 shows the 17 global goals for sustainable development.



Figure 3: United Nation Sustainable Development Goals Illustration, as the Goals that committed by 193 country leaders, September 2015.



Figure 4: The 17 Global Goals for Sustainable Development.

No Poverty



Figure 5: The Global Goals for Sustainable Development, No Poverty.

It is clear to see that in the area where Geothermal Project location, in Indonesia, has the effect on economy, that provide works at certain types ie. construction, security, administration, logistic, safety, supplier, cleaner and perhaps engineering etc all other support work with the right training and the need of employee can be fulfilled by the locals first, as it is making sense and if there were not skill set available then the people will be hired from outside and by giving training to the locals to prepare to fill in the position when this person ready. With work provides by the project also creating other economic activities and for sure creating jobs inside or outside the project. Figure 5 shows the global goals for sustainable development, no proverty.

So, the impact is real to cut the poverty, giving the local the opportunity to do the economic activity. Whether it is direct or indirectly to the Project, the growth of economy can be observed. The additional work or even the new type of works as before the project exists for sure more traditional type of works are common as farmers, logging and or the typical work in the remote or village area.

Gender Equality and Reduces Inequalities

These two goals are still not easy to measure. Having the variety cultural background and traditions are so diversity throughout the archipelago. Indonesia has so many ethics background over 300 tribes, with majority of Javanese. Even within the majority, the range of high education of women is not uniform. This will be an honest statement, a tricky one for Indonesia to measure but there is niche group that some female geoscientists and engineers work in STEM/STEAM more specific in Geothermal Industry. Figure 6 shows the global goals for sustainable development, Gender equality. Figure 7 shows the global goals for sustainable development, reduced inequalities.



Figure 6: The Global Goals for Sustainable Development, Gender Equality.



Figure 7: The Global Goals for Sustainable Development, Reduced Inequalities.

One of the schedules that we have is to get the real data on how many females in the geothermal work force in the and in related industries.

It does not say we are against it, Indonesia has the women hero to fight for the Equality, Kartini, the familiar hero for the nation, fighting to get the same education for girls back in the colonial time, she had been fighting for emancipation since 1900. Back in the days, pre-colonialism, most of society in Indonesia were led by the women and only few left as the maternalism, Padangnese (tribe in West Sumatera) is the obvious one which is still valid until now.

In one side we have particular figure and the reality, the percentage is still unknown, how many real numbers are female have higher education and still holding the tradition practice, which is a norm as you do just how to manage the life.

Climate Action



Figure 8: The Global Goals for Sustainable Development, Climate Action.

The Geothermal Energy has been known as a friendly kind of source of energy, it is known produced much less CO_2 emissions compared to the conventional energy sources, coal, fossils fuels. Geothermal is classified as renewable energy and the waste mostly 99.99% is water. Figure 8 shows the global goals for sustainable development, climate action.

BRIEF HISTORY OF GEOTHERMAL INDONESIA

Period 1918 - 1945:

The Geothermal Exploration was first proposed in 1918. The further work was done by the colonial Geological Survey of Indonesia (GSI), the initial exploration drilling in Kamojang in 1926.

Period 1945 - 1970:

Geothermal exploration (1970–1980) During the first PELITA (first 5-year development plan, 1969 – 1974).

In 1969, a PLN group, Indonesian State Power Company (Power Research Institute) undertook a geothermal reconnaissance survey of Sulawesi (Radja, 1970).

Period 1970 - 2000:

Between 1970 and 1972, the K. Sikidang sector of the Dieng volcanic complex was investigated under the auspices of a USAID program, involving US Geological Survey staff and collaborate with Indonesian counterpart group of VSI/ITB/PLN. The prospect carries a certain volcanic risk, as indicated by its history of phreatic eruptions and gas hazards (Simkin and Seibert 1994).

Exploration Drilling program was done to 80 m depth, encountering a temperature of 145◦C at the bottom (Radja, 1975). of Dieng, Gunung Tampomas, Gunung Salak and Gunung Perbakti, K. Kamojang, and the Cisolok prospect (Zen and Radja, 1970).

From 1974 Pertamina, The Indonesian State Oil Company entered geothermal exploration, became responsible for all geothermal exploration in Java (Dieng) and Bali, in line with Presidential Decree PD 16/1974.3.1. Now, it has own branch Pertamina Geothermal Energy (PGE).

The Volcanological Survey (VSI) Group completed a geothermal inventory of Sumatra, Sulawesi, and the Halmahera Islands (Radja, 1985; Soetantri, 1986).

There was also the establishment of PLTP Gunung Salak. Mount Salak PLTP is located in Gunung Halimun Salak National Park, West Java. It commenced operations in 1994. The plant, operated jointly by Unocal Geothermal Indonesia (later on taken over by Chevron) and PT Pertamina, is capable of generating 375 MW of electricity.

In 1984 Amoseas Indonesia Inc (a joint venture between Chevron Corp and Texaco Inc) under a Joint Operating Contract to Pertamina, the Indonesian National Oil Company, began developing the Darajat geothermal resource. The commercial operations of Darajat began in November 1994, with capacity near 145 MW.

Period 2000 - up to now, 2019

Up to the year of 2003 re-drilling development and production wells was occurred. Then in 1983, PLTP (Geothermal Power Plant) Kamojang Unit 1 with a capacity of 30 MW officially declared by President Soeharto as the first geothermal field in Indonesia, followed by the inauguration of PLTP Units 2 & 3 (2 x 55 MW) in 1988 continued later in 2003 – 2007 with PLTP Unit 4 (60 MWe).

Lahendong Geothermal Power Plant is located in North Sulawesi. It was first operated in 2004. Operated by PT Pertamina Geothermal Energy (PGE,) producing electricity up to 80 MW. It consists of four units: Lahendong I, Lahendong II, Lahendong III and Lahendong IV. At Darajat the completion and upgrading of Unit III in 2009, gives total capacity of 271 MW.

Three projects were completed in 2018, in North Sumatra and West Java. The three projects are PLTP Sarulla in North Sumatra with a capacity of 110 MW, then PLTP Sorik Marapi in North Sumatra with capacity of 20 MW and PLTP Karaha in West Java with a capacity of 30 MW.

The government's target by December 2018 that geothermal utilization would increase by 1,858.5 MW. With those additions, the total geothermal power capacity in Indonesia would become 2,023.5 MW.

Education and Training

Since most of the earlier works were not listed in the scientific literature, thesis and diploma reports of Indonesian Geothermal graduate students attending the University of Auckland between 1979 and 2003 became an important source of information and were used as reference of many geothermal development (Hochstein and Browne).

Post 2000, ITB open the Geothermal Program to fill in the growing Geothermal Industry.

THE BENEFIT AND ROLE OF WING

WING is an International Member of International Geothermal Association (IGA), and WING members participative in their own national Geothermal associations and communities.

We would like to be partners in promoting gender Equality and women's empowerment in the industry. So far, we have been supported by NZTE/MFAT and Jacobs to be able to run some of the program for the major event, but the WING itself is run by volunteers. We are hoping companies and other parties who is in the industry can participate and play the role as well.

WING Indonesia will also conduct the research and survey to find out how many women are in the Geothermal Industry in Indonesia. It will be a good track record to have and it is a good will in participating also in the advocate for the increase of MWs. produced from Geothermal. To work together with all others Geothermal components, the government as regulator, the universities as education provider and also research organization, the fund manager, investors, legal consultants and other to achieve more electricity/energy source from Geothermal and also the awareness that Geothermal is great way to reduce the Carbon emissions to decrease the Global Climate, to act on Climate Change.

REFERENCES

Hochstein, P. M., Sudarman, S., (2008), "History of Geothermal exploration in Indonesia from 1970 to 2000," Science Direct Geothermics 37, 220–266.

https://www.un.org/sustainabledevelopment/sustainable-development-goals/

WING Indonesia documentation, 2019

GEOTHERMAL ENERGY DEVELOPMENT COMPARISON AMONG TOP GEOTHERMAL PRODUCERS

Dorman P. Purba[1], Ribka F. Asokawaty[3], Daniel W. Adityatama[1], Rany C. Putri[4], Riviani Kusumawardani[3], Mukhamad Umam[2]

[1]PT. Rigsis Energi Indonesia
[2]PPSDM Cepu
[3]Bandung Institute of Technology
[4]Trisakti University
Email: dorman.purba@rigsis.com

ABSTRACT

Indonesia currently hold a second place for the most installed geothermal power plant capacity with 1,924.5 MWe, second only to the USA. Government of Indonesia through RUEN (Rencana Umum Energi Nasional) set target for 7,200 MWe geothermal plant installed capacity in 2025 to ensure that Indonesia's energy mix will be more independent from the volatile fossil fuel price. However, with the current rate, it seems to be a daunting task to achieve that target, especially considering the first geothermal power plant in Indonesia was installed back in 1983. This very slow rate of development is concerning, as other countries such as Turkey and Kenya are able to accelerate their development rate in the recent time. Turkey in particular installs around 1,000 MWe in 10 years. This paper reviewed the energy mix and market of the top 5 geothermal countries, their typical geothermal system, current development strategy, and their roadmaps for development. The challenges for each country geothermal energy development was also discussed. Kenya and Turkey geothermal energy development are also discussed even though they are not in the top 5. To conclude, this study discussed what other countries do differently with Indonesia regarding the policy or technology, and what can Indonesia learns from them in order to accelerate and increase the geothermal energy portion in its energy mix.

Keywords: Production, geothermal energy

INTRODUCTION

The geological setting of Indonesia makes Indonesia has the largest geothermal Indonesia. Badan Geologi (2019) stated that total geothermal potential in Indonesia is 25.39 GW (Figure 1). But unfortunately, if we compare to the other geothermal producers in the world, the utilization is only 7.6% of its potential (Figure 2). The first geothermal power plant in Indonesia was the Kamojang Unit 1 at Kamojang, West Java Province, with a capacity of 30 MW; the plant began successfully operating in 1983. Despite the fluctuating development in geothermal electricity in the past, as of 2014, Indonesia's installed geothermal capacity was approximately 1401 MW, making it the economy with the third-largest installed geothermal capacity in the world. And in 2018, Indonesia successfully added its capacity to 1949 MW, making it the second largest installed geothermal capacity in the world with five years rate since first installation was 6 MW/ year. And currently the rate of geothermal installed capacity is 56 MW/year. (Figure 3). This success stemmed largely from government efforts to continuously improve several factors in order to create an environment conducive to wide private sector participation. But it needs more comprehensive study to meet Indonesia's geothermal future target in 2025, that is 7,200 MW installed capacity.

This study will identify the factors that effect the rate of geothermal in top geothermal producers in the world. So, it can be a recommendation for better geothermal future in Indonesia. We must know first, in simplified load curves of electricity (Figure 4), geothermal is a base load energy, and cannot be compared directly with other energy, such as coal or fuel.

IDENTIFYING THE NEEDS OF GEOTHERMAL STAKEHOLDERS IN INDONESIA

Figure 5 shows the key elements of successful energy development (ESMAP, 2013). Information, institutions, policies, and finance take control directly to the outcome of geothermal development project or program. The stakeholders of geothermal could be government, investors, and the social community. From an investor's point of view, the strength of each factors works to increase the expected return or reduce risk. From the government's standpoint, these factors may determine the level of investment in the geothermal energy or, indeed, whether or not such investments will happen at all. From the social community's perspective, geothermal will open a lot of job opportunity or impact to economic growth in the prospect area.

This study was started from reviewing literature and workshop/ seminar so the needs of geothermal stakeholders could be identified. The ESMAP key elements of successful energy development will be

the base of the base key factors and sub key factors. Then these factors be identified for each country to find the success factors and barriers to meet the goal of this study (Figure 6).

COMPARISON ON OTHER TOP GEOTHERMAL PRODUCERS

Basic Situation

United States

United States is located on active extensive margin (most of it is transform) geological setting with fault controlled geothermal system. The first utilization of geothermal energy in US was started from 1960 (Yellowstone). The 5 years rate since its first installation was only 4 MW/year, but now the mean installation rate is 62 MW/year. And currently, US is the largest installed capacity in the world (3591 MW, 2018).

New Zealand

New Zealand is located on active margin geological setting with low terrain geothermal system. The first utilization of geothermal energy in New Zealand was started from 1958. The 5 years rate since its first installation was very rapid (38 MW/year), but now the mean installation rate is only 17 MW/year. And currently, New Zealand geothermal installed capacity is 1,005 MW (2018).

Philippines

Philippines is located on active margin (most of it is subduction) geological setting with high terrain geothermal system. The first utilization of geothermal energy in Philippines was started from 1986. The 5 years rate since its first installation was 109 MW/year, but now the mean installation rate is 46 MW/year. And currently, Philippines is the third largest installed capacity in the world (1,903 MW, 2018).

Mexico

United States is located on active extensive margin (most of it is transform) geological setting with fault controlled geothermal system. The first utilization of geothermal energy in Mexico was started from 1973. The 5 years rate since its first installation was 15 MW/year, but now the mean installation rate is 20.7 MW/year. And currently, US is the largest installed capacity in the world (951 MW, 2018).

Turkey

United States is located on active margin geological setting with low – medium enthalpy geothermal system. The first utilization of geothermal energy in Turkey was started from 1984. The 5 years rate since its first installation was only 3 MW/year, but now the mean installation rate is 63.2 MW/year. And currently, Turkey installed capacity is 1,115 MW (2018).

Kenya

Kenya is located on active extensive margin (most of it is extensive rift) geological setting with low – high enthalpy geothermal system. The first utilization of geothermal energy in US was started from 1981 (Olkaria). The 5 years rate since its first installation was only 9 MW/year, but now the mean installation rate is 30.2 MW/year. And currently, Kenya installed capacity is 1,150 MW (2018).

Energy Mix and Electricity Market

Energy price did not have big impact to the energy mix percentage and installed capacity rate in other top geothermal producers.

Informations

Governments of US, New Zealand, and Philippines have a well-organized geothermal database. But only Kenya which has a very good access to geothermal resources because the prospect areas are nearby. While the secure and exclusive rights to resources are easily gave by the government in US, Philippines, and Turkey.

Institutions

Most of countries which have geothermal energy have geothermal institution. But only a few are serious into it. Those are US, New Zealand, and Philippines. As in institutions, research and development for geothermal that supported by government are in US, New Zealand, Philippines, and Mexico. And the US and New Zealand government willingness to support human resources should be appreciated.

Policies

Breakdown could be seen in Table 1.

Finance

It was a tricky thing. Through this item we could see how serious of governments towards the renewable energy. And only US and Turkey which are very serious into it.

Technical

The transmission network grid in US, New Zealand, Philippines, and Turkey has been planned well. And the contracts are open for private (free market).

CONCLUSIONS

If only from the installed capacity rate, Indonesia is the third rank under Turkey and US. So, we have to learn from US and Turkey, especially from the government policies to accelerate the geothermal development program. In order to accelerate the development of geothermal electricity in Indonesia,

the efforts of the government to address some issues by establishing the new Geothermal Law of 2014 are highly appreciated. Although the power of local government to regulate indirect use of geothermal resources has been revoked, but the local government has maintained the responsibility to regulate direct use of geothermal resources, then harmonizing regulations and authorities in terms of prioritizing utilization of resources should be regulated. However, when viewed from the total potential, Indonesia ranks last. We still have plenty rooms for improvements.

This study recommends following:

1. Government should consider to build a good database (subsurface and drilling) using independent verification consultants and/or to follow standards for resource certification procedures that have been applied in some economies/countries until an International Standard for Resources Certification is established to create credible resource assessment.
2. Even though geothermal and coal are base load power generator, but currently in Indonesia, geothermal could not compete with coal from the tariff, except the government is committed to the renewable energy to give financial incentive for cleaner energy or add more carbon tax for fossil fuel generator

REFERENCES

Centre, A. P. (2015). "Policy Success Factors for Geothermal Electricity Deveopment in The APEC Region". Tokyo: Asia Pacific Energy Research Centre.

Effendi, P. (2019). "Indonesian Geothermal Development: Opportunities with Workable Challenges". Bandung, West Java, Indonesia: ITB International Geothermal Workshop.

Gehringer, M., & Lokhsa, V. (2012). "Geothermal Handbook: Planning and FInancing Power Generation". Washington: The WORLD BANK Group.

IEA. (2016). "Energy Policies of IEA Countries". France: International Energy Agency.

Prambudi, N. A. (2017). "Geothermal power generation in Indonesia, a country within the ring of fire: Current status, future development, and policy". Renewable and Sustainable Energy Reviews.

Primana, J. R. (2019). "The Role and Implementations of Bappenas in Encouraging the Development of Renewable Energy". Bandung, West Java, Indonesia: ITB International Geothermal Workshop.

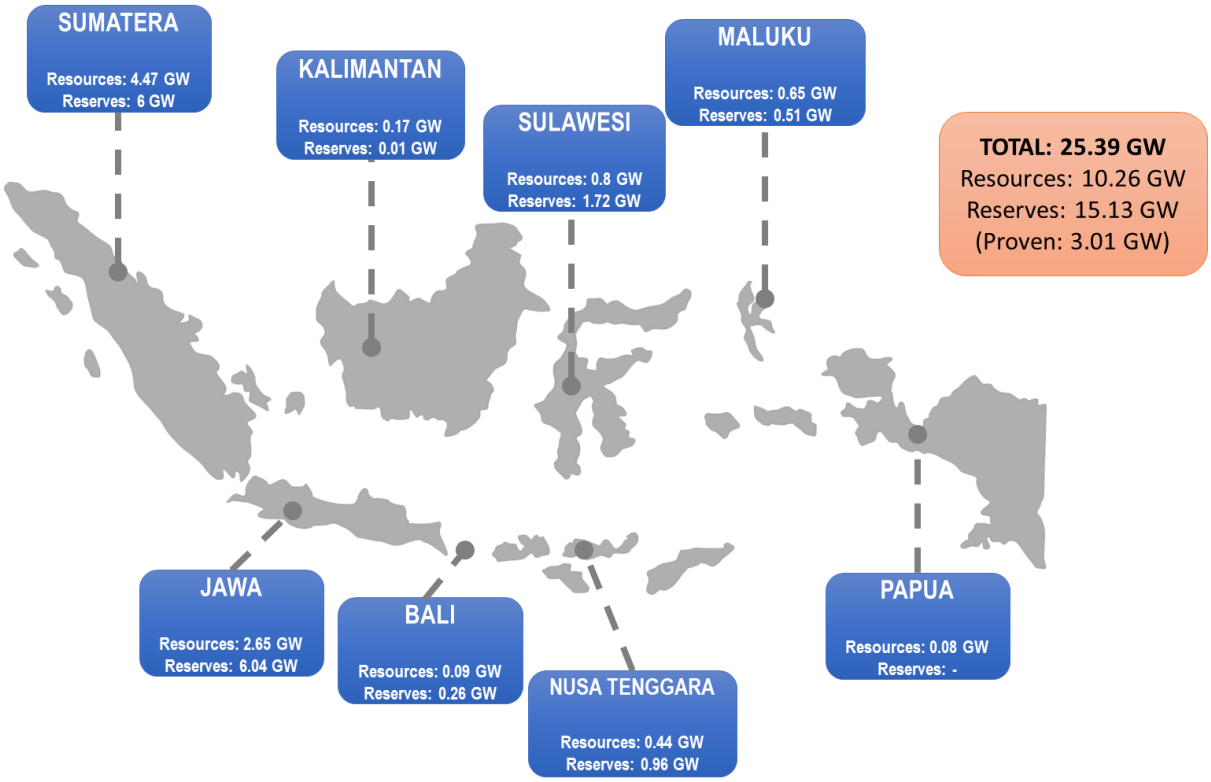


Figure 1: Geothermal Potential of Indonesia (Badan Geologi in Primana, 2019).

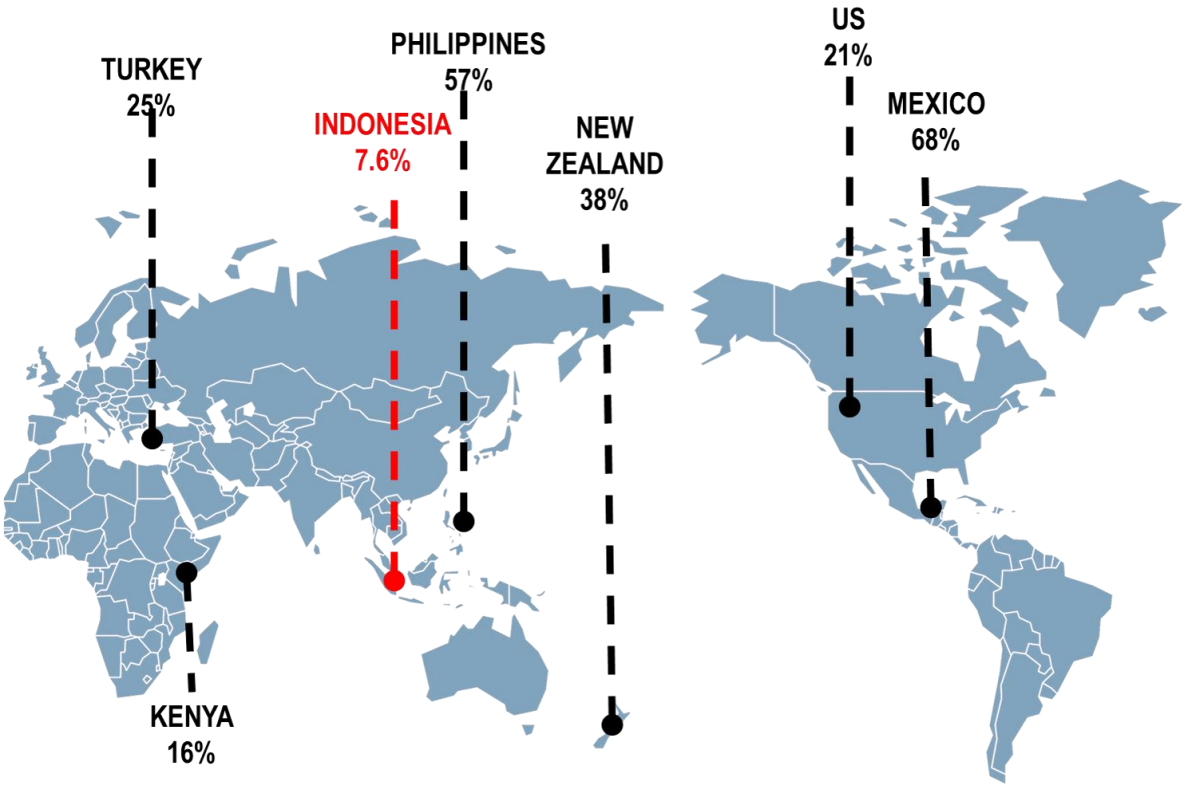


Figure 2: The Utilization of Geothermal in The World.

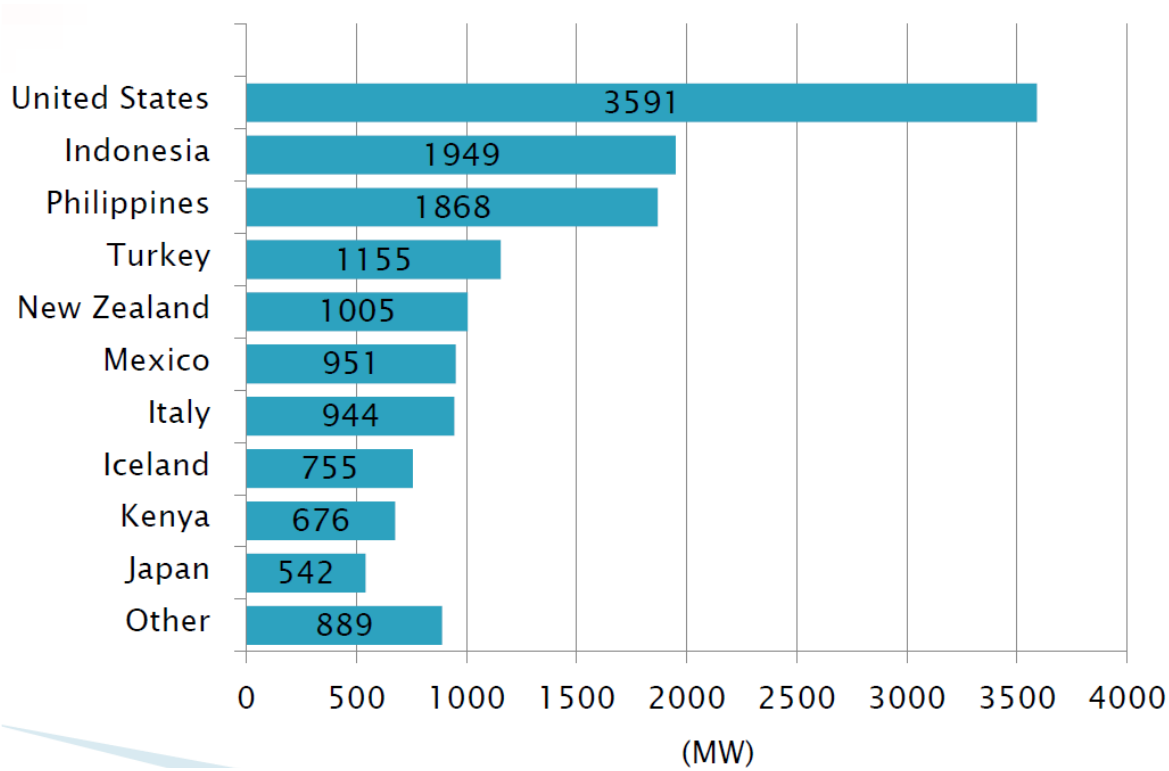


Figure 3: Installed Capacity of Geothermal Countries.

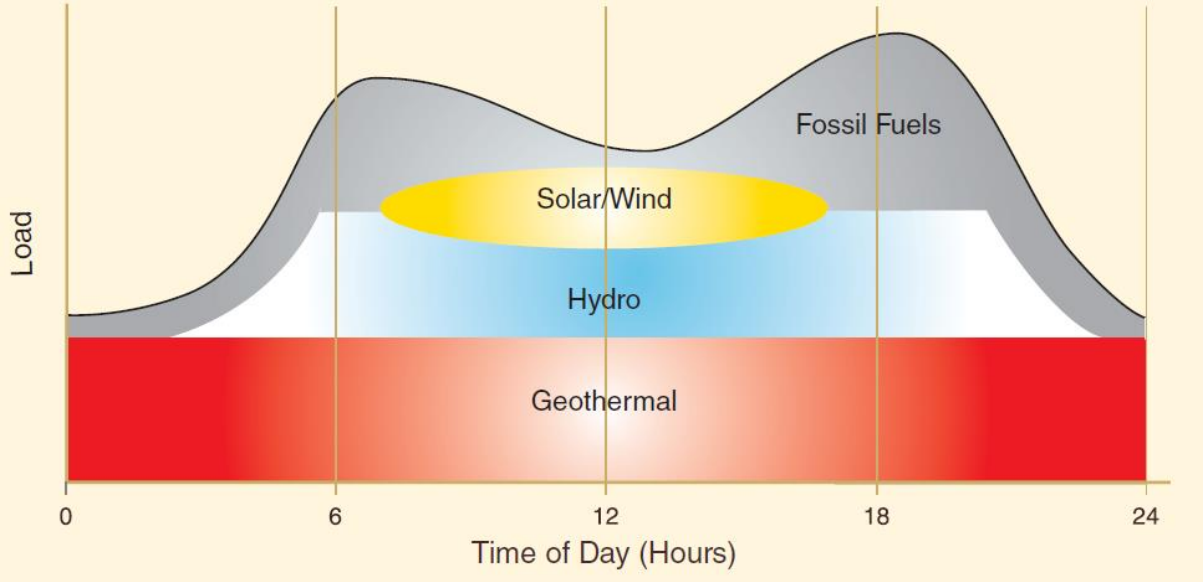


Figure 4: Simplified Load Curve with Typical Fuel Sources (Gehringer and Lokhsa, 2012).

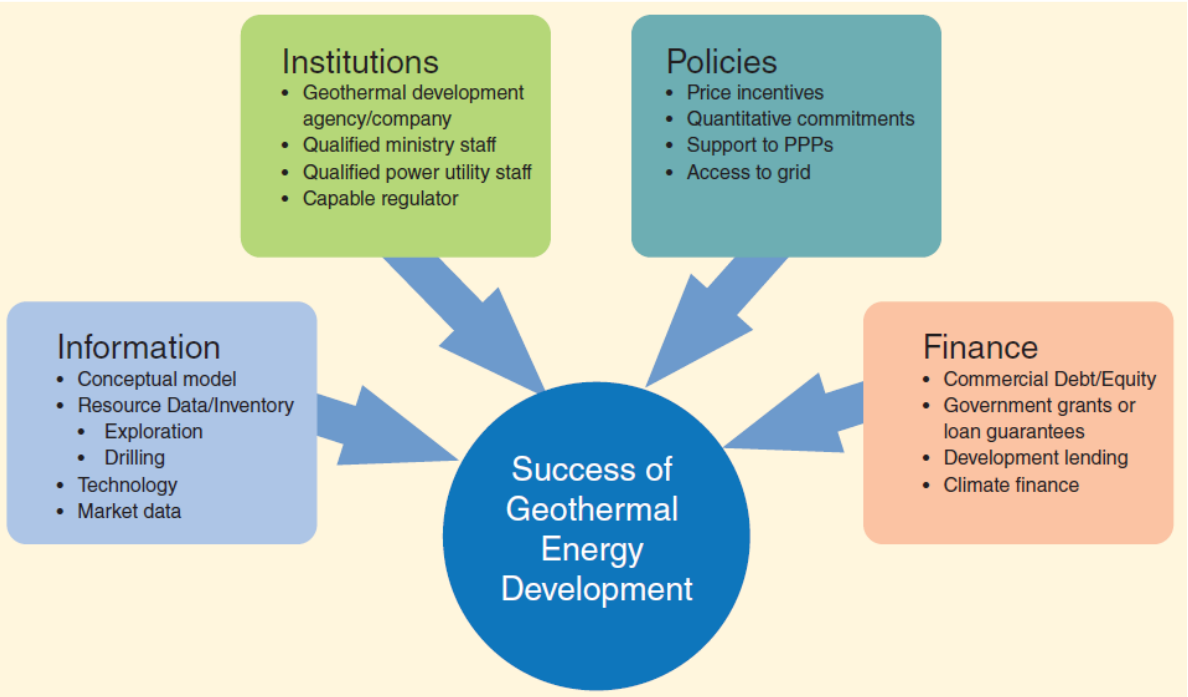


Figure 5: Key Elements of Successful Geothermal Energy Development.

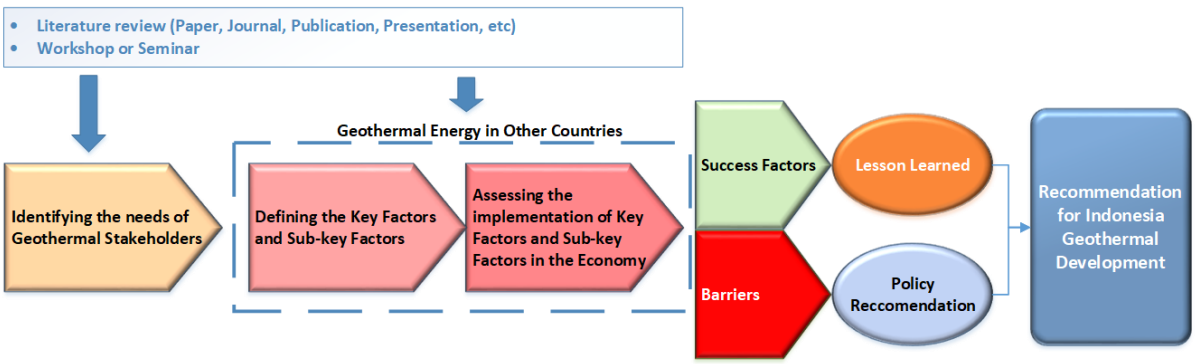


Figure 6: Methodology of study.

Table 1: Geothermal electricity development, assessment policy success factors.

Comparation Item	Indonesia	US	New Zealand	Phillipines	Turkey	Kenya	Mexico
Informations							
Database							
Access to Geothermal Resources							
Secure and Exclusive Rights to Resources							
Institutions							
R & D							
Institutions							
HRD							
Policies							
Legal Basis							
The Government Strategy							
The Government Commitment to Investors							
Permitting Time Limits							
One-Stop Permitting							
Inter-Agency Coorperation							
Finance							
Financial Incentives							
Technical							
Transmission Network							
Electricity Sales Contracting							

UTILIZATION OF MULTI-CRITERIA DECISION ANALYSIS (MCDA) IN SELECTING CONTRACT TYPES FOR GEOTHERMAL EXPLORATION DRILLING PROJECT IN INDONESIA

Farhan Muhammad[1], Vicki Agustino[1], Dorman Purba[1], Daniel Adityatama[1], Ruly Husnie[2], Mukhamad F. Umam[2], Ribka Asokawaty[4]

[1]Rigsis Energi Indonesia,
[2]Geo Dipa Energi,
[3]PPSDM Migas Cepu
[4]Geothermal Master Program ITB
Email: farhan.muhammad@rigsis.com

ABSTRACT

One of the important factors is achieving a successful drilling campaign is by having proper drilling contracts that is fitting with the current company's organizational capability. This leads to the question on which type of contract is the best for a certain drilling project, especially in the exploration phase in Indonesia. This issue is currently on the rise in geothermal industry in Indonesia due to Government of Indonesia's effort to achieve 7,200 MWe geothermal plant installed capacity in 2025. However, there is no absolute answer to that question as the decision making to choose the drilling contract type is usually involving more than one criterion. Therefore, it is necessary to use decision-maker's preferences to differentiate between alternatives.

Several drilling contract type for geothermal exploration project in Indonesia that is commonly known are discrete contract, integrated project management contract (IPM), and semi-IPM where usually the selection of contracts is primarily based on the organizational capability company has at the time. However, based on literature reviews, there are several other ways for drilling contract types that do not really fit into the three categories mentioned previously and might improve the drilling performance.

This paper discusses the application of Multi-Criteria Decision Analysis (MCDA) in assisting the decision-making process in drilling contract type selection. MCDA is considered as one of complex decision-making (DM) tool involving both quantitative and qualitative factors. It has been widely applied in various fields such as; energy and environment, business, economy and production.

The study initiated by defining clear objectives of drilling contract. Several drilling contract scenarios or alternatives are then identified to be examined where most of scenarios are developed based on published literature related to case in Indonesia. Sensitivity analysis is conducted to test whether conclusions are sensitive to changes in the model.

Keywords: Drilling contract, geothermal

BACKGROUND

Indonesia, as one of the countries with the greatest potential for geothermal energy in the world, faces various challenges in utilizing this energy source. Since the first geothermal power plant was installed on the Kamojang field in 1930, Indonesia until the end of 2018 has only managed to use less than 7%, namely 1948.5 MW, of its total potential geothermal energy that is estimated at 28.5 GW (EBTKE, 2018). Figure 1 shows the history and target of geothermal energy development in Indonesia.

Many studies have discussed various challenges in developing geothermal energy in Indonesia, where the high resource risk in the exploration phase is considered one of the main challenges (IGA, 2014; Darma, et al., 2010; Ngugi, 2014; Purba, Adityatama, Umam, & Muhammad, 2019). The level of risk is high due to the uncertainty of the existence of economic resources in the subsurface combined with the high upfront drilling cost, which makes investors think more carefully before investing.

Moreover, managing a high-cost geothermal drilling project might become more complex in the exploration phase due to shortage of personnel. It is realistic to view that a geothermal company most likely still has not yet fully establish a team to run a drilling campaign in that early stage of project. In order to address this issue, the geothermal company need to choose the most suitable drilling contract type since it precedes the performance of work and governs the operator-contractor relationship (Williams, Schaffner, & Co, 1989). By choosing the right type of contract to its current situation, a geothermal company may expect to successfully manage the drilling risk and complete the exploration phase in a timely manner that eventually could accelerate the development of geothermal energy in Indonesia.

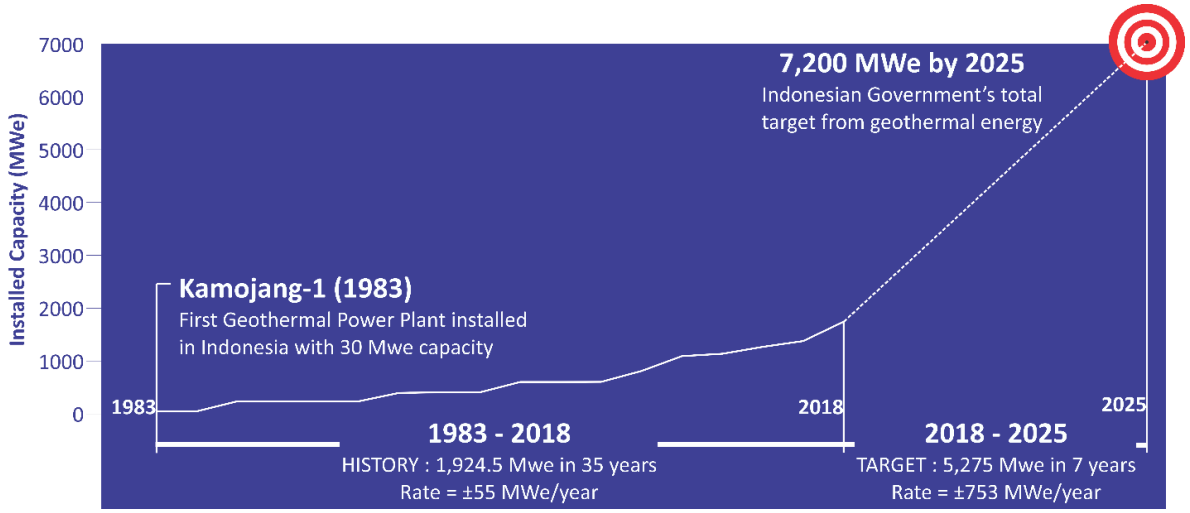


Figure 1: History and 2025 target of Indonesia geothermal development.

Consequently, the decision maker will need a reliable decision-making tool to assist him or her in choosing the type of drilling contract that is appropriate in accordance with the project characteristics and capabilities of the team that will manage the project. It is very natural if the decision maker wants the type of contract that can produce wells with the smallest possible risk, cost and effort. But then again, decision makers will find that getting the ideal conditions in accordance with it is often unrealistic so that compromise is needed on several criteria to still produce the most optimum decision in achieving the objectives related to the type of drilling contract to be used.

RESEARCH OBJECTIVES AND QUESTIONS

This study aims to investigate whether Multi-Criteria Decision Analysis (MCDA), a decision-making (DM) tool, is applicable to assists the decision maker in selecting drilling contract type for geothermal exploration project in Indonesia.
To achieve the objective, this study explores several questions as follow:

1. What are the key activities in a geothermal drilling project?
2. What kind of drilling contract types available in the market?
3. What kind of DM tool is available to select the right type of drilling contract for geothermal exploration project?
4. Are there any previous work or publication exercising MCDA in selecting drilling contract?
5. What are the objectives of decision maker in a contract type selection?
6. Is MCDA tool relevant to assist decision maker in selecting drilling contract type for geothermal exploration project?
7. What is the limitation of application of MCDA in this case?

METHOD

The main method used in this study is literature review and group discussion. The study initiated by group discussion to understand the situation and dilemma faced by the decision maker in choosing the right type of drilling contract. defining objectives of the drilling contract. Several drilling contract scenarios or alternatives are then identified to be examined where most of scenarios are developed based on published literature related to case in Indonesia. Sensitivity analysis is conducted to test whether conclusions are sensitive to changes in the model.

RESULTS AND DISCUSSION

Before exercising the application of MCDA in the drilling contract selection process, the authors of this study discussed a scenario that would be used as an example case. The discussion process mainly includes exploration drilling situation and the types of contracts that exist in Indonesia, which are described in the following sections.

Geothermal Exploration drilling in Indonesia

The understanding of the drilling project cycle and the geothermal project cycle is very important for any decision maker to enable him/her to get the most suitable type of contract for the project. Figure 2 shows an illustration of the stages of geothermal energy development projects in Indonesia in accordance with government regulations in Indonesia. In general, geothermal energy development projects in Indonesia are divided into 2 main phases, namely the exploration phase and the development phase (Figure 2).

In the exploration phase the purpose of drilling is to prove the existence of economic geothermal reserves in the sub-surface that have been initially mapped through geology, geochemistry and geophysical (3-G) surveys. Because in this phase the

level of uncertainty is still high, generally geothermal companies (developer) will only commit to drill 3-5 wells, depending on the area of interest size. After conducting exploration drilling or test drilling, the developer will conduct well testing and assess the size of the economic reserves that can be developed. Once agreement met between the developer and the government regarding the development plan, the project will continue into the development phase where the number of wells will increase according to the MW target amount.

Regarding the geothermal exploration drilling project in Indonesia, some discussion notes obtained from authors experiences were:

1. The drilling risk is still high due to very minimum sub-surface data. This creates a more challenging situation of the drilling planning stage.
2. In Indonesia, the number of drilling personnel and drilling contractors who have experience in geothermal drilling is far less than oil and gas. This made geothermal developers must compete to get experienced geothermal drilling personnel when the level of certainty in the project is still very high. Umam et al (2018) mentioned how the difference nature of geothermal to oil and gas drilling requires competency adjustment when personnel from one of the industries migrates to the other.
3. Developing companies that are undergoing an exploration phase on geothermal fields are often new companies in the geothermal industry so they have not gained the trust of the drilling contractors.

Drilling Contract

By definition, Williams, Schaffner, & Co (1989) stated that a contract is a deliberate engagement between competent parties with a lawful consideration or cause to do or not to do a particular thing; and the obligation of a contract is found in the terms in which the contract is expressed. They also mentioned that the key words of any contract are the same, which are: promise, agreement, obligation, performance, and consideration.

Several reasons why a company need to have a correct type of drilling contract are (de Wardt & van Gils, 1994; Isa, Hartono, Jayanto, & Putra, 2017):

1. To produce and maintain cost-effective quality wells.
2. To achieve highest safety standard in the process of well construction.
3. To comply with local government regulation and with company's policy.

In Indonesia drilling industry, both petroleum or geothermal, there has not yet been a standard for drilling contract type or name. However, International Association Drilling Contractor (IADC) has been providing forms or template of several types of drilling contract through their website (IADC, 2018).

In this study, several types of drilling contract that has been found through literature study and authors experiences are summarized as follow:

Based on Contract Type

1. Discrete contract

This is a term that recently used by drilling personnel in Indonesia referring to the most conventional type of drilling contract where the geothermal developer is contracting separately with the rig contractor and every other service company. This kind of approach may create a lot of contract documents, 15-23 in estimate.

2. Integrated contract

This is a term used by drilling personnel in Indonesia in describing the type of contract that brings together several drilling services into a single contract. This is done with the aim of facilitating coordination with drilling service companies because developers only need to communicate with one project coordinator. Companies that become contract leaders can be in the form of drilling rig company or other drilling service companies such as directional drilling, cementing, or other services. This kind of approach is expected to result in less document, 4-5 in estimate.

Based on Payment Scheme

1. Day rate

This is the conventional method scheme where the drilling rig and service companies are paid based on working days. The unit may be in a form of day rate or another unit rate. This type put the risk more toward on the developer, which force the developer to establish a competent internal drilling team. In Indonesia, companies that use this type are usually companies that have long been in the geothermal industry and have had experience developing geothermal fields (Isa, Hartono, Jayanto, & Putra, 2017).

2. Footage

This scheme allows the developer to pay the rig company and service companies based on contractor performance, which is footage drilled. This type put the risk more toward on the rig contractor and drilling service companies, which force the contractors to allocate the risk in their quotation.

3. Turnkey

This is the most uncommon type of drilling contract in Indonesia. The payment scheme is very simple,

the contractor will only be paid when the well is delivered as per agreed specification. This is uncommon due to the risk is almost fully absorbed by the contractor, which makes the contractor put a high quotation to the developer to compensate the risk.

Regarding the various types of contracts, the authors discuss the following points:

1. In general, the authors believe that in Indonesia geothermal developers who choose the type of discrete-day rate contract are companies that have high confidence in their internal drilling team capability.
2. For new geothermal companies in Indonesia, there is a tendency to choose the type of integrated-day rate contract, for example SOL (Sarula), SAE (Batu Raden), SGE (Jaboi) and KS Orka (Sorik Marapi and Sokoria).

Decision-making Process

Multiple Criteria Decision Analysis (MCDA) is one of the DM tool that has been widely used in many industries, including geothermal industry (Greco, Ehrgott, & Figueira, 2016; Khan, 2019; Cook, Fazeli, & Davidsdottir, 2019). The difference between MCDA and other DM or DA tool such as Financial analysis, Cost-benefit analysis and Cost-effectiveness analysis is it does not require monetized measurements, thus make it more applicable to more complex decision-making situation (Raith, 2018).

When trying to make a good decision, a person must weigh the positives and negatives of each option and consider all the alternatives (WebFinance Inc., 2019). This is also what the decision maker must do when trying to make decision on which type of drilling contract is the best for the project situation that he managed at the time. Some studies (Yadav & Paudel, 2017) describes MCDA as follows:

1. It does not provide the "right" answer
2. It does not provide an objective analysis
3. It does not relieve decision makers of the responsibility of making difficult judgements
4. It assists the decision makers to confidently making a decision by:
    a. Gain a better understanding of the problem faced.
    b. Organizing and synthesizing the entire range of information.
    c. Integrating objective measurements with value judgements.
    d. Making explicit and managing the decision maker's subjectivity.
    e. Ensuring that all criteria and decision factors have been taken properly into account.

MCDA application in drilling contract selection for geothermal exploration project.

As discussed in Introduction, this study aims to exercise the application of MCDA in assisting the decision-maker in the drilling contract type selection process. As to authors knowledge, so far there has not yet any publication on this kind of MCDA application.

Define Alternatives

The first step of applying this method is to define as many as possible unique alternative ways the decision maker will consider for contracting drilling contractors (Table 1).

Define Objectives and Criteria

The next step is to define objective of the decision. In this study, the objective of this "Getting Suitable Drilling Contract Type" decision analysis is to determine the most optimum alternative for drilling contract that gives minimum cost, minimum risk, minimum effort and maximum peace of mind. Figure 3 shows the value tree and the criteria of the decision analysis.

Based on the value tree, the criteria measurement is described as follow:

1. Cost

a. ***"Cost per well"*** is the cost of wells which includes tangible and intangible costs but does not cover infrastructure costs and the costs of internal drilling teams. In this study a discrete contract with a day rate scheme is used as a baseline where other types of contracts will experience an increase in costs due to handling fees and risk compensation. This cost assumption uses figures from studies that have been carried out by EBTKE (Purwanto et al, 2018) and is expressed in US Dollar. Table 2 shows the cost per well assumptions used in this study. The least the cost the better.

b. ***"Tender/procurement duration"*** is the duration, expressed in month, required to conduct the procurement process in obtaining contract for drilling rig and other drilling services. The duration of contract is correlate directly to the cost. The longer the procurement process the higher the cost of internal drilling personnel,

therefore the least the duration the better.

c. ***"Cost of drilling personnel"*** is the total cost that need to be spent to maintain or sustain all of drilling personnel in the geothermal developer organization to run the exploration drilling project. The least the cost of drilling personnel the better. Table 3 shows the assumption used in estimating the cost of drilling personnel of each alternative.

2. **Effort**

a. **"Number of contract document"** shows the quantity of contract document required as the consequence of the selected alternative. The main component of effort where it expressed "peace of mind" when using the alternative. The least contract document required the least effort from the geothermal developer, which, in this study, is preferable. The assumption used in this study is based on author experiences and on Hartono (2019) paper.

b. ***"Number of contractor reps"*** is the total number of representative sent by the drilling contractors. This number is directly related to number of contracts. The authors of this study assume that geothermal developer prefers to communicate with less people to avoid confusion and minimize man-hours consumption. The less the number of contractor reps the better.

"Number of internal drilling personnel" *shows how many drilling personnel assigned in the project from geothermal developer side that already shown in*

c. Table 4 "cost of drilling personnel". It expresses the difficulties geothermal developer must handle in the recruitment process due to limited supply of experienced geothermal drilling personnel in Indonesia. The less drilling personnel required the better.

3. **Risk**

a. ***"Potential market response"*** is the one of the main components of risk where it expressed "certainty" of successful tender process. The decision-maker from geothermal developer may choose any contract he or she prefers but the remaining question is whether there are any contractors that willing to participate in the tender process. The value of this criterion is using direct rating resulted from authors discussion. Alternative with the highest market response is preferable.

b. ***"Potential dispute"*** expresses the likelihood of dispute between parties involved in the contract as consequences of type of contract selected. Authors of this study believe that discrete type has the lowest possibility of dispute due to each service company contracting directly to the geothermal developer. The lower the likelihood of potential dispute the better. Same as "potential market response" criterion, the "potential dispute" is valued using direct rating in a subjective way by the authors.

c. ***"Overall risk toward geothermal company"*** shows how the alternative put risk to the geothermal developer. Same as the two aforementioned risk criterion, this criterion is valued using direct rating in a subjective way by the authors and is shown in the performance matrix criteria.

Criteria measurement and performance matrix

Based on discussion above a performance matrix of each criteria that can be measured can be developed as shown in Table 2 below.

Table 3 below shows matrix of scores for each criterion which for the quantifiable criteria the value is be derived using the linear function.

Specify the weights for each different criterion

The next step is to define the weights chosen for each criterion. "Cost per well" criterion and "Potential dispute" are given the highest weight in this study due to authors believe in the exploration phase, where uncertainty is still high the geothermal developer prefers to spend minimal investment, avoid conflict with business partners and tends to share risk. Moreover, the developer also wants to have a successful procurement process, which is indicated by market response and procurement duration. That is the reason why "Potential market response" and "Tender/procurement duration" weight ranked the second and third consecutively. The detailed work is shown in

Table 4 below.

Overall Score for each alternative

The last step is deriving the overall scores for each of the alternatives for the decision problem given by our value tree. Table 5 and Figure 4 below shows the overall score.

Authors initial expectation is to see the alternative 1-DU to come up as the best decision since it gives the lowest well cost and the lowest potential of contract dispute. However, Figure 4 above shows that the highest score is alternative 2-ISU. It does make sense since alternative 2-ISU cost is not significantly different from alternative 1-DU and still ranked second in term of potential dispute. The winning points of alternative 2-ISU from alternative 1-DU in the “number of contract document” and “number of drilling personnel required”.

CONCLUSION

The MCDA method is applicable for selecting drilling contract types in geothermal exploration projects in Indonesia. The author of this study has applied this method by acting as a decision-maker, which means other decision makers can apply this method by adjusting the value tree, performance matrix and criterion weight according to the available data and their own personal judgment.

REFERENCES

Cook, D., Fazeli, R., & Davidsdottir, B. (2019). "The need for integrated valuation tools to support decision-making - The case of cultural ecosystem services from geothermal areas". Ecosystem Services 37, 100923.

Darma, S., Poernomo, A., Pramono, A., Brahmantio, E. A., Kamah, Y., & Suhermanto, G. (2010). "The role of Pertamina Geothermal Energy (PGE) in completing geothermal power plants-achieving 10,000 MW in Indonesia". World Geothermal Congress. Bali: IGA.

de Wardt, J. P., & van Gils, J. M. (1994). "Strategies and Structures for Drilling and Service Contracts in the 1990's". 1992 SPE/IADC Drilling Conference. New Orleans: Society of Petroleum Engineers.

EBTKE. (2018, September 6). "Buka IIGCE 2018, Menteri ESDM Paparkan Terobosan Pengembangan Panas Bumi Indonesia". (K. E. Mineral, Producer) Retrieved June 2, 2019, from Direktorat Jendral Energi Baru Terbarukan dan Konservasi Energi (EBTKE): http://ebtke.esdm.go.id/post/2018/09/06/2014/buka.iigce.2018.menteri.esdm.paparkan.terobosan.pengembangan.panas.bumi.indonesia

Greco, S., Ehrgott, M., & Figueira, J. R. (2016). "Multiple Criteria Decision Analysis State of the Art Surveys Second Edition". London: Springer.

IADC. (2018). "IADC Contracts". (I. Headquarters, Producer) Retrieved June 3, 2019, from International Association of Drilling Contractors: https://store.iadc.org/product-category/contracts

IGA. (2014). "Best practices guide for geothermal exploration". Bochum, Germany: International Geothermal Association.

Isa, B., Hartono, Y., Jayanto, C., & Putra, W. M. (2017). "A non IPM Contract for Exploration Drilling in PT Sorik Marapi Geothermal Power". The 5th Indonesia International Geothermal Convention & Exhibition (IIGCE) 2017 . Jakarta: EBTKE.

Khan, I. (2019). "Power generation expansion plan and sustainability in a developing country: A multi-criteria decision analysis". Journal of Cleaner Production 220, 707-720.

Ngugi, P. K. (2014). "Risks and risk mitigation in geothermal development". Short Course VI on Utilization of Low-and Medium-Enthalpy Geothermal Resources and Financial Aspect of Utilization. Santa Tecla: UNU-GTP.

Purba, D. P., Adityatama, D. W., Umam, M. F., & Muhammad, F. (2019). "Key Considerations in Developing Strategy for Geothermal Exploration Drilling Project in Indonesia". 44th Workshop on Geothermal Reservoir Engineering. Stanford: Stanford University.

Raith, A. (2018, March). "Lecture notes ENERGY 722 Semester 1. Introduction to Decision Making". Auckland, New Zealand: The University of Auckland.

WebFinance Inc. (2019). "Dictionary". Retrieved June 1, 2019, from BusinessDictionary: http://www.businessdictionary.com/definition/decision-making.html

Williams, D. W., Schaffner, W. R., & Co, P. (1989). "Integrity and Trends in Current Drilling Contracts: Risk vs Reward". SPE/IADC Drilling Conference. New Orleans: SPE/IADC.

Yadav, M., & Paudel, C. R. (2017). "Multi Criteria Analysis for Comparison of Infrastructure Analysis". Pokhara, Nepal.

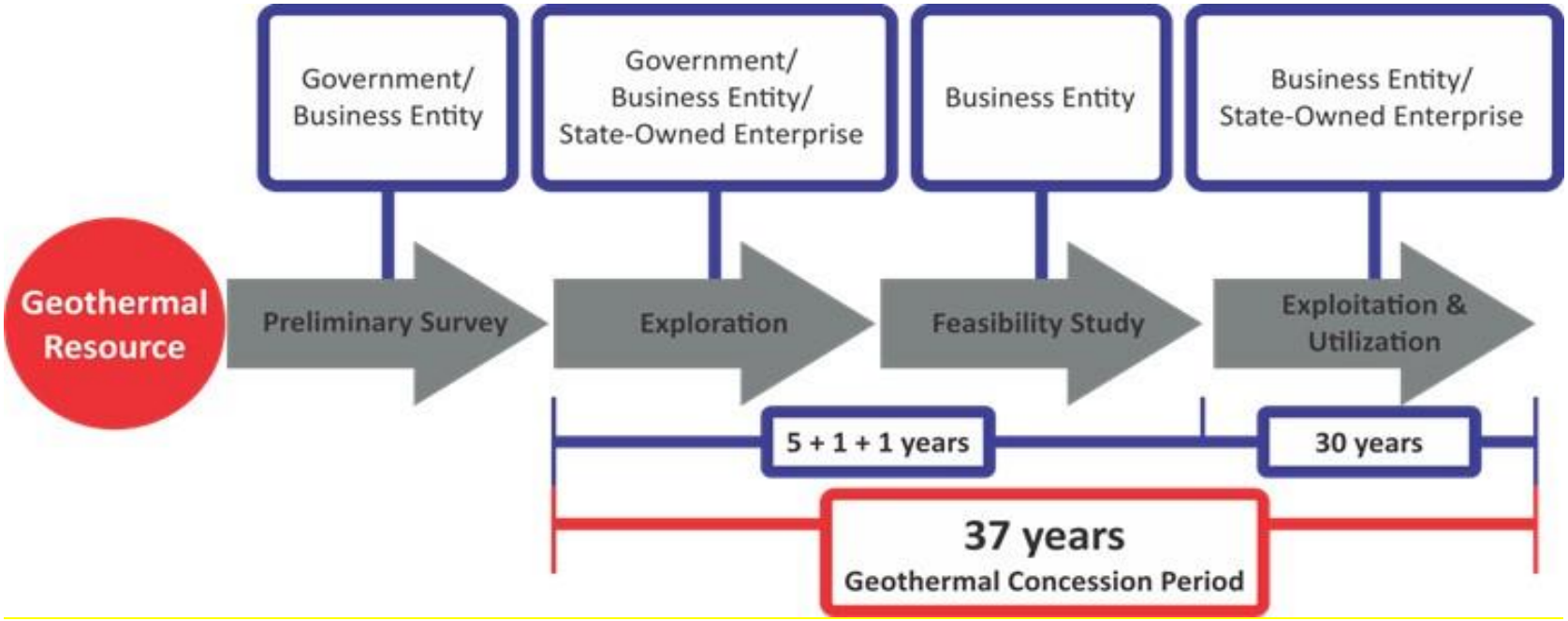


Figure 2: Geothermal energy development projects in Indonesia are divided into 2 main phases, namely the exploration phase and the development phase.

Table 1: Consideration of decision maker for contracting drilling contractors.

No	Alternative Name	Contract type	Alternative description
1	**1-DU**	Discrete + Unit Rate	• the conventional contract type where the geothermal company has contract with rig company and all other drilling services. • there will be more than **20 contract documents**: list attached • the compensation scheme will use **unit rate or day rate** since it almost impossible to apply footage scheme with 20 different parties, which makes more risk toward the geothermal company.

2	**2-ISU**	Integrated service + Unit Rate	• Recently in Indonesia geothermal drilling community, this type often called Bundled service or Semi-IPM contract. • in this alternative, rig contract is separated from other services contract, where all of the drilling services is integrated into a single contract document. • There will be **5 contract documents**: Rig contract, integrated services contract, equipment inspection contract, casing purchase contract and wellhead purchase contract • the compensation scheme is using **day rate** which makes more risk toward the geothermal company.
3	**3-ISF**	Integrated service + Footage	• Recently in Indonesia geothermal drilling community, this type often called Bundled service or Semi-IPM contract. • in this alternative, rig contract is separated from other services contract, where all of the drilling services is integrated into a single contract document. • There will be **4 contract documents**: Rig contract, integrated services contract, casing purchase contract and wellhead purchase contract • the compensation scheme is using **footage** which makes more risk toward the rig and service company.
4	**4-SubU Rig**	Sub contracted + Unit Rate (Rig as leader)	• Recently in Indonesia geothermal drilling community, this type often called IPM contract. • in this alternative, **rig act as the leader** and subcontracting other services such as directional drilling, cementing, wireline logging, etc. • There will be **4 contract documents**: Rig/IPM contract, equipment inspection contract, casing purchase contract and wellhead purchase contract • the compensation scheme is using **day rate** which makes more risk toward the geothermal company
5	**5-SubU SC**	Sub contracted + Unit Rate (Service company as leader)	• Recently in Indonesia geothermal drilling community, this type often called IPM contract. • in this alternative, **service company act as the leader** and subcontracting other services such as directional drilling, cementing, wireline logging, etc. • There will be **4 contract documents**: IPM contract, equipment inspection contract, casing purchase contract and wellhead purchase contract • the compensation scheme is using **day rate** which makes more risk toward the geothermal company.

6	**6-SubF Rig**	Sub contracted + Footage (Rig as leader)	• Recently in Indonesia geothermal drilling community, this type often called IPM contract. • in this alternative, **rig act as the leader** and subcontracting other services such as directional drilling, cementing, wireline logging, etc. • There will be **3 contract documents**: Rig/IPM contract, casing purchase contract and wellhead purchase contract • the compensation scheme is using **footage** which makes more risk toward the IPM company/drilling contractor.
7	**7-SubF SC**	Sub contracted + Footage (Service company as leader)	• Recently in Indonesia geothermal drilling community, this type often called IPM contract. Sometimes it can also be interpreted as a turnkey contract. • in this alternative, **service company act as the leader** and subcontracting other services such as directional drilling, cementing, wireline logging, etc. • There will be **4 contract documents**: IPM contract, equipment inspection contract, casing purchase contract and wellhead purchase contract • the compensation scheme is using **footage** which makes more risk toward the IPM company/drilling contractor.
8	**8-Turnkey Rig**	Full turnkey (Rig as the leader)	• The drilling of a well for a fixed lump sum price • This type of contract is not common in Indonesia geothermal industry recently. This type of contract sometimes Full IPM with **footage** compensation scheme • The leader can be **rig or any other service company** that has the capability to run the full IPM project where the risk is fully borne by the IPM contractor • Only need **1 contract document**: Turnkey contract
9	**9-Turnkey SC**	Full turnkey (Service company as the leader)	• The drilling of a well for a fixed lump sum price • This type of contract is not common in Indonesia geothermal industry recently. This type of contract sometimes Full IPM with **footage** compensation scheme • The leader can be **rig or any other service company** that has the capability to run the full IPM project where the risk is fully borne by the IPM contractor • Only need **1 contract document**: Turnkey contract

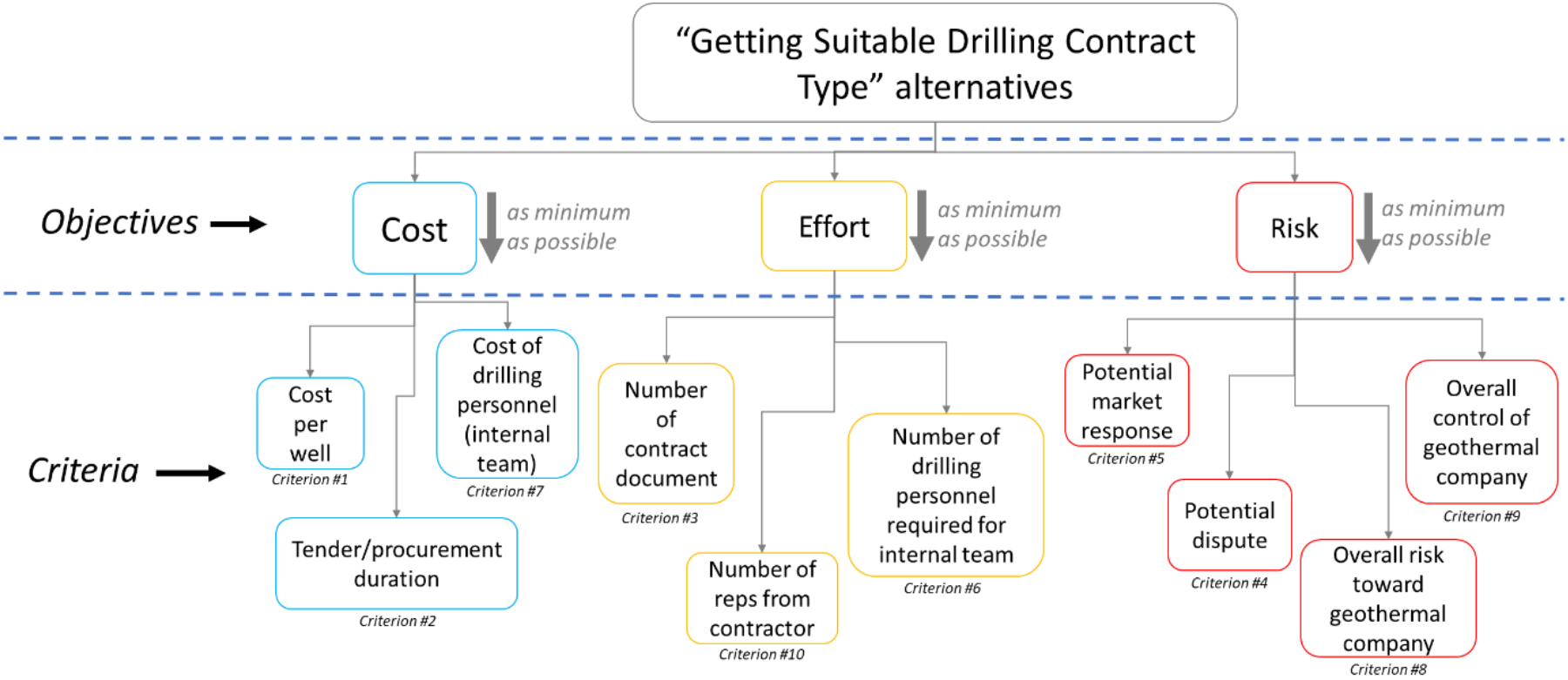


Figure 3: the Value tree and the criteria of the decision analysis.

Table 2: The cost per well assumptions used in this study.

			Mark up percentage	*25%*	*25%*	*50%*	*50%*	*75%*	
No	Alternative Name	Contract type	Baseline well cost (standard hole with 2,000m depth)	Handling fee applied by rig	Handling fee applied by service companies	Footage risk compensation applied by rig	Footage risk compensation applied by service companies	Turnkey risk applied by the contractor	Total
1	1-DU	Discrete w/ Unit Rate	$5,860,000	0	0	0	0	0	$5,860,000
2	2-ISU	Integrated service w/ Unit Rate	$5,860,000	0	$487,845	0	0	0	$6,347,845
3	3-ISF	Integrated service w/ Footage	$5,860,000	0	$487,845	$1,552,900.0	$975,690	0	$8,876,435
4	4-SubU Rig	Sub contracted w/ Unit Rate (Rig as leader)	$5,860,000	$487,845	0	0	0	0	$6,347,845
5	5-SubU SC	Sub contracted w/ Unit Rate (Service company as leader)	$5,860,000	0	$776,450	0	0	0	$6,636,450
6	6-SubF Rig	Sub contracted w/ Footage (Rig as leader)	$5,860,000	$487,845	0	$2,930,000	0	0	$9,277,845
7	7-SubF SC	Sub contracted w/ Footage (Service company as leader)	$5,860,000	0	$776,450.0	0	$2,930,000	0	$9,566,450

8	8-Turnkey Rig	Full turnkey (Rig as leader)	$5,860,000	$487,845	0	0	0	$4,395,000	$10,742,845
9	9-Turnkey SC	Full turnkey (Service company as leader)	$5,860,000	0	$776,450.0	0	0	$4,395,000	$11,031,450

Table 3: The assumption used in estimating the cost of drilling personnel of each alternative.

		Monthly payment	$ 3,000	$ 3,000	$ 4,000	$ 9,000	$ 14,000	$ 9,800	$ 12,000	$ 12,000		
Alternative name	Estimate tender/procurement duration (months)	Total number of drilling personnel required	Procurement specialist (head count)	Contract Engineer (head count)	Drilling Engineer (head count)	Sr. Drilling Engineer (head count)	Day Drilling Supervisor (head count)	Night Drilling Supervisor (head count)	Drilling Superintendent (head count)	Drilling Manager (head count)	Monthly Cost	Total Cost during the exploration drilling project
1-DU	9	14	2	2	3	1	2	2	1	1	$ 104,600	$ 1,464,400
2-ISU	11	11	1	1	2	1	2	2	1	1	$ 94,600	$ 1,513,600
3-ISF	12	5	1	1	1	1	0	0	0	1	$ 31,000	$ 527,000
4-SubU Rig	16	11	1	1	2	1	2	2	1	1	$ 94,600	$ 1,986,600
5-SubU SC	16	11	1	1	2	1	2	2	1	1	$ 94,600	$ 1,986,600
6-SubF Rig	18	5	1	1	1	1	0	0	0	1	$ 31,000	$ 713,000

7-SubFSC	18	5	1	1	1	1	0	0	0	1	$ 31,000	$ 713,000
8-Turnkey Rig	20	3	1	0	0	1	0	0	0	1	$ 24,000	$ 600,000
9-Turnkey SC	20	3	1	0	0	1	0	0	0	1	$ 24,000	$ 600,000

Table 4: Cost of drilling personnel.

PERFORMANCE MATRIX	Criterion-1	Criterion-2	Criterion-3	Criterion-4	Criterion-5	Criterion-6	Criterion-7	Criterion-8	Criterion-9	Criterion-10
ALTERNATIVES	Estimated cost per well	Estimate tender/procurement duration	Number of contract document	Potential dispute	Potential market response	Number of personnel required from geothermal company	Cost of drilling personnel hired by geothermal company	Overall risk toward thegeothermal company	Overall control of geothermal company on the project	Number of project coordinator/reps provided by the contractor
	USD	*months*	*count*	*direct rating*	*direct rating*	*count*	*USD*	*direct rating*	*direct rating*	*count*
1-DU	5,860,000	9	20	95	95	14	1,464,400	40.0	90.0	8
2-ISU	6,347,845	11	5	75	75	11	1,513,600	40.0	80.0	2
3-ISF	8,876,435	12	4	30	30	5	527,000	70.0	60.0	2
4-SubU Rig	6,347,845	16	4	60	65	11	1,986,600	50.0	50.0	1
5-SubU SC	6,636,450	16	4	65	60	11	1,986,600	50.0	50.0	1
6-SubF Rig	9,277,845	18	3	40	35	5	713,000	60.0	35.0	1
7-SubF SC	9,566,450	18	3	45	40	5	713,000	60.0	35.0	1
8-Turnkey Rig	10,742,845	20	1	10	10	3	600,000	90.0	5.0	1
9-Turnkey SC	11,031,450	20	1	10	10	3	600,000	90.0	5.0	1

Table 5: The overall scores for each of the alternatives for the decision problem.

MATRIX OF SCORE *[using linear function = 100/(best-worst)*(criterion_value - best)+100]*	**Criterion-1**	**Criterion-2**	**Criterion-3**	**Criterion-4**	**Criterion-5**
ALTERNATIVES	**Estimated cost per well**	**Estimate tender/procurement duration**	**Number of contract document**	**Potential dispute**	**Potential market response**
1-DU	100.0	100.0	0.0	100.0	100.0
2-ISU	90.6	81.8	78.9	76.5	76.5
3-ISF	41.7	72.7	84.2	23.5	23.5
4-SubU Rig	90.6	36.4	84.2	58.8	64.7
5-SubU SC	85.0	36.4	84.2	64.7	58.8
6-SubF Rig	33.9	18.2	89.5	35.3	29.4
7-SubF SC	28.3	18.2	89.5	41.2	35.3
8-Turnkey Rig	5.6	0.0	100.0	0.0	0.0
9-Turnkey SC	0.0	0.0	100.0	0.0	0.0

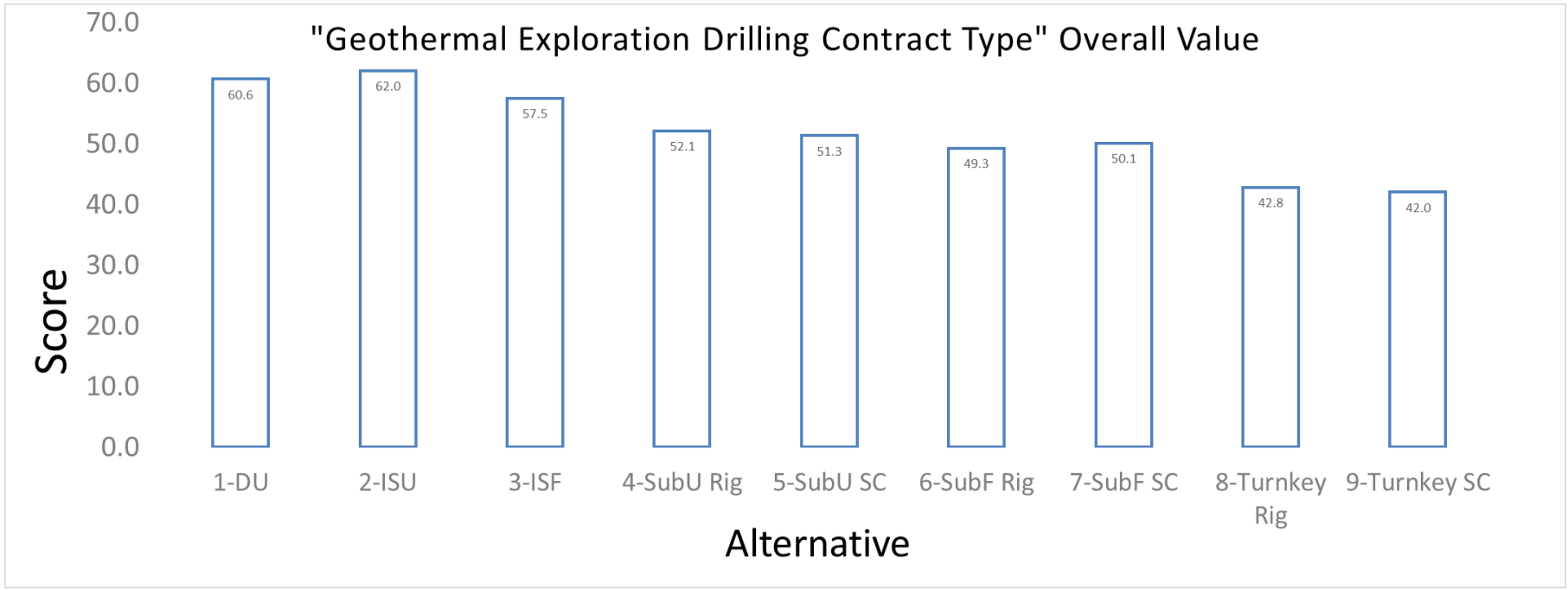


Figure 4: Histogram of the overall scores for each of the alternatives for the decision problem.

JAVAN LEOPARD IN SEGS CONCESSION AREA: THE HARMONY BETWEEN WILDLIFE AND GEOTHERMAL

Misbah Satria Giri[1], Senjaya Mercusiana[1], Nur Indah Ristiana[2], Ali Sahid[3], Willy Ekariyono[3]

[1] Gunung Halimun Salak National Park Staff
[2]Spatial Analyst of Indonesia Herpetofauna Foundation
[3] Star Energy Geothermal Salak Staff
Gunung Halimun Salak National Park Office – West Java
Email: satriagr1@gmail.com

ABSTRACT

Javan Leopard (Panthera pardus melas), considered as the most adaptable species amongst Felidae. Javan Leopard which remains biggest cat species in Java after Javan Tiger's extinction was claimed in 1980s. Several National park are justified as the habitats for Javan Leopard and Gunung Halimun Salak National Park (GHNSP) is one of them. The results of the study carried out in the last few years, leopards spread almost throughout the GHSNP area. Based on that study GHSNP is the largest habitat for leopards on the island of Java.

The Star Energy Geothermal Salak, Ltd (SEGS) concession area is on the west side of the Mount Salak. This area is an animal corridor that connects between the Mount Salak and Mount Halimun. On several occasions, direct encounters with leopards are quite common around some of the SEGS's consession area. This study tried to monitor the presence of leopards within the area of geothermal exploitation activities as well as against the population. From July to September 2018, at least 10 individuals found, 6 males and 4 females recorded by camera traps. The density of leopards in the study area is 5,5 individual/km^2. This number is higher than previous research. In the previous research, the number of individuals caught on camera was 5 individuals. Two of the same individuals discovered in 2017-2018 in a row at the same 2 locations, this indicates the leopard habitat in the area had not been disturbed. The highest encounter of leopards found at 06.00-10.00 am and 02.00-04.00 pm. This data is quite interesting, most of big cats are nocturnal animals but based on an analysis, leopards in the SEGS consession area are categorized as crepruscular animals, active during the day and night. These data also show that leopard activity is not significantly affected by geothermal activities which highly in normal working hour from the morning to evening.

Keywords: Javan leopard, geothermal, national park

BACKGROUND

Electrical energy is one of the primary needs in everyday life for both human daily needs and industry (Juwito et al., 2012). The main sources of energy generation in Indonesia today are mostly met from fossil energy. While the amount of fossil energy reserves, especially petroleum, continues decline because efforts to add new reserves are slower than the decline in existing reserves, this occurs as a result of massive exploitation carried out so far (Mary et al., 2017). In order to continue providing energy needs in the future, the government tried to find solutions for developing other alternative energy, especially from renewable and one of them is geothermal energy (Raehanayati, 2013).

Geothermal is energy produced from heat stored in rocks beneath the earth's surface. The easiest characteristic to see geothermal potential is through the presence of volcanoes. Salak Mountain is one of the volcanoes in the western region of Java Island (Global Volcanism Program, 2007). The mountains which included then Sunda volcanic arc is characterized by high geothermal activity. Volcanic activity on Mount Salak is limited to phreatic eruptions (Giri, et al. 2018) it is a great potential, which is the basis of utilization of geothermal energy by Star Energy Geothermal Salak, Ltd (SEGS).

Since 2003, Mount Salak Forest area has become a part of Mount Halimun-Salak National Park (Ario, 2007). This makes the total area increased to 113 thousand hectares Gunung Halimun Salak National Park (GHSNP). Later on this total area reduced to 87.000 Ha in 2016, so that this conservation area became the largest lowland mountain rainforest in Java. Therefore, The Mount Salak Landscape was supposed to be one of the best habitats for various wildlife species including Leopard (*Panthera pardus melas*).

P. p. melas, a carnivore that functions as the top predator on Java. According to Simber (1998) animals that become top predators have a very important role as an umbrella and flagship species in an ecosystem. Large carnivores used as umbrella species when associated with conservation area management. These animals need extensive space, so by protecting them it will automatically protect the habitat of various other species (Balme et al. 2009).

To conduct the umbrella species conservation will certainly correlated with other species habitat conservation. The importance of Javan leopard conservation activities is due to the increase in IUCN conservation status which is currently classified as "Critically endangered" (Ario et al. 2008). Javan leopard trade status according to CITES included in Appendix I groups (forbidden traded) and prohibited from being hunted (Nowell & Jackson 1996).

Javan leopard population estimates across the island of Java by Ario et al. (2008) ranged from 363-525 individuals, whereas according to KLHK (2016) the estimated population of *P.p. melas* as many as 491-596 individuals. Estimated density of *P.p. melas* in GHSNP in 2003 as many as 1 individual per 6.67 km2 while in 2007 the estimated density was 1 individual per 6.5 km2 (Harahap & Sakaguchi 2003; Ario 2007). Wibisono et al. (2018) states that there were only three national parks in Java with potential habitats that can accommodate the lives of 50 individuals *P.p. melas*, namely GHSNP, Ujung Kulon National Park, and Meru Betiri National Park. From three of these national parks in Java Island, only GHSNP has the potential to accommodate 100 individuals *P.p. melas*. The highly potential capacity of habitat *P.p. melas* in the Halimun Salak Mountain National Park area makes an interest to undertake conservation of the species.

On the other hand, the occurrence of deforestation and degradation forest area is the major disturbance to wildlife habitat, especially *P.p. melas*. Decrease in population *P.p. melas* is caused by hunting and especially habitat deforestation. According to Carolyn et al. (2013) between 2003 and 2011 GHSNP forest cover experienced a mild degradation of 6,197.13 ha and severe degradation of 1,200.15 ha. In addition, Ilyas et al. (2014) stated that there had been a decreased GHSNP forest cover area of 6,272 ha in the period between 2000 and 2010. The results of the study proved that without planned and systematic real efforts in the conservation of Javan leopards, there was 17 location led Javan leopard local extinction in 20 years (1988-2008) or 26% in Central Java (Gunawan, 2010).

The logical consequence of industrial development will be to open land because it requires a working area. Human activity is a necessity in its implementation. Therefore, in addition to hunting and deforestation, non-forestry activities, in this case geothermal utilization activities have a potential impact on the existence of *P. p. melas*. This study conducted to determine the implications of geothermal activities to the population of *P. p. melas* around the SEGS consession area.

MATERIALS AND METHODS

Study Area

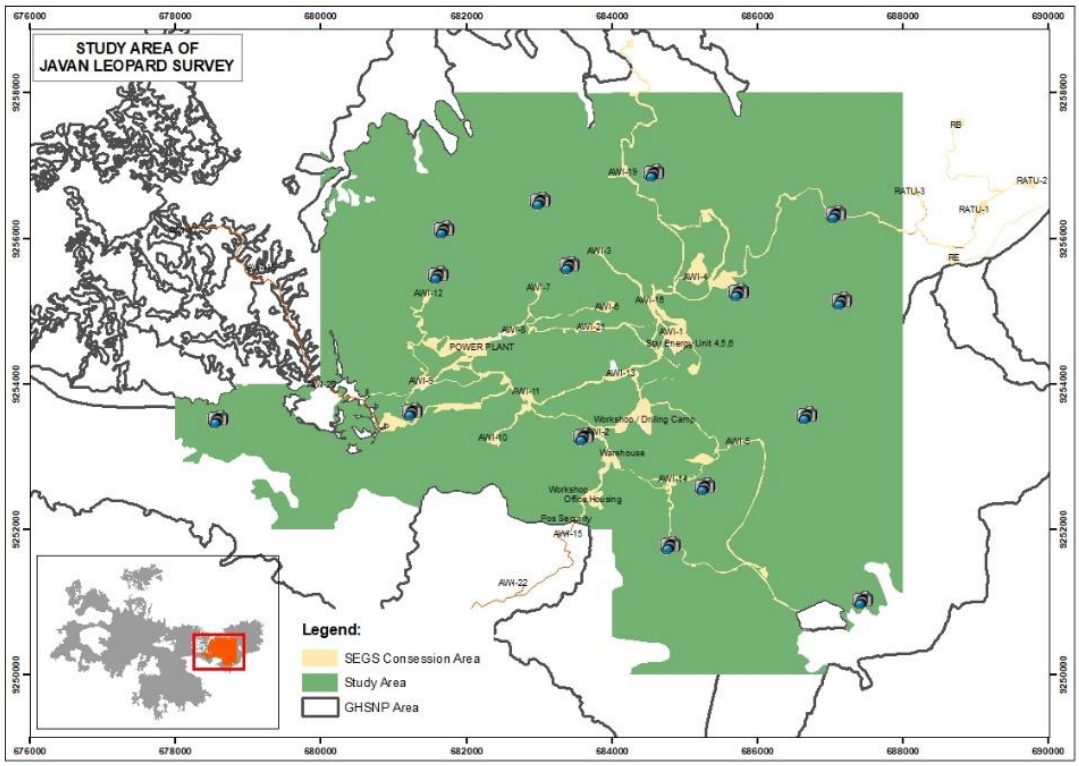


Figure 1: Activity Location and camera installation point.

The permit area for SEGS geothermal land usage or RoW (Right of Way) is 228 ha. The study area is a conservation forest area around the SEGS consession area, covering of 54.5 km^2, between 800 – 1800 m asl.

Based on the working area of the GHSNP, the location of study area was at Gunung Butak Resort, Gunung Salak II Resort, Kawah Ratu Resort, and Gunung Kendeng Resort. Administratively the location is located at Bogor and Sukabumi Regency, West Java Province.

Data Collection

Study of existence and population *P.p. Melas* is carried out using camera traps. Data collection is carried out for 71 days from 30 July - 12 October 2018. Figure 1 shows the camera installation point. Figure 2 shows the Busnel camera trap used in this study.



Figure 2: Busnel Camera trap used in this study.

Camera was installed in pairs on each predetermined grid. The total number of the grids divide into 15 area, each area cover of 2 x 2 km^2. The camera placed on each area that previously already identified as *P.p. melas* habitat. Their habitat had some indicators of their presence such as footprint, feces, scratches and the existences of animal's prey. The camera records 24 hours for 71 days.

Data Analysis

Data had been analyzing both qualitatively and quantitatively. Qualitative data analyzed mainly by crosschecking, summarizing, synthesizing, and descriptive characterization (Newing et al., 2011).

The results of the camera records identified to determine the differences of each species, so that the number of individual leopards could identified in the study area. Furthermore, quantitative analysis was carried out to determine population distribution, relative density, abundance of prey, as well as the pattern of activity of leopards at the study location. Data is processed using several software, namely: Presence, Jim Sanderson and Density Program. This software is used to estimate the density or size of animal population from capture-recapture data collected using an array of 'detectors'. Distribution mapping is done using ArcGis software. Figure 3 shows the spots pattern on black leopard.



Figure 3: Spots pattern on black leopard.

RESULTS AND DISCUSSION

Camera Capture

The camera trap is a combination of an automatic digital camera with passive infra-red moving-heat sensor. The infra-red sensor is used to detect any endothermic animal movement in front of the camera. When an endothermic animal is moving passes through infrared sensor, then the electronic system will immediately activate the camera to capture the image of moving object (Ario, 2007).

The total time of camera installation (day trap) is 71 days with an average active camera based on the result were 54.6 days. Within that active camera period, 436 images were capture. There were 21 type of objects captured can be identified including humans and other objects that could not be identified. Figure 4 shows the one of P. p. melas trapped on camera.



Figure 4: One of P. p. melas trapped on camera.

Based on the study results, there were interesting finding that the most frequent objects that captured by the camera is human (77 times) with a proportion of up to 17.6%. This shows that human (local

people) presence in the study location is quite high. On the one hand this finding shows one form of disruption to wildlife habitat especially *P. p. melas*.

The most common type of wildlife is Wild Boar (*Sus scrofa*). These animals are the most resistant to all types of habitats and quite resistant to disturbances compared to other wildlife. *P. p. melas* is on 4th position with 33 records. Table 1 shows the ten of the most objects trapped on camera.

Table 1: Ten of the most objects trapped on camera.

Object	Total
People	77
Sus scrofa	51
Paradoxurus spp	50
Muntiacus muntjak	46
Panthera pardus melas	**33**
Arborophila javanica	29
Tragulus javanica	19
Rattus spp	17
Tupaia spp	15
Mydaus javanensis	12

P. p. Melas has a variety of habitat types, because it has a high tolerance for climate and food variations (Lekagul & McNeely, 1977). Ario et al. (2008) mention that the total habitat area estimation is *P. p. melas* an area of 2,267.9-3,277.3 Km2. *P. p. melas* inhabit various forest areas on Java Island both primary forests, secondary forests, and production forests. Research results on habitat's suitability *P. p. melas* by Malau (2013) at Gunung Botol Resort, *GHSNP* was found that this area has 3,258.84 ha of area included in the class of high suitability to support life *P. p. melas*.

Study location of *P. p. melas* at SEGS consession area divide into 15 grids. Cameras were installed in pairs on each grid. 13 of the 15 grids installed by the camera managed to capture images *P. p. melas*, so the occupancy rate in this study area by 86%. Camera on two grids does not capture the objects though this survey found several indicators of the trace. Camera on these two grids captures several other species that potential to be prey like *S. scrofa, M. muntjak,* dan *M. javanica*.

Density and Population Estimation

P. p. melas can be identified and differentiated based on body size, gender, and point pattern on the body. Spot characteristics are the most effective way to identify (Ario, 2007). Leopard spots have the same function as fingerprints for human, each individual has a different pattern. Figure 5 shows the grids in the study area

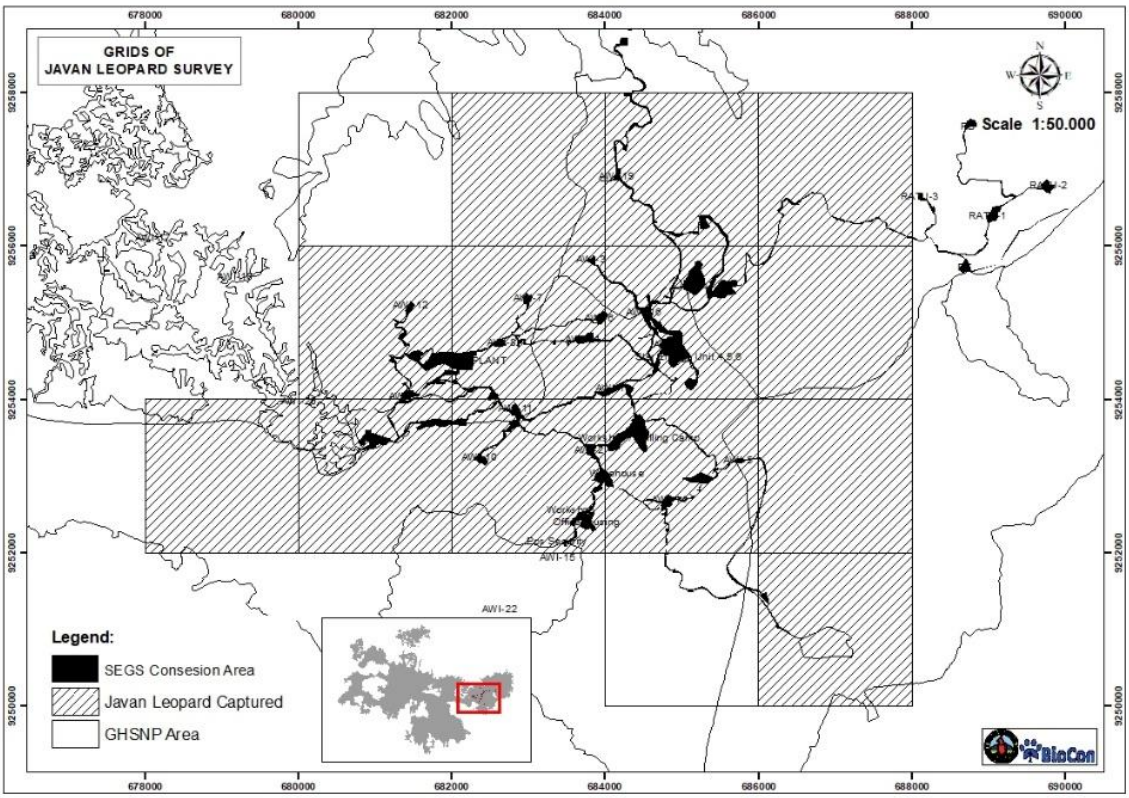


Figure 5: grids area in the study area.

Based on the analysis of 33 photos *P. p. melas*, identified 10 different individuals. These individuals consist of 6 males (4 black leopards and 1 apparent-spots leopard) and 4 females (2 black leopards and 2 apparent-spots leopard). 7 out of 10 individuals P. p. melas identified are black leopards, this is an interesting finding. Based on observations of *P. p. melas* in the mountain halimun region, the frequency of leopard apparent-spots is far more than the black leopard. We cannot analyze it further, so it is interesting finding to do further research to uncover this phenomenon.

P.p. melas has the highest density when Java tigers became extinct in the mid-1900s (Hoogewerf 1970). In 1990, the results of the study stated that *P. p. melas* spread over 12 conservation areas including national parks, nature reserves, wildlife parks and hunting parks. (Santiapillai and Ramono, 1992). Estimated density of *P.p. melas* in Gunung Gede Pangrango National Park 1 individual per 6 km2 (Ario 2006). Estimated density of *P. p. melas* in GHSNP in 2003 1 individual per 6.67 km2 whereas in 2007 the estimated density was 1 individual per 6.5 km2 (Harahap & Sakaguchi 2003; Ario 2007). Estimated population range of *P. p. melas* in Java Island ranges from 363-525 individuals (Ario et al. 2008). In 2013, LIPI estimated the population of *P. p. melas* around 491-596 individuals (KLHK 2016). Figure 6 shows the footprint of P. p. Melas.



Figure 6: Footprint, one indicator of the presence of P.p. melas found around the river.

The scope of the study area around this SEGS consession area is 54.5 km^2. The relative density can be calculated in which resulted in one individual of javan leopard per 5.5 km^2 area. This parameter value is smaller than previous research's which stated that the relative density in this region is 6.5 km2 per individual. The results of this study could be followed up by conducting a survey of the entire Mount Salak landscape so that extrapolation can be carried out to estimate the number of individuals in the entire GHSNP area.

Based on the results of the study, it was found that 72.7% of camera recordings were found in 2 grids, One of them (42.4%) encounter highest *P.p. melas* are in the quarry area. In line with the results of previous studies by Ario (2007) which stated the highest findings *P. p. melas* in the SEGS consession area are located in the Quarry location. The other region that produces the highest record is the halimun-salak coridor area. This location is estimated to be a transition region of P. *p. melas* between the landscape of Mount Halimun and Mount Salak.

Prey Abundance

Several species of Javan leopard's prey in GHSNP are deer, wild boar, Javan hedgehog, surili, black langur, coyote, partridge, squirrel, porcupine, lingsang, langur, civet civet, Javan gibbon, quail gonggong, skunk, java thorn rat, Pangolin (Harahap & Sakaguchi 2003; Yanti 2011). Based on the results, there were 10 species of Javan leopard's prey in GHSNP based on feces analysis, this including; deer, wild boar, Javan hedgehog, surili and langur (Gunawan et al., 2012). Whereas in the TNGGP, the prey animals are wild boar, mouse deer, civet civet, jungle fowl, Javanese horn, Javan slow loris, surili, langur, long-tailed monkey, antelope, anteater, porcupine and mountain squirrel (Ario 2006; Nugroho 2013; Rustiadi 2015). Figure 7 shows the prey abudance-SEGS consession area.

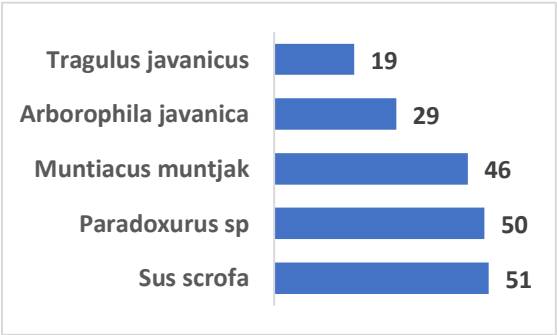


Figure 7: Prey abundance-SEGS consession area.

P. p. melas is a true carnivorous animal, these animal prey on almost all types of food. Its ability to climb and swim the choice of prey is increasingly widespread. In this survey found 18 types of prey recorded by camera traps. The type of prey consists of species in the mammal and aves class.

The five types of prey with the highest abundance were *S. scrofa* (18%), *Paradoxurus sp* (17%), *M. muntjac* (16%), *A. javanica* (10%), *T. javanicus* (7%). *S. scrofa* are most commonly find in this region, traces of hoods are always find at every survey. These animals usually move in groups with extensive habitat preferences. The content of the soil is rich in nutrients causes pig prey to be very abundant.

Diversity of *P. p. melas* preys inside SEGS consession area is the "moderate" category with an indices value of 2.439. While the evenness of the

type of prey is included in the "high" category with a value of 0.844. Diversity indices included in the category of "moderate" shows the condition of preys at SEGS consession area towards to stable. Geothermal activities are not too disturbing to the presence of prey animals around the area. This is in line with the high number of camera catches and the ease of finding traces of prey animals in the study area.

Diversity indices and evenness indices are two different things. Evenness indices values range from 0 to 1. Maximum values show relatively even numbers for all species. Evenness indices value of prey type P. p. melas in the study area close to 1, means that the number of prey populations at that location is even relative, there are no dominan individuals compared to other types.

Beside the animals prey captured by camera, primates are another type of animals that have potentially as *P.p melas* prey. There were at least four types of primates in GHSNP, namely: Javan gibbon (*Hylobates moloch*), Surili (*Presbytis comata*), Lutung (*Trachypthecus auratus*), and Long-tailed Monkey (*Macaca fascicularis*).

Activity Pattern

P. p. melas is a wandering animal (Dir PPA 1978) and an arboreal animal where dominant activities such as eating, sleeping, mating and hunting are carried out on trees (Alderton 1998). Leopards are generally quiet and have territory with signs of urine, feces, presence and scratches. Leopards are solitary animals except during the mating and caring season. Nocturnal active though sometimes they're hunting during the day. Hunting time occurs between 15.00-20.00 and 03.00-06.00 (Hoogerwerf 1970). Figure 8 shows the graph of activity patterns P. p melas by time.

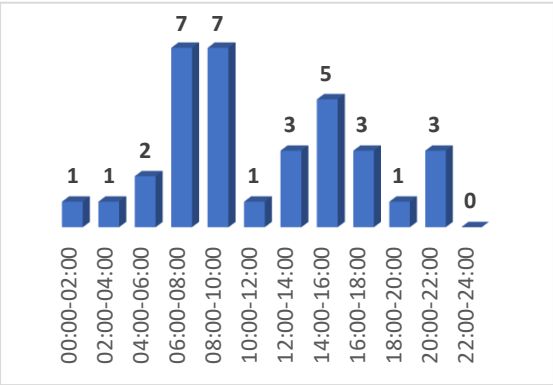


Figure 8: Graph of activity patterns P. p. melas by time.

In Figure 8, *P. p. melas* is not only active at night. In contrast, the highest encounter based on the camera catches is in the morning before noon (6:00 - 10:00 am) and afternoon before evening (02: 00-4: 00 pm). Meaning *P. p. melas* activities inside SEGS consession area not only at night (nocturnal) but also during the day (diurnal). The behavior of wildlife that has an active nature during the day and night is usually called crepuscular.

Based on the camera recording *P. p. melas* are not trapped at night in the hours of 22.00 pm - 01.00 am. Most other animals are not active at this time. This shows that most wildlife uses this time to rest. Only a few recorded nocturnal animals such as civets (*Paradoxurus sp*), Linsang (*Prionodon linsang*), and forest rats (*Rattus sp*). Figure 9 shows the comparison of activity patterns P. p. melas and its prey.

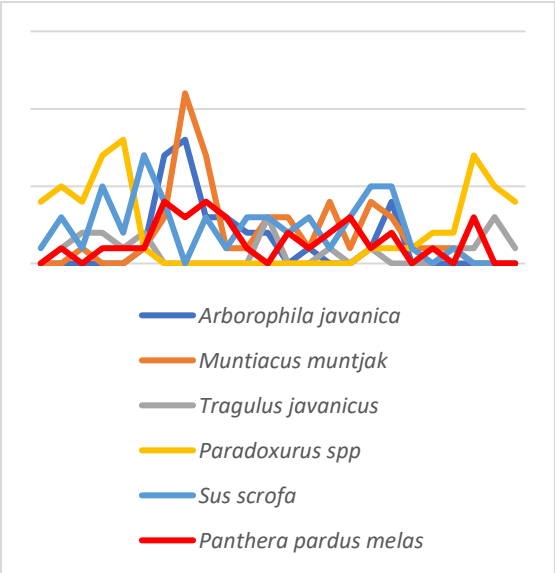


Figure 9: Comparison of activity patterns P. p. melas and its prey.

The study area that located on the western side of Mount Salak has topographic characteristics in the form of mountain's terrain with varying heights and slopes. Supported by high rainfall throughout the year causing the availability of water in the form of rivers and tributaries spread evenly. Generally, the condition of forest cover as a wildlife habitat in this region is still quite good. With such habitat characteristics, water and habitat conditions are not limiting factor for the movement of wildlife. It most likely the movement of wildlife was restricted by the locations with steep topography and slopes.

Preference for habitat selection by *P. p. melas* are influenced by the presence of prey, availability of shelter and water sources. With habitat characteristics as explained before, the pattern of activity is *P. p. Melas* is influenced by the behavior and movement of prey animals.

The pattern of javan leopard activity inside SEGS consession area was driven by several prey species such as *M. muntjac, S. scrofa, and Paradoxurus sp* (Figure 9). *M. muntjac* is generally active in the

morning to evening while *S. scrofa* and *Paradoxurus sp* are more active at night even though they are also found during the day. So that it can be determine that prey activity affects the behavior of *P. p. melas* in the study area.

Javan Leopard Around Geothermal Facility

P. p. melas is not only found in the lowlands, but also found at altitudes above 1,000 meters above sea level. As stated in Nugroho's research (2013), Habitat *P.p melas* in Gunung Ciremai National Park spread at an altitude of 1000-1500 masl. *P. p. melas* is a species that is very adaptable. *P. p. melas* can live from lowland forests to mountain forests reaching a height of more than 2,000 m above sea level. Inhabiting various forest areas on Java, both primary and secondary forests, not even a few living in production forests (plantations). *P. p. Melas* is more tolerant than tigers at extreme temperatures and dry environments (Santiapillai and Ramono 1992). Spatial utilization of *P. p. melas* is influenced by various factors, which one is prey. The spatial utilization in Gunung Gede Pangrango National Park that *P. p. Melas* used more industrial forest areas because it has a high number of species and individual prey (Nugroho 2013).

Spatial utilization of *P. p. melas* in Gunung Ciremai National Park (TNGC) are known to use two slope classes where very steep slopes used by *P. p. melas* as a place of hiding and place of birth, while the undulating class is used for hunting activities (Nugroho 2013). Ario (2007) states that the highest activity is *P. p. melas* in GHSNP is located at Quarry location and the results of his research also found that human activity did not affect the presence of *P.p. melas.*

Notes regarding direct encounter of *P. p. melas* quite often around SEGS geothermal facilities. There are several points with a high frequency of encounters such as Quarry, Batu Nonjol, and Awi 8. The time of encounter is quite varied between morning, afternoon and evening. This is in line with the activity pattern of *P. p. melas* based on the camera traps. Afternoon is an active time for geothermal activities, the mobility of personnel at this hour is quite high. This shows that geothermal utilization at SEGS consesion area does not significantly interfere with the presence and population of *P. p. melas.*

One of the facilities utilized by *P. p. melas* for their activity is a steam and brine pipelines in warm temperature due to covered by calcium silicate and aluminium cladding. SEGS area altitute and high rainfall make the air temperature at SEGS area quite low. *P. p. melas* using a steam and brine pipelines to warm his body.

The development of geothermal utilization over time referred as a form of environmentally friendly energy utilization. Geothermal fluids used to convert heat energy into electrical energy, returned to the reservoirby injection to be re-used again (renewable). In addition, SEGS minimizes forest clearing in its concession area, only total of 228 Ha or 2.28% was using from 10.000 Ha of consession area inside forrest conservation. Minimizing the land usage have implication to reduce tree cutting for construction of geothermal facilities; office, well pads, power plant, and operation roads as best practice for geothermal development. This is a guarantee to reduce disruption to habitat and wildlife populations. Figure 10 shows the multilevel piping in SEGS facilitis.



Figure 10: Multilevel piping in SEGS facilities.

The environmentally friendly development commitment also proven by several design facilities such as multilateral and directional well and multilevel piping system. Multilateral and directional well allows to drilled several wells on a well pad area. In one area, one site can accommodate up to 10 wells (Awi-1).

Multilevel piping designed to provide the pipelines construction does not using extensive land usage, as consequences, this will minimized forest clearing and tree cutting. The pipe height from the surface is about one to two meters. With this system, the presence of pipes does not limit the movement and path of *P. p. melas*. This is indicated by several encounters of *P. p. melas* on the edge and when crossing the operational road.

CONCLUSION

Conservation Forrest around the SEGS conssesion area which part of GHSNP is still in good condition. This makes the area a good habitat for *P. p. melas*. Occupancy rate of *P. p. melas* as much as 86% in the study area. Some disturbances still occur, detected by the finding of animal snare and the frequency of public activities from local people recorded on the camera.

Based on the analysis, that was identified 10 different individuals of *P. p. melas*. Then the relative density can be calculated in which results in one individual of javan leopard per 5.5 km2 area. Relative density *P. p. melas* is higher than previous research.

Direct encounter *P. p. melas*s quite often around SEGS geothermal facilities. During morning until afternoon is an active working time for geothermal activities, the mobility of personnel at this hour is quite high. On the other side, most frequent camera captured the javan leopard in between activities active in the morning before noon (6:00 - 10:00 am) and afternoon before evening (02:00 - 4:00 pm). This shows that geothermal activities at SEGS consession area does not significantly affect the presence and population of *P. p. melas*.

An environmentally friendly of geothermal development commitment proved by several design facilities that pay attention to the presence of wildlife. The design for pipelines at a distance of one to two meters from the surface with multilevel pipe let *P. p. melas* easy to crossing operational roads beneath the pipelines. Multilateral and directional well also contribute as a significant factor to minimize land usage and tree cutting.

With these types of the above design and commitment, the harmony between wildlife and geothermal activities could maintain in a good relation. The wildlife habitat keep in sustain condition and geothermal activities run in optimal production of electricity.

ACNOWLEDGMENT

This study is a collaboration between GHSNP and SEGS, Ltd. We want to thank Ir. Awen Supranata as head of the GHSNP who has provided full support in this study. Many thanks also to Irwan Januar Kusuma Hasbullah as Asset Manager SEGS for the support and all facilities provided during the survey. Furthermore, PEH colleagues, forest police, and GHSNP staff were involved both last but not least, colleagues, students, communities, and communities who are members of the PSSEJ Volunteer so that all these activities and study could accomplished safely.

REFERENCES

Ario A. (2006). "Survey of Javan Leopard Jawa (Panthera pardus melas) using camera trap in Bodogol Gunung Gede-Pangrango Natural Reserve. [Research Report]". Conservation International Indonesia, Jakarta. [Indonesia].

Ario A. (2007). "The Javan Leopard (Panthera pardus melas) Among the Human Pressures: A Preliminary Assessment for their Habitat and Preys in Gunung Halimun-Salak National Park". Conservation International Indonesia.

Ario, A., Sunarto, S. & Sanderson, J. (2008). "Panthera pardus ssp. Melas". http://dx.doi.org/10.2305/IUCN.UK.2008.RLTS.T15962A5334342.en

Carolyn, R. D., Baskoro, D. P. T., & Prasetyo, L. B. (2013). "Analisis Degradasi untuk Penyusunan Arahan Strategi Pengendaliannya di Taman Nasional Gunung Halimun Salak Provinsi Jawa Barat". Majalah Ilmiah Globe 15(1), 3947.

Giri, M. S., Mercusiana, S., Permasih I., Kurniawan H., Wasana, D. (2018). "Eksplorasi Fauna di Koridor Halimun Salak". Balai GHSNP. Sukabumi. Indonesia.

Global Volcanism Program, (2007). "Report on Salak (Indonesia)". In: Wunderman, R (ed.), Bulletin of the Global Volcanism Network, 32:9. Smithsonian Institution. https://doi.org/10.5479/si.GVP.BGVN200709-263050.

Gunawan, H., (2009). "Ekologi Macan Tutul (Panthera pardus melas Cuvier 1809) dan Masalah konservasinya". Paper disampaikan pada Seminar Penyusunan Strategi dan Rencana Aksi Konservasi Macan tutul di Hotel Safari, Taman Safari Indonesia.

Gunawan, H. (2010). "Habitat Dan Penyebaran Macan Tutul Jawa (Panthera pardus melas Cuvier, 1809) Di Lansekap Terfragmentasi Di Jawa Tengah". Disertasi Program Doktor Sekolah Pascasarjana Institut Pertanian Bogor. Not Published.

Gunawan, H., R. Wienanto, A. Riyanti dan Eman. (2012). "Teknik Konservasi Satwa Karnivora Puncak Macan Tutul Jawa (Panthera pardus melasCuvier 1809)". Laporan Penelitian pada Pusat Litbang Konservasi Dan Rehabilitasi, Badan Penelitian dan Pengembangan Kehutanan, Kementerian Kehutanan. Bogor. Not Published.

Harahap S. A. and Sakaguchi, N. (2003). "Monitoring Research on the Javan Leopard Panthera pardus melas in Tropical Forest, Gunung Halimun National Park, West Java". Research and Conservation of Biodiversity in Indonesia, Vol. XI. Bogor.

Hoogerwerf, A. (1970). "Udjung Kulon, The Land of The Last Javan Rhinoceros". E.J. Brill. Leiden, Netherlands. 252p.

Ilyas, M., Munibah, K., & Rusdiana, O. (2014). "Analisis Spasial Perubahan Penggunaan Lahan dalam Kaitannya dengan Penataan Zonasi Kawasan Taman Nasional Gunung Halimun Salak". Majalah Ilmiah Globe, 16(1), 33-42.

Juwito A. F., Pramono H., Haryono T. (2012). Renewable Energy Optimization of Electrical Power Generation toward the Energy Self-Sufficient Village in Margajaya. Jurnal Ilmiah Semesta Teknika; Vol. 15, No. 1, 22-34, Mei 2012.

Ministry of Environmental and Forestry. “Strategi dan rencana aksi konservasi macan tutul jawa (Panthera pardus melas): 2016±2026”. Jakarta, Indonesia: Direktorat Jenderal Konservasi Sumberdaya Alam dan Ekosistem, Kementerian Lingkungan Hidup dan Kehutanan Republik Indonesia; 2016.

Lekagul, B. and J. A. McNeely. (1977). “Mammals of Thailand”. Kurusapha Ladprao Press. Bangkok, 747 pp.

Malau PW. (2013). “Kesesuaian Habitat Macan Tutul Jawa (Panthera pardus melas Cuvier, 1809) di Resort Gunung Botol Taman Nasional Gunung Halimun Salak, Provinsi Jawa Barat [skripsi]”. Bogor (ID): IPB.

Mary R T., Armawi A., Hadna A. H., Pitoyo A. J. (2017). “Panas Bumi Sebagai Harta Karun Untuk Menuju Ketahanan Energi”. Jurnal Ketahanan Nasional: Vol.23, No.2, Agustus 2017, Hal 217-237.

McGregor T, al Hikmani K, Hammer M. (2011). “Expedition report: Status of the Arabian Leopard (Panthera pardus nimr) in Dhofar Sultanate of Oman”. Biosphere expedition.

Newing H, Eagle CM, Puri RK. (2011). “Conducting research in Conservation: A Social Science Perspective”. Routledge, London.

Nowell K, Jackson P (1995) “New Red List Categories for Wild Cats”. Cat News, 23, 21–27.

Nugroho J. (2013). “Analisis Pola Penggunaan Ruang dan Parameter Demografi Macan Tutul Jawa di Taman Nasional Gunung Ciremai [tesis]”. Bogor (ID): IPB.

Raehanayati, Rachmansyah, Arief, Maryanto, Sukir. (2013). “Studi Potensi Energi Geothermal Blawan- Ijen, Jawa Timur Berdasarkan Metode Gravity”. Jurnal Neutrino. 31. 10.18860/neu.v0i0.2444.

Rustiadi A, Prihatini W. (2015). “Macan tutul Jawa (Panthera pardus melas Cuvier, 1809) dan mangsa potensialnya di Bodogol, Taman Nasional Gunung Gede Pangrango”. Pros Sem Nas Masy Biodiv Indon 1(2):236-241. DOI: 10.13057/psnmbi/m010211

Santiapillai, C. and W.S. Ramono. (1992). “Status of the leopard (Panthera pardus) in Java, Indonesia”. Tigerpaper 19: 1-5.

UN ESCAPE (United Nation Economic and Social Commission for Asia and The Pacific). (2007). “Saving the Flagship Species of North-East Asia: Nature Conservation Strategy of NEASPEC”. United Nations Publication: Bangkok (TH).

Wibisono HT, Wahyudi HA, Wilianto E, Pinondang IMR, Primajati M, Liswanto D. (2018). “Identifying priority conservation landscapes and actions for the Critically Endangered Javan leopard in Indonesia: Conserving the last large carnivore in Java Island”. PLoS ONE 13(6): e0198369. https://doi.org/10.1371/journal.pone.0198369.

Yanti E. (2011). “Kajian Karakteristik Habitat dan Pola Sebaran Spasial Macan Tutul Jawa (Panthera pardus melas Cuvier, 1809) di Taman Nasional Gunung Halimun Salak [skripsi]”. Bogor (ID): IPB.

COMPARISON OF GLOBAL APPROACHES TO GEOTHERMAL RESOURCE RISK MITIGATION

Muchsin Chasani Abdul Qadir

The World Bank
Jakarta - Indonesia
Email: mqadir@worldbank.org

ABSTRACT

Geothermal is a clean and renewable energy source that can produce a reliable baseload power on 24/7 basis. Despite its abundant resources in the "ring of fire" countries, only limited known reserves which have been exploited and producing electricity. There are many reasons, which vary in many countries, for the slow pace of geothermal power development. A widely recognized obstacle of geothermal power development is the high resource risk during exploration as the initial stage of development. Exploration and confirmation of geothermal resources for power generation is high-risk and requiring a large upfront capital. Exploration drilling is normally financed by project owner's equity which may not be recovered if the resource is not confirmed or too small to be developed.

There are several approaches in many countries and regions which have been established to address the geothermal resource risk. The use of public finance, arrangement of public and private finance, and insurance are common mechanism as the approach to response on the resource risk challenge. This paper will compare and analysis the geothermal resource risk mitigation facility in country level such as Iceland, Indonesia, Japan, Kenya, New Zealand, the Philippines, Turkey, and the United States of America. Similar facilities at region level such as Latin America, East Africa, African Rift, and Eastern Europe/Central Asia will also be discussed in this paper.

Keywords: Resource risk, geothermal, mitigation

INTRODUCTION

Geothermal energy is developed through successive phases, starting with preliminary surveys and surface studies followed by exploration drilling to confirm the availability and temperature of resources, which if successful, will be followed by delineation drilling to confirm the extent and productivity of the reservoir as well as the feasibility of its exploitation. Once the resource has been confirmed and financial viability established, project finance can be structured to cover production drilling and power plant construction, after which operation can start. Figure 1 illustrates the risk profiles and capital requirements for different stages of geothermal development.

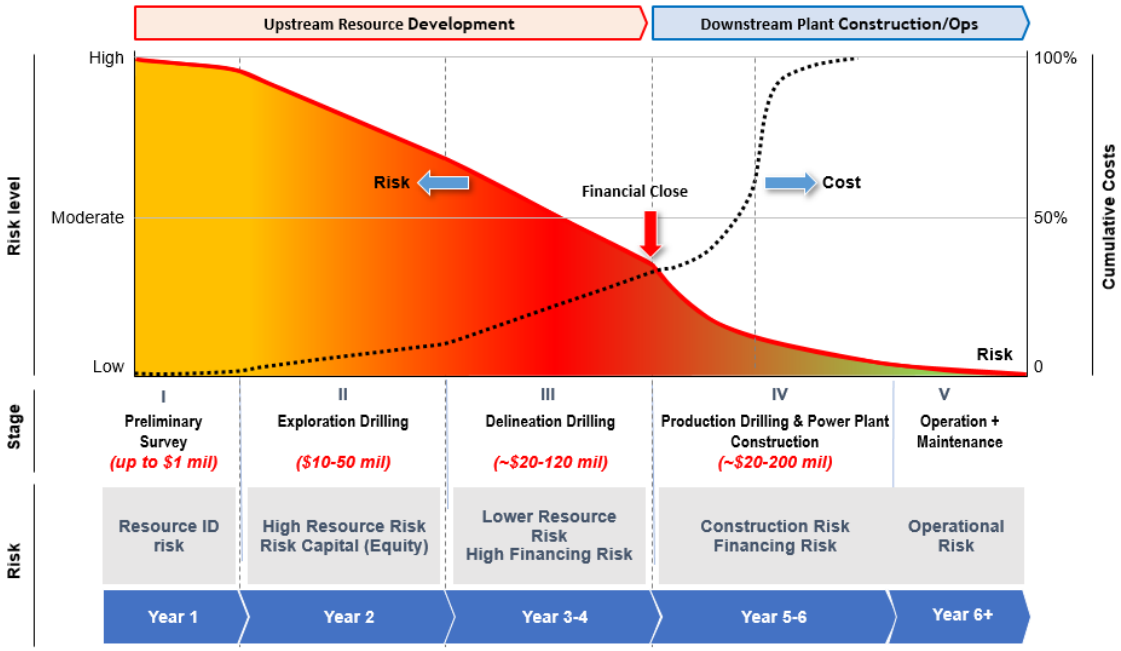


Figure 1: Stage-wise Risk Profiles and Capital Requirements for Geothermal Development (Modified from ESMAP/World Bank, 2011).

Resource risk (also known as exploration drilling risk) and the required large upfront risk capital is the key barrier to geothermal development. Exploration drilling normally requires project owner's equity or corporate finance, which may not be recovered if the drilling result reveals that the resource is not sufficient or economically viable for exploitation. Exploring and confirming geothermal resources for power generation is financially high-risk and costly. For an example in Indonesia, it is expected that an exploration drilling program will cost US$30 million assuming a minimum of three wells for a greenfield development and at least two wells producing an acceptable level of steam for the site exploration to provide satisfactory proof or resource availability. Even though the costs for exploration drilling are relatively modest compared to the total cost of developing all stages of a geothermal operation, it is the riskiest phase of the operation and finding this initial capital has proven to be challenging for developers.

RESOURCE RISK MITIGATION APPROACHES

A number of countries has already developed specific schemes to address geothermal resource risks and mobilize required capital for exploration drilling and resource confirmation. The ESMAP/World Bank report has identified four risk mitigation approaches based on the separation of the development responsibilities and financing burden at different stages of geothermal development cycle between the public and private sectors. A clear risk mitigation scheme has led to shift the resource risk to the party which is better to handle it in a given country. The ESMAP report identified four types of approaches that have been used in various countries to mitigate geothermal resource risk:

1. **Government**, acting as the total project developer from upstream to downstream (exploring, discovering, building and operating the project) and taking on the full resource and other project risks through state-owned enterprises or other government-backed entities. A clear government's commitment to support geothermal development with sufficient capacity to provide the necessary financial support has been proven to allow an accelerated geothermal growth in a country. Government could also mobilize cheap and concessional public funding to absorb geothermal resource risks and enhance the viability of projects in markets that may not been attractive for private sector with the commercial funding.

   Under this approach, resource risk has not been the only hurdle; other risk is a continuous commitment by government to support geothermal development. When the government could not maintain a high level of support and investment into geothermal development, the geothermal industry sometimes grew slowly and may even have become stalled at various stages. Some governments may not be able to mobilize concessional public funding to invest in geothermal development. Limited knowledge on the geothermal sector and coordination issues among government entities could also hinder the geothermal growth at the desired pace.

   Government or state-owned-enterprises (SOE) that develop full-scale geothermal development of both the upstream (resources) and the downstream (power plants) will absorb all the risks associated with geothermal projects, including the early stage exploration risks. Sometimes, an SOE will require a sovereign guarantee for the mobilized public finance and it also means that the government ultimately bears the risk of project failure. An exception would be when some grants are available for early stage of development from development partners outside the country, in which the resource risk would be borne by the grant provider. However, the size of the grants might not be adequate to finance the full exploration drilling program.

2. **Cost-shared drilling** between public and private entities with the resource risk is shifted to the public sector.

   Cost-shared drilling has successfully reduced resource risk in several countries and has helped in mobilizing financing for geothermal exploration/resource confirmation. Cost-shared drilling typically is applied through one of the following two forms:

   • Cost-shared of exploration drilling between the public and private sectors.
   The high-risk capital for early stage of exploration drilling will be provided by the government. This support will be expected to leverage the private finance to cover the remaining exploration fund. It will also reduce the exposure of geothermal developers to the project failure due to resource risk.

   A common scheme in this scenario is that the government provides a grant to cover some parts of exploration drilling budget. The grant for exploration drilling aims to sufficiently incentivize the private developers to mobilize private financing to undertake the geothermal development. A concessional loan may also be available from public funding sources through the government to lower the financing cost for geothermal exploration drilling.

   Recently, a typical geothermal risk mitigation facility with a contingent grant is developed in some countries and region. The contingent grant

is provided to cover some portion of exploratory drilling and will be forgiven in case for unsuccessful exploration which will not lead to any development. For successful exploration project which will continue to the development, the developer will have to repay the grant with some premium to allow the sustainability of the facility.

With this cost-shared scheme, the risk of project failure will be shared between the government and the private developer under circumstance that the geothermal project is not technically and economically justified for the next development.

• **Government-led exploration drilling to facilitate later private project development**. The government agencies or SOEs take responsibility to obtain surface data from 3G surveys and subsurface data from exploration drilling to confirm the geothermal resource and reduce the investor risk. It will then facilitate the entrance of private sector to develop the remainder of the project (i.e., through the development of the rest of the steam field, as well as power plant construction and operation). For a geothermal project with confirmed resource, the government will offer the development license to the developers. A project with confirmed resource will increase its commercial viability and thus will also attract private developers to bid for the license. In some cases, the developer which obtains the license shall repay part or all of the cost incurred by the government for exploration drilling. The government will then use the recovered cost to fund another exploration project.

In this scheme, all the risks during the exploration drilling stage will be borne and absorbed by the government.

3. **Geothermal resource risk insurance.** Insurance for a geothermal drilling process is common which will cover the developers from any drilling problems such as failure of well components, mud losses while drilling, stuck pipe, etc. Geothermal resource risk insurance is designed differently with drilling insurance to insure the productivity of a well. Megawatt capacity or a combination of flow rate and enthalpy can be defined as the parameters of well productivity. Based on the agreed success criteria by the developer and the insurance company, the premium then will be set up by the insurer based on the likelihood of payouts. The developer will pay a premium up-front prior the exploration drilling.

   Upon the completion of exploration drilling followed by various well tests, the actual productivity of well can be compared with the previous agreed success criteria. If the result is lower than the agreed parameter, it will trigger a payment from the insurance company to cover the losses by the developer.

   However, the application of geothermal resource risk insurance is still limited to date. There are two reasons that made the resource insurance is not popular scheme: (i) geothermal is a small sector compared to oil & gas and insurance company needs a large scale of portfolio to share the risk and made the coverage to be efficient, and (ii) due to the high uncertainty and risk during the exploration phase, the insurance usually offers the resource risk insurance with a high premium which may not be affordable to some developers. Figure 2 shows the geothermal development growth in Japan and the United State.

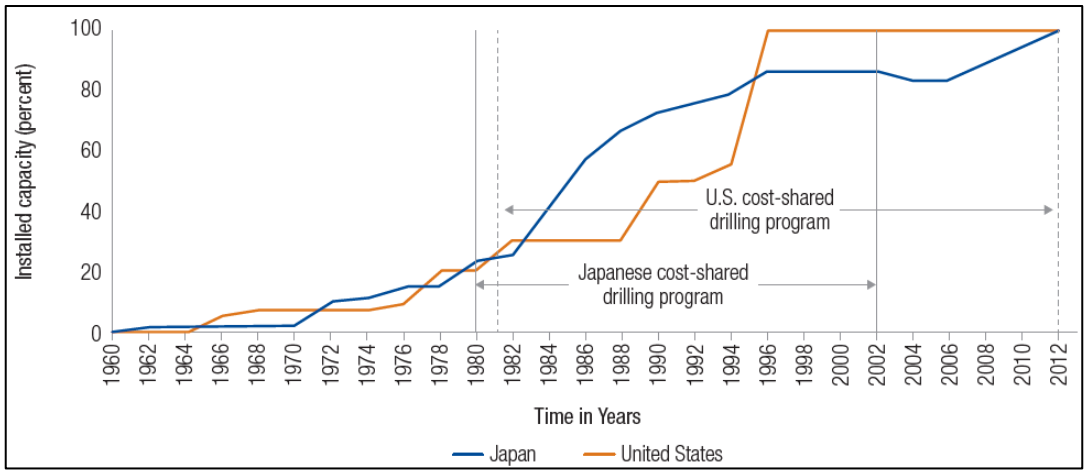


Figure 2: Geothermal Development Growth in Japan and the United States as Result of Cost-Shared Drilling Program. Source: ESMAP/World Bank, 2018.

4. **Early-stage fiscal incentives.**
   The government may provide fiscal incentives for the developers during the exploration stage to reduce the financial exposures by the developers. It can be provided in a form of tax credits, exemption of duties, etc. For the case of Indonesia, the government provides exploration incentives on the exemption of duty on imported material/equipment, tax allowance for the income tax, loss carry forward for tax deduction, and exemption on sales tax.

   Though fiscal incentives are not a purely resource risk mitigation scheme, they reduce the amount of risk capital during the exploration stage. These incentives will also reduce the exposure by the developers on the potential losses from unsuccessful exploration. Instead of being considered as risk mitigation facility, fiscal incentives are more appropriate as supporting financial facility on the geothermal exploration. Usually, the amount of fiscal incentives is minor compared to overall exploration budget. The developers will still hold the major risk on geothermal resource and project failure. The government has only risk of losing small tax revenue in the exploration stage but can hope of receiving more tax revenue from profitable geothermal projects at later stage. Non-fiscal incentives such as the Fit in Tariff, obligation for utility companies to purchase renewable power, and Renewable Portfolio Standards have also made significant contribution to the accelerated development of geothermal projects in some countries.

RISK MITIGATION FACILITIES: COUNTRY IMPLEMENTATION

By the end of 2018, the worldwide installed capacity of geothermal power generation reached 14,600 MW. The world's leading geothermal countries, in terms of installed capacity, are the USA, Indonesia, the Philippines, Turkey, and New Zealand. The risk mitigation policies and strategies for the top 5 geothermal countries were presented below. As the geothermal development pioneers, Iceland and Japan are also discussed and adding Kenya as an emerging geothermal producer in Africa.

Iceland. Commencing in 1940s, the government has encouraged geothermal exploration and research for the geothermal utilization. The work started by the State Electricity Authority, which later continued by the National Energy Authority (Orkustofnun) which was established in 1967. The work has been able to acquire geothermal resource knowledge and led to the utilization for geothermal power and space heating. While the National Energy Authority is still responsible for state sponsored exploration, a new state institute namely Iceland GeoSurvey is now becoming a key player to conduct survey for private energy developers (Orkustofnun, 2010). Figure 3 shows the geothermal development stages at various scenarios. Figure 4 shows the top 10 geothermal countries 2018.

Government / Public Sector as Total Geothermal Project Developer

Stage of development	I Surface reconnaissance	II Exploratory/ test drilling	III Production drilling	IV SAGS and power plant	V Operation and maintenance
Financing	Public funding	Public funding	Public funding	Public funding	
Developer	Public sector	Public sector	Public sector	Public sector	Public sector

Government / Public Sector led Exploration Drilling

Stage of development	I Surface reconnaissance	II Exploratory/ test drilling	III Production drilling	IV SAGS and power plant	V Operation and maintenance
Financing	Public funding	Public funding	Private funding	Private funding	
Developer	Public sector	Public sector	Private sector	Private sector	Private sector

Cost-Shared Exploration Drilling

Stage of development	I Surface reconnaissance	II Exploratory/ test drilling	III Production drilling	IV SAGS and power plant	V Operation and maintenance
Financing	Public funding Private funding	Public funding Private funding	Private funding	Private funding	
Developer	Private sector	Private sector	Private sector	Private sector	Private sector

Figure 3: Geothermal Development Stages at Various Scenarios. Source: ESMAP/World Bank, 2018.

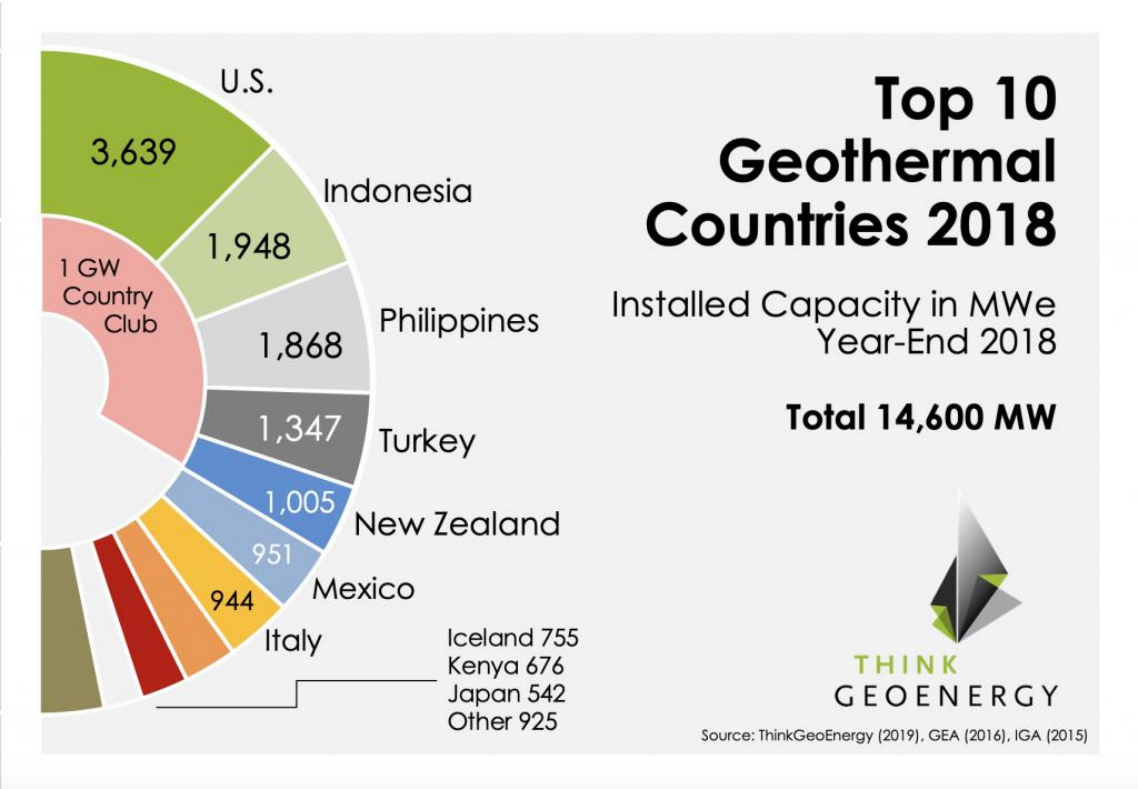


Figure 4: Top 10 Geothermal Countries 2018. Source: ThinkGeoEnergy.

The Icelandic government has also set up a Geothermal Fund in 1961 to encourage geothermal development. The fund provides grants to the State Electricity Authority to conduct reconnaissance and exploration drilling. It also provided loans to communities and farmers for exploratory and appraisal drilling covering up to 60% of the drilling expenses. The loan would be converted to grant for unsuccessful drilling. The fund was merged with the Electricity Fund and named the Energy Fund in 1967. Over 350 loans have been issued since its early establishment in 1940s that led to the use of geothermal across Iceland (Ketilsson et. al, 2015).

Indonesia. Early geothermal development was commenced in 1919 by Volcanological Society of Netherland East Indies with 5 shallow wells were drilled during 1926 – 1928 at Kamojang. There was no more study until 1971 when the Volcanological Society of Indonesia, national oil company Pertamina, and Geothermal Energy of New Zealand Ltd continued studying the Kamojang Project. Some additional wells were drilled and resulted in operation of the first geothermal power plant with capacity 250 kW in 1978 (Swandaru, 2015).

Pertamina was officially assigned by the government to conduct geothermal survey and exploration in 1974. The assignment to Pertamina was strengthened in 1981 by giving it the sole right on behalf of the government to undertake geothermal exploration and exploitation for power generation in Indonesia. Under this assignment, Pertamina was allowed to have a cooperation with other parties in a form of Joint Operation Contract (JOC). Pertamina developed the steam facility and supplied it to the power stations operated by PLN. During that period, only national utility company PLN (and its subsidiaries) had the right to develop the power stations. The first participation by private sector happened in 1980s when Pertamina appointed Amoseas Indonesia Inc and Unocal Geothermal Indonesia (later acquired by Chevron Indonesia) to manage its two concession areas and sell the steam to PLN. In 1992, the government allowed private sector participation for the development of power generation facilities. The regulation encouraged Pertamina to issue new JOCs with private developers on its 4 concession areas with larger scope to include developing upstream - downstream and selling the electricity to PLN.

The government took over the geothermal sector authority from Pertamina, and leaving 14 prospective geothermal projects to Pertamina, when the first Geothermal Law issued in 2003. Under this regime, the geothermal exploration responsibility was covered by the government and the developers. The government carried out surface studies (geology, geophysics, geochemistry) and tendered out the concession to both public and private developers. The high risk of exploration drilling was then borne by the winning of the concession tender. A Geothermal Fund Facility (GFF) was established by the Government in 2011 to provide loan to local government and geothermal developers in carrying out exploration program. While the facility could be an incentive for exploration financing which is not

available in commercial financing, the facility was not equipped with the risk mitigation facility which is highly needed during exploration stage. The GFF was managed by Government Investment Centre, an entity under Ministry of Finance (MoF). Since it was managed by government entity, provision of risk mitigation facility could mean a "state's financial lost". The terms of the facility were also considered not attractive by the developers. There was no disbursement at all on this facility until it was transfer to PT. SMI, a non-bank financial institution under MoF, in 2015.

The new Geothermal Law was issued in 2014 to improve the sector and accelerate more development. Under this regime, the government and both public/private developers play different roles in geothermal exploration stage. There are 4 pathways in conducting exploration as below:

- The government conducts surface studies through Geological Agency and tendered out the concession. The winning developer will be granted geothermal license and conduct exploration drilling at its own risk.
- The government conduct surface studies and government exploration drilling. Later, a concession tender will be carried out based on surface and subsurface information.
- The government appoints private developers to conduct preliminary survey and exploration drilling. The developer will have a privilege to win the concession tender at later stage.
- The government assigns public developers (Pertamina Geothermal Energy, Geo Dipa Energi, and PLN) to undertake geothermal exploration and exploitation.

The Infrastructure Financing for Geothermal Sector, a new label of GFF under PT. SMI, is equipped with the risk mitigation facility for geothermal exploration. The fund can be used for the financing of government sponsored drilling prior to concession tender. Public developers can also access the fund for their exploration program. Any unsuccessful exploration by public developers, the government will provide forgiveness up to 50% of the exploration loan. Under the on-going Geothermal Energy Upstream Development (GEUDP) Project, the World Bank is supporting PT. SMI for the government drilling at 4-5 geothermal sites and leveraging the facility with additional Climate Funds (Clean Technology Fund and Global Environment Facility). However, private developers do not have access to this exploration financing facility managed by PT. SMI. The facility can only provide loans to private sector for the development of geothermal power plants. The World Bank is currently discussing with the government to prepare a risk mitigation facility at exploration stage which can be accessed by both public and private developers.

Japan. The country is considered one of the pioneers in geothermal development when the first shallow well was drilled in 1919 and followed by the geothermal power production of 1.12kW in Beppu, Kyushu Island in 1925 (Nakashima et al., 2015). A significant geothermal development happened during 1970s until 1999 resulting in more than 500 MW geothermal power generation capacity. Government provided support with cost-shared drilling scheme and it was successfully stimulated geothermal projects during that period. NEDO, a government enterprise, also provided support on the nation-wide survey and technology development. The government suspended budget support for geothermal technology development in 2003 and the other budget supports for geothermal was rapidly declined. Consequently, there was no new development in Japan for about 20 years and made the installed geothermal power capacity remained at 536 MW against total potential resource of 23.47 GW.

The Fukushima earthquake and subsequent closure of nuclear power plants in Japan have renewed government policy on the geothermal energy. This renewable energy has been expected to replace the nuclear power as a base load energy. The government introduced the Feed-In Tariff for several renewable energy including geothermal depending on the size of the project. FIT of 27.3JPY/kW during first 15 years is given to geothermal projects with capacity higher than 15,000kW with large conventional flush power plant. A higher FIT rate at JPY42/kW during first 15 years is given to projects with capacity below 15,000kW with small binary power plant (Yanagisawa, 2013).

Table 1: JOGMEC's Financial Support for Development Nakashima et al (2015).

.

Stage	Support	
	National Company	**Local Company**
Surface Survey	Subsidy up to 75% of the survey cost.	Subsidy up to 100% of the survey cost.
Investigation Wells (Early Exploration Drilling)	Subsidy up to 50% of the survey cost.	Subsidy up to 100% of the survey cost.
Additional Exploration Drilling	Investment up to 50% of the equity capital of the company	
Development (Production Drilling & Power Plant)	Provision of liability guarantee up to 80% of the development expenses.	

Considering the high-risk profile of early geothermal development, in 2012 the Government assigns JOGMEC (Japan Oil, Gas and Metals National Corporation), a government enterprise, to take additional function to support geothermal

resource development. JOGMEC support on resource development includes a) Promotion and support for geological surveys (providing subsidies for geothermal resource development surveys by Japanese companies), b) Provision of financial assistance to Japanese companies (providing equity capital and liability guarantees for exploration and development of geothermal resource by Japanese companies), c) Collecting and providing information (collecting and providing information related to geothermal resources), and d) Technological developments (developing of technologies related to the exploration, drilling, evaluation and management of geothermal reservoirs). Table 1 below provides detail of government financial support for geothermal development.

As of March 2018, JOGMEC has provided subsidy program of total 27 projects and has been helping new geothermal energy development at Japan.

Kenya. The geothermal development has been commenced since 1950s and reached install capacity of power generation at 676 MW as of 2018, against total potential of about 10 GW. During 2010 – 2018, a growth of over 300% has increased of 500 MW geothermal plant capacity. Additional 560 MW is expected from Olkaria project through PPP arrangement between Kenya Electricity Generating Company (KenGen) and private sector. KenGen and the Geothermal Development Company (GDC) are the government enterprises which have been playing major roles in the geothermal development (Omenda & Mangi, 2016). GDC was established as a government's Special Purpose Vehicle to undertake surface studies, exploration, appraisal and production drilling, develop and manage proven geothermal fields, and enter into steam sales or joint development business with IPP developers. KenGen, which was established earlier to develop power generation facilities, also plays major role in the geothermal sector in Kenya. In the latest development, both entities offer the IPP developers to construct the power plants on Built-Operate-Transfer (BOT) or Built-Operate-Own-Transfer (BOOT) scheme (Omenda, 2012).

The government is responsible to conduct surface studies and exploration drilling before offering the geothermal prospects to IPP developers. The exploration program includes drilling of at least 3 deep wells. The government also takes responsibility of resource assessment by drilling additional 6-9 wells to reach 30-50% of required steam capacity (Mariita, 2007). KenGen and GDC are the government entities which are assigned to conduct those activities.

The government of Kenya provides significant financial support for the geothermal development, particularly during early stage of development and exploration. The financial support from state budget is transferred to KenGen and GDC to conduct geothermal drilling and purchase of equipment, including drilling rigs. The government also facilitates geothermal development with tax exemptions on equipment / machinery, grants, concessional climate funds, and soft loans from multilateral and bilateral development banks. A Feed in Tariff policy was also introduced by the government in 2008 and was revised in 2012 to include a fixed tariff for geothermal (Shammah et al., 2017).

New Zealand. Three government entities worked together in commencing the geothermal exploration and development after the World War II. The Department of Scientific and Industrial Research (DSIR) conducted the exploration, the Ministry of Works performed the design and construction of field facilities, and the Electricity Department developed the stations and facilities for the transmission and distribution of electricity. This effort was successfully resulting in commissioning of Wairakei power plants in 1958 as one of the first geothermal power plant in the world. The development of geothermal resources by the government entities continued until 1990s. In 1987, the Electricity Department had been reorganized as the state-owned Electricity Corporation of New Zealand (ECNZ). Another state-owned entity, Contact Energy Ltd, was established in 1996 for the development of geothermal and given Wairakei and Ohaaki projects. The Electricity Industry Reform Act of 1998 had caused privatization of Contact Energy and splitting of ECNZ into 3 state-owned entities (GeothermEx, 2010). The government continues its support for geothermal exploration and development through GNS Science (formerly DSIR) and Mighty River Power (one of the ECNZ's successors). Major geothermal development happened because of the government involvement, through its entities, in conducting reconnaissance and exploration drilling. The resource risk associated with exploration drilling was borne by the government. Some of those entities are still undertaking geothermal exploration projects today.
The resource risk for current existing geothermal projects was covered by the government through surface exploration, drilling of exploratory wells, and resource assessment made by DSIR and Ministry of Works in the decades of the 1950s through early 1980s.

The Philippines. The geothermal exploration was commenced in 1960s by the Commission of Volcanology by conducting an inventory of hot springs areas in the country. A significant progress on geothermal exploration happened in 1970s when the Philippines National Oil Company (PNOC) established Energy Development Corporation (EDC) a subsidiary dedicated for geothermal development. A private developer, Unocal

Philippines (later became Philippine Geothermal Production Company, Inc and then acquired by Chevron Geothermal Philippines Holding, Inc), also played a major role in the upstream geothermal business. For all geothermal projects at that time, the National Power Corporation (NPC) was the only entity to have the right on developing power stations. The combination of public and private participation has resulted in significant geothermal development in the Philippines during 1970s until early 1980s.

After a decade without any new development, the geothermal sector was scaling up again after the establishment of the Department of Energy (DOE) in 1992. The government offered power generation contracts to private developers with BOT scheme where the steam would be supplied by EDC and the electricity would be sold to NPC. A major development took place since then on the arrangement that EDC supplying the steam to NPC and private developers which developing and operating the geothermal power stations (ESMAP/World Bank, 2016).

The privatization policy on energy sector was introduced early 2000s. On the geothermal sector, PNOC-EDC was privatized in 2006 and followed by selling some of NPC's geothermal power stations to Aboitiz Power Renewables, Inc (APRI). After privatized, EDC also took over some of NPC's geothermal plants (Ogena, 2011). This policy resulting domination of private sector in the geothermal industry with minimum government involvement. Later in 2017, Chevron's geothermal assets were sold to the consortium of Ayala Corp and Star Energy Geothermal Holding.

The Renewable Energy Act was issued in 2008 to provide additional fiscal and non-fiscal incentives to further develop all renewable energy sources of energy, including geothermal. While the government still owns the geothermal resource and has full control and supervision over the exploration, development and utilization of the geothermal resource, an eligible developer may obtain Geothermal Service Contract / Operating Contract from the DOE. The Act incorporates a number of non-fiscal incentives such as the Feed in Tariff (but not including geothermal), Renewable Portfolio Standard, net metering, green energy option, and priority dispatch. On the fiscal incentives, the government provides Income Holiday Tax, Duty Free Importation, Special Realty Tax, Net Operating Loss Carry Over, Corporate Tax Rate, Zero Percent Value Added Tax Rate, Accelerated Depreciation, Cash Incentives for Missionary Electrification, Tax Exemption on Carbon Credit, and Tax Credit on Domestic Capital Equipment and Services. The government also provides preferential financing packages for geothermal development through the Development Bank of the Philippines, Land Bank of the Philippines, and Philippines Exim Bank, as duly recommended and endorsed by the DOE (Penarroyo, 2010).

In many ways, the geothermal development experience from the Philippines brings a good example of a balance between private and public partnerships that influenced the major scale-up geothermal development.

Turkey. The geothermal exploration was started in early 1960s by the government focusing on high enthalpy projects for power generation. A number of medium – high enthalpy prospects were discovered in 1970s – 1980s. Later, the central government was gradually withdrawing from power generation business and let the private sector to take more roles on this sector (Serpen et al., 2010). The early works on the exploration drilling was carried out by the General Directorate of Mineral Research and Exploration (MTA). In 1998, the Turkish Petroleum International Company (TPIC) was established by Turkey's national oil company with additional mandate to conduct geothermal drilling (Kaya, 2012). Exploration and drilling surveys rapidly increased since 2005 supported by continuous budget increased. Three new drilling rigs were purchased to accelerate geothermal exploration drilling (Dagistan, et al., 2015). Nevertheless, the geothermal development was still growing in slow pace. Until 2010, only less than 100 MW of geothermal power stations were installed.

The significant progress on geothermal development happened after the issuance of Renewable Energy Resources in 2005 which introduced a Fit in Tariff for geothermal at US$ 10.5 cents/kWh. A privatization policy later was implemented under the Geothermal Law issued in 2007, allowing private sector to play a major role in the sector. All the geothermal prospects which have completed the exploration surveys and drilling in various degrees shall be tendered out by MTA to private developers. The initial role of MTA during early stage exploration has mitigated some resource risk of the geothermal projects. As of 2018, installed geothermal power capacity in Turkey has reached 1347 MW and made Turkey as the 4th largest geothermal producer in the world.

The European Bank for Reconstruction and Development (EBRD) and the Clean Technology Fund (CTF) developed the PLUTO program to support exploratory drilling investments in Turkey (US$ 100 million from the EBRD and US$25 million from the CTF). The main objective is to help mitigate the early risks of geothermal projects and to provide comfort to lenders interested in providing finance at early and later stages of geothermal project development, with expectation of result at least 60 MW geothermal power projects to be developed.

Phase 1 will finance exploratory drilling, utilizing the CTF funds, and will be provided for the exploration stage. Soft loans of up to US$5 million for each project are offered with a 3-year grace period and a 7-year repayment period. PLUTO will provide up to US$2 million per well, with the developer required to provide at least 50 percent equity. If initial drilling is successful, EBRD will be available to finance the final stages of the drilling and the construction of the power plant as the second phase. **Phase 2** will provide loans to private-sector investors as a bridging fund at early stage of development of geothermal power plants.

With the on-going Turkey Geothermal Development Project, the World Bank is currently supporting Turkey's geothermal sector in providing a risk sharing mechanism for resource validation in the early stage of exploration and confirmation drilling. The project also provides financing for the production drilling stage, steam gathering facilities, and power plant construction stage.

The United States. The first commercial geothermal power plant was commissioned in 1960 at The Geysers, which continues to operate successfully until today and has grown into the largest geothermal development in the world with capacity of 750 MW. The country continues to be the world leader in geothermal production with total installed capacity of 3,639 MW as of 2018.

The peak of geothermal development growth with additional capacity more than 2,000 MW took place during 1980s – 1995. In this period, the government (federal and many states) have established various supports to reduce the financial risk of exploration and lower the exploration drilling cost for both power generation and direct use. These supports have been provided in the form of grants, loans, guaranteed loans, or industry cost sharing, and tax incentives (Bloomquist, 2005). Table 2 below summarizes the incentives for geothermal development in the USA.

Table 2: The USA Government Supports for Geothermal Development (Bloomquist (2005), Robertson-Tait (2008))

Incentives	Features
A. Loan Programs	
The Geothermal Loan Guarantee Program (GLGP)	Effective in 1975 and became the most successful program. Loan guarantees could be granted for up to 75% of the project costs with the Federal government guaranteeing up to 100% of the amount borrowed. Amended in 1980 to increase the loan size up to 90%.
	Loans were limited to $100 million per project.
The User Coupled Confirmation Drilling Program	Initiated in 1980 as cost-share expenses for exploration drilling and reservoir engineering. The facility was structured to serve as a loan guarantee. The developers would use its own equity or commercial financing. On a completely unsuccessful project, the government's cost-share was 90%.
Feasibility Study Loans	Loans would be available for up to 90% of the cost for feasibility study and preparing necessary licenses application.
Industry-Coupled Case Studies Program	This cost-share mechanism covered 20% to 50% of the exploration and reservoir confirmation costs. In exchange, developers had to provide drilling and well data.
The Loans for Geothermal Reservoir Confirmation Program	Loans were provided for surface exploration and the drilling of one or more exploratory wells. It was designed to replace the User Coupled Loan Program
B. Financial Assistance Programs	
Technical Assistance Grant Program	To provide assistance to potential developers of geothermal energy who had little or no expertise in the geothermal field to promote the rapid geothermal development.
The Program Research and Development Announcement	Initiated to provide funds for much more detailed feasibility studies such as detailed engineering and economic feasibility studies.
California State	Funding has come from geothermal royalties on state lands and the states' share of Federal royalties. Supports included, for example, resource assessment, drilling, technical assistance, regulatory compliance, technology development and demonstration and enhanced injection.
C. Taxation	
Investment Tax Credit	A Federal tax credit of 10% of new capital investment in renewable power generation.
Production Tax Credit	It provides a tax credit of $0.019 (recently increased from $0.018) per kW-hour of energy generated from renewable sources.
D. Utility Policy	
Public Utilities Regulatory Policy Act (PURPA)	Obligation by utilities to purchase the power output from geothermal power plants at its avoided cost.
Renewable Portfolio Standards (RPS)	Ensuring the electricity suppliers to have a minimum amount of supply from renewable energy including geothermal.
Renewable Energy Certificates or Credits (REC)	These credits accrue to the generator or the utility, and can be traded. Utilities will offer higher prices for RE power if they retain the RECs (rather than the developer).

While PURPA and tax credit approaches have been in use since the 1980s, the RPS, REC and carbon credit mechanisms are relatively new, and probably represent the future of legislative approaches to geothermal risk reduction.

RISK MITIGATION FACILITIES: REGION IMPLEMENTATION

There are several resource risk mitigation facilities at a region level to support the early stage of geothermal development for the countries at the region. Several key programs worldwide can be summarized as follows.

- The Geothermal Development Fund (GDF) for Latin America by KfW provides grants to cover the costs of surface studies and exploration drilling. The current facility is funded at about €50 million with expectation to catalyze the development of at least 7 projects in Central and South America with an estimated capacity of at least 350 MW. Funding is available to private companies, public institutions, or PPPs for early stage projects (surface studies which may include 1 slim hole) and confirmation drilling (preferably a 3-wells program). The eligible projects will receive 40% of eligible costs (maximum of €600,000 for surface studies as non-recoverable grants and €5.8 million for drilling projects as contingent grants, repayable if the wells are successful).
- The Geothermal Risk Mitigation Facility for East Africa (GRMF) managed jointly by the African Union Commission, German Federal Ministry for Economic Cooperation and Development, the European Union-Africa Infrastructure Trust Fund and the UK Department for International Development (DfID) provides grants to cover eligible allowable costs (20% of infrastructure preparation, 80% of surface studies, 40% of exploration drilling and testing for confirmation wells), and 30% on follow-on activities (additional drilling, well head generation unit, long term discharge testing, updating reservoir evaluation, and conducting Feasibility Studies). Funds are provided on a reimbursement basis, requiring developers to have funds available upfront. There is no requirement to repay any of the GRMF grants. The facility began in 2012 with the size of €115 million. As of mid-2017, GRMF is in its fourth round of applications, and it is expected that the next (fifth) round will be the last.
- The long-standing African Rift Geothermal Development Program (ARGeo) is a multi-donor funded risk mitigation facility, capacity building and knowledge sharing platform for Kenya, Tanzania, Ethiopia, Uganda, Rwanda and Eritrea to promote geothermal development for electricity generation.

  ARGeo has two major components: **Technical Assistance Grants** for surface exploration and identification of drilling targets at geothermal prospects in Kenya (Silali), Ethiopia (Tendaho-Dubti), Uganda (Kibiro) and Tanzania (Ngozi-Mbeya). Grants are provided by ARGeo to procure scientific equipment and software, and to undertake exploration by local parties and/or international consultants. **The second component** is related to regional networking, information systems, policy advice, capacity building and awareness creation.

  GeoFutures Facility was recently introduced to improve the risk mitigation instrument for East Africa. The supports provided by this facility are presented as below:

Table 3: Features of GeoFutures Facility (Robertson-Tait et al. (2017)).

Facility	Coverages
Pillar 1 - Technical Assistance	
Enabling environment for geothermal development and respond to specific technical needs of projects.	Grant of 100% from eligible costs.
Pillar 2 – Direct Finance	
Focused exploration work (de-risking of the selection of well locations and drilling targets, such as detailed geophysical surveys and temperature gradient surveys)	Grant of 40% from eligible costs.
Infrastructure development (roads, drilling pads and water supply)	Contingent grant of 40% from eligible costs to be repaid when projects are developed.
The first exploratory drilling (at least the first well, and possibly the first 2 or 3 wells)	Grant of 40% from eligible costs.
Pillar 3 – Risk Mitigation Instruments	
Due Diligence Facility (due diligence study to underwrite the resource risk)	The facility will cover 60% of the due diligence costs which are assumed to be about US$150,000. This fund would be issued as a contingent loan that would be recoverable (repaid) in the event of a successful project.
Premium Payment Facility (payment for the premium of insurance)	The premium rates are likely to be in the range of 15-25% of total drilling cost. This means that premiums may be $8.4 million per project, assuming a drilling cost of $7 million per well, a 20% premium, and that a 6-well program that would be insured. The facility will cover 60% of the premium cost. The funds provided to cover the premium costs will be repaid by the project in the event of a successful project, and by the insurers in the event of an unsuccessful project, ensuring that this facility will be replenished and recycled many times over without recourse to public funds

- The earlier WB-supported Geothermal Energy Development Program (GeoFund) for countries in the Eastern Europe and Central Asia Region channeled Global Environment Facility (GEF) grants to improve geothermal policies, with expected follow-on funding envisaged for a Geological Risk Insurance (GRI) component to be designed to mitigate the geological risks associated with geothermal energy exploration and operation (though this did not materialize).

CONCLUSIONS

The high resource risk is perceived as a major barrier to geothermal development worldwide because it could make geothermal development stalled in its initial stages. This risk also makes difficult in mobilizing required financing for the early exploration drilling. A large number of geothermal developments have been undertaken by government through its entities including national oil companies and state-owned enterprises.

Cost sharing of resource risks between the public and private sectors has enabled risk capital and private expertise to be mobilized towards geothermal drilling. Cost sharing is a win-win situation in that it reduces the burden on public finances while catalyzing geothermal development by the private sector. It is also relatively straight forward to implement, monitor, and manage.

Although it can also help attract risk capital to geothermal projects, the experience with geothermal well productivity insurance schemes is limited, and the results have been mixed. While an insurance scheme does not require explicit government support, the high uncertainty at the exploration stage and the relatively small pool of available projects has made it difficult to diversify geothermal resource risks through a market mechanism without the imposition of high insurance premiums.
Risk mitigation schemes, while critically important for tackling a major barrier to getting a geothermal development initiated, may not be sufficient, if implemented in isolation, to lead to successful execution throughout the multiple stages of development in a geothermal project. For this reason, it is important that any specific risk mitigation instrument is applied in coordination with other incentives that enhance the overall investment climate for geothermal development.

Five funding instruments options which have been applied in several countries might be applicable to support the geothermal exploration stage: loan guarantee, lending support mechanism to buy down the cost of financing, concessional loans, contingent grants, grants, technical assistance, tax incentives, and resource risk insurance. Policy incentives such as attractive tariff and ensured offtake on the geothermal electricity also contribute the creation of attractive investment climate for the geothermal industry.

REFERENCES

Bloomquist, G., (2005). "The Evolution of U.S. Policy Designed to Encourage Geothermal Development Provision of Access and Encouraging Project Development". Proceedings World Geothermal Congress 2005.

Boyd, Tonya et al., (2015). "The United States of America Country Update 2015". Proceedings World Geothermal Congress 2015.

Dagistan, Hayrullah et al., (2015). "Geothermal Explorations and Investigations by MTA in Turkey". Proceedings World Geothermal Congress 2015.

Carey, Brian et al., (2015). "2010 – 2015 New Zealand Country Update". Proceedings World Geothermal Congress 2015.

The ESMAP/World Bank, (2012). "Geothermal Handbook: Planning and Financing Power Generation".

The ESMAP/World Bank, (2016). "A Global Survey: Comparative Analysis of Approaches to Geothermal Resource Risk Mitigation".

The ESMAP/World Bank, (2018). "Opportunities and Challenges for Scaling Up Geothermal Development in LAC".

Fronda, Ariel et al., (2015). "Geothermal Development in the Philippines: The Country Update". Proceedings World Geothermal Congress 2015.

Gehringer, M., (2017). "Alternative Design of Geothermal Support Mechanism and Risk Mitigation Funds".

GeothermEx, (2010). "An Assessment of Geothermal Resource Risks in Indonesia". The World Bank report.

Handoko, Bayu et al., (2015). "History of Joint Operation Contract in Indonesia". Proceedings World Geothermal Congress 2015.

Imolauer, K., Ueltzen, Maria., (2015). "Risk Mitigation Systems in Comparison".

Kaya, T., (2012). "Geothermal Project Development in Turkey - An Overview with Emphasis on Drilling". GRC Transactions, Vol. 36, 2012.

Ketilsson, Jonas et al., (2015). "Legal Framework and National Policy for Geothermal Development in Iceland". Proceedings World Geothermal Congress 2015.

Lund, J., Bloomquist, G., (2012). "Development of Geothermal Policy in the United States – What Works and What Doesn't Work". Proceedings

37th Workshop on Geothermal Reservoir Engineering, Stanford University.

Mariita, N., (2007). "Hurdles to Financing Geothermal Development in ARGeo Countries with Special Focus on Kenya". GRC Transactions, Vol. 31, 2007.

Nakashima, Hidefumi et al., (2015). "On the Japan's Geothermal Energy Development and the Role of JOGMEC". Proceedings World Geothermal Congress 2015.

Ogena, M. S (2011), "Philippine Geothermal Industry Updates 2011". Proceedings of the 9th Asian Geothermal Symposium, 7-9 November 2011.

Omenda, Peter (2012). "Geothermal Development in Kenya: A Country Update – 2012".

Omenda, Peter and Mangi, Peketsa (2016), "Country Update Report for Kenya 2016". Proceedings, 6th African Rift Geothermal Conference.

Orkustofnun (2010), "Geothermal Development and Research in Iceland".

Penarroyo, Fernando (2010), "Renewable Energy Act of 2008: Legal and Fiscal Implications to Philippine Geothermal Exploration and Development". Proceedings World Geothermal Congress 2010.

Robertson-Tait et al. (2008). "Managing Geothermal Resource Risk – Experience from the United States". Workshop on Geological Risk Insurance, World Bank GEOFUND Project.

Robertson-Tait et al. (2015), "An Evaluation of Risk Mitigation Approaches for Geothermal Development".

Robertson-Tait et al. (2017), "The GeoFutures Facility: A Proposed Geothermal Risk Mitigation Instrument for East Africa". GRC Transactions, Vol. 41, 2017.

Serpen, Umran et al. (2010), "2010 Present Status of Geothermal Energy in Turkey". Proceeding of 35th Workshop on Geothermal Reservoir Engineering, Stanford University, 2010.

Shammah, Kiptanui et al. (2017). "Subsidies in Kenya's Geothermal Sub-Sector". GRC Transactions, Vol. 41, 2017.

Speer, Bethany et al. (2014). "Geothermal Exploration Policy Mechanisms: Lessons for the United States from International Applications". NREL Technical Report.

Swandaru, Roy (2015), "The History of the Earliest Geothermal Power Plants in Indonesia". Proceedings World Geothermal Congress 2015.

Yanagisawa, Norio (2013), "Geothermal Development Progress in Japan after Earthquake, 2011". Proceedings Australian Geothermal Energy Conferences 2013.

RAPID ENVIRONMENTAL AND SOCIAL IMPACT ASSESSMENT TO AVOID HIGH-RISK AREAS IN GEOTHERMAL EXPLORATION AND DEVELOPMENT

Agustina Parwitosari, Ninin Kania Dewi, Muchsin Chasani Abdul Qadir

The World Bank
Jakarta - Indonesia
Email: aparwitosari@worldbank.org, ndewi@worldbank.org, mqadir@worldbank.org

ABSTRACT

Geothermal energy is believed to be one of the most beneficial sources of energy in comparison with the conventional sources in many aspects. In Indonesia, geothermal resource is one of the largest potential sources of renewable energy with an estimated potential of 29 GW, which would be able to support the country's target of achieving 23% renewable energy generation plant capacity by 2025. Furthermore, the production of geothermal energy has relatively low emissions of greenhouse gases (GHG) and airborne particulate matters and will curb the country's dependence on fossil fuels for electricity generation.

The fact that most of the geothermal potential is in or close to forest areas has raised societal concerns about environmental and social impacts, especially in forests that play an important role in supplying fresh water, harbor endangered wildlife, or have high cultural or religious values. This paper will propose a preliminary desktop screening process as a complement of a rapid environmental and social assessment on geothermal project development through a macro and micro level risk assessment of some geothermal projects in Indonesia, focusing on the potential impact of the development to the forest areas. The result of screening and risk assessment will provide early information on the potential and likelihood of environmental and social impacts on the geothermal power development.

Keywords: Environmental and social impact, geothermal, exploitation

BACKGROUND

GeoFor-Indonesia Technical Assistance is a World Bank project for promoting sustainable geothermal power development in Indonesia. The report presents the results of a Strategic Environmental and Social Assessment of Geothermal Development in Conservation and Forest Areas, undertaken as part of this World Bank assistance.

Geothermal resources are one of Indonesia's largest potential sources of renewable energy with an estimated potential of 29 GW, which would be able to support Indonesia's target of achieving the production of 23% of its energy mix through new and renewable energy production by 2025. Furthermore, the production of geothermal energy has relatively low emissions of greenhouse gases (GHG) and airborne particulate matters and will curb the country's dependence on fossil fuels for electricity generation. The development of geothermal power provides a significant opportunity to address Indonesia's power shortages and increase its electrification rates, especially in remote parts of the country, whilst meeting international commitments towards reducing GHG emissions.

Unlocking the potential of geothermal power in Indonesia, however, has been hampered by a lack of capital investment in exploration and project development as well as by policy restrictions. The Geothermal Law No. 27/2003 defined geothermal development as a mining activity, only allowing its development in protection and production forest and non-forest areas. Furthermore, a prolonged permitting process and complex compliance requirements associated with working in forest areas, have delayed or cancelled many proposed geothermal power developments. In order to stimulate the industry, a major revision of the law in 2014 (Geothermal Law No. 21) removed substantial barriers when geothermal was no longer defined as a mining activity and allowed geothermal power development in certain conservation areas not previously available for development.

The fact that most of the geothermal potential is located in or close to forest areas has raised societal concerns about environmental and social impacts, especially in forests that play an important role in supplying fresh water, harbor endangered wildlife, or have high cultural or religious values. How these social and environmental impacts and risks vary between geothermal power projects is poorly understood, and thus a key focus of the study. The report further assesses the current regulatory framework for geothermal power development in Indonesian forests and makes recommendations on risk avoidance and mitigation. Subsequently, the Bank conducted preliminary desktop screening for several proposed geothermal exploration and development sites not only with the focus on the biodiversity and potential impacted forests, but also in the presence of cultural heritage, indigenous peoples, nature and degree of public concern and interest and legacy issues. The ultimate objective is to further stimulate the development of a clean energy source in Indonesia by de-risking it through avoidance of high-risk areas from environmental

and social perspective as well as effectively mitigating social and environmental impacts through good management.

PRELIMINARY DEKSTOP SCREENING

The full screening must be conducted through a comprehensive site visit and engagements with relevant stakeholders such as the communities, local government officials, local CSOs/NGOs. However, there are few steps that the developers can do to better prepare an informed site visit and engagements. The preliminary desktop screening requires an in-depth discussion by a team of operation/drilling specialist, social safeguard specialist and environmental safeguard specialist based solely on the secondary data in public domain.

BIODIVERSITY AND POTENTIAL IMPACTED FORESTS

The initial information on biodiversity and potential impacted forests can be obtained from several sources, namely the forestry status in 2017 Ministry of Energy and Mineral Resources (ESDM) publication "Potensi Panas Bumi Indonesia", in addition to data extracted from Integrated Biodiversity Assessment Tool (IBAT) www.ibat-alliance.org specific for the proposed geothermal exploration and development sites. Information on the existence of IUCN management areas or IUCN red list, key biodiversity areas, potential impacted forests can be obtained. The site visit will look at the potential impact to natural habitat and to define the terms of reference for further study to assess the degree of threat to identified natural habitats (particularly critical natural habitats).

CULTURAL HERITAGE

Internet searching is the best place to start. Any information on the previous environmental studies, such as UKL-UPL (Environmental Management and Monitoring Measures) or cultural research in the proposed area could also be used as reference. The site visit and consultations with the communities and local stakeholders will verify the information.

INDIGENEOUS PEOPLES (IP)

The preliminary screening for IP is conducted using the list of IP published by the Social Ministry, 2010 and EgiMap tools (World Bank IPs Screening Study in 2010) as well as 4 characteristics of IP in the Bank Safeguards Policies/Environmental Social Framework:

- Self-identification as members of a distinct indigenous social and cultural group and recognition of this identity by others; and
- Collective attachment to geographically distinct habitats, ancestral territories, or areas of seasonal use or occupation, as well as to the natural resources in these areas; and
- Customary cultural, economic, social, or political institutions that are distinct or separate from those of the mainstream society or culture; and
- A distinct language or dialect, often different from the official language or languages of the country or region in which they reside.

NATURE AND DEGREE OF PUBLIC CONCERN AND INTEREST

Initial information on the nature and degree of public concern and interest can be obtained from initial stakeholder engagement or public consultation reports. Media coverage can also serve as resources to find out the main public concerns and interests.

LEGACY ISSUES

It is imperative to have the knowledge of legacy issues in the proposed geothermal exploration and development areas. Examples of legacy issues are the history of conflict and previous issues on land use. By being aware of the legacy issues, the site visit and engagement to verify the information can be designed to acquire more data related to the issues.

CONCLUSION

The outcome of preliminary desktop screening will then be verified during site visit and the final screening results will be used to make the decision for the investment. It is expected that geothermal development in Indonesia will fully consider avoidance of high-risk areas from environmental and social perspective as well as effectively mitigating social and environmental impacts through good management.

REFERENCES

The World Bank. (2017), "Rapid Environmental and Social Assessment of Geothermal Power Development in Conservation Forest Areas of Indonesia".

The World Bank. (2017), "Environmental and Social Framework".

The World Bank. (2000), "Biodiversity and Environmental Assessment Toolkit".

Kementerian Energi dan Sumber Daya Mineral. (2017), "Potensi Panas Bumi Indonesia".

PT SMI. (2019), "Geothermal Risk Resource Management Project Environmental and Social Management Framework".

THE INVOLVEMENT OF LOCAL INSTITUTION AND COLLABORATION WITH GEOTHERMAL INDUSTRY IN INCREASING LIVELIHOOD OF THE PROJECT AFFECTED PEOPLE

Erwin Patrisa Floris and Ismoyo Argo

PT. Supreme Energy Rantau Dedap
MenaraSentraya, 23rd Floor, Jakarta Selatan
Email: Erwin-Patrisa@supreme-energy.com, Ismoyo-Argo@supreme-energy.com

ABSTRACT

The project's development, either conducted by the Government or private sector, often cannot be spare from adverse impact to environment and social that may lead to loss of income sources or other means of livelihood to the Project Affected Peoples (PAPs). On the other hand, in the view of national and international regulations, the project's initiator is required to avoid environmental damages, social conflict, and severe long terms hardship toward the local community upon the appropriate measures are carefully planned and carried out through the project's Environmental and Social Management System.

Considering project development generally affecting the local community, therefore a mitigation of environment and social impacts needs to establish to reduce the adverse impact of the project activities to the local communities. The environment and social impact mitigation are deem to ensure improvement or at least restored the social and ecological conditions. The key challenge is how to balance between project investments with the risks such projects can pose to adverse impact and social conflict to the local communities. States, parastatals and companies making investments, must take increased responsibility.

Through the implementation of social risks mitigation process and impact mitigation expected could be implement more participatory and effective. The project has established collaboration with local institution, namely Komite Desa especially in managing local recruitment, local supplier & grievance mechanism. The role of Community Committee is to connect between the interests of the project and the local constituents, which are manage through the local customs. The Company also runs the Integrated Social Development Program to boost up the Livelihood of the Project Affected People. We, simply call it as "a perfect blend of customary stakeholders and corporate governance"

Keywords: CSR, geothermal

INTRODUCTION

The development of a project, whether undertaken by the Government, donors, or the private sector, is often inevitably avoided from the negative impacts of both physical and social environments. On the other hand, the initiator of a development project is required to avoid any adverse effects to the physical and social environments wherever possible. This is due to the negative impacts of a development project. The disruption of the existence and harmony of socio-cultural entities and livelihoods sources belonging to the local community, until the occurrence of disruption to health and safety at the community around the project area.

The potential negative impact of the development of an area in the area of the development of the region a project in the community sphere. Therefore, an appropriate effort from each project initiator is needed to prevent, minimize, or mitigate any possible physical and social environmental impacts. Efforts to prevent and mitigate the impacts of project development should be planned, implemented consistently and systematically within an integrated environmental and social management system.

One of the most important things to considering setting up a construction project that will be implement. It aims to ensure that the environmental and social mitigation management strategies that will be develop by the company will be conducted in mitigating efforts environmental and social.

Initiative attempts to maintain harmony with local cultural customs as well as establishing a model of collaborative relationships with local government institutions are viable strategy to apply to geothermal energy industry projects. This is due to the fact that the nature of the geothermal energy utilization and development industry is carried out for a long and sustained period of time so that it is necessary to maintain a harmonious relationship between the project and the local community where the project operations are located.

INVOLVEMENT OF LOCAL INSTITUTION AND COLLABORATION WITH SUPREME ENERGY IN RANTAU DEDAP PROJECT

The Rantau Dedap Geothermal Project will help opening up a somewhat remote regions in South Sumatra Province, providing employment opportunity to around 1,200 people as well as providing opportunity to local businesses during the construction period. The CO2 emission free electricity generated by the plant will be able to provide electricity to some 130 thousand households.

The Project needs total around 124.5 hectares (ha) of land located in the Districts of Muara Enim, Lahat, and the City of Pagar Alam, which comprise of 9.5 ha private lands and 115 ha lands within Bukit Jambul Gunung Patah Protection Forest Area. The total of 157 households were affected, comprise of 57 PAHs whose private lands and/or crops were affected, and 100 PAHs within the protection forest whose coffee plantations were affected and eligible for crop compensation. None of the 157 households required physical displacement of housing and commercial assets. The process of land acquisition were adopting negotiation (willing seller willing buyer) settlements, and was done by COMPANY's Relations team from February 2011 until November 2017. The 115 ha of lands belonging to the Ministry of Environment and Forestry, assigned to PT Supreme Energy Rantau Dedap (COMPANY) through Forest Lend Use Permit (FLUP) for Exploitation dated September 22, 2017. The lands within the protection forest required for the development of well pads, access roads, pipelines and other facilities have been scattered cultivated by 100 households for coffee plantations since 1980s, by Semendo peoples, who were shifted from the nearby Segamit village. The 9.5 ha private belonging to 57 households are required to accommodate the access road improvements spoil disposal locations and the construction campsite.

Socio-economic baseline survey in 2014 stated that 112 of 153 directly Project Affected Peoples (DPAP) were eligible to be included in the Integrated Social Development Program (ISDP) for livelihood restoration. The ISDP has been implemented since 2015. The first stage of implementation was focused on the Capacity Building Program, particularly on the Life Skill improvement for the DPAP.

Project Stakeholders

During the project development, the Company sets up the Social Management System and determine the project stakeholders as Stakeholders are those 'external' to COMPANY operation who have an interest or can influence project operations, such as affected individuals and communities, local government authorities, non-governmental and other civil society organizations, academia, media nd other interested or affected parties. Stakeholders such as contractors, suppliers, distributors and customers of COMPANY, who are considered 'internal' to COMPANY operational activities are not addressed in this SEP, as they are part of the core business function, subject to national regulations and established company policies and procedures.

The framework helps to ensure that adequate information is provided to the project-affected people and other stakeholders in a culturally appropriate and timely manner and that these groups are provided sufficient equal opportunity to voice their opinions and concerns with regard to COMPANY project operations.

Local Institution

The Geothermal of Rantau Dedap project, in Muara Enim and Lahat District including the City of Pagar Alam, South Sumatra, is one of the largest geothermal energy projects in the world. Since its inception the project has worked closely with customary institutions and local government, especially in terms of project socialization, public consultation, and land acquisition, recruitment management of local workers and suppliers, grievance mechanisms, CSR programs and so on.

The Company management does the Involvement of the Local Institution. This institution may consist of:

1. Local Government (from the hamlet up to regency/ district).
2. Local law enforcer.
3. Local religious leader.
4. Local youth leader.
5. Local community leader.
6. Academia.
7. Project-related stakeholder (in SERD Integrated Social Development Program terms: Coffee off-taker).
8. Others.

In order to have harmonious project execution, local institutions no. #1 until no. #5 was being unite by the Company in the form of *Komite Desa* of Village Community. This committee mainly will focus on of project socialization, public consultation, and land acquisition, recruitment management of local workers and suppliers, grievance mechanisms and CSR programs issues.

While the #6 and no. #7 was focusing on CSR Programs Implementation specifically in Integrated Social Development Programs (ISDP). This program aims to make sure to improve the livelihood of the Project Affected People after being disturb by the Company project activities.

Management of Local Institutions

The Village Committee Forum was established and facilitate by Supreme Energy. Organizational forum of this committee has the organizational structure as follows:

Organizational Structure:

- Patrons:
  - Camat in 3 Subdistricts around PLTP Rantau Dedap
  - Danramil Semendo
  - Kapolsek Semendo
  - Danramil Kota Agung
  - Kapolsek Kota Agung
  - Danramil Dempo Selatan
  - Kapolsek Dempo Selatan
  - Religious Leader of Semendo Darat Ulu
  - Youth Leader of Semendo Darat Ulu
  - Religious / Community Leader of Semendo Darat Ulu
  - Youth Leader of Semendo Darat Ulu
  - Religious / Community Leader of Kota Agung
  - Youth Leader of Kota Agung
- COMMITTEE Members:
  - 3 Village Heads as Semendo Darat Ulu District Representative;
  - 2 Village Heads as Sub-District Representative of Kota Agung.

Selection and is determined based on a consensus between the sub-district in the working area of the project. However, the Company also reserves the right to review candidates for Members of the Committee to be recommended by the Sub-district Heads. After the Company has given the approval of the Membership of the Committee, PT SERD has issued a Decree approving the stewardship of the Village Committee Forum.

In carrying out its functions to conform to the expected objectives, the main Tasks of the Village Committee were prepared as follows:

Duties of the Committee:

- Coordinate and communicate continuously to bridge the Company's needs with the community;
- Communicate/disseminate information provided by the Company and/or that has been approved by the Company and is intended for public/public consumption;
- Helping to prepare the local hiring process and verification of local suppliers according to the needs and demands of the Company;
- When requested by the Company, the Committee may facilitate the Company's needs in accordance with the capacity and scope of the Committee's territory;
- Socialize, coordinate, and supervise CSR programs implemented by the Company.

Implementation of the Duties of the Committee

- Hold meetings on an ad hoc basis tailored to the conditions and needs of the Company in the field;
- Together the Company and the Local Government hold a stakeholder meeting every October used to discuss, discuss and formulate the Company's CSR programs for the following year;
- Create a database/list prospective worker from each Kecamatan/Desa, in accordance with the territorial authority covered by the Committee;
- The Committee and its members shall keep the commitment and confidentiality of the information provided by the Company.

The committee also serves as the advisor on grievance mechanism status and supporter for Company program.

One of the company programs was the Integratde Social Developent Programs (“ISDP”), the program has set the target to improve the livelihood of the Project Affected People (PAP). The PAP was already calssified as:

Directly Project Affected People (Priority-1 & Priority-2)

This category will fall to those who are directly impacted by the Project land acquisition and having above 10% of total productive land acquired and having than 10% of total productive land (and thus significantly impacted by land acquisition) based on the 2017 SERD Land Procurement Documentation or are defined as vulnerable households residing in the WKPB. The comprehensive definition will follow:

a. Priority 1 (P1): those who are members of Affected Households (AHs) directly impacted by the Project land acquisition and having above 10% of total productive land acquired (and thus significantly impacted by land acquisition) based on the 2017 SERD Land Procurement Documentation or are defined as vulnerable AHs regardless of the extent of impacts.

b. Priority 2 (P2): those who are members of Affected Households directly impacted by the Project land acquisition and having than 10% of total productive land (and thus not significantly impacted by land acquisition) based on the 2017 SERD Land Procurement Documentation or are defined as vulnerable households residing in the WKPB.

b. Indirectly Project Affected People (Priority-3): This category will fall to those who are indirectly impacted by the Project (i.e: residents of villages and hamlets within the Project area as well as residing within the WKP).

c. Women and Vulnerable People
During the land acquisition process, the Company has identified 121 directly affected households that have been considered as vulnerable group of people in the project area. The basis for vulnerability considerations are as follows:

- Households with incomes less than the South Sumatra Provincial Rate for full term employment (IDR 30 million per annum) and lies under poverty line (IDR 391,178 per month per capita).
- Women headed households without any other earning members.
- Households headed by elderly, or with disabled children.

Besides that, the Woman Organization (PKK in Bahasa) in Pagar Alam City, Lahat and Muara Enim Regency is included as indirect affected stakeholder of this project.

Involvement of Local Institutions in Improvement of Project Affected People Livelihood

Rantau Dedap farmer's especially direct affected people (DAP) are mostly situated at Rantau Dedap people was have mono-culture livelihood, which is depends on the coffee production.

Undoubtedly, the project's existence has resulted in direct impact on the lives and livelihood of the landowners. Thus, empowerment of the people as landowners as well as affected people directly affected by SERD project is an important part of the effort in improving the livelihood of the households and to push it to become better and more independent. Empowered and independent people are expected to be able to achieve their goals. Almost all of the people expect to have better livelihood so that they can provide for their family's economy. This effort is the commitment of PT SERD to show its function to the society living in the area.

PT Supreme Energy Rantau Dedap (SERD) is committed to empower the people, particularly people affected by the geothermal project. The commitment is done by conducting agriculture training and practices as well as other activities. The agriculture training focuses on coffee plant and other plants cultivated by the local. The stress on coffee is due to the fact that most of the affected people in Segamit and Tunggul Bute villages have their lands planted with coffee. Based on Impact Monitoring Report, first phase of coffee training has resulted in some social economical changes of the landowners participating and implementing the training. Nevertheless, there are still more landowners that have not received the training and have not implemented the training received. Therefore, at this stage, to make the training for the affected people effective, strategies are made by creating several target groups each consisting a maximum of 25 affected people. The group will be given intensive training and the implementation monitored as well as the results are reported for analysis as to how effective the effects of the training are on the economic and social lives of the affected people. Additionally, to add to their income and other alternative livelihood, the training also includes horticulture training.

The attention to other than coffee is an effort to provide the people with other source of income. Some of the people do other than coffee. There are those who do paddy, vegetables, and fruits. These plants produce results, but in terms of production capacity, the result is not to the maximum.

The training provided is expected to yield knowledge as well as confidence and motivation to the people to the importance of knowledge and confidence in cultivation, processing and marketing produce particularly coffee produce. The training that includes Q&A sessions is expected to draw important feedback in terms of the kinds of problems the people are facing and their expectations of the follow-ups of the training.

Purpose

1. To provide knowledge, skills in agriculture, particularly coffee and its post-harvest process.
2. To seek information on the problems faced by farmers in conducting cultivation of coffee or other types of plants.
3. To seek information on the hopes of the farmers and farming groups for similar activities or follow-ups related to people empowerment.

Benefits

1. The training is expected to increase the knowledge of the farmers on coffee cultivation and how it can increase their income.
2. The training is expected to increase their confidence in the importance of harvesting ripe coffee and processing the coffee beans using wet processing system.
3. The training has fostered interest of the farmers to do important things such as getting Bank loans.
4. Foster sense of trust and support between PT SERD and the people for their benefit and common progress.

Implementation Method

The training begins by logging participants based on the previous data. Special participants of the training are the people who have been related to PT Supreme Energy Rantau Dedap at the time of planting transfer on the lands used as the facility of PT Supreme Energy Rantau Dedap.

The training is given in two phases. First, the training materials is delivered indoors followed by discussion or Q&A. Second, it involves field work to implement parts of the theory given. The field practice done around the settlement or plantation is easily accessible by the people. It is expected the plantation is visible by the people around the location of the field practice. It also includes discussion to see directly problems occurring in the plantation.

The training is deemed successful. It can be seen from the participants involved in both villages (Segamit Village, Semendo Darat Ulu Sub-district, Muara Enim District and Tunggul Bute Village, Kota Agung Sub-district, Lahat District). All invited participants were present. The Sub-district apparatuses consisting of representatives of the Head of Sub-districts, Head of the Sub-district Police and the Head of Regional Military also attended the training. Village apparatuses, forestry officers and popular figures also attended the training. Figure 1 shows the basic training of coffee cultivation by UNSRI expert.



Figure 1: Basic Training of Coffee Cultivation by UNSRI Expert.

Previously, the farmers mixing both red & green picking during harvest, which lead to poor green bean quality, increasing post-harvest processing time due to longer drying to get the right moisture content according to the international standard.

Directly affected people located scattered across the 4 village: Rantau Dedap, Tunggul Bute, Segamit & Karang Endah. Current farmer's selling price for their coffee is IDR 18,000-20,000 based on existing coffee quality.

Some of coffee are taken as sample for further analysis & market development. Robusta coffee is the most cultivated variety of coffee in the area of Segamit, Tunggul Bute and Karang Endah. Most of the villagers get their livelihood mainly from coffee harvest. Most of the villagers become a coffee farmers more than 10 years and many has been inherited their plantation from their ancestors.

Coffee plantation most of them are quite well maintained to prove that its farmers do the good agricultural/ coffee practices such as topping and prunning of the unproductive branches. Only several farmer they didn't trim off their plantation due to the lack of resources. Unfortunately, most of the farmers does not practice the selective harvesting of red cherry. Most of the farmers are picking both red & green cherry, in which categorized as low coffee quality. Farmers know about the information if red cherry picking is the best process for coffee handling. Unfortunately local buyers does not count the good quality of bean. On this situation farmers decide not to make selective picking redchery.

Last crop was less production due to the bad weather condition, rainy season during blooming of coffee flowers and preventing the development of its cherry.

Most of farmers sell their bean to the local intermediaries with low price for commercial grade coffee industry. Farmers owning small pulper machine is identified, meaning that it make the drying process much shorter in the highland area in which intensive raindrop frequency on certain months happend.

There is no other better option of marketing for good quality of bean, there fore farmers could not get better revenue from their harvest. There is no incentive for farmer to improve their soil plantation fertility, because price of harvest will not compensate. There was another interesting issue that picking red bean may increase of coffee stealing in the village. (interview with farmers in Tunggul Bute).

Identified one processing unit of coffee pulping with good drying processed unit in Yayasan hamlet, Segamit. On interview it was revealed that marketing is still on development process. Some time cooperatives wont give good price and does not have resources to buy.

However on the second batch of coffee collected during the survey showed that two samples showed it was harvested mix of unripe and red cherry. Another one sample still on drying processed.

From samples recieved and cupping testing, showed that coffee originally has very much potential to be classified as grade 1 or fine robusta. But farmers need to have technical assistance on processing and more importantly a better or higher price as compensation or incentive should follow. There fore

alternative market chanelling is need. Figure 2 shows the coffee plant trees over 100 years old.



Figure 2: Over 100 hundred-year-old coffee plant trees. The tree is a potential source of superior seeds of Typical Semendo.

Evaluation

a. Robusta
Robusta coffee are collected from several farmers and intermediaries in green bean condition.

Quality analysis based on physical characteristic that current coffee quality grade is grade 2-3 based on SNI (Indonesian National Coffee Standard). This 2-3 physical grade character are dominant in primary defect (black bean, off flavor and high impurities).

The current green bean reprocessed to improve the physical quality by sorting process, further drying and roasting. Sensory evaluation deployed by cupping test and application of coffee serving: *tubruk*, espresso and cappuccino (Table 1).

b. Arabica Coffee
Arabica coffee planted in several block of coffee field in Semende with limited area (Table 2). Based on site survey observation at Akram processing area:

- West Sumatra origin, around Pagaralam.
- The farmers have less knowledge on several Arabica variety.
- Some farmers are practising red bean picking.
- Fully wash process implemented at Akram processing at Rantau Dedap.
- Pulper & Drying Facility are deployed.

Table 1: Result of Curatorial Analysis Existing Robusta Green Bean.

Sample	Grade	Treatment	Remark
Biji Beras Robusta	Grade 2-3 physical Grade	Drying to ensure moisture content at 11-12%.	Upgrade quality meet local market quality
		Sorting out defect bean Up grading **Grade 1-up**	For export quality need advance processing "polishing"
Biji Robusta (Roasted)	Sensory Analysis: - Roasting at medium level to dark - May meet as fine grade	**Test Cup** Good balance, complexity, chocolate, spicy, low bitterness, long finishing, clean cup ***Tubruk* Serving** Ideal with average thickness and sweet after taste **Espresso Serving** Delicious, comfortable, sweet and consistent **Cappuccino Serving** Strong flavor, delicious, completely blended with milk, comfortable and sweet after taste.	Upgraded quality bean profile meet as single origin coffee or as blending component

Cupping and Sensory Training (Physical & Sensory Aspect)

A training program for quality champion delivered on 2018, this training designed to deliver quality understanding both physical and sensory quality. Figure 3 shows the physical & sensory training.



Figure 3: Physical & Sensory Training.

These trainers representing of each group, upon completion this training, the participants expected to share their knowledge to other members of the groups and play as quality control role among the groups.

From the training, we identify there are 4 four participants that could be local quality tester, since they have a good Physical & Sensory knowledge and talent. Figure 4 shows the taste of flavor wheel.

Table 2: Result of Curatorial Analysis Existing Arabica Green Bean.

Sample exist	**Quality Analysis**	**Treatment**	**Notes**
Arabica Grain Coffee Arabica Green Bean	Normal quality as grain coffee as result of wet process No indication of extended fermentation (spoil or fungi) High moisture content >30%	Drying grain coffee to reach moisture <20% Hulling	Coffee sample has potential special market for local roaster
Arabica Roasted	Sensory Quality: - Roasted at medium level - Has potential as fine grade	**Test Cup** Sweet, fruity, good balance, chocolate, spicy, fruity, good finishing, clean cup ***Kopi Tubruk* Serving** Strong character, balance, sweet, fruity **V60 process** Sweet soft, fruity	Upgraded Quality Coffee has profile as single origin or blend component

Table 3: Potential Market for Raw Green Bean.

Potential Buyer	Market Orientation	Cooperation term	Remark
PT. Fortunium	Export to China & South Korea	Supply Chains based on trade contract 1-2 year	Grade 1 SNI Tonnage: 5-10 MT Payment Scheme: advance payment Note: LOI attached
Rumah Kopi Ranin	Export market alternative micro lot Domestic Market	Post-harvest upgrading (contract farming)	Grade: fine grade Quantity: 250-300 kg/6 month
Others trader (Indokom)	Domestic Market/Export Market	Regular Term	Grade: Commercial: 200 ton minimum for Arabica

Market Development

Potential market for Robusta Sumatra origin is exist both for local market and export market. For Arabica, even though having good sensory result, need extra effort to introduce to the market. The option to introduce to local coffee house is realistic and feasible. This development aligns with newly Geographical Index (IG) recognized so that trading route initiated. Figure 5 shows the Indonesia coffee area map.

Based on market study of upgraded quality green bean & sample of green bean (Table 3) accepted by several potential buyer.

The current off takers of the product are:

1. Rumah Kopi Ranin – Bogor.
2. Supreme Energy Rantau Dedap Office – Jakarta.
3. Marubeni Office – Jakarta.

CONCLUSIONS

From baseline study that had been made on 2016 and the series of training in 2017 – 2018, the livelihood of the Semendo people had been increased significantly on coffee production aspects. It shows during the grand harvest 2017 and 2018 the production could reach 3000 – 4000 kg/ha. The quality of the bean had been increased, the water contains was decreased from 17 – 18 % to 14 – 15 % but still need to improve until 12 – 13 % as per Indonesian Standard. The size grading also improved since the Company also support them with manual coffee size grader. The farmers continue to pick only read cherry for best grade coffee bean. Figure 5 shows the current coffee quality in Rantau Dedap quality station.

Instead of the above facts, there are plenty of room for improvement:

1. All farmers should have an equal coffee quality knowledge.
2. Initiation to have small coffee processor by village coffee tester.
3. Improving Serving capability.
4. Need to initiate event of coffee serving or landscape plantation.
5. Need a workshop to develop handcraft skill.
6. Initiate coffee farming as tourism destination for coffee addict or hobby based on sport such as cycling.

REFERENCES

Kvam, R. (2017), "Meaningful stakeholder consultation". IDB series on environmental and social risk and opportunity (IDB Monograph; 545)

LRQA &Rumah Kopi Ranin. (2017), "Social Dimesion Stry in a cup of Semendo Coffee". ISDP report of SERD (2017)

Supreme Energy Rantau Dedap Company Procedure. (2014), "Stakeholder Engagement Plan"

Supreme Energy Rantau Dedap Company Procedure. (2014), "Committee Principles and Policies"

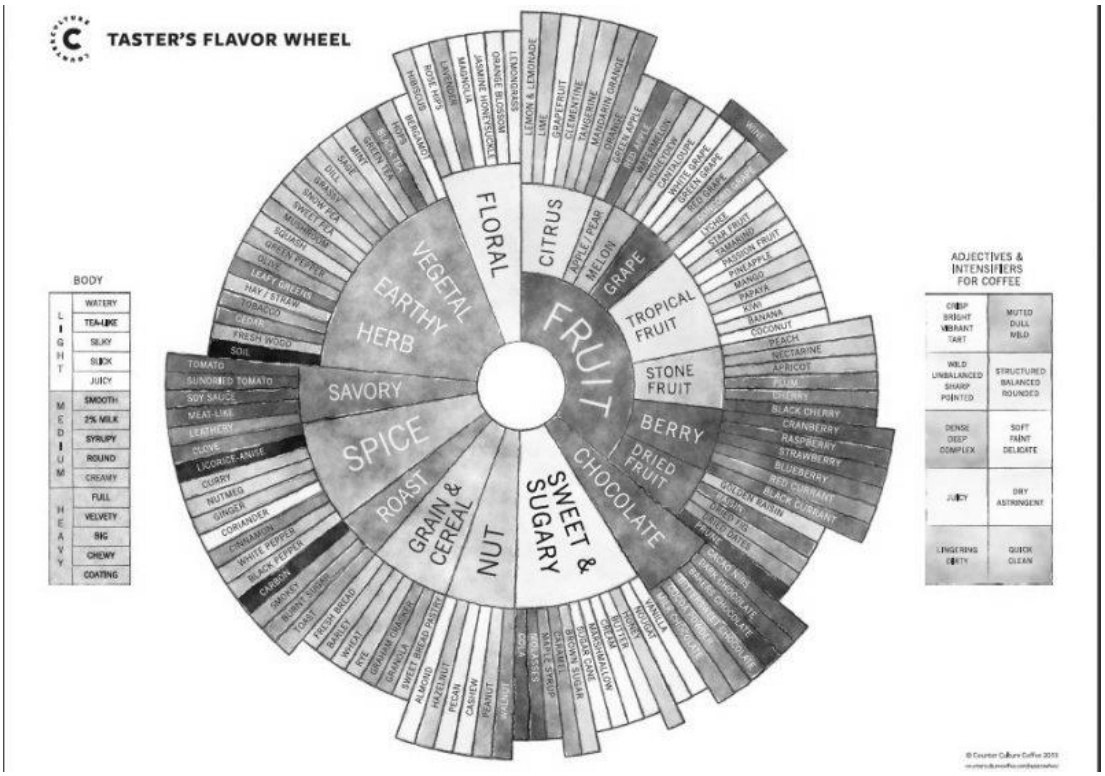


Figure 4: Taste of Flavor Wheel.

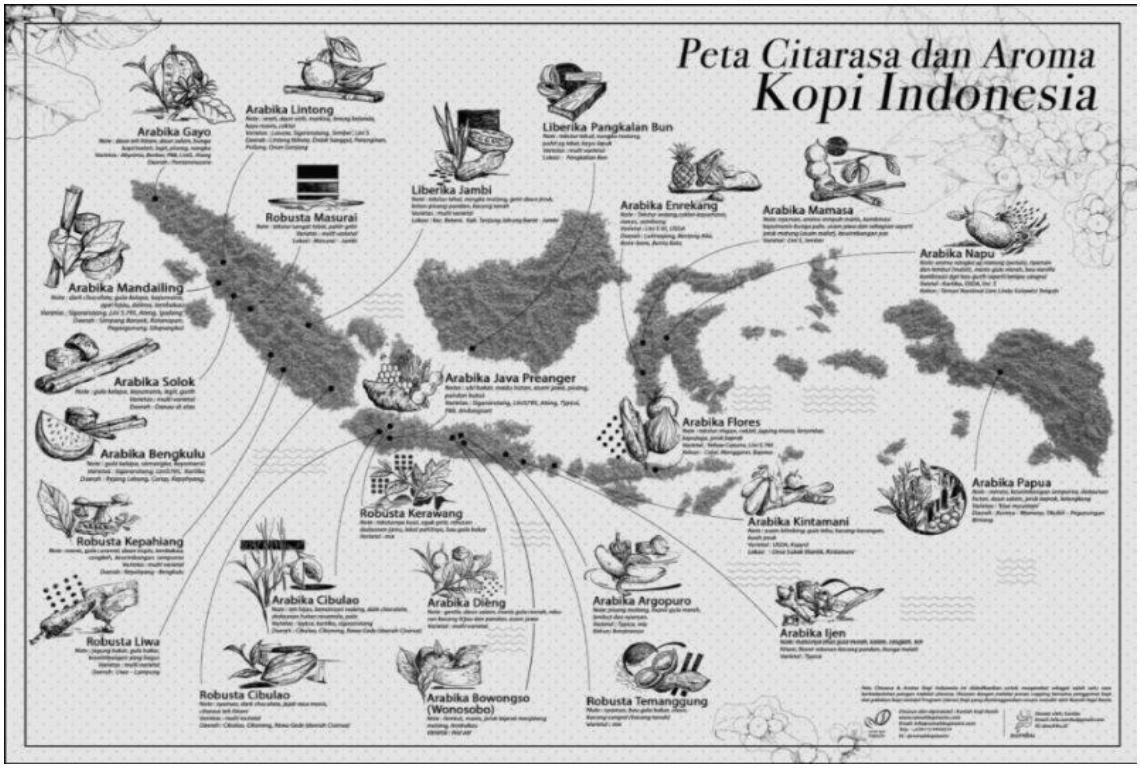


Figure 5: Indonesia Coffee Taste and Area Map.



Figure 6: Current Coffee Quality in Rantau Dedap Coffee Station.

SROI ANALYSIS TO MEASURE THE IMPACT OF CSR PROGRAM CASE STUDY IN STAR ENERGY GEOTHERMAL SALAK

Dali Sadli Mulia, Fernando Eka Satria, and Reva Sasistiya

Star Energy Geothermal Salak, Limited
Sentral Senayan II, lt.24
JL Asia Afrika No.8 Jakarta
Email: dali.mulia@starenergy.co.id

ABSTRACT

Corporate social responsibility program is a common practice in geothermal industry. CSR programs are implemented to address community issue as well as part of operational requirement. CSR is set not only to fulfill company's requirement or regulation but also to show its business strategy performance. However, it is still complicated to measure the CSR benefit or its impact to the company. Thus, Star Energy Geothermal Salak, Limited (SEGS), the largest geothermal operator in Indonesia which located at National Park of Halimun Salak, West Java, is piloting the implementation of a quantitative method in measuring the success or evaluation of CSR portfolio by using Social Return of Investment method (SROI). It shows that the impact of CSR program can be determined by key factors such as quantify variable measurement, stakeholder expectation, and beneficiary acceptance. CSR in economic development program obtain higher SROI score rather than CSR in environment. SROI result also show that the stakeholder expectation in CSR is less significant compare to beneficiary acceptance. It is recommended to use SROI approach not only in evaluation stage but also in planning process.

Keywords: CSR, Social return on investment, Geothermal

BACKGROUND AND LITERATURE REVIEW

Star Energy operates a 377 MW geothermal field in the Salak area, Sukabumi, enough to provide the electricity needs of more than 300,000 households in Indonesia. As the largest geothermal energy producer in Indonesia, Star Energy believes that encouraging community self-reliant and maintaining natural and clean, safe and healthy environment can be harmonized with efforts to produce renewable electricity in Indonesia. Based on social mapping studies around the Star Energy Geothermal Salak operation area, there were three vulnerable groups in the community, consisted of farmers, youth and poor families. One of the main social issues is communities limited capability to improve their livelihood and conflict between agricultural land and conservation areas.

In order to help resolving the issue, SEGS implemented corporate social responsibility program which called as Promoting Sustainable Integrated Farming, Small Enterprise Cluster and Microfinance Access Program (PRISMA). The PRISMA program consisted of training (soft skill and technical skill), technical assistance, strengthen institutional capacity building, facilitate to access to market and finance and provide technical support such as infrastructure, production facility and technology. The program objectives are to improve community livelihood by increasing skill and knowledge on their business, to encourage their entrepreneurial mindset and to maintain community acceptance toward the company and to ensure business continuity.

To measure the impact of CSR programs to business continuity was challenging. Some methodology and approach are usually used by company, such as The Academy of Business in Society argue to CSR Impact approach in measuring the performance, the 5R tools and ISO 26000 standard. In this article, SROI approach will be observed to measure the CSR impact. Social return on investment (SROI) is a method for measuring values that are not traditionally reflected in financial statements, including social, economic and environmental factors. They can identify how effectively a company uses its capital and other resources to create value for the community. While a traditional cost-benefit analysis is used to compare different investments or projects, SROI is used more to evaluate the general progress of certain developments, showing both the financial and social impact on the corporation. SROI is useful for corporations because it improves program management through better planning and evaluation. It also increases the corporation's understanding of its effect on the community and it allows for better communication regarding the value of the corporation's work (both for internal and to external stakeholders). Philanthropists, venture capitalists, foundations and other non-profits may use SROI to monetize their social impact, in financial terms. Impact of the program quantified into monetary value or monetized. This value then compared with program costs to determine whether the program is worth the investment.

For example, ratio SROI Rp 5: Rp 1 shows that by investing Rp1, the program generates social impact

Rp 5. The higher the SROI ratio (above 1), the better. It means the value of benefits the program exceeds the investment value. If the SROI ratio is below 1, the value of the program benefits lower than the investment value.

Social impacts are intangible. The measurement can't be done by measuring the tangible impact for money. For example, the impact of increasing farmers' income. Social impact such as reputation, community acceptance, reduced disruption/social conflict towards operations, changing behavior, and others should be measured by value of money so we can quantify the impact.

SROI is needed to assist management in analyzing the effectiveness of the Program and make decisions based on it, including the decisions to determine the strategy, intervention, scope, and budget of the CSR program. Results of SROI can be communicated to stakeholders so they get complete information on the social impact of the program. This can help management and stakeholders to manage risk, to identify opportunities, to develop ways to improve investment performance, to increase the benefits of the program, to strengthen image and to build branding. SROI also helps provide information about whether a program is financially feasible or not, or if it has a short or long-term benefit.

SROI can help identify parties who receive benefits and the amount of the benefits so it can help to decide whether the program is distributed equitably to target beneficiaries or centralized on one or a group of beneficiaries or even reach those who are not in the beneficiary target (Table 1).

The CSR program description

The Promoting Sustainable Integrated Farming, Small Enterprise Cluster and Microfinance Access (PRISMA), hereinafter referred as the Program is funded by Star Energy Geothermal Salak, Limited (SEGS), and implemented together partnering with Sahabat Cipta Foundation (SC) who act as facilitator or service provider. PRISMA is implemented in the SEGS operating area, around Mount Halimun-Salak (Bogor and Sukabumi Regencies) which includes 6 villages in 3 sub-districts.

The PRISMA program main objective is to contribute in improving socio-economic conditions with target community as measured indicators are:

1. Increased knowledge and skills of the target community in business activities.
2. Increased positive behavior in the socio-economic life of the community.
3. Increased public acceptance of SEGS social investment performance.

To achieve the goal, the Program interventions are:

1. Training (to increase knowledge, skills and motivation).
2. Mentoring (to ensure new knowledge and skills acquired applied in accordance with the specified criteria).
3. Strengthening farmer/business group organization.
4. Facilitate to access of various business services (raw materials, markets, etc).
5. Provision of technical assistance (pilot infrastructure, production facilities & equipment).

Table 1: Location, sector, beneficiaries' number and implementing partners.

Regency	Sub-district	Village	Sector	Beneficiaries number	Implementing partner
Bogor	Pamijahan	Ciasihan	Hydroponic	9	SC
		Ciasmara	Fisheries	18	Dejeefish & SC
		Ciasmara	Cattle fattening	9	Jaya Laras Sentosa
		Pasarean	Cattle fattening	10	Jaya Laras Sentosa
Sukabumi	Kalapanunggal	Palasari Girang	Cattle fattening	15	Jaya Laras Sentosa
		Pulosari	Cattle fattening & feedmill	26	Jaya Laras Sentosa
	Kabandungan	Cipeteuy	Cattle fattening	12	SC

METHODOLOGY

The program impact assessment methodology with the SROI method refers to principles and guidelines for evaluating SROI Network UK & Social Value International. The type of SROI used is evaluation, which is an assessment based on the impact (output, outcome) generated by stakeholders or beneficiaries. The implementation of this study includes 6 stages, as follows:

1. Identify the scope of the Program's impact assessment.
2. Description of program intervention in the scope of the impact assessment.
3. Determine the expected chain of results or changes.
4. Identification of key stakeholders and impact mapping.
5. Identify inputs, processes, and outputs/outcomes.
6. Asses impact value.
7. SROI Calculation.

We conducted impact assessment on the Program implemented in the period November 2015-December 2017 which include:

1. Cattle fattening in Kalapanunggal District, Sukabumi Regency with target beneficiaries:
    a. Gemah Ripah Farmers Group.
    b. Ucing Gering Farmers Group.
    c. Sabilulungan group (with diversification of cassava business for feed).

2. Cattle fattening in Cipeutey Village, Kabandungan District, Sukabumi Regency with target beneficiaries:
    a. Cooperative Corridor Community Network (Jarmaskor).
    b. Group of sheep breeders.

3. Freshwater and aquaponic aquaculture in Pamijahan District, Bogor Regency with the target beneficiary: Mina Asmara Group.

4. Hydroponic vegetable cultivation in Ciasihan Village, Pamijahan District, Bogor Regency with targeted beneficiaries: Hydroponic Communities

In addition, there are also monitoring reports that summarize progress of output achievement and outcome indicators based on a logical framework for the purpose of evaluating program performance.

RESULT AND DISCUSSION

The results of the SROI study show the present value of the program's impact for 3 years (2015-2017) is Rp5,370,000,000, while the investment value of the Program is Rp 3,611,000,000. SROI ratio (ratio between the value of the impact and value of investment) of the Program for 2015-2017 (3 years) is 1.49, meaning that every Rp1 invested, the Program provides benefits of Rp1.49. So, the PRISMA Program is feasible for social investment. The value of SROI for each year shows > 1. Thus, the value of the program benefits exceeds the value investment every year.

Among the PRISMA Program interventions in this study, the impact value from the cattle fattening group, Sabilulunganis the largest (Rp1,979,000,000). This is because the intervention can be replicated by reaching the indirecr beneficiaries through job creation, for those who work as a daily workforce. At the second rank is Ucing Geuring cattle fattening group (Rp1,126,000,000), followed with Jarmaskor cooperative at the third (Rp1,088,000,000). Those groups have big member numbers and bussiness diversitification.

In short, the Program impact value will increase along with beneficiaries' number increase, program replication reaches indirect beneficiaries, and the existence of diversification or value-added business. Overall, the PRISMA Program made a positive impact on communities around the SEGS operation area. The results of this SROI study can be used by SEGS as internal and external communication material and as well as for evaluation purposes program in planning social investment in the future, and in improving relationships between stakeholders and strengthen SEGS branding.

The lessons learned from this study included:

1. The SROI study plan should have been integrated into the strategy, logical framework, and program work plan so SROI indicators can be incorporated into the program's monitoring and evaluation system.
2. The program's monitoring and evaluation system does not record changes (observation of behavior change) on beneficiaries on a regular basis and can be validated with the results of observations in the field.
3. Program managers can use SROI projection to take decisions whether the program is worth the investment before the program is implemented.
4. Monitoring the value of SROI can also be done periodically before the program ends to determine the value of the provisional impact of the program so that program managers can evaluate and make improvements if found in the SROI ratio <1.
5. Technical errors in conducting surveys in the field, such as errors in data input or invalid data may occur. For this reason, the quality control of survey data is very high important and must be done at least two stages, first by quality control staff and second by quality control

supervisors. Data verification also needed until the phase analysis and reporting.

Based on the results of the analysis, conclusions and learning of this SROI study, Sahabat Cipta recommended to SEGS the following short-term follow-up steps:

1. Arrange the program's communication material (e.g infographics and presentation slides) which summarizes the impact of the PRISMA Program based on the results of this SROI study for delivered to program stakeholders (government, media, organizations civil, business associations, etc).
2. Integrating SROI into the new CSR program after the PRISMA Program.
3. Conduct observations on the beneficiaries-behavior changes regularly and consistent referring to the SROI work plan and monitoring system as well as evaluation of new programs.

Based on the findings when conducting SROI studies, technical recommendations can be considered for a new CSR program as following:

a) Define program objectives, outputs and outcomes explicitly with indicators measurable (qualitative and quantitative).
b) Integrate other objectives, such as securing operations into program objectives.
c) Arrange the program monitoring and evaluation plan in detail with reference to program objectives, outputs and outcomes. Schedule and monitoring tools and strategies implementation and implementation must be included in the plan.

If the new program is a continuation of the PRISMA Program with intervention and beneficiaries of the same program, strengthen mentoring by dividing between technical/cultivation assistance and mentoring management/institution. Business feasibility analysis, business plan preparation, and recording business finance must be done consistently and completely.

CONCLUSION

With reference to the objectives of the SROI study, it can be concluded that:

1. This study has achieved its goal, to measure social performance and to determine values impact and the ratio of Social Return on Investment Program (SROI) PRISMA in Salak.
2. The present value of the impact of the Program for 3 years (2015-2017) is Rp 5,370,000,000, while the investment value of the Program is IDR 3,611,000,000.
3. The value of SROI in The PRISMA program for 2015 to 2017 (3 years) is 1.49. This means that every Rp1 invested, the Program provides benefits of Rp1.49. So, the PRISMA Program is feasible for social investment.
4. In the 3rd year, grades Program benefits exceed the value of the investment.The value of SROI for each year shows> 1. Thus, the value of the benefits of the Program exceeds the value of the investment every year.
5. Among the PRISMA Program interventions in this study, the impact value of cattle fattening group Sabilulungan is the biggest (Rp1,979,000,000). This is supported by the intervention which replicated the program and reach indirect beneficiaries through job creation, i.e. those who work as daily laborers (peeler, enumerator, drying, and cassava suppliers). The second biggest impact value is Kucing Geuring group (Rp1,126,000,000). They have more members compared to the Gemah Ripah cattle group. On the thirs is sheep group Jarmaskor Cooperative (Rp1,088,000,000). Apart from the relatively large number of members, this group has add benefits by diversifying business (organic liquid fertilizer, savings and loans, for the production of sheep).
6. The impact value of the Program will increase if:
    a. The number of beneficiaries increased.
    b. Program replication reaches indirect beneficiaries.
    c. The existence of diversification or value- added business.
7. Overall, the PRISMA Program has had a positive impact on communities around the SEGS operation area.

The results of this SROI study can be used as an effective internal and external communication material for SEGS's program evaluation, social investment planning in the future, and to improve relations between stakeholders as well strengthen SEGS branding.

ACKNOWLEDGEMENT

The highly appreciations are given to: Dani Hamdani (Yayasan Sahabat Cipta) and Yayasan KEHATI to provide report and data in this study. Hopefully the partnership established in implementing the CSR program can provide benefits for all.

REFERENCES

Emick K., (2016), "Measuring the ROI of CSR – The 5 R Framework", Linkedin, 7 December 2016.

Nicholls J., Lawlor E., Neitzert E., Goodspeed, 2012, "A guide to Social Return on Investment", 2nd ed. UK

BUFFERZONE PROGRAM AS A STRATEGIC IMPLEMENTATION OF COMMUNITY DEVELOPMENT PROGRAM BASED ON SECURITY IN DARAJAT FOREST AREA

Maraden H. Panggabean, Dali Sadli Mulia, and Panji Pranadikusumah

Star Energy Geothermal Darajat II, Limited
Darajat – Kabupaten Garut
Email: maraden@starenergy.co.id, dali.mulia@starenergy.co.id, panji@starenergy.co.id

ABSTRACT

Operation area of Star Energy Geothermal Darajat II, Limited (SEGD) is a National Vital Object or "Objek Vital Nasional" (OBVITNAS) located between Papandayan Mountain Nature Park and Darajat Protection Forest Area, Garut. Deforestation that occurs around SEGD operation area is increasing due to horticulture farming quickly and massively. This condition leads to negative impact to environment such as landslide, deceasing water source.

Due to both the social economic condition of the people who are, living around the SEGD operation area and decreasing of forest resource caused horticultural farming, conflict between the company and the community may occur and this potential to disrupt SEGD by demonstration, road blockade by the community. For this reason, a comprehensive, participatory, and sustainable forest management strategy is highly required. Security-based Community Development through Bufferzone program is one of the strategies for managing and securing forest areas by using the approaches of community empowerment, environmental sustainability, and involving the stakeholders in economic development.

The aim is to create a harmonious relationship among the company, the community and stakeholders in forest resourtces management. The Rehabilitation "Bufferzone" program is implemented in an integrated manner starting from social mapping, inventorying natural and forest resources, stakeholder mapping, joint planning with stakeholder on forest management, implementing community-based environmental management awareness program, implementing rrehabilitation and conservation (by commodity change and land location transfer), and mentoring community/farmers as well as monitoring and evaluation periodically. These efforts are to restore the forest function, so it could function ecologically and economically.

By this bufferzone program, Farmers/Community will get benefit not only from MPTS and coffee harvest but also protection from potential landslide, at the end surrounding community secures SEGD operation from community disruption.

Keywords: Community development, Darajat geothermal field

BACKGROUND

In accordance with the Decree of the Minister of Energy Mineral Resources number 2288/K /07/MEM/2008, Star Energy Geothermal Darajat II, Limited (SEGD) which is formerly Chevron Geothermal Indonesia, .Ltd has been established as National Vital Objek or "Objek Vital Nasional" (OBVITNAS) in the energy and mineral resources sub-sector Geothermal. OBVITNAS is the area or location, building, installation and / or business that involves the needs of many people, and / or as significant source of state revenue. (Presidential Decree number 63 of 2004).

As OBVITNAS that manages geothermal, SEGD has an important role for both the nation and state in terms of economic, political, social, cultural, defense and security. Given the strategic role, SEGD as OBVITNAS requires more robust security system in order to minimize the risk and safety impacts caused by threats.

SEGD area is located "Taman Wisata Alam" (TWA) – Darajat Block of Papandayan Mountain, located at an altitude 1750-2000 m above sea level. This area is under e administrative area of Garut district, West Java Province. Currently, land of Forest Darajat has lack of endemic tree. This occurs because many conversions of protected forest (endemic/forest tree) into horticultural conventionally and intensively by the community. This condition is very harmful to the environment that lead to landslide and flood in rainy season, and decreasing water source in dry season. Based on social economy condition of the community residing in Darajat forest area, increasing complexity of the society's problem, and the declining of forest resources capacity has emerged various forms of threats and harassment against the security of SEGD, such as: demonstration, roadblocks.

As stated in Presidential Decree No. 63 year 2004, security is all efforts, works, and activities within the framework of prevention, deterrence, tackling, and law enforcement against any threats and harassment directed to Vital National Object. The implemented security system should be able to minimize the risk and safety impacts caused by threats and security problems.

Given the strategic role, SEGD as OBVITNAS requires more robust security system in order to minimize the risk and safety impacts caused by threat and security problem. The stakeholders and community in the area around the company's operation should be involved. it is because the forest area protection/safeguarding is responsibility of all related parties.

For the above reason, a comprehensive, participatory and sustainable forest management is highly required. Community Development security based through bufferzone program is one of the forest management strategies. It consists of security by community through the approach of community empowerment, environmental sustainability, and economic development. The objectives of Bufferzone program are to create a harmonious relationship between the company and the community living around the company as well as stakeholders in the forest resources management. All that be held is to both secure company's operation area known as OBVITNAS and to restore forest function ecologically, economically and socially.

RESEARCH METHOD

Based on social and economic condition of community, environmental safety, and stakeholder condition, there are a chance to execute the partnership for securing forest area, then implemented BufferZone program by using Research and Development (R&D). R & D is the research method used to produce a particular product and test the effectiveness of the product. To be able to produce certain product, it is used the need analysis. In order to function in society at large, the research to test the product's effectiveness is also necessary. Longitudinal research and development carried out in stages and multiple years.

DISCUSSION RESULT

SEGD operating area is located at "Taman Wisata Alam" (TWA). It it a tropical highland forest which has a very high biodiversity with the structure of a complex ecosystem.

Existing condition in Darajat forest is lack of endemic/forest tree. This occurs because many conversions from forest tree into horticultural tree conventionally by the community. People living around the Darajat forest area plants horticultural on critical area in terms of landslide. This condition is very dangerous especially where there are nearby SEGD's facility. Based on the condition, securing forest in operation area of SEGD becomes priority. Security and forest management is not only an obligation of the company, but also a shared responsibility. It is therefore necessary to build forest's management and security system in a comprehensive and sustainable way by involving stakeholders. Management and security system of forest area is implemented based on the development of the company's internal security and private security involving the stakeholders, with the principles of partnership, environmental management and, community development. Bufferzone program is a program that could be implemented in forest area management and protection. The program is implemented by the principles of community empowerment that is centered in the target communities. It is also based on the active participation of the community and stakeholders and conducted in a sustainable manner. The environmental management's principle is implemented by community-based environmental management to implement safeguards movement. This management is to carry out forest rehabilitation and conservation over critical land. While the partnership principle is built based on trust, mutual understanding, mutual agreement, and a joint security program, so that all stakeholders can take benefit from the program.

Management and Security System of Darajat Forest Areas through BufferZone Program

Based on the existing condition in Darajat forest area, management and security must be immediately implemented to increase the carrying capacity of the forest as to function ecologically, economically and socially.

The efforts that applied are to establish multi stakeholder partnership system in the management and security of the area in a way of participatory and sustainable forest.

In the early stages, stakeholders carry out surveys and identify environmental condition, land, and crops in a critical location. Later, conducted joint planning of Bufferzone program to carry out the rehabilitation and conservation on that critical land through the conversion of horticultural crops become endemic forest plants. Also MPTS as Puspa Surian Cinnamon, Damar, avocado, and jackfruit. Notably for growers located in critical areas, it is implemented social management program in form of conversion of location and profession in collaboration with LMDH and Perhutani KPH Garut.

To increase public participation and stakeholder in the security and management system, it is then implemented community capacity building both softskills and hard skills through community-based environmental management program on an ongoing basis with all stakeholder participation. There is also the movement to save the environment through rehabilitation and conservation towards the critical land. The most important program is to realize

sharecroppers located around SEGD and stakeholders to join this program.

Security and management of forest areas through BufferZone is a synergy program of systematic, comprehensive, and sustained multi stakeholder by the community and stakeholder's participation. It provides awareness to the community living around the forest to join the program in implementing environmental safeguards by implementing disaster mitigation and attention to observe sustainability aspects in every activity by Building security and management system of forest areas to improve security and safety as well as forest resources; Building a multi-stakeholder partnership in the security and management system of forest areas; Improving community's knowledge, skills, and attitudes who live around the forest, especially when implementing the rehabilitation and conservation of forest areas; Activating forest village community institution for private security of the community; Carrying out the rehabilitation and conservation, especially in the critical land; Implementing transfer commodities, and social management to tenant farmers on critical land; Mentoring social and techniques for securing and managing forest areas.

Darajat Forest Area Management and Security Model through BufferZone Program

Security and Management of forest areas model is the development of the internal security SEGD as OBVITNAS, which is developed by private security in cooperation with stakeholders and farmer communities around SEGD.

This model is a synergy between the Darajat Geothermal Energy Star II, Ltd. through a Corporate Social Responsibility, UNINUS through community service program, Perhutani KPH Garut as Block Darajat protected area manager and the Institution of Forest Village Community Mekar Lestari, Karyamekar Village Pasirwangi District, Garut.

Security-Based Community Development Strategies through Bufferzone Program

Security-based community development is a strategy through forest rehabilitation "Bufferzone" program. This program is a forest resource management with core target is farmers surrounding SEGD area. By this program, the farmer would get benefit from rehabilitation (i.e: coffee and MPTS tree), community could be mitigated/protected from potential landslide, and eventually surrounding farmers/villager will triggered to secure Darajat area as OBVITNAS.

Bufferzone program is implemented participatory and sustainable by approaching ecology, partnership, community empowerment is shown in Figure 1.

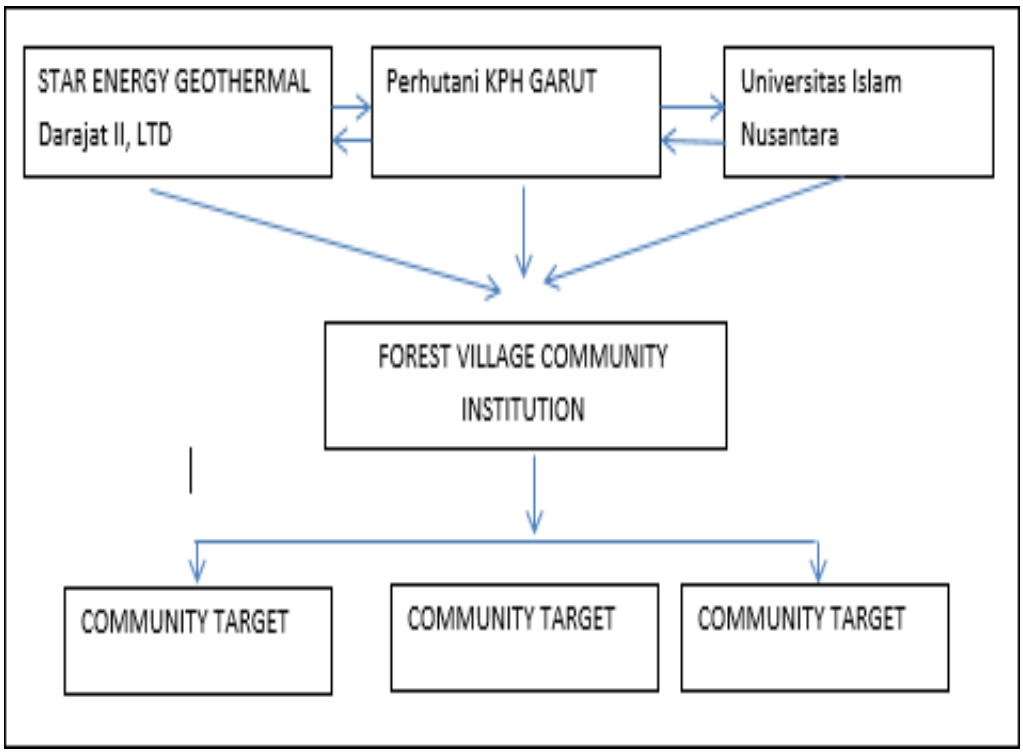


Figure 1: Model of darajat forest area management through Bufferzone program.

- Awareness efforts on the forest resource management and security which is OBVITNAS
- Capacity building through trainings, both formal and informal. Trainings both hard skill but also soft skill in terms of managing and maintaining the environment, and to build social capital in the community
- Build and enable institutions in society, especially in forest resource management
- Technology implementation in forest area management
- Economic development assistant/mentoring to farmers under Forest Village Community institution (LMDH)
- Infrastructure and related assistance for commodities change
- Marketing networks and partnership development;

The Implementation of Management and Security Actitivies as well as Forest Management Through BufferZone Program

In general, all forest resource and security management are implemented by Figure 2.

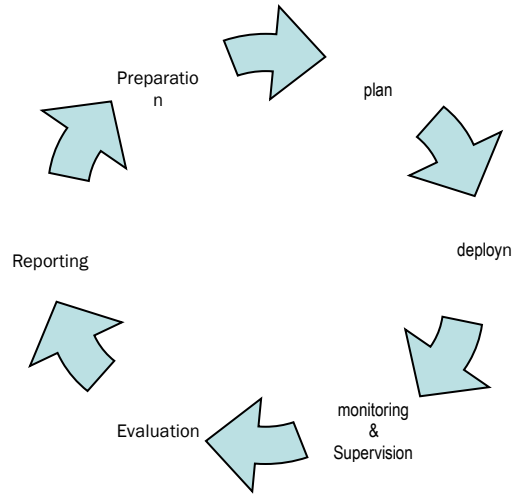


Figure 2: Cycle of Darajat forest management through bufferzone program.

Preparation

- The identification of community target is the community living around SEGD as obvitnas;
- Needs assessment for rural community about environmental management;
- Synchronization program over environmental management with stakeholders;
- The identification of community target, land, and its condition;
- The identification of partners for mentoring.

Plan

- Needs and problems mapping of environmental management in the community and disaster mitigation;
- oint-planning, planning phases, and the implementation of the program;
- Program proposal to all partner institutions.

Implementation

- Activities socialization to all stakeholders;
- LMDH capacity development and community target;
- Strengthening institutional communities;
- Environmental Rescue movement through rehabilitation and conservation on critical land;
- Facilities and infrastructure provision, transfer commodity as well as location and profession;
- LMDH and community empowerment through productive activities;
- Technical and social assistance to LMDH and community target.

Monitoring and Supervision

- Monitoring is carried out on the entire process at a time when activities are ongoing;
- Regular supervision is carried out when there is less optimal work, so it needs efforts to improve performance of the implementers.

Evaluation

- Formative evaluation is performed during the process when the activities take place;
- Summative evaluation is carried out when the activities end;
- Final program is evaluated together.

Reporting

- Reports are submitted to all partner institutions.
- Held in the mid and at the end of the program.

CONCLUSION

Given SEGD operation area as “Object Vital Nasional” (OBVITNAS) in Papandayan TWA and protected forest area, the forest resource management thru commodity change (horticultural with coffee/MPTS and endemic) by Bufferzone program is very important. Community will get benefit, not only financial from MPTS and coffee harvest but also protection from potential landslide, at the end surrounding community secures SEGD operation from community disruption. Therefore, it is necessary to build a security based on surrounding community/farmers by managing forest

resource comprehensively, participatory and sustainability. The most important thing is to encourage community and stakeholder participate in Forest rehabilitation to protect environment from landslide and decreasing water source that all these to be carried over to next generation.

Bufferzone program is security-based community empowerment program, which has positive impact on maintaining OBVITNAS. It is a private security strategy with the community and stakeholders based on the principles of environmental conservation and community development partnership. It is done by increasing the knowledge, skills, and attitude of the community living in SEGD operation area, implementing environmental protection movement to carry out the rehabilitation and conservation on critical land, change commodity, transfer location and also change profession. The most important thing is to raise the awareness of stakeholders towards the forest management and to utilize forest wisely with the goal of common security and sustainability. Thus, that forests can function ecologically, economically and socially.

RECOMMENDATION

It is recommended to have synergy activity on both security and forest resources management in accordance with the community/farmer characteristics and specific local development such as: commodity change, land location transfer and profession change. Hence, partnership development with organizations/other agencies shall be implemented to enhance benefit of forest resources as well as security by community.

ACKNOWLEDGEMENT

Special gratitude and highest appreciation given to: Star Energy Geothermal Darajat II. Ltd., Universitas Islam Nusantara, Perhutani KPH Garut and LMDH Mekar Lestari. May our partnership since implementing this security and management program in the forest area could provide benefits to all parties.

REFERENCE

Okke, R., Ibrahim, D., Panji, P., (2017). “The Joint Forest Management as a Multi-Stakeholder Implementation of Corporate Social Responsibility,” *Journal of Community Service Vol 7 No. August 1st, 2017. P-ISSN 2088-6977 E-ISSN 2584-1487.*

EMPOWERMENT OF QUAIL BREEDER (EAGLE FEED SUPPLIER) TO EAGLE CONSERVATION CENTER IN GEOTHERMAL KAMOJANG AREA WITH UTILIZING FECES TO BE FERTILIZER AS AN ADDITIONAL VALUE

Darussalam

PT Pertamina Geothermal Energy
Bekasi, Indonesia
Email: darus.ti08@gmail.com

ABSTRACT

The presence of geothermal company with renewable energy should give positive impact to environment and social community such as conducting Corporate Social Responsibility (CSR) program. PT Pertamina Geothermal Energy (PGE) has real concern for the environment and community that one of the implementations is the Kamojang Eagle Conservation Center (KECC) as CSR program. In KECC, the conserved eagles get feed namely quail that it supplied by 50 quail breeders. On the other hand, quail farms certainly have waste such as quail feces which if not handled properly it can pollute the environment.

The innovation of using quail feces into fertilizer can be an added value for breeders as well as efforts to handle the waste. In addition, nowadays there is still gap between supply and demand of fertilizer in Indonesia so it can be alternative fertilizer to fulfil the demand. As the results of research by Riza Zainuddin Ahmad et al. (1997: 3-4), the contents of quail feces have nutrients that are useful for plants such as Water (H2O), Potassium Chloride (KCI), Magnesium (Mg), Manganese (Mn), Cation Exchange Capacity (CEC), C organic, Nitrogen (N), Potassium (K), Calcium (Ca), and Phosphor (P). Hence creating fertilizer from quail feces can be an alternative fertilizer that is environmentally friendly for farmers.

The fertilizer marketing itself has a great opportunity which is supported by close to the potential market where the Geothermal Kamojang Area is surrounded by agricultural and plantation areas.

Therefore, empowering quail breeders to utilize of quail feces as fertilizer could be not only handling wastes but also an additional income. On the other side, it can be alternative fertilizer for farmers moreover this empowerment program increasing the positive image of company that improve the social community and environmental sustainability.

Keywords: Fertilizer, Quail, Social, Environment, Empowerment, Added Value, Breeder, Farmer.

INTRODUCTION

As one of realization about environment concern, PT Pertamina Geothermal Energy (PGE) was build up the Kamojang Eagle Conservation Center (KECC) with IUCN standard (International Union for Conservation of Nature). This program realized through the PGE Kamojang Regional Corporate Social Responsible (CSR) that synergized with West Java BBKSDA and the Indonesian Raptor Forum. Figure 1 shows the Eagle in KECC. Figure 2 shows the quail as feed for eagles in KECC.



Figure 1: Eagle in KECC.



Figure 2: Quail as feed for eagles in KECC.

The existence of this KECC does not only preserve eagles but also has a continuing effect on feeding businesses for eagles, which are currently supplied by 50 quail farmers. Figure 3 shows the Quails in farm.



Figure 3: Quails in Farm.

The existence of quail farms certainly has problems such as quail feces. Improper handling of quail feces can pollute the environment such as air pollution (odor) and changes in environmental ecosystems.

Regarding on that, correct handling of quail feces is an important matter and even an innovation is needed in order the waste can be an added value for farmers. Such alternative for that is by making fertilizer.

DATA AND METHOD

The Kamojang area itself located in agricultural and plantation such as paddy fields and vegetable plantations so that quail feces to be fertilizer has a close and potential market.

From the results of the study by Riza et al. (1997: 3-4), the contents of quail feces have nutrients that useful for plants such as water (H_2O), Potassium chloride (KCI), Magnesium (Mg), Manganese (Mn), Cation Exchange Attachment (CEC), C Organic, Nitrogen (N), Potassium (K), Calcium (Ca) and Phosphorus (P). Nutrients level that contained in it able to increase if it stored as shown in Table 1.

Based on the Table above, to get the value of certain nutrient level, it is necessary to store with the right time. Quoting the results of the study by Kusuma (2012: 8), the use of quail feces as fertilizer on vegetable mustard plants had a significant effect on plant length variables that is 17 days after planting (dap) and on leaf area variables, besides giving a very significant effect on plant length variables (10 days, 24 days and 31 days after planting), it also gave effects to plant gross weight, plant net weight and plant dry weight.

The giving of 15 tons/ha quail feces fertilizer resulted the highest variable to the plant length (24 and 31 dap) while the provision of quail manure 20 to/ha gave the highest variable to plant length (10 dap and 17 dap), leaf area, weight dirty plants, net weight of plants and dry weight of plants (Table 2).

Quoting from the article, the process of making fertilizers from quail feces starts from preparing materials including:

1. 10 kg of dry quail feces.
2. 50 ml EM4 (a mixture of microorganism cultures consisting of dotositensi bacteria, lactobacillus sp, Streptomyces sp; cellulose decomposing fungi, phosphate and yeast solvent bacteria that can increase the decomposition of waste).
3. 10 tablespoons of sugar.
4. 2 liters of water.

Table 1: H_2O, KCl, C Organic, N total, P, Ca, Mg, Mn and KTK within quail feces with different storing time.

Storage	Level										
Duration	cl	H2O	KCl	C. Org	N.tot	P	Ca	Mg	K	Mn	KTK
0 Day	1	7,80	6,50	2,10	0,19	60,07	10,40	6,20	0,62	0,40	4,38
	2	7,90	7,30	1,70	0,18	60,11	10,50	6,40	0,59	0,45	4,40
	3	7,70	6,30	1,90	0,17	60,08	10,60	6,30	0,62	0,44	4,39
	Average	7,60	7,00	1,00	0,18	60,09	10,50	6,30	0,61	0,43	4,39
2 Month	1	8,10	7,40	6,30	0,49	48,45	6,30	6,70	0,40	0,93	16,39
	2	8,30	7,30	5,90	0,46	48,51	6,40	7,00	0,39	0,97	16,34
	3	8,20	7,50	6,40	0,47	48,60	6,50	6,70	0,38	0,98	16,35
	Average	8,20	7,40	6,20	0,47	48,52	6,40	6,80	0,39	0,96	16,36
6 Month	1	8,30	7,50	5,70	0,26	20,54	10,50	6,50	0,50	0,95	18,30
	2	8,40	7,60	6,10	0,27	20,61	10,40	6,90	0,54	0,96	18,37
	3	8,50	7,40	6,00	0,25	20,59	10,60	7,00	0,55	0,97	18,35
	Average	8,40	7,50	5,90	0,26	20,58	10,50	6,80	0,53	0,96	18,34

Table 2: Test result of difference mean value that influenced by difference dosage of quail feces fertilizer to height of plant (cm) which observed 10 dap (X1), 17 dap (X2), 24 dap (X3), and 31 dap (X4).

Treatment (ton/ha)	X1 cm	X2 cm	X3 cm	X4 cm
0	14,70	20,11	24,70	30,60
10	15,93	22,44	28,59	35,91
15	16,96	22,73	30,61	38,10
20	17,90	25,27	30,30	37,23
25	16,33	22,65	29,61	36,60

The fertilizer manufacturing process is:

1. Prepare 10 kg of quail feces on black tarpaulin plastic.
2. Prepare a solution with a mixture of 1 liter of water added 50 ml of EM4 and 10 tablespoons of sugar then stirred evenly.
3. Pour the mixture solution in quail feces gradually while stirring evenly until the water content reaches 60% which is marked by good cohesive when it stirred with solution when being clenched.
4. Soak in black tarpaulin plastic for 3 weeks. Check every couple day to see the development of fermentation. Fermentation is characterized by an increase in temperature which is 40^{o}-60^{o}C, but if the temperature is too high then do a reversal and close it again.
5. After 3 weeks the fermentation is complete without temperature increase and foul odor.
6. Dry the quail feces waste that has been fermented to dryness. Geothermal steams can be used to dry the dry quail feces in order accelerate the drying process.
7. Milled quail waste that has dried until it becomes flour and ready to use.

As summarized in Figure 4.

RESULT

Based on information from article, quail farmers could get additional income around Rp 800,000.00 – Rp 1,000,000.00 (Rp 1,500.00/kg) from selling the quail feces only without processed into fertilizer.

From 1,500 quails could get 15-20 sacks per week. The price for each sack is valued at Rp 20,000.00 and can be harvested 4-5 times a month.

Whereas based on information from article, quail feces that have been made as fertilizer are sold for Rp 2,500.00/kg or Rp 32,500 per sac. The price of quail feces fertilizer is cheaper than the other non-subsidy fertilizer i.e:

- Urea fertilizer (Rp 5,000.00/kg)
- SP-36 (Rp 5,000.00/kg)
- NPK (Rp 9,000.00/kg)
- KCI ((Rp 6,000.00/kg); and
- ZK (Rp 8,900.00/kg).

In addition, the geothermal steams that used for drying process could accelerate the process faster than manual and overall reduce time to produce the quail feces fertilizer.

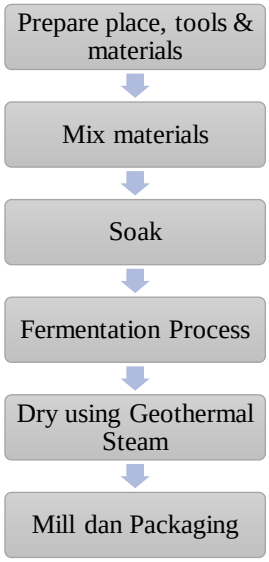


Figure 4: Procedure of making fertilizer from quail feces.

CONCLUSION

Utilization of quail feces as fertilizer in addition to handling waste can also provide additional income for farmers with fertilizer prices of Rp 2,500.00/kg. Empowerment of quail breeders, suppliers of CCEK eagle feed by making fertilizers, can improve breeder's welfare while increasing PGE's positive image in CSR activities in the form of concern for the community and the environment.

In addition, quail feces fertilizers have a great market opportunity to be an alternative fertilizer that is environmentally friendly for farmers around the Kamojang area and even extends to Bandung and Garut Regencies and farmers afford to buy this fertilizer which the price is cheaper than the other non-subsidy fertilizer.

REFERENCES

Ahmad, R., Z., et al., (1997), "Peningkatan Nilai Unsur Hara Tinja Burung Puyuh Melalui Penyimpanan", Seminar Nasional Peternakan dan Vereriner, page 3-4.

Maria, E., K., (2012), "Pengaruh Takaran Pupuk Kandang Kotoran Burung Puyuh Terhadap Pertumbuhan dan Hasil Tanaman Sawi Putih

(Brassica Juncea L.)", Jurnal Ilmu Hewani Tropika Vol 1. No. 1, page 8.

http://www.peksigunaraharja.com/artikel/ada-manfaat-pada-feses-puyuh,accessed 8/10/2018.

https://www.pertanianku.com/raup-untung-jutaan-rupiah-dari-kotoran-burung-puyuh-kok-bisa, accessed 8/10/2018.

http://www.rudipuyuhindramayu.com/2018/01/jual-kotoran-puyuh.html, accessed 15/10/2018.

https://republika.co.id/berita/ekonomi/korporasi/18/01/26/p35r64415-yuk-lihat-penampakan-elang-di-wisata-edukasi-pusat-konservasi-kamojang, accessed 15/10/2018.

https://harga.web.id/harga-pupuk-subsidi-non-subsidi-dan-organik.info, accessed 28/06/2018.

Resources and Management



This page is intentionally left blank



NUMERICAL MODEL OF WAYANG WINDU GEOTHERMAL SYSTEM TO OPTIMIZE PRODUCTION STRATEGY

Riza Pasikki, Boyke Bratakusuma, and Mulyadi

Star Energy Geothermal Wayang Windu Ltd
Wisma Barito Pacific 11th floor, Jl. S Parman Kav 62-63, Jakarta 11410 Indonesia
Email: riza.pasikki@starenergy.co.id

ABSTRACT

A full field numerical simulation model has been developed for Wayang Windu for forecasting field performance under range of production scenarios. The quality of the history match obtained for well pressure (steam zone and liquid) and enthalpy gave confidence that the newly developed model is a reasonable predictive tool to evaluate alternative exploitation strategies, with the main focus to evaluate capacity of reservoir to support additional 60 MW development by 2024. The area of commercial reservoir interpreted from numerical model has excluded the northwestern region of the developed field that was previously defined as potential commercial reservoir extension based on resistivity anomaly distribution. Therefore, development strategy to drill in the northwestern region was not included in reservoir forecast. Two basic development strategies were included: (1) shallow drilling in the northern steam cap supported by several shallow wells in the central area which represents production strategy currently applied in Wayang Windu field; and (2) mixed shallow and deep wells. In both development strategies, the southern Windu reservoir compartment was reserved exclusively for brine and condensate injection.

Numerical modeling indicated that steam cap alone cannot support 227 MW generation until the end of contract life. Maintaining a right balance between production from steam cap and deep brine reservoirs is a critical to the successful management of the liquid dominated geothermal reservoir such as Wayang Windu. Based on the model, the current production scheme of producing 95% from steam cap reservoir and 5% from brine reservoir has caused rapid pressure decline in the steam cap reservoir section while deep-brine reservoir pressure relatively unchanged. As the result, water level in the reservoir has inclined to the shallower depth from initial depth of around +450 m ASL elevation. Model's response is consistent with recent measured pressure-temperature data from deep wells. The preferred resource development strategy is combination of shallow and deep drilling which outperforms shallow drilling strategy because of: 1) more balanced extraction from steam cap and brine reservoir sections promotes steam cap growth; and 2) less production interference due to larger well separation. The model suggests that production plateau of 227 MW could be sustained until end of contract life. The upside potential of reservoir was also tested with the same drilling strategy, wherein 60 MW generation is added to the existing 227 MW generation by 2024. The model confirms the opportunity for Unit-3 development should the > 60 milli-Darcy permeability be encountered in deep brine reservoir section.

Keywords: Numerical model, natural state, Wayang Windu geothermal field

INTRODUCTION

Recent assessment has been conducted by Reservoir Management Group to evaluate whether Wayang Windu geothermal resource could support organic growth of adding 60 MW power plant to the existing 227 MW power plant operation until year 2040. This resource assessment is based on the existing integrated conceptual model of geothermal field upon evaluations of geology, geochemistry, geophysics, downhole well and discharge well data. A large number of big-hole development wells and several slim-hole exploratory wells have been drilled in and around the field, providing data on subsurface temperatures, pressures, fluid chemistry, and subsurface geology and reservoir properties. Therefore, the location, shape and appropriate extent of Wayang Windu geothermal system have been defined reasonably well and many key characteristics of the system have been interpreted with a reasonable degree of confidence. The proven resource covers an area of 22 sq. km (Figure 1) and is closely associated with northeasterly trending volcanic domes on the southern slope of Gunung Malabar. This most likely conceptual model has been converted into a numerical model to evaluate resource performance under different generation scenarios. The new Wayang Windu numerical model has been constructed using Tough2 reservoir simulator and has been calibrated against initial reservoir pressure and temperature. In addition, it has also been calibrated against historical production parameters during 18 years of commercial operations at 110 and 227 MW loads.

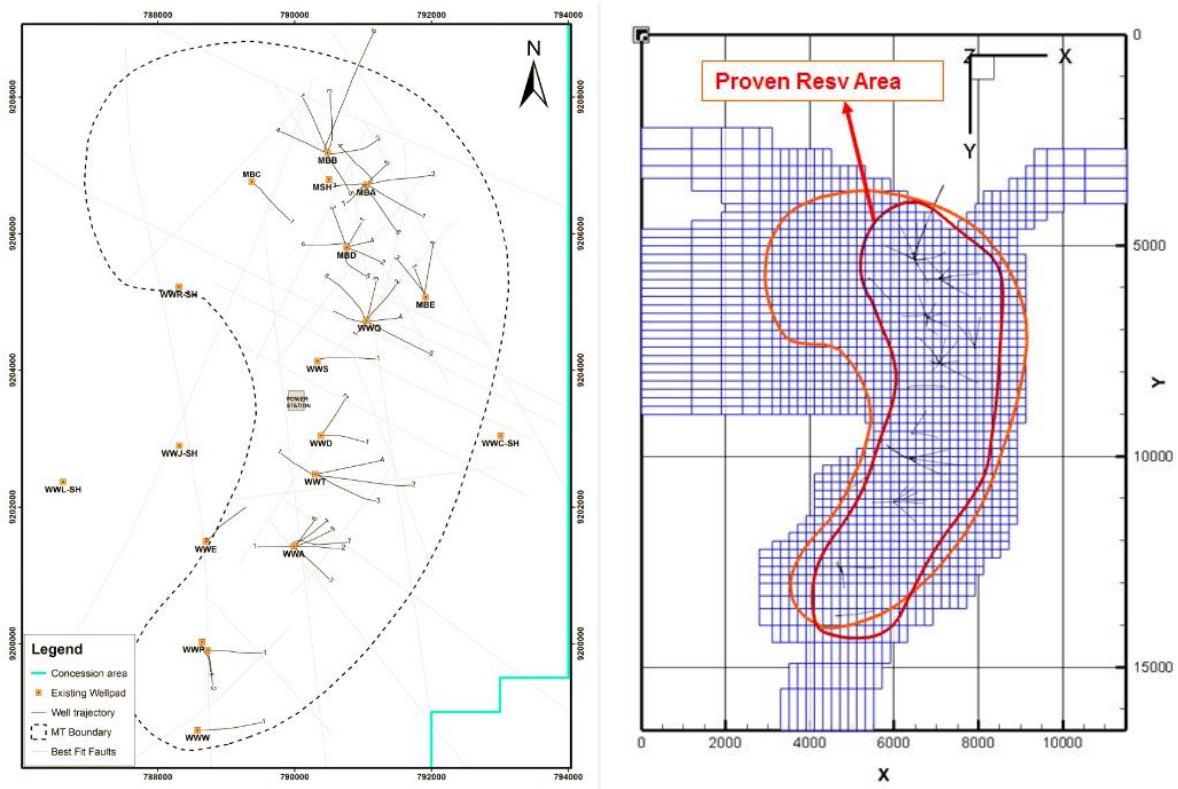


Figure 1: Map view of Wayang Windu resource (left) and Model Geometry (right).

To represent better the naturally fractured nature of the Wayang Windu reservoir, the numerical model is constructed using dual porosity approach. With this approach, the model composed by two permeable media one of them is the rock matrix and the other the fractures. The matrix contains most of the pore space but its permeability is much lower than the fractures. The fractures, on the other hand contain a very small pore space but their permeability is large. The two media are connected in each modeling block through a very important link named the matrix-fracture interface. Neighboring fracture elements are connected to each other and this makes possible for the fluid to flow throughout the reservoir. Throughout the numerical model rock and fluid properties are specified and the production history is simulated by imposing mass extraction and injection on specific fracture blocks where the wells are completed. Pressure is monitored and compared to actual measured pressure variations and the quality of the match is conventionally associated to the quality of the model to predict future behavior.

NUMERICAL MODEL VARIABLES

The variables required to characterize a geothermal fractured reservoir will be discussed and their center point value presented in this section.

Model Geometry

The grid was set to allow future investigation of reservoir performance under both base and optimistic resource areas. Therefore, the model grid covered potential reservoir area extension to the northwest as indicated by low resistivity anomaly from magnetotelluric (MT) data. As shown in Figure 1, the model grid extended 11.5 km in the east-west direction, 16.5 km north-to-south. There are totally thirteen layers in vertical direction to cover reservoir section from an elevation of 1,200 to -1,700 m SL and each layer of the model is divided into 40 by 59 blocks or 2,360 blocks with a typical size of 200 by 200 by 200 m. The reason for this coarse discretization is that the implementation a dual porosity model creates very small fracture elements. Wells are completed in these fracture elements and typical flow rates of geothermal wells are in the range of 10's of kg/s of steam. These large flow rates are not numerically compatible with too small fracture blocks as the numerical solution becomes extremely slow and numerically unstable. Using dual porosity method with MINC (Multiple interacting continua) of 2 (from layer 1 to 4) and 4 (from layer 5 to 13), the model was partitioned to have a total of 30,680 blocks.

Porosity

General approach of declining porosity with increasing depth due to increased compaction was taken with the assigned matrix porosity of 3.0 – 12.5%. Unlike the unfractured oil and gas reservoir where fluids contained in porosity and only flows through porous space, Geothermal's reserve is heat (not mass) that uniformly distributed and flows through rock and porous space. Therefore, unlike the unfractured oil and gas reservoir where fluids contained in porosity and only flows through porous

space, Geothermal's reserve is heat (not mass) that uniformly distributed and flows through rock and porous space. Therefore, unlike the unfractured oil and gas reservoir where detailed porosity is important to show location of reserve, the detailed porosity is less important for geothermal and average values are enough. In addition, the existence of fracture system in geothermal reservoir reduces importance of detailed description on matrix porosity distribution and allows reliance on average values. In naturally fractured reservoir, it is commonly assumed that most porosity is located in the matrix while the fractures provide large scale permeability but negligible porosity. The smaller volume element in the model are fracture elements that consist of void volume with no rock volume, this means that their local porosity in 100%. The bulk porosity for the fracture, however, is set at 1%. This value is a compromise that results from being small enough to represent the expected low fracture volume but high enough to avoid numerical instability.

Fracture Permeability

Fracture permeability is a bulk property of the fractured medium. It is created by the combined action of fractures each one with very different local permeability values. The horizontal fracture permeability distribution on the model is initially interpreted using a property of the region close to the well called Productivity Index (PI) using the following equations:

$$PI' = \frac{2\pi kh}{\ln\left(\frac{r_e}{r_w}\right) + S - 0.5}$$

$$k = \sqrt{k_x^2 + k_y^2}$$

PI : Permeability Index (m3)
r_e : drainage radius (m)
r_w : well radius
S : skin
kh : fracture permeability (milli Darcy – meter), where h is model block thickness
k_x : horizontal fracture permeability in X direction
k_y : horizontal fracture permeability in Y direction

PI's measured in the wells based on Pressure-Temperature-Spinner (PTS) survey and calibrated with historical production data were set as basis for initial distribution of fracture permeability in numerical model. The assigned permeability was then calibrated with natural state and production history. There was no anisotropy for horizontal fracture permeability within the block model so that k_x was equal to k_y. In most of blocks the vertical fracture permeability was set at half of horizontal permeability. A map view of the central point cases for horizontal fracture permeability at the sea level is shown in Figure 2. At current reservoir model, the low fracture permeability figures of < 10 milli-Darcy were assigned to the northwestern region that was previously indicated by low-resistivity anomaly data as potential commercial reservoir extension. Low permeability distribution to the northwest area of proven reservoir was required to obtain good matches on pre-exploitation state and during production period at given boundary conditions especially reasonable upflow strength as explained at later section of this paper.

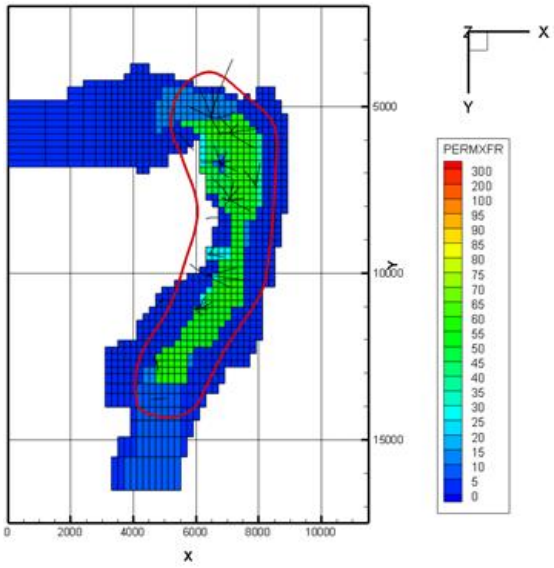


Figure 2: Fracture Permeability at the sea level.

Matrix-Fracture Connection

The single-phase volumetric flow between matrix and fractures is formulated in with this equation:

$$Q = \frac{\sigma\, k_{ma}\vartheta}{\mu}\,(P_{ma} - P_{fr})$$

$$\sigma = \frac{C}{L^2}$$

Q : volumetric flow rate
σ : shape factor
k_{ma} : matrix permeability
μ : viscosity
V : the bulk volume of matrix
P_{ma}, P_{fr} : matrix and fractures pressure respectively
L : Fracture spacing
C : Shape factor constant. Tough2 simulator uses 60.

The matrix fracture connection is therefore controlled by the product of shape factor and matrix permeability (σk_{ma}). Matrix permeability can be measured in cores. For geothermal systems it is orders of magnitude smaller than fracture permeability. In current model it assumed that the matrix permeability was isotropic. This means that

values in the three main directions are the same in each simulation block. Matrix permeability currently assigned was quite homogenous: 8 micro-Darcy from the top of reservoir to +400 m SL depth (steam cap reservoir section) and 5 micro-Darcy for all blocks located below +400 m SL (liquid reservoir section).

The effect of changes in matrix permeability can be offset by simultaneous changes in shape factor such that σk_{ma} remains constant. The effect of fracture spacing and matrix permeability is directly dependent on one another. The term that controls the effectiveness of the matrix-fracture connection is given by product of matrix permeability over fracture spacing squared:

$$\sigma k_{ma} = \frac{C k_{ma}}{L^2}$$

The "shape factor" is nothing else that the area of interface between matrix and fracture per unit volume divided by the average distance of the fluid in the matrix to the interface. We do not know the actual geometry of the fracture system and there is no proven method to measure fracture spacing from logs. In order to define the range on possible values and based on experience, we know that the actual value is larger than the inverse of fracture density measured in image logs but smaller than the average distance between feed zones in wells.

Permeability Multipliers in X, Y, Z directions

These three variables are used to specify the presence of a barrier or an enhanced flow channel. This is done by multiplying the area of contact between neighboring blocks by the respective parameter. A low value causes the connection of neighboring blocks to be made weaker as expected for barriers. A large value increases the interface area making possible to create enhanced flow paths. A value of 1 will not create any change. Permeability multiplier of 0.1 was applied in the model to help creating two horizontal semi-permeable barriers that help increase the pre-exploitation temperature gradient below mean sea level (0 m SL) in liquid regions of the reservoir.

Multiple Interacting Continua (MINC)

The simulator (TOUGH2) makes possible to discretize even further the matrix blocks in order to model in intra-matrix gradients in pressure, temperature and saturation. A parameter called MINC controls whether we discretize the matrix or not. For this case we have elected to use MINC to 2 - 4 on Wayang Windu Model.

NATURAL STATE MODELING

The variables required to characterize a geothermal fractured reservoir will be discussed and their center point value presented in this section. Geothermal reservoir is dynamical wherein the upflow, thermal losses to surface, hot springs/fumaroles and discharge/recharge to lateral aquifers take place even before start exploitation. Therefore, initial state (natural) simulation is a must in numerical modelling of geothermal reservoir. This is done by placing mass/heat sources and sinks in a 3-D permeable medium and running simulation until steady state is achieved (>150,000 years of simulation time). Important variables to adjust on natural state modeling include:

- Location, strength of inflows (rate, enthalpy).
- Fracture permeability distribution.
- boundary conditions (aquifer, outflow, heat loss).

Measured downhole pressure and temperature from the wells from pre-exploitation stage provide reliable constrains for calibration of natural-state model. The variables are changed by trial and error until a good match on initial pressure and temperature achieved. Results of natural state match are not affected by storage terms (porosity, initial water saturation) and fracture-matrix connectivity terms (fracture spacing, matrix permeability). Therefore, the later step called "production-history matching" was used to calibrate the storage and fracture-matrix connectivity terms.

Boundary Conditions

Boundary conditions at depth consisted of an impermeable and constant-temperature (300ºC) boundary condition in the simulation cells located at the bottom face of the model. The upper boundary condition was also an impermeable and constant-temperature (20ºC), acts as heat sink. The interface was located in the upper face of the uppermost block in each block column and the distance of the boundary condition to this interface equals the difference in elevation between this upper face and the surface.

Natural recharge occurs at the bottom of the model in three sources located in the deepest block (Figure 3). The first one at north called Gambung upflow injecting 29 kg/s of fluid at enthalpy of 1402 kJ/kg. The second natural recharge called Wayang upflow located at central parts of field near to WWA wellpad location, injecting 1432 kJ/kg fluid at rate 11.6 kg/s. Geochemical evidence indicates that this was the most equilibrated upflow to Wayang Windu system. Initial Chloride concentration in the deep reservoir was approximately 12,000 ppm with low gas concentration of 0.2 wt. % and the temperature in the upflow was about 310ºC. The southernmost upflow is located at Gunung Windu near to WWF and WWW wells, injecting 1432 kJ/kg fluid at rate 8 kg/s. This part of the field was distinguished by its brine and gas chemistry. The deep brine contains relatively low chlorides approximately 7,000 ppm and enriched with gas with concentration up to 10%.

Total upflow rate was 49 kg/s. To capture the geochemistry evidence, discontinuity of high fracture permeability distribution was applied to the area near to WWW and WWF wells.

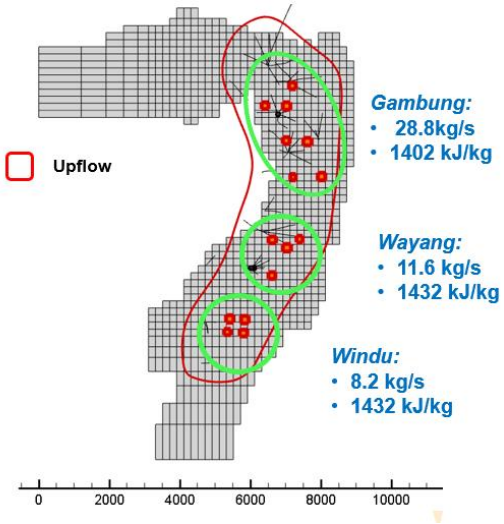


Figure 3: Upflow distributions and strengths applied in Wayang Windu Reservoir Model.

The outflows were located north, close to MBB wellpad in the uppermost block. It was simulated as the wells on deliverability with a back pressure of 10 bara. Four constant pressure boundaries are also attached to the reservoir model act as mass sinks toward northeast, northwest and west directions at layer 4 (elevation 500 m ASL), 6 (100 m), 7 (-100 m) and 9 (-500 m). Productivity Index (PI) of the simulated wells for outflow and the pressure of the constant-pressure boundaries are adjusted to obtain good match of pre-exploitation pressure.

Initial Pressure and Temperature

There are 12 wells in Wayang Windu where the pre-exploitation downhole pressure and or temperature are available: MBD-2OH, MBD-4, MBE-2, WWQ-2, WWQ-3OH, WWQ-5, WWS-1, WWD-1, WWT-1, WWA-2, WWF-1 and WWW-2. From initial state simulation, good agreement between measured and modeled initial pressure and temperature obtained for all these wells. Figure 4 shows the example of initial pressure and temperature match at MBD-2 well. In addition, the thermodynamic initial conditions below have been successfully reproduced in natural-state modeling:

- Steam to liquid contact before exploitation was located at +400 m SL.
- At the shallow reservoir section (800 to 400 m ASL), initial temperature at central and south was higher than that at north reservoir part, consistent with measured initial steam cap pressure distribution (Figure 5).
- In the liquid reservoir section at southern part of field, the axis of high temperature in the model was consistent with observed high-temperature (exceed 300°C) trend of NE to NNE orientation and passes through the traces of WWA and WWT wells (Figure 6).

One key insight provided by natural-state simulation is that the NW region previously defined as potential reservoir extension based on anomaly resistivity distribution is least likely to be part of Wayang Windu commercial reservoir extension. With reasonable boundary conditions, low fracture permeability need to be assigned on NW region to obtain acceptable initial pressure and temperature matches.

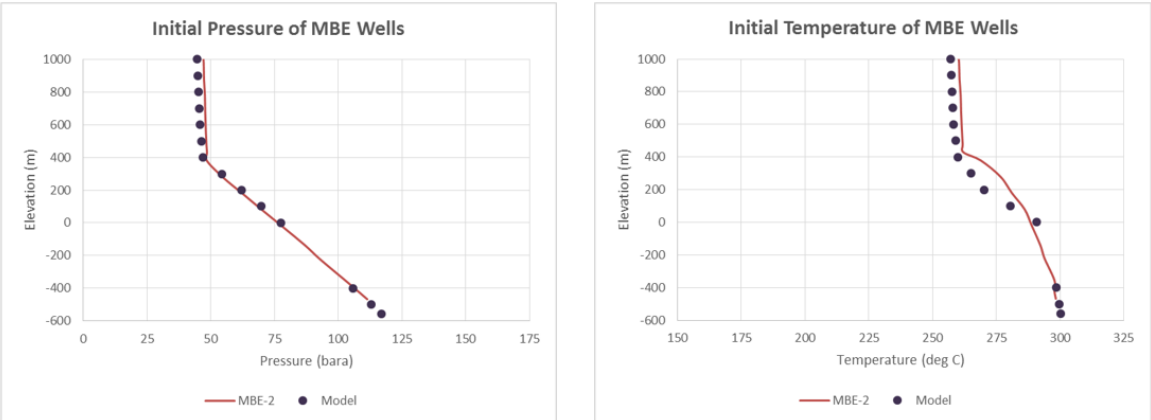


Figure 4: Initial pressure and temperature match on MBE-2 well.

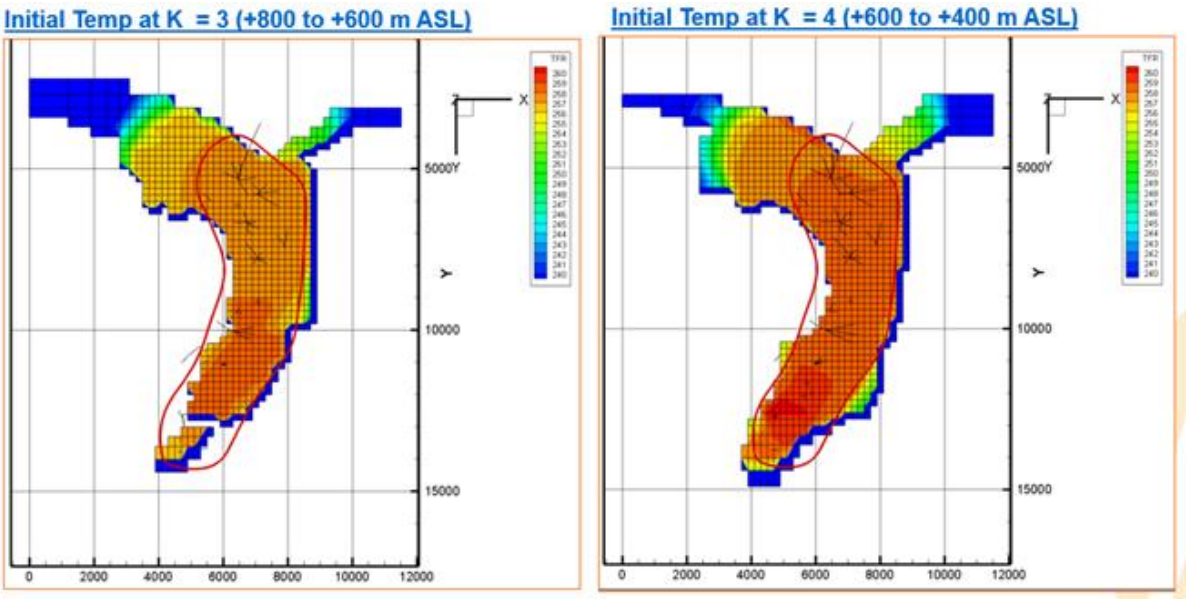


Figure 5: Initial Temperature at Shallow (Steam Cap) Reservoir Section, 800 to 400 m ASL elevation.

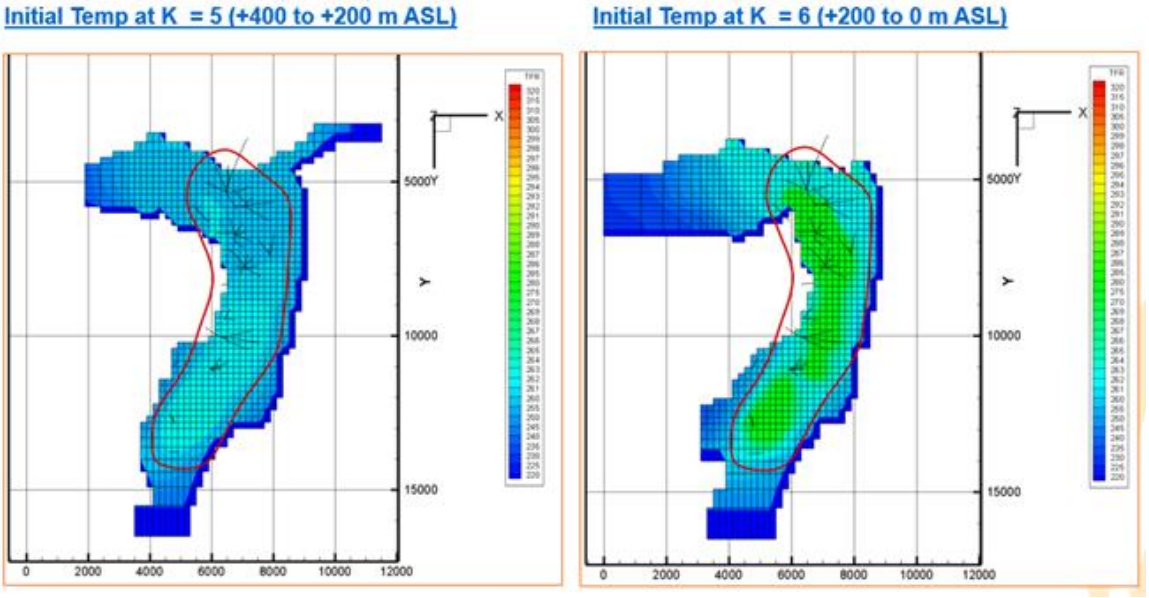


Figure 6: Initial Temperature at Liquid Reservoir Section from 400 to 0 m ASL elevation.

PRODUCTION HISTORY MATCH

The second step of model calibration is called production history match. Stabilized pressure, temperature and saturation resulted from natural state simulation was used as the initial condition for production simulation. Historical data of production rate, brine and condensate injection rate, as well as enthalpy of injected brine and condensate within year 2000 – 2018 time interval were imposed to run the model. History match was then done using three main variables from 22 production wells: steam cap pressure, liquid pressure and discharge enthalpy measured in the individual wells. In addition, historical evolution of superheat was also used to constrain the model.

Figure 7 shows an example plot comparing the simulated steam cap reservoir pressure profiles with the measured pressures obtained from MBD-1 well. These measured pressures were the shut-in wellhead pressures taken at wells that have steam feedzone at central and north parts of the field. The simulated pressure was corrected to the wellhead pressure using vapor static pressure gradient. Good matches with measurements for wells at north (MBA, MBB, MBD and MBD) are obtained.

However, historical steam cap pressure on central wells (WWQ) on the period of year 2000 to 2016 could not be matched (Figure 8). Further attempts to improve the match have not been done considering reliability of available shut in wellhead pressure data of WWQ wells to represent the steam cap pressure. All WWQ wells are drilled to penetrate the deep liquid reservoir section. Unlike the dry steam wells

at north part of the field (MBA, MBB, MBD, MBE), the WWQ wells require longer period of time to reach stabilized wellhead pressure under shut in condition, especially those that are weak wells. For WWQ wells, steam cap pressure match was focused on the event wherein the wells were shut in for long period of time such as during field shut down for five months due to landslide incident in 2015. Despite some discrepancies, the good matches with measured data at the end of production simulation were obtained in WWQ wells, which is important to proceed with the next step of reservoir forecasts. Overall, the model could reconstruct the change of pressure decline at the steam cap reservoir due to change of field generation from 110 to 227 MW in 2009. Simulated steam cap pressure decline rates of 0.4 bar per year before 2009 and around 1.0 bar per year after 2009 are consistent with field observation.

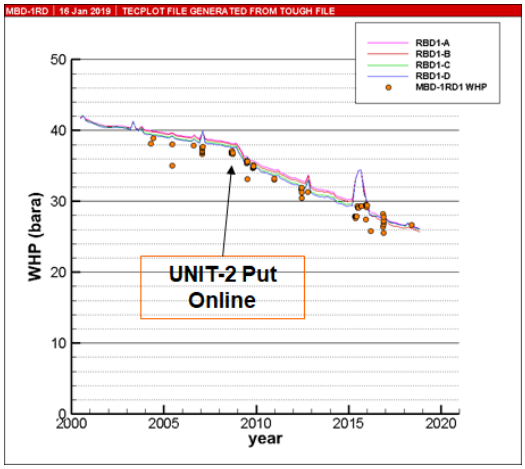


Figure 7: Steam cap pressure match on MBD-1.

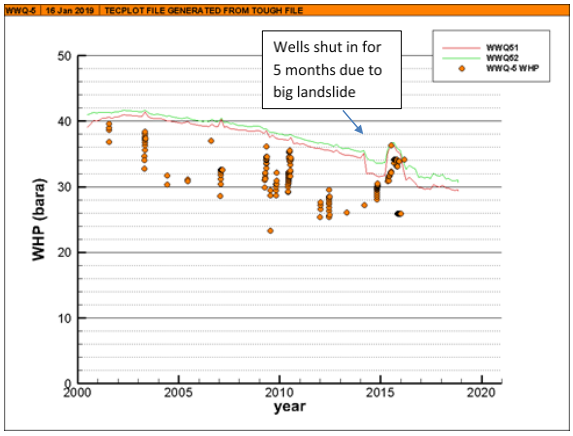


Figure 8: Steam cap pressure match on WWQ-5 Well.

Unlike steam cap pressure trend, amount of data to constrain pressure trend in the liquid reservoir section was relatively limited. With the absence of the continuous down-hole pressure measurement system from dedicated monitoring well, trends of liquid reservoir pressure only derived from sporadic shut-in PT surveys. Figure 9 shows example of reasonable match obtained between model and measured liquid reservoir pressure trend in WWD-1 and WWD-2 wels. Liquid reservoir pressure has been relatively stable with maximum total pressure drop of 5 bar over 18 years of field production. This mostly caused by the existing field production strategy in which 95% of production comes from steam cap reservoir and only 5% of steam comes from deep brine reservoir. Imbalance extraction between steam cap and deep brine reservoirs has not been the most optimum way to develop the field as steam cap reservoir experience high pressure decline rate but very low-pressure decline rate at the liquid reservoir. As the result, steam to liquid contact in the reservoir become shallower (Figure 10). Continuing this production strategy will cause steam feedzones to flood and eventually drop steam production.

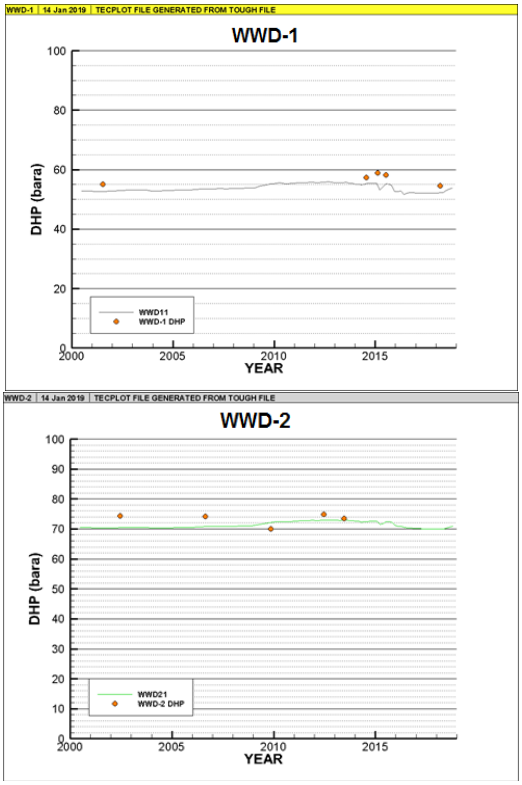


Figure 9: Liquid pressure match on WWD-1 and WWD-2 Wells.

Besides pressure-decline trends, the discharge enthalpy trends observed on the wells also provided additional constraint for calibrating the numerical model. Throughout the period of production, the enthalpy of the dry steam wells on MBA, MBB, MBD and MBE pads remained constant and the model was able to match the enthalpy pattern well.

Initial liquid saturation was one of the unknown in the steam cap reservoir part and we relied on the superheat information to constrain it. Timing of development, area and degree of superheat as being measured in the wellbore are matched by adjusting initial water saturation parameters. Fracture-to-matrix connection parameters were also adjusted to obtain superheat match. General distribution of superheat degree in the model has been consistent

with field measurement. The highest superheat degree of 20 ºC occurs in the area around MBB pad and the other areas of steam cap have maximum superheat degree of 10 ºC (Figure 11). The results of the history matching showed that the newly developed reservoir model successfully simulated behavior of the reservoir under historical conditions of production and injection. Pressure decline trends determined from the well surveillance have been matched. Enthalpy trends measured from the production wells have been closely simulated by the numerical model. The model was sufficiently calibrated for use in forecasting future reservoir behavior under different production scenarios.

RESERVOIR FORECAST

Forecast Methodology

The quality of pre-exploitation and history matches obtained on the wells give confidence that the newly developed numerical model was a reasonable tool to evaluate alternative Wayang Windu development strategies. The in-house Star Energy program called ToughRunner was used. This program runs reservoir simulator (Tough2) and Wellbore Simulator (Geoflow) in forecast mode. Initially, the program reads pressure for the feed zones from the TOUGH input file and then calculates enthalpy using temperature or saturation data also from the input file. This is just an approximation for flowing enthalpy. The reservoir pressures and enthalpies are then used to calculate the peak wells deliverability using Geoflow with the Duns correlation. The program calculates the peak capacity of all production wells, whether open or closed, and adds up the peak capacities of open wells to obtain the peak production capacity of the field. It then compares this peak capacity with the steam requirement for the field. If the peak capacity is more than the requirement, all wells will be throttled proportionally to match the steam requirement. Otherwise, make-up wells will be opened until the steam requirement is satisfied. Make-up wells will only be activated when their deliverability is greater than or equal to some specified economic limit, which is currently set at 6 kg/s of steam production. When no more make up wells are available or all available make up wells are not economic to drill then the turbine will operate at a lower pressure reducing the steam demand. This is defined as the turbine operating in “floating” mode and marked as “end of production plateau period”. At this point, the turbine inlet pressure will be reduced. For current reservoir forecast, 2 psi of pressure-drop was applied. A drop in turbine inlet pressure produces a drop in separator pressure in all separators attached to that turbine. This produces a drop in the wellhead pressure for the connected wells. The pressure drop between separator and turbine and also between separators and wells is updated using the formula.

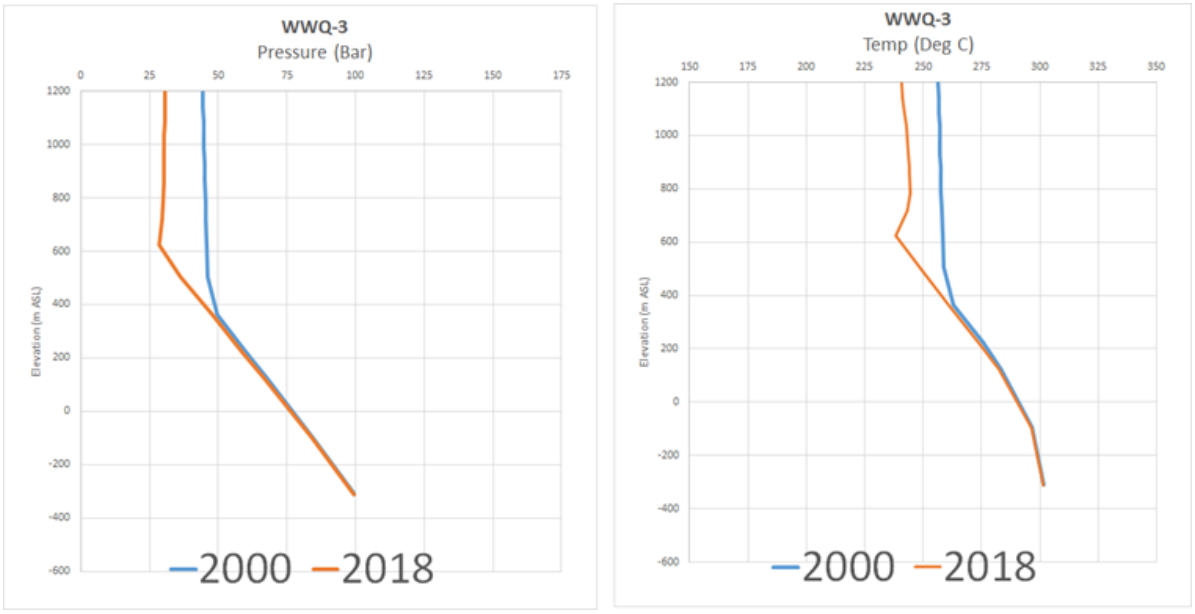


Figure 10: Comparison of Reservoir Pressure and Temperature between pre-exploitation and 2018.

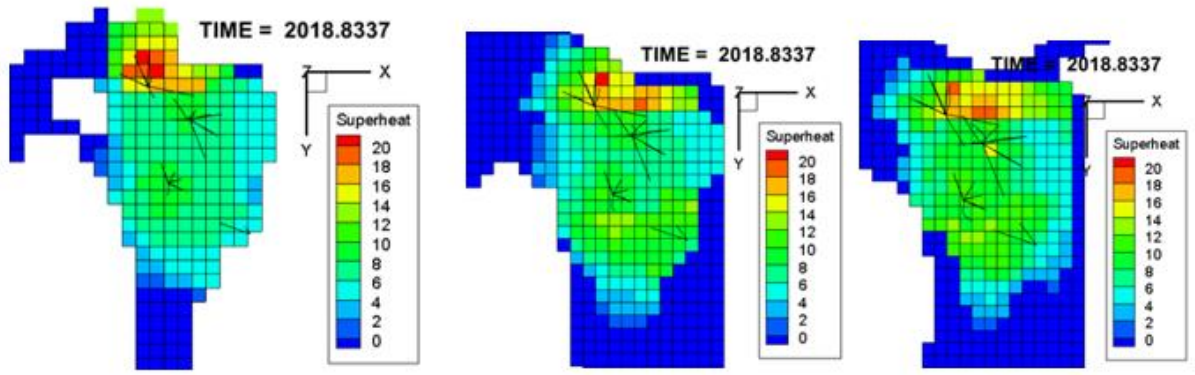


Figure 11: Map view of modeled superheat at K=1 - 3 (1200 to 600 m) at northern steam cap reservoir.

$$\Delta p_{new} = \Delta p_{old} \left(\frac{W_{new}}{W_{old}} \right)^2 \frac{p_{old}}{p_{new}}$$

Therefore, output from reservoir forecast included: 1) forecasted steam production profile (or can be converted into forecasted power generation profile) and 2) the predicted number of make-up wells to sustain steam extraction during production plateau period.

One key information required to conduct reservoir forecast using ToughRunner is the value of PI (productivity index) at each feedzone of the wells. For the existing wells, the PI of each permeable zone has been calibrated with the historical evolution of pressure and enthalpy (2). For the future make-up wells, the PI was calibrated using current average production of the existing wells. In forecasting reservoir performance with the current model, all new wells were assumed to be operated at a constant wellhead pressure of 13 bar and separation pressure of 11.5 bar.

Forecast Results

Using the calibrated numerical model, reservoir performance forecasts were done for three (3) different production scenarios:

Scenario-1: Continue 227 generation and future make-up wells are only steam wells drilled to the maximum depth of +400 m SL. It was assumed that the make-up wells are situated mostly in the northern part of the field. The model suggests that the 227 MW of production plateau would only sustain until year 2031 with total required number of make-up wells of 21. Forecasted decline rate of 4.9% from the model was consistent with the observed natural decline rate of 5% (Figure 12). Natural decline rate is defined as the decline rate that excludes production decline due to flow assurance issues in the wellbore such as scaling. It is typically calculated by plotting the well production rate right after the well clean-out programs. Numerical model with Tough2 is not capable of simulating the chemical reactions lead to scale development in the wellbore and therefore, the actual decline rate taken for quality check of forecasting simulation was the decline rate where the impact of wellbore scaling was neglected.

Scenario-2: Continue 227 MW generation and future make-up wells include brine wells drilled to maximum depth of -400 m SL. The ratio between number of steam and brine wells on future make-up wells was set at 2:1. It is assumed that the make-up wells are widely distributed across the field. With this development scenario, the model suggest that the production plateau of 227 MW could sustain until end of contract life or longer. Totally 20 make-up wells required to maintain 227 MW generation until year 2040. A more balance extraction between steam cap and brine reservoir sections in Development Scenario 2 promotes steam cap growth as indicated by increased enthalpy. In addition, Scenario 2 has less production interference than Scenario 1 due to higher well separation. As a result of steam cap expansion and less production interference, Development Scenario 2 outperforms Scenario 1 in terms of longer production plateau period and less aggressive drilling program requirement.

Scenario-3: Increase generation to 287 MW in 2023 and future make-up wells include brine wells (at ratio between steam and brine wells of 2:1) drilled to maximum depth of -400 m ASL. Distribution of candidate wells for future drilling program was similar to the one used in Scenario-2. The results from the model suggest that the Wayang Windu reservoir is capable of supporting 287 MW generation (the existing 227 MW plus the proposed additional 60 MW generation), provided that the fracture permeability with magnitude of > 60 milli-Darcy can be found in deep reservoir section (0 to -400 m ASL elevation) as per currently assigned to the reservoir model. The model suggests that 27 make-up wells required to support steam supply demand for the growth case in Scenario-3.

Production brine form Scenario-3 is higher than that of Scenario-2 which leads to higher steam cap expansion rate as indicated by earlier change of produced enthalpy from liquid into dry steam.

SUMMARY

The numerical model of Wayang Windu reservoir recently developed with Tough2 simulator has been calibrated with measured initial state conditions and historical production over 18 years with reasonable result. First key takeaway from modelling exercise was the confirmation of northern reservoir boundary which excluded the potential NW reservoir extension that was previously indicated by resistivity anomaly distribution from MT data. Spending cost for drilling the delineation well to NW area can therefore be prevented. Modelling also helps the asset team to understand that the cause of recently observed inclining water level in the wellbore was the inclining water level in the reservoir due to imbalance fluid extraction between steam cap and liquid reservoir sections. Increasing production from the liquid reservoir section is a key for future reservoir management in Wayang Windu. Drilling future make-up wells to the brine reservoir section is critical to support both; 1) continuance of 227 MW generation until end of contract life and 2) supporting organic growth. Therefore, it is prudent to establish drilling capability given the generally lower success rate in drilling into deep reservoir to date. In addition, risks related to sustainability of future deep brine wells to produce from the deep liquid feedzones should also be addressed. Calcite scales have been formed in several deep wells which reduce or prevent flow from deep brine feedzones in the wellbore. Downhole scale inhibition technology will be established to mitigate the risk.

REFERENCES

Parini, M. and F. Jarach. (1987), "Evaluation of geothermal resources with mathematical modeling combined with a probabilistic approach", Proceedings, 8th International Conference on Alternative Energy Sources, Miami.

O'Sullivan, M. and Pruess, K. (2000), "Geothermal Reservoir Simulation: The State-of-practice and Emerging Trends", Proceedings, World Geothermal Congress, Kyushu, Japan.

Finsterle, S., and Pruess, K. (1997), "Application of Inverse Modelling to Geothermal Reservoir Simulation", Proceeding, 22nd Workshop on Geothermal Reservoir Engineering, Stanford University, Stanford, CA.

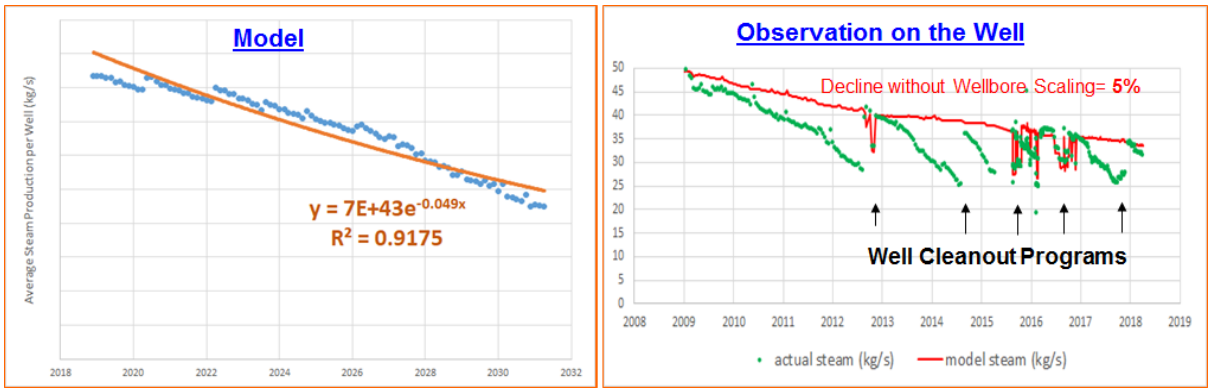


Figure 12: Forecasted and observed and production decline rates from the model and the observed well.

DARAJAT UNIT 2 AND UNIT 3 UPSTREAM PRESSURE OPTIMIZATION

Agus Riyadi and Sigit Winarno

Star Energy Geothermal Darajat II, Ltd
Sentral Senayan II, 26th Floor, South Jakarta, Indonesia
Email: agus.riyadi@starenergy.co.id; sigit.winarno@starenergy.co.id

ABSTRACT

Darajat Unit 2 and Unit 3 are geothermal power plants operated by Star Energy Geothermal Darajat II, Limited (SEGD) located in Garut, West Java, Indonesia. These power plants produce electricity 95 MW and 121 MW during full load and 90 MW and 116 MW during Take or Pay (TOP). TOP is a minimum generation accepted by PLN based on Energy Sales Contract. To generate electricity, power plant requires the production of geothermal steam supplied from subsurface resources.

Unit 2 and Unit 3 turbines require steam production for approximately 370 kg/s during full load and 350 kg/s during TOP and upstream steam pressure average at 17.9 barg. With a typical steam decline rate and the current upstream steam pressure around 17.9 barg, Darajat steam supply is calculated to fall in to a deficit situation around Q1/Q2 2018 (using full load scheme) or the end of December 2018 (using TOP scheme). Considering this steam supply calculation and potential deficit consequence, steam production optimization is required to maintain maximum electricity generation. In order to resolve the problem above, Lean Sigma project team was formed to execute the steam production optimization. The Lean Sigma is a method that relies on a collaborative team effort to improve performance by systematically removing waste and reducing variation adopted by SEGD. The project is divided into DMAIC phase (Define, Measure, Analyze, Improve and Control) process.

As the result of this project, Unit-2 and Unit-3 upstream pressure can be optimized by reducing the pressure from 17.9 to 17.39 barg as an average with a duration of five months. Upstream optimization of Unit 2 and Unit 3 can extend steam shortages until the end of August 2018 (using full load scheme) or end of April 2019 (using TOP scheme). This steam production optimization project contributes potential cost savings USD 2,624,620 to company.

Keywords: Optimization, Production, Power Plant, Darajat

INTRODUCTION

Star Energy Geothermal Darajat II, Ltd is one of the steam dominated geothermal largest in the world. It is located in Garut Regency, West Java Province, Indonesia, about 35 km southeast of Bandung (capital city of West Java Province. Comprises three geothermal power plants; Unit 1 (55MW), Unit II (95 MW), Unit 3 (121 MW) and 271 MW in total of three geothermal power plants. Figure 1 shows the location of Darajat geothermal.

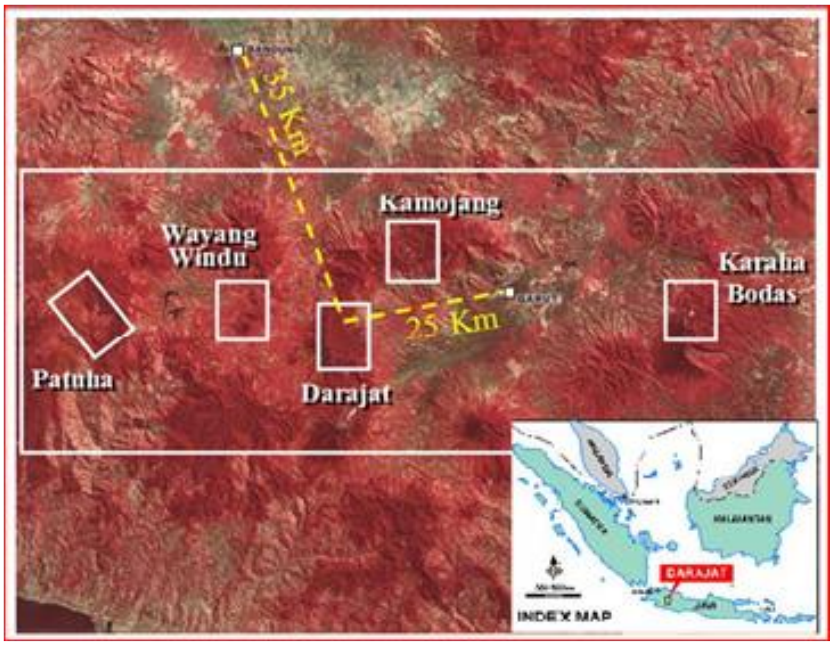


Figure 1: Location of the Darajat Geothermal field relative to other volcanic activities and other geothermal fields.

Star Energy Geothermal Darajat II, Ltd supplies steam to Unit 1 which owned by and operated by PLN (Indonesia's National Electricity Company) under its subsidiary PT. IP (Indonesia Power), and to Units II and III, which are owned and operated by Star Energy Geothermal Darjat II, Ltd. The total steam produced to run these three units is 476 kg/s in average. Unit I started to operate commercially in 1994, Unit II in 2000 and Unit III in 2007.

Maintaining the steam supply to meet the target generation has become a huge challenge experienced by the Darajat Geothermal Field in the last 20 years. The high decrease in flow rate and reservoir pressure is the main factor that influencing the availability of steam supply to meet the needs of the power plant.

Darajat Unit 2 and Unit 3 has potential steam shortage around Q1/Q2 2018 according to latest steam supply forecast by RM team as per bussines plan. The steam shortage has potential impact to generation Unit 2 and Unit 3. The Star Energy Geothermal Darajat, Ltd has formed the Lean Sigma team to address this problem to by performing Unit 2 and Unit 3 upstream pressure optimization program, so above mentioned steam shortage can be avoided.

Unit 2 and Unit 3 currently supported 25 production wells which interface operated on 14.03 barg for Unit 2 and 16.38 barg for Unit 3 while upstream pressure is operated 17.77 barg for Unit 2 and 18.04 barg for Unit 3. This high-pressure difference causes a bottleneck effect so that steam production from the well becomes inefficient. During Darajat Lean Sigma VSM (Value Stream Map) a process to identify optimization operation on Star Energy Geothermal Darajat, Ltd, the team looks at an opportunity to eliminate those bottleneck effect at the meeting point between the power plant and steam field by optimizing steam differences between the upstream and downstream pressure located on power plant area in order to maximize the well production and reserve steam buffer from several Units 2 and Unit 3 wells. Figure 2 shows the schematic of Darajat unit 2 and unit 3.

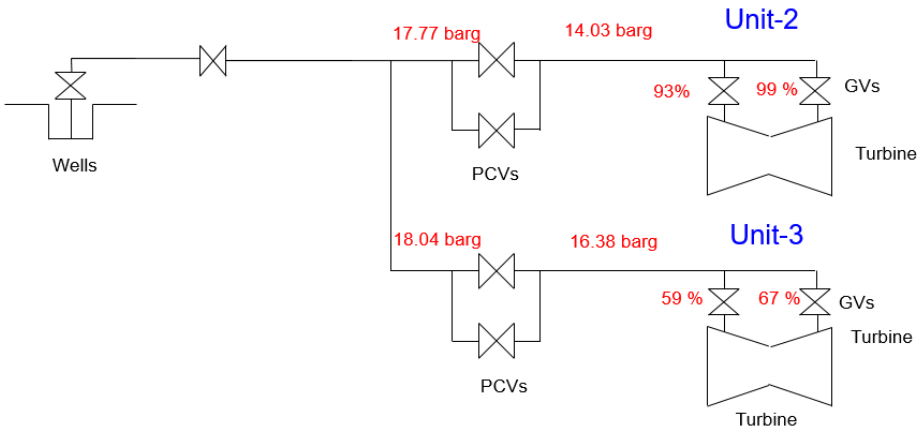


Figure 2: Darajat Unit 2 and Unit 3 Power Plant Operation Schematic.

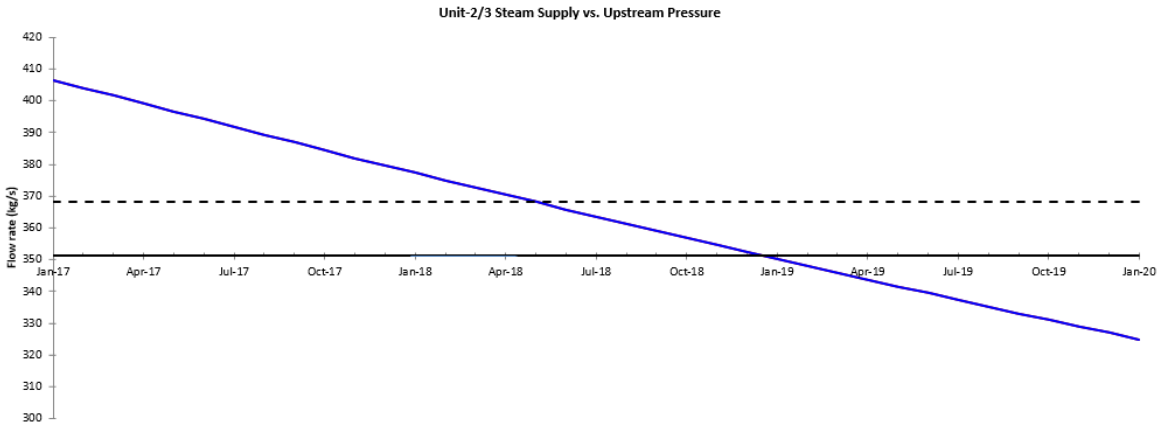


Figure 3: Darajat Steam shortage-based figure as per steam production forecasting.

DARAJAT UNIT 2 AND UNIT 3 OPERATION

During monitoring of steam production, to maintain generation target, steam flow rate shall be maintained at approximately 370 kg/s for both Darajat Unit 2 and Unit 3. As the natural resources this steam flow rate has typical decline or shortage. And if the problem of shortage is maintained to continue, the steam supply will facing the condition where the amount of steam supply production is not able to produce the amount of electricity required production. The typical Darajat Unit 2 and Unit 3 decline rate can be shown as per Figure 3 below.

The Figure 3 made based on Darajat Unit 2 and Unit 3 well data (flow, pressure and temperature and other parameters).

LEAN SIX SIGMA PROCESS

Lean six sigma process is operation management concept that is synergy of lean and six sigma. With lean six sigma process company can get "speed" that lean has while "quality" from six sigma has. This methodology directs the company to eliminate of waste that occur in the processes and acquisition of quality in output that minimizes the creation of defective products. The goal is to increase company profits, provide sustainability, and provide added value. Lean Six Sigma process is divided into 4 phases and called DMAIC (Define, Measure, Analyze, Improve and Control). DMAIC is the heart of the lean six sigma analysis that ensures the voice of the customer runs throughout the process so that the products produced satisfy the customer.

Define (D)

Define (D) phase is to determine problems, determining customer requirement. During this phase does not use statistic approach, tools such as causal diagrams (Cause and Effect Chart), Pareto Chart (Pareto Chart), Input, Process, Output (IPO) diagram are often used in this phase.

Measure (M)

Measure (M) is the phase of measuring the current level of performance. Before measuring the level of performance usually first conduct an analysis of the measurement system used.

Analyze (A)

The analysis phase (A) is the phase of finding and determining the root or the cause of a problem. Problems that arise are sometimes very complex so that it is confusing which one we will and will not complete.

Improved (I)

Improve (I) is the phase of increasing the process (x) and eliminating the causes of defects. Whereas in the development phase I (Improve) involves a lot of experimental design test (Design of Experiment) or abbreviated as DoE.

Control (C)

Control (C) is the phase of controlling process performance (x) and ensuring defects do not reappear.

- Helps reduce variability.
- Monitor performance at all times.
- Enables correction processes to prevent rejection.

PROGRAM IMPLEMENTATION

After team formed then conduct meeting, study and workshop. Team used the rule of practice that exist on lean sigma process. Project Contract containing commitment from of the project team, project sponsor, project champion and facilitator has been made on early of the project. Input-Process-Output (IPO) diagram has been made during this Define (D) phase to identify input and output this lean sigma process (Figure 4).

After completing Define (D) phase team moved to Measure (M) stage to determine base line data. As team agreed based line data was capture 3 months Darajat upstream pressure data of Unit 2 (Figure 5) and Unit 3 (Figure 6) data from January 1st, 2018 to 26th March 2018. Summary of based line can represent on the below chart (Table 1).

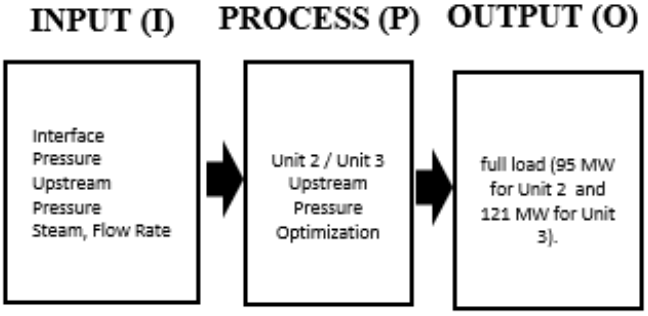


Figure 4: Unit 2 / Unit 3 Upstream Pressure Optimization IPO Diagram.

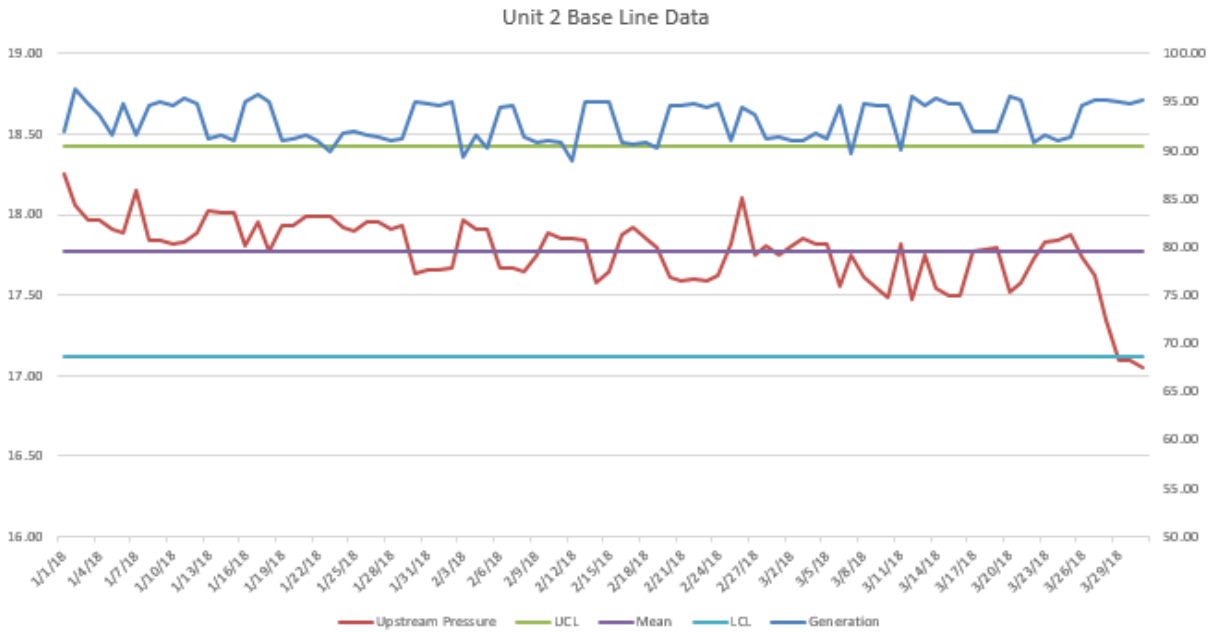


Figure 5: Unit 2 Upstream Pressure Based Line Data.

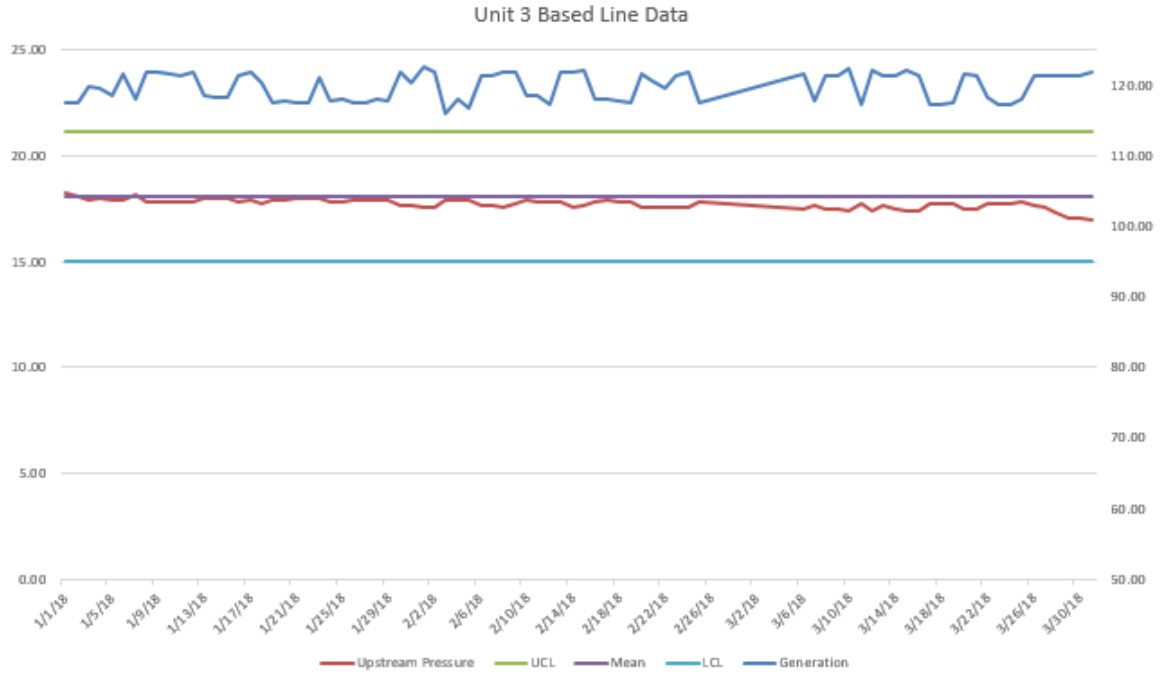


Figure 6: Unit 3 Upstream Pressure Based Line Data.

Table 1: Based line data Unit 2 and Unit 3 Upstream pressure optimization.

	U/S Press	I'face Pres	MW	U/S Press	I'face Press	MW
	PIT-428	PIT-403A	MWG	PIT-428	PIT-407	MW-GRS
SD	0.22	0.09	1.99	1.02	0.05	3.18
UCL	18.42	14.30	98.94	21.10	16.54	128.82
Mean	17.77	14.03	92.96	18.04	16.38	119.30
LCL	17.12	13.76	86.99	14.97	16.23	109.77

Team also processed statistical data to get statistical representation of based line data. Standard Deviation (SD), Upper Control Limit (UCL), mean and Lower Control Limit (LCL) has been determined as followings table:

COPQ (Cost of Poor Quality) of this lean sigma project is determined based on the gap between desire an actual of production line that already compensate with decline rate that can be represent on Figure 7 below. Total COPQ is equal of triangle shifting area between the actual line and desired line crossing with time interval. Based assumption of electrical price, base and desired upstream pressure, current steam consumption and time during optimization. Total COPQ of this lean sigma project is equal to USD 2,400,000.

During Analyze (A) phase team brainstormed to get idea for optimization process. Team used 6M principle (Man, Material, Machine, Method, Measurement and Mother Nature or Environment. Team used Fish Bone to determined possible aspect of 6M and identify whether is categorized as Noise (N), Constant (C) or Experimental or (X). After all aspect was identified team then decided only aspect that will impact to Unit 2 and Unit 3 upstream pressure optimization process. The Fish Bone is used for this analyzed process and result can be represent on Figure 8 below.

Improvement, (I) phase was made base on brainstorming across the team and formulized into SOP (Standard Operating Procedure). Figure 9 below shows brainstorming result of this optimization process.

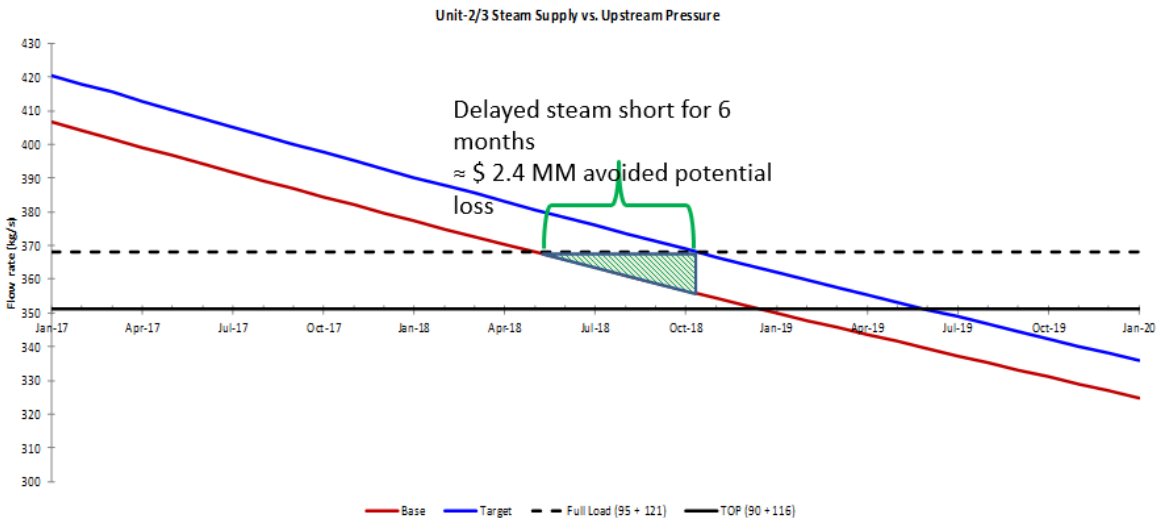


Figure 7: Unit 2 / Unit 3 Upstream Pressure Optimization COPQ calculation.

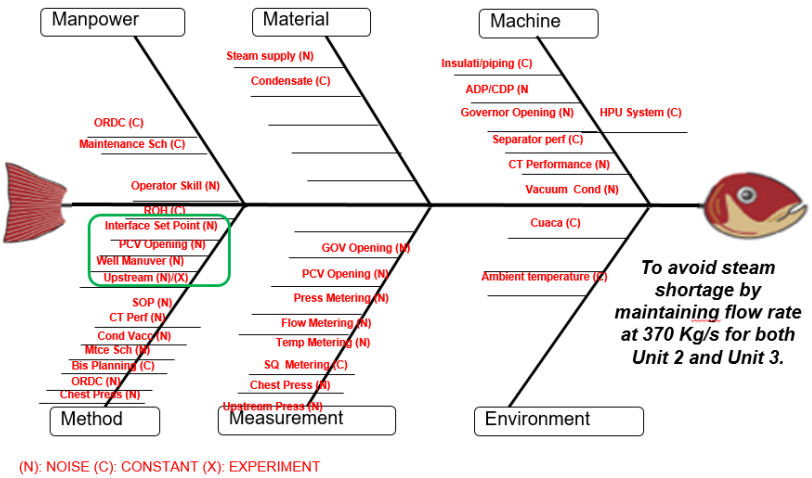


Figure 8: Fish Bone Diagram Unit 2 and Unit 3 Upstream Pressure Optimization.

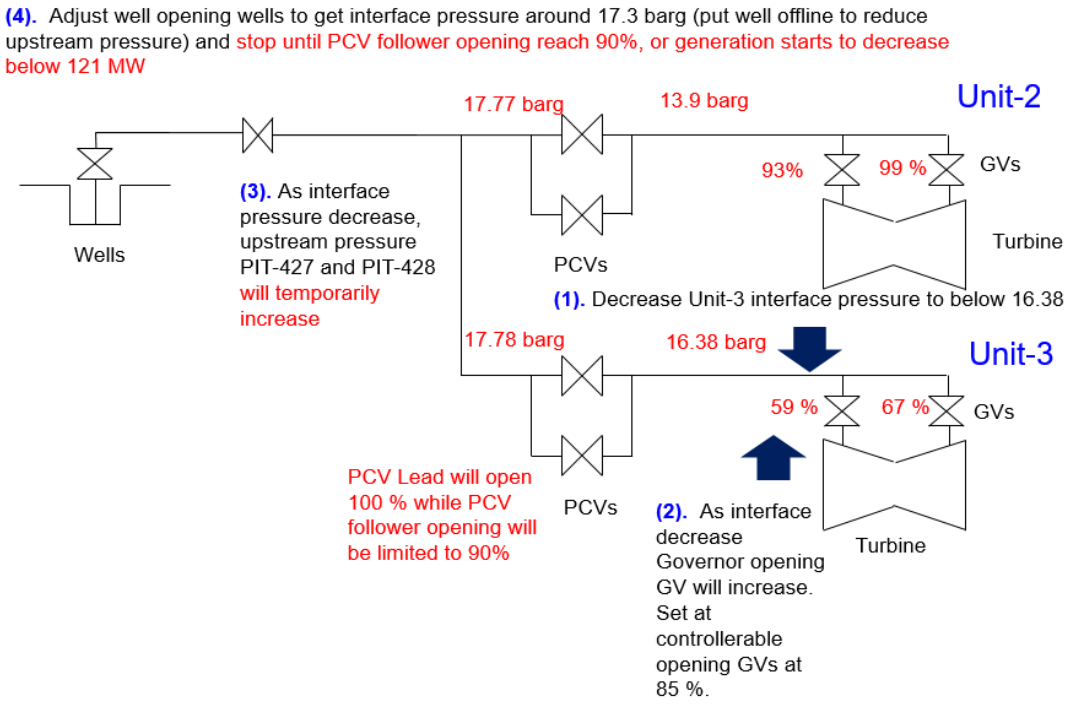


Figure 9: Optimization Scenario as result of Improvement (I) Phase.

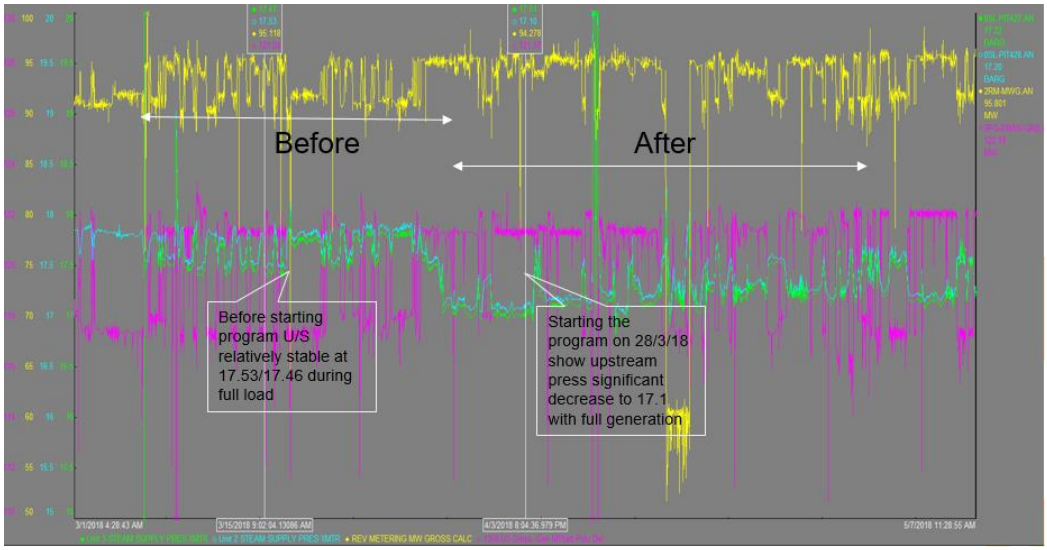


Figure 10: Implementation result of Unit 2 and Unit 3 Upstream Pressure Optimization.

Detail of optimization process can be summarized as followings:

1. Decrease Unit 3 interface pressure to below 16.3 barg.
2. As interface pressure decreased governor opening will increase. Increase interface pressure until governor opening reach 85 %.
3. As interface pressure decrease, upstream pressure PIT-427 and PIT-428 will temporary increase but decrease afterwards.
4. Adjust well opening of to get interface pressure around 17.3 (put well offline if required to reduce upstream pressure) and stop until PCV-follower reach 90% and/or Unit 3 generation start to decrease below 121 MW.
5. Unit 2 was not consider to be altered current parameter due to current governor opening was already stable above 90 % opening.

The above process then formulized through SOP and team then conduct testing and implementation process on Control (C) phase.

TEST RESULT AND IMPLEMENTATION

The SOP result form of Improvement (I) phase was tested three days starting 27 March 2018 to 30 March 2018. To get desired optimization parameter, Unit 2 and Unit 3 generation was set to maximum

generation (95 MW for Unit 2 and 121 MW for Unit 3). Operating parameter such as Interface pressure, turbine inlet pressure, governor opening and PCV opening was adjust as per recommendation that formulized on Standard Operation Procedure (SOP). Based on testing result, team observed upstream pressure was significantly decrease as Figure 10 below. As this test was successfully conducted, team then decided to maintain optimized upstream pressure.

Improvement of the Unit 2 and Unit 3 upstream pressure optimization can be represented statistical data below (Table 2 and 3).

Table 2: Improved Performance in Comparison with the Baseline – Before.

	U/S Press	I'face Pres	MW	U/S Press	I'face Press	MW
	PIT-428	PIT-403A	MWG	PIT-428	PIT-407	MW-GRS
SD	0.22	0.09	1.99	1.02	0.05	3.18
UCL	18.42	14.30	98.94	21.10	16.54	128.82
Mean	17.77	14.03	92.96	18.04	16.38	119.30
LCL	17.12	13.76	86.99	14.97	16.23	109.77

Table 3: Improved Performance in Comparison with the Baseline – After.

	U/S Press	I'face Pres	MW	U/S Press	I'face Press	MW
	PIT-428	PIT-403A	MWG	PIT-428	PIT-407	MW-GRS
SD	0.17	0.28	8.24	0.18	0.06	1.44
UCL	17.77	14.99	117.46	17.73	16.41	125.25
Mean	17.26	14.15	92.73	17.21	16.24	120.93
LCL	16.76	13.31	68.01	16.68	16.07	116.61

In order to maintain sustain improvement, data collection plan and behavior action plan need to be determined as followings (Table 4)

Table 4: List of Key Metric or KPI to be monitored.

Data to be Collected	Key Metric/KPI #1	Key Metric/KPI #2
Metric or KPI Name	Upstream Pressure	Unit generation
Unit	BarG	MW
Data Collector	Rudy Heryadi	Shift Leader
Frequency	Daily	Daily
Source of Data	PI, DCS	PI, DCS
Method of presentation	Chart, Report	Chart, Report
Action	When Pressure Increase	When Generation Decrease

REALIZED FINANCIAL BENETIF

As part of Control (C) phase, team determined financial benefit from this Darajat Unit 2 and Unit 3 upstream pressure optimization process. Accrual Financial Benefit (AFB) verification also claimed to Lean Sigma process champion and financial team as cost avoidance for approximately US $ 2,624,620. This calculation has been has been made based on trapezoidal area starting April to August 2018. Detail of realized financial benefit can be represent as table below (Table 5).

Table 5: Accrual Financial Benefit (AFB) result of Unit 2 and Unit 3 upstream pressure optimization process.

Month/Year	**Cost Avoidance**	**Cumulative**
Apr-18	$345,768.71	$345,769
May-18	$447,818.82	$793,588
Jun-18	$527,895.53	$1,321,483
Jul-18	$619,475.29	$1,940,958
Aug-18	$683,661.18	$2,624,620
Totals:	**$2,624,620**	

Above calculation has been made based on asumption:

1. Specific Stem Consumption (SSC) is 1.7 kg/s.
2. Using Darajat Unit 2 and Unit 3 typical steam production decline rate.
3. Use electrical price as per contract.

CONCLUSIONS

1. Darajat Unit 2 and Unit 3 has potential steam shortage during early year 2018.
2. Team lean sigma tools has been successfully used to address the Darajat Unit 2 and Unit 3 steam shortage.
3. Unit 2 and Unit 3 Upstream pressure can be optimized form 17.77 barg to 17.26 for Unit 2 and 18.04 barb to 17.21 barg with the same unit optimum generation.
4. Lean sigma project has been successfully claimed USD 2,624,620 for this lean sigma optimization project.

REFERENCES

Comstock, D., (2011), "Lean Sigma Green Belt". Variance Reduction International, Inc

George, M., L., Rowlands, D., Price, M., and Jones, E., R., (2005), "Lean Six Sigma Pocket and Tool Books."

Yamin, W., Choiri, M., Goesmano, A., and Nurfahmiawati, T., (2015), "Darajat Unit II/III Interface Debottlenecking Project", Proceedings World Geothermal Congress, 1-2.

PRE-FEASIBILITY STUDY OF WELLHEAD GENERATING UNIT IN WATER DOMINATED SYSTEM

Muhammad Alwy Dahlan[1], Heru Berian Pratama[2], and Nenny Miryani Saptadji[2]

[1]Petroleum Engineering Study Program, Faculty of Mining and Petroleum Engineering,
Institut Teknologi Bandung
[2]Geothermal Engineering Study Program, Faculty of Mining and Petroleum Engineering,
Institut Teknologi Bandung
Jl. Ganesha No. 10, Bandung, West Java, Indonesia. 40132
Email: alwydahlan.ad@gmail.com

ABSTRACT

The development of geothermal fields needs 5-6 years from the first well drilled until the operation of the central power plant. Between the gap years, the wells will be shut in and will be re-opened when the power plant is ready. However, there is an alternative to utilize the wells with Wellhead Generating Unit (WGU), the small power plant which can generate the electricity as soon as the drilled productive wells completed. Therefore, the investor and developer will earn an early return on investment. The objective of this study is to decide the preferable scheme for the installed capacity of WGU with economic consideration. Correspondingly, this study uses two types of WGU, backpressure and condensing turbine. Full factorial experimental design with Monte Carlo simulation is used to calculate and design the backpressure and condensing turbine. Steam fraction, mass flow rate, turbine inlet pressure, and turbine exhaust pressure are the parameters to be analyzed in the Monte Carlo Simulation. The economic feasibility of the project is based on capital expenditure, decline curve analysis, and electricity price. The result of probability, P10, P50, and P90 of gross power output for the backpressure and condensing turbine are 6.8, 8.4, 10 MWe and 13.6, 16.7, 19.9 MWe respectively. Then, the P10, P50, and P90 of Specific Steam Consumption (SSC) are 3.82, 3.95, 4.09 kg/s/MWe and 1.93, 1.97, 2.02 kg/s/MWe respectively. Based on the economic evaluation, the best type of WGU is condensing turbine with the P10, P50, and P90 of Internal Rate of Return (IRR) are 12%, 16%, 21% respectively and the P10, P50, and P90 of Net Present Value (NPV) are 1.1 MUSD, 3.6 MUSD, 6.0 MUSD respectively over 30 years of WGU lifetime. This paper is the first study for designing the WGU combined with an economic study based on the technical evaluation to propose the best option to develop the field.

Keywords: Wellhead Generating Unit, Experimental Design, Economic Feasibility

INTRODUCTION

In the early phase of development, some exploration wells have a chance to become productive wells after conducted by several well testing. However, to complete the construction of the central power plant need more extended time from the first accomplished exploration well. The wells will be shut in during construction, or in another word, it will be disposed of wasteful steam. Hence, the steam will be utilized immediately after completing the drilled wells to reduce those losses with Wellhead Generating Unit (WGU). WGU will turn the steam into electricity.

In WGU, steam is extracted from the well and converted to electricity at the wellhead (Saitet and Kwambai, 2015). Different from the conventional power plant, the construction of WGU is placed on a portable unit, generally known as skid mounted. Because of this, it is easy to move to another place. The other characteristics of WGU that make it more attractive for certain applications are the re-usability, modest capital investment, and rapid power production capability (Sutter et al., 2012). The most promising applications of WGU include on-site industrial use, electricity supply in remote areas, as a tool for developing geothermal fields, and peak units for larger utilities (Sutter et al., 2012). For this study, WGU will be applied to a specific geothermal system; it is the water-dominated system.

Water-dominated system is represented by the reservoir system of Lumut Balai Field. Calculation and design of WGU will be based on data in this field. In the Lumut Balai field, the current capacity of the installed power plant is 55 MWe and will be operated commercially (Commercial on Date) on July 2019. Therefore, the next development can be considered by using the WGU as alternative power plants.

Table 1: Case studies of WGU application worldwide.

Year	Field	Country	Capacity	Type of WGU	Objectives
1966	Matsukawa	Japan	1 × 450 kW	Backpressure Turbine	18 months well testing to assess the corrosion effects on various materials from exposure of geothermal steam and its condensate
1969	Namafjall	Iceland	1 × 3 MW	Backpressure Turbine	First project utilization of geothermal resources
1978	Kamojang	Indonesia	1 × 250 kW	Backpressure Turbine	First project utilization of geothermal resources
1982	Los Azufres	Mexico	5 × 5 MW	Backpressure Turbine	Test the new field
1995	Miravalles	Costa Rica	1 × 5 MW	Backpressure Turbine	Provide electricity during well-drilling phase and well testing with real time flow condition
2011	Olkaria	Kenya	1 × 5 MW	Condensing Turbine	The first project to accelerate the utilization of geothermal resource in Kenya
2012	Eburru	Kenya	1 × 2.5 MW	Condensing Turbine	Pilot project of WGU with shut in wells in Eburru since 1990

Determination of WGU capacity needs to be done before it can be applied in the field. The proper installed capacity of WGU can be approached by experimental design. In this study, the installed capacity of WGU will be calculated by full factorial experimental design with Monte Carlo simulation to get the probabilistic result. Full factorial in Experimental Design (ED) is a systematic way of involving several factors where it is necessary to investigate the combined effects of the factors on a response variable (Myers et al., 2009).

The study of probabilistic approach for calculation and design of WGU was done by Ahmad et al. in 2017. In the previous study, the calculation and design of WGU were in the vapor-dominated system with Kamojang field as its representative data. The type of WGU used was only a backpressure turbine and there was no economic feasibility evaluation for the utilization of WGU. However, this study used two types of WGU, they are backpressure and condensing turbine for comparison. Then, the economic feasibility evaluation was used to determine the best type of WGU for the geothermal system. In addition, the economic calculation was based on decline curve analysis to get more realistic value over the lifetime of WGU. The Experimental Design (ED) was used to find the location of borehole optimally in the geothermal field (Seidler et al., 2015). The application of systematic ED was used to approach a geothermal reservoir simulation model to generate probabilistic resource assessment results (Quinao, 2015). The experimental design was also applied in geothermal resource assessment in Ciwidey-Patuha, West Java, Indonesia (Ashat and Pratama, 2018).

The first objective of this study is to determine technical empiric equations of gross power output for the backpressure and condensing turbine represented by the probabilistic result, P10, P50, and P90. The second objective is to determine technical empiric equations of Specific Steam Consumption for the backpressure and condensing turbine represented by the probabilistic result, P10, P50, and P90. Then, the third objective is to propose the best type of WGU with economic consideration based on the technical evaluation, especially for this geothermal system.

WELLHEAD GENERATING UNIT

WGU is the small power plant compared to the conventional power plant and can generate electricity from 1 to 15 MW, with the largest offered being 25 MW (McHugh et al., 1985). As the name suggests, WGU placed on the same wellpad as the location of production wells. Therefore, WGU uses short pipelines to transport the production fluids from one or a group of wells to the generating unit.

There are several types of commercial WGU, depending on the characteristics of the geothermal resource being developed and the kind of conversion cycle being used. The major types of WGU are backpressure wellhead units, condensing wellhead units, and binary wellhead units. For this study, only two types of WGU are used for designing. They are a backpressure turbine and a condensing turbine.
Table 1 shows some examples of case studies of WGU application worldwide. The table also shows the different capacities, types, and objective of

WGU for geothermal resources development. WGU is not a new technology because since 1966 it has been used in Matsukawa, Japan with backpressure tubine for well testing (Lund, 2005). In Kamojang, Indonesia, the utilization of WGU began in 1978 with backpressure turbine (Suryadarma, et al., 2010). The other utilizations of backpressure turbine are in Los Azufres, Mexico (Hiriart, 1983) and in Miravalles, Costa Rica (Moya & Dipippo, 2011). While, the utilization of condensing turbine is in 2011 and 2012 for pilot projects of geothermal resources development in Olkaria and Eburru, Kenya (Saitet and Kwambai, 2015).

The most characteristic feature of a wellhead generating facility is its modular construction. The turbine-generator modules are assembled at the factory on one or more skids (McHugh et al., 1985). Therefore, they will easily and securely be transported and used as a unit. And because of the modular construction, the space requirements of a wellhead power plant could be a minimum of 60 m by 30 m with the typical size of wellpads measure approximately 100 by 100 m (Kiptanui et al., 2016).

Other advantages of WGU that make it more attractive in the geothermal industry are as follow. Because of their size and packaging, WGU can be operated faster, which is only about 6 months while conventional plants need 2-3 years. Hence, the use of WGU can allow the investors to earn their revenue in a shorter period. Moreover, WGU can be used in areas with complex topographic conditions or remote areas.

Furthermore, there are some disadvantages from using WGU; those are WGU can still be categorized as a new technology, its spare parts are still limited in the market, then the capital cost and operating cost are relatively high per MW of installed capacity. There are new problems in operation and maintenance if there are many WGU spread in one field, also new problems on handling brine or condensate disposal if the wells produce two-phase fluid (Saptadji, 2018).

Backpressure Turbine

Backpressure turbine is the simplest type and, in capital cost, the cheapest of the wellhead conversion system. Backpressure turbine only consists of a separator, steam turbine-generator, transformers, and electrical distribution modules. The fluid flow from the wells will be going through separator. Then, separated steam will flow through the turbine and exhausted to the atmosphere. The schematic of the backpressure turbine as shown in Figure 1.

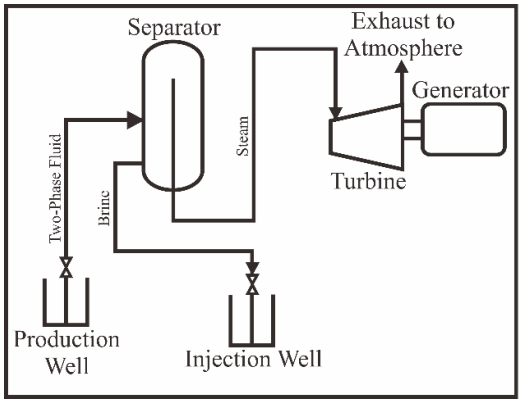


Figure 1: Schematic of backpressure turbine (modified from Sutter, 2012).

The efficiency of a backpressure turbine plant is less than a condensing turbine plant (Kiptanui, 2016). Other concern about this type of WGU is the noisy sound from exhaust steam because of greater different pressure between the inside turbine and atmospheric pressure. Besides all of its deficiency, the backpressure turbine is still attractive because of the economic reason for testing new well in the first development project.

Condensing Turbine

Condensing turbine has a more complex component than backpressure turbine because it has more additional components, such as a condenser, cooling tower, and condensate pumps. Then, the capital cost of this type is higher than the backpressure turbine. The additional components also result in more efforts to move these units to another location, and it will take times longer for the relocation. The use of a condensing turbine can be generated power from the steam become doubled or more than backpressure turbine.

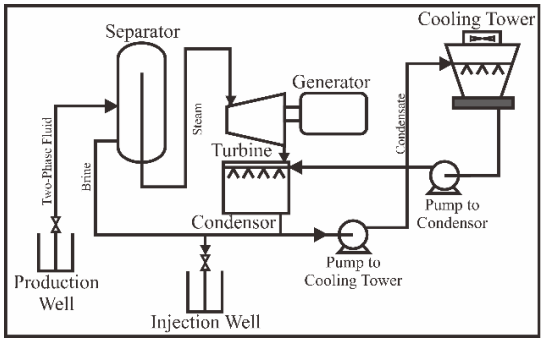


Figure 2: Schematic of condensing turbine (modified from Sutter, 2012).

The schematic of the condensing turbine shown in Figure 2. Condensing turbine with the type of single flash system is used for this study. Two-phase fluid from the wells flows into the separator to separate the steam and brine. The steam from the separator will going through the turbine to generate the

electricity. Then, brine or condensate will be injected back into the reservoir.

METHODOLOGY

The methodology used for this study as presented in Figure 3. Start from determining the gross power output and specific steam consumption (SSC) of WGU until the economic feasibility calculation for choosing the best type of WGU.

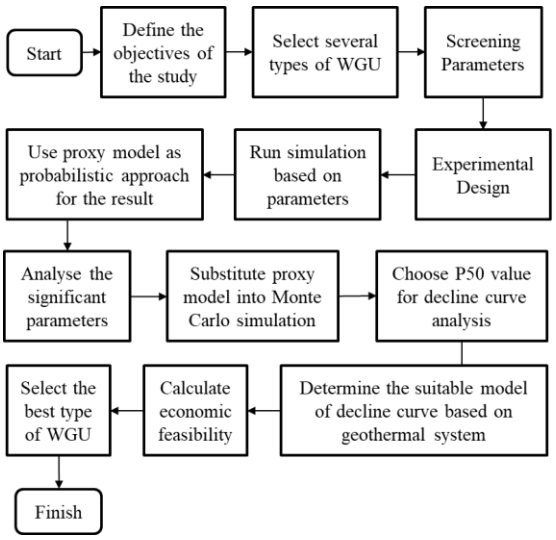


Figure 3: Experimental design and economic feasibility workflow of WGU.

The objectives of this study are fulfilled by the calculation of gross power output and SSC to determine the size of the installed capacity of WGU. All parameters which affect the performance of WGU will be chosen. For this study, full factorial experimental design with Monte Carlo simulation is used to calculate and design WGU. Significant parameters are analyzed by the Pareto Chart. Then, the first-order polynomial application will be selected as the proxy model. For economic feasibility, the type of WGU which gave the higher profit will be chosen for this geothermal system.

Technical Section

The Lumut Balai geothermal project is located on Sumatera Island, South Sumatra Province, Penindaian village, sub-district of Semende Darat Laut, Muara Enim regency, about 292 km southwest of Palembang.

The reservoir in the Lumut Balai is represented the condition. Well test data that has been performed in each well of Lumut Balai field is tabulated in Table 8. The gray rows in the table are the production wells data used for input data of WGU calculation and design. The data tabulated in Table 8 is the result of well test data in the condition of the shut-in wells.

Gross power output generated by turbine-generator can be calculated by Equation (1) (Dipippo, 2008 and Saptadji, 2018):

$$W_e = \frac{x \times \dot{m} \times \eta_t \times (h_{TIP} - h_{cond.})}{1000} \quad \text{…….(1)}$$

where W_e is the gross power output in MWe, x is the steam fraction in the wellhead, $\dot{m}$ is the total mass flow rate in kg/s, η_t is isentropic turbine efficiency in percentage, h_{TIP} is specific steam enthalpy at turbine inlet pressure in kJ/kg, and $h_{cond.}$ is specific steam enthalpy at condenser in kJ/kg.

Table 2: Well test data of Lumut Balai Field.

Well	Results			
	Well Head Pressure (bara)	Total Mass Rate (kg/s)	Dry-ness	Enthalpy (kJ/kg)
LMB -X.1	6	133	0.17	1045
LMB -Y.1	6	132	0.15	1006
LMB -Z.1	6	256	0.15	1035
LMB -Z.2	6	240	0.16	1042

SSC determines power plant performance. SSC is the amount of steam in kg/s consumed by power plant to generate 1 MW of electricity. The lower value of SSC indicates the greater efficiency of power plant. SSC can be calculated by Equation (2) (Dipippo, 2008 and Saptadji, 2018) as follows:

$$SSC = \frac{x \times \dot{m}}{W_e} \quad \text{……(2)}$$

where *SSC* is specific steam consumption in kg/s/Mwe, x is the steam fraction in the wellhead, $\dot{m}$ is the total mass flow rate in kg/s, and *We* is the gross power output in MWe.

Four significant parameters which affect the calculation of gross power output and SSC will be chosen based on Equation (1) and (2). Four significant parameters used in this calculation are steam fraction (x), mass flow rate (ṁ), turbine inlet pressure (TIP), and turbine exhaust pressure (TEP). The mass flow rate which flowing to turbine will affect the number of electricity generating capacity. For backpressure turbine, the inlet and outlet pressure of turbine will affect the enthalpy of the fluid. Whereas, for condensing turbine, the turbine inlet pressure and condenser pressure will affect the enthalpy of the fluid. The parameters of backpressure turbine are tabulated in Table 3, and the parameters of condensing turbine are tabulated in Table 4. The parameters are taken from Firanda, et al. in 2015, Long, et al. in 2012, Ahmad et. al. in

2017, and Dipippo in 2008. The low and high values in parameters are categorized on data in Lumut Balai Field as the representative of this geothermal system.

Table 3: Parameters of backpressure turbine.

Parameters	Low (-1)	High (+1)	Reference
Steam Fraction	0.15	0.19	Firanda, et al., 2015
Mass flow rate (kg/s)	132	256	Firanda, et al., 2015
Turbine Inlet Pressure (bar abs)	6	6.5	Long, et al. 2012
Turbine Exhaust Pressure (bar abs)	0.8	1	Ahmad et al., 2017

Table 4: Parameters of condensing turbine.

Parameters	Low (-1)	High (+1)	Reference
Steam Fraction	0.15	0.19	Firanda, et al., 2015
Mass flow rate (kg/s)	132	256	Firanda, et al., 2015
Turbine Inlet Pressure (bar abs)	6	6.5	Long, et al. 2012
Turbine Exhaust Pressure (bar abs)	0.08	0.12	Dipippo, 2008

Experimental Design

Full Factorial experimental design with Monte Carlo simulation is used to calculate and design the backpressure turbine and condensing turbine. ED is the study of the effect on a response of k factors, each at two levels. These are commonly known as 2^k factorial experiments (Walpole et al., 2012) where k is the number of parameters. The parameters are often denoting the levels as "high" and "low" in dimensionless variables, i.e., +1 for low and -1 for high. Experimental design concept will be applied in WGU to calculate the gross power output and SSC with probabilistic approach based on several significant parameters.

A two-level, four-parameter full factorial design requires 2^4 or 16 simulation runs. This is shown in Table 5. The simulation of ED was using Minitab 18™ software. The order shown in the RunOrder column used to collect data which contains the randomized order of the runs.

Probabilistic approach of polynomial response or proxy models is used to define the simulation results and the tested parameters in Table 2 and 3. Equation (3) shows a first-order polynomial approximation of the simulations from the design.

$$y = \beta_0 + \beta_1 A + \beta_2 B + \beta_3 C + \beta_4 D + \beta_5 AB + \beta_6 AC + \beta_7 AD + \beta_8 BC + \beta_9 BD + \beta_{10} CD + \beta_{11} ABC + \beta_{12} ABD + \beta_{13} ACD + \beta_{14} BCD + \beta_{15} ABCD \quad \text{.....(3)}$$

where y is simulation results, βs are the regression coefficients, A is the coded variable that represents x, B is the coded variable that represents $\dot{m}$, C is the coded variable that represents *TIP*, and D is the coded variable that represents *TEP*. The regression model can be used to predict the response at any point in the space spanned by the factors in the design (Myers et al., 2009).

Table 5: A two-level, four-parameter full factorial design.

StdOrder	RunOrder	x	$\dot{m}$	TIP	TEP
7	1	-1	1	1	-1
2	2	1	-1	-1	-1
3	3	-1	1	-1	-1
4	4	1	1	-1	-1
6	5	1	-1	1	-1
9	6	-1	-1	-1	1
15	7	-1	1	1	1
14	8	1	-1	1	1
12	9	1	1	-1	1
8	10	1	1	1	-1
1	11	-1	-1	-1	-1
13	12	-1	-1	1	1
11	13	-1	1	-1	1
10	14	1	-1	-1	1
16	15	1	1	1	1
5	16	-1	-1	1	-1

Economical Section

A preferable scheme for the installed capacity of WGU between backpressure and condensing turbine is decided by the economic feasibility. The economic feasibility will be evaluated by using financial model. A financial modeling is concerned with the development of tools supporting firms, investors, intermediaries, governments etc. in their financial-economic decision making, including the validation of the premises behind these tools and the measurement of the efficacy of these tools (Spronk, 1996). In this study, the financial model is divided into four calculation sheets, namely, Investment Cost and Expense, Loan Schedule, Income Tax, and Cash Flow, modified from Randle, in 2005. Figure 4 depicts the structure and interrelationships between the calculation sheets in the financial model.

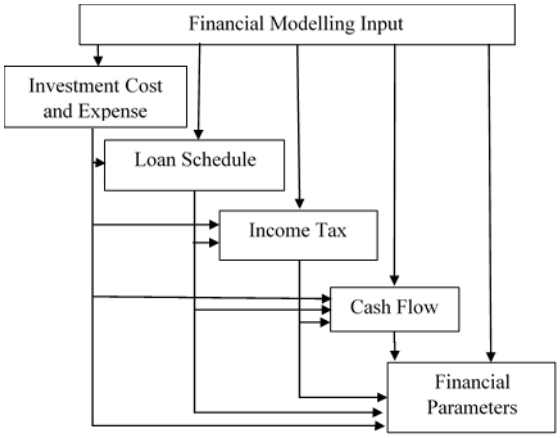


Figure 4: Financial model structure (Modified from Randle,2005).

Technical and financial assumptions

Table 6: Technical assumption to build financial model.

Technical Parameters	Value	Unit	References
Wellhead Economic Life	30	Years	Sarmiento, 2013
Number of Production Well	1	Well	-
Number of Injection Well	1	Well	-
Capacity Factor	90	%	Sarmiento, 2013

Table 7: Financial assumption to build financial model.

Financial Parameters	Value	Unit	References
Depreciation	8	Years	PMK No. 21/PMK. 11/2010
Depreciation Rate	25	%	PMK No. 21/PMK. 11/2010
Equity : Loan	30 : 70	%	Serdjuk, 2013
Loan Period	20	Years	Quinlivan, 2015
Interest	4	%	Quinlivan, 2015
Interest During Construction	4	%	Quinlivan, 2015
Tax Rate	25	%	Constitu-tion No. 36/2008
Discount Rate	10	%	Quinlivan, 2015

In the pre-feasibility stage, an investment analyst generally does not have accurate data on technical and financial aspects. Therefore, assumptions that refer to accurate references are needed. The assumptions used in financial modeling are divided into two parts, technical and financial assumptions. Table 6 summarizes the technical assumptions for building a financial model taken from Sarmiento in 2013. Then, Table 7 tabulates the financial assumptions used in calculating the financial model taken from Ministry of Finance Regulations No.21/2010 and No. 36/2008, Serdjuk in 2013, and Quinlivan in 2015. In technical and financial assumptions, there is no allocation and cost for make-up well because this study wanted to know the effect of decline curve on the performance and economics of WGU for a certain period.

Revenue

The results of ED and polynomial approximation used to be a good substitute in Monte Carlo simulation. Then, the P50 result of gross power output will be the input for declining curve analysis over 30 years. The suitable model of decline curve for this field is the model of harmonic decline curve because this model is suitable in the field with vapor dominated. The hyperbolic exponent (b) is the rate of change at the rate of decline with time. This means that "b" is the second derivative of the rate of production with time. If the value of b is equal to 1, the equation becomes the equation for the harmonic decline. The equation for the harmonic decline model is shown in Equation (4) (Modified from Arps, 1945) below:

$$W_e = \frac{W_{ei}}{(1+d_i t)} \quad \text{.....(4)}$$

where, W_e is current gross power output, W_{ei} is initial gross power output (start of production), d_i is initial nominal of decline rate when $t = 0$, t is cumulative time since start of production.

The area under the decline curve of W_e versus time between t_1 and t_2 is a measure of the cumulative gross power output (C_{We}) during a certain period can be expressed as (Modified from Arps, 1945):

$$C_{We} = \int_{t_1}^{t_2} W_e \, dt \quad \text{.....(5)}$$

Substituting the gross power output from Equation (4) to Equation (5) that describes the harmonic decline curve, and integrating gives:

$$C_{We(t)} = \left(\frac{W_{ei}}{d_i}\right) \ln\left(\frac{W_{ei}}{W_e}\right) \quad \text{.....(6)}$$

where $C_{We(t)}$ is cumulative gross power output at time t, W_{ei} is initial gross power output (start of production), d_i is initial nominal of decline rate when $t = 0$, and W_e is gross power output at time t.

The area below the decline curve multiplied by the electricity price is the total revenue of WGU, which

decreased every year. This study did not assume the constant total revenue every year, but it will be following the decline curve analysis and made it more realistic calculation.

Investment cost and expense

The first calculation in financial modeling is Investment Cost and Expense. From this calculation, the equity, loan, and income tax of the project can be estimated. Investment and Expense are built from cost estimation. The estimated cost of a geothermal project can affect the risk and viability of a geothermal project. Many factors cause the cost of geothermal development to vary greatly from one location to another location and from one project to another project. According to Purwaningsih, et al. in 2017, several aspects could affect the investment cost component in geothermal projects, including:

1) Size of the plant.
2) Power plant technology.
3) Knowledge of the resource.
4) Location.
5) Schedule and delay.
6) Chemistry of the geothermal water.
7) Environmental policies.
8) Tax incentive.
9) Markets.
10) Financing options and costs.

The cost assumptions for the financial model are summarized in Table 8, where *c* is the installed capacity of WGU in MW. The economic assessment in this study is assumed by excluding the exploration cost. Exploration cost is the cost spent in the early development stage, such as exploration survey, exploration wells, land access, reservoir modeling study, etc. This study only considers the required drilling wells for production and injection wells in the development stage. The exception to exploration cost was made because in this study only wanted to focus on the things that matter in the development of a WGU.

The production well and injection well costs are taken from Purwanto et. al, 2018. The Capital Costs, in USD per kW, are included the separators, turbines, generators, well connections, civil works, and everything that supported the running of the WGU. The Operation & Maintenance Costs, in US¢ per kWh, are calculated based on the gross power output generated by the WGU. The Capital Cost and Operation & Maintenance Cost of backpressure turbine in the form of the equation are modified from Sanyal, 2005, Long et al., 2012, and Environmental Protection Agency (EPA), 2015. The Capital Cost and Operation & Maintenance Cost of condensing turbine also in the form of the equation are taken from Sanyal, 2005. Then, the transmission cost, in USD per kW, is taken from Asian Development Bank (ADB) and the World Bank, 2015.

Depreciation was also considered in this study. Depreciation is accounted for tangible and intangible investments. Tangible investment is an investment spent to buy tangible items and having a life span, so there is a decrease in value in the form of depreciation due to the use of assets over time whereas intangible investment is an investment that is spent to pay for services provided by other parties to complete work. Although intangible investment is not visible but has a useful life of more than one year, so it can be categorized as an asset and has a decline in value from time to time called amortization.

Table 8: Cost Assumptions.

Parameters	Price	Unit	References
Capital Cost			
Production Well Injection Well	4 – 6	MUSD per Well	Purwanto et al., 2018
Backpressure Turbine	$1500\times e^{-0.003(c-0.5)}$ ……(7)	USD per kW	Sanyal, 2005 and Long et al., 2012 (Modified)
Condensing Turbine	$2500\times e^{-0.003(c-5)}$ ..……...(8)	USD per kW	Sanyal, 2005
Transmission	66	USD per kW	ADB and the World Bank, 2015
Operation & Maintenance Cost			
Backpressure Turbine	$e^{-0.0025(c-0.5)}$ …….(9)	US¢ per kWh	Sanyal, 2005 and EPA, 2015 (Modified)
Condensing Turbine	$2e^{-0.0025(c-5)}$ ……...(10)	US¢ per kWh	Sanyal, 2005

Loan schedule

Capital Loan is calculated from total capital multiplied by the percentage of loans from the beginning of the project until before the Commercial Operation Date (COD). Before COD, the loan was added by Interest during Construction (IDC) because there was no revenue. In the Loan schedule, annual repayment is determined since the project has been operating commercially.

Income tax

Geothermal developers are required to pay tax from the net income of geothermal utilization to the government. Based on Constitution No. 36/2008, a tax is imposed 25% of net income. Net income is calculated from revenue minus the depreciation result, interest deduction, and expense.

Cash flow

Cash flow is calculated annually from start of the project until 30 years of utilization. Cash flow is built through revenue plus loan capital and reduced by investment costs, interest from loans, income tax, and annual loan repayment. Furthermore, the estimation of cumulative cash flow is needed in determining when the developers will begin to gain a profit.

Financial parameters

The financial parameters are used to evaluate the financial feasibility of a geothermal project. In general, the financial parameters that are often used in considering investment decisions are Net Present Value (NPV) and Internal Rate Return (IRR) (6, 2010). The feasibility criteria based on NPV and IRR are explained as follows:

1) Net Present Value (NPV)

Net Present Value (NPV) is the sum of a time series of cash flow in present values using a nominated discount rate over the project life. If the value is less than 0, the project will be rejected. However, if the value is greater than 0, the investment is more attractive than the discount rate. It is useful for comparing options within a project (Quinlivan, 2015).

2) Internal Rate of Return (IRR)

Internal Rate of Return (IRR) is the discount rate at which the Net Present Value of all the cash flows from a project equal to zero. It is useful for comparisons between different projects (Quinlivan, 2015).

3) Pay Out Time (POT)

Pay Out Time (POT) is the required time to recover all cost in a project. The longer times of POT are usually not desirable for investment position to undertake the project (Purwaningsih et al., 2017).

RESULT AND DISCUSSION

Technical Result and Analysis

The other data to complete the design of water dominated system are wellhead pressure and turbine efficiency. The wellhead pressure is 8 bara taken from GeothermEx, 1998 and the assumption of turbine efficiency is 85% taken from Dipippo, 2008. After creating 16 models based on parameter condition in Table 5, doing the simulations, and calculating the gross power output and SSC, the results of backpressure turbine are summarized in Table 9, and the results of condensing turbine are summarized in Table 10.

Table 9: Simulation design run and gross power output and SSC results of backpressure turbine.

Run-Order	x -	$\dot{m}$ kg/s	TIP bara	TEP bara	We Mwe	SSC kg/s/Mwe
1	-1	1	1	-1	10.6	3.63
2	1	-1	-1	-1	6.6	3.82
3	-1	1	-1	-1	10.0	3.82
4	1	1	-1	-1	12.7	3.82
5	1	-1	1	-1	6.9	3.63
6	-1	-1	-1	1	4.6	4.30
7	-1	1	1	1	9.5	4.06
8	1	-1	1	1	6.2	4.06
9	1	1	-1	1	11.3	4.30
10	1	1	1	-1	13.4	3.63
11	-1	-1	-1	-1	5.2	3.82
12	-1	-1	1	1	4.9	4.06
13	-1	1	-1	1	8.9	4.30
14	1	-1	-1	1	5.8	4.30
15	1	1	1	1	12.0	4.06
16	-1	-1	1	-1	5.4	3.63

Table 10: Simulation design run and gross power output and SSC results of condensing turbine.

Run-Order	x -	$\dot{m}$ kg/s	TIP bara	TEP bara	We Mwe	SSC kg/s/Mwe
1	-1	1	1	-1	20.5	1.87
2	1	-1	-1	-1	13.1	1.91
3	-1	1	-1	-1	20.1	1.91
4	1	1	-1	-1	25.4	1.91
5	1	-1	1	-1	13.4	1.87
6	-1	-1	-1	1	9.5	2.08
7	-1	1	1	1	18.9	2.03
8	1	-1	1	1	12.4	2.03
9	1	1	-1	1	23.4	2.08
10	1	1	1	-1	26.0	1.87
11	-1	-1	-1	-1	10.3	1.91
12	-1	-1	1	1	9.8	2.03
13	-1	1	-1	1	18.5	2.08
14	1	-1	-1	1	12.1	2.08
15	1	1	1	1	24.0	2.03
16	-1	-1	1	-1	10.6	1.87

The maximum and minimum result of the gross power output of backpressure turbine based on Table 9 is 4.6 MWe and 13.4 MWe respectively. Then, the maximum and minimum result of SSC of

backpressure turbine based on Table 9 is 3.63 $^{kg/s}/_{MWe}$ and 4.30 $^{kg/s}/_{MWe}$ respectively.

The maximum and minimum result of the gross power output of condensing turbine based on Table 10 is 9.5 MWe and 26.0 MWe respectively. Then, the maximum and minimum result of SSC of backpressure turbine based on Table 10 above is 1.87 $^{kg/s}/_{MWe}$ and 2.08 $^{kg/s}/_{MWe}$ respectively.

The polynomial approximation response was analyzed by Minitab 18^{TM} to generate the gross power output (*We*) and SSC responses of backpressure and condensing turbine. The first-order polynomial equation of backpressure turbine is:

$$We = 8{,}377 + 0{,}9855\,x + 2{,}677\,m + 0{,}2254\,TIP - 0{,}4753\,TEP + 0{,}3150\,x*m + 0{,}02651\,x*TIP - 0{,}05592\,x*TEP + 0{,}07203\,m*TIP - 0{,}1519\,m*TEP + 0{,}001376\,TIP*TEP + 0{,}008474\,x*m*TIP - 0{,}01787\,x*m*TEP + 0{,}000162\,x*TIP*TEP + 0{,}000440\,m*TIP*TEP + 0{,}000052\,x*m*TIP*TEP \quad (11)$$

$$SSC = 3{,}953 + 0\,x - 0\,m - 0{,}1071\,TIP + 0{,}2246\,TEP - 0\,x*m + 0\,x*TIP - 0\,x*TEP + 0\,m*TIP - 0\,m*TEP - 0{,}01277\,TIP*TEP - 0\,x*m*TIP - 0\,x*m*TEP - 0\,x*TIP*TEP - 0\,m*TIP*TEP - 0\,x*m*TIP*TEP \quad (12)$$

The first-order polynomial equation of condensing turbine is:

$$We = 16{,}75 + 1{,}970\,x + 5{,}352\,m + 0{,}2024\,TIP - 0{,}6830\,TEP + 0{,}6296\,x*m + 0{,}02381\,x*TIP - 0{,}08035\,x*TEP + 0{,}06469\,m*TIP - 0{,}2183\,m*TEP + 0{,}001778\,TIP*TEP + 0{,}007610\,x*m*TIP - 0{,}02568\,x*m*TEP + 0{,}000209\,x*TIP*TEP + 0{,}000568\,m*TIP*TEP + 0{,}000067\,x*m*TIP*TEP \quad (13)$$

$$SSC = 1{,}973 + 0\,x - 0\,m - 0{,}02395\,TIP + 0{,}08051\,TEP - 0\,x*m + 0\,x*TIP - 0\,x*TEP + 0\,m*TIP + 0\,m*TEP - 0{,}002159\,TIP*TEP - 0\,x*m*TIP + 0\,x*m*TEP - 0\,x*TIP*TEP - 0\,m*TIP*TEP + 0\,x*m*TIP*TEP \quad (14)$$

Minitab 18^{TM} also generated the pareto chart to detect the most sensitive parameters which affect the results. The term significance level (α-level) is used to refer to a pre-chosen probability. Conventionally, 0.05 chosen as α-level which means it was set at a 95% confidence level. Figure 5 and 6 show the pareto chart of the effect of *We* and SSC by backpressure turbine respectively.

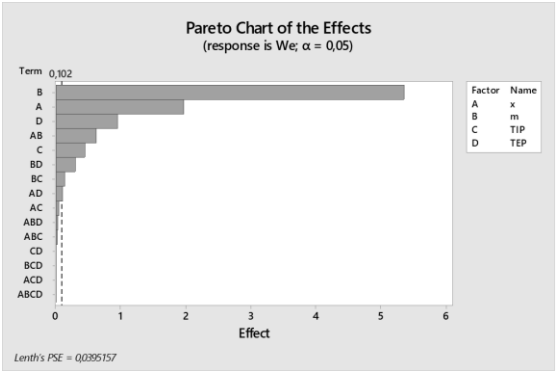


Figure 5: Gross Power Output Pareto Chart of backpressure turbine.

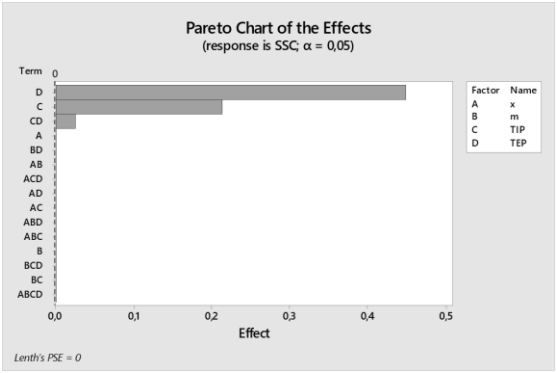


Figure 6: SSC Pareto Chart of backpressure turbine.

The most sensitive parameter which affects gross power output is mass flow rate (5.3), and the most sensitive parameter which affects SSC is TEP (0.45) even if this parameter cannot be changed because TEP of backpressure turbine is atmospheric pressure which depends on the elevation of power plant and environmental condition.

Then, Figure 7 and 8 show the pareto chart of the effect of gross power output and SSC by condensing turbine respectively.

The most sensitive parameter which affects gross power output is mass flow rate (10.7), and the most sensitive parameter which affects SSC is TEP (0.16).

Furthermore, both of first-order polynomial equation of backpressure and condensing turbine will be run by Monte Carlo simulation. After doing around 50,000 iterations by using the spreadsheet, the simulation was randomly sampling the probability distribution function as the result of gross power output and SSC. The frequency of random sampling appeared in a certain value range will be calculated automatically by the simulation. The accuracy of a Monte Carlo simulation results is a function of the number of realizations. The confidence limit was chosen on the value of P10,

P50, and P90. Based on the central limit theorem, P50 estimation has more chance of occurring than the P10 and P90 estimations.

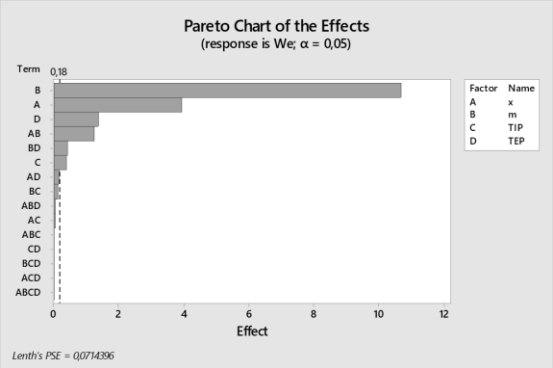


Figure 7: Gross Power Output Pareto Chart of condensing turbine.

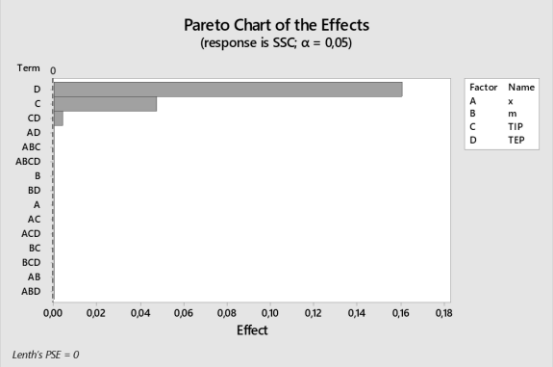


Figure 8: SSC Pareto Chart of condensing turbine.

The probabilistic approach was done by Monte Carlo Simulation on the proxy models given in Equation (11) and (12). The cumulative distribution function for gross power output and SSC of backpressure turbine is shown in Figures 9 and 10 respectively and it was tabulated with the cumulative percentage of P10, P50, and P90 in Tables 11 and 12 respectively.

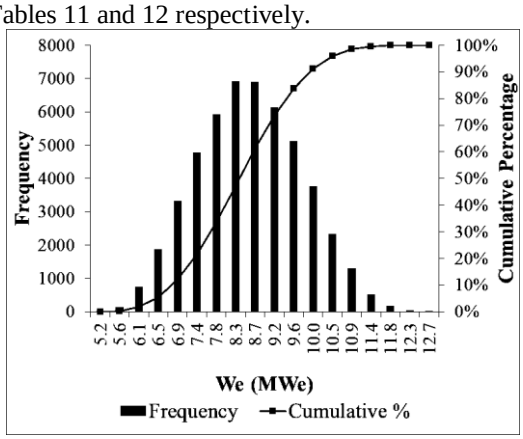


Figure 9: Cumulative distribution function for gross power output of backpressure turbine.

Table 11: Cumulative percentage of P10, P50, and P90 for gross power output of backpressure turbine.

Probability Percentage	Values	Units
P10	6.8	MWe
P50	8.4	MWe
P90	10.0	MWe

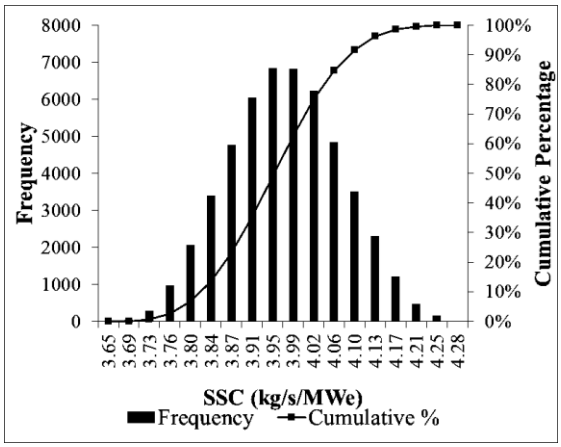


Figure 10: Cumulative distribution function for gross power output of condensing turbine.

Table 12: Cumulative percentage of P10, P50, and P90 for SSC of backpressure turbine.

Probability Percentage	Values	Units
P10	3.82	$^{kg/s}/_{MWe}$
P50	3.95	$^{kg/s}/_{MWe}$
P90	4.09	$^{kg/s}/_{MWe}$

The cumulative distribution function; P10, P50, and P90 for the gross power output of backpressure turbine is 6.8, 8.4, and 10.0 MWe respectively. The cumulative distribution function; P10, P50, and P90 for SSC of backpressure turbine is 3.82, 3.95, and 4.09 kg/s/MWe respectively. The P50 estimation has more chance of occurring than the P10 and P90 estimations as shown in Figures 9 and 10.

The probabilistic approach was done by Monte Carlo Simulation on the proxy models given in Equation (13) and (14). The cumulative distribution function for gross power output and SSC of condensing turbine is shown in Figures 11 and 12 respectively and it was tabulated with the cumulative percentage of P10, P50, and P90 in Tables 13 and 14 respectively.

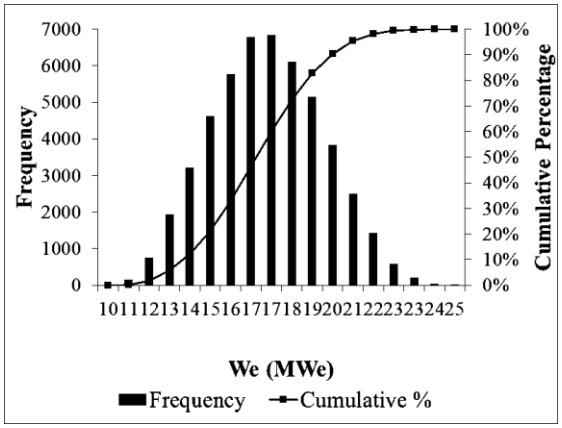


Figure 11: Cumulative distribution function for gross power output of condensing turbine.

Table 13: Cumulative percentage of P10, P50, and P90 for gross power output of condensing turbine.

Probability Percentage	Values	Units
P10	13.6	MWe
P50	16.7	MWe
P90	19.9	MWe

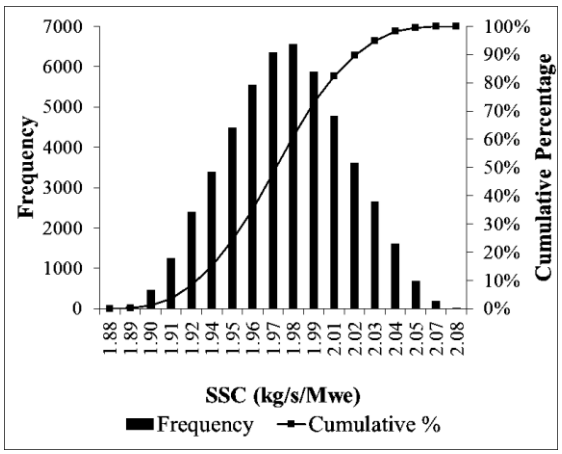


Figure 12: Cumulative distribution function for SSC of condensing turbine.

Table 14: Cumulative percentage of P10, P50, and P90 for SSC of condensing turbine.

Probability Percentage	Values	Units
P10	1.93	$^{kg/s}/_{MWe}$
P50	1.97	$^{kg/s}/_{MWe}$
P90	2.02	$^{kg/s}/_{MWe}$

The cumulative distribution function; P10, P50, and P90 for the gross power output of condensing turbine is 13.6, 16.7, and 19.9 MWe respectively. The cumulative distribution function; P10, P50, and P90 for SSC of condensing turbine is 1.93, 1.97, and 2.02 kg/s/MWe respectively. The P50 estimation has more chance of occurring than the P10 and P90 estimations as shown in Figures 11 and 12.

Economic Assessment

The P10, P50, and P90 values of gross power output for backpressure turbine and condensing turbine are used as the base case of economic calculation in decline curve analysis. This study assumed the value of decline rate is 3% per year as stated in Purwaningsih et al., 2017. Figure 13 shows the production decline curve of backpressure turbine and Figure 14 shows the production decline curve of condensing turbine. Integral calculations from 0 to 30 years are performed to calculate the area of each decline rate then multiplied by the electricity price to get the total revenue.

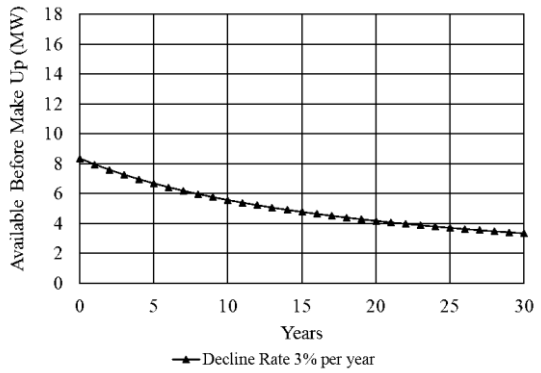


Figure 13: Production decline curve of backpressure turbine.

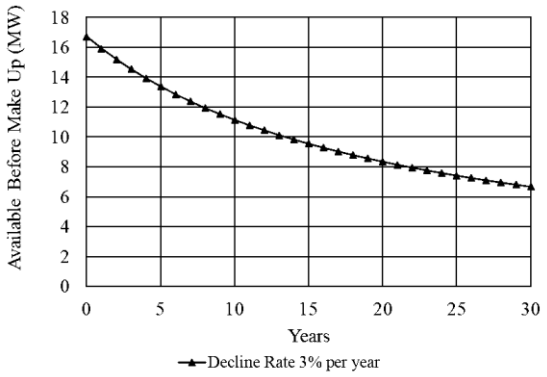


Figure 14: Production decline curve of condensing turbine.

For this study, the electricity price is determined by the P50 values of IRR. The probabilistic results from Monte Carlo simulation were done by the spreadsheet in Microsoft Excel. Figures 15 and 16 show cumulative distribution function of IRR for backpressure turbine and Figures 20 and 21 show cumulative distribution function of IRR for condensing turbine. Then, all the probabilistic results were tabulated in Table 15. The P50 value of backpressure and condensing turbine is 16% and the ideal IRR desired by the company is 16% (Poernomo, 2012). Therefore, the value of the IRR will be set at 16%.

Table 15: IRR for backpressure and condensing turbine.

Probability Percentage	Backpressure Turbine	Condensing Turbine
P10	12%	12%
P50	16%	16%
P90	20%	21%

The calculation of electricity prices was done by adjusting the value of the IRR. The electricity price of backpressure turbine and condensing turbine is 7.7 US¢/kWh and 8.6 US¢/kWh respectively. Then, the calculation of total revenue was done by multiplying the electricity price with the area below the curve. The total revenue earned for 30 years has decreased in value because the calculation of total revenue is based on the decline curve analysis.

Based on the P10, P50, and P90 values, the capacity of backpressure turbine is 3, 4, 5 MW respectively and the capacity of condensing turbine is 6, 8, 10 MW respectively. Calculation of capital cost and expense is conducted for 30 years WGU operation. Tables 16 and 17 show required capital cost and expense of backpressure and condensing turbine respectively for 30 years utilization. The total capital cost of a backpressure turbine is less than a condensing turbine as well as the total expense. Meanwhile, if total capital cost is calculated per MW, the backpressure turbine requires more slightly higher capital cost per MW than the condensing turbine because the cost of production and injection well is included in the calculation of capital cost while using backpressure turbine can only generate 4 MW of electricity.

Table 16: Capital cost and expense of backpressure turbine.

Parameters	Minimum	Most-likely	Maximal
Capital Cost			
Production Well	$ 4,000,000.00	$ 6,000,000.00	$ 8,000,000.00
Injection Well	$ 4,000,000.00	$ 6,000,000.00	$ 8,000,000.00
Power Plant	$ 8,973,040.46	$ 11,892,484.55	$ 14,776,679.09
Transmission line	$ 396,000.00	$ 528,000.00	$ 660,000.00
Total Capital Cost	$ 17,369,040.46	$ 24,420,484.55	$ 31,436,679.09
Expense			
Operation and Maintenance Cost per Year	$ 518,422.46	$ 687,782.42	$ 855,440.12
Total Expense	$ 13,997,406.38	$ 18,570,125.37	$ 23,096,883.11
Power Generation Capacity	6 MW	8 MW	10 MW
Capital Cost/MW	**$ 2,894,840.08**	**$ 3,052,560.57**	**$ 3,143,667.91**

Table 17: Capital cost and expense of condensing turbine.

Parameters	Minimum	Most-likely	Maximal
Capital Cost			
Production Well	$ 4,000,000.00	$ 6,000,000.00	$ 8,000,000.00
Injection Well	$ 4,000,000.00	$ 6,000,000.00	$ 8,000,000.00
Power Plant	$ 31,729,285.57	$ 38,701,542.38	$ 47,799,874.09
Transmission line	$ 858,000.00	$ 1,056,000.00	$ 1,320,000.00
Total Capital Cost	$ 40,587,285.57	$ 51,757,542.38	$ 65,119,874.09
Expense			
Operation and Maintenance Cost per Year	$ 1,045,953.61	$ 1,359,393.56	$ 1,682,116.82
Total Expense	$ 31,378,608.15	$ 40,781,806.79	$ 50,463,504.54
Power Generation Capacity	13 MW	16 MW	20 MW
Capital Cost/MW	**$ 3,122,098.89**	**$ 3,234,846.40**	**$ 3,255,993.70**

Figure 17 shows the cumulative cash flow of backpressure turbine. The cash flow of all cases will be decreased overtimes because as mentioned above, the total revenue in each year will be decreased while the developer should pay all the bills, such as loan payment, interest, O&M cost, and income tax. From the 21st-year, the cash flow is increased because the loan payment is completed. This result can be used as a consideration for the development of WGU under this condition. On the other hand, the POT is shown at the fifth year. The cumulative cash flow of the condensing turbine had the same results as those in the backpressure turbine as shown in Figure 22.

The probabilistic results calculation was done by the spreadsheet in Microsoft Excel. Figures 18 and 19 show cumulative distribution function of NPV for backpressure turbine and Figures 23 and 24 show cumulative distribution function of NPV for condensing turbine. Then, Table 19 shows the P10, P50, and P90 of NPV for backpressure and condensing turbine. Based on the NPV criteria, both backpressure and condensing turbine project are interesting to develop. The most prominent information is a condensing turbine giving NPV greater than a backpressure turbine. Therefore, condensing turbine is the best type of WGU to be applied in Lumut Balai Field.

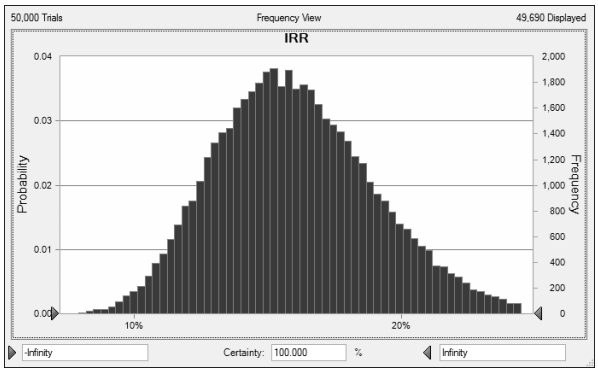


Figure 15: Distribution function of IRR for backpressure turbine.

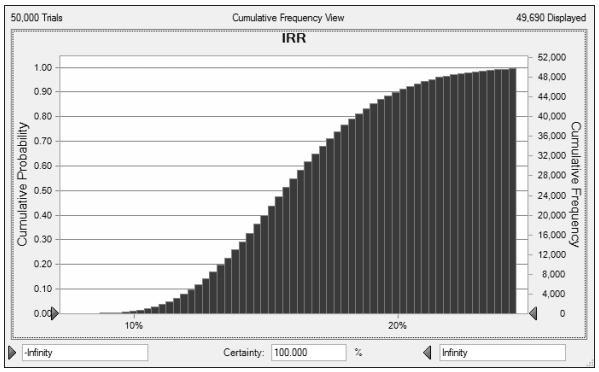


Figure 16: Cumulative distribution function of IRR for backpressure turbine.

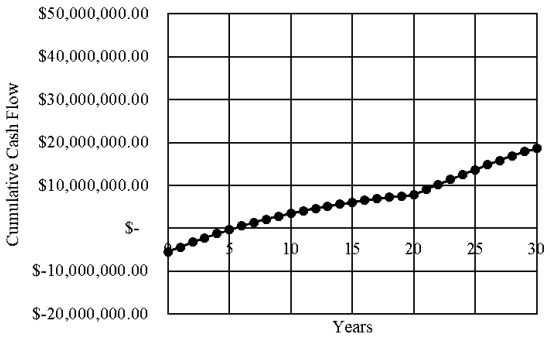


Figure 17: Cumulative cash flow of 3% decline rate per year for backpressure turbine.

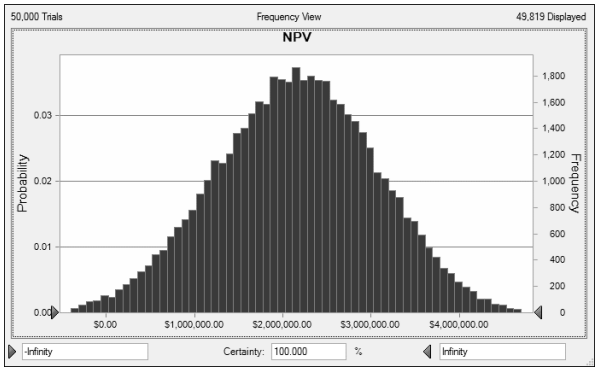


Figure 18: Distribution function of NPV for backpressure turbine.

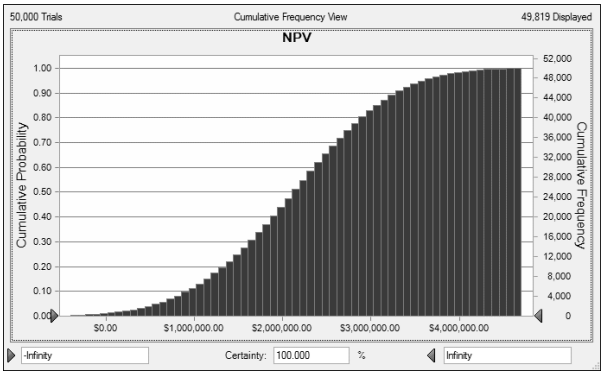


Figure 19: Cumulative distribution function of NPV for backpressure turbine.

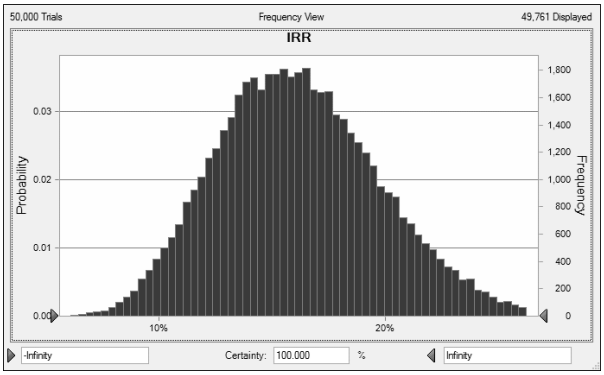


Figure 20: Distribution function of IRR for condensing turbine.

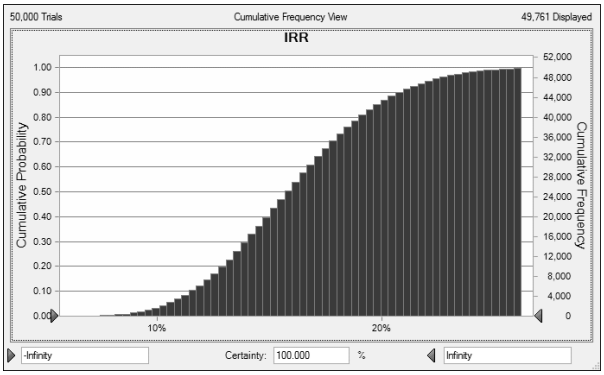


Figure 21: Cumulative distribution function of IRR for condensing turbine.

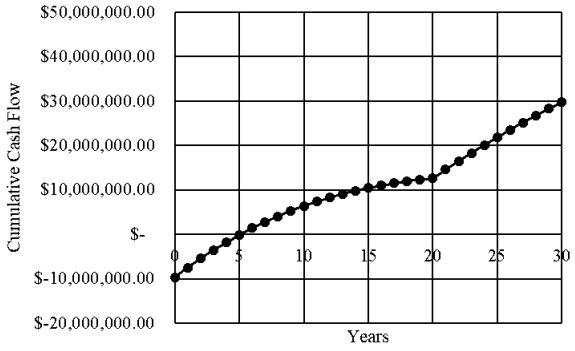


Figure 22: Cumulative cash flow of 3% decline rate per year for condensing turbine.

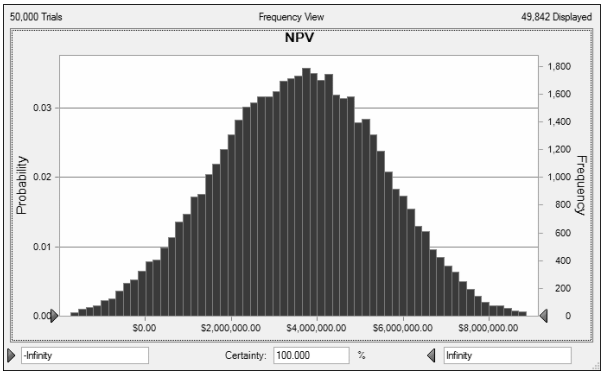


Figure 23: Distribution function of NPV for condensing turbine.

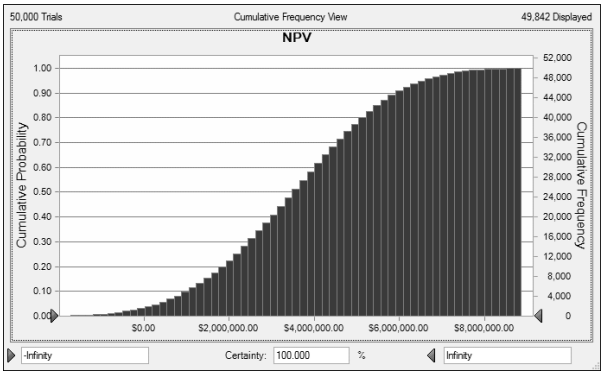


Figure 24: Cumulative distribution function of NPV for condensing turbine.

CONCLUSION

Full factorial experimental design with Monte Carlo simulation for gross power output and Specific Steam Consumption with 50,000 iterations has been successfully applied to calculate and design the backpressure and condensing turbine. The financial model has also been successfully applied to propose the best type of WGU for this geothermal system. The results of this study are as follow:

1. The result of probability, P10, P50, and P90 of gross power output for the backpressure and condensing turbine are 6.8, 8.4, 10 MWe and 13.6, 16.7, 19.9 MWe respectively.
2. The result of probability, P10, P50, and P90 of Specific Steam Consumption (SSC) for the backpressure and condensing turbine are 3.82, 3.95, 4.09 kg/s/MWe and 1.93, 1.97, 2.02 kg/s/MWe respectively.
3. Based on the economic evaluation, the best type of WGU is condensing turbine with the P10, P50, and P90 of Internal Rate of Return (IRR) are 12%, 16%, 21% respectively and the P10, P50, and P90 of Net Present Value (NPV) are 1.1 MUSD, 3.6 MUSD, 6.0 MUSD respectively over 30 years of WGU lifetime.

RECOMMENDATION

Several recommendations are required to get better result in calculation and design, either in technical or financial section. The recommendations are as follow:

1. More detailed and up-to-date well test data which affect the performance of WGU to generate the electricity are required, such as the content of Non-Condensable Gas (NCG) in every well, to get more realistic calculation.
2. The application of binary wellhead unit for another comparison of wellhead generating unit type for this geothermal system.
3. If the economic assessment is including the exploration cost, the calculation can use more than one unit of WGU to get its economic feasibility.
4. The comparison of calculation between the utilization of WGU since early rather than just shut-in the well can be conducted to get the value of lost revenue in Lumut Balai Field.
5. Other experimental designs and response surface methods, such as two-level fractional factorial design and three-level factorial design, can be applied to this study as a comparison with the two-level factorial design.

REFERENCES

Ahmad, A., Gunowijoyo, F., and Pratama, H. (2017). "Probabilistic Approach: Back Pressure Turbine for Geothermal Vapor-Dominated System". IOP Conference Series: Earth and Environmental Science 103 012011. DOI: https://doi.org/10.1088 /1755-1315/103/ 1/012011.

Arps, J.J., (1945). "Analysis of Decline Curves". Trans. AIME 160, 228–247. DOI: https://doi.org/10.2118 /945228-G

Ashat, A., Pratama, H.B., (2018). "Application of experimental design in geothermal resources assessment of Ciwidey-Patuha, West Java, Indonesia". IOP Conference Series: Earth and Environmental Science 103 012009. DOI: https://doi.org/10.1088/1755-1315/103/1/012009

Asian Development Bank and The World Bank. (2015). "Unlocking Indonesia's Geothermal Potential. Mandaluyong City, Philippines". ISBN: 978-92-9254-901-5.

Constitution, Indonesia. (2008). "Perubahan Keempat atas Undang-undang Nomor 7 Tahun 1983 Tentang Pajak Penghasilan". [Constitution No.38/2008]. Retrieved from https://jdih.esdm.go.id/.

Danar, Agus and Sukhyar, R. (2010). "Energi Panas Bumi di Indonesia: Kebijakan Pengembangan dan Keputusan Investasi". Badan Geologi Kementerian Energi dan Sumber Daya Mineral, Jakarta. ISBN: 978-979-18509-8-8.

DiPippo, R. (2008). "Geothermal Power Plant Second Edition: Principles, Applications, Case Studies and Environmental Impact". Butterworth-Heinemann, Oxford. ISBN: 978-0-7506-8620-4.

Environmental Protection Agency (EPA). (2015). "Technology Characterization: Steam Turbines". Retrieved from http://www.epa.gov/

Firanda, Eric, et al. (2015). "The Effect of Well Elevation on Production in Lumut Balai Field". Proceedings World Geothermal Congress, Melbourne, Australia.

Hiriart, Gerardo. (1983). "One Year Experience with Portable Back-Pressure Turbines in Los Azufres". Proceedings Ninth Workshop Geothermal Reservoir Engineering Stanford University, Stanford, California, December 1983.

Kiptanui, Shammah, & Kipyego, Ezekiel. (2016). "Viability of Wellhead Power Plants in Accelerating Geothermal Development in Kenya: Case og Menengai". Proceedings, 6th African Rift Geothermal Conference, Addis Ababa, 2nd – 4th November 2016.

Lund, John W. (2005). "100 Years of Geothermal Power Product". Proceeding Thirtieth Workshop on Geothermal Reservoir Engineering Stanford University, Stanford, California, January 31-February 2, 2005.

McHugh, J., & Bodylski. (1985). "A Generic Overview of Geothermal Wellhead Generating Units". GRC Bulletin, May.

Ministry of Finance Regulation, Indonesia. (2010). "Pemberian Fasilitas Perpajakan dan Kepabeanan untuk Kegiatan Pemanfaatan Sumber Energi Terbarukan". Ministry of Finance Regulation No. 21 of 2010, Retrieved from https://jdih.kemenkeu.go.id/.

Moya, P., & DiPippo, R. (2011). "Miravalles PGM-29 Wellhead Unit, Guanacaste, Costa Rica: Technical and Environmental Performance Assessment". Short Course on Geothermal Drilling, Resource Development and Power Plants.

Myers, R., Montgomery, D., and Anderson-Cook, Christine. (2009). "Response Surface Methodology: Process and Product Optimization Using Designed Experiments", 3rd ed. John Wiley & Sons, Inc., New Jersey. ISBN 978-0-470-17446-3.

Purwaningsih, Fitri O., et al., (2017). "Make-up Wells Drilling Cost in Financial Model for a Geothermal Project". IOP Conference Series: Earth and Environmental Science 103 012010. DOI: https://doi.org/10.1088/1755-1315/103/1/012010.

Purwanto, Eko Hari., (2018). "Geothermal Drilling in Indonesia: A Review of Drilling Operation, Evaluation of Well Cost and Well Capacity". Proceedings, The 6th Indonesia International Geothermal Convention & Exhibition 2018, Cendrawasih Hall- Jakarta Convention Center Indonesia, September 5th -8th ,2018. In press.

Poernomo, A., (2012). "23 Proyek Panas Bumi Terancam Merangkak". Berita Satu, Retrieved from http://www.beritasatu.com

Randle, James B. (2005). "Financial Modelling of Geothermal projects". Proceeding World Geothermal Congress 2005, Abtalya, Turkey, April 24-29, 2005.

Quinao, J., and Zarrouk, S. (2015). "Application of Experimental Design and Response Surface Methods in Probabilistic Geothermal Resource Assessment: numerical simulation and volumetric methods". Proceedings World Geothermal Congress 2015, Melbourne, Australia, 19-25 April 2015.

Quinlivan, Paul, et al., (2015). "Assessing Geothermal Tariffs in the Face of Uncertainty, a Probabilistic Approach". Proceedings World

Geothermal Congress 2015, Melbourne, Australia, 19-25 April 2015.

Saitet, Daniel, & Kwambai, Clety. (2015). "Wellhead Generating Plants: KenGen Experience". Proceedings World Geothermal Congress. Melbourne, Australia, 19 – 25 April 2015.

Saptadji, Nenny. (2018). "Teknik Geotermal". Penerbit ITB, Bandung. ISBN: 978-602-5417-76-4.

Sarmiento, Zosimo F. Benedikt Steingrímsson, Gudni Axelsson. (2013). "Volumetric Resource Assesment". Presented at "Short Course V on Conceptual Modelling of Geothermal Systems", organized by UNU-GTP and LaGeo, in Santa Tecla, El Salvador, February 24 - March 2, 2013.

Seidler, R., Bücker, H.M., Padalkina, K., Herty, M., Niederau, J., Marquart, G., (2015). "Optimal Experimental Design for Finding Optimally Located Boreholes in Geothermal Engineering". World Geothermal Congress 2015. pp. 1–3.

Serdjuk, Martina, et al., (2013). "GEOLEC: Geothermal Investment Guide. Europe". The Intelligent Energy Europe Programme of the Europe Union.

Spronk, Jaap; Hallerbach, Winfried. (1996). "Financial modelling: Where to go? With an illustration for portfolio management". European Journal of Operational Research 99, 1997, pp 113-125.

Suryadarma, et al. (2010). "Sustainable development of the Kamojang geothermal field". Elsevier Ltd. DOI: https://doi.org/10.1016/j.geothermics. 2010. 09.00.

Sutter, J., Kipyego, E., and Mutai, D. (2012). "The Use of Portable Geothermal Wellhead Generators as Small Power Plants to Accelerate Geothermal Development and Power Generation in Kenya". GHC Bulletin, February 12.

Walpole, R., Myers, R., Myers, S., Ye, K. (2012). "Probability & Statistics for Engineers and Scientists, 9th ed". Pearson Education, Inc. Prentice Hall, Boston. ISBN: 978-0-321-62911-1.

PROBABILISTIC METHOD: A NEW APPROACH FOR DETERMINING THE NUMBER OF MAKE-UP WELLS IN FEASIBILITY STUDY

Feri Vernando Salim[1], Heru Berian Pratama[2], and Nenny Miryani Saptadji[3]

[1]Petroleum Engineering Study Program, Institut Teknologi Bandung, Indonesia
[2,3]Geothermal Engineering Study Program, Institut Teknologi Bandung, Indonesia
10 Ganesha Street, Bandung, West Java, Indonesia
Email: ferivernando.fv@gmail.com

ABSTRACT

The uncertainty and risk during presuming the number of make-up wells in the feasibility study is caused by the lack of information about the wells and the field properties. The source of the uncertainty is the different characteristics in the wells, such as the enthalpy, mass flow rate, decline rate, and other features. Therefore, the number of make-up wells should be estimated accurately to cover the uncertainty and reduce the risk. The method often used for calculating the number of wells is a deterministic approach that involves only a single value for every parameter. Since the result of this method is a single value, the uncertainties of the field parameters cannot be captured. Hence, the new way that applies the 2-level full factorial design of experiment approach is proposed to quantify the uncertainties. With the help of Minitab and the combination with Monte Carlo Simulation, the uncertainties will be covered, and the range of geothermal well number is the result. The proposed method has been successfully used to calculate the number of wells in the case study of Karaha-Talaga Bodas field. Based on the research, the most significant factors for determining the make-up well number in this field are the decline rate and make-up well capacity. The minimum number of the make-up well should be drilled for developing 30 MW in this field are four wells. Also, the learning curve is obtained in this study to predict the number of make-up well required for various power plant capacity developed.

Keywords: Operational, make-up wells, experimental design

INTRODUCTION

The production of steam or fluid from the geothermal reservoir will be followed by the decreasing of pressure and temperature. Also, it will result in the decreasing of steam production and electric power generated by the power plant. Therefore, the addition of new wells which are make-up wells is a must for covering the production decline of the geothermal field. The decline model, decline rate, and make-up well capacity are the factors that affect the number of make-up wells. Since the wells drilled are not always successful, the drilling success rate should be embroiled for presuming the number of geothermal wells during the planning process. However, the field variables cannot be predicted or are found in varying values (GeothermEx, 1998).

The determination of the number of make-up wells is conducted in the feasibility study (FS). Not only in a specific area but also the world, the uncertainty of FS is estimated to be at a medium level and sourced from the data in the previous phases (Gehringer and Loksha, 2012). The risk for each stage can be observed in Figure 1. All data from the pre-survey, exploration, and test drilling and the uncertainties in them should be analyzed in this phase. Since the feasibility study document is contained of the exploitable reserve, development strategy, and the financial flow of the project (Parada, 2016), the result of economics should be very sensitive of the number of wells due to the 40% portion of drilling cost from the whole geothermal project investment (Thorhallsson and Sveinbjornsson, 2012). Therefore, the correct method for determining the make-up well number should be settled to reduce the risk of development strategy and financial flow on the next stages.

Nowadays, the method used in calculating the number of make-up wells is the deterministic approach (Arps, 1945). The decline type, decline rate, make-up well capacity, and drilling success rate are employed to estimate the number of make-up wells a geothermal field. However, there is high uncertainty in each parameter above. Directly in one area, the difference in well flow rate and enthalpy can be found. The use of a single value of every parameter above can lead to the individual value of the number of make-up wells that also have high uncertainty. Therefore, to overcome the risks due to those uncertainties, the probabilistic method can be applied to the calculation of the number of make-up wells to minimize the effect of uncertainty. Even though the numerical simulation method is used for estimating the number of geothermal wells, a more straightforward approach with high accuracy is offered by this probabilistic method.

The application of the probabilistic method had been widely used in the geothermal industry. Application of experimental design and response surface method was established in a preliminary result of geothermal resource assessment (Jaime J. Quinao and Zarrouk, 2014). The location of a wellbore in the geothermal

area had been optimized by experimental design (Seidler et al., 2015). The design of experiment method was used in assessing the reserve or "field size" in a geothermal greenfield (Pasikki et al., 2016). The utilization of Placket-Burman design was also applied in uncertainty parameters reservoir vapor-dominated (Rachman, 2016). The probabilistic approach had been employed in geothermal backpressure turbine application (Ahmad et al., 2018). The implementation of experimental design was done in Ciwidey resource assessment (Ashat and Pratama, 2018). The experimental design had been implemented in 3D natural state model for Karaha-Talaga Bodas geothermal area (Prabata et al., 2019). However, none of these sources have applied the experimental design for determining the number of make-up well. The new insight in estimating the number of make-up wells will be brought by this paper.

Based on several reasons above, the probabilistic method that utilizes two levels of full-factorial experimental design is proposed to cover the field properties uncertainty in this study. Design of experiment result is a proxy equation. The proxy equation will be combined with Monte Carlo Simulation to get the range number of geothermal wells that should be considered during the development of the geothermal field. There will be a case study in Karaha-Talaga Bodas area to apply the method. Karaha-Talaga Bodas is the field with a high level of uncertainty due to the brine-underlain steam cap system. Also, there are published papers about Karaha-Talaga Bodas geothermal area that can be used as the reference for the case study. During the field study, the probabilistic method is utilized to find the number of make-up wells that will be divided into P10, P50, and P90 number.

In sum, the objectives to obtain in this research are the followings.

1. To establish a method using the probabilistic approach for estimating the number of make-up wells in a geothermal area.
2. To determine the most significant factor in determining the number of make-up wells.
3. To estimate the range of make-up well number needed in a geothermal area.
4. To build a learning curve to predict the number of make-up wells required for various power plant capacity in a geothermal area.

BASIC THEORY

Production Decline Calculation Method

Make-up well in geothermal is quite similar to the infill drilling well in petroleum. Make-up well is the back-up or addition of geothermal fluid to the geothermal power plant due to the production decline. Since the contract capacity of the power plant must be fulfilled during the production phase, the production decline should be covered by the addition of production from the new production well that is called as make-up well.

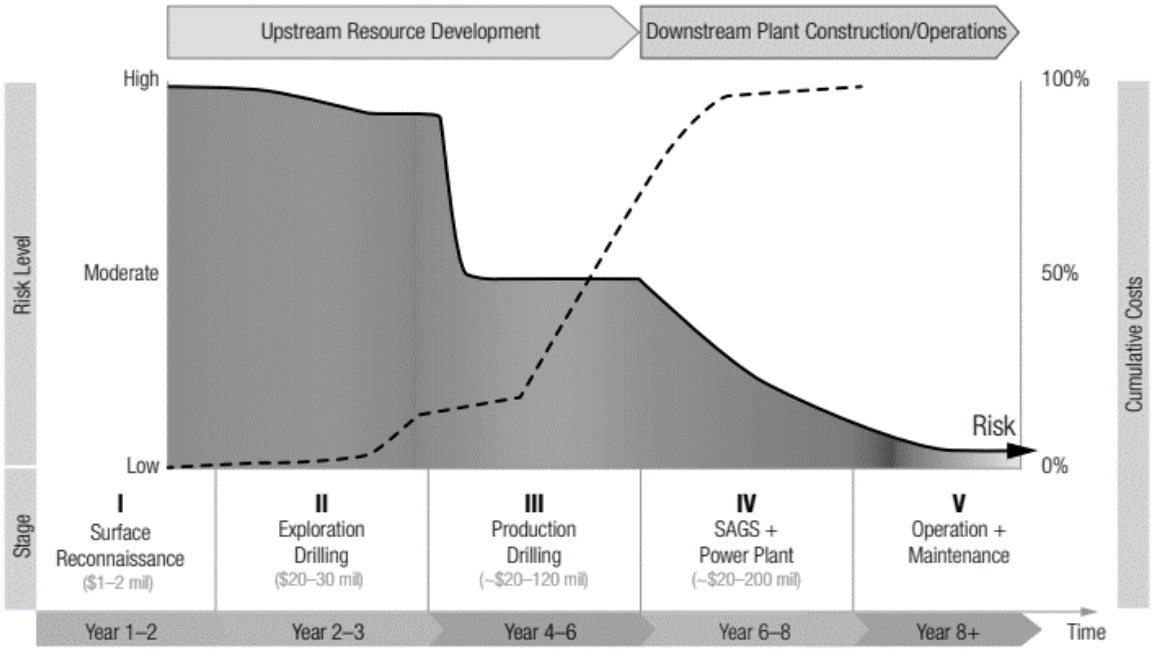


Figure 1: Geothermal Development Phases and The Risk (Gehringer and Loksha, 2012).

The determination of the make-up well number required is related to the production decline model. The production decline model in the geothermal industry is adopted from the one used in the petroleum industry by cause of similar condition (Hidayat, 2016). The decline curve analysis in the petroleum industry had been done by Arps in 1945. There are three types of decline curve proposed by Arps (1945), which are exponential, hyperbolic, and harmonic declines. The basic decline curve model is shown in Eq. 1.

$$\frac{1}{q}\frac{dq}{dt} = -bq^d \quad \ldots(1)$$

$$Q_{existing} = Qe^{-bt} \quad \ldots(2)$$

$$Q_{existing} = \frac{Q_i}{(1 + b_i t)} \quad \ldots(3)$$

b and d are the constants that must be determined based on production data. Three equations were developed from Eq.1. b is the decline rate. They are the exponential, hyperbolic, and harmonic decline models. When d=0, the decline curve is the exponential model. When 0<d<1, the result is the hyperbolic model. When d=1, the model is a harmonic decline model. Eq.2 is the exponential decline, and Eq.3 is the harmonic decline model. $Q_{existing}$ is the current production flow rate. Qi is the initial flow rate. D is the decline rate (%/year). Di is the initial decline rate. T is the production time (year). Hence, these equations are modified to meet the geothermal industry condition. The decline models used in the geothermal industry are the followings.

$$MW_{existing} = MW_i \; x \; e^{-bt} \quad \ldots(4)$$

$$MW_{existing} = \frac{MW_i}{(1 + b_i t)} \quad \ldots(5)$$

Mwexisting is the current production of electrical capacity (Mwe). Mwi is the initial production of electrical capacity (Mwe).

The principle for estimating the number of make-up wells is the minimum MWexisting applied in a geothermal area. If the actual production electrical capacity is lower than the contract capacity or the capacity limit agreed, then the make-up well should be drilled to cover the production decline.

Experimental Design

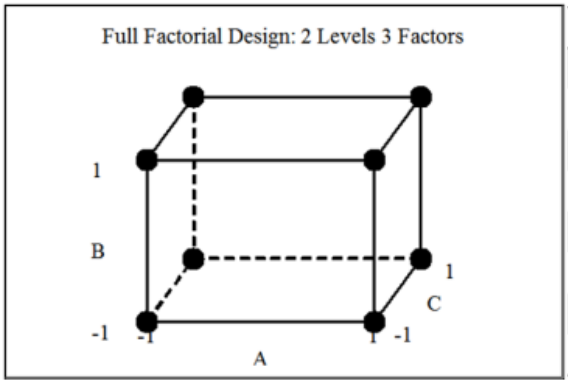
The experimental design was founded between the 1920s and 1930s by Ronald A. Fisher (Telford, 2007). Design of experiment or also known as the experimental design is a thorough process of the test in which the deliberate modifications are applied, and the variations in response variables are observed. The main point of this design is to determine the independent variable, dependent variable, and nuisance effect and to find out in what way these variables interact. Therefore, the result is the causal relationship between the independent and dependent variables (Fisher, 1971).

There are four basic principles of experimental design; they are randomization, replication, blocking, and size of experimental units (Casler, 2015). The function of randomization is to spread the uniqueness of every variable and to avoid the subjectivity of the researcher towards the allocation of independent variables for specific treatments (Cox, 2009). There are four aims of doing replication, they are estimating, reducing, and controlling the experimental error, and adding broader insight into the experimental process (Casler, 2015). Blocking is the act to protect the effect of "super-randomization." Therefore, the effect nuisance factor can be avoided due to the batch-to-batch variability. Nuisance factor is the factor outside the independent factor that can affect the response variable but cannot be measurable (Telford, 2007). The size of the experiment units is the measurement of how the large the scope of the plot that is involved in the experiment. The larger the size, the lower the variance that will be obtained. However, the asymptotic value will occur at some point in the plot size (Casler, 2015).

The experimental design method used in this paper is the 2^k factorial experiments. k is the number of factors involved during the experiment. The value of k is denoted between "high" and "low" value (Walpole, 2007). The dimensionless number of high and low values that are represented by "1" and "-1" is used on this 2-level factorial design. For example, if there are three factors, which are A, B, and C, are included to the experiment, the change of value for every factor will be evaluated to the shift in the response variable. Based on the 2^k factorial design, the eight runs will be resulted by the three factors. The example of 2^k factorial design can be observed in Figure 2. Not only 2^k factorial design, but also there are more complex experimental design, such as Central Composite Design and Box-Behnken Design (Myers et al., 2009).

$$y = \alpha_0 + \alpha_1 A + \alpha_2 B + \alpha_3 C + \alpha_4 AB + \alpha_5 AC + \alpha_6 BC + \cdots \quad \ldots(6)$$

The proxy equation is the response of the result of the experimental design such as in Eq.6. This equation is the causal relationship between the factors involved and the response variable. α is the coefficient that represents the significance of the factors. The bigger the α is, the more significant the factor regardless of the coefficient sign ("+" or "-").



Run	A	B	C
1	-1	-1	-1
2	+1	-1	-1
3	-1	+1	-1
4	+1	+1	-1
5	-1	-1	+1
6	+1	-1	+1
7	-1	+1	+1
8	+1	+1	+1

Figure 2: Example of 2-level full factorial design with three factors (Jaime Jose Quinao and Zarrouk, 2014).

METHODOLOGY

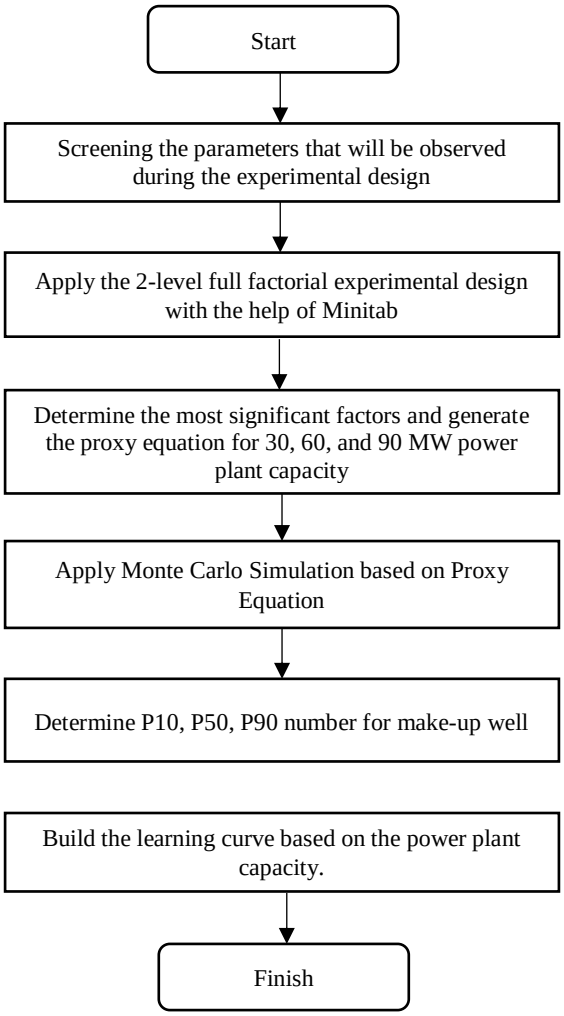


Figure 3: Flow chart of the research.

Based on Figure 3, the first step is determining the observed variables for experimental design. Since the objective of this method is to capture the uncertainties of the field properties, the variables should be the high-level of uncertainty factor. Then the principles of experimental design are applied to each observed factor and its response. By utilizing Minitab, the result of significance for every observed factor will be shown on the Pareto chart. From the chart, the most significant factor for determining the number of make-up wells can be answered. Not only the Pareto chart, the proxy equation that is the causality between the observed factors and the responses is one of the results in this experimental design. The format of the proxy equation is on Eq.6.

This proxy equation is combined with Monte Carlo Simulation to get the P10, P50, and P90 number of the geothermal well. P10 is the most optimistic number. Meanwhile, P90 is vice versa. The whole process is done for 30, 60, and 90 MW power plant capacity. From the range of value, the learning curve can be built to predict the number of wells needed for the particular geothermal area.

CASE STUDY

Field Overview

Karaha-Talaga Bodas (KTB) Geothermal Field is the partially vapor-dominated system in West Java with the brine reservoir and the steam cap overlying it (Allis' et al., 2000). The drilling process in this field had shown that the temperature results were in the range of 250ºC until 350ºC (Powell, Moore, & Cumming, 2002). In 2009, 14 wells had been drilled in this geothermal field (Darma et al., 2010).

Based on Figure 4, the distribution of the steam is from the south until the northern area. The thickest steam cap is located in the southern region. The heat source is estimated between the Saat Crater and the Talaga Bodas lake (Prabata et al., 2019). The location of the upflow zone is approximated in the southern area. It is verified by the appearance of some geothermal manifestations such as fumaroles, acid lake, thermal spring, and the high concentration of SO_4 and Cl in the fluid of the southern area (Prabata et al., 2019) whereas the outflow zone is predicted in the eastern region (Pamoyanan, Cicilap, and Cipancing) (GeothermEx, 1998).

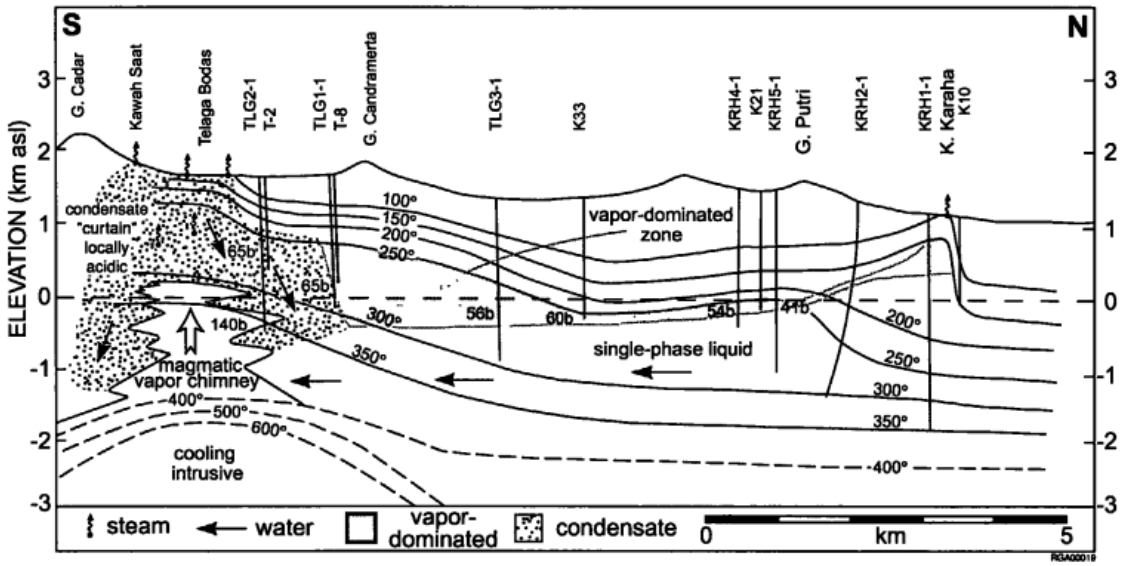


Figure 4: Karaha-Talaga Bodas Conceptual Model (Allis' et al., 2000).

Based on the previous operator of this field, which is Karaha Talaga Bodas Company, the reserve of Karaha-Talaga Bodas is 260 MW (GeothermEx, 1998). However, further study showed that the potential reserve of this field is 116 MWe (Prabata et al., 2019). Based on Geothermal Directorate of Indonesia, the potential reserve of Karaha is 30 MW, and the Talaga's is 80 MW (Kementerian Energi dan Sumber Daya Mineral, 2017).

Currently, KTB is operated by Pertamina Geothermal Energy (PGE) with the contract capacity of 220 MW with PLN (Handoko et al., 2015). The commercial operation date for 30 MW power plant was on April 6th,2018 (Wijayanto, 2018). Naturally, the properties of this field vary greatly. It will also affect the well-properties that have been drilled. A well that was drilled to the steam zone had very different output compared to the brine zone well. The variation and uncertainty that were occurred should be considered in determining the number of wells.

Well Data Analysis

There are the data that should be analyzed before using it in the calculation. The following data in Table 1 are the result of well testing in Karaha-Talaga Bodas Geothermal Field. In Figure 5, it is shown that the Karaha part is in the north, and Talaga-Bodas part is in the south region. From the data, it can be observed that the Karaha part of this field is a liquid-dominated area. Meanwhile, the Talaga Bodas part is a vapor-dominated area. Therefore, the more north (Karaha), the more liquid-dominated can be found in this field. K-33, T-2, and T-8 well are the core holes. Therefore the three wells are not considered as the data for the calculation of the number of development wells. KRH 2-1RD data cannot be used as productive well. It is due to the wellhead pressure is too low to be commercialized. The same thing has also happened in KRH 3-1ST. Besides, the acidity and salinity if this well is relatively high. The chloride content of this well is about 40,780 mg/L, and the pH is about 2.2 (GeothermEx, 1998). The pH of TLG 1-1ST2 is also low (< 3). NCG (Non-Condensable Gas) content of TLG 2-1 is also too high (± 17 wt%). The condition of high salinity, high acidity, and high NCG content cannot be considered as proven area (Sarmiento and Steingrímsson, 2011). Therefore, the data that are used for the experimental design is from KRH 4-1, KRH 5-1, and TLG 3-1.

KRH1-1 ST2 is the non-productive well with compressed-liquid fluid. Based on the PT profile, the thickness of the reservoir zone is 1783 m, with the highest temperature of 300°C. KRH2-1 RD is the sidetrack workover of the KRH2-1. Based on the flow test, the fluid characteristic of this well is compressed liquid. The reservoir thickness and temperature are respectively 1171 m and 269°C. KRH4-1 is productive well with two-phase fluid. Based on the flow test, the fluid temperature is higher than the boiling point with the highest temperature of 263°C. The reservoir thickness of KRH4-1 is 846 m. KRH5-1 is productive well too. The feed zone of this well is sourced from two feed zones, which are the vapor and the liquid dominated zones. KRH5-1 is categorized as a two-phase high temperature well with the highest temperature of 272°C. The thickness of the reservoir zone, which is divided into vapor, and the liquid-dominated region is 1513 m (Prabata et al., 2017).

Table 1: Flow Testing Data of Karaha-Talaga Bodas (GeothermEx, 1998).

Well	Well Size	Results		
		WHP (bara)	Total Mass Rate (kg/s)	Enthalpy (kJ/kg)
Karaha				
KRH 1-1ST	Normal Size	Not sustain to flow		
KRH 2-1RD	Normal Size	4	100.8	1163
KRH 3-1ST	Normal Size	5	37.8	1628
KRH 4-1	Normal Size	8	34.6	2210
KRH4-2RD	Normal Size	No flow test conducted		
KRH 5-1	Normal Size	8	25.5	1396
K-33	Slim Hole	10	2.4	2035
Talaga				
TLG 1-1ST2	Normal Size	10	8.2	2559
TLG 2-1	Normal Size	8	5.3	2675
TLG 3-1	Normal Size	8	15.7	2559
T-2	Slim Hole	16	3.4	2675
T-8	Slim Hole	8	2.8	2652

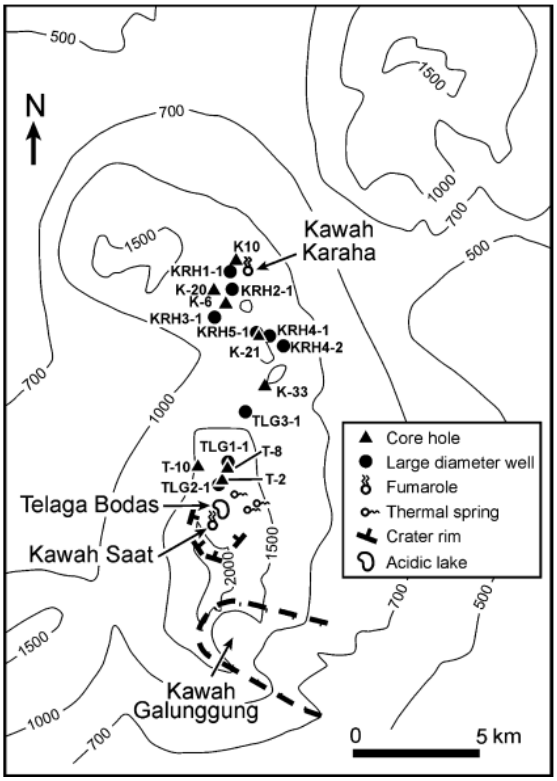


Figure 5: Karaha-Talaga Bodas Map (Nemčok et al., 2007).

TLG1-1 ST2 is a high-temperature vapor-phase well. The highest temperature and reservoir thickness of this well are respectively 289ºC and 791 m. TLG2-1 is a high-temperature vapor-phase well. Based on the chemical rig test, the presence of Non-Condensable Gas (NCG) and H_2S are relatively high in this well (10.3 wt% and 844 ppmw). The highest temperature of this well is 353ºC, and the reservoir thickness is 1433 m. TLG3-1 is productive well with two-phase fluid. Based on the rig test sample, the concentration of NCG and H2S is relatively low (0.5 wt% and 360 ppmw). The highest temperature of TLG3-1 is 289ºC. The reservoir is divided into two zones, which are the vapor and liquid dominated zones, with the thickness of 1092 m. The summary of the well characterizations can be observed in Table 2.

Table 2: Well Characterization (Prabata et al., 2017).

Well	Reservoir Thickness (m)	Highest Temperature (ºC)	Fluid Type
TLG1-1	791	289	Single phase – Vapor
TLG2-1	1433	350	Single phase – Vapor
TLG3-1	1092	286	Two-phase
KRH1-1	1783	235	Compressed-Liquid
KRH2-1	1171	269	Compressed-Liquid
KRH4-1	846	263	Two-phase
KRH5-1	1513	272	Two-phase

RESULT AND DISCUSSION

Application of Experimental Design

The drilling of make-up wells is necessary to cover the production decline of the geothermal area. The production decline is happened due to the declining of reservoir performance. Therefore, the number of new wells should be drilled during the operational period to fulfill the power plant capacity contract. However, the number of these make-up wells must be estimated while reviewing the project planning. Determining the number of make-up wells is related to the current performance of the reservoir during the production period, but there is not enough data related to the production history on the project planning phase. In other words, the data from well testing and other fields must be utilized as much as possible.

The formula for calculating the production decline in Eq.4 and 5 are utilized for the application of experimental design on the make-up well. Three factors are observed to the change of the response. The three factors are the decline curve model, decline rate, and make-up well capacity. Since it is the 2-level full factorial, the minimum and maximum values of the three factors above are determined for the factorial design.

The decline model is based on Eq.4 and Eq.5. The decline rate is the assumption based on the average decline rate for the vapor-dominated geothermal area in Indonesia (Purwaningsih et al., 2017). The well capacity or make-up well capacity is assumed based on the well testing data used The wellhead pressure is assumed to be at 8 bara; the turbine inlet pressure is considered as much as 6.8 bara; and the condenser pressure is 0.012 bara (Pertamina Geothermal Energy, 2012). The separator pressure is assumed the same as the turbine inlet pressure. The turbine efficiency is the average values of the study done by Dickson and Fanelli (2003). The result of the calculation is shown in Table 3.

Table 3: The Generated Power by The Wells.

Well	Generated Power (MWe)
KRH4-1	12.9
KRH5-1	4.4
TLG3-1	7.2

The minimum and maximum values are chosen from the result of well capacity calculation of the three estimated producing wells. The parameters/factors observed are summarized in Table 4. To analyze these three factors above, the 2-level (maximum and minimum) full factorial is applied with the help of Minitab Software. The entire runs are 8 runs for 30 MW development capacity in 30 years. The design and results are shown in Table 5. From the table, there are standard order and run order. The standard order is the fulfillment of random interaction between factors and the avoidance of order-dependence interaction.

The examples of make-up well calculations are shown in Figure 6. Only based on the result of the factorial design, it can be said that the decline model, whether it is exponential or harmonic, is not significant for predicting the number of make-up wells needed. However, it must be confirmed by the Pareto chart of the experimental design. The results of the Pareto chart are depicted in Figure 7.

Table 4: Observed Factors for the Number of Make-Up Wells Experimental Design.

Factors	Min (-1)	Max (1)
Decline Model	Exponential	Harmonic
Decline Rate (%/year)	1	3
Well Capacity (MW)	4.4	12.9

The examples of make-up well calculations are shown in Figure 6. Only based on the result of the factorial design, it can be said that the decline model, whether it is exponential or harmonic, is not significant for predicting the number of make-up wells needed. However, it must be confirmed by the Pareto chart of the experimental design. The results of the Pareto chart are depicted in Figure 7.

Table 5: 2-Level Factorial Design and The Result of Make-Up Well Experimental Design for 30 MW Power Plant Capacity.

Std Order	Run Order	Decline Model	Decline Model	Well Capacity	The Number of Make-Up Wells
4	1	1	1	-1	7
8	2	1	1	1	3
3	3	-1	1	-1	7
1	4	-1	-1	-1	3
6	5	1	-1	1	1
7	6	-1	1	1	3
5	7	-1	-1	1	1
2	8	1	-1	-1	3

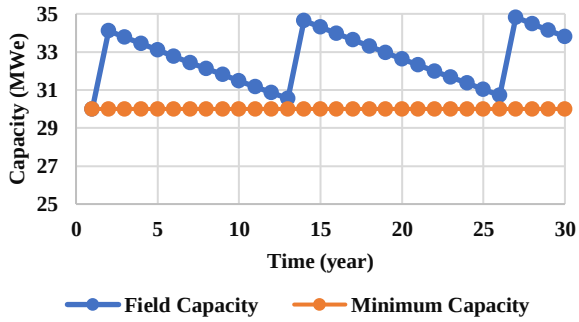


Figure 6: Calculation of Make-Up Well Number using Exponential Decline Curve, 4.4 MWe Well Capacity, and 1%/year Decline Rate.

According to the Pareto chart, it is approved that the decline model is not significant. Meanwhile, the most significant variables are the make-up well capacity and the decline rate. The interactions between the observed factors are also included in the Pareto chart. The causal relationships between the observed and the response variables are found on Eq. 7.

$$30\ MW_{nMU} = 3.5 + 1.5*D_Rate - 1.5*Well_Cap - 0.5*D_Rate*Well_Cap \quad \text{.....(7)}$$

The R^2 is 100%. The higher the value of R^2 is better the result of the model. The standard deviation (S) of the equation is 0. S value is the representation of the standard deviation of the distance between the data values and the fitted values. The fitted values are the results of the proxy equation. The lower S values are more representative of the model. The reason behind 100% R^2 and 0 S is the involvement of all variables might affect the equation. The more variables and its combination included, the higher the value of R^2. The condition of S is vice versa. All distance between the data values and fitted values had been involved in the model. The only parameter not included is ABC. Therefore, the coverage of data variations by the equation is nearly perfect, and the distance between data values and the estimation values had been involved in the proxy equation.

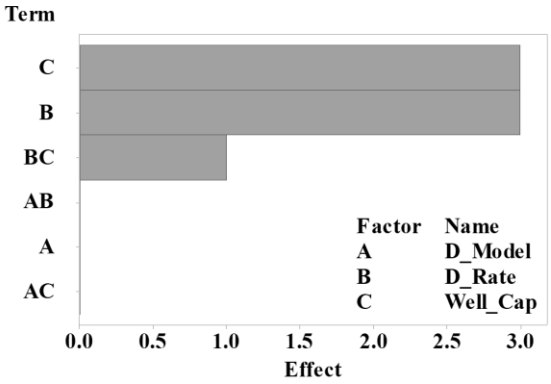


Figure 7: Pareto Chart of Make-Up Well Experimental Design for 30 MW Power Plant Capacity.

The above equation is combined with the Monte Carlo simulation to get the range of make-up well number in Karaha-Talaga Bodas area for each scenario of power plant capacity. The results of the Monte Carlo simulation are pictured in Figure 8. By the result, at least three make-up wells required for covering the production decline of Karaha-Talaga Bodas 30 MW power plant capacity.

The drilling process is not always successful. There is a gap between the number of wells drilled with the successful one. Therefore, it is essential to add new observed factor which drilling success rate. The drilling success rate is the ratio between the number of successful wells with the number of wells drilled. The observed variables are equal; the difference is only on the addition of the drilling success rate. Sanyal and Morrow had studied that the expected drilling success rate for the operational phase is higher than 90% in several geothermal areas in the world (2011). The new composition of the factors is shown in Table 6.

The factorial design is shown in Table 7. As in Table 7, the result is equal to the previous one. The decline model is not significant. As evidence, the Pareto charts are illustrated in Figure 9. Appertaining to the Pareto chart results both on the case considering the drilling success rate and the one is not, it can be concluded that the number of make-up wells is greatly influenced by the decline rate and the make-up well capacity in Karaha-Talaga Bodas area. Meanwhile, no effect is affected by the decline model. Therefore, either the exponential or the harmonic decline model can be applied to this field. The proxy equation of the experimental design is interpreted on Eq. 8. The R^2 is 100%, and the S value is 0.

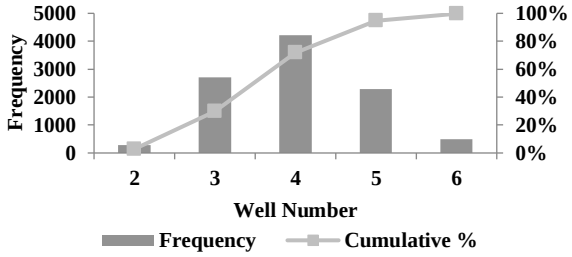


Figure 8: Monte Carlo Simulation Result of Make-Up Wells Experimental Design for 30 MW Power Plant Capacity.

Table 6: Observed Factors for the Number of Make-Up Wells Experimental Design with DSR.

Factors	Min (-1)	Max (1)
Decline Model	Exponential	Harmonic
Decline Rate (%/year)	1	3
Well Capacity (MW)	4.4	12.9
DSR	0.9	0.95

The same step is applied. The proxy equations will be combined with the Monte Carlo simulation. With 10000 iterations, all possible number of make-up wells are counted in the simulation. The results of the simulation are given in Figure 10. From the results, the probabilistic numbers are obtained. The most optimistic numbers of the make-up well in Karaha-Talaga Bodas for 30 MW power plant capacity are three wells. These numbers are the number of make-up wells should be drilled in this field.

$$30\ MW_{nMU} = 4.5+1.5*D_Rate - 1.5*Well_Cap - 0.5*D_Rate*Well_Cap \ldots\ldots\ldots (8)$$

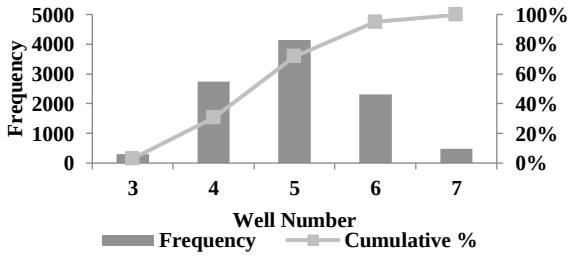


Figure 10: Monte Carlo Simulation Result of Make-Up Wells Experimental Design for 30 MW Power Plant Capacity considering DSR.

Table 7: 2-Level Full Factorial Design and The Result of The Make-Up Wells Number Experimental Design for 30 MW Power Plant Capacity considering DSR.

Std Order	Run Order	Decline Model	Decline Rate	Well Capacity	Drilling Success Rate	The Number of Make-Up Wells
16	1	1	1	1	1	4
7	2	-1	1	1	-1	4
11	3	-1	1	-1	1	8
3	4	-1	1	-1	-1	8
15	5	-1	1	1	1	4
14	6	1	-1	1	1	2
8	7	1	1	1	-1	4
2	8	1	-1	-1	-1	4
6	9	1	-1	1	-1	2
5	10	-1	-1	1	-1	2
12	11	1	1	-1	1	8
13	12	-1	-1	1	1	2
4	13	1	1	-1	-1	8
1	14	-1	-1	-1	-1	4
10	15	1	-1	-1	1	4
9	16	-1	-1	-1	1	4

Learning Curve for Predicting the Number of Make-Up Wells

The same method can be applied to various values of power plant capacity. In this study, a similar approach is utilized for 60 MW and 90 MW power plant capacity. The results are summarized and used for building the learning curve.

All results from the probabilistic method are summarized in Table 8. As acquired from Table 8, the drilling success rate for all outcomes is not in the range of the assumption applied before (90%-95%). The learning curves are built for the probabilistic method of the make-up well number. The linear functions of the learning curve can be observed in Figure 12 and 13. The level of confidence for each function is considered high due to the R^2 values of more than 0.98. The same as the previous type of well, the results from the learning curve are juxtaposed to the numerical simulation result of the prior study in Table 9. The numerical simulation was done in two production scenarios. The scenarios are the production from the steam zone and the mixed zone. The higher decline rate was found in steam zone production. Therefore, the requirement of make-up wells is higher in the steam zone production than in the mixed zone production. Since the production scenario in this paper is not specified before, the results of the probabilistic method and the previous study of numerical simulation are not comparable. However, the outcomes of the probabilistic approach are still in the combined range of both production scenarios. Thus, this method can even be used to estimate the number of make-up wells.

Only the value of drilling success rate for the most pessimistic result in 90 MW scenario (93%) is included in the range. The reason behind this case is the different assumption used for estimating the drilling success rate between Sanyal and Morrow and this paper. The value of drilling success rate during the operational phase is determined by the accumulation of all wells drilled until this phase, as shown in Figure 11. However, the success rate values that are shown in Table 8 only includes the number of make-up wells without adding up from the previous stages.

Table 8: Summary of The Make-Up Well Number Result.

Power Plant Capacity (MWe)	Percentile	Well Number		Success Rate (%)
		DSR	Non-DSR	
30	P10	4	3	75
	P50	5	4	80
	P90	6	5	83
60	P10	6	5	83
	P50	8	7	88
	P90	10	9	90
90	P10	8	7	88
	P50	11	9	82
	P90	14	13	93

Although the comparison is not valid due to a substantially different assumption, the numerical simulation results are just for validating the logical result of the probabilistic method. The assumption of the numerical simulation is shown in Table 10. Therefore, either numerical simulation or this probabilistic method can be utilized. The decision is depended on the confidence level. If the field data is already established with precision values, the deterministic result combined with the numerical

simulation is the most suitable way. If the case is vice versa, then the probabilistic method is a wise choice.

As a consideration, the drilling success rate is not applied to all values compared to the learning curve result. Notably, all number of wells from the numerical simulation is successful well in being reached during the development or operational phase.

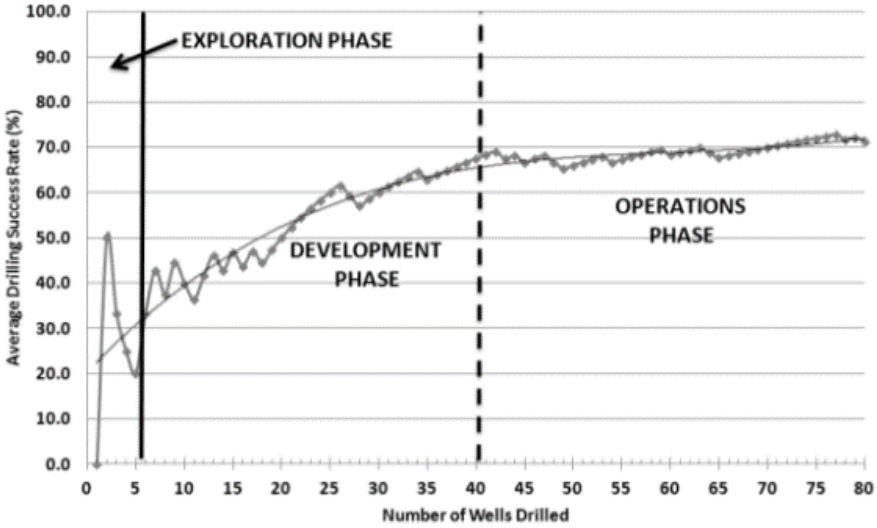


Figure 11: Average Drilling Success Rate vs. Number of Wells in Kamojang Field, Indonesia (Sanyal and Morrow, 2012).

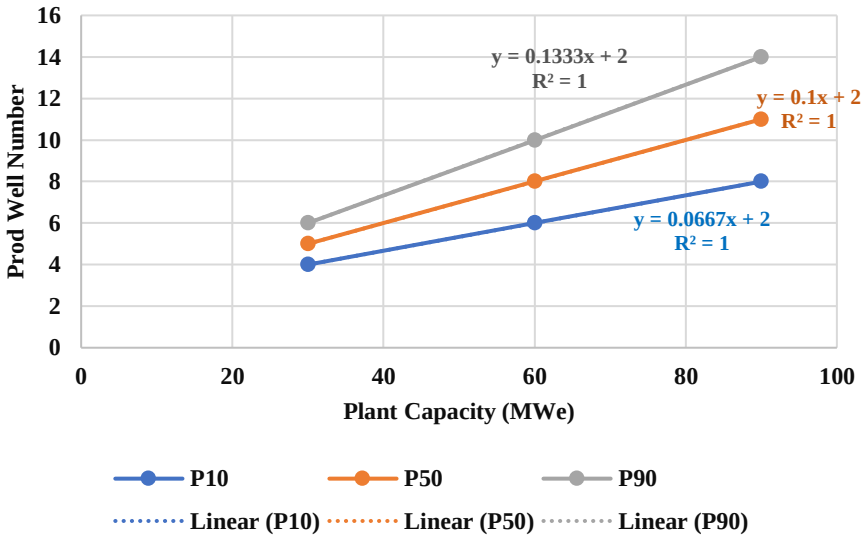


Figure 12: The number of make-up wells vs. power plant capacity (with DSR).

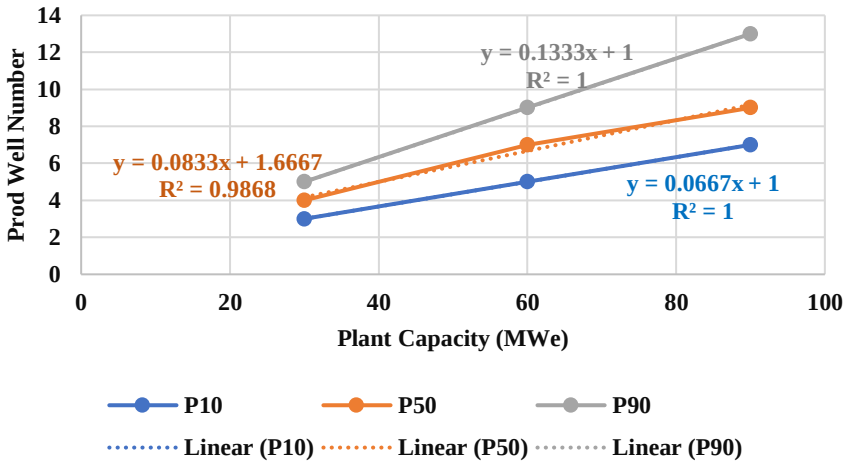


Figure 13: The Number of Make-Up Wells vs Power Plant Capacity (Without DSR).

Table 9: The comparison between the learning curve and the previous study for the make-up well number.

Power Plant Capacity (MWe)	Frequency Cumulative	Well Number		
		Learning Curve (Non-DSR)	Numerical Simulation	
			Steam Zone	Mixed Zone
30	P10	3	3	2
	P50	4		
	P90	5		
6.60	P10	5	4	2
	P50	7		
	P90	9		
110	P10	9	22	9
	P50	11		
	P90	16		
150	P10	12	-	16
	P50	15		
	P90	21		

Table 10: Assumption Used in Numerical Simulation (Prabata et al., 2017).

Parameter	Unit	Value
Wellhead Pressure	barg	10
Separator Pressure	barg	7.5
Turbine Inlet Pressure	barg	6
Condenser Pressure	bara	0.08
Turbine Eff.	%	80
Produced fluid enthalpy	kJ/kg	2300
Injectivity	kg/s	55.56
Make-Up Well Capacity	MW	7

CONCLUSION

The new method for estimating the number of make-up wells has been established. The findings based on the result of this study are the followings.

1. The most significant factors for estimating the number of make-up wells are the decline rate and the make-up well capacity.
2. The minimum number of wells required to drill for 30 MW power plant capacity in Karaha-Talaga Bodas are four make-up wells.
3. The learning curve for predicting the number of geothermal wells for various power plant capacities has been built in the linear function (R^2>0.98).

RECOMMENDATION

There are several recommendations to upgrade the quality of this research. The recommendations are the followings.

1. The data utilized must be the most updated one. The well testing data in this paper are the data from the year 1998. There are many possibilities that the real-time field data are very different from the data in this paper. Therefore, the result cannot be representative of the existing conditions, especially for the decline rate of the field.
2. The method should be applied to other field data to validate the robustness of the approach.
3. For the learning curve, it can be re-evaluated by adding more values of power plant capacity as the reference data to observe the real trendline for the learning curve.
4. The other experimental design and response surface method such as 3-level full factorial, Central Composite Design, Box-Behnken Design, and the other can be applied to this study as a comparison to the 2^k factorial design. The comparison can be made by utilizing the residual plot, error, standard deviation, and R^2 of each experimental design or surface response method.
5. By combining the method with economic analysis, the negotiation of funding between the field operator and the investor/buyer can be more flexible.
6. The number of iterations should be tested with several values to get enough number of iterations for this probabilistic approach. The test can be done by comparing the result of Monte Carlo

Simulation between the different number of iterations.

7. The well size is not considered in this research. The categorization by using well size will be the excellent choice to get a more accurate number of geothermal wells based on the size.
8. The drilling success rate is quite optimistic in this research. The data of drilling success rate can be modified using the case in Indonesia.

REFERENCES

Ahmad, A.A., Guwowijoyo, F.X., Pratama, H.B., (2018). "Probabilistic approach: Back pressure turbine for geothermal vapor-dominated system", in: IOP Conference Series: Earth and Environmental Science. pp. 1–7. https://doi.org/10.1088/1755-1315/103/1/012011

Allis, R., Moore, J., Petty, S., DeRocher, T., (2000). "Karaha-Telaga Bodas, Indonesia: A Partially Vapor-Dominated Geothermal System". Geotherm. Resour. Counc. Trans. 24, 7.

Arps, J.J., (1945). "Analysis of Decline Curves". Trans. AIME 160, 228–247. https://doi.org/10.2118/945228-G

Ashat, A., Pratama, H.B., (2018). "Application of experimental design in geothermal resources assessment of Ciwidey-Patuha, West Java, Indonesia", in: IOP Conference Series: Earth and Environmental Science. pp. 0–10. https://doi.org/10.1088/1755-1315/103/1/012009

Casler, M.D., (2015). Fundamentals of Experimental Design: Guidelines for Designing Successful Experiments". Agron. J. 107, 692. https://doi.org/10.2134/agronj2013.0114

Cox, D.R., (2009). "Randomization in the Design of Experiments". Int. Stat. Rev. Rev. Int. Stat. 77, 415–429.

Darma, S., Harsoprayitno, S., Setiawan, B., (2010). "Geothermal Energy Update: Geothermal Energy Development and Utilization in Indonesia". Presented at the World Geothermal Congress 2010, Bali, Indonesia, p. 13.

Dickson, M.H., UNESCO (Eds.), (2003). "Geothermal energy: utilization and technology", Renewable energies series. Paris.

Fisher, S.R.A., (1971). "The Design of Experiments", 8th ed. Hafner Publishing Company, New York.

Gehringer, M., Loksha, V., (2012). "Geothermal Handbook: Planning and Financing Power Generation. Energy Sector Management Assistance Program (ESMAP)", Washington DC.

GeothermEx, (1998). "Assessment of The Geothermal Resource in The Karaha-Talaga Bodas Area, Indonesia". GeothermEx, Inc., Richmond, California.

Handoko, B.T., Permana, J., Yosodiningrat, B., Tohari, M.A., Satyajit, D., (2015). "History of Joint Operation Contract in Indonesia", in: World Geothermal Congress 2015. Presented at the World Geothermal Congress 2015, Melbourne, Australia, p. 4.

Hidayat, I., (2016). "Decline Curve Analysis for Production Forecast and Optimization of Liquid-Dominated Geothermal Reservoir". IOP Conf. Ser. Earth Environ. Sci. 42, 012024. https://doi.org/10.1088/1755-1315/42/1/012024

Kementerian Energi dan Sumber Daya Mineral, (2017). "Potensi Panas Bumi Indonesia Jilid 1". Direktorat Panas Bumi.

Myers, R.H., Montgomery, D.C., Anderson-Cook, C.M., (2009). "Response Surface Methodology", 3rd ed. Wiley, United States of America.

Nemčok, M., Moore, J.N., Christensen, C., Allis, R., Powell, T., Murray, B., Nash, G., (2007). "Controls on the Karaha–Telaga Bodas geothermal reservoir, Indonesia". Geothermics 36, 9–46.

Parada, A.F.M., (2016). "Phases of Geothermal Development, in: SDG Short Course I on Sustainability and Environmental Management of Geothermal Resource Utilization and the Role of Geothermal in Combating Climate Change". UNU-GTP and LaGeo, Santa Tecla, El Salvador, p. 5.

Pasikki, R., Cita, F., Hernawan, A., (2016). "Application of experimental design (ED) in geothermal greenfield size assessment", in: Proceedings: The 4th Indonesia International Geothermal Convention & Exhibition.

Pertamina Geothermal Energy, P.G.E., (2012). "Project Design Document for Karaha Unit 1" PT. Pertamina Geothermal Energy.

Prabata, W., Berian, H., Sutopo, (2017). "Aplikasi Permodelan Numerikal Reservoir Pada Studi Skenario Pengembangan Lapangan Geothermal Karaha-Talaga Bodas, Jawa Barat, Indonesia" (Master's Degree Thesis). Institut Teknologi Bandung, Bandung, West Java, Indonesia.

Prabata, W., Sutopo, Pratama, H.B., (2019). "Experimental design and response surface method application in resources assessment: case study Karaha-Talaga bodas, West Java", Indonesia. IOP Conf. Ser. Earth Environ. Sci. 254, 012026. https://doi.org/10.1088/1755-1315/254/1/012026

Purwaningsih, F.O., Husnie, R., Afuar, W., Abdurrahman, G., (2017). "Make-up wells drilling cost in financial model for a geothermal project". IOP Conf. Ser. Earth Environ. Sci. 103, 012010. https://doi.org/10.1088/1755-1315/103/1/012010

Quinao, Jaime Jose, Zarrouk, S., (2014). "Applications of Experimental Design and Response Surface Method in Probabilistic Geothermal Resource Assessment – Preliminary Results", in: SGP-TR-202. Presented at the Thirty-Ninth Workshop on Geothermal Reservoir Engineering, Stanford University, California, p. 12.

Quinao, Jaime J., Zarrouk, S.J., (2014). "Applications of Experimental Design and Response Surface Method in Probabilistic Geothermal Resource Assessment – Preliminary Results", in: Proceedings, Thirty-Ninth Workshop on Geothermal Reservoir Engineering Standford University, Stanford, California, February 24-26,2014. pp. 1–12.

Rachman, R.H., (2016). "Application Methods Experimental Design (Plackett-Burman) in Uncertainty Parameters Reservoir Vapour Dominated, in: SGP-TR-209". Presented at the 41st Workshop on Geothermal Reservoir Engineering, Stanford University, Stanford, California, p. 12.

Sanyal, S.K., Morrow, J.W., (2012). "Success and The Learning Curve Effect in Geothermal Well Drilling – A Worldwide Survey 8".

Sanyal, S.K., Morrow, J.W., (2011). "An Investigation of Drilling Success in Geothermal Exploration, Development and Operation". Geotherm. Resour. Counc., Transactions 35, 5.

Sarmiento, Z.F., Steingrímsson, B., (2011). "Resource Assessment I: Introduction and Volumetric Assessment", in: Short Course on Geothermal Development in …. pp. 1–15.

Seidler, R., Bücker, H.M., Padalkina, K., Herty, M., Niederau, J., Marquart, G., (2015). "Optimal Experimental Design for Finding Optimally Located Boreholes in Geothermal Engineering", in: World Geothermal Congress 2015. pp. 1–3.

Telford, J.K., (2007). "A Brief Introduction to Design of Experiments". Johns Hopkins APL Tech. Dig. 27, 9.

Thorhallsson, S., Sveinbjornsson, B.M., (2012). Geothermal Drilling Cost and Drilling Effectiveness". Presented at the Short Course on Geothermal Development and Geothermal Wells, UNU-GTP and LaGeo, Santa Tecla, El Salvador, p. 10.

Walpole, R.E. (Ed.), (2007). "Probability & statistics for engineers & scientists", 8th ed. Pearson Prentice Hall, Upper Saddle River, NJ.

Wijayanto, Nanang, (2018). "PGE Berhasil Operasikan PLTP Karaha". https://ekbis.sindonews.com/read/1302087/34/pge-berhasil-operasikan-pltp-karaha-1525112696 (accessed on June 23rd, 2019).

HOW TO MANAGE THE GEOTHERMAL FIELD IN ACHIEVING SUSTAINABLE POWER OUTPUT BASED ON RESERVOIR CHARACTERISTICS AND UNIQUE PROBLEMS CASE STUDY: GEOTHERMAL FIELDS IN INDONESIA

Akbar Dwi Wahyono and Heru Berian Pratama

Geothermal Engineering Study Program, Institut Teknologi Bandung, Indonesia
Jl. Ganesha No.10, Bandung, West Java, Indonesia. 40132
Email: adwiwahyono07@gmail.com

ABSTRACT

Various practices and application of the latest advanced technology and strategic management tools have significantly contributed immensely to the management of geothermal resource in Indonesia. Distinct characteristics of geothermal reservoir in Indonesia has provided both key issues and opportunities in achieving sustainable performance throughout its lifespan. Geological setting in Western tectonics margin in Sumatra, Southern margins in Java-NTB and Northeastern margin in Minahasa are believed to be essential in resulting diverse reservoir characteristics. However, it is still unclear whether the distinct reservoir settings would yield such difference in specific response to the change of production strategies and eventually should have diverse in reservoir management applied to the corresponding geothermal fields.

Therefore, we investigated this case by reviewing its reservoir characteristics and unique problems of some geothermal fields in Indonesia. The method used is providing a statistical evidence by comparing different reservoir settings and characteristics in the way managing its resource sustainability in Ulubelu, Kamojang and Lahendong. Each field represents diverse regional settings which resulting distinct reservoir characteristics and its unique problems.

By the review, all of three geothermal fields are sharing the similarity of negative effect on pressure support programs. Relocation of reinjection wells has been a mandatory program conducted to avoid thermal breakthrough in these fields. Some fields evidently possess the unique reservoir response (i.e Kamojang), where other is becoming a projection (i.e Lahendong) of future reservoir response to the other field (I,e Ulubelu). In the end, the recommendation on how to manage the geothermal resource to achieve sustainability throughout its lifespan has been provided.

Keywords: Reservoir characteristics, reservoir management, vapor dominated, two-phase, liquid dominated reservoir

INTRODUCTION

Several authors have discussed the sustainability and renewability of geothermal resources (Hanano et al., 1990; Hanano, 2003; Stefansson, 2000; Wright, 1999; Cataldi, 2001; Axelsson et al.,2004; Rybach and Mongillo, 2006; Rybach, 2007). According to Stefansson (2000) the concept of "renewable" attributes to property of the energy resource, whereas "sustainable" attributes to the way the resource is utilized. Sustainable operation is characterized by equilibrium as it is not possible to extract more energy out of the system than the amount of the energy entering into the system. Therefore, sustainable exploitation can only be achieved with a renewable energy resource.

The initial hypothesis on renewability of geothermal resource state that eventually the renewability will affect the sustainability of geothermal resource and vice versa. Evidently, in many cases the company production strategy or "sustainability factors" eventually will evoke the renewability of the resource during years of production, thus, we can understand the way the developers dealing with such change.

In this paper, the practices in achieving sustainability of geothermal exploitation through resource management of geothermal fields in Indonesia will be reviewed and summarized based on its individual reservoir characteristics and unique problems. By assessing the parameter of reservoir characteristics and the unique problem, the effectiveness and efficiency of management programs that have been applied to the corresponding geothermal fields can be fairly reviewed.

As a law of "large numbers" in statistics for the interest of validity in representing the general cases by collecting the sufficient amount of research sample, therefore, we provide each examples of vapor dominated, two-phased dominated and a case of water dominated geothermal fields in Indonesia. It supposedly represents the general cases in geothermal reservoir management programs.

The objective is to get some lesson learned for the new prospective geothermal power plant in Indonesia such as Lumut Balai, Karaha Bodas,

Muara Laboh and etc. should they have to mitigate the potential problems and manage to sustain their resource in the foreseeable future based on these several cases in the more mature fields.

GEOTHERMAL RESERVOIR CHARACTERISTICS OF INDONESIA WESTERN TECTONIC MARGIN, SOUTHERN MARGIN AND MINAHASA MARGIN

Budihardi (1998) mentioned that based on the origin of geothermal systems in Indonesia due to the difference of the tectonic subduction dynamic play upon the western margin of Sumatra and southern margin of Java-NTB, the geothermal systems in Indonesia evidently have distinct reservoir characteristics. Shallower and oblique subduction plate in Sumatra resulted in felsic-rich magma by relatively shallow magmatism which produced mostly andesitic-rhyolite hosted reservoir rocks. Whereas deeper and parallel subduction plate in Southern of Java-NTB caused mafic-rich magma by relatively deeper magmatism, thus, mainly reservoir hosted in andesitic-basaltic rocks.

The rate of subduction of the Indo Australia Plate beneath the Eurasian Plate is 6-7 cm/year, with the highest rate in West Java. This subduction, which developed in the early Tertiary, has controlled the volcanic activity in Java and also the structural trend. In Java, there are four different structure trends i.e. N-S (Sunda trend), NE-SW (Meratus trend), E-W (Java trend), and NW-SE (Sumatera trend). The Sumatera, Meratus, and Sunda trends consist of normal and strike-slip faults, while the Java trend consists of thrust-reverse faults and folds (Pulunggono et al., cited in Fauzi et al., 2015).

These structural controls of geothermal fields were also believed to be decisive in resulting distinct reservoir characteristics. The great Sumatra regional strike slip fault as a result of shallow and oblique subduction created volcanism in geological setting of pull apart basin, subsequently, had sediment rocks as hosted reservoir. Whereas Southern margin, fault controls are dominantly in local scale and in caldera, depression system, resulted in volcanic rocks hosted reservoir.

Furthermore, in geomechanics point of view, explained the difference pressure regimes of both characteristics within the geothermal reservoir and its response during the exploitation period. In Sumatra where the reservoir is supposedly shallower and greater effective porosity, the pressure regime is expected below the Java-NTB geothermal regions, whereas, tighter and deeper reservoir were expected dominantly in Southern margin which most of the fracture permeability dictated by local faults.

However, based on Mahon et al., (2000) originally all geothermal fields had hot brines contained sodium chloride as the major water constituent in the reservoirs, however, through the geological time scale the boiling hot brines exceeded its steam saturation within the reservoir then it naturally began the evolution to become vapor dominated reservoir. This matured geothermal system evidently show a hydrostatics pressure lower than the water dominated system. In this case, the distinction of Western or Southern regional geological setting might not sufficiently affect in determining pressure regime, otherwise the evolution of the reservoir fluids through times that change the pressure regime.

Meanwhile, in Minahasa tectonic area according to Hamilton (1990) on tectonic of Sulawesi, the Kshaped island of Sulawesi comprise of northern arms of tertiary sediments and volcanic-arc rocks. The North Arm can be divided into 3 compartments; the NE-SW trending compartments (Minahasa compartments), the central E-W trending segment (Gorontalo compartments) and the N-S trending compartment or Neck. The Minahasa compartment is part of Sangihe Ridge that created inner volcanic arc in which Lahendong situated.

The magmatic evolution of Minahasa compartment derived from tholeitic series to alkali series that is typical orogenic tectonic environment. The basement rock is composed of interbedded carbonate sediments and volcanic rock deposited in the middle Miocene to Pliocene. The Lahendong geothermal field and Tompaso geothermal prospect separated by the NE-SW strike slip fault. The Lahendong geothermal filed located in the Pangalombian caldera and the Tompaso placed in the southern part of Tondano caldera (Siahaan et al., 2005.

INDONESIA GEOTHERMAL FIELD CASES

Reservoir Management in Kamojang

Renewability

Kamojang geothermal field belongs to Southern tectonic margin, which implied to the reservoir rock comprise of interbedded pyroclastics lavas and basaltic andesite (Utami. P, 2000).

The field is characterized by typical vapor-dominated systems at its natural state, thus, it mostly produces 100% steam. However, Kamojang reservoir has a water saturation in the order of 25-35%. The enthalpy of the fluid is around 2800 kJ/kg, with reservoir pressures of 30-34 bars and temperatures of 235-250 °C. Values of permeability-thickness of production area range from 500 to 140,000 Darcy-meter where the productive wells display values greater than 4900 Darcy-meter (GENZL, 1992). According to Suryadarma et al., (2010) the general distribution of

permeability (K) is subdivided into three zones, namely. high K-zone, moderate K-zone, and low Kzone (Figure 1).

Sustainability

The 35 years of continuous commercial production have led to slight dropping in the reservoir pressure and temperature within the production sector. As a result, some of the 33 production wells show production decline and prone to approach the superheated conditions (Suryadarma et al., 2010).

The aftermath of 15 years of production, all wells at Kamojang estimated to decline at an annual harmonic rate of 4.2%, while the reservoir pressure declined by 5 bar (Sanyal et al., 2000). By contrast, the constant operation of steam supply from 1982 to 2009 has resulted decline of reservoir pressure from initial conditions by about 17% to 25% (an average of 0.35 Ksc/year or 1.06%/year). Over the 27-year operation, the average reservoir declined in pressure is 8.5 Ksc (8.34 bar). Meanwhile, temperatures have dropped from initial conditions by about 2% to 7% (average 0.71ºC/year or 0.29%/year) and over 27 years the temperature reservoir drop is about 14 ºC on average (Suryadarma et al., 2010).

Since 2000, when further reservoir decline in pressure started to be anticipated as a result of major increase in mass withdrawal, three deep unproductive wells have been revitalized into reinjection wells to adjust with the total field production. Another strategy on preserving the reservoir pressure is to operate different productive wells alternately. The advantage of this strategy is evidenced in the stabilization output of producing wells and in the increase of wellhead pressure. Shortly, the immediate response taken by the company is to recover the mass production corresponding to increase in the steam output.

At present, Kamojang wells produce dry to superheated steam. The capacity of the wells varies from 20 to 110 ton/hour of steam. From 2010 to 2013, eight wells were used for the disposal of condensate from the power plants. The reinjection strategy is to use four wells but if steam production rate is found to decrease, reinjection will be transferred to other wells that are near the declining area. This strategy has been successful in minimizing productivity decline (Suryadarma et al, 2010).

Monitoring Program

To monitor the reservoir performance, wellhead static pressure is one of the parameters measured during well testing and reservoir monitoring programs. Downhole measurement is also done for this purpose by using conventional Kuster gauge mechanical tools. Pressure and temperature are also monitored continuously for accuracy using electric digital wire line logging.

Meanwhile, tracer tests have used deuterium as natural tracer, and tritium and methanol as artificial tracers. They have been performed to observe the pattern of fluid flow in the reservoir.

Sustainability Measurements

Data management is conducted to collect pressure build up data, well productivity history, well deliverability data, and reservoir performances. Those data that combine with the update of geoscience data are used to develop a numerical reservoir model. A three dimensional reservoir model started development in 2006 and was undergoing update in 2009. The first 3D model shows that the steam supply for 140 MW is safe until the end of the contract of Units 1, 2 and 3. Simulation also shows that exploitation at Unit 4 does not influence the steam supply of Units 1, 2 and 3 (Suryadarma et al., 2010).

Unique Problems and Mitigation

The imbalance of discharge and recharge induces decreases of deep brine level to the deeper parts of the reservoir. As the steam withdrawal too fast to be replaced by boiling deeper brine, therefore superheated zone started to be found in some production wells. Up until 2010, eight deep unproductive wells have been used for reinjection to prevent the superheated zone extended. Three of those are situated in the center of the field and in the low permeability zone but the other two are in medium permeability. However, this reinjection strategy has not yet given impact to sustain the productivity, except to wells KMJ33, KMJ-18, KMJ-40 gave a good response from reinjection program to minimize the decline of productivity.

Some reinjection wells gave adverse response i.e. made further decline in production, as in KMJ-11. To anticipate it, repositioning the reinjection wells were taking into account as change in reinjection strategy. In Figure 2 we can see the production performance before injections taken place, the decline 0.88%/year harmonic. Then during injection period (2001 – 2006) the decline rate increased to be 7.4%/year exponential. During the next period (2006 – 2008), increasing of injection rate by active injection well KMJ-13 caused increasing decline rate into staggering 14.58%/year harmonic. Afterwards, from the 2009 until 2010, reduction of injection rate has displayed a good response to reduce decline rate to be 0.18%/year exponential.

Reservoir Management in Ulubelu

Renewability

Ulubelu is a representative of geothermal field which heavily controled by Sumatran Fault situated

in the Northern tectonic margin. Ulubelu reservoir is inferred to be situated in a graben which consisting mainly of andesitic lavas and pyroclastics (Suharno, 2013). The presence of various structures inside the graben contributed to the relatively homogeneous reservoir properties which established through well logs data although geological structures controls the permeability distribution. Permeability value were generally ranged from moderate to good but uniformly distributed. Single phase brine with the average temperature of 250°C is proven to be main fluids which dominated the reservoir. In some wells there were observed boiling fluids, however it is believed that boiling zone did not occur within the reservoir condition. As consequences the production fluids produce moderate enthalpy (Yuniar, D, M., et al., 2015).

Sustainability

Ulubelu, a relatively new operating geothermal field in Indonesia, is being operated since the end of 2011 with installed capacity of 110 MW. Production wells for unit 1 and 2 are spread into 3 clusters named B, C, and D. There are 4 operating production wells in each of Cluster B and C while 3 wells in cluster D (Figure 3). Other clusters present in the surrounding of production wells for upcoming unit 3 and 4. The average enthalpy of production fluids from the wells is around 1100 kJ/kg, which can be turned into 20% of dryness at the separator. The required steam consumption to generate 110 MWe which turbine inlet pressure was set in approximately 6.5 bar is around 800 t/h. During the process 3000 t/h brines is produced.

Reinjection wells were programmed for pressure support within the reservoir, thus, 5 reinjection wells supposedly accommodate injection fluids of brine and condensate from units 1 and 2, up until 2015. The injection strategy was to inject as far as possible from the production zone while still inside the reservoir. The main consideration behind this scenario is to prevent rapid thermal breakthrough that would lower the fluids enthalpy of the production zone. However, current injection wells are situated in relatively close proximity to the production zone. New injection clusters are intended to accommodate brine from both recent productions and the prospective productions of the upcoming unit 3 and 4. Hot brine from the separator is injected to 4 wells, two of which are located in cluster A while the other two are in cluster F. Meanwhile, condensate is injected through a well in cluster A. Both injections are gravitational with the help of additional pressure from the separator (Yuniar, D, M., et al., 2015).

Monitoring Program

Reservoir performance monitoring is highly critical in Ulubelu as development of Unit 3 and 4 are underway. The aim of monitoring is also for securing steam supply for existing contract of Unit 1 and 2 power plants. Reservoir monitoring are conducted mainly by observations of surface data, physical and chemical data of wells**.**

Changes have occurred in observed production wellhead pressure (especially in wells in cluster B, C, and D) which may indicate a premature decline in reservoir pressure, or, may also be a transient response of reservoir due to early production.

Production rate and enthalpy are monitored from daily data and changes are observed from tracer dilution test data. Injection tracer test was also conducted as a part of reservoir monitoring to determine the effects of reinjection wells. Slight decrease in enthalpy of production fluids was observed at all production wells. Fluid chemistry surveillance indicated that chemical and thermal breakthrough from reinjected fluids might have caused the decline in enthalpy (Yuniar, D, M., et al., 2015).

The decrease in chloride and silica content from the baseline until August 2012 is observed in Clusters C and D, which is interpreted as the aftermath of cold condensate water influx from one of the injection wells. Meanwhile, the trends of increasing in chloride and decreasing in silica content which indicated as result of brine injection return from cluster A and F had been observed since August 2012 until December 2013.

There is a potency of steam cap development as indicated by steam entry from the shallower depth observed in cluster B. Although it's not quite significant but it will become benefit to steam gain extraction. Meanwhile, the decrease of NCG trends observed in production wells supported the conclusion regarding indication of injection return and early stage of steam cap development (Giriarso, J, P. et al., 2015).

Unique Problems and Mitigation

The highest concentrations of NCG concerted in the cluster B as shown in Figure 4, with the largest NCG 1.26% (wt) in well UBL-3. Meanwhile, the lowest value of NCG was found in the cluster C well UBL-5 with a value of 0.3% (wt) (Mulyanto et al., 2015).

The presence of a thin vapor zone concentrated in the vicinity of wells at cluster B attributed to the distinct NCG distribution pattern in Ulubelu compare to geochemical distribution pattern in other fields. However, this vapor zone has not produced excess enthalpy yet, thus, no significant additional contribution to the steam production rate and discharge enthalpy in cluster B (Mulyanto et al., 2015).

The existence of the steam cap is quite interesting in reservoir management because this zone has the potential to thicken and extend due to the pressure and water level drop. It may change the reservoir management strategy that currently applied.

Reservoir Management in Lahendong

Renewability

Lahendong is the only geothermal prospect in the Minahasa tectonic margin which being exploited. The reservoir rock in the Lahendong geothermal system are mostly andesite as a part of the unit of Pra-Tondano (Koestono, H, et al., 2010). The temperature of Lahendong Field is in the range of 280 – 320°C.

Utami et al., (2005) divided the northern and southern zone in terms of reservoir characteristics. The northern zone (Linau Zone) has acidic fluid from 570 – 370 masl which is confirmed by Volcanology Survey of Indonesia's drill hole. The reservoir rock is found in the the southern zone (Lengkoan Zone) has medium permeability with 2 reservoir layers. The shallow one extends from 450 – 250 masl while the deep reservoir extends from 150 – 1150 mbsl with temperatures more than 300°C. The north zone characterized by two-phase fluid with dryness ranging from 30 – 50 %, whereas production wells in the southern zone are characterized by fluid dryness more than 50% with several wells having dryness up to 90% (Permana, T, et al., 2015). The increasing dryness in both zone is believed due to the developing of steam cap as a result of reservoir pressure drawdown during years of production.

Sustainability

Development of this field was 80 MWe electricity generation consisted of 4 power plant units. In 2001, the first unit was commissioned and produced 20MWe electricity until present, followed by second unit in 2007, third unit in 2009 and the latest unit in 2012. Total production fluids of this field is around 1100 t/h with 600 t/h of steam and 500 t/h of brine from 10 production wells. Lahendong field implements cold injection system with brine and condensate injection combined in one injection cluster (Cluster LHD-7) which consists of three injection wells shown in Figure 5 (Prabowo et al., 2015).

Extensive exploitation of the Lahendong geothermal field has had an impact on the reservoir. Since 2001, 37 geothermal wells have been drilled to support 80 MW electricity generation by 4 power plants. This condition leads to several consequences on that reservoir which is reflected by reservoir chemical characterization changes. Usually the physical changes of the reservoir (i.e temperature and pressure) occur afterwards.

Monitoring Program

The southern zone has been exploited for almost more than 12 years and the major problem is limited downhole measurement data that can be used in a reservoir monitoring program. Therefore, geochemical monitoring is implemented in a reservoir monitoring program. The monitoring program consisted of liquid enthalpy monitoring, chloride and sulphate monitoring, NCG monitoring and Liquid-gas geothermometry monitoring. Several consequences on that reservoir which is reflected by reservoir chemical characterization were evidently show changes.

Meanwhile, in order to determine the effect of injection to the reservoir, two tracer injection surveys were conducted in Lahendong field (Prabowo et al., 2015). First survey was implemented in 2006 by using tritium as tracer fluid. The last survey was performed in 2014 using NDSA as tracer fluid. The tracer injection survey objectives are determining injection fluid path, breakthrough time, mass recovery and thermal breakthrough to the reservoir.

Unique Problem and Mitigation

Comparison with the initial condition of geochemical database, all of the production wells in cluster 4 suffered a decrease in enthalpy. LHD-10 had the deepest decline in enthalpy of about 1,000kJ/kg wells which shown in Figure 6 (Prabowo, et al., 2015). Based on tracer profile curve (Figure 7), all production well monitored is affected by the injection from well LHD-7.

Based on the result of tracer test analysis, to reduce negative effect of Lahendong Field reinjection strategy for production wells in north block, the injection rate should be controlled around 25 kg/s below 50 kg/s (Prabowo et al., 2015). However, the reduction of injection rate would impact the reservoir pressure in south area where the mass recovery actually much lower. For compensation, some of the injection should be split off from northern boundary (cluster LHD-7) to other area especially southern boundary where mass extraction is high.

Other strategy that could be implemented to maintain reservoir pressure and temperature is change the cold injection strategy into hot injection strategy. This strategy would reduce the reservoir temperature decline and maintain reservoir pressure by injecting high mass rate to the reservoir. The main considerations of this strategy are the possibility of scaling in the pipeline and the high investment cost in order to change the pipeline design.

DISCUSSION

All three geothermal fields have been run by the same developer which is Pertamina Geothermal Energy. The company's experience and expertise in managing diverse resource have been reflected by the steady power output of all three fields.

The fact that regional tectonics play huge role in determining the diverse resource characteristics in Kamojang (Southern tectonic margin), Ulubelu (Western margin) and Lahendong (Minahasa tectonic margin) has all evidently created diverse reservoir management treatment taken by the company. It is done to accommodate each of reservoir responses during the years of massive mass withdrawals.

The similarity of the three cases is boiled down to the effect of reservoir pressure support program or reinjection. Thermal breakthrough were all observed in all fields, thus, the dynamic of production injection strategy is played an important role in achieving sustainable production by carefully considering the behavior of the reservoir.

The response of Kamojang reservoir dealing with pressure drawdown is uniquely created superheated zone in some area of production. This is common problem encountered in vapor dominated geothermal field. The management of reinjection strategy can be tricky sometimes, PGE has been repositioning the reinjections well at many times to prevent the enlargement of superheated zone while at the other hand to avoid thermal breakthrough in production section.

Whereas, in Lahendong, the evolution of liquid dominated reservoir into two phase dominated have been observed by increasing of fluid enthalpy in production wells. This provide both key issue and opportunity to the developer. The evolution brings side effect of increasing in fluid acidic in some production wells, evidently observed some decline in chloride simultaneously by increasing in sulphate. The evolution also brings opportunity which is the increasing in fluid enthalpy in well head, thus, additional steam fraction in wellhead will bring efficiency in fluid production capacity.

Relatively a new operating geothermal field in Indonesia, Ulubelu, is experiencing the Lahendong type of evolution but it is still in the earlier phase. Some of the increasing NCG content in production wells were all observed, this indicated that boiling in reservoir have been massively increase. However, this not contribute significantly to the steam production rate and wells discharge enthalpy in some production wells, as no excess enthalpy was found. The existence of the steam cap may change the reservoir management strategy that currently applied to exploit the expected excess fluids enthalpy in reservoir.

Overall, the comparison of management reservoir program in each field is summarized in table 1.

CONCLUSION

1. Regional tectonics play huge role in determining the diverse resource characteristics in Kamojang (Southern tectonic margin), Ulubelu (Western margin) and Lahendong (Minahasa tectonic margin) has all evidently created diverse reservoir management treatment taken by the company.
2. All of three geothermal fields are sharing the similarity of the negative effect on pressure support programs. Relocation of reinjection wells has been a mandatory program conducted to avoid thermal breakthrough.
3. The response of Kamojang reservoir dealing with pressure drawdown is uniquely created superheated zone in some area of production.
4. In Lahendong, the evolution of liquid dominated reservoir into two phase dominated have been observed by increasing of fluid enthalpy in production wells
5. Ulubelu, is experiencing the Lahendong-type of evolution but it is still in the earlier phase. It evinces in increasing NCG and boiling in reservoir (i.e steam cap developing), but the fluid enthalpy in production wells has not increase significantly.
6. The recommendation on how to manage the geothermal resource to achieve sustainability throughout its lifespan is as follows:

    - Identify the renewability of the geothermal field by intensively and gradually assessing the geothermal resource through some integrated reservoir studies
    - Careful consideration in proposing the development scenario which suit to the reservoir characteristics to better maintain its sustainability by not excessively withdrawing massive fluids
    - Delicately arrange the reservoir monitoring program periodically, to accommodate the surveillance of both physical and chemical change within reservoir.
    - Identify the common and unique problems observed in daily, quarterly or yearly surveillance program.
    - Propose an effective mitigation program (i.e relocation injection wells, scaling inhibitor etc.) to the identified problems.
    - Carefully evaluate the mitigation program.
    - Conducting the sustainability measurement (i.e well modelling, flow

modelling and reservoir modelling) to get optimum scenario in sustaining the power output.
- Lesson learned of reservoir management program in some similar geothermal fields.

REFERENCES

Axelsson, G., Stefansson, V., Bjornsson, G., (2004). "Sustainable utilization of geothermal resource for 100–300 years. In: Proceedings 29th Workshop on Reservoir Engineering", Stanford University, Stanford, California, USA, January 26–28, 9 pp.

Cataldi, R., (2001). "Sustainability and renewability of geothermal energy". In: International Scientific Conference on Geothermal Energy in Underground Mines, Ustron, Poland, 4 pp.

Fauzi, A., Permana, H., Indarto, S., and Gaffar, E.Z, (2015). "Regional structure control on geothermal systems in West Java, Indonesia". Proceedings of the WGC 2015, Melbourne, Australia, 14 pp.

Giriarso, J, P., Puspadianti, A., Mulyanto, Hartanto, D, B., and Siahaan, E, E., (2015). "Intial Geochemical Monitoring Ulubelu Geothermal Field". Proceedings of the World Geothermal Congress 2015, Melbourne, Australia.

GENZL, (1992). "Reservoir review and simulation of the Kamojang field relating to production decline and steam supply for an additional 1 x 55 MW unit", Unpublished, PERTAMINA in house report.

Hamilton W., (1990). "Convergent-plate Tectonics Viewed from the Indonesian Region", Journal of the Indonesian Association of Geologists, Vol.12, No.1. Hanano, M., 2003. Sustainability steam production in the Matsukawa geothermal field, Japan. Geothermics 32, 311–324.

Hanano, M., Takahashi, M., Hirako, Y., Nakamura, H., (1990). "Longevity evaluation for optimum development in a liquid dominated geothermal field: effect of interaction of reservoir pressure and fluid temperature on steam production at operating conditions". Geothermics 19 (2), 199 – 211.

Koestono, H., Siahaan, E, E., Silaban, M., and Franzson, H., (2010). "Geothermal Model of the Lahendong Geotermal Field, Indonesia", In: Proceeding World Geothermal Congress 2010, Bali, Indonesia.

Mahon, T., Harvey, C., and Crosby, D., (2000). "The Chemistry of Geothermal Fluids in Indonesia and Their Relationship to Water and Vapor Dominated System", In: Proceedings 2000. WGC, Kyushu-Tohoku, Japan, pp. 1389-1394.

Mulyanto, Puspadianti, A., Giriarso, J, P., and Hartanto, D, B., (2015). "The Initial State Geochemistry as Baseline for Geochemical Monitoring in Ulubelu Geothermal Field, Indonesia". Proceedings of the World Geothermal Congress 2015, Melbourne, Australia.

Permana, T., Mulyanto, and Hartanto, D, B., (2015). "Geochemical Change during 12 Year Exploitation of the Southern Part of Lahendong Geothermal Field, Indonesia". Proceedings of the World Geothermal Congress 2015, Melbourne, Australia.

Prabowo, T., Yuniar, D, M., Suryanto, S., and Silaban M., (2015). "Tracer Test Implementation and Analysis in Order to Evaluate Reinjection Effect in Lahendong Fields". Proceedings of the World Geothermal Congress 2015, Melbourne, Australia.

Rybach, L., Mongillo, M.A., (2006). "Geothermal sustainability, a review with identified research needs". Geothermal Resources Council Transactions 30, 1083–1090.

Siahaan, E, E., Soemarinda, S., Fauzi, A., Silitonga, T., Azimudin, T., Raharjo, I, B., (2005). "Tectonism and Volcanism Study in the Minahasa Compartment of North Arm of Sulawesi Related to Lahendong Geothermal Field, Indonesia". In: Proceeding World Geothermal Congress, Antalya, Turkey.

Stefansson, V., (2000). "The renewability of geothermal energy". In: Proceedings 2000. World Geothermal Congress, Kyushu-Tohoku, Japan, pp. 883–888.

Subir K. Sanyal, A. Robertson-Tait, James W. Lovekin, Philip J. Brown, (2000). "Assessment of Steam Supply for the Expansion of Generating Capacity from 140 MW to 200 MW Kamojang Geothermal Field, West Java, Indonesia". In: Proceeding WGC 2000, Kyushu, Japan, 2195 – 2200.

Suharno, (2013). "Review of the Rendingan-UlubeluWaypanas (RUW) Geothermal Field, Lampung, Indonesia", Geothermal Resources Council Transactions Vol.37, 471-478.

Suryadarma, Dwikorianto, T., and Zuhro, A., (2010). "Lesson Learned from Kamojang Geothermal Steam Field Management: from the Beginning Until Now". In: Proceeding World Geothermal Congress 2010, Bali, Indonesia.

Utami, P., (2000). "Characteristics of the Kamojang Geothermal Reservoir (West Java) as Revealed by Its Hydrothermal Alteration Mineralogy". In: Proceedings 2000. World Geothermal Congress, Kyushu-Tohoku, Japan, pp. 19211926.

Utami, P., Browne, P.R.L., Simmons, S.F., and Suroto. (2005). "Hydrothermal Alteration Mineralogy of the Lahendong Geothermal System, North Sulawesi", Proceedings, New Zealand Geothermal Workshop.

Wright, P.M., (1999). "The sustainability of production from geothermal resources". In: Lectures presented at the United Nations University Geothermal Training Programme, Reykjavik, Iceland, September, 42pp.

Yuniar, D, M., Hastuti, P, and Silaban, M., (2015). "Ulubelu, First Year Reservoir Monitoring". Proceedings of the World Geothermal Congress 2015, Melbourne, Australia.

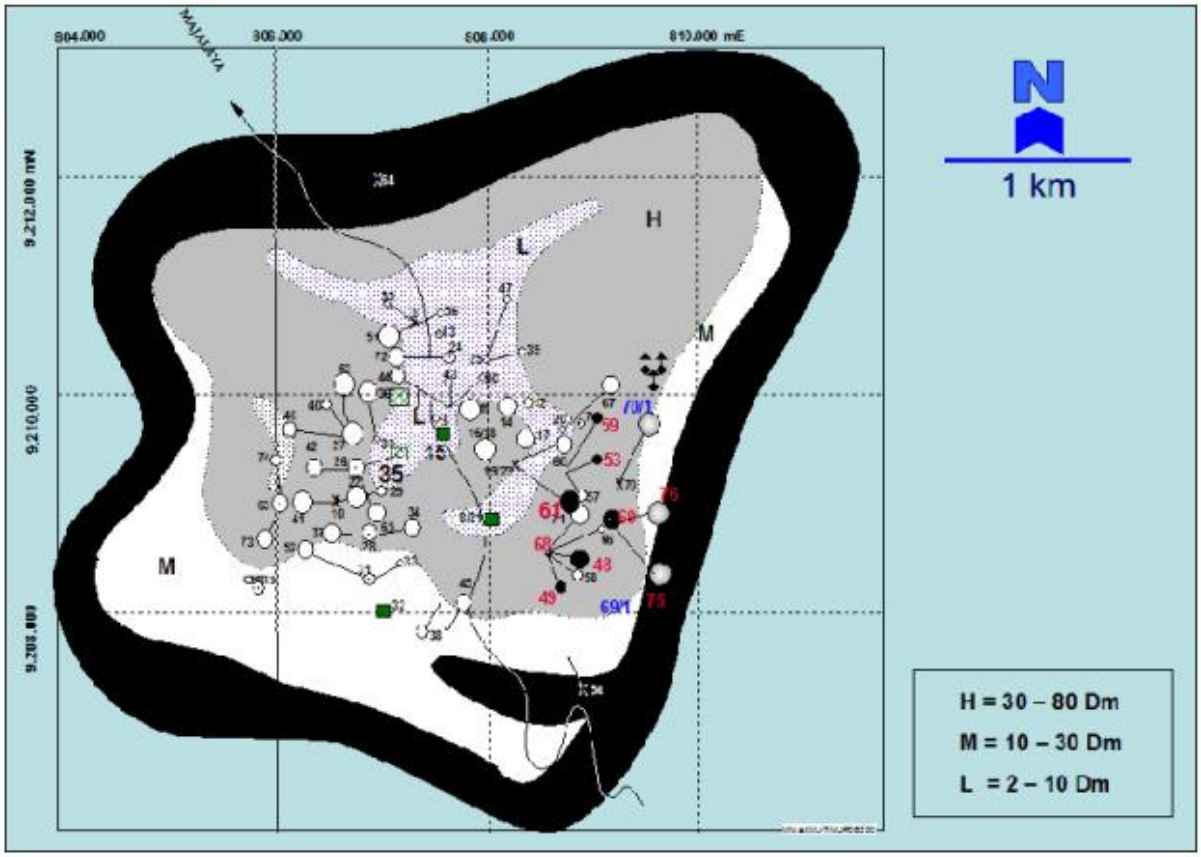


Figure 1: Distribution of permeability thickness in Kamojang geothermal field (GENZL, 1992).

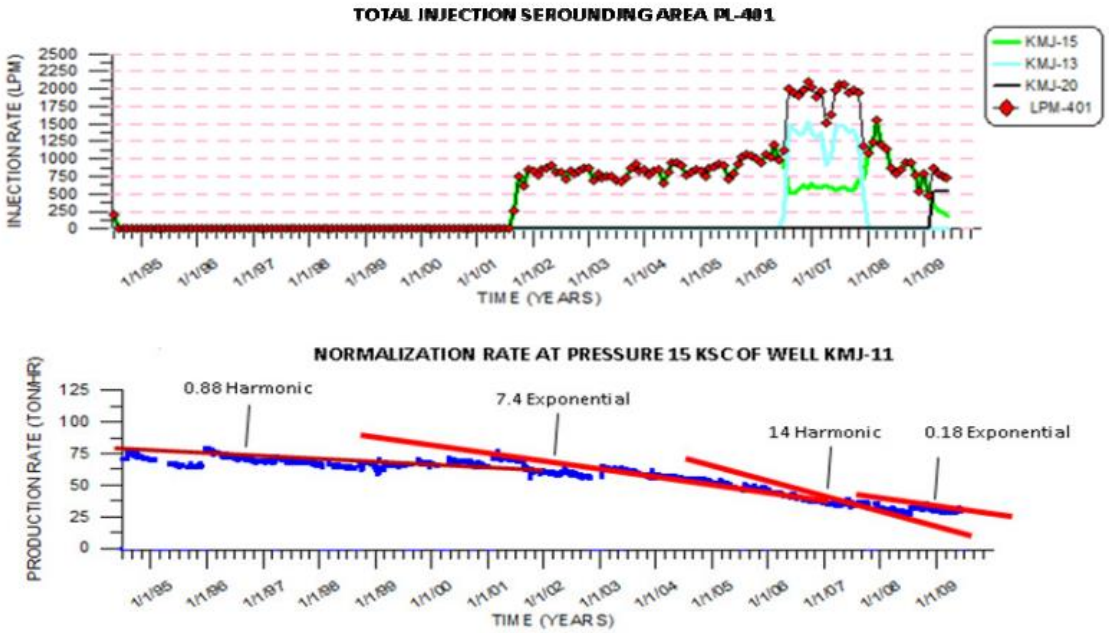


Figure 2: The comparison initial feed zone pressure of the wells to the beginning of start of Unit-4 commercial operation in 2008 (Suryadarma et al., 2010).

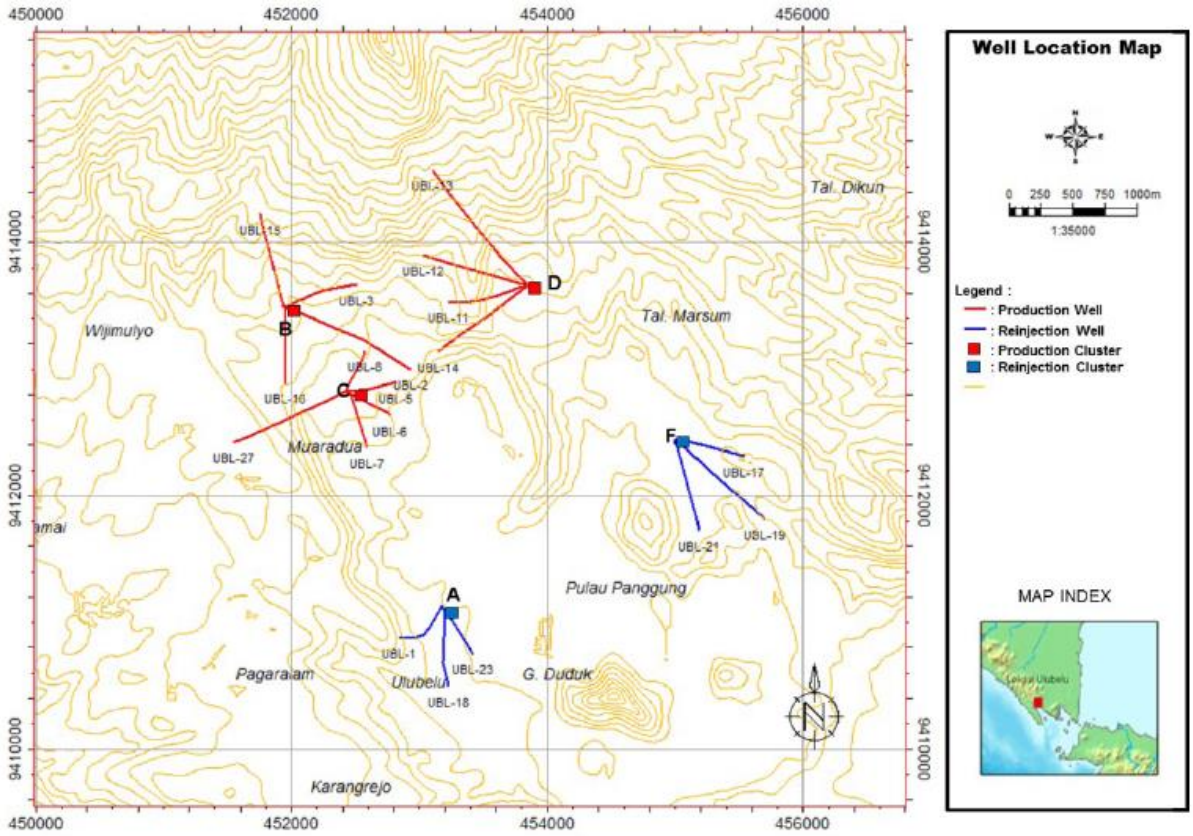


Figure 3: Ulubelu Production and Injection Well Map (Mulyanto et al., 2015).

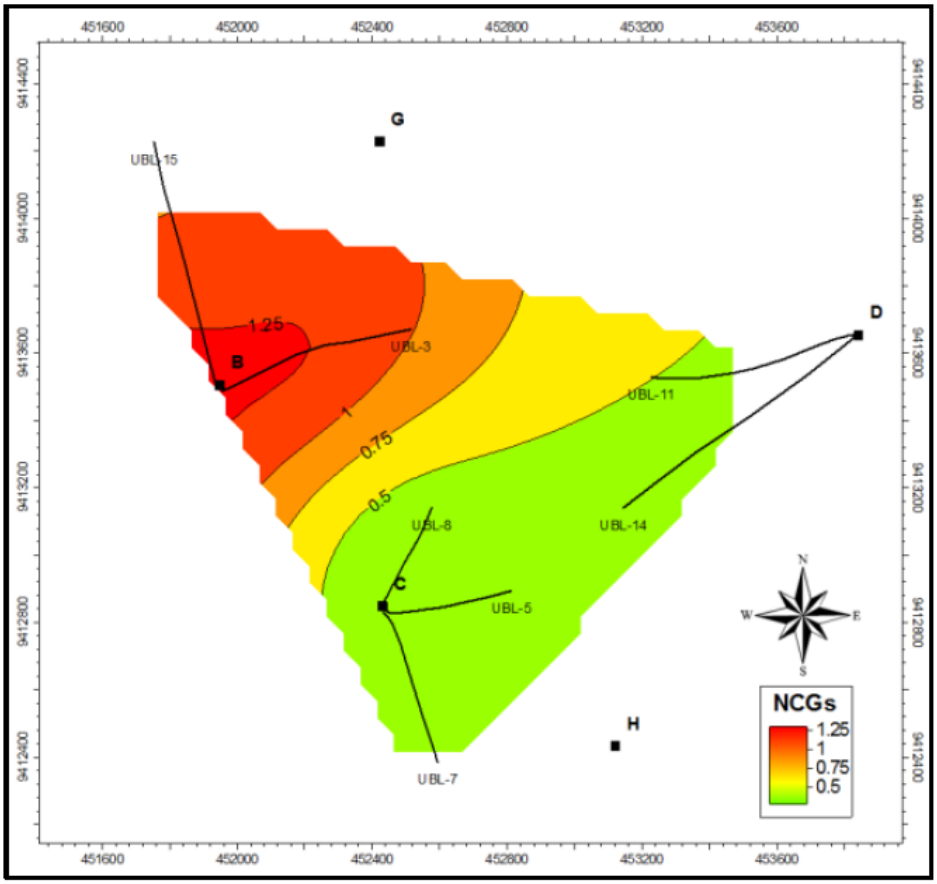


Figure 4: Ulubelu NCG contour map (Mulyanto, et al., 2015).

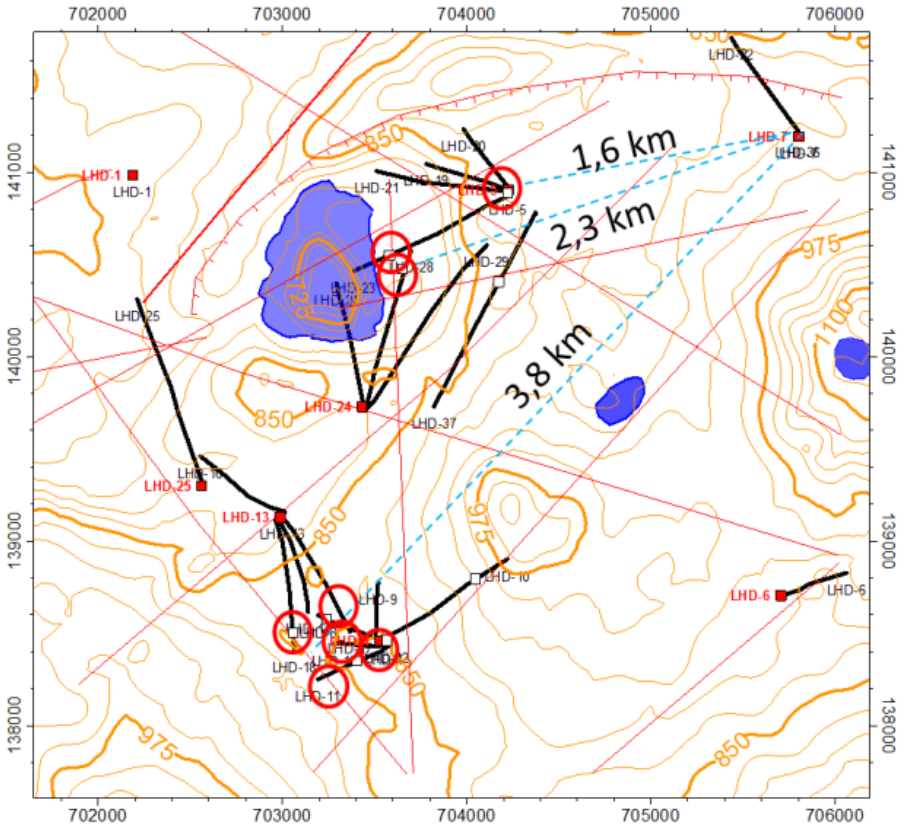


Figure 5: Well Direction and Location of Lahendong Field (Prabowo, et al., 2015).

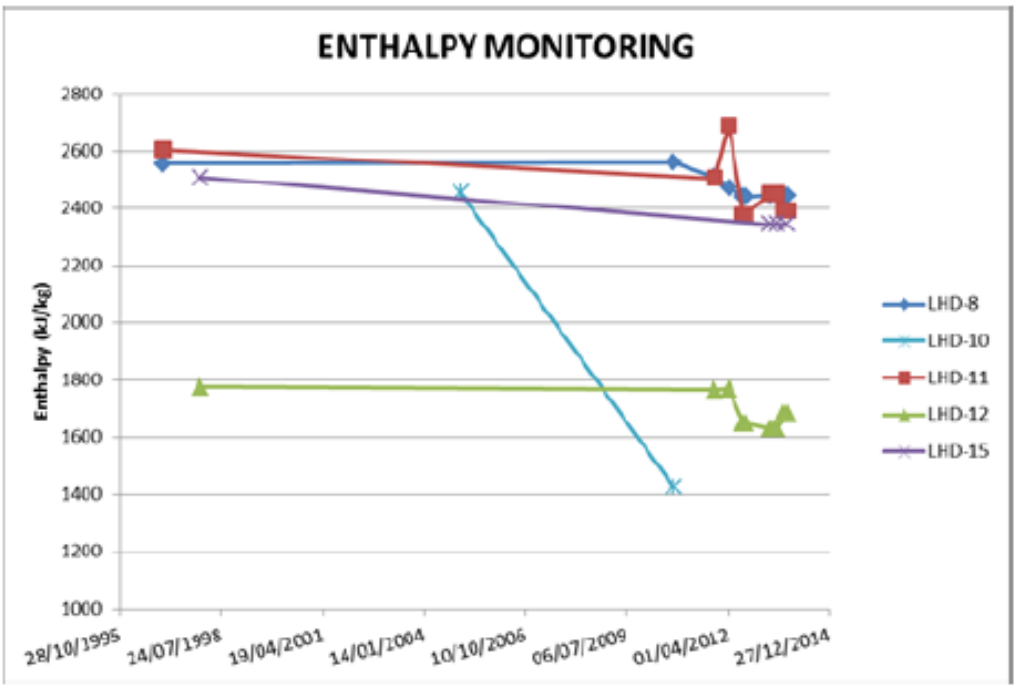


Figure 6: Graph of enthalpy monitoring in cluster 4 Lahendong Geothermal Field (Permana, T, et al., 2015).

Table 1: The comparison of the Kamojang, Ulubelu, and Lahendong geothermal field in terms of reservoir characteristics, renewability (i.e fluid production), sustainability (fluid extraction and reinjection), monitoring program that have been applied and each unique problem that has been encountered.

Field Name	Reservoir Characteristics	Fluid Production	Reinjection	Monitoring	Unique Problems
Kamojang	Vapor dominated ~245°C	- mostly produces 100% steam - the fluid enthalpy of t is around 2800 kJ/kg	- reinjection in the closest zone which most severe decline pressure - reformulating reinjection strategy due to mixing problem - reduce the condensate water injection	Surveillance activities: - quantity of steam produced - geochemistry of reservoir fluid - microgravity - seismicity - PT static, PTS - tracer Test: radioactive, fluorescent, and chemical tracers	- well production decline rate 3-4% per year - reservoir temperature decrease: mixing with cooler fluids - scalling (silica) steam pipeline, gathering and production wells - pressure drop - superheated area enlargement - thermal breakthrough
Ulubelu	Liquid dominated reservoir ~250°C	- average enthalpy 1100 kJ/kg with 20% of dryness - 800 t/hr. steam from total 3000 t/hr brines is required to generate 110Mwe	- current injection clusters are located relatively near the production zone - New injection clusters are planned to accommodate brine from both current production (relocation) and the production of the upcoming unit 3 and 4	Monitoring activities: - geochemistry monitoring in production fluids - geothermometer monitoring (fluids from wells) - pressure and temperature monitoring in Wellhead	- increasing in total NCG at production wells - low temperature fluid inclusion, indicated by increasing sulphate water while chloride content is decreasing significantly - thermal breakthrough
Lahendong	Two phase ~280 - 320°C	- total of 1100 t/h with 600 t/h of steam and 500 t/h of brine to generate 80 MWe - - average enthalpy 2600 kJ/kg	- need to reduce in cool injection rate or replace strategy with hot fluid injection	Surveillance activities: -quantity of steam produced - short-term micro seismic - tracer test - geochemistry monitoring	- acid fluids, depleted chloride content and high sulphate in production wells - pressure drawdown dramatically - thermal breakthrough

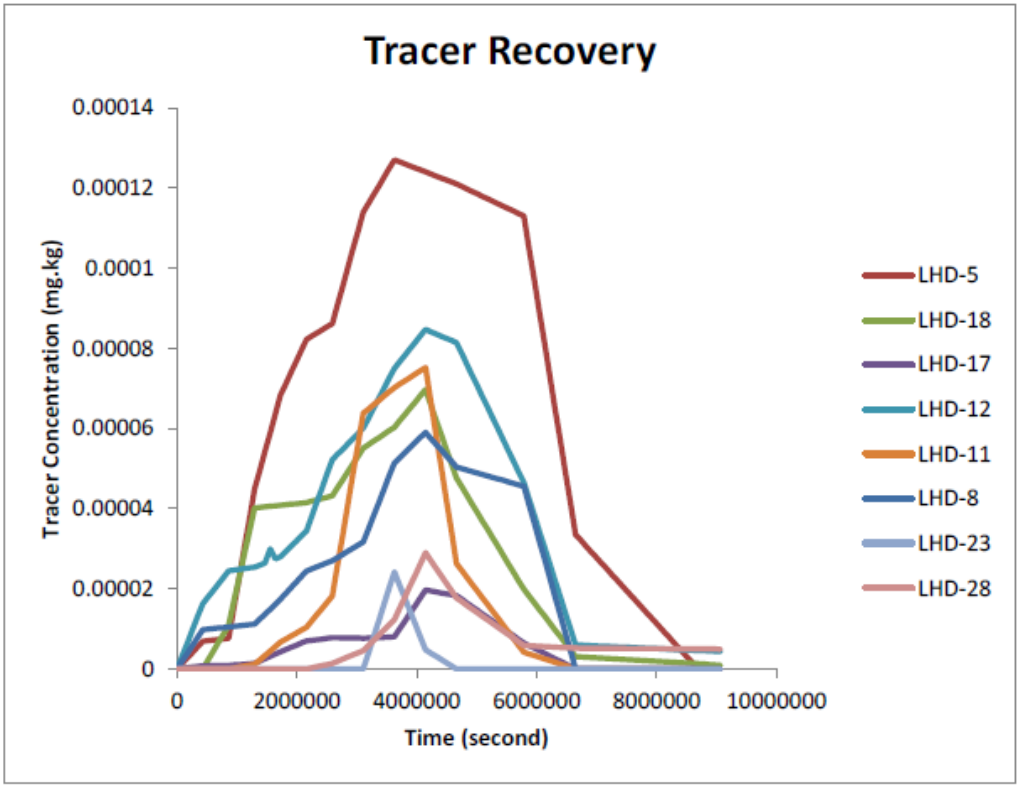


Figure 7: Tracer Profile Curve of Lahendong Field 2013 (Prabowo, et al., 2015).

Social, Politics, Economics and Community



This page is intentionally left blank



CERTIFIED EMISSION REDUCTION ISSUANCE PROGRESS OF CLEAN DEVELOPMENT MECHANISM GEOTHERMAL PROJECT IN INDONESIA

Muhyidin

Star Energy Geothermal Darajat II, Limited
Sentral Senayan II, 25th floor. Jl.Asia Afrika No.8, Jakarta 10270. Indonesia
Email: muhyidin@starenergy.co.id

ABSTRACT

Indonesia is the biggest geothermal resources in the world with potential 29 GW. As of first quarter 2018, installed capacity of geothermal project in Indonesia is 1,924.5 MW. Currently Indonesia is the second highest of geothermal producer after United State of America, that previously Philippine is in that position. The government of Indonesia has commitment through Presidential Decree No.79/2014 on National Energy Policy to increase renewable energy and target to minimum 23% of primary energy mix (geothermal targeted to 7% by 2025).

Geothermal project in Indonesia has contributed 32.91% of total certified emission reduction (CER) with total emission reduction 11,311,630 ton CO_2e. Indonesia is the biggest of CER issuance in the world in geothermal sector or equal to 82.77% of total CER issuance. Currently there are 13 clean development mechanism (CDM) projects registered & approved at United Nations Framework Convention on Climate Change (UNFCCC) secretariat and only 4 of them with CER issued status.

Since 29 May 2019, there is no more additional CER issuance from geothermal project in Indonesia. The last issuance is from Wayang Windu Phase 2 geothermal project with total CER issuance is 1,681,431 ton CO_2e. Some challenges and opportunities discussed in this paper to share the best practice and knowledge among project participants.

Keywords: Emission reduction, geothermal

INTRODUCTION

Asia and the Pacific countries has achieved rapid economic expansion in the recent years and has become a major source of greenhouse gas (GHG) emissions with more than half of the world's population and high rates of economic growth, the region is especially vulnerable to the effects of climate change (ADB, 2015). Indonesia, as part of Asia, is the fourth most populous nation in the world, following China, India and the United States. The population grew from 119 million in 1971 to 219 million in 2005 and it is projected that Indonesia population will reach 300 million in 2030 (KLH, 2010). Despite continuous, the multi-decade economic growth, approximately 11% of Indonesia's population is living below the poverty line. To lift people out of poverty, the Government of Indonesia is promoting economic development projected to average at least 5% per year in order to reduce the poverty rate to below 4% by 2025 as mandated by the Indonesia Constitution (KLHK, 2016).

In line with population growth and economic growth, it will increase the energy consumption. In Indonesia, the energy consumption still dominated by energy from fossil fuel. The discrepancy between high-energy consumption from fossil fuel and speed to find new resources, the fossil fuel energy will no longer available and Indonesia will depend on the import energy. This fossil fuel energy consumption automatically will increase subsidize from Government (EBTKE, 2015). The use of non-renewable energy especially from fossil fuel energy has increased the potential of global warming.

Diversification of new and renewable as the primary of national energy supply and fossil fuel energy as contributor paradigm should be set clearly. The government of Indonesia has commitment through Presidential Decree No.79/2014 on National Energy Policy to increase renewable energy. Renewable energy (include geothermal) currently only 7.7 % from the primary energy mix and targeted to minimum 23% or equal to 45 GW on 2025 (geothermal targeted to 7% by 2025).

Indonesia has renewable resources with potential more than 443 GW. Its potential such as hydro energy 75 GW, geothermal 29 GW, solar energy 207 GW, wind energy with 60.6 GW, and bioenergy with more than 102 GW. Indonesia is also known as the biggest geothermal resources in the world with total potential 29 GW (ESDM, 2018). As o first quarter 2018, Indonesia become the second largest world geothermal producer with total 1,924.5 MW installed capacity, shifting second position previously occupied by Phillipines. Additional installed capacity in 2018 came from Karaha Unit 1 (30 MW) and Sarulla Unit 3 (110MW). The following second semester from Sorik Marapi Modullar Unit 1 (20 MW on August 2018), Sorik Marapi Modullar Unit 2 (30 MW on December 2018), Lumut Balai Unit 1 (55 MW on December 2018) and Sokoria Unit 1 (5 MW on December

2018) (ESDM, 2018). Table 1 show installed capacity of geothermal plant in the world.

Table 1: Installed Capacity of World Geothermal Plant (Thinkgeoenergy.com, 2018).

No	Country	Total MW
1	United States	3,591
2	Indonesia	1,925
3	Philippines	1,868
4	Turkey	1,155
5	New Zealand	980
6	Mexico	951
7	Italy	944
8	Iceland	755
9	Kenya	676
10	Japan	542
11	Other	889

CDM projects from geothermal sector in Indonesia has contributed in national GHG emission reduction. It has reduced 11,311,630 ton CO_2e (32.91%) from total CER issuance from all industries in Indonesia. Table 2 showed CDM register status from geothermal projects in Indonesia. There are 13 CDM projects registered with total amount of reduction is 7,437,880 ton CO_2e / year based on Project Design Document (PDD). Meanwhile, Lahendong Unit 5 & Unit 6 Geothermal Project with CDM project reference number 9519, initial registration request on 11 Jan 2013, has not been approved by UNFCCC and currently in pending publication status. Sibayak Geothermal Power Plant has not got CDM project reference number and currently in validation terminated status (UNFCCC, 2019).

Table 2: CDM register status from geothermal projects in Indonesia (UNFCCC, 2019).

No.	Registration project title	Registered
1	Darajat Unit 3 Geothermal Project	11-Dec-06
2	Lahendong II-20 MW Geothermal Project	19-Dec-09
3	Kamojang Geothermal	16-Dec-10
4	Wayang Windu Phase 2 Geothermal Power Project	2-Dec-10
5	Patuha Geothermal Project	21-Dec-12
6	Project Ulubelu Unit 3 - 4 PT. Pertamina Geothermal Energy	15-May-12
7	Project Lumut Balai Unit 1 - 2 PT. Pertamina Geothermal Energy	22-May-12
8	Gunung Rajabasa Geothermal Power Plant	18-Sep-12
9	Liki Pinangawan Muaralaboh Geothermal Power Plant	31-Oct-12
10	Rantau Dedap Geothermal Power Plant	21-Nov-12
11	Project Lumut Balai Unit 3 - 4 PT. Pertamina Geothermal Energy	19-Sep-12
12	Project Kamojang Unit 5 PT. Pertamina Geothermal Energy	28-Nov-12
13	Project Karaha Unit 1 PT. Pertamina Geothermal Energy	27-Nov-12

Compared to other industry, CDM geothermal project in Indonesia contributed to 32,91% of total CER issuances from other industries and it is only 4 of 13 CDM project which has got CER issuance. It means those 9 CDM projects have not been run and verified by Designated Operational Entity (DOE) as per approved PDD. Currently there are 49 CDM projects in Indonesia with CER issuance status with total 34,373,731 ton CO_2e (UNFCCC, 2019). Detail of CDM project with total CER issuance showed at Table 3 below.

Table 3: CDM Project in Indonesia with total CER issuance and number of project (UNFCCC, 2019).

No	CDM Project in Indonesia	Total CER (ton CO_2e)	Total Project
1	Biomass Energy	895,962	7
2	Cement	8,863,083	1
3	Energy Efficiency Industry	1,124,545	1
4	Energy Efficiency Supply Side	17,154	1
5	Fossil Fuel Switch	743,933	1
6	Fugitive	3,110,798	1
7	Geothermal	11,311,630	4
8	Hydro	6,282,516	7
9	Landfill Gas	128,941	1
10	Methane Avoidance	1,696,813	21
11	Nitrate Oxide (N_2O)	125,937	2
12	Perfluorocarbon (PFCs) and Sulphur hexafluoride (SF6)	71,342	1
13	Solar	1,077	1
	Total	34.373.731	49

Eventhough Indonesia is the biggest country on CER issuance achievement from geothermal sectors; there are some opportunity for improvement to get more CER issuance from this sector. Total CER issuance from geothermal project per country described in Table 4.

Table 4: Total CER issuance of geothermal project per country (UNFCCC, 2019).

No	Country	Total CER (ton CO_2e)	Total Project
1	Nicaragua	171,541	1
2	Papua New Guinea	215,424	1
3	El Salvador	1,413,621	2
4	Indonesia	11,311,630	4
5	Guatemala	208,953	1
6	Kenya	345,628	1
7	China	28,330	1
	Total	13,695,127	11

METHOD

This research is descriptive qualitative method to describe and explain the CER issuance progress of CDM geothermal project in Indonesia by data collection method, review of literature, and interview & discussion. The rationale of this qualitative approach was to explore and describe the experiences and perspective of some CDM projects participants to contribute in national emission reduction.

Best practice sharing session among CDM participants already conducted in April 2018 at Sentral Senayan office. This session was coordinated by Pertamina Geothermal Energy (PGE) and attended by geothermal company under PGE joint operation contract. There was no competition in this CDM project, and some of companies share their best practice and CDM update. Star Energy group also has formal and non-formal sharing on CDM topic to discuss the progress.

This study will contribute to the literature on the sources of geothermal project as a lower emission energy sources, its initiative GHG emission reduction program implementation and best practices in contribution to national GHG emission reduction.

RESULT & DISCUSSION

Even though geothermal projects in Indonesia are the biggest CER contribution among other geothermal industries in the world (82.6% of CER contribution in all geothermal industries in the world is from Indonesia), room for improvements to have more CER from geothermal project is achievable. There are 13-registered CDM project from geothermal power plant in Indonesia, but only 4 of them already got CER issuance from UNFCCC secretariat. The highest CER issuance was from Darajat Unit 3 project with the last issuance was on 18 August 2017 with total 801,111 ton CO_2e. The second largest CER issuance was from Wayang Windu Phase 2 Geothermal Power Project with the last issuance was on 29 May 2019 with total 1,681,431 ton CO_2e. It means there are no additional CER issuance from geothermal project in Indonesia since 29 May 2019 (UNFCCC, 2019). The detail CER issuance from geothermal sector described in Table 5.

Table 5: CER issuance of CDM project from geothermal sector in Indonesia (UNFCCC, 2019).

CDM Project Title	Total CER	Percentage
Darajat Unit 3	6,260,609	55%
Lahendong II-20 MW Geothermal Project	216,304	2%
Kamojang Geothermal	92,691	1%
Wayang Windu Phase 2 Geothermal Power Project	4,742,026	42%
Total	11,311,630	100%

There are some reasons why CDM project from geothermal sectors in Indonesia were not run smoothly mainly due to some projects have not been implemented, transition of company name change registration, end of crediting period and some registered project have not completed verification audit on their CDM monitoring report. There are 3 CDM project with status those projects have not been implemented which are: Gunung Rajabasa Geothermal Power Plant, Liki Pinangawan Muaralaboh Geothermal Power Plant and Rantau Dedap Geothermal Power Plant.

Kamojang Geothermal CDM project with installed capacity 60 MW, the status is that verification contract has been terminated since 12 August 2015. Last day of the last monitoring period was on 28 February 2011 with total CER issuance was 92,691 ton CO_2e with latest issuance on 18 November 2011.

There are 3 geothermal projects with status end of first crediting period which are: Lahendong II-20 MW Geothermal Project (18 December 2016), Kamojang Geothermal (15 December 2017 but terminated on 2015), and Wayang Windu Phase 2 Geothermal Power Project (1 December 2017). Based on interview with employee Wayang Windu that their project currently in progress of renewal second crediting period to UNFCCC secretariat.

Darajat Unit 3 Geothermal Project is the pioneer of CDM project in Indonesia. This project was registered to UNFCCC since 11 December 2006. Start of first crediting period was 14 June 2007 and end of first crediting period was 13 June 2014. Darajat Unit 3 also pioneer in renewal of crediting period. The PDD of second crediting period is approved on 5 September 2015. Its second crediting period is 14 June 2014 until 5 October 2019 with amount of reduction is 753,136 ton CO_2e/year based

on approved PDD. Darajat Unit 3 initially operated by Chevron Geothermal Indonesia, Ltd (CGI) and as per 1 April 2017 this company was sold to Star Energy Geothermal Darajat II, Limited (SEGD). Chevron Limited and Chevron Products UK Limited (registered in the United Kingdom) registered as Project Participants (PP) of Darajat Unit 3. Chevron Products UK Limited has withdrawn from this project since 31 October 2018. The other issue is that Chevron Limited also has been sold to other company. SEGD has difficulty in coordination and communication to this new company to ask them also to withdrawn as part of transition process in change name of PP.

The change name of project participants consuming times. Since 2017, the process has not finished yet due to involving some stakeholders such as Delegation of National Authority (DNA) Indonesia and project participants at United Kingdom (UK). This process was not planned due to corporate action. The change name of project participants also not included during the purchase agreement between CGI and SEGD. Due to registered name of project participants of Darajat Unit 3 still under CGI, some monitoring period of CDM activities cannot be processed by SEGD as new owner/operator of Darajat Unit 3. It can become lesson learnt to other CDM project at geothermal sector to properly plan this administrative process if any corporate action in the future. Since Monitoring Report (MR) #13 until now, Darajat Unit 3 cannot be verified by DOE to have CER issuance from UNFCCC. Summary of Darajat Unit 3 CER issuance can be seen in the Table 6 below.

Darajat Unit 3 has total CER achieved 4,697,905 ton CO_2e during 1st crediting period (14 June 2007 – 13 June 2014) and during 2nd crediting period (14 June 2014 – 5 October 2019) total CER achieved is 1,562,704 ton CO_2e . Potential CER during period 1 Jul 2016 - 5 Oct 2019 is in progress while waiting the change name of PP from CGI to SEGD at UNFCCC secretariat.

Lahendong II-20 MW Geothermal Project had initial registration request of PDD on 4 August 2009 and registered on 19 December 2009 with amount of reduction is 66,713 ton CO_2e/year. PP of this CDM project in Indonesia is Perusahaan Listrik Negara (PLN) and PP in Netherlands are International Bank for Reconstruction and Development (IBRD) as Trustee of Netherlands CDM Facility (NCDMF) & Netherlands' Ministry of Infrastructure and the Environment (IenM). Both PP from Netherland have withdrawn from this project (UNFCCC, 2019).

There are 3 MR that have been verified by DOE with total CER issuance are 216,304 ton CO_2e. MR period 1 January 2013 – 18 December 2016 (1st crediting period) has not been verified by DOE. Summary of Lahendong II-20 MW Geothermal Project CER issuance can be seen in the Table 7.

Table 6: Summary of Darajat Unit 3 CER Issuance (UNFCCC, 2019).

Category	Cover Period	CER (tCO_2e)
Monitoring Report #1 (CER issued on 11 Jun 2009)	14 Jun 2007 – 31 Aug 2007	90,804
Monitoring Report #2 (CER issued on 25 May 2011)	1 Sep 2007 – 1 Nov 2008	737,846
Monitoring Report #3 (CER issued on 25 May 2011)	2 Nov 2008 – 31 Jul 2009	501,310
Monitoring Report #4 (CER issued on 17 Apr 2012)	1 Aug 2009 – 31 Oct 2010	889,337
Monitoring Report #5 (CER issued on 11 Dec 2012)	1 Nov 2010 – 31 Dec 2011	838,969
Monitoring Report #6 (CER issued on 15 Apr 2013)	1 Jan 2012 – 30 June 2012	362,546
Monitoring Report #7 (CER issued on 16 Jun 2013)	1 July 2012 – 31 Dec 2012	345,420
Monitoring Report #8 (CER issued on 13 Jun 2014)	1 Jan 2013 – 30 Jun 2013	346,094
Monitoring Report #9 (CER issued on 15 Aug 2014)	1 Jul 2013 – 31 Dec 2013	263,040
Monitoring Report #10 (CER issued on 4 Dec 2015)	1 Jan 2014 - 13 Jun 2014	322,539
Monitoring Report #11 (CER issued on 5 Jan 2017)	14 Jun 2014 - 30 Jun 2015	761,593
Monitoring Report #12 (CER issued on 18 Aug 2017)	1 Jul 2015 - 30 Jun 2016	801,111
Total CER		6,260,609

Table 7: Summary of Lahendong II-20 MW Geothermal Project CER Issuance (UNFCCC, 2019).

Category	Cover Period	CER (tCO_2e)
Monitoring Report #1 (CER issued on 14 Mar 2014)	19 Dec 2009 – 31 Dec 2010	84,960
Monitoring Report #2 (CER issued on 14 Mar 2014)	1 Jan 2011 – 31 Dec 2011	63,817
Monitoring Report #3 (CER issued on 14 Mar 2014)	1 Jan 2012 – 31 Dec 2012	67,527
Total CER		216,304

Table 8: Summary of Kamojang Geothermal Project CER Issuance (UNFCCC, 2019).

Category	Cover Period	CER (tCO_2e)
Monitoring Report #1 (CER issued on 18 Nov 2011)	16 Dec 2010 – 28 Feb 2011	92,691

Kamojang Geothermal CDM Project 3028 was registered since 16 December 2010 with amount of reduction 402,780 ton CO_2e/year. PP of this CDM project in Indonesia are Perusahaan Listrik Negara (PLN) and PT Pertamina Geothermal Energy. PP in United Kingdom of Great Britain and Nothern Ireland are EcoSecurities International Ltd and EcoSecurities Group Plc.

Total CER issued from Kamojang Geothermal is 92,691 ton CO_2e. Latest CER issuance was on 18 November 2011 and until now there is no additional CER issuance. The verification contract has been terminated and the last communication with UNFCCC secretariat was on August 2015. There are 2 monitoring reports with status is awaiting issuance request. Period 1 March – 31 July 2011 had emission reduction 182,908 ton CO_2e and period 1 August 2011 – 30 September 2012 with emission reduction 408,199 ton CO_2e. Both monitoring reports can not be processed due to the verification contract has been terminated. Table 8 show summary of Kamojang Geothermal Project CER issuance.

Wayang Windu Phase 2 Geothermal Power Project is the second highest CER issuance after Darajat Unit 3 with total 4,742,026 ton CO_2e or 42% from total CER issuance in Indonesia from geothermal sector. Summary of Wayang Windu Phase 2 CER issuance is shown in Table 9 below. The latest CER issuance was on 29 May 2019 with total 1,681,431 ton CO_2e (period 1 January 2015 – 1 December 2017).

Commercial Operation Date (COD) of Wayang Windu Phase 2 is on 4 Mar 2009 while their CDM registration was on 2 December 2010, so during that period the CER cannot be claimed into CDM project under UNFCCC. Carbon credits developed by carbon offset which are not yet certified called Voluntary Emission Reduction (VER). The opportunity to commercialize the real and verifiable reductions for project which have not been operational prior the successful registration at UNFCCC secretariat. In this case, emission reduction from the COD to the registered date was under VER. The VER has been verified by external parties so it can be commercialized as carbon trading (Muhyidin, 2018). Wayang Windu Phase 2 Geothermal Power Project currently in progress for 2nd crediting period renewal process. The end of 1st crediting period was on 1 December 2017. Table 9 show summary of Wayang Windu Phase 2 Geothermal Power Project CER Issuance.

Even thought, CDM project from geothermal sector have opportunity to get some fund from carbon trading and can contribute to national emission reduction, some challenges to run this project shall be handled properly. Some challenges of CDM geothermal project in Indonesia were: a) financial barriers, b) carbon market, c) international CDM regulation and policy, d) capacity building and knowledge, e) local regulation and policy, and f) unspecific domestic policy related to CDM (DNPI, 2014).

Current situation of registered CDM project from geothermal sectors are described to explore the challenges and figure out the best practice to solve it. There are 3 of registered CDM project from geothermal sectors which have not been implemented. They are Gunung Rajabasa Geothermal Power Plant, Liki Pinangawan Muaralaboh Geothermal Power Plant, and Rantau Dedap Geothermal Power Plant.

Gunung Rajabasa Geothermal Power Plant was operated by PT Supreme Energy Rajabasa (SERB). This CDM project was registered since 30 May 2012 same with Liki Pinangawan Muaralaboh Geothermal Power Plant. SERB has started the engineering design for civil constructed since August 2012. On April 2014, SERB just receive Borrow Use Permit of Protection Forest (IPPKH) permit from the Ministry of Forestry. This permit is a final requirement for the commencement of construction work in the area of the protection forest. In 2014, SERB focused on engineering design related to Jetty construction, piping systems, sea water facilities, pumping facilities, and facilities for the supply of electricity generators. The construction activity of Jetty began in early 2015 and was completed by the end of 2015 (SE, 2019).

Liki Pinangawan Muaralaboh Geothermal Power Plant was operated by PT Supreme Energy Muara Laboh (SEML). By the end of 2013, SEML has completed the exploration drilling program covering 6 wells. In 2014, construction of admin and accommodation building was completed on September 2014. By the end of 2015, SEML has completed the Engineering, Procurement, and Construction (EPC) tender process, and construction of geothermal power plants began in 2016 and estimated electricity production in 2019 (SE, 2019).

Rantau Dedap Geothermal Power Plant was operated by PT Supreme Energy Rantau Dedap (SERD). This CDM project has been registered since 24 July 2012. By the end of 2013, about 14 kilometers of road has already been opened and civil construction has been finished its original scope on July 2014. In November 2014, SERD reached financial closing to get USD 50 million facility agreement from the Asian Development Bank (2016) supported by the Clean Technology Fund, for the exploration of Rantau Dedap geothermal project. The exploration drilling continued until early 2015 and completed 6 wells. In 2016, SERD completed the feasibility study report, and EPC tender (SE, 2019).

The current challenges of Darajat Unit 3 Geothermal Project are on the transition of project participant names due to divestation process. Formerly the project participants from the host party (The Government of Indonesia) are Chevron Geothermal Indonesia, ltd and PT Darajat Geothermal Indonesia. After divestation, the project participant become Star Energy Geothermal Darajat II, limited (SEGD). While project participants from other party (The Government of the United Kingdom of Great Britain & Northern Island) are Chevron Limited and Chevron Products.

Since April 2017, SEGD as new operator of Darajat Unit 3 Geothermal Project was in progress of changing the project participant name including coordinated with UNFCCC, Government of Indonesia and Chevron. The MR #13 and MR #14 currently can't be submitted to DOE for verification, due to the participant name has not been changed formally at UNFCCC secretariat.

Lahendong II-20 MW Geothermal Project and Wayang Windu Phase 2 Geothermal Power Project are currently in progress of renewal for second crediting period in its CDM project. The end of first crediting period of Lahendong II-20 MW Geothermal Project was on 18 December 2016 while Wayang Windu Phase 2 Geothermal Power Project ended its first crediting period on 1 December 2017.

Since August 2017, there was only 1 monitoring report from Wayang Windu Phase 2 Geothermal Power Project achieved CER from register CDM project from geothermal sector. The current CER issuance is on 29 May 2019 with total amount 1,681,431 ton CO_2e. Currently Wayang Windu is still in progress renewal of second crediting period.

Past experience from Darajat Unit 3 Geothermal Project on its journey of second crediting period approval, it takes about 2 years since formal notification to UNFCCC secretariat on 10 December 2013 until renewal date of PDD approval from UNFCCC secretariat on 5 September 2015. It took time especially on preparing contract for consultant service, interview validator with CDM members, Ministry of Energy and Mineral Resources and National Council for Climate Change (DNPI) until supporting document and submit renewal of PDD report to DOE.

Darajat Unit 3 Geothermal Project is in progress for renewal of third crediting period until approval by UNFCCC secretariat with ultimate deadline by October 2020. Before renewal process, the transition process of project participant name from CGI to SEGD shall be done so the renewal process can be further processed to UNFCCC secretariat.

Table 9: Summary of Wayang Windu Phase 2 Geothermal Power Project CER Issuance (UNFCCC, 2019).

Category	Cover Period	CER (tCO_2e)
Monitoring Report #1 (CER issued on 2 Feb 2012)	2 Dec 2010 – 22 May 2011	379,773
Monitoring Report #2 (CER issued on 27 Apr 2012)	23 May 2011 – 31 Oct 2011	329,762
Monitoring Report #3 (CER issued on 28 Dec 2012)	1 Nov 2011 – 31 May 2012	444,255
Monitoring Report #4 (CER issued on 21 May 2013)	1 Jun 2012 – 31 Dec 2012	401,492
Monitoring Report #5 (CER issued on 15 May 2015)	1 Jan 2013 – 31 Dec 2014	1,505,313
Monitoring Report #6 (CER issued on 29 May 2019)	1 Jan 2015 – 1 Dec 2017	1,681,431
Total CER		4,742,026

Patuha Geothermal Project was operated by PT Geo Dipa Energi. This project was registered since 12 December 2012. The estimated CER from this CDM project based on approved PDD was 263,851 ton CO2e. Currently there is no CER issuance yet from this project that has been verified by DOE.

The rest of registered CDM projects under PT Pertamina Geothermal Energy (Project Ulubelu Unit 3 – 4, Project Lumut Balai Unit 1 – 2, Project Lumut Balai Unit 3 – 4, Project Kamojang Unit 5, and Project Karaha Unit 1) have not got CER issued due to those project have not been verified by DOE. These projects have been upgraded to Gold Standard CDM project since February 2013. The Gold Standard is a standard for creating high quality emission reduction projects in the CDM, Joint Implementation (JI) and Voluntary Carbon Market. Its objective is to add branding, a label to existing and new carbon credits generated by projects which can then be brought and traded by countries that have a binding legal commitment according to the Kyoto Protocol.

Sarulla Operation, one of the geothermal project that already reached full commercial operation of its 3x110 MW, have not been registered yet as CDM project at UNFCCC secretariat. The commercial operation of the first unit was operated on 18 March 2017, the unit 2 in November 2017 and unit 3 in May 2018. The potential of CER from this geothermal project will be more contribute in national emission reduction.

CONCLUSION

CDM project from geothermal sectors in Indonesia has significant contribution to national emission reduction. Current CER from all geothermal sectors was 11,311,630 ton CO_2e or 32.91% of all total CER from all sector include biomass, cement, fossil fuel switch, hydro, methane avoidance, etc.

Only 30.77% (4 of 13 registered CDM projects achieved CER issuances from UNFCCC secretariat. It means still have opportunity from all registered CDM project from geothermal sector to get more CER to contribute in national emission reduction program.

Regular best practice sharing and discussion among CDM project participants need to be conducted to update and share best practice among participants so that CDM project implementation can be run smoothly and higher CER can be achieved.

REFERENCES

Asian Development Bank (2016), "Emission Trading Schemes and Their Linking – Challenges and Opportunities in Asia and the Pacific", *pg. 102*

Chevron Geothermal Indonesia (2015), "Project Design Document 0673: Darajat Unit III Geothermal Project", *pg.4.*

Dewan Nasional Perubahan Iklim (2014), "Bunga Rampai Mekanisme Pembangunan Bersih (CDM) di Indonesia 2005 – 2014", *pg.26-76.*

Direktorat Jenderal Pengendalian Perubahan Iklim, Kementrian Lingkungan Hidup (2015), "Rencana Strategis Ditjen PPI Tahun 2015-2019", *pg.26.*

Kementrian Lingkungan Hidup (2010), "Second National Communication to the UNFCCC", *pg.ix - V-12.*

Kementrian Lingkungan Hidup dan Kehutanan (2016), "First Nationally Determined Contribution Republic of Indonesia", *pg.2.*

Ministry of Energy and Mineral Resources, Dirjen EBTKE (2015), "Potensi dan Peluang Investasi Energi Baru, Terbarukan dan Konservasi Energi", *pg.1.*

Ministry of Energy and Mineral Resources (2018), "Energi Hijau". *Pg.9.*

Ministry of Energy and Mineral Resources (2018), "Kini Indonesia Menjadi Produsen Listrik Panas Bumi Terbesar Kedua Dunia".

Ministry of Energy and Mineral Resources (2018), "Capaian 2017 dan Outlook 2018 Subsektor Ketenagalistrikan dan EBTKE", *pg.2.*

Ministry of Energy and Mineral Resources (2018), "Energi Hijau". *Pg.9.*

Muhyidin (2018), "Opportunity and Challenges of Clean Development Mechanism Geothermal Projects in Indonesia to Contribute in National Emission Reduction". *Pg.5. Proceeding of the 6th Indonesia International Geothermal Convention & Exhibition (IIGCE) 2018.*

Prihantono, Dwita (2006), "Renewable Energy/Energy Efficiency and the CDM", *pg.10.*

Spalding-Fecher, et al (2012), "Assessing the Impact of the Clean Development Mechanism", *pg. 23-56.*

Supreme Energy (2018), "Company PT Supreme Energy Muara Laboh, PT Supreme Energy Rajabasa, and PT Supreme Energy Rantau Dedap".

Think Geoenergy (2018), "Indonesia Reaches 1,925 MW Installed Geothermal power Generation Capacity".

UNFCCC (2019), "CDM Insights: Database for PAs and PoAs".

UNFCCC (2019), "Project 2876: Lahendong II-20 MW Geothermal Project".

UNFCCC (2019), “Project 0673: Darajat Unit III Geothermal Project”.

UNFCCC (2019), “Project 3028: Kamojang Geothermal”.

UNFCCC (2019), “Project 3193 *:* Wayang Windu Phase 2 Geothermal Power Project”.

LITHIUM IN BRINE WATERS FROM THE INDONESIAN GEOTHERMAL SYSTEMS: COULD IT MEET THE NATIONAL NEEDS OF MAKING LITHIUM BATTERIES?

Niniek Rina Herdianita[1,2], I Gusti Bagus Eddy Sucipta[1,2], and Aditya Yuda Kencana[1]

[1]Department of Geology, Faculty of Earth Science and Technology (FITB)
[2]Petrology, Volcanology and Geochemistry Research Group, Faculty of Earth Science and Technology (FITB),
Bandung Institute of Technology (ITB)
Jl. Ganesha No.10, Bandung 40132
Email: herdianita@gl.itb.ac.id

ABSTRACT

Lithium (Li) is an alkali metal which is the lightest metal. Lithium is an important metal, because Li, along with nickel (Ni) and cobalt (Co), is the main material in making batteries, especially for electric vehicles. Early 2019 electric-vehicle battery factory was built in Morowali, Central Sulawesi. Ni, Co and especially Li's supply needs to be found in Indonesia.

Lithium is not present as a free element in nature. It is as a compound in rocks and also found in brine water or salt water, including geothermal fluids. A small number of Li is contained in geothermal brine water from New Zealand, Iceland and Chile.

As Indonesia has a large amount of geothermal resources, Li might also be good metal resources. This paper gives the value of Li content in several geothermal fluids in Indonesia, either as surface manifestation or brine reservoir waters. The research is based on desktop study and the goal is to understand the type of geothermal system carrying Li anomalies in their geothermal brine water.

Keywords: direct use, geothermal, Lithium

INTRODUCTION

Lithium (Li) is the lightest metal belongs to alkali metal. Lithium has excellent electrical conductivity (i.e. low resistivity) and it is also the most electronegative metal (British Geological Survey, 2016). Lithium is an important metal, because Li, along with nickel (Ni) and cobalt (Co), is the main material in making batteries, especially for electric vehicles. Early 2019 electric-vehicle battery factory was built in Morowali, Central Sulawesi. Ni, Co and especially Li's supply needs to be found in Indonesia.

Lithium is not present as a free element in nature, but as a compound in rocks. Granite and Pegmatite are referred to as the main sources of Lithium carrier. Lithium is also found in brine water or saltwater, namely in salt fields, on oil fields and from geothermal fluids (Kay, 2018). Figure 1 shows the proportion of Li's existence in nature. Lithium is mostly found in salt deposits (referred to as continental brine), such as in the Andes mountain region which includes Argentina, Chile and Bolivia; here the average Li content is around 0.14% (Kay, 2018). A small number of Li is contained in geothermal brine water from New Zealand, Iceland and Chile. The Salton Sea geothermal field in Southern California is the most famous example of the presence of Li deposits from geothermal brine water. Concentration of Lithium in several geothermal areas including Reykjanes, Iceland; Wairakei, New Zealand; Cesano, Italy; Alsace, France; Kyushu, Japan; and Salton Sea, USA, in the range of 12 to 350 ppm (Garrett, 2004). In addition, Li extraction has also been carried out from brine water in oil fields (oil field brines); this adapted the Li extraction technology from geothermal brine.

Indonesia has a large geothermal potential, which is equal to nearly 30 GW (KESDM, 2017) with different geothermal systems. Geothermal fluids that emerge on the surface as geothermal manifestations on average contain Lithium less than 20 mg/L (Nicholson, 1993). The content of Lithium in geothermal fluid is highly dependent on subsurface reservoir rocks. Lithium is taken up into chlorite, quartz, and probably also onto clays in near-surface reactions (Duchi, et al., 1987a, b; in Nicholson, 1993). Li, Rb, Cs attain greatest concentration (of the order of 1-10 mg/kg) in areas with host rocks of rhyolitic and andesitic composition (including sedimentary environments with similar rock chemistry), and are significantly lower (~<0.1 mg/kg) in fluids from basaltic areas (Ellis, 1979; in Nicholson, 1993).

This paper gives the value of Li content in several geothermal fluids in Indonesia, based on desktop study. The samples were taken from surface manifestation and brine reservoir waters.

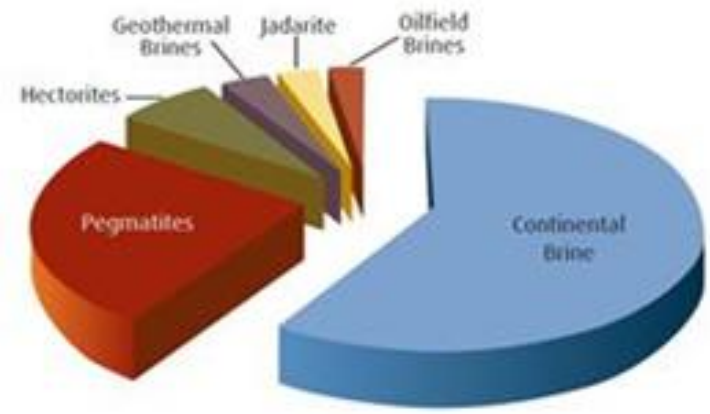


Figure 1: The proportion of Li's existence in nature. The largest sources of Li are salt water (salt fields) and rocks of Pegmatite (Evans, 2009 in ALS, -). Jadarite and hectorite are silicate minerals carrying Li.

GEOTHERMAL SYSTEM OF INDONESIA

There are more than 260 geothermal systems in Indonesia, that is located in Sumatera, Java, Bali, Nusa Tenggara, Sulawesi, Maluku, and non-volcanic area, such as Kalimantan and Papua. Most of geothermal system is associated with Quarternary volcanic arc (Pusat Sumber Daya Geologi (PSDG)/Geological Survey of Indonesia). Hochstein and Sudarman (2008) classify geothermal system in Indonesia into 6 types, i.e.: vapour-dominated system (e.g. Kamojang and Darajat), volcanic geothermal system with magmatic steam plume surrounded by neutral-pH hot fluids (e.g. Dieng Sikidang and Dieng Sileri), vapour layer system with partially liquid-saturated layers on top and liquid-saturated substratum (e.g. Wayang-Windu), vapour layer in the setting of a volcanic geothermal system (e.g. Patuha and Telaga Bodas-Karaha). Liquid-dominated system with major fault zone (e.g. Silangkitang), and liquid-dominated system beneath a stratovolcano associated with a concealed outflow plume (e.g. Citaman and Cisolok).

Furthermore Hochstein and Sudarman (2015) divide an explored geothermal system that associated with stratovolcanoes into 3 types: Sibayak, Kawah Ijen, and Ulubelu types. Sibayak type has reservoir near the conduit(s) of two small stratovolcano and associated with caldera, Kawah Ijen type. The characteristic of this type is that the system consist of a group of stratovolcano system with advective flow beneath the flanks, then Ulubelu type that is characterised of having a large outflow structure.

Geological Survey of Indonesia (PSDG) classified hydrothermal system into four stratovolcano, volcanic complex, caldera, and graben-volcanic and intrusions.

LITHIUM IN INDONESIA GEOTHERMAL SYSTEM

Table 1 shows the concentration of Lithium in several geothermal systems in Indonesia. Samples were taken in surface manifestation and well separators or weirbox.

Exploited geothermal systems, such as Dieng and Wayang Windu, seem to have higher Lithium in their brine water. The chloride brine water from deep reservoir can contain up to 70 mg/L Lithium. However, the system with dominantly steam (vapour dominated system), such as Kamojang and Darajat, has only less than 2 mg/L Lithium. High Lithium anomaly in brine water is probably due to intensely circulation of water in a close system during geothermal exploitation.

In greenfield geothermal systems with chloride water discharging as surface manifestations, such as Tampomas, Lawu and Geureudong, Lithium can dissolve in the thermal waters of up to 25 mg/L. However, if the surface thermal water is bicarbonate type, the Lithium dissolving in the water is less than 10 mg/L only. This might be due to dilution of meteoric cold water or mixing with condensate water. The other reason is probably relating to the type of reservoir lithology that interacts with thermal water. In this paper, the different rock composition is not explained yet.

Regarding to the type of geothermal system, it is previously shown that the liquid dominated system can have higher Lithium in reservoir water, compared to the vapour dominated system. Furthermore, Table 1 shows that the non-volcanic geothermal system, such as Limbong and Bittuang, seems to have higher dissolving Lithium in thermal water (as surface manifestation) than in the volcanic geothermal system. This might be control of reservoir lithology. Host rocks of granite, granodiorite and sandstone seem to contribute more Lithium into thermal water, compared to host rock of metamorphic and volcanic rocks.

.

Table 1: Lithium in Indonesia geothermal fields.

Location	Area	Geothermal System Type	Sample Type	Water Type	Lithology Reservoir	Li (mg/L)	Sources
Cibingbin	West Java	Non volcanic?	Surface	Cl	-	5.8	-
Cilayu	West Java	Non volcanic?	Surface	Cl	-	< 0.4	-
Cipacing	West Java	Non volcanic?	Surface	HCO_3	-	0.4 - 1.6	-
Tanggeung-Cibungur	West Java	Non volcanic?	Surface	SO_4-Cl	-	< 1.0	PSDG, 2017
Krakal-Wadas Malang-Wadas Lintang	Central Java	Non volcanic?	Surface	Cl	-	< 0.3	-
Sajau, Sebakis, Semolon, Mengkuasar	North Borneo	Non volcanic	Surface	HCO_3-Cl	-	< 3.2	Meiliani, 2018
Kandangan	South Borneo	Non volcanic	Surface	HCO_3, SO_4	-	< 0.01	Meiliani, 2018
Sungai Batuq, Dondang	East Borneo	Non volcanic	Surface	HCO_3-Cl	-	< 0.1	Meiliani, 2018
Sape, Nanga Dua	West Borneo	Non volcanic	Surface	HCO_3	-	< 0.1	Meiliani, 2018
Kadidia	Sulawesi	Non volcanic	Surface	H HCO_3, Cl-HCO_3	Granite	< 0.10	Kurniawan, 2015
Kadidia	Sulawesi	Non volcanic	Surface	Cl	-	1,37	Kurniawan, 2015
Napu	Sulawesi	Non volcanic	Surface	HCO_3, Cl-HCO_3	Phyllite	< 0.7	PSDG, 2017
Toare	Sulawesi	Non volcanic	Surface	HCO_3, Cl-HCO_3	Granite	< 4.2	PSDG, 2017
Parara-Pincara	Sulawesi	Non volcanic	Surface	HCO_3, Cl-HCO_3	Granite	< 0.5	PSDG, 2017
Limbong	Sulawesi	Non volcanic	Surface	HCO3, Cl-HCO3	Granite	0.4 - 8.3	PSDG, 2017
Bituang	Sulawesi	Non volcanic	Surface	Cl	Sandstone	7.0 - 11	PSDG, 2017
Maranda	Sulawesi	Non volcanic	Surface	HCO_3, Cl-HCO_3	Metamorphic rocks	0.2 - 3.7	PSDG, 2017
Tambu	Sulawesi	Non volcanic	Surface	Cl	Sandstone	5,90	PSDG, 2017
Tambu	Sulawesi	Non volcanic	Surface	HCO_3, Cl-HCO_3	-	< 1.3	PSDG, 2017
Dolok Marawa	-	Non volcanic	Surface		-	0.5 - 0.9	PSDG, 2017
Lainea	Sulawesi	Non volcanic	Surface	HCO_3	Phyllite, sandstone, limestone	< 0.75	PSDG, 2017
Pohuwato	Sulawesi	Non volcanic?	Surface	Cl	Granodiorite	10-12	PSDG, 2017
Tulehu	Moluccas	Non volcanic	Wellbore	Cl	-	5-13	-
Ransiki	Manokwari, Irian	Non volcanic	Surface	HCO_3	-	< 0.6	-
Dieng	Central Java	Volcanic	Wellbore	Cl	Volcanic rocks	32-68	Fathoni, 2016
Tangkuban Perahu	West Java	Volcanic	Surface	-	Volcanic rocks	0.3 - 8.8	Nasution, et al., 2004
Kamojang	West Java	Volcanic	Surface	-	Volcanic rocks	< 0.8	Mahon, et al., 2000
Darajat	West Java	Volcanic	Wellbore	Cl	Volcanic rocks	1,4	Mahon, et al., 2000
Salak	West Java	Volcanic	Wellbore	Cl	Volcanic rocks	12,4	Mahon, et al., 2000
Wayang Windu	West Java	Volcanic	Wellbore	Cl	Volcanic rocks	33,0	Mahon, et al., 2000
Tampomas	West Java	Volcanic	Surface	Cl- HCO_3	Volcanic rocks	< 1.3	Rahayudin, et al., 2018
Tampomas	West Java	Volcanic	Surface	Cl	Volcanic rocks	21,3	Rahayudin, et al., 2018
Gunung Ciremai	West Java	Volcanic	Surface	HCO_3-Cl, SO_4	-	< 0.4	Herdianita, et al., 2010
Cidanau, Banten	West Java	Volcanic	Surface	HCO_3-Cl, SO_4	-	< 1.6	Alam, et al., 2014
Malingping	West Java	Volcanic	Surface	HCO_3- SO_4	-	< 0.3	PSDG, 2017
Subang	West Java	Volcanic	Surface	HCO_3-Cl	-	< 7.0	-
Subang	West Java	Volcanic	Surface	Cl	-	18.3	-

Table 1: Continued.

Location	Area	Geothermal System Type	Sample Type	Water Type	Lithology Reservoir	Li (mg/L)	Sources
Dieng	Central Java	Volcanic	Surface	HCO_3, SO_4, Cl-HCO_3, Cl- SO_4	Volcanic rocks	< 0.88	Ramadhan, et al., 2010
Lawu	East Java	Volcanic	Surface	SO_4	Volcanic rocks	5,00	Fathoni, 2016
Lawu	East Java	Volcanic	Surface	Cl	Volcanic rocks	3.0 - 12.5	Fathoni, 2016
Lawu	East Java	Volcanic	Surface	HCO_3	Volcanic rocks	1.0 - 3.1	Fathoni, 2016
Hululais	Sumatera	Volcanic	Surface	Cl	-	0.5 - 5.4	-
Hululais	Sumatera	Volcanic	Surface	HCO_3- SO_4	-	< 0.5	-
Sungai Penuh	Sumatera	Volcanic	Surface	Cl	-	3 - 5	Silitonga, dkk., 2015
Gunung Kaca	Sumatera	Volcanic	Surface	HCO_3-Cl	-	2.0 - 2.4	PSDG, 2017
Permis	Sumatera	Volcanic	Surface	Cl	-	0.5	PSDG, 2017
Rajabasa	Sumatera	Volcanic	Surface	Cl	Volcanic rocks	1.3 - 7.5	Mussofan, et al., 2015
Rajabasa	Sumatera	Volcanic	Surface	HCO_3-Cl, SO_4	Volcanic rocks	< 0.15	Mussofan, et al., 2015
Kepahiang	Sumatera	Volcanic	Surface	HCO_3-Cl, SO_4	Volcanic rocks	< 0.8	PSDG, 2017
Geureudong	Aceh	Volcanic	Surface	Cl	-	25.3	PSDG, 2017
Geureudong	Aceh	Volcanic	Surface	HCO_3-Cl, HCO_3- SO_4	-	< 0.6	PSDG, 2017
Talang	West Sumatera	Volcanic	Surface	HCO_3-Cl, SO_4	Volcanic rocks	< 1	-
Talang	West Sumatera	Volcanic	Surface	Cl	Volcanic rocks	5-10	-
Ulubelu	South Sumatera	Volcanic	Surface	SO_4	Volcanic rocks	< 0.01	Sunaryo, et al., 1993
Ulubelu	South Sumatera	Volcanic	Surface	Cl	-	1.2 - 2.3	Sunaryo, et al., 1993
Sibualbuali	North Sumatera	Volcanic	Surface	HCO_3-Cl	Volcanic rocks	0.5 - 0.7	Gunderson, et al.
Donotasik	North Sumatera	Volcanic	Surface	HCO_3-Cl, Cl	Volcanic rocks	4.4 - 7.4	Gunderson, et al.
Namora-I-Langit	North Sumatera	Volcanic	Surface	HCO_3-Cl, Cl	Volcanic rocks	< 4.2	Gunderson, et al.
Silangkitang	North Sumatera	Volcanic	Surface	Cl	Volcanic rocks	6.3 - 6.5	Gunderson, et al.
Sipoholon	North Sumatera	Volcanic	Surface	HCO_3, SO_4, HCO_3- SO_4	-	< 0.8	Nukman and Hochstein, 2019
Lahendong	Sulawesi	Volcanic	Wellbore	Cl	-	< 2.3	Permana, 2016
Lahendong	Sulawesi	Volcanic	Wellbore	SO_4-Cl	-	0.8 - 5.2	Permana, 2016
Mataloko	Flores	Volcanic	Wellbore	Cl- SO_4, SO_4	-	< 0.04	Dahlan, et al., 2011
Songa-Wayaua	-	Volcanic	Surface	Cl	-	0.13 - 8.60	PSDG

CONCLUSION

The anomaly of Lithium in geothermal system is affected by several factors, such as type of geothermal system and type of thermal water. The main factor controlling the dissolving Lithium into thermal water is lithology of geothermal reservoir. Therefore, the influenced of lithology needs to further study

ACKNOWLEDGEMENT

The authors are grateful to Riset Program Penelitian, Pengabdian kepada Masyarakat dan Inovasi ITB (P3MI-ITB) 2019 for supporting this research.

REFERENCES

Alam, B. Y. C. S., Itoi, R., Taguchi, S., and Yamashiro, R. (2014). "Hydrogeochemical Characterization and the Origin of Hot Springs in the Cidanau Geothermal Field, West Java, Indonesia". Proceeding Thirty-Ninth Workshop on Geothermal Reservoir Engineering Stanford University.

ALS laboratory, -. Lithium: Analysis in Pegmatites, Jadarite, Clays, Carbonates, Sediments and Brine. Geochemistry Technical Note.

Dahlan, Eddy, M., Anna, Y., (2011). "Monitoring Sumur-Sumur Eksplorasi Lapangan Panasbumi

Mataloko, Provinsi Nusa Tenggara Timur". Proceeding Hasil Kegiatan Pusat Sumber Daya Geologi Tahun 2011.

Garrett, D.E., (2004). "Handbook of Lithium and Natural Calcium Chloride, their deporits, processing, uses, and properties". Elsevier Academic Press, pp. 476.

Gunderson, R. P., Dobson, P. F., Sharp, W. D., Pudjianto, R., and Hasibuan, A. (1995). "Geology and Thermal Features of the Sarulla Contract Area, North Sumatra, Indonesia". Proceeding World Geothermal Congress 1995.

Gunderson, R.,Ganefianto, N., Riedel, K., Azwar, L. S., and Suleiman, S. (2000). "Exploration Results in the Sarulla Block, North Sumatra, Indonesia". Proceeding World Geothermal Congress 2000.

Haryanta, T., (2015). "Geologi dan Studi Geokimia Air Panasbumi Daerah Wae Sano dan Sekitarnya, Kecamatan Sano Nggoang, Kabupaten Manggarai Barat, Flores, Provinsi Nusa Tenggara Timur". Skripsi Program Studi Teknik Geologi, ITB.

Herdianita, N. R., Julinawati, T., and Amorita, I. E. (2010). "Hydrogeochemistry of Thermal Water from Surface Manifestation at Gunung Ciremai and Its Surrounding, Cirebon, West Java – Indonesia". Proceeding World Geothermal Congress 2010.

Hochstein, M.P. and Sudarman, S. (2008). "History of Geothermal Exploration in Indonesia from 1970 to 2000". Geothermics, 37, 220-266.

Hochstein, M. P. and Sudarman, S. (2015). "Indonesian Volcanic Geothermal Systems". Proceeding World Geothermal Congress 2015.

Kay, A., (2018). "Types of Lithium Brine Deposits". https://investingnews.com/daily/resource-investing/battery-metals-investing/lithium-investing/lithium-deposit-types-brine-pegmatite-and-sedimentary/ (6 March 2019).

KESDM (Kementerian Energi dan Sumber Daya Mineral), (2017). "Potensi Panas Bumi Indonesia". Direktorat Panas Bumi, Dirjen EBTKE - KESDM, ISBN 978-602-50394-0-9 dan 978-602-50394-1-6.

Mahon, T., Harvey, C., and Crosby, D. (2000). "The Chemistry of Geothermal Fluids in Indonesia and Their Relationship to Water and Vapour Dominated Systems". Proceeding World Geothermal Congress 2000.

Mussofan, W., Powell, T., Sutrisno, L., and Sihotang, M. A. (2015). "Geochemistry Model of Chloride Springs Origin near Sea Coastal Area: Case Study from Rajabasa Geothermal Field". Proceeding World Geothermal Congress 2015.

Nasution, A., Aviff, M., Nugroho, S., Yunis, Y. dan Honda, H., (2015). "The Preliminary Conceptual Model of Tolehu Geothermal Resource, Based on Geology, Water Geochemistry, MT and Drilling". Proceedings World Geothermal Congress 2015, Melbourne, Australia.

Nasution, A., Kartadinata, M. N., Kobayashi, T., Siregar, D., Sutaningsih, E., Hadisantono, R., Kadarstia, E. (2004). "Geology Age Dating, and Geochemistry of the Tangkuban Parahu Geothermal Area, West Java, Indonesia". Journal of the Geothermal Research Society of Japan, Vol. 26, No. 3, p. 285-303.

Nicholson, K., (1993). "Geothermal Fluids Chemistry and Exploration Techniques", Springer-Verlag, Berlin.

Nukman, M. and Hochstein, M. P. (2018). "The Sipoholon Geothermal Field and Adjacent Geothermal System along the North-Central Sumatra Fault Belt, Indonesia: Rreview on Geochemisty, Ttectonics, and Natural Heat Loss". Journal of Asian Earth Sciences, 170. 10.1016/j.jseaes.2018.11.007.

Purnomo, B.J. dan Pichler, T., (2014). "Geothermal systems on the island of Java, Indonesia", Journal of Volcanology and Geothermal Research, -

PSDMBP (Pusat Sumber Daya Mineral, Batubara, dan Panas Bumi), Badan Geologi. (2017). "Potensi Panasbumi Indonesia". Jakarta: Direktorat Jendral EBTKE.

Rahayudin, Y., Kashiwaya, K., Susmanto, A., Tada, Y., Iskandar, I., and Koike, K. (2018). "Estimation of Fluid-rock Interaction Process and Recharge Area of the Tampomas Geothermal Field, West Java, Indonesia by Water Chemistry". Proceedings 43rd Workshop on Geothermal Reservoir Engineering Stanford University.

Ramadhan, Y., Channel, K., and Herdianita, N. R. (2013). "Hotwater Geochemistry for Interpreting the Condition of Geothermal Reservoir, Dieng"

Plateau Case, Banjarnegara-Wonosobo Regency, Central Java.Indonesian Journal of Geology, Vol. 8, No. 2.

Silitonga, T. H., Siahaan, E. E., Sasradipoera, D. S., Pelmelay, C., and Timisela, D. P. (2015). "Exploration Strategy in Kerinci Geothermal Procpect located inside the National Park of Indoensia". Proceeding World Geothermal Congress 2015.

Sunaryo, Hantono, D., Ganda, S., and Nugroho. (1993). “Exploration Result of the Ulubelu Geothermal Prospect, South Sumatra, Indonesia”. Proceeding 15th NZ Geothermal Workshop.

West Japan Engineering Consultants. (2011). “Study on Geothermal Power Development in Hululais, Indonesia”. Final Report, Study on Economic Partnership Projects in Developing Countries in FY2010

Wibowo, A.E.A., (2014). “Karakteristik Fluida Panas Bumi Non Vulkanik di Pulau Sulawesi dan Pemanfaatannya untuk Pembangkit Listrik dengan Siklus Kalina”. Tesis Program Studi Magister Teknik Panas Bumi, ITB.

Tipe Sistem Panasbumi di Indonesia dan Estimasi Potensi Energinya,

http://psdg.geologi.esdm.go.id/buletin_pdf_file/Bul%20Vol%204%20no.%203%20thn%202009/3.%20Sistem%20panas%20bumi%2 0p.%20Kasbani.pdf.

WELL TARGETING BASED ON TEMPERATURE AND STRUCTURAL MODEL IN GEOTHERMAL FIELD BY USING PETREL SOFTWARE

S. Mulyani and D. Juandi

Schlumberger
Wisma Mulia Building 45th floor, Jakarta, Indonesia
Email: smulyani@slb.com

ABSTRACT

Well targeting is important stage during geothermal development. To plan geothermal well, target is defined based on reservoir boundary and high permeability distribution, which approached by 3D structural and temperature model using Petrel®, a state-of-art and interactive modelling software to design well path while displaying those models.

The objective of this study is to show the workflow of well targeting based on structural and temperature model by using integrated modeling software. All information used for this project is published data from relevant website.

Field X was selected as reference for this project. Located on gently sloping alluvial cover, this field lies inside the margin of sedimentary basin. The regional stratigraphy of this field consists of granitic rocks as basement, and sequence of sedimentary deposits as basin fill. Structurally, four fault systems have been identified with several fracture patterns. High temperature gradient in basement and reservoir rocks 70ºC/Km, with maximum temperature 197ºC. Data used for this study are: geological map, lithological intersection, and lineament structure from surface mapping, topography point from geophysical survey, basement depth from gravity survey, alteration, lithological zone, and temperature data from exploration wells.

The workflow utilizes all information start with preparing data, building models of faults, lithology and temperature, then digitizing well for the next target. Data preparation done by collecting all information from website and load them into correct location. Structural model was built as framework for the model, based on topography, basement and lineament data by using structural modeling method. Lithological model was created based on geological map, and intersection information by using geometrical modeling method. Temperature model was defined based on well data by using kriging interpolation method. Geothermal resource then being identified to be used as well target. The result of this study is well plan information based on resource and fault position.

Keywords: 3D modelling, PETREL Software, well targeting

INTRODUCTION

In an exploration stage for Geothermal project, well target identification could be the highest risk task. Moreover, there is no single formula that indicates the drilling location because each project must be based on site specific condition (Santos, P., 2011). There are several approaches used to well targeting such as: anomaly hunting, anomaly stacking and conceptual model targeting. For this paper, the approach that has been using is the conceptual model. Basically, this approach done by integrating data sets from all geoscientist discipline to constrict a physical model, by avoiding artificial perception of reliability and characterize anomaly by explicitly illustrating how data sets constrain geothermal target parameters (Cumming, 2009).

A conceptual model usually consisted by main components: heat source, production reservoir, sealing cap rock, up flow & outflow zones, and the recharge & discharge zones. By having this model for well targeting, the well will directly test the properties of the model (i.e. temperature value), and any revision based on the updated well results can be directly included for the next assessment. To be more specific, this study aims to show the well targeting workflow based on structural geological model and the temperature model by using single integrated modeling software.

To get successful drilling of any geothermal well, correct siting and design of the well based on clear understanding of the target is vital. The well itself can give essential access for both energy extraction and information collection during geothermal utilization and research. In this study, the well targeting discussion will be focused on the production well that drilled with the purpose to enabling production of geothermal energy from a specific target in reservoir. Generally, production wells are designed for spontaneous discharge through boiling in high temperature reservoirs, or for the application of downhole pumps in lower temperature reservoirs. The principal drilling targets are in fact structures, volumes, permeability and sufficiently high temperature to maintain productive wells (Axelsson, G. & Franzon, H. 2012). So, information about geothermal system of the field really needed to get correct understanding.

Based on nature and geological setting, the geothermal systems of reference field X that used

for this study classified as Hot Dry Rock (HDR) or Enhanced Geothermal System (EGS). This system consists of rocks volumes that have been heated to useful temperatures by volcanism or abnormally high heat flow but have low permeability or are virtually impermeable. Therefore, they cannot be exploited in a conventional way (Axelsson, G. & Franzon, H. 2012).

REFERENCE FIELD

To show the workaround in this study, several free data was collected and loaded into software. Based on the location of those available data, field X was selected as reference study area.

Location

The site is located around 350 km south of Salt Lake City, Utah USA. It is unpopulated place with total of project area about 19 x 12.5 km^2 (Figure 1).

Stratigraphy

Geomorphology of the project area is a gently sloping alluvial cover, between Mineral Mountains to Milford valley (Simmons et al., 2018). The site lies inside the southeast margin of the Great Basin in a broad zone that is characterized by elevated heat flow. The regional stratigraphy consists of folded and imbricated Paleozoic-Mesozoic carbonates and clastic. These have been overprinted by eruption of Tertiary-Recent ages with mafic-felsic magmatic rocks. The local lithology is divided into two defined units, they are: comprising crystalline basement rocks and the overlying basin fill sedimentary deposits.

The basement rocks are dominated by Miocene age granitic rocks which make up the core of the Mineral Mountains. The basin fill consists of a layered sequence of poorly consolidated sedimentary deposits that is more than 3000 m thick in the deepest part of the basin. The deepest part of the basin fills with depth around 1200 m to the contact with the basement, consist of volcaniclastic sandstones and gravels, lacustrine sediments, tuffaceous deposits, and localized flows of andesitic lavas. At shallower depths, the strata consist of calcareous lacustrine deposits made of siltstone and sandstone dominate. The geological map and cross section of the site based on the integration study show the boundary between both units (Figure 2).

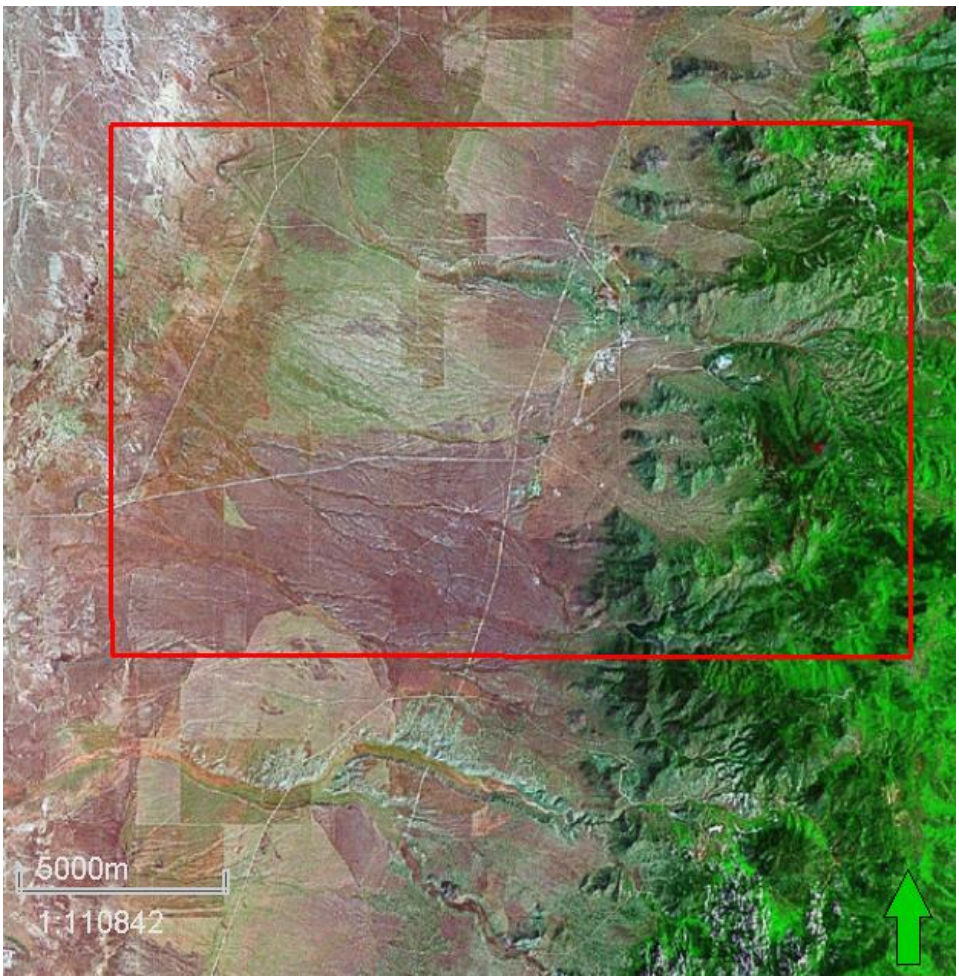


Figure 1: Project boundary (square box) of study area.

Structural Geology

The geological structures in this site is comparatively simple. Four faults and fault systems have been identified, based on field observations, seismic reflection, and correlation of drill logs. Those faults are attributed to basin and range extension, which have dominated the region since the Eocene (Simmons, et al., 2018). The Opal Mound and Negro Mag faults are relatively short length structures that intersect at an orthogonal angle to form the boundaries of the Roosevelt Hot Springs reservoir. The Mineral Mountains West fault system comprises a series of parallel north-south trending, normal fault segments with small offsets. The traces of these three faults are exposed at the surface. The fourth fault is unnamed, but it is the most significant fault in the site. This fault marks the contact between overlying basin fill and the underlying crystalline basement rock, forming an inclined ramp that dips ~20-35° west apparently accommodated a large amount displacement in the relatively distant past (mid-Miocene), but it is now inactive having rotated to a low-angle during uplift and exhumation of the Mineral Mountains more than six million years ago (Coleman et al., 2001). Figure 3 shows several faults that will be modeled in this project.

Geothermal System

Understanding of the heat flow and temperature gradients for this site is based on analysis of temperature profiles from approximately 100 wells drilled with 200 to 4000 m depth. A geometrically simple thermal structure has been defined and shown by Figure 4, that reflecting high conductive heat flow (50-70°C/km) in the basement rocks around and through the reservoir. This area is surrounded by more than 100 km3 granitoid rock with temperature more than 175°C. In this system, the structural geology which is the opal mound fault forms the eastern boundary for this large conductive thermal regime (Simmons, et al., 2018).

Geohydrological condition in this site shows shallow unconsolidated basin fill forms the primary aquifer, ranging in thickness from 100 to more than 500 ft. New groundwater well test data confirm transmissivities that range from 240 to 1600 ft2/day, which is ample groundwater supply for future geothermal activities. The groundwater resources for the site are confined to basin fill sediments that overlie the granitoid basement rocks. Beneath the deep drill site, the groundwater elevation is approximately 5100 ft and the depth to water is between 200 and 500 ft, consistent with new transient electromagnetic (TEM) data. Within the vicinity of the site, the groundwaters contain a significant proportion of Roosevelt Hot Springs waters, which makes them non-potable, chemically benign, and highly suitable for Enhance Geothermal System (EGS) heat transfer experiments (Simmons et al., 2018).

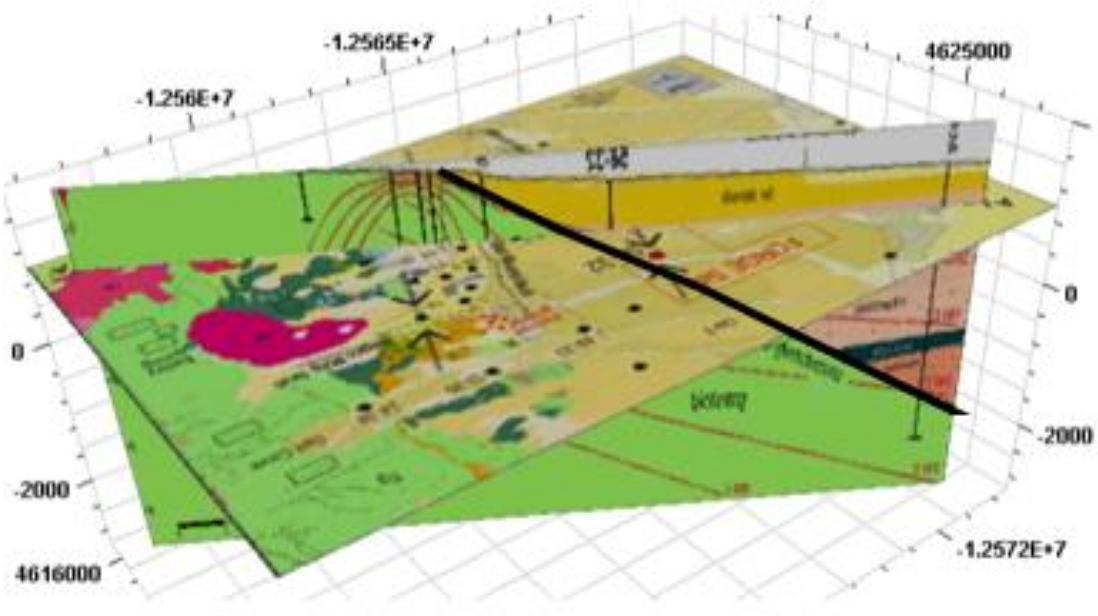


Figure 2: Geologic map (upper) and cross section (lower) of the site. The bold curve line is the boundary of basement and sedimentary fills.

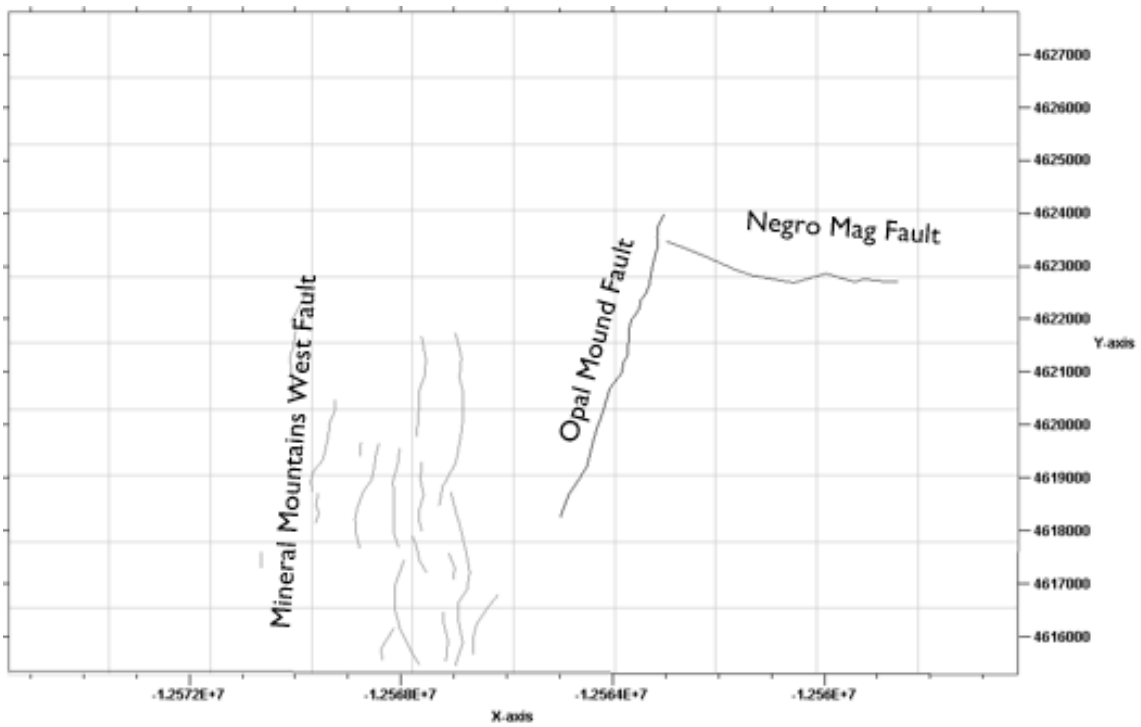


Figure 3: Location of several faults used in project.

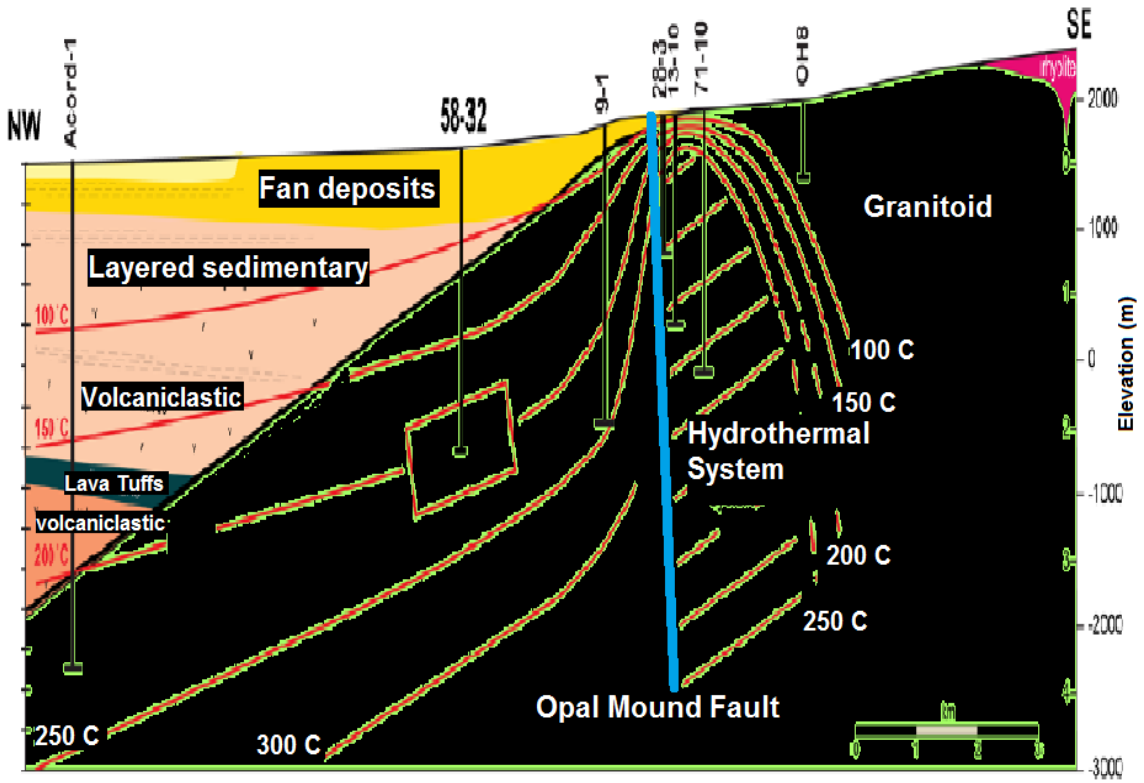


Figure 4: Thermal structure in the basement rocks (granitoid) with Opal Mound faults as eastern boundary of thermal regime (Modified from Simmons et al., 2018).

DATA AND METHODOLOGY

Source of data being used in this project is published website from US department (i.e. www.gdr.openei.org). There are several kinds of data that has been collected and then loaded into integrated modeling software Petrel®. Below is detail explanation about available data and the workaround to utilize them.

Available Data

All collected data can be classified into two categories: surfaces data and well data. Surfaces data is all information acquired above the earth surfaces, such as geological surface mapping, gravity survey, chemical sampling for temperature information and remote sensing. Well data acquired from deep drilling beneath earth surface, that can provide information about lithology, confirm the faults location and measured temperatures.

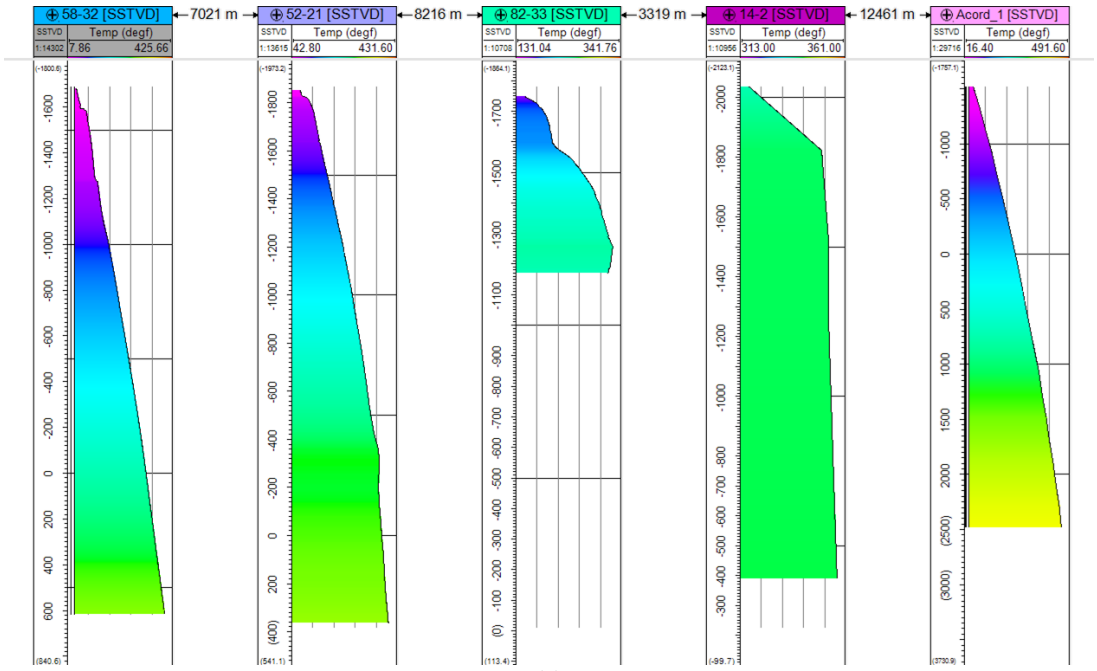
To create structural and lithological model, data that needed are: geological map, lithological intersection, topography elevation, basement depth from gravity data, and lineament polygon that represents fault location. To build temperature model, there are two main data obtained from well drilling: temperature logs and temperature contours at certain levels (Figure 5). Both temperature data will be combined as upscaled data to get understanding of temperature values in three-dimensional model.

Workflow

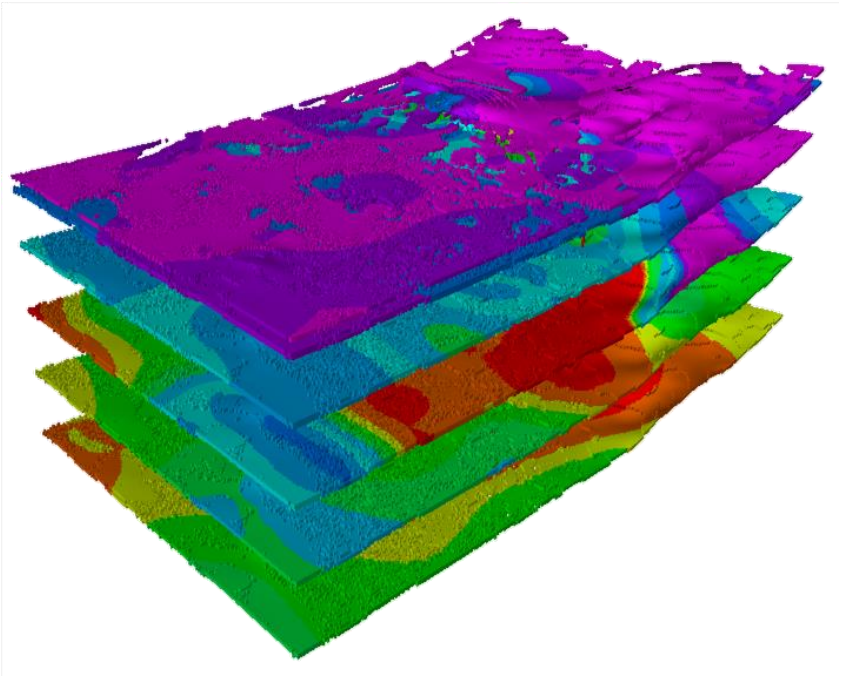
The workaround that has been done to finish the project starting with create 3D model of structural, lithology and temperature model. Based on those models, the well targets and plan were designed. Workaround for the 3D modeling of this geothermal field was adapted from study conducted in Aydin, Turkey, which used Petrel® as the modeling software (Akar, S. et al., 2011). With four main steps including: data input, structural modeling, property modeling (lithology and temperature) and quality check for the results (Licup et al, 2017).

Data preparation

All data were loaded inside software based on their format and confirmed that they had correct location. Quality checking was done by comparing all data position and their value to avoid anomaly data. For some points data such as topography elevation points were interpolated into topography surface. Lithological contact was digitized from geological section and changed into lithological surface. Figure 6 showing surface of basement depth in the bottom, lithological surface of lithological section in the middle, and topography map in the top as main input to build lithological model.



(a)



(b)

Figure 5: Available temperature data that used to create temperature model: (a) well temperature logs and (b) temperature contours.

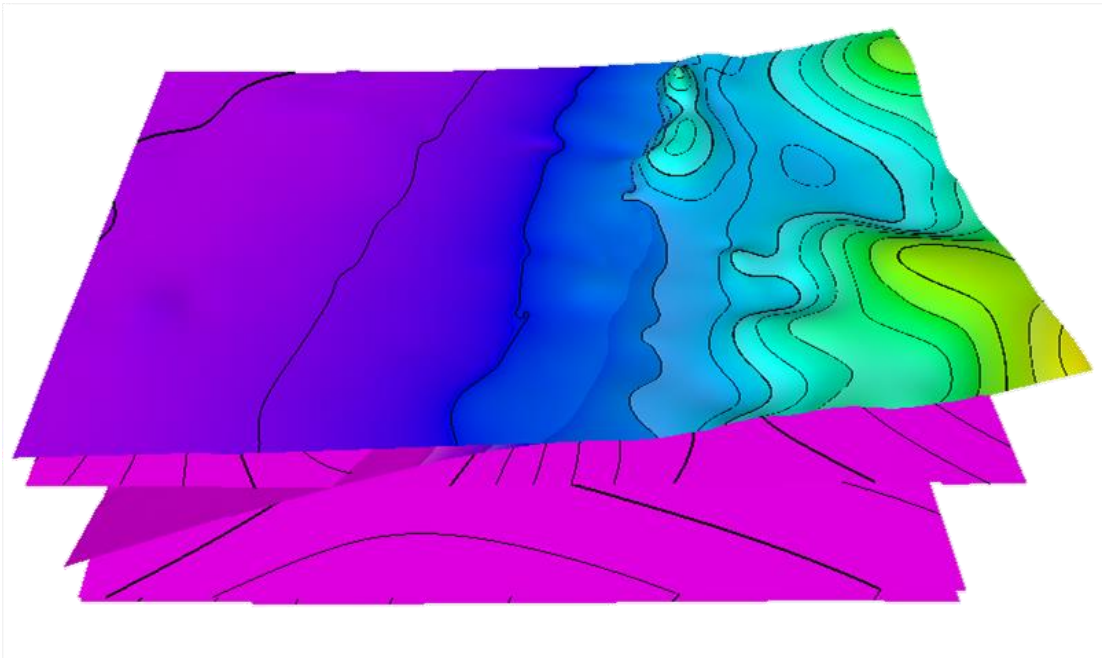


Figure 6: Lithological surfaces data that used to create lithological (facies) model. They are: basement, sedimentary fills, and topography.

Model building

To create structural model, the main inputs are topography surface, basement surface and fault lineaments. Polygon boundary for the model was obtained from the outline of topography surface. Process that being used to utilize those data is structural framework and simple gridding. Results of this process are fault planes in the project field.

Lithological model was created by using lithological surfaces from lithology intersection and the existing structural model. The process called geometrical modeling with assign value between surfaces as method. The result is lithological model with facies zone in three-dimensional view.

The workaround in this study which difference from the previous one is temperature model building. Input data for this model is combination between temperature log and temperature contour points.

Data combination was done by using scale up process data, and the algorithm to distribute those values into 3D model are kriging. This algorithm was chosen because there are many temperature points data that available from data combination process. Moreover, there is no additional input data or trend that used during interpolation data.

Well plan digitizing

Well targeting decided based on the location of high temperature zone and position of the faults plane which representing high permeability area. In this study, well head position has been decided by using existing one of exploration well near the fault location. Then, well path was designed nearly perpendicular to the faults plane.

There are three targets created along fault plane in vertical line order. Three points were selected to see the comparison between well paths that designed based on those targets. By using well plan designer function, starting point was selected as well head then being hold to certain depth (TVD). From that point, curve well path was chosen to point target and finalize by extending the well path to certain depth (MD) value. Three-dimensional view of well path and well report are the results of well design process.

MODEL RESULTS

There are three models that will be discussed in this project, they are structural, lithology and temperature models. For the main result is well plan and well report based on existing those models. Each result was analyzed at the same 3D grid structural model as follows.

Structural Model

Faults plane were created based on faults lineament in the topography surface (Figure 7). There are two faults (Opal Mound & Negro Mag) and one system fault (Mineral Mountains West Fault) that has several associated faults plane. All planes created with relatively vertical position due to interpretation of their dip from lithological section data. Opal Mound Fault has single plane with strike direction relatively North-South. This fault identified as permeability zone where the targets will be placed. Negro Mag fault has single plane in East-West direction and relatively perpendicular with Opal Mound fault. As group of faults, Mineral Mountain West faults plane are shorter with similar strike direction North-South. This whole structural model consists of three main surfaces: topography, basement rock, and bottom plane (Figure 8).

Lithology Model

Lithology model was built based on contact boundary of each units that given by geological section data. Using the structural model as skeleton, lithological information was distributed with certain constrain limit. In this model, the biggest portion of lithology model, at bottom part is constructed by granitoid as basement rock. Contact of granitoid with other sediment fills interpreted from gravity survey data. Basin formed by this igneous rock then filled by volcaniclastic rocks, from oldest to the youngest are: old volcaniclastic, lava tuffs, young volcaniclastic and fan deposits. This model shows that the granitoid is exposed in the earth surface with higher elevation than volcaniclastic rocks (Figure 9).

Temperature Model

Result for temperature model is distribution of temperature values inside the existing structural model. There are many point temperature data from temperature contour data at level: 200m, 1000m, 2000m, 3000m and 4000m below earth surface. This data combined by more accurate data from well drilling from 5 wells, resulting final temperature model. Ranges values of temperature is surface temperature to 300ºC as shown in Figure 10.

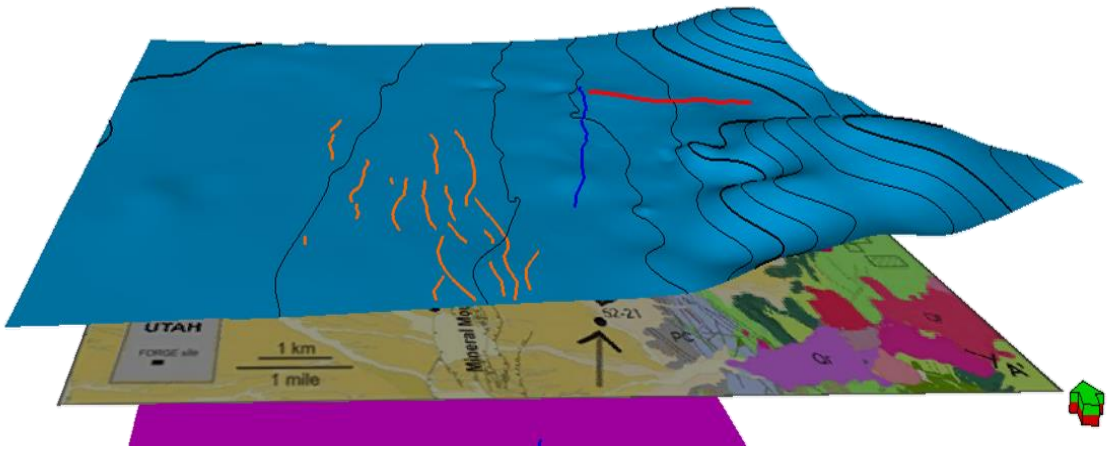


Figure 7: Fault lineament in topography surfaces which digitized based on geological map.

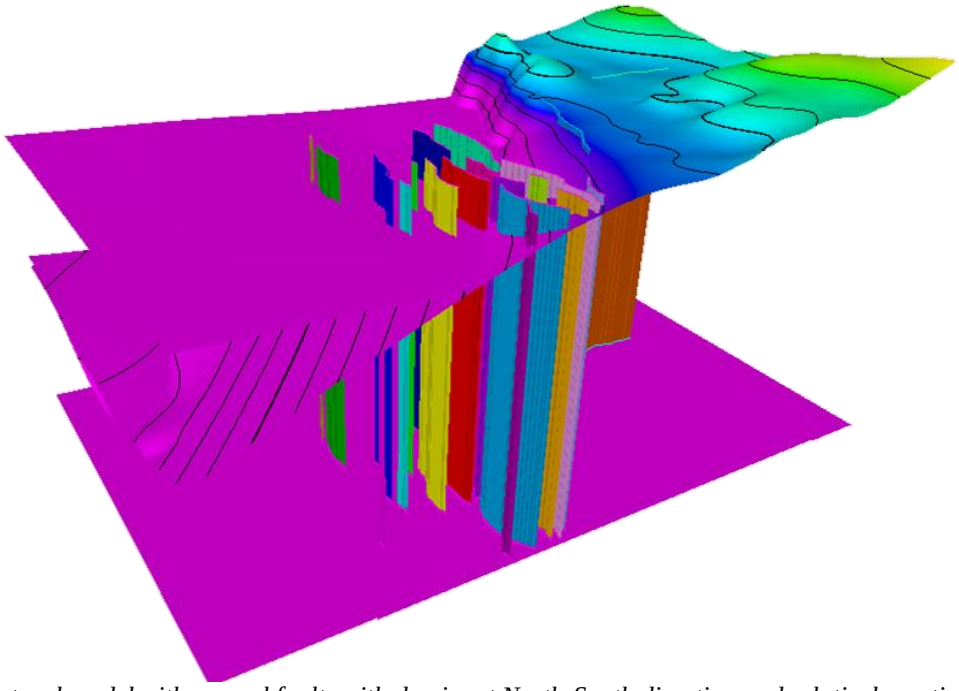


Figure 8: Structural model with several faults with dominant North-South direction and relatively vertical plane.

To understand more about temperature model, the whole cube can be filtered at certain values. For the example, to get highest temperature zone in the site then the temperature model was filtered to show high temperature bodies (Figure 11). This zone will be used as one of parameter to limit the area that chosen as well-target.

Well Target and Plan

Based on all models created in this study, zone of interested was delineated. The first parameter that used to decide location of well target is temperature model. Bottom limit of temperature that selected is 250ºC. By filtering the temperature model at that number, high temperature body was obtained. Then, the second parameter used as reference to put well targets is fault position that represent high permeability zone. Opal mound fault was selected as the well targets due to its position as boundary of high temperatures regime in that area. It was assumed that this fault has good permeability and was not sealing. Well head then being selected from existing well, which is well plan B. To get low inclination for the well path, well targets put at the fault plane with perpendicular position towards well head. It can be achieved by drawing a vertical intersection through the well head and perpendicular with the fault plane (Figure 12).

The other parameter that used for well targets are lithological model. Based on temperature model that has been selected, the zone of interest located in granitoid (basement rock). Figure 13 shows the lithology model that has been filtered based on high temperature values.

Well targets put along fault plane at vertical intersection created in Figure 12. There are three targets put in the zone of interest. Lithological surfaces (fan deposits & old volcaniclastic) placed above and bottom as guidance for well path design. Figure 14 shows the temperature model that has been filtered with higher temperature values (>250ºC) so the well targets can be placed easier.

After well targets have been identified, a new well path design was created. By using three available well targets, there are three well path that can be generated from the same well head, they are: plan B0, B1 and B2. Some numbers that need to be identified for each well path are starting point, first measuring depth (MD) to start the curve path, target position, and final MD as the end of well. Starting point for all well path are same point, with coordinate position x, y and z are: -12563322, 4618310.3 and 1825 m. The first measuring depth where the path starts becoming curve for plan B0 and B1 is 600m, while plan B2 is 50 m because the well target was shallower. The position of well head toward each well target that have been created will define the value of inclination, azimuth and dogleg severity. The inclination values for well plan B0, B1 and B2 are: 73º, 87º and 94º. All of well plan have the same azimuth value, which is 291º (North-East). The values of dogleg severity for plan B0, B1 and B2 are: 1.02º, 1.38º and 1.56º. Figure 15 shows the well path design for all well plans.

Detail of well reports for all well plan can be seen in *Appendix A.* The well report provided as table list with information about coordinate position for important point from the well path with value of inclination, azimuth and dogleg severity.

DISCUSSION

By comparing all well path design, one well path was selected as the main well plan. There are several parameters to choose the best well plan in this study: length of horizontal well path, shallower true vertical depth or measuring depth and small dogleg severity. More horizontal well path, more fractures can be hit to get more permeable zones from structural discontinuities. Shallower well path can reduce the drilling cost. Smaller dogleg severity will make the drilling program getting easier than big value of dogleg severity. Based on those parameters, well plan B2 was chosen. This well plan has more horizontal path and shallower target. Compared with the others well plan, it has bigger value of dogleg severity. However, the value is still acceptable since the value is still less than 3°.

To get more accurate well target position, better understanding about conceptual model can be very significant. Each study case can have different parameters to select the best well plan. The combination of more parameters that have correlation with good production (i.e. temperatures, water composition and permeability) should give better idea for the well targeting. Since there is no single workaround that can be applied for all cases, this study can be one of reference to be used for well planning in geothermal field.

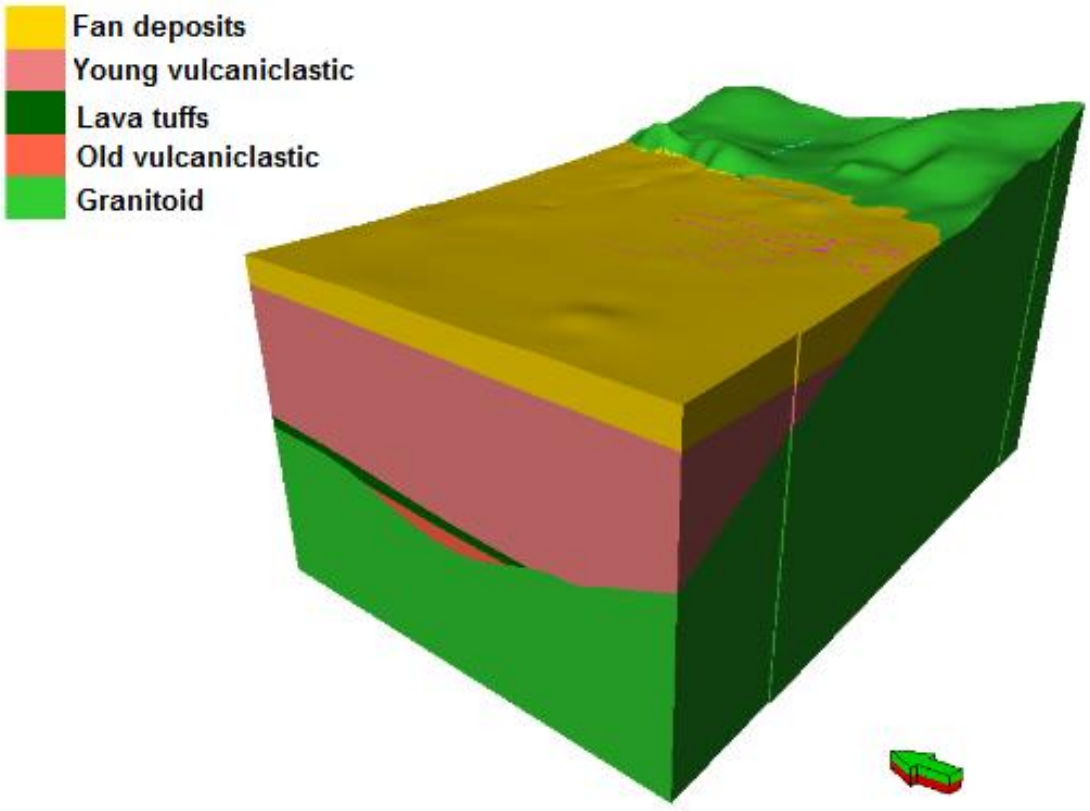


Figure 9: Lithology model consist of two main facies: granitoid as basement rock and sedimentary fills from volcaniclastic rocks.

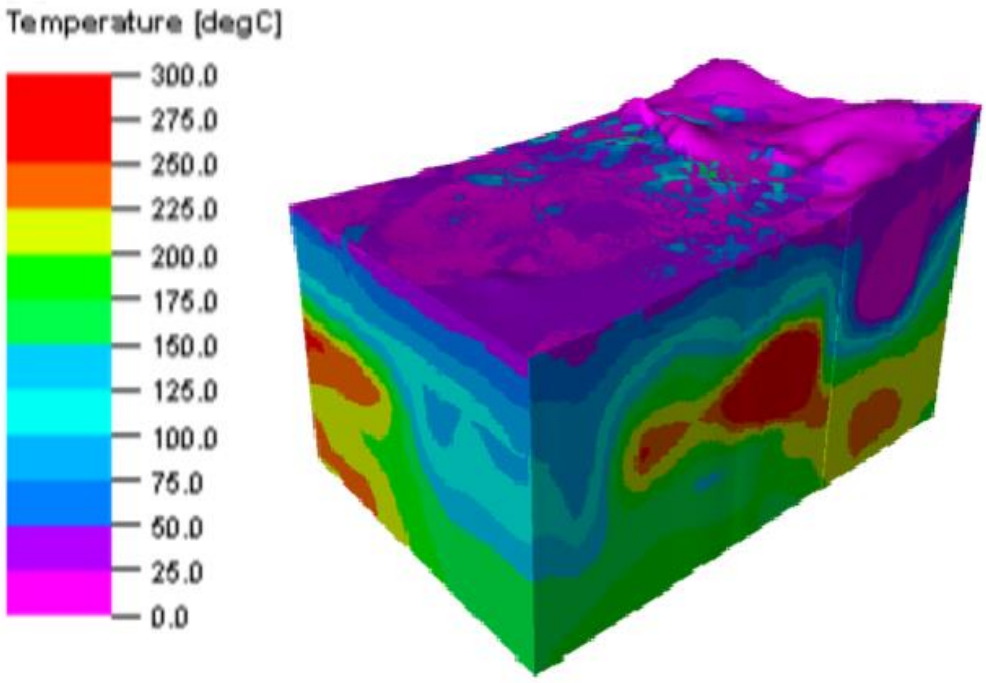


Figure 10: Temperature model created by using temperature contour points data and temperature well data by using kriging algorithm and resulting temperature values that reach 300º C.

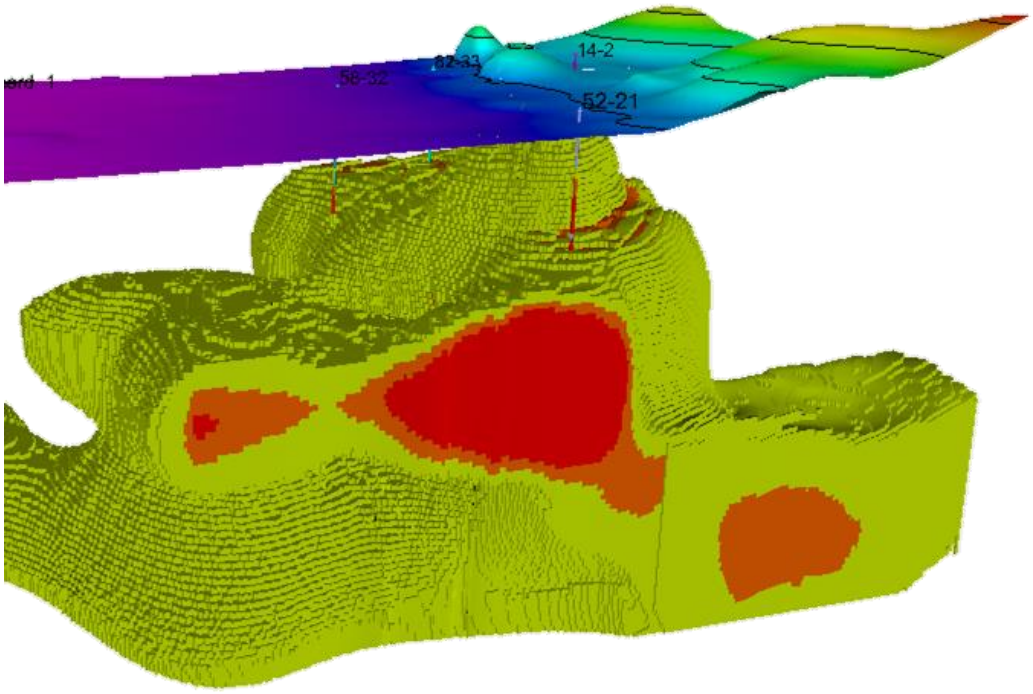


Figure 11: Temperature model that has been filtered to see high temperature bodies in the field, three-dimensionally.

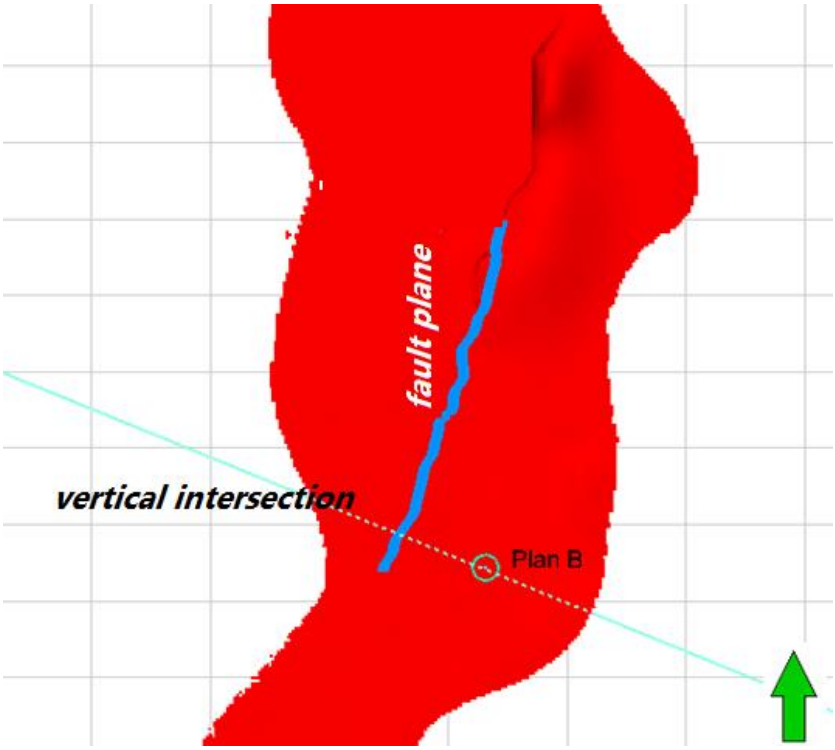


Figure 12: Vertical intersection that perpendicular to fault plane and pass the well head. Selected area is highest temperature zone to place well targets.

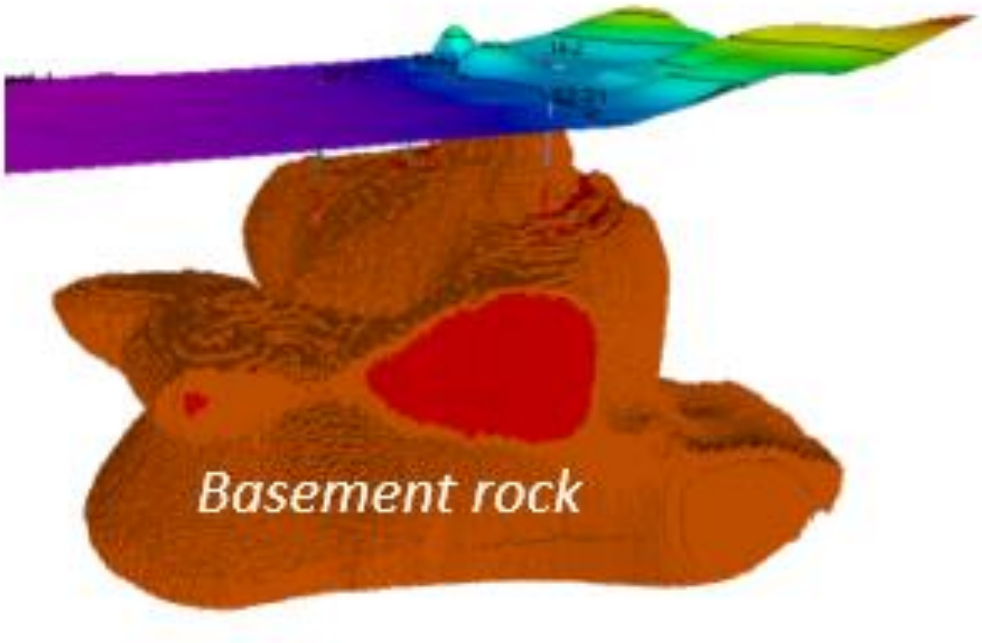


Figure 13: Lithology model that has been filtered based on high temperature model to see zone of interest.

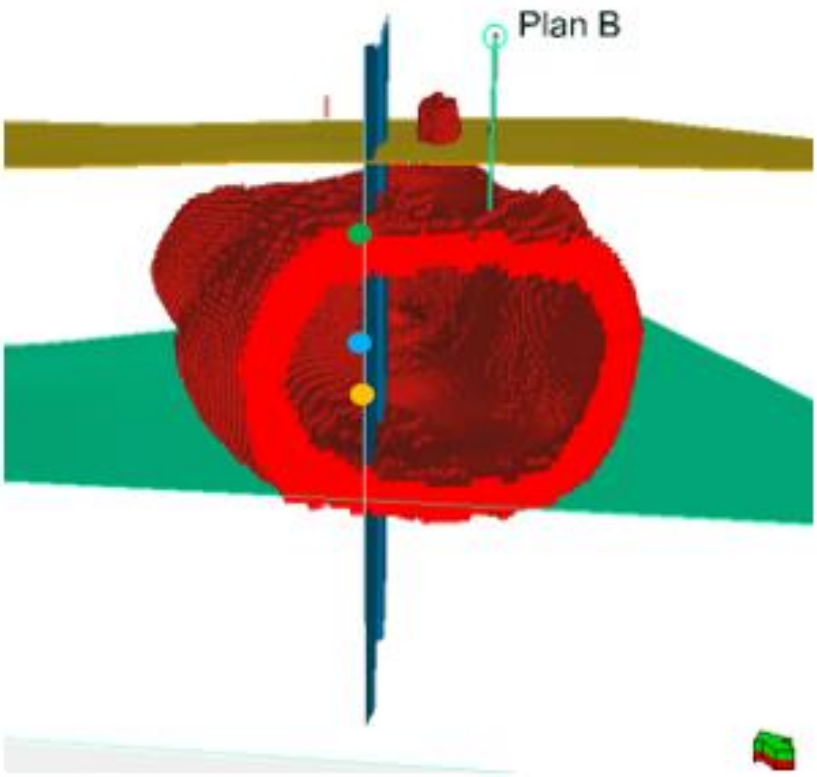


Figure 14: Vertical intersection from side view to see zone of interest when selecting well targets place.

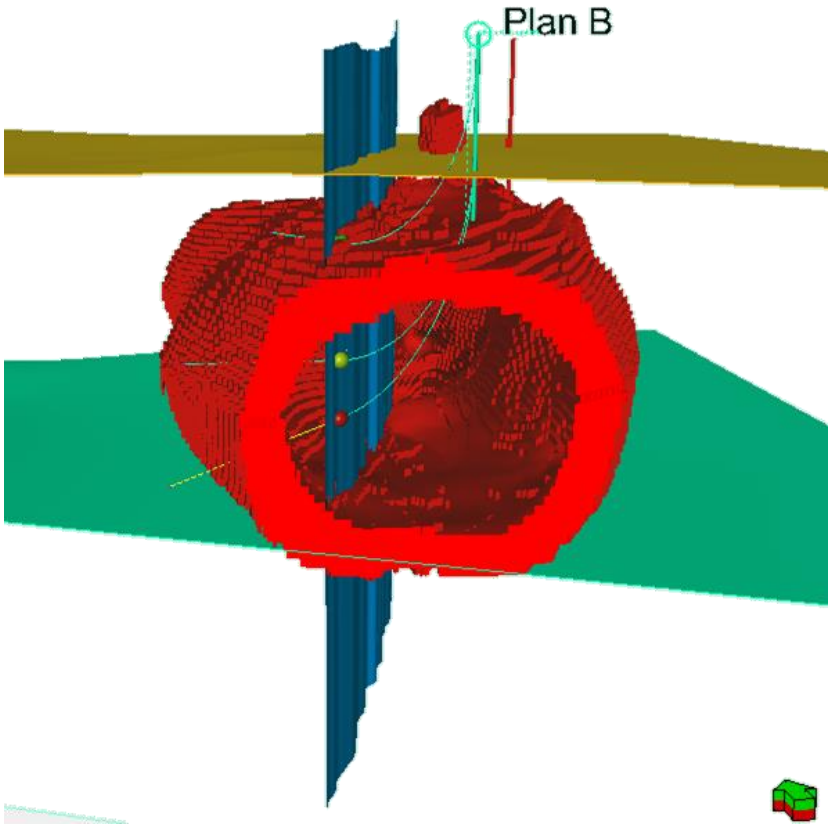


Figure 15: Well design of plan B2 (above), plan B1 (middle) and plan B0 (bottom).

CONCLUSIONS

Well targeting and well path planning can be done by using single software where the conceptual model (structural, lithology and temperature model) have been built. Three-dimensional view of well plan based on 3D subsurface model provides better understanding for designing the well path accurately. Moreover, the values of parameters listed at well report can be used to select the best well plan based on drilling regime and cost assumption. Finally, better well plan design in geothermal field can maximize the production and minimize the risk or the cost of well drilling.

ACKNOWLEDGEMENTS

The authors would like to thank you for the managements of Schlumberger who allowing us to use the software and the machine in the preparation of this manuscript.

REFERENCES

Akar, S., Atalay, O., Kuyumcul, C., Solarog'lul, U.Z.D., Colpan, B., Arzuman, S., (2011). "3D Subsurface Modeling of Gümüs¸köy Geothermal Area, Aydın, Turkey". GRC Transactions, Vol. 35.

Axelsson, G & Franzon, H., (2012). "Geothermal Drilling Targets and Well Siting". Short Course on Geothermal Drilling, Resource Development and Power Plants", organized by UNU-GTP and LaGeo, in Santa Tecla, El Salvador, March 11-17, 2012

Coleman, D.S., Walker, J.D. Bartley, J. M., and Hodges, K.V. "Thermochronologic evidence of footwall deformation during extensional core complex development, Mineral Mountains, Utah". The Geologic Transition, High Plateaus to Great Basin-A symposium and field guide, AAPG Pacific Section Guidebook,78 (2001), 155-168.

Cumming, W., (2009). "Geothermal resource conceptual models using surface exploration data". Thirty-Fourth Workshop on Geothermal Reservoir Engineering Stanford University, 2009, SGP-TR-187.

Licup, A.C. Jr., Sarmiento, Z.F., Omac, X.L., Maneja, F.C., Chandra, V.R., M.B. Esberto, M.J.Z., Villareal, Balthasar, A.S.J., Mulyani, S., Sari, P.S., Jhonny,P.P., Juandi, D., (2017). "Geothermal 3D Subsurface Modeling – A Case Study from Sorik Marapi Field, Indonesia". PROCEEDINGS, The 5th Indonesia International Geothermal Convention & Exhibition 2017.

Santos, P., (2011). "Geothermal Well Target Approaches in the Exploration Stage". Short Course on Geothermal Drilling, Resource Development and Power Plants", organized by UNU-GTP and LaGeo, in Santa Tecla, El Salvador, January 16-22, 2011.

Simmons, S., Moore, J., Allis, R., Kirby, S., Jones, C., Bartley, J., Kleber, E., Knudsen, T., Miller, J., Hardwick, C., Rahilly, K., Gwynn, M., McLennan, J., Forbes, B., Podgorney, R., Pankow, K., Wannamaker, P., and Fischer, T. (2018). "A Revised Geoscientific Model for FORGE Utah EGS Laboratory". Proceedings, 43rd Workshop on Geothermal Reservoir Engineering Stanford University, Stanford, California, February 12-14, 2018.

APPENDIX A

Section	Station	MD (m)	TVD (m)	INCL (deg)	AZIM (deg)	EW (m)	NS (m)	DLS (deg/30m)	DeltaMD (m)	DeltaTVD (m)	X (m)	Y (m)	Z (m)
StartPoint	StartPoint	0.00	0.00	0.00	291.13	0.00	0.00				-12563322	4618310.3	1825.(
HoldToTV	HoldToTVD	50.00	50.00	0.00	291.13	0.00	0.00	0.00	50.00	50.00	-12563322	4618310.3	1775.(
Target	Target	1863.03	1152.31	94.01	291.13	-1102.78	426.17	1.56	1813.03	1102.31	-12564729	4618853.8	672.
HoldToMD	HoldToMD	2500.00	1107.80	94.01	291.13	-1695.54	655.17	0.00	636.97	-44.51	-12565485	4619145.9	717.

MD, INCL, AZIM | MD, INCL, DLS | TVD, INCL, AZIM | INCL, AZIM, DLS | Hold or Curve to Target | Target | TVD, INCL, DLS | MD, AZIM,

Input target: Targets B2 | Link to target | X: -12564729.27 | Y: 4618853.88 | Z: 6

Section	Station	MD (m)	TVD (m)	INCL (deg)	AZIM (deg)	EW (m)	NS (m)	DLS (deg/30m)	DeltaMD (m)	DeltaTVD (m)	X (m)	Y (m)	Z (m)
StartPoint	StartPoint	0.00	0.00	0.00	291.13	0.00	0.00				-12563322	4618310.3	1825.00
HoldToTV	HoldToTVD	600.00	600.00	0.00	291.13	0.00	0.00	0.00	600.00	600.00	-12563322	4618310.3	1225.00
Target	Target	2494.59	1845.63	87.03	291.13	-1103.18	426.33	1.38	1894.59	1245.63	-12564729	4618854.1	-20.6
HoldToMD	HoldToMD	4000.00	1923.64	87.03	291.13	-2505.70	968.10	0.00	1505.41	78.01	-12566518	4619545.0	-98.64

MD, INCL, AZIM | MD, INCL, DLS | TVD, INCL, AZIM | INCL, AZIM, DLS | Hold or Curve to Target | Target | TVD, INCL, DLS | MD, AZIM, DL

Input target: Targets B1 | Link to target | X: -12564729.78 | Y: 4618854.1 | Z: -20.

Section	Station	MD (m)	TVD (m)	INCL (deg)	AZIM (deg)	EW (m)	NS (m)	DLS (deg/30m)	DeltaMD (m)	DeltaTVD (m)	X (m)	Y (m)	Z (m)
StartPoint	StartPoint	0.00	0.00	0.00	291.14	0.00	0.00				-12563322	4618310.3	1825.0
HoldToTV	HoldToTVD	600.00	600.00	0.00	291.14	0.00	0.00	0.00	600.00	600.00	-12563322	4618310.3	1225.0
Target	Target	2739.43	2204.60	73.09	291.14	-1109.32	428.85	1.02	2139.43	1604.60	-12564737	4618857.3	-379.(
HoldToMD	HoldToMD	4500.00	2716.68	73.09	291.14	-2680.70	1036.01	0.00	1760.57	512.08	-12566741	4619631.7	-891.(

MD, INCL, AZIM | MD, INCL, DLS | TVD, INCL, AZIM | INCL, AZIM, DLS | Hold or Curve to Target | Target | TVD, INCL, DLS | MD, AZIM, D

Input target: Targets B0 | Link to target | X: -12564737.62 | Y: 4618857.3 | Z: -37

Appendix A. Well report of plan B2 (above), plan B1 (middle) and plan B0 (bottom). Each well path correlates with its well target with specific number of inclinations, azimuth and dogleg severity.

3D GEOLOGICAL MODELLING WORKFLOW USING LEAPFROG GEOTHERMAL: PRELIMINARY STAGE

Claudio R.I. Ponggohong, Suryantini, and Angga B. Pratama

Geothermal Master Program Institut Teknologi Bandung
Energy Building, Ganeca Street 10, Bandung, Indonesia
Email: criponggohong@gmail.com

ABSTRACT

Modelling in geothermal is very important to determine the surface and subsurface of the geothermal field. The modelling software is needed to process and integrate geoscience data to simplify modelling. Visualization of the 3D Geological model in this study was made using Leapfrog Geothermal. The data used is data from the literature that has been previously published. This study uses geological map data, geological cross-section and downhole temperature from published papers. Based on the data available, the workflow used in building this 3D geological model included delineating each lithological contact boundary on the geological map which were then constrained using a geological cross section and polylines. Leapfrog uses the Radial Base Function (RBF) interpolation to create 3D models. 3D modelling can reduce uncertainty in drawing subsurface conditions, especially the geometry of the Geothermal system components.

Keywords: 3D Modelling, Geological Modeling, Geothermal System, Leapfrog Geothermal.

INTRODUCTION

The key to the success of exploration is there is a clear perspective on the description of surface and subsurface conditions and understanding the characteristics of Geothermal systems in the area.
The first step to build 3D geothermal system is create a geological model.

The conceptual model of Geothermal systems is used to describe and illustrate the geological conditions and delineation of important processes that occur in a geothermal field. There is never one answer and conceptual models are used to explore different thoughts or options. The process is an iterative process to create a model, evaluate and update if required. Basically, a conceptual model is dynamic and is based on geoscientists and engineer's interpretation and the data to hand. The construction of a conceptual model must be updated as information increases.

The modelling software is needed to process and integrate geoscience data to simplify modelling. Leapfrog Geothermal software has been developed to model and visualize geothermal systems in 3D.

The technology was originally developed for the mining industry (Cowan & Beatson, 2002) but recently the technology has been adapted for the geothermal industry (Milicich et al., 2010).

There are two basic forms of models. Firstly, there are discrete models which describe quantities that occur in discontinuous units such as geology and alteration. Secondly there are continuous models that describe numeric quantities such as temperature, pressure, contaminant levels etc. (Newson et al., 2012). This paper discusses the workflow to build discrete 3D geological model using Leapfrog Geothermal software.

METHOD

Leapfrog Geothermal uses fast 3D interpolation to derive a continuous function from the data which is evaluated at any point in the model (Alcaraz et al., 2015). The model is created by combining geological maps and cross sections that are digitized using polyline. The 3D conceptual model built on this paper uses data from a published paper by Prasetyo et al., 2015.

This 3D model was built with the following workflow: Preparing Data, Topography, Geological Map, Cross Section, 3D Geological Model.

RESULT AND DISCUSSION

Preparing Data

All the data used in this paper are public data derived from literature review. The study area located in North Sulawesi Province. Figure 1 shows the workflow to build 3D geological model. To build 3D geological model, need to prepare data that shows in Table 1.

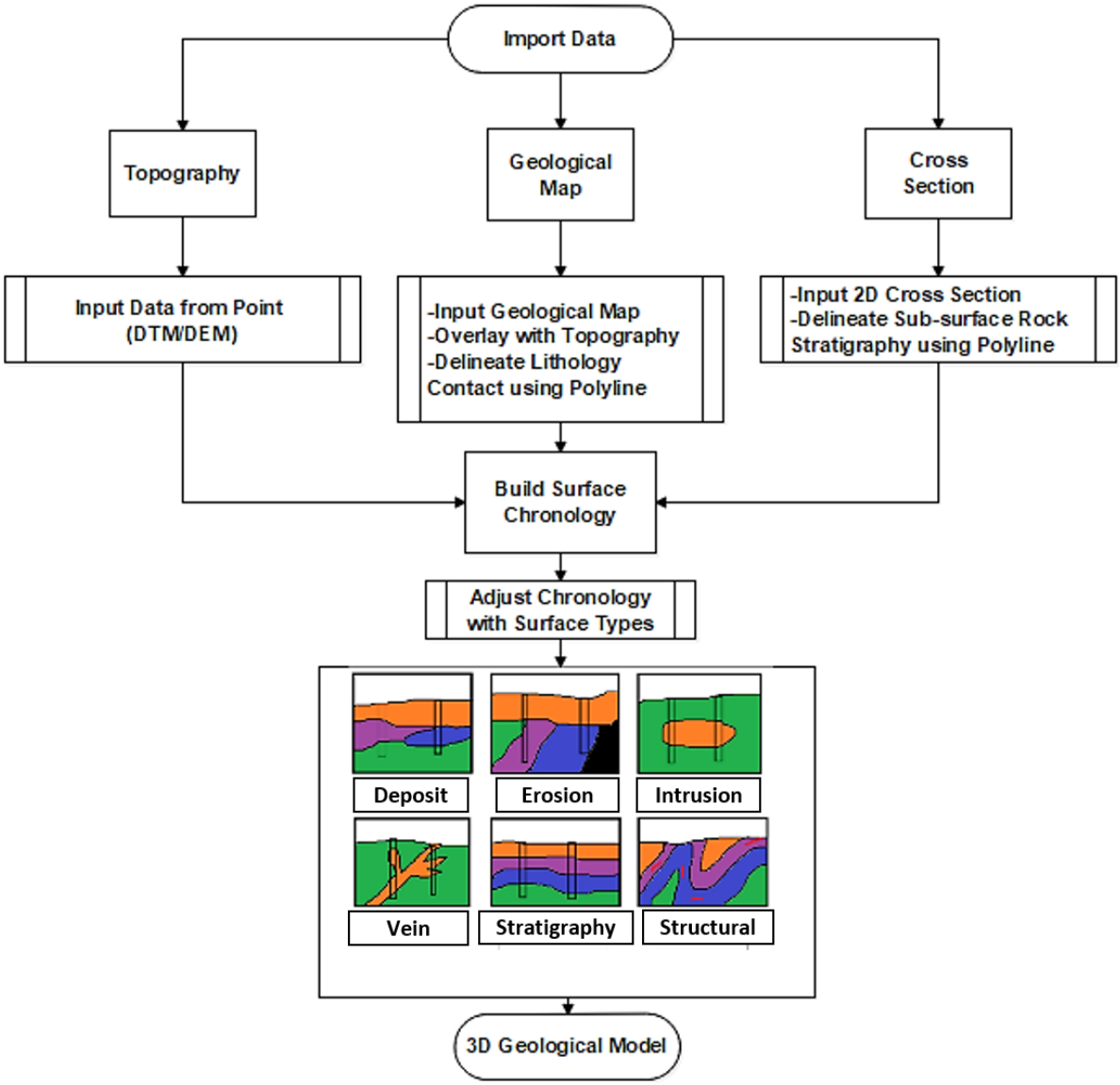


Figure 1: Workflow to Build 3D Geological Model.

Table 1: Type of Data to Build 3D Geological Model.

Type of Data	Purpose	Source
DTM/DEM	To Build Topography in 3D	Derived from Public Satellite Data
Geological Map	Delineate Each Lithology Contact on The Surface	Derived from the Literature Review
Traditional 2D Cross Section	Delineate Sub-surface Rock Stratigraphy	Derived from the Literature Review

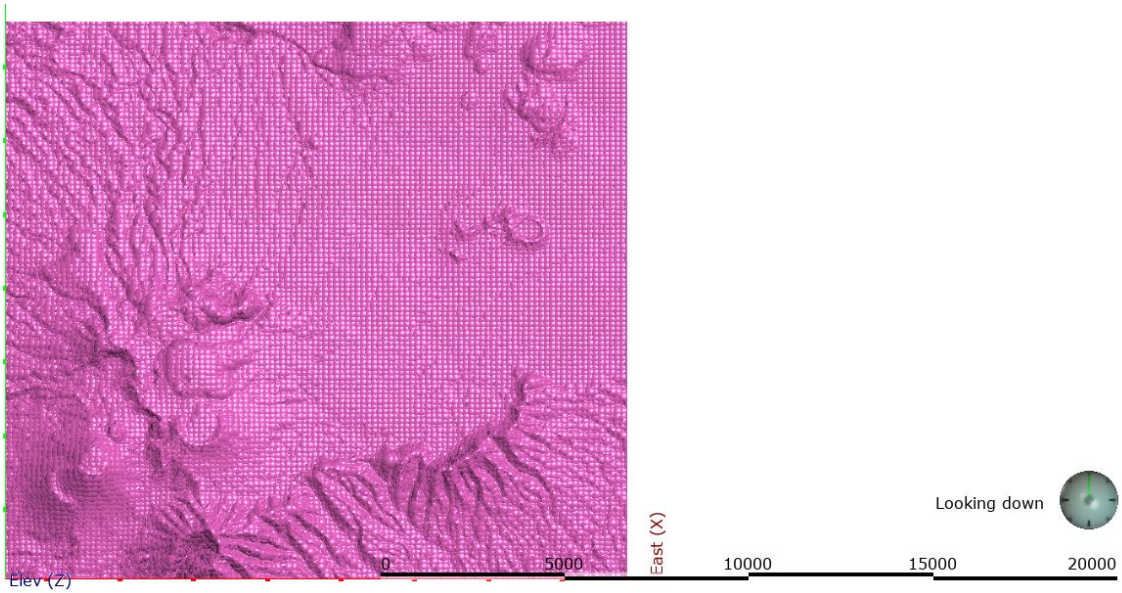


Figure 2: Topography Point from DEM.

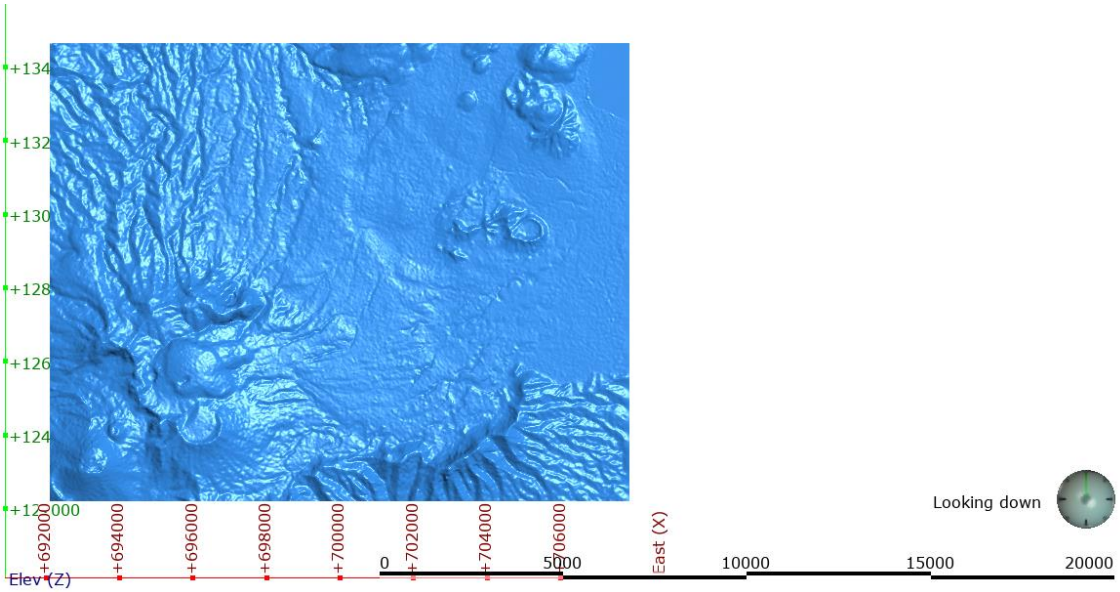


Figure 3: Final Topography Point Model.

Topography

The first step to create the topography is importing the topography point from DTM/DEM data. The result of importing topography data shows in Figure 2. Next step is creating the topography from point (shows in Figure 3). The Topography surface in Leapfrog is unique relative to other surfaces in Leapfrog in 2 ways (Leapfrog Geothermal Fundamentals):

- The Topography surface will automatically act as the upper boundary of 3D model
- All GIS data in the model is automatically draped onto the Topography surface providing it with reliable elevation data

Geological Map

Figure 4 is a geological map that was made by Ganda and Sunaryo (as cited in Prasetyo, 2015) and further detailed study of the structure was added by Siahaan (as cited in Prasetyo, 2015). The geological studies divided the lithology into 7 different formations (Prasetyo 2015):

- Tondano Formation (Tt): Interlayers of pyroclastic breccias, andesite lava, and tuff. These rocks carved the morphology on the south eastern part of the field. This lithology is the oldest unit in the field.
- Tondano Tuff (Tf): This unit comprise mainly tuff and pumice formed during the formation of the Tondano caldera. It can be compared to ignimbrite that formed during the erratic explosion of Tondano volcano.

- Lengkoan Lava (Qlk): Lengkoan mountain range is located on the northern side and consist mainly of andesite lava.
- Rindengan 1 (Qrd1): A series of interbedded layers of pyroclastic breccia, lapilli, tuff. This unit forms the flat morphology and covers the most part of the prospect area.
- Rindengan 2 (Qrd2): Interlayers of andesite lava and breccia; volcanic bomb and lapilli from proximals to the Rindengan mountain.
- Sempu (Qsp): Interbedded layers of pyroclastic breccias and andesite lava from Sempu volcanic centre located in the south part of the map.
- Tondano Lake deposit (Qal): Alluvium and lake deposit that consists of fine grain sandstone with thin layer of tuff. These sediments occur in the vicinity of Lake Tondano on the eastern side of the map.

The surface of model is digitized from the geological map using polyline tools, the results shown in Figure 5.

Cross Section

The Sub-surface model is digitized from 2D cross section (Figure 6) using polyline tools, the results shown in Figure 7. There is a well trajectory in Figure 6, but because it does not have enough data, the well trajectory is not shown on the model.

3D Geological Model

The 3D geological model is created by combining geological map and cross sections that are digitized using polyline (Figure 5 and 7). Lithology arrangement from the oldest to the youngest are shown in Figure 8. Figure 8A shows the volume of the Pre-Tondano (Tb), Figure 8B shows the volume of the Tondano Tuff (Tt), Figure 8C shows the volume of the Lengkoan (Qlk), Figure 8D-8F shows the volume of the Rindengan 1-3 (Qrd1-3), Figure 8G and 8H shows the volume of the Sempu 1 and 2 (Qsp1&2), Figure 8I shows the volume of the Soputan (Qst), Final 3D geological model shown in Figure 7J.

CONCLUSION

This 3D geological model is built on an academic perspective that relates to published data. The model created is a model in the early stages of exploration. The details and confidence in the model depend on the quality of the data. A comprehensive model will improve operator confidence and support drilling strategies in Geothermal field.

ACKNOWLEDGEMENT

We would like to thank SEEQUENT for providing 3D Geological Modelling software Leapfrog Geothermal license which enable this research.

REFERENCE

Alcaraz, S. A., Chambefort, I., Pearson, R., & Cantwell, A. (2015), "An Integrated Approach to 3-D Modelling to Better Understand Geothermal Reservoirs". *Proceeding WGC 2015, Melbourne, Australia.*

Cowan, J., & Beatson, R. (2002), "Rapid geological modelling". *Applied Structural Geology for Mineral Exploration and Mining, International Symposium*

Milicich, S. D., Dam, M. A. Van, Rosenberg, M. D., Rae, A. J., & Bignall, G. (2010), "'Earth Research" 3-Dimensional Geological Modelling of Geothermal Systems in New Zealand – a New Visualisation Tool". *Proceeding WGC 2010, Bali, Indonesia.*

Newson, J., Mannington, W., Sepulveda, F., Lane, R., Pascoe, R., Clearwater, E., & Sullivan, M. J. O. (2012), "Application of 3D Modelling and Visualization Software to Reservoir Simulation : Leapfrog Geothermal and TOUGH2". *Proceeding 37th Workshop on Geothermal Reservoir Engineering, Standford, California, USA.*

Prasetyo, I. M., Koestono, H., & Thamrin, M. H. (2015), "Clay Alteration Study from Wells of Tompaso Geothermal Field, North Sulawesi , Indonesia". *Proceeding WGC 2015*, Melbourne, Australia.

Seequent. "Leapfrog Geothermal Fundamentals".

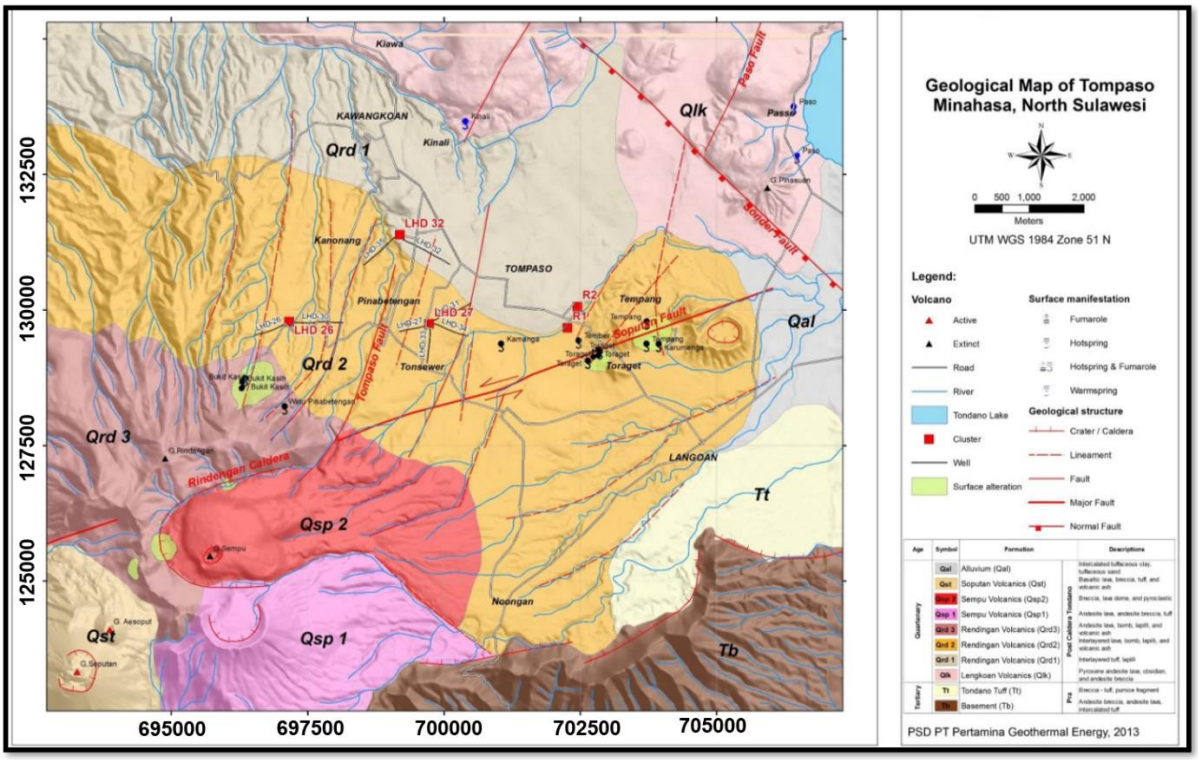


Figure 4: Geological Map of Study Area (Prasetyo et al., 2015).

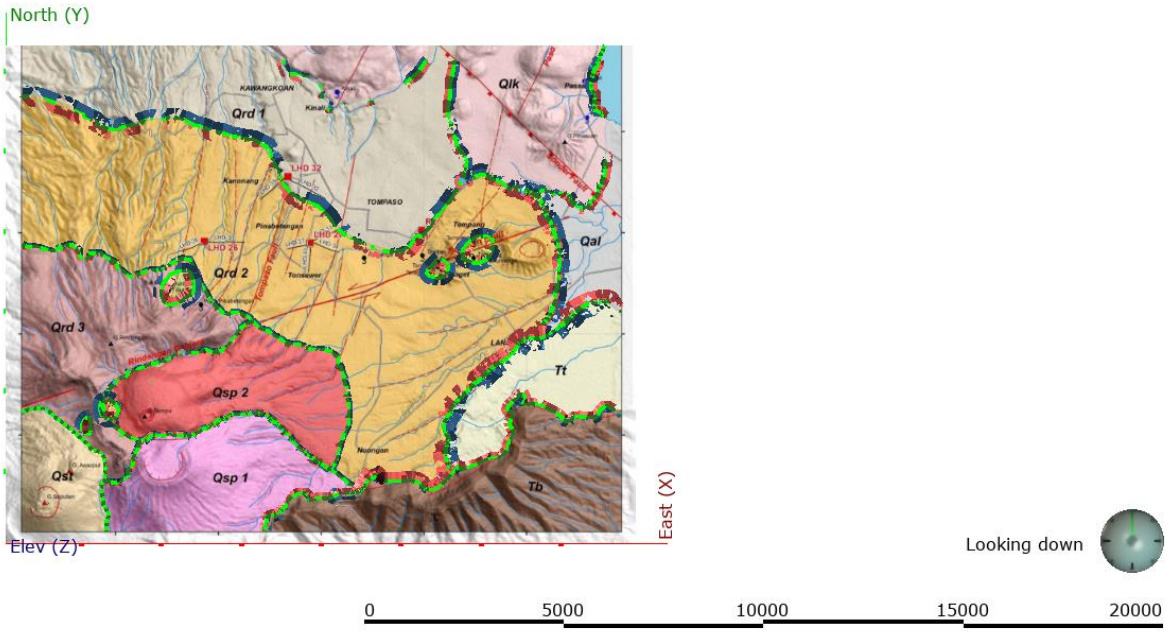


Figure 5: Delineate Geological Map using Polyline Tools.

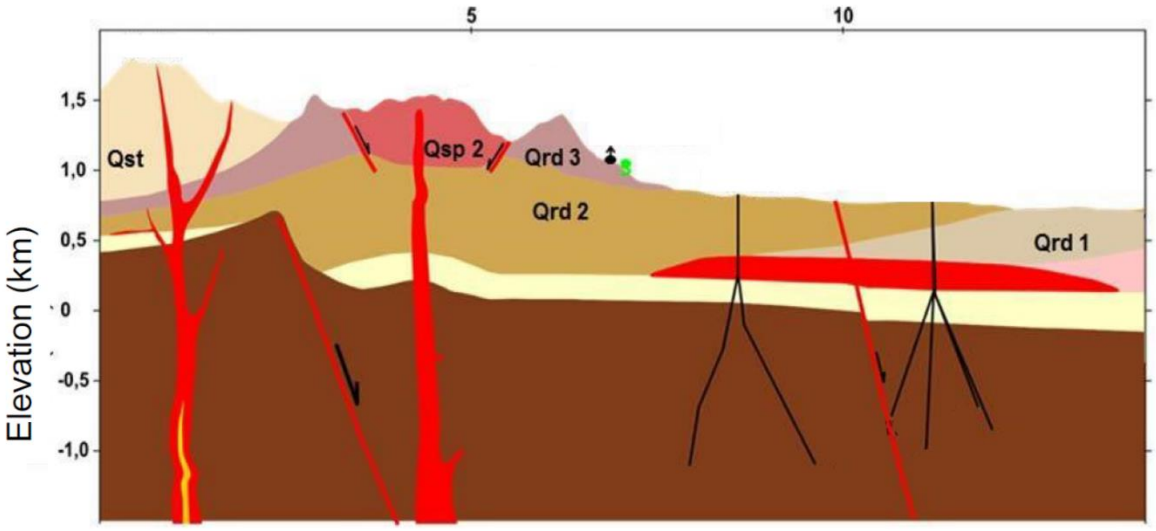


Figure 6: Cross Section of Study Area (Prasetyo et al., 2015).

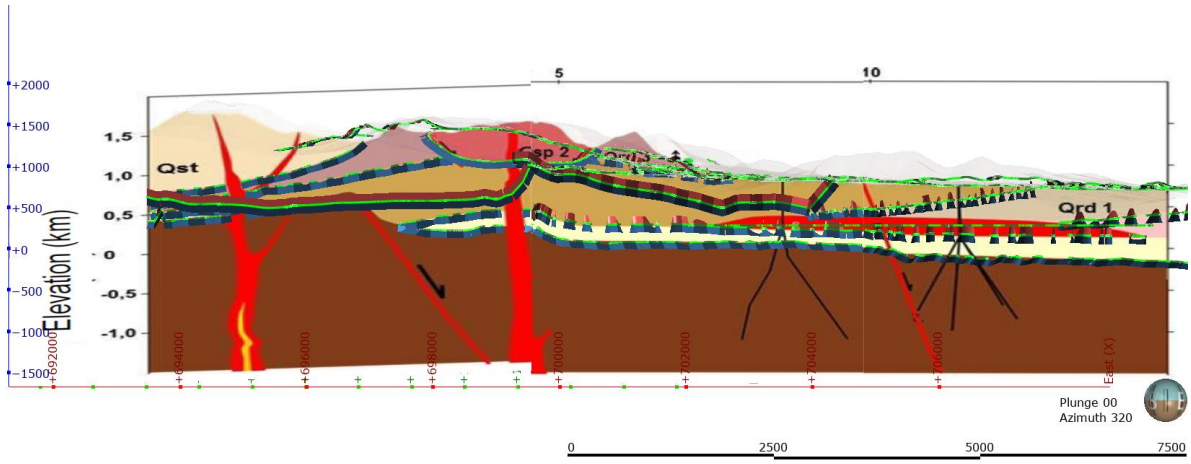


Figure 7: Delineate Sub-surface Lithology Contact using Polyline Tools.

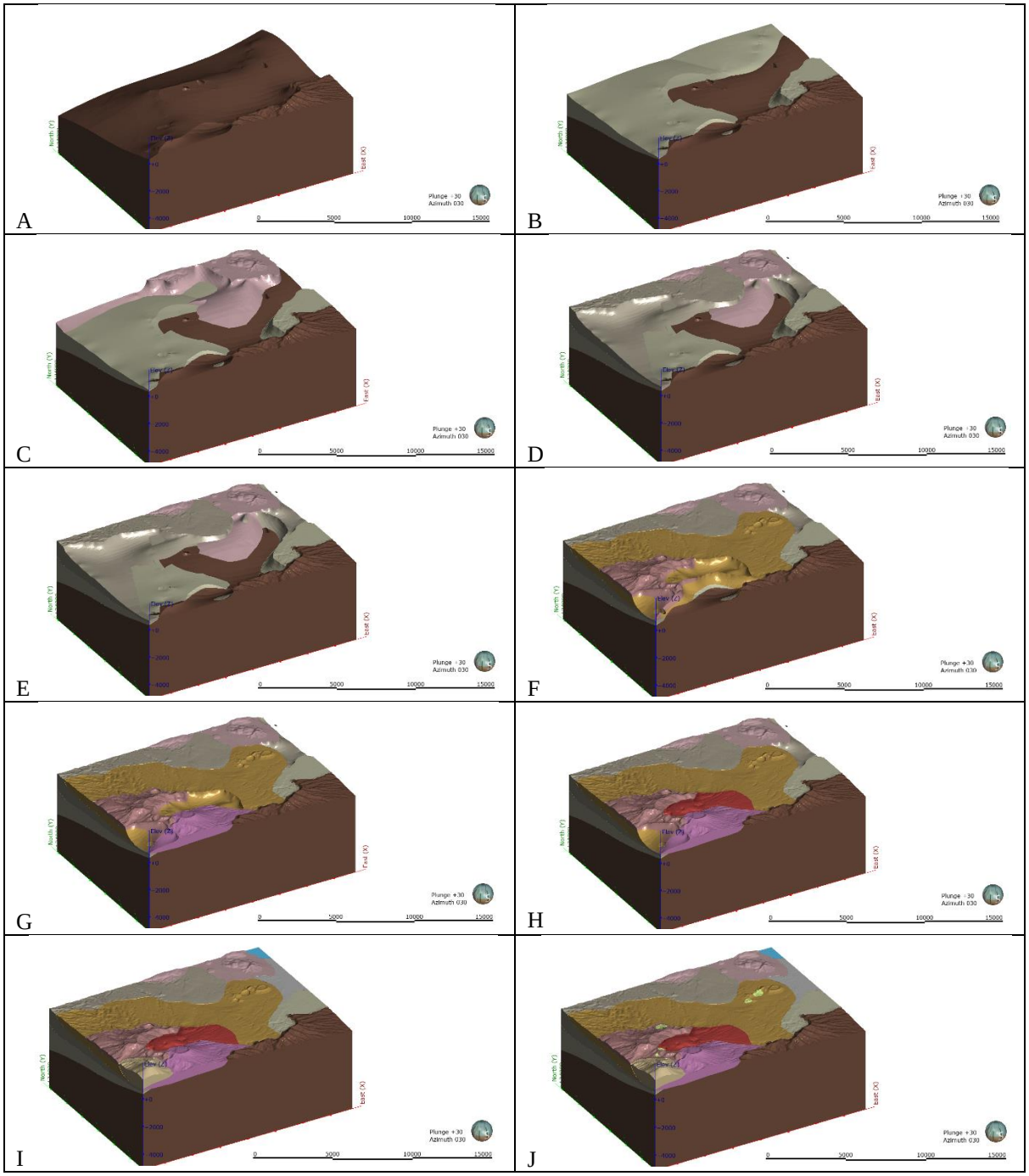


Figure 8: Volume of the 3D Geological Model.

HIV AIDS PROGRAM IN THE GEOTHERMAL COMPANY: A STRATEGIC WAY TO SUSTAINABLE GEOTHERMAL OPERATION IN FACING THE THREAT OF GLOBAL PANDEMIC

Deddi Ekaputra Rangan, Sandriana Tadjoeddin, Rahmat D. Gulo, Jedi Rijendra, Afrionaldi, and Stevano Dihart

Star Energy Geothermal (Wayang Windu) Ltd
Desa Margamukti, Kecamatan Pangalengan, Kabupaten Bandung, West Java, Indonesia
Email: Deddi.Rangan@starenergy.co.id

ABSTRACT

Star Energy Geothermal Wayang Windu Limited (SEGWWL) showed a strong commitment in HIV prevention programs in the workplace and also in the community around the company. SEGWWL works closely with Association of VCT Counselors (PKVHI) who are competent NGO in the field of HIV AIDS. There are 11 elements of the HIV AIDS program that were developed to make this program effective and have a significant impact. The HIV AIDS program is one of the health promotion and prevention programs, as part of the 4 pillars of occupational health. Strengthening HIV AIDS programs is very necessary in the workplace and in the community because HIV AIDS still has poor stigmatization and discrimination, while most people with HIV AIDS are people of productive age who can still work well. The existence of stigmatization and discrimination is the impact of the lack of correct knowledge about this disease, on the other hand stigmatization and discrimination will lead to increasing new cases of HIV. Internally within the company, procedures and policy are developed that demonstrate management's commitment on HIV AIDS and passion for eliminating stigmatization and discrimination. For external programs to the community, good cooperation with stakeholders, will be the key to success for outreach to key populations. Mapping the area at high risk of HIV transmission in the Pangalengan sub-district area was highly appreciated from elements of stakeholders. The program plays important role to sustainability of geothermal operation. SEGWWL received appreciation for the implementation of this HIV AIDS program by receiving the Platinum Award eight times from the Ministry of Manpower of the Republic of Indonesia and the ARROW Award (ASEAN Red Ribbon of Outstanding Workplace) in 2018 provided by the ASEAN Business Coalition on AIDS and ASEAN Secretariate in Kuala Lumpur Malaysia.

Keywords: HIV AIDS, Occupational Health, Stigmatization, Discrimination, Sustainability, Award

BACKGROUND

Indonesia is one out of three countries that has seen an increase in HIV/AIDS along with the Philippines and Russia. While the world trend is decreasing, Indonesia failed to reduce the transmission of the human immunodeficiency virus and mitigate the harm. Thus far, it has only managed to diagnose 47 percent of people living with HIV from an estimated 640,443 HIV positive cases; only 32 percent of people living with HIV received antiretroviral drugs from 301,959 diagnosed HIV positive cases and less than 1 percent of people living with HIV has been successfully treated and exhibited undetectable HIV in their blood.

This gap is immense compared with 90 percent of the target for each indicator as urged by the United Nations Agency on AIDS (UNAIDS), which aims to eliminate HIV as a public health threat by 2030. Stigma and discrimination against people with HIV/AIDS remain strong in Indonesia. Such stigma elicits an irrational or fear-driven negative attitude, behavior, and judgment toward people living with HIV and those perceived to be living with HIV.

According to the Basic Health Research (Riskesdas) 2018, 65.2 percent of Indonesians have a poor understanding of HIV/AIDS. Misunderstanding or lack of knowledge about HIV/AIDS has contributed to public fear, stigma, and discrimination. People must understand that HIV/AIDS can be prevented and managed so that people living with HIV can live as healthily as normal people.

Health workers have the credibility to inform society and convince them to destigmatize HIV/AIDS. Thus, health facilities are pivotal to help put an end to stigmatization and discrimination. They must be strengthened to empower people living with HIV. There are three important messages for health workers to circulate in society.

The total number of working people in Indonesia in February 2019 is 129.37 million people. That represents 48.44% of the total population of Indonesia (267.05 million). Of the 129.37 million people who worked, 41.78% worked in the formal sector (53.09 million people). While the remaining 58.22% worked in the informal sector (73.98 million people).

The Ministry of Manpower of the Republic of Indonesia issued regulation number 68 in year 2004 concerning the prevention and management of HIV AIDS in the workplace. This regulation targets workers who work in the formal sector, although it does not rule out the possibility of workers in the informal sector. In this regulation employer are required to develop HIV AIDS prevention and management program in the workplace, which work with labour union and government within the tripartite framework. With this regulation, Star Energy Geothermal (Wayang Windu) Ltd (SEGWW) is also required to develop HIV AIDS prevention and management program in the workplace because SEGWW is bound by the applicable laws and regulations in the territory of Indonesia. Thus, the beginning of the development of HIV AIDS program in the workplace was due to compliance with government regulation. However, from the risk aspects of transmission of HIV infection, the SEGWW work area is quite remote and the character of the geothermal sector workers in Indonesia meets the criteria of a high-risk group for HIV transmission, namely high-risk men mobile with money in macho environment (4M).

HIV AIDS prevention is also one of the seventeen goals of sustainable development goals (SDG), namely goal number 3 (good health and well-being for people). The purpose of this goal is to Ensure healthy lives and promote well-being for all ages. One point is to prevent the spread of HIV AIDS and reduce the occurrence of new infections. In the long term, it is hoped that the HIV AIDS pandemic can be ended. SEGWW is committed to support the Indonesia government in achieving SDG goals, because the goals are believed will have a good impact on the company and ensure better health status of workers and their families, and ultimately guarantee the sustainability of the geothermal operation and business.

HIV AND AIDS

History of the Disease

The history of the HIV and AIDS pandemic began in illness, fear and death as the world faced a new and unknown virus. It is widely believed that HIV originated in Kinshasa, in the Democratic Republic of Congo around 1920 when HIV crossed species from chimpanzees to humans. Up until the 1980s, it was not known how many people were infected with HIV or developed AIDS. HIV was unknown and transmission was not accompanied by noticeable signs or symptoms. While sporadic cases of AIDS were documented prior to 1970, available data suggests that the current epidemic started in the mid- to late 1970s. By 1980, HIV may have already spread to five continents (North America, South America, Europe, Africa and Australia). In this period, between 100,000 and 300,000 people could have already been infected. Figure 1 shows the diagram listing of sustainable development goals.



Figure 1: A diagram listing the 17 Sustainable Development Goals.

In 1981, cases of a rare lung infection called Pneumocystis carinii pneumonia (PCP) were found in five young, previously healthy gay men in Los Angeles. At the same time, there were reports of a group of men in New York and California with an unusually aggressive cancer named Kaposi's Sarcoma. In December 1981, the first cases of PCP were reported in people who inject drugs. By the end of the year, there were 270 reported cases of severe immune deficiency among gay men - 121 of them had died.

In June 1982, a group of cases among gay men in Southern California suggested that the cause of the immune deficiency was sexual and the syndrome was initially called gay-related immune deficiency (or GRID). Later that month, the disease was reported in haemophiliacs and Haitians leading many to believe it had originated in Haiti. In September, the CDC used the term 'AIDS' (acquired immune deficiency syndrome) for the first time.

In January 1983, AIDS was reported among the female partners of men who had the disease suggesting it could be passed on via heterosexual sex. In May, doctors at the Pasteur Institute in France reported the discovery of a new retrovirus called Lymphadenopathy-Associated Virus (or LAV) that could be the cause of AIDS. In June, the first reports of AIDS in children hinted that it could be passed via casual contact but this was later ruled out and it was concluded that they had probably directly acquired AIDS from their mothers before, during or shortly after birth. By September, the CDC identified all major routes of transmission and ruled out transmission by casual contact, food, water, air or surfaces. The CDC also published their first set of recommended precautions for healthcare workers and allied health professionals to prevent "AIDS transmission". In November, the World Health Organization (WHO) held its first meeting to assess the global AIDS situation and began international surveillance.

In April 1984, the National Cancer Institute announced they had found the cause of AIDS, the retrovirus HTLV-III. In a joint conference with the Pasteur Institute they announced that LAV and HTLV-III are identical and the likely cause of AIDS. A blood test was created to screen for the virus with the hope that a vaccine would be developed in two years. In July, the CDC state that avoiding injecting drug use and sharing needles "should also be effective in preventing transmission of the virus."

In March 1985, the U.S Food and Drug Administration (FDA) licensed the first commercial blood test, ELISA, to detect antibodies to the virus. Blood banks began to screen the USA blood supply. In April, the U.S. Department of Health and Human Services (HHS) and the World Health Organization (WHO) hosted the first International AIDS Conference in Atlanta Georgia. Ryan White, a teenager from Indiana, USA who acquired AIDS through contaminated blood products used to treat his haemophilia was banned from school.

In May 1986, the International Committee on the Taxonomy of Viruses said that the virus that causes AIDS will officially be called HIV (human immunodeficiency virus) instead of HTLV-III/LAV.

In February 1987, the WHO launched The Global Program on AIDS to raise awareness; generate evidence-based policies; provide technical and financial support to countries; conduct research; promote participation by NGOs; and promote the rights of people living with HIV. In March, the FDA approved the first antiretroviral drug, zidovudine (AZT), as treatment for HIV. In April, the FDA approved the western blot blood test kit, a more specific HIV antibody test. In July, the WHO confirmed that HIV could be passed from mother to child during breastfeeding. In October, AIDS became the first illness debated in the United Nations (UN) General Assembly.

In 1988, the WHO declared 1st December as the first World AIDS Day.

Epidemiology

In 2017, 36.9 million people people globally were living with HIV. Sub Saharan Africa is still the region with the highest HIV prevalence. An estimated 7.5% of adults in the region have HIV. HIV prevalence among pregnant women aged 15-24 years is also high. This shows that HIV has spread to the general population, not only concentrated in high-risk groups.

In Asia the HIV epidemic is still concentrated in the Injecting Drug Users (IDU), men have sex with men (MSM), and sex workers (heterosexual and homosexual) along with their regular customers and sex partners. In this area effective preventive programs have not been adequate.

In Indonesia, since the first time discovered in 1987 until December 2018, HIV AIDS has been reported by 460 (89.5%) of the 514 regencies in all provinces. The number of HIV cases reported from 2005 to 2018 increase in each year. The cumulative number of HIV infections reported as of December 2018 is 327.282. There are 5 provinces with the highest number of HIV infections: DKI Jakarta (58.877), East Java (48.241), West Java (34.149), Papua (32.629) and Central Java (27.629).

The highest cumulative percentage of AIDS is in the age group 20-29 years (32,3%), then followed by group of 30-39 years (30, 9%), 40-49 years (13,4%), 50-59 years (5%), and 15-19 years (3,3%). There are

5 provinces with the highest number of AIDS: Papua (22.538), East Java (19.829), Central Java (10.111), DKI Jakarta (9.932), and Bali (7.990).

The highest number of AIDS according to work type is non-professional staff/employee (16.867), housewife (16.405), private entrepreneur/business owner (14.899), farmers/fisherman (5.670), and unskilled laborers (5.154).

Most mode of transmission is through risky sexual intercourse: heterosexual (70,3%), use of non-sterile syringes (8,4%), homosexuals (6,6%). and perinatal transmission (2,9%).

Etiologic Agent

HIV is the etiologic agent of AIDS; it belongs to the family of human retroviruses (Retroviridae) and the subfamily of lentiviruses.The four retroviruses known to cause human disease belong to two distinct groups: the human T lymphotropic viruses (HTLV)-1 and HTLV-2, which are transforming retroviruses; and the human immunodeficiency viruses, HIV-1 and HIV-2, which cause cytopathic effects either directly or indirectly. The most common cause of HIV disease throughout the world, and certainly in the United States, is HIV-1, which comprises several subtypes with different geographic distributions. The currently defined groups of HIV-1 (M, N, O, P) and the HIV-2 groups A through H each are likely derived from a separate transfer to humans from a nonhuman primate reservoir. HIV-1 viruses likely came from chimpanzees and/or gorillas, and HIV-2 from sooty mangabeys. The AIDS pandemic is primarily caused by the HIV-1 M group viruses. Although HIV-1 group O and HIV-2 viruses have been found in numerous countries, including those in the developed world, they have caused much more localized epidemics.

Pathogenesis of HIV Infection

Infection with HIV starts without symptoms or ill-feeling and is accompanied by slight changes in the immune system. This stage spans up to three months after infection until seroconversion where HIV-specific antibodies can be detected in individuals following recent exposure. The outcome of infection and duration for disease progression with clinical symptoms may vary greatly between individuals, but often it progresses fairly slowly. It takes several years from primary infection to the development of symptoms of advanced HIV diseases and immunosuppression. Figure 2 shows the structure of HIV.

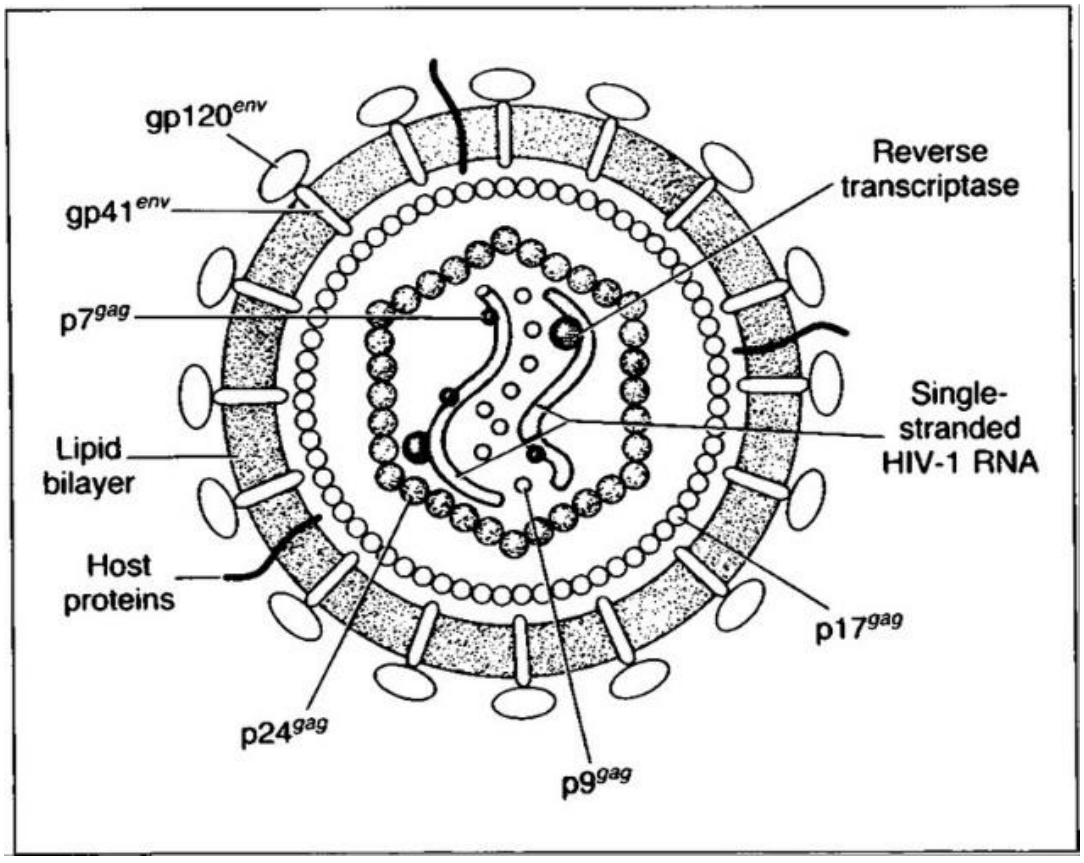


Figure 2: Structure of HIV-1, including the gp120 envelope, gp41 transmembrane components of the envelope, genomic RNA, enzyme reverse transcriptase, and p24 core protein (capsid).

During primary infection, although individuals may look healthy, the virus is actively replicating in the lymph nodes and blood stream of infected individuals. As a result, the immune system may get slowly damaged by the burst of viral load in their bodies. Symptomatic stage of disease indicates the late phase of HIV disease (AIDS) where individuals may be susceptible to other opportunistic infections (OIs), such as infections with *Mycobacterium avium*, *Mycobacterium tuberculosis*, *Pneumocystis carinii*, CMV, toxoplasmosis and candidiasis. It is agreed that infected individuals develop an AIDS status when their plasma HIV load is high and the CD4+ T count is less than 200 mm. The availability of the highly active antiretroviral therapy (HAART) may question the dilemma as to whether everyone who seroconverts to HIV will develop AIDS.

One mechanism HIV weakens the immune system is by infecting and destroying CD4+ T cells, which in turn leads to immunodeficiency at later stage of disease. HIV attaches to the CD4+ protein on the surface of these and other cells to gain entry. However, the presence of CD4+ molecules alone proves to be not enough to allow viral entry into other cell types such as monocytes and dendritic cells. Therefore, a second doorway is needed for the virus to gain access to infect cells. This led to the discovery of the chemokine receptor as essential coreceptors for HIV-1. There are different types of these coreceptors for different cell types that HIV variants can use for infection of cells. Two main chemokine receptors have been identified to play a major role in HIV entry, CCR5 and CXCR4 (or fusin). The discovery of chemokine receptors as essential coreceptors required for HIV entry has to a large extent rationalised the basis of cellular tropism and better-defined HIV entry into different cells. CCR5 is present on a broad range of cells that can be infected by HIV, including T cells, monocytes and macrophages. Different HIV strains may be encountered in the body of the patients which can be classified into three variants: M-, T- and dual-tropic. Mtropic HIV variants can infect monocytes, macrophages and T lymphocytes through using CCR5 (R5), but not T cell lines as these express primarily CXCR4. T-tropic variants, which use CXCR4 (X4) as their principal coreceptor readily, infect T-cell lines and T lymphocytes but not macrophages. Dual-tropic strains of HIV-1 utilise CCR5 and CXCR4 (R5X4) to enter macrophages and T celllines, respectively, but they can also utilise combinations of major and minor coreceptors.

Macrophages act as major reservoirs for HIV-1 in tissues of the body. HIV infected macrophages may be found in brain, lungs, lymph nodes, skin, bone marrow and blood of seropositive individuals. They are the main source of productive infection in brain, and HIV infected macrophages in lymph nodes produce large amounts of viral particles. Infection with HIV-1 persists for weeks or months after commencement of highly active retroviral therapy (HAART). Monocytes/macrophages are believed to serve as vehicles for dissemination of HIV between different tissues of the body. Progression of acute HIV-1 infection to AIDS is accompanied by immune dysregulation and susceptibility to OIs. Figure 3 shows the window detection of HIV.

Window Period

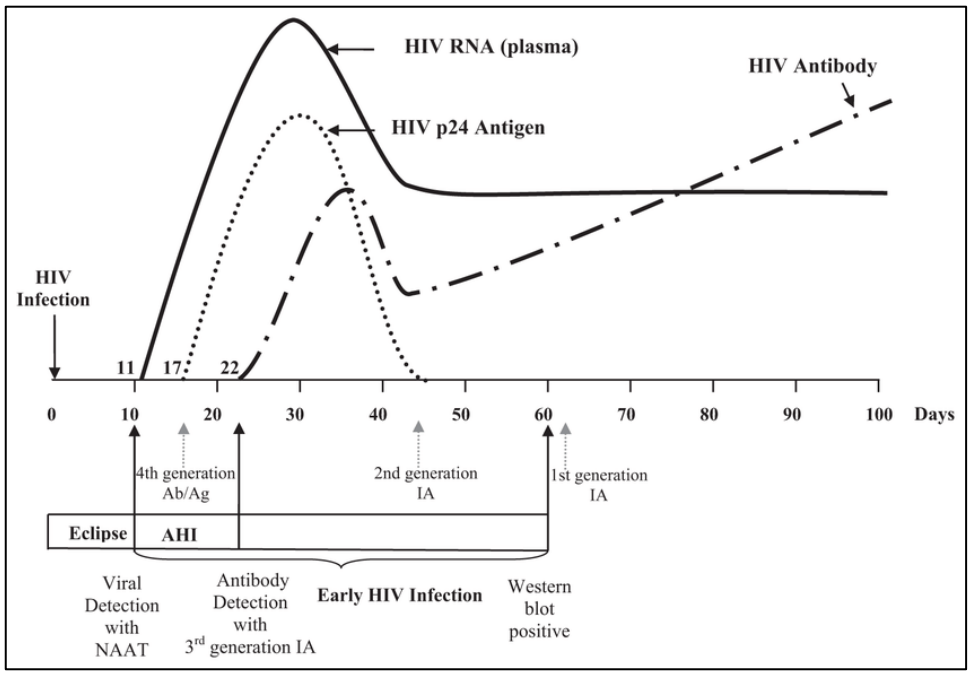


Figure 3: Window of detection of HIV markers early in HIV infection and window period of different generations.

Most people infected with HIV do not know that they have become infected. HIV infected persons develop antibodies to HIV antigens usually 6 weeks to 3 months after being infected. In some individuals, the test for the presence of these antigens may not be positive until 6 months or longer (although this would be considered unusual). This time -- during which people can be highly infectious and yet unaware of their condition -- is known as the "the window period". Seroconversion is when a person recently infected with HIV first tests sero-positive for HIV antibodies. Some people have a "glandular fever" like illness (fever, rash, joint pains and enlarged lymph nodes) at the time of seroconversion. Occasionally acute infections of the nervous system (eg. aseptic meningitis, peripheral neuropathies, encephalitis and myelitis) may occur.

The ESSE Mnemonic

HIV AIDS transmission is actually very limited. In addition to risky sex, transmission can be through the use of sharing needles together for more than one person and blood transfusions. Viruses are also easily transmitted from mother to child, for example through breastfeeding. The easy assumption of HIV AIDS transmission cannot be separated from the stigma that still exists regarding this disease.

Exit, Sufficient, Survive, Entry (ESSE), which are four necessary conditions for HIV to be transmitted from a Person Living with HIV (PLHIV) to another person who is uninfected, someone with an unknown status, or another PLHIV. The infection process starts when the virus exits the body through body fluids like: blood, breast milk, rectal fluid, semen, and vaginal fluid. These body fluids allow HIV to survive outside the body, but they need to immediately enter the other person's body for a new infection or a co-infection to occur.

HIV can only be transmitted among humans, and contrary to popular belief, mosquitoes are not part of our family tree. The first essential step for an infection to start is for the virus (embedded in body fluids) to exit the body in sufficient numbers. The amount of virus that exists in the body is known as the viral load. Among the different body fluids, only blood, seminal fluid, vaginal fluid, rectal fluid, and breastmilk are the reported means of HIV transmission. Other body fluids like saliva, tears, sweat, or urine contain negligible traces of the virus, which are not enough to successfully transmit infection. By knowing which body fluids have the sufficient amount of the virus, we know which behaviors or incidents could expose us to HIV. For instance, unprotected penetrative anal sex exposes someone to semen, rectal fluid, or even blood if one gets a laceration. Having anal sex without a condom exposes a person to higher risks, especially if it is done with someone (a stranger or your current partner) with an unknown serostatus.

Viruses are infectious agents that can only replicate themselves inside the living cells of other organisms. This is why HIV does not survive for long outside the human body. Conversely, this is the reason it is not possible to get infected with the virus by mere contact with infected body fluids. Our skin is our first line of defense from pathogens (disease-causing organisms). An intact skin and mucosa provide us optimum protection. However, cuts and/or wounds would limit the protection they provide. In airtight syringes and needles, the absence of oxygen allows the virus to live longer. And during sex (particularly during penetration), there is an immediate contact between the fluids and the possible route of entry of the virus. This is a major factor why unprotected penetrative sex poses a high risk for HIV transmission. Infection can be prevented if one engages in safe and satisfying sex practices, which include using condoms and lubes for penetrative sex, and performing less risky sexual practices. Avoiding sharing of needles or taking care so as not to get pricked by used needles are also measures in preventing HIV infection. In all cases, wearing condoms and making sure sterilized equipment are used at all time are major prerequisites in mitigating risks of getting infected with HIV. The risk of getting HIV varies widely depending on the type of exposure or behavior (such as sharing needles or having sex without a condom). Some exposures to HIV carry a much higher risk of transmission than other exposures. For some exposures (Table 1), while transmission is biologically possible, the risk is so low that it is not possible to put a precise number on it. But risks do add up over time. Even relatively small risks can add up over time and lead to a high lifetime risk of getting HIV. In other words, there may be a relatively small chance of acquiring HIV when engaging in a risk behavior with an infected partner *only once;* but, if *repeated many times*, the overall likelihood of becoming infected after repeated exposures is actually much higher.

Clinical Manifestation of HIV/AIDS

The clinical consequences of HIV infection encompass a spectrum ranging from an acute syndrome associated with primary infection to a prolonged asymptomatic state to advanced disease. It is best to regard HIV disease as beginning at the time of primary infection and progressing through various stages. Active virus replication and progressive immunologic impairment occur throughout the course of HIV infection in most patients. With the exception of the rare, true, "elite" virus controllers or long-term nonprogressors, HIV disease in untreated patients inexorably progresses even during the clinically latent stage. It is estimated that 50–70% of individuals with HIV infection experience an acute clinical syndrome ~3–6 weeks after primary infection.

Table 1: Estimated Per-Act Probability of Acquiring HIV from an Infected Source, by Exposure Act.

Type of Exposure	Risk per 10,000 Exposures
Parenteral	
Blood Transfusion	9,250
Needle-Sharing During Injection Drug Use	63
Percutaneous (Needle-Stick)	23
Sexual	
Receptive Anal Intercourse	138
Insertive Anal Intercourse	11
Receptive Penile-Vaginal Intercourse	8
Insertive Penile-Vaginal Intercourse	4
Receptive Oral Intercourse	Low
Insertive Oral Intercourse	Low
Other^	
Biting	Negligible
Spitting	Negligible
Throwing Body Fluids (Including Semen or Saliva)	Negligible
Sharing Sex Toys	Negligible

Acute human immunodeficiency virus (HIV) infection, also known as primary HIV infection, is the period just after initial HIV infection, generally before seroconversion. Although some patients remain asymptomatic, acute HIV infection often manifests with transient symptoms related to high levels of HIV viral replication and the subsequent immune response. Because symptoms of acute HIV infection (e.g., fever, rash, malaise, sore throat) mimic other, more prevalent conditions, such as influenza, misdiagnosis is common. Furthermore, patterns of care for patients seeking medical attention for acute HIV infection are largely unknown.

At least 50 (and up to 90) percent of patients with acute HIV infection develop symptoms consistent with acute infection, although timing and duration are variable. For most symptomatic patients, acute illness develops within one to four weeks after transmission, and symptoms usually persist for two to four weeks. Acute HIV infection is often described as mononucleosis-or influenza-like, with the most prevalent symptoms being fever, fatigue, myalgias/arthralgias, rash (typically an erythematous maculopapular exanthem), and headache (Table 2 and 3). Patients also may experience anorexia, pharyngitis, lymphadenopathy, mucocutaneous ulcerations, diarrhea, or a combination of these symptoms. Severe manifestations of acute HIV infection (e.g., meningoencephalitis, myelitis), although rare, have been described. CD4 lymphocyte counts exhibit a marked transient decrease during acute infection. There have been case reports of patients with acute infection presenting with opportunistic infections, such as esophageal candidiasis. Physical examination is nondiagnostic but may be notable for hepatosplenomegaly.

Symptoms of AIDS are caused by the deterioration of the immune system and the decline of CD4+ T cells, which are the immune system's key infection fighters. As soon as HIV enters the body, it begins to destroy these cells. Some common symptoms include:

- Diarrhea that lasts for more than a week
- Dry cough
- Memory loss, depression and neurological disorders
- Pneumonia
- Profound, unexplained fatigue
- Rapid weight loss
- Recurring fever or profuse night sweats
- Red, brown, pink or purplish blotches on or under the skin or inside the mouth, nose or eyelids
- Swollen lymph glands in the armpits, groin or neck
- White spots or unusual blemishes on the tongue, in the mouth, or in the throat

Because people with AIDS have weakened immune systems, they're more prone to infections, called opportunistic infections. Opportunistic infections are caused by organisms that typically don't cause disease in healthy people but affect people with damaged immune systems. These organisms attack when there's an opportunity to infect.

Deterioration of the immune system is caused by the decline in CD4+ T cells, which are key infection fighters. As soon as HIV enters the body, it begins to destroy these cells.

Symptoms of opportunistic infections common with AIDS include:

- Coma
- Coughing and shortness of breath
- Difficult or painful swallowing
- Extreme fatigue
- Fever
- Mental symptoms such as confusion and forgetfulness
- Nausea, abdominal cramps and vomiting
- Seizures and lack of coordination
- Severe, persistent diarrhea
- Severe headaches

- Vision loss
- Weight loss

Many opportunistic infections associated with AIDS cause serious illness. Some may be prevented. Below is a list of infections and how they affect the body.

Table 2: Diagnostic Value of Signs and Symptoms in Acute HIV Infection.

Sign/Symptom	Sensitivity * (%)	Specificity † (%)	Positive Likelihood Ratio ‡	Negative Likelihood Ratio§
Mucocutaneous ulcerations	2 to 37	85 to 97	2.2	0.9
Rash	51 to 58	66 to 82	2.1	0.6
Myalgias/ arthralgias	49 to 60	69 to 74	1.9	0.6
Anorexia/ weight loss	32 to 54	68 to 86	1.9	0.7
Fever	80 to 88	50 to 56	1.8	0.3
Severe central nervous system manifestations	25	82	1.4	0.9
Fatigue/ malaise	68 to 78	38 to 51	1.3	0.6
Headache	54 to 55	56 to 57	1.3	0.8
Lymphadenopathy	38	71	1.3	0.9
Pharyngitis	43 to 44	51 to 77	1.2	0.9
Gastrointestinal distress	12 to 49	60 to 91	1.2	0.9

Table 3: Differential Diagnosis of Acute HIV Infection.

Most Common	Less Common	Least Common
Epstein-Barr virus	Acute viral hepatitis	Acute cytomegalovirus infection
Influenza	Drug reaction	Acute toxoplasmosis
Streptococcal pharyngitis	Primary herpes simplex infection	Brucellosis
Viral/noninfectious gastroenteritis	Secondary syphilis	Disseminated gonococcemia
Viral upper respiratory tract infection		Measles
		Meningitis/encephalitis
		Primary immunodeficiencies
		Rubella
		Travel-related pathogens (e.g., malaria, typhoid)

Opportunistic Infections

- Cryptoccoccal Meningitis is a yeast-like fungus infection that usually involves the brain and lungs, although it can affect almost any organ. The fungus that causes this condition is found in soil throughout the world. It is most common in soil contaminated by bird droppings. This disease most often occurs when a person's CD4+ T cell count falls below 100 cells per cubic millimeter of blood.
- HIV-related Encephalopathy is a term for diseases that alter brain function or structure, leading to problems with cognitive function, or mental processes, and memory. In people with HIV and AIDS, encephalopathy is usually caused by an infectious agent, such as a bacteria, virus or prion. Encephalopathy most often occurs when a person's CD4+T cell count falls below 50 cells per cubic millimeter of blood. Toxoplasma-seropositive patients who have a CD4+T cell count of less than 100 cells per cubic millimeter of blood should be treated with prophylaxis to prevent developing encephalopathy.
- Progressive Multifocal Leukoencephalopathy (PML) is a rare disorder of the nervous system caused by a common human polyomavirus, JC virus. It leads to the destruction of the myelin sheath that covers nerve cells. The myelin sheath is the fatty covering that acts as an insulator on nerve fibers in the brain. Symptoms include mental deterioration, vision loss, speech disturbances, inability to coordinate movements, paralysis and ultimately coma. In rare cases, seizures may occur. This disease can occur when the CD4+T cell count falls below 200 cells per cubic millimeter of blood.
- Toxoplasmosis occurs when a parasite infects the brain. Symptoms include confusion or delusional behavior, severe headaches, fever, seizures and coma. It can affect the eye, causing eye pain and reduced vision. Toxoplasmosis most likely occurs when the CD4+ T cell count falls below 100 cells per cubic millimeter of blood. Preventative treatment — usually with trimethoprim-sulfamethoxazole, also called Septra and Bactrim — may be administered when the CD4+ T cell count falls below 100 cells per cubic millimeter of blood.
- Cytomegalovirus (CMV) commonly affects the eye's retina, causing blurry vision and in severe cases, blindness. Other common symptoms include chronic diarrhea and nerve problems. It is most likely to occur when a person's CD4+ T cell count falls below 100 cells per cubic millimeter of blood.
- Cryptosporidiosis is a parasite that can cause chronic diarrhea. Other symptoms include stomach cramps, nausea, fatigue, weight loss, appetite loss, vomiting and dehydration. This infection is difficult to treat and there is no definitive effective treatment. Symptom control and treatment of HIV are necessary.
- Mycobacterium Avium Complex is a bacterial infection that can cause persistent fever, night sweats, fatigue, weight loss, anemia, abdominal pain, dizziness, diarrhea and weakness. The bacteria that cause this infection is found in water, dust, soil and bird droppings. This disease most likely occurs when the CD4+T cell count falls below 50 cells per cubic millimeter of blood. Preventive treatment, usually with azithromycin, is administered when CD4+ T cells are less than 50 cells per cubic millimeter of blood.
- Candidiasis is an infection caused by the candida fungi. Also known as a yeast infection, it's the most common HIV-related fungus infection. It can affect the entire body, but most commonly occurs in the mouth, called thrush, or vagina. An overgrowth of yeast in the vagina can cause irritation, itching, burning and thick white discharge.
- Herpes Simplex Virus causes genital herpes, which are painful blisters in the genital area, or cold sores. Severe conditions are more common in the advanced stage of AIDS.
- Human Papilloma Virus (HPV) can cause warts on the anus, cervix, esophagus, penis, urethra, vagina and vulva. Studies have shown that certain types of HPV can contribute to the development of cervical and anal cancer. Individuals with HIV and AIDS are at increased risk for developing precancerous and cancerous lesions.
- Liver Disease is one of the leading causes of death among AIDS patients, especially liver disease caused by the hepatitis B and hepatitis C virus. Many drugs used in the treatment of HIV and AIDS can cause liver disease or hepatitis. It is important that patients infected with hepatitis receive treatment and follow-up care.
- Coccidiomycosis is caused by inhaling an infective fungus called Coccidioides immitis, found mainly in contaminated soil in the southwestern United States, Mexico, Central America and parts of South America. The lungs are most commonly affected by this infection. In severe cases, it can involve the kidneys, lymph system, brain and spleen. Symptoms include cough, weight loss and fatigue. Meningitis is a common complication when left untreated.
- Histoplasmosis almost always involves the lungs, although other organs may be affected. The fungus that causes this condition is found in southern parts of the United States and South America. It is usually found in soil contaminated with bird droppings and must be inhaled to cause infection. Signs and symptoms include high fever; weight loss; respiratory complaints; an enlarged liver, spleen, or lymph

nodes; depressed production of white cells, red blood cells and platelets from the bone marrow; and life-threatening, unstable, low blood pressure.

- Pneumocystis carinii occurs when a fungus infects the lungs. Symptoms may include fever, cough, difficulty breathing, weight loss, night sweats and fatigue. It is most likely to occur when the CD4+ T cell count falls below 200 cells per cubic millimeter of blood. Preventative treatment may be administered when the CD4+ T cell count falls below 200 cells per cubic millimeter of blood. Treatment is usually trimethoprim-sulfamethoxazole, also called Septra or Bactrim, dapsone or atovoquone.
- Recurrent Pneumonia is bacterial infection to the lungs, which may lead to problems ranging from a mild cough to severe pneumonia. Recurrent pneumonia is most likely to occur when the CD4+ T cell count falls below 200 cells per cubic millimeter of blood.
- Tuberculosis (TB) is a serious, and often deadly, bacterial infection that primarily infects the lungs. TB is transmitted when a person with active TB coughs or sneezes, releasing microscopic particles into the air. If inhaled, these particles may transmit the condition. Once infected by TB, most people remain healthy and develop only latent infection. People with latent infection are neither sick nor infectious. However, they do have the potential to become sick and infectious with active TB. It can occur at any CD4+ T cell level but especially when the CD4+ T cell count falls below 350 cells per cubic millimeter of blood.
- Non-Hodgkin's lymphoma is a disease in which tumors develop from white blood cells in the lymphatic system. It is another common disease associated with AIDS.
- Candidiasis is the most common HIV-related fungus infection. It can affect the entire body, but most commonly occurs in the mouth (thrush) or vagina. An overgrowth of yeast causes white patches on gums, tongue or lining of the mouth, pain, difficulty in swallowing and loss of appetite. Candida in the esophagus, trachea, bronchi or lungs is AIDS defining.
- Kaposi’s Sarcoma is the most common AIDS-related cancer. It causes reddish-purple lesions that usually appear on the skin. They also can appear on the lymph nodes, mouth, gastrointestinal tract and lungs.
- Shingles are caused by a reactivation of the chicken pox virus. It may cause a painful rash or blisters that follow the path of nerves.

Testing for HIV Infection

HIV testing may take place at any level of the health-care system, and a diagnosis can be established for a majority of individuals on the same day. Many people will access HIV testing in their community or in primary care facilities. The degree of infrastructure required for the assay format, such as need for reliable electricity and climate-controlled testing rooms, as well as the staff skills and competencies required, will determine how complex an assay can be used in a given testing setting.

With the evolution of HIV enzyme-linked immunosorbent assays (ELISA) from first to third generation tests, the window period (i.e., the time between transmission and production of HIV antibodies when an HIV ELISA test result may be falsely negative) for confirming HIV infection through antibody testing has narrowed from approximately 56 to 21 days. However, because acute HIV infection occurs before the appearance of HIV antibodies, it can be diagnosed only by demonstrating the presence of p24 antigen or HIV viral RNA, which can be detected as early as 14 to 15 days and 11 to 12 days after infection, respectively.

Rapid diagnostic tests (RDTs) are so called as they produce a test result quickly, usually in less than 30 minutes. The broad class of HIV-1/2 RDTs includes lateral-flow (immunochromatographic) and vertical-flow (immunofiltration) assay formats, which detect the presence of HIV-1/2 antibodies and/or HIV p24 antigen. RDTs are not only quick but also are easier to perform than assays that require a laboratory. With training, both health-care professionals and lay providers can perform HIV testing with high accuracy and reliability using RDTs. Most RDTs and their accompanying reagents can be stored between 2 and 30 °C. They do not require any additional equipment and, thus, do not need to necessarily be performed in a laboratory. This means that RDTs are suited for use in both community- and facility-based settings, including sites with limited infrastructure that process low numbers of specimens daily.

For people over 24 months of age, HIV is typically diagnosed through the detection of HIV antibodies (a serological marker) and/or HIV p24 antigen rather than direct detection of the components of the virus itself (virological markers). Serological assays used for HIV diagnosis detect HIV-1/2 antibodies, with fourth generation assays incorporating detection of both HIV-1/2 antibodies and HIV p24 antigen. When initial HIV testing cannot discern a diagnosis, supplemental assays may be used, such as assays that detect HIV p24 antigen only or assays that can detect specific types of HIV-1/2 antibodies. Most RDTs can be performed with capillary whole blood collected by a finger-stick procedure using a lancet. This means that phlebotomy by venepuncture is not necessarily required. Always refer to the manufacturer's instructions for use, however, for specific recommendations on specimen collection. Certain other RDTs are validated for use with oral fluid specimens. Results for RDTs are visually read

and interpreted by the operator. The appearance of a control line and test line(s) signifies a reactive result, while the appearance of only a control line signifies a non-reactive result. As with any visually read assay, a second reader should independently read and interpret the test results to mitigate any reading errors.

RDTs are designed for qualitative (yes or no) detection of antibodies and/or antigen, rather than quantitative detection of the amounts of antibodies, irrespective of the intensity of the test line(s). However, RDTs may show faint test lines, and so users may have difficulty interpreting these types of test results. It is critical to follow the manufacturer's instructions for use, which usually say to read any band, irrespective of its intensity, as reactive. Some studies have observed that faint lines can be associated with false reactivity, but this is not always the case. Any visually read assay is prone to inter-reader variability and potential differences in interpretation. Therefore, it is suggested that the relative intensity of the test line(s) be scored on a scale of 0 (no line), +/− (possible line), 1+ (weak line), 2+ (strong line). Figure 4 shows the detecting HIV infection.

For a period of about 10 days following HIV infection, known as the **eclipse period**, no currently available serological or virological assay can detect any marker of HIV infection. The end of the eclipse period is marked by the appearance of HIV RNA or DNA detectable by nucleic acid testing (NAT) and then HIV p24 antigen, detectable by immunoassay (IA). The period prior to detection of HIV-1/2 antibodies is often referred to as “acute infection”. The number of HIV virus particles rises rapidly during acute infection and may be associated with higher infectivity and rate of transmission. As the level of HIV-1/2 antibodies increases, these antibodies form immune complexes with free HIV antigen circulating in the bloodstream. Thus, free HIV antigen is captured (complexed) and, therefore, unable to bind to monoclonal antibody presented on the test device. As a result, the level of detectable HIV antigen decreases. The detection of HIV-1/2 antibodies by serological assay signals the end of seroconversion and, therefore, the window period for diagnosis.

The duration of the window period depends on three main factors: (1) the genetics of the virus, (2) the genetics and immunocompetence of the host, and (3) what exactly the assay detects (antigen, antibodies). In particular, the format of the assay determines its ability to detect early HIV antibodies (including IgM, IgA, IgG); this may also depend on the specimen type, such as oral fluid, venous or capillary whole blood and serum/plasma. The shortest window period is generally observed with fourth generation serological assays, followed by third and then second generation assays, with first generation assays having the longest window period. Among RDTs, those using oral fluid specimens exhibit the very longest window period, irrespective of their generation, likely because the concentration of HIV-1/2 antibodies is lower in oral fluid than in other specimen types. However, they have been successfully used in many settings, particularly where high HIV incidence is not expected.

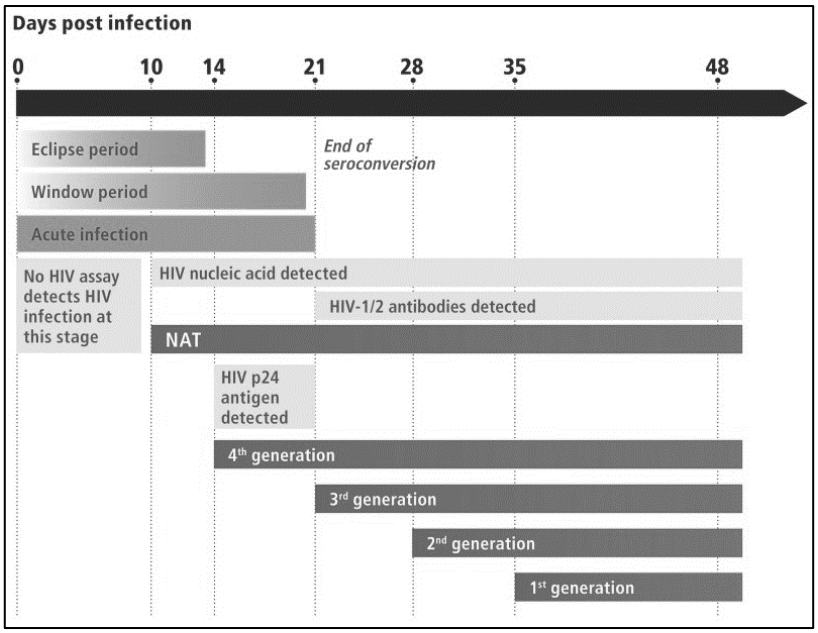


Figure 4: Detecting HIV-infection with various formats and generations of in vitro diagnostics over the natural history of infection.

Prevention of HIV Infection

Individuals can reduce the risk of HIV infection by limiting exposure to risk factors. Key approaches for HIV prevention, which are often used in combination, are listed below.

Male and female condom use

Correct and consistent use of male and female condoms during vaginal or anal penetration can protect against the spread of sexually transmitted infections, including HIV. Evidence shows that male latex condoms have an 85% or greater protective effect against HIV and other sexually transmitted infections (STIs).

Testing and counselling for HIV and STIs

Testing for HIV and other STIs is strongly advised for all people exposed to any of the risk factors. This way people learn of their own infection status and access necessary prevention and treatment services without delay. WHO also recommends offering testing for partners or couples. Additionally, WHO is recommending assisted partner notification approaches so that people with HIV receive support to inform their partners either on their own, or with the help of health care providers.

Testing and counselling, linkages to tuberculosis care

Tuberculosis (TB) is the most common presenting illness and cause of death among people with HIV. It is fatal if undetected or untreated and is the leading cause of death among people with HIV, responsible for more than 1 of 3 HIV-associated deaths. Early detection of TB and prompt linkage to TB treatment and ART can prevent these deaths. TB screening should be offered routinely at HIV care services and routine HIV testing should be offered to all patients with presumptive and diagnosed TB. Individuals who are diagnosed with HIV and active TB should urgently start effective TB treatment (including for multidrug resistant TB) and ART. TB preventive therapy should be offered to all people with HIV who do not have active TB.

Voluntary medical male circumcision (VMMC)

Medical male circumcision, reduces the risk of heterosexually acquired HIV infection in men by approximately 60%. This is a key prevention intervention supported in 15 countries in Eastern and Southern Africa (ESA) with high HIV prevalence and low male circumcision rates. VMMC is also regarded as a good approach to reach men and adolescent boys who do not often seek health care services. Since the 2007 WHO recommendation for VMMC as an additional prevention strategy, over 18 million adolescent boys and men in ESA were provided a package of services including HIV testing and education on safer sex and condom use.

Antiretroviral drug use for prevention

A 2011 trial has confirmed that if an HIV-positive person adheres to an effective ART regimen, the risk of transmitting the virus to their uninfected sexual partner can be reduced by 96%. The WHO recommendation to initiate ART in all people living with HIV will contribute significantly to reducing HIV transmission.

Pre-exposure prophylaxis (PrEP) for HIV-negative partner

Oral PrEP of HIV is the daily use of ARV drugs by HIV-negative people to block the acquisition of HIV. More than 10 randomized controlled studies have demonstrated the effectiveness of PrEP in reducing HIV transmission among a range of populations including serodiscordant heterosexual couples (where one partner is infected and the other is not), men who have sex with men, transgender women, high-risk heterosexual couples, and people who inject drugs. WHO recommends PrEP as a prevention choice for people at substantial risk of HIV infection as part of a combination of prevention approaches. WHO has also expanded these recommendations to HIV-negative women who are pregnant or breastfeeding.

Post-exposure prophylaxis for HIV (PEP)

Post-exposure prophylaxis (PEP) is the use of ARV drugs within 72 hours of exposure to HIV in order to prevent infection. PEP includes counselling, first aid care, HIV testing, and administration of a 28-day course of ARV drugs with follow-up care. WHO recommends PEP use for both occupational and non-occupational exposures and for adults and children.

Harm reduction for people who inject and use drugs

People who inject drugs can take precautions against becoming infected with HIV by using sterile injecting equipment, including needles and syringes, for each injection and not sharing drug using equipment and drug solutions. Treatment of dependence, and in particular opioid substitution therapy for people dependent on opioids, also helps reduce the risk of HIV transmission and supports adherence to HIV treatment. A comprehensive package of interventions for HIV prevention and treatment includes:

- Needle and syringe programmes;
- Opioid substitution therapy for people dependent on opioids and other evidence-based drug dependence treatment;
- HIV testing and counselling;
- HIV treatment and care;
- Risk-reduction information and education and provision of naloxone;
- Access to condoms; and

- Management of STIs, tuberculosis and viral hepatitis.

Elimination of mother-to-child transmission of HIV (EMTCT)

The transmission of HIV from an HIV-positive mother to her child during pregnancy, labour, delivery or breastfeeding is called vertical or mother-to-child transmission (MTCT). In the absence of any interventions during these stages, rates of HIV transmission from mother-to-child can be between 15–45%. MTCT can be nearly fully prevented if both the mother and the baby are provided with ARV drugs as early as possible in pregnancy and during the period of breastfeeding.

WHO recommends lifelong ART for all people living with HIV, regardless of their CD4 count clinical stage of disease, and this includes women who pregnant or breastfeeding. In 2017, 80% of the estimated 1.1 million pregnant women living with HIV globally received ARV treatments to prevent transmission to their children. A growing number of countries are achieving very low rates of MTCT and some (Armenia, Belarus, Cuba and Thailand) have been formally validated for elimination of MTCT of HIV as a public health problem. Several countries with a high burden of HIV infection are also progressing along the path to elimination.

Cost of HIV Treatment

While effective, ARV treatment does not represent a cure for HIV infection, and treatments must be taken for the duration of a patient's lifetime. Patients are typically treated with a combination of drugs, including at least two nucleoside reverse transcriptase inhibitors (NRTIs) and at least one drug from the other, more potent drug classes (commonly called the ''third-agent'' treatment). Third agents are treatments from the non-NRTI, protease inhibitor, and integrase inhibitor drug classes and are responsible for the large improvement in the treatment of HIV disease by combination therapy observed in the last 2 decades. These combinations are costly; the most popular combination (efavirenz/emtricitabine/tenofovir) is published to have an average wholesale price of USD 2,253.88 per 30 tablets in the United States. Despite the high cost of ARVs, studies have shown early combination treatments to be cost-effective because they reduce the economic burden of illness associated with AIDS-related hospitalizations and death and increase patients' quality of life. Thus, HIV disease has created a large economic burden, with annual costs of care for HIV-infected patients in the US estimated to be USD 19,912 in 2006 dollars and discounted lifetime costs estimated at USD 385,200 (2004 dollars).

The majority of pharmaceutical companies do not use one global price for their products. Actual pricing data on ARVs shows the variation for countries with different socio-economic status. For example, the average price per patient per year paid by lower income countries for lopinavir/ritonavir 133/33mg is USD 500, whereas the price for the same product in middle-income countries is USD 1134 (WHO, 2008). For four of the ARV regimens (the lowest/highest priced first-line ARV combinations and the lowest/highest priced second-line ARV combinations) large price differences between countries were found, even those which had the same income and prevalence. For instance, Congo in 2007 paid USD 95 for lamivudine 150mg+nevirapine 200mg+stavudine 30mg, whereas Nigeria paid more than three times (USD 334) for the same ARV combination. Both are low-income countries with a prevalence of 1.2% and 3.1% respectively in the same region (Sub-Saharan Africa). Furthermore, there were also large differences between countries procuring both the same innovator products. For instance, Morocco paid USD 1,053 for the innovator ARV combination of lamivudine, zidovudine and efavirenz, whereas the lowest price for the same innovator combination was USD 513.

The United States President's Emergency Plan for AIDS Relief (PEPFAR) is supporting ART treatment in many countries across the globe; their estimated costs per patient per year for 2006–2009 were USD 436; the cost components included were similar to those in the present study. A report from Zambia suggests that the cost for a first-line HAART (highly active antiretroviral therapy) regimen is USD 488 per patient per year, which also includes diagnostics. A systematic review conducted in 2011 on unit costs for delivery of ART and prevention of mother-to-child transmission of HIV estimated that the median cost of ART per patient per year was USD 792 for lower-middle-income countries and USD 1454 for uppermiddle-income countries; about 47% of the costs were spent on antiretroviral drugs alone. The Multi-country Analysis of Treatment Costs for HIV/AIDS (MATCH) in 2010-–2011, which included all the components of service delivery, revealed that the costs ranged from USD 208 to USD 682 per person per year across the countries studied (Ethiopia, Malawi, Rwanda, South Africa and Zambia).

In India, the cost per person per year is comparatively less when compared to PEPFAR-supported treatment sites across 12 countries. The use of generic drugs, bulk procurement of drugs and reagents at a national level, and reduction in drug costs over the years has contributed to a low cost for commodities. The lower cost in India may also be attributed to efficient use of general health systems. Also, India has the capacity to scale up its ART services, using the country-owned domestic drug manufacturing base. The estimated cost for ART services is USD 133.89 per patient per year, of

which 66% (USD 88.6) is for antiretroviral drugs and 34% (USD 45.23) is for non-ART recurrent expenditures. Of the total non-ART expenditure of USD 45.23 per person per year, USD 32.51 (72%) is borne by the NACP and the remaining USD 12.72 (28%) is borne by health systems. Figure 5 shows the conceptual framework of the socio-economic impact of HIV/AIDS.

Impact on Business Sustainability

The impact of the HIV/AIDS epidemic goes far beyond the household level. Firms and businesses may also be affected as HIV-infected people are usually in the prime working years and are involved in the process of production. If HIV prevalence reaches a high level in a country or within a firm, the impact of the disease may be dramatic for the business or firm involved. As HIV infection progresses to AIDS, affected workers are likely to be absent from the workplace more and more often. The periods of absenteeism may affect the productivity of the firm, especially if the worker occupies an important position in the firm and consequently is more difficult to replace. Firms that have a health programme may find themselves responsible for substantial medical costs. The insurance scheme of the firm may become more expensive as insurance companies increase the costs of coverage in response to high HIV prevalence rates in firms. Higher costs could impede saving for investment. HIV/AIDS in the workplace may also lead to increased funeral expenses for workers.

High levels of absenteeism seem to be one of the characteristics of the impact of HIV/AIDS on firms. For example, a study of 15 different establishments in Ethiopia found that the companies were experiencing considerable absenteeism. The number of HIV/AIDS-related illnesses was 53 percent of all reported illnesses, totalling 15,363 incidents over a five-year period. In Namibia, NamWater, the largest water purification company, announced in 2000 that HIV/AIDS was crippling its operations. They reported a high staff turnover from HIV-related deaths, increasing absenteeism and a general loss of productive hours.

Firms and companies are facing substantial cost increases resulting from HIV/AIDS that threaten their viability. The situation has been documented in Botswana, Kenya and Uganda. The annual cost of AIDS per employee was estimated to range from USD 49 for a Kenyan sugar firm to USD 300 for the Uganda Railway Corporation. The extent to which people living with HIV/AIDS will continue to be part of the workforce depends largely on the type of work performed, the stage of the disease and the existing policies in the relevant companies. Workers in physically demanding jobs may find it more difficult to maintain their jobs when they become ill. The response of businesses to the HIV/AIDS epidemic has taken many forms. Some companies have increased medical care and instituted prevention programmes to help workers avoid contract-ing the virus. As mentioned above, a cost-benefit study by Rosen and others (2003), concluded that company investment in prevention and treatment would result in a net gain for most companies. Many companies are attempting to cut costs and prevent new HIV infections at the same time. Prevention programmes usually include AIDS education for workers and their families, treatment of sexually transmitted diseases (STDs) and distribution of condoms (Simon and others, 2000).

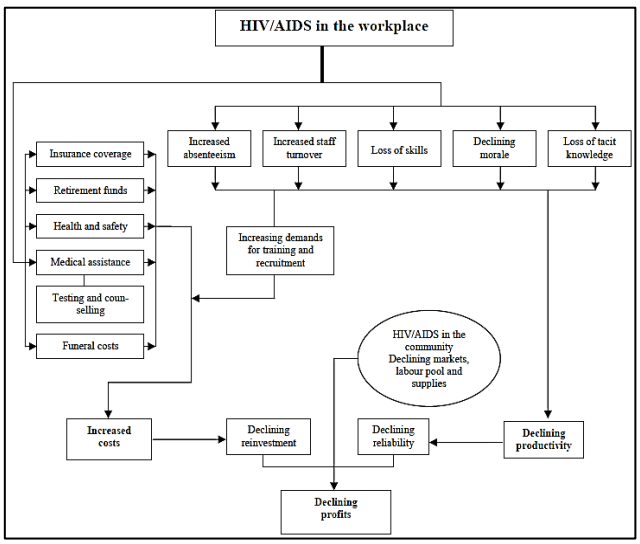


Figure 5: Conceptual framework for the socio-economic impact of the HIV/AIDS epidemic on firms. (Source: UNAIDS, Global Business Council on HIV/AIDS and Prince of Wales Business Leaders Forum, The Business Response to AIDS: Impact and Lessons Learned. Geneva, 2000).

HIV AIDS PREVENTION AND MANAGEMENT PROGRAM (HAPMP) AT STAR ENERGY GEOTHERMAL (WAYANG WINDU) LTD

Refer to Indonesia Director General of Man Power Regulation No.Kep/75/DK/PPK/IX/2010, there are 11 elements in the implementation of the HAPMP in each company operating in the territory of Indonesia.

HAPMP Policy

Each company must have a written document on HAPMP in the workplace. SEGWW has procedures regarding HAPMP that have been implemented since 2011. The purposes of this procedure are:

- To protect healthy employee(s) from the threat of HIV and AIDS, on the other hand also to protect employee(s) who positively diagnosed of HIV AIDS from mishandling in treatment, include protect the confidentiality matter.
- To comply with governmental rule and regulation, especially regulation of Indonesia Minister of Labor and Transmigration No.68 / 2004.
- To keep and improve employee(s) safety and health.

Education and Training Program

SEGWW has carried out various training and education for employees regarding HIV AIDS. Among them is the training of HIV AIDS peer educators to employees and contractors. Peer educator training is able to develop non-medical people who can become information disseminating agents to peers and the community about HIV AIDS and the danger of stigmatization and discrimination, in ways and languages that are easily understood by peers. SEGWW has also included the HIV AIDS subcommittee within the structure of the occupational health and safety team.

Efforts to avoid stigma and discrimination

SEGWW do not carry out compulsory HIV testing either in the pre-employee medical check-up, annual medical check-up, or pre-retirement medical check-up. In addition, all medical information is stored confidentially in employee medical records that can only be accessed by medical personnel. SEGWW treats HIV positive worker in the same way as seronegative worker. SEGWW Health Guidelines and Company-Labour Agreement (CLA) emphasize that all workers and families of workers diagnosed with HIV AIDS will receive appropriate treatment and be borne by the company.

In addition, at SEGWW, the work environment is measured every year under the industrial hygiene program, which measures the parameters of the work environment, such as indoor air quality, dust levels, the number of bacteria and fungi in the room, and etc. This program will greatly create a healthy working environment for workers both HIV-infected and seronegative workers.

Support and care programs for HIV and AIDS employees such as social support, Voluntary Counseling and Testing (VCT), treatment, referral systems, etc.

SEGWW have a occupational health clinic equipped with complete facilities for VCT- both HIV pre-test and post-test. This includes a closed counseling room which guarantees confidentiality, examination rooms, ambulance vehicle and medicine rooms. In addition, medical personnel are also certified as VCT counselor issued by the Ministry of Health of the Republic of Indonesia. SEGWW has had cooperation with many major hospitals around the company's location and throughout Indonesia that allows referral if there are cases that require further consultation and treatment by specialists doctor at hospital. Figure 6 shows the SEGWW's procedure of prevention and management HIV/AIDS.

Budget Allocation for HAPMP

The annual budget fluctuates according to operational needs in the field. However, it has become a SEGWW commitment that HAPMP must always be carried out. The allocated budget can be spread to several departments, depending on the events and occasions carried out, not only allocated in HR-Medical department. For example, HAPMP related to the community around the company can be covered by the budget in External Relation department.

Socialization and communication the contents of HAPMP policy to all employees

Every year, we always provide updated counseling materials on HIV AIDS and HAPMP policy to all employees. SEGWW also establish good communication with the Manpower Office and the local Health Office to find out if there are updates on regulations related to HIV AIDS in the workplace in Indonesia.

	8.0 HEALTH, SAFETY & ENVIRONMENT OCCUPATIONAL HEALTH	PROCEDURE TIER : 03
starenergy	MEDICAL TECHNICAL PREVENTION AND MANAGEMENT OF HIV AIDS IN THE WORKPLACE	Doc : SHE-8.0-OHE-MT-106 Rev : 04

REVISION HISTORY

REV	DATE	ORIGINATOR	REVIEWED	APPROVED	DESCRIPTION
00	Oct - 11	Deddi Ekaputra R	Soedarmadji	Heribertus Dwiyudha	New procedure
01	Dec - 14	Esuh/Deddi ER	Soedarmadji	Rully Wirawan	No changes still valid
02	Oct - 15	Dewi Kania	Sandriana T	Walda H	Change on numbering structure & format tier Bilingual reformat
03	1 Sept 17	Acknowledge by	KTPB	Ismail H.	Compliness to requirment of EBTKE
04	16 Jan. 2019	Rahmat D. Gulo	Dr. Soedarmadji Dr. Deddi ER	Ismail Hidayat	Update Refference and Responsibility

Note: In the event of any conflict between the English and the Bahasa Indonesia version of this procedure, then the English version shall prevail and be used for interpretation and settlement of any dispute.

Figure 6: SEGWW's Procedure of Prevention and Management of HIV AIDS in the Workplace.

Data of number of employees who have been given counseling or participated in discussions about HIV AIDS in the workplace in the past year

The record of the number of employees who have received socialization regarding HAPMP policy and updates on knowledge about HIV AIDS is always documented so that further plans can be made for employees who have not received information and updates on knowledge about HIV AIDS. The goal is that all workers who work in SEGWW area understand about HIV AIDS, do not practice behaviors that are at risk of contracting HIV, and do not discriminate and stigmatize seropositive people.

Regular evaluation of policy and the effectiveness of program implementation through HIV risk-related behavioral questionnaires for employees in the company

Every year, we conduct a measurable survey to determine the level of employee understanding about HIV AIDS, especially regarding risky behavior. The results of the questionnaire were analyzed so that it would be known which aspects still needed to be sharpened in HAPMP for the following years.

Special occupational health and safety procedure in the prevention of HIV transmission in the workplace

SEGWW has several special procedures related to prevention of HIV transmission in the workplace, including procedures for needle stick injury and procedures for handling hazardous waste including medical waste. There has been an incident of a needle stick injury that happened to a medical personnel in 2010. By referring to the needle stick injury procedure, we took medical steps to anticipate the risk of contracting HIV for the incident, including doing VCT and sending to hospital for more consultation and examination by an infection specialist doctor.

Reporting to local authority in charge for Man Power

Regularly every three months, SEGWW sends a report to the man power agency about HAPMP program. It aims to establish good communication

and harmonious cooperation between the private sector and the government that monitors it. The objective is that HAPMP can run well and achieve the target to achieve 3 zero: zero new infection, zero death related AIDS, and zero discrimination among workers.

Develop HAPMP for community surrounding the company (schools, community health center, red district area)

SEGWW regularly educates about HIV AIDS every year, including efforts to not stigmatize and discriminate against people suffering from HIV AIDS to schools around the company. The education is also conducted at the community health center. Various breakthroughs were also carried out in the dissemination of HIV AIDS information, including using community radio broadcasts in the Pangalengan area. In addition, key population groups in the Pangalengan area were also being the target of data collection and education on HIV AIDS. The key population includes commercial sex workers, transvestites, men who have sex with men (MSM), and IV drug users. In order to empower community health centers, SEGWW also provides HIV rapid test kit to community health center in the Pangalengan area. In 2011, SEGWW provided assistance to the Indonesian team incorporated in Rumah Cemara, an institution that accommodates homeless drug users and teenagers with HIV and AIDS to go to the "Homeless World Cup" world soccer championship in Paris, France. All of that shows the concern of SEGWW for people with HIV in society so that they remain productive and dignified.

AWARDS

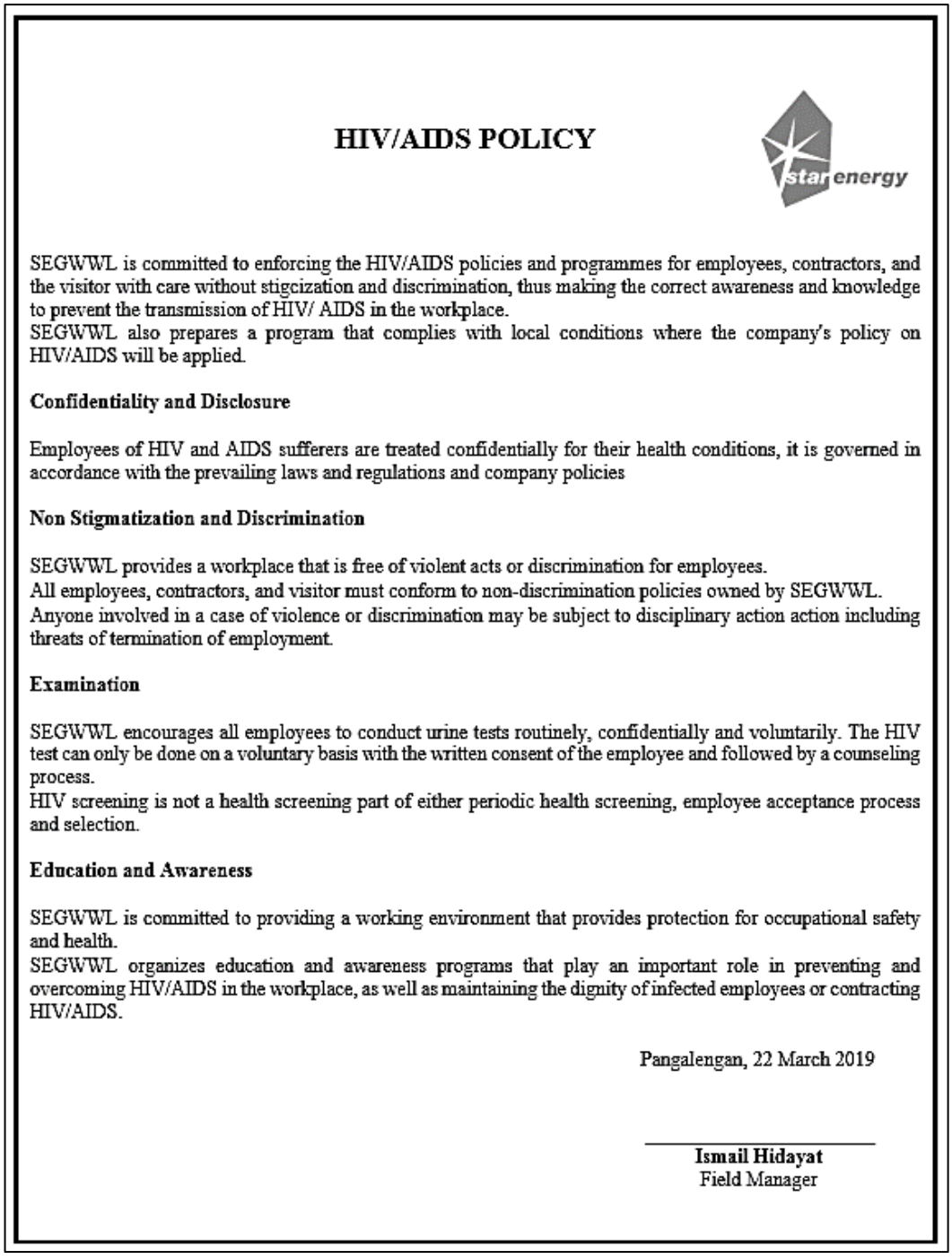
Appreciation was given to the Republic of Indonesia government, in the form of a platinum award which was the highest award for the implementation of the P2HIV program. I've got this award since 2010-2019 (9 times in a row). in 2018, a number of people received the ARROW (ASEAN Red Ribbon for Outstanding Workplace) award as an appreciation for companies that run HIV AIDS programs in the workplace. This success is a pride for all people, but on the other hand it becomes a whip to continue to innovate so that the P2HIV program can continue to sharply anticipate the dangers of the global pandemic HIV AIDS.

DISCUSSION

HIV AIDS has become an unresolved world problem. Even in African countries, this disease has caused a huge economic burden. Various efforts have been made by world bodies to reduce the rate of new HIV infections. In some countries these efforts appear to have produced results, but in several other countries including Indonesia, the rate of new HIV infections continues to increase from year to year. HIV AIDS is a disease that has a bad stigma for sufferers, so they often get discrimination from other people, including at work. Stigma and discrimination against people with HIV / AIDS remain strong in Indonesia. Such stigma is irrational or fear-driven negative attitude, behavior, and judgment toward people living with HIV and those who are perceived to be living with HIV. Such stigma and discrimination are stigmatized and discriminated against cause anxiety, depression, guilt, isolation, low self-esteem, family dynamics disruption, physical and emotional violence, intensification of grief, and loss of social support.

Self-stigma bundled with discrimination prevents people from accessing education and information on preventive behavior, refute risk, refuse to test, not seeking health assistance, delay treatment, and not adhering to therapy. This health-avoiding behavior results in increasing the HIV rate of transmission, declining of patient quality of life and a higher risk of AIDS-related death. Stigma and discrimination are clearly the cause of efforts to reduce the rate of new HIV infections hampered. In the context of occupational health, HIV AIDS programs fall into the pillars of preventive and promotive, from 4 pillars of occupational health (preventive, promotive, curative, and rehabilitative) efforts. In Indonesia, the labor ministry plays an active role in providing regulations that require every company to develop HIV AIDS prevention and management programs (HAPMP) in the workplace. This program is very appropriate because the number of workers in Indonesia is 48.44% of the total population in Indonesia. Based on data from the Ministry of Health in 2018, the majority of HIV cases occur in people of productive age between 20 - 59 years. This poses a big challenge for companies, including the geothermal industry. Of course, Indonesia does not want to be like countries in Africa which, due to the concentrated HIV AIDS epidemic, have caused many businesses to be disrupted due to the many workers who have to be absent for doing treatment (high rate of absenteeism). For example, in Ethiopia where 53% of employee absenteeism is caused by HIV and AIDS related diseases. In Namibia, the largest water purifier company in the country, NamWater, its business has been severely reduced by HIV AIDS suffered by its workers. Geothermal industries in Indonesia must anticipate the risk of this global HIV AIDS pandemic early on. In Indonesia, the geothermal industry is included in the high risk category of HIV AIDS transmission, because it is dominated by men who have relatively high income (compared to the average income of workers in other sectors), mobile, in a remote and macho work environment (4M principle). The essential of prevention is always better than cure. Aspects of risk management threat of the global HIV AIDS pandemic must always be assessed and

incorporated into measurable and planned programs. Eleven elements of the program included in HAPMP can adequately cover a variety of critical points in the risk of HIV transmission in the workplace. The participation of all workers and also synergy with the community around the company is the key to the success of the program. SEGWW from 2009 until now has carried out this HAPMP program. SEGWW has achieved various national and international awards, i.e the 9th consecutive Platinum Award (national highest award), and the Arrow (ASEAN Red Ribbon of Outstanding Workplace) Award which is a regional award in ASEAN. The main objective of HAPMP in Indonesia is three zero: Zero new HIV infection, Zero Stigma and Discrimination, and Zero AIDS-related deaths among workers.



HIV/AIDS POLICY

SEGWWL is committed to enforcing the HIV/AIDS policies and programmes for employees, contractors, and the visitor with care without stigcization and discrimination, thus making the correct awareness and knowledge to prevent the transmission of HIV/ AIDS in the workplace.
SEGWWL also prepares a program that complies with local conditions where the company's policy on HIV/AIDS will be applied.

Confidentiality and Disclosure

Employees of HIV and AIDS sufferers are treated confidentially for their health conditions, it is governed in accordance with the prevailing laws and regulations and company policies

Non Stigmatization and Discrimination

SEGWWL provides a workplace that is free of violent acts or discrimination for employees.
All employees, contractors, and visitor must conform to non-discrimination policies owned by SEGWWL.
Anyone involved in a case of violence or discrimination may be subject to disciplinary action action including threats of termination of employment.

Examination

SEGWWL encourages all employees to conduct urine tests routinely, confidentially and voluntarily. The HIV test can only be done on a voluntary basis with the written consent of the employee and followed by a counseling process.
HIV screening is not a health screening part of either periodic health screening, employee acceptance process and selection.

Education and Awareness

SEGWWL is committed to providing a working environment that provides protection for occupational safety and health.
SEGWWL organizes education and awareness programs that play an important role in preventing and overcoming HIV/AIDS in the workplace, as well as maintaining the dignity of infected employees or contracting HIV/AIDS.

Pangalengan, 22 March 2019

Ismail Hidayat
Field Manager

Figure 7: SEGWW's HIV AIDS Policy.

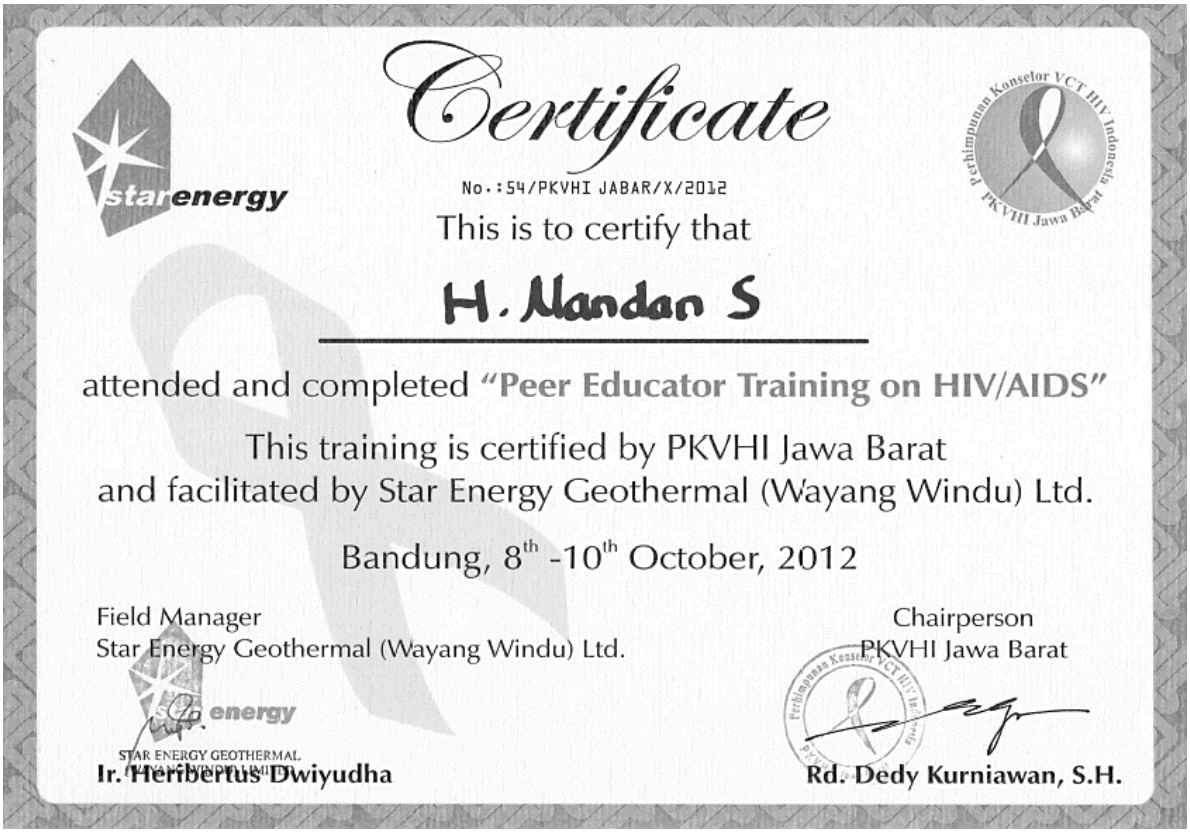


Figure 8: Sample of HIV AIDS Peer Educator Training facilitated by SEGWW.

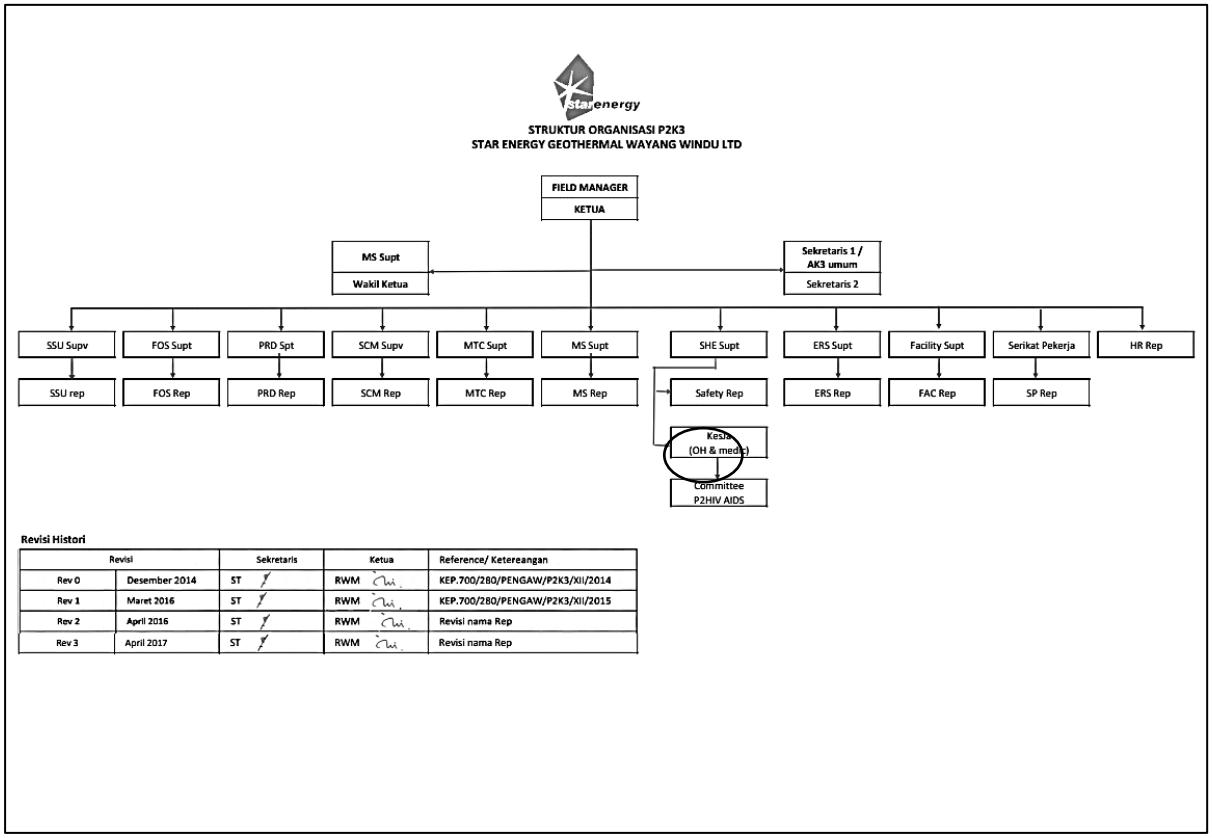
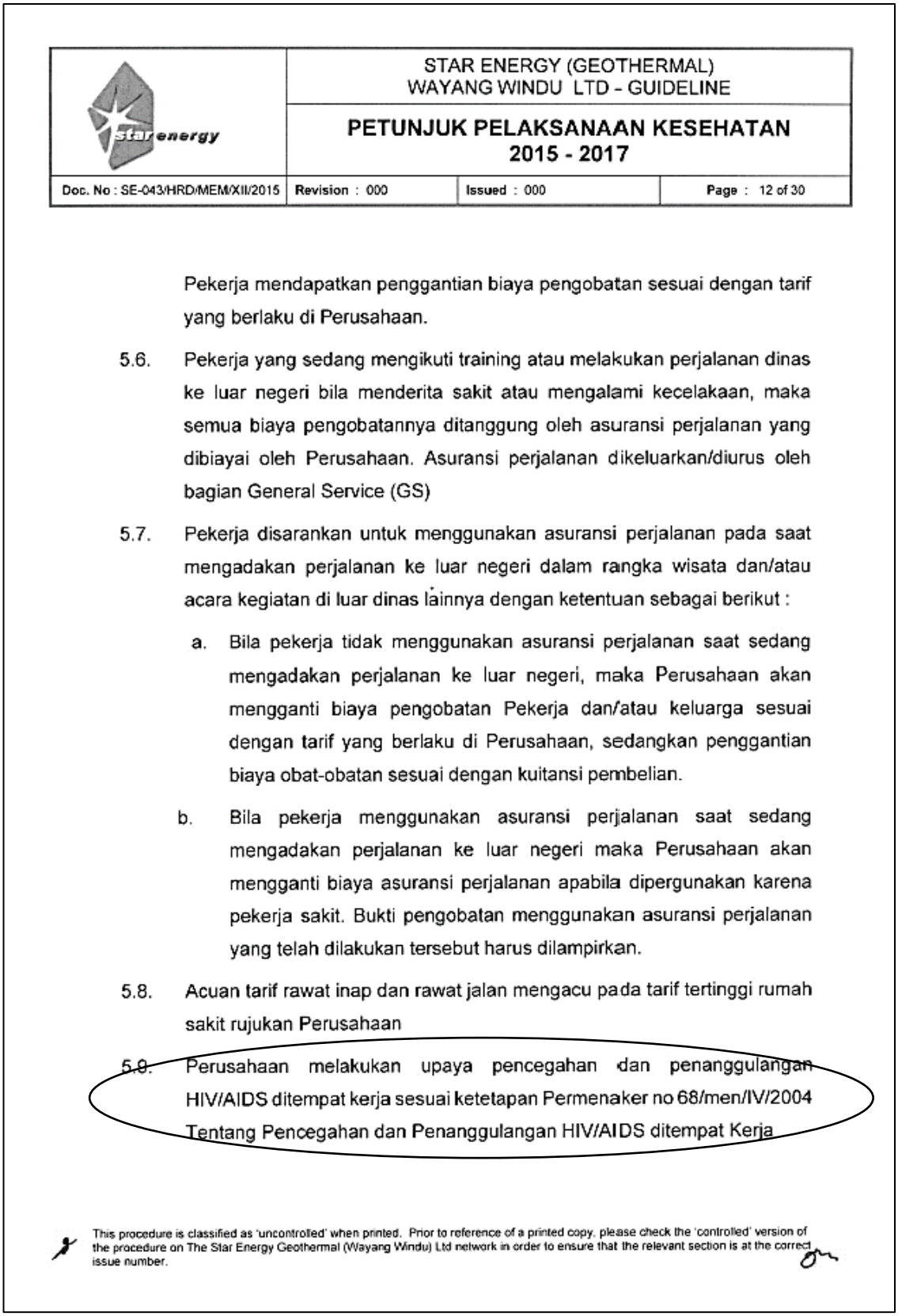


Figure 9: HAPMP Subcommitee is included within Structure of Occupational Health and Safety.



STAR ENERGY (GEOTHERMAL)
WAYANG WINDU LTD - GUIDELINE

PETUNJUK PELAKSANAAN KESEHATAN 2015 - 2017

Doc. No : SE-043/HRD/MEM/XII/2015	Revision : 000	Issued : 000	Page : 12 of 30

Pekerja mendapatkan penggantian biaya pengobatan sesuai dengan tarif yang berlaku di Perusahaan.

5.6. Pekerja yang sedang mengikuti training atau melakukan perjalanan dinas ke luar negeri bila menderita sakit atau mengalami kecelakaan, maka semua biaya pengobatannya ditanggung oleh asuransi perjalanan yang dibiayai oleh Perusahaan. Asuransi perjalanan dikeluarkan/diurus oleh bagian General Service (GS)

5.7. Pekerja disarankan untuk menggunakan asuransi perjalanan pada saat mengadakan perjalanan ke luar negeri dalam rangka wisata dan/atau acara kegiatan di luar dinas lainnya dengan ketentuan sebagai berikut :

a. Bila pekerja tidak menggunakan asuransi perjalanan saat sedang mengadakan perjalanan ke luar negeri, maka Perusahaan akan mengganti biaya pengobatan Pekerja dan/atau keluarga sesuai dengan tarif yang berlaku di Perusahaan, sedangkan penggantian biaya obat-obatan sesuai dengan kuitansi pembelian.

b. Bila pekerja menggunakan asuransi perjalanan saat sedang mengadakan perjalanan ke luar negeri maka Perusahaan akan mengganti biaya asuransi perjalanan apabila dipergunakan karena pekerja sakit. Bukti pengobatan menggunakan asuransi perjalanan yang telah dilakukan tersebut harus dilampirkan.

5.8. Acuan tarif rawat inap dan rawat jalan mengacu pada tarif tertinggi rumah sakit rujukan Perusahaan

5.9. Perusahaan melakukan upaya pencegahan dan penanggulangan HIV/AIDS ditempat kerja sesuai ketetapan Permenaker no 68/men/IV/2004 Tentang Pencegahan dan Penanggulangan HIV/AIDS ditempat Kerja

This procedure is classified as 'uncontrolled' when printed. Prior to reference of a printed copy, please check the 'controlled' version of the procedure on The Star Energy Geothermal (Wayang Windu) Ltd network in order to ensure that the relevant section is at the correct issue number.

Figure 10: SEGWW Health Guideline states clearly that it will cover the costs of medical treatment and care for HIV AIDS cases.



Figure 11: Indoor Air Quality Measurement provided in yearly Industrial Hygiene Program.

REFERENCES

Haryawan, A., G., (2018), "Stigma Still Thwarts HIV Prevention" [online], (https://www.thejakartapost.com/academia/2018/12/26/stigma-still-thwarts-hiv-prevention.html, accessed on June 25, 2019).

Badan Pusat Statistik, (2019), "Keadaan Angkatan Kerja di Indonesia February 2019," Katalog: 2303004, executive summary.

Komisi Penanggulangan HIV dan AIDS Nasional, (2015), "Strategi dan Rencana Aksi Nasional 2015-2019: Penanggulangan HIV dan AIDS di Indonesia," 45.

United Nations Development Programme, (2019), "Goal 3: Good health and well-being," [online], (https://www.undp.org/content/undp/en/home/sustainable-development-goals/goal-3-good-health-and-well-being.html, accessed on June 26, 2019)

Avert, (2019),"History of HIV and AIDS Overview"[online],(https://www.avert.org/professionals/history-hiv-aids/overview, accessed on June 26, 2019)

UNAIDS, (2018), "Global HIV and AIDS Statistics-2018 Fact Sheet".

Kementerian Kesehatan Republik Indonesia, (2019), "Laporan Perkembangan HIV AIDS".

Naif, H., M., (2013), "Pathogenesis of HIV Infection," Infectious Disease Reports, 5 (Suppl 1):e6

World Health Organization, (1993), "Fact Sheet 1 HIV AIDS: The Infection," [online], (https://www.who.int/hiv/abouthiv/fact_sheet_hiv.htm, accessed on June 27,2019).

De Castro, M., (2017), "Triangle of Self-Care: The Essentials of HIV Transmission" [online], (http://www.loveyourself.ph/2017/02/triangle-of-self-care-esse-ntials-of.html,accessed on June 27,2019).

Centers for Disease Control and Prevention, (2015), "HIV Risk Behaviors," [online], (https://www.cdc.gov/hiv/risk/estimates/riskbehaviors.html,accessed on June 27,2019).

Kasper, Dennis L., et al., (2015), "Human Immunodeficiency Virus Disease: AIDS and Related Disorders," Harrison's Principles of Internal Medicine, 19th edition.

Chu, C., Selwyn, P., A., (2010), "Diagnosis and Initial Management of Acute HIV Infection," American Family Physician, 10, 1239-1244.

University of California San Fransisco, (2019), "AIDS Signs and Symptoms," [online], (https://www.ucsfhealth.org/conditions/aids/signs_and_symptoms.html,accessed on June 28,2019).

World Health Organization, (2015), "Diagnostics for HIV Diagnosis," [online], (https://www.ncbi.nlm.nih.gov/books/NBK316024/, accessed on June 28,2019).

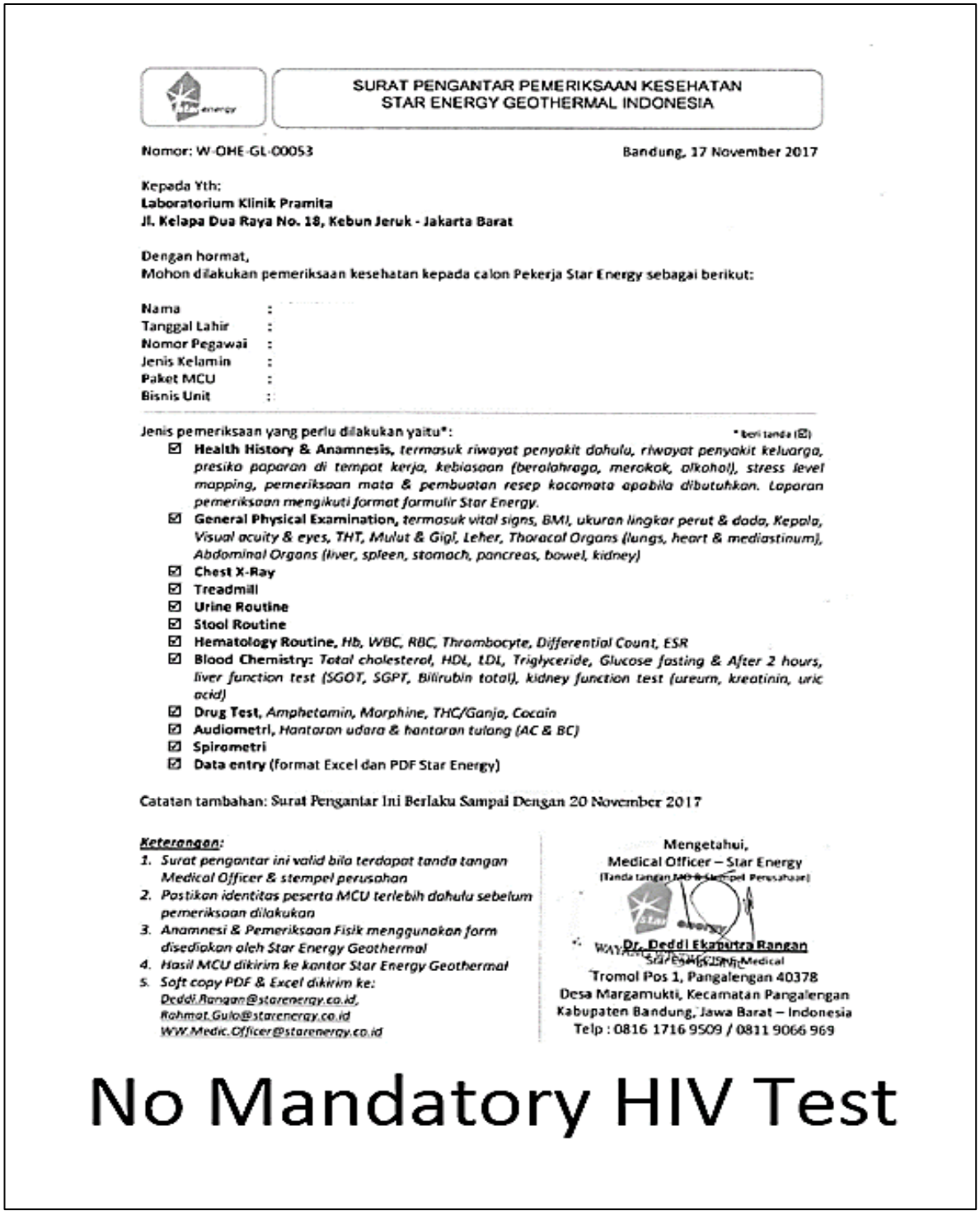
World Health Organization, (2018), "HIV AIDS," [online], (https://www.who.int/news-room/fact-sheets/detail/hiv-aids, accessed on June 28,2019).

Solem, C., T., Snedecor, S., J., Khachatryan, A., Nedrow, K., Tawadrous, M., et al., (2014), "Cost of Treatment in a US Commercially Insured, HIV-1–Infected Population," PLoS ONE, 9(5),1-2.

Wirtz, V., J., Forsythe, S., S., et al., (2008), "The Cost of Antiretrovirals, Maximizing Value for Money." Results for Development Institute.

Agarwal, R., Rewari, B., B., Shastri, S., Nagaraja, S., B., Rathore, A., S., (2017), "Delivery of antiretroviral treatment services in India: estimated costs incurred under the National AIDS Control Programme," WHO South-East Asia J Public Health. ;6(1):94–98.

United Nations Department of Economic and Social Affairs/Population Division, (2004), The Impact of AIDS.



SURAT PENGANTAR PEMERIKSAAN KESEHATAN
STAR ENERGY GEOTHERMAL INDONESIA

Nomor: W-OHE-GL-00053 Bandung, 17 November 2017

Kepada Yth:
Laboratorium Klinik Pramita
Jl. Kelapa Dua Raya No. 18, Kebun Jeruk - Jakarta Barat

Dengan hormat,
Mohon dilakukan pemeriksaan kesehatan kepada calon Pekerja Star Energy sebagai berikut:

Nama :
Tanggal Lahir :
Nomor Pegawai :
Jenis Kelamin :
Paket MCU :
Bisnis Unit :

Jenis pemeriksaan yang perlu dilakukan yaitu*: * beri tanda (☑)

- ☑ **Health History & Anamnesis,** *termasuk riwayat penyakit dahulu, riwayat penyakit keluarga, presiko paparan di tempat kerja, kebiasaan (beralahraga, merokok, alkohol), stress level mapping, pemeriksaan mata & pembuatan resep kacamata apabila dibutuhkan. Laporan pemeriksaan mengikuti format formulir Star Energy.*
- ☑ **General Physical Examination,** *termasuk vital signs, BMI, ukuran lingkar perut & dada, Kepala, Visual acuity & eyes, THT, Mulut & Gigi, Leher, Thoracal Organs (lungs, heart & mediastinum), Abdominal Organs (liver, spleen, stomach, pancreas, bowel, kidney)*
- ☑ **Chest X-Ray**
- ☑ **Treadmill**
- ☑ **Urine Routine**
- ☑ **Stool Routine**
- ☑ **Hematology Routine,** *Hb, WBC, RBC, Thrombocyte, Differential Count, ESR*
- ☑ **Blood Chemistry:** *Total cholesterol, HDL, LDL, Triglyceride, Glucose fasting & After 2 hours, liver function test (SGOT, SGPT, Bilirubin total), kidney function test (ureum, kreatinin, uric acid)*
- ☑ **Drug Test,** *Amphetamin, Morphine, THC/Ganja, Cocain*
- ☑ **Audiometri,** *Hantaran udara & hantaran tulang (AC & BC)*
- ☑ **Spirometri**
- ☑ **Data entry** (format Excel dan PDF Star Energy)

Catatan tambahan: Surat Pengantar Ini Berlaku Sampai Dengan 20 November 2017

Keterangan:

1. *Surat pengantar ini valid bila terdapat tanda tangan Medical Officer & stempel perusahan*
2. *Pastikan identitas peserta MCU terlebih dahulu sebelum pemeriksaan dilakukan*
3. *Anamnesi & Pemeriksaan Fisik menggunakan form disediakan oleh Star Energy Geothermal*
4. *Hasil MCU dikirim ke kantor Star Energy Geothermal*
5. *Soft copy PDF & Excel dikirim ke:*
   Deddi.Rangan@starenergy.co.id,
   Rahmat.Gulo@starenergy.co.id
   WW.Medic.Officer@starenergy.co.id

Mengetahui,
Medical Officer – Star Energy
(Tanda tangan MO & Stempel Perusahaan)

Dr. Deddi Ekaputra Rangan
Star Energy Geothermal Medical

Tromol Pos 1, Pangalengan 40378
Desa Margamukti, Kecamatan Pangalengan
Kabupaten Bandung, Jawa Barat – Indonesia
Telp : 0816 1716 9509 / 0811 9066 969

No Mandatory HIV Test

Figure 12: SEGWW's sample of pre-employment medical check-up item.

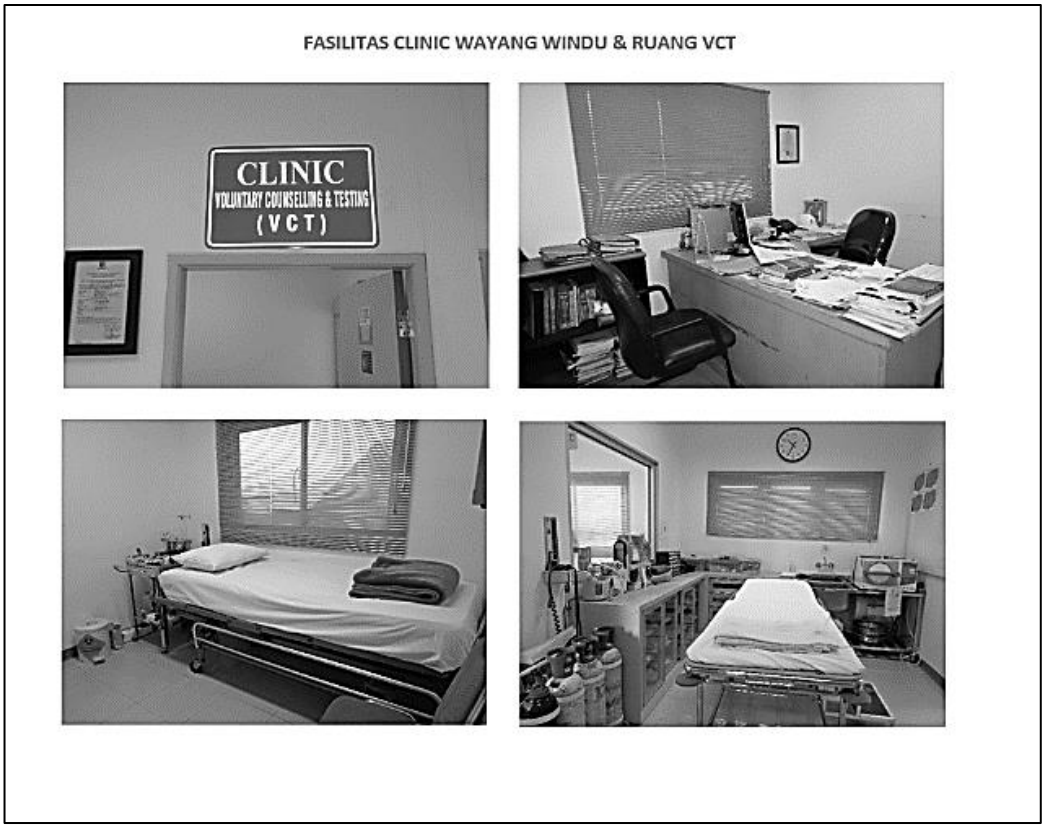


Figure 13: SEGWW's VCT room, examination room, and emergency room.



Figure 14: SEGWW's occupational health clinic, drug store, and ambulance vehicle.



Family Health International

DEPARTEMEN KESEHATAN REPUBLIK INDONESIA

SERTIFIKAT

No. 597456/ H/ DL/ 001471/ VIII/ 2007

Menteri Kesehatan Republik Indonesia berdasarkan Peraturan Pemerintah Nomor 101 Tahun 2000, serta ketentuan-ketentuan pelaksanaannya, menyatakan bahwa :

Nama : Dr. Deddi Eka Putra R

NIP/NRP :

Tempat dan Tanggal lahir :

Pangkat/Golongan : Konselor VCT

Instansi : Chevron

TELAH BERHASIL

Menyelesaikan Pelatihan Konseling dan Tes secara Sukarela (VCT) bagi Konselor Profesional yang diselenggarakan oleh Family Health International dan Ditjen PP & PL Departemen Kesehatan RI tanggal 06 September 2006 s/d 11 September 2006 bertempat di Balikpapan dengan jumlah 64 jam pelatihan @ 45 menit senilai 1 kredit.

Jakarta, 11 September 2006

An. MENTERI KESEHATAN REPUBLIK INDONESIA
KEPALA PUSDIKLAT SDM KESEHATAN

Dra. Nasirah Bahaudin. MM
NIP: 140 165 648

Figure 15: Certificate of VCT counselor.

BUDGET HIV AIDS PROGRAM TAHUN 2011-2023

TAHUN	BUDGET (Rp)
2011	90.700.000
2012	78.783.000
2013	93.735.000
2014	29.890.000
2015	38.000.000
2016	13.000.000
2017	35.000.000
2018	10.000.000
2019	40.000.000
2020	42.000.000
2021	44.100.000
2022	46.305.000
2023	48.620.250

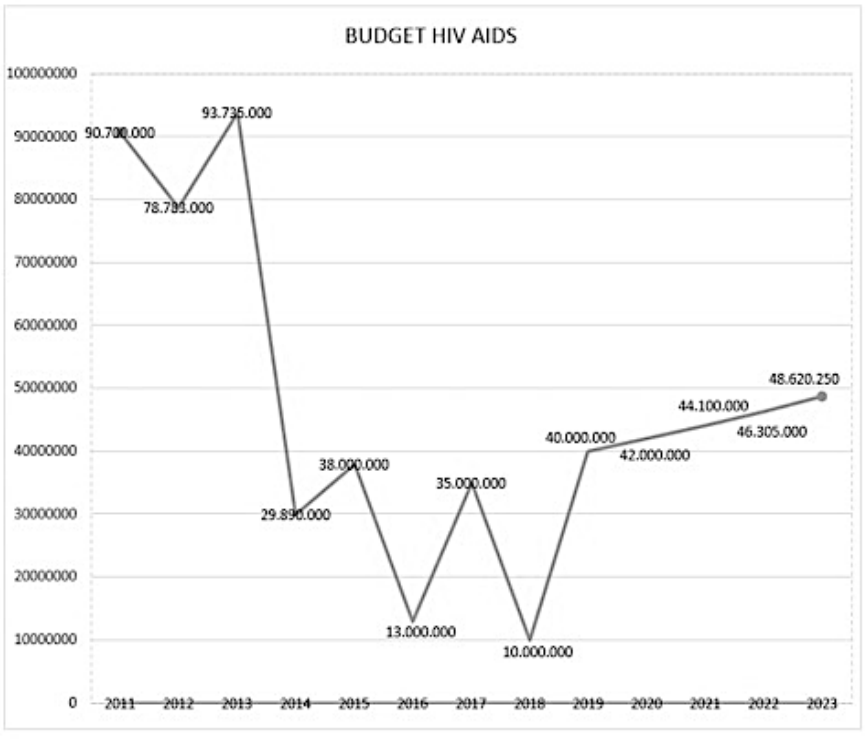


Figure 16: SEGWW's budget of HAPMP.



Figure 17: Socialization of HAPMP Policy and Update Knowledge About HIV AIDS to SEGWW Employee.

38 Djamaludin K Prod
39 Hariyanto MTC

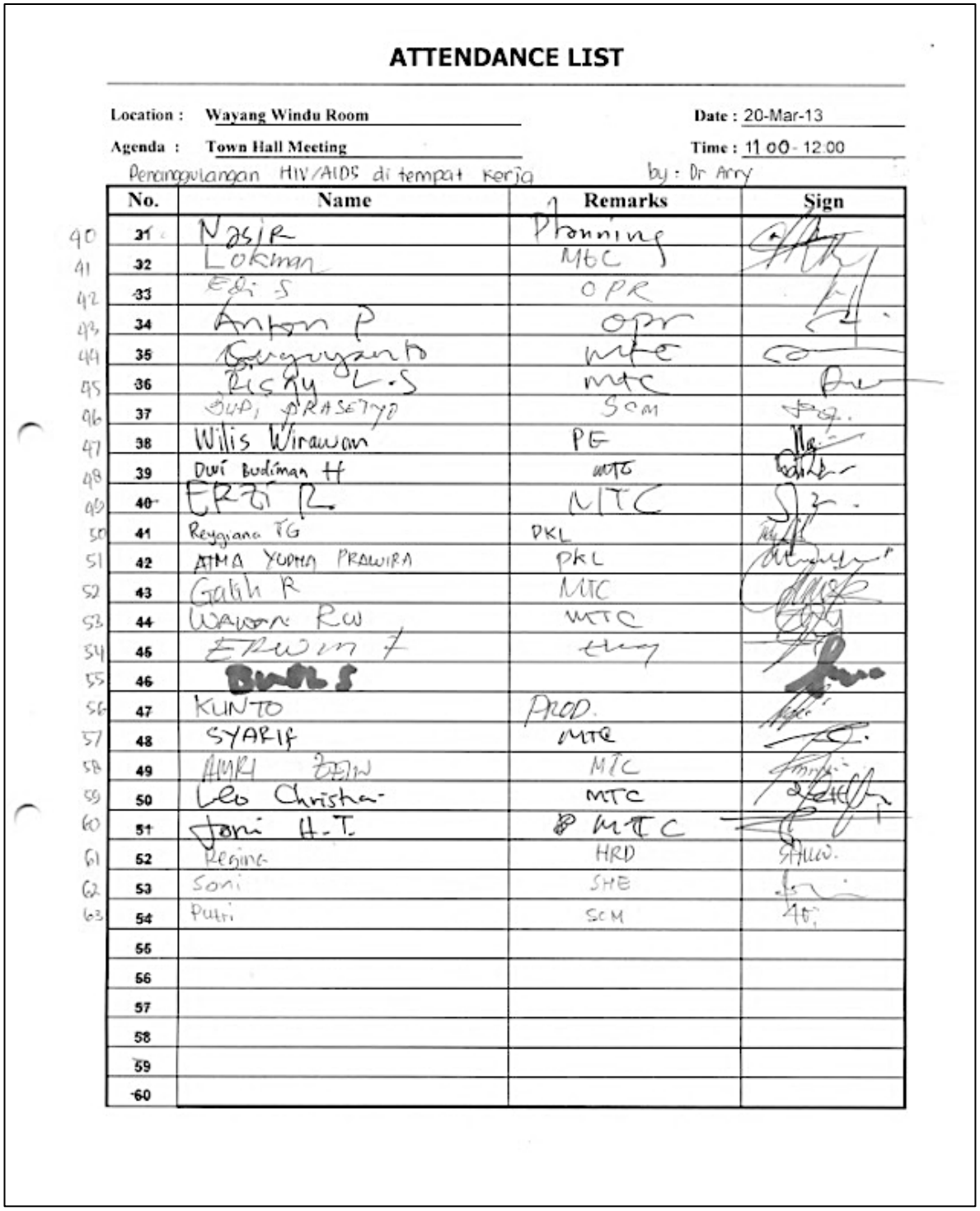
ATTENDANCE LIST

Location : Wayang Windu Room **Date :** 20-Mar-13

Agenda : Town Hall Meeting **Time :** 11.00 - 12:00

Sosialisasi Penanggulangan HIV/AIDS di tempat kerja by: Dr Arry

No.	Name	Remarks	Sign
1	[illegible]	[illegible]	
2	M SEDIAWAN	FAD	
3	WAHYU MULYANA	MTC	
4	[illegible]	FAD	
5	dr. Dedi ER	HR	
6	Esuh.S	HR	
7	[illegible]	[illegible]	
8	TRISNA	FAD	
9	[illegible]	[illegible]	
10	[illegible]	SHE	
11	ARIYA P	SBS (MTC)	
12	M. Rizky	SHE	
13	[illegible]	IT	
14	Salsa Pretiwi Muryani	Lab	
15	Pirman Nur Alam	Engg	
16	Sidik Setiadi	Eng.	
17	Ricky kurnia	Eng.	
18	Arini F.	SHE	
19	Dewi. Malasari	FAD	
20	Nayla Srofi. H	FAD	
21	Dewi Kania	Field opr	
22	Reni HF	FAD	
23	AGUS MULYADI	PROD	
24	Deny. Kurniawan	Eng	
25	Munggang H.P	Eng.	
26	Sulaeh	Eng	
27	Yusmi Anto	MTC	
28	Argo W	MTC	
29	Burhan Sjah Putra	[illegible]	
30	Ardisyah P	MTC	
31	Dea PN Falah	Prod	
32	A. Lutfi	MTC	
33	Sugiyanto	MTC	
34	Dedy S	MTC	
35	Sandi	OPR	
36	Zahid. A	OPR	
37	Fajri H	MTC	



ATTENDANCE LIST

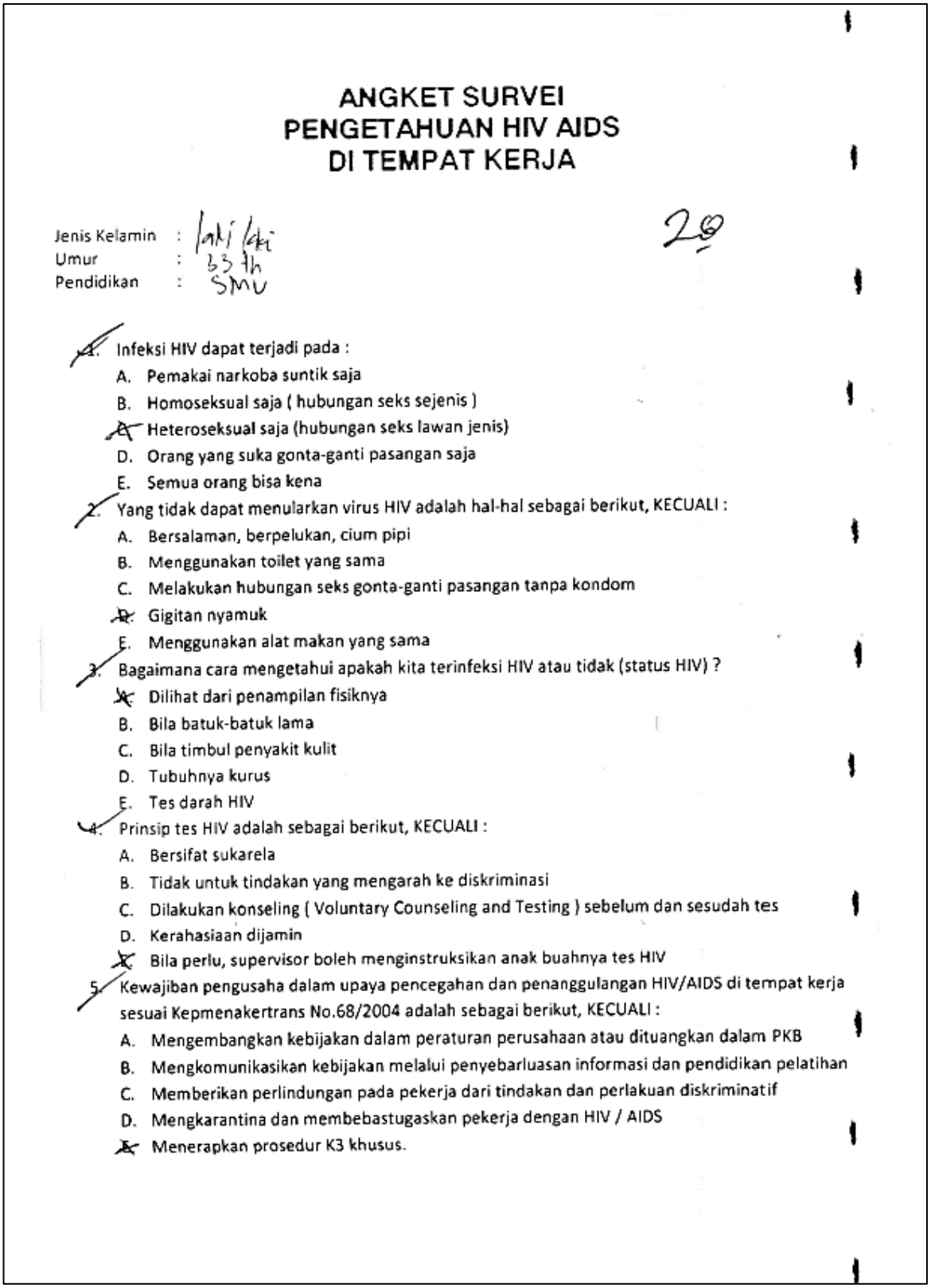
Location : Wayang Windu Room — Date : 20-Mar-13

Agenda : Town Hall Meeting — Time : 11.00 - 12.00

Penanggulangan HIV/AIDS di tempat Kerja — by : Dr Arry

No.	Name	Remarks	Sign
31	Nasir	Planning	
32	Lokman	MTC	
33	Edi S	OPR	
34	Anton P	OPR	
35	Suryanto	MTC	
36	Risky L.S	MTC	
37	Supi Prasetyo	SCM	
38	Wilis Wirawan	PE	
39	Dwi Budiman H	MTC	
40	Erri R.	MTC	
41	Reygiana TG	DKL	
42	Atma Yudha Prawira	DKL	
43	Galih R	MTC	
44	Wawan RW	MTC	
45	Erwin F	MTC	
46	[redacted]		
47	Kunto	PROD.	
48	Syarif	MTC	
49	Amri Dian	MTC	
50	Leo Christian	MTC	
51	Joni H.T.	MTC	
52	Regina	HRD	
53	Soni	SHE	
54	Putri	SCM	
55			
56			
57			
58			
59			
60			

Figure 18: Attendace list of employees who attend socialization on HAPMP policy and update on HIV AIDS.



ANGKET SURVEI
PENGETAHUAN HIV AIDS
DI TEMPAT KERJA

Jenis Kelamin : laki laki
Umur : 33 th
Pendidikan : SMU

29

1. Infeksi HIV dapat terjadi pada :
   A. Pemakai narkoba suntik saja
   B. Homoseksual saja (hubungan seks sejenis)
   C. Heteroseksual saja (hubungan seks lawan jenis)
   D. Orang yang suka gonta-ganti pasangan saja
   E. Semua orang bisa kena
2. Yang tidak dapat menularkan virus HIV adalah hal-hal sebagai berikut, KECUALI :
   A. Bersalaman, berpelukan, cium pipi
   B. Menggunakan toilet yang sama
   C. Melakukan hubungan seks gonta-ganti pasangan tanpa kondom
   D. Gigitan nyamuk
   E. Menggunakan alat makan yang sama
3. Bagaimana cara mengetahui apakah kita terinfeksi HIV atau tidak (status HIV) ?
   A. Dilihat dari penampilan fisiknya
   B. Bila batuk-batuk lama
   C. Bila timbul penyakit kulit
   D. Tubuhnya kurus
   E. Tes darah HIV
4. Prinsip tes HIV adalah sebagai berikut, KECUALI :
   A. Bersifat sukarela
   B. Tidak untuk tindakan yang mengarah ke diskriminasi
   C. Dilakukan konseling (Voluntary Counseling and Testing) sebelum dan sesudah tes
   D. Kerahasiaan dijamin
   E. Bila perlu, supervisor boleh menginstruksikan anak buahnya tes HIV
5. Kewajiban pengusaha dalam upaya pencegahan dan penanggulangan HIV/AIDS di tempat kerja sesuai Kepmenakertrans No.68/2004 adalah sebagai berikut, KECUALI :
   A. Mengembangkan kebijakan dalam peraturan perusahaan atau dituangkan dalam PKB
   B. Mengkomunikasikan kebijakan melalui penyebarluasan informasi dan pendidikan pelatihan
   C. Memberikan perlindungan pada pekerja dari tindakan dan perlakuan diskriminatif
   D. Mengkarantina dan membebastugaskan pekerja dengan HIV / AIDS
   E. Menerapkan prosedur K3 khusus.

Figure 19: A sample of questionnaire about HIV AIDS and risky behavior.

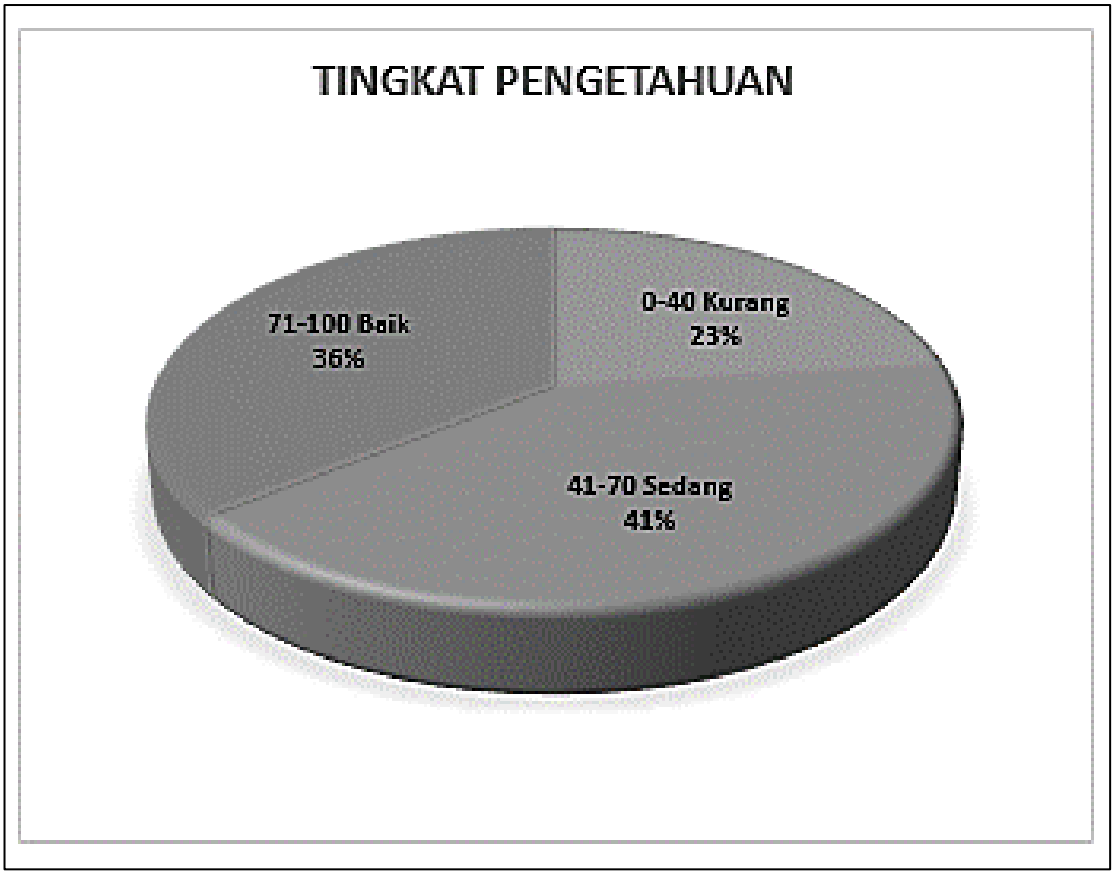


Figure 20: Analysis of participant level of knowledge about HIV AIDS: good (36%), fair (41%), low (23%).

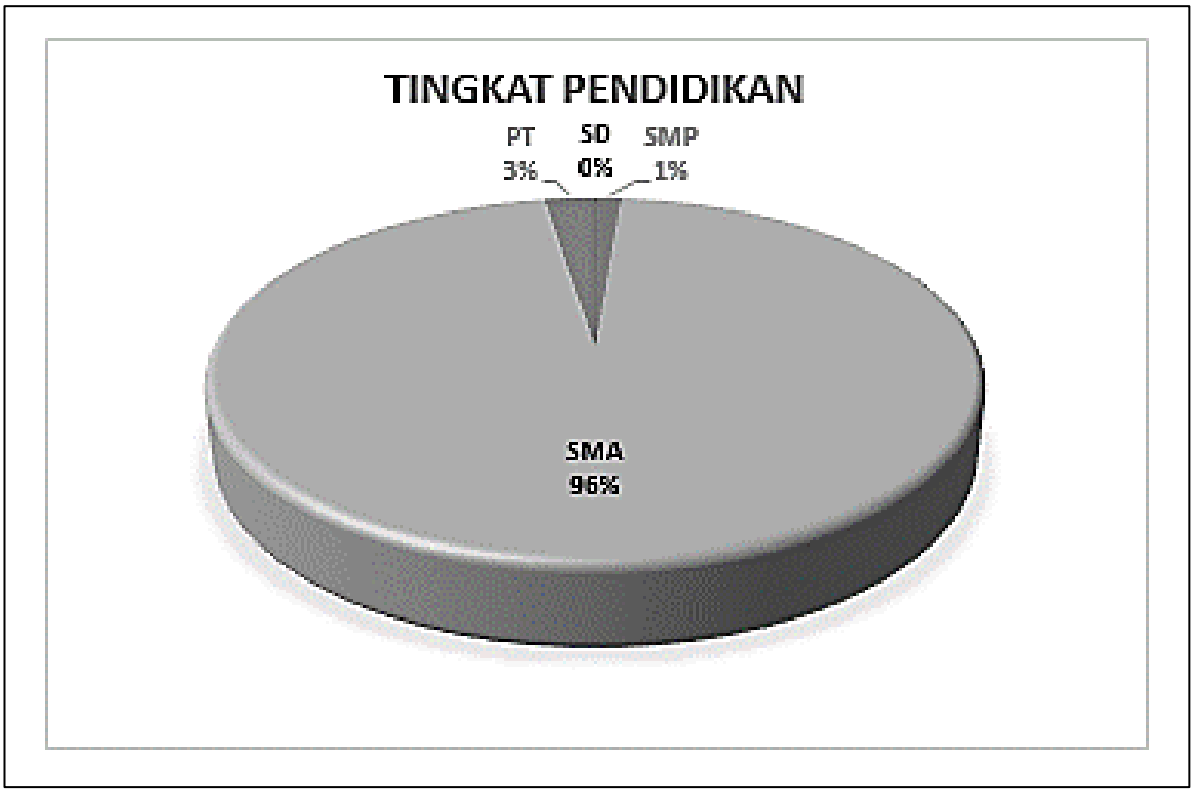


Figure 21: Analysis of questionnaire participant education level: University (3%), Senior High School (96%), Junior High School (1%).



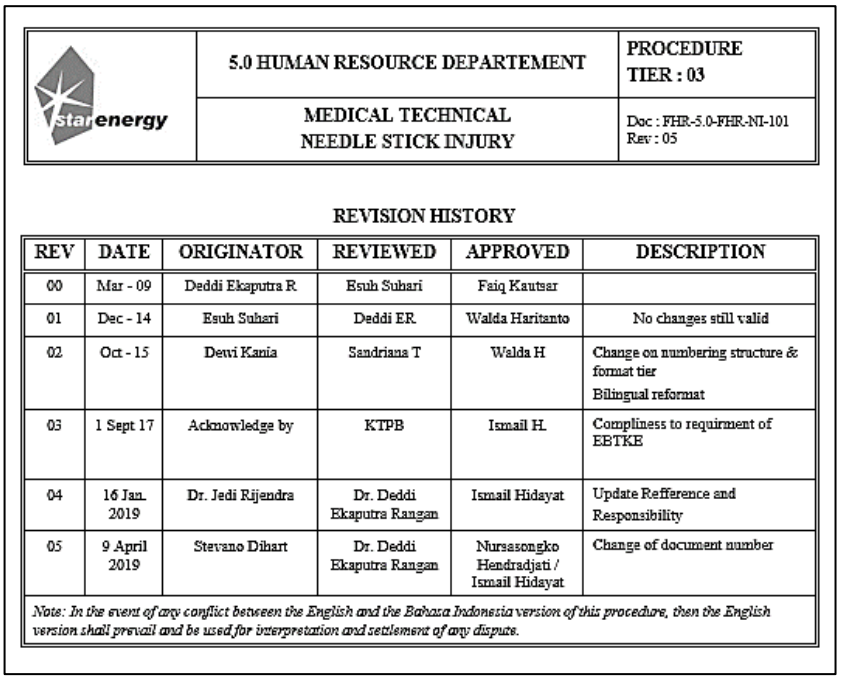
	8.0 SAFETY, HEALTH & ENVIORNMENTAL ENVIRONMENTAL	PROCEDURE TIER : 03
starenergy	WASTE MANAGEMENT	Doc : SHE-8.0-EPE-WM-100 Rev : 05

REVISION HISTORY

REV	DATE	ORIGINATOR	REVIEWED	APPROVED	DESCRIPTION
00	Feb - 05	Dufiroh	Paul Taylor	WWMSC	
00	Sep - 06	Dufiroh	Paul Taylor, Rully Wirawan	Dufiroh	Convert from WWE-11.01.01, status returned to Rev 00
01	May - 09	Muhamad Rizky	Huri Kustino, Roby Dominggus, Dufiroh	Faiq Kautsar	Revised as PROPER 2009 inspection suggestion Change on company name & logo Change on numbering structure
02	Jun - 11	Muhamad Rizky	Huri Kustino	Faiq Kautsar	Change based on internal audit finding W-O-MTW-PI-10077
03	Jul - 15	Sandriana T	Walda H	Rully Wirawan	Change on numbering structure and format tier Bilingual reformat
04	May - 17	Martalena	dr. Soedarmadji	Rully Wirawan	Revision of content
	1 Sept 17	Acknowledge by	KTPB	Ismail H.	Compliness to requirment of EBTKE
05	Jan-19	Soni Sopian Sonjaya	Dr. Soedarmadji	Ismail H.	Change the document title General Review Update the document references table

Note: In the event of any conflict between the English and the Bahasa Indonesia version of this procedure, then the English version shall prevail and be used for interpretation and settlement of any disputes.

Figure 22: SEGWW's procedure of waste management (including medical/infectious waste).



	5.0 HUMAN RESOURCE DEPARTEMENT	PROCEDURE TIER : 03
starenergy	MEDICAL TECHNICAL NEEDLE STICK INJURY	Doc : FHR-5.0-FHR-NI-101 Rev : 05

REVISION HISTORY

REV	DATE	ORIGINATOR	REVIEWED	APPROVED	DESCRIPTION
00	Mar - 09	Deddi Ekaputra R	Esuh Suhari	Faiq Kautsar	
01	Dec - 14	Esuh Suhari	Deddi ER	Walda Haritanto	No changes still valid
02	Oct - 15	Dewi Kania	Sandriana T	Walda H	Change on numbering structure & format tier Bilingual reformat
03	1 Sept 17	Acknowledge by	KTPB	Ismail H.	Compliness to requirment of EBTKE
04	16 Jan 2019	Dr. Jedi Rijendra	Dr. Deddi Ekaputra Rangan	Ismail Hidayat	Update Refference and Responsibility
05	9 April 2019	Stevano Dihart	Dr. Deddi Ekaputra Rangan	Nursasongko Hendradjati / Ismail Hidayat	Change of document number

Note: In the event of any conflict between the English and the Bahasa Indonesia version of this procedure, then the English version shall prevail and be used for interpretation and settlement of any disputes.

Figure 23: SEGWW's procedure of needle stick injury.

STAR ENERGY GEOTHERMAL (WAYANG WINDU) LTD.
Office: Tromol Pos 1 Desa Margamukti - Kecamatan Pangalengan
Kabupaten Bandung - Jawa Barat 40378
Phone: 022-5979552, Fax: 022- 5979910

LAPORAN PEMELIHARAAN KESEHATAN
STAR ENERGY GEOTHERMAL WAYANG WINDU (LTD)

Periode : Oktober - Desember 2018

Kepada Yth :
Kepala Dinas Tenaga Kerja
Kabupaten Bandung
Di
Tempat

I Identitas Perusahaan

1. Nama Perusahaan	:	Star Energy Geothermal Wayang Windu Ltd
2. Alamat Perusahaan	:	Jl. Jend. S. Parman kav 62-63, Slipi, Jakarta 11410
3. Jenis Usaha	:	Pembangkit Listrik Tenaga Panas Bumi
4. Kepemilikan / Status	:	
5. Nomor Pendaftaran Perusahaan	:	
6. Jumlah Tenaga Kerja + Keluarga		
- Lajang	:	20 Orang
- Berkeluarga	:	121 Orang
- Suami	:	8 Orang
- Istri	:	113 Orang
- Anak	:	266 Orang
Jumlah		528 orang

II Kepesertaan

Tenaga Kerja	:	141 Orang
		Perempuan : 18 Orang
		Laki - Laki : 123 Orang
Tenaga Kerja + Keluarga	:	528 Orang
Jumlah anak yang ditanggung perusahaan	:	266 Orang

III Paket Layanan Kesehatan

1. Rawat Jalan Tingkat Pertama		
- Dokter Umum	:	Ya
- Dokter Gigi	:	Ya
- Obat - obatan	:	Ya
- Imunisasi Dasar	:	Ya
- Keluarga Berencana	:	Ya
- Lab Sederhana	:	Ya
- Radiologi	:	Ya
- USG	:	Ya
- Pemeriksaan Kehamilan	:	Ya
2. Rawat Jalan Tingkat Lanjutan		
- Pemeriksaan Dokter Spesialis	:	Ya
3. Pelayanan Gawat Darurat	:	Ya
4. Penunjang Diagnostik Lanjutan		

	- EKG	: Ya
	- EEG	: Ya
	- USG	: Ya
	- CT Scanning	: Ya
IV	Total Kunjungan	
	- Oktober 2018	: 74 Orang
	- November 2018	: 82 Orang
	- Desember 2018	: 80 Orang
V	Top Ten Disseases	
	Common Cold	: 44
	Myalgia / Muscle Spasm	: 30
	Acute Pharyngitis	: 20
	URTI	: 16
	Hypertension	: 15
	Gastritis Duodenitis	: 11
	Pulpitis	: 10
	Stomatitis	: 10
	Gout	: 8
	Acute Conjuntivitis	: 7

Bandung, 02 Januari 2018

Ismail Hidayat
Field Manager

4. Progam kegiatan Pencegahan dan penanggulangan HIV AIDS

Nama Dokter Pemeriksa : dr. Deddi Ekaputra Rangan
No. Register SKP Dokter : KEP.177/PPK&K3-PNK3/KK/IX/2015
Nama Perusahaan : Star Energy Geothermal (Wayang Windu) Ltd
Alamat Perusahaan :Desa Margamukti, Kec Pangalengan, Kab Bandung, Jawa Barat 40378

No	Aktifitas	Waktu dan tempat	Jumlah peserta kegiatan
1	Kegiatan Donor Darah	Star Energy Geothermal Wayang Windu - SSC	58 Orang
2	VCT HIV - AIDS	Star Energy Geothermal Wayang Windu - SSC	21 Orang

Dokumentasi :
Donor Darah



VCT - HIV AIDS



Dokter Pemeriksa
Kesehatan Tenaga Kerja

dr. Deddi Ekaputra Rangan

Figure 24: Sample of 3 pages report of occupational health doctor to man power agency, include HAPMP.



Figure 25: Sponsorship of Rumah Cemara (institution for people living with HIV AIDS) to participate in Homeless World Cup in 2011.



Figure 26: Various activity to community, including to schools, "red district area", and community health center.



Figure 27: Award ceremony as appreciation: Platinum Award (national level) and ARROW Award (ASEAN level).

GEOTHERMAL SALT FACTORY (GSF) DESIGN IN PARANGWEDANG GEOTHERMAL, BANTUL, SPECIAL REGION OF YOGYAKARTA

Alfian Gilang[1], Mohammad Hassan Jauhari[2], Yusril Ihza[2], and Maria Theresia Kristiati[2]

[1]Geological Engineering, UPN "Veteran" Yogyakarta
[2]Petroleum Engineering, UPN "Veteran" Yogyakarta
Jl. SWK 104 Lingkar Utara, Yogyakarta, 55283
Email: gilanggumelar88@gmail.com

ABSTRACT

Indonesia has the largest geothermal energy potential in the world with potential value ± 28 GWe, but the potential of geothermal low enthalpy is still not utilized properly. On the other hand, improvement in the salt industry needs to be done because the salt industry in Indonesia has not been able to meet domestic salt demand. Domestic salt supply deficit is caused by the salt industry in Indonesia just relies on salt traditional farmers who are very dependent on the sunlight and the absence of a modern and sustainable salt-making industry. Therefore, the authors made a salt factory design using low enthalpy geothermal by utilizing Parangwedang geothermal as a heat source energy. Parangwedang geothermal located in Special Region of Yogyakarta with existence manifestation is hot spring. Based on previous research, the potential of Parangwedang geothermal was 10 MWe. The reservoir rock may have a temperature range 115°C and the hot spring fluid temperature 43°C. The hot spring distance from the seashore is 403 meters with elevation reach 8 meters. The method used in this study is literature study and data collection in the field. Literature data obtained from various sources then compiled and grouped for the design of the salt factory that utilize low enthalpy geothermal energy. This factory system will involve two pumps, one of which will drain the hot water from the Parangwedang hot spring and the other will drain the water from the ocean to salt production pan. A boiling tank and condenser are used to boil the sea. Hot water from the boiling tank is used for drying the salt brine and brine is dried in the salt pan. In the result, the authors calculated factory production capacity, the GSF production capacity is ± 14 ton salt each year.

Keywords: Salt Factory, Low Enthalpy Geothermal, Parangwedang Hot Spring.

INTRODUCTION

Indonesia is one of the countries that have the largest potential of geothermal energy in the world with a potential of 11,073 MW and reserves of 17,506 MW (ESDM, 2017), this potential energy still needs to be exploited to meet energy diversification in Indonesia in accordance with Presidential Regulation No. 5 of 2006 about the National Energy Policy that geothermal energy in 2025 has a role of 5% on national energy consumption. There are two types of geothermal energy utilization models, namely indirect use of geothermal energy high enthalpy and direct use of geothermal low enthalpy. In Indonesia, indirect use is used for electricity generation while direct use is only used for hot spring tourism, so the potential of geothermal low enthalpy in Indonesia is still not utilized properly (Hassan, 2009).

On the other hand, Indonesia still needs to modernize in the industrial field, one of which is the salt industry. Salt is Indonesia's strategic commodity whose demand continues to increase along with the increase in population (Jami et al, 2017), modernization in the salt industry needs to be done due to salt production in Indonesia not yet able to meet domestic salt needs. Referring to the Ministry of Trade's data in 2018 during January-February Indonesia's salt imports have reached 299 thousand tons. The main cause of the domestic salt supply deficit lies in the Indonesian salt-making industry which relies solely on traditional pond farmers who are too dependent on climate and weather (Jami et al, 2017). Therefore, the researchers propose making FGSF a low enthalpy geothermal salt producer.

One of the low enthalpy geothermal fields in Indonesia is the Parangwedang geothermal field, Bantul, DIY whose manifestations are located at 8º 01 '27.26' 'south latitude and 110º 19' 40.84 'east longitude, and ± 74 meters from the shoreline. GSF was designed in Parangtritis by utilizing geothermal energy from the Parangwedang hot spring. This proposal will describe the geological review of Parangwedang hot springs, design, work mechanism and estimated production capacity of GSF (Geothermal Salt Factory).

THEORY

Low Enthalpy Geothermal Utilization in Indonesia

The 300 low-high enthalpy locations that have been identified in Indonesia (Fauzi, 2015), their utilization is still far from 5% (Table 1). In fact, Presidential Regulation No. 5 of 2006, mandates that in 2025 geothermal energy has a role of 5% of national energy consumption. In addition, the use of low enthalpy geothermal energy in Indonesia is still

very minimal, most of which are only used for hot water baths and water tourism, whose benefits are still very low for the economy, even though enthalpy low heat can be used for various things, one of which is for energy salt factory.

The stratigraphy of Parangtritis and its surrounding areas is composed of Tertiary rocks such as volcanic clastic sedimentary rocks, volcanic rocks, and carbonate clastic sediments, and Quaternary sediments (Idral et al, 2003). The pattern of geological structures is mostly related to the tectonic event in the Java Trench, including a major NE-SW normal fault, called Opak normal fault (Figure 1). Additionally, there are also SE-NW Bantul normal fault and NE-SW Parangkusumo strike-slip fault around the Parang Wedang, The Parangkusumo fault, showing strike of N 300°W and dip of 80° (Juliarka, 2016).

The manifestation of Parangwedang located ± 403 meters from the shoreline with elevation ± 8 meters above sea level (Figure 2). In a previous investigation, it was known that hot water tastes salty, colorless, odorless, neutral pH (7.49), surface temperature 49ºC at air temperature 28.2ºC, while sub-surface temperature based on geo-thermometer SiO2 is estimated at ± 115ºC (Idral et al, 2003). Based on the SiO_2 (ac) geothermometer, the estimation of the subsurface temperature is around 115 ºC which is included in the low enthalpy. With an estimate of the prospect of around 4 km^2 from the results of pseudo-type resistance and with a cut-off temperature of 90 ºC, and with the formula:

$$Q = 0.2317 \times A \times (Tag - Tcut\text{-}off) \quad (1)$$

So, the potential of Parangtritis geothermal resources is around 10 MWe with geothermal reservoir depth at 600 meters (Idral et al, 2003).

Table 1: Classification of the distribution of geothermal energy in Indonesia (Fauzi, 2015).

Location	Classification (Mwe)	
	Low enthalphy <100 -190 ºC	*High enthalpy* >190 ºC
Sumatera	2951	8636
Jawa & Bali	1663	5373
Nusa Tenggara	862	537
Kalimantan	145	-
Sulawesi	1696	1146
Maluku & Papua	569	442
Total	**7886**	**16134**

Parangwedang Low Enthalpy Geothermal Potential

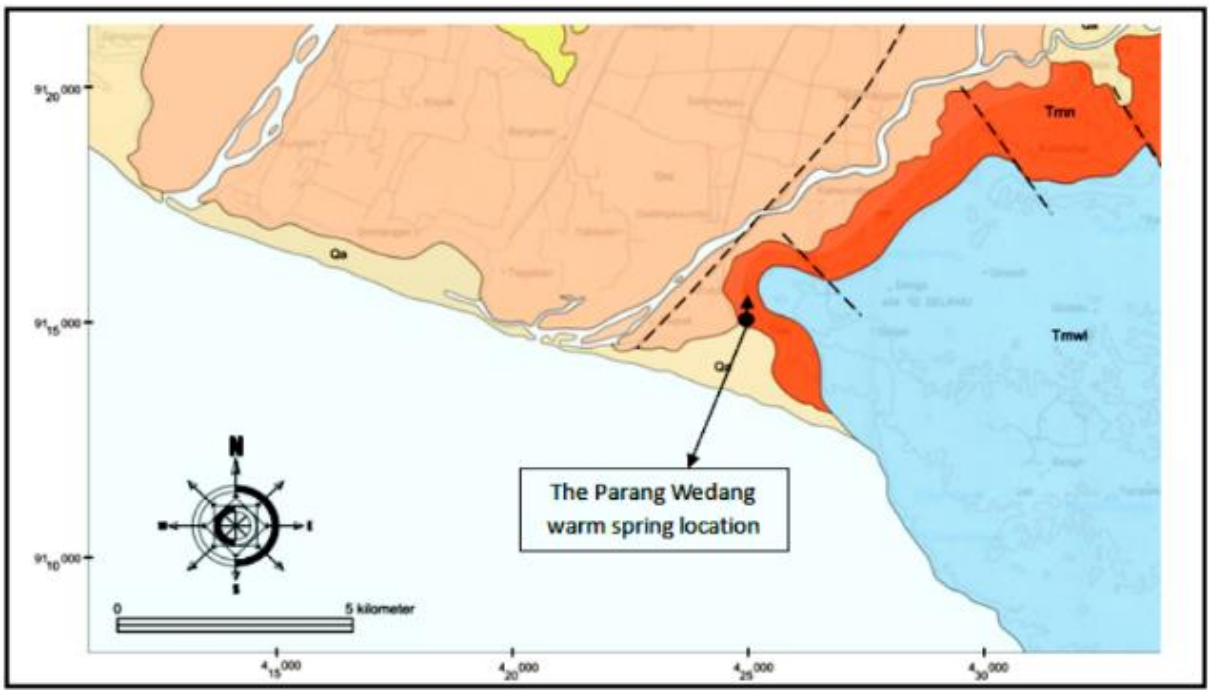


Figure 1: Surface geological map of the Parang Wedang area showing the distribution of lithologies, faults and warm springs (Restu, 2016).

Indonesia Salt Production Conditions

The Indonesian government always imports salt annually to meet domestic salt needs, this is because Indonesia only relies on traditional salt farmers who only depend on weather and climate (Figure 4). In addition, the amount of land used for salt ponds is also decreasing because a lot of salt land has been converted into settlements. Based on Badan Pusat Statistik data in 2018, Indonesia's salt imports in the period (January-February 2018) reach 299 thousand tons with a value of US $ 9.5 million. The volume of imports rose 62% from the same period the previous year with only 184 thousand tons and in the last three years (2015-2018) there has been an increase in salt imports year to year. Figure 3 shows the Indoensia salt import 2010 - 2017



Figure 2: The research area (yellow rectangle) located in Parangwedang, Bantul, DIY.



Figure 3: Indonesia Salt Import 2010-2017 (Processed from BPS, 2019).

Parangtritis Salt Potential

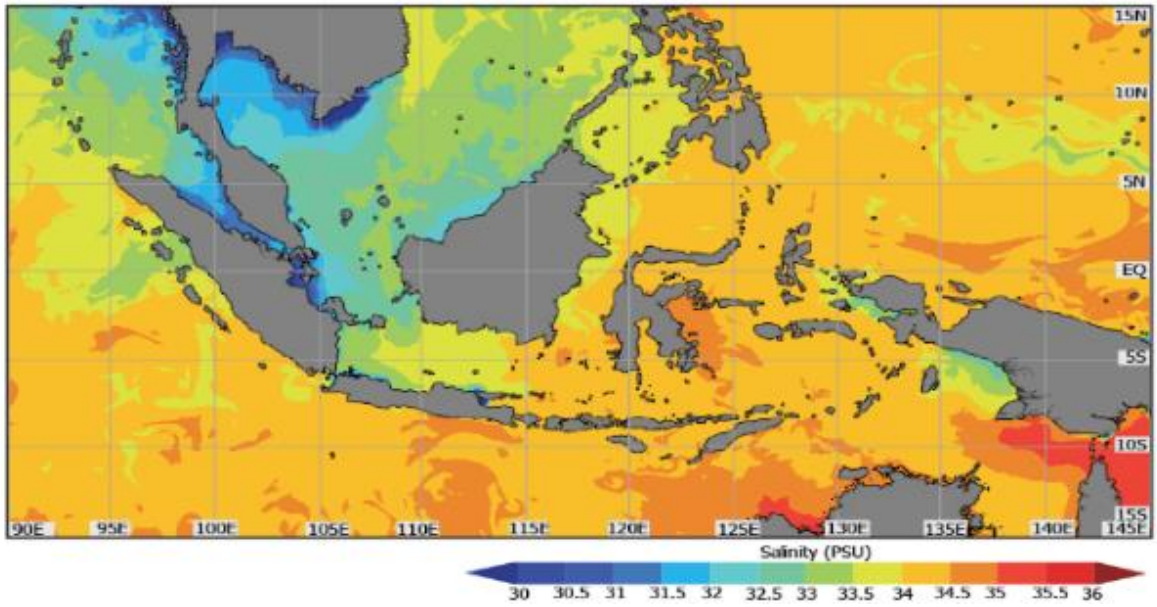


Figure 4: Indonesia Seawater Salinity Maps (BMKG, 2018).

Geographically, Parangtritis Beach is in Parangtritis Village, Bantul Subdistrict, D. I. Yogyakarta which is located at the coordinates of 7º 59 '15 "- 8º 1' 58" South Latitude and 110º 20 '37 "East Longitude. (Handoyo, 2017). From Figure 4 (appendix), it can be seen that Parangtritis beach, which is the southern coast of Yogyakarta, has a salinity content ranging between 34-34,5 PSU, which according to the Directorate of Coastal Community Empowerment and Business Development, sea salinity that can be used to make salt is usually it only ranges from 30-35 PSU, so it can be seen that Parangtritis beach has great potential to be developed into a national salt production center. According to Rilley (1975) with the seawater specific gravity of ± 1.0258 kg/liter obtained NaCl concentration of ± 29.6959 g / liter.

METHOD

The method used in this study is literature observation and data collection in the field. Literature data obtained from various sources then compiled and grouped for the design of the salt factory that utilize low enthalpy geothermal energy in Yogyakarta.

Data on geothermal energy potential is obtained based on the calculation of the geothermometer around the Parangwedang manifestation and estimation of temperature value in the reservoir rock and surface, as a form of geological and geochemical survey results. Other data obtained from observations in the field and satellite images from BMKG and Google Earth such as the distance between the sea and Parangwedang hot spring, salinity level, altitude. This study obtained a model of a salt factory that utilizes low enthalpy geothermal in Parangwedang Yogyakarta.

RESULT AND DISCUSSION

GSF (Geothermal Salt Factory) Design

The factory design (Figure 5) adopts basic working principles, conduction and convection using a heat exchanger, this factory uses the evaporator (boiler/pre-heating tank) to vaporize seawater into highly viscous salt water, then the viscous solution will be deposited at a deposition site (Figure 6). Where the main processes of GSF are as follows:

1. Seawater is filtered first to remove impurities such as sand, soil, and other contaminants to ensure that only pure seawater enters the boiler (pre-heating tank).
2. After that, the water will enter the boiler where the boiler will be set to be under a pressure of 1 atm to reduce the boiling point of seawater at 51ºC (the boiler will be modified with a heat exchanger to transfer heat from the hot fluid to the boiler), after boiling seawater and evaporates, the boiler will make seawater with a high salt concentration.
3. Furthermore, the viscous/saturated seawater will be channeled towards the open pan which is the evaporator to be collected and deposited (open pan is also heated using continuous hot fluids).
4. After that, when seawater passes through the saturated phase, it will naturally appear on the surface of the salt crystals in the salt pan and salt can be harvested manually.
5. Then hot water that has been used will be injected to the injection well.

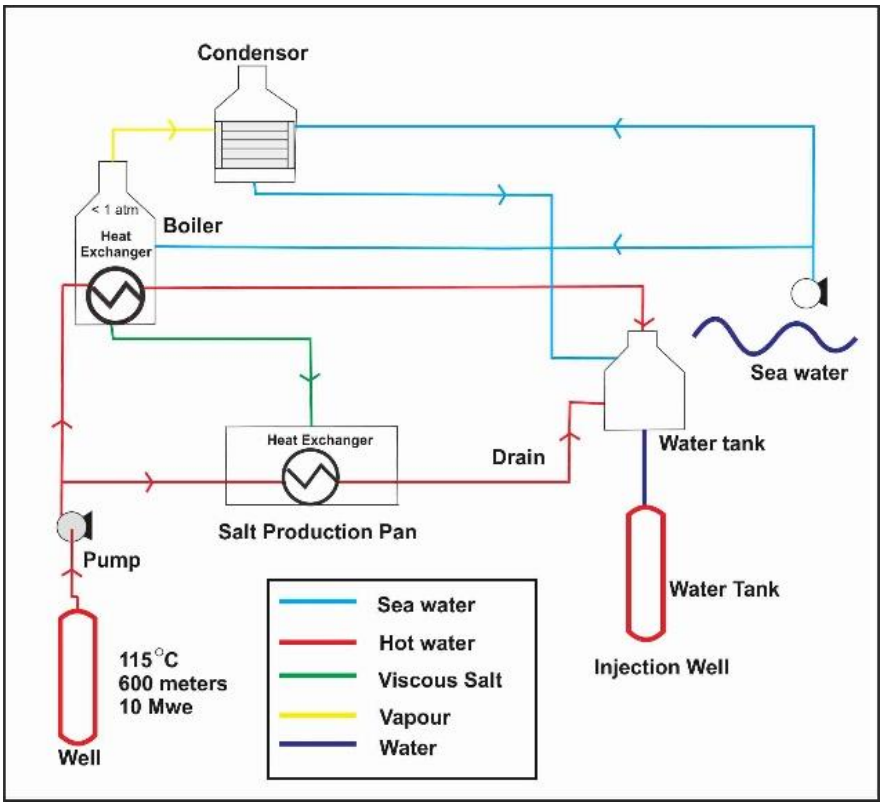


Figure 5: Schematic Diagram of GSF.

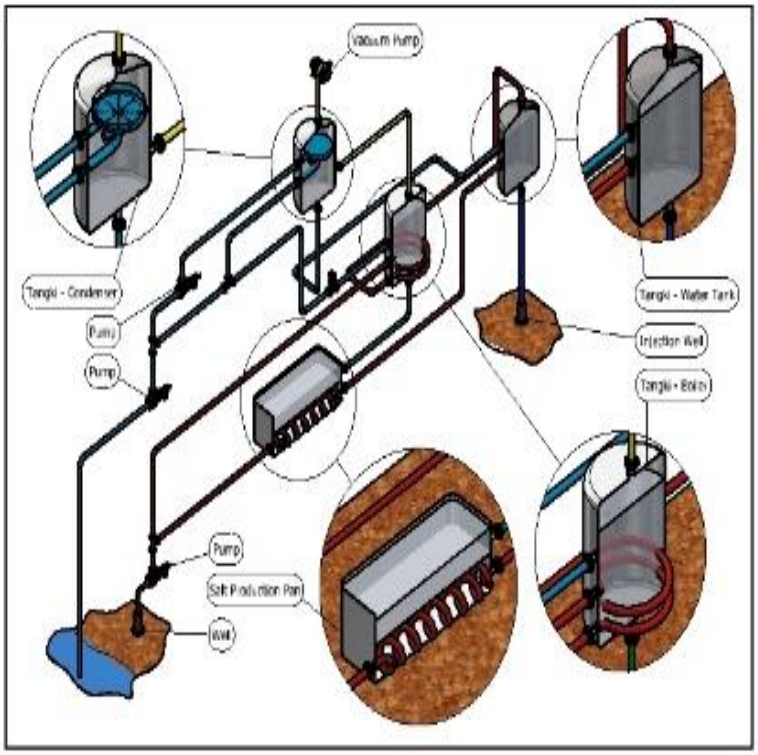


Figure 6: 3D Design of GSF.

GSF (Geothermal Salt Factory) Production Capacity

The working principle of a salt production pan and boiler that is modified by a heat exchanger is to move heat energy from hot water to evaporate seawater through two mechanisms, namely conduction and convection. The process of conduction and convection heat transfer can be explained by Fourier and Newton law equations as follows:

$$q_c = -kA\,\frac{dT}{dX} \qquad (2)$$

$$q_h = hA(\,T_i - T_O) \qquad (3)$$

The Factory Production Capacity is calculated by determining the evaporation rate (g /s) in salt production pan, with the following equation (Akridge, 2007):

$$E = \frac{q}{\alpha} \qquad (4)$$

E = Evaporation Rate (g/s)
q = Heat Transfer Rate (MJ/s)
α = Latent Heat (MJ/kg)

Whereas q is sought from Fourier law equation assuming steady state flow, the material made of copper (k=386,0 W/mK), area 2 m × 1 m and thickness 0,05 m

$$q_c = -kA\,\frac{(T_O - T_i)}{\Delta X} \qquad (5)$$

Where, latent heat can be determined based on equations (Akridge, 2007):

$$\alpha = 2{,}501 - 0{,}002361 \times \mathrm{T} \qquad (6)$$

T= average temperature (ºC)

Assuming the average temperature of hot water at reservoir conditions is 115ºC, then q_c = 10 MW, α = 2.300315 MJ / kg and evaporation rate of E = 4347.2 g /s. After determining E, we can find the production capacity of GSF with equation (Akridge, 2007):

$$m_s = m_w(1{,}52 \times 10^{-4}S + 9{,}50 \times 10^{-3}S) \quad (8)$$

Where m_s is the mass (kg) of salt crystallized, m_w is the mass (kg) of the water evaporated, and S is the initial salt concentration of the brine in wt% NaCl. We assume that the initial salt concentration of the brine is 10 %, we can find that the capacity production of GSF is ± 14 ton/year.

SWOT Analysis

Based on the results of data analysis that has been done with a SWOT analysis. The results are following:

Strength:

1. The south coast in Yogyakarta (Parangtritis and its surroundings) has great potential to be processed into quality salt.
2. The opportunity to utilize low enthalpy geothermal energy in Indonesia is very large. Because only 5% of geothermal energy in Indonesia has been utilized.
3. The design of this salt plant does not require solar heat, so the production process will not be affected by bad weather (rainy season).
4. Salt is one of the strategic commodities in Indonesia and the demand for domestic salt consumers is very high, this demand comes from industry, cosmetics, food ingredients and even pharmaceuticals.

Weakness:

1. Heavy plant maintenance process due to problems such as scale and corrosion
2. Requires large capital.
3. Salt farmers in Yogyakarta have long left their jobs as salt farmers.
4. The surrounding community still does not know about this technology.

Opportunity:

1. The market for salt commodities is still large. National export and industrial needs are still large.
2. Geothermal utilization and increased salt production are activities supported by the central government. The governor of DIY representing the regional government even expects Jogja to produce quality salt.
3. The free trade system has also been running, providing an opportunity to get bigger consumers.

Threat:

1. Non-detailed regulations regarding the utilization of low enthalpy geothermal.
2. Complex business licensing.
3. Increasingly expensive maintenance costs for salt mills and tools that support this industry

CONCLUSION

From the research it can be obtained that:

1) GSF is a modern, efficient and environmentally friendly factory that adopts two basic working principles, conduction and convection. This factory does not depend on sunlight. So the production process will not be affected by bad weather.

2) After calculating the evaporation rate (*E*), the estimated production capacity of salt from GSF is ±14 ton salt each year.

RECOMMENDATION

This concept would be more advanced if this design could be integrated into a salt factory pilot project and require a detailed concept in process engineering aspect.

REFERENCES

Akridge, G. D. (2007). "Methods for Calculating Evaporation Rates During Salt Production". Journal of Archaeological Science. 35: 1453-1462.

BMKG. (2018). "Peta Maritim". [Online]. (http://peta-maritim.bmkg.go.id/static/ diakses pada tanggal 24/10/2018).

BPS. (2018). "Impor Garam". [Online]. (https://www.bps.go.id/ diakses pada tanggal 14/06/2019).

ESDM. (2017)." Potensi Panas Bumi Indonesia Jilid 1". Published by Direktorat Panas Bumi, Ditjen EBTKE.

Fauzi, A. (2015). "Geothermal resources and reserves in Indonesia: an updated revision". Journal Geothermal Energy Science. 3: 1-6.

Handoyo, G, Agus A.D, Subardjo. (2017). "Peta Kerawanan Tsunami Serta Rancangan Jalur Evakuasi di Pantai Desa Prangtritis Kecamatan Kretek Kabupaten Bantul Daerah Istemewa Yogyakarta". Jurnal Kelautan. 10 (2): 117.

Hassan, A. (2009). "Mesin Pengering Produk Pertanian Bertenaga Panas Bumi". Jurnal Teknik Lingkungan. 10 (2): 153-160.

Idral, A., E. Suhanto, E. Sumardi, D. Kusnadi, and T. Situmorang. (2003). "Penyelidikan Terpadu Geologi, Geokimia Dan Geofisika Daerah Panas Bumi Parangtritis". Colloquium result of inventory Event of Ministry of Mineral Resource year 2003.

Jami, A.S, Suharno, Netty, T. (2017). "Faktor-Faktor Yang Memengaruhi Permintaan Dan Efektivitas Kebijakan Impor Garam Indonesia". Buletin Ilmiah Litbang Perdagangan. 11 (1) : 43-68.

Juliarka, Bela Restu, and Sintia Windhi Niasari. (2016). "Geothermal Exploration Using Geochemical Data; Study Case: Parang Wedang Geothermal Field, Indonesia". AIP Conference Proceedings (2016).

Konthandaraman, C.P. Fundamentals of Heat and Mass Transfer Revised Third Edition. (2010). New Delhi: New Age International Publishers.

THE SIGNIFICANCE OF DRILLING DATA MANAGEMENT TO IMPROVE GEOTHERMAL DRILLING OPERATION

Daniel Adityatama[1], Riviani Kusumawardani[2], Dorman Purba[1], Farhan Muhammad[1], and Ribka Asokawaty[2]

[1]PT Rigsis Energi Indonesia
[2]Geothermal Master Program ITB
Equity Tower, Jl Jend. Sudirman, SCBD, Jakarta
Email: daniel.adityatama@rigsis.com

ABSTRACT

Drilling is one of the major cost components in geothermal exploration and development. Effective and cost-efficient drilling significantly contribute to the success of geothermal development. Key factors in reducing drilling costs are optimising operations, utilising manpower to its fullest potential, and also benchmarking with other drilling activities to evaluate one's performance objectively. This is possible if the information regarding the previous drilling activities is stored and easily gathered and analysed before making plans for the drilling campaign.

The importance of drilling data analysis and drilling data management have been a subject of study and discussion since the 1980s, but it is still not that common in geothermal drilling, especially in Indonesia. The purpose of this paper is to summarise the definition and examples of drilling data management in a more well-established industry such as oil and gas from various studies in the past, assess the advantages of having a proper drilling database or data management system, and how can the data be used for potentially improving future drilling operation. A case study of converting legacy data from previous drilling campaign of two geothermal fields in Java into a database is also discussed to demonstrate how legacy drilling data can be used to evaluate drilling performance.

Keywords: Drilling, data management

INTRODUCTION

Geothermal Development in Indonesia

Indonesia's National Energy Plan (Rencana Umum Energi Nasional / RUEN) dictates that the renewable energy should reach 23% from the total Indonesia's energy mix (Kementerian ESDM 2017), in which around 7,200 MW or 16% is originating from geothermal energy (Umam, et al. 2019). With the installed geothermal power plant capacity at around 1,950 MW at the end of 2018, the 5,000 MW increase in ~6 years period is a bold target to say the least (Purba, et al. 2019). One of the reasons of this slow development rate is the high upfront cost required during exploration, with drilling as the main contributor. Therefore, it is important to have lower cost per MW by having acceptable drilling cost per well. (GeothermEx 2010, Purba, et al. 2019).

Drilling operation in geothermal with its many uncertainties, requires a lot of experiences before reaching the most optimum condition. The heterogeneity of the subsurface condition compared to oil and gas poses another challenge for geothermal drilling, making lessons learned from previous drilling operation are invaluable to improve the whole drilling planning and operation. However, most of the time the drilling data from previous drilling campaigns are neglected, or just stored in the company's hard drive / server without proper structuring. This makes drilling analysis difficult if not impossible to carry out, as the drilling engineer has to dig piles of folders and files just to find some parts of information. In oil and gas industry, the awareness for having a proper drilling database and data management system is widely known and has been a popular topic for years (Hanley, et al. 2011, Iyoho, Meize, et al. 2005, Shi, et al. 2015, Sumbal, et al. 2017). However, as far as the authors' knowledge the importance of drilling database in geothermal, let alone drilling data management system in Indonesia has not been a serious concern.

Optimizing Drilling Operation to Reduce Drilling Cost

As drilling is one of the biggest contributors in total geothermal project cost, it is imperative to address the optimisation of the drilling activity, especially as drilling has high risk due to uncertainties during operation. One way to optimise drilling planning and execution is by analysing previous drilling operations, or in drilling engineering is known as drilling analysis (Figure 1). However, Iyoho et al. (2004), assert that drilling analysis is not routinely practised as it should be. One of the main reasons that drilling analysis is seems like being ignored is that most of the time the company lack of an organized knowledge-based data-management system that can seamlessly cross-correlate relevant drilling and geologic parameters.

Another concern is it is widely believed that there is a lack knowledge retention in oil and gas industry, with drilling in particular (Sumbal, et al. 2017). There is generation gap between drilling engineers, and it is critical to have a proper record of lesson

learned and processes to ensure transfer knowledge between drilling engineers (Damski 2014). Authors of this study believe that if in the well-established sector such as oil and gas the lack of knowledge retention is apparent, then it is safe to assume that it will be the same in the less-established industry like geothermal. Therefore, without a proper record of lesson learnt, process description, field knowledge, and a proper drilling analysis of previous drilling operations data, it will be difficult if not impossible to optimise / improve any future drilling planning.

The data recorded may vary from daily activity report, bit performance, survey log, mud logging data, etc. However, more often than not, the previous drilling data and report are stored in various formats and inconsistent folder. This might lead to the following problems:

- Engineers have to manually dig in into folders and sort piles of data or report to find information they need. This is time consuming, and if the folder location is not consistent, other personnel who is not familiar with the availability or location of the data will have a hard time to find the information.
- Existing drilling data / report might be in different format, making it difficult to collect, compare, and analyse.

Purpose of the Study

As discussed in previous section, optimising geothermal drilling is not possible without learning from previous drilling operation. However, lessons learned and data from previous campaign or operation are often neglected due to there is no proper database or data management system which in turn discourage engineers to look up for the information or data. Therefore, the purpose of this paper is as follow:

- Summarise the drilling data management definition and concept from literatures and previous studies;
- Assessing the potential advantages of having a proper geothermal drilling database or data management system;
- Exploring how the data from previous drilling operations can be used for improving future drilling planning;
- What can be done with the legacy/historical drilling data that have not been stored properly.

Literature review regarding current geothermal drilling in Indonesia, basic drilling data management, and drilling analysis from petroleum industry was carried out. A case study from a geothermal field in Central Java which has been drilled in the past and will be drilled for future expansion is also investigated to demonstrate how the legacy data can still be utilised for future drilling planning

Figure 2.

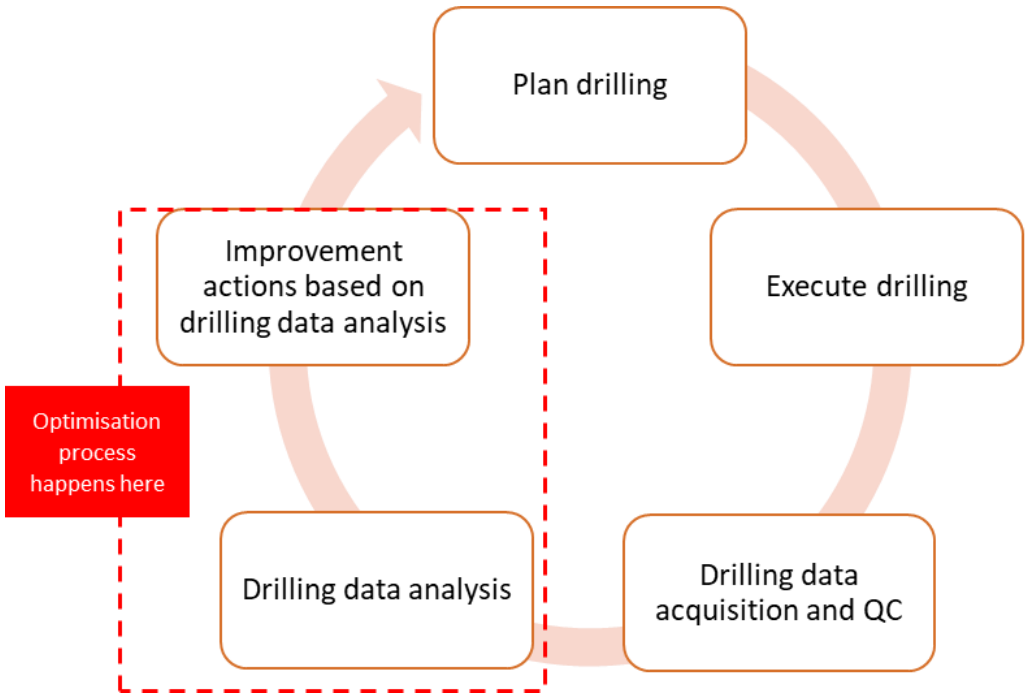


Figure 1: Drilling planning and operation cycle.

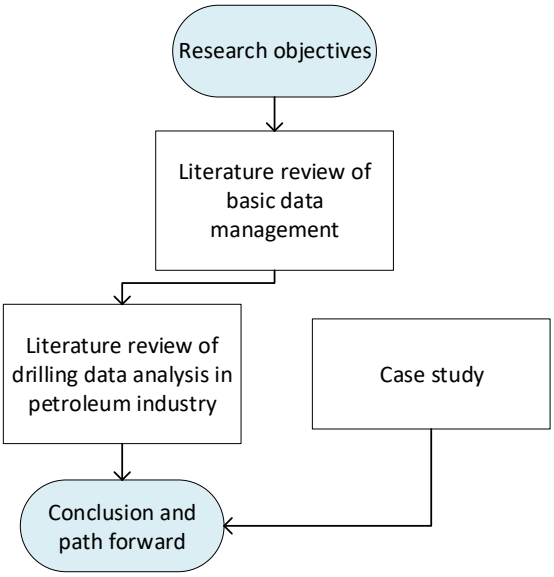


Figure 2: Methodology flowchart of this study.

WHAT IS DATA MANAGEMENT

Definition of data itself is varied depending on the source or context, but to put it simply, it can be defined as facts, numbers or other entities that has no context or purpose on its own. Data should be organised into a meaningful context and become information. The information then can be interpreted, analysed, and used for various purpose such as decision-making, evaluation, etc. and become knowledge. Hence, the data itself is practically unusable unless organised into a database or documents.

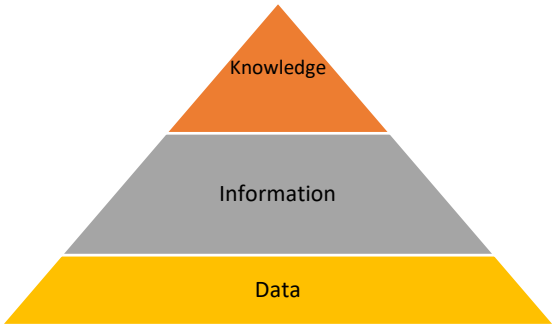


Figure 3: Illustration of data, information, and knowledge (modified from Damski, 2014).

Data management can be described as "the practice of collecting, keeping, and using data efficiently and cost-effectively" (ORACLE 2019). However, the term data management in drilling operation is unclear, as sometimes streaming the real-time mud logging data from drilling site to the headquarter office or collecting the data (reports, mud logging data, e-log data, etc.) and storing them inside company's hard drive or server is considered enough as a form data management. Damski (2014) asserts that it is not enough in a business sense, as it is just an expense without any Return of Investment (ROI). After the information extracted from the data can be used to generate decision to improve the business process of the company, then the cost spending for the data management will become make sense (Figure 4). Collecting or acquisitioning and storing the data from previous drilling operations will only become additional cost with no value if the data is not analysed to deliver business intelligence improve business process (productivity, safety, etc.) of the company.

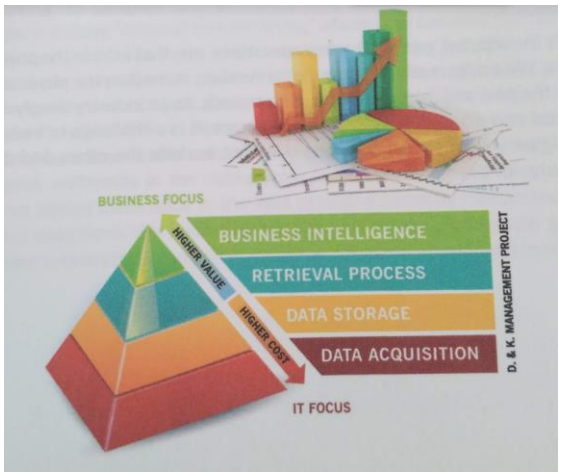


Figure 4: Cost vs value in data management (modified from Damski, 2014).

However, as stated in the previous section, the business intelligence part can only be done if the data is available and easy to access / retrieve. With the readily available and processed data, the difference between two decisions is just a matter of business intelligence or data interpretation, which in turn can provide better drilling program, drilling cost estimation, etc.

Data Management in Drilling

Damski (2014) described that for drilling operation, the data management process can be summarised into the following steps **(**

Figure 9**)**:

- Data acquisition
- Data QC
- Data storage
- Data retrieval
- Data analysis

Data Acquisition

Generally, there are two types of data source in drilling; one is the manually-filled report and the other is automatic report from the sensors such as mud logging unit. The manual report may range from morning meeting, daily drilling report (DDR) in a form of spreadsheet file or some sophisticated software such as Peloton's WellView™, Halliburton's OpenWells®, etc. Irrespective of the method, the manual report is involving a person in the rig to type or fill the form. This is also occurred

for other data record such as geology, bit, cost, drilling fluid, etc.

The electronic data from sensors on the other hand, are collected real time and may or may not directly transmitted to the office for storage and plotting. For both of these data types, the data reliability is crucial. This makes quality control of the data become important and will be discussed int the later section.

Data Storage

Data storage in drilling is a very interesting topic. As far as authors know, many geothermal companies store drilling data or reports in folders inside their servers or computers. However, in IT perspectives, data such as reports, presentations, images, even excel files are considered "unstructured" data, as it is not stored in a structured manner and most of the time have different and inconsistent format, thus making it harder to store and retrieve (Figure 5). Databases, on the other hand, are considered as "structured" data, as they possess formal method to organise and retrieve the data (Damski 2014).

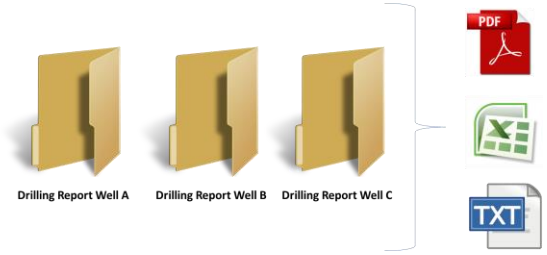


Figure 5: Illustration of commonly data storage in companies.

To address this, companies can obtain a database system that converts the information inside their files into a database such as provided by ORACLE, MySQL, etc. To access / retrieve the data, users or engineers can use a SQL (Structured Query Language) or use a graphic interface or application.

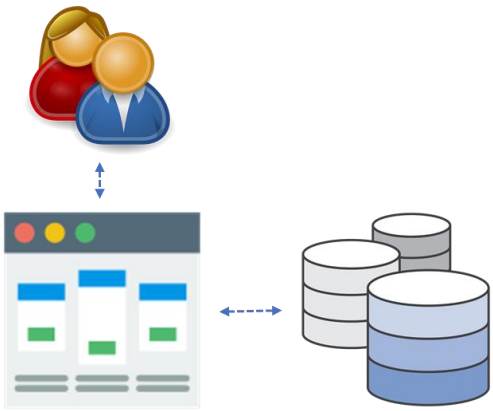


Figure 6: Simplified concept of how user access data in database via interface/application.

Data QC

Data QA/QC process is very important due to that any bad data (inconsistent or even wrong) will also be used for analysis. There is a famous adage in IT world "garbage in – garbage out"; where any incorrect or poor-quality input will generate nonsense output or garbage. As stated in the Data Acquisition section, the manual report quality is highly dependent on the person in the rig site. This is more complicated than it sounds because usually the person filling the manual report (company man or drilling supervisor) has to supervise the operation, and at the end of his shift he has to create a report. If the drilling supervisor is not aware of the utilisation of the data from his report, he might miss or skimp through some information that he thinks is not important. Even if the drilling supervisor is aware or has been briefed previously on what to input in the report, based on authors experience there are a lot of occurrence when some details were missed in the report simply because of the drilling supervisor was too occupied in supervising the operation, and reporting was just become an afterthought. Similar thing in automatic (sensor-based) report, as faulty or not calibrated sensor will give wrong reading. Overall, Damski (2014) described that the most common errors in drilling database are as follow:

- Wrong datum / unit
- Inconsistency (e.g. one engineer can code one particular operation in one well and another code in the same operation in different well, making comparison difficult).
- Dispersed data source
- Outliers / anomaly
- Bad relationships between data entities.

The QC process is often overlooked by people despite its significance. Acquiring the data relatively easy, but without proper QA/QC, the analysis result can be incorrect or misleading.

Data Retrieval

After the data is stored in some databases, the following tasks is how to easily retrieve it. In unstructured data such as reports, presentation, and images stored in folders, retrieving the data is no easy task. In a database, it can be done using a language called Standard Query Language (SQL). However, SQL itself is sometimes seems like a domain for IT engineer, and seems like a foreign land for a drilling engineer. Therefore to simplify things for the user, it is important to have graphical interface to query or retrieve the required data.

Data analysis can be described as "methods to inspect, transform and model data aiming to detect patterns, develop explanations, test hypotheses, highlighting useful information, suggest conclusions and support decision making" (Damski

2014, Iyoho, Millheim, et al. 2004). The primary objective of the whole data management (and data analysis in particular) is how will this benefit or improve the whole business. The drilling data analysis can be used to reflect the condition in the past, present, and future (Figure 10). In day-to-day drilling operation, the company will need all three of them. The past can be used as historical basis to understand past performance, to plan future wells, and to forecast potential problems. It also helps to aid decision making in the present condition, especially if the occurring problems had been occurred in the past operation.

ANALYSING DRILLING DATA

Drilling Process

As stated earlier in previous section, the drilling data (both in the past or in the current time) is crucial in every stage of well life cycle. One approach for quality management and continuous improvement is PDCA (Plan, Do, Check, Act) cycle (Johnson 2002, Sokovic, Pavletic and Pipan 2010). Figure 1 illustrates the cycle of drilling a well, and it resembles the PDCA cycle. Without a proper drilling database, every stage of well life cycle will be disturbed. There will be no data, information, and lessons learned from previous drilling operation to aid in improving the next drilling plan. The execution stage will also be disturbed, as every problem encountered during operation will be a new problem, since there is no record on problems in the past and how to address or mitigate them. The possible improvement and utilisation of drilling data analysis is discussed in the later section.

The drilling data is crucial in the planning and evaluation phase of drilling operation. The engineer can use the historical data (after they are collected, organised, and quality controlled) to identify what and where problems are encountered in the past, what and where improvements can be made in future planning. There are some tools to improve drilling planning via analysis of historical data (Damski 2014):

- Productive time analysis;
- Process control analysis;
- Non-productive (NPT) analysis;
- Best Composite Time (BCT) analysis and technical limit;
- Bit performance analysis;
- Learning curve analysis;
- Benchmark analysis.

In oil and gas industries, several works have been carried out to propose the methodology for drilling analysis. One of them is "10-step methodology" proposed by Iyoho et al. (2004). These steps are as follow:

1. **Define project objectives and scope.** In order to understand the context, targets, and design a plan. This stage should provide answer for the following questions: where are we now? Where do we want to be? What is possible? How do we get there?
2. **Data selection and QA/QC**. The comparable sets of data are identified, compiled, and checked for their integrity prior to the subsequent analysis.
3. **Best Composite Time (BCT)**. The best time recorded for each discreet sequential activity (rig up, make up bit, run in hole, etc.) from comparable well data are identified and added up to create an "ideal well" drilling time. Then this BCT can be used for future drilling planning. Note that BCT is not technical limit in terms of what is possible, in terms of what has been done.
4. **Best Composite Cost (BCC)**. After BCT is identified, it is then converted to the total cost to better analyse the financial target.
5. **Learning Curve-Analysis**. This step is carried out to analyse the performance, progress and accomplishment in general and in specific areas of the drilling.
6. **Major Operations Analysis**. In this step, a time breakdown analysis is carried out for major operations and drilling phases to identify NPT and problems during drilling.
7. **Detailed Problem Analysis & Opportunity Identification**. This step evaluate the trouble-time duration and occurrence / repetitiveness, thus in turn can identify area for improvement.
8. **Peer Review, Design Changes, and Technology Scouting**. Peer review is carried out to study the possibility of optimising drilling process through design changes, adopting new technology, etc.
9. **Economic Benefit Evaluation**. The possible improvement options from step 8 are assessed for the most cost-effective solution.
10. **Recommendation and Follow-up**. The result from step 9 is converted into series of recommendations and measure the financial impact as they are implemented to continuously improve the BCT and BCC.

Activity Reporting

The drilling reports, both manually-inputted daily drilling report and mud-logging or other sensor-based data are an essential part of understanding the drilling operation and analyse it. However, most of the time, the daily report is only used for daily morning meeting, and "discarded" if there is no apparent problem during the operation. With the rise of proper drilling data management system and BI

tools, people are starting to realise the importance of this historical data.

However, even if the company realised the significance of this historical data and with the aid of sophisticated activity reporting software, sometimes it is still difficult to accurately take advantage of the information. One of the main reasons is the improper activity data reporting and the lack of operational activity coding process. (Nakagawa, Damski and Miura 2005). Several studies in the past have tried to identify what are the barriers that hinder the use of historical data and how to mitigate it (Nakagawa, Damski and Miura 2005, Damski 2014).

It can be seen that the activity coding process is crucial for the historical data analysis, however, as it is not standardised in geothermal industry in Indonesia, this can cause some inaccuracies due to the following reasons:

- Not detailed enough to differentiate different activities, or excessively detailed thus making the one making the report to identify the right code;
- Inconsistent coding due to different people inputting the activity report;
- Differences on when to start / end the activity code in reporting;
- Inconsistent coding for trouble time.

Therefore, it is highly imperative that for a proper drilling activity reporting, the company should establish a dedicated team to assess their activity coding system, set standards, carry out training, and socialize the significance of proper drilling activity report throughout the organization.

CASE STUDY

Problem

A geothermal company in Indonesia has no database of their previous drilling operation. The legacy data available are just reports in various format (mostly spreadsheet, and in the form of single daily drilling report with no summary). The problem arises when the company wants to carry out next drilling campaign for power plant expansion. The inconsistent and unstructured report make it very difficult to do drilling performance analysis.

Solution

A preliminary data management was then carried out to organise, data QC and cleansing, and implement a system to convert the spreadsheet report into one integrated historical database.

Figure 12 shows the examples of the daily drilling report, directional survey, and bit performance. Note that all of the reports have not been summarised yet prior to the data management implementation.

Figure 13 shows the data management flowchart for company's legacy data.

Implementation and Challenges

The data management started with sorting and organise the reports, data quality check, creating a single format for each type of reports, and establishing a uniform activity coding system. However, as the drilling was carried out in 1998 and the original drilling team is not in the company anymore, several challenges regarding reliability of the data were faced during the process. Those challenges are described in Figure 8.

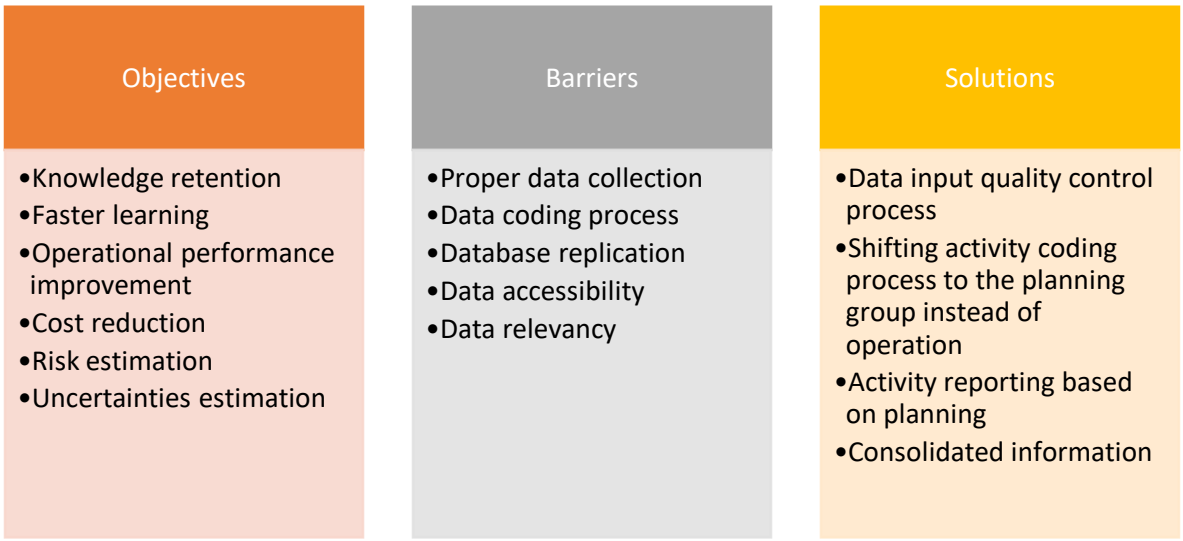


Figure 7: Barriers and potential solution to take fully advantages of historical drilling activity data (modified from Nakagawa et al., 2005).

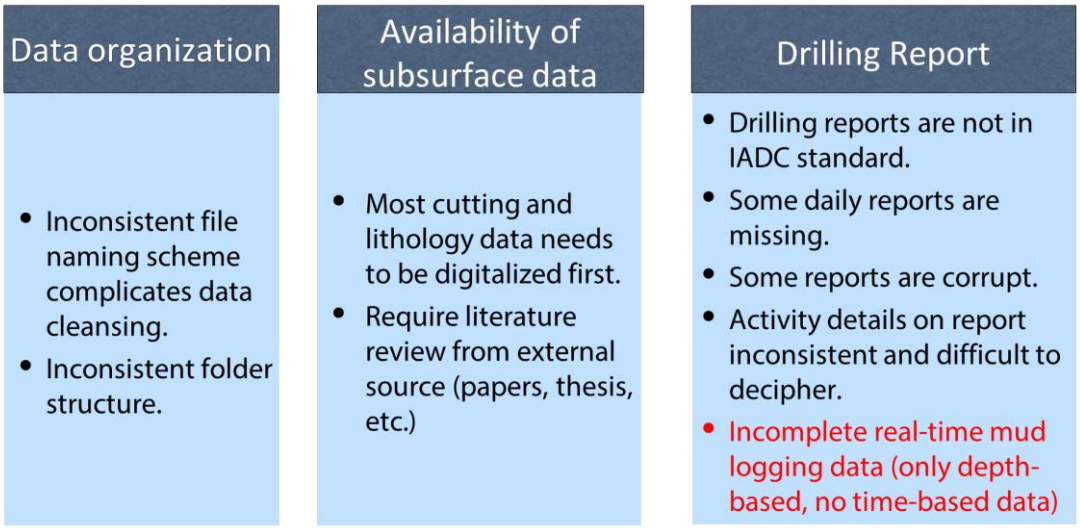


Figure 8: Challenges faced during data management process.

The basic drilling data analysis could be conducted by BI tools such as Microsoft PowerBI or Sisense, but for the quick setup and readily available tools in the company, Microsoft Excel was then used. Several examples of the information that were extracted after the data management process is shown in Figure 14. Note that it is practically not possible to be done without data cleansing and establishing uniform activity coding process first.

Results and Lessons Learned

The implementation of the data management shows that the pile of seemingly impossible to use data can be utilised to extract useful information to aid for future drilling campaign. The format is proven to be relatively easy to use with run-of-the-mill software such as Microsoft Excel. However, to fully take benefit from the whole data management process in the future, several points of improvement are identified:

- Employ fit-to-purpose business intelligence process to extract the critical information required for future drilling campaign decision making.
- Assess the activity code to ensure that it is already fit with the company needs.
- Utilise drilling activity reporting software, or establish standardised daily drilling report spreadsheet (adopting IADC or other standards) to ease drilling report input to database.
- QA/QC all drilling report immediately prior to inputting to database to ensure accuracy and reliability.

SUMMARY AND CONCLUSIONS

This study has summarised the drilling data management concept and advantages from various sources, mostly from more established industry such as oil and gas. From the literature study and case study, several points are obtained:

- It is important to have proper & structured drilling data in the form of database.
- Proper database can be further developed into fully-fledged Drilling Data Management.
- A good Drilling Data Management will greatly aid in conducting drilling data analysis and business intelligence to improve business process. Without it, the whole data management will only be an extra cost with no value for the company.
- A legacy drilling data can still be used to analyse past performance and obtain lessons learned, but require a lot of post-event quality control. Therefore, it is advised to apply proper quality control process from the early phase of drilling data management.

REFERENCES

Damski, C., (2014), "Drilling Data Vortex: Where the bits meet the bits". Australia: Genesis Publishing and Services Pty Ltd.

GeothermEx, (2010), "An Assessment of Geothermal Resource Risks in Indonesia". Working Paper, Richmond, California: GeothermEx, Inc.

Hanley, C., J. Kubicki, M. Lumpkin, and L. Tompkins, (2011), "Development of a Global Drilling Performance Database." SPE/IADC Middle East Drilling Technology Conference and Exhibition. Muscat, Oman: SPE International.

Iyoho, A. W., K. K. Millheim, B. K. Virginillo, A. R. Adeleye, and M. J. Crumrine, (2004), "Methodology and Benefits of a Drilling

Analysis Paradigm." IADC/SPE Drilling Conference 2004. Dallas, Texas: SPE International.

Iyoho, A. W., R. A. Meize, K. K. Millheim, and M. J. Crumrine, (2005), "Lessons from Integrated Analysis of GOM Drilling Performance." Offshore Technology Conference 200. Houston: SPE International.

Johnson, C. N., (2002), "The benefits of PDCA." Quality Progress (Proquest) 35 (5). https://search.proquest.com/openview/6fb24b731a9c0c8bafd90096fd751e76/1?pq-origsite=gscholar&cbl=34671.

Kementerian ESDM, (2017), "Rencana Umum Energi Nasional." Kementerian Energi dan Sumber Daya Mineral Republik Indonesia. Accessed June 2, 2019. https://www.esdm.go.id/id/publikasi/ruen.

Nakagawa, E., C. Damski, and K. Miura, (2005), "What is the Source of Drilling and Completion Data?" Asia Pacific Oil & Gas Conference and Exhibition. Jakarta: SPE International.

ORACLE, (2019), "What is Data Management?" ORACLE. Accessed June 5, 2019. https://www.oracle.com/database/what-is-data-management/.

Purba, D. P., D. W. Adityatama, M. F. Umam, and F. Muhammad, (2019), "Key Considerations in Developing Strategy for Geothermal Exploration Drilling Project in Indonesia." PROCEEDINGS, 44th Workshop on Geothermal Reservoir Engineering. Stanford: Stanford University.

Shi, X., Y. Zhou, P. Song, Q. Zhao, H. Jiang, Z. Huo, G. Yang, and X. Zhai, (2015), "Integrated Drilling Database Enables Automated Drilling Engineering Design." SPE/IATMI Asia Pacific Oil & Gas Conference and Exhibition. Nusa Dua, Bali: SPE International.

Sokovic, M., D. Pavletic, and K. K. Pipan, (2010), "Quality Improvement Methodologies - PDCA Cycle, RADAR Matrix, DMAIC and DFSS." Journal of Acheivements in Materials and MAnufacturing Engineering (International OCSCO World Press) 43 (1).

Sumbal, M. S., E. Tsui, E. See-to, and A. Barendrecht, (2017), "Knowledge retention and aging workforce in the oil and gas industry: a multi perspective study." Journal of Knowledge Management (Emerald) 21 (4): 907-924. doi:10.1108/JKM-07-2016-0281.

Umam, M. F., J. Susilo, D. P. Purba, and D. W. Adityatama, (2019), "Design of Geothermal Drilling Training Curriculum as the Implementation of the National Competence Standard on Onshore Drilling." PROCEEDINGS, 8th ITB International Geothermal Workshop 2019. Bandung: Institut Teknologi Bandung.

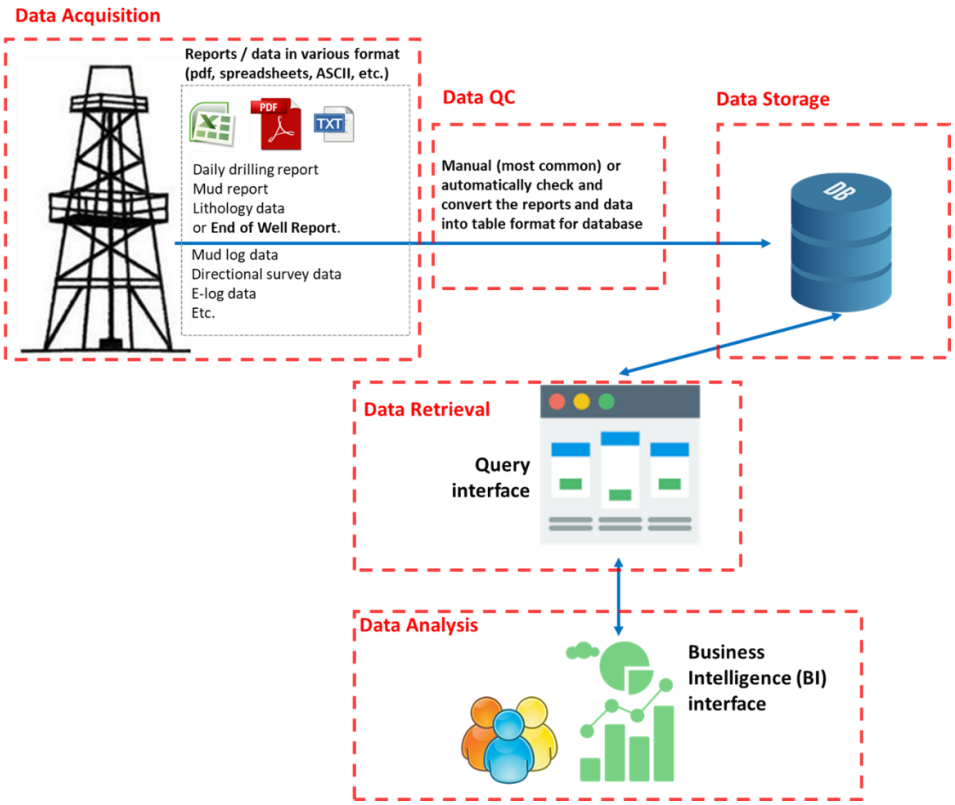


Figure 9. Steps of drilling data management. Modified from Damski (2014).

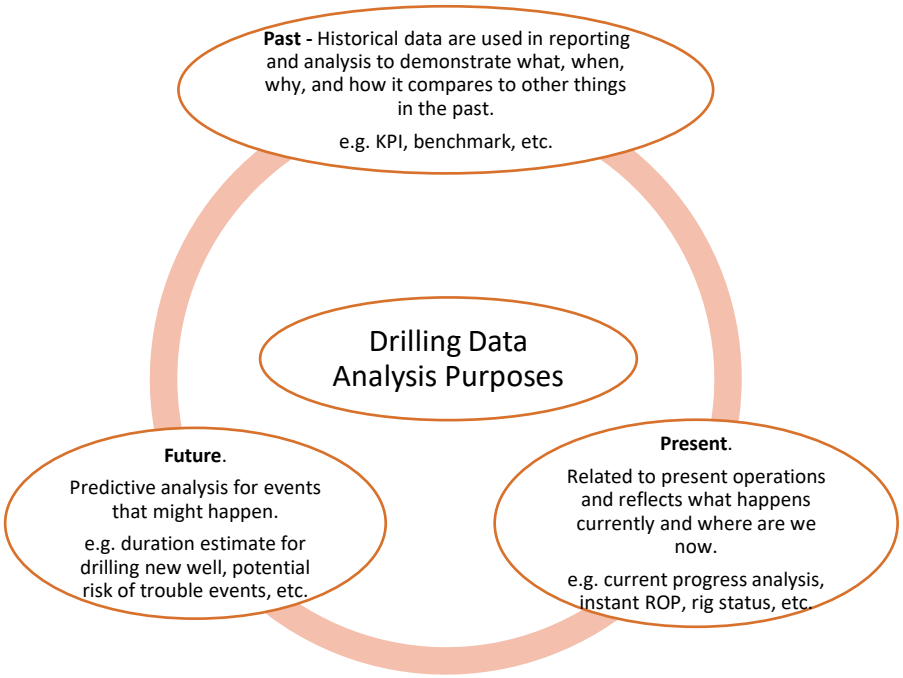
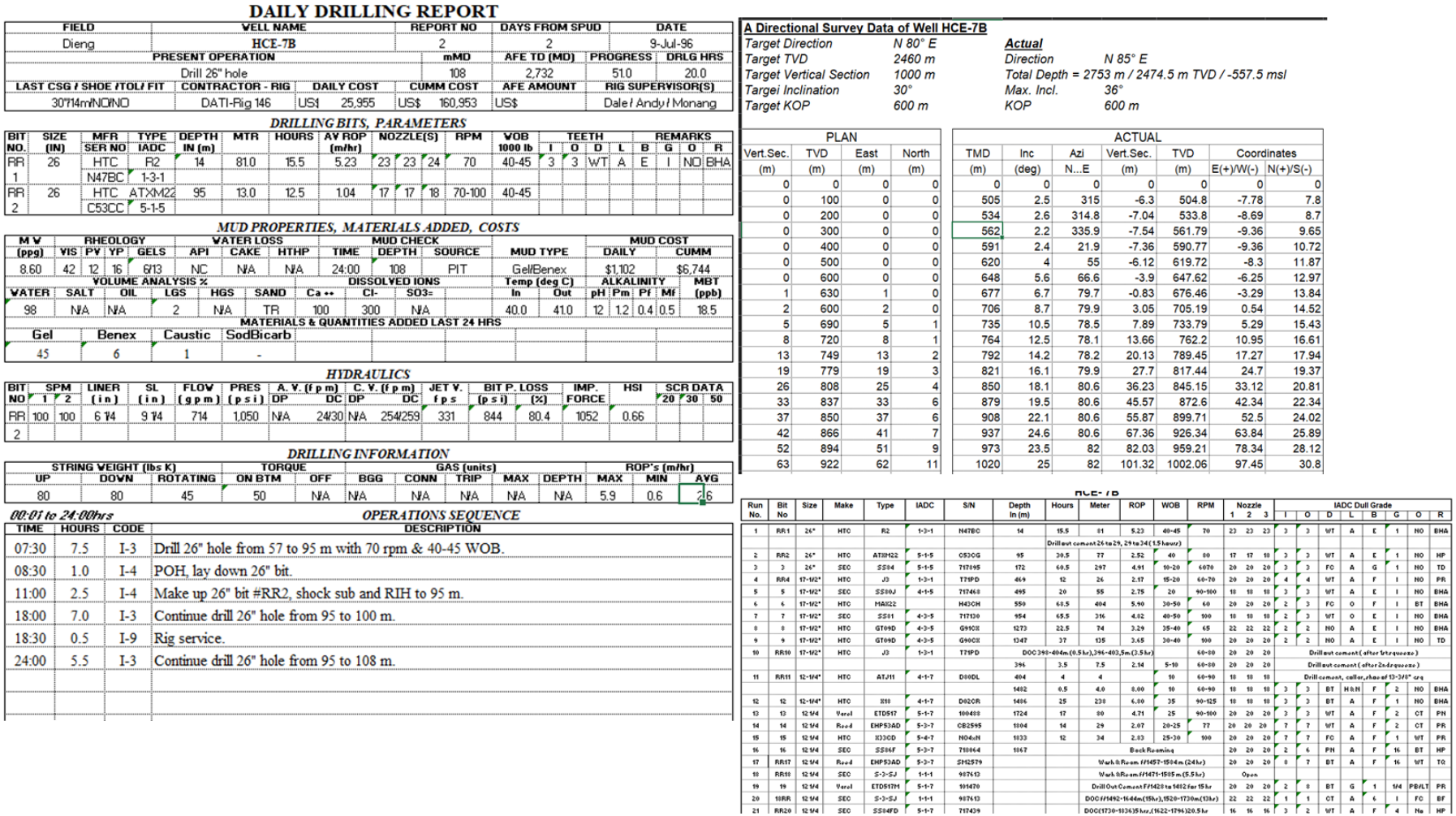


Figure 10. Basic purposes of drilling data analysis.



Figure 11. 10 steps drilling analysis flowchart (Iyoho, Millheim, et al. 2004).



DAILY DRILLING REPORT

FIELD	WELL NAME	REPORT NO	DAYS FROM SPUD	DATE
Dieng	HCE-7B	2	2	9-Jul-96

PRESENT OPERATION	mMD	AFE TD (MD)	PROGRESS	DRLG HRS
Drill 26" hole	108	2,732	51.0	20.0

LAST CSG / SHOE /TOL/ FIT	CONTRACTOR - RIG	DAILY COST	CUMM COST	AFE AMOUNT	RIG SUPERVISOR(S)
30"/14m/NO/NO	DATI-Rig 146	US$ 25,955	US$ 160,953	US$	Dale / Andy / Monang

DRILLING BITS, PARAMETERS

BIT NO.	SIZE (IN)	MFR / SER NO	TYPE / IADC	DEPTH IN (m)	MTR	HOURS	AV ROP (m/hr)	NOZZLE(S)	RPM	WOB 1000 lb	TEETH I	O	D	L	B	G	O	R
RR 1	26	HTC N47BC	R2 1-3-1	14	81.0	15.5	5.23	23 23 24	70	40-45	3	3	WT	A	E	I	NO	BHA
RR 2	26	HTC C53CC	ATXM22 5-1-5	95	13.0	12.5	1.04	17 17 18	70-100	40-45								

MUD PROPERTIES, MATERIALS ADDED, COSTS

MW (ppg)	RHEOLOGY VIS	PV	YP	GELS	WATER LOSS API	CAKE	HTHP	MUD CHECK TIME	DEPTH	SOURCE	MUD TYPE	MUD COST DAILY	CUMM
8.60	42	12	16	6/13	NC	N/A	N/A	24:00	108	PIT	Gel/Benex	$1,102	$6,744

VOLUME ANALYSIS % WATER	SALT	OIL	LGS	HGS	SAND	DISSOLVED IONS Ca ++	Cl-	SO3=	Temp (deg C) In	Out	ALKALINITY pH	Pm	Pf	Mf	MBT (ppb)
98	N/A	N/A	2	N/A	TR	100	300	N/A	40.0	41.0	12	1.2	0.4	0.5	18.5

MATERIALS & QUANTITIES ADDED LAST 24 HRS

Gel	Benex	Caustic	SodBicarb
45	6	1	-

HYDRAULICS

BIT NO	SPM 1	2	LINER (in)	SL (in)	FLOW (gpm)	PRES (psi)	A. V. (fpm) DP	DC	C. V. (fpm) DP	DC	JET V. fps	BIT P. LOSS (psi)	(%)	IMP. FORCE	HSI	SCR DATA 20	30	50
RR 1	100	100	6 1/4	9 1/4	714	1,050	N/A	24/30	N/A	254/259	331	844	80.4	1052	0.66			
2																		

DRILLING INFORMATION

STRING WEIGHT (lbs K) UP	DOWN	ROTATING	TORQUE ON BTM	OFF	GAS (units) BGG	CONN	TRIP	MAX	DEPTH	ROP's (m/hr) MAX	MIN	AVG
80	80	45	50	N/A	N/A	N/A	N/A	N/A	N/A	5.9	0.6	2.6

00:01 to 24:00hrs ***OPERATIONS SEQUENCE***

TIME	HOURS	CODE	DESCRIPTION
07:30	7.5	I-3	Drill 26" hole from 57 to 95 m with 70 rpm & 40-45 WOB.
08:30	1.0	I-4	POH, lay down 26" bit.
11:00	2.5	I-4	Make up 26" bit #RR2, shock sub and RIH to 95 m.
18:00	7.0	I-3	Continue drill 26" hole from 95 to 100 m.
18:30	0.5	I-9	Rig service.
24:00	5.5	I-3	Continue drill 26" hole from 95 to 108 m.

A Directional Survey Data of Well HCE-7B

Target Direction	*N 80° E*	***Actual***	
Target TVD	*2460 m*	*Direction*	*N 85° E*
Target Vertical Section	*1000 m*	*Total Depth = 2753 m / 2474.5 m TVD / -557.5 msl*	
Targei Inclination	*30°*	*Max. Incl.*	*36°*
Target KOP	*600 m*	*KOP*	*600 m*

PLAN Vert.Sec. (m)	TVD (m)	East (m)	North (m)	ACTUAL TMD (m)	Inc (deg)	Azi N...E	Vert.Sec. (m)	TVD (m)	Coordinates E(+)/W(-)	N(+)/S(-)
0	0	0	0	0	0	0	0	0	0	0
0	100	0	0	505	2.5	315	-6.3	504.8	-7.78	7.8
0	200	0	0	534	2.6	314.8	-7.04	533.8	-8.69	8.7
0	300	0	0	562	2.2	335.9	-7.54	561.79	-9.36	9.65
0	400	0	0	591	2.4	21.9	-7.36	590.77	-9.36	10.72
0	500	0	0	620	4	55	-6.12	619.72	-8.3	11.87
0	600	0	0	648	5.6	66.6	-3.9	647.62	-6.25	12.97
1	630	1	0	677	6.7	79.7	-0.83	676.46	-3.29	13.84
2	600	2	0	706	8.7	79.9	3.05	705.19	0.54	14.52
5	690	5	1	735	10.5	78.5	7.89	733.79	5.29	15.43
8	720	8	1	764	12.5	78.1	13.66	762.2	10.95	16.61
13	749	13	2	792	14.2	78.2	20.13	789.45	17.27	17.94
19	779	19	3	821	16.1	79.9	27.7	817.44	24.7	19.37
26	808	25	4	850	18.1	80.6	36.23	845.15	33.12	20.81
33	837	33	6	879	19.5	80.6	45.57	872.6	42.34	22.34
37	850	37	6	908	22.1	80.6	55.87	899.71	52.5	24.02
42	866	41	7	937	24.6	80.6	67.36	926.34	63.84	25.89
52	894	51	9	973	23.5	82	82.03	959.21	78.34	28.12
63	922	62	11	1020	25	82	101.32	1002.06	97.45	30.8

HCE-7B

Run No.	Bit No	Size	Make	Type	IADC	S/N	Depth In (m)	Hours	Meter	ROP	WOB	RPM	Nozzle 1	2	3	IADC Dull Grade I	O	D	L	B	G	O	R
1	RR1	26"	HTC	R2	1-3-1	N47BC	14	15.5	81	5.23	40-45	70	23	23	23	3	3	WT	A	E	1	NO	BHA
								Drill out cement 26 to 29, 29 to 34 (1.5 hours)															
2	RR2	26"	HTC	ATJ22	5-1-5	C53CG	95	30.5	77	2.52	40	80	17	17	18	3	3	WT	A	E	1	NO	HP
3	3	26"	SEC	SS84	5-1-5	717895	172	60.5	297	4.91	10-20	6070	20	20	20	3	3	FC	A	G	1	NO	TD
4	RR4	17-1/2"	HTC	J3	1-3-1	T71PD	469	12	26	2.17	15-20	60-70	20	20	20	4	4	WT	A	F	I	NO	PR
5	5	17-1/2"	SEC	SS80J	4-1-5	717468	495	20	55	2.75	20	90-100	18	18	18	3	3	WT	A	E	I	NO	BHA
6	6	17-1/2"	HTC	MA122		H43CH	550	68.5	404	5.90	30-50	60	20	20	20	2	3	FC	O	F	I	BT	BHA
7	7	17-1/2"	SEC	SS81	4-3-5	717130	954	65.5	316	4.82	40-50	100	18	18	18	2	3	WT	O	E	I	NO	BHA
8	8	17-1/2"	HTC	GT09D	4-3-5	G91CX	1273	22.5	74	3.29	35-40	65	22	22	22	2	2	NO	A	E	I	NO	BHA
9	9	17-1/2"	HTC	GT09D	4-3-5	G90CX	1347	37	125	3.65	30-40	100	20	20	20	2	2	NO	A	E	I	NO	TD
10	RR10	17-1/2"	HTC	J3	1-3-1	T71PD	DOC 390-404m (0.5 hr), 396-403.5m (3.5 hr)					60-80	20	20	20	Drill out cement (after 5 to squeeze)							
							396	3.5	7.5	2.14	5-10	60-80	20	20	20	Drill out cement (after 2nd squeeze)							
11	RR11	12-1/4"	HTC	ATJ11	4-1-7	D80DL	404	4	4		10	60-90	18	18	18	Drill cement, collar, shoe of 13-3/8" csg							
							1402	0.5	4.0	8.00	10	60-90	18	18	18	3	3	BT	H & H	F	2	NO	BHA
12	12	12-1/4"	HTC	X18	4-1-7	D02CR	1406	25	238	6.80	35	90-125	18	18	18	3	3	BT	A	F	1	NO	BHA
13	13	12 1/4	Varel	ETD517	5-1-7	100488	1724	17	80	4.71	25	90-100	20	20	20	3	3	WT	A	F	2	CT	PN
14	14	12 1/4	Reed	EHP53AD	5-3-7	OB2595	1804	14	29	2.07	20-25	77	20	20	20	7	7	WT	A	F	2	CT	PR
15	15	12 1/4	HTC	XDGOD	5-4-7	N04JN	1833	12	34	2.83	25-30	100	20	20	20	7	7	FC	A	F	1	WT	PR
16	16	12 1/4	SEC	SS86F	5-3-7	718064	1867		Back Reaming				20	20	20	2	6	PN	A	F	16	BT	HP
17	RR17	12 1/4	Reed	EHP53AD	5-3-7	SH2579			Work & Ream f/1457-1504 m (24 hr)				20	20	20	8	7	BT	A	F	16	WT	TQ
18	RR18	12 1/4	SEC	S-3-SJ	1-1-1	987613			Work & Ream f/1471-1505 m (5.5 hr)				Open										
19	19	12 1/4	Varel	ETD517M	5-1-7	101470			Drill Out Cement F/1428 to 1492 for 15 hr				20	20	20	2	8	BT	G	1	1/4	PB/LT	PR
20	18RR	12 1/4	SEC	S-3-SJ	1-1-1	987613	DOC f/1492-1644m (15hr), 1520-1730m (13hr)						22	22	22	1	1	CT	A	4	I	FC	BF
21	RR20	12 1/4	SEC	SS84FD	5-1-7	717439	DOC (1730-1836) 5 hr, (1622-1796) 20.5 hr						16	16	16	3	2	WT	A	F	4	No	HP

Figure 12. Example of legacy drilling report (daily drilling report, survey, and bit performance).

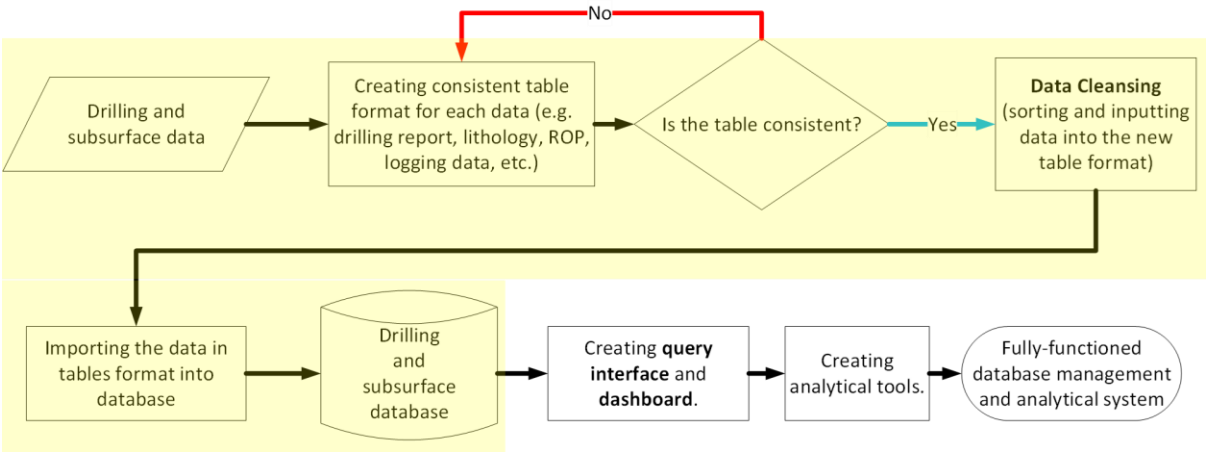


Figure 13. Data management flowchart. Current progress is highlighted in yellow.

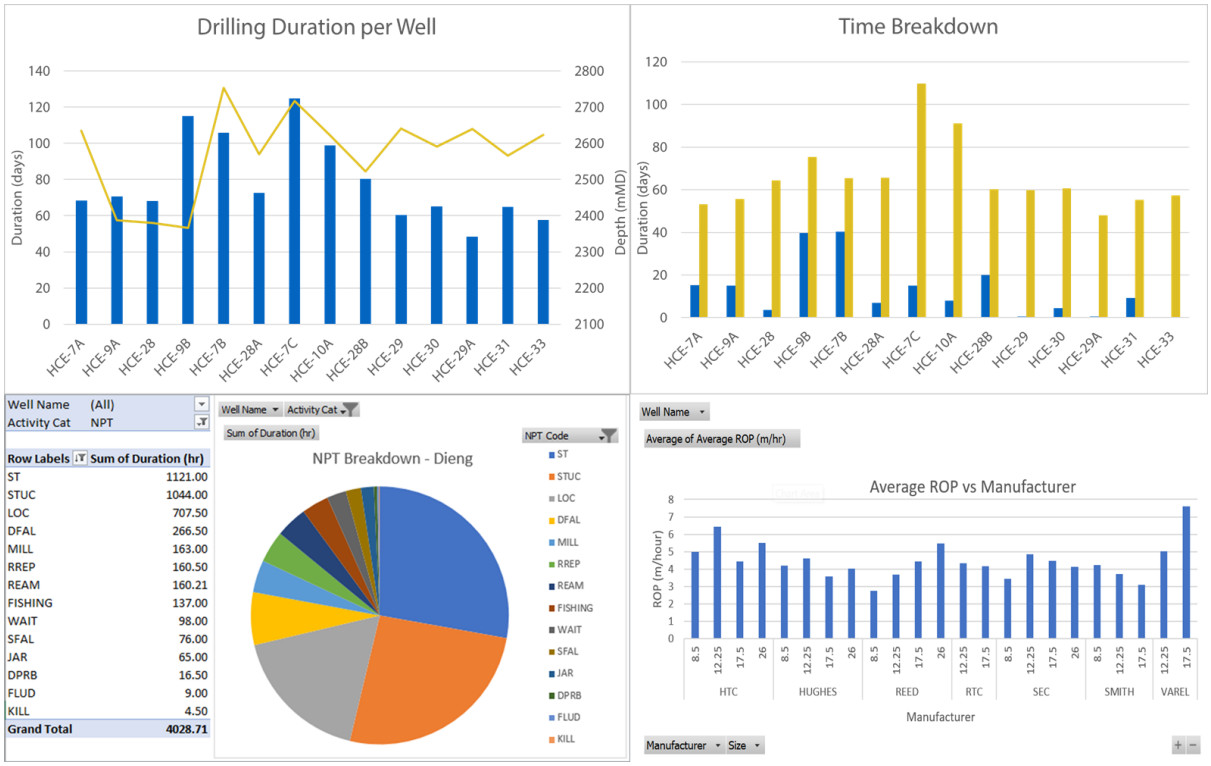


Figure 14. Several informations that can be extracted after data cleansing process on the legacy data.

A REVIEW OF GEOHEAT AS NEW ZEALAND'S GEOTHERMAL DIRECT USE STRATEGY

Wini Rizkiningayu

New Zealand Trade and Enterprise Organization
New Zealand Embassy, Sentral Senayan 2 10th Floor,
Gelora Bung Karno, Jl Asia Afrika no.8 Jakarta 10270
Email: wini.rizkiningayu@nzte.govt.nz

ABSTRACT

New Zealand has a long history of geothermal electricity generation. Today, geothermal energy produces almost 20% of New Zealand's electricity supply. New Zealand's main geothermal generating capacity is situated in the Taupo Volcanic Zone. Power companies in New Zealand generate roughly 7,500 GWh per year from 19 power plants located in over 8 high-temperature fields. Geothermal power forms a key role in decarbonizing the New Zealand's electricity Market.

However, the contribution of Geothermal extends beyond electrification with geothermal direct use. It has been applied to substitute or complement fossil fuel to provide heat in many activities in New Zealand. Depends on the temperature of Geothermal fluid available, the direct use has been applied in timber industries, food processing, green house agriculture, aquaculture, heating, tourism, and health. Currently there is about 8 PJ/y of energy in direct geothermal applications, which contribute to technological advancement, regional social and economic development, local community employment and environmental impact.

The application of Geothermal Direct Use in New Zealand is strategically outlined in a policy called Geoheat. Geoheat attempt to optimize Geothermal direct use to supply new and existing businesses with heat; to attract industries to take advantage of New Zealand's geothermal assets with the flow on environmental benefits; to create employment in the ventures that use the geothermal energy and business that service the ventures; as well as to empower the socioeconomic of tangata whenua (Maori community).

The paper aims to review the formulation and implementation of New Zealand's Geoheat which might be of benefit for Indonesia. The paper will discuss Geoheat from the following point of view: the strategy formulation and the underlying principles, mapping of stakeholders, its relationship to other existing strategies and processes, and action plan to implement the strategy.

Keywords: Direct use, geoheat, New Zealand

GEOTHERMAL IN NEW ZEALAND

In New Zealand, Geothermal plays important role in energy generation of the country with current installed capacity of 900MW, enabling it to provide approximately 17% of the electricity (New Zealand Electricity Authority, 2018). Some of the earliest large-scale use of geothermal in the world were in New Zealand, with Wairakei being the first geothermal plant opened in 1958. At that moment, Wairakei was the second large-scale plant existing worldwide, with the first being Valle del Diavolo 'Devil's Valley' plant in Larderello, Italy in 1911.

As the petrochemical fuel price rises and electricity demand grows, Geothermal energy has been described as one of the most attractive and reliable sources of energy. With around 1000MW resource can be used for electricity generation, geothermal energy contributes to the supply of renewable energy in New Zealand. Geothermal energy is heavily independent to weather, making it as one of the most reliable sources of renewable energy as well, above wind, solar, and even hydroelectricity. Geothermal power stations in New Zealand has load factors of 95%, compared to typical load factors of 30 – 50% for hydro and wind power stations. The 60 years old Wairakei power station even has operated at load factor for more than 90% for over 40 years with low operating cost.

Geothermal energy is a relatively low-cost and indigenous generation option that can contribute to New Zealand's growing demand for electricity. It is uniquely reliable, with geothermal power stations typically achieving load factors of 95%, compared to typical load factors of 30 – 50% for hydro and wind power stations. Wairakei Power Station has operated at a load factor of more than 90% for over 40 years with low operating costs. This inherent reliability makes geothermal generation a valuable component in a diverse electricity supply system such as New Zealand's.

Not only that New Zealand has a long history of utilizing high temperature geothermal resources for electricity generation, it has also even longer history of geothermal direct use.

DIRECT USE OF GEOTHERMAL IN NEW ZEALAND

Direct use of geothermal heat can be traced back to early Māori use of geothermal springs and pools for bathing, healing, cooking, and community life. Geothermal plays inseparable role in the Māori community. The first geothermal field in Aotearoa (New Zealand) was described upon a legend of the high priest Ngatoroirangi. He was caught in a blizzard while climbing Mount Ngauruhoe. In Hawaiki, his sisters Te Pupu and Te Hoata heard his prayers for help and sent fire to save him from freezing. In the wake of this fire, a path of geothermal fields remains.

With high and moderate to low enthalpy resources, geothermal heat is widely use directly (without a heat pump or power plant) for many purposes such as heating buildings, industrial processes, domestic heating, greenhouses, aquaculture, public baths and pools. The type of direct use depends on the temperature of the geothermal fluid available. Some examples of different uses across the temperature range are shown against the thermometer (Figure 1).

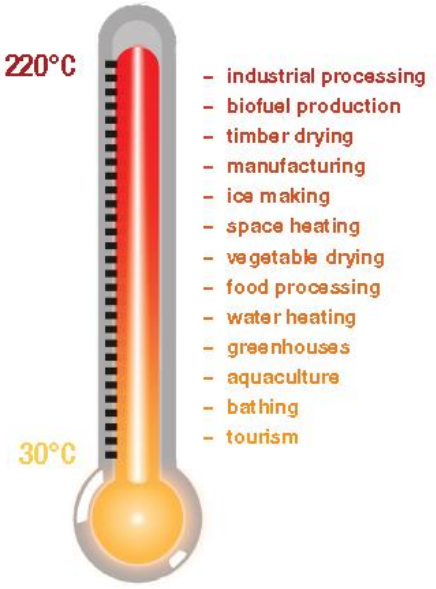


Figure 1: Various direct use of geothermal based on the temperature of the resources.

Industrial and non-industrial sector can use geothermal direct use for most of the heat reliant process instead of, or as a supplement, to other energy sources, such as electricity or fossil fuels. In New Zealand, several businesses that are using geothermal heat include the Tenon timber drying facility in Taupō, the Miraka milk processing facility at Mokai, the Asaleo tissue manufacturing plant in Kawerau and a cut flower grower at Horohoro, near Rotorua.

The largest geothermal direct user in the world is the Norske Skog Tasman pulp and paper mill at Kawerau industrial estate in New Zealand. With an installed capacity of 210 MWt and an annual energy use of 7.5PJ, the plant uses geothermal fluids to generate clean process steam for paper drying, a source of heat in evaporators, timber drying and increasingly for electricity generation.

GEOHEAT STRATEGY

In discussing and reviewing the strategy, the material below until the chapter 'Relation to the strategy' are taken from NZGA, Geoheat strategy for Aotearoa NZ 2017-2030, 2017 and NZGA, Action Plan 2018-2019 Geoheat strategy for Aotearoa NZ 2017-2030, 2017.

Background

On 2011, GNS Science, one of the crown research institute, wrote a roadmap for geothermal direct use in New Zealand (Carey and Climo, 2012). It was presented as a paper and keynote address at the 2012 New Zealand Geothermal Workshop. There was sufficient interest shown such that GNS Science staff and the then New Zealand Geothermal Association (NZGA) President, Brian Carey, pursued the development of the roadmap into strategy.

With GNS Science's geothermal research funding, team from GNS Science and Environmental Management Services Limited (now Mitchell Daysh) were developing and writing the Strategy through several sector consultation. Involving the sector was considered important to the ultimate uptake of the Strategy. The entire strategy development process aimed to be inclusive, stakeholder-led, non-partisan and unbiased. For this, the New Zealand geothermal association (NZGA) was deemed as the appropriate host for the Strategy.

Strategy Formulation

The Geoheat Strategy seeks to drive an increase in the utilization of direct geothermal heat to derive value for New Zealand. The goal is to develop and implement a Strategy that will establish continuous and sustainable growth in the direct use of geothermal energy. There are several crucial factors in formulation the strategy, namely:

1. Collaborative and consultative formulation process with related stakeholders
2. Clear scoping and focusing of what the strategy will encompass
3. SMART goal and success factor.

These 3 important factors are considered critical in shaping and formulating the strategy in order to be sustainable and successful. Each factor will be discussed separately on this paper.

Collaborative and consultative formulation process with related stakeholders

To achieve success, the strategy formulation needs to consider the involvement of stakeholders in direct geothermal energy. Stakeholders, with their different role, are central to the formulation of the strategy. They serve as regulators, executioners, suppliers, service, commercial side, user, as well as the affected local community.

The stakeholders in direct geothermal energy use are mapped below (Figure 2)

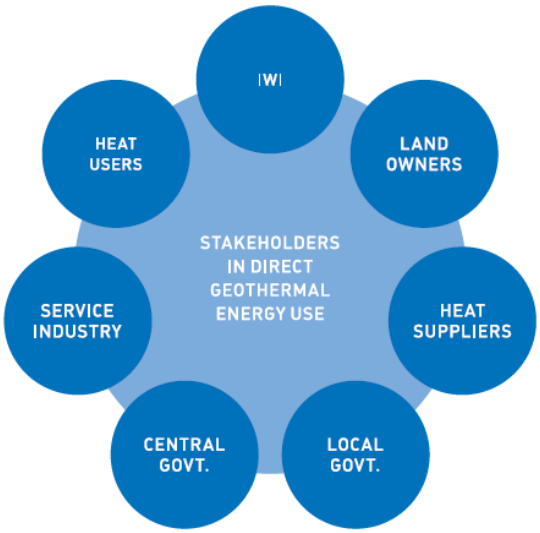


Figure 2: Mapping of Geoheat Stakeholders.

In the background section, we have discussed how several forum i.e workshops serve as cross sector consultation in creating the strategy. Participants in these forums are the stakeholders in direct geothermal energy use as defined above. The collaborative and consultative formulation process are the heart of Geoheat formulation, with the stakeholders involved as follow:

1. Local and indigenous communities: Iwi, Māori Landowners and Māori Trust Representatives
2. Central Government Agencies:
   • Ministry of Business, Innovation and Employment
   • Energy Efficiency and Conservation Authority
   • GNS Science
   • Te Puni Kokiri
   • New Zealand Trade and Enterprise
3. Regional and Local Government
   • Bay of Plenty Regional Council
   • Waikato Regional Council
   • Rotorua Lakes Council
   • Taupō District Council
   • Kawerau District Council
4. NZGA Members and Conference Participants from the Geothermal Sector
   (at the New Zealand Geothermal Workshop 2015)
5. NZGA Industry Groups
   •Direct heat
   •Power and industrial heat
   •GHANZ — the Geothermal Heat-pump Association of NZ
6. Regional Development Agencies
   • Bay of Connections
   • Northland Inc. (Preliminary Discussions)
7. District Development Agencies
   • Grow Rotorua
   • Enterprise Great Lake Taupō
   • Kawerau Enterprise Agency Incorporated

Through the consultation with above stakeholders, the Strategy has been developed in a consultative and collaborative way and reflects the inputs and views of multiple people across New Zealand with an interest in geothermal future

Through 2015, several workshops were held with a broad cross-section of interested parties and stakeholders, including:

1. NZGA Generation and Industrial Heat Interest Group - 3 August 2015 (Wairakei).
2. Bay of Connections Governance Group - 10 August 2015 (Taupō).
3. Waiariki Māori Geothermal Advisory Group - 9 September 2015 (Rotokawa).
4. 2015 New Zealand Geothermal Workshop 18 and 19 November 2015 (Wairakei).

These workshops serve as cross sector consultation in creating the strategy. It is recognized that cross sector consultation is part of the collaborative work in the strategy formulation to enable a wholesome, more comprehensive and inclusive approach towards formulating a strategy that will drive geothermal direct use for benefit of all stakeholders involved.

Clear scoping and focusing of the strategy

Due to the wide possibility for geothermal direct use activity areas, defining clear scope and focus is important to the strategy success. The strategy will encompass direct geothermal energy activity focusing on higher temperature primary geothermal energy.

The scopes of the strategy are on direct use both in industrial and residential, with defined areas across New Zealand. Electricity generation (including directly fostering electricity generation) and geothermal heat pumps are excluded from the scope. Although the geothermal ground sourced or water sourced heat pump sector was excluded, the Geothermal Heat Pump Association of New Zealand (GHANZ) is developing its own strategy that responds to the unique characteristics of that sector. In regard to the geothermal electricity sector, it is understood that this strategy will bear a strong

association where electricity and direct heat installations share a geothermal resource. In some cases, direct geothermal use will occur in conjunction with a geothermal electricity operation where the direct use might not standalone, and there are opportunities to explore further.

Considering the different feasibility, priority and importance of various geothermal direct use project and future project across New Zealand, the strategy will define the focus activities in the scoped area. During the consultative process with the stakeholders, it is decided that the Geoheat strategy will have primary and secondary focus. The primary focus will be zooming in on commercial scalability of geothermal direct use in 3 areas in New Zealand, in line with the regional energy plan and regulation. While the primary focus will be the main agenda, secondary focus will still be road mapped under Geoheat strategy albeit the lesser priority.

PRIMARY FOCUS
- Direct use of geothermal energy
- Industrial and commercial scale developments
- Regional focus on Northland, Waikato and Bay of Plenty geothermal resources

SECONDARY FOCUS
- Residential scale use
- Geothermal resources in other regions of New Zealand

With this clear scoping and focus, the activities derived from the strategy is expected to be more effective.

SMART goal and success factor

In order to achieve its purpose, Geoheat strategy are guided by well-defined goals. SMART criteria need to be met when formulating the strategy goals so that the goals reflect the original purpose of the strategy. The SMART criteria are defined below:

1. Specific
2. Measurable
3. Action-oriented
4. Reasonable
5. Time bound

With the criteria in mind and the initial purpose of the strategy to serve development of geothermal direct use in New Zealand, the strategy will have been successful if, by 2030:

1. Annual direct primary geothermal energy use has increased by 7.5 PJ in new projects in the period 2017–2030; and
2. Geothermal direct use business operations are employing (directly and indirectly) an additional 500 people associated with new projects in the period 2017–2030.

To measure the goal, the strategy is equipped with success factors. These seven success factors identified through stakeholder engagement and consultation. These success factors aim to provide strategic direction for activities undertaken under this Strategy. The seven success factors are:

1. Funding: Government, industry and other sectors invest in developing geothermal energy projects.
2. Awareness: Everyone thinks geothermal first; it is intrinsically linked to New Zealand's national identity.
3. Expertise: New Zealand has readily accessible, world-leading capability.
4. Policy: National, regional and district level policy are aligned to enable sustainable geothermal utilization.
5. Geothermal Resources Information: Data is accessible on resources and uses.
6. Market & Economics: Geothermal energy is integrated in business structures as a clear value proposition generating advantage, including through 'green' branding.
7. Technology: Best practise application of technologies and generation of innovative ideas.

<u>Underlying Principles</u>

For Geoheat strategy to be able to be executed sustainably in day to day basis, guiding principles need to be set. The guiding principles acts as a compass in formulating the strategy, providing clear values and principles. It will as well provide a clear framework in defining action, decision-making and behaviors.

The four underlying principles that governs actions, decision-making and behavior in Geoheat strategies are Kaitiakitanga; Shared; Integrated; and Focused. Kaitiakitanga is Maori philosophy for guardianship and sustainability. In this strategy, geothermal development is founded on sustainable business and resource use models, recognizes kaitiaki (guardianship), and supports current and future generations. Shared principles govern that the strategy responsibility is shared, information will be open, and benefits will be mutual. Integrated principles mean that: Sectors, organizations and disciplines support and complement each other in the pursuit of a common goal. The last principle, focused, meaning that the strategy's focus is direct use growth, building on strengths and current successes, to deliver maximum benefit to New Zealand.

The Strategy is a SHARED responsibility for mutual benefit that INTEGRATES sectors, organizations and disciplines. Future growth is underpinned by the

principle of KAITIAKITANGA, with a long-term, sustainable vision. The Strategy is FOCUSED on commercial and industrial scale direct use of the higher temperature Central North Island and Northland geothermal resources but doesn't discount lower temperature resources in other regions or domestic scale use. Figure 3 shows the geoheat success factors and underlying principle, while Figure 4 shows strategy implementation scheme.

The following graphic presents these principles, together with seven success factors identified through stakeholder engagement and consultation.

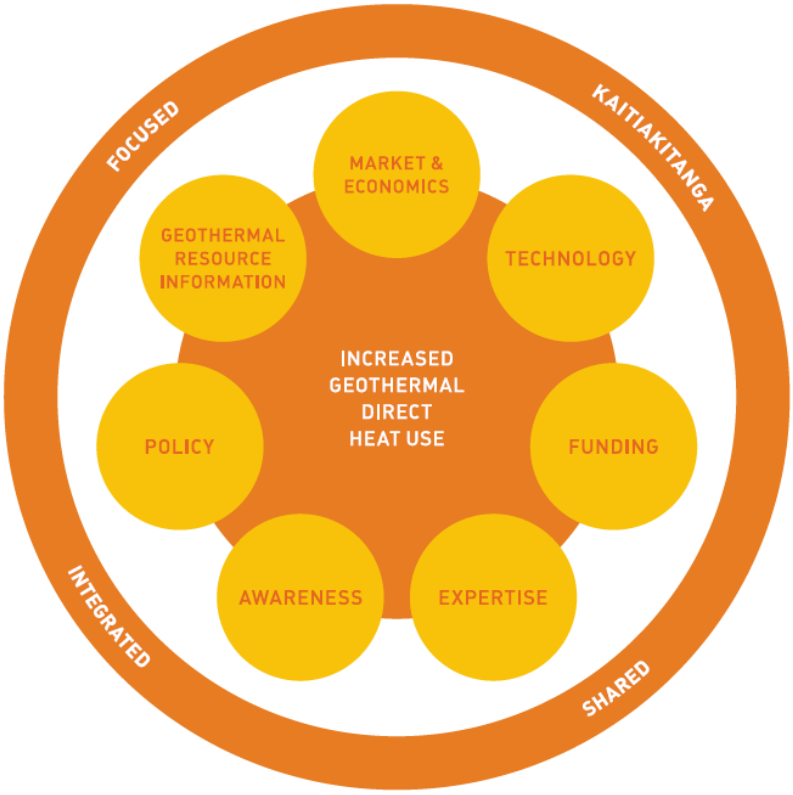


Figure 3: Geoheat success factors and underlying principles.

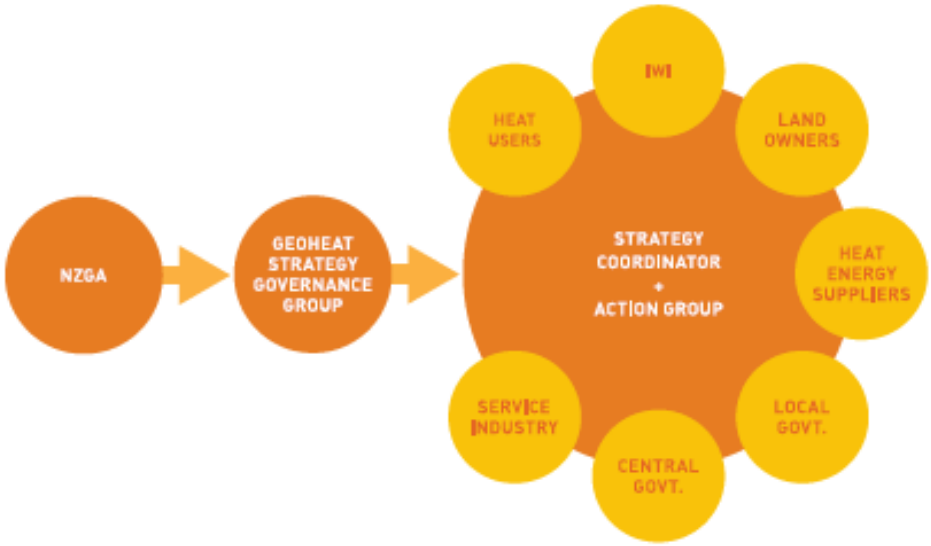


Figure 4: Strategy implementation scheme.

Implementations and Action plans

In relation to the strategy implementation, mapped stakeholders are essential for executing priority action. These stakeholders will strategically take role and accountability in driving, maintaining, executing and evaluating such strategy.

This strategy implementation is illustrated in above's scheme in driving the actions. In order to realize this scheme and to build a strong foundation for successful implementation, five key steps are needed:

1. Establish a Geoheat Strategy governance group.
2. Strategy coordination.
3. Establish Geoheat Strategy Action group.
4. Establish center for geothermal direct use advocacy and activity.
5. Identify and prioritize workplan for implementation of strategy actions.

The strategy is pushed by the NZGA (New Zealand Geothermal Association Board) as project Sponsor. The strategy will be guided and directed by Geoheat Strategy Governance Group that consists of cross-sector representatives (industry, Tangata Whenua, government, heat users, etc.) who guide and direct strategy implementation. To do the day to day basis action and implementation, the governance group appoint a dedicated role of Strategy Coordinator is responsible for coordinating and ensuring the Strategy outcomes are delivered, and reports to the Governance Group. Aside from the central role, the coordinator will facilitate an action group consists of interested person who drive strategy actions and activities. The strategy coordinator will establish a multiple sector and interests' engagement, ensuring cross sector relationship and coordinate activities to drive success.

Geoheat Strategy Governance Group

As an inclusive strategy, Geoheat require participation, consultation, oversight and guidance from a governing committee consist of identified stakeholders. The inclusion of related stakeholders in the committee also aims to provide accountability of implementation. The committee consists of people in relevant fields to geothermal direct use i.e industry and technology/science expertise, Tangata Whenua, Central Governmental, Local Government, regional representation (Northland, Waikato, Bay of Plenty), economic development and end users of heat, will also provide accountability for implementation. Seed funding of $30,000 is provided from joint funding — NZGA and GNS Science funding from Geothermal Resources of New Zealand Research Program.

Strategy Coordination

To do the day to day basis action and implementation, the governance group appoint a dedicated role of strategy coordinator is responsible for coordinating and ensuring the Strategy outcomes are delivered, and reports to the Governance Group. The primary focus for the role is to coordinate, communicate, enthuse, engage and organize the implementation of regional strategies, action plans and an investment attraction campaign, that will drive and convert interest into investment in geothermal direct use projects. Aside from the central role, the coordinator will facilitate an action group consists of interested person who drive strategy actions and activities. The strategy coordinator will establish a multiple sector and interests' engagement, ensuring cross sector relationship and coordinate activities to drive success. The role would be supported by the Geoheat Strategy Governance Group, and funded by support from regional government, industry, and possible Central government funding.

Establish Geoheat Strategy Action Group

As discussed above, the strategy coordinator's role is also to facilitate an action group – a group of interested persons to take ownership over key actions and priorities and drive input into various sectors. GNS Science will initially assist to establish this group.

Establish a center for geothermal direct use advocacy and activity

To simplify access to expertise, information, and advice, a direct use geothermal research and advisory hub for New Zealand is needed. The center can be initially formed virtually with online presence / virtual center. This centre will be the responsibility of Geoheat Strategy Governance Group, with sources of funding from NZGA, Regional and Central Government funding sources with support from industry, to cover the estimated incidental cost of $10,000.

Identify and prioritize workplan for implementation of strategy action

To pursue its goal, Geoheat strategy identified workplan and action through the stakeholder engagement and consultation process. A list of priority order provides a strong base for strategy implementation, with on-the-go review, addition, and re-prioritizing by strategy coordinator with guidance from Governance Group.

Action plans

To specify the actions and activity, Geoheat strategy was accompanied by a set of action plan document detailing activity under overall guidance of the strategy. The action plan document is intended to be

reviewed and renewed every 2-3 years to ensure the deliberation, effectiveness and target achievement.

The overarching objective of the action plan is defined as: “Three new medium to large scale (minimum 30 jobs) direct geothermal projects are committed and in development by December 2019”. To fulfill the objective, four key priority actions are identified and needed to be driven by strategy coordinator through 2018-2019:

1. Develop a stock take of supply side assets, infrastructure and geothermal resources to create a communicable picture of geothermal opportunities in New Zealand.
2. Target commercial and industrial scale projects on brownfield sites where geothermal capacity exists.
3. Undertake domestic and international market analysis for large heat users.
4. Develop market value propositions for geothermal heat suppliers.

The governance group identify ranged of prioritized activity to support the key priority tasks. These activities will be implemented by the Geoheat Strategy Action Group across a range of areas, including funding, awareness, expertise, policy, market and technology.

These action areas were identified as barriers to the development of direct geothermal energy use in New Zealand and were flagged during strategy development as action areas.

The action areas have been split into two categories:

1. Ongoing activity – business as usual or needs to be maintained to build critical mass. Able to be undertaken by interested individuals or organizations.
2. Beyond 2019 – less urgent, more complex and/or requiring substantial funding, or currently beyond the mandate of individuals/interested organizations.

There are 6 identified action areas are:

1. Building action groups
   Action group is a cluster of 'like minds’, created with the aim to assist with growth of geothermal energy use. The action group is formed with the insight that a united, connected and cooperative group consist of relevant people in the industry can affect far greater change than individual efforts.

2. Network and connect
   The strategy governance group, strategy coordinator and the action groups need to raise the profile of geothermal direct use. This can be achieved by maintaining and growing connections and networks. The end goal is that through network and connect, a mechanism to provide interaction between potential geothermal heat users and heat suppliers can be established.

3. Maori Economic Development
   To involve and connect with Māori economic interests and entities to explore geothermal direct use opportunities is of a paramount importance. The inclusivity of this strategy includes exploring opportunities for Māori knowledge, resources and people to contribute to research, science, technology and economic development using geothermal direct use.

4. Engage Expertise
   One of the important action items is to identify consultants with expertise to assist in the development of geothermal energy projects. Database of the willing and abled consultant is prepared in advance should the need arise.

5. Showcase
   The strategy action will include showcase activities, highlighting existing success stories in geothermal energy use. The aim is to increase awareness and stimulate further development, as well as to share information. It is realized that only by sharing lessons learned, future projects can learn from and build on past successes. One of the concrete steps is by collecting data that enables effective monitoring of the strategy goals and actions.

6. How-to guide
   To gain the best insight so that future geothermal direct use project can be more effective and impactful, a 'how-to' reference guide needs to be developed. It is identified that the complexity of developing geothermal direct use can be a significant barrier especially on small scale project. To reduce this, the how to guide is aimed to provide the concise advice, information on regulatory requirement as well as the available technology and resources.

Relations to other existing strategy

To guarantee the sustainability and success of the strategy, Geoheat Strategy needs to coexist and relate to other strategy in energy space in New Zealand. The strategy simply cannot work in silo and need to align with broad range of activity within the energy space across central and local government, and other sectors as well. The collaborative ability with other strategy will influence Geoheat’s success.

In the national New Zealand energy space, there are many elements that work collaboratively, namely national energy policy, geothermal business growth

agenda, research, political (minister & councilors), and executive (central government, district and regional councils). These elements play significant role not only in shaping the energy policy and implementation in general, but also in ensuring that specific strategy as Geoheat can be implemented and be sustained. Thus, it is of importance that Geoheat is part of the ecosystem, strategies and processes. The diagram below shows how the Geoheat Strategy relates to various areas of activity.

Geoheat strategy is being influenced by national, regional and local strategy and activity - especially in the processes and outcomes. The strategy will also need to advocate back to the executive (central, district and regional government and council), political side, research side, business growth agenda as well as national energy policy to improve outcomes for direct geothermal use. The Strategy will later drive a series of direct actions that are aimed at generating new direct geothermal projects. In the monitoring and evaluation side, the mechanism of effectiveness review will be established to drive Geoheat as a nimble and responsive strategy.

TAKEAWAYS FOR INDONESIA

As the second largest geothermal producer in the world with second biggest geothermal potential, geothermal is and will be playing a big role in the national energy mix. There is a big potential of not only utilizing geothermal as energy source for electricity market but also to develop geothermal direct use. The potential of geothermal ranging from high enthalpy geothermal resource to medium to low enthalpy. The way geothermal energy has been applied to substitute or complement fossil fuel to provide heat in many activities in New Zealand can also be applied in Indonesia. There are many resources with varied temperature of geothermal fluid available, generally around the mountainous areas with surrounding agricultural, plantation, forestry, as well as fisheries and tourism sites. This would enable various application of geothermal direct use i.e in drying and preservation processes of agricultural products (tea, coffee, cocoa, coconut, etc), growing agent sterilization, breeding products pasteurization (milk, etc), heating room, hot spring bathing, and other utilizations including leather tanning industry, metal, etc. (Suyanto et al, 2010). Figure 5 shows the relation to other energy.

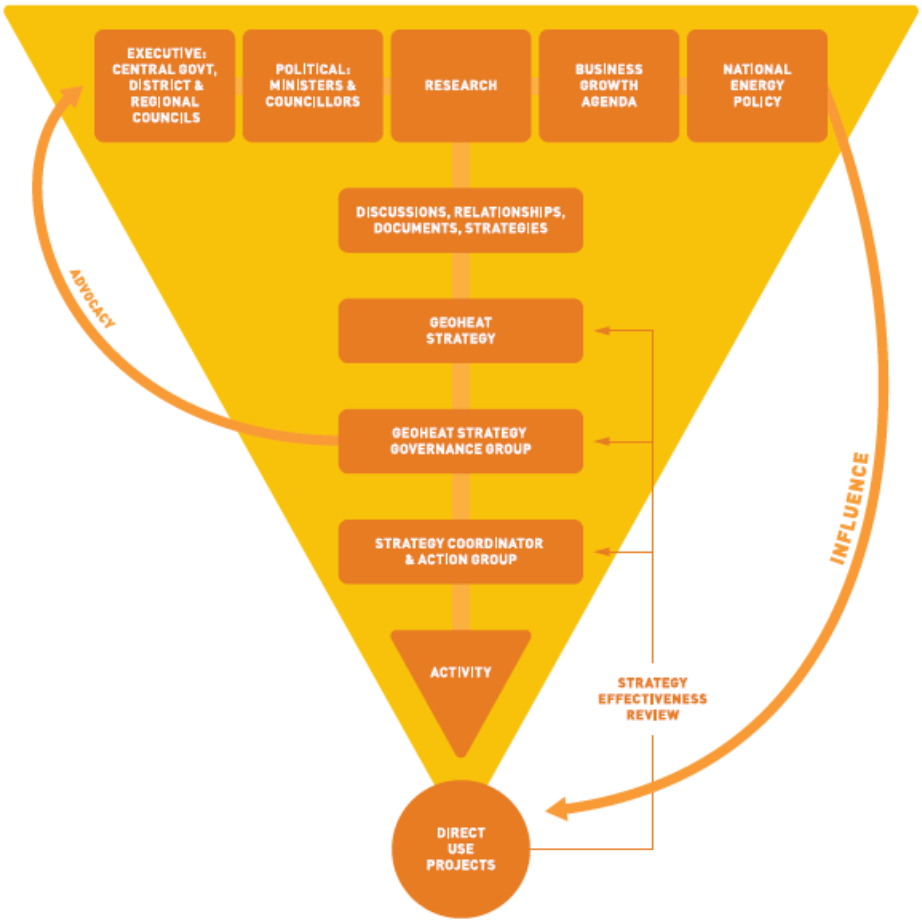


Figure 5: Relation to other strategy.

Regardless the potential and possibility, geothermal direct use application Indonesia is pale on comparison to worldwide direct use trend, and even very small compared to the Indonesia's geothermal electricity generation application, even though having vast resource potential. (Taqwim et al., 2015).

Taqwim et al.,2015 argued that the reason behind lacking geothermal direct use are derived from the 3 factors:

1. Direct-use applications are not presently viewed as an attractive proposition for development.
2. Implementing regulations and policy framework that sets out detailed rules and systems are still not available.
3. There are no schematic and strategic plans for long-term direct-use development.

The 3 main challenges mentioned above are heavily interconnected with one another. Lack of attractive proposition foe development of geothermal direct use heavily tied to the unavailability of supporting policies and regulation, moreover the strategic plan.

The presence of such strategy like New Zealand's Geoheat could drive the development of geothermal direct use by providing a clear strategic plans and roadmap, which later can prove the economic case and influence the central regulation and policy framework. By having such strategy in place, made by neutral party and involving related stakeholders, geothermal direct use in Indonesia could be moved from being the less attractive project into an effort of an economically feasible projects that foster inclusive energy.

Main takeaways from the strategy reviewed above are:

Stakeholders

Stakeholders is the backbone of Geoheat strategy. Not only that the formulation process started with identifying and mapping the stakeholders, the process in strategy formulation is significant in making sure that the stakeholders are all being consulted in developing the strategic plans, leading into the future ownership and shared accountability in the future strategy.

It is best to note that Geoheat strategy is facilitated by New Zealand Geothermal Association (NZGA) as a neutral party, and the initial development was led by GNS as the crown research institute. This shows the importance of geothermal association, in Indonesia's case, INAGA (Indonesia Geothermal Association) as a neutral platform hosting the strategy. GNS as the crown research institute – equivalent of BPPT (Indonesian agency for assessment and application of technology) and LIPI (Indonesian Institute of Sciences) – shows the importance of government research agency in driving the agenda.

Other heavily involved stakeholders is of Maori community - be it through the iwi (largest social unit in Maori community), Māori Landowners and Māori Trust Representatives shows that the indigenous community is the inseparable part of any energy strategy or policy. As the effort on making renewable energy – especially in this case, geothermal – as an inclusive energy, the strategy needs to consider the active involvement of local community and indigenous people surrounding the geothermal resources. There's need of empowerment and inclusion so that the direct use of geothermal would benefit not only the industry and government but also the local community. One of the main obstacles in developing geothermal in Indonesia is society rejection. Previous experiences in various countries have shown that community rejection or public opposition can significantly delay or even stop the geothermal powerplant project (Reith, Kölbel, Schlagermann, Pellizzone, & Allansdottir, 2013; Wallquist & Holenstein, 2015). Thus, the inclusivity of local community and indigenous people are essential in developing the geothermal direct use. The inclusivity will lead into social benefit. Geothermal activity has an influence on economic growth in various ways, such as increase power supply, increase government revenue, reduce unemployment rate, extension of CSR programs, improve infrastructures and increase in tourism sector (Elizabeth, 2011). This social benefit can be optimized should the strategy is formulated consultatively and executed with local community and indigenous community.

The stakeholders then are also involved in the Geoheat strategy governance group as well as in the action group. This involvement is possible when all the related stakeholders are embraced from the early stages of strategy preconception until execution, and the shared ownership and accountability will help ensuring the strategy achieved its success.

Economic case

The unattractive proposition of the current direct-use projects in Indonesia are mainly related to the lack of investment security that corresponds to the project sustainability of a long-term direct use business project (Taqwim et al, 2015). It is clear that the case of direct use in Indonesia is not yet economics. The importance of having a strategy that can showcase and support the economics case is of importance. By working with commercial stakeholders, the strategy will be built upon the steady economics case and assessment.

The first important step in building the economic case would be to stock take on available geothermal resource for direct use and assess the economic case. Working with current geothermal developer that want to diversify the business in geothermal direct use or extending the CSR arms into a more commercial and sustainable business can be a good start. State owned enterprise such as Pertamina Geothermal Energy with current establishment of geothermal direct use in Kamojang field can be a good pilot project in assessing the economic possibility.

Economic assessment cannot be separated from the elements of stakeholder, business model and potential assessment. As discussed before, the successful strategy as well is greatly tied into stakeholder identification, mapping and consultative process. Economic assessment will take into account local community acceptance, cost of unrest, as well as government aspect (taking into account central policy and local/ district regulation, etc). With the right knowledge and insight of the local livelihood and potential, the right choice of geothermal direct usage can be made. Coupled with the geothermal resource potential capacity assessment, scalability option and financial feasibility calculation from geothermal developer, effective and economic business model can be established.

The Geoheat strategy reflects the sufficient mastery of economical and non-economic value of geothermal direct use project, thus able to focus the entire strategy into a clear focus and priority. The clarity enabled a more focused approach, success factor and related action areas to support the projects. It even goes into granular detail of which areas in New Zealand that this strategy will focus on, the scope of geothermal direct use project, how to focus and in what manner, and the timeline for the activities. For example, the strategy will focus on commercial and industrial geothermal direct use project with goal of increasing the usage by 7.5 PJ and creating 500 additional direct and indirect employment, with regional focus on Northland, Waikato and Bay of Plenty. This clarity can only be achieved because during the formulation of the strategy, it is decided that these are the economical criteria to boost the growth of geothermal direct use.

Conducive energy ecosystem

Geoheat strategy is an inseparable part of New Zealand's national energy policy as well as regional and district regulation and energy plan. With advocacy, action, and influence mechanism, the strategy is part of the intertwined mechanism of energy sector in the country. The strategy cannot walk in silo with disregards to other strategy, policies and regulation. Without supportive policy from central, regional and district government, the Geoheat strategy will not be able to be realized. The importance of having a supportive energy ecosystem in fostering geothermal direct use is paramount.

In Indonesia, there is no specific policy and regulation on geothermal direct use yet. If the government and the industry would develop and foster geothermal direct use, in parallel with the strategy, government need to establish a conducive energy ecosystem, including supportive policy and regulation from both central and local government.

CONCLUSION

Geoheat strategy is considered an effective and comprehensive strategy in fostering the geothermal direct use in New Zealand, it is a schematic approach with clear economic case that involves all stakeholders in its formulation, execution and evaluation. The strategy relates and works collaboratively to other strategy, regulation and policy in the New Zealand energy ecosystem.

There are three takeaways from Geoheat strategy should Indonesia want to pursue the path of developing geothermal direct use: the importance of stakeholders, economic case, and conducive energy ecosystem. These will help addressing the challenge of why Indonesia's performance on direct use of geothermal is still lacking despite the current potential.

REFERENCES

Elizabeth, G., M., (2011), "Social aspects of geothermal development - A case of Olkaria geothermal project in Kenya". Naivasha: Kenya Electrical Generating Company Ltd - KenGen.

New Zealand Geothermal Association, (2017), "Geoheat Strategy for Aotearoa NZ 2017-2030"

New Zealand Geothermal Association, (2017), "Action Plan 2018-2019 Geoheat Strategy for Aotearoa NZ".

New Zealand Electricity Authority, (2018), "Electricity in New Zealand", p.30

Suyanto, Surana, T., Agustina, L., Subandriya, A., (2010), "Development of Direct Use Application by BPPT"

Taqwim, S., Pratama, H., B., Nugraha, T., (2015), "Schematic Approach to Boost Geothermal Direct Use Development in Indonesia"

Reith, S., Kölbel, T., Schlagermann, P., Pellizzone, A., & Allansdottir, A., (2013), "Public acceptance of geothermal electricity production". GEOELEC: Deliverable, 44.

DEVELOPING INTEGRATED GEOTOURISM IN UNGARAN'S GEOTHERMAL MANIFESTATION

Dhinar Luhung Anggita and Yanuar Dian Anugrah

Department Geological Engineering, Diponegoro University
Prof. Soedarto st., Tembalang, Semarang, Indonesia
Email: dhinarlanggita@gmail.com

ABSTRACT

The abundance of potential geothermal in Indonesia has a direct impact on villager's economy aspect surrounding the area, also for Ungaran Mountain that reaching potential reserves approximately 55 MW and will be developed by State Electricity Enterprise (Central Java Governor's audience, 2019). Mount Ungaran is one of quarter volcano in the east of North Serayu Mountain. The existence of these old volcano activities can be shown by the presence of geothermal manifestation, in this area including fumarole, hot spring, steaming ground, and hydrothermal alteration. Some manifestations are quite well-known by tourists such as fumarole in Gedong Songo temple. With the appearance of tourist attraction and manifestation, a more optimal plan to increase number of tourists is needed. Therefore, this research was carried out to develop potential geotourism in Ungaran Mountain using GIS process to get geotourism map and track for tourists that has minim hazard, geological survey, and previously validated data. The result, much of manifestations suitable for geotourism e.g. Gedongsongo, Derekan, Nglimut, and Diwak (from the highest to lowest score) but one of them need more structural develop in economical and educational ascpects because of inadequate land cover for tourists reaching the location, which is Kaliulo maifestation. The route plan for the tour is from center city of Semarang - Nglimut – Gedong Songo – Diwak – Derekan – Kaliulo – center city of Semarang. It concludes that Mount Ungaran has much manifestation to be explore as potential geotourism classification by Kubalikova 2013.

Keywords: Geotourism, Ungaran field, surface manifestation

INTRODUCTION

Mount Ungaran is one of quarter volcano in the east of North Serayu Mountain which located in the Central Java province about 30 km southwest of Semarang, Indonesia. It has geothermal potential approximately 55 MW (Central Java Governor's audience, 2019) and is still undeveloped geothermal prospect. The existence of these old volcano activities can be shown by the presence of geothermal manifestation, in this area including fumarole, hot spring, steaming ground, and hydrothermal alteration (Nukman, 2009). Some manifestations are quite well-known by tourists such as fumarole in Gedongsongo temple. To more increase villager's economy, developing others geothermal manifestation as geosite will bring advantages for surrounding the area and make Mount Ungaran as a new geotourism in Indonesia. Geotourism is Tourism relating specifically to geology and geomorphology and the natural resources of landscape, landforms, fossil beds, rocks and minerals, with an emphasis on appreciating the processes that are creating and created such features. (Dowling and Newsome, 2006). Therefore, geosite analysist in Ungaran manifestation is needed to divide between suitable areas and developing areas also draw up geotrack map plan.

METHOD

The method used in this study is geotourism potential mapping based on geothermal manifestation in Mount Ungaran. The data taken consisted of the level of feasibility of geothermal manifestations as geosite based on Kubalikova (2013) classification. This data is processing with GIS based on an analysis of previous research data, books and other scientific journals combined with the author's idea, to obtain prospective geosite which can be developed and geotourism map.

KUBALIKOVA CLASSIFICATION

This classification based on geomorphological assessment. The criteria are divided into five groups with numerical method for calculation. The first group (scientific and intrinsic values) is based on the principles "geologically based" and "integrity of place" and geology and geomorphology oriented definitions of geotourism. The second group of criteria (educational values) comes out from the fact that most of the definitions of geotourism emphasize the educational issues; this group is based on the principles "environmentally educative", "protection and enhancement of destination appeal", "interactive interpretation and evaluation". The third group of criteria (economic values) considers the principles "tourist satisfaction", "tourist satisfaction", "locally beneficial", "market selectivity and diversity", "community involvement and benefit". The fourth group (conservation value) is based on the principles "sustainable", "land use and planning" and "conservation of resources" and partly on the geoconservation principles. The last group of the criteria (added values) comes out of the

fact that geotourism does not consider only the natural aspects, but also cultural and aesthetic aspects of the site.

In the final calculation from each group, it is done on average towards the value which shows whether it is feasible to be a geotourism area or not. If the final value is obtained more than 50%, then the area is considered suitable as a geotourism area, whereas if the value is less than 50% it is considered inappropriate (Mark, 2016).

$$\text{Precentage (\%)} = \frac{\text{Scoring from Each Group Total}}{\text{Total Score (18.5)}} \text{ x } 100\%$$

DATA

Geology and Manifestation Ungaran

Manifestation Ungaran is located in Gedongsongo, Nglimut, Diwak, Derekan and Kaliulo based on Yudianto (2014) and Yuanita (2015). Although Kendalisodo manifestation is not examined because not from Ungaran geothermal system (Aribowo and Nurohman, 2012). Manifestation that shows up are fumarole, steaming ground, hot spring, and alteration (Figure 1).

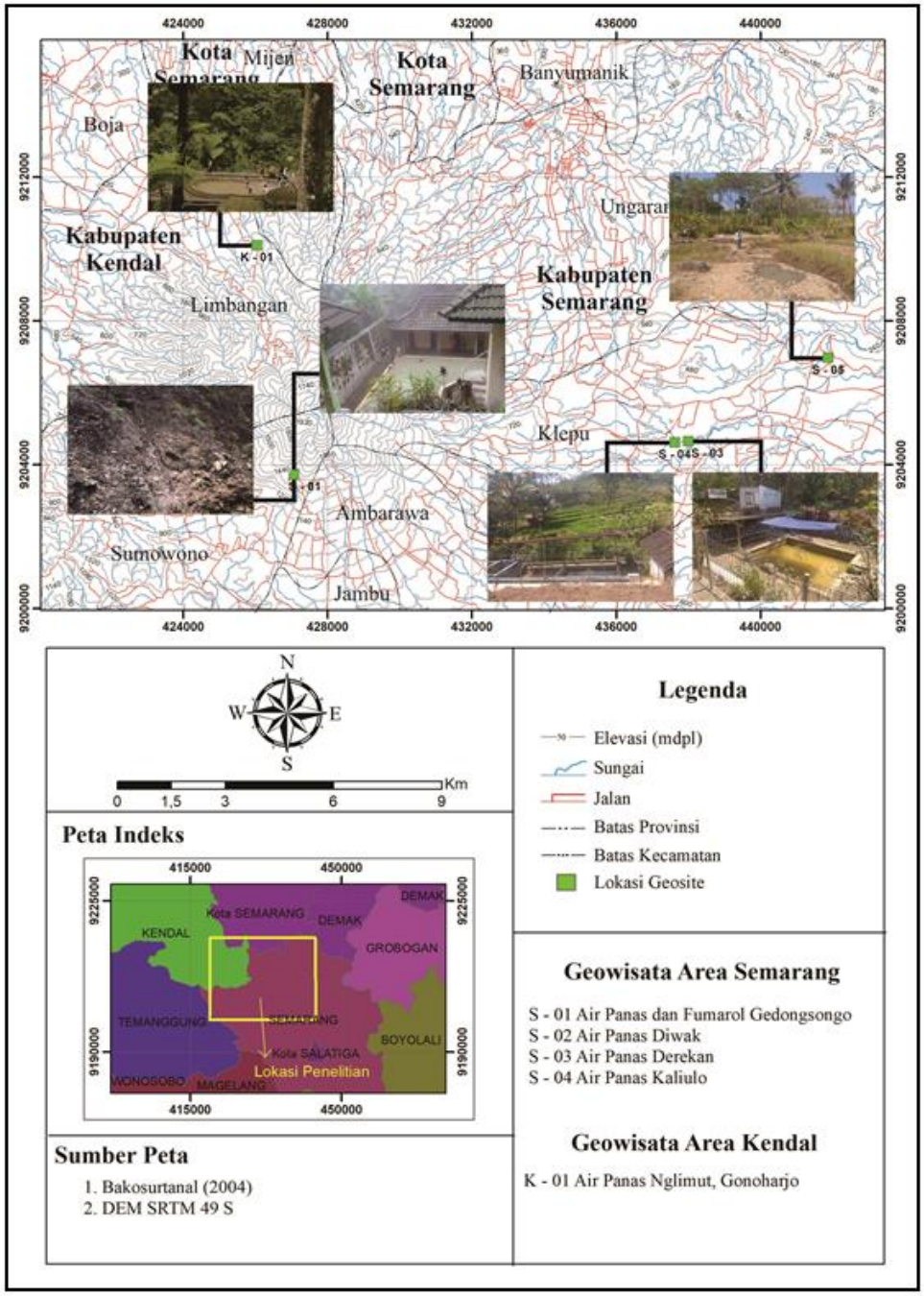


Figure 1: Location of Ungaran Manifestation Map.

Gedong Songo Manifestation

As the nearest place from Mount Ungaran, manifestation in Gedongsongo has much variarities included fumarole, hot spring, steaming ground, and alteration. Gedong Songo is located in the coordinates x: 427010 and y: 9203713. This area is composed of volcanic breccia that has been altered. Based on field, showed composition minerals, e.g. kaolinite, smectite, and illite that located in alteration zone of Argillic – Advance Argillic Zone (Figure 2). Fumarole area named "Kawah Dasamuka" shows sulphate deposit formed and spend out acid sulphate. This place is quite well-known as tourist attraction through hindu's temple.

Nglimut Manifestation

Manifestation in Nglimut is hot spring that spend out bicarbonate water. It is located in Gonoharjo with the coordinates x: 426027 and y: 9210091. This place used as tourist attraction through addition family facilities e.g. swimming pool, camping ground, and villa. Near the hot spring there is waterfall showed relict lithology before alteration which is volcanic breccia (Figure 3).

Diwak Manifestation

Manifestation in Diwak is hot spring that spend out bicarbonate water. It is located in Karangjati near Kalisori River with the coordinates x: 437595 and y: 9204629. Near the hot spring there is waterfall called "Curug Nangka" that showed lithology surrounding area which is volcanic breccia (Figure 4).

Derekan Manifestation

Manifestation in Derekan is hot spring that spend out bicarbonate water. It is located in Karangjati near Derekan River with the coordinates x: 438002 and y: 9204663. This place used as tourist attraction through additional historical temple hindu's temple called "Candi Ngempon". This place shows fresh lithology stopsite that composed flow volcanic breccia (Figure 5).

Kaliulo Manifestation

Manifestation in Kaliulo is hot spring that spend out bicarbonate water. It is located in Klepu near Kaliulo River with the coordinates x: 441768 and y: 920693. This area has volcanic breccia stopsite that has been altered (Figure 6). This place has not become tourism area and not well-known place.

Kubalikova Classification Value

From calculating percentage from each manifestation, shows that Kaliulo has < 50% (44.595%) from the classification (Table 1). It shows that Kaliulo is not appropriate to become geosite. The highest score is 81.081% from Gedongsongo manifestation. It because the place has become popular tourism area in Semarang. This manifestation located around hindu's temple along with the many historical stories behind this manifestation. The second place is Derekan in 75.676% because there is hindu's temple that increasing educational values for Derekan manifestation. The third is Nglimut in 64.865% because this place is recommended by the government so increase conservation values. The fourth is Diwak in 63.51% because it has waterfall near manifestation so it can be increase economical values for tourist attraction.



Figure 2: Volcanic Breccia Outcrop Alterated (alteration mineral showed e.g illit, kaolinite, smectite).

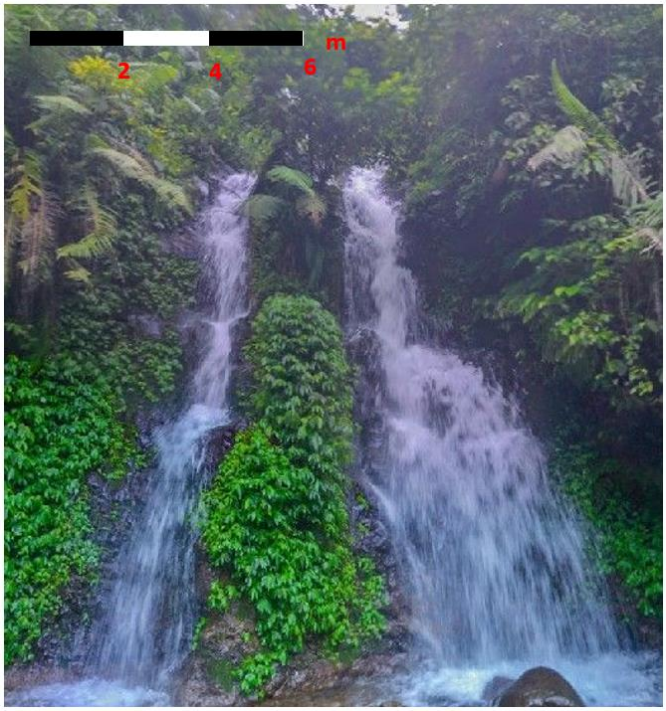


Figure 3: Waterfall Near Nglimut Hot Spring Shows Volcanic Breccia as a lithology around the area.

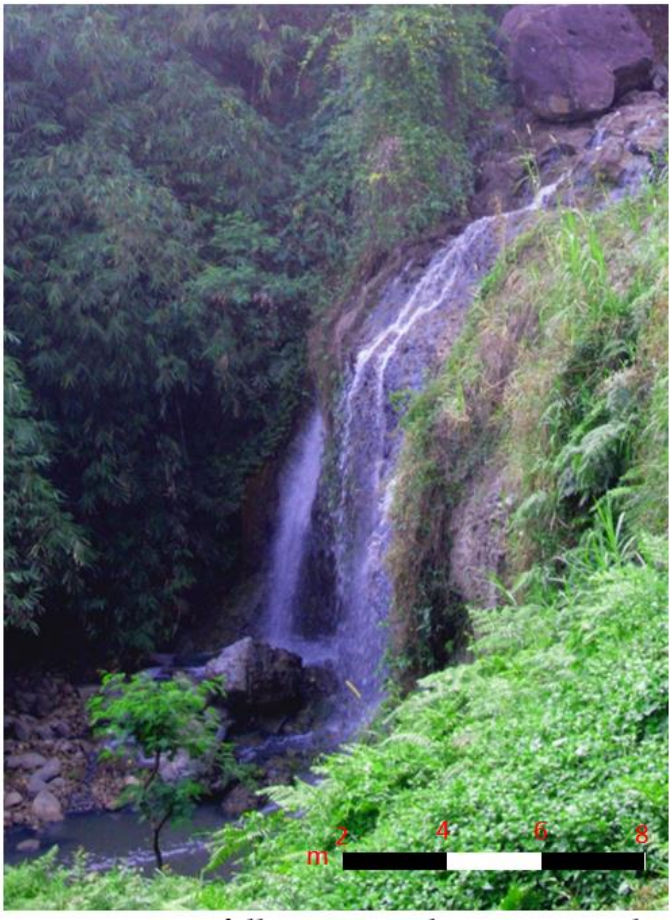


Figure 4: Waterfall Near Diwak Hot Spring Shows Volcanic Breccia as a lithology around the area.



Figure 5: Flow Volcanic Breccia Stopsite in Derekan River.



Figure 6: Altered Volcanic Breccia Stopsite in Kaliulo River.

DISCUSSION

Developed Geosite

According to Ungaran manifestation value as geosite, Kaliulo hot spring has the lowest score in 44.595%. It shows that Kaliulo is not appropriate to become geosite although this place has geological stopsite that is very unique to be visited. To increasing the percentage, developing economical values e.g. by building infrastructure that occupies tourism needs or making local products that have high selling value and educational values e.g. by making knowledge board about Kaliulo manifestation to increase the awareness of tourists also can be some optional recommend to make Kaliulo manifestation suitable as a potential geosite.

Geotourism Track Plan

Potential geosite on Ungaran's geothermal manifestations can be described through a geotrack map that has been compiled (Figure 7). These geosites can be visited within one day of travel. The purple trajectory shows the journey assumed to start from the center of Semarang City. The first recommended geosite to visit is the Nglimut hot spring, because of the morning atmosphere in the cool mountainous area around Nglimut and offers beautiful views of Mount Ungaran. Geosite Nglimut hot springs also provide food for breakfast. Then next is visiting Geosite Gedongsongo. In this Geosite there are geothermal manifestations in the form of fumaroles, steam ground, hot springs, and alterations. With the highest value of feasibility, this Geosite can be visited for quite a long time because

there are also historical value buildings in the form of temples and various souvenirs from Ungaran region. Next is visiting the Geosite Diwak and Derekan which are relatively close to each other. At the Diwak and Derekan Geosite there are hot springs and Nangka waterfalls around the location which can also be an alternative for excursions. The Derekan geosite also found a historic site in the form of a temple building similar to the one in Gedongsongo. The last visit was Geosite Kaliulo. Kaliulo Geosite is relatively new and has the smallest feasibility value of 44.595% and not too much development. After visiting Geosite Kaliulo, it can be continued by returning to the city center of Semarang by passing the main road of Jend. Sudirman Street. Routes that are passed in all Geosite can be reached by motorbike or car. For bus use, it is limited to small buses that can pass Geosite Nglimut and Gedongsongo, besides that it cannot be passed by bus.

The distance from the center of Semarang City to Geosite Nglimut is as far as 32 km or can be reached during the journey of approximately 60 minutes. Then the distance from Geosite Nglimut to Geosite Gedongsongo is 25 km and can be reached in approximately 55 minutes. The distance from Geosite Gedongsongo to Geosite Diwak is 17 km or can be reached in approximately 50 minutes. For the distance from Diwak to Derekan Geosite only 3 km or about 10 minutes travel time. While for the distance from Derekan to Kaliulo Geosite is as far as 6.5 km which can be reached during the journey of approximately 15 minutes. Finally continued with the journey back to the center of Semarang City within 34 km or about a 50 minutes trip.

CONCLUSION

Based on Kubalikova classification calculation in five geothermal manifestations (Gedong Songo, Nglimut, Diwak, Derekan, and Kaliulo) on Mount Ungaran, the suitable geosite is Gedong Songo, Derekan, Nglimut, and Diwak (from the highest score to the lowest). Kaliulo hot spring is unappropriate to be geosite with value percentage 44.595%. Developing economical and educational values are some optional recommend to increase the percentage. To reach entire geosite optional geotrack plan for one day travel is started from center city of Semarang - Nglimut – Gedong Songo – Diwak – Derekan – Kaliulo – Center city of Semarang.

REFERENCES

Aribowo, Y. & Nurohman, H. (2012), "Studi Geokimia Air Panas Area Prospek Panasbumi Gunung Kendalisodo Kabupaten Semarang, Provinsi Jawa Tengah", TEKNIK, 33, 32-36

BAKOSURTANAL, (2004), "SHP Jalan, Sungai, Batas Kecamatan – Kabupaten Indonesia", Jakarta

Central Java Governor's audience, (2019), "PLTP Ungaran Segera dibangun", JawaPos.com, Jan 22th 2019.

Dowling, R. K., & Newsome, D. (Eds.). (2006). "Geotourism". Oxford: Elsevier Ltd.

Kubalikova, L. (2013). "Geomorphosite Assessment for Geotourism Purposes", Czech Jounral of Tourism, 2, 80-104

Mark, S. R. (2016), "Romancing the Wild: Cultural Dimensions of Ecotourism, by Robert Fletcher", Journal of Sustainable Tourism, 24, 1-2

Nukman, M. (2009). "Overview of Gedongsongo Manifestation of the Ungaran Geothermal Prospect, Central Java, Indonesia: a Preliminary Account", Geothermal Reservoir Engineering Proceedings, 34, SGP-TR-187

Yudianto, H. & Setyawan, A. (2014), "Interpretasi Struktur Bawah Permukaan Daerah Manifestasi Panasbumi Gedong Songo Gunung Ungaran Menggunakan Metode Magnetik", Youngster Physics Journal, 2, 39-48

Yuanita, E., Harmoko, U., Hananto, N. D., Handayani, L. (2015), "Karakterisasi Daerah Panas Panas Bumi Diwak dan Derekan Berdasarkan Pengukuran Audio-Magnetotelurik", RISET Geologi dan Pertambangan, 25, 23-29

Table 1: Ungaran Manifestation Values as Geosite Based on Kubalikova (2013).

	Gedongsongo	Nglimut	Diwak	Derekan	Kaliulo
Scientific and Intrinsic Values					
Integrity	1	1	1	1	1
Rarity (number of similar sites)	1	0.5	0.5	0.5	0.5
Diveristy	1	0.5	0.5	0.5	0.5
Scientif Knowledge	1	0.5	1	0.5	0.5
Educational Values					
Representativeness and Visibility	1	1	1	1	0.5
Exemplarity	1	1	1	1	0.5
Existing Educational Products	1	0.5	0.5	0.5	0
Actual Use of a Site for Educational Purposes	1	0.5	0.5	1	0.5
Economical Values					
Accessibility	0	0.5	0.5	0.5	0.5
Presence of Tourist Infrastructure	1	1	1	1	0
Local Products	1	0.5	0	0.5	0
Conservation Values					
Actual Threats and Risks	0.5	1	1	1	1
Potential Threats and Risks	0.5	0.5	0.5	0.5	0.5
Current Status of a Site	1	1	1	1	1
Legislative Protection	1	0.5	0.5	1	0
Added Values					
Cultural Values	0.5	0	0	1	0
Ecological Values	1	1	1	1	1
Aesthetic Values	0.5	0.5	0.25	0.5	0.25
PERCENTAGE (%)	**81.081**	**64.865**	**63.51**	**75.676**	**44.595**

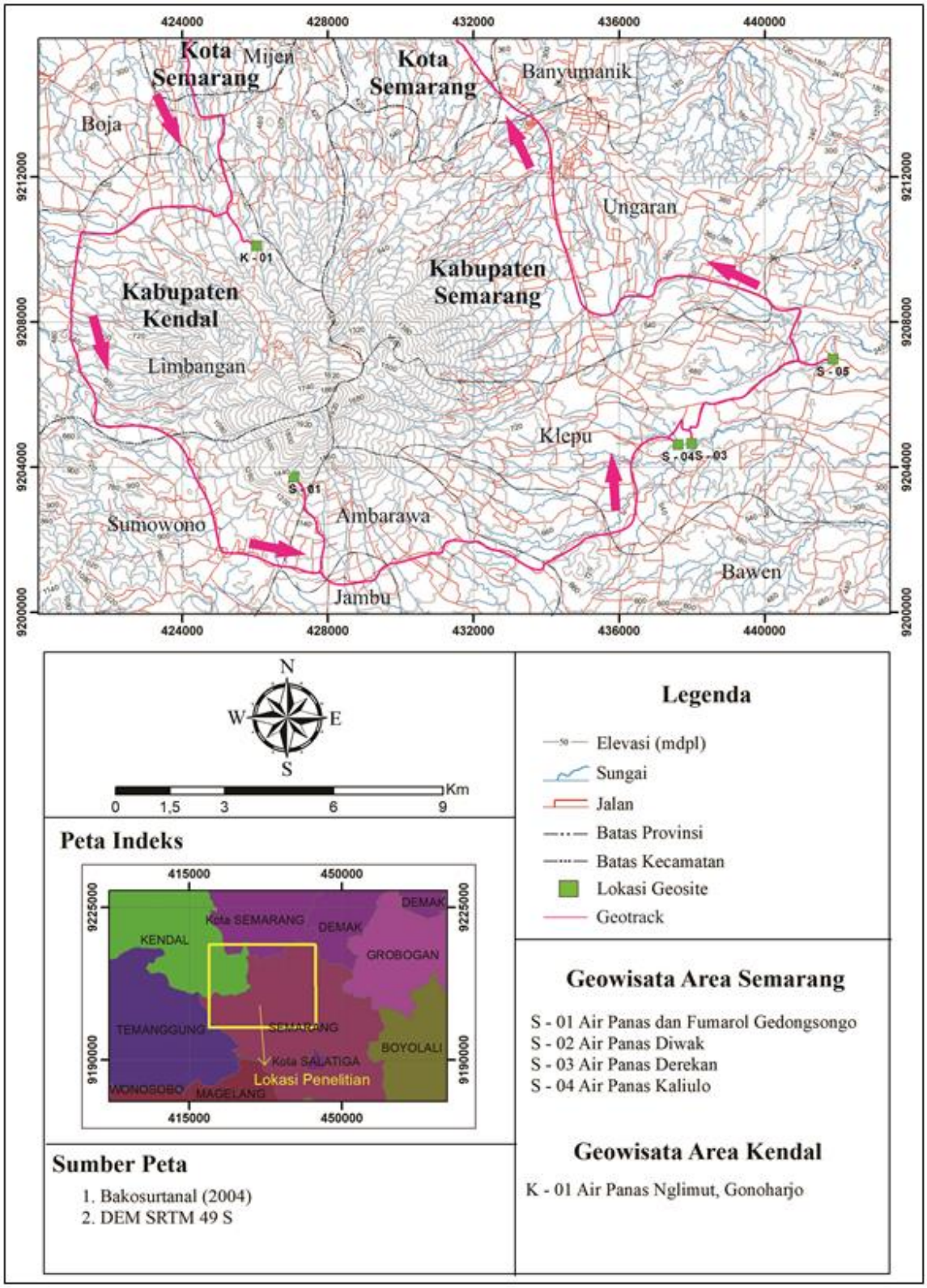


Figure 7: Geotrack Map Plan for Getourism in Mount Ungaran Manifestation.

GEOTOURISM PROSPECT SELECTION USING ANALYTICAL HIERARCHY PROCESS (AHP): CASE STUDY IN TELOMOYO GEOTHERMAL AREA, INDONESIA

Aulia Umami and Alfath Zain

Geological Engineering, Faculty of Mineral Technology,
Institute of Science & Technology AKPRIND Yogyakarta, Indonesia
Jl. Kalisahak No. 28, Kompleks Balapan, Yogyakarta, DIY 55222
Email: auliaumami051@gmail.com

ABSTRACT

Telomoyo geothermal area is created in a volcano quarter complex, Semarang, Central Java. Telomoyo geothermal areas have two locations that have the potential for geothermal energy, which is located in the Umbul Temple and Dukuh Temple. This is indicated by the presence of geothermal manifestations in the form of several hot spring that appear in the area. Based on the geological and environmental conditions, in addition to having geothermal energy potential, this area also has other potential in the form of geotourism potential. Therefore, this research was conducted to select the potential of geotourism which has more prospects from the two potential geothermal energy locations using the analytical hierarchy process (AHP) method.

Analytical hierarchy process (AHP) is a decision-making technique based on various criteria. This AHP analysis technique can handle any complex, multicriterion, and multiperson problems. In AHP, the problem is decompossed into a hierarchical structure and are given the weights based on its level of importance. Then this strength is one alternative that can be used to make a decision.

In the AHP method it consists of alternatives, main criteria and subcriteria. Alternatives here are Dukuh Temple and Umbul Temple. There are three main criteria used in this study, namely geoscience, infrastructure, and social-culture. Subcriteria that have high weight are subcriteria of geological resources in the form of geothermal energy. Subcriteria for geological risk and environmental subcriteria play a role as a threat assuming the availability of existing geothermal energy potential, so it is not possible to develop geothermal energy commercially and to exploit the environment. While the criteria that act as supporting factors for developing geotourism potential are infrastructure criteria because they are considered not to have many obstacles. The results showed that potential geothermal areas with the potential for geotourism development were the Umbul Temple area.

Keywords: Geotourism, Telemoyo geothermal field

INTRODUCTION

Geothermal is a natural resource that has an important role in national development, because this energy source can be updated and environmentally friendly. Indonesia has geothermal reserves of 27,189 MW or around 40 percent of the world's potential, but only 807 MW of the total potential is used to meet energy needs, and that is mostly used for electricity needs. Currently geothermal is used as a substitute for the main energy of oil and gas, it is not yet optimal because of the lack of socialization in terms of geothermal energy. In addressing this, there are other ways to utilize geothermal energy. so that not only has a high selling value, but also an innovation in entrepreneurship based on science and technology, namely by making tourist attractions with geological nuances in the geothermal area of Telomoyo, Central Java.

Tourism activities are closely related to natural environmental problems that cannot be separated from the nuances of geology and ecosystems. Both are a network of systems that are interrelated with natural law, forming a place where humans settle and form a natural order in which people live in society. It is in this society that humans are able to develop social, economic and cultural life. Availability of strong socio-economic support, human culture can create various types of guidance that refers to aspects of space, time, and science / technology. Not all natural tourist attractions match the pattern of tourism development that seeks to bring in as many tourists as possible. Because the high and low carrying capacity of the environment will be very dependent on the terrain topography and rests on the geological order. The scientific discipline of geology as a tourism resource needs to be used to produce a sustainable geological tourist attraction.

The purpose of this assessment is not only to provide information about the resources of geothermal prospects in certain areas but also to provide information about which areas will be developed in the near future. Therefore, the prospect of geothermal geotourism must be ranked to determine the development of its priorities. By ranking this priority, it is expected that the government can build development plans and regulations for a region, including the development of geothermal geo-tourism prospects. Considering that priority ranking

is multicriteria decision-making produced by assessing several very different factors and knowledge, the Analytical Hierarchy Process (AHP) method is chosen for the ranking process. This paper describes the AHP application in the selection process and prioritizes the prospect of geotourism in the Telomoyo geothermal area. The area studied is shown in Figure 1.

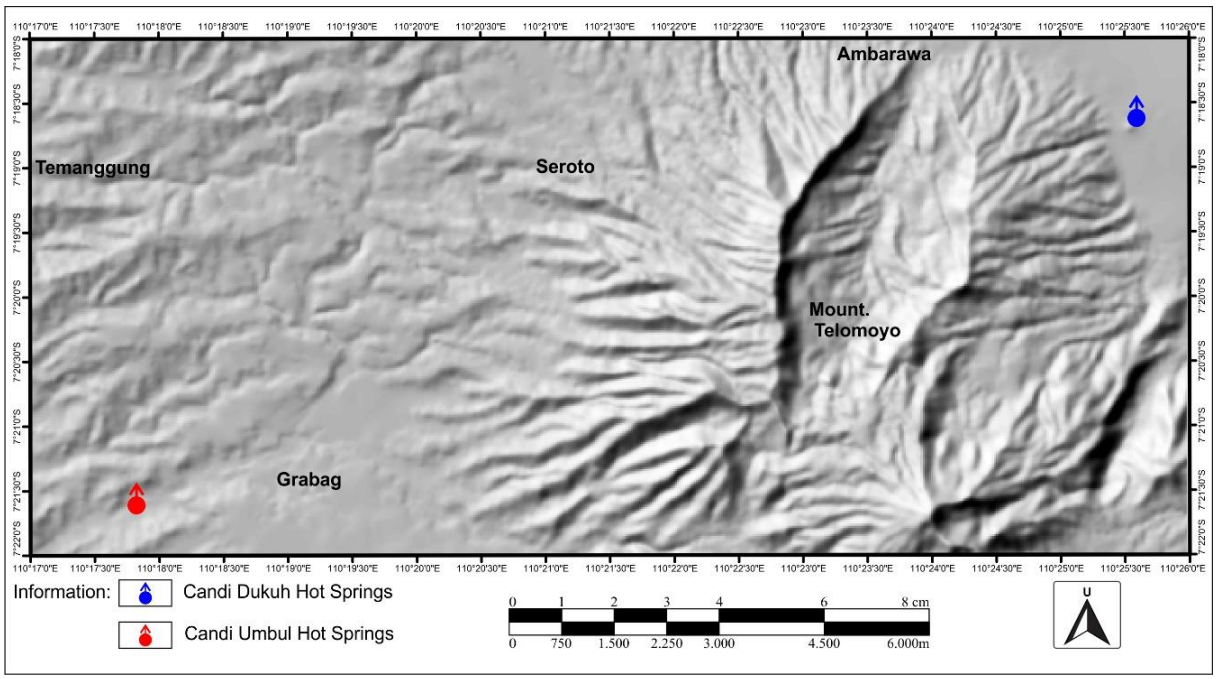


Figure 1: Location map of Candi Umbul and Candi Dukuh Geotourism Prospect in theTelomoyo Geothermal Area.

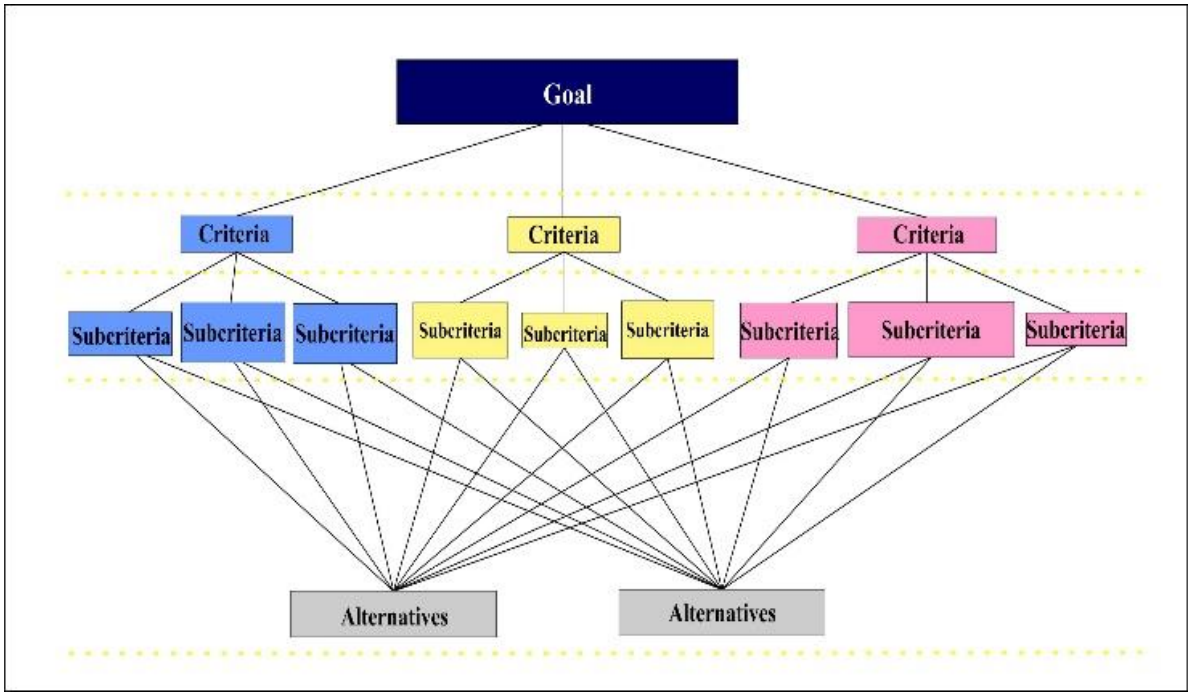


Figure 2: The hierarchical stucture in the AHP method.

DATA AND METHOD

The Analytical Hierarchy Process (AHP) method is a stage or method of decision making that was first developed by Thomas Saaty. This method is used to solve decision-making problems in different environments, where decision making is compared with different criteria. AHP method forms the weight of decisions by compiling criteria and subcriteria in a hierarchical structure.

Factor identification and hierarchy creation

The hierarchy is based on several main components, namely goals, criteria, subcriteria, and alternatives. However, the selection of components in the making of hierarchies is adjusted to the needs for the main purpose so that they are more subjective. The initial stage of hierarchical making is the main objective followed by making criteria based on the assessment factor of an object of research. A hierarchy is an abstraction of the structure of a system that studies the interaction functions between components and their effects on the system. The hierarchy arrangement or decision structure is carried out to describe the system elements or alternative decisions identified. The following is an example of making a hierarchy presented in Figure 2.

Table 1: The fundamental scale comparison assessment in the AHP method by Saaty (1987)

Scale	Intencity of Importance	Explanation
1	Similar	Both elements are equally important
3	A little more important	One element is a little more important than the other elements
5	More important	One element is more important than the other elements
7	Very important	One element is totality more important than the other elements
9	Absolutely important	One element is absolutely important than the other elements
2,4,6,8	Intermediate value	Values between two values of adjacent considerations
1/n	The opposite	If for activity I gets one number compared to activity J, then J has the opposite value compared to I

Comparative matrix processing

By comparing each element with other elements in pairs so that the value of the level of importance of the elements in the form of qualitative opinions is obtained. To change these results into a form of quantitative opinion, the rating scale is used. Comparisons are made based on decision-making policies by assessing the importance of one element to another. The pairwise comparison process starts from the hierarchy level which is intended to choose an alternative, for example A, then the criteria elements to be compared are taken for example A1, A2, and A3. Then the arrangement of the elements to be compared will look like in Table 2 below.

Table 2: Pairwise comparison matrix.

	A1	A2	A3
A1	1		
A2		1	
A3			1

After an assessment with a comparison matrix, then proceed with normalizing the data. Data normalization is done by dividing the elements in each column with the total number per column in question, then the normalized relative weight values are obtained. After that, proceed with calculating the eigenvalue of the vector and testing its consistency, if it is not consistent then the data retrieval needs to be repeated. The eigenvalue of the vector in question is the maximum eigen vector value obtained from each eigen vector per line. Eigen vector values per line are obtained by dividing the total score on the line of each criterion by the number of columns. The maximum eigen vector value (λmaks) is obtained by summing the multiplication of the total score in each criterion column with eigen vector per line.

Next is to calculate the consistency index value (CI) using the following formula:

$$\mathrm{CI} = \frac{\lambda\mathrm{maks} - \mathrm{n}}{n - 1}$$

After obtaining the CI value, then proceed with calculating the consistency ratio value (CR) using the following formula:

$$\mathrm{CR} = \frac{\mathrm{CI}}{RI}$$

The value of the Random Consistency Index (RI) can be obtained from table 3 by Saaty (1980) as follows:

Table 3: Value of the Random Consistency Index (RI) by Saaty, 1980.

N	1	2	3	4	5	6	7
RI	0	0	0.58	0.9	1.21	1.24	1.32

The consistency ratio is considered consistent if it is less than or equal to 10% or 0.1.

Then proceed with determining the feasibility assessment for each alternative based on the assessment of criteria and subcriteria based on the assessment table that has been modified from Kubalikova, 2013 (Table 4).

RESULT AND DISCUSSION

Factor identification and hierarchy creation

The hierarchy is based on several main components, namely goals, criteria, subcriteria, and alternatives. However, the selection of components in the making of hierarchies is adjusted to the needs for the main purpose so that they are more subjective. The initial stage of hierarchy creation is the main objective followed by the making of criteria based on the assessment factor of a geothermal prospect area. The main objective is to find out which geothermal prospect areas have the most potential to be developed geotourism in the area. Furthermore, it is done by determining the selection criteria. The criteria here consist of 3 criteria, namely geoscience, infrastructure, and socio-culture. Each criterion has 3 subcriteria. And finally, the determination of alternatives. Alternatives here are 2 locations in the Telomoyo geothermal prospect area, namely Umbul Temple Hot Spring and Dukuh Temple Hot Spring which will be compared to which areas have the most potential to be developed geo-geography. The hierarchical structure has been arranged in Figure 3.

Table 4: Geotourism feasibility assessment method (modification from Kubalikova, 2013).

Criteria	Subcriteria	Scale	Explanation
Geoscience	Resources	0	Has no geothermal energy potential
		0.5	Derived from a non-volcanic geothermal system
		1	Derived from a volcanic geothermal system
	Geothermal System	0	Do not have a geothermal energy system
		0.5	Located in the Outflow Zone in geothermal systems
		1	Located in the Upflow Zone in the geothermal system
	Geological Risk	0	The location is prone to geological disasters and dangerous for humans
		0.5	The location is prone to geological disasters but can be handled
		1	Safe and harmless location for humans
Infrastructure	Access to Location	0	Difficult to reach by public transportation or private vehicles
		0.5	Easy to reach by private vehicle but difficult to reach by public transportation
		1	Easily accessible by public or private vehicles
	Facilities	0	There are no adequate facilities and infrastructure
		0.5	There are already facilities and infrastructure but inadequate
		1	There are already adequate facilities and infrastructure
	Land Properties	0	Densely populated area
		0.5	Areas have a rare population density
		1	Areas have very rare population densities
Social and Culture	People responses	0	People oppose the creation of geotourism
		0.5	The people do not have any response to the proposal for making geotourism
		1	The people support the proposal for making geotourism
	Small industries deman for activity	0	Reject
		0.5	Indifferent
		1	Support
	Environment	0	The environment is polluted
		0.5	The environment is partly polluted
		1	The environment is still beautiful and has not been polluted

Alternative assessment and criteria

Based on predetermined parameters, a 3x3 matrix will be made, which is a comparison between the three criteria for the purpose of the goal. The assessment parameters are based on Table 1 by Saaty, 1987. The criteria assessment in this case study has been presented in the form of an assessment table in Table 5.

Then the table rating is normalized according to the normalization of data in the AHP method so that we can determine the parameter weight of each criterion.

From the assessment data above, it will be normalized to assess the relative weighting of the criteria. The normalized data is presented in Table 6. The following is a normalized calculation of the reative weight:

1: 1,343	= 0,745	1 : 9	= 0,111
0,143 : 1,343	= 0,106	5 : 7	= 0,714
0,2 : 1,343	= 0,149	1 : 7	= 0,143
7 : 9	= 0,778	1 : 7	= 0,143
1 : 9	= 0,111		

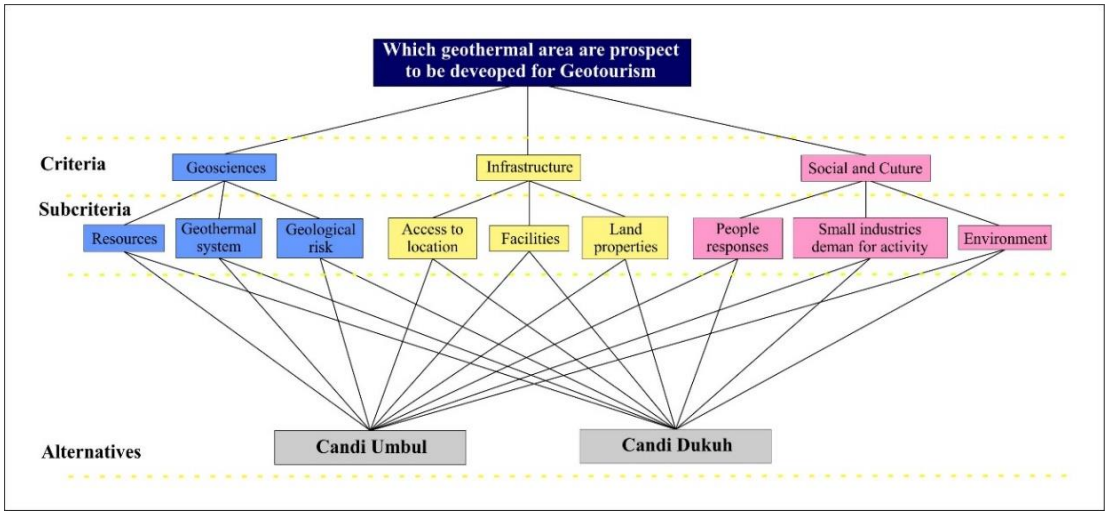


Figure 3: The hierarchical structure of geotourism prospect selection in Telomoyo geothermal area.

Table 5: Parameters of assessment criteria.

	Geoscience	Infra-structure	Social-Culture
Geoscience	1	7	5
Infra-structure	0,143	1	1
Social-Culture	0,2	1	1
ΣScore	1,343	9	7

Table 6: Normalization of assessment data for relative weights of criteria.

Focus	Geoscience	Infra-structure	Social-Culture	ΣScore	Eigen vector	Weight of criteria
Geoscience	0,745	0,778	0,714	2,237	0,746	74,56
Infra-structure	0,106	0,111	0,143	0,360	0,120	12,01
Social-Culture	0,149	0,111	0,143	0,403	0,134	13,43

Calculation of eigen vector values and consistency testing

Calculate the eigen value of the vector and test its consistency, if it is not consistent then the data retrieval needs to be repeated. The eigen value of the vector in question is the maximum eigen vector value obtained from each eigen vector per line. The maximum eigen vector value (λmaks) is obtained by summing the results of multiplying the number of columns with eigen vector.

λ_{maks} = (1,343 x 0,746) + (9 x 0,120) + (7 x 0,134)
= 1,001 + 1,081 + 0,94
= 3,022

Because the matrix has 3 rows (has a number of columns = 3), the consistency index value (CI) obtained is:

$$CI = \frac{\lambda_{maks} - n}{n-1}$$
$$= \frac{3,022-3}{3-1}$$
$$= 0,011$$

Because n = 3, so the RI value = 0.58 based on the Saaty scale table, then:

$$CR = \frac{CI}{RI}$$
$$= \frac{0,011}{0,58} = 0,019$$

(CR value < 0.1 the result of the calculation is consistent)

Assessment of the potential feasibility of geotourism in the Telomoyo geothermal area

Based on the results of the analysis using the geological site assessment classification for the geotourism area by Kubalikova (2013) which has been modified, the assessment scores obtained from each sub-criteria and criteria presented in Table 7-10.

Criteria and alternative priority determination

Based on the results of calculations obtained from the previous steps, then prioritizing the criteria and alternatives is presented in Table 11-12. Based on the two calculation tables above, it can be seen that the Alternative Umbul alternative has the highest score on the assessment of alternative feasibility and criteria, while Candi Dukuh has a lower score than the Umbul Temple.

CONCLUSIONS

Based on a series of calculations that have been made, conclusions that can be drawn to answer the objectives of this study are as follows:

1. The area of the Telomoyo geothermal prospect has two locations that have the potential to be developed as geotourism areas, namely Umbul Temple Hot Spring and Dukuh Temple Hot Spring.
2. Based on research using the AHP method, the location of Umbul Temple has more potential to be developed as a geotourism area than the location of the Umbul Temple. This is evidenced by the results of calculating the alternative feasibility of Umbul Temple is always higher than the results of the calculation of the alternative feasibility of Dukuh Temple.

REFERENCES

Kubalikova, L., (2013), "Geomorphosite Assessment for Geotourism Purposes" Czech Journal of Tourism, 2, 80-104.

Kubalikova, L., Kirchner, K., (2016), "Geosite and Geomorphosite Assessment as a Tool for Geoconservation and Geotourism Purposes: A Case study from Vizovicka vrchovina Highland" Geoheritage, 8, 5-14.

Saaty, R., W., (1987), "The Analytic Hierarchy Process- What it is and how it is used" Math Modelling, Vol.9, 3-5, 161-176.

Saaty, T., L., (1990), " How to make decision: The Analytical Hierarchy Process" Europian Journal of Operational Research, 48, 9-26.

Saaty, T., L., (2008), "Decision making with the Analytic Hierarchy Process" Int. J. Services Science, Vol.1 no.1.

Saputro, T., C., (2018), "Geologi dan Potensi Goa Ngantap Sebagai Geosite Baru Di Kawasan Karst Geopark Gunung Sewu, Kabupaten Wonogiri, Provinsi Jawa Tengah" Thesis, Department of Geological Engineering. Gadjah Mada University, Yogyakarta.

Suryantini, Wibowo, H., (2010), " Geothermal Prospect Selection Using Analytical Hierarchy Process (AHP): A Case Study in Sulawesi Island, Indonesia," Jurnal Geologi Indonesia, 254, vol.5 No.4 December 2010, 241-254

Table 7: Assess the feasibility of Geoscience criteria

	Resources	Geothermal System	Geological Risk	Score
Candi Umbul	1	1	1	3
Candi Dukuh	1	1	0,5	2,5

Table 8: Assess the feasibility of Infrastructure criteria

	Access to Location	Facilities	Land Properties	Score
Candi Umbul	0,5	0,5	0,5	1,5
Candi Dukuh	0,5	0,5	0	1

Table 9: Assess the feasibility of Social-Culture Criteria

	People Responses	Small industries deman for activity	Environment	Score
Candi Umbul	1	1	1	3
Candi Dukuh	1	1	0,5	2,5

Table 10: Total value of feasibility criteria

	Geoscience	Infra Structure	Social Culture	Score
Candi Umbul	3	1,5	3	7,5
Candi Dukuh	2,5	1	2,5	6

Table 11: Alternative AHP Candi Umbul

Alternative (Candi umbul)	Value of feasibility (A)	Maximum feasibility value	A/A value max	Weight of criteria	Score
Geoscience	3	3	1	74,558	74,558
Infra Structure	1,5	1,5	1	12,012	12,012
Social Culture	3	3	1	13,430	13,430

Table 12: Alternative AHP of Candi Dukuh

Alternative (Candi Dukuh)	Value of feasibility (A)	Maximum feasibility value	A / A value max	Weight of criteria	Score
Geoscience	2,5	3	0,833	74,558	62,132
Infra Structure	1	1,5	0,667	12,012	8,008
Social Culture	2,5	3	0,833	13,430	11,192

USING CONTINUOUS WAVELET TRANSFORM FOR ENHANCING MAGNETOTELLURIC DATA IN GEOTHERMAL EXPLORATION

Haidar Firdaus Avicienna, Yunus Daud, and Nauval Ivanditho

Undergraduate Program in Geophysics, Faculty of Mathematics and Natural Sciences, Universitas Indonesia
Universitas Indonesia, Kampus UI, Depok
Email: Haidar.firdaus@ui.ac.id

ABSTRACT

The presence of noise in magnetotelluric data can produce a bias in its interpretation. To eliminate this noise, a remote station that is far from interference is needed. Assuming that the remote station is almost free from noise, the data from remote station can be used to reduce the noise from measurement station. However, adding an additional station means there will be an increase in exploration cost. Also, adding a remote station itself can be challenging and time-wasting since finding an area that is free from interference is quite hard to do, especially for geothermal exploration area in Indonesia that usually have difficult terrain and access. To answer this, we need a technology that can reduce noise from magnetotelluric data and improve the data quality while keeping the cost and time of exploration as low as possible. By using continuous wavelet transform method, the noise from magnetotelluric data can be reduced without the need to use a remote station which makes exploration becomes more efficient.

Keywords: Geothermal, Exploration, Magnetotelluric, Noise, Continous Wavelet Transform.

INTRODUCTION

The magnetoteluric (MT) method is one of the geophysical methods that measures the electromagnetic (EM) fields emitted by the earth. The EM fields can be categorized into two main categories. The first category refers to high frequency signals (frequencies above 1Hz) which are produced by lightning activity and are associated with electromagnetic waves produced by conductive ionosphere and earth. While on the second category, EM is produced because of the activity of the solar wind with the Earth's magnetic field fabricates magnetohydrodynamic waves that propagate in the atmosphere through the ionosphere of the magnetosphere (McPherson, 2005)

According to Manoj (2003), measured MT data can be divided into signals and noise. The signal is a measured component of the electric and magnetic field which is connected through the impedance transfer function. Noise is an additional component in the electric or magnetic field which is measured but not interconnected. Madden (1964) mentions that all MT data cannot be predicted as noise.

Fontes (1988) divides noise into coherent and incoherent. Coherent noise in MT data is caused by noise at the origin of the source which produces MT data where noise is read by electric fields and magnetic fields such as lightning and power lines. Inherent noise is caused by the existence of unreadable noise on electric field or magnetic field but also can be caused by random noise such as vibrations by vehicles or strong winds that affect plants so that they move the roots of trees and produce seismic vibrations.

Noise can damage or reduce the value of impedance in a measured magnetic field (Sims et al, 1971). The usual way to solve this problem, according to Gamble (1979), is to install a remote station. Where this station is used by using assumption that the origin of noise is different so that it can eliminate bias significantly. The flaw of this method is it will slightly increase the cost and time of acquisition because the user needs to add an additional area for the remote station, which often times is placed faraway and can be difficult to access.

Zhang (1997) give another option to eliminate noise by using continuous wavelet transform (CWT) on data with high frequency signal in time series. The method is done by increasing the signal-to-noise ratio in determining function response directly by selecting useful signal parts only. Larnier (2016) with CWT has also demonstrated as a good tool in reducing noise in computational tensor, even in the case of one station. In the process, Larnier consider the noise and natural transient properties of MT from two types of signals, geomagnetic pulsation and sferics.

The CWT method can be used as the basis for the development of the MT method using one station, especially in difficult-to-reach installation areas to reduce the cost and time required for processing. Therefore, further research on CWT is considered necessary and becomes important to resolve the problems. Favorably, the results can be an additional reference for research purpose to reduce noise in MT data.

SIGNAL SOURCES FOR MT

Magnetotelluric method uses natural electromagnetic fields as the source. According to Manoj (2003), the advantages of using natural terrain is the source continues to exist at the desired frequency (~ 10^{-4} up to 10^{4}Hz). Through this, it is certain that MT penetration can reach ~ 100km. However, the uses of natural resources causes a long measurement time because natural waves sources are difficult to predict and also susceptible to noise, especially at frequencies close to the value of 0.1 to 1 Hz.

Natural EM waves can come with several variations and sources that range from the earth's core to outer space (Vozoff, 1991), while Manoj added that the signal source used in the MT method is only the EM field from outside the earth. The reason is because variations in the magnetic field produced in Earth are very small, making it difficult to be used properly. Looking at the characteristics of the source frequency, it can be divided into two categories. High frequency signals (frequencies above 1Hz) are usually produced by lightning activity and are associated with electromagnetic waves produced by ionosphere and conductive earth. While on the other category, EM is produced because of the activity of solar wind with the earth's magnetic field so as to produce magnetohydrodynamic waves that propagate through the atmosphere through the ionosphere of the magnetosphere, this category has a signal frequency <1Hz (McPherson, 2005). Both of these categories can be described by using spectra analysis as in Figure 1.

It is known that electromagnetic fields with frequencies above 1 Hz come from meteorological activities such as lightning activity. The signal that produced from lightning activity is also known as sferics. Sferics propagate in guide waves as transverse electric (TE) waves, transverse magnetic (TM) waves, and transverse electric magnetic (TEM) waves which can be amplified or weakened, depending on the frequency.

When a magnetic storm occurs, large amount of sun's plasma released and causes a change in the sporadic magnetic field of the earth resulting in high magnetic field variations.

NOISE SOURCES FOR MT

Manoj (2003) said that the obtained MT data is not only in the form of signal but also noise. Noise is an additional component in the electric or magnetic field which is measured but not interconnected. Madden (1964) mentions that all MT data that cannot be predicted and not follow the signal trend as a noise. Changes that cannot be predicted on amplitude and phase are also called noise. The existence of this noise can ruin the data, thus giving confusion in making the actual conceptual model and influencing the value of the signal to noise ratio.

Fontes (1988) divides noise into coherent and incoherent. Coherent noise in MT data is caused by noise at the origin of the source which produces MT data where noise is read by electric fields and magnetic fields as lightning or power lines. Inherent noise is caused by the existence of unreadable noise on electric field or magnetic field but also can be caused by random noise such as vibrations by vehicles or strong winds that affect plants so that they move the roots of trees and produce seismic vibrations. This classification from Fontes is summarized in Table 1.

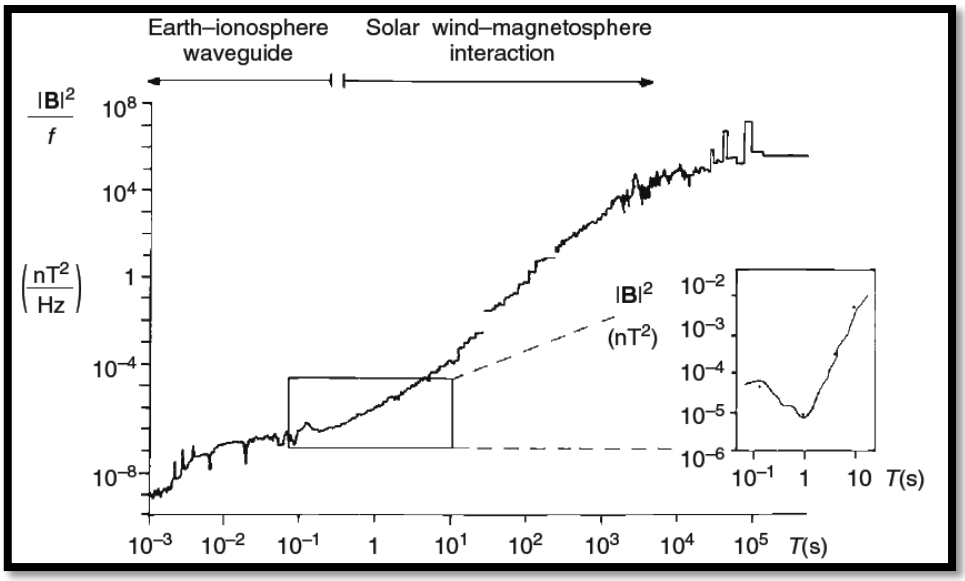


Figure 1: Signal in Magnetotellurics. (Manoj, 2003).

Table 1: Noise classification of magnetotellurics methods. (Fontes et al., 1988)

Time Domain				Frequency Domain
Regular		Irregular		
Coherent (Random noise, linear trend)	Non-Coherent (repeating pulse)	Coherent (Spike)	Non-Coherent (Spike)	50-60 Hz, Dead band

While the other noise classification is summarized in Table 2.

Table 2: Noise classification based on its influences. (Simpsons and Bahr, 2005)

Cultural Noise	Meteorological	Sensor
Electricity Powerline, Automobile	Wind storm, Lightning, Temperature	White noise, Temperature

NOISE REDUCTION USING CONTINOUS WAVELET TRANSFORM METHODS

Noise reduction in MT data can be done in various ways, one of which is through continuous wavelet transform (CWT). CWT method has several advantages, such as low-entropy, multi-resolution, de-correlation and more flexibility than other methods (Deasy et al, 2002). The method in CWT basically includes three stages: the decomposition of original signal by wavelet transform, obtaining wavelet coefficient as a boundary, and finally reconstructs the wavelet coefficient to get a useful signal after noise recovery is done.

CWT method will estimate the impedance by using the connection of fields and impulse tensor element as follows:

$Ex(t) = Zxx(t)*Hx(t)+Zxy(t)*Hy(t)$ (1)

$Ey(t) = Zyx(t)*Hx(t)+Zyy(t)*Hy(t)$ (2)

Where E is the electric field, H is the magnetic field, and Z is the impedance tensor. Z can be converted to apparent resistivity ($\rho\alpha$) and phase(Φ) by using equation as follows:

$$\rho_a = |Z|^2/(\mu\omega) \quad (3)$$

$$\phi = \arctan\left(\frac{\Im(Z)}{\Re(Z)}\right) \quad (4)$$

Where $\mu = 4\mu 10^{-7}$H/m is the magnetic permeability and $\omega = 2\mu f$ with f as the frequency signal. The value of these can be used in analyzing the electrical properties of the subsurface.

Then, from equation 1 can be continued by using *wavelet transform* to become:

$Ex(a,\tau) = Zxx(\tau)*Hx(a,\tau)+Zxy(\tau)*Hy(a,\tau)$ (4)

$Ey(a,\tau) = Zyx(\tau)*Hx(a,\tau)+Zyy(,\tau)*Hy(a,\tau)$ (5)

Where $E(a,\tau)$ and $H(a,\tau)$ is the *wavelet transform* from electric field and magnetic field.

Wavelet coefficient can be obtained based on dilatation $a > 0$ (describing frequency) and translation τ (time) through *wavelet* transformation, which can be formulated as follows:

$$\mathcal{W}_\psi[s](a,\tau) = \int_{-\infty}^{+\infty} dt \frac{1}{a}\psi * \left(\frac{t-\tau}{a}\right) s(t) \quad (6)$$

Where s is the analyzed signal and ψ is the *mother wavelet. Mother wavelet* is determined by the type of MT source signal.

Data processing using CWT was first known in the execution of seismic data by Goupillaud (1984). CWT has been widely used in research to analyze non-stationary processing and has been proven to be an efficient tool in researching magnetoteluric data (Zhang & Paulson, 1997; Garcia & Jones, 2008; Escalas et al., 2013; Larnier et al., 2016).

RESULT

The study data is processed with filters that have been made to change the time series data in the time domain into a time-frequency domain using the continuous wavelet transform method. After that, analysis of the existence of the noise will be carried out in the time frequency domain to produce data that are cleared from noise.

The impedance from the data will be estimated to get the resistivity and phase values by using equations 3 and 4. The values of resistivity and phase are displayed in the apparent resistivity curve.

The processed data will be compared with the results before the filter is done to ensure that the filter works properly as shown in Figure 2. From Figure 2, it can be seen that in the unfiltered image (left) there is noise as proved by an analysis of the time-frequency domain. The noise is then removed so that it will becomes the right image.

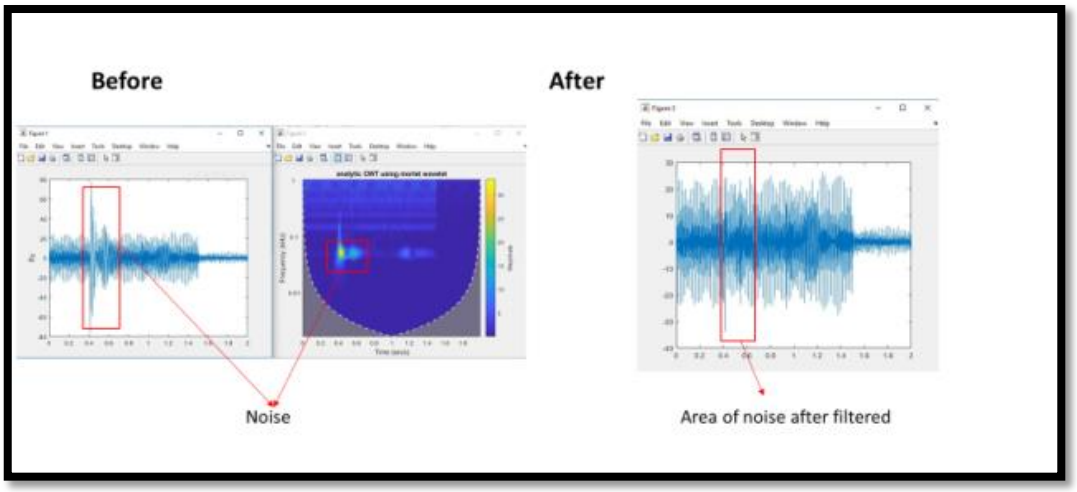


Figure 2: Comparation of time series data; unfiltered (left) and filtered (right).

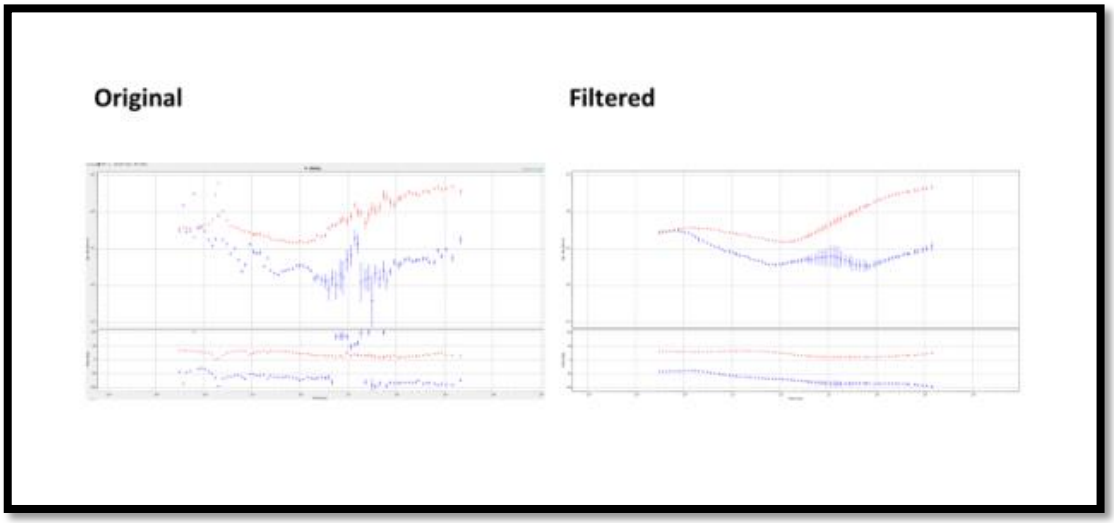


Figure 3: Comparation of apparent resistivity curve unfiltered (left) and filtered (right).

Based on the results of filtered data obtained the curve shown in Figure 3. It can be seen from Figure 3 that the comparison of the unfiltered data (left) and filtered data (right), Continuous wavelet transform filter that has been made can eliminate noise in the MT data from the original data where from the looks of it still looked in disarray but already has a good TE and TM trend. The results of the filtered curve also show that there is a curve splitting between the TE and TM curves. This curve splitting can be caused by several things, for example, a displacement.

The results of curves and time series on original data that have been filtered show that the filters that have been made can eliminate noise in magnetotellurics data.

CONCLUSION

Based on the results of research conducted by the CWT method, it has proved to be useful for characterizing noise in magnetotellurics data, hence enhancing the quality of the data. Existing noise can be analyzed and filtered using this method. This is evidenced by the results of pseudo resistivity curves and phases of research that are better than before filtering. Therefore, CWT method can become an alternative in removing noise-influenced magnetotelluric data.

REFERENCES

Deasy, J., O., Wickerhauser, M., V., Picard, M. (2002). "Acclerating Monte Carlo Simulation of Radiation Theraphy Dose Distribustions using Wavelet Threshold De-noising". Med Phys, 29(10): 2366-2373.

Escalas, M., P., Queralt, J., Ledo, A., Marcuello, (2013), "Polarization Analysis of Magnetotelluric Time Series using a Wavelet-based Scheme: A Method for Detection and Characterisation of Cultural Noise Sources". Physics of the Earth and Planetary Interiors. 218: 31–50.

Fontes, S., L., Harinarayana, T., Dawes G., J., K., Hutton, V., R., S., (1987), "Processing of Noisy

Magnetotelluric Data Using Digital Filters and Additional Data Selection Criteria". Physics of the Earth and Planetary Interiors, 52 (1988): 30-40.

Gamble, T., D., Goubau, W., M., Clarke, J., (1979), "Magnetotellurics with Remote Reference". Geophysics, 44(1): 53-68.

Garcia, X., Jones, A., G., (2008), "Robust Processing of Magnetotelluric Data in The AMT Dead Band using The Continuous Wavelet Transform". Geophysics, 73(6): 223–F234.

Goupillaud, P., Grossmann, A., Morlet, J., 1984, "Cycle-octave and Related Transforms in Seismic Signal Analysis". Geoexploration, 23: 85–102.

Larnier, H., Sailhac, P., Chambodut, A., (2016), "New Application of Wavelets in Magnetotelluric Data Processing: Reducing Impedance Bias". Earth Planet Science, 68(70).

Madden, T., Nelson, P., (1964, reprinted 1986), "A defence of Cagniard's magnetotelluric method". In Society of Exploration Geophysicists, Geophysics Reprint Series, No. 5., ed. Vozoff.

Manoj, C., (2003), "Magnetotelluric Data Analysis using Advances in Signal Processing Techniques". Hyderabad: National Geophysical Research Institute.

McPhershon, R., L., (2005), "Magnetic Pulsation Their Source and Relationship to Solar Wind and Geomagnetic Activity". Surv Geophys, 26(5): 545-592.

Sims, W., E., Bostick, F., X., J., Smith, H., W., (1971), "The estimation of magnetotelluric impedace tensor elements from measured data". Geophysics, 36(5): 938-942.

Simpson, F., Bahr, K., (2005), "Pratical Magnetotellurics". Cambrige: Cambrige University Press.

Vozoff, K, (1991), "The Magnetotelluric Method in Electromagnetic Methods in Applied Geophysic". Ed by M.N Nabighian, Society of Exploration Geophysics, Tusla, USA.

Zhang, Y., Paulson, K., V., (1997), "Enhancement of signal-to-noise ration in natural source transient magnetolluric data with wavelet transfrom". Pure Apllied Geophysics, 149 405-419.

GEOTHERMAL DIRECT UTILIZATION FOR FROST PROTECTION ON POTATO CROPS IN DIENG PLATEAU, CENTRAL JAVA

Farizky Hisyam and Afifah Nurul Maulina

Brawijaya Volcano & Geothermal Research Center, Department of Physics, Brawijaya University
Jalan Veteran, Malang, East Java, 65145, Indonesia
Email: hishamfarizky@gmail.com

ABSTRACT

Dieng Plateau is prominent potato producer in Indonesia, especially in Central Java. However, there is problem found, i.e. phenomenon of frost or locally called *embun upas* which occurs during dry season (July to September). The frost occurs due to soil surfaces that lose heat radiation. The frost damages the potato crops and causes losses up to hundreds of million rupiah for the farmers. On the other hand, it is known that Dieng plateau is one of regions with high geothermal potential in Indonesia. The study was conducted to utilize geothermal potential directly for preventing damage to potato plants due to frost. For case study, this research was conducted at potato cultivations in Kejajar, Wonosobo and Batur, Banjarnegara. Based on characteristic of frost formation, including appearance of inversion layer, the most appropriate method for frost protection is active method, i.e. heater. Heater emits heat energy to compensate the loss heat due to radiation during night. The released warm air ascends by convection and radiation. Hence, the surrounding air gets warmer. Instead of using fossil fuel for burning, geothermal direct use in heater able to reduce the fuel consumption and suppress the total cost required. Total heat energy requirement to prevent frost around 140 W/m^2. Analysis both in thermal and mass equilibrium showed that this total energy could be provided by flowing 11.146 kg/s brine along pipes into heaters and obtaining warm air with mass rate 44.092 m^3/s. The system's efficiency could be increased by adding the number of heater or combining with other active methods (i.e. irrigation). Applying the cascade system to harness the remaining heat for another geothermal direct utilization was also possible. Therefore, this study could be an alternative solution for frost protection in Dieng plateau.

Keywords: Dieng plateau, frost protection, geothermal direct use, heater, potato crops

INTRODUCTION

Indonesia is a country blessed with enormous geothermal energy because it is located on the "Ring of Fire". The 2011 Ministry of Energy and Mineral Resources' (MEMR) report shows that Indonesia has a geothermal potential of 29,215 MWe which constitutes 40% of the world's geothermal potential

(Asian Development Bank and The World Bank, 2015). The Government of the Republic of Indonesia through Law No. 21 of 2014 has regulated the use of geothermal energy in Indonesia both indirectly (electricity needs) and indirectly (non-electricity needs). However, the direct use in Indonesia is still very low. Based on reports of the world's direct use of geothermal energy in 2015 Indonesia is still around 2.30 MWt or equivalent to 11.3 GWh/year (Lund, 2015).

Generally, geothermal energy in Indonesia is concentrated in mountainous areas with agricultural, plantation, forestry, and tourism which the heat has the potential to be used directly (Surana, 2010). Among of them is geothermal energy in Dieng, Central Java. The Dieng geothermal field has 250 MWe of geothermal potential with 60 MWe of which is used for electricity generation (Harijoko et al., 2015). Because the soil is fertile and the climate is cool, around the geothermal field it is intensely cultivated in agriculture (Hino et al., 2013).

One of the most important commodities from Dieng is potatoes (*Solanum tuberosum L.*). It is noted that the Dieng plateau is the largest potato producer in the province of Central Java. Based on 2014 horticultural production statistics Central Java itself is the largest potato producing province in Indonesia, which is around 21.68 percent of all potato production in Indonesia. Furthermore, the 2016 statistics show that Banjarnegara is the regency with the largest potato production in Central Java (974,667 quintals) followed by Wonosobo in third place (508,464 quintals). In 2017, 793,934 quintals of which were produced from 4,508 ha of land in Batur District, Banjarnegara and 462,340 quintals of potatoes produced from 2,858 ha of land in Kejajar District, Wonosobo.

The cool climate and high elevation allow during the dry season the air temperature at night until the dawn can reach freezing point and ice sheets (frost) form which is known by the local community as *embun upas* (Figure 1).



Figure 1: Frost impact on potato leaves in Dieng plateau (Radarbanyumas.co.id, 2016).

Even though it melts after the sun shines, frost damages the potato plant tissue. This is indicated by the color of the leaves of the potato plant being blackish brown. Usually, if the leaf dries up it will also be followed by the stem. If the potato plants affected by frost are still under 60 days, it is certain that they will totally damage (Mongabay, 2018). As a result, farmers experience crop failure. The loss is estimated at hundreds millions of rupiah per hectare (Detiknews, 2014). A number of frost prevention scenarios have been proposed, ranging from active to passive methods. Efforts to replace potato plants with other types of plants have been carried out. However, with more favorable economic reasons, farmers are still reluctant to switch from potatoes (Ngabekti et al., 2007). Pradana et al. (2018) suggests that one scenario provides heating temperature near the ground at night, in order to prevent the temperature cools below the frost point. However, this preparedness plan has more financial or investment needed, especially the fuel used.

Therefore, in this paper a feasibility study of geothermal direct use in Dieng Plateau will be conducted as an alternative solution for frost protection.

DIENG GEOTHERMAL FIELD

Dieng Plateau is physiographically located in the depression zone of South Serayu. Generally the relief of the area is mountains and plateau with moderate to steep slopes with an elevation range of 1,500-2,000 m a.s.l. As depicted by Dieng geological map in Figure 2, the regional structure in the Dieng region is a caldera controlled by faults with the SE-NW trend. Dieng geothermal resources are located in volcanic mountain ranges composed of Quaternary andesitic volcanic rocks (Layman, 2002). The Dieng geothermal field is a dominant water geothermal system. The temperature of the Dieng field reservoir can reach 300 ^{o}C. Hence, Dieng is categorized as a high-temperature reservoir system. A number of geothermal manifestations found in the Dieng region are solfatara, hotspring, mudpool, fumarole, and moffet (Wibowo et al., 2015). With the relatively high content of dissolved silica in reservoir fluid, scaling silica has great potential to be deposited on the surface (Utami et al., 2014).

Based on the Schmidt-Fergusson climate classification, Dieng has type A or wet climate. The average rainfall is more than 3,500 mm/year where the wettest rainfall is recorded in January and the driest in August. The annual temperature ranges from 19.3 to 20.6 ^{o}C. Air humidity ranges from 86.6% with a minimum of 53% and a maximum of 100%. Because of its location on the plateau, during the dry season (July-September) temperatures reach very low values. Even at dawn, it can reach freezing point (Ngabekti et al., 2007).

FROST AND ITS PROTECTIONS

Frost is formed on a clear, calm night and the ground cools rapidly due emitting infrared radiation. At that time, the ground becomes much cooler than the ambient air. Thus, it will be observed that the air temperature will increase with increasing altitude. This is known as radiation inversion. The air that is in direct contact with the cold surface will cool down by conduction. The air will reach dew point, i.e. temperature where the water vapor begins to condense. If the dew point is precisely or below freezing point, water vapor will be deposited to form ice. Ice crystals that form on the ground or other objects are known as frost. Frost can also occur in cold air blowing towards the area and recovering the warm air in the area. It is associated with cloudy conditions, strong winds, and no radiation inversion.

In tropical regions like Indonesia, ice can be found in places with high elevations. When frost is formed,

plants can be injured by plant tissue damage (Snyder and de Melo-Abreu, 2005). This has a significant impact on production. Basically, frost prevention in crops is maintaining plant tissues in condition above critical temperature (Evans, 1999). The recommended critical temperature is the highest freezing temperature for vegetables. The critical temperature of a plant varies depending on the type and phase of its growth. Potatoes have a critical temperature of -0.8 ºC (Snyder and de Melo-Abreu, 2005).

Frost can be prevented by two mechanisms, i.e. active and passive method. Passive methods are those that act in preventive and long term whilst the active methods are temporary and energy required (Snyder and de Melo-Abreu, 2005). One of active methods which well-known as frost prevention for 2,000 years is heaters or orchard heater. Conventional heaters work by creating convection currents around the surface of the ground through radiation from the heat energy of oil or gas burning in the heater.

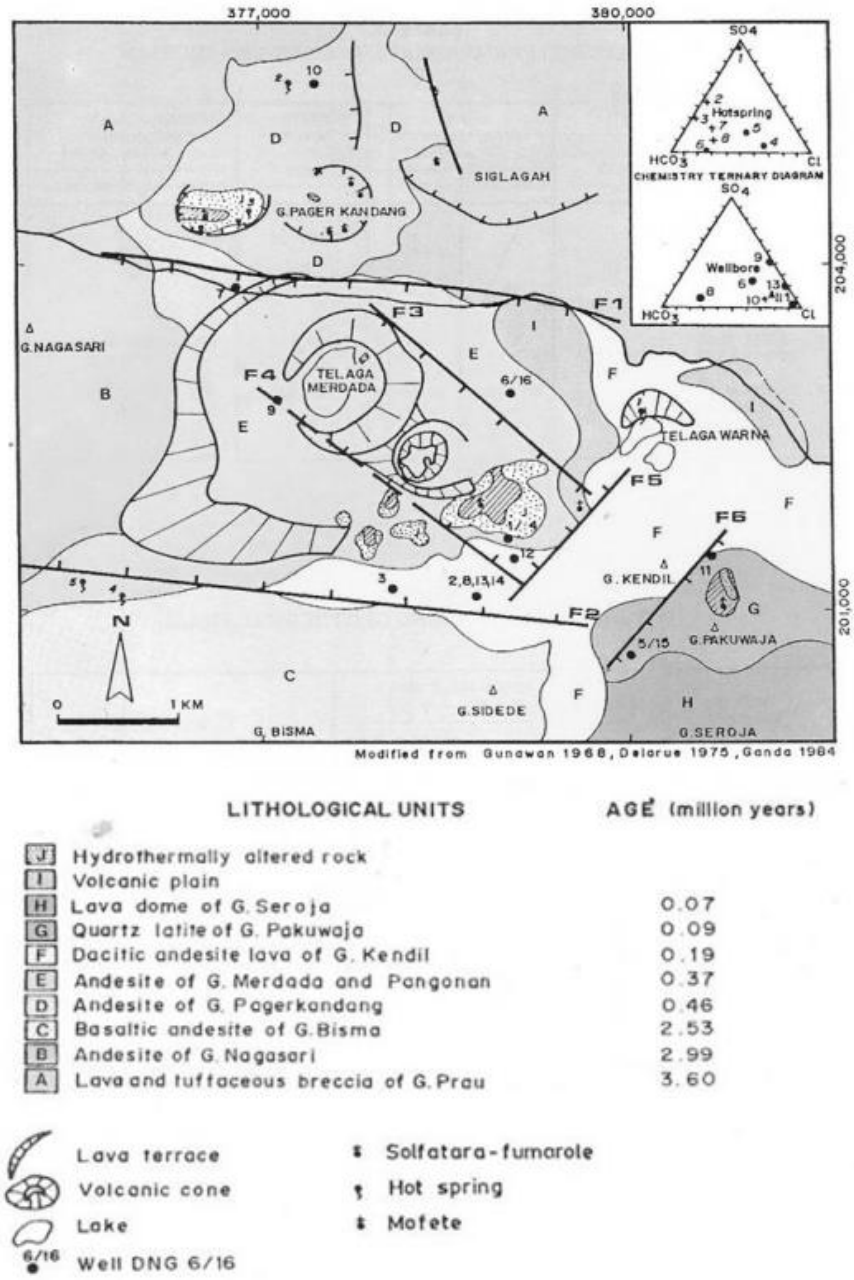


Figure 2: Geological map of Dieng geothermal field (Boedihardi, 1992 in Hino et al., 2013).

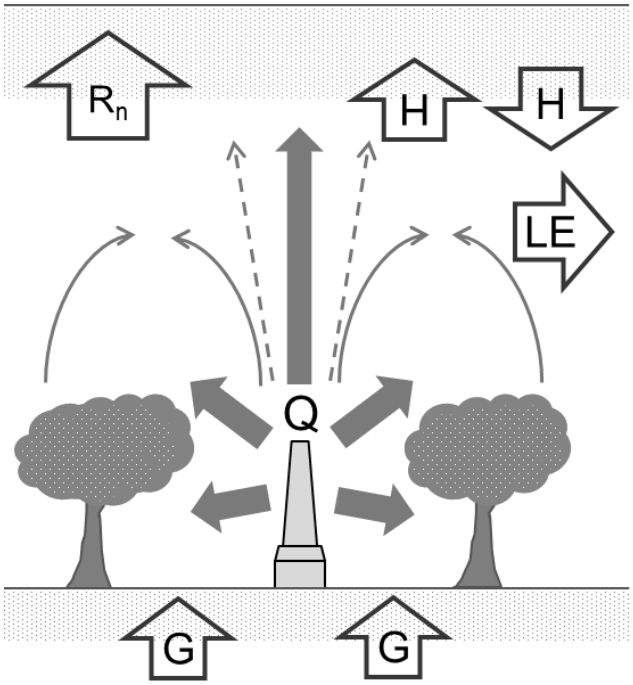


Figure 3: Energy fluxes and thermal circulation around a heater (modification from Snyder and de Melo-Abreu, 2005). Abbreviation: nett radiation (Rn), vertical and horizontal sensible heat flux (H), conductive heat flux from the ground (G), latent heat (LE), and energy added by heater (Q).

The created heat energy would compensate the lost heat energy from the crops. The heat energy would be captured by crops and ambient air. Then, it would help increasing temperature above the critical point. Conventional heater emits high concentrated smoke in large quantities which can trigger severe pollution. Therefore, heaters are also known as smudge pot. Initially there is assumption that the smoke would trap the heat which radiated into the space. However, currently research proved that the smoke impact in preventing heat loss have no significant effect and could be neglected. In addition to the issue of emissions, conventional heaters also have their drawbacks, which are relative costly compared to other active methods (Evans, 1999).

If frost occurs, the natural energy losses from a crop are bigger than the energy gains (Snyder and de Melo-Abreu, 2005). This causes the air temperature to drop. As shown in Figure 3, energy is mainly lost to net radiation (Rn) and the losses are partially replaced by sensible (H) and ground (G) heat fluxes towards the surface. Furthermore, the released latent (LE) heat can also replace some of the energy loss. Therefore, heaters provide energy (Q) to replace the net loss radiation. If sufficient heat is added to the cultivation area, all of the losses are replaced so the temperature will not fall below its critical point.

Dieng's topography is both mountains and hills. Generally frost hits the land found in valleys and alluvial plains. Frost is formed at night when the valley releases heat radiation faster than the mountain slopes due to cold air drainage, which is the flow of cold air from the slope to the valley (Pradana et al., 2018). As a result, warm air on the surface of the valley will rise to the upper air layer so that an inversion layer is formed. The absence of wind accelerates the cold air down into the valley. Thus, the valley area will experience more intensive frost than on the slopes.

The existence of this inversion layer (Figure 4) will be advantageous if the applied frost protection method is the active method, i.e. heaters. Due to the inversion layer, hot air from the heater will not easily escape into space, but will be trapped near the ground and replace the heat that has been released during the radiation process. The stronger the inversion layer, the less heat energy would be required. In some cases it is only necessary to increase the air temperature by several degrees celcius to minimize crop damage due to frost (Evans, 1999).

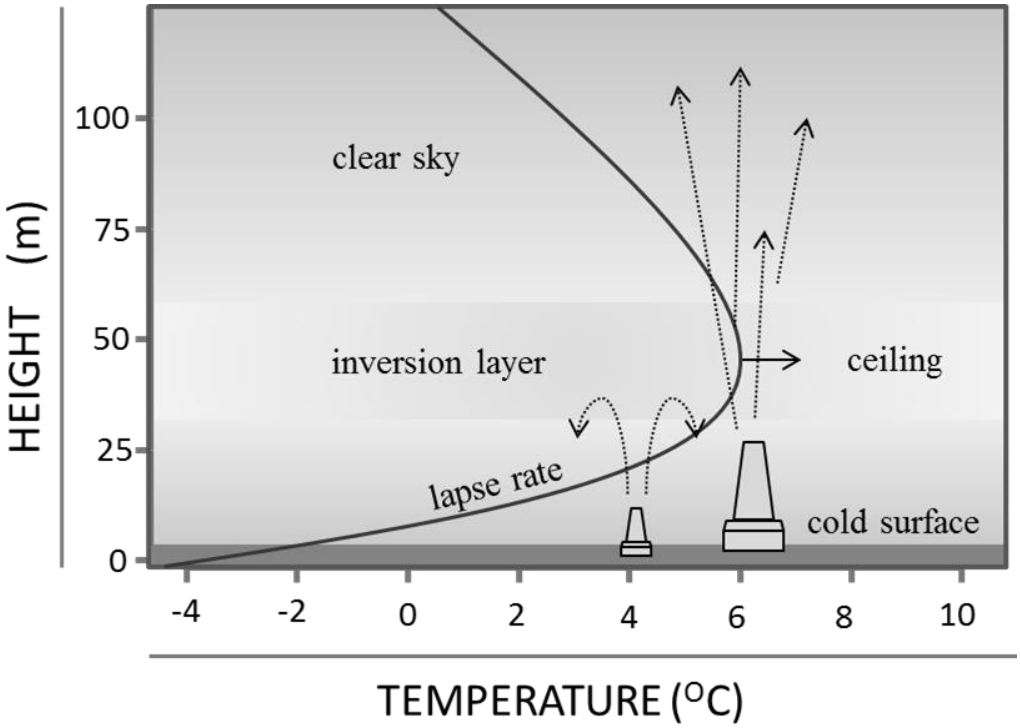


Figure 4: Temperature profile during frost night and the effect of output heater in heat distribution and heat loss from a heater (modification from Snyder and de Melo-Abreu, 2005).

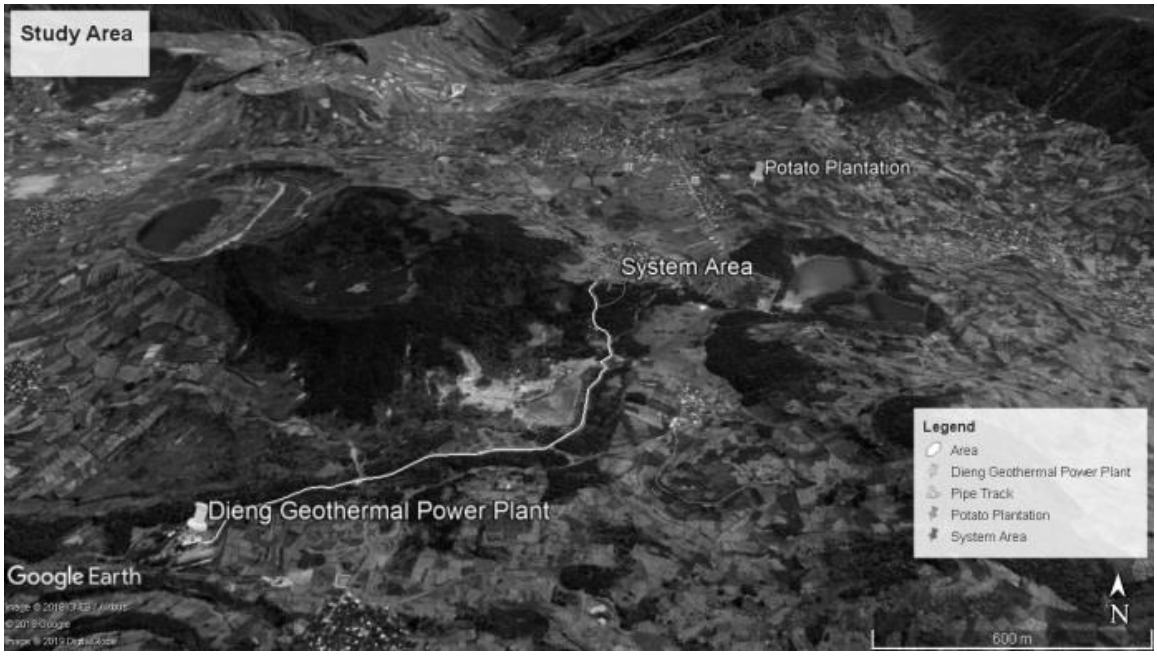


Figure 5: Satellite imagery of study area

METHODOLOGY

The study was conducted in the Dieng geothermal area which comprises potato cultivations in the Kejajar District, Wonosobo Regency and Batur District, Banjarnegara Regency, Central Java (Figure 5). The data used are Google Earth satellite imagery, the distribution of geothermal manifestations, and data of production wells. Satellite imagery is used to determine the location of the potato cultivations. The cultivations are scattered near geothermal facilities. Potato land was chosen based on access to geothermal pipes installed in the field and topographic factors. Data on geothermal manifestations were obtained through literature study papers. The fluid parameters obtained are then used to analyze the heat and fluid mass flow rate balance. Hence, the brine and hot air discharge parameters required to prevent frost formation are obtained.

RESULT AND DISCUSSION

Heat and Mass Balance Analysis

Fundamentally, direct use of geothermal energy is harnessing of heat energy from brine. Therefore, an analysis of energy and mass balance between brine and cold air is required. Heat exchange between the brine and cold air will take place inside the heat exchanger. This will satisfy the energy and mass equilibrium equations as follows:

$$q_{brine} \times \rho_{brine} \times c_{brine} \times (T_{in\ brine} - T_{out\ brine}) = q_{air} \times \rho_{air} \times c_{air} \times (T_{out\ air} - T_{in\ air}) \quad (1)$$

where q_{brine} is the brine flow rate and q_{air} is the air flow rate. The description of other parameters along with the values used in the analysis and calculations are summarized in Table 1.

Snyder and de Melo-Abreu (2005) calculated that the heat losses due to thermal radiation are between -90 W/m^2 and -50 W/m^2. This loss is replaced with downward heat flux and ground fluxes which each can reach 20 to 40 W/m^2. This depends on local conditions. Therefore, the energy needed to prevent freezing becomes 20 to 40 W/m^2. However, 75-85% of the substituted heat will be lost due to radiation into space as well as buoyant convective forces over plants or stack effect (Evans, 1999). The heat energy that can be released by the heater produces 140 to 240 W/m^2. This depends on fuel, combustion rate, and number of heaters.

Assuming from the previous calculation results that the energy needed to prevent frost is 140 W/m^2. Converting this value yields 1,400,000 W per hectare. This heat can be achieved by flowing hot air with flow rate of 44.092 m^3/s and brine with flow rate of 11.146 kg/s.

Table 1: Summary of system parameters.

Parameter	Symbol	Unit
Density of brine	ρ_{brine}	1,050 kg/m^3
Specific capacity of brine	c_{brine}	4,187 J/kg ^{o}C
Inlet temperature of brine	$T_{in\ brine}$	60 ^{o}C
Outlet temperature of brine	$T_{out\ brine}$	30 ^{o}C
Density of air	ρ_{air}	1.05 kg/m^3
Specific capacity of air	c_{air}	1,008 J/kg ^{o}C
Inlet temperature of air	$T_{in\ air}$	5 ^{o}C
Outlet temperature of air	$T_{out\ air}$	35 ^{o}C

Furthermore, brine temperature efficiency can be obtained by the following equation:

$$\eta_h = \frac{T_{in\ brine} - T_{out\ brine}}{T_{in\ brine} - T_{in\ air}} \times 100\% \quad (2)$$

Whilst the efficiency of air temperature is obtained from the equation:

$$\eta_c = \frac{T_{out\ air} - T_{in\ air}}{T_{in\ brine} - T_{in\ air}} \times 100\% \quad (3)$$

From the parameters obtained each shows that the average temperature efficiency is the average of the two equations above and yield value 54.55%.

Design System

In general there are 5 components in the heater systems that utilize geothermal energy directly:

1. Pump
2. Pond
3. Heat Exchanger
4. Heater
5. Pipe

The system arrangement is illustrated in the Figure 6.

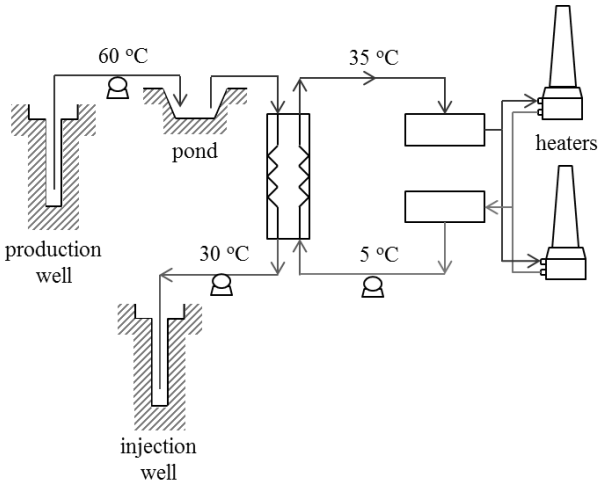


Figure 6: Schematic diagram of heater system for frost prevention with direct geothermal utilization.

This system commences from production wells. The brine used has an initial temperature of 60 °C. The brine will be pumped from production wells and flowed to a pond. This pond aims to reduce the levels of dissolved silica in brine thereby reducing the potential for scaling in brine pipes to be distributed to injection wells (Wahyudityo et al., 2013). After passing the pond, brine is redistributed through the heat exchanger. For another scenario with lower costs, the brine used in the system can also come from the remaining brine from the power plant. Therefore, before brine is re-injected through injection wells, the remaining heat from brine is utilized optimally.

Heat exchangers are the most important instrument in direct use of geothermal energy. The heat exchanger will transfer heat from the brine to cold air. The type of heat exchanger that is recommended to be used is shell and tube heat exchangers (Figure 7) which are usually used for high pressure systems (Jubaedah et. al., 2015). However, there are a number of things that need to be considered in the shell and tube type heat exchanger, i.e. problems with fouling, greater approach temperature between incoming and outgoing fluid temperature, and the large size (Lund, 1998).

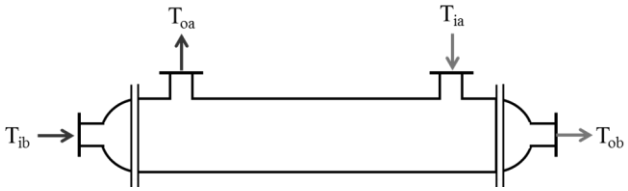


Figure 7: Design of shell and tube heat exchanger.

Leaving from the heat exchanger, the brine will flow back through the pipe to be injected into the injection well. The brine is in 30 ^{o}C temperature condition when injected. The heat transferred to cold air will increase the temperature of cold air until reach temperature around 35 ^{o}C. The cold air from the ambient air will be sucked and flowed through the heater. The cold air collected will be pumped towards the heat exchanger. Then, cold air that has warmed will be distributed through another pipe to be released into the surrounding air via heaters. Thus, the heater will work like an air circulation device by convection, i.e. cold air will be sucked and hot air will be emitted. Important to be noted, the heater will not work continuously. The heater will work if the temperature at the night suddenly drops dramatically to close to the critical temperature. Therefore, the heater needs to be installed with a thermostat whose function as a temperature sensor. When the thermostat detects changes in temperature to critical temperatures, the system will automatically work. Installing a thermostat as a temperature sensor will certainly facilitate the operation of the heater system without having to monitor it directly all the time. Figure 8 shows the heat design.

For pipes used in distributing fluids, it is recommended to use pipes equipped with insulators to minimize the effect of heat loss. To distribute brine from the main source to the heat exchanger the stainless-steel zinc alum pipe is used. The use of this pipe is also equipped with thermal insulation using glass wool. Pipes are located above the ground intentionally. This makes easier to detect the presence of pipes as well as to avoid damage to the pipe if there is an excavation around the pipe. Meanwhile, for pipes that connect heat exchanger to heaters in potato fields, PPR pipes with smaller diameter are used. Furthermore, because the distance of the production well to the heat exchanger reaches 2.2 kilometers whilst the distance between the heat exchanger to the potato field is around 1.2 km, a pressurized pipe system is needed to overcome the possibility of losing head pressure.

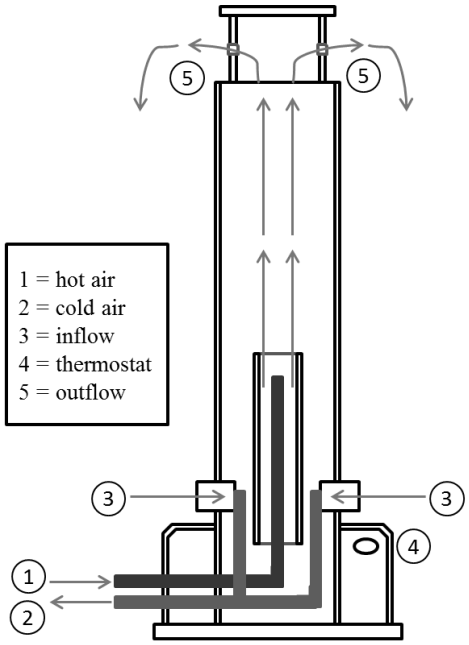


Figure 8: Design of heater.

CONCLUSION

Frost in the research area can be prevented by heat which is generated from heaters that directly utilize geothermal energy. For one hectare of potato cultivation area, heat is obtained by flowing brine with a discharge of 11.146 kg/s and transferred to the air flow with a discharge 44.092 m^3/s. However, there is no absolutely perfect method of frost prevention. The method offered in this study is an alternative solution to prevent frost on the Dieng plateau. Either appropriate management or combination other methods (active and passive) are required in order to improve heaters efficiency.

Potatoes are promising agricultural product in the future. Demand for potatoes will continue to increase along with the emergence of a variety of processed potato products. Dieng area can be the center of the largest potato supplier in Indonesia. The existence of a geothermal heater system as a frost protection in Dieng is expected to minimize losses due to frost. For other direct geothermal utilization, beside the “frost season”, geothermal energy can be used directly to sterilize potato seeds and to process potato products that are able to prosper the local farming community. By this handling, it is expected that the heat energy remain from the brine will be fully utilized.

If the results of this study will be applied, it is necessary to analyze the previous costs. Last, for

better result and improvement, recalculating of required heat to protect plant from frost Dieng plateau by considering local climate parameter is needed.

ACKNOWLEDGEMENT

The author would like to thank Mr. Sukir Maryanto, Ph.D, who has been willing to review and give suggestion in this research. Appreciation is also given to Mr. Dadang Jaiz, ST who helped in providing civil material references in this study.

REFERENCES

Ahren, D., C., (2009), "Meteorology Today: An Introduction to Weather, Climate, and the Environment Ninth Edition". Belmont. Brooks/Cole.

Asian Development Bank and The World Bank, (2015), "Unlocking Indonesia's geothermal potential". Mandaluyong City, Philippines.

BPS-Statistics of Banjarnegara Regency, (2018), "Banjarnegara Regency in Figures".

BPS-Statistics of Wonosobo Regency, (2018), "Wonosobo Regency in Figures".

Detiknews, (2014), "Musim Kemarau, Kristal Es Embun Beku Muncul di Dieng", https://news.detik.com/berita/d-2676735/musim-kemarau-kristal-es-embun-beku-muncul-di-dieng accessed in 11 June 2019.

Dinas Pertanian dan Perkebunan Jawa Tengah, (2017), "Statistik Hortikultura Provinsi Jawa Tengah tahun 2016".

Euis, J., Bambang, T., P., Abdurrachim, (2015), "Study of Geothermal Utilization for Milk Pasteurization in Pangalengan, Indonesia". Proceedings, World Geothermal Congress 2015, Melbourne, Australia.

Evans, R., G., (1999), "Frost protection in orchards and vineyards," Northern Plains Agricultural Research Laboratory, USDA – Agricultural Research Service, Sidney.

Harijoko, A., Hapsari, K., Wibowo, Y., T., Atmaja, R., W., Nupratama, M., I, (2015), "The Sulfide Mineral Deposit in the Geothermal Pipes of Dieng Geothermal Field, Indonesia," Proceedings, World Geothermal Congress 2015, Melbourne, Australia.

Hino, T., Itoi, R., Tanaka, T., Pambudi, N., A., Khasani, (2013), "Natural State Modeling of Geothermal Reservoir at Dieng, Central Java, Indonesia," GRC Transaction, 37, 831-836

Kementerian Pertanian Direktorat Jenderal Hortikultura, (2015), "Statistik Produksi Hortikultura tahun 2014".

Layman, E., B., Agus, I., Warsa, S., (2002), "The Dieng Geothermal Resource, Central Java, Indonesia," Geothermal Resources Council Transactions, 26, 573-579.

Lund, J., W., (1998), "Geothermal Direct-Use Equipment Overview". GHC Bulletin. 1-6.

Lund, J., W., Boyd, T., L., (2015), "Direct Utilization of Geothermal Energy 2015 Worldwide Review". Proceedings, World Geothermal Congress 2015, Melbourne, Australia.

Mongabay, (2018), "Embun Beku Bisa Terjadi Lagi di Dieng, Petani Kentang Rugi. Kenapa?" https://www.mongabay.co.id/2018/07/10/embun-beku-bisa-terjadi-lagi-di-dieng-petani-kentang-rugi-kenapa/ accessed in 11 June 2019.

Ngabekti, S., Setyowati, D., L., Sugiyanto, R., (2007), "The Level of Environmental Damage in Dieng Plateau for Database to Conservation Action," Jurnal Manusia dan Lingkungan, Vol. 14, No. 2, 93-102.

Pradana, A., Rahmanu, Y., A., Prabaningrum, I., Nurafifa, I., Hizbaron, D., R., (2018), "Vulnerability assessment to frost disaster in dieng volcanic highland using spatial multi-criteria evaluation," IOP Conf. Series: Earth and Environmental Science, 148, doi:10.1099/1755-1315/148/1/012002.

Republic of Indonesia, (2014), Law No.21/2014 about Geothermal.

Snyder, R., L., de Melo-Abreu, J., P., (2005). "Frost protection: fundamentals, practice, and economics". Food and Agriculture Organization of the United Nations. Rome.

Surana, T., Atmojo, J., P., Suyanto, Subandriya, A., (2010), "Development of geothermal energy direct use in Indonesia," GHC Bulletin, 11-15.

Utami, W., S., Herdianita, N., R., Atmaja, R., W., (2014). "The Effect of Temperature and pH on the Formation of Silica Scaling of Dieng Geothermal Field, Central Java, Indonesia," Proceedings, Thirty-Ninth Workshop on Geothermal Reservoir Engineering, Stanford, California.

Wahyudityo, R., Harto, A., W., Suryopratomo, K., (2013), "Analisis Scaling Silika pada Pipa Injeksi Brine di Lapangan Panas Bumi Dieng dengan Studi Kasus di PT. Geo Dipa Energi," Teknofisika, 2, 7-14.

Wibowo, A., T., Thasril, M., Sirait, P., (2015), "Production Test Analysis of XYZ-Well at Dieng Geothermal Field Using Horizontal Discharge Lip Pressure Method with Russel James Equation and Hiriart Equation". Proceedings, World Geothermal Congress 2015, Melbourne, Australia

INDONESIA GEOTHERMAL DASHBOARD WITH PLANT INFORMATION MANAGEMENT SYSTEM (PIMS)

Kadar Aditama

DCS Specialist, SIL Power Plant, Sarulla Operation Ltd.
Silangkitang Village, Pahae Jae District, North Tapanuli Regency, North Sumatera Province, Indonesia
Email: kadar.aditama@sarulla-geothermal.com

ABSTRACT

The internet and modern technology increasingly are shaping the manufacturing industry. Digitalization already has changed the manufacturing way. It's called Industry 4.0, the networked factory.

Industry 4.0 wants to take data collection to new levels, monitoring all along the manufacturing process, collecting and storing information from individual measurements to offsets sent to the machines to production results.

Indonesia has 40% of the world's potential geothermal resources, estimated at 28,000 megawatts (MW). With an achievement of 1,924.5 MW it put Indonesia in third place in the world after the Philiphines and United States in utilizing geothermal power.

EBTKE as a representative of the government has a function to monitor every exploitation and utilization of geothermal activities until it is converted into electricity, must have a "Big Screen" that can access all Geothermal Power Plants for monitoring amount of steam coming out from reservoir and the MW productivity.

In line with Indusrty 4.0, IndONEsia Geothermal Dashboard with Plant Information Management System (PIMS) is a set of hardware and software modules designed for plant-wide monitoring and analysis, also it can handles the collection, storage, and retrieval of numerical and string data of process value from each Geothermal Power Plant throughout Indonesia by using technology information an Internet and combined to OPC (Object Link Embedding for Process Control) specifies the communication of real-time data between Control System devices from different manufacturers (ie DCS, PLC, SCADA).

Keywords: Information system, geothermal

WHAT IS PLANT-WIDE MONITORING

The term "plant-wide" applies to an information system in two ways. The first function is that of collecting information from various data sources throughout the actual manufacturing process, including the administrative infrastructure around the plant. The information system should then condition and archive the data. Data conditioning refers to a variety of techniques that include, but are not limited to, averaging, filtering, correlating time stamps, creating combined calculated values, and aggregating raw data.

The second application of the "plant-wide" term refers to the re-presentation of the conditioned data throughout the mill. While using a system like this may seem like an obvious idea, there are many facilities that fall far short of this ideal.

Production processes were largely re-instrumented and put under the control of computer based Distributed Control Systems (DCSs) or Programmable Logic Controllers (PLCs). Some of these systems had the ability to archive data, some did not. Initially these systems were offered by a variety of vendors and the exchange of data was either not considered, or discouraged. It is not unusual to see incompatible Control Systems from different vendors within a single facility.

APPLICATION PIMS FOR ONE DASHBOARD GEOTHERMAL POWER PLANT'S (GPP) MONITORING

Every exploitation and utilization of geothermal activities will be monitored from wide-monitoring system on the EBTKE Head Office. Based on the readiness for every operator's Geothermal Power Plant as owner eligible to share their process and generation information from site area. Then it will be mapped to "big-screen" of Indonesia Geothermal Dashboard.

By using PIMS, it will provide EBTKE with a clear business-directed focus, integrating production data across the enterprise to deliver operational information to the Head Office, both EBTKE and Operator GPP as owner. Figure 1 shows the illustration of display clustered chart., while Figure 2 shows the template Big-Screen monitoring systems.

The primary function of PIMS is to store and manage data gathered from the PCS(s) and serve it to clients. It provides the following functionality:

- PCS Data Gathering using OPC for process data transfer, in terms of point data (DA).

- The Real-time Database provides high performance real-time storage for process and plant data. It provides flexible, user-defined calculations and aggregations.
- An optimized, long-term Historian provides efficient storage and fast retrieval of vast amounts of plant data, over very long time periods.
- A suite of easy-to-use configuration tools is provided to build, deploy and manage the PIMS environment.
- Industry standard open data interfaces, with OPC interface, as a standard interface to communicate between numerous data sources, avoid access conflicts in industrial control systems, and allow any client to access any OPC-compatible device.

Most suppliers of industrial data acquisition and control devices, such as Programmable Logic Controllers (PLCs) and Programmable Automation Controllers (PACs), are designed to work with the OPC Foundation standard.

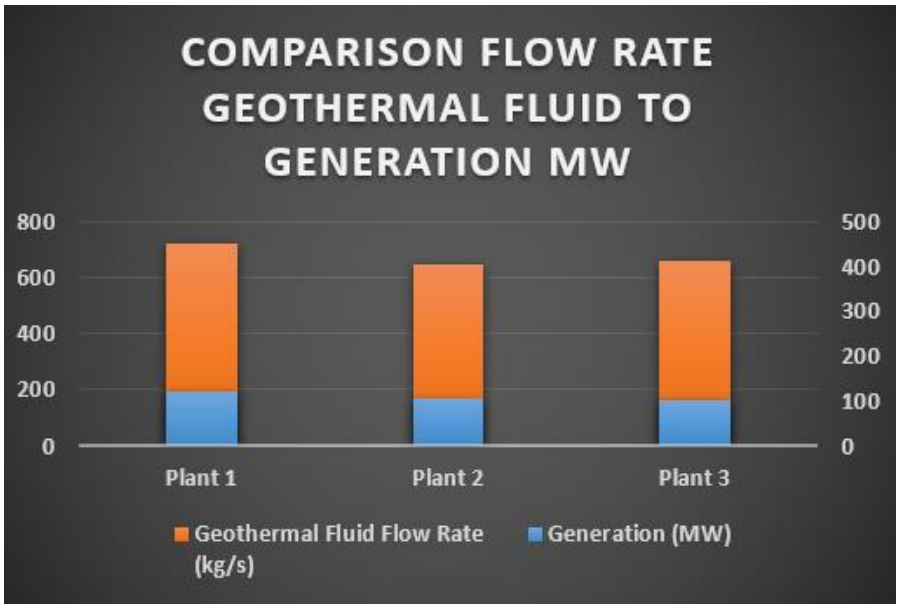


Figure 1: Illustration of display Clustered Chart for Comparation Flow Rate Geothermal Fluid to Output Generation MW from all Operator GPP.



Figure 2: Template Big-Screen "Indonesia Geothermal Dashboard" monitoring system.

OPC LINKED A VARIOUS CONTROL SYSTEM ACROSS THE OPERATOR GPP

OPC is a software interface interoperability standard that allows secure and reliable exchange of data between Windows programs and industrial hardware devices. It is platform-independent and ensures the continuous flow of information across multiple vendor devices.

Object Linking and Embedding (OLE) for process control (OPC) is a set of standards developed by a joint collaboration of leading automation industry suppliers. OPC's primary mission is to define a uniform interface for use with any organization or custom software package. Figure 3 shows the overall view of configuration OPC.

OPC was designed to provide a common bridge for Windows-based software applications and process control hardware. Standards define consistent methods of accessing field data from plant floor devices. This method remains the same regardless of the type and source of data. An OPC Server for one hardware device provides the same methods for an OPC Client to access its data as any and every other OPC Server for that same and any other hardware device. The aim was to reduce the amount of duplicated effort required from hardware manufacturers and their software partners, and from the SCADA (Supervisory Control And Data Acquisition) and other HMI (Human-Machine Interface) producers in order to interface the two. Once a hardware manufacturer had developed their OPC Server for the new hardware device their work was done to allow any 'top end' to access their device, and once the SCADA producer had developed their OPC Client their work was done to allow access to any hardware, existing or yet to be created, with an OPC compliant server.

OPC servers provide a method for many different software packages (so long as it is an OPC Client) to access data from a process control device, such as a PLC or DCS. Traditionally, any time a package needed access to data from a device, a custom interface, or driver, had to be written.

The purpose of OPC is to define a common interface that is written once and then reused by any business, SCADA, HMI, or custom software packages.

Once an OPC Server is written for a particular-device, it can be reused by any application that is able to act as an OPC client. OPC servers use Microsoft's OLE technology (also known as the Component Object Model, or COM) to communicate with clients. COM technology permits a standard for real-time information exchange between software applications and process hardware to be defined.

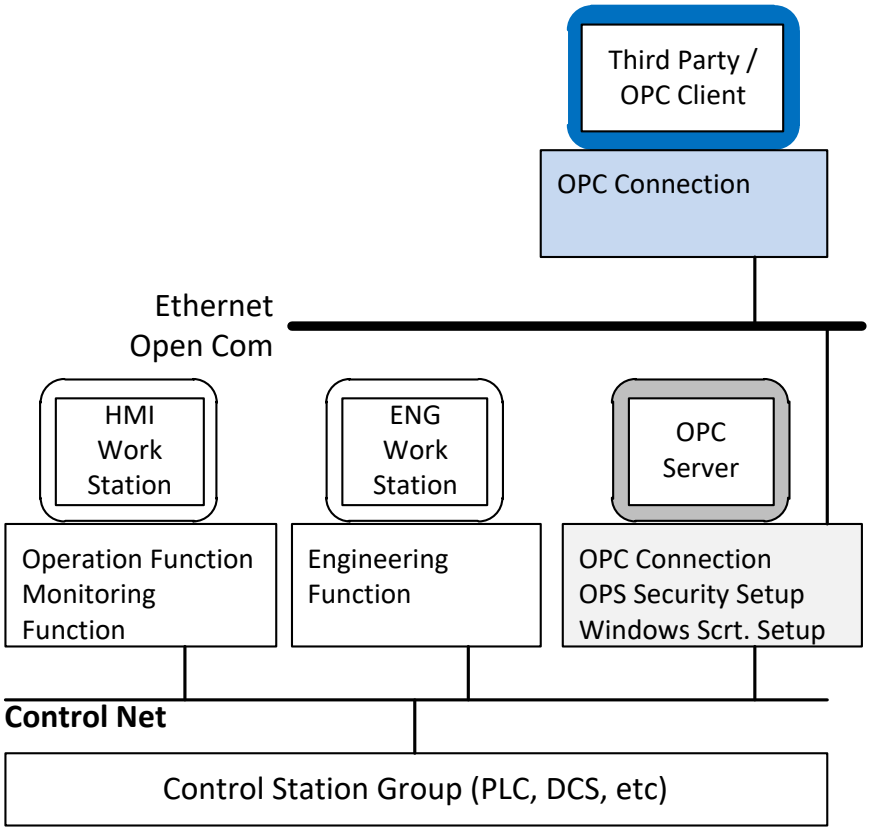


Figure 3: Overall View of Configuration OPC.

COM / DCOM

The underlying layer of the OPC Data Access (DA) specification is based on Microsoft's COM/DCOM technology, which enables inter-process communication in a variety of programming languages for the Windows operating system. In modern operating systems, processes are encapsulated to provide increased stability and security. COM provides a communication interface layer that allows local and remote procedure calls between processes. DCOM (Distributed COM) is the natural extension of COM to support communication among objects on networked computers.

DCOM can achieve security transparency, making distributed applications secure without any security-specific coding or design in either the client or the component. This is because DCOM lets developers and administrators configure the security settings for each component. Just as Windows operating systems allow administrators to set Access Control Lists (ACLs) for files and directories, DCOM also stores ACLs for components. These ACLs indicate which users or groups of users have access to a component of a certain class. Figure 4 shows the conceptual of OPC.

PIMS SYSTEM COMPONENTS

The system forms a multi-tier architecture with OPC servers normally providing the raw process data. This data is first managed and accumulated within the PIMS server. There may be multiple PIMS servers at this level. The data then becomes available to the PIMS/Explorer and/or the PIMS/Web applications. Figure 5 shows the PIMS communication through OPCS, while Figure 6 shows the PIMS systems component configuration.

CONCLUSIONS

While different industries often use different specialized devices, control systems, and applications, they all share a common and it can be captured by OPC interface. And all variables mapped by OPC Server shares to PIMS, which PIMS clients handle multiple PIMS servers transparently from each Geothermal Power Plant (GPP). Finally, all process and generation value from all Operator GPP integrated to big-screen and archived to big-data storage on the EBTKE Head Office, we called Geothermal Industry 4.0.

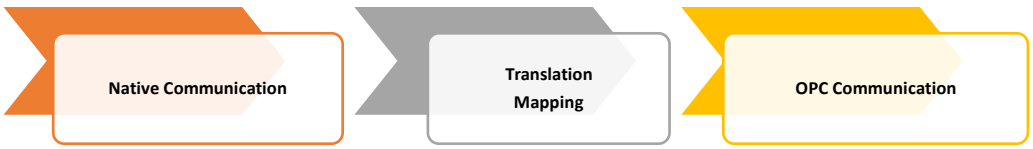


Figure 4: Conceptual OPC Communication based on Microsoft's COM/DCOM Technology.

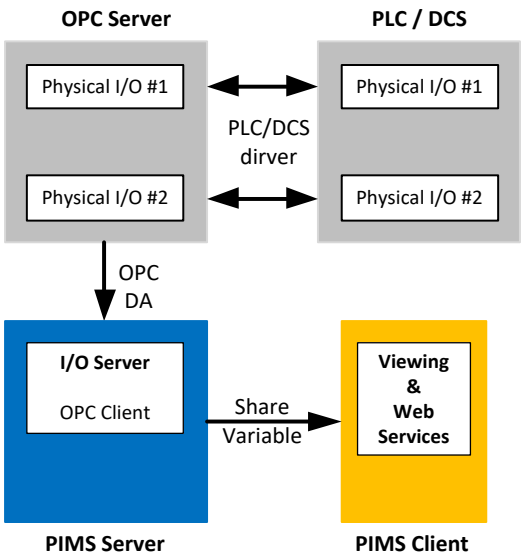


Figure 5: PIMS Communication with Local Control System through OPC.

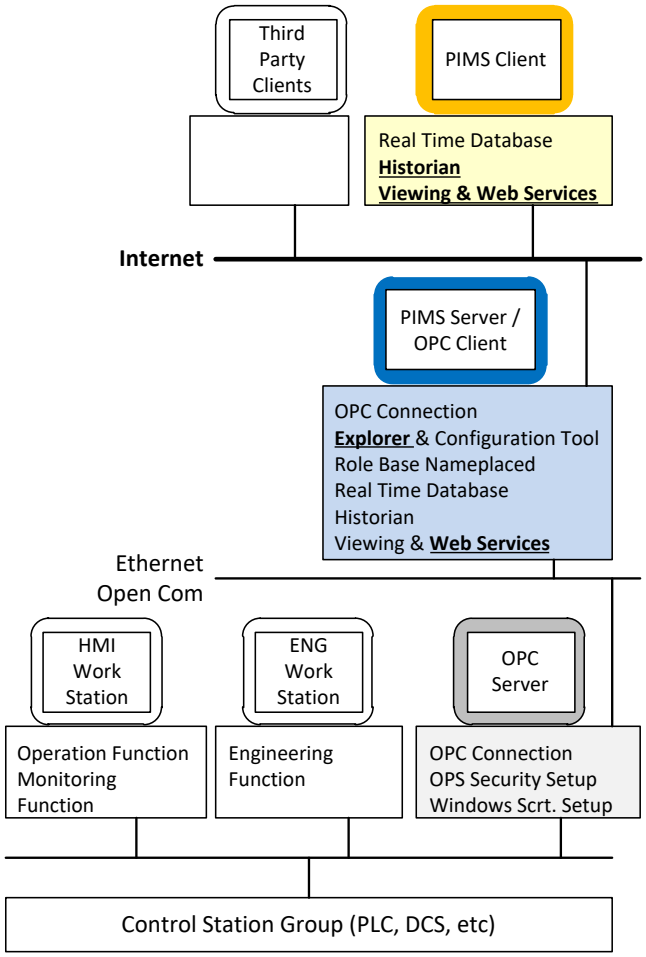


Figure 6: PIMS System Components Configuration.

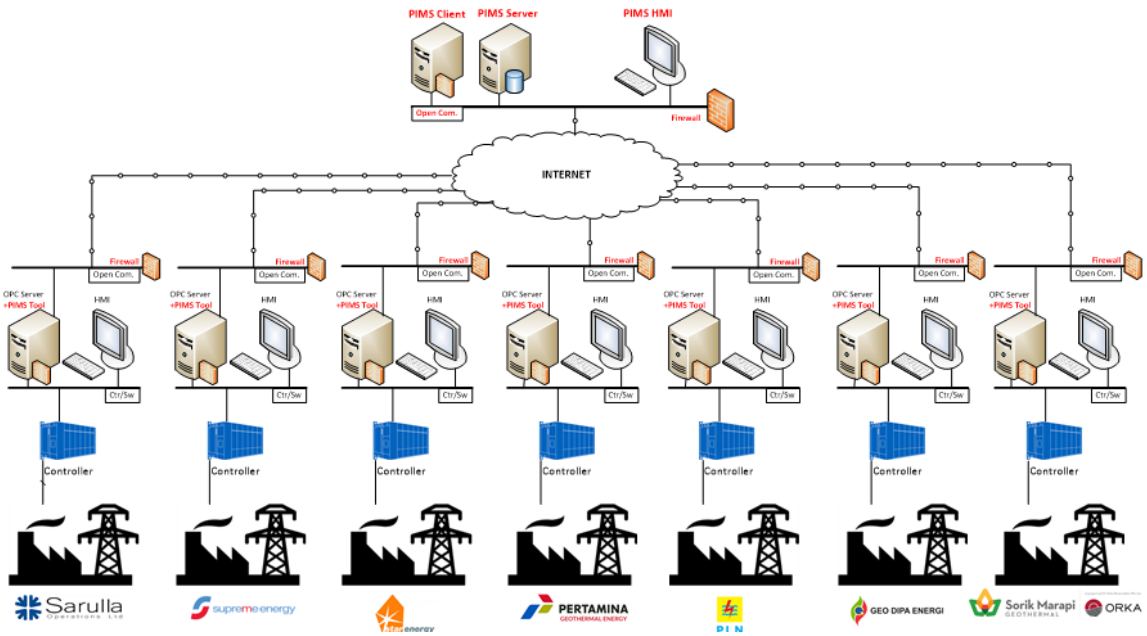


Figure 7: System Integration Communication and Configuration overall Indonesia's Geothermal Power Plant.

REFERENCES

Yokogawa, (2007), "Exaquantum/Plant Information Management System", 8th Edition February 05, 2007.

OPC Foundation, (2010), "OPC Foundation and MTConnect Institute Announce a Memorandum of Understanding", Archived from the original on June 6, 2016, Retrived May 30, 2019.

Dataparc, (2016), "3-Key Benefits of Plant Information Management Systems", http://www.dataparc.com/2015/06/16/3-key-benefits-of-plant-information-management-systems-pims/, Retreived May 30, 2019.

I-FIELD IMPLEMENTATION FOR ENERGY EFFICIENCY IMPROVEMENT IN DARAJAT UNIT II AND III POWER PLANTS

Wibisono Yamin, Otto Hari Karyawan, and Agus Riyadi

Star Energy Geothermal Darajat II, LIMITED
Sentral Senayan II, 24th Floor, Jl. Asia Afrika 8, Jakarta, Indonesia 10270
Email: wibisono@starenergy.co.id

ABSTRACT

Star Energy Geothermal Darajat II, LIMITED (SEGD II) operates steam field and two power plants, Unit II and III with capacity of 95 and 121 MW respectively and provides steam for Unit I which is operated by PT Indonesia Power.

To ensure a reliable and sustainable power plant operation, SEGD II implements i-field (integrated field) program that is composed of Real Time Simulation Technology (RTST) and Decision Support Center (DSC). This program offers data processing system, real-time analysis, and collaborative decision-making process; the first of its geothermal application in the world.

Through i-field, within the first five years of its implementation, SEGD II succeeded in improving energy efficiency (energy savings) and energy conservation (additional steam reserves) by a total of 1,258 GWh which was able to delay the need for drilling of 4 new wells. This total saving is equivalent to Rp113.5 billion. The program also succeeded in identifying additional 9.5 GWh energy saving opportunity (Star Energy Geothermal Darajat II, Limited, 2018). Utilization of appropriate technology that goes hand in hand with effective collaboration between departments has been successful in supporting the implementation of energy efficiency programs in SEGD II.

Keywords: Operation, improvement, Darajat geothermal field

BACKGROUND

Star Energy Geothermal Darajat II, Limited (SEGD II) operates Unit II and III power plants with a total generation of 216 MW and supplies geothermal steam to a 55 MW Unit I power plant owned by PT Indonesia Power. In 2018, total average house-load of Unit II and III was 7.25 MW (PT Rekayasa Engineering, 2018) . The electricity produced is transmitted to the Java-Madura-Bali grid. Figure 1 shwos the location of Darajat.

Sustaining electricity generation to meet grid energy demand with a reliable and efficient production system is the key to running profitable geothermal power plant. In line with this objective, SEGD II keep striving to improve performance of its production system, among others, by developing integrated performance analysis tool. This effort is done on the basis of the following contexts:

- Natural decline of steam reserves and aging production equipment after more than 20 years of exploitation period requires advanced energy efficiency and conservation efforts.
- The need for integrated reservoir management and plant operation strategy to achieve optimum and sustained production levels, both technically and commercially.
- The need for accurate, accessible and integrated production system monitoring and analysis in order to accelerate decision making process in response to changes of unit's performance and reserves conditions while maintaining operational reliability and efficiency.
- Management's commitment to implement energy efficiency and emission reduction. As stated in the SHE Policy, energy efficiency target is 40 MWH per year (Star Energy Geothermal Darajat II, LIMITED, 2018).

Several constraints faced in its implementation include:

- The spread of historian data on different platforms, without a common communication hub. Plant operation data such as gross generation, fluids flowrate, pressure and temperature, and performance of equipment are monitored through DCS and PI (Plant Information), while data and simulations of reservoir/wells capabilities are stored in excel-based platforms.
- Steam supply management occasionally is unable to take into account surface facilities capability in sufficient detail. This causes the optimization potential, or worse, the consequential generating disruption is not well identified during well maneuvers.
- Inaccuracies of steam flowrate measurement between the supply side (production wells) and receiver (power plant), which is not properly reconciled. On the other hand, the existing production system model was static. This results in incorrect predictions on production system performance and response.

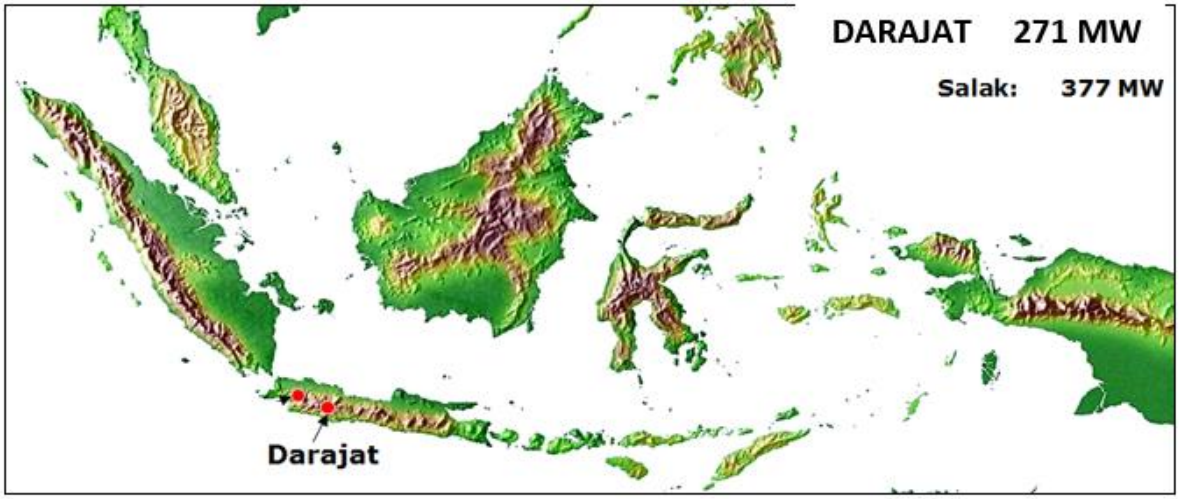


Figure 1: Location of Darajat Geothermal Field in Garut, West Java (Star Energy Geothermal Darajat II, Limited , 2018).

These challenges inspired the development of an integrated wells - surface facilities model that is directly connected to real-time monitoring system that provides:

a. Accurate process simulation tool to test various operation scenarios and to identify improvement opportunities
b. Steam availability forecasting in the respective scenario.
c. Data measurement reconciliation to detect and compensate meter inaccuracy.
d. Collaborative space to display key operating data in real-time basis, as well as KPI dashboard.

This development plan later became a project known as *i-field*, that was commissioned in 2014. The program consists of Real Time Simulation Technology (RTST) and Decision Support Center (DSC) – an integration of operation monitoring system, real-time simulation, and collaborative decision-making process.

DEVELOPMENT

Concept and Vision

To ensure reliability and availability of the plants, SEGD II has applied PI (Plant Information) system since 2007 that enables plant personnel to supervise and collect historical data of running plants. Nevertheless, FE and O&M team identified some opportunities to improve the current operations to achieve higher KPI out of: efficient steam consumption and longer reservoir lifetime, house-load reduction, higher reliability and availability, early identification of failure, and better Predictive Maintenance.

To achieve this target, an analytical layer of operations was deemed necessary to sits above supervisory control and historical data. Previously, the analytical process came in separate ways, incorporated in personal computers, and required some time to gather all information. In some cases, the time required to acquire data reached weeks and even months. When system upset occurs, delayed decision may impact to higher Loss of Production Opportunity (Figure 2). This condition triggered the development of *i-field* program, envisioned in Figure 3.

The program was set to allow privilege to drill deeper to study steam field and power plant, and increase system efficiency through a common platform, in prompt time.

This common platform was then titled: Decision Support Center (DSC), an integrated tool such as historian, trending wizards, overall data acquisition, real time KPI, simulation process to allow decisions to be made at shorter period of time, and to predict future problems. By then, the operations will be able to maximize production with detailed consideration of asset lifetime.

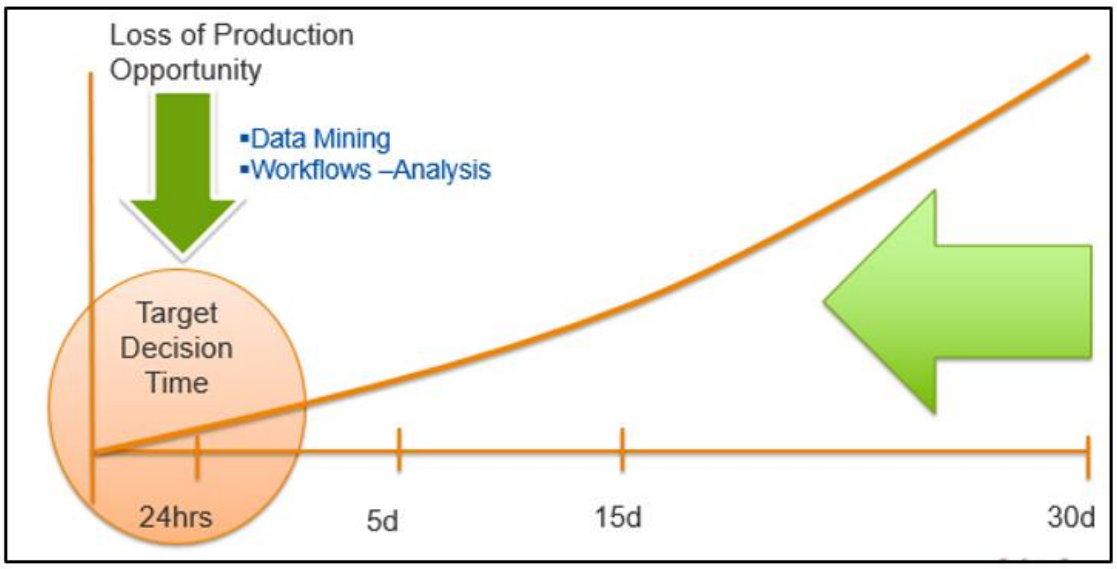


Figure 2: Loss of Production Opportunity Comes at Delayed Decision (Star Energy Geothermal Darajat II, LIMITED, 2014).



Figure 3: i-field Vision (Star Energy Geothermal Darajat II, Limited, 2018).

Design

Planning of *i-field* implementation started with infrastructure design, in 2013. In accordance with the initial concept that combines real time analytics tool and collaborative decision-making process, *i-field* structure design was planned with the following scope (Figure 4):

- Data interfacing protocol – allow data transfer across networks and various platforms (PI, reservoir data, maintenance data)
- Real time simulation layer – a computer model that runs dynamically and is continuously calibrated based on actual data.
- Web visualization – display KPI-based real-time analysis results to facilitate gap identification.
- Decision Support Center – facilitates collaborative, cross functional decision making.

Interconnection between data platforms and analytic tool within *i-field* program is shown in the infrastructure diagram on Figure 5.

Data taken in real time from various platforms is fed into the simulation tool that run dynamically and are continuously calibrated (RTST). Analysis results and recommendations are then displayed through KPI-based web visualization, so that operational gap can be known directly in real time. Based on the available information, decision making process will be carried out cross functionally involving all related

teams, in the Decision Support Center. After planning stage was approved by management, next development continued to execution phase.

Execution

Execution process took place through several steps:

1. Workshop involving multi-departments that directly supports production: Operation, Maintenance, Reservoir, and Engineering. This workshop aimed to agree on:
   - Operation and reservoir data needed in the simulation.
   - Scope of modeling: steam-field and power plant.
   - Details of model, software, hardware and installation detailed plans.
   - Dashboard for operating parameters and Key Performance Indicators.
   - Procedure or workflow of Decision Support Center.



Figure 4: i-field Implementation Scope (Star Energy Geothermal Darajat II, Limited, 2018).

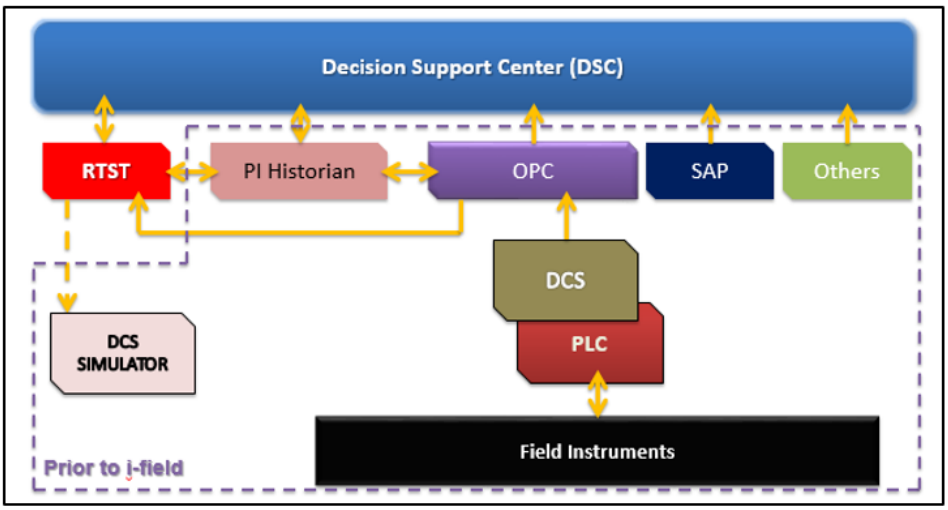


Figure 5: i-field Infrastructure (Star Energy Geothermal Darajat II, LIMITED, 2014).



Figure 6: i-field Implementation Milestones (Star Energy Geothermal Darajat II, Limited, 2018).

Selected software and aplication for *i-field* are:

- RTST: Optiramp® (Statistics & Control, Inc.) – able to perform mass and heat balance (process) and power/electrical models.
- Web Visualization: PI Vision® (OSIsoft, LLC) and OptiRamp® Web Analytics (Statistics & Control, Inc.) – additional feature of readily installed PI System™; a visualization tool to quickly, easily and securely access all PI data.

2. Software installation and continued with RTST (steam field and power plant) and Web Visualization dashboard development.
3. Hardware and Decision Support Center (DSC) room installation
4. Development of Standard Operating Procedure for decision making process carried out in the DSC.

The *i-field* installation was completed in October 2014. Execution milestones are shown in Figure 6.

FEATURES AND WORKFLOW

KPI Dashboard

Web visualization of KPI dashboard shows critical information of operating parameters such as:

- Power plants actual generation including carbon emission
- Generation outlook and expected date to reach Business Plan target
- Reliability, availability and efficiency of plants
- Exception reports such as unit's backpressure and production wells with changes above certain variance

This KPI-based visualization provides general overview on the actual health of steam field and power plants. The web visualization allows DSC team to drill deeper on each indicator to get the corresponding detailed information, just by a single click.

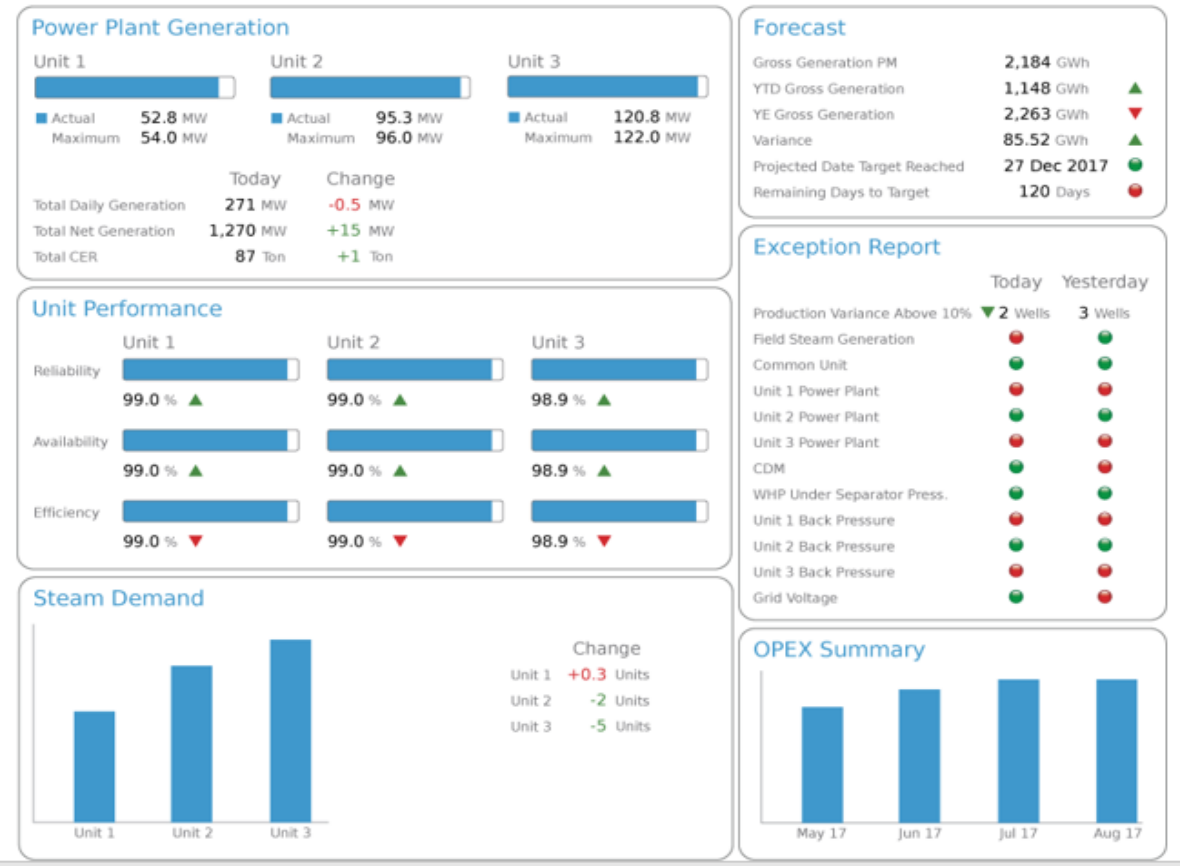


Figure 7: i-field KPI Dashboard (Star Energy Geothermal Darajat II, Limited, 2018).

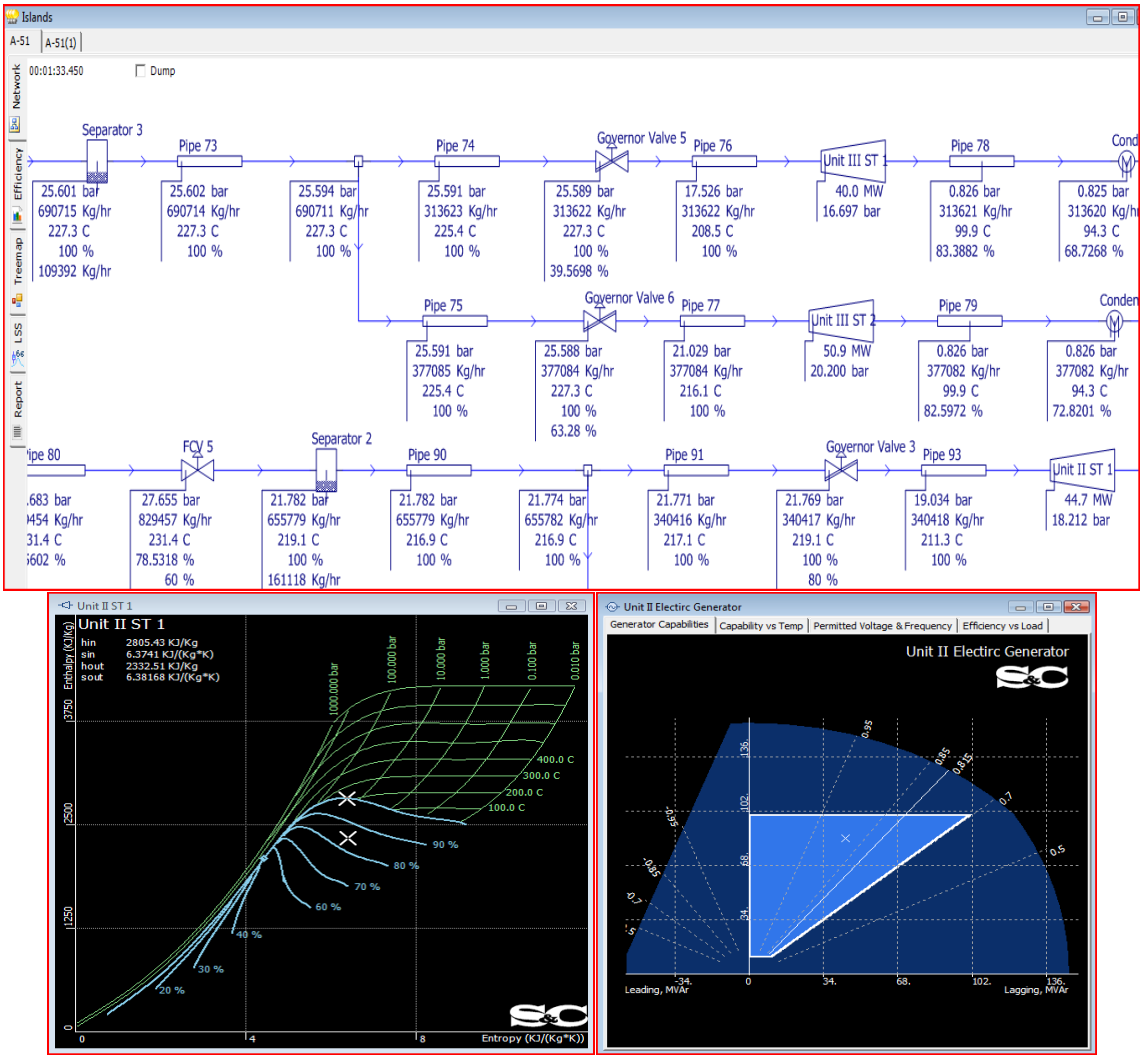


Figure 8: i-field Real Time Simulation Technology (Star Energy Geothermal Darajat II, Limited, 2018).

Real Time Simulation Technology Feature

Optiramp® suite for Real Time Simulation Technology (RTST) is made of several primary components (Statistics & Control, Inc., n.d.):

- Data Foundation that collects data from multiple sources—including Microsoft Excel, CSV files, Rational SCADA, Oracle databases, Microsoft SQL Server, and PI System—using standard OPC and ODBC protocols
- Modeling & Simulation accurately models system (both hydraulic and electrical processes) total value stream and dynamically simulates the operation in real time. This feature continuously updates via auto-tuning to reflect current conditions.
  Auto-tuning compares model coefficients with real-time data and automatically updates the model to become highly accurate, reducing the level of errors in the final model/simulation results. With this capability, the simulator is able to forecast system behavior and optimize the current operating mode.
- Optimization & Forecasting. The simulator has integrated optimization, predictive analytics, and forecasting algorithms. With this capability, the simulator is able to forecast system behavior and optimize the current operating mode.

Decision Support Center (DSC) Feature

DSC refers to a multimedia room where the centralized operations intelligence monitoring is located. KPI review, forecasting, process simulation and making decision are carried out collaboratively in the room.

Workflow

In order to sustain *i-field* implementation, organization capability (DSC Team) was established to drive the base business and start returning values to capital expended.

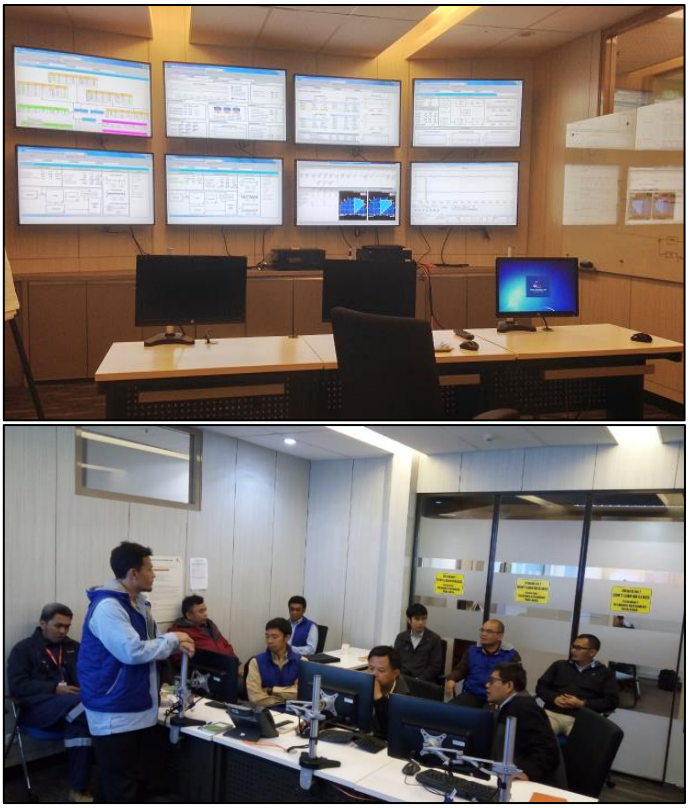


Figure 9: SEGD II DSC Room & Meeting (Star Energy Geothermal Darajat II, Limited, 2018).



Figure 10: i-field Process Workflow (Star Energy Geothermal Darajat II, Limited, 2018).

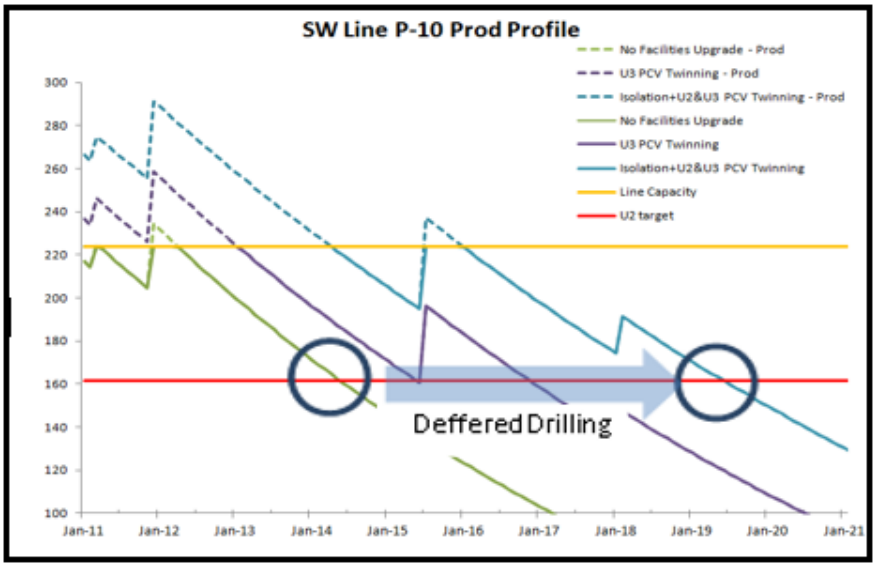


Figure 11: Optimization in Adding Steam Reserves (Star Energy Geothermal Darajat II, Limited, 2018).

DSC team leader facilitates daily discussion involving representatives' personnel from O&M, FE, and Reservoir/Production. DSC team member consists of:

- Operations Analyst - Leader
- Maintenance Analyst
- Facility Engineer
- Production Engineer

The collaborative discussion in DSC focuses on: increasing steam production, house-load

optimization, increasing the availability of steam reserves, and optimizing the ratio of steam consumption to production MW.

Daily meeting at DSC is set at 08.00 – 09.00, reviewing KPI Dashboard and system performance. Any gap or findings identified is transformed into action items (DSC opportunity list) to be acted upon by respected parties with agreed timeframe.

Inside the DSC, specific technical team can be assembled to handle particular operational issues/ concern. Specific tasks of the team include:

- Study/review certain operating maneuver plan by using RTST
- Discuss the studies progress in Generation Support Team (in relation to Steam Supply) and Plant Performance.
- Reliability Monitoring Team (in relation to Power plant).
- Deliver study report in Generation Support Team (GST) and Plant Performance & Reliability Monitoring Team (P2RM) meetings, where further actions are to be formulated.

i-field workflow is presented in Figure 10.

RESULTS AND SIGNIFICANCES

With Real Time Simulation technology (RTST), various scenario of steam field operation modes can be tested with accurate results, without restraints.

i-field (RTST) was utilized in verifying the outcome of a debottlenecking project in Darajat in 2014. Impact of the designed piping modification on lower well head pressures and higher production wells deliverability was modeled in numerous scenarios, prior to commissioning. The simulation was able to confirm the optimization impact on increasing steam reserves that was equivalent to the production of 4 wells, which in turn deferred the need for make-up well drilling to 2019 thus saved capital expenditure of USD 40 million. In addition, this method helped enhance the "Readiness to Operate" of the facility during handover.

With a real-time and integrated model between plant and wells, the simulator was capable to validate the accuracy of wells deliverability curves. This feature is instrumental in preventing over- or under-estimation of production capacity. This data is used by the Reservoir team to allocate resources for well testing activities. A valid prediction of well production will improve accuracy of plant generation forecast, reasonable business plan, and correct drilling plan.

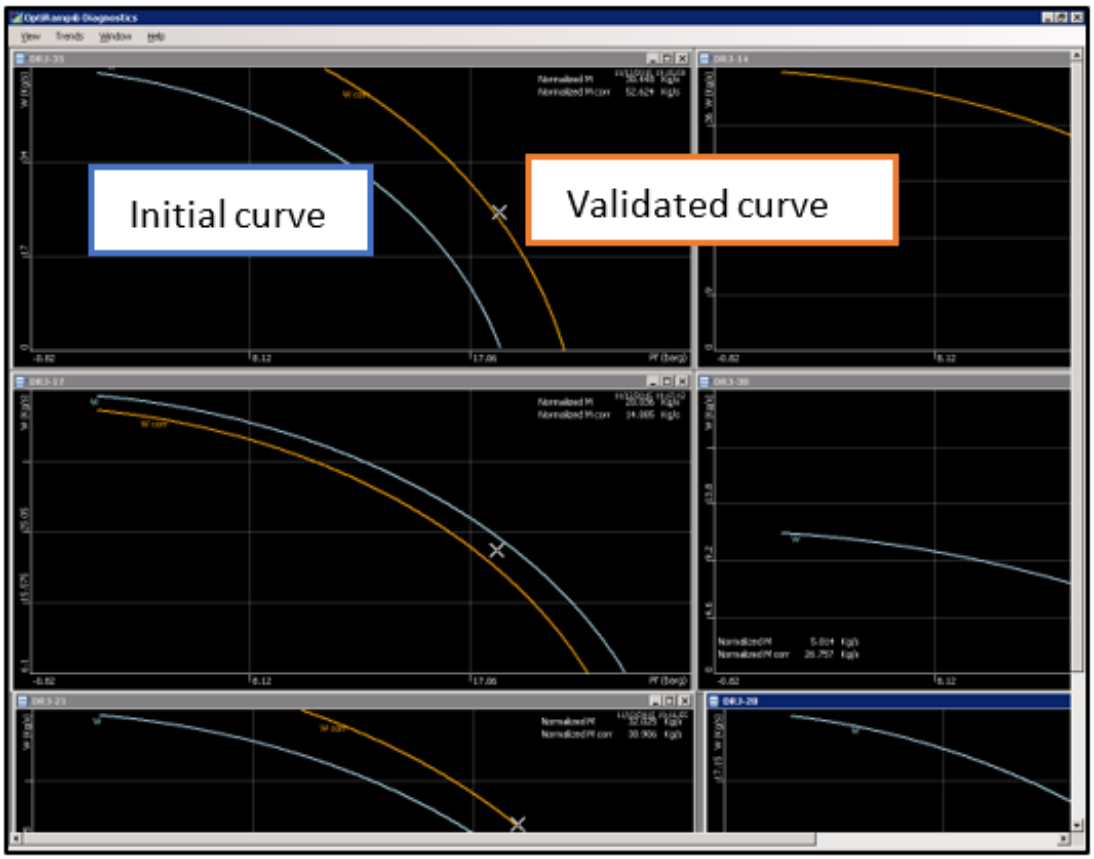


Figure 12: Auto Update of Well Deliverability Curves (Star Energy Geothermal Darajat II, LIMITED, 2015).

The next advantage of RTST is the ability to perform data reconciliation of the actual process variables. One of the examples was its capability to identify inaccuracy problems of steam flowrate measurement that helped facilitate Maintenance team in prioritizing resources for calibration.

The following table shows that the RTST was successful in detecting 8 inaccurate steam flow meters, out of a total of 30 installed in wellheads.

RTST has been used in predicting plants operating points that provide the most optimum combination of generation and steam reserves (length of exploitation period).

Simulation results show that (Star Energy Geothermal Darajat II, Limited, 2018):

- The optimum generation load set of Unit III is 118 MW instead of its rated capacity 121 MW.
- Although annual revenue is less than the baseload by USD 2 million, the number of wells for sustaining production for 20 years' period is fewer by 12 wells.
- Net savings reached USD 24 million.

This information provides alternative regarding optimum operation of the plant from full economic life cycle perspective.

Daily discussions in Decision Support Center has helped SEGD II to accelerate decision-making process and follow-up actions; this led to the completion of efficiency and reliability improvement efforts in shorter period of time. This can be seen from the results of *i-field* implementation against the initial target as below (Table 1):

Table 1: i-field KPI achievement (Star Energy Geothermal Darajat II, Limited, 2018)

KPI	Target	Result 2018	Remarks
Plants reliability	≥ 98%	99,88%	realized
Additional steam reserves	20 kg/s	49 kg/s	realized
House load reduction from initial	1%	7%	realized

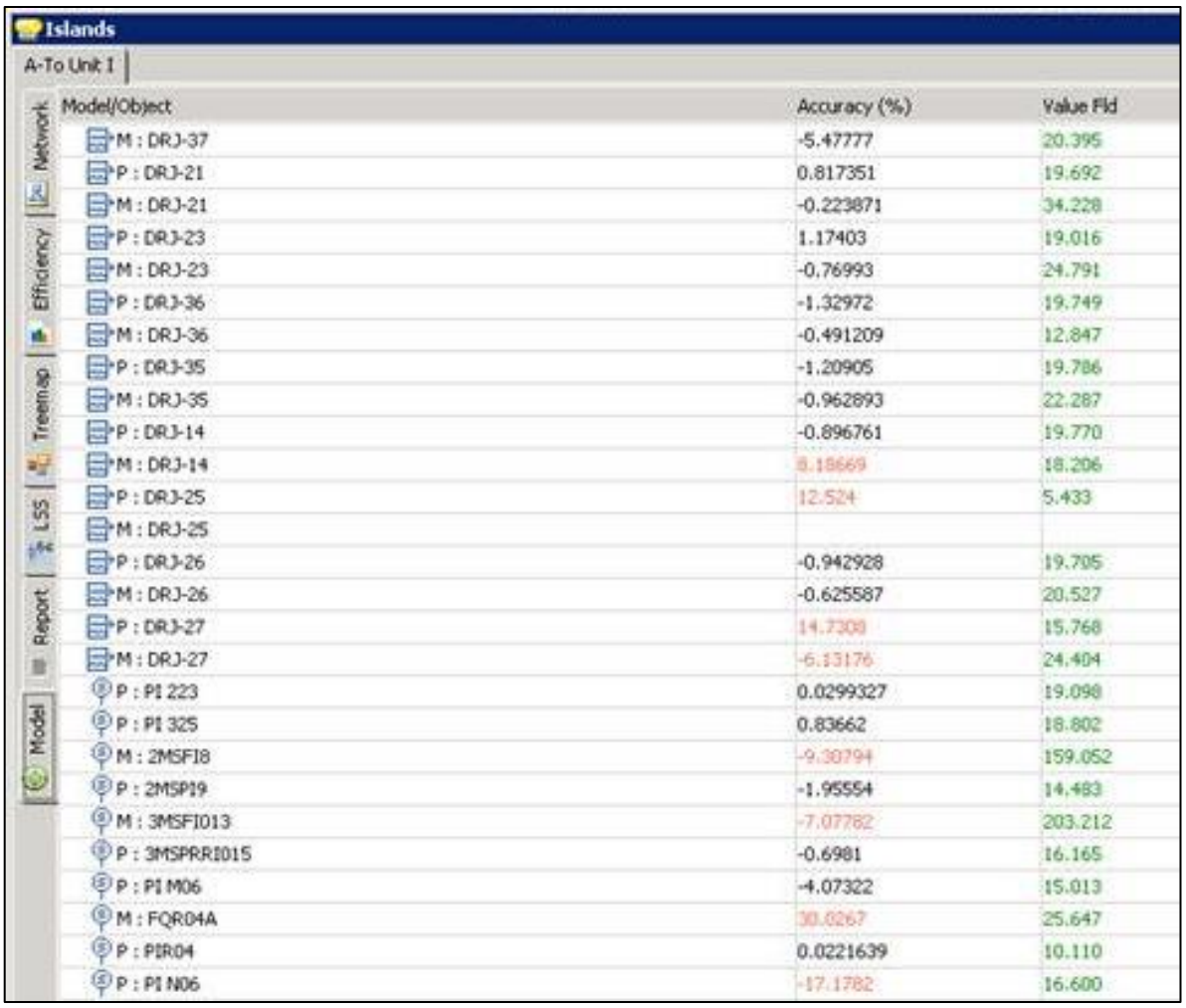


Figure 13: Instrumentation Error Detection (Star Energy Geothermal Darajat II, LIMITED, 2011).

The significance of *i-field* implementation for energy efficiency and conservation in SEGD II, which in turn reducing emissions, is driven by the following factors (Star Energy Geothermal Darajat II, Limited, 2018):

1. SEGD II is one of the 10 largest Geothermal Power Plants (GPP) in the world and also the first plant to achieve Clean Development Mechanism Certified Emission Reduction from the United Nations. This efficiency and emission reduction program are important in maintaining SEGD II position as a world-class company.
2. SEGD II production contract in Darajat steam field lasts until 2040, where the sustainability of operations requires reliable and efficient equipment, as well as excellent conservation of steam energy (reservoir).
3. This IT-based application of GPP operation management was awarded the 2018 National Energy Efficiency - Subroto Award in special innovation category. Subroto Award is the highest prize given by the Ministry of Energy and Mineral Resources of Republic of Indonesia to stakeholders who have outstanding achievements in advancing the energy sector.

CONTINUAL IMPROVEMENT

From the observation of *i-field* implementation over the past three years it is known that there are opportunities for greater impact through expanding the scope of simulations to other supporting production systems. In relation to this, SEGD II developed next plan as part of *i-field* continual improvement that comprises (Star Energy Geothermal Darajat II, Limited, 2018):

1. Include Gas Removal System in RTST. Improvement of ejector efficiency is expected to reduce motive steam consumption equivalent to 8 GWh per year.
2. Include Cooling Water System in RTST. Improvement of cooling efficiency has a potential to save 1.5 GWh equivalent per year from condenser vacuum betterment.
3. Include RTST module as part of operator/ engineer competency development training.

The total potential savings from energy efficiency improvement is amounting 9.5 GWh per year which is equivalent to USD 500,000 (Rp7 billion).

CONCLUSIONS

i-field is a vision to improve production with combination of advance data acquisition system, technology of real time simulation system and collaborative platform.

SEGD II *i-field* program consists of:

- Real Time Simulation Technology (RTST) to perform mass and heat balance (process) and power/electrical models dynamically.
- Web Visualization: platform to display KPI performance in real-time basis, such as: reliability and availability, steam consumption, and house-load.
- Decision Support Center (DSC), a multimedia room where the centralized operations intelligence monitoring, KPI review, forecasting, process simulation and decision making are carried out collaboratively.

Lesson learnt from *i-field* project execution and deployment:

- Access to real time and integrated process data and analytics tool, and fit-for-purpose workflows will improve decision making capabilities.
- Proper Operation Assurance (OA) by involving stakeholders early in development stage, and selection of fit-for-purpose enabling technology, helps to ensure successful project outcome: “Readiness to Operate”.

i-field implementation provides benefits to the Operation and Reservoir Team with:

- Initial identification of potential failures.
- Predictive Maintenance planning.
- More efficient steam consumption and increase of steam reserves.
- Identification of optimum plants operating point.
- Sustainable development provides potential savings of 9.5 GWh per year.
- Real time well decline rate monitoring; more than prediction.
- Steam buffer capacity calculation for better forecasting and business planning.

REFERENCES

PT Rekayasa Engineering, (2018), "Laporan Akhir Audit Energy Star Energy Geothermal Darajat II, Limited". Jakarta: PT Rekayasa Engineering.

Star Energy Geothermal Darajat II, Limited, (2018), "Asset Overview, s.l.: Star Energy Geothermal Darajat II, Limited".

Star Energy Geothermal Darajat II, LIMITED, (2011), "Base Business: GPO i-field implementation (UPDATE 2014 AND

PLANNING)", Jakarta: Star Energy Geothermal Darajat II, LIMITED.

Star Energy Geothermal Darajat II, LIMITED, (2014), "Base Business: i-field Communication package for GPO-I implementation", Jakarta: Star Energy Geothermal Darajat II, LIMITED.

Star Energy Geothermal Darajat II, LIMITED, (2015), "i-field implementation 2015 Update", Jakarta: Star Energy Geothermal Darajat II, LIMITED.

Star Energy Geothermal Darajat II, LIMITED, (2018), "Environmental Policy, Garut: Star Energy Geothermal Darajat II, LIMITED".

Star Energy Geothermal Darajat II, Limited, (2018), "Implementasi i-field Dalam Peningkatan Efisiensi Energi Pada PLTP Darajat Unit 2 dan Unit 3". Jakarta, s.n.

Statistics & Control, Inc., n.d. Optiramp Digital Power Solutions. [Online] Available at: http://optiramp.com/digital-power [Accessed 6 23 2019].

GEOTHERMAL WELL ANALYSIS USING UNDERBALANCE DRILLING MODULE ON LANDMARK HALLIBURTON WELLPLAN SOFTWARE

Wisnu Adi Nugroho[1], Ali Imran Rangkuti[1], Fernando Marpaung[2], Samuel Halomoan Silitonga[2], Frankly Hardytanputra[3], Muhammad Sinar[4], Beno Marfianto[5], Randy Janitra[6], Muhammad Taufiq Qurrahman[6], and Deshinta Putri[6]

[1]Pertamina Drilling Service Indonesia, Jakarta
[2]Landmark Halliburton, Tangerang
[3]Institut Teknologi Bandung, Bandung
[4]Universitas Trisakti, Jakarta
[5]Institut Teknologi Sains Bandung, Bandung
[6]Geotech System Indonesia
Email: Wisnu.nugroho@pertamina.com, Ali.rangkuti@pertamina.com, Fernando.Marpaung@halliburton.com, Samuel.HalomoanSilitonga@halliburton.com, franklyhardytanputra@gmail.com, muhammadsinar17@yahoo.com, benomarfianto@gmail.com, randy_janitra@yahoo.com

ABSTRACT

Geothermal drilling faced many challenges due to its natural characteristics, the formation characteristic is a sub-normal type formation which has highly fractured rock properties. If we use normal drilling methods, we will face the most common problems e.g. lost circulation and stuck pipe. Hence, Underbalance Drilling method is performed. Underbalance drilling is the most effective way to drill geothermal wells. Underbalance drilling is a method where the hydrostatic head of the drilling fluid is intentionally designed to be lower than the pressure of the drilled formations, in this case we use foam injection and air drilling methods. This paper aims to describe the study case based on Underbalance Drilling Module Application on a geothermal well execution using Landmark Halliburton Wellplan Software from one of our clients.

Landmark Halliburton Well plan Software provided the module where user will be able to optimize liquid pump and gas injection rates and also control the bottom and surface pressure. For the result, user can quickly determine pressure, ECD, velocity and cutting transport ratio profiles, also other relevant hydraulic calculations for multi-phase fluid circulation operations. Landmark Halliburton Wellplan Software were proven to be able to provide the best and the most efficient option for client's operation wells.

Keyword: Wellplan Software, Halliburton, Underbalance Drilling, Foam, Air Drilling

INTRODUCTION

Basically, Geothermal drilling techniques similar with oil and gas drilling, what differs them is the rock formation. In Indonesia, Geothermal field characteristic igneous rocks associated with volcanos where igneous rocks have the compact characteristic but has high permeability towards fractures. Due to potential of fractures to be found, hence the potential of loss circulation or no return flow equal no cutting is higher than on oil and gas field (sedimentary rocks) where when the loss circulation happened, cutting won't be uplifted and increasing the stuck pipe potential. To prevent stuck pipe, hole cleaning needs to be done. Hole cleaning performed when lost circulation is using aerated drilling and foam also known as underbalance drilling due to lower density compared to water density (1 gr/cc).

The hydrostatic head of the drilling fluid during underbalanced drilling (UBD) is intentionally designed to be lower than the pressure of the formations that are being drilled. Underbalanced drilling prevents formation damage that can occur during conventional, or overbalanced drilling processes.

The negative differential pressure obtained during underbalanced drilling between the reservoir and the wellbore encourages production of formation fluids and gases. In contrast to conventional drilling, flow from the reservoir is driven into the wellbore during underbalanced drilling, rather than away from it.

Although initially more costly, underbalanced drilling, also known as managed-pressure drilling, reduces common conventional drilling problems, such as lost circulation, differential sticking, minimal drilling rates and formation damage. Additionally, underbalanced drilling extends the life of the drill bit because the drilling gases cool the bit while quickly removing cuttings.

The hydrostatic head of the fluid may naturally be less than the formation pressure, or it can be induced by adding different substances to the liquid phase of the drilling fluid (generally), such as: Natural gas, Nitrogen and Air.

THEORETICAL

Because air is the ideal low density drilling medium, air drilling provides many advantages in underbalanced drilling methods. To achieve the best results and greatest economy, several factors must be considered for air drilling. The best conditions for air drilling involve hard, dry formations that produce relatively few formation liquids. Once the formation is completely dry, or the influx of liquids is small enough to be absorbed in the air stream, the drill cuttings return to the surface as dust. The process allows for the immediate and sustained evaluation of hydrocarbons. Figure 1 shows the operating envelope.

Other advantages of air drilling are low cost, increased rate of penetration, extended bit life, superior control in cavernous and lost circulation areas, and minimal damage to liquid-sensitive pay zones. Figure 2 shows the minimum oxygen of combustion

The drill string always remains on the bottom when gas is encountered, which is a tremendous advantage in well control. If no gas is in the hole when a trip is made, no gas will be in the hole when the new bit is returned to the bottom. Sometimes holes filled with mud will allow gas to enter the well bore because of reduced hydrostatic pressure, creating well control issues. With air drilling, gas that has already been penetrated will enter the well bore on trips, but the amount of gas is a known quantity that can easily be jetted away from the rig and operating personnel. Increased rate of penetration occurs because the low density of air or gas used minimizes hydrostatic pressure and aids with fracturing. The rate of penetration in air drilling has been recorded at up to 200 ft/hr compared to 30 ft/hr in conventional drilling.

To establish pressure control, a rotating control head with a rotating inner seal assembly is used in conjunction with the rotating table. An important factor to successful underbalanced drilling, drilling and completion operations must remain underbalanced at all times during operation. To accomplish this, pre-planning and onsite engineering are critical to the success of underbalanced drilling procedures.

During underbalance drilling, there are some problem that usually happens. Underbalanced Drilling Problems such as:

1. Underbalanced Drilling cannot be used in most shale environment;
2. Wellbore stability problems. It happens when Wellbore pressures are lower in underbalanced drilling than overbalanced drilling operations; this may cause wellbore instability due to mechanical borehole collapse.
3. Liquid Influx problem. Liquid influx includes water inflow and oil production. Water inflow can cause mud ring problems during air/gas drilling, the mud ring can grow till the drill string is trapped. Excess water inflow increases flowing bottom-hole pressure and reduce gas velocity resulting in lowering carrying capacity which cause stuck pipe.
4. The surface equipment should be able to handle the maximum rate of oil production safely at certain pressure, if the oil production rate is too high to handle, the underbalanced drilling should be converted to overbalance drilling.
5. Directional Drilling Difficulties;
6. Safety Issues such as downhole fires/explosions and vibration & noise.
7. Economic considerations.

For this case Wellplan software provide many modules for UBD analysis, such as UB Operating Envelope, UB Minimum Oxygen Combustion, UB Pressure Profile, UB Mixture Density, UB Liquid Hold Up, UB annular Velocity Profile, UB Cuttings Transport Ratio, UB Gas Deviation Factor, UB Fanning Friction Factor, UB Flow Pattern, UB Summary, Foam Quality, and Foam Viscosity.

DATA

The main problem in this case is that there is total zone loss on the drilling operation in the hole section caused user need to replace the mud with air drilling but doesn't change the drilling tools.

The following data from well-x that needs to be input on underbalance module:

1. Trajectory & Casing (See on Appendix-A).
2. BHA.
3. Circulating Pressure & Pump.

RESULT AND DISCUSSION

Result

Result from simulation using Wellplan Underbalance Module can be seen using several important parameters in underbalance drilling such as:

1. Operating Envelope

Operating envelope showed the result of Gas Rate range and Optimum BHP on certain Liquid Rate (foam). In this case, Wellplan suggests to use Liquid Rate at the rate of 850 gpm, hence we will be able to obtain lower BHP (Table 1 – 3).

Table 1: Bottom Hole Assembly Data in well-x.

Section Type	Length	MD	OD	ID
	(ft)	(ft)	(in)	(in)
Bit	1	7,545.90	12.25	
Mud Motor	29.53	7,544.90	8	3
Sub	3	7,515.40	8	3.24
Drill Collar	28.67	7,512.40	8	2.5
Sub	3	7,483.70	7.92	3.24
Sub	3	7,480.70	8	3
Drill Collar	90	7,477.70	8	2.5
Sub	3	7,387.70	6.625	3
Drill Collar	90	7,384.70	6.5	2.5
Heavy Weight	210	7,294.70	5	3
Jar	6.34	7,084.70	6.5	2.75
Heavy Weight	501.84	7,078.40	5	3
Drill Pipe	6,576.52	6,576.50	5	4.276

Table 2: Specification Pump 1 in Well-x.

Pump Name	National - 10-P-130 - TRIPLEX	
Volume per Stroke	4.309	gal/stl
Max. Speed	140	spm
Max. Discharge Pressure	3,325.00	Psi
HorsePower Rating	1,300.00	hp
Volumetric Efficiency	100.00	%
Max. Pump Rate	603.30	gpm

Table 3: Specification Pump 1 in Well-x.

Pump Name	Gardner Denver - PZL (PZ-11)	
Volume per Stroke	4.74	gal/stl
Max. Speed	115	spm
Max. Discharge Pressure	4,529.00	Psi
HorsePower Rating	1,600.00	hp
Volumetric Efficiency	100.00	%
Max. Pump Rate	545.20	gpm

2. Minimum Oxygen for Combustion

This feature shows the range percentage of oxygen analyzation that wouldn't cause oxygen combustion.

3. Pressure Profile

Shows pressure profile analyzation on string and annulus towards pore pressure and fracture gradient.

4. Mixture Density

Shows gas-liquid fluid density analyzation towards depth, temperature, and pressure well.

5. Liquid Holdup

It shows air fluids rate simulation (aerated and mud), shows when the fluids were injected from the surface. Mud will flow faster than aerated drilling this caused by density mud is higher than aerated fluids. Nevertheless, when the backflow to annulus through surface, aerated fluids will flow faster than the mud due to lower aerated fluids density.

6. Annular Velocity Profile

Annular velocity profile shows flow rate between fluids mixture (mud and aerated fluids), fluids (mud), gas (aerated fluids), and cutting. We can see than aerated fluids graphics has highest velocity compared to another graphics due to the lowest density. Cutting graphic coincide with liquid graphic shows that cutting flow rate is synchronize with the liquid.

7. Cuttings Transport Ratio

Shows cutting transport ratio towards pump rate used.

8. Gas Deviation Factor

Gas deviation shows transformation of liquid phase into gas. Simulation performed thorough inputting temperature values as 80 F and rate injection as 1500 scfm. We can see that fluids still on its liquid phase (Gas deviator factor <1).

9. Fanning Friction Factor

Fanning friction factor shows friction experienced by fluid when inside the string (showed by green line), drilling fluid friction inside the string is bigger than inside the annulus due to annulus surface (open hole. We can also see when the fluids are reaching the casing shoe of the previous track where there's a change in open hole diameter from open hole to the casing.

10. Flow Pattern

Shows flow pattern on annulus and string towards certain gas rate. Figure 3 shows the annular velocity profile.

11. Summary

Shows final results of underbalance system, liquid holdup, and circulation time.



Figure 1: Operating Envelope as one of the results from Wellplan Underbalance Module.

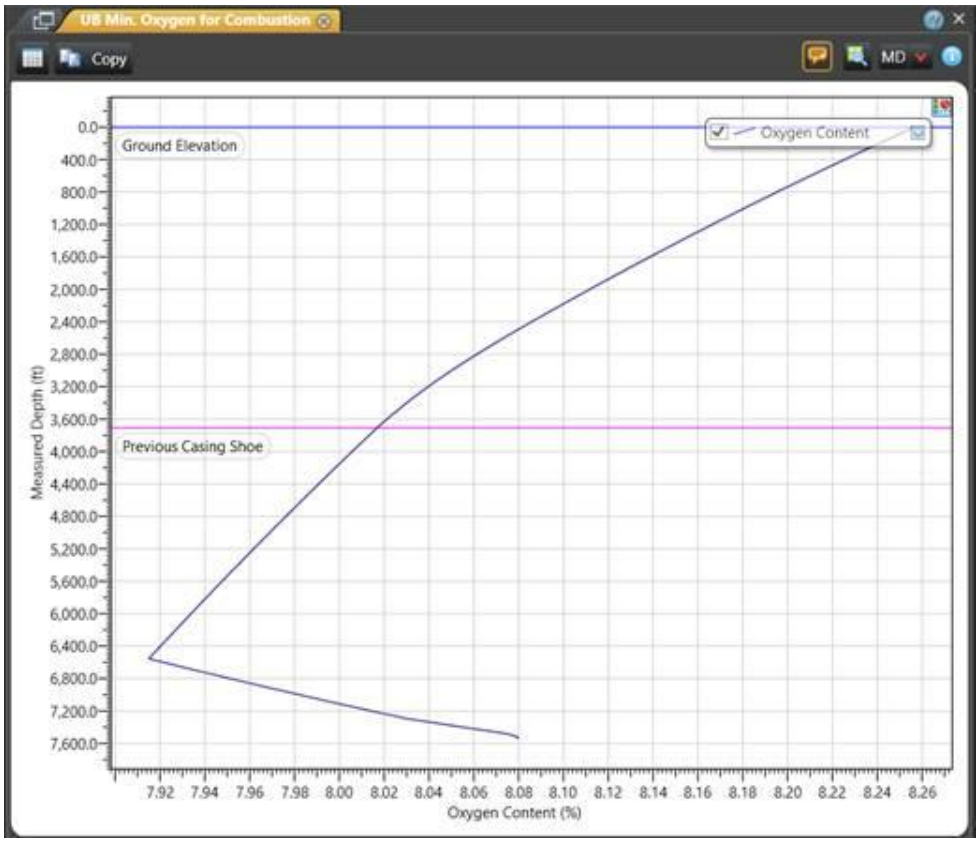


Figure 2: Minimum Oxygen for Combustion as one of the results from Wellplan Underbalance Module.

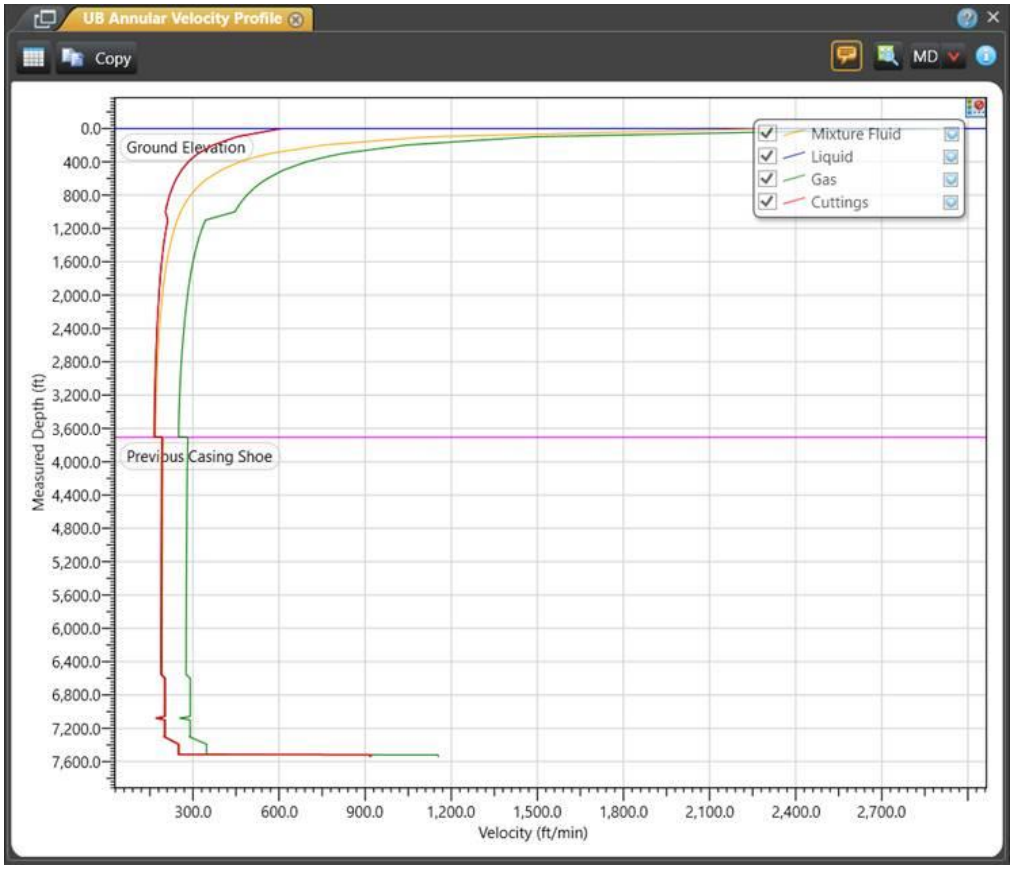
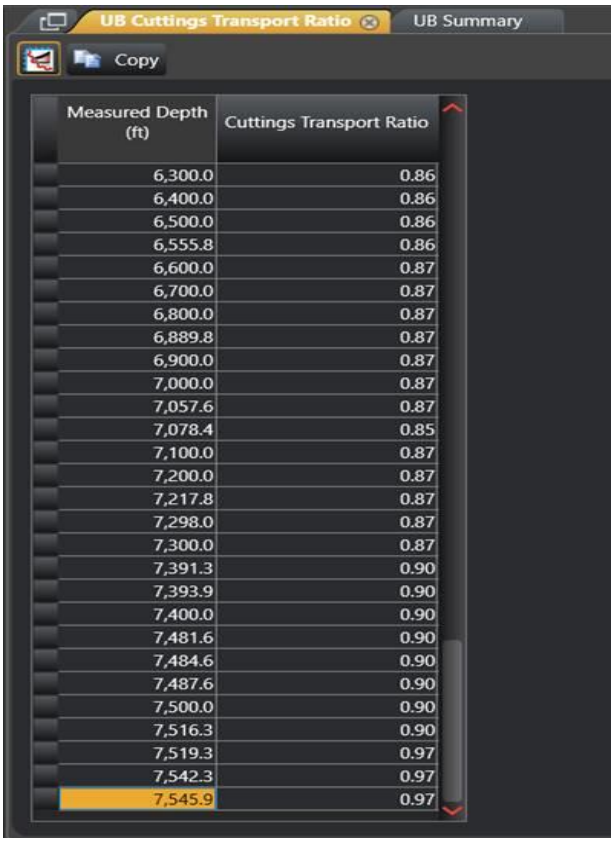


Figure 3: Annular Velocity Profile as one of the results from Wellplan Underbalance Module.



Measured Depth (ft)	Cuttings Transport Ratio
6,300.0	0.86
6,400.0	0.86
6,500.0	0.86
6,555.8	0.86
6,600.0	0.87
6,700.0	0.87
6,800.0	0.87
6,889.8	0.87
6,900.0	0.87
7,000.0	0.87
7,057.6	0.87
7,078.4	0.85
7,100.0	0.87
7,200.0	0.87
7,217.8	0.87
7,298.0	0.87
7,300.0	0.87
7,391.3	0.90
7,393.9	0.90
7,400.0	0.90
7,481.6	0.90
7,484.6	0.90
7,487.6	0.90
7,500.0	0.90
7,516.3	0.90
7,519.3	0.97
7,542.3	0.97
7,545.9	0.97

Figure 4: Cutting transport ratio on Wellplan Underbalance Module.

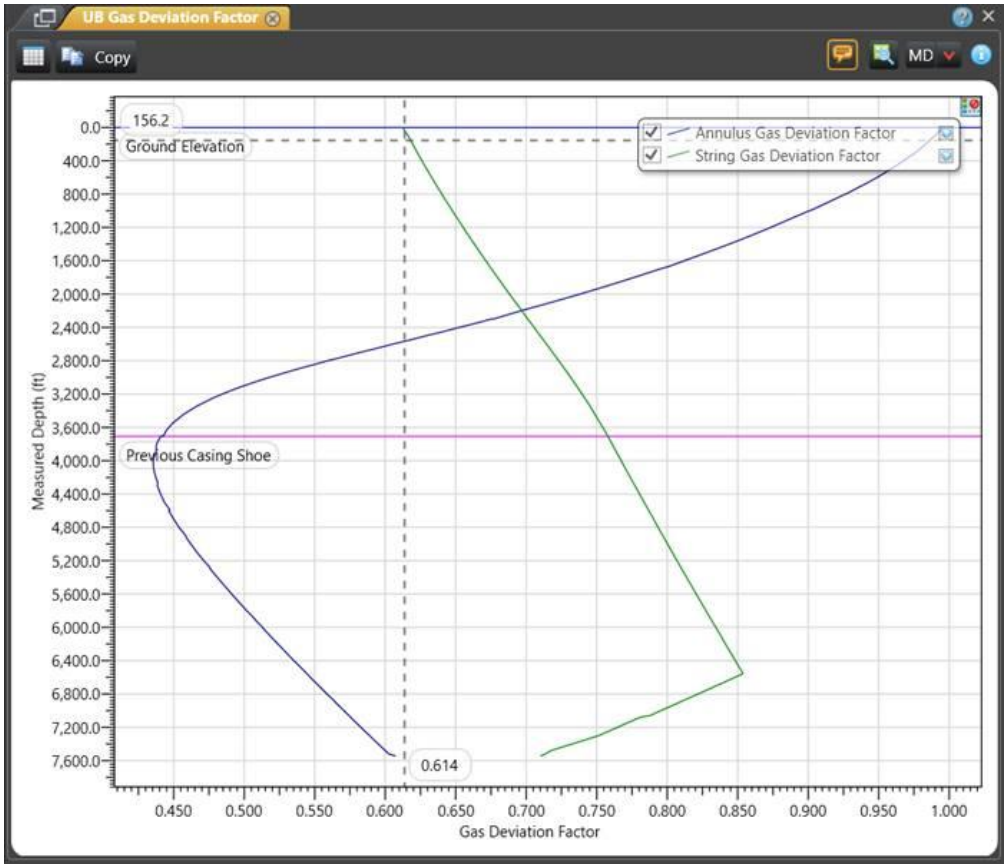


Figure 5: Gas Deviation Factor on Wellplan Underbalance Module.

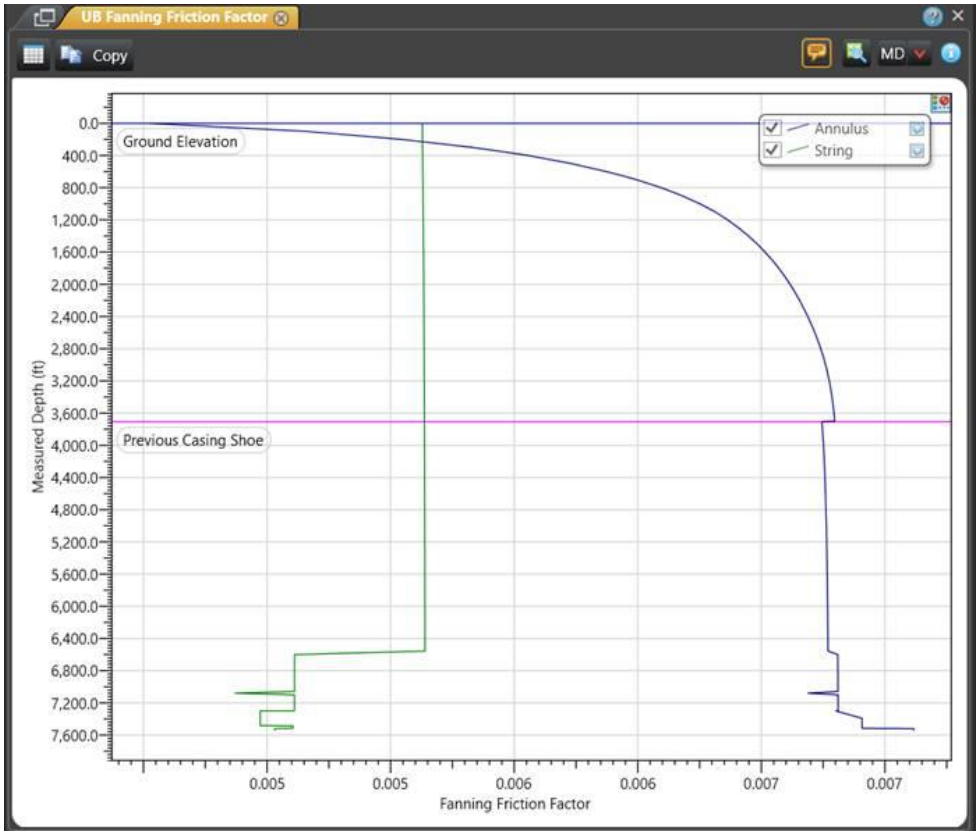


Figure 6: Fanning Friction Factor on Wellplan Underbalance Module.

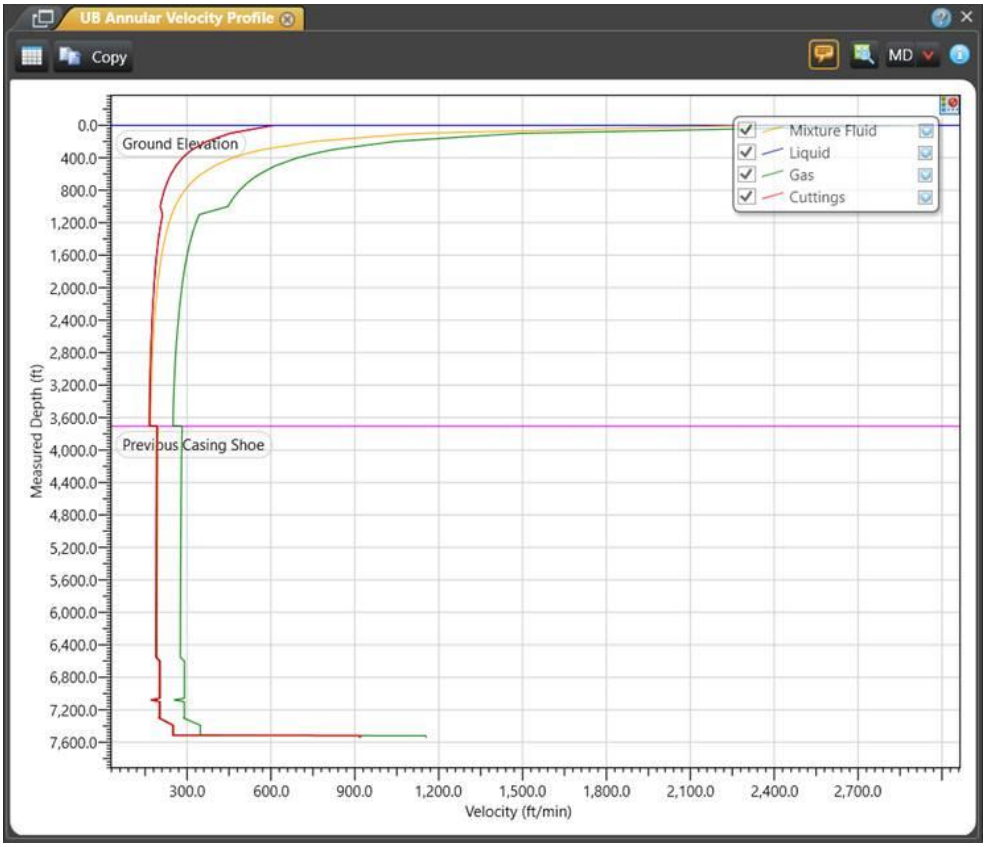


Figure 7: Flow Pattern on Wellplan Underbalance Module.

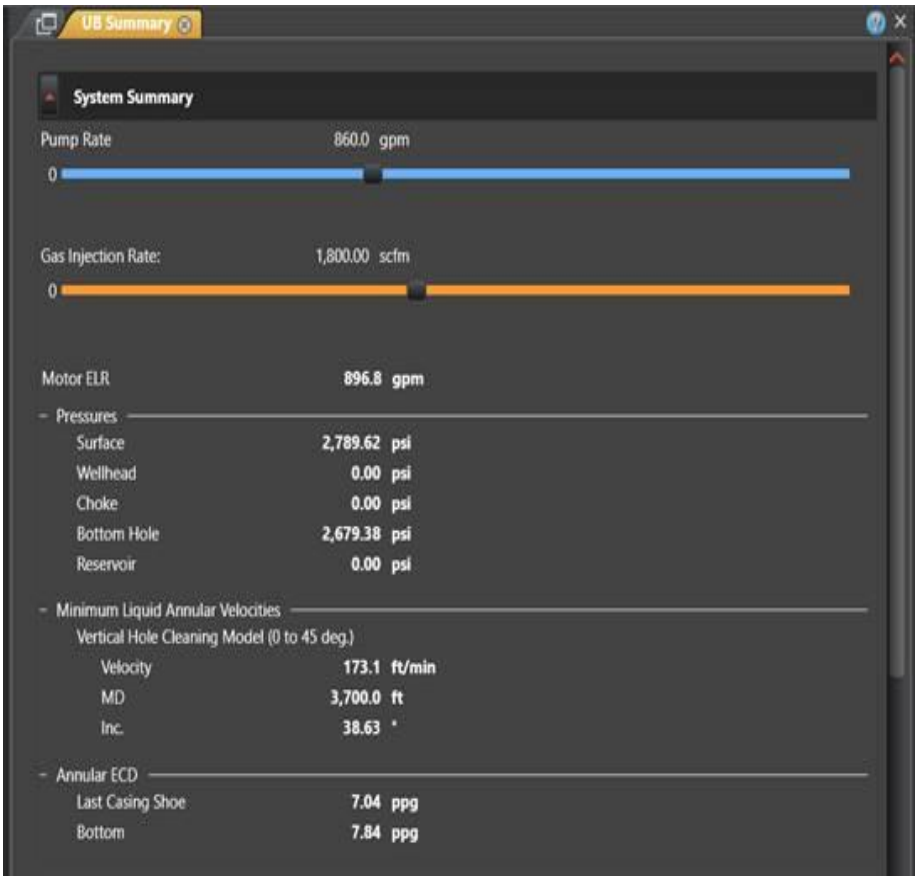


Figure 8: Summary showed by Wellplan Underbalance Module.



Figure 9: Summary showed by Wellplan Underbalance Module.

After that, a comparison is made between the simulation value and the actual value, then see what the error value is.

Table 4: Comparison between fluid simulation vs fluid actual after run software.

	Fluid Simulation	Fluid Actual	Error Value (%)
Name	Water Polymer	Water Polymer	
Mud Base Type	Water	Water	
Base Fluid	Water	Water	
Rheology Model	Power Law	Power Law	
Temperature (F)	80	80	n/a
Pressure (psi)	14.7	14.7	n/a
Density	8.7 ppg	8.75 ppg	0.571
n'	0.5	0.5	0
K'	0.02089	0.02089	0

Table 5: Comparison between summary simulation vs summary actual after run software.

	Summary Simulation	Summary Actual	Error
Pump Rate (gpm)	860	860	
Gas Injection (scfm)	1800	1800	
Press. Surface (psia)	2789.62	2075.82	34.39
Press. Wellhead(psia)	0	0	
Press. Choke (psia)	0	0	
Press. Bottom Hole (psia)	2679.38	2181.3	22.8
Press. Reservoir (psia)	0	0	
Velocity (ft/min)	173.1	186.4	7.1
MD (ft)	3700	7100	
Inc (°)	38.63	39	0.95
Annular ECD Last Casing Shoe	7.04	4.69	
Annular ECD Bottom	7.84	6.38	
Foam Surface Annulus	0.25	0.9497	73.68
Foam Surface String	0.95	0.1087	88.56
Foam Bottom Annulus	0.96	0.087	90.94
Foam Bottom String	0.96	0.0686	92.85

Table 6: Comparison between simulation vs actual after run software.

Cutting Transport Ratio				**Error**
Simulation		**Actual**		
MD (ft)	**Ratio**	**MD (ft)**	**Ratio**	**(%)**
6500	0.86	6500	0.915	6.01
6600	0.87	6600	0.917	5.13
6700	0.87	6700	0.92	5.43
6800	0.87	6800	0.92	5.43
6900	0.87	6900	0.92	5.43
7000	0.87	7000	0.92	5.43
7100	0.87	7100	0.923	5.74
7200	0.87	7200	0.92	5.43
7300	0.87	7300	0.92	5.43
7400	0.9	7400	0.921	2.28
7500	0.9	7500	0.922	2.39

CONCLUSION

Simulation performed using Wellplan software specifically underbalance module on this research is similar with actual data when underbalance drilling is performed. It's also validated with the actual data with error margin in Table-4, Table-5, Table-6. Other concerns beside the analysis could create an error on the list. Otherwise, Landmark Underbalance Module in Wellplan Software could give users a very accurate and efficient ways for the operation activity.

REFERENCES

Al-Yami, A.S., Schubert, J., Medina, C., and Ok-Youn (2010), "Drilling Expert System for the Optimal Design and Execution of Successful Cementing Practices," paper IADC/SPE 135183 presented at the 2010 Asia Pacific Drilling Technology Conference and Exhibition held in Ho Chi Minh City, Vietnam, November 1-3.

Al-Yami, A.S., Schubert, J., and Beck, G. (2011). "Expert System for the Optimal Design and Execution of Successful Completion Practice Using Artificial Bayesian Intelegence" paper SPE 143826 presented at the 2011 Brasil Offshore Conference and Exhibition held in Macae, Brazil, June 14-17.

Korb, K., B., and Nicholson, A.E., (2004), "Bayesian Artificial Intelligence, Boca Raton, FL: Chapman and Hall/CRC.

APPENDIX

Appendix A. Well Trajectory in well x.

MD (ft)	Inc (°)	Azi (°)	MD (ft)	Inc (°)	Azi (°)
0	0	0	3,508.50	32.9	33.15
293.3	0	0	3,606.90	35.4	34.15
621.4	0	0	3,650.60	37.9	36.65
654.2	0.83	0.42	3,672.50	39	38.45
752.6	3.33	2.08	3,902.20	39	39
778.8	4	3.67	4,230.30	39	39
949.5	4	4	4,558.40	39	39
1,638.40	4	4	4,886.50	39	39
2,261.80	4	4	5,247.40	39	39
2,327.40	5.58	4.79	5,870.70	39	39
2,425.80	8.01	6.8	5,985.50	39	39
2,524.30	10.48	9.25	6,855.00	39	39
2,622.70	12.96	11.72	7,183.00	39	39
2,721.10	15.44	14.2	7,511.10	39	39
2,819.50	17.93	16.69	8,206.70	39	39
2,918.00	20.42	19.18	8,823.50	39	39
3,016.40	22.92	21.67	9,151.60	39	39
3,114.80	25.41	24.17	9,479.60	39	39
3,213.20	27.91	26.66	10,103.00	39	39
3,311.70	30.4	29.16	10,792.00	39	39
3,410.10	33.4	31.9	11,513.80	39	39

PRODUCTION BEHAVIOR COMPARISON OF CO2 AND WATER AS WORKING FLUID AS POSSIBILITY OF ENHANCED GEOTHERMAL SYSTEM IN SIBAYAK AND DARAJAT, INDONESIA

Roynaldo Lumban Batu[1], Ignatius Bernadi[2], Cynthia Dewi Susanto[2], and Jose Prima Boang Manalu[1]

[1]Geological Engineering Department of Diponegoro University
[2]Chemical Engineering Department of Diponegoro University
Jl. Prof Soedarto, Semarang, Central Java, Indonesia 50275
Email: roylumbanbatu@students.undip.ac.id

ABSTRACT

Sibayak and Drajat both are the geothermal fields located in North Sumatra and West Java, Indonesia that has been in operation for a long time. The amount of mass produced to the surface without being returned to the reservoir causes reservoir pressure to decrease. Decreasing pressure and low permeability values led to the testing of Enhanced Geothermal Systems (EGS) in Sibayak and Darajat field. EGS is a method created to increase the production of a geothermal system by fluid injection. At certain geothermal temperature and pressure conditions, the flow and heat transfer behavior of using CO2, chemical interaction effects between CO2 and reservoir rocks would be considerably different from using water. Numerical simulation is used to evaluate mass flow and heat extraction rates from enhanced geothermal injection-production systems that are operated using either CO2 or water as working fluid. Favorable fluid properties by comparing CO2 towards water are chemically CO2 is poor solvent for rock minerals, fluid circulation in wellbores has large compressibility and expansivity, and ease of flow in reservoir has lower viscosity. Simulation studies showed heat extraction rates for CO2 as compared to water for a reservoir temperature of 200°C is larger approximately 50%. From environmental aspect, re-injection of residual CO2 will reduce the greenhouse gases to the environment.

Keywords: Sibayak ,Drajat, CO2, Water, Enhanced Geothermal System

INTRODUCTION

Darajat is spatially associated with andesitic stratification which has erosion, Mount Kendang. Volcanics found in the reservoir comprise mostly intermediate to mafic compositions, but younger formations are found in the central part of the area consisting of hornblende andesite lava, obsidian riolite and associated ash tufa (Rejeki et al., 2010). The main geological structure, identified in remote sensing images and aerial photography, is the Kendang, Gagak, Cibeureum, Cipanday and Ciakut faults (Rejeki et al, 2010). Other geological structures are inferred from MEQ alignment. Based on the analysis, it is known that the trend of the geological structure is dominated by the direction of NE-SW and NW-SE.

Geothermal power plants in geothermal systems Darajat has produced steam for electricity in Indonesia. Chevron Geothermal Indonesia Ltd. managing the facility found a tendency to decrease pressure in the reservoir. This is caused by continuous steam extraction from the reservoir. Analog with oil and gas reservoirs where 20-30% of oil and gas are easily extracted, in a geothermal reservoir, around 80% of thermal energy is reserved in hot rocks. A geothermal system is said to fail if it does not have fluid availability to extract energy from a heat source to the surface (Pardede and Elsworth, 2015). There are five characteristics of the geothermal system that produce: Heat source, Permeability, Availability of sufficient fluid, Cap rock, Natural recharge system.

Darajat is one of the geothermal fields located in West Java, Indonesia. Currently Darajat supplies steam to produce 260 MWe from 3 power generating units (Rejeki et al, 2010). Geographically, the location of the work area of the Panasbumi Darajat is at coordinates 7° 11 "9" LS to 7° 15 "40" LS, and 107° 41 "54" to 107° 45 "40" BT. Physiographically, the Darajat field is located along the eastern side of various volcanic centers, which are nearly 30 km long, which includes the active volcanoes of Mount Papandayan (which last erupted in November 2002) and Mount Guntur (the last erupted in 1840). Darajat is located at an altitude of 1,750-2000 meters above sea level and is located about 9 kilometers southwest of the Kamojang geothermal field and 10 km east of the Wayang Windu geothermal field. Figure 1 shows the geological structure identified with MEQ alignment, while Figure 2 shows the physiographic map of Darajat.

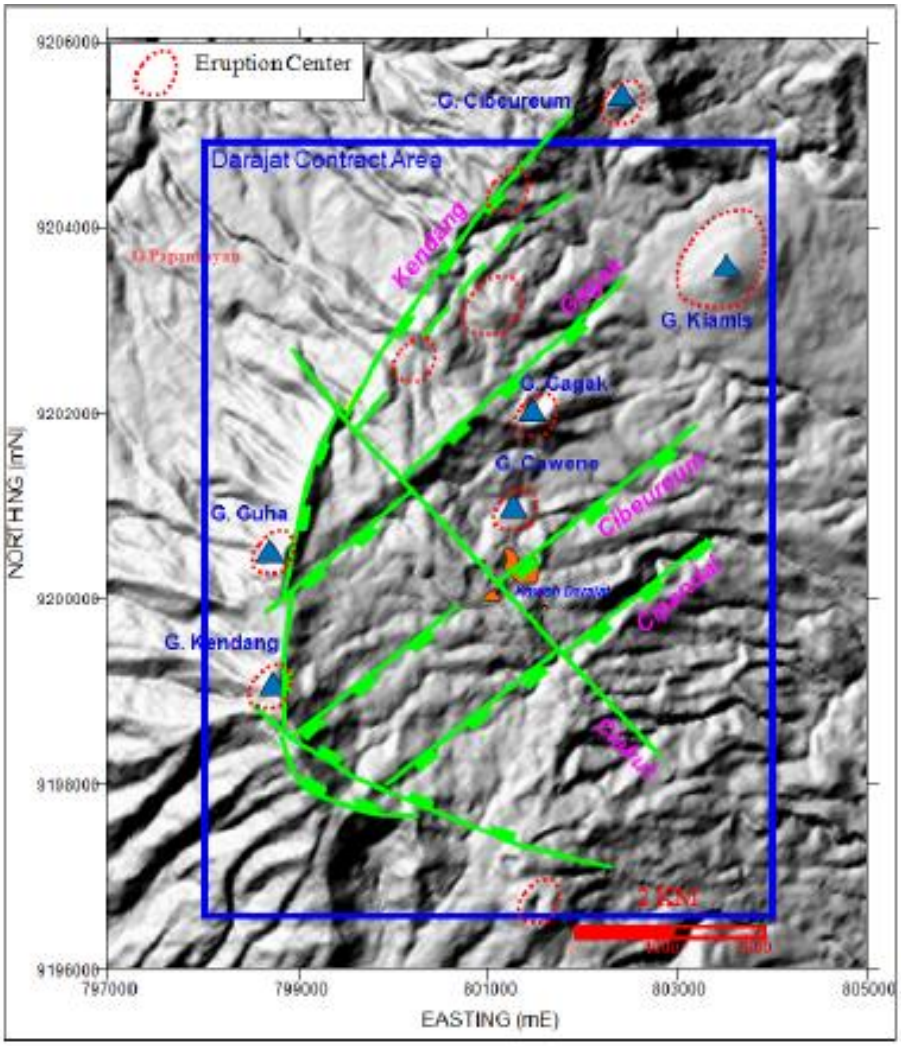


Figure 1: Geological structure identified by MEQ alignment. Based on the analysis, it is known that the geological structure trend is dominated by the NE-SW and NW-SE directions (Rejeki et al, 2010).

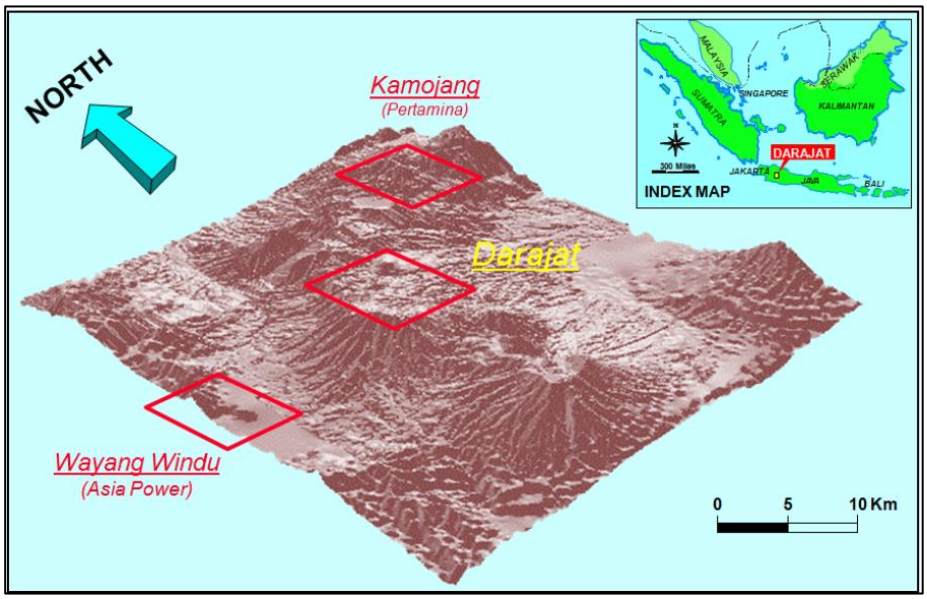


Figure 2: Physiographic map of Darajat and the surrounding area.

If one or more of the characteristics mentioned above are lacking, efforts need to be made so that production can still be carried out to the fullest. Especially if a geothermal system has no permeability and does not have enough fluid. The Darajat geothermal field has been operating for a long time, the amount of mass produced to the surface without being returned to the reservoir causes reservoir pressure to decrease. This resulted in the production and pressure of wells also decreased in the Darajat geothermal system. Therefore, it is necessary to conduct a feasibility analysis of the application of the EGS method to the Darajat geothermal system (Pardede and Elsworth, 2015). EGS is a method in geothermal systems which has the role of maximizing the production of geothermal wells. The mechanism of this method generally consists of 3 stages, namely field identification, reservoir creation, and reservoir management. The feasibility study of this seminar was conducted at Darajat field, Indonesia, which has been produced for decades which has experienced a decline in production Geothermal systems are found in regions with relatively normal geothermal gradients, especially on the edges of the plate where geothermal gradients usually have a temperature range higher than the average temperature (Dickson and Fanelli, 2004).

Enhanced geothermal system (EGS) is a method created to increase the production of a geothermal system (Pardede and Elsworth, 2015). Not only for geothermal production in Indonesia, research on EGS is needed in developing the potential of geothermal systems in a country, especially in areas that have faults and active volcanic activity Making this reservoir is at the core of the use of the EGS method. Reservoir production begins by drilling injection wells on hot dry rock. The injection well serves to reinject the brine after the (heat) energy is extracted (brine injector) or to inject the remaining water from the process in a power plant called condensate (condensate injector) into the gothermal field.

EXPERIMENTAL METHODS

Field Identification

In making the EGS reservoir there are stages in the form of determining the field, reservoir creation and reservoir management. Need to have preliminary geological, geo-chemical and numerical studies must be developed. Subsequently is to drill and exploratory well to measure and confirm properties of the reservoir priori. The decision as to which to drill will depend on the level of confidence and the funding available to the project developer.

Creation of Reservoir

Making the reservoir is at the core of the use of the EGS method. Reservoir production begins by drilling injection wells on hot dry rock. The injection well serves to reinject the brine after the (heat) energy is extracted (brine injector) or to inject the remaining water from the process in a power plant called condensate (condensate injector) into the gothermal field. An injection well must not affect other injection wells, and there is no backflow even though water and mud have been pumped into the wellbore and no contamination or cement is found on the springs around the site. The given fluid must have enough pressure and temperature to create fractures. Operations continue to be carried out until there is sufficient crack volume to create reservoirs (fluid, temperature, volume, and sustainability). The resulting circulation allows water to flow through an enhanced reservoir, taking in situ heat. Hot water is then pumped to the surface through a production well (U.S Department of Energy, 2012).

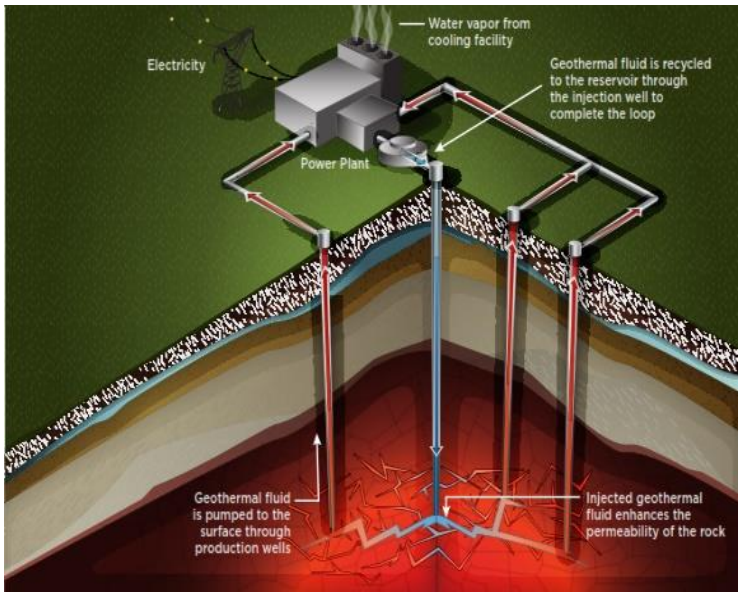


Figure 3: The mechanism of Enhanced Geothermal System (U.S Department of Energy, 2012).

RESULT AND DISCUSSION

Darajat Field's Well

Measurement of temperature and pressure with depth is important data on geothermal wells. The profile of PT Darajat geothermal wells is shown in Table 1. This measurement is inside the geothermal wellbore. This PT Profile data serves as input data for numerical simulations along with other reservoir characteristics data.

Table 1: Profil PT Sumur Panas Bumi Darajat (Pardede dan Elsworth, 2015).

Meas. Depth (m)	Elevation (masl)	T (deg.C)	P (barg)
3.4	1769.2	225.0	24.7
50.0	1722.6	225.3	24.7
100.0	1672.7	225.4	24.8
150.0	1622.7	225.6	24.9
200.0	1572.7	225.7	24.9
250.0	1522.7	225.8	25.0
300.0	1472.7	226.0	25.1
350.0	1422.8	226.0	25.1
400.0	1372.8	226.2	25.2
450.0	1322.9	226.4	25.3
500.0	1273.4	226.5	25.3
550.0	1224.6	226.6	25.4
600.0	1176.4	226.8	25.4
650.0	1129.1	226.9	25.5

From the research by Eylem and O'Sullivan on the Darajat field, the value of the fracture spacing used was estimated to be 5m, such a value as used in the Darajat geothermal field modeling project (Pardede and Elsworth, 2015).

Porosity and Permeability

Porosity and permeability are very important in the management of geothermal reservoirs. Porosity is the ratio of vacuum to the overall volume. Permeability is the ability to flow through rocks. Permeability is the interconnection of void space. The interrelated porosity will still produce low permeability (Pardede and Elsworth, 2015).

Low porosity means that the surface contact between fluid and rock is small, making it difficult to extract thermal energy from the earth's layer. In geothermal systems, liquids heat up when they come into contact with rock surfaces through conductive heat transfer. Rocks act as thermal storage. Hot water or steam then flows through the wellbore to the surface because of the pressure difference when transferring heat convective (Pardede and Elsworth, 2015).

One Darcy corresponds to the slow flow of single-phase fluid which has a 1cP viscosity and a flow rate of 1 cm3 / s through a 1 cm2 cross section. Typical permeability for geothermal reservoirs is 10 - 70 milliDarcy. For the purpose of this study, permeability and porosity are considered constant and not affected by water injection. The mechanical and chemical impacts of injection water in the reservoir were not taken into account in this study. The permeability used for the Darajat geothermal system is 0.1 Darcy (Pardede and Elsworth, 2015).

Thermal Drawdown

Thermal drawdown occurs in the reservoir because water is injected and interacts with hot rocks (Pardede and Elsworth, 2015). Two important variables for this study are distance and permeability of fractures, because this is a characteristic of the Darajat geothermal system (Pardede and Elsworth, 2015). Throughout this study, these two things are considered constant.

Thermal drawdown is analogous to pouring cold water continuously on a hot stone that is being heated. There is a level of rock that is refilled with heat because there is convection by water flowing on the surface. If these two levels are not in equilibrium, Thermal drawdown can occur (Pardede and Elsworth, 2015).

Modeling with TOUGH2

The models used in this study are single injection wells and single production wells. Direct water flow from one well to another and spread around the well. By using geothermal models made by Gan Quan, Darajat geothermal simulation data is run on existing models. This model has a geometry of 1500x600x15 m and is used in previously published papers. The injection well in this study will be called DRJ-A. While production wells are referred to as DRJ-B. The distance between the two wells is 1 km.

EOS 1 TOUGH2

EOS is the equation used in the TOUGH2 numerical simulation. EOS 1 is one of ten modules available to be selected in TOUGH2, EOS 1 specifically for water fluid, water with trackers. ParaView which is used to preview .vtk files is publicly available and is suitable for viewing results from TOUGH2 simulations. The results of TOUGH2 are visualized through ParaView and plot. Power is calculated by data on the results of mass flow rates and specific enthalpies (Pardede and Elsworth, 2015).

The pressure profile shows an overall increase in the reservoir (Figure 4). The pressure gradient also increases significantly as the pressure difference between injection and production wells. Fluid flow in porous media in the reservoir is driven by pressure gradients (Pardede and Elsworth, 2015).

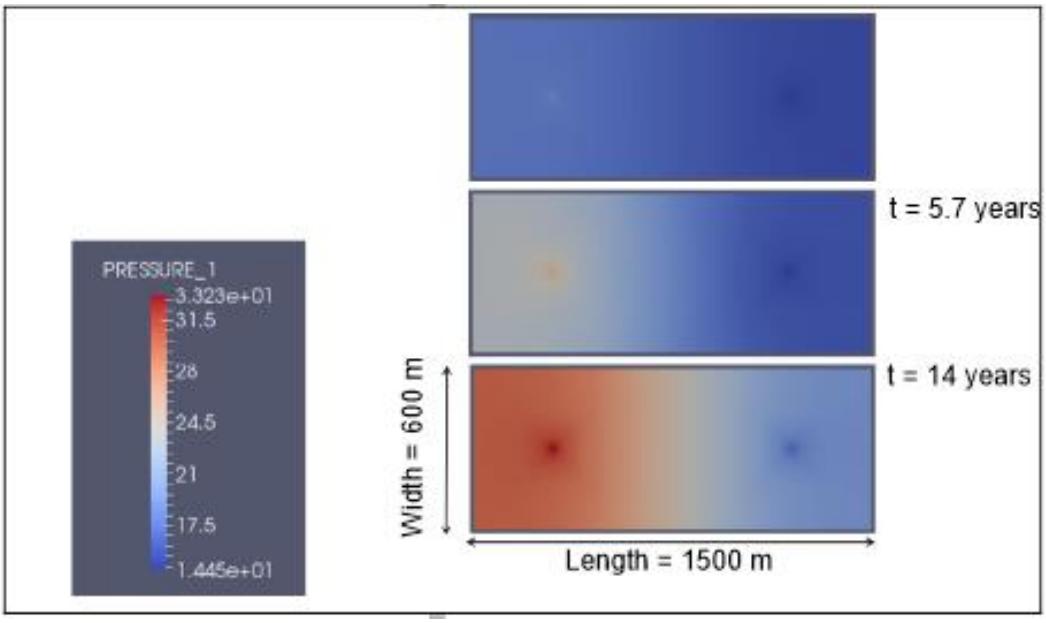


Figure 4: Pressure's changes Distribution Due to Fluid Injection (Pardede and Elsworth, 2015).

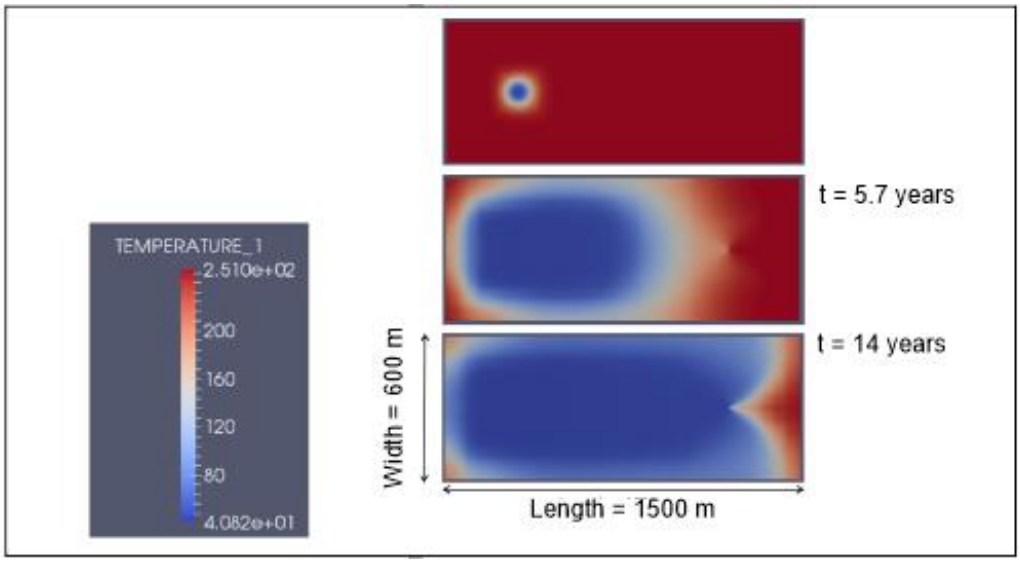


Figure 5: Temperature Distribution Shows Thermal Drawdown (Pardede and Elsworth, 2015).

The temperature distribution profile shows thermal withdrawal in the reservoir. It appears that initially the reservoir temperature is uniform ~ 250℃. Because water continues to be injected at 20 kg / s, the area around the injection also cools down which is shown in blue (Figure 4). This cooled area continues to grow outward and finally reaches the production well area. Thermal withdrawal completely cools the reservoir after about 32 years of continuous water injection at 40 ° C (Pardede and Elsworth, 2015).

Simulation results are presented on the production of mass and enthalpy flow rates over time (Figure 5). The water injection flow rate is constant at 20 kg/s and enthalpy is 1.08 x 10^5 J/kg. Production of the mass flow rate jumped at the beginning and fell in 33 hours but remained constant around 20 kg/. The enthalpy of the resulting liquid decreases after three years of continuous injection (Pardede and Elsworth, 2015).

The amount of steam produced in this well produces 21.6 MWth with equation

$$P_{th}=m*h=20\frac{kg}{s}*1{,}08*\frac{10\text{^}6J}{kg}=21.6MW_{th} \quad \text{..... (1)}$$

This is the thermal power produced from the production of steam and hot water. Taking into account the efficiency of a steam turbine power plant, which is about ~ 0.3, power. And electricity is obtained 6.48 MWe

$$Pe=\eta * Pth= 0.3 * 21.6\ MWth= 6.48\ MWe \quad \text{... (2)}$$

Results of the Feasibility Study with Injection Water

Based on EGS testing in the Darajat field precisely at the DRJ-A injection well and the DRJ-B production well, the results of the feasibility study are known if without injection, the thermal power output of the DRJ-B itself is 16.2 MWth. Compared to 21.6 MWth for injection conditions, where power increases due to injection. Without injection, DRJ-A is also capable of producing steam and provides 7.6 MWth thermal output. While with injection, the DRJ-A will inject water to produce a negative power of -4 MWth. In total, 23.8 MWth of heat power without injection still provides more power compared to injection with a total thermal output of 17.6 MWth (Pardede and Elsworth, 2015). So, it is concluded from the results of the feasibility study that EGS is feasible to be done in the Darajat field but not as expected.

Comparison of CO2 and water as working fluid

After it was discovered of feasibility that EGS is feasible but not as expected, so there are the idea for using CO_2 instead of water. The idea of using as a working fluid at high pressures introduces a new concept in the operation of EGS plants. CO_2 has chemical and thermal/physical properties that make it an attractive option as a heat transfer medium. In EGS plants that use water as their working fluid, water losses are a drawback for commercial operation, but in plants run with CO_2 fluid losses could result in geological sequestration of CO_2, which would be a secondary benefit. In addition to the potential to store CO_2 in the reservoir, the most important benefit of using CO_2 as working fluid for EGS is that the actual heat flow rate from a given reservoir could be up to five times larger than the heat flow rate achievable using the formation brine as working fluid. *(Olasolo et al, 2015)*

According to the literature of Olasolo et al, 2015, CO2 is not an ionic dissolution product, so it does not cause substantial dissolution problems. Pruess, 2006 had conducted quantitative exploration from an EGS plant *(Olasolo et al, 2015)*. And this can be done hypothetically that the Darajat area can be a heat extraction ratio of approximately 50% higher than water. For EGS plants with water as their working fluid, most of the pressure difference between the injection well and the production well goes into moving the fluid (with its high viscosity) in the immediate vicinity of the injection well. By contrast, the viscosity of CO_2 increases much less at low temperatures, so most of the pressure is available for use in the production well. *(Olasolo et al,2015)*. According to Pruess, 2006 when the working pressure is supercritical, the heat extraction ratios can be maintained for considerably longer in systems that use CO_2 as their working fluid than in systems that use water. As might be expected, for subcritical pressures a much lower heat extraction ratio is obtained, because the density of gaseous CO_2 is much lower than that of supercritical CO_2. And in the low pressures CO_2 is inefficient and is not considered a viable alternative to water as a working fluid. However, it is much more efficient at medium and high pressures. It is noteworthy that if high pressures are used the heat extraction ratios are very high in the first ten years but then gradually decrease over time, whereas at medium pressures the extraction ratios are lower but remain much more stable over the passage of time. *(Olasolo et al,2015)*. And from environmental aspect, EGS geothermal operating with closed circulation also provide environmental benefit such as minimal greenhouse gas or other kind a emission (Table 2).

Table 2: Comparison of CO2 and water as working fluids in an EGS type geothermal plant (Olasolo et al, 2015)

Fluid Properties	CO_2	H_2O
Chemical	Not an iomic dissolution /precipitation problems	An ionic cissolution product.
Fluid circulation in wells	High compressible and expandable	Low compressibility. Moderate expandibility
Ease of flow in the geothermal reservoir	Low viscosity and expandable	High viscosity and density
Heat transmission	Low spesific heat level	High specific heat level
Fluid losses	Could result in beneficial geological CO_2	A hindrance for development of geothermal reservoir.

CONCLUSION

Favorable fluid properties by comparing CO_2 towards water are chemically CO_2 is poor solvent for rock minerals, fluid circulation in wellbores has large compressibility and expansivity, and ease of flow in reservoir has lower viscosity. Simulation studies showed heat extraction rates for CO2 as compared to water for a reservoir temperature of 200°C is larger approximately 50%. From environmental aspect, re-injection of residual CO_2 will reduce the greenhouse gases to the environment.

REFERENCES

Bronto, S., and Hartono, U., (2006), "Potensi sumber daya geologi di daerah Cekungan Bandung dan sekitarnya", Jurnal Geologi Indonesia, Vol. 1 No. 1, 9-18.

Department of energy, U. S., (2012), "Enhanced Geothermal System (EGS)". Southwest,

Washington D.C: Geothermal technologies Office.(https://energy.gov/eere/geothermal/how-enhanced-geothermal-system-works, accesed 24 October 2017).

Cladouhos, T., T., Petty, S., Nordin, Y., Moore, M., Grasso, K., Uddenberg, M., Swyer, M., (2013), "Microseismic monitoring of Newberry Volcano EGS Demonstration". Stanford, California: Proceedings, Thirty-Eight Workshop on Geothermal Reservoir Engineering Stanford University.

Dickson, M., H., and Fanelli, M., (2004), "What is Geothermal Energy", Instituso Geoscienze. CNR. Pisa.

Faridah, Sri Ana, N., and Krisbiantoro, A., (2014), "Analisis distribusi temperature permukaan tanah wilayah potensi panasbumi menggunakan teknik penginderaan jark jauh di Gunung Lamongan, Tiris-Probolinggo, Jawa Timur". Journal Berkala Fisika 17, No.2, 67-72.

Glassley, W., E., (2011), "Geothermal energy: renewable energy and the environtment. Florida", CRC Press Taylor&Francis Group, 270-272

Hochstein, M., P., and Browne, P., R., L., (2000), "Surface Manifestation of Geothermal Systems with Volcanic Heat Sources" In Encyclopedia of Volcanoes, H. Sigurdsson, B. F. Houghton, S.R., McNutt, H., Rymer dan J. Stix (eds.), Academic Press.

Pardede, F., and Derek E., (2015), "Feasibility of Enhanced Geothermal System in Darajat, Indonesia". Pennsylvania: Energy and Geo-Environmental Engineering (EGEE), 494.

Rejeki, S., Nordquist, G., Fitriyanto, A., and Rohrs, D., (2010), "Geological Conceptual Model Update of the Darajat Geothermal Field, Indonesia". Bali Proceedings World Geothermal Congress, 1-6.

Van der Hoorn, K., Heijnen, L., J., Gankema, M., E., Nitters, G., (2012), "Hydraulic Fracturing in Limestone: A Case Study of Two EGS Projects in The Netherlands". Stanford, California: Proceedings, Thirty-Seventh Workshop on Geothermal Reservoir Engineering Stanford University, 194-202.

Olasolo, P., Juarez, M., Sebastiano, A., Liarte, "Enhanced geothermal systems (EGS): A review". Renewable and Sustainable Energy Reviews, 56, 133-144.

Pruess, K., (2006), "Enhanced geothermal systems (EGS) using CO2 as working fluid – a novel approach for generating renewable energy with simultaneous seques- tration of carbon.Geothermics 2006", 35, 351–367.

UTILIZATION OF GEOTHERMAL MANIFESTATION AS THE POTENTIAL OF THE LOMBONGO REGIONAL GEOMETIC, BONEBOLANGO REGENCY, PROVINCE OF GORONTALO

Miftahul Jannah and Muhammad Rizqy Gau

Faculty of Engineering, Universitas Diponegoro Universitas Diponegoro, Jalan Prof. Soedarto, Tembalang, Semarang, 50275, Jawa Tengah
Email: Muhammadrizqygau@gmail.com, mifta0021@gmail.com

ABSTRACT

Bone Bolango Regency, Province of Gorontalo, is one of the regions with potential geothermal manifestations, one of which is hot water. This research is motivated by the fact that Bonebolango District has geothermal manifestations as a sign of the existence of an active geothermal system whose capacity is planned to be developed by 20 mw of the total potential used to meet energy needs. Most of it is used for electrical energy needs, in addition to the electrical energy needs of potential manifestations such as hot springs, steamy soil, and mud pools can be used as geotourism potential but less attention, with this background the research aims to optimize the natural potential (geology) in the form of hot springs are of added value to the economic well-being of local communities, and provide good management advice in terms of geology and tourism. The research method is carried out secondary data collection. Then supported by direct survey data in the field according to the parameters needed in the study. Geomorphologically in the area is a Volcanic Mountain Unit, Denudational and Fluvial, with lithology in the form of andesite rocks and diorite intrusions. The temperature of the hot springs in the geotourism area is measured on the 420C-480C field. This hot spring is controlled by a horizontal fault passing through the surrounding rock. Hot water bathing as a form of geotourism which will be optimized further is a hot spring bath in the middle of the beauty of tropical rainforest in Gorontalo. In the future promotion must be more aggressively carried out through existing media, then spatial planning by procuring attractive lodging around hot springs, structuring kiosks as support, and in terms of tourism can be added to the performance of local culture shown to tourists who come.

Keywords: Direct use, surface manifestation

INTRODUCTION

Bone Bolango Regency, Province of Gorontalo is included in the geothermal manifestation group. The geothermal system that occurs in Bone Bolango Regency occurs due to magmatism and the formation of active faults caused by the movement of micro and macro plates. Geothermal is a natural resource that has an important role in national development, because the source of this geothermal energy can be renewed.

Geothermal is also one of the energy sources whose utilization can be used for a long time and is environmentally friendly so it is very supportive in the development process. Geothermal symptoms that occur in this study area are characterized by the appearance of three groups of relatively hot springs located close together, namely are the Libungo and Lombongo groups and those located far in the eastern part of the research area, the Pangi group.

Geothermal energy can be used to meet energy needs, for example for electrical energy needs. Regions that have geothermal prospects can be indicated by the potential of the existence of hot springs as well as those found in Bone Bolango Regency. Bone Bolango Regency is an area that is beginning to develop and is in dire need of geotourism which is still lacking in attention to support mining in the area.

Geotourism is a type of tourism that is sustainable and is highly related to geological processes such as geological structure, geological history, and the shape of the existing landscape in a location. These places are very good if used as a place to travel, for example, hot springs found in research areas that can be used as geotourism for hot springs.

In geotourism there are several things that need to be developed, among them are from the preservation and uniqueness of a geotourism place. It must be developed because it greatly affects the tourists who come to the geotourism location. In addition, geotourism must be geologically based, which means that geotourism is a tourist object formed due to the influence of geological processes and can be of interest by tourists, for example from the unique types of rock present in the geotourism.

The aim of geotourism itself is to increase knowledge about geo-tourism regional geological potential, preserve the earth by preserving relics - inheritance as in ancient times. The benefits of geotourism, among others, can encourage visitors to be more aware and understand the geological conditions in the geotourism area and can add insight. For local people, geotourism can be useful

as a job opportunity and help the economy of the community around the geotourism area.

The purpose of this study is to optimize the potential of nature (geology) in the form of hot springs to be an added value for the economic welfare of local communities, while being able to minimize the potential for natural damage and provide good management advice in terms of geology and tourism.

LITERATURE REVIEW

The research area is an area where there are two subductions, namely is the subduction of the Sulawesi sea and East Sangihe in the northern part of the North Sulawesi Arm and in the eastern and southern parts of the North Arm of Sulawesi. This activity resulted in the formation of plutonic rocks and young volcanic cones caused by the implications of magmatism and volcanic activity.

Litology/Stratigraphy

Stratigraphy/sequence of rocks from old to young are Gamping Tandaka (Tmgt), Andesite Bilungala (Tmab), Bone Granite (Tmgb), Diorit Bone (Tmdb), Old Pinogoe Andesite (QTap 1), Pinogoe pyroclastic (QTpp), Young Pinogoe Andesite (QTap 2), and Aluvium (Qa). Gamping Tandaka (Tmgt), revealed to the west of the Lombongo hot spring, yellow-brownish white, hollow and containing fossils. This rock is of Lower Tertiary age and contact with younger rocks in the form of incongruity. Andesite The center of the eruption is unknown, partially amplified, weathered and oxidized in the form of limonite, the color is grey.

In the Upper Miocene there is an orogenesis that produces Bone granite batolites with a spread in the north and northwest. As the formation of Bone granite batolites, in the Upper Miocene also formed Diorit Bone plutonic rocks, revealed in the north and northeast, with harmonious contact above andesite Bilungala (Tmab). At the time of the Pliocene there was an initial eruption of G. Pinogoe which produced Old Pinogoe andesite lava (Tqap 1), revealed fresh and well and formed a gentle slope towards the north of the Bone river. The second eruption of G. Pinogoe occurred in the Late Tertiary Period resulting in a pyroclastic flow, namely is Pyroclastic G. Pinogoe (QTpp) which was revealed in the middle to the north 24 of the Bone rivers. Figure 1 shows the location of research area, while Figure 2 shows the geological map of Suwawa.

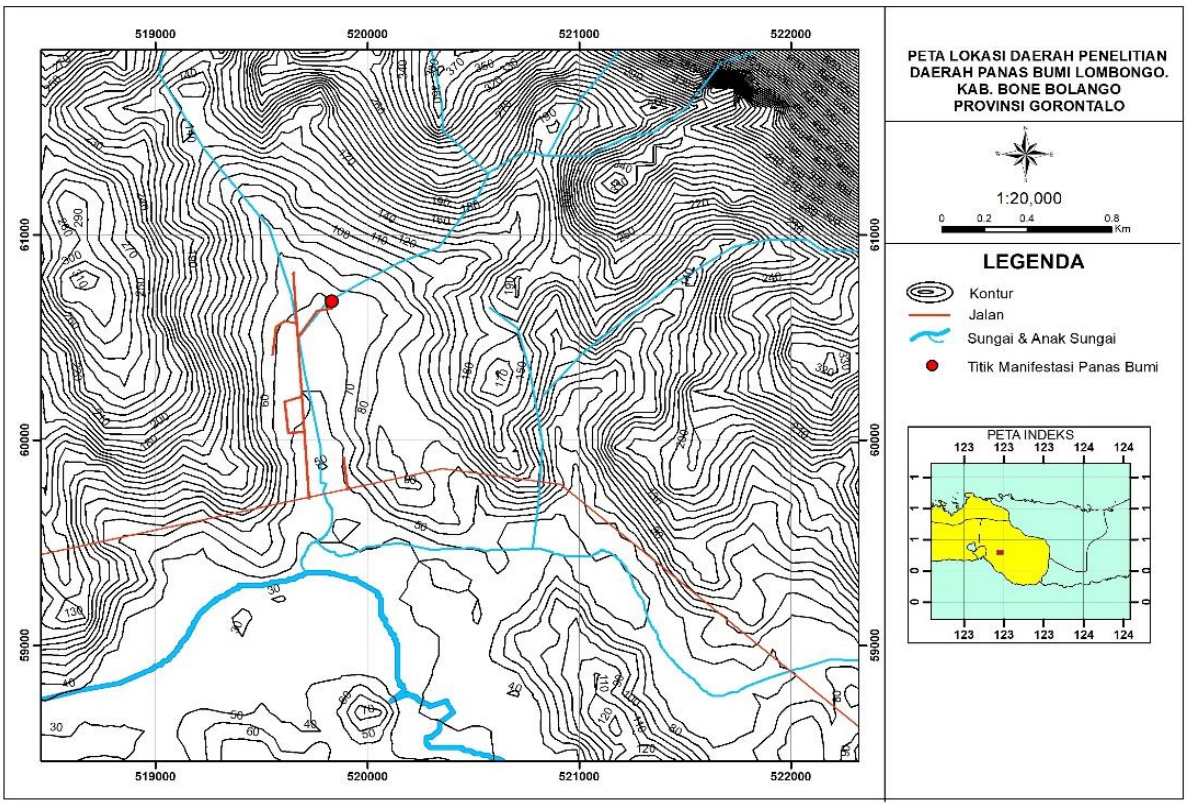


Figure 1: Map of the research area.

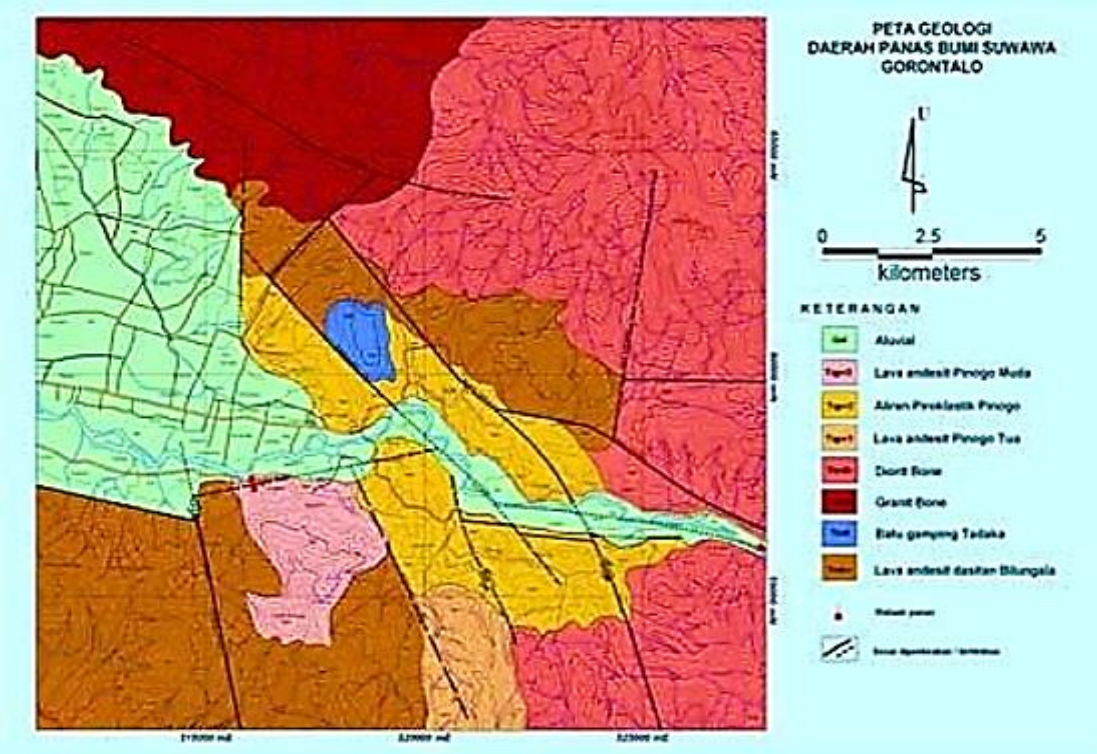


Figure 2: Suwawa geological map (T. Apandi & S. Bachri, 1997).

Geomorphology

The morphology of the Suwawa geothermal area based on the shape of the landscape, river flow patterns, erosion rates and rock types can be grouped into 3 (three) morphological units, namely are lowland morphological units (SDR), volcanic morphological units of G. Balangga and Pinogoe (SVBP) and G. Mogi and Lompotoo volcanic morphology units (SVML). (Brahmantyo, 2009).

Geological Structure

Some faults that developed in the study area include the Lombongo fault in the form of a sliding normal fault, northwest-southeast to west-east, having a pattern similar to the distribution of Tertiary plutonic rocks, and is the oldest fault. Furthermore, the Lombongo fault was evaluated to become a normal second order fault. Batunobatuo fault in the form of a sliding and directed normal fault F 3300 E. The Gorontalo fault has a west-southeast direction and forms a fault trap in the form of accumulation of lake deposits in the west outside the mapping area. The fault trap has formed the west-east depression zone, producing several second-order faults, including the Libungo and Bone / Pangi faults.

METHODOLOGY

The methodology carried out in this study is primary data and secondary data. Primary data is obtained by direct survey in the field by looking at the condition of the research area according to the parameters needed in research such as lithology, structure, impact, development and others. Then to strengthen the data generated from the primary data, secondary data collection was carried out with a literature study in the form of regional geology to determine the geological conditions of the study area as well as observations using remote sensing to determine the location conditions of the research area.

RESULT AND DISCUSSION

In the research area, the Lombongo region has manifestations of geothermal energy. the geothermal manifestations are in the form of hot springs. Based on the study of Regional Geology, the Geothermal System that occurs in Bone Bolango Regency occurs due to magmatism activities and the formation of active faults that occur due to the influence of micro and macro plate movements, where the appearance of hot springs is interpreted from existing diorite rock fractures in the form of diorite, where when in the study area there is a diorite rock outcrop, and also controlled by a horizontal faults passing through the surrounding rock, this is characterized by the presence of waterfalls around the geotourism site, then viewed from the topography of the research area based on topographic maps and conditions the geomorphology of the hydrogeological conditions around Lombongo is a recharge area located in the mountains in the northern part which is included in the tropical rain forest and is a volcanic landscape. Figure 3 shows the workflow.

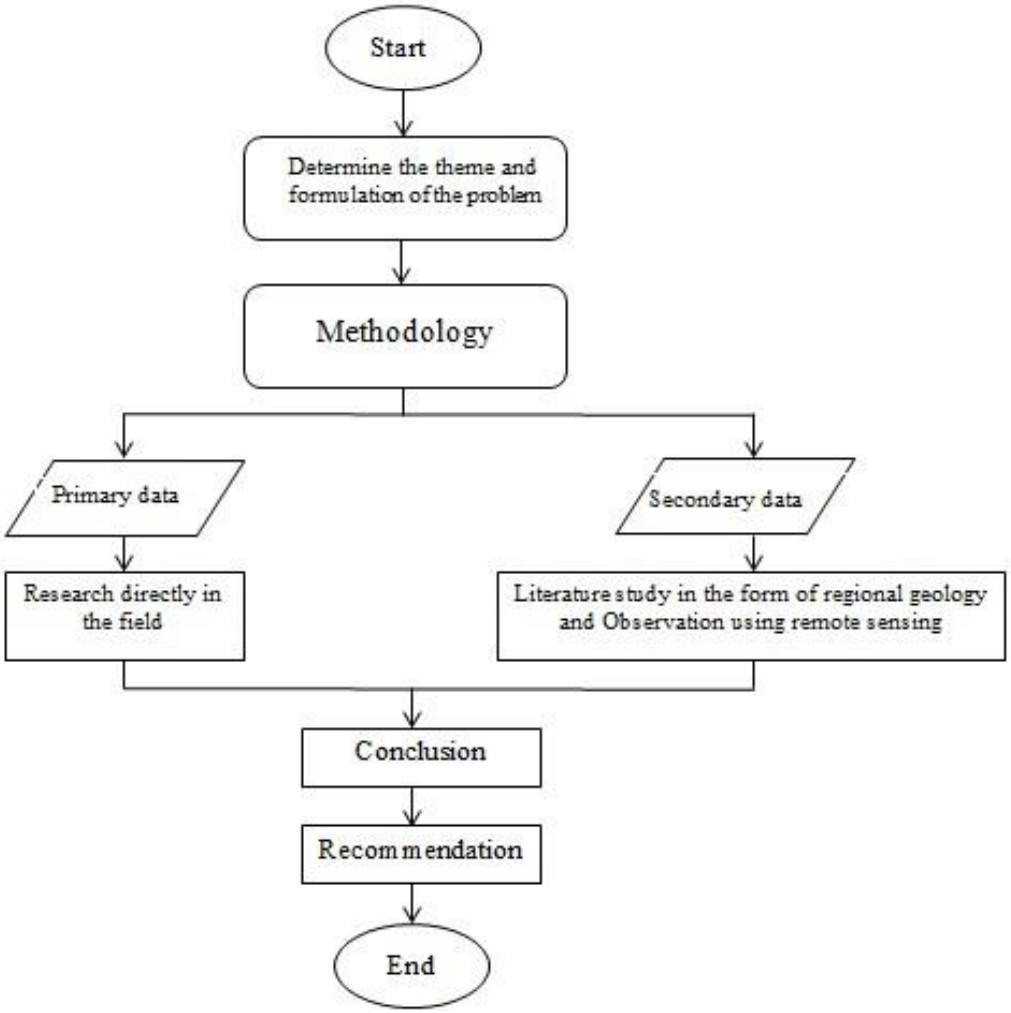


Figure 3: Workflow.

From the first table, show The characteristics of the heat in the study area have a temperature measured in the field 420C-480C, and based on secondary data has a neutral pH with the dominance of sulfate ions, sulfate water which has a neutral pH is interpreted due to the influence of Ca ions high enough in this hot water. This table also shows that in Bonebolango district, besides Lombok which is the object of research, there are also surface manifestations of geothermal which can be utilized further. Figure 4 shows the waterfall area around geotourism.

This geothermal manifestation in the form of hot springs which is used as an object of geotourism is a form of Geothermal Direct Use in Bonebolango Regency, which is a business activity to utilize energy and / or geothermal fluids for non-electric purposes, both for public interest and for its own sake. Or in short, utilizing geothermal energy for purposes other than electricity generation which are adjusted to the required temperature. The potential for direct use depends on the characteristics of the reservoir source and the natural conditions around it.

The hot spring bath of Lombongo as a form of geotourism that will be further optimized is a hot spring bath in the middle of the beauty of the tropical rainforest in Gorontalo. Optimization in welcoming good geotourism in The hot spring bath of Lombongo is expected to provide an output of benefits which include:

1. Benefits in nature preservation, and geological phenomena that become tourist attractions;
2. Achievement of tourist satisfaction through tourism experience and enrichment of knowledge gained during the tour;
3. Increasing the economic welfare of the community;
4. The realization of sustainable tourism management.

In fulfilling the benefits that are to be achieved, optimization can be done in the first aspect of benefits, natural sustainability and geological phenomena that become a tourist attraction can be achieved by structuring organic, non-organic, and residual waste in several corners of the tourist site and increasing power Tourist attraction can be promoted through existing media media added by staging local culture that is shown to tourists who

come. Figure 5 shows the arrangement conditions stall around geotourism site.

The second aspect of benefits, optimization can be done with a good information system, for example about the history of the formation of geological collisions, which tourists are expected to understand the natural process processes that occur. With this information, people are also expected to be aware not to damage the beauty of the environment around geotourism.



Figure 4: Waterfall in the area around Geotourism.



Figure 5: Arrangement conditions stall around the geotourism site.

This things can also add an Education Tour which is a form of packaging tour that is suitable for geotourism. The Education Tour is a tour that is intended to provide an overview, comparative study or knowledge about the field of education or science that he visits. This education tour is carried out to develop insights and knowledge for the actors. Actors who take educational trips usually don't attach too much importance to excessive luxury in carrying out travel activities. But it requires more self-enrichment, in the form of new knowledge and experience.

In achieving the third benefit in the form of meeting the needs of the surrounding community, spatial planning can be carried out, which includes the community making attractive lodging around the hot springs, structuring kiosks to support the income of the surrounding community.

Then in order to realize sustainable tourism management can be optimized by cleaning the bathing pool every week, which can be seen in tourist hot spring baths that lack attention from tourism managers, this is in accordance with the research objectives of optimizing natural potential in the form of springs heat becomes an added value for the economic well-being of the local community, and it can also be through the management of hot springs not only as a bathing facility but also as hydrotherapy, as well as being able to minimize the potential for natural damage and provide good management advice on the geology and tourism.

In the future, it is hoped that the Lombongo will become one of the Geotourism destinations that has high attraction with the realization of the optimization that is to be achieved. Figure 6 shows the hot water pool conditions.



Figure 6: Hot water pool conditions.

CONCLUSION

Geothermal manifestations in the form of hot springs which are used as objects of geotourism are a form of Geothermal Direct Utilization in Bonebolango Regency. The temperature of hot springs in the geotourism area is measured on the 420C-480C field and based on secondary data has a neutral pH with the dominance of sulfate ions, sulfate water which has a neutral pH is interpreted as a result of the influence of Ca ions high enough in this hot water. This hot spring is controlled by a horizontal fault fault passing through the surrounding rock. Hot water bathing as a form of geotourism which will be optimized further is a hot spring bath in the middle of the beauty of tropical rainforest in Gorontalo. In the future promotion must be more aggressively carried out through existing media, then spatial planning by providing attractive lodging around hot springs, structuring kiosks as support, and in terms of tourism can be

added to the performance of local culture that is shown to tourists who come. Figure 7 shows the geotourism entrance.



Figure 7: Geotourism entrance.

RECOMMENDATION

Based on the conclusions from the research that has been done, suggestions or recommendations can be given as follows:

- To the management, in order to optimize tourist attractions that have been made into geotourism that can provide more information in the form of education about geological phenomena in order to be an attraction for tourists.
- To tourists, to always maintain cleanliness at the geotourism location and make good use of existing facilities at the geotourism location.
- To the government, to provide positive support to develop geotourism potential, both from technology and the utilization of geothermal energy sources.

REFERENCES

Apandi, T., and Bachri, S., (1997), "Geological Maps of Kotamoagu, Sulawesi Sheets, Sulawesi, Scale 1:250.000", Geological Research and Development Center, Bandung.

Berno, T., and Bricker, K., (2001), "Sustainable Tourism Development: The Long Road from Theory to Practice". International Journal of Economic Development, 3(3), 1–18.

Brahmantyo, B., (2009), "Indonesian Geography Expedition. Bakosurtanal", Jakarta.

Geothermal Potential Book in Indonesia Volume 2, (2017), "Ministry of Energy and Mineral Resources". Not published.

Hermawan, H., (2018), "Geotourism as a Model for the Use of Environmental Geological Wealth". STP AMPTA Yogyakarta.

Manyoe, I., N., (2019), "Geological Study of the Lombongo Geothermal Region in Bone Bolango Regency, Gorontalo Province". Geomine Journal, 5 (1), 10–18.

Simanjuntak, T.O., (1986), "Sedimentology and Tectonics of The Collision Complex in The East Arm of Sulawesi", University of London, UK.

INVESTIGATION AND PRELIMINARY STUDY OF GEOTOURISM PROSPECTS IN GEOTHERMAL AREA: A CASE STUDY IN NGEBEL GEOTHERMAL PROJECT, EAST JAVA, INDONESIA

Fathoni Tri Kurniawan, Muhamad Fauzan Tanjung, and Ilham Arifal Guntoro

Geological Engineering Department, Diponegoro University
Semarang, Indonesia
Email: fathonitri@student.undip.ac.id

ABSTRACT

Ngebel is a district located on the western side of Mount Wilis, Ponorogo Regency, East Java Province. Mount WIlis itself is a volcano which is one of the Quartenary Volcanoes of Java. This area is located at an elevation of 832 masl and is 190 km from Surabaya City. There is a volcanic lake, known as Lake Ngebel, which is the main tourist destination in the Regency. Aside from being a tourist destination, this area has a geothermal potential in an amount of 120 MWe, according to Government data. One form of social support is the development of this area into a geotourism area, which brings a lot of education and economic improvements of the surrounding community. This journal aims to provide an overview of Lake Ngebel Area as geotourism prospects within some interesting geothermal manifestations. Some of the methods used are literature studies and field data collection and comparison with other geothermal areas in Indonesia. The results of those methods show that this area has an attractive landscape and is very prospective to be developed as a leading geotourism area. Besides the main area, there are also hot springs in this area such as Padusan Tirto Husodo and some interesting tourism places. The area for several years has also been developed as a conservation area in the form of conservation forests and production forests.

The concept of the development of geotourism areas proposed in this journal follows values such as Ecological, Educational, and Cultural Values. All of these values can be implemented with the introduction of the Region as a very prospective geological area with strong local cultural wisdom and environment-based tourism. From the research, we believe that geotourism initiation can bring some beneficial effects to the local community.

Keywords: Geotourism, direct use, Ngebel geothermal field

INTRODUCTION

Objectives

This journal has several objectives including: 1) knowing the location of the ideal tourist location in the Ngebel area; 2) analyze the quality and quantity of each existing tourist spot; 3) provide an overview of the existing geothermal potential and its effects on tourist spots and communities; 4) provide recommendations on each tourist spot, both socially and culturally.

Ngebel Area

Ngebel is a district located on the western side of Mount Wilis, Ponorogo Regency, East Java Province. Mount WIlis itself is a volcano which is one of the Quartenary Volcanoes of Java. This area is located at an elevation of 832 masl and is 190 km from Surabaya City. There is a volcanic lake, known as Lake Ngebel, which is the main tourist destination in the Regency. This area is well known as an area that has several potentials, one of those potentials is geothermal potential. According to a data from Ministry of Energy and Mineral Resources from 2017, Ngebel area has amount of 120 MWe energy. This amount is also proven by the presence of manifestations, such as hot pools, hot springs, Mud pools, and altered rocks. These conditions has already drawn some geothermal company to explore and exploit the potential of the area. Even some company has already done some early exploration, for neccesities in next step:Drilling and Production.

Geotourism

Some of the geothermal potential development found to be very complicated, especially in social side, where oppositions from society rise up in the early or middle phase of geothermal development, especially when drilling process is about to begin. There are many solutions to decrease social challenge on this kind of development, one of those solutions is Geotourism.

Geotourism is a concept of tourism activities which relies on Geological spots visit (Hendratno, 2002). Two important elements in geoturism concept are conservations and educations through appreciations a learning (Newsome & Dowling, 2010 in Kubalíková and Kirchner, 2016). Geotourism potential is presented in geodiversity but through exploration and exploitation, only those potential can be used for geotourism purposes (Pralong & Reynard, 2005 in Kubalíková and Kirchner, 2016). Geodiversity is a concept of diversity of earth features and its systems. Human activities and environments are linked through geodiversity because geodiversity contains geological, natural processes, landforms, landscapes, soils, climates,

and others as fundamental elements in affecting human activities (Kubalíková and Kirchner, 2016). Cultural and economics sides of society also the affected by geodiversity because of elements in geodiversity is found to support each other to form conditions for human life, i.e groundwater will be fundamental for residential places, or mountainous landscapes found to be suitable places to grow agriculture. One of the products formed by geodiversity is geoturism potentials, which its parameter is: 1) geological, 2) geomorphological, 3) soil features (Gray, 2004).

Some of important terms used about Geotourism are geomorphsite and geosite based on Kubalíková and Kirchner (2016). Geosite means some sites on earth/ geosphere that represents geological history based on its prevailing feature, i.e. volcanic, or geothermal (Reynard, 2004, in Kubalíková and Kirchner, 2016). Geomorphsite means geosites that had been defined as landforms comes along with several values thanks to human perceptions. Geomorphsites values can be divided into two main values, there are scientific and added values, where scientific values contain information about genesis, process, evolutions, and dynamics of geomorphsites, while added values contains socials, cultural, aesthetics, ecological, economical, and others (Panizza, 2001 in Kubalíková and Kirchner, 2016).
The concept of geodiversity, geosites, geomorphsites, and geotourisms are very important, also could be applied on some of geothermal area where geodiversity is rich that appear as geosite and geomorphsites that have potentials to be developed as geotourism. In this case, preliminary studies are needed to explore and exploit the geotourism potentials. In this study, we proposed a concept that will be used as a "tool" In order to educate the people that live within or around the geothermal area.

GEOLOGICAL OVERVIEW

Ngebel Geothermal Area is located in Ngebel District. Surrounded by hills and Mountains such as Tunggangan, Kemlangan, and Tumpakkencono. This region has interval 15 (gentle) to 70 % (steep) of Slope. Its temperatures ranging from 22 degrees Celsius to 32 degrees Celsius with rainfall of 1,907-4,593 mm/year. It is located on the western slope of Wilis Mountains.

Geological Condition

According to Geological Map of Madiun, Java published by Center of Geological Research and Development (1992). The north to the east is formed from the Ngebel Morphocyte composition. This lithological Uni consists of andesitic volcanic breccia, pyroxene, andesite horlene and diorite, tuff and volcanic conglomerates. Figure 1 shows the geological map of Ngebel. The west to the south is formed from the Jeding-Patukbanteng, which includes andesite pyroxene lava, volcanic breccias, and tuff-pumice.

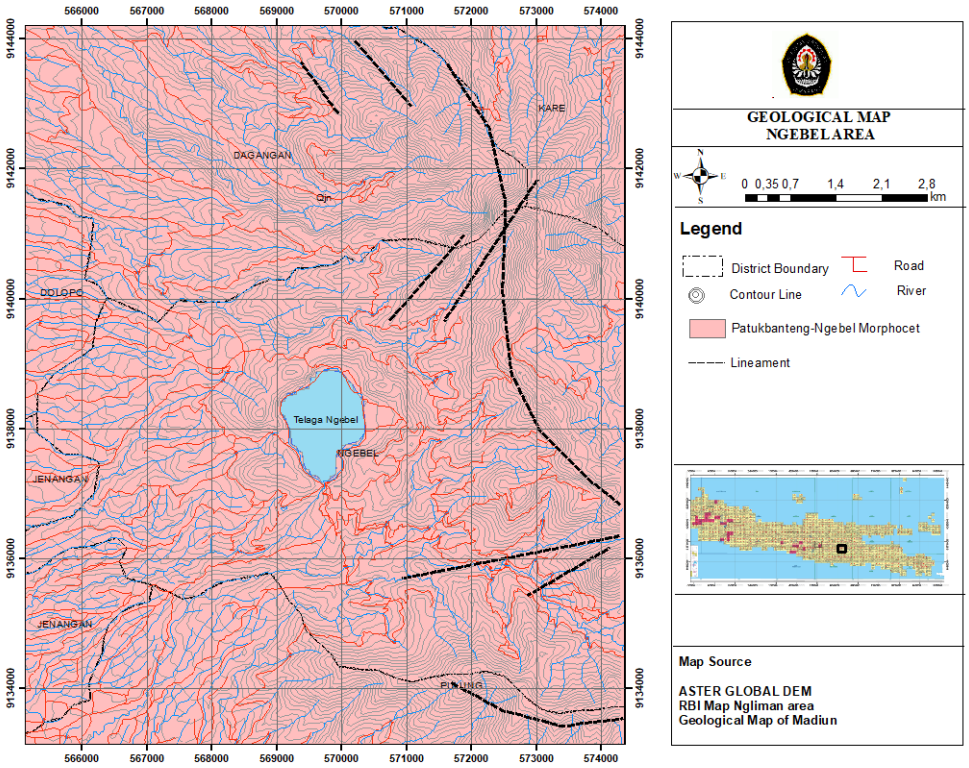


Figure 1: Geological Map of Ngebel Area (Hartono, 1992).

METHODOLOGY AND DATA

The preparation of this journal uses the method of Literature study, and Field Observations. From literature studies and observations in the field, Preliminary plans can be made in the Ngebel Lake area. Those two main methods are done in some steps. First is Gathering ideal references and appropriate secondary data. Comparisons with other geothermal prospect areas were also carried out. Then a field study is carried out to find out certain data such as road access, existing social roles in tourism. From this data a qualitative and quantitative analysis is carried out to determine whether existing tourism spots meet the rules in Geotourism. Then after conducting this analysis recommendations were made, those final recommendations consider current and future tourism development challenges.

COMPARISON WITH OTHER GEOTHERMAL FIELDS

Comparison are done to look for the parameters that can be considered in developing the geotourisms plan in Ngebel Geothermal Area. Those parameters are: 1) Area must be a located at residences area; 2) Area are in contact with protected rainforest; 3) society of the geothermal area development isn't well understood about geothermal activity and development,

1. Bedugul Geothermal Field

Bedugul Geothermal Field is located in Bali Province. The project of geothermal development has been suspended since 2005, where some oppositions come from public communities in Bali, also with the support from Bali House of Representatives. The reason is those prospects area is located in sacred forest in BAli, also because of the forest act as water recharge area, so it must remain undisturbed. In society's opinion, geothermal development activity in the Bedugul Geothermal Field could disturbed the nature balance of the forest and also disturbed the cultural activity (Richter, 2015).

2. Kamojang Geothermal Field

Kamojang Geothermal Field is at West Java Province. It comprises 21 km^2 area by size, and its electric potential are estimated around 300 MWe (Sudarman, 1995, in Utami, 2000). Studies show that Geothermal development is accepted by Local community. In Kamojang, direct use utilization is present in order to give opportunities to society who comes and stay after Kamojang WKP (Wilayah Kerja Panas Bumi) area are developed. Direct use utilization can be found in Kamojang are educative geo-tourism, such as a beautiful landscape enriched with agricultural activity i.e. Tea garden and hot water bathing activity has given a good potential of geotourism for visitor, and also direct use utilization in agricultural activity, i.e. Oyster Mushroom cultivated (Suyanto et al, 2010; Fadli et al. 2015).

3. Lawu Geothermal Field

Lawu Geothermal Field is located at two Province, Central and East Java Province. This Field development has been suspended since 2016. The reasons of the protest are based on the WKP area are located at Lawu conservational forest where many people depend on it as life resources, i.e. water, food, and also the Lawu area act as the center of spiritual activity in Java. Some activity has done to decrease community's disagreement on these developments but those action found to be not successful.

4. Dieng Geothermal Field

Dieng Geothermal Field is located in Central Java Province. Located at Volcanic island arc subduction zone from subduction of Indo-Australia and Eurasia tectonic plates, Geothermal development there is accepted by local community. Educative geotourism and direct uses of geothermal are the ways of community to take their parts in geothermal activities in Dieng Geothermal Area, where society developed a special interest in tourists activity, also by geothermal exploitation of the company, some of the unexploited fluids are used by people as direct uses utilization, i.e. Bathing, also in Dieng visitor could find many kinds of local products. Some of the geotourism activity can be seen in Kawah Sikidang Dieng, where local people build a semipermanent house to sold sulphuric mud in bottles or handicrafts as local products of Kawah Sikidang, also by built photobooth like- infrastrucutres, the visitors can take photos. The geotourism activity of Kawah Sikidang is also enriched with the knowledge of local people who know about the history of natural geothermal activity and its development. (Geomagz, 2015; Diengnesia, 2016).

GEOTOURISM PROSPECT SITE CONDITIONS

Social conditions data in the study area were collected into several groups. Among them are education, health, and community work Ngebel District has a population of 23558 persons in 2017 (BPS, 2017). Obtained data shows that the educational condition in the area is relatively good, there are educational facilities such as Elementary School, Middle School and High School. Next, if viewed from the health condition of the community, it is also considered good. In Ngebel Subdistrict there are decent health facilities such as Posyandu, Clinics and Puskesmas. Then if viewed from the work of the community, the employment of the agricultural sector is the most, besides also found other sectors such as trade and tourism. (BPS, 2017).

Economic conditions

Ngebel District where the geothermal prospect location is found to have various economic characteristics. The population in the Ngebel area mainly works in the agricultural sector (around 70% of the population works in this sector). Generally produced agricultural products are rice, corn and vegetables and teak wood.

Cultural conditions

People in the Ngebel area still maintain their cultural traditions. At the research location, precisely at Ngebel Lake, there are celebrations such as Larung Sesaji as offerings. This offering is carried out on every 1 Muharram (Suro). In addition, the Reyong Parade (Ponorogo typical art) was also held.

Infrastructure Conditions

The condition of facilities in the Ngebel area is mostly in damaged condition, so that it is in a lightly damaged condition. Even some tourist attractions are lacking of adequate facilities. The hot springs and springs are three flavors, and the waterfall is a tourist attraction which still don't have adequate facilities.

Access to the geotourism location also suffered damage due to landslides and incapabilities of road. Road which lightly damaged are 3% of all road, 24% are in moderate damage and 11% are in severe damage.

QUALITATIVE ANALYSIS

According to Gray (2004), Qualitative analysis is an analysis to observe, and describe geosites, mostly about it is geological and tourism potential. There are 4 (four) geosites which has ideal characteristic in Ngebel Geothermal Area. Figure 2 shows the Tirtohusodo pools.

Padusan Tirtohusodo (Tirtohusodo hot Pools, TH)

Tirtohusodo hot pools are one example of geothermal manifestation found in Ngebel area. Those spots are located at coordinates 570084 Easting, 9135886 Northing and has elevation 612 masl. These spots are located in Jagir Lor Village, Ngebel District, Ponorogo Regency administratively. Located 3 kilometers from Lake Ngebel, this pool can be accessed by car on motorcycle through local road. According to data from Ministry of Energy and Mineral Resource in 2017, this hot springs has 71,8 degree celcius temperature and its pH is 6,87, and lies on same structure lineament on Lake Ngebel area. Currently, this spring is widely used for bathing by residents and tourists from Ngebel Lake, and is also believed to be efficacious for various diseases.



Figure 2: Tirtohusodo Pools.

Geotourism potential can be found in this spot are:

a. Good place in learning about geothermal activity and its dynamics that showed by its manifestations,
b. As balneology spots in Ngebel area,
c. Beautiful landscape surrounding hot springs,
d. Others.

Through further developments, the geotourism potential can be created are:

a. By adding some information signs, some tourism will know the significance of this pool in Ngebel area,
b. A place to find local products of Geotourisms, like sulfur powder, or sulfuric mud for healty skin,
c. Others.

Lake Ngebel (LD)

Lake Ngebel is located in the sentral-proximal zone of Wilis-Liman Mountain. Located Ngebel district. Geographically this spot is located in 568750E, 9138072N and on 650 metre asl. Lake Ngebel is believed to be the leftover of past volcanic processes that forming a depression where surface water and shallow groundwater accumulated. Ngebel Lake is the main tourist destination in this district. This lake can be accessed through the provincial road from Ponorogo City Center or from Dolopo District, Madiun. Ngebel Lake is geologically formed by Plinian and Phreatomagmatic eruptions on Plistocene era. The eruption forms the crater of Ngebel Lake, which was a new parasitic crater,

which differs characteristically from Main Crater of the mountain in South East. Figure 3 shows the Ngebel lake.

Geotourism potentials can be found in this place are:

a. Good place for nature-based adventuring,
b. A good place for enjoying the beautiful view of volcanic lake,
c. Others.

Through further developments, the geotourism potential can be created are:

a. By adding the presence of information signs, information of the Geological and Ecological in Lake Ngebel will reach the visitors,
b. By presence of local tour guide, visitor will get more information,
c. Others.



Figure 3: Lake Ngebel.

Toyomerto Waterfall (TY)

Toyomerto or Selorejo waterfall is located in pupus village, ngebel district, ponorogo regency, east java province. Located approximately 6 (six) kilometers from Lake Ngebel to the east.

This waterfall is located between two hills namely Nglengko hill and Mount manyutan. Both are located in the wilis mountain range which spans from Madiun to Ponorogo. This waterfall comes from a spring on mount manyutan. Flows from this waterfall spans and continue into River Catur in Madiun. Figure 4 shows the Toyomerto waterfall.

Geotourism potentials can be found in this place are:

a. Good place for nature-based adventuring,
b. A good place for enjoying the beautiful view of waterfall,
c. Others.

Through further developments, the geotourism potential can be created are:

a. By adding the presence of information signs about waterfall on entrance, the tourist will learn about landscapes around waterfall,
b. Others.



Figure 4: Toyomerto Waterfall.

Widodaren Waterfall (WD)

Widodaren Waterfall is located in Talun Village, Ngebel District, Ponorogo Regency, East Java Province. Located approximately 3 (three) kilometers from Telaga Ngebel sub-district to the east. This waterfall can be accessed from Tirtohusodo Pools in about 1,5 kilometres.

To arrive at this waterfall combing the outskirts of the bridge of Talun Village through paddy fields in the right and left of the river.

Geotourism potentials can be found in this place are:

a. Good place for nature-based adventuring,
b. A good place for enjoying the beautiful view of waterfall,
c. Others.

Through further developments, the geotourism potential can be created are:

a. By adding the presence of information signs about waterfall on entrance, the tourist will learn about landscapes around waterfall,
b. Others.

QUANTITATIVE ANALYSIS

Quantitative analysis is done by giving some scores to several parameter and subparameter from 0 – 1. Quantitative Analysis is done by calculating some aspects of 4 geosites. Some Scores are gathered from Kubalikova (2013) (Table 1 and 2).

From the quantitative analysis, there are some parameters which needed to be improved in order to construct a geotourism plans In Ngebel Area. From the scientific and intrinsic values, can be seen that the range of the values is 75-100%. Those variations because some threat could happen differently in some sites i.e. the human activity who throw garbage in the sites. The acts that need is to raise the integrity and scientific values of the sites. But according to scores based on the classification, four sites has good value on Scientific and Intrinsic aspects. Figure 5 shows the Widodaren waterfall.



Figure 5: Widodaren Waterfall.

From the educational values, the values are ranged from 37,5-100%. Low values are because lack of educational values (in this case, low values is present on Toyomerto). Lots of action is needed to give visitors more information about the sites, the information may come from the information boards, flyers, brochures, websites, or even by serving a guide in geotourism sites.

From the economical values, the values are ranged from 50-100 %. According to these scores range, Low accessibility happened because road access to tourism place is not good enough, even in bad conditions. Low values of local product are also present because of the society in this area have a little or no awareness on each of Tourism place. The acts need to do are by increasing the accessibility and presence of local products value. Accessibility as parts of infrastructures is needed by building a safe trail/ tracks to reach the geotourism sites, as well as to serving local product of each sites, in order to serving visitors something to bought to their relations as gifts.

From the conservational values, the values are ranged from 62,5 – 100%. Such high values are present on those area because some Geosites like Lake Ngebel and Tirtohusodo pool are on good condition. The acts need to be done is just to determine the regulations how to keep the area keep conserved when the geotourism activity is about to begin, to keep the area from any threats of destructions that could lower the values of geotourisms itself.

Added values are presents because of the difference in cultural, aesthetical, and ecological in each site. The presence of added values could relate the abiotic features and processes to cultural issues as biotic features (Kubalíková, 2013). Some actions needed to take in order to increase the attractions on Geotourism prospect at this area such as renovating sites which in the bad conditions and repairing some road access.

RESULTS AND DISCUSSION

Geotourism in the form of special interest trips is the main thing in the development of geotourism in WKP Ngebel. According to Hall and Weller (1992) in Hendratno (2002), in its implementation Geotourism in this form must fulfill several things including:

Rewarding, which is the appreciation of an object and tourist attraction that it visits, which is manifested in the desire of tourists to be able to learn to understand or even take part in activities related to the project.

Enriching, containing aspects of enrichment and being able to improve the ability of each geosites

Adventurism (adventure), which contains aspects of involving tourists for adventure

Learning (learning process), which contains aspects of education through a learning process that is followed by tourists towards educational activities in the geosites.

From the important aspects given, the development of geotourism must fulfill the following points:

- The geotourism concept of the curiosity of the society and visitor about the nature of geothermal activity in the Ngebel Geothermal Area,
- The geotourism concept must serve the activity of geotourism to the society and the visitors,

- How to engage the Society as the organizer of geotourism activities?
- How long will it take to build the infrastructure for those geotourism plans?
- The geotourism concept must be answer how to rises up the conservational value as reward for nature.

Therefore, there is a prospect of geotourism that is ideal for the Ngebel region, namely Geothermal Tourism based on Geodiversity. The intended geodiversity is combining geological, cultural, social and economic aspects in the research area. Social and economic synergy is able to empower the surrounding community while cultural aspects are able to provide added value to the development of existing geosites. In line with the development of geotourism in other WKP, there are several unique and new tourism potentials that are able to meet the expectations of tourists: 1) sightseeing as part of trip agenda, 2) opportunities, 3) scientific learning or educational study interest, and 4) curiosity and ambitions to see something unusual (Erfurt-Cooper, 2010).

The four tourism potentials in the Ngebel and surrounding areas which have been described in the analysis are able to be moved to be the main prima donna for educate the society and visitors who live within the Bukit Daun differently based on their geological, geomorphological, and soil features uniqueness, such as:

- Lake Ngebel with a high quantitative score (97.5%), is able to provide information about past volcanic activity on Mount Wilis. Lake Ngebel tourism development is also able to provide information about positive ecological relations between protected forest areas, lakes and surface water. Besides that, culturally, this placealso has more values including the location of Larung Sesaji and other major district events. This added value will provide an opportunity to involve the surrounding community.
- Tirtohusodo pool, with a relatively high quantitative score (83%). With the development of geotourism, it is able to provide information to tourists and the public about geothermal systems working in this area, and their impact on surrounding areas such as hydrothermal alteration.
- Toyomerto Waterfall is able to provide information about volcanic activity, the geological structure of the surrounding area or even the unique lithological features found in waterfalls. In addition, ecologically, it can also be explained about the relationship of waterfalls to ecosystems in their surroundings. However, it is necessary to develop both physically and empowering the community around the waterfall considering that from the quantitative aspect (score of 58%), the development of a waterfall becomes an ideal geotourism spot which is quite difficult.
- WidodarenWaterfall is able to provide information about volcaic activity, the geological structure of the surrounding area or even the unique lithological features found in waterfalls. In addition, ecologically, it can also be explained about the relationship of waterfalls to ecosystems in their surroundings.

CHALLENGES

There are 5 questions to be performed by the developers of Geotourism area in the Ngebel Geothermal project with the aim of becoming socialization of natural sciences, environmental education, and the preservation of geological based nature that later can be realized as sustainable tourism, namely:

1. How is the preparation we need to do in the development of the Geotourism geothermal Ngebel project? The basis of this question is that there is usually a conflict between the surrounding citizens and the developers in a populated area where the local community is concerned if their territory is in large exploitation and can interfere with the balance of nature and harm the community.
2. How to make the community take part in geo-tourism activities and help the maintainer? To create education-based geo-tourism, environmental education, the community must be an organizer of tourism activities, so they should know the local conditions of the location of geo-tourism and help the tourists contain Some natural potential as a tourist attraction and the provision of resident houses that can be called as lodging/Homestay.
3. How can further development management and activities be implemented? On the further development of this geo-tourism party developers and stakeholders are responsible for the development because it has more knowledge of the geologic aspect, ecological aspects, environmental aspects that are able to maintain the balance Nature and no party is harmed, realizing the satisfaction of tourists means the management of geo-tourism can provide the satisfaction of the birth and inner to tourists who visit it in the area.
4. How is the infrastructure development needed to develop geo-tourism areas? The importance of infrastructure development as a visitor to the creation of a comfortable tourist area and can improve the economy of people who live near the region, in addition, can provide good service in activities Better and safer tourism, it is a return benefit for the tourism activities that can be felt by the community.

5. How to do geoconservation of the Ngebel Geothermal area? Conservation sites are the relationship and the final responsibility between my sweetened interests, the developers, the community, and tourists to maintain a balance of nature well in the context of protecting natural beauty for recreation (tourism), or as Understanding of natural value, conservation efforts are It has been done even though everyone has diversity in addressing it, the action that needs to be done is to serve sanitation facilities, as well as serve the Functionarian staff is to serve sanitary facilities and office staff.

CONCLUSION

The conclusions from this publications Ngebel Geothermal Area is that area contains some sites/places that have high potentials to be developed in geotourism, they are Lake Ngebel, Tirtohusodo Pools, Toyomerto Waterfall, and Widodaren Waterfall. Those geosites have decent characteristic quantitatively and qualitatively but need to be utilized with collaboration of Stakeholder, company developer, and society are needed to construct a geotourism activity that based on rewarding, enriching, adventuring, and learning.

ACKNOWLEDGEMENTS

Authors want to say thanks to Mr. Parmo as Local Resident in Ngebel District for giving information about Ngebel tourism potential. And for some colleagues in Geological Engineering Department who gives some supports to author when finishing this research.

REFERENCES

Badan Pusat Statistik Kabupaten Ponorogo, (2017), "Kabupaten Ponorogo dalam Angka". Jakarta: BPS

Badan Pusat Statistik Kabupaten Ponorogo, (2017), "Kecamatan Ngebel dalam Angka", Jakarta: BPS

Hartono, B. (1992). "Geological Map of Madiun, Java". Centre of Geological Research and Development

Hendratno, A., (2002), 'Perjalanan Wisata Minat Khusus Geowisata Gunung Merapi (Studi di Lereng Merapi Bagian Selatan, Yogyakarta)', Jurnal Nasional Pariwisata, vol. 2, no. 2, hh7-23.

Kubalikova, L., (2013), 'Geomorphosite Assessment for Geotourism Puposes', Czech Journal of Tourism, vol. 2, no. 2, hh80-1

Kubalikova, L., Kirchner, K., (2016), 'Geosite and Geomorphosite Assessment as a Tool for Geoconservation and Geotourism Purposes: a Case Study from Vizovicka vrchovina Highland (Eastern Part of Czech Republic)', Geoheritage, hh5-14.

Priatna, (2015), "Panas Bumi Dieng", GEOMAGZ-Majalah Geologi Populer, Badan Geologi, dilihat pada 10 Juli 2017, <http://geomagz.geologi.esdm.go.id/panas-bumi-dieng/>.

Putra, Ilham, D., Haq, Fadliyatul., Irvan, H., M., Hendratno, A., (2017), "Preliminary Study of Geotourism Plans in Geothermal Area: A Case Study in Bukit Daun Geothermal Project". Proceedings Indonesia International Geothermal Convention and Exhibition 2017.

Utami, P., Widarto, D., S., Atmojo, J., P., Kamah, Y., Browne, P., R., L., Warmada, I., W., Bignall, G., Chambefort, I., 2015, "Hydrothermal Alteration and Evolution of the Lahendong Geothermal System, North Sulawesi", Proceedings World Geothermal Congress, hh1-10.

Table 1: Kubalikova Classiffication.

Scientific and intrinsic values	
integrity	0 - totally destroyed site,
	0.5 - disturbed site, but with visible abiotic features,
	1 - site without any destruction
rarity (number of similar sites)	0 - more than 5 sites,
	0.5 - 2-5 similar sites,
	1 - the only site within the area of interest
diversity (number of different partial features and processes within the geosite or geomorphosite)	0 - only one visible feature/processes,
	0.5 - 2-4 visible features/processes,
	1 - more than 5 visible features/processes
scientific knowledge	0 - unknown site,
	0.5 - scientific papers on national level,
	1 - high knowledge of the site, monographic studies about the site
Educational values	
representativeness and visibility/clarity of the features/ processes	0 - low representativeness/clarity of the form and process,
	0.5 - medium representativeness, especially for scientists,
	1 - high representativeness of the form and process, also for the laic public
exemplarity, pedagogical use	0 - very low exemplarity and pedagogical use of the form and process, 0.5 - existing exemplarity, but with limited pedagogical use,
	1 - high exemplarity and high potential for pedagogical use, goedidactics and geotourism
existing educational products	0 - no products,
	0.5 - leaflets, maps, web pages,
	1 - info panel, information at the site
actual use of a site for educational purposes (excursions, guided tours)	0 - no educative use of the site,
	0.5 - site as a part of specialized excursions (students),
	1 - guided tours for public
Economical Values	
accessibility	0 - more than 1000 m from the parking place,
	0.5 - less than 1000 m from the parking place,
	1 - more than 1000 m from the stop of public transport
presence of tourist infrastructure	0 - more than 10 km from the site existing tourist facilities,
	0.5 - 5 – 10 km tourist facilities,
	1 - less than 5 km tourist facilities
local products	0 - no local products related to a site,
	0.5 - some products,
	1 - emblematic site for some local products
Conservation values	
actual threats and risks	0 - high both natural and atrophic risks,
	0.5 - existing risks that can disturb the site,
	1 - low risks and almost no threats
potential threats and risks	0 - high both natural and athrophic risks,
	0.5 - existing risks that can disturb the site,
	1 - low risks and almost no threats
current status of a site	0 - continuing destruction of the site,
	0.5 - the site destroyed, but now with management measures for avoid the destruction,
	1 - no destruction
legislative protection	0 - no legislative protection,
	0.5 - existing proposal for legislative protection,
	1 - existing legislative protection (Natural monument, Natural reservation…)
Added values	
cultural values: presence of historical/archaeological/ religious aspects related to the site	0 - no cultural features,
	0.5 - existing cultural features but without strong relation to abiotic features,
	1 - existing cultural features with the strong relations to abiotic features
ecological values	0 - not important,
	0.5 - existing influence but not so important,
	1 - important influence of the geomorphologic feature on the ecologic feature

Table 2: Scoring on Each Geosites based on Kubalikova (2013).

Geosites		TY	TH	LN	WD
Scientific and Intrinsic Values					
Integrity		1	1	1	1
Rarity		0,5	1	1	0,5
Diversity		0,5	1	0,5	0,5
Scientific Knowledge		1	1	1	1
Score		75	100	87,5	75
Educational Values					
Representativeness and Visibility/ Clarity of the Features / Processes		0,5	1	1	0,5
Exemplarity, Pedagogical use		0	1	1	0,5
Existing Educational Products		0	1	1	0,5
Actual Use of a Site for Educational Purpose		1	1	1	1
Score		37,5	**100**	**100**	62,5
Economical Values					
Acessibility (A)		0,5	1	1	0,5
Presence of Tourist Infrastructure		0,5	1	1	0,5
Local Community Product		0,5	0,5	1	0,5
Score		**50**	**83**	**100**	**50**
Conservational Values					
Actual Threat and Risk		0,5	0,5	1	0,5
Potential Threat and Risk		0,5	0,5	1	0,5
Current Status of a Site		1	1	1	1
Legislature Protection		0,5	0,5	1	0,5
Score		62,5	62,5	100	62,5
Additional Values					
Presence of Cultural Value		0,5	0,5	1	0,5
Ecological Value		1	1	1	1
Aesthetic: Amount of Colour; Stucture of Space and Viewpoints		0,5	0,5	1	0,5
Score		66	66	100	66
OVERALL SCORE (%)		58,2	82,3	97,5	63,2

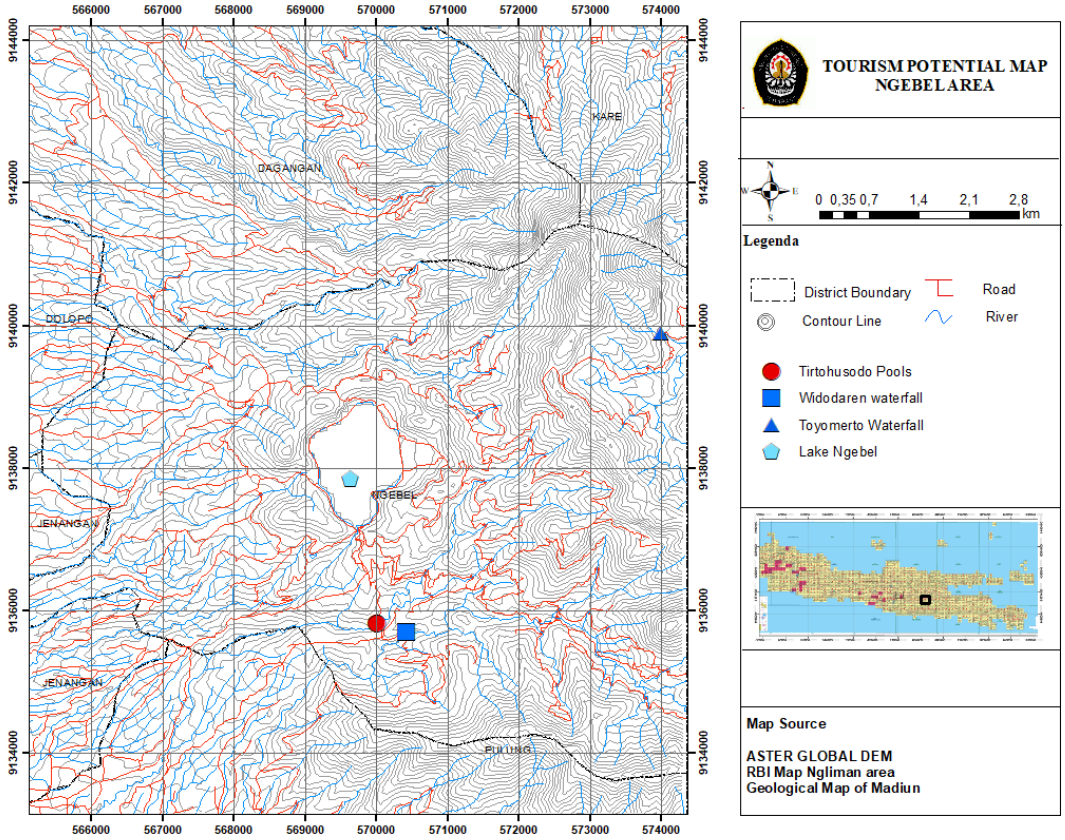


Figure 6: Tourism Map and Geosites Locations.

INTEGRATION OF GEOTHERMAL MANIFESTATION AND GEOTOURISM AS A CATALYST TOWARDS EDUCATING SOCIETY, ECONOMIC GROWTH AND SUSTAINABLE DEVELOPMENT BASED ON GEOTHERMAL ENERGY

Muhammad Ali Akbar Velayati Salim, and Astri Yunita

Universitas Diponegoro
Email: research.aliakbar@gmail.com, astriyunita26@gmail.com

ABSTRACT

Indonesia government national energy policy projects that 7,200 MW of electricity is targeted to be available in 2025 from geothermal energy production. In the wake of renewable energy trends among the industries and corporates alike, it is crucial to embrace the society in a way that empowers people's economy while also conserving natural ecosystem; these factors tend to influence the development rate of geothermal energy. While the integration of geothermal manifestation and geotourism has been implemented, rejection of geothermal power plant construction still arises in some areas, lagging the development of geothermal energy in some ways. This study intends to synthesize solution to the problems arising from the pros and cons found in related cases of integration of geothermal manifestation & power plant construction with geotourism. It is conducted by methodologically studying literatures from scientific journals and previous studies that discuss about relevant topics. Analysis is carried out by reviewing the general sub district geothermal manifestation and geotourism integration to guideline the stakeholders and general public. From the results, it is concluded that in order to integrate geothermal manifestation with geotourism, certain components in line with UNESCO's International Congress of Geotourism AROUCA Declaration are compulsory, such as: a) Preplanning of various aspects ranging from Environmental Impact Analysis, effective land use determination between production and geopark area, tourist attractions establishment based on geothermal manifestation, etc.; b) Eco-friendly construction method; c) Active involvement and employment of local citizens in establishing the geopark; d) Integrating and prioritizing the use of technology and mobile application over the use of traditional information posters; e) Providing easily understood, intelligible, and accessible knowledge; f) Building local identity and promote authenticity and uniqueness in the area. This ensures that the environment and its inhabitants obtain social justice, environmental integrity and sustainable economic development while also having a better understanding of geothermal energy development.

Keywords: Geothermal manifestation, geotourism, sustainable development, social awareness.

INTRODUCTION

In recent years, the market for geothermal power has increased sharply, especially in emerging markets because - due to economic growth - more and more communities in low-income rural areas have access to electricity. Many governments are also increasingly emphasizing their focus to reduce dependence on expensive and non-environmentally friendly fossil fuels.

Indonesia is one of these developing countries that is facing an increase in demand for electricity as much as 10% annually (especially on islands outside Java) and therefore this country needs additional capacity to produce electricity of approximately 6 Giga Watts per year. Indonesia's electricity ratio - that is the percentage of Indonesian households connected to the electricity grid - is around 80.38% at the end of 2013, implying that there are still around 50 million Indonesians who do not have access to electricity. The Indonesian government has high expectations for geothermal energy. Indonesia has the one of the largest geothermal reserves in the world, therefore the Government aims to increase the role of geothermal energy as a producer of electricity. Because energy demand has risen sharply in Indonesia due to population growth combined with the structural expansion of the economy has led to an increasing number of middle class and also industrialization and new investments - the Government has recently efforts to facilitate investment in geothermal expansion after all this time tend to ignore this sector. In the past the situation was reversed, the government relied on coal, natural gas and crude oil to fuel power plants. In line with this past, the government has also ignored the potential of other renewable energy sources (such as hydroelectric energy, solar power, biofuels and biomass). The private sector is also less interested in investing in renewable energy sources in Indonesia because the country's investment climate is complicated. Moreover, the cheap abundance of coal in Indonesia makes investment in renewable energy less attractive.

Indonesia government national energy policy projects that 7,200 MW of electricity is targeted to be available in 2025 from geothermal energy production. In the wake of renewable energy trends among the industries and corporates alike, it is crucial to embrace the society in a way that empowers people's economy while also conserving

natural ecosystem; these factors tend to influence the development rate of geothermal energy. While the integration of geothermal manifestation and geotourism has been implemented, rejection of geothermal power plant construction still arises in some areas, lagging the development of geothermal energy in some ways. This study intends to synthesize solution to the problems arising from the pros and cons found in related cases of integration of geothermal manifestation & power plant construction with geotourism.

METHODOLOGY

This research was conducted by gathering literature studies related to geoturism and geological conditions in regions with geothermal prospects, methodologically studying literatures from scientific journals and previous studies that discuss about relevant topics. For study case purposes, Gedongsongo (which is located in Ungaran, Semarang) is selected to analyze what constitutes an integration of geopark geotourism and geothermal manifestation, how it creates prosperity, opens economic opportunities and educate geothermal energy to the society.

GEOLOGICAL SETTING

The study location is located in the Gedongsongo temple area of Mount Ungaran located in Semarang Regency, Central Java. Ungaran is a volcanic complex formed due to tectonic-volcanic depression (volcano-tectonic depression). The depression is in the form of a big curve and elongation whose formation is strongly influenced by tectonic and volcanic processes in highland areas with material in the form of volcanic products (Bemmelen, 1970). Mount Ungaran is located in the easternmost part of the North Serayu Mountains with an altitude of 2,050 masl. Mount Ungaran in the middle to the north it forms a weak bumpy hill, the rocks are arranged by Ungaran Tua volcanic broth and sedimentary Kalibiuk Formation alluvial in the north. The composition of rocks found on Mount Ungaran quite varied, consisting of olivine basal, andesite pyroxene, hornblende andesite and gabbro (Rezky et al., 2012).

Basically, the evolution of Mount Ungaran is divided into three periods, namely, The Oldest Ungaran, Old Ungaran, and Young Ungaran. Each period distinguished by the volcano-tectonic collapse process. First period, The Oldest Ungaran Mountain formed in the Lower Plestocene whose products consists of pyroclastic flow and basaltic andesite lava. Mountain eruption products The Oldest Ungaran is deposited as Middle Damar and Upper Damar Formation.

Then followed by andesitic tuffs and andesitic pyroclastic. The growth period of the Oldest Ungaran Mountain ends with destruction of its body in the Early Pleistocene. The second period, Old Ungaran was formed and the product consists of andesitic basalt. Old Ungaran Mountain eruption products is then deposited above Damar Formation in an inconsistent manner called Notopuro Formation. In the second period it ends with the occurrence of volcano-tectonic fault system so that Old Mount Ungaran was destroyed. In the period these two produces three block sections surrounded by a fault system ring, where the Notopuro Formation is folded and several parasitic cones occur such as Mount Turun, Mount Kendalisodo and Mount Mergi. Period third, Mount Ungaran is formed through the center of the Old Ungaran eruption that produces a lot of lava flows that compose between basaltic and andesitic. Figure 1 shows the study case location.

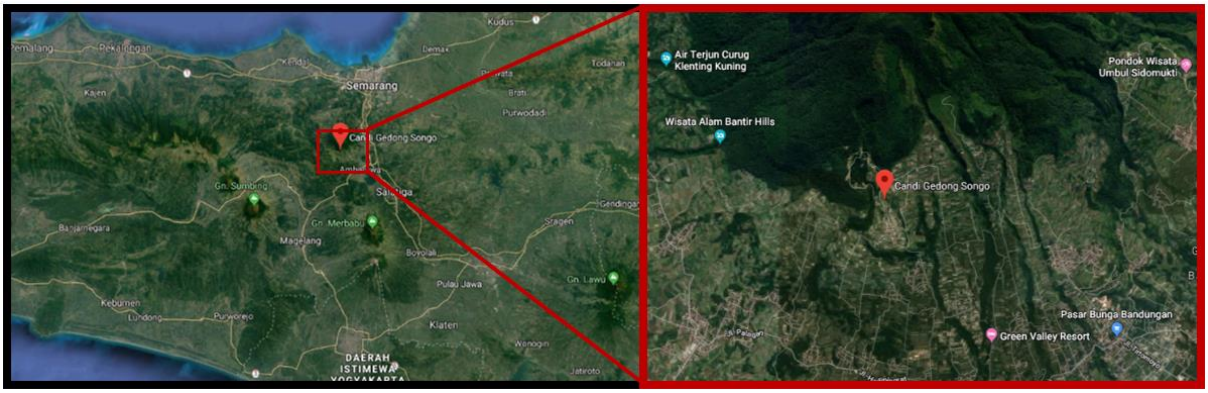


Figure 1: Location of study case research area.

MANIFESTATION

Thermal manifestations of Gedongsongo are in the form of fumaroles, hot springs and steaming ground. The active thermal manifestations mostly occur in the western part of a small creek on the southern flank of Ungaran summit. Measured temperatures made using a thermistor at the vent of fumaroles (size 0.75 m x 0.50 m) reaches 85 ºC (measured in November 2008) with significant mass flow rate. The fumarole discharges from steep cliff; whereas steaming ground (45 m x 30 m) with similar temperatures coexists in higher topography. This suggests that fumaroles were formed due to heated ground water which in bisected topography. The temperature of hot spring (eastern part) and steaming ground (southern part) reaches about 40 ºC and 50 ºC, consecutively. In the eastern part of the creek exist relic manifestations. There are many dead trees covered by sulphur and mud. The sulphur odor can be recognized at very close distance, and there are tiny fractures over the ground also covered by sulphuric mud interpreted as relic warm or hot spring channel mouth. The altered ignimbrite and andesitic rocks reveal a high alteration intensity (0.8 of 1 AI of Browne, 1999) and pervasive silica replacement is also present; there are not many feldspar left. Relic epidote also appears at some outcrops. The distribution of manifestations shows a N-S alignment, parallel with steep cliff (and small creek) which possibly formed due to a collapse structure or normal faulting as commonly occur in volcanic regions. This permeable structure is considered to control the convective heat transfer. A silicified fracture indicating a normal fault is found at the relic steaming ground at northern part. There is no relic epidote in this site (Sinuhaji, 2014).

GEOTOURISM

Geotourism (geotourism) is a special interest tourism by utilizing all the potential of natural resources, so that it is necessary to increase enrichment of insight and understanding the process of the natural phenomenon (Nainggolan, 2016).

Geotourism is a form of special interest tourism activity that focuses primarily on the geological appearance of the earth's surface as well as what it contained in it in order to encourage understanding educational purposes of the environment, nature and culture, and further as a form of appreciation, conservation activities, and having concern for the sustainability of local wisdom.

In order to join the Global Geopark Network (GGN) forum, UNESCO has set several criteria that must previously be met in line with UNESCO's International Congress of Geotourism AROUCA Declaration, including: (1) Size of regional parameters. The size of the regional parameters that will be used as a geopark must have clear limits, large surface area to cover cultural and economic development activities. In addition, the area proposed as a geopark must have an important and international geological heritage site, has scarcity, scientific value and beauty. Including the integration with the wisdom of the cultural governance of the surrounding local community; (2) Management management. The geopark principle includes the existence of a management body and a comprehensive development plan; (3) Economic development. One of the strategic goals of geopark formation is to stimulate economic activity and promote sustainable development. Geotourism destinations is often expected to be a pillar of national economic development; (4) Educational aspects. A geopark must provide and support equipment and activities for the development of science, especially geo-science knowledge and concepts of protection to the public. Some basic infrastructure, such as information centers, museums, and the development of geopark routes are important to support public educations; (5) Environmental conservation aspects. Aside from being a protected area, the geopark is a means of local socio-economic development. Geopark area managers are responsible for ensuring the protection of geological heritage that has been carried out in accordance with local traditional values and in accordance with applicable regulations. The enlightenment of geological phenomena that have historical value is indispensable in the management of geopark.

DISCUSSION

Geotourism can be used as a medium for the dissemination of natural science, environmental education, and nature conservation which in the end is expected to realize sustainable geological tourism development. Principles that must be considered in geotourism planning, development and management should be the following management guidelines.

The first principle, the geological object that is used as an attraction for geotourism is in fact a result of geological processes. Geotourism requires natural and natural landscapes, not artificial or artificial human nature. Authenticity in nature-based attractiveness has been alluded to in the criteria of natural tourist attraction that have been previously stated. That the criteria for natural tourist attraction must have a value of authenticity (originality and authenticity). The physical aspects that are used as tourist attractions can be in the form of geological conditions, types of rocks along with the mineral content in them, or other things that are still related to geology. Figure 2 shows the Gedongsongo surface manifestation.



Figure 2: Gedongsongo surface geothermal manifestations

The second principle is that geotourism management must be sustainable, meaning that the development and management of geotourism must be sustainable so that its sustainability can be maintained. Not only in tourism, in any business, long-term sustainability is a main consideration in management. The concept of long-term development in question is sustainable development. Sustainable development is development to meet the needs of the present without damaging or decreasing the ability of future generations to fulfill their needs (World Commission on Environment and Development, 1987 and the United Nations Commission for Sustainable Development 1999). A more specific formulation in sustainable tourism is fulfilling current tourism needs while protecting and increasing opportunities to meet future tourism needs, while preserving natural sustainability, fair to the economic and social culture of the community. This principle is considered in managerial to manage all resources in such a way, so that the economy, social, and aesthetic needs can be fulfilled while maintaining the values of cultural wisdom, important ecological protection, diversity of biological elements and other life support systems (Insula in Berno & Bricker, 2001).

The third principle, the effort to make geotourism a special interest tourism activity by utilizing all the potential of natural resources, so that it is necessary to increase enrichment of insight and understanding the process of natural physical phenomena. Examples of geotourism objects are volcanoes, lakes, hot springs, beaches, rivers, etc. which of course have aspects in the field of education as geodiversity knowledge of the diversity of the earth that needs to be preserved (Nainggolan, 2016).

Geotourism destinations should be equipped with clear and easy to understand information systems. With a good information system, for example about the history of the formation of geological collisions, tourists are expected to understand the processes of natural processes that occur. With the information, the community is also expected to be aware not to damage the beauty of the environment around geotourism.

Education Tour is a form of packaging tour that is suitable for geotourism. The Education Tour is a tour that is intended to provide an overview, comparative study or knowledge about the field of education or science that he visits. This education tour is carried out to develop insights and knowledge for the actors. Actors who take educational trips usually don't attach too much importance to excessive luxury in carrying out travel activities. But it requires more self-enrichment, in the form of new knowledge and experience.

The fourth principle is a locally beneficial. Which means that the existence of geotourism is expected to be able to provide benefits to the community / community around it. These benefits can be in the form of positive impact contributions that can be enjoyed such as: economic growth, progress in socio-cultural values, improvement of environmental quality or others (Hermawan, 2016; Hermawan, 2016).

With geotourism, it is expected that the development process in these tourist areas will increase. One management model that is suitable for geotourism by adopting community / community-based tourism, otherwise known as Community Based Tourism (CBT). In CBT, tourism is initiated with local communities, developed by local communities, and benefits from tourism are expected to be enjoyed by local communities themselves.

The fifth principle is Tourist satisfaction. Realizing tourist satisfaction means that geotourism management can provide birth and inner satisfaction for tourists who visit it. Tourist satisfaction can be obtained by good tourism management, at least able to present a beautiful, unique, original and valuable tourist attraction along with appropriate supporting

facilities and excellent service (Hermawan, 2017). Improved safety is also considered a very appropriate effort in ensuring tourist satisfaction with tourist destinations.

CONCLUSION

In conclusion, geotourism is presented as a solution on how to utilize geological resources along with its various dynamics for tourism activities, educational and social awareness and environmentally sound economy. The paradigm in geotourism management is how tourism management is able to optimize the potential of nature (geology) to be an added value for the economic well-being of local communities, while at the same time being able to minimize the potential for natural damage.

In order to integrate geothermal manifestation with geotourism, certain components in line with UNESCO's International Congress of Geotourism AROUCA Declaration are compulsory, such as: a) Preplanning of various aspects ranging from Environmental Impact Analysis, effective land use determination between production and geopark area, tourist attractions establishment based on geothermal manifestation, etc.; b) Eco-friendly construction method; c) Active involvement and employment of local citizens in establishing the geopark; d) Integrating and prioritizing the use of technology and mobile application over the use of traditional information posters; e) Providing easily understood, intelligible, and accessible knowledge; f) Building local identity and promote authenticity and uniqueness in the area. This ensures that the environment and its inhabitants obtain social justice, environmental integrity and sustainable economic development while also having a better understanding of geothermal energy development.

REFERENCES

ASEAN Community Based Tourism Standard, (2016), Jakarta: ASEAN Secretariat

Berno, T., and Bricker, K., (2001), "Sustainable Tourism Development: The Long Road from Theory to Practice". International Journal of Economic Development.

Hague, Browne, P., R., L., (1999), "Hydrothermal Alteration". Lecture note 655.611, Geothermal Institute, Auckland University

Hermawan, H., (2016), "Dampak Pengembangan Desa Wisata Nglanggeran Terhadap Ekonomi Masyarakat Lokal". Jurnal Pariwisata

Hermawan, H., (2016), "Dampak Pengembangan Desa Wisata Nglanggeran Terhadap Sosial Budaya Masyarakat Lokal". In Seminar Nasional Ilmu Pengetahuan dan Teknologi Komputer Nusa Mandiri Pertama Tahun 2016

Hermawan, H., (2017)., "Pengaruh Daya Tarik Wisata, Keselamatan dan Sarana Wisata Terhadap Kepuasan serta Dampaknya terhadap Loyalitas Wisatawan : Studi Community Based Tourism di Gunung Api Purba Nglanggeran". Wahana Informasi Pariwisata : Media Wisata

Hose, T., (2008), "Towards a history of geotourism: definitions, antecedents and the future". In The history of geoconservation, (Eds.) C. Burek, C Prosser, Geological Society, Bath,

Naidoo, P., Ramseook-Munhurrun, P., and Seegoolam, P., (2011), "An Assessment of Visitor Satisfaction with Nature-Based Tourism Attractions". International Journal of Management and Marketing Research, The Institute for Business and Finance Research.

Nainggolan, R., (2016), "Informasi Geologi Lingkungan Berbasis Partisipasi Masyarakat debagai Kawasan Geowisata Danau Toba di Kabupaten Samosir". Jurnal Penelitian Pendidikan Sosial Dan Humaniora,

Rezky, Y., Zarkasyi, A., Risdianto, D., (2012), "Sistem panas bumi dan model konseptual daerah panas bumi Gunung Ungaran, Jawa Tengah". Buletin Sumber Daya Geologi, 7 (3), 109 – 117

The International Congress of Geotourism, (2011), "Arouca Declaration". The International Congress of Geotourism

UNESCO, (2006), "Guidelines and Criteria for National Geoparks seeking UNESCO's assistance to join the Global Geoparks Network (GGN)"

UNESCO, (2008), "Members of the Global Geoparks Network". UNESCO Global Geopark Network (GGN)

Van Bemmelen, R., W., (1970), "The Geology of Indonesia". Martinus Nijhoff, The Hague

This page is intentionally left blank



ISBN 978-602-52132-2-9



Asosiasi Panasbumi Indonesia (API)
Apartemen Menteng Square, BR-9 Tower B
Jl. Matraman No 30 E, Jakarta Pusat - 10320 Indonesia
Email: api.inaga@yahoo.co.id